

THE PHYSICAL REVIEW

A JOURNAL OF EXPERIMENTAL AND
THEORETICAL PHYSICS

CONDUCTED BY
THE
AMERICAN PHYSICAL SOCIETY

BOARD OF EDITORS

Managing Editor JOHN T. TATE, University of Minnesota, Minneapolis
I. S. BOWEN, R. S. MULLIKEN, H. D. SMYTH, E. U. CONDON, C. J. DAVISSON,
F. K. RICHTMYER, K. F. HERZFELD, A. W. HULL, F. W. LOOMIS

VOLUME 35, SECOND SERIES
JANUARY-JUNE, 1930

THE PHYSICAL REVIEW
MINNEAPOLIS, MINN.

Composed, Printed and Bound by
The Collegiate Press
George Banta Publishing Company
Menasha, Wisconsin

CONTENTS

JANUARY 1, 1930

An X-Ray Search for the Origin of Ferromagnetism - - - - -	J. C. STEARNS	1
Form of the X-Ray Diffraction Bands for Regular Crystals of Colloidal Size - - - - -	CARLETON C. MURDOCK	8
Spectral Phenomena in Spark Discharges - - - - -	J. W. BEAMS	24
Vibrational Quantum Analysis and Isotope Effect for the Lead Oxide Band Spectra - - - - -	SYDNEY BLOOMENTHAL	34
Fine Structure Analysis of the Bands in the <i>A</i> and <i>D</i> Systems of Lead Oxide - - - - -	ANDREW CHRISTY AND SYDNEY BLOOMENTHAL	46
Laboratory Method of Producing High Potentials - - - - -	G. BREIT, M. A. TUVE AND O. DAHL	51
Application of High Potentials to Vacuum-Tubes - - - - -	M. A. TUVE, G. BRIET AND L. R. HAFSTAD	66
Anode Spots and their Relations to the Absorption and Emission of Gases by the Electrodes of a Geissler Discharge - - - - -	C. H. THOMAS AND O. S. DUFFENDACK	72
Electron Velocities in High Frequency Discharge in Hydrogen - - - - -	CHARLES J. BRASEFIELD	92
Secondary Electrons of High Velocity from Metals Bombarded with Cathode Rays - - - - -	PAUL BERTHOLD WAGNER	98
Electrodynamic Damping in Pulsating Stars - - - - -	ROSS GUNN	107
Letters to the Editor - - - - -		112
Book Reviews - - - - -		118

PROCEEDINGS OF THE AMERICAN PHYSICAL SOCIETY

Chicago Meeting, November 29 and 30, 1929; Minutes and Abstracts 1-42; Author Index - - -	119
Berkeley Meeting, December 7, 1929; Minutes and Abstracts 1-18; Author Index - - -	132

JANUARY 15, 1930

Probability and Critical Potentials for the Formation of Multiply Charged Ions in Hg Vapor by Electron Impact - - - - -	WALKER BLEAKNEY	139
Experiments on the Reported Fine Structure and the Wave-Length Separation of the $K\beta$ Doublet in the Molybdenum X-Ray Spectrum - - - - -	SAMUEL K. ALLISON AND JOHN H. WILLIAMS	149
Intensity Maxima in the Continuous Helium Spectrum - - - - -	JANE M. DEWEY	155
Schottky Effect and Contact Potential Measurements on Thoriated Tungsten Filaments - - - - -	NEIL B. REYNOLDS	158
Temperature Dependence of Field Currents - - - - -	N. A. DE BRUYNE	172
Variable Flow in Pipes - - - - -	H. BATEMAN	177
Ionic Mobilities in Cl_2 and in Cl_2 -Air Mixtures - - - - -	LEONARD B. LOEB	184
On Mechanical and Magnetic Factors Influencing the Orientation and Perfection of Bismuth Single-Crystals - - - - -	ALEXANDER GOETZ	193
Letters to the Editor - - - - -		208

FEBRUARY 1, 1930

Capture of Electrons by Alpha-Particles - - - - -	ARTHUR H. BARNES	217
Relative Intensities of Super-Multiplet Lines - - - - -	JAMES H. BARTLETT, JR.	229
Extension of the Spectrum of Thallium II - - - - -	STANLEY SMITH	235
Ionization in the Upper Atmosphere; Variation with Longitude - - - - -	E. O. HULBURT	240
Surface Heat of Charging - - - - -	KARL F. HERZFELD	248
Change of Spacing of Positive Column Striations with Temperature - - - - -	F. M. SPARKS AND CHARLES T. KNIPP	259
Persistence of Velocity and the Theory of Second Order Gas Reactions - - - - -	LOUIS S. KASSEL	261
Young's Modulus Determined with Small Stresses - - - - -	DAROL K. FROMAN	264

Rochelle Salt as a Dielectric - - - - -	C. B. SAWYER AND C. H. TOWER	269
Sedimentation Equilibria of Colloidal Particles - - - - -	NORRIS JOHNSTON AND LYNN G. HOWELL	274
Letters to the Editor - - - - -	- - - - -	283
Book Reviews - - - - -	- - - - -	287

PROCEEDINGS OF THE AMERICAN PHYSICAL SOCIETY

Des Moines Meeting, December 30 and 31, 1929; Minutes and Abstracts 1-32; Author Index - - -	289
--	-----

FEBRUARY 15, 1930

Sodium and Magnesium Lines in the Far Ultraviolet, and the Quantitative Application of the Irregular Doublet Law to Isoelectronic Sequences - - - - -	J. E. MACK AND R. A. SAWYER	299
New Measurements in the Fourth Positive CO Bands - - - - -	ROGER S. ESTEY	309
Fine Structure of the Beryllium Fluoride Bands - - - - -	F. A. JENKINS	315
Relativity and Aether Drift - - - - -	W. F. G. SWANN	336
Spatial Distribution of Photoelectrons - - - - -	S. E. SZCZENIEWSKI	347
Reflection of Beams of the Alkali Metals from Crystals - - - - -	JOHN B. TAYLOR	375
Emission of Positive Ions from Tungsten and Molybdenum - - - - -	LLOYD P. SMITH	381
On the Early Stages of Electric Sparks - - - - -	ERNEST O. LAWRENCE AND FRANK G. DUNNINGTON	396
New Regularity in the List of Existing Nuclei - - - - -	HENRY A. BARTON	408
Black Bodies in the Extreme Infrared - - - - -	C. HAWLEY CARTWRIGHT	415
Peltier and Thomson Effects for Bismuth Crystals - - - - -	H. D. FAGAN AND T. R. D. COLLINS	421
Shatter Oscillations, Their Nature and Theory - - - - -	E. H. KENNARD	428
Letters to the Editor - - - - -	- - - - -	434

MARCH 1, 1930

Nuclear Spin and Hyperfine Structure - - - - -	H. E. WHITE	441
Second Spark Spectrum of Antimony, and a Note on the First Spark Spectrum of Tin - - - - -	R. J. LANG	445
Emission Spectrum of Benzene in the Region 2500-3000A - - - - -	J. B. AUSTIN AND IAN ARMSTRONG BLACK	452
Note on the Theory of the Interaction of Field and Matter - - - - -	J. R. OPPENHEIMER	461
Effect of End Losses on the Characteristics of Filaments of Tungsten and other Materials - - - - -	IRVING LANGMUIR, SAUNDERS MACLANE AND KATHARINE B. BLODGETT	478
Absorption Coefficient for Slow Electrons in Cadmium and Zinc Vapors - - - - -	ROBERT B. BRODE	504
Cohesion in Monovalent Metals - - - - -	J. C. SLATER	509
Stability of Metallic Crystal Lattices - - - - -	R. H. CANFIELD	530
Influence of Temperature on Polarization Capacity and Resistance - - - - -	E. E. ZIMMERMAN	543
On the Solution of Certain Cases of the General Equation of Diffusion - - - - -	R. L. PEEK, JR.	554
Letters to the Editor - - - - -	- - - - -	562
Book Reviews - - - - -	- - - - -	566

MARCH 15, 1930

Separation of Angles in the Two-Electron Problem - - - - -	G. BREIT	569
Interpretation of Pauli's Exclusion Principle - - - - -	E. U. CONDON AND J. E. MACK	579
X-Ray Scattering Powers of Nickel and Oxygen in Nickel Oxide - - - - -	RALPH W. G. WYCKOFF	583
Effect of Hyperfine Structure Due to Nuclear Spin on Polarization of Resonance Radiation - - - - -	A. ELLETT	588
Spectroscopic Evidence of Two Types of Ammonia Molecule - - - - -	JOSEPH W. ELLIS	595
Afterglow in Air - - - - -	JOSEPH KAPLAN	600
Infrared Absorption of Some Organic Liquids - - - - -	E. K. PLYLER AND THEODORE BURDINE	605
Measurement of the Dielectric Constant and Index of Refraction of Water and Aqueous Solutions of KCl at High Frequencies - - - - -	F. H. DRAKE, G. W. PIERCE, AND M. T. DOW	613
Measurements of the Dielectric Constants of Conducting Media - - - - -	JEFFRIES WYMAN, JR.	623
On the Anomalous Rotation of the Sun - - - - -	ROSS GUNN	635
Simple Equation for the Joule-Thomson Effect in Real Gases - - - - -	JAMES A. BEATTIE	643
Letters to the Editor - - - - -	- - - - -	649
Book Reviews - - - - -	- - - - -	654

PROCEEDINGS OF THE AMERICAN PHYSICAL SOCIETY

New York Meeting, February 21, 22, 1930; Minutes and Abstracts 1-63; Author Index - - -	656
---	-----

CONTENTS

V

APRIL 1, 1930

Plasmoidal High-Frequency Oscillatory Discharges in Non-Conducting Vacua - R. W. WOOD	673
Ionization of Helium by Potassium Positive Ions - - - - - RICHARD M. SUTTON AND J. CARLISLE MOUZON	694
On the Potential Relations in the Striated Positive Column of Electrical Discharges through Hydrogen - - - - - JOHN ZELENY	699
On the Distribution in Time of the Scintillations Produced by the α -Particles from a Weak Source - - - - - N. FEATHER	705
L Series Spectra of the Elements from Calcium to Zinc - - - - - C. E. HOWE	717
Cybotatic (Molecular Group) Condition in Liquids: the Nature of the Association of Octyl Alcohol Molecules - - - - - G. W. STEWART	726
Barkhausen Effect, II. Determination of the Average Size of the Discontinuities in Magnetization - - - - - RICHARD M. BOZORTH AND JOY F. DILLINGER	733
Measurement of the Intensity of High Frequency Magnetic Fields - - - - - ROY H. MORTIMORE	753
On the Fundamental Constitutive Equations in Electromagnetic Theory - - - - - C. KAPLAN AND F. D. MURNAGHAN	763
Equilibrium between Matter and Radiation - - - - - LOUIS S. KASSEL	778
On the Interaction of Stark Effect and Electron Spin in Alkali Atoms - - - - - VLADIMIR ROJANSKY	782
Alternating Intensities and Isotope Effect in the Blue-Green Absorption Bands of Li_2 - - - - - A. HARVEY AND F. A. JENKINS	789
Intensity Measurements in the Arc Spectrum of Thallium - - - - - O. U. VONWILLER	802
Frequency of Occurrence of the Disintegrative-Synthesis of Oxygen 17 from Nitrogen 14 and Helium - - - - - WILLIAM D. HARKINS AND A. E. SCHUE	809
Some Investigations into the Velocity of Sound at Ultrasonic Frequencies using Quartz Oscillators - - - - - CHARLES D. REID	814
Velocity of Propagation of Longitudinal Waves in Liquids at Audio-Frequencies - - - - - LOUIS G. POOLER	832
Dielectric Constant and the Molecular Structure of CS_2 - - - - - C. T. ZAHN	848
Variation of Dielectric Constant with Temperature, I. Electric Moments of the Carbon Bisulphide and Nitrous Oxide Molecules - - - - - CHRISTIAN H. SCHWINGEL AND JOHN W. WILLIAMS	855
Numerical Determination of Characteristic Numbers - - - - - W. E. MILNE	863
Letters to the Editor - - - - -	868
Book Reviews - - - - -	871

APRIL 15, 1930

On the Use of the Energy-Momentum Principle in General Relativity - - - - - RICHARD C. TOLMAN	875
On the Use of the Entropy Principle in General Relativity - - - - - RICHARD C. TOLMAN	896
On the Weight of Heat and Thermal Equilibrium in General Relativity - - - - - RICHARD C. TOLMAN	904
Determination of Electron Distributions from Measurements of Scattered X-Rays - - - - - ARTHUR H. COMPTON	925
Two Notes on the Probability of Radiative Transitions - - - - - J. R. OPPENHEIMER	939
Boundary Conditions and the Meaning of Wave Groups in Wave Mechanics - - - - - H. A. WILSON	948
Heat of Dissociation of Carbon Monoxide - - - - - JOSEPH KAPLAN	957
Band Spectrum of Silver Chloride - - - - - BROOKS A. BRICE	960
Relation between the Intensity and Position of the Overtones of Some Organic Liquids - - - - - P. E. SHEARIN	973
Magnetic Susceptibility of Rubidium - - - - - C. T. LANE	977
Secondary Electrons from Contaminated Surfaces - - - - - PAUL L. COPELAND	982
Thomson Effect in Zinc Crystals - - - - - L. A. WARE	989
E. M. F., Resistance, and Capacitance Phenomena in Photovoltaic Cells Containing Grignard Reagents - - - - - H. E. HAMMOND	998
Thermal Convection - - - - - R. W. BABCOCK	1008
Letters to the Editor - - - - -	1014
Book Reviews - - - - -	1017

MAY 1, 1930

Electron Distribution of Magnesium Oxide - - - - - E. O. WOLLAN	1019
Predissociation of Diatomic Molecules from High Rotational States - - - - - D. S. VILLARS AND E. U. CONDON	1028

New Measurements on the Fourth Positive Bands of Carbon Monoxide - - - -	L. B. HEADRICK AND G. W. FOX	1033
Absorption Bands of Ammonia Gas in the Visible - - - -	RICHARD M. BADGER	1038
Evidence for Quantization from the Electric Polarization of Acetic Acid Vapor - - -	C. T. ZAHN	1047
An Extension of Van Vleck's Theory of Dielectric Polarization - - - -	C. T. ZAHN	1056
On a New Photoelectric Effect in Alkali Cells - - - -	ERICH MARX	1059
Oscillations in the Glow Discharge in Neon - - - -	GERALD W. FOX	1066
Conductivity of a High Frequency Discharge in Hydrogen - - - -	CHARLES J. BRASEFIELD	1073
On the Cathode of an Arc Drawn in Vacuum - - - -	R. TANBERG	1080
Reflection of Lithium Ions from Metal Surfaces - - - -	R. B. SAWYER	1090
Zodiacal Light and the Gegenschein as Phenomena of the Earth's Atmosphere - - -	E. O. HULBURT	1098
Polar Molecules, Their Contribution to Energy Loss in Dielectrics - - - -	F. HAMBURGER, JR.	1119
Letters to the Editor - - - -		1125
Book Reviews - - - -		1135

MAY 15, 1930

Space-Distribution of X-Ray Photoelectrons Ejected from the <i>K</i> and <i>L</i> Atomic Energy-Levels - - -	CARL D. ANDERSON	1139
Hyperfine Structure in Neutral Manganese, Mn I - - -	H. E. WHITE AND R. RITSCHL	1146
Mean Lives of Lines of Mercury Triplet $2^3P_{012} - 2^3S_1$ - - -	ROBERT H. RANDALL	1161
Hydrogen Atom in the Stark Effect - - - -	FRANCIS G. SLACK	1170
A Possible Origin of the Band at 2540 in the Spectrum of Mercury Vapor - - -	R. ROLLEFSON	1177
Ionization of Hydrogen by Single Electron Impact - - - -	WALKER BLEAKNEY	1180
Electron Energy Losses in Mercury Vapor - - - -	CASTLE W. FOARD	1187
Motion of Slow Positive Ions in Gases - - - -	JAMES S. THOMPSON	1196
Absorption Coefficient for Slow Electrons in Gases - - - -	C. E. NORMAND	1217
On the Concentration of Metastable Mercury Atoms - - - -	E. GAVIOLA	1226
Most Probable 1930 Values of the Electron and Related Constants - - -	ROBERT A. MILLIKEN	1231
Uniform Positive Column of an Electric Discharge in Mercury Vapor - - -	THOMAS J. KILLIAN	1238
Absorption of Resonance Radiation in Mercury Vapor - - - -	ANCIL R. THOMAS	1253
Dispersion Formula and Raman Effect for the Symmetrical Top - - -	MORRIS MUSKAT	1262
Location of the Electromotive Force in the Photovoltaic Cell - - -	W. NORWOOD LOWRY	1270
Viscosity of Compressed Gases - - - -	JAMES H. BOYD, JR.	1284
Letters to the Editor - - - -		1298
Book Reviews - - - -		1301

JUNE 1, 1930

Penetration of a Potential Barrier by Electrons - - - -	CARL ECKART	1303
Quantum Mechanics of Electrons in Crystals - - - -	PHILIP M. MORSE	1310
An Extension of Houston's and Slater's Multiplet Relations - - -	S. GOUDSMIT	1325
Resonance Separations in Configurations of Type p^6s and d^9s - - -	O. LAPORTE AND D. R. INGLIS	1337
Singlet-Triplet Interval Ratios for sp , sd , sf , p^6s and d^9s Configurations - - -	E. U. CONDON AND G. H. SHORTLEY	1342
Intensities of Vibration-Rotation Bands with Special Reference to Those of HCl - - -	J. L. DUNHAM	1347
Raman Effect in HCl-Gas - - - -	R. W. WOOD AND G. H. DIEKE	1355
Photoelectric and Thermionic Properties of Platinum Coated Glass Filaments - - -	A. KEITH BREWER	1360
Role of the Core Metal in Oxide Coated Filaments - - - -	E. F. LOWRY	1367
On the Theory of the Solar Corona - - - -	E. O. HULBURT	1379
Distribution of Non-Reacting Fluids in the Gravitational Field - - -	MORRIS MUSKAT	1384
Recombination of Ions in Air and Oxygen in Relation to the Nature of Gaseous Ions - - -	OVERTON LUHR	1394
Letters to the Editor - - - -		1405
Book Reviews - - - -		1410
Erratum - - - -		1414

PROCEEDINGS OF THE AMERICAN PHYSICAL SOCIETY

Washington Meeting, April 24 to 26, 1930; Minutes and Abstracts 1-114; Author Index - -	1415
---	------

JUNE 15, 1930

Possible Effects of Nuclear Spin on X-Ray Terms - - - - -	G. BREIT	1447
On the Reflection of the $K\alpha$ Line of Carbon from a Glass Mirror - - - - -	J. THIBAUD	1452
Molybdenum L -Series Wave-Lengths by Ruled Gratings - - - - -	J. M. CORK	1456
Independence of X-Ray Absorption on Temperature - - - - -	J. A. BEARDEN	1463
Effect of an Electric Field on the X-Ray Diffraction Pattern of a Liquid - - - - -	RONALD L. MCFARLAN	1469
Resolving Power of Calcite for X-Rays and the Natural Widths of the Mo $K\alpha$ Doublet - - - - -	SAMUEL K. ALLISON AND JOHN H. WILLIAMS	1476
Vibrational Quantum Analysis of the Blue-Green Bands of Magnesium Oxide - - - - -	P. N. GHOSH, P. C. MAHANTI AND B. C. MUKKERJEE	1491
Zeeman Effect in the OH Bands - - - - -	GERALD M. ALMY	1495
Zeeman Effect in the Red CaH Bands - - - - -	WILLIAM W. WATSON AND WILLIAM BENDER	1513
Infrared Absorption of some Organic Liquids Under High Resolution - - - - -	R. BOWLING BARNES	1524
Quantum Kinetics and the Planck Equation - - - - -	GILBERT N. LEWIS	1533
Contribution to the Quantum Mechanical Theory of Radioactivity and the Dissociation by Rotation of Diatomic Molecules - - - - -	OSCAR KNEFLER RICE	1538
Perturbations in Molecules and the Theory of Predissociation and Diffuse Spectra, II - - - - -	OSCAR KNEFLER RICE	1551
Concerning the Absorption Method of Investigating β -Particles of High Energy: The Maximum Energy of the Primary β -Particles of Mesothorium 2 - - - - -	N. FEATHER	1559
Motion of Electrons in Carbon Monoxide - - - - -	H. B. WAHLIN	1568
Magnetic Susceptibility of Gases. I. Pressure Dependence - - - - -	FRANCIS BITTER	1572
Letters to the Editor - - - - -		1583
Book Reviews - - - - -		1588
Index to Volume 35 - - - - -		1589

THE PHYSICAL REVIEW

AN X-RAY SEARCH FOR THE ORIGIN OF FERROMAGNETISM

BY J. C. STEARNS

RYERSON PHYSICAL LABORATORY, UNIVERSITY OF CHICAGO

(Received November 19, 1929)

ABSTRACT

A sensitive null method, employing two crystals and two ionization chambers, was used to detect any change in intensity of an x-ray beam reflected from a magnetic crystal, when this magnetic crystal was magnetized. This method was capable of detecting from 1.0 to 0.1 percent change in intensity, according to the intensity of the reflected beam. Crystals of magnetite and silicon steel were used. No change of intensity was observed, although the theoretical change was several times that which could have been detected. The change in intensity of the x-ray beam was computed on the basis of the alteration of the structure factor due to orientation of electronic orbits by the magnetic field. It is concluded that electrons revolving in orbits within the atom cannot account for ferromagnetism. The models of Honda and Ehrenfest are briefly discussed. On the basis of present atomic models and present experimental evidence it appears that the ultimate magnet should be identified with the spinning electron.

SEVERAL experiments have been reported¹ in which x-rays have been used to study the nature of the ultimate magnetic particle. From these it has been concluded that the most minute crystal aggregations in solid iron are not oriented by a magnetic field, that the ultimate magnet cannot be a group of atoms such as the chemical molecule, and finally, that the atom as a unit cannot account for ferromagnetism. On the basis of present atomic models three possible ultimate magnetic particles remain: the atomic nucleus, the spinning electron, or electrons revolving in inner orbits. The following experiment was performed primarily to ascertain whether electrons revolving in the inner orbits may be responsible for ferromagnetism.

THE EXPERIMENT

The apparatus used is indicated in Fig. 1. It is essentially a refinement of that employed by A. H. Compton and Rognley. The x-ray tube had a water-cooled molybdenum target, and could be operated at 35 milliamperes

¹ M. de Broglie, *Le Radium* 10, 186 (1913). K. T. Compton and E. A. Trousdale, *Phys. Rev.* 5, 315 (1915). A. H. Compton and Oswald Rognley, *Phys. Rev.* 16, 464 (1920). T. D. Yensen, *Phys. Rev.* 31, 714 (1928).

and 50 kilovolts. One portion of the x-ray beam fell on C' , a crystal of magnetite or silicon steel, which reflected the $K\alpha$ line into ionization chamber I' . Another portion of the beam passed above C' and was incident upon C'' , a calcite crystal, from which the $K\alpha$ line was reflected into chamber I'' . The electrodes of the ionization chambers were connected to the same pair of electrometer quadrants, while one chamber was maintained at a positive and the other at a negative potential. S' and S'' were adjustable slits. An intense beam of x-rays was allowed to fall upon the crystals, and the slits were adjusted until the electrometer charged up at a very slow rate. With other conditions unaltered the crystal C' was magnetized and the rate of deflection of the electrometer again taken. In order to make a comparison of successive readings, two readings taken with the electromagnet unenergized alternated with two successive readings with the magnet energized. From a set of twenty-five to fifty readings for each order the mean change of

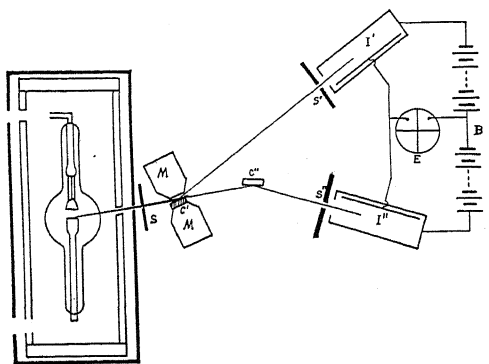


Fig. 1. Diagrammatic sketch of apparatus.

rate due to magnetization was determined. A sheet of aluminium, which absorbed four percent of the beam was then placed in front of S' and the resulting change in the rate at which the electrometer was being charged observed. Then: $\text{Change of rate due to magnetization} / \text{Change in rate due to absorption by aluminium} \times 4 = \text{percent change in intensity due to magnetization}$.

The electromagnet M had a laminated core about which were wound five thousand turns of number 23 copper wire. The air gap was about 2 mm. Demagnetization was secured by successively reversing and gradually decreasing the current. The magnetic induction was measured by means of a commercial flux meter. The calcite crystal was fixed to a non-magnetic mounting which was placed outside the magnetic field and could be rotated independently of the electromagnet and the magnetic crystal. The x-ray tube was mounted inside a heavy wrought iron pipe, the ends of which were closed by iron plates one inch in thickness. The ionization chambers were duplicates, and each was filled with argon.

DISTURBING EFFECTS AND THEIR ELIMINATION

It was necessary to mount the crystal C' with unusual care in order to avoid motion of the crystal relative to the incident beam when the magnet

was energized. It was found also that the establishing of the magnetic field sufficient in strength to produce magnetic saturation in the crystal shifted the electrometer needle through several degrees, and changed the current sensitivity of the electrometer. By using a mica needle plated with a suitable combination of gold and platinum this effect was overcome. In testing the sensitivity the deflection rates were compared with and without the magnetic field, using radium emanation tubes as a source of ionization.

Before the tube was enclosed in the iron pipe, the field in the region of the x-ray tube was found to be sufficient to move the focal spot 0.2 or 0.3 mm. This shift produced a change in the intensity of the reflected x-rays of the order of 1 percent, which changed in sign with a reversal of the field. When the tube was placed in the iron pipe, tests showed the shielding to be adequate.

CALCULATION OF CHANGE IN REFLECTION DUE TO ORIENTATION OF AN ELECTRON ORBIT

The following method was used in computing the theoretical change in the intensity of the reflected beam due to K or L electrons being oriented by an external field so that their magnetic moments were parallel to this field. A. H. Compton² shows that

$$W_n = K F_n^2, \quad (1)$$

where W_n is the total energy diffracted by a small crystal and F_n is the structure factor of the atom, while the subscript n refers to the order in question, and K is a factor of proportionality. If the primed letters refer to the energy and structure factor respectively when the crystal is magnetized and the unprimed letters to the same quantities when the magnetic crystal is unmagnetized, then

$$\frac{W'}{W} = \frac{(F_n')^2}{(F_n)^2} = \frac{[F_n + (F_n' - F_n)]^2}{(F_n)^2} = 1 + \frac{2\Delta F_n}{F_n}. \quad (2)$$

neglecting higher powers of ΔF_n . To calculate the change in intensity it is thus necessary to know the number of atoms affected by the magnetic field and the structure factors of the atom for the order in question when the crystal is magnetized and unmagnetized respectively.

The structure factor³ for the n th order of an electron moving at random over the surface of a spherical shell of radius r is

$$F_{en} = \frac{\sin 2\pi nr/D}{2\pi nr/D}, \quad (3)$$

where D is the grating space of the crystal. If magnetizing the crystal perpendicular to the reflecting face causes the orbit of an electron to lie in the plane of the reflecting face, its structure factor becomes unity, since the waves reflected by it are in phase with those from the middle of the atomic

² A. H. Compton, "X-rays and Electrons" p. 125.

³ Reference 2, p. 148.

layer. If without the magnetic field the orientation of the orbit is random, then

$$\Delta F_{en} = 1 - \frac{\sin 2\pi nr/D}{2\pi nr/D} \quad (4)$$

If, however, the crystal is magnetized parallel to the reflecting face, and the electron in question moves in a circle whose plane is perpendicular to the reflecting face, the structure factor for this electron becomes a Bessel function of the zero order,

$$F_{en}' = J_0(2\pi nr/D) \quad (5)$$

ΔF_{en} is then found in the same manner as in the preceding case.

If ΔF_{en} is the change in structure factor for each electron whose orbit is turned by the magnetic field, and if f is the number of electronic orbits per atom thus turned, the average change in structure factor is

$$\Delta F_n = f\Delta F_{en} \quad (6)$$

From Eq. (2) it follows that the ratio of the intensities when the crystal is magnetized and unmagnetized respectively is

$$(W'/W) = 1 + 2f(\Delta F_{en}/F_n) \quad (7)$$

To find the ratio f of the number of orbits oriented to the number of atoms, we may assume that each electronic orbit has a magnetic moment of one Bohr magneton. This ratio then becomes

$$\frac{1}{5589} \times \frac{\text{saturation intensity of magnetization}}{\text{number of atoms per molecule}} \times \frac{\text{molecular weight}}{\text{density}}$$

On this basis, in the case of magnetite, half of the atoms will have one atom oriented, i.e. $f=0.5$ while for silicon steel three orbits per two atoms will be turned around, i.e. $f=1.5$.

The structure factor F_n of the atom for any order may be determined if the structure factor for the first order is known and if the relative intensity reflected in each order is known. Equation (1) could then be used to give the structure factor. The ratio Z/F of the atomic number to the structure factor for the first order does not vary greatly with different atoms. In the cases of sodium and chlorine this ratio is 1.45 and 1.25 respectively. It is thus reasonable to assume the structure factor for the first order of the iron atom to be about 20 and that of the oxygen atom to be about 6.5. The intensities for the first three orders from the 110 planes of iron have been measured, thus permitting direct substitution* in (1) to find the atomic structure factor for orders 1 and 2. In the case of magnetite we may make use of the fact that the experimental values of F , for reflecting planes that are similar and similarly placed, are experimentally found to vary approximately inversely as the order. In computing the results for magnetite it has accordingly been assumed that $F_n = 20/n$ for the iron atom and $6.5/n$ for the oxygen atom.

* In making this substitution it is necessary to note that the factor K of Eq. (1) includes the trigonometric factor $(1 + \cos^2 2\theta)/\sin 2\theta$ (cf. A. H. Compton, reference 2).

For silicon steel these considerations are sufficient for determining $\Delta F_{en}/F_n$; but for magnetite it is necessary to know how a change in atomic structure factor will affect the intensity when the planes are neither similar nor similarly placed. Bragg⁴ has shown that the 110 planes may be represented by a single plane having a weight

$$56 + 112 \cos \pi n/4 + 168 \cos \pi n + 128 \cos \pi n/2,$$

where n is the order of the spectrum. The first three terms are the contributions due to the iron atoms, while the last term represents the contribution of the oxygen atoms. One may assume that both the oxygen and iron atoms are affected by the magnetic field or that either the iron or oxygen atoms have their electronic orbits oriented by the applied field. The first assumption seems the more reasonable and is the one here employed. It is seen that in the fourth order the planes made up of oxygen atoms cooperate with those made up of iron atoms, and a maximum change in intensity would result if only the oxygen atoms were influenced. This is due to the fact that the change in intensity per oxygen atom is greater than that per iron atom and the total number of atoms affected in either case must be the same. If only the iron atoms were influenced the effect would still be detectable, while the result given in the table is that based on the assumption that both iron and oxygen atoms are turned about by an external magnetic field. In the case of the fifth order all the planes may be represented by a plane of iron atoms of weight 90. In the sixth order all the 110 planes may be replaced by planes of iron atoms of weight 224 with planes of oxygen atoms of weight 128 midway between the iron planes. If both kinds of atoms are affected by the magnetic field the change in intensity would be too small to detect, while if the inner orbits of the iron atoms alone are oriented there should be a detectable increase in the intensity of the reflected x-ray beam. On the other hand a change in the oxygen atom alone should produce a decrease in intensity which would have been detected. Thus, by considering the fourth, fifth and sixth orders of magnetite, all possible cases have been considered, and the magnitude of the theoretical effect found is great enough for detection by the method employed whichever atom is affected by the magnetic field. The radii used for the K and L orbits were computed by use of Bohr's formula.

It appears that any reasonable assumptions regarding atomic structure factor or magnetic moment per electron orbit must lead to a predicted effect of the order of magnitude here calculated.

EXPERIMENTAL RESULTS

In the following table both the theoretical and experimental results are given. In the first column on the left the order is given. In the next column is given the theoretical ratio, $I'/I(K)$, of the integrated intensities reflected by the crystal when it is magnetized and unmagnetized respectively, assuming that the K electrons are the ones that orient themselves when the field is applied. In the next column is the same ratio for the case of the L electrons, while the last gives the experimental value.

⁴ W. H. Bragg, Phil. Mag. 30, 305 (1915).

TABLE I. Ratio of x-ray reflection from magnetized to that from unmagnetized crystals.

1. Magnetized perpendicular to the reflecting face			
Order	<i>Magnetite (111) Plane</i>		Experiment I'/I
	Calculated I'/I(K)	Calculated I'/I(L)	
1	1.0000	1.0000	
2	1.0000	1.0003	1.0001+ .0002
3	1.0006	1.0020	0.9999+ .0002
4	1.0070	1.0230	0.9998+ .0001
5	1.0015	1.0100	1.0002+ .0001
6	1.0030	1.0210	1.0001+ .0004
7	1.0050	1.0280	0.9988+ .0015
	<i>Silicon steel (110 Plane)</i>		
	Calculated I'/I(K)	Calculated I'/I(L)	
1	1.0000	1.0012	1.0001+ .0001
2	1.0009	1.0100	0.9999+ .0001
2. Magnetized parallel to the reflecting face			
	<i>Magnetite (111) Plane</i>		
	Calculated I'/I(K)	Calculated I'/I(L)	
4	0.9980	0.9100	1.0002+ .0010
5	0.9970	0.8900	0.9997+ .0004
6	0.9950	0.8000	1.0004+ .0003
	<i>Silicon steel (110 Plane)</i>		
	Calculated I'/I(K)	Calculated I'/I(L)	
2	1.0000	0.9993	1.0003+ .0006

In the above table the probable error of the mean is quoted.

It will be seen that the apparent changes in intensity of x-ray reflection due to magnetization are very small, and are of the magnitude to be expected from the probable error. There is thus no evidence for any change whatever in the reflecting power of these magnetic crystals due to magnetization. This conclusion is a considerable extension of the negative result of A. H. Compton and Rognley, for whereas in their experiments magnetite only was used, and this was magnetized only to one third saturation, here both the magnetite and the iron crystals were magnetically saturated. Moreover, these authors gave 1 percent as the precision of the experiment, whereas the more precise of the present experiments may probably be relied upon to 0.1 percent.

SIGNIFICANCE OF THE NEGATIVE RESULTS

Compton and Rognley¹ pointed out that a change of intensity of less than one percent in the fourth order when the crystal was only one third saturated was to be interpreted as meaning that the ultimate magnetic particle could not be the molecule or the atom as a whole unless the atom is surprisingly isotropic. The present data set a lower limit to the maximum displacement of atoms from their normal positions which could have occurred due to magnetization without being detected by this experiment. This distance could not have changed by as much as 1/2000 of the grating space without producing an effect that would have been detected by this experiment. It is also very improbable that the electrons revolving in inner orbits can account for ferromagnetism. In the fourth order in the case of magnetite the theoretical value is 35 times the experimental value, while in the second order for silicon steel the theoretical value is 9 times the experimental change.

Honda⁵ ascribes the magnetic property of an atom to the nucleus. Within the nucleus he pictures electrons and protons as revolving in opposite senses. This gives a large magnetic moment and a small angular momentum which would enable the nucleus to be oriented by an applied field. Such a system would be dynamically unstable. Further, as pointed out by Compton and Rognley, the magnetic properties of a substance are vitally affected by temperature, chemical combination and modification of the crystal structure as in the case of the Heusler alloys. On the other hand we cannot, by the most drastic of physical or chemical means, affect the radiation from radioactive substances, thus indicating that the nucleus is not influenced by external conditions. Thus while the results of this experiment are compatible with the theory of Honda, auxiliary evidence seems to indicate that the nucleus cannot be the ultimate magnet.

Ehrenfest has attempted to identify the ultimate magnet with an electron moving within a fixed orbit. In the absence of a magnetic field either sense of revolution is equally probable, while the application of an external magnetic field increases the probability that the sense of revolution of the electron will be such as to produce a magnetic moment in the direction of the field. When one tries to picture the process of magnetization, he is forced to imagine the orbits as turning suddenly, or the electron as suddenly reversing its direction in the orbit. If the whole orbit is able to turn it is difficult to conceive of it as a fixed orbit. If one is to account for hysteresis, energy must be dissipated when the probability of orientation in different directions changes. It then becomes difficult to see how hysteresis can be greatly reduced when the change in direction of magnetization is effected by means of a rotating magnetic field instead of an alternating field.

THE SPINNING ELECTRON AS THE ULTIMATE MAGNET

The results of other investigators indicate that neither minute crystal aggregations nor the chemical molecule nor the Rutherford type of atom as a whole can account for ferromagnetism. This experiment shows that it is highly improbable that electrons revolving in any of the orbits are responsible for ferromagnetism. Auxiliary evidence is against the conclusion that the nucleus may account for magnetic properties. It therefore appears that the ultimate magnetic particle should be identified with the spinning electron, as was long ago suggested by Parson⁶; and in accord with Uhlenbeck and Goudsmit's⁷ hypothesis of the origin of certain spectroscopic phenomena.

The author wishes to thank Professor A. H. Compton for proposing the problem, and Dr. R. D. Bennett for constructive suggestions during the course of the experimental work. The kind cooperation of Dr. T. Y. Yensen of the Westinghouse Electric and Manufacturing Company, Professor L. W. McKeehan of Yale University, and Mr. Norman Goss of the American steel and Wire Company in supplying large crystals of iron and silicon steel has made the completion of the work possible.

⁵ Honda, "Theory of Magnetism," p. 192.

⁶ A. L. Parson, *Smithsonian Misc. Collections*, Nov., 1915.

⁷ Goudsmit and Uhlenbeck, *Nature* 117, 264 (1926).

THE FORM OF THE X-RAY DIFFRACTION BANDS FOR REGULAR CRYSTALS OF COLLOIDAL SIZE*

BY CARLETON C. MURDOCK
CORNELL UNIVERSITY

(Received October 23, 1929)

ABSTRACT

The form of the diffraction bands of a very fine uniform crystalline powder has been computed for the (1, 0, 0), the (1, 1, 0) and the (1, 1, 1) planes for cubical and octahedral crystals of the regular system. The shape of the bands is approximately that of the Gauss error curve. Both the shape and the half intensity breadth vary from band to band and the variations are characteristic of the shape of the crystals. There is definite correlation between the form of the band and the direction of the corresponding Bragg planes with respect to the external features of the crystal. The mean breadth of the bands is nearly the same for cubical and octahedral crystals having the same volume. The values of the constant of Scherrer's equation are in general smaller than those computed by other investigators for the cubical case.

Secondary maxima.—A case is found in which secondary maxima of the intensity function would be sufficiently intense to be directly observable. It is pointed out that such an effect might lead to a false interpretation of the crystal structure of a very fine crystalline powder.

WHEN monochromatic x-rays are diffracted by a fine crystalline powder the diffraction bands are found to have a measurable width which is a function of the fineness of the powder. The effect is closely analogous to the low resolving power of a diffraction grating having a small number of lines. In this case we can regard the crystals as three dimensional gratings, the shape and size of which influence the form of the observed diffraction band. Scherrer¹ investigated the case of crystals of the regular (cubic) crystallographic system which are cubical in shape and gave for the half intensity breadth, B , of a diffraction band produced by the powder method,

$$B = \frac{K\lambda}{D \cos(\theta_0/2)} \quad (1)$$

in which λ is the wave-length of the incident x-rays, D , the length of one edge of the cube, and θ_0 , the angle between the diffracted and the incident ray. K is a constant whose value Scherrer found to be $2 [\log 2/\pi]^{1/2}$. Two other investigators treating more general cases have obtained results which reduce to Eq. (1) for the case of cubical crystals. They obtained slightly different values of the coefficient K . Seljakow² investigated the case of crystals of any

* This investigation was supported by a grant from the Heckscher Foundation for the Advancement of Research at Cornell University.

¹ P. Scherrer, *Nachr. Gesell. Wiss. Göttingen* (1918), p. 190.

² N. Seljakow, *Zeits. f. Physik* 31, 439 (1925).

crystallographic system whose shape is a parallelopiped geometrically similar to the unit cell and whose edges are parallel to the crystallographic axes. v. Laue³ treated the case of parallelopipeds which have edges parallel to the crystallographic axes but which are not necessarily similar to the unit cell. His development brought out two interesting facts; viz. that the breadth of the diffraction bands depends upon the shape as well as upon the size of the parallelopiped; and in the general case, that the breadth is a function of the Miller indices of the band.

Considerable use has been made of Scherrer's equation in estimating the size of crystalline powders. Particular interest attaches to the investigation of colloidal preparations of such elements as gold, silver and nickel. These elements crystallize in face-centered cubic lattices and are normally of the octahedral form. In the investigations cited above no attempt has been made to determine the shape of the diffraction band. The shape of the band should depend upon the Miller indices of the band, the shape of the crystals, and, if the crystals are not of uniform size, upon the distribution of size. It seemed desirable to investigate the theoretical breadth and shape of several diffraction bands for crystals of octahedral as well as cubical shape.

The general procedure for computations of this sort is given by v. Laue³ and in the following discussion his notation is generally followed. Assume a parallel beam of monochromatic x-rays incident upon a crystal in a direction which we shall specify by the unit vector s_0 . Consider the rays diffracted by the crystal in the direction of the unit vector s . The intensity of the diffracted beam may be expressed⁴ as a periodic function of the quantities A_i defined by $A_i = k \mathbf{a}_i \cdot \mathbf{H}$; $i=1, 2, 3$ in which $k=2\pi/\lambda$ and $\mathbf{H}=\mathbf{s}-\mathbf{s}_0$. $\mathbf{a}_1, \mathbf{a}_2$ and \mathbf{a}_3 represent the three primitive vectors of the space lattice. In the case of fine powders the extinction effect is negligible⁵ and each unit cell of the crystal may be regarded as diffracting in the direction of \mathbf{s} rays which are identical except for phase. In the expression for the total intensity of the diffracted beam, A_1, A_2 , and A_3 represent the phase differences between rays diffracted by cells adjacent respectively along the three crystallographic axes of the crystal. The principal maxima of the function occur when the phase differences, A_i , are integral multiples of 2π , i.e. when $A_i=2\pi h_i$; $i=1, 2, 3$ in which the quantities h_i are integers. It will be noted that h_1, h_2 , and h_3 are respectively n times the Miller indices of the Bragg planes of the crystal where n is the order number.

In the cubic system, the magnitudes of the three vectors \mathbf{a}_i are equal and we can write $|\mathbf{a}_i|=a$. This makes it possible to regard A_1, A_2 , and A_3 as the projections on the three crystallographic axes of a vector, $\mathbf{A}=ka\mathbf{H}$. Consider a rectangular cartesian system in which A_1, A_2 , and A_3 are the coordinates with axes parallel to the crystallographic axes of the crystal. We will designate the space thus defined as A -space. Each point, A_i , of this space deter-

³ M. v. Laue, *Zeits. f. Krist.* **64**, 115 (1926).

⁴ M. v. Laue, *Enc. Math. Wiss.* **5**, 459.

⁵ R. J. Havighurst, *Phys. Rev.* [2] **28**, 882 (1926).

mines a value of the intensity function. The points $2\pi h_i$ in A -space form a lattice which is geometrically similar to Ewald's reciprocal lattice.⁶ Each such point corresponds to a principal maximum of the diffraction pattern.

Since H is the difference of two unit vectors, s and s_0 , its numerical value is $2 \sin(\theta/2)$ in which θ is the angle between the two vectors, s and s_0 , i.e. the angle of diffraction. It follows that A , the numerical value of A , may be expressed by

$$A = ka |H| = (4\pi a/\lambda) \sin(\theta/2). \quad (2)$$

The direction of A is that of H and depends only upon the directions of the incident and diffracted rays. The vector A is therefore independent of the size, shape and orientation of the crystal. If the incident beam falls upon a crystalline powder, the same vector A pertains to the ray diffracted by each crystal in the direction determined by the angle θ . To each crystal of the powder there corresponds an A -space with axes parallel to the crystallographic axes of the crystal. The total intensity of the beam diffracted through the angle θ by the powder is the sum of the values of the intensities determined in the A -spaces of the several crystals by the vector, A .

The intensity function is determined by the size and shape of the crystal, the crystal lattice and the structure factor. Consider a large number, N , of crystals of uniform size, shape, space lattice and structure. Then the same intensity function, J , will pertain to the A -spaces of all the crystals and the total intensity will be found by integrating J between such limits as to include all possible orientations of the crystallographic axes. For the purpose of carrying out this integration, it is convenient to specify the orientation in terms of the direction of A_0 , the radius vector of the point $2\pi h_i$ in A -space corresponding to the diffraction maximum, h_i , with which we are concerned. Let ϕ be the polar angle between the directions of A and A_0 ; ξ , the azimuth angle about the direction of A as a pole; and ψ , that about the direction of A_0 as a pole. The total intensity, I , will then be represented by

$$\begin{aligned} I &= N \frac{\int_0^\pi \int_0^{2\pi} \int_0^{2\pi} J(A_i) \sin \phi \, d\phi \, d\xi \, d\psi}{\int_0^\pi \int_0^{2\pi} \int_0^{2\pi} \sin \phi \, d\phi \, d\xi \, d\psi} \\ &= \frac{N}{4\pi} \int_0^\pi \int_0^{2\pi} J(A_i) \sin \phi \, d\phi \, d\psi \end{aligned} \quad (3)$$

since $J(A_i)$ is invariant with respect to ξ . This double integral is the same as that representing the integral over the surface of the sphere in A -space whose center is the origin and whose radius is A . It will be convenient to consider I as this surface integral.

The intensity function⁴ for the case of a crystal whose shape is a cube with edges parallel to the crystallographic axes is well known. Expressed in terms

⁶ P. P. Ewald, *Zeits. f. Krist.* 56, 129 (1921).

of the intensity diffracted by one unit cell per unit solid angle in the specified direction, it is given by

$$J = \frac{\sin^2 \frac{1}{2} M A_1}{\sin^2 \frac{1}{2} A_1} \cdot \frac{\sin^2 \frac{1}{2} M A_2}{\sin^2 \frac{1}{2} A_2} \cdot \frac{\sin^2 \frac{1}{2} M A_3}{\sin^2 \frac{1}{2} A_3} \quad (4)$$

in which M is the number of unit cells along one edge of the cube. The principal maxima of J occur when $A_i = 2\pi h_i$ and the value of J at these maxima is $J_0 = M^3$. Because of its structure the intensity of the rays diffracted by a unit cell will vary with the direction thus causing the various principal maxima to have different intensities. In a study of the variation of intensity within a diffraction band, we compare the surface integrals over spheres in A -space which comprise a very thin spherical shell and we may neglect the variation of the structure factor with respect to A within this shell. This is accomplished by measuring the intensity function in terms of its maximum value at $A_i = 2\pi h_i$ for the band, h_i , under investigation and gives

$$J' = J/J_0. \quad (5)$$

Let us investigate the intensity function for an octahedron consisting of a simple cubic lattice with axes x, y, z along the diagonals of the octahedron and a single diffracting particle at each point of the lattice. Let M be the number of diffracting particles along a diagonal. We will take M to be an odd integer. We will specify the points of the lattice by the coordinate whole numbers n_1, n_2, n_3 measured parallel to the x, y, z axes respectively in terms of the length of the unit cell i.e. $x = n_1 a, y = n_2 a, z = n_3 a$. The points having a particular value of n_3 form a square parallel to the x, y plane whose diagonals extend from $-(m - |n_3|)$ to $(m - |n_3|)$ in which $m = 1/2 (M - 1)$. In this square the points having a particular value of n_2 form a row which extends from $n_1 = -n_1''$ to $n_1 = n_1''$ in which $n_1'' = m - |n_2| - |n_3|$. The resultant of the rays diffracted in the direction of s by the $(2n_1'' + 1)$ points comprising the n_2, n_3 row will be in phase with that diffracted in this direction by the central point, $0, n_2, n_3$, of the row. The contribution of any point, n_1, n_2, n_3 to this resultant is $\cos(n_1 A_1)$ multiplied by the amplitude. Measured in terms of the ray diffracted in the direction of s by any point, the resultant is $\sum_{-n_1}^{n_1} \cos(n_1 A_1)$. As we now proceed to combine the resultant rays from the various rows of the n_3 square, we are combining rays having unequal amplitudes whose values are symmetrically distributed about the central row, $0, n_3$. Each component ray has the phase of the central point of its row. The resultant will therefore have the same phase as that of the ray diffracted by the central point $0, 0, n_3$ of the n_3 square and will be

$$\sum_{-n_2'}^{n_2'} \{ \cos(n_2 A_2) \sum_{-n_1}^{n_1} \cos(n_1 A_1) \}$$

in which $n_2' = m - |n_3|$. Similarly we may combine the rays from all such squares and obtain P , the resultant amplitude of the ray diffracted by the octahedron in the direction of s .

$$P = \sum_{-m}^m \left\{ \cos(n_3 A_3) \sum_{-n_2'}^{n_2'} \left[\cos(n_2 A_2) \sum_{-n_1'}^{n_1'} \cos(n_1 A_1) \right] \right\}. \quad (6)$$

Principal maxima of P occur when $A_1 = 2\pi h_1$, $A_2 = 2\pi h_2$, $A_3 = 2\pi h_3$ where h_1 , h_2 , h_3 are integers. The value of these maxima is $P_0 = (4m^3 + 6m^2 + 8m + 3)/3$ and the intensity function measured in terms of the intensity at a maximum is $J' = P^2/P_0^2$. (7)

An investigation of the variation of P with respect to M shows that if P is expressed in terms of new variables, $u_i = 1/2 M(A_i - 2\pi h_i)$, it is approximately independent of M in the neighborhood of the point $2\pi h_i$. If we now write the expression for J_∞' , the limit of J' as M approaches ∞ , the summations of Eq. (6) become definite integrals which may be evaluated. The result of the integration is

$$J_\infty' = 6 \left\{ \frac{(u_1^2 - u_2^2)u_3 \sin u_3 + (u_2^2 - u_3^2)u_1 \sin u_1 + (u_3^2 - u_1^2)u_2 \sin u_2}{(u_1^2 - u_2^2)(u_2^2 - u_3^2)(u_3^2 - u_1^2)} \right\}. \quad (8)$$

An investigation of Eq. (8) shows that the distribution of the values of J_∞' about the origin of u_i is nearly spherical i.e. J_∞' is approximately a single valued function of $u = (u_1^2 + u_2^2 + u_3^2)^{1/2}$. For any given value of u , maxima or minima occur if (a) $u_j = u_k = 0$, (b) $u_i = u_j$, $u_k = 0$, or (c) $u_i = u_j = u_k$. On the sphere in A -space whose radius is u and whose center is $2\pi h_i$ these maxima and minima occur at intersections with diameters parallel respectively to (a) the axes of the space lattice, (b) the diagonals of squares bounding the unit cells, and (c) the diagonals of the unit cells. The values of J_∞' for these three conditions are given by

$$\left. \begin{aligned} \text{(a)} \quad J_\infty' &= \frac{6}{u_i^3} (u_i - \sin u_i), & u &= u_i \\ \text{(b)} \quad J_\infty' &= \frac{3}{u_i^3} (\sin u_i - u_i \cos u_i), & u &= \sqrt{2} u_i \\ \text{(c)} \quad J_\infty' &= \frac{3}{4u_i^3} [(1 + u_i^2) \sin u_i - u_i \cos u_i], & u &= \sqrt{3} u_i \end{aligned} \right\} \quad (9)$$

and are shown as functions of u in curves Ia, Ib, and Ic of Fig. 1. For values of $u > 5.7$, minima at which $J_\infty' = 0$ occur at other points on the sphere. It follows that when $u < 5.7$ all values of J_∞' must lie in the narrow strip enclosed between the curves and when $u > 5.7$, in that enclosed between the curves and the line $J_\infty' = 0$.

The nature of the approximation involved in using Eq. (8) instead of Eq. (7) is shown by curves Ia, Ib and Ic of Fig. 2. Here the corrections which must be applied to J_∞' in order to obtain the value of J' for the case, $M = 11$ are plotted against u . The correction curves for larger values of M are of the same general form with maxima and minima approximately at the same values of u , but they have smaller values for the ordinates. The correction for any

value of u is approximately inversely proportional to M^2 . For values of M which ordinarily occur these corrections are small.

The secondary maxima of the function J' defined by Eqs. (6) and (7), lie on the diagonals of the cubes of the lattice formed in A -space by the principal maxima points, $2\pi h_i$. At the centers of these cubes where three such diagonals intersect there occur secondary maxima at which the intensity is approximately three times that at the neighboring secondary maxima. The large ordinate at $u=29.9$ in curve Ic of Fig. 2 is due to such a large secondary maximum. In the derivation of Eq. (6), M was assumed to be odd. If M were even, no secondary maxima would occur at these points in A -space.

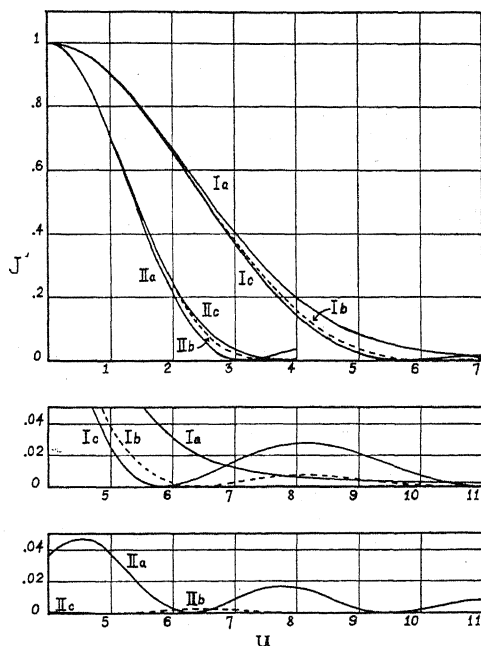


Fig. 1. The intensity function, J'_∞ , plotted against u ; (I), for octahedral crystals; (II), for cubical crystals. u is measured parallel to the radius vector A_0 of (a) the (1, 0, 0) maximum, (b) the (1, 1, 0) maximum, (c) the (1, 1, 1) maximum.

Substituting the coordinates of these points, $(2\pi h_i - \pi)$, for A_i in Eq. (6) we obtain $P = (-1)^m (3/M) (M^2 + 1) / (M^2 + 5)$ which gives a value of J approximately $9/M^2$ times that at the neighboring principal maxima. Colloidal crystals have been examined by x-rays⁷ for which the equivalent value of M was as small as 9. Crystals of this size, having octahedral shape and a simple cubic lattice would form an x-ray powder spectrogram in which these large secondary maxima should be directly observable as faint diffraction bands. The principal maxima points, $2\pi h_i$, form in A -space a simple cubic lattice, geometrically similar to the reciprocal lattice⁸ of the crystal. If we include the large secondary maxima points, $(2\pi h_i - \pi)$, the reciprocal lattice becomes body-centered. Since the reciprocal lattice of a face-centered crystal is a body-

centered lattice, the observed diffraction pattern would be similar to that of a face-centered crystal. The relative strengths of the bands would be very much like that observed in the diffraction pattern of sodium fluoride.

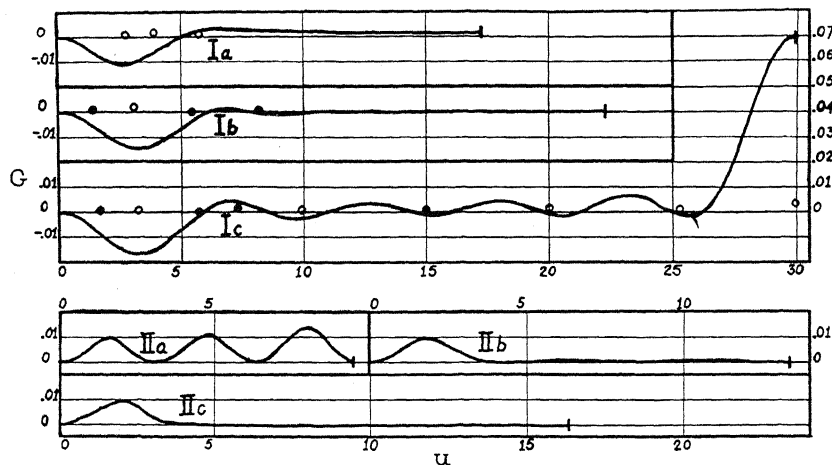


Fig. 2. The correction function, $G(M, u_i) = J' - J_\infty'$ plotted against u ; for a simple cubic lattice; (I) octahedral crystals, $M=11$; (II) cubical crystals, $M=6$. The small circles show corresponding values for a face-centered lattice. u is measured parallel to the radius vector A_0 of (a) the (1, 0, 0) maximum, (b) the (1, 1, 0) maximum, (c) the (1, 1, 1) maximum.

The intensity function in the case of a cubical crystal may be treated in the same way as in the case of an octahedral crystal. If we express J' of Eq. (5) in terms of u_i and take the limit as M approaches ∞ we obtain

$$J_\infty' = \frac{\sin^2 u_1}{u_1^2} \cdot \frac{\sin^2 u_2}{u_2^2} \cdot \frac{\sin^2 u_3}{u_3^2}. \quad (10)$$

The conditions for maxima and minima of this function are similar to those for Eq. (8). Curves IIa, IIb, and IIc of Fig. 1 show the corresponding maxima and minima as functions of u . In this case additional minima at which $J_\infty' = 0$ occur for values of $u > 3.3$. Curves IIa, IIb, and IIc of Fig. 2 show the corrections to be added to J_∞' to obtain the value of J' for the case, $M=6$. Here also the correction for a particular value of u is inversely proportional to M^2 .

Since crystals having face-centered lattices are of particular interest, the intensity functions have been developed also for diffracting particles at the points of a face-centered lattice. In the octahedral case, the result is

$$J' = \left[\frac{P+Q}{P_0+Q_0} \right]^2 \quad (11)$$

in which

$$Q = \sum_{-m+1}^{m-1} \left\{ \cos(n_3 A_3) \frac{1}{4} \sum_0^{n_2'-1} \left[\cos(n_2 A_2 + \frac{1}{2} A_2) \sum_0^{n_1''} \cos(n_1 A_1 + \frac{1}{2} A_1) \right] \right\}$$

⁷ R. Zsigmondy, "Kolloidchemie," Leipzig 1920, p. 406.

⁸ cf. A. L. Patterson, Zeits. f. Physik 44, 596 (1927).

+ two other terms formed from the first by a rotation of subscripts and $Q_0 = 4m^3 + 6m^2 + 2m$. The limit of J' as M approaches ∞ is identical with J_∞' as given by Eq. (8). The corrections to be added to J_∞' to obtain J' are so small that the curves have not been drawn. The points indicated by the small circles in Fig. 2 indicate some of the values for $M = 11$.

In the case of crystals of cubical shape with a face-centered lattice

$$J' = \left(\frac{R+S}{R_0+S_0} \right)^2 \quad (12)$$

in which $R = J^{1/2}$ as given by Eq. (4), $R_0 = M^3$,

$$S = \frac{\sin \frac{1}{2}MA_1}{\sin \frac{1}{2}A_1} \cdot \frac{\sin \frac{1}{2}(M-1)A_2}{\sin \frac{1}{2}A_2} \cdot \frac{\sin \frac{1}{2}(M-1)A_3}{\sin \frac{1}{2}A_3}$$

+ two other terms formed from the first by rotation of subscripts and $S_0 = 3M(M-1)^2$. The limit of J' as M approaches ∞ is identical with J_∞' as given by Eq. (10). The corrections to be added to J_∞' to obtain J' are larger than in

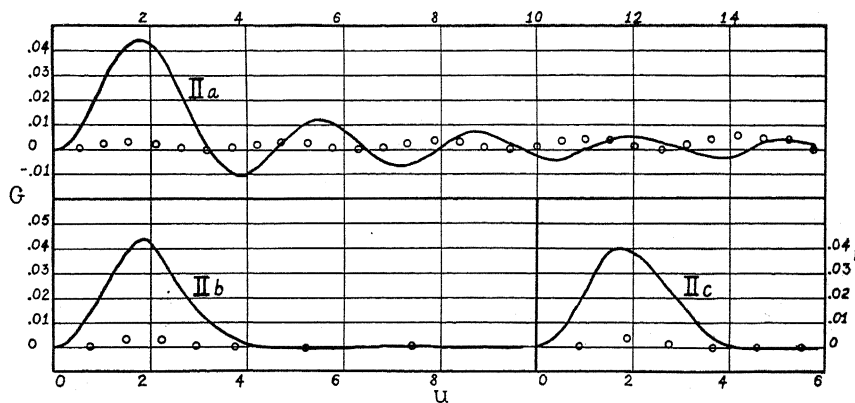


Fig. 3. The correction function, $G(M, u) = J' - J_\infty'$ plotted against u for a face-centered lattice and cubic crystals, $M=10$. The small circles show corresponding values for a simple cubic lattice. u is measured parallel to the radius vector A_0 of (a) the (1, 0, 0) maximum, (b) the (1, 1, 0) maximum, (c) the (1, 1, 1) maximum.

the other cases studied. The curves are shown in Fig. 3 for $M=10$. As in the other cases the positions of the maxima of these curves vary but slightly with M . In this case the ordinates are approximately inversely proportional to M . For the purpose of comparison, corrections for the case of the cubical shape with a simple cubic lattice for $M=10$ are shown in Fig. 3 by small circles.

The narrow limits, between which all values of the intensity function must lie as shown in Fig. 1, make it possible to select an integrable function of u which closely approximates J . An approximate solution of our problem may be obtained by substituting this function for J in Eq. (3) and performing the integration. An investigation⁹ of the case of octahedral crystals by this

⁹ C. C. Murdock, Phys. Rev. [2] 31, 304 (1928).

method gave the value of the constant K of Eq. (1) as 1.6 when D was measured through the center of the octahedron from corner to corner. The investigation showed that the value of K was different for the various diffraction bands. The method of procedure, however, is not suitable for the study of this variation or for the determination of the form of a diffraction band.

Let us represent the function, J_{∞}' , by the expression, $e^{-u^2/p^2} + F(u_i)$ in which the value of p is so selected that the first term approximates J_{∞}' for the case under consideration. We may now express J of Eq. (3) as

$$J = J_0 J' = J_0 \{ J_{\infty}' + G(M, u_i) \} = J_0 \{ e^{-u^2/p^2} + F(u_i) + G(M, u_i) \} \quad (13)$$

in which $G(M, u_i)$ represents the correction to be added to J_{∞}' in order to obtain J' . The ordinates of Figs. 2 and 3 are values of G for the particular cases shown. We will use u^2 in place of ϕ as the variable of integration.

$$\begin{aligned} u^2 &= u_1^2 + u_2^2 + u_3^2 \\ &= \frac{1}{4} M^2 [A^2 + 4\pi^2 h^2 - 4\pi(h_1 A_1 + h_2 A_2 + h_3 A_3)] \\ &= \frac{1}{4} M^2 [A^2 + 4\pi^2 h^2 - 4\pi h A \cos \phi] \end{aligned}$$

in which $h^2 = h_1^2 + h_2^2 + h_3^2$. Therefore $d(u^2) = \pi h A M^2 \sin \phi d\phi$.

In terms of u^2 the limits of integration of Eq. (3) become v^2 and w^2 where $v = \frac{1}{2} M(A - 2\pi h)$ and $w = \frac{1}{2} M(A + 2\pi h)$. These limits are such that the integration may be considered as a surface integration over the surface of a sphere in A -space whose diameter is $2A$. In changing variables from A_i to u_i we shifted the origin to the point, $2\pi h_i$, associated with the diffraction band, h_i , with which we are concerned. We also changed the scale of the space by the factor $1/2 M$. In terms of the new scale, the diameter of the sphere of integration is $AM = w + v$. The diameter of the sphere which passes through the point $2\pi h_i$ is $2\pi h M = w - v$. The point $2\pi h_i$ is not the only point on the surface of this sphere at which a principal maximum of J occurs. For example on the sphere of integration for the (1, 1, 1) diffraction band there are eight points, $2\pi h_i$, corresponding to the following values of h_i ; 1, 1, 1; -1, 1, 1; 1, -1, 1; 1, 1, -1; 1, -1, -1; -1, 1, -1; -1, -1, 1; and -1, -1, -1. Let N' represent the number of such points. Since J is a periodic function of A_i , the integration indicated in Eq. (3) includes the values of J in the neighborhood of all these points and the contribution to the integral in the neighborhood of each point is identical. J_{∞}' is not a periodic function. It can approximate $J_0 J$ only in the neighborhood of the point, $2\pi h_i$. In its integration the limits should be fixed so as to include $1/N'$ times the area of the sphere and the integral should be multiplied by N' . It will not be found necessary to specify exactly the upper limit of this integration. Its order of magnitude may be ascertained by taking the upper limit of u^2 as r^2 , where r represents the radius of a circle whose area is $1/N'$ times the area of the sphere. Thus $\pi r^2 = 4\pi^2 h^2 M^2 / N'$ and $r^2 = 4\pi^2 M^2 h^2 / N'$. The value of h^2 / N' is $1/6$ for the (1, 0, 0) and the (1, 1, 0) diffraction bands, but has a larger value for each of the other bands. The upper limit of integration is therefore of the order of magnitude of $2/3 \pi^2 M^2$ or larger.

Making these substitutions in Eq. (3) we obtain

$$I = \frac{NN'J_0}{4\pi^2 h A M^2} \left[\int_{v^2}^{r^2} e^{-u^2/p^2} d(u^2) + \int_{v^2}^{r^2} f(u, v) d(u^2) + \int_{v^2}^{r^2} g(M, u, v) d(u^2) \right] \\ = \frac{NN'J_0}{4\pi^2 h A M^2} [U + V + W], \quad (14)$$

in which $f(u, v) = 1/2\pi \int_0^{2\pi} F(u_i) d\psi$, the average value of F with respect to ψ , $g(M, u, v) = 1/2\pi \int_0^{2\pi} G(M, u_i) d\psi$ and U , V , and W represent respectively the three integrals of the equation.

The first integral, U , of Eq. (14) has the same value for each band, h_i , and may be written

$$U = \int_{v^2}^{r^2} e^{-u^2/p^2} d(u^2) = p^2 e^{-v^2/p^2} \quad (15)$$

if r^2/p^2 is large. Since $r^2/p^2 \geq \frac{2}{3}\pi^2 M^2/p^2$ and M^2/p^2 is of the order of 10 for the smallest colloidal crystals so far studied,⁷ this assumption is justified.

The second integral, V , of Eq. (14) varies from band to band. It may be evaluated graphically by the following method. Contour plots are made of the function, $F(u_i) = J_\infty' - e^{-u^2/p^2}$ for a number of values of u . These may be made on the surfaces of spheres, the radii of which are taken as equal to u . It has been found more convenient, however, to make plots which are the projections of such spherical plots upon planes tangent to the sphere and perpendicular to the direction of the vector A_0 . From these plots the curves for $F(u_i)$ at various values of u and v are plotted as functions of ψ and integrated by inspection to obtain the values of $f(u, v)$. These values are then plotted as functions of u^2 for various values of v and the integrals evaluated graphically.

It is not practicable to carry out this process to the upper limit of integration. For large values of u , the value of f becomes small but remains finite and small errors in the function produce large errors in the integral due to the fact that the integration is performed with respect to the square of u . If s^2 is the upper limit of the graphical integration it leaves a part, $\int_{s^2}^{r^2} f(u, v) d(u^2)$, unevaluated. By properly choosing the value of s , the error involved in neglecting this part of the integral may be compensated in making the experimental observations. In an experiment the incident radiation will not be strictly monochromatic. Moreover there will be some generally scattered radiation. Both of these effects will give a background intensity superimposed upon that which we are computing. In practice the intensity is measured on either side of a diffraction band and from these data the background intensity is estimated for the points in the band on the assumption that there are no maxima or minima in the background intensity in that region. If the value of s is taken two or three times the largest value of v used, this assumption is also justified for $\int_{s^2}^{r^2} f(u, v) d(u^2)$ and the part of the intensity proportional to it will be automatically subtracted from the measured intensity as part of the background correction.

The third integral, W , of Eq. (14) may be evaluated by the method used for the evaluation of V . If, however, G can be approximated by an integrable function of u , it will be simpler to proceed as in the case of J_∞' . An examination of the correction curves of Figs. 2 and 3 shows that the (a), (b) and (c) curves of each set are practically identical for the smaller values of u and that for the larger values, two curves of each set have small ordinates. Advantage may be taken of this to approximate G by the function $Cu^2e^{-u^2/p^2}$ which gives as a first approximation

$$W = Cp^2(p^2 + v^2)e^{-v^2/p^2}. \quad (16)$$

C is a function of M . It may be expressed for the various cases studied as shown in Table I.

TABLE I.

	Cube	Octahedron
Simple lattice	$C = 1/(3M^2)$	$C = -1/(2M^2)$
Face-centered lattice	$C = 1/(3M)$	$C = 0$

The remainder, $G - Cu^2e^{-u^2/p^2}$, may now be integrated by the method described for the evaluation of V .

Since W depends upon M , which, in general, can only be known as a result of the solution of our problem, we will first investigate the case in which W is negligible. If $W = 0$, Eq. (14) may be written

$$I = \frac{NN'J_0L}{4\pi^2hAM^2}, \quad (17)$$

in which $L = U + V$. L is the surface integral over the sphere of $N'J_\infty'$. The only quantities in the second member of Eq. (17) which depend upon v , are L and A . If, therefore, we measure the intensity in terms of its maximum value, I_0 , for which $v = 0$, we obtain

$$I' = I/I_0 = L'A_0/A, \quad (18)$$

in which $L' = L/L_0$ and L_0 represents the value of L when $v = 0$. The factor A_0/A may be written by Eq. (2) as $\sin(\theta_0/2) \div \sin(\theta/2)$ in which θ_0 is the value of θ corresponding to the maximum, h_i . In this form it is seen to be determined by directly observable quantities. Within a diffraction band θ differs only slightly from θ_0 and the factor may be written $1/(1 + \frac{1}{2} \cot(\theta_0/2) \Delta\theta)$ where $\Delta\theta = \theta - \theta_0$. Since this factor is unsymmetrical with respect to $\Delta\theta$ it introduces asymmetry in the diffraction band. It is due to the fact that the integrations for values of v which are numerically equal but of opposite sign, are performed over spheres of different areas. In the graphical process for the evaluation of V another source of asymmetry occurs. It is due to the curvature of the spherical surface. No case has yet been found in which this second asymmetry is large enough to be taken into consideration. Because of the small value of

s used in the evaluation of V an integration in the spherical surface is practically the same as an integration in the tangent plane perpendicular to the vector, A_0 . If the integration is performed in this plane, the asymmetry due to curvature does not appear in the result.

We may now write Eq. (18) as

$$L' = [1 + \frac{1}{2} \cot(\theta_0/2) \Delta\theta] I'. \quad (19)$$

In this form there are collected in the second member the experimentally observable factors and the first member is a symmetrical function which may be computed for any band h_i from the integrals U and V of Eq. (14). U is the same for all bands. If V is integrated over the tangent plane it will vary from band to band due to the variation of the direction of the vector A_0 . This is, however, the same for all bands having the same Miller indices. It follows that the function L' will be the same for all orders of a diffraction band and need only be computed for one order.

The function L' has been computed for the (1, 0, 0), the (1, 1, 0), and the (1, 1, 1) diffraction bands in the cases of cubical and octahedral crystals. In the cubical case, the value of p was taken as $\sqrt{3}$, contour plots were made for eight values of u , and the graphical integration performed to the limit $s^2 = 90$. In the octahedral case the value of p was taken as 3, contour plots were made for eleven values of u , and the graphical integration performed to the limit $s^2 = 120$. Table II gives the resulting values of L' as determined. The uncertainty in the values due to the errors of the operation are of the order of ± 0.005 . Since L' is a symmetrical function the values are given for the positive values of v only.

TABLE II.

v	Cube L'			v	Octahedron L'		
	(1, 0, 0)	(1, 1, 0)	(1, 1, 1)		(1, 0, 0)	(1, 1, 0)	(1, 1, 1)
0	1.000	1.000	1.000	0	1.000	1.000	1.000
1	.728	.692	.680	1	.874	.891	.905
1.41	.500	.445	.466	2	.591	.631	.673
1.73	.333	.300	.333	2.6	.428	.456	.504
2	.221	.211	.268	3.2	.292	.305	.348
2.5	.074	.123	.170	4	.177	.145	.170
3	.027	.089	.131	5	.105	.060	.051
3.5			.094	6	.064	.046	.020
4	.054	.072	.069	7	.039	.040	.025

Experimentally we measure the width of a diffraction band in terms of differences in the angle of diffraction. By the definition of v , and by Eq. (2), we obtain

$$v = \frac{1}{2} M(A - 2\pi h) = (2\pi a M / \lambda) [\sin(\theta/2) - \sin(\theta_0/2)].$$

If we substitute $d/d\theta (\sin \theta/2) \Delta\theta$ for $\sin(\theta/2) - \sin(\theta_0/2)$ we obtain

$$v = (\pi a M / \lambda) \cos(\theta_0/2) \Delta\theta.$$

Let v' represent the value of v for which $I' = 1/2$ and, following Scherrer, let B represent the half intensity breadth of a diffraction band, measured in radians. Then

$$v' = (\pi a M / \lambda) \cos (\theta_0 / 2) (B / 2)$$

and

$$B = (2v' / \pi) \cdot \lambda / (Ma \cos (\theta_0 / 2)). \quad (20)$$

This is identical with Eq. (1) obtained by Scherrer since $Ma = D$, the length of the crystal along a crystallographic axis. Thus we obtain for the value of K , $2v' / \pi$. For comparing crystals of different shape, it is convenient to measure the size of the crystal in terms of D' , the cube root of the volume. D' may be used in place of D in Scherrer's equation, if a suitably modified constant K' is used in place of K . For the cubical shape $D' = D$ and $K' = K$. For the octahedral shape $D'^3 = 1/6 D^3$ and $K' = K/6^{1/3}$. Table III shows the values of v' , K and K' as computed from the data of Table II.

TABLE III.

Indices	Cube		Octahedron		
	v'	$K = K'$	v'	K	K'
(1, 0, 0)	1.41	0.90	2.32	1.48	0.81
(1, 1, 0)	1.32	0.84	2.45	1.56	0.86
(1, 1, 1)	1.36	0.87	2.62	1.67	0.92

These values are in general smaller than the results of previous investigations. Scherrer's value of K as computed from Eq. (1) is 0.94. Seljakow² obtained 0.92 and v. Laue³ 0.90 for the value of K for the cubical case. The previous investigation⁹ of the octahedral case gave $K = 1.6$ or $K' = 0.88$, a value 7 percent less than Scherrer's value of K . This difference was attributed to the shape of the crystal and it was concluded that the values of the crystal volumes which have been estimated by the use of Scherrer's equation were too large by 20 percent if the true shape of the crystals was octahedral. It now appears that the smaller value of K was due not so much to the shape of the crystals as to the method of computation. An examination of Table III shows that the mean values of K' in the cubical case and in the octahedral case are practically the same. Both Seljakow² and v. Laue³ used methods which may be regarded as the substitution of a function of u for the intensity function.

The results shown in Table III illustrate the dependence of the half intensity width of a diffraction band upon the indices of the band. The numerical order of the values of K in the two cases is different. In the cubical case the largest value of K is that of the (1, 0, 0) band while in the octahedral case it is that of the (1, 1, 1) band. In each case, the value of K for the diffraction band which is associated with a Bragg plane, parallel to a face of the crystal, is larger than the values which are associated with the other planes.

The shape of the crystals not only influences the relative width of the diffraction bands but also the form of the bands. This is shown in Fig. 4 in which

L' is plotted against v/v' , or what is the same thing, $2\Delta\theta/B$. On this scale the half intensity width of all the diffraction bands is 2 and their shapes can be directly compared.

The upper halves of all the curves are practically the same and are sufficiently approximated by the exponential relation $L' = e^{-(v/1.2v')^2}$ which is

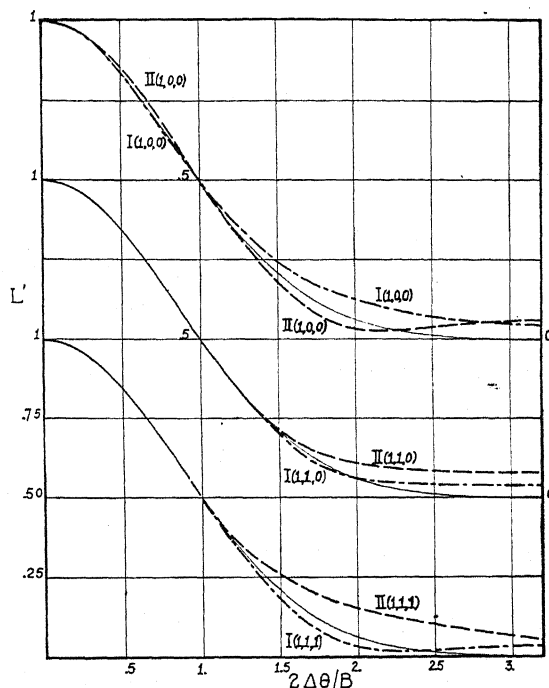


Fig. 4. The (1, 0, 0) (n), the (1, 1, 0) (n) and the (1, 1, 1) (n) diffraction bands for, (I) octahedral crystals, (II) cubical crystals. The scales are such that the maximum intensity is 1 and the half intensity breadth is 2. The unbroken line shows the corresponding Gauss error curve.

plotted in unbroken lines in the figure. The lower halves of the curves show marked variations. Three types occur:

- (a) that illustrated by I(1, 1, 1) and II(1, 0, 0), falls slightly below the exponential curve to a minimum and then rises to a secondary maximum;
- (b) that illustrated by I(1, 1, 0) and II(1, 1, 0) follows the exponential curve until well below the half intensity point and then becomes nearly parallel to the v/v' axis;
- (c) that illustrated by I(1, 0, 0) and II(1, 1, 1) lies well above the exponential curve throughout the lower half of the curve and continues to approach the axis of v/v' to the limits of the computation.

There is a correlation between the type of curve and the Bragg plane associated with the diffraction band. Type (a) occurs when the Bragg plane is parallel to the faces of the crystal, the (1, 0, 0) for the cube and the (1, 1, 1) for the octahedron. These are the same bands which show large values of K .

Type (c) occurs when the Bragg planes are perpendicular to lines connecting opposite corners of the crystal, the (1, 1, 1) for the cube and the (1, 0, 0) for the octahedron. Type (b) occurs for the (1, 1, 0) band in both cases. In both the cube and the octahedron the (1, 1, 0) planes are perpendicular to lines connecting the centers of opposite edges of the crystal. The extension of this correlation to the case of crystals of dodecahedral shape would suggest that in this case the (1, 1, 0) diffraction band would be of type (a).

These results have been obtained by assuming that the third integral, W , of Eq. (14) was negligible. This will not be true if M is very small. By Eq. (20) and Table II we may now estimate the value of M and compute corrections to account for the finite value of W . If $W \neq 0$, we must write in place of L' of Eqs. (18) and (19), $(L + W)/(L_0 + W_0)$ in which W_0 is the value of W when $v = 0$.

If W is small compared with L_0 we may write $(L + W)/(L_0 + W_0) = L' + (W/L_0) - (W_0/L_0) L'$ and compute W by Eq. (16) taking $p^2 = (1.2v')^2 = L_0$. This gives for the correction to be applied to L' ,

$$\Delta L' = W/L_0 - (W_0/L_0)L' = Cv'^2 \{ (v/v')^2 e^{-v^2/p^2} - 1.2^2 (L' - e^{-v^2/p^2}) \}. \quad (21)$$

This may be readily computed. C is given in Table I; v' in Table II; v/v' are the abscissa of Fig. 4; and e^{-v^2/p^2} are the corresponding ordinates of the unbroken line curves of Fig. 4.

At the half intensity point, Eq. (21) reduces to $\Delta L' = \frac{1}{2} Cv'^2$. If we assume the slope at the half intensity point to be that of the unbroken line curve we obtain for the correction to be applied to v' ,

$$\Delta v' = 0.72 Cv'^3. \quad (22)$$

Thus v' may be corrected for the finite value of W by multiplying it by the factor $(1 + 0.72 Cv'^2) = (1 + 1.8 CK^2)$. Since K and K' are proportional to v' this same correction factor may be applied to them and also to the values of D and M as computed by Scherrer's equation.

Eqs. (8) and (10) have been derived for the face-centered, as well as for the simple lattice. They may be shown to hold for the body-centered lattice as well. It follows that J' , its integral, L , and the results shown in Tables II and III and Fig. (4) hold for any of these space lattices. However, the corrections to these results computed by Eqs. (21) and (22) vary with the space lattice. The corrections have been derived on the assumption that the diffracting material is concentrated at the points of the lattice. Actually these points are merely centers of space distributions of diffracting material. Since the corrections depend upon the distribution of diffracting material within the unit cell, a more exact determination of W than that given by Eq. (16) does not seem to be warranted by the assumptions.

It has been assumed throughout the discussion that the crystalline powder is made up of crystals of uniform size. In practice this assumption is frequently not justified. Any attempt to determine the size distribution from the x-ray diffraction pattern requires a knowledge of the theoretical form of

the band for the case of uniform size. Indeed it was this requirement which instigated this investigation. The closeness with which the form of the diffraction bands agrees with the Gauss error curve as shown in Fig. 4 makes it possible to assume this form for the purpose of estimating the distribution of particle size. The (1, 1, 0) band is particularly suitable for this purpose. It is hoped that studies of the form of the (1, 0, 0) and (1, 1, 1) bands together with studies of the relative width of the bands will lead to information as to the shape of the colloidal crystals in cases where there is approximate uniformity of shape.

The shape of the x-ray diffraction bands of a very fine uniform crystalline powder has been computed for the (1, 0, 0), (1, 1, 0) and (1, 1, 1) planes of cubical and octahedral crystals of the regular system. The results are shown in Fig. 4 plotted to such scales that the maximum ordinate is 1 and the half intensity breadth, 2. The coefficient K of Eq. (1) which relates the half intensity breadth of a band to the size of the crystal has been computed for each case. The values are shown in Table III. In comparing these theoretical results with experimental data, one must take care to comply with the following conditions.

- (a) The experimental data must be corrected for "background" radiation and instrumental errors.
- (b) The corrected data must be multiplied by the asymmetrical factor, $[1 + \frac{1}{2} \cot(\theta_0/2) \Delta\theta]$ of Eq. (19).
- (c) An approximate value of M should be computed by Eq. (20) and Table III.
- (d) The corrections to the ordinates of Fig. 4 may then be computed by Eq. (21) and Table I and the approximate value of M may be corrected by the factor $(1 + 1.8 CK^2)$.

I wish to express my thanks to Sir William Bragg and to the managers of the Royal Institution for putting at my disposal the facilities of the Davy-Faraday Laboratory where the work of this investigation was started. I wish also to acknowledge the valuable assistance of Miss M. A. Ewer who carried out a considerable part of the computations.

SPECTRAL PHENOMENA IN SPARK DISCHARGES

By J. W. BEAMS

ROUSS PHYSICAL LABORATORY, UNIVERSITY OF VIRGINIA

(Received November 29, 1929)

ABSTRACT

Two methods are described for measuring the differences in the time of appearance of the spectrum lines in sparks. The first is a refinement of the Kerr cell method previously used and a detailed description of its use is included. The criticisms of Gaviola of the method are shown not to apply. The second method makes use of a rapidly rotating mirror which either reflects the dispersed light of the spark to a photographic plate or the undispersed light to the slit of a spectrograph. In either case the position of the beginning of a line on the photographic plate gives its time of appearance. The method of Henriot and Hunguenard was used to rotate the mirror. Photographs of sparks are shown with the mirror rotating 1830 r. p. s. However, higher rotational speeds have been used. It is concluded that the Kerr cell method is superior for examining the air lines in the initial stages of the spark; while the rotating mirror method is better in studying the appearance and duration of the metallic lines which are not present in the very first stages of the spark discharge.

ALTHOUGH the electric spark in air has been the subject of a very large number of careful investigations, most of the mechanisms in the various stages of the discharge still remain obscure. This state of affairs probably results from the fact that the essential phenomena of the spark occur in such a short interval of time that the apparatus used in most cases failed to separate them into their component parts. However, during the last few years considerable progress has been made in the study of the various stages of the spark, due largely to the development of several methods of investigation that make it possible to study processes occurring in from 10^{-6} to 10^{-9} sec. It is the purpose of this paper to describe two independent methods of investigating the spark discharge and to record some of the results obtained.

When the sparking potential is first applied across a spark gap the discharge does not take place instantaneously, but a certain average time is required for the initiation of the discharge.¹ This time—usually called the time lag of the spark—is decreased by increasing the overvoltage and becomes in some cases of the order of magnitude of 10^{-8} sec.²

When once the discharge is initiated and the effective resistance across the gap starts falling, very little is definitely known of the process except

¹ Sir J. J. Thomson, *Conduction of Electricity Through Gases*, Cambridge University Press, 2nd Edition, p. 431.

² P. O. Pedersen, *Ann. d. Physik* **71**, 317 (1923); Rogowski, *Archiv f. Electrotech.* **16**, 496 (1926); Torok, *Jour. A.I.E.E.* **47**, 177 (1928); Beams, *Jour. Franklin Inst.* **206**, 809 (1928); L. B. Loeb, *Science* **59**, 509 (1929)—Suggests a possible explanation of these short time lags.

that the potential across the gap does not fall instantaneously to zero but decreases at a finite and measurable rate.³

If the light emanating from the spark in air during its initial stages is examined spectroscopically, it is found that all the spectrum lines do not appear simultaneously. In general the air lines appear first, followed by the spark lines of the metal with the metallic arc lines appearing last. Observations on these phenomena were first made by Schuster and Hemsalech,⁴ while they were studying the duration of lines in metallic sparks. Their method consisted essentially in projecting the spectrum on a rapidly moving photographic film and measuring the relative positions of the various parts of the lines. Other workers⁵ have observed the spark in a rotating mirror with similar results. The time resolving power of their methods, however, was not sufficient to give anything but rough qualitative results. Recently⁶ a method based upon the findings of Abraham and Lemoine⁷ that the Kerr effect in some liquids disappears very quickly after the electric field producing it is relaxed, has been successfully used to measure the order of appearance of spectrum lines in condensed discharges. By this method the values for the differences in the time of appearance of the various air lines themselves as well as the lines of a few metals were measured directly in terms of the velocity of light.⁸ Since that time the method has been considerably refined and the observations on the air lines repeated. These values have also been confirmed by a rotating mirror method within the limits of precision of the latter method.

The experimental arrangement, except for refinements and details, is essentially the same as that previously described. The method, however, has been recently questioned⁹ on the basis that oscillations of large amplitude should exist that would complicate the results.* Since in the work care was taken to investigate experimentally the magnitude of the oscillations present and, since the writer believes the method might find applications to other experiments, it will be described somewhat more in detail.

In Fig. 1 light from the spark *A*, made parallel by a lens *L*, plane polarized by a Nicol prism *N*₁, passes through a Kerr cell *K*, made by immersing two parallel metallic plates in CS₂, into a second Nicol prism *N*₂ crossed with

³ Lawrence and Beams, *Phys. Rev.* **32**, 483 (1929).

⁴ Schuster and Hemsalech, *Phil. Trans.* **193A**, 212 (1900).

⁵ E. C. C. Baly, *Spectroscopy* **2**, 153 Longmans (1927).

⁶ Brown and Beams, *J.O.S.A.* **11**, 11 (1925).

⁷ Abraham and Lemoine, *Comptes Rendus* **129**, 206 (1899).

⁸ Beams, *Phys. Rev.* **28**, 475 (1926).

⁹ Gaviola, *Phys. Rev.* **33**, 1023 (1929).

* Note: In the writer's opinion the questions raised by Gaviola (*loc. cit.*) and by L. V. Hamos [*Zeits. f. Physik* **52**, 549 (1928)] concerning the "electro-optical shutter" have been adequately investigated and reported [Beams and Lawrence, *Jour. Franklin Inst.* **206**, 169, (1928)]. The cause of the discrepancy in the values in the difference in the average lags of the Faraday effect as observed by Beams and Allison, [*Phys. Rev.* **29**, 161 (1927)] and Allison, [*Phys. Rev.* **30**, 66 (1927)], which Dr. Gaviola claims no attempt was made to explain, was investigated and discussed by Allison in the paper referred to and shown to be due to the effect of wave-length upon the lag.

respect to N_1 . If a potential is applied across the plates of K and the plane of polarization of the light makes an angle (45° in these experiments) other than zero or 90° with the lines of force, light can pass N_2 because of the double refraction in K .¹⁰ This double refraction produced in CS_2 by the electric field is called the Kerr effect. If μ_1 and μ_2 are the refractive indices for the

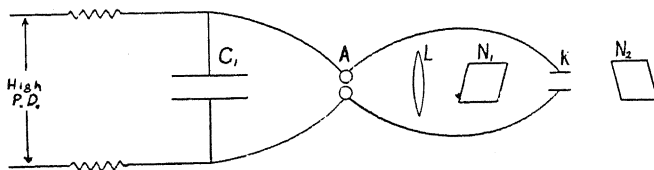


Fig. 1

two rays then their phase difference after passing through the Kerr cell K is $D = 2\pi l / \lambda (\mu_1 - \mu_2) = 2\pi B l E^2$, where λ is the wave-length of the light, B is a constant for a given substance, wave-length and temperature, l is the length of the light path through the liquid, and E is the electric field strength. The intensity of light passing N_2 is

$$I = A \sin^2 D/2 = A \sin^2 \pi B l E^2$$

where A is a constant. As a result, for comparatively small values of D (6° to 16°) as used in most of these experiments, the intensity of light passing N_2 varies approximately as the fourth power of the field strength.

If an electric potential is slowly applied across the spark gap A in air until the spark discharge takes place, it has been previously found that no light from the spark intense enough to be detected by the eye passes N_2 , provided the lead wires are not too long and are approximately the same length as the light path. The Kerr effect in K therefore effectively vanishes by the time that the light reaches the cell, or the light from the spark is too faint to be observed for a certain time after the beginning of the discharge. If, however, the lead wires from A to K were lengthened, the light path remaining fixed, light passes N_2 . When the light was examined spectroscopically it was found that the spectrum lines for any given substance appeared in a definite order which was not a function of their wave-length or of their intensity when measured over the entire duration of the spark.

Fig. 2 shows schematically the arrangement used to measure the time between the appearance of the lines directly in terms of the velocity of light. The arrangement in Fig. 1 is merely modified to allow the light to pass to a movable trihedral mirror system M_1 before entering the cell. The mirror system, designed by Professor L. G. Hoxton, returns a beam of light parallel but displaced. The three mirrors silvered on the front surface are mutually perpendicular and mounted on a steel frame which slides on a wooden track 23 meters in length. The optical system was adjusted (with Nicol prisms uncrossed) until the intensity of the light passing N_2 remained constant while the mirror system was moved throughout the length of its track.

¹⁰ Kerr, Phil. Mag. 1, 337 (1875); 8, 85 (1879).

The lead wires from A to K were either symmetrical and equal in length or one of the leads was removed and one side each of A and K grounded with short wires to high capacity grounds as shown in Fig. 2. The lead can be lengthened or shortened over the ranges being investigated by a sliding copper bar T . The inductance and capacity of both the lead wires and K were made as small and uniformly distributed as conveniently possible. In some of the experiments a resistance $R = (L/C)^{1/2}$ (app. 500 ohms),

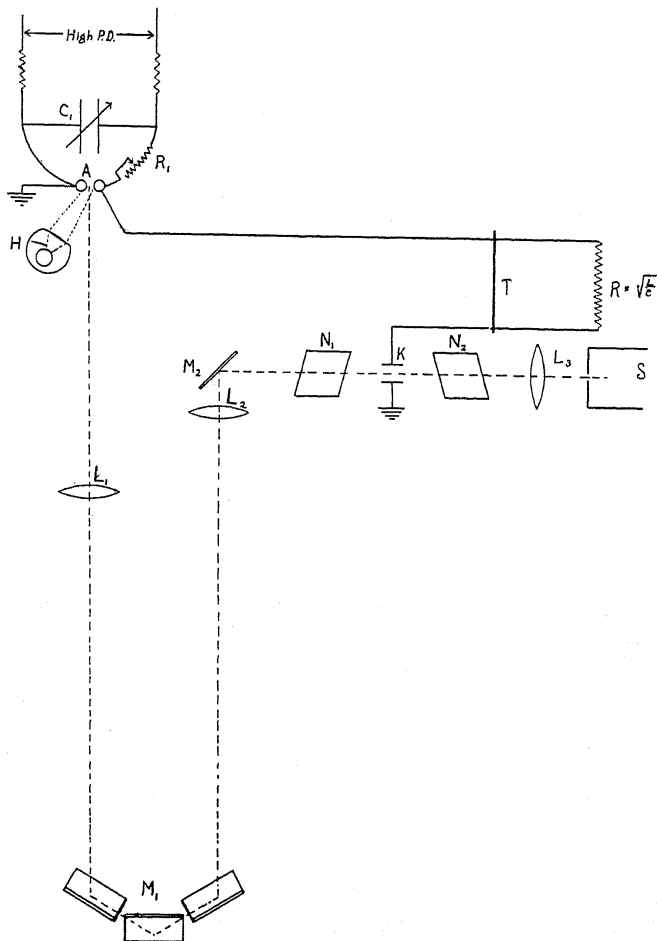


Fig. 2

where L and C are the inductances and capacities per unit length of the wire, is attached across the open ends to prevent possible reflections of the initial transients; while a variable capacity C_1 (0.0005 to 0.005 microfarads) and variable resistance R_1 were used to change the conditions in the spark. The circuit containing C_1 is in a plane at right angles to the Kerr cell circuit to avoid unnecessary inductive coupling. The spark gap A was illuminated by a source of ultra-violet light H placed vertically over it and in

a direction at right angles to the direction in which the light of the spark is observed. This reduces the time lag and causes the spark to jump at approximately the same potential each time.

When the spark at *A* takes place, the potential across it does not fall to its low later value instantaneously.³ Some recent unpublished work done by Dr. L. B. Snoddy in this laboratory indicates that the exact rate of fall of potential is not completely independent of the circuital factors, as, for example, the rate at which energy is fed into the spark, but that under the conditions here used the potential probably falls to half value within the limits of 10^{-9} to 3×10^{-8} sec. Of the remainder of the potential-time curve very little is definitely known. The fall of potential travels along the lead wires at approximately the velocity of light and starts discharging *K* at a time equal to the length of lead wire divided by the velocity of light after the beginning of the fall of potential across *A*. Now since it is possible to reduce the capacity of *K* to a comparatively small value (4 cm) the rate of fall of potential across *K* follows roughly the rate of fall across *A* but at a definite time later.*

If the exact rate of fall of potential across *K* were definitely known, it would then be possible to compute the time of optical cut-off, since a possible lag in the Kerr effect of CS_2 is at least short enough to be here neglected.¹¹ Such computations show that the intensity of the light passing *N*₂ has dropped to $1/e$ of its value by the time that the potential across *K* falls to 0.77 of its original magnitude. The cell is therefore effectively closed before the potential across *K* drops to half value. If, then, the amplitude of oscillations in the Kerr cell does not exceed $1/2$ the initial potential, when once the cell closes, it does not again effectively re-open.

The fact that the amount of light passing *N*₂ after the first optical cut-off was too small to effect the results obtained could easily be tested experimentally. The lead wire from *A* to *K* was lengthened until one or two lines appeared in the field of view. Then as the mirror system *M*₁ was slowly moved backward increasing the optical path, the intensity of the lines showed no rapid decreases and, when once they disappeared, did not reappear while the light path was lengthened over 30 meters. This shows that there are no effective short oscillations. Oscillations of longer period were also tested for by placing a mirror rotating at 2000 revolutions per second behind the cell and observing the light flashes passing *N*₂. The rotating mirror could easily resolve less than 10^{-7} sec, yet the spark appeared when reflected from the mirror as a single sharp image.

It was very easy, however, to introduce oscillations large enough to cause trouble by adding inductance and capacity or by sufficiently lengthening the lead wire from *A* to *K*. In fact, with a cell of 4 cm capacity and about 16 meters of lead wire the oscillations become very troublesome, although

* Note: By carefully purifying the CS_2 smaller cells than 4 cm can be used without sacrificing intensity of light passing *N*₂ for as is well known the dielectric strength of CS_2 can be considerably increased by careful purification.

¹¹ Beams and Lawrence, Jour. Franklin Inst. 206, 169 (1928).

longer wires than this have been used successfully. When a low resistance (5.2 ohms) thermocouple galvanometer was placed in series with K and the lead wires lengthened, the readings of the galvanometer, which gave an indication of the magnitude of the oscillations present, increased relatively fast for the first 2 or 3 meters, then increased slowly as more wire was added. Similar observations were made with a wave meter having a vacuum tube voltmeter as an indicator, by means of which an estimate of the amplitude of the oscillations could be obtained. The frequency of course decreased with increase of wire path. A method making use of Lichtenberg figures¹² was also used to get the maximum potential that was applied across the cell after the initial field is relaxed. The method as used here is only approximate but it indicated that the potential never attained more than one half its original value over the wire path range used, at least in the investigation of the air lines.

The fact that the oscillations in K did not have an amplitude greater than one-half the initial potential of the spark might at first seem surprising, but when consideration is taken of the resistance in the spark in its initial stages, the high frequency resistance of the wires, corona losses, etc., this relatively large damping is to be expected. The resistance of the spark gap during its initial stages is not known, but it must fall from a very large value to a comparatively small one in less than the time required for the potential to drop to a low value. If then one-fourth the oscillation period of the Kerr cell circuit is of the same general order of magnitude as that of the time required for the resistance and potential to fall in the spark, the oscillation in the Kerr cell will be highly damped during a part of its first quarter of a period. As the lead wires are lengthened the inductance and capacity of the Kerr cell circuit are increased and hence the amplitude of oscillations, which occur after the initial transient has discharged the Kerr cell, is increased. An increase of lead wire also increases the period of the oscillations as was observed. If, therefore, very long leads are used, it is necessary to introduce resistance. The addition of resistance lengthens the time of optical cut-off, but in most of the work, especially when long leads are used, the cut-off can be slowed down considerably without the introduction of serious complications. The oscillating circuit containing C_1 and A can be changed over a fairly wide range without producing undesirable oscillations in K . This results from the fact that when once the potential across A falls to a low value and the air in the gap is ionized, it does not again rise to a value that, when applied across K , will cause an appreciable amount of light to pass N_2 . This condition holds, of course, only when the oscillations in C_1 , as in all these experiments, are rapid enough to prevent complete deionization in the gap between half oscillations. Also, since the circuit containing C_1 is not coupled to the circuit containing K except through the spark gap A , oscillations of amplitude large enough to give trouble should not be induced in K even for narrow bands of harmonics, as these, under the given conditions, have too little energy to be effective.

¹² P. O. Pedersen, K. Danske Vidensk. Selkab. 1, 11 (1919); 4, 7 (1922); 8, 10 (1929).

The light after leaving N_2 either is focused on the slit of a spectroscope so that the length of the spark is parallel to the slit, or else the image is examined by means of a direct vision prism. The direct vision prism resolves most of the lines without a slit because of the fact that the spark starts as a narrow thread and expands radially. The air lines appear the full length of the gap. Table I gives the time of appearance of the strong air lines (since it was necessary to use a spectrograph of large light-gathering power and

TABLE I.

Wave-length	Classification ¹³		Intensity	Interval (sec. $\times 10^8$)
5011	$1^3P_1' - 1^3S_1'$	N II	3	0.8
5007	$1^3S_1' - 1^3P_2'''$	N II	4	
5005	$1^3D_3' - 1^3F_4'$	N II	10	
5001	$\begin{cases} 1^3D_2' - 1^3F_3' \\ 1^3D_1' - 1^3F_2' \end{cases}$	$\begin{matrix} \text{N II} \\ \text{N II} \end{matrix}$	10	
4643	$1^3P_2' - 2^3P_1$	N II	8	1.4
4631	$1^3P_2' - 2^3P_2$	N II	10	
5680	$1^3P_2' - 1^3D_3'$	N II	10	
5676	$1^3P_0' - 1^3D_1'$	N II	6	
5667	$1^3P_1' - 1^3D_2'$	N II	8	

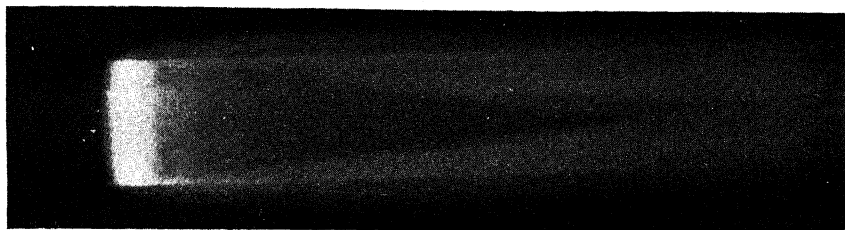
fairly wide slit, the members of the above groups of lines were not clearly resolved.) with respect to the first line that appears. The observations could be repeated with a precision of 3×10^{-9} sec. It will be noted that the order of appearance is not a function of intensity or of wave-length and therefore not the result of the electro-optical dispersion in K . This dispersion in double refraction should make the lines seem to appear in the order of increasing wave-length, but as previously pointed out, is too small to produce serious error under the experimental conditions. When the lead wires were lengthened, the spark lines of the metal appeared as points on the electrodes, followed in turn by the metallic arc lines. The fact that the metallic lines appear in the field of view as points introduces the greatest difficulty in determining the time of their appearance; in fact, some of the previous values for the metallic lines are perhaps somewhat in error due to this cause. Photometric measurements on the rate of increase of intensity of these metallic lines have been attempted but without much success. The rate of evaporation of the metal is apparently variable but a more serious difficulty arises because of the uncertainties of the photographic plate when illuminated with light flashes of short duration.¹⁴ The Clayden effect and other effects that are probably related to it make practically all photographic measurements of light intensities with flashes as short as 5×10^{-8} sec. very unreliable. For example, if a photographic plate is slightly fogged by a weak light as is sometimes done to photograph faint sources of light¹⁵

¹³ Fowler and Freeman, Proc. Roy. Soc. A114, 662 (1927).

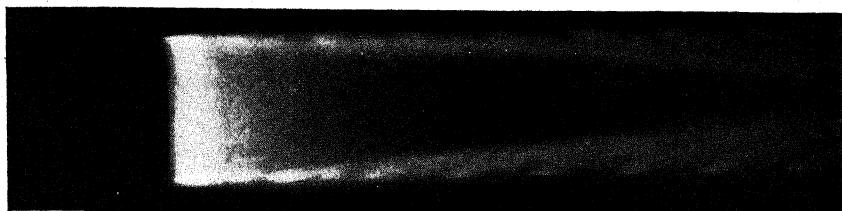
¹⁴ R. W. Wood, Astrophys. J. 17, 361 (1903). Lüppo-Cramer Grundlagen d. Photographischen Negativverfahren Halle 1, 608 (1927).

¹⁵ R. W. Wood, Astrophys. J. 27, 379 (1908).

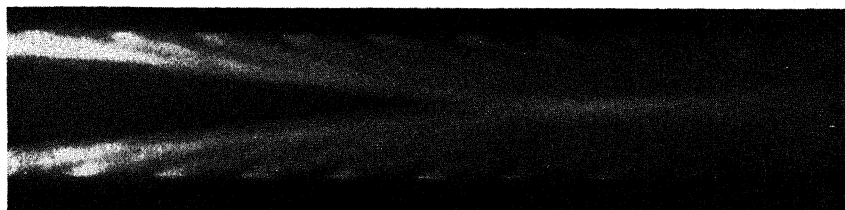
and then illuminated with a short flash, the image of the flash on the plate is usually reversed. Even when the plate is exposed to the flash alone and care is taken to prevent, as far as possible, fogging by other light, any developer fog is reversed. The intensity of the light is always a factor; a



A. Mg gap. = 7 mm



B. Bi gap = 8 mm



C. Bi gap = 8 mm



D. Bi

Fig. 3

faint flash produces a reversal, while a more intense flash gives the ordinary image with usually a reversal around its edges. Attempts have been made to eliminate these troubles but, in the case of flashes less than 5×10^{-8} sec. in duration without much success.

Because of these difficulties with the Kerr cell method when used for observing the metallic lines, as well as the fact that its precision decreases in

the later stages of the spark, a search has been recently made for an independent and complementary method of study. The method finally adopted has been made possible by the development by Henriot and Hunguenard¹⁶ of a means of obtaining high rotational speeds. A mirror 12×12 mm is mounted on a cone shaped piece of metal which rides on a whirling cushion of air. With this arrangement the angular speed is in general limited only by the viscosity of the gas, its molecular velocity and the strength of the rotating parts.

The light from the spark passes through a lens, is reflected by a rotating mirror and falls upon a photographic plate placed at the focus of the lens. Fig. 3, A. B. C. give traces of the image of a spark between magnesium electrodes and bismuth electrodes, each moving 1,300,000 cm/sec. perpendicular to its length. In each case the constants of the circuit are the same. It will be specially noted that the spark first appears as a bright streak completely across the gap. This bright streak fades out very quickly, but the luminosity persists near the electrodes and gradually moves toward the center of the gap. The visible spectrum of the bright streak is composed of air lines and that of the luminous streamers emanating from the electrodes, metallic lines. In the bismuth spark the curved metallic streamers which start from the cathode each half oscillation and move with diminishing velocity until they reach the moving vapor front are very distinct on the original plate. These streamers have been previously observed by several experimenters,⁵ but whether they are jets of luminous vapor or pulses of luminosity in the vapor has not yet been completely settled.

Fig. 3 D shows the image of the spark moving parallel to its length. A narrow portion is isolated by a slit perpendicular to the spark to prevent overlapping errors. It will be noted that the spark starts as a thread and expands radially. When the slit was removed or moved to allow only the light from near and including that on the surface of the electrode to reach the plate, and the light dispersed by a prism just before reaching the rotating mirror, the time of appearance of the various spectrum lines could be observed. Similar observations were made when the moving image of the spark fell upon the slit of a spectrograph. The photographs show plainly that the air lines appear first, followed by the spark and later by the arc lines. The technique, however, is not yet developed to a stage where the members of the metallic arc triplets can be distinctly separated, due probably to the photographic errors previously discussed. The limiting factor here seems to be intensity and not angular speed because it is not especially difficult to obtain rotational speeds of 4000 r. p. s. and this can be multiplied several times by simply allowing the light to be reflected from stationary mirrors back to the rotating mirror again. The work, however, is being continued with a better arrangement than that previously used.

The above experiments together with those performed by other investigators^{5,17} show definitely that the various spectrum lines in the spark appear

¹⁶ Henriot and Hunguenard, *Jour. d. Phys. et Ra.* 8, 443 (1927).

¹⁷ Locher, *J.O.S.A.* 17, 91 (1928).

at different times after the beginning of the discharge where by the appearance of a line is meant the time required for the line to become visible through the observing apparatus. However, there is a disagreement in the values obtained by Locher and the writer using similar methods. The difference perhaps lies partly in the larger Kerr cell used by Locher, which would lengthen the time for his cell to cut off. This probably explains, in part at least, why he could not completely extinguish the air lines with lead wires of the same length as his light path, for the intensity of the light passing his cell at maximum voltage was considerably less than that used by the writer so that any errors due to light intensity are in the wrong direction to explain the difference. He also had no way of slowly varying his light path which has been found essential in the above work in testing for troublesome oscillations, or of measuring his time directly in terms of the velocity of light.

The principal factors that determine the appearance of a spectrum line during the initial stages of a spark discharge through a gas must be the average time required to put the atom in the properly excited state by the discharge, the average time it remains excited, and the rate with which it radiates energy when once it starts radiating. In the case of the air lines the sum of the last two factors would be expected from the general results of canal ray experiments¹⁸ to be of the right order of magnitude to explain the observed time between the appearance of the groups of nitrogen lines. This then suggests that in the first stages of the discharge through air where a large number of atoms must be ionized before the potential can fall to a value which will effectively close the cell, that there is a correspondingly large number of atoms multiply ionized and excited to the upper energy levels of the strong air lines. Also, the distribution of excited atoms among the various upper levels of the strong lines probably does not change during the initial stages of the spark. It is possible to study the effect that the average time an atom holds its energy has upon the appearance of spectrum lines in the case of the arc triplets of zinc and cadmium. These triplets have the same upper energy level and therefore should be independent of the conditions of excitation in the discharge. In previous work⁷ these lines were found to appear at different times but it has not yet been possible to increase the time-resolving power of the rotating mirror method to a point where a difference in the time of appearance of the lines can be observed. This is necessary before definite conclusions should be drawn because it will then be possible to change the excitation conditions over a very much wider range than was possible with the Kerr cell method and thus make certain any possible effect of the discharge.

The writer is indebted to Professors L. G. Hoxton and C. M. Sparrow of this Laboratory and to Professor E. O. Lawrence of the University of California for many valuable criticisms of part of the work. He is also very grateful to Mr. A. J. Weed, instrument maker, for help in the construction of apparatus.

¹⁸ Wien, *Ann. d. Physik* **66**, 229 (1921); **73**, 483 (1924). McPetrie, *Phil. Mag. Series 7*, **1**, 1082 (1926).

VIBRATIONAL QUANTUM ANALYSIS AND ISOTOPE EFFECT FOR THE LEAD OXIDE BAND SPECTRA*

BY SIDNEY BLOOMENTHAL

RESEARCH DEPARTMENT, RADIO CORPORATION OF AMERICA, NEW YORK CITY†

(Received November 19, 1929)

ABSTRACT

Each strong line (Pb^{206}O) in the band spectrum emitted by a uranium lead arc in air is represented by three lines ($\text{Pb}^{208}, ^{207}, ^{206}\text{O}$ with relative intensities in agreement with Aston) in the band spectrum from an ordinary lead arc. The first and second orders of a 21 ft. Rowland grating were used to make this comparison. The observed separations between corresponding band lines of isotopic molecules are in good agreement with the theory of the isotope effect in band spectra with PbO as the emitter.

New measurements of the wave-lengths of the band heads were made from moderate dispersion spectrograms of the ordinary lead arc in air. The bands in the near ultra-violet form a new system**

$$\nu = 30,197.0 + [530.6(\nu' + \frac{1}{2}) - 1.05(\nu' + \frac{1}{2})^2] - [722.3(\nu'' + \frac{1}{2}) - 3.73(\nu'' + \frac{1}{2})^2].$$

Three other systems in the visible have been discussed already by Mecke. Evidence in favor of combining two of these systems (*C* and *B*) into one is presented. All of the band systems have a common lower state.

INTRODUCTION

THE lead arc in air gives a fairly bright band spectrum consisting of a large number of heads all degrading towards longer wave-lengths. The same spectrum appears with compounds of lead subjected to a variety of conditions of excitation, and consequently there has been a great deal of speculation concerning the identity of the emitter.¹ Using low and moderate dispersion, Eder and Valenta² photographed the bands excited upon the introduction of lead chloride into an oxygen illuminating gas flame. They gave wave-length measurements of the heads to four figures, and believed that lead oxide was the emitter. Using the same method of excitation, Lamprecht³ photographed the visible region at moderate dispersion, and in addition the yellow green region at high dispersion, failing however to resolve the fine structure completely.

Grebe and Konen⁴ photographed the spectrum of a carbon arc containing ordinary lead chloride at high dispersion, and repeated using uranium lead

* Paper presented at the Annual Meeting of the A. P. S., New York City, Dec. 28, 1928 (cf. Phys. Rev. 33, 285 (1929)).

† This work was done at Ryerson Physical Laboratory of the University of Chicago.

** The symbol ν is used in this work for the vibrational quantum number.

¹ H. Kayser, Handbuch der Spektroskopie, VI 256.

² J. M. Eder und E. Valenta, Atlas Typischer Spektren 17, Wien, new printing 1924.

³ H. Lamprecht, Zeits. f. Wiss. Phot. 33, 10, 16 (1911).

⁴ L. Grebe und H. Konen, Phys. Zeits. 22, 546 (1921).

chloride. They limited themselves to a narrow region in the blue and found that the isotope effect was evident only as a slight wave-length shift and difference in the degree of sharpness of the band spectrum lines compared.

The first part of the present work deals with the vibrational quantum analysis of the lead oxide bands. New measurements of the wave-lengths of the band heads, believed to be more accurate than existing data, are used for most of this analysis. The isotope effect served to guide this part of the work.

In the second part the observed isotope effects will be discussed in detail, and it will be shown that the comparison of the single lines from uranium lead (Pb^{206}O) with the corresponding lines in the triplets $\text{Pb}^{208}, ^{207}, ^{206}\text{O}$ from ordinary lead is in quantitative agreement with the fact that ordinary lead contains isotopes 208, 207, 206.⁵ This comparison furnishes a direct test of the theory of the isotope effect in band spectra.

While this work was in progress, and after preliminary reports on the isotope effect had been issued,⁶ a short paper by Mecke⁷ appeared dealing with his independent work based on Lamprecht's data, leading to a vibrational quantum analysis. These data are not quite complete since Lamprecht gives no measurements of the bands in the red and near ultra-violet. Further details of Mecke's work will be taken up later.

EXPERIMENTAL PROCEDURE

Measurements were made from moderate dispersion spectrograms of the ordinary lead arc in air. In addition comparisons and measurements were made from high dispersion spectrograms in the study of the band structure and isotope effect, and these spectra were taken first with an ordinary lead arc and then with a uranium lead arc. The uranium lead used originated in Belgian Congo ores, and had an atomic weight of 206.1.

The arc electrodes were copper rods $\frac{1}{2}$ " in diameter. A bead of a molten alloy of copper and lead was formed on both the upper (—) and lower (+) electrodes while the arc was in progress by melting pure thin copper wire and lead filings. With the proper proportions of lead and copper in each of the two beads, the arc had a blue color and emitted the lead oxide bands in a satisfactory manner. Fresh lead filings were added at intervals of several hours to prevent the appearance of the green tinge denoting strong emission of the copper spectrum. Copper lines were present on the spectrograms but did not interfere seriously with the work. The red copper oxide bands, generally recorded in a few minutes when the copper arc itself is used, were weak or entirely absent. The current carried was three amperes supplied at 220 volts with a suitable series resistance.

Spectrograms were taken with the Hilger Littrow-mounted E1 prism spectrograph, having a dispersion with the glass optical system of approximately 21A/mm at 6500A to 6A/mm at 4400A, and with the quartz system of 14A/mm at 4200A to 5.8A/mm at 3200A. The resolution of the structure

⁵ F. W. Aston, *Nature* 120, 224 (1927).

⁶ S. Bloomenthal, *Phys. Rev.* 33, 285 (1929). *Science* 69, 229, 676 (1929).

⁷ R. Mecke, *Die Naturwissenschaften* 17, 122 (1929).

lines is incomplete and the heads are single and fairly sharp except where overlapping is great. Exposure of one hour sufficed with the E1.

The high dispersion work was done in the first and second orders of the six inch 21 ft. Rowland concave grating having about 14,500 lines per inch and set up in a Rowland mounting. The dispersion in the first order is about 2.63A/mm. The exposure time was usually in excess of 15 hours. Fine grained plates were used in most of the photographic work. Iron lines were placed on the plates before and after exposure. Shifts due to temperature changes were minimized by an efficient system of temperature control consisting of thermostat, fan and heating unit with a mercury current break actuated by a sensitive relay circuit.

Reductions of the measurements of the moderate dispersion plates were made using the Hartmann⁸ formula and an automatic Monroe calculating machine. The residuals were small, generally of the order of 0.02A. The formula was applied to only about 200A of the plates at any one time. Kayser's "Schwingungszahlen" served to convert the corrected measurements to vacuum wave-numbers. The iron line wave-lengths selected by the International Astronomical Union served as standards⁹ in most of the reductions.

VIBRATIONAL QUANTUM ANALYSIS

In making the assignment of v values the new data on band head wave-lengths, which are believed to be better than the older data, were used. These were supplemented, however, where necessary by older values. This assignment is in agreement with the observed isotope effects (to be described later) using half integral values for the vibrational quantum number following Mulliken,¹⁰ who first found them necessary in the analysis of the BO band spectra. The suggestions of Birge¹¹ proved useful in evaluating the constants in the empirical frequency equations by means of a consideration of the first and second differences of the wave-numbers in the usual two dimensional matrix diagram.

Assuming that the head is close to the band origin, where the change in rotational energy is approximately zero, one employs the following formula for the frequency of a band head

$$\nu = \nu^0 + \omega_e'(v' + \frac{1}{2}) - x'\omega_e'(v' + \frac{1}{2})^2 + \omega_e''(v'' + \frac{1}{2}) - x''\omega_e''(v'' + \frac{1}{2})^2$$

where ω_e is the frequency of vibration for infinitesimal amplitude and v is the vibration quantum number which takes integral values 0, 1, 2,.... Primes (') and double primes (') refer, respectively, to the quantity indicated in the upper and lower electronic states.

Mecke assigned the bands in the wave-length region covered by Lamprecht's data to three systems A , B and C . The bands of the C system were extremely weak on the plates taken by the writer, and hence no measure-

⁸ A. Hartmann, *Astrophys. J.* 8, 218 (1898).

⁹ H. Kayser, *Op. Cit.* VII 405.

¹⁰ R. S. Mulliken, *Phys. Rev.* 25, 259 (1925).

¹¹ R. T. Birge, *Nat. Res. Council Bulletin* 57, 11, 123 (1926).

ments were made on such heads. The writer has found an additional system *D* in the region 3209—3594Å which was not photographed by Lamprecht. The band head data and vibrational quantum assignments for the *A*, *B* and *D* systems are given in Tables I, II and III.

The data apply to band heads. In the case of PbO the origin of each band as shown by the results of the following paper lies close to the head. *I* is the relative photographic intensity of the band as a whole, λ the wave-length in air in international Angstroms and ν the vacuum wave-number. *O-C* is the difference between the observed wave-number and the value calculated from the proper empirical formulas given below. Under remarks brackets [] denote masking by a band of higher frequency whose ν values are enclosed. In some cases of masking it was not possible to secure the measurement of a head and the value of the wave-number calculated from the appropriate empirical formula is given in brackets. In such instances the relative intensity estimate was made from the plate enlargement, although the head was not measured. In cases where a measured wave-number value is classified in two systems, evidence justifying this has been found in extensive overlapping of the fine structure examined at high dispersion. The wave-number data for systems *A*, *B* and *D* are from new measurements.

When the suitable ν' and ν'' values are inserted, the following formulas give the wave-number of a classified band head to within a small difference from the measured value.

For heads in system *A*

$$\nu = 19,863.3 + [451.7(\nu' + \frac{1}{2}) - 3.33(\nu' + \frac{1}{2})^2] - [722.3(\nu'' - \frac{1}{2}) - 3.73(\nu'' + \frac{1}{2})^2]$$

For heads in system *B*

$$\nu = 22,289.8 + [496.3(\nu' + \frac{1}{2}) - 2.33(\nu' + \frac{1}{2})^2] - [722.3(\nu'' + \frac{1}{2}) - 3.73(\nu'' + \frac{1}{2})^2]$$

For heads in system *D*

$$\nu = 30,197.0 + [530.6(\nu' + \frac{1}{2}) - 1.05(\nu' + \frac{1}{2})^2] - [722.3(\nu'' + \frac{1}{2}) - 3.73(\nu'' + \frac{1}{2})^2]$$

Because of the fact that the isotope effect is unresolved at moderate dispersion, the constants given in these formulas are but approximations.

It is evident from inspection of these equations that all three systems have a common final state, which is probably the normal state of the PbO molecule. The systems *A*, *B* and *D* arise then from transitions from 2.5, 2.8, and 3.7 volt electronic levels, respectively, to this common lower state.

Mecke's equations based on Lamprecht's data are

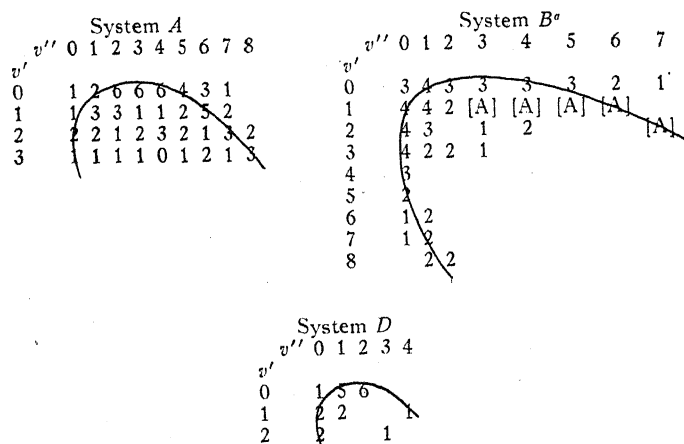
$$(A) \quad \nu = 19,877 + [445(\nu' + \frac{1}{2}) - 1(\nu' + \frac{1}{2})^2] - [722(\nu'' + \frac{1}{2}) - 3.5(\nu'' + \frac{1}{2})^2]$$

$$(B) \quad \nu = 22,293 + [498(\nu' + \frac{1}{2}) - 1.4(\nu' + \frac{1}{2})^2] - [722(\nu'' + \frac{1}{2}) - 3.5(\nu'' + \frac{1}{2})^2]$$

$$(C) \quad \nu = 24,875 + [537(\nu' + \frac{1}{2}) - 15(\nu' + \frac{1}{2})^2] - [722(\nu'' + \frac{1}{2}) - 3.5(\nu'' + \frac{1}{2})^2]$$

System *D* is missing from Mecke's analysis since Lamprecht failed to secure wave-number data below 3740Å. Although the new equations of *A* and *B* are similar numerically to Mecke's, the writer believes that his equations

TABLE I. The A bands. New data and vibrational quantum analysis.



^a The intensity data of Table I for system B comes from Lamprecht's data. [A] denotes masking by A heads. These superposed bands are unusually strong in some cases.

v'	v''	I	λ Hd. (I.A)	ν (cm ⁻¹)	O-C (cm ⁻¹)	Remarks
0	7	1	6720.32	14,876.2	-4.3	
2	8	2	6620.23	15,101.1	-.1	
1	7	2	6524.25	15,323.2	-2.3	
3	8	3	6433.63	15,539.0	6.2	
0	6	3	6427.73	15,553.3	2.6	
2	7	333	6342.01	15,763.5	-.4	
1	6	5	6250.75	15,993.4	-2.3	
3	7	1		[16,195.6]		[0,5]
0	5	4	6160.52	16,227.9	-.4	
2	6	1d		[16,434.1]		
1	5	2		[16,673.3*]		[Pb 6002.0]
3	6	2		[16,865.8]		[0,4]
0	4	6	5910.74	16,913.7	.3	
2	5	2	5842.13	17,112.3	.6	
1	4	1d		[17,358.4]		[0,3]
3	5	1		[17,543.5]		[0,3]
0	3	6	5677.78	17,607.6	1.7	
2	4	3	5617.65	17,796.1	-.7	
1	3	1		[18,050.9]		[0,2]
3	4	0		[18,228.5]		[0,2]
0	2	6d	5459.38	18,312.0	6.2	also 2,7 B
2	3	2	5407.18	18,468.8	-.5	also 1,6 B
1	2	3	5331.11	18,752.6	1.7	
3	3	1		[18,921.1]		[0,1]
0	1	2	5258.26	19,012.4	-.9	
2	2	1	5211.98	19,181.2	8.1	
1	1	3	5138.18	19,457.4	-1.0	
3	2	1	5093.19	19,628.6	7.6	
0	0	1	5068.78	19,723.1	-5.0	
2	1	2	5024.21	19,898.1	-1.4	
1	0	1		[20,233.1]		[0,2 B]
3	1	1	4916.62	20,333.5	-5.1	
2	0	2	4850.12	20,612.1	-.6	
3	0	1	4747.81	21,047.7	-3.4	

* Eder and Valenta give λ 5998A ($\nu=16,667.6$).

fit the new data better than Mecke's do the data of Lamprecht. Mecke assigned the three systems *A*, *B* and *C* to a $^3\pi \rightarrow ^3\Sigma$ transition, but the fine structure analysis to be reported in a companion paper does not justify this

TABLE II. *The B bands. New data and vibrational quantum analysis.*

v'	v''	<i>I</i>	λ Hd. (I.A)	ν (cm ⁻¹)	O-C (cm ⁻¹)	Remarks
0	7	1	5770.01	17,326.2	-3.3	
0	6	1	5553.83	18,000.6	-.9	
2	7	2	5459.38	18,312.0	4.1	also 0,2 A
1	6	2	5407.18	18,488.8	1.6	also 2,3 A
0	5	3	5353.82	18,673.1	-4.7	
1	5	0		[19,168.1]		[2,2 A]
0	4	6	5162.31	19,365.8	3.3	
1	4	0		[19,853.2]		[0,3]
0	3	6	4983.79	20,051.4	3.6	
2	4	1	4916.80	20,341.0	-.3	
1	3	0		[20,545.7]		[2,0 A]
0	2	6	4816.90	20,754.5	.5	
2	3	1	4753.55	21,031.1	2.3	
1	2	2	4706.43	21,241.6	4.1	
0	1	5	4657.98	21,462.5	-.2	
3	3	1	4647.49	21,511.1	4.2	
2	2	1		[21,733.4*]		[1,1]
1	1	6	4553.71	21,954.0	-1.0	
0	0	1	4509.23	22,170.5	6.7	
3	2	1	4499.99	22,216.1	-.7	
2	1	1	4454.80	22,441.4	-.7	
1	0	5	4410.38	22,667.4	.5	
3	1	0		[22,922.7†]		[2,0]
2	0	4	4317.06	23,157.4	-1.8	
3	0	4	4229.01	23,639.6	-2.0	
4	0	2	4145.93	24,113.3	1.5	

* Lamprecht gives $\lambda 4597.9$ ($\nu = 21,743$) (doubtful)

† Lamprecht gives $\lambda 4358.3$ ($\nu = 22,938$)

designation. Furthermore it has been noticed that practically all the bands belonging to system *C* can be accounted for equally well as members of *B*.

It has been remarked previously that the bands of system *C* in the region from 4280Å to 3740Å were not sufficiently strong to be measured on the

TABLE III. *The D bands. New data and vibrational quantum analysis.*

v'	v''	<i>I</i>	λ Hd. (I.A)	ν (cm ⁻¹)	O-C (cm ⁻¹)	Remarks
1	4	1	3594.16	27,815.0	-.3	
0	2	6	3485.68	28,680.6	1.1	
2	3	1	3442.76	29,038.2	4.6	
0	1	5	3401.92	29,386.9	0	
1	1	2	3341.83	29,915.2	.1	
0	0	1	3320.68	30,105.7	3.7	
1	0	2	3264.36	30,625.1	-4.9	
2	0	2	3209.21	31,151.3	-4.5	

plates taken by the writer. On the other hand, Lamprecht's data do not extend beyond 3740Å where the heads of the *D* system occur. Thus the older data in this region cannot be corrected to conform to the measurements made by the writer. Employing, therefore, Lamprecht's data for all the heads of

the bands in this region an equation for the *B* system is found including practically all of the heads of system *C*.¹² The equation is

$$\nu = 22,292 + [495.7(v' + \frac{1}{2}) - 2.05(v' + \frac{1}{2})^2] - [722.3(v'' + \frac{1}{2}) - 3.73(v'' + \frac{1}{2})^2]$$

The observed minus calculated values obtained from this equation are well within the experimental error of the measurements given by Lamprecht. It is obvious that this equation differs but little from the equation for the *B* system

TABLE IV. *Unidentified heads in the lead oxide band Spectrum.*^b

λ Hd. (I.A)	ν (cm ⁻¹)	<i>I</i>	Investigators	Remarks
6680	14,966	2 ^a	Eder and Valenta	also 6677.77 (1) S.B
6476	15,437	2	Eder and Valenta	also 6475.78 (1) S.B
6288	15,899	1	Eder and Valenta	b
6210	16,099	2	Eder and Valenta	b
6021	16,604	1	Eder and Valenta	b
5858	17,066	1	Eder and Valenta	d
4784.9	20,893	2	Lamprecht	b
4694	21,289	1	Eder and Valenta	c 4692.94 (1) S.B.
4632	21,583	2	Eder and Valenta	d
4619	21,644	1	Eder and Valenta	d
4369.4	22,880	1	Lamprecht	e
4281.2	23,351	1	Lamprecht	b
4156.3	24,053	2	Lamprecht	b
4036.2	24,769	2	Lamprecht	b
3950.6	25,306	1	Lamprecht	e
3878.3	25,777	1	Lamprecht	e
3839.6	26,037	1	Lamprecht	e
3804.9	26,275	1	Lamprecht	f 3810.61 (1) S. B.
3771.8	26,505	1	Lamprecht	e
3748	26,673	1	Eder and Valenta	d
3736.3	26,757	1	Lamprecht	e
3557	28,106	1	Eder and Valenta	f 3554.43 (1) S.B.

^a Observed also by Lamprecht but not by S. B.

^b Observed also by Eder and Valenta but not by S. B.

^c Observed also by S. B. but not by Lamprecht.

^d Observed by neither Lamprecht nor S. B.

^e Observed by neither Eder and Valenta nor S. B.

^f Observed also by both Eder and Valenta and by S. B.

^g The relative intensity estimates for Eder and Valenta's data were made by the writer from an examination of the PbO spectra in the Atlas.

^h These unidentified heads cannot be accounted for even if Mecke's system *C* is included with the other three systems. Many of these heads represent, no doubt, the superposition of a number of lines.

based upon the new data. However, until new data are obtained one may reasonably assume that thus far only three systems are known to be present in the spectrum of PbO, namely *A*, *B*, and *D*.

Table I illustrates the experimental intensity data. Comparison with the Franck-Condon theory is postponed until a fine structure analysis yields further data concerning the molecular constants of PbO.

BAND STRUCTURE AND ISOTOPE EFFECT

Under high dispersion each band consists apparently only of a *P* and *R* branch, which run coincident near the head of each band. Because of the fine

¹² The heads not included in *B* are 4281.2A, 4156.3A and 4036.2A.

scale of the band structure and overlapping of series, it is difficult to make accurate measurements of the wave-lengths of the individual lines. The bands in the red, yellow and green, photographed already at high dispersion with the uranium lead arc as source, appear to offer the best possibilities for a fine structure analysis. Such an analysis has been made already for some of the bands, and the results are given in a subsequent paper in collaboration with Dr. A. Christy.

The expression for the separation in wave-numbers between the corresponding band spectrum lines of two isotopic diatomic molecules¹³ is

$$\nu_2 - \nu_1 = (\rho - 1) \left[(v' + \frac{1}{2}) w_{e1}' - (v'' + \frac{1}{2}) w_{e1}'' \right] - (\rho^2 - 1) \left[(v' + \frac{1}{2})^2 x_1' w_{e1}' - (v'' + \frac{1}{2})^2 x_1'' w_{e1}'' \right] - (\rho^2 - 1)(\nu_1 - \nu_{Hd})$$

where $\rho = (\mu_1/\mu_2)^{1/2}$ and $\mu_1 = m_1 m / m_1 + m$, $\mu_2 = m_2 m / m_2 + m$. m_1 and m_2 are the masses of the isotopic atoms and m is the mass of the common kind of atom in the molecules $m_1 m$ and $m_2 m$. Subscript 1 refers to the constant for the more abundant and subscript 2 to that for the less abundant molecule. In our case m_1 is the mass of Pb^{208} , and m_2 the mass of Pb^{207} . For convenience one can make the following abbreviations.

$$\begin{aligned} \Omega &= (\rho - 1) \left[(v' + \frac{1}{2}) w_{e1}' - (v'' + \frac{1}{2}) w_{e1}'' \right] \\ O &= -(\rho^2 - 1) \left[(v' + \frac{1}{2})^2 x_1' w_{e1}' - (v'' + \frac{1}{2})^2 x_1'' w_{e1}'' \right] \\ \tau &= (\rho^2 - 1)(\nu_1 - \nu_{Hd}). \end{aligned}$$

The subscript 1 is dropped above since the isotope effect is unresolved at moderate dispersion.

$$\nu_2 - \nu_1 = \Omega + O + \tau.$$

Neglecting the rotational contribution τ and also the term O , the approximate magnitude of the (vibrational) isotope effect can be calculated simply by the relation

$$\nu_2 - \nu_1 = (\rho - 1)(\nu - \nu^0)$$

where ν^0 is the wave-number of the band system origin. ρ for PbO is $[(208 \times 16)(207 + 16)/(208 + 16)(207 \times 16)]^{1/2} = 1.000173$. This is approximately equal to $[(207 \times 16)(206 + 16)/(207 + 16)(206 \times 16)]^{1/2}$. Hence in the A system where $\nu^0 = 19,863.3$ and ν for the head of the 0,5 band is 16,227.9, then $\nu_2 - \nu_1 = -0.63 \text{ cm}^{-1}$. This is close to the observed value -0.68 ± 0.05 determined by direct comparison of the lines $Pb^{206}O$ from uranium lead with the lines $Pb^{208, 207, 206} O$ from ordinary lead. If Pb_2 were the emitter, then

$$\rho = [(208 \times 207)(207 + 207)/(208 + 207)(207 \times 207)]^{1/2} = 1.0015,$$

and the isotope separation $\nu_2 - \nu_1$ for the 0,5A band ought to be about 5.5 wave-numbers, almost nine times as large as the value actually observed.

¹³ R. S. Mulliken, Phys. Rev. 25, 119 (1925) and F. W. Loomis, Nat. Res. Council Bulletin 57, 11, 123 (1926). The last term in this formula is only an approximation.

Figure 1 illustrates the isotope effect observed near the head of the $\lambda 5677.78\text{\AA}$ (0,3A) band. The upper microphotometer record was secured from a spectrogram taken with uranium lead of atomic weight 206.1 in the arc. Below is the record of the same region on a spectrogram taken with ordinary lead (atomic weight 207.2) in the arc. A Moll microphotometer, which records automatically was used. The central reference line is a lead arc line of wave-length 5692.329\AA which probably shows a small atomic isotopic effect. The light vertical lines serve to identify the corresponding

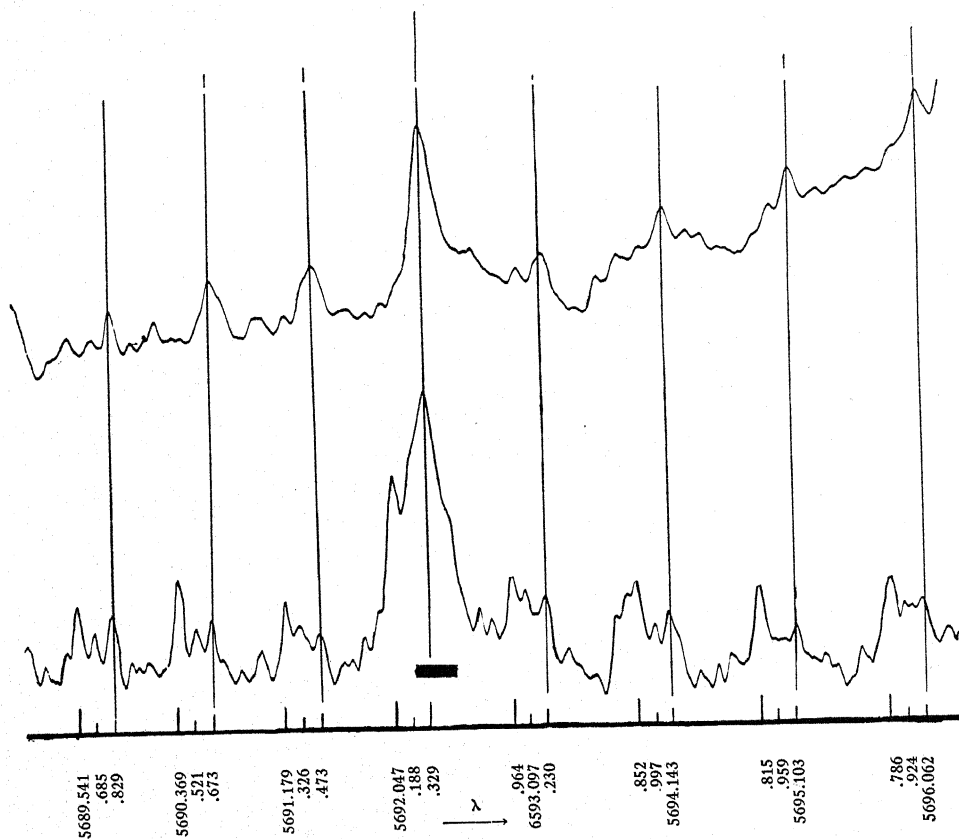


Fig. 1. Isotope effect in the $\lambda 5677.78$ (0,3 A) band of PbO. Above, Pb^{206}O from uranium lead. Below, $\text{Pb}^{208}, ^{207}, ^{206}\text{O}$ from ordinary lead. Isotopic displacement -0.428 wave-numbers.

lines in the two spectra, namely Pb^{206}O . The lines Pb^{208}O and Pb^{207}O are apparently absent from the upper trace. Isotope 208 is the most abundant in ordinary lead, and hence Pb^{208}O gives the strongest lines. Aston gives 208 (7), 207 (3), and 206 (4) as the composition of ordinary lead, and the results of this investigation are in agreement with these relative abundancies. The wave-lengths of the series lines are given in the lower part of the figure.

Figure 2 gives a similar comparison near the head of the $\lambda 6160.52\text{\AA}$ (0,5A) band. Just as in the case of the 0,3 band, the lines Pb^{206}O are on the long wave-length side of the lines Pb^{207}O . The *P* and *R* lines are coincident

in the middle of the picture and begin to diverge both on the far left and far right side, causing the lines to become fuzzy. The single lines Pb^{206}O in the upper spectrum were secured with a heavy exposure in order to bring out weak lines of other isotopic molecules that might possibly be present. This was done in an attempt to satisfy Dr. C. S. Piggot's¹⁴ wish for a reliable qualitative analysis of uranium lead from the Belgian Congo. Data of this

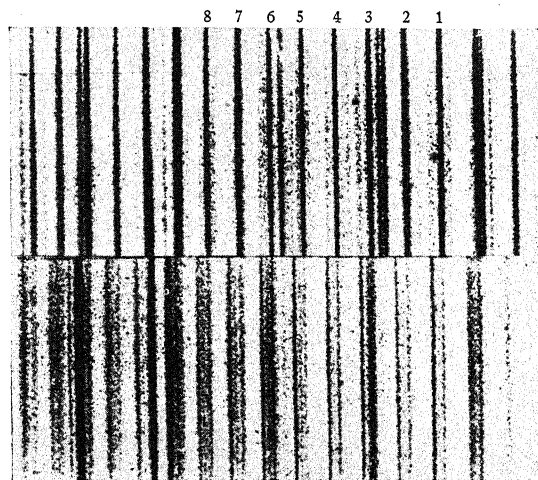


Fig. 2. Isotope effect in the $\lambda 6160.52\text{A}$ (0,5 A) band of PbO .

nature are necessary in estimating the age of uranium minerals. It is evident from inspection of Fig. 2 that 206 is the principal isotope in the uranium lead sample used. This is to be expected from its atomic weight of 206.1.

Table V gives the measured wave-lengths of the band lines examined in Fig. 2. The first order of the grating was used. The numbers above the lines Pb^{206}O in Fig. 2 correspond to those under "group" in Table V.

TABLE V. Wave-lengths of lines in the 6160.52 A (0,5A) band.

Group	Pb^{206}O	Pb^{207}O	Pb^{208}O
1	6204.916	6204.685	6204.434
2	3.327	3.077	2.800
3	1.717	1.461	1.174
4	0.117	6199.890	6199.653
5	6198.583	8.369	8.108
6	7.086	6.827	6.577
7	5.662	5.386	5.125
8	4.213	3.973	3.707

Figure 3 illustrates the isotope effect observed in one of the *D* system bands. The band lines in the upper half of the figure are the lines Pb^{206}O from uranium lead. These are shifted $0.036 \pm 0.01\text{A}$ on an average approximately to longer wave-lengths with respect to the lower lines $\text{Pb}^{208, 207, 206}\text{O}$ from

¹⁴ C. S. Piggot, Jour. Wash. Acad. of Sciences 18, 10, 269 (1928).

ordinary lead, which are unresolved in this region. Table VI gives the wave-length data. These begin, reading from right to left, with the second line on the short wave-length side of the reference line in Fig. 4. It is to be noted that here the isotope effect is unresolved although the second order of the grating was used. This is in marked contrast to the effects observed in system *A*, but is in agreement with the shift calculated on the basis of the vi-

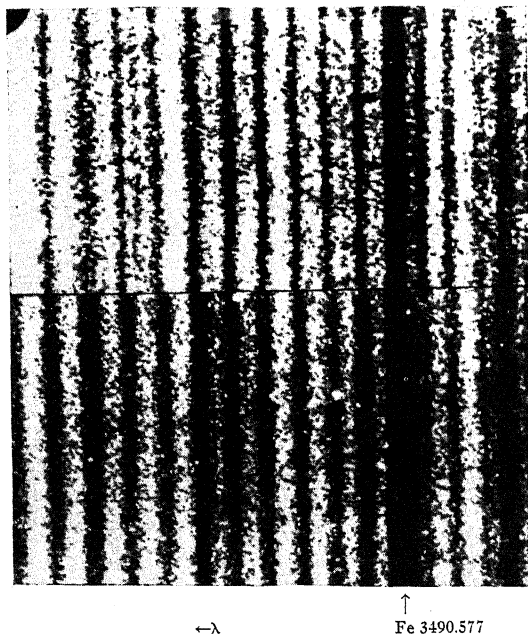


Fig. 3. Isotope effect in the $\lambda 3485.68\text{\AA}$ ($0,2 D$) band of PbO. Upper spectrogram, uranium lead oxide. Lower spectrogram, ordinary lead oxide.

brational assignment for the *D* bands. The calculated shift is -0.271 cm^{-1} for Pb^{208}O as compared with Pb^{207}O while the value measured is $-0.30 \pm 0.08\text{ cm}^{-1}$. The minus sign indicates that the lines from the molecules containing the lighter isotope are displaced towards lower frequencies with respect to the radiations from the molecules containing the heavier isotope.

TABLE VI. Wave-lengths of lines in the $\lambda 3485.68\text{\AA}$ ($0,2D$) band.
 Pb^{206}O $\text{Pb}^{208, 207, 206}\text{O}$ (unresolved)

(From uranium lead)	(From ordinary lead)
3490.106	3490.078
.372	.343
Fe 3490.577	Fe 3490.577
.632	.579
.922	.895
1.236	1.168
.501	.458
.807	.773
2.108	2.081
.443	.390

Table VII gives a comparison between the observed isotope effects and the values calculated as the sum $\Omega + O + \tau$.

In the 0,3 band of system *A* the lines which we now recognize as Pb^{208}O and Pb^{206}O were measured by Lamprecht in 1911, who designated them as lines of series I and III in his tables of wave-lengths. The lines Pb^{207}O , which form the intermediate series, are missing from the data of Lamprecht, since he used lower dispersion and resolving power than did the writer.

TABLE VII. Isotope effects observed by direct comparison of Pb^{206}O from uranium lead with $\text{Pb}^{206,207,208}\text{O}$ from ordinary lead, and the values calculated as the sum $\Omega + O + \tau$.*

in Band	$\nu - \nu_{\text{Hd.}}$ (cm^{-1} approx.)	$\lambda_2 - \lambda_1$ (I.A.) Observed	$\nu_2 - \nu_1$ (cm^{-1})	Ω	<i>O</i> Calcu- lated (cm^{-1})	τ	$\nu_2 - \nu_1$ (cm^{-1}) Calcu- lated	Observers	Remarks
0,5A	- 78	$0.255 \pm .02$	$-0.68 \pm .05$	-0.648	+0.039	-0.027	-0.636	S. B.	Resolution into Triplets
0,3A	- 47	$0.141 \pm .02$	$-0.43 \pm .06$	-0.398	+0.016	-0.016	-0.398	S. B.	Resolution into Triplets
3,0B	-116	$-0.055 \pm .02$	$+0.31 \pm .11$	+0.238	-0.010	-0.040	+0.188	Grebe and Konen	Not Resolved
0,2D	- 36	$0.036 \pm .01$	$-0.30 \pm .08$	-0.267	+0.008	-0.012	-0.271	S. B.	Not Resolved

* The isotope effect calculated here is that of Pb^{208}O and Pb^{207}O and is approximately the same as that of Pb^{208}O and Pb^{207}O numerically.

Dr. R. S. Mulliken suggested this problem and gave a good deal of important advice in the course of this investigation. Consequently the writer takes this opportunity to thank him. To Drs. Gale, Compton, Harkins, Piggot, Hoag and Christy, the writer feels indebted for many helpful hints. The uranium lead of atomic weight 206.1 was a gift from the Wolcott Gibbs Memorial Laboratory of Harvard University, and the writer is indebted through Dr. Mulliken to Dr. L. P. Hall for making about 20 grams of pure material extracted from Belgian Congo uranium ores available.

When Dr. Mecke was informed of the present investigation, he very kindly agreed to leave further work on the fine structure analysis to the writer.

FINE STRUCTURE ANALYSIS OF THE BANDS IN
THE A AND D SYSTEMS OF LEAD OXIDEBY ANDREW CHRISTY AND SYDNEY BLOOMENTHAL
RYERSON PHYSICAL LABORATORY, UNIVERSITY OF CHICAGO AND RADIO
CORPORATION OF AMERICA, NEW YORK CITY

(Received November 19, 1929)

ABSTRACT

The bands of the *A* and *D* systems of PbO are composed of single *R* and *P* branches only. The combination principle has been applied to the lines of these branches and the rotational constants of the molecule have been determined. The bands of PbO have been assigned previously to three systems, *A*, *B*, and *D*, all three having the final state in common. The nuclear separation of this final state is found to be 1.9207×10^{-8} cm, that of the upper state of *A*, 2.0927×10^{-8} cm, and of the upper state of *D*, 2.0424×10^{-8} cm. No *Q* branches have been found in either of the two systems, indicating that all the electron states involved have the same value of Δ . It is shown that the electronic levels of the two systems investigated are singlets. All the electron states involved are, in all probability, $^1\Sigma$ states.

THE purpose of this work is to determine the rotational constants of the lead oxide molecule and if possible its electron states. The vibrational analysis and the isotope effect are treated in the preceding paper, in which it is also shown that practically all the bands in the spectrum of PbO may be assigned to three systems, *A*, *B*, *D*, all having the final electron states in common.

The following bands were used for the fine structure analysis:

0, 2 $\lambda 5459.4$ <i>A</i> system	0, 5 $\lambda 6160.5$ <i>A</i> system
0, 3 $\lambda 5677.8$ <i>A</i> system	0, 2 $\lambda 3485.7$ <i>D</i> system

The spectrograms¹ from which the lines were measured were taken with a sample of uranium lead of atomic weight 206.1. The stronger lines, therefore, are due to Pb²⁰⁶O. In addition to these, however, there are, near the head of each band, especially in those of *A*(0,2), *A*(0,3), and *A*(0,5), fainter lines due to Pb²⁰⁸O. It cannot be determined with any certainty whether or not lines due to Pb²⁰⁷O are present. If the lines of Pb²⁰⁸O are due to the fact that the uranium lead has been contaminated with ordinary lead, we should expect the lines of Pb²⁰⁷O to appear with intensity approximately half as great as those of Pb²⁰⁸O.² Since most rocks contain traces of ordinary lead, it may be that in the process of extraction uranium lead has been contaminated with ordinary lead. Furthermore the atomic weight of pure uranium lead was found to be 206.06³ while the atomic weight of the sample

¹ For a detailed account of the experimental work, see preceding paper.

² Aston, *Nature* 120, 224 (1927). Ordinary lead consists of isotopes 208, 207, 206, in the ratio of 7, 3, 4.

³ G. Kirsch, "Geologie und Radioaktivitat" p. 138.

from which these spectrograms were made was 206.1, indicating that the sample used must have contained traces of ordinary lead.

The lines of the $\lambda 5677.8$ Å and $\lambda 6160.5$ Å bands were measured from first order plates, those of the other two from second order plates. The measurements of individual lines are considered to be accurate to within 0.1 cm^{-1} .

The bands of the two systems which were examined consist of single R and P branches, indicating that we have to do with a transition between two singlet electron levels having the same $\Lambda(^1\Sigma - ^1\Sigma$ or perhaps $^1\Pi \rightarrow ^1\Pi)$. In the more favorable cases, for large rotational quantum numbers, lines from the R and P branches fall in such a way as to form close doublets, the doublets becoming single lines as they approach the head. All the bands of PbO so far investigated degrade to the red.

Assuming rotational terms of the form

$$\text{const} + BJ(J+1) - DJ^2(J+1)^2 + \dots$$

where⁴ $B = B_v = B_0 - \alpha v = B_e - \alpha(v + 1/2)$, we may define the usual combination differences $\Delta_2 F'(J)$ and $\Delta_2 F''(J)$ as

$$R(J) - P(J) = \Delta_2 F'(J)$$

and

$$R(J-1) - P(J+1) = \Delta_2 F''(J)$$

$\Delta_2 F(J)$ being

$$\Delta_2 F(J) = 2(B - 2D) + 4(B - 3D)J - 12DJ^2 - 8DJ^3 + \dots$$

$\Delta_2 F'(J)$ should be the same for the (0,2), (0,3), and (0,5) bands of the A system, and $\Delta_2 F''(J)$ should be the same for the (0,2) band of the A system and for the (0,2) of D , since both these systems have the final level in common. These combinations have been found and tested for over thirty members, at least, of the R and P branches in each of the above bands. Samples of values for $\Delta_2 F^{(0)'}(J)$ of the A system for the three bands mentioned above are given in Table I, while the corresponding values of $\Delta_2 F^{(2)''}(J)$ of (A) and (D) are given in Table II.^{4a} The values of $\Delta_2 F^{(3)''}(J)$ (A), $\Delta_2 F^{(5)''}(J)$ (A) and $\Delta_2 F^{(0)'}(J)$ (D), for small, medium, and large values of J , are given in Table III, columns 2, 3, and 4. The correct value of J is given in column 1 of the latter three tables. The occasional large discrepancies between the corresponding $\Delta_2 F$ values in Tables I and II are due partly to over-lapping of the two branches R and P , especially in the regions near the head, and partly to the superposition of lead and copper lines or their ghosts on the lines of the bands. It is thought inadvisable at present to give more complete tables of $\Delta_2 F$ values or tables of the wave-numbers of the lines which have been measured in all these bands. These tables will be given later, when a more thorough investigation of these three systems of the PbO molecule has been made.

⁴ The symbol v is used in this work for the vibrational quantum number.

^{4a} In $\Delta_2 F^{(0)'}$, $\Delta_2 F^{(2)''}$, etc., the subscript of F indicates the value of the vibrational number v .

The constants of the molecule were obtained by the graphical method outlined on pp. 172-173 of the Report.⁵ The values of $\Delta_2 F/J$ were plotted

TABLE I. Samples of values of $\Delta_2 F^{(0)}$ for $A(0,2)$, $A(0,3)$, and $A(0,5)$.

J	$A(0,2)$	$A(0,3)$	$A(0,5)$
10		10.8	
11		11.2	
12		12.8	
20		21.1	21.2
21		21.8	22.0
22		23.2	23.0
35	36.4	36.6	36.1
36	37.5	37.8	37.2
37	38.9	38.7	39.1
47	48.7	48.9	48.8
48	49.7	50.1	49.8
49	50.7	51.0	50.9
56	57.8	57.9	57.8
57	59.3	58.9	58.9
58	59.9	59.8	59.9
66	67.7	67.9	68.0
67	68.6	68.8	68.9
68	69.7	69.9	69.7
76	77.9	77.8	
77	79.0	79.1	
78	79.7	79.7	

TABLE II. Samples of values of $\Delta_2 F^{(2)}$ of $A(0,2)$ and $D(0,2)$.

J	$A(0,2)$	$D(0,2)$
25		29.8
26		31.3
27		33.2
36	44.1	43.9
37	45.3	45.5
38	46.9	46.7
47	57.4	57.3
48	58.4	58.4
49	59.7	59.5
56	68.6	68.1
57	69.4	69.3
58	70.5	70.5
65	78.8	79.0
66	79.8	79.2
67	81.1	81.4
74	89.1	
75	90.8	
76	91.9	
83	100.0	
84	101.1	
85	102.5	

against J , and from this plot the values of B and D were calculated. The value of D found by this method is the same, within experimental error,

TABLE III. Values of $(A)\Delta_2 F^{(3)}$, $(A)\Delta_2 F^{(5)}$, and $(D)\Delta_2 F^{(0)}$, for small medium and large J .

J	$(A)\Delta_2 F^{(3)}$	$(A)\Delta_2 F^{(5)}$	$(D)\Delta_2 F^{(0)}$
11	13.7		
12	14.9		
18	22.1	22.0	
19	23.4	23.2	
23	28.2	27.5	24.8
24	29.7	29.1	25.8
25	30.8	30.4	26.5
41	49.9	49.0	44.9
42	51.1	50.5	45.6
43	52.4	51.4	46.8
66	79.5	78.4	71.6
67	80.8	79.6	72.4
68	81.8	80.9	73.5
75	90.2		
76	91.4		
77	92.4		

⁵ National Research Council Bulletin, Report on "Molecular Spectra in Gases," Vol. 11, part 3, 1926.

as that obtained by the formula $D=4B_0^3/\omega_0^2$. The constants of the molecule for the three electronic levels are given in Table IV.

TABLE IV. Rotational constants of the $Pb^{206}O$ molecule.

Final states of systems A and D*		
$B_0''=0.3063\text{ cm}^{-1}$		$B_2''=0.3025\text{ cm}^{-1}$
$B_3''=0.3007\text{ cm}^{-1}$		$B_5''=0.2967\text{ cm}^{-1}$
$D_0''=2.203\times 10^{-7}\text{ cm}^{-1}$		$\alpha''=0.0019$
$r''_0=1.9207\times 10^{-8}\text{ cm}$		
Initial state of A		
$B_0'=0.2579\text{ cm}^{-1}$		$D_0'=2.7856\times 10^{-7}\text{ cm}^{-1}$
$\alpha'=0.0022$		
$r_0'=2.0927\times 10^{-8}\text{ cm}$		
Initial state of D		
$B_0'=0.2707\text{ cm}^{-1}$		$D_0'=2.8183\times 10^{-7}\text{ cm}^{-1}$
$\alpha'=0.0006$		
$r_0'=2.0424\times 10^{-7}\text{ cm}$		

* These systems have the final state in common.

It is estimated that the values of B are accurate to within 0.1 percent, hence the calculated values of r_0 (nuclear separation) should be accurate to within 0.05 percent. In this analysis the value of B_0'' was not obtained directly but was extrapolated from the known values of B_2'' , B_3'' , and B_5'' . Since B_2'' was obtained from two bands, i.e. 0,2 of (A) and 0,2 of (D), twice as much weight was given to this value as to the two others.

R. T. Birge⁶ has found the following empirical equation from a study of a large number of bands: $2B_0\alpha/\alpha=1.4\pm 2$. Substituting the corresponding values for the lower electronic level of the A system we find: $2\times 3.73\times 30616/722.3\times 0.0183=1.7$. Using this value for the above fraction, α for the upper electronic levels for the systems A and D was calculated. In calculating r_0 , the atomic weight of uranium lead was taken to be 206.06.⁴ In all the calculations the values of the auxiliary constants used are those given by Birge.⁷

It has been remarked above that in all the bands investigated no Q branches were observed.⁸ The absence of a strong Q branch indicates that $\Delta\Lambda=0$.⁹ The only possibilities, therefore, are that we are dealing with such transitions as $^1\Sigma\rightarrow^1\Sigma$, $^1\Pi\rightarrow^1\Pi$, $^1\Delta\rightarrow^1\Delta$, etc. It has been stated that the bands of the A and D systems consist of single R and P branches. Thus it is not possible that either the upper or lower levels of the system or both are narrow multiplets, for, in that case, we would expect additional branches to appear. It is evident, therefore, that the levels in question are singlets. (The bands of the B system have also been examined with this fact in mind. As far as can be ascertained from a cursory investigation of enlargements

⁶ R. T. Birge, Phys. Rev. 31, 919 (1926).

⁷ R. T. Birge, Phys. Rev. Supplement 1, 1 (1929).

⁸ R. Mecke, Die Naturwissenschaften 17, 133, stated that the three systems A, B, and C are probably due to a $^3\Pi\rightarrow^3\Sigma$ transition, the upper electron states of A, B, and C being the components of the $^3\Pi$ state. It has been shown in the preceding paper that practically all the bands assigned by Mecke to system C are actually members of system B. This work shows that system A is not due to a $^3\Pi\rightarrow^3\Sigma$ or even to a $^1\Pi\rightarrow^1\Sigma$ transition.

of these bands, their appearance is similar to those of the other systems. If there is a Q branch in these B bands, it must be very weak.)

R. S. Mulliken⁹ has given the theoretical intensities to be expected in transition between two singlet electronic levels, both of which have the same value of Λ . The equations are:

$$i_Q = a(2J+1)\Lambda^2/J(J+1)$$

$$i_P = a(J^2 - \Lambda^2)/J$$

$$i_R = [a(J+1)^2 - \Lambda^2]/J+1$$

In these equations the Boltzmann factor has been omitted, since for low values of J and B and high temperatures this factor is essentially equal to 1. It may be shown readily from the above equations that if $\Lambda = 1, {}^1\Pi \rightarrow {}^1\Pi$, there is a weak Q branch; the intensity of the first Q line is three times as great as that of the first R line, the intensities of the other Q lines, however, decrease rapidly for higher values of J . For $\Lambda = 2, {}^1\Delta \rightarrow {}^1\Delta$, we have qualitatively the same result but the first Q line is very much stronger, and the intensities of the other lines decrease less rapidly.

It is obvious from an examination of the plates and enlargements of these bands that we do not have a ${}^1\Delta \rightarrow {}^1\Delta$ transition, for in that case a Q head should be strong enough to show and there is no evidence of such head in our plates. The only alternative, therefore, is that the bands are due either to ${}^1\Pi \rightarrow {}^1\Pi$ or ${}^1\Sigma \rightarrow {}^1\Sigma$ transitions. In our opinion the latter is the more reasonable as it seems improbable that all the electron states of this molecule should be ${}^1\Pi$ states with no ${}^1\Sigma$ state present. For a final decision, however a more accurate study of the bands must be made, with plates of greater dispersion.

It has been shown in the preceding paper that the three known systems of the PbO molecule, A , B , and D , have the final state in common, hence we may reasonably assume that this state is the normal state of the molecule. The nuclear separation $r_0 = 1.9207 \times 10^{-8}$ cm., while larger than that of other oxides¹⁰ so far investigated, is comparatively small for such a heavy molecule. This seems to indicate that the normal state is fairly stable.

If we assume that in the formation of PbO only the four electrons of Pb in the P shell are greatly influenced by the O atom, then the configuration of outer electrons in the PbO molecule should resemble that of CO with a ${}^1\Sigma$ state as the normal state of the molecule. It appears to us that the data on hand are neither sufficiently accurate nor extensive to warrant any further conclusions as to the electron states of PbO. The fine structure analysis of the bands is being continued in Ryerson laboratory, in order to determine this and other related points.

In conclusion the writers wish to acknowledge their indebtedness to Professor R. S. Mulliken, who proposed this problem, for his advice and many helpful suggestions.

⁹ R. S. Mulliken, Phys. Rev. 29, 391 (1927). See also Hönl and London, Zeits. f. Physik 33, 803 (1925), for the derivation of these equations. The equations as given here are in terms of the final quantum number J .

¹⁰ Compare CO, 1.15×10^{-8} cm, and TiO, 1.619×10^{-8} cm.

A LABORATORY METHOD OF PRODUCING
HIGH POTENTIALS

BY G. BREIT, M. A. TUVE, and O. DAHL

DEPARTMENT OF TERRESTRIAL MAGNETISM, CARNEGIE INSTITUTION OF WASHINGTON

(Received November 19, 1929)

ABSTRACT

Details are given of the experimental arrangement by which, using Tesla coils in oil, very high potentials have been produced and measured. Excited at the rate of 120 sparks per second Tesla coils have been operated at 3,000,000 volts in ordinary transformer oil at atmospheric pressure. In oil under a pressure of 500 pounds per square inch, voltages as high as 5,200,000 have been produced with intermittent excitation. These voltages (peak values) are measured by a simple capacity-potentiometer, in which an insulated electrode "picks up" a known fraction of the total voltage, this fractional voltage being measured by means of a sphere gap. Measurements are given of the voltage-distribution along Tesla coils. Calculations and measurements of the efficiency and power-output of such coils show that at 120 sparks per second, a coil operating at 5,000,000 volts provides sufficient power, if used to accelerate helium nuclei in a suitable vacuum-tube, to yield the equivalent of about 2,600 grams of radium.

THE importance of obtaining sources of high-speed electrons and atomic nuclei for physical investigations is so obvious that an explanation of the aim of the present work is hardly needed. It may be permitted however to say a few words about the part played by experiments with penetrating radiations in the past and to mention briefly some of the current problems for the solution of which the development of new and more powerful sources than have been available appears to be essential.

The Rutherford-Bohr atomic model was suggested by experiments on the scattering of α -particles. Their penetrating nature made it possible to obtain a simple interpretation of the results. The understanding of the nature of the solid state has received its main stimulus from experiments following Laue's discovery. Here the penetrating x-ray quanta offer direct and clear information; similarly with the Compton effect and with Rutherford's nuclear disintegration experiments. These very important experimental facts forming the foundation of modern theoretical conceptions have come out of experiments employing high-energy quanta, electrons, and α -particles. The historical reason for the importance of high-energy experiments is, of course, that classical physics corresponds to energy-jumps of zero-value so that the larger the energy concerned the more radical the departure from classical physics and the more interesting the phenomenon. Quantum mechanics has explained in recent years all of the fundamental facts in ordinary atomic structure. According to current theoretical opinion it is highly improbable that one shall find a serious contradiction to the present theoretical scheme by studies of line and band spectra. Apparently

the main unsolved questions at present are Dirac's $\pm m$ difficulty and the combined relativistic treatment of matter and electrodynamics. The first of these as shown by Klein becomes particularly pronounced for potential walls of high absolute value. It may be hoped that light may be thrown on the question by studies on nuclei by means of particles with high kinetic energy.

The precise form of the equation for one electron is intimately concerned with the $\pm m$ difficulty. It will be noted that by studying the intensity of scattering of recoil-electrons by hard γ -rays, Skobeltzin¹ has recently obtained evidence for preferring Dirac's equation for a free electron to the older Schroedinger form. His intensities agree with the calculations of Klein-Nishina, which use Dirac's equation, rather than with the older calculations of Dirac employing the Schroedinger equation without spin. It is not altogether clear at present to what extent Skobeltzin's experiments prove the validity of Dirac's equation or deal only with the presence of the electronic spin. It is clear however that when repeated with still more penetrating radiation they will give very important evidence. The practical approach to the combined treatment of matter and the electromagnetic field is also in all probability to be obtained by studying systems containing two particles in a state of rapid relative motion. Experiments on atomic nuclei giving their energy-levels, conditions for disintegration, etc., may be expected to offer new and valuable evidence for these still unsolved theoretical points and may besides suggest quite different questions and difficulties which do not come up in dealing with phenomena outside atomic nuclei.

We have thought it worth while therefore to construct high-potential equipment of convenient laboratory dimensions to make it possible to perform experiments on high-velocity particles. The electrical problem of producing high potentials was solved without much difficulty over two years ago.² The construction of high-potential vacuum (x-ray) tubes has proved more difficult but is at present sufficiently advanced to make a progress-report of interest and to show that the Tesla coils used for producing high potentials are suited for supplying the potentials to vacuum-tubes. The details of the electrical arrangement not having been published before we have divided the matter into two parts the present paper being concerned with the electrical arrangements and the one following with the construction and experiences with high-potential vacuum-tubes.

The apparatus used for producing high potentials is old and well-known under the name of Elihu Thomson or Tesla coils. Since their invention Tesla coils have been known to give possibilities of producing with limited means potentials of the order of one million volts.³ They have commonly been used in air, the insulating qualities of which constituted a limitation on their performance. It is difficult to construct Tesla coils of sufficiently large dimensions to prevent corona and sparking in air. The energy con-

¹ D. Skobeltzin, *Nature* **123**, 411 (1929).

² G. Breit and M. A. Tuve, *Nature* **121**, 535 (1928).

³ M. Wolfke, *Phys. Zeits.* **24**, 249 (1923).

sumed in the corona and sparking is so large that the Tesla coil ceases to operate as a resonance-transformer on account of the high damping and loses most of its advantages. If the dimensions of the coil are sufficiently large to prevent corona its electrostatic capacity becomes inconveniently large and necessitates unnecessarily cumbersome primary circuits. The main point in the operation of Tesla coils is therefore to prevent corona and sparking by using the high-potential parts of the coil in a medium of high dielectric strength. For a number of years two of us had in mind the possibility of using Tesla coils in a vacuum or in some other insulating medium. The method described here employs transformer oil which we have found sufficient for roughly five million volts when used under pressure and three million volts at atmospheric pressure. These figures are somewhat arbitrary, simply being the voltages obtained in the laboratory and not representing final limits in the voltages obtainable with oil. No doubt still higher voltages can be obtained by using oil for insulation. The practical advantages of oil over vacuum for preliminary trials are obvious when the question of repairs, changes in design, and baking out of metal parts is considered. The ultimate possibility of using Tesla coils in a vacuum is of course not excluded.

EXPERIMENTAL ARRANGEMENTS

The principles underlying the operation of a Tesla coil are well known and need not be explained here in detail. The important thing is that two resonant oscillatory electrical circuits, the primary and the secondary, are coupled magnetically to each other. The primary circuit has a large capacity and a small inductance while the secondary (the Tesla coil) has a large inductance and a small capacity. The condenser of the primary circuit is charged to a high potential (of the order of 30 or 60 kv) and is allowed to discharge suddenly through a spark-gap and the primary inductance. An oscillatory discharge takes place. The secondary circuit being in resonance with the primary the energy is transferred with fair efficiency to the secondary before the damping appreciably reduces the amplitudes of oscillation. In the set-ups used the peak-voltage of the secondary circuit corresponds roughly to the transfer of one-fourth of the energy of the primary condenser to the secondary. The resonant frequencies of the coils used have been of the order of 100,000 cycles per second.

Figure 1 shows the arrangement for a Tesla coil in oil under pressure, with which over 5,000,000 volts were obtained. The condenser is fed on rectified current supplied by an x-ray machine. The primary gap is of the stationary type.* The use of rectified current is advisable if power consumption and large charging currents of the primary condenser are to be avoided. The arrangement can also be used without a rectifier, the primary condenser being then fed by a transformer and discharged through a syn-

* It can be made cheaply out of ten-inch hollow zinc-balls used for decoration purposes and usually furnished in the form of two hemispheres. For long and continued use heavier electrodes are preferable.

chronous gap. For our highest voltages we have been forced to use the rectifier because our power-lines have the unusually small capacity of 50 KVA.

The synchronous gap has been used up to 3,000,000 volts secondary output. The transformer was fed on 60-cycle alternating current and the condenser was discharged 120 times per second. No pressure had to be applied to the oil for this voltage. Even at low voltages, however, we find it convenient to use the rectifier when possible because by so doing a weak spot in the insulation of the secondary can be detected before electrical breakdown causes too much damage. In our experiments with oil at atmospheric pressure, corona at the ends of the Tesla coil limited the voltage obtainable to about 3,000,000. With the high-pressure arrangement corona has not given any serious difficulty. Insulation between turns limited the voltage in this case to about 5,000,000 volts.

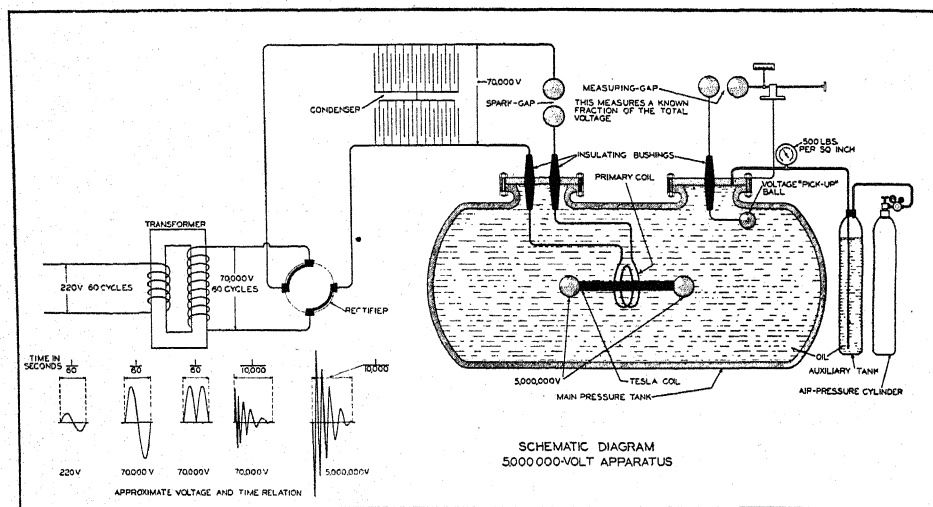


Fig. 1. Schematic diagram Tesla coil in oil under pressure.

Power-supply for the primary condenser.—For the production of 3,000,000 volts we used a small transformer giving about 30,000 volts and operating on 60 cycles with approximately a 3-kilowatt rating, kindly loaned to us by the Washington Navy Yard. For the intermittent production of the higher voltages we used a 10-KVA Kelley-Koett x-ray machine operating on a 220-volt 60-cycle supply. This or any other reliable x-ray machine contains the transformer mechanical rectifier and controls needed for charging the condenser. A potential of 120,000 volts could be supplied by the machine. In our experience we have rarely used it above 70,000 volts.

Condenser.—The work was begun by using a set of glass-in-oil Telefunken condensers loaned by the Washington Navy Yard; these had previously been used in a high power Navy spark-transmitter. Sixteen of these sufficed for the production of 3,000,000 volts. The capacity of each was 0.038 microfarad and each unit stood 15,000 volts (peak). For higher voltages however

we constructed a special condenser similar to that used by Anderson for exploding wires. Lead foil 0.003 inch thick was applied to each side of 200 glass plates. The plates are 40 inches square of somewhat irregular thickness approximating one-eighth inch, being ordinary B-grade double-strength window-glass. They are assembled in wooden racks in air and constitute a generally useful as well as comparatively inexpensive piece of laboratory equipment. Figure 2 shows a condenser including part of the lower and most

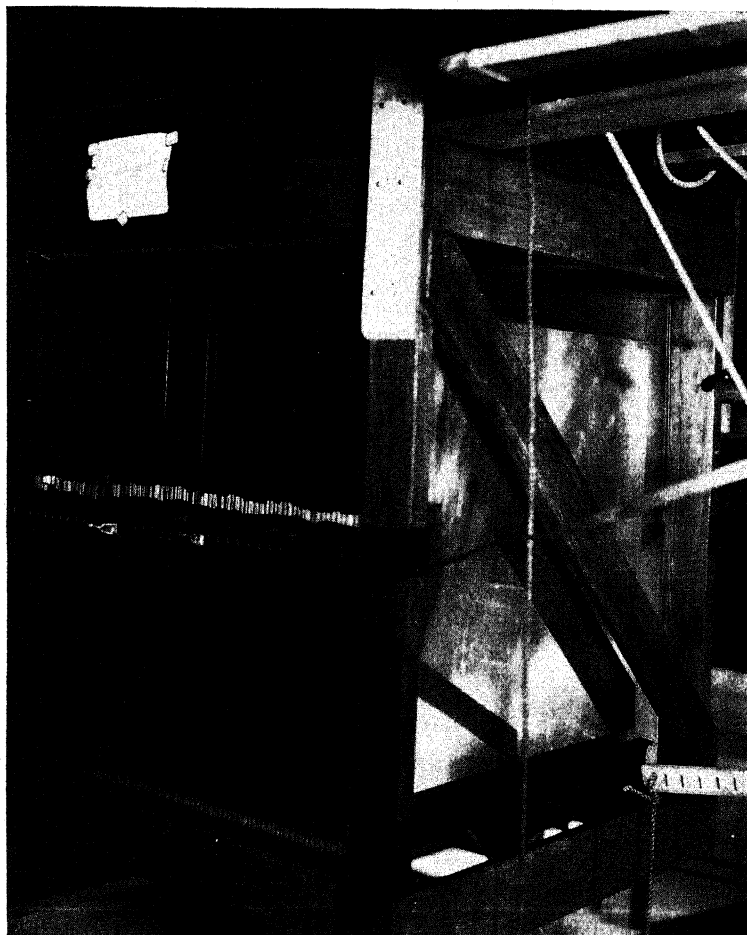


Fig. 2. View of section of the glass-plate condenser ($C = 1.6\mu f$, 30,000 volts).

of the upper rack. The plates are spaced one-half inch apart. For reasons which are somewhat obscure it is essential that the plates be spaced to prevent breakage when the condenser is discharged. We found it very convenient to fasten the lead foil to the plates simply by an oil-film. Any lubricating oil of a not too heavy consistency is satisfactory, but linseed oil seems to be the most convenient material for this purpose both on account of being easily squeezed into a thin film under the lead foil and because it dries around

the edges. A margin of about 4 inches is left on the glass around the foil, allowing the plates to go up to a sufficiently high potential and yet providing a safety-gap around the edge of the glass plate. In two years we have not had a single puncture of the plates although the condenser has been repeatedly at the flash-over point. In case of breakage however the plates can be taken out of the racks with relative ease. Pieces of rubber tubing inserted between plates close to the edges help to secure a uniform distance between them. The side of the racks shown in the figure is provided with two pieces of angle brass (only one is visible) which serve as supports for the connectors to the plates and as bus-bars. The opposite side (not shown in the figure) has each bus-bar split into two insulated sections thus allowing the use of the plates either all in parallel, in two sections in series, or in four sections in series. The capacity of all plates in parallel is about 1.6 microfarads. The maximum voltage which can be used with the plates in parallel varies between 30,000 and 40,000 volts depending on the type of external circuit. As a rule a high inductance in the external circuit allows one to use a

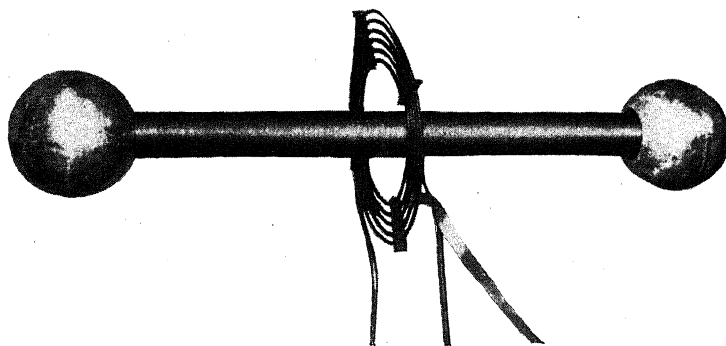


Fig. 3. Tesla coil and primary, showing the spun-zinc balls which serve as corona-shields at the ends of the Tesla coil.

higher voltage on the condenser. If the voltage exceeds this limit a local flash-over occurs around the edge of a plate when the primary gap discharges. The exact nature of the flash-over is hard to explain but it is undoubtedly due to transients. When it occurs the primary circuit becomes inefficient but in our experience no particular damage to the condenser takes place. With the four sections in series we have used this condenser without flash-over at 120,000 volts.

Primary of Tesla transformer.—This as shown in Figure 3 is made of several turns of spirally-wound copper tubing. Some of the most efficient circuits employ only two turns.

Tesla coil.—This is shown also in Figure 3. It is convenient to wind a high-voltage Tesla coil on a piece of Pyrex glass tubing as supplied by the Corning Glass Works with an approximate diameter of 8 cm and length of about one meter. The wire is generally wound without spacing and always in a single layer. The ends are protected by approximately spherical caps, those shown in the figure being 25 cm in diameter. When the Tesla coil is

immersed in oil it is important to eliminate the air which is likely to be trapped between the wires and the glass. If silk-covered wire is used soaking in oil is often sufficient to draw it in by capillary action. Vacuum impregnation is often advisable. For this purpose the coil is put in a tin tray and inserted into a horizontal piece of 6-inch pipe. The pipe is closed, exhausted, and oil is let in slowly with the vacuum-pump running. When the tray is full the pump is disconnected, the tray is taken out, and the coil is ready for use. Our best coils were made of No. 38 or No. 40 B.S. gauge copper wire, 5,000 to 7,000 turns. Either double silk, silk enamel, or the especially heavily enameled No. 40 wire (made by the General Electric Company) are satisfactory. It often happens that there are flaws in the insulation of the wire. These cause sparks between turns as soon as the coil is used and the coil is often burned out at such points. Having thus found out the weak points a few turns are unwound, the wire is scraped carefully at the ends, and is spliced; such a repaired coil is usually better than a fresh one. Insulation between turns usually gives no trouble up to 3,000,000 volts peak.

A screw is fixed permanently in the ball so that the ball can be screwed as a whole into a tapped hole in a brass end-piece fixed on the axis of the Tesla at its end. Incidentally, Houston's water putty made by the Gold Medal Polish Company (Racine, Wisconsin) provides a very convenient means for fastening attachments to Pyrex tubing. In most of our experiments the Tesla coil has been supported in the oil by a loop of silk fish-line at each end, which stands the full voltage to ground without trouble.

Oil and high-pressure tank.—Light transformer oil (not switch oil) purified by passing through a centrifuge has been used. Most of the oil employed by us has the trade name Transil 10 C. At its best clean oil is broken by about 46,000 volts across a 1-mm gap; in thicker layers its apparent dielectric strength is always less than this. The effective dielectric strength also depends to a large extent on the state of the electrodes between which the discharge takes place. No exact quantitative values can be assigned to it in our experience except by allowing a considerable safety-factor. It has proved possible to improve the performance of the oil by continued and judicious use. A preliminary discharge is often likely to take place while using a Tesla coil before the dielectric strength of pure oil is reached. We find it advantageous to "break in" the oil by allowing such discharges to occur. The procedure in this "breaking in" process is to bring up the Tesla voltage gradually. For very low voltages the caps on the ends of the coil show no discharge. As the voltage is brought up occasionally a corona "tree" shoots out from one of the caps into the oil. If the voltage is held at such a value that the "tree" occurs only seldom, the "trees" disappear after continued use. The voltage may then be brought up higher, "trees" occurring again occasionally and again disappearing after continued running. This process cannot be continued indefinitely but it is quite essential in improving the performance and obtaining as high a potential as possible. If the "trees" refuse to disappear it is often advisable to lower the potential to a point where they occur less frequently and to make them disappear

there. The "breaking in" of the oil and cap surface can be done either with a Tesla using 60-cycle excitation with a synchronous primary gap, or else by the intermittent primary sparks produced when using the x-ray machine. We have no special evidence of the superiority of either method. The synchronous gap is likely to shorten the time required but it is also likely to carbonize the oil if too heavy discharges occur. Its main danger lies in burning out the fine wire of the Tesla at points where the insulation on the wire is defective. We have obtained 3,000,000 volts with a Tesla used on 60-cycle synchronous gap excitation, the ends of the Tesla being protected by 5-inch spun copper caps. The mode of oscillation of the coil was such that the middle of it was at ground while the ends were at each instant at equal and opposite potentials. Each 5-inch cap was therefore at 1,500,000 volts corresponding to a gradient of 240,000 volts per cm. We did not find it practical to use much higher gradients in oil at atmospheric pressure, the performance of the apparatus becoming unreliable due to the corona from the caps. Also the apparent gradient to which the oil may be brought up depends on the caps used. An increase in the diameter of the caps makes it possible to bring them up to a somewhat higher potential. However the gain in potential is always less than would be calculated from the diameter. The exact reason for this we do not know but the obvious difficulty of having a perfectly shaped light metal sphere of large diameter, and of keeping it clean and polished, has probably much to do with it. The nature of the "breaking in" process we also do not know much about. It may be connected with removing dirt or microscopic particles of moisture from the electrodes or even with a local purification of the oil due to driving moisture or small air bubbles away from regions in which the electric field is large. Our main concern with regard to the production of high voltages has been the purely practical one of using oil at as high a value of the electric field as possible in order to test the voltage and power-output limitations of the method.

To improve the performance of the oil beyond that which was obtainable by ordinary purification and "breaking in" at atmospheric pressure we resorted to the pressure-method.⁴ The pressure container is shown to scale in proportion to the Tesla coil in Figure 1. It is a hammer-welded iron tank originally made by the M. W. Kellogg Company of Jersey City for use as a steam separator. It is designed for a working pressure of 450 pounds per square inch in accordance with the standard boiler safety-code. [The importance of precautions in the use of high pressures in large containers cannot be over-emphasized.]

The tank was furnished with solid manhole plates which were later machined with proper openings for the insulating bushings and peep-holes (not shown in the figure). A peep-hole was put in each manhole plate. Each hole, three inches in diameter is covered with two-inch plate-glass. The inside of the tank was illuminated with two automobile headlights, current being supplied through an ordinary spark-plug screwed into a third manhole of the crab type in one head of the tank. This third manhole has been

⁴ F. Koch, *Elektr. Zeits.* **36**, 85 and 99 (1915).

omitted in the figure. The pressure was applied to the oil by means of a carbon dioxide cylinder shown in the figure as "air-pressure cylinder." On account of the increase of volume of the tank under internal pressure and on account of the compressibility of the oil it is necessary to supply extra oil (several gallons) when pressure is applied. This is done by connecting the carbon dioxide pressure-cylinder to the auxiliary oil tank shown in the figure.

The "breaking in" of the oil is essential also in this high-pressure arrangement. It is difficult to give exact figures for the improvement in the dielectric strength due to pressure. Roughly a factor of two is correct in our experience. The limitation which we encountered in the use of Tesla coils in oil under pressure was due to insulation between turns and not to "trees" (corona) off the caps. With longer Tesla coils it would be doubtless possible to exceed our voltages. The maximum which we obtained was 5,200,000 volts. The coil was wound with ordinary No. 40 enameled and silk-covered wire. The caps were 20 cm in diameter and the length of winding was approximately 90 cm. The mode of oscillation was again the half wave-length, that is, middle at ground and ends at opposite potentials. The application of pressure improves the insulation between turns as well as the insulation around the caps, there apparently always being a film of oil between turns. The improvement for the caps, however, proved to be so large that they offered no serious difficulty. The oil is purified at intervals by means of a Hydroil centrifugal purifier.

Measurement of high potentials.—We have used two methods of estimating the potentials. The first was used purely qualitatively although it can be developed into a quantitative one. It consisted in observing the deflection of a cathode-ray beam in a low voltage cathode-ray oscillograph. The latter was of the Johnson type made by the Western Electric Company giving cathode rays of 300-volt velocity observed visually on a fluorescent screen. The cathode-ray tube was put vertically in a wooden box the outside surface of which served as a support for a set of vertical grounded wires. These allowed only horizontal fields to affect the cathode rays. The sensitivity of the tube to electric fields inside the shield was determined experimentally by putting it in known fields produced by an electron-tube oscillator. One centimeter deflection on the screen could after the calibration be interpreted as a known electric field. When the cathode-ray box was put in the neighborhood of the Tesla coil the deflection on the screen was observed and the oscillating electric field due to the coil thus determined.⁵ From a knowledge of the potential distribution on the coil and the distances involved the numerical value of the potential can be computed. The difficulty of this method lies in the extreme weakness of the trace on the fluorescent screen

⁵ For this experiment the Tesla coil was supported in an open wooden tank containing the oil, although for experiments at atmospheric pressure we now use a 1500-gallon steel gasoline storage tank with about one-fourth of the cylindrical surface cut away. No particular loss of efficiency is occasioned by operating these high-frequency coils inside of a metal tank. This is clear, of course, from the results with the thick-walled high-pressure tank.

due to the extremely short duration of the high potential on the Tesla coil. The visibility of the trace being so low no quantitative measurements could be made. The estimates thus formed were checked however by measurements by the second method. Photographic registration of the cathode ray, as in the Dufour cathode-ray oscillograph, would make the first method quantitative and we mention it mainly for this reason.

The second method can be described as a capacity-potentiometer or "pick-up" measurement. The principle is shown in Figure 1. The manhole on the right of the high-pressure tank is provided with an insulating bushing which supports a voltage "pick-up" ball. Since the potential on the Tesla coil alternates with a high frequency (approximately 100,000 per second) the potential assumed by the pick-up ball is determined by the capacities between the Tesla coil and the ball as well as between the ball and the ground. In order to know the potential of the coil it is sufficient therefore to measure the potential on the "pick-up" system and to determine the ratio of the potential on the coil to the potential on the "pick-up." The measurement of the potential on the "pick-up" system is made by means of a sphere-gap and the ratio of the two potentials is determined at low voltages where the potential of the Tesla coil can be measured directly. The direct measurements of the Tesla-coil voltages in the low range have been made in two ways. The most direct method is to connect a sphere-gap across the coil. In doing this care is taken to have the high-potential lead to the sphere-gap removed as far as possible from the "pick-up" ball so as not to change the relative distribution of capacities. Since this can never be done perfectly, although in general it leads to underestimating the true voltage, we have also determined the potential ratio, or calibration-factor, by a somewhat different method free from this objection.

The second way of determining the calibration-factor makes use of the fact that the potential at the middle of the Tesla coil is the same as that of the ground, and that a small capacity around a small section of the coil at its middle does not change appreciably the voltage-distribution along the coil. Thus the coil is provided with taps exactly at the middle as well as at one and two centimeters to each side of the middle. The coil is excited by sustained oscillations from an electron-tube oscillator. A bifilar electrometer is connected across the middle tap and one of the others, and another bifilar electrometer is connected across the measuring gap. The ratio of the two measured potentials gives therefore the ratio of the potential across one centimeter of the Tesla coil at its middle to the "pick-up" potential. In order to determine the calibration-factor it is now only necessary to find the ratio of the potential across the whole Tesla coil to the potential across a centimeter of it at its middle. This was determined by finding the potential distribution along the coil by special experiments.

It may be shown by calculation that the change in the resonant frequency of a Tesla coil when a capacity is connected across a section of it is proportional to this capacity and the square of the voltage across the section in question. This calculation presupposes that the change of frequency dealt

with is small. Model Tesla coils were built with taps and the "detuning" effects were observed when a small fixed condenser was connected across the various sections. The square roots of the detuning effects $(\Delta C)^{1/2}$, when ΔC is the capacity-change required to retune an oscillator coupled to the Tesla coil, gave the potentials across the separate sections and hence by addition the potential distribution along the coil. The magnitude of the fixed capacity used was varied so as to make sure that it was small enough and not sufficient to cause partial resonance of a part of the coil which would vitiate the measurements. The condenser employed to produce the capacity-changes was made of two circular plates about 5 cm in diameter separated by a thin sheet of mica and thus had a fairly small capacity to ground. This capacity was sufficient to require a correction because it was found that if the condenser was connected to one of the taps it had a measurable detuning effect on the Tesla coil. This detuning effect was therefore ascertained for all the

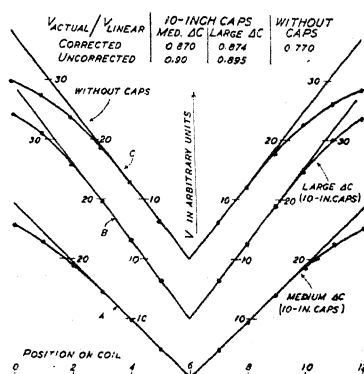


Fig. 4. Voltage-distribution curves for Tesla coils (points are plotted for corrected data only; the uncorrected points are almost indistinguishable from these on the scale of the figure).

taps and corrected for by subtracting it from the detuning effect of connecting the condenser across two adjacent taps. The remaining number gave the detuning due to a capacity across the two taps without having a capacity to ground. This correction reduced the resulting form-factor only two or three percent, however, (see Figure 4). When different condensers were used the voltage-distribution curves corrected for the capacity to ground of the "probing condenser" checked closely for different capacities of the condenser used. Such measurements were made on Tesla coils wound with different sizes of wire and with different caps on the ends. The voltage-distribution curves proved to be independent of the size of wire used for winding the Tesla coil. Experiment shows however that it depends appreciably on the capacity load at the ends and that it is different for different sizes of caps used. The results can be expressed most conveniently in terms of the ratio of the average slope of the voltage-length curve to the maximum slope at the middle of the coil. For coils of the dimensions used by us this ratio or "form-factor"

is 0.77 for coils without caps (Figure 4C), 0.82 for 5-inch cast bronze caps, 0.87 for 10-inch caps. The voltage-distribution thus becomes more linear as the capacity-load at the ends is increased, as would be expected. Knowing the "form-factor" of the coil we obtain the potential across the coil from the potential across one centimeter of it at the middle by multiplying the latter potential by the length of the coil in centimeters and by the "form-factor."

We have ascertained the effects of the capacity of the electrometers used in the measurements by connecting a third electrometer either at the measuring sphere-gap or at the tap across the middle of the Tesla coil. These effects are small and corrected for. The calibrating-factors obtained by the first or second method of measuring the Tesla-coil voltage agree very closely. In both cases we also have made sure that the "pick-up" voltage is due to the potential on the Tesla coil itself rather than to induction from the primary and calibrating circuits by partially or completely detuning the primary circuits from the Tesla coil. This reduces the "pick-up" voltage to zero.

Every calibrating-factor depends on the setting of the measuring gap because the capacity of the "pick-up" system to ground is affected by the distance between the two measuring spheres. A curve for the calibrating-factor against the "pick-up" gap setting is plotted and used in the calculation of the voltage. The corrections due to this cause are of the order of 5 to 10 percent in our set-ups. The measurement of the "pick-up" voltage in actual operation consists in determining the separation between the spheres at which sparks definitely pass between them. The potential across the gap is then obtained from the data of Peek.⁶ The potentials of the secondary gap are generally of the order of from 30,000 to 100,000 volts thus allowing one to make fairly accurate gap-settings. Since voltage-measurements by a sphere-gap may be subject to corrections due to local conditions such as air ionization, surface condition of gap, etc., as a precaution we have checked one of our gaps on 60 cycles against an electrostatic voltmeter and found the results to be in agreement with Peek's data. For our measuring gaps we always employ 25-cm (10-inch) diameter spheres, which are known from the work of Peek to be reliable indicators in the range of voltages used. A sphere-gap does not give as consistent readings immediately after polishing as it does after a number of sparks have passed. Freshly polished spheres will spark occasionally at a greater separation than will "used" spheres for a given voltage. We have always taken measurements with gaps in the "used" condition, leading to lower rather than higher voltage-estimates.

It may be observed that if the oil should become partially conducting under the influence of high electric fields the "pick-up" method would be seriously vitiated and would tend to give exaggerated values to the Tesla voltage. We have taken care therefore to make sure that this is not the case.

⁶ F. W. Peek, Jr. Dielectric phenomena in high-voltage engineering (McGraw-Hill, 1920) Chapter IV; Trans. A. I. E. E. **34**, 1857 (1915); J. Franklin Inst. **197**, 1 (1924) and **199**, 141 (1925); Smithsonian Inst. Report for 1925, 169 (1926). Also L. W. Chubb and C. Fortescue, Proc. A. I. E. E. **32**, 627 (1913).

Our main evidence lies in the fact that the measured Tesla voltages, with a given primary setting, are independent of the position of the "pick-up" (each position of course being separately calibrated at low voltage) as long as there are no "trees" from the caps in the oil. Since at low voltages used in the electrometer-calibrations there is absolutely no possibility of a non-uniform oil-conductivity we conclude that the oil-conductivity is uniform also when high potentials are used unless a visible breakdown occurs as shown by "trees" or bolts in the oil. In the second place we find that the measured Tesla-coil voltage is proportional to the potential to which the primary condenser is charged which is determined by the setting of the primary gap. This again would not be the case if the conductivity of oil and invisible discharges played any part in the measurements. If insufficient care is exercised in preventing corona in air or the discharges along the surface of the oil from the high-potential connections of the measuring gap, too low values of the Tesla voltage may result. The only deviations from linearity which we have observed have been due to these causes.

Data on the efficiency of Tesla coils.—We have made rough measurements of the potentials developed by Tesla coils with various sizes of caps in terms of the potential of the primary gap. The measurements given in the table were all made with a primary voltage of 6500 and with half wave-length excitation of the Tesla coil. V_T represents the total voltage between caps, measured by the capacity-potentiometer method. Each cap is therefore charged to a voltage $V_T/2$ above ground. The primary circuits and the coils may be rated either from the point of view of having a certain maximum usable primary potential or else on the basis of having a certain maximum number of plates for the primary condenser. For this reason we tabulate both the ratio V_T/V_P giving the voltage gain-factor of the Tesla over the primary and applying therefore to the case when the primary potential is the limitation, and also $C_P V_P^2/V_T^2$ expressed in micro-microfarads. The latter figure gives the effective capacity of the Tesla coil which for this purpose is defined to be such a capacity C_T which would attain a voltage V_T if all of the energy $C_P V_P^2/2$ of the primary condenser were transferred to the capacity C_T . The point is that a given number of plates available for the primary condenser whether used all in parallel or in several groups in series gives roughly the same maximum value of $C_P V_P^2$ and therefore if the limitation lies in the primary condenser a small value of $C_P V_P^2/V_T^2$ is an advantage.

It is seen from the table that if the primary voltage is fixed a small primary inductance and a large primary condenser constitute the best circuit. If however the number of glass plates available for the condenser is limited it is perhaps at times better to use a reasonably large number of primary turns and therefore less primary capacity but a higher voltage by subdividing the condenser into sections used in series. A too large number of sections in series is of course not practical, leading to overvoltages and increase of circuit-inductance. A too small primary inductance however is also frequently harmful, leading to explosion-like flash-overs of the con-

denser. The use of the table is therefore only to select rough values for the circuit-constants. The best arrangement is found afterwards by trial. The table applies to the particular circuits which were made up of the Telefunken condensers and therefore takes account of the particular lead-inductances used with them.

The table shows the relatively high energy efficiency of the Tesla coil, which is capable of storing in its very small capacity about one-fourth of the energy of the primary circuit. This is made clear by comparison of the

TABLE I. *Data on efficiency of Tesla coils.*

Caps	Primary turns	Primary capacity in microfarads	Transformation ratio V_T/V_P	$C_P V_P^2 V_T^2$ in micro-microfarads
No. 36 double silk-covered wire				
5-inch	2	0.19	101	19
	3	.13	85	18
6-inch	2	.26	104	24
	3	.16	106	14
8-inch	2	.33	106	29
	3	.22	99	22
	4	.15	83	22
10-inch	2	.41	121	28
	3	.30	112	23
	4	.20	94	23
No. 40 General Electric enameled wire				
5-inch	3	0.45	162	17
	4	.33	147	15
	5	.23	115	17
	6	.19	87	25
6-inch	4	.48	123	32
	5	.37	113	29
	6	.27	97	29
8-inch	4	.60	131	35
	5	.45	118	32
	6	.33	107	29
10-inch	5	.54	137	29
	6	.45	119	32

last column of the table with the calculated capacities of the caps (remembering that each cap is charged only to $V_T/2$ above ground). Now a capacity of 1.5 microfarads at 30,000 volts contains 675 joules so that 170 joules can be put into the capacity of the Tesla coil. Even if it should be dissipated in one ten-thousandth second (about 10 cycles at a frequency of 10^5) this gives an instantaneous power of 1.7×10^3 kilowatts. By direct tests we find that a Tesla coil is able to feed about 20 megohms without having its voltage decreased to less than about half. Since insulation, rather than electrical efficiency, is the limiting factor at high voltages, the voltage under load may

be brought up to that obtained without load by supplying extra power in the primary circuit. At 5,000,000 volts the power-consumption through 20 megohms is 1.2×10^8 kilowatts. The instantaneous power available in a Tesla coil is therefore of the order of one thousand kilowatts and at the high potentials produced the coil is capable of delivering fairly efficiently an instantaneous current of 5×10^6 volts/ 2×10^7 ohms = 0.25 ampere. If now the coil is used on 60-cycle current, that is, with 120 primary sparks a second, and if only 10^{-6} second during each discharge (roughly one tenth of a cycle) is counted as effective in feeding a high-potential x-ray tube, the average current is $120 \times 10^{-6} \times 0.25$ ampere = 3×10^{-5} ampere. If only one spark a second is used an average current of 2.5×10^{-7} ampere can be drawn. The synchronous-gap excitation thus gives 1.9×10^{14} five-million-volt electrons per second and the one spark-a-second excitation gives 1.5×10^{12} electrons. For comparison with radioactive sources we recall that the number of α -particles emitted by a gram of radium per second is about 3.5×10^{10} . Thus at 5,000,000 volts one spark a second has sufficient power to drive 0.75×10^{12} α -particles equivalent to 21 grams of radium, and 120 sparks a second would be equivalent to 2600 grams. Such α -particles would have an energy of 10,000,000 electron volts, at least 2,000,000 volts higher than the highest energy α -particles obtainable from radioactive sources. We may conclude therefore that the amount of energy which may be drawn from Tesla coils is sufficient to obtain sufficient numbers of high-velocity particles for disintegration-experiments.

We are greatly indebted to Lieutenant William Klaus formerly of the Washington Navy Yard for arranging the loan of the apparatus with which this work was begun and to the Potomac Electric Power Company for a temporary loan of 400 gallons of transformer oil. Our particular thanks are due to our colleague, J. A. Fleming, for his energetic support and to B. Howard Griswold of Alexander Brown and Sons, Baltimore, Maryland, for temporary financial assistance.

THE APPLICATION OF HIGH POTENTIALS TO
VACUUM-TUBES

BY M. A. TUVE, G. BREIT, AND L. R. HAFSTAD

DEPARTMENT OF TERRESTRIAL MAGNETISM, CARNEGIE INSTITUTION OF WASHINGTON

(Received November 22, 1929)

ABSTRACT

A brief progress-report is made on the results so far obtained in the development of vacuum-tubes to which the very high voltages produced by Tesla coils (greater than 10^6 volts) can be applied. One cascade tube has been constructed which withstood repeatedly a voltage of 1,400,000 volts, and others have been used at lower voltages. This method, originally developed by Coolidge, gives promise of being suitable for voltages of several million, and eventually perhaps even higher. No effort has been made so far to use these tubes with a definite and controlled emission, since experience has shown that single-section tubes operated at several hundred kilovolts have approximately the same voltage-limitation with or without hot cathodes. The chief difficulty with very high-voltage tubes is that of preventing the uncontrollable (cold-cathode) emission which limits the voltage which can be applied. An electrodeless tube which withstood 1,000,000 volts is briefly described.

THIS paper is a brief progress-report giving some of our experiences and the results so far obtained in the development of vacuum-tubes to withstand the high voltages so readily produced by means of Tesla coils. Many different designs of tubes have been constructed, with different kinds of electrodes and variations in vacuum technique, and in general our conclusions parallel those of others working on similar problems using other high-voltage sources. It is very difficult to apply more than 300 to 400 kilovolts to a single two-electrode tube, whatever the design or treatment within practical limits. The reason for this is not known exactly at present. The main difficulties are presumably uncontrollable emission and accumulation of charges on the glass walls resulting in punctures and short-circuiting of the voltage source. We have succeeded, however, in applying Tesla voltages of considerable magnitude to vacuum-tubes by two methods, and these results seem interesting enough to merit a brief description.

(1). *The cascade-tube method*—This is essentially the method developed by Coolidge.¹ We have found it possible to use much smaller tubes for the same voltages by immersing them in oil. Figure 1 shows a picture of a 6-section tube used successfully at 850,000 volts. The overall length is 34 inches; the bulbs are of 100-cc size. A tube of similar design with fifteen 300-cc bulbs and having an overall length of 7 feet has gone up repeatedly to 1,400,000 volts. This tube is shown in Figures 2 and 3. Such tubes are at present always used by us on the pumps. The pump system is an ordinary diffusion or Langmuir pump arrangement. The electrodes are copper tubes

¹ W. D. Coolidge, J. Frank. Inst. 202, 693 (1926).

with rounded ends of as large a radius of curvature as possible, the electrodes being rounded by "spinning" the ends in. We have used Pyrex glass for these tubes for mechanical reasons, although it is quite possible that other glass may prove more advantageous. We have preferred to use each section at a somewhat smaller voltage and to increase the number of

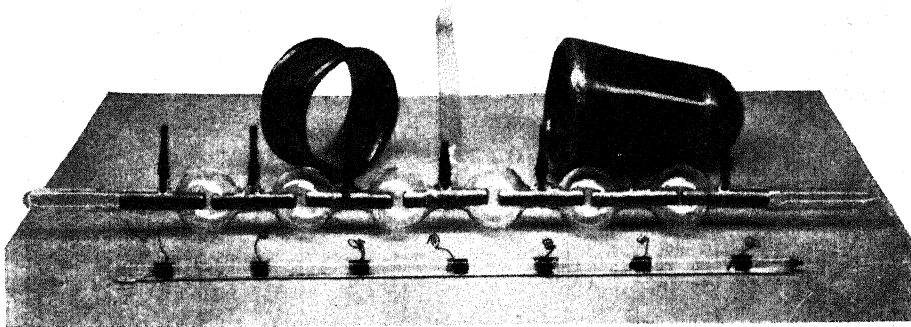


Fig. 1. Six-section tube, with potentiometer and typical shields unmounted.

sections rather than to design each section for operation at the limiting value of 250 or 300 kilovolts, although this no doubt can be done later even with small sections such as we are using. The essential points in the design of tubes are: (a) the subdivision of the whole tube into sections; (b) the uni-

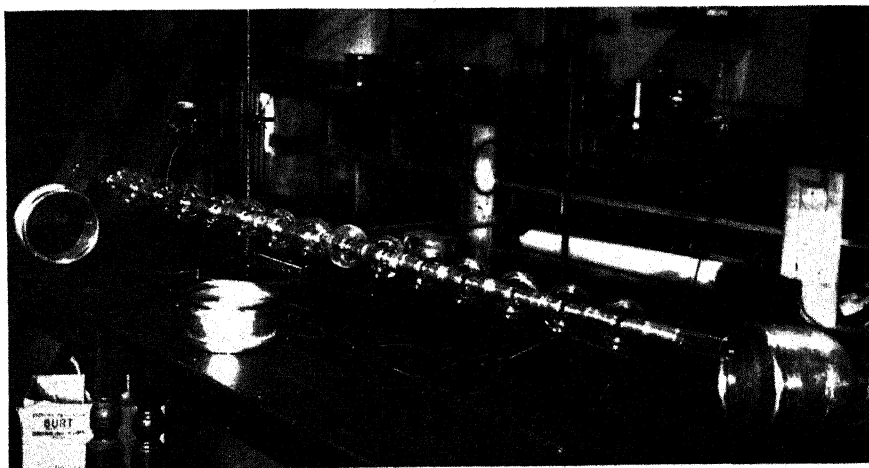


Fig. 2. Fifteen-section tube.

form distribution of voltage between sections by means of a potentiometer or some other electrical circuit; and (c) electrostatic shielding of the sections outside of the vacuum. The type of potentiometer used is shown in Figure 1. The glass tube is filled with a weak solution of salt in water. The concentration of salt is adjusted by trial until the potentiometer connected

across the Tesla coil produces a measurable effect on the voltage, for example until it reduces the total voltage by one quarter or somewhat more. The taps of the potentiometer are connected to the successive electrodes of the vacuum-tubes. In operation the potentiometer is put inside the shields.

The type of shield used is also shown in Figures 1, 2, and 3. The 15-section tube, each section of which was $4\frac{3}{4}$ inches long, had shields $3\frac{3}{4}$ inches long, the diameter of each shield being about 8 inches. The spacing between shields was about 1 inch. Experience showed that shielding of bulbs at high potentials is quite necessary. This may apply only to the high-frequency alternating type of potential we are using.

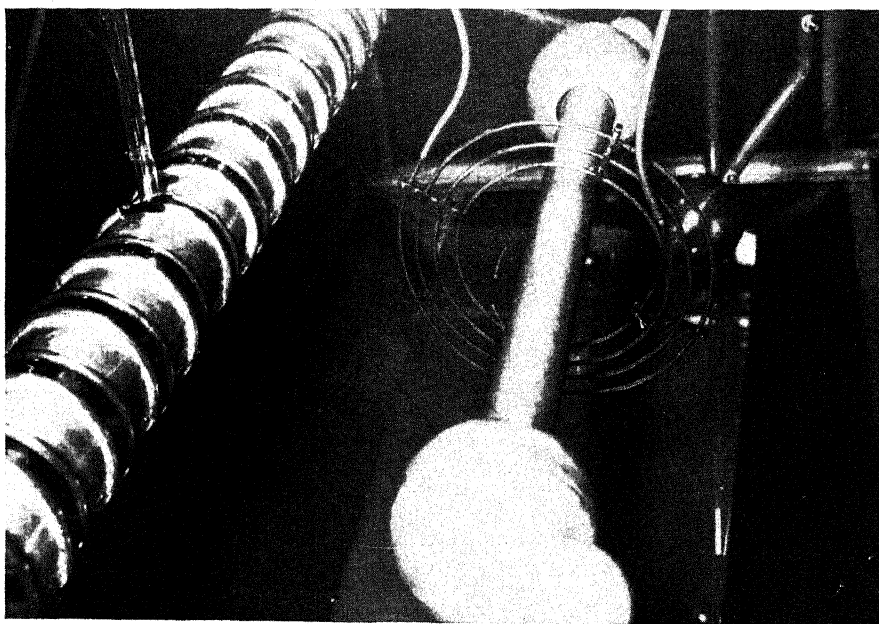


Fig. 3. Fifteen-section tube mounted in steel tank showing shields in position; Tesla coil in place but oil pumped out.

As is seen in Figure 1 the connections to the electrodes were made through waxed joints. There was thus no question of an extremely high vacuum since the tube as a whole could not be baked. The electrodes themselves (copper) were prebaked at 950°C in a quartz-tube furnace. The tube was also torched with a gas flame while evacuated, before the electrodes were put in. Carbon-dioxide snow in alcohol was used on the trap for keeping down the pressure of Hg and other condensable vapors. No refrigerant was used during the first half-hour of pumping, in order to pump out most of the water-vapor. Liquid air on the trap obviously might be quite dangerous in case of an accident, since the tubes are tested under oil. As indicative of the rather low degree of vacuum required it may be of interest to mention that the 15-section tube withstood 1,000,000 volts without trouble only 4 hours after

it was assembled and the pumps started. This was without torching any of the glass parts.

An important point about bringing up a tube to a high voltage is "breaking in" as in the case of x-ray tubes on direct current or low-frequency alternating current. When a potential is first applied the tube may flash at one-half of the potential which it stands without puncture after it is broken in. Our procedure is to bring the potential up cautiously until the tube flashes. Then the potential is lowered until the flashing weakens appreciably. After a few minutes running or less the flashing disappears. The potential is brought up until the tube flashes again and the procedure is repeated. In cases where one of a set of bulbs shows bad flashing it is sometimes helpful to break this section in by itself. There is of course an approximate limit which a given size of bulb of a given design will not exceed. The potential which can be applied to the whole tube is however rather accurately equal to the potentials which may be applied to the bulbs separately. Thus the bulbs act independently. The "breaking in" procedure may at times be carried out safely by letting the tube flash and allowing it to rest for a minute or two. Then the potential is applied again. The flash is often weaker or absent. It seems that it is important to pump off the gases evolved during a flash. The "breaking in" of a tube is somewhat similar to the "breaking in" of oil described in the preceding article. The "breaking in" lasts, that is, if a tube is broken in one day it can be broken in to the same voltage on the next day in a much shorter time. At times no "breaking in" the next day is required. In all of these experiments we use the intermittent voltage-excitation by means of a stationary primary gap and direct current on the primary condenser described in the preceding article. It may be that the same tubes would be subjected to more danger if used on other and more continuous sources of potential.

It will be noticed that the increase in the potential applied to the 15-section tube over that used on the earlier 6-section one was not proportional to the number of sections and was especially out of proportion to the total lengths. It might be supposed that the use of tubes with many sections is disadvantageous. No such limitation was responsible for the insufficiently high voltage applied to the larger tube. One of the shields which was insufficiently well supported, fell on the tube and caused a puncture at the point of contact with the glass during the "breaking in" process. The flashing at 1,400,000 volts was not due to lack of additivity in the action of the bulbs, because the bulbs when tried separately flashed at about 100,000 volts per bulb. This relatively bad performance of the bulbs was in all probability due to partial contamination of the electrodes with mercury which occurred during an accident to the tube. The amount of work involved in taking the electrodes out, baking them, and putting them in again being considerable, the tube was repaired without removing the electrodes. Since the electrodes in the 15-section tube were larger and more nicely rounded than in the 6-section tube and since the bulbs in it were also larger there is every reason to expect at least one-sixth of 850,000 volts per section when care is taken

to have uncontaminated electrodes. It must also be mentioned that one of the 15 sections was not used because of a defect in the potentiometer at that section. The additivity of potentials which may be applied to the bulbs separately when they are connected in series seems thus to be demonstrated. We expect therefore that a 2,000-kilovolt tube can be constructed without serious difficulty.

So far we have tried hot cathodes in single-section rather than cascade tubes. The puncture-voltage was independent of whether a hot cathode was used or not. The evidence is that its use will not make the operation on the cascade principle more difficult.

(2) *Electrodeless tubes*—These have been mentioned by us in a previous publication.² Under proper conditions a spherical Pyrex bulb immersed in oil between electrodes does not puncture when a million volts is applied to the electrodes. The arrangement is shown in Figure 4. The exact conditions for successful operation of such bulbs are still not certain. The evidence

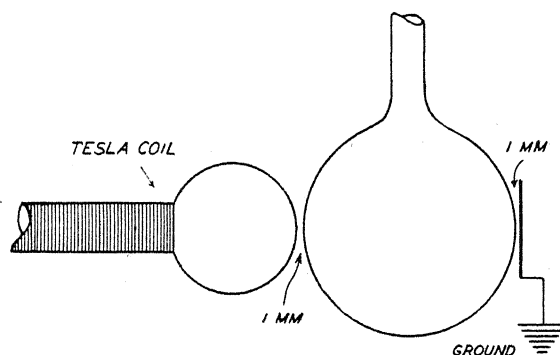


Fig. 4. Diagrammatic sketch showing the arrangement for electrodeless tube.

seems to be however that a partially electrically conducting-layer on the inside surface of the glass, in our case due to carbonized oil, is essential. The fluorescence patches of long duration observed with this type of bulb are quite similar to those occurring with the cascade-bulbs.

(3) *Miscellaneous experience*—Long tubes, with one electrode at each end put inside the Tesla, puncture readily. The high-frequency field produced by the Tesla is thus insufficient to prevent accumulation of charges inside the tube.

Sealed off commercial Coolidge tubes at times stand a higher Tesla voltage than would be expected from their behavior on direct current. This however is not always true. It was impossible in our experience to exceed 400 kilovolts without bad flashing. One 220-kilovolt deep therapy tube was punctured at 400 kilovolts.

An extraordinarily good vacuum is not essential in securing good operation of single-section tubes up to say 300,000 volts. Extreme precautions

² G. Breit and M. A. Tuve, *Nature* 121, 535 (1928).

with regard to vacuum technique do not suffice in our experience to bring about anything but very erratic improvements beyond this figure.

One quite definite type of failure is that shown by "straight" tubes, whether single or cascade, made by enclosing the electrodes in ordinary drawn Pyrex tubing of a diameter not much larger than that of the electrodes themselves, instead of in bulbs. Such a rigid design of tube would be mechanically very desirable, but 10-section and 20-section tubes made in this way have failed well under 500,000 volts, the glass wall shattering inward from longitudinal striae or bubbles in the glass without puncturing through to the outside. Violent flashing then limits the voltage which can be applied. The striae are usually invisible before the shattering takes place.

The authors take pleasure in recording their indebtedness to O. Dahl, whose assistance during a part of this tube-work has been invaluable, and again to J. A. Fleming for his support of the work.

ANODE SPOTS AND THEIR RELATIONS TO THE
ABSORPTION AND EMISSION OF GASES BY THE
ELECTRODES OF A GEISSLER DISCHARGEBY C. H. THOMAS AND O. S. DUFFENDACK
UNIVERSITY OF MICHIGAN

(Received September 23, 1929)

ABSTRACT

In a Geissler discharge containing H_2 , N_2 , CO, mixtures of hydrogen and the rare gases or mixtures of mercury vapor in the rare gases at pressures of 0.5 to 12 mm and electrode separation of 4 to 30 cm, the anode glow breaks up into a number of bright hemispherical spots, more or less symmetrically arranged when the polarity of a direct current discharge is reversed. Anode spots do not form in O_2 , A or Ne but faint spots form in He which contain a trace of H_2 . It is shown that one necessary condition for the formation of spots is the emission of gas from the surface of the anode. As many as 75 spots arranged in 5 concentric rings have been observed on an anode 34 mm in diameter. Conditions governing the number, size and duration of the spots have been determined. Spots formed on all the metals tried; Fe, Ni, Al, Cu, Hg and brass. The formation of anode spots has been used to prove that in a Geissler discharge between cold electrodes, the cathode absorbs gas and the anode emits gas at rates which are functions of the current density, gas pressure, kind of gas and electrode temperature. It is shown that the increase of the potential drop of a discharge with time, is due almost wholly to an increase in the gas content of the cathode, and that the potential drop immediately after starting a discharge is lowered by previously degassing the cathode by means of an induction furnace or by using this electrode as anode.

INTRODUCTION

ALTHOUGH hundreds of investigations have been carried out during the past fifty years on some part or other of the Geissler discharge, a complete understanding of the phenomena which occur therein is still lacking. Among these phenomena is the "clean up" or disappearance of the gas. It has long since been postulated that the electrodes absorb gas but in the past no direct proof of this has been given although the several explanations^{1,2,3,4} of the phenomena of cathode sputtering have as their bases the absorption of gas by the cathode or the existence of gas in it.

That certain gases diffuse through certain metals is shown by the diffusion of hydrogen through palladium. Yamada⁵ has shown by spectroscopic analysis that absorption of hydrogen in palladium produced a uniform expansion of the space lattices by 2.9 percent. He found no evidence that the absorbed hydrogen had reacted with the palladium.

¹ Hittorf, Wied. Ann. 21, 126 (1884).² Kingdon and Langmuir, Phys. Rev. 22, 148 (1922).³ Berliner, Weid. Ann. 33, 291 (1888).⁴ Kohlschutter, Jahrb. d. Radioakt. 4, 353 (1912).⁵ Yamada, Phil. Mag. 45, 241 (1923).

Baum⁶ has made microphotographs of silver cathodes which had been used in a Geissler discharge of 3000 volts in which he found that gas molecules had penetrated to a depth of 1.5 mm.

In some recent experiments, one of the writers has had occasion to investigate an alternating current Geissler discharge in hydrogen. He found that during one half of the cycle of alternating current the discharge did not strike. During the succeeding half cycle, the discharge struck when the voltage had attained the sparking potential of the gas for the existing pressure-distance conditions. A check on the history of these electrodes showed that they were of the same metal and that they had been subjected to the same treatment except that a direct current discharge in hydrogen had previously been passed between them. The discharge struck with A.C. when the electrode previously used as anode in the D.C. discharge was negative.

This experiment shows that the use of an electrode as anode or cathode changes its sparking potential. Later in this paper, it will be shown that this difference in sparking potential was due mainly to a difference in the amounts of gas absorbed in each electrode. During the investigation of this difference in sparking potential, the anode spots appeared. The term anode spots is used throughout this paper to apply to the hemispherical bright spots which were more or less symmetrically arranged on the cathode side of the anode.

The appearance of anode spots has been previously reported by Lehmann⁷ who found them in a discharge in air in a tube of wide diameter, and by Mackay⁸ who found more elaborate patterns in helium. Neither author attempted any explanation of the formation of the anode spots.

OBJECT

In the light of this information, it seemed advisable to make the following investigations: (1) A determination of the cause of anode spots; (2) A study of their characteristics; (3) An application of the phenomenon of anode spots to the study of emission and absorption of gases by the electrodes of a Geissler discharge; (4) A study of the effect of gas absorbed in the electrodes on the potential drop of the discharge.

APPARATUS

The vacuum system consisted of the usual pumps, mercury cut-off and liquid air trap. The gas pressure in the system was determined by means of two McLeod gauges whose combined range extended from 30 mm to 2×10^{-5} mm of mercury. A gas storage and purifying system was connected by suitable stopcocks to the vacuum system so that either all parts could be evacuated to a high degree or purified gas could be admitted to the experimental tube.

Figure 1 is a diagram of the experimental tube most used. The tube proper was 63 cm in length and 6 cm in diameter. Electrical connections were made

⁶ Baum, *Zeits. f. Physik* 40, 690 (1926).

⁷ Lehmann, *Ann. d. Physik* 7, 8 (1902).

⁸ Mackay, *Phys. Rev.* 15, 309 (1920).

to the movable electrode through a capillary glass tubing which supported it. By means of a magnetic force on a cylinder of soft iron which was fastened to this capillary shaft, the one electrode could be moved through a distance of 30 cm. The electromagnet for moving this electrode was mounted on a screw device which permitted a slow regular movement of the electrode.

Electrodes of several sizes, shapes and thicknesses were used as well as similar electrodes with different degrees of polish. In several cases, extreme care was taken that no foreign material touched the electrode surface except the steel tool with which it was turned down. The electrodes were supported on glass stoppers in such a way that only one half inch of metal was exposed behind each electrode. Thus the distortion of the electric field was reduced to a minimum. The glass stoppers were ground to fit another tube of the same length as the first but of a diameter 4 cm larger than the latter. A third glass stopper which supported a spiral tungsten filament was interchangeable with the stopper which carried the fixed cold electrode.

A direct current motor-generator set supplied the potential which was regulated by changing the resistance in the circuit of the field exciter. The voltage across the tube was measured on a Jewell voltmeter of range 0 to 500

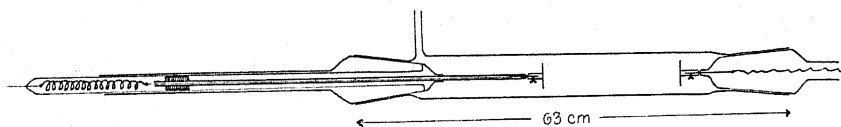


Fig. 1. Experimental tube.

volts. This voltmeter was equipped with suitable external resistances by means of which the voltage range could be extended up to 2000 volts. A resistance of 3000 ohms was placed in series with the experimental tube. By means of a reversing switch the direction of the discharge through the experimental tube was easily changed.

PROCEDURE

Whenever any appreciable sputtered material appeared on the inner walls of the tube or when a change of electrodes was made, the tube was disassembled and cleaned with aqua regia. Subsequently, the tube was mounted in its usual position and the glass stoppers were turned until the electrodes were parallel and symmetrically placed as judged by the eye after which the ground glass joints were sealed with De Khotinsky cement. The necessary precautions were taken for the removal of water vapor and occluded gases and for the exclusion of mercury vapor from the tube.

Extreme care was exercised in order to obtain pure hydrogen, carbon monoxide, argon, neon and helium. However, in no case was it possible to remove all traces of hydrogen from helium, possibly because the system and tube had previously been used for hydrogen.

The electrode separation was determined by measuring the relative position of the soft iron cylinder on the shaft which supported the movable

electrode. By this method the electrode separation could be easily determined within one half a mm regardless of the condition of the discharge tube proper.

When the gas, tube, and electrodes were properly prepared, the gas was admitted slowly to the tube through a liquid air trap until the desired pressure was attained. In the cases in which the effects of complete degasification of electrodes were investigated, the discharge was set up in the tube within a few seconds after the gas was admitted to the tube in order that the electrodes might have little time for absorption of the gas.

The ordinary procedure was to allow the one electrode to serve as cathode for a given time at a given current. This is called the period of "soaking" during which the cathode absorbed gas through positive ion bombardment. The polarity of the electrodes was then reversed so that the electrode which had been soaked as cathode now became the anode. Anode spots then formed on the anode if the pressure-electrode distance conditions were suitable. The discharge was then maintained at a constant current or potential during the period of the existence of these spots on the anode.

As soon as the last spot disappeared from the anode, the discharge was stopped, since it is assumed that for a given current, the spots disappeared when the rate of evolution of the gas from the anode had decreased to a critical value. Within a few seconds after the discharge was stopped, as mentioned above, the process was repeated. Thus a series of observations which showed the effects of the soaking of the cathode on the characteristics of the anode spots were obtained.

It was observed early in this investigation that the number of spots which appeared under similar conditions of current, pressure, etc., was different depending on whether the current was increased or decreased in order to obtain the desired value. This was to be expected since the spots often formed in patterns such that a considerable change in current was necessary to change the pattern. It was necessary, therefore, to use the same applied potential difference at each closing of the switch in order to obtain consistent results in the number of spots which were formed on the anode.

Throughout the work, particular attention was paid only to the one electrode for which the gas content and previous treatment had to be known at all times.

Photographs were taken at an angle of 30 degrees with the axis of the tube. Sometimes difficulty was encountered in obtaining a satisfactorily stationary pattern. The photographs of the spots which are presented in the succeeding parts of this paper were obtained with an exposure of one-fifth second on a Voigtlander camera which had an F 4.5 lens.

RESULTS

Presentation and discussion of photographs: The photographs presented in Figure 2 were chosen because they show the relative difference in the size of the spots. In pictures *a*, *b*, *c*, and *d*, the electrodes were 41 mm in diameter, while those in pictures *e*, *f*, *g*, and *h* were 34 mm in diameter. In picture *g*, the

spots were rotating rapidly under the influence of their own magnetic field. Picture *h* which was taken perpendicular to the axis of the tube shows the hemispherical form of the spots and their appearance back of a striation.

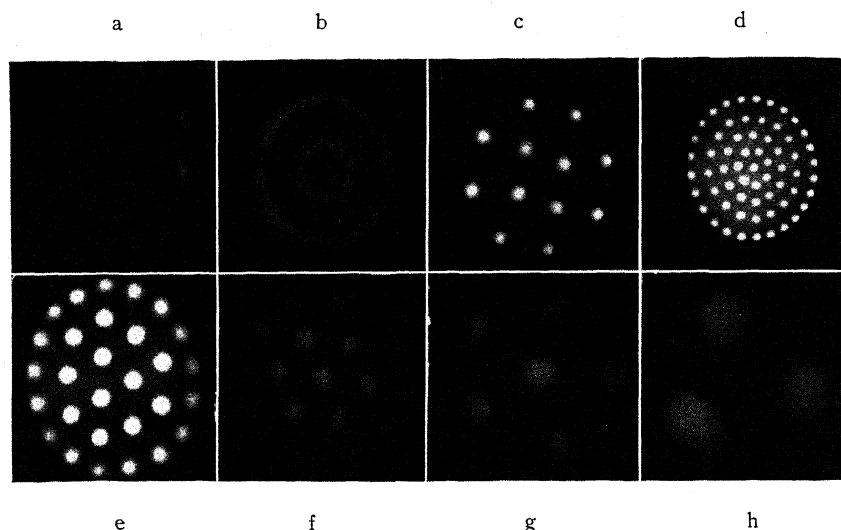


Fig. 2. Typical patterns of anode spots.

The experimental conditions for the patterns which are presented in Figure 2 are given in Table I.

TABLE I.

Pattern	Kind of gas	Gas pressure in mm Hg	Electrode separation in cm	Potential drop in volts	Current in milliamperes
<i>a</i>	nitrogen	0.41	10.5	825	17
<i>b</i>	hydrogen	2.25	16.9	880	125
<i>c</i>	hydrogen	5.8	12.3	625	275
<i>d</i>	hydrogen	3.3	14.7	881	180
<i>e</i>	(argon 90%) (hydrogen 10%)	9.0	10.8	690	240
<i>f</i>	hydrogen	3.1	13.2	920	160
<i>g</i>	hydrogen	3.35	14.3	1240	200
<i>h</i>	hydrogen	2.55	18.3	902	85

Results for different gases. Anode spots did not form in any gas when the electrodes had been sufficiently degassed provided that mercury vapor was excluded from the tube and that the discharge was set up within two minutes after the admission of the gas. In general, anode spots formed in hydrogen, nitrogen, carbon monoxide, air, and in certain gas mixtures. Spots did not form in oxygen, pure argon or pure neon. The formation of very weak spots in helium which contained a trace of hydrogen will be discussed later.

In a discharge in hydrogen, the spots formed over a gas pressure range of from 0.6 to 12 mm. The gas pressure limits varied with different gases; but in all gases, the lower pressure value was limited by the possible electrode separa-

tion and the higher pressure value was limited by the limit of the current which was available from the generator. Hydrogen was different from other gases in that, for a given pressure, the spots formed over a comparatively wide range of electrode separation which in some cases was as much as 20 cm. When striations were present in the hydrogen discharge, the spots appeared when the anode was placed in the dark space between the striations. The spots disappeared and reappeared as the anode was moved through the bright part and the dark part of the striations respectively. In case the configuration of spots was made up of several rings, the outside ring disappeared first as the anode was moved through a striation which, for the smaller electrodes, was conical in shape.

When a well-degassed electrode was allowed to remain in hydrogen for a few minutes, spots which lasted as long as a second or two were formed at the first passage of the discharge. This observation shows that the metal of the electrodes absorbed hydrogen even in the absence of an electric field. Degasification of the electrodes by means of the induction furnace after they had been used in hydrogen gas was almost as difficult as was the degasification of new electrodes.

The anode spots formed easily in nitrogen over a pressure range of 0.4 to 14 mm of mercury for available electrode separation and current limits. In nitrogen, however, the spots formed only at the beginning of the positive column within a range of two cm at most. As the anode was moved farther into the Faraday dark space, the spots gradually disappeared. When the anode was moved farther into the positive column, the configuration of spots became unstable and finally merged into the positive column. This peculiarity of limitation of the formation of spots to the neighborhood of the beginning of the positive column in nitrogen and other gases which gave a strong positive column make it impracticable to carry out as extensive investigations in these gases as in hydrogen.

Anode spots formed very readily when the anode was placed near the beginning of the positive column of a discharge in carbon monoxide. The spots which were greenish white in color in this gas, formed over a pressure range of 0.4 to 15 mm of mercury for the electrode separation and current limits of the apparatus. For a given period of "soaking" of the cathode in carbon monoxide, the spots lasted much longer than in either hydrogen or nitrogen. Moreover, degasification of electrodes, subsequent to their use in carbon monoxide discharge, was much more difficult than that of electrodes used in hydrogen or nitrogen.

No anode spots were formed in pure oxygen under any conditions. In mixtures of oxygen and carbon monoxide, spots did not form until the carbon monoxide content of the mixture had reached about 30 percent. Then anode spots which were characteristic of carbon monoxide were formed.

An electrode was "soaked" to saturation in carbon monoxide. The carbon monoxide was then removed from the tube and oxygen was substituted. Under these conditions, spots which were characteristic of carbon monoxide formed on the anode which was then full of carbon monoxide. Such spots

lasted for three or four minutes. This observation is direct proof that the anode spots are formed by gas being evolved from the anode under electron bombardment. The previous observation that 30 percent carbon monoxide in oxygen was necessary for anode spot formation precluded any possibility of the formation of these spots by any small amount of residual gas.

Anode spots were not formed in pure argon or pure neon. In these gases there was a tendency for the positive column to separate into two or more parts which rotated with respect to the axis of the tube. These streamers ended in bright spots on the anode which, however, were not of the same nature nor of the same origin as the anode spots now under investigation.

In argon, neon, and helium, the presence of mercury vapor given off from a mercury surface in the tube permitted the formation of bright anode spots. Bright anode spots also were formed when ten and five percent hydrogen was present in argon and neon respectively. Since no arrangement was made in the present apparatus for mixing and circulating the gases in the discharge tube, the above percentages may be somewhat in error. However, they are of the correct order of magnitude.

When the helium was apparently pure except for a small trace of hydrogen, very weak yellow anode spots appeared. These weak spots in helium were much larger than those for a corresponding pressure in another gas. However, these spots were symmetrically arranged and had all the characteristics of true anode spots. Bright anode spots appeared on the anode in a discharge in helium to which two tenths of one percent hydrogen had been added.

Effect of the metal of the electrodes. The effect of the metal on the formation of anode spots was studied only qualitatively. Anode spots formed on electrodes of iron, nickel, copper, aluminum, and brass. Electrodes of iron were used almost entirely for the quantitative study because its rate of sputtering was low. However, electrodes of nickel produced no noticeable change in the characteristics of the spots from those observed on iron electrodes. The thickness of the electrodes was found important only insofar as it affected the change of temperature of the electrodes.

The anode spots were not symmetrically arranged on the anode when impurities were present on the surface of the anode or when a new electrode was used as anode without previous degassing. However, the use of a new untreated electrode for a few minutes as cathode put it into such a condition that a symmetrical pattern of spots was formed when it was subsequently made anode.

The use of a barium coated electrode as cathode resulted in a decrease in the potential drop across the tube. As cathode it gave a symmetrical arrangement of spots on an uncoated electrode used as the anode; but when it was used as anode the spots were very unsymmetrically arranged, due most probably to the non-uniformity of the barium oxide layer.

Unsymmetrically arranged anode spots were formed on a carbon anode. The effects of local heating produced bright anode spots on the carbon. The carbon electrode could not be outgassed with the induction furnace. More-

over, the surface of the carbon could not be made to absorb gas uniformly by reversing the direction of the current because the discharge from the cathode was concentrated on several small areas on the carbon surface of the sleeve of this electrode. On the whole, the carbon electrode was unsatisfactory both as a cathode and as an anode. Nevertheless, anode spots were formed on its surface from the occluded gases.

Faint anode spots which were symmetrically arranged appeared on the surface of an anode of mercury in hydrogen and in the rare gases.

Rotation of the anode spots. The spots were seldom stationary on the anode for any length of time. Under the influence of the magnetic field which was set up by the passage of the current through the tube, the pattern of spots rotated with respect to the central axis of the tube, sometimes in a clockwise direction and at other times in a counter clockwise direction. The angular velocities of the spots in the various rings were not the same, the outer ring having the largest. At times the direction of rotation in two concentric rings was opposite. An increase in the distance between the electrodes increased the tendency for rotation of the pattern.

A solenoid placed coaxial with the tube, and away from the anode, so that a part of the field was radial to the electrode, could change the rotational velocity of the spots in the rings and even reverse the direction of rotation. When a solenoid was placed perpendicular to the axis of the tube in the immediate region of the anode, the configuration of spots was deformed by the magnetic forces so that the spots then appeared in a deformed circular pattern which also rotated rapidly during the application of the magnetic field of the solenoid. An unstable and unsymmetrical pattern of spots always formed when the walls of the tube in the neighborhood of the anode were badly sputtered.

Size and shape of electrodes. Circular electrodes of 41 mm and 34 mm in diameter were used. Under the same experimental conditions, the size of the spots was larger on the larger electrodes.

The use of a small spiral incandescent tungsten cathode did not destroy the symmetry of the anode pattern of spots when this cathode was placed on the line of the axis of the anode.

That the pattern of spots was governed primarily by the shape of the anode was proved by the use of a circular cathode and a triangular anode on which the spots formed in a triangular pattern which contained as many as four distinct triangles with their sides parallel to the edges of the anode. When the electrodes were placed so close that the form of the cathode influenced the field at the anode the spots on the anode were equally spaced on the sides of the triangles, but when the electrode separation was increased to some extent, the spots, except those forming the vertices of the triangles, tended to concentrate toward the middle of the sides of the triangles, but even then the form of the triangle was not destroyed.

When the electrodes were not parallel, an asymmetrical arrangement of spots always resulted. Under these conditions, the angular velocity of a spot was not uniform. Its angular velocity was greatest where the separation of the electrodes was greatest.

When the electrodes were parallel their centers were not on the same horizontal lines. The pattern of spots was displaced from one edge of the anode.

Size and intensity of anode spots. In general the size of the spots increased with an increase in the gas content and temperature of the electrode, with a decrease in the gas pressure, with an increase in the size of the electrode, and slightly with a decrease of the distance between the electrodes. The size of the spots definitely decreased with an increase in current and voltage. It also decreased with an increase in the age of the spots, although, for constant potential, the current decreased during their life.

Figure 3 is composed of two photographs of patterns of anode spots in hydrogen at 2.6 mm pressure and electrode separation of 17.2 cm. The pattern on the left was formed by 210 milliamperes at 1300 volts and the pattern

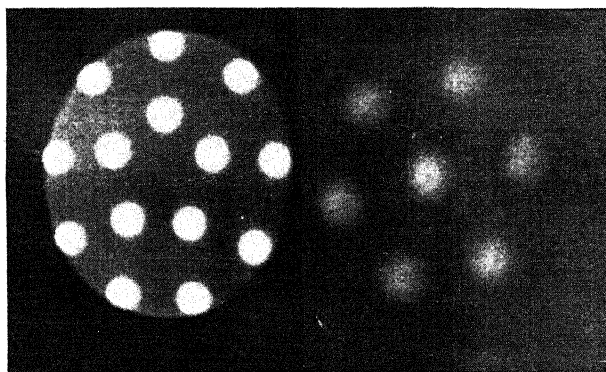


Fig. 3. Change of number of spots with change in current and voltage.

on the right by 30 milliamperes and 725 volts. These photographs show the change in the number and in the intensity of the spots with a change of current and voltage.

The change of the size of the spots with the change of temperature of the anode is shown in Figure 4. These photographs were taken as a discharge

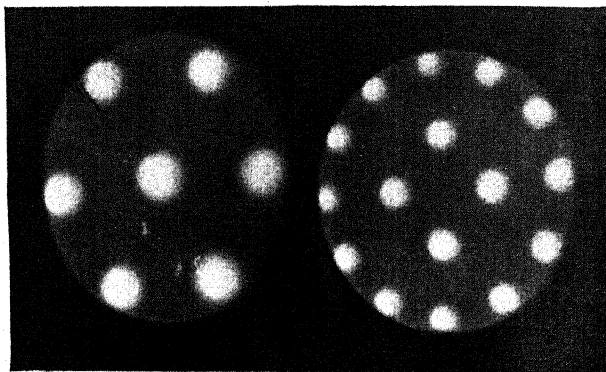


Fig. 4. Change in size and number of spots with change in temperature of anode.

passed through hydrogen at a pressure of 2.45 mm between electrodes separated 17.7 cm. The picture on the right is that of an anode which was saturated with gas by means of soaking it previously as cathode. This picture was taken after the electrode had cooled to room temperature, with a current of 115 milliamperes at 1120 volts. The picture on the left was taken while the anode was still red hot from its previous use as cathode, with a current of 115 milliamperes and 1100 volts.

The intensity of the spots increased with an increase in current and voltage. To a small degree, it depended on the kind of gas. Hydrogen gave brighter spots than nitrogen. The intensity was quite high when a rare gas was mixed with hydrogen or mercury vapor.

Factors which influence the number of spots. The number of spots which appeared in the pattern on the anode increased with an increase of pressure, with an increase in current, with an increase in the amount of gas in the surface of the anode up to a saturation value, and slightly with an increase of distance between the electrodes. An example of the increase in the number of spots with an increase in current and voltage is given in Figure 3 above. The number of spots decreased with an increase of the temperature of the anode within certain limits. An example is given in Figure 4.

The same pattern of spots was obtained after a thirty second period of soaking of the electrode as when the electrode was soaked ten minutes provided that the temperature change in the electrode during this latter period was not over two hundred degrees. This indicates that the condition of the surface layer or near surface layer governed the number of spots and that this layer quickly reached saturation.

Mention has already been made of the observation that spots were formed from gas which was absorbed by mere contact with the metal. The following experiment showed that spots were also formed by gas which diffused to the surface of the anode. The cathode was soaked with hydrogen gas until saturation was reached, then it was used as anode until the spots disappeared. Immediately afterward the tube was evacuated to a pressure less than 2×10^{-4} mm at which pressure it remained for forty-eight hours. At the end of this period, hydrogen was again passed into the tube until a pressure of 3.3 mm was reached. Forty spots in four rings were present when the discharge was established within a few seconds after the gas was admitted. At the end of 25 seconds the number of spots had decreased to 30 in three rings. The remainder of the spots disappeared simultaneously at 30 seconds.

The large number of spots which appeared under the above conditions and the short life of the spots indicate that the gas, which had penetrated to a considerable depth in the electrode diffused to the surface or to the layers immediately underneath the surface. Since a considerable amount of gas was given off from the anode only during a thirty second period, one may conclude that the gas which diffused to the surface, was held there

by the molecular forces of the metal. Since no similar effect was observed when a degassed electrode was treated in a similar manner, it is not probable that these spots were formed from hydrogen absorbed while the electrodes were subjected to the low gas pressure given above.

Application of the phenomenon of anode spots to the study of the rates of absorption and emission of gases by the electrodes of a Geissler discharge: Let us assume that the cathode of a direct current Geissler discharge absorbs gas under the influence of positive ion bombardment at a rate which is a function of the number and energy of the positive ions which strike and of the gas content of the cathode at that particular moment. Let us further assume that the anode emits its absorbed gas under the influence of electron bombardment at a rate which is a function of the velocity of the electrons at the moment of striking, of the number striking, of the gas content of the anode, and of the kind of gas.

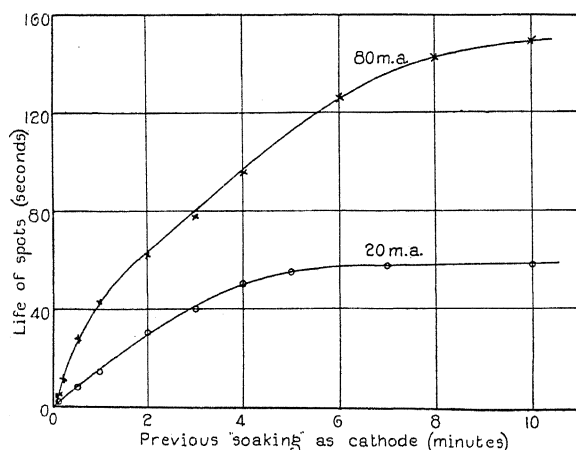


Fig. 5. Life-soaking curves for different soaking currents.

In order to test the validity of the above assumptions a series of experiments was carried out in hydrogen. Typical results are given in Fig. 5. The lower curve was obtained by subjecting the cathode to soaking in 3mm of hydrogen with a current of 20 milliamperes for different periods. At the end of each of these periods of soaking, the direction of the discharge was reversed and a current of 110 milliamperes was passed through the discharge until the last spot had disappeared from the anode. The lower curve of Figure 5 shows that, with a soaking current of 20 milliamperes, the life of the spots approached a constant value with a soaking period of 5 minutes. However, when a soaking current of 80 milliamperes was used the life of the spots was relatively longer as shown in the upper curve.

We believe that the differences in the lives of the spots for different soaking currents were due to differences in the rates of the absorption and in the total amount of gas absorbed. This difference in absorption was due to the difference in the temperature of the cathode during positive ion bombardment

and to the difference in the energy of the impinging positive ions under the two conditions.

Many similar curves were obtained in hydrogen with both the small and the large experimental tubes. The rates of absorption and emission of hydrogen changed with the change of conditions in the electrode. However, for a series of runs on the same day, the same type of curves was obtained. It was not possible to retrace the curves backwards because of a change in the temperature of the electrode in the long periods of soaking. For soaking currents between 20 and 80 milliamperes the curves fell between those given in Figure 5.

Since the charge on the walls of the tube influences the electric field at the anode and since the ratio of the random current to the drift current in the tube governs the anode drop, it was deemed advisable to investigate the effect of the diameter of the tube on the anode spots. To this end a tube of 10 cm was substituted for the tube of 6 cm diameter. The use of the larger tube resulted in a greater stability and uniformity of the pattern of the spots, less rotation of the spots and a longer period of use before cleaning was necessary. However, no appreciable difference appeared in the life-soaking curves which were obtained from the different tubes when the walls of the tubes were equally free from sputtered material. It was to be expected that a greater electrode separation would be required for the larger tube, because the length of the negative glow increase with an increase in the diameter of the tube.

It was possible to obtain curves as those given in Figure 5 only in hydrogen because in all gases having a strong positive column the change in the potential drop across the tube with the change in the gas content of the electrodes altered the position of the beginning of the positive column to such an extent that the anode was soon out of the narrow region in which the formation of anode spots was possible. However, in the case of carbon monoxide gas, the anode was moved through a small distance in order to keep it in the region of the anode spots. This method showed that the life of the spots for carbon monoxide, for a given amount of soaking, was considerably longer than that of hydrogen for similar soaking. This observation is only qualitative because the potential drop across the tube changed with the change in the distance of electrode separation.

Figure 6 contains the life-soaking curves for the same electrodes under the same conditions except that the curves were taken on consecutive days in the order given in the figure. Curve I, was obtained with new electrodes which had been carefully degassed by heating in vacuo by means of the induction furnace. Between the time of obtaining curves I and II, a discharge was maintained in the tube for short periods which totaled four hours after which the electrodes were again degassed by heating in vacuo. A similar procedure took place between the time of taking the data given in the consecutive curves of Figure 6. These curves show that the life of the spots increased with the use of and the degassing of the electrodes. On the assumption that a certain rate of evolution of gas from the anode is neces-

sary for the formation of anode spots, these curves show that the anode evolves gas for a longer time above that rate when the electrode is used in a discharge and is subsequently degassed.

In order than an electrode, under constant current conditions, evolve gas above a certain rate for a longer period, it must contain a greater amount of

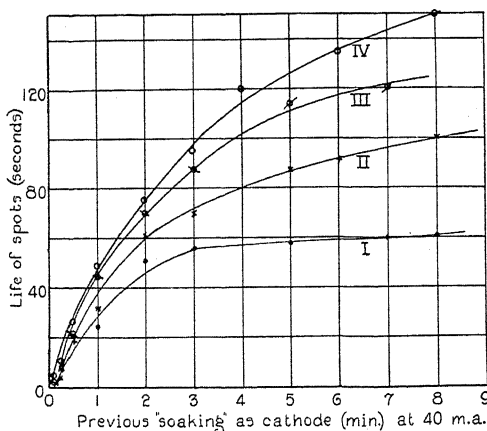


Fig. 6. Life-soaking curves showing effect of aging of electrode.

gas to begin with or the rate of evolution of gas must be more gradual or both conditions must be fulfilled. For this we give the following explanation.

It is certain that some of the gas ions which are driven into the anode structure by considerable electrical force are more difficult to remove than are the molecules of the original occluded gas. Hence, degassing by means of heating

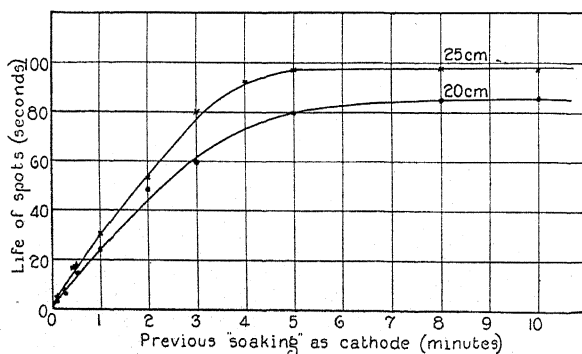


Fig. 7. Life-soaking curves for different electrode separations.

in vacuo may not be so efficient in removing such gas molecules. Therefore, the electrode may contain more gas to begin with even after the same period of degassing than it did before it was used so much as cathode. On the other hand, the spacing of the molecules of the metal may be so changed by use and subsequent degassing, that the hydrogen molecules will then be absorbed more readily as they strike the cathode in the form of positive ions. Also they may penetrate deeper into the metal of the cathode.

Experimental evidence, which supports this hypothesis, is given by Yamada⁵ who found that absorption of hydrogen in palladium resulted in a uniform expansion in the space lattices and by Baum⁶ who found that hydrogen ions under the influence of 3000 volts not only penetrated a silver cathode to some distance but that they also produced fissures in the crystal structure of the metallic electrode.

The life soaking curves which are presented in Figure 7 were obtained from data in which the experimental conditions except the change in electrode separation were kept constant, as nearly as possible. These curves show that the life of the spots increases with an increase in the electrode separation. This increase of the life of the spots with increase of electrode separation was not due to temperature increase or aging effect of electrodes because the data for the curve at 20 cm were obtained immediately after that used in the curve at 25 cm.

Since the electrode contained approximately the same amount of gas in both cases at the end of similar periods of soaking, and since the number of electrons striking the anode was also the same, this difference in the life of the spots for different electrode separations must have been due primarily to a difference in the velocity of the electrons at impact on the anode by which the rate of evolution of gas would have been different.

This change in the velocity of impinging electrons could have been produced by a difference in the electric field depending on the position of the anode especially if it was placed near the beginning of the positive column. Moreover, a change in the anode drop of potential may produce a greater change in the energy of impact of an electron on the anode than that which corresponds to a change of V in the relation $eV = 1/2 mv^2$. For instance, if the anode drop of potential is just greater than the ionizing potential of the gas, some of the electrons will make ionizing collisions with the gas molecules in the region of anode space charge, and will thus lose most of their energy. Such electrons will then strike the anode with much less energy than that of the electrons which make only elastic collisions with molecules because their velocities are below that which corresponds to the velocities necessary for ionization or excitation of the gas molecule.

Change of potential with the change in the gas content of the electrode. In Figure 8 are given the time-voltage curves during the life of the anode spots for a constant current of 110 milliamperes in hydrogen at 3 mm pressure and electrode separation of 22 cm. The anode in the discharge from which the data for these curves were taken was soaked at 40 milliamperes for the different periods given in this figure. These curves show that the anode spots disappeared in each case at approximately the same voltage. When the experiment was continued beyond the time of the disappearance of the spots the potential drop approached a constant value of which there is some evidence in these curves. (The curves in the Figure 9 show this more plainly.) We believe that the constant potential drop was determined by the conditions in the tube reaching a state of equilibrium, that is, the change in the gas content of the electrodes must have reached a steady state. These curves

also show that, at least within given limits, the potential drop, immediately after the initiation of the discharge was lowered by an increase in the soaking period of the cathode. Each of these curves corresponds to the determination of one point of the life-soaking curve such as given in Figure 6.

The differences in the potential drop for the discharge as shown in these curves were due almost entirely to different amounts of gas in the electrodes. Different amounts of gas were obtained in each electrode by varying the time of reversal of the current during which the cathode absorbed gas and the anode emitted gas. Degassing the cathode by means of an induction furnace resulted in a lower maintaining potential at the beginning than that given in curve VI of Figure 8.

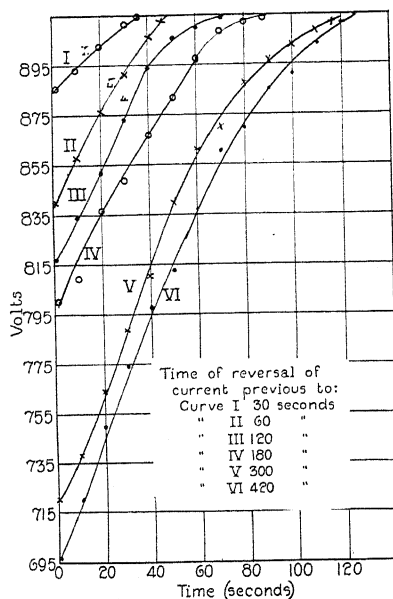


Fig. 8. Time-voltage curves during life of spots.

That the differences in the maintaining potential which are evident in the several curves and in each single curve at different times, were due almost wholly to the processes at the cathode was proved by the following experiment. Two new iron electrodes *A* and *B* were degassed in vacuo by an induction furnace to an equal degree. Then electrode *A* was made cathode and electrode *B* anode in a discharge of 100 milliamperes in hydrogen at 2.8 mm pressure. The variation of the voltage with time is given in curve I, Figure 9.

Since both electrodes were degassed to begin with most of the change in potential difference was due to absorption of gas at the cathode since electron bombardment could free few gas molecules from the already degassed anode.

Upon reversal of the direction of the discharge at the end of three minutes, results were almost identical with those given in curve I although in this case

the cathode was a degassed electrode but the anode contained gas as a result of previous use as cathode for three minutes. Thus we found that degassed cathode and anode produced the same time voltage characteristics as a degassed cathode and a gas filled anode. From this we conclude that the evolution of gas from an anode under electron bombardment has little or no effect on the potential drop of the discharge.

Subsequently, electrode *A* which contained some gas was made cathode and the results given in curve II of Figure 9 were obtained. The main difference in the curves I and II is a higher starting potential difference when the cathode contained some gas. The irregularity of curve I between 60 and 100 seconds is typical of the curves obtained with new electrodes which were degassed by the induction furnace. We believe the change in potential to

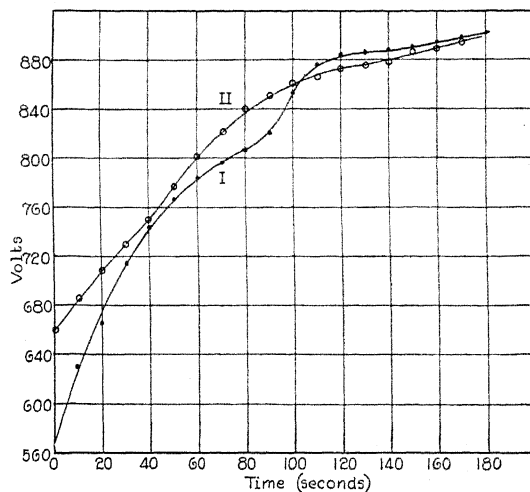


Fig. 9. Time-voltage curves with new electrodes.

be due to evaporation of impurities from the surface of the cathode, impurities which were brought to the surface of the metal during the first heat treatment.

DISCUSSION OF RESULTS

Summing up the behavior of the anode spots, we see that their formation and existence must depend on the joint action between the gases released from the anode and the electron stream to the anode. From their magnetic behavior and from their dependence on the distance between the electrodes, we deduce that they must be the manifestations of a splitting up of the electronic current into discrete and more or less stable "rays" or current-beams. Also, since their life was, within limits, proportional to the length of time the electrode had previously been used as cathode, since their number decreased with the time that the electrode was used as anode, since no spots formed on a well outgassed anode, and since spots having the color characteristic of carbon monoxide formed in a discharge in oxygen on an anode previously

soaked in carbon monoxide, we infer that gas must escape from the anode in order that the formation of electron beams and their resultant anode spots be possible.

On the assumption that one necessary condition for the formation of anode spots is the evolution of a certain amount of gas from the surface of the anode when it is subjected to electron bombardment, we shall now give an explanation of the formation of the anode spots.

When no gas is liberated by the anode, the electrons form a space charge sheath which limits the more intense part of the field to within a short distance of the anode,⁹ of the order of a few millimeters at the pressure used. Outside the sheath the electric intensity is so small that the drift velocity of the electrons due to the field is not sufficient to keep them in relatively straight paths parallel to the axis of the tube, and they scatter by successive collisions with the gas molecules until the slowly drifting stream fills the cross section of the tube.

When these electrons enter the sheath, their increased speed causes them to fall to the anode in nearly straight lines. It is, then, in this sheath, where the field is large, that there is any possibility of formation of electron beams; and the chance of their formation increases as the sheath increases in thickness.

If, now, gas is emitted from the anode, the molecules will either already be ions, or will soon become ions by collision with electrons, and these ions will partially neutralize the electronic space charge, thus increasing the sheath thickness and decreasing slightly the anode fall of potential, and therefore making the formation of beams more probable. Inasmuch as one positive hydrogen molecular ion neutralizes the space charge of three hundred or more electrons a small quantity of gas from the anode will cause a large change in sheath thickness, and under these conditions the electrons will move in straight paths for a centimeter or more before striking the anode.

Only a small portion of the current will be concentrated in the spots, for the gas will scatter many electrons to the other parts of the anode. These rays will be the favored paths, however, and the fastest electrons, those which have suffered few collisions, will travel therein. These faster electrons will create more ions than the other scattered ones, and so, a short time after the discharge is started, these beams will act as separate phenomena superimposed on the back-ground of scattered electrons, having their own potential distribution, their own motions, and their constant current density. This current is probably due predominantly to the ions created by the original electron beam in the gas coming from the anode. For this reason, and because the gas from the anode increases the sheath thickness, it is probable that the number of spots or beams present is proportional to the amount of gas evolved by the anode.

Since anode spots form only at the beginning of the positive column in gases which have a strong positive column and since they form before the first striation and in each dark space between successive striations when

⁹ Langmuir, *Gen. Elec. Rev.* 27, 767 (1924).

striations occur in the tube, it is now necessary to show why the spots form on the anode when it is placed in these positions.

Langmuir⁹ explains how an electron sheath around an anode may be broken down suddenly, through its neutralization by positive ions which are formed in the space charge sheath, to such an extent that the anode drop falls discontinuously to a lower value. He found that, when breakdown occurred, the anode glow usually appeared in the form of a sharply defined hemispherical region several times more luminous than the surrounding region. In this explanation, he assumes that very few gas molecules are present in the electron space charge sheath so that only a small fraction of the electrons which pass through this sheath make ionizing collisions. He further assumes that the gas molecules which are present in this sheath come into the sheath from the region on the outside of the anode sheath.

However, it is apparent from his theory that the breakdown of the electron sheath will be brought about the more easily the greater the concentration of gas molecules in the space charge sheath since a larger percentage of the electrons then make ionizing collisions with the gas molecules in their passage through the space charge sheath. Thus we see that the emission of gas from the anode will assist in the neutralization of the space charge sheath, which results in an increase in its thickness and a decrease in the total anode drop of potential.

It is evident from the preceding discussion that the electron space charge sheath will increase in thickness or breakdown (in the sense as used by Langmuir) more easily in the regions where the field is small. Therefore, the anode spots, whose appearance is due to the increase in the thickness of the electron space charge sheath of the anode or to its breakdown, will form when the anode is placed in the region at the beginning of the positive column where the electric field has not yet attained the maximum value of the positive column. In the dark space regions between striations, the field is again small. Therefore, these dark space regions between striations will also be favored regions for the formation of anode spots.

A field which is below that necessary for the production of an anode glow by ionization is excluded from this consideration. Consequently, the region of the Faraday dark space is excluded because there the anode drop of potential is too low to produce ionization, so that one would not expect the formation of anode spots.

We believe that anode spots do not form in oxygen because the oxygen ions, on striking the cathode, react with the metal of the cathode to form stable compounds which are not decomposed under subsequent electron bombardment of the anode.

Since the rare gases, helium, neon, and argon do not react chemically with any substance under any condition, and since very little gas was evolved in the degasification of electrodes subsequent to their use in these rare gases, we infer that these gases are not absorbed by the metal of the electrodes in amounts which are capable of producing anode spots. We believe that very weak yellow anode spots were formed in helium which contained a trace of

hydrogen whose presence could be detected by means of a direct vision spectroscope because the anode space charge sheath was not sufficiently broken down by the presence of a few hydrogen ions to permit the formation of bright spots.

Considering the effects of absorption of hydrogen by an electrode in a mixture with the rare gases and the production of hydrogen ions by collision with excited atoms, we have been able to explain, to our own satisfaction, the formation of bright anode spots when 10 percent, 5 percent and two tenths of one percent of hydrogen is present in argon, neon and helium, respectively.

When mercury is present in the discharge tube, sufficient mercury molecules are present on the surface of the anode to bring about the formation of anode spots in each of the rare gases. Anode spots appeared under similar conditions of the gas as those described by MacKay⁸ who photographed the spots in a discharge in helium containing mercury vapor. MacKay reports in the same paper the formation of spots of similar nature when mercury was excluded from the discharge tube. In that event, the helium which he used must have had, as impurity, hydrogen to the extent about two tenths of one percent. From the nature of the spots formed when a trace of hydrogen was present in the helium, it is doubtful if anode spots will be formed at all in pure helium.

Since anodes spots are formed by beams of electrons we would expect these beams to be influenced or even rotated by the application of a suitable external magnetic field. We offer the following explanation for their rotation in the absence of a magnetic field.

The drift current approaches the anode in the form of a frustum of a cone rather than in the form of a cylinder so that there will be present in the tube a small resultant radial magnetic field which will be sufficient under certain conditions to set the whole pattern in rotation. As the electrodes are separated farther apart, the influence of the electrodes on the drift current will be less, so that some of the drift current will approach the anode at a greater angle with the axis of the tube in a manner which may be likened to the change of the lines of electric force. Then the radial component of the magnetic field will be greater so that the angular velocity of the pattern will be increased.

In order to explain the change of sense of rotation of the pattern, the rotation in the opposite sense in consecutive rings and even the formation of a stable pattern, one would have to consider, in addition to the component of the magnetic field already discussed, the magnetic field set up by the diffusion of the electrons to the walls.

Since a given rate of emission of gases from the anode is necessary for the formation of anode spots, this phenomenon can be used as a measure of the rate of emission of gas from the anode and indirectly as a measure of gas absorption by the cathode. By the application of this method, we find that a cathode absorbs certain gases in proportion to the time of soaking up to a certain saturation value which is determined by the current and voltage of soaking, the temperature of the cathode and the previous treatment of the

electrode. We also find that the anode emits both absorbed and original occluded gas when it is subjected to electron bombardment.

Finally, in consideration of the evidence which follows, we believe that the absorption of hydrogen gas by the cathode of a Geissler discharge increases the potential drop across the tube until saturation of the cathode with gas is reached.

1. The potential drop increased with time until it reached approximately a constant value which depended upon the current density and the temperature of the cathode, in almost the same way that the life of the anode spots increased with an increase in the period of soaking of the cathode for a similar current density.

2. Degassing an electrode previous to its use as cathode either by having it serve as anode in a Geissler discharge or by heating it in vacuo with induction currents resulted in a decrease in the potential necessary to maintain the discharge for a short time after the discharge had struck. This decrease was a function of the amount of gas which had been emitted from the electrode in degassing.

3. After a discharge had been discontinued for a time, the potential drop was always lower at the second initiation of the discharge than it was just previous to the time of its discontinuation.

4. Although the cathode contained different amounts of gas to begin with in different experiments under the same conditions, the potential drop approached the same limit in each case as the cathode approached saturation in absorption of gas.

5. Experiments under identical conditions, except that in one case the anode was full of gas and in the other it was thoroughly degassed, gave almost identical time voltage curves. This we take to be good evidence that the emission of gas from the anode has little or no effect on the potential drop of a discharge.

We wish to express our indebtedness to L. B. Headrick and Dr. P. M. Morse for helpful suggestions in this work.

ELECTRON VELOCITIES IN A HIGH FREQUENCY DISCHARGE IN HYDROGEN

BY CHARLES J. BRASEFIELD
UNIVERSITY OF MICHIGAN

(Received November 20, 1929)

ABSTRACT

A high frequency discharge in hydrogen was obtained by applying undamped high frequency voltages to the movable external electrodes of a cylindrical discharge tube. The mean velocity of the electrons in the discharge was determined from the ratio of the densities of certain singlet and triplet lines of the molecular spectrum of hydrogen. It was found (1) that the electron velocity increases as the voltage between electrodes is increased, the gas pressure and the frequency of oscillation being constant; (2) for a given voltage between electrodes, the electron velocity is, in general, greater the longer the wave-length of oscillation; (3) the electron velocity decreases as the pressure is increased. The paper concludes with a discussion of the mechanism of the high frequency discharge in which an explanation of its behavior is proposed.

INTRODUCTION

IN THE study of any sort of gaseous discharge, one of the more important items of interest is the mean velocity of the electrons in the discharge and its variation under different conditions. The high frequency discharge with external electrodes is a very peculiar type of gaseous discharge. Studies have been made of numerous characteristics of this discharge, such as the striking and maintaining potentials¹ and the conductivity² but to the writer's knowledge no one has succeeded in determining the mean electronic velocity in the discharge. As a matter of fact, it would appear to be extremely difficult, if not impossible, to make such measurements by the ordinary method applied in arcs and glow discharges, namely, the Langmuir exploring electrode method. It has been suggested³ that the mean electron velocity in a high frequency discharge in hydrogen might be determined from the ratio of the densities of certain singlet and triplet lines of the molecular spectrum of hydrogen. This method has been employed with more or less success in the present work.

APPARATUS

To produce the high frequency oscillations, two U. X. 852 75-watt tubes were used in push pull in an ordinary Colpitts circuit, which is shown diagrammatically in Fig. 1. The plate voltage was supplied by a 2 KW, 3000 volt transformer, T_1 , and measured by an electrostatic voltmeter, V .

¹ R. L. Hayman, Phil. Mag. 7, 586 (1929) and others.

² H. Steinhauser, Zeits. f. Physik 54, 788 (1929).

³ C. J. Brasefield, Phys. Rev. 34, 437 (1929).

One quarter ampere fuses, F , protected the plates from overloading. The radio frequency chokes, $R.F.C.$, were made of #30 B. & S. copper wire, $S.C.E.$, wrapped on 3-inch bakelite tubing; 65 turns for 15, 25, and 50 meters, 180 turns for 100 meters, and 300 turns for 200 meters. The mica condensers C_1 had a capacity of $0.002 \mu f.$ and could stand 2500 volts. The variable air condensers C_2 had a capacity of $0.00045 \mu f.$ and were carefully calibrated. The inductance L was a coil of $3/16$ inch copper tubing 3.5 inches in diameter; 2 turns for 15 meters, 3 turns for 25 meters, 5 turns for 50 meters, 10 turns for 100 meters, and 30 turns for 200 meters. The electrodes surrounding the discharge tube were of sheet copper 2 cm wide. Copper ribbon $1/4$ inch wide was used for wiring the tank circuit and the tank current was measured by a 0-15 ampere radio frequency ammeter A (thermocouple type). The grid leak, $G.L.$, was a 40,000 ohm wire wound resistor to dissipate about 100 watts. The filament current was supplied by a 175 watt, 12 volt transformer T_2 , across whose secondary were the by-pass condensers C_3 ($0.002 \mu f.$).

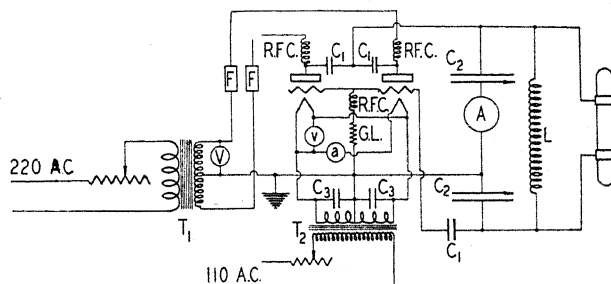


Fig. 1. Diagram of oscillatory circuit.

The discharge tube was of Pyrex glass, 30 cm long and 4.5 cm in diameter, with an optical glass window sealed into one end. Hydrogen was admitted to one end of the tube by means of a platinum tube and was pumped out at the other end, thus insuring a continuous flow of pure hydrogen. The platinum tube was 20 cm long, 1 mm in diameter with 0.1 mm walls. It was surrounded by a glass jacket through which commercial hydrogen was flowed. On heating the platinum tube to a dull red heat (about $600^\circ K$) by passing a current of about 16 amperes through it, an adequate flow of hydrogen was obtained through the discharge tube. The pressure could be varied either by changing the temperature of the platinum tube or by means of a valve which regulated the rate of pumping. Pressures were measured by a McLeod gauge.

PROCEDURE

The voltage between electrodes, which is equal to the voltage across the condensers C_2 was calculated from the formula $E = I/2\pi fC$ where E is the voltage across the condensers, I is the current through them in amperes, f is the frequency of oscillation and C is the capacity in farads of the two

condensers in series. The condensers C_2 were always adjusted so as to be of equal capacity. Hence, the ammeter A was at a potential node and its readings were independent of its capacity to earth.

A series of runs was taken at frequencies of oscillation corresponding to 15, 25, 50, 100, and 200 meters wave-length. The pressure was kept constant at 0.03 mm and the distance between electrodes was 5 cm. For each run, the tank current I , and consequently the voltage between electrodes E , was varied between the widest limits possible. The minimum voltage was

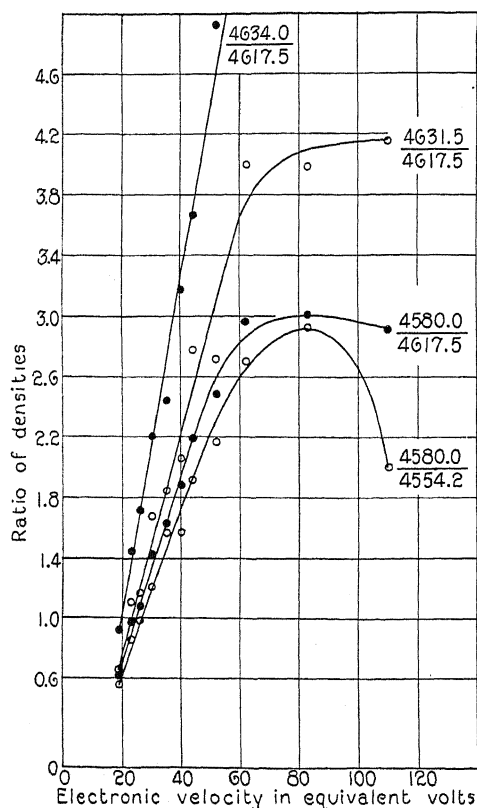


Fig. 2. Variation in the ratio of the densities of singlet and triplet lines with the electronic velocity (taken from Phys. Rev. 34, 437 (1929)).

approximately that at which the discharge first struck. The maximum voltage was determined by the output of the oscillator, that is, the voltage at which the plates of the valves became red hot.

Between these limits, photographs were taken of the discharge at regular intervals. The spectrograph used was a fairly fast two-prism glass instrument. Exposures were taken on Cramer Hi-Speed plates and were all of five minutes duration. Microphotometric traces were then made of all the spectra by means of a Moll self-registering microphotometer. From these traces, the density of the singlet line 4631.5 and the triplet line 4617.5 were

obtained by use of the relation: $\text{density} = \log d/d-h$, where d is the total galvanometer deflection in the absence of a line and h is the height of the peak on the trace corresponding to the line.

From the ratio of the densities of these two lines, the electron velocity could easily be determined since the variation in this ratio with electron velocity is already known³ (see Fig. 2). It might be remarked that although the curves of Fig. 2 were obtained using electrons of uniform velocity, they also can be used to find the *mean* electronic velocity; for the contribution to the ratio of the densities of 4631.5 to 4617.5 of those electrons whose velocity is greater than the mean will be balanced by the contribution of the elec-

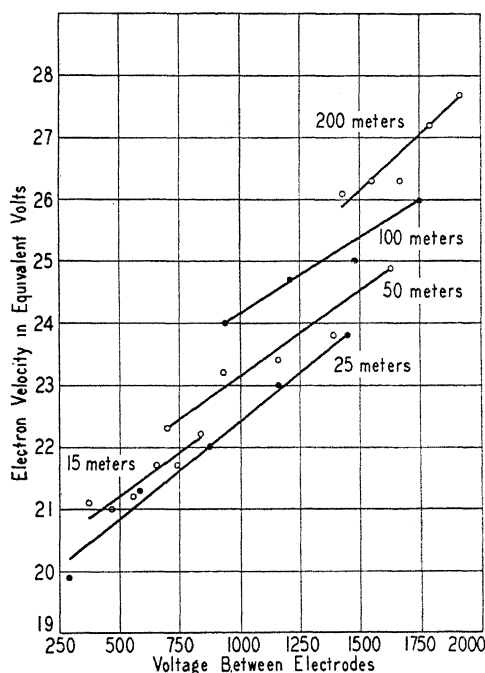


Fig. 3. Variation in electron velocity with voltage between electrodes and frequency of oscillation.

trons whose velocity is less than the mean—provided always, that the mean velocity lies on the straight part of the curves.

RESULTS

Variation of electron velocity with voltage and frequency. The variation in electron velocity with voltage between electrodes and frequency of oscillation is shown in Fig. 3. At all wave-lengths, the electron velocity increases as the voltage between electrodes is increased. Moreover, for a given voltage between electrodes, the electron velocity, in general, increases with the wave-length of the oscillation. (The electron velocities at 15 meters seem to be an exception to this). The error in this method of finding electron velocities

is estimated at 2 volts while the experimental error is something under 0.5 volts. In other words, if two electron velocities were found to be 20 and 24 volts, they both might be in error by 2 volts, but their difference would not be in error by more than 0.5 volts.

Variation of electron velocity with gas pressure. To find the variation of electron velocity with gas pressure, a series of exposures were taken at various pressures between 0.01 mm and 0.06 mm. The wave-length of the oscillations was 25 meters, distance between electrodes 7 cm and voltage between electrodes 1020 volts. Since the ratio of the densities of the singlet and triplet lines varies with pressure as well as with electron velocity, it was necessary to correct the values of the ratio of 4631.5 to 4617.5 for the change in pressure. To the writer's knowledge, there has been only one attempt to find the effect of pressure on the excitation of the secondary spectrum. The results presented in that paper⁴ were of such a nature that the correcting factor could only be calculated roughly. Very approximately, then, it was found that the mean electron velocity decreased from 25 volts at 0.01 mm to 23 volts at 0.06 mm. pressure.

Variation of electron velocity with distance between electrodes. In general, a change in the distance between electrodes produced only a slight change in the electron velocity. At 15, 50, and 100 meters, increasing the distance between electrodes seemed to produce a slight increase in electron velocity, while at 25 and 200 meters, a slight decrease in electron velocity was found.

DISCUSSION

It is not difficult to understand why the mean electron velocity should increase when the voltage between electrodes is increased, and decrease when the pressure is increased; but at first one does not see why the electron velocity should increase when the wave-length of the oscillations is increased. To understand this, it will be necessary to consider more in detail the functioning of a high frequency discharge with external electrodes.

In a direct current Geissler tube discharge, with cold cathode, we know that the discharge is started by a few stray electrons in the gas which, under the action of the electric force between electrodes, produce more electrons by ionizing gas molecules. In this way, the number of electrons is increased to the point where the discharge strikes. Because of the unidirectional current, it is essential that there be a source of electrons, namely, the cathode. This source of electrons would not have been necessary, however, if the direction of the applied electric force were reversed before the electron cloud had time to disperse (by leakage along the walls of the tube, recombination with positive ions, etc.). This condition of affairs is obtained by applying high frequency electric forces to the discharge and since a source of electrons is no longer necessary we are able to use external electrodes.

Before a high frequency discharge will strike, however, a second condition must be fulfilled, namely, that the electrons shall attain ionizing velocity before they reach the end of the discharge tube. As a matter of fact, they

⁴ P. Lowe, Trans. Roy. Soc. Can. 20, 217 (1926).

probably must attain ionizing velocity before they have travelled the distance between the electrodes, since it is in this interval that they are under the influence of the electric forces. If, now we keep the voltage applied to the electrodes constant and increase the wave-length of the oscillations, it is evident that the time required for the electric force to reach its maximum value becomes longer and longer. Consequently, it will take the electron more time to reach ionizing velocity at the longer wave-lengths than it does at shorter wave-lengths. In other words, if an electron is to reach ionizing velocity in the same time at two different wave-lengths, the applied voltage must be increased for the longer wave-length, which means that the minimum striking potential will increase with the wave-length of the oscillation. This fact has been verified in the present experiments (see Fig. 3) as well as in those of others.¹

It has also been shown by others² that a discharge has its maximum conductivity under the same conditions that give the minimum striking potentials. Hence, by referring to Fig. 3, we must conclude that the conductivity of the discharge decreased with increasing wave-length. So if the discharge were operated at two different wave-lengths of oscillation, but with the same voltage applied to the electrodes, we would expect to find a smaller drop in potential along the positive column of the discharge which had the greatest conductivity. That is, for equal voltages applied to the electrodes, there will be a smaller drop in potential along the positive column of the discharge when it is operated at shorter wave-lengths. Consequently, at shorter wave-lengths, we would expect to find smaller electron velocities. This explains why, for a given voltage applied to the electrodes, the electron velocity increases with the wave-length of the oscillations.

The writer wishes to express his appreciation to the Grigsby-Grunow Company of Chicago, Illinois, which has supported this investigation. He is also indebted to several members of the Department of Physics for their interest in this work and especially to Mr. J. S. Owens, who assisted in the experimental work.

SECONDARY ELECTRONS OF HIGH VELOCITY FROM
METALS BOMBARDED WITH CATHODE RAYSBY PAUL BERTHOLD WAGNER
STANFORD UNIVERSITY

(Received November 20, 1929)

ABSTRACT

The magnetic spectra of high-speed secondary electrons emitted by Au, Ag, and Al, when bombarded with cathode rays of from 16 to 40 kv., have been photographed and densitometered. Beginning at the high-velocity end, the density is zero down to energy eV_0 , equal to that of a primary ray, then rises rapidly to a maximum at about $0.94eV_0$ for Au or Ag, or $0.85eV_0$ for Al, and then declines. The density is everywhere continuous. Its first derivative may be discontinuous at eV_0 , but nowhere else.

Thin targets show spectra sufficiently like those of thick targets to indicate that most of the secondary electrons come from very near the surface: for Au, within 0.2 micron even up to 40 kv; for Ag, over 0.2 micron only above 20 kv; for Al, over 0.5 micron only above 20 kv.

OBITUARY NOTICE

It is with great regret that we must record the death of the brilliant and promising young scientist whose work is described here. With his great enthusiasm for research, his conscientious thoroughness both instinctive and cultivated by his early education in Germany, and his unusually likable personality, he had every prospect of success and enjoyment in scientific research, and his death was a great loss, both to science and to his friends.

This paper is taken from his thesis for the degree of Master of Arts. As his death occurred in the sinking of the *San Juan*, on his way home to Los Angeles, just after handing in the thesis, he never had an opportunity to condense it for publication. This duty was therefore performed by the instructor, D. L. Webster, with whom he had done the research, but from whom only very little help was ever needed by such an original and able man as Paul Wagner.

I. INTRODUCTION

LITTLE work has been done on secondary electron emission at voltages ranging from 16 to 40 kv. At lower velocities, 10–12,000 volts, investigation has been carried on by Becker¹ (10–1,000 volts) and by Stehberger² (1,000–12,000). Both used the opposing field method. Plotting against the opposing voltage the number of secondary electrons having energy enough to overcome it, Becker obtained, for lower primary velocities, curves of the following general characteristics: for opposing voltages from zero to about 36 volts there is a rapid falling off in intensity; as the opposing voltage reaches higher values the intensity decreases gradually and uniformly, and at an opposing voltage equal to the primary voltage it suddenly drops to zero. This led Becker to distinguish between three types of electrons involved in the process of secondary emission; these he called "secondary" electrons,

¹ A. Becker, Ann. d. Physik 78, 228 (1925).

² K. H. Stehberger, Ann. d. Physik 86, 825 (1928).

"rediffused" electrons and "reflected" electrons. This classification was accepted by Stehberger. The distinction between secondary and rediffused electrons was based by Becker on the fact that his curves are straight from about 36 volts onward to primary voltages. Denoting by $N(V)dV$ the number of electrons having energies between V and $V+dV$, Becker's curves imply that $N(V)$ is constant except below 36 volts. This constant value gives the number of the electrons Becker calls rediffused; the excess over this, at voltages less than 36 volts, is composed of what he calls secondary electrons. The reflected electrons, finally, are those which have practically the primary energy.

Becker and Stehberger found that the upper limit of energy at which there is an appreciable number of what they call secondary electrons is 36 volts, whatever the nature or thickness of the target and whatever the primary voltage (within the range stated above). They concluded that these secondary electrons are electrons of the target material knocked out by primary and rediffused electrons, that rediffused electrons are primary electrons which have suffered a large number of small encounters with an atomic nucleus. Becker finds that for higher primary velocities the number of reflected electrons diminishes. Stehberger, being unable to apply opposing fields up to the higher primary velocities, made the assumption that reflection completely ceases for these higher primary velocities, basing his assumption on Becker's results for lower velocities.

There is arbitrariness in Becker's distinction between secondary and rediffused electrons, for we are not at all assured that the number of rediffused electrons does remain constant within the interval from zero to 36 volts. In this paper, therefore, the term "secondary" will be used from now on in a broader sense, denoting all the electrons coming from a target bombarded by primary electrons.

M. Baltruschat and H. Starke³ find that for voltages larger than 6,000 volts the number of fast electrons increases, and that at 30,000 volts even 80 percent of them possess velocities of the order of magnitude of the primary velocities.

Chilinsky⁴ did some work on the magnetic velocity spectra of secondary electrons produced from silver by primary electrons of 5 to 20 kv, and found that most of outgoing electrons had velocities about 0.8 of the primary value, and that the intensity in the spectrum fell off sharply at about 0.9 of the primary velocity.

Egon Lorenz⁵ carried on investigations, on the x-rays from the back of a tungsten target. He covered a wide range of voltages, up to 83 kv, and compared the spectrum of this so-called "stem-radiation" with that of the focal-spot radiation. The spectra are similar, but the entire stem-radiation spectrum is displaced, towards longer wave-lengths. Thus it approaches the axis at a point which is displaced from the short-wave limit of the focal spot.

³ Baltruschat and H. Starke, *Phys. Zeits.* **23**, 403, (1922).

⁴ S. Chilinsky, *Phys. Rev.* **28**, 429 (1928).

⁵ Egon Lorenz, *Zeits. f. Phys.* **51**, 71 (1928).

Beyond this point, it is true, there is a weak intensity extending as far as the focal spot limit, but Lorenz attributes this small amount of radiation to general scattered rays. He then interprets the apparent short-wave limit of the stem radiation by the hypothesis that the primary electrons eject electrons from the L (or other) levels of the target atoms, and that these secondary electrons cause the stem radiation; the short-wave limit of the focal-spot and stem spectra would then differ by just the frequency corresponding to the amount of energy required to extract these electrons. For instance Lorenz observes that at 22.4 kv primary voltage this difference in energy or voltage corresponds to the M level; and at 83.3 kv, to the L level. He states that this can be explained by the known fact "that the greater the energy of rays, the larger is the proportion of them absorbed in higher levels of any series in comparison with that in the other levels." Lorenz concludes that, if the primary cathode-ray energy is about 40 times that of, say, the M level, absorption would cease in that level and proceed to the next higher that is, the L level.

If Lorenz's explanation of his data is correct, it demands revision of current ideas on some other points. Each L electron ejected as a secondary electron must leave an L vacancy in an atom at the focus, and the filling of this vacancy will often, if not usually, cause the emission of a quantum of x-rays of one of the L lines. At 83 kv, an L quantum from tungsten carries off only about a tenth of the energy brought into the focus by the primary cathode ray, and the percentage of L vacancies causing L quantum emission may not be over 50 percent. Even so, however, if the number of secondary electrons is 20 or 30 percent of the number of cathode rays, and if they are chiefly from the L levels, we should expect 1 or 2 percent of the cathode ray energy to reappear as L -series radiation from the focus, as a result of the ejection of only such L electrons as escaped from the target, and much more as a result of the ejection of other L electrons not so directed as to leave the target. This is a considerably greater amount of energy than the total radiation from tungsten at 83 kv (about 0.75 percent). Thus this comparison, and also comparison with other data on line-emission efficiencies,⁶ lead to serious doubt about the hypothesis that many of the high-speed secondary electrons are ejected L electrons.

However, some of the secondary electrons must be of this type, and a further test is needed. For this purpose, the magnetic velocity spectrum suggests itself, and the next question is what to look for in it.

The secondary-electron velocity suggested by Lorenz's stem-radiation spectra, at least as a maximum, is that which would occur if all the kinetic energy possessed by a cathode ray as it enters the target is transferred to an L electron, which then loses only enough energy to escape from the atom. Most ejected L electrons, however, should have less kinetic energy than this maximum, for two reasons. First, most of the atoms from which the L electrons are ejected are not at the surface of the target, and there are energy

⁶ D. L. Webster, Proc. Nat. Acad. of Sci. 14, 330 (1928). Data here indicate that when an 80 kv. electron strikes a block of silver, it has a line-emission efficiency of only about 0.1 percent.

losses along the paths of both the primary and secondary electrons. And second, in the act of ejection, the cathode ray should probably not transfer all its energy to the L electrons. It may be possible to eliminate the former of these causes for deficiency of energy, if the target can be made thin enough, but the latter is inherent in the atomic process. Thus even with an infinitely thin target, the energy limit described above might at best be looked for in the velocity spectrum only as a discontinuity in the first derivative of the intensity; and with a thick target, only in the second derivative.

These predictions are somewhat discouraging, but not completely so. For even if the secondary electrons were of uniform velocity, like the primary, the discontinuity in the x-ray spectrum of the stem-radiation would still be only in its first derivative. And uniform velocity means, for the velocity spectrum, not simply a finite discontinuity in some derivative, nor even in the intensity function itself, but in its first integral. In general, the order of the lowest derivative in the stem-radiation spectrum, having a finite discontinuity, should be two units higher than that in the velocity spectrum. Thus the better of the two spectra, as evidence on the question in hand, should be the velocity spectrum, which ought therefore to be explored thoroughly. And regardless of all such hypotheses as are discussed above, such exploration will surely improve our understanding of the process of secondary electron emission.

II. APPARATUS AND METHODS

The apparatus used here was of the well-known type for semicircular focussing of a magnetic spectrum, as described by Robinson,⁷ and is illustrated in Figures 1 and 2. The source of the secondary electrons to be

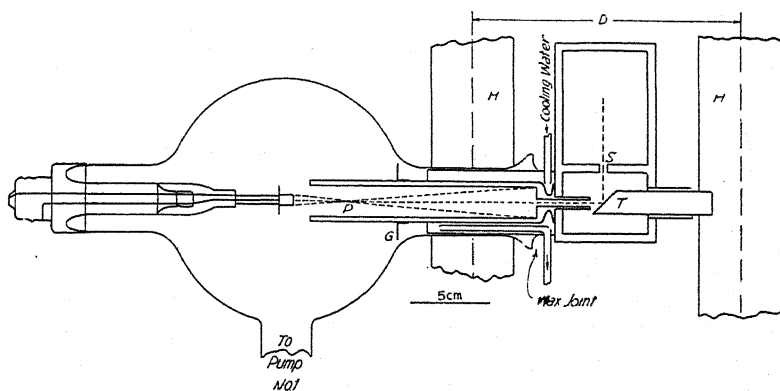


Fig. 1

analyzed into a spectrum is the target, T , shown from two directions in Figs. 1 and 2. The familiar magnetic focussing of the electrons is illustrated in Fig. 2, while Fig. 1 shows how the primary rays came along the lines of the magnetic field, as in Chilinsky's apparatus. Thus they travelled in straight

⁷ H. Robinson, Proc. Royal Soc. A104, 455 (1923).

lines, from the Coolidge cathode in the glass bulb at the left, to the target *T*. The current producing this field ran in a pair of Helmholtz coils, indicated in Fig. 1 by the broken segments marked *H*. The brass box, in which the electrons made their semicircular paths, communicated with the glass bulb only through the very narrow slit *S*, and both of the chambers needed very good vacuum. Therefore, even though a test showed that the pump leading from the box alone would evacuate the bulb satisfactorily, a pump from the bulb was added as a precaution.

The target was sometimes a solid rod of aluminum as shown here, sometimes a brass rod with copper, silver, or gold soldered to it, and sometimes a brass tube, 7 cm deep, with a bore of 1 cm diameter, covered at the end with aluminum, silver, or gold leaf, to make a thin target. In each case, the primary rays struck the target at 45° , and the secondary rays used left it at the same angle, being thus 90° from the primary. The thicknesses of the thin targets were: Al 0.53×10^{-4} cm, Ag 0.18×10^{-4} cm, Au 0.23×10^{-4} cm.

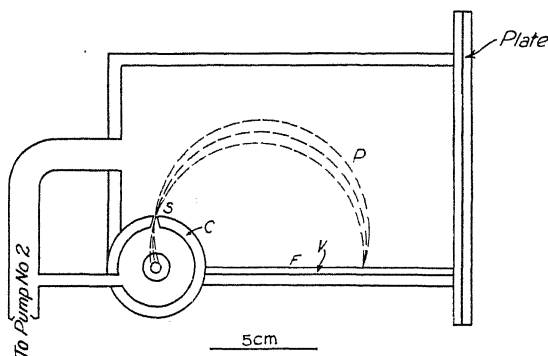


Fig. 2

Some other numerical data were as follows: slit *S*, 1.4 cm by 0.025 cm; diameter of hole through which the cathode rays approached the target, 0.2 cm; fraction of the cathode rays going through this hole, about 5 percent; radius of the Helmholtz coils, 17 cm; center of whole Helmholtz coil system, at the center of an electron path of radius 5 cm; non-uniformity of field (by test coil) not over 0.9 percent from its value at the center, anywhere on a radius of 6 cm.

The voltage applied to the primary cathode rays was obtained by connecting the cathode to the negative line of the D.C. system of the laboratory, and the brass box to the neutral line, which was grounded. It could be held constant to better than 0.3 percent, and the fluctuations due to the primary A.C. were far less than this.

For final use, spectra were photographed at four voltages, 16, 20, 30, and 40 kv, the first two with 1 ma (of which, as noted above, only about 5 percent reached the target), and the last two with 0.6 ma. To insure constancy of voltage and magnetic field in each exposure, the following procedure was adopted. First, the film was inserted, the box closed, and the ap-

paratus pumped to a high vacuum. Second, the current in the Helmholtz coils was set for a value such as to deflect secondary electrons of primary velocity into semicircles of 5 cm radius, and it was watched carefully thereafter. Then the high voltage was turned on, adjusted, and watched by another observer, usually Mr. B. G. Eaton, to whom hearty thanks is due for the care with which he rendered this assistance. Third, the filament was heated gradually, taking about half a minute to heat, so as to avoid voltage disturbances due to slight evolution of gas, and it was maintained at the right temperature for 5 minutes. Finally, the filament current was shut off, then the high voltage, and last the magnetizing current. Thus all the electrons had a primary voltage and deflecting field, each uniform to 0.3 percent, so that no discontinuity in the magnetic spectrum could be blurred by any lack of constancy involving energy changes as great as 1 percent.

Beyond tests for discontinuities, however, this work is purely qualitative although the conditions of exposure and development of the films were kept as constant as possible, to facilitate the comparisons of films. Especial care in this respect was applied to pairs of films, for thick and thin targets of the same metal at the same voltage, which were developed together.

Along with all the ordinary sources of photographic errors, it was unfortunately not found possible to eliminate entirely the effect of stray light from the filament. Tests without high voltage, however, (thus omitting the cathode rays) showed that the most serious fogging by such light occurred only in the low-velocity region. In the high-velocity region, say above half the primary ray energy, where most of the secondary electrons appeared, the fog was very light and practically constant. Thus, fortunately, it can be neglected in discontinuity tests or in qualitative comparisons confined to this high-velocity part of the spectrum.

III. RESULTS

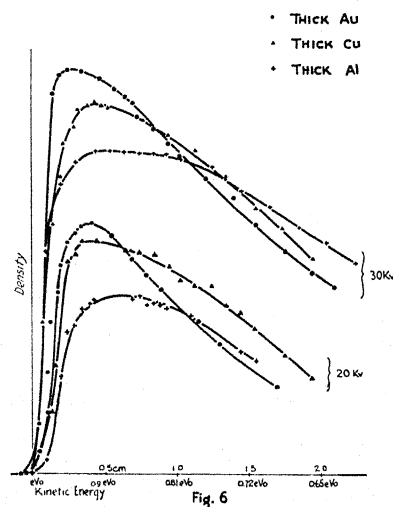
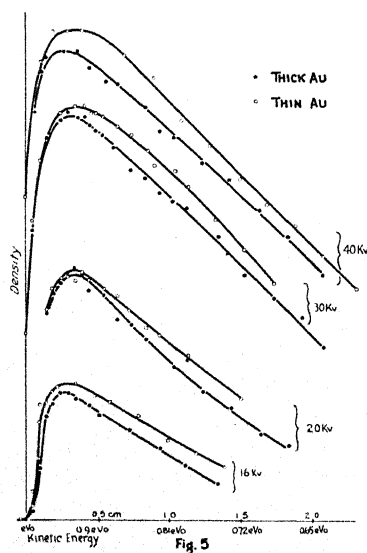
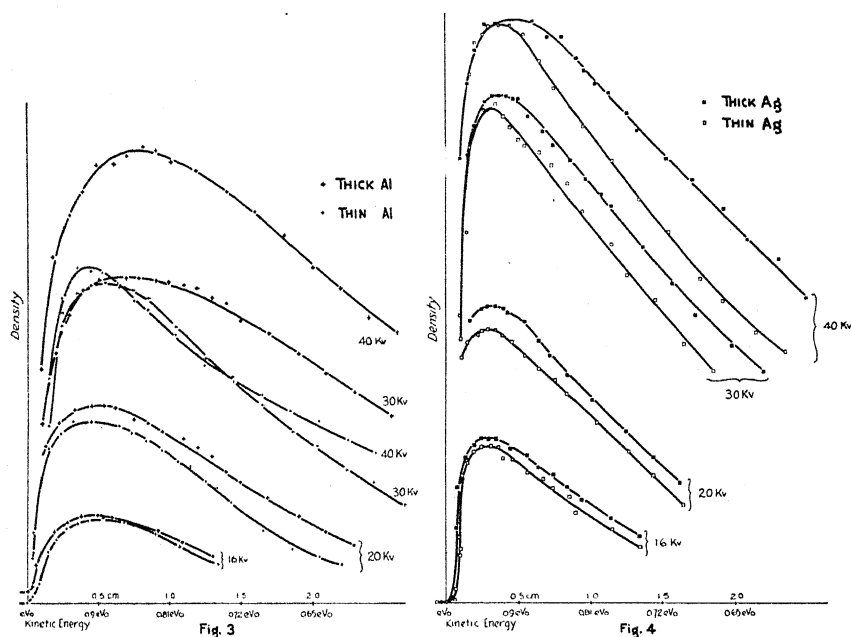
Some densitometer graphs, comparing thick and thin targets of Al, Ag, and Au are shown in Figs. 3, 4, and 5 respectively; and some for thick targets only, of Al, Cu, and Au, in Fig. 6.

As will be seen on inspection of these graphs, *all these spectra are continuous.*

With regard to discontinuities in the derivatives of density or number of electrons with respect to velocity, it is evident that *there is apparently a real discontinuity in the first derivative, in every spectrum, at its high velocity end which is always found on measurement to occur at a velocity equal to that of the primary cathode rays. Aside from this point, however, no discontinuities have been found.*

First-derivative discontinuities would of course be much easier to detect than second, of the same relative proportions. Considering now only the thick targets, it has already been noted that we cannot expect to find any evidence of electrons ejected from the inner orbits, except in second-derivative discontinuities. Therefore, so far as we can tell here, such electrons may constitute several percent of the secondary electrons. But if they con-

stituted a majority, it would be a different matter. If, for example, in gold at 20 kv the majority of the secondary electrons were ejected from the M



Figs. 3, 4, 5 and 6

levels, we should expect to find relatively few electrons of energy greater than $(20-4)$ kv, or $0.8eV_0$, and just below this energy we should expect the density to begin to increase rapidly. The facts, however, are totally different

from any such prediction, not only in this spectrum, but in all the spectra. We must, therefore, conclude that, although some of the secondary electrons undoubtedly do arise from ejections from the inner orbits, they are a very small minority.

Turning now from discontinuity tests to qualitative information on other matters, still on thick targets, we find for all these elements, Al, Cu, Ag, and Au (as Chilinsky found for Ag up to 20 kv) that most of the high-speed secondary electrons have very high speeds. In terms of kinetic energy the maximum densities in these spectra occur at energy values bearing nearly constant ratios to the primary energy, eV_0 . For Al, this optimum energy eV_m is about $0.85 eV_0$; for Cu, about $0.90 eV_0$; for Ag and Au, each about $0.94 eV_0$. The probable errors in these ratios are several percent, of course, especially for Cu, for which relatively few photographs were made.

Below the optimum energy, in every case, the density declines rapidly, reaching half its maximum somewhere around 0.6 or $0.7 eV_0$. Part of this decline may result from a decline in the photographic effect per electron, though not if each electron causes development of one grain, as may be possible. These statements on densities give, of course, only a qualitative idea of the laws governing the number of electrons per unit energy interval, but this number must vary in a manner roughly similar to these densities.

Since the conclusions drawn here differ radically from those of Lorenz, a question arises, whether the difference is due to theoretical assumptions in the interpretation of the data, or to some hidden source of experimental error. From the present data on the velocity spectra of the secondary electrons, we may predict roughly the form of the x-ray spectrum of the stem radiation they might excite. Considering only gold, as the element most like Lorenz's tungsten, the outstanding feature is the concentration of the secondary electrons in the general region around $0.9 eV_0$, ± 0.1 . The x-rays due to such electrons would not be expected to show any very sharp short-wave limit, but the general form of their spectrum would be much like that of the x-rays from the focal spot, except that it would be shifted to wave-lengths about 10 percent longer, and blurred out by ± 10 percent, more or less. Considering the short-wave limit more carefully, what it should show, as noted above, is a finite discontinuity in a derivative of order two units higher than that of the discontinuous derivative in the velocity spectrum. Therefore, since the velocity spectrum has its discontinuity in its first derivative, the x-ray spectrum should start, as measured from its short-wave limit, more or less like the curve $y=x^3$. In other words, it should have a graph which runs very low near the limit, and curves upward rather sharply at a wave-length somewhat greater. It is, therefore, not inconceivable that this sharp upward curvature might occur in the region where most of the secondary electrons would have their individual short-wave limits, that is, around 10 percent above the true short-wave limit. This is just about the region where Lorenz found a strong upward curvature in each of his spectra, assuming it to be a short-wave limit and assuming the weak radiation of still shorter wave-lengths to be stray rays from the focal spot. Thus

it may well be that the only cause for difference between his conclusions and the present lies in these assumptions, and that the data are consistent within the limits of reasonable experimental errors.

Turning now to the thin-target velocity spectra, they prove somewhat disappointing. Differences from the corresponding thick-target spectra are found only in Al and Ag, and there only above 20 kv. However, some recent theoretical work by Bothe,⁸ on the stoppage of cathode rays in matter, throws light on this point. In thick targets, only very few cathode rays are stopped far short of their normal range, by large losses of energy; but practically all of them are deflected by nuclear attractions without much energy loss, in very short distances. Thus, at the speeds used here, they have completely lost all sense of direction before they have gone a micron. Qualitative calculations on rather loose assumptions related to those of Bothe, make it quite reasonable to expect many of the cathode rays deflected back out of the metal to have had very short paths within it. Such deflected cathode rays (or rediffused, as Becker would call them) should therefore have two characteristics in common with the secondary electrons observed here: first, that each electron should retain a large fraction of its initial kinetic energy; and second, that a metallic film, whose thickness is small compared to the range of a cathode ray in the metal, should nevertheless be thick enough to give practically the same velocity spectrum as a thick target. The agreement of theory and observation here tends to confirm the view that most of these high-speed secondary electrons are rediffused cathode rays.

With regard to how thin a target must be, to give "single scattering," and really give the velocity spectrum of an infinitely thin target, it seems probable that this requirement of thinness is considerably more severe than that for obtaining a "thin-target" x-ray spectrum. For velocity spectrum work, these spectra show that 0.2 micron gold is "thick" even at 40 kv; likewise 0.2 micron silver and 0.5 micron aluminum are each thick at 20 kv. To consider such films really "thin" from this viewpoint, these voltages must be greatly exceeded.

⁸ W. Bothe, *Zeits. f. Physik* 54, 161 (1929). Mr. Wagner had not seen Bothe's work, but this application of Bothe's theory tends to confirm the views Mr. Wagner expressed, as to the origin of the secondary electrons, and is therefore a reasonable extension of his paper.

Physics Department
Ewing Christian College
Allahabad

ELECTRODYNAMIC DAMPING IN PULSATING STARS

BY ROSS GUNN

NAVAL RESEARCH LABORATORY, WASHINGTON, D. C.

(Received November 29, 1929)

ABSTRACT

Small radial pulsations of stars are shown to be highly damped by electrodynamic forces when the star has a magnetic field unless the star is very diffuse. The author's theory of the permanent magnetic field of the sun indicates that the field is produced by regenerative means which is initiated by a small field arising from some more fundamental mechanism. The small initial field is probably produced by the rotation of the star combined with a separation of charge, although it may conceivably arise in other ways. Thus rotating stars will have a magnetic field and cannot pulsate, and conversely stars which pulsate can have no magnetic field and probably do not rotate. This is in accord with the idea that Cepheid variables, being youthful giants, are so large that they would be unstable under rotation. These considerations appear to remove the difficulties encountered by Eddington in his detailed theory of star pulsations.

A CLASS of stars known as Cepheid variables are observed to go through regular periodic changes in their brightness, color and spectrum. It appears that the variation must be due to a variation of surface temperature rather than to eclipses or a rotation of the star, for observation shows that the rise in surface temperature is much more rapid than its decline. The astronomical observations are well explained by the pulsation theory which was first proposed by Shapley and later worked out in detail by Eddington.¹ This theory attributes the observations to a periodic radial expansion and contraction of the star under the joint action of gravitation, radiation and gaseous pressure. In this theory it is supposed that a star is in internal equilibrium and that the pressure at any level due to the weight above it is just balanced by the outward gaseous and radiation pressure. Let the entire star be uniformly compressed. On removing the constraint the internal radiation and gaseous pressures will expand the star and the inertia of the moving material will cause it to expand beyond its equilibrium position. This may give rise to an oscillation which can be sustained if energy is supplied in phase with the variation and if it is of sufficient magnitude to overcome the dissipative forces. Eddington has examined the problem and finds that if the pulsation of Cepheid variables is to be explained satisfactorily nearly all stars should pulsate and the phenomena should be more generally observed than is actually the case. In the treatment of the subject of star oscillations no account has been taken of electrodynamic forces and as we shall see presently these forces may be large and always act in such a manner that they tend to damp out very rapidly any radial oscillation of a star.

¹ Eddington, *Internal Constitution of the Stars*, Cambridge Press (1926).

Indeed, the present paper shows that radial oscillations of a star can exist only under very special conditions; conditions which appear to be satisfied in the youthful giant stars.

In an earlier paper² the writer outlined a theory of the origin of the magnetic fields of the sun and earth. The theory showed that any highly ionized star having radial temperature or gravitational symmetry would be expected to build up a large magnetic field by regeneration if a small initial magnetic field were present to start the regenerative process. All stars possess the requisite radial temperature and gravitational symmetry and it is only necessary to produce a small initial field to bring about their complete magnetization. The small initial field might be attributed to a "magnetic collision" with the stray magnetic field of another star or in some other way. Earlier work on the sun³ indicates, however, that a star's magnetic field is more or less confined by the diamagnetic action of the ions in the stars atmosphere which execute long free paths. It seems more reasonable to consider the initial field as arising from gyromagnetic effects or from the gross rotation of the star combined with a slight gravitational or thermal separation of charge. Such an assumption leads to the correct sign for the magnetic field of the sun and earth. The general conclusion is that any star which possesses appreciable angular momentum will be magnetized. We must therefore examine what effect a magnetic field may have on the stability of a star and in particular we shall examine the effects produced by the magnetic field when the star is subject to a small symmetrical radial oscillation.

Assume for simplicity that the magnetic field inside a star is uniform and consider the forces acting on a ring of star material which lies in a plane perpendicular to the magnetic field and which expands and contracts radially with the star itself. In order to keep the essential physics before us let us also assume that the ring has a mean equilibrium radius R_0 and that any expansion or contraction of the ring will set up elastic restoring forces which are proportional to the displacement of the ring from the equilibrium position. On account of the symmetry we may describe the process by writing down the equations of motion for the material enclosed by unit volume of the ring. In addition to the inertial and elastic forces, account must be taken of the dissipative forces and in the following we shall consider only those of electromagnetic origin. Consider an expanding ring of star material. As the ring expands the magnetic flux enclosed by the ring is increased and an electromotive force is induced. This electromotive force produces a current in the closed circuit of the ring which is always in such a direction as to oppose the motion. Suppose the ring is expanding outward with a velocity V . Then the electric field E produced by the motion is

$$E = V \times B \quad (1)$$

where B is the constant impressed magnetic field intensity of the star. The force F acting on unit volume of material is by aid of (1)

² Gunn, Phys. Rev. 34, 335 (1929).

³ Gunn, Phys. Rev. 33, 614 (1929).

$$\mathbf{F} = \mathbf{i} \times \mathbf{B} = \sigma(\mathbf{V} \times \mathbf{B}) \times \mathbf{B} \quad (2)$$

where \mathbf{i} is the current density and σ is the conductivity. For the purposes of the rough calculations in this paper the classical expression for conductivity can be used and Eq. (2) reduces (in the special case where the ring expands in a plane perpendicular to the impressed magnetic field) to

$$\mathbf{F} = -\sigma B^2 \mathbf{V} = -\frac{N e^2 \lambda B^2}{2(3mkT)^{1/2}} \mathbf{V} \quad (3)$$

where N is the number of ions per cm^3 , e the ionic charge (e.m.u.), λ the mean free ion path, m the mass, k the Boltzmann constant and T the absolute temperature. It has been shown previously⁴ that the expression for the electrical conductivity given by Eq. (3) breaks down and the conductivity decreases greatly when the mean free path of the ion approaches (in numerical value) the radius of the circle generated by the ion as it spirals about the impressed magnetic field. It has also been shown³ that in the outer surface layers of the sun the mean free paths of the ions are longer than this critical radius and the conductivity of the region low. Thus the currents flowing in a very diffuse star or in the outermost layers of the star are small and the resulting damping is probably unimportant.

If we measure r from the equilibrium position of the ring, the equation of motion for a typical volume element is

$$\rho \frac{d^2 r}{dt^2} + \sigma B^2 \frac{dr}{dt} + K^2 r = 0 \quad (4)$$

where ρ is the density of the star material and K^2 is a constant which must be determined by a complete analysis or by observation of the free period of oscillation. With $2u = (B^2 \sigma / \rho)$ and $v^2 = K^2 / \rho$ the solution of (4) is of the form

$$r = C_1 e^{[-u + (u^2 - v^2)^{1/2}]t} + C_2 e^{[-u - (u^2 - v^2)^{1/2}]t} \quad (5)$$

and may represent a completely damped pulse, a critically damped oscillation or a free oscillation depending on the value of the coefficients. From Eq. (5) it is seen that any mean displacement will be reduced to roughly one e^{th} its initial value in a time

$$t = \frac{1}{u} = \frac{2\rho}{B^2 \sigma} \quad (6)$$

and if the system is oscillatory it will oscillate with a frequency

$$f = \frac{1}{2\pi} \left(\frac{K^2}{\rho} - \frac{B^4 \sigma^2}{4\rho^2} \right)^{1/2} \quad (7)$$

It will be noted in passing that the frequency of oscillation is sensitive to changes in the value of B , for σ will have fairly large values in any ordinary

⁴ Gunn, Phys. Rev. 32, 133 (1928).

star. It must be remembered that Eq. (6) only applies to rings which expand at right angles to the magnetic field. In all other orientations the damping will be somewhat less and there is a tendency for the star to expand more at the magnetic poles than at the equator. In fact, closed circuits in a plane containing the magnetic axis might be expected to produce no damping of the type we have considered. Moreover, certain types of oscillation can be conceived wherein any typical current ring suffers no change in area but takes on successive elliptical forms. Such an oscillation would induce no current and electrodynamic forces would not be important.

It will be necessary to consider an actual case to determine the importance of electrodynamic forces. The only star which we definitely know possesses a magnetic field is the sun and earlier work,^{2,3} has indicated that its internal magnetic field intensity was not less than 10^4 gauss. We shall apply a disturbing force to the sun in such a manner as to set it in radial oscillation and calculate by Eq. (6) and (3) the time it will take the oscillation to die out. We will take representative values of the quantities as follows:

$$\begin{array}{lll} B = 10^4 \text{ gauss} & \rho = 1.4 \text{ gm/cm}^3 & N = 10^{23} \text{ ions/cm}^3 \\ e = 1.59 \times 10^{-20} \text{ e.m.u.} & \lambda = 10^{-6} \text{ cm} & \\ m = 10^{-27} \text{ gms} & k = 1.37 \times 10^{-16} & T = 10^7 \text{ degrees} \end{array}$$

which leads to a value of $\sigma = 6.25 \times 10^{-6}$ e.m.u. Thus by Eq. (6) the time for the mean solar displacement to be reduced to $1 e^{th}$ of its initial value is 4.5×10^{-3} seconds. It is therefore clear that no oscillation can take place and the sun is in stable equilibrium. It must be emphasized that this conclusion is only true for small oscillations which produce no appreciable change in the impressed magnetic field. When the oscillations are large the problem offers mathematical difficulty but qualitatively it appears that large oscillations would be damped out much less rapidly than small ones and that the surface layers will reach equilibrium well before the deeper ones. If it is assumed that the numerical values which have been chosen in the case of the sun are representative of stars in general, it is doubtful if any star having a magnetic field can oscillate over any extended period of time. We must therefore interpret the occurrence of true pulsating stars to mean that the star does not have a magnetic field or that it is so diffuse that the ion free path is long and the magnetic field reduces the electrical conductivity almost to zero.

The writer's theory of the origin of the permanent magnetic fields of the sun and earth is based on a regenerative action which requires a small initial magnetic field to trigger it off. The small initial field is most simply accounted for by a rotation of the star and it seems correct to assume that every rotating star is highly magnetized. Conversely, a star which has no magnetic field would not be expected to rotate. The foregoing considerations definitely suggest that a true pulsating star does not rotate. Appeal to observation shows that all the stars that are suspected of being true

pulsating bodies are youthful giants which astronomers believe would break up if they were possessed of any great amount of angular momentum. This observed fact seems to bear out the conclusion that true radial pulsation of a star is possible and the argument shows that the existence of such entities in the universe does not necessarily mean that all stars should be unstable and exhibit a radial pulsation.

Jeans⁵ has concluded that the pulsation theory is inadequate to explain the observations and chooses to think of the variables as stars in the process of breaking up to form binary systems. Consideration of electrodynamic damping might be favorable to this theory if it can be shown that the probability of rotation for a star is very much greater than the observed probability for the occurrence of a nonpulsating star. Unless some such statistical relation be established the considerations of this paper appear to support the ideas of Shapley and Eddington as formulated in their pulsation theory. While it is too early to decide whether the present considerations support or disprove the pulsation theory of Cepheid variables, it appears that electrodynamic forces play an important part in stabilizing a star and they must be considered in any complete study of its history. The possibility that electrodynamic loading of the type we have considered may account for certain observed features of Novae is now being investigated.

⁵ Jeans, *Astronomy and Cosmogony*, Cambridge Press (1928).

LETTERS TO THE EDITOR

Prompt publication of brief reports of important discoveries in physics may be secured by addressing them to this department. Closing dates for this department are, for the first issue of the month, the twenty-eighth of the preceding month; for the second issue, the thirteenth of the month. The Board of Editors does not hold itself responsible for the opinions expressed by the correspondents.

Effect of Red Light on Stopping Potentials of Photoelectrons Liberated by Blue Light

In "Naturwissenschaften" (41, 806-807, October 11, 1929) was published a note by Erich Marx, announcing observations which seemed to show that red light superimposed on blue light falling on a photoelectrically sensitive potassium surface had the effect of decreasing the maximum kinetic energy of emission of the electrons liberated by the shortest wave blue light. This is a most surprising and important result, if true. Details of the experiment were missing, but the only care necessary to observe this effect seemed to be that of preventing light from striking the anode directly or indirectly while determining the stopping potentials of the photoelectrons. In fact, Marx explained that the phenomenon was easily observed qualitatively, on any commercial potassium cell.

Now, since most commercial model photoelectric cells are of the central anode type and require upwards of a hundred volts, at least, to produce saturation of the photoelectric current, shifts ranging from a fraction of a volt to a few volts in the voltage-current relation can only be detected at a voltage where the current approaches zero. Hence, it is undoubtedly at the foot of the stopping potential curves that Marx claims to have observed the effect of the red light superimposed on the blue. But, as rather carefully pointed out by Millikan [Phys. Rev. 7, 18, 355 (1916)] and quite generally proven by experimental results, this part of the curve for a given anode is not a function of the cathode at all and can only be affected by a change in light frequency. Certainly there exists no sound reason for only the highest frequency of the incident light being altered, so the so-called "new photoelectric phenomenon" of Marx is hard to reconcile with experience or theory.

Such an apparent reduction of the retarding

potential as cited above, however, would be produced if some of the incident or reflected light fell on an anode sensitive more to red light than to blue, and it seems highly probable that such was the case. For, in the first place, Marx stressed the importance of preventing light from falling on the anode, a precaution unnecessary if the anode were not light sensitive and one practically impossible to put into effect. In the second place, it is a matter of common observation that the anodes of potassium photoelectric cells frequently respond better to red light than the cathodes, a fact which suggested to Campbell [Phil. Mag. 6, 633 (1928)] a method of making red-sensitive potassium cathodes. Undoubtedly the sensitivity of the anode to red is due to a thin film of potassium spontaneously deposited thereon, and these films naturally respond to light of longer wave-length than the bulk metal or heavy layer of the cathode [Ives and Olpin, Phys. Rev. 34, 117 (1929)]. Whenever potentials are applied to retard electrons released at the cathode they accelerate at the same time any electrons liberated from the anode, and the measured current will be the difference between the number of electrons reaching and leaving the cathode. Since potassium, in bulk form or thick layers, responds well to blue light but not to red light, whereas potassium in the form of thin films on metals, responds well to red light, it is at once evident that if any scattered light fell on the anode, the presence of red light will occasion a greater reverse current and consequently the voltage at which the current becomes zero will be less than for blue light alone.

In order, therefore, to make a complete check of the "Marx phenomenon," a cell having an anode absolutely insensitive to

light should be used. I had available such a cell, made by preparing the cathode in a separate chamber and then slipping it into place within a nickel anode coated with soot. The cathode was not coated with potassium but with sodium, sensitized by the introduction of small amounts of sulphur and oxygen until the response to red light was far greater than that of potassium-hydride cells [Olpin, Abs. 57, Bull. Am. Phys. Soc. vol. 4, No. 2

a tungsten filament, and the red light similarly produced by using a No. 29-Ek Wratten filter. The photoelectric currents were read on a high sensitivity Leeds and Northrup galvanometer.

The results of this test are shown in Fig. 1. There was absolutely no effect of the red light on the electrons emitted with maximum kinetic energy, but an increase in the number of slower electrons. The voltage-current curve

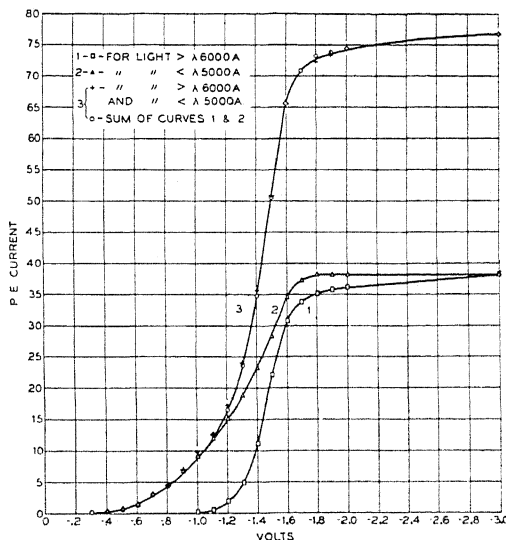


Fig. 1.

(April 6, 1929) Phys. Rev. 33, 1081 (1929)]. These alterations from the Marx experiment may be criticized, but there seems to be no reason for expecting potassium to behave differently from sodium in the property under discussion, unless it be the fact that potassium is far more likely to pass by vaporization to the anode than is sodium. The blue light was produced by inserting No. 49-EK Wratten filter in the path of radiations from

for both red and blue light falling simultaneously on the surface was exactly the sum of the voltage-current curves for the two colors of light used separately. This was found to be equally true when yellow light was used in place of the red.

A. R. OLPIN

Bell Telephone Laboratories, Inc.

New York, New York,

December 5, 1929

The Origin of Snowflakes

Experiments begun in 1920 on the conditions governing the origin and growth of snowflakes have now met with some success. It has been found possible to produce an opalescent cloud of snowflakes, to put individual particles of this cloud under microscopic observation within about five seconds of their inception, and to control their growth

up to a diameter about four times that at which their outlines become distinguishable.

The experimental method consists in passing a current of cold dry gas—obtained by the evaporation of liquid oxygen or liquid air—into a mixing tee where it may meet a current of air and saturated water vapor supplied at a temperature a few degrees above 0°C .

The mixture passes immediately into the top of a vertical observing chamber kept at a few degrees below zero, thence down through the chamber and out by horizontal lateral passages. The bottom of the chamber is made of a glass plate with a fine scale engraved or etched on its upper surface. A microscope objective under the plate is placed so as to form a magnified image of the scale and of any deposit that may occur on it, in the focal plane of an eyepiece or on a photographic film. Illumination is downward through the observing chamber. With these arrangements, the admission of the moist air to the mixing tee is accompanied by a reddening and darkening of the field of view, and in a few seconds the glass receives a deposit of particles of the order of 5×10^{-4} cm in diameter—too small to permit observations on their shape with the optical system used. An additional supply of vapor to the chamber results in the visible and rapid growth of these particles to sizes which display definite outlines. Diameters of 2×10^{-3} cm are frequent. The particles thus grown may be held under observation for a minute or more, and photographed.

After the process of growth has started, it is not possible to bring onto the plate an additional deposit of particles of the original size. The opalescence occurs as usual, but produces only a further growth of the particles already on the plate. This indicates that snowflakes, like raindrops, grow at the expense of their smaller neighbors, and implies that the equi-

librium vapor pressure above a particle of ice decreases with increasing dimensions. The opposite effect has been observed by Farnsworth [Phys. Rev. **34**, 684 (1929)] in the case of small copper crystals growing at the expense of a large one.

The crystalline character of the deposit is obvious from an inspection of the photographs. Many of the particles show twinning, and a few appear to be aggregates. More common than either of these are forms without internal markings, perfectly transparent, revealing in their outlines the symmetry characteristic of the hexagonal system. The symmetry is not merely that of external form, for when these crystals are made to grow, each of the six faces advances at the same rate, so that the outline remains similar to itself. This observation indicates that the faces are alike in physical properties, and that therefore the particles are monocrystalline. The deposits also contain abundant material for the study of the so-called cubic crystals which have been reported occasionally by observers of naturally formed ice crystals.

The method is probably applicable to the formation and growth of small single crystals of substances other than water, and affords a means of studying problems of crystal structure in the light of the kinetic theory.

JOHN MEAD ADAMS

Department of Physics,
University of California at Los Angeles,
December 10, 1929.

Inhomogeneities in Crystals

Ever since Griffiths proposed the existence of internal flaws in apparently perfect crystals as an explanation of certain anomalies in their behavior, various workers have attempted experimental verifications of this hypothesis. There have likewise been attempts to justify it on theoretical grounds and thus bring it within the domain of regular and predictable phenomena.

The subject derives its importance from its bearing on the validity of some highly fundamental physical measurements. Among these are the refined determinations of compressibility such as those of Bridgeman and the determinations of x-ray wave-lengths based on the assumption that the calcite crystal is perfect and homogeneous. Other determinations affected are those of all elastic

constants, thermal and electrical conductivities and densities. All the data of crystal energetics are subject to large and unpredictable errors if internal inhomogeneities exist.

Mehl and Canfield in a note (Nature, Sept. 28, 1929) have discussed the question of voids in crystals and conclude that the experimental evidence, particularly the recent measurements of x-ray wave-lengths with a ruled grating (Beardon, Proc. Nat. Acad. **15**, 6 (1929)) cannot be reconciled with their existence.

The most important recent paper supporting the inhomogeneity hypothesis is by Zwicky (Proc. Nat. Acad. **15**, 11 (1929)) who contends not for the presence of voids but for planes of altered density occurring at fairly regular intervals within the lattice and di-

viding it into a sort of mozaic. He has previously secured experimental evidence of such structure on the *surface* of etched metal crystals. The paper here referred to is devoted to a theoretical treatment of the subject, resulting in a prediction of the required phenomenon, and it is this to which the present writer wishes to take exception.

In setting out on his discussion the author makes (in substance) the following steps of reasoning:

Crystals in general contract laterally when they are elongated in one direction. Hence, if we picture the crystal as built up of planes of atoms, the withdrawal of neighbor planes permits the atoms of a given plane to come closer together. Hence the atoms of any one plane would draw nearer together if that plane were isolated and allowed to come to its equilibrium configuration.

This reasoning is fallacious. The elongated crystal is not in equilibrium, but has had work done on it by external forces; the configuration it assumes is determined by the condition that the work done by the external forces shall be a minimum. As a matter of fact the process of withdrawing the neighbor planes *pulls* the atoms of the given plane into closer proximity. A plane of atoms when isolated might expand or contract from its

dimensions in the lattice, depending on the density of packing of the atoms in the plane. For example a (111) plane of a homo-polar face-centered cubic lattice would expand; a (100) plane would contract. Since the remainder of the proof rests on the argument already outlined it requires no comment. Although the reasoning is called thermodynamic, it is in reality dynamic, with the words "free energy" substituted for "potential energy."

As regards the experimental evidence, there can be little doubt that an actual mozaic structure does exist on the *surface* of a crystal. In fact the effect is to be expected as a result of the surface energy, as the present writer hopes to show in a paper now in preparation. But it must be emphasized that the experimental evidence now at hand establishes the existence of *surface inhomogeneities only*. The non-agreement of predicted tensile strengths with experimental values—the main prop of the mozaic argument—is susceptible of too many other explanations to serve as *prima facie* evidence of internal inhomogeneities.

R. H. CANFIELD

Naval Research Laboratory,
Bellevue, Anacostia, D. C.,

December 20, 1929.

A New Relativity Theory of the Unified Physical Field

I have succeeded in applying to the above question what appears to be an important new conception regarding the significance of relativity mathematics with noteworthy results. I have abandoned altogether the quasi-geometrical interpretation with such hazy notions as parallel displacement in a curved space of n dimensions. Instead, we construct an indeterminate vector field by means of Eddington's displacement rule (considered now as an association rule), and identify it at every point with the velocity a material particle might have if present there and then. Vector lines in this field are necessarily the orbits of material particles under any physical conditions.

We now construct an indeterminate tensor field, and by its means define the invariant magnitude of the elementary arc of these vector lines. Actual physical vector and tensor fields are necessarily determinate at every point, and these are defined as usual by applying the association rule round a closed

loop. This gives the usual symmetric and antisymmetric field tensors.

When the antisymmetric field tensor vanishes the vector lines reduce to Einstein's so-called geodesics. The electric field is given by the antisymmetrical tensor, and here the vector lines become mathematically equivalent to the known orbit equations. Maxwell's first set of field laws are identically satisfied, and the set referring to electric charge and current are approximately true for small fields. In strong fields in the neighborhood of atomic nuclei the electron orbits reduce again to geodesics, independent of negligible radiation due to their acceleration, and Maxwell's second set of laws no longer holds. This is obviously very strong support for our theory. But further; the introduction of field laws which reduce to Einstein's in the pure gravitation field appear to lead to a principle of selection among the orbits in nuclear regions.

Before leaving England this summer, the

writer prepared a hurried account of the above theory intended for publication in the Proceedings of the Royal Society. It unfortunately gave no explanation of the mathematics which latter were faulty at one point. A careful and complete revision has now

proved the soundness of the theory, and publication will follow as quickly as possible.

WILLIAM BAND

Physics Department,
Yenching University, Peking,
December 19, 1929.

The Microstructure of Some Magnetic Alloys of High Platinum Concentration

In a recent paper [Phys. Rev. **34**, 1217 (1929)] the writer has described an attempt to measure the magnetic properties of ferromagnetic atoms in a somewhat isolated state. The method used was to study alloys of platinum with a small percentage of cobalt. Alloys of 5% cobalt and 10% cobalt were both ferromagnetic. Provided these alloys are solid solutions, which was believed to be the case, the cobalt atoms in them could be regarded as mostly isolated from one another by the intervening platinum atoms.

A microscopic study of these alloys has since been made. The diagram of thermal equilibrium has not been obtained for the Pt-Co series, although Carter has investigated many high-platinum alloys and believes platinum and cobalt form an isomorphous series of solid solutions. However, it was necessary to be sure that two solid solutions did not exist together in a given alloy, with the result that a particular cobalt alloy would generally consist of a cobalt-rich phase plus a platinum-rich phase, or of a platinum-cobalt mixed crystal in pure platinum; in this case, increased platinum concentration would not mean further isolation of cobalt atoms, but a different proportion of the two phases.

Sections of each alloy were prepared, polished and etched with hot aqua regia. Wires in the hard-drawn state showed, under the microscope, that their crystals were elongated and distorted in the direction of strain. In the annealed state, however, each alloy showed the polygonal polycrystal pattern characteristic of pure metals or single solid solutions. If two phases were present in, say, the 10% cobalt-90% platinum alloy, they would have to exist in nearly equal proportions or one phase might be present in a

small quantity between the grain boundaries. The 5% cobalt alloy, however, showed the same structure, although it, too, could not contain equal amounts of the two phases. In neither alloy was the characteristic eutectic structure of one phase imbedded in the other present. The sections were etched a little at a time and examined at each stage, but intercrystalline material was never detected. The sections etched uniformly, but the 5% cobalt several times more slowly than the 10% cobalt; as the acid more readily attacks cobalt, this again indicated that the cobalt atoms were distributed over all the crystals uniformly, the cobalt concentration in the 5% alloy being less throughout and the resistance to the acid hence greater. For comparison, a section of an annealed wire of pure platinum was similarly examined, and its microstructure was practically identical with that of the cobalt alloys. The alloys must, therefore, be solid solutions of cobalt in platinum, and the cobalt atoms in them isolated.

Platinum possesses a face-centered cubic lattice, while cobalt is hexagonal for lower temperatures and face-centered cubic at higher ones (about 600°C). As transformation points are generally rapidly lowered by alloying, e.g., the Curie point, these high-platinum alloys might be expected to have the cubic structure. High magnification (1300 times), revealed definite cubic formations in many of the crystals.

F. W. CONSTANT,
National Research Fellow.

California Institute,
Pasadena, California,
December 17, 1929.

Recombination of Electron and Alpha-Particle

The writers have computed by quantum mechanical means the probability of recombination between an electron and a hydrogen atomic ion or an alpha-particle, when the final state is the hydrogen atom or

helium ion in some quantum state. The initial wave function used is that developed by Mott,¹ and represents a unidirectional

¹ Mott, Proc. Roy. Soc. A118, 542 (1928).

beam of electrons travelling toward a nucleus with velocity v . The final wave function is the usual one for the atom in one of its quantum states.

The matrix element of the moment corresponding to this transition is proportional to the target area of recombination, $q(v, \nu_i)$, discussed by Mohler.²

The calculations indicate that the target area for recombination of an electron and a nucleus of charge Ze is

$$q = 6.10 \times 10^{-11} Z^8 \exp \left[\frac{\pi k - 4k \tan^{-1}(1/k)}{v\nu^2 \sin h \pi k} \right]$$

where V is the electronic energy of motion relative to the nucleus in volts, ν is the frequency of the radiated light in wave-numbers, $k = 3.67 Z/V^{1/2}$, and the final state is the normal state. This agrees remarkably well with the theoretical and experimental formulas given in the recent summary by Seeliger.³ No approximations have been made in the derivation of this formula.

The q 's for the upper states are similar expressions, none of them showing any maxima in the range of V between zero and infinity. Therefore the maxima obtained by Davis and Barnes must be due to some mechanism involving more than one electron and one alpha-particle. The explanation offered by E. Q. Adams⁴ might be the correct one, despite

Barnes's⁵ objection. For the quantum mechanics indicates that processes not involving the electrical forces between the nuclei hold equally well for single nuclei, with the quantities giving the relative proportions of the resulting end products appearing as probabilities. In other words, if a stream of electrons falling on N alpha-particles creates n He⁺ ions in time t , then when this same stream of electrons falls on one alpha-particle, there is a probability n/N that this one alpha-particle will become a He⁺ ion in time t .

The authors have carried through this reasoning by probabilities from the beginning and have obtained an equation substantiating Adams's result. Since, however, the values of all the constants involved are not known, it is impossible to know at present whether this mechanism will account for the observed peaks.

E. C. G. STUECKELBERG
PHILIP M. MORSE

Palmer Physical Laboratory,
Princeton, N. J.,
December 15, 1929.

² Mohler, Phys. Rev. Supplement 1, 217 (1929).

³ Seeliger, Phys. Zeits. 30, 354 (1929).

⁴ E. Q. Adams, Phys. Rev. 34, 537 (1929).

⁵ Barnes, Phys. Rev. 34, 1224 (1929).

BOOK REVIEWS

Müller-Pouillet's *Lehrbuch der Physik*. 11. Aufl. 2. band. *Lehre von der Strahlenden Energie (Optik)*. 2. Hälfte. 1 & 2. teil. KARL WILHELM MEISSNER, editor. Pp. xvi+xvi+929 to 2392. Figs. 625 to 1345. Friedr. Vieweg & Sohn, Braunschweig, 1929.

After some delay following the death of Dr. Lummer, the editorship of this standard text and reference work has been assumed by K. W. Meissner. Three times the bulk of the corresponding sections of the previous edition (1909), the new half-volume impresses one again with the rate at which the research workers in the field of optics have been outdistancing the publishers. The editor has carefully subdivided the field, and with the cooperation of several of the most able German physicists presents here a work thorough, well organized, and readable, that develops experimental and theoretical optics up to 1924-1925 and, in a few outstanding sections, further.

About a third of the space is given to spectroscopy, including chapters on spectroscopic apparatus and methods, by Meissner, Hettner, Czerny, and Gehrcke; series spectra, by Paschen; band spectra, by Kratzer; x-ray spectroscopy, by Coster; Zeeman effect, by Back; and the foundations of the quantum theory of atomic structure, by Pauli. The prospective reader who is led by the author's name and the publisher's date, to expect a unified present-day account of atomic theory in this last chapter, will be disappointed. There is an apology elsewhere (p. 1483) for this chapter, written in 1924, and there are excellent concise appendices on the introduction of the Goudsmit-Uhlenback magnetic electron and the fundamental work of Schroedinger and Heisenberg. But there is no sufficient excuse given for publishing, under the date 1929, of a good deal of obsolete material, in this chapter (e.g., Art. 11, *Die Grenzen der heutigen Form der Quantentheorie*) and others.

The older electromagnetic-optical phenomena are handled mainly by Buchwald and Ladenburg. Kohn has an exhaustive treatise on photometry.

J. E. MACK

PROCEEDINGS
OF THE
AMERICAN PHYSICAL SOCIETY

• MINUTES OF THE CHICAGO MEETING, NOVEMBER 29 AND 30, 1929

The 159th regular meeting of the American Physical Society was held in Chicago, Illinois at the Ryerson Physical Laboratory of the University of Chicago on Friday and Saturday, November 29 and 30, 1929. The presiding officers were Professor Henry G. Gale, President of the Society, and Dr. W. F. G. Swann, Vice-President.

On Friday evening the Physical Society had a dinner at the Quadrangle Club. There were about one hundred members present. The after dinner speakers were Dr. W. F. G. Swann, Dr. Dayton C. Miller and Professor A. J. Dempster.

At the regular meeting of the Council held on Friday, November 29th, 1929, one was elected to fellowship, one was transferred from membership to fellowship, and one hundred and fifty-two were elected to membership. *Elected to Fellowship:* John B. Whitehead. *Transferred from Membership to Fellowship:* William V. Houston. *Elected to Membership:* T. E. Allibone, Emerson D. Bailey, William Baldwin Jr., E. G. Bangratz, LeRoy L. Barnes, Milton Bergstein, Arthur Bernhart, Donald K. Berkey, Luther M. Bingaman, Francis Birch, Heaton P. Blakeslee, Charles D. Bock, Gilbert F. Boeker, Isabel Boggs, Thomas H. Briggs Jr., Leslie E. Brooking, William F. Brown Jr., O. H. Caldwell, C. Wesley Carnahan, A. B. Carr, Randle V. Cartwright, Margaret L. Clark, Philip Constantinides, Trevor R. Cuykendall, Beryl H. Dickinson, James F. Duncan, J. R. Dunning, M. A. Easley, Sister Mary Edwina, Alexander Efron, Charles D. Ellis, John H. Findlay, Arthur W. Fleming, Hazel M. Fletcher, Arthur E. Focke, J. Franck, Austin R. Frey, Harold Q. Fuller, James W. Givens Jr., A. T. Goble, Martin Grabau, Newton M. Gray, John P. Hagen, August Hagenbach, Sigmund Hammer, O. Philip Hart, Charles D. Hartman, Alexander Harvey, Clifford E. Harvey, Edgar R. Hauser, Thomas Hazen, C. M. Hebbert, Jesse C. Hendricks, Willard H. Hickok, A. F. Horlacher, D. S. Hughes, Lewis H. Humason, Malcolm C. Hylan, H. F. Kaiser, Roy J. Kennedy, W. Jay Kennedy, James R. Kershaw, George E. Kimball, Harold L. Knowles, Matsui Kumiyasu, A. M. Kuethe, Olive M. Lammert, Charles C. Lauritsen, Glenn Q. Lefler, Lewis Larrick, Urner Liddel, Tate Lindsey, Erwin F. Lowry, Janet M. MacInnes, Homer E. Malmstrom, Louis Marick, D. E. Marshall, Tanaka Masamichi, F. A. Maxfield, Ronald L. McFarlan, R. T. McGoldrick, Edwin M. McMillan, Harold Mestre, Earl R. Miller, John S. Millis, Carol G. Montgomery,

Howard R. Moore, Neal D. Newby, J. L. Nickerson, Foster C. Nix, Will V. Norris, Helen B. Notestein, Leonard M. Onsgard, Herbert N. Otis, F. L. Partlo, John V. Pennington, William M. Pierce, Milton S. Plesset, Richard G. Poindexter, Wilson M. Powell Jr., Simeon A. Ratner, John J. Rheins, Charles E. Rich, Donald E. Richardson, H. P. Robertson, Walter W. Roehr, Harry Rolnick, Donald C. Rose, Jenny Rosenthal, Philip W. Rounds, Edward W. Samson, A. Sandow, S. P. Sashoff, Edwin G. Schneider, Harold F. Schwede, Raymond W. Sears, Shirleigh Silverman, William W. Sleator, F. Raymond Smith, John F. Smith, Letha A. Smith, David L. Soltau, Wayne T. Sproull, John R. Stehn, Louis Strait, Kuno Takuji, Tutomu Taraka, John B. Taylor, James S. Thompson, John A. Tiedeman, John S. Tobin, John W. Todd, A. H. Toepfer, Charles B. Vance, Robert J. Van de Graaff, Frank L. Verweibe, Alice M. Vieweg, Donald S. Villars, Worth Wade, Henry Walther, William H. Watson, Wayne Webb, Max Wehrli, Thomas W. B. Welsh, W. W. Wetzell, Mary A. Wheeler, John L. Wilson, E. O. Wollan, Ralph W. G. Wyckoff, Imaoka Yoshio, Suga Yosuke, and Rolland M. Zabel.

The regular scientific session consisted of forty-two papers, five of which—Nos. 1, 16, 17, 21, 38—were read by title. The abstracts of these papers are given on the following pages. An AUTHOR INDEX will be found at the end.

W. L. SEVERINGHAUS, *Secretary*

ABSTRACTS

1. Thermal expansion of "Carboloy." PETER HIDNERT, *Bureau of Standards*. Measurements have been made on the linear thermal expansion of two samples of "Carboloy" (a new tool material) purchased several months ago from Carboloy Company, Inc., 350 Madison Ave., New York City. An interferometer was used in the determinations at various temperatures between 20° and 400°C. The following results were obtained.

Sample	Heating	Average Coefficients of Expansion per Degree Centigrade				
		20 to 60°C $\times 10^{-6}$	20 to 100°C $\times 10^{-6}$	20 to 200°C $\times 10^{-6}$	20 to 300°C $\times 10^{-6}$	20 to 400°C $\times 10^{-6}$
1374 I	First	5.2	5.3	5.5	5.6	5.9
	Second	5.1	5.2	5.6	5.7	6.0
1375 I	First	5.0	5.2	5.5	5.8	6.0
	Second	4.9	5.2	5.5	5.8	6.0

The coefficients of expansion of "Carboloy" are larger than the corresponding coefficients of tungsten. For the range from 20° to 400°C, the average coefficient of expansion of the two samples of "Carboloy" is approximately 30 percent greater than the coefficient of expansion of tungsten.

2. Young's modulus determined with small stresses. DAROL K. FROMAN, *University of Chicago*. (Introduced by A. J. Dempster.)—An interferometer method, similar to that used by E. G. Grüneisen (*Ann. d. Physik* **22**, 801, (1907)), was used to determine the extensions of metallic rods under small stresses. The applied stresses ranged in value from less than 1 kg/cm² to the smallest usually used in commercial testing, about 300 kg/cm². For the substances examined, Young's Modulus was found to increase very rapidly as the stress increased from zero, to reach a maximum at a comparatively small stress, and then to decrease almost exponentially to the ordinary value. The maximum elasticity was found to be from 10 to 30

percent higher than that at large stresses. The annealing of the rods is probably connected with this divergence from Hooke's Law with small stresses, as slight differences were found on reannealing some of the rods.

3. The construction of a master clock with light controlled contacts. J. V. HOFFACKER, *Purdue University*. (Introduced by K. Lark-Horovitz.)—Mercury contacts for controlling circuits periodically by means of pendulums, because of their unreliability and their effect on the period of the pendulum, have been replaced by photoelectric cells influenced by beams of light interrupted periodically by the swinging pendulums. But since selenium cells are equally sensitive to light when operating with direct or alternating current they can be used with a specially constructed relay employing alternating current from lighting mains as the only source necessary. Low resistance selenium cells transformer coupled and high resistance cells as grid leaks in triodes have been used successfully. The relayed current rectified by a dry rectifier is used to keep the pendulum itself going so that no clockwork is necessary to operate repeater clocks.

4. The Nernst heat theorem. HERBERT J. BRENNEN, *Northwestern University*. The Gibbs-Helmholtz equation requires that the limit of $(\partial U/\partial T)=0$, as T approaches zero. Nernst makes the further assumption that the limit of $(\partial A/\partial T)=0$, as T approaches zero. On putting: $U=U_0-bT^2-2cT^3$ -etc., integrating the Gibbs-Helmholtz equation and using Nernst's assumption, one finds: $A=U_0+bT^2+cT^3$ +etc. Whence, $Q=A-U=2bT^2+3cT^3$ +etc.; where A , Q , U and T have their usual significance. Hence, for small values of T , as a first approximation: $(\partial \log Q/\partial \log T)$ is equal to two, which is double that demanded by the Carnot heat theorem. In order to account for this discrepancy, it is suggested that: (1) since U is a function of the volume as well as the temperature, both U and T be regarded as independent variables and A , a dependent variable; (2) the Gibbs-Helmholtz equation be generalised to: $A-U=T(\partial A/\partial T)+KU(\partial A/\partial U)$ where K is a constant. This equation becomes identical with that of Gibbs and Helmholtz when $U=0$ or when A is independent of U .

5. Porous plug measurements with air. J. R. ROEBUCK, *University of Wisconsin*.—In an earlier article (Proc. Amer. Acad. 60, 537, (1925)) I described apparatus and methods used for measuring the Joule-Thomson coefficient over 25 to 280°C and 1 to 215 atm. The present work extends the data down to -150°C. The measurements give isenthalpic curves in a pressure-temperature field. The derivative $(dT/dp)_h=\mu$ =Joule-Thomson coefficient has been plotted as a function of p and T over the whole field. The original curves were used to spread C_p at 1 atm. over the 215 atm. range. With the aid of data on (pv) for air taken from the literature, the free-expansion (Joule) coefficient $(dT/dp)_u=\eta$ has been calculated over -100° to +200°C and 1 to 100 atm. These again give the elastic coefficient $1/v(dv/dp)_t=\gamma$ and $(du/dv)_t=\lambda$ over this field. λ can be used to calculate the correction to the constant volume air temperature scale, which is being done. This completes the work with air, and the apparatus is being rebuilt into a closed system to measure pure gases of which the first is to be helium.

6. The function of the base metal in oxide coated filaments. E. F. LOWRY, *Westinghouse Elec. & Mfg. Co., East Pittsburgh*.—Measurements on a number of UX-281 Radiotrons with oxide coated platinum-iridium filaments and others having oxide coated "Konel" filaments show that the base or core metal plays an important part in the behavior of such filaments. Konel, an alloy of nickel, cobalt, iron and titanium, has a much higher thermal emissivity than platinum and therefore, when operated at 4 watts per cm², reaches a temperature about 150°C lower than that reached by oxide coated platinum with the same energy input. Nevertheless, oxide coated Konel filaments give slightly higher emissions than oxide coated platinum filaments under like conditions of input energy. This anomalous behavior requires a modification of the present theory of oxide emission. This requirement is met by assuming that the source of the electron emission is a layer of metallic barium in contact with the base metal and that the electrons diffuse through the pores in the oxide coating which is a rather good non-conductor. This hypothesis serves as a satisfactory basis of explanation for the varied and somewhat confusing phenomena of oxide emission.

7. Photoelectric behavior of solid and liquid mercury. DUANE ROLLER, *University of Oklahoma*.—With monochromatic light, the photoelectric threshold for solid mercury, freshly distilled in vacuum, was found at $2750 \pm 25\text{Å}$ for all temperatures between -190°C and the melting point. The threshold for liquid mercury at room temperature was at $2735 \pm 10\text{Å}$, confirming the value established earlier by Kazda and by Hales. The emission for monochromatic light was independent of the temperature between -190° and -40°C . There was no indication of a change in the crystal structure of mercury in this region of temperatures. The emission for the solid phase was always somewhat higher than that for the liquid at room temperature, possibly due in part to a change in the optical absorptivity of the mercury surface with change in phase. A study of the optical absorptivity of solid mercury is in progress. Between -39° and 0°C the emission was about 75 percent of that at room temperature but showed hysteresis with successive warming and cooling of the mercury. Thus a further study of liquid mercury between melting and room temperatures is needed. Most of this work was done at the California Institute of Technology.

8. Spatial distribution of photoelectrons. S. SZCZENIOWSKI, (*International Education Board Fellow*) *University of Chicago*.—The perturbation of a hydrogen-like atom by a plane polarized electromagnetic wave is considered on the basis of Dirac's equations, and perturbed wave-functions are obtained. These functions lead by a method similar to that used by Sommerfeld in his "Wellenmechanisches Ergänzungsband," to a formula for the spatial distribution of the photoelectrons, but differing from his in the first approximation, by a factor equal to $5/9$. This factor follows from a consideration of the normalization factors for the spherical harmonics, which were not introduced by Sommerfeld. A second approximation has also been obtained showing the influence of electron spin. This formula differs from that obtained by Carrelli (Zeits. f. Physik 56, 694, (1929)) in that the spin and some other terms not considered by Carrelli appear.

9. Electron velocities in an electrodeless discharge. CHARLES J. BRASEFIELD, *University of Michigan*.—A high frequency discharge in hydrogen was obtained by applying high frequency voltages to the movable external electrodes of a cylindrical discharge tube. By observing the change in the ratio of the densities of certain singlet and triplet lines of the secondary spectrum (see Phys. Rev. 34, 437 (1929)), the mean electronic velocity in the discharge was studied as a function of (1) the frequency of oscillation, (2) voltage between electrodes, (3) distance between electrodes and (4) gas pressure. Observations were made at frequencies of oscillation corresponding to the wave-lengths 15, 25, 50, 100 and 200 meters. For example, at 0.03 mm pressure with 1400 volts applied to the electrodes, the electronic velocity increases from 23.7 volts at 25 meters to 25.8 volts at 200 meters. At 25 meters and 0.03 mm pressure, the electron velocity increases from 20.8 volts to 23.7 volts as the voltage between electrodes is increased from 500 volts to 1400 volts. Finally, at 25 meters with 1000 volts between electrodes, the electron velocity increases from 22.7 volts to 24.7 volts as the pressure is reduced from 0.06 mm to 0.01 mm. It appears that conditions in the electrodeless discharge should be quite similar to those in the positive column of an ordinary Geissler tube discharge. This probably explains why such small changes in electronic velocity were observed.

10. Motion of electrons in carbon monoxide. H. B. WAHLIN, *University of Wisconsin*.—In a paper which appeared in an earlier issue of the Physical Review [21, 517 (1923)] it was shown that the mobility of electrons in CO obey the equation $U = A/[B + V]^{1/2}$ with a high degree of accuracy. Shortly after the appearance of this paper K. T. Compton showed that the equation for the mobility should be of the form $U = A/[1 + (1 + BV^2)^{1/2}]^{1/2}$. Application of this equation to the data presented earlier shows that for low fields the Compton equation holds within the limits of experimental error. At values of X/P above 0.4 volts/cm/mm pressure a systematic deviation from this equation appears due probably to a decrease in the electronic free path with increasing electron velocity. The electron free path in thermal equilibrium with the gas and at a pressure of 1 mm is found to be 0.069 cm.

11. Slow caesium ions in hydrogen and helium. J. S. THOMPSON, *University of Chicago*, (Introduced by A. J. Dempster).—The motion of positive caesium ions in hydrogen and helium has been examined for ion velocities ranging from 3 to 600 volts. Three different experimental arrangements were used in which the ions traversed a known gas path and in which any weakening of the bundle could be observed. No absorption of 10 to 600 volt ions was observed for gas pressures up to 0.030 mm of Hg. At the highest pressure the ions make 20 collisions without deflections from their original directions. Below 10 volts and for pressures above 0.010 mm a definite weakening of the bundle sets in and increases rapidly with the pressure. In all cases studied the ions were retarded, and the velocity distribution produced has been measured. The final velocities show an approximate probability distribution about a mean retardation. This distribution becomes more nearly that of the error curve for smaller velocities and higher pressures. The large absorption of the caesium ions observed by Ramsauer is accounted for on the basis of this retardation. Lithium ions in helium show considerable scattering which decreases as the velocity is increased and rises rapidly as the velocity is reduced below 50 volts.

12. Ionization efficiency of electrons in potassium vapor. J. KUNZ AND A. HUMMEL, *University of Illinois*.—Using a direct method in which a beam of electrons is projected into a field-free chamber, the number (N) of positive ions formed per electron per centimeter path per unit pressure has been measured and plotted against the energy of the primary electron. Scattering of the primary beam was prevented by means of a magnetic field of 350 to 400 gauss parallel to the beam. A small transverse electric field was employed to drive the positive ions to the collecting plate. Two other plates served to make this field uniform in the region from which the ions were collected. For potassium vapor N was found to have three maxima occurring at 40, 81, and 122 volts accelerating potential. The second and third maxima are respectively 18 percent and 11 percent greater than the first. N is approximately 20 times the value of N for argon. The curve for argon has a maximum value for N of 0.108 appearing at 88 volts which compares with the maximum 0.113, at approximately 125 volts, observed by Compton and Van Voorhis.

13. A study of the ions produced in mercury vapor by electron impact. WALKER BLEAKNEY, *University of Minnesota*.—In a recent paper (Phys. Rev. 34, 157 (1929)) a method was proposed for analyzing the primary results of ionization by electron impact. The method has been applied to a quantitative study of the five mercury ions Hg^+ , Hg^{2+} , Hg^{3+} , Hg^{4+} and Hg^{5+} . The results show that the fraction of the current carried by the Hg^+ ion falls rapidly from 100 percent at electron velocities between 10.4 and 30 volts to about 70 percent at 100 volts, and then approaches a nearly constant value of about 60 percent for increasing electron speeds. At 300 volts the fractions of the total positive ion current carried by the five ions, in order, are 59, 26, 11, 3.5, and 0.5 percent respectively. The results have been reduced to number of ions per electron per cm path per mm pressure at 0°C as a function of the electron velocity. These data show a distinct maximum of magnitude about 21 for the Hg^+ ion in the neighborhood of 50 volts while the value at 300 volts has dropped to half as much. Maxima also appear for Hg^{2+} and Hg^{3+} at 115 and 210 volts respectively.

14. Absorption of lithium ions in mercury vapor. I. W. COX, *University of Chicago*, (Introduced by A. J. Dempster).—The absorption of 25 to 300 volt lithium ions in passing through mercury vapor at various pressures up to 48×10^{-4} mm was observed by two different methods. In the first method the ions described a semicircular path in a magnetic field and the decrease as the pressure was increased was observed. In the second method the ions, after this magnetic analysis, described a straight path to a collecting chamber and the decrease in the number entering the circular aperture of the collecting chamber was observed as the pressure was increased. A consistent difference was found in the absorption coefficients given by the two methods. It was also altered by a change in the aperture of the collecting chamber in method 2. This indicates that the collisions with the mercury atoms are not elastic, but that a large fraction of the deflections are through small angles. Ionic diameters deduced from the absorption depend on the apertures of the apparatus used. The ions collected are not slowed

up appreciably, and there is a dependence of the absorption observed with any particular aperture on the velocity of the ions.

15. The reflection of lithium ions from metal surfaces. R. B. SAWYER, *University of Chicago*. (Introduced by A. J. Dempster.)—Experiments have been performed on the reflection of lithium ions from reflectors of platinum foil and of nickel crystals deposited on tungsten foil (Rupp, *Ann. d. Physik* [5], 1, 801 (1929)). Movable ground joints in the tube were entirely eliminated. Readings were taken with both cold and hot reflectors. Spodumene was used as a source of ions and reflection was studied in the meridian plane only. Superposed on a diffuse scattering of ions were two reflected beams. One was reflected nearly specularly, as found by Read (*Phys. Rev.* 31, 155 (1928)) and Gurney (*Phys. Rev.* 32, 467 (1928)), the angle of maximum reflection, however, being independent of accelerating potential. The other beam appeared only at voltages above 200 or 250 and was composed of ions most of which had retained 80 percent or more of their original energy. This beam was found between the incident beam and the normal to the surface, at angles independent of the accelerating potential up to 700 volts. This independence of angle on voltage forbids diffraction interpretations. A tentative explanation consists in supposing specular reflection from the (110) planes of the nickel crystals, but the agreement is not entirely satisfactory.

16. Secondary emission of nickel under positive ion bombardment in the positive column in neon. W. UYTERHOEVEN AND M. C. HARRINGTON, *Princeton University*.—An attempt is made to measure the secondary emission under positive ion bombardment of metal collectors in the positive column under conditions as near as possible to those in the cathode fall. A combination of a fixed collector and a movable one opposite the first, was used. The movable one was given a negative potential and the ion current to it compensated; then the potential of the fixed electrode was varied and the corresponding change in current to each measured. The results obtained so far show that for an accelerating potential of about -150v , the secondary emission can reach 50 p.c. of the total current collected on a negatively charged electrode. (*Proc. Nat. Ac. Sc.* 15, 32 (1929)). The electron mean free path seems to depend markedly on the degree of ionization of the gas, the measured values being less than the gas kinetic values (e.g. 50 p.c.). A large fraction of the electron emission from the metal is apparently due to the impact of metastable atoms on the collector. (Oliphant, *Proc. Roy. Soc. A* 124, 228 (1929)), but for higher accelerating potentials of the positive ions their effect becomes more and more important (Penning, *Physica*, 8, 13 (1928)).

17. Zeeman effect in $\lambda 5211$ MgH band. G. M. ALMY, F. H. CRAWFORD AND E. L. HILL, (*National Research Fellow*), *Harvard University*.—The Zeeman effect for molecules lying between Hund's cases (a) and (b) has been treated theoretically by the quantum mechanics, and the results applied to the MgH band at $\lambda 5211$. For states near case (a) the theory predicts the usual splitting into $(2J+1)$ magnetic substates. When the magnetic separations are comparable with the doublet separations (very high fields or small doublet intervals) a Paschen-Back effect sets in corresponding to uncoupling of the electronic spin and the rest of the molecule with a degeneration of the term system into that of a symmetrical top superposed on that due to practically free spin. In a $^3\Sigma$ state (neglecting rho-type doubling) this degeneration is sensibly complete at all fields. The theory is verified quantitatively in the $\lambda 5211$ MgH band. In the earlier lines the size of the fine structure patterns agrees numerically with calculations. In the higher lines the Paschen-Back effect causes a filling in of the normal doublet interval with an unresolved band in addition to the appearance of outer wings which move out and become fainter with field. Pattern widths, separation of components, and line displacements, where observable, have been measured from plates taken at fields between 5000 and 28000 gauss. No detailed intensity calculations have been made.

18. A magneto-optic method of chemical analysis. FRED ALLISON AND EDGAR J. MURPHY, *Alabama Polytechnic Institute*.—This is a refinement of a method previously reported by one of us (Allison, *Phys. Rev.* 30, 66 (1927) and 31, 313(A) (1928)). Each chemical compound produces a minimum of light at a point characteristic of the compound. The surprising result

has been found that this characteristic minimum does not disappear until the concentration has been reduced to less than one part in 10^{10} . The method thus affords a very sensitive and rapid means of chemical analysis. A large number of such analyses has been made. The presence of compounds, instead of elements, is detected. Each inorganic compound is characterized by either a single minimum or two or more close minima. The number of these minima, with few exceptions, is the same as the number of known isotopes of the metallic element of the compound. The investigations have been confined to a number of organic liquids and an extensive series of nitrates, chlorides, sulphates and hydroxides in solution. The positions of the minima are some inverse function of the chemical equivalent of the metallic element of the inorganic compounds. The effect is no doubt a time effect, but a complete interpretation must await further investigations, which are in progress.

19. The absorption spectrum characteristic of vitamin A. JAY W. WOODROW AND H. L. CUNNINGHAM, *Iowa State College*.—The absorption spectra of substances containing vitamin A were obtained in the region from 290 to 350 $m\mu$ by means of a sensitive photoelectric spectrophotometer. Fresh cod-liver oil and spinach juice gave prominent absorption bands with maxima at 310 and 326 $m\mu$ with minor bands at 320, 330 and 337 $m\mu$. When the oils were extracted with ether, the bands were shifted toward the shorter wave-lengths by 3 $m\mu$ but their relative intensities remained the same. These bands were obtained with cod-liver oil, spinach juice, egg yolk and butter, all of which are known to be rich in vitamin A. Peanut oil which is rich in vitamin D but contains no vitamin A, gave the characteristic vitamin D bands at 270, 280 and 290 $m\mu$ but gave no indication of the bands in the neighborhood of 326 $m\mu$. Bubbling air through the cod-liver oil at a temperature of 90°C for an hour or exposing it to the ultra-violet light from a quartz mercury arc for 20 min., either of which will destroy most of the vitamin A, caused the disappearance of the absorption bands at 310, 320, 326 and 330 $m\mu$.

20. A new absorption band of atmospheric oxygen and the vibrational frequency of the normal molecule. HAROLD D. BABCOCK, *Mount Wilson Observatory*.—Four possible absorption bands in the "atmospheric" system of oxygen have been sought with air paths of 40 to 70 kilometers, (0, 1), (2, 1), (2, 2), (1, 1). The last has been discovered; the others are not yet established. The intensity of (1, 1) is roughly 1/2500 that of (0, 0). Over 30 lines are identified and 26 are accurately measured. Wave-number differences are taken from these to corresponding lines in (0, 0), (1, 0), (2, 0) and (3, 0). Eliminating the rotational effect and using the known spacing of the vibrational levels in excited O_2 , these combinations give $1556.31 \pm 0.05 \text{ cm}^{-1}$ as the most probable value of the vibrational frequency of the normal molecule having 1 unit of vibrational energy. Results from *P* branches are more concordant than from *R* branches, which show a slight linear dependence on the upper vibrational state. The new value is compared with the Raman displacement, and its usefulness is discussed in other relations such as, calculation of isotopic displacement and of heat of dissociation. The data also help to establish a test for the consistency of solar standards of wave-length.

21. On the active nitrogen glow. RICHARD RUEDY, *Toronto*.—With strong afterglows in N_2 the 3 prominent bands can be seen for several seconds; such a persistence is longer than the time necessary for the recombination of N atoms (the formation of H_2 being taken as a basis of comparison) and considerably longer than the life of metastable systems. However, the potential energy curve for the initial state of the afterglow bands shows that, although emission of light takes place when during their oscillations the atoms have reached their greatest elongation, dissociation is likely to occur at the inner turning point, particularly for the smaller heats of dissociation which have found favor since it was shown that no Xe lines could be obtained in the afterglow, (*Trans. R. Soc. Can.* **22**, 303 (1928)). This dissociation process provides for the afterglow the necessary number of atoms, and eventually for metastable atoms. The real excitation potential of level *A* seems to be below 7 volts. In a 1 to 2 l bulb an initial intensity of the glow, corresponding to about one candle, can be obtained at a few mm Hg, and a total intensity of a few candles. This corresponds to 10^{17} emission processes initially, or to 10^{14} radiating molecules per cm^3 (10^{-3} mm Hg), an insufficient amount for ordinary absorption measurements.

22. The excitation of certain nitrogen bands by positive ion impact. H. D. SMYTH AND E. G. F. ARNOTT, *Princeton University*.—In the sources of light usually used for the study of band spectra excitation is chiefly by electron impact. It is now generally agreed that an electron impact does not alter the rotational nor vibrational momentum of a molecule. However, it might be expected that in excitation by positive ion impact both the vibrational and rotational momentum might be altered. We have, therefore, undertaken the study of the intensities of band spectra excited in nitrogen by the impact of mercury ions. Mercury canal rays pass through the cathode of a discharge tube into an atmosphere of nitrogen. The feeble light excited is found to consist almost exclusively of the negative nitrogen bands. In the two bands ($\lambda 4278$ and $\lambda 3914$) which have been photographed with a small grating, the lines corresponding to the lowest rotational states are definitely weaker than in comparison photographs taken with an electrodeless discharge. In fact the first two lines of the *R*-branch and the first line (perhaps the first two) of the *P*-branch are entirely missing. Theoretically one might expect one more line of the *P*-branch than of the *R*-branch to be missing. The investigation is still in a very preliminary stage.

23. The spectrum of singly ionized indium. R. J. LANG, *University of Alberta* AND R. A. SAWYER, *University of Michigan*.—The indium spectrum has been excited in a hollow cathode discharge in helium, using the same technic as in the authors' previous work with gallium. The spectrum has been photographed throughout the entire photographic region. The first spark spectrum is a two electron spectrum with singlet and triplet terms of which the chief combinations have been identified. Enough higher terms have been found to permit the calculation of approximate term values. The deepest term, $(5s^2)^1S$, is placed at 152350 cm^{-1} corresponding to an ionization potential of 18.81 volts.

24. Intensity measurements in neon spectrum. H. N. SWENSON, *University of Illinois*.—The Ornstein method of photographic photography has been applied to a study of the neon discharge. Special emphasis was placed upon elimination of errors in the optical system and in the development of plates. Density screens were prepared by sputtering platinum films of various densities on quartz plates. This screen was placed in an optical system similar to that of Ornstein and vibrated electrically to eliminate possible errors due to non-uniformity. Development was carried out at constant temperature and with forced circulation of developer around the plate. Intensity ratios were obtained for 19 lines in the region from 5800\AA to 6700\AA . The discharge was excited by a 10,000 volt transformer, the pressure being 2 mm. The intensity ratios for multiplets which are transitions from the same upper level, are not in agreement with the values of Dorgelo or those predicted by the Ornstein-Burger intensity rules, but show marked agreement with values recently published by Ende using electron impact excitation.

25. Intensity relations in some of the stronger multiplets of chromium I and chromium II. CEDRIC E. HESTHAL, *Ohio State University*.—The relative intensities of thirteen multiplets in the spectrum of chromium I and of five multiplets in the spectrum of chromium II have been determined by photographic photometry. The method used was that described by G. R. Harrison in the *Journal of the Optical Society* (17, 389 (1928); 18, 287 (1929)). Numerous violations of the intensity formulas which have been derived by H. N. Russell, R. de L. Kronig and others are found. In some multiplets all the lines appear anomalous while in other multiplets only a fraction of the lines are abnormal. In general, the violations are more numerous than those observed by Harrison in titanium and fewer than those observed in iron and nickel by Ornstein, showing that perturbations increase with atomic number among the elements of the iron group. The intensities of multiplets forming two triads have also been determined and the equivalent excitation temperatures for these calculated. For one of these triads the method fails showing that this triad does not obey the formulas of R. de L. Kronig while for the other, temperatures between 2800°K and 4800°K were observed for different exposures. Data have been obtained to show that the equivalent excitation temperature is not the same for multiplets having final states in different regions of the atom.

26. Relations between hyperfine structure separations. S. GOUDSMIT AND R. F. BACHER, *University of Michigan*.—The quantum mechanics conception of a spinning electron in an s -state makes it probable that its interaction energy with a nuclear moment i is simply proportional to the average of $i \cos(i \cdot s)$. In some cases where the hyperfine structure is mainly caused by an s -electron one can evaluate this cosine. This gives relations between the hyperfine structures of different levels which agree well with observations on Tl II (McLennan).

The large hyperfine structures in Tl II are due to the presence of the deeply penetrating single $6s$ -electron, those of Tl I are much smaller ($6s^2$). In Tl III only the normal state $6s$ will show a very large hyperfine structure which must be about 8 cm^{-1} . In more complicated cases one can only tell that the interaction energy will be proportional to $ij \cos(i \cdot j)$ which causes the interval rule to be valid for hyperfine structure.

27. Relativity transformation of an oscillation into a traveling wave, and de Broglie's postulate in terms of velocity angle. VLADIMIR KARAPETOFF, *Cornell University*.—The author has previously described a method of representation of space-time relationships in restricted relativity, by means of oblique coordinates (J.O.S.A. and R.S.I. 13, 155 (1926)). The theory has been applied to the following problem: Two observers, S and S' , are moving at a relative velocity q . The S' observer has in his system a set of pointers oscillating in synchronism and in phase with one another. It is required to describe the motion as seen by the observer S . By drawing two sine waves in the Lorentzian plane, it is shown graphically that for the S observer the pointers do not swing in synchronism, but form a traveling wave whose velocity of propagation, u , is connected with q by the familiar relationship $uq = c^2$, where c is the velocity of light.

Introducing the so-called velocity angle, α , determined by the relationship $\sin \alpha = q/c$, various other properties of the traveling wave, as seen by S , have been deduced, such as the apparent frequency at a point in space, the apparent amplitude and its velocity of propagation, the Fitzgerald contraction of the oscillating system, the slowing down of the frequency of oscillation, the group velocity of "super-light" waves, and de Broglie's quantum principle. The article appeared in the *Journal of the Optical Society of America* for November, 1929.

28. The significance of the Michelson-Morley-Miller experiments in relation to the restricted theory of relativity. W. F. G. SWANN, *Bartol Research Foundation*.—While aether drift experiments originally suggested the line of thought which leads to the formulation of the restricted theory of relativity, it would seem that the fundamental significance of that theory does not depend primarily upon these experiments. The most logical origin of the transformation of the restricted theory is to be found as a special case of the general theory, and the purpose of the present paper is to show how, with this in view, the fundamental working content of the restricted theory, the invariance of laws under the Lorentzian transformation, is something which has no fundamental relation to the question of whether the aether drift experiments do or do not give a positive result.

29. Electron distribution in magnesium oxide. ERNEST O. WOLLAN, *University of Chicago*. (Introduced by A. H. Compton.)—The intensity of x-rays reflected from powdered crystals of magnesium oxide were measured for all lines out to $\theta = 45^\circ$. The values of the structure factor, F , were calculated and plotted against $\sin \theta$. Using the values of F from this curve as coefficients in the Fourier Series given by Compton ("X-Rays and Electrons") the radial electron distribution for the atoms of magnesium and oxygen was determined. The electron distribution curves for these atoms are very similar to the curves by Havighurst (Phys. Rev. 29, 1 (1927)) for NaCl and NaF. However, the data indicate that the number of electrons associated with magnesium and oxygen is more nearly that of the neutral atoms than that of the ions, whereas Havighurst concludes that the lattice points are occupied by ions. A recalculation of some of Havighurst's data brings results which are in closer agreement with those of the author.

30. The efficiency of x-ray fluorescence. A. H. COMPTON, *University of Chicago*.—A review of the published data describing the intensity of fluorescent x-rays shows that the various observers agree that the number of quanta of fluorescent x-rays emitted by a radiator is con-

siderably less than the number of quanta which it absorbs from the primary beam. The values of the efficiency of fluorescence that appear in the literature are for the most part, however, found not to be quantitatively reliable. New experiments give values of the "fluorescence yield," or ratio of the number of fluorescent K quanta to the number of photoelectrons ejected from the K shell, of 0.68 for a molybdenum radiator, 0.56 for bromine, 0.54 for selenium, and 0.37 for nickel. The values seem to be independent of the wave-length of the exciting rays. These measurements agree within experimental error with Auger's values of the fluorescence yield, based on his count of the frequency of occurrence of the compound photoelectric effect, and thus indicate that it is this effect which makes the fluorescence yield less than unity. Knowledge of the fluorescence yield gives an expression for calculating the relative intensity of two x-ray beams of different wave-length, in terms of the ionization currents obtained, and other factors.

31. Efficiency of production of continuous spectrum x-rays. WARREN W. NICHOLAS, *Bureau of Standards*.—There is a large discrepancy between the efficiency estimated by Kulenkampff (*Handbuch der Physik* vol. 23), who found $k=8\pm2\times10^{-10}$ in the formula, $\text{efficiency}=kZV$, where Z is the atomic number of the anticathode material and V is the potential across the tube in volts and the more recent experimental determination by Rump, who found k to be about 15×10^{-10} . This discrepancy makes desirable a closer consideration of some of the secondary processes (reflection of cathode rays from anticathode, etc.) occurring in both gas filled and hot cathode x-ray tubes, as well as a further examination of corrections for absorption (including absorption in the anticathode) and for asymmetric spatial distribution of x-ray energy. A correction of Rump's data on this basis leads to a value of k about 10×10^{-10} . Some estimates of actual x-ray energy, both continuous and characteristic, obtained outside a tube are obtained incidentally.

32. Absolute measurement of certain x-ray wave lengths. J. M. CORK, *University of Michigan*.—An x-ray vacuum spectrograph employing a plane glass grating 30,000 lines per inch and having a distance between grating and photographic plate of one meter has been used to obtain the absolute wave-length value of the L -series emission lines for elements molybdenum (42) to antimony (51). In addition many other lines are present due to extraneous sources in the x-ray tube. These wave lengths have been previously accurately measured by many observers employing the crystal method. A comparison of the two sets of values is made bearing on the question regarding the Avogadro number and electronic charge. The results obtained for the wave-lengths of the two molybdenum lines $L\alpha$ and $L\beta_1$, are respectively 5.3943 and 5.1658 A.U., indicating for e the value 4.821×10^{-10} e.s.u.

33. The index of refraction and absorption coefficient of gold for the $K\alpha$ line of carbon. ELMER DERSHEM, *University of Chicago*.—An experimental curve showing the intensity of reflected radiation plotted against glancing angle of incidence was obtained for a sputtered gold surface and the $K\alpha$ line of carbon ($\lambda=44.6\text{\AA}$) by the use of methods and apparatus previously described (*Phys. Rev.* 34, 1015 (1929)). The absorption coefficient (μ) of gold leaf for this wave-length was measured and a value of the extinction coefficient (κ) determined from the relation $\kappa=\mu\lambda/4\pi$. The experimental value being $\kappa=0.0086$. A computation by the use of the Drude-Lorentz dispersion formula gives $1-n=\delta=0.009$ for the case of gold and this wave-length. These values of κ and δ were substituted in a modified form of the Fresnel reflection equations and a theoretical curve relating reflected intensity and glancing angle was thus obtained. To secure perfect agreement with the experimental curve either κ or δ or both must have smaller values. Hence curves are also computed with various pairs of arbitrarily assigned values of κ and δ which show the effect of changes in the values of these constants upon the theoretical curve.

34. Diffraction of x-rays in liquids and the effect of temperature. E. W. SKINNER, *University of Iowa*.—Fourteen liquids have been examined for x-ray scattering both at room temperature and close to their boiling points. Results for principal maxima are as follows: 1. Change in intensity. a. Heptylic acid, cyclohexane, benzene, octane, lauryl alcohol, and 2-7 dimeth-

ylactane show a decrease in intensity with increase in temperature. b. Mesitylene, di-n-propyl carbinol, tertiary butyl alcohol, 4 hydroxy 1-3 dimethylbenzene, 2 hydroxy 1-3 dimethylbenzene, 2-2-4 trimethylpentane, phenol, and naphthalene show an increase in intensity with increase in temperature. 2. An increase in molecular dimensions at higher temperatures was found, and, in general, the change is in agreement with the expected change in density due to expansion. 3. Change in peak width. The large peak common to all liquids thus far examined in this laboratory, appears to be wider at higher temperatures in all cases which is in agreement with existing theories of temperature effect in crystal scattering. All results are shown to be in agreement with the theory of the cybotactic condition except that an additional effect is needed to account for (1b).

35. Polarization of x-rays from thin aluminium anti-cathodes. BALEBAIL DASAN-NACHARYA, *University of Chicago*. (Introduced by A. H. Compton.)—An electron-beam 5 mm in diameter falls on thin aluminum foils of thickness varying from $6-250 \cdot 10^{-8}$ cm, mounted on a cylindrical frame-work attached to a glass tap and regulated from outside. A graphite plate on an ionization spectrometer served to measure the polarization. The voltages varied from 27-56 KV. For a given voltage, polarization increases slowly at first with diminution of thickness but rises exponentially for thicknesses smaller than $2.5 \cdot 10^{-4}$ cm. For different voltages the form of the curves remains the same, but the value of the polarization slightly diminishes with increase of voltage. The maximum polarization obtained was 47.5 percent. It looks likely that for a thickness of about $5 \cdot 10^{-6}$ cm the polarization would be complete.

36. A relation between the Compton effect and the diffraction by electrons. JAKOB KUNZ, *University of Illinois*.—In the Compton effect a quantum of radiation of momentum $h\nu/c$ is transformed into the momentum of an electron mv and into a weaker quantum of radiation of momentum $h\nu'/c$. If we assume that the reversed process also is possible and that an electron strikes a quantum head on, then we obtain: $mv = h\nu'/c = h/\lambda$, or $\lambda = h/mv$, which is the relation given by wave mechanics for the diffraction of electrons.

37. Paschen-Back effect of hyperfine structure. S. GOUDSMIT AND R. F. BACHER, *University of Michigan*.—By replacing the quantum vectors (s, l, j) and the magnetic moments (sg, lg, jg), of the ordinary multiplet theory by those of the hyperfine structure theory ($i, j, f; ig, jg, fg$), it is possible to adapt the work of Heisenberg, Jordan and Darwin on Zeeman effect and intensities in any field strength, to the study of the Zeeman effect of hyperfine structure. The thallium line ($6p^2P_{1/2} - 7s^2S_{1/2}$) $\lambda 3776$ is an example of incomplete Paschen-Back effect which can be treated quantitatively with the above method. The calculated splitting up of this line in a field of 43350 gauss is in cm^{-1} . $-3.00, -2.52, (-1.43), -(1.20), (+1.28), (+1.36), +2.45, +3.08$. Measurements by Professor E. Back and Dr. J. Wulff at Tuebingen give $-3.02, -2.54, (-1.42), (-1.22), (+1.35 \text{ strong}), +2.43, +3.10$. Without hyperfine structure the Zeeman effect would have been $(\pm 1.36), \pm 2.71$.

38. Rectifier characteristics and detection diagrams. RICHARD RUEDY, *Toronto*.—The average current I_m obtained per cycle when, in addition to the constant voltage E , the potential $E_0 \sin \omega t$ is applied to a rectifier possessing the characteristic curve $I = f(E)$, has been calculated and compared with experiment for different $f(E)$. The curve $I = ce \exp [E/e_c]$ giving at open circuit a voltage independent of E applies to all types of vacuum tubes when the A.C. voltage does not exceed a few tenths of a volt, or 0.5 volts in the case of oxide-coated emitters. The curve $I = I_0/E$ gives $I_m = I_0/(E^2 - E_0^2)^{1/2}$, and applies to certain types of glow and arc discharges in which an a.c. e.m.f. is superimposed upon d.c. Parabolic curves, for which the increase in I is independent of E , represent the actual current I_m better than the theoretical curves $I = CE^{3/2}$.

39. A new equation of state. HERBERT J. BRENNEN, *Northwestern University*.—Dieterici (Ann. d. Physik 66, 826 (1898)) put forward the equation of state: $P(V-b) = RT \exp(-A/RT)$ where P, V and T are the pressure, volume and temperature, respectively, and A, b and R are parameters. However, limit (PV/T) , as V becomes infinite, is equal to R and has the same value for one mole of all substances. Hence, we may replace RT by a new variable E and

Dieterici's equation becomes a two parameter equation. Since, a straight line intersects this equation in three real finite points at temperatures below the critical temperature, mathematical theory demands, in general, three parameters which makes Dieterici's equation, in general, mathematically absurd. Accordingly, I propose the new equation: $P(V-b) = RT \exp [-A(V-b)/RTV^n]$ which, for large values of V becomes identical with the equation (Proc. Nat. Acad. Sci. 15, 11-18, Jan. (1929)) already proposed by me, and where n is the third or missing parameter. This new equation predicts that the Law of Corresponding States is true only for substances having the same values of the critical ratio, RT_c/P_cV_c .

40. On the origin of the line absorption spectra of the rare earths. OTTO LAPORTE, *University of Michigan*.—In the rare earth group of elements the configuration $4f^n$, $4f^{n-1}5d$, $4f^{n-1}6s$ will compete in the formation of the lowest terms. For neutral atoms or ions of low order, terms with $5d$ and $6s$ electrons will be most stable; for higher ionizations, terms due to $4f$ will be lowest, as is easily seen by comparing the slopes of the Moseley curves of the three configurations in question. Consequently, there will be intermediate stages of ionization, where the Moseley lines of the $4f^n$ and $4f^{n-1}5d$ terms cross, and spark spectra, for which the frequency of the allowed transition $4f^n - 4f^{n-1}5d$ lies in the visible or at least at much longer wave-lengths than is usual for ions of (say) third or fourth order. The sharp absorption lines exhibited by rare earths in the liquid or crystal state are believed to be due to this transition. The fact that the absorption lines of gadolinium, recently measured by Freed and Spedding (Phys. Rev. 34, 945, (1929)) lie farther towards the violet than those of any other rare earth may be understood in analogy to the group-theoretical ionization potentials as obtained by Peierls (Zeits. f. Physik 55, 738, (1929)).

41. Further experiments on the disintegrative synthesis of oxygen of atomic weight 17 from nitrogen of atomic weight 14. WILLIAM D. HARKINS, *University of Chicago*, AND ARTHUR E. SCHUB, *Bell Telephone Laboratory*.—By the method of Harkins and Ryan (J. Am. Chem. Soc. 45, 2095 (1923)) approximately 34,000 photographs of alpha ray tracks from thorium C and C' were taken as they appeared in a modified Wilson-Shimizu apparatus. Two disintegrative syntheses were given by 270,000 tracks of 8.6 cm and 145,000 tracks of 4.9 cm range in air. The gas used was nitrogen. It may be assumed that the alpha-particle attaches itself to the nitrogen nucleus, thus forming the nucleus of an atom of fluorine, which in less than a millionth of a second emits a fast hydrogen particle (proton) thus giving an oxygen nucleus of mass 17. By the use of the same general procedure Blackett (Proc. Roy. Soc. A107, 349 (1925)) obtained eight, and Harkins and Shadduck (Proc. Nat. Acad. Sci. 12, 707 (1926)) obtained two such disintegrative syntheses. In this work 38 "collisions" of the alpha-particle were found in which the alpha-particle is deflected by more than 90° , while in the work of Harkins and Shadduck about 30 such collisions were found. If it is assumed that only such approximately direct impacts give a probability of a disintegrative-synthesis, then the possibility that the nitrogen thus transformed has an atomic weight of 15 seems negligible. A special search was made for the much more numerous short range hydrogen particles assumed by some workers to be emitted, but none of these were found. Thus far in this laboratory about 8 disintegrative syntheses per million long range alpha-particles, have been observed. Thus about eight protons per million long range alpha-particles were obtained in nitrogen, while Rutherford and Chadwick observed two with aluminum. However their scintillation method is not exactly comparable.

42. An isotope of nitrogen, atomic weight 15. S. M. NAUDÉ, *University of Chicago*. (Introduced by Elmer Dershem).—(The abstract of this paper appeared as a Letter to the Editor, (Phys. Rev. 34, 1498 (1929)). The following slight corrections should, however, be made in the calculated value of the wave-lengths of the isotope heads: Q_1 heads: 2155.263($N^{14}O^{17}$), 2155.753($N^{16}O^{16}$), 2156.744($N^{14}O^{18}$). P_1 heads: 2156.498($N^{14}O^{17}$), 2156.978($N^{16}O^{16}$), 2157.949($N^{16}O^{18}$). For the (0,0) band the calculated shifts of the P_1 head are for $N^{14}O^{17}$, $N^{14}O^{18}$ and $N^{16}O^{16}$, -2.595 cm^{-1} , -4.952 cm^{-1} and -3.375 cm^{-1} respectively. This corresponds to the wave-lengths 2269.536A, 2269.659A and 2269.577A.

The third from the last paragraph of the letter should read as follows: "The effect on the (0, 0) band is very difficult to observe owing to its smallness. The wave-lengths of the displaced heads found are 2269.60($N^{18}O^{16}$) and 2269.70($N^{14}O^{18}$) which correspond within experimental error with the calculated shift. The displaced head due to the $N^{14}O^{17}$ molecule could not be observed."

AUTHOR INDEX

- Allison, Fred and Edgar J. Murphy—No. 18
 Almy, G. M., F. H. Crawford and E. L. Hill—
 No. 17
 Arnott, E. G. F.—see Smyth
 Bacher, R. F.—see Goudsmit
 Babcock, Harold D.—No. 20
 Bleakney, Walker—No. 13
 Brasefield, Charles J.—No. 9
 Brennen, Herbert J.—Nos. 4, 39
 Cox, I. W.—No. 14
 Cork, J. M.—No. 32
 Compton, A. H.—No. 30
 Crawford, F. H.—see Almy
 Cunningham, H. L.—see Woodrow
 Dasannacharya, Balebail—No. 35
 Dershem, Elmer—No. 33
 Froman, Darol K.—No. 2
 Goudsmit, S. and R. F. Bacher—Nos. 26, 37
 Harkins, W. D. and Arthur E. Schuh—No. 41
 Harrington, M. C.—see Uyterhoeven
 Hesthal, Cedric E.—No. 25
 Hidnert, Peter—No. 1
 Hill, E. L.—see Almy
 Hoffacker, J. V.—No. 3
 Hummel, A.—see Kunz
 Karapetoff, Vladimir—No. 27
 Kunz, J.—No. 36
 ——— and A. Hummel—No. 12
 Lang, R. J. and R. A. Sawyer—No. 23
 Laporte, Otto—No. 40
 Lowry, E. F.—No. 6
 Murphy, Edgar J.—see Allison
 Naudé, S. M.—No. 42
 Nicholas, Warren W.—No. 31
 Roebuck, J. R.—No. 5
 Roller, Duane—No. 7
 Ruedy, Richard—Nos. 21, 38
 Sawyer, R. A.—see Lang
 Sawyer, R. B.—No. 15
 Schuh, Arthur E.—see Harkins
 Skinner, E. W.—No. 34
 Smyth, H. D. and E. G. F. Arnott—No. 22
 Swann, W. F. G.—No. 28
 Swenson, H. N.—No. 24
 Szczeniowski, S.—No. 8
 Thompson, J. S.—No. 11
 Uyterhoeven, W. and M. C. Harrington—
 No. 16
 Wahlin, H. B.—No. 10
 Wollan, Ernest O.—No. 29
 Woodrow, Jay W. and H. L. Cunningham—
 No. 19

PROCEEDINGS
OF THE
AMERICAN PHYSICAL SOCIETY

MINUTES OF THE STANFORD MEETING, DECEMBER 7, 1929

The 160th regular meeting of the American Physical Society was held in the main lecture room of the Physics Department of Stanford University, Stanford University, California, on Saturday, December 7, 1929. There were fifty members in attendance.

There was no business of importance transacted at the meeting except the announcement by the secretary that the 164th meeting of the American Physical Society would be in affiliation with Section B of the Pacific Division of the American Association for the Advancement of Science, at the University of Oregon, Eugene, Oregon, in the period from June 18 to 21, 1930.

Papers were presented in the morning from ten until twelve-thirty, and in the afternoon from one-thirty until four-thirty. There were no papers read by title, and the relatively short program gave ample time for discussion, making the meeting a great success.

Abstracts of the 18 papers presented are given in the following pages. An Author Index will be found at the end.

L. B. LOEB, *Local Secretary for the Pacific Coast*

ABSTRACTS

1. The blue-green absorption bands of Li_2 . A. HARVEY AND F. A. JENKINS. *University of California*.—The absorption spectrum of lithium vapor contained in a nickel tube, and maintained at temperatures varying from 650°C to 900°C , has been examined under both high and low dispersion. Employing a tube 1 m long at the lower temperatures, we have identified the band heads due to the less abundant isotope molecule, Li^6Li^7 , which accompany the (1,0), (2,0) and (3,0) bands of the stronger Li^7Li^7 system. The isotope displacements agree with their calculated values within the error of measurement (calculated: 2.08, 4.32, 6.30Å; observed: 2.06, 4.47, 6.37Å. This checks the assignment of vibrational quantum numbers and the equations for the vibrational energy previously given (Phys. Rev. **34**, 1286 (1929)). Measurements of the band heads are necessarily inaccurate, because the head occurs at a low rotational quantum number. More satisfactory data may be obtained with the band lines, which are well resolved in the first order of the 15-foot grating. It has been possible to establish definitely that each band has the three-branch structure expected for a $^4\Pi \rightarrow ^1\Sigma$ transition, by using an unambiguous graphical method due to Loomis (Phys. Rev. **32**, 223 (1928)). Quantitative measurements will be made of the alternating intensities previously reported, and the rotational isotope effect in the (0,0) band investigated.

2. Why does molecular hydrogen reach equilibrium so slowly? HARVEY HALL AND J. R. OPPENHEIMER, *University of California*.—The uncatalyzed conversion ortho-para in gaseous hydrogen may be investigated quantum mechanically. A molecule of parahydrogen may be converted by collision with any other molecule to orthohydrogen; but the probability for this

conversion is small, because the conversion is induced by the very small interaction of nuclear magnetic moment with the magnetic moment of the rotating molecule. Furthermore, two molecules of parahydrogen may be converted to orthohydrogen by the interchange of nuclei between the molecules; this effect depends upon the overlapping of the wave functions for the nuclei which interchange; and its relative probability may be shown to be small, in comparison with the probability of a gas kinetic collision, of the order

$$e^{-(M/m)^{1/2}}$$

where M is the mass of the proton, and m that of the electron. The consideration of both effects shows that parahydrogen should, at N. P. T., be half converted to orthohydrogen in a period of the order of 10^8 seconds.

3. The Carbon isotope, Mass 13. A. S. KING AND R. T. BIRGE. *Mount Wilson Observatory and University of California*.—A systematic study of the carbon isotope is in progress, with the following results to date. (1) The isotope has been found in the 2-0 ($\lambda 4382$) band of C_2 , and in the 1-0 ($\lambda 3590$) band of CN, in addition to the original 1-0 band of C_2 and 0-0 band of CN. (2) Much stronger exposures of the 1-0 C_2 isotope band ($\lambda 4744$) have been obtained, in both first and second order spectra, showing at least fifteen lines suitable for measuring the isotope shift. (3) The large perturbation in line P_{33} ($\lambda 4731.8$) of the 1-0 C_2 band, does not appear in the corresponding isotope line, in agreement with theory. (4) The "staggering" in the main 1-0 C_2 band, caused by the absence of alternate rotational levels, is not present in the isotope band, again in agreement with theory. (5) The $\lambda 4744$ isotope band, as excited in the furnace, is at least ten times as strong, relative to the main band, as in the arc, where it has not as yet been observed with certainty. The relative intensity of the isotope band is thus a function of excitation conditions, and this fact may well invalidate all estimates of relative isotope abundance, based on relative spectral intensity.

4. The vibrational isotope effect. RAMOND T. BIRGE. *University of California*.—Gibson (*Zeits. f. Physik* 50, 692 (1928)) has formulated a beautiful method for calculating the vibrational isotope shift which is theoretically sound, and is the only accurate method available in the region of high values of the vibrational quantum number (n). The writer has added the details necessary for its precise numerical application, and has tested it on the absorption bands of Cl_2 previously treated by Elliott (*Proc. Roy. Soc. A123*, 629 (1929)), and of ICl , previously treated by Gibson (*loc. cit.*) and by Patkowski and Curtis (*Trans. Faraday Soc.* in press). In both these cases the theory is used to determine the correct n' numbering of the bands. The present results definitely require the half quantum numbers of the new mechanics. For Cl_2 they show that Elliott's n' numbering should be decreased by two units. For ICl they show, (1) that the main absorption progression arises from the $n''=0$ level, in apparent contradiction to a temperature experiment by Gibson (indicating the $n''=1$ level) which, however, the writer believes can be otherwise explained: (2) that Gibson's n' numbering should be decreased by one unit. Both of these latter results agree with Patkowski and Curtis' conclusions, based on a less rigorous method of calculation.

5. Equivalent temperatures in the electric arc as measured by multiplet intensities. GEORGE R. HARRISON, *Stanford University*.—It has been shown by Langmuir, Nottingham, and others, that probe measurements in the positive column of the electric arc indicate equivalent electron temperatures lying between 5000 and 70,000A, the electrons having a Maxwellian velocity distribution. Engwicht and the writer have previously shown that corrections corresponding to temperatures in the neighborhood of 8000A had to be applied to the intensities of multiplets have widely separated upper states when measured in the titanium arc under average conditions. New studies have been made of the effect of changing excitation conditions on the relative intensities of multiplets in triads, and excitation temperatures between 3000 and 15,000A have been found for the positive column of the titanium arc. The curves relating current density and electron temperature are similar to those obtained by Nottingham with the Langmuir probe for cadmium, copper, and other arcs. While probably less accurate than the probe method, the intensity method gives an excellent check on its results. The most consistent data are obtained when multiplets with common lower states are chosen, so that the most accurate self-reversal corrections can be made if required.

6. **Photographic photometry in the extreme ultra-violet.** PHILIP A. LEIGHTON AND GEORGE R. HARRISON, *Stanford University*.—The work of one of us (J.O.S.A.11, 341 (1925)) on characteristics of photographic emulsions coated with fluorescent substances when exposed to ultra-violet light has been extended to the extreme ultra-violet. Slow, medium, and fast emulsions coated with various oils have been exposed in a vacuum spectrograph under controlled conditions. Several combinations have been found which exhibit uniform contrast throughout the region 1000–3,000Å, with quite uniform sensitivity. The great difficulty of producing known variations of intensity in the extreme ultra-violet makes it desirable to find photographic materials which obey the reciprocity law accurately for use in this region. The best conditions to be fulfilled appear to be: 1. Selection of an emulsion obeying the reciprocity law accurately at wave-lengths near 4,000Å; 2. Coating it with a substance which fluoresces near this wave-length, does not absorb its own fluorescence light, and completely absorbs in a thin layer all light of wave-lengths 1,000–3,000Å. It is shown that the behavior of a given combination of emulsion and fluorescent substance in the extreme ultra-violet can often be predicted from a knowledge of the characteristics of each in the fluorescence region.

7. **The broadening of spectrum lines during early stages of spark discharges.** FRANK G. DUNNINGTON AND ERNEST O. LAWRENCE. *University of California*.—The voltage across a spark gap drops to a relatively small value in 10^{-8} sec. after the beginning of the discharge. The cross-section of the discharge during periods of the magnitude of 10^{-7} sec. after breakdown, however, has not been observed, but there is evidence that it is small and therefore that the discharge current density is enormous. Such large initial ionic densities should be evidenced by large Stark effect broadening of spectrum lines in the early stages of sparks. Using the Beams electro-optical shutter we have photographed the light emitted by sparks during 5×10^{-7} sec. after breakdown. As expected all spectrum lines are diffuse, the spark doublets ($3d_{1,2}-4f$) of Mg, ($3d_1-4f_1$, ($3d_2-4f_2$) of Cd and Zn for example, having a breadth of approximately 40Å. From existing data on the Stark effect of Mg it is calculated that the average ionic field producing the here observed Stark effect broadening is about 600,000 volts/cm, and that approximately 1/2 of the molecules in the path of the discharge are ionized. The luminosity of the metallic vapor was observed to spread from the cathode at a velocity of 1.2×10^{-8} cm/sec.

8. **The effective collision cross-section of cadmium and zinc atoms for slow electrons.** ROBERT B. BRODE. *University of California*.—The variation with the electron velocity of the effective collision cross-section or the absorption coefficient, α , has been measured in the vapors of cadmium and zinc and found to follow a curve of the type previously found for mercury. (Proc. Roy. Soc. 125, 134, (1929)). The cadmium curve has a maximum at about 40 volts, $\alpha = 130$, and a minimum at about 25 volts, $\alpha = 126$, followed by a steady rise with decreasing velocity to the limit of accurate measurements, 1 volt, $\alpha = 700$. The zinc curve has a very flat maximum at about 50 volts, $\alpha = 76$, a minimum at about 36 volts, $\alpha = 74$, followed by a steady rise to $\alpha = 500$ at 1 volt. As in mercury vapor a very small change in the general slope is observable in both of the curves just beyond the first resonance potential. The magnitude of the maximums are in the order ; Cd, $\alpha = 125$; Zn, $\alpha = 75$ and Hg, $\alpha = 60$. Other related properties of these atoms such as the molar refractivity and the critical potentials show this same irregularity in order.

9. **A direct measurement of molecular velocities.** I. F. ZARTMAN, *University of California*.—The molecules whose velocities are to be measured are vaporized in an electrically heated crucible. A sharply defined molecular beam is formed by two rectangular slits, one of which is placed in the cover of the crucible, the other 3.8 cm above the crucible slit. A steel cylinder, 9.41 cm inside diameter, which is rotated by an electric motor has a slit in its periphery and supports a glass collecting plate (which has been coated with a thin uniform deposit of the substance to be investigated) on the inner face diametrically opposite the slit. The entire assembly is operated in a vacuum of less than 10^{-4} mm and at speeds varying between 120 and 240 r.p.s. The molecules in the group entering the cylinder possess a distribution of velocities. These molecules pass to the opposite side of the cylinder and are collected on the glass plate in the form of a velocity spectrum whose density is measured with a microphotometer. The

velocity v of the molecules $= \pi d^2 n / s$ where d = diameter of the cylinder, n = r. p. s., and s = displacement of the molecules. Three runs taken with Bi at 800°C indicate that it vaporizes as a monatomic molecule. The displacement corresponding to the most probable speed in the beam at 120 r. p. s. is 0.7 cm. Other substances are now being investigated.

10. Experiments on the reported fine structure of the molybdenum K_β lines. SAMUEL K. ALLISON AND J. H. WILLIAMS. *University of California*.—Davis and Purks (Proc. Nat. Acad. Sci. 14, 172, (1928)) have investigated the K-spectrum of molybdenum with a double x-ray spectrometer and obtained a complete resolution of the K_β doublet with both crystals reflecting in the second order. They report a new line $K_{\beta'}$, 24 seconds of arc (0.17 X.U.) on the long wave-length side of K_{β_1} . The intensity of this new line appears to be about 1/3 that of K_{β_1} . An attempt has been made to study this new line using a double spectrometer with both crystals in the second order, and one in the second and one in the third order. Experiments were carried out at 42.7 kv and 45.6 kv. No positive evidence could be obtained for a satellite of K_{β_1} in the reported position. From the curves obtained it appears that if such a satellite is present at the voltages stated above, its intensity must be less than 1/10 that of K_{β_1} . An average of eight determinations of the wave-length separation of β_1 and β_2 gives $\Delta\lambda = 0.572 \pm 0.003$ X.U. Previous values obtained with the single spectrometer were 0.563 X.U. (Allison and Armstrong, Phys. Rev. 26, 701, (1925)) and 0.565 X.U. (Larsson, Phil. Mag. 3, 1136, (1927)).

11. The electric space charge in the lower atmosphere. JOSEPH G. BROWN. *Stanford University*.—During the past year continuous records of space charge have been obtained 7.5 meters above the earth's surface. Obolensky's method of gathering all the ions from a known volume of air and measuring the residual charge has been used. The mean value of the positive charge has been about 0.10 E. S. U. per cubic meter. This value lies between Obolensky's and Kahler's. The air was quite free from dust which gives large negative charges, or smoke which gives large positive charges. If the air is still the space charge is remarkably constant, but if in motion sudden changes occur. This fact has led to the conclusion that most variations at a given point are due to different bodies of air which have different charges. At night when the air becomes saturated the positive space charge decreases and negative charge often occurs. During rain large positive or negative charge results. The mean diurnal variation is almost the reciprocal of the temperature variation, though there is a decided tendency to agree with the potential gradient. Sudden changes in space charge are accompanied by corresponding changes in potential gradient, though many changes in potential gradient are not accompanied by changes in space charge.

12. Variation of the electric potential gradient in the lower atmosphere. JOSEPH G. BROWN. *Stanford University*.—The mean electric field is characterized by a negative surface charge and a positive space charge. The mean distribution of the positive space charge can be inferred from the values of the potential gradient at different elevations, since $d^2 V / dh^2 = -4\pi\rho$. Approximate computation shows that 50 percent of the charge is in the first kilometer, 18 percent in the second, etc., Variations in mean distribution will cause variations in potential gradient at any point by changing the relative magnitudes of the space charges (a) in horizontal layers and (b) in vertical columns. Expansions and convection currents will produce such changes in distribution and hence determine potential gradients. Continuous records of potential gradient and space charge have been obtained for a year 7.5 meters above the surface and their diurnal variations compared with the diurnal system of convection as inferred from the meteorological elements. In general upward currents near the surface correspond with increased charge and potential gradient, while downward correspond with decreased. General expansion and overflow above correspond with decreased charge and potential gradient, while cooling and inflow above correspond with increased. This is in agreement with the theory. Dust, smoke, and condensation are important factors but are believed to be of secondary importance in determining the mean diurnal variation.

13. **The multiple crystal x-ray spectrograph.** JESSE DUMOND AND HARRY KIRKPATRICK, *California Institute of Technology*.—An x-ray spectrograph designed to obtain increased intensity and contrast in spectra of scattered x-rays has been designed and built. The instrument consists of fifty small units each containing a Seeman wedge and calcite crystal. The units are closely spaced on the arc of a circle of one-half meter radius and are oriented with great precision so that the spectra from the different units are exactly superposed. The spectra are photographed on a film bent to conform to an arc of the same circle. The geometry of the instrument is such that when the crystals are oriented so as exactly to superpose one spectral line from all of them, all wave-lengths and all orders are exactly in superposition. The instrument can take two forms having respectively a virtual point source and a real point source. The form having the virtual point source is the one here described. Beside the gain in intensity and contrast the instrument permits the study of scattered radiation over a wide range of scattering angles with almost perfect homogeneity of scattering angle.

14. **Adjustments and tests of the multiple crystal x-ray spectrograph.** HARRY KIRKPATRICK AND JESSE DUMOND, *California Institute of Technology*.—The technique of adjusting the crystals of the multiple crystal x-ray spectrograph is described and some improvements in design are suggested. Preliminary results obtained from a setting of seventeen of the crystals show that very good resolution is possible. The lines have a breadth of less than half an X.U. the dispersion being about 0.2 mm per X.U. The lines resulting from the superposition of seventeen crystals are not appreciably broader than the lines from one crystal and are seventeen times as intense showing that the superposition is practically complete. A preliminary test using the instrument to investigate the Compton effect for Mo K radiation scattered at 90 degrees from a paraffine scatterer with extremely homogeneous scattering angle confirms the result obtained by one of the authors for 180 degrees scattering that the so-called Compton line is diffuse. According to the work of Bergen Davis a fine line structure may be superposed on this broad diffuse structure though no theory has been yet given to account for such fine lines in the Compton shifted position. Attempts are being made to locate these lines with the multiple crystal spectrograph.

15. **Photographs of single crystals of ice, grown from the vapor.** JOHN MEAD ADAMS, *University of California at Los Angeles*.—The abstract of this paper appears as a Letter to the Editor in this issue, p. 113.

16. **Valence electrons in the diamond.** M. L. HUGGINS AND RUTH PARRISH, *Stanford University*.—Previous calculations of density of scattering power for x-rays by means of Fourier series have involved the assumption that the structure can be resolved into two face-centered cubic structures, with the atoms oriented in the same way in both, and with three mutually perpendicular planes of symmetry passing through each atomic center. By taking the origin at a center of symmetry, midway between two atoms, this doubtful assumption need not be made. The resulting curves of density of scattering power show a small peak midway between each two neighboring carbon atoms. These peaks may be due to the electron pairs constituting the valence bonds.

17. **A method of calculating complex spectra.** WILLIAM V. HOUSTON, *California Institute of Technology*.—It is possible to build up, in a step by step process, the proper functions to represent any spectral term in the zero approximation. The coefficients occurring in these functions can be determined once for all by solving a set of simple simultaneous equations. From these functions, it is easy to compute the first approximation to the energy levels by integration over radial functions and spherical harmonics. If the radial integrals are not carried out, the integrals over the spherical harmonics still suffice to determine a number of relationships between the energies of the various multiplets. The accuracy of the determination is best when there are no other electron configurations with nearly the same energy as the one under consideration. The step by step process of setting up the functions gives at once the correlation between atomic terms and the ionic terms with which they are associated. It is then possible to apply the electron spins as a further perturbation. This leads to a determination of relationships between interval ratios in a multiplet and the interval ratios between multiplets.

18. The mobilities of gaseous ions in Cl_2 and Cl_2 -air mixtures. LEONARD B. LOEB, *University of California*.—Work of the early investigators and of Herbert Mayer indicates that the presence of traces of Cl_2 reduces the mobility of the negative ion below that of the positive ion, a fact which appeared inconsistent with a theory of Condon and Loeb. No other investigations of mobilities of *both* ions in pure Cl_2 had been undertaken. The possibility that the discrepancy between theory and observation in earlier work was caused by HCl made a more careful investigation imperative. Cl_2 carefully prepared by heating CuCl_2 and free from both HCl and H_2O was used. It was found that the values of the mobilities in pure Cl_2 on the new absolute standard for positive and negative ions was 0.654 and 0.510 cm/sec per volt/cm respectively. A study of mixtures of dry air and Cl_2 showed that traces of Cl_2 less than 0.1 percent reduce the negative mobility below that of the positive ion. The positive mobilities were little affected by the presence of Cl_2 , so that positive ions obey Blanc's law in Cl_2 -air mixtures, indicating the absence of disturbances due to dipole moments in Cl_2 as is to be expected. The behavior of the negative ion shows a clustering effect of considerable magnitude which has no simple electrochemical explanation.

AUTHOR INDEX

- Adams, John Mead—No. 15
Allison, S. K. and J. H. Williams—No. 10
Birge, R. T.—see King
——— No. 4
Brode, Robert B.—No. 8
Brown, Joseph G.—Nos. 11, 12
DuMond, Jesse—see Kirkpatrick
——— and Harry Kirkpatrick—No. 13
Dunnington, Frank G. and Ernest O. Lawrence—No. 7
Hall, Harvey and J. R. Oppenheimer—No. 2
Harrison, George R.—No. 5
——— see Leighton
Harvey, A. and F. A. Jenkins—No. 1
Houston, William V.—No. 17
Huggins, M. L. and Ruth Parrish—No. 16
Jenkins, F. A.—see Harvey
King, A. S. and R. T. Birge—No. 3
Kirkpatrick, Harry—see DuMond
——— and Jesse DuMond—No. 14
Lawrence, Ernest O.—see Dunnington
Leighton, Philip A. and George R. Harrison—
No. 6
Loeb, Leonard B.—No. 18
Oppenheimer, J. R.—see Hall
Parrish, Ruth—see Huggins
Williams, J. H.—see Allison
Zartman, I. F.—No. 9

HANDY REFERENCE CARDS

of the most probable values of the
GENERAL PHYSICAL CONSTANTS

as estimated by Raymond T. Birge in the first issue of

The Physical Review Supplement

Tables of the values of the general physical constants taken from Birge's article will be printed on two stiff cards, $8\frac{1}{2} \times 11$ ", bound together with linen tape.

Price 75 cents

JOHN T. TATE, *Editor*
PHYSICAL REVIEW SUPPLEMENT
University of Minnesota
Minneapolis, Minnesota

Back Numbers Wanted of the PHYSICAL REVIEW



We will pay \$2.00 each for copies of the January, February, April and May issues of Volume 7, 1916; also \$1.00 for copies of the January, 1927, issue.

Send to the Physical Review, 1500 University Ave. S. E.,
Minneapolis, Minnesota.

Please Mention the PHYSICAL REVIEW when Writing to Advertisers

THE PHYSICAL REVIEW

PROBABILITY AND CRITICAL POTENTIALS FOR THE FORMATION OF MULTIPLY CHARGED IONS IN HG VAPOR BY ELECTRON IMPACT

BY WALKER BLEAKNEY

PHYSICAL LABORATORY, UNIVERSITY OF MINNESOTA

(Received December 15, 1929).

ABSTRACT

With a type of apparatus previously reported the procedure is described for measuring the probability of the formation of multiply charged ions in mercury vapor as a function of the velocity of the incident electron.

Critical potentials for the formation of multiply charged ions. New results together with those of an earlier paper place the minimum or ionizing potentials for the formation of Hg^+ , Hg^{2+} , Hg^{3+} , H^{4+} , and Hg^{5+} by a single impact at 10.4, 30, 71, 143, and 225 volts respectively. A brief correlation of these results with those of other observers is given.

Relative numbers of multiply charged ions. A set of curves is given showing the fraction of the total positive ion current carried by each type of ion as a function of the electron velocity. Another set of curves shows the fraction of the total number of ions carrying one, two, three, four, and five charges. The fraction for Hg^+ drops to a nearly constant value of 78 percent while the value for Hg^{2+} approaches 16 percent of the total number beyond 150 volts. At 400 volts the values for the five ions in order are 77, 16.5, 4.4, 1.3 and 0.8 percent respectively.

Quantitative measure of the number of ions produced and effective cross-sectional area of the Hg atom. Curves are given representing the number, N , of each type of ion, per electron, per cm path, per mm pressure at 0°C as a function of the electron velocity. The values of N for Hg^+ , Hg^{2+} , Hg^{3+} , and Hg^{4+} have maxima of 20.8, 3.2, 0.72, 0.15 at 50, 115, 210, and 400 volts respectively. The effective cross-sectional area of the Hg atom toward an ionizing collision of a given type is obtained by dividing the appropriate value of N by the number of molecules per cc. The maximum value of this area for Hg^+ is about 60 percent of the kinetic theory value.

A discussion is given of the meaning of the area under the peaks in the e/m analysis curves and its effect on the accuracy of the interpretation of the data.

I. INTRODUCTION

BEFORE our knowledge of the probability of ionization in gases by electron impact can be complete it is necessary to investigate the critical potentials for the formation of multiply charged ions, and the effective cross-sectional area of the molecule or atom toward an ionizing collision as a function of the energy of the incident electron. Heretofore the types of apparatus used by investigators in this field have been such that the total number of unit positive charges was observed and not the actual number of ions formed since

an ion may carry several positive charges. It is important, therefore, to study separately the probability of the formation of ions having one, two, three, or more charges. Until recently no direct experimental method had been devised capable of such an investigation. The success of any method requires that only the primary products be examined, that is, the pressure of the gas must be such that there is little chance of an electron colliding twice and the current density of electrons must be so low that there is also little chance of an ion being struck a second time. The scheme proposed in a recent paper¹ lends itself very well to work of this kind. As yet a study has been made of mercury vapor only. A preliminary report² of some of the results has already been made.

II. APPARATUS AND PROCEDURE

The apparatus used in the present experiment has already been described¹ in considerable detail and the reader is referred to this paper for the principles and details of the design. A plan view is shown in Figs. 1 and 2 for convenience in the discussions which follow.

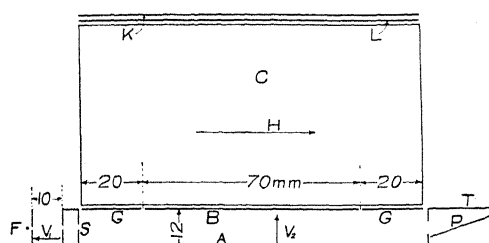


Fig. 1. Side view of apparatus.

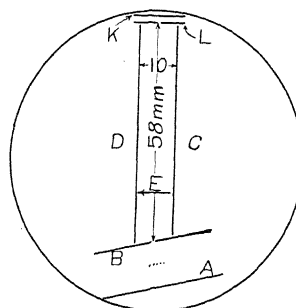


Fig. 2. End view.

The pressure of the mercury vapor was controlled by regulating the temperature of a trap in the exhaust line containing liquid mercury. The data for the pressure of the vapor corresponding to the temperatures used were taken from the International Critical Tables. The best temperature at which to work was found to be in the neighborhood of -20°C or a pressure of 1.81×10^{-5} mm Hg. Temperatures in this region were maintained either by a mixture of NaCl and ice or by solid CCl_4 . The latter melts at -24°C . The temperature of the ionization chamber was measured by means of a thermocouple and was always found to be about 45°C . Since the mean free path of the atoms was much greater than the diameter of the connecting tube a pressure correction for diffusion was made to get the true pressure in the tube.

The electron current required in most cases was about 3×10^{-7} amperes. It was measured by means of a galvanometer of 4,000 megohms sensitivity. A potential (usually about 90 volts) was applied to the plate P positive with respect to the surrounding box of a magnitude sufficient to give a saturation current. The galvanometer measured the current to the box and plate com-

¹ W. Bleakney, Phys. Rev. **34**, 157 (1929).

² W. Bleakney, Phys. Rev. **35**, 123 (1930).

bined, thus obviating any correction due to ions being formed inside the box. It is believed that secondary electrons escaping from this arrangement were quite negligible. The positive ion current arriving at the plate *B* was measured with a Leeds and Northrup galvanometer of 110,000 megohms sensitivity. Saturation current to this plate was observed with a field V_2 as low as 0.3 volts per cm. The field strength used for the final runs was 3.3 volts per cm. The current to the plate *K* was measured with a Compton electrometer at a sensitivity of 2000 mm per volt. For the larger currents a direct deflection was observed by shunting the instrument with India ink resistances. For very small currents the time required to deflect through a given distance on the scale was measured.

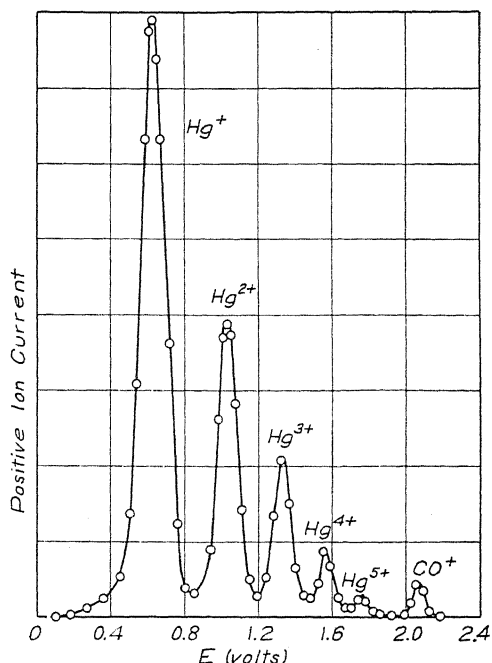


Fig. 3. A typical e/m analysis curve. $V_1 = 350$ volts. $p = 1.8 \times 10^{-6}$ mm Hg.

A set of preliminary runs was taken at various values of the field V_2 . It was found that the relative sizes of the peaks remained unchanged between 1.2 and 3.5 volts per cm. A second set of preliminary runs was taken at various pressures, the results showing that the effects of scattering and neutralization were negligible at the pressures finally used. The final set of runs was then taken at electron velocities ranging from 20 to 500 volts.

III. RESULTS

In Fig. 3 is shown a curve typical of a large number obtained with the apparatus. The electrometer current is plotted as a function of the crossed field E . In this instance the accelerating potential for the electrons V_1 was set at 350 volts, the drawing out field V_2 at 3.3 volts per cm, and the pressure was that corresponding to saturated mercury vapor at -20°C or 1.8×10^{-6} mm

Hg. The magnetic field furnished by the solenoid amounted to 400 gauss. The curve distinctly reveals the five mercury ions Hg^+ , Hg^{2+} , Hg^{3+} , Hg^{4+} , and Hg^{5+} . Only one impurity shows up to any extent and its ionization potential was found to be 14.5 volts. It seems certain then that it is a singly charged ion and its position indicates a molecular weight of 28. These two facts are strong evidence for its being a CO^+ ion.

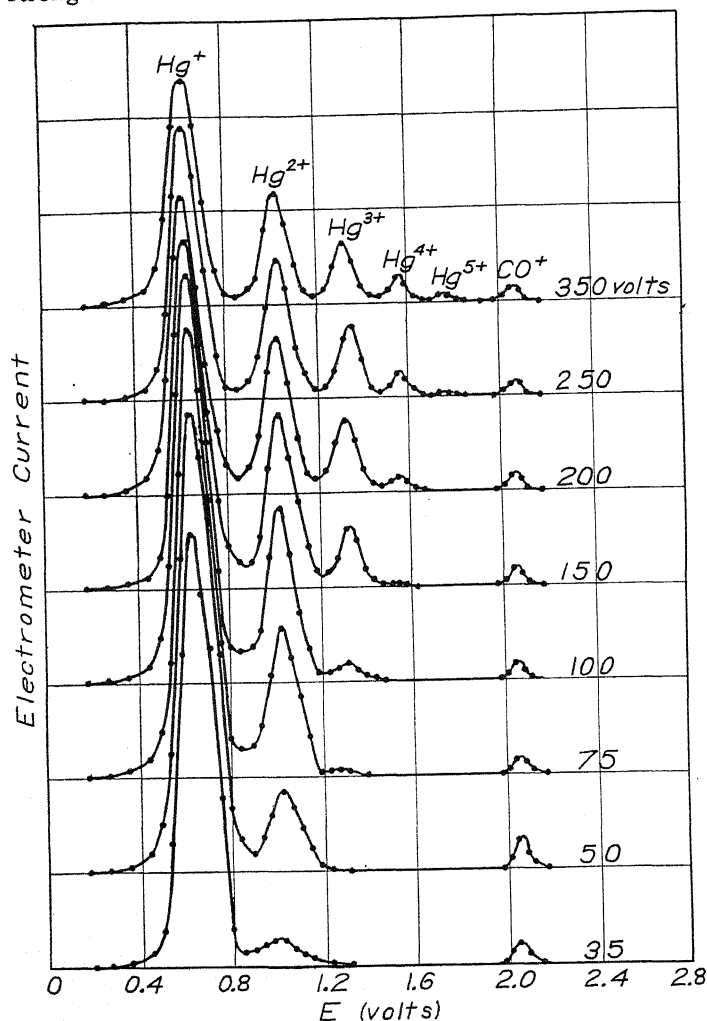


Fig. 4. A series of e/m analysis curves taken at various electron velocities.

Figure 4 illustrates a series of curves taken at electron velocities ranging from 35 to 350 volts. The ordinates of the different curves have been reduced to correspond to the same pressure and the same electron current throughout.

Critical potentials for the formation of multiply charged ions at single impact. If the areas under the peaks are plotted as a function of the electron velocity and the curves extrapolated to zero area the minimum or critical potentials for the formation of the different ions at a single collision are obtained. These

values may be called the ionization potentials for single impact. To the four values reported in the first paper¹ there is now added a fifth. The curves are shown in Fig. 5. The ionization potential for Hg^{5+} was difficult to determine with any accuracy because of the proximity of the Hg^{4+} peak and a very

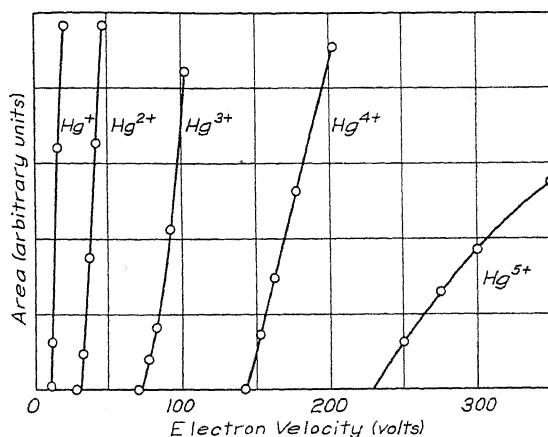


Fig. 5. Curves showing the ionization potentials at single impact.

slight impurity which coincided with the Hg^{5+} peak. Assuming the value of Hg^+ to be 10.4 volts the values, with the estimated probable errors, of Hg^{2+} , Hg^{3+} , Hg^{4+} , and Hg^{5+} are placed at 30 ± 1 , 71 ± 2 , 143 ± 3 , and 225 ± 5 volts respectively. There has been observed only slight evidence for the Hg^{6+} ion while Hg^{7+} and Hg^{8+} , if any are formed, are completely masked by the CO^+ impurity.

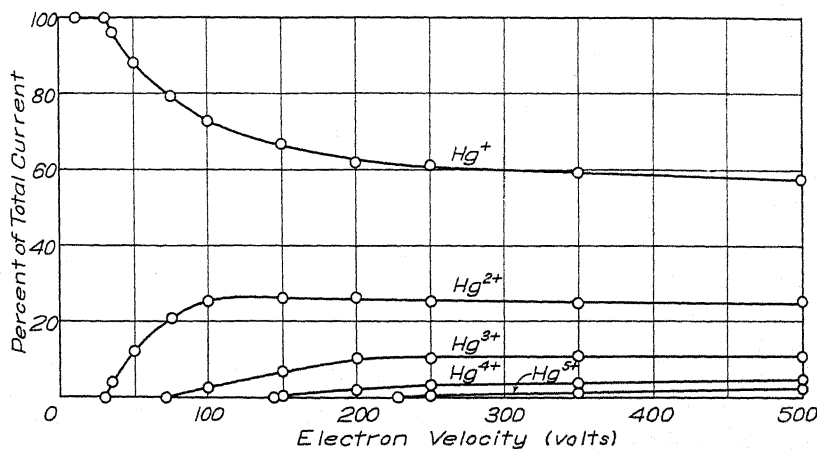


Fig. 6. Percent of total current carried by each type of ion.

Relative numbers of multiply charged ions. It will be assumed that the area under each peak of the e/m analysis curves is proportional to the current due to that particular type of ion and the validity of this assumption will be examined later. The curves of Fig. 6 representing the fractions of the total

current due to the different ions are obtained by plotting the area under each peak divided by the total area as a function of the electron velocity. Between 10.4 and 30 volts the positive ion current is 100 percent singly charged, and the effect of the appearance of the other ions is to lower this value to a nearly

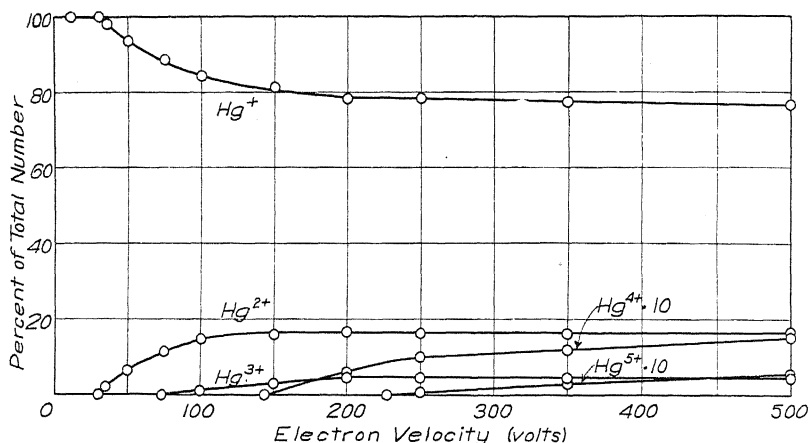


Fig. 7. Percent of total number of ions having one, two, three, four and five charges.

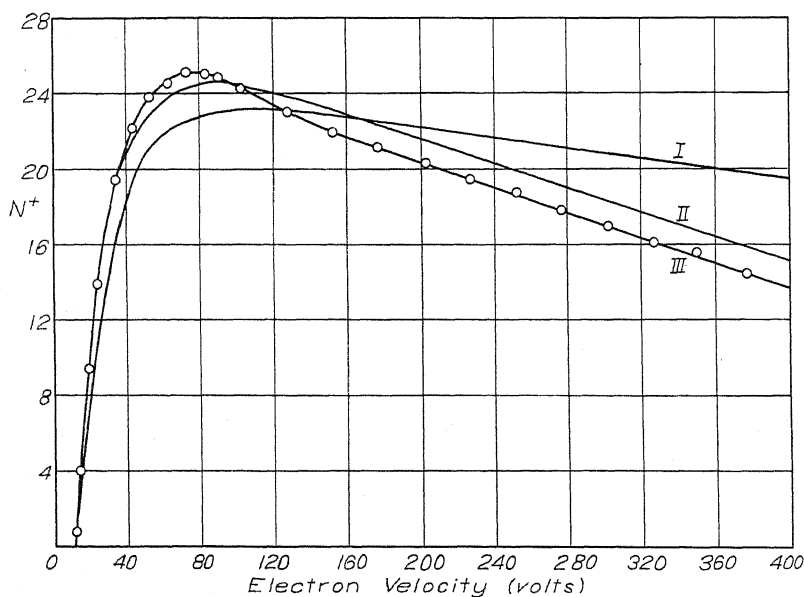


Fig. 8. Total number of positive charges, N^+ , per electron per cm path per mm pressure at 0°C. constant one of 59 percent at the higher velocities. The fractions of the total current due to Hg^{2+} and Hg^{3+} reach maximum values of 27 and 11 percent respectively.

To find the relative abundance of the different ions in *number* it is necessary to consider the total area under the first peak, one half the area under the

second, one third the area under the third, and so forth, as fractions of the sum. The curves of Fig. 7 show the results of this calculation. The ordinates for the fourth and fifth ions are here multiplied by 10. It will be noticed, for instance, that while at 300 volts the current due to Hg^+ is only 60 percent of the total yet 78 percent of the ions actually formed are singly charged.

Quantitative measure of the number of ions and the effective cross-sectional area of the Hg atom. As has been stated before the total number of positive charges arriving at the plate *B* was measured. Let the number of positive charges formed per electron per cm path per mm pressure at 0°C be denoted by N^+ .

The values of N^+ are indicated in Fig. 8 as a function of the electron velocity. The curves of two other observers are shown for comparison. Curve I,

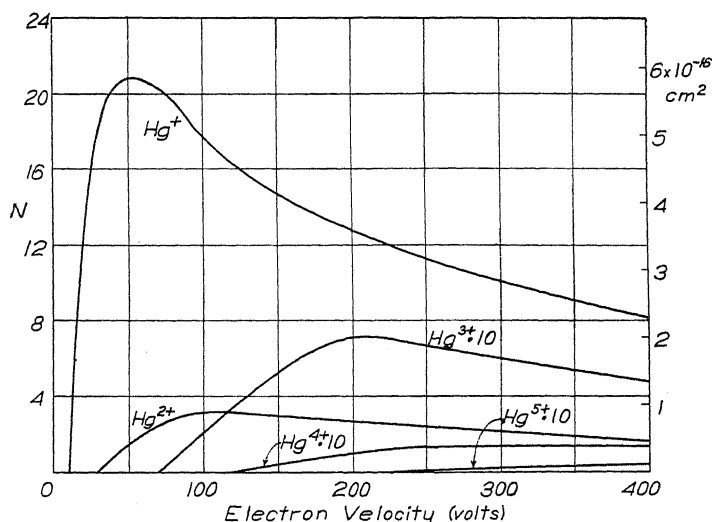


Fig. 9. Number of Hg^+ , Hg^{2+} , Hg^{3+} , Hg^{4+} , and Hg^{5+} ions per electron per cm path per mm pressure at 0°C and effective cross-sectional area of the Hg atom.

reduced to 0°C , is from the work of Compton and Van Voorhis.³ Curve II, corrected to conform to the pressure and temperature data used in this article, is taken from the paper by T. J. Jones.⁴ Curve III was obtained by the author and was used in the calculations which follow. Curves II and III agree fairly well as indeed they should since they were obtained by the use of the same type of apparatus. The maximum in the curve found in the present experiment has a magnitude of 25.2 at 75 volts compared to 24.6 at 90 volts as observed by Jones. Beyond the maximum the results of Jones are consistently higher than curve III. At present an attempt is being made in this laboratory with a new apparatus to measure the quantity N^+ with greater accuracy. If such a determination should prove different from the results here given the following results may be easily revised to conform to the new data.

³ K. T. Compton and C. C. Van Voorhis; Phys. Rev. **26**, 436 (1925) and **27**, 724 (1926).

⁴ T. J. Jones, Phys. Rev. **29**, 822 (1927).

Having measured the total number of positive charges and the fraction due to each type of ion it is possible to calculate the actual number of each type by taking values from the curves of Fig. 6, multiplying by the corresponding N^+ from Fig. 8 and dividing by the number of charges on the ion. These results have been plotted in Fig. 9 where N is the number of ions per electron per cm path per mm pressure at 0°C as a function of the electron velocity. The ordinates for the last three ions have been multiplied by 10. Now if the number N be divided by the number of atoms per cc the quotient is the effective cross-sectional area of the Hg atom toward an ionizing collision. This area is indicated by the scale on the right margin of Fig. 9. The kinetic theory value for this area is in the neighborhood of $10 \times 10^{-16} \text{ cm}^2$ depending on one's choice of the recorded values for the diameter of the mercury atom. Although the total positive ion current exhibits a maximum at an electron velocity of about 75 volts yet when the ions are examined separately the maximum yield for Hg^+ occurs at 50 volts. Maxima for Hg^{2+} , Hg^{3+} and Hg^{4+} appear at 115, 210, and 400 volts respectively.

IV. DISCUSSION

Because of its complicated structure there has been no theoretical treatment worked out to predict the ionization potentials in mercury vapor. Of course the first, 10.4 volts, is well known from a host of critical potential experiments. The determination by Lawrence⁵ is probably the most accurate, and his value agrees with spectroscopic measurements. Smyth,⁶ using a method of positive ray analysis, found doubly charged ions appearing at 19 volts while Carroll,⁷ from an analysis of the spectrum of Hg II, gets the same value. These values represent the energy necessary to remove the second electron after the first is gone. If the energy required to remove the first is included they are in satisfactory agreement with the value given by the present investigation.

It was assumed, earlier, that the area under any peak in the e/m analysis curve was proportional to the current due to that type of ion. Suppose the ions are traveling in the x direction and the slit has a width dy . Then for any particular setting of the field E the electrometer measures the number of ions which fall between y and $y+dy$ a quantity which is equivalent to dn/dy where n is the total number of charges between y_0 and y . This is the quantity which is plotted as a function of E , and measuring the area under the curve is equivalent to performing the integration,

$$\int_{E_0}^{E_1} (dn/dy) dE$$

a quantity which has dimensions different from that which we wish to find. The integral which we would like to find is

$$\int_{E_0}^{E_1} (dn/dy)(dy/dE) dE$$

⁵ E. O. Lawrence, Phys. Rev. **28**, 947 (1926).

⁶ H. D. Smyth, Proc. Roy. Soc. **A102**, 283 (1922).

⁷ J. A. Carroll, Phil. Trans. Roy. Soc. **A225**, 365 (1925).

and only in case dy/dE is equal to a constant is the area as measured proportional to the current. The analytical expression for dy/dE can be found from the equations of motion but it is not simple and it involves the unknown initial velocity distributions of the ions. The numerical value therefore can only be roughly approximated. It was thought, therefore, that an experimental attack might prove more fruitful.

Professor Tate pointed out that if the factor by which the area under a peak must be multiplied to get the current is the same for all the peaks then this factor is equal to the total current entering the analyzing chamber divided by the total area under the curve. It was decided, therefore, to measure the current and area at various electron velocities to see if the ratio remained constant when different peaks were involved. The current issuing from the first slit was measured with the high sensitivity galvanometer while the electrometer measured the current through the second slit in the usual way. The experimental error of such a determination is rather large because of the low intensity of the current to the galvanometer. Ten runs were made with electron velocities ranging from 20 to 70 volts. Below 30 volts only the single ion is formed while below 70 volts only single and double ions may exist. In these runs the ratio of current to area showed a maximum deviation of 3 percent from the mean and displayed, moreover, no systematic variation with increasing numbers of doubly charged ions. Tests at higher electron velocities gave similar results although the experimental error was greater. The conclusion is that the area is proportional to the current within the experimental error of this test. It should be pointed out, however, that the experimental error for the determination of the ratio for the second peak alone is perhaps ten or twelve percent since it contains at most only about one fourth of the total area. In general the smaller the peak the less certain are the measurements.

Another test was made by connecting the galvanometer to the plate *C* Fig. 2, and measuring the current arriving at this plate as a function of the field *E*. With $E=0$ all the positive ions issuing from the lower slit fell upon *C*. As *E* was increased a point was reached at which singly charged ions were prevented from reaching the plate and the remainder was measured by the galvanometer. Here, also, the accuracy is not great because the separation of the ions is not precise at the current densities required, but the results agreed substantially with the previous test.

The original data as represented by the curves in Fig. 4 can be reproduced quite accurately. It is in the interpretation that great care must be exercised lest errors creep in. It is believed that the results as represented by the curves in Figs. 5 and 6 are very close to the true values.

The calculation of the probability of formation of the different types of ions is dependent on the measurements of the total ionization and different observers are somewhat at variance on these values. The results obtained in the present work are in fair agreement with those of Jones, and Compton and Van Voorhis (see Fig. 8) but are not at all in agreement with those of von

Hippel.⁸ It is argued by him that a crossed field due to contact potentials swept out the multiply charged ions before they were measured and hence his results apply to Hg^+ only. Even so, the author cannot correlate von Hippel's data with the present work, and it appears that his theory that the maximum yield occurs at twice the ionization potential is untenable.

Smyth,⁶ who was the first to investigate the multiply charged ions in mercury vapor by means of a mass spectrograph, states that at the higher velocities the number of doubly charged ions is nearly equal to the number singly charged. From the appearance of his curves it is probable that it is the *current* which is nearly equal in the two cases. If this be true then both Jones and von Hippel have misinterpreted Smyth's data.

It seems to be quite generally assumed that the classical kinetic theory value for the mean free path of an electron is $4(2)^{1/2}$ times the mean free path of an atom of the gas. This value has apparently been used by Hughes and Klein,⁹ Compton and Van Voorhis,³ Jones,⁴ and others in their calculations. It seems to the author that this is not the true kinetic theory value for high speed electrons such as were used in all of these experiments, the more appropriate value being

$$\lambda = 1/\pi r^2 N$$

where N is the number of atoms per cc and πr^2 is the kinetic theory value of the cross-sectional area of an atom. The difference in the two points of view is very marked in the case of mercury. The maximum effective cross-sectional area of a mercury atom toward an ionizing collision of the first type calculated on the basis of the latter argument is at least 60 percent of the kinetic theory value, while Jones, and Compton and Van Voorhis on the basis of their calculations get a little over 30 percent for any type of ion. It is interesting to note in the curves of Compton and Van Voorhis that mercury vapor gives the largest yield of positive charges of any gas used and it is among the lowest in probability of being ionized and yet the kinetic theory value for the size of the mercury atom does not differ greatly from the others.

The author has been unable to check the calculations for curve 2, Fig. 3, in the paper by Jones⁴ and it is believed that this curve is in error. It also seems that a correction for diffusion due to the large difference in temperature between trap and tube should have been made in the pressure before calculating the values for curve 1 of this same figure.

It is essential to point out that while the number of Hg^+ ions, for instance, has been measured yet what electron was removed in its formation is unknown. This fact makes a theoretical explanation of the observed phenomena even more difficult.

Work on hydrogen and the rare gases has been started and it is hoped that these results may be reported in the near future.

Many thanks are due Professor John T. Tate for his ever present interest and timely suggestions in the prosecution of this problem.

⁸ A. v. Hippel, Ann. d. Physik 87, 1035 (1928).

⁹ A. L. Hughes and E. Klein, Phys. Rev. 23, 450 (1924).

EXPERIMENTS ON THE REPORTED FINE STRUCTURE AND THE WAVE-LENGTH SEPARATION OF THE $K\beta$ DOUBLET IN THE MOLYBDENUM X-RAY SPECTRUM

BY SAMUEL K. ALLISON AND JOHN H. WILLIAMS
UNIVERSITY OF CALIFORNIA, BERKELEY

(Received November 26, 1929)

ABSTRACT

A nomenclature is suggested for describing the possible positions of the double x-ray spectrometer. A position may be defined by (n_A, n_B) where n_A is the order of reflection on crystal A ; n_B the order on B . n_A is to be considered always positive. n_B is negative if the position of crystal B for the reflection of a wave-length incident upon it is such that by turning B through an angle of less than 90° the reflecting surface of B can be made parallel to that of A , and the given wave-length be reflected in this parallel position. If this convention be adopted it is shown that general equations for the instrument may be easily set up. Experiments on the separation of the $K\beta_1$ doublet of molybdenum at the position (2, 2) at 43-46 kv and 22 m.a. show that if the line $K\beta'$ reported by Davis and Purks¹ exists, its intensity is less than 1/10 that of β_1 at these voltages. An average of eight determinations of $\Delta\lambda$ for MoK, β_1, β_2 gives 0.572 ± 0.003 XU.

SUMMARY OF PREVIOUS WORK

THE doublet character of the $K\beta_1$ line in x-ray spectra has been noted by various experimenters.¹ Allison and Armstrong obtained a considerable separation of the doublet for molybdenum in the 5th order of a single crystal ionization spectrometer, and found $\Delta\lambda = 0.563$ XU. The intensity ratio β_1/β_2 was found to be 2/1. Larsson achieved a separation of the doublet photographically and found $\Delta\lambda = 0.565$ XU. Kellström investigated the doublet in the second order and obtained good separations in palladium and silver, and a very good separation was obtained by Enger and photometered, for the case of rhodium. Davis and Purks, using a double spectrometer, obtained a complete separation of the doublet with both crystals reflecting in the second order. They report a new line $K\beta'$, 0.172 XU. (24 seconds of arc at the dispersion used) to the long wave-length side of $K\beta_1$, and of intensity about 1/3 to 1/2 that of β_1 . The voltage at which their tube was operated was not stated in their report. The photographs taken

¹ M. de Broglie, *Compt. Rend.* **170**, 1053 and 1245 (1920); Durrant and Patterson, *Bull. Nat. Res. Counc. USA* Vol. 1, part 6, p. 393 (1920); Crofutt, *Phys. Rev.* **24**, 100 (1924); Allison and Armstrong, *Phys. Rev.* **26**, 701 (1925); Leide, *Compt. Rend.* **180**, 100 (1925); Thesis, Lund (1925); Ehrenberg and von Susich, *Zeits. f. Physik* **42**, 823 (1927); Larsson, *Phil. Mag.* **3**, 1136 (1927); Kellström, *Zeits. f. Physik* **41**, 516 (1927); Enger, *Zeits. f. Physik* **46**, 826 (1928); Stenman, *Zeits. f. Physik* **48**, 349 (1928); Edlén, *Zeits. f. Physik* **52**, 364 (1928); Davis and Purks, *Proc. Nat. Acad. Sci.* **14**, 172 (1928); J. Valasek, *Phys. Rev.* **34**, 1231 (1929). The same author has also reported, in a paper read at the Dec. 1929 meeting of the Amer. Phys. Soc., that attempts to find the fine-structure lines announced by Davis and Purks were unsuccessful.

by Enger in rhodium were obtained at 50–60 kv and no such line is indicated on them. An attempt has been made to study this new line in molybdenum, using a double x-ray spectrometer.

APPARATUS

Several standard molybdenum target tubes supplied by the General Electric Co. for crystal analysis work were used in the course of the experiments. These tubes were cooled by a pump circulating kerosene through the hollow target; the kerosene after entering and leaving the target through insulated glass tubes, was cooled by passing through a copper spiral immersed in running water. The target and the cathode of the tube were at potentials above and below ground respectively. The focal spot was at a distance of 53 cm from crystal *A*, and the radiation used was taken off at an angle of 8° with the target face. A description of the double spectrometer used has been previously published.² The horizontal angular width of the beam (angular width in a plane perpendicular to the axes of rotation of the crystals) was determined by the width of the slits of the instrument, which were 35 cm apart. These slits were 1.5 and 1.8 mm wide in various experiments. The voltmeter which measured the voltage across the x-ray tube was connected between the cathode side of the tube and ground, and therefore measured only half the total potential drop across the tube. It was found by trial that the potential of the anode above ground was very nearly equal to that of the cathode below ground so that the indication of the voltmeter needed only to be multiplied by two. The tube current in all experiments was 22 m.a., the voltage in some was 43 kv and in some 46 kv. In the course of the experiments three different sets of calcite crystals were used.

NOMENCLATURE FOR THE DOUBLE X-RAY SPECTROMETER

Since two crystals are used in the double x-ray spectrometer, we have found it convenient to specify their positions by giving two numbers n_A and n_B which represent the orders in which crystals *A* and *B* are reflecting respectively. The corresponding glancing angles are θ_A and θ_B . The sign of n_A is to be taken as positive in all cases. The sign of n_B is determined as follows. If the position for crystal *B* for the reflection of a given wave-length incident upon it is such that by turning *B* through an angle less than 90° the reflecting surface of *B* can be made parallel to that of *A*, and the given wave-length reflected in this parallel position, n_B is negative. If an angle greater than 90° must be traversed in order to bring the crystals to this type of parallel position, n_B is positive. According to this convention, so-called "parallel position_{act}" (Ehrenberg and Mark³ Case I; Schwarzschild⁴ Case II) are special cases of a number of positions in which n_B is to be considered negative. Using this convention, we may write for the dispersion *D*,

² Williams and Allison, J.O.S.A. & R.S.I. 18, 473 (1929).

³ Ehrenberg and Mark, Zeits. f. Physik 42, 807 (1927).

⁴ Schwarzschild, Phys. Rev. 32, 162 (1928).

$$D \equiv \frac{d\theta_B}{d\lambda} = \frac{n_A}{2d \cos \theta_A} + \frac{n_B}{2d \cos \theta_B} \quad (1)$$

in which $d\theta_B$ is the angular range on crystal B corresponding to the wave-length range $d\lambda$, and d is the grating space (assumed to be the same on both crystals).

If the absolute value of n_B is greater than that of n_A and n_B is negative, D is negative, and the sense of rotation of crystal B to pass from shorter to longer wave-lengths is the reverse of that for cases in which D is positive. This is the case, for example, in the position $n_A = 1$, $n_B = -2$, which we designate as the $(1, -2)$ position. Here the dispersion is negative, and for molybdenum K radiation its magnitude is only slightly greater than that from a single crystal reflecting in the first order.

Using the conventions suggested here, Schwarzschild's equation⁵ for the "geometric breadth" $\delta\theta_B$, in the case in which the two axes of rotation lie in the reflecting faces of the crystals and are parallel, may be written

$$\delta\theta_B = \frac{1}{2} D \lambda \phi^2. \quad (2)$$

In the preceding equation, $\delta\theta_B$ is the angular range through which crystal B may be turned while reflecting the wave-length λ . D is the dispersion defined by (1). ϕ is one-half of the maximum angle between any two rays incident on crystal A in a plane parallel to the axis of rotation of A . In other words, if the only restraint upon the divergence of the x-ray beam is that it must pass through two equal rectangular apertures separated by a distance L , whose height, or dimension in a plane parallel to the axis of rotation of the crystal is h , then $\phi = h/L$.

If the geometric width $\delta\theta_B$ has been made small in comparison to the observed width, and can be neglected, the following equation holds for the width observed for any line in the spectrum at any position of the crystals:

$$W = (W_A^2 + W_B^2 + D^2 W_\lambda^2)^{1/2}. \quad (3)$$

In this equation W represents the half width at half maximum in angular measure of the observed "rocking curve," W_A the half width at half maximum in angular measure of the curve (assumed Gaussian error curve) representing the intensity of reflection from crystal A as a function of the deviations from the Bragg angle, W_B is the analogous quantity for crystal B , D is defined in (1) and W_λ is the half width at half maximum of the line in question in linear measure.

ATTEMPT TO FIND THE LINE $K\beta'$

Some of the curves we have taken which have the most direct bearing on the intensity of the line $K\beta'$ are shown in Fig. 1. These curves were all

⁵ Schwarzschild expressed this equation in the form $\delta\theta_B = 1/2(\tan \theta_1 \pm \tan \theta_2)\phi^2$ in which the negative sign was to be chosen when the crystals are in a position where "the first incident and the last reflected rays are on opposite sides of the first reflected ray." This agrees with our method of designating the sign of n_B .

taken in the (2, 2) position (both crystals in the second order, reflecting faces not parallel).

Curve (a). This curve was taken at 43 kilovolts and 22 milliamperes. The rate of deflection of the electrometer observed on a scale 225 cm from the instrument was 0.744 mm per second at the highest point of $K\beta_1$. At the base-line point on the short wave-length side it was 0.163 mm per second. The voltage sensitivity of the electrometer on the scale at this distance was 4.5 meters per volt. The capacity of the insulated system was not accurately known but was of the order of magnitude of 10^2 cm. The width of the lines

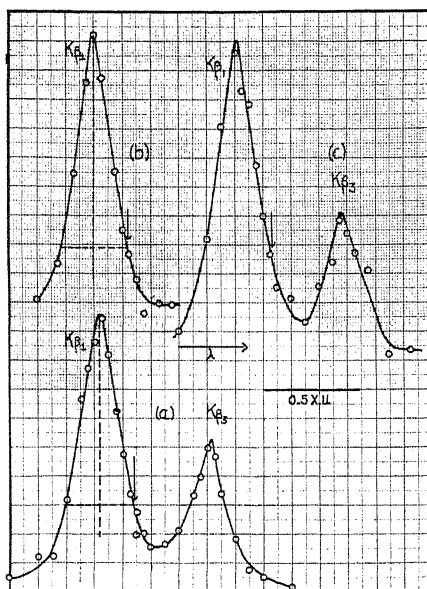


Fig. 1. Typical curves bearing on the intensity of $K\beta'$.

to be expected from geometric sources may be calculated from Eq. (2). The vertical adjustment of the two crystal faces was made by observing the reflection of a beam of light from their faces. This beam was made horizontal by passing through two narrow slits held on a cathetometer and was very nearly perpendicular to the reflecting crystal surfaces. The crystal was then tilted about a horizontal axis until the reflected beam was in the same horizontal plane as the incident beam. This adjustment was accurate to 2 minutes of arc. ϕ was calculated from the height of the focal spot (3 mm) and the height of crystal B (18 mm) and the distance from the target of the tube to crystal B (71 cm). This gives $\phi = 0.0147$, $\delta\theta_B = 9.5$ seconds of arc. The half width at half maximum of the curve for β_1 is approximately 15.5 seconds of arc; the preceding calculation shows that this cannot be explained as due to geometrical causes only. We do not wish to take up the question of the width of x-ray lines here, leaving this for a later publication. The half

width at half maximum of the curve at $(1, -1)$ for these crystals was 3.1 seconds of arc.

Curve (b). This curve was taken with the same arrangement as that of curve (a) except that a vertical stop 7.5 mm high was introduced at a distance of 48 cm from the target. This gives $\delta\theta_B = 5.2$ seconds of arc from Eq. (2). The voltage was 43 kv. The rate of deflection of the electrometer (scale and sensitivity as for curve (a)) at the highest point on the peak was 0.398 mm per second; at the lowest point shown on the short wave-length side it was 0.093 mm per second. The half width of the peak at half maximum is about 14 seconds. An accident to the x-ray tube prevented continuing the curve to cover β_3 .

Curve (c). This curve was taken on a different set of crystals and with a different target from that used in curves (a) and (b). The voltage was 46 kv. The rate of deflection of the electrometer (same arrangement as for (a) and (b)) at the highest point of β_1 was 0.475 mm per second; at the lowest point on the short wave-length it was 0.162 mm per second. The value of ϕ and consequently of $\delta\theta_B$ was the same as that for curve (a). For various unknown reasons the curve (c) is less reliable (as indicated by the scattering of the points) than curves (a) and (b). The half width at half maximum of the curve at $(2, -2)$ for the crystals used was 1.5 seconds of arc.

The vertical arrows in Fig. 1 show the angular positions at which β' should appear (24 seconds of arc to the long wave-length side of β_1) according to the results of Davis and Purks.¹ In curves (a) and (b) the total intensity here is about 1/5 of that at the maximum. In these curves, the vertical dotted line represents the center of the line $K\beta_1$; the horizontal dotted line its width at an angular distance of $24''$ from the center. It is evident that within the accuracy of the readings the curve is symmetrical in this region about an ordinate through its maximum. We can therefore obtain no positive evidence for the presence of the line $K\beta'$ at the voltage used.

A rough estimate of the maximum possible intensity in the form of the line $K\beta'$ which could be present in our curves may be obtained by assuming a Gaussian error curve for β' symmetrical about the position indicated, and of the same half width as that for β_1 . The distortion of the symmetry of β_1 which would be thus produced can be plotted by adding up the contributions from β_1 and the supposed β' at various abscissae. Proceeding by this method the conclusion was reached that the curves (a) and (b) could not have failed to show evidence of a line in the specified position of intensity 1/10 that of β_1 . Our conclusion is therefore that there is no line at this position of intensity greater than 1/10 that of β_1 under the conditions of the experiment.

DETERMINATION OF THE WAVE-LENGTH SEPARATION OF THE DOUBLET $K\beta_1, \beta_3$ IN MOLYBDENUM

In the course of the investigation many curves have been taken of the doublet in question in various positions of the double spectrometer. Eight of the most reliable of these have been selected for the purpose of obtaining an accurate value of $\Delta\lambda$ for this doublet. The results are shown in Table I.

TABLE I. Observations on the wave-length separation of β_1, β_3 .

Position n_A	n_B	Dispersion from Eq. (1)	$d\theta_B$ obs.	Av. $d\theta_B$	$\Delta\lambda$ calc.	Weight
1	1	68.46"/XU	39.1"	39.1"	0.5711XU	2
1	2	103.8	61.0 61.2 59.5	60.6	.5835	9
1	3	140.7	80.0	80.0	.5687	4
2	2	139.2	78.5 77.0	77.8	.5587	8
2	3	176.0	101.5	101.5	.5766	5

The weights assigned in the last column of Table I are the products of the number of observations for a given position by $(n_A + n_B)$ for that position, since it was supposed that higher dispersion gave more accurate results. The weighted mean of the measurements shown in Table I is

$$\Delta\lambda = 0.572 \pm 0.003 \text{ XU}$$

in which the probable error has been computed according to the usual methods.⁶ This value is slightly higher than the values 0.563 XU observed by Allison and Armstrong¹ and 0.565 XU observed by Larsson.¹ In general the effect of greater resolution of a close doublet should be to increase the estimate of its wave-length separation. The errors in the value quoted must be mainly due to two factors (1) the uncertainty of the electrometer readings, and (2) the fact that a change of temperature of the crystals might have taken place between the time of reading one peak and the time for the next.

⁶ For instance, Birge, Phys. Rev. Supp. 1, 1 (1929), pp. 5-6.

THE INTENSITY MAXIMA IN THE CONTINUOUS
HELIUM SPECTRUM

BY JANE M. DEWEY

EASTMAN LABORATORY, UNIVERSITY OF ROCHESTER

(Received December 9, 1929)

ABSTRACT

The position of the maxima of the continuous spectrum of helium was measured with an arc in which measurements of ion concentration was made. The displacement of the maxima to the red by stray fields in the gas was calculated from the formula $E = -2e(eF)^{1/2}$ given by Robertson and Dewey and more recently by Kudar. The observed displacement is always larger than the calculated. Reasons for this are discussed.

IN A paper in this journal¹ H. P. Robertson and the author suggested an explanation of the displacement of the maxima of continuous atomic spectra to the red of the limit of the spectral series. It was assumed that the effect is due to the stray fields set up in the gas by the ions and free electrons, and the least energy for which aperiodic orbits are possible was calculated from the complete formula for the Stark effect on the basis of the classical quantum theory. Kudar² has recently obtained the same value for this limit of the continuous spectrum from general reasoning on the basis of the quantum mechanics. It is not possible to carry through the calculation in quantum mechanics as the complete equation is not soluble and is known to give no discrete states unless some restriction is imposed. Since the quantum mechanics must go over into ordinary mechanics for large quantum numbers, or atomic states of energy close to zero, the classical mechanics should give the correct formula for the displacement of the spectral limit. The uncertainty which it introduces lies rather in the fact that it gives no information as to the relative probabilities of the various transitions which are possible.

EXPERIMENTAL PROCEDURE

The spectrum of a hot cathode helium arc very similar to that described in an earlier paper³ was photographed, with a Hilger E3 quartz spectrograph, and the position of the maximum intensity in the continuous spectra determined with a recording microphotometer. The cathode of the arc was a cylinder of platinum foil, coated with barium oxide and heated by a current put through it lengthwise. A Langmuir exploring electrode used to measure the electron concentration was placed in the center of the cylinder with its axis perpendicular to the axis of the cylinder. One photograph on which the intensity of the continuous spectra could be measured was obtained with a

¹ Robertson and Dewey, *Phys. Rev.* **31**, 973 (1928).

² Kudar, *Zeits. f. Physik* **57**, 705 (1929).

³ Dewey, *Phys. Rev.* **32**, 918 (1928).

Schüler tube containing a similar electrode. Even when the exploring electrode was small (1 mm of seven mil wire) the discharge tended to avoid its neighborhood, as could be seen by visual observation of the tube. This was probably due to recombination of the ions on the glass insulation of the electrode and to the cooling effect of the electrode. As the curves from which the electron temperatures and concentrations were obtained were regular and obtained without difficulty, the removal of electrons by the electrode itself cannot have caused a serious disturbance. The most serious difficulty in the measurement of ion concentration was that it sometimes caused a sudden increase in the current which melted the glass insulation from the electrode. The ion concentration which could be obtained in the tube was limited by the heating effect.

Helium was chosen rather than an alkali metal to avoid the possibility of the atomic spectrum being complicated by unresolved bands or continuous molecular spectra. The helium recombination spectra have been observed by Paschen⁴ and more recently by Mohler and Boeckner.⁵ For purposes of photometric measurement they have the serious disadvantage of being accompanied by bands. Mohler and Boeckner report that the bands are greatly reduced in intensity by the addition of a trace of mercury to the helium but in the discharges used in this investigation this did not appear to be the case. It was not found possible to eliminate the bands in any way except by the reduction of both pressure and ion concentration, which also reduced the intensity of the recombination spectra. The arc was more suitable than the Schüler tube as the bands were strong only when a high current was put through the arc. The tube used by Mohler⁶ and by Mohler and Boeckner apparently would give better spectra but has the disadvantage that the ion concentration must be measured by an indirect method. Probably the bands were weakened on the one plate taken with a Schüler tube on which the intensity of the continuous spectra could be measured by some impurity accidentally present. This was the first plate taken with a newly set up Schüler tube and all subsequent exposures showed very strong bands. The difficulty of estimating the intensity of the continuous spectrum when bands appear on the plate can be seen on the excellent reproductions which accompany Paschen's paper. The bands are strongest in the neighborhood of the $2p$ limit but the weak bands in the ultra-violet also make measurements on the $2s$ limit difficult. The small dispersion of the spectrograph used made measurements at the $2p$ limit of parhelium impossible. The range of ion concentrations included in these results is small and the estimated fields uncertain but, as it was necessary to discontinue the investigation, it seemed worthwhile reporting such results as were obtained.

Table I gives the results. The field is calculated from the formula of Holtsmark,⁷ taking account of the presence of both ions and electrons by doubling

⁴ Paschen, Berl. Sitzb. Math. Phys. K. 1926, p. 135.

⁵ Mohler and Boeckner, Bureau of Standards Jour. of Research 2, 489 (1929).

⁶ Mohler, Phys. Rev. 31, 187 (1928).

⁷ Holtsmark, Ann. d. Physik 58, 577 (1919), Phys. Zeits. 20, 162 (1919) and 25, 73 (1926). The formula used is $F = 3.9n^{2/3}e$. This gives the most probable field. The mean field is somewhat larger.

the electron concentration. This probably gives too small a field. Under "displacement of maximum" the distance in cm^{-1} of the maximum intensity of the continuous spectrum from the limit of the spectral series for zero field

TABLE I

Series limit	Electron concentration	Calculated field (e.s.u. per cm)	Displacement of maximum observed	Displacement of maximum calculated
2p	3.6×10^{12}	0.69	160 cm^{-1}	91 cm^{-1}
2s	3.6×10^{12}	0.69	140	91
2p	5.1×10^{12}	0.87	175	105
2s	9.1×10^{12}	1.3	185	125
2s	1.1×10^{13} *	1.4	205	130

* Schüller tube.

is given. From the formula $E = -2e(eF)^{1/2}$ the calculated displacement is obtained, where F is the field and e the charge on the electron.

DISCUSSION

The displacement of the limit observed is in every case larger than that calculated. This is to be expected from the serious error in the electron concentrations introduced by the avoidance of the neighborhood of the exploring electrode by the discharge. Since the intensity of the continuous spectrum increases as the square of the electron concentration the spectrum observed will be essentially the spectrum of the region of the discharge in which the concentration is highest. All other sources of error, both in measurement and in calculation, will probably result in discrepancies in the same direction, but it is probable that this error is so large as to mask all others. One source of error in the calculation may be large. Oppenheimer⁸ has pointed out that there is a possibility of dissociation, and therefore of recombination on the basis of the new mechanics even when the energies of the ions and electrons do not permit it according to classical mechanics. The general argument that the results of the two types of mechanics must approach each other for large quantum number makes it improbable that this introduces serious error, although it is conceivable that it might. It is not possible to estimate the magnitude of the effect from Oppenheimer's or Kudar's formulae as for the upper excited states of the atom the change in energy due to the field is as large as the total energy of the states even for small fields and cannot be calculated from perturbation theory.

A more complete study of the effect would be desirable, accompanied if possible by a determination of the field in the source by an independent method, such as the intensity of forbidden lines appearing in its spectrum, as it appears to give a reasonably direct method of estimating the ion concentrations in stellar sources.

These measurements were made in Palmer Physical Laboratory, Princeton University, while the author was a fellow of the National Research Council. She is greatly indebted to Dr. K. T. Compton for his interest in the work as well as for extending to her the privilege of working in the laboratory.

⁸ Oppenheimer, Phys. Rev. 31, 66 (1928).

SCHOTTKY EFFECT AND CONTACT POTENTIAL
MEASUREMENTS ON THORIATED
TUNGSTEN FILAMENTS

BY NEIL B. REYNOLDS

PALMER PHYSICAL LABORATORY, PRINCETON UNIVERSITY

(Received December 7, 1929)

ABSTRACT

The Schottky effect for thoriated tungsten filaments is investigated and Schottky's relation that $\log i \propto (V)^{1/2}$ is verified at high fields, but fails at gradients below 10000 volts/cm, even for fully activated surfaces. This lack of saturation at low fields is accentuated by the effect of bombardment with high velocity positive ions, such bombardment apparently producing a surface roughening and consequently increased fields in local areas. Investigation with low accelerating and retarding voltages, while varying the temperature and state of activation of the filament, allows a comparison of the contact potential and the work function at the absolute zero of temperature (ϕ_0) for the thoriated surface. The two values (contact potential and ϕ_0) are found to vary with a one-to-one correspondence if ϕ , the work function at the temperature of measurement, be allowed a temperature coefficient. This coefficient is much larger than can be attributed to the specific heat of the electrons in the metal. The electrons with high velocities show a Maxwellian velocity distribution. Near the zero of potential there are certain anomalous effects and a "patch surface" is postulated which, in a qualitative manner, explains this behavior and the lack of current saturation with voltage gradients below a limiting value.

SCHOTTKY,¹ many years ago, derived an equation to explain the increase of saturation thermionic current with anode voltage. This relation has been verified by many investigators for pure metallic electron emitters, especially in the last few years. With one or two exceptions, the analogous effect with composite cathodes has been neglected, and the present paper deals with the current-voltage relations for thoriated tungsten filaments over a range of anode potentials from retarding potentials of 10 volts to accelerating potentials of 5000 volts, corresponding to potential gradients of nearly 500000 volts/cm.

A number of tubes were used in these experiments, varying slightly in detail but of the same general design. A 1.6 mil thoriated tungsten filament was stretched in the center of a cylindrical nickel or molybdenum anode. This was constructed in three pieces, on the guard ring principle. An alkaline earth metal was vaporized on the wall of the tube as a getter. The tube was given the best possible exhaust, baked, the metal parts degassed, and then sealed off from the pumping system. The tube was so designed that it could be completely immersed in liquid air.

The temperature of the filament was determined from the watts input according to the latest temperature scale of Jones.² Since all three parts of the

¹ W. Schottky, *Phys. Zeits.* **15**, 872 (1914); also *Zeit. f. Physik* **14**, 63 (1923).

² H. A. Jones, *Phys. Rev.* **28**, 202 (1926).

anode were maintained at the same potential but currents were measured only to the center cylinder, the effects of filament cooling at the leads and of field distortion at the edges were eliminated. Currents were measured by galvanometers and a Rawson multimeter, with a system of shunts giving a measuring range from 1 ampere to 5×10^{-11} amperes. Batteries, a 1500 volt dc generator and a 20000 volt full wave rectifier gave a complete range of anode potentials.

Langmuir and others³ have described the methods of manipulation of thoriated tungsten cathodes. In these experiments the state of activation of the filament was controlled by allowing thorium to diffuse to the surface at lower temperatures, or by raising the temperature and removing it by evaporation. It is practically impossible to obtain a completely deactivated thoriated filament even by flashing at very high temperatures since diffusion occurs while the filament is cooling. In the present instance it was possible to obtain values of θ as low as 0.30 (θ = fraction of the surface covered).

Becker⁴ has distinguished between the amount of barium present on a tungsten filament and the amount effective in lowering the work function. Since in the experiments reported in the present paper the emission obtained from the filament was used as the criterion of θ according to Langmuir's relation that $\log i \propto \theta$, there is no contradiction and θ might more properly be defined as the fraction of the tungsten covered with thorium atoms which are effective in lowering the work function.

Becker and Mueller⁵ reported that partially activated thoriated and caesiated tungsten surfaces obeyed Schottky's relation,

$$\log i = \log i_0 + \frac{K}{T} \left(\frac{dV}{dx} \right)^{1/2}$$

at high electric fields, but deviated from this as zero potential was approached. They discussed the nature of the fields to be expected close to non-homogeneous surfaces and concluded that poor saturation was to be expected from partially activated cathodes. This effect has been known for some time, but as a subject of detailed study it has been neglected. Dushman⁶ and others in their calculations of the electron emission from composite surfaces have projected the $\log i$ vs. $(F)^{1/2}$ line from high fields to zero potential and assumed this as the current emitted at zero field. Since this extrapolated value was several times greater than the current actually obtained, some doubt was thrown on the procedure and it was thought important to investigate in detail the relation between electron current and anode voltage so as to obtain some sort of an explanation of the departures at low fields and perhaps a work-

³ I. Langmuir, Phys. Rev. 22, 357 (1923); S. Dushman and J. Ewald, Phys. Rev. 29, 857 (1927).

⁴ J. Becker, Phys. Rev. 33, 1082 (A) (1929).

⁵ J. Becker and D. Mueller, Phys. Rev. 31, 431 (1928).

⁶ Dushman and Ewald, Reference 3; K. Kingdon, Phys. Rev. 24, 510 (1924); Dushman, Dennison and Reynolds, Phys. Rev. 29, 903 (1927).

ing picture of the surface. The procedure and results will be briefly stated, and the theory and conclusions left for consideration at the end of the paper.

Figure 1 shows two typical curves obtained at the same temperature with two values of θ , $\theta_A > \theta_B$. It will be observed that above V_1 both curves follow

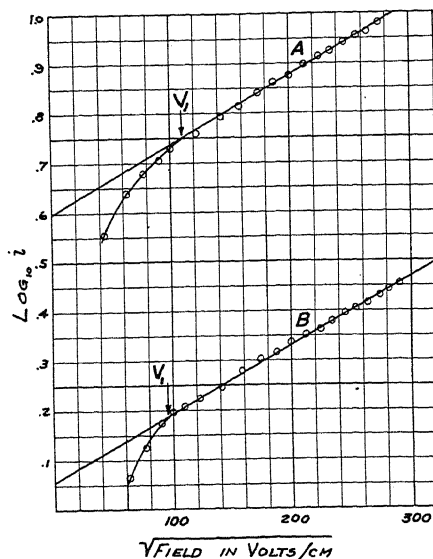


Fig. 1. Typical curves, for two partially activated thoriated filaments, $\theta_A > \theta_B$.

straight lines of approximately the same slope. The theoretical slope can be calculated from the field gradient at the filament surface, as derived from the tube dimensions. The observed slopes varied somewhat, running on the aver-

TABLE I. From tube geometry, $T[\Delta \log i / \Delta(V)^{1/2}] = 18.4$.

Run	Temp.	θ	$[\Delta \log i / \Delta(V)^{1/2}]$	$T[\Delta \log i / \Delta(V)^{1/2}]$
28	1045°K	1.0	0.0189	19.77
27	1101	1.0	.0184	20.40
26	1295	1.0	.0138	17.90
87	1350	1.0	.0141	19.05
88	1350	1.0	.0148	19.95
91	1350	0.5	.0150	20.25
101	1350	1.0	.0146	19.70
102	1350	1.0	.0150	20.25
116	1350	0.9	.0143	19.30
107	1375	0.9	.0136	18.70
108	1375	0.9	.0142	19.52
92	1450	0.8	.0145	21.02
112	1450	1.0	.0141	20.45
114	1450	0.9	.0165	23.90
32	1500	0.6	.0127	19.06
Average				19.93

age about 10 percent higher than the calculated. Table I gives results for various runs at different temperatures and values of θ .

The position of the critical field V_1 must next be considered. This varied slightly from run to run, and the discussion of the effect of positive ion bombardment will show one reason for this variation. However, under the best vacuum conditions, the point of departure from the straight line was constant at about 10000 volts/cm. This appeared to be a limiting minimum value, independent of the temperature and of the state of activation of the filament. So, between $\theta=0.30$ and $\theta=1.0$, and between $T=1100^\circ\text{K}$ and $T=1600^\circ\text{K}$, Schottky's relation held with very fair accuracy for fields greater than 10000 volts/cm, and this limiting value was characteristic only of the surface thorium on tungsten.

It is interesting to note that in Becker and Mueller's paper, Fig. 5 shows the curve approximating to a Schottky straight line at high voltages but departing from it at about 15000 volts/cm, which is in fair agreement with the results obtained here.

The portion of the curves between V_1 and V_0 , the zero of applied potential, presents something of a puzzle. The results vary a great deal, but averaging a large number of runs and eliminating possible complicating factors, there seems to be a certain amount of regularity. Curves *A* and *B* of Fig. 1 illustrate this. It will be noted that curve *A* approaches the dotted straight line more gradually than does curve *B*. These are two runs at the same temperature, where $\theta_A > \theta_B$. This example and numerous others lead to the generalization that the point of departure, V_1 , is approximately independent of θ , but as θ is decreased, the curve falls away more and more steeply. So far, attempts exactly to analyze this portion of the data have failed, yielding only this observed qualitative result.

Removal of liquid air from around the tube resulted in the liberation of small amounts of gas. Thoriated tungsten surfaces are very sensitive indicators of the presence of the least traces of even chemically inert gases, since positive ions produced by electron impacts are accelerated to the filament and remove thorium, reducing θ and consequently the emission obtainable at a given temperature. With "residual gas" ions, this effect becomes important at around 40–50 volts. After such *low voltage bombardment*, the general nature of the $\log i$ vs. $(V)^{1/2}$ curves was unchanged, but was shifted vertically downward due to the decrease in the emission current. However, if *bombardment at 400 volts or higher* was maintained for a considerable period of time (15–60 minutes), subsequent $\log i$ vs. $(V)^{1/2}$ curves in good vacuum exhibited marked changes.

Figure 2 illustrates this. Curve *A* is a normally activated filament. Curve *B* was taken after positive ion bombardment at 400 volts. The filament was then flashed at 2800°K and reactivated and curve *C* taken. This last has been shifted downward in the figure for purposes of spacing. Actually the upper parts of *B* and *C* practically coincide, while at low voltages the currents of *C* are considerably higher than those of *B*.

The effect of bombardment was a semi-permanent one. Subsequent activation and deactivation by temperature (below 2700°) shifted the curve along the current axis but did not otherwise alter its unique character. Flashing at

2700°K or higher, where rapid sintering of tungsten is known to take place, destroyed the effect of bombardment and subsequent activation produced normal $\log i$ vs. $(V)^{1/2}$ curves.

When gas was present in the tube and a run was made, first with ascending and then descending voltages, bombardment occurred while readings were being taken and the curve would not retrace its original path. When the maximum potential used was 1000 volts or higher, the return curve was actually higher than the ascending one, but broke away sooner and crossed the first. A second ascending curve retraced the previous descending one, returning still higher and giving a second sort of hysteresis loop. Thus a filament which at low fields gave higher emission currents than a bombarded one which

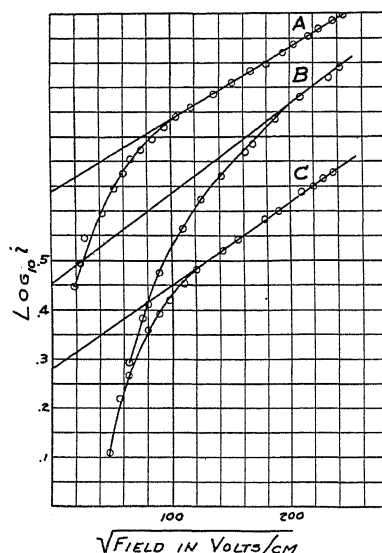


Fig. 2. Curves illustrating effect of positive ion bombardment at 400 volts. Curve A, normally activated filament; B, after bombardment; C, after reactivation. Curve C is shifted downward from practical coincidence with A.

had less thorium present, actually produced less current than the bombarded filament when fields of the order of hundreds of thousands of volts per centimeter were applied. The indication was that something other than the amount of thorium present determined the emission.

A study of the diffusion characteristics of the bombarded filament throws some light on this behavior. Subsequent to severe bombardment, diffusion of thorium to the surface of the wire from the interior occurred at temperatures much lower than in normal thoriated tungsten filaments. The activation rate at 1800°K was about that expected in a normal wire at 2100°K. It is known that diffusion of thorium in tungsten occurs most readily in fine grain structures, presumably along the crystal boundaries. An explanation suggests itself, that the effect of the bombarding positive ions may have been to rup-

ture the surface of the tungsten, producing a superficial fine crystal structure which facilitated the diffusion of thorium atoms. If this had also produced some sub-microscopic roughening, there would have been points where the field strength would have been greatly increased. This would account for a more rapid increase of the current with applied voltage, and an apparent, but not an actual deviation from Schottky's relation.

It was not possible during the course of this investigation to repeat these experiments with a pure tungsten filament and verify this hypothesis, free from the complicating influence of the thorium. However, Bartlett⁷ has reported similar results with pure tungsten, giving curves resembling those shown here. He reported difficulty in eliminating gas, and stated that his procedure was to flash the filament and then bombard his anode to red heat to remove gas. Only after this process was he able to obtain satisfactory results. He had only 1000 volts available and was able to go only to about 60000 volts/cm. Up to this point his curves were steeper than the theoretical Schottky line, but were rounding over and approaching this slope. His degassing schedule was an ideal one to produce positive ion bombardment of his filament. It seems possible that the lack of saturation he reports may be the same phenomenon noted here—a roughening of the surface by a positive ion “sand blast”—and that if he had continued to higher fields the curves might have straightened out along the conventional Schottky line. The highest fields used by Bartlett are of about the same order of magnitude as the point of departure of the bombarded curves in the present investigation.

II. LOW AND RETARDING POTENTIALS

If the electrons emitted from a filament at a given temperature all had zero or a constant initial velocity normal to the emitting surface, at a certain anode potential the current should rise abruptly from zero to its full value, and then remain constant, subject to the increase predicted by Schottky's equation, as the potential is increased. It has been shown by several investigators⁸ that the emitted electrons have an initial velocity distribution given by Maxwell's equation (via Schottky)

$$i = i_0 \frac{2}{\pi^{1/2}} \left[\left(\frac{Ve}{KT} \right)^{1/2} e^{-Ve/KT} + \int_{(Ve/KT)^{1/2}}^{\infty} e^{-x^2} dx \right].$$

Thus, if complicating effects such as voltage drop along the cathode be eliminated, the current should break at a definite potential, and as the anode is made more negative the current should fall away so as to make the $\log i$ vs V plot substantially a straight line. The sharp break point defines the absolute zero of potential, i.e., the state at which the anode and cathode are at the same potential, and the difference of this from the zero of applied voltage gives the contact difference of potential (CDP) between the anode and cathode materials. Comparison of two different cathodes or states of surface of the

⁷ R. S. Bartlett, Proc. Roy. Soc. A121, 456 (1928).

⁸ Davisson and Germer, Phys. Rev. 24, 666 (1924); Germer, Phys. Rev. 25, 795 (1925).

cathode with the same anode provides a method of determining changes in the contact potential of a material.

This method was used in examining thoriated tungsten filaments with accelerating and retarding fields in the neighborhood of zero field. Figure 3 shows a typical curve. It will be noted that the left hand portion of the curve follows a straight line, and that after passing through the transition region near zero, the points again approach the nearly straight line saturation value. It was decided to consider the intersection of these two lines, as the experimentally determined zero of potential as a basis for the determination of contact potential differences. This is designated in Fig. 3 as V_c . A justification of this will be given in the discussion to follow.

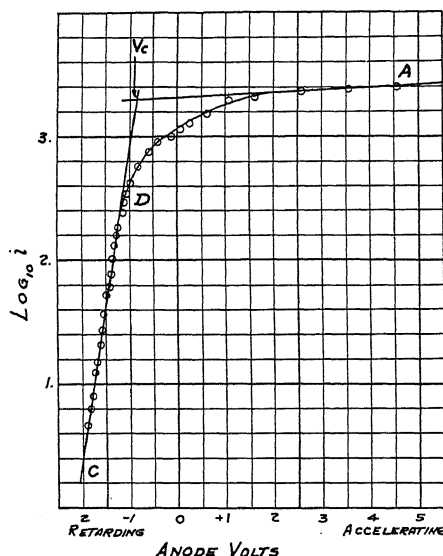


Fig. 3. Typical curve for determining contact potentials.

That part of the straight line just to the left of V_c is a theoretical, not an experimentally obtained curve, since the plotted curve falls away from it before V_c is reached. One cause of this deviation is the voltage drop along the filament cathode. The length of the center anode cylinder of the tube was 2.8 cm, and the difference in the cathode potential opposite the upper and lower ends was considerable and varied with the filament temperature. For this, a first order correction was applied. This was accomplished by first determining the potential of the mid-point of the filament. Then since the current from the most negative end was greater than from the most positive end, and the contribution of each element of the filament did not vary linearly along the filament, a method of graphical integration was used to determine what may be designated as the potential of the effective mid-point of the filament. This is the potential, which applied to a unipotential cathode would give the same observed current. The correction showed that only a part of the devia-

tion near zero could be attributed to the effect of filament drop since, whereas the correction was effective over only a few tenths of a volt range, the observed deviation extended over a range of one or more volts on either side of the determined zero. The effect of the correction on the retarded straight portion of the curve was simply to produce a small lateral shift, altering the actual value of the contact potential break but not the slope of the $(\log i)/V$ line.

Taking this corrected point as zero, and calculating from the filament temperature the fraction of the corresponding saturation current having different initial velocities, a series of points was obtained from Maxwell's distribution law coinciding with the corrected experimental line within the limits of experimental error. Over a 500°C temperature range this effect was verified. At least those electrons with high initial velocities had a Maxwellian velocity distribution. It will be shown later that the apparent deviation of the low velocity electrons (those contributing to the curve near zero voltage) from this distribution was not an actual deviation but was the result of quite another phenomenon.

The low electronic work function of a composite surface, such as thorium on tungsten, has generally been attributed to the effect of the contact difference of potential existing between the thorium and tungsten atoms at their point of contact.⁹ Whether the electrons come from the tungsten and are aided in their escape by local fields due to the thorium film, or whether they come from the thorium atoms themselves, it is impossible to state with certainty. Since the currents obtained from the thoriated tungsten are slightly greater than those from a pure thorium filament at the same temperature, and some tens of thousands of times greater than from pure tungsten, it seems reasonable to assume that the emission is that from thorium, modified by the proximity of the tungsten base.

Dushman's¹⁰ derivation of the thermionic emission equation leads to the result:

$$i_0 = AT^2 e^{-b_0/T}$$

where $b_0 = (e\phi_0/K)$, or $\phi_0 = (K/e b_0)$, and ϕ_0 is the work function of the surface at the absolute zero of temperature. From this equation, it is seen that the value of ϕ_0 for any condition of cathode surface can be found from the slope of the line obtained by plotting $(\log i - 2 \log T)$ against $1/T$. This value of ϕ_0 varies with the amount of thorium present on the surface, ranging from 4.5 volts ($b_0 = 52400$) for pure tungsten, to 2.6 volts ($b_0 = 30500$) for a completely activated filament.

In a preceding paragraph it was pointed out that the difference of the abscissa coordinate V_c from the zero of applied potential V_0 gave a measure of the contact difference of potential between cathode and anode materials. By measuring this difference for different values of θ , to each of which corresponded a definite value of ϕ_0 obtained as just described, a relation was arrived

⁹ O. W. Richardson, *Phil. Mag.* **43**, 557 (1922).

¹⁰ Dushman, *Phys. Rev.* **21**, 623 (1923).

at connecting the change in contact potential with the change in ϕ_0 for a range of surface conditions. Measurements of the C.D.P. were also made over as wide a range of temperatures as the measuring instruments and other limiting conditions allowed. Since the C.D.P. should be related to ϕ , the work function at the temperature of measurement, while ϕ_0 should be a constant independent of temperature, and presumably

$$\phi = \phi_0 + \pi(T),$$

a study of the change of the C.D.P. with temperature should give an insight into the nature of the function $\pi(T)$. Results are tabulated in Table II.

TABLE II. Results showing variation of ϕ with temperature.

I	II	III	IV	V	VI	VII	VIII
Run	Temp.	ϕ_ϕ	Observed π_θ	π_1	Corrected π_θ	Deviation (IV-VI)	Deviation %(IV-VI)
57	1175°K	2.85 v	(-)0.3 v	0.08 v	0.30 v	0	0
73	1175	2.73	.4	.30	.18	-.22	—
75	1175	2.68	.3	.28	.10	-.20	—
78	1295	2.68	.3	.28	.36	-.06	16.7
66	1320	3.14	.9	.39	.90	0	0
56	1350	2.85	.5	.28	.68	-.18	26.5
61	1350	2.74	.6	.49	.57	-.03	5.3
59	1350	3.18	1.1	.55	1.01	-.09	8.9
76	1350	2.66	.6	.57	.49	-.11	22.5
84	1375	3.60	1.4	.43	1.48	-.08	5.4
86	1400	2.70	.6	.53	.64	-.04	6.2
63	1450	3.58	1.6	.65	1.62	-.02	1.2
83	1475	3.60	1.7	.73	1.70	0	0
72	1500	2.84	1.1	.89	.99	-.11	11.1
77	1500	2.65	.7	.68	.80	-.10	12.5
68	1550	3.79	2.1	.94	2.05	-.05	2.4
82	1575	3.60	2.0	1.03	1.91	-.09	4.7
64	1660	3.58	1.9	.95	2.07	-.12	5.8
70	1755	3.79	2.4	1.24	2.48	-.08	3.2
Average							-7.8%

Column III gives the value of ϕ_0 for different values of θ as obtained from the emission data. Column IV lists the contact potential differences from the measurements with retarding fields. These are denoted by π_θ , since they represent results for varying values of θ . Let ϕ_1 denote the value of ϕ_0 for $\theta = 1$ and ϕ_θ for any given value of θ ; π_1 and π_θ the corresponding C.D.P. values. Then it is assumed that $\Delta\pi_\theta = \pi_\theta - \pi_1 = \Delta\phi_\theta = \phi_\theta - \phi_1$. Hence $\pi_1 = \pi_\theta - \Delta\phi_\theta$.

Thus, from the observed values of π_θ , an averaged plot of π_1 was obtained as a function of the temperature. These values of π_1 are given in column V. This smoothed curve was used to give corrected values of π_θ , from the observed $\Delta\phi_\theta$. Column VI shows these corrected results, for comparison with the originally observed values of C.D.P. (π_θ). The best justification for this process is the agreement between columns IV and VI. The last two columns give the actual and percentage deviations of IV and VI. In VIII, those cases have been omitted for which the values of $(\pi_\theta - \Delta\phi_\theta)$ were of the order of magnitude of the probable errors of measurement.

In most cases in the experiments, the measurements with retarding fields were made at 0.05 volt intervals throughout the critical range. However, due to the approximation in the correction for filament drop, no claim is made to an accuracy of better than 0.1 volt. The actual magnitude of the measured C.D.P. between the filament and nickel anode can have very little significance. The nickel was at all times positive to the filament. It was noted that after long operation it was impossible to reproduce the earlier readings, an effect traceable to evaporation of thorium to the anode and a consequent shift in the potential of the nickel surface.

The foregoing calculations were based on the assumption that $\Delta\phi_0 = \Delta\pi_0$, and the reasonably close agreement resulting seems to justify this assumption. This seems to be a direct experimental support of Richardson's theory of the essential identity of contact difference of potential and difference of work functions. From this viewpoint, the data of column V are of considerable qualitative interest. They may be interpreted as giving the temperature coefficient of ϕ .

Previous investigators have failed to show conclusively that the work function changes with the temperature. Germer¹¹ obtained what appeared to be evidence for such a change, but later attributed it to temperature effects inherent in the anode. Whatever the effect in pure metals—tungsten, platinum, and the like—it is small, and the conclusion reached is that the electrons which produce the thermionic current do not share in the temperature equilibrium in the metal. If they did have a share in the specific heat of the solid they should, by the equipartition theory, contribute an amount at most of the order of $2kT$, an effect barely detectable in these experiments. The results obtained here indicate a temperature coefficient of ϕ of the order of 2×10^{-3} volts per degree, or in the neighborhood of $20kT$. To attribute this to degrees of freedom is obviously absurd.

The constancy of ϕ_0 in the emission equation is not to be doubted, and the method by which the work function is here determined precludes obtaining the value of ϕ and analyzing it for temperature dependence. DuBridge¹² has pointed out that since, for composite surfaces, A in the equation is not constant, and ϕ_0 is by definition a constant, any temperature coefficient of ϕ will be concealed in A . No effort has been made as yet to study the mutual dependence of A and ϕ in a quantitative way.

III. THEORETICAL TREATMENT

Langmuir and also Richardson and Young¹³ have considered a patch surface to account for lack of saturation of electronic and photoelectric currents from thin electropositive films. Becker and Mueller¹⁴, in their paper on thoriated and caesiated filaments, calculated that at non-homogeneous surfaces the fields between the two types of atoms should produce the observed depar-

¹¹ Germer, Reference 8.

¹² DuBridge, Proc. Nat. Acad. Sci. 14, 788 (1928).

¹³ Langmuir, General Electric Rev. 504 (1920); Young, Proc. Roy. Soc. A104, 611 (1923).

¹⁴ Becker and Mueller, Reference 5.

tures from Schottky's plot at low applied fields. While any concrete representation of phenomena of atomic behavior may be questioned, the following considerations apparently do offer a tentative explanation of the effects set forth in the foregoing sections of this paper. These considerations were suggested by Dr. K. T. Compton in discussing the interpretation of the present work. It was learned later that the same idea had been carried to a partial quantitative stage a number of years ago by Langmuir and Mott-Smith, but not published.

The work function of a surface is the work required to remove an electron from the surface to infinity. The Thomson method of images furnishes a way of calculating this work, which can be expressed to a first approximation as

$$\phi = - \int_0^{\infty} (e^2/4x^2) dx.$$

But this leads to an infinite value for ϕ . This difficulty is overcome by assuming that within some small distance x_0 some other law applies, while beyond it the relation given above holds good. Langmuir¹⁵ has shown that whether the force between the surface and x_0 be assumed to be constant or to increase parabolically from zero, the result is the same and the work to reach x_0 is $W = e^2/4x_0$ and then

$$\phi = \frac{e^2}{4x_0} + \frac{e^2}{4x_0} = \frac{e^2}{2x_0}.$$

A simple calculation will show that the work required to remove an electron to a distance $10 x_0$ is 19/20 that needed to remove it to infinity. Thus the factors operating in this region close to the surface are the ones most effective in modifying the work function of the metal and the emission of electrons.

For a perfectly smooth, homogeneous surface, the electric field is constant at any distance outside it, and the work function is constant over it. If, instead of the surface being homogeneous, it consisted of single, isolated atoms of one metal distributed regularly over the surface of the foundation metal, the electric field at atomic distances would be disturbed by the effect of the contact potential between the two metals. However, at a distance of several atomic diameters the field would be very nearly uniform and consequently ϕ would be nearly constant for the whole surface.

The third possible distribution capable of any sort of study would consist of patches of the electropositive material distributed at random over the surface of the other. If such a patch consisted of many hundreds of atoms, it would appear to an electron at a distance $10 x_0$ normally out from the center of the patch as an infinite plane, and the field acting on the electron, and consequently the work function as applied to that electron would be a perfectly definite magnitude, characteristic of the patch material. Between the patch and the basic metal there would be a potential difference equal to the

¹⁵ Langmuir, Trans. Am. Electrochem. Soc. 29, 125 (1916).

C.D.P. between the two metals. Let Fig. 4-I represent such a surface. The shaded portions are patches of thorium and the adjacent areas tungsten.

Between these two there is a potential difference of about two volts (assumed since ϕ_0 for full activation is 2.6 volts and for clean tungsten is 4.5 volts). There will be lines of force originating on the thorium, as shown on the diagram. The effect of the fields of force will be to aid electrons to escape from the tungsten but to hinder their escape from the thorium. Since we assume the electrons under consideration to come exclusively from the thorium, the first effect can be ignored. The retarding action will be more pronounced near the edge of the thorium areas, falling off rapidly as we move toward the center of the patch, and becoming fairly constant and negligible over the central portion.

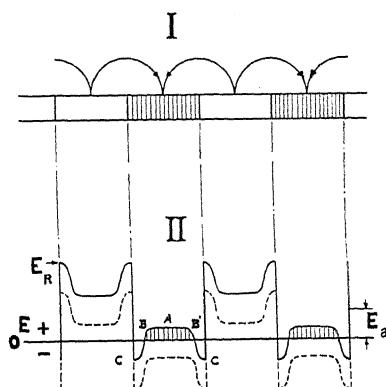


Fig. 4.

Let the dotted line of Curve II-Fig. 4 represent the field resulting from the C.P.D. between thorium and tungsten. The exact shape of the field distribution is indeterminate, but the one shown should be approximately correct. Assume for the present the electrons all to have zero initial velocities. If an external field E_a be applied, the combined effect of this and the "patch field" will be that of the solid line (Fig. 4-II). The shaded area represents the portion of the field accelerating electrons away from the surface. The length defined by it along the abscissa axis represents the part of the thorium covered surface from which electrons can escape from the surface under the influence of the applied field E_a . As E_a is increased from zero, emission begins as soon as the heavy solid line appears above the E_0 axis. Since the center portion of this curve is shown as flat, the area from which electrons can escape increases first rapidly with the voltage, then more and more slowly until finally the whole of the resultant field is in the direction to accelerate electrons away from the metal. At this point, the whole area of the thorium patch is an effective emitter, and the applied field is just strong enough to overcome the maximum field between thorium and tungsten at the point of contact of the two areas. This critical field is independent of the fraction of the surface covered with thorium so long as there remain exposed lines of contact of the two metals.

It should be characteristic only of the C.D.P. between the two metals concerned, and should vary for different pairs of elements.

If now the electrons be assumed to have a Maxwellian distribution of velocities, characteristic of the temperature, investigation with retarding fields should show a perfectly normal distribution curve for the portion BAB' and since we have assumed this line nearly flat, falling off sharply at B and B' , the distorting effect of the patch field should be a minimum. As zero is approached and the shoulder of the curve BC begins to emit, the Maxwellian curve will be distorted by the increasing effective area of the thorium brought into action.

Application of this analysis to the typical curve of Fig. 3 shows agreement of the postulated theory and the experimental result throughout the length of the curve. Retarding fields show a Maxwellian distribution. In the neighborhood of zero potential a saturation current is reached, modified by the neutralization of the patch field by the applied field and by the Schottky effect. The patch effect is less and less important with increasing fields until at the point V_1 (Fig. 1) the whole patch area emits and above this there is saturation emission, increased by the Schottky correction. It will be evident that for some distance above V_1 Schottky's relation will apply only approximately, as the field effective in reducing the surface work function is the difference between the field applied and the field due to the proximity of the tungsten, which is non-uniform over the area of the thorium patch. At very high applied voltages, where the patch field becomes negligible, Schottky's equation should represent the results with very satisfactory accuracy.

The choice of the point V_c as the zero of potential in the contact potential curve (Fig. 3) may need some justification. The point D , lying as it does on the actual curve, would seem at least an equally appropriate reference point, since only *changes* in contact potential are involved. However, the accuracy with which it can be determined is much less. Moreover, this point is modified by the velocity distribution of electrons and is therefore dependent on the temperature. Its sharpness of definition depends upon the shape of the shoulder of the curve E_R (Fig. 4-II). The extrapolated intersection at V_c is much less open to these objections. Also, due to the steepness of the slope of the portion CD (Fig. 3) and the flatness of AV , the uncertainty in the line AV due to its actual curvature introduces only a slight error in the determination of the hypothetical zero of potential at V_c .

It is important to note that the necessity of assuming a patch field even for a fully activated surface leads to the conclusion that the tungsten is never fully covered, but that there exist a maximum number of thorium areas distributed over the surface. If the break at V_1 (Fig. 1) is a constant for thorium on tungsten and this field is equal to the maximum retarding field exerted on electrons at the edge of the thorium areas by the tungsten atoms, this field should be of the order of magnitude of the C.D.P. (circa 2 volts) divided by some length which is of the same magnitude as that of the patches. For any different combination of elements, this critical field V_1 should have a different constant value. Thus for caesium on tungsten it should be larger, presumably in proportion to the larger contact difference in potential.

On the basis of this theory there seems to be a real significance to Dushman's extrapolation of the Schottky line to zero field to obtain i_0 . This represents the emission from the actual area of electropositive metal present, free from the effects of both the "patch field" and the applied field, and is characteristic of the work function of the surface under consideration.

I take pleasure in acknowledging my indebtedness to the Charles A. Coffin Foundation, since most of the present investigation was carried out while holding one of its Fellowships at Princeton University. Also I tender sincere thanks to Professor K. T. Compton, under whose direction this research was conducted, and whose contributions were many and invaluable; to Dr. S. Dushman, of the General Electric Research Laboratories, for suggestions and criticism; to others in the Laboratories of that company for assistance in preparing apparatus; and to Mr. Robert W. Graves for aid and collaboration during part of the work.

Note added with proof: Since sending this paper to the publisher, these results have been discussed with Dr. Langmuir who has extended his calculations on the properties of a patch surface and reaches conclusions which are in complete disagreement with the observed facts on the Schottky effect. The explanation of this inconsistency between the theoretical deductions and the observations is to be included in a joint report in preparation by Dr. Langmuir and Professor Compton to be published in a forthcoming number of the Physical Review Supplement.

THE TEMPERATURE DEPENDENCE
OF FIELD CURRENTS

BY NORMAN A. DE BRUYNE*

TRINITY COLLEGE, CAMBRIDGE, ENGLAND

(Received November 12, 1929)

ABSTRACT

The increase in the field current observed by Millikan and Eyring to take place at about 1000°K is shown to be of the order of magnitude of the thermionic emission to be expected from a thoriated filament at this temperature. The author considers that the results of Millikan and Lauritsen are inconclusive and do not definitely establish the existence of a dependence of field currents upon temperature. The author has carried out new experiments using an improved method of investigation and has been unable to detect any temperature variation in the field current. His contention is not that no temperature variation exists but that no real variation has yet been observed.

ALL investigators¹ are agreed that from 80°K to 1000°K the auto-electronic, or field, emission is independent of temperature. There is however a difference of opinion about the existence of a temperature dependence above 1000°K . Millikan and Eyring² observed an increase in the emission at this temperature but, by separating out the thermionic from the field current in a mixed emission, I found³ that the field current showed no systematic increase with temperature and therefore concluded that the increase observed by Millikan and Eyring was due to the occurrence of a thermionic emission. Millikan and Lauritsen⁴ have recently stated that the increase in emission observed by Millikan and Eyring "is about a billion times too large to be so interpreted;" this statement is evidently based on the emission characteristics of pure tungsten and disregards the fact that Millikan and Eyring used thoriated filaments. The thermionic emission from a thoriated tungsten filament is in fact of the order of magnitude of the increase observed by Millikan and Eyring, as may be seen from the following considerations.

THE RESULTS OF MILLIKAN AND EYRING

The diameter of the filament used by Millikan and Eyring was 0.00123 cm. Its length is not stated but from the relative dimensions in their diagram it appears to have been of the order of 5 cm, giving a surface area of 0.019 cm.⁵

* Fellow of Trinity College, Cambridge.

¹ J. E. Lilienfeld, *Ber. d. Sächs. d. Wiss.* **72**, 31 (1920). B. S. Gossling, *Phil. Mag.* **1**, 609 (1926). R. A. Millikan and C. F. Eyring, *Phys. Rev.* **27**, 51 (1926).

² R. A. Millikan and C. F. Eyring, *Phys. Rev.* **27**, 51 (1926).

³ N. A. de Bruyne, *Proc. Cambs. Phil. Soc.* **24**, 347 (1928).

⁴ R. A. Millikan and C. C. Lauritsen, *Phys. Rev.* **33**, 598 (1929).

⁵ S. Dushman, *Gen. Elect. Rev.* **26**, 156 (1923).

Thermionic emission from a fully thoriated wire at 1100°K is⁵ 2.51×10^{-6} amps per cm^2 corresponding to an emission of 4.77×10^{-8} amps from an area of 0.019 cm^2 . The Schottky effect at a field of 0.7×10^6 volts per cm would increase the thermionic emission to 1.35×10^{-6} amps; at this field Millikan and Eyring observed an increase in the emission of 0.02×10^{-6} amps. At a field of 1.0×10^6 volts/cm the thermionic emission would be 2.58×10^{-6} amps while the observed increase was 3.0×10^{-6} amps. The thermionic emissions have been computed for a fully thoriated surface, but taking into account the uncertainties in the measurements the observed increases appear to be of the order of magnitude of the possible thermionic currents, even if the surface were not completely thoriated. The experiments of Millikan and Lauritsen do not therefore establish the existence of a dependence of the autoelectronic emission on temperature.

THE RESULTS OF MILLIKAN AND LAURITSEN

Millikan and Lauritsen⁴ have recently published some new data in which proper allowance can be made for the thermionic emission taking into account the Schottky effect. Unfortunately the new data are limited to one graph in which only two points are relevant. Up to 800°K the current was constant at 4.6×10^{-8} amperes, at 1130°K (a temperature at which the thermionic current was negligible) the current was 5.6×10^{-8} amperes, at higher temperatures a thermionic current set in. These results therefore show a temperature variation which cannot be explained as due to a thermionic emission. Yet the position as left by the publication of Millikan and Lauritsen's paper is far from satisfactory, since it is impossible to have any confidence in a conclusion based on a few measurements of an effect in which it is extremely difficult to obtain reproducible results.

AUTHOR'S FIRST RESULTS

I first repeated Millikan and Lauritsen's experiment. A constant voltage was applied to a tube and the filament temperature was raised and lowered rapidly in fixed steps, the emission being noted at each step. The voltages used varied between 12,000 and 23,000 volts. A number of experimental runs were carried out. The results were quite inconclusive; two showed an increase in the autoemission at 1100°K of the order of magnitude observed by Millikan and Lauritsen, one showed a decrease in the emission, but the majority gave a series of widely scattered points through which it was impossible to draw any smooth curve; in general the spontaneous fluctuations in the emission were found to be of the order of magnitude of the increase observed by Millikan and Lauritsen. In plotting characteristics showing the variation of emission with field these fluctuations are far less disturbing because of the tremendous increase in the current produced by a comparatively small rise of field, but in an experiment such as this where the field is kept constant the spontaneous variations become relatively important. It was obvious that a new method of attack was required, and it was decided to obtain a continuous record of the galvanometer deflection.

RESULTS BY IMPROVED METHOD OF INVESTIGATION

The author observed that in some tubes the filament changed its shape considerably when heated and that such distortion was accentuated when a strong field was applied. The same difficulty has been noted by I. Langmuir and K. H. Kingdon⁶ in their work on contact potentials. The author therefore used tungsten wire of 0.02 mm diameter instead of the finest wire available. The filament of length was formed into a stable sharp angled loop inside a cylindrical anode closed at one end. The filament leads were encased in glass leaving only the filament exposed. The tubes were exhausted under the same conditions as a transmitting valve, the filament was outgassed and the anode was kept at bright red heat for twenty minutes before sealing off. After sealing off the filament was lit for some time with an applied anode voltage of 10,000 volts.

The galvanometer deflection was recorded photographically on a rotating drum which revolved once in about two minutes. A constant voltage from a valve rectifier set was applied to the experimental tube and the filament temperature was raised, for periods of about ten seconds, from room temperature to some other higher temperature which was fixed for each run. The periods when the filament was hot were recorded on the drum by the lighting of a small lamp which left a trace on the photographic paper. A calibration and zero line were also recorded. In all the curves the time axis increases from right to left.

Fig. 1. Galvanometer record. Applied potential 5,500 volts, filament heating current 0 and 0.235 amp.

Fig. 1 shows the record obtained when the voltage was too low to produce an autoemission. The small regular rises in the emission correspond to the periods when the filament temperature was raised to 0.235 amps [giving a temperature of 1600°K approximately]; 5500 volts were applied to the anode. It will be seen that at 5500 volts a measurable thermionic emission begins at a filament current of 0.235 amps.

Figs. 2, 3, 4, 5 show results obtained with an applied potential of 17,800 volts (corresponding to a field strength of 1.4×10^6 volts per cm). The first signs of any correlation between the emission and the periods of heating occur between a filament current of 0.220 and 0.230 amps. i. e. between 1550°K and 1600°K; it is in just this temperature range that a thermionic current is to be expected.

Figs. 6, 7, 8, 9, 10 show results obtained at an applied potential of 14,800 volts corresponding to a field of 1.2×10^6 volts per cm. Here again the first signs of any increase occur when the filament current is raised to 0.230 amps, corresponding to a filament temperature of 1590°K. Thus no measurable

⁶ I. Langmuir and K. H. Kingdon, *Phys. Rev.* 34, 129 (1929).

increase in the autoemission takes place up to about 1600°K at which temperature a thermionic emission sets in.

It seems probable that the electrons pulled out by strong fields must come in the main from energy levels lower down than those from which the ther-



Fig. 2. Filament heating current 0 and 0.190 amp.

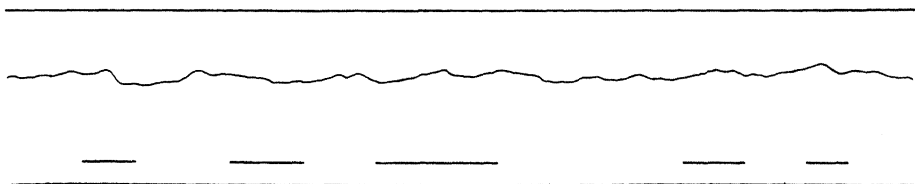


Fig. 3. Filament heating current 0 and 0.200 amp.

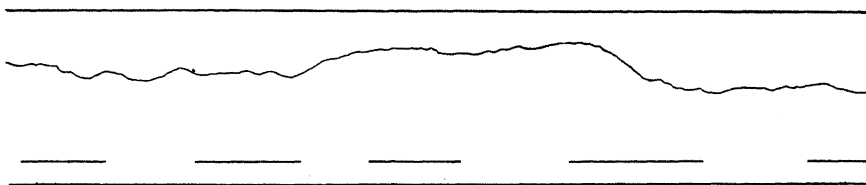


Fig. 4. Filament heating current 0 and 0.220 amp.



Fig. 5. Filament heating current 0 and 0.231 amp.

Figs. 2, 3, 4, 5. Galvanometer records with 17,800 volts applied to filament. The top horizontal line represents a current of 2 microamperes, the irregular line gives the electronic emission, the broken lines the periods of heating the filament, and the bottom line the galvanometer zero.

mionic emission takes place, since within the limits of experimental error the autoemission is independent of temperature. Unfortunately Sommerfeld's theory can give no information on the temperature dependence, beyond showing that it must be small, since no exact measurement of the applied field is yet possible.

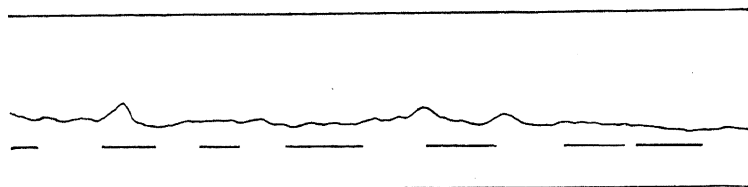


Fig. 6. Filament heating current 0 and 0.195 amp.

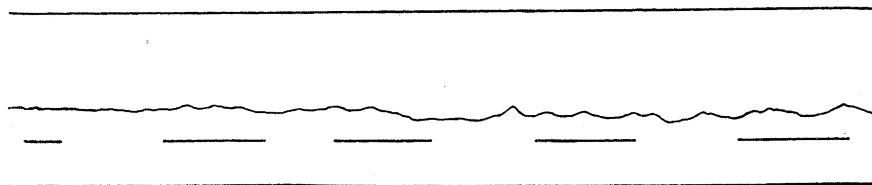


Fig. 7. Filament heating current 0 and 0.202 amp.

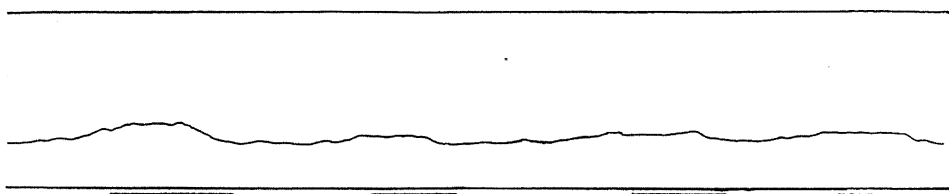


Fig. 8. Filament heating current 0 and 0.230 amp.

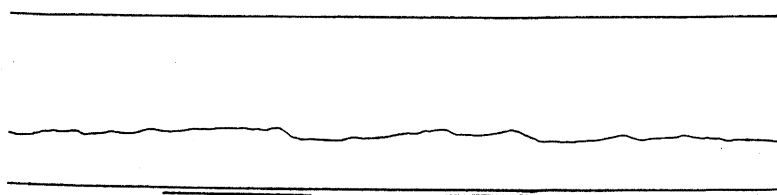


Fig. 9. Filament heating current 0 and 0.235 amp.

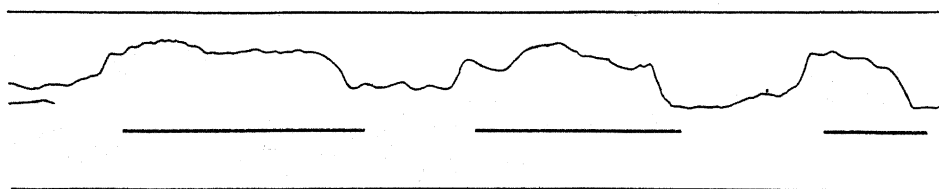


Fig. 10. Filament heating current 0 and 0.248 amp.

Figs. 6, 7, 8, 9, 10. Galvanometer records with 14,800 volts applied to the filament. The top horizontal line represents a current of 2 microamperes, the irregular line represents the electronic emission, the broken lines the periods of heating of the filament, and the bottom line the galvanometer zero.

I wish to acknowledge gratefully a grant from the Government Grant Committee of the Royal Society for the purchase of the drum camera used in this investigation.

VARIABLE FLOW IN PIPES

BY H. BATEMAN

CALIFORNIA INSTITUTE OF TECHNOLOGY, PASADENA

(Received December 9, 1929)

ABSTRACT

The problem considered is that of finding a variable pressure gradient or forced motion of the pipe in a longitudinal direction which, at the time when it ceases to act, will have produced a prescribed distribution of velocity over the cross-section of the pipe. The subsequent changes in the distribution as the motion decays are also investigated and the cases examined point to the conclusion that an initial velocity profile with curvature of one sign will retain this property as it changes into the profiles for the different stages of the decaying motion.

INTRODUCTION

THE subject of variable flow in pipes is of much importance in engineering and has been studied experimentally in the case when the motion is turbulent. The problems which arise in connection with the metering of gases have been ably discussed by Hodgson,¹ Swift,² Judd and Pheley.³ Accelerated flow without pulsations has been studied by Gibson⁴ and Aisenstein⁵ who express the time necessary to reach a velocity v in the form

$$t = (K/2V) \log \frac{V+v}{V-v}$$

where V is the final velocity of steady flow under the force or pressure gradient which produces the constant acceleration and K is a coefficient which has one value for the Poiseuille régime and another value for the Venturi or turbulent régime, K depending in each case upon the value of the Reynolds number at time t .

We shall study here problems relating to flow in the Poiseuille régime when the acceleration is variable. For simplicity the compressibility of the fluid is neglected. This is undoubtedly a defect because in the particularly interesting case of rapid oscillations the motion will be complicated by the propagation of waves.

The propagation of waves in water has been much studied in connection with the phenomenon of water hammer in pipes and need not be discussed here. The propagation of air waves along a pipe, when viscosity is taken into consideration, has been studied theoretically by Stokes, Kirchhoff and Rayleigh.⁶

¹ Hodgson, Proc. Inst. Civil Engineers **204**, 108 (1916-17).

² Swift, Phil. Mag. (7) **5**, 1 (1928).

³ Judd and Pheley, Mech. Eng., **45**, 223, 270 (1923).

⁴ Gibson, "Water hammer in hydraulic pipe lines," p. 50.

⁵ Aisenstein, Trans. Amer. Soc. Mech. Eng. **51**, 67 (1929).

⁶ See Lamb's Hydrodynamics, pp. 612-617.

The recent experiments of Simmons and Johansen⁷ indicate, however, that there is need of further mathematical investigations. The author is considering the problem of pulsations when both viscosity and compressibility are taken into consideration but the work is not sufficiently advanced to warrant publication.

1. *Free decay, motion initially prescribed.* 'A long straight pipe of uniform cross-section has its ends attached by flexible connections to two reservoirs containing water, the pipe itself being supposed to be at any time completely filled with water.

The pipe is now moved in the direction of its length with a varying velocity $P(t)$. If u is the velocity of the water at the point (x, y, z) at time t the direction of motion being that of the axis of x , the equation of motion of the water relative to axes fixed relative to the reservoirs is

$$\rho \frac{\partial u}{\partial t} = \mu \left(\frac{\partial^2 u}{\partial y^2} + \frac{\partial^2 u}{\partial z^2} \right) - \frac{\partial p}{\partial x} + \rho X$$

where p is the pressure, ρ is the density of the water, μ its viscosity and X the external force per unit mass. If the water is treated as incompressible and the pipe as rigid, the equation of continuity

$$\frac{\partial \rho}{\partial t} + \frac{\partial}{\partial x} (\rho u) = 0$$

reduces to $\partial u / \partial x = 0$ and implies that $u = F(y, z, t)$. We shall assume moreover that ρ and μ are constants independent of position and of the time t .

If we write $u = U + P(t)$ where U is the velocity of the water relative to the pipe, the equation for U is

$$\rho \frac{\partial U}{\partial t} = \mu \left(\frac{\partial^2 U}{\partial y^2} + \frac{\partial^2 U}{\partial z^2} \right) - \frac{\partial p}{\partial x} - \rho \frac{dP}{dt} + \rho X$$

and so the motion relative to the pipe is the same as if the pipe were at rest and the fluid acted upon by an additional body force $-P'(t)$ per unit mass or an equivalent pressure gradient $\rho(P't)$. When p and X are zero the free motion in an oscillating pipe is relatively the same as the forced motion in a stationary pipe when the external force or pressure gradient fluctuates in the prescribed manner.

The transfer of motion from an oscillating plane to an adjoining liquid has been studied by Stokes,⁸ Rayleigh⁹ and other writers. Stokes showed that when the frequency of oscillation is high the motion in the fluid rapidly diminishes in intensity as the distance from the plane increases. This indicates that if fluid bounded by parallel plane walls is set in motion by a rapidly fluctuating pressure gradient which oscillates about a zero value, the

⁷ Simmons and Johansen, British Advisory Committee for Aeronautics, R & M. 957 (1925).

⁸ Stokes, *Cambr. Phil. Trans.* 9 (1850).

⁹ Rayleigh, *Phil. Mag.* (6) 21, 697 (1911).

distribution of velocity over the cross-section will be approximately uniform except in the immediate neighbourhood of the walls, where rapid variations are to be expected. This result has been extended by S. F. Grace¹⁰ to the case of flow in a pipe of circular section. For a pipe of radius 1 cm there is approximate uniformity in the distribution of velocity over a large part of the cross-section if the period of oscillation is less than six seconds. The velocity moreover, lags 90° in phase behind the force producing the motion.

The existence of a phase lag indicates that the water may still be moving when the driving force has ceased to act. If, then, we go back to the case of the moving pipe we can say that the water may still be moving when the pipe is brought to rest. The velocity distribution at this time ($t=0$, say) may, indeed, be prescribed more or less arbitrarily so long as the velocity at the boundary is zero. Some interesting questions now arise with regard to the manner in which the velocity profile changes as the motion dies down.

Suppose, for instance, that the velocity profile has initially curvature of only one sign so that, when the velocity at each point of the cross-section is represented by an ordinate MQ , the locus of Q is everywhere concave to the plane of the section. It is interesting to inquire whether at some later time t the velocity profile can be partly convex to the plane of the section. This question is an interesting one because in his studies of the stability of an inviscid incompressible fluid in rectilinear motion between parallel planes Lord Rayleigh¹¹ found that a steady motion, without changes in the sign of the curvature of the velocity profile, was stable for small oscillations but that a profile with changes in the sign of the curvature might be unstable.

The question has been studied for the case of flow between parallel planes $z = \pm a$, the free motion being represented by

$$u = c_1 e^{-s} \cos \theta + c_3 e^{-9s} \cos 3\theta + c_5 e^{-25s} \cos 5\theta + \dots$$

where $s = \nu \pi^2 t / 4a^2$ and $\theta = \pi z / 2a$. The expansion was limited to the first three terms and the coefficients c_1, c_3, c_5 were chosen so that the coefficients of z^2 and z^4 in the Taylor series for u were initially zero. This gives an initial distribution of velocity with curvature of one sign and a nearly constant value for a large part of the cross-section. The numerical work gave no indication of a change in sign of the curvature at any point of the profile as it changed with the time. The profile, in fact, gradually approached the shape of the cosine curve $u = k \cos \theta$ which differs only slightly in shape from the parabola characteristic of steady motion.

The question was also examined by assuming that at time $t=0$

$$d^2u/dz^2 = -\cos \theta [(\alpha \cos^2 \theta + \beta)^2 + \gamma^2]$$

where α, β and γ are constants. Again there was no indication that at a later time t it would be legitimate to write

¹⁰ Grace, Phil. Mag. (7) 5, 933 (1928).

¹¹ Rayleigh, Proc. London Math. Soc. 10, 4 (1879); 11, 57 (1880); 19, 67 (1887); 27, 5 (1895); Phil. Mag. 34, 59 (1892); 26, 1001 (1913); 28, 609 (1914). See also, L. Prandtl, Ziets. f. Angew. Math. und Mech. 1, 431 (1921).

$$d^2u/dz^2 = -\sigma \cos \theta [\cos^2 \theta - \cos^2 \theta_1][\cos^2 \theta - \cos^2 \theta_2]$$

where θ_1 and θ_2 are real angles.

In the work of Grace the oscillations were undamped. To discuss a type of variable motion which ceases at time $t=0$ we first consider the case in which

$$\begin{aligned} P(t) &= (-\nu t)^{-1/2} \exp(m^2/4\nu t) & t < 0, \\ P(t) &= 0 & t > 0, \end{aligned}$$

where $\nu = \mu/\rho$ is the kinematic viscosity. Since $\partial u/\partial t = \nu \partial^2 u/\partial z^2$ and

$$P(t) = K \int_0^\infty e^{\xi^2 \nu t} \cos(m\xi) d\xi, \quad t < 0,$$

where $K = 2/\sqrt{\pi}$, an appropriate solution is

$$u = K \int_0^\infty e^{\xi^2 \nu t} \cos(m\xi) \cosh(z\xi) \operatorname{sech}(a\xi) d\xi \quad t < 0.$$

As $t \rightarrow 0$, $u \rightarrow u_0$, where

$$\begin{aligned} u_0 &= K \int_0^\infty \cos(m\xi) \cosh(z\xi) \operatorname{sech}(a\xi) d\xi \\ &= \frac{(2K/a) \cosh(m\pi/2a) \cos(z\pi/2a)}{\cosh(m\pi/a) + \cos(z\pi/a)}. \end{aligned}$$

When $\sinh^2(m\pi/2a) = \frac{1}{2} u_0$ is approximately constant over a considerable part of the cross-section. If, however, we take $\pi^2 m^2/4a^2 = 1/32$, we have the result that u_0 is approximately proportional to

$$\frac{65 \cos \theta}{4 + 128 \cos^2 \theta}.$$

When $z=0$ this fraction is equal to $65/132$ and when $z=2a/3$ the fraction is equal to $65/72$. It should be noticed that the maximum value of $P(t)$ occurs when $2\nu t = -m^2$, the maximum value being $(m^2 e/2)^{-1/2}$. Hence a small value of m corresponds to a large maximum velocity of the walls.

The present result confirms our statement that the fluid may still be moving when the pipe has ceased to move.

To discuss the decay of the motion when $t > 0$ we expand u_0 in the form

$$u_0 = H \sum_{s=0}^{\infty} (-)^s e^{-mS} \cos(zS)$$

where $S = \pi(2s+1)/2a$ and $H = 4\sqrt{\pi}/a$. The velocity at time t is then

$$u = H \sum_{s=0}^{\infty} (-)^s e^{-mS - \nu S^2 t} \cos(zS).$$

Since u satisfies the equation $\partial u / \partial t = \nu \partial^2 u / \partial z^2$ the velocity $u^{(n)}$ corresponding to a function

$$P^{(n)}(t) = \frac{\partial^n}{\partial t^n} P(t)$$

$$u^{(n)} = \nu^n \frac{\partial^{2n} u}{\partial z^{2n}}$$

is

$$= K \nu^n \int_0^\infty e^{\xi^2 \nu t \xi^{2n}} \cos(m\xi) \cosh(z\xi) \operatorname{sech}(a\xi) d\xi \quad (t < 0)$$

$$= H \nu^n \sum_{s=0}^\infty (-)^s + n S^{2n} e^{-mS - \nu S^2 t} \cos(zS) \quad (t > 0).$$

An initial distribution of velocity

$$\bar{u}_0 = H \sum_{s=0}^\infty (-)^s \phi(-\nu S^2) e^{-mS} \cos(zS)$$

will, with a suitable form of the function ϕ , be produced by a velocity of the walls varying up to time 0 according to the law

$$\bar{P}(t) = \phi\left(\frac{\partial}{\partial t}\right) P(t).$$

2. *Forced motion.* We next consider the equation

$$\rho \frac{\partial u}{\partial t} = \mu \frac{\partial^2 u}{\partial z^2} - \frac{\partial p}{\partial x}, \quad (\mu = \rho \nu)$$

for the rectilinear flow of an incompressible viscous fluid of constant density ρ when the pressure gradient $\partial p / \partial x$ varies with the time. For convenience we write

$$-\frac{\partial p}{\partial x} = \left(\frac{2\mu}{\pi}\right) \int_0^\infty e^{-\nu m^2 t} \cos ma \cdot dm \int_0^\infty \cos mv \phi(v) dv$$

where $\phi(v)$ is an even function for which Fourier's integral formula may be used with confidence. The corresponding expression for u is then

$$u = (2/\pi) \int_0^\infty e^{-\nu m^2 t} (\cos mz - \cos ma) (dm/m^2) \int_0^\infty \cos mv \phi(v) dv.$$

It should be noticed that at time $t=0$ we have

$$-\frac{\partial p_0}{\partial x} = \mu \phi(a)$$

$$u_0 = \int_z^a ds \int_0^s \phi(v) dv.$$

If, on the other hand we write $f(m)$ instead of $\int_0^\infty \cos mv \phi(v) dv$ and take $f(m)=1$ we have

$$-\frac{\partial p}{\partial x} = \mu(\pi \nu t)^{-1/2} e^{-a^2/4\nu t}, \quad \text{and}$$

$$u = (\pi \nu t)^{-1/2} [F(a, t) - F(z, t)], \quad \text{where}$$

$$F(z, t) = \int_0^z (z-s) e^{-(s^2/4\nu t)} ds.$$

A short table of values of $F(z, t)/2\nu t$ is given below. For convenience n has been written for $z/2(\nu t)^{1/2}$ and values of e^{-n^2} are also included. The fifth figure in the decimal may be slightly incorrect.

TABLE I

n	$F(z, t)/2\nu t$	$\exp(-n^2)$
0	0	1
0.1	0.00999	0.99005
0.2	0.05974	0.96079
0.3	0.08866	0.91393
0.4	0.15587	0.85214
0.5	0.24009	0.77880
0.6	0.33992	0.69768
0.7	0.45361	0.61263
0.8	0.57959	0.52729
0.9	0.71611	0.44486
1.0	0.86156	0.36788
1.1	1.01436	0.29820
1.2	1.17313	0.23693
1.3	1.33668	0.18452
1.4	1.50399	0.14086
1.5	1.67401	0.10540
1.6	1.84608	0.07731
1.7	2.02000	0.05557
1.8	2.19489	0.03916
1.9	2.37055	0.02705
2.0	2.54666	0.01832

For the case in which $a=2$ the distribution of velocity has been calculated at times t for which $2(\nu t)^{1/2}$ has the values 1, 2, 4, respectively and compared with the parabolic distribution for steady flow. In each case the velocity is compared with the axial value c . The third time is beyond that at which the pressure gradient is a maximum. It will be noticed that while the pressure gradient is increasing the distribution of velocity differs only slightly from the distribution for steady flow. When t is large we have $F(z, t) = z^2/2 - z^4/48\nu t$, approximately, and so in the final stages of the motion the distribution of velocity again differs only slightly from the parabolic distribution.

TABLE II
 z/a

$2(\nu t)^{1/2}$	0	0.2	0.4	0.6	0.8	1	
1	1	0.9384	0.7724	0.5393	0.2751	0	u/c
2	1	0.9307	0.8191	0.6054	0.3273	0	u/c
4	1	0.9584	0.7512	0.6307	0.3508	0	u/c
Parabola	1	0.96	0.79	0.64	0.36	0	u/c

3. The analysis for rectilinear flow in a tube of circular section is very similar to that for flow between two parallel walls. The equation of motion is now

$$\rho \frac{\partial u}{\partial t} = \mu \left(\frac{\partial^2 u}{\partial r^2} + \frac{1}{r} \frac{\partial u}{\partial r} \right) - \frac{\partial p}{\partial x},$$

where r is the distance of a point from the axis of the tube. We shall commence with a study of forced motion.

If

$$-\frac{\partial p}{\partial x} = \mu \int_0^\infty e^{-\nu m^2 t} J_0(ma) m dm \int_0^\infty J_0(mv) \psi(v) v dv$$

where $\psi(v)$ is a function for which the inversion formula of Hankel may be used with confidence, the corresponding expression for u is

$$u = \int_0^\infty e^{-\nu m^2 t} [J_0(mr) - J_0(ma)] (dm/m) \int_0^\infty J_0(mv) \psi(v) v dv$$

and at time $t=0$ we have

$$\begin{aligned} -\frac{\partial p}{\partial x} &= \mu \psi(a) \\ u_0 &= \int_r^a (ds/s) \int_0^s v \psi(v) dv. \end{aligned}$$

Another particular case of interest is that in which

$$\begin{aligned} -\partial p / \partial x &= (\mu / 2\nu t) \exp [-a^2 / 4\nu t] = \mu \int_0^\infty e^{-\nu m^2 t} J_0(ma) m dm \\ u &= \int_t^\infty (d\tau / 2\tau) [\exp (-r^2 / 4\nu t) - \exp (-a^2 / 4\nu t)]. \end{aligned}$$

Next, taking the case of free motion, let us suppose that the velocity of the pipe at time t is given by the function $P(t)$, where

$$\begin{aligned} P(t) &= (-1/2\nu t) \exp (g^2/4\nu t) & t < 0 \\ P(t) &= 0 & t > 0 \end{aligned}$$

Since

$$P(t) = \int_0^\infty e^{\nu m^2 t} J_0(mg) m dm \quad t < 0$$

an appropriate solution is

$$u = \int_0^\infty e^{\nu m^2 t} J_0(mg) m dm [I_0(mr) / I_0(ma)], \quad t < 0$$

with the usual notation for the Bessel function with imaginary argument.

As $t \rightarrow 0$, $u \rightarrow u_0$, where

$$u_0 = \int_0^\infty J_0(mg) m dm [I_0(mr) / I_0(ma)]$$

IONIC MOBILITIES IN Cl_2 AND IN Cl_2 -AIR MIXTURES

BY LEONARD B. LOEB

UNIVERSITY OF CALIFORNIA, BERKELEY

(Received December 9, 1929)

ABSTRACT

Work of early investigators and of Herbert Mayer indicates that the presence of traces of Cl_2 reduces the mobility of the negative ion below that of the positive ion, a fact which appeared inconsistent with a theory of Condon and the writer. No investigations of mobilities of both ions in pure Cl_2 have been reported. The possibility that the discrepancy between theory and observation in Mayer's results was caused by HCl in the Cl_2 made a more careful investigation imperative. Cl_2 carefully prepared and free from both HCl and H_2O was used. It was found that the values of the mobilities in pure Cl_2 on the new absolute standard for positive and negative ions was 0.654 and 0.510 cm/sec per volt/cm respectively. A study of mixtures of dry air and Cl_2 showed that traces of Cl_2 less than 0.1 percent reduce the negative mobility below that of the positive ion. The positive mobilities were little affected by the presence of Cl_2 so that while positive ions obey Blanc's law in Cl_2 -air mixtures the negative ion shows a marked clustering effect. No disturbances due to dipole moments were observed for positive ions in Cl_2 as is to be expected.

INTRODUCTION

IN ATTEMPTING to determine something of the nature of the gaseous ions a study of mobilities of ions in gaseous mixtures has shown itself to be of value.¹ Later investigations have shown that beyond the more important conclusions already drawn from this study, further investigations will add but little of importance, until a much greater control of minute traces of impurity can be had.^{1,2} This appears to be the more so in view of the recent researches of Erikson.³ Before concluding the work on mixtures and turning to a new method of attack on the ion problem it was felt essential to study one more gas, to wit: chlorine, in view of certain apparent discrepancies in data and theory. So far ionic mobilities in pure chlorine have been studied by only one observer, Wahlin,⁴ and that for the *negative ion* only. His value for the negative ion mobility constant was 0.73 cm/sec per volt/cm. The interest in Cl_2 lies in the fact that all observers have reported⁵ that the *negative* mobility in Cl_2 appeared to be *less than* the *positive* mobility while according to Condon

¹ L. B. Loeb, Phys. Rev. **32**, 81 (1928).

² DuSault and Loeb, Proc. Nat. Acad. Sci. **14**, 384 (1928).

³ H. A. Erikson, Phys. Rev. **34**, 635 (1929).

⁴ H. B. Wahlin, Phys. Rev. **19**, 173 (1922).

⁵ To date no accurate observations on *both* ions in Cl_2 have been made. The effect of Cl_2 in mixtures of low percentage Cl_2 with other gases inferred by early observers and one very uncertain result of Mayer's at 8 cm pressure were the only data on which such assertions could be founded.

and the writer⁶ this should not occur for gases having a low dipole moment fairly symmetrically placed inside of the molecule, as in Cl_2 .

EARLY ATTEMPTS OF THE WRITER

In closing the work on the mobilities in mixtures for the spring of 1928 Miss L. DuSault and the writer therefore made a study of Cl_2 . In this case ordinary *grease lubricated stopcocks* were employed, and the Cl_2 was fractionated from a large tank loaned by the Chemistry department, liquid air being used, together with cooling traps to remove moisture. Two interesting facts were found in this work which was carried on with Cl_2 and occasionally Cl_2 mixed with H_2 , using pure H_2 as a control gas for calibrating the apparatus. The one fact was that Cl_2 yielded a positive mobility constant of 0.617 cm/sec per volt/cm and a negative mobility constant of 0.466 cm/sec per volt/cm under the conditions used. This is one of the cases where the negative mobility relative to the positive mobility is as low as it has ever been observed and appeared contrary to the theory of Condon and Loeb. Further certain uncontrollable irregularities were observed in some of these cases in which the presence of traces of Cl_2 in pure H_2 caused phenomenally high values of the positive ion mobilities. An analogous result had been observed to a smaller extent in the SO_2 - H_2 ² mixtures, but in the case of Cl_2 the values of the positive mobility were so high, (i.e. in one or two cases three times the normal mobility in H_2) that a further study seemed suitable.

In all these studies it was observed that when the ionization chamber was opened for cleaning to remove the last traces of Cl_2 a strong odor of HCl was present, even after prolonged pumping. This was found to be due to the extensive reaction of Cl_2 with the organic stopcock grease which emitted HCl for hours after exposure to Cl_2 .

On resuming work in the fall of 1928, the abnormally high positive mobilities persisted in an unpredictable fashion, even after all the apparatus up to the mercury vapor pump had been carefully cleaned. At this stage of the work it had never been found essential to place a liquid air trap between the pump and the chamber as Hg vapor has no material effect on the ions. It then was suspected that the Cl_2 acting on the Hg had produced HgCl_2 which on heating in the pump gave off Cl_2 and so produced the spurious high values mentioned. On cleaning the pump and using fresh Hg no more values of this sort were observed. The facts which seemed apparent as far as the high values of positive mobilities were concerned could be summed up as follows. The presence of either traces of SO_2 or more especially Cl_2 from the mercury vapor pump in traces sometimes seemed to cause this effect which could never be controlled. It became an urgent problem to attempt to discover the cause of this effect if possible.

The low values of the negative mobilities in Cl_2 relative to the positive values, and the practically non-polar nature of Cl_2 , led the writer to look for this lowering in the presence of HCl due to stopcock greases and due to HCl in the Cl_2 from the tank which could not be removed by fractionation.

⁶ L. B. Loeb, Phys. Rev. 32, 95 (1928). Also Kinetic Theory of Gases, p. 478.

THE PREPARATION OF PURE Cl_2

Beginning in the spring of 1929 and extending well into the autumn attempts were made to develop a system for generating Cl_2 free from H_2O and HCl , and devise greaseless stopcocks. The trouble with the use of mercury seal stopcocks lay in the large number of cocks required, the dangerous nature of large quantities of Cl_2 gas in case of failure of the mercury seal stopcocks and the constant "freezing" of such stopcocks with large pressure differences and constant use. The problem was finally solved as follows.

For the apparatus a large number of mercury seal type of stopcocks of a high quality were made for this work by Mr. L. B. Clark, then departmental glass blower. The design of these is shown in Figure 1. In place of ordinary

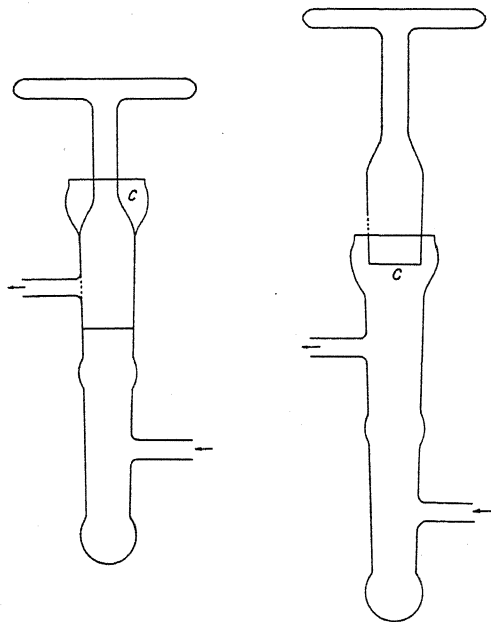


Fig. 1. Design of mercury-seal stopcocks.

lubricants a paste of P_2O_5 and water was made by dissolving as much P_2O_5 in a small amount of water as possible. This was achieved by heating to 250 or 300°C in a porcelain dish. The paste on cooling was like a very thick syrup in consistency. Trouble was experienced at first in that the P_2O_5 of *best quality* for drying tubes furnished by standard chemical concerns *contained marked amounts of P_2O_3* . On mixing with water local heating and steam production resulted in the reduction of P_2O_3 to P, which on heating or otherwise changed to the red form. The presence of this substance was confirmed by the dull red color, the odor and the flashes of flame at the surface of the paste as the temperature rose above 250°C. It might be noted that the pink color taken on by P_2O_5 in drying trains as it hydrates where organic matter is avoided is due to

the formation of this substance. By either getting a good grade of P_2O_5 , which rarely happens, or by subliming the P_2O_5 for long hours at a reasonably low temperature, (below the melting point so as not to attack the glass) in a stream of O_2 the pentoxide may be prepared free from such substances. In the results to be given earlier measurement were made with P_2O_5 lubricant containing red phosphorus. The fear that Cl_2 might react in traces with P led to the use of later lubricants treated as above and free from this source of trouble. As it turned out the results were apparently not influenced by this impurity.

In using P_2O_5 paste as a lubricant care must be taken to have the moisture of the air kept from the paste on the stopcocks. Accordingly the surface of the P_2O_5 was covered with a pure mineral oil in the cup part C of the stopcocks. The system was always first dried out carefully before lubricating and replacing the stopcocks. As long as the gases inside were dry the lubricant on the beautifully ground stopcocks made for us behaved very well even under pressure differences of 1 atmosphere and with frequent turning. Gradually however the lubricant "worked" out of the cocks on constant use, (25 to 50 turnings over a period of a week) and had to be renewed.

The Cl_2 was generated by a method previously used by Professor Rollefson of the Chemistry department. $CuCl_2$ deprived of most of its water by heating and stirring under a hood was placed in heavy Pyrex glass bulbs surrounded by heating coils. These were heated in vacuo gradually beginning at $200^\circ C$ for some 10 to 20 hours increasing the temperature step by step to 250° in 3 hours, to 300° in 3 more hours, to 350° in 4 hours and held at close to 400° for some 4 hours. Under these conditions no more water or HCl was observed to come off and Cl_2 began to appear. The temperature was then raised rapidly to from 450° 500° and the first fraction of Cl_2 was run down the drain by using a Nelson oil pump which permits the exhaust being run into a drainpipe of the sink directly. The pump with liquid air trap protecting it was then cut off and the Cl_2 generated into a trap cooled with liquid air. After enough had distilled over, the heat was reduced and the first fraction of the Cl_2 run into the trap protecting the pump by opening the proper stopcock. The central fraction was then distilled into a storage trap adjoining the mobility apparatus and kept frozen with liquid air until needed. The last fraction and the material in the protecting trap to the pump were then rapidly exhausted through the pump to the drain by warming the traps with the hand. The oil in pumps used this way needs frequent changing to prevent rusting of the pump due to the HCl from the reaction of the oil with Cl_2 . In this way the experiments were carried on with no exposure to Cl_2 on the part of the workers although dangerously large quantities of liquid Cl_2 were used. When in removing the last parts of Cl_2 -air mixtures by the Cenco and diffusion pumps from the ionization chamber into the air of the room the noxious effects of the Cl_2 in the room were considerably ameliorated by the free use of NH_4OH about the escape vents. The NH_3 gas by protecting mucous membranes from the action of HCl saved all the Cl_2 workers from bad chlorine colds.

THE MEASUREMENTS

In other respects the measurements were carried out by the standard methods employed by the writer^{1, 2, 7} in other mixtures, except for the use of a liquid air trap between the mercury vapor pump and ionization chamber. A brand new freshly gold plated chamber was used for this work with a spring contact device to insure good metallic contact between the upper plate and the outside. In the previous designs the contact had been made by the pressure of the threads in the tube supporting the upper plate against the threads of the supporting rod. The chamber was made gas tight as before by a pressure joint on a lead gasket. To prevent slow leaks the *outside* of the lead joint at the gasket was covered with an oily heavily chlorinated hydrocarbon called commercially chloracosan, which does not react with Cl_2 and is employed medicinally for use in chlorine applications, as it does not react to form HCl . This was kindly suggested to the writer by Dr. Felix Lengfeld, formerly of the University of California.

The measurements were nearly all made using an auxiliary field with 12 volts between gauze and lower plate over 1.2 cm. The plate distance used was about 1.0 cm, and in most cases the alternating potential at which the ions crossed was fixed so as to be 30-40 volts. Where the ions crossed at lower or higher alternating potentials correction was made for the interpenetration of

TABLE I. *New measurements; pure Cl_2 , Autumn 1929.*

	Mobility constant (reduced to 760 mm, 20°C)	
	K+	K-
	0.600	0.448}
	0.582	0.422}
		Stopcock lubricant free from red P
	0.600	0.532}
	0.606	0.490}
		Stopcock lubricant contained red P
	0.598	0.473 average

TABLE II. *First measurements of tank Cl_2 , Spring, 1928 (in collaboration with L. DuSault).*

Ion	Mobility Constants				Average
K+	0.612	0.594	0.632	0.631	0.617
K-	0.472	0.452	0.456	0.482	0.466

fields^{2, 8} by multiplying by a factor corresponding to the change in mobility for the same alternating potential produced by a corresponding change in the auxiliary field. The same sort of correction was applied to the few results using an auxiliary field of 6 volts. The corrected results for the mobility constant for pure chlorine are listed below with comments.

⁷ L. B. Loeb, Proc. Nat. Acad. Sci. 13, 510 (1927); 14, 193 (1928); 14, 384 (1928); 15, 146 (1929).

⁸ L. B. Loeb, Jour. Franklin Inst. 196, 537, and 771 (1923). Ann. d. Physik 84, 689 (1927).

THE MOBILITIES OF IONS IN Cl_2 .

It is seen from Tables I and II that the values of the mobilities were closely the same in the early measurements and in those with purer Cl_2 . It is also seen that the presence of red P in the lubricant did not change the values within the limits of error. The values were all averaged together, the newer values being weighted twice the old ones. This gives the final values as 0.604 cm/sec per volt/cm for positive ions and 0.471 cm/sec per volt/cm for negative ions under the experimental conditions mentioned above. Corrected for the effects of the interpenetrating fields^{2, 8} the mobilities in terms of the old accepted air standard of 1.4 and 1.8 cm/sec per volt/cm, and on the new absolute scale come out in cm/sec per volt/cm as

+ ions	- ions	
0.544	0.424	old scale
0.654	0.510	new absolute scale

The negative value obtained is lower than that of Wahlin⁴ obtained at lower pressures with undefined conditions of auxiliary field strength, and about of the order observed by Mayer's confessedly uncertain values at 8 cm pressure.⁹

THE WORK IN MIXTURES OF Cl_2 AND AIR

In spite of Mayer's work on the air mixtures from 1 to 4.5 percent Cl_2 , it was considered worthwhile to extend measurements in the mixture to higher concentrations using the pure Cl_2 . To study the effects of mixtures of dry air and Cl_2 the following set of values were observed for a field strength from 30-40 volts for bringing ions across, and an auxiliary field of 10 volts/cm. The uncorrected values were used to give the comparison of the mobilities with those computed from the law of mixtures of Blanc,¹⁰ using the reciprocals of the mobilities instead of the mobilities as is the custom in the more recent work.¹

TABLE III. Mobilities in mixtures of Cl_2 and air.

Mol fraction <i>f</i> of Cl_2	Mobility constants		Mol fraction <i>f</i> of Cl_2	Mobility constants	
	$K+$	$K-$		$K+$	$K-$
1.00	0.604	0.471	0.0011	1.61	1.46
0.427	0.905	0.676	0.0003	1.40	1.34
0.238	1.13	0.838	0.0001	1.48	1.48
0.119	1.25	0.91	trace	1.63	1.74
0.052	1.53	1.19	0.0000	1.61	2.00
0.025	1.51	1.20			

If the reciprocal of the mobility be written $R_f = 1/K_f$ (virtually the resistance to motion of the ion), then in a mixture containing a mol fraction *f* of Cl_2 , the reciprocal of the mobility according to Blanc's¹⁰ law should be given by

$$R_f = fR_{\text{Cl}_2} + (1-f)R_{\text{air}},$$

⁹ Herbert Mayer, Phys. Zeits. 27, 513 (1926) and 28, 637 (1926).

¹⁰ A. Blanc, Jour. Physique 7, 825 (1908).

where R_{Cl_2} and R_{air} , are computed from the observations above, using the data actually observed for an auxiliary field of 10 volts/cm and an alternating field of 30-40 volts. The results are thus merely relative and not absolute, but could be reduced to absolute values by using the appropriate factors given in the reduction of the observed mobility in Cl_2 to the absolute scale.

The results observed are shown by the experimental points as crosses for positive ions and circled points for negative ions joined by the dashed lines in Figure 2. The full straight lines are computed from the Blanc's law above for this mixture and appropriately labelled as to sign.

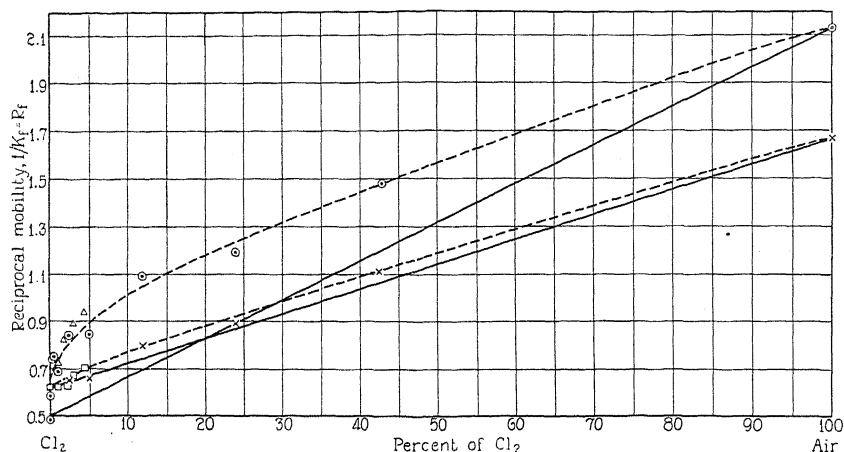


Fig. 2. Reciprocal of mobility as function of concentration of Cl_2 in a Cl_2 -air mixture.

The early measurements of Mayer⁹ from 1 to 4.5 percent Cl_2 are indicated by the triangles for negative ions and squares for positive ions. The positive observations of Mayer were multiplied by a factor to make Mayer's low positive values in air and air- Cl_2 mixtures coincide with the writers' for pure air. The reason for Mayer's low positive values in air lies in the fact that Mayer's apparatus due to lack of experimental facilities contained impurities which gave him a low positive mobility in air compared to negative values, (i.e. some organic vapors from his ebonite insulators). It is seen that Mayer's points for the negative ions agree remarkably well with the writers, considering the differences in technique used, and that on reduction to the same scale Mayer's positive ions show the same relative change in mobility as the writer's within experimental uncertainty.

DISCUSSION

It is seen at once that the positive mobilities lie along the Blanc's law curve within the limits of experimental accuracy. This indicates that the *positive ions do not react specifically with Cl_2 molecules to form clusters*. As the dielectric constant of Cl_2 is low the effect of dielectric attractions observed in gases like HCl , SO_2 and NH_3 ^{1,7} are absent as shown by agreement with

Blanc's law. It is further seen that the *negative ions have mobilities which drop from values of 2.00 to about 1.4 cm/sec for concentrations less than 1/2 of one percent*. The negative ions suffer therefore a very large, (perhaps the largest), decrease of mobility observed for additions of traces of any active gases to gases like air. This means not only a *specific cluster formation of Cl₂ about the negative ions but also a large cluster and a stable one*. It is also clear that this is due to some electrochemical affinity which is not caused by a high dielectric constant, for that of Cl₂ is low.

According to Blanc's law for Cl₂ the positive and negative ions should have equal mobilities at about 20 percent. This is also the value at which the positive and negative mobilities were *observed* to be equal for HCl. In these experiments traces of Cl₂ too small to measure made the mobilities of positive and negative ions equal. In Mayer's results as observed, due to an abnormal lowering of Mayer's positive mobilities by other impurities, the two mobilities were found equal at about 1 percent. This result as Mayer⁹ has already pointed out indicates that the lowering of the negative mobility in his experiments was not due to HCl. The writer's work confirms this conclusion further by the use of Cl₂ free from HCl.

No trace of the capricious high positive mobilities with traces of Cl₂ were observed in the later experiments of the writer, even with the absence of the liquid air trap near the diffusion pump, and with the use of hydrogen as in earlier work. This may indicate that such results as mentioned earlier in this paper for Cl₂ and possibly also for SO₂² were due to imperfect electrical contacts in these reactive gases. In any case they were not reproduced in the present work and their uncontrollable appearance must be taken as an indication that they are spurious, and to be regarded with caution.

CONCLUSIONS

The conclusions to be drawn from these results are as follows: (1) The high irregular positive mobilities mentioned elsewhere in SO₂² and found in preliminary work in Cl₂ appear to be of a spurious origin, and must not be regarded seriously. (2) Cl₂ has no effect on the positive ion other than that predicted by Blanc's law and the mobility of this ion varies in Cl₂-air mixtures in much the same fashion as in H₂²-air or CO₂-air mixtures. There is no indication of a stable large cluster formation about the positive ion in Cl₂ and no indication of the effect of a high dielectric constant, as is to be expected as Cl₂ is said to be non-polar. (3) The negative ion shows a marked affinity for Cl₂ molecules. Cl₂ obviously forms a large and stable cluster about the negative ion even when present in minute traces. (4) The lowering of the mobility of the negative ion below that of the positive ion for traces of Cl₂ *must be ascribed to this cluster formation, due to a totally unexplained electro-chemical mechanism. It cannot be accounted for by the existence of an unsymmetrical dipole of large moment in the Cl₂ molecule*, which is a viewpoint put forward by Condon and Loeb⁶ to explain the decrease of the negative mobility below the positive mobility in the cases of HCl, SO₂, H₂O, H₂S and other substances. It is surprising that this type of action should occur with the *Cl₂ molecule* since this *molecule* appears to have satisfied the strongly electronegative tendency of the

Cl_2 atoms relative to its other physical reactions in its formation. The chemical reactivity of Cl_2 on the other hand is due to a low heat of dissociation, and supposedly not to other properties of the Cl_2 molecule. The action on the negative ion is presumably analogous to the action of ethyl ether or NH_3 on the positive ions, yet how and why it takes place is in no sense clear.

With this work the writer is closing his investigation of mobilities in mixtures using the methods in which the mobilities of *unknown carriers are determined in gases where the carriers make 10^7 or more impacts with neutral gas molecules in the time of measurement.* In such cases purities of substances are required that are beyond chemical control. It is hoped that a new method which is being developed will enable the mobilities of ions of a known nature to be studied under conditions where impurities do not play the important role which they play in the usual measurements.

In concluding the writer desires to express his sincere thanks to his colleague Professor J. H. Hildebrand for his valuable advice in solving some of the many chemical difficulties encountered, to Miss L. DuSault who cooperated in the earlier measurements, and finally to his friend and research assistant Commander T. Lucci, late of the Italian Navy for his untiring assistance in the tedious work of preparation of and measurements in pure Cl_2 .

ON MECHANICAL AND MAGNETIC FACTORS INFLUENCING THE ORIENTATION AND PERFECTION OF BISMUTH SINGLE-CRYSTALS

BY ALEXANDER GOETZ
CALIFORNIA INSTITUTE, PASADENA

(Received December 12, 1929)

ABSTRACT

Method of producing crystals of bismuth.—A method is described which permits the production of single crystals of metals, with practically no limit to size or to desired orientation, thus indicating that all external mechanical influences are avoided. Furthermore, the method permits the zone of formation in a growing crystal to be subjected to a strong magnetic field.

Mechanical factors influencing the orientation and perfection of crystals.—A systematic study of the conditions in which the seed-crystal transfers its orientation to the rod is made. Experiments with artificially distorted seeds, etc., show that crystalline units must already exist in the liquid state. It is shown that this "liquid crystal" is destroyed at about 10° above the melting point. It is suggested that these units are identical with elementary units of a crystal as treated theoretically by Zwicky and observed by the author.

The influence of a magnetic field on a forming crystal.—Crystals in the three main orientations to the directions of the field lines (20,000 Gauss) were grown, one-half with, the other half without field. No change in the orientation between both halves could be observed as long as no secondary influence was present. However, crystals grown without a predetermined orientation indicated a preference for an orientation in which the direction of the smallest diamagnetic susceptibility (along the trigonal axis) was parallel to the lines of force. The fact that this influence, though much smaller than the orienting forces of a seed, exists, supports the assumption of "block-phase" slightly above the melting point.

INTRODUCTION

THERE are several reasons why a systematic investigation of the factors influencing the orientation and perfection of a metal crystal seems to be important. One of these reasons is the fact that certain methods of growing crystals succeed only for certain orientations, though the orientation is forced on the growing crystal by inoculation with a seed-crystal. Then it can happen that the desired orientation is only maintained over a short region or does not even start. In a previous paper,¹ Goetz and Hasler came to the same conclusion as Kapitza:² namely, that a growing crystal is very sensitive to any mechanical stress. Such stresses exist in almost every known method of crystal production. This necessitates the development of a new method which allows also the decision to be made as to whether this extremely sensitive region is in the solid part of the growing crystal or in the still liquid state.

¹A. Goetz and Maurice F. Hasler, Proc. Nat. Acad. 15, 646 (1929).

²P. Kapitza, Proc. Royal Soc. A119, 358 (1928).

Furthermore, it seemed to be interesting to see if directional forces of other than mechanical or thermal, especially magnetic, nature would show any influence when applied to the zone of formation. In spite of several papers written on this subject, no investigations excluding secondary effects have been systematically made. The results correlated from these papers contradict each other to some extent also.

THE METHOD OF PRODUCING CRYSTALS

After investigating the conditions for an unrestricted growth of Bi crystals by means of all known methods, it was found that these conditions can be summarized as follows:

(1) No strain of any kind should be applied to the zone of formation of the growing crystal.

(2) The crystal should not have any oxide-coat which can be the cause of stress.

(3) The speed of growth should be uniform.

(4) The heat gradient over the crystal should be uniform and its position within the crystal constant over the whole length.

(5) If the orientation of the crystal is to be predetermined by inoculation, it is necessary to obtain thermal equilibrium at the transition between seed-crystal and inoculated metal.

There is no method known which fulfills all these conditions equally well. However Kapitza's method, with which he produced the crystals finally used for his measurements, comes nearest, but it cannot be used for long crystals and does not satisfy condition (2).

Condition (1) seemed to me the most important one, and a large number of experiments were performed to fulfill it satisfactorily. One of the main troubles was that the molten metal (as soon as it was free from oxide) stuck to the walls of the container, thus interfering with the change of volume at crystallization. Many different arrangements were tried. For instance, a trough of thin paper was made in which the molten Bi was poured. When heated the paper carbonized, yet kept its shape sufficiently until the metal crystallized. The strength of these troughs was so small that the crystallizing metal could break them easily. Very uniform crystals were obtained by this method but the external shape was quite irregular. Finally, it was found that smooth troughs of Acheson graphite worked as well as the troughs of carbonized paper without having the disadvantage of losing their shape after the crystallization of the metal.

The final arrangement based on the previous experiences was the following: The troughs were shaped out of large blocks of Acheson graphite from a region free from fissures. The troughs had a length of 30 cm, were 0.4 cm wide and shaped rectangularly. Special precautions had to be observed in shaping to avoid deformations caused by the flexibility of the material. To fulfill condition (2) it was necessary to place the trough *G* in a glass or quartz tube *C* (in Fig. 1) which had at one end a ground-glass cone in which a little glass dome with a capillary was fitted. The cross-section of *C* was circular

over the whole length to within 3 cm of the cone, where it was as shown in the cross section (Fig. 1) elliptical to give more space above the trough. *F* was an electric furnace (chromel wire coiled around a quartz-tube) with two end plates, through the holes of which went the tube *C*, in such a manner that it did not touch the walls. The tube was supported at one end by means of the V-shaped adjustable holder *A* in which the tube glided over graphite wedges. The other end of the tube was supported at the clamp *O* which was a part of the driving arrangement fulfilling condition (3) (not shown in Fig. 1, because its design has already been published¹.) The connection between *O* and *C* was made with a rubber-tube *N* which absorbed to some extent the vibrations of the motor.

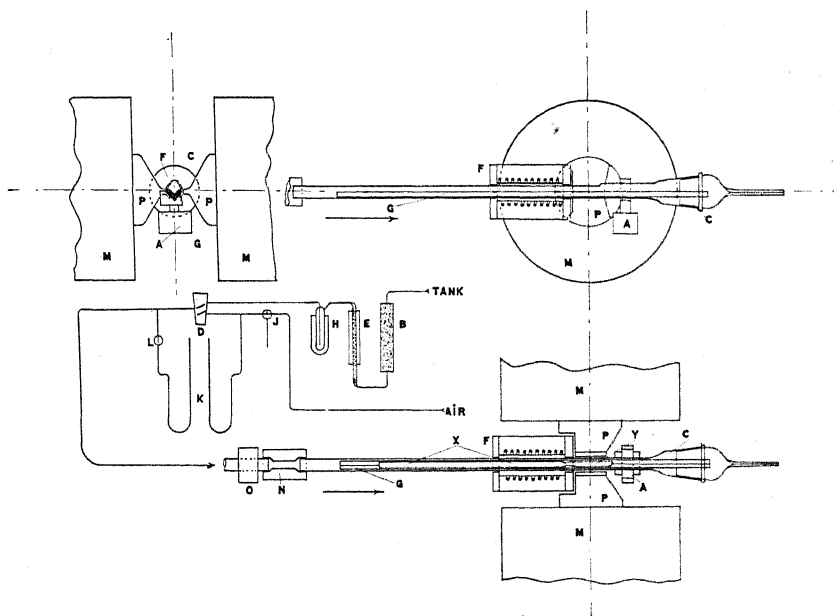


Fig. 1. Diagram of essential features of the apparatus.

The method of producing crystals was as follows: Round metal rods of 2–3 mm diameter were first made in glass tubes as described in another paper.¹ After the glass was taken off, the rods were cut down to a standard length of 120 mm (first generation).

The clamp *O* was then disengaged from the driving mechanism and moved towards the right so that the tube *C*, and with it the trough *G*, came out of the furnace *F* as far as possible. The glass dome was then removed and the rod placed in the trough. Then the tube was closed and the clamp *O* was put back into such a position that the end of the rod came out of the furnace *F* for a short distance. The furnace was restrictively heated so as not to melt the end of the rod. After the tube had come to thermal equilibrium with the furnace, the clamp *O* was engaged with the driving apparatus which moved

it in the direction of the arrow at a rate of 5 mm/min. To reduce the oxide at the surface of the rod a constant flow of hydrogen was sent through the tube. It soon became apparent that the purity of the hydrogen and the constancy of the flow were of great importance for the uniformity of the crystals, which made a rather elaborate arrangement necessary. The hydrogen was first taken from a tank with a reduction valve. To separate dust from the gas, it was then sent through a gas filter *B* and then through a heated tube with palladiumized asbestos to oxidize the impurities; thereafter through the trap *H*, cooled by liquid air, and then through the valve *D*. From here it went into the tube, over the metal and escaped through the capillary in the dome. The rate of flow could be measured by one of the manometers *K*.

By this arrangement, it was possible to keep the thickness of the oxide coat over the whole length of the crystal practically constant, since the factors determining the rate of reduction, temperature (very important), flow of hydrogen, and speed of the trough through the furnace could all be controlled. It soon became apparent that a perfect reduction is highly undesirable, because as soon as the last surface layer is gone, the surface tension of the liquid metal becomes so large that it coagulates into large drops and thus destroys entirely the uniform cross-section of the crystal. This effect made it necessary to provide an arrangement which permitted the production of a very thin oxide layer over the crystal. For this purpose, compressed air was used, which went first through the valve *J*, then through the stopcock *D* which opened the way to *C* either for the hydrogen or the air. For making the change between these two gases as fast as possible, every unnecessary apparatus-volume not exposed to the direct flow was avoided. Therefore, the hydrogen manometer, for instance, could be closed with the stopcock *L* as soon as the air-flow, which was measured by the manometer *K* (right), started.

For producing the "second generation," the rod was placed in the trough, as mentioned above, and the furnace heated to about 310°. To prevent coagulation, the first few millimeters were placed so that they did not melt, then the hydrogen flow was turned on at a pressure of 20–25 mm water-column and the motor started. Thus the metal rod melted into the shape of the trough and was reduced so that the surface became very bright. As soon as the other end of the rod entered the furnace the hydrogen-flow was stopped and the air-flow started to cover this part with an almost invisible coat which fixed the shape of the end of the rod and thus prevented the metal from running forward under the influence of surface tension.

This second generation was, in general, monocrystalline, but the orientation was at random. To predetermine the orientation the method of inoculation by a seed-crystal was used. For this purpose, the metal rod obtained by the previous methods was placed again in the trough, the latter being placed in the furnace, again under a flow of hydrogen, so as to melt the right end of the rod. The thin oxide-coat kept the end in shape, since the temperature (about 290°) of the furnace was so low that no appreciable reduction occurred. As soon as the end was liquid (Fig. 2a), the glass dome of *C*

was removed, a hooked steel needle was introduced and the oxide coat taken off the end of the liquid rod (Fig. 2b). The hydrogen flow prevented a re-oxidation of this point, whereas the oxide-hull of the rest kept the rod in shape. Then the seed-crystal, the end of which was cleaved immediately before using, was brought into the trough (Fig. 2c). The liquid end of *X* and the left end of *Y* were brought into contact very carefully, so that they united over a small region (Fig. 2d). Again coagulation had to be avoided by pulling the seed-crystal out a trifle so as to produce a little constriction between *X* and *Y*. (Fig. 2e). The glass dome of *C* was then replaced, the tube itself pushed back into the furnace for annealing the transition (Fig. 2f) and the hydrogen-flow was replaced by an air-flow. This process was necessary in order to protect the very delicate junction between *X* and *Y* by a uniform oxide coat (see later). After the rod and the seed-crystal reached

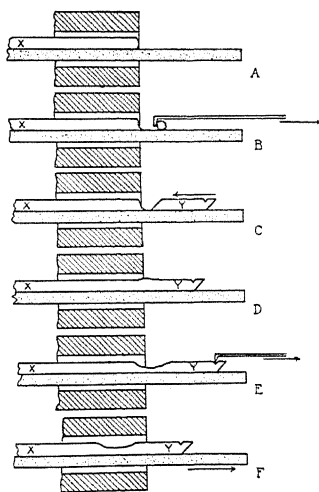


Fig. 2. Method of inoculating rod with seed crystal.

thermal equilibrium, corresponding to the new position in the furnace, the motor was started and thus the crystal started to grow. As soon as the junction came out of the furnace, the air flow was replaced by hydrogen to prevent a thickening of the oxide coat on *X*. It was found that this oxide coat had to be very thin, almost invisible to the eye, and had to be very uniform over the whole rod. For fulfilling this condition, it was necessary to start the hydrogen rather exactly at the moment at which the junction started to crystallize. The moment at which the air inside *C* was replaced by hydrogen could easily be observed on account of the difference of viscosity of the two gases. The storage pressure of the hydrogen indicated by the manometer *K* (left) was large as long as the rest of the air had to flow through the capillary of *C*, but went down to a constant value as soon as the tube contained only hydrogen. The opposite was the case if the hydrogen was replaced by air.

Thus the third generation of the crystal was obtained. After the whole rod crystallized, it was taken out of the trough very carefully and etched with diluted nitric acid. If all precautions had been observed carefully, the crystal obtained was perfectly uniform in shape and orientation, and not the smallest alien crystal could be observed. The orientation of the crystal was

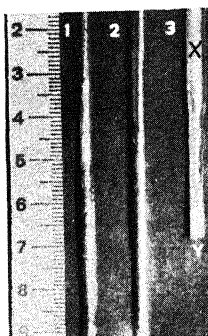


Fig. 3. Crystal 1 shows first "generation" after removing the glass cover. It is polycrystalline and shows many regions of twinning. Crystal 2 is second "generation," its core being singly-crystalline. However, its surface contains many crystals in twin orientations due to oxide stress. Crystal 3 is third "generation" (X) with the seed-crystal (Y) in orientation P_1 . The rod is a single crystal.

exactly the one of the seed crystal, no matter which orientation that had. It was found also that this method had no limitations in the matters of the lengths and the cross-sections of the crystal. Fig. 3 shows a photograph of the first three generations of crystals.

As has been mentioned above, the whole investigation was undertaken to study the factors influencing the orientation and perfection of these

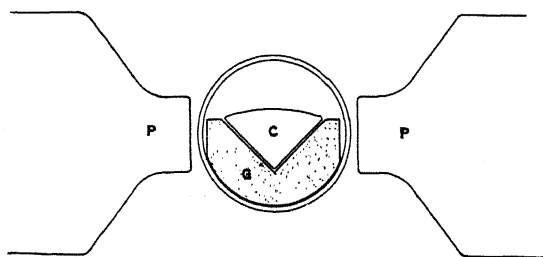


Fig. 4. Cross-section of arrangement for crystallization in a magnetic field.

crystals with special regard to the influence of a transverse magnetic field. The method just described allowed a very exact location of the zone in which the crystal formed. If the temperature of the furnace was high enough, this zone was outside the furnace; hence it was possible to bring it between the pole-pieces of an electromagnet M . The pole-pieces P were shaped so as to concentrate the field between two edges and thus across the crystal over a

length of 18 mm. This distance was necessary to allow for the unavoidable uncertainty in the exact position of the zone of formation. Fig. 4 shows an enlarged cross-section of the arrangement whereas Fig. 5 is a top view photograph which shows the crystal *C* lying in the trough *G* as it comes out of the furnace *F* and crystallizes between the pole pieces *P* of the magnet *M*.

This method has the disadvantage that the direction of the lines of force cannot be changed relative to the rod. Nevertheless, it is possible to change the orientation in the rod by inoculation with different seed crystals. This, allowed the study of the influence of the field at different angles with regard to the trigonal axis.

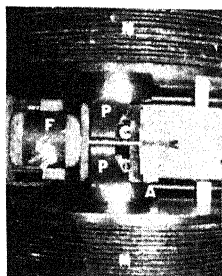


Fig. 5. Top view of the formation of the single crystal *C* carried in the trough *G* between the pole pieces *PP* of the magnet *M* after being molten in the furnace *F*.

MECHANICAL FACTORS INFLUENCING THE ORIENTATION AND PERFECTION OF CRYSTALS

For studying the kinds of influences preventing a perfect growth of Bicrystals, about 500 crystals were grown under circumstances which were changed systematically. The results concerning the disturbances involved in the artificial growth by inoculation can be summarized as follows.

Two different kinds of mischief in the production of single crystals have to be separated, (a) the fact that the rod consists of several crystals with different orientations, and (b) the fact that the inoculation of the rod by a seed-crystal does not succeed. All experiments were performed at a constant speed (exact to about 0.2 percent), in absence of vibration, and at a constant temperature (exact to 2°).

The failure of an inoculation can consist of

- (1) That the orientation of the rod has no relation whatsoever to the seed crystal;
- (2) That the orientation of the rod is partly the same as the seed crystal;
- (3) That the orientation of the rod is the twin orientation of the seed crystal.

The first case occurred in general if the contact between rod and crystal was bad. It was quite remarkable how an almost invisible layer of oxide between both parts destroyed entirely the influence of the seed crystal,

although they may have congealed and formed a unit after solidification. Case (2) can have the same cause as (1). If the face of contact between both parts was partly contaminated by oxide, then one half grew in the orientation of the seed crystal, whereas the other half, separated from the seed by contamination, formed one or several new centers of crystallization which produced new crystals which grew together with the inoculated one. There may be still another cause which will be discussed later. The most interesting case is (3). Here one can have a perfect crystal, the orientation of which is the same throughout, only that the perfect cleavage of the seed plane is replaced by one of the imperfect cleavage planes. The same effect may occur in case (2), where one can obtain the parallel growth of two crystals with interchanged planes.

It is well known that almost any deformation in a Bi crystal results in the production of twin-lamellae^{3,4} where the (111) plane is replaced by one of



Fig. 6.

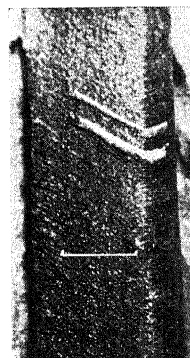


Fig. 7.

Twin lamellae caused by distortion in Bi single crystals. The illumination under the microscope was such as to show the original orientation of the crystal dark (Fig. 7) or bright (Fig. 6). The white line in Fig. 7 corresponds to 1 mm.

the (11 $\bar{1}$) type. The change takes very little energy because the rhombohedral symmetry of Bi is almost a cubic one. Fig. 6 and Fig. 7 illustrate this effect on two artificially distorted crystals of Bi, which show the appearance of the twin lamellae differently illuminated. Thus the conclusion is easily reached that the twinning occurred in case (3) at the point where seed and rod came in contact. A close investigation of this effect brought out the following facts.

If the seed-crystal is not perfect, i. e. if it contains twin lamellae which are easily observed under the microscope after etching (3) the rod will grow frequently in the twin orientation. It is furthermore very hard to avoid the twinning effect if one cleaves crystals in special orientations, as was shown by x-ray diagrams, but it is possible by careful handling to extend the twinned region not farther than a few tenths of a mm beyond the cleaved plane. Thus

³ P. Mügge, *Jahrbuch d. Mineralogie* 1, 183 (1886).

⁴ A. Goetz, *Proc. Nat. Acad.* in press.

in order to inoculate the rod with an undisturbed seed, it is only necessary to bring the trough, after the contact between rod and seed is made (Fig. 2 e) far enough into the furnace so that the imperfect end of the seed is melted (Fig. 2 f). Then the unhurt part of the seed reinoculates its imperfect part and the rod starts to crystallize in the desired orientation.

However, it was very surprising that case (3) occurred very often, even though this precaution was taken, i.e. the rod crystallized in the twin orientation in spite of a perfect seed.

Closer investigation showed that this effect had two reasons. One should expect that if one inoculates with well twinned seed crystals i.e. where distinct regions of the crystal have either the normal or the twin orientation as shown in Fig. 6 and 7, one would obtain rods of both orientations depending on the position of the point up to which the seed was melted. But it was discovered that *the rod grows in an orientation possessed by a region of the seed which was already molten*. This process is shown schematically in Fig. 8 where X is the molten rod and Y the seed crystal having the twin-lamellae $t, t \dots$. In case the seed Y was molten up to point 1, X grew in the orientation corresponding to the seed. If Y was molten up to point 2, X grew in the twin orientation.

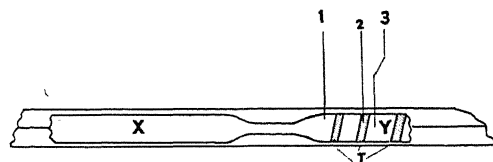


Fig. 8.

tation. But if Y was liquidified up to point 3, where the twin lamella was doubtlessly melted, X grew still in the twin orientation. This experiment could be repeated as often as desired. The maximum distance still effective between the border of the lamella and the end of the molten region was, in general, several millimeters. Fig. 9 shows an enlarged photograph of the transition between seed and rod. The illumination of the crystal is such as to show the parts of the desired orientation bright. The dark crystal is the seed (right) which shows three good intersections of twin lamellae. The white half to the left is the beginning of the inoculated rod, which shows the same orientation as the twin lamellae of the seed-crystal. The sharp transition shows how far the seed was melted. The original end of the seed had one twin lamella which was melted about 0.5 mm beyond its left border, but was still able to determine the orientation of the rod. The faint black lines on the left crystal are twin lamellae in the rod which were produced later to show that they have the original orientation of the seed indicated by their dark appearance.

This phenomenon shows that the forces determining the orientation of a crystal are not destroyed at the melting point and exist within the liquid as long as the temperature is near to that of the melting point.

The study of the conditions of successful inoculation with untwinned crystals (or seeds melted far beyond the limits of the imperfections) revealed

another phenomenon which points in the same direction. As mentioned above it was necessary (to preserve the perfect shape of the rod) to pull the seed a little away from the rod (Fig. 2 d) so that the junction was constricted (Fig. 2 e). It goes without saying that this constriction concerned only the region where the metal was molten entirely. It was found, nevertheless, in almost all cases, that the rod grew in the twin orientation of the seed if the crystallization was started from the position of the trough in Fig. 2 e. After the crystal was finished, it was etched and the region where the twin orientation occurred could be determined easily. It started always close to point 1 (Fig. 4 e) i.e. at the beginning of the constriction, no matter whether the melted region of the seed reached still farther or not.

The only way to avoid this twinning effect in the liquid was to anneal the liquid junction at temperatures much higher than the melting point; hence the

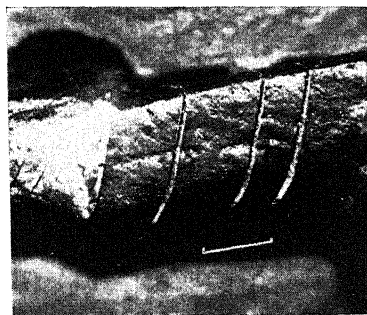


Fig. 9. Seed crystal with twin lamellae (right), inoculated crystal (left) grew in twin orientation although the twinned region of the seed was molten. The white line corresponds to 1 mm.

trough had to be backed into the furnace (Fig. 2 f) and kept in that position for 5-7 minutes before the crystallization was started.

This effect shows that within the temperature region of the "liquid crystal," the twinning occurs just as well as in the solid state with the only difference that the little energy necessary for changing the shape of the liquid rod (determined by its surface tension and the shape of the thin oxide cover) is already sufficient to produce the effect.

The fact that the orientation of a crystal is not destroyed immediately after melting could be shown in another experiment. If a polycrystalline rod (first generation) was put into the trough and was run through the furnace with the usual speed, but a maximum temperature which was only slightly above the melting point, a polycrystalline rod was obtained which had the same position and the same orientation of the different prominent crystal elements as it had before it entered the furnace although it had been molten and recrystallized. As soon as the temperature was higher, an entirely different polycrystalline combination occurred.

The high sensitivity to any stress applied to the transition between solid and liquid metal causes another effect which is highly undesirable. If a single crystal rod which is covered by oxide was placed in the trough and pulled through the furnace, a rod was generally obtained which was monocrystalline at the core but polycrystalline at the surface, an observation which was also made by Kapitza². Under the microscope, it was observed that the alien crystals have the shape of thin stripes running along the rod, each of them starting at a wrinkle in the oxide coat produced by the shrinking of the metal at the moment of melting. As soon as the rod crystallized, these wrinkles were stretched out again, but the pressure necessary for this process was sufficient to cause twinning if the oxide coat was sufficiently thick. The alien crystals produced by this cause were only at the surface and could be removed by etching. The effect was different if the rod was free from oxide and the oxide coat was produced around the rod in the molten state. Then the whole hull was too small for the solid form and it had to be split by the solidifying metal, which caused pressures which were very often able to start an entirely new orientation. Hence it was necessary to grow the metal in a reducing atmosphere so that the oxide coat was too thin to affect the structure of the crystal, but sufficient to preserve the shape of the molten rod.

With regard to the orientation which is produced by these stresses, the following can be said: Any tension longitudinal with regard to the rod results in an orientation in which the trigonal axis is normal to the rod. If the original orientation is already such, the tension has no influence at all. If the stresses are not very large, the new orientation is obtained by twinning which places the trigonal axis in a direction in which the energy needed for overcoming the obstacles of thermal contraction is smaller. This is the reason as already stated in another paper,¹ crystals, the trigonal axes of which are parallel to the rods, are very difficult to obtain with the usual methods, which apply either longitudinal tensions or lateral compressions to the zone of formation due to the expansion of the metal at the moment of crystallization. The method described avoids these influences and allows the growth of all possible orientations equally well. However, the opposite effect can be shown, where a longitudinal compression prevents the perfect growth of a crystal, the axis of which is normal to the rod. If a rod was covered with a heavy oxide coat and inoculated with a seed, the axis of which was normal to the rod, the last end of the rod had an orientation in which the axis became more parallel to the rod. The obvious reason is that the oxide at the end of the rod formed a kind of sack, the end of which prevented the longitudinal expansion and thus exerted a longitudinal compression, which resulted in an orientation of maximum contraction parallel to it.

THE INFLUENCE OF THE MAGNETIC FIELD UPON THE CRYSTALLIZATION.

Since the orientation and perfection of these crystals could be influenced mechanically when in the molten state, it seemed worth while to study whether or not a magnetic field applied to the zone of formation would produce any effects.

The way in which the magnetic field was applied has already been described. The tests were made as follows: The crystal (third generation), with an already definite orientation, was put into the trough and the tube pulled back into the furnace so far that the left end of the crystal did not melt. The temperature of the furnace was increased so much that the transition between liquid and solid crystal was approximately at the middle of the pole pieces when the crystal reached its thermal equilibrium, a process which took in general, 5 minutes. Then the magnetic field was excited and the driving mechanism started at the same time. Thus the molten part of the rod crystallized again within a transversal magnetic field of a strength of 20,000-21,000 gauss.

It is obvious that there are three different possible orientations of the crystal with respect to the rod, or to the direction of the lines of force. These orientations which differ fundamentally are as sketched in Fig. 10. This

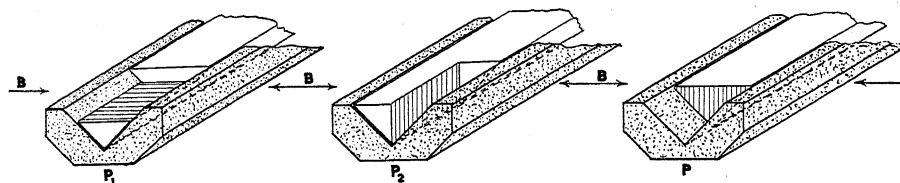


Fig. 10.

shows the trough G (dotted) with the crystal, the latter cut parallel to its main cleavage plane. These three main orientations are:

Name	Trigonal axis to field		(111) plane to field	
	rod	field	rod	field
P_1	\perp	\perp	\parallel	\parallel
P_2	\perp	\parallel	\perp	\perp
P_3	\parallel	\perp	\perp	\parallel

As long as the conditions of growth were not influenced accidentally, *no influence of the magnetic field upon the crystallographic orientation could be observed, no matter which of the above main orientations was introduced into the field.* It is to be mentioned however, that this result can only be obtained if one succeeds in avoiding any secondary influence. Any shock, for instance caused by the sudden excitation of the magnet, transferred to the trough or to the furnace will immediately produce a change in orientation.

Moreover, crystals, the orientation of which had not been predetermined, were grown in a magnetic field to find out whether there exists an influence of the field on the first originating center of crystallization. In fact, indications were found which point toward a preference of an approximate parallelism of the trigonal axis and the lines of force. However, these results seem not to be precise enough for a definite statement, since first the number of measured crystals produced this way was not large enough that the results could be considered statistically; and second, it is known that the direction of the

heat-gradient with relation to the rod can predetermine the orientation aside from any mechanical influence. Thus, the non-inoculated crystal may not have been entirely free to grow in any orientation because the apparatus did not allow a change of the direction of the heat-gradient with respect to the rod. On the other hand, it is certain that these predetermining influences are extremely small because they cannot affect, in any way, the growth of an inoculated crystal. However, the influence of the applied field showed itself to be smaller than the orienting forces of an inoculating crystal and may be similar in magnitude to the orienting forces of the gradient, which makes it possible that the effects produced by the latter fog the former.

DISCUSSION

The results obtained by the above observations may be able to explain a number of experiences of other authors. It has been already suggested in a previous paper¹ that the extended experiments of Hoyem and Tyndall⁵ on single zinc crystals may find their explanations in the effect of the stress applied to the zone of formation by the weight of the liquid column hanging from the crystal. The variation of the successfulness of an inoculation with the temperature of the molten metal can thus be explained, because the length of the liquid column depends upon that temperature and herewith its weight.

Moreover the lack of success of several methods of Kapitza² and his explanation thereof is confirmed and becomes understandable as soon as one realizes that in the case of liquid bismuth, the interchange of the main cleavage plane with an $(11\bar{1})$ plane is exactly the effect which occurs in any plastic deformation of solid bismuth. It seems that there are only two alternate interpretations possible: First, one could assume that the twinning force of the crystal becomes infinitely small in the neighborhood of the melting point so that the smallest strain, as given, for instance, by the surface tension of the liquid metal, is sufficient to start the twinning; or second, in view of the observed facts one might assume that the twinning effect occurs within the melted region, which would mean that the crystal is not destroyed entirely after melting, but that it consists still of units which preserve their orienting power. The first makes it impossible to explain the fact that qualities can be "inherited" by a growing crystal from the molten region of a seed crystal or to explain the preservation of a polycrystalline structure in a bar heated above the melting point. These units exist apparently only over a small range of temperature, since the phenomena through which one infers their presence disappear entirely about 10° above the melting point (annealing of the liquid metal).

One is perhaps not entirely wrong in assuming that these units are of the same nature as the "blocks" in a Bi-crystal described by the author in a recent paper⁴ in connection with the theoretical considerations of Zwicky.⁶ In this case, one considers that the melting crystal disintegrates first into its

⁵ A. G. Hoyem and E. P. T. Tyndall, *Phys. Rev.* **33**, 81 (1929).

⁶ F. Zwicky, *Proc. Nat. Acad.* **15**, 253, 000 (1929).

blocks which exist within a state of equilibrium of dissociation with the liquid metal at each temperature. This "block phase," however, exists only over a small range of temperature.

There are several indications in experiments of other authors which are in favor of this hypothesis. Boydston⁷ found in observing the thermal e.m.f. of Bi-crystals of different orientations that the e.m.f.'s characteristic for the crystalline state did not disappear exactly at the melting point, but continued for a few degrees. Thus (to quote his own words) "it appears, in fact, as if some crystalline arrangement still persists in the molten metal . . ."

Futhermore, Traube and vonBehren have shown⁸ that the dissolving of a crystal into an almost saturated solution results in separating particles of ultra-microscopic size from the crystal, "submicrons," which exist for a considerable length of time. The parallelism between the melting process and the process of dissolving into a saturated solution does not need to be mentioned.

Finally, it is possible to connect the observations by Stewart and his collaborators⁹ concerning the "cybotactic" state of matter with these results. It seems as if there is no principal difference between the "block-phase" and the "cybotaxis."

Regarding the extremely small energy needed for influencing the orientation in a liquid crystal, I was surprised to find no orientating effect caused by the magnetic field on a crystal with a predetermined orientation. This however, does not contradict necessarily, experiments which were performed by Plücker¹⁰ and Leduc.¹¹ From experiments on polycrystalline Bi solidified in a magnetic field, Plücker finds that among the individual crystals, one direction is predominant, that is where the trigonal axis is parallel to the lines of force. A result of this kind should be expected, if there is any positive effect, because of the anisotropic diamagnetism of Bi, as the trigonal axis is known to be parallel to the most "paramagnetic" direction. The observations of Leduc¹¹ point in the same direction. He crystallized Bi in spherical glass containers which could be suspended within a field of 4-5000 Gauss. These Bi balls were polycrystalline without doubt, but suspended in the field they turned into a direction in which the "average main axis" of the conglomerate was parallel to the lines of force. If the ball was formed outside the field, no prediction about its zero position in the field could be made, but as soon as the sphere had crystallized within the field, the zero position was the same as its position during crystallization. The explanation of this effect is obviously the same as of Plücker's observations, although, the orientation of the conglomerate was not measured by Leduc.

It seems surprising that Welo did not find any effect of this kind in a recent study.¹² It may be due to the fact that his way of casting his disk in a

⁷ R. W. Boydston, *Phys. Rev.* **30**, 911 (1927).

⁸ J. Traube and W. von Behren, *Sx. f. Phys. Chem.* **A138**, 85 (1928).

⁹ G. W. Stewart and R. M. Morrow, *Phys. Rev.* **30**, 232 (1927).

¹⁰ S. Plucker, *Pogg. Ann.* **76**, 583 (1849).

¹¹ M. A. Leduc, *C. R.* **140**, 1022 (1905).

¹² L. A. Welo, *Phys. Rev.* **34**, 296 (1929).

mould with good thermal conductivity produced a polycrystallization so rapid that the orienting effect was very small.

Our own observations make a directional effect, in a crystal which crystallizes completely in a magnetic field, probable with a sign which agrees with Plücker's and Leduc's experiments. They show, however, that this effect is so small that it cannot overcome the orienting forces of a seed-crystal.

The presence of the magnetic effect shows furthermore, that the orientation of a crystal must exist already in the liquid state provided that the crystal unit has still freedom to move with regard to the rod. This supports again the existence of the above "block-phase." The insensibility of the inoculated crystal shows further that the growing crystal, if under stable conditions, must have an already ordered section of the liquid ahead of it. Then the orienting effect of a magnetic field is too small to break up the liquid arrangement.

Nevertheless, it was found that the magnetic field influences considerably other properties of a Bi crystal formed in it, as stated already by the author and his collaborators^{13, 14, 15}. More extensive results will be published soon.

I feel very much indebted to Dr. R. A. Millikan for the interest he showed in this investigation, and I should like to express my thanks to my assistants, Mr. M. F. Hasler and Mr. A. B. Focke for their very helpful assistance.

¹³ A. Goetz, *Phys. Rev.* **32**, 322 (1928).

¹⁴ A. Goetz and M. F. Hasler, *Phys. Rev.* **34**, 549 (1929).

¹⁵ A. Goetz, R. C. Hergenrother and A. B. Focke, *Phys. Rev.* **34**, 546 (1929).

LETTERS TO THE EDITOR

Prompt publication of brief reports of important discoveries in physics may be secured by addressing them to this department. Closing dates for this department are, for the first issue of the month, the twenty-eighth of the preceding month; for the second issue, the thirteenth of the month. The Board of Editors does not hold itself responsible for the opinions expressed by the correspondents.

Hyperfine Structure in the Spectra of Neutral Manganese

A light source, designed by Schüler, operated at liquid air temperatures in conjunction with a prism spectrograph and silvered Fabry-Perot etalons is being used to study the hyperfine structures in the spectral lines of neutral manganese. At 4000Å a resolving power of approximately one million is obtained. The observed fine-structure patterns although identical in appearance with those found in praseodymium (Phys. Rev. **34**, 1397, 1929) are in general a fifth to a tenth as wide. Patterns of from 2 to 6 components are found, some degrading toward the red and others toward the violet. For example, $\lambda 4030$ has the fine-structure components,

Int.	10	9	8	7
$\Delta\lambda$	0	+0.0122	+0.0230	+0.0317
$\Delta\nu$	0	-0.0751	-0.1416	-0.1951
			6	5
			+0.0379	+0.0420
			-0.2333	-0.2585

degrading toward longer wave-lengths while $\lambda 4018$ has the

Int.	10	9	8	7
$\Delta\lambda$	0	-0.0152	-0.0274	-0.0377
$\Delta\nu$	0	+0.0941	+0.1696	+0.2333
			6	5
			-0.0456	-0.0516
			+0.2822	+0.3193

components degrading toward the violet. Since the well-known gross structure of Mn I and II in general shows strictly *LS* coupling, an excellent opportunity for the study of the role played by *s*, *p*, and *d* electrons in producing hyperfine structure presents itself. The $^6S_{5/2}$ ($3d^5 4s^2$) term is apparently quite narrow. With a nuclear angular momentum $(5/2)(h/2\pi)$ for Mn, the $^6P_{43}$, $^6P_{33}$ ($3d^5 4s 4p$) and the $^6D_{43}$ ($3d^5 4s$) terms are each broken into six *normal* components with

separations 0.116, 0.107, 0.082, 0.068, 0.052 and 0.075, 0.066, 0.054, 0.038, 0.025, and 0.099, 0.086, 0.069, 0.054, 0.040 cm^{-1} respectively. While the $^6P_{43,33,23}$ terms each have six components, the $^6D_{43,33,23,13,12}$ and $^6P_{33,23,13}$ terms have 6, 6, 6, 4, 2 and 6, 6, 4 components respectively, as would be expected with $i=2\frac{1}{2}$. The total fine-structure separation 0.348 cm^{-1} for $^6D_{43}$ ($3d^5 4s$) is due chiefly to the 4s electron, the 3d electrons contributing very little. To this the 4p electron contribution is (a) added to give the $^6P_{43}$ ($3d^5 4s 4p$) separation 0.414 cm^{-1} and (b) subtracted to give the $^6P_{33}$ ($3d^5 4s 4p$) separation 0.258 cm^{-1} .

The total separations of the fine structures for the three terms $^6D_{43,33,23}$ are found to be proportional to the $\cos si$, when $J \geq i$ and $\cos Ji=1$, as predicted. The fine structures that have as yet been photographed are found to be in excellent agreement with the "Theoretical Interpretation of Hyperfine Structure" given by one of the authors (H. E. W. in a Letter to the Editor, Phys. Rev. **34**, 1288, (1929)). The value of i for manganese appears to be $(5/2)(h/2\pi)$ as is also the case for lanthanum and praseodymium. The ratio between gross-structure and fine-structure is about 20,000:1 the same order of magnitude as the ratio between the mass of a manganese atom and five times the mass of an electron. This indicates that if the nuclear spin is due to negative charges, as seems to be the case from the *normal* order of the fine structure, they must carry with them the total mass of the nucleus in space quantization.

H. E. WHITE
R. RITSCHL

Physikalisch-Technische
Reichsanstalt

December 7, 1929.

The Unified Field-Theory and Schwarzschild's Solution

Vallarta¹ has investigated, with negative results, the consistency of Einstein's unified field-theory with the generalized relativity theory of 1916 as regards the gravitational equations in a spherically symmetrical field. It appears, however, that he made a slip toward the beginning of his calculation. The expressions for the potentials should be

$$\phi_i = 2Ax_i - \frac{W'x_i}{Wr} \quad (i=1, 2, 3)$$

instead of simply the first term. As a result, Vallarta's expressions for $V_{\beta\gamma}^\alpha$ and $V^{\alpha\beta\gamma}$ are wrong. When the necessary corrections are applied, Vallarta's gravitational equations

$$\frac{\partial V^{\alpha\beta\gamma}}{\partial x_\gamma} + V^{\sigma\beta\gamma}\Gamma_{\gamma\sigma}^\alpha + V^{\alpha\sigma\gamma}\Gamma_{\sigma\gamma}^\beta + V^{\alpha\beta\sigma}\Gamma_{\sigma\gamma}^\gamma = 0 \quad (1)$$

yield, for the case $\alpha=\beta=4$

$$dU/dr = U/r - U^2/r$$

where U is the square-root of the coefficient of dr^2 in the fundamental quadratic differential form. The solution of this differential equation,

$$U = \frac{1}{1 - (m/r)},$$

where m is a constant, is identical with Schwarzschild's solution for the coefficient itself. The agreement extends, therefore, as far as the first power of m/r .

For the cases $\alpha=\beta=i$ ($i=1, 2, 3$), one of the consequences to be deduced from (1) is the differential equation

$$W(U-1) - rW' = 0$$

where W is the square-root of the coefficient of dt^2 in the fundamental quadratic form. This is satisfied, though, of course, not uniquely, by a function identical with Schwarzschild's solution for the coefficient itself:

$$W = 1 - (m/r),$$

the approximation being of the same order as in the case of U . It must be borne in mind however, that the implications of (1) have by no means been exhausted.

It would indeed be surprising, in view of the basic similarity between Vallarta's and Schwarzschild's metrical assumptions, and in view also of the relation between Einstein's theories of 1916 and 1929, were results wholly at variance with Schwarzschild's solution obtainable from Vallarta's problem.

MEYER SALKOVER

Department of Mathematics,
University of Cincinnati
December 31, 1929.

¹ M. S. Vallarta, Proc. Nat. Acad. Sci. 15, 784 (1929).

Limiting Resolving Power of a Crystal Grating

From time to time one sees in the literature reports of unsuccessful attempts to find certain fine structures in x-ray spectral lines. These attempts are generally made by the single crystal photographic method, but the following considerations apply to other spectrometers, either single or double crystal type.

The resolution is limited by the "tolerance" angle of the crystal. This "tolerance" angle, namely, possible deviations from Bragg's Law, is determined by the parallel crystal method on the double spectrometer. The crystals used by Davis and Purks (Proc. Nat. Acad. Sci. Feb. 1928) in analyzing the structure of the $\text{MoK}\alpha_1$ line gave a rocking curve of 6 seconds at half-maximum, at first order. The corresponding width at second order would be 2" of arc. The tolerance angle of one of these crystals was $6/2^{1/2} = 4''$, at first order and $2/2^{1/2} = 1.4''$ at second order.

The Bragg law of crystal reflection is $\lambda = 2d \sin \theta$, so $d\lambda = 2d \cos \theta d\theta$. The fine structure displacement is represented by $d\lambda$. In the case of the $\text{MoK}\alpha_1$ fine structure the observed displacement was 0.085 x.u. This gives the angular displacement $d\theta = 3$ seconds of arc. This deviation is less than the tolerance angle of the best crystal at first order and of course the structure would be entirely washed out. Such fine structure is beyond the power of a single crystal analysis, no matter how great the distance between slits or the distance of the photographic plate.

The above applies also to double crystal analysis. Unless the tolerance angle at any order is less than the fine structure displacement, the structure will not be observed.

The width of rocking curve given here is for fine calcite. The corresponding curve for good rock-salt is 600 seconds (Davis and

Stempel, Phys. Rev. May, 1922). Rock-salt is of course not suited to fine structure work.

In general no crystal should be used for fine structure observation until its tolerance angle has been determined. Many specimens of calcite give quite wide rocking

curves and are unsuited to this type of experiment.

BERGEN DAVIS

Department of Physics,
Columbia University,
January 4, 1930.

The Third Law of Thermodynamics

R. H. Fowler admits the practical utility of the concept of absolute entropy but maintains that no theoretical significance is to be attached to the concept. This viewpoint seems at variance with the one in vogue at the present time in physics.

If we treat absolute entropy as an operational concept the only question that needs to be considered in connection with the Third Law, is whether it is ever necessary to assume the entropy of the pure stable crystalline form of a substance different from zero at 0°K in order to calculate the correct value of the entropy from the thermal data. Difficulties might be anticipated in the case of elements in which the atoms have j values different from zero where it might prove necessary to add a term $R \ln (2j+1)$ to the value obtained from the thermal data. In the case of the sodium atom (Rodebush, Proc. Nat. Acad. 13, 185 (1927)) and the oxygen molecule (Giauque and Johnstone, Jour. Am. Chem. Soc. 51, 2300 (1929)) it has been shown that the thermal data alone lead to the correct value, so that apparently no correction factors are likely to be needed for electronic moments.

In the case of nuclear spins the situation is otherwise. Here theoretically the thermal data alone should still give the correct value of the entropy but practically only in the case of hydrogen (Rodebush, Proc. Nat. Acad. 15, 678 (1929)) can the correct value of the en-

trophy be obtained in the customary manner. For all hydrogen compounds we shall presumably have to add arbitrarily the quantity $R \ln 2$ per gram atom of hydrogen to the thermal entropy. In the case of other elements having nuclear spins the term $R \ln (2s+1)$ may be omitted from the entropy of elements and compounds alike for all thermodynamical calculations.

It is not to be doubted that in the case of an element such as sodium which has a nuclear spin of several half units, that a heat effect due to the change in orientation of the nuclear spins will appear at low temperatures, but the heat effect will be so small and the temperature so low that it will probably elude observation, although the corresponding entropy change is, of course, not negligible. The more or less prevalent idea that no appreciable entropy changes occur at very low temperatures is evidently not justified.

The only other case that needs to be noticed is that of elements which are isotopic mixtures. If we consider the separation of isotopes as a process which is realizable thermodynamically then we shall have to consider the isotopic mixture as a solution and solutions together with supercooled liquids are unstable forms of matter at 0°K and the Third Law does not apply to them.

W. H. RODEBUSH

University of Illinois,
December 23, 1929.

Note on Hartree's Method

Hartree's method of self-consistent fields, for determining atomic models, has seemed to many persons to stand rather apart from the main current of quantum theory; in spite of the papers of Gaunt and the writer, showing its connection with Schrödinger's equation, it has seemed to contain arbitrary and empirical elements. It appears, however, that it has a very close relation to the variation method. That principle states that, if one has an approximate wave function con-

taining arbitrary parameters or arbitrary functions, one will have the best approximation to a solution of Schrödinger's equation if one chooses the parameters or functions so that the energy is stationary with respect to slight variations of them. Suppose one sets up an approximate wave function for a general problem of the motion of electrons among stationary nuclei, by assuming a product of functions of the various electrons: $u = u_1(x_1) \cdots u_n(x_n)$; suppose further that

one apply the variation principle by varying separately each of the functions u_i , leaving the others constant. The n variation equations so obtained prove to be those for the motion of the n electrons, each in a separate electrostatic field; and the field for each electron is obtained by adding the densities u_i^2 for all the other electrons, and finding by electrostatics the field of this charge and of the nuclei. Thus this field is self-consistent in the sense of Hartree; the result is a generalization of his method to more complicated problems than atomic ones.

For atoms, Hartree's procedure differs in the one detail that instead of taking the field so obtained (which would not be quite spherically symmetrical), he averages over all directions, to get a real central field for each electron to move in. This process also can be partly, although not entirely, justified by variation methods. If one demands that the functions u_i be solutions of a central field problem—that is, that they be products of spherical harmonics of the angles, by functions of r —and vary only the function of r , then one finds that the potential should be averaged over all orientations; but with a certain weighting function, not used by Hartree, depending on the spherical harmonic occurring in the wave function of the electron for which we are finding the potential. That is, Hartree's method could be slightly changed in this matter, with slight improvement of the results; but, except for this, it is definitely the best method, in the sense of variation principle, using central fields.

Closer examination shows that the potential we have found differs from Hartree's merely in being slightly dependent on the m , as

well as the n and l , of the electron one considers. As a result, the energy levels of the different electrons of the same n and l , but different m , will differ slightly, an effect without physical meaning. In an earlier paper of the writer (Phys. Rev. **32**, 343, 1928), it is shown that essentially this same dependence on m results in only a small error, and further, that this effect has a very close connection with the resonance terms, and that by considering these also, the energy again becomes independent of m . It would therefore not be sensible to make this slight improvement in Hartree's method without at the same time making the more important one of considering resonance. If one wished to do this, one could again use variation methods, to derive a new method similar to self-consistent fields: one would demand that the wave function be written not as $u_1(x_1) \cdots u_n(x_n)$, but as a linear combination of such functions with permuted indices, so arranged as to have proper symmetry relations; and one would then vary the u_i 's to make the energy a minimum. This would give a method similar to Hartree's, but really an improvement on it. Some preliminary calculations by Drs. Zener and Guillemin indicate that it may really be feasible to carry through this improvement. Their method differs from that sketched here only in that they represent the u_i 's by simple analytic forms containing parameters, which they vary, instead of determining them by numerical solutions of a differential equation.

J. C. SLATER

Leipzig, Germany

December 19, 1929.

An X-Ray Study of Molecular Orientation in the Kerr Effect

Perhaps the most successful theory of the Kerr effect for liquids is that which assumes a tendency toward definite orientation of the molecules under the influence of an electric field. Such a tendency towards uniform orientation should affect the x-ray diffraction pattern of the liquid by increasing the intensity of the x-rays observed at the peak of the diffraction curve. It is the purpose of this experiment to investigate the existence of such an effect.

Since, in observing the Kerr effect, the light beam is at right angles to the applied field it was thought best to arrange the path of the

x-ray beam as nearly at right angles to the applied field as possible. In order to accomplish this the following method was devised. The liquids used were placed in a cylindrical glass cell one end of which was covered by a thin window of cellophane on whose inner side thin aluminum leaf was fastened. A beam of unfiltered x-rays from a molybdenum tube operated at 35 K.V. was reflected from this face, the cell replacing the crystal of an ordinary Bragg spectrometer. Measurements of the intensity of the reflected beam were made in the ordinary manner used in crystalline reflection, namely by turning the cell through

an angle θ , and the ionization chamber through 2θ , where θ is the grazing angle of incidence on the cell. The intensity of the reflected x-rays from an empty cell was less than 15 percent of the intensity observed at the same angle when the cell was filled. Soller slit sets were used to collimate both the incident and reflected beams. The reflection curves obtained for benzene and nitrobenzene were found to be practically the same as the corresponding liquid diffraction curves obtained by other methods.

The Kerr effect is most strongly shown by nitrobenzene when a rapid succession of practically instantaneous sparks are passed through it. Since full-wave rectification was used in obtaining the high potential for the x-ray tube it was thought desirable to synchronize the electric impulses across the cell with the peaks of the x-ray pulses. This was done by connecting a water rheostat in parallel with the tube, and connecting the aluminum leaf of the cell to this rheostat. In order to sharpen the electric impulse across the cell a spark gap was inserted between the rheostat and the cell, and a jet of air was blown between the balls of this gap. The other end of this cell was covered with a grounded brass plate.

All observations of the effect of the electric field were made with the cell at the grazing angle corresponding to maximum reflected intensity. Readings were taken alternately with and without a field of 13 K.V. per cm across the cell. Four groups of readings of 25 pairs each were obtained for nitrobenzene, the increases in intensity being 1.8, 2.5, 2.1, and 2.9 percent respectively for each of the four groups. The average increase with the field was thus found to be 2.3 percent, with a probable error of 0.5 percent. The effect thus

observed is between four and five times the probable error.

With a field applied to the cell in the manner described above benzene shows little or no Kerr effect. Hence, if the Kerr effect is due to partial molecular alignment, benzene—under the field applied to nitrobenzene—would not be expected to show a change in intensity of the peak maximum. Four groups of readings of 25 pairs each, taken alternately with and without the field in precisely the same manner as nitrobenzene, showed for benzene changes in intensity of -0.4 , $+0.3$, -0.3 , and -0.6 percent. The negative sign is used to indicate the variations in the opposite direction to that of nitrobenzene. The average change in intensity for all readings is -0.3 percent which is well within the probable error. This lack of any definite shift in intensity with the field rules out the possibility that the effect observed for nitrobenzene might be due to a slight bending of the cellophane window as a result of electrostatic forces of attraction.

The results here given show for nitrobenzene an increase in intensity of the peak maximum of an amount that is approximately five times the probable error, while for benzene any change observed lies not only well within the probable error but also is, for the most part, in a direction opposite to that of nitrobenzene. It would thus seem that for nitrobenzene there occurs, when the proper type of electric field is present, a small but detectable tendency of the molecules to align themselves in a common direction.

RONALD L. MCFARLAN

Ryerson Physical Laboratory,
The University of Chicago,
December 21, 1929.

A Comparison of the Reflection Spectra of $\text{SmCl}_3 \cdot 6\text{H}_2\text{O}$ at Room Temperature and at that of Liquid Air with its Absorption Spectra at Low Temperatures

In a communication to Nature¹ we discussed a change which we observed in the absorption spectrum of a single crystal of $\text{SmCl}_3 \cdot 6\text{H}_2\text{O}$ as we lowered the temperature to that of liquid hydrogen. Many lines or bands which were prominent in the spectrum at room temperature practically disappeared at the temperature of liquid hydrogen and

others which were extremely faint increased in intensity as the temperature was lowered. We ascribed this change in relative intensity to the presence of different electronic configurations of Sm^{+++} in the solid state in thermal equilibrium. (This interpretation is in accord with the magnetic behavior of Sm^{+++} .)

¹Freed and Spedding, *Nature*, April 6 1929).

At present we wish to report the most general features of the reflection spectra

obtained by reflecting a continuous spectrum from the surfaces of many small crystals of the same salt. The reflected spectrum has the characteristics of an absorption spectrum. The lines which we attribute to the electronic modification stable at the low temperature, that is those which are prominent only at the low temperatures in absorption are found relatively much more intense at room temperature in reflection. In addition, the lines in the reflection spectra are accompanied by satellites about 160 cm^{-1} toward the red. The reflection spectrum at room temperature also contains narrow diffuse bands which were not observed in absorption.

At the temperature of liquid air, these bands sharpen and become resolved into multiplets consisting of very narrow lines. At this temperature, many new lines make their appearance and they tend to cluster on both sides of the lines which are found in the absorption spectrum. Satellites accompany the prominent lines at intervals of about 160 cm^{-1} at the temperature of liquid air also.

Our method of photographing the reflection spectra does not exclude the simultaneous appearance of the absorption spectrum. (We intend to eliminate this spectrum in our future work.) However, the astonishing intensification of the "low temperature" lines in the reflection spectrum at room temperature cannot be ascribed to any spurious experimental influence because we are considering relative intensities only.

A fluorescence or an unusual reflecting power appears to take place on the violet side of a number of the lines in the reflection spectrum at the temperature of liquid air which do not occur in absorption.

The force fields in the surface are definitely different from those within the crystal. It is conceivable that in the surface there is a higher concentration of the "low temperature modification" than corresponds to an equilibrium distribution within the crystal. It is also possible that the absorption coefficient of this particular modification may be greater under these conditions.

The large number of entirely new lines which occur in the reflection spectrum may possibly be due to the fact that the electrostatic fields to which the Sm^{+++} ions within the crystal are exposed are no longer regular in direction and in magnitude in the surface so that any "forbidden" electronic jumps within the crystal are no longer "forbidden" in the surface. In other words, the probability of transition between certain states has been increased. We are investigating this phenomenon further.

SIMON FREED
FRANK H. SPEDDING

University of California,
Berkeley, California,
Chemistry Department.

December 19, 1929.

An Observed Periodicity in the Packing Fraction

It is found that a single oscillatory curve can be fitted to the packing fraction data taken by Aston, eliminating the necessity of the two branches at the small mass number end (Proc. Roy. Soc. **A115**, 487 (1927)). Points of maxima are located at mass numbers 6, 10, 13, 17, 21, 25, \dots , and minima are found for the elements whose mass number is an integral multiple of four.

The mass number of the atom was assumed to be given by the expression $4n+x$, where $n=0, 1, 2, 3, \dots$ and $x=1, 2, 3$ or 4. Since the packing fraction represents an average mass defect per proton it is evident that in the $4n+1$ type of atom, the one proton is loosely connected to the core of the nucleus probably existing as a satellite in the form of a neutron. In the $4n+2$ type the two protons

are a little more tightly bound to the core. Similarly for the $4n+3$ atom. And finally for the $4n+4$ type of atom we find maximum packing, the four protons probably forming an alpha-particle which goes into the center of the nucleus. These conclusions were arrived at after a calculation of the change in packing fraction per proton produced by the "x" portion of the atom had been made wherever possible. Curves were plotted showing the effect of the value of "x" on this change in the packing fraction, these being used to determine the points of maxima and minima.

The fact that the packing becomes greater for the $4n+4$ atoms with an increase in mass number indicates that the alpha-particle actually goes into the center of the nucleus each time "x" becomes equal to four. This

was suggested by Aston. This continues up to about mass number eighty. A definite oscillation for the kryptons is observed. For the heavier elements the data are not accurate enough to show any oscillation if it is present. Aston has attributed the general rise in the curve beyond mass number eighty to the increasing complexity of the nuclear structure. If this oscillation continues for the heavier elements, we might still have the alpha-particle forming in the nucleus as before but instead of going into the center they begin to form satellites around the now

"filled up" center of the nucleus. For the heaviest elements these satellites may be far enough from the core to render them unstable and thus produce atomic disintegration with the ejection of alpha-particles and electrons. More accurate packing fraction data are needed to determine definitely whether this periodicity exists for the heavy elements.

HOWARD OLSON

Department of Physics,
Colorado College,
January 13, 1930.

The Unified Field Equations and Schwarzschild's Solution. II.

All of the implications of Eq. (1) of the previous note¹ have since been worked out. Another consequence of the case $\alpha = \beta$ ($\alpha, \beta = 1, 2, 3$) is

$$\frac{W''}{UW} + \frac{W'}{Wr} \left(\frac{2}{U} + \frac{1}{U^2} - \frac{U'r}{U^2} - 1 \right) - \frac{U'}{U^2r} + \frac{1-U}{U^2r^2} = 0. \quad (1)$$

The only other non-trivial case so far not considered is $\alpha \neq \beta$ ($\alpha, \beta = 1, 2, 3$); this yields

$$\frac{W''}{UW} + \frac{W'}{Wr} \left(\frac{2}{U} - \frac{2}{U^2} - \frac{U'r}{U^2} - 1 \right) - \frac{U'}{U^2r} - \frac{2(1-U)}{U^2r^2} = 0. \quad (2)$$

If for U is substituted the solution obtained in the previous note

$$U = 1/(1-m/r),$$

both (1) and (2) are seen to have as a particular solution

$$W = C \left(1 - \frac{m}{r} \right), \quad (3)$$

where C is a constant. On subtracting (2) from (1) and reducing, we get

$$W'r = W(U-1) = \frac{mW}{r-m} \quad (4)$$

which was found in the previous note as a consequence of the case $\alpha = \beta$ ($\alpha, \beta \neq 4$). The general solution of (4) is (3); and if the reasonable boundary condition

$$\lim_{r \rightarrow \infty} W = 1$$

is applied—the corresponding condition is already satisfied by $U=$, the constant C becomes unity, and we find, unambiguously,

$$W = 1 - \frac{m}{r}.$$

MEYER SALKOVER

University of Cincinnati,
January 11, 1930.

¹ See page 209, this issue.

On the Vibration Frequencies of HCl and HBr in the Liquid State

Modified scattering of the mercury 4047 line by HCl in the liquid has already been reported (Science, March 29, 1929). We have repeated our measurements with greater accuracy and have also measured a modified line from liquid HBr, at -75°C . Calling ν_1 the observed modified line, ν_0 the molecular frequency and λ_0 the corresponding wavelength, the results are (reduced to vacuum):—

Liquid	ν_1	ν_0	λ_0
HCl	21924	2781	3.595 μ
HBr	22226	2479	4.033 μ

The value of ν_0 for gaseous HCl is 2886 (Wood, Phil. Mag. 7, 744 (1929); Colby, Phys. Rev. 24 (1), 53 (1929)), and for gaseous HBr is 2559 (Imes, Astrophys. J. 50, 251 (1919)). Comparing these with the above values, we see that ν_0 is shifted to the smaller frequencies in the liquid, 105 wave-numbers in the case of HCl and 80 in the case of HBr.

The Lorentz-Lorenz theory affords an explanation of frequency differences of a molecule in different physical states (see e.g. Wolf and Herzfeld, Handbuch der Physik).

Thus, letting ν_0' refer to the liquid, there is the relation

$$\nu_0' = \left(\nu_0^2 - \alpha \frac{Ne^2p}{m} \right)^{1/2}$$

where N is the number of molecules per unit volume in the liquid, p the number of resonating particles of charge e and mass m in a molecule, and α times the polarization per unit volume is the Lorentz force, α being $4\pi/3$ for a spherical cavity. But α when calculated from the above observed frequencies in the gas and in the liquid comes out not around $4\pi/3$ but 0.20 for HCl and 0.16 for HBr. In fact, using $4\pi/3$ for α makes the last term larger than ν_0^2 for these molecules.

However, this calculation is made with

The Reflecting Powers of Atoms for X-rays of Different Wave-lengths

In the course of measurements of atomic F -curves¹ experiments have been made to find out whether the scattering power of an atom changes with the wave-length of the x-rays used. It might be expected that such a wave-length effect, if it exists, would be most conspicuous in the neighborhood of characteristic frequencies of the diffracting atom. With this in mind, the F -curves of NiO have been mapped for molybdenum, copper and nickel radiation and points have been determined upon the curves of the metals iron, copper and nickel for molybdenum, copper, nickel and iron rays. This has been done by comparing the relative intensities of powder lines from these substances with the intensity of a standard NaCl reflection. Though the scattering powers thus obtained are not necessarily correct in absolute value, nevertheless as long as the F of the standard NaCl reflection is either constant or changes in a regular fashion with increasing wave-length, the relationships they show amongst themselves will be significant.

Earlier measurements from this laboratory² have shown that the scatterings of metallic iron and copper for copper K -radiation are less than for the $K\alpha$ line of molybdenum. Additional observations have shown (1) that the scattering power of a particular atom decreases with increasing wave-length as this wave-length approaches a critical excitation value for the scatterer; (2) that F is a minimum for this longest exciting radiation;

4.77×10^{-10} e.s.u. for e , that is, it assumes that the vibrating atom is H^+ . But we know that HCl and HBr do not have this structure. Dennison has, indeed, introduced into band spectrum theory the "effective charge," which he finds for HCl to be $0.199 \times 4.77 \times 10^{-10}$ e.s.u. (Phys. Rev. **31**, 503 (1928)). Using this value for e , and retaining $\alpha = 4\pi/3$, we now calculate $\lambda_0' = 3.578\mu$, in quite good agreement with our measured 3.595μ .

These results and others will be presented at greater length later.

E. O. SALANT
A. SANDOW

Physics Department,
Washington Square College,
New York University,
January 13, 1930.

(3) that this number then rises to a maximum for a wave-length equal to that characteristic of the scatterer; and (4) that thereafter it appears to fall slowly with further increase in wave-length. Thus, for example, the approximate values of Table I are obtained assuming $F(220, \text{NaCl}) = 15.62$.

TABLE I.

Wave-length	Fe $F(110)$	Ni $F(200)$	NiO $F(220)$	Cu $F(220)$
Mo $K\alpha$	15.87*	—	18.28	14.28*
Cu $K\alpha$	11.48	13.70	15.83	11.53
Ni $K\alpha$	9.77	14.48	16.88	11.18
Fe $K\alpha$	13.45	—	—	—

* See footnote 2.

The absorption coefficients of the diffracting powders enter into these determinations. The sequence of Table I is obtained, however, whether either experimental coefficients are used or those calculated by the general formula of Jönsson.³

The usual theory of the intensity of reflection from ideally imperfect crystals, to

¹ C. G. Darwin, Phil. Mag. **43**, 800 (1922); etc.; A. H. Compton, X-rays and Electrons (New York, 1926) Chap. V.

² A. H. Armstrong, Phys. Rev. **34**, 931 (1929).

³ E. Jönsson, Uppsala Univers. Årsskrift, 1928.

which these data are legitimately referable indicates that F , the ratio of the scattering of an atom to that of a single electron, may be expected to be constant for constant values of $\sin \theta/\lambda$. In other words, it will be the same for a particular reflection no matter what wave-length is employed.

The observed departures from this constancy probably have more than one cause. Thus the minimum in F which occurs at the critical absorption wave-length of the scattering atom is most naturally accounted for if energy which otherwise would be coherently scattered is utilized in the production of the secondary radiation. At the same time, the fact that maxima in F are always obtained at characteristic wave-lengths of the scatterer suggests some sort of resonance. Such

resonance, if it exists, cannot be sharp, however, for F falls away only slowly with longer wave-lengths.

It is apparent that photographs of RbBr made by Mark and Szilard⁴ with strontium and bromine radiations are expressions of variations in F of the same nature as those just described.

Detailed results of these experiments will be published soon.

RALPH W. G. WYCKOFF

Rockefeller Institute for Medical Research,
New York City,
January 7, 1930.

⁴ H. Mark and L. Szilard, *Zeits. f. Physik.* **33**, 688 (1925).

THE PHYSICAL REVIEW

THE CAPTURE OF ELECTRONS BY ALPHA-PARTICLES

BY ARTHUR H. BARNES

PHYSICS LABORATORIES, COLUMBIA UNIVERSITY

(Received December 24, 1929)

ABSTRACT

A stream of electrons is superposed upon a beam of alpha-particles. The alpha-particles are then deflected by a magnetic field and counted by the scintillation method. Alpha-particles which have captured electrons will not be deflected to the point where observation is made, and consequently, the decrease in scintillations will indicate the number of captures which occur.

Probability of capture as function of relative velocity.—It is found that electrons are captured when their velocity equals that of the alpha-particle, and also, at a series of discrete velocities both greater and less than that of the alpha-particle. Counting scintillations due to singly charged particles showed that at certain of these discrete velocities one electron is captured. At the other velocities two electrons are captured. This was determined by counting scintillations due to neutral particles which had passed undeflected through the magnetic field. Both single and double capture occur at zero relative velocity, the latter predominating as the electron density is increased.

Calculation of the kinetic energy of the electron with respect to the alpha-particle corresponding to each of the velocities at which single capture occurs, gives a series of energy values which can be associated with the energy levels in the ionized helium atom. Similarly, for the case of double capture, the sum of the kinetic energies due to each of the two electrons, corresponds to the energy of the quantum states of both the parhelium and orthohelium types of atom. There is indication that the hitherto unobserved ground state of orthohelium is being formed. The conclusion is reached that in order for capture to occur, it is necessary that the electron, due to some external field, possess a kinetic energy, which, with respect to the nucleus, is either zero, or equal to the energy of one of the quantum states of the atom. In the latter case double the normal energy must be radiated, and the question arises as to whether it is radiated as two quanta of normal frequency, or as one quantum of twice that frequency.

There is evidence that the *penetrating power* of the singly charged and neutral particles is less than that of the nucleus alone.

Time required for capture of electron by alpha-particle.—The construction of one of the tubes used permitted the time during which the alpha-particle was in the electron stream to be made less than 3×10^{-10} sec without appreciably decreasing the percent of capture. The electron density under these conditions was of the order of 10^7 electrons per cc.

IN A previous report¹ an experiment was described which showed that an electron is captured by an alpha-particle only at definite relative velocities.

¹ Bergen Davis and A. H. Barnes, Phys. Rev. 34, 152 (July 1, 1929).

The series of energy values associated with these velocities was shown to correspond to the energy levels in the ionized helium atom.

The present paper gives the details of the experiment (which were omitted in the preliminary announcement) and presents additional information obtained with a new experimental arrangement.

FIRST EXPERIMENTAL TUBE

Two experimental tubes were constructed. The first tube is shown diagrammatically in Figure 1. The alpha-particle source is polonium deposited upon a pointed copper rod placed at *S*. A thin glass window *W*, 0.0005 cm thick, allows the alpha-particles to enter the tube. By thus placing the radioactive source outside the tube, contamination difficulties were entirely avoided.

After passing through the tube, the alpha-particles leave it by means of another window placed at *Y*, or if a sufficient magnetic field be applied at *M*, they will be deflected and pass out through a window at *Z*. The latter windows are each 0.001 cm thick. Zinc sulphide screens are placed outside the windows. Aluminum foil 0.0004 cm thick was placed before each screen to shield it from the light of the filament. The air is exhausted from the spaces between screen and window and also from the space between source and window.

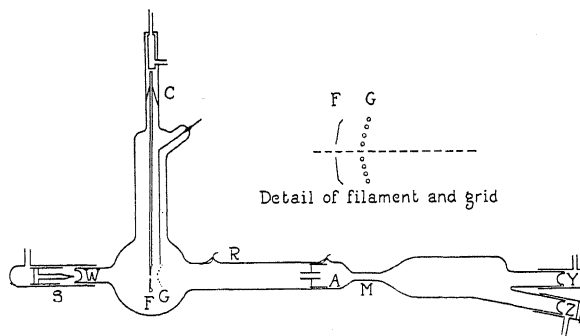


Fig. 1. Diagram of first experimental tube. *S*, radioactive source; *W*, thin glass window; *F*, filament; *G*, grid; *R*, lead to silvered surface; *A*, second anode; *M*, magnetic field; *C*, copper seals; *Y*, and *Z*, zinc sulphide screens.

The source of the electrons is a large oxide-coated filament *F*, 2.5 cm square and made slightly concave. A hole 0.5 cm in diameter allows the alpha-particles to pass through. The current necessary to heat the filament was about 150 amperes and entered the tube through water-cooled copper seals at *C*.

The first anode *G*, is placed one cm from the filament and takes the form of a conical spiral of 60 mil tungsten wire. The diameter of the inner and outer turn is 0.4 cm and 2.5 cm respectively. The spacing between turns is 0.4 cm. The second anode *A*, is a nickle cylinder 0.5 cm in diameter and 3 cm long. It is placed 18 cm behind the grid *G*.

The inside of the glass vessel is silvered and the conducting layer grounded to prevent accumulation of charge on the walls. All metal parts were out-gassed in a vacuum furnace before being placed in the tube. The tube was evacuated, baked, and sealed off.

Electrons leaving the filament are accelerated to any desired velocity by the potential impressed upon the grid G . Due to the shape of the grid and filament, those electrons which pass through the grid will converge and proceed along the axis of the tube towards the anode A . The alpha-particle does not enter into a region of relatively great electron density until it reaches the point of convergence of the electron stream. If an electron is captured at this point, the alpha-particle will arrive at the magnetic field with a decreased charge, and consequently will not be deflected to the lower screen at Z . The decrease in scintillations observed at Z will therefore determine the number of captures which occur.

PROCEDURE AND RESULTS

The procedure followed with this tube was to vary the magnetic field until the alpha-particles were deflected to the lower screen Z . The potential applied to the grid G , and cylinder C , was then varied in small steps and the corresponding change in the number of alpha-particles arriving at Z was determined. During most of the runs the current to G was 60 milliamperes and to A , 0.08 milliamperes.

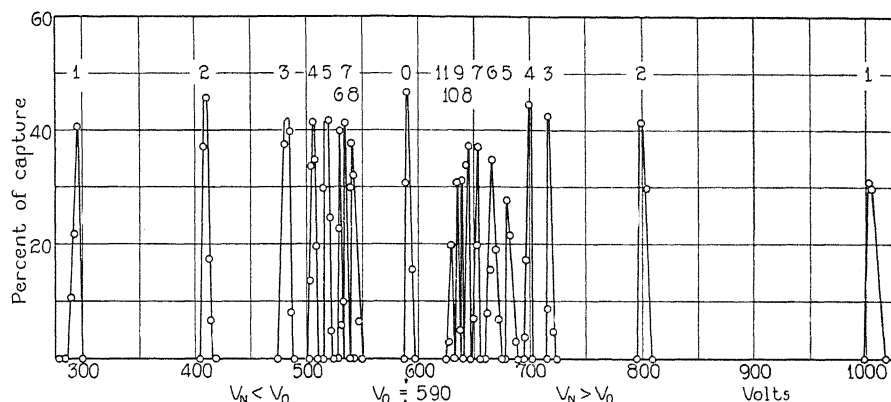


Fig. 2. Electron capture as a function of accelerating voltage.

It was found that capture takes place when the velocity of the electron is equal to that of the alpha-particle also at a series of definite electron velocities both greater and less than that of the alpha-particle. A curve showing the relation between capture and applied voltage as obtained with this tube is given in Figure 2. It consists of a double series of sharp maxima grouped on each side of a central peak. The velocity of the electrons corresponding to the voltage at which the central peak occurs is 1.44×10^9 cm/sec. This agrees closely with the calculated velocity of the alpha-particle after passing through the window of the tube.

If v is the velocity of an electron and u the velocity of an alpha-particle, then the kinetic energy of the electron with respect to the alpha-particle will be,

$$W = \left(\frac{1}{2}\right)m(v-u)^2$$

where m is the mass of the electron.

Let V_n and V_0 be the potential differences through which electrons must fall to acquire the velocities v , and u , respectively, then,

$$eV_n = mv^2/2$$

and,

$$v = (2eV_n/m)^{1/2}$$

similarly,

$$u = (2eV_0/m)^{1/2}$$

substituting,

$$W = \left(\frac{1}{2}\right)m \left(\frac{2e}{m}V_n - \frac{4e}{m}V_n^{1/2}V_0^{1/2} + \frac{2e}{m}V_0 \right) \\ = e(V_n^{1/2} - V_0^{1/2})^2$$

or,

$$\frac{W}{e} = (V_n^{1/2} - V_0^{1/2})^2 = E_n$$

where E_n is the energy expressed in volts when V_n and V_0 are in volts.

If in this equation we substitute for V_0 the voltage which will accelerate an electron to a velocity equal to that of the alpha-particle, and for V_n successively the voltages at which the observed peaks occur, then we arrive at a series of energy values which correspond to the energy levels in the ionized helium atom.

Table I gives the voltages of the observed peaks and the corresponding values of E_n . The last column gives the values of E_n as calculated from Bohr theory. There are of course two sets of observed values for E_n corresponding to the two cases in which $V_n > V_0$ and $V_n < V_0$.

TABLE I. Values of E_n for which capture takes place.

n	$V_n < V_0$	E_n	$V_n > V_0$	E_n	Mean of E_n	$E_n = 54.16/n^2$
1	295	50.6	1005	54.9	52.0	54.16
2	410	16.7	800	15.6	16.2	13.54
3	483	5.33	720	6.45	5.67	6.01
4	505	3.29	700	4.71	4.00	3.38
5	519	2.28	681	3.27	2.77	2.16
6	531	1.56	667	2.41	1.98	1.50
7	535	1.34	653	1.59	1.46	1.10
8	538	1.19	645	1.23	1.21	.84
9			638	.96		.67
10			635	.88		.54

It thus appears that the probability that an alpha-particle will capture an electron is great only when the kinetic energy of the electron with respect to the alpha-particle is either zero, or equal to the energy of one of the quantum states of the ionized helium atom. It is to be noted that the kinetic energy here referred to is that due to the applied field only.

The effect of varying the potential of the second anode A , with respect to the first G , was investigated. It was found that if the potential of A was made greater or less than that of G , then to maintain the condition for capture, it was also necessary to change the potential of G . Thus if the potential of A is decreased, then to maintain capture, it is necessary to increase the

potential of *G*. Another result of making the potential of *A* different from that of *G* is a considerable broadening of the peaks, especially when *A* is at a higher potential than *G*. These effects indicate that capture is taking place at some point between the first and second anodes, and that the velocity of the electrons is the governing factor.

It will be noticed that the peaks do not continue to the central peak as they might be expected to do, but stop abruptly at about the tenth energy level. It was thought that this might be due to re-ionization caused by collisions with the molecules of residual gas in the tube. This effect was investigated with the second tube and will be discussed later.

An alpha-particle which has picked up one electron will be deflected to the lower screen *Z*, when the magnetic field is doubled. If it has picked up two electrons it will pass through the magnetic field without deflection and arrive at the upper screen *Y*. It should therefore be possible to observe an increase in scintillations corresponding to every decrease.

When this procedure was tried no increase could be detected. It was further found that with the magnetic field entirely removed, a decrease in scintillations on the upper screen occurred at the same voltages at which decreases had formerly occurred on the lower screen. This effect indicated that the penetrating power of a singly charged or neutral particle was less than that of the nucleus alone.

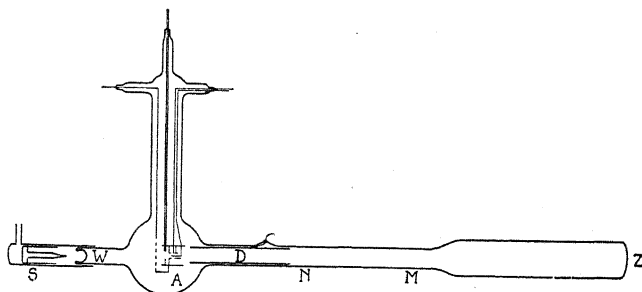


Fig. 3. Diagram of second experimental tube. *S*, radioactive source; *W*, thin glass window; *A*, filament-anode system; *M*, magnetic field; *Z*, zinc sulphide screen.

SECOND EXPERIMENTAL TUBE

The second tube was constructed with four objects in view.

1. The reduction of the time of passage of an alpha-particle through the electron stream to a known small value.
2. The detection of scintillations due a singly charged and neutral particles.
3. The investigation of the effect of varying the velocity of the alpha-particle.
4. The investigation of the captureless intervals located on each side of the central peak.

The construction of the second tube is shown diagrammatically in Figure 3 and Figure 4. The electron source is an oxide-coated filament *F*, in the form of a flat disk with a 0.4 cm diameter hole at its center to allow the passage of the alpha-particles. Two mm in front of the filament is placed a plate *P*, with

0.5 cm diameter hole exactly opposite the hole in the filament. A 60 mil tungsten wire *T*, extends for one cm along the axis of the tube to a point within one mm of the plate *P*. Surrounding the wire is a cylinder *C*, 0.5 cm in diameter and 0.5 cm long. A second cylinder *D*, 2 cm in diameter and 10 cm long is placed 1 cm behind the first cylinder and on the same axis. The whole assembly is held rigidly in place and mutually insulated. Separate leads are brought out from each of the elements.

Zinc sulphide is placed on the inside of the flattened end of the tube at *Z*. The window used to admit the alpha-particles was of very nearly the same thickness (0.0005 cm) as that used on the first tube, so that the velocity of the alpha-particles in each tube was very nearly the same. The tube was evacuated and sealed off.

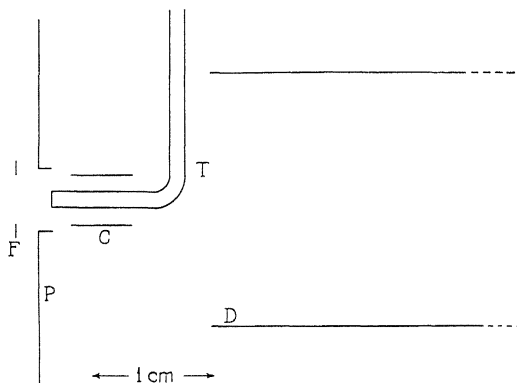


Fig. 4. Detail of filament-anode system in second tube. *F*, filament; *P*, plate; *T*, wire; *C*, cylinder; *D*, cylinder.

If the anode assembly (*P*, *C*, *D*, and *T*) is all put at the same potential the electrons leaving the filament will be accelerated by the field between the filament and the plate *P*, and wire *T*. Some will pass between this wire and the cylinder *C*, and so on to the larger cylinder at *D*. If however, the cylinder *C*, is put at filament potential, the field existing between *C* and *T* will be sufficient to deflect all the electrons which pass *P*, to the wire *T* near its end. The length of path which the electrons can possibly travel is thus limited. Furthermore every electron which reaches the wire *T*, must cross the paths of the alpha-particles.

PROCEDURE AND RESULTS WITH SECOND TUBE

The effect on capture of various arrangements of the anode system was tried. The plate *P*, wire *T*, and cylinders *C*, and *D*, were put at the same potential and the percent of capture determined. The cylinders *C* and *D*, were then put at filament potential and it was found that the percent of capture remained practically unchanged.

Under the latter conditions the greatest length of path possible for the electrons was approximately 5 mm, and since the velocity of the alpha-particle as it passes through this region is 1.45×10^9 cm/sec it follows that the process of capture must take place in less than 3×10^{-10} sec.

In the second tube the scintillations due to both singly charged and neutral particles could be detected. It was possible to count the increase in scintillations due to alpha-particles which had captured one electron and therefore struck the screen at a point midway between the center and the edge. It was also discovered that at certain voltages neutral particles were produced. They, of course, were not deflected by the magnetic field and struck the center of the screen.

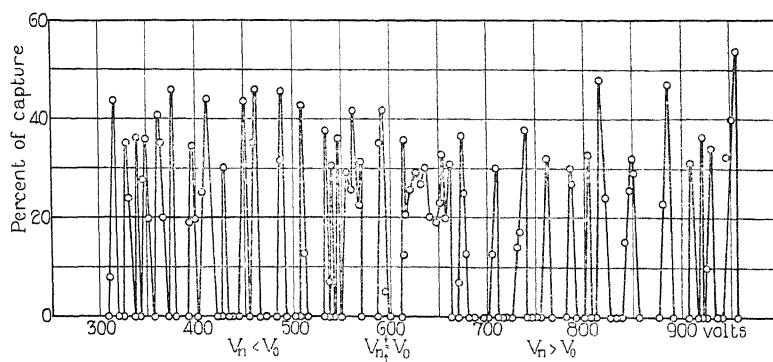


Fig. 5. Double electron capture as a function of accelerating voltage.

It was found by observing at the center of the screen that there exists a whole series of voltages at which double capture occurs. A curve showing the relation between this type of capture and the applied voltage is given in Figure 5. There exists also an independent series of values at which single capture occurs, (Figure 6.). With the first tube it was not possible to separate

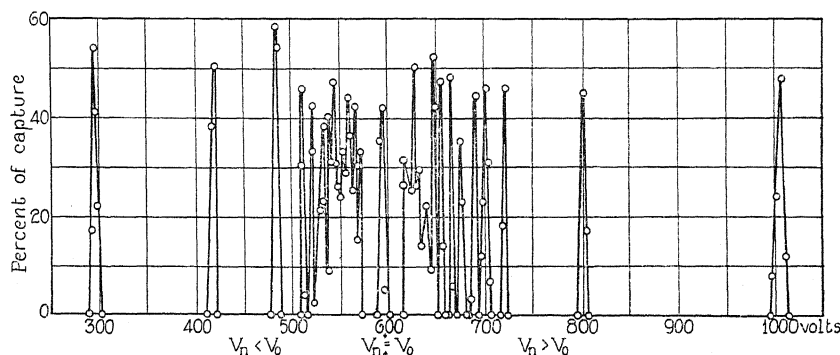


Fig. 6. Single electron capture as a function of accelerating voltage.

these two types of capture, (since only a decrease in scintillations could be observed) and consequently some of the peaks which were thought due to single electron capture were in reality due to double capture. The peak found at 410 volts for example was at first attributed to single capture. The second tube showed however, that this was a voltage at which double capture occurred, and that the single capture peak was at 418 volts.

The most striking feature of the curves is the narrowness of the peaks. This indicates that capture takes place at a point where the electrons are moving with a very uniform speed and direction. The electron velocity at this point will in general be somewhat less than that corresponding to anode potential. The observed voltage across the tube will therefore not indicate the true velocity at the point of capture. This condition introduces an error in the determination of the location of the peaks and consequently also in the calculated energy values. It should be possible to design an arrangement in which the electron velocity at the point of capture was very exactly known and so obtain correct values for the energy levels.

The whole range of voltage was investigated and the single capture peaks separated from those due to double capture. A revised table showing single capture voltages and the corresponding energy values is given in Table II.

TABLE II. Values of E_n for single capture.

n	$V_n < V_0$	E_n	$V_n > V_0$	E_n	Mean of E_n	$E_n = 54.16/n^2$
1	293	51.8	1005	54.9	53.3	54.16
2	418	14.8	800	15.6	15.2	13.54
3	481	5.53	719	6.45	5.99	6.01
4	508	3.16	700	4.71	3.93	3.38
5	519	2.31	689	3.72	3.01	2.16
6	531	1.56	673	2.69	2.12	1.50
7	535	1.39	662	2.02	1.70	1.10
8	540	1.12	652	1.51	1.31	.84
9	—	—	645	1.21	—	.67
10	—	—	637	.53	—	.54

Applying the energy relation given above to the case of the double capture peaks it is possible to calculate the kinetic energy of each electron with respect to the alpha-particle. If double capture takes place under conditions similar to that for single-capture, then the sum of the kinetic energies of each of the two electrons, (as acquired from the applied field, but with respect to the alpha-particle) should correspond to the energy of one of the quantum states of the helium atom.

Table III shows the voltages at which double capture occurs and the corresponding relative kinetic energy of one and of two electrons.

TABLE III. Values of E_n for double capture.

$V_n < V_0$	E_n	$2E_n$	$V_n > V_0$	E_n	$2E_n$	Mean of $2E_n$
315	43.0	86.0	955	43.5	87.0	86.5
327	38.6	77.2	930	38.4	76.8	77.0
338	35.4	70.8	921	36.0	72.0	71.4
347	32.1	64.2	907	33.6	67.2	65.7
360	28.4	56.8	885	29.7	59.4	58.1
375	25.0	50.0	848	24.1	48.2	49.1
395	19.5	39.0	815	18.0	36.0	37.5
410	16.4	32.8	803	16.4	32.8	32.8
428	13.0	26.0	783	13.5	27.0	26.5
448	10.5	21.0	760	10.8	21.6	21.3
460	8.25	16.5	738	8.2	16.4	16.5
486	4.60	9.20	708	5.3	10.6	9.90
507	3.24	6.48	672	2.60	5.20	5.84
533	1.49	2.98	661	1.96	3.96	3.47
537	1.25	2.50	652	1.51	3.02	2.76

The second value (77 volts) given in the last column of the table agrees with the observed total energy of the parhelium type of atom ($54.2 + 24.5$ volts). It is suggested that the first value, 86.5 volts, may correspond to the ground state of orthohelium, a configuration hitherto unobserved, but which might be formed under the special transition conditions peculiar to this experiment.

It is also probable that the remaining values constitute a double series, consisting of the energy levels of both the parhelium and orthohelium types.

No significance is to be attached to the fact that the peaks in Figures 2, 5, and 6, do not rise much above 50 percent. It was discovered after these curves had been taken that by a suitable adjustment of the position of the radioactive source it was possible to increase capture to over 90 percent.

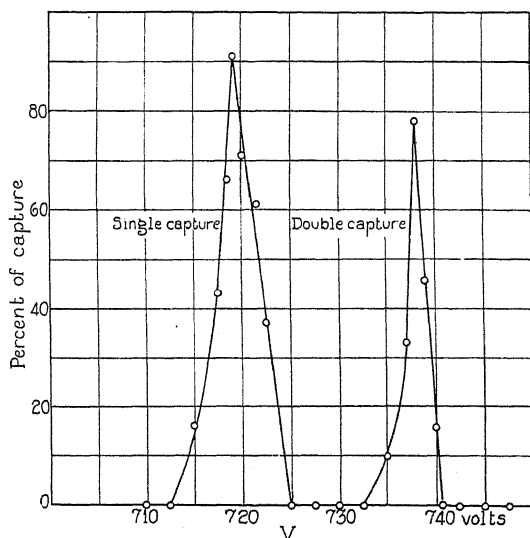


Fig. 7. Typical peaks.

Two typical peaks taken under these conditions are shown in Figure 7. The peak at 719 volts is one due to single capture. The 738 volt peak is due to double capture.

The explanation of this dependence of capture on the position of the source is that the electron stream is not uniformly distributed over the area through which the alpha-particles are passing. Thus, if there is always a portion of the observed alpha-particles which pass through a region where the electron density is always too low for capture to occur, it will be impossible by merely increasing the current to the anode to make the percent of capture rise above a certain value. If however, the position of the source is so adjusted that all the alpha-particles which fall within the field of view of the microscope, (2.4 mm in diameter) must pass through the region of maximum electron density, then by increasing the current to the anode it is possible to make capture approach 100 percent.

The effect of gradually increasing the current to the anode T , when the voltage is held at one of the peak values is illustrated in Figure 8 and Figure

9. The curve in Figure 8 is taken at the single capture peak at 719 volts. Figure 9 is the curve obtained at the double capture peak occurring at 738 volts.

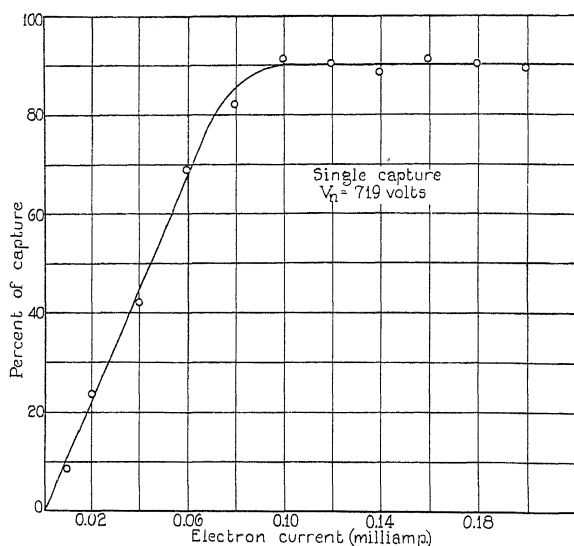


Fig. 8. Capture as a function of electron current. A curve taken at the 719 volt single capture peak.

Since these voltages are relatively close together, the electron density for a given anode current is probably not very different in each case, and there-

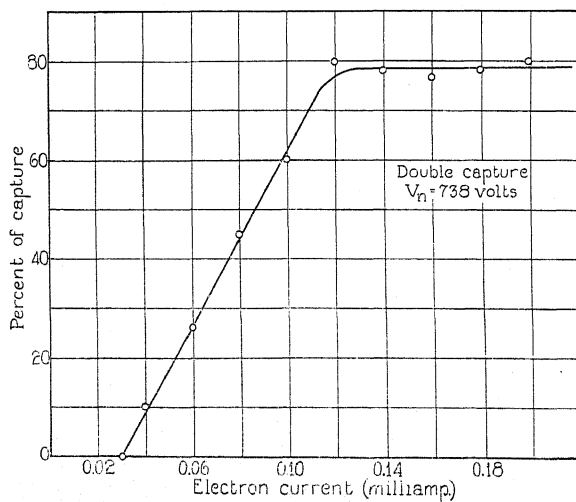


Fig. 9. Capture as a function of electron current. A curve taken at the 738 volt double capture peak.

fore the percentage of capture should be a rough indication of the relative probabilities of single and double capture.

Further information on this question is given in Figure 10 which shows a series of three curves taken at the 590 volt peak which corresponds to zero relative velocity of electron and alpha-particle. Curve (1) shows the manner in which the number of single captures varies with the current going to the anode *T*. It was obtained by counting increases in scintillations due to singly charged particles striking the screen at the midway point. Curve (2) shows the variation with current of the number of neutral particles which strike the screen at its center. Curve (3) shows the total decrease in scintillations as observed at the lower edge of the screen. The ordinates in this case are not given in percent but in the observed variation in scintillations per minute.

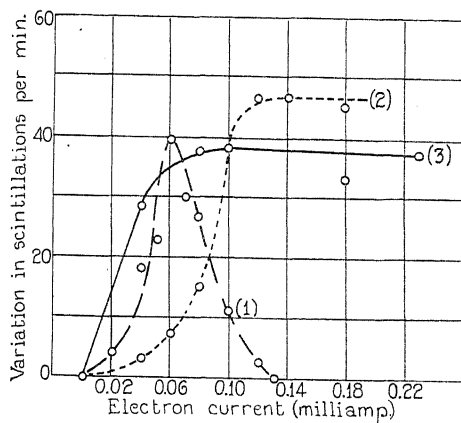


Fig. 10. Capture at zero relative velocity as a function of electron current. (1), single electron capture; (2), double electron capture; (3), total decrease of doubly charged alpha-particles.

For single capture, (Figure 8) saturation is reached when only 0.1 milliampere of current flows to the anode *T*. The order of magnitude of the electron density under these conditions is about 10^7 electrons per cc, which corresponds to an average distance between electrons of 4.6×10^{-3} cm. The process of capture must therefore involve some mechanism, which, when the energy condition is satisfied is effective over a relatively large region of space.

With the second tube it was possible to investigate the effect of reducing the velocity of the alpha-particles. Two different velocities were tried by interposing aluminum foil between the radioactive source and the window. The resultant velocities of the alpha-particles were 1.35×10^9 cm/sec and 1.21×10^9 cm/sec. The whole series of peaks was found to shift in each case. Several of the peaks were located in their new position and the corresponding energy levels calculated by means of the energy relation already given. A comparison of these values with the values found at the higher alpha-particle velocity showed very good agreement.

The intervals on each side of the central peak where no capture occurs were found to be much narrower with the second tube than with the first. Whereas with the first tube they were 40 volts wide, with the second they

were only about 22 volts wide. In other words capture terminated at the tenth energy level in the first tube and at about the fifteenth energy level in the second. If these captureless intervals were due to re-ionization by collision with the residual molecules of gas in the tube, then the width of the intervals should be dependent on the length of path between the point of capture in the electron stream and the magnetic field. To test this the magnet was placed in two positions along the tube at M , and at N , (Figure 3) such that the distance ($A - M$) was double the distance ($A - N$). It was impossible to detect any change in the width of the interval under these two conditions. These captureless intervals must therefore be due to some cause other than collisions of this kind.

CONCLUSION

In the type of recombination taking place in this experiment the electron does not fall from rest into a given energy level (except in the special case when the velocities of electron and alpha-particle are equal). It has an initial kinetic energy, due to the applied field, equal to that of the energy level at which it is captured. Twice the normal energy must therefore be radiated, and the question arises as to whether it is radiated as two quanta of normal frequency, or as one quantum of double that frequency.

The striking result of this experiment is the discovery that electron capture is governed by a definite energy condition. In order for capture to occur, it is necessary that the electron, due to some external field, possess a kinetic energy, which, with respect to the nucleus, is either zero, or equal to the energy of one of the quantum states of the atom.

It has been shown that electron capture takes place in less than 3×10^{-10} sec in a region where the electron density is probably not greater than 10^7 electrons per cc. Probably the time involved is actually much less than this. The process of capture must therefore involve some mechanism whose action is extremely rapid, and when the energy condition is satisfied, effective over a relatively great region of space. When the energy condition is not satisfied the capture mechanism either does not function at all, or operates in such a manner that the probability of capture is relatively very small. The inference to be drawn is that under certain energy conditions, the mutually effective radius of action of the electron and the nucleus may be relatively very great, while under other energy conditions it is very small.

The results of this experiment are based upon the counting of over 700,000 alpha-particle scintillations.

In conclusion, the writer wishes to express his appreciation and gratitude to Professor Bergen Davis for suggesting this research, and for his continued interest and encouragement throughout the course of the experiment. Many thanks are also due to the other members of the department of Physics.

THE RELATIVE INTENSITIES OF SUPER-MULTIPLYET LINES

BY JAMES H. BARTLETT, JR.
INSTITUT F. THEORETISCHE PHYSIK, LEIPZIG

(Received December 27, 1929)

ABSTRACT

A simple method is described by which one may construct wave functions for the case of (*jj*) coupling. The wave functions for $(2p)^2$, so determined, agree with those given in a previous paper, when one sets the electrostatic interaction equal to zero. It is shown how the ordinary multiplet intensity formulae may be modified to give the relative intensities in a super-multiplet for (*jj*) coupling. The modified formulae, applied to the transition $(2p)^2 \rightarrow 2p3s$, give relative intensities in agreement with those found in the above paper, for this limiting case. The sum-rules hold quite generally for non-equivalent electrons, and it is shown to what degree they hold for a transition such as $(2p)^2 \rightarrow 2p3s$.

ON THE basis of the Darwin-Pauli theory of the spinning electron it has been found possible^{1,2} to calculate the relative intensities of super-multiplet lines for certain transitions, such as $(ds \rightarrow fs)$ and $(2p\ 2p \rightarrow 2p\ 3s)$. The intensities so found are dependent upon the strength of the electrostatic interaction between the electrons, as compared with that of the magnetic interactions between spin and orbital angular momenta. In the limiting case of strong electrostatic interaction, or (*ls*) coupling, these intensities agree with those calculated from the formulae for relative intensities within an ordinary multiplet. In the other limiting case, that of (*jj*) coupling, where the spin-orbit interaction is predominant, analogous formulae can be set up and the intensities so obtained would agree with those found from more general formulae when the electrostatic interaction is set equal to zero. The difficulties involved in obtaining these general formulae for any degree of coupling have already been mentioned in a previous paper.² Accordingly, it seems expedient to calculate the theoretical intensities for the two limiting cases and to use some suitable method of interpolation when comparing with experiment.

1. THE WAVE FUNCTIONS AND ENERGY VALUE FOR (*jj*) COUPLING

For simplicity, we shall at first deal with only two electrons. For (*jj*) coupling, we are to consider as a perturbation the magnetic interaction between each electron and its own orbit. Each electron can be considered

¹ W. V. Houston, Phys. Rev. 33, 297 (1929).

² J. H. Bartlett Jr., Phys. Rev. 34, 1247 (1929). A sign error in the matrix components of the intercombination lines should be corrected. Both c_1 and c_8 should have the opposite sign. None of the conclusions of the paper are invalidated, to our degree of approximation. Furthermore, in the roots ϵ_3 and ϵ_4 , one should substitute +8 for -8.

separately during this perturbation calculation and then the product functions, or a linear combination thereof, will represent the total system. As usual, we group those functions together which have a common $m = \sum m_l + m_s$, where m_l and m_s refer to the projections of l and s , the azimuthal and spin quantum numbers, on a preferred axis. For an externally undisturbed system, terms with different m 's cannot combine, since m represents a constant of the motion. The wave functions are written

$$\psi_\alpha^m = R_{ln}(r) P_l^{m-1/2} S_\alpha; \quad \psi_\beta^m = R_{ln}(r) P_l^{m+1/2} S_\beta.$$

The two possible values of the spin variable are S_α and S_β respectively, and

$$P_l^{m_l} = (l - m_l)! \sin^{m_l} \theta \left(\frac{d}{d \cos \theta} \right)^{l+m_l} \frac{(-\sin^2 \theta)^l}{2^l l!} e^{i m_l \phi}.$$

Let

$$\gamma_{ln} = \frac{\hbar^2}{16\pi^2} \frac{Ze^2}{m_0^2 c^2} \int R_{ln}^2 \frac{1}{r^3} d\tau \quad \text{and} \quad \epsilon = \frac{\Delta E}{\gamma_{ln}}.$$

For the perturbation arising from the interaction between spin and orbit, the secular equation is:

$$\begin{vmatrix} m - \frac{1}{2} - \epsilon & (l - m + \frac{1}{2})^{1/2} (l + m + \frac{1}{2})^{1/2} \\ (l - m + \frac{1}{2})^{1/2} (l + m + \frac{1}{2})^{1/2} & -m - \frac{1}{2} - \epsilon \end{vmatrix} = 0.$$

The roots are $\epsilon_1 = l$ and $\epsilon_2 = -l - 1$, and the corresponding wave functions are:

$$\begin{aligned} \psi_1^m &= (1/2l+1)^{1/2} [(l+m+\frac{1}{2})^{1/2} \psi_\alpha^m + (l-m+\frac{1}{2})^{1/2} \psi_\beta^m] \\ \psi_2^m &= (1/2l+1)^{1/2} [-(l-m+\frac{1}{2})^{1/2} \psi_\alpha^m + (l+m+\frac{1}{2})^{1/2} \psi_\beta^m]. \end{aligned}$$

One sees that, for the state l , $j = m_{\max} = l + \frac{1}{2}$ and for the state 2, $j = m_{\max} = l - \frac{1}{2}$.

The calculation thus far deals with coupling of the type $(s_1 l_1) = j_1$. In order to treat coupling of the type $(j_1 j_2) = j$ one must construct antisymmetric wave functions from products of functions such as ψ_1^m and ψ_2^m . For instance, set³

$$\psi_{j_1 j_2}^m = \left(\frac{1}{2} \right)^{1/2} \begin{vmatrix} \psi_{j_1}^{m_1}(1) & \psi_{j_1}^{m_1}(2) \\ \psi_{j_2}^{m_2}(1) & \psi_{j_2}^{m_2}(2) \end{vmatrix}.$$

If now, for a given m , the vectors j_1 and j_2 combine to give only one j , then the state is not degenerate for (jj) coupling and will be represented, except perhaps for a sign factor, by a function of the above type. Just as frequently, however, one finds a degeneracy and the correct wave functions for a given value of j are found by taking linear combinations, the coefficients being

³ In the more general case of more than two electrons, the antisymmetric functions will have the determinant form. See J. C. Slater, Phys. Rev. (being published). The notation used above is similar to that of the paper to which reference is here made.

determined from a perturbation calculation, the electrostatic interaction between the electrons being the perturbation. This degeneracy is for a given set $(j_1 j_2)$ combining to give different j 's. If one should take the wave functions for the same j , as determined by this process, but for different sets $(j_1 j_2)$, and repeated the process, this would give the correct wave functions for (ls) coupling. This is to be expected, since it should make no difference in which order the various perturbations are applied. In the previous paper,² the reverse order was employed, and the results agree, both for energy values and for wave functions.

The total energy of the two-electron system for (jj) coupling is given by

$$E = E(n_1 l_1) + \gamma_{l_1 n_1} \epsilon(j_1) + E(n_2 l_2) + \gamma_{l_2 n_2} \epsilon(j_2).$$

This agrees with the work of Goudsmit⁴ if we make $\gamma = a/2$.

2. SELECTION RULES

Let us denote the set of quantum numbers $(nljm)$ by p . Then the matrix element for a transition involving two electrons will be a linear combination, in the zeroth approximation, of matrix elements of the type

$$z(p_1 p_2; p_3 p_4) \sim \delta(p_2 p_4) z(p_1 p_3) + \delta(p_1 p_3) z(p_2 p_4) - \delta(p_2 p_3) z(p_1 p_4) - \delta(p_1 p_4) z(p_2 p_3). \quad (1)$$

Thus, whether the coupling be of the (ls) (jj) type, as long as the wave functions are formed by the linear combinations of functions of the unperturbed system, then two-electron jumps are not permitted. This is true for any number of electrons, but only as a first approximation. According to Pauli's exclusion principle, no two electrons can have the same p and so, for any transition, we have only one term on the right-hand side of equation (1). Let this term be the first, i.e. $p_2 = p_4$. That is, for one of the two electrons, all four quantum numbers remain the same, and for the other, the ordinary selection rules hold. In the (jj) coupling case, therefore, j_1 can change by 0, ± 1 and j_2 does not change. If $p_1 = p_3$ instead, then $\Delta j_1 = 0$ and $\Delta j_2 = 0, \pm 1$.

3. INTENSITIES

Consider the transition $(n_1' l_1' j_1' m_1'; n_2 l_2 j_2 m_2) \rightarrow (n_1'' l_1'' j_1'' m_1''; n_2 l_2 j_2 m_2)$. The z -matrix will be a linear combination of a number of "unperturbed" z -matrices, which have the form $\int [R_{l_2 n_2}(2)]^2 r_2^2 dr_2 \int R_{l_1' n_1'}(1) R_{l_1'' n_1''}(1) r_1^2 dr_1 \int P_{l_1'}^*(1) z_1 P_{l_1''}(1) d\omega_1$ corresponding to the term $z(p_1 p_3)$ in Eq. (1). Thus, the radial integration gives a common factor and, since this is the only way in which the principal quantum numbers can enter, they have no influence on the relative intensities in a super-multiplet. It makes, therefore, no difference in the relative intensities as to whether the electrons are or are not equivalent. The equivalence is manifested, however, in the disappearance of certain states with the result that certain intensity sums are not proportional to statistical weights of the corresponding states.

⁴ S. Goudsmit, Phys. Rev. 31, 946 (1928).

For (jj) coupling, j_2 plays the same role as s , and j_1 the same role as l , respectively, in (ls) coupling. We can introduce a notation analogous to the Russell-Saunders notation, namely, $r(j_1)_j$, where $r=2j_2+1$. The j_1 labels the valence electron, and r is the multiplicity. Even when the two electrons are equivalent, there is no ambiguity as to which is the valence electron, unless $j_1=j_2$. In this case one must double the intensity as calculated from the formulae to be given, to allow for the two possibilities.

The ordinary multiplet formulae can now be rewritten in terms of j_1 and j_2 instead of l and s . In the ordinary multiplet theory the statistical weight of an $r(l)$ state is $r(l+1)$, e.g. a 3D state has a degeneracy of fifteen. For (jj) coupling, the statistical weight of an $r(j_1)$ state is $r(2j_1+1)$, except for equivalent electrons with $j_1=j_2$, where it becomes $2rj_1$. The degeneracy of a $ps\ ^4(1/2)$ state is eight, that for a $(2p)^2\ ^4(3/2)$ state is twelve, and that for a $(2p)^2\ ^4(1/2)$ the same as for $(2p)^2\ ^2(3/2)$, namely eight.

The formulae in terms of j_1 and j_2 follow:

$$\begin{aligned}\Delta j_1 = \pm 1 \quad J_{-1} &= G_j A_{j-1, j_1-1}^{j, j_1} = \frac{C}{4jj_1} P(j, j_1) P(j-1, j_1) \\ J_0 &= G_j A_{j, j_1-1}^{j, j_1} = \frac{C}{4jj_1} \frac{2j+1}{j+1} P(jj_1) Q(jj_1) \\ J_{+1} &= G_{j-1} A_j^{j-1, j_1} = \frac{C}{4jj_1} Q(jj_1) Q(j-1, j_1) \\ \Delta j_1 = 0 \quad J_0 &= G_j A_{j, j_1}^{j, j_1} = \frac{C}{4jj_1} \frac{2j+1}{j+1} \frac{2j_1+1}{j_1+1} R^2(j) \\ J \pm 1 &= G_j A_{j-1, j_1}^{j, j_1} = G_{j-1} A_j^{j-1, j_1} = \frac{C}{4jj_1} \frac{2j_1+1}{j_1+1} P(j, j_1) Q(j-1, j_1)\end{aligned}$$

where

$$\begin{aligned}P(j) &= (j+j_1)(j+j_1+1) - j_2(j_2+1) \\ -Q(j) &= (j-j_1)(j-j_1+1) - j_2(j_2+1) \\ R(j) &= j(j+1) + j_1(j_1+1) - j_2(j_2+1).\end{aligned}$$

The A 's are the squares of matrix elements. For any super-multiplet, or group of lines belonging to a transition such as $sp \rightarrow pp$, the value of C is the same for all lines. The sum of intensities from any state with equivalent electrons over all the states (with non-equivalent electrons) to which transitions can be made is, for a given super-multiplet, proportional to the statistical weight of the initial state. If these sums be taken horizontally, then in general the vertical sums will not be proportional to the corresponding statistical weights due to the exclusion of certain states which would be possible if the electrons were not equivalent.

As examples of applications of the formulae we give below the results (1) for a case with two non-equivalent electrons, and (2) for two equivalent electrons,

TABLE I. Relative intensities in the super-multiplet $dp \rightarrow ds$, for (jj) coupling.

$\begin{matrix} d\mathcal{P} \\ ds- \end{matrix}$	$4(\frac{1}{2})$			$4(\frac{3}{2})$				$6(\frac{1}{2})$		$6(\frac{3}{2})$				Sums	
$4(\frac{1}{2})$	j	2	1	3	2	1	0	3	2	4	3	2	1		
	2	5	5	14	5	1	0	0	0	0	0	0	0	30	
	1	5	1	0	5	5	2	0	0	0	0	0	0	18	48
$6(\frac{1}{2})$	2	0	0	0	0	0	0	$7\frac{7}{9}$	$2\frac{2}{9}$	0	$6\frac{2}{9}$	$7\frac{7}{9}$	6	30	72
	3	0	0	0	0	0	0	$6\frac{2}{9}$	$7\frac{7}{9}$	18	$7\frac{7}{9}$	$2\frac{2}{9}$	0	42	
Sums		10	6	14	10	6	2	14	10	18	14	10	6		
		16		32				24		48					
		48						72							

 TABLE II. Relative intensities in the super-multiplet $(2p)^2 \rightarrow 2p3s$ for (jj) coupling.

$(2p)^2$	$2p3s$	$4(\frac{1}{2})$		$2(\frac{1}{2})$		Sums		
		j	1	2	1	0		
	$4(\frac{3}{2})$	0	$2 \cdot 2 = 4$	0	0	0	4	
		2	$2 \cdot 5 = 10$	$2 \cdot 5 = 10$	0	0	20	24
	$4(\frac{1}{2})$	2	5	5	0	0	10	16
		1	1	5	0	0	6	
	$2(\frac{3}{2})$	2	0	0	10	0	10	16
		1	0	0	2	4	6	
	$2(\frac{1}{2})$	0	0	0	$2 \cdot 2 = 4$	0	4	4
	Sums		20	20	16	4		
			40		20			

It is seen that the total intensity in a given system is proportional to the multiplicity of that system. For non-equivalent electrons both horizontal and vertical sums are proportional to the corresponding statistical weights, e.g. $4(1/2):4(3/2):6(1/2):6(3/2)=8:16:12:24$. For the equivalent electrons, the sums from the $(2p)^2$ states are likewise proportional to the statistical weights, e.g. $4(3/2):4(1/2):2(3/2):2(1/2)=12:8:8:2$.

However, this is not so for the sums from the $2p3s$ states, but would be true if the two p electrons were not equivalent. It should be noted that the $4(1/2)$ and $2(3/2)$ states of the $(2p)^2$ configuration have the same energy, but differ in the value of j which the valence electron has. (In the one case, $j_1=1/2, j_2=3/2$ and in the other case $j_1=3/2, j_2=1/2$ where j_1 denotes the

valence electron). The intensities given above for the transition $(2p)^2 \rightarrow 2p3s$ agree with those found from the general formulae of the previous paper,² when one sets the electrostatic interaction equal to zero.

As to the comparison with experiment, the observed intensities vary greatly from observer to observer, perhaps due to the excitation conditions. Furthermore, in some cases the identification of terms is in question. However, the intensities given by Mack⁵ for the super-multiplet $d^9p \rightarrow d^9s$ in Ge V and SnV are not in any marked disagreement with what one should expect from Table I. Where (jj) coupling is not realized, it may sometimes be possible to interpolate between this case and that of (ls) coupling. This question, as well as the allied ones of term-crossing and co-ordination to series limits, is beyond the scope of the present paper, but in all probability can be treated by obtaining the general formulae for a few simple cases and by then applying the method of induction. The calculations involved are not impossibly complicated for two electrons.

In conclusion, I wish to thank Professor Slater for helpful suggestions, and Harvard University for the renewal of my Parker Travelling Fellowship.

⁵ J. E. Mack, Phys. Rev. 34, 17 (1929).

AN EXTENSION OF THE SPECTRUM OF Tl II

BY STANLEY SMITH

DEPARTMENT OF PHYSICS, UNIVERSITY OF ALBERTA

(Received December 12, 1929)

ABSTRACT

The spectrum of singly ionized thallium has been obtained by using the metal in a hollow cathode discharge in helium. Spectrograms have been made from 1900Å. to 8000Å. The newly found terms here reported are $6s8d^3D_{1,2,3}$, $6s8d^1D_2$, $6s9s^3S_1$, $6s10s^3S_1$, $6s6f^3F_{2,3,4}$, $6s7f^3F$ and an unclassified term $2s^0$. Absolute term values have been calculated from the sequence $6s6d^3D_2$, $6s7d^3D_2$, $6s8d^3D_2$. The ionization potential is found to be 20.30 volts. Tables of term values and of about sixty newly classified lines are given. Fourteen new multiplets arising from the fine structure of the terms are also tabulated.

1. INTRODUCTION

THE spectrum of singly ionized thallium has been investigated by Rao, Narayan, and Rao,¹ by McLennan, McLay, and Crawford² and by Smith.^{3,4} A further publication by McLennan, McLay and Crawford⁵ has not only extended the number of known terms but has also revealed the fine structure character of some of the terms. A very interesting feature of the fine structure of the Tl II terms was found to be the relatively large values of the differences between the term components as compared with those previously found by Back and Goudsmit⁶ for Bi I and by Jackson⁷ for Cs I. McLennan, McLay and Crawford were able to account for the observed structure of the Tl II lines by assuming that the nucleus has a spin of quantum number $\frac{1}{2}$, as Jackson had previously found to be the case for the nucleus of Cs I.

The further progress in the elucidation of the Tl II spectrum which is here reported, has been made by examining the spectrum obtained from a hollow cathode discharge in helium.

2. EXPERIMENTAL

As the Schüller lamp and the experimental details of its use have been previously described by Schüller,⁸ Paschen⁹ and Sawyer¹⁰ it is not necessary to enter into any detailed account of the apparatus. There is, however,

¹ K. R. Rao, A. L. Narayan, A. S. Rao, Indian Journ. Phys. **2**, 467 (1928).

² J. C. McLennan, A. B. McLay, M. F. Crawford, Trans. Roy. Soc. Can. **22**, 241 (1928).

³ S. Smith, Proc. Nat. Acad. Sci. **14**, 951 (1928).

⁴ S. Smith, Phys. Rev. **34**, 393 (1929).

⁵ J. C. McLennan, A. B. McLay, M. F. Crawford, Proc. Roy. Soc. **A125**, 570 (1929).

⁶ E. Back and S. Goudsmit, Zeits. f. Physik **43**, 321 (1927) and **47**, 174 (1928).

⁷ D. A. Jackson, Proc. Roy. Soc. **A121**, 432 (1928).

⁸ H. Schüller, Zeits. f. Physik **35**, 323 (1926).

⁹ F. Paschen, Sitz. Preuss. Akad. Wiss. **32**, 536 (1928).

¹⁰ R. A. Sawyer and F. Paschen, Ann. d. Physik **84**, 1 (1927).

in the carbon at the closed end and a semi-circular carbon stop was inserted in the open end to correspond with the remaining piece of carbon at the other end, so that when the electrode was put into the tube with its axis horizontal and the thallium was melted, the carbon acted as a trough to hold some of the molten metal. On replacing the electrode the cleaning process with the oxygen discharge was continued, care being taken to prevent the thallium from melting. The tube was then pumped out to a hard vacuum and the

helium made to circulate through the apparatus. A heavy discharge was then passed through the tube until the thallium became molten, when half the metal ran out on to the outside aluminum electrode leaving the carbon cylinder half full of thallium with an untarnished surface.

A potential difference of about 1500 volts was applied to the electrodes by means of a variable voltage transformer in series with a rectifying valve. The spectrum from 1900Å to 8000Å was photographed by means of a two meter grating arranged on a Rowland mounting and giving a dispersion of about 8.5Å per mm in the first order. A Hilger interchangeable spectrograph was also used with quartz and glass trains. Neither of these instruments, although the best at the disposal of the writer, gives sufficiently large dispersion or high resolution for an accurate investigation of the fine structure. Consequently the fine structure separations measured are, at the best, only accurate to about one-half of a unit of wave-number.

3. RESULTS

The newly found terms are $6s8d^3D_{1,2,3}$, $6s8d^1D_2$, $6s9s^3S_1$, $6s6f^3F_{2,3,4}$, $6s7f^3F$, an unclassified term here denoted by 2_3^0 and $6s10s^3S_1$. The last mentioned term is given tentatively as only the $6s7p^3P_{0,1,2}$ - $6s10s^3S_1$ combinations have as yet been found.

The term values given in Table I are arrived at by taking $6s^2S_0$ to be 164,600, a value which makes the Rydberg denominators of the three $6snd^3D_2$ terms vary in much the same way as do the corresponding terms of Hg I. The ionization potential of singly ionized thallium would then appear to be 20.30 volts.

The tabulated term values in the case of terms for which the fine structure differences have been measured are the averages of the term values of the two components, the fine structure intervals being listed on the right hand side of the table. To make the table as complete as possible all the previously found terms and fine structure intervals are also included.

Reference might be made to the abnormal nature of the $6s6f^3F$ terms. It will be noticed that the partial inversion of the terms differs from that of the $6s5f^3F$ terms. Written in the order of descending magnitude the 5 F terms are F_3 , F_2 , F_4 while for the 6 F terms the order is F_4 , F_2 , F_3 . The unclassified term 2_3^0 has a value very close to the estimated value of the $6s8p^3P_2$ term, but the intensity relations observed for its combinations with $6s6d^3D_{2,3}$ suggest that the inner quantum number is 3 and not 2. More over if 2_3^0 were identified as $6s8p^3P_2$ a strong combination with $6s7s^3S_1$ would be expected at ν 37559. There is, indeed, a line of intensity 0 at λ 2661.74 or ν 37558.3 but it is difficult to believe this could actually be $6s7s^3S_1$ - $6s8s^3P_2$.

Table II contains the newly classified lines of Tl II and Table III shows in detail the new fine structure multiplets which have as yet been observed.

I wish to express my thanks to Dr. R. A. Sawyer through whose courtesy the essential parts of the Schüler lamp apparatus were made in the Department of Physics at the University of Michigan. My thanks are also due to

TABLE II. *New classified lines of Tl II.*

λ I A air	ν	Int.	Classification
5642.75	17717.0	4	$6p6p^1D_2 - 6s6f^3F_3^0$
4946.67	20210.0	3	
4945.55	20214.6	2	$6p7p^1P_1^0 - 6s8d^1D_2$
4660.99	21488.7	3	$6s7p^1P_1^0 - 6s8d^3D_2$
§4340.43	23032.7	1	$1_1^0 - 6s9s^3S_1$
4339.65	23036.9	1	
4292.4	23290.5	1	$6p^2\ ^1D_2 - 6s7f^3F^0$
4291.5	23295.3	2	
4274.96	23385.5	10	$6s7p^3P_2^0 - 6s9s^3S_1$
4274.20	23389.6	2	
3955.94	25271.3	1	$1_1^0 - 6s8d^3D_2$
3955.45	25274.4	3	
3910.05	25567.9	1	
3909.49	25571.6	0	$6s7p^3P_2^0 - 6s8d^3D_1$
3909.15	25573.8	1	
3901.72	25622.5	9D	$6s7p^3P_2^0 - 6s8d^3D_2$
*3887.24	25717.9	?	$6s7p^3P_2^0 - 6s8d^3D_3$
3869.81	25833.8	2	
3869.19	25837.9	5	$6s7p^3P_1^0 - 6s9s^3S_1$
3868.59	25841.9	2	
3852.10	25952.5	3	$6s6d^3D_3 - 2_3^0$
3851.67	25955.4	2	
3837.49	26051.3	2	$6s7p^3P_0^0 - 6s9s^3S_1$
3836.81	26056.0	4	
3794.08	26349.4	10D	$6s6d^3D_2 - 2_3^0$
3724.79	26839.5	0	$6s7p^3P_1^0 - 6s8d^1D_2$
3619.43	27620.8	2	$6s6d^1D_2 - 2_3^0$
3567.56	28022.4	3	
3567.21	28025.1	0	
3567.06	28026.3	0	$6s7p^3P_1^0 - 6s8d^3D_1$
3566.75	28028.8	2	
3560.77	28075.8	5	
3560.40	28078.7	4	$6s7p^3P_1^0 - 6s8d^3D_2$
3540.05	28240.1	3	
3539.78	28242.3	2	$6s7p^3P_0^0 - 6s8d^3D_1$
3369.13	29672.8	10	$6s6d^3D_3 - 6s6f^3F_4^0$
3365.43	29705.4	1	$6s6d^3D_3 - 6s6f^3F_3^0$
3364.12	29717.0	2	$6s7p^3P_2^0 - 6s10s^3S_1$
3322.30	30091.0	2	
3321.94	30094.3	1	$6s6d^3D_2 - 6s6f^3F_2^0$
3321.17	30101.2	4	
3320.80	30104.6	3	$6s6d^3D_2 - 6s6f^3F_3^0$
3291.09	30376.4	6	$6s6d^3D_1 - 6s6f^3F_2^0$
3186.60	31372.4	2	$6s6d^1D_2 - 6s6f^3F_3^0$
3186.26	31375.7	1	
3107.73	32168.5	0	$6s7p^3P_1^0 - 6s10s^3S_1$
3086.53	32389.5	00	$6s7p^3P_0^0 - 6s10s^3S_1$
2833.27	35284.6	6	$6s6d^3D_3 - 6s7f^3F^0$
2801.85	35680.2	5	$6s6d^3D_2 - 6s7f^3F^0$
2780.25	35957.4	3	$6s6d^3D_1 - 6s7f^3F^0$
2705.55	36950.1	3D	$6s6d^1D_2 - 6s7f^3F^0$
λ I A vac			
†1413.12	70765	2	$6s6p^1P_1^0 - 6s8d^1D_2$
1310.22	76323	1	$6s6p^3P_2^0 - 6s7d^3D_2$
1169.07	85538	0	$6s6p^3P_1^0 - 6s7d^3D_1$
1162.56	86017	1	$6s6p^3P_2^0 - 6s8d^3D_3$
1018.81	98153	00	$6s6p^3P_0^0 - 6s8d^3D_1$
817.11	122382	8	$6s^2\ ^1S_0 - 1_1^0$
792.29	126216	5	$6s^2\ ^1S_0 - 6s7p^1P_1^0$

§ This line may be $H\gamma$.

* This line falls in the region of halation caused by the helium line $\lambda 3888.64$: its intensity is therefore difficult to estimate.

† This line is attributed to Tl IV by Rao¹¹, but not by Mack.¹²

¹¹ K. R. Rao, Phys. Soc. London Proc. **41**, 361 (1929).

¹² J. E. Mack, Phys. Rev. **34**, 17 (1929).

TABLE III. *Fine structure multiplets of Tl II.*

F	$6s7p^3P_0^0$ $\frac{1}{2}$	$6s7p^3P_1^0$ $\frac{1}{2}$ $1\frac{1}{2}$	$6s7p^3P_2^0$ $1\frac{1}{2}$ $2\frac{1}{2}$
$6s9s^3S_1$			
$\frac{1}{2}$	26051.3 (2)	25837.9 (5) 25833.8 (2)	23385.5 (10)
$1\frac{1}{2}$	26056.0 (4)	25841.9 (2) 25837.9 (5)	23389.6 (2) 23385.5 (10)
F	$6s7p^3P_0^0$ $\frac{1}{2}$	$6s7p^3P_1^0$ $\frac{1}{2}$ $1\frac{1}{2}$	$6s7p^3P_2^0$ $1\frac{1}{2}$ $2\frac{1}{2}$
$6s8d^3D_1$			
$\frac{1}{2}$	28242.3 (2)	28028.3 (2) 28025.1 (0)	25573.8 (1)
$1\frac{1}{2}$	28240.1 (3)	28026.3 (0) 28022.4 (3)	25571.6 (0) 25567.9 (1)
F	$6s7p^3P_1^0$ $\frac{1}{2}$ $1\frac{1}{2}$		1^0 $\frac{1}{2}$ $1\frac{1}{2}$
$6s8d^3D_2$			
$1\frac{1}{2}$	28078.7 (4)		25271.3 (1)
$2\frac{1}{2}$	28075.8 (5)		25274.4 (3)
F	$6s6d^1D_2$ $1\frac{1}{2}$ $2\frac{1}{2}$		$6s6d^3D_2$ $1\frac{1}{2}$ $2\frac{1}{2}$
$6s6f^3F_3^0$			
$2\frac{1}{2}$	31375.7 (1)		30104.6 (3)
$3\frac{1}{2}$	31372.4 (2)		30101.2 (4)
F	$6s7p^1P_1^0$ $\frac{1}{2}$ $1\frac{1}{2}$	F	$6p^2\ ^1D_2$ $1\frac{1}{2}$ $2\frac{1}{2}$
$6s8d^1D_2$			
$1\frac{1}{2}$	20214.6 (2)	$6s7f^3F_3^0$ $2\frac{1}{2}$	23290.5 (1)
$2\frac{1}{2}$	20210.0. (3)	$3\frac{1}{2}$	23295.3 (2)
F	2_3^0 $2\frac{1}{2}$ $3\frac{1}{2}$		$6s6d^3D_2$ $1\frac{1}{2}$ $2\frac{1}{2}$
$6s6d^3D_3$			
$2\frac{1}{2}$	25955.4 (2)	$6s6f^3F_2^0$ $1\frac{1}{2}$	30094.3 (1)
$3\frac{1}{2}$	25952.5 (3)	$2\frac{1}{2}$	30091.0 (2)

Dr. R. J. Lang for his advice in the assembling of the apparatus and in putting it into operation.

Finally I gratefully acknowledge a grant from the National Research Council of Canada which assisted very substantially in the prosecution of this work.

IONIZATION IN THE UPPER ATMOSPHERE
VARIATION WITH LONGITUDE*

BY E. O. HULBURT

NAVAL RESEARCH LABORATORY

(Received December 20, 1929)

ABSTRACT

Continuing a former paper (Phys. Rev. **34**, 1167 (1929)) the present paper gives theoretical calculations of the changes in the ionization in the upper atmosphere with longitude. The electrical conductivity of the upper atmosphere is about 1.4×10^{-5} at noon equinox at the equator and an order of magnitude less at night. The maximum density of electrons y_m varies with the latitude θ and longitude ψ , measured from noon equinox at the equator according to $y_m = 3.14 \times 10^8 \cos \theta (0.18 \sin \psi + \cos \psi)$ for the daylight hours. At night the expression is more complex. The values of y_m yield skip distances of short wireless waves roughly in accord with observation in the day but somewhat too great at night. The theory puts the shortest skip distance at 40 minutes past noon and observation in temperate zones gives 2 p.m.; the agreement is good, but not perfect.

IN A recent paper¹¹ the ionization in the upper atmosphere was worked out over the entire earth. The ionization, assumed to be caused by the ultra-violet light of the sun, was shown to explain certain facts of wireless wave propagation and of terrestrial magnetism. The variation of the ionization with latitude was described in some detail, less space being given to the variation with longitude. This paper presents the longitude calculations, and is therefore a direct continuation of the earlier paper, the nomenclature, numbering of paragraphs, equations, figures, tables and references being carried on from that paper.

33. It is assumed that the temperatures of the upper atmosphere for longitudes along the equator are given by the values of T of column 2, Table I, the degrees of latitude of column 1 being now degrees of longitude measured from high noon. For example, at 60° longitude, i.e., at 8 a.m. or 4. p.m. T is 360°K . At any point in the day hemisphere of longitude ψ and latitude θ the angular distance ζ from equatorial noon is $\cos \zeta = \cos \theta \cos \psi$ and $T = 220 + 280 \cos \zeta$. Everywhere in the night hemisphere T is 220°K . From the values of T the ionic recombination coefficient α is known at all points. The critical level z_c is nearly independent of the longitude; for example, at the equator z_c descends from the noon value of 150 km to 147 km at night, and the diurnal change at high latitudes is less.

34. In the S region the y, z curves for various longitudes were calculated for the daylight hours by the method of sections 10 and 11. The method neglected gravity diffusion of the ions and assumed that equilibrium existed between the rate of production and the rate of loss as expressed by

* Published with the permission of the Navy Department.

¹¹ Hulburt, Phys. Rev. **34**, 1167 (1929).

$$q \cos \psi - \alpha n y^2 = 0. \quad (19)$$

The curves for the equator are given in Fig. 4. ("Gravity diffusion" is a short expression for "temperature diffusion of the ions to attain gravitational

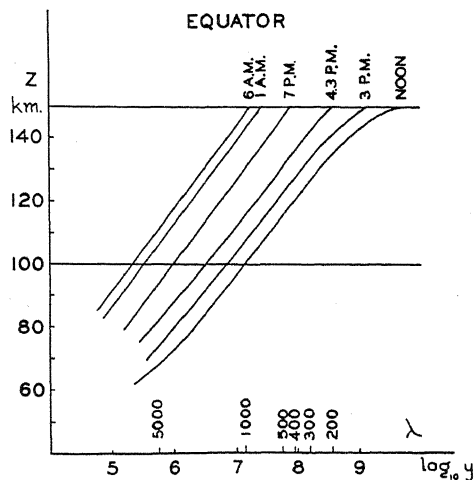


Fig. 4. Theoretical values of the density y of ion pairs in the S region of the upper atmosphere at the equator.

equilibrium.") Apart from the neglect of gravity diffusion (19) is an approximation because as the earth turns under the sun equilibrium in general does not exist. The more complete expression is

$$dy/dt = q \cos \omega t - \alpha n y^2, \quad (20)$$

where t is the time measured from high noon and ω is the angular velocity of rotation of the earth on its axis; $\omega = 7.28 \times 10^{-5}$ radians sec^{-1} . α and q are functions of the longitude ωt . Even if α and q are assumed to be constant with respect to t we are unable to solve (20) and must turn to approximate methods.

At noon at the equator $y = 5 \times 10^9$ for $z = 150$ km. At 1 p.m. y is 4.8×10^9 from (19). If there were no production of ions after 12 o'clock and the ions at 1 p.m. were those of noon decreased by recombination, y at 1 p.m. would be 1.5×10^9 , as found from (20) with $q = 0$. Since this is less than one third the value of y (19) we see that the ions at 1 p.m. are mainly those formed by the sunlight at 1 p.m. rather than those left over from noon. Therefore, the maximum value of y at $z = 150$ km is reached within less than 20 minutes after noon. Similarly, it is found that the maximum of the ionization occurs later as z becomes less until at $z = 100$ km the maximum is near 1 o'clock. Thus, except for the small shift in the maximum, (19) gives values of y which are approximately correct during the day until about 4 p.m. After 4 p.m. (19) gives values of y which are too low; for example, it would make $y = 0$ at 6 p.m., whereas at this hour many of the ions formed during the day still exist, and indeed continue to do so all night. From (19) and from (20) with $q = 0$ it comes out that at about 4.7 p.m. the number of ions in equilibrium with the

ultra-violet radiation is equal to the number left over from the earlier hours. We therefore calculate the y, z curve for 4.3 p.m. by means of (19), assume no more production of ions and calculate the y, z curves for various hours through the night from (20), with $q=0$. The night-time y, z curves for the equator are given in Fig. 4. In like manner the y, z curves throughout day and night were determined for all latitudes. The curves of Fig. 4 are probably not plotted entirely correctly, those at night being lifted up too much. Due to the cooling and contraction of the atmosphere at night and at the higher latitudes, mentioned in sections 17 and 19, the upper atmosphere is lower than at equatorial noon. The decrease in height from noon to midnight is about 25 and 15 km at 140 and 100 km, respectively. This would bring the night y, z curves closer to the noon curve than are shown in Fig. 4.

35. The height z at which a wireless wave of wave-length λ is totally reflected (refracted) at normal incidence is found by putting the refractive index μ equal to zero in the expression $\mu^2 = 1 - 2ye^2\lambda^2/\pi m$, solving for y and determining z from the y, z curve. The values of y for total reflection of waves of length 5,000, 1,000, 500, 400, 300, and 200 m are marked along the X -axis of Fig. 4. It is seen, for example, that the height reached by 1,000 m waves increases on the equator from 100 km at noon to 140 km at midnight and to 150 km in the early morning before dawn, with similar increases in the heights reached by the other long waves. The heights for total reflection at latitudes 40° , 60° , and 70° are, respectively, 5, 12, and 19 km greater than the corresponding heights at the equator. But due to the shrinkage of the atmosphere at night and at the higher latitudes the increase in the height is probably less. On the whole the heights reached by the longer waves change but little with the latitude and the time of day. This is in accord with the facts as far as they are known. It must be remembered that the observation of the height reached by wireless waves gives always an "apparent height" which is in general greater than the true height. This is due to the group velocity retardation of the wave in the ionized region of the atmosphere. Therefore, the interpretation of a height measurement is always open to some uncertainty and, in the case of the echo experiments, is often ambiguous for it is sometimes difficult to know where the echo has come from.

36. The absorption of wireless waves calculated from the y, z curves showed that in the region below the height of total reflection the intensity of 500 m waves, for example, was reduced to $1/\epsilon'$ th by passage through 20, 25 and 80 km of the medium at noon at latitudes 0° , 40° and 60° respectively. These values are, if anything, below those inferred from qualitative observation. A suitable number of electrons which undoubtedly exist in this region may be called upon to give the correct absorption. The absorption of 5,000 m waves is greater than is observed if the y, z curve is assumed to continue according to the arbitrary formula of section 10 below the height where these long waves are reflected. We may conclude, as is quite reasonable, that y becomes small and that the formula is not valid in the levels below 70 km at equatorial noon.

For 500 m waves the absorption at 4 p.m., 7 p.m. and midnight was about 0.3, 0.07 and 0.01 of the noon values. The absorption thus decreases fairly rapidly at sunset, but perhaps not quite rapidly enough. It is well known that the intensity of broad-cast waves received at some distance increases rather sharply at sunset, passing within less than two hours from its low daylight value to a high night value. Although the observations are only qualitative it would seem that they might call for a more pronounced change at sunset than the y, z ion curves can give. Electrons in the S region will disappear rapidly after sunset and may account for the sharp change in the wireless phenomena. Since 1 electron is equivalent to about 10^6 ions as far as absorption is concerned and to 10^5 ions for refraction purposes, it is possible to have the absorption in the daylight S region controlled by electrons and the refraction by ions.

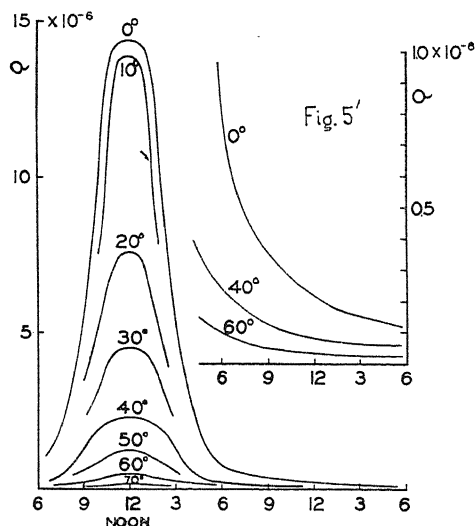


Fig. 5. Theoretical values of the electrical conductivity σ of the upper atmosphere.

In this connection an interesting difficulty appears. Experiments with long waves indicate that the polarization of the received wave varies more or less rapidly with the time during the day and the night. The explanation usually given is that the upper atmosphere contains electrons which are influenced by the earth's magnetic field and cause magnetic double refraction and absorption of the wave. Ions are too heavy to give rise to appreciable double refraction except for very long waves beyond the normal wireless range. Electrons produced by the ultra-violet light of the sun, in all probability, exist in the levels below 150 km during the day, but one would expect them to disappear very rapidly at night. For example, the rate of decrease of the electron density y_e due to attachment of the electrons to oxygen molecules of density n' is $dy_e/dt = -bn'y_e$ where $b = 7 \times 10^{-14}$. At 120 km at night $n' = 1.72 \times 10^{11}$. Thus $\log_e y_e/y_0 = -0.012t$ and in 10^3 seconds or 17 minutes y_e becomes very small. The decrease is greater at the lower heights. The diffusion of electrons down from higher levels is inappreciable. Therefore, if the observations de-

mand electrons in the 70 to 140 km levels at night we shall conclude that something has been left out of the present theory. It is possible that the interference of a number of rays may give rise to changes in the polarization of the received wave quite apart from magnetic double refraction effects.

37. From the y, z curves the values of the electrical conductivity σ of the S region were calculated by means of (12) and were plotted in Fig. 5 for various longitudes and latitudes. In Fig. 5' the night values of σ are given on a larger scale. Summing up the values of σ over the light and dark hemispheres gives the ratio of the total night to day conductivity to be $1/20$; this value was used in section 18. The electrical conductivity of copper is 5.9×10^{-4} and of mercury is 1.06×10^{-5} c.g.s.e.m. u. The conductivity of a 1 cm^2 column vertically upward through the S region of the atmosphere is about 1.4×10^{-5} at equatorial noon and 10^{-6} at sunset, and is therefore equivalent in these two cases to that of 14 and 1 mm of mercury, respectively.

38. Concerning the variation of the D ions with longitude there is little to add to what has already been said in sections 13 to 16. The calculations of the D ions were on the whole pretty rough because so many simplifying assumptions were made. To improve the calculations appears to be intricate and the mathematical difficulties promise to be appreciable. At equatorial noon the magnetic susceptibility of each cm^3 of the D region is about two orders of magnitude greater than that of bismuth, bismuth being the most strongly diamagnetic substance known.

39. The electrons were shown¹ to attain their maximum density y_m at a height of 190 km at summer noon. The y_e, z curve for noon at $\theta = 17^\circ$ (as at Washington, D. C., on June 22) is given in curve 1, Fig. 2, reference 1, in which $y_m = 3 \times 10^5$. We use this curve and adopt the simplifying assumption (reference 1, page 1029) that during changes in the curve, which occur during the day and night, the electron density y_e at each point on the curve changes in the same proportion. This enables all the calculations of the y_e, z curve to be reduced to a calculation of the changes in y_m . The physical justification for this assumption lay in the fact that most of the electrons were produced somewhere above the maximum and diffused rapidly downward to build up their maximum density approximately at a height where the loss due to attachment to oxygen molecules became greater than the supply due to diffusion from above, the loss increasing and the rate of diffusion decreasing as z became less. Therefore, if the rate of production q grew less y_e diminished at all points of the curve, and the assumption is that y_e diminishes equally at all points of the curve. Using the calculations of reference 1, page 1030, and changing them to refer to the somewhat higher day temperatures of the present paper, the total loss sec^{-1} of electrons above y_m due to attachment is 1.59×10^8 or $530 y_m$. The loss due to the recombination of electrons with positive ions is negligible; this is fortunate, for the recombination term involves a y_m^2 which would make the equation hard to solve. The loss due to the electrical drift downward during the day with velocity v is $250 y_m$, using an average value $v = 250 \text{ cm sec}^{-1}$ among the values of v of column 9, Table I. The loss due to gravity diffusion across the maximum is $166 y_m$, but this we leave

out. For gravity diffusion can not occur in its full extent simultaneously with the electrical drift as it involves molecular collisions which interfere with the drift. Therefore the rate of loss is approximately $(530 + 250) y_m = 780 y_m$.

The total number of electrons above the maximum is $5.76 \times 10^{11} = 1.95 y_m$. The rate of production is $q \cos \theta \cos \omega t$ where q is the rate at equatorial noon equinox, i.e., the sun directly overhead. Then

$$dy_m/dt = q \cos \theta \cos \omega t - 780 y_m / 1.95 \times 10^6. \quad (21)$$

Solving

$$y_m = \frac{q \cos \theta}{16 \times 10^{-8} + \omega^2} (\omega \sin \omega t + 4 \times 10^{-4} \cos \omega t). \quad (22)$$

Putting $t=0$, $y_m = 3 \times 10^5$, $\theta = 17^\circ$ and $\omega = 7.28 \times 10^{-5}$ in (22) gives $q = 130$, and (22) becomes

$$y_m = 3.14 \times 10^5 \cos \theta (0.18 \sin \omega t + \cos \omega t). \quad (23)$$

With this expression the values of y_m were calculated over the daylight hemisphere and are plotted in the full line curves of Fig. 6. The maximum value of y_m occurs at about 40 minutes past noon. Formula (23) is not valid at night for the sunset to sunrise voltage E reverses in sign at sunset and hence the downward daytime electrical drift velocity v changes after sunset to an up-

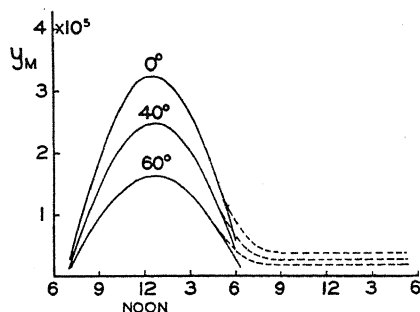


Fig. 6. Theoretical values of the maximum electron density y_m in the upper atmosphere.

ward velocity. At night (18) is used. (23) gives too low values of y_m as sunset is neared, for at this time the rate of loss of the electrons grows less because the downward electrical drift diminishes due to the decreasing E and the attachment coefficient diminishes due to the cooling temperature. Therefore the night curves, calculated from (18) and plotted in the dotted lines of Fig. 6 were joined to the day curves at 5 p.m.

40. The skip distance $2s$ for a wireless wave of length λ is given approximately by

$$2s = 2h(\pi m / y_m e^2 \lambda^2 - 1)^{1/2}, \quad (24)$$

where e and m are the electronic mass and charge, respectively, and h is the value of z for y_m . h was taken to be 190 km with the sun directly overhead, to be 140 km along the sunset and sunrise longitudes and to vary between these limits over the day hemisphere according to $\cos \theta \cos \omega t$. During the night the electrons move upward with a velocity roughly 250 cm sec^{-1} or 9 km hr^{-1} . Therefore h increases 9 km each hour during the night being 140 km at night-

fall and 210 km 8 hours later. With these values of h and with y_m from the curves of Fig. 6, the values of $2s$ for $\lambda 32$ meters were calculated from (24) and are plotted in Fig. 7. The skip distances for other short wireless waves calculated from (24) are approximately proportional to those for $\lambda 32$ meters. During the day the skip distance of Fig. 7 agree within 50 percent with the observed values as far as they are known; in the small hours of the night the calculated values appear to be on the whole 1.5 to 2 times too great.

Equation (24) is not exact for it leaves out of account the magnetic field and the curvature of the earth; the neglect of the first gives too long and of the second too short skip distances, the error due to the approximations being in general less than 30 percent. (24) also assumes sharp reflection of the wave at a height h and therefore neglects refraction by ions and electrons below y_m . The inclusion of this refraction will lessen the calculated skip distances. The

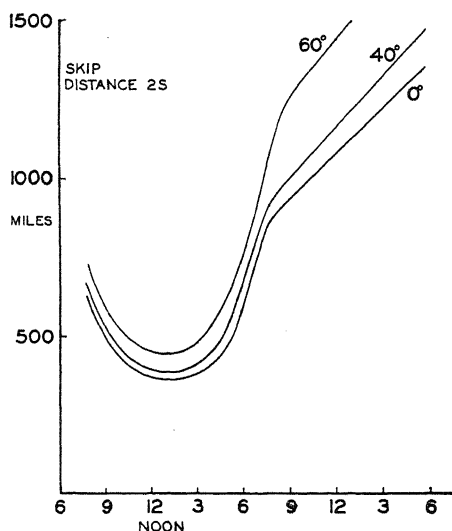


Fig. 7. Calculated values of the skip distance $2s$ for a 32 meter wireless wave.

skip distances of Fig. 7 are a minimum at 40 minutes past noon, the time when y_m is a maximum. Observation in temperate latitudes puts the shortest skip distance at about 2 o'clock. The agreement between theory and experiment is therefore good but not perfect. It is difficult to give a satisfactory explanation of the slight discrepancy; perhaps the value of the attachment coefficient is a little high, or perhaps there are shifts in the distribution of the ionization below the maximum which cause a warping of the ray paths.

41. In conclusion, it may be stated that an ionization produced by the ultra-violet light of the sun has been worked out which accounts in a general way for wireless wave propagation phenomena over the earth and for the part of the earth's magnetic field of external origin and its diurnal variations. We can not regard, however, the ionization which has been obtained as a unique solution of the problem of the ionization of the upper atmosphere. The ionization can be modified within limits in a number of ways without disturbing

the present conclusions, and probably some modification may be desirable for the numbers of ions and electrons which have been used may be slightly too great.

With the sun directly overhead D is 1.5×10^{16} atomic nitrogen ion pairs from 150 to 180 km, or the ion density is 10^{10} . From the relation¹²

$$\mu^2 = 1 - ye^2\lambda^2 / (1 - He\lambda / 2\pi cm)\pi m, \quad (25)$$

it is seen that 10^{10} atomic nitrogen ions give the same refraction for 40 meter waves as 3.2×10^5 electrons. Therefore at equatorial noon either the ions or the electrons will account for the wireless skip distances equally well, but both the 3.2×10^5 electrons and the 10^{10} ions are unnecessary, although to be sure there is no objection to having both if they are at different levels. Early in the morning and late in the afternoon the refraction of the ions falls below that of the electrons, as calculated from the values of y and y_e of the foregoing paragraphs, and at night it rises above the electronic refraction. If the observational facts of short wireless waves call for a refraction predominately electronic there are several ways in which the refractive effects of the ions may be decreased without disturbing the present development. One may keep the same number of ions and suppose that, say, one-half are molecular ions. This will decrease their refraction, change the drift currents and modify the calculations throughout, but will not change any of the values by as much as 100 percent. Or, one may decrease the number of ions and assume higher noon temperatures. In illustration, let us suppose that the number of ions were $1/2$ and the noon temperatures 2 times the respective values which have been used. This will multiply the day values of σ and E by $1/4$ and $3/2$, respectively. The currents in the D and S regions for day and night, instead of being, respectively, about 11.6, 8.7, 2.3 and 0.6, become 6, 3, 2.5 and 0.5 millions of amperes. The steady current around the earth and the diamagnetism are unchanged.

On the other hand one can not be entirely certain that it is the ions which should be reduced. Actually the ions will give very closely the same skip distance-wave-length relation as the electrons. Therefore if the refraction of short wireless waves were due to ions rather than to electrons the skip distance theory¹² would be unchanged. In this case it would be an "ion limitation" theory rather than an "electron limitation" theory. A sufficient number of electrons could be assumed such that by their magnetic double refraction and absorption they would account for the dip in the wireless range curve at $\lambda 200$ meters¹³ and the polarization phenomena. It is doubtful whether at the present time the observational data permit a final decision among the various possibilities. We may express the view, based on the complexity of wireless wave behavior, that some complex modification may be the one which will best account for all of the facts. That is, that perhaps the ions and electrons are present in such numbers that their refractions are about equal, and that during certain hours of the day or night and at certain latitudes the refraction of wireless waves is controlled by electrons and at other times and latitudes by ions.

¹² Taylor and Hulburt, Phys. Rev. 27, 189 (1926), equation 2.

THE SURFACE HEAT OF CHARGING

BY KARL F. HERZFELD

PHYSICAL LABORATORY, JOHNS HOPKINS UNIVERSITY

(Received December 24, 1929)

ABSTRACT

In recent papers by Bridgman, Langmuir and Tonks, and the author, the deviation of the constant A of *thermionic emission* from the theoretical value has been linked with the surface heat of charging and the *temperature variation of the photoelectric threshold*. In the present paper, at least a part of this effect is explained by the heat expansion of the material together with the dependency of the *work function* on the volume. Numerical calculations both for the deviations of A and for the temperature change of the threshold are made and compared with experiments. Before deciding whether the explanation given here is complete it will be necessary to calculate the space-charge effect of the electrons in the transition layer on the surface of the metal.

I. INTRODUCTION

THERE is considerable interest shown in the discussion of the formula for the thermionic emission, to which Richardson gave the form

$$i = BT^2 e^{-b/T}. \quad (1)$$

Equivalent to this, but better suited for our purpose, is the formula for the equilibrium density of the electron gas.

$$c = AT^{3/2} e^{-q/kT}. \quad (2)$$

in which A should be a universal constant^{1,2}

$$A = (2\pi mk)^{3/2} / Nh^3. \quad (3)$$

Here the exponent $3/2$ of T comes about by putting the specific heat of the electron gas equal to $3R/2$, the specific heat of the electrons in the metal zero.³

Independent of this assumption, one can give general formulas connecting vapor pressure and heat of evaporation.^{4,5,6} For example Lane² and Schottky⁷ write in generalization of (2)

¹ O. W. Richardson, Proc. Cambr. Phil. Soc. 11, 286 (1901); Phil. Mag. 28, 633 (1919); Proc. Roy. Soc. A91, 530 (1915); Phys. Rev. 23, 153 (1923).

² M. v. Laue, Jahrb. d. Rad. 15, 205, 257 (1918); S. Dushman, Phys. Rev. 21, 623 (1923). The same formula had been found by K. F. Herzfeld, Phys. Zeits. 14, 1119 (1913) but he had made no applications of it.

³ A. Sommerfeld Zeits. f. Phys. 47, 1 (1928).

⁴ O. W. Richardson, The Electron theory of Matter, Cambridge, 2 ed., 1916 p. 445.

⁵ W. Rodebush, Phys. Rev. 23, 774 (1924); H. A. Wilson, Phys. Rev. 23, 38 (1924).

⁶ C. Davisson and L. H. Germer, Phys. Rev. 20, 300 (1922); 30, 634 (1924).

⁷ W. Schottky, Handb. d. Experimentalphysik, Vol. XIII, Leipzig 1928, p. 30.

$$c = AT^{3/2}e^{-\mu_s/kT} \quad (4)$$

where μ_s is the chemical potential of the electrons in the metal instead of their potential energy (in other words, the assumptions leading to (2) are equivalent to say $\mu_s = q$) and then proceeds to allow for μ for example a linear variation with T . This procedure is thermodynamically quite correct but leaves the question why μ is a linear function of T unanswered.

As a next step, one can introduce the specific surface heat of charging as the specific heat which enters into the thermodynamical equations.^{6,8,9} It has been shown that such an effect might change the apparent value of A , the value of which agrees well experimentally with (3) in many cases but by no means always.

One can on the other hand consider the fact that the mutual potential energy which holds the electrons in the lattice will depend on the lattice distance and if heat expansion occurs will accordingly depend on the temperature.¹⁰ This is closely connected with the temperature variation of the long-wave-length limit of the photoelectric effect. How to treat such a case has been discussed in a short paper¹¹ but no formulas have been given and some remarks there seem now incorrect.

Bridgman,¹² in a paper that appeared before the one last mentioned has shown quite clearly how the two effects of a variation of the photo-electric stopping potential with temperature and the surface heat of charging are connected and will modify A .

The present paper, while using a different scheme of thermodynamical calculations than Bridgman because it seems simpler, is intended to supplement it by showing just what values the surface heat of charging must have.

We propose first to give the calculations for a somewhat simplified case, in the second part we will discuss a few subtle points to justify our method of procedure.

II. CALCULATIONS FOR A SIMPLIFIED CASE

1. The free energy.

Consider a piece of metal, insulated and surrounded by vacuum. Call the number of electrons the metal contains in excess of the neutral state n , the free electrons in the vacuum n' . Let p be the pressure, V the volume of the metal, V_0 its normal volume when neutral and at zero pressure, $\Delta = (V - V_0)/V_0$.

We then write the formula for the free energy F of the whole system.

$$F = U(V) - nq(V) - \frac{1}{2}en\phi - T\Phi\left(\frac{h\nu}{kT}\right) - Tn\tilde{\Phi} + n'(\mu_G - kT).$$

⁸ L. Tonks and I. Langmuir, *Phys. Rev.* **29**, 524 (1926); L. Tonks, *Phys. Rev.* **32**, 284 (1928).

⁹ P. W. Bridgman, *Phys. Rev.* **27**, 143 (1926).

¹⁰ O. W. Richardson, *Phil. Mag.* **23**, 594 (1912).

¹¹ K. F. Herzfeld, *Sommerfeld Festschrift*, Leipzig, 1928, p. 143.

¹² P. W. Bridgman, *Phys. Rev.* **31**, 90 (1928).

Here $U(V)$ is simply the (elastic) energy of the neutral metal. On account of deviations from neutrality, there is additional energy, an unelectric part¹³ $-nq(V)$ and an electric part $(-1/2)en\phi$. In contradiction to Schottky¹³ but in accord with Eckardt¹⁴ we call electric only the part of the field due to excess charges and having accordingly a long range. This part can be changed by connecting the plate with outside sources. Accordingly $\phi = 0$ means that there is no field of long range present. The energy then necessary to remove an electron is called the unelectric part $\tilde{q}(V)$. Φ is the integral

$$\Phi\left(\frac{h\nu}{kT}\right) = \int_0^T \frac{dT}{T^2} \int_0^T C_v dT \quad (5)$$

for the specific heat of the metal and will be usually a Debye function. Through ν , it will depend on the volume. We assume, (for the discussion of this assumption see under III) that ν does not depend explicitly on the charge.

$n\tilde{\Phi}$ would be the corresponding integral taken over the specific heat of the electrons in the usual sense, as calculated by Sommerfeld.³ $\partial(n\tilde{\Phi})/\partial n$ corresponds to the part variable with temperature in Sommerfeld's expression of $2kT \ln A$ (which has as physical meaning just the electron part of our $\partial F/\partial n$) and is negligible up to 3000° ($2 \cdot 10^{-3}$ compared with 1, although it accounts for Thomson- and thermoelectric effects).

Finally, μ_G is the usual expression for the chemical potential of the electron gas

$$\mu_G = kT \ln c + (3/2)kT \ln T + kT \ln A. \quad (6)$$

2. Equilibrium formula.

In equilibrium, F will be a minimum in respect to the possible variations, namely of n (electron emission) and of volume. The first condition will give the equilibrium concentration, the second the equation of state of the charged metal (in making this latter variation, we neglect the fact that an increase of the volume of the metal will decrease the volume of the electron gas).

$$0 = -\left(\frac{\partial F}{\partial n}\right)_v = q(V) + \frac{1}{2}e\phi + \frac{1}{2}en\frac{\partial \phi}{\partial n} + T\frac{\partial}{\partial n}(n\tilde{\Phi}) + \mu_G \quad (7)$$

$$0 = -p = \left(\frac{\partial F}{\partial V}\right)_n = \frac{\partial U}{\partial V} - n\frac{\partial q}{\partial V} - \frac{1}{2}en\frac{\partial \phi}{\partial V} - \frac{h}{k}\Phi\frac{\partial \nu}{\partial V} - Tn\frac{\partial \tilde{\Phi}}{\partial V}. \quad (8)$$

As at least in first approximation $n\partial\phi/\partial n = \phi$ and as we have decided to neglect $\tilde{\Phi}$, we get from (7)

$$-\mu_G = q(V) + e\phi \quad (9)$$

¹³ W. Schottky, Handb. d. Exp. Phys. Vol. XIII, 2 half p. 14 Leipzig 1928.

¹⁴ C. Eckardt, Zeits. f. Physik 47, 38 (1928).

¹⁵ In this we include the part of the internal electron pressure effect which does not depend on temperature, namely $-W_i$ (Sommerfeld) so that $q = W_a - W_i$.

or

$$c = AT^{3/2} e^{-(q(V) + e\phi)/kT} \quad (10)$$

which for constant volume of the metal, is identical with the usual form (2).

The problem is then to find $q(V)$. Here we use the following approximations: As U refers to the neutral metal, we introduce the common compressibility κ and write, using a familiar development in powers of Δ

$$U(V) = U_0 + V_0 \Delta^2 / 2\kappa. \quad (11)$$

Furthermore, we assume

$$q(V) = q_1 - q_2 \Delta \quad (12)$$

with the expression

$$q_2 = -V_0 \partial q / \partial V.$$

This gives

$$\frac{\Delta}{\kappa} + \frac{nq_2}{V_0} - \frac{1}{2} en \frac{\partial \phi}{\partial V} + \frac{h\nu}{kV_0} \Phi' \gamma = 0 \quad (13)$$

using Gruneisen's result,^{15a} that

$$-\gamma = (V_0/\nu) \partial \nu / \partial V \quad (14)$$

is a constant, namely about 1-3 for many metals.

Using the expansion coefficient α for the uncharged metal ($n=0$), which is according to Gruneisen given by

$$\int_0^T \alpha dT = -\kappa \frac{h\nu}{kV_0} \gamma \Phi' \quad (15)$$

we find

$$\Delta = \int_0^T \alpha dT - nq_2 \frac{\kappa}{V_0} + \frac{1}{2} en \kappa \frac{\partial \phi}{\partial V}. \quad (16)$$

For the approximately neutral metal, $n=0$, $\phi=0$, we have

$$c = AT^{3/2} e^{-q_1/kT} \exp \left[\frac{-q_2}{kT} \int_0^T \alpha dT \right]. \quad (17)$$

The last factor is the deviation from the formula (2). It is simply the change in q due to the total expansion of the metal up to T .

Equation (17) can be written for sufficiently high temperature

$$c = A' T^{3/2} e^{-q_1/kT} \quad (18)$$

$$A' = A \exp \left[\frac{q_2}{kT} \int_0^T \alpha dT \right] = A e^{q_2 \alpha / k} \quad (19)$$

^{15a} E. Gruneisen, Ann. d. Physik 39, 257 (1912).

3. Calculation of q_2 and numerical value of A' .

It is possible to get an estimate of q_2 . We have first to remember that q is a difference between the potential energy of an electron in the metal (Sommerfeld's W_a) and the effect of the internal pressure. (W_i according to Sommerfeld.) Therefore

$$-q_2 = V_0 \frac{\partial W_a}{\partial V} - V_0 \frac{\partial W_i}{\partial V}$$

Bethe¹⁶ attempts a theoretical calculation of W_a ; it is composed of a contribution from the positive ions, which is, for a given size of the ions, proportional to their number per unit volume and which we call therefore

$$W_a^+ + V_0/V$$

and a contribution from the electrons, inversely proportional to the distance, or

$$W_a^-(V_0/V)^{1/3}.$$

Finally, W_i is proportional to the $2/3$ power of the number of electrons per cm^3 .

If we assume that compression does not change the total amount of electrons per atom, we have (W_a^+ , W_a^- , W_i^0 constants)

$$q = W_a^+ \frac{V_0}{V} + W_a^- \left(\frac{V_0}{V} \right)^{1/3} - W_i^0 \left(\frac{V_0}{V} \right)^{2/3}. \quad (20)$$

Then

$$q_2 = W_a^+ + \frac{1}{3} W_a^- - \frac{2}{3} W_i^0. \quad (21)$$

According to Bethe's calculations for nickel, W_a^+ is about 13 volts, W_a^- 6 volts, W_i^0 15 volts, which would make $q_2 \sim 5$ volts.

If we write $\alpha = \alpha' \times 10^{-5}$, $q_2 = +q_2'$ volt, we have

$$e^{q_2 \alpha / k} = 10^{0.059 q_2' \alpha'} \quad (22)$$

From this it follows: A is always apparently increased $A' > A$. For $q_2' \alpha' < 10$ the factor multiplying the theoretical A is not larger than 3, which is within the limits of the experiment. If the above estimate of q_2 is correct, this means for metals with low expansion coefficient ($\alpha' < 2$), that the theoretical value of A can be made to fit the results.

But we have to expect much higher A 's if α' is larger. $\alpha' = 9$ (linear expansion coefficient 3), $q_2' = 5$ means already $A' = A \cdot 10^{2.25} \sim 180A$; $\alpha' = 15$, $q_2' = 6$ means $A' = 30.000A$.

While this is in the right order of magnitude,^{18,19} we can give no reason why a large A' should always go with a high q_1 .

¹⁶ H. Bethe, Ann. d. Physik **87**, 55 (1928).

¹⁷ The factor $\exp[-(1/k) \partial(n\Phi)/\partial n]$ which is responsible for the thermoelectric effects has been neglected.

¹⁸ C. Zwikker, Proc. Amst. Ac. **24**, 1 (1926); A. L. Du Bridge, Phys. Rev. **31**, 236 (1928); **32**, 961 (1928).

¹⁹ A. L. Du Bridge, Proc. Nat. Ac. **14**, 788 (1928); I. Langmuir and K. H. Kingdon, Phys. Rev. **34**, 129 (1929).

4. Temperature change of the heat of evaporation.

We are first going to calculate the heat of evaporation of the electron and show that the deviation can be interpreted as a contribution of the specific surface heat of charging, not to C_v , but to $C_p - C_v$.

The heat of evaporation of an electron at constant volume of the metal would be

$$q(V) + 3RT/2 + e\phi \quad (23)$$

the middle part coming from the specific heat of the electron gas. The contribution of the specific heat of the electrons in the metal has been neglected.

At constant pressure, we have to add to (23)

$$T^2 \left(\frac{\partial}{\partial V} \frac{\mu}{T} \right)_{T,n} \left(\frac{\partial V}{\partial T} \right)_{p,n}$$

or take simpler

$$T^2 \left(\frac{\partial}{\partial T} \frac{\mu(p, T)}{T} \right)_{p,n} + \frac{3}{2} RT. \quad (24)$$

This is, with

$$\mu(p=0, T) = -q_1 - \frac{h\nu}{k} q_2 \frac{\gamma}{V} \kappa \Phi' \quad (25)$$

from (7) for the uncharged plate, $n=0$, leads after a short calculation to the following formula in which the value of Φ has been introduced

$$q_1 - q_2 \frac{\gamma}{V_0} \kappa \left(C_v T - \int_0^T C_v dT \right) + \frac{3}{2} RT. \quad (26)$$

Instead of the last $3RT/2$, $2RT$ or $5RT/2$ might have to be introduced, depending on which heat is actually measured.⁶

The interesting point is that for moderate temperatures, $C_v T - \int_0^T C_v dT$ is a constant or, in the presence of zeropoint energy in the vibrations of the solid, even zero. The exponent $-q_1/RT$ in (3) gives therefore at moderate temperatures the real heat of evaporation (apart from the member $3RT/2$, which is due to the electron gas).

In making this statement, we have again neglected the increase with temperature of the kinetic energy of the electrons in the metal as too small to detect. We can expect to find a change of the heat of evaporation with temperature:

(a) at high temperature, where C_v increases

$$C_v = C^0 + C' T$$

$$C_v T - \int_0^T C_v dT = \frac{C'}{2} T^2, \quad \Delta q = -q_2 \frac{\gamma}{V_0} \kappa \frac{C'}{2} T^2.$$

This increase will not modify greatly the last factor in (17) because it occurs at high temperatures ($1/T$).

(b) at low temperatures, where quantum effects appear in the specific heat, there will be an increase in the heat of evaporation (apart from $3RT/2$) with decreasing temperature up to the amount

$$q_2 \gamma \kappa N h \nu / V_0.$$

The value of the specific surface heat of charging at constant pressure follows from (26) to be

$$q_2 \frac{\gamma k}{V_0} T \frac{\partial C_v}{\partial T}$$

(C_v specific heat of the metal at constant volume.) Bridgman^{9,12} has shown that if (2) is valid and A' different from A , the specific surface heat of charging must be 0 and there must exist an entropy difference between the charged and the uncharged surface at zero temperature contrary to Nernst's heat theorem. In the case considered here the specific surface heat of charging is zero at zero temperature, takes then positive values and decreases to zero again for high temperatures. Accordingly (2) is valid at very low temperatures with the theoretical A , ceases to be valid afterwards and becomes valid again at high temperatures with $A' > A$. This hump of the specific heat at low temperatures is then responsible for the deviation of A' from A . If one would extrapolate formula (2) with A' different from the theoretical value to zero temperature one would find an entropy difference. A very similar situation is present in a number of chemical reactions. The whole situation is bound up with the fact that the expansion coefficient disappears at zero temperature which fact itself is again connected with Nernst's theorem.

Numerical calculations for the case of potassium give the following result: We use

$$\gamma = 1.34^{20} \quad \kappa^{21} = 35.6 \times 10^{-12} \quad V_0 = 45 \quad h\nu/k = 99^{22}$$

and for $C_v - (1/T) \int_0^T C_v dT$ tables given by Simon.²³

If we take $q_2 = 5$ volt we find

T	$\beta\nu/T$	$CT - \int C dT$ (cal/Mol)	Δq (millivolts)
495	0.2	0	0
198	0.5	8	1.7
99	1	36	7.8
49	2	92	20
20	5	170	37
10	10	196	43

²⁰ E. Grüneisen, Handb. d. Phys. X p. 29, Berlin 1926.

²¹ Reference 20, p. 38.

²² A. Eucken, Handb. d. Exp. VIII, Leipzig 1929, p. 245.

²³ F. Simon, Handb. d. Physik X Berlin, 1926.

5. Photoelectric threshold.

Offhand, one could be doubtful whether the photoelectric threshold is determined by the energy or the free energy of the electrons in the metal. But Bridgman has proved the connections between threshold and contact potentials, and there is no doubt that the contact potentials are determined by the free energy or, more exactly, the chemical potential μ .

The temperature variation of the threshold is then given by

$$q_1 + q_2 \frac{\gamma}{V_0} \kappa \frac{h\nu}{k} \Phi' = q_1 - q_2 \frac{\gamma}{V_0} \kappa \int_0^T C_v dT = q_1 - q_2 \int_0^T \alpha dT.$$

That means, that for an increase of 100°C and $q_2 \sim 5$ volts, the change in the photoelectric threshold is as follows.

K	Al	Mg	Zn	Cu	Ag	Au	Fe	Ni	Pt	Pb	Sb	
125	36	39	43	25	29	21	17	23	15	43	18	millivolts.

Comparing this with experiments, it seems reasonable that such a change could not be detected in the work of Millikan and Winchester²⁴ who heated Al, Mg, Zn, Cu, Ag, Au, Fe, Ni, Pb, Sb 100° and of Varley and Unwin²⁵ who varied the temperature of Pt 300°, corresponding to changes of less than 50 millivolts. It is more astonishing that Millikan and Winchester²⁴ found no change for Al between 50 and 350° (110mv) and Ladenburg²⁶ for Au, Pt, Ir up to 860° (150mv) and that Dember²⁷ could not detect any effect on K on heating it to 67°, but it is difficult to estimate how much a change in the long-wave-length limit would affect the current measured by these investigators.

Recently Du Bridge²⁸ detected a change in current upon heating platinum to 1200° and narrowed down the wave-length shift to a region between 1943-1973Å; 30Å would correspond to 90 while $q_2 \sim 5$ V would lead to 180mv. Measurements of Suhrmann²⁹ give a few percent shift in Ag, Au, Pt between room temperature and liquid air. Finally Ives³⁰ has found a shift for K in the same interval of 220mv while $q_2 = 5$ would give 250 (actually it should be less on account of the smaller coefficient of expansion at low temperatures). It seems therefore that the present theory gives the right order of magnitude.

It should be mentioned in conjunction with the fact that the oxide-coated cathodes have a particularly high A' , that Koppius³¹ found a very strong variation of their threshold with the temperature.

²⁴ R. A. Millikan and G. Winchester, *Phil. Mag.* **14**, 188 (1907).

²⁵ W. M. Varley and F. Unwin, *Proc. Roy. Soc. Edinburgh* **27**, 117 (1907).

²⁶ R. Ladenburg, *Verh. d. D. Phys. Ges.* **9**, 165 (1906).

²⁷ H. Dember, *Ann. d. Physik* **23**, 957 (1907).

²⁸ L. A. DuBridge, *Phys. Rev.* **29**, 451 (1927).

²⁹ R. Suhrmann, *Zeits. f. Physik* **33**, 63 (1925); see also A. Becker, *Ann. d. Physik* **78**, 83 (1924).

³⁰ H. E. Ives, *Journ. Am. Opt. Soc.* **8**, 551 (1924); H. E. Ives and A. L. Johnsrud, *Journ. Am. Opt. Soc.* **11**, 565 (1925).

³¹ O. Koppius, *Phys. Rev.* **18**, 443 (1921).

III. JUSTIFICATION OF METHOD OF PROCEDURE

1. We have made our calculations as if the evaporating electron were taken from the interior and have not said anything in particular about the surface. Here we have to distinguish two steps in the equilibrium condition (7) we have put the expression for the thermodynamical potential of an electron deep in the interior of the vessel equal to one in the gas. But as Schottky pointed out, this is justified as the numerical value of μ (not the form of μ) must be the same for an electron in the interior as it is in the surface on account of the internal equilibrium of the electrons. On the other hand, the particular expression for the potential energy (q) in the interior, as calculated by Bethe, might be wrong; this value might be influenced by the surface. But it seems reasonable that this would not change the order of magnitude of q_2 , and our calculation does not claim more.

2. We did not include, "electrical contributions," as we defined the Volta potential ϕ as being due to the total charge and we assume this to be zero (compensation for Volta potential in the actual thermionic experiment). The difference between this case and the usual case, for example in the thermodynamics of gases where differentiation at constant pressure (analogous to ϕ) and constant volume (analogous to en) makes a difference even for $n=0$, comes from the fact that

$$pV = nkT$$

and therefore $\partial(pV)/\partial n = kT$ even for $n=0$ while here $ne\phi$ is proportional to n^2 and therefore $[\partial(ne\phi)/\partial n]_{n=0} = 0$.

The reason we have deviated from Schottky's¹³ definition, which amounts here to saying that the non-electric part in the differences of the (total and free) energy is the one remaining, if the two places to be compared were brought to the same potential, is the following: With this definition all differences in potential energy of the electron would belong to the electrical part. Indeed, the electrical potential of a place is defined only by the work necessary to bring a test charge (electron) there. Accordingly the difference in potential energy q inside and outside of the metal would belong entirely to the electrical part, which does not seem advisable. On the other hand, it is always possible, by measuring at a sufficient distance, to state whether a (large) body is charged. We define as the non-electric part of the (free or total) energy of an electron in respect to a (large) body the part which would be alone present if the body as a whole were uncharged.

In passing, it may be said that this together with the emphasis that in measuring thermionic currents one has always to correct for the Volta potential, that is one always takes care to have $\phi=0$, gives a clear view of the situation in the presence of surface layers.

3. We have assumed that Φ or the specific heat C_v of the metal at constant volume depends upon n only indirectly through the volume. If we now drop this assumption, (8) and (13) remain unchanged, but in (7) we must add

$$-T \left(\frac{\partial}{\partial n} \Phi \right)_{v,T} = -\frac{h}{k} \Phi' \frac{\partial \nu}{\partial n}$$

which then produces finally on the right hand side of (17) another factor

$$\exp \left[\frac{h}{k^2 T} \Phi' \frac{\partial \nu}{\partial n} \right].$$

Now we can write, for a plate containing N atoms, at sufficiently high temperature

$$\frac{h}{k^2 T} \Phi' \frac{\partial \nu}{\partial n} = -\frac{h}{k^2 T} 3Nk \frac{kT}{h\nu} \frac{\partial \nu}{\partial n} = -3N \frac{\partial \ln \nu}{\partial n}$$

or better

$$-\partial(\Sigma \ln \nu) / \partial n$$

where the sum is to be extended over all the vibrations which make up the heat movement of the plate. Therefore³²

$$\exp \left[\frac{1}{R} \left(\frac{\partial \Phi}{\partial n} \right)_{v,T} \right] = \prod_i \exp \left[- \left(\frac{\partial \ln \nu_i}{\partial n} \right)_v \right].$$

If we would assume that the removal of an electron affected only three vibrations (in a primitive picture the vibrations of one atom), we could say safely that the new frequency would lie between half and the double of the original frequency, or

$$\left| \frac{\partial \ln \nu_i}{\partial n} \right| < 1 \quad i=1,2,3 \quad \frac{\partial \ln \nu_i}{\partial n} = 0 \quad i>3.$$

Then, the additional factor in (19) would lie between e^{-3} and e^3 1/20 and 20. If, as will be the case, the change affects all vibrations, it still seems reasonable that

$$\left| \sum \frac{\partial \ln \nu}{\partial n} \right|$$

will be not much larger than 3 and therefore, a direct influence of a removal of electrons on the specific heats at low temperature will probably not influence A' as strongly as the indirect effect through the volume.

4. The most important assumption however that we have made is the omission of a part of q which would be explicitly dependent on temperature. Now the part in the potential energy of an electron which is due to the surrounding charges, as calculated by Bethe,¹⁶ is not dependent directly on temperature (the heat movements of the positive ions will upon averaging have no effect of the first order). But there might be another contribution³² due to

³² W. Schottky, reference 13, p. 96f. See also E. D. Eastman, Jour. Am. Chem. Soc. **48**, 552 (1926), C. Zwicker, Physica, **9**, 321 (1929).

an electric double layer or space charge, which might be formed on the surface of the metal where the electron density drops gradually off. This might depend on T , not in the part farther in, where the electron density is still high, the electron gas degenerate and therefore its μ independent of T , but in the outside layers. How much these contribute, can not be estimated until a calculation has been made.

The only thing to be said is that the part discussed previously gives the right order of magnitude.

IV. OTHER APPLICATIONS

The method which we have developed here can be applied similarly to an ordinary solution, in which the mutual potential energy between the solvent and the dissolved molecules depends on the distance between them and accordingly varies indirectly with the temperature on account of the heat expansion of the solvent.

CHANGE OF SPACING OF POSITIVE COLUMN STRIATIONS WITH TEMPERATURE

By F. M. SPARKS AND CHARLES T. KNIPP
UNIVERSITY OF ILLINOIS

(Received December 19, 1929)

ABSTRACT

Cassen's prediction (Phil Mag. 268, 948, Nov. 1926) that the separation of the striations in a discharge tube should increase almost linearly with the absolute temperature is verified for the wide blue striations. For the narrow striations, the separation first decreases, but in general reaches a minimum, after which the separation increases as predicted.

FROM theoretical considerations, Cassen¹ predicts that the distance between striations in the positive column of a discharge tube should increase almost linearly with the absolute temperature, and that the addition of an impurity may greatly change the spacing.

A vertical discharge tube was heated in a liquid bath contained in a large vertical glass tube. An electric heating coil was placed in the bottom of the bath and the temperature controlled by an external resistance. Two thermometers were placed in the bath at different heights to obtain the temperature. A large flask was connected to the discharge tube to minimize the change in pressure due to change in temperature of the tube. To secure steady striations which could be measured with a cathetometer, a potential of 3000 volts from small storage cells was used. The current was controlled by a water resistance and measured with a milliammeter.

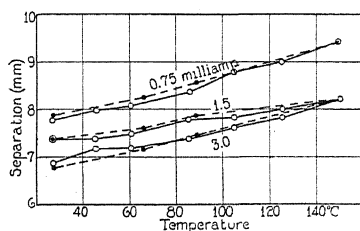


Fig. 1. Wide striations at a pressure of 1 mm Hg.

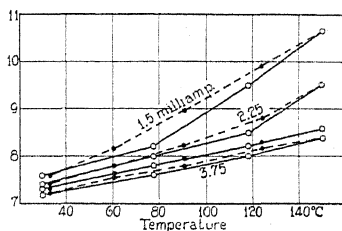


Fig. 2. Wide striations at a pressure of 1 mm Hg.

Hydrogen was used in the discharge tube because it gives striations over a much greater range of conditions than the other ordinary gases. Only the blue striations were obtained, these being due to impure hydrogen.² The pressures used were such that both the wide and the narrow blue striations appeared.³ To detect any temperature lag or change in character of the gas, the separations were noted with both increasing and decreasing temperature.

The separation was gotten by measuring across several striations and

¹ B. M. Cassen, Phil Mag. 268, 948 (1926).

² Handbuch der Physik, vol. 14, p. 298.

³ Handbuch der Physik, vol. 14, p. 300.

dividing this distance by the number of striations measured. The separation in millimeters was plotted against the temperature of the bath in degrees Centigrade. Measurements were made for different values of the current because the separation varies with current.⁴

Figure 1 shows three curves, obtained at the same time, for current values of 0.75, 1.5, and 3 milliamp. Measurements were begun at room temperature, the unbroken line indicating readings with increasing temperature, and the broken line being for decreasing temperature. Figure 2 shows another set of curves, for currents of 1.5, 2.25, 3, and 3.75 milliamp. Both these sets of curves are for the wide striations, at pressures of about 1 mm Hg. Figures 3 and 4 represent data for the narrow striations, at pressures of 2.5 and 1.7 mm.

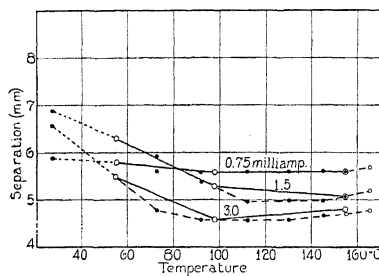


Fig. 3. Narrow striations at a pressure of 2.5 mm Hg.

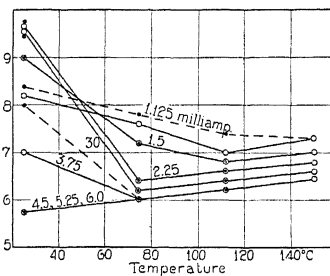


Fig. 4. Narrow striations at a pressure of 1.7 mm Hg.

In Fig. 3 the readings were begun at 155°C, the temperature lowered to 55°, then increased to 165°, and the last readings at room temperature were made the next day. In Fig. 4 no reading was made for a current of 6 milliamp. at 150° because the cathode became too hot. Figures 1 and 3 were made with prepared hydrogen, using one discharge tube, and Figs. 2 and 4 with commercial hydrogen, using a different tube.

Figures 1 and 2, representing the wide striations, agree with Cassen's prediction that the separation should increase almost linearly with the temperature. Figures 3 and 4, representing the narrow striations, show that the separations may first decrease but that they reach a minimum value and then increase linearly with the temperature. The curves for current values of 4.5, 5.25 and 6 milliamp. in Fig. 4 show only an increase in separation, which is in exact accord with the prediction. However, the minimum value of the separation seems to be shifted toward lower temperatures as the current is increased so that these curves might be expected to be similar to the others in the same figure, but with a minimum at some temperature below room temperature. Figure 3 also shows the shifting of the minimum to the left with increasing current. The deviation from Cassen's predictions might be explained by saying that his simplifying assumptions are valid only under certain conditions.

A series of curves was also plotted for hydrogen at 2.5 mm, after successive additions of impurity. The general shape of the curves was similar to those of Fig. 3, but they were shifted down to smaller values of separation, reaching a minimum, and then were shifted up to greater values.

⁴ Handbuch der Physik, vol. 14, p. 301.

PERSISTENCE OF VELOCITY AND THE THEORY
OF SECOND ORDER GAS REACTIONS

BY LOUIS S. KASSEL*

GATES CHEMICAL LABORATORY, CALIFORNIA INSTITUTE

(Received December 10, 1929)

ABSTRACT

R. H. Fowler has stated that if, in second order gas reactions, it is supposed that reaction occurs whenever two reactant molecules collide with sufficient velocity, then the deviation from the Maxwell distribution law which would result is so great that this law cannot be used in calculating the rate of the reaction. It is shown that this view is sometimes in error, and that in a mixture of molecules of nearly equal mass reacting in this way the molecular velocities do not diverge appreciably from the predictions of the Maxwell law.

IT IS an experimental fact that the rates of all the known second order gas reactions can be represented, at least within a factor of 5 or 10, by the simple expression $Ze^{-E/RT}$, where Z is the number of collisions between reactant molecules, calculated in accordance with the methods of kinetic theory, and E , the energy of activation, is an experimental constant for each reaction. There are a number of simple theories which are able to predict an equation of this form. In particular, if it is assumed that reaction occurs at every collision for which the relative velocity parallel to the line of centers at the instant of collision is at least V_0 , it is found¹ that the rate is $Ze^{-E_0/RT}$, where $E_0 = MV_0^2/2$ and M is the reduced molecular weight $M_1M_2/(M_1+M_2)$. If it is supposed that the reaction occurs whenever the relative velocity of the collision exceeds V_0 , regardless of its direction with respect to the line of centers, it is found that the rate is given by $Ze^{-E_0/RT}(1+E_0/RT)$. Since in actual cases E_0/RT is about 40, the form of this equation is not experimentally distinguishable from a simple exponential, though of course the predicted rate, for an experimentally determined temperature coefficient, is rather larger. This latter mechanism has been considered recently by Fowler² from the standpoint of persistence of velocity;³ he has concluded that if reaction were to occur at every collision the number of high velocity molecules present in the gas would fall far below the Maxwell quota, so that the rate of reaction would be substantially less than that calculated; if the mechanism of any actual second order reaction were of this simple type, and if the theory were subject to the correction suggested by Fowler, then we should expect the rate to be very considerably increased by the addition of an inert gas, which would tend to maintain the Maxwell quota, and an effect of this kind has not been observed.

* National Research Fellow in Chemistry.

¹ See, for example, Tolman, *Statistical Mechanics*, (1927) p. 272.

² R. H. Fowler, *Statistical Mechanics*, (1929), p. 461.

³ Jeans, *Dynamical Theory of Gases*, (1925), pp. 260, 275, 312.

It seems, however, that when the molecular masses are nearly equal Fowler's correction is actually inappreciable; qualitatively this is so because in most of the collisions with relative velocity of V_0 or more, each of the colliding molecules has velocity of about $\frac{1}{2}V_0$; hence if reaction did not occur, each of them would leave the collision with velocity about $\frac{1}{2}V_0$, and, since this is very much greater than the mean velocity of all the molecules, in the vast majority of cases each of them would next collide with a slower molecule; at such a collision the relative velocity could not be greater than V_0 , so that reaction could not occur. Fowler has written, "A certain proportion of collisions with relative energy more than ξ will concern at least one molecule whose last collision was also one of the same class. This is the phenomenon of the *persistence of velocities*." This, however, is not exactly what Jeans has meant by the term; he has taken as a measure of the persistence the ratio of the expected component of velocity after the collision in the direction of the original velocity to this original velocity, and found for this ratio a value of about 40 percent. Fowler is interested not in this, but in the value of the proportion mentioned in the preceding quotation, which is a very different thing.

Since an exact calculation would involve the quadrature of some rather cumbersome integrals, it will be considered sufficient to show that the effect in question is very small. First we notice that almost all of the collisions with relative velocity greater than V_0 have relative velocity less than $9V_0/8$; the ratio of the number which exceed this limit to the number which exceed V_0 is about $e^{-17E_0/64RT}$, which is of the order of 10^{-4} .⁴ We shall use the methods given by Jeans.⁵ Instead of the three velocity components for each of the two molecules which are involved in the collision, we take three for the center of gravity, and three for the relative velocity. When we do this, we find that, both before the collision and afterwards, the relative velocity of each molecule is about $\frac{1}{2}V$. Jeans' treatment shows that the motions of the centers of gravity of the various collision complexes obey the Maxwell law for molecules of the appropriate mass, and that there is no correlation between the relative velocity of the collision and the velocity of the center of gravity of the colliding molecules. Since this is so, we can calculate the chance that the relative velocity of the center of gravity and the next molecule with which either of the original ones will collide shall exceed any specified value. We have seen that only in a negligible fraction of the collisions which concern us will the relative motion of the center of gravity of the colliding molecules and either of the molecules exceed $9V_0/16$. Now it is plainly necessary (though not sufficient), in order for the relative velocity of the next collision to exceed V_0 , for the relative velocity of the colliding molecule and the center of gravity of the two original molecules to exceed $7V_0/16$. This chance is easily calculated as about 10^{-3} . Hence we may state confidently that the proportion in which Fowler is interested is less than one in a thousand, and may be neglected. A similar treatment can be given for the case that the relative velocity along the line of

⁴ In all the following calculations, the value 40 will be used for E_0/RT .

⁵ Jeans, reference 3, p. 35.

centers must exceed a critical value for reaction to occur. Hence the simple expressions $Ze^{-E_0/RT}$ and $Ze^{-E_0/RT}(1+E_0/RT)$ are the correct rate expressions for the mechanisms which have been described when the molecular masses are nearly equal.

When the masses of the two molecules are very different, the situation is entirely changed, and the correction discussed by Fowler becomes of importance. Thus in a collision between a molecule of hydrogen and a molecule of iodine, where the ratio of the masses is about 127, the hydrogen contributes practically all the velocity of the collision; in a large fraction of all the collisions with relative velocity greater than V_0 , the hydrogen molecule itself has a velocity greater than this value, and can be expected to produce another collision of the same type if it survives the first one. The correction would be most important when the concentration of hydrogen was much less than that of iodine; then hydrogen molecules would have been expected to execute fairly long series of collisions with iodine, all with relative velocity greater than V_0 , if the system did not react; the reaction mechanism which has been postulated would cut off these series at the first member, and the rate would therefore be much less than that given by the naive calculation. There is no experimental evidence for such behavior, which indicates either that this is not the mechanism of the reaction or that if it is, then reaction occurs only at a small fraction of the collisions for which the energy condition is satisfied.

With regard to the question of the actual mechanism of second order reactions, the writer does not believe that either of these simple mechanisms is correct. It seems likely to him as it does to Fowler also, that translational, vibration, and rotational energy must all be considered, and that in most cases the effective target area for reaction will be small compared to the kinetic theory cross-section.

YOUNG'S MODULUS DETERMINED WITH SMALL STRESSES

BY DAROL K. FROMAN

RYERSON PHYSICAL LABORATORY, UNIVERSITY OF CHICAGO

(Received December 19, 1929)

ABSTRACT

An interferometer method similar to that used by E. Grüneisen was used to determine the extensions of metallic rods of brass, steel, copper, aluminum and nickel under small stresses. The largest stresses applied were considerably less than those usually used in commercial testing. For the substances examined Young's Modulus was found to increase very rapidly as the stress increased from zero, reach a maximum at a comparatively small stress, and then to decrease almost exponentially to the ordinary value. The annealing of the rod may be connected with this divergence from Hooke's law with small stresses, as slight differences were found on reannealing some of the rods used.

IT HAS been known¹ for some time that the value of Young's Modulus computed from the velocity of weak longitudinal vibrations in rods was appreciably higher than that obtained by ordinary static methods. The differences expected in the adiabatic and isothermal moduli² are small compared to those found experimentally by dynamic and static methods, although values found by these methods are often quoted as the adiabatic and isothermal moduli respectively.³ Therefore it was decided to measure the elasticity statically at small stresses, comparable with those in a sound wave. Following E. Grüneisen⁴ an interferometer was used to determine the strain.

In Fig. 1 the rods *A* are under test and the plates *B* are fixed to their ends. There is a universal joint at the point *C*. *G* and *H* are plates with holes and lock screws to clamp them to the rods. The holes are bevelled so that contact with the rods *A* can be made at one point only. By means of rods *P* the plate *G* supports another plate *E*, having a circular hole in its centre under which is supported a three-quarter silvered mirror *T*. The plate *H* has three leveling screws supporting a plate *Q*, on which is placed the other interferometer mirror *R*, similar to *T*. *N* is a right-angled prism held in position by a fixed external support and *L* is a mirror also supported from the outside. *S* is the source of light, a mercury arc, used with a filter *F*.

Monochromatic light is incident on *L* and reflected through the partly silvered mirrors to *N*, which totally reflects it to the telescope *M*. The telescope is adjusted for parallel light and circular interference fringes can be produced by making the mirrors *R* and *T* parallel with each other. The telescope is equipped with an eye-piece having both movable and fixed cross

¹ R. J. Lang, Proc. Roy. Soc. Can. 16, 163 (1907). G. W. Pierce, Am. Acad. Proc. 63, 1 (1928). E. Grüneisen, Ann. der Physik 22, 801 (1907).

² G. F. C. Searle, "Experimental Elasticity" p. 22.

³ E. Grüneisen, reference 1, p. 843.

⁴ E. Grüneisen, reference 1, p. 826.

hairs. W is a scale pan attached to the center of the lowest plate by means of a universal joint not shown in the diagram. As weights are applied at W the rods A stretch, the mirrors separating by the extension in the length from G to H . This causes the fringes to move out from their center. Three vanes not shown in the diagram are clamped to the bottom plate. These move in an oil bath to damp the motion of the apparatus after the application of a weight at W .

Measurements were made by taking the diameters of two successive fringes in the arbitrary units of the screw attached to the movable cross hair. Then a weight was applied to W and the number of fringes passing the cross

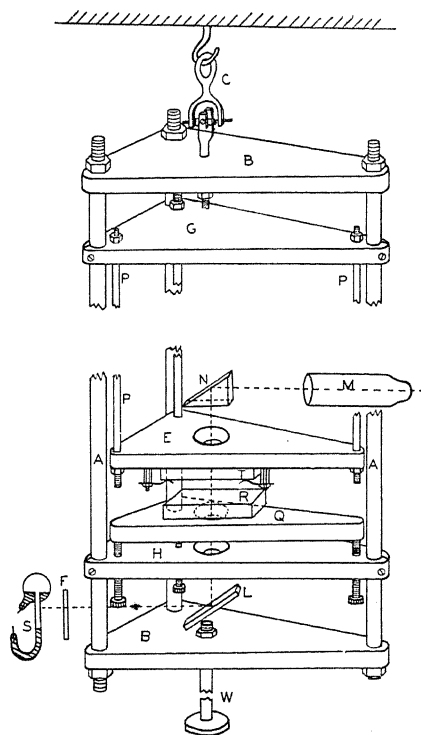


Fig. 1. Diagram of interferometer.

hairs counted. The diameter of the fringe which remained between the positions previously occupied by the two fringes measured was then taken. If readings were taken on fringes further from the center than the fourth or fifth, no appreciable error was introduced by taking the fractional fringe shift as proportional to the displacement over the width of one fringe. Thus if d_1 and d_2 be the diameters of two successive fringes, and, on the application of a weight, n fringes and a fraction pass the cross hairs, if d_3 be the diameter of a fringe occupying a position between d_1 and d_2 , then the fringe shift is $n + (d_3 - d_1)/(d_2 - d_1)$.

Since a shift of one fringe is caused by a motion of the mirrors R and T of one-half wave-length, the extension in the part of the rods from G to H can be computed, and Young's Modulus found in the usual way by dividing the stress by the strain.

Care was taken to keep the apparatus at a nearly constant temperature as the difference in the lengths of the rods P and A produces a different thermal expansion. The two sets of rods must be of the same material, also, so that their thermal expansion coefficients will be equal. It was found that if one set were of brass and the other of steel, temperature changes of one degree

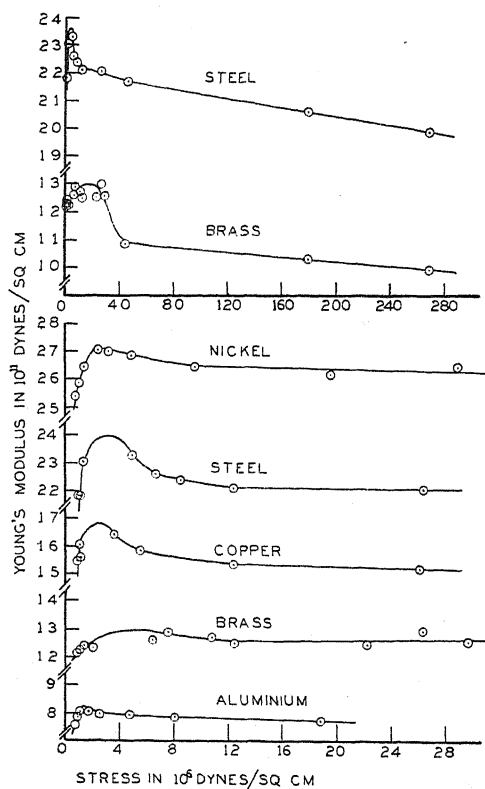


Fig. 2. Curves of Young's Modulus.

per hour were quite sufficient to invalidate the results since it required two or three minutes to take a reading.

After a reading was taken the weight was removed and the diameters of the fringes checked to see if the rods had returned to their original lengths. if they had not, the reading was thrown out. It was found quite easy to measure the displacement of the mirrors to one two-hundredth of a wave-length.

The stress on the rods was adjusted to any desired value by applying weights at W and the elasticity measured by applying a small additional

weight and measuring the shift in the fringes. The stress was computed from the sum of the original weights at W , one-half of the small additional weight and the weight of the parts of the apparatus supported by the rods including one-half of their own weight.

In this way Young's Modulus was determined for five materials at various stresses. The rods used were about 40 cm long and 0.95 cm in diameter. In Fig. 2 curves of Young's Modulus against stress are plotted for the various materials.

Professor Huntley of Armour Institute, Chicago, kindly determined Young's Modulus for two of the specimens at three very much higher stresses than it was possible to use with the apparatus just described. The rods used were cut from the same piece as the ones tested with the interferometer. These values are the three with largest stresses plotted in Fig. 2 for steel and brass, respectively. By means of Kundt's tube the velocity of sound was measured in each material. The air in the tube was carefully dried and Young's Modulus, E , calculated from the relation

$$v = \sqrt{E/d},$$

where v is the velocity of sound and d is the density. The values obtained by this method are given in Table I.

TABLE I. *Young's Modulus as determined from velocity of sound.*

Material	$v(\text{cm/sec})$	$d(\text{gm/cm}^3)$	$E(\text{dynes/cm}^2)$
Brass	3.63×10^5	8.45	11.1×10^{11}
Steel	5.15×10^5	7.81	20.75
Copper	3.89×10^5	8.61	13.01
Aluminum	5.155×10^5	2.70	7.19
Nickel	4.905×10^5	8.82	21.25

For two of the materials rods were excited into longitudinal vibrations at various frequencies up to 17000 per second, by a method described by Boyle and Lehmann.⁵ The rods were cut in half and each glued, end on, to a thin piece of quartz cut with its faces perpendicular to an electric axis. This constituted a parallel-plate condenser which was connected in parallel with the variable condenser in the tank circuit of an ordinary five watt radio oscillator. Then the faces of the quartz disc were vibrated longitudinally by the piezo-electric pressures and the frequency of the electric oscillations varied until the rods came into resonance. If this frequency were in the audible range of frequencies the rods gave off a distinct sound. A precision wave-meter was used to determine the frequency of the Hertzian oscillations which was, of course, the frequency of the mechanical vibrations of the rod. In agreement with Professor Pierce,⁶ this was found to be constant at all of the frequencies tried and the same as that given by Kundt's tube, although the stresses were probably much smaller.

⁵ Boyle and Lehmann, Trans. Roy. Soc. Can., Sect. III, Vol. XIX (1925).

⁶ Pierce, Am. Acad. Proc. 63, 40 (1928).

A set of steel rods were annealed in an electric furnace and the tests again carried out. Young's Modulus was found to be slightly higher for each value of the stress that it was previously. Otherwise the behavior was exactly similar.

From these results it appears that Hooke's Law does not hold exactly for very small stresses but that Young's Modulus has a maximum at some small but finite stress. The elasticity decreases rapidly to the ordinary value as the stress is increased from this value and decreases even more rapidly as the stress is decreased from the point of maximum elasticity. It will be noted that Young's Modulus determined from the velocity of sound is somewhat lower than the values from the interferometer method but higher in the cases of brass and steel, than the values obtained with large stresses.

In conclusion the author wishes to acknowledge with thanks the assistance given by Professor Huntley of Armour Institute, mentioned above, and to thank Professor Dempster of this Laboratory for his untiring interest in the problem and his many very valuable suggestions.

ROCHELLE SALT AS A DIELECTRIC

BY C. B. SAWYER AND C. H. TOWER
THE BRUSH LABORATORIES, CLEVELAND

(Received November 6, 1929)

ABSTRACT

Both saturation and hysteresis appear in Braun tube oscillograms made at various temperatures with a condenser whose dielectric consists of Rochelle salt slabs cut perpendicular to the *a*-axis. The dielectric constant for such slabs may reach a value of 18,000. Curves are also given, showing the variation in mechanical and electrical saturation with temperature. These correspond in only a general way to the piezoelectric constant's variation with temperature. Certain marked peculiarities are noted in the resulting mechanical deformation when Rochelle salt is excited with alternating potentials. Clear Rochelle salt half-crystals have been produced up to forty-five centimeters in length.

THE remarkable physical properties of Rochelle salt, the most piezoelectric active of all crystalline substances, have been reported by other authors.¹ Comparatively small plates and few crystals were used in their determinations.

Work at this laboratory has been carried on for a number of years on Rochelle salt with a view towards commercialization. It has, therefore, been necessary to produce large clear crystals in quantity. Clear, flawless half-crystals are grown up to 45 cm in length and 2 kg in weight.

The dielectric strength and insulation value of plates from such crystals is very high. Many hundreds of plates (mostly perpendicular to the *a*-axis of the crystal) have been produced and their electrical properties measured. Thus a Rochelle salt plate 4.75 mm thick shows a dielectric constant of 18,000 when tested at 15°C at 60 volts 60 cycles alternating current. The highest previously reported value which has come to the attention of the authors is about 1380.² An air condenser of area and capacity equal to that of the crystal plate would have a plate separation of only 0.00475 mm, if 1380 be taken as the crystal dielectric constant; and 0.000262 mm (0.0001") if 18,000 be taken. It is thus evident that a comparatively thin layer of cement or dehydrated Rochelle salt between the body of the crystal and the foil electrode will introduce a very large error in the determination of the dielectric constant. Any adhesive such as balsam in xylol, Japan Gold size, or beeswax dissolved in benzol with a small addition of rosin, may be used in dilute solution for attaching the foil. It is important, subsequently, to

¹ Frayne, *Phys. Rev.* **21**, 348 (1923); Isley, *Phys. Rev.* **24**, 569 (1924); Laurey and Morgan, *J. Am. Chem. Soc.* **46**, 2192-6, (1924); Pockels, *Encyklopadie der Math. Wiss.* Vol. 5, Part 2; Valasek, *Phys. Rev.* **17**, 475 (1921); **19**, 478 (1922); **20**, 639 (1922) and **24**, 560 (1924). Voigt, *Lehrbuch der Kristallphysik*, Chap. 8, Leipzig (1910).

² Valasek, *Phys. Rev.* **19**, 488 (1922).

rub down the foil very thoroughly to bring it as close to the crystal surface as possible.

A series of Braun tube oscillograms was obtained. For this purpose, and for all other results reported in this paper, a crystal plate was employed measuring about $8.5 \times 5.5 \times 0.5$ cm, cut with its plane perpendicular to the

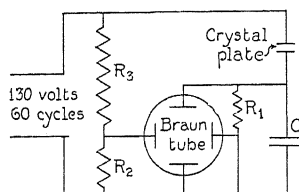


Fig. 1. Schematic connection of Braun tube. Capacity of crystal plate 0.004 to 0.2 Mf; of C 0.7 Mf. $R_1 = 0.45$ megohms; $R_2 = 3180$ ohms; $R_3 = 31800$ ohms.

a-axis, and its long edges parallel to the c-axis. All measurements and oscillograms were carried out with 60 cycle current from the power lines. All vertical deflections are on the same scale as in Fig. 2.

Fig. 1 shows the connections employed with the Braun tube for obtaining crystal oscillograms. At the left is a resistance acting as a voltage divider. To the right is the crystal plate under test, connected in series with a con-

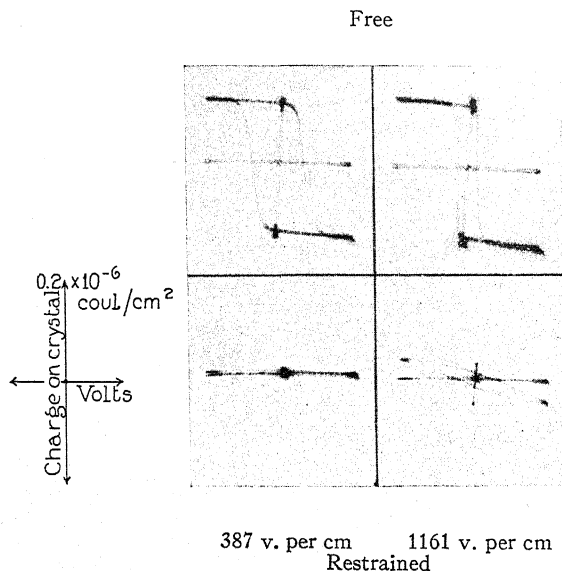


Fig. 2. Oscillograms of crystal plate, free and restrained. Temperature 15° C; frequency 60 cycles per sec.

denser giving voltages proportional to the charge on the crystal. The resulting oscillograms, such as shown in Fig. 2, have ordinates proportional to crystal charge and abscissae proportional to applied voltage.

Fig. 2 shows comparative oscillograms of a plate when entirely free, and of the same plate restrained by cementing it between two thick aluminum

plates, thus very largely precluding mechanical motion due to piezo-activity. The left-hand vertical pair is for 387 peak volts per cm; the right-hand vertical pair is for 1161 peak volts per cm. The upper pair is unrestrained; the lower pair is restrained. Dielectric constants calculated from these oscillograms show exceedingly interesting and suggestive values: from the left-hand oscillogram (restrained plate) about 430; from the left-hand oscillogram (free plate) in the saturated range about 330; from the same oscillogram for a complete cycle, excluding saturation range 10,500; and for maximum instantaneous value not less than 200,000.

Such enormous values of the dielectric constant in connection with less efficient foiling of the crystal plates, may account in part for the previously observed storage battery effect. Supplementary tests indicate that little

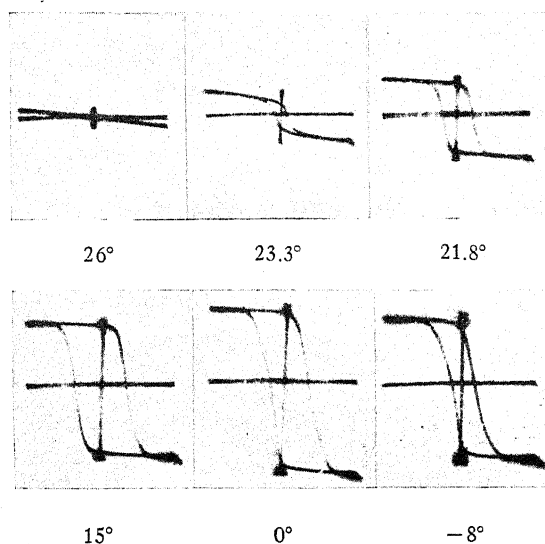


Fig. 3. Hysteresis and saturation of Rochelle salt plate II. Potential gradient in dielectric 387 (peak) volts per cm; frequency 60 cycles per sec.

change in the value of the dielectric constant is to be looked for as a result of improvement in foiling. In these supplementary tests, electrodes of saturated Rochelle salt solution were used and results did not differ significantly from those obtained from a carefully foiled plate. Moreover these large values of the dielectric constant of Rochelle salt have been observed in many hundreds of plates of various dimensions from many different crystals. Determination of the dielectric constant was usually made by applying 112 volts of 60 cycles alternating potential to the free crystal plate and noting the resulting current. In addition, circuit resonance and condenser substitution methods served to check this first method, all three giving results in substantial agreement.

Fig. 3 comprises a series of comparative oscillograms made from the same crystal plate at different temperatures as indicated. Proceeding from top

left to bottom right it is evident that as the temperature is decreased both the voltages and charges required for saturation greatly increase. So also do the areas of the hysteresis loop. Here again the method of applying the foil electrodes to the crystal is of great importance as the shape and area of the loop will vary somewhat with this factor.

All of the oscillograms were made with the greatest care. A second crystal plate gave results identical with the first. Two other plates of the same dimensions as before but with their long edges cut at 45° to the *c*-axis, showed no essential differences in the derived oscillograms. Though no special humidity precautions were observed, the resistance of the plates, at 100 volts constant potential, never fell below many megohms.

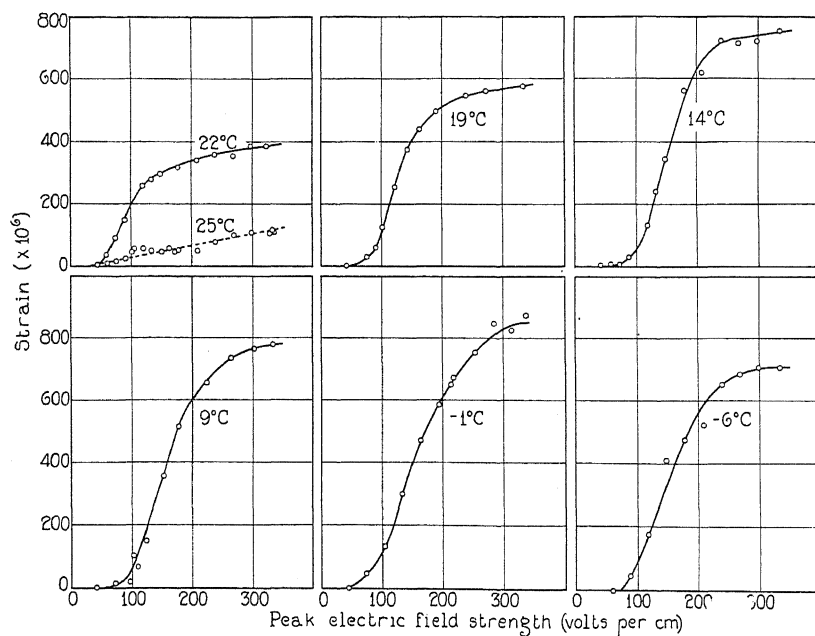


Fig. 4. Temperature variation of saturation effect and piezoelectric constant.

If a standard plate—its long edge being cut parallel to *c*-axis—is electrified with an alternating potential, it will be deformed and such deformation can be observed and measured conveniently with a microscope. For the results shown in Fig. 4, one short edge of the plate was cemented to a large lead block and various values of 60 cycle potential were applied to the electrodes. The alternating motion produced under these conditions lies in the plane of the plate and is perpendicular to the *c*-axis. The relation between total deformation and electrification is shown for various temperatures.

Saturation is again in evidence and saturation values again increase greatly with decrease in temperature. Keeping close pace with it is the voltage required to produce saturation. But it is very noteworthy that considerable voltage must be applied before the crystal shows appreciable deformation.

Fig. 5 shows the close relationship existing at different temperatures between: 1st, volts per cm required for mechanical saturation; 2nd, the energy loss per cubic centimeter per cycle; 3rd, the charge per cubic centimeter required for electrical saturation. Though not shown in this figure, these curves are followed closely by those of the voltage required for electrical saturation and of the deformation at mechanical saturation. No determina-

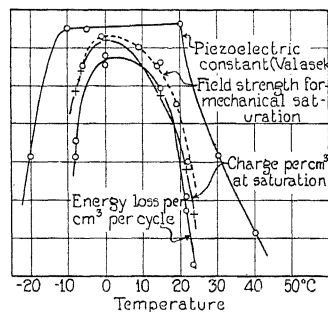


Fig. 5. Properties of Rochelle salt at various temperatures.

tions of the piezoelectric constant were made, but Valasek's³ most recent curve of the temperature variation of the piezo-electric constant is included for the sake of comparing temperature variation of this property with those of the others.

It has been the great privilege of the authors to carry on this work begun under the very able leadership of the late Charles F. Brush, Jr.

³ Valasek, Science Vol. LXV No. 1679, p. 235 (1927).

SEDIMENTATION EQUILIBRIA OF COLLOIDAL PARTICLES*

BY NORRIS JOHNSTON AND LYNN G. HOWELL**
CALIFORNIA INSTITUTE OF TECHNOLOGY, PASADENA

(Received December 9, 1929)

ABSTRACT

The purpose of this work was to find the distribution law of colloidal particles for sedimentation equilibrium in large cells, in which uniform concentrations had been observed by Burton, Porter and Laird. We took great care to eliminate effects which might prevent an equilibrium state. Gold particles prepared by the Zsigmondy nuclear method were allowed to settle several days in a quartz cell in a carefully controlled thermostat bath. The steady state was determined by taking visual ultra-microscopic counts on different days. The La Place-Perrin exponential law of distribution was found to hold as demanded by the kinetic theory.

INTRODUCTION

UNTIL recent years it seemed quite well established that colloidal particles obey in their Brownian movement and related phenomena the simple laws of the kinetic theory when no forces operate between the particles. Thus, in the early work on sedimentation equilibria with colloids in a gravitational field, Perrin¹ and Westgren² found results in agreement with the familiar La Place-Einstein distribution law, which the molecules of the atmosphere obey; namely:

$$\log n = \log n_0 - Nvg h(\rho_1 - \rho_2)/RT.$$

In this equation n is the concentration of particles at the height h above a given point of reference, n_0 is the concentration of particles at the reference point, v is the volume of a particle, ρ_1 is the density of the particles, ρ_2 is the density of the medium in which the particles are dispersed, g is the gravitational acceleration constant, R is the gas constant and T is the absolute temperature. Each of the two above-mentioned men used cells constructed of microscope slides and cover glasses, the depth of the cells used by Perrin being in general about 0.1 mm. The very careful work of Westgren, who observed through ranges as great as 1.1 mm in thin cells of presumably much greater depth than the range of observation, yielded a value of N which checks very closely the accepted value.

* This paper contains results obtained in an investigation on the La Place-Perrin Law of the Distribution of Suspensions listed as Project No. 34 of the American Petroleum Institute Research. Financial assistance in this work has been received from a research fund of the American Petroleum Institute donated by Mr. John D. Rockefeller. This fund is being administered by the Institute with the cooperation of the Central Petroleum Committee of the National Research Council.

** American Petroleum Institute Research Fellows.

¹ Perrin, "Brownian Movement and Molecular Reality," page 41.

² Westgren, *Zeits. f. Phys. Chemie* 89, 63 (1915).

However, later workers in the field of colloids noticed that the particles in larger containers often remained in suspension over long periods of time without any apparent sedimentation. This seemed to be in contradiction with the La Place-Einstein law and investigations on distributions in sols five millimeters or more in depth were carried out by Burton,³ Porter⁴ and Laird,⁵ who reported a uniform distribution throughout the greater portion of the sol. In attempts to explain such a distribution, Burton suggested the existence of electrical forces acting between the particles while Porter assumed that his sol was so concentrated that the osmotic pressure of the colloidal solution no longer followed the simple law of dilute solutions; in other words, he introduced a volume term which acts like the b in van der Waal's equation. Although Porter introduced the b term arbitrarily, he suggested that if it should have a physical significance, in order to get the requisite size he must assume a concentration of the liquid upon the particles of the suspension. Others have suggested that the apparent contradiction might be due to insufficient precautions in the eliminating of convection or insufficient time in waiting for the attainment of the equilibrium of colloids in deep cells. Kraemer⁶ has made a very illuminating discussion of the whole field, so that it is hardly necessary to present a great amount of critical detail.

At this point, it might be well to mention that Rinde⁷ has determined the equilibrium distribution of gold colloids in a high centrifugal field produced by an ultra-centrifuge. The range shown in his plot extends over a distance of more than three millimeters and although the exponential law seems to hold in a layer about 0.5 mm thick, there is a slight deviation from this law in the remainder of the distance.

Since some knowledge of the electrical nature of colloids had already been gained from the study of electrocapillary phenomena, the possibility of forces acting between colloidal particles in such a manner as to become manifest in sedimentation equilibria was of great interest. In fact, the possibility of any factor which would upset the La Place-Einstein law seemed very important for the understanding of all phenomena in which finely divided matter is in contact with liquid. Thus, it seemed worth while for us to attack the problem of sedimentation equilibria in deep cells taking great care to eliminate spurious effects, which might account for a uniform distribution, in particular to avoid convection currents in the sol, to prepare colloids with little variation in size, and to wait a sufficient time for equilibrium to be attained.

EXPERIMENTAL WORK

In our work, we used gold sols enclosed in a cell 8.3 mm in height. This cell was constructed of quartz which is much more insoluble in water than glass.

³ Burton and Bishop, *Proc. Roy. Soc. A*100, 414 (1922); Burton and Currie, *Phil. Mag.* 47, 721 (1924).

⁴ Porter and Hedges, *Phil. Mag.* 44, 641 (1922).

⁵ Laird, *Jour. Phys. Chem.* 31, 1034 (1927).

⁶ Kraemer, "Colloid Symposium Monograph," Vol. V, p. 81.

⁷ Rinde, *Diss. Upsala*, p. 200 (1928).

It is important not to pollute the sol since gold sols are quite sensitive to electrolytes as regards stability. The colloidal solution was allowed to settle undisturbed for several days inside a thermostat system which was capable of holding the temperature constant to within a few thousandths of a degree Centigrade. It was necessary that temperature gradients, which cause disturbing convection currents in the cell, be avoided. The distribution curve was then found by taking visual ultra-microscopic counts at successive levels within the cell's height. The thermostat control was so little affected by the heat from the arc and the observer during the period of observation that there was a temperature rise of only a few thousandths of a degree Centigrade. Thus, the distribution could be determined and compared on different days.

A cross section of the cylindrical quartz cell is shown in Figure 1.

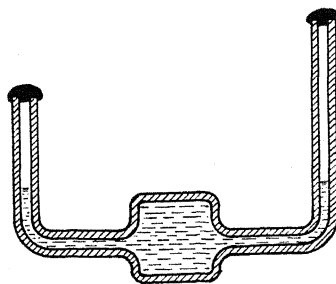


Fig. 1. Cross section of cylindrical quartz cell.

The vertical wall was made of tubing about 8 or 9 mm in inside diameter, the ends of which were ground in order that flat plates could be fused on to form the top and bottom of the cell. The two small L-shaped tubes were sealed into opposite sides of the tubing in order to make possible cleaning and filling of the cell. After the filling with colloidal solution, these side tubes were closed with sealing wax as shown in the diagram.

A great amount of effort was spent on the phase of the problem having to do with temperature control. In the final system, the cell was clamped inside a trough well insulated thermally inside the wooden case marked *C* in the photograph in Figure 2. The cell was immersed in a stream of water, pumped through the trough from a large thermostat tank whose dimensions were 16" \times 18" \times 27". The connections between the trough and the tank were made inside the insulating material shown in the lower left hand corner of the photograph. The temperature of the water in the trough was obtained by means of the Beckmann thermometer *B*. A view of the assembled apparatus is shown from the opposite side in the photograph in Figure 3, in which the tank is marked *T*. The water was kept in turbulent motion in the tank by means of a large stirring propellor which was rotated by the motor as seen in the photograph. Immersed in this tank was a thermostat regulator made of glass tubing filled with carbon tetrachloride, which has a high thermal coefficient of expansion. This regulator operated a relay to the heating element by means of a vacuum tube circuit mounted on the top of the tank near-by the

relay. With this circuit practically no current flowed through the mercury contact in the regulator.

In Figure 3 a part of the optical system can be seen mounted on the sturdy wooden frame to the left of the tank. The entire optical system was built on the heavy metal carriage *L*. The colloidal solution was illuminated by means of the carbon arc *A*, the light from which was passed through the copper chloride absorption cell *H* in order that the beam which was transmitted should have little heating effect. Next the beam was passed through a paraboloidal condensing lens, a 16 mm microscope objective and a glass window in the trough immediately in front of the cell. The beam was transmitted into the cell through the curved wall and was brought to a focus in a fairly small pencil inside the cell. Observations were made with the microscope *M* in Figure 2, suspended on the carriage directly above the cell. This microscope consisted of the vertical tube made of Bakelite for thermal insulation, an objective with a focal length of 16 mm immersed in the water of the trough, and a hyperplane eyepiece containing a scale divided into squares, one of

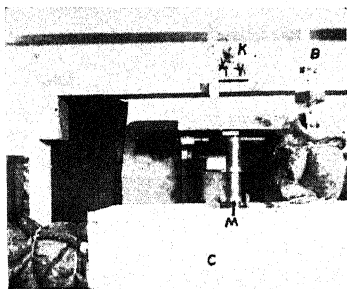


Fig. 2.

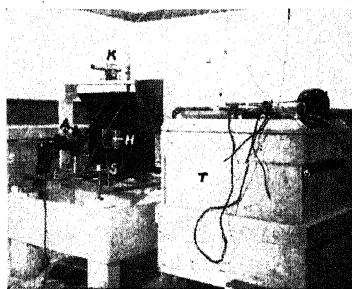


Fig. 3.

which was divided into smaller squares. The focal plane of the microscope fell within the pencil of light inside the cell and counts of the numbers of colloids inside squares could be made. Various levels in the cell could be observed by raising or lowering the entire carriage by means of four screws upon which were mounted divided heads. Two of these screws *S* can be seen in Figure 3. Large changes in height could be read from the screw-heads while small changes could be read by means of the cathetometer *K*.

Gold sols were prepared by the Zsigmondy nuclear method,⁸ which was used by Westgren and is perhaps the most highly recommended for obtaining particles closely uniform in size. The La Place-Einstein law is, of course, valid only for particles having a definite radius and a definite mass. The nuclear sol was formed by the reduction of gold chloride by phosphorus dissolved in ethyl alcohol. The nuclei were enlarged in two steps by the reduction of gold chloride upon the particles by means of hydrogen peroxide (30 percent). The sol upon which observations were made was obtained by diluting this gold sol. In this preparation, it was highly important to obtain water low in both sus-

⁸ Rinde, Diss. Upsala, p. 25 (1928).

pendent matter and electrolyte content. A special still was constructed which employed the partial condensation of steam from water treated with potassium permanganate and potassium carbonate. The steam was passed through a settling chamber and a tin condensation tube. The water was collected in a Jena glass bottle.

RESULTS

We shall show distribution curves for two different sols which contained particles approximately the same size, but were different in initial concentration. The temperature control for the more dilute sol was not as good all of the time as might have been desired. Also, one or two small bubbles were observed in the top of the cell when it was removed. However, the consistency of

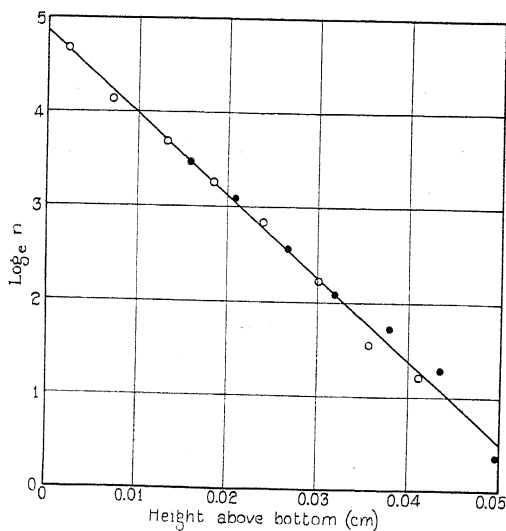


Fig. 4.

the results would indicate that no serious disturbances were set up, as one may see in Figure 4 where logarithms of concentration values are plotted as ordinates, and in Figure 5 where the same concentration values are plotted in the ordinate direction. Each of the points shown is taken from 50 counts with the exception of the two lowest points marked with circles which are taken from 25 counts. The points marked with dots were taken after about 3 days of sedimentation while the points marked with circles were taken from the same sol after about 5 days. The concentration at the end of 5 days in the upper regions was roughly one-half percent of the highest concentration observed. Such a value is even lower than the lowest point shown, so that the distribution curve lies very close to the zero axis in the upper part of the cell. This portion of the curve was somewhat higher as observed at the end of three days of sedimentation, the concentration near the top being almost as great as that shown by the lowest point plotted and also being greater than the concentration in an intermediate region. This latter would indicate that there might

have been a slight disturbance in the upper regions which was of practically no consequence in the immediate neighborhood of the bottom, where, after all, the bulk of the particles in which one is interested was located. The impor-

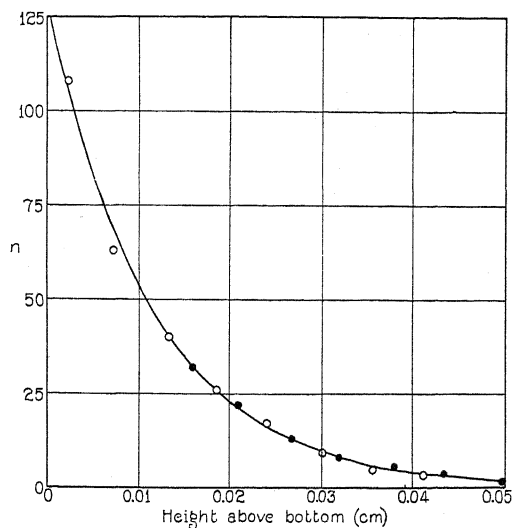


Fig. 5.

tant fact is that a steady state was reached and the distribution of the particles in this state was exponential. The slope of the curve shown in Figure 4 is 87; the temperature was 26.5°C.

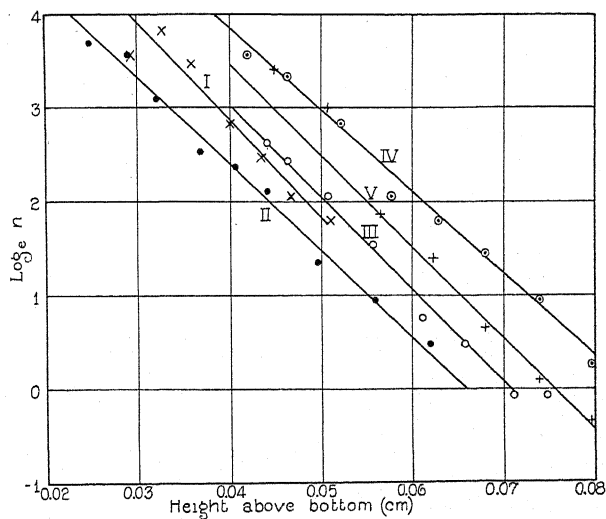


Fig. 6.

The second sol which was of higher concentration was unusually stable and the cell was allowed to remain in the thermostat for a period of about two

weeks. During the first three days of sedimentation, the two extreme temperatures observed differed by only 0.005°C , so that for long periods of time, the temperature was scarcely seen to vary on the Beckmann thermometer. The temperature was maintained at 26.5°C . Curves I to V shown in Figure 6 were obtained after sedimentation periods of 3, 5, 8, 9, and 10 days respectively. At each level marked by a point, a total of 50 counts was taken. It should be mentioned that the counts were made with quite a little difficulty due to the scattering of light near the bottom of the cell (in a large measure from the dense layer of colloids), the shifting of the light pencil due to changes of the arc, and the psychological factor attendant with such counts. However, the slopes of the curves are fairly consistent and the average is 96. The relative displacements of the curves were perhaps in a large measure due to the experimental error in locating the bottom with respect to the points, although it is not certain that actual shifts of the distribution did not occur. Certainly, it is more difficult to avoid slight disturbances in the regions observed in Figure 6 than those in Figure 4 since these regions are further removed from the damping surface at the bottom. In any case, whether the displacements were real or not, the effect was certainly of no prime importance as regards the distribution law which is seen to be exponential in character. In this solution the colloidal particles became remarkably scarce in the upper regions. On the ninth day, the concentrations observed in the main body of the sol were of the same order as those observed on the fifth day for the other sol, and thus were relatively slight since the latter sol was much the less concentrated of the two initially. This scarcity of particles is important since the distribution curve should approach the zero axis very rapidly upwards. The slight upward displacement of the experimental curve above the theoretical curve in the upper regions might be due to the lateral diffusion of particles into the cell from the side arms, the presence of particles differing in size or density from the bulk of the gold particles, and perhaps the presence of undetected slight movements of the sol.

DISCUSSION

As has been pointed out by others, it is likely that both Burton and Porter did not take sufficient precautions against disturbing convection currents. Burton and Bishop,⁹ working with copper colloids, used a large tube 94 cm long without much care in this respect. Burton and Currie,¹⁰ working with gamboge, arsenious sulphide, Bredig copper and Bredig silver colloids, repeated the work using 145 cm tubes immersed almost completely in a thermally insulated bath. They state that this bath was stirred "from time to time" and that the temperature of the room varied slowly over a range of 7°C during the period of four months of sedimentation. It is very doubtful if such conditions were satisfactory. Porter and Hedges¹¹ working with gamboge particles, fractionally centrifuged to obtain uniformity in size, reported that

⁹ Reference 3.

¹⁰ Reference 3.

¹¹ Reference 4.

although the distribution was uniform in the greater portion of their cell's height, the concentration diminished near the top as the top was approached. We, also, found a similar distribution in our early work when there were disturbing currents. In addition, however, we found an increase in concentration near the bottom. It is unfortunate that Porter did not investigate the region in the immediate neighborhood of the bottom, although it is quite surprising he found no appreciable increase in concentration in the lowest level he reached. Barkas¹² working under Porter stated that convection currents were quite a disturbing factor in his work. It is very easily seen how there could be a settling of particles in the neighborhood of a surface even though convection currents were stirring up the particles in the central portion of the sol since the frictional drag at the surface would prevent appreciable currents from being set in motion in that neighborhood. Thus one might expect to find the diminishing concentration near the top.

Then there is the phase of the problem which concerns the time necessary for sedimentation equilibrium to be attained. The theoretical work on sedimentation has been done by Mason and Weaver¹³ and Fürth.¹⁴ Weaver¹⁵ laid down the general rule that equilibrium should be attained within the time that it takes a particle to settle twice the depth of the cell according to Stokes' law. Later Fürth¹⁶ stated more rigorously that the necessary time is proportional to the cell depth when RT/NXl is large, and proportional to the square of the cell depth when this quantity is small. In this expression, which is called α by Mason and Weaver, X is the resultant gravitational force acting on the particle and l is the cell depth. Fürth estimated that it would take a number of years for equilibrium to be attained in Burton's work. As already stated, the time of sedimentation was only four months. It must be mentioned that the whole problem in Burton's case is very indefinite since he did not use particles of uniform size. As pointed out by others, since Porter does not state the length of time allowed for sedimentation, it is quite possible that he did not wait long enough for equilibrium conditions. Fürth pointed out the similarity between Porter's curve and the theoretical transient state curve. In our work, we have calculated the time necessary for a gold particle to settle twice the height of the cell for the sol of Figure 4, taking the slope of the equilibrium curve to be 87. The value of the radius obtained from the La Place-Einstein equation is 3.6×10^{-6} cm. From Stokes' law, the time of settling a distance of twice our cell depth, or 1.66 cm is 76 hours or about three days. A steady state was apparently reached in our work in about 3 to 5 days. Thus, it seems that the Weaver rule holds roughly in our case. Our value of α is 0.014.

Burton¹⁷ explained the uniform distribution curve by assuming that the colloidal particles are electrically charged and repel each other. Porter

¹² Barkas, *Trans. Far. Soc.* 21, 66 (1925).

¹³ Mason and Weaver, *Phys. Rev.* 23, 412 (1924).

¹⁴ Fürth, *Zeits. f. Phys.* 40, 351 (1927).

¹⁵ Weaver, *Phys. Rev.* 27, 499 (1926).

¹⁶ Fürth, *Zeits. f. Physik* 45, 83 (1927).

¹⁷ Burton, "The Physical Properties of Colloidal Solutions," p. 87.

criticised this theory by stating that the particles would tend to move to the walls of the containing vessel in such a case.

Burton¹⁸ also suggested that the settling of colloids may be prevented by Brownian movement and defined as the "critical radius," that radius for which the particle is displaced by Brownian movement in one second the same distance through which it would fall in one second according to Stokes' law. Particles with radii smaller than this so-called critical radius would remain in suspension without sedimentation. Now, of course, as Kraemer has pointed out, Brownian movement takes place in no favored direction and it is obvious from our results that settling did take place. The critical radius of gold is several times our radius since Burton gives 28×10^{-8} cm as the critical radius of platinum, which is heavier than gold.

Porter has suggested that his results were due to the fact that his sol was no longer dilute. His concentration of gamboge particles was of the order of 10^7 per cc. From our work, the concentration represented by the highest point plotted in Figure 5 is of the order of 4×10^8 per cc. Porter's value of concentration seems far too low to justify his assumption of a concentrated sol, especially in comparison with the concentrations used by the earlier workers.

Porter has also suggested that there are three distinctive regions in a colloidal solution: the Gibbs layer located very close to the surface, the "Perrin layer" in which the colloids are distributed exponentially in a layer a fraction of a mm in thickness near the top of the vessel, and finally "a layer of one or two millimeters' thickness (in the particular cases studied in this paper), in which a further change of concentration occurs which can not be calculated in the way adopted by Perrin." The third region is close above the principal part of the sol in which the concentration is constant. From our results, we have concluded that in the case of particles more dense than water in deep cells the particles are distributed in a "Perrin layer" extending from the bottom upwards. Whether this layer extends appreciably up through the main body of the sol should depend upon the height of the vessel, the radius and the density of the particles, and the initial concentration of the particles. Certainly if one should look for an anomaly in the distribution law due to high concentration, the logical region to investigate is that near the bottom of the cell where high concentrations may be obtained. In fact Constantin¹⁹ working with high concentrations of gamboge particles found a deviation from the exponential law in the lower portion of the range which he investigated.

In conclusion, it seems that the work on colloidal suspensions leading to a uniform distribution was very likely not free from spurious effects and that there is no change in distribution law in increasing the height of a cell. Such a conclusion is certainly in harmony with the bulk of the other work related to this phase of the study of colloidal particles.

We wish to express our gratitude to the American Petroleum Institute for the funds furnished for this research, to Dr. R. A. Millikan for his interest as director of this project, to Mr. A. A. Grubb for his aid in the experimental work and to Dr. M. E. Nordberg for constructing the quartz cells.

¹⁸ Burton, Alexander's "Colloid Chemistry," Vol. I, p. 165.

¹⁹ Constantin, Comptes Rendus 158, 1171 (1914).

LETTERS TO THE EDITOR

Prompt publication of brief reports of important discoveries in physics may be secured by addressing them to this department. Closing dates for this department are, for the first issue of the month, the twenty-eighth of the preceding month; for the second issue, the thirteenth of the month. The Board of Editors does not hold itself responsible for the opinions expressed by the correspondents.

Inhomogeneities in Crystals (A Reply)

Dr. R. H. Canfield¹ has published in a letter of the above title some objections to my theory of the mosaic structure of crystals. His arguments are based on a very serious misunderstanding of my considerations.² In order to clear up the case, I shall repeat here the general method which enabled me to find configurations of lower energy than that of the crystallographically ideal crystal. For the sake of an unambiguous illustration, I shall give the energy changes involved for the very specific case of an NaCl crystal.

Using the notations of loc. cit., we have $d_0 = 5.6\text{\AA}$ for the lattice constant of NaCl. The lattice constant of an isolated (100) plane "in equilibrium," which is not sandwiched in between other (100) planes, is $d = 0.94d_0$. The outline of my method for finding the configurations of low energy given in loc. cit. p. 818 is literally this.

" α) Contract (an arbitrary plane 100) II so that its spacing is changed from d_0 to d .

β) Fill the gaps which have been opened by α between the two remaining parts I and II of the crystal.

γ) Rearrange the relative position of I and II in a certain way."

If we disregard the polarizability of the atoms for a moment, then the process α involves an energy change $\epsilon_\alpha = \epsilon_1 + \epsilon_2$, where ϵ_1 represents the (negative) energy of contraction of the plane II under its own forces. ϵ_2 is the positive energy which has to be supplied in order to annihilate the energy of the plane II relative to the remaining parts I and II. It is easily seen that ϵ_2 if taken per cm^2 is approximately equal to $2\sigma = 300$ ergs where σ is the theoretically derived surface energy of NaCl. The value for $\epsilon_1 \cong -220$ ergs/ cm^2 may be obtained from curves published by I. E. Lennard-Jones and B. M. Dent³

for instance. It is $\epsilon_1 + \epsilon_2 > 0$ as Mr. Canfield justly remarks. Otherwise an NaCl crystal would fall apart.

The step β involves a negative energy change which is easily seen to be 12 percent of 2σ approximately. This yields $\epsilon_\beta \cong -36$ ergs/ cm^2 . The rearrangement γ in our specific case is a very simple process. Exchange all the positive ions with all the negative ions in part I of the crystal. This leaves the relative energy between I and the plane II unaltered. It involves, however, a small negative change of energy of I relative to II; namely, $\epsilon_\gamma \cong -20$ ergs/ cm^2 .

Finally, we have to consider the polarizability of the ions. In the ideal crystallographic configuration, the ions are in locations where the electric field strength is zero. The ions (e) of our II plane, however, are subjected to fields of the order of $E = 4e/d_0^2$ e.s.u. due to the rearrangement γ of the relative position of I and II. We therefore have lowered in this way, the energy of an ion in the II-plane by an amount $|\delta\epsilon_i| = \alpha E^2/2 = 8\alpha e^2/d_0^4$ where α is the polarizability of the ion. The average value of α for the couple Na^+ and Cl^- may be taken equal to that of Ne and A with sufficient accuracy. This results in $\alpha = 10^{-24} \text{ cm}^3$. We therefore obtain $\delta\epsilon_i = -1.8 \times 10^{-13}$ ergs/ cm^2 . As there are $n = 1.3 \times 10^{15}$ ions per cm^2 , we have $\epsilon_4 = n\delta\epsilon_i = -230$ ergs/ cm^2 . This value has in reality to be multiplied by a factor of the order of three, because of the fact that the ions in the two neighboring planes of II are also subjected

¹ R. H. Canfield, Phys. Rev. **35**, 114 (1930).

² F. Zwicky, Proc. Nat. Acad. Sci. **15**, 816 (1929). Will be referred to as loc. cit.

³ I. E. Lennard-Jones & B. M. Dent, Proc. Roy. Soc. A**121**, 259 (1928).

to the same high fields. In any case the, figures show conclusively that the total change in energy is $\epsilon = \epsilon_a + \epsilon_b + \epsilon_c + \epsilon_d < 0$ which verifies my general contention for the case of rock-salt.

The principle which led me to the conception of the mosaic structure might be called the *principle of the slight asymmetries in complex configuration* such as atoms, molecules, and crystals. *Indeed, due to the deformability of the atoms and molecules, nature, according to the above, definitely favors configurations which are somewhat asymmetrical.* I owe to Professor O. Stern the remark that this principle might apply to cases like $\text{H}_2\text{O} = (\text{HO}^- + \text{H}^+)$.

The trivial consideration mentioned by Mr. Canfield that under the proper circumstances, certain planes like (111) have a tendency to expand has not escaped my attention. Indeed, I have thought out its consequences long ago. One of them I have mentioned, loc. cit. p. 820, "In regard to the space groups characterizing the primary and the secondary (mosaic) structure, it must be remarked that they are not necessarily the same, etc."

In regard to the experimental evidence which we have secured so far, I can mention here only that it supports my conception of a *spacial* mosaic structure. It is not a surface

phenomenon only as Mr. Canfield seems to think. Moreover, if an indirect argument is wanted, I may mention the quantitative agreement which can be obtained on the basis of my theory with some of the important phenomena related to the *slipping strength* (not the tensile strength). For all further detailed information, I have to refer the reader to several articles by my collaborators and myself which will be published presently. A complete representation of my theory is now in preparation for the *Helvetica Physica Acta*.

Finally, I wish to make a remark in regard to the development of the theory. Mr. Canfield intimates that I had secured direct experimental (optical) evidence for the mosaic structure first, and then developed a theory "resulting in a prediction of the required phenomenon." I can only state that the exact contrary is true, inasmuch as *all* the experimental investigations at this Institute dealing with the mosaic structure have been undertaken at my suggestion to check the theoretical predictions and *all* the evidence obtained is posterior to the development of the essentials of the theory.

F. ZWICKY

Norman Bridge Laboratory of Physics,
California Institute of Technology,
Pasadena, California,
January 23, 1930.

The Effect of Dilution upon the Raman Spectra of Nitric Acid

Photographs of the Raman spectra of dilute and concentrated solutions of nitric acid in water obtained in this laboratory last May show striking differences in the frequencies of the lines scattered in the two cases. Lines which are strong in commercial 70 percent acid become weak and ultimately disappear as the acid is diluted, and other lines, weak in the concentrated acid grow strong, reach a maximum intensity and disappear as the dilution becomes infinite. In a recent note to *Nature* (124, 762 (1929)) I. R. Rao reports similar results. As Rao points out, the effect can be attributed to dissociation. The lines which are strong in the concentrated acid and which disappear upon dilution are very probably due to the HNO_3 molecule. Those which are greatly enhanced by dilution can be attributed to the NO_3^- ion.

Four infra-red frequencies, two forming a doublet, give rise to the strong scattering in

the concentrated acid, and hence may be associated with the HNO_3 molecule. They are 618, 669, 937, and 1293 cm^{-1} . One transition, at 1034 cm^{-1} , grows enormously strong with dilution, reaching its greatest strength, approximately, in mixtures of equal volumes of water and commercial acid. Rao attributes the doublet at 618 and 669 cm^{-1} (given by him as 630 and 689 cm^{-1}) to the NO_3^- ion. On the plates obtained by the author this pair behave exactly as do 937 and 1293 cm^{-1} disappearing completely in a 25 percent solution of the commercial acid. At this dilution 1034 cm^{-1} is still of high intensity. Rao reports, in addition, a Raman frequency at 3319 cm^{-1} and attributes it to the HNO_3 molecule. No such frequency was found on the present plates. The doublet transition 618 and 669 cm^{-1} which is strongly excited by the mercury line 4358 appears only feebly excited by 4046 in concentrated acid. An

interpretation of this as a singlet transition excited by the 3650 mercury line would give a scattering frequency of 3328 cm^{-1} . It is possible that this corresponds with Rao's reported 3319 cm^{-1} transition which he attributed to the HNO_3 molecule.

The variation of the intensity of the lines with dilution is clear cut and is believed to be the second optical indication of the formation of different molecular or ionic species by the dilution of strong acids. The first was obtained years ago by Pfund (*Astrophys. J.* **24**, 19 (1906)), who observed differences in the infra-red frequencies, reflected from surfaces of fuming and dilute sulphuric acid. The

effect undoubtedly affords a new probe into the processes of dissociation in solution and will be particularly useful in cases where the strong absorption of water makes the solution opaque to the infra-red. The Raman work is being extended to salts, other acids and electrolytes, and in collaboration with Professor Ellis the infra-red absorption spectra, as a function of concentration, are being studied.

E. L. KINSEY

University of California at Los Angeles,
Los Angeles, California,
January 16, 1930.

Note on Electron Scattering in Atomic and Molecular Hydrogen

The theoretical scattering formula in the paper on Electron Scattering in Atomic and Molecular Hydrogen in the *Physical Review* of September 1st, 1929, refers to the number of electrons scattered between the angles θ and $\theta+d\theta$, whereas the experimental points represent the scattering in the solid angle between θ and $\theta+d\theta$. In order to make the experimental points refer to the quantity given by the theoretical formula they must be divided by a factor proportional to the sine of θ . When this is done to the results for inelastic scattering the points are in much better agreement with the theoretical curve. But when the proper correction is applied to the results for elastic scattering the agreement with the theoretical curve is not as good as that given in the paper. The departure from

the curve at small angles is probably due to the influence of adsorbed gas on the slits of the apparatus. Some evidence of this was found during the experimental work but it was not a factor which could be accurately determined and corrected for. It would be of about the right amount to account for the observed departure at small angles. At large angles the observed scattering would differ from that predicted by the formula. The explanation of this effect is not clear, unless it is due to the scattering from molecular hydrogen. It is hoped to obtain further information on these points with an apparatus of different design.

GAYLORD P. HARNWELL

Princeton University,
January 14, 1930.

Evidence of the Presence of Element 87 in Samples of Pollucite and Lepidolite Ores

Element 87 is peculiarly well placed in the periodic table for detection by a new and very sensitive method recently reported by us. (*Phys. Rev.* **35**, 124 (1930).) We have accordingly made a search for this element in samples of pollucite and lepidolite ores supplied by the Research Laboratory of the General Electric Company, and we have consistently found minima at points of the scale which correspond to an element of the atomic weight and the valence ascribed to eka-caesium. We have studied the substance in the chloride, sulphate, nitrate and hydroxide compounds, in each case finding the minima at points of the scale characteristic of an element of the chemical equivalent of eka-caesium. Since the same element in different compounds produces its character-

istic minima of light at different points of the scale, the fact that minima are observed in each of the four compounds at the points appropriate to element 87 affords evidence of considerable weight for its presence in the sample under test. The element appears to have several isotopes, as judged by the number of its characteristic minima. The method employed is sufficiently delicate to detect less than one part of a compound in 10^{10} parts of water. The work is still in progress.

FRED ALLISON
EDGAR J. MURPHY

Department of Physics,
Alabama Polytechnic Institute,
January 11, 1930.

Voltage Intensity of $\lambda 2537$ in Mercury

In a recent paper (Phys. Rev. 34, 1352 (1929)) note was made that the curve (Fig. 3) showing the relation between the voltage of the electrons and the intensity of the radiation from mercury vapor apparently was a composite of two curves, one with a maximum at about 5.5 volts and the other with a maximum at about 5.95 volts. Since the whole radiation from the beam was focused on the photographic plate it was not possible to decide whether these two maxima are characteristic of $\lambda 2537$ alone or whether at about 5.7 volts a new radiation, possibly a molecular band, was added to $\lambda 2537$. In this connection it was thought significant that in critical potential measurements under similar conditions a critical potential at 5.7 volts is always found.

The purpose of the present letter is to present results which indicate that the curve given in the paper referred to is characteristic of $\lambda 2537$ alone, and that no light of other wave-length is responsible for the appearance of two maxima in that curve.

The light from the excitation tube was

passed through a 2.9 cm path of a solution of 1 part of glacial acetic acid to 200 parts distilled water. This cell absorbed about 95 percent or more of light of wave-length shorter than 2350A and about 75 percent of light of wave-length 2537A. This would decrease any light of wave-length less than 2350A to $\frac{1}{4}$ or less of its former relative importance. A curve was taken with the cell in place and it checked the two previous runs as closely as they checked each other. This indicated that there was no appreciable amount of light of wave-length less than 2350 affecting the photographic plate.

A spectrograph was made of a monochromatic illuminator. The slit of the illuminator was removed and the beam of light from the tube was used as a slit. A special ultra-violet plate made by the Eastman Kodak Company was used to emphasize any light in this wave-length region, but no light was found other than $\lambda 2537$.

FLOYD C. OSTENSEN

University of Minnesota,
January 20, 1930.

BOOK REVIEWS

Advanced Laboratory Practice in Electricity and Magnetism. EARLE M. TERRY. Second Edition, 1929. Pp. 318, figs. 175. McGraw-Hill Book Co., New York. Price \$3.00.

This is a second and somewhat larger edition of Professor Terry's well-known manual for use in a course which in many institutions is called "Electrical Measurements." The introduction a dozen or so years ago of the use of audiofrequency oscillatory currents into laboratory experiments and the development of very sensitive telephone receivers revolutionized the methods (and the theory) of the measurement of capacitance, and self and mutual inductance. The first edition of this book was outstanding in its use of these newer methods. In the new edition the number of experiments has been increased by about 25 percent, most of the new ones being on three-element vacuum tubes and oscillatory circuits. These new experiments have been so planned that they may be used in a course on radio communication. The extensive use of vacuum tubes in many types of physical measurements makes it desirable to give in our advanced laboratory courses experiments in this field. The same clearness that was characteristic of the presentation of both the theoretical and the experimental parts of the first edition is shown in the additions.

The manuscript for this edition was finished by Professor Terry before his death and the responsibilities connected with the publication were undertaken by Professor H. B. Wahlin, a colleague in the University of Wisconsin.

O. M. STEWART

The Electromagnetic Field. MAX MASON AND WARREN WEAVER. Pp. xiii+390. University of Chicago Press, 1929. Price \$6.00.

In his attempt not to discourage the student with lengthy analysis and fine reasoning the author of the average text on electromagnetism glosses over many delicate logical difficulties in a way that often proves very disturbing to the thoughtful reader. The authors of the present volume, on the other hand, have attempted to present the fundamentals of the classical electromagnetic theory with as great a degree of mathematical rigor as the subject permits, and have been exceptionally successful in achieving their objective. Their argument requires in many places the closest attention on the part of the reader, but any effort on his part is well repaid by the very much clearer understanding of the subject which he gains. The treatment is necessarily quite mathematical, and the close analysis of the subject which the authors have undertaken has necessitated a rather annoying recourse to subscripts and accents. The book is hardly one which can be recommended as an introductory text in electromagnetism but to the advanced student who is looking for a rigorous development and critical study of the subject it should prove invaluable.

The very elegant treatment of the difficult subject of dielectrics in electrostatic fields merits particular commendation. In so far as the potential theory aspect is concerned it leaves little to be desired. On the other hand the equally difficult subject of stresses in dielectrics and on conducting surfaces, which is perhaps more puzzling to the student than any other part of electrostatics, has hardly received an adequate presentation.

The authors make no attempt to develop the relation between electrodynamics and the special relativity theory, nor do they make any use of four-dimensional vector analysis. Instead of the significant three-dimensional vector notation of Gibbs they have preferred to use the parentheses, brackets, divs and curls which European writers generally employ. They have been careful to avoid any mention of lines of force either electric or magnetic, a procedure which can hardly be claimed to increase rigor while it deprives the reader of the aid of a convenient geometrical picture. A feature much to be commended is the placing of an introduction at the beginning of each part of each chapter and of a concluding paragraph at the end. In this way the reader is given an idea of the aim of each part before he enters upon

the analytical details and he gains from the conclusion at the end a perspective which he might otherwise miss.

The book is divided into four chapters each of which contains several parts. The titles of the chapters are "Coulomb's Law and Some Analytic Consequences," "The Electrostatic Problem for Conductors and Dielectrics," "Magnetostatics" and "The Maxwell Field Equations." In addition to the formulation of Maxwell's equations the last chapter takes up the activity equation, electromagnetic waves, retarded potentials, and the concept of electromagnetic mass. The discussion of the activity or energy equation is especially clear and searching. At the end of the book are a mathematical appendix on vector analysis, a formula index and a general index.

While the book contains much analysis the physics of the subject is by no means neglected and every difficult point is carefully and fully explained. The process of averaging in the case of a dielectric, for instance, is discussed in much detail with illustrations drawn from outside the subject of electromagnetism. The whole work gives every evidence of the most careful and painstaking preparation. It constitutes unquestionably the foremost critical study of electromagnetic theory in the English language.

LEIGH PAGE

PROCEEDINGS
OF THE
AMERICAN PHYSICAL SOCIETY

MINUTES OF THE DES MOINES MEETING, DECEMBER 30 AND 31, 1929

The Thirty-first Annual Meeting (the 161st regular meeting) of the American Physical Society was held in Des Moines, Iowa at the Hotel Fort Des Moines on Monday and Tuesday, December 30-31, 1929. The presiding officers were Professor Henry G. Gale, President of the Society, and Professor P. W. Bridgman. The average attendance was about 150.

On Tuesday morning Professor Henry G. Gale delivered the presidential address, his subject being, "The Interplay between Theory and Experiment in Modern Spectroscopy."

The annual joint session with Section B was held on Tuesday afternoon. The presiding officer was Professor Charles E. Mendenhall, Vice-President of Section B. The program consisted of the address of the Retiring Vice-President of Section B, Professor P. W. Bridgman, on the subject, "Permanent Elements in the Flux of Present Day Physics." In addition there were two invited papers, "Polarization of Matter Waves" by A. Landé, University of Tübingen (Germany), (Ohio State University 1929-1930) and "The Wave Mechanics of Collision Processes" by L. H. Thomas, University of Cambridge (England), (Ohio State University, 1929-1930).

On Monday evening, December 30, there was a dinner for the members of the Society and Section B and their friends in the Hotel Fort Des Moines, attended by seventy-five persons.

Annual Business Meeting. The regular annual business meeting of the American Physical Society was held on Tuesday afternoon, December 31, 1929 at three o'clock. A canvass of the ballots for officers resulted in elections for the year 1930 as follows:

President:	Henry G. Gale
Vice-President:	W. F. G. Swann
Secretary:	W. L. Severinghaus
Treasurer:	George B. Pegram
Members of the Council, Four	L. W. McKeehan
year term:	D. L. Webster
Members of the Board of the Physical	F. W. Loomis
Review, Three year term:	K. F. Herzfeld
	A. W. Hull

The Secretary reported that during the year there had been 261 elections to membership. The deaths of 4 members had been reported during the

year; 30 had resigned and 38 had been dropped. The membership of the Society as of December 31, 1929 was as follows: Members: 1834; Fellows: 532; Honorary Members: 6; Total Membership: 2372. The numbers are approximate because they include elections and transfers at the November and December meetings. In the year there had been a net increase of 197 members and a net increase of 12 fellows.

The Treasurer's financial report for the year 1929 was presented by the Secretary.

The Managing Editor presented the financial report for the Physical Review for the year 1929 and for the Physical Review Supplement for May 1, 1929 to November 30, 1929. The reception of the Supplement by the members of the Society and others was reported to be very gratifying. A greatly increased speed of publication of papers and letters for the Physical Review was also reported. The number of pages printed increased over last year as did also the cost per page of printing. An operating loss of approximately \$2400 in the publication of the Physical Review for 1929 was reported.

At this session the Council announced that in the week of June 16th the Society would hold a meeting at Ithaca, New York, by invitation from Cornell University. This meeting is to be of a somewhat less formal nature affording more time for discussion of the papers presented.

Meeting of the Council: At its meeting held on Monday morning, December 30, 1929, six persons were elected to fellowship, five were transferred from membership to fellowship and forty-six were elected to membership.

Elected to Fellowship: Robert d'E. Atkinson, James A. Beattie, Edward Mack Jr., Thomas H. Osgood, Hugh S. Taylor, and J. W. Williams.

Transferred from Membership to Fellowship: Gaylord P. Harnwell, Robert B. Lindsay, Harry B. Maris, Jonas B. Nathanson and E. P. T. Tyndall.

Elected to Membership: Homer G. Anderson, Soichiro Asao, Robert F. Bacher, James W. Ballard, Fred J. Beck Jr., Lowell C. Beers, Claud E. Cleeton, Howard L. Cobb, Samuel G. Cook, William F. Drea, Charles Foster, Darol K. Froman, Willard Geer, Yu Ming Hsieh, Hugh H. Hyman, Ellis A. Johnson, Matthew T. Jones, E. B. Jordan Jr., Walter H. Jordan, Louis S. Kassel, Ray W. Kenworthy, P. W. Ketchum, Jackson G. Kuhn, Frances M. Lemery, John A. Madigan, Kyuzi Matukawa, Iwao Miyake, Lawrence D. Montgomery, Herbert D. Owens, Everett R. Phelps, L. R. Philpott, Robert M. Pinkerton, Cyrus A. Poole, G. W. Presnell, W. R. Pyle, Bernhard A. Rose, Herman M. Roth, Otto Rothenstein, L. A. Sanderman, H. W. B. Skinner, Masamichi So, Roy R. Sullivan, Hisao Suzuki, Ryoza Tajime, Vernon Thornton and Tameiti Yasaki.

The regular program of the American Physical Society consisted of 32 papers. Numbers 4, 9, 16, 18, 19, 20, 22, 24, 26 and 28 were read by title. The abstracts of these papers are given in the following pages. An *Author Index* will be found at the end.

W. L. SEVERINGHAUS, *Secretary*.

ABSTRACTS

1. X-ray scattering by mixtures of organic liquids. A. WESLEY MEYER, *University of Iowa*.—The x-ray scattering curves for the following mixtures were obtained; n-ethyl alcohol—methyl cyclohexane, n-butyl alcohol—orthodimethylcyclohexane, quinoline-phenol, cyclo-hexane—tetranitromethane and phenol-water. All mixtures but the last one are totally miscible, and it is a solution with either large water content or high phenol content but is an emulsion at other concentrations, but may be dissolved by heating. The resulting curves have peaks to which Bragg's Law is applied to obtain the spacings of the molecules in the cybotactic groups. The results indicate that in every case of solution there is a single type of cybotactic group in which both kinds of molecules participate. The molecular spacing of the group is intermediate between the spacings of the pure liquids and dependent upon the number of each kind of molecule present. In the phenol-water emulsion curves, two spacings were found corresponding to those of saturate phenol water, and saturate water phenol, agreeing with the common belief that the molecules of the constituents of an emulsion do not intermingle, except in large groups, the constituents in this case being the two saturate solutions. The conclusion concerning solutions agrees with that obtained in cases of solid solutions such as alloys.

2. Dependence of viscosity in liquids upon the molecular space arrangement as shown by x-ray diffraction. R. L. EDWARDS, *Miami University* and G. W. STEWART, *University of Iowa*.—It has become possible to make a comparison between the physical condition of a liquid and its viscosity. Twenty-one octyl alcohols made under the direction of Professor E. Emmet Reid of Johns Hopkins were examined by x-rays. The "perfection" of the molecular groups were estimated by the magnitude of the secondary diffraction peaks which evidently depend upon the planar spacing of diffraction centers in the direction of the length of the molecules rather than diametrically. The coefficients of viscosity were obtained by the measurements of Professor E. C. Bingham of Lafayette College. When the OH group is in a fixed position and a methyl group of the octyl alcohol is placed in the possible positions in the molecule, the variation in the coefficient of viscosity varies in a manner similar to that of the magnitude of the secondary peak. The agreement is striking because the variations are large. The interpretation made is in accord with the obvious effects that grouping of molecules to any extent would have. The need of the incorporation of the cybotactic condition or molecular grouping in any theory of viscosity of liquids is emphasized.

3. The extent of noticeable cybotactic condition in a liquid as exhibited by triphenol-methane. G. W. STEWART, *University of Iowa*.—By means of the comparison of the chief x-ray diffraction peak of triphenolmethane in powdered crystal form with that occurring with the liquid, an approximate estimate may be made of the extent of the condition of molecular space grouping throughout the liquid. Areas of the diffraction curves were determined, the experiments being made with thicknesses of material, equal as determined by weight. It was found that the total diffracted energy in the chief diffraction peak of the first order was greater with the liquid than the crystal. Properly interpreted this means that the effective groupings of the molecules in the liquid are approximately of the same extent in the liquid as in a finely powdered crystal. Ignorance concerning the exact nature of the grouping and the structure factors prevent any quantitative comparison.

4. The structure of certain *K* series emission lines. J. VALASEK, *University of Minnesota*.—Recently, Davis and Purks have reported several new satellites near the $K\alpha_1$ and α_2 emission lines of Ni, Cu, and Mo, and $K\beta_1$ of Mo, using a double-crystal spectrometer. The writer has attempted to confirm these results in Siegbahn's laboratory, using a new single-crystal spectrometer designed by Siegbahn. With the slit 0.03 mm wide and the plate at 3 meters, the resolving power in the first order was equal to that of the double-crystal spectrometer in the first order. According to the curves given by Purks, some of the satellites should be perceptible in the first order. Microphotograms were made of the following lines: $K\alpha_1$ and α_2 of Cu, Mo, and Ag, and $K\beta_1$ of Mo. No satellites were found. Lack of time prevented observations in the second order.

5. Fine structure in K x-ray absorption spectra. BEN KIEVIT, JR. and GEO. A. LINDSAY *University of Michigan*.—The K x-ray absorption spectra of the free elements Ca, Cr, Mn, Co, Ni, Cu and Zn have been photographed and for each of these elements an extended fine structure has been obtained. This fine structure, consisting of six or seven secondary edges, extends over an energy range of some 200 volts. In every instance the element was used as the absorbing screen except in the case of manganese where it was present in the alloy manganin. Indications are that the alloy screen gives the same result as the element alone. A KCl crystal served as reflector to obtain the spectra. Additional exposures were made with copper and with zinc, using the [111] face of calcite as reflector in order to increase the dispersion in this region of shorter wave-lengths. An attempt is made to account for the observed phenomenon on the basis of multiple ionization. The atom absorbs energy sufficient to remove a K electron to the first permissible unoccupied orbit and also to eject an outer electron. One is led to the conclusion that probably similar fine structure might be obtained for all elements under suitable conditions.

6. The intensity of reflection of the $K\alpha$ line of carbon from a quartz surface. ELMER DERSHEM and MARCEL SCHEIN, *University of Chicago*.—The $K\alpha$ line of carbon ($\lambda=44.6\text{\AA}$) was reflected from a polished quartz surface and the intensity of the reflected radiation measured for glancing angles of incidence between $1^\circ 15'$ and 8° . The apparatus and methods have been previously described (Phys. Rev. 34, 1015 (1929)). The curve obtained by plotting the experimental values of reflected intensity against glancing angle of incidence is compared with various curves computed from the theoretical value of the index of refraction given by the Drude-Lorentz dispersion formula and values of the absorption coefficient obtained by the extension to this long wave-length region of various well-known empirical formulas relating to x-ray absorption. A calculated curve which is in good agreement with the experimental curve may be secured by the use of a mean of the values of the absorption coefficient for this wave-length in quartz which are given by the different empirical formulas.

7. An x-ray search for the origin of ferro-magnetism. J. C. STEARNS, *University of Denver*.—A sensitive null method, employing two crystals and two ionization chambers, was used to detect any change in the intensity of the Molybdenum $K\alpha$ reflected from a magnetic crystal when this crystal was magnetized. This method was capable of detecting from 1.0 to 0.1 percent change in the intensity, according to the intensity of the reflected beam. Crystals of magnetite and silicon were used. The change in the intensity of the x-ray beam was computed on the basis of the alteration of the structure factor due to the orientation of the electronic orbits by the magnetic field. The experimental results indicate that there is no change in the reflecting power of crystals of magnetite or silicon steel due to magnetization. It is concluded that electrons revolving in inner orbits within the atom cannot account for ferro-magnetism. On the basis of present atomic models and present experimental evidence it appears that the ultimate magnet should be identified with the spinning electron.

8. Magnetic properties of thin films of cobalt. E. P. T. TYNDALL and W. W. WERTZBAUGHER, *University of Iowa*.—The films are deposited electrolytically on brass tubes from a 3% solution of cobalt ammonium sulphate with the addition of boric acid. The magnetic properties are largely dependent on the amount of boric acid present in the solution. Films deposited from solutions nearly saturated with boric acid show almost complete magnetic saturation at $H=200$ gauss ($I_{\max}=1300$ c.g.s. units) and have very high remanence, about 98% of the maximum intensity of magnetization. The reciprocal of the coercive force is roughly proportional to the film thickness for films from 30 to 130 $m\mu$ thick, in approximate agreement with the relation previously found for iron (Phys. Rev. 30, 681 (1927)). Films from less acid solutions depart considerably from this relation. The properties of the films are undoubtedly partly due to occluded hydrogen, the effect of which is at present being investigated by heating the films.

9. Will the magnetic pole vanish? F. W. WARBURTON, *University of Oklahoma*.—By considering the parallel plate condenser and the long solenoid as sources of uniform electric

and magnetic fields respectively, the physical picture of the behavior of dielectrics and of magnetic media (in terms of displacement charge and of the equivalent magnetization current appearing at the respective surfaces) is very evident. The picture is simple and obviates the need of defining and using the fictitious magnetic unit pole even in elementary presentations. E , like B , is dependent on the medium, while D and H are the fields when dielectrics and magnetic media are absent. Non-uniform fields may be considered by the superposition of simpler cases. Were the charge on a condenser rather than the potential difference maintained constant a potential $V' = \int D ds$ would be useful as well as the ordinary potential $V = \int E ds$. Somewhat similarly a scalar magnetic potential $\phi' = \int H ds$, related to ampere-turns, is rather more useful than $\phi = \int B ds$, because it is the current in the solenoid and therefore H , not B , that is externally controlled. H and B can be derived from the corresponding vector potentials, A' and A .

10. Reflection of zinc atoms from NaCl crystals. HAROLD A. ZAHL, *University of Iowa*.—Zinc atoms issuing from a boiler at a temperature of 600°C are in part specularly reflected from a clean cleavage surface of a rock-salt crystal. Measurements, by means of a rotating sector disc-velocity-filter, of the velocity of the specularly reflected beam show that it contains atoms of but one velocity (or at least a very limited range of velocities). This velocity varies with the angle of incidence as shown below.

θ	vel(m/sec)			Average	$\phi \times 10^{14}$
22.5	763	736	761	753	4.4
45.0	666	672	683	674	12.1
67.5	712	689	695	699	22.2

An equation of the form $\lambda = h/mv = 2d(1 - 2\phi/mv^2 - \cos^2\theta)^{1/2}$ will not represent these results if ϕ is a constant. If it is assumed that ϕ varies with the angle of incidence then of course the equation may be made to fit. Values of ϕ calculated on this assumption are given in the table.

11. Specular reflection of atoms from crystals. A. ELLETT, *University of Iowa*.—The existence of specularly reflected nearly monochromatic beams of atoms and the behavior of these beams on reflection from two crystals in succession (Phys. Rev. **34**, 493, (1929)) is most readily understood as a wave or diffraction phenomenon. Neither the previous observations on cadmium nor those just reported on zinc can be represented by the equation $\lambda = h/mv = 2d(1 - 2\phi/mv^2 - \cos^2\theta)^{1/2}$ if ϕ is supposed to be constant. If it is assumed that ϕ varies with the angle of incidence and this equation used to calculate the appropriate values, we find

θ	22.5°	45°	67.5°
$\phi_m \times 10^{14}$	4.4	12.1	22.2
$\phi_{cd} \times 10^{14}$	4.84	13.2	19.6

The fact that the values obtained run roughly parallel may be significant. These values of ϕ correspond to the existence of a repulsive force acting upon the impinging atom and to values of the refractive index for phase waves $\mu = [1 - 2\phi/(mv^2)]^{1/2}$ less than unity. Both Davisson and Germer and Farnsworth have reported dispersion of the refractive index for electron waves, but the range of variation is much less than that found here.

12. Secondary electrons from contaminated metal surfaces. PAUL L. COPELAND, *University of Iowa*.—Small quantities of grease, or gases, or foreign metal upon a metallic surface have in the past been the cause of many spurious electrical effects. Stuhlmann and Compton cite a spurious contact potential difference of some 60 volts. Using electron reflection as a tool some of the properties of such surfaces have been investigated. The presence of surface impurities on a tungsten wire greatly increases reflection or secondary emission when electrons strike the filament. Surface fields are set up retarding the reflected electron; in some cases the film actually is an insulating layer which breaks down under a potential difference of some 50 volts, which may account for the results of Stuhlmann and Compton.

13. Electron energy losses in mercury vapor. CASTLE W. FOARD, *State University of Iowa*.—An improved magnetic spectrum method was used to determine the energy losses

sustained by slow speed electrons in mercury vapor. Electron energies up to 60 volts were used, the main region of interest being from 0 to 25 volts. The energy losses detected, below that required for ionization, were; 4.9, 5.4, 6.7, 7.7, 8.8, 9.8 volts. These correspond to practically all the transitions of a valence electron from the basic 1S level up to each of the higher levels to 4P. No evidence of other losses such as are observed by the photoelectric method was found. At voltages above 10.4, the ionization potential, electrons seem to be able to give up any quantity of energy in excess of that required for ionization, the higher losses being favored. A very interesting loss of 11.07 volts has been found, which has not been recorded heretofore. It begins to be resolved at about 18 volts, and grows steadily with increasing voltage in much the same manner as the 6.7 volts loss. It is thought that this loss involves the displacement of both valence electrons from their normal levels.

14. On the electric arc drawn in vacuum. RAGNAR TANBERG, *Westinghouse Elect. Mfg. Co.* (Introduced by J. Slepian).—In an electric arc drawn in vacuum, the cathode only contributes vapor to the maintenance of the arc, if the arc is of sufficiently short duration. The speed of the vapor emitted from the cathode spot is of the order of 15×10^5 cm/sec. and the temperature calculated from this molecular velocity is of the order of 500,000°K. Low voltage and high voltage vacuum arc forms have been observed, depending upon the location of the cathode spot relative to the anode. The low-voltage form appears when the cathode spot is so located as to discharge the cathode vapor into the arc stream. The highly ionized cathode vapor in this case prevents the development of negative space charges which otherwise would build up. The high voltage form appears when the path of the cathode vapor does not coincide with the arc stream. Motion of the arc in a transverse magnetic field between solid metal electrodes in a direction opposite to that which would be expected from ordinary electrodynamic considerations has been observed and explained by the bending of their path by the magnetic field and subsequent impingement on the cathode surface of some of the positive ions in the cathode vapor.

15. Voltage-intensity relations of the cadmium spectra. DEVER COLSON, *University of Iowa*.—The critical potentials for different spectrum lines are given by spectrum analysis. Qualitative observations of these critical potentials have been made by Ruark and Chenault and Esclanton and have been used for the differentiation of the different orders of the spark spectra of cadmium. The present work gives more exactly the critical potentials of the more prominent arc and spark lines and traces their behavior as a function of the energy of the impacting electron. The existence of 2^3D orbits suggested but not adopted by Von Salis is indicated.

16. Absorption of light by flames containing sodium. C. D. CHILD, *Colgate University*.—The intensity of sodium light from a series of flames into which a saturated solution of sodium chloride is sprayed was found to vary approximately as the square root of the number of flames. As the amount of sodium in the flames is diminished the ratio between the light from several flames and that from one becomes greater. These observations may be explained by assuming; first, that the number of sodium atoms in the flame which are able to emit light in a given direction or to absorb light going in that direction is very much less than the total number of sodium atoms in the flame and secondly that even this limited number is greatly diminished by the process of absorbing sodium light which is going in the direction considered. A possible explanation for these assumptions is that atoms emit light in a direction which bears a definite relation to the orientation of the atom at the time it is emitting the light and absorbs only light which is going in the same direction.

17. The use of homogeneous coordinates in physics and chemistry. HERBERT J. BRENNEN, *Northwestern University*.—It is shown that homogeneous coordinates can be advantageously used in the following cases: 1. A generalisation of the third law of thermodynamics. 2. Equations of state. 3. A generalisation of the phase rule to take account of the change of vapor pressure of a substance, at constant temperature, with the size of the particle. In order to take account of the change of vapor pressure of a substance at constant temperature with the

total pressure on the system, the phase rule may be still further generalised by the introduction of a new coordinate the total pressure on the system. 4. The restricted theory of relativity where the four planes are: $X=0$, $Y=0$, $Z=0$ and $\mathcal{G}=0$, where \mathcal{G} is the product of the velocity of light and the time. 5. The general theory of relativity where we have four surfaces analogous to the four planes in the restricted theory. Hence, by the use of homogeneous coordinates, four dimensional relativity becomes a problem in a space of three dimensions.

18. Zodiacal light and magnetic storms. E. O. HULBURT, *Naval Research Laboratory*.—From April, 1853, to April, 1855, Rev. George Jones, U. S. N., observed the zodiacal light every night, weather and other things permitting. A comparison of his record with the Greenwich magnetic storm list gave the following results: In this period there were 26 magnetic storms, or storm groups, and 23 periods of abnormal zodiacal light, 16 of which followed within 3 days after a magnetic storm. 10 storms occurred on dates for which there were no zodiacal light observations, and there were 7 cases of abnormal zodiacal light with no accompanying magnetic storms listed. The abnormalities in the light were mainly fluctuations, and sometimes an unusual brilliance or distribution in the heavens. The correspondence between zodiacal light behavior and magnetic disturbance indicates, but does not prove, that the light comes from particles originating from the terrestrial atmosphere, in accord with the views of Barnard and others. It seems possible to sketch out a qualitative theory by considering the behavior of the high flying terrestrial ions under the influence of gravitation, light pressure and the terrestrial magnetic field.

19. Changes in the ozone concentration of the atmosphere. RICHARD RUEDY, *Toronto*.—An ozone layer equivalent to 3 mm being situated in the atmosphere above altitude 40 km, that is being contained in a column equivalent to not more than 100 m of air at sea-level, corresponds to a volume percentage of 10^{-3} to 10^{-4} , a value agreeing roughly with that calculated from Nernst's theorem for thermal equilibrium at 6000° . At concentrations of this order, the natural thermal decomposition of O_3 cannot be neglected as has been proposed, when explaining the decrease of O_3 towards the equator. It becomes also apparent in cyclonic, or anti-cyclonic, conditions, owing to the heat radiated to, or from, the troposphere. During the "ultra-violet outburst's" of the sun, as proposed for explaining auroras and magnetic storms, the ozone-building radiations could reach 6 times, the destructive radiations but 1.2 times their stationary values. The daily measurements recently made at Arosa, Marseille, Oxford, etc. do not exhibit an increase in O_3 for the few days preceding or following the strongest magnetic storms. (October 15, 1926, July 7/8, and October 18, 1928). If the outburst lasted only for one-half hour, the increase would have been smaller than the error of observation (0.01 cm); on the other hand, increases by 0.04 cm are observed in the absence of magnetic storms.

20. Electrodynamical damping in pulsating stars. ROSS GUNN, *Naval Research Laboratory, Washington, D. C.*—Small radial pulsations of stars are shown to be highly damped by electrodynamic forces when the star has a magnetic field. The author's theory of the permanent magnetic field of the sun indicates that the field is produced by regenerative means which is triggered off by a small initial field. The small initial field probably arises from the rotation of the star combined with a separation of charge, although it may conceivably arise in other ways. Thus rotating stars will have a magnetic field and cannot pulsate, and conversely stars which pulsate have no magnetic field and do not rotate. Cepheid variables are observed to pulsate and therefore have no magnetic field and do not rotate. This is in keeping with the idea that Cepheid variables, being youthful giants, are so large that they would be unstable under rotation. These considerations appear to remove the difficulties encountered by Eddington in his detailed theory of star pulsations.

21. The analysis of cosmic-ray observations. LE ROY D. WELD, *Coe College*.—Millikan and Cameron find evidence of several distinct absorption coefficients for the cosmic rays in deep lakes, suggesting a spectrum of definite wave-lengths. In this paper, a general method of least-square adjustment of non-linear observation equations is adapted to the analysis of the cosmic-ray absorption curve, in order to determine the most probable values of the two constants for each component of the radiation.

22. Mass-weight ratio of metals under strain. P. I. WOLD, *Union College*.—The late Dr. Charles F. Brush conducted work for years on the mass-weight ratio of metals. One of his methods of experimentation consisted in weighing certain alloys while they were subjected to very considerable pressure. He found losses in weight amounting to as much as one part in 40,000. Measurements have been carried on for the last two years on alloy specimens, which he had prepared, to see if independent observers could reproduce his results. On such specimens changes amounting to about one part in 150,000 were obtained. The curves of weight against pressure show the same characteristics as obtained by Dr. Brush. While the changes are small, they are substantially larger than can be ascribed to the errors of the balance or to temperature changes.

23. The surface tension of molten glass at temperatures near the melting point. W. B. PIETENPOL AND H. H. SCOTT, *University of Colorado*.—A new method has been devised by which the surface tensions of a number of glasses of different composition have been determined throughout a range of temperature of approximately 200°C. just above the softening points. The method is termed "The Bulb Method" and is similar to the soap bubble experiment in which the excess of pressure within the bubble can be balanced against a small head of liquid in a manometer. It was found that the weight of the glass bulb needed to be considered and a formula is developed giving the relation between surface tension and pressure in which the correction factor is introduced. Throughout the range to which the method is applicable, it is found that the surface tension of glass varies but slightly with temperature. The magnitude of the surface tension for different glasses is of the order of 250 to 350 dynes per cm.

24. Thermal expansion of lead. PETER HIDNERT AND W. T. SWEENEY, *Bureau of Standards*.—Data by Hidnert and Sweeney on the linear thermal expansion of one sample of cast lead and various lead-antimony alloys between 20 and 60°C were published in 1924 by Vinal, "Storage Batteries." Since then additional determinations were made on three samples of cast lead over various temperature ranges between 20 and 300°C. The following results were obtained:

Sample ¹	Lead content Percent	Average coefficients of linear expansion per Degree Centigrade				Difference in length before and after Expansion test Percent
		20 to 60°C. $\times 10^{-6}$	20 to 100°C. $\times 10^{-6}$	20 to 200°C. $\times 10^{-6}$	20 to 300°C. $\times 10^{-6}$	
1215 ²	99.8	{ 29.0	28.9	29.7	30.9	−0.01
		—	28.8	29.4	31.0	.00
1144	99.9	28.3	28.6	29.5	31.2	.00
1001 ³	—	29.2	29.6	31.2	32.5	+ .02

¹ Samples 1215 and 1144 were cast in sand molds, and sample 1001 in a pre-heated steel mold.

² Values given on second horizontal line were obtained on a second test.

³ Sample 1001 cast from same ingot as sample 1215.

The differences obtained in the coefficients of expansion are evidently due to variations in the methods of casting.

25. Two different types of association of alcohol molecules in the liquid state. G. W. STEWART, *University of Iowa*.—By x-ray diffraction studies of liquid alcohols, including twenty-one octyl alcohols, eleven primary n-alcohols, and nine additional isomers of primary normal alcohols, evidence is obtained of two types of association of molecules. When the OH group is attached to the terminal carbon atom or the one adjacent thereto, the molecules are associated primarily in pairs with the OH group adjoining and the median lines of two chains in the same line. At the same time there is a more or less orderly lateral arrangement of these pairs of OH groups. When the OH group is attached to any other carbon atom in the chain, then the double molecules disappear and the association is side by side. There is no exception to these conclusions in the liquids studied.

26. On the theory of the solar corona. E. O. HULBURT, *Naval Research Laboratory*.—The outer atmosphere of the sun is assumed to be composed mainly of charged particles, which are actuated by gravitation, radiation pressure and the magnetic field of the sun. By distillation along the lines of magnetic force the particles collect in the lower latitudes of the solar outer atmosphere and by their diamagnetism and drift currents reduce the magnetic field approximately to zero in this region, leaving a stray field at the poles. Thus the coronal streamers, prominent during sun-spot minima, are regarded as owing their form to the magnetic field of the sun. Whereas the wide-spreading structureless coronal luminosity expending out from the lower latitudes is due to an accumulation of ionization which reduces the magnetic field to a low value and permits the radiation to blow the particles out to great distances. During maximum solar activity there is sufficient ionization of the outer atmosphere to reduce the magnetic field to a low value even at the poles, and hence the outer atmospheric spray extends roughly equally in all directions, in accord with the appearance of the corona.

27. Resistance of an electrolytic conductor at various frequencies. D. E. RICHARDSON, *University of Chicago*. (Introduced by J. Barton Hoag.)—The resistance of a conductor, as defined by the ratio of electrical energy converted into heat and the square of the current, is a function of the frequency of the current because of the non-uniform current density throughout the cross-section of the conductor. Classical electrical theory offers an equation for this skin effect. This has been verified for metallic conductors for frequencies up to one megacycle. Using a calorimetric method, the equation is now verified in a particular case of electrolytic conduction (30% solution of H_2SO_4) for frequencies up to eight megacycles (37 m). It is concluded that the resistivity of this electrolytic conductor is independent of the frequency up to eight megacycles, since this assumption was made in the derivation of the equation. Measurements of the currents were made by comparing photometrically the intensities of two filaments, one carrying the high frequency currents, the other direct current.

28. Change of spacing of positive column striations with temperature. F. M. SPARKS AND CHAS. T. KNIPP, *University of Illinois*. Cassen (Phil. Mag. 268, 948 (1926)) predicts that the separation of the striations in the positive column of a discharge tube should increase almost linearly with the absolute temperature. A discharge tube was heated in a liquid bath, the temperature range being from room temperature to 165°C . Hydrogen was used in the tube, but only the blue striations, due to impure hydrogen (Handbuch der Physik, vol. 14, p. 298) were obtained. To detect any temperature lag or any change in the characteristics of the gas the separations were noted with both increasing and decreasing temperature. The resulting curves showed no appreciable lag. Cassen's prediction is verified for the wide striations, at pressures around 1 mm Hg, but for the narrow striations, above 1.5 mm, the separation decreases with increasing temperature. However, the separation, in general, reaches a minimum value, and then begins to increase with increasing temperature. A series of temperature-separation curves were plotted for hydrogen at 2.5 mm, using three different values of current, after successive additions of impurity. The general shape of the curves remained the same, but were shifted to smaller values of separation, reaching a minimum, and then were shifted back to greater values.

29. A glass window mounting for withstanding pressures of 30,000 atmospheres. THOS. C. POULTER, *Iowa Wesleyan College*. The range in the field of optical study at high pressures has been extended from approximately 4,000 atmospheres to 30,000 atmospheres or even higher by the development of a window mounting that will withstand these higher pressures. This window mounting consists of a piece of glass 12 mm in diameter and 8 mm in thickness and having one of its flat surfaces placed over a 6 mm hole in a polished surface of hardened "high speed" steel disk. No gasket material is used between the steel and the glass. Since the flowing of the gasket material under pressure was the main source of unequal strains in the windows causing them to break, the piece of "high speed" steel is held in place by means of a large screw which in turn carries another window similarly mounted so as to catch flying materials in case the first window shatters.

30. Magnetostriction measurements using a heterodyne beat method. A. B. BRYAN AND C. W. HEAPS, *The Rice Institute*. Two circuits oscillating with radio frequency produce a beat note which is itself made to beat slowly with a tuning fork. A photographic record of this slow beat is obtained on a moving photographic film. A parallel plate condenser in one of the oscillating circuits has its capacity changed by the magnetostriction of a nickel wire supporting one of the plates. From the photographic record the magnetostriction can be accurately determined. A search coil around the nickel wire picks up Barkhausen discontinuities which are then amplified and recorded on the film simultaneously with the magnetostriction effect and a time scale. Indications are that a Barkhausen discontinuity is accompanied by a sudden change in the length of the nickel wire. The apparatus detects a length change of about 10^{-7} cm in the length of the wire and can be used for a very rapid cycle of magnetization. Magnetostrictive hysteresis is to be investigated in different materials.

31. Diffraction of molecules. OTTO STERN, *Hamburg University*. (Introduced by W. L. Severinghaus.)

32. Deflection of hydrogen positive rays by calcite. A. J. DEMPSTER, *University of Chicago*. A series of photographs of the reflection patterns of hydrogen canal rays from a calcite crystal has been obtained with different angles of incidence showing a gradual alteration in the pattern with angle. Patterns have been obtained from three different calcite crystals. A charging up of the surface was observed in one case, as shown by the deflection of the negative ions in the canal ray beam. The amount of the deflection is of the order of magnitude required by the first of the Laue equations, $a(\alpha - \alpha_0) = \lambda$, if $\lambda = 0.0017\text{\AA}$, as given by the de Broglie formula. The lines in the patterns in many cases form arcs of circles passing through the center. This suggests the reflection of the rays at the planes belonging to various zones as found with x-rays in Laue spot photographs. The angles at which reflection occurs when small are influenced very greatly by any surface energy or change of refractive index, even if very small. Radiation is excited in the calcite by the impact of the canal rays, which issues outside of a critical angle of approximately 0.01 radian with the surface. The refractive index deduced agrees with that of radiation of the wave-length of the $K\alpha$ calcium line.

AUTHOR INDEX

- | | |
|--|--|
| Brennen, Herbert J.—No. 17 | Pietenpol, W. B. and H. H. Scott—No. 23 |
| Bryan, A. B. and C. W. Heaps—No. 30 | Poulter, Thomas C.—No. 29 |
| Child, C. D.—No. 16 | Richardson, D. E.—No. 27 |
| Copeland, Paul L.—No. 12 | Ruedy, Richard—No. 19 |
| Colson, DeVere—No. 15 | Schein, Marcel—see Dershem |
| Dempster, A. J.—No. 32 | Scott, H. H.—see Pietenpol |
| Dershem, Elmer and Marcel Schein—No. 6 | Sparks, F. M. and C. T. Knipp—No. 28 |
| Edwards, R. L. and G. W. Stewart—No. 2 | Stearns, J. C.—No. 7 |
| Ellett, A.—No. 11 | Stern, Otto—No. 31 |
| Foard, Castle W.—No. 13 | Stewart, G. W.—Nos. 3, 25 |
| Gunn, Ross—No. 20 | ——— see Edwards |
| Heaps, C. W.—see Bryan | Sweeney, W. T.—see Hidnert |
| Hidnert, Peter and W. T. Sweeney—No. 24 | Tanberg, Ragnar—No. 14 |
| Hulburt, E. O.—Nos. 18, 26 | Tyndall, E. P. T. and W. W. Wertzbaugher—No. 8 |
| Kieviet, Ben Jr. and Geo. A. Lindsay—No. 5 | Valasek, J.—No. 4 |
| Knipp, C. T.—see Sparks | Warburton, F. W.—No. 9 |
| Lindsay, Geo. A.—see Kieviet | Weld, LeRoy D.—No. 21 |
| Meyer, A. Wesley—No. 1 | Wertzbaugher, W. W.—see Tyndall |
| | Wold, P. I.—No. 22 |
| | Zahl, Harold A.—No. 10 |

THE PHYSICAL REVIEW

SODIUM AND MAGNESIUM SPARK LINES IN THE FAR ULTRA-VIOLET, AND THE QUANTITATIVE APPLICA- TION OF THE IRREGULAR DOUBLET LAW TO ISOELECTRONIC SEQUENCES

BY J. E. MACK¹ AND R. A. SAWYER
UNIVERSITY OF MINNESOTA AND UNIVERSITY OF MICHIGAN

(Received January 13, 1930)

ABSTRACT

New levels in Na III, Mg IV, and Mg V are identified through the transition $2s \leftarrow 2p$. The value of the negative term $2s2p^5\ ^3P$ of O I is predicted.

The relativistic screening number $\sigma_2(L_{21}L_{22})$, is 3.19 for $Z=10, 11$ compared with the value 3.49 for heavier atoms, usually considered independent of Z . The difference is probably due to outer screening.

Wentzel's result $\sigma_1(n, l+1) - \sigma_1(n, l) = 0.58 \cdot 2'n$ for the first order screening number σ_1 in x-rays is applied instead of the usual qualitative form of the irregular doublet law to determine the rate of dependence of the transition energy $2s^22p^5 \leftarrow 2s2p^6$ upon Z in the fluorine-like isoelectronic sequence. The extremely high result, $49 \cdot 10^3 \text{cm}^{-1}$, is verified by the new Na III and Mg IV data. Certain regularities in the curves showing the rates of dependence of the irregular doublet transition frequencies upon the atomic number in isoelectronic sequences, as functions of the number of electrons present, may be used for interpolation of these rates.

SEVERAL new lines and some old ones, due to the transition $2s \leftarrow 2p$ in the spark spectra of sodium and magnesium, have been photographed with the University of Michigan's one meter vacuum spectrograph and classified.²

Due to the necessity of breaking down the rare gas shell $2p^6$, the several times ionized atoms in this part of the periodic table require more energy for excitation than any others of the same stage of ionization except those isoelectronic with helium and hydrogen. Attempts to obtain the lines of Na IV and Al IV and extend the scheme of Mg III have been thus far unsuccessful. The failure to obtain the PP^o group of Na IV expected at $244 \cdot 10^3 \text{cm}^{-1}$, in the face of the success with Mg V, may be attributed to the inconvenient physical properties of sodium. We had to insert the sodium as a

¹ National Research Fellow.

² We are indebted to Messrs. R. F. Bacher and G. R. Miller for aid in the photographic work.

TABLE I. Lines and new levels in sodium and magnesium.

SODIUM					
Lines			New Levels ($\cdot 10 \text{ cm}^{-1}$)		
(Bowen)	Int λ	Int λ ν ($\cdot 10 \text{ cm}^{-1}$)	Assignment	Na III	
2 372.04	3	372.16	$2s^2 2p^6 \text{ } ^1S_0 - 2s^2 p^5 3s \text{ } ^1P_1^{\circ}$		0
1 376.34	2	376.63	$1S_0 - \text{ } ^3P_1^{\circ}$		138
	1	378.34	$2s^2 2p^5 \text{ } ^2P_{1/2}^{\circ} - 2s^2 p^6 \text{ } ^2S_{1/2}$		26431
	1	380.33	$2P_{1/2}^{\circ} - \text{ } ^2S_{1/2}$		
MAGNESIUM					
Lines			New Levels ($\cdot 10 \text{ cm}^{-1}$)		
(Mil. Bow.)	Int λ	Int λ ν ($\cdot 10 \text{ cm}^{-1}$)	Assignment	Mg IV	
2 231.6	2	231.71	$2s^2 2p^6 \text{ } ^1S_0 - 2s^2 p^5 3s \text{ } ^1P_1^{\circ}$		0
	1	234.25	$1S_0 - \text{ } ^3P_1^{\circ}$		221
	1	276.28	$2s^2 2p^5 \text{ } ^2P_{1/2}^{\circ} - 2s^2 p^6 \text{ } ^2S_{1/2}$		31162
5 320.9	1	320.90	$2P_{1/2}^{\circ} - \text{ } ^2S_{1/2}$		
4 323.2	2	323.20	$2s^2 2p^5 \text{ } ^2P_{3/2}^{\circ} - 2s^2 p^6 \text{ } ^2S_{1/2}$		0
	0	338.48	$2P_{3/2}^{\circ} - \text{ } ^2S_{1/2}$		161
	1	349.07	$2s^2 2p^4 \text{ } ^3P_2 - 2s^2 p^5 \text{ } ^3P_2^{\circ}$		254
	1	351.03	$3P_1 - \text{ } ^3P_0^{\circ}$		28326
	1	352.13	$3P_1 - \text{ } ^3P_1^{\circ}$		28507
0 352.9	2	353.03	$3P_{1,2} - \text{ } ^3P_{1,2}^{\circ}$		28580
	1	354.19	$3P_0 - \text{ } ^3P_0^{\circ}$		
0 355.3	1	355.31	$3P_1 - \text{ } ^3P_2^{\circ}$		

core in a hollow aluminum electrode, whereas whole electrodes were easily made of magnesium.

Table I shows all the lines, $\lambda < 380$ of Na, and $\lambda < 360$ of Mg, that have ever been detected. The already classified Na II and Mg III lines are included for completeness.³ The present assignment of Mg $\lambda\lambda 320, 323$ has been suggested among other possibilities by Turner.⁴ Now the quantitative applicability of the irregular doublet law (Part III, below), and the relative unlikelihood of the strong occurrence of such x-ray transitions as $s^2p^5s^2 \leftarrow sp^6s^2$ in magnesium alone, make this assignment certain. The intensity relations, especially when examined in connection with those given in Millikan and Bowen's first paper on far ultra-violet spectra, (Table I, Mg, first column) are most satisfactory.

Table II gives the relativistic screening numbers $\sigma_2(2s^22p^4$ or $2s2p^5)$ for oxygen-like systems and $\sigma_2(2s^22p^5)$ for fluorine-like systems, respectively, as functions of the atomic number Z . The number σ_2 is calculated from the Sommerfeld formula $\Delta\nu = \alpha^2 R(Z - \sigma_2)^4 / n^3 l(l+1)$, which applies in these cases if $\Delta\nu$ is the doublet separation or the overall separation of the triplet.⁵ The frequency of the transition $2s \leftarrow 2p$, is given in the next to last column, while the last column shows the differences in the frequency of the transitions $2s \leftarrow 2p$ for successive members of each isoelectronic sequence. The extraordinarily high values of these differences will be discussed below (Part III). The numbers in parentheses are interpolated. Backward extrapolation of the next to last column to the arc spectra shows that O I $sp^5\ ^3P$ lies about $15 \cdot 10^3 \text{ cm}^{-1}$ above the lowest state $s^2p^3\ ^4S$ of O II, and F I $sp^6\ ^2S$ about $16 \cdot 10^3 \text{ cm}^{-1}$ above the lowest state $s^2p^4\ ^3P$ of F II. Neither of these negative levels has been observed.

The mean error in wave-length separations is about 0.03A, which at 300A amounts to 30 cm^{-1} . Thus the screening numbers at the bottom of each sequence in Table II are uncertain by about 0.03, while those at the top are perhaps ten times as accurate. Only in F II is it possible to distinguish, with the available measurements, between the values of the s^2p^4 and the sp^5 screening.

³ Detailed references to sources of spectroscopic data are omitted. The x-ray references may be found in Handbuch der Physik 21, 338; optical spectra, in the forthcoming University of Michigan term tables. Of special importance for this paper are the following:

F I: (the tentative assignment of $s^2p^5 \leftarrow sp^6$ is wrong). H. Dingle, Roy. Soc. Proc. A 117, 40 (1928).

F I, F II: I. S. Bowen, Phys. Rev. 29, 231 (1927).

Ne II: H. N. Russell, K. T. Compton, and J. C. Boyce, Nat. Acad. Sci. Proc. 14, 280 (1928).

Ne III: J. C. Boyce and K. T. Compton, Nat. Acad. Sci. Proc. 15, 656 (1929).

Na II: I. S. Bowen, Phys. Rev. 31, 967 (1928).

Mg III: J. E. Mack and R. A. Sawyer, Science 68, 1761 (1928).

Mg lines: R. A. Millikan and I. S. Bowen, Phys. Rev. 23, 1 (1924).

⁴ L. A. Turner, Phys. Rev. 32, 727 (1928).

⁵ S. Goudsmit, Phys. Rev. 31, 946 (1928).

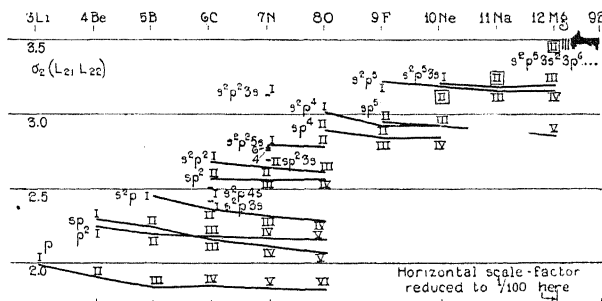
TABLE II. Application of the doublet laws to oxygen- and fluorine-like spectra.

Oxygen-like isoelectronic sequence.				
Z	$s^2p^4 \ ^3P$ $\Delta\nu(\text{cm}^{-1})$	$sp^5 \ ^3P$ $\Delta\nu(\text{cm}^{-1})$	$\sigma_2(s^2p^4)$ 3.010 2.976	$\sigma_2(sp^5)$ 2.957
8 O I	226	486		
9 F II	492			
10 Ne III	904		2.94 (2.90)	
11 Na IV	(1560)		2.85	
12 Mg V	2540			
			$s^2p^4 \ ^3P_{1/2} - sp^5 \ ^3P_2$ $\nu(\cdot 10 \text{ cm}^{-1})$	$s^2p^4 \ ^3P_{1/2} - sp^5 \ ^3P_2$ $\nu(\cdot 10 \text{ cm}^{-1})$
			16480	16480
			20430 (24378)	20430 (24378)
			28326	28326
				3950
				mean 3948
Flourine-like isoelectronic sequence.				
Z	$s^2p^5 \ ^2P$ $\Delta\nu(\text{cm}^{-1})$		$\sigma_2(s^2p^5)$ 3.216 3.194	$s^2p^5 \ ^2P_{1/2} - sp^6 \ ^2S_{1/2}$ $\nu(\cdot 10 \text{ cm}^{-1})$
9 F I	408			
10 Ne II	782			
11 Na III	1380		3.15	21627
12 Mg IV	2210		3.17	26431
				31162
				diff.
				4804
				4731

II. ON THE REGULAR DOUBLET LAW

Fig. 1 shows the screening numbers from Table II, with the other relativistic $2p$ -screening numbers, calculated with the aid of the Goudsmit separation factors.⁵ The assumption of normal coupling, where necessary for calculating the screening, is well justified.⁶ The fourth power formula is applied throughout, for it is a good approximation to call the $2p$ -electrons non-penetrating. All principal quantum numbers omitted in the notation are 2. The $1s^2$ shell is present in each configuration. Within the limits of experimental error, all the values decrease smoothly toward horizontal asymptotes.⁷ The p^2 and sp^2 curves are considerably flatter than their neighbors.

The addition of an s -electron to s^2p^5 makes a change only on the order of 0.01 in the $2p$ -screening, quite in contrast with the case where less than five $2p$ -electrons are present, as in N I, for instance, where the presence of a $3s$ -electron alters the screening by half a unit. This often-noted constancy



of the many closed shells, are probably sufficient to account for the discrepancy.⁹

III. ON THE IRREGULAR DOUBLET LAW

Heretofore the irregular doublet law has been applied to optical spectra only in the following qualitative rule: In an isoelectronic sequence, the transition frequency $\nu(n, l) - \nu(n, l+1)$ is approximately a linear function of the atomic number Z .

The irregular doublet law for x-rays can be stated, following Wentzel, in a refined form¹⁰ as

$$\sigma_1(n, l+1) - \sigma_1(n, l) = 0.58 \cdot 2^l n \quad (1)$$

for inner electrons; where n and l have their usual spectroscopic meaning, R is Rydberg's energy constant, and $\sigma_1 = Z - n (\nu_{\text{red}}/R)^{1/2}$. If $5 \cdot 10^{-5}(Z - \sigma_2)^4$ may be neglected compared with ν/R , as it may be for our purposes among the light elements with which we are concerned,¹¹ then ν_{red} is the same as ν , the energy required to remove the electron.

From Eq. (1) and the definition of σ_1 , we have

$$\nu_{\text{red}}(n, l) - \nu_{\text{red}}(n, l+1) = 0.58 \cdot 2^l R [0.58 \cdot 2^l + 2(Z - \sigma_1(n, l+1))/n] \quad (2)$$

$$\frac{\Delta}{\Delta Z} [\nu_{\text{red}}(n, l) - \nu_{\text{red}}(n, l+1)] = \frac{0.58 \cdot 2^{l+1} R}{n} \left[1 - \frac{\Delta}{\Delta Z} \sigma_1(n, l+1) \right] \quad (3)$$

for inner electrons.

With the aid of the newly found data we can study (Table III and Fig. 2) the frequency of the irregular doublet transition $2s \leftarrow 2p$ as a function of the atomic number (Z) and the net charge (indicated by a roman numeral), for systems of one to nine electrons. The rows labeled "upper config." and "lower config." in Table III show the electron configurations between which the transition takes place. All omitted principal quantum numbers are 2. The $1s^2$ shell is present except in the configurations marked () or (1s). The row $(Z+1) \text{ II}$ gives the transition frequency¹² (in terms of the Rydberg constant) for the first spark spectrum isoelectronic with the arc spectrum of atomic number Z . The row $(Z+1) \text{ II} - Z \text{ II}$ (row A) gives the rate at which the transition frequency for first spark spectra depends upon Z , while the row $(Z+1) \text{ II} - Z \text{ I}$ (row B) gives the rate at which the transition frequency depends upon Z in each isoelectronic sequence. The organization

⁹ The importance of such disturbances is shown, for instance, by the fact that the separations for some of the one-electron doublets among the heavier atoms actually have negative values. The case of Hg II $5f^2 F \Delta \nu = -257$ (F. Paschen, Preus, Akad. Sitzungsber. p. 536 (1928)) is especially striking.

¹⁰ G. Wentzel, Zeits. f. Physik 16, 41 (1926); A. Sommerfeld, "Atombau" 4th ed. p. 459.

¹¹ At $Z=10$, Ne II, "reduction" decreases the $-2s$ term (L_{11}) from $3.563R$ to $3.509R$, and the $-2p$ term (L_{21}) from $1.592R$ to $1.585R$.

¹² In the optical part, the frequency given is the difference between the lowest level in the lower configuration and the lowest level of the same multiplicity in the upper configuration.

TABLE III. Transition frequencies $2s \leftarrow 2p$. (Unit-Rydberg constant).

Upper config. Lower config. Z	$(\)_s$ 1	$(1s)_s$ 2	p 3	sp s^2 4	sp^2 s^2p 5	sp^3 s^2p^2 6	sp^4 s^2p^3 7	sp^5 s^2p^4 8	sp^6 s^2p^5 9	41	$1s^2sp^63s^3p^6$ etc. (L_{11}) $1s^2sp^63s^3p^6$ etc. (L_{21}) 73	91
(Z+1)II	0	0.17	0.29	0.67	0.68	0.84	1.10	1.50	1.971	...	18.4	...
Same, reduced									1.924	...	16.9	...
A (Z+1)II-ZII		0.17	0.12	0.38	0.01	0.16	0.26	0.40	.47	mean	mean	mean
B (Z+1)II-ZI	0	0.08	0.16	0.28	0.25	0.26	0.29	0.36 ^a	.44 ^a	.47	.49	.53
(Z+1)II σ (2p)								7.48		"	"	"
$\Delta\sigma_1/\Delta Z$										14.2	19.9	22.4
										mean 0.23	mean 0.16	mean 0.14

^a (Z+2)III - (Z+1)II is used here because the configurations sp^5 , sp^6 are unknown in the arc spectra.

of Table III will be made clear by a comparison of columns 8 and 9 with the last two columns of Table II (e.g. $216270 \text{ cm}^{-1} = 1.971R$, and $48040 \text{ cm}^{-1} = 0.44R$). Table III is divided by vertical lines into an optical part (left) and an x-ray part (right); column 9 must be included in both parts because of the double role of the L levels of Ne II. Elements 42 Mo, 74 W, and 92 U are chosen as samples for the x-ray part.

No modification of the meaning of any quantity is needed in putting the x-ray data in row $(Z+1)II$. But for clearness the "reduced" values are used in the rest of the x-ray part of the table, which means simply that the complicating effects of the relativity and spin corrections are eliminated.

There are no direct data on isoelectronic sequences of x-ray spectra, such as would be required to fill the spaces ditto-marked in the table. But all the difference between the quantity that belongs in such a space, and the quantity recorded just above it, is due to the influence of an outer electron. The presence of such an electron can have but little influence on an x-ray energy level, and clearly the subtraction of one L -level from another to determine the transition frequency, would tend to cancel out this little influence. So we can confidently conclude that the numbers in the spaces marked with ditto marks in row B should be very nearly the same as those above them in row A .

The ordinary $L_{21}L_{22}$ first order x-ray screening number, and its rate of dependence on Z (e.g. $(14.8 - 7.48)/(41 - 9) = 0.23$) are given in the last two rows.

We shall now show that the values of the numbers in italic type, column 9, are in quite close agreement with values that may be calculated for them simply by the use of the x-ray data to the right of the lines in Table III, the irregular doublet law, and the ionizing potential¹³ of Ne I.

The quantities appearing in the row $(Z+1)II$ reduced and row A of Table III are simply the $\nu_{\text{red}}(2, 0) - \nu_{\text{red}}(2, 1)$ in Eq. (2) and its derivative in Eq. (3), respectively. So as long as we confine ourselves to inner electrons (i.e. to x-ray levels) the quantities in row A are given by Eq. (3). And so are the quantities in row B , from our discussion of the ditto marks. Thus, using the average slope of σ_1 from the last row of the table, we have directly from Eq. (3):

$$\begin{aligned} (\text{italic numbers, Table III}) &= 0.58R (1 - 0.23) \\ &= 0.45R \\ &= 49 \cdot 10^3 \text{ cm}^{-1} \end{aligned}$$

an extraordinarily high value for the rate of dependence of an irregular doublet transition upon Z in an isoelectronic sequence, but in good agreement with the experimental data.

Fig. 2 shows the rate of dependence of the transition frequency $2s \leftarrow 2p$ upon the number of electrons present, for the cases we have been considering: Table III, row A , (first spark spectra)¹⁴ and row B (isoelectronic sequences)

¹³ Or any other data that gives the σ_1 's of Ne.

¹⁴ The abscissae for this curve are shifted by half a unit, since it is a first difference curve.

The change in scale factor masks the fact that the curve for the x-ray part of the figure, is almost horizontal. Three facts readable from Fig. 2 are worth pointing out here:

1). The extrapolability of the x-ray curve to $0.45R$ for the fluorine-like sequence, which has been discussed above.

2). The uselessness of attempts to apply Wentzel's regularity to outer electrons.¹⁵

3). The smoothness of the isoelectronic sequences curve, compared with the successive first spark spectra curve, from $Z=1$ to $Z=9$. Wide irregularities occur in the optical part of row *A* curve, superimposed upon the general upward trend with increasing Z that might be expected due to the increasing differences in screening between $2s$ and $2p$, as the K and L shells are being added. It is often pointed out that such irregularities can be explained

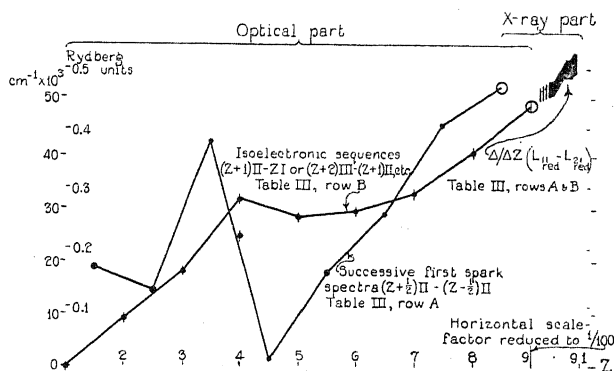


Fig. 2. Rates of dependence of the transition frequency $2s \leftarrow 2p$ upon the atomic number, in successive first spark spectra (*A*) and in isoelectronic sequences (*B*).

qualitatively by considerations based on the discrete changes in the number of electrons present: such as the formation of stable configurations at 2 and 4 and the neglect of higher multiplicities at 4, 5, and 6. To the first degree of approximation these irregularities are absent in the row *B* curve, because the differences in an isoelectronic sequence involve identical electron structures. Quite generally it appears that isoelectronic sequence irregular doublet transition curves such as the row *B* curve, depart from linearity only by a slight upward curvature, with a peak wherever the lower configuration is a Pauli shell.¹⁶ (See the $4s \leftarrow 4p$ data, below).

The irregular doublet we have been considering ($2s$, $2p$) is uniquely favored for the quantitative application of the law to isoelectronic sequences,

¹⁵ E.g., B. C. Mukherjee and B. B. Ray, *Zeits. f. Physik* **57**, 345 (1929).

¹⁶ If we used $sp \leftarrow p^2$ in the beryllium-like sequence (the isolated point at 4, $0.22R$ in Fig. 2) we would eliminate the peak at 4. (Such a choice would also make the row *A* curve smoother, lowering the ordinate at 3.5 and raising that at 4.5 by $0.11R$). Similarly in the $4s \leftarrow 4p$ list below, the choice of $3d4s \leftarrow 3d4p$ instead of $4s^2 \leftarrow 4s4p$ would lower the ordinate for the 20-electron sequence to 0.110 .

for only here is it possible to excite an electron from a normally closed shell (here $2s^2$) in increasingly heavy atoms even up to those wherein the next shell with the same principal quantum number (here $2p^6$) is normally closed. But we can apply the regularities we have found for $2s \leftarrow 2p$, somewhat more crudely in other sequences. For instance, the following shows (in part) the rate of dependence upon Z in isoelectronic sequences, of the frequency $4s \leftarrow 4p$, analogous to Table III, row B :

lower config.													
No. electrons	1	• • • 11	12	13	• • • 18	19	20	21	• • • 27	28	29	30	
rate	0	.059	.069	.074	.089	.111	.185 ¹⁶	.116	.133	.147	.161	.219	

At 30 the experimental data stops, the $4s^2$ shell being so stable that there is no data on optical transitions involving $4s$ electrons for $Z > 30$; whereas the $4p$ electrons do not become inner electrons until $Z = 36$. It is not possible to calculate the rate in the sequence joining x-ray and "semi-optical" spectra (the bromine-like sequence in the case $4s \leftarrow 4p$) from Eq. (3) with the same accuracy as in the $2s \leftarrow 2p$ case, for the curvature and uncertainty in the x-ray, σ_1 curves increases with increasing principal quantum number.¹⁷ The rate for $4s \leftarrow 4p$ in the bromine-like sequence from Eq. (3) is about $0.58 \cdot 2(1 - .4)/4 = .17$.

Interpolations in such tables as this, allowing for the peaked but otherwise smooth character of the curves, should be quite reliable.

¹⁷ A. Sommerfeld, "Atombau" p. 460.

NEW MEASUREMENTS IN THE FOURTH POSITIVE
CO BANDS

BY ROGER S. ESTEY

WASHINGTON SQUARE COLLEGE, NEW YORK UNIVERSITY

(Received October 28, 1929)

ABSTRACT

That part of the fourth positive system of CO lying between 1970A and 2800A has been remeasured together with sixteen bands not previously observed. An equation for the band heads is given, the constants of which yield the values $D' = 12.00$ volts, $D'' = 11.17$ volts for the heat of dissociation.

Modifications in values of frequency have been small, while those of intensity have been rather large. Some discrepancies have been removed. Revision of intensity estimates permits a far more accurate comparison than previously with Condon's theory of intensity distribution and shows the superiority of Morse's $U(r)$ function. Using this function, the distribution of intensity among the bands of the fourth positive system agrees perfectly with Snow and Rideal's value of the moment of inertia for the normal state, $I_0'' = 15.0 \times 10^{-40}$ g cm².

The quantum assignment of Asundi's infra-red electronic bands has been revised.

INTRODUCTION

THE fourth positive band system of CO, which extends at least from 2800A to 1300A, has never been completely measured by any one investigator. The work on this system prior to 1926 is fully described by Birge.¹ His paper analyzes data taken by Deslandres (42 bands), Bair (22 bands), Duncan (14 bands), Lyman (100 bands), and Leifson (12 bands), all under low dispersion. Subsequent to 1926 papers have appeared on the energy levels of CO,^{2,3} the mode of dissociation,⁴ CO in active nitrogen,⁵ the isotope effect,⁶ and a series of papers on the structure of the various systems.^{7,8,9,10}

The initial vibrational levels of this system are the same as the final levels of the Angstrom bands and of the new bands analyzed by Herzberg,⁷ and Johnson and Asundi,⁸ while the final levels are the same as those of the Cameron bands and several absorption systems. These relationships are shown in Fig. 1, which diagrams the electronic energy levels for neutral CO. In addition to the bands just mentioned there are shown the third

¹ Birge, Phys. Rev. **28**, 1157 (1926).

² Hopfield and Birge, Phys. Rev. **29**, 922 (1927).

³ Duffendack and Fox, Astrophys. J. **65**, 214 (1927).

⁴ Hogness and Harkness, Phys. Rev. **32**, 936 (1928).

⁵ Knauss, Phys. Rev. **32**, 417 (1928).

⁶ Birge, Phys. Rev. **34**, 379 (1929).

⁷ Herzberg, Zeits. f. Physik **52**, 815 (1929).

⁸ Johnson and Asundi, Proc. Roy. Soc. **A123**, 560 (1929).

⁹ Asundi, Proc. Roy. Soc. **A124**, 277 (1929).

¹⁰ Asundi, Nature **123**, 47 (1929).

positive and the three *A* systems. Asundi⁹ has contributed two other new systems, the five *B* and an unnamed system in the near infra-red. The absorption and emission systems described by Hopfield and Birge are also shown.

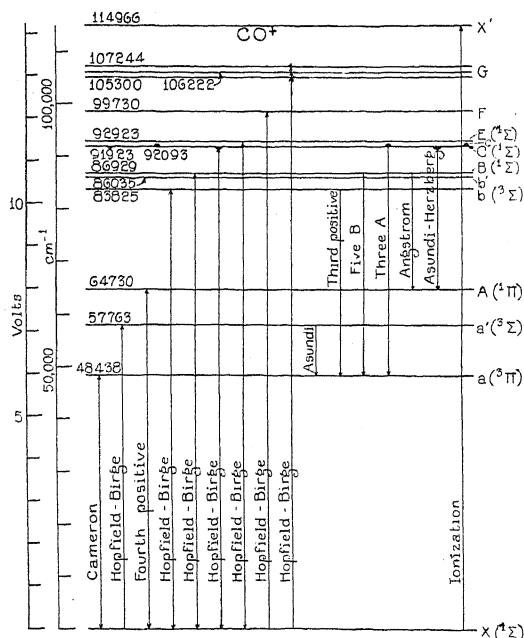


Fig. 1. Energy level diagram for neutral CO.

Asundi's vibrational analysis¹¹ of the infra-red system requires revision with respect to the initial state. The upper electronic level is at 57763 cm⁻¹ (Birge, private communication) rather than at 58927, and the most recent value¹² for ω_0' is 1173 cm⁻¹. This yields the equation for the infra-red bands

$$\nu = 9325 + (1173n' - 9n'^2) - (1726.5n'' - 14.4n''^2).$$

Accordingly the initial quantum numbering must be increased by one unit and the band called 1, 0 by Asundi is really the 2, 0 band.

The present knowledge of the fourth positive band system is somewhat inaccurate because it has been measured under low dispersion only, and because of a lack of satisfactory wave-length standards in the region which it occupies. Therefore it seemed advisable to remeasure as many bands as could be reached with a quartz spectrograph.

EXPERIMENTAL DETAILS

The CO bands were excited at 0.3 mm pressure in a water-cooled U-shaped discharge tube, the straight portion of which was viewed end on. This straight portion was 23 cm long and 6 mm in diameter. Large iron

¹¹ His equation is $\nu = 10489 + (1155n' - 9n'^2) - (1726.5n'' - 14.4n''^2)$.

¹² Mulliken, Phys. Rev. 32, 186 (1928).

electrodes permitted an input of 1.2 amperes at 2200 volts from a 3 KVA power transformer. Magnesium carbonate in an electrically heated side tube served as a source of CO_2 which later broke down to CO in the discharge. The vapor pressure of CO_2 over magnesium carbonate is constant at constant temperature. In this way fresh gas was provided as rapidly as required by the clean-up of the electrodes.

The pictures were taken on Hilger Schumann plates, or oiled Eastman 40's with a Hilger E 1 quartz spectrograph. This instrument has a dispersion of 3.91Å/mm at 2800Å and 1.21Å/mm at 1970Å, the limits of the range covered in this investigation.

Copper arc and spark lines and nickel spark lines as listed by Shenstone^{13,14,15} served as standards below 2500Å, while in the region above this iron standards as listed in volume VII of Kayser and Konen, "Handbuch der Spektroskopie," were used. The transformations between wave-lengths and wave-numbers were made with the aid of Kayser's "Tabelle der Schwingungszahlen."

RESULTS

The new measurements on the band heads are shown in the following table.

TABLE I. *Fourth positive bands of CO.*

$\lambda(\text{Å})$	$\nu(\text{cm}^{-1})$	I	n', n''	O-C	$\lambda(\text{Å})$	$\nu(\text{cm}^{-1})$	I	n', n''	O-C
2799.7	35708.2	9	9 22	+ 1.6	2356.5	42422.3	4	5 15	+1.1
2785.4	35890.3	8	4 18	- 4.8	2337.9	42760.1	7	8 17	+0.7
2742.6	36450.7	6	11 23	+14.1	2332.5	42860.0	3	4 14	+2.0
2740.0	36486.0	4	7 20	- 4.0	2311.5	43249.2	8	7 16	+0.5
2712.1	36860.5	4	{ 6 19 10 22? }	{ - 7.7 -15.8 }	2286.1	43728.5	7	6 15	-0.5
2698.3	37049.7	6	13 24	- 4.2	2273.9	43963.4	3	9 17	-0.2
2684.0	37247.4	3	5 18	+10.1	2272.3	43994.0	1	12 19	+4.4
2680.8	37291.5	5	9 21	+15.5	2261.7	44200.0	9	5 14	-0.2
2662.9	37541.8	4	12 23	+ 4.6	2247.2	44486.6	7	8 16	-0.8
2661.5	37561.7	4	15 25	+ 3.0	2238.3	44663.8	9	4 13	+1.3
2659.6	37587.9	4	4 17	- 9.6	2221.5	45001.4	10	7 15	-0.8
2630.0	38011.4	6	11 22	\pm 0.0	2215.8	45115.9	3	3 12	+0.1
2598.3	38474.8	4	10 21	- 1.8	2196.8	45506.4	10	6 14	-1.6
2594.5	38531.5	1	16 25	+10.3	2173.0	46004.7	9	5 13	-0.1
2567.8	38932.8	5	9 20	- 0.1	2150.2	46492.6	8	4 12	\pm 0.0
2556.0	39111.7	3	12 22	- 0.3	2137.0	46779.9	5	7 14	-1.2
2538.6	39379.7	4	8 19	- 0.4	2128.3	46971.1	8	3 11	-0.2
2521.8	39642.7	3	14 23	- 7.9	2113.1	47309.6	9	6 13	-2.9
2509.9	39830.1	8	7 18	+11.8	2107.2	47440.3	7	{ 2 10 9 15 }	{ -0.8 -3.8 }
2492.9	40102.1	8	10 20	- 0.3	2089.9	47834.0	10	5 12	-0.8
2483.8	40248.8	3	6 17	+ 1.3	2086.9	47901.5	1	1 9	-0.4
2463.2	40584.6	10	9 19	+ 0.3	2067.6	48349.4	10	4 11	+1.3
2458.0	40671.5	2	5 16	+ 3.8	2046.3	48852.9	10	3 10	+0.5
2433.9	41057.5	9	8 18	+ 0.5	2025.8	49347.8	9	2 9	+0.1
2424.1	41239.3	5	11 20	+ 1.7	2011.8	49690.6	8	5 11	+0.2
2407.6	41552.0	7	7 17	+ 1.3	2005.8	49838.2	5	1 8	+4.2
2394.2	41754.2	3	10 19	+ 0.3	$\lambda(\text{vac.})$				
2393.1	41773.9	4	13 21	- 4.5	1990.8	50230.9	10	4 10	+1.7
2381.6	41975.3	6	6 16	- 0.2	1970.0	50761.7	8	3 9	+2.6
2365.5	42261.9	5	9 18	+ 0.7					

¹³ Shenstone, Phys. Rev. 28, 449 (1926).

¹⁴ Shenstone, Phys. Rev. 29, 380 (1927).

¹⁵ Shenstone, Phys. Rev. 30, 255 (1927).

The assignment of vibrational quantum numbers (n' , n'') is substantially that given by Birge. A few bands given by him were not measured because of overlapping by other bands. Otherwise, all bands given by Birge, as well as many new bands, have been measured and quantum numbers assigned.

The new measures on fifty-eight bands yield the equation¹⁶

$$\nu = 64729.60 + (1497.63 n' - 17.262 n'^2) - (2149.08 n'' - 12.761 n''^2).$$

The column headed "O-C" in Table I lists the observed minus calculated values of the band heads as calculated from this equation. Unfortunately it was possible to measure bands of relatively large quantum numbers only. For this reason the equation written above probably does not express the origin of the system and the bands near it as well as the former equation¹⁶ does, although for the region represented by the bands of Table I the new equation is probably the better.

The plates showed clearly the presence of a single P , Q , and R branch in each band. The bands degrade to the red. Although they were unresolved at the origin and it was impossible to determine how many lines were missing, there is no reason to doubt the correctness of the assumption that these bands result from a $^1\Pi$ to $^1\Sigma$ transition.

DISCUSSION

Accuracy in our present methods of evaluating the heat of dissociation of a molecule from data on vibrational energy levels depends on our ability to extrapolate to $\omega_n = 0$ the $\omega_n:n$ curve. Fortunately in many cases including this one the $\omega_n:n$ curve is nearly linear over the known range, which facilitates extrapolation. The data in this paper, being more accurate and extensive, yield a more reliable extrapolation and provide a more certain value of the heat of dissociation than that previously reported.¹⁷ The heat of dissociation of a CO molecule in the normal state, as now determined, is 11.17 volts. To raise a CO molecule to the $^1\Pi$ level and dissociate it there requires 12.00 volts.

The large extent of the fourth positive system affords both opportunity and difficulty in discussing vibrational intensity relations. Table I gives, under the heading " I ", simple visual estimates of intensity, allowing as well as possible for overlapping bands and for large variations in plate sensitivity over the range considered. Fig. 2 shows in a graphical manner the intensities of the observed bands. The diameters of the circles are proportional to the intensities of the corresponding bands.

A theory has been given by Condon¹⁸ which predicts, from a knowledge of certain band constants including the moment of inertia, which bands of a system will be the most intense. A $U(r)$ curve (potential energy as a function of r) is drawn for each of the two electronic states involved. Such a curve

¹⁶ The next most recent equation (I.C.T. Vol. 5, p. 412) is $\nu = 64765 + (1499.0n' - 17.24n'^2) - (2154.7n'' - 12.70n''^2)$. $D = 11.2$ volts.

¹⁷ Birge and Sponer, Phys. Rev. **28**, 259 (1926).

¹⁸ Condon, Phys. Rev. **28**, 1182 (1926).

shows the extremes between which a molecule with a given amount of energy can vibrate. Condon's theory is based on the assumption that the molecule spends most of its time in an extreme position and that as a consequence the transitions between the extreme positions are the most probable. Since the $U(r)$ curve represents these extremes, transitions drawn between the upper and lower of two $U(r)$ curves of a molecule are according to the theory the most probable, and on an n', n'' diagram (cf. Fig. 2) they fall on a smooth curve roughly parabolic in form with the vertex near the origin of the system. If the constants and the function on which the $U(r)$ curves are based are correct, then the theoretical intensity distribution curve should pass through the most intense bands observed. The $U(r)$ function used by Condon in

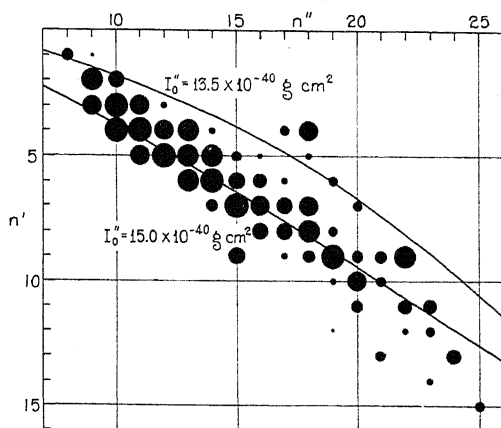


Fig. 2. Intensities of band heads. The intensity of each band as listed in Table I is proportional to the diameter of the corresponding circle on the n', n'' diagram. Intensity distribution curves based on Morse's $U(r)$ function are plotted for two values of I_0'' . The observed distribution of band intensities agrees with $I_0'' = 15.0 \times 10^{-40} \text{ g cm}^2$.

developing his theory is a power series, and for computing purposes the polynomial composed of the first three terms is used. In the particular case of the CO molecule this polynomial is satisfactory only over a very small range of r near r_0 . An intensity curve using $I_0'' = 14.9$ appears in Condon's paper.¹⁸ This curve fits near the origin, but for quantum numbers higher than $n'' = 10$ the upper branch becomes concave upward while the trend of the bands in this region is concave downward.

Fortunately another form of $U(r)$ function is available¹⁹ which has the following properties: (a) when r is zero, U is very large, (b) when r is r_0 , U is at its only minimum, (c) when r is very large, U is asymptotic to D , the heat of dissociation, and (d) when the quantum theory is applied, the function yields the correct expression for the vibrational energy levels. This function is given by the expression

$$U = A + De^{-2a(r-r_0)} - 2De^{-a(r-r_0)},$$

where A is the constant which moves the entire curve up or down on the energy scale, D is the heat of dissociation, $a = 0.2454(M\omega_0 x)^{1/2}$, where M is

¹⁹ Morse, Phys. Rev. **34**, 57 (1929).

the reduced mass in terms of the atomic weights; and r and r_0 are nuclear separations, the latter corresponding to the special case of zero vibrational energy.

Theoretical intensity curves are drawn on Fig. 2 corresponding to $U(r)$ curves computed from the following constants:

	A	D	a	r_0
Initial	97500	32500	2.67	1.24
Final	91394	91394	2.29	1.09
	91394	91394	2.29	1.15

Curves corresponding to two values of the moment of inertia ($I_0'' = 15.0 \times 10^{-40}$ g cm², giving $r_0'' = 1.15A$, and $I_0'' = 13.5 \times 10^{-40}$, giving $r_0'' = 1.09$) appear on Fig. 2 because at the time the figure was first drawn Snow and Rideal's paper²⁰ giving $I_0'' = 15.0 \times 10^{-40}$ had not appeared and it seemed probable that the lower value of I_0'' was about right.^{9,21} The intensity curve corresponding to the lower value of the moment of inertia does not fit the observed bands very well, while the intensity curve corresponding to the larger value is an excellent fit, especially in the center of the diagram. For low quantum numbers the fit is really better than the figure would indicate because bands observed by others with a vacuum spectrograph are not shown since the diagram shows only the data of the author.

The intensity distribution among the bands of the fourth positive system is very distinct evidence in favor of the larger value of the moment of inertia if we assume that the $U(r)$ function given above is essentially correct. The evidence strongly favors this assumption and the intensity distribution can therefore be taken as good evidence from the electronic bands for the correctness of the infra-red value of the moment of inertia for the normal state. This represents a new and useful check on the value of this constant.

Babcock²² has estimated the prevalence of O¹⁶ relative to O¹⁸ as 1250:1. If we assume that C¹² has an atomic weight 12.000 and that C¹² and C¹³ are the only factors influencing the atomic weight (12.003) of carbon,²³ then they are prevalent in the ratio of 333:1. This calculation shows, in harmony with the experimental findings of King and Birge²⁴ that C¹³O¹⁶ is much more prevalent than C¹²O¹⁸ or C¹³O¹⁸. Therefore the calculated positions of several favorably located band heads of the C¹³O¹⁶ molecule have been examined on a heavily exposed plate, but no isotopic heads have been found. This does not cast doubt on the isotopic heads reported by Birge on the fourth positive absorption plates taken by Hopfield, but merely goes to show that absorption spectra show these faint bands more readily than do emission spectra.

I wish to express my appreciation for the advice and assistance of Professor R. S. Mulliken.

²⁰ Snow and Rideal, Proc. Roy. Soc. A125, 462 (1929).

²¹ Lowry, J.O.S.A. & R.S.I. 8, 647 (1924). A numerical error appears in this paper (Lowry, private communication) and a recalculation of Lowry's data by the writer gives $I_0 = 13.0 \times 10^{-40}$ g cm².

²² Babcock, Phys. Rev. 34, 540 (1929).

²³ Birge, Phys. Rev. Sup. 1, 1 (1929).

²⁴ King and Birge, Phys. Rev. 34, 376 (1929).

FINE STRUCTURE OF THE BERYLLIUM FLUORIDE BANDS

By F. A. JENKINS

DEPARTMENT OF PHYSICS, UNIVERSITY OF CALIFORNIA

(Received December 24, 1929)

ABSTRACT

Wave-length measurements of BeF bands.—New wave-length measurements have been made of the rotational lines of the BeF bands in the regions $\lambda\lambda 3009.5$ – 3026.3 , 2908.9 – 2927.8 , and 3126.1 – 3140.8 , which include all the stronger lines of the (0, 0), (1, 0) and (0, 1) bands. The source was a cored carbon arc run at atmospheric pressure. The Harvard 21-foot grating was used in the second order, giving a linear dispersion of 0.97 Å per mm and an effective resolving power of nearly 100,000. The wave-numbers of the lines in the six branches of each band are tabulated for rotational quantum numbers up to about $K=50$ in the R branches, 45 in the Q branches, and 30 in the P branches. Visual intensity estimates are also included.

Term analysis of BeF bands.—The rotational structure is found to be that characteristic of a ${}^2\Pi \rightarrow {}^2\Sigma$ electronic transition, with a relatively small value of $\Delta E/B$, +15.667, in the Π state. The combination relations among the lines of the (1, 0), (0, 0) and (0, 1) bands are satisfied within the experimental error in every case where exact agreement is to be expected. The R - Q , Q - P relations show a small combination defect, which is referred to Λ -type doubling in the initial state. This doubling is slightly greater for the levels involved in the low-frequency sub-band, and therefore it is assumed that the ${}^2\Pi$ state is normal. Rotational terms having the same K in the initial state draw rapidly together as the rotation increases, due to the loose coupling of the spin with the molecular axis. Quantitative agreement is obtained between the observed term-differences, ΔF , and their values calculated by the theoretical energy formulas derived by Hill and Van Vleck for the transition from case a to case b type of spin coupling. Equations capable of representing all the lines in a given band are deduced.

Constants of BeF molecule.—The following values for the more important molecular constants are obtained: $B^{(0)'} = 1.41060 \text{ cm}^{-1}$, $B^{(0)''} = 1.47928$, $\alpha' = 0.01610 \text{ cm}^{-1}$, $\alpha'' = 0.01685$, $D^{(0)'} = -8.301 \times 10^{-6} \text{ cm}^{-1}$, $D^{(0)''} = -8.209 \times 10^{-6}$, $\beta' = 1.060 \times 10^{-8} \text{ cm}^{-1}$, $\beta'' = 2.903 \times 10^{-8}$, $I_e' = (19.50 \pm 0.03) 10^{-40} \text{ g cm}^2$, $I_e'' = (18.59 \pm 0.03) 10^{-40}$, $r_e' = 1.390 \times 10^{-8} \text{ cm}$, $r_e'' = 1.357 \times 10^{-8}$, $\omega_e' = 1172.56 \text{ cm}^{-1}$, $\omega_e'' = 1265.62$, $x_e' = 0.007488$, $x_e'' = 0.007206$, $\nu_e = 33,233.61 \text{ cm}^{-1}$, $\Delta E = 22.10 \pm 0.1 \text{ cm}^{-1}$.

INTRODUCTION

BAND spectra are known for a large number of diatomic alkaline earth halides,¹ the most familiar being those of the fluorides, such as CaF. In general, the rotational structure of these bands is so finely spaced that there seems to be little hope of carrying out a detailed fine structure analysis, even

¹ For the experimental material on the alkaline earth halides, other than BeF, see H. Kayser, "Handbuch der Spectroscopie," Vols. 5, and 6, and S. Datta, Proc. Roy. Soc. 99A 436 (1921). General treatments of the relations between the electronic states, molecular constants, etc., have been given by R. Mecke, Zeits. f. Physik 42, 390 (1927) and by R. C. Johnson, Proc. Roy. Soc. 122A, 161, 189 (1929).

with spectrographs of the highest resolving power. The most favorable case for analysis is the lightest molecule of this class, BeF, for which, owing to its small moment of inertia, the spacing of the lines in a band should be great enough to permit almost complete resolution. A band system due to this molecule was first reported by Datta² in 1922. Its bands are shaded toward the red and lie completely in the ultra-violet, the head of the strongest occurring at $\lambda 3009.6$. Datta undertook a study of the fine structure of this band, and was able to identify three fairly regular series of lines. It is obvious, however, from an examination of his reproduction, and of the curves obtained, that the resolving power he used (third order of a 10-foot grating) was insufficient for a satisfactory quantum analysis of the band structure. Each of his series, as will appear in the present work, represents the blending of two or more true series. For the analysis to be reported here, new plates were taken, having a dispersion and actual resolution from 2 to 3 times greater than those attained by Datta. This comparatively small advantage has made possible a complete and satisfactory interpretation of the rotational structure.

The BeF bands were first considered from the standpoint of the quantum theory by Mulliken.³ Vibrational quantum numbers were assigned, and an equation derived for the frequencies of the heads, as measured by Datta. The molecule BeF was classed with a number of one-valence-electron emitters of band spectra, such as BO, CN, CO⁺, N₂⁺, the spectra of which appeared to be qualitatively similar. From such considerations, it was concluded that the ultra-violet BeF system represents a $^2\Pi \rightarrow ^2\Sigma$ electron jump, analogous to the α bands of BO, the red CN bands, etc. The latter are of the double double-headed type, the first head in each pair being formed by an *R*, and the second by a *Q* branch.⁴ Each of the BeF bands has only 3 heads, the first two forming a close pair of nearly equal intensity, and the third being somewhat weaker. It has therefore been assumed that the second and third heads are those of the *Q* branches, the second *R* head being too faint to be observed. On this view, the two *Q* heads should represent approximately the double origin of the band and from these $\Delta E \cong 35 \text{ cm}^{-1}$ for the $^2\Pi$ state. A revised interpretation of the formation of the heads has recently been given by Jevons.⁵ From a critical study of Datta's measurements, especially with regard to the variation of the mutual separations of the heads with vibrational quantum number, he concluded that the first pair of heads is formed by two closely parallel *R* branches and the third by one of two *Q* branches. Evidence for a second *Q* head was found on the writer's spectrograms early in the present work, but it appeared later during the analysis that this apparent head is merely a fortuitous accumulation of lines at the point in question.

In beginning the analysis of a band of complex structure, it is very desirable to have as a starting point an approximate idea of the type of band

² S. Datta, Proc. Roy. Soc. 101A, 187 (1922). An excellent reproduction of the band system as a whole is given.

³ R. S. Mulliken, Phys. Rev. 26, 561 (1925).

⁴ F. A. Jenkins, Proc. Nat. Acad. 13, 496 (1927).

⁵ W. Jevons, Proc. Roy. Soc. 122A, 216 (1929).

structure, i.e. number of branches, approximate electronic separation, etc. According to the revised interpretation by Jevons, the rotational structure of the BeF bands should resemble that of the green MgH bands, where the electronic doublet separation is relatively small, and the corresponding branches of the two sub-bands draw rapidly together with increasing rotational quantum number. Bands showing this type of "rotational distortion" are fairly numerous⁶ and, as in BeF, three heads are usually observed, one of the Q branches not forming a head due to the distortion effect. Such a structure is characteristic of a ${}^2\Pi \rightarrow {}^2\Sigma$ or ${}^2\Sigma \rightarrow {}^2\Pi$ transition, in which the ratio of the doublet energy difference, ΔE , to the constant B , is small (i.e. less than about 20). A point strongly opposed to the previous interpretation, with $\Delta E/B$ large, appeared in the fact that, although the bands are closely grouped in sequences the distance from the R head to the origin would be extremely small (3 cm^{-1}). This would violate the rule of Birge and Mecke, according to which a small change in the vibration frequency during the transition is always accompanied by a small change in the moment of inertia. It therefore seemed probable that in BeF the $\Delta E/B$ is small. By postulating that the bands are of the MgH type, preliminary investigations of the structure⁷ showed that Jevons' scheme is essentially correct.

EXPERIMENTAL PROCEDURE

The spectrograms were obtained in the second order of the 21-foot grating at Harvard University, giving a dispersion of 0.97\AA per mm in the region investigated. An arc in air between carbon poles, both cored with a mixture of BeKF_3 and powdered carbon, gives not only the BeF, but also the BeO band system with considerable intensity in the flame surrounding the poles.⁸ Therefore, the BeO bands were also obtained on these plates. The rotational quantum analysis of the latter system has been given by Miss J. E. Rosenthal and the writer,⁹ and also independently by Bengtsson.¹⁰ In the former article will be found a brief description of the experimental details pertaining to the spectrograms used in the present investigation, since the BeF and BeO spectra were photographed simultaneously. Two sets of plates were of use for our purpose, one showing the stronger sequence $\Delta v = 0$ ¹¹ with the best possible resolution (slow, fine-grained plates) and another on which the 0 sequence is considerably over-exposed, but the sequences $+1$ and -1 are of satisfactory

⁶ R. S. Mulliken, Phys. Rev. **32**, 388 (1928).

⁷ The main results embodied in the present article were given in a paper before the American Physical Society, Washington Meeting, April, 1929. Cf. Phys. Rev. **33**, 1090 (1929) (Abstract).

⁸ Jevons, ref. 5, finds that the oxide bands are relatively stronger in the outer part of the flame.

⁹ J. E. Rosenthal and F. A. Jenkins, Phys. Rev. **31**, 705 (Apr. 1928) (Abstract), Phys. Rev. **33**, 163 (1929).

¹⁰ E. Bengtsson, Arkiv. för Mat. Astro. och Fysik, **20A**, No. 21, p. 1, June 1928.

¹¹ The nomenclature used here conforms with the revised system recently proposed (Mulliken, private communication). In this v represents the vibrational quantum number, formerly n .

intensity. The first heads of the three sequences are, according to Mulliken's assignment: $\lambda 3009.582$ (0), $\lambda 2908.994$ (-1) and $\lambda 3126.116$ (+1). Doublets with a separation of 0.04\AA are resolved on these plates. The iron arc comparison spectrum shows no relative displacement on the two sets. An enlargement of part of the 0 sequence from the first set is shown in Fig. 1, accompanied by a Fortrat diagram of the (0, 0) band, according to our complete analysis.

In order to take full advantage of the combination principle, it was necessary to study bands which would yield agreements in the term-differences of

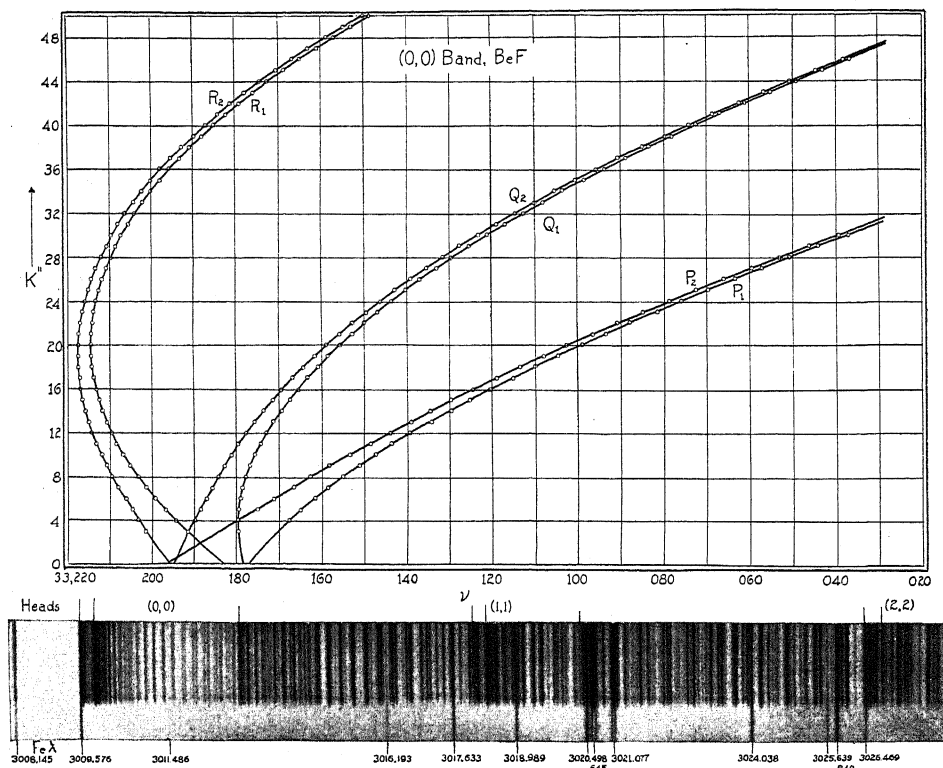


Fig. 1. (0, 0) band of BeF. The spectrum has been enlarged to practically the same scale as the diagram, but the correspondence of the lines with points on the diagram is not exact throughout, because the latter is on a scale of frequencies.

both the initial and the final states. Accordingly, wave-length measurements were made of the lines in the first band of each of the three above-mentioned sequences, i.e. in the (0, 0), (1, 0) and (0, 1) bands. The secondary Fe wave-length standards given by Fabry¹² were used throughout. The measurements included every line in each sequence as far as the first head of the third band in that sequence. This was necessary because, as will be apparent in Fig. 1, many lines of the first band are intermingled with those of the second. In

¹² Ch. Fabry, Int. Crit. Tables, Vol. V, p. 275.

general, our wave-lengths agree well with those of Datta.² Table I gives the wave-numbers in vacuum of all lines assigned to the above three bands. A large number of measured lines belonging to the second bands of the sequences are not given, because they represent only certain parts of these bands and would be of little value for the present purpose. Although there is an element

TABLE I. Wave-number and intensity data for BeF bands.

R_2 head, $\lambda_{air} = 3009.582$			(0, 0) band R_1 head, $\lambda 3009.873$		Q_1 head, $\lambda 3013.011$	
K''	R_2	R_1	Q_2	Q_1	P_2	P_1
3	33,201.42 ²¹	33,191.43 ¹⁰	33,190.66 ²³	—	—	—
4	203.21 ²²	194.24 ¹¹	189.85 ²⁴	33,179.45 ^{24d}	33,179.76 ²²	33,167.42 ^{23d}
5	205.06 ²⁰	196.73 ^{1d}	188.44 ¹¹	179.45 ^{24d}	174.92 ¹⁰	164.92 ²³
6	206.71 ²¹	199.14 ¹¹	187.03 ²⁴	178.97 ²¹	171.26 ²⁴	161.41 ²⁴
7	207.84 ²³	201.42 ²¹	185.74 ²²	178.59 ¹¹	166.59 ²⁴	158.30 ²⁵
8	209.47 ^{4d}	203.21 ²²	184.14 ^{24d}	177.64 ²⁵	161.41 ²⁴	154.82 ²¹
9	210.71 ⁴⁴	205.06 ²⁰	182.74 ²³	176.76 ¹²	156.87 ²²	151.03 ¹²
10	211.77 ^{3d}	206.71 ²¹	180.96 ^{24d}	175.65 ²⁵	153.18 ¹¹	147.13 ¹⁰
11	213.11 ⁴³	208.38 ²³	179.45 ^{24d}	174.17 ²³	148.42 ^{22d}	143.36 ^{23d}
12	214.18 ^{75d}	209.47 ^{4d}	177.64 ²⁵	172.82 ¹²	143.89 ²²	138.93 ^{44d}
13	214.95 ²²	210.71 ⁴⁴	175.65 ²⁵	171.26 ²⁴	138.93 ^{44d}	134.32 ²³
14	215.69 ²²	211.77 ^{3d}	173.53 ¹²	169.30 ^{24d}	134.32 ²³	129.57 ^{23d}
15	216.36 ²¹	212.44 ²²	171.26 ²⁴	167.42 ^{23d}	129.57 ^{23d}	125.00 ²³
16	216.65 ²¹	213.11 ⁴³	169.30 ^{24d}	165.33 ¹³	124.22 ¹²	120.13 ^{11d}
17	216.94 ²¹	213.75 ²²	166.59 ²⁴	163.08 ¹³	118.78 ^{24d}	115.02 ^{22d}
18	217.41 ^{45d}	214.18 ^{75d}	164.05 ¹³	160.77 ²⁴	113.51 ¹²	109.75 ²³
19	217.41 ^{45d}	214.18 ^{75d}	161.41 ²⁴	158.30 ²⁵	107.81 ²⁴	104.48 ¹²
20	217.41 ^{45d}	214.18 ^{75d}	158.56 ²⁵	155.58 ²⁵	102.36 ¹²	099.04 ¹²
21	217.41 ^{45d}	214.18 ^{75d}	155.58 ²⁵	152.59 ²⁵	096.54 ^{3d}	093.44 ²³
22	216.94 ²¹	214.18 ^{75d}	152.59 ²⁵	149.87 ^{24d}	090.71 ^{10d}	087.67 ^{11d}
23	216.36 ²¹	213.75 ²²	149.28 ¹⁴	146.61 ¹³	084.82 ²⁴	081.83 ^{12d}
24	215.69 ²²	213.11 ⁴³	145.93 ¹³	143.36 ^{23d}	078.58 ^{13d}	075.89 ¹¹
25	214.95 ²²	212.44 ²²	142.48 ¹⁴	139.96 ¹³	072.37 ²⁴	069.49 ^{22d}
26	214.18 ^{75d}	211.77 ^{3d}	138.93 ^{44d}	136.47 ¹³	065.89 ¹³	063.30 ^{12d}
27	213.11 ⁴³	210.71 ⁴⁴	135.10 ¹³	132.77 ¹³	059.46 ¹²	057.09 ¹³
28	211.77 ^{3d}	209.47 ^{4d}	131.19 ²⁴	128.94 ¹⁵	052.86 ¹²	050.52 ^{25d}
29	210.71 ⁴⁴	208.38 ²³	127.20 ¹³	125.00 ²³	046.12 ^{14d}	043.70 ¹²
30	209.47 ^{4d}	207.02 ¹²	123.01 ¹⁴	120.82 ²⁴	039.08 ¹⁴	036.84 ¹⁴
31	207.84 ²³	205.44 ¹²	118.78 ^{24d}	116.72 ¹²	—	—
32	205.98 ¹²	203.98 ^{3d}	114.28 ¹³	112.38 ^{13d}	—	—
33	203.98 ^{23d}	202.14 ²⁴	109.75 ²³	107.81 ²⁴	—	—
34	202.14 ²⁴	200.03 ²⁵	105.07 ¹³	103.14 ¹³	—	—
35	200.03 ²⁵	197.79 ^{24d}	100.22 ¹³	098.30 ^{13d}	—	—
36	197.79 ^{24d}	195.66 ¹⁴	095.27 ^{13d}	093.44 ²³	—	—
37	195.27 ¹⁴	193.23 ¹³	090.20 ^{12d}	088.41 ^{12d}	—	—
38	192.58 ¹³	190.66 ¹³	084.82 ²⁴	083.17 ¹²	—	—
39	189.85 ²⁴	187.93 ¹³	079.49 ¹³	077.82 ¹³	—	—
40	187.03 ²⁴	185.10 ¹³	073.91 ¹⁴	072.37 ²⁴	—	—
41	184.14 ^{24d}	182.08 ¹³	068.20 ¹⁴	066.69 ¹³	—	—
42	180.96 ^{24d}	178.97 ²¹	062.44 ¹⁴	060.96 ¹³	—	—
43	177.64 ²⁵	175.65 ²⁵	056.61 ¹⁴	054.98 ¹³	—	—
44	174.17 ²³	172.10 ¹²	050.52 ^{25d}	048.97 ¹³	—	—
45	170.39 ¹³	168.60 ¹²	044.20 ^{13d}	042.72 ^{13d}	—	—
46	166.59 ²⁴	164.92 ²³	037.90 ¹²	036.43 ¹⁵	—	—
47	162.74 ¹²	160.77 ²⁴	—	—	—	—
48	158.56 ²⁵	156.87 ²²	—	—	—	—
49	154.50 ¹¹	152.59 ²⁵	—	—	—	—
50	149.87 ^{24d}	148.42 ^{22d}	—	—	—	—
51	145.58 ¹²	143.89 ²²	—	—	—	—
52	140.85 ¹²	138.93 ^{44d}	—	—	—	—
53	136.12 ¹¹	134.32 ²³	—	—	—	—
54	131.19 ²⁴	129.57 ^{23d}	—	—	—	—
55	125.94 ¹¹	—	—	—	—	—

TABLE I. (Continued)

R_2 head, $\lambda 3126.116$			(0, 1) band		Q_1 head, $\lambda 3130.369$	
K''	R_2	R_1	Q_2	Q_1	P_2	P_1
5			31,941.19 ¹			
6			940.39 ²			
7			939.28 ²	31,932.20 ¹		
8	31,963.42 ⁵ <i>d</i>	31,957.34 ² <i>d</i>	938.24 ² <i>d</i>	931.45 ³ <i>d</i>		
9	964.92 ³	959.12 ²	937.37 ¹	930.95 ² <i>d</i>		
10	966.43 ³	961.64 ⁵ <i>d</i>	935.89 ²	929.89 ³ <i>d</i>		
11	967.96 ³	963.42 ⁵ <i>d</i>	934.40 ³ <i>d</i>	929.01 ² <i>d</i>		
12	969.38 ³	964.92 ³	932.99 ³ <i>d</i>	928.60 ⁵ <i>d</i>	31,899.20 ¹	31,894.22 ¹
13	970.72 ³	966.43 ³	931.45 ³ <i>d</i>	927.06 ²	894.72 ¹	889.94 ²
14	971.81 ⁴ <i>d</i>	967.96 ³	929.89 ³ <i>d</i>	925.60 ¹	890.60 ⁰	886.24 ²
15	972.78 ⁴	969.38 ³	928.60 ⁵ <i>d</i>	924.48 ⁵ <i>d</i>	886.24 ²	881.65 ⁰ <i>d</i>
16	974.32 ³ <i>d</i>	970.72 ³	926.47 ²	922.73 ⁵	881.65 ⁰ <i>d</i>	877.37 ⁰
17	975.02 ⁴	971.43 ³ <i>d</i>	924.48 ⁵ <i>d</i>	921.14 ⁴	876.74 ²	873.22 ²
18	975.66 ⁴ <i>d</i>	972.78 ⁴	922.73 ⁵	919.36 ³	872.42 ⁴	868.52 ⁰
19	976.64 ⁵ <i>d</i>	973.75 ³ <i>d</i>	920.70 ⁴	917.44 ⁵	867.65 ² <i>d</i>	863.70 ² <i>d</i>
20	977.28 ² <i>d</i>	974.32 ³ <i>d</i>	918.65 ³	915.54 ³ <i>d</i>	862.18 ³ <i>d</i>	859.12 ¹
21	977.95 ²	975.02 ⁴	916.39 ³	913.50 ⁴	857.32 ¹	853.83 ² <i>d</i>
22	978.55 ⁰	975.66 ⁴ <i>d</i>	914.09 ³	911.24 ⁴ <i>d</i>	851.95 ⁰	849.12 ⁰
23	979.10 ⁵ <i>d</i>	976.08 ² <i>d</i>	911.77 ⁴ <i>d</i>	909.07 ⁵ <i>d</i>	846.99 ²	844.11 ¹
24	979.10 ⁵ <i>d</i>	976.64 ⁵ <i>d</i>	909.07 ⁵ <i>d</i>	906.64 ⁵	841.86 ¹	839.08 ¹
25	979.34 ²	976.78 ³	906.64 ⁵	904.16 ³	836.50 ¹	833.46 ² <i>d</i>
26	979.34 ²	976.78 ³	904.16 ⁵	901.47 ⁵	831.07 ⁰	
27	979.34 ²	976.78 ³	901.47 ⁵	898.80 ² <i>d</i>		
28	979.10 ⁵ <i>d</i>	976.78 ³	898.40 ² <i>d</i>	895.98 ⁰		
29	979.10 ⁵ <i>d</i>	976.64 ⁵ <i>d</i>	895.41 ⁵	893.02 ⁵ <i>d</i>		
30	978.55 ⁰	976.08 ² <i>d</i>	892.12 ¹	889.94 ²		
31	977.95 ²	975.66 ⁴ <i>d</i>	888.94 ¹	886.79 ¹		
32	977.28 ² <i>d</i>	975.02 ⁴	885.60 ¹ <i>d</i>	883.61 ¹		
33	976.64 ⁵ <i>d</i>	974.32 ³ <i>d</i>	882.24 ⁴ <i>d</i>	880.31 ³		
34	975.66 ⁴ <i>d</i>	973.75 ³ <i>d</i>	878.70 ¹	876.74 ²		
35	975.02 ⁴	972.78 ⁴	875.05 ¹	873.22 ²		
36	973.75 ³ <i>d</i>	971.81 ⁴ <i>d</i>	871.40 ¹	869.50 ⁵		
37	972.78 ⁴	970.72 ³	867.65 ² <i>d</i>	865.84 ²		
38	971.43 ³ <i>d</i>	969.38 ³	863.70 ² <i>d</i>	862.18 ³ <i>d</i>		
39	970.06 ¹	967.96 ³	859.71 ²	858.14 ³ <i>d</i>		
40	968.64 ¹	966.43 ³	855.57 ² <i>d</i>	853.83 ² <i>d</i>		
41	966.95 ³ <i>d</i>	964.92 ³	851.26 ¹	849.92 ² <i>d</i>		
42	965.31 ⁴	963.42 ⁵ <i>d</i>	846.99 ²	845.49 ¹		
43	963.42 ⁵ <i>d</i>	961.64 ⁵	842.52 ⁰	841.07 ²		
44	961.64 ⁵	959.79 ² <i>d</i>	838.04 ¹ <i>d</i>	836.50 ² <i>d</i>		
45	959.79 ² <i>d</i>	957.80 ² <i>d</i>	833.45 ²	831.97 ³		
46	957.34 ² <i>d</i>	955.62 ²				
47	954.84 ³ <i>d</i>	953.43 ²				
48	952.79 ³	951.07 ³				
49	950.39 ³	948.56 ³				
50	947.63 ³	945.97 ²				
51	945.03 ³	943.32 ²				
52	942.13 ²	940.39 ²				
53	939.28 ²					

of arbitrariness in reporting the data in this way, that is in giving only lines assigned to the P , Q and R branches, it should be emphasized that every line of measurable intensity up to the head of the second band is accounted for and included in Table I. It is true that, due to the complexity of the structure blends of two or more lines are frequent, and the same wave-number often occurs several times in the table. It will be shown below, however, that this

TABLE I. (Continued)

R_2 head, $\lambda 2908.994$			(1, 0) band R_1 head, $\lambda 2909.300$		Q_1 head, $\lambda 2911.700$	
K''	R_2	R_1	Q_2	Q_1	P_2	P_1
4			—	34, 334.17 ¹ 2		
5			—	333.80 ² 3		
6			34, 341.22 ² 2	333.05 ² 3		
7			339.19 ² 3	332.22 ¹ 1		
8			337.60 ¹ 2d	331.55 ² 4		
9			336.01 ² 3d	329.87 ² 2		
10			333.80 ² 3	328.20 ² 2	34, 306.27 ² 5	34, 300.19 ¹ 1
11			331.55 ² 4	326.50 ¹ 3	301.07 ² 2	295.61 ² 5d
12			329.53 ² 4d	324.63 ² 4	296.22 ² 3d	291.08 ² 3
13			327.03 ¹ 3	322.53 ² 3d	291.08 ² 3	286.38 ¹ 1
14			324.63 ¹ 4	320.35 ² 5	285.68 ² 4	281.21 ² 4d
15			321.58 ¹ 2	317.95 ² 3d	280.69 ² 1	276.61 ² 4d
16	34, 365.95 ² 5d	—	318.79 ¹ 3	315.24 ¹ 2	274.37 ² 4	270.55 ¹ 1
17	365.95 ² 5d	34, 362.28 ² 5d	315.99 ¹ 3d	312.63 ² 5d	268.66 ¹ 1	265.24 ² 3d
18	365.28 ¹ 2d	362.28 ² 5d	312.63 ² 5d	309.33 ² 4	262.67 ¹ 0	259.39 ² 5d
19	364.71 ¹ 2	361.75 ² 2	309.33 ² 4	306.27 ² 5	256.56 ¹ 1	253.19 ¹ 2
20	363.87 ¹ 2	360.98 ¹ 2	305.76 ² 5	302.81 ² 3	250.38 ² 3	247.19 ¹ 3
21	363.09 ¹ 2	360.00 ¹ 3	302.07 ¹ 2	299.34 ¹ 2	244.12 ¹ 0	240.76 ¹ 3
22	361.75 ² 2	359.14 ² 4	298.27 ² 3d	295.61 ² 5d	237.27 ² 2	233.94 ¹ 1d
23	360.54 ¹ 1	357.94 ¹ 3	294.39 ¹ 2	291.68 ¹ 3	230.55 ¹ 3	227.55 ¹ 3
24	359.14 ² 4	356.50 ¹ 2	290.14 ¹ 2	287.66 ² 4d	223.56 ¹ 2	220.88 ² 3d
25	357.49 ¹ 3	354.95 ¹ 2d	285.68 ² 4	283.40 ¹ 3	216.56 ¹ 3	213.84 ² 3
26	355.71 ¹ 2	353.28 ¹ 3	281.21 ² 4d	278.83 ¹ 3	209.54 ¹ 1	207.11 ¹ 0
27	353.90 ¹ 2d	351.53 ² 3d	276.61 ² 4d	274.37 ² 4	202.56 ¹ 3d	199.42 ¹ 4
28	351.53 ² 3d	349.31 ² 4d	271.90 ¹ 3d	269.55 ² 4	194.40 ¹ 1d	192.13 ¹ 3
29	349.31 ² 4d	346.97 ² 4d	266.74 ¹ 3	264.60 ¹ 3	186.47 ¹ 2	184.38 ² 5
30	346.97 ² 4d	344.63 ¹ 3	261.49 ¹ 3	259.39 ² 5d	178.55 ² 2	176.55 ¹ 2d
31	344.16 ¹ 3	341.95 ¹ 2d	256.07 ¹ 2	254.15 ¹ 3	170.40 ¹ 0	168.30 ¹ 0
32	341.22 ² 2	339.19 ² 3	250.38 ² 3	248.57 ¹ 4	161.97 ² 3d	159.95 ¹ 1
33	338.27 ¹ 2	336.01 ² 3d	244.87 ¹ 3	243.04 ¹ 3	153.93 ² 1	151.83 ¹ 2
34	335.00 ¹ 2	333.05 ² 3	239.08 ¹ 1	237.27 ² 2	—	—
35	331.55 ² 4	329.53 ² 4d	233.09 ¹ 3d	231.26 ¹ 4	—	—
36	328.20 ² 2	326.03 ¹ 2	226.88 ¹ 3	225.23 ¹ 2	—	—
37	324.32 ² 4	322.53 ² 3d	220.88 ² 3d	218.89 ¹ 4d	—	—
38	320.35 ² 5	317.95 ² 3d	213.84 ² 3	212.32 ¹ 3d	—	—
39	316.30 ¹ 2	314.30 ¹ 2	207.11 ¹ 0	205.57 ¹ 5d	—	—
40	311.79 ¹ 1	310.05 ¹ 2	200.24 ¹ 1	198.64 ¹ 2	—	—
41	307.48 ¹ 2	305.76 ² 5	193.07 ¹ 3	191.70 ¹ 3	—	—
42	302.81 ² 3	301.07 ² 2	185.77 ¹ 4	184.38 ² 5	—	—
43	298.27 ² 3d	296.22 ² 3d	178.55 ² 2	177.13 ¹ 1	—	—
44	293.03 ¹ 1	291.08 ² 3	170.90 ¹ 0	169.31 ¹ 3	—	—
45	287.66 ² 4d	286.16 ¹ 3	163.17 ¹ 1	161.97 ² 3d	—	—
46	282.46 ¹ 1	280.69 ² 1	155.40 ¹ 3	153.93 ² 1	—	—
47	277.16 ¹ 0	275.06 ¹ 1	147.21 ¹ 0	145.97 ¹ 0	—	—
48	270.96 ¹ 1	269.55 ² 4	—	—	—	—
49	265.24 ² 3d	263.54 ¹ 1	—	—	—	—
50	259.39 ² 5d	257.53 ¹ 1d	—	—	—	—

does not materially detract from the certainty of our interpretation of the band structure. Following each wave-number in Table I, a superscript gives the number of times a given value appears, or in other words the number of lines of the band coinciding so closely as to be unresolved and measured as a single line. The last number gives a rough measure of the intensity, on a scale 0 to 5, from eye estimates made during the measurements. These are only strictly comparable for lines near together. The letter *d* indicates a particularly wide or diffuse line. Thus, for example, the line $R_1(26)$ in the (0, 0) band

is given as $33,211.77^4 3d$, since it is a diffuse line formed by the near coincidence of $R_1(26)$, $R_2(28)$, $R_1(14)$, $R_2(10)$, and is of intensity 3 on the scale employed. Regularities in the intensities, as well as the significance of the designations R_2 , R_1 , K , etc., will be discussed below in connection with the quantum analysis.

INTERPRETATION OF THE DATA

Solution of band structure. In attacking the problem of sorting out the various branches, it was noticed from the outset that a short series of very strong lines appears in the region between the second and third heads of each band, and another at some distance beyond the third head (See Fig. 1). These lines are sharp only for a few members, becoming diffuse and soon separating into doublets at each end. Since the separation of adjacent lines in the first of these series is slightly less than that of the close double head, which is that formed by the branches R_2 and R_1 according to the provisional interpretation, it appeared that these strong lines must have about the separation of the so-called "natural" doublets of the R branch. These doublets are formed by pairs of lines with the same value of K^{13} in the $^2\Pi$ state, and the components approach each other as the rotation increases to the point where the spin axis becomes coupled nearly as in Hund's case b .⁶ With the doublets spaced so that the second component of one falls on the first component of the next, the above-mentioned series show exactly the aspect they should. This is the strongest of the series identified by Datta. Similarly, the second series is formed by an analogous coincidence in the doublets of the Q branch. With this opening, it was a simple matter to identify two series of doublets, those of the R and Q branches. The approximate assignment of rotational quantum numbers to these lines in the $(0,0)$ band was then obtained in the following way. The first differences of the *mean* wave-numbers for the Q doublets were plotted against an arbitrary numbering, and extrapolated to zero spacing. This gives roughly the position of the band origin, ν_0 , and a revised numbering of the Q lines, (starting with 1 at the point of convergence) which is correct to one or two units. The slope of the line is 2 ($B' - B''$). Next, taking the mean values of the R doublets, we use the formula for the distance H from the (mean) R head to the origin.

$$H = B' - \frac{(B')^2}{B' - B''}.$$

One thus obtains approximate values of both B' and B'' , and also an idea of the assignment of quantum numbers to the R lines, from the relation $K_{head} = B'/(B' - B'')$, to the nearest whole number. The method of working with mean values of the natural doublets recommends itself for such preliminary work, since these follow very nearly the simple relations in a band with singlet R , Q and P branches.

¹³ K is used here for the resultant of Λ and N , where Λ measures the effective component of the resultant orbital angular momentum along the nuclear axis, and N the angular momentum of the nuclei (K formerly j_k , Λ formerly σ_k , N formerly m). Also J will here replace the former j (quantum number of the total angular momentum).

To be certain of the true K assignment, recourse must be had to the combination principle. To this end, the above process was repeated for the (1,0) band, and the R and Q series identified, with their approximate numbering. By suitably shifting the relative numbering in these series, both in the (0, 0) and (1, 0) bands, two sets of $R-Q$ differences were found which agreed throughout the observed range. These represent the combination differences $R_m(K) - Q_m(K+1) \cong \Delta_1 F''(K)$, of the final state $v'' = 0$. In a $^2\Sigma$ state, one has¹⁴

$$\Delta_1 F''(K) = 2B''(K+1) + 4D''(K+1)^3 + \dots, \quad (1)$$

where D can be approximated by the theoretical relations given on p. 327. Correcting for the cubic term, which is small, there results a series of quantities practically linear in K , which may be used to determine the final true assignment of K values. In agreement with the theoretical requirement for an odd molecule, the K values appeared definitely to be whole numbers. These $R-Q$ combination agreements obtained between the (0, 0) and (1, 0) bands were afterwards proved to be unique by the method of Pomeroy.¹⁵ This is a systematic procedure for trying all possible relative numberings for the four branches,¹⁶ which eliminates the possibility of a fortuitous agreement yielding false combination differences. Three other possible assignments were indeed found, with the short range of lines then available, but all of these gave a relative numbering far outside the range of possible error in the preliminary assignment reached by the method first described. Considering finally the (0, 1) band, it was found that with but a slight shift in the preliminary numbering, satisfactory equality could be obtained with the differences $R_m(K) - Q_m(K) = \Delta_1 F'_m(K)$ from the (0, 0) band.

In identifying the remaining lines of the bands, a convenient procedure described by Loomis and Wood¹⁷ was followed. Having the lines of a portion of a given branch, one derives an empirical formula in K to fit the wave-numbers of these members, using again the mean value of each doublet. The deviations of all observed lines from this equation are then plotted; at least of all which lie within a few cm^{-1} on either side of each calculated value. Such a diagram is shown in Fig. 2 for the Q lines of the (0, 0) band. The series stand out clearly among the extraneous lines, and the proper line to choose in each case is apparent. The method has the added advantage that any other series with approximately the same spacing as those used, such as the so-called "satellite" series, will reveal their presence. By this means, the Q branches were extended to small values of K , the low-frequency components converging in the third head, and the high-frequency components extending into the comparatively simple portion beyond this head. The low K lines of the R branches could then be found by adding the appropriate combination

¹⁴ This expression for $\Delta_1 F''$, the difference between adjacent rotational terms of the lower state, is derived directly from the term formula, Eq. (3) below.

¹⁵ W. C. Pomeroy, Phys. Rev. **29**, 59 (1927).

¹⁶ I am indebted to Mr. S. W. Nile, New York University, for performing this lengthy calculation.

¹⁷ F. W. Loomis and R. W. Wood, Phys. Rev. **32**, 223 (1928).

differences $\Delta_1 F''(K)$, computed from Eq. (1), to the mean values $Q_m(K+1)$. Adding and subtracting half the doublet separation for $Q(K+1)$, the R lines going up to the head were identified as a series of weak lines not previously assigned. The location of this series was clearly not that to be expected if the doubling of $R(K)$ was assumed to be the same as that of $Q(K)$. This is a proof that the large doubling is in the initial state, and that the transition is ${}^2\Pi \rightarrow {}^2\Sigma$, and not ${}^2\Sigma \rightarrow {}^2\Pi$. This statement will be evident if one refers to the energy level diagram of Fig. 3.

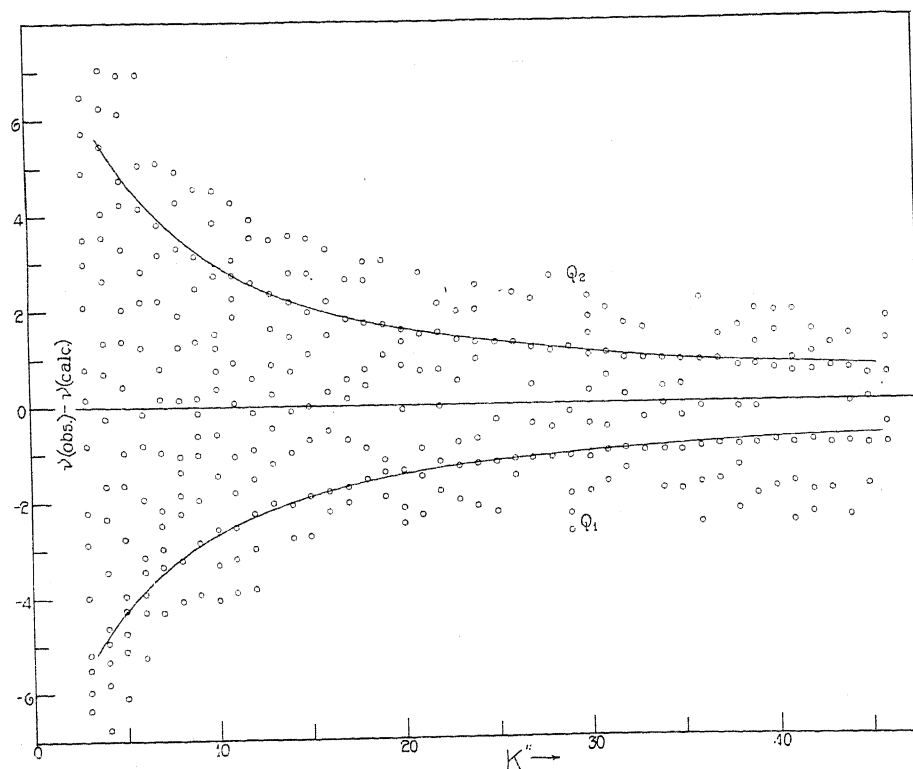


Fig. 2. Deviations of lines in the (0, 0) band from the approximate formula for the mean wave-numbers of the Q doublets: $Q_m(K) = \nu_0 - B' + (B' - B'')(K + \frac{1}{2})^2 + (D' - D'')(K + \frac{1}{2})^4 = 33,185.80 - 0.0685(K + \frac{1}{2})^2 - 0.0920 \times 10^{-6}(K + \frac{1}{2})^4$. The curves give the deviations of the theoretical values of $Q(K)$, calculated by Eq. (11).

The R branches are comparatively free from overlapping by extraneous lines, but their extension to values of K lower than that of the head could not be satisfactorily done in the weaker bands (0, 1) and (1, 0), especially the latter, where the value of K_{head} is smallest. Graphs of the type shown in Fig. 2 were used to identify the Q and P branches in all three bands. The preliminary equation for finding the P branches was based on the approximate relation

$$P_m(K) = Q_m(K-1) - [R_m(K-1) - Q_m(K)]. \quad (2)$$

This is strictly true only in the absence of the well-known Λ -type doubling associated with ${}^2\Pi$ states. A systematic deviation from the predicted positions of the P lines was in fact found, of nearly the same magnitude for the components P_2 and P_1 . The observed lines were slightly displaced toward lower frequencies from the values calculated by Eq. (2).

Analysis of rotational terms. The lines given in Table I comprise six branches for each band, three of which, R_1 , Q_1 and P_1 , are to be correlated with terms of the initial and final states in which the spin vector, $S=1/2$, when completely uncoupled from the nuclear axis, stands parallel to the resultant vector K of the orbital and nuclear angular momenta. Similarly, for R_2 , Q_2 and P_2 , S is anti-parallel to K in both states. In the lower state, ${}^2\Sigma$, there is no component, Λ , of the orbital angular momentum along the molecular axis, and hence no interaction of the spin with this axis, even at very low values of K . The rotational terms may then be represented by

$$F_2(J) = BK(K+1) + D[K(K+1)]^2 + \dots \quad (3)$$

In this case each level is a degenerate pair, $F_2(K-1/2)$ coinciding with $F_1(K+1/2)$, where F_1 and F_2 designate terms having S parallel and antiparallel to K , respectively. If this degeneracy is removed by the rotation, we have ρ -type doubling, but in the present case no evidence for this doubling was found, as explained below, under *Intensities*.

In the initial state, ${}^2\Pi$, the situation is more complicated. At high speeds of rotation, the condition is almost the same as in the ${}^2\Sigma$ case, levels of the same K coming close together. In Fig. 3, the tendency of these levels to approach each other is evident, even when K is relatively small. With decreasing K , the corresponding levels diverge more and more, as the interaction of the spin with the molecular axis becomes stronger. In the limit of no rotation if the doublet is normal, S is anti-parallel to Λ for F_1 terms (${}^2\Pi_{1/2}$), and parallel for F_2 (${}^2\Pi_{3/2}$). If it is inverted, S is parallel to Λ for F_1 terms (${}^2\Pi_{3/2}$) and antiparallel for F_2 (${}^2\Pi_{1/2}$). In either case the set of lower energy is designated F_1 . Two methods are available for distinguishing a normal from an inverted doublet. There should be more missing lines in the ${}^2\Pi_{3/2}$ than in the ${}^2\Pi_{1/2}$ sub-band. In the present case these could not be determined, due partly to the numerous cases of superposition, and partly to the faintness of the first few lines in a branch. An alternative criterion is available in the magnitude of the Λ -type doubling. In case *a*, this is always much larger for ${}^2\Pi_{1/2}$ than for ${}^2\Pi_{3/2}$.¹⁸ It was impossible in our case to detect this doubling for low values of K , and at larger values the type of coupling approaches case *b* rapidly. Van Vleck has shown¹⁸ that in the strict case *b* the Λ -type doubling should be equal for ${}^2\Pi_{1/2}$ and ${}^2\Pi_{3/2}$. That this is not exactly true in the BeF bands, even for very large K , can be most directly shown by comparing the natural doublet separation for $Q(K)$ with that for $R(K-1)$ and $P(K+1)$. The Q branch separations are noticeably smaller, which shows that the Λ -type doubling is greater in the F_1' states (see Fig. 3). The difference is not great, however, and is only

¹⁸ J. H. Van Vleck, Phys. Rev. 33, 467 (1929). R. S. Mulliken, Phys. Rev. 33, 507 (1929).

considerable for high K values, as will be seen in Fig. 4, which represents graphically the course of these natural doublet separations. In the absence of confirmatory evidence from the missing lines, it seemed best to assume that the $^2\Pi$ state is normal.

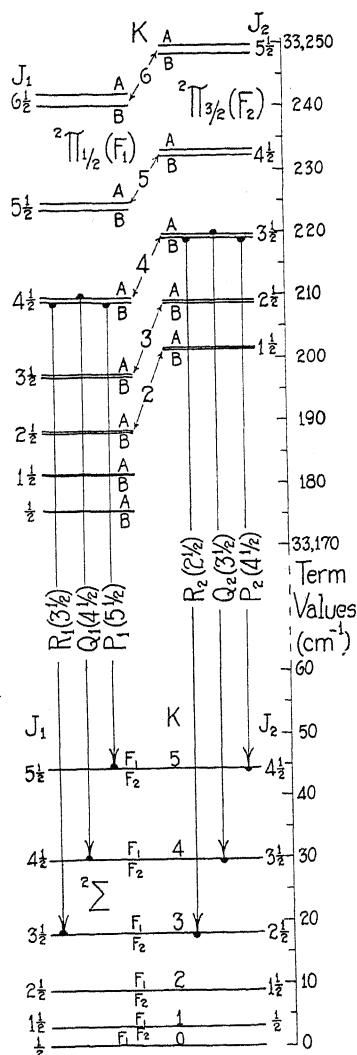


Fig. 3. First few rotational terms in the initial and final states $v=0$, drawn to scale according to Eqs. (3) and (4). The transitions shown by the vertical arrows give the natural doublets $R(K-1)$, $Q(K)$ and $P(K+1)$, (here $K=4$) which have the same doublet separation, except for slight differences in the A-type doubling for $F_1'(K)$ and $F_2'(K)$. The latter doubling, to be visible, is magnified 100-fold.

The effect of the transition from case a at low rotational speeds to case b at high speeds upon the energy formula for doublet states was first studied quantitatively by Kemble.¹⁹ The resulting equations were tested with the OH

¹⁹ E. C. Kemble, Phys. Rev. 30, 387 (1927).

bands, and gave excellent agreement except at the lowest values of K . Slight discrepancies were to be expected, because the formulas were based on the old quantum theory. More recently, Hill and Van Vleck,²⁰ using the new mechanics, have obtained a convenient closed formula for the energy throughout the transition from case a to case b , applicable to both normal and inverted doublets. Aside from their statement that somewhat better agreement with experiment is obtained in the case of OH than found by Kemble, this formula appears not to have been applied in any specific case. It is therefore desirable to see how well it is capable of giving the observed rotational terms in Be F. Denoting by λ the ratio $\Delta E/B\Lambda$, and introducing the term in $D[K(K+1)]^2$ appropriate to case b (since this is appreciable only at higher values of K) the equations of Hill and Van Vleck may be written

$$F_2(J) = B(K^2 - \Lambda^2) + \frac{B}{2} [4K^2 + \lambda(\lambda - 4)\Lambda^2]^{1/2} + D[K(K+1)]^2 + \dots$$

$$F_1(J-1) = B(K^2 - \Lambda^2) - \frac{B}{2} [4K^2 + \lambda(\lambda - 4)\Lambda^2]^{1/2} + D[K(K-1)]^2 + \dots$$
(4)

The J in each case is that appropriate to the value of K in the same equation, that is, $J_2 = K - 1/2$, $J_1 = K + 1/2$. For a $^2\Pi$ state, $\Lambda = 1$ always. The constant $B = h/8\pi^2 Ic$ is best determined from the initial state combination differences at relatively high K , where case b is approximated. Thus, one has

$$\Delta_1 F'_m(K) = 2B'(K+1) + 4D'(K+1)^3 + \dots$$
(5)

Taking $\Delta_1 F'_m(K)$ as the mean of the combination differences $R_m(K) - Q_m(K)$ and $Q_m(K+1) - P_m(K+1)$, to eliminate the effect of Λ -type doubling, the constants²¹ $B^{(0)'}$ and $B^{(1)'}$, were evaluated by least squares from the ΔF 's between $K=20$ and 30. For this purpose, the effect of the term in $(K+1)^3$ was first allowed for by using the accurate values of $D^{(0)'}$ and $D^{(1)'}$ obtained from the theoretical relations²²

$$D^{(v)} = D_e + \beta(v + \frac{1}{2})$$

$$D_e = -4B_e^3/\omega_e^2$$

$$\beta = \frac{\alpha^2}{6\omega_e} + \frac{20\alpha B_e^2 - 32x_e B_e^3}{\omega_e^2}$$
(6)

The equation for β is taken from Kemble's work,²³ and is in a more convenient form than that given by Pomeroy.¹⁵ The ω_e and x_e were taken from Jevons' work,⁵ and α was approximated from preliminary results. An analogous com-

²⁰ E. L. Hill and J. H. Van Vleck, Phys. Rev. 32, 250 (1928).

²¹ The vibrational quantum number v to which a constant refers will be indicated as a superscript, in parentheses.

²² The subscript e indicates that the constant refers to the *equilibrium* position of the nuclei ($v = -\frac{1}{2}$).

²³ E. C. Kemble, Jour. Opt. Soc. Am. 12, 1 (1926). The possibility of getting this convenient expression for β was kindly called to my attention by Prof. R. T. Birge.

putation with $\Delta_1 F''$, using Eq. (1), gave the constants $B^{(0)''}$ and $B^{(1)''}$ of the final state.

Since it was impossible to obtain observed values of the separations of the lowest levels, it was necessary to choose a value for λ such that Eqs. (4) fit the

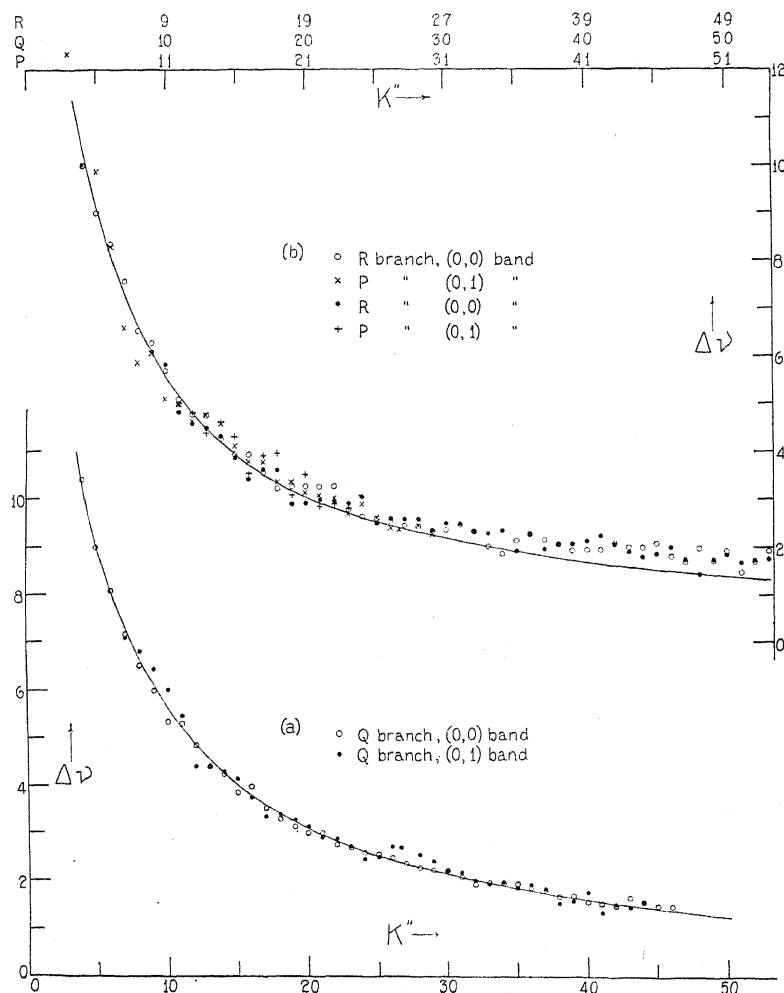


Fig. 4. Separation of the natural doublets as a function of rotational quantum number. In (a) the curve gives the theoretical separations from Eq. (7). The curve in (b) gives the best representation of the empirical separations in the Q branches, to show their divergence from those in the R and P branches at high values of K .

data for higher K most exactly. If this can be done, we have the electronic difference in the upper state for zero rotation, ΔE , since by definition $\lambda = \Delta E/B$. Instead of calculating the actual $F(J)$ values, it is more convenient to use the expression derived from Eqs. (4) for the natural doublet separation.²⁴

²⁴ The equation for Δ given by Hill and Van Vleck applies not to the actual doublets, but to a mean value of the separation for two adjacent ones.

$$\Delta = F_1'(K) - F_2'(K) = B' \left[\frac{1}{2} \{ 4K^2 + \lambda(\lambda - 4) \}^{1/2} + \frac{1}{2} \{ 4(K+1)^2 + \lambda(\lambda - 4) \}^{1/2} - 2(K + \frac{1}{2}) \right] \cong B' \left[\{ 4(K + \frac{1}{2})^2 + \lambda(\lambda - 4) \}^{1/2} - 2(K + \frac{1}{2}) \right]. \quad (7)$$

The best representation of Δ from the Q branches, shown graphically in Fig. 4(a) is obtained with $\lambda = +15.667$, assuming a normal doublet. If the doublet is taken as inverted, an equally good fit is obtained with $\lambda = -11.667$. With $B' = 1.4108$ (see p. —), this gives for the electronic separation in the $^2\Pi$ state $\Delta E = +22.10$ cm $^{-1}$ if it is normal, -16.46 if inverted. A change of ± 0.1 cm $^{-1}$ in these quantities makes the agreement with the observed Δ curves definitely less exact.

The rotational terms, $F(J)$ are not found directly from the spectrum, but only their differences, ΔF . Table II contains these quantities for all cases in which agreements between different sets are to be expected. Strict equality should only be found for corresponding differences in two bands with a common vibrational state, for example $R_2(K) - Q_2(K)$ in the (0, 0) and (0, 1) bands. The agreement of the differences $R - Q$ with $Q - P$ is only approximate, due to the Λ -type doubling in the initial state. It seemed best, for purposes of comparison with the theory, to eliminate the effect of this

TABLE II. Agreements in the combination differences.

$R_2(K) - Q_2(K)$ $= \Delta_1 F_2' - \delta F_2(K + \frac{1}{2})$		$R_1(K) - Q_1(K)$ $= \Delta_1 F_1' - \delta F_1(K + \frac{1}{2})$		$R_2(K) - Q_2(K+1)$ $= \Delta_1 F_2'' - \delta F_2(K+1)$		$R_1(K) - Q_1(K+1)$ $= \Delta_1 F_1'' - \delta F_1(K+1)$	
	(0,0) (0,1)	(0,0) (0,1)		(0,0) (1,0)		(0,0) (1,0)	
17	50.4 50.5	50.7 50.3		52.9 53.3		53.0 53.0	
18	53.4 53.0	53.4 53.4		56.0 56.0		55.9 56.0	
19	56.0 56.0	55.9 56.3		58.9 58.9		58.6 58.9	
20	58.8 58.6	58.6 59.2		61.8 61.8		61.6 61.6	
<hr/>							
21	61.8 61.6	61.6 61.5		64.8 64.8		64.3 64.4	
22	64.4 64.5	64.3 64.4		67.7 67.4		67.6 67.5	
23	67.1 67.3	67.1 67.0		70.4 70.4		70.4 70.3	
24	69.8 70.0	69.8 70.0		73.2 73.5		73.2 73.1	
25	72.5 72.7	72.5 72.6		76.0 76.3		76.0 76.1	
<hr/>							
26	75.2 75.2	75.3 75.3		79.1 79.1		79.0 78.9	
27	78.0 77.9	77.9 78.0		81.9 82.0		81.8 81.9	
28	80.6 80.7	80.5 80.8		84.6 84.8		84.5 84.7	
29	83.5 83.7	83.4 83.6		87.7 87.8		87.6 87.6	
30	86.5 86.4	86.2 86.1		90.7 90.9		90.3 90.5	
<hr/>							
31	89.1 89.0	88.7 88.9		93.6 93.8		93.1 93.4	
32	91.7 91.7	91.6 91.4		96.2 96.3		96.2 96.2	
33	94.2 94.4	94.3 94.0		98.9 99.2		99.0 98.7	
34	97.1 97.0	96.9 97.0		101.9 101.9		101.7 101.8	
35	99.8 100.0	99.5 99.6		104.8 104.7		104.3 104.3	
<hr/>							
36	102.5 102.4	102.2 102.3		107.6 107.3		107.2 107.1	
37	105.1 105.1	104.8 104.9		110.5 110.8		110.1 110.2	
38	107.8 107.7	107.5 107.2		113.1 113.2		112.8 112.4	
39	110.4 110.4	110.1 109.8		115.9 116.1		115.6 115.7	
40	113.1 113.0	112.7 112.6		118.8 118.7		118.4 118.4	
<hr/>							
41	115.9 115.7	115.4 115.0		121.7 121.7		121.1 121.4	
42	118.5 118.3	118.0 117.9		124.3 124.3		124.0 123.9	
43	121.0 120.9	120.7 120.6		127.1 127.4		126.7 126.9	
44	123.6 123.6	123.1 123.3		130.0 129.9		129.4 129.1	

TABLE II. (Continued)

$Q_2(K+1) - P_2(K+1)$ $= \Delta_1 F_2' + \delta F_2(K + \frac{1}{2})$		$Q_1(K+1) - P_1(K+1)$ $= \Delta_1 F_1' + \delta F_1(K + \frac{1}{2})$		$Q_2(K) - P_2(K+1)$ $= \Delta_1 F_2'' + \delta F_2(K+1)$		$Q_1(K) - P_1(K+1)$ $= \Delta_1 F_1'' + \delta F_1(K+1)$	
(0,0)	(0,1)	(0,0)	(0,1)	(0,0)	(1,0)	(0,0)	(1,0)
9 27.8	28.5	29.6	29.7	29.6	29.7
10 31.0	30.8	32.5	32.7	32.3	32.7
11 33.8	33.8	33.9	34.4	35.6	35.3	35.2	35.4
12 36.7	36.7	36.9	37.1	38.7	38.5	38.5	38.3
13 39.2	39.3	39.7	39.4	41.3	41.4	41.7	41.3
14 41.7	42.4	42.4	42.8	44.0	43.6	44.3	43.7
15 45.1	44.8	45.2	45.4	47.0	47.2	47.3	47.4
16 47.8	47.7	48.1	47.9	50.5	50.1	50.3	50.0
17 50.5	50.3	51.0	50.8	53.1	53.3	53.3	53.2
18 53.6	53.1	53.8	53.7	56.2	56.1	56.3	56.1
19 56.2	56.5	56.5	56.4	59.0	59.0	59.3	59.1
20 59.0	59.1	59.2	59.7	62.0	61.6	62.1	62.1
21 61.9	62.1	62.2	62.1	64.9	64.8	64.9	65.4
22 64.5	64.8	64.8	65.0	67.8	67.7	68.0	68.1
23 67.4	67.2	67.5	67.6	70.7	70.8	70.8	70.8
24 70.1	70.1	70.5	70.7	73.6	73.6	73.9	73.8
25 73.0	73.1	73.2	76.6	76.1	76.7	76.3
26 75.6	75.7	79.5	78.7	79.4	79.4
27 78.3	78.4	82.5	82.2	82.2	82.2
28 81.1	81.3	85.1	85.4	85.2	85.2
29 83.9	84.0	88.1	88.2	88.2	88.1

TABLE II. (Continued)

K	$R_2(K) - P_2(K)$ $= \Delta_2 F_{2B}$		$R_1(K) - P_1(K)$ $= \Delta_2 F_{1B}$		$R_2(K-1) - P_2(K+1)$ $= \Delta_2 F_2''$		$R_1(K-1) - P_1(K+1)$ $= \Delta_2 F_1''$	
	(0,0)	(0,1)	(0,0)	(0,1)	(0,0)	(1,0)	(0,0)	(1,0)
12	70.3	70.2	70.5	70.7	74.2	74.1
13	76.0	76.0	76.4	76.5	79.9	79.9
14	81.4	81.2	82.2	81.7	85.4	85.7
15	86.8	86.5	87.4	87.7	91.5	91.6
16	92.4	92.7	93.0	93.3	97.6	97.3	97.4
17	98.2	98.3	98.7	98.2	103.1	103.3	103.4	102.9
18	103.9	103.2	104.4	104.3	109.1	109.4	109.3	109.1
19	109.6	109.0	109.7	110.0	115.0	114.9	115.1	115.1
20	115.1	115.1	115.1	115.6	120.9	120.6	120.7	121.0
21	120.9	120.6	120.7	121.2	126.7	126.6	126.5	127.0
22	126.2	126.6	126.5	126.5	132.6	132.5	132.4	132.4
23	131.5	132.1	131.9	132.0	138.4	138.2	138.3	138.3
24	137.1	137.2	137.2	137.6	144.0	144.0	144.3	144.1
25	142.6	142.8	143.0	143.3	149.8	149.6	149.8	149.4
26	148.3	148.3	148.5	155.5	154.9	155.4	155.5
27	153.6	153.6	161.3	161.3	161.2	161.2
28	158.9	158.9	167.0	167.4	167.0	167.1
29	164.6	164.7	172.7	173.0	172.6	172.8

doubling by defining the ΔF 's in terms of the centers of the doublet levels. Reference to Fig. 3 will show that to obtain these ΔF 's, the differences between actual lines must be corrected by an amount proportional to the

combination defect $[R(K) - Q(K+1)] - [Q(K) - P(K+1)]$, which we will call $2\delta F$. According to the theory,¹⁸ the Λ -type doubling, and hence the combination defect, should be proportional to $(J + \frac{1}{2})^2$. Graphs of $2\delta F$ against J for F_1' and F_2' states gave curvessimilar to that obtained by Loomis and Wood¹⁷ for the Na_2 bands, in which the defect could be satisfactorily represented as proportional to $(J + \frac{1}{2})^2$. Hence a simple method of taking the Λ -type doubling into account in the energy formulas is to give slightly different values of B to the F_A and F_B levels. Their difference can be found from the combination defect by the relation¹⁷

$$2\delta F = [F_A'(J+1) - F_B'(J+1)] + [F_A'(J) - F_B'(J)] \\ \cong 2[F_A'(J + \frac{1}{2}) - F_B'(J + \frac{1}{2})] = 2(B_A' - B_B')(J + \frac{1}{2})^2. \quad (8)$$

The values of $B_A' - B_B'$ obtained in this way were, for F_1' states, $+0.00046$, and for F_2' , $+0.00028$. The corrections, δF_1 and δF_2 , to be applied to the

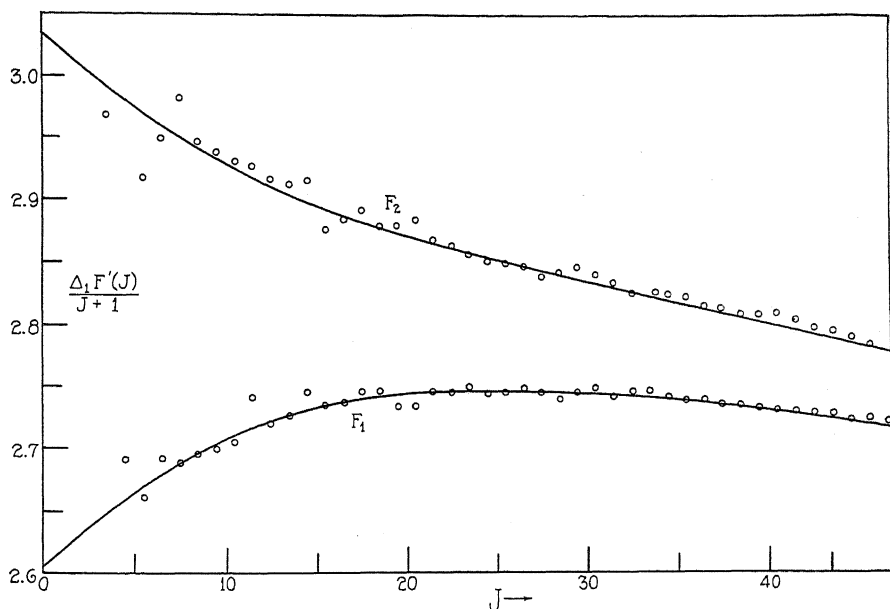


Fig. 5. Comparison of $\Delta_1 F'(J)/(J+1)$ with the theoretical curves (Eq. (10)). Data from the (0, 0) band.

combination differences to obtain the quantities $\Delta_1 F'$ are indicated above each column in Table II.

The formula for $\Delta_1 \hat{F}'$ may be found from Eqs. (4) as follows:

$$\frac{dF_i(J)}{dJ} = \Delta_1 F_i(J - \frac{1}{2}) = 2B'(J + \frac{1}{2}) [1 \pm (4(J + \frac{1}{2})^2 + \lambda(\lambda - 4))^{-1/2}] \\ + 4D'(J + \frac{1}{2} \pm \frac{1}{2})^3 + \dots \quad (9)$$

The upper sign applies to F_2 and the lower to F_1 . This formula was tested in several cases, and agreed with the observed ΔF 's within a few hundredths cm^{-1} . For a graphical comparison of the theory with the empirical results, it is more convenient to divide the ΔF 's throughout by $(J+\frac{1}{2})$. Thus, to a close approximation

$$[\Delta_i F_i'/(J+\frac{1}{2})]/(J+\frac{1}{2}) = 2B'[1 \pm \{4(J+\frac{1}{2})^2 + \lambda(\lambda-4)\}^{-1/2}] + 4D'(J+\frac{1}{2} \pm \frac{1}{2})^2. \quad (10)$$

In Fig. 5 are plotted the observed quantities $\Delta F/(J+1)$ against J , and the curve represents the theoretical values from Eq. (10). Although systematic discrepancies are evident, especially at high J , it is probable that these could be somewhat reduced by slight adjustments of the constants. This was not attempted, but it is clear that the theory accounts remarkably well for the rather complicated variation of the ΔF 's. Not only do the two sets draw together in the proper way, but they show the expected downward trend at large J values due to the term in D' .

The term-formulas (4) are surprisingly simple, considering the complexity of the uncoupling phenomenon involved. They permit the representation of all the lines of a complex band of this kind by comparatively compact and convenient formulas. Taking Eqs. (3) for the terms of the lower state, and Eqs. (4) for those of the upper, and forming the appropriate differences for the several branches, one obtains expressions of the form:

$$\nu = a + bK + c/2[4K^2 + \lambda(\lambda-4)]^{1/2} + dK^2 + eK^3 + fK^4. \quad (11)$$

TABLE III. Values of coefficients for each branch.

Lines	a	b	c	d	e	f
$R_2(K-1)$	$\nu_0 - B_2B'$	B''	B_2B'	$B_2B' - B''$	$2(D' + D'')$	$D' - D''$
$R_1(K-2)$	$\nu_0 - B_1B' - 2B''$	$3B''$	$-B_1B'$	$B_1B' - B''$	$-2(D' - 3D'')$	$D' - D''$
$Q_2(K)$	$\nu_0 - B_2A'$	$-B''$	B_2A'	$B_2A' - B''$	0	$D' - D''$
$Q_1(K-1)$	$\nu_0 - B_1A'$	B''	$-B_1A'$	$B_1A' - B''$	0	$D' - D''$
$P_2(K+1)$	$\nu_0 - B_2B' - 2B''$	$-3B''$	B_2B'	$B_2B' - B''$	$2(D' - 3D'')$	$D' - D''$
$P_1(K)$	$\nu_0 - B_1B'$	$-B''$	$-B_1B'$	$B_1B' - B''$	$-2(D' + D'')$	$D' - D''$

The coefficients to be used for each branch are given in Table III. The origin, ν_{00} of the (0, 0) band was found by applying these equations to several lines of each branch, the average of a number of consistent values being 33,187.21 cm^{-1} . Eq. (11), taken in connection with our final values of the constants, listed below, represents all the lines of the (0, 0) band quite accurately, the largest consistent deviation being about 0.2 cm^{-1} . Errors of this size would not be noticeable in a diagram on the scale of that in Fig. 1. Small systematic trends are apparent, however, when the lines are represented graphically by the method illustrated in Fig. 2. Nevertheless, the formulas reproduce the observed lines to the same order of accuracy as do the more familiar ones applicable to bands of simpler structure.

The molecular constants resulting from the present study of the band structure are given in Table IV. All are expressed in cm^{-1} units.

TABLE IV. *Molecular constants.*

Initial state, $^2\Pi$ (normal)	Final state, $^2\Sigma$
$\Delta E = 22.10$	
$B_{1A}^{(0)} = 1.41083$	
$B_{1B}^{(0)} = 1.41037$	$B^{(0)} = 1.47928$
$B_{2A}^{(0)} = 1.41074$	
$B_{2B}^{(0)} = 1.41046$	
$\alpha = B^{(0)} - B^{(1)} = 0.01610$	0.01685
$D^{(0)} = -8.301 \times 10^{-6}$	-8.209×10^{-6}
$\beta = D^{(1)} - D^{(0)} = 1.060 \times 10^{-8}$	2.903×10^{-8}

Defining B_e as the value of $h/8\pi^2 I_e c$ for the non-vibrating molecule, we have $B^{(v)} = B_e - \alpha(v + \frac{1}{2})$, whence $B_e = B^{(0)} + \alpha/2 = 1.48770$ in the lower state. Using the relation $I_e = 27.66/B_e$ given by Birge,²⁵ the equilibrium value of the moment of inertia in the less excited state becomes $(18.59 \pm 0.03) 10^{-40} \text{ g cm}^2$, and the corresponding internuclear distance 1.357\AA . In the more excited state, these quantities are, respectively, $(19.50 \pm 0.03) 10^{-40} \text{ g cm}^2$ and 1.390\AA .

Intensities. The intensity in each branch rises to a maximum at about $K=20$, and then falls off slowly in the usual way. On our plates, the first few lines were too faint to be observed. The two components of each natural doublet are, as far as can be judged, of equal intensity. Because of the great amount of overlapping in the P branches and the outer part of the Q branches it is difficult to compare the relative intensities of the various branches. By considering only the weaker lines in the regions where blends are frequent, an approximation can be made, however. The P branches have about the same intensity as the R —perhaps slightly less. The Q lines are much stronger, with about twice the intensity of the R lines of the same rotational quantum number.

Mulliken's scheme⁶ for $^2\Pi \rightarrow ^2\Sigma$ transitions predicts certain satellites of the strong branches, and two further branches, for which $\Delta K = \pm 2$. All of these should be relatively weak when $\Delta E/B$ is small. In the absence of ρ -type doubling in the final state, his satellites $^R Q_{21}$ and $^Q P_{21}$ coincide with the strong branches R_2 and Q_2 respectively. Similarly, $^Q R_{12}$ and $^P Q_{12}$ coincide with Q_1 and P_1 . Our failure to observe these satellites is the most important evidence for the absence of appreciable ρ -type doubling in the $^2\Sigma$ state of BeF. Of Mulliken's double R - and double P -form branches, which may be called S_{21} and O_{12} , the former is definitely absent, and therefore almost certainly the latter as well. Our graphical investigations by the method of Fig. 2 show no evidence for the presence of the satellites Q_{2B2A} and Q_{1B1A} , which violate the selection principle for Λ -type doubling, but which are, however, found in the OH bands.

Vibrational structure. Jevons⁵ has derived the following equations to represent the heads of some 45 bands of this system.

²⁵ R. T. Birge, Phys. Rev. Supplement 1, 62 (1929).

$$\begin{aligned}
 R_2 \text{ heads: } \nu &= 33,217.3 + 1153.3\nu' - 5.88\nu'^2 - 1247.1\nu'' + 11.21\nu''^2 - 4.92\nu'\nu'' \\
 R_1 \text{ heads: } \nu &= 33,214.3 + 1153.9\nu' - 5.67\nu'^2 - 1247.1\nu'' + 11.50\nu''^2 - 5.36\nu'\nu'' \\
 Q_1 \text{ heads: } \nu &= 33,179.9 + 1163.8\nu' - 8.78\nu'^2 - 1256.5\nu'' + 9.12\nu''^2.
 \end{aligned}$$

The coefficients in the third equation, except the constant term, apply equally well to the band origins, since the head of the Q_1 branch occurs at a very small value of K . Assuming that the vibrational constants are the same in ${}^2\Pi_{3/2}$ and ${}^2\Pi_{1/2}$, the variation with ν of the distance from the Q_1 head to the origin is probably negligible. Inserting the constant, ν_0 , evaluated above, the equation for origins becomes

$$\nu_0 = 33,187.21 + 1163.8\nu' - 8.78\nu'^2 - 1256.5\nu'' + 9.12\nu''^2 \quad (12)$$

The vibration frequency for infinitesimal amplitudes is, accordingly, $\omega_e = \omega^{(0)} + x\omega^{(0)} = 1265.62$ in the final state, and 1172.58 in the initial state. The electronic frequency, ν_e of the system-origin is obtained as the constant term when Eq. (12) is transformed to express ν_0 as a function of $(\nu + \frac{1}{2})$. We find $\nu_e = 33,233.61$.

Morse²⁶ has recently found an empirical relation connecting the constants $\omega^{(0)}$ and $r^{(0)}$, which is useful as a check on the correctness of our analysis. According to this rule, $\omega^{(0)}r^{(0)} = 3000 \pm 120 \text{ Å}^3/\text{cm}$. In the present case the product is 3159 and 3176 in the upper and lower states, respectively. Another important rule, due to Birge²⁷ requires that $2xB^{(0)}/\alpha = 1.4 \pm 0.2$. From our constants, this ratio for BeF is 1.32 in the upper state, and 1.27 in the lower.

CONCLUSIONS

This is the first analysis of a band structure of the contracting doublet type in a spectrum other than that of a diatomic hydride. Due to the much closer spacing of the lines (the moment of inertia is 13 times that of OH), the actual resolving power available was not far above the minimum required for an unambiguous proof of the structure by the application of the combination principle. In view of the various agreements with the theory, and especially of the graphical proofs of the reality of the different line series, it is thought that our results are justified in all their more essential respects. Several investigators^{1,5} have drawn conclusions concerning the electronic states of other alkaline earth halides from a study of the positions and intensities of the heads in the numerous band systems of these molecules. As stated above, these systems appear to be beyond the reach of our present spectrographs, as far as the rotational structure is concerned. It should be emphasized that bands due to entirely different types of electronic transitions may show an almost identical gross structure. For example, the BeF bands described here show very nearly the same relative spacing and intensity of the three heads in each band as do the blue-green TiO bands recently analysed by Christy,²⁸ although the states involved are even of a different mul-

²⁶ P. M. Morse, Phys. Rev. **34**, 57 (1929).

²⁷ R. T. Birge, Phys. Rev. **31**, 919 (1927) (Abstract).

²⁸ A. Christy, Phys. Rev. **33**, 701 (1929).

tiplicity; the transition is $^3\Pi \rightarrow ^3\Pi$. Therefore, unless one brings every available type of evidence to bear, it seems that conclusions based on a study of the band heads alone must be regarded as highly speculative.

The $^2\Pi \rightarrow ^2\Sigma$ system of BeF constitutes the entire known spectrum of this molecule. Although it has not as yet been obtained in absorption, it appears probable, from analogy with the iso-electronic molecule CN, that the $^2\Sigma$ state is the normal electronic configuration. The band systems in the visible region due to a number of other alkaline earth halides have been found in absorption.²⁹ Mulliken³⁰ has given a provisional assignment of quantum numbers to the individual electrons in BeF as follows: in the $^2\Sigma$ state, $(2s\sigma)^2 (3p\sigma)^2 (2p\pi)^4 (3s\sigma)$, and in the $^2\Pi_i$ state, $(2s\sigma)^2 (3p\sigma)^2 (2p\pi)^4 (3p\pi)$. The assignment given for $^2\Sigma$ is identical with that for the $^2\Sigma$ state (normal state) of BO, CN and CO^+ . For the $^2\Pi$ state, however, the arrangement differs from that proposed for the inverted $^2\Pi$ states of BO, etc., which are designated $(2s\sigma)^2 (3p\sigma)^2 (2p\pi)^3 (3s\sigma)^2$, $^2\Pi$. This difference in interpretation is based on the fact that ΔE in the $^2\Pi$ state is much smaller for BeF than for the others ($\Delta E = 126, 56, 126$). No contradiction to Mulliken's conclusions is therefore contained in our assumption of a normal $^2\Pi$ state, with $\Delta E = 22.10$.

In conclusion, it is a pleasure to acknowledge several valuable suggestions in connection with this work from Professors R. T. Birge and R. S. Mulliken, as well as assistance in the measurements and computations from Mr. S. W. Nile and Professor F. W. Doermann.

²⁹ J. M. Walters and S. Barratt, Proc. Roy. Soc. 118A, 120 (1928).

³⁰ R. S. Mulliken, Phys. Rev. 32, 286 (1928).

RELATIVITY AND AETHER DRIFT¹

By W. F. G. SWANN

BARTOL RESEARCH FOUNDATION OF THE FRANKLIN INSTITUTE

(Received January 10, 1930)

ABSTRACT

While aether drift experiments originally suggested the line of thought which led to the formulation of the restricted theory of relativity, it would seem that the fundamental significance of that theory does not depend primarily upon these experiments. The most logical origin of the transformation of the restricted theory is to be found as a special case of the general theory, and the purpose of the present paper is to show how, with this in view, the fundamental working content of the restricted theory, the invariance of laws under the Lorentzian transformation, is something which has no fundamental relation to the question of whether the aether drift experiments do or do not give a positive result.

THE general belief thirty years ago that the Michelson-Morley-Miller experiment gave a "null" result led to a formulation of the restricted theory of relativity in a form in which the actual space and time measures of observers in two relatively moving systems S and S' were considered, and in which postulates were stated and a law of transformation from one set of measures to the other was derived such as to insure that both observers would measure the same velocity c in all directions for the velocity of light. The transformations are the well-known transformations first derived by Larmor and Lorentz in electromagnetic theory, and are of the form

$$x' = \beta(x - vt) ; y' = y ; z' = z ; t' = \beta \left(t - \frac{v}{c^2} x \right) \quad (1)$$

where
$$\beta = \left(1 - \frac{v^2}{c^2} \right)^{-1/2} .$$

The desire to provide for the null effects in other experiments which had been attempted and which might yet be attempted to detect the earth's "absolute motion" led to the further postulate that the same transformation of measures which served to conceal from the observers any difference as regards the propagation of light in their two systems would also serve to conceal from them any analogous difference as regards any other experiments which they might perform. The postulate was completely provided for by the more widely embracing postulate that the laws of nature² are invariant under the Lorentzian transformation (1), at least this is the case if the two sets of

¹ Presented at the Chicago Meeting of the American Physical Society, November 30, 1929

² The more detailed significance of the content of this statement will be discussed in an article "Relativity and Electrodynamics" now in process of publication in the Physical Review Supplement.

coordinates specified in (1) correspond to the actual measures of observers in the two systems. There are, in fact, two aspects to the restricted theory of relativity as usually understood. The first, which we shall call (*A*), which takes (1) as relations between the actual measures of observers in the two systems, and the second which we shall call (*B*) which concerns itself with the form of physical laws as expressed in the first instance, at any rate, in *one* system of coordinates. In its general form, aspect *B* may be said to imply that "There exists a way of assigning numbers to identifiable points in space-time (there exists a set of coordinates) such that if the laws of nature are expressed in terms of them, they will be found to be invariant under the Lorentzian transformation (1); so that if there exists one set of coordinates in which the statement is true, there exists an infinity of all others, obtainable from the first by Lorentzian transformations, in which the statement is also true." But there will also be a multifold infinity of other sets of coordinates such that if the laws be expressed in terms of these, the statement will not be true.

The test of the forms of the physical laws is the problem of a single observer, who needs for his purpose no collaboration of an obliging assistant sailing through heaven with half the velocity of light. It must be maintained most emphatically that the aspect *B* involves no implication that the different systems obtainable from each other by Lorentzian transformation have anything to do with the actual measures of observers traveling with the corresponding velocity v in relation to the first named system. The quantity v is simply an arbitrary parameter in the equations of transformation, a parameter which does its duty by enabling the transformation to say something about the laws by itself disappearing from the transformed equations. There is no v in the original equations in x, y, z, t , and although v goes into the equations when they are expressed in terms of x', y', z', t' , it mysteriously disappears when everything is boiled down. Even in the case of the electromagnetic equations, where, for example the density ρ in the old equations becomes replaced by $\beta\rho(1 - u_x v/c^2)$, in the transformed equations, u_x being the x component velocity of the electricity in the undashed system, and where v consequently *appears* to take part in the final equations, it actually disappears owing to the fact that the quantity $\beta\rho(1 - u_x v/c^2)$ turns out to be the quantity which, in the dashed system, plays the part of ρ' the electric density in that system.

Having found the forms of the laws in one system of coordinates, the question as to whether or not they are invariant under (1) is a matter to be tested with pen and paper, and not by experiment. *Experiment does play a part in the whole procedure, but its part is played in formulating the laws in one system of coordinates only.*

One immediately commences to wonder what elements are concerned in the question of whether or not *our* system of measures is such that the laws when expressed in terms of them may be expected to be invariant. In order to bring out the essentials of some of the elements here involved, let us consider what the situation would have been if laws had been of such

a type that they were invariant under the Lorentzian transformation when written down in terms of a system of coordinates x, y, z, t , obtainable from ours which we shall call x'', y'', z'', t'' , by the transformation

$$x'' = x - vt; y'' = y; z'' = z; t'' = t \quad (2)$$

i.e., the transformation which a mid-Victorian physicist would have made to allow for what he believed to be a motion of his system of coordinates through space with velocity v . Then, of course, if the laws were written down in the same form but in the double dashed system, they would be wrong. However, if v were of the order of 18 miles per second, which is the sort of velocity we talk about when considering aether drift experiments, it would be necessary to measure to one part in 10^8 , i.e., to an accuracy of v^2/c^2 in order to find the errors in the erroneous laws. Even in our doubled dashed system of coordinates we should consequently discover these laws, although we ought not to. This statement needs some amplification.

If the laws are true when written down in terms of x, y, z, t , i.e., in the system of coordinates which we shall call S , they will also be true when written down in the same form in x', y', z', t' , (the system S') as given by (1), since they are supposed invariant under that transformation. Suppose now, we write them down in the same form, but in x'', y'', z'', t'' , (the system S''). What will be the situation? If we neglect quantities of the order v^2/c^2 , we may write

$$\left. \begin{aligned} x'' &= x'; y'' = y'; z'' = z' \\ t'' &= t' + \frac{v}{c^2}x = t' + \frac{v}{c^2}(x'' + vt'') \\ \text{i.e., } t'' &= t' + \frac{v}{c^2}x'' = t' + \frac{v}{c^2}x' \end{aligned} \right\} \quad (3)$$

Now let there be any experiment which involves the measurement of the differences of the coordinates of two points (denoted by subscripts 1, and 2) which difference remains constant for all values of t' and so of t'' . Such a measurement we shall call a measurement of type I. Then, it is obvious that, excluding the order v^2/c^2 ,

$$x_2'' - x_1'' = x_2' - x_1'; \quad y_2'' - y_1'' = y_2' - y_1'; \quad z_2'' - z_1'' = z_2' - z_1'.$$

Again, suppose that the experiment involves the measurement of the difference between two times at a fixed value of x', y', z' , and hence at a fixed value of x'', y'', z'' . We shall call this a measurement of type II. It is obvious that, in this case, to the order referred to

$$t_2'' - t_1'' = t_2' - t_1'.$$

Now practically all accurate experiments in the field in question involve measurements included in the above types. Thus, suppose for example, we should perform an experiment on the variation of e/m with velocity; and, to fix our ideas, suppose the measurements are made by the usual

magnetic deflection experiment, followed by a compensation of the magnetic deflection by an electrostatic deflection to determine the velocity ω of the electrons. We here use ω to denote the velocity of the electron as distinct from the very much smaller velocity v associated with the transformation. *It is to be distinctly understood that it is the same experiment which is being discussed in the two systems of measures S' and S'' .* The magnetic deflection involves the measurements of lengths which are constant for all time during the experiment, and it also involves the measurement of a magnetic field. The lengths in question involve measurements of the type I, and consequently they are the same excluding the order v^2/c^2 whether they are measured in S' or S'' . As regards the magnetic field, we may trace its measurement according to any consistent scheme, with the same ultimate conclusions. Suppose it is measured by the time of oscillation of a magnet whose moment is subsequently determined by allowing it to vibrate in the vicinity of another similar magnet. The experiment involving the measurement of the time of vibration is one in which two times are recorded at a fixed position, and so is a measurement of type II. The moment of inertia of the magnet involves its dimensions and density. The measurements of the dimensions are of type I. The measurement of density may be regarded as the comparison of the linear dimensions (measurement of type I) of a kilogram of the material, and of the standard kilogram, the equality of the two kilograms being tested by a dynamic method.³ For example, it may be tested by annulment of velocity at impact after traveling with equal and opposite velocities. In this test the velocity as tested in S'' is related to that tested in S' by the relation

$$\frac{dx''}{dt''} = \left(\frac{dx'}{dt'} \right) / 1 + \left(\frac{v}{c^2} \right) \left(\frac{dx'}{dt'} \right)$$

which is easily derivable from (3). In general dx'/dt' would be much less than v , so that $dx''/dt'' = dx'/dt'$ except for quantities of an order less than v^2/c^2 . A similar set of arguments applies to the determination of the moment of the magnet by measuring its time of vibration in the field of a similar magnet, and the net result of all these considerations is that the magnetic field as measured by use of the system of units S' will come out the same as that obtained by using the system S'' , if we neglect v^2/c^2 . A similar conclusion will readily be seen to follow for measurement of the electric field utilized in the determination of ω , the electronic velocity. Hence the net result of all of these considerations is that, exclusive of the order v^2/c^2 , an observer using the system S' will measure values of e/m and of ω which are the same as those obtained by using the system S'' .

It is quite true that the values of ω would be different to a higher order if they could be measured directly in S' and in S'' . For if $x_2' - x_1'$ is the distance travelled by the electron in the time $t_2' - t_1'$ as measured in S' , the velocity ω' as measured in that system is

³ The simple and actually used method of comparison of masses by comparison of weight involves logical complications which would require too much space to unravel here

$$\omega' = \frac{x_2' - x_1'}{t_2' - t_1'}$$

while in S'' , it is

$$\begin{aligned}\omega'' &= \frac{x_2'' - x_1''}{t_2'' - t_1''} = \frac{x_2' - x_1'}{t_2' - t_1' + \frac{v}{c^2}(x_2' - x_1')} \\ &= \frac{x_1' - x_1'}{(t_2' - t_1')\left(1 + \frac{v}{c^2}\omega'\right)}\end{aligned}$$

i. e.,

$$\omega'' = \omega' / \left(1 + \frac{v\omega'}{c^2}\right)$$

which, since ω' may be comparable with c , results in ω'' differing from ω' by quantities of the order $\omega'v/c$. However, it is never in any such way as this that velocities are measured. Even in the measurement of a velocity such as that of light, which approaches most nearly the direct measurement of a velocity, the back and forth journeys of the light are both involved, so that terms involving v/c to the first order become eliminated.

If, in a manner analogous to that adopted above for the e/m experiment we may trace through the kind of experiments whose performance leads to the formulation of the electromagnetic equations, we shall find that if the electromagnetic equations are true when expressed in the measures of S' , the *experiments used to test them* will give the same results in S'' as S' exclusive of the order v^2/c^2 , so that the observer in S'' will discover the equations, although, strictly speaking he ought not to. We must again emphasize that in the above it is the *same* experiments which are supposed discussed in the of S' and S'' units.

It is perhaps worth while pointing out that the electromagnetic equations, when written down in the same form in S' and S'' are not equivalent in all respects up to but excluding v^2/c^2 . Thus if the set expressed in S'' be transformed to S' it will differ from the set originally written down in S' in that in certain places the magnetic fields will have added to them or subtracted from them terms of the order vE/c , and the electric fields will experience corresponding additions or subtractions of the order vH/c . Moreover, terms of the order $\omega'v/c^2$ will make their appearance, where ω' is the velocity of the electricity in S' . All that is maintained is that all experiments so far performed to detect quantities even of the order v/c are experiments falling under classes I and II. This may not seem obvious at first sight in all cases; but if the actual calculations associated with any test be carried completely through to the point where the comparison is between quantities actually measured, it will be found to be true. There are respects in which the electro-

magnetic equations when written down in S' and S'' would differ in their conclusions to the order v/c as regards *ideal* experiments. Thus the wave equation for E is contained in the equations, and in one dimension in free space it is

$$\frac{\partial^2 E'}{\partial t'^2} = c^2 \frac{\partial^2 E'}{\partial x'^2} \quad (4)$$

in S' while, in the same form in S'' it is of course

$$\frac{\partial^2 E''}{\partial t''^2} = c^2 \frac{\partial^2 E''}{\partial x''^2}$$

where E'' refers to the quantity which is defined in S'' in the same manner as E' is defined in S' .

This equation, on transformation to S' by (3) gives

$$\frac{\partial^2 E''}{\partial t'^2} = c^2 \left(\frac{\partial}{\partial x'} - \frac{v}{c^2} \frac{\partial}{\partial t'} \right)^2 E''$$

i.e.,

$$\left(1 - \frac{v^2}{c^2} \right) \frac{\partial^2 E''}{\partial t'^2} = c^2 \left(\frac{\partial^2 E''}{\partial x'^2} - \frac{2v}{c^2} \frac{\partial^2 E''}{\partial x' \partial t'} \right)$$

the general solution of which is

$$E'' = f_1(x' + c_1 t') + f_2(x' - c_2 t')$$

where, excluding terms of the order v^2/c^2

$$c_1 = c - v$$

$$c_2 = c + v$$

and f_1 and f_2 are arbitrary functions. The general solution of (4) is of course

$$E'' = f_1(x' + ct) + f_2(x - ct).$$

Thus, anyone who measured the velocity of a wave directly in the system S' , by measuring the distance travelled by the wave front in one direction in a measured time, would obtain a result differing to the order v/c from that obtained if he had measured the velocity of the same wave in S'' . As already remarked, however, it is not by such procedures that accurate experiments are made.

In view of the foregoing considerations it is not remarkable that we should be led to discover a great scheme of regularity like the electromagnetic scheme lying, as it were, within one part in 10^8 of what our measurements in S'' would predict if we made them with infinite accuracy. Having discovered the scheme of equations, the discovery of its invariance under the Lorentzian transformation is a matter for pen and paper rather than for experiment.

Now, of the two aspects *A* and *B* of the restricted theory of relativity it is *B* which contains the whole of the usefulness of the theory as a working tool. When we study new branches of physics we examine the laws we propose, to see whether they satisfy the mathematical criterion of invariance.⁴ The test, as has been stated, is one of pen and paper, and has no relation whatever to the question of what would happen to measuring apparatus if a velocity were imparted to it.

An example of a class of problem in which, at first sight, we appear to utilize the correspondence between the actual measures and the corresponding Lorentzian system of coordinates, is afforded by the problem leading to the deduction of the Fresnel coefficient on the basis of the theory of relativity. The argument normally proceeds by our taking our stand in imagination in a system of axes moving with the medium. In this system we write for the propagation of a wave along the axis of x ,

$$P = P_0 \sin 2\pi\nu(t - x/V) \quad (5)$$

where V is the velocity applicable to the medium at rest. On applying the Lorentzian transformation to a system S' , specified by (1), equation (5) becomes replaced by

$$P = P_0 \sin 2\pi\nu'(t' - x'/V') \quad (6)$$

where

$$\left. \begin{aligned} \nu' &= \beta\nu(1 - v/V), \quad \beta = (1 - v^2/c^2)^{-1/2} \\ \text{and} \quad V' &= V(1 - v/V)(1 - vV/c^2)^{-1} \end{aligned} \right\} \quad (7)$$

The quantity ν' gives the modification of the original frequency as a result of the Doppler effect, generalized into relativistic form, and V' gives the velocity of the wave in the moving medium when that velocity, which is $-v$ in this case, is measured relative to one who does not participate in the motion of the medium.

The foregoing argument *appears* to involve the principle that if we moved with the medium, the propagation would take place in our frame of reference as it would take place for a medium at rest. The transformation then represents the phenomenon as viewed by one who does not participate in the motion of the medium, and appears to involve something concerned with a relation between the actual measures in the two systems. This conclusion is only apparent, however. The picture of the observer moving along with the medium is one which really plays no part in what we actually do in our mathematical derivation. If we concentrate specifically on what we really do, the story assumes a different aspect as follows: Eq. (5) represents the propagation of the wave with respect to a medium at rest in our axes. We are interested in using the Lorentzian transformation to discover, if possible, the form of the law of propagation when the medium is in motion in our axes. Our criterion is that we must produce a law of propagation which is invariant under the Lorentzian transformation. Now

⁴ I hold no brief for the procedure we adopt, my object here is simply to say what it is.

we may regard our transformation which resulted in (6) as representing the mathematical technique of discovering a suitable invariant law, minus v being the velocity of the medium in our S' system of axes. For we know that a further transformation of the Lorentzian type will leave (6) invariant in form. The equation will, in fact, become

$$P = P_0 \sin 2\pi \bar{v}(\bar{t} - \bar{x}/\bar{V})$$

where

$$\bar{v} = \beta_2 v' (1 - v_2/V'), \quad \beta_2 = (1 - v_2^2/c^2)^{-1/2}$$

$$\bar{V} = V' (1 - v_2/V') (1 - v_2 V'/c^2)^{-1}$$

and v_2 refers to the velocity associated with the second transformation. Remembering that if $-\bar{v}$ the velocity of the medium in the barred system of coordinates, is given by:

$$-\bar{v} = -\frac{v + v_2}{(1 + vv_2/c^2)}$$

and using (7) we readily find that

$$\bar{v} = \bar{\beta}_2 v (1 - \bar{v}/V), \quad \bar{\beta}_2 = (1 - \bar{v}^2/c^2)^{-1/2}$$

$$\bar{V} = V (1 - \bar{v}/V) (1 - \bar{v}V/c^2)^{-1}$$

showing that the second transformation leaves the form (6)–(7) unchanged. The important thing to realize is that the foregoing technique of discovering an invariant law has nothing whatever to do with the question of what would happen in the case of an observer who, with his measuring instrument, participated in the motion of the medium. All that we have said would be applicable if the said measuring instruments were rendered utterly unrelated to their former selves as a result of causing them to move with the medium. There is only *one* set of measuring instruments in mind in the whole argument the set associated with the observer who measures the velocity $-v$ for the medium.

Now the Michelson-Morley-Miller experiment is one sensitive to the order v^2/c^2 ; and a positive result from it invalidates conclusions drawn from the aspect A , but leaves untouched the aspect B , which is the only one of practical use, and which can stand absolutely independent of A .

The aspect B says absolutely nothing about what should happen in the Michelson-Morley-Miller experiment. It has no story to tell as to what happens to things when set in motion, except to this very limited extent: If we knew the complete laws of nature we could predict what happens to a body as a result of changing its motion in any assigned way; and, the aspect B does place upon the complete laws the requirement of invariance. Apart from this, the aspect B is perfectly content if the Michelson-Morley-Miller experiment gives a positive result.

But while one might accept all of the above arguments, he might well say "Yes, but is it not a remarkable thing that the laws of Nature should

be invariant under transformation (1) unless there is something fundamental behind the story?" The old developments of the transformation based upon the postulate of invariance of light velocity, and the relation between the measures of observers in different systems, did place *something* behind the story, even though that something itself did not rest on anything very obvious. The answer to this question is to be found in the general theory of relativity. However, even in this remark we must be careful. It is customary to say that the restricted theory is a special case of the general theory; but, it is only the aspect *B* which is a special case of it. Aspect *A* is not contained in it as a necessary consequence at all. Let us probe the matter a little more deeply.

Perhaps the most concise statement of the general theory applicable to the case in hand is to the effect that it maintains that the laws of nature take the form of differential equations involving the coordinates of things, or quantities expressible in terms of these quantities and involving in addition the derivatives of certain quantities $g_{\mu\nu}$, which satisfy equations usually written

$$G_{\mu\nu} = 0 \quad (8)$$

which are invariant under any point transformation of coordinates, in the sense that if we make an arbitrary transformation, Eq. (8) come back to the same form in new $g_{\mu\nu}$'s which we shall denote by dashed quantities and which are related to the old $g_{\mu\nu}$'s, in such a way as to make

$$\sum \sum g_{\mu\nu} dx_\mu dx_\nu = \sum \sum g_{\mu\nu}' dx_\mu' dx_\nu' \quad (9)$$

ds^2 is usually written for either of the quantities occurring in (9). Moreover, the general theory of relativity demands that the laws of nature shall be invariant under an arbitrary of transformation. An example of such a set of laws is the equation of the geodesic.

$$\frac{d^2 x_\mu}{ds^2} + \frac{1}{2} \sum_{\alpha=1}^4 \sum_{\nu=1}^4 \sum_{\lambda=1}^4 \left\{ g^{\mu\lambda} \left(\frac{\partial g_{\alpha\lambda}}{\partial x_\nu} + \frac{\partial g_{\nu\lambda}}{\partial x_\alpha} - \frac{\partial g_{\alpha\nu}}{\partial x_\lambda} \right) \right\} \frac{dx_\alpha}{ds} \frac{dx_\nu}{ds} = 0 \quad (10)$$

where $g^{\mu\lambda} = \frac{\text{minor of } g_{\mu\lambda}}{g}$, and $g = \begin{vmatrix} g_{11} & g_{12} & g_{13} & g_{14} \\ g_{41} & g_{42} & g_{43} & g_{44} \end{vmatrix}$.

In the first place, I would remark that the invariance as understood in (10) is a very different kind of thing from the invariance as understood in the restricted theory. If in (10), the derivatives of the g 's were inserted as functions of the coordinates, the resulting equation would not be invariant under any transformation of coordinates. It is not as invariant as all that. It would not, in general, be invariant even under the Lorentzian transformation. By the invariance of (10) we mean⁵ that on an arbitrary transformation it comes back to the same form in new g 's which are related to the old g 's by (9).

⁵ A fuller discussion of the significance of invariance in the general theory will be given in a paper "Relativity and Electrodynamics" now in process of publication in the Physical Review Supplement.

Now if there is a region of space in which the g 's become

$$\left. \begin{aligned} g_{\mu\nu} &= 0 \quad \text{if } \mu \neq \nu \\ g_{11} &= g_{22} = g_{33} = -g_{44}/c^2 = -1 \end{aligned} \right\} \quad (11)$$

so that, using x, y, z, t , instead of x_1, x_2, x_3, x_4

$$ds^2 = -dx^2 - dy^2 - dz^2 + c^2 dt^2 \quad (12)$$

then, since it is a characteristic of the Lorentzian transformation that it leaves (12) invariant, i.e. that it leaves the new g 's as $-1, -1, -1, c^2$ if the old g 's were $-1, -1, -1, c^2$, we see that in a region where the g 's are of the form (11) such equations as (10) or, of course, any other equations invariant in the sense of the general theory will be invariant not only in that sense but in the more drastic sense of the restricted theory for the Lorentzian transformation. For the form (11), which makes all the g 's constants, requires all the terms involving g 's to vanish in the system of coordinates in which (11) holds, and consequently the invariance of (12) under the Lorentzian transformation insures the disappearance of the g 's from equations (10) when expressed in any system of coordinates derivable from the former set by a Lorentzian transformation. We may then say that if in any set of laws we have g 's such functions of the coordinates that the ds^2 as given by

$$ds^2 = \sum g_{\mu\nu} dx_\mu dx_\nu$$

reverts at infinity to (12), or to something transformable to that form; then, when expressed in terms of the coordinates applicable to the form (12) the special theory will hold in the form B . This is perhaps the most logical birth-place of the special theory. The special theory will not hold however, in a system of coordinates derivable from one of the Lorentzian set by a transformation which is not a Lorentzian transformation. To illustrate the matter let us consider the problem of astronomical motion, in which it is customary to take such solutions of (8) as give a line element of the symmetrical form:

$$ds^2 = -\gamma^{-1} dr^2 - r^2 d\theta^2 - r^2 \sin^2 \theta d\phi^2 + c^2 \gamma dt^2 \quad (13)$$

where

$$\gamma = 1 - 2m/r.$$

If we go off to infinity, γ becomes unity, and the line element assumes the ordinary polar form transformable to the form

$$ds^2 = -dx^2 - dy^2 - dz^2 + c^2 dt^2 \quad (14)$$

by the ordinary transformation for polar coordinates. We should therefore conclude that in the coordinates x, y, z, t , occurring in (14) the special theory should hold for all differential equations to which the g 's of (13) were in the more general case applicable.

Suppose however, that taking (13) and before proceeding to infinity we make a single transformation equivalent in Cartesian coordinates to

$$x'' = x + vt, \quad y'' = y; \quad z'' = z, \quad t'' = t. \quad (15)$$

The new g 's appropriate to the new expression of the line element would be solutions of (8), for no transformation would rob them of this property since (8) is invariant under any transformation. In proceeding to the solution of any problem in these coordinates, we should, of course, obtain exactly the same differential equations as we obtained before⁶ but transformed to the dashed system of coordinates specified by (15). We should obtain exactly the result which would be obtained by a mid-Victorian physicist who had somehow or other been led to the differential equations which he considered as applicable to the subject when referred to axes at rest and had then corrected them because he learned that the solar system was moving through space with a velocity v . When we proceed to infinity, however, with our x'' , y'' , z'' , t'' , coordinates, we no longer obtain a line element of the form (14) but one obtainable from it by the transformation (15); and the form of this line element tells us immediately that the restricted theory even in the aspect B will not hold in the coordinates in terms of which that line element is expressed.

Thus, all that the general theory predicts as regards the restricted theory, is that, if we make a transformation back from x'' , y'' , z'' , t'' , to x , y , z , t , we shall find ourselves in a set of coordinates such that at infinity the laws expressed in terms of them will be invariant under the Lorentzian transformation, so that they will also be invariant in any coordinates obtained from these coordinates by a Lorentzian transformation. They will not, however, be invariant when expressed in the double dashed coordinates. Further, the general theory, at least without further hypothesis, has no story to tell as to the relation between different Lorentzian systems of coordinates and the corresponding measuring rods, etc. I am perfectly aware of the fact that the equivalence of the line element ds and the ds of experimental measurements is frequently stressed. I merely wish to point out that such equivalence amounts to an extra postulate, and a postulate not essential to the main content of the general or restricted theories—a postulate moreover which leads to such dangerous conclusions as are involved in the “red shift” of the spectrum lines of the sun, and which appears to place upon the theory a burden of prediction greater than it need bear.

⁶ We here refer to the differential equations typified in the astronomical problem by the equations obtained from (10) by substituting the appropriate values of the g 's.

THE SPATIAL DISTRIBUTION OF PHOTOELECTRONS

BY S. E. SZCZENIOWSKI*

RYERSON PHYSICAL LABORATORY, UNIVERSITY OF CHICAGO

(Received December 6, 1929)

ABSTRACT

The perturbation of a hydrogen-like atom by a plane polarized electromagnetic wave is considered on the basis of Dirac's equation, and perturbed wave functions are obtained. These functions lead by a method similar to that used by Sommerfeld in his "Wellenmechanisches Ergänzungsband" to a formula for the spatial distribution of the photoelectrons. To the first approximation this formula differs from that given by a factor 5/9 in the second term. The angle between the average direction of the emission of the photoelectrons and the electric vector of the incident wave appears therefore to be equal to $h\nu/cmv$ instead of the value $(9/5)(h\nu/cmv)$ given. The factor 5/9 follows from the consideration of the normalizing factors for the spherical harmonics, which were not introduced by Sommerfeld. A second approximation has also been obtained showing the influence of electron spin. This approximation differs from that obtained by Carrelli in that the spin and some other terms not considered by Carrelli and also the factor 5/9 appear.

THE photoelectric effect has been treated theoretically on the basis of the wave mechanics by G. Wentzel,¹ G. Beck² and by A. Sommerfeld,³ who gave a better approximation than the first two authors. However, all these authors have started either from the ordinary form of the Schrödinger equation (Wentzel, Beck) or from the form which takes into account the magnetic field but does not consider the relativity and spin effects. It is therefore of some interest to make the corresponding calculations on the basis of the wave equation given by Dirac. By means of this equation the relativity corrections and the spin influence can be found.

The computations in the present paper will proceed in a manner closely similar to the one used by Sommerfeld in his book.

I. PERTURBATION OF A HYDROGEN-LIKE ATOM BY AN ELECTROMAGNETIC WAVE

Dirac has shown⁴ that the Hamiltonian expression for one electron can be written in the form

$$H = (p_0 + eA_0/c) + \rho_1(\sigma, p + eA/c) + \rho_3 mc. \quad (1)$$

In this expression ρ_1, ρ_3 are four-row matrices, σ is a vector four-row matrix, whose components $\sigma_1, \sigma_2, \sigma_3$ are ordinary four-row matrices which satisfy the following relations

* Fellow of the International Education Board.

¹ G. Wentzel, *Zeits. f. Physik* **40**, 574 (1926); **41**, 828 (1926).

² G. Beck, *Zeits. f. Physik* **41**, 443 (1927).

³ A. Sommerfeld, *Atombau und Spektrallinien*, *Wellenmechanisches Ergänzungsband*, p. 207.

⁴ P. A. M. Dirac, *Proc. Roy. Soc. A* **117**, 610 (1928); **118**, 351 (1928).

$$\begin{aligned}\sigma_1\sigma_2 &= i\sigma_3 = -\sigma_2\sigma_1 \\ \sigma_2\sigma_3 &= i\sigma_1 = -\sigma_3\sigma_2\end{aligned}\quad (2)$$

$$\begin{aligned}\sigma_3\sigma_1 &= i\sigma_2 = -\sigma_1\sigma_3 \\ \sigma_1^2 &= 1; \quad \sigma_2^2 = 1; \quad \sigma_3^2 = 1.\end{aligned}\quad (3)$$

Similar relations are valid for ρ_1, ρ_3 ; moreover all σ 's are commutable with all ρ 's.

The parenthesis $(\sigma, p + eA/c)$ stands for a scalar product of the two vectors σ and $p + eA/c$. A is the vector potential, A_0 the scalar potential.

To the Hamiltonian (1) correspond two mutually adjoint functions, ψ and ϕ , each of which has four components.

To obtain Dirac's equations it is to be assumed that

$$p_0 = \frac{i\hbar}{2\pi c} \frac{\partial}{\partial t} \quad (4)$$

and p is to be interpreted as a vector operator, whose components are given by the relations

$$p_x = -\frac{i\hbar}{2\pi} \frac{\partial}{\partial x}; \quad p_y = -\frac{i\hbar}{2\pi} \frac{\partial}{\partial y}; \quad p_z = -\frac{i\hbar}{2\pi} \frac{\partial}{\partial z}. \quad (5)$$

Then simultaneously

$$(p_0 + eA_0/c)\psi + \rho_1(\sigma, p + eA/c)\psi + \rho_3 mc\psi = 0 \quad (6)$$

$$\phi(-p_0 + eA_0/c) + \phi\rho_1(\sigma, -p + eA/c) + \phi\rho_3 mc = 0. \quad (7)$$

In the Eqs. (6) and (7) the following notation has been used. If μ is a four rowed matrix, then

$$\mu\psi = \sum_{k=1}^4 \mu_{ik}\psi_k \quad (i=1,2,3,4) \quad (8)$$

$$\phi\mu = \sum_{k=1}^4 \phi_k\mu_{ki} \quad (i=1,2,3,4) \quad (9)$$

If the matrices ρ and σ are hermitian, as, for instance, those given by Dirac,⁴ ϕ is the conjugate complex function to ψ . This will be the case in the present paper. The operators p_0 and p in Eq. (7) operate backwards.

Dirac has shown, also, that the electric charge and current densities are given by

$$\rho = -e\varphi\psi \quad (10)$$

and

$$J = ec\phi\rho_1\sigma\psi. \quad (11)$$

In these expressions $\phi\psi$ stands for $\sum_{k=1}^4 \phi_k\psi_k$ and $\phi\mu\psi$ for $\sum_{i,k=1}^4 \phi_i\mu_{ik}\psi_k$.

It will be convenient to use the equations of second order, which correspond to the Eqs. (6) and (7) and in the present case will be equivalent to

them. These equations were also derived by Dirac and can be written in the form

$$\left\{ -\left(\frac{i\hbar}{2\pi c} \frac{\partial}{\partial t} + \frac{eV}{c} \right)^2 + \left(-\frac{i\hbar}{2\pi} \nabla + \frac{eA}{c} \right)^2 + m^2 c^2 \right\} \psi + \frac{e\hbar}{2\pi c} (\sigma, H) \psi + \frac{ie\hbar}{2\pi c} \rho_1 (\sigma, E) \psi = 0 \quad (12)$$

$$\left\{ -\left(-\frac{i\hbar}{2\pi c} \frac{\partial}{\partial t} + \frac{eV}{c} \right)^2 + \left(\frac{i\hbar}{2\pi} \nabla + \frac{eA}{c} \right)^2 + m^2 c^2 \right\} \phi + \frac{e\hbar\phi}{2\pi c} (\sigma, H) - \frac{ie\hbar}{2\pi c} \phi \rho_1 (\sigma, E) = 0 \quad (13)$$

In these equations ∇ stands for a vector operator with components $\partial/\partial x$, $\partial/\partial y$, $\partial/\partial z$; H and E are the magnetic and electric field intensities which correspond to the scalar potential $V=A_0$ and the vector potential A , whereas (σ, H) and (σ, E) are scalar products of vectors σ and H or σ and E respectively.

The point of departure for the following considerations will be an undisturbed hydrogen-like atom in the k -th quantum state, consequently V will be equal to Ze/r , where Ze is the charge of the nucleus. The corresponding initial proper functions will be denoted by ψ_k and ϕ_k . As in the present case ϕ_k is always the conjugate complex function to ψ_k it will be sufficient to consider only the functions ψ .

Accordingly the initial conditions are described by the equations

$$\left\{ -\left(\frac{i\hbar}{2\pi c} \frac{\partial}{\partial t} + \frac{eV}{c} \right)^2 + \left(-\frac{i\hbar}{2\pi} \nabla \right)^2 + m^2 c^2 \right\} \psi_k + \frac{ie\hbar}{2\pi c} \rho_1 (\sigma, E_0) \psi_k = 0 \quad (14)$$

where E_0 designates the intensity of the electrostatic field of the nucleus.

Eq. (14) can be written in the form

$$\frac{1}{c^2} \frac{\partial^2 \psi_k}{\partial t^2} - \Delta \psi_k - \frac{4\pi ieV}{\hbar c^2} \frac{\partial \psi_k}{\partial t} - \frac{4\pi^2 e^2 V^2}{\hbar^2 c^2} \psi_k + \frac{4\pi^2 m^2 c^2}{\hbar^2} \psi_k + \frac{2\pi ie}{\hbar c} \rho_1 (\sigma, E_0) \psi_k = 0 \quad (15)$$

It will be now supposed that the atom is disturbed by a plane polarized electromagnetic wave, whose field can be derived from the vector potential

$$A = A_x = a \cos 2\pi\nu \left(t - \frac{z}{c} \right)$$

It is known that

$$H = \text{curl } A ; \quad E = -\text{grad } A_0 - \dot{A}/c \quad (16)$$

and therefore

$$\begin{aligned} H_x = H_z = 0 ; \quad H_y &= a \cdot (2\pi\nu/c) \sin 2\pi\nu(t - z/c) \\ E_y = E_z = 0 ; \quad E_x &= a \cdot (2\pi\nu/c) \sin 2\pi\nu(t - z/c). \end{aligned} \quad (17)$$

Eqs. (17) correspond to an electromagnetic wave, which proceeds in the direction of the z axis and is polarized in the yz plane.

If the values (17) are applied to Eq. (12) it assumes the form

$$\begin{aligned} & \frac{1}{c^2} \frac{\partial^2 \psi}{\partial t^2} - \frac{4\pi^2 e^2 V^2}{h^2 c^2} \psi - \frac{4\pi i e V}{h c^2} \frac{\partial \psi}{\partial t} - \Delta \psi - \frac{4\pi i e a}{h c} \cos 2\pi \nu \left(t - \frac{z}{c} \right) \frac{\partial \psi}{\partial x} \\ & + \frac{4\pi^2 e^2 a^2}{h^2 c^2} \psi \cos^2 2\pi \nu \left(t - \frac{z}{c} \right) + \frac{4\pi^2 m^2 c^2}{h^2} \psi + \frac{4\pi^2 \nu e a}{h c^2} \sin 2\pi \nu \left(t - \frac{z}{c} \right) \sigma_2 \psi \\ & + \frac{2\pi i e}{h c} \rho_1(\sigma, E_0) \psi + \frac{4\pi^2 i e a \nu}{h c^2} \rho_1 \sigma_1 \psi \sin 2\pi \nu \left(t - \frac{z}{c} \right) = 0. \end{aligned} \quad (18)$$

It is convenient to introduce exponentials instead of sines and cosines in Eq. (18). Moreover the term with a^2 as a factor can be neglected, since usually the amplitude a of the disturbing wave is very small. Then

$$\begin{aligned} & \frac{1}{c^2} \frac{\partial^2 \psi}{\partial t^2} - \frac{4\pi^2 e^2 V^2}{h^2 c^2} \psi - \frac{4\pi i e V}{h c^2} \frac{\partial \psi}{\partial t} - \Delta \psi + \frac{4\pi^2 m^2 c^2}{h^2} \psi + \frac{2\pi i e}{h c} \rho_1(\sigma, E_0) \psi \\ & - \frac{2\pi i e a}{h c} \frac{\partial \psi}{\partial x} [e^{2\pi i \nu(t-z/c)} + e^{-2\pi i \nu(t-z/c)}] - \frac{2\pi^2 i e a}{h c^2} [e^{2\pi i \nu(t-z/c)} \\ & - e^{-2\pi i \nu(t-z/c)}] \sigma_2 \psi + \frac{2\pi^2 e \nu a}{h c^2} [e^{2\pi i \nu(t-z/c)} - e^{-2\pi i \nu(t-z/c)}] \rho_1 \sigma_1 \psi = 0. \end{aligned} \quad (19)$$

Eq. (19) can be simplified by the introduction of a perturbation parameter $\chi = -2\pi i e a / h c$. On account of the factor a this parameter is a small quantity, so that all the terms, which have a power of a larger than unity as a factor can be neglected. Therefore it can be assumed that

$$\psi = \psi_k + \chi v + \dots \quad (20)$$

In the expression above ψ_k denotes the proper function for the initial state of the atom and therefore

$$\psi_k = \bar{\psi}_k e^{-2\pi i E_k t / h} \quad (21)$$

where E_k is the proper energy of the atom in the initial state and $\bar{\psi}_k$ is a function of the spatial coordinates only. On account of Eq. (20) the substitution of (21) into Eq. (19) leads to

$$\begin{aligned} & \frac{1}{c^2} \frac{\partial^2 v}{\partial t^2} - \frac{4\pi^2 e^2 V^2}{h^2 c^2} v - \frac{4\pi i e V}{h c^2} \frac{\partial v}{\partial t} - \Delta v + \frac{4\pi^2 m^2 c^2}{h^2} v + \frac{2\pi i e}{h c} \rho_1(\sigma, E_0) v \\ & + \frac{\partial \bar{\psi}_k}{\partial x} \left\{ \exp \left[-\frac{2\pi i}{h} (E_k + h\nu) t + 2\pi i \nu \frac{z}{c} \right] \right. \\ & + \exp \left[-\frac{2\pi i}{h} (E_k - h\nu) t - 2\pi i \nu \frac{z}{c} \right] \left. \right\} \\ & + \frac{\pi \nu}{c} \left\{ \exp \left[-\frac{2\pi i}{h} (E_k - h\nu) t - 2\pi i \nu \frac{z}{c} \right] \right. \end{aligned} \quad (22)$$

$$\begin{aligned}
& -\exp\left[-\frac{2\pi i}{h}(E_k+h\nu)t+2\pi i\nu\frac{z}{c}\right]\bigg\}\sigma_2\psi \\
& +\frac{i\pi\nu}{c}\bigg\{\exp\left[-\frac{2\pi i}{h}(E_k-h\nu)t-2\pi i\nu\frac{z}{c}\right] \\
& -\exp\left[-\frac{2\pi i}{h}(E_k+h\nu)t+2\pi i\nu\frac{z}{c}\right]\bigg\}\rho_1\sigma_1\bar{\psi}=0
\end{aligned}$$

The terms with the squares of χ were omitted, according to the former assumption.

The form of Eq. (22) suggests that

$$v=v_+e^{-(2\pi i/h)(E_k+h\nu)t}+v_-e^{-(2\pi i/h)(E_k-h\nu)t}. \quad (23)$$

If z/λ is written instead of $\nu z/c$ then, on account of (23) Eq. (22) takes the form

$$\begin{aligned}
& -\frac{4\pi^2}{h^2c^2}(E_k\pm h\nu)^2v_{\pm}-\frac{4\pi^2e^2V^2}{h^2c^2}v_{\pm}-\frac{8\pi^2eV}{h^2c^2}(E_k\pm h\nu)v_{\pm}-\Delta v_{\pm} \\
& +\frac{4\pi^2m^2c^2}{h^2}v_{\pm}+\frac{2\pi ie}{hc}\rho_1(\sigma, E_0)v_{\pm}+\frac{\partial\bar{\psi}_k}{\partial x}e^{\pm 2\pi iz/\lambda} \\
& \mp\frac{\pi\nu}{c}e^{\pm 2\pi iz/\lambda}\sigma_2\bar{\psi}_k\mp\frac{i\pi\nu}{c}e^{\pm 2\pi iz/\lambda}\rho_1\sigma_1\bar{\psi}_k=0.
\end{aligned} \quad (24)$$

All upper signs in this equation belong together; the same applies to the lower signs.

Eq. (24) can be written in the form

$$\begin{aligned}
\Delta v_{\pm}+\frac{4\pi^2}{h^2c^2}[(E_k\pm h\nu+eV)^2-m^2c^4]v_{\pm}-\frac{2\pi ie}{hc}\rho_1(\sigma, E_0)v_{\pm} \\
=\frac{\partial\bar{\psi}_k}{\partial x}e^{\pm 2\pi iz/\lambda}\mp\frac{\pi}{\lambda}e^{\pm 2\pi iz/\lambda}\sigma_2\bar{\psi}_k\mp\frac{i\pi}{\lambda}e^{\pm 2\pi iz/\lambda}\rho_1\sigma_1\bar{\psi}_k.
\end{aligned} \quad (25)$$

Since

$$(E_k\pm h\nu+eV)^2-m^2c^4=(E_k\pm h\nu+eV+mc^2)(E_k\mp h\nu+eV-mc^2) \quad (26)$$

and, except for very great values of ν , the expression $E_k\pm h\nu+eV$ is nearly equal to mc^2 , it follows that the Eq. (25) differs from that given by Sommerfeld⁵ only by the terms connected with the electron spin.

However, it is to be remembered that in Eq. (25) the functions v_+ and v_- stand for four components each. Furthermore in Sommerfeld's equations e is the electron charge, whereas in the present paper e denotes the absolute value of the electron charge. This explains the difference of signs, since eV stands for Sommerfeld's $-U$.

The solution of the Eq. (25) can be assumed in the form of an infinite series of the proper solutions of the undisturbed problem. However it is to

⁵ A. Sommerfeld, reference 3, p. 195, Eq. (8).

be taken into account, that the hydrogen atom has a continuum of proper functions for electron energies greater than mc^2 in addition to a discrete set of proper functions for electron energies less than mc^2 . Accordingly

$$v_{\pm} = \sum_i B_i^{\pm} \bar{\psi}_i + \int B^{\pm}(E') \bar{\psi}(E') dE'. \quad (27)$$

However, the expansion of the right side of the Eq. (25) into a corresponding series of proper functions meets a difficulty pointed out by Darwin.⁶ Darwin has shown that the proper functions of the hydrogen atom form an incomplete set of orthogonal functions and that therefore it is not possible to develop an arbitrary four component function into a series of these proper functions. To do this the number of orthogonal solutions must be doubled. It means that in order to go through the calculations the existence of the solutions which correspond to the negative proper energies of the electron must be admitted. These solutions are obtained if the sign of the electron charge in Dirac's equation is changed from negative to positive and it is clear that they have no physical meaning. Therefore it is to be remembered that only those terms of the above mentioned series expansion which correspond to positive proper energies are to be taken into account in further considerations.

According to these considerations the series expansion can be written in the following form

$$\begin{aligned} \frac{\partial \bar{\psi}_k}{\partial x} e^{\pm 2\pi i z/\lambda} \mp \frac{\pi}{\lambda} e^{\pm 2\pi i z/\lambda} \sigma_2 \bar{\psi}_k \mp \frac{i\pi}{\lambda} e^{\pm 2\pi i z/\lambda} \rho_1 \sigma_1 \bar{\psi}_k \\ = \sum_i A_i^{\pm} \bar{\psi}_i + \int A^{\pm}(E') \bar{\psi}(E') dE'. \end{aligned} \quad (28)$$

The integrals in the equation above are to be extended from $E' = mc^2$ to $E' \rightarrow \infty$ and from $E' = -mc^2$ to $E' \rightarrow -\infty$, but only the integrals within positive limits have a physical meaning.

The functions $\bar{\psi}_i, \bar{\psi}(E')$ are solutions of the undisturbed Eq. (14) and therefore

$$\begin{aligned} -\frac{4\pi^2}{h^2 c^2} E_i^2 \bar{\psi}_i - \Delta \bar{\psi}_i - \frac{8\pi^2}{h^2 c^2} E_i eV \bar{\psi}_i - \frac{4\pi^2 e^2 V^2}{h^2 c^2} \bar{\psi}_i \\ + \frac{4\pi^2 m^2 c^2}{h^2} \bar{\psi}_i + \frac{2\pi i e}{hc} \rho_1(\sigma, E_0) \bar{\psi}_i = 0. \end{aligned} \quad (29)$$

Similar equation is valid for $\bar{\psi}(E')$

The Eq. (29) leads to

$$\Delta \bar{\psi}_i - \frac{2\pi i e}{hc} \rho_1(\sigma, E_0) \bar{\psi}_i = -\frac{4\pi^2}{h^2 c^2} [(E_i + eV)^2 - m^2 c^4] \bar{\psi}_i. \quad (30)$$

⁶ G. Darwin, Proc. Roy. Soc. A118, 654 (1928).

If Eqs. (27), (28) and (30) are substituted into (26), then it is found that

$$B_j^\pm = \frac{h^2 c^2}{4\pi^2} \frac{A_j^\pm}{(E_k \pm h\nu + eV)^2 - m^2 c^4} \quad (31)$$

$$B^\pm(E') = \frac{h^2 c^2}{4\pi^2} \frac{A^\pm(E')}{(E_k \pm h\nu + eV)^2 - (E' + eV)^2}.$$

On account of these relations Eqs. (20) leads to

$$\begin{aligned} \psi = & \bar{\psi}_k e^{-2\pi i E_k t / h} - \frac{h c i e a}{2\pi} \left\{ \left[\sum_j \frac{A_j^+ \bar{\psi}_j}{(E_k + h\nu + eV)^2 - (E_j + eV)^2} \right. \right. \\ & + \left. \int \frac{A^+(E') \bar{\psi}(E') dE'}{(E_k + h\nu + eV)^2 - (E' + eV)^2} \right] e^{-2\pi i (E_k + h\nu) t / h} \\ & + \left[\sum_j \frac{A_j^- \bar{\psi}_j}{(E_k - h\nu + eV)^2 - (E_j + eV)^2} \right. \\ & + \left. \left. \int \frac{A^-(E') \bar{\psi}(E') dE'}{(E_k - h\nu + eV)^2 - (E' + eV)^2} \right] e^{-2\pi i (E_k - h\nu) t / h} \right\}. \end{aligned} \quad (32)$$

From Eq. (10) the electric charge density is

$$\begin{aligned} \rho = & -e \bar{\phi}_k \bar{\psi}_k + \frac{h c i e a}{2\pi} \left\{ e^{2\pi i \nu t} \left[\sum_j \frac{A_j^+ \bar{\phi}_j \bar{\psi}_k}{(E_k + h\nu + eV)^2 - (E_j + eV)^2} \right. \right. \\ & - \sum_j \frac{A_j^- \bar{\phi}_j \bar{\psi}_k}{(E_k - h\nu + eV)^2 - (E_j + eV)^2} \left. \right] + e^{-2\pi i \nu t} \left[\sum_j \frac{A_j^+ \bar{\phi}_j \bar{\psi}_k}{(E_k + h\nu + eV)^2 - (E_j + eV)^2} \right. \\ & - \sum_j \frac{A_j^- \bar{\phi}_j \bar{\psi}_k}{(E_k - h\nu + eV)^2 - (E_j + eV)^2} \left. \right] \left. \right\}. \end{aligned} \quad (33)$$

According to the former assumptions the terms whose coefficients are proportional to a^2 were neglected, furthermore the integrals, which correspond to the continuous spectrum are not written out.

From Eq. (33), which is very similar to the one given by Sommerfeld⁷ the dispersion formulas could be obtained in the usual way.

As long as $h\nu \ll mc^2$

$$(E_k \pm h\nu + eV)^2 - (E_j + eV)^2 \cong 2mc^2(E_k - E_j \pm h\nu) \quad (34)$$

because the energy values include the energy mc^2 , so that on the one hand eV is negligibly small with regard to E_k or E_j (except for the K -levels of the heavy elements) and on the other hand each of these terms differs only negligibly (with the same exception) from mc^2 (the energy mc^2 in electron-volts is of the order of $5 \cdot 10^5$).

With that simplification the Eq. (33) leads to the usual dispersion formula. Only when $h\nu$ begins to be comparable with mc^2 and especially for the

⁷ A. Sommerfeld, reference 3, p. 197.

heaviest elements does Eq. (33) give results differing appreciably from the usual dispersion formula. As $h\nu$ is equal to mc^2 for $\lambda \cong 24XU$ it follows that the difference begins to be appreciable for X-rays of the order of 0.1A.

According to Eq. (28) the value of A_j^\pm is given by

$$A_j^\pm = \frac{1}{C_j} \left\{ \int \bar{\phi}_j \frac{\partial \bar{\psi}_k}{\partial x} e^{\pm 2\pi i z/\lambda} d\tau \mp \frac{\pi}{\lambda} \int e^{\pm 2\pi i z/\lambda} \bar{\phi}_j \sigma_2 \bar{\psi}_k d\tau \right. \\ \left. \mp \frac{i\pi}{\lambda} \int e^{\pm 2\pi i z/\lambda} \bar{\phi}_j \rho_1 \sigma_1 \bar{\psi}_k d\tau \right\}. \quad (35)$$

Eq. (35) is obtained if Eq. (28) is multiplied by $\bar{\phi}_j$ on the left-hand side and integrated over the whole space. Furthermore the normalizing integrals

$$\int \bar{\phi}_j \bar{\psi}_j d\tau = C_j \quad (36)$$

are to be used. The integrations in the expressions (36) extend over the whole space.

II. THE PHOTOELECTRIC CURRENT

The photoelectric current excited in a given direction by an electromagnetic wave incident on a hydrogen like atom can now be found on the basis of Eq. (32). Only the photoelectric emission from a single atom will be considered here. To calculate this emission, those excited states of the atom which belong to the continuous spectrum are to be considered. Therefore in the present case the sums in Eq. (32) can be omitted as irrelevant. The values of the coefficients $A^\pm(E')$ are given by the formulas

$$A^\pm(E') = \frac{1}{C(E')} \left\{ \int \bar{\phi}(E') \frac{\partial \bar{\psi}_k}{\partial x} e^{\pm 2\pi i z/\lambda} d\tau \mp \frac{\pi}{\lambda} \int \bar{\phi}(E') \sigma_2 \bar{\psi}_k e^{\pm 2\pi i z/\lambda} d\tau \right. \\ \left. \mp \frac{i\pi}{\lambda} \int \bar{\phi}(E') \rho_1 \sigma_1 \bar{\psi}_k e^{\pm 2\pi i z/\lambda} d\tau \right\} \quad (37)$$

where

$$C(E') = \lim_{\Delta_n E' \rightarrow 0} \frac{\int \Delta_n \bar{\phi}(E') \Delta_n \bar{\psi}(E') d\tau}{\Delta_n E'} \quad (38)$$

(the integral extends over the whole space) and

$$\Delta_n \bar{\phi}(E') = \int_{\Delta_n E} \bar{\phi}(E') dE'; \quad \Delta_n \bar{\psi}(E') = \int_{\Delta_n E} \bar{\psi}(E') dE' \quad (39)$$

(see Fuess⁸).

In Eq. (32) the term $\bar{\psi}_k e^{-2\pi i E_k t/\hbar}$ can be also omitted. This term represents the initial k -th quantum state of the atom and therefore its radial part contains an exponential of the type $e^{-\mu r}$, where μ is a real positive number.

⁸ E. Fuess, Ann. d. Physik 81, 281 (1926).

Since $\mu \sim 10^9$ this exponential vanishes very rapidly with increasing r . (The same applies to the terms of the sums in Eq. (32)). On the other hand the radial parts of the functions $\bar{\varphi}(E')$ have as a factor an exponential $e^{\mu' r}$ where μ' is purely imaginary. They vanish therefore only slowly with growing r . It follows that for the values of r great compared with the atomic dimensions (and it is these values that are to be considered for the photoelectric effect) only the integrals in Eq. (32) are to be taken into account.

According to Sommerfeld⁹ the integrands of these integrals can be separated into three factors

$$a) \frac{A^{\pm}(E')}{(E_k \pm h\nu + eV)^2 - (E' + eV)^2}; \quad b) \bar{\psi}(E') \quad \text{and} \quad c) e^{-2\pi i(E_k \pm h\nu)t/\hbar}.$$

In the factor (a) only V depends upon the coordinates, but, as V is equal to eZ/r it can be safely omitted in the computations. The factor (a) then becomes a constant, i.e. it depends only upon E' .

The factor (c) gives the dependence of $\bar{\psi}$ upon the time. The expression $E_k \pm h\nu$ in the exponent can be interpreted as the energy of the photoelectron. The kinetic energy of the photoelectron is

$$\epsilon = E_k \pm h\nu - mc^2.$$

If the $+$ sign is taken this can be written in the form $\epsilon = h\nu - J$ where $J = mc^2 - E_k$ is the ionization potential. The corresponding expression with the $-$ sign becomes negative. Hence there cannot be given a physical interpretation to the corresponding parts of ψ unless the possibility of existence of states with negative total energy is admitted. The existence of these states has already been admitted to obtain an expansion of the right side of the perturbed Eq. (25) into a series of the proper functions of the undisturbed problem. The factor $E_k - h\nu$ could then be written in the form $-(-E_k + h\nu)$ and the negative kinetic energy of the photoelectron, which evidently has no physical significance would be $\epsilon' = -(-E_k + h\nu) - (-mc^2)$ or $\epsilon' = -(h\nu - J)$. This forms an analogue to Einstein's photoelectric equation.

According to the above considerations these parts of ϕ which correspond to the $-$ sign in the expression $E_k \pm h\nu$ can be omitted, the more so, that the parts with the $+$ sign will be incomparably greater than the parts with the $-$ sign on account of the expression $(E_k + h\nu + eV)^2 - (E' + eV)^2$ in the denominator of the integrands, which tends to zero with E' tending to $E_k + h\nu$.

The factor (b) is the really interesting one for the determination of the spatial distribution of the photoelectrons. Moreover it must be added that only the radial parts of the functions ψ have the continuous spectra. The directional parts have only the discrete proper functions. Therefore on account of the foregoing considerations the following expressions are properly to be used in the subsequent calculations (because A_j^{\pm} and $A(\pm E')$ should be explicitly written as A_{jkm}^{\pm} and $A_{km}^{\pm}(E')$)

⁹ A. Sommerfeld, reference 3, p. 209.

$$\psi \cong -\frac{hc\epsilon_0 e a}{2\pi} e^{-2\pi i(E_{k_0} + h\nu)t/\hbar} \left\{ \sum_k \sum_m \int \frac{A_{km}^+(E') \bar{\psi}_{km}(E') dE'}{(E_{k_0} + h\nu + eV)^2 - (E' + eV)^2} \right\}. \quad (40)$$

To avoid the divergence of the integral in (40) the integration can be performed according to Wentzel¹⁰ along a path which extends slightly around the pole $E' = E_{k_0} + h\nu$ into the positive part of the complex plane E' .

Darwin¹¹ has shown that the solutions of Dirac's equations for a central electrostatic field can be written in the form

$$\begin{aligned} \bar{\psi}_{km}^{(1)} &= -iF_k P_{k+1}^m & \bar{\psi}_{km}^{(3)} &= (k+m+1)G_k P_k^{m+1} \\ \bar{\psi}_{km}^{(2)} &= -iF_k P_{k+1}^{m-1} & \bar{\psi}_{km}^{(4)} &= (-k+m)G_k P_k^{m+1} \end{aligned} \quad (41)$$

and

$$\begin{aligned} \bar{\psi}_{km}^{(1)} &= -i(k+m)F_{-k-1} P_{k-1}^m & \bar{\psi}_{km}^{(3)} &= G_{-k-1} P_k^m \\ \bar{\psi}_{km}^{(2)} &= -i(-k+m+1)F_{-k-1} P_{k-1}^{m+1} & \bar{\psi}_{km}^{(4)} &= G_{-k-1} P_k^{m+1}. \end{aligned} \quad (42)$$

The functions P_k^m are spherical harmonics defined in the following way

$$P_k^m = (k-m)! \sin^m \theta \left(\frac{d}{d \cos \theta} \right)^{k+m} \left(\frac{\cos^2 \theta - 1}{2^k \cdot k!} \right) \cdot e^{im\phi}. \quad (43)$$

It can be shown that

$$P_k^{-m} = (-1)^m P_k^{m*} \quad (44)$$

so that only the values of P_k^m for positive m need to be known. Furthermore

$$\int_0^\pi \int_0^{2\pi} P_k^m P_k^{m*} \sin \theta d\theta d\phi = \frac{4\pi}{2k+1} (k+m)!(k-m)!. \quad (45)$$

The functions F_k and G_k depend upon the radius r only and satisfy the relations

$$\begin{aligned} \frac{2\pi}{h} \left(\frac{E+eV}{c} + mc \right) F_k + \frac{dG_k}{dr} - \frac{k}{r} G_k &= 0 \\ -\frac{2\pi}{h} \left(\frac{E+eV}{c} - mc \right) G_k + \frac{dF_k}{dr} + \left(\frac{k+2}{r} \right) F_k &= 0. \end{aligned} \quad (46)$$

For a hydrogen-like atom with the nuclear charge Ze the potential V is equal to eZ/r and so, if the following notation is used

$$\frac{2\pi}{h} \left(\frac{E}{c} + mc \right) = A^2; \quad \frac{2\pi}{h} \left(\frac{E}{c} - mc \right) = B^2; \quad \frac{2\pi e^2 Z}{hc} = \gamma = Z\alpha \quad (47)$$

where α is the Sommerfeld fine structure constant, then instead of (46)

$$\begin{aligned} \left(A^2 + \frac{\gamma}{r} \right) F_k + \frac{dG_k}{dr} - \frac{k}{r} G_k &= 0 \\ \left(B^2 + \frac{\gamma}{r} \right) G_k - \frac{dF_k}{dr} - \frac{k+2}{r} F_k &= 0. \end{aligned} \quad (48)$$

¹⁰ G. Wentzel, Zeits. f. Physik 40, 574 (1926).

¹¹ C. G. Darwin, reference 6.

The solutions (41) and (42) correspond to different values of the inner quantum number j . For the solution (41) $j = k + \frac{1}{2}$, for (42) $j = k - \frac{1}{2}$. Moreover, for the solution (41) $-k-1 \leq m \leq k$ which leads to $2k+2$ different solutions, whereas for the type (42) one has $-k \leq m \leq k-1$ i.e. $2k$ different solutions. In each case there are $2j+1$ solutions as it should be.

In the subsequent calculations the normalizing integrals for the proper functions (41) and (42) are used. These integrals were given by Darwin¹² For the solution (41)

$$C'_{km} = \int \bar{\phi}_{km} \bar{\psi}_{km} d\tau = 4\pi(k+m+1)!(k-m)! \int_0^\infty (F_k^2 + G_k^2) r^2 dr \quad (49)$$

and for the solution (42)

$$C''_{km} = \int \bar{\phi}_{km} \bar{\psi}_{km} d\tau = 4\pi(k+m)!(k-m-1)! \int_0^\infty (F_{-k-1}^2 + G_{-k-1}^2) r^2 dr. \quad (50)$$

It is also to be noted that the solutions (41) and (42) form an orthogonal set of functions, i. e.

$$\int \bar{\phi}_{kmj}(E) \bar{\psi}_{k'm'j'}(E') d\tau = 0 \quad (51)$$

except for $E=E'$, $k=k'$, $m=m'$ and $j=j'$ (j -inner quantum number).

Darwin has also shown that for $E < mc^2$ a hydrogen-like atom has a set of discrete proper values of E , which correspond to the solutions (41) and (42). For $E > mc^2$ there are solutions for each value of E . This last condition corresponds to the existence of a continuous spectrum. It can be shown that in this latter case F_k and G_k are complex functions, which to the first approximation correspond to spherical waves diverging from the nucleus (or converging towards the nucleus).

To find the approximate forms of F_k and G_k for $r \rightarrow \infty$ all terms in Eqs. (48) with r in the denominator can be omitted in the first approximation. This leads to

$$A^2 F + dG/dr = 0; \quad B^2 G - dF/dr = 0 \quad (52)$$

with both A^2 and B^2 positive. Hence

$$A^2 F + \frac{1}{B^2} \frac{d^2 F}{dr^2} = 0; \quad B^2 G + \frac{1}{A^2} \frac{d^2 G}{dr^2} = 0 \quad (53)$$

and

$$F = ae^{iABr}; \quad G = be^{iABr}. \quad (54)$$

These values of F and G substituted into Eqs. (52) give

$$a = -ibB/A = -ibp \quad (55)$$

p is a small quantity and so $\bar{\psi}^{(1)}$ and $\psi^{(2)}$ are small compared with $\bar{\psi}^{(3)}$ and $\bar{\psi}^{(4)}$.

¹² C. G. Darwin, reference 6.

In the second approximation a and b can be considered as varying slowly with r and so all terms with a/r^2 , a'/r and a'' and analogous terms for b are to be omitted. If the values (53) and (54) are substituted into Eqs. (48) the above assumption leads to

$$a' + \frac{a}{r} \left[1 - \frac{i\gamma}{2} \left(\frac{A}{B} + \frac{B}{A} \right) \right] = 0 \quad (56)$$

and the same equation for b

If one puts

$$\frac{\gamma}{2} \left(\frac{A}{B} + \frac{B}{A} \right) = \delta \quad (57)$$

then the Eq. (56) takes the form

$$a' + \frac{a}{r} (1 - i\delta) = 0 \quad (58)$$

whence

$$a = C e^{i\delta \log r} / r. \quad (59)$$

Therefore finally

$$\begin{aligned} F &= -i p C e^{i(ABr + \delta \log r)} / r \\ G &= C e^{i(ABr + \delta \log r)} / r. \end{aligned} \quad (60)$$

On the basis of the notations (47) it can easily be found that AB is usually of the order 10^9 , whereas δ is, for high speed photoelectrons and low atomic numbers, small compared with unity. As the $\log r$ varies much more slowly than r it follows that $\delta \log r = \tau$ can be considered to this approximation as a constant.

All is now prepared for the actual calculation of the coefficient $A_{km}^+(E')$ in Eq. (40). These coefficients are given by Eq. (37), which, written in the developed form is

$$\begin{aligned} C_{km}(E') A_{km}(E') &= \int \bar{\phi}_{km}^{(1)}(E') \frac{\partial \bar{\psi}_{k_0}^{(1)}}{\partial x} e^{2\pi i z / \lambda} d\tau \\ &+ \int \bar{\phi}_{km}^{(2)}(E') \frac{\partial \bar{\psi}_{k_0}^{(2)}}{\partial x} e^{2\pi i z / \lambda} d\tau \\ &+ \int \bar{\phi}_{km}^{(3)}(E') \frac{\partial \bar{\psi}_{k_0}^{(3)}}{\partial x} e^{2\pi i z / \lambda} d\tau + \int \bar{\phi}_{km}^{(4)}(E') \frac{\partial \bar{\psi}_{k_0}^{(4)}}{\partial x} e^{2\pi i z / \lambda} d\tau \\ &- \frac{\pi}{\lambda} \left[-i \int \bar{\phi}_{km}^{(1)}(E') \bar{\psi}_{k_0}^{(2)} e^{2\pi i z / \lambda} d\tau + i \int \bar{\phi}_{km}^{(2)}(E') \bar{\psi}_{k_0}^{(1)} e^{2\pi i z / \lambda} d\tau \right. \\ &\left. - i \int \bar{\phi}_{km}^{(3)}(E') \bar{\psi}_{k_0}^{(4)} e^{2\pi i z / \lambda} d\tau + i \int \bar{\phi}_{km}^{(4)}(E') \bar{\psi}_{k_0}^{(3)} e^{2\pi i z / \lambda} d\tau \right] \quad (61) \end{aligned}$$

$$-\frac{i\pi}{\lambda} \left[\int \bar{\phi}_{km}^{(1)}(E') \bar{\psi}_{k_0}^{(4)} e^{2\pi iz/\lambda} d\tau + \int \bar{\phi}_{km}^{(2)}(E') \bar{\psi}_{k_0}^{(3)} e^{2\pi iz/\lambda} d\tau \right. \\ \left. + \int \bar{\phi}_{km}^{(3)}(E') \bar{\psi}_{k_0}^{(2)} e^{2\pi iz/\lambda} d\tau + \int \bar{\phi}_{km}^{(4)}(E') \bar{\psi}_{k_0}^{(1)} e^{2\pi iz/\lambda} d\tau \right].$$

The Eq. (61) follows from (37) if it is remembered that, according to Dirac¹³

$$\sigma_2 = \begin{vmatrix} 0 & -i & 0 & 0 \\ i & 0 & 0 & 0 \\ 0 & 0 & 0 & -i \\ 0 & 0 & i & 0 \end{vmatrix} \quad \text{and} \quad \rho_1 \sigma_1 = \begin{vmatrix} 0 & 0 & 0 & 1 \\ 0 & 0 & 1 & 0 \\ 0 & 1 & 0 & 0 \\ 1 & 0 & 0 & 0 \end{vmatrix}. \quad (62)$$

To simplify the calculations it will be supposed that the hydrogen-like atom considered is initially in the normal unexcited state. According to Darwin two possibilities are then to be considered¹⁴.

Either

$$\bar{\psi}_{k_0}^{(1)} = \frac{-i\gamma}{1+(1-\gamma^2)^{1/2}} P_1^0 r^\beta e^{-r/a_0} \quad \bar{\psi}_{k_0}^{(3)} = r^\beta e^{-r/a_0} \quad (63)$$

$$\bar{\psi}_{k_0}^{(2)} = \frac{-i\gamma}{1+(1-\gamma^2)^{1/2}} P_1^1 r^\beta e^{-r/a_0} \quad \bar{\psi}_{k_0}^{(4)} = 0$$

OR

$$\bar{\psi}_{k_0}^{(1)} = \frac{-i\gamma}{1+(1-\gamma^2)^{1/2}} P_1^{-1} r^\beta e^{-r/a} \quad \bar{\psi}_{k_0}^{(3)} = 0 \quad (64)$$

$$\bar{\psi}_{k_0}^{(2)} = \frac{-i\gamma}{1+(1-\gamma^2)^{1/2}} P_1^0 r^\beta e^{-r/a_0} \quad \bar{\psi}_{k_0}^{(4)} = -r^\beta e^{-r/a_0}$$

In the equations above β denotes $(1-\gamma^2)^{1/2}-1$ and a_0 is equal to a/Z where a is the radius of the first Bohr orbit.

Accordingly either

$$\frac{\partial \bar{\psi}_{k_0}^{(1)}}{\partial x} = \frac{-i\gamma}{1+(1-\gamma^2)^{1/2}} \frac{\partial}{\partial r} (r^{\beta-1} e^{-r/a_0}) P_1^0 r \sin \theta \cos \phi \quad (r P_1^0 = z) \\ \frac{\partial \bar{\psi}_{k_0}^{(2)}}{\partial x} = \frac{-i\gamma}{1+(1-\gamma^2)^{1/2}} \frac{\partial}{\partial r} (r^{\beta-1} e^{-r/a_0}) P_1^1 r \sin \theta \cos \phi - \frac{i\gamma}{1+(1-\gamma^2)^{1/2}} r^{\beta-1} e^{-r/a_0} \\ \frac{\partial \bar{\psi}_{k_0}^{(3)}}{\partial x} = \frac{\partial}{\partial r} (r^\beta e^{-r/a_0}) \quad (r P_1^1 = x + iy) \\ \frac{\partial \bar{\psi}_{k_0}^{(4)}}{\partial x} = 0 \quad (65)$$

¹³ P. A. M. Dirac, Proc. Roy. Soc. **117**, 680 (1928).

¹⁴ C. G. Darwin, l. c.

or

$$\begin{aligned}
 \frac{\partial \bar{\psi}_{k_0}^{(1)}}{\partial x} &= -\frac{i\gamma}{1+(1-\gamma^2)^{1/2}} \frac{\partial}{\partial r} (r^{\beta-1} e^{-r/a_0}) P_1^{-1} r \sin \theta \cos \phi + \frac{i\gamma}{1+(1-\gamma^2)^{1/2}} r^{\beta-1} e^{-r/a_0} \\
 \frac{\partial \bar{\psi}_{k_0}^{(2)}}{\partial x} &= -\frac{i\gamma}{1+(1-\gamma^2)^{1/2}} \frac{\partial}{\partial r} (r^{\beta-1} e^{-r/a_0}) P_1^0 r \sin \theta \cos \phi \quad (-r P_1^{-1} = x - i\gamma) \\
 \frac{\partial \bar{\psi}_{k_0}^{(3)}}{\partial x} &= 0 \\
 \frac{\partial \bar{\psi}_{k_0}^{(4)}}{\partial x} &= -\frac{\partial}{\partial r} (r^\beta e^{-r/a_0}).
 \end{aligned} \tag{66}$$

These two possibilities will be considered separately.

The integrals in Eq. (61) differ from zero only for certain definite values of k and m . The next step of the computations consists in determining these values.

On account of the appearance of the factor $e^{2\pi iz/\lambda}$ in the integrands there are two possible ways of performing the computations. Either as Sommerfeld has done, one can develop the function $e^{2\pi i r \cos \theta / \lambda}$ into a series of powers of $r \cos \theta / \lambda$ and then can calculate the possible values of the coefficients $A_{km}(E')$ on the basis of this expansion or one can start from the function $e^{2\pi i r \cos \theta / \lambda}$ itself. This last method was used recently by Carrelli.¹⁵ Both these methods lead to the same results on account of the absolute and uniform convergence of the series

$$1 + \frac{x}{1!} + \frac{x^2}{2!} + \frac{x^3}{3!} + \dots \tag{67}$$

for all points of the x plane. The series (67) can be therefore integrated term by term, which gives the same result as the integration of the function e^x itself. The same applies to the products of the exponential by various spherical harmonics and the products of the expansion (67) by these harmonics.

Carrelli finds the coefficients $A_{km}(E')$ in the form of the functions of a quantity R equal to

$$\lambda/2\pi (1/a_0 + iAB)$$

and then develops these functions into series of R . Sommerfeld's method leads immediately to the power series of R as the value for $A_{km}(E')$. It is obvious that both these power series are identical.

Carrelli has computed only the coefficients $A_{11}(E')$ and $A_{21}(E')$ on the basis of the Schrödinger equation and in his calculations took into account only the first two terms of the power series expansions for each of these coefficients. These terms were of the order of $1/R^2$ and $1/R^4$ for the coefficient $A_{11}(E')$ and of the orders of $1/R^3$ and $1/R^5$ for the coefficient $A_{21}(E')$.

¹⁵ A. Carrelli, *Zeits. f. Phys.* **56**, 694 (1929).

To be consistent Carrelli should also find the first term of the expansion, which corresponds to the coefficient $A_{31}(E')$, whose order is $1/R^4$ and the first term of the expansion for $A_{41}(E')$ which is of the order of $1/R^5$. These last two terms were neglected by Carrelli and this invalidates his result. To appreciate the influence of the above mentioned terms one has to consider that in Carrelli's case the perturbed wave function can be written in the form

$$\psi = A_{11}Q_1^1 \cos \phi + A_{21}Q_2^1 \cos \phi + A_{31}Q_{31}^1 \cos \phi + A_{41}Q_4^1 \cos \phi \quad (68)$$

where Q_k^m denote the spherical harmonics used by Carrelli. The values of the harmonics in (68) are

$$\begin{aligned} Q_1^1 &= \sin \theta & Q_2^1 &= 3 \sin \theta \cos \theta \\ Q_3^1 &= (3/2) \sin \theta (5 \cos^2 \theta - 1) & Q_4^1 &= (5/2) \sin \theta \cos \theta (7 \cos^2 \theta - 3) \end{aligned} \quad (69)$$

whence

$$\begin{aligned} \psi = \sin \theta \cos \phi \left\{ A_{11} + 3A_{21} \cos \theta + \frac{15}{2}A_{31} \cos^2 \theta \right. \\ \left. - \frac{3}{2}A_{31} + \frac{35}{2} \cos^3 \theta A_{41} - \frac{15}{2}A_{41} \cos \theta \right\}. \end{aligned} \quad (70)$$

It follows, that the terms omitted by Carrelli were

$$-\frac{3}{2}A_{31} \quad \text{and} \quad -\frac{15}{2}A_{41} \cos \theta.$$

In the present paper Sommerfeld's method of computation will be used. To obtain the degree of approximation comparable with that of Carrelli the exponential $e^{2\pi i r \cos \theta / \lambda}$ will be developed into a power series, whose first four terms will be retained. Thus

$$e^{2\pi i r \cos \theta / \lambda} = 1 + \frac{2\pi i r}{\lambda} \cos \theta - \frac{2\pi^2 r^2}{\lambda^2} \cos^2 \theta - \frac{4\pi^3 i r^3}{3\lambda^3} \cos^3 \theta. \quad (71)$$

To find the values of k and m for which Eq. (61) differs from zero it is sufficient to take into account the orthogonality relations for the functions P_k^m , as Sommerfeld has done. Those relations are

$$\int_0^\pi \int_0^{2\pi} P_k^m P_l^{n*} \sin \theta d\theta d\phi = 0 \quad \left(\begin{matrix} k \neq l \\ m \neq n \end{matrix} \right). \quad (72)$$

Furthermore in Eqs. (65) and (66) $\frac{1}{2}(e^{i\phi} + e^{-i\phi})$ can be written instead of $\cos \phi$. The values of the functions P_k^m for those values of k and m which enter into consideration in this paper are given below

$$\begin{aligned} P_0^0 &= 1 & P_1^1 &= \sin \theta e^{i\phi} \\ P_1^0 &= \cos \theta & P_2^1 &= 3 \sin \theta \cos \theta e^{i\phi} \\ P_2^0 &= 3 \cos^2 \theta - 1 & P_3^1 &= 3 \sin \theta (5 \cos^2 \theta - 1) e^{i\phi} \end{aligned}$$

$$\begin{aligned}
P_3^0 &= 3(5 \cos^3 \theta - 3 \cos \theta) & P_4^1 &= 15 \sin \theta (7 \cos^3 \theta - 3 \cos \theta) e^{i\phi} \\
P_4^0 &= 3(35 \cos^4 \theta - 30 \cos^2 \theta + 3) & & \\
P_2^2 &= 3 \sin^2 \theta e^{2i\phi} & & \\
P_3^2 &= 15 \sin^2 \theta \cos \theta e^{2i\phi} & & \\
P_4^2 &= 15 \sin^2 \theta (7 \cos^2 \theta - 1) e^{2i\phi}.
\end{aligned} \tag{73}$$

It will be supposed now that the initial state of the atom is given by Eqs. (63) and (65). The two types of the solutions, given by the Eqs. (41) and (42) have to be considered separately. The reasoning quite similar to that of Sommerfeld shows that for the solution (41) the coefficients $A'_{km}(E')$ (the accent is used to denote the first type of the solution) are different from zero for

$$\begin{aligned}
k=0 & \quad m=-1 & k=3 & \quad m=\pm 1 \\
k=1 & \quad m=\pm 1 & k=4 & \quad m=\pm 1 \\
k=2 & \quad m=\pm 1 & &
\end{aligned} \tag{74}$$

Similarly for the solution (42) the coefficients $A''_{km}(E')$ (two accents denote the second type of solution) are different from zero for

$$\begin{aligned}
k=1 & \quad m=-1 & k=4 & \quad m=\pm 1 \\
k=2 & \quad m=\pm 1 & k=5 & \quad m=\pm 1 \\
k=3 & \quad m=\pm 1 & &
\end{aligned} \tag{75}$$

It is to be noted that for the term $-4\pi^3 i r^3 \cos^3 \theta / 3\lambda^3$ in the expansion (71) only the integrals in Eq. (61) with the greatest absolute value were taken into account.

For the sake of brevity the following notations are used in the subsequent calculations (κ is equal to AB).

$$\int_0^\infty \frac{\partial}{\partial r} (r^{\beta-1} e^{-r/a_0}) e^{-i\kappa r} r^2 dr = Q_1 \tag{76} \quad \int_0^\infty r^\beta e^{-r/a_0} e^{-i\kappa r} r^2 dr = Q_6 \tag{81}$$

$$\int_0^\infty \frac{\partial}{\partial r} (r^{\beta-1} e^{-r/a_0}) e^{-i\kappa r} r^3 dr = Q_2 \tag{77} \quad \int_0^\infty \frac{\partial}{\partial r} (r^\beta e^{-r/a_0}) e^{-i\kappa r} r dr = Q_7 \tag{82}$$

$$\int_0^\infty \frac{\partial}{\partial r} (r^{\beta-1} e^{-r/a_0}) e^{-i\kappa r} r^4 dr = Q_3 \tag{78} \quad \int_0^\infty \frac{\partial}{\partial r} (r^\beta e^{-r/a_0}) e^{-i\kappa r} r^2 dr = Q_8 \tag{83}$$

$$\int_0^\infty r^\beta e^{-r/a_0} e^{-i\kappa r} dr = Q_4 \tag{79} \quad \int_0^\infty \frac{\partial}{\partial r} (r^\beta e^{-r/a_0}) e^{-i\kappa r} r^3 dr = Q_9 \tag{84}$$

$$\int_0^\infty r^\beta e^{-r/a_0} e^{-i\kappa r} r dr = Q_5 \tag{80} \quad \int_0^\infty \frac{\partial}{\partial r} (r^\beta e^{-r/a_0}) e^{-i\kappa r} r^4 dr = Q_{10}. \tag{85}$$

If the values (73) of the spherical harmonics and the normalizing integrals (49) and (50) are taken into account then with regard to Eq. 61 it follows after some easy calculations that

$$A'_{0,-1}(E') = \frac{\pi}{\lambda} Q_5 \left(i + \frac{\gamma p}{6} \right) + \frac{\pi^2}{3\lambda^2} Q_6 (2p + i\gamma) \quad (86)$$

$$A'_{1,1}(E') = -\frac{i\gamma p}{12} Q_1 + \frac{\pi^2}{30\lambda^2} i\gamma p Q_3 + \frac{Q_7}{6} - \frac{\pi^2}{15\lambda^2} Q_9 + \frac{i\pi^2}{15\lambda^2} \gamma p Q_6 - \frac{\pi\gamma}{6\lambda} Q_5 \quad (87)$$

$$A'_{1,-1}(E') = \frac{i\gamma p}{12} Q_1 - \frac{\pi^2}{30\lambda^2} i\gamma p Q_3 - \frac{Q_7}{6} + \frac{\pi^2}{15\lambda^2} Q_9 - \frac{2\pi^2}{3\lambda^2} Q_6 + \frac{\pi\gamma}{6\lambda} Q_5 \quad (88)$$

$$A'_{2,1}(E') = \frac{\pi\gamma p}{30\lambda} Q_2 + \frac{i\pi}{\lambda} Q_8 - \frac{\pi^2}{15\lambda^2} i\gamma Q_6 - \frac{2i\pi^3}{105\lambda^3} Q_{10} \quad (89)$$

$$A'_{3,1}(E') = -\frac{\pi^2}{210\lambda^2} i\gamma p Q_3 - \frac{\pi^2}{105\lambda^2} Q_9 \quad (90)$$

$$A'_{2,-1}(E') = -\frac{\pi\gamma p}{30\lambda} Q_2 - \frac{i\pi}{\lambda} Q_8 + \frac{\pi^2}{15\lambda^2} i\gamma Q_6 + \frac{2i\pi^3}{105\lambda^3} Q_{10} \quad (91)$$

$$A'_{3,-1}(E') = -\frac{\pi^2}{210\lambda^2} i\gamma p Q_3 + \frac{\pi^2}{105\lambda^2} Q_9 \quad (92)$$

$$A'_{4,1}(E') = -\frac{2i\pi^3}{2835\lambda^3} Q_{10} \quad (93)$$

$$A'_{4,-1}(E') = \frac{2i\pi^3}{2835\lambda^3} Q_{10} \quad (94)$$

$$A''_{1,-1}(E') = \frac{i\gamma p}{6} Q_1 - \frac{\pi^2}{15\lambda^2} i\gamma p Q_3 + \frac{i\gamma p}{2} Q_4 - \frac{Q_7}{3} + \frac{2\pi^2}{15\lambda^2} Q_9 + \frac{2\pi^2}{3\lambda^2} Q_6 \\ + \frac{\pi}{\lambda} Q_5 \left(ip - \frac{\gamma}{6} \right) \quad (95)$$

$$A''_{2,1}(E') = \frac{\pi\gamma p}{30\lambda} Q_2 + \frac{i\pi}{15\lambda} Q_8 + \frac{\pi\gamma p}{6\lambda} Q_5 - \frac{\pi^2}{15\lambda^2} i\gamma A_6 - \frac{2i\pi^3}{105\lambda^3} Q_{10} \quad (96)$$

$$A''_{2,-1}(E') = -\frac{\pi\gamma p}{30\lambda} Q_2 - \frac{\pi\gamma p}{6\lambda} Q_5 - \frac{i\pi}{5\lambda} Q_8 - \frac{2\pi^2}{3\lambda^2} Q_6 (p + i\gamma) + \frac{2i\pi^3}{35\lambda^3} Q_{10} \quad (97)$$

$$A''_{3,1}(E') = \frac{\pi^2 i\gamma p}{105\lambda^2} Q_3 - \frac{2\pi^2}{105\lambda^2} Q_9 + \frac{\pi^2}{15\lambda^2} i\gamma p Q_6 \quad (98)$$

$$A''_{3,-1}(E') = -\frac{2\pi^2}{105\lambda^2} i\gamma p Q_3 + \frac{4\pi^2}{105\lambda^2} Q_9 \quad (99)$$

$$A''_{4,1}(E') = -\frac{2i\pi^3}{945\lambda^3} Q_{10} \quad (100)$$

$$A''_{4,-1}(E') = \frac{2i\pi^3}{567\lambda^3} Q_{10} \quad (101)$$

$$\left. \begin{aligned} A''_{5,1}(E') &= 0 \\ A''_{5,-1}(E') &= 0 \end{aligned} \right\} \quad (102)$$

If it is taken into account that

$$\frac{\partial}{\partial r}(r^\beta e^{-r/a_0}) = \left(\beta r^{\beta-1} - \frac{r^\beta}{a_0} \right) e^{-r/a_0} \quad (103)$$

and

$$\frac{\partial}{\partial r}(r^{\beta-1} e^{-r/a_0}) = \left((\beta-1)r^{\beta-2} - \frac{r^{\beta-1}}{a_0} \right) e^{-r/a_0} \quad (104)$$

then with the notation $q = 1/a_0 + i\kappa$ and

$$S = \int_0^\infty r^\beta e^{-qr} dr \quad (105)$$

it can be shown by integration by parts that

$$Q_1 = -\frac{S}{a_0 q} (1 + a_0 q) \quad (106) \quad Q_6 = \frac{2S}{q^2} \quad (111)$$

$$Q_2 = -\frac{S}{a_0 q^2} (2 + a_0 q) \quad (107) \quad Q_7 = -\frac{S}{a_0 q} \left(1 + \gamma^2 \frac{i a_0 k}{2} \right) \quad (112)$$

$$Q_3 = -\frac{2S}{a_0 q^3} (3 + a_0 q) \quad (108) \quad Q_8 = -\frac{2S}{a_0 q^2} \left[1 + \frac{i\gamma^2}{2} \left(i + \frac{a_0 k}{2} \right) \right] \quad (113)$$

$$Q_4 = S \quad (109) \quad Q_9 = -\frac{6S}{a_0 q^3} \quad (114)$$

$$Q_5 = \frac{S}{q} \quad (110) \quad Q_{10} = -\frac{24S}{a_0 q^4} \quad (115)$$

The expressions (106) (115) were simplified by taking into account the fact that β is equal to $(1 - \gamma^2)^{1/2} - 1$ or approximately to $-\gamma^2/2$ and is therefore very small. Accordingly it was put equal to zero in all the Q 's with the exception of Q_7 and Q_8 whose values, on the evidence of the expressions (86)-(102) are the most important ones. Therefore in the expressions (112) and (113) β was put equal to $-\gamma^2/2$.

On the basis of Eqs. (41) and (42) together with (40) one can write if the radial parts of the functions $\psi_{km}(E')$ which are common to all terms on account of the expressions (60), are omitted

$$\begin{aligned} \bar{\psi}_3 \sim & A'_{0,-1}(E')(0-1+1)P_0^{-1} + A'_{1,-1}(E')(1-1+1)P_1^{-1} \\ & + A'_{1,1}(E')(1+1+1) \cdot P_1^1 + A_{2,1}(E')(2+1+1)P_2^1 + A'_{2,-1}(E')(2-1+1)P_2^{-1} \\ & + A'_{3,1}(E')(3+1+1)P_3^1 + A'_{3,-1}(E')(3-1+1)P_3^{-1} + A'_{4,1}(E')(4+1+1) \cdot P_4^1 \\ & + A'_{4,-1}(E')(4-1+1)P_4^{-1} + A''_{1,-1}(E')P_1^{-1} + A''_{2,1}(E')P_2^1 \\ & + A''_{2,-1}(E')P_2^{-1} + A''_{3,1}(E')P_3^1 + A''_{3,-1}(E')P_3^{-1} + A''_{4,1}(E')P_4^1 \\ & + A''_{4,-1}(E')P_4^{-1} = P_1^1 \cdot 3A'_{1,1}(E') + P_1^{-1} [A'_{1,-1}(E') + A'_{1,-1}(E')] \\ & + P_2^1 [4A'_{2,1}(E') + A''_{2,1}(E')] + P_2^{-1} [2A'_{2,-1}(E') + A''_{2,-1}(E')] \\ & + P_3^1 [5A'_{3,1}(E') + A''_{3,1}(E')] + P_3^{-1} [3A'_{3,-1}(E') + A''_{3,-1}(E')] \\ & + P_4^1 [6A'_{4,1}(E') + A''_{4,1}(E')] + P_4^{-1} [4A'_{4,-1}(E') + A''_{4,-1}(E')]. \end{aligned} \quad (116)$$

and

$$\begin{aligned}
 \psi_4 \sim & A'_{0,-1}(E')(0-1)P_0^0 + A'_{1,1}(E')(-1+1)P_1^2 + A'_{1,-1}(E')(-1-1)P_1^0 \\
 & + A'_{2,1}(E')(-2+1)P_2^2 + A'_{2,-1}(E')(-2-1)P_2^0 + A'_{3,1}(E')(-3+1)P_3^2 \\
 & + A'_{3,-1}(E')(-3-1)P_3^0 + A'_{4,1}(E')(-4+1)P_4^2 + A'_{4,-1}(E')(-4-1)P_4^0 \\
 & + A''_{1,-1}(E')P_1^0 + A''_{2,1}(E')P_2^2 + A''_{2,-1}(E')P_2^0 + A''_{3,1}(E')P_3^2 + A''_{3,-1}(E')P_3^0 \\
 & + A''_{4,1}(E')P_4^2 + A''_{4,-1}(E')P_4^0 = -P_0^0 A'_{0,-1}(E') + P_1^0 [A'_{1,-1}(E') \\
 & - 2A'_{1,1}(E')] + P_2^0 [A'_{2,-1}(E') - 3A'_{2,1}(E')] + P_2^2 [A'_{2,1}(E') - A'_{2,-1}(E')] \\
 & + P_3^0 [A'_{3,-1}(E') - 4A'_{3,1}(E')] + P_3^2 [A'_{3,1}(E') - 2A'_{3,-1}(E')] \\
 & + P_4^0 [A'_{4,-1}(E') - 5A'_{4,1}(E')] + P_4^2 [A'_{4,1}(E') - 3A'_{4,-1}(E')].
 \end{aligned} \quad (117)$$

With regard to $\bar{\psi}_1$ and $\bar{\psi}_2$ it is to be remembered that they are small, of the order of p , when compared with $\bar{\psi}_3, \bar{\psi}_4$. Therefore it is sufficient to compute for them only the terms with the greatest absolute values and hence only the terms with the coefficients $A'_{1,-1}(E'), A'_{1,1}(E')$ and $A''_{1,-1}(E')$ are considered. Thus

$$\begin{aligned}
 \bar{\psi}_1 = & -p \{ P_2^1 A'_{1,1}(E') + P_2^{-1} A'_{1,-1}(E') + P_0^{-1} (1-1) A''_{1,-1}(E') \} \\
 = & -p \{ P_2^1 A'_{1,1}(E') + P_2^{-1} A'_{1,-1}(E') \}
 \end{aligned} \quad (118)$$

and

$$\begin{aligned}
 \bar{\psi}_2 = & -p \{ P_2^2 A'_{1,1}(E') + P_2^0 A'_{1,-1}(E') + P_0^0 (-1-1+1) A''_{1,-1}(E') \} \\
 = & -p \{ P_2^2 A'_{1,1}(E') + P_2^0 A'_{1,-1}(E') - P_0^0 A''_{1,-1}(E') \}.
 \end{aligned} \quad (119)$$

If Eqs. (86) (102) and (106) (115) are taken into account and substituted into Eqs. (116) (119) then after some calculation

$$\bar{\psi}_1 = -p \sin \theta \cos \theta \cos \phi \quad (120)$$

$$\bar{\psi}_2 = -p \sin^2 \theta \cos \phi e^{i\phi} \quad (121)$$

$$\begin{aligned}
 \bar{\psi}_3 = & \left(1 + \gamma^2 \frac{i a_0 \kappa}{2} \right) \sin \theta \cos \phi - \frac{i \gamma p}{2} (1 + a_0 q) \sin \theta \cos \phi + \frac{i \gamma p a_0 q}{2} \sin \theta e^{-i\phi} \\
 & + \frac{4\pi i}{\lambda q} \sin \theta \cos \theta \cos \phi \left[1 + \frac{i \gamma^2}{2} \left(i + \frac{a_0 \kappa}{2} \right) \right] + \frac{\pi \gamma p}{\lambda q} (2 + a_0 q) \sin \theta \cos \theta \cos \phi \\
 & - \frac{\pi \gamma a_0}{\lambda} \sin \theta \cos \theta \cos \phi - \frac{12\pi^2}{\lambda^2 q^2} \sin \theta \cos^2 \theta \cos \phi \\
 & + \frac{2\pi^2}{\lambda^2 q^2} (3 + a_0 q) i \gamma p \sin \theta \cos^2 \theta \cos \phi - \frac{2\pi^2}{\lambda^2} \frac{a_0}{q} i \gamma p \sin \theta \cos^2 \theta e^{i\phi} \\
 & + \frac{\pi a_0}{2\lambda} \sin \theta (\gamma e^{i\phi} + 2 i p e^{-i\phi}) - \frac{2\pi^2}{\lambda^2} \frac{a_0}{q} \sin \theta \cos \theta (2 p e^{-i\phi} - i \gamma e^{i\phi}) \\
 & - \frac{32 i \pi^3}{\lambda^3 q^3} \sin \theta \cos^3 \theta \cos \phi
 \end{aligned} \quad (122)$$

$$\psi_4 = \frac{\pi i a_0}{\lambda} - \frac{i \gamma p a_0 q}{2} \cos \theta. \quad (123)$$

In the Eq. (123) only the terms with the greatest absolute values were taken into account, the rest can be safely omitted to the present approximation. Moreover in all the four Eqs. (120)–(123) the common factor $-S/a_0 q$ was omitted.

The Eqs. (120), (121), (122) and (123) represent a spherical material wave diverging from the considered atom, whose amplitude depends upon the direction in space. This can be seen at once if one takes into account the neglected common radial factors. Therefore the spatial distribution of the photoelectrons (whose kinetic energy and velocity do not depend upon the direction of emission as can be seen from the foregoing discussion) is given by the intensity of these waves or by the density of electric charge emitted in a considered direction, which is equal to

$$-e\bar{\phi}\bar{\psi} = -e(\bar{\phi}_1\bar{\psi}_1 + \bar{\phi}_2\bar{\psi}_2 + \bar{\phi}_3\bar{\psi}_3 + \bar{\phi}_4\bar{\psi}_4). \quad (10)$$

It is to be remembered that ϕ is conjugate complex with regard to ψ . According to the relations (120)–(123)

$$\begin{aligned} \phi\psi \sim & p^2 \sin^2 \theta \cos^2 \phi + \frac{\pi^2 a_0^2}{\lambda^2} + \frac{\gamma^2 p^2}{4} a_0^2 q q^* \cos^2 \theta - \frac{\pi a_0^2}{2\lambda} \gamma p (q + q^*) \cos \theta \\ & + \sin^2 \theta \cos^2 \phi + \frac{16\pi^2}{\lambda^2 q q^*} \sin^2 \theta \cos^2 \theta \cos^2 \phi - \frac{4\pi i}{\lambda q q^*} (q - q^*) \sin^2 \theta \cos \theta \cos^2 \phi \\ & + \frac{2\pi a_0 k \gamma^2}{\lambda q q^*} (q + q^*) \sin^2 \theta \cos \theta \cos^2 \phi + \left[\frac{2\pi i \gamma^2}{\lambda q q^*} (q - q^*) \right. \\ & \left. - \frac{\pi \gamma^2 a_0 k}{\lambda q q^*} (q + q^*) \right] \sin^2 \theta \cos \theta \cos^2 \phi - \frac{12\pi^2}{\lambda^2 q^2 q^{*2}} (q^2 + q^{*2}) \sin^2 \theta \cos^2 \theta \cos^2 \phi \\ & + \frac{a_0 i \gamma p}{2} (q^* - q) \sin^2 \theta \cos^2 \phi + \frac{2\pi \gamma p}{\lambda} \left(a_0 + \frac{q + q^*}{q q^*} \right) \sin^2 \theta \cos \theta \cos^2 \phi \\ & - \frac{2\pi a_0 \gamma}{\lambda} \sin^2 \theta \cos^2 \theta \cos^2 \phi + \frac{i \gamma p a_0}{2} (q e^{-i\phi} - q^* e^{i\phi}) \sin^2 \theta \cos \phi \\ & + \frac{\pi a_0}{\lambda} (\gamma \cos \phi + 2p \sin \phi) \sin^2 \theta \cos \phi + \frac{6\pi^2 i}{\lambda^2 q^2 q^{*2}} (q^{*2} - q^2) \gamma p \sin^2 \theta \cos^2 \theta \cos^2 \phi \\ & - \frac{2\pi^2}{\lambda^2} \frac{a_0 i \gamma p}{q q^*} (q - q^*) \sin^2 \theta \cos^2 \theta \cos^2 \phi - \frac{4\pi^2}{\lambda^2} \frac{a_0 p}{q q^*} (q e^{i\phi} + q^* e^{-i\phi}) \sin^2 \theta \cos^2 \theta \cos \phi \\ & + \frac{2\pi^2}{\lambda^2} \frac{a_0 i \gamma}{q q^*} (q^* e^{i\phi} - q e^{-i\phi}) \sin^2 \theta \cos^2 \theta \cos \phi \\ & + \frac{32}{\lambda^3 (q q^*)^3} i \pi^3 (q^3 - q^{*3}) \sin^2 \theta \cos^3 \theta \cos^2 \phi \end{aligned} \quad (124)$$

$$-\frac{2\pi^2 a_0 i \gamma p}{\lambda^2} \sin^2 \theta \cos^2 \theta \cos \phi (e^{-i\phi}/q - e^{-i\phi}/q^*)$$

$$+\frac{48i\pi^3}{\lambda^3 q q^*} \left(\frac{1}{q} - \frac{1}{q^*} \right) \sin^2 \theta \cos^3 \theta \cos^2 \phi.$$

If on the other hand the initial state of the atom is described by Eqs. (64) and (66) then it is found that for the solutions of the type (41) the coefficients $A'_{km}(E')$ are different from zero for

$$\begin{array}{lll} k=0 & m=0 & k=3 \quad m=0, -2 \\ k=1 & m=0, -2 & k=4 \quad m=0, -2 \\ k=2 & m=0, -2 & \end{array} \quad (125)$$

whereas for the type (42) $A''_{km}(E')$ differ from zero for

$$\begin{array}{lll} k=1 & m=0 & k=3 \quad m=0, -2 \\ k=2 & m=0, -2 & k=5 \quad m=0, -2 \\ k=3 & m=0, -2 & \end{array} \quad (126)$$

After some calculations quite similar to the ones given previously for the foregoing possibility it follows that in this second case

$$\bar{\psi}_1 = p \sin^2 \theta \cos \phi e^{-i\phi}$$

$$\bar{\psi}_2 = -p \sin \theta \cos \theta \cos \phi \quad (127)$$

$$\bar{\psi}_3 = \frac{\pi i a_0}{\lambda} - \frac{i \gamma p a_0 q}{2} \cos \theta \quad (128)$$

$$\bar{\psi}_4 = - \left\{ \left(1 + \frac{\gamma^2 i a_0 q}{2} \right) \sin \theta \cos \phi - \frac{i \gamma p}{2} (1 + a_0 q) \sin \theta \cos \phi + \frac{i \gamma p a_0 q}{2} \sin \theta e^{i\phi} \right. \quad (129)$$

$$+ \frac{4\pi i}{\lambda q} \sin \theta \cos \theta \cos \phi \left[1 + \frac{i \gamma^2}{2} \left(i + \frac{a_0 q}{2} \right) \right] + \frac{\pi \gamma p}{\lambda q} (2 + a_0 q) \sin \theta \cos \theta \cos \phi$$

$$- \frac{\pi \gamma a_0}{\lambda} \sin \theta \cos \theta \cos \phi - \frac{12\pi^2}{\lambda^2 q^2} \sin \theta \cos^2 \theta \cos \phi + \frac{2\pi^2}{\lambda^2 q^2} (3 + a_0 q) i \gamma p \sin \theta \cos^2 \theta \cos \phi$$

$$- \frac{2\pi^2}{\lambda^2} \frac{a_0}{q} i \gamma p \sin \theta \cos^2 \theta e^{-i\phi} + \frac{\pi a_0}{2\lambda} \sin \theta (\gamma e^{-i\phi} + 2 p i e^{i\phi}) \quad (130)$$

$$\left. - \frac{2\pi^2}{\lambda^2} \frac{a_0}{q} (2 p e^{i\phi} - i \gamma e^{-i\phi}) \sin \theta \cos \theta - \frac{32 i \pi^3}{\lambda^3 q^3} \sin \theta \cos^3 \theta \cos \phi \right\}$$

Therefore in this case

$$\phi \psi = p^2 \sin^2 \theta \cos^2 \phi + \frac{\pi^2 a_0^2}{\lambda^2} + \frac{\gamma^2 p^2 a_0^2 q q^*}{4} \cos^2 \theta - \frac{\pi a_0^2 \gamma p}{2\lambda} (q + q^*) \cos \theta$$

$$\begin{aligned}
& + \sin^2 \theta \cos^2 \phi + \frac{16\pi^2}{\lambda^2 q q^*} \sin^2 \theta \cos^2 \theta \cos^2 \phi - \frac{4\pi i}{\lambda q q^*} (q - q^*) \sin^2 \theta \cos \theta \cos^2 \phi \\
& + \frac{2\pi a_0 \kappa \gamma^2}{\lambda q q^*} (q + q^*) \sin^2 \theta \cos \theta \cos^2 \phi + \left[\frac{2\pi i \gamma^2}{\lambda q q^*} (q - q^*) \right. \\
& \left. - \frac{\pi \gamma^2 a_0 \kappa}{\lambda q q^*} (q + q^*) \right] \sin^2 \theta \cos \theta \cos^2 \phi - \frac{12\pi^2}{\lambda^2 (q q^*)^2} (q^2 + q^{*2}) \sin^2 \theta \cos^2 \theta \cos^2 \phi \\
& + \frac{a_0 i \gamma p}{2} (q^* - q) \sin^2 \theta \cos^2 \phi + \frac{2\pi \gamma p}{\lambda} \left(a_0 + \frac{q + q^*}{q q^*} \right) \sin^2 \theta \cos \theta \cos^2 \phi \\
& - \frac{2\pi \gamma a_0}{\lambda} \sin^2 \theta \cos \theta \cos^2 \phi + \frac{i \gamma p a_0}{2} (q e^{i\phi} - q^* e^{-i\phi}) \sin^2 \theta \cos \phi \\
& + \frac{\pi a_0}{\lambda} \sin^2 \theta \cos \phi (\gamma \cos \phi - 2p \sin \phi) + \frac{6\pi^2 i}{\lambda^2 (q q^*)^2} (q^{*2} - q^2) \gamma p \sin^2 \theta \cos^2 \theta \cos^2 \phi \\
& + \frac{2\pi^2 a_0 i \gamma p}{\lambda^2 q q^*} (q^* - q) \sin^2 \theta \cos^2 \theta \cos^2 \phi - \frac{4\pi^2}{\lambda^2} \frac{a_0 p}{q q^*} (q e^{-i\phi} + q^* e^{i\phi}) \sin^2 \theta \cos^2 \theta \cos \phi \\
& + \frac{2\pi^2}{\lambda^2} \frac{a_0 i \gamma}{q q^*} (q^* e^{-i\phi} - q e^{i\phi}) \sin^2 \theta \cos^2 \theta \cos \phi \\
& + \frac{32 i \pi^3}{\lambda^3 (q q^*)^3} (q^3 - q^{*3}) \sin^2 \theta \cos^3 \theta \cos^2 \phi \\
& - \frac{2\pi^2 a_0 i \gamma p}{\lambda^2} \sin^2 \theta \cos^2 \theta \cos \phi (e^{-i\phi}/q - e^{i\phi}/q^*) \\
& + \frac{48 i \pi^3}{\lambda^3 q q^*} \left(\frac{1}{q} - \frac{1}{q^*} \right) \sin^2 \theta \cos^3 \theta \cos^2 \phi.
\end{aligned} \tag{131}$$

According to G. Wentzel¹⁶ the average of the expressions (124) and (131) is to be taken to find the real spatial distribution of the photoelectrons. Therefore this distribution is given by

$$\begin{aligned}
\phi \psi \sim & p^2 \sin^2 \theta \cos^2 \phi + \frac{\pi^2 a_0^2}{\lambda^2} + \frac{\gamma^2 p^2 a_0^2 q q^*}{4} \cos^2 \theta - \frac{\pi a_0^2 \gamma p}{2\lambda} (q + q^*) \cos \theta \\
& + \sin^2 \theta \cos^2 \phi + \frac{16\pi^2}{\lambda^2 q q^*} \sin^2 \theta \cos^2 \theta \cos^2 \phi - \frac{4\pi i}{\lambda q q^*} (q - q^*) \sin^2 \theta \cos \theta \cos^2 \phi \\
& + \frac{\pi a_0 \kappa \gamma^2}{\lambda q q^*} (q + q^*) \sin^2 \theta \cos \theta \cos^2 \phi + \frac{2\pi i \gamma^2}{\lambda q q^*} (q - q^*) \sin^2 \theta \cos \theta \cos^2 \phi \\
& + \frac{a_0 i \gamma p}{2} (q^* - q) \sin^2 \theta \cos^2 \phi - \frac{12\pi^2}{\lambda^2 (q q^*)^2} (q^2 + q^{*2}) \sin^2 \theta \cos^2 \theta \cos^2 \phi
\end{aligned}$$

¹⁶ G. Wentzel, l. c.

$$\begin{aligned}
& -\frac{2\pi\gamma a_0}{\lambda}(1-p)\sin^2\theta\cos\theta\cos^2\phi \\
& +\frac{2\pi\gamma p}{\lambda}\left(\frac{q+q^*}{qq^*}\right)\sin^2\theta\cos\theta\cos^2\phi+\frac{i\gamma pa_0}{2}(q-q^*)\sin^2\theta\cos\phi \\
& +\frac{\pi a_0\gamma}{2}\sin^2\theta\cos^2\phi+\frac{6\pi^2 i(q^{*2}-q^2)}{\lambda^2(qq^*)^2}\gamma p\sin^2\theta\cos^2\theta\cos^2\phi \\
& -\frac{4\pi^2}{\lambda^2}a_0 p\left(\frac{q+q^*}{qq^*}\right)\sin^2\theta\cos^2\theta\cos^2\phi+\frac{2\pi^2}{\lambda^2}\frac{a_0 i\gamma}{qq^*}(q^*-q)\sin^2\theta\cos^2\theta\cos^2\phi \\
& +\frac{32i\pi^3}{\lambda^3(qq^*)^3}(q^3-q^{*3})\sin^2\theta\cos^3\theta\cos^2\phi \\
& +\frac{48i\pi^3}{\lambda^3 qq^*}\left(\frac{1}{q}-\frac{1}{q^*}\right)\sin^2\theta\cos^2\theta\cos^2\phi.
\end{aligned} \tag{132}$$

If the notations used by Sommerfeld are adopted, then

$$a_0 = a/Z; \quad q = Z/a + i\kappa; \quad \gamma = \alpha Z \tag{133}$$

and so

$$\begin{aligned}
q+q^* &= 2Z/a; & q-q^* &= 2i\kappa; & qq^* &= Z^2/a^2 + \kappa^2; \\
q^2-q^{*2} &= 4i\kappa Z/a; & q^2+q^{*2} &= 2(Z^2/a^2 - \kappa^2); & q^3-q^{*3} &= 2i\kappa(3Z^2/a^2 - \kappa^2);
\end{aligned} \tag{134}$$

Moreover, according to Eq. (55)

$$p = \frac{B}{A} = \left(\frac{E' - mc^2}{E' + mc^2} \right)^{1/2} = \frac{\kappa}{A^2} \cong \frac{\kappa h}{4\pi mc} = \frac{\alpha \kappa a}{2} \tag{135}$$

but $E' - mc^2$ is equal to the kinetic energy of the photoelectron, $E' \sim mc^2$ and therefore

$$p \cong \left(\frac{mv^2}{4mc^2} \right)^{1/2} = \frac{v}{2c}. \tag{136}$$

Substitution of these values into Eq. (132) leads

$$\begin{aligned}
\phi\psi &\sim \sin^2\theta\cos^2\phi\left(1+p^2+\frac{\pi a\alpha}{\lambda}\right) + \sin^2\theta\cos\theta\cos^2\phi\left\{\frac{8\pi\kappa}{\lambda(Z^2/a^2+\kappa^2)}\right. \\
& +\frac{2\pi\alpha Z^2}{\lambda(Z^2/a^2+\kappa^2)}\frac{p}{a}-\frac{2\pi\kappa\gamma^2}{\lambda(Z^2/a^2+\kappa^2)}-\frac{2\pi a\alpha}{\lambda}(1-p)\left.\right\} + \sin^2\theta\cos^2\theta\cos^2\phi \\
& \cdot \left\{\frac{48\pi^2\kappa^2}{\lambda^2(Z^2/a^2+\kappa^2)^2}-\frac{8\pi^2}{\lambda^2(Z^2/a^2+\kappa^2)}+\frac{4\pi^2 a\alpha\kappa}{\lambda^2(Z^2/a^2+\kappa^2)}-\frac{24\pi^2 p a\alpha\kappa Z^2/a^2}{\lambda^2(Z^2/a^2+\kappa^2)^2}\right. \\
& \left.-\frac{8\pi^2 p}{\lambda^2(Z^2/a^2+\kappa^2)}\right\} + \sin^2\theta\cos^3\theta\cos^2\phi\left\{\frac{256\pi^3\kappa^3}{\lambda^3(Z^2/a^2+\kappa^2)^3}-\frac{96\pi^3\kappa}{\lambda^3(Z^2/a^2+\kappa^2)^2}\right\} \\
& +\frac{\pi^2 a^2}{Z^2\lambda^2}-\frac{\pi a\alpha p}{\lambda}\cos\theta+\frac{a^2\alpha^2 p^2}{4}\left(\frac{Z^2}{a^2}+\kappa^2\right)\cos^2\theta.
\end{aligned} \tag{137}$$

According to Sommerfeld and to the Eqs. (47)

$$\kappa = \frac{2\pi m v}{h(1-v^2/c^2)^{1/2}}; \quad a = \frac{h^2}{4\pi^2 m c^2} \quad (138)$$

$$\frac{Z^2}{a^2} + \kappa^2 = \frac{8\pi^2 m v}{h} \quad (139)$$

furthermore

$$p^2 \approx \epsilon/2mc^2 = (h\nu - I_0)/2mc^2 \quad (I_0 - \text{ionization potential}) \quad (140)$$

and

$$\pi a \alpha / \lambda = h\nu / 2mc^2. \quad (141)$$

If these values are substituted into Eq. (137) then

$$\begin{aligned} \phi\psi = & \sin^2 \theta \cos^2 \phi \left(1 + \frac{h\nu}{mc^2} - \frac{I_0}{2mc^2} \right) + \frac{2v}{c} \left(1 - \frac{\alpha^2 Z^2}{8} + \frac{v^2}{c^2} + \frac{h\nu}{4mc^2} \right. \\ & \left. - \frac{h\nu}{c^2 m v} \right) \sin^2 \theta \cos \theta \cos^2 \phi + \frac{3v^2}{c^2} \left(1 - \frac{h\nu}{3mv^2} \right) \sin^2 \theta \cos^2 \theta \cos^2 \phi \\ & + \frac{4v^3}{c^3} \left(1 - \frac{3h\nu}{4mv^2} \right) \sin^2 \theta \cos^3 \theta \cos^2 \phi + \frac{\pi^2 a^2}{Z^2 \lambda^2} - \frac{h\nu}{4mc^2} \cdot \frac{v}{c} \cos \theta \\ & + \frac{h\nu}{8mc^2} \frac{v^2}{c^2} \cos^2 \theta. \end{aligned} \quad (142)$$

The term $-\alpha^2 Z^2/4$ in the parenthesis after $3v^2/c^2$ was omitted, because other terms of the same order have been also omitted for the present approximation.

If the right side of the Eq. (142) is divided by $1 + h\nu/mc^2 - I_0/2mc^2$ then to the same degree of approximation

$$\begin{aligned} \phi\psi = & \sin^2 \theta \cos^2 \phi \left\{ 1 + \frac{2v}{c} \left(1 - \frac{\alpha^2 Z^2}{8} + \frac{I_0}{2mc^2} + \frac{v^2}{2c^2} - \frac{3h\nu}{4mc^2} - \frac{1}{2} \frac{h\nu}{cmv} \right) \cos \theta \right. \\ & \left. + \frac{3v^2}{c^2} \left(1 - \frac{h\nu}{3mv^2} \right) \cos^2 \theta + \frac{4v^3}{c^3} \left(1 - \frac{3h\nu}{4mv^2} \right) \cos^3 \theta \right\} \\ & + \frac{\pi^2 a^2}{Z^2 \lambda^2} - \frac{h\nu}{4mc^2} \frac{v}{c} \cos \theta + \frac{h\nu}{8mc^2} \frac{v^2}{c^2} \cos^2 \theta \end{aligned} \quad (143)$$

On the basis of Eq. (143) one can calculate, as Sommerfeld has done, the angle of the cone surrounding the z axis inside of which half of the electrons are emitted. Then to Sommerfeld's degree of approximation

$$\theta = \pi/2 - v/2c. \quad (144)$$

This result agrees with the elementary calculation of the basis of the quantum hypothesis.¹⁷ Sommerfeld's result differs by the factor 9/5 before

¹⁷ A. H. Compton, X-rays and Electrons, London, 1927, p. 240.

$-v/2c$ which is due, as can be seen by repeating his calculations, to the neglecting of the normalizing factors for the spherical harmonics. Thus, instead of the harmonics

$$P_k^m(\cos \theta) \quad (145)$$

in the formula (4) on the 210th page of the "Wellenmechanisches Ergänzungsband," the functions

$$\left[\frac{(k-m)!}{(k+m)!} \frac{2k+1}{2} \right]^{1/2} P_k^m(\cos \theta) \quad (146)$$

ought to be used, otherwise the formula (7) on the page 212 is not correct. The same remark applies to the result of Carrelli.

To calculate the angle θ with a higher degree of accuracy one can start from the equation given by Sommerfeld

$$\int_0^{2\pi} \int_0^\theta \phi \psi \sin \theta d\theta d\phi = \int_0^{2\pi} \int_0^\pi \phi \psi \sin \theta d\theta d\phi. \quad (147)$$

To simplify the notations the relation (143) can be written in the form

$$\phi \psi = \sin^2 \theta \cos^2 \theta (1 + b \cos \theta + c \cos^2 \theta + d \cos^3 \theta) + A - B \cos \theta + C \cos^2 \theta. \quad (148)$$

Eq. (147) leads then to

$$2 \cos \theta + 4A \cos \theta + b \cos^2 \theta - \frac{2 \cos^3 \theta}{3} = \frac{b}{2} + \frac{d}{6} - 2B. \quad (149)$$

If it is supposed that θ is equal to $\pi/2 - x$, then from (149) it follows that

$$\sin x = \frac{b}{4} + \frac{d}{12} - B - \frac{5b^3}{192} - \frac{Ab}{2} \quad (150)$$

whence, on account of (143)

$$\sin x = \frac{v}{2c} \left(1 - \frac{\alpha^2 Z^2}{8} + \frac{I_0}{2mc^2} + \frac{3v^2}{4c^2} - \frac{7h\nu}{4mc^2} - \frac{1}{2} \frac{h\nu}{cmv} - \frac{2\pi^2 a^2}{Z^2 \lambda^2} \right). \quad (151)$$

If it is supposed that the photoelectrons are emitted from the K-level only, which conforms with the initial assumptions in this paper then

$$\frac{I_0}{2mc^2} = \frac{RhZ^2}{2mc^2} = \frac{\alpha^2 Z^2}{4} \quad (152)$$

and so Eq. (151) can be written in the following form

$$\sin x = \frac{v}{2c} \left(1 - \frac{5\alpha^2 Z^2}{8} - \frac{h\nu}{4mc^2} - \frac{1}{2} \frac{h\nu}{cmv} - \frac{2\pi^2 a^2}{Z^2 \lambda^2} \right). \quad (153)$$

According to Birge¹⁸ $\alpha = 7.283 \times 10^{-3}$ and $h/mc = 0.02428\text{\AA}$. If moreover the value of λ is given in Ångström units, then finally

¹⁸ R. T. Birge, Phys. Rev. Suppl., July 1929.

$$\sin x = \frac{v}{2c} \left(1 - 3,53 \cdot 10^{-5} Z^2 - \frac{v}{4c} - \frac{0.006}{\lambda} - \frac{5.50}{Z^2 \lambda^2} \right). \quad (154)$$

Eq. (154) shows that the increase of the frequency of the incident radiation causes a decrease of $\sin x$ from the value $v/2c$. However, this effect becomes appreciable only for very high frequencies such as correspond to very hard x-rays, and γ -rays. This does not apply to the last term in the brackets, namely $5.50/Z^2 \lambda^2$, which becomes of importance even for ordinary x-rays in the case of low values of Z . Therefore for helium and especially for hydrogen the value of $\sin x$ should be markedly less than $v/2c$. For both these gases and for x-rays of the order of 1\AA the coefficient A in Eq. (149) becomes of the order of unity and so instead of Eq. (159) it follows that

$$\sin x = \frac{b}{4(1+2A)} \left\{ 1 + \frac{d}{36} - \frac{4B}{6} - \frac{b^2}{48} \frac{(5+12A)}{(1+2A)^3} \right\} \quad (155)$$

whence finally

$$\sin x = \frac{v}{2c(1+2A)} \left\{ 1 - 3.77 \times 10^{-5} Z^2 - \frac{v}{4c} - \frac{0.002}{\lambda} - \frac{v^2}{12c^2} \frac{5+12A}{(1+2A)^3} \right\} \quad (156)$$

where

$$A = \frac{\pi^2 a^2}{Z^2 \lambda^2} = \frac{2.75}{Z^2 \lambda^2}. \quad (157)$$

The formulas (154) and (156) do not agree with the results obtained recently by Williams, Nuttall and Barlow¹⁹ but they represent fairly well the results of other authors.²⁰ However, the experimental methods used to find the spatial distribution of photoelectrons cannot as yet claim a high degree of accuracy and it seems therefore well to wait for a final decision till more experimental data are available.

It is to be noted that the angle of the maximum emission of photoelectrons does not coincide with the above computed $\theta = \pi/2 - x$. This angle can be calculated from the formula

$$\frac{d}{d\theta}(\phi\psi) = 0. \quad (158)$$

In the first approximation this leads to the value

$$\theta_1 = \pi/2 - v/c \quad (159)$$

which differs from the corresponding value of Sommerfeld

$$\theta_1 = \pi/2 - 9v/5c \quad (159')$$

by the disappearance of the factor $9/5$.

¹⁹ E. J. Williams, *Nature*, **121**, 134 (1928). E. J. Williams, J. M. Nuttall and H. S. Barlow, *Proc. Roy. Soc.* **121**, 611 (1928).

²⁰ A. Sommerfeld, *l.c.* p. 225, fig. 20.

In the second approximation it can be found that according to Eqs. (158) and (148)

$$\theta_1 = \pi/2 - x_1$$

where

$$\sin x_1 = \frac{b}{2} + \frac{cb}{2} - \frac{5b^3}{16} - \frac{B/\cos^2 \phi}{2} \quad (160)$$

or according to Eqs. (148) and (143)

$$\sin x_1 = \frac{v}{c} \left\{ 1 - \frac{11h\nu}{4mc^2} + \frac{5\alpha^2 Z^2}{8} + \frac{1}{2} \frac{h\nu}{cmv} - \frac{h\nu}{8mc^2} \frac{1}{\cos^2 \phi} \right\}. \quad (161)$$

Hence finally by using the formerly given values of h/mc and α

$$\sin x_1 = \frac{v}{c} \left(1 + 3.53 \cdot 10^{-5} Z^2 - \frac{v}{4c} - \frac{0.067}{\lambda} - \frac{0.003}{\lambda \cos^2 \phi} \right). \quad (162)$$

It can be readily seen from this formula that for very hard x-rays the value of $\sin x_1$ begins to be appreciably smaller than v/c , but for the same values of v and λ the values of $\sin x_1$ increases with the increase of Z .

The independence of the maximum of photoelectric emission from the value of A can be readily understood with regard to the fact that Eq. (148), if coefficients B and C are neglected represents a superposition of an emission given by the term

$$\sin^2 \theta \cos^2 \phi (1 + b \cos \theta + c \cos^2 \theta + d \cos^3 \theta)$$

which shows a pronounced maximum and an emission independent from the direction in space, represented by the term A .

The values of the angles of maximum photoelectric emission which follow from the data of Loughridge²¹ agree fairly well with the formula (162). This formula ceases to be valid for ϕ nearly equal $\pi/2$ or $3\pi/2$.

The author wishes to express his gratitude to the International Education Board for the granting of a fellowship.

Note added during the proof. The average forward momentum of the photoelectrons can be calculated readily from the Eq. (148). It appears to be equal to $bmv/5$ or, if the ionization energy is neglected, so that

$$b = \frac{4h\nu}{c} / mv$$

equal to $0.8h\nu/c$. According to Williams (Proc. Roy. Soc. 121, 611, 1928) an average momentum $0.8h\nu/c$ of photoelectrons in the direction of the x-ray beam corresponds to a constant momentum $5/4$ ($0.8h\nu/c$) in the direction of the x-ray beam, superimposed on the radial momenta of the photo-

²¹ D. H. Loughridge, Phys. Rev. 30, 488 (1927).

electrons distributed proportionally to $\sin^2 \theta \cos^2 \phi$. It follows that this additional component of momentum is equal to the momentum of the photon.

It is to be noted that all the results of this paper were obtained by neglecting the term $-i\delta \log r$ in the exponential of the formula (56). The value of δ is according to Eq. (57)

$$\delta = \frac{\gamma^2}{2} \left(\frac{A}{B} + \frac{B}{A} \right) = \gamma^2 \frac{c}{v}. \quad (163)$$

The smaller the value of δ , the smaller the effect of its neglect. It follows that the results of this paper are more exact, the greater the velocity of the photoelectrons and the smaller the atomic number.

The calculations of this paper can be repeated taking δ into account, which causes the wave functions representing the photoelectrons to take the form

$$\psi \sim r^{-i\delta} e^{-i\kappa r} / r. \quad (164)$$

The calculations are easy but rather long; they lead to the result that to the first approximation

$$\phi\psi \sim \sin^2 \theta \cos^2 \phi \left\{ 1 + \frac{2v}{c} \left(1 + \frac{\delta Z}{2a\kappa} \right) \cos \theta \right\}. \quad (165)$$

It follows that for $\delta Z / 2a\kappa \ll 1$ or $(v/c)^2 \gg (\alpha Z)^3 / 2$ the terms with δ can be neglected and the formula (143) is then valid.

Thus for comparatively slow photoelectrons and high atomic numbers the formula (165) is to be applied instead of (143), whereas this latter formula is valid for high speed photoelectrons and low atomic numbers. Eq. (165) ceases to be valid for very slow photoelectrons, because the use of the asymptotic formula (164) is then not justified.

THE REFLECTION OF BEAMS OF THE ALKALI METALS FROM CRYSTALS

BY JOHN B. TAYLOR*

GENERAL ELECTRIC COMPANY, SCHENECTADY, N. Y.

(Received January 9, 1930)

ABSTRACT

Beams of lithium, potassium, and caesium were reflected from crystals of sodium chloride and lithium fluoride, as a means of studying the wave nature of these atoms. Incident angles from 2° to 60° were investigated. Although one one-hundredth percent of specular reflection could have been detected, no trace of such a reflection or of diffraction was found. The measured angular distribution of reflected atoms followed closely the cosine law. Apparatus, and the detecting device depending on positive ion emission by which this sensitivity of measurement was obtained, are described.

THE reflection of a beam of atoms from a crystal or ruled grating has for some time been recognized as a means of investigating the wave nature of the atoms.¹ Recently the author has described a method of detection and intensity measurement of molecular beams.² This method has proved so reliable and sensitive that it gave opportunity for a very detailed study of the reflection of the alkali metals from crystals. This has been done, using the detector for measuring the angular distribution of the atoms reflected when a beam of alkali metal atoms is allowed to fall upon a crystal.

Reflection experiments have already been carried out for a few atoms. Knauer and Stern³ have obtained specular reflection of helium and hydrogen molecules from sodium chloride and potassium chloride crystals. In addition they have measured distinct surface diffraction beams arising from the crossed grating. These occur, within the present limits of the experiment, at the angle calculated from the surface grating formula using the de Broglie wave-length, $\lambda = h/mv$, obtained from the velocity and mass of the helium atom. Johnson⁴ has shown that hydrogen atoms are specularly reflected from sodium chloride. Kirschbaum⁵ also reports experiments with hydrogen atoms. No evidence of diffraction was found in either case. Ellett, Olson, and Zahl⁶ have obtained specular reflection of cadmium, mercury, arsenic, and antimony from sodium chloride crystals. Certain features of their results not in

* National Research Fellow, University of California, Berkeley, California.

¹ O. Stern, *Zeits. f. Physik* **39**, 762 (1926).

² J. B. Taylor, *Zeits. f. Physik* **57**, 242 (1929).

³ F. Knauer and O. Stern, *Zeits. f. Physik* **53**, 779 (1929); O. Stern, *Naturwiss.* **21**, 391 (1929).

⁴ T. H. Johnson, *J. Frank. Inst.* **206**, 301 (1928).

⁵ H. Kirschbaum, *Ann. d. Physik* **2**, 213 (1929).

⁶ A. Ellett and H. F. Olson, *Phys. Rev.* **31**, 643 (1928); Ellett and Zahl, *Phys. Rev.* **31**, 1122 (1928).

agreement with a surface grating action are yet to be explained. They also report a trial of reflection of sodium from sodium chloride. No regular reflection was observed.

In the present work, beams of lithium, potassium and caesium have been reflected from crystals of sodium chloride and lithium fluoride. The most probable de Broglie wave-lengths in question, at furnace temperatures of 900° , 500° , and 450°K respectively, vary from about 0.2×10^{-8} cm for lithium to 0.07×10^{-8} cm for caesium. No trace of specular reflection or diffraction has been found. On the contrary the intensity of reflection measured at various angles with the surface follows almost exactly the cosine law of Knudsen; i.e. all of the atoms are reflected diffusely from the point of incidence. One-tenth of one percent specular reflection could easily have been observed in the

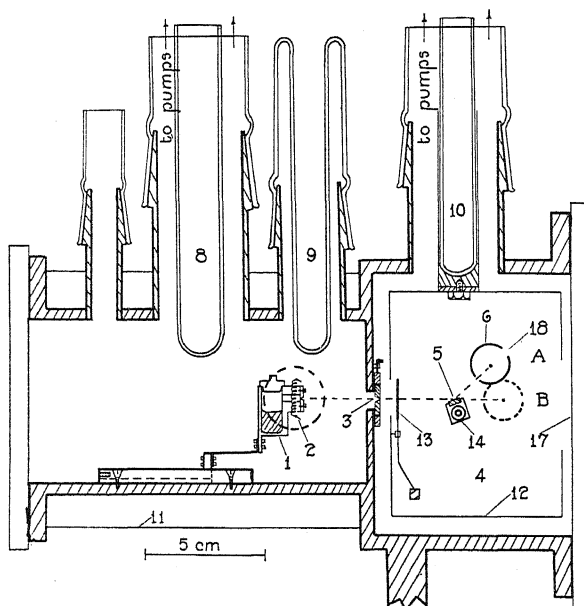


Fig. 1. Section of apparatus showing path of beam to crystal and detector.

present experiments. In some cases one one-hundredth of a percent could have been detected. In the other experiments mentioned the specular reflection has varied from almost one hundred percent⁷ in the case of helium, to 10 to 20 percent in the case of cadmium, and one or two percent for atomic hydrogen.

APPARATUS

The beam forming arrangement, furnace, slits, etc. are practically the same as have been described previously.⁸ Figure 1 gives a schematic view

⁷ Recent experiments of O. Stern about to be published, and as described to the author in private communication.

⁸ J. B. Taylor, *Zeits. f. Physik* 52, 846 (1929); 57, 242 (1929).

of the situation. Atoms of the alkali metal evaporate through a fine slit in the steel oven (1) which is heated by radiation or by electron bombardment from the tungsten spiral (2). The beam is then formed by a second slit (3) and passes into the reflection chamber (4). Here it impinges on the crystal surface (5). The reflected atoms are received on the filament of the detector (6) which can be moved to intercept and measure the number of atoms leaving the crystal at any angle.

In the sketch the detector in position (4) observes the specular beam. The detector was a platinum cylinder eighteen \times fifty mm with a coaxial pure tungsten filament 0.05 mm in diameter. The cylinder was held ten volts negative to the filament and at a temperature of about 1500°K. Every alkali metal atom striking the filament leaves as a positive ion.⁹ Thus the positive ion current is at once a measure of the intensity of the beam or of the reflected atoms at the point. The detector is carried on the ground joint (7) Fig. 2, by

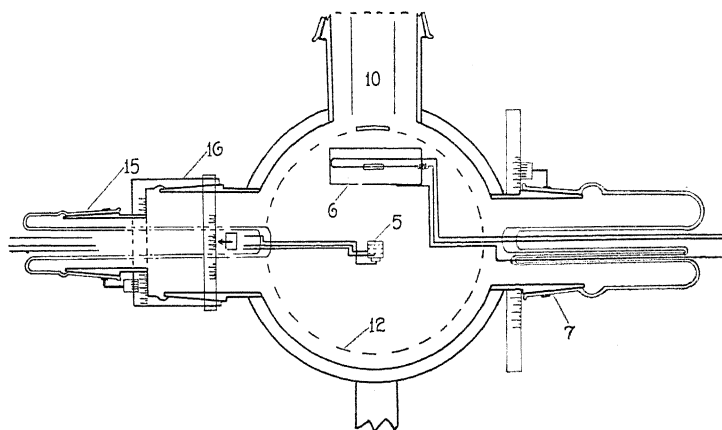


Fig. 2. End view of detecting chamber showing mounting and motions of crystal and detector.

which it may be moved to cover various angles of reflection. For lithium the detector filament was oxygen on tungsten.

The oven and crystal chambers were evacuated separately by two large Langmuir pumps. Liquid air traps (8), (9), (10), served to protect the chambers from grease vapors from the joints. The walls of the apparatus were held below room temperature by the water jacket (11). Added protection is given the detector and crystal by a sheet copper shield (12) cooled by liquid air from the trap (10). (13) is a shutter operated by action of a small magnet on an iron lever. It allowed interruption of the beam at any instant.

The crystal (5) is carried in the holder and heater (14). A tungsten spiral running through the body of the holder allows heating the crystal by radiation to at least 500°C. The holder is mounted on the ground joints (15) and (16) Fig. 2. (15) is eccentric in (16) so that by turning (16) the crystal can be

⁹ I. Langmuir and K. H. Kingdon, *Proc. Roy. Soc.* **21**, 380 (1923).

raised into or lowered out of the path of the beam. By turning (15) the crystal is rotated on an axis through its surface and coaxial with the motion of the detector, to set the crystal at any incident angle with the beam.

Since the detector motion is coaxial with the crystal motion, the filament remains equidistant from the crystal at all angles and the positive ion currents require no correction for distance.

Graduations on the various joints permitted accurate readings of the angular settings.

Crystals used. Natural crystals of sodium chloride were used in a few experiments. Later to secure more perfect crystals, they were grown from the melt by the excellent method of Kyropolous.¹⁰ Single crystals 3 to 5 cm in diameter were easily made in a few hours. Lithium fluoride was first purified by this method from an impure melt, and then crystalized from a melt of the pure product. The crystals were held at 2 to 300°K until ready for use. After cleaving they were immediately inserted in the apparatus and evacuation and heating begun at once.

During the reflection experiments the crystals were held at temperatures varying from room temperature to about 500°C. The elevated temperatures were to prevent if possible the momentary condensation or adsorption of alkali metal atoms on the crystal surface, and to insure a surface free from adsorbed gases.

The crystals used were 5 to 10 mm × 6 mm.

PROCEDURE

The oven was loaded and the experiment begun as described⁸ previously, with the addition of the crystal introduction. After five to eight hours pumping and heating of the crystal the oven was brought gradually to a temperature giving the desired beam intensity. This changing oven pressure could be readily followed by moving the detector into the path of the beam, (position *B* in Fig. 1), with the crystal lowered. In addition when the desired intensity was reached the detector filament was moved by 0.01 to 0.05 mm steps through the beam to measure its intensity from point to point. Thus in size and intensity the incident beam was accurately known. Fig. 3 gives examples of such measurements. The small displacements of the filament during this measurement were controlled by use of a traveling microscope with eyepiece micrometer. Through the glass window (17) and the detector opening (18), the filament could be seen as a bright line against the scale.

The width of the beams striking the crystal was changed in different trials from 0.05 mm to 1 mm. The maximum intensity in the undeflected beam at *B* was varied from 30 cm full galvanometer sensitivity to about 60 meters equivalent deflection. These latter were measured with galvanometer shunted to one-thirtieth of full sensitivity. The galvanometer had a full sensitivity of 4×10^{-11} amps. per mm.

Then by means of the joint (16) the crystal was raised into and parallel to the beam. This could be done very accurately by noting the decrease in gal-

¹⁰ S. Kryopolous. *Zeits. f. Anorg. Chemie* **154**, 308 (1926).

vanometer deflection as the crystal intercepted half of the beam. Next with the shutter (13) closed the crystal was turned to whatever incident angle desired, the shutter opened and observations begun. Incident angles from 2° to 60° were investigated. By joint (7) the detector was moved around the crystal, the intensity of the reflected atoms at any angle being recorded immediately by a certain steady galvanometer deflection. In the neighborhood of the expected specular reflection the steps could be made in fractions of a degree and the whole region explored a number of times to remove any question as to the character of the reflection. Readings could also be made by setting the detector at a given angle and then rotating the crystal to investigate any preferred angles of reflection.

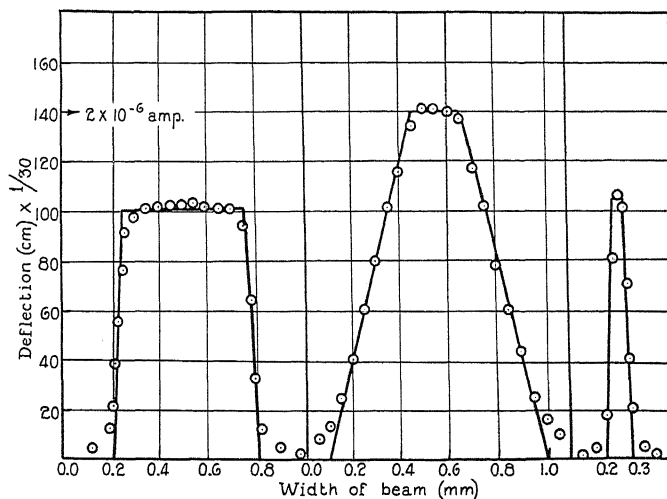


Fig. 3. Examples of intensity measurements of beams used. Solid lines are the geometrical beams constructed from the slit arrangements.

At any angle of reflection, if the shutter was closed the galvanometer deflection fell at once to zero.

At any time the crystal could be lowered and a check made on the constancy of the incident beam.

At the larger beam intensities one-tenth percent of specular reflection would have given 30 to 60 mm galvanometer deflection. However in no case was there the slightest indication of specular reflection.

Fig. 4 shows a reflection measurement with potassium from sodium chloride at an incident angle of 15° . The reflection from lithium fluoride and at other intensities of the main beam gave similar data.

An interesting critical temperature phenomenon was noted in the course of the experiments. If the crystal was allowed to cool, a temperature range was reached where the reflection at any angle fell very quickly practically to zero. This temperature where almost all the incident atoms were condensing on the crystal varied, as to be expected, with the incident beam intensity. It

is apparent that the combination of beam and detector offers a precise method of studying surface condensation and evaporation phenomena.

The experiments made so far on the reflections of atoms from crystals have led to no explanation of the efficiency of reflection. The great ease with which the alkali metal atoms are adsorbed on surfaces is believed to explain at least in part their failure to be specularly reflected or diffracted. To avoid this, the possibility is suggested of employing crystals which may be heated to

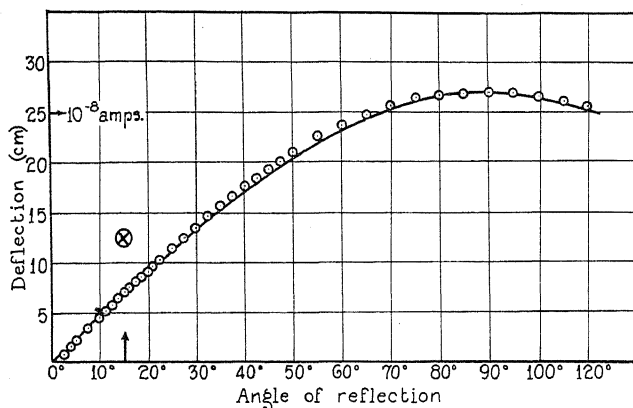


Fig. 4. Showing measured angular distribution of reflection (points) as compared to a cosine distribution (solid curve); the incident beam making an angle of 15° with crystal. Cross indicates intensity which would have been measured at 15° if one-tenth percent of the incident atoms had been specularly reflected.

still higher temperatures than in these experiments, or crystals on which the adsorbing forces are much smaller. However unless unusual conditions as to reflecting surface can be secured, it may not be possible to detect an appreciable specular reflection of the alkali metal atoms.

The writer wishes to express his appreciation of support from the National Research Council and to Professor G. N. Lewis for the facilities so kindly made available at the University of California.

THE EMISSION OF POSITIVE IONS FROM
TUNGSTEN AND MOLYBDENUM

BY LLOYD P. SMITH

DEPARTMENT OF PHYSICS, CORNELL UNIVERSITY

(Received November 25, 1929)

ABSTRACT

An examination of the positive ion emission from tungsten and molybdenum has been made in which it was sought to determine the following points: (1) The nature of the ions emitted at various temperatures; (2) the temperature variation of the positive ion current; (3) the theory of positive ion emission with regard to where and how the ions are formed; (4) the positive ion work function for these metals; (5) whether the work function, determined by experiment, checks with that calculated by a simple cyclic process involving the thermionic work function, the ionizing potential, and the latent heat of evaporation of the metal.

The mass spectrum for tungsten and molybdenum filaments taken at moderate temperatures (1700° to 2000°K) has shown that the emitted ions consist of sodium, the two isotopes of potassium, and aluminum. At high temperatures these impurities disappear and finally both tungsten and molybdenum filaments yield positive ions of their own metal. The latter confirm a report by Wahlin. The temperature variation of the positive ion current at high temperature yields a value of 6.55 volts for the positive ion work function of tungsten and 6.09 volts for that of molybdenum. These values disagree widely from the values 10.88 volts and 9.26 volts calculated from the simple cyclic process mentioned above. This suggests that the ions are formed as a by-product of an irreversible recrystallization of the metal. Theoretical considerations show that the ions are emitted from the metal and are not formed after a neutral atom evaporates.

UNTIL recently, it has been thought that any positive ion emission from metals was due entirely to ionized atoms of one or more impurities which existed in the metal. O. W. Richardson¹ has shown that most metals contain a very small amount of potassium which is driven out of the metal as the temperature is raised. He obtained rather erratic results from tungsten and did not give any data concerning molybdenum. His work was carried on for temperatures below 2,000°K. J. J. Thomson² investigated the positive ion emission from platinum by crossed electric and magnetic fields and found in addition to those of alkaline impurities, ions having an atomic weight of 27 which he concluded were ionized CO molecules. More recent work³ has shown definitely that platinum contains potassium and sodium as impurities which are ionized and emitted at high temperatures.

During the summer of 1927 the author attempted to perfect a plotron having a grid extremely well insulated. It was found during the course of this investigation that part of the electric leakage to the grid was due to positive

¹ O. W. Richardson. *Emission of Electricity From Hot Bodies*.

² J. J. Thomson, *Camb. Phil. Proc.* **15**, 64 (1908).

³ Barton, Harnwell, and Kunsman, *Phys. Rev.* **27**, 739 (1926).

ions arising at the filament. These ions persisted even after the filament was flashed to some $3,000^\circ$ and then well aged. An investigation of the nature of these high temperature ions and the variation of the positive ion current with temperature was undertaken. After the work was begun it was noted that Jenkins⁴ had found that the tungsten cathode of a Coolidge x-ray tube was a source of positive ions. Mitra⁵ carried on the investigation and obtained data on the temperature variation of the positive ion current using a commercial type of radio tube having a tungsten filament, but did not attempt to determine the positive ion work function. The author has given a preliminary report⁶ on such a work function.

MASS SPECTROGRAPH

The apparatus for obtaining the mass spectrum of the ions is shown diagrammatically in Fig. 1. It consisted essentially of a copper tube *A* in the form of a half torus ring spun from sheet copper. The diameter of the cross section was approximately 2.5 cm. Caps having the slits *S*₁ and *S*₂ were placed over the ends. The slit *S*₁ was about 0.8 mm wide and 8 mm long. The slit

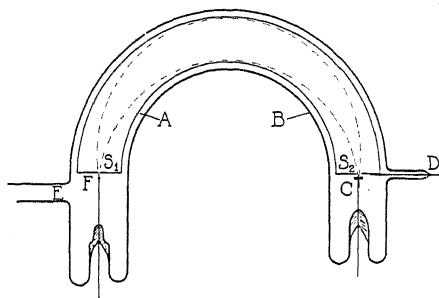


Fig. 1. Diagram of mass spectrograph.

*S*₂ was somewhat larger being about 3 mm wide and 1 cm long. A wire filament of the metal under investigation having a length of about 1.4 cm was placed at *F*, parallel to the slit *S*₁ and about 5 mm away from it. Ions passing through *S*₁ and bent by the magnetic field on an arc whose radius was 6.95 cm were focused at *S*₂. Those passing through *S*₂ were collected on the electrode *C* which was connected to a quadrant electrometer. The accelerating potential was applied between *D* and *F*. The copper tube together with the filament leads and collector leads were all sealed into a glass tube *B* which was exhausted at *E*. A pressure less than 10^{-6} cm of Hg was maintained. The tube was placed between poles of an electromagnet having pole pieces of large diameter. The field in the region occupied by the tube was found to be uniform and its intensity was determined by careful flip coil measurements.

In determining the mass spectrum, the field intensity was set at a given value and the accelerating potential was varied very slowly but continuously

⁴ Jenkins, *Phil. Mag.* **47**, 1025 (1924).

⁵ Mitra, *Phil. Mag.* **5**, 67 (1928).

⁶ Smith, *Phys. Rev.* **33**, 279 (1929).

by a mechanical device. The presence of a particular ion was noted by a drift of the electrometer. When it began to drift, the rate of drift for various accelerating potentials was taken and from these data the voltage yielding the maximum rate of drift was obtained. The voltage across the filament was measured and one half of this drop was added to the voltage producing maximum drift to yield the true accelerating potential.

NATURE OF THE IONS

From the accelerating potential corresponding to a given electrometer current, the atomic weight W was computed by means of the expression $W = (1/V) [RH/144.5]^2$ where R is the radius of the path traversed in cm, H is the field intensity in gauss, and V is the accelerating potential in volts. The electrometer current in arbitrary units was plotted against W to give a mass spectrogram. A typical mass spectrum for tungsten at moderate temperature is shown in Fig. 2. The peak at $W = 23.1$ is due to sodium ($W = 23.0$) and could

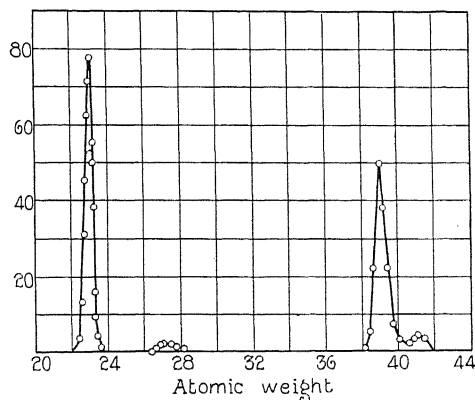


Fig. 2. Mass spectrum from tungsten at moderate temperatures (1600–2000°K).

be detected at a temperature of about 1700°. The peaks at $W = 39$ and 41.1 were also present at this temperature. They are undoubtedly due to the two isotopes of potassium occurring at $W = 39$ and 41 . The only element falling in this region is calcium ($W = 40.07$). No evidence of calcium ions has been found and in fact it would be quite improbable that any appreciable amount of calcium would be ionized at these temperatures for its ionization potential is too high (6.09 volts). The peak occurring at $W = 27.2$ did not show up until temperatures over about 2,000° were reached. This atomic weight compares well with aluminum ($W = 27.0$), and since the ionizing potential of aluminum is 5.9 volts we would not expect to find it until a higher temperature is reached than would yield either potassium or sodium ions whose ionizing potentials are 4.3 and 5.1 volts respectively. As mentioned before, J. J. Thomson found ions of atomic weight 27 emitted from platinum and concluded that they were ions of CO molecules ($W = 28$). It seems improbable that these were really positively ionized CO molecules because the ionizing potential of such molecules is of the order of 14 volts, much too high to have any ions of CO present

below the melting point of platinum. It therefore seems extremely likely that aluminum was present as an impurity.

Fig. 3 is the mass spectrum obtained from molybdenum. It shows the presence of the same impurities as existed in the tungsten. This spectrum does not show as high a resolution as the one for tungsten but this is doubtless due to the fact that it was obtained at a higher temperature and the voltage drop along the filament broadened the peaks. It is interesting to note that

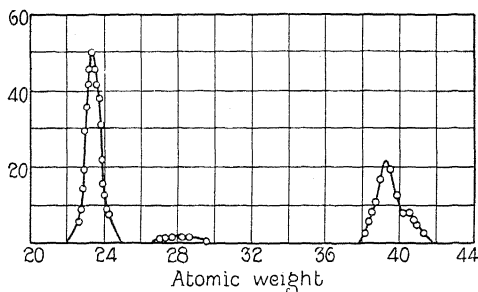


Fig. 3. Mass spectrum from molybdenum at moderate temperatures.

these impurities are present in extremely small amounts. A spectroscopic analysis was made on the samples of tungsten and no trace of the impurities here detected was found, which indicates that each was probably present in an amount less than 1 part in 100,000 and certainly less than 1 part in 10,000.

These ions which are emitted at moderate temperatures become less in number as time of heating increases and they can be gotten rid of quite

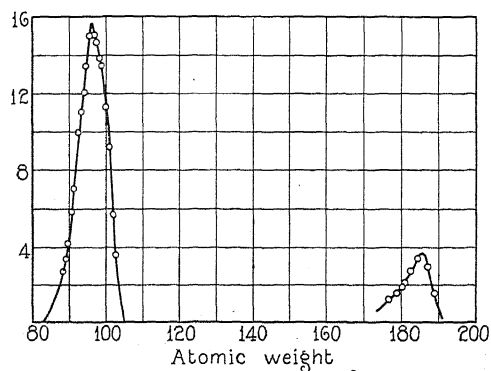


Fig. 4. Mass spectrum of molybdenum and tungsten at high temperatures.

rapidly if the filament is aged at higher temperatures. As the temperature is increased a point is found where no ions of impurities are emitted. On further increasing the temperature to about 2500° for tungsten and 2300° for molybdenum new ions are emitted. The spectrum curves for molybdenum and tungsten at these temperatures are plotted in Fig. 4. These spectra leave no doubt that the high temperature ions from tungsten found by Jenkins and the author are really tungsten ions, and that molybdenum also emits positive ions

of molybdenum. While this paper was being prepared Wahlin reported in a brief note⁷ that he had found tungsten, molybdenum, tantalum, and rhodium to emit positive ions of their own metal. The results given here corroborate his results for tungsten and molybdenum.

No trace of doubly ionized atoms was found nor was there any evidence of ions which were singly charged but having a mass of two or more atoms of the material, although they were looked for. It appears that the ion of the metal is emitted as a singly ionized atom.

VARIATION OF EMISSION WITH TEMPERATURE

To obtain the magnitude of the positive ion current for a given temperature, the form of tube shown in Fig. 5 was used. The current to the lower cylinder was measured. For tungsten, the temperature was determined from the current through a given sized filament as given by Langmuir and Jones.⁸

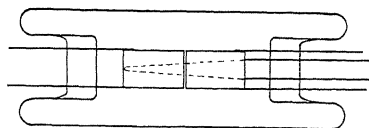


Fig. 5. Tube used to measure the positive ion current.

For molybdenum the temperature was determined from data kindly supplied by S. Dushman giving the watts per cm^2 as a function of the temperature. Volt-ampere characteristics of two hair pin filaments were taken. They had the same diameter but different lengths, and were electrically welded to identical lead wires. By a method of differences the cooling effect of the leads was eliminated and the temperature of the center of the longer filament was obtained as a function of the current through it.

The magnitude of the positive ion current from tungsten at a given temperature depends on the heat treatment through which the filament has passed. Furthermore there exists a decay with time which is slow after the filament has been allowed to age for a time and has been carried over the range

TABLE I. *Variation of positive ion current with temperature.*

Tungsten		Molybdenum	
Current per cm^2	Temp. $^{\circ}\text{K}$	Current per cm^2	Temp. $^{\circ}\text{K}$
5.39×10^9	2390	2.43×10^9	2300
9.71	2450	3.89	2340
18.3	2500	5.71	2375
25.1	2560	7.79	2400
62.6	2585	9.71	2420
79.2	2635	13.6	2460
113.	2670	17.3	2470
168.	2715	20.4	2490
276.	2760	24.3	2500
424.	2800	29.1	2520

⁷ Wahlin, Phys. Rev. **34**, 164 (1929).

⁸ Langmuir and Jones, General Electric Rev. p. 510, June 1927.

of temperatures to be used. Hence in the case of tungsten no final value of the current at a given temperature can be given. After a few hours aging at about 2300°, molybdenum seemed to give values that were reproducible. These values could be duplicated after aging for several hours more at 2300°. Table I shows data for tungsten and molybdenum obtained after some 5 hours aging.

POSITIVE ION "WORK FUNCTION"

In determining electronic work functions it has been customary to make use of the usual electron emission formula

$$I = AT^2 e^{-(\phi_- e/kT)}.$$

The work function ϕ_- is found by plotting $\log I - 2 \log T$ against $1/T$ and determining the slope of the straight line thus found. This procedure however would be incorrect for determining the work function for positive ions because of the difference in the process involved in the evaporation of ions. We shall therefore deduce an expression which should be applicable for the evaporation of ions.

Following Bridgman⁹ we take a neutral metal composed of n atoms at 0° absolute and raise its temperature to T and evaporate m ions reversibly at the equilibrium pressure. At this temperature we then have a positive ion gas, a negative surface charge, and the remaining neutral metal. Let the entropy of one atom in the condensed state be denoted by s_1 , the entropy of one evaporated ion by s_2 and the entropy to be associated with the heat of surface charging produced by the evaporation of one ion by s_2' . The entropy before evaporation is then ns_1 and the entropy after the evaporation of m ions is $ms_2 + ms_2' + (n-m)s_1$. Since the entropy after evaporation minus the entropy before evaporation must equal the change of entropy during evaporation we have,

$$(mL/T) = m(s_2 + s_2') + (n-m)s_1 - ns_1$$

where L is the latent heat of evaporation of one ion, the metal being isolated. This expression reduces to

$$(L/T) = s_2 + s_2' - s_1. \quad (1)$$

Using essentially the same expressions for s_1 , s_2 and s_2' as Bridgman, Eq. (1) becomes—

$$\begin{aligned} \frac{L}{T} = k \left[\frac{5}{2} + \log_e \frac{(2\pi M)^{3/2} k^{5/2}}{h^3} + \frac{5}{2} \log_e T - \log_e P \right] \\ + \int_0^T \frac{C_{pp}}{T} dT - \int_0^T \frac{C_{pm}}{T} dT + s_p \end{aligned} \quad (2)$$

where p is the equilibrium vapor pressure of the ion gas; M is the mass of one ion; C_{pm} is the heat capacity, at constant pressure, of an ion in the condensed

⁹ Bridgman, Phys. Rev. 27, 173 (1926).

state; $C_{p\rho}$ is the heat capacity associated with the surface heat of charging produced by the evaporation of one ion, and s_ρ is the entropy associated with the surface heat of charging at $T=0$.

The latent heat of evaporation may be expressed as a function of the temperature by the relation⁹

$$L_T = L_0 + (5/2) kT + \int_0^T C_{p\rho} dT - \int_0^T C_{pm} dT \quad (3)$$

Combining Eqs. (2) and (3) we have:

$$\log_e p = -\frac{L_0}{kT} + \frac{5}{2} \log_e T + \log_e \frac{(2\pi M)^{3/2} k^{5/2}}{h^3} + \frac{s_\rho}{k} + \frac{1}{k} \left[\int_0^T \frac{C_{p\rho}}{T} dT - \frac{1}{T} \int_0^T C_{p\rho} dT \right] - \frac{1}{k} \left[\int_0^T \frac{C_{pm}}{T} dT - \frac{1}{T} \int_0^T C_{pm} dT \right].$$

This reduces to

$$\log_e p = -\frac{L_0}{kT} + \frac{5}{2} \log_e T + \log_e \frac{(2\pi M)^{3/2} k^{5/2}}{h^3} + \frac{1}{k} \int_0^T \frac{dT}{T^2} \int_0^T C_{p\rho} dT + \frac{s_\rho}{k} - \frac{1}{k} \int_0^T \frac{dT}{T^2} \int_0^T C_{pm} dT. \quad (4)$$

Under equilibrium conditions just as many ions condense as are evaporated per second, hence we may take the rate at which ions strike the surface of the metal at the equilibrium pressure as the rate of evaporation. It may be shown that at the pressure p the number of ions striking unit area per sec is

$$n = p / (2\pi M k T)^{1/2}$$

where M is the mass of the atom concerned. If some of the ions striking the metal are not condensed but are reflected then the number emitted must be $n = (1-r)p / (2\pi M k T)^{1/2}$ where r is a reflection coefficient. The positive ion current will be given by

$$I = ne = \frac{pe(1-r)}{(2\pi M k T)^{1/2}}$$

or

$$\log_e p = \log I + \frac{1}{2} \log_e 2\pi M k T - \log_e e - \log (1-r). \quad (5)$$

Making use of (5), Eq. (4) becomes:

$$\log_e I = -\frac{L_0}{kT} + 2 \log_e T + \log_e M + \log_e 2\pi k + \log_e \frac{k}{h^3} + \log_e e + \log_e (1-r) + \frac{1}{k} \int_0^T \frac{dT}{T^2} \int_0^T C_{p\rho} dT + \frac{s_\rho}{k} - \frac{1}{k} \int_0^T \frac{dT}{T^2} \int_0^T C_{pm} dT$$

or

$$\log_e I = -\frac{L_0}{kT} + 2 \log_e T + \log_e M + \log_e \frac{2\pi k^2 e}{h^3} + \log_e (1-r) \\ + \frac{1}{k} \int_0^T \frac{dT}{T^2} \int_0^T C_{pp} dT + \frac{s_p}{k} - \frac{1}{k} \int_0^T \frac{dT}{T^2} \int_0^T C_{pm} dT. \quad (6)$$

The integral containing C_{pm} has been evaluated¹⁰ for tungsten and molybdenum. Making use of the evaluation for tungsten and changing to logarithms to the base ten, Eq. (6) becomes

$$\log_{10} I + 0.363 \log_{10} T + 1.64 \times 10^{-4} T = \frac{-\phi_{+0}e}{2.303kT} + \frac{1}{2.303k} \int_0^T \frac{dT}{T^2} \int_0^T C_{pp} dT \\ + \frac{s_p}{2.303k} + \log_{10} (1-r) + 12.43. \quad (7)$$

Where $\phi_{+0} = L_0/e$ is the equivalent difference of potential through which an ion must be moved. The corresponding equation for molybdenum is,

$$\log_{10} I + 0.453 \log_{10} T + 2.70 \times 10^{-4} T = \frac{-\phi_{+0}e}{2.303kT} + \frac{1}{2.303k} \int_0^T \frac{dT}{T^2} \int_0^T C_{pp} dT \\ + \frac{s_p}{2.303k} + \log_{10} (1-r) + 12.76. \quad (8)$$

If it were known how C_{pp} varied with the temperature then the above equation would show exactly how the positive ion current varies with the temperature and the work function ϕ_{+0} could be found by putting all functions of T on the left hand side of the equation except the term containing ϕ_{+0} and plotting it against $1/T$. The slope of the straight line so obtained would yield ϕ_{+0} .

Langmuir and Tonks¹¹ have shown that the surface heat of charging for the removal of electrons from a surface is very small i.e., of the order of 0.04 volts, at 2270°. Although the fact that it is small does not mean that it cannot vary rapidly with the temperature, we shall for the present assume $C_{pp} = 0$.

Fig. 6 shows the result of plotting the data for tungsten according to Eq. (7). Curve I is that obtained by plotting the data for tungsten given in Table I. The points lie very close to a straight line. Curve II was obtained after a sample of tungsten had aged some 30 hours and the rate of decay of the positive ion current had become very small. The point to be noticed is that even though a decay has taken place and the positive ion current has become smaller for a given temperature it has the same temperature variation as it had for considerably less aging, for the slopes of the lines I and II are the same. Curve III shows the result of plotting the data given by Mitra according to Eq. (7). As is evident, the curve so obtained has a slope almost identi-

¹⁰ Jones, Langmuir and Mackay, Phys. Rev. 30, 201 (1927).

¹¹ Langmuir and Tonks, Phys. Rev. 29, 524 (1927).

cal to that of Curves I and II. The fact that it is displaced relative to the other lines does not yield any definite information because the area of emission used by him was not given. Since the slopes of these curves are the same the work function ϕ_{+0} is definitely determined. Eq. (7) represents each of the Curves I and II with suitable change in the constant term. A discussion concerning the value of the constant term will be given later.

As stated before, molybdenum after suitable aging gave reproducible results. The data given for Mo in Table I were plotted according to Eq. (8). Fig. 7 shows how well these data give a straight line thus determining a value for ϕ_{+0} for Mo.

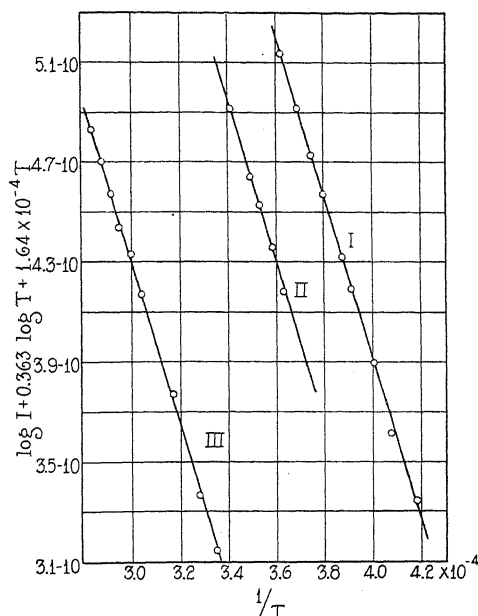


Fig. 6. Curves for determining the positive ion work function of tungsten.

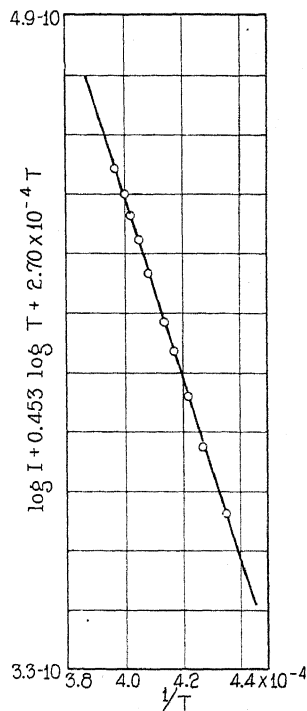


Fig. 7. Work function curve for molybdenum.

From Curve I, Fig. 6, ϕ_{+0} for tungsten is 6.55 volts, ϕ_{+0} determined from Curve II is 6.60 volts and from Mitra's data $\phi_{+0} = 6.55$ volts. It cannot be inferred that ϕ_{+0} is determined with an accuracy suggested by these figures for a slightly different line through the points yields a considerably different ϕ_{+0} as regards the third place, but 6.55 volts is undoubtedly a good representative value. The curve for molybdenum gives $\phi_{+0} = 6.09$ volts.

The constant term that must appear in Eq. (7) to represent the data plotted in Curve I, Fig. 6, is 6.51. If Curve II is considered to have the same slope as Curve I then the constant term for it is 6.28. From the curve for Mo it is found that the constant term of Eq. (8) must be 6.90.

Two serious difficulties now present themselves. The first is in regard to the constant terms just determined. Each of them is respectively much smaller than the numerical term appearing on the right side of Eqs. (7) and (8). On the assumption that the entropy associated with the surface heat of charging is zero, the constant 12.43 in Eq. (7) must be reduced to the value obtained (about 6.5) solely by the magnitude of the reflection coefficient r . To yield the proper constant, r would have to be so great that only 1 ion out of about 100,000 striking unit area would be condensed. It appears, however, that there is no quantitative evidence for such high values of r . For the evaporation of atoms, it has been found that satisfactory results are obtained when r has been assumed to be equal to or nearly zero, and even in thermionic emission r is probably not greater in order of magnitude than 0.5. Even if it had not been assumed that the entropy associated with the surface charge was zero, it is not likely that it would contribute a negative entropy constant term in Eqs. (7) and (8). Such a negative entropy would mean that heat would be developed when the metal surface became negatively charged and seems improbable. In fact evidence is presented later to indicate that heat is absorbed in the process of charging a metallic surface negatively.

The second difficulty seems more serious than the first. If we consider an inclosure in which molybdenum say is in equilibrium with its radiation at a given temperature T we may carry out the following cycle. Remove an electron and positive ion from the metal thus requiring an amount of work $\phi_{-T} + \phi_{+T}$ where ϕ_{-T} and ϕ_{+T} are the respective work functions at the temperature T , then allow the electron and ion to recombine thus producing a neutral atom and yielding an amount of energy corresponding to its ionizing potential V . Then let the atom condense on the metal thus yielding the heat of condensation. This is a reversible cycle and the sum of all the energy transfers should vanish thus:

$$\phi_{+T} + \phi_{-T} = V + U_T \quad (9)$$

where U_T is the heat of evaporation at the temperature T . Güntherschulze¹² has made use of such a cycle to compute ϕ_{+0} for those elements where the remaining data were available. With the ϕ_{+0} determined as above for molybdenum, all the terms of the cycle are known. U_T has been determined by Langmuir and Tonks,¹¹ V has been determined from the spectral series for molybdenum.¹³ At zero degrees, $\phi_{-0} = 4.42$ volts, $V = 7.35$ volts, $U_0 = 6.33$ volts. We note then that

$$V + U_0 = 7.35 + 6.33 = 13.68$$

$$\phi_{+0} + \phi_{-0} = 6.09 + 4.42 = 10.51$$

and that the cycle (9) *fails to close* by some 3.17 volts. Although the ionization potential for tungsten has not been determined it can be estimated as about 7.1 volts, and $U_0 = 8.31$ volts while $\phi_{-0} = 4.53$. For tungsten we have

¹² Güntherschulze, Zeits. f. Physik 31, 507 (1925).

¹³ Compton and Mohler, Nat. Res. Council Bulletin No. 48, 81.

$$V + U_0 = 7.1 + 8.31 = 15.41$$

$$\phi_{+0} + \phi_{-0} = 6.55 + 4.53 = 11.08.$$

Again the cycle does not close by some 4.33 volts.

Since the value of ϕ_{+0} which has been determined depends so greatly on the theoretical equation used, and the effect of a possible surface heat of charging and its variation with temperature, a check was made by computing the values occurring in Eq. (9) at a given temperature. In order to do this the Clausius-Clapeyron equation,

$$L_T = T(V - v_0)(dp/dT) \quad (10)$$

was used, where L_T is the heat of evaporation at the temperature T , V the volume of the vapor, v_0 the volume of the metal and p is the vapor pressure. Neglecting v_0 and setting $V = kT/p$ we have

$$L_T = \frac{kT^2}{p} \frac{dp}{dT} = kT^2 \frac{d(\log_e p)}{dT}. \quad (11)$$

We may express p in terms of the positive ion current by the relation (5), obtaining:

$$\log p = \log \left\{ \frac{\beta}{1-r} IT^{1/2} \right\} \quad (12)$$

where β is a constant. If r does not depend on T then Eq. (11) becomes:

$$L_T = kT^2 \frac{d}{dT} (\log_e IT^{1/2}).$$

This gives L_T in terms of the positive ion current measured and the temperature, and does not depend on any assumptions made concerning the surface heat of charging. Changing to logarithms to the base 10 and expressing L_T in terms of volts we have:

$$\phi_{+T} = 1.987 \times 10^{-4} T^2 \frac{d}{dT} (\log_{10} IT^{1/2}). \quad (13)$$

The values of $\log_{10} IT^{1/2}$ were plotted against T for molybdenum and the slope of this curve was determined at 2350°K. Using this slope, ϕ_{+} at 2350° was found to be 5.43 volts.

The electron work function ϕ_{-} at 2350° was computed from Eq. (3) assuming that the specific heat of the electrons in the condensed state was zero. Its value was found to be 4.92 volts. The value of U at 2350° was also computed by means of Eq. (3) in which the integral, $\int_0^T C_{pm} dT$ for Mo was obtained from the work of Jones, Langmuir, and Mackay.¹⁰ At $T = 2350^\circ$, U was found to be 5.41 volts. It is readily seen that if these values are substituted in the cycle (9) it still *fails to close* by some 2.45 volts. The failure of the cycle to close is, therefore, not due principally to our lack of knowledge concerning the surface heat of charging.

Under the assumption that C_{pp} equals zero Eq. (3) assumes the form

$$L_T = L_0 + \frac{5}{2}kT - \int_0^T C_{pm}dT. \quad (14)$$

The value of $\int_0^T C_{pm}dT$ for Mo was determined as stated above. Converting L_T to volts, Eq. (14) becomes,

$$\phi_{+T} = \phi_{+0} - 2.71 \times 10^{-4}T - 5.37 \times 10^{-8}T^2 + 0.019. \quad (15)$$

If C_{pp} is really zero then Eq. (15) should yield the same value of ϕ_{+} at 2350° as Eq. (13). Using the value of ϕ_{+0} already determined (6.09), ϕ_{+T} from Eq. (15) at 2350° is 5.17 volts as compared with 5.43 volts determined from Eq. (13). The difference between these two values represents a contribution due to surface charging, thus indicating that heat is absorbed in the process. By combining Eqs. (13) and (3) it would be possible to determine an empirical value for the $\int_0^T C_{pp}dT$ which in turn would modify the equation used to determine ϕ_{+0} and therefore yield a slightly different value for ϕ_{+0} . It does not seem desirable to do this until the theoretical form of C_{pp} is determined because the empirical relation could be expressed in several different forms which have no obvious theoretical significance.

It should be noted that ϕ_{+T} as expressed in Eq. (13) is independent of the reflection coefficient as a result of the *assumption* that r was independent of T . It is not at all unreasonable to suppose that r varies somewhat with the temperature but it would have to vary with *extreme* rapidity to yield a value of ϕ_{+0} which would satisfy the energy cycle (9). Such an extreme variation in r is not found in the evaporation of neutral atoms or electrons and therefore may be regarded as untenable in the case of ionic evaporation. It is therefore apparent that in Eqs. (7) and (8) there are no terms missing which change violently with the temperature and thus yield a value of ϕ_{+0} sufficiently large to close the energy cycle (9).

POSSIBLE EFFECTS OF THE FILAMENT SURFACE

It is well known that the condition of the filament surface affects the electron emission very greatly. The ordinary thermionic work function of a filament can be varied within wide limits by allowing a monatomic layer of foreign atoms to deposit on its surface. Such a layer of thorium on tungsten reduces the work function from 4.53 volts to 2.69 volts. On the other hand a layer of oxygen on tungsten increases it to 9.2 volts. Since the positive ion work function is related to the electron work function by Eq. (9) it follows that impurities on the surface would effect the positive ion work function materially. It could be supposed for example that the positive ions were really coming from small patches of the filament which were coated with oxygen atoms. For a tungsten filament coated with oxygen $\phi_{-0} = 9.22$ volts. Using this value of ϕ_{-} in Eq. (9), ϕ_{+0} comes out to be 6.2 volts which agrees fairly well with the value 6.55 volts determined by experiment.

If surface contamination is the cause of the discrepancy between the work function determined experimentally and that calculated from the cycle, it

is difficult to see how it could be due to oxygen. In the first place, as far as the writer is aware, it is impossible to keep oxygen atoms on the surface of tungsten at temperatures above 2300° or 2400°. In order to be sure that oxygen was not playing any part in the positive ion emission, a small amount of oxygen was admitted while the tungsten was emitting positive ions but the ion current was not affected until sufficient oxygen was admitted sensibly to cool the filament. A small amount of argon was admitted in the same way but the only effect was to decrease the ion current if an excessive amount was admitted. Argon is chemically inactive and its only action was probably a cooling of the filament.

It might be supposed that the surface of the filament was rough and jagged when looked at through a microscope and that the ions were being emitted from these microscopic points in the same way as electrons are emitted from cold metals. In the latter phenomenon, however, the electrons are emitted from the points because the field strength is extremely high at the point. In the case of positive ions however the voltage applied between the collector and filament was never greater than 150 volts and Mitra has shown that the ion current saturates very well thus making the correction for the Schottky effect very small. Furthermore tungsten undergoes a recrystallization at about 2800°K and filaments that have been made rough by ion bombardment can be made smooth again by raising the temperature above 2800°K. No extraordinary behavior of the ion current was noted in the neighborhood of this temperature.

RECOMBINATION AT THE FILAMENT SURFACE

If an appreciable amount of recombination took place at the surface of the filament, then it would be possible that the positive ion current as measured would not correspond to the actual rate of emission. The rate of recombination would be a function of the temperature and would modify the ion current in such a way that the measured ion current would not yield the true work function. The order of magnitude of this rate can be calculated from the Thomson theory of recombination. Such a calculation shows that at 2500°K the fraction of the ion current actually emitted which would be removed by recombination is 6.5×10^{-7} . It is therefore seen that recombination does not measurably influence the measurement of the positive ion current.

PROBABLE IONIZATION OF ATOMS AFTER EVAPORATION

One may reasonably ask whether the ions might not be formed from atoms after they evaporated. Ions certainly exist in the vapor of metal in equilibrium with the metal itself, if the temperature is high enough even though the metal emits electrons but no ions. The concentration of positive ions in such a vapor may be obtained from Saha's ionization equation, and some idea of the rate of formation of ions in such a vapor may be obtained by calculating the number of collisions which occur with sufficient energy to ionize, and the number formed by the action of radiation from the hot metal. Such calculations have been made by the writer with the result that the maxi-

num rate of formation of ions from neutral atoms in the vapor is entirely negligible compared to the ion currents measured.

PHOTOELECTRONS FROM THE COLLECTING ELECTRODE

The effect of radiation from the filament in producing photoelectrons from the collecting electrodes which would thereby influence the ion current measured has been investigated in several ways. In the first place Jenkins applied a magnetic field at right angles to the ion current in his Coolidge x-ray tube which was of sufficient strength to prevent electrons leaving the cathode from arriving at the target when a positive potential was applied to it equal to the negative potential used to collect the ions. This had no effect on the ion current which could be true only if heavy ions alone were conducting the current. Similar magnetic experiments performed by the writer produced no effect on the ion current. Collecting electrodes of different metals were used but they produced no changes in the ion current or the variation of it with temperature. The photoelectric effect does not therefore account for a measurable part of the current observed.

POSSIBILITY OF AN APPARENT WORK FUNCTION

It appears then that positive ions of the metal are actually emitted from the metal and the amount of heat required to emit them is less than the amount deduced from cycle (9) the latter of which should be the true heat required. It seems necessary in order to overcome this discrepancy to assume that the value of ϕ_+ obtained from cycle (9) is the true work function for positive ions while the value ϕ_+ determined from the positive ion current is an apparent work function, just as it was necessary to assume in the Sommerfeld¹⁴ theory of the Richardson effect that the true electron work function is W_a , and the value ϕ_{-0} determined by actual measurement is only apparent. In the Sommerfeld theory

$$\phi_{-0} = W_a - W_i$$

Where W_a is the true work required to remove an electron from the metal and W_i is the maximum energy which the electrons already have in the metal due to their high velocities acquired as a result of the velocity distribution law of the Fermi Statistics. It should be pointed out that W_a should not replace ϕ_- in cycle (9) because ϕ_- actually represents the work required to remove an electron which already has the energy W_i . The term W_i occurs implicitly in cycle (9) in the heat of condensation term U , since in condensing the atoms together to form the metal, part of the heat U must have been used up in giving the free electrons the energy W_i .

In the case of positive ions, the degeneracy condition which gave the electrons their high internal energy W_i , is not fulfilled due to their large mass, and their internal energy is the relatively small amount given by classical theory. Hence the question concerning a W_i for ions does not arise. However if it is to be assumed that ϕ_{+0} is an apparent work function then there must

¹⁴ Sommerfeld, *Zeits. f. Physik* 47, 27 (1928).

exist a source of energy of an amount ψ , which is not included in one of the terms in Eq. (9) and the magnitude of which is equal to that required to close the cycle (9). Such an amount of energy could not be supplied through the agency of a force field tending to repel the ion from the metal since such energy would be implicitly included in the work function ϕ_+ .

It may be that tungsten and molybdenum slowly recrystallize in an irreversible manner at high temperatures yielding the necessary energy ψ to emit an ion. The ions would thus be emitted as a secondary effect. In all probability some electrons and atoms would be emitted as a result of the recrystallization but the number thus emitted would be small compared with the number actually emitted per second per cm^2 and would not therefore measurably effect the heat of evaporation of atoms or the electron work function. This may readily be seen by noting that at 2500°K , 3.52×10^{16} atoms of Mo evaporate per sec per cm^2 while only 1.53×10^{11} ions are emitted.

It must be concluded from the foregoing investigation that some, if not all, hot metals emit positive ions of their own metal as well as neutral atoms and electrons. The analysis made above shows that the mechanism of emission of electricity from hot metals is not clearly understood especially as regards the emission of positive ions, for, unlike the evaporation of electrons and neutral atoms, the evaporation of ions is not strictly represented by an equation based upon thermodynamical arguments under equilibrium conditions.

The writer wishes at this time to express his appreciation of the constant help he has received from Professor R. C. Gibbs under whose direction this work was carried out, of the valuable suggestions received from Professor E. H. Kennard and of help given from time to time by other members of the Cornell faculty interested in this work.

ON THE EARLY STAGES OF ELECTRIC SPARKS

BY ERNEST O. LAWRENCE AND FRANK G. DUNNINGTON
UNIVERSITY OF CALIFORNIA

(Received January 3, 1930)

ABSTRACT

With the Kerr-cell electro-optical shutter of Abraham-Lemoine and Beams, phenomena in the early stages of sparks between electrodes of Zn, Cd and Mg have been studied. It was found that, during $50(10^{-8})$ sec after beginning of the sparks, the spark doublet lines $3d_{1,2}-4f_{1,2}$ of Zn have widths of 45A, while the corresponding lines of Cd and Mg are about 30A in width. The luminosity of the metallic vapors of Zn, Cd and Mg was observed to spread from the electrodes with speeds of $2.1(10^5)$ cms/sec, $1.5(10^5)$ cms/sec, and $1.2(10^5)$ cms/sec, respectively. Photographs of the early stages of single sparks with exposure times as short as $4(10^{-8})$ sec were obtained. The snapshots showed that during these short intervals of time after beginning of a spark the discharge is confined to a filament having a cross-section at the anode of $5(10^{-4})$ cm² which broadens out to four times this size at the cathode. From the circuit constants and these dimensions of the discharge it was accordingly estimated that the discharge current density attained the magnitude of $1.7(10^6)$ amps/cm². The asymmetry of the photographed images of the sparks disappeared when the exposure times were extended to include a complete cycle of the discharge, thereby proving the satisfactory operation of the shutter.

Assuming that the broadening of the lines to be due to the Stark effect of inter-ionic fields and with the aid of existing data on the Stark effect behavior of the lines, it was calculated that the average inter-ionic field was 10^6 volts/cm. This result in turn implies that the average separation of the ions was $3.8(10^{-7})$ cm and therefore that 1/3 of the molecules in the path of the discharge were ionized. Approximately the same degree of ionization follows from the assumption that 1/2 of the discharge current is carried by the positive ions moving towards the cathode with the observed velocity of $2.1(10^5)$ cms/sec.

Four more or less independent methods of estimating the temperature of the early periods of the spark from the present observations lead to values of the order of magnitude of $10,000^\circ\text{K}$ which point to thermal ionization as a prominent feature of such discharges.

INTRODUCTION

ELECTRIC sparks have been studied extensively for a long time and yet much remains to be understood concerning the physical process involved. One of the great remaining mysteries¹ centers around the observations of Pedersen,² Rogowski,³ Torok,⁴ Beams,⁵ Peek,⁶ Burawoy⁷ and others that sparks sometimes break down in time intervals of about 10^{-8} sec after ap-

¹ Loeb has proposed a solution of the difficulty, *Science* **69**, 509 (1929).

² Pedersen, *Ann. d. Physik* **71**, 317 (1923).

³ Rogowski, *Archiv. f. Electrotech.* **16**, 496 (1926).

⁴ Torok, *Jour. A. I. E. E.* **47**, 177 (1928).

⁵ Beams, *Jour. Frank. Inst.* **216**, 809 (1928).

⁶ Peek, *A. I. E. E. Trans.* **34**, 2, 1857 (1915).

⁷ Burawoy, *Archiv. f. Electrotech.* **26**, 14 (1926).

plication of electric fields. Their work and the work of Lawrence and Beams⁸ made it clear, moreover, that during such short time intervals the voltage across a spark gap drops from its initial high value to low values characteristic of arcs. Thus, the interesting high voltage processes which distinguish a spark from an arc occur during such short intervals of time that they are not easily susceptible to experimental observation.

However, several experimental methods have been developed which have contributed valuable information of the above mentioned sort. Pedersen² used Lichtenberg figures to measure spark lags, Rogowski³ developed a high speed cathode ray oscillograph and studied time variations of potential across spark gaps, Torok,⁴ Peek⁶ and others used surge or transient voltages of very short duration in their studies of sparks, and Anderson and Smith⁹ devised a revolving mirror camera and obtained interesting information on the early phenomena occurring during the "explosion" of wires. The adaptation by Beams¹⁰ of the electro-optical shutter of Abraham and Lemoine¹¹ to the studies of the relative time of appearance of spectrum lines in spark discharges has perhaps pointed to one of the best ways to the attack of the problem of the early stages of sparks, because the Kerr cell optical shutter makes it possible to view sparks during the desired short intervals of time.

The present paper is concerned with such an experimental study in which, for example, snapshots of single sparks with exposure times as short as $4(10^{-8})$ sec. have been obtained, which show interesting features of the early state of affairs in the discharge.

APPARATUS

The apparatus (Fig. 1) consisted essentially of a spark gap *SG*, with condenser *C* in parallel, connected across a source of high voltage *T*, and an electro-optical shutter placed in the optical path between the spark gap and the light recording device at *P*. The latter was either a spectrograph or a camera. When the spectrograph was used, the source of high voltage was

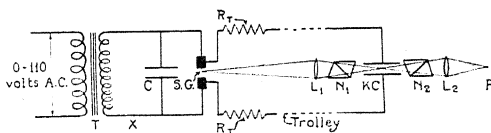


Fig. 1. Experimental arrangement.

simply a 25,000 volt 1 KW transformer which supplied a 60 cycle voltage of any value up to its maximum. When the camera was used a high voltage kenotron (KM-1) rectifying tube was inserted at *X* together with a resistance of about 500,000 ohms. The electrodes of the spark gap made of Zn, Cd or Mg were shaped so that the spark jumped between two parallel faces

⁸ Lawrence and Beams, *Phys. Rev.* **32**, 478 (1928).

⁹ Anderson and Smith, *Astrophys. J.* **64**, 295 (1926).

¹⁰ Beams, *Phys. Rev.* **28**, 475 (1926).

¹¹ Abraham and Lemoine, *Comp. Rend.* **130**, 245 (1900).

6 mm apart. The dimensions of these faces were, when using the spectrograph 3×6 mm (the short dimension being perpendicular to the optical path), and when using the camera, 3×3 mm. The spectrograph was a Hilger constant deviation type having a dispersion of about 36Å per millimeter at 4900Å. The camera consisted of a plate holder and bellows to exclude light, no lenses other than L_1 and L_2 being necessary.

The electro-optical shutter which was the heart of the apparatus was essentially the same as that described by Beams,¹⁰ but with certain minor though important modifications. A Kerr cell consisting of parallel plates 9.5 cm long, 1.2 cm wide and 0.5 cm apart immersed in carbon bisulphide and situated between crossed Nicol prisms N_1 and N_2 was attached to the terminals of the spark gap by wires of variable length. This system operated as an optical shutter controlled by electrical means in the following manner. With no voltage on the Kerr cell, the carbon bisulphide was not doubly refracting and hence light could not pass through the crossed Nicols. Upon application of a potential across the cell the liquid became doubly refracting and a fraction of the light was passed, within a limited range of voltages the amount of light passed being proportional to the fourth power of the voltage. Now since the voltage which was impressed across the gap and condenser was also impressed across the Kerr cell, by the time the voltage had built up to a value sufficient to cause a breakdown of the gap the shutter was open. When the gap broke down the voltage across it dropped to a relatively small value in a time interval at least not greater than 10^{-8} sec. A resulting discharge wave was propagated along the wires to the Kerr cell causing a lowering of the voltage across the plates at a time after the spark breakdown approximately equal to the length of wire in one lead from SG to KC divided by the velocity of light. At about the same time that this discharge wave started from the gap, light from the spark began to be emitted and traveled towards the Kerr cell system. A part of the light which reached the cell before the wave was transmitted, while all of the light reaching the shutter thereafter was rejected. Thus it was possible to observe the light from the spark from its beginning up to any desired time of cut off determined by the lengths of the trolley leads. The times of cut off in the present experiments ranged from practically zero to 50 (10^{-8}) sec. after beginning of the spark.

The modifications in the electro-optical shutter had to do with the control of oscillations. It is obvious that if oscillations should exist in the Kerr cell circuit after the voltage is supposedly reduced to a low value, light from later periods of the spark would be transmitted, thereby producing spurious results. Because previous work has been questioned¹² on this basis, it is believed worthwhile to give some of the details and show proof that the shutter operated in the manner outlined above. The methods used to control the oscillations in the trolley circuit were as follows

(1) *Reduction of coupling between the condenser-spark gap circuit and the trolley-Kerr cell circuit to a minimum.* Upon breakdown of the gap, the dis-

¹² Gaviola, Phys. Rev. 33, 1023 (1929).

charge of the condenser C through the gap is oscillatory. If the coupling between this condenser-spark gap circuit (hereinafter referred to as the condenser circuit) and the spark-gap-trolley-Kerr cell circuit (hereinafter referred to as the trolley circuit) were appreciable, forced oscillations would be produced in the latter. With this in mind the length of path in common between the two circuits was reduced to a minimum by taking off the leads to the trolley circuit by taps in the electrodes about a millimeter back from the sparking surfaces. The coupling was further reduced by taking off these leads to the trolley in a plane at right angles to the condenser circuit.

(2) *Maintaining the fundamental wave-length of the condenser circuit always considerably under that of the trolley circuit.* The trolley circuit consisting of distributed inductance and capacity has a fundamental oscillatory period of its own. It is obvious that even though the coupling were small, the effect in the trolley circuit of oscillations in the condenser circuit would be much greater at or near resonance. To avoid the effect of harmonics as well as that of the fundamental oscillations of the condenser circuit, its wave-length was adjusted so as to be considerably less than that of the trolley circuit. The wave-length of the condenser circuit was calculated and checked by a wavemeter. That of the trolley circuit was obtained by comparison with the condenser circuit by resonance in the following manner. The trolley leads to the gap were disconnected and joined together and the plane of the leads was turned so as to increase the mutual inductance of the circuits. For every set of condenser circuit constants that gave a wave-length within the range of that of the trolley circuit, a position of the trolley could be found that allowed light to pass. Approximate calculations showed that such resonance between the circuits involved fundamentals and not harmonics of the condenser circuit.

(3) *Damping of the oscillations in the trolley circuit.* Even though the trolley circuit were free of all outside disturbances, the charge stored by its distributed capacity previous to a breakdown of the spark would oscillate upon the shorting of the gap by the spark. If these oscillations were critically damped by the insertion of sufficient resistance R_c , the rate of fall of voltage across the Kerr cell would thereby be greatly diminished. However, this impasse to arranging the circuit so that the shutter closes with great rapidity free of appreciable oscillations is only apparent. The intensity of the light passed by the shutter is proportional to the fourth power of the voltage. Hence were the amplitude of the voltage on the first reversal only damped to a value one half the original voltage, the light passed per unit time would be only a sixteenth that at the original voltage. Thus, since the delay in the voltage-drop caused by damping is small until the region of critical resistance is reached, it is possible to damp the oscillations sufficiently without appreciably delaying the closing-time of the shutter. Exact calculations being difficult, the best value for the damping resistance was found experimentally by finding the value which gave the smallest observed distance of migration of the metallic vapor out from the electrodes (see results). The value found was 500 ohms (250 ohms distributed over each lead from spark gap to Kerr cell).

Oscillations were apparent when using resistances considerably below this value. Increasing the damping resistance produced little effect until values of over 1000 ohms were reached when the slowing down of the rate of closing of the shutter became observable

That the shutter was effectively closing at times close to those calculated from the wire path was definitely proved by the direct photographs of the spark (see results). When the time of cut off was made equal to or less than that of a half cycle of the condenser circuit, the pictures obtained were assymmetric relative to the cathode and anode, the images of the discharge being narrower and more intense near the latter electrode. This experimental observation constitutes indisputable evidence that the shutter operated in the manner outlined above.

THE EXPERIMENTS

The initial experiments were concerned with observations of spectra emitted during early stages of the spark. An image of a portion of the spark near one electrode was projected through the optical shutter and was focused lengthwise on the slit of the spectrograph and photographs of the spark spectra of Zn, Cd and Mg were obtained with the shutter closing at various times after the beginning of the sparks. In order to obtain sufficient blackening of the photographic plates it was necessary to expose for from 3 to 10 minutes. Since 120 sparks occurred per sec. the photographs represent the integrated spectra of the beginning of a large number of sparks. The general features of the results were the same for the three metals studied and therefore only the data on Zn are here exhibited. Fig. 2h shows the spectrum of the Zn spark obtained with the Nicol prisms uncrossed, being consequently the ordinarily observed spark spectrum. The Zn spark doublet 4912-24Å and the arc lines 4680Å, 4722Å and 4811Å together with several air lines are prominent. 2a exhibits the spectrum observed with the shutter closing $19 (10^{-8})$ sec after the beginning of the spark—a spectrum which bears little resemblance to 2h. As the experiments of Schuster-Hemsalech¹³, Beams¹⁰ and others have shown, the metallic lines of the spark are absent in its early stages, the spectrum being that of air with a strong continuous background. Taking into account the dependence on wave-length of the photographic sensitivity of the plate and the absorption in the optical system it is estimated that the maximum intensity of the continuous spectrum occurred well below 4600Å. It is of particular significance to note the extreme diffuseness of the air lines during this early period of the spark which is attributed to the Stark effect of the inter-ionic fields

Fig. 2b shows the spectrum photographed with the shutter closing $27 (10^{-8})$ sec after the beginning of the spark. In this photograph, as in all the others, light which produced the lower ends of the spectrum lines came from the region of the spark adjacent to one of the electrodes and the length of the lines represents about 2 mm of the gap. The continuous background at this later time appears definitely to be most intense near the electrodes.

¹³ Schuster and Hemsalech, *Phil. Trans.* 193A, 189 (1900).

This photograph indicates also that the position of maximum intensity of the continuous spectrum shifts to a slightly longer wave-length at this later time. This photograph also shows the first appearance of the Zn metallic spark doublet 4912-24A as a very diffuse region of luminosity near the electrodes. The broadening of the lines is more easily seen in 3g which is

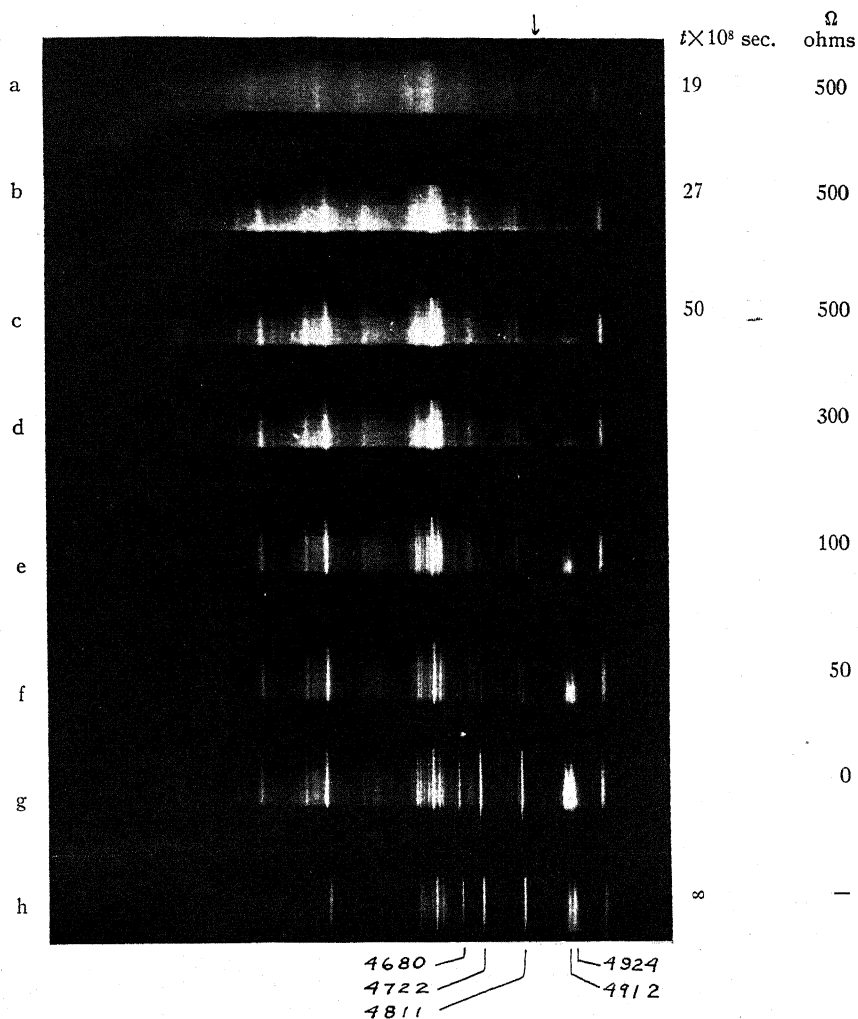


Fig. 2. Photographs of spectra emitted during various intervals of time after beginning of sparks between Zn electrodes in air.

a magnified section of 2c. It was estimated from these observations that each of the *spark lines during this early period of the discharge were broadened symmetrically to a total width of 45A*. The widths of the corresponding lines of Cd and Mg were observed to be somewhat less—approximately 30A.

Fig. 2c shows that at the later time of 50 (10^{-8}) sec after the beginning of the spark, the metallic spark lines were emitted at a greater distance from

the electrodes. This observation gives at once a measure of the average velocity of migration of the metallic ions away from the electrode surfaces. From several such observations it is found that *during the first 27 (10^{-8}) sec the average velocity of migration of the metallic ions away from the electrode surface is $2.1 (10^5)$ cms per sec.* The corresponding observed velocities for Cd and Mg ions were 1.2×10^5 cm/sec and 1.5×10^5 cm/sec respectively. Due to photographic difficulties, these values however are much less accurate than that for Zn.

The above mentioned spectra were taken with a distributed resistance in series with the Kerr cell of 500 ohms. Reducing this resistance to 300 ohms produced no perceptible change—as shown by the spectrum 2d which was taken under the same conditions as 2c excepting that the resistance was reduced to the lower value. On reducing the resistance to 100 ohms, 50 ohms and practically zero, however, a marked effect resulted as shown by Fig. 2e, f and g. From the fact that the luminosity of the spark lines extended further from the electrodes in the latter cases and that even the arc lines were in evidence, it is concluded that the oscillations were of sufficient magnitude to reopen the shutter at a later time. Careful examination showed that the operation of the shutter was sensibly independent of the damping resistance over the range 300 to 1000 ohms. Inserting resistance in excess of 1000 ohms over damped the discharge of the Kerr cell to such an extent that its effective time of closing was perceptibly delayed. Though it was not possible to make an accurate estimate, a calculation from the dimensions of the circuit agreed with the above values as being the right order of magnitude to damp the oscillations to the extent desired.

Our photographs fail to show the metallic arc lines at all, during 50 (10^{-8}) sec after beginning of the spark, a result not in agreement with the observations of Beams¹⁰ and Locher.¹⁴ A faint haze of luminosity near the electrode of wave-length near 4811A shown in 2c might easily have been thought to be due to the Zn arc line 4811A. However, measurements show that it is nearer 4817.5A. The origin of this line is uncertain at the present time as there are no well known Zn or air lines of this wave-length.

The photographs 2a, b, c, show a diffuse air line near 4865A (indicated by arrow) which occurs only in these very early periods of the discharge. 2a shows it extending practically across the spectrogram while in 2b and 2c it is confined successively nearer the lower edge. As will be evident in the discussion, very intense ionization and accompanying high temperature exists in the early period of the spark and it is probable that this line therefore is due to an ionized constituent of the air. There are many examples in the literature of lines which appear only under such conditions.¹⁵

For the purpose of measuring the cross-section of the discharge during its early development in order to obtain an estimate of the current density, direct snapshots of the spark of the requisite short exposures were attempted. A kenotron and a one-half megohm resistance inserted in series with the

¹⁴ Locher, J.O.S.A. and R.S.I. 17, 91 (1928).

¹⁵ Handbuch der Physik 21, p. 434.

condenser made it possible to apply known differences of potential across the spark gap resulting in single sparks. Images of the spark projected through the Kerr cell and focused on a photographic plate are shown in Fig. 3. The polarity indicated in all the photographs is that of the first half cycle. 3a is a series of single sparks taken with the Nicol prisms uncrossed (with the

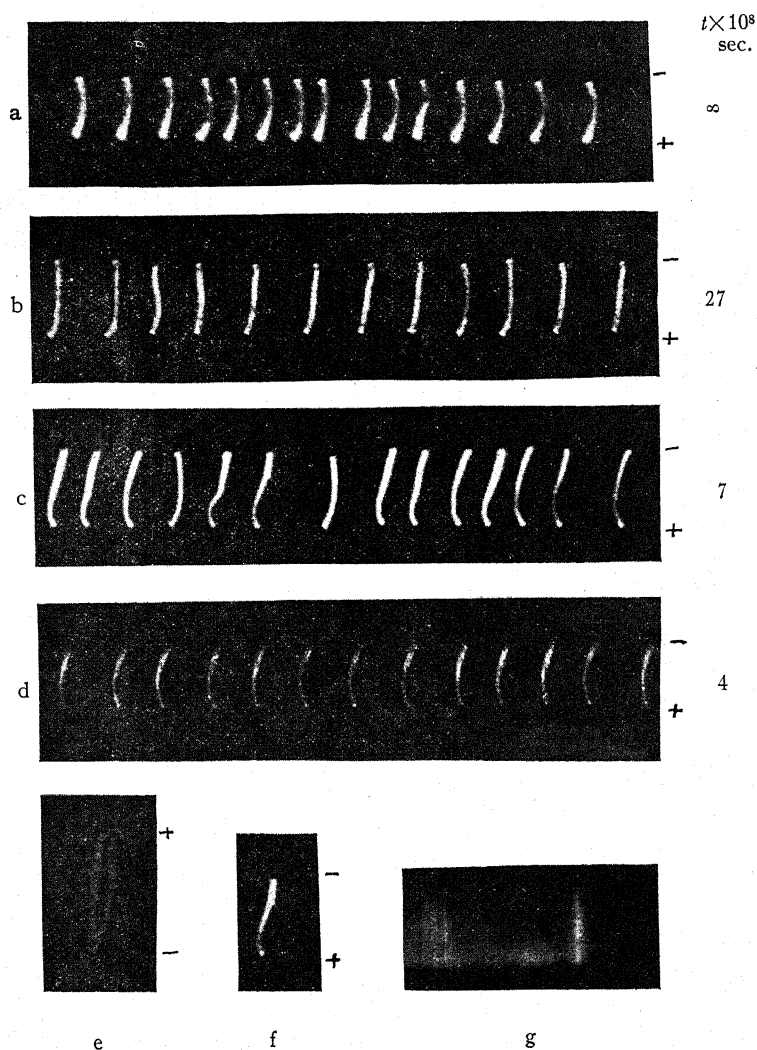


Fig. 3. Photographs of the early stages of sparks between Zn electrodes.

shutter continuously open) and therefore represent images of completed sparks. 3d shows the spark during the first 4 (10^{-8}) sec of its existence. To obtain these photographs it was necessary to have a condenser capacity of 0.004 mf in order to maintain the oscillations in the spark circuit out of resonance with the Kerr cell circuit. It is seen that *the discharge is confined*

to a very narrow filament near the anode which widens out towards the cathode. Measurement of the plates showed that the average diameter of the discharge at the anode was 0.25 mm and at the cathode 0.5 mm. Since the period of oscillation of the spark was $26 (10^{-8})$ sec, these photographs represent the form of the discharge during the earlier part of the first half cycle. Changing the condenser capacity to 0.008 mf, the photographs of 3c were obtained with the shutter closing $7 (10^{-8})$ sec after the breakdown of the potential across the gap. In this instance the period of oscillation was $36 (10^{-8})$ cm and consequently these are pictures of approximately the first quarter cycle of the discharge. The dissymmetry of the discharge is still evident, though not as marked as in the shorter exposures,—the average diameter of the discharge at the anode being 0.45 mm and at the cathode 0.5 mm. Another interesting feature of these photographs is the presence of a *very bright spot of luminosity close to the anode*, indicating an intensity of light there greatly in excess of that of the central section of the filament. 3b was obtained with the shutter closing at $27 (10^{-8})$ sec. In this instance the shutter closed after the setting in of the second half cycle, as the period of oscillation remained at $36 (10^{-8})$ sec. As was to be expected, this photograph shows a more nearly symmetrical filament with minute intense spots of light at both electrodes, that at the cathode being less intense than the one at the anode because the cut off occurred at about the middle of the second half cycle. The average diameter of the filaments is 0.5 mm. It is perhaps not amiss to emphasize again that *these observations of the asymmetry of the discharge during the first half cycle are indisputable evidences that the electro-optical shutter functioned in the manner outlined above and that oscillations were of inappreciable magnitudes.*

Thus during the period of $23 (10^{-8})$ sec between the closing of the shutter for groups d and b, the cross-section of the discharge at the anode was observed to vary from $4.9 (10^{-4})$ sq cms to $1.9 (10^{-3})$ cm² and since during these periods the average discharge currents (estimated from the circuit constants) were 800 and 1100 amps respectively, *the average current density varied from $1.7 (10^6)$ amps per cm² to $5.8 (10^6)$ amps per cm².* These enormous current densities produced the great brilliance of the spark which made possible the short exposure photographs of the present experiments.

The path of breakdown of the sparks usually were along the lines of force. When the electrode surfaces were flat with sharp edges the sparks jumped from edge to edge along the curved lines shown in many of the photographs. When the edges were rounded off the sparks jumped between the middle of the electrode surfaces along the straighter lines of force in that region. However, interesting exceptions have been observed during the first $3Q (10^{-8})$ sec of the spark as shown in Fig. 3, e and f. 3f shows a sharp spur protruding from the main filament of the discharge of the sort that might arise from an ion path initiated by a high velocity particle. The spur is bent away from the anode and luminosity is seen to extend outside the main discharge from the spur to the cathode, as though positive ions formed along the path of the spur produced additional luminosity during their

passage to the cathode. 3e shows a case where the spark took two simultaneous paths, the bifurcation suggesting that the spark breakdown was initiated at the cathode. Examples of bifurcation at the anode and also in the middle of the gap, however, have been observed.

DISCUSSION

There can be little doubt that large broadening of spectrum lines produced by high current densities is due to the Stark effect of inter-ionic fields.¹⁶ The width of the spark doublets of Mg, Cd and Zn observed in the early stages of the spark therefore can serve as a measure of the average ionic fields, and in turn, the average number of ions per cc in the discharge. Such an estimate requires an independent knowledge of the Stark effect behavior of the lines. Now the spark lines in question result from transitions between the hydrogen like energy levels $3d_{1,2}$ and $4f_{1,2}$ and indeed are very similar to the corresponding line 4686Å of ionized helium. It is therefore to be expected that the metallic spark lines should exhibit a Stark effect closely resembling the observed Stark effect of the corresponding He line. Several experimental measures of the Stark effect of the He line in question have been made, the most recent being that of Foster¹⁷ who finds that the maximum displacement of the components from the undisplaced position is about 2.4Å per 100,000 volts/cm field. The results of Nagaoka and Sugiura¹⁸ show that the corresponding line 4811Å of Mg is broadened to a width of about 2Å on each side of the undisplaced position in an average field of 116,000 volts/cm, a fact which supports the expectation that the corresponding lines of He, Zn, Cd and Mg should exhibit nearly the same Stark effect. From the total width of 45Å observed in the present experiments then it can be concluded with considerable confidence that *the average ionic field during the early stage of the Zn sparks here studied was approximately 10^6 volts per cm.*

From this value for the average ionic field and the inverse square law it follows that the average separation of the ions was approximately 3.8 (10^{-7}) cm and therefore that the total number of ions and electrons was about $1.8 (10^{19})$ per cc. *Thus, about 33 percent of the molecules in the path of the discharge were ionized.* Anderson and Smith⁹ have found an equally great degree of ionization during the early stages of the "explosion" of wires.

The present experimental data lead to a second and independent estimate of the ionic density. The average velocity of migration of the metallic spark luminosity, and therefore presumably of the positive ions away from the anode was observed. Assuming that the positive ions moved towards the cathode with this speed and carried one-half the discharge current, it follows that there were necessarily present about $0.82 (10^{19})$ positive ions per cc. Thus, this second estimate indicating 30 percent ionization is in excellent agreement with the first.

¹⁶ An excellent resume of the subject of the broadening of spectrum lines is to be found in volume 21 of the "Handbuch der Physik."

¹⁷ Foster, Astrophys. Jour. **62**, 229 (1925).

¹⁸ Nagaoka and Sugiura, Jap. Jour. of Phys. **3**, 46 (1924).

The objection might be raised perhaps that, because of the far greater mobility of the electrons, they carry most of the current of the discharge and consequently it is not valid to assume that half the current is carried by the positive ions. Loeb¹ states, for example, that the electrons have about 1000 times the mobility of the positive ions. However, such estimates are made with the assumption that the density of the ions is small compared to the density of the neutral molecules, a state of affairs existing in low current-density discharges. The above results make it clear that in the early stages of sparks because of the high degree of ionization a pumping action of the ions produces a general flow of both ions and neutral molecules resulting thereby in a greater mobility of the ions than calculated in the usual manner. Moreover, a simple calculation shows that the high current density of the discharge produced a magnetic field as great as 20,000 Gauss which exerted a great influence on the trajectories of the electrons. Thus, if the velocity of the electrons were 10^8 cms/sec perpendicular to the magnetic field, it is calculated that the magnetic field caused them to travel in curved paths with radii of curvature $3 (10^{-4})$ cm. The effect of the magnetic field was consequently to increase greatly the paths traversed by the electrons in passing from cathode to anode, thereby producing a great reduction of their general drift velocity (mobility). Space charge effects played an unknown though probably important part also in keeping the electron current and the positive ion current at the same order of magnitude.

Several independent estimates of the temperature may be made as follows.

(1). From the degree of ionization the effective temperature of the discharge can be calculated after the manner of Saha.¹⁹ We have the reaction-isochores

$$\log \frac{x^2}{1-x^2} P = -\frac{5050 V_i}{T} + 2.5 \log T - 6.69.$$

where x is the fractional number of the atoms ionized, P is the pressure in atmospheres, V_i is the ionization potential in volts and T is the absolute temperature. Taking for x the here-observed value $1/3$, for V_i 9.3 volts, the ionization potential of Zn, and for P , 10 atmospheres, there results for the temperature of the discharge the value of $13,500^\circ\text{K}$. A higher assumed value for V_i corresponding to ionization of O or N would lead to a correspondingly higher estimate of the temperature. However, the observations were taken in the proximity of the electrode where the metallic vapor predominated. From the observed spreading of the filament of the discharge during the course of time, from the work of Anderson and Smith on exploded wires, and from other considerations, it appears that the assumed pressure is right in order of magnitude.

(2). It is also possible to make a rough estimate of the temperature of the discharge from knowledge of the rate of dissipation of energy in the spark. Professor J. W. Beams has kindly let us see some of his revolving mirror

¹⁹ Saha, Proc. Roy. Soc. A99, 135 (1921).

photographs of sparks in advance of publication from which we deduce that the sparks we worked with had a duration of the order of magnitude of 10^{-5} sec, and therefore that about one one-hundredth of the energy of the discharge was dissipated in the spark during the first 10^{-7} sec. Knowing in addition the capacity of the condenser, the voltage at breakdown, the specific heat of the, and the volume of the gas heated, an elementary calculation leads to 5000°K as the temperature of the discharge. This estimate is somewhat lower than that resulting from Saha's equation, a fact that is to be accounted for by the assumption that only $1/100$ of the energy stored in the condenser is dissipated in 10^{-7} sec. Beams has shown in his revolving mirror photographs that the first cycle of the spark discharge has a period about 1.5 times longer than the period of later oscillations and therefore that the resistance and rate of energy dissipation is greater at the beginning of the spark. This fact was also taken into account in estimating the current density in the above calculations.

(3). As has been pointed out above, the high degree of ionization produced a general flow of ions and neutral molecules to such an extent that the observed velocity of migrations of the ions probably also measured the average velocity of the molecules. An estimate of the temperature then follows from

$$(3/2)kT = (1/2)mv^2$$

where k is Boltzman's constant, T is the temperature, m is the mass of a Zn atom and v is the observed velocity. Such an estimate yields a temperature of $10,900^{\circ}\text{K}$.

(4). Finally, an estimate of the temperature may be made from the intensity distribution in the continuous spectrum of the discharge. From the observation that the intensity was a maximum well below 4600\AA , it is concluded that the discharge temperature was considerably above 6200°K . This value is least reliable of all because many sources of error in estimating light intensities were not carefully investigated.

Thus, four more or less independent estimates of the temperature of the sparks obtained from the data of the present experimental study agree in indicating that it is of the order of magnitude of $10,000^{\circ}\text{K}$. This result points to thermal ionization as the main process in the early stages of sparks as has been suggested by Slepian.²⁰

²⁰ Slepian, *Phys. Rev.* **31**, 1123 (1928).

A NEW REGULARITY IN THE LIST OF EXISTING NUCLEI

BY HENRY A. BARTON

DEPARTMENT OF PHYSICS, CORNELL UNIVERSITY

(Received January 13, 1930)

ABSTRACT

In the absence of a theory of nuclear constitution, a search for regularities in the list of existing nuclear types is of value. Aston's data form a fairly complete list up to atomic number 61. Previous investigations disclosed evidence of several types of regularity. A new type has been observed in which most of the known nuclei in the range studied fall into three clusters, each characterized by a two dimensional symmetry. More specifically, when the nuclei are plotted as points whose ordinates and abscissas indicate the number of protons and electrons respectively in their constitution, there exists for each cluster a center (P, E) such that if there is a nuclear type $(P-X, E-Y)$ there is, in general, also a symmetrical type $(P+X, E+Y)$. A consideration of the relatively few departures from this rule within the clusters leads to a list of *predicted isotopes* as yet undiscovered. A possible physical interpretation of the new type of regularity is tentatively suggested. The considerations advanced apparently do not apply to a number of points scattered through the regions between the clusters.

INTRODUCTION

THERE is no comprehensive theory of the structure of atomic nuclei. The present position is one in which it is very desirable to examine the available data in search of empirical laws with which to simplify the statement of what is known. The list of nuclei embracing all known isotopes of all elements which actually exist, in contra-distinction to those conceivable nuclei which do not, presents a fruitful field for such a scrutiny. Any rule or regularity of occurrence which can be found will facilitate the development of a satisfactory theory. Beck¹ has pointed out that Aston's work has now furnished a body of excellent data² covering nearly all elements up to atomic number 61. A knowledge of the isotopes of many elements heavier than this is as yet lacking so that the data do not have the completeness which is necessary, or at least most desirable, when it is a question of the existence or non-existence of each possible nucleus. Only that part of the list of elements which lies below atomic number 61 is considered in the present paper. For such a list presented in significant tabular form the reader is referred to Beck's papers.

The considerations which Beck advances lead to valuable rules in addition to those already noted by others.³ The work of Harkins,⁴ based on evidence

¹ G. Beck, *Zeits. f. Physik* **47**, 407 (1928); **50**, 548 (1928).

² F. W. Aston, *Phil. Mag.* **49**, 1191 (1925); *Proc. Roy. Soc. A* **115**, 487 (1927), p. 509.

³ A summary of speculations about nuclear constitution and structure is given by E. N. da C. Andrade, "The Structure of the Atom," Chap. VII.

⁴ W. D. Harkins, *Science* **70**, 433 and 463 (1929). *Zeits. f. Physik* **50**, 97 (1928). Also many earlier papers references to which are made in the two cited.

concerning the relative abundance⁵ of the elements in the earth's crust and in meteorites, has been particularly fruitful in establishing rules governing the existence and stability of nuclear types. The kinds of regularity pointed out by these and other authors deal with the numbers of α -particles, protons, and electrons in the nuclei. For example, the fact that mass increments of four units together with charge increments of two units occur frequently in almost any sort of classification gives strong evidence of the existence of

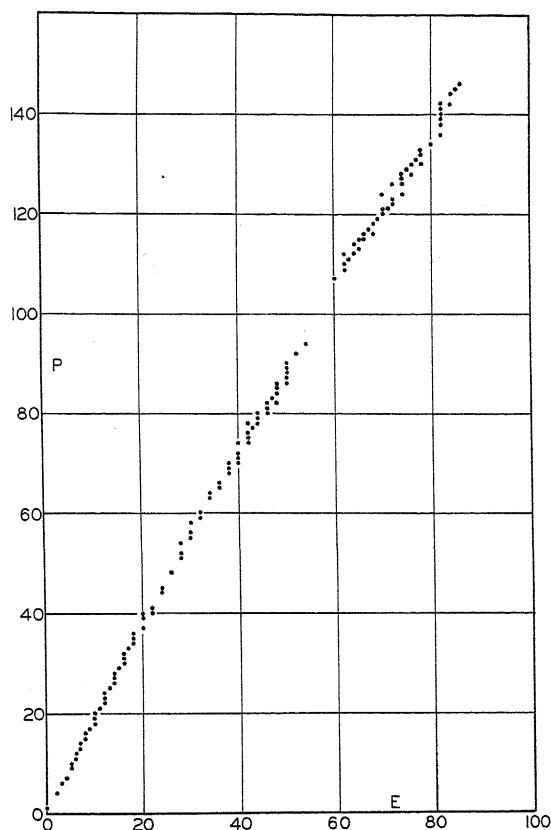


Fig. 1. Constitution of all known nuclear types in the range of elements below atomic number 61.

nuclei which differ from one another merely in the number of integral α -particles they contain. Other rules are, for example, the tendency for the number of nuclear electrons to be even, the limitation to two isotopes in the cases of elements of odd number, etc.

A NEW TYPE OF REGULARITY

The writer has recently observed an altogether different type of regularity which does not seem to be described in the literature. It appears when a

⁵ F. W. Clark, "The Data of Geochemistry," Bulletins 491 (1911) and 616 (1915), U. S. Dept. of the Interior. "Evolution and Disintegration of Matter," U. S. Geol. Surv., Prof. Paper 132-D (1924). W. D. Harkins, J. Am. Chem. Soc. 39, 856 (1917).

suitable chart is made of the constitution of the existing nuclei. Fig. 1 is such a chart in which a point is plotted for each nucleus opposite the ordinate P representing the number of protons it contains and the abscissa E representing the number of electrons it contains. P , the number of protons, is approximately equal to the atomic mass. E stands for *all* of the nuclear electrons whether constituting α -particles or not, so the atomic number, or nuclear charge, Z , is equal to $P - E$. The chart was compiled from Aston's data.

It is evident even on this small scale chart that there are three clusters of points separated by regions of relatively low density, i.e., where the ratio of the number of actual to conceivable nuclei is relatively small. The clusters themselves are individually of interest. A superficial examination of a small

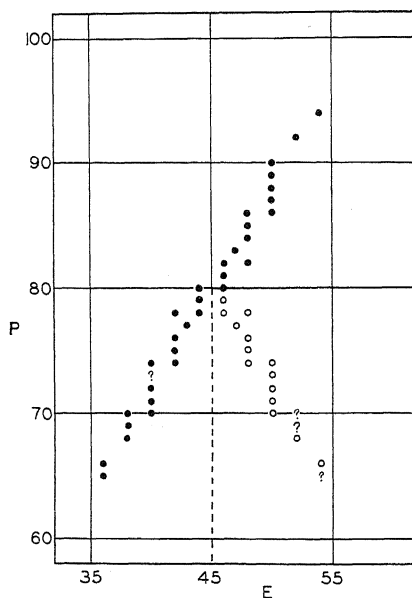


Fig. 2. Enlargement of the middle portion of the chart in Fig. 1 to show the two-dimensional symmetry of the cluster. (Cluster II.)

chart such as Fig. 1 gives little basis for specifying the limits or centers of the clusters. On a larger scale, however, it is apparent that in each group there exists a regularity in the form of a two dimensional symmetry about a definite point near the center of gravity of the clusters. For example, Fig. 2 shows the region of Fig. 1 occupied by the middle cluster. The solid dots are the same as those of Fig. 1. The circles show the positions occupied by the dots in the upper right quadrant if that quadrant is rotated 180° around the axis of symmetry $P = 80$. The extent of the symmetry can now be estimated at a glance. In this cluster, evidently centered at $(P, E) = (80, 45)$, the symmetry is perfect except that in the cases of four out of the thirty-two points plotted, the symmetrically located positions are vacant. Such vacant positions are indicated by question marks.

Similar charts of the clusters in the regions of heavier and lighter elements respectively are shown in Figs. 3 and 4. In the cluster made up of heavier elements, it is noteworthy that the symmetry, centering at (124,72) consists largely of two long diagonal lines of points. One of these, starting at (124, 74), runs one way to (112,62), and the other starting at (124, 70), runs the other way to (136,82). The one represents the isotopes of tin and the other the isotopes of xenon. Although two positions are vacant in the case of xenon, the end positions of the two lines are symmetrical, and in each case, the outer end is followed by several points in a vertical row.

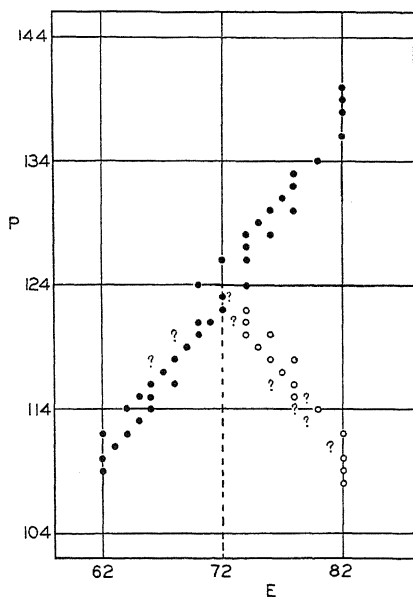


Fig. 3. Cluster III; heavier elements.

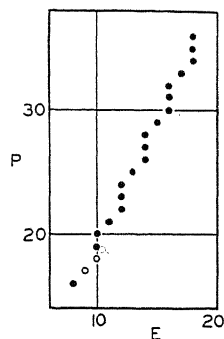


Fig. 4. Cluster I; lighter elements.

The cluster in the region of lighter elements presents so simple a type of symmetry that the center cannot be located without ambiguity. The point (25,13) would serve as well as (27,14). The discovery of the new oxygen isotopes⁶ (shown by circles) would tend to shift one's estimate of the "center of gravity" of the cluster downward.⁷

Aston has recently published the result of some further experiments with the mass spectrograph.^{8,9} These must be considered now in so far as they

⁶ W. F. Giaque and H. L. Johnson, *Nature* **123**, 318 and 831 (1929). *J. Am. Chem. Soc.* **51**, 1436 (1929).

⁷ It is interesting to note that the new oxygen isotopes are nuclei which would have been predicted by extrapolation of the obvious step-like regularity of the cluster.

⁸ F. W. Aston, *Nature* **120**, 224 (1927); **122**, 167 and 345 (1928).

⁹ The writer was not aware of these when he published a preliminary notice. (*Phys. Rev.* **34**, 1228 (1929)). He wishes to take this opportunity of also acknowledging his error in including in that notice a nuclear type ($80+11$, $45+7$) which has not been shown to exist. Beck has postulated its existence on fairly firm grounds. However, the writer wishes to confine himself to Aston's experimental data with the addition of the isotopes 17 and 18 of oxygen, 15

affect the symmetry of the clusters. New isotopes of lead, mercury, germanium and zinc are announced. It is not of interest for the present purpose to add the corresponding points to Fig. 1. In fact, lead and mercury are above the range of elements investigated. The isotopes of germanium and zinc alter only Cluster II. To bring Fig. 2 up to date it would be necessary to add points corresponding to the additional isotopes of germanium and zinc, namely (73, 75, 76, 71 and 77) and (67 and 65) respectively. The previously known isotopes were of course already plotted in Fig. 2. None of the new points falls into a position symmetrical with one already existing. The symmetry of this cluster is thereby considerably impaired although strong evidence of the tendency remains.

Aston states⁸ that it is impossible to exclude the possibility that the mass spectrum lines representing some of these isotopes really represent hydrides of the previously known isotopes. Germanium is known to be like carbon in its tendency to form unstable hydrogen compounds, so it would be expected that such hydrides would appear in the discharge tube in the same way as CH , CH_2 , etc. appeared when compounds of carbon were present. The symmetry considerations would be helped if this were found to be the case. On the other hand, it may be that here is an example of the danger of working with only partially gathered data. The relative abundance of the new isotopes is obviously very small since they escaped discovery in Aston's previous study of germanium. It is possible that symmetrical nuclear types of the same order of abundance (very faint isotopes of strontium) may yet be found to restore a high degree of symmetry to the cluster. It is because of these reservations that the cluster has been plotted without, rather than with, the new data.

DISCUSSION

The boundaries of the three clusters as represented in Figs. 2, 3, and 4 are of course, arbitrarily chosen. However, it can be said that there is good evidence of symmetry just inside these boundaries and little of such evidence just outside. There remain, then, the regions below and between the clusters in which fall the points of a number of very common nuclei, among them hydrogen, helium, carbon, calcium, and iron. In these regions no evidence of symmetry has been discovered, so that no claim for applicability over the whole list of natural elements can be made for the type of regularity described in this paper.

Alternative points of view may be taken with regard to the departures from perfect symmetry within the clusters. The vacant positions may be vacant only through lack of data. On the other hand, the existing points symmetrical to these vacant positions may represent nuclei not properly belonging to the cluster in some sense which we do not now know how to define. The first alternative may at least be adopted tentatively. On this

of nitrogen, and 13 of carbon discovered through the band spectra of compounds of these elements. See Ref. 6; also A. S. King and R. T. Birge, *Nature* **124**, 127 (1929); *Phys. Rev.* **34**, 376, 379 (1929); S. M. Naudé, *Phys. Rev.* **34**, 1498 (1929).

basis it is predicted that the question marks in Figs. 2 and 3 represent isotopes which should still be found, perhaps in very small quantity. A list of the isotopes so predicted is given in Table 1.

TABLE I

P, E	Z	Element	Remarks
		(Cluster II)	
73,40	33	As	Note 1
90,52	38	Sr	
91,52	39	Y	Note 1
95,54	41	Nb	Note 2
		(Cluster III)	
108,62	46	Pd	
118,66	52	Te	
120,68	52	Te	
125,72	53	I	Note 1
127,73	54	Xe	
133,79	54	Xe	
132,76	56	Ba	
134,78	56	Ba	
135,79	56	Ba	Note 3
137,81	56	Ba	

Note 1. Gives this odd element two isotopes at usual mass interval of two units.

Note 2. Isotopic constitution entirely unknown. Atomic weight of 93.1 would suggest strongly the two isotopes 93 and 95 following the rule for odd elements referred to in Note 1.

Note 3. Atomic weight of 137.37 indicates existence of some isotopes lower than the known 138.

At the foot of the table are some notes as to independent reasons for expecting these isotopes to exist or not to exist in the several cases.

The additional isotopes of germanium and zinc, to which reference has already been made, would demand, on the basis of symmetry, the isotopes 83, 84, 85, 87 and 89 of strontium and 93 and 95 of zirconium.

Even if complete data do not make the symmetry perfect, it is nevertheless a strongly marked tendency and calls for explanation. There is probably not sufficient basis as yet for the serious advancement of a theory. As a point for discussion, however, the suggestion which follows is not out of order.

Consider, for example, the middle cluster whose center is at the point (P_2, E_2) representing a conceivable nucleus consisting of 80 protons and 45 electrons. That this nucleus apparently does not exist is a matter of no concern. Suppose that at an early stage in the evolution of the matter from which terrestrial matter was drawn, there were formed fairly abundantly nuclei of constitution $(2P_2, 2E_2)$, i.e., (160, 90) containing just twice as many protons and electrons as the center of the symmetrical cluster. Such a nucleus has not been found to exist in the earth's crust and may hypothetically be regarded as unstable. Suppose there to be a tendency on the part of this nuclear type to break into just two nearly (but not precisely) equal parts. The products of any one such event would be $(80+X, 45+Y)$ and, since the second part is postulated to contain the rest of the nuclear matter, $(80-X, 45-Y)$. Obviously there would thus come into existence always two nuclei symmetrically located X, Y and $-X, -Y$ units respectively from the sym-

metry center (80, 45). The possible values X , Y would presumably be governed by nuclear forces of cohesion. That is, like a crystal, the nucleus might have particular surfaces of division more probable than others.

To explain the three observed clusters, three transitory parent nuclear types must be postulated. They would have the constitutions: a) (248, 144) representing an element a little beyond uranium and, therefore, almost certainly unstable; b) (160, 90) falling near the upper region of the rare earths; and c) possibly (54, 28) the lesser isotope of iron, or (50, 26) an unknown isotope of chromium.

Nothing has thus far been said about the relative abundance of the nuclear types. On the basis of the suggestion that symmetrical nuclei are natal twins, the observed symmetry of existence would be expected to extend itself to a like symmetry of abundance. Roughly speaking this is not found to be the case. A test of such a consideration is difficult when the elements involved are different chemically. It is possible, however, to observe whether the course of abundance of the isotopes of tin corresponds symmetrically to that of the isotopes of the symmetrically located element xenon. Aston places the tin isotopes in the order 120, 118, 116, 124, 119, 117, 122, 121, 112, 114, 115. A comparison of the symmetrical order for xenon with the observed order of that element is given below:

Expected from symm.	128, 130, 132, 124, 129, 131, 126, 127, 136, 134, 133
Found by Aston	129, 132, 131, 134, 136, 128, 130, 126, 124

It may well be the case that an initial symmetry of abundance has ceased to exist on account of differences in the stability of the several nuclear types, and only the symmetry of existence remains as a relic of the originating process.

Before concluding, it should be acknowledged that the suggestion outlined may be entirely supplanted by an assumption of inherent symmetry in the rules governing the stability of the nuclei. Probably no more explicit statement in this vein may be made for the present.

BLACK BODIES IN THE EXTREME INFRA-RED

BY C. HAWLEY CARTWRIGHT
CALIFORNIA INSTITUTE, PASADENA

(Received December 30, 1929)

ABSTRACT

Absorbing power of various materials of wave-lengths greater than 50μ .—For blackening a receiver of a thermocouple for radiation for obtaining pure rotation band spectra, it is desirable to use a material that is an efficient absorber of the extreme infra-red but a poor absorber of radiation of shorter wave-lengths. The absorbing power of 25 materials were tested for radiation of wave-lengths near 4μ and greater than 50μ . Of all the materials tested, white lead, litharge, red phosphorus, powdered glass, copper sulphide, and celestite were found the best for covering a receiver to absorb the extreme infra-red radiation. The 25 materials were tested by painting them on a receiver of a thermocouple which was exposed to extreme infra-red radiation. The same receiver and thermocouple were used throughout the experiment. A D'Arsonval type galvanometer was improved by using a quartz suspension and replacing each conducting lead with silver leaf or gold plated silver ribbon 1μ thick wound in a spiral.

Glass as a source of extreme infra-red radiation.—Hot glass made a good source of extreme infra-red radiation when used with a cold thin glass shutter.

INTRODUCTION

While working with thermocouples and radiometers in the extreme infra-red, it was found that nothing was known quantitatively of the absorbing qualities of the materials used for blackening the receiver. Since the efficiency of the receiver depends on its absorbing power, it was fundamentally important to know the relative merits of the various materials suitable for blackening a receiver. Twenty-five such materials were selected and comparisons made of their respective absorbing powers for both extreme and near infra-red radiation. It was desired to find a material that was black for infra-red radiation of wave-length greater than 50μ and a poor absorber of shorter radiation and especially adapted for coating a thermocouple or radiometer. Some materials that had no practical usefulness were also tested to see if any were exceptional absorbers of the extreme infra-red.

The experimental difficulties encountered in working with radiation of longer wave-length than 50μ is due mostly to the very small amount of energy available in that region and the interference of the large amount of shorter radiation. Various means are used to filter out the shorter radiation. A black body at 1000°K radiates 57 percent of its energy between 2μ and $5\mu^1$ and only 0.08 percent of its energy in wave-lengths greater than 50μ . Increasing the temperature to 2000°K increases the energy between 2μ and 5μ 12-fold while radiation of 70μ is only increased $2\frac{1}{2}$ times; the proportion is less favorable at 3000°K .

¹ L. L. Holladay, J.O.S.A. 17, 333 (1928).

The small amount of energy available makes it desirable to use a material that is an efficient absorber of long waves; also, it would be desirable if the material were a poor absorber of the near infra-red. The desirability of a material depends on the type of receiving apparatus. For thermocouples, the material should be a good heat conductor, so that it will quickly heat the metal receiver. For radiometers, it is better to use a poor heat conductor so that the back side of the vane will be cool; also, it is better to have a high temperature gradient.^{2,3}

A material that absorbs the extreme infra-red well could be used as a source, if the temperature is not too high to alter the physical or chemical state of the material, so that Kirchoff's law would no longer apply. Here, too, it would be an advantage to use a material that is a poor absorber of the short infra-red.

THE EXPERIMENTAL ARRANGEMENT

The apparatus was essentially that used by most investigators of pure rotation band spectra with regard to the method of isolating the long wavelengths. Fig. 1 shows schematically the apparatus. The source of radiation

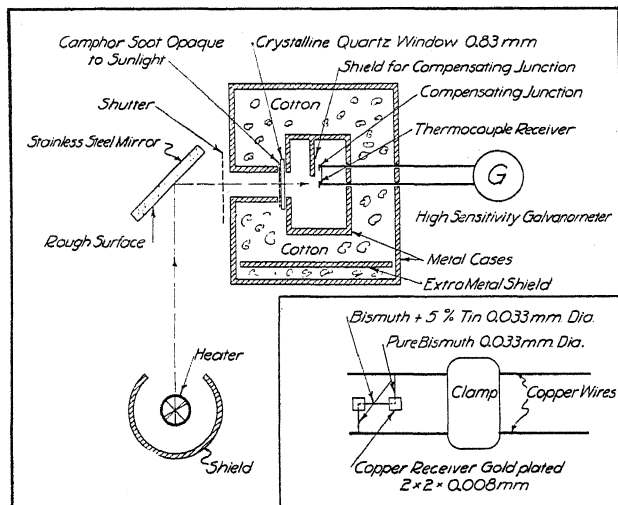


Fig. 1. Apparatus.

consisted of an electric heater painted with ground glass in tartaric acid and sugar. The temperature was held constant at 1000°K . The radiation was reflected from a stainless steel mirror that had been ground rough with emery. The average depth of the pits was about 8μ and since the reflection was at 45° , the effective depth was about 6μ . A crystalline window 0.83 mm thick was sooted with camphor smoke, so that it was opaque to sunlight. The thermocouple was a balanced type and was shielded from stray radiation and conduction. The wires were 0.033 mm in diameter and had a high ther-

² G. Hettner, *Zeits. f. Physik* **47**, 499 (1928).

³ Paul S. Epstein, *Zeits. f. Physik* **54**, 537 (1929).

moelectric power. The receivers were gold plated copper 2 mm by 2 mm and 0.008 mm thick. The receivers were waxed to the thermojunctions. Two shutters, one of metal and one of microscope cover glass 0.014 mm thick were used separately and in combination. The galvanometer had a sensitivity of 11 mm microvolt when critically damped. It was found desirable to rebuild the galvanometer in order to get more reliable measurements. The silver ribbon suspension was replaced by a quartz fiber and the conducting leads were each made from a narrow strip of silver leaf. The galvanometer with this arrangement was much improved for there was practically no zero shift even for deflections of two feet at a meter scale distance. Another advantage of this arrangement was that the silver leaf damped out forced vibrations due to earth tremors. A more rugged and simple construction, suggested by Mr.

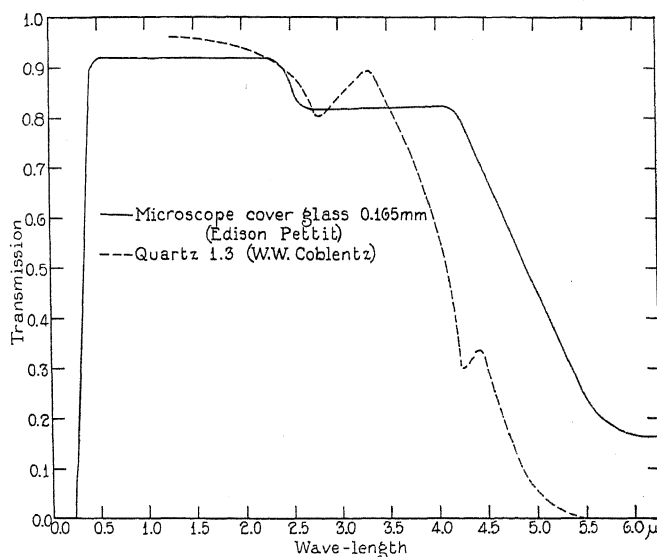


Fig. 2. Transmission of quartz and thin glass, 0-6.2 μ .

Julius Pearson, consisted of making each conducting lead of a gold plated silver ribbon rolled to 1 μ thickness and wound into a flat spiral.

Fig. 2^{4,5} shows the transmission curve for quartz and a microscope cover glass. The quartz becomes opaque at 5 μ but transmits wave-lengths greater than 50 μ except for a narrow absorption band at 78 μ . The microscope cover glass remains opaque to long wave-lengths.

Four groups of readings were taken, using (1) the metal shutter to exclude all radiation, (2) the glass shutter to exclude all of the extreme infra-red but only a small fraction of the near infra-red, (3) the glass shutter always in and moving the metal shutter to find the effect of the near infra-red, and (4) the metal shutter again to see if conditions had remained constant during the

⁴ Edison Pettit, *Astrophys. J.* **61**, 163 (1926).

⁵ W. W. Coblentz, *B. S. Bull.* **2-3**, 462 (1906).

experiment. Designating by V the energy below 5μ that is received by the thermocouple without any shutter, I the energy above 50μ under the same conditions, and k the fraction of energy below 5μ either reflected or absorbed by the glass shutter, the four groups become:

$$(1), V+I; \quad (2), kV+I; \quad (3), (I-k)V; \quad (4), V+I.$$

(2) and (4) are redundant but are useful as a check and for taking averages. Thus: $(2)-(1)=(3)$ and $(2)+(3)=(1)=(4)$.

The value of k can be seen from Fig. 2 to be between 0.15 and 0.20. The value of k was determined experimentally by using an additional window of microscope cover glass 0.008 mm thick, and using the metal shutter to find V and the glass shutter to find kV . The value of k was found to be 0.18. This value depends on the particular apparatus and in a small way on the material used to blacken the receiver.

The table shows the relative blackness or absorbing power of the different materials tested.

TABLE I. *Absorbing power of various materials.*

Substance	Radiation absorbed for			Substance	Radiation absorbed for		
	$\lambda < 5\mu$ V	$\lambda > 50\mu$ I	I/V		$\lambda < 5\mu$ V	$\lambda > 50\mu$ I	I/V
1. Litharge	10.8	4.3	.40	14. Copper sulphate crystals from solution	15.0	4.1	.27
2. Ground Glass	11.9	4.7	.40	15. Wellsbach mantle material	8.9	3.1	.35
3. Powdered Glass	11.7	5.0	.43	16. Platinum Black	18.2	4.4	.24
4. White Lead 2 Pb				17. Tartaric Acid and Sugar	16.0	3.9	.24
CO ₃ · Pb(OH) ₂	14.9	4.9	.33	18. Talc H ₂ MgSi ₄ O ₁₂	12.5	3.8	.30
5. White Lead in lacquer	14.3	4.4	.31	19. Water glass	12.1	3.7	.31
6. Red Phosphorus	18.3	5.0	.27	20. Tellurium, powdered	19.2	3.3	.17
7. Red Phosphorus from a match box	17.7	5.1	.29	21. India Ink	18.8	3.8	.20
8. Celestite, powdered SrSO ₄	14.7	4.6	.31	22. Lacquer	8.6	3.0	.35
9. Brucite, powdered Mg(OH) ₂	11.4	4.2	.37	23. Castor Oil	8.8	2.8	.32
10. Angelsite, powdered PbSO ₄	14.2	4.2	.30	24. Glycerine	11.2	3.1	.28
11. Copper Sulphide	17.1	5.2	.30	25. Turpentine	8.1	0.2	.02
12. Copper Oxide	13.8	4.4	.32	26. Clean Receiver	2.9	0.2	.07
13. Silver Sulphide	12.8	4.4	.34				

Some of the materials were selected because they were transparent to near infra-red, some because they had been used by investigators of the extreme infra-red. The powdered materials were painted on the receiver by mixing them with one part turpentine and five parts alcohol. After a material was tested, the receiver was carefully cleaned and painted with another material. Care was taken to replace the thermocouple in the apparatus in the same place each time. The absorbing materials were painted with uniform thickness on the receiver and in each case the thickness of the coat was about 0.01 mm as estimated under a microscope.

Water glass was very unsuitable for a delicate thermocouple for it caused the heavy receiver used here to curl. The glue mixed with the red phosphorus taken from a match box also caused the receiver to curl.

Item 25 in the table shows that turpentine did not absorb the long waves. To determine whether they were reflected or transmitted by the turpentine, a receiver painted with white lead in lacquer was covered with turpentine. The far infra-red was absorbed equally well which showed that turpentine is transparent to long wave-lengths.

The absorbing power of a receiver depends on the thickness of the absorbing material. A copper receiver tarnished with H_2S , so that it appeared quite black was about 50 percent efficient in the near infra-red and only 25 percent efficient in the extreme infra-red, compared with a 0.01 mm coat of copper sulphide painted on the receiver. The physical state of the receiver affects its absorbing power. A receiver, electroplated rapidly with copper, so that the surface was rough, absorbed the far infra-red well; it had a ratio of $I/V=0.28$. A heavy coat of platinum black electroplated on a receiver had the same absorption as if it were painted on the receiver.

The transmission of crystalline quartz, hard rubber, and a cellulose paper used for wrapping candy was also tested to compare their merits as window material. The cellulose paper is very strong and gas tight. The same apparatus was used and the radiation made to shine through the sample being tested. The following table shows the percentage of radiation transmitted by the three samples, used as extra windows:

Material	V	I	I/V
Cellulose paper, 0.033 mm	47%	37%	0.79
Crystalline quartz, 0.83 mm	70	23	0.33
Hard Rubber, 1.2 mm	11	6	0.55
Without an extra window	100	100	0.30

The reflection of the far infra-red from a glass surface was tested by replacing the rough mirror by a piece of plate glass. The ratio of the number of waves reflected from the plate glass to the number reflected from the rough steel mirror was 31 percent.

CONCLUSION

It is to be noticed that the absorptive power of the materials tested was an integrated effect extending over the entire far infra-red.

Litharge, powdered glass, white lead, copper sulphide, celestite, and red phosphorus were the best absorbers of radiation longer than 50μ .

The physical state of the receiver determined its efficiency. A very thin coat of the absorbing material in most cases was an inefficient absorber of the extreme infra-red waves. A very poor absorbing material such as copper or platinum will absorb if the surface is sufficiently rough.

For radiometers, the absorbing material is better when mixed with turpentine and alcohol and painted on the vanes. Very delicate fly-wing radiometers were made in this manner, weighing only 0.04 mg. The vanes were double and a sputtered mica mirror was used.

For thermocouples, absorbing material is better if it is mixed with lacquer. The thermocouples must be in vacuum to be steady; in some cases an increase of 60 times the sensitivity was obtained by evacuation.

The high absorption in glass of the extreme infra-red and its low absorption of the near infra-red suggested its use as a source. Such a source was made by covering with glass two platinum wires that were separated 4 mm. The wires were heated by an electric current and the hot portion of glass between the two wires served as a source of extreme infra-red radiation. This source was tested in a vacuum spectrometer⁶ and found to be satisfactory.

A convenient method of filtering out the near infra-red is to grind the windows with emery so that the pits are about 4μ deep. The apparatus can be aligned with visible light by covering the rough surface with turpentine.

Although a tarnished metal surface is not an efficient absorber of the extreme infra-red, it may be desirable to sacrifice efficiency for the extra speed with which the thermocouple will come to thermal equilibrium,—particularly if the readings are recorded photographically. The receiver of a thermocouple can be improved by pressing it against the surface of a file to make the surface rough. A thermocouple with tarnished silver receivers reached equilibrium in one second. White lead is especially desirable for blackening a receiver for it is white to visible light and allows almost perfect alignment of the apparatus.

⁶ Badger and Cartwright, *Phys. Rev.* 33, 696 (1929).

PELTIER AND THOMSON EFFECTS FOR
BISMUTH CRYSTALSBY H. D. FAGAN AND T. R. D. COLLINS
PHYSICS LABORATORY, UNIVERSITY OF IOWA

(Received November 20, 1929)

ABSTRACT

The Peltier and Thomson effects are directly measured (the former against copper) in single crystal rods almost covering the entire orientation range. For the first effect the Voigt-Thomson symmetry relation is definitely not substantiated, while for the latter the data do not provide an adequate test, though it appears likely that there is a deviation here also.

The following values are found: at a temperature of 27°C , $\pi(\parallel\text{vs.}\perp)=13.8$, $\pi(45^{\circ}\text{vs.}\perp)=8.6$ microvolts; at a temperature of 48.5°C , $\sigma_{\parallel}-\sigma_{\perp}=43$, $\sigma_{45}-\sigma_{\perp}=26.5$ microvolts/ $^{\circ}\text{C}$. These values are all in fair agreement with values deduced from thermal e.m.f. temperature data of the writers and of previous observers.

INTRODUCTION

BRIDGMAN¹ and Boydston² have recently measured the thermal e.m.f. of bismuth crystals of various orientations³ against a reference metal. From these results are deduced by the usual thermodynamic relations, values of the Peltier e.m.f. between the reference metal and a crystal of any orientation or between two crystals of different orientations; likewise the differences in the Thomson coefficients for the two parts of the above combination are deduced. In the investigation described below the Peltier e.m.f. against copper and the Thomson coefficient of bismuth crystals, covering most of the possible orientation range, were measured directly. Two sets of crystals were used, the first for measurement of Peltier coefficient, the other for all the other measurements, which included determination of specific resistance, mean thermoelectric power (between 0° and 100°C) against both copper and constantan, and the Thomson effect. From such data it should be possible to test the validity of the Voigt-Thomson symmetry relation for the directly observed Peltier e.m.f. and Thomson coefficient and to make comparison with the indirectly determined values of these same quantities.

APPARATUS AND EXPERIMENTAL METHOD

The method for determining the Peltier e.m.f. is essentially that of Caswell,⁴ or Barker.⁵ The two thermo-junctions (Cu-Bi and Bi-Cu) are isolated

¹ P. W. Bridgman, (a) Proc. Amer. Acad. of A. and S. **61**, 101 (1926); (b) Proc. Amer. Acad. of A. and S. **63**, 351 (1929).

² R. W. Boydston, Phys. Rev. **30**, 911 (1927); also gives reference to earlier work.

³ Orientation is used as usual to define the angle between the length of the specimen and the principal crystallographic axis, which for bismuth is perpendicular to the plane of best cleavage.

⁴ A. E. Caswell, Phys. Rev. **33**, 379 (1911).

⁵ H. C. Barker, Phys. Rev. **31**, 321 (1910).

from each other by placing them in separate Dewar flasks each containing the same amount of calorimetric fluid, a heating coil, a stirrer, and a copper-constantan thermocouple. See Fig. 1 (a). Current from the battery B_2 may be passed in either direction around the Bi-Cu circuit. The purpose of the heating coils is made clear below. By obvious manipulations of switches S_1 and S_2 it is possible to read the temperature in either flask, or to detect a very minute difference in temperature between the flasks. The heating coils, L and R , are wound of No. 36 constantan wire on thin mica sheets, while the leads, which go through the surface of the liquid and through holes in the flask covers, are of No. 2 constantan. The calorimetric fluid is "Finol," a light oil of low specific heat and high mobility. The amount contained in each

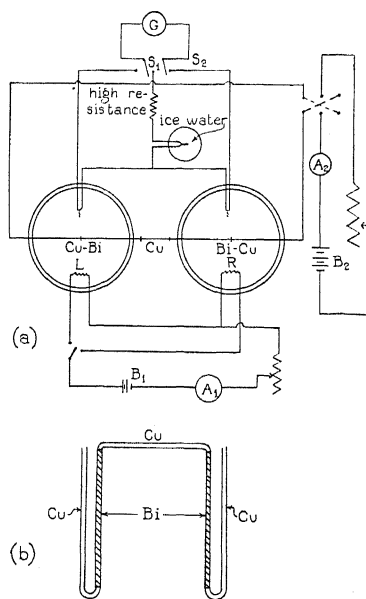


Fig. 1. Diagram of apparatus and electrical connections.

flask is about 150 cc. Stirring is done by glass propellers (not shown in Fig. 1) running at the rate of about 1 r.p.s.

The construction of the two bismuth copper junctions, in which the effect is measured, is apparent from the vertical section shown in Fig. 1(b). The two bismuth portions are parts of one crystal rod cut in two. The two ends adjacent to the cut are used to form the two Bi-Cu junctions in the flasks. The copper is No. 6 wire of commercial grade. The bismuth-copper connections are made without solder by fusing the bismuth directly to the copper, using zinc chloride as a flux. To take a reading a known constant current is sent in one direction through the bismuth-copper circuit. Heat is absorbed at the junction where current passes from bismuth to copper. To compensate for this loss of heat (and for the generation of heat at the other junction) current is passed through the appropriate heating coil. This current is con-

tinually so regulated that the flasks show no temperature difference. In about an hour no further adjustment is necessary. The reading of A_1 is then recorded. The current in the main (bismuth-copper) circuit is then reversed, but kept at the previous value, and the procedure above repeated. Caswell has shown that in this case the Peltier e.m.f. is given in volts by

$$\pi = \frac{i_R^2 R + i_L^2 L}{4I}$$

in which i_R , i_L = current (amperes) in right and left heaters, respectively; R , L = resistance (ohms) of right and left heaters respectively; I = current (amperes) in main circuit. This relation is valid provided the following conditions are satisfied.

1. The heat capacities of the two flasks and their contents are the same. This condition was met by making the two as nearly identical as possible.

2. The rate of loss of heat from each flask must be approximately the same. This was tested from time to time during the investigation and found to be satisfactory.

3. The temperature difference between the flasks and their surroundings must be small. The oil in the flasks never exceeded 2°C above room temperature at the end of any run.

For measuring the Thomson coefficient the method of Nettleton,⁶ as modified by Ware,⁷ was used. Measurements of the same specimen made on Ware's apparatus and the writers' agree well. The resistance of each crystal with one end at about 0° and the other at about 100°C is a necessary datum for determining the Thomson coefficient, and from it the specific resistance (at 48.5°C) can be computed. To do this the average cross section of a crystal is found from its measured mass and length, and assumed density (9.78 gm/cm³). The crystals were from 6 to 10 cm long and from 5 to 10 mm² cross sectional area.

With the temperature gradient established along a crystal the thermal e.m.f. was measured with a potentiometer. The reference metal is copper, since the ends of the specimen were fused or soldered to copper blocks. Dividing this e.m.f. by the temperature difference gives the mean thermoelectric power. This is approximately the thermoelectric power at the mean temperature, 48.5°C. The thermoelectric power against constantan was measured in a similar fashion.

The two sets of bismuth crystals were grown by drawing them from a crucible full of molten bismuth. This method and the apparatus have been described by Linder.⁸ The modifications in the procedure mentioned by Boydston and by Hoyem⁹ and Tyndall were also followed. The crystals of

⁶ H. R. Nettleton, *Proc. Lond. Phys. Soc.* **29**, 59 (1916-17).

⁷ In connection with unpublished work in this laboratory by L. A. Ware on the Thomson Effect in zinc crystals.

⁸ E. G. Linder, *Phys. Rev.* **29**, 554 (1927).

⁹ R. W. Boydston, *Phys. Rev.* **30**, 911 (1927); A. G. Hoyem and E. P. T. Tyndall, *Phys. Rev.* **33**, 81 (1929).

one set (for Peltier Effect) were 30 cm long and from 2.5 to 3.0 mm in diameter. The others have been described above. The material used was Mallinckrodt C. P. bismuth with the following analysis:¹⁰

Zn 0.01%	Cu 0.00%	Fe 0.00%
Pb 0.00%	As 0.000%	Ag 0.04%

RESULTS AND DISCUSSION

Measurements of Peltier e.m.f. against copper were made on fourteen single crystals ranging in orientation from 16° to 90°. For a majority of the crystals five readings were taken. For two, however, six readings were taken, while for three crystals, only four were taken. The arithmetic mean of all the readings on one specimen is the adopted value. The results are shown graphically in Fig. 2, in which the observed Peltier e.m.f. in millivolts is plotted

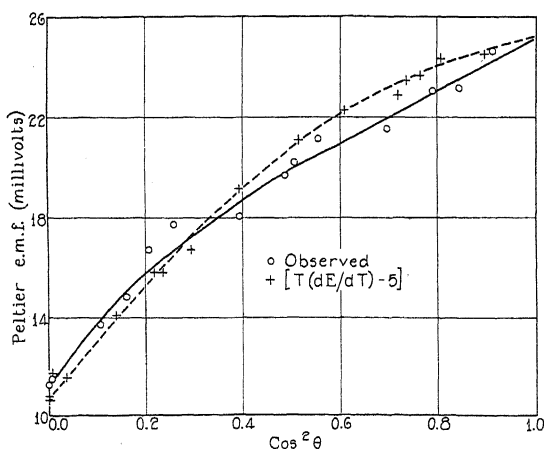


Fig. 2. Peltier e.m.f. as function of orientation angle.

(circles) against the square of the cosine of the orientation angle. By substituting in $\pi = Te$, in which $T = 300^\circ\text{A}$ and e is the mean thermoelectric power (at 48.5°C) against copper,* previously mentioned, it is possible to obtain values of the Peltier e.m.f. Values obtained in this way are plotted (as crosses) in the same figure. Before plotting, each value has been arbitrarily reduced by 5 millivolts, since any constant difference between the two sets of data can readily be ascribed to the use of different samples of reference metals (a copper block in one case and a copper wire in the other). These two curves are probably in agreement within experimental error. Such plots should yield straight lines to satisfy the Voigt-Thomson symmetry relation.

¹⁰ The bismuth used by Boydston had this same stated analysis. The omission of Ag 0.04% is due to an oversight on his part. It seems certain, however, that the content of Ag in the crystals used in this investigation must be much less than 0.04%. This point is considered later.

* The value of e at 27°C should be used, of course, but it was not determined and probably does not differ much from the value at 48.5°C .

It is obvious that the experimental relation is not linear in either case. Moreover Bridgman¹¹ finds a very similar deviation from linearity for the thermoelectric power (as a function of $\cos^2\theta$) of bismuth crystals against copper, and therefore for the indirectly determined Peltier e.m.f.

TABLE I. Peltier e.m.f. (millivolts) at 27°C.

Junction	Directly * observed	$T(dE/dT)^*$	$T(dE/dT)^*$ (Bridgman)	$T(dE/dT)^{**}$	$T(dE/dT)^{**}$ (Boydston)
M-Bi ₀	25.1	30.2	32.2	18.2	20.2
M-Bi ₄₅	19.9	25.6	25.9	13.1	11.6
M-Bi ₉₀	11.3	15.7	17.2	3.3	3.0
Bi ₀ -Bi ₉₀	13.8	14.5	15.1	14.9	17.2
Bi ₄₅ -Bi ₉₀	8.6	9.9	8.7	9.8	8.6

* Reference metal, M, copper.

** Reference metal, M, constantan.

Table I presents a comparison of previous work with the present, the subscript for Bi being the value of θ . The data in the second and third columns are obtained from the two curves in Fig. 2. To compute Bridgman's values use is made of his empirical formulas¹² for thermal e.m.f. as a function of temperature. The fifth column is obtained from a plot of the observations on thermoelectric power against constantan, previously mentioned. By interpolation in Boydston's Fig. 3 the thermoelectric power (against constantan) is found for 27°C, and from this the values in the last column are easily computed. All the results in this table are found to be in fair agreement, when allowance is made for the fact that in the upper 3 rows of data a different reference metal (or different specimen of the same metal) was used. In the lower two rows the results are typical of bismuth alone and an absolute comparison is allowable. It will be seen that the directly observed values are lower than those computed from $\pi = TdE/dT$. The agreement with this relation is, however, probably as good as is usually obtained. There seems little doubt that the deviation from the Voigt-Thomson symmetry relation is real for the Peltier effect in these crystals. Boydston finds no deviation (at 27°C) and one must conclude that the bismuth used by Boydston differed from ours in spite of having the same stated analysis.

The specific resistance at 48.5°C is plotted in Fig. 3 against $\cos^2\theta$. The line drawn represents Bridgman's latest results, changed to 48.5°C, however, assuming a temperature coefficient of resistivity of 0.0044. With the exception of four points, the results are satisfactory and indicate that the crystals are not badly strained and that the bismuth is very pure, since both strains and impurities seem to affect the specific resistance seriously.¹³ The three high points may be ascribed to slight accidental strains occurring during growth or in the subsequent handling of the crystals. This seems probable also because crystals of intermediate orientations are very easily deformed.

¹¹ Reference 1, (b).

¹² Reference 1, (b), p. 383.

¹³ See discussion by Bridgman, reference 1, (b) pp. 386-389.

Ware has shown for zinc crystals that a deformation which is large enough to raise the specific resistance has a negligible effect on the Thomson coefficient. It might be expected, therefore, that the group of crystals of Fig. 3 would give consistent and satisfactory results for the Thomson coefficient. This is,

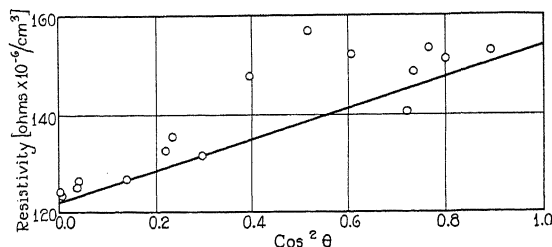


Fig. 3. Specific resistance as function of orientation angle.

however, not the case as is evident on reference to Fig. 4, particularly for orientations less than about 50° . These data, moreover, do not provide an adequate test of the Voigt-Thomson symmetry relation. In spite of this an attempt has been made to draw a smooth curve through the observations. Assuming that -8.5 microvolts/ $^\circ\text{C}$ is a reasonably certain value for σ_\perp (i.e. for $\theta = 90^\circ$), it is possible to make comparison with Bridgman's latest data. The values of σ for $\theta = 45^\circ$ and $\theta = 0^\circ$ for a temperature of 48.5°C have

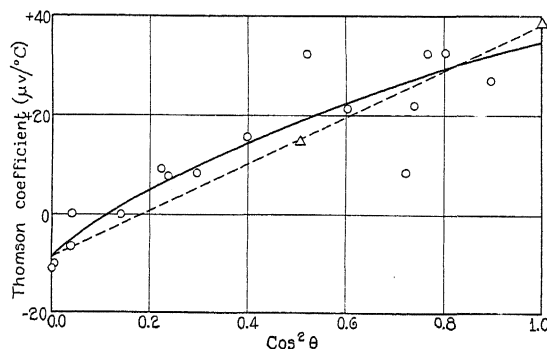


Fig. 4. Thomson coefficient as function of orientation angle.

been computed from formulas deduced by Bridgman¹⁴ from his thermal e.m.f. data. These values are plotted as triangles in Fig. 5. Our curve gives $(\sigma_\perp - \sigma_\parallel) = 43$ microvolts/ $^\circ\text{C}$ at 48.5°C , dependent on a very uncertain extrapolation to $\cos^2\theta = 1$. Boydston's data give $(\sigma_\perp - \sigma_\parallel) = 57.5$, and Bridgman's, 48. At 43.5°C Caswell¹⁵ finds 58 microvolts/ $^\circ\text{C}$ for polycrystalline bismuth, a value considerably in excess of what might be expected from the above stated values for crystals. Laws¹⁶ finds a much lower value, 10 microvolts/ $^\circ\text{C}$.

¹⁴ Reference 1, (b) pp. 384, 385.

¹⁵ Caswell, Phys. Rev. 12, 235 (1918).

¹⁶ Laws, Phil. Mag. [6] 7, 560 (1904).

It seems certain, from the investigations of the two writers just mentioned, that a small admixture of tin raises the Thomson coefficient to a very great extent. It therefore seemed desirable to make an analysis of the bismuth. This was done spectroscopically using the spark spectrum and the general procedure of Meggers, Kiess, and Stimson.¹⁷ A small quartz spectrograph was used the dispersion of which was such that the length of spectrum between 3400 and 2600A was 1.5 cm. About 120 spectrograms were taken of three crystals¹⁸ with normal, low, and high Thomson coefficients, respectively, as judged from the curve of Fig. 4. Between exposures a two millimeter piece was clipped from each of the two portions of the crystal between which the spark occurred. All of the spectrograms, except one, were identical and indicated a material of high purity. A very faint and diffuse line which might be the "raie ultime" of silver (3281A) was present in all the spectrograms. No trace of 3383A, another very sensitive silver line, was found. Moreover, comparison of these spectrograms with others taken in this laboratory of bismuth known to contain far less than 0.04 percent Ag, has led to the conclusion that the silver content is much lower than the figure stated in the analysis. Certainly the crystals examined showed no difference from each other and no detectable inhomogeneity in composition between different parts of the same crystal. In the one exceptional case mentioned above one of the electrodes consisted of a portion (one end) which had been accidentally fused and was probably contaminated with solder. Several lead and tin lines were easily identified in this spectrogram.

In conclusion the writers wish to express their thanks to Prof. E. P. T. Tyndall for suggesting this work and for his advice and interest during its prosecution.

¹⁷ Meggers, Kiess and Stimson, *Sci. Pap. Bur. Stand.* **18**, 235 (1922-23).

¹⁸ $\cos^2\theta = .894$, $\sigma = 27$; $\cos^2\theta = .517$, $\sigma = 32.4$; $\cos^2\theta = .719$, $\sigma = 8.5$.

SHATTER OSCILLATIONS, THEIR
NATURE AND THEORY*BY E. H. KENNARD
CORNELL UNIVERSITY

(Received December 30, 1929)

ABSTRACT

Shatter oscillations are an apparently novel type in which the pressure sinks periodically to the minimum value which the liquid can sustain, the liquid mass becoming then porous or "shattered"; they tend to be much slower but more powerful than purely elastic vibrations and the wave-form is very different, pressure impulses alternating with long intervals of quiet. An experimental case is described and the general theory of such oscillations is developed. Further experiments are needed.

AN EXPERIMENT

SEVERAL years ago the writer was privileged to witness some interesting experiments upon liquid oscillations in the plant of the Goulds Pumps Company at Seneca Falls, N. Y., which were of an astonishing and apparently little-known type. It is the purpose of this paper to describe them briefly, together with the theory proposed by the author, in the hope that some physicist may be induced to make a detailed study of the phenomena and so to find out whether the theory is correct and adequate.

In the most interesting experiment a pipe 31 m long and full of water was connected at one end to a tank which contained a considerable mass of water and over it air at a pressure of about 4 atmospheres (the pressure of the atmosphere included). At the other end of the pipe was a small pump with its

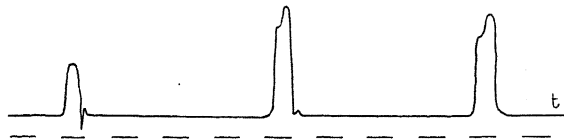


Fig. 1. Indicator record showing pressure distribution.

discharge valve removed and its suction valve blocked shut, so that it served merely to "fan" the water with an approximately simple-harmonic motion. A recording gauge recorded the pressure of the water in the pipe at a point near the pump.

Under the circumstances one might expect the water column to oscillate like a "closed organ pipe" (i.e. open only at the tank end, where the pressure must have been sensibly constant); the speed of sound in water in such a pipe being about 1360 m per sec, the fundamental period should be around 0.091 sec. Nothing of the sort was observed. At suitable pump speeds oscillations

*Part of this paper was read before the National Academy of Sciences; an abstract of this part appears in *Science*, 70, 618 (1929).

did occur, and of enormous amplitude, but they were much slower than the slowest possible elastic oscillation, and the distribution of pressure was of the remarkable type shown in Fig. 1, which is copied from one of the actual indicator cards. Isolated "humps" of pressure appeared at intervals, in the figure one every 0.7 second, separated by long quiet intervals during which the pressure seemed to be about zero (certainly below atmospheric); the humps always occurred during discharge strokes of the pump (which are shown by horizontal lines in the diagram, four per oscillation in that case). The maximum pressure was usually around 25–30 atmospheres but in one case it rose to 75 atmospheres before the gaskets blew out of the pump and stopped the experiment.

Now the direction in which to look for an explanation of this phenomenon seems obvious enough. In an ordinary elastic oscillation a compression is followed by an equal rarefaction, but water cannot withstand a tension of 20–30 atmospheres; under special conditions tensions up to 5 atmospheres have been observed, but in practice, according to what appears to be the opinion of engineers, the pressure never sinks below zero (i.e. one atmosphere below atmospheric)—at all events no appreciably lower pressures were ever observed in these experiments, although the indicator was often capable of showing them.

We have, then, a case, apparently new in hydrodynamical theory, of large-amplitude oscillations in a liquid whose pressure cannot sink below a certain critical pressure, p_0 . It was at first naively supposed that under these circumstances large gaps might form in the liquid mass; for instance, in the present case, that the column might break loose from the pump and retreat several feet down the pipe. But a little reflection shows that this cannot happen when the minimum pressure is really quite definite. For in order to form such a gap the layer of liquid on one side or the other of it must at some time experience an acceleration directed away from the incipient gap, and, since by hypothesis the pressure is p_0 in the gap and cannot become less than this in the liquid, no force producing such an acceleration can be developed by pressure differences in the liquid (although it could arise, of course, from gravity in a non-horizontal column, and large gaps could then form). For theoretical purposes the situation might be idealized satisfactorily by assuming that when the pressure sinks to p_0 the elasticity drops discontinuously to zero. What happens in practice, however, must be that the liquid mass does break, at many closely spaced points, in consequence of local inhomogeneities of composition or of state and under the action of cohesive forces, so that the liquid becomes full of small crevices or, as we shall call it, "shattered." We shall study this process a little more closely.

THEORY OF SHATTERING IN A LIQUID COLUMN

The point at which the pressure first sinks to the minimum value, p_0 , must be one where, momentarily,

$$\frac{\partial p}{\partial t} < 0, \quad \frac{\partial u}{\partial x} = -\frac{1}{\epsilon} \frac{\partial p}{\partial t} > 0, \quad (1)$$

in which p =pressure, t =time, ϵ =elasticity, u =particle velocity, x =distance along the column. Continuity being assumed, p will then proceed to reach p_0 at neighboring points and a shattered region will form in which $p=p_0$ and is thus uniform, so that $\partial u/\partial t=0$. In this region, according to (1), $\partial u/\partial x > 0$ (see also below, after Eq. (2)); the liquid will therefore expand at a constant rate through enlargement of the crevices so long as the shattered condition persists. The boundaries of the region, which we shall call "shatter-fronts," advance thru the liquid with a speed V which can easily be calculated. During an interval dt let the shatter-front advance positively a distance Vdt from a point P to P' ; then at the beginning of dt the pressure was p_0 at P and $p_0 + (Vdt) \partial p/\partial x$ at P' , whereas at the end of dt it has risen at P' by an amount, actually negative, $(\partial p/\partial t) dt$ and has now become p_0 ; thus $(Vdt) \partial p/\partial x + (\partial p/\partial t) dt = 0$ and

$$V = -\frac{\partial p}{\partial t} / \frac{\partial p}{\partial x} = \epsilon \frac{\partial u}{\partial x} / \frac{\partial p}{\partial x}. \quad (2)$$

A second and rather peculiar condition for the propagation of the shatter-front arises from the condition that the liquid must be left behind it in an expanding condition (or at least not in a contracting one, since then the pressure would immediately rise above p_0 again). In the same notation, at the beginning of dt let the particle velocities at P and P' resp. be u and $u + (Vdt) \partial u/\partial x$; then at the end of dt the velocity is still u at P (because of the uniformity of pressure), but at P' it has changed by $(\partial u/\partial t) dt$. The condition stated then requires that the final velocity at P' shall exceed that at P , or that $u + (Vdt) \partial u/\partial x + (\partial u/\partial t) dt \geq u$; and, since $\partial u/\partial t = -(1/\rho) \partial p/\partial x$ where ρ is the density and the speed of sound is $c = (\epsilon/\rho)^{1/2}$, we have by (2):

$$k^2 \left(\frac{\partial u}{\partial x} \right)^2 \geq \left(\frac{\partial p}{\partial x} \right)^2, \quad V^2 \geq c^2, \quad (3)$$

where $k = (\epsilon\rho)^{1/2}$. It follows that the shatter-front moves with a speed above that of sound; its progress therefore depends upon conditions in the liquid due to other causes than what may be going on in the shattered region.

In its advance the shatter-front may eventually come to a point where the first of Eqs. (3) is no longer satisfied. It will then turn into a "reconsolidating front" and immediately start back in the opposite direction, for the higher pressures in the adjacent unbroken region will accelerate the liquid toward the shattered region. As the reconsolidating front reaches each point in the shattered region, the crevices suddenly close up and the liquid already present undergoes an impulsive acceleration and compression which give to it both the particle velocity u and the pressure p that obtain on the unbroken side of the advancing front. For convenience let us resolve conditions in the unbroken column as usual into two wave-trains moving in opposite directions; let the unbroken column lie on the left, toward $-x$, and let u_1, p_1 be particle velocity and pressure in the wave-train moving positively and u_2, p_2 the corresponding quantities in the other wave-train. Then by the usual laws for elastic waves

$p_1 = ku_1$, $p_2 = -ku_2$, and at the front $p = p_1 + p_2$, $u = u_1 + u_2$. Here u_1 , p_1 , referring to the "incident" waves, are determined by conditions to the left and can be regarded as known, while u_2 and p_2 can be regarded as referring to waves "reflected" from the boundary of the shattered region and are to be found. Let U = velocity of advance of the reconsolidating front and in the shattered region let u_s = particle velocity and f = degree of shattering or fraction of the space that is empty of liquid, both taken at a point just ahead of the advancing front. Then in time dt the front sweeps over a section PP' of length Udt ; during this time the liquid flowing in at P , of volume $u dt$ per unit of cross-section, must fill up not only the crevice-space $fUdt$ but also the space $(1-f)Udt$ $(p-p_0)/\epsilon$ emptied through compression of the liquid already in the section PP' and the space emptied by the outflow past P' of a volume $u_s dt$ of the shattered column. Hence

$$u = \left[f + (1-f) \frac{p-p_0}{\epsilon} \right] U + u_s. \quad (4)$$

(We assume u/U small so that terms in u^2 or u/U can be neglected, as in the ordinary theory of sound.) During the same interval dt the difference in pressure at the ends of the section PP' must impart to the liquid already in it the additional momentum acquired as its velocity changes impulsively from u_s to u ; whence,

$$p - p_0 = \rho U (1-f) (u - u_s). \quad (5)$$

From these two equations we find:

$$(p - p_0)^2 + \frac{\epsilon f}{1-f} (p - p_0) = k^2 (u - u_s)^2, \quad (6)$$

$$\frac{1}{U^2} = \frac{1-f}{c^2} \left[1 - f + \frac{\epsilon f}{p - p_0} \right] = \frac{1}{c^2} \left[1 + f^2 + f \left(\epsilon \frac{1-f}{p - p_0} - 2 \right) \right]. \quad (7)$$

Equation (6) expresses the "boundary condition" that must hold under these conditions at the junction of shattered and unbroken regions. Eq. (7) gives U , and shows, among other things, that $U < c$ under the conditions assumed, since $\epsilon/(p - p_0)$ will be many times greater than 2.

The reconsolidating front in its turn will disappear upon meeting either a similar front moving in the opposite direction or an obstruction, with resulting final elimination of the shattered region (as a third alternative, of course, it might also be overtaken and destroyed by a fresh shatter-front). When two reconsolidating fronts meet, with pressure and particle velocity p , u in the one moving positively and approaching from the left and p' , u' in the other one, then at the point of meeting these quantities will change impulsively to certain values p_m , u_m . Let us resolve the motion on each side into positive and negative wave-trains, with respective pressures $p_1 = (p + ku)/2$, $p_2 = (p - ku)/2$ on the left, and $p_1' = (p' + ku')/2$, $p_2' = (p' - ku')/2$ on the right. Then, after the two fronts meet, these wave-trains advance as usual and by

their superposition determine subsequent conditions in the liquid; after the lapse of a very short time the trains will overlap a little at the point of meeting and will produce there the following values:

$$p_m = p_1 + p_2' = \frac{1}{2}(p + p') + \frac{k}{2}(u - u'), \quad u_m = \frac{p_1}{k} - \frac{p_2'}{k} = \frac{1}{2}(u + u') + \frac{1}{2k}(p - p') \quad (8)$$

The case in which the reconsolidation front is stopped by an obstruction, such as the closed end of the pipe, can be handled by putting $u_m = 0$ in the last equations and eliminating p' and u' ; this gives the usual impact formula:

$$p_m = p + ku. \quad (9)$$

The extension of the theory just developed to the three-dimensional case is easy, but for completeness we shall sketch it. The boundary of the shattered region is in this case a closed surface which may move either as a shatter-front or as a reconsolidating front, or in part as one and in part as the other; the theory developed above will apply provided we take the x -axis along the normal to the surface, with the single exception that we must also take account of expansion due to the component of particle velocity tangential to the surface. The tangential acceleration vanishes because over the surface $p = p_0$ and is constant. One finds thus as the conditions for the advance of a shatter-front, in the unbroken liquid just ahead of it:

$$\text{div } u > 0, \quad k^2(\text{div } u)^2 = \left(\frac{\partial p}{\partial n}\right)^2, \quad (1'), (3')$$

n denoting distance along the normal to the front (which is also the direction of ∇p), and for V , the speed of advance of the front along its normal:

$$V = -\frac{\partial p}{\partial t} / \frac{\partial p}{\partial n} = \epsilon(\text{div } u) / \frac{\partial p}{\partial n}; \quad V^2 \leq c^2. \quad (2'), (3'')$$

When the boundary starts back through the shattered region as a reconsolidating front, we have as boundary conditions for the determination of p and u in the unbroken liquid,

$$(p - p_0)^2 + \frac{\epsilon f}{1 - f}(p - p_0) = k^2(u_n - u_{sn})^2, \quad (6')$$

in exact analogy with (6), n denoting the component normal to the front, and also, owing to the absence of pressure gradient over the front,

$$u_t = u_{st}, \quad (6'')$$

the t denoting the vector component tangential to the front. These equations are equivalent to three scalar ones and suffice to determine the reflected wave in terms of the variables describing the incident waves and the conditions in the shattered region. The value of U , the speed of advance of the front along its normal, is given as before by Eq. (7).

EXPLANATION OF THE EXPERIMENT

In the light of these theoretical developments the course of the oscillation described at the beginning of the article is believed to be as follows. The enormous gradient implied by the momentary high pressure at the pump sets the water into rapid motion toward the tank; this phase should last about $0.091/4 = 0.023$ sec. Then as the pressure sinks to p_0 a shatter-front sweeps quickly along the pipe and a considerable section of the column becomes shattered and remains so, the crevices widening steadily, for a considerable time. Some photographs of the column taken thru a short glass section of the pipe seemed to confirm the prediction of the theory as to its condition during this phase. Finally, as the reconsolidating front arrives at the pump and the now rapidly moving column is brought to rest, a "water-hammer" results and the high hump of pressure is thereby restored.

Unfortunately the mathematical discontinuity in the equations seems to preclude obtaining any simple solution as an illustrative case. The best method of attack seems to be to start with an assumed hump of pressure and determine the motion of the liquid by approximate methods of calculation. It seems most profitable, however, for such a calculation, rather laborious at best, to be undertaken in conjunction with a repetition of the experiment in which simultaneous pressure records are obtained at several points along the pipe, in order to obtain a complete check on the theory. No projected experiment of this sort is known to the writer at the present moment.

LETTERS TO THE EDITOR

Prompt publication of brief reports of important discoveries in physics may be secured by addressing them to this department. Closing dates for this department are, for the first issue of the month, the twenty-eighth of the preceding month; for the second issue, the thirteenth of the month. The Board of Editors does not hold itself responsible for the opinions expressed by the correspondents.

Atomic Stability as Related to Nuclear Spin

As is well known, the stability of an ordinary atom nucleus is very great. For example almost head-on collisions between α -particles with velocities greater than $0.055c$ (ten thousand miles per second) with nitrogen or argon nuclei, commonly do not disrupt the nucleus, though it is true that in certain collisions the α -particle adds itself to a nitrogen nucleus and a proton is emitted at high speed. Such a high stability in a body of high positive charge does not seem probable on the basis of electrostatic forces alone, so the existence of powerful forces (partly magnetic) associated with spin and other types of quantized momenta, may be assumed. In the extra-nuclear atom, magnetic moments are associated with both orbital and with spin angular momentum, and the stability is greatest when the resultant of each of these sets of momenta is zero, or if $L=0$ and $S=0$.

The problem may be approached from the standpoint of known nuclear relations. In 1917 the writer assumed the electrons in nuclei to be associated in pairs (J. Am. Chem. Soc. 39, 859 (1917), Phys. Rev. 15, 73 (1920)), and it was also shown (Phil. Mag. 43, 305 (1921)) that in almost all atoms the total number of electrons (the electronic number) is even. In addition the number of protons is in general found to be even. Such pairing suggests the relation of antiparallel spins.

It has been shown (loc. cit.) that all atomic species fall into four classes, if oddness and evenness in the number (N) of nuclear electrons, and the number (P) of protons is used as the basis of the classification. The general stability of the atoms of each class is represented by the abundance in the meteorites, in which the abundance follows very general relations, and on earth, where segregation has been more effective. See table at bottom of page. The numbers in parentheses represent later work in which species of smaller abundance have been detected.

Both the abundance and the number of known species are very much higher for class 1 than for the other classes. In fact the abundance in the meteorites for this class is 19 times that for all of the other three classes. For this class alone the known values of the quantum number i , which represents the resultant angular momentum ($ih/2\pi$), are all equal to zero, while for all of the other three classes all of the known values are greater than zero.

In class 1 the nuclear spins (in units $h/2\pi$) have been found to be zero for helium, carbon 12, oxygen 16, and for those isotopes of zinc and of cadmium which belong to class 1 (have even isotopic number). In class 2 the known values are: Li >0 ; F, $1/2$; Na $\geq 5/2$; Cl, $5/2$; La, $5/2$; Pr, $5/2$; Cs >0 ; I, large; Tl, $1/2$;

Class	N	P	Z	Meteor- ites	Earth	Number species	Nuclear spin number	Examples
1	Even	Even	Even	95.4	87.4	71 (73)	0	O ¹⁶ , C, He, Cd (even isotopes)
2	Even	Odd	Odd	2.1	10.8	33	$1/2$ to $9/2$	F, La, Bi
3	Odd	Odd	Even	2.5	1.8	18 (25)	$1/2$	Cd (odd isotopes)
4	Odd	Even	Odd	0.0	0.0	3	1	N ¹⁴

and Bi, 9/2. In class 3 the odd isotopes of cadmium are supposed by Schüler and Bruck to exhibit a value of 1/2.

Class 4 represents the most unstable of all nuclei, since only three species of this type are thus far known, and all of these have only a minute abundance. The only one of these for which the spin is known is nitrogen 14, for which the spin is 1.

Unfortunately, the interpretation of the nuclear spin in terms of intra-nuclear spins, and possibly of other intra-nuclear momenta, is uncertain, though the present values seem to indicate that only the proton spins are apparent. This seems peculiar in view of the fact that the pairing of the electrons is more apparent than that of the protons. It may be possible that the nucleus is too densely packed to allow an electron spin, but it is also pos-

sible that the present apparent absence of electron spins is fictitious.

It may be assumed that one important factor in nuclear stability is to be found in the relations of the intra-nuclear spins, and also of any other types of angular momentum. Since these relations are unknown it has seemed important to show that all known data indicate that: *In general high nuclear stability is associated with zero nuclear angular momentum (zero spin).* The relations of the atomic species indicate that the limits of stability are related to other quantities, and are a function of the relation between Z and N/P , and of some other variables.

WILLIAM D. HARKINS

University of Chicago,
January 28, 1930.

The Unified Field Theory and Schwarzschild's Solution: A Reply

I have read with a great deal of interest Mr. Salkover's criticism (Phys. Rev. 35, 209 (1930)) of my paper on Einstein's unified field theory and the Schwarzschild solution (Proc. Nat. Acad. 15, 784 (1929)). I agree with Mr. Salkover that the expression for the electromagnetic potential which I used in my paper for the calculation of the tensor $V_{\beta\gamma}{}^{\alpha}$ was not correctly copied from the previous paper by Wiener and myself there referred to (Proc. Nat. Acad. 15, 802 (1929): communicated in May, 1929). The expression given in the latter paper of course agrees with that calcu-

lated by Mr. Salkover, and also with the value of the tensor $\Lambda_{\mu\nu}{}^{\sigma}$ reported in my paper. This mistake, while vitiating my results on the Schwarzschild solution, in no way affects our previously announced conclusions, in particular the non-existence in the unified theory of an electrostatic field with spherical symmetry.

M. S. VALLARTA

Massachusetts Institute of Technology,
Cambridge, Mass.,
February 3, 1930.

Scattering of Light in Sodium Vapor

An artificial chromosphere was constructed in the following manner: Sodium vapor was admitted into a cylindrical glass shell, like the region between the walls of an unsilvered Dewar flask, and a filament was inserted along the axis of the cylinder. The filament is considered to be the photosphere, and the sodium vapor shell the chromosphere. When a spectroscope was directed through the shell of vapor, at right angles to the axis, at the continuous background furnished by the filament, the "Fraunhöfer" lines were observed. When the shell was lowered so only the upper part of the cylinder was in front of the slit, resonance radiation was seen, corresponding to the flash spectrum. It was observed that the D lines appeared in absorption at lower

vapor densities than those for which they appeared in emission.

This is in accord with the work of J. Q. Stewart and the author, (Astrophys. J. January, 1930). The reason for this is not understood. It is probably not due to quenching of resonance radiation by the hydrogen present in the sodium, since kinetic theory calculations indicate that it is necessary to assume effective collision radii of order 10^{-6} cm before a collision frequency is obtained comparable to the unloading time of the $2P$ state of sodium; though the work of Mannkopf (Zeits. f. Physik 36, 315 (1926)) leaves some doubt on this point. Since in the experiments of R. W. Wood (Physical Optics, Pp. 575 et seq.) the vapor density was not

accurately known, his experiments cannot given an answer to this problem. While in the present experiment feeble resonance radiation may have been lost through experimental difficulties, such as reflections from the glass surfaces, yet the result is what one would expect on the assumption that pure scattering is not the only process at work in the production of the cores of "absorption" lines, whereas scattering alone produces the edges.

Further evidences for this assumption are discussed in the paper referred to above. It would be interesting to know whether resonance radiation has even been observed at as low vapor densities as to produce just observable absorption.

S. A. KORFF

Palmer Physical Laboratory,
Princeton University,
January 28, 1930.

The Heat of Dissociation of Oxygen

In a recently written paper on the heat of dissociation of carbon monoxide, the writer has pointed out that the energy of the 1D_2 level in the oxygen atom is 1.3 volts. This value agrees well with the one given recently in Nature by McLennan and Crawford. Since the heat of dissociation of oxygen can be calculated from band spectrum data if the energy of the 1D level is known, it is proposed here to point out the source of this new value for the 1D level. The resulting heat of dissociation is equal to 5.7 volts and it lies between the limits set by Professor Birge in his Faraday symposium paper.

In the above mentioned paper, reasons were advanced for the correctness of a linear extrapolation of the vibrational levels associated with the F level of CO. Such an extrapolation yields a value of 2.5 volts for the total energy of the products of dissociation from this level. At the time that the paper was written, the writer was not aware of the fact that Fowler and Selwyn had determined the energy of the 1D_2 carbon atom. Consequently the value of 1.3 volts for the energy of the 1D_2 oxygen atom, proposed by McLennan and Crawford, was used to predict a

value of 1.2 volts for the energy of the 1D_2 carbon atom. This however is exactly equal to the value found by Fowler and Selwyn, so that the above work is really independent evidence that the energy of the 1D oxygen atom is 1.3 volts.

The new value of the heat of dissociation of oxygen follows immediately from the theoretical prediction that the products of dissociation from the B level of oxygen are a normal oxygen atom and one in the 1D level. This has already been used by both Herzberg and Birge in their discussions regarding the heat of dissociation of oxygen. Since that total energy in the B level is known exactly and is equal to 7.0 volts, it follows that the heat of dissociation of oxygen is 5.7 volts. It is believed that, in view of the nature of both the present evidence and that of McLennan and Crawford, this low value for the heat of dissociation is correct to within 0.1 volt.

JOSEPH KAPLAN

University of California at Los Angeles,
February 2, 1930.

A Remark on Hyperfine Structure

An error which has crept into the literature of the theory of hyperfine structure might easily cause misunderstanding and indeed in some places has already led to incorrect deductions.

The problem is to determine what is the direction of the magnetic field produced at the nucleus by a spinning electron in its orbit. For large values of l the classical theory will give the correct result and elementary considerations show, that the magnetic field has the opposite direction of the mechanical moment l . The field produced by the spin is parallel to the spin-vector s , but for large values of l

may be neglected. This result means that a spinning proton will be in its most stable state when its mechanical moment i is opposite to j , from which follows that the produced hyperfine splitting will be "regular," the lowest level having the smallest total resultant f .¹

It is obvious that the orbital picture can

¹ For the complete classical expression and its quantum mechanical equivalent see L. Pauling and S. Goudsmit, *The Structure of Line Spectra*, Chapter XI, McGraw-Hill, to appear soon.

not be used for an s state, where $l=0$. Here one should use a model that comes nearer to the results of the quantum mechanics. An s state is then a spherically symmetric charge distribution and the spin may be represented by a current distribution within this charge distribution. The result is that the magnetic field at the nucleus is now *opposite* to the spin direction, in complete agreement with the quantum mechanics calculations of Fermi (Nature **125**, 16, 1930). One thus also expects "regular" hyperfine structure if protons interact with an s electron. (For details, especially in more complicated configurations, see S. Goudsmit and R. F. Bacher, Phys. Rev. **34**, 1501, 1929).

Jackson (Proc. Roy. Soc. **A121**, 432, 1928) in his paper on the hyperfine structure of caesium used incorrect results for both s and p states. He assumes his fine structures to be all inverted, which causes his deductions about the nuclear moment of caesium being $\frac{1}{2}$ to be quite uncertain. Also Hargreaves (Proc. Roy. Soc. **A124**, 568, 1929) in his paper dealing with the quantum mechanics treatment of the interaction between nuclear magnetism and the electron orbit, seems to

have adopted this incorrect result when he compares his expressions with the results obtained by Jackson. It must be mentioned here that the derivations of Hargreaves clearly show that the minus sign entering in his final formula must be an accidental error.

Finally the same error occurs in the important papers of White (Phys. Rev. Dec. 1929 and Feb. 1930) and causes his deductions about the origin of the nuclear magnetism to be incorrect.

Actually "inverted" fine structure² occurs in Cd and probably in Li an explanation of which can not yet be given with certainty.

I hope that this letter will prevent further spreading of this unfortunate mistake.

S. GOUDSMIT

Department of Physics,
University of Michigan,
February 12, 1930.

² "Inverted" means here when the fine structure appears as if it were due to a negative particle in the nucleus. Certain fine structures are inverted because of complications in the electron configurations. (See S. Goudsmit and R. F. Bacher, l.c.)

Doublets in the Vibration Spectrum of Cyclohexane

Infra-red and visible absorption spectra and Raman scattered spectra have shown that the C-H bands of organic compounds are often made up of more than one component. In particular the spectrum of cyclohexane is of interest. The writer has already shown that the second, fifth, sixth and seventh members of the C-H anharmonic series* of this liquid are doublets of comparable intensities. By means of the Raman effect the fundamental band has also been shown to be a doublet by Petrikaln and Hochberg, Ganesan and Venkateswaran, and Daure. The writer has thus far failed to resolve the third and fourth members, probably largely because of the relatively great widths of the component lines. In attempting to resolve the third band a recording quartz spectrograph with a slit width equivalent to 0.006μ was used, but only a single broad band was obtained. A Hilger El spectrograph with neocyanine stained

plates was employed when trying to resolve the 0.93μ band. This band occurs in the region of the spectrum for which the plate is relatively insensitive. Considerable halation resulted from an overexposure of the $0.85-0.90\mu$ region for which the plate is very sensitive. Even when the intensity of the spectrum in this region was cut down by placing a cell of neocyanine solution before the slit of the spectrograph, the broad region of absorption near 0.93μ could not be resolved into a doublet. Although no precise measurement could be made upon the center of the band it seems certain that it has a somewhat lower value than 0.93μ which had been previously determined thermally.

In spite of the inability to separate the components of these two bands, the frequency separations of the remaining five are sufficient to permit us to arrive at some interesting conclusions. In the table are shown the wavelength values λ , λ' , their frequencies ν , ν' , the doublet separations $\delta\nu$, the first differences in the frequencies of the members of the separate series $\Delta\nu$, $\Delta\nu'$, and the second differences $\Delta'\nu$, $\Delta'\nu'$. Since it has been necessary to

* Although the term series is used here, we are in reality dealing with an n' progression according to the general theory of band spectra.

assume reasonable data for the doublet structure of the third and fourth bands these have been bracketed in the table.

further supporting this interpretation has been submitted for publication). In that instance it was assumed that the constant

TABLE I.

n	λ	λ'	ν	ν'	$\delta\nu$	$\Delta\nu$	$\Delta\nu'$	$\Delta'\nu$	$\Delta'\nu'$
1	3.50 μ	3.40 μ	2860cm ⁻¹	2940 cm ⁻¹	80cm ⁻¹	2860cm ⁻¹	—	2940cm ⁻¹	—
2	1.77	1.74	5650	5750	100	2790	70cm ⁻¹	2810	130cm ⁻¹
3	*[1.21]	[1.19]	[8270]	[8400]	[130]	2620	170	2650	160
4	*[0.930]	[0.917]	[10750]	[10900]	[150]	2480	140	2500	150
5	0.763	0.753	13100	13280	180	2350	130	2380	120
6	0.653	0.644	15300	15520	220	2200	150	2240	140
7	0.575	0.567	17390	17640	250	2090	110	2120	120

* 1.20 ± 0.01 and 0.93 ± 0.01 are the values observed thermally for these unresolved bands.

Since the $\delta\nu$ values are not the same for all of the bands the two broad components cannot be regarded as P and R branches of single bands.

Within the limits of certainty of the $\delta\nu$ values we may conclude that there is a linear relation between these values and n . From this we conclude that the coefficients of n differ in the two anharmonic formulas which relate ν and ν' independently to n . Furthermore, it can be seen that $\delta\nu$ will not extrapolate to zero when n equals zero, and from this fact we conclude that a constant term must appear in one or both of the equations. An inspection of the $\Delta\nu'$ and $\Delta'\nu'$ columns of the table indicates that the equation for the components of higher frequency requires no constant term. We are led therefore to the remarkable conclusion that a subtractive constant term must be included in the equation relating the lower frequency components to n . We have then $\nu_n' = a'n - bn^2$; $\nu_n = -c + an - bn^2$; $\delta\nu = c + (a' - a)n$. It is impossible to say whether there is any small change in the b coefficient.

The writer has already pointed out an instance in the case of ammonia in solution in which an additive constant must be included in the formula which relates a set of anharmonic overtones to their fundamental. (Jl. Franklin Inst. 208, 507 (1929). A paper

term is a measure of the energy which goes to change the molecule to a form with slightly greater potential energy. In the present instance we are forced to conclude that a drop in the potential energy of the vibrator which yields the ν_n frequencies supplies the additional energy which the quantum lacks to produce the vibration. The behavior of the molecule in this respect is in a way similar to its behavior when producing an anti-Stokes line in a Raman spectrum. In the latter instance however the energy which the molecule gives up as it drops to a lower quantized level goes to increase the magnitude of the scattered quantum.

The data of the table cannot be used to decide whether we are dealing with a single kind of C-H vibrator which shifts at times to a lesser value of the restoring force, or with two distinct types of C-H vibrators. The writer however still inclines to his previous viewpoint that vibrations of one of the hydrogen atoms bonded to each carbon atom contribute to one component of the doublet series whereas vibrations of the second hydrogen atom contribute to the other component.

JOSEPH W. ELLIS

Physics Department,
University of California at Los Angeles,
February 4, 1930.

Secondary Emission from Metals by Impact of Metastable Atoms and Positive Ions

In studying the positive column of the noble gases, using plane sounding electrodes, some phenomena were observed, which could not be explained by the theory proposed by Langmuir¹ and applied by himself and Mott Smith² to the mercury arc. The simplest in-

terpretation of the observed discrepancies, was to assume a secondary electron emission

¹ Langmuir, G. E. Rev. 26, 731 (1923).

² Langmuir and Mott Smith, G. E. Rev., 27, 449, etc. (1924).

from a negatively charged plane electrode, amounting to from 40 to 50% of the measured current. This value was obtained by comparing the measured current i_m and the current i_c , calculated from the observed thickness of the space-charge layer with the usual equations.³ We have succeeded in proving directly that there is an electron emission from the electrode of that magnitude, and that it is principally due to impact of metastable atoms on the collecting electrode.

A plane circular collecting electrode (Ni) with a guard-ring was placed in the positive column of a neon discharge ($p=0.02$ mm) with hot cathode. At the center of the metal disk was a small hole, and behind this a Faraday box. The arrangement was such that the box was practically completely shielded from the radiation in the discharge. It was thought that a comparison of the ion current coming through the hole with the apparent ion current density on the central disk would give a measure of the secondary electron emission from the latter. Indeed, the chance for a secondary electron liberated in the Faraday box to get out is so small, that the current recorded at the box was supposed to be a pure positive ion current, provided the plate is sufficiently negative with respect to the gas ($-125v$) to keep out all electrons coming from the discharge. The experimental results were much more complicated than expected. Using different arrangements of potentials we proved that neutral particles, diffusing out of the main discharge through the gap between disk and guard-ring, caused a considerable electron emission from the metal parts behind the collector. This suggested that the secondary emission referred to above was due principally to the action of metastable atoms on the collector.⁴

More quantitative results were obtained in the same tube with another arrangement. Opposite to the plane collector with the guard ring, mentioned above, was a small hollow cylindrical one, whose axis was perpendicular to the plane collector. The near end, covered with Ni gauze, was exposed to the discharge, the sides and other end being shielded by glass. This cylinder was movable in the direction of its axis, i.e., perpendicular to the sur-

face of the disk collector. Suppose the cylinder at a potential $V_c = -125v$ with respect to the gas; it is then collecting a certain positive ion current i_c . The potential of the plate, V_p , originally $-75v$ with respect to the gas, is now made more negative and the variation of i_c is studied as a function of V_p . As long as the plate is positive with respect to the cylinder, no secondary electrons from the plate can reach the latter, since in falling through the positive space charge layer on the disk they can only acquire an energy corresponding to V_p . When the potential of the plate reaches V_c , the ion current i_c shows a decrease due to incoming electrons originating in the space charge sheath on the plate. The mean free path of the electrons with a velocity corresponding to V_p depends on the degree of ionization and can be determined experimentally in each case by varying the distance between the cylinder and the plate, all other conditions remaining the same. Knowing the electron mean free path and the secondary electron current at a given distance, the secondary emission from the plate can be computed and is found to be from 40 to 50% of the total current i_p .

When the current voltage curve of the secondary electrons is differentiated, a velocity distribution curve is obtained which shows that most of the electrons have at least an energy corresponding to V_p ; it follows that they must be liberated at the plate or at a very small distance from it. In addition to the energy, acquired in falling through the space charge sheath, they possess energies of a few volts which are probably initial energies of emission. Some velocity distribution curves show that there are also electrons produced in the sheath at some distance from the plate, but only in small numbers. The interpretation proposed earlier⁵ that the electrons are principally due to photoelectric ionization in the sheath has to be given up. The experiments are continued with an improved apparatus to study the influence of different factors on the secondary emission.

W. UYTERHOEVEN
M. C. HARRINGTON

Palmer Physical Laboratory,
Princeton, N. J.,
February 10, 1930.

³ Uytterhoeven, Phys. Rev. 31, 931 (1928); Proc. Nat. Ac. Sc. 15, 32 (1929).

⁴ Oliphant, Proc. Roy. Soc. A124, 228, 1929.

⁵ Morse and Uytterhoeven, Phys. Rev. 31, 827 (1928); see also de Groot Naturwiss. 17, 13 (1929).

Predictions of Manganese Hyperfine Structure

In a recent letter to the Physical Review H. E. White (Phys. Rev., 35, 208, 1930) announces that he has obtained an analysis of the hyperfine structure of the manganese arc spectrum. His letter contains the results for three levels and mentions that he has been able to analyze many more.

With the aid of the theoretical considerations given in a previous paper (S. Goudsmit and R. F. Bacher, Phys. Rev. 34, 150, 1929) it is possible to predict the hyperfine structure for a number of manganese levels from the few data given by White. Here follow the predictions for the separation factors¹ and the total separations:

$3d^5 4s^1 {}^6D$	$J=4\frac{1}{2}$	$A=0.0139$	$\nu\Delta=0.384^2$
	$3\frac{1}{2}$.015	.29
	$2\frac{1}{2}$.016	.25
	$1\frac{1}{2}$.022	.19
	$\frac{1}{2}$.058	.17
4D	$3\frac{1}{2}$	-.011	-.21
	$2\frac{1}{2}$	-.009	-.14
	$1\frac{1}{2}$	-.005	-.05
	$\frac{1}{2}$	+.025	+.08
$3d^5 4s 5s {}^8S$	$3\frac{1}{2}$.020	.40
6S	$2\frac{1}{2}$.022	.33

These predictions are based on the following assumptions and will, therefore, be correct only if the assumptions are.

(a). The $3d$ electrons give no appreciable contribution to the fine structure. The fact mentioned by White, that the $3d^5 4s^2 {}^6S$ level shows no fine structure does not prove that the contribution of the $3d$ electrons will be

¹ The separation factor A is the proportionality constant which one obtains if one applies the interval rule to the splitting up of the level. It is only then strictly a constant when the interval rule holds. The validity of the vector model and of the interval rule for hyperfine structure was for the first time pointed out with certainty in the bismuth spectrum (E. Back and S. Goudsmit, Zeits. f. Physik 43, 321, 1927) it formed in fact the basis for the analysis of its hyperfine structure and the determination of the nuclear moment, later confirmed by the Zeeman effect.

² Value given by White.

small in all other configurations too, though it is probable.

(b). The addition of the $4s$ electron does not affect the resultant spin of the already present $3d$ electrons. This means that in the expression for A ,

$$A = a \cdot (s/S) \cos(s, S) \cdot (g-1),$$

$(s/S) \cos(s, S)$ is equal to $+1/5$ for the 6D and $-1/5$ for the 4D . This is verified by the formulas for the multiplet separations themselves (S. Goudsmit and C. J. Humphreys, Phys. Rev. 31, 960, 1928) in which this same cosine occurs.

The contribution of the $5s$ electron is estimated to be about one tenth of that of the $4s$ electron.

The contribution of a p electron is of a more complicated type and general expressions which I obtained for it can only be applied to a few simple cases. For two electrons, one being in an s state, the complete expression for A becomes:³

$$A = a \frac{1}{2}(g-1) + b \left[(2-g) + \frac{l(l+1)}{2(l-1/2)(l+3/2)} \left\{ \frac{1}{2}(g-1) - 3(2-g)\Gamma/2L(L+1) \right\} \right].$$

The hyperfine structures in Tl II (J. C. McLennan, A. B. McLay, and F. M. Crawford, Proc. Roy. Soc. A125, 570, 1929) and in Cd (H. Schüller and H. Brück, Zeits. f. Physik 56, 291, 1929) are not yet known with enough accuracy to test the second part of this formula.

S. GOUDSMIT

Department of Physics,
University of Michigan,
February 12, 1930.

³ The constants a and b measure the interaction energy of the nucleus with the s electron and the p electron respectively. Unpublished calculations of H. Casimir give for b in a hydrogenic case

$$b = R\alpha^2 Z^3 g(i) / n^3 l(l + \frac{1}{2})(l+1)$$

in which $g(i)$ is the Landé g -value for the nucleus and thus expected to be of the order $1/1840$.

THE PHYSICAL REVIEW

NUCLEAR SPIN AND HYPERFINE STRUCTURE

By H. E. WHITE¹

PHYSIKALISCH-TECHNISCHE REICHSANSTALT, BERLIN

(Received January 27, 1930)

ABSTRACT

Assuming that hyperfine structure in spectral lines has its origin in the coupling of a nuclear spin with electron resultant J , a comparison between gross structure and hyperfine structure is made from the following relation, $\Delta\nu_g/\Delta\nu_f = m_k/4im_e$. For those atomic systems for which the electron configurations show LS or jj coupling, the agreement with the above equation is quite as good as would be expected. For electronic configurations which do not show LS or jj coupling it is doubtful whether such a comparison of gross structure with hyperfine structure can be suitably made. From the meagre data as yet available, one is led to suspect that nuclear spin is due to the last electrons, protons, or both (most probably electrons) added to the nucleus in atomic construction. These electrons should, in accordance with the principles of the wave-mechanics, have a *probability density* spherically symmetrical about the nucleus. The difference between the electrons associated with the nucleus and the outer electrons is that the nuclear electrons carry with them in space quantization the total mass of the atom.

THE splitting up of ordinary energy levels into a number of hyperfine structure components is quite generally attributed to a nuclear angular momentum. Observations indicate that this nuclear spin, whether due to electrons, protons, or to both electrons and protons, carries with it in space quantization the total mass of the nucleus. Assuming the nuclear spin to be a rotation of the nucleus as a whole, Jackson² has derived the following equation for the approximate shift in energy of ordinary energy levels due to nuclear spin.

$$\Delta\nu_g/\Delta\nu_f = m_k/2m_e. \quad (1)$$

Here $\Delta\nu_g$ is a gross or multiplet structure separation, $\Delta\nu_f$ the corresponding hyperfine structure separation, m_e the mass of an electron and m_k the mass of the nucleus. Since this formula was derived for a nuclear spin of $i = \frac{1}{2}$ a quantum of energy, it may be made general for all values of i by replacing the constant 2 in the above equation with $4i$. This gives

¹ National Research Fellow.

² Jackson, Proc. Roy. Soc. A121, 432 (1928).

$$\Delta\nu_a/\Delta\nu_f = m_k/4im_e \quad (2)$$

which for $i = \frac{1}{2}$ reduces to equation (1).

Jackson has shown² that in the simple case of a so called *one electron system*, like caesium, an electron spin doublet separation ($\Delta\nu_a$), for example $^2P_{1/2} - ^2P_{3/2}(6p)$, is to be compared with the hyperfine separation ($\Delta\nu_f$) of one of the terms, 2P . The ratio $\Delta\nu_a/\Delta\nu_f$, as compared with computed values from Eqs. (1) and (2), is in reality in quite good agreement (Table I).

From a discussion with Dr. Schüler³ it appears that the hyperfine structure of $\lambda 5486$, $^3S_1 - ^3P_{0,1,2}$, in singly ionized lithium may be accounted for by assigning an angular momentum, $i = \frac{1}{2}$, to the nucleus of Li.⁷ From the observed hyperfine structure, the $^3S_1(1s2s)$ term and the $^3P_2(1s2p)$ term have normal doublet separations of about 0.60 cm^{-1} and 0.45 cm^{-1} respectively (error $\pm 0.10 \text{ cm}^{-1}$). The splitting up of these terms is shown in Fig. 1. In

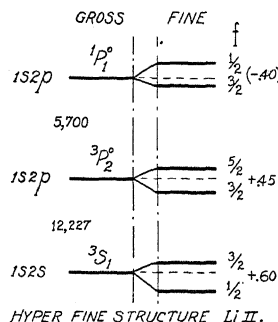


Fig. 1.

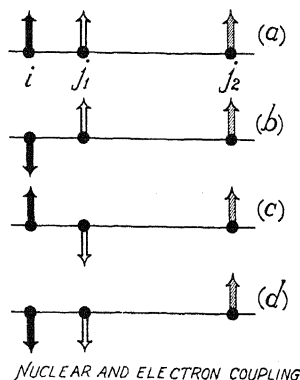


Fig. 2.

this case of a nucleus and two electrons, it may be shown by the use of Fig. 2 which gross structure and which hyperfine structure separations are to be compared with each other. The left hand vector i , in Fig. 2, may be taken to represent the nuclear angular momentum, $\frac{1}{2}$, of Li,⁷ and j_1 and j_2 may be taken to represent $1s$ and $2p$ electrons respectively. In the space quantization of these three vectors the coupling between j_1 and j_2 produces the gross-structure energy levels, whereas the coupling between j_1 and i and between j_2 and i produces the hyperfine energy levels. For the term 3P_2 of Fig. 1, all three vectors i , j_1 and j_2 , Fig. 2(a), are parallel as shown.⁴ When i is now inverted, to position Fig. 2(b), the shift in energy to the term 3P_2 is observed to be about 0.45 cm^{-1} . Owing to the relative nearness of the $1s$ electron

³ Schüler, Zeits. f. Physik.

⁴ With the apparent need of the new quantum number f to represent an energy level, it is suggested that this quantum number precede the ordinary term designation as a subscript for example, $_{3/2}^3D^0_2$. If the electron configuration is given, it is desirable to include the nuclear spin, for example, $_{7/2}^3S_1$. A radiated hyperfine structure line would be designated, $_{3/2}^3S_1 - _{5/2}^3P^0_2$.

to the nucleus, this shift in energy is almost entirely due to the coupling between j_1 and i . When from $_{5/2}^3P_2$, Fig. 2(a), the vector j_1 is inverted to position Fig. 2(c), the shift in energy to $_{3/2}^1P_1$ is observed to be about -7000 cm^{-1} . The inversion now of i to position $_{1/2}^1P_1$, Fig. 2(d), should produce, although not yet observed, a shift of about -0.4 cm^{-1} . The inverted hyperfine structure in this 1P_1 term follows from the hypothesis that, while the separation arises from the coupling between j_1 and i , space quantization must take place between nuclear spin, i , and electron resultant, J .⁵ The ratio $\Delta\nu_g/\Delta\nu_f$ is given in Table I along with the values obtained for other elements.

Making quite the same arguments given above for lithium, a correlation between gross structure and hyperfine structure may be made for an atomic system having a number of valence electrons, for example, manganese, Mn I. Using again Fig. 2, vector i is taken to represent the nuclear angular momentum $i = 5/2$ of manganese, vector j_1 to represent a $4s$ electron and, vector j_2 to represent the resultant angular momentum of all of the rest of the electrons outside of the nucleus, for example $3d^5$, 5D_4 , of Mn II. With all three vectors parallel as in Fig. 2(a) the atom is in state $^7D_{9/2}(i_{5/2}3d^54s)$. The inversion of vector i to position (b), $^6D_{9/2}(i_{5/2}3d^54s)$, produces a shift in energy of about 0.50 cm^{-1} . An inversion, however of vector j_1 from position (a) to position (c), $^4D_{7/2}(i_{5/2}3d^54s)$, produces a shift in energy of $-6,244 \text{ cm}^{-1}$. The ratio $\Delta\nu_g/\Delta\nu_f = 12,488$ is in quite good agreement with the calculated value 10,100.

In order to account for the observed hyperfine structure of the principal doublet of caesium, Jackson² assigned an angular momentum of $i = \frac{1}{2}$ to the nucleus of caesium. It is interesting to note that the observations are equally well explained by assuming greater values of i . From values of nuclear spin found in other elements $1/2$, $5/2$ and $9/2$, and the last two columns of Table I, excluding Tl and Cd, the value $i = 5/2$ seems to be, although the evidence is not strong, the more probable for caesium.

TABLE I.
A comparison of gross structure with hyperfine structure.

Element	i	Electron Config.	Terms	$\Delta\nu_g$	$\Delta\nu_f$	$\Delta\nu_g/\Delta\nu_f$	$m_k/4im_s$
Li ⁷ II	$\frac{1}{2}$	$1s2p$	$^3P_2^\circ - ^1P_1^\circ$	7,000	0.45	15,555	6,440
Mn I	$2\frac{1}{2}$	$3d^54s$	$^6D_{4\frac{1}{2}} - ^4D_{3\frac{1}{2}}$	6,244	.50	12,488	10,100
Mn I	$2\frac{1}{2}$	$3d^54p4s$	$^8S_{3\frac{1}{2}} - ^6S_{2\frac{1}{2}}$	9,984	.60	16,640	10,100
Cs I	$\frac{1}{2}$?	$6p$	$^2P_{3/2}^\circ - ^2P_{1/2}^\circ$	554	.01	55,400	122,000
Cs I	$2\frac{1}{2}$?	$6p$	$^2P_{3/2}^\circ - ^2P_{1/2}^\circ$	554	.01	55,400	24,500
Cs I	$4\frac{1}{2}$?	$6p$	$^2P_{3/2}^\circ - ^2P_{1/2}^\circ$	554	.01	55,400	13,600
Tl I	$\frac{1}{2}$	$6p$	$^2P_{3/2}^\circ - ^2P_{1/2}^\circ$	7,793	.40	19,480	187,600
Tl II	$\frac{1}{2}$	$6s6p$	$^3P_2^\circ - ^1P_1^\circ$	13,935	3.5	3,980	187,600
Cd I	$\frac{1}{2}$	$5s5p$	$^3P_2^\circ - ^1P_1^\circ$	11,864	.25	47,460	103,000

The ratios $\Delta\nu_g/\Delta\nu_f$, given in Table I for Tl I and Tl II, are decidedly not in agreement with the calculated value 187,600. From Zeeman effect data on $\lambda 3776$ of Tl I⁶ the nuclear spin is quite certainly $1/2$. The enormous hyperfine

⁵ H. E. White, Phys. Rev. 34, 1404 (1929).

⁶ Schüller and Brück, Zeits. f. Physik 56, 291 (1929).

structure separations in Tl II as compared with the small separations found in Tl I are undoubtedly due to the strong coupling between i and the deep penetrating $6s$ electron for Tl II, in contrast with the coupling and penetration of a $6p$ electron in Tl I. In Tl II, it would appear that the difficulty arises in the uncertainty of the coupling between the two valence electrons. Since the terms do not indicate either LS or jj coupling, it is doubtful whether such a comparison of gross structure with hyperfine structure can be suitably made for such cases. It has been interesting to note, however, for all observed hyperfine structure, that the space quantization between electron resultant J and the nuclear spin i always follows the interval rule, i.e., a Ji coupling where the intervals are proportional to $\cos Ji$. The exact form of the constant multiplier of i in equation (2) depends largely upon the distribution of charge causing the nuclear spin. Even with the meagre data as yet available, one is led to suspect that the nuclear spin is due to the last added electrons, protons, or both electrons and protons. From observations electrons alone seem to be the most probable.⁵ These electrons should, in accordance with the principles of the wave mechanics, have a probability density spherically symmetrical about the nucleus and might be thought of as a charged shell over the surface of the nucleus. The difference between the electrons associated with the nucleus and the outer electrons is that the nuclear electrons carry with them in space quantization the total mass of the atom.

The author wishes to take this opportunity to thank Dr. Paschen for his interest in and criticism of this paper.

THE SECOND SPARK SPECTRUM OF ANTIMONY AND A NOTE ON THE FIRST SPARK SPECTRUM OF TIN

BY R. J. LANG

UNIVERSITY OF ALBERTA, EDMONTON, CANADA

(Received January 30, 1930)

ABSTRACT

Some sixty lines of the vacuum spark spectrum of antimony have been classified as transitions between the following terms of Sb III: $(s^25p)^2P$, $(s^26p)^2P$, $(s^26s)^2S$, $(s^27s)^2S$, $(s^28s)^2S$, $(s^25d)^2D$, $(s^26d)^2D$, $(s^24f)^2F$, $(s^25f)^2F$, $(s^25g)^2G$, $(s^26g)^2G$, $(s5p^2)^4P$, 2D , 2S , 2P and $(5p^3)^4S$. Corresponding to the deepest term value an ionization potential of approximately 24.7 volts is calculated. A note on SN II gives the terms 4P and 2S from the $(s5p^2)$ configuration and new value for the terms: $(s^27s)^2S$, $(s^28s)^2S$, $(s^27d)^2D$ and $(s^26f)^2F$.

THE vacuum spark spectrum of antimony has been measured over the range 6600 to 600A and also the Paschen hollow-cathode spectrum from 5200 to 1950A. By means of these two measurements it has been possible to separate the first and second spark spectra rather definitely from one another and thus to arrive at a classification for the latter. Work on the first spark spectrum is now in progress and will be reported on later. The measurements of the vacuum spark spectrum below 2500A were made on a two-meter grating mounted in a vacuum spectrograph giving a dispersion of 4.5A per mm. Above 2000A several instruments were used. The vacuum spark and hollow cathode spectra were measured in Edmonton on a two-meter Rowland grating kindly loaned to the author by Professor Smith. The vacuum spark spectrum was also measured in Michigan by the author using a Hilger E_2 quartz spectrograph made available through the courtesy of the Department of Physics. The author is also indebted to Professor R. A. Sawyer of Michigan for a plate of the vacuum spark in the region from 5300 to 6600A made on a large Hilger glass spectrograph. A few wave-lengths are taken also from Schippers measures given by Kayser.

In a previous report¹ the author gave three multiplets for Sb III all of which turn out to be real but the first one given was improperly classified as $(s^26s)^2S-(s^26p)^2P$. It should have been $(s5p^2)^2S-(s^26p)^2P$. It thus corresponds very satisfactorily to the doublet in As III at 4200A. A paper on As III and Sb III appeared later in the Indian Journal of Physics.²

Some important electron configurations and resultant terms expected in the spectrum of Sb III are as follows:

¹ Lang, Phys. Rev. 32, 737 (1928).

² Pattabhiramiah and Rao, Indian Journ. Phys. 3, 437, 1929

Configuration	Terms	Configuration	Terms
(s^25p)	2P	$(s5p^2)$	$^4P, ^2PDS$
(s^26s)	2S	$(s5p5d)$	$^4PDF, ^2PDF$
(s^25d)	2D	$(s5p6s)$	$^4P^2P$
(s^24f)	2F	$(5p^3)$	$^4S, ^2PD$
(s^25g)	2G	$(s5p6p)$	$^4PSD, ^2SPD$

TABLE I. Empirical term values in Sb III.

Odd Terms			Even Terms		
$(s^25p)^2P_{\frac{3}{2}}$	200272	6576	$(s5p^2)^2D_{1\frac{1}{2}}$	123744	1270
$(s^25p)^2P_{1\frac{1}{2}}$	193696		$(s5p^2)^2D_{2\frac{1}{2}}$	122474	
$(s^24f)^2F_{2\frac{1}{2}}$	118940		$(s^26s)^2S_{\frac{1}{2}}$	107321	
$(s^24f)^2F_{3\frac{1}{2}}$	118567	373	$(s5p^2)^2S_{\frac{3}{2}}$	106852	5392
$(s^26p)^2P_{\frac{3}{2}}$	85550		$(s5p^2)^2P_{\frac{3}{2}}$	105624	
$(s^26p)^2P_{1\frac{1}{2}}$	83882		$(s5p^2)^2P_{1\frac{1}{2}}$	100232	
$(s^25f)^2F_{3\frac{1}{2}}$	64055	-55	$(s^25d)^2D_{1\frac{1}{2}}$	101450	1567
$(s^25f)^2F_{2\frac{1}{2}}$	64000		$(s^25d)^2D_{2\frac{1}{2}}$	99883	
$(5p^3)^4S_{1\frac{1}{2}}$	51259		$(s^27s)^2S_{\frac{1}{2}}$	57143	
			$(s^26d)^2D_{1\frac{1}{2}}$	55589	237
			$(s^26d)^2D_{2\frac{1}{2}}$	55352	
			$(s^28s)^2S_{\frac{1}{2}}$	36882	
			$(s^25g)^2G$	35966	
			$(s^26g)^2G$	25812	
Even Terms					
$(s5p^2)^4P_{\frac{3}{2}}$	145906	3596			
$(s5p^2)^4P_{1\frac{1}{2}}$	142310				
$(s5p^2)^4P_{2\frac{1}{2}}$	136952	5358			

TABLE II. Comparison of term values.

Term	Element	4	5	6	7	8
2S	In I			22295	10366	6031
	Sn II			15205	7841	5194
	Sb III			11924	6349	4098
$^2P_{\frac{1}{2}}$	In I		46668	14811	7808	
	Sn II		29426	11553		
	Sb III		22252	9506		
$^2D_{1\frac{1}{2}}$	In I		13775	7620	4832	
	Sn II		11575	6867	4342	
	Sb III		11272	6176		
$^2F_{2\frac{1}{2}}$	In I		6960			
	Sn II		7104	4511		
	Sb III	13215	7111			
2G	In I					
	Sn II					
	Sb III		3996	2868		

TABLE III. Combinations, intensities and discrepancies in the spectrum of Sb III.

Odd Terms	$(s^2p)^2P_{\frac{3}{2}}$	$(s^2p)^2P_{\frac{1}{2}}$	$(s^2f)^2F_{\frac{7}{2}}$	$(s^2f)^2F_{\frac{5}{2}}$	$(s^2p)^2P_{\frac{3}{2}}$	$(s^2p)^2P_{\frac{1}{2}}$	$(s^2f)^2F_{\frac{7}{2}}$	$(s^2f)^2F_{\frac{5}{2}}$	$(s^2p)^2P_{\frac{3}{2}}$
Even Terms	200272	193696	118940	118567	85550	83882	64055	64000	51259
$(s^2p)^2P_{\frac{3}{2}}$ 145906	12 2	2 1							10 -2
$(s^2p)^2P_{\frac{1}{2}}$ 142310	15 -2	10 -2							10 -4
$(s^2p)^2P_{\frac{3}{2}}$ 136952		12 0							12 0
$(s^2p)^2D_{\frac{3}{2}}$ 123744	20 1	10 -1			12 5	5 3		15 -3	8 1
$(s^2p)^2D_{\frac{5}{2}}$ 122474		20* -6				15 5	15 -2	3 -3	20* 1
$(s^2s)^2S_{\frac{1}{2}}$ 107321	30 1	40 0			30 0	40 0			
$(s^2p)^2S_{\frac{1}{2}}$ 106852	20 0	30 0			30 0	50 0			
$(s^2p)^2P_{\frac{3}{2}}$ 105624	10 -3	10 0							
$(s^2d)^2D_{\frac{3}{2}}$ 101450	40 -2	20 0	1 -4	3 -15?	3 0	1 -1		20 0	
$(s^2p)^2P_{\frac{1}{2}}$ 100232	15 -2	20 0							
$(s^2d)^2D_{\frac{5}{2}}$ 99883		40 4	1 -6			5 3	20 0	5 1	
$(s^2s)^2S_{\frac{1}{2}}$ 57143	10 -3	15 -3			15 1	30 -1			
$(s^2d)^2D_{\frac{3}{2}}$ 55589	10 -3	8 -2			20 1	15 0			
$(s^2d)^2D_{\frac{5}{2}}$ 55352		15 -4				50 0			
$(s^2s)^2S_{\frac{1}{2}}$ 36882					3 0	5 0			
$(s^2g)^2G$ 35966			50 0	50 0			40 -1	40 -1	
$(s^2g)^2G$ 25812			5 3	5 0			1 -2	1 3	

* Classified twice.

TABLE IV. *Classified lines of Sb III.*

Classification	λ (I.A.)	I	ν
$(s^25p)^2P_{\frac{1}{2}} - (s^26d)^2D_{1\frac{1}{2}}$	691.18	10	144680
$^2P_{1\frac{1}{2}} - ^2D_{2\frac{1}{2}}$	722.86	15	138340
$^2P_{1\frac{1}{2}} - ^2D_{1\frac{1}{2}}$	724.81	8	138105
$(s^25p)^2P_{\frac{1}{2}} - (s^27s)^2S_{\frac{1}{2}}$	698.69	10	143126
$^2P_{1\frac{1}{2}} - ^2S_{\frac{1}{2}}$	732.33	15	136550
$(s^25p)^2P_{\frac{1}{2}} - (s5p^2)^2P_{1\frac{1}{2}}$	999.62	15	100038
$^2P_{\frac{1}{2}} - ^2P_{\frac{1}{2}}$	1056.58	10	94645
$^2P_{1\frac{1}{2}} - ^2P_{1\frac{1}{2}}$	1069.93	20	93464
$^2P_{1\frac{1}{2}} - ^2P_{\frac{1}{2}}$	1135.43	10	88072
$(s^25p)^2P_{\frac{1}{2}} - (s^25d)^2D_{1\frac{1}{2}}$	1011.94	40	98820
$^2P_{1\frac{1}{2}} - ^2D_{2\frac{1}{2}}$	1065.90	40	93817
$^2P_{1\frac{1}{2}} - ^2D_{1\frac{1}{2}}$	1084.06	20	92246
$(s^25p)^2P_{\frac{1}{2}} - (s5p^2)^2S_{\frac{1}{2}}$	1070.43	20	93420
$^2P_{1\frac{1}{2}} - ^2S_{\frac{1}{2}}$	1151.49	30	86844
$(s5p^2)^4P_{2\frac{1}{2}} - (5p^3)^4S_{1\frac{1}{2}}$	1056.58	10	94645
$^4P_{1\frac{1}{2}} - ^4S_{1\frac{1}{2}}$	1098.34	10	91047
$^4P_{\frac{1}{2}} - ^4S_{1\frac{1}{2}}$	1166.96	12	85693
$(s^24f)^2F_{2\frac{1}{2}} - (s^26g)^2G$	1073.76	5	93131
$^2F_{3\frac{1}{2}} - ^2G$	1078.10	5	92755
$(s^25p)^2P_{\frac{1}{2}} - (s^26s)^2S_{\frac{1}{2}}$	1075.82	30	92952
$^2P_{1\frac{1}{2}} - ^2S_{\frac{1}{2}}$	1157.74	40	86375
$(s^24f)^2F_{2\frac{1}{2}} - (s^25g)^2G$	1205.20	50	82974
$^2F_{3\frac{1}{2}} - ^2G$	1210.64	50	82601
$(s^25p)^2P_{\frac{1}{2}} - (s5p^2)^2D_{1\frac{1}{2}}$	1306.69	20	76529
$^2P_{1\frac{1}{2}} - ^2D_{2\frac{1}{2}}$	1404.18	20	71216
$^2P_{1\frac{1}{2}} - ^2D_{1\frac{1}{2}}$	1429.57	10	69951
$(s5p^2)^2D_{1\frac{1}{2}} - (5p^3)^4S_{1\frac{1}{2}}$	1379.58	8	72486
$^2D_{2\frac{1}{2}} - ^4S_{1\frac{1}{2}}$	1404.18	20	71216
$(s5p^2)^2D_{1\frac{1}{2}} - (s^25f)^2F_{2\frac{1}{2}}$	1673.89	15	59741
$^2D_{2\frac{1}{2}} - ^2F_{2\frac{1}{2}}$	1710.23	3	58472
$^2D_{2\frac{1}{2}} - ^2F_{3\frac{1}{2}}$	1711.84	15	58417
$(s^25p)^2P_{\frac{1}{2}} - (s5p^2)^4P_{1\frac{1}{2}}$	1725.33	15	57960
$^2P_{1\frac{1}{2}} - ^4P_{2\frac{1}{2}}$	1762.30	12	56744
$^2P_{\frac{1}{2}} - ^4P_{\frac{1}{2}}$	1839.32	12	54368
$^2P_{1\frac{1}{2}} - ^4P_{1\frac{1}{2}}$	1946.13	10	51384
$^2P_{1\frac{1}{2}} - ^4P_{\frac{1}{2}}$	2091.85	2	47791
$(s^26p)^2P_{\frac{1}{2}} - (s^28s)^2S_{\frac{1}{2}}$	2054.10	3	48668
$^2P_{1\frac{1}{2}} - ^2S_{\frac{1}{2}}$	2127.00	5	47000
$(s5p^2)^2D_{1\frac{1}{2}} - (s^26p)^2P_{1\frac{1}{2}}$	2507.71	5	39865
$^2D_{2\frac{1}{2}} - ^2P_{1\frac{1}{2}}$	2590.13	15	38597
$^2D_{1\frac{1}{2}} - ^2P_{\frac{1}{2}}$	2617.17	12	38199
$(s^25f)^2F_{3\frac{1}{2}} - (s^26g)^2G$	2614.20	1	38241
$^2F_{2\frac{1}{2}} - ^2G$	2617.63	1	38191
$(s^25d)^2D_{1\frac{1}{2}} - (s^25f)^2F_{2\frac{1}{2}}$	2669.39	20	37450
$^2D_{2\frac{1}{2}} - ^2F_{2\frac{1}{2}}$	2785.87	5	35884
$^2D_{2\frac{1}{2}} - ^2F_{3\frac{1}{2}}$	2790.27	20	35828

TABLE IV (Continued)

Classification	λ (I.A.)	I	ν
$(s^26p)^2P_{\frac{3}{2}} - (s^26d)^2D_{1\frac{1}{2}}$	3336.61	20	29962
$^2P_{1\frac{1}{2}} - ^2D_{2\frac{1}{2}}$	3504.07	50	28530
$^2P_{1\frac{1}{2}} - ^2D_{1\frac{1}{2}}$	3533.45	15	28293
$(s^26p)^2P_{\frac{3}{2}} - (s^27s)^2S_{\frac{3}{2}}$	3519.06	15	28408
$^2P_{1\frac{1}{2}} - ^2S_{\frac{3}{2}}$	3738.90	30	26738
$(s^25f)^2F_{3\frac{3}{2}} - (s^25g)^2G$	3559.18	40	28088
$^2F_{2\frac{1}{2}} - ^2G$	3566.25	40	28033
$(s^26s)^2S_{\frac{3}{2}} - (s^26p)^2P_{1\frac{1}{2}}$	4265.09	40	23439
$^2S_{\frac{3}{2}} - ^2P_{\frac{1}{2}}$	4591.89	30	21771
$(s5p^2)^2S_{\frac{3}{2}} - (s^26p)^2P_{1\frac{1}{2}}$	4352.16	50	22970
$^2S_{\frac{3}{2}} - ^2P_{\frac{1}{2}}$	4692.91	30	21302
$(s^24f)^2F_{2\frac{3}{2}} - (s^25d)^2D_{2\frac{3}{2}}$	5247.71	1	19051
$^2F_{2\frac{3}{2}} - ^2D_{1\frac{1}{2}}$	5717.3	1	17486
$^2F_{3\frac{3}{2}} - ^2D_{1\frac{1}{2}}$	5845.5	3	17102
$(s^25d)^2D_{1\frac{1}{2}} - (s^26p)^2P_{1\frac{1}{2}}$	5690.8	1	17567
$^2D_{2\frac{1}{2}} - ^2P_{1\frac{1}{2}}$	6246.7	5	16004
$^2D_{1\frac{1}{2}} - ^2P_{\frac{1}{2}}$	6287.6	3	15900

In Table I the terms which have been located together with the empirical term values and separations are given. All of the term values rest upon an arbitrary choice of 64000 cm^{-1} for the value of $(s^25f)^2F_{\frac{3}{2}}$. Experience has shown that one can probably arrive at as good or even better values for the terms by a comparison such as is given in Table II than by the use of a Rydberg formula applied to two P or two S terms such as are available in this instance. The deepest F terms are not absolutely certain since the combination with the deepest normal D terms is not very satisfactory. The same may also be true of the second G terms and the third S terms, the last depending upon one combination only since no others fall within the range of measurements. Hence until some of these terms can be established more certainly it seemed as well to estimate the value of the basic term.

In Table III the intensities of observed combinations are shown and under each intensity the discrepancy between the observed wave-number and the wave-number calculated from the values assigned to the energy levels is given. In Table IV a list of all the lines which have been classified in the spectrum of Sb III is given. Throughout this report all wave-lengths above 2000\AA are given in I.A. (air) below this value in I.A. (vacuum) while all wave-numbers are reduced to vacuum values. Corresponding to the deepest term of this spectrum an ionization potential of 24.7 volts is found.

A NOTE ON SN II

The hollow cathode spectrum of tin was also photographed between 6000\AA and 2000\AA in an endeavor to find more terms from the $(s5p^2)$ con-

figuration. Out of the total of nine terms (4P , 2D , 2S , 2P) arising from this configuration none but 2D had been located.³

The $(s^25p)^2P - (s5p^2)^4P$ multiplet in In I had already been found⁴ and those for Sn II and Sb III were located by the use of the doublet laws. The multiplet in Sn II is taken from the spectrum of the hollow cathode. It occurs but very weakly in the vacuum spark spectrum. That for Sb III is taken from the vacuum spark spectrum and the only abnormality is the weak intensity of one of the lines in this multiplet.

TABLE V. *Multiplets and terms in the spectrum of Sn II.*

Configuration	$\lambda(\text{\AA})$	I	ν	$\Delta\nu$	Term values	
$(s^25p)^2P_{\frac{3}{2}} - (s^27s)^2S_{\frac{1}{2}}$ $^2P_{1\frac{1}{2}} - ^2S_{\frac{1}{2}}$	1158.21	2	86340		$(s^25p)^2P_{\frac{3}{2}}$	117704
	1218.19	4	82089	4251	$^2P_{1\frac{1}{2}}$	113451*
$(s^26p)^2P_{\frac{3}{2}} - (s^28s)^2S_{\frac{1}{2}}$ $^2P_{1\frac{1}{2}} - ^2S_{\frac{1}{2}}$	3930.37	2	25435		$(s^27s)^2S_{\frac{1}{2}}$	31363
	4071.79	2	24552	883		
$(s^25d)^2D_{1\frac{1}{2}} - (s^26f)^2F$ $^2D_{2\frac{1}{2}} - ^2F$	3537.56	1	28260		$(s^28s)^2S_{\frac{1}{2}}$	20778
	3620.54	1	27613	647		
$(s^25p)^2P_{1\frac{1}{2}} - (s5p^2)^2D_{1\frac{1}{2}}$ $^2P_{1\frac{1}{2}} - ^2D_{2\frac{1}{2}}$ $^2P_{\frac{3}{2}} - ^2D_{1\frac{1}{2}}$	1699.50	12	58841	4252	$(s^27d)^2D_{1\frac{1}{2}}$	17367
	1811.23	15	55211	622*	$^2D_{2\frac{1}{2}}$	17327
	1831.85	12	54589			
$(s5p^2)^2D_{1\frac{1}{2}} - (s^26f)^2F$ $^2D_{2\frac{1}{2}} - ^2F$	2448.93	1	40821		$(s^26f)^2F$	18043
	2486.95	2	40197	624		
$(s^25p)^2P_{\frac{3}{2}} - (s5p^2)^4P_{1\frac{1}{2}}$ $^2P_{1\frac{1}{2}} - ^4P_{2\frac{1}{2}}$ $^2P_{\frac{3}{2}} - ^4P_{\frac{3}{2}}$ $^2P_{1\frac{1}{2}} - ^4P_{1\frac{1}{2}}$ $^2P_{1\frac{1}{2}} - ^4P_{\frac{3}{2}}$	2151.57	12	46462		$(s5p^2)^4P_{\frac{3}{2}}$	73196
	2209.70	10	45241	1954	$^4P_{1\frac{1}{2}}$	71242
	2246.11	10	44508		$^4P_{2\frac{1}{2}}$	68210
	2368.26	15	42211	1957	$(s5p^2)^2D_{1\frac{1}{2}}$	58863
	2483.48	12	40254		$^2D_{2\frac{1}{2}}$	58240*
$(s^25p)^2P_{\frac{3}{2}} - (s5p^2)^2S_{\frac{1}{2}}$ $^2P_{1\frac{1}{2}} - ^2S_{\frac{1}{2}}$	1223.73	10	81717		$(s5p^2)^2S_{\frac{1}{2}}$	35986
	1290.89	20	77465	4252		
$(s^26p)^2P_{\frac{3}{2}} - (s^27d)^2D_{1\frac{1}{2}}$ $^2P_{1\frac{1}{2}} - ^2D_{2\frac{1}{2}}$ $^2P_{1\frac{1}{2}} - ^2D_{1\frac{1}{2}}$	3465.73	3	28846	884		
	3570.09	8	28002			
	3575.31	4	27962	40		

* Green and Loring.

The $(s^25p)^2P - (s5p^2)^2D$ multiplet seems well established in Sn II and Sb III. One peculiarity worth mentioning is that the position of this multiplet in the spectrum of Sn II is almost exactly the same as in Si II⁵. However, there seems little doubt that in Sn II this group has been correctly classified³ for when a tin spark in nitrogen, excited by a 2200 volt transformer joined to the 110 volt A.C. mains, was photographed between 2000A and 1250A but nine tin lines were found including the three lines of this multiplet, and every one of these lines except one (1290.90A) had been classified as arising from transitions involving the deepest 2P levels of the atom of Sn II.

³ Green and Loring, Phys. Rev. 30, 574 (1927).

⁴ Lansing, Phys. Rev. 34, 597 (1929); Sawyer and Lang, Phys. Rev. 34, 712 (1929).

⁵ Fowler, Trans. Roy. Soc. A225, 26 (1925).

In regard to the $(s^25p)^2P - (s5p^2)^2S$ doublet it may be stated that the line (1290.90A) together with another line at 1223.79A which occurs in the vacuum spark, but unable here to pass the fluorite window, have the separation of the deepest 2P terms. There seems little doubt that these two lines represent this doublet as has been suggested.³

The remaining $(s^25p)^2P - (s5p^2)^2P$ multiplet in Sn II has not been located with any certainty. There is one possibility worth mentioning, however. The $(s^25p)^2P - (s^27s)^2S$ doublet³ occurs with too great intensity in the vacuum spark and the 2S term is greater than one would expect. Another pair of weaker lines, one of which had not been resolved from a stronger tin line, probably represent this doublet and the stronger pair represents one-half of the missing multiplet. However, it must be said that there is not complete agreement yet between Sn II and Sb III in regard to these terms of the $(s5p^2)$ configuration and it does not seem possible to obtain this at the present time. When the arc spectrum of indium has been studied below 2000A it should be possible to obtain this agreement. An attempt to do this is now in progress. One or two other minor alterations have been made in the spectrum of Sn II all of which are shown in Table V.

The author takes this opportunity of thanking the Research Council of Canada for a grant to carry on this research.

THE EMISSION SPECTRUM OF BENZENE
IN THE REGION 2500-3000ABY J. B. AUSTIN* AND IAN ARMSTRONG BLACK†
DEPARTMENT OF CHEMISTRY, YALE UNIVERSITY

(Received January 25, 1930)

ABSTRACT

The ultra-violet emission band spectrum of benzene vapor has been observed with a Tesla discharge as a means of excitation. The wave-lengths of over 100 bands lying between 2400 and 3000A have been measured with an accuracy of $\pm 0.5A$. It is found that the measurements are in general in agreement with those of McVicker, Marsh and Stewart. All the bands except the faintest and most diffuse ones may be represented by the following equations:

$$1/\lambda = 37485 + 924m - 161n$$

$$1/\lambda = 37398 + 924m - 162n$$

$$1/\lambda = 37485 - 986m - 162n$$

$$1/\lambda = 37425 - 986m - 162n$$

$$1/\lambda = 36479 - 991m - 162n$$

$$1/\lambda = 36412 - 991m - 162n$$

where m and n are integers.

The evidence supporting the conclusion that the bands are due to benzene and not to some decomposition product is summarized. The applicability of the data to spectroscopic analysis is also discussed.

INTRODUCTION

THE general features of the spectra obtained from the vapor of benzene and its simple derivatives under the excitation of the Tesla discharge have been described by McVicker, Marsh and Stewart,¹ who have designated them as Tesla luminescence spectra to distinguish them from the absorption and fluorescence spectra. The present research was undertaken as an extension of their work; it was hoped, on the purely chemical side, to develop the suggestion made by them that a means of ascertaining the identity and quantity of any impurity present could be elaborated. In this regard it has been shown that such a method would be unwieldy in practice, except perhaps for routine work on a large number of samples; moreover, the number of likely impurities which yield satisfactory spectra under these conditions is rather small. On the other hand, it was felt that more comprehensive data on the Tesla luminescence spectra, particularly on the spectrum of benzene which is noteworthy for the sharpness of its bands and the absence of any continuous background, might be obtained, which with the increased accuracy would lead to some theoretical interpretation of the observed regularities. In this object some success has been achieved and the present work describes the results for benzene; the results for the simple derivatives will be published in the near future.

* From a dissertation presented by J. B. Austin to the Graduate School of Yale University, June 1928, in candidacy for the degree of Doctor of Philosophy.

† Commonwealth Fellow 1926-1928.

¹ McVicker, Marsh and Stewart, J. Chem. Soc. 123, 642 (1923).

EXPERIMENTAL METHOD

The methods employed differed from those of McVicker, Marsh, and Stewart in many ways, the most significant difference being the use of much lower pressures of the vapor. They used benzene vapor at pressures as high as 65 mm of Hg and were forced to use a steam jacket to prevent condensation; in the present work the pressures ranged from 0.01 to 0.10 mm which yielded satisfactory results at room temperature. In its final form our apparatus was fitted with internal electrodes whereas the previous practice used external ones. The general scheme for producing and maintaining these low pressures was to place the liquid benzene in a side limb of the discharge tube, to immerse it in liquid air to freeze the liquid to a solid cake, and then to seal the side limb and evacuate the system with a mercury diffusion pump until the residual air was so attenuated that a discharge could not be produced. The liquid air bath was then partially removed to allow the frozen benzene to warm slightly so that its vapor at low pressure could continuously diffuse through the discharge tube to a liquid air trap where it was condensed. In this manner equilibrium between speed of pumping and rate of sublimation was soon established and could be modified to give pressures between the limits of 0.01 and 0.10 mm. This method of maintaining a constant flow of vapor in the tube helped to remove any decomposition products as soon as they were formed and in conjunction with the low kinetic energy, and consequent small molecular disruptive power of the Tesla discharge gave some assurance that the spectrum originated in the benzene molecule. As a further precaution against contamination a new tube and liquid air trap were used for each exposure.

The first attempt to obtain the desired spectrum was made with the so-called "electrodeless" discharge, produced by placing the discharge tube in a helix of stout brass rod through which the current from a 1 KW Thordarson transformer was passed. A few trials sufficed to show that the spectrum obtained under these conditions was not that of the undecomposed molecule, but was due apparently to molecular fragments. Moreover, this discharge was very sensitive to slight fluctuations in pressure; with the pressure above a certain limiting value the free electrons and ions did not seem to attain a velocity sufficiently high to excite the rest of the vapor; with pressures too low the intensity of the glow suffered appreciably. At times this discharge showed a tendency to form a shell adjacent to the inside wall of the tube which electrically shielded the interior and caused a luminescent cylinder to form; the dark core of this cylinder rendered the discharge quite unsuitable for photographing.

It is interesting to note that the exciting coil and discharge tube grew quite warm during the passage of the current through the former; at the end of a run the latter invariably cracked, the cracks following the helix around the tube; whether the rupture of the glass was caused by thermal or electrical strain was not determined.

The next attempt was made with electrodes of lead foil wrapped around a Pyrex tube. This set-up yielded a satisfactory spectrum but endless trouble

was experienced with the breakdown of the glass along the surface between the electrodes. The presence of air streaks in the glass made trouble certain.

Finally it was decided to install internal electrodes, a procedure which had hitherto been regarded as hazardous because of the possibility of excessive decomposition of the vapor. Such electrodes, however, proved the

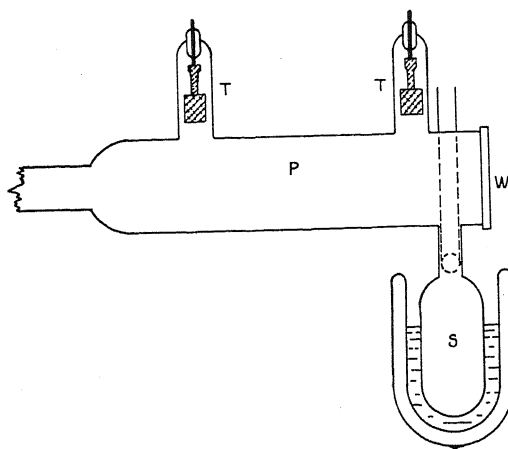


Fig. 1. Discharge tube.

most satisfactory of all the arrangements tried and in most cases caused no greater decomposition than the other types. This system was used to obtain all the results herein reported. Fig. 1 shows the discharge tube which consisted of a cylinder of Pyrex, *P*, with a quartz window, *W*, sealed on at one end with de Khotinsky cement; the other end was connected to a vacuum

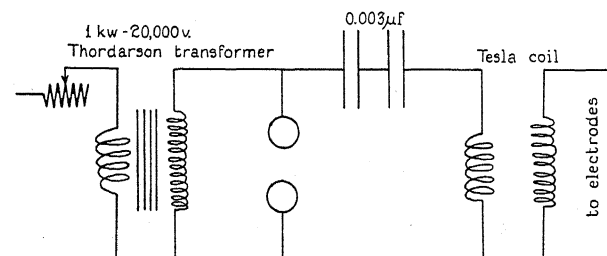


Fig. 2. Electrical connections.

system and a mercury diffusion pump. The electrodes, *T*, were cylinders of aluminum attached to tungsten seals; a side bulb, *S*, held the benzene.

The electrical system is shown in Fig. 2. When properly tuned this circuit gave a potential of about 120,000 volts as estimated from the spark produced between metal points.

SPECTROSCOPIC AND PHOTOGRAPHIC METHODS

In this work two spectrographs were employed:

(a) A Hilger size C quartz spectrograph, giving a photograph 200 mm in length for the range 2100A to 7000A. On this instrument exposures ranging from 3 to 12 hours were made; a plate exposed for 12 hours was used for the final measurements. For comparison, the spectrum of a mercury arc was superposed on the middle of the benzene spectrum with the aid of a reducing stop on the slit.

(b) A Hilger E_1 quartz spectrograph (Littrow mounting) giving a spectrum 140 mm in length for the region 2500A to 3000A. The spectrum of the mercury arc was superposed on these plates as on the others.

All photographs were taken on Eastman 33 plates of a special thin glass so that they could conform to the curvature of the plate holder without danger of breaking. In the earlier stages of the work Nujol and transformer oil were tried as sensitizers but were later discarded since they did not appreciably enhance the intensities of the ultra violet lines and were not deemed of sufficient value to warrant the extra trouble.

The spectra obtained with the smaller instrument extended almost 150A farther into the ultra-violet than those from the larger one; on the latter no bands were measured beyond 2600A while on the former they were recorded as far as 2471A. This difference is probably due to the greater absorption of the thicker quartz prism in the big spectrograph. On the other hand the large Hilger resolved some of the bands and permitted greater accuracy in measurement; hence, to obtain a complete spectrum of considerable accuracy the data obtained with the two instruments have been combined.

WAVE-LENGTH MEASUREMENTS

All plates were measured on a Société Genevoise ruling engine whose ruling mechanism had been replaced by a plate holder and a fixed telescope with cross hair attachment. The screw head was graduated in divisions of 0.005 mm with a vernier which allowed readings to be made to 0.001 mm. Tests on the accuracy of the screw showed that any deviations or flaws in it were negligible compared to other errors. The wave-lengths of the unknown lines were calculated by means of the parabolic interpolation formula:

$$\lambda_i = \lambda_0 + as_i + bs_i^2$$

where λ_0 , a and b are constants determined from the mercury lines² and s_i is the reading of the measuring engine corresponding to the i^{th} line. This formula proved to be as accurate as the observations for ranges of 200A in the lower visible and ultra-violet and involved much less labor than the Hartmann formula. The whole spectrum was covered in overlapping sections of 200A.

Each plate was measured in the center of the spectrum to avoid any error due to curvature of the lines. The further precaution was taken of having

² Kayser, *Tabelle der Hauptlinien der Linienspektra* J. Springer, Berlin 1926.

TABLE I.

λ in A A & B	$1/\lambda$ in cm^{-1} A & B	$1/\lambda$ in mm^{-1} McV., M. & S.	λ in A A & B	$1/\lambda$ in cm^{-1} A & B	$1/\lambda$ in mm^{-1} McV., M. & S.
2471.1*	40456		2777.2	35996	
2483.0*	40262		2789.4	35839	3586
2528.5*	39537		2800.2	35701	3570
2541.5*	39335		2810.6	35569	
2547.3*	39245		2812.3	35535	3554
2551.6*	39179		2815.2	35511	
2562.5*	39013		2817.2	35485	
2571.9*	38870		2820.0	35450	
2585.1*	38672		2822.6	35417	3542
2589.0*	38613		2824.7	35391	3537
2595.0*	38524		2828.1	35349	
2599.9*	38452		2830.2	35322	
2602.6	38411		2832.9	35289	3528
2608.7	38321		2834.5	35269	
2613.6	38250		2835.7	35254	
2619.8	38159		2837.9	35227	3521
2624.8	38086		2841.0	35188	
2629.8*	38014		2848.6	35094	3512
2631.1*	37996		2852.9	35041	3504
2641.7*	37843		2854.4	35023	
2647.8*	37776		2857.5	34985	3498
2649.0*	37739		2866.5	34875	
2657.5	37618	3765	2895.5	34526	3454
2663.6	37532	3752	2898.1	34496	
2667.4	37478		2900.6	34465	3445
2667.9	37472		2903.7	34428	
2668.4	37465		2909.1	34364	3438
2669.1	37455		2911.9	34331	
2673.5	37393	3741	2914.5	34301	
2678.6	37321		2917.6	34264	3428
2684.6	37233		2920.5	34230	3422
2685.6	37224	3725	2922.8	34203	
2689.2*	37175	3717	2925.5	34172	
2690.2	37061		2930.4	34115	3411
2696.2	37078	3708	2932.9	34086	
2701.7	37002	3703	2937.0	34038	3405
2702.2	36995		2951.0	33876	3390
2705.1*	36956		2961.0	33763	3376
2707.7*	36921	3693	2980.6	33540	3357
2714.0*	36835	3686	2983.5	33507	
2718.6*	36773		2985.9	33481	
2727.8	36648	3666	2989.5	33440	
2729.6	36624		2995.1	33378	3339
2734.6	36557		2998.5	33340	
2736.5	36532		3003.4*	33286	
2739.1	36497	3652	3009.5	33218	3322
2740.5	36478		3012.8*	33182	
2743.7	36436		3018.6*	33118	3308
2745.4	36413	3642	3052.7*	32748	
2747.3	36388	3636	3060.6*	32664	
2751.2	36337		3068.3*	32582	3257
2752.7	36317		3074.2	32519	
2755.9	36275		3075.5*	32506	
2757.7	36251	3625	3080.1	32457	3242
2759.6	36239		3085.6	32399	
2763.4	36176		3090.4*	32349	
2764.9	36157	3611	3095.1*	32300	
2771.7	36068		3102.0*	32228	3229
2775.4	36020	3602	3158.1	31654	

each of us independently measure each plate twice, once when it was run along the measuring engine forward and once backward; in this way each line was approached from both sides. The agreement obtained in these sets of observations was most satisfactory, the difference rarely exceeding $\pm 0.5\text{\AA}$ and in most cases being less than $\pm 0.25\text{\AA}$. The four measurements of each line have been averaged and converted to wave numbers in vacuo.

PREPARATION OF BENZENE

Merck's product was shaken six times with concentrated sulfuric acid; at the end of this treatment no color was imparted to fresh acid. The benzene was then washed successively with concentrated sodium hydroxide, dilute sodium hydroxide, and distilled water, until the final wash water was neutral to litmus. The resulting product was dried over sodium for 25 hours and redistilled from the same. A large fraction came over at a constant temperature and this was taken for use. B. P. 80.0°C at 760 mm Hg pressure.

RESULTS

The general scheme of the bands is shown in the photograph, Fig. 3. The following table gives the average results obtained from the two spectrographs. Lines observed only on the smaller spectrograph are marked with an asterisk. The results of McVicker, Marsh, and Stewart are given for comparison.

While a rough notion of the relative intensities of the bands may be gathered from Fig. 3, a more exact measure for the most prominent band groups is given in the microphotograph, Fig. 4. This was made on a Koch-Goos microphotometer from a plate taken on the large spectrograph. The ratio of length on this curve to length on the plate is 2:1.

It was found that all the principal bands could be accounted for with an accuracy of $\pm 3\text{ cm}^{-1}$ by the following equations:

$$1/\lambda = 37485 + 924m - 161n$$

$$1/\lambda = 37425 - 986m - 162n$$

$$1/\lambda = 37398 + 924m - 161n$$

$$1/\lambda = 36479 - 991m - 162n$$

$$1/\lambda = 37485 - 986m - 162n$$

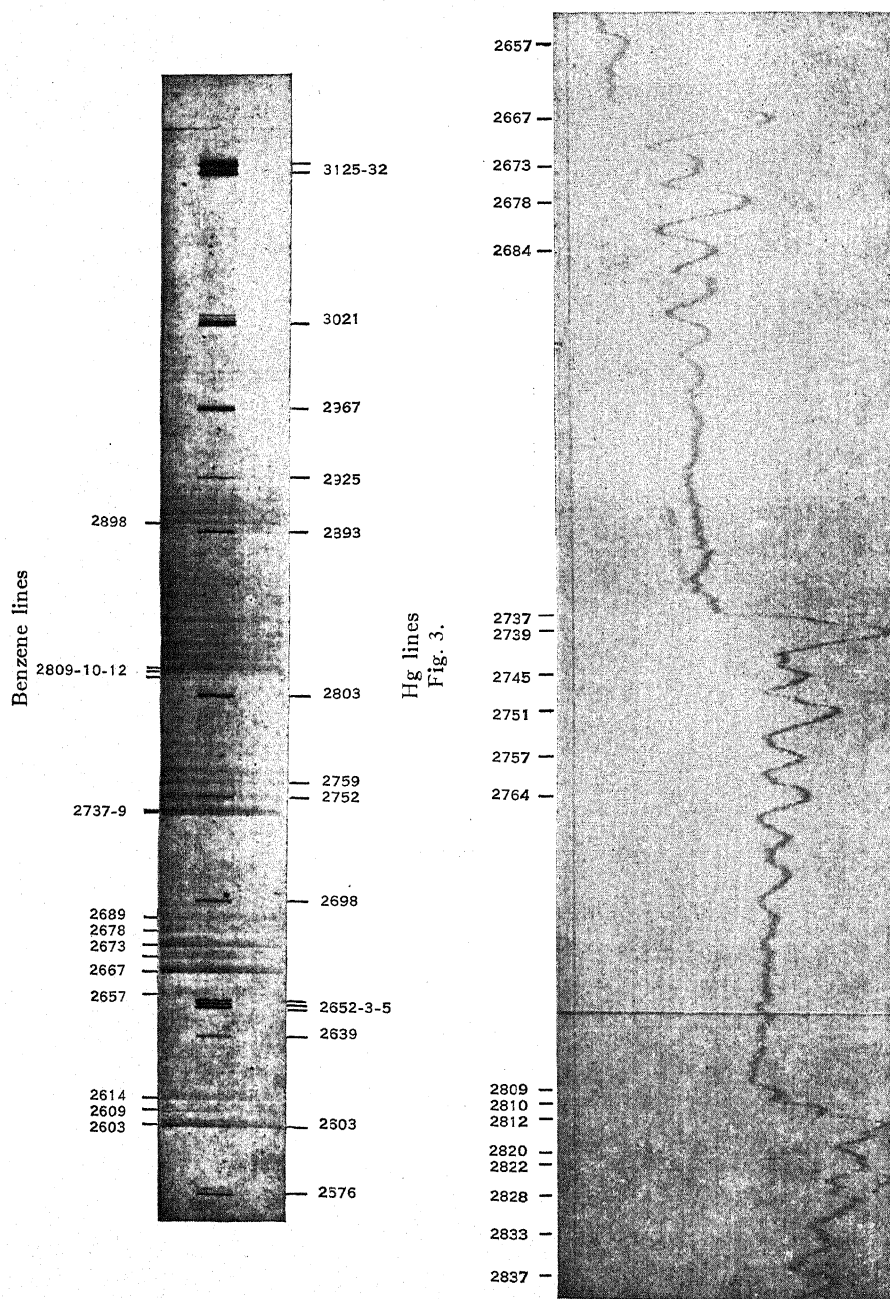
$$1/\lambda = 36412 - 991m - 162n$$

where m and n are assigned integral values. In one band (2667.4) some of the fine structure was observed, the wave-length difference being about $\pm 0.5\text{\AA}$. This agrees with the value reported by Henri³ in the absorption spectrum. It is interesting to note in this connection that the wave-number differences 991 and 162 cm^{-1} appearing in these equations are found also in the Raman spectrum of benzene. It is hoped that before long some definite significance can be attached to these values.

It may be well to review the evidence supporting the assumption that this spectrum originates in the benzene molecule for in spite of all precautions some decomposition did occur. At the end of the 12 hour runs the surfaces of

³ Henri, *Structure des Molecules*, Paris, 1925, p. 109.

the aluminum electrodes were found to be covered with a layer of carbon and the discharge tube showed a very thin film of a shellac-like substance adher-



ing to the walls. However, despite the appearance of these products there is little doubt that the spectrum observed is actually that of benzene. Apart

from the fact that the decomposition products seem non volatile, the following considerations point to the same conclusion.

First, it was observed that conditions which produced the greatest visible decomposition gave spectra of low intensity. Thus, for example, as the pressure is lowered decomposition is decreased while the intensity of the glow is increased. This is just what is to be expected since, for a given energy input, the larger the amount of energy used in molecular rearrangements, the smaller will be the fraction of the total energy as light.

Second, the regularity exhibited by the spectrum seems to militate against any decomposition hypothesis, for this regularity implies a uniformity in the system which produces it; if this system is a benzenoid molecule, its symmetry is easily understood, but if it is produced by some dissociation or rearrangement under the stress of the discharge then it is necessary to postulate an absolute uniformity of decomposition which would be hard to concede from a theoretical view point and would certainly not account for the fact that several decomposition products are actually found.

Aside from these considerations, which involve only the emission spectra, the results can be checked with the spectra in solution. For instance, Dickson⁴ has observed the fluorescence spectrum of benzene in alcohol solution. It is well known that a solvent shifts the spectrum of a substance in solution but this shift is generally a translation of the system as a whole so that the relative positions of the bands remain unchanged. It is found that if 19 units of wave-number are added to the values given by Dickson the broad bands of his spectrum coincide with the principal emission bands which we have observed.

Even more convincing is the agreement between the absorption and emission spectra of the vapor, which prove to have identical band arrangements. The emission spectrum should include the bands found in absorption but the far ultra-violet part of the former is lacking due to the absorption by unexcited benzene molecules in the discharge tube. However, it is found that the most refrangible emission band group coincides with the bands of the red end of the absorption spectrum as determined by Henri.⁵ This arrangement is shown in the following table.

TABLE II.

Absorption Bands of benzene vapor after Henri λ	Emission Bands of benzene vapor (A & B) λ	Absorption Bands of benzene vapor after Henri λ	Emission Bands of benzene vapor (A & B) λ
2528.6	2528.6	2599.9	2599.7
2541.7	2541.5	2603.0	2602.6
2552.5	2551.7	2610.2	2610.1
2589.0	2588.7	2613.9	2613.5
2595.2	2595.2		

⁴ Dickson, Zeit. Wiss. Photo. 10, 166 (1912).

⁵ Henri, J. de Phys. et Rad. 3, 181 (1922).

This check is sufficient to establish the fact that the carrying structure is the same, and, since no decomposition is to be expected, nor indeed is any found, in the absorption work, it follows that both spectra are due to undecomposed benzene.

The foregoing considerations, in addition to demonstrating that the benzene molecule is the carrier of the spectrum, also indicate a very satisfactory agreement between our work and the known absorption and fluorescence spectra. It may be of interest to conclude with a comparison of our results with those of McVicker, Marsh and Stewart. Taking the results from both spectrographs we have recorded the wave-length of about 110 bands and in addition to more than doubling the known number of emission bands have given evidence of two new band systems in the far ultra-violet. We do not claim to have measured all the bands in the spectrum, however, for in many cases bands could be seen on the plates with the naked eye which were not susceptible of measurement under the microscope. We have also shown that many of the lines reported by McVicker, Marsh, and Stewart are really doublets. A number of our measurements when expressed in wave numbers seem to be about 30 units smaller than those of the corresponding lines in the work of McVicker, Marsh, and Stewart. This is interesting on account of the fact that in the comparison made between their results and Hartley's values for the absorption of benzene approximately 20 units were added to the latter in order to make the regularities coincide.

In conclusion the authors wish to express their thanks to Dr. John Johnston at whose suggestion the work was undertaken, to Dr. A. E. Ruark who gave valuable assistance with the experimental work, to Professor Uhler for much help in the spectroscopic and photographic work and for suggesting the methods of measurement and calculation, to Professor McKeehan who kindly placed the resources of the Sloane Physics Laboratory at our disposal. The authors wish also to thank the Commonwealth Fund for the fellowship which one of them held and without which he would have been unable to undertake this research.

NOTE ON THE THEORY OF THE INTERACTION
OF FIELD AND MATTERBY J. R. OPPENHEIMER
BERKELEY, CALIFORNIA

(Received November 12, 1929)

ABSTRACT

The paper develops a method for the systematic integration of the relativistic wave equations for the coupling of electrons and protons with each other and with the electromagnetic field. It is shown that, when the velocity of light is made infinite, these equations reduce to the Schroedinger equation in configuration space for the many body problem. It is further shown that it is impossible on the present theory to eliminate the interaction of a charge with its own field, and that the theory leads to false predictions when it is applied to compute the energy levels and the frequency of the absorption and emission lines of an atom.

THE relativistic theory of the interaction of electrons and protons with each other and with the electromagnetic field has been developed in two papers.¹ The theory is developed in close analogy to the corresponding classical theory: the field is on the one hand determined by the configuration of the charges; and the motion of the charges is affected by the field. The interaction between two charges is not then, on this theory, expressed directly as a function of the configuration of the charges, but as the effect on each of the charges of the field induced by the other. On the classical theory this procedure involves grave difficulties, because each charge reacts also with its own field. The proper energy of this interaction is, for point charges infinite; and it depends upon the motion of the charge. On the classical theory one tried to avoid this difficulty by ascribing to the elementary charges a finite size; but it was not possible to carry through the theory in a way that was not completely arbitrary; nor was it possible to make the work relativistically invariant. One of the purposes of the present paper is to see in how far these difficulties persist in the quantum theory, and in what measure they render impossible the application of the theory.

We may recapitulate briefly the main points of divergence between the present quantum theoretic treatment and the classical theory. In the first place the state of the matter is here represented, not by a trajectory, but by a wave function. Further, the Hamiltonian for the matter is that derived from Dirac's linear wave equation, and not from the quadratic wave equation which would follow from the classical relativistic Hamiltonian. Finally, both the material waves and the electromagnetic waves are quantized, the matter

¹ W. Heisenberg and W. Pauli, *Zeits. f. Physik* 56, 1 (1929); *ibid.* in press. The second of these two papers is referred to in this work as LC. I am greatly indebted to Professor Heisenberg and Professor Pauli, not only for the opportunity of seeing their work before its publication, but also for their very valuable criticism and advice.

to make the particles satisfy the exclusion principle, the field to make the quanta satisfy the Einstein-Bose statistics. This procedure leads to a formal difficulty; for the fourth Maxwell equation

$$\operatorname{div} \mathbf{E} - 4\pi\rho = 0 \quad (1)$$

is inconsistent with the quantum conditions, according to which there are functions of the electromagnetic potentials which do not commute with $\operatorname{div} \mathbf{E}$ but which must commute with the charge density. The two papers of Heisenberg and Pauli are distinguished chiefly by different methods of resolving this difficulty. In the former paper new terms were added to the fourth Maxwell equation to make the new equation consistent with the quantum conditions; in obtaining physical results these terms were to be made to vanish. In the second paper a much more satisfactory method has been used, which takes advantage of the fact that the left hand side of (1) is a constant of the motion for all systems involving matter and radiation; and it is shown that this constancy follows from the gauge invariance of the Hamiltonian for all such systems. The solution of the dynamical problem thus reduces to finding a wave function for the coupled system of field and matter, which makes the Hamiltonian for the coupled system a diagonal matrix, and which in addition makes the left hand side of (1) vanish. The wave function has thus to satisfy not only the Hamiltonian wave equation, but also a series of wave equations which express the fact that (1) is satisfied at all points in space. It is from this set of wave equations that we shall start in this paper; we shall write them first in the form given in LC Eq. (68), in which the wave function is taken as a function of the Cartesian coordinates

$$q_P = (q_P^{(1)}, q_P^{(2)}, q_P^{(3)}); P = 1, 2, \dots, N$$

and spin variables

$$\sigma_P; P = 1, 2, \dots, N$$

of the N particles in the system, the number of quanta

$$M_{r\lambda}$$

of frequency

$$\nu_r$$

vector of propagation $\mathbf{K}_r = (K_r^1, K_r^2, K_r^3)$; $K_r = \nu_r/c$ and polarization λ , and finally a third set of variables P_{r3} , which are essentially the constant components of the electric field parallel to the vectors of propagation \mathbf{K}_r . We shall first show that it is possible to eliminate the P_{r3} 's from the wave equations in such a way that (1) is automatically satisfied. The reason why this is possible is that the condition (1) determines $\operatorname{div} \mathbf{E}$ precisely—instead of determining only the relative probabilities of different values of $\operatorname{div} \mathbf{E}$,—when the configuration of the charges is known, so that the values of the P 's so determined can be put at once into the Hamiltonian. When this is done the variables Q_{r3} canonically conjugate to the P 's must disappear from the Hamiltonian, since otherwise the Hamiltonian would not be consistent with (1);

we shall show that this is in fact the case, and then proceed to an investigation of the resulting Hamiltonian.

It should be observed that the wave functions must satisfy, in addition to the wave equations in configuration space, the condition that they be antisymmetric in all the electrons of the system, and antisymmetric in all the protons of the system. Only wave functions satisfying these conditions are to be considered in this paper; and it will therefore be unnecessary to indicate the antisymmetry of the wave functions explicitly. The fact that electrons and protons satisfy the exclusion principle is largely irrelevant to the difficulties discussed in this work; for these difficulties persist even in the one-electron problem. On the other hand it is to be hoped that the resolution of the errors in the present theory will make the heuristic postulate of the exclusion principle unnecessary.

We shall look for a solution of the wave equation in which both wave function and characteristic values are expanded in powers of v/c . It has already been shown by Breit² that, when the interaction of the particles may be treated as small, and radiation processes may be neglected, that these interaction terms give a contribution to the energy of the system, which, in second order in v/c , agrees with that computed from Breit's equation.³ We shall not retain the assumption that the interaction terms are small, and shall show, somewhat more generally, that when the proper energy terms are systematically neglected, the characteristic energy levels and the wave function are determined by Breit's equation. This equation is, of course, not relativistically invariant; and it takes no account of radiation processes. In order to remedy these defects one must retain the proper energy terms; and we shall show that it is then possible to make a *formally* satisfactory theory to give the shape and position of all spectral lines, and the energy of the normal state. The theory, is, however, wrong, since it gives a displacement of the spectral lines from the frequency predicted on the basis of the nonrelativistic theory which is in general infinite. This displacement arises from the infinite interaction of the electron with itself; this interaction depends upon the state of the material system; and the difference in the energy for two different states is not in general finite. Thus the present theory gives no more than the nonrelativistic theory of Jordan, Klein and Wigner.⁴ It seems improbable that Breit's equation gives the energy levels of an atom correct to second order terms in v/c ; but we shall see that there is ground for supposing that it does give the separation of the fine structure levels correctly in this order. On the other hand the displacement in the frequency of the spectral lines which arises from the proper energy should be of the second order in v/c , and is thus larger than the natural line breadth, which is of the third order; and on the present theory it is not possible to compute this displacement. We shall return later to a consideration of these difficulties.

² G. Breit, Phys. Rev. 34, 553 (1929).

³ Breit, *ibid.*, Eq. (6).

⁴ P. Jordan and O. Klein, Zeits. f. Physik 45, 751 (1927). P. Jordan and E. Wigner, *ibid.* 47, 631 (1928).

1. The condition that the left hand side of (1), regarded as an operator on the wave function ψ of the variables

$$q_P, \sigma_P, M_{r\lambda}, P_{r3}$$

shall make the wave function vanish at every point in space, gives a series of wave equations

$$I \quad C_r \Psi = \left[P_{r3} + \sum_P e_P v^{r0}(q_P) \right] \psi(q_P, \sigma_P, M_{r\lambda}, P_{r3}) = 0$$

which must hold for all values of the K_r consistent with the boundary conditions. Here the v^{r0} are functions defined in LC (54):

$$v^{r0}(q_P) = \frac{2}{\pi} (ck_r^3 L^3)^{-1/2} \sin \pi k_r^{(1)} q_P^{(1)} \sin \pi k_r^{(2)} q_P^{(2)} \sin \pi k_r^{(3)} q_P^{(3)} \quad (2)$$

Here L is the length of the fundamental cube, or Hohlraum, and is taken finite in LC to avoid the introduction of a continuous manifold of normal coordinates; in all our results we shall make L become infinite. Furthermore the Hamiltonian for the coupled system, regarded as an operator on the same wave function, gives the wave equation

$$\begin{aligned} II \quad & \left\{ -E + \sum_r \left[\sum_{\lambda=1,2} M_{r\lambda} \hbar \nu_r + \pi \nu_r P_{r3}^2 \right] + \sum_{P=1}^N \left[\frac{\hbar c}{2\pi i} (\alpha^P \text{grad}_P) + m_P \alpha_0^P c^2 \right] \right\} \psi \\ & + \left\{ \sum_{P=1}^N [e_P A_0^0(q_P) + e_P (\alpha^P \cdot A^0(q_P))] \right\} \psi \\ & + \left\{ i \sum_r \sum_{\lambda=1,2} \sum_{P=1}^N \mu_P^{r\lambda} [(M_{r\lambda} + 1)^{1/2} \Delta_{r\lambda}^{-1} - M_{r\lambda}^{1/2} \Delta_{r\lambda}] \right\} \psi \\ & + \left\{ \sum_r \sum_{P=1}^N \mu_P^{r3} Q_{r3} \right\} \psi = (+H - E) \psi = 0. \end{aligned}$$

Here A_0^0 is the external scalar potential, and A^0 the external vector potential; and $\Delta_{r\lambda}$ is an operator which transforms $M_{r\lambda}$ into $M_{r\lambda} - 1$, and leaves all other variables unchanged; the α^p 's are operators which operate only on σ_p , and are derived from the Dirac matrices $\alpha_{p\sigma}^i$ by the definition

$$\alpha_i^P F(\sigma_P) = \sum_{\rho_P} \alpha_{\sigma_P}^i \rho_P F(\rho_P); \quad \alpha_0^P F(\sigma_P) = \sum_{\rho_P} \alpha_{\sigma_P}^0 \rho_P F(\rho_P).$$

Further the Q_{r3} are canonically conjugate to the P_{r3} so that

$$[P_{r3} Q_{r'3}] = \frac{\hbar}{2\pi i} \delta_{rr'} \quad (3)$$

Finally the functions $\mu_P^{r\lambda}, \mu_P^{r3}$ are defined in LC (59):

$$\mu_P^{r3} = e_P c \left(\frac{\nu_r}{2} \right)^{1/2} \sum_{i=1}^3 \alpha_i^P v_i^{r3}(q_P)$$

$$\mu_P^{r\lambda} = e_P c \left(\frac{\hbar}{2\pi\nu_r} \right)^{1/2} \sum_{l=1}^3 \alpha_l^P v_l^{r\lambda}(q_P); \lambda=1,2 \quad (4)$$

$$v_l^{r\lambda}(q_P) = \left(\frac{8}{L^3} \right)^{1/2} F_{l\lambda}^r \cos \pi k_l q_P^{(l)} \sin \pi k_{l'} q_P^{(l')} \sin \pi k_{l''} q_P^{(l'')};$$

$$l=1,2,3.$$

$$\lambda=1,2,3.$$

The square matrix $F_{l\lambda}^r$ is given by the scheme

$$\begin{array}{c|ccc} & \lambda = & 1 & 2 & 3 \\ \hline l & & & & \\ 1 & & \epsilon_2^r / (\epsilon_1^2 + \epsilon_2^2)^{1/2} & \epsilon_1 \epsilon_3 / (\epsilon_1^2 + \epsilon_2^2)^{1/2} & \epsilon_1 \\ 2 & & -\epsilon_1 / (\epsilon_1^2 + \epsilon_2^2)^{1/2} & \epsilon_2 \epsilon_3 / (\epsilon_1^2 + \epsilon_2^2)^{1/2} & \epsilon_2 \\ 3 & & 0 & -(\epsilon_1^2 + \epsilon_2^2)^{1/2} & \epsilon_3 \end{array} \quad (5)$$

where the ϵ_l^r 's are the direction cosines of the vector \mathbf{K}_r . It should be observed that

$$\frac{\hbar c}{2\pi i} (\mathbf{a}^P \cdot \text{grad}_P) e_P v^{r0}(q_P) = \frac{\hbar}{2\pi i} \mu_P^{r3}. \quad (6)$$

This equation, together with (3), shows that

$$[HC_r] = 0 \quad (7)$$

for all r , so that all the C_r 's are constants of the motion. The equations I and II are those given⁵ in LC (68).

From I we see that the wave function must be singular in the P 's. We may avoid the use of singular functions by making a contact transformation from the variables P to Q , and writing the wave function as:

$$\psi(q_P, \sigma_P, M_{r\lambda}, Q_{r3}).$$

For we may then solve (3) by taking

$$P_{r3} = \frac{\hbar}{2\pi i} \frac{\partial}{\partial Q_{r3}}.$$

If now we set

$$\psi(q_P, \sigma_P, M_{r\lambda}, Q_{r3}) = e^{-2\pi i / \hbar \sum_r \frac{1}{p} \sum_p e_p v^{r0}(q_p) Q_{r3}} \phi(q_P, \sigma_P, M_{r\lambda}, Q_{r3}) \quad (8)$$

the equations I give us

$$\frac{\partial \phi}{\partial Q_{r3}} = 0 \quad (9)$$

for all r so that

$$\phi = \phi(q_P, \sigma_P, M_{r\lambda}).$$

⁵ In LC (68) the A 's are dropped,

Further the Hamiltonian II becomes

$$\begin{aligned}
 & e^{-2\pi i/\hbar} \sum_r \sum_P e_P v^{r0}(q_P) Q_{r3} \left\{ -E + \sum_r \left[\sum_{\lambda=1,2} M_{r\lambda} \hbar v_r + \pi \nu_r \sum_{P,P'}^N e_P e_{P'} v_0^{r0}(q_P) v^{r0}(q_{P'}) \right] \right. \\
 & + i \hbar \sum_r \sum_P \nu_r e_P v^{r0}(q_P) \frac{\partial}{\partial Q_{r3}} - \frac{\hbar^2}{4\pi} \sum_r \nu_r \frac{\partial^2}{\partial Q_{r3}^2} + \sum_P \left[\frac{\hbar c}{2\pi i} (\alpha^P \text{grad}_P) + m_P c^2 \alpha_0^P \right] \\
 & - c \sum_r \sum_P e_P (\alpha^P \text{grad}_P) v^{r0}(q_P) Q_{r3} + \sum_P e_P [A_0^0(q_P) + (\alpha^P \cdot A^0(q_P))] \\
 & + \sum_r \sum_P \mu_P r^3 Q_{r3} + i \sum_r \sum_{\lambda=1,2} \sum_P \mu_P r^\lambda [(M_{r\lambda} + 1)^{1/2} \Delta_{r\lambda}^{-1} \\
 & \left. - M_{r\lambda}^{1/2} \Delta_{r\lambda}] \right\} \phi(q_P \sigma_P M_{r\lambda}) = 0.
 \end{aligned} \quad (10)$$

The terms in Q drop out because of (6); the terms in $\partial/\partial Q$ give nothing because of (9). The equations I and II thus reduce to the single system

$$\begin{aligned}
 & \left\{ -E + H_0 + \sum_{r\lambda} M_{r\lambda} \hbar v_r + i \sum_{r\lambda P} \mu_P r^\lambda [(M_{r\lambda} + 1)^{1/2} \Delta_{r\lambda}^{-1} - M_{r\lambda}^{1/2} \Delta_{r\lambda}] \right\} \phi = 0 \\
 & H_0 = \sum_P \left\{ \frac{\hbar c}{2\pi i} (\alpha^P \text{grad}_P) + m_P c^2 \alpha_0^P + \rho_P [A_0^0(q_P) + (\alpha^P \cdot A^0(q_P))] \right. \\
 & \left. + \pi \sum_{P'} \sum_r e_P e_{P'} \nu_r v^{r0}(q_P) v^{r0}(q_{P'}) \right\}.
 \end{aligned} \quad (11)$$

It is this system which we must now investigate.

The terms

$$G(q_P, q_{P'}) = \sum_r \pi \nu_r v^{r0}(q_P) v^{r0}(q_{P'})$$

may readily be evaluated,⁶ and give for $L \rightarrow \infty$

$$G(q_P, q_{P'}) \rightarrow -\frac{1}{2r_{PP'}}; \quad r_{PP'} = |\mathbf{q}_P - \mathbf{q}_{P'}|. \quad (12)$$

The terms for p and p' different give the electrostatic interaction of the two particles; the terms for $p=p'$ give the infinite electrostatic proper energy of the particles; on the present theory it is not possible, as it was on the non-relativistic theory,⁴ to eliminate these terms; the physical ground for this impossibility has already been indicated, and lies in the fact that the field acting on any particle is the sum of the fields induced by all particles; it is a consequence of the principle of superposition for the field. These electrostatic proper energy terms do not, however, interfere with the application of the theory, since they are constants, and may be dropped from (11) without altering the form of the wave function. We shall find other infinite proper

⁶ W. Heisenberg and W. Pauli, *Zeits. f. Physik* 56, 1 (1929). Eq. (115); G. Breit, reference 2 Eq. (57). Breit has independently evaluated the P_{rs} terms in the Hamiltonian; and I am much indebted to him for informing me of his result.

energy terms in the course of the work; but these will turn out not to be constants, but to depend upon the configuration of the system; dropping them does alter the form of the wave function.

If we now neglect the coupling between matter and the light quantum field the wave equation reduces to

$$\left[-E + H_0 + \sum_{r\lambda} M_{r\lambda} h\nu_r \right] \phi = 0 \quad (13)$$

and for the case that no quanta are present we have

$$\left\{ -E + \sum_P \left[\frac{hc}{2\pi i} (\alpha^P \cdot \text{grad}_P) + m_P c^2 \alpha_0^P + e_P [A_0^0(q_P) + (\alpha^P \cdot A(q_P))] \right] - \sum_{PP'} \frac{e_P e_{P'}}{2r_{PP'}} \right\} \phi(\sigma_P, q_P) = 0. \quad (14)$$

We shall show that the terms which we have neglected in (12) are small of the order $(v/c)^2$; and by neglecting other terms of the same order, (13) can be considerably simplified. For consider first the equation

$$\left\{ -E + \sum_P \left[\frac{hc}{2\pi i} (\alpha^P \cdot \text{grad}_P) + m_P c^2 \alpha_0^P \right] \right\} \phi = 0. \quad (15)$$

For N -free uncoupled particles. If we choose all matrices $\|\alpha_{\sigma_P}^i\|$ of the form

$$\begin{pmatrix} 0 & 0 & b & a \\ 0 & 0 & c & d \\ \bar{b} & \bar{c} & 0 & 0 \\ \bar{a} & \bar{d} & 0 & 0 \end{pmatrix} \quad (16)$$

and all the $\|\alpha_{\sigma_P}^0\|$ of the form:

$$\begin{pmatrix} +1 & 0 & 0 & 0 \\ 0 & +1 & 0 & 0 \\ 0 & 0 & -1 & 0 \\ 0 & 0 & 0 & -1 \end{pmatrix} \quad (16)$$

and satisfying of course

$$[\alpha^{\mu,P} \alpha^{\nu,P'}] = 0 \text{ for } P \neq P'; [\alpha^{\mu,P} \alpha^{\nu,P}] = 2\delta_{\mu\nu} \quad (17)$$

then any $\phi(\sigma_P)$ in which n of the σ_P 's have either of the values 3 or 4 will be small compared with any of the ϕ 's for which all of the σ_P 's have the values 1 or 2 of the order $(v/c)^n$. Now the terms

$$- \sum_{PP'} \frac{e_P e_{P'}}{2r_{PP'}} \quad e_P A_0^0(q_P)$$

in (14) do not involve the α^P 's, while the terms

$$e_P (\alpha^P \cdot A(q_P))$$

are small of the order v/c ; thus as v/c is made to vanish, all the solutions of (14) vanish except those for which all the σ_p 's have the values 1 or 2; and (14) reduces to

$$\left[-E + \sum_P \left\{ m_P c^2 + e_P A_0^0(q_P) - \frac{\hbar^2}{8\pi^2 m_P} \Delta_P - \sum_{P'}' \frac{e_P e_{P'}}{2r_{PP'}} \right\} \right] \phi(\sigma_P q_P) = 0 \quad (18)$$

for all σ_p 's = 1 or 2 and

$$\phi(\sigma_P q_P) = 0 \text{ for any } \sigma_P = 3 \text{ or } 4$$

which is the Schroedinger equation for the N -body problem.⁷ It would thus be possible to take (18) as the starting point for our systematic solution of (11) in powers of v/c . We shall not do this, however, as it would complicate the analysis, and lead to no new results. We shall thus give up the assumption that the α 's are written in the form (16), and take for our zero'th approximation to (11), the solutions of (14).*

2. We may write the equations (11) *seriatim*:

$$\sum_{r\lambda} M_{r\lambda} = M = 0; (-E + H_0)\phi = -i \sum_{r\lambda P} \mu_P^{r\lambda} \phi(1_{r\lambda}); \quad \phi = \phi(0_{r\lambda}) \quad (11.1)$$

$$M=1 \quad \left\{ \begin{aligned} (-E + \hbar\nu_r + H_0)\phi(1_{r\lambda}) &= +i \sum_P \mu_P^{r\lambda} \phi - \left[i \sum_{r'\lambda'} \sum_P \mu_P^{r'\lambda'} \phi(1_{r\lambda}, 1_{r'\lambda'}) \right] \\ &- 2^{1/2} i \sum_P \mu_P^{r\lambda} \phi(2_{r\lambda}) \end{aligned} \right. \quad (11.2)$$

$$M=2 \quad \left\{ \begin{aligned} &(-E + \hbar(\nu_r + \nu_{r'}) + H_0)\phi(1_{r\lambda}, 1_{r'\lambda'}) = +i \sum_P [\mu_P^{r\lambda} \phi(1_{r'\lambda'}) \\ &+ \mu_P^{r'\lambda'} \phi(1_{r\lambda})] - i \sum_{r''\lambda''} \sum_P \mu_P^{r''\lambda''} \phi(1_{r\lambda}, 1_{r'\lambda'}, 1_{r''\lambda''}) \\ &- 2^{1/2} i \sum_P [\mu_P^{r\lambda} \phi(2_{r\lambda}, 1_{r'\lambda'}) + \mu_P^{r'\lambda'} \phi(1_{r\lambda}, 2_{r'\lambda'})] \end{aligned} \right. \quad (11.3)$$

$$\left\{ \begin{aligned} &(-E + 2\hbar\nu_r + H_0)\phi(2_{r\lambda}) = +2^{1/2} i \sum_P \mu_P^{r\lambda} \phi(1_{r\lambda}) \\ &- i \sum_{r'\lambda'} \sum_P \mu_P^{r'\lambda'} \phi(2_{r\lambda}, 1_{r'\lambda'}) - 3^{1/2} i \sum_P \mu_P^{r\lambda} \phi(3_{r\lambda}) \end{aligned} \right. \quad (11.4)$$

etc.

Now for fixed r , and fixed K_r ,

$$\mu_P^{r\lambda} = 0(c^{-1/2})$$

whereas

$$\nu_r = 0(c).$$

⁷ It is possible to write the two component wave equation when the magnetic interactions are retained up to the order $(v/c)^2$, as has been shown by Breit, reference 2.

* We shall not make explicit use of the fact that the α 's are in the form (16); we shall, however, retain the assumption that the α 's are small of the order v/c , to obtain $\mu_P^{r\lambda} = 0(c^{-1/2})$.

Thus we should expect $\phi(1_{r\lambda})$ to be small of the order $c^{-3/2}$, $\phi(1_{r\lambda}, 1_{r'\lambda'})$ to be of the order c^{-3} , and so on, and we should try to find a solution of (11) of the form

$$\begin{aligned} E &= E^{(0)} + E^{(1)} + E^{(2)} \dots \\ \phi(M_{r\lambda}) &= \phi^{(0)}(M_{r\lambda}) + \phi^{(1)}(M_{r\lambda}) \dots \end{aligned} \quad (19)$$

with

$$\begin{aligned} E^{(n)} &= 0(c^{-n}) \\ \phi^{(n)}(M_{r\lambda}) &= 0(c^{-n-3/2M}). \end{aligned}$$

It should be observed that in general there will be certain frequencies for which $\phi(1_{r\lambda})$, $\phi(1_{r\lambda}, 1_{r'\lambda'})$ etc. will not converge uniformly for $c \rightarrow \infty$; and that for these frequencies the expansions (19) will be illegitimate. The frequencies for which this convergence is non-uniform are those for which

$$+E - \sum_{r\lambda} M_{r\lambda} h\nu_r$$

is a characteristic value of the homogeneous equations

$$(H_0 - \lambda)\phi = 0. \quad (20)$$

Such frequencies will not occur if (20) has no solutions for $\lambda < E$, i.e. if the material system is in a normal state; but in general the expansions (19) must be modified; we shall return to this modification later, and shall see that it gives a satisfactory theory of the absorption and emission of radiation; but for the present we shall assume that the atom is in a normal state, so that (19) is justified.

On the present theory there is no normal state for the matter, because states of infinite negative energy are possible; one may in fact show that, on the present theory, Dirac jumps to such states from states of positive energy, jumps in which the energy and momentum lost by the matter are taken up by the field, are not only possible, but infinitely probable. But that the theory should predict this is a token of an error in the theory; and since the Dirac jumps do not seem to be *directly* responsible for the difficulties with which we are, in this work, most concerned, we shall for the present neglect them.

We shall first give a complete solution for the case that we drop all proper energy terms, for the case, that is, that in all double sums of the form

$$\sum_{PP'} F(q_P, \sigma_P, q_{P'}, \sigma_{P'})$$

we may set the terms with p equal to p' equal to zero. This solution is not unique beyond terms of the second order in v/c ; for in the higher orders it is no longer possible uniquely to separate proper energy and interaction energy. But we may readily obtain a possible solution:

$$\phi(M_{r\lambda}) = \prod_{r\lambda} \left[\frac{-i \sum_P \mu_P r\lambda}{h\nu_r} \right]^{M_{r\lambda}} \phi \quad (21)$$

where

$$\left[-E + H_0 - \sum_{r\lambda} \sum_{PP'} \frac{\mu_P^{r\lambda} \mu_{P'}^{r\lambda}}{h\nu_r} \right] \phi = 0. \quad (22)$$

For if we put these values, for example, in (11.2) we get

$$\begin{aligned} & \frac{+i \sum_P \mu_P^{r\lambda}}{h\nu_r} \left[-E + H_0 - \sum_{r'\lambda'} \sum_{PP'} \frac{\mu_P^{r'\lambda'} \mu_{P'}^{r'\lambda'}}{h\nu_{r'\lambda'}} + h\nu_r \right] \phi \\ & + \frac{i}{h\nu_r} \left[H_0, \sum_P \mu_P^{r\lambda} \right] \phi = i \sum_P \mu_P^{r\lambda} \phi. \end{aligned} \quad (23)$$

Now in

$$\sum_P [H, \mu_P^{r\lambda}] = \sum_{PP'} \left[\left(\frac{hc}{2\pi i} (\alpha^P \cdot \text{grad}_P) + m_P c^2 \alpha_0^P + e_P (\alpha^P \cdot A(q_P)) \right), \mu_P^{r\lambda} \right] \quad (24)$$

and in

$$\sum_{PP'} \mu_P^{r'\lambda'} \mu_{P'}^{r'\lambda'}$$

we may put

$$\sum_{PP'} \rightarrow \sum'_{PP'}$$

so that

$$\sum_P [H, \mu_P^{r\lambda}] = 0 \quad (25)$$

and (11.2) is satisfied. In a similar way it may be shown that all the equations (11) are satisfied.

We may evaluate the terms

$$\sum_{r\lambda} \frac{\mu_P^{r\lambda} \mu_{P'}^{r\lambda}}{h\nu_r} = e_P e_{P'} \frac{c^2}{2\pi} \sum_{ll'} \alpha_l^P \alpha_{l'}^{P'} \sum_{r\lambda} \frac{v_l^{r\lambda}(q_P) v_{l'}^{r\lambda}(q_{P'})}{\nu_r^2}$$

in (22) by observing that for $l \neq l'$

$$\sum_{r\lambda} \frac{v_l^{r\lambda}(q_P) v_{l'}^{r\lambda}(q_{P'})}{\nu_r^2} = \frac{\partial}{\partial q_{l'}^{l'}} \frac{\partial}{\partial q_P^{l'}} F(q_P q_{P'}) ; \Delta_P F = \frac{\pi}{c^2 r_{PP'}}$$

and

$$\sum_{r\lambda} \frac{v_l^{r\lambda}(q_P) v_l^{r\lambda}(q_{P'})}{\nu_r^2} = \frac{-\pi}{2c^2 r_{PP'}} - \frac{\partial^2}{\partial q_P^{l_P} \partial q_{P'}^{l_P}} F(q_P, q_{P'})$$

so that

$$\sum_{r\lambda} \frac{\mu_P^{r\lambda} \mu_{P'}^{r\lambda}}{h\nu_r} = \frac{-e_P e_{P'}}{4} \left\{ \frac{(\alpha^P \cdot \alpha^{P'})}{r_{PP'}} + \frac{(\alpha^P \cdot \mathbf{r}_{PP'}) (\alpha^{P'} \cdot \mathbf{r}_{PP'})}{r_{PP'}^3} \right\} \quad (27)$$

This gives for ϕ_0

$$\left\{ -E + H_0 + \frac{1}{4} \sum_{PP'} \frac{e_P e_{P'}}{r_{PP'}^3} [(\alpha^P \cdot \alpha^{P'}) r_{PP'}^2 + (\alpha^P \cdot \mathbf{r}_{PP'}) (\alpha^{P'} \cdot \mathbf{r}_{PP'})] \right\} \phi = 0 \quad (28)$$

This is the equation used by Breit.³ It is patently not relativistically invariant; this means that the proper energy terms are not invariant, and forces us to

retain these terms, at least in part. Furthermore, we have not, in the deduction of (28), used the fact that the atom is in its normal state; in spite of this there is no sign, in the solution, of processes involving the emission or absorption of radiation; for these processes arise from the interaction of the particles with their own field. We have, therefore, to consider the solution of (11) when the proper energy is not neglected; the retention of these terms will preserve the invariance of the theory, and give us an account of radiation processes, but it leads to results in contradiction with experiment; it makes the validity of (28), even to the second order in v/c , doubtful.

3. We can readily find a solution of the form (19) when E^0 and ϕ^0 correspond to a normal state for the matter; but we cannot find this solution in closed form; nor is there an equation in configuration space, corresponding to (28), for ϕ . If we put (19) in (11.2) etc. we get

$$\phi^{(0)}(1_{r\lambda}) = i \sum_m \frac{b_{0m}^{r\lambda} \phi_m^{(0)}}{h\nu_r + E_m^{(0)} - E_0^{(0)}}; \left\{ \begin{array}{l} b_{0m}^{r\lambda} = \sum_p \int \cdots \int dq_1^{(1)} \cdots dq_N^{(3)} \\ \left[\sum_{\sigma' \cdots \sigma N} \bar{\phi}_{\sigma'}^{(0)} \mu_P^{r\lambda} \phi_{\sigma}^{(0)} \right] \\ (H_0 - E_m^{(0)}) \phi_m^{(0)} = 0 \end{array} \right. \quad (29)$$

and further

$$\begin{aligned} \phi^{(0)}(1_{r\lambda}, 1_{r'\lambda'}) &= - \sum_{mn} \frac{b_{0m}^{r\lambda} b_{mn}^{r'\lambda'} \phi_n^{(0)}}{[h\nu_r + E_m^{(0)} - E_0^{(0)}][h(\nu_r + \nu_{r'}) + E_n^{(0)} - E_0^{(0)}]} \\ &\quad - \sum_{mn} \frac{b_{0m}^{r'\lambda'} b_{mn}^{r\lambda} \phi_n^{(0)}}{[h\nu_{r'} + E_m^{(0)} - E_0^{(0)}][h(\nu_r + \nu_{r'}) + E_n^{(0)} - E_0^{(0)}]} \quad (30) \\ \phi^{(0)}(2_{r\lambda}) &= - 2^{1/2} \sum_{mn} \frac{b_{0m}^{r\lambda} b_{mn}^{r\lambda}}{[h\nu_r + E_m^{(0)} - E_0^{(0)}][2h\nu_r + E_r^{(0)} - E_0^{(0)}]} \cdot \text{etc.} \end{aligned}$$

Further $E_{(0^1)}$ and $\phi_{(0^1)}$ vanish, and

$$\begin{aligned} E_0^{(2)} &= - \sum_{r\lambda} \sum_m \frac{|b_{0n}^{r\lambda}|^2}{h\nu_r + E_m^{(0)} - E_0^{(0)}} \\ \phi_0^{(2)} &= \sum_{r\lambda} \sum_m \sum_{n=0} \frac{b_{0m}^{r\lambda} \bar{b}_{mn}^{r\lambda} \phi_n^{(0)}}{[h\nu_r + E_m^{(0)} - E_0^{(0)}][E_n^{(0)} - E_0^{(0)}]} \end{aligned}$$

Moreover $\phi^1(1_{r\lambda})$, $\phi_{(0^3)}$ and $E_{(0^3)}$ vanish, and

$$\phi^{(2)}(1_{r\lambda}) = i \sum_{r'\lambda'} \sum_{mk} \sum_{n \neq 0} \frac{b_{0m}^{r'\lambda'} \bar{b}_{mn}^{r'\lambda'} b_{nk}^{r\lambda} \phi_k^{(0)}}{[h\nu_{r'} + E_m^{(0)} - E_0^{(0)}][h\nu_r + E_k^{(0)} - E_n^{(0)}][E_n^{(0)} - E_0^{(0)}]} \quad (32)$$

$$\begin{aligned} E_0^{(4)} &= - \sum_{r\lambda} \sum_{r'\lambda'} \sum_{mk} \sum_{n \neq 0} \frac{b_{0m}^{r'\lambda'} \bar{b}_{mn}^{r'\lambda'} b_{nk}^{r\lambda} \bar{b}_{k0}^{r\lambda}}{[h\nu_{r'} + E_m^{(0)} - E_0^{(0)}][h\nu_r + E_k^{(0)} - E_n^{(0)}][E_n^{(0)} - E_0^{(0)}]} \\ &\quad \text{etc.} \end{aligned}$$

The terms

$$-E_0^{(3)}\phi^{(0)}(1_{r\lambda})$$

and

$$-i \sum_P \sum_{\lambda' r'} \mu_P^{r' \lambda'} \phi^{(0)}(1_{r\lambda} 1_{r' \lambda'}) - 2^{1/2} i \sum_P \mu_P^{r\lambda} \phi^{(0)}(2_{r\lambda})$$

in the equation for $\phi^{(3)}(1_{r\lambda})$ cancel, so that

$$\phi^{(3)}(1_{r\lambda}) = 0$$

and

$$\phi_0^{(5)} = 0, \quad E_0^{(5)} = 0.$$

The expansion for $E^{(0)}$ and $\phi^{(0)}$ can be continued, and only terms of even order in v/c appear.

It will be observed that the interaction terms in (31)

$$- \sum_{r\lambda} \sum_m [h\nu_r + E_m^{(0)} - E_0^{(0)}]^{-1} \left\| \int \bar{\phi}_n^{(0)} \mu_P^{r\lambda} \phi_0^{(0)} d\mathbf{q} \right\| \left\| \int \phi_n^{(0)} \mu_{P'}^{r\lambda} \phi_0^{(0)} d\mathbf{q} \right\| \quad (33)$$

$$\left[\text{we write } \int d\mathbf{q} \text{ for } \int \dots \int dq_1^{(1)} \dots dq_N^{(3)} \sum_{\sigma' \dots \sigma_N} \right]$$

differ from those computed for the second order from (28):

$$- \sum_{r\lambda} \sum_m (h\nu_r)^{-1} \left\| \int \bar{\phi}_n^{(0)} \mu_P^{r\lambda} \phi_0^{(0)} d\mathbf{q} \right\| \left\| \int \bar{\phi}_n^{(0)} \mu_{P'}^{r\lambda} \phi_0^{(0)} d\mathbf{q} \right\| \quad (34)$$

It is possible to express

$$\sum_{r\lambda} \frac{\mu_P^{r\lambda} \mu_{P'}^{r\lambda}}{h\nu_r + E_m^{(0)} - E_0^{(0)}}$$

in terms of the confluent hypergeometric functions, but the expressions are too complicated to be suitable for calculation.

The proper energy terms

$$- \sum_{r\lambda} \sum_P \sum_m \frac{\left| \int \bar{\phi}_m^{(0)} \mu_P^{r\lambda} \phi_0^{(0)} d\mathbf{q} \right|^2}{h\nu_r + E_m^{(0)} - E_0^{(0)}} = - \sum_{r\lambda P m} T_{0m,P}^{r\lambda}$$

do not exist, although both

$$\sum_{r\lambda} T_{0m,P}^{r\lambda}$$

and

$$\sum_m T_{0m,P}^{r\lambda}$$

converge; for large ν_r ,

$$\sum_m T_{0m,P}^{r\lambda} = 0(1)$$

and for large E

$$\sum_{r\lambda} T_{0m,P}^{r\lambda} = 0(1).$$

The energy level of the normal state is thus infinitely displaced by the interaction of the particles with the field; the question which we have now to consider is whether or not the energy differences between two states are displaced by a finite or an infinite amount.

In order to answer this question we must treat the case of energies which do not correspond to a normal state for the matter; and we have to modify (19), and take account of the emission of radiation by the system. And for this purpose it is convenient to make the dimensions L of the Hohlraum infinite, because that makes the physical interpretation of the solution more immediate. For then ν_r becomes continuous and we may normalize the $v_i^{r\lambda}(q_p)$ to the intervals $\Delta\nu\Delta\omega$, where $\Delta\omega$ is the element of solid angle of the unit vector ϵ_r . Furthermore we may treat here, to simplify the writing, the case that E corresponds to the first excited state of the atom, so that there is only one energy E_0 lower than E for which (20) is soluble.

We define the energy of the normal state by

$$E_0 = E_0^{(0)} + E_0^{(2)} + E_0^{(4)} \dots \quad (35)$$

where $E_0^{(2)}$ and $E_0^{(4)}$ are given by (31) and (32), and we define the corresponding wave function

$$u_0 = \phi_0^{(0)} + \phi_0^{(2)} + \phi_0^{(4)} \dots \quad (36)$$

where $\phi_0^{(2)}$ is given by (31). We can then extend this definition formally to obtain the energy and wave function of excited states:

$$\begin{aligned} E_m &= E_m^{(0)} + E_m^{(2)} + E_m^{(4)} \dots ; \\ E_m^{(2)} &= - \int d\nu_r \int d\omega_r \sum_{\lambda} \sum_n \frac{|b_{mn}^{r\lambda}|^2}{h\nu_r + E_n^{(0)} - E_m^{(0)}} \\ u_m &= \phi_m^{(0)} + \phi_m^{(2)} + \phi_m^{(4)} \dots \text{etc.} \end{aligned} \quad (37)$$

But in the expressions for $E_m^{(2)}$ etc, and $\phi_m^{(2)}$ etc, the integrals over ν are now improper, and we have to displace the path of integration around the singularities. This is equivalent to replacing

$$\frac{1}{h\nu + E_n^{(0)} - E_m^{(0)}} \text{ for } E_n^{(0)} < E_m^{(0)}$$

by

$$\frac{1}{h\nu + E_n^{(0)} - E_m^{(0)}} \pm i\pi\delta(h\nu + E_n^{(0)} - E_m^{(0)}) \quad (38)$$

and then taking the principal value of the integrals over ν . Then in general all the E_m 's except E_0 are complex. We now transform the $\phi(M_{r\lambda}, q_p\sigma_p)$ by the formulae

$$\phi(M_{r\lambda}, m) = \sum_{\sigma_P} \int \cdots \int dq_1^{(1)} \cdots dq_N^{(3)} u_m(q_P, \sigma_P) \quad (39)$$

$$\phi(M_{r\lambda}, q_P, \sigma_P)$$

and introduce

$$\mu_{mn}^{r\lambda} = \sum_{\sigma_P} \int \cdots \int dq_1^{(1)} \cdots dq_N^{(3)} \bar{u}_m \mu_P^{r\lambda} u_n. \quad (40)$$

Then if the $\phi(M, m)$ satisfy the equations, which follow from (11):

$$(-E + E_m)\phi(0, m) = -i \int d\nu_r \int d\omega_r \sum_{\lambda} \sum_P \mu_{0m, P}^{r\lambda} F_1(\omega_r, \lambda) \delta\left(\nu_r + \frac{E_0 - E}{h}\right) \\ - \int d\nu_r \int d\omega_r \sum_{\lambda} \sum_P \mu_{nm, P}^{r\lambda} \int d\nu_r' \int d\omega_r' \sum_{\lambda'} \sum_{P'} \mu_{0n, P'}^{r'\lambda'} F_2(\omega_r, \omega_r', \nu_r', \lambda, \lambda') \delta\left(\nu_r + \nu_r' + \frac{E_0 - E}{h}\right) + \cdots \quad (41)$$

$$\phi(1_{r\lambda}, 1m) = i \sum_{P_n} \mu_{nm, P}^{r\lambda} \phi(0, n) \left\{ \frac{1}{-E + h\nu_r + E_m} + \frac{i\pi\delta_{m0}}{h} \delta\left(\nu_r + \frac{E_m - E}{h}\right) \right\} \\ + F_1(\omega_r, \lambda) \delta\left(\nu_r + \frac{E_m - E}{h}\right) - i \sum_P \int d\nu_r' \int d\omega_r' \sum_{\lambda'} \mu_{0m, P}^{r\lambda} \\ F_2(\omega_r', \omega_r, \nu_r', \lambda, \lambda') \delta\left(\nu_r + \nu_r' + \frac{E_0 - E}{h}\right) \cdots \quad (42)$$

$$\phi(1_{r\lambda}, 1_{r'\lambda'}, m) = i \sum_{P_m} \left\{ \mu_{nm, P}^{r'\lambda'} \phi(1_{r\lambda}, n) + \mu_{nm, P}^{r\lambda} \phi(1_{r'\lambda'}, n) \right\} \\ \left\{ \frac{1}{-E + h(\nu_r + \nu_r') + E_m} \pm \frac{i\pi\delta_{m0}}{h} \delta\left(\nu_r + \nu_r' + \frac{E_m - E}{h}\right) \right\} \\ + F_2(\omega_r, \omega_r', \nu_r', \lambda, \lambda') \delta\left(\nu_r + \nu_r' + \frac{E_0 - E}{h}\right) \cdots$$

where now the functions F are completely arbitrary, then the $\phi(M_{r\lambda}, q_P, \sigma_P)$ satisfy (11); for each choice of these F 's we can obtain a solution of (11). Now the terms

$$\frac{\mu_{nm, P}^{r\lambda} \phi(0, n)}{-E + h\nu_r + E_m} \text{ etc.}$$

give a radiation field which does not extend to infinity; and the terms

$$\frac{\pm i\pi \mu_{nm, P}^{r\lambda}}{h} \phi(0, n) \delta_{m0} \delta\left(\nu_r + \frac{E_0 - E}{h}\right) \text{ etc.}$$

represent outgoing⁸ electromagnetic waves, so that by the choice of the F 's

⁸ P. A. M. Dirac, *Zeits. f. Physik* **44**, 585 (1927).

we may determine the radiation incident upon the system. The simplest case is that in which only quanta of the single frequency

$$\nu = \frac{1}{h}(E - E_0) = \nu_r \quad (43)$$

are incident upon the system, so that all the F 's vanish except

$$F_1(\omega, \lambda).$$

For this case

$$\phi(0, m) = + \frac{i \sum_{\lambda} \sum_P \int d\omega_r \mu_{0m, P}^{\tau\lambda} F_1(\omega, \lambda)}{E - E_m} = \frac{iG_m^{\nu}}{E - E_m}. \quad (44)$$

Now by hypothesis E is to be chosen that only one $E_m - E$, that for $m = 1$, say, is to be small, so that only

$$\phi(0, 1) = \frac{iG_1^{\nu}}{E - E_1} \quad (45)$$

is large. The probability of absorption to this state is thus proportional to

$$\frac{|G_1^{\nu}|^2}{|E - E_1|^2} = \frac{|G_1^{\nu}|^2}{|h\nu + E_0 - E_1|^2} \quad (46)$$

so that the shape of the absorption line is given by

$$\frac{\text{const.}}{\left| \nu + \frac{1}{h}(E_0 - E_1) \right|^2} \quad (47)$$

since G_r^{ν} , varies slowly with ν .

If we evaluate E_0, E_1 to the second order in v/c , and drop the higher terms—and this is equivalent to neglecting transitions in which more than one quantum plays a part—(47) reduces to

$$\frac{\text{const.}}{\left[\nu + \frac{1}{h}(E_0^{(0)} - E_1^{(0)}) + \frac{1}{h}(E_0^{(2)} - \frac{1}{2}E_1^{(2)} - \frac{1}{2}\bar{E}_1^{(2)}) \right] + \frac{1}{4h^2} |E_1^{(2)} - \bar{E}_1^{(2)}|^2} \quad (48)$$

The absorption line is thus of the same shape as that predicted on the basis of the correspondence principle, and that found, for this case, by Dirac³, and the half-breadth of the line is

$$\left| \frac{E_1^{(2)} - \bar{E}_1^{(2)}}{2h} \right| = \frac{\pi}{h} \int d\omega \sum_{\lambda} |b_{01}^{\tau\lambda}|^2 = \frac{1}{4\pi\tau_1} \quad (49)$$

where τ_1 is the natural life time of the state 1.

The center of the absorption line is displaced to the red from $(1/h)(E_1^{(0)} - E_0^{(0)})$ by an amount

$$\begin{aligned} & \frac{1}{h} \left(E_0^{(2)} - \frac{1}{2} E_1^{(2)} - \frac{1}{2} \bar{E}_1^{(2)} \right) \\ &= \frac{1}{h} \int d\nu \int d\omega \sum_{\lambda} \sum_n \left\{ \frac{|b_{1n}^{\lambda}|^2}{h\nu + E_n^{(0)} - E_1^{(0)}} - \frac{|b_{0n}^{\lambda}|^2}{h\nu + E_n^{(0)} - E_0^{(0)}} \right\} \\ &\sim \frac{1}{h} \int d\nu \int d\omega \sum_{\lambda} \sum_n \sum_{PP'} \left\{ \frac{\mu_{1n,P}^{\lambda} \mu_{n1,P'}^{\lambda}}{h\nu + E_n^{(0)} - E_1^{(0)}} - \frac{\mu_{0n,P}^{\lambda} \mu_{n0,P'}^{\lambda}}{h\nu + E_n^{(0)} - E_0^{(0)}} \right\}. \quad (50) \end{aligned}$$

Here the principle values are to be taken for all improper integrals over ν . The terms for $p \neq p'$ are just those to be expected from (33) for the displacement of the energy levels by the magnetic interaction of the particles. The terms

$$\frac{1}{h} \int d\nu \int d\omega \sum_{\lambda} \sum_n \left\{ \frac{|\mu_{1n,P}^{\lambda}|^2}{h\nu + E_n^{(0)} - E_1^{(0)}} - \frac{|\mu_{0n,P}^{\lambda}|^2}{h\nu + E_n^{(0)} - E_0^{(0)}} \right\} \quad (51)$$

must be ascribed to the effect of the interaction of the particle with its own field. They may be compared with the formula obtained⁸ for the same effect by Dirac, who finds a displacement

$$\frac{1}{h} \int d\nu \int d\omega \sum_{\lambda} \frac{|\mu_{01,P}^{\lambda}|^2}{h\nu + E_0^{(0)} - E_1^{(0)}}. \quad (52)$$

There does not appear to be any justification for this result, because in its derivation terms were neglected that are of the same order as those retained. But it is of interest to observe that the integral in (52) exists, and gives a finite displacement of the line of the second order in v/c . This displacement is thus larger than the natural line breadth, which is of the third order. It can be computed⁹ when the u 's are known. Thus for the first Lyman doublet of hydrogen we find the same displacement, in this order, for both components; it turns out to be

$$+ \frac{ch}{32\pi^2 e^2} \frac{1}{\tau_1} = \frac{ch}{32\pi^2 e^2} A_{10}$$

which is about forty times the line breadth. The fact that this term, and the similar terms in (51), are the same, in second order, for the two components of the doublet, suggests that the formulae (33) in which the proper energy is neglected, will give the atomic fine structure splitting correct to the second order.

If we try to compute the displacement from (51), we find that the integrals over ν diverge logarithmically for high frequencies. One can readily

⁹ The calculations of the displacements predicted by the results of Dirac were carried through in collaboration with Harvey Hall; and I am indebted to him for permission to quote them here. One must use the retarded potentials to obtain a convergent integral.

see that this is not the result of the neglect of higher order terms, nor of any of the approximations made in the work. The theory thus leads to the false prediction that spectral lines will be infinitely displaced from the values computed by the Bohr frequency condition. The behavior of the expression (51) calls for some comment. As the formula stands, the integral over ν diverges absolutely; this may be verified by evaluating the terms for a free particle. But the question arises whether it is possible so to rearrange the order of the integration over ν the summation over n , and the two integrations involved in the evaluation of the μ_{mn} 's by (40), that the limit $n \rightarrow \infty$, $\nu \rightarrow \infty$ exists. This cannot be effected by an interchange of the sum over n and the integral over ν ; but there is a procedure which, when the E 's in the resonance denominators of (51) are dropped, does give an absolutely convergent result. This procedure was suggested by Heisenberg, who showed that, if we first perform the integration over ν and ω and the summation over λ , then sum over all the states n of the same energy, then sum these up to some large but finite energy E , take the difference of the two terms for the state (0) and the state (1), then perform the two integrations over the configuration space, and finally allow E to become infinite, the limit $E \rightarrow \infty$ exists, and (51) tends to zero. But if we try to apply this procedure to (51) when the E terms are not dropped, we get for the leading term the divergent result

$$4e_p^2/hc \cdot (E_1^{(0)} - E_0^{(0)})/h \cdot \int^\infty dx/x \quad (53)$$

Nor is there any method for obtaining an absolutely convergent expression for (51). It should be observed that (53) gives us another justification for using (33) to get the fine structure separations correct to the second order.

One can see quite simply that (47) ought not to give a finite line displacement. For consider two states of a free particle; in one let the particle be at rest; in the other let it have the velocity v . Then if the energy of the particle at rest be E , the energy of the moving particle in proper coordinates moving with the particle will also be E . But we know how this energy transforms under a Lorentz transformation; in the original coordinates it will be

$$E\beta \quad \beta = [1 - (v/c)^2]^{-1/2}$$

and in the same coordinates the difference in energy of the two states, which gives the line displacement, will be

$$E(\beta - 1)$$

But this can only be finite if E is finite which, by (31), it is not.

We have treated these difficulties in some detail, because they show that the present theory will not be applicable to any problem where relativistic effects are important, where, that is, we cannot be guided throughout by the limiting case $c \rightarrow \infty$. The theory can thus not be applied to a discussion of the structure of the nuclei. It appears improbable that the difficulties discussed in this work will be soluble without an adequate theory of the masses of electron and proton; nor is it certain that such a theory will be possible on the basis of the special theory of relativity.

THE EFFECT OF END LOSSES ON THE CHARACTERISTICS OF FILAMENTS OF TUNGSTEN AND OTHER MATERIALS

BY IRVING LANGMUIR, SAUNDERS MACLANE AND KATHARINE B. BLODGETT
GENERAL ELECTRIC COMPANY, SCHENECTADY, NEW YORK

(Received September 20, 1929)

ABSTRACT

The leads of a tungsten filament in vacuum cool the ends of the filament and so affect the voltage, candle power, electron emission and other properties of the filament. For long filaments, where there is a central portion at a uniform temperature T_m , the temperature distribution near the lead is derived. A method for determining T_0 , the temperature of the lead-filament junction, is given. Tables and formulas are presented which allow ready calculation of the effect of the leads on the properties of any long tungsten filament for which the current and diameter are known. From the more general results it has been found that the decrease in voltage due to the cooling of one lead may be represented by $\Delta V = 0.154 (T_m/1000) - 0.081 (T_0/1000) - 2.1 \cdot 10^{-3} T_0 T_m - 0.056$. There is an extension of the theory to cover the cases of filaments in gases, filaments of other materials, etc.

Part II of the paper gives figures from which may be found the properties of filaments so short that the first theory does not apply. Some experimental checks of the theory are given.

In general the results and the methods of application have been placed first, and the mathematical derivations have been placed at the end of each part.

For a short filament with leads cooled in liquid air a negative slope of the volt-ampere characteristic when the central temperature is much smaller than T_m is observed.

PART I. THE LONG FILAMENT

THE extensive use of tungsten filaments in research and industry makes it important to consider how the cooling effects of the leads influence the characteristics of such filaments. For wide ranges of temperature the characteristics of hypothetical filaments which are not cooled by leads may be found from tables of the properties of tungsten¹⁻⁷. The magnitudes of the lead losses have been evaluated experimentally^{1, 8, 9} and by theoretical methods.¹⁰ It is felt that there is still a place for a systematic treatment

¹ W. E. Forsythe and A. G. Worthing, *Astrophys J.* **61**, 146 (1925).

² C. Zwikker, *Royal Acad. Amsterdam* **34**, No. 5 (1925).

³ H. A. Jones and I. Langmuir, *G. E. Review* **30**, 310, 354, 408 (1927).

⁴ H. A. Jones, *Phys. Rev.* **28**, 202 (1926).

⁵ I. Langmuir, *Phys. Rev.* **7**, 154 (1916).

⁶ I. Langmuir, *Phys. Rev.* **7**, 302 (1916).

⁷ I. Langmuir, *G. E. Review* **19**, 208 (1916).

⁸ A. G. Worthing, *Journ. Frank. Inst.* **194**, 597 (1922).

⁹ T. H. Amrine, *Trans. Ill. Eng. Soc.* **8**, 385 (1913).

¹⁰ A. G. Worthing, *Phys. Rev.* **4**, 524 (1914); R. Ribaud and S. Nikitine, *Ann. de Physique* **7**, 5 (1927); V. Bush and K. E. Gould, *Phys. Rev.* **29**, 337 (1927).

which may be conveniently applied to a filament operated under any ordinary conditions.¹¹

Temperature distribution. For most tungsten filaments the cooling effect of the leads does not extend appreciably to the central portion of the filament. The absolute temperature, T_m , of this portion may be calculated from the diameter of the filament and the current through it.¹² The temperature of other parts of the filament is best expressed as a fraction, θ , of T_m . Thus $\theta = T/T_m$, where T represents the absolute temperature of any point of the filament.

We may consider the effect of each lead independently, since the two effects do not overlap. Of fundamental importance is the variation of θ with x , the distance from the lead. This is shown later to be governed by the equation,

$$\phi = ad\theta/dx \quad (1)$$

where ϕ is a function of θ , and is given by Eq. (30). a is a parameter of the dimension of length, and depends on T_m and the filament diameter D .

TABLE I. Values of a_0 for various values of T_m . (For ' a ' use Eq. (2).)

$T_m(^{\circ}K)$	$a_0(\text{cm})$	T_m	a_0	T_m	a_0
600	5.84	1700	0.646	2800	0.275
700	4.08	1800	.582	2900	.261
800	3.01	1900	.527	3000	.247
900	2.33	2000	.481	3100	.235
1000	1.863	2100	.441	3200	.223
1100	1.524	2200	.406	3300	.213
1200	1.274	2300	.377	3400	.209
1300	1.084	2400	.351	3500	.195
1400	.936	2500	.329	3600	.187
1500	.821	2600	.309	3655	.183
1600	.724	2700	.291		

a_0 , the value of a for $D = 0.01$ cm (4 mil approx.) is given in Table I. a for other values of D may be found from

$$a = a_0(D/0.01)^{1/2}. \quad (2)$$

Integration of (1) gives

$$(x/a)_0^{\theta} = \int_0^{\theta} d\theta/\phi. \quad (3)$$

The values of $(x/a)_0^{\theta}$ for various values of θ are tabulated in the second column of Table II. Note that a is effectively a unit of length. The symbol $(x/a)_0^{\theta_2}$ will in general represent the distance, expressed in a -units, from a point at temperature $\theta_1 T_m$, to a point at temperature $\theta_2 T_m$. To obtain dis-

¹¹ I. Langmuir, Trans. Faraday Soc. **17**, 634 (1922). See also references (7) p. 210, (6) p. 312, (3) p. 356. In these papers formulas for ΔV and ΔV_H are given. They were derived by methods similar to the ones used in this paper.

¹² Ref. (3), p. 312, Table I, column 4.

tance in a -units, divide the distance x in cm by the value of a , in cm, found from Table I.

TABLE II. Values of $(x/a)_0^\theta$ and $\beta(\theta_0)$.
For $n > 4$: $\beta(\theta_0) = (x/a)_0^\theta$. For $n = 1.2$, see columns 3 and 6.

θ	$(x/a)_0^\theta$	$\beta(\theta_0)$ $n=1.2$	θ	$(x/a)_0^\theta$	$\beta(\theta_0)$ $n=1.2$
0.0	0.000	0.000	0.7	0.7394	0.464
.1	.0419	.040	.8	.9766	.532
.2	.1110	.102	.85	1.1354	
.25	.1522	.137	.9	1.3592	.598
.3	.1974	.172	.95	1.7260	.630
.4	.2999	.245	.99	2.5535	.654
.5	.4200	.320	.999	3.7224	.659
.6	.5628	.392	1.000		.660

The temperature distribution near a cooling lead is represented by the curve farthest to the right (labeled 0.995) in Fig. 2 (Part II). The increment in the abscissa $(x/a)_0^\theta$ from the ordinate θ_2 to ordinate θ_1 gives the distance along the filament from a point at temperature $\theta_1 T_m$ to a point at temperature $\theta_2 T_m$.

In practice the junction of lead and filament will be at a temperature $T_0 = \theta_0 T_m$. The exact determination of this temperature is rather difficult. If the leads are short and fairly heavy we may assume $T_0 = T_R$, where T_R is the room temperature. The error due to this assumption in the value of any filament-property for the whole filament¹³ computed by the methods of this paper will be less than 1 percent when the length of the lead is less than a certain maximum length l_0 . We find that l_0 is given approximately by

$$l_0 = 0.32(x/a)(D_L/0.1)^2(\lambda_L/0.586)/A. \quad (4a)$$

A is the filament current in amperes and (x/a) represents the half length of the filament. D_L is the lead diameter in cm. λ_L is the thermal conductivity of the lead in watts $\text{cm}^{-1} \text{deg}^{-1}$. For nickel leads $\lambda_L/0.586 = 1$, for tungsten leads $\lambda_L/0.586 = 2.73$, for molybdenum $\lambda_L/0.586 = 2.49$.

Thus with nickel leads for which $D_L = 0.1$ cm and $l < 1.6$ cm, used with a 20 cm filament of $D = 0.02$ cm for which the highest operating temperature is $T_m = 2400^\circ$ we may assume $T_0 = T_R$, since we find $A = 4.02$,¹² $x/a = 20.2$, and thence from Eq. (4a) $l_0 = 1.6$ cm.

For leads such as those used in incandescent lamps it is sufficiently accurate for many purposes to assume that $T_0 = (1/4)T_m$.

If desired we may evaluate $\Delta T = T_0 - T_R$ in terms of the lead length l . We find that

$$\Delta T = l \cdot A (0.586/\lambda_L)(0.1/D_L)^2 (\Delta T_0). \quad (4b)$$

$(\Delta T)_0$ is the value of ΔT for a nickel lead for which $D_L = 0.1$ cm, $l = 1$ cm and $A = 1$ amp. It is given in Table III as a function of the value of T_m for the filament. Note that these values are for a filament of constant current,

¹³ Such as the voltage or the candle power of the whole filament.

and hence that the diameter of a filament for which $\Delta T = (\Delta T)_0$ is smaller for the higher temperatures in the table.

The data from Table III are not dependable above $T_0 = 1000^\circ$, where radiation loss is appreciable, nor when the resistance loss in the lead is large.

TABLE III. $(\Delta T)_0 = T_0 - T_R$ for nickel leads when $A=1$, $D_L=0.1$, $l=1$.

$T_m(^{\circ}\text{K})$	$(\Delta T)_0$	T_m	$(\Delta T)_0$	T_m	$(\Delta T)_0$
1000°	21°	1800°	45°	2800°	80°
1200	26	2000	51	3000	87
1400	32	2200	58	3200	95
1600	38	2400	65	3400	102
		2600	72		

The actual temperature distribution of the filament is given by (cf. Eq. (3))

$$(x/a)_{\theta_0}^{\theta} = \int_0^{\theta} d\theta/\phi - \int_0^{\theta_0} d\theta/\phi. \quad (5)$$

To find the distance from the lead, x , of a point of known temperature θ , we may evaluate the two integrals above by means of Table II, and then obtain x from $(x/a)_{\theta_0}^{\theta}$ by using Table I. Conversely we may find the temperature θ of a point at any given distance, x .

By the use of data on the characteristics of tungsten filaments as functions of temperature,^{1, 3} and from the temperature distribution along a filament as found above, the properties of the filament at each point can be calculated. For example, we can determine the electron emission, the radiated energy, the luminous intensity, et cetera, at each point.

The effect of lead losses on filament characteristics. Many filament properties which are functions of the temperature would be strictly proportional to the length of the filament if the temperature were everywhere uniform. Let h be a quantity which measures some one of these properties *per unit length* at any given absolute temperature T . For example, h may represent the voltage drop per cm or the electron emission per cm of length. Let h_m be the value of h at the temperature T_m . Nearly all the properties of tungsten which we shall need to consider vary in proportion to some definite power of the temperature over rather wide ranges. Thus we may put

$$h = h_m \theta^n \quad (6)$$

$$n = (dh/h)(T/dT) \quad (7)$$

where n is approximately constant.¹⁴

If a filament of length $2x$ were all at its maximum temperature T_m the value H_m of any property for the whole filament would be

$$H_m = 2xh_m. \quad (8)$$

¹⁴ For values see Ref. 3, p. 354 Table II or Ref. 1, p. 153 Table I-B.

The cooling effect of the leads makes H , the actual value of the property for the whole filament, less than H_m . ΔH , the amount of this decrease due to one lead, may be thought of as the total value of the property over a short length of uncooled filament. Designate by ΔV_H the voltage drop across this length. ΔV_H is then the volt-equivalent of ΔH , and the fractional decrease of H_m can thus be expressed as a fraction of the total voltage V_m

$$\Delta V_H/V_m = \Delta H/H_m. \quad (9)$$

The ratio H/H_m is a measure of the extent to which the cooling effect changes the property. We have

$$H/H_m = (H_m - 2\Delta H)/H_m = (V_m - 2\Delta V_H)/V_m. \quad (10)$$

The factor 2 accounts for two leads.

TABLE IV. Values of $B_1 = \int_0^1 (1 - \theta^n) d\theta / \phi$.

n	B_1	n	B_1	n	B_1
1	0.583	9.0	1.626	20	2.032
1.2	0.660	10	1.682	22	2.079
2.0	0.882	11	1.728	24	2.124
3.0	1.076	12	1.772	25	2.145
4.0	1.217	13	1.813	26	2.165
5.0	1.329	14	1.850	28	2.203
5.1	1.339	15	1.885	30	2.238
6.0	1.421	16	1.918	35	2.315
7.0	1.500	17	1.949	40	2.384
8.0	1.566	18	1.978	50	2.497
		19	2.006	60	2.589

If V is the actual voltage drop (in volts) and ΔV the value which ΔH has when the property measured by H is voltage

$$H/H_m = (V + 2\Delta V - 2\Delta V_H)/(V + 2\Delta V). \quad (11)$$

It will be shown later that the value of ΔV_H is given by

$$\Delta V_H = 1.812 \cdot 10^{-5} T_m^{1.3} [B_1 - \beta(\theta_0)]. \quad (12)$$

B_1 is given in Table IV. It is a function of n , the temperature exponent for the property H in question. For $n > 5$, B_1 is given by the equation

$$B_1 = 0.5170 + 1.1660 \log_{10} n - 0.0591/n + 0.2224/n^2 + 0.0140/n^3 - 0.468/n^4 + \dots \quad (13)$$

The coefficient of Eq. (12), $1.812 \cdot 10^{-5} T_m^{1.3}$, is given in Table V.

$\beta(\theta_0)$ in Eq. (12) is a function of θ_0 . It is independent of n if $n > 4$ and $\theta_0 < 0.5$, and is given by

$$n > 4, \theta_0 < 0.5 \quad \beta(\theta_0) = (x/a)_{\theta_0}^{\theta_0}. \quad (14)$$

This value of x/a is to be taken directly from Table II for $\theta = \theta_0$. For $n = 1.2$ (the exponent for resistance and the only important small value of n) $\beta(\theta_0)$ is given in the third column of Table II.

TABLE V. $1.812 \cdot 10^{-5} T_m^{1.3}$

T_m	$1.812 \cdot 10^{-5} T_m^{1.3}$	T_m	$1.812 \cdot 10^{-5} T_m^{1.3}$
1000°	0.1439	2300°	0.4250
1100	.1629	2400	.4493
1200	.1825	2500	.4737
1300	.2024	2600	.4985
1400	.2229	2700	.5236
1500	.2438	2800	.5490
1600	.2651	2900	.5744
1700	.2869	3000	.6003
1800	.3091	3100	.6266
1900	.3316	3200	.6528
2000	.3544	3300	.6797
2100	.3777	3400	.7066
2200	.4011	3500	.7337

Since the current is constant, the voltage has the same temperature exponent as the resistance. Hence ΔV may be found from Eq. (12) by setting $n = 1.2$. In many cases to apply Eq. (11) it may be easier to find the theoretical voltage $V_m = V + 2\Delta V$ directly from the resistivity at T_m and the filament dimensions. The wattage *input* depends on the resistance of the filament and hence ΔV_H in this case is to be found for $n = 1.2$. The wattage *radiated* on the other hand depends on $n = 5.1$ or thereabouts.¹⁵

Method of application. In finding the value of B_1 for Eq. (12) from the value of n , we notice that for most properties of tungsten n is not constant as was assumed, but varies slightly with the temperature. We must take a mean value of n , that is, its value at some effective temperature T_E . This temperature is roughly that at which $h = h_m/2$. This temperature and the corresponding value of n may be found directly.¹⁴

As an alternate method to find T_E we note that for some properties h may be quite accurately expressed as

$$h = CT^k e^{-b/T}. \quad (15)$$

Thus for candle power Wiens' law (using a Crova wave-length) gives $k = 0$, $b = 25200^\circ$. The Richardson-Dushman equation for the electron emission from pure tungsten has $k = 2$, $b = 52600^\circ$. The rate of evaporation of a tungsten filament is expressed by Eq. (15) with $k = 0$, $b = 94100^\circ$. Setting $h = h_m/2$ in Eq. (15) and using Eq. (6) to evaluate the term in k , we find approximately

$$b/T_E = b/T_m + [1 - k/n] \log_e 2. \quad (16)$$

Differentiating Eq. (15) and comparing with Eq. (7) we see that

$$n = k + b/T. \quad (17)$$

Hence from Eq. (16) and the values of the constants given above we obtain the following equations for effective values of n in terms of T_m

$$\text{candle power } n = 25200^\circ/T_m + 0.7 \quad (18)$$

¹⁵ Ref. 3, p. 312, Table I, column 5.

$$\text{electron emission } n = 52600^\circ/T_m + 2.6 \quad (19)$$

$$\text{evaporation } n = 94100^\circ/T_m + 0.7. \quad (20)$$

The decrease in the rate of evaporation near the leads is ordinarily not a matter of experimental interest, but under certain conditions its effects may be directly observed. Nitrogen or carbon monoxide in the presence of a tungsten filament at very high temperatures gradually disappears because every atom of tungsten which evaporates combines with a molecule of the gas to form a stable and non-volatile compound. Thus the rate of "clean-up" of the gas depends on the total amount of metal that evaporates.

The direct application of Eq. (12) as outlined above is the most accurate method for the evaluation of ΔV_H . In many cases where only approximate results are desired ΔV_H may be found from the following empirical equations, which were found to fit the data calculated from Eq. (12). The deviation from the results of Eq. (12) is less than the amount tabulated for the given range. The actual error of the results may in some cases be larger than this, due to approximations in the derivation of Eq. (12).

TABLE VI. $\Delta V_H = P(T_m/1000) - Q(T_0/1000) - R$ volts.

<i>H</i> is	<i>P</i>	<i>Q</i>	<i>R</i>	Range— <i>T_m</i>	Range— <i>T₀</i>	Range— <i>θ₀</i>	Max. error (volts)
Voltage*	0.154*	0.081*	0.056*	1000–2500°	any values	0.1–0.5	0.004
Candle Power	.338	.182	–.004	600–3500	300–1400°	.1–.5	.01
Electron emission	.440	.158	.072	1000–3500	300–900	.07–.5	.009
Evaporation	.480	.160	.060	1500–3500	300–900	.07–.5	.008
Watts radiated	.293	.160	.084	1100–3000	300–900	.1–.4	.01

* For voltage (Watts input) a term $-2.1 \cdot 10^{-8} T_0 T_m$ is to be added to the right hand side of Eq. (21).

In many cases with short, heavy leads $T_0 = 300^\circ$. In these circumstances the following approximate equations hold.

TABLE VII. $\Delta V_H = P_0(T_m/1000) - S$ volts (22)

<i>H</i> is	<i>P₀</i>	<i>S</i>	Range— <i>T_m</i>	Max. error (volts)
Voltage	0.148	0.080	1000–2500	0.004
Candle Power	.338	.051	600–3500	.01
Electron Emission	.439	.119	1000–3500	.007
Evaporation	.477	.103	1500–3500	.001
Watts radiated	.287	.121	1000–3100	.01

Computation of T_m . If we know the diameter of a filament and the current through it, T_m may be obtained directly from Tables which give temperature tabulated against current divided by $d^{3/2}$.¹²

If the diameter is not known, but if the length $2x$ is known, the voltage V and amperage A corresponding to the temperature we wish may be found. Assuming that the filament is all at the maximum temperature T_m , we compute $VA^{1/3}/(2x)$ and find a first approximation for T_m .¹⁶ For

¹⁶ Ref. 3, p. 312, Table I, column 6 gives $VA^{1/3}/(2x)$ as a function of T .

this value of T_m there is a certain voltage correction ΔV . This gives us a much better value, $V+2\Delta V$, for the voltage if the filament were all at T_m . $(V+2\Delta V) A^{1/3}/(2x)$ then gives us a second approximation for T_m . As many approximations as desired may be made.

Shorter filaments. With shorter filaments the cooling effects of the two leads overlap, and the temperature at any point may be found approximately by adding the cooling effect of each lead at that point. With still shorter filaments these temperatures and the values of H/H_m found as above are in error. The amount of the error depends on n , the temperature exponent of the property in question. Part II, Table X gives in column 2 the maximum value of the half length $(x/a)_{0\%}^0$ for which the error in H/H_m is less than 1 percent. Column 3 gives similar information for 5 percent error. For details see Part II.

DERIVATION OF THE EQUATIONS

The fundamental differential equation giving the temperature distribution near a cooling lead is⁸

$$A^2 r + [\lambda(d^2 T/dx^2) + (d\lambda/dT)(dT/dx)^2] \pi D^2/4 = w. \quad (23)$$

The symbolism is explained in Table VIII. The terms $A^2 r$ and w correspond respectively to the rate of production of energy and the rate of radiation

TABLE VIII. *Symbols.*

A	Filament current in amps	w	$=h$ for power radiated
D	Filament diameter (cm)	r	$=h$ for resistance
D_L	Lead diameter (cm)	v	$=h$ for voltage drop
l	Length of lead (cm)	H	Value of any property for the whole filament
x	Distance along filament (cm)	H_m	Value of H if the whole filament were at T_m
a	Unit of length (cm) Table I	V	$=H$ for voltage drop
a_0	a for $D=0.01$ cm	H_c	Value of H if the whole filament were at T_c
sub m	Value at the uncooled central portion of the filament	n	Temperature exponent for any property $=d \log h/d \log T$
sub c	Value at the center of the filament (Part II)	ρ	$=n$ for resistance
T	Absolute temperature	ω	$=n$ for radiation
T_R	Room temperature	k	$=n$ for thermal conductivity
$T_0 = \theta_0 T_m$	Lead-filament junction temperature	ϕ	$=ad\theta/dx$
ΔT	$=T_0 - T_R$	ΔV_H	see Eq. (12)
θ	$=T/T_m$	B_1	Table IV
$(x/a)_{\theta_1}^{\theta_2}$	Distance in a -units from point at θ_1 to point at θ_2	B_{15}	Value of B_1 for $\omega=5$
λ	Thermal conductivity of filament	$\beta(\theta_0)$	Table II
λ_L	Thermal conductivity of lead	τ_0	$=T_0/T_c$
h	Value of any property per cm of filament length		

of energy per unit length of filament, while the expression involving λ corresponds to the net rate of conduction of energy into an element of the filament.

An inspection of tables giving the characteristics of tungsten filaments as functions of the temperature shows that it is possible to express Eq. (23) in a much simpler form.³

The resistance of a tungsten filament can be expressed quite accurately over a wide range of temperatures by the equation $r = cT^\rho$, where c is a constant and $\rho = 1.20$ (for the range between 600°–3,000°K). Similarly the radiated power may be expressed approximately by the relation $w = c'T^\omega$, where ω is fairly constant, having the values, 5.65 at 1,000°K, 5.12 at 1700°, 4.93 at 2,000°, 4.71 at 2,400° and 4.48 at 3,000°. In the majority of experiments in which it is desired to calculate the cooling effect of the leads the temperature of the hottest part of the filament will probably be below 2,400°. By averaging the values of this exponent from 2,000° to 400°, weighing each in proportion to the corresponding value of w , the effective exponent is found to be 5.1. We shall, therefore, take this to be the value of ω . Even at very high filament temperatures, where the effective exponent would be about 4.7, we shall see that the error made by using $\omega = 5.1$ is practically negligible.

The heat conductivity of tungsten at temperatures from 1,300 to 2,500° has been given by Forsythe and Worthing.¹ It ranges from 0.93 watts $\text{cm}^{-1} \text{deg}^{-1}$ at 1,300° to 1.21 at 2,500°. We find that the empirical equation

$$\lambda = 0.840(T/1000)^{0.4} \quad (24)$$

expresses the values of λ at the 13 observed points given in their table (at 100° intervals) within an error of 0.0022 or about 0.2 percent.

This equation is used throughout this paper.

In the central uncooled portion w_m , the power radiated per unit length, is equal to $A^2 r_m$, where r_m is the resistance per unit length at this place. Since A is constant throughout the length of the filament, the temperature exponent of $A^2 r$ is the same as that of r , that is ρ . Hence we can replace the first term in Eq. (23) by $w_m \theta^\rho$. Similarly w may be replaced by $w_m \theta^\omega$. From Eq. (24) we obtain the relation $\lambda = \lambda_m \theta^{0.4}$, where λ_m is the thermal conductivity at temperature T_m . Using the values of λ and $d\lambda/dT$ from this relation, we obtain from Eq. (23)

$$d^2\theta/dx^2 + 0.4(d\theta/dx)^2/\theta = (\theta^{\omega-0.4} - \theta^{\rho-0.4})/a^2 \quad (25)$$

where a is a parameter defined by

$$a^2 = \pi D^2 \lambda_m T_m / 4 w_m. \quad (26)$$

We can replace w_m by its value v_m^2/r_m where v_m is the voltage drop per cm at temperature T_m . The factor $r_m D^2$ which then occurs in the equation is independent of D and varies as $T_m^{1.2}$ (it is in fact the function R' given by Jones and Langmuir).³ Thus

$$r_m D^2 = 7.89 \cdot 10^{-9} T_m^{1.2}. \quad (27)$$

From Eqs. (24), (26), (27)

$$a = 1.812 \cdot 10^{-5} T_m^{1.3} / v_m. \quad (28)$$

In computing a from this equation v_m was found from Tables of characteristics.¹³ Since $v_m \propto D^{-1/2}$, we obtain Eq. (2).

In Eq. (25) set $\omega=5.1$, $\rho=1.2$ and substitute ϕ as defined by Eq. (1) for x

$$\phi d\phi/d\theta + 0.4\phi^2/\theta = \theta^{4.7} - \theta^{0.8}. \quad (29)$$

By taking as new variables ϕ^2 and $\log \theta$ this equation becomes linear and may be solved in the usual way to give

$$\phi^2 = (3 - 5\theta^{2.6} + 2\theta^{6.5})/6.5\theta^{0.8}. \quad (30)$$

The constant of integration, 3, is fixed by the condition that $d\theta/dx=0$, and therefore $\phi=0$ at $\theta=1$, the center of the filament.

For values of θ close to unity (30) may be expanded in terms of $Z=1-\theta$

$$\phi^2 = 3.9Z^2 - 4.81Z^3 + 3.715Z^4 - 0.8886Z^5 + 0.4068Z^6 + 0.27Z^7 + \dots \quad (31)$$

Temperature distribution. When $\theta \leq 0.6$ the integral in Eq. (2) may be found by expanding $1/\phi$ in the series

$$1/\phi = 1.472\theta^{0.4} [1 + (5/6)\theta^{2.6} + (25/24)\theta^{5.2} - (1/3)\theta^{6.5} + 1.447\theta^{7.8} - (5/6)\theta^{9.1} + \dots]. \quad (32)$$

Integration gives

$$(x/a)_0^\theta = 1.0514\theta^{1.4} + 0.3067\theta^4 + 0.2323\theta^{6.6} - 0.0621\theta^{7.9} + 0.231\theta^{9.2} - 0.117\theta^{10.5} + \dots \quad (33)$$

When $\theta \geq 0.6$ Eq. (31) gives

$$1/\phi = 0.5064 [1 + 0.6167Z + 0.0941Z^2 - 0.1809Z^3 - 0.227Z^4 - 0.172Z^5 + \dots] / Z. \quad (34)$$

Integrating we obtain the indefinite integral, and find the integration constant by comparison with Eq. (33) at $\theta=0.6$, where both series are sufficiently convergent to give results accurate to 1 part in 1,000

$$(x/a)_0^{1-Z} = 0.2247 - 1.1660 \log_{10} Z - 0.3123Z - 0.0238Z^2 + 0.0305Z^3 + 0.0287Z^4 + 0.0174Z^5 + \dots \quad (35)$$

Column 2, Table II was calculated from Eqs. (33) and (35).

Lead-filament junction temperature. The rate of flow of heat, Q , in watts, past any point of the filament is equal to the integral, from that part to the center, of the difference between the heat generated by resistance and that lost by radiation.

$$Q = w_m a \int_{\theta}^1 (\theta^{1.2} - \theta^{5.1}) d\theta / \phi. \quad (36)$$

Setting $w_m = Av_m$, substituting for a from Eq. (28), and integrating

$$Q = (1.812 \cdot 10^{-5} T_m^{1.3}) 6.5^{-0.5} (3 - 5\theta^{2.6} + 2\theta^{6.5})^{0.5} A \quad (37)$$

where θ corresponds to the temperature of the point in question.

For short fairly heavy leads at temperatures below 1,000°K the resistance loss and radiation loss in the lead are negligible. All the heat that flows into the lead from the filament must flow out at the cold end, which may be assumed to be at room temperature. Taking the heat conductivity of nickel leads as constant at 0.586 watts cm⁻¹ deg⁻¹, the leads have a constant temperature gradient given by

$$\lambda_L(dT/dl)\pi D_L^2/4=Q. \quad (38)$$

Consequently for the total temperature difference $\Delta T = T_0 - T_R$ for the leads we obtain

$$\Delta T = 4lQ/(\pi D_L^2 \lambda_L). \quad (39)$$

Eqs. (37) and (39) give Eq. (4b) for ΔT in terms of $(\Delta T)_0$. To find the latter we notice that the lead temperature θ_0 has little effect on Q . Setting $\theta_0 = 0.24$, $A = 1$, $l = 1$, $D_L = 0.1$, $\lambda_L = 0.586$, we obtain from Eqs. (37) and (39)

$$(\Delta T)_0 = 145 [1.812 \cdot 10^{-5} T_m^{1.3}]. \quad (40)$$

Eq. (40) was used in conjunction with Table V to compute Table III.

Filament characteristics. We have

$$2\Delta H = H_m - H = 2a \int_{\theta_0}^1 (h_m - h) d\theta/\phi. \quad (41)$$

Applying Eqs. (6) and (28) and substituting for h_m/v_m the equal ratio H_m/V_m , where V_m is the voltage drop that would exist between the ends of the filament if it were all at the temperature T_m

$$\Delta V_H = \Delta H(V_m/H_m) = 1.812 \cdot 10^{-5} T_m^{1.3} \int_{\theta_0}^1 (1 - \theta^n) d\theta/\phi. \quad (42)$$

ΔV_H is a convenient symbol for the expression $\Delta H(V_m/H_m)$. It represents the voltage across a section of uncooled filament of such length that H_m for this section would equal the decrease caused by the cooling effect of the lead. The advantage of this nomenclature is that it requires no knowledge of filament diameter or length.

By breaking up the integral of Eq. (42) into

$$B_1 = \int_0^1 (1 - \theta^n) d\theta/\phi \quad (43)$$

and

$$\beta(\theta_0) = \int_0^{\theta_0} (1 - \theta^n) d\theta/\phi \quad (44)$$

we obtain Eq. (12).

In evaluating B_1 , we meet the difficulty that we must use two different series for $1/\phi$, one for small and the other for large values of θ . Let $1/\phi_1$

be the value of $1/\phi$ given by the first six terms only of the series in Eq. (32) and $1/\phi_2$ by the first six terms only of the series in Eq. (34). We have

$$\begin{aligned} 0 &\leq \theta \leq 0.5 & \phi &= \phi_1 \\ 0.5 &< \theta < 0.65 & \phi_1 &= \phi = \phi_2 \\ 0.65 &\leq \theta \leq 1 & \phi &= \phi_2. \end{aligned}$$

Since the series are equivalent between 0.5 and 0.65 we may put

$$B_1 = \int_0^t (1-\theta^n) d\theta / \phi_1 + \int_t^1 (1-\theta^n) d\theta / \phi_2$$

where $0.5 < t < 0.65$. A simple transformation gives

$$B_1 = \int_0^t (1-\theta^n) (1/\phi_1 - 1/\phi_2) d\theta + \int_0^1 (1-\theta^n) d\theta / \phi_2. \quad (45)$$

The value of $1/\phi_1 - 1/\phi_2$ is practically zero for values of θ between 0.5 and 0.65, and therefore the value of the first integral is not dependent on the actual value of t . Even at $\theta = 0.1$ the value of $1/\phi_1 - 1/\phi_2$ is only 0.117, but at $\theta = 0$ it becomes 0.573. Thus the larger part of the first integral is for values of $\theta < 0.1$. In this range θ^n may be neglected in comparison with unity for all large values of n . Even if $n = 1$ the error in neglecting θ^n will be small.

Calling the first integral of Eq. (45) F_1 , we have

$$\begin{aligned} F_1 &= \int_0^t d\theta / \phi_1 - \int_0^t d\theta / \phi_2 \\ &= (x/a)_0^t - \int_0^t d\theta / \phi_2. \end{aligned} \quad (46)$$

Designate the right hand side of Eq. (35) by F_2 . From the derivation of this equation

$$F_2 + C = \int d\theta / \phi_2$$

C being a constant of integration. Hence

$$\int_0^t d\theta / \phi_2 = [F_2 + C]_{\theta=0}^{\theta=t} = [F_2 + C]_{z=1}^{z=1-t} = F_2(1-t) - F_2(1).$$

But from Eq. (35) $F_2(1-t) = (x/a)_0^t$. Hence from Eq. (46)

$$F_1 = F_2(1) = -0.0348$$

the numerical value being found by setting $z = 1$ in the expression for F_2 in Eq. (35). Due to the definition of ϕ_2 this value is not affected by the missing terms of the series.

Putting the value of $1/\phi_2$ from Eq. (34) in the second integral of Eq. (45), we find

$$B_1 = -0.0348 + 0.5064 \sum_{p=1}^6 A_p \int_0^1 (1-\theta^n)(1-\theta)^{p-2} d\theta$$

where A_1, A_2, A_3 are the coefficients, 1, 0.6167, etc., in the series in Eq. (34). This reduces to

$$B_1 = 0.2247 + 0.5064 \int_0^1 (1-\theta^n) d\theta / (1-\theta) - 0.3123 / (n+1) \\ - 0.0477 [(n+1)(n+2)]^{-1} + 0.1833 [(n+1) \cdots (n+3)]^{-1} \cdots \quad (47)$$

the coefficients of the next two terms being 0.6894 and 2.092.

If n is an integer we have

$$\int_0^1 (1-\theta^n) d\theta / (1-\theta) = 1 + \frac{1}{2} + \frac{1}{3} + \frac{1}{4} + \cdots + 1/n \quad (48)$$

and for other values of n the integral can be expressed in terms of gamma functions. For $n=1.2$, its value is 1.1216. For large values of n the integral is given by the series

$$\int_0^1 (1-\theta^n) d\theta / (1-\theta) = 0.5772 + \log_e n + 1/2n \\ - [12n(n+1)]^{-1} - [12n(n+1)(n+2)]^{-1}. \quad (49)$$

Inserting this value in Eq. (47) and expressing as a series in reciprocal powers of n we obtain Eq. (13).

In computing Table IV for values of n less than 5, Eq. (47) was used but Eq. (13) was found more convenient for the larger values.

To evaluate $\beta(\theta_0)$ we note that in general $\theta_0 < 0.5$ and hence that for fairly large n the term θ^n is negligible, and Eq. (14) holds. For ΔV , when $n=1.2$, $\beta(\theta_0)$ for the third column of Table II was obtained by using the series expansions of $1/\phi$ given by Eqs. (32) and (34).

Application under other conditions. For filaments in the presence of gas, or for filaments of materials other than tungsten there will be changes in the values used in Eq. (29) for ω , ρ and k , where k is the temperature exponent of the thermal conductivity. By methods similar to the derivation of Eq. (30) we find that the general expression for ϕ is

$$\phi^2 = 2\theta^{-2k} [(1-\theta^{\rho+k+1})/(\rho+k+1) - (1-\theta^{\omega+k+1})/(\omega+k+1)]. \quad (30a)$$

The integral B_1 in Eq. (12) may be found by numerical integration or by direct integration in some cases. Thus, when $\omega+k+1=2(\rho+k+1)$, ϕ^2 is a perfect square, and

$$B_1 = (\omega-\rho)^{-1/2} \{ \psi[(n+k+1)/(\rho+k+1)] - \psi[(k+1)/(\rho+k+1)] \} \quad (50)$$

where $\psi(x) = d \ln \Gamma x / dx$ is the logarithmic derivative of the gamma function. Table IVa gives some values of B_1 obtained in some of these ways.

TABLE IVa.
 $B_1 = \int_0^1 (1 - \theta^n) d\theta / \phi$ for various exponents ω, ρ, k, n

ω	ρ	k	n	B_1
5.1	0.0	1.0	5.1	1.695
4.3	1.85	-.4	20.	4.079
6.0	1.0	1.0	1.0	0.371
4.0	1.0	1.0	1.0	0.428
4.0	1.0	1.0	5.0	1.118
4.0	1.0	1.0	10.0	1.486
4.0	1.0	1.0	20.0	1.871
4.0	1.0	1.0	40.0	2.264
3.8	1.2	0.4	27.2	2.522

Data such as those in Table IVa show that the variation of B_1 with ω is small and may be represented thus

$$\text{For } n = \rho \quad B_1 = B_{15} [1 + 0.077(5.0 - \omega)] \quad (51a)$$

$$\text{For } n = 20 \quad B_1 = B_{15} [1 + 0.100(5.0 - \omega)] \quad (51b)$$

where B_{15} is the value of B_1 for $\omega = 5.0$. B_{15} may be found by these equations from tables of B_1 such as Table IVa. Fig. 1 is a plot of B_{15} as abscissa against ρ as ordinate for constant values of k . The full lines are for voltage correction, $n = \rho$. The dotted lines are for $n = 20$.

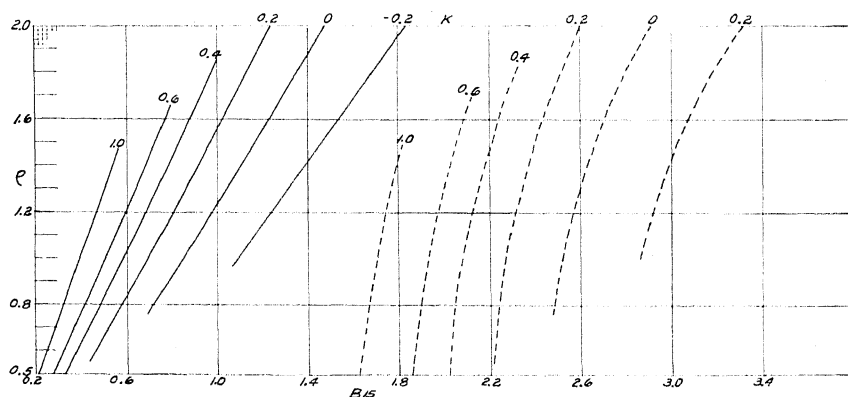


Fig. 1. Plot of B_{15} ($\omega = 5$) against ρ for constant k .
 Full lines $n = \rho$. Dotted lines $n = 20$.

The deviations of B_1 found from Fig. 1 from the value of B_1 , for the same n , found in Table IV may be expressed as a fraction, N , of the latter value. The variation of N with n , for constant values of ω, ρ and k may be approximately expressed by

$$N(n) = N(20) - \alpha(20 - n) [N(20) - N(\rho)] / (20 - \rho) \quad (51c)$$

where

n	ρ	5	10	30	40
α	1	0.42	0.27	0.15	0.11

We may find B_1 for any exponents n , ω , k and ρ by finding $N(20)$ and $N(\rho)$ for the appropriate values of ω , k and ρ from Fig. 1 and Eqs. (51a) and (51b). Eq. (51c) and Table IV then give the desired B_1 .

Other metals. From Eq. (26) and the derivation of Eq. (28) we see that

$$a = (\lambda_m T_m R_m / v_m)^{1/2} \quad (28a)$$

where R_m is the resistivity of the metal in question at the temperature T_m . We then have

$$\Delta V_H = (\lambda_m T_m R_m)^{1/2} [B_1 - \beta(\theta_0)]. \quad (12a)$$

The Wiedemann-Franz law states that, at a given temperature, λR , and hence the coefficient in Eq. (12a), is approximately the same for most metals and alloys. This coefficient is thus given by $1.812 \cdot 10^{-5} T_m^{1.3}$ in Table V. Consequently the magnitude of ΔV_H may be found for any metal which obeys this law with the help of Fig. 1 and the assumption that the change of $\beta(\theta_0)$ is similar to that of B_1 .

End losses from filaments in the presence of gas. Gas around a filament causes a loss of heat by conduction and increases the voltage required to reach a given T_m . Eq (12a) shows that for a fixed T_m , ΔV_H is the same for filaments in gas and vacuum except for the variation in the values of B_1 and $\beta(\theta_0)$. The latter may be evaluated by considering the conduction loss to be part of the radiation loss w in Eq. (23). Thus if at T_m the conduction loss is $1/4$ of the radiation loss, and if the conduction loss varies as $T^{1.7}$,¹⁷ the effect on B_1 may be represented as a change in the effective value of ω from 4.6 to 3.8, which by Table IVa means an increase of about 15 percent in the values of B_1 given in Table IV. In general the values of ΔV_H for vacuum hold with fair accuracy for small gas pressures, but the temperature distribution is altered.

For new filament materials or other new conditions there will be no accurate knowledge of the filament characteristics and the temperature exponents for the application of the above method, which method nevertheless will, we hope, still be capable of indicating whether or not lead losses are important in any given case.

PART II. LEAD LOSSES IN SHORT FILAMENTS

Temperature distribution. Shorter filaments do not admit the assumption, made for most of the results of Part I, that the central portion of the filament is not cooled by the leads. Even the calculation of temperature distribution by adding the effects of the two leads is not very good in these cases. Thus when x/a , the filament half length, is 1.53, for which the cooling effect of one lead at the other gives $\theta = 0.994$, the long filament case gives a central temperature corresponding to $\theta = 0.85$, while the true value is $\theta = 0.8$. Theoretically the maximum temperature T_m can only be attained in an infinitely

¹⁷ These conditions are approximately those for a filament of 0.007 cm diameter at $T_m = 2900^\circ$ in 10 mm of N_2 . See I. Langmuir and G. M. J. Mackay, J. Amer. Chem. Soc. 36, 1717 (1914). For larger filaments the conduction losses are relatively smaller.

long filament (cf. Eq. (35)). A "short filament" is one for which this fact invalidates the conclusions of Part I.

Let T_c be the actual temperature at the center of the filament, and let the larger value T_m still indicate the temperature of a hypothetical portion uncooled by leads as calculated from the current and diameter of the filament. Let $\theta_c = T_c/T_m$.

Eq. (1) holds as before with a more complicated value for ϕ . If $(x/a)_{\theta_0}^{\theta_c}$ is the distance from the center to a lead at temperature $T_0 = \theta_0 T_m$, we have, as before

$$(x/a)_{\theta_0}^{\theta_c} = \int_{\theta_0}^{\theta_c} d\theta/\phi \quad (52)$$

a has the same values as before, and is given in Table I.

Table IX gives the values of $(x/a)_{\theta_0}^{\theta_c}$ for various values of θ_c . Fig. 2 gives the plot of $(x/a)_{\theta_0}^{\theta_c}$ as abscissa against θ as ordinate, for constant values of θ_c . The value of θ_c for any curve is of course the intercept on the θ axis.

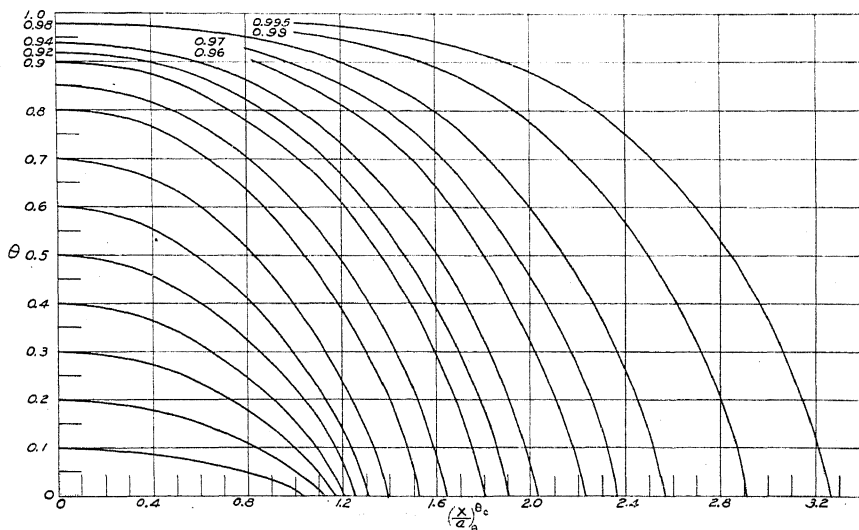


Fig. 2. Plot of $(x/a)_{\theta_0}^{\theta_c}$ against θ for constant values of θ_c .

These curves are temperature distribution curves. Thus if $\theta_c = 0.8$ the curve with that intercept gives us the temperature (θ) at any distance, $(x/a)_{\theta_0}^{\theta_c}$, from the center. To find for any filament the value of θ_c , we need know only one point on the temperature distribution curve. Thus for a filament of known length and of known lead temperature, a point having the coordinates $(x/a)_{\theta_0}^{\theta_c}$, θ_0 is determined on the plot. This point lies on some temperature distribution (constant θ_c) curve—probably not one of these drawn. The value of θ_c may readily be found, however, by interpolating between the two nearest curves. By continuing this interpolation down to the x/a scale, the value $(x/a)_{\theta_0}^{\theta_c}$ is found. This is the value that would obtain if the given

filament were prolonged until its leads were at 0°K, and were left otherwise unchanged. If desired, $(x/a)_{\theta_c}^{\theta_0}$ may be found from θ_c by interpolating in Table IX.

Of course the value of any property h at any point of the filament may be found by first finding the temperature at that point, then applying published data on filament characteristics.^{1,3}

TABLE IX. Relation between the temperature $T_c = \theta_c T_m$ at the center of a short filament with leads at °K and the length $(2x)$ of the filament.

θ_c	$(x/a)_{\theta_c}^{\theta_0}$	θ_c	$(x/a)_{\theta_c}^{\theta_0}$	θ_c	$(x/a)_{\theta_c}^{\theta_0}$
0.005	0.7325	0.4	1.2065	0.94	2.031
.01	.8262	.5	1.2510	.95	2.118
.03	.9221	.6	1.3077	.96	2.225
.05	.9704	.7	1.3905	.97	2.365
.1	1.0401	.8	1.5280	.98	2.565
.2	1.1154	.85	1.6399	.99	2.912
.3	1.1645	.9	1.802	.995	3.261
		.92	1.899	.999	4.074

The effect of lead losses on characteristics. If all the filament were at the actual maximum temperature, T_c , the value H_c of any property for the whole filament would be

$$H_c = 2h_c x = 2ah_c(x/a)_{\theta_c}^{\theta_0}. \quad (53)$$

h_c is the value of the property in question for 1 cm of filament at temperature T_c . The ratio of the actual value for the whole filament, H , to the hypothetical value is H/H_c . The value of this ratio when $\theta_0 = 0$ we designate as $(H/H_c)_0$. If $n > 4$, H is independent of θ_0 for constant θ_c for all the practical range. Hence, applying Eq. (53)

$$H = 2ah_c(x/a)_{\theta_c}^{\theta_0}(H/H_c)_0. \quad (54)$$

H , and hence H/H_c , is a function of n , the temperature exponent of the property in question. In Fig. 3, ordinates $(H/H_c)_0$ are plotted against abscissae $(x/a)_{\theta_c}^{\theta_0}$ for constant values of n (the full lines). The scale for $(x/a)_{\theta_c}^{\theta_0}$ at the top, and the scale for θ_c on the bottom may be used interchangeably. They correspond as in Table IX.

For a given filament, knowing x , a , and θ_0 , $(x/a)_{\theta_c}^{\theta_0}$ is determined from Fig. 2. Fig. 3 then yields $(H/H_c)_0$ for the value of n corresponding to the property in question. H may then be found from Eq. (54).

For $n \leq 4$, H is not independent of θ_0 . For $n = 1.2$, the resistance-exponent, the dotted lines at the top of Fig. 3 give the value of H/H_c [not $(H/H_c)_0$] for constant values of $\tau_0 = \theta_0/\theta_c$. Note however that this is still given in terms of the abscissa $(x/a)_{\theta_c}^{\theta_0}$.

For values of x/a less than 1.0, and hence not in Fig. 2, H/H_c is constant at the value for $x/a = 1.0$.

It is to be remarked that for $T_c < 1000^\circ\text{K}$ none of the given data apply accurately, nor is the temperature distribution accurate. This is because of the uncertainty in the value of λ here.

Limits of long filament case. Table X gives the smallest value of $(x/a)_0^{\theta_c}$ for which the errors in H/H_c made in applying the long filament instead of the short filament case are less than the percentage at the head of the column. The errors of course depend somewhat on the value of n for the property under consideration. A (+) after the value of n indicates that the long filament case gives too large a value of H/H_c , or of H ; that is, too

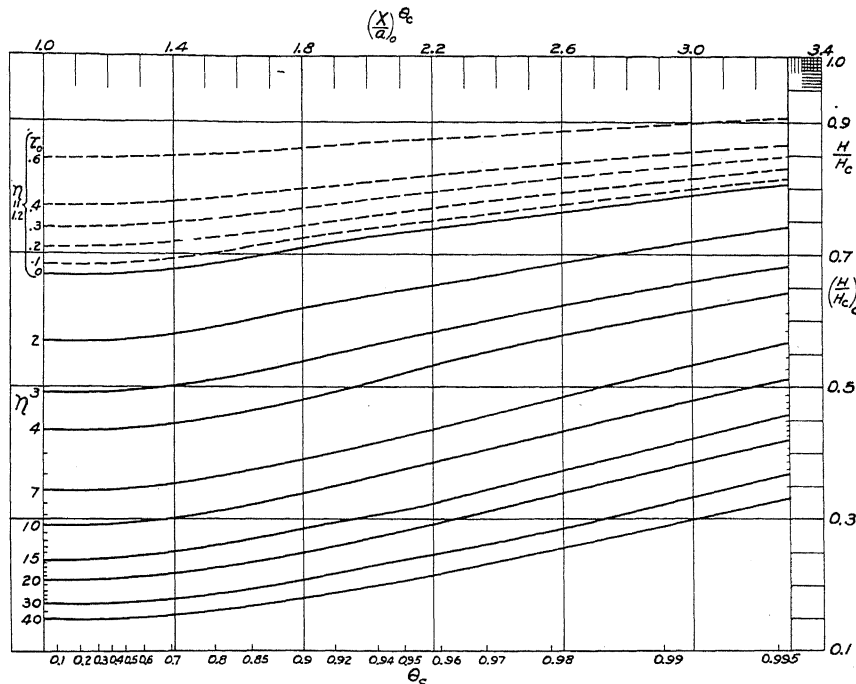


Fig. 3. Full lines $(H/H_c)_0$ for constant n against $(x/a)_0^{\theta_c}$ and θ_c . Dotted lines H/H_c for $n=1.2$ constant τ_0 against $(x/a)_0^{\theta_c}$ and θ_c .

small a value of B_1 . In the neighborhood of $n=5$ the sign of the error changes. For $n=1$ (temperature distribution) the long filament case gives too high temperatures, even when the cooling effects of the two leads are added.

Lead temperatures may be found with sufficient accuracy for most cases from Table III of Part I. For high accuracy or for very short filaments Eqs. (36) and (39) may be applied directly, using Eq. (55).

TABLE X. Errors in H/H_c made in assuming a filament to come under Part I. This table gives approximately the smallest value of $(x/a)_0^{\theta_c}$ for which the error made by that assumption is less than the percentage given at the head of the column.

n	1 percent	5 percent	n	1 percent	5 percent
1.0 (+)	1.9	1.6	10 (-)	2.8	2.3
1.2 (+)	1.9	1.7	15 (-)	2.9	2.6
4 (+)	1.9	1.8	20 (-)	3.0	2.7
5 (\pm)	1.6	1.6	30 (-)	3.2	3.0
7 (-)	2.3	2.0	40 (-)	3.3	3.0

Computation of temperature distribution. Eq. (30) holds with a new constant of integration determined by the condition $\phi = ad\theta/dx = 0$ when $\theta = \theta_c$ (the maximum temperature):

$$1.3\phi^2 = \theta^{-0.8}(\theta_c^{2.6} - 0.4\theta_c^{6.5} - \theta^{2.6} + 0.4\theta^{6.5}). \quad (55)$$

The integration in Eq. (52) is best carried out by series approximations. *Case I.* $\tau = \theta/\theta_c$ is small

$$(x/a)_0^{\theta_c} = \theta_c \int_0^{\tau} d\tau/\phi. \quad (56)$$

Expressing Eq. (55) in terms of τ , then expanding $1/\phi$ by the binomial theorem and integrating the resulting series term by term

$$(x/a)_0^{\theta_c} = 0.8144A^{0.5}\theta_c^{0.1}\tau^{1.4} [1 + 0.175A\tau^{2.6} + 0.0795A^2\tau^{5.2} - 0.0354A\theta_c^{3.9}\tau^{6.5} + \dots] \quad (57)$$

where $A = 1/(1 - 0.4\theta_c^{3.9})$.

In Eq. (57) $\tau^{9.2}$ has been neglected. If $\theta \leq 0.6\theta_c$ the error is less than 1 percent. If in this series we set $\theta_c = 1$, we get the series of Eq. (33) of Part I. *Case II.* $\sigma = 1 - \tau = (\theta_c - \theta)/\theta_c$ is small and θ_c is also small.

Eq. (55) may be expanded in terms of σ to give

$$\phi^2 = 2\theta_c^{1.8}\sigma(1 - \theta_c^{3.9})(1 - \sigma)^{-0.8} [1 - 0.8\sigma(1 - 2.438\theta_c^{3.9}) + 0.16\sigma^2(1 - 24.78\theta_c^{3.9}) + 0.016\sigma^3(1 + 229\theta_c^{3.9}) + \dots].$$

Terms of the form $(1 - b\theta_c^{3.9})/(1 - \theta_c^{3.9})$ were expanded by the binomial theorem, and $\theta_c^{7.8}$ and higher powers neglected. Expanding $1/\phi$ and integrating

$$(x/a)_0^{\theta_c} = \theta_c \int_0^{\sigma} d\sigma/\phi = \theta_c^{0.1}(1 + \frac{1}{2}\theta_c^{3.9})(2\sigma)^{0.5} [1 - 0.33\theta_c^{3.9}\sigma - 0.024\sigma^2(1 - 10\theta_c^{3.9}) - 0.0034\sigma^3(1 + 5.38\theta_c^{3.9})]. \quad (58)$$

This is accurate when σ^4 and $\theta_c^{7.8}$ may be neglected in comparison with unity. At $\theta_c = 0.56$ this error is about 1 percent.

Case III. σ is small and θ_c large.

Let $z = 1 - \theta$ and $z_c = 1 - \theta_c$. z and z_c are both small. Expanding (55) by the binomial theorem

$$1/\phi = 0.5064(1 - 0.4z - 0.12z^2 + \dots)(z^2 - z_c^2)^{-0.5} [1 + 1.0167C_1 + C_2 + \dots]. \quad (59)$$

where

$$\begin{aligned} C_1 &= (z^3 - z_c^3)/(z^2 - z_c^2) \doteq z [1 + (1/2)(z_c/z)^2] \\ C_2 &= 1.5504C_1^2 - 0.930(z^4 - z_c^4)/(z^2 - z_c^2) \\ &\doteq [0.621 + 1.008(z_c/z)^2]z^2 \end{aligned}$$

substituting, multiplying Eq. (59) out, collecting like terms and integrating

$$(x/a)_{\theta_c}^{\theta_c} = \int_{z_c}^z dz/\phi = 0.5064(1+0.852z_c^2) \operatorname{arc} \cosh (z/z_c) + 0.3123(z^2 - z_c^2)^{0.5} \\ + 0.2574z_c \operatorname{arc} \cos (z_c/z) + 0.0239z(z^2 - z_c^2)^{0.5} \quad (60)$$

This series is good if $\theta_c \geq -0.7$; $\theta \geq 0.5$.

Case IV. θ_c is nearly unity.

We may choose z small enough for series (60) to converge, but at the same time much larger than z_c . The small quantity z_c then has little effect on the integral from 0 to $1-z$. To evaluate this integral we may neglect z_c entirely and use Eq. (35) of the long filament case, which, by the choice of the integration constant, gives the value of $(x/a)_0^{\theta}$. z as chosen above is sufficiently small for this series also to converge. Adding Eqs. (35) and (60), expressing $\operatorname{arc} \cosh (z/z_c)$ as a logarithm and $\operatorname{arc} \cos (z_c/z)$ as a series, and remembering that z is much larger than z_c , we obtain

$$(x/a)_{\theta_c}^{\theta_c} = 0.5757 - 1.16596 \log_{10} z_c + 0.4043z_c + 1.9z_c^2. \quad (61)$$

The coefficient of the last term was chosen empirically so as to compensate for the missing terms. Note that the result is independent of the specific value of z , as long as it has such a value as to make the derivation valid.

Thus we can obtain $(x/a)_0^{\theta}$ by Case I and $(x/a)_{\theta_c}^{\theta_c}$ by Case II or III. These two methods overlap in the admissible values of θ except for intermediate values of θ_c , when neither Case II nor Case III is very good. Numerical integration was used for accurate results in this region. The value of $(x/a)_0^{\theta_c}$ may be obtained by Case IV or by the formula

$$(x/a)_{\theta_c}^{\theta_c} = (x/a)_0^{\theta_c} + (x/a)_{\theta_c}^{\theta_c}.$$

Table VII and Fig. 2 were obtained by the above methods.

Filament characteristics. Assuming as in Part I that the value of the property in question varies as the n th power of the temperature, we have

$$H = 2h_c \int_0^x (T/T_c)^n dx = 2ah_c J \quad (62)$$

where

$$J = (1/\theta_c^n) \int_0^{\theta_c} \theta^n d\theta/\phi - (1/\theta_c^n) \int_0^{\theta_0} \theta^n d\theta/\phi. \quad (63)$$

If $n > 4$, θ^n becomes rapidly smaller with decreasing θ . Hence we may neglect the second integral to obtain

$$J = (1/\theta_c^n) \int_0^{\theta_c} \theta^n d\theta/\phi. \quad (64)$$

From Eqs. (53) and (62)

$$(H/H_c)_0 = J/(x/a)_0^{\theta_c}. \quad (65)$$

There are two limiting cases to be considered.

Case I. θ_c is small.

We may neglect $\theta_c^{6.5}$ in Eq. (55). Introducing $\tau = \theta/\theta_c$ we obtain from Eqs. (63), (53), (62), (52), and (55)

$$H/H_c = \frac{\int_{\tau_0}^1 \tau^{n+0.4} d\tau (1-\tau^{2.6})^{-0.5}}{\int_{\tau_0}^1 \tau^{0.4} d\tau (1-\tau^{2.6})^{-0.5}}.$$

The value of θ_c has cancelled out. If $\tau_0 = \theta_0/\theta_c$ is held fixed, then H/H_c is independent of θ_c . Hence in Fig. 3 the values for $x/a < 1.0$ are the same as those given for $x/a = 1.0$.

Case II. θ_c is large.

As θ_c approaches unity we get the transition from the short filament to the long filament case. When $z_c = 1 - \theta_c$ can be neglected entirely, Eqs. (64) and (43) give

$$(x/a)_{0^c}^{\theta} - \theta_c^n J = B_1. \quad (66)$$

From Eq. (62)

$$H = 2a h_m (\theta_c^n J).$$

Thus when (66) is satisfied the value of H increases in direct proportion to the increase of length. This is because the central portion, to which the increased length is added, is at practically constant temperature.

The degree to which Eq. (66) is satisfied is a measure of the approximation involved in assuming that the filament is long. To construct Table VIII the true values of J as found below were compared with the value calculated from Eq. (66). For $n=0$ the short filament temperature distributions were compared with those obtained from the long filament case by adding the cooling effect of the two leads.

Evaluation of J . If θ_c and hence $D = 0.4 \theta_c^{3.9} (1 - 0.4 \theta_c^{3.9})^{-1}$ is small, we set $y = (\theta/\theta_c)^{2.6}$ in Eq. (64) and obtain, using Eq. (55)

$$J = \theta_c^{0.1} M (1/5.2)^{1/2} (1 - 0.4 \theta_c^{3.9})^{-1/2} \quad (67)$$

where

$$M = \int_0^1 y^p dy (1-y)^{-1/2} [1 - Dy(1-y^{3/2})(1-y)^{-1}]^{-1/2} \quad (68)$$

and $n = 2.6p + 1.2$. M may be expanded as a power series in D

$$M = G_0 + (1/2)G_1 D + (3/8)G_2 D^2 + (5/16)G_3 D^3 + \dots \quad (69)$$

where

$$G_k = \int_0^1 y^{p+k} (1-y)^{-1/2} [(1-y^{3/2})(1-y)^{-1}]^k dy. \quad (70)$$

Each of these integrals may be expanded in terms of $u=1-y$, and then integrated by means of gamma functions.

$$\begin{aligned}
 G_0 &= \pi(-1/2)\pi(p)/\pi(p+1/2) \\
 G_1 &= \frac{3\pi(-1/2)\pi(p+1)}{2\pi(p+3/2)} [1 - (1/8)(p+5/2)^{-1} \\
 &\quad - (1/32)(p+5/2)^{-1}(p+7/2)^{-1} + \dots] \\
 G_2 &= \frac{9\pi(-1/2)\pi(p+2)}{4\pi(p+5/2)} [1 - (1/4)(p+7/2)^{-1} \\
 &\quad - (1/64)(p+7/2)^{-1}(p+9/2)^{-1} + \dots] \\
 G_3 &= \frac{27\pi(-1/2)\pi(p+3)}{8\pi(p+7/2)} [1 - (3/8)(p+9/2)^{-1} \\
 &\quad + (3/64)(p+9/2)^{-1}(p+11/2)^{-1} + \dots].
 \end{aligned} \tag{71}$$

As θ_c and D become larger the series of Eq. (69) does not converge rapidly. A better series may be obtained by setting

$$M = G_0(1 - g_1 D - g_2 D^2 - \dots)^{-1/2} \tag{72}$$

and determining the value of each g_i in terms of the G_k 's by expanding Eq. (72) and equating coefficients with Eq. (69).

If θ_c is very small, D may be neglected entirely. For the case $n=0$, Eqs. (69), (71), (67) give

$$J = (x/a)_{\theta_c}^{\theta_c} = 1.309(\theta_c)^{0.1}. \tag{73}$$

This is useful in determining the smaller values of Table VII.

When $0.9 \leq \theta_c < 1$ even series (72) does not give accurate results. The values of J here were determined by means of Simpson's rule. The difficulties due to the infinite integrand at $\theta = \theta_c$ were avoided by an integration by parts.

If n is small, θ_c may not be neglected as in Eq. (64). The most important case is $n=1.2$ (the exponent for resistance). The values of J may be found from Eq. (63), the first integral being evaluated by the methods above, and the second integral by a series similar to that of Eq. (57). This holds over the useful range $\theta_0 \leq 0.6 \theta_c$.

A similar method might be used for other small values of n . The calculations for the second integral may be simplified by neglecting $\theta^{0.5}$ in Eq. (55). At $\theta_0 = 0.6 \theta_c$ the error made thus is less than 3 percent for any short filament ($\theta_c \leq 0.94$). Since this integral is a correction term, the approximation is justified. By substituting $u = 1 - 0.4\theta_c^{3.9} - (\theta/\theta_c)^{2.6}$, the integral is reduced to a form which may be evaluated in terms of elementary functions for $n=1.2, 2.5, 3.8, 5.1$ and 6.4 . Interpolation may be used for intermediate values of n .

For $n \geq 4$ Eq. (64) is valid, unless high accuracy is desired. When $n=10$, $\theta_c=0.7$, $\theta_0=0.5$, the error is less than 1 percent.

Experimental checks. Several lamps were made up to test the short filament theory by experiment. Filament L was a straight filament 1.6 cm long, $D=0.0256$ cm, cut from a length of wire that had been aged 24 hours at 2400° . It was welded to nickel leads 5 cm long, $D_L=0.254$ cm. The temperature distribution along this filament was measured by means of an optical pyrometer mounted on a carriage that could be moved along a horizontal scale which gave the position of the pyrometer accurately to 0.001 inch. The pyrometer had previously been calibrated against a standard lamp.

The curves in Fig. 4 show the temperature distribution for three different currents. The solid lines indicate the observed values, and a comparison of T_c in each case with the corresponding value of T_m listed in the corner of

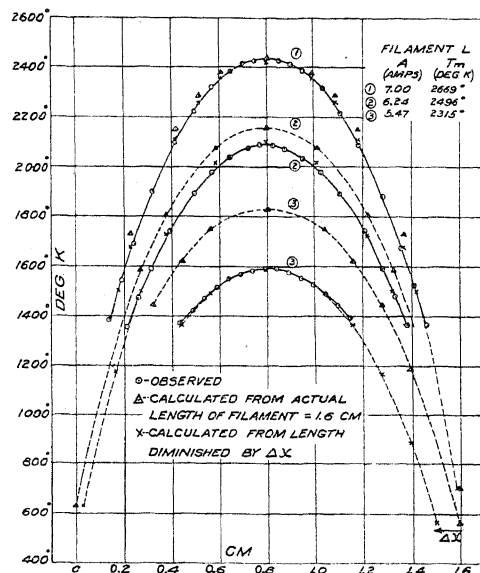


Fig. 4. Temperature distribution for filament L , $D=0.0256$ cm, $2x=1.6$ cm, wire aged throughout its length. Experimental and theoretical curves.

the graph, shows that the center of the filament is greatly cooled by the leads; in other words, filament L is a "short filament."

The temperature distribution was calculated from the short filament theory and the results shown in the curves marked by triangles. In Curve 1 where $\theta_c=0.912$ and $T_m-T_c=234^\circ$, the agreement with experiment is fairly good. In the more nearly extreme cases of Curve 2 where $\theta_c=0.836$, $T_m-T_c=408^\circ$, and Curve 3 where $\theta_c=0.687$, $T_m-T_c=725^\circ$, the temperatures given by the theory are too high. We attribute this departure from the observed values to an error in the value of λ at the cool ends of the filament. The heat conductivity of tungsten is not accurately known at temperatures below incandescence, and if we have used values of λ in this range that are too low, so that the calculated temperature gradient near the leads is too steep, the resulting T_c will be too high. An error from this source becomes important

only when the short filament theory is put to the severe test of predicting T_c in cases where T_c is much less than T_m .

Since T_c must be known before either the voltage or the candle-power of a filament can be calculated, the following empirical addition to the theory has been devised, to be used in those cases in which T_c can be determined only by calculation. To compensate for the error that results from using values of λ that are too low, we proceed as if the length of the filament were shortened by an amount Δx such that the heat loss by conduction will be increased above Q_λ , the value corresponding to λ , by an amount $\psi = 4Q_\lambda\Delta x/(\pi D^2)$. Q_λ is given by Eq. (37) which for $\theta_0 = 0.24$ becomes approximately

$$Q_\lambda = 0.6654 A \theta_c (1.812 \cdot 10^{-5} T_m^{1.3}) \quad (74)$$

It has already been pointed out, in connection with the derivation of Eq. (40), that changes in θ_0 have little effect on the factor 0.6654. θ_c supplies approximately the factor by which Q_λ must be reduced when the integration in Eq. (36) is carried only to θ_c instead of to 1. The term in brackets is given in Table V. Values of ψ derived from the data of Fig. 4 are given in Table XI. They were calculated using those values of Δx which made the theoretical and observed curves coincide at 1500°; the theoretical curves are indicated by crosses. ψ is tabulated as a function of T_0 , since the error is greater at low lead temperatures.

TABLE XI.

$T_0 =$	300°	400°	500°	600°
$\psi =$	471	367	263	159

From Table V and Table XI one can calculate

$$\Delta x = \pi D^2 \psi / (4Q_\lambda) \quad (75)$$

and subtract Δx from the actual half length x of the filament before calculating T_c . This correction applies to calculations of T_c only, and the maximum values to be used are $0.15x$ for leads in air, and $0.22x$ for leads in liquid air.

Fig. 5 is a plot of the volt-ampere characteristics of filament G, 1.928 cm in length, $D = 0.0103$ cm. The curves labelled air, using the bottom scale for voltage are for the bulb at room temperature, 300°K. The curves labelled liquid air, using the top scale for voltage, are for the bulb immersed in liquid air.

The course of the liquid air observations for low voltages is interesting. For $450^\circ < T_c < 1200^\circ$ and $T_m \approx 2,000^\circ$, the current decreases with increasing voltage. This phenomenon has been obtained with all short filaments which have been tried in liquid air.

Thus for one value of the current there are in some cases three possible values of the central temperature of the filament. With a low temperature the heat generated is small and so the small temperature gradient is sufficient to carry away the heat and maintain equilibrium. Likewise, with a

higher central temperature the heat generated is greater and the larger temperature gradient is necessary to preserve stability. Hence it is possible that all three central temperatures may be stable. The phenomenon may be explained in more detail by assuming that below $1,200^\circ\lambda$ is larger than the value given by Eq. (24). Analysis shows that the general form of Eq. (73), which gives $(x/a)_0^{\theta_c}$ for small θ_c , is

$$(x/a)_0^{\theta_c} \propto \theta_c^{(1+k-\rho)/2}. \quad (73a)$$

If k , the thermal conductivity exponent, is less than 0.2, then by Eq. (73a) the temperature distribution curves of Fig. 2 will cross near $\theta=0$ and $x/a=1$. Thus $(x/a)_0^{\theta_c}$ and hence also T_m and A decrease with increasing θ_c for small values of the latter. This is essentially the phenomenon observed above.

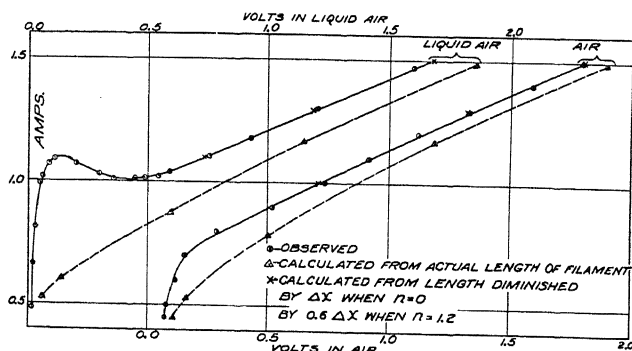


Fig. 5. Volt-ampere characteristics of filament G , $D=0.0103$ cm, $2x=1.928$ cm, wire aged throughout its length. Experimental and theoretical curves.

To obtain the calculated voltages, marked by crosses on the curves in Fig. 5, a correction of $0.6\Delta x$ subtracted from x was found sufficient to compensate for the decreased voltage drop along the ends of the filament due to the lower temperature which we assume to exist in this region. Thus for $n=0$, (temperature distribution) the correction is Δx ; for $n=1.2$ it is $0.6\Delta x$; and for higher values of n no correction is needed.

Example of the calculations. To illustrate the method of calculating lead losses, consider filament G running at a current of 1.295 amps. From $D=0.01030$ cm we find $D^{3/2}=0.001045$, $A/D^{3/2}=1239$, thence $T_m=2222^\circ(12)$. Table I gives by interpolation $a_0=0.400$, whence, as $D^{1/2}=0.1015$ we find from Eq. (2) that $a=0.406$. To determine the lead junction temperature, we find in Table III that $(\Delta T)_0=59^\circ$ and hence with $l=5$ cm and $D_L=0.254$ cm Eq. (4b) gives $\Delta T=59^\circ$. Thus $T_0=359^\circ$, and by interpolation in Table XI $\psi=410$. Table IV gives $(1.812 \cdot 10^{-5} T_m^{1.3})=0.4064$, so that from Eq. (75) we have $\Delta x=0.100$ cm if we put $\theta_c=1$. The half-length $x=0.964$, therefore $x'=x-\Delta x=0.864$. Dividing by $a=0.406$ we have $(x'/a)_{\theta_0}^{\theta_c}=2.128$. Since $T_0=359^\circ$ we find θ_0 by dividing by T_m , and have $\theta_0=0.1616$. We then find

the point of coordinates 2.128, 0.1616 on Fig. 2, and drawing through it a curve parallel to the given curves we obtain the intercepts $\theta_c = 0.959^{18}$ and $(x'/a)_0^{\theta_c} = 2.220$. Multiplying θ_c by T_m we find $T_c = 2131^\circ$.

Eq. (54) shows that the voltage of a short filament is given by

$$V = A(H/H_c)8xp_c/(\pi D^2) \quad (76)$$

ρ_c is the resistivity at T_c and is $61.12 \cdot 10^{-6}$ ohm cm^{18} . To find H/H_c we must first obtain τ_0 by dividing 359° by T_c to obtain 0.168. From Fig. 3 for abscissa $(x'/a)_0^{\theta_c} = 2.220$ we find $H/H_c = 0.766$. We substitute for x in Eq. (76) the corrected value $x - 0.6\Delta x = 0.904$ and obtain $V = 1.315$ volts. The experimental value was $V = 1.330$.

To find the candle power we use Eq. (54) to give

$$\text{Candle power} = H_c = 2aDC_c'(H/H_c)_0(x/a)_0^{\theta_c} \quad (77)$$

C_c' , the specific candle power of tungsten at T_c , is found to be 47.3 international candles $\text{cm}^{-2(18)}$. From Eq. (18) using T_c instead of T_m we find the effective value of n to be 12.53. From Fig. 3 for abscissa $(x'/a)_0^{\theta_c} = 2.220$ we then find $(H/H_c)_0 = 0.362$. $(x/a)_0^{\theta_c}$ is obtained from $(x'/a)_0^{\theta_c}$ by multiplying by $x/(x - \Delta x)$ to give 2.477. We thus obtain $H_c = 0.355$ international candles. We did not measure the candle power in this instance, but in other instances similar calculations of candle power gave results that were in good agreement with experimental values.

Discussion of experimental checks. In ordinary practice the ends of a filament are "unaged," that is, they can never be heated to the temperature which a filament must once have before the properties become those of "aged" tungsten. It is known⁶ that heating tungsten wire for one minute to a temperature of about 1500° causes the cold resistance to be lowered 15 to 20 percent, and presumably the heat conductivity would be increased at the same time by about the same amount. The filaments used for experimental checks were made from wire that had been previously aged throughout its length, in order to obtain uniform results, for the properties of unaged wire vary from sample to sample and depend on the history of the filament. It has been shown that in the case of aged tungsten the heat conductivity at the cool ends of the filament is higher than the values used in the theory. But where the filament is unaged in this region, the heat conductivity is lower than in the case of the aged filament which tends to restore λ to the values used in the theory so that in general the short filament theory may be used without the correction Δx to calculate lead losses from filaments that are made in the ordinary way.

¹⁸ Where θ_c comes out to be less than 0.95 it is well to substitute θ_c equal to the calculated value instead of unity in Eq. (74), and thus arrive at a second approximation for Δx from Eq. (75).

THE ABSORPTION COEFFICIENT FOR SLOW ELECTRONS
IN CADMIUM AND ZINC VAPORS

BY ROBERT B. BRODE

DEPARTMENT OF PHYSICS, UNIVERSITY OF CALIFORNIA

(Received January 27, 1930)

ABSTRACT

The variation with the electron velocity of the absorption coefficient, α , or the effective collision cross-section has been measured in the vapors of cadmium and zinc and found to follow a curve of the type previously found for mercury. The cadmium curve has a maximum at about 40 volts, $\alpha=130$, and a minimum at about 25 volts, $\alpha=126$, followed by a steady rise with decreasing velocity to the limit of accurate measurements, 1 volt, $\alpha=700$. The zinc curve has a very flat maximum at about 50 volts, $\alpha=76$, a minimum at about 36 volts, $\alpha=74$, followed by a steady rise to $\alpha=500$ at 1 volt. The magnitudes of the maximums are in the order: Cd, $\alpha=130$; Zn, $\alpha=75$; and Hg, $\alpha=60$. Other related properties of these atoms, such as the molar refractivity and the critical potentials, show this same irregularity in order.

THE measurement of the absorption coefficient for electrons in the noble gases, Ar, Kr and Xe,¹ has shown that the shape of the curves obtained is the same for all three of these. Similar measurements in the vapors of the alkali metals² have shown that these elements also have a characteristic type of curve. Mercury has been studied by Brode,^{3,7} Maxwell,⁴ Beuthe,⁵ and Jones.⁶ All of these observers except Beuthe have found a curve with values of the absorption coefficient in excellent agreement. Cadmium and zinc were also studied at the same time with the first measurements of mercury.³ These observations were shown by subsequent experiments⁷ to be unreliable, due to secondary and reflected electrons which were present in the form of apparatus used for the first measurements.

The apparatus, Fig. 1, used for the measurements of cadmium and zinc was of the same design as that described in the measurements of mercury.⁷ About half of the measurements in cadmium vapor were made with the apparatus used for the mercury measurements. The mean radius of the path was 15 mm and the final slit was 0.5 mm wide. The rest of the observations in cadmium were made with an apparatus in which the mean radius of the path was 10 mm and the width of the final slit 1.0 mm. All of the measurements in zinc were made with this same apparatus.

¹ C. Ramsauer, Ann. d. Physik 72, 345 (1923).

² R. B. Brode, Phys. Rev. 34, 673 (1929).

³ R. B. Brode, Roy. Soc. Proc. A109, 397 (1925).

⁴ L. R. Maxwell, Proc. Nat. Acad. Sci. 12, 509 (1926).

⁵ H. Beuthe, Ann. d. Physik 84, 949 (1927).

⁶ T. J. Jones, Phys. Rev. 32, 459 (1928).

⁷ R. B. Brode, Roy. Soc. Proc. A125, 134 (1929).

The control of the temperatures, the neutralization of the earth's field, the deflecting magnetic field, and the arrangement of the electrical circuits was the same as previously described in the mercury⁷ and alkali² metal

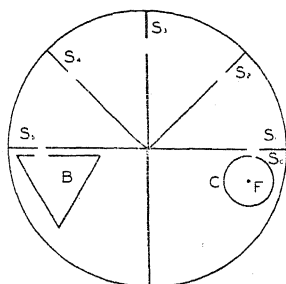


Fig. 1. Diagram of apparatus.

papers. The pressure of the gas was obtained from the vapor pressure at the temperature of the lower furnace which contained the supply of metal. This pressure was corrected for thermal effusion and the observations were

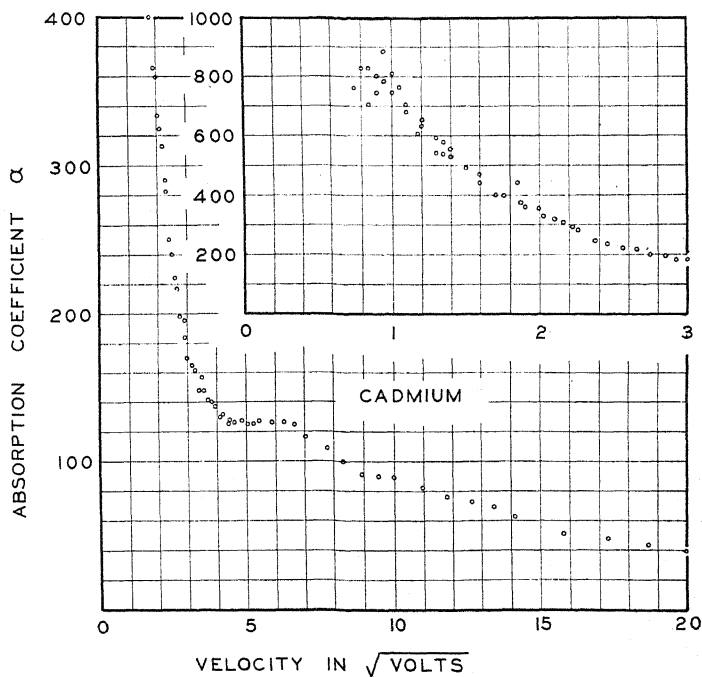


Fig. 2. The absorption coefficient α for electrons in cadmium vapor as a function of the velocity of the electrons.

reduced to 0°C and 1 mm of Hg pressure. The constants of the vapor pressure equation were taken from those given in the International Critical Tables.⁸

⁸ International Critical Tables, Vol. III, p. 205.

These constants for zinc and cadmium are much more accurately determined than those for the alkali metals. The principle source of uncertainty in the values of the absorption coefficients is not due to the vapor pressure constants in this case but to the determination of the temperature. From the uncertainty in the temperature, not over 2°C , the resulting absorption coefficients might be in error by about 5 percent. Small differences in the temperature could be measured to 0.1°C .

Samples of the metals were used which were over 99 percent pure. These were distilled several times in vacuum and finally into the apparatus, which had previously been baked at 500°C for several hours, and the metal

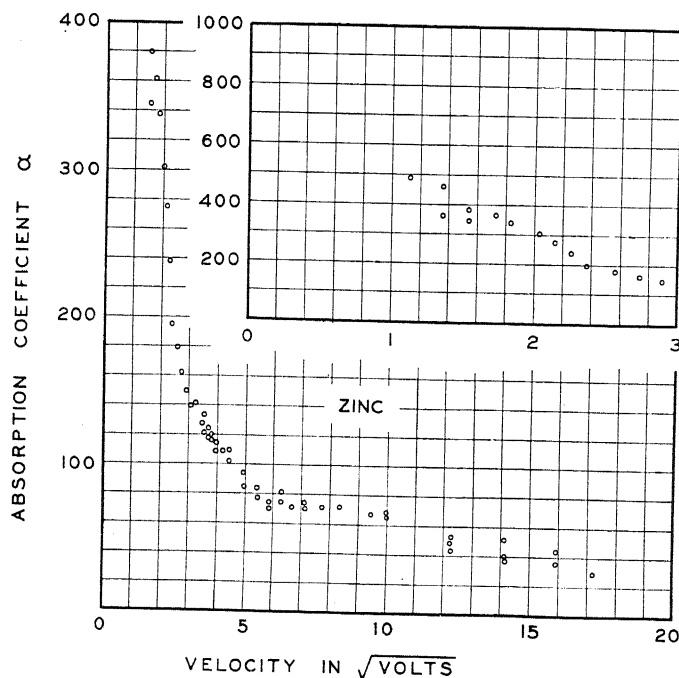


Fig. 3. The absorption coefficient α for electrons in zinc vapor as a function of the velocity of the electrons.

parts glowed by an induction furnace. This treatment was effective in removing the gases absorbed in the cadmium and zinc as measurements of the absorption coefficient were constant over a period of two months in a closed apparatus.

By plotting the log of the ratio of the current at the end of the path to the current from the slit in the cylinder, S_e , against the pressure, a straight line was obtained. The slope of the line gave the value of the absorption coefficient for unit pressure. Figs. 2 and 3 show the resulting values of the absorption coefficient for cadmium and zinc. Each point is the result of measurements at from 3 to 5 different pressures. Due to increasing leakage currents above 300°C , the data obtained with zinc were not as consistent as

those obtained with cadmium. The data taken with the two different experimental arrangements in cadmium are shown on the graph and are seen to be in excellent agreement. In the upper right portion of each graph the low velocity measurements are plotted. In cadmium the measurements were taken to 0.5 volts but, due to the leakage currents at the higher temperature used with zinc, the measurements could not be extended to 1.0 volt in zinc. There is an indication that the absorption coefficient in cadmium ceases to rise as rapidly below one volt as above one volt.

The opening of the final slit determines the maximum angle through which an electron may be deflected without being measured as absorbed. In

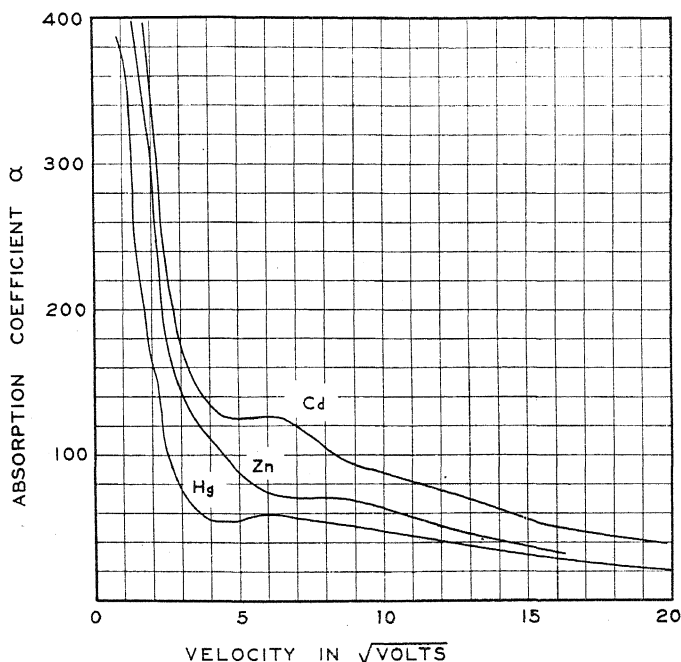


Fig. 4. The absorption coefficient α for electrons in cadmium, zinc and mercury vapors as a function of the velocities of the electrons.

cadmium two systems of slits and chambers were used with different limiting angles but the values of the absorption coefficient were not changed. Measurements by several observers on mercury⁷ gave results that are quite consistent although the chambers used were geometrically quite different. This would indicate that the number of electrons scattered through small angles is only a small fraction of the total number of scattered electrons. These results are not in agreement with the measurements of Arnot⁹ which indicate that a large fraction of the electrons of 82 volts velocity in mercury vapor are scattered in small angles. An apparatus with an adjustable aperture is being constructed to test this point.

⁹ Arnot, Roy. Soc. Proc. A125, 660 (1929).

In Fig. 4 the curves for cadmium and zinc are compared with that for mercury. The values of α for mercury⁷ have been changed from those due to vapor pressure data in Landolt and Börnstein's tables used in the original report to the data given in the International Critical Tables¹⁰ from which the vapor pressure data for cadmium and zinc were also taken. This involves an increase of about 10 percent in the values of α . The character of all the three curves is the same; a very large effective cross-section for slow electrons which decreases rapidly with increasing velocity to a minimum, then rises slightly to a faint maximum followed by a steady decrease with further increase in velocity.

The curves indicate that cadmium is the largest of the three, zinc is next, and mercury is the smallest. This is the order of size to be expected rather than that of increasing atomic weight. The classical scattering of electrons due to the polarization of the atom by a passing electron was shown by Zwicky¹¹ to give the right order of magnitude for the absorption coefficients in the noble gases at velocities above the maximum in the curves. The absorption coefficient was proportional to the molar refractivity. The molar refractivities for these elements are Cd = 20.0 Zn = 14.6, and Hg = 13.7. This same agreement between the absorption coefficients and molar refractivity is found in the alkali vapors. The effective size of an atom is also indicated by its ionization potential. Helium, with the highest ionization potential, has one of the smallest effective cross-sections of any observed atom while caesium, with the lowest ionization potential, has the largest effective cross-section. The ionization potentials of the elements studied in this paper are Cd 8.9 volts, Zn 9.4 volts and Hg 10.4 volts. In the curves of elements not in the same row of the periodic table and therefore of different shape, it is not always easy to designate one as larger than the other. In general, however, it seems to be true that the magnitude of the absorption coefficient or the effective collision cross-section of an atom is proportional to the molar refractivity and inversely proportional to the ionization potential.

¹⁰ International Critical Tables, Vol. III, p. 206.

¹¹ F. Zwicky, *Phys. Zeits.* 24, 171 (1923).

COHESION IN MONOVALENT METALS

By J. C. SLATER

JEFFERSON PHYSICAL LABORATORY, HARVARD UNIVERSITY

(Received January 27, 1930)

ABSTRACT

The theory of metallic structure, of Sommerfeld, Heisenberg, and Bloch, is carried far enough to explain cohesive forces, and calculations are made for atoms with one valence electron, particularly metallic sodium. The numerical results, though rough, are in qualitative agreement with experiment. It is found that the forces in general are of the same nature as those met in ordinary homopolar binding, discussed by Heitler and London; except that the purely electrostatic force from penetration of one atom by another is relatively more important, the valence effect from the exchange of electrons relatively less important, than in diatomic molecules.

As a preliminary to the calculation, the relations of the methods of Heisenberg and of Bloch are discussed, and it is shown that they are essentially equivalent in their results when properly handled. Remarks are made both about conductivity and ferromagnetism. In connection with conduction, it is shown that a definite meaning can be given to free electrons, that they are necessary to conduction, and that a method can be set up for computing their number, which is rather small compared with the number of atoms. Ferromagnetism is discussed in connection with a recent paper of Bloch. It is shown that a metal like an alkali cannot be ferromagnetic, for atoms at such a distance that the interatomic forces keep the metal in equilibrium, are too close to be magnetic. For ferromagnetism, rather, it seems necessary to have one group of electrons responsible for cohesion, and another group, of smaller orbit and therefore relatively farther apart, producing the magnetism; a situation actually found only in the iron group and the similar groups.

I. INTRODUCTION

A CRYSTAL of a metal is an enormous molecule, with electronic energy levels depending on the positions of all the nuclei, just as the electronic energy of a diatomic molecule depends on the internuclear distance. In this paper, in which we are interested in cohesive forces, we must find this energy of the lowest state in terms of the size of the crystal. We limit ourselves to geometrically similar arrangements of the nuclei, with changing scale. From the minimum of the curve, we find the heat of dissociation, grating space, and compressibility of the metal. But also we can investigate the wave function of this lowest state, and obtain information about the electric and magnetic properties of the metal. In this way we are naturally led to a discussion of the calculations of Heisenberg¹ and of Bloch on these subjects; in order to be sure that we really understand the arrangement of energy levels, we discuss the relationships of their methods, and arrive at a consistent picture combining them.

¹ W. Heisenberg, *Zeits. f. Physik* **49**, 619 (1928);
F. Bloch, *ibid.* **52**, 555 (1929).

As for the results, one naturally asks first, what are the forces holding a metal together? Are they ordinary attractions on account of penetration of atoms, or valence forces, or electrostatic forces of ionic attraction, or van der Waals forces, or some special sort not found in other cases? This question cannot be answered categorically; no doubt all the forces are simultaneously present, and the problem is to find the relative magnitudes. The tentative result at which we arrive is that the simple penetration of one atom by another is the most important part of the effect. But valence effects are also present, although weakened by having the valences shared by many neighbors, and are responsible for a considerable fraction of the attraction. Although these actual magnitudes may not be verified by more accurate calculation, still we have discussed the problem in enough detail so that the general relations can be understood in any case.

The other question one will ask is, what is the situation of the electrons in the metal? Can one give a meaning to the question, how many free electrons are there? The answer, from whichever side we look at the question, seems to be the same. Most of the valence electrons are at any time attached to their atoms. These electrons cannot take part in conduction; they could do it only by having a whole file of such electrons simultaneously jump to the next atom in line, a most unlikely occurrence. But a few electrons at any time—calculation suggests a few percent—will be detached from their atoms, leaving an equal number of positive ions behind them; and they are what, by all rights, one should call free electrons. These electrons, and the positive ions left behind, can take part in conduction. First, the free electrons can move easily from one atom to the next. Second, a bound or associated electron on one of the atoms next a positive ion can jump to that ion, leaving its own atom ionized. We are thus led precisely to the dual theory of conduction, by free and by associated electrons, which Professor Hall² has suggested and elaborated. When we look at the metal by the method of Heisenberg, these results become clear. In that method, a wave function consists of the assignment of electrons to atoms. We find that we must go beyond Heisenberg, in assigning sometimes two electrons to one atom, sometimes none, instead of always one; for we need such states to solve the problem of the stationary states of the metal. That is, we introduce free electrons. And when we consider transitions from one state to another, it is easy to see that these transitions can result in conduction only when such free electrons are present. On Bloch's scheme, where we describe directly the velocity, rather than the position, of the electrons, it is less easy to see the relation; but here too one can show that, if there are no free electrons, the velocities of all electrons must compensate, so that there is no net current. Since this paper is not primarily about conduction, we do not go into these points with any detail.

The only metals specifically treated are those with one valence electron per atom, and that in an *s* state; that is, the alkalis. And it is assumed that they can be replaced by single valence electrons moving in non-coulomb

² E. H. Hall, *Proc. Nat. Acad.*, 1920-1921.

fields. This can be easily justified. It is to be noted that the other metals are more complicated, not merely by having more electrons, but by having them in p or d orbits, thus introducing new degeneracies. The actual calculations of cohesion have been carried through for sodium, with satisfactory results. They are only done roughly, however; the primary purpose of this paper is to make clear the general relations, rather than to attempt accurate calculations. The work is being carried further by Dr. Bartlett, and I wish to thank him for help on some of the calculations used in this paper. The work described here has been done while the writer was on leave, working in Leipzig. He wishes to thank Professor Heisenberg for his courtesy in extending the privileges of his laboratory, and for a number of illuminating conversations on the subject of the paper; and also to thank Harvard University for granting leave, and the Guggenheim Foundation for the assistance of a fellowship.

2. COMPARISON OF HEISENBERG'S AND BLOCH'S METHODS

The problem of a metal must be attacked by perturbation theory, and the unperturbed functions which we use can be set up in two quite different ways, one used by Heisenberg, the other by Bloch, either giving us a finite set of unperturbed functions. We regard the perturbation problem in the following way: we seek those linear combinations of these functions which, in the sense of the variation method, form the best approximations to solutions of Schrödinger's equation. This problem is solved by computing the matrix of the energy operator with respect to these functions, and solving the equations

$$\sum_k (H(i/k) - \delta(i/k)W)S(k) = 0$$

for the coefficients $S(k)$ to be used in making the linear combinations, and the energy values W of the resulting terms. (The term $\delta(i/k)$ must be given a slightly different form if the unperturbed functions are not orthogonal). This differs from the more conventional method: there one starts with an infinite, complete set of unperturbed functions, instead of our finite set, but solves only as a power series in the non-diagonal terms of the energy matrix, breaking off after the second power in all ordinary applications. It resembles more closely the quite different method ordinarily used with degenerate systems, where one takes only very few unperturbed states, but correctly solves the problem of combining them. For a nearly degenerate problem like the present one, with a great many states near together, the conventional method of developing in series will not work well, for the series do not converge well, and we are forced to use something like the present method. The justification comes simply from the assumption that the lowest states can be well approximated by such a linear combination of Heisenberg's or Bloch's functions (which correspond to having the atoms in their normal states). Surely this is not exact; for better results we should have to consider also the excited states of the atoms. But also certainly it is a fair approximation for the lowest states of the metal.

Heisenberg's functions, amplified in a simple way, form good approximations when the crystal is extended, for they are derived from the separated atoms. Bloch's functions on the other hand come by analogy with the free electron theory of Sommerfeld, and are good approximations when the crystal is compressed. The actual solutions of the perturbation problem are of course linear combinations of either Heisenberg's or Bloch's functions, not individual ones, and one gets the same final result whichever set one starts with (for the two sets of functions can be written as linear combinations of each other). But the fact that in the limiting cases the functions of one of the two sets become rather good approximations can be used, along with interpolation, to derive the general nature of the real stationary states. This comparison is made in the present section, and is illustrated by the interesting case of H_2 , where the calculations can be made exactly. At the outset, we must recognize two facts: first, that we must amplify Heisenberg's method by including polar states, to make it general enough to agree with Bloch's and to permit conductivity; second, that although Bloch has the proper set of functions, he has nowhere attempted to solve the perturbation problem, but has merely taken his unperturbed functions as being correct, which amounts to getting the energy to the accuracy of the conventional "first order perturbations."

The first step in either Heisenberg's or Bloch's method, as we apply them, is to write an approximate solution as a product of functions of the individual electrons. Heisenberg takes, for these separate functions, the wave functions of electrons attached to individual nuclei; the number of such functions is the product of the number of nuclei, multiplied by the number of different sets of quantum numbers we consider for an individual nucleus. If we restrict ourselves to s states, there are then only two states per nucleus, corresponding to the two orientations of the spin. For nucleus a , we denote these two³ by $u_\alpha(a/x)$, $u_\beta(a/x)$, and we have such a function for each nucleus $a \ b \ \dots \ n$. Bloch takes, on the other hand, combinations of these functions:

$$u_\alpha(klm/xyz) = \sum_{g_1 g_2 g_3} e^{2\pi i(kg_1/G_1 + lg_2/G_2 + mg_3/G_3)} u_\alpha(g_1 g_2 g_3/xyz),$$

where $g_1 g_2 g_3$ are the coordinates of a particular nucleus, $G_1 G_2 G_3$ the dimensions of the rectangular crystal, and $u_\alpha(g_1 g_2 g_3/xyz)$ the wave function (as used by Heisenberg) for an electron moving around the nucleus situated at $g_1 g_2 g_3$. The function with k, l, m represents an electron, in general moving in the direction k, l, m , but pausing at the various atoms on the way. There are as many sets k, l, m allowed as there are atoms in the crystal; for larger k, l, m the function proves to be merely a repetition of one already counted.

³ We use here for convenience in writing Pauli's notation u_α, u_β for the spin, rather than the more explicit but more cumbersome notation $u(n/x_i) \delta(m_s/m_{si})$ used in a previous paper. See J. C. Slater, Phys. Rev. **34**, 1293 (1929). The method used in the present paper is described, as applied to atoms, in the paper referred to; it should be understood that, although we speak here of using Heisenberg's and Bloch's methods, our actual procedure is quite different from that of these authors.

Now we actually set up the product of functions mentioned in the previous paragraph: we pick one out and let it be a function of the coordinates x_1 of the first electron, a second for the coordinates x_2 of the second, and so on to the n th, and multiply them all together. By the exclusion principle, no function can be chosen more than once. Then we form an antisymmetric combination, by permuting the indices of the electron coordinates, and adding the permuted functions with appropriate signs, obtaining essentially a determinant. These antisymmetric functions are the ones with which we start our perturbation calculation. Many such functions can be set up: there are $2n$ functions of a single electron, of which only n are to be chosen for each antisymmetric function, so that there are $(2n)!/(n!)^2$ different functions. Our perturbation problem is that of finding which linear combinations of these functions most nearly satisfy the wave equation. We may note the restriction of Heisenberg's method as he uses it; he does not include polar states. That is, he does not allow for example the two functions $u_\alpha(a/x)$, $u_\beta(a/x)$ to appear together in any product. This greatly limits the number of functions; but although the terms obtained by it certainly represent the lowest energy levels, since it requires energy to form a positive and a negative ion from two neutral atoms, we do not make this limitation.

Having set up the unperturbed functions, we next make linear combinations of them, by the method described in a previous paragraph. This process can be simplified by using a property of the spin. Every unperturbed function has a certain definite component M_s of spin along the axis, equal to $(n_\alpha - n_\beta)/2$, where n_α is the number of electrons with positive component of spin, n_β the number with negative. If now we neglect the magnetic interaction between the spins and the orbital motion, the problems with each value of M_s can be handled separately: the components $H(i/j)$ from a function with one value to a function with another are zero. The states with a given M_s include, as one readily sees, all those states whose total spin S is equal to or greater than M_s (for just these S 's can be so oriented, on the vector model, as to give a component M_s along a fixed axis). Thus by solving each such problem, and comparing, we can identify the spin of each term.⁴

The two methods can be illustrated by the case of H_2 . Here there are $4!/(2!)^2 = 6$ different wave functions. On Heisenberg's method, the four functions for an individual electron can be symbolized by $(\alpha\alpha)$, $(\beta\alpha)$, $(\alpha\beta)$, $(\beta\beta)$; two of these are to be picked out for each antisymmetric wave function. Thus the six are $(\alpha\alpha)(\alpha\beta)$; $(\alpha\alpha)(\beta\alpha)$, $(\alpha\beta)(\beta\beta)$; $(\alpha\alpha)(\beta\beta)$, $(\beta\alpha)(\alpha\beta)$; $(\beta\alpha)(\beta\beta)$. They are arranged, first, by M_s : the first has the value 1, the next four the value 0, and the last -1. Thus the terms consist of one triplet and three singlets. Among the four terms with $M_s = 0$, the first two are polar (and not considered by Heitler and London, or Heisenberg), the last two are non-polar. Immediately one finds that the sum of these non-polar functions is the component of the triplet. We are then left with three functions: the

⁴ This is essentially the method used in the paper already quoted. It has already been applied by Bloch to problems in the theory of metals. See F. Bloch, *Zeits. f. Physik*, **57**, 545 (1929).

two polar ones, and the difference of the non-polar ones, from which to find our three singlets. The difference of the polar ones is antisymmetric in the nuclei, giving one state; their sum, and the difference of the non-polar functions, give two functions symmetrical in the nuclei, between which we finally solve the simple perturbation, resulting now in a quadratic secular equation, and obtain the two remaining singlet states. The energy levels as a function of the distance of separation are plotted in Fig. 1. The energy level of the lowest, $^1\Sigma S''$, is almost exactly as given by Heitler and London, but its wave function contains quite an appreciable contribution from the polar state. The triplet is just the repulsive state of Heitler and London. The other two levels are essentially polar. They go at infinite separation to the energy of $H^+ + H^-$, greater than the other limit by the ionization potential less the electron affinity of H (this rough approximation gives $-\frac{1}{4}Rh$ for the electron

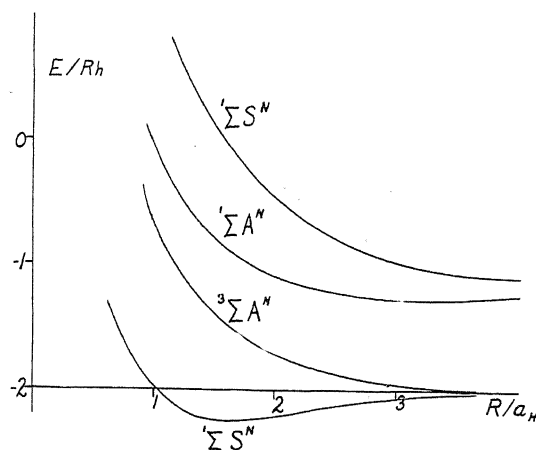


Fig. 1. Energy levels of H_2 .

affinity, so that the terms go to $5/4Rh$). The lower of these has a minimum; it is presumably the polar part which, by combination with other functions, leads to the experimentally known B state of the molecule. We notice that at large separations the functions behave just like Heisenberg's (extended) unperturbed functions: a triplet and a singlet are non-polar, and go to the lower energy; while two singlets are polar, and go to the higher level.

Next we consider Bloch's method for the same problem. His functions for one electron, for this case, are

$$u_a(0/x) = u_a(a/x) + u_a(b/x)$$

$$u_a(1/x) = u_a(a/x) - u_a(b/x),$$

with similar functions for β . (These do not follow quite directly from the general formulas given above; Bloch's functions must be slightly modified for finite systems, for they apply rather to infinite but periodic ones.) The discussion of multiplicity given above goes through without change, if we only substitute 0, 1 for a, b . We can easily show by direct calculation

that the resulting unperturbed antisymmetric functions are linear combinations of those found by Heisenberg's method. For example, for $M_s=1$, there is only one function by either method, so these must be identical, except for a numerical factor. By Heisenberg's method the function is

$$u_\alpha(a/x_1)u_\alpha(b/x_2) - u_\alpha(b/x_1)u_\alpha(a/x_2).$$

By Bloch's it is

$$\begin{aligned} & u_\alpha(0/x_1)u_\alpha(1/x_2) - u_\alpha(1/x_1)u_\alpha(0/x_2) \\ &= [u_\alpha(a/x_1) + u_\alpha(b/x_1)][u_\alpha(a/x_2) - u_\alpha(b/x_2)] \\ &\quad - [u_\alpha(a/x_1) - u_\alpha(b/x_1)][u_\alpha(a/x_2) + u_\alpha(b/x_2)] \\ &= -2[u_\alpha(a/x_1)u_\alpha(b/x_2) - u_\alpha(b/x_1)u_\alpha(a/x_2)]. \end{aligned}$$

We can set up the whole perturbation problem in these functions; and the solution can be carried out as easily as before, leading of course to just the same answers. The interesting question now is, how closely do Bloch's individual functions approximate the correct ones, for small values of R ? The functions are respectively as follows: a singlet with both electrons in the state 0; a singlet and triplet with one in the state 0, the other in the state 1; and a singlet with both in the state 1. The state 0 corresponds to the lowest vibrational state on Sommerfeld's theory, the state 1 to the next higher one, so that the first state has on the simple interpretation only the zero-point vibrational energy, the next two have each one quantum, and the last two. Examination of the actual wave functions shows that they agree quite closely with the functions of Bloch: the lowest one is made, it is true, by combination of the (00) and (11) states, both being S^N , but the coefficient of the first is about eight times as large as that of the second, when R is such that the energy is at its minimum. The next two are made up of the (01) states. The highest is about eight parts of (11) to one of (00). The energies also show, for high compression, the behavior expected: the two states which should have one quantum of vibrational energy draw together, and the one with two quanta is just about twice as far above the lowest state as those with one. Even the spacing of these levels is just about what would be calculated on Sommerfeld's theory for an electron vibrating in a region the size of the molecule. Thus we see that Bloch's unperturbed functions form fairly good approximations to the real functions for the compressed state, as Heisenberg's do for the extended state.

We can now return to the general case, and make use of the fact that Heisenberg's functions approximate the real wave functions well for large separations, Bloch's for small. First, for the extended system, the energy is the ionization energy, on account of having many ions as well as neutral atoms. For a metal, it requires about 6 volts to form a positive and negative ion from two neutral atoms. Thus if all the atoms were ionized, we should have $n/2$ such pairs, or an energy per atom, or per electron, of about 3 volts. This measures the extension of the group of terms, for large R . It is a simple problem in permutations to find the number of terms of each multiplicity

with each energy value in the limit. The one term of highest multiplicity will approach the lowest limit, for large R ; it must be entirely nonpolar, for all spins point in the same direction, so that no two electrons can be in the same atom. For the next lower multiplicity, only one electron has a reversed spin; it is the only one which can be in an atom with another electron, so that there can be just one pair of atoms ionized. Following out, we easily see that terms of lower and lower multiplicity, in the limit of large R , lie higher and higher, and at the same time are more and more spread out. They spread in such a way that there are terms of each multiplicity way down to the bottom limit, although not to the top. As we shall see later, for R large but not infinite, in the normal case, the really lowest terms have small spins; but near them are many terms with large spin.

For the compressed system, the arrangement is as given by Bloch's theory. The total extension of the group of terms increases with $1/R^2$; for ordinary values of R , it is of the order of the mean zero-point energy, times n , which is decidedly larger than 3 volts $\times n$. Thus not only do the curves tend upward for decreasing R , giving repulsive energy levels, but they are definitely doing this at the actual size of the metal. The general physical interpretation of this repulsion is obvious: the valence electrons act here approximately as a perfect gas, and the energy levels are those of such a gas as it is compressed adiabatically against gas pressure, the energy varying therefore as $V^{-2/3}$ or as $1/R^2$. Here the terms of high multiplicity lie in the center of the pattern; those of lower spin also average in the center, but are more and more spread out. Since the terms of high spin are so low for large R , but not for small R , they must be even more repulsive than the others. The possibility seems very remote that any terms except those with very low multiplicity could be so low as to have minima, and come into the question for the normal state. We see that for cohesion we are interested only in the very lowest fraction of the whole set of terms. These terms almost all will go to the lowest energy level at infinite separation; they become in this limit non-polar. And the accuracy with which one can compute the lowest states of H_2 from Heitler and London's non-polar functions suggests that here too this may be possible. Accordingly for our actual calculation of these lowest states, we shall use Heisenberg's method with only non-polar functions. We shall find here, as we expect from our qualitative discussion, that the terms of low multiplicity really do lie below, some of them being attractive; while those of high multiplicity are repulsive, the highest spins lying highest. Finally we shall consider the effect of polar terms, and conclude that it is really small on the low energy levels, although not on the wave functions; for it is the polar character of the wave functions which makes conductivity possible.

3. ELECTRIC AND MAGNETIC PROPERTIES

Conductivity. In the introduction we have mentioned the interpretation of electric conduction on Heisenberg's and on Bloch's scheme. One notices that a single one of Bloch's functions implies conduction—the diagonal term

of the momentum matrix is different from zero—whereas with Heisenberg's functions we must have a continual change from one stationary state to another. But it is particularly important to notice that, without polar states, or free electrons, no conduction is possible; we cannot set up combinations of non-polar states with a resultant momentum. For example, with two electrons, we can set up an arbitrary non-polar function $c_1u(a/x_1)u(b/x_2) + c_2u(b/x_1)u(a/x_2)$. If now we compute the momentum, whose operator is $\hbar/2\pi i(\partial/\partial x_1 + \partial/\partial x_2)$, the only possibly significant terms are the cross terms, like

$$\begin{aligned} & c_1c_2 \frac{\hbar}{2\pi i} \int u(a/x_1)u(b/x_2) \left(\frac{\partial}{\partial x_1} + \frac{\partial}{\partial x_2} \right) u(b/x_1)u(a/x_2) dv_1 dv_2 \\ &= c_1c_2 \frac{\hbar}{2\pi i} \left\{ \int u(b/x_2)u(a/x_2) dv_2 \int u(a/x_1) \frac{\partial}{\partial x_1} u(b/x_1) dv_1 \right. \\ & \quad \left. + \int u(a/x_1)u(b/x_1) dv_1 \int u(b/x_2) \frac{\partial}{\partial x_2} u(a/x_2) dv_2 \right\}. \end{aligned}$$

On account of the penetration of one atom by the other, the integrals $\int u(b/x_2)u(a/x_2) dv_2$ are not zero. The integral $\int u(a/x_1)(\partial/\partial x_1)u(b/x_1) dv_1$ is also different from zero. But it is exactly cancelled by $\int u(b/x_2)(\partial/\partial x_2)u(a/x_2) dv_2$, as one can show by Green's theorem, so that the whole is zero. On the other hand, if we set up a polar combination like $c_1u(a/x_1)u(a/x_2) + c_2u(b/x_1)u(b/x_2)$, we again get two terms, but now they add, and give a current. As another example, we can take the term of maximum multiplicity in any system. In this term, we have seen by Heisenberg's scheme that each atom has just one electron, so that we expect no conduction. But in Bloch's scheme, each value k, l, m has just one electron. Since each such value is balanced by one with $-k, -l, -m$, having opposite momentum, the total momentum is zero, and there is again no current.

We can now see the importance of considering exactly the wave functions, as well as the energy levels, of the lowest state. In the ordinary low states there will, of course, be no current. But near the lowest state, if there is to be conductivity, there must be combinations of polar states, having a current, which are assumed in the presence of a field, and whose added energy comes simply from the kinetic energy of the electrons and the self-induction. Such states are possible only on account of the presence of positive and negative ions, with the resulting free and associated electron conductivity.

Magnetism. The lowest state of H_2 is the non-magnetic $^1\Sigma$, and we have found such a situation in general. In the region where the lowest states have their minimum, the metal must surely be in a compressed state, Bloch's arrangement of energy levels must be a good approximation, and the states of large spin must lie very high. We are thus led to the quite general conclusion that the outer electrons, which are largely if not entirely responsible for both cohesion and conduction, cannot produce ferromagnetic effects. If a metal is to be ferromagnetic, there must then be other electrons than these

outer ones which are responsible for it, and these others must have smaller orbits, so that at the equilibrium distance of the outermost ones, the inner ones will be relatively further apart, and can be treated as an extended rather than as a compressed system. It is a very attractive hypothesis to suppose that in the iron group the existence of the $3d$ and $4s$ electrons provides in this way the two electron groups apparently necessary for ferromagnetism; for it is only in the transition groups that we have two such sets of electrons, and this criterion would go far toward limiting ferromagnetism to the metals actually showing it.

We next ask just how such inner electrons could be ferromagnetic. Certainly the general trend of the terms of high spin to the low energy values at large R is an essential part of the question: there will be terms of large spin near the lowest level. Bloch⁵ has discussed the problem, concluding that for large R 's the terms of high spin actually lie lower than those of smaller spin (he does not specifically discuss the dependence on R , but his energy formulas all contain it parametrically). This conclusion, however, is not correct; Bloch has merely computed diagonal values of the energy, with respect to his functions, and for large R these by no means form approximations to the actual energy values. From the correct treatment of the problem as we have given it, it is plain that at all R 's there are terms of low multiplicity as low as those of high spin, or lower. It may be, however, that the mere presence of so many low terms of high multiplicity may be enough, on account of their high *a priori* probability and large number, to insure that the terms of large spin should be well represented at ordinary temperatures, even though there are low terms of zero spin, and so produce ferromagnetism. If, however, this should prove on calculation not to give the right effect, we should be led to consider Heisenberg's assumption that the normal order of terms is inverted in ferromagnetic atoms, the terms of high multiplicity lying lowest. He has shown by a general argument that electrons of large total quantum number (which the $4s$ electrons of iron have) have an exchange integral of the opposite sign to that found in hydrogen, so that the order of the non-polar terms would be reversed. This we should fit into our scheme in the following way: although this exchange integral is anomalous at large R , it presumably changes sign and becomes normal at smaller R ; for first, Heisenberg's general argument only applies at large R ; and second, our condition that the energy levels should approach those of Bloch at small R , with the terms of large spin lying high, seems quite general. Thus we should assume that the terms at small R lie as in Fig. 1: but that at a considerable value of R , there is a crossing over (in this case the ${}^3\Sigma A^N$ crossing and lying under the ${}^1\Sigma S^N$), described by a change in the sign of the exchange integral K used in the next section from negative to positive. By assuming the existence of an inner group of electrons with these properties, we seem to secure a consistent picture of ferromagnetism. On the other hand, of course it is always possible that ferromagnetism is connected with the fact that the valence electrons of iron have an orbital angular momentum different from zero.

⁵ F. Bloch, *Zeits. f. Physik*, 57, 545 (1929).

4. COHESION

We are now prepared to begin the actual calculation of the lowest stationary states. We make several simplifications, which we later remove. First, we consider only non-polar states, in Heisenberg's scheme, and disregard exchange integrals except between adjacent atoms; this is the approximation also made by Heisenberg. Finally, for the present, we consider a linear lattice, n atoms uniformly spaced along a line, rather than a space lattice. Our problem, of course, is to compute the matrix of the energy with respect to the wave functions we have chosen, and then solve the problem of making proper linear combinations. The computation of the matrix is simple. By a fundamental formula of the previous paper mentioned above, the diagonal components are a sum, first, of the energies of the separate atoms, which we need not consider; next, a sum over all adjacent pairs, as the pair of atoms a and b , of integrals $J(a/b)$, which is essentially the diagonal energy E_1 of Heitler and London; finally, a sum over all adjacent pairs which have the same spin, of terms $-K(a/b)$, where K is the exchange integral E_2 of Heitler and London. Further, it is easy to show that all non-diagonal terms are zero, except those for which the distributions in the two states differ only by the exchange of an adjacent α and β ; in such cases, the term is $-K$. In the normal case, to which we shall refer specifically, J and K as functions of R are both negative, K numerically greater than J . But in Heisenberg's case, K must be taken to be positive for large R , although presumably negative for small R .

To illustrate by H_2 , we have one state with both spins parallel; then the energy is $J-K$. Next we have the problems with one parallel, the other anti-parallel; there are two such states (the two polar ones being omitted). Each has the diagonal energy J , and the non-diagonal energy between them is $-K$. Thus the equations for the linear combinations are

$$\begin{aligned}(J-W)S(1)-KS(2) &= 0 \\ -KS(1)+(J-W)S(2) &= 0,\end{aligned}$$

giving energy values $W=J\pm K$, the first evidently being the singlet, the second the component of the triplet.

In the general case, the computation of the matrix is no more difficult; the real problem is the solution of the linear equations for the S 's. We cannot do this exactly; but we adopt two methods of approximation, one holding for larger spins, the other for smaller spins. We first discuss the former.

Method for large spins. First we take the problem where all spins are parallel, $n_\alpha=n$, $n_\beta=0$. Here there is but one state. Since with our linear lattice there are $(n-1)$ adjacent pairs, and all spins are parallel, the energy is simply $(n-1)J-(n-1)K$. Since J and K are normally both negative, but K numerically greater than J , this is a positive energy for all values of R , and results in a repulsive term. For Heisenberg's case, on the other hand, K is positive, and this term is attractive. Next we take the problem $n_\alpha=n-1$, $n_\beta=1$. There are now n unperturbed wave functions: the one electron β can

be attached to any of the n atoms. We number the functions by the number of the atom where the electron is, only decreased by $\frac{1}{2}$: we have $u_{1/2} \cdots u_{n-1/2}$. Each of these functions will have the diagonal energy $(n-1)J - (n-3)K$, since two of the adjacent pairs now have opposite spins, except for the two functions $u_{1/2}$ and $u_{n-1/2}$ where our β electron is at an end of the lattice, and the energy is $(n-1)J - (n-2)K$. Also, all non-diagonal terms will be zero except those between terms of adjacent number, as for example between those symbolized by

$$\begin{aligned} & \cdots \alpha \alpha \alpha \beta \alpha \alpha \alpha \cdots \\ \text{and} & \cdots \alpha \alpha \alpha \alpha \beta \alpha \alpha \cdots, \end{aligned}$$

and which differ by just one interchange of an α and β . As a result, the perturbation equations will be

$$\begin{aligned} & [(n-1)J - (n-2)K - W]S\left(\frac{1}{2}\right) - KS\left(\frac{3}{2}\right) = 0 \\ & -KS\left(\frac{1}{2}\right) + [(n-1)J - (n-3)K - W]S\left(\frac{3}{2}\right) - KS\left(\frac{5}{2}\right) = 0 \\ & -KS\left(\frac{3}{2}\right) + [(n-1)J - (n-3)K - W]S\left(\frac{5}{2}\right) - KS\left(\frac{7}{2}\right) = 0 \\ & \cdots \cdots \cdots \\ & -KS\left(n - \frac{3}{2}\right) + [(n-1)J - (n-2)K - W]S\left(n - \frac{1}{2}\right) = 0 \end{aligned}$$

These equations are easily solved; they occur, for example, in the problem of a string weighted at equal intervals,⁶ the S 's being the displacements of the weights. To solve, we merely assume $S(k) = \frac{\cos}{\sin}(\alpha k)$. The first and last equations give boundary conditions. They become like the others if we introduce an $S(-\frac{1}{2})$ and $S(n+\frac{1}{2})$, the first equation becoming

$$-KS(-\frac{1}{2}) + [(n-1)J - (n-3)K - W]S(\frac{1}{2}) - KS(\frac{3}{2}) = 0,$$

and if we further set $S(-\frac{1}{2}) = S(\frac{1}{2})$ and $S(n+\frac{1}{2}) = S(n-\frac{1}{2})$. These are then the boundary conditions; and to satisfy them we must take

$$S(k/p) = \cos p\pi k/n, \quad \text{where } p=0, 1, \cdots, n-1.$$

Now we substitute this form in our difference equations; and we get for W

$$-K\left(\cos \frac{p\pi}{n}(k-1) + \cos \frac{p\pi}{n}(k+1)\right) + [(n-1)J - (n-3)K - W(p)] \cos \frac{p\pi k}{n} = 0,$$

from which in each case

$$W(p) = (n-1)J - (n-3)K - 2K \cos \frac{p\pi}{n}.$$

⁶ See, for example, Rayleigh's "Theory of Sound."

We now have the transformation coefficients $S(k/p)$ and the energy values $W(p)$ for the rotation of axes to the p th stationary state; the W 's are the exact energy levels. They are evidently distributed between the values $W(0) = (n-1)J - (n-1)K$, and $W(n-1) = (n-1)J - (n-3 - 2 \cos \pi(n-1)/n)K = (n-1)J - (n-5)K$, almost, for large n . Obviously $W(0)$ is the energy of the level of highest multiplicity, which we have found before. Thus the levels $1 \cdots (n-1)$ are those of next to highest multiplicity.

Next we take the problem with two electrons of spin β . There are $n(n-1)/2$ such terms: each of the two indistinguishable β 's can be on any one of the n atoms, so long as they are not on the same atom. Now it is convenient to denote states by the two atoms, say i and j (each going from $\frac{1}{2}$ to $n - \frac{1}{2}$) on which electrons β are. Our problem becomes analogous to that of a square membrane loaded at equally spaced points. The diagonal terms of the energy are all $(n-1)J - (n-5)K$, unless one of the β 's is at an end of the lattice, or unless the two β 's are adjacent. There are four non-diagonal terms for transitions from each wave function: for $i \rightarrow i \pm 1$, or for $j \rightarrow j \pm 1$. A typical equation can be written

$$\begin{aligned} & -KS(i, j-1) \\ & -KS(i-1, j) + [(n-1)J - (n-5)K - W]S(ij) - KS(i+1, j) \\ & -KS(i, j+1) = 0. \end{aligned}$$

This we satisfy by a product of cosine functions, $S(ij/pq) = \cos(p\pi i/n) \cos(q\pi j/n)$. We easily find that these exactly satisfy the boundary conditions when i or $j = \frac{1}{2}$ or $n - \frac{1}{2}$. There remains the condition when i is nearly equal to j . If $i = j \pm 1$, the diagonal energy is $(n-1)J - (n-3)K$, since the two β 's are together; on the other hand, since the β 's cannot be on the same atom, the coefficients $S(jj)$ and $S(j+1, j+1)$ vanish, so that only two transitions, rather than four, are possible. If now we define an $S(jj)$ and $S(j+1, j+1)$, we can make the equations of the same form as the general one, if only $S(jj) + S(j+1, j+1) = 2S(j+1, j)$. This furnishes our second boundary condition, which is evidently along the diagonal of our square "membrane." Unfortunately we cannot satisfy this condition exactly with our cosine functions; closer investigation shows that one must have much more complicated functions, with hyperbolic cosines, to satisfy it exactly, and one cannot carry the method through for the general case. Approximately, however, we can easily take care of our condition. If the p and q are not too great, so that the "wave-length" of the waves in our membrane is large, we can replace our condition by a differential one: it states that the amplitude at a point next the diagonal is the mean of the two adjacent values on the diagonal, and this very nearly means that the normal derivative of the function, at right angles to the diagonal, is zero. This we can satisfy by making our function symmetrical about the diagonal, or using $\cos(p\pi i/n) \cos(q\pi j/n) + \cos(q\pi i/n) \cos(p\pi j/n)$. We may expect this to hold best for small p and q , not so well for large values. It is clearly not right; for example, it yields $n^2/2$ functions, instead of the correct number $n(n-1)/2$.

Our function is an exact solution of the difference equations, if not of the boundary condition; and we find for the energy

$$W(p, q) = (n-1)J - (n-5)K - 2K \left(\cos \frac{p\pi}{n} + \cos \frac{q\pi}{n} \right),$$

where p, q go from 0 to $n-1$, but each pair is counted only once. The term of highest multiplicity comes from $p=q=0$; the $(n-1)$ terms of next highest value are those with either p or $q=0$, but the other not; the remaining terms are of multiplicity smaller by two.

This result can now be generalized without trouble: if we have many β 's, the energy levels are given by

$$W = (n-1)J - (n-1-2n_\beta)K - 2K \sum_{i=1}^{n_\beta} \cos \frac{p_i\pi}{n}, \quad p_i = 0 \cdots n-1.$$

The terms where one or more p_i 's equal zero are those whose total spin is greater than $(n_\alpha - n_\beta)/2$; those with all p_i 's different from zero are those whose total spin equals $(n_\alpha - n_\beta)/2$. The latter value is evidently enormously greater than the other: every spin has enormously more terms than any higher spin. Thus the terms of a given component of spin along the axis, and those of the same total spin, are approximately the same. We can at once find the distribution in energy of the terms of a given spin. They evidently cluster about the value $(n-1)J - (n-1-2n_\beta)K$; they are distributed about this value like the displacements of a point simultaneously acted on by a sum of n_β periodic vibrations of equal amplitudes but arbitrary phases. This gives, of course, approximately a Gauss distribution. The width of the distribution curve can be derived very easily: we compute the mean square deviation of the energy from its mean, $(W - \bar{W})^2 = 4K^2 [\sum \cos(p_i\pi/n)]^2$, the average being taken when each p varies independently from 0 to n . We can take this variation to be continuous rather than discrete. Then the product terms in the square of the sum of cosines all average to zero, the square terms average to $\frac{1}{2}$, and the result is $2K^2 n_\beta$. These results may be compared with those obtained by Heisenberg on the group theory, and which as Bloch has shown can also be found from the present method. In the notation of the present paper, putting the number of neighbors of each atom equal to 2, and leaving out the terms in J , Heisenberg finds

$$\begin{aligned} \bar{W} &= -(n - 2n_\beta + 2n_\beta^2/n)K \\ (\overline{W - \bar{W}})^2 &= 2K^2 n_\beta (1 - n_\beta/n)(1 + 2n_\beta/n - 2(n_\beta/n)^2). \end{aligned}$$

Our formulas agree with these exact ones to terms in n_β but no further, as we expect from the fact that our approximations hold only for small n_β . For small p 's, as we have seen, our results should be good even for large n_β ; for the case of ferromagnetism, when on Heisenberg's hypothesis the terms are reversed, these are the lowest terms, so that this result should be very useful here. In the normal case, however, the lowest terms are those of large p , and these are the ones we need for cohesion. About these lowest terms, we

can be fairly sure that they lie higher than the lowest ones we have found, or $(n-1)J - (n-1-4n_\beta)K$, since the mean lies higher than the mean we found. For zero spin, for example, we can be fairly sure that the term lies above $(n-1)J + nK$. But this value need not be a very good approximation; we actually find, by the method of the next section, that the lowest term for zero spin is about $(n-1)J + 0.290nK$. Fortunately even this has a positive coefficient for K , and is so an attractive rather than a repulsive term.

Method for zero spin. For zero spin, $n_\alpha = n_\beta = n/2$, and there are $n!/(n/2!)^2$ terms. We adopt quite a different method of classifying them. Before, most of the terms of a given n_β had nearly the same diagonal energy; but now the range of energy is large, from $(n-1)J$ for the state with alternating α 's and β 's so that there are no parallel spins, to $(n-1)J - (n-2)K$ for the state where all the α 's come at one end of the lattice, all the β 's at the other. With this large range, we find it convenient to classify terms by their diagonal energies; and we find as we should expect, that for the lowest states of the perturbed system we must consider most the low unperturbed states. We do not need to take into account all states: we find that approximately (though by no means exactly) the terms can be divided into a number of non-combining sets, and we set up one such set in the following way. We commence with the lowest state, of energy $(n-1)J$, where α 's and β 's alternate. Next we consider the $n-1$ states which combine with it, coming from interchanging one pair, and each having the energy $(n-1)J - 2K$, except those from the two end pairs, with energy $(n-1)J - K$. We leave these two out, retaining for our set the $n-3$ states which have the energy $(n-1)J - 2K$. Each of these has $n-3$ states with which it combines, coming from interchange of one of the $n-3$ adjacent pairs with opposite spins. Of these $n-3$, the two in which the new interchanged pair is next the one already interchanged have the energy $(n-1)J - 2K$; the one in which the pair already interchanged is changed back has the energy $(n-1)J$; the two where the end pair is interchanged have the energy $(n-1)J - 3K$; and the remaining $n-8$ have the energy $(n-1)J - 4K$. We retain for our set only these $n-8$ terms of energy $(n-1)J - 4K$. So we proceed, asking which terms combine with those already set up, and retaining just those whose energy is $-2K$ greater than for those with fewer interchanges. We find that a term of our set, with the energy $(n-1)J - 2pK$, has non-diagonal terms to p terms of the set of energy $(n-1)J - 2(p-1)K$ and to $(n-3-5p)$ terms of the set of energy $(n-1)J - 2(p+1)K$. Evidently so long as p is small, the terms we leave out of the set and yet which combine with terms of the set are comparatively few. It is only for the large p 's that we make serious error by leaving out these terms, and for large p the diagonal energy is high enough so that for the lowest states of the perturbed system these unperturbed states are unimportant. Thus we may reasonably believe that the low energy levels found by solving this restricted problem will be approximately some of the low levels of the actual problem. We can at least be sure of the following: by the variation principle, they can be no lower than the actual stationary states.

The other sets of non-combining terms which we can set up are easily described, and are of considerable physical interest. Instead of starting from the state with spins alternating, we start from a state where the spins alternate up to a given point; there the sequence is interrupted, and alternation commences again, so to speak, in the opposite phase, as

$$\cdots \alpha \beta \alpha \beta \alpha \beta \alpha \beta \alpha \cdots$$

With a few such interruptions in the course of the crystal, the energy is very little above the really lowest state; yet a great many individual interchanges would be required to pass to the lowest state. With such a state to start with, we proceed just as we did before, and construct a whole system of states; and the non-diagonal terms between this and the first system come only from high values of p , involving many interchanges, and can be neglected. Physically, at the interruption of phase, one essentially has a slight interruption of crystal structure. Our catalogue of all possible states of the metal includes not only that where it is one perfect crystal, but also where it is composed of many smaller crystals not perfectly joined together. Obviously each problem can be treated separately; physically it would take a very long time to change from one to the other. And obviously each problem will give us essentially the same set of energy levels.

We now take our set of wave functions, and try to solve the perturbation problem between them. For each value of p , we have many wave functions; and we look for those particular solutions for which all these functions have the same coefficient $S(p)$. Afterwards we shall show that we really find the lowest solutions this way. Then, remembering the number of transitions with non-diagonal term K from a given state, computed above, we have for a typical equation

$$-KpS(p-1) + [(n-1)J - 2pK - W]S(p) - K(n-3-5p)S(p+1) = 0.$$

This set of difference equations for the S 's is somewhat similar to what we had before; it also corresponds to a weighted string. But now the properties, and hence the wave-length, change from point to point, and we seek the various overtones. The equation is a close analogue to Schrödinger's equation, in many ways; the fact that it is a difference equation rather than a differential one is quite immaterial. To solve, we assume $S(p) = e^{\int \alpha dp}$, where α is to vary slowly with p . Then $S(p) = e^\alpha S(p-1)$, etc., so that we have

$$\begin{aligned} -Kp + e^\alpha [(n-1)J - 2pK - W] - e^{2\alpha} K [n-3-5p] &= 0, \\ e^\alpha &= \frac{-[(n-1)J - 2pK - W] \pm \{[(n-1)J - 2pK - W]^2 - 4K^2 p [n-3-5p]\}^{1/2}}{-2K [n-3-5p]}. \end{aligned}$$

The equation expresses e^α as a function of p , for any particular W . Now we must remember that there are essentially boundary conditions; the S 's must remain finite for $p=0$ and $p=\text{an extreme value}$. To tell how to apply this condition, we must investigate the solution we have found.

The ratio e^α of successive coefficients is real or complex, according as $[(n-1)J - 2pK - W]^2$ is greater than or less than $4K^2p[n-3-5p]$. Regarded as a function of p , the limiting cases, where the two are equal, come from $(n-1)J - W = 2pK \pm 2K[p(n-3-5p)]^{1/2}$. The right hand side, plotted as a function of p , forms an ellipse; the straight line represented by the left side intersects the ellipse in two points, or in none, depending on the value of W . The region of W where it intersects can be found by computing the maximum and minimum ordinates of the ellipse; that is, the values of $(n-1)J - W$ for which $(d/dp)(2pK \pm 2K[p(n-3-5p)]^{1/2}) = 0$. This gives $p = (n-3)/10 [1 \pm (1/6)^{1/2}] = (n-3) \times (0.0592, 0.1408)$. At these two limits, substituting, $W = (n-1)J + (n-3)K \times (0.290, -0.690)$. For values of W between these limits, there is a range of p for which e^α is complex, and the solution is oscillatory; outside this region, which is closed, the solution is in any case exponential. To satisfy our boundary conditions, now, we have a problem much like that with Schrödinger's equation in one dimension; and boundary conditions can be satisfied only if there is an oscillatory region. As a result, the actual energy levels of the problem must lie between the limits given. Closer examination shows that a "quantum condition" can be applied, and that between these limits there are just the number of energy levels there should be. We now have the lowest level: it lies arbitrarily close to our lower limit, or is

$$W = (n-1)J + 0.290(n-3)K,$$

as we stated in the last section. In this lowest state, we can show without trouble that the unperturbed wave functions with p near $0.0592(n-3)$ are represented most strongly. Thus the value of p is really quite small; relatively few pairs are interchanged, and we are safely in the region where we can treat the different systems separately.

We have solved our problem for the lowest state in which all terms of the same p have the same coefficient. We can now investigate the effect of removing this assumption, varying the coefficient of one function of a given p in one direction, varying the rest to keep the same total representation for functions of this p , and calculating the change in the energy. When we do this, we find the energy to be a minimum with respect to such variation; in fact, the changes of energy compensate each other to a higher order, showing that the problem is nearly degenerate with respect to these coefficients. Thus we may be rather confident that we have a good approximation to the lowest non-polar states. It is of course obvious that this method becomes worse as we go to higher states.

It is instructive to ask what ordinary perturbation theory would give us for the lowest state. The lowest unperturbed state has the diagonal energy $(n-1)J$; this represents the ordinary first order perturbation calculation. Now we pass to the second order calculation. The lowest state is not degenerate, so that we can use the power series development method. The next term in the expansion is $\sum_j (H_{ij}H_{ji})/(E_1 - E_j)$, summed over all excited states j . Now there are non-diagonal terms H_{1j} only to the $n-1$ states with $p=1$.

Thus the H_i 's are all equal to $-K$, and the energy differences are all given by $E_i = E_1 - 2K$. Thus we have as second approximation

$$W = (n-1)J + (n-1)\frac{K^2}{2K} = (n-1)J + \frac{1}{2}(n-1)K.$$

This differs from our result in having the factor $\frac{1}{2}$ rather than 0.290; we have only the first term of a series development, but it is reassuring that agreement is as good as it is. For finding the order of magnitude, we could use this term alone; we shall find this simple method useful with the space lattice.

Effect of polar states. One can make an estimate, by a method like that used here, of the effect of the polar states in depressing the non-polar ones, which alone we have considered so far. We can build up a series of states by starting with a given non-polar state; then removing one of the electrons to an adjacent atom, producing a positive and a negative ion; then removing a second; and so on. The series of states so found behave formally like those used above. If we solve the problem by the previous method, or by the second order perturbation method, we get a further depression of the lowest state, which again can be written as

$$(n-1) \times \frac{\sum \text{square of non-diagonal term}}{\text{energy difference}}.$$

The non-diagonal term which comes in here is presumably of the same order of magnitude as before, although it is a somewhat different integral. But the diagonal energy difference is now essentially an ionization energy, which is of the order of several volts, rather than the fraction of a volt that K is. Thus the effect on the energy is a number of times smaller than what we found before, and we can neglect it. It is not worth while calculating more accurately, in this approximation; for with H_2 , it appears that on account of the lack of orthogonality of the wave functions, the actual depression of the energy is very much less than this rough method would indicate, although the effect on the wave function is about what we should expect. One can reasonably believe for this reason that the polar states in the crystal depress the energy only very little. But we recall that their effect on the wave function is to introduce free electrons. By our rough method described above, we infer that the fraction of free electrons is of the order of 1 percent, for reasonable choice of the constants. This could easily be in error by a factor of 10 either way; but at least we see that a definite meaning can be attached to the number of free electrons, and that there is a definite procedure for calculating this number.

Normalization and orthogonality. We have not considered the lack of orthogonality of the wave functions, resulting in factors like the $1/1 \pm S$ of Heitler and London. When one tries to do this, one immediately strikes a difficulty which appears insurmountable: the factor in the denominator, instead of being like $1+S$, is like $1+nS+\dots$, where n is the number of

atoms, so that the term nS is enormous compared with unity. On examination of simple cases, it appears that the remaining terms, coming from other permutations than the simple interchange, are also important, in many cases the terms almost cancelling each other. Further, in every expression for energy, like the simple $(J \pm K)/(1 \pm S)$, there are more terms in the numerator, also of great importance. But the simple cases give no suggestion of how to treat the general case. The key to this difficulty comes from Bloch's method. For example, the term of maximum multiplicity has one function, which can be expressed either by Heisenberg's or Bloch's functions. But the difference is that Bloch's functions are really orthogonal, unlike Heisenberg's, so that we meet no such difficulty. Of course, the same terms occur, but now in the normalization of the individual functions. And the numerators, and denominators like $1 + nS + \dots$, appear as products of n factors, each of approximately a simple Heitler and London form; further, all but one or two of these factors of the denominator cancel against equal factors in the numerator, giving very simple results. Essentially the same method can be used with the other states; for this method is one for treating a determinant of Heisenberg's wave functions, and converting it into a determinant of Bloch's functions; and all of our wave functions are products of two such determinants. When we calculate in our case, it appears that the terms S will have small effect; we are roughly half way between the cases $1 + S$ and $1 - S$, and the effects of S nearly average out. This method at the same time gives the proper way of considering more distant pairs, as well as adjacent ones; these contribute the further terms in the numerators, as $J \pm K + \dots$. We see from the next paragraph that these more distant pairs are really quite important.

Method for space lattice. So far, we have spoken about a linear lattice of atoms, rather than a space distribution. We now extend this theory to a crystal; but we shall not carry it through in the same detail. We consider only the problem of zero spin, and use our second order perturbation approximation. Let us take the body-centered cubic lattice, which the alkalis have. The lowest unperturbed state of this lattice can be set up much as with the linear one: we let the electrons at the corners of the cubes have the spin α , those at the centers the spin β . Then each electron is surrounded by eight others of opposite spin, so that if we consider only adjacent pairs, the diagonal energy of this state is $4nJ$, where there are n electrons, $4n$ pairs. This lowest state now has non-diagonal terms, each equal to $-K$, to the $4n$ states obtained by interchanging an adjacent pair. Each of these states has two misplaced spins, each surrounded by 7 spins of the same sign, so that the energy has a term $-14K$. Thus for our perturbation problem, we have a non-diagonal energy $-K$, an energy difference $14K$, and $4n$ non-diagonal terms, so that the perturbed energy is $4nJ + (4nK^2/14K) = 4nJ + (2/7)nK$.

This formula is rather significant. We compare the energy with that of the lowest state of the diatomic molecule, $n=2$, which is $(n/2)J + \frac{1}{2}nK$. We observe that for the crystal the coulomb interaction, the term J , has a coefficient eight times as great: each atom has eight neighbors instead of one, each

penetrating. On the other hand, the valence term K has a coefficient only $2/7$, instead of $1/2$. The valence, so to speak, is spread out among all the neighbors, and weakened in the process. It is partly on this account that we can say that the coulomb interaction is the more important part of the cohesive force, in metals.

We have considered only those pairs with smallest separation, and they give a definite attraction. But in this lattice, there are not only the eight nearest atoms at distance R ; there are also six, in directions parallel to the edges of the cube, at distance of $1.155R$, and these have parallel spins, producing therefore a repulsion. In the diagonal energy, each pair will then contribute an energy $J-K$, a positive amount, so that the diagonal energy of the lowest state is $4nJ+3n(J(1.155R)-K(1.155R))$. The next higher diagonal energy also will differ from this not merely by $-14K(R)$, but also by an amount $12K(1.155R)$, because by interchange of two spins some of these repulsive terms are removed. Thus the lowest energy level, counting also these pairs, is

$$4nJ(R)+3n(J(1.155R)-K(1.155R))+\frac{4nK^2(R)}{14K(R)-12K(1.155R)}.$$

This results, on computation, in a much weakened attraction. If we were to consider in succession the effects of pairs at greater and greater distance, we should come in succession to attracting atoms with antiparallel spin, and repulsive ones with parallel, so that the successive approximations to the energy would oscillate, falling first above, then below, the true value.

Application to sodium. For the sodium crystal, approximate calculations have been carried out, to test these formulas. These were made by taking a simple analytical expression for the wave function of the valence electron of sodium, and computing the integrals J and K . The details of the calculation will not be given here. The first thing that one notices is that, for Na, J is several times larger in proportion to K than in hydrogen. It is this fact, taken together with the increased coefficient of the J term, that results in the importance of the coulomb term. It is also significant in connection with the question, why do the alkalies, and metals in general, form metallic lattices, while hydrogen does not? We can see the essential answer from our energy formulas of the previous page. For substances where J is the important term, the coefficient of J will be greater, and the energy lower, for the crystal than for the same number of atoms in diatomic molecules, and the crystal will be the stable form. For hydrogen, on the other hand, the valence term K is the important one. Here the coefficient in the molecular form is greater; and even if the metallic form of such a substance were stable in the sense of having a minimum of energy for some definite size, as seems quite possible, still the energy in the molecular state would be lower. The atoms in the crystal would tend to form pairs, resulting in a molecular lattice; the molecules would repel each other, and would be held together only by van der Waals forces, which have been neglected in this paper. This seems to be exactly what hydrogen does.

The numerical values for Na are approximately as follows. If we take only the adjacent pairs, the minimum comes at $R=4.9a_H$ approximately, rather seriously less than the correct value 7; this can partly be explained by the observation that the best atomic wave function for use in the crystal would be more extended than that determined from the free atoms, which are here used. The energy at this point comes out about -40 kg cal/gm mol, the coulomb term supplying about four fifths of this; the observed heat of vaporization is 26.4 kg cal, so that this gives, as we should expect, too large a value. If now we consider the repulsive pairs at distance of $1.155 R$, the situation is quite changed. In the first place, the energy is reduced from -40 to about -9 kg cal. When we remember that these two values are the first two terms of a series, whose value oscillates on both sides of the answer, it seems very reasonable that the final result should be not far below the experimental value. The problem of properly computing this energy must be done by the method, using Bloch's functions, described in the preceding section. In the next place, the minimum of the curve is greatly broadened: for quite a range of values, from $R=4.9$ (the previous minimum) to $R=7$, the energy stays about constant, the change of the attractive term being just about balanced by the relatively more rapid change of the smaller repulsive effect. (For smaller R 's, a situation can be found when the denominator $14 K(R) - 12 K(1.155 R) = 0$, so that the function becomes infinite; but this is without physical significance.) No doubt a persistence of this effect in the final answer helps to correct the improperly low grating space we have already found. It also is interesting in connection with the compressibility. The alkalies are remarkably compressible, and if we compute the compressibility for the case where only adjacent pairs are considered, the result is too small by a factor of 2 or 3. On the other hand, considering the next set of atoms, our very broad maximum would give much too great a compressibility. Here again it seems that our result may oscillate, perhaps approaching eventually something near the right value.

THE STABILITY OF METALLIC CRYSTAL LATTICES*

BY R. H. CANFIELD
NAVAL RESEARCH LABORATORY

(Received January 22, 1930)

ABSTRACT

The first sections of this paper are a partial repetition and amplification of Born's theory of homopolar crystal lattices, without, however, making any assumption about the law of force between atoms other than that the force is central and that diatomic molecules are possible. The mathematical work is supplemented with graphical illustrations. If the lattice is in equilibrium as regards (a) displacement of one atom, (b) unidirectional extension of the entire lattice, and (c) simple shear of the entire lattice, it is shown that each of these postulates leads to a restrictive condition on the symmetry and pattern of the possible lattices, thus accounting for the high symmetry actually observed. Finally if the equilibria *a*, *b*, *c*, are stable, there are three series of terms in W'' , corresponding to elastic constants, which must be positive. Making use of these series, it is shown that the lattice is likewise in equilibrium against motion of one portion *en bloc* relative to another portion and hence that "mosaic" crystals cannot be configurations of minimum potential energy.

INTRODUCTION

THE primary purpose of this paper is to determine whether there is any theoretical basis for the existence of a mosaic structure in crystals of metals or other crystals containing atoms of only one kind. This periodic inhomogeneity for which "mosaic" seems the best short equivalent, has been proposed by various workers¹ as accounting for the non-agreement between calculated and observed tensile strengths of crystals.

Zwicky¹ and his collaborators, e.g. Evjen,³ have made numerical calculations of the energy changes due to the formation of these mosaic structures in ionic lattices, and find that they are to be expected. Zwicky² has also published a general thermodynamic proof intended to apply to crystals of any kind, which the writer⁴ has criticized. The subject will be dealt with more fully in the closing paragraphs of this paper.

The present paper is an attempt to deal with the same problem, for metallic lattices only, in a rigorous manner.

The preliminary steps are elementary and a recapitulation of other work; but it is hoped that this feature may be of some value to others who have found Born's⁵ classical treatment "nicht ganz einfach zu lesen." The method and notation here introduced will be used by the writer in other papers.

* Published by permission of the Navy Department.

¹ Notably Zwicky, Phys. Zeits. 24, 131 (1923).

² Zwicky, Proc. Nat. Acad. Sci. 15, 11 (1929).

³ Evjen, Phys. Rev. 34, 1385 (1929).

⁴ Canfield, Phys. Rev. 35, 1 (1930).

⁵ Born, "Atomtheorie Des Festen Zustandes," Leipzig, 1923.

FUNDAMENTAL STATEMENTS

Let us regard the atoms of a homopolar lattice as centers of mutual forces. Whatever wave-functions are in the background of this behavior we do not enquire. Neither do we concern ourselves with whether or not the atoms are charged. We merely assume that all the atoms are alike and that each two of them exert mutual forces on each other, independent of the presence of other atoms, such that at great distances they attract, and at very small distances they repel each other. At very great distances the force of attraction, and all its derivatives, vanishes. Finally, the mutual force has a potential.

We then represent the mutual energy W of two atoms in terms of their distance r by a curve like Fig. 1. In the absence of kinetic energy the two atoms will form a molecule, their centers being at a distance r_e . If they possess relative kinetic energy less than W_e , they will execute vibrations, the amplitude being represented by ρ . Due to the energy curve not being in general a parabola (i.e. not obeying Hooke's Law), these vibrations are neither iso-

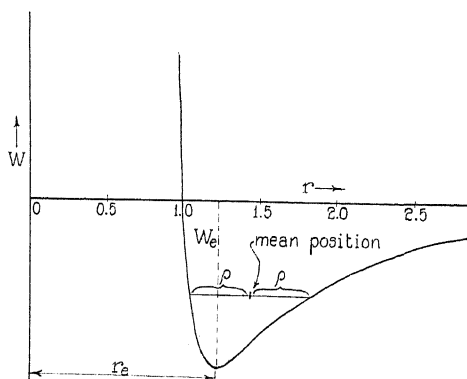


Fig. 1.

chronous nor simply harmonic. The theory of the vibration of such an anharmonic oscillator is part of the theory of molecular spectra.

Our present problem is the application of this energy curve to those polyatomic molecules called crystals.

We next picture an aggregation of atoms in space occupying the points of a regular geometric space lattice and forming a crystal. For the time being we are not concerned with the exact configuration of this lattice. We fix our attention on a single atom of this lattice. We now construct spherical surfaces with this atom as center, such that all of the surrounding atoms fall on one or another of these surfaces. We select some distance, say the distance to the nearest neighbor atom, as a parameter and call it r_0 . The number of atoms at the distance r_0 we call $2n_1$. We designate the shells in the order of their radii by subscripts 1, 2, \dots , and their radii by k_1r_0 , k_2r_0 , \dots , k_ir_0 ; the number of atoms in the i th shell is $2n_i$.

Referring now to Fig. 2, an energy diagram for our selected atom, we put on it the ordinates corresponding to the various groups of neighbors at dis-

tances $k_i r_0$ and label each ordinate with the corresponding n_i . (It is plain that since the energy of each pair of atoms is W_i , the energy of each atom due to its neighbors at $k_i r_0$ is only $n_i W_i$ instead of $2n_i W_i$). Then the energy of one atom in the lattice is

$$U = \sum_{i=1}^{i=\infty} n_i W_i. \quad (1)$$

We may quite simply refer to n_i as the number of *bonds* of length $k_i r_0$ associated with each atom in the lattice.

Still assuming that the *type* of the lattice is fixed, it is next of importance to find how the crystal attains a configuration of a certain density. We are of course assuming that the atoms are at rest. Actually they are in vibratory motion but it can be shown that the amplitude of vibration is small com-

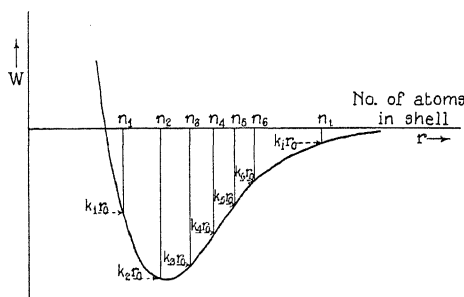


Fig. 2.

pared with r_0 and thus the fixed positions correspond pretty closely with the average positions of the atoms over a period of time. It is plain that a change in r_0 will result in a dilatation of the entire lattice to correspond; the equilibrium configuration will be that for which a small change in r_0 results in no change of energy. We therefore differentiate Eq. (1) as follows:

$$\partial U / \partial r_0 = \sum_i n_i \partial W_i / \partial r_0 = \sum_i n_i k_i W_i' = 0 \quad (2)$$

where $W_i' = [\partial W / \partial r]_{r=k_i r_0}$ and $\partial W / \partial r_0 = k_i W_i'$.

In more graphic terms, the array of ordinates in Fig. 2 is horizontally expanded or contracted, until, each ordinate being weighted with the corresponding number n_i , their sum is a minimum.

It will be of interest at this point to study the diagrams in Fig. 3. Diagram A is a plot of the number of bonds of length r or less than r for an atom in a face-centered cubic lattice; diagram B for a body-centered, and C for a simple cubic lattice. The dotted lines represent the same functions calculated on the assumption of uniformly distributed matter.

Several points of interest are at once apparent. There are almost always more bonds, shorter than any specified length, in a face-centered than in a body-centered cubic lattice, and more in the latter than in a simple cubic. It

is just this characteristic that is implied by the words "close-packing" applied to the two former types. Thus if atoms were rigid spheres attracting each

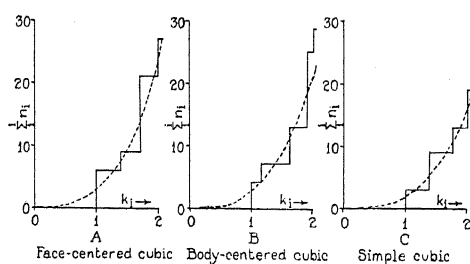


Fig. 3

other according to an inverse power of r , and therefore possessing an energy curve like Fig. 4, they would inevitably choose one of the configurations of

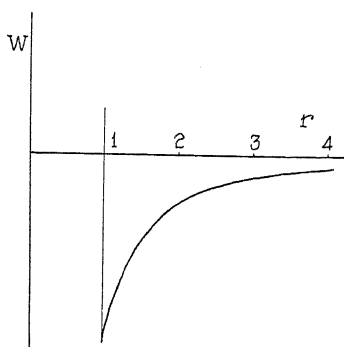


Fig. 4

closest possible packing, i.e., the face-centered cubic or close-packed hexagonal (practically equivalent).

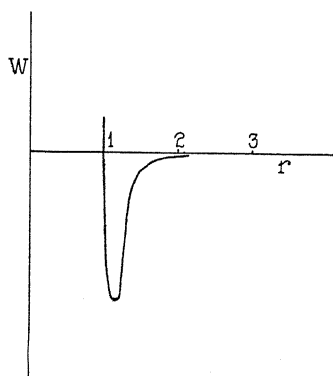


Fig. 5

On the other hand, if the energy curve were like Fig. 5, they would choose the body-centered cubic type, since here there is room for the first two groups

of the body-centered lattice, containing 7 bonds and thus more negative potential energy than the face-centered type, which would have only one group containing 6 bonds in the deep loop of the diagram.

We thus already see a clue to the explanation of the different types of lattices. The expression for dU in terms of the second power of dr_0 yields a formula for the compressibility of the crystal. This is of course positive, since the configuration is one of stable equilibrium. The expression is

$$dU = \frac{1}{2} dr_0^2 \sum n_i k_i^2 W_i''.$$

EQUILIBRIUM AGAINST VARIOUS DISPLACEMENTS

1. *Displacement of a single atom.* We have already established the manner in which the atoms place themselves on a lattice of a certain type and with a certain density, i.e., equilibrium as regards dilatation and change of lattice type. It is next in order to study equilibrium against a displacement of one atom from its correct position, for if the lattice is not in stable equilibrium against such displacements, thermal agitation will destroy it. Referring to

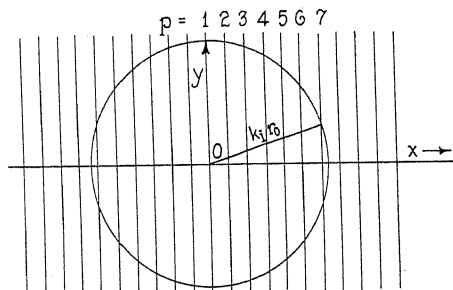


Fig. 6

Fig. 6, the atom O under consideration is shown at the center of the i th sphere. Atom O suffers a displacement dx . The atoms in the shell i are arranged in groups p for which all the atoms in any group p lie in the same plane perpendicular to x . The number of atoms lying in the p th plane of the i th shell is n_{ip} and their bonds to O all make the same angle θ_{ip} with the X -axis. Evidently $\sum_p n_{ip} = 2n_i$. The change in energy dU due to the motion dx is then (only taking account of the atoms in shell i)

$$dU_i = \left(W_i' \sum_p n_{ip} \cos \theta_{ip} \right) dx.$$

For all the shells i we then have

$$dU = \left(\sum_i (W_i' \sum_p n_{ip} \cos \theta_{ip}) \right) dx = 0. \quad (3)$$

But we already have an equation (Eq. (2)) of the form

$$\sum_i A_i W_i' = 0,$$

and since these are two linear equations in the W_i' their coefficients must be proportional or else the coefficients of Eq. (3) must be zero. The latter is the only possible alternative* and thus we have for any i ,

$$\sum_p n_{ip} \cos \theta_{ip} = 0 \quad (4)$$

as a restrictive condition on the configuration.

Put into words this means that an atom in the lattice must lie at the center of gravity of each of the concentric surrounding shells of atoms. Most, if not all, of the known crystalline elements obey this condition, so that it cannot be called highly restrictive.

Having disposed of the terms involving dx we now develop dU_i in terms of dx .² Referring again to Fig. 6, it will be seen that $dU_i = \frac{1}{2}(W_i'' \sum_p n_{ip} \cos^2 \theta_{ip}) dx^2$, in which the coefficients of W_i'' are always positive. But W_i'' may be either positive or negative, so we have no *a priori* knowledge of whether $\sum dU_i$ is positive or negative. If negative the lattice is in unstable equilibrium. Since we know, however, that actual lattices are actually in stable equilibrium we have the strongest reasons for believing that

$$\sum_i \left(W_i'' \sum_p n_{ip} \cos^2 \theta_{ip} \right) > 0 \quad (5)$$

and we can hereafter use this series for comparison.

2. *Equilibrium against uniform extension in one direction.* We now assume that the whole lattice is uniformly stretched in the X -direction at the same time not permitting it to contract laterally. Let the amount of stretch per unit length be ϵ . Referring again to Fig. 6, we see that bond ip is stretched an amount $\epsilon k_i r_0 \cos^2 \theta_{ip}$. Hence

$$dU_i = k_i W_i' \epsilon r_0 \sum_p n_{ip} \cos^2 \theta_{ip}$$

where θ_{ip} is now confined to values between $-\pi/2$ and $+\pi/2$. If equilibrium exists

$$\sum_i k_i W_i' \sum_p n_{ip} \cos^2 \theta_{ip} = 0.$$

Comparing the above expression with Eq. (2) as before, it is plain that we have the same two alternatives; but since the coefficients of W_i' in the above expression are definitely positive, each one must be the same multiple of the corresponding coefficient in Eq. (2), i.e.

$$\sum_p n_{ip} \cos^2 \theta_{ip} = a n_i \quad (6)$$

where a is the same constant for every different value of i , but not the same for different directions of the axis of elongation.

This result may be put into more familiar terms by saying that the planar moment of inertia of every shell of atoms with respect to a given YZ plane is

* For $\sum_p n_{ip} \cos \theta_{ip} \leq n_i$, while n_i becomes a smaller and smaller fraction of $k_i n_i$.

the same fraction of $k_i^2 r_0^2 n_i$ for that shell. In particular it will be noticed as a result of familiar properties of moments of inertia, that the principal axes of inertia have the same directions for all shells, and the principal moments of inertia are in the same proportion. This constitutes a very severe restriction on the pattern of the lattice.

The terms in ϵ^2 are now to be evaluated. By a similar reasoning to that employed in the previous paragraphs, we find

$$dU_i = \frac{1}{2} W_i'' k_i^2 \left(\sum_p n_{ip} \cos^4 \theta_{ip} \right) \epsilon^2 r_0^2$$

or

$$dU = \frac{1}{2} \epsilon^2 r_0^2 \sum_i k_i^2 W_i'' \sum_p n_{ip} \cos^4 \theta_{ip}$$

and since we have experimental evidence that crystals are in stable equilibrium against just such an extension as this, we are justified in concluding that

$$\sum_i k_i^2 W_i'' \sum_p n_{ip} \cos^4 \theta_{ip} > 0. \quad (7)$$

The series in Eq. (7) is proportional to the elastic constant c_{11} for the X -axis we have selected.

3. *Equilibrium against shear.* Imagine the lattice distorted parallel to the XY plane, the displacements being given by $dy = \epsilon x$, $dx = 0$, $dz = 0$. This is a simple shearing distortion. The first order terms in the energy-change are of the type

$$dU_i = \epsilon r_0 k_i W_i' \sum_p \cos \theta_{ip} \sin \theta_{ip} \sum_q \cos \phi_q$$

where ϕ_q is the angle between the XY plane and the plane through the X -axis which contains the atom in question, and where the summation with respect to q means summation over the atoms lying in the circle of intersection of the plane p and the shell i . This expression may be rewritten:

$$dU_i = \frac{\epsilon W_i'}{k_i r_0} \sum_r x_r y_r$$

where the summation is over the atoms of the i th shell. For all the shells:

$$dU = \epsilon r_0 \sum_i k_i W_i' \sum_r \frac{x_r y_r}{k_i^2 r_0^2}$$

and if this latter expression equals zero we have:

$$\sum_i k_i W_i' \sum_r \frac{x_r y_r}{k_i^2 r_0^2} = 0.$$

Comparing this equation with Eq. (2) as before, we find the two only compatible if

$$\sum_r x_r y_r = f n_i k_i^2 r_0^2 \quad (8)$$

where f is the same constant for each value of i , but varies with the orientation of the coordinate frame. It turns out that Eq. (8) is a consequence of Eq. (6), as a simple calculation will demonstrate. Thus, equilibrium against shear introduces no restriction on the lattice geometry beyond what was already imposed by the equilibrium against unidirectional elongation. (This might have been directly inferred from the theory of elasticity).

The expression for dU in terms of ϵ^2 must be greater than zero if the equilibrium against shear is stable. The corresponding inequality is:

$$\sum_i k_i^2 W_i'' \sum_p \sin^2 \theta_{ip} \cos^2 \theta_{ip} \sum_q \cos^2 \phi_q > 0. \quad (9)$$

The series in Eq. (9) is proportional to the elastic constant c_{66} for the axes selected.

4. *Equilibrium against displacement of a large portion of the lattice.* The principal object in deriving the equations of the preceding paragraphs was not to prove that crystals can exist, for we know this from observation, but to obtain certain series in W_i' and W_i'' of which the sums are known to vanish, or be positive respectively, and which can be used for comparison with other series in W_i' and W_i'' of which the behavior is not known from observation.

We now draw another picture of our lattice, Fig. 7, in which we once more show all the atoms lying on a series of equidistant planes, each plane

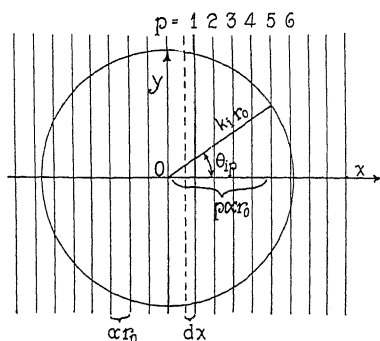


Fig. 7.

containing an equal number of atoms. (For some lattices the planes may not be equidistant, or equally densely packed, but there will always be a repetition of the same distances in the same order, and the argument is but little affected). The X -axis is an arbitrary line in space as before. Though the transverse planes may be very close together and contain each but a few atoms, nevertheless the lattice can always be resolved into such a series of planes with finite separation and perpendicular to an arbitrary axis. The distance between planes is αr_0 .

Now we elect to remove the portion of the lattice lying to the right of 0 by a distance dx from the portion to the left. In so doing we elongate every bond crossing the gap dx by an amount $dx \cos \theta_{ip}$.

We must also notice that if $k_i \cos \theta_{ip} = \alpha$, only the atoms lying in the plane through 0 have their bonds affected. But if $k_i \cos \theta_{ip} = 2\alpha$, then the plane through 0 and also its neighbor on the left contain atoms whose bonds are lengthened; and in fact if $k_i \cos \theta_{ip} = p\alpha$ there are p planes to the left of 0, and including 0, containing atoms whose i th bonds are lengthened by the operation. So if there are N atoms in each plane

$$dU_i = NW_i' dx \sum_p n_{ip} p \cos \theta_{ip}$$

But $p = k_i \cos \theta_{ip} / \alpha$ hence

$$dU_i = \frac{Nk_i W_i' dx}{\alpha} \sum_p n_{ip} \cos^2 \theta_{ip}$$

and

$$dU = (Ndx/\alpha) \sum_i W_i' k_i \sum_p n_{ip} \cos^2 \theta_{ip} \quad (10)$$

where θ_{ip} takes on values between $-\pi/2$ and $+\pi/2$.

But Eq. (6) told us that $\sum_i [W_i' k_i \sum_p n_{ip} \cos^2 \theta_{ip}] = 0$. Hence in Eq. (10) $dU = 0$. Hence the lattice is in equilibrium against the assumed displacement.

We now develop dU in terms of dx^2 as follows:

$$\begin{aligned} dU_i &= \frac{1}{2} N dx^2 W_i'' \sum_p n_{ip} p \cos^2 \theta_{ip} \\ &= \frac{1}{2} \frac{N dx^2 W_i'' k_i}{\alpha} \sum_p n_{ip} \cos^3 \theta_{ip} \end{aligned}$$

whence

$$dU = (N dx^2 / 2\alpha) \sum_i k_i W_i'' \sum_p n_{ip} \cos^3 \theta_{ip} \quad (11)$$

The question whether the equilibrium we have been discussing is stable depends on whether the series in Eq. (11) is positive.

To settle this matter we shall require the series of Eq. (7) for purposes of comparison. Let us use the letter S for the latter series and the letter S' for the series of Eq. (11). If we now refer to Fig. 2 we see that for the first few terms W_i'' is positive, and for all the remainder out to infinity W_i'' is negative. Let us say that W_μ'' is the last positive term. Then we may write $S = S_A - S_B$ where S_A is a terminating series ending with W_μ'' , and S_B is an infinite series of positive terms starting with $-W_{\mu+1}''$. The fact that $S > 0$ implies that $S_A > S_B$. Similarly we divide S' into two parts S_A' and S_B' the division being at the same term as for S . Let the i term of S be S_i and the i term of S' be S_i' . Then

$$\begin{aligned} \frac{S_i}{S_i'} &= \frac{k_i^2 W_i'' \sum_p n_{ip} \cos^4 \theta_{ip}}{k_i W_i'' \sum_p n_{ip} \cos^3 \theta_{ip}} \\ &= \alpha \cdot \frac{k_i W_i'' \sum_p p n_{ip} \cos^3 \theta_{ip}}{k_i W_i'' \sum_p n_{ip} \cos^3 \theta_{ip}} \end{aligned}$$

Let $S_i/S'_i = t_i$. Evidently $\alpha < t_i < \alpha q_i$ where q_i is the largest integer in k_i/α , i.e., the largest value of p . Also $t_i < t_{i+1}$.*

We may now write the two series as follows:

$$S = S_A - S_B = \sum_1^{\mu} t_i S'_i - \sum_{\mu+1}^{\infty} t_i S'_i$$

$$S' = S_A' - S_B' = \sum_1^{\mu} S'_i - \sum_{\mu+1}^{\infty} S'_i.$$

Then

$$\alpha < S_A/S_A' < t_{\mu} < \alpha q_{\mu} \leq \alpha q_{\mu+1} < S_B/S_B'.$$

or

$$S_A/S_A' < S_B/S_B'.$$

But

$$S_A > S_B$$

hence

$$S_B/S_A' < S_B/S_B'$$

or

$$S_A' - S_B' > 0.$$

The expression in Eq. (11) is therefore positive, and the equilibrium is stable. In other words, any displacement of a portion of the perfect lattice directly away from another portion sets up a restoring force. If the crystal does not extend to infinity to right and left, the effect will only be to make S_B and S_B' terminating series, and the inequalities will be even more pronounced. It only remains to carry through a similar argument with respect to a lateral displacement of one portion of the lattice relative to the other. It turns out that, using a similar notation and procedure to that which preceded,

$$S = \sum_i k_i^2 W_i'' \sum_p \cos^2 \theta_{ip} \sin^2 \theta_{ip} \sum_q \cos^2 \phi_q \quad (\text{Eq. 9})$$

$$= \alpha \sum_i k_i W_i'' \sum_p p \cos \theta_{ip} \sin^2 \theta_{ip} \sum_q \cos^2 \phi_q$$

and

$$S' = \sum_i k_i W_i'' \sum_p \cos \theta_{ip} \sin^2 \theta_{ip} \sum_q \cos^2 \phi_q.$$

From which, as before, we find that $dU > 0$ and the equilibrium is stable with respect to this displacement too.

POSSIBLE CLASSES OF SYMMETRY IN HOMOPOLAR CRYSTALS

In this section we shall discuss rather briefly the consequences of Eqs. (4) and (6), so far as they affect the symmetry properties of homopolar lattices as defined in the opening paragraph.

The meaning of Eq. (4) is that any atom in the lattice must lie at the center of gravity of any group of atoms which are situated on the surface of a

* For large values of k , t approaches $(4/5)k$; there may be isolated values of i for which $t_i > t_{i+1}$ but these are very rare. It is impossible to imagine a W function for which this slight departure from rigor would invalidate the general conclusion.

sphere with the atom in question at its center. It is plain that the atoms of such a group must display at least all the elements of symmetry of the crystal as a whole. (They may display additional elements of symmetry, but here we are concerned with minimum requirements.)

The elements of symmetry, so far as they affect our present argument, are: (1) a center of symmetry; (2) an axis of symmetry, either digonal, trigonal, tetragonal or hexagonal; (3) a plane of symmetry. The properties of these as they affect the center of mass are as follows:

1. The center of gravity coincides with a center of symmetry if one exists.
2. Any axis of symmetry contains the center of gravity.
3. Any plane of symmetry contains the center of gravity.

Since all elements of symmetry of points on a sphere contain the center of the sphere, it is sufficient that the elements of symmetry shall determine a point, to make that point the center of gravity. This then may be accomplished in the following ways:

- (1) A center of symmetry.
- (2) Two axes of symmetry of any order.
- (3) An axis of symmetry and a plane of symmetry which does not contain the axis.
- (4) Three non-collinear planes of symmetry.

Any class of symmetry, then, which displays at least one of the four combinations of symmetry elements listed above, fulfills the requirements of

TABLE I.†

Class (Dana)	Symbol (Schoenflies)	Class (Dana)	Symbol (Schoenflies)
I. Triclinic System		V. Cubic	
Asymmetric	C_1	*Tetartohedral	T
*Normal	C_i	*Pyritohedral	T^h
II. Monoclinic System		*Tetrahedral	T^d
Clinohedral	C_2	*Plagihedral	C
Hemimorphic	C_2^h	*Normal	O^h
*Normal		VI. Hexagonal.	
III. Orthorhombic		(Rhombohedral Division)	
Hemimorphic	C_2^v	*24	C_3
*Sphenoidal	V	*Trirhombohedral	C_3^v
*Normal	V^h	Ditrigonal Pyramidal	C_3^v
IV. Tetragonal		Trapezohedral	D_3
Tetartohedral	S_4	*Rhombohedral	D_3^d
*Sphenoidal	V^d	(Hexagonal Division)	
Pyramidal Hemimorphic	C_4	*23	C_3^h
*Pyramidal	C_4^h	*Trigontype	D_3^h
Hemimorphic	C_4^v	Pyramidal Hemimorphic	C_6
*Trapezohedral	D_4	*Pyramidal	C_6^h
*Normal	D_4^h	Hemimorphic	C_6^v
		*Trapezohedral	D_6
		*Normal	D_6^h

*Indicates classes which conform to barycentric symmetry condition of Eq. (4) in text.

† Table copied from Wykoff: "The Structure of Crystals", N. Y. 1924.

Eq. (4). In Table I are listed the 32 recognized classes of crystal symmetry. Those classes which obey Eq. (4) are designated with asterisks. Of the 32

classes, 21 obey this condition. All the known space lattices of crystal elements fall into the 21 classes with the possible exception of graphite, of which the lattice is still the subject of discussion.

We still have to discuss the consequences of Eq. (6), which imposes a restriction far more severe than Eq. (4).

Eq. (6) demands that the principal axes of inertia of each sphere of atoms concentric with a selected atom shall have the same directions (this also follows from symmetry considerations) and that the principal planar moments of inertia shall be in the same proportion. So far as the writer can determine, this condition is satisfied by the five classes of the cubic system and none other. The hexagonal close-packed arrangement may be said to satisfy the condition 'approximately', i.e. the first departure is in the shell $i=3$, and involves the transfer of two atoms from a shell containing twelve, to a shell of about 6 percent smaller radius. Just what meaning can be attached to this 'approximate' fulfilment of such a condition is not clear. It may mean that this small departure from equilibrium can be balanced by a minute polar force-field superposed on the central force-field which we have postulated in the first paragraph of the Fundamental Statements above.

It may finally be remarked that if Eq. (2) has a solution r_0 for a particular lattice type, and if this lattice type satisfies Eqs. (2) and (4), and if $\sum n_i W_i$ is smaller for this configuration than for any of the other configurations satisfying Eqs. (1), (2) and (4), then the inequalities expressed by Eqs. (5) and (7) show that no lattice obtained by a homogeneous deformation of the given lattice can satisfy the given conditions. Moreover, since the validity of these inequalities is only increased by leaving out terms beyond the first few terms in the summations, all departures from complete geometrical perfection in the interior of a homopolar crystal are unstable.

At points near the surface of a crystal, particularly for points nearer to the surface layer than the distance at which $W_i''=0$, the above statement is not true; the writer hopes to make those surface conditions the subject of a future paper.

MOSAIC STRUCTURES

The displacement of one portion of a crystal *en bloc* relative to the other portion may be said to be the purest type of inhomogeneous deformation. From the two cases of this kind which we have considered above, in conjunction with the postulated stability against homogeneous deformation, it is possible to show that any conceivable picture of inhomogeneous deformation leads to an increase of energy in the second order terms of the displacements. Among others, it is possible to show that the equilibrium is stable against a uniform or non-uniform contraction of a single lattice plane.

Two types of variation from perfect symmetry are conceivable mosaic structures. The first is obtained by some sort of inhomogeneous deformation of an originally perfect lattice. Our conclusions given above show that any such configuration involves a greater energy than the original.

The second is obtained by some such inhomogeneous deformation forming gaps in the lattice into which additional atoms are inserted. To show that this results in a preferred configuration it is necessary not merely to show (a) that the new atom has a negative potential energy greater than the positive energy created by the deformation, but also (b) that the net decrease in energy thereby effected is greater than what would result from adding one more atom in a normal way to the structure of the perfect lattice. Zwicky⁶ in replying to the author's⁴ criticism his general thermodynamic argument for all crystals, recapitulates his calculations for an ionic lattice (rock salt), and establishes the condition (a) above; but he does not show that condition (b) is satisfied as well.

Evjen² has calculated the case of inhomogeneous deformation of a rock-salt lattice and finds as we do here for a homopolar lattice, that the energy terms in the second powers of the displacements are positive. He does, however, find that when terms of the third and fourth powers are included, it is possible to find a secondary minimum in the energy which may be lower than the original minimum.

In concluding the author wishes to express to Professors K. F. Herzfeld and F. D. Murnaghan his appreciation of their comments on certain portions of this paper.

⁶ Zwicky, *Phys. Rev.* 35, 3 (1930)

THE INFLUENCE OF TEMPERATURE ON POLARIZATION CAPACITY AND RESISTANCE

BY E. E. ZIMMERMAN

EDGEWOOD ARSENAL, EDGEWOOD, MARYLAND

(Received January 16, 1930)

ABSTRACT

The temperature coefficients of polarization capacity and resistance have been determined for gold and plain platinum electrodes in 0.63, 1.50 and 2.42 N solutions of sulphuric acid and also at different frequencies for 1.46 N concentration. To reduce the electrodes to a condition representing minimum capacity, a method of thermal treatment was employed and found quite effective. Values of the angle of phase difference have been computed for the various conditions under which measurements were made.

During the process of reducing the electrodes to a condition representing minimum capacity, the value of polarization capacity decreased to about one-half the original value and the resistance increased to a few times the original value. The angle of phase difference increased 15 or 20 degrees. After the electrodes were conditioned, consistent and reproducible values of capacity and resistance could be obtained.

The temperature coefficient of capacity is about twice as great with platinum as with gold electrodes and is apparently independent of concentration. Phase difference changes only slightly with temperature, but increases with concentration. The absolute values of the slopes of the curves, capacity versus temperature and resistance versus temperature, decrease with increasing frequency. The temperature coefficient of capacity, however, increases with frequency for platinum electrodes and decreases in the case with gold electrodes.

THERE has been a limited amount of investigation of the effects on polarization capacity and polarization resistance caused by changes in temperature. Sheldon, Leitch and Shaw¹ determined the temperature coefficient of capacity for cells consisting of $\text{Pt}|\text{H}_2\text{SO}_4|\text{Pt}$ and $\text{Hg}|\text{H}_2\text{SO}_4|\text{Pt}$. Schönherr² studied the influence of temperature on the reduction of the electrodes to a condition corresponding to minimum capacity. The work herein described was an investigation to determine the nature and magnitude of changes in polarization capacity and resistance as influenced by changes in temperature, under various conditions with respect to the concentration of the electrolyte, the frequency of the applied voltage and the material and condition of the electrodes.

APPARATUS AND EXPERIMENTAL PROCEDURE

Measurements were made by means of the Wheatstone bridge and auxiliary apparatus, diagrammatically represented in Fig. 1. The low-power vacuum tube oscillator which had a frequency range from 600 to 4000

¹ Sheldon, Leitch and Shaw, *Phys. Rev.* (1) 2, 401 (1895).

² Schönherr, *Ann. d. Physik u. Chemie* 6, 116 (1901).

cycles per second was loosely coupled to the bridge by means of a step-down transformer in order to maintain the voltage across the polarization cell at or below the value corresponding to minimum or initial-capacity. Minimum or initial-capacity is that value of polarization capacity characteristic of the cell when the applied voltage is sufficiently low that further decrease in voltage does not result in any appreciable decrease in the value of polarization capacity. With respect to variations in capacity as influenced by variations in voltage, Wien³ found that the polarization capacity was constant at the minimum value if the voltage across the cell was 0.05 or less. Wolff⁴ found the capacity nearly constant for voltages less than 0.1 volt. In the present work, in order to ascertain whether or not variations in applied voltage were influencing the measurements, the voltage across the polarization cell was measured by means of a vacuum tube voltmeter and was found to be less than the critical value. Also, resistance was inserted in the leads to the bridge without decreasing the measured value of capacity. All values of polarization capacity recorded in this paper are, therefore, thought to be

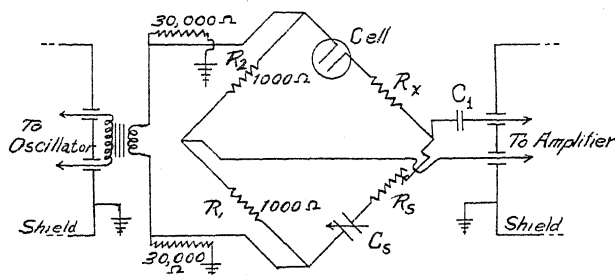


Fig. 1. Bridge and auxiliary apparatus.

minimum values insofar as the influence of the voltage applied to the cell is concerned.

The resistances, R_1 and R_2 , in the ratio arms of the bridge were maintained equal in order to minimize the effects of distributed capacity and inductance although with the type of bridge used and at the comparatively low values of frequency, effects of distributed capacity and inductance were negligible. The condenser, C_1 , was a fixed condenser and served to prevent any direct current through the cell.

Fig. 2 is a diagram of the polarization cell. The cell consisted of a container in the form of a test tube, with a pair of similar electrodes mounted by inserting through the perforated stopper the glass tubes into which the wire electrodes were sealed. The thermometer was similarly mounted with the center of the bulb in the same horizontal plane as the faces of the electrodes, the thermometer and electrodes being securely fastened together so that the faces of the electrodes were coplanar and about 3 mm apart. The end of any glass tube containing an electrode was ground transversely to the length so that the exposed circular cross-section of the wire electrode was

³ Wien, Ann. d. Physik u. Chemie 58, 37 (1896).

⁴ Wolff, Phys. Rev. 27, 755 (1926).

flush with the end of the tube. Gold and plain platinum electrodes were used, the gold having a diameter of 2 mm and the platinum a diameter of 0.623 mm. Under the conditions of the experiment, the capacity of polarization cells with electrodes as described was within the range from 0.03 to 0.7 microfarads and the corresponding range of polarization resistance was from 4000 to 500 ohms. For any particular test the electrolyte was an aqueous solution of sulphuric acid of desired concentration, which had been heated to free it of absorbed gases. The temperature of the cell was controlled by immersing it in an oil or water bath, the temperature of which could be controlled at will.

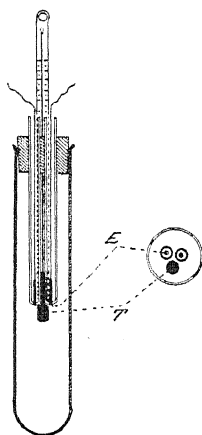


Fig. 2. Polarization cell. *E*, electrode. *T*, bulb of thermometer.

Data were obtained for any one set of conditions by making a series of measurements as the temperature was increased through a range from 0°C to a maximum of 90 or 95°C and then decreased through the same range.

THE EFFECT OF THERMAL TREATMENT ON STABILIZATION OF THE ELECTRODES

As have other experimenters,⁵ the writer found that cells having freshly surfaced electrodes do not give consistent and reproducible values of capacity and resistance. Incidentally, in attempting to duplicate results for rising and falling temperatures of a cell with freshly surfaced⁶ electrodes, it was found that the effect of any so-called temperature run such as that described above was to decrease considerably the values of capacity and increase the values of resistance. The value of the capacity at 0°C after the cell had been taken through the range of temperatures was reduced to a value which was from 40 to 60 percent of the original value at that temperature on starting the run. More marked changes took place in the resistance, the final value of which might be as much as four times greater after the conditioning runs. After

⁵ Gordon, Göttingen Diss. 72 (1896-97); Orlich, Diss., Berlin (1896); Wolff, reference 4.

⁶ The electrodes were surfaced by filing with a fine-grained file.

two or three such runs with a cell, values of capacity and of resistance obtained with falling temperature were in agreement with those obtained with rising temperature. Schönherr,⁷ also, found by increasing the temperature of the cell through a considerable range and then decreasing it through the same range that the final value of capacity was much less than the original value.

The manner in which polarization capacity and resistance change for freshly surfaced platinum electrodes when the cell is subjected to a series of runs is shown by the curves of Fig. 3. Curve *A* shows the relation between capacity and temperature for the initial run and curve *B* shows the relation

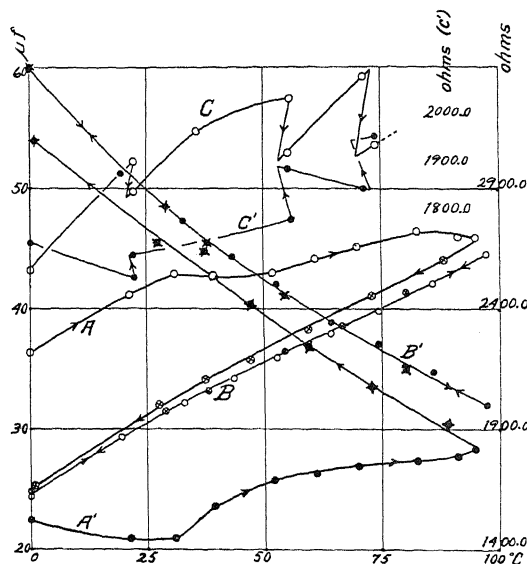


Fig. 3. Capacity-temperature and resistance-temperature curves for platinum electrodes while in the process of being conditioned. For explanation of curves, see text. Values of capacity are in microfarads per sq cm for one electrode and the plotted values of resistance represent total resistance of the cell. To obtain resistance per sq cm for one electrode, the values as plotted should be multiplied by 0.0015. Open circles, without and with crosses, represent values of capacity for increasing and decreasing temperature, respectively, while filled-in circles represent values of resistance, circles with projections being values obtained with decreasing temperature. For all curves, the concentration was normal and the frequency was 1020 cycles per second.

for the third run, the second having given results nearly the same as the third. The corresponding curves showing the development of polarization resistance⁸ are *A'* and *B'*, respectively. It may be noted in curve *B* (capacity)

⁷ Schönherr, reference 2.

⁸ Values of resistance are in all cases the measured values of the total resistance of the polarization cell without deducting for the resistance of the electrolyte which was assumed negligibly small in comparison with the resistance of polarization. A test of the validity of this assumption was made by varying the spacing between the electrodes and noting the effect on resistance. When the spacing was increased to 16 times the original value, the resistance

and in curve B' (resistance) that the agreement between the values of capacity and of resistance for rising temperature and the corresponding values for falling temperature is reasonably good. This same fact is also well emphasized in the curves of Fig. 4, in nearly all of which the values obtained with rising temperature are in very good agreement with those obtained with falling temperature. The one prominent exception in the curves of Fig. 4 is in the case of curves C (capacity-temperature for 0.63 N solution, with plain platinum electrodes) and C' (the corresponding curve for resistance). The lack of agreement in this case is due to the fact that these curves represent the first run of the series with the platinum electrodes and there had been only one run made to condition the electrodes previous to taking the data for these curves. The one run was not sufficient fully to condition the electrodes. In fact, in curves B and B' which are plotted from measurements made during a run following that for curves C and C' , there is still lack of complete agreement between the rising and falling-temperature branches of the curves.

When cells with gold electrodes were treated similarly, the effect was similar, excepting that the gold electrodes were more readily conditioned and did not require as many conditioning runs as did the platinum electrodes.

Success in duplication of results in making measurements of polarization capacity and resistance was possible only when the electrodes were fully conditioned. The writer found the method of thermal treatment as described above to be quite effective in accomplishing this and it is, moreover, a method which requires much less time than that of leaving the electrodes in the electrolyte to age for several days. Just what the condition of the electrode is when it has minimum capacity for a given set of conditions, is not definitely known. It doubtless represents a certain condition with respect to absorbed gas and also with respect to the condition of the surface. As have other experimenters, the writer observed that the electrodes undergo a change in color as they become conditioned, changing from a bright to a dull color. It was also observed that the electrodes could be conditioned in an electrolyte of given concentration and then be used in an electrolyte of different concentration and yet have capacity according to the second concentration.

In curves A and A' , Fig. 3, on the rising-temperature branches of the curves, attention is called to the fact that at a temperature of about 31° , the capacity underwent a rather sudden decrease and the resistance a sudden increase. The cause for these changes was a drop of about 1° in the temperature of the cell at this point after which, although the temperature was

increased only 3.5 percent. Also, the platinum electrodes which were used during the experimental work were finally platinized and the total resistance was determined. The value thus determined, when corrected for concentration, was not in any case more than 5 percent of the total resistance of the cell with plain platinum electrodes. Since part of the resistance of the cell as measured with platinized electrodes was resistance of polarization for platinized platinum, the value of the resistance of the electrolyte thus determined was somewhat too large. Consequently, 5 percent is a liberal estimate of the outside limit of the approximation.

again brought to its former value, the values of capacity and of resistance had undergone the changes noted. Later, in order to investigate this effect further, the electrodes were again freshly surfaced and the data represented in curves C and C' were obtained. In taking the data for these curves, the temperature was purposely permitted to fall 1 or 2 degrees at three different points on the ascending parts of the curves. The curves show that apparently the reversal of the temperature gradient with reference to the electrode and the electrolyte is effective in decreasing the capacity and increasing the resistance and also that a change in capacity is accompanied by a corresponding and closely related change in resistance.

During the conditioning process in case of the cell with platinum electrodes the phase difference, i.e., $\tan^{-1}\omega RC$, where ω is $2\pi \times$ frequency, R is polarization resistance and C is polarization capacity, increased from 27° to 40° and in case of the cell with gold electrodes the phase difference increased from 12° to 35° . The initial low value of phase difference in the latter case is probably due to the fact that the gold electrodes had previously been heated to the melting point, while in the case with the platinum electrodes, the electrodes had been freshly surfaced by filing, only. The electrode, then, having the property of polarization capacity, may be regarded as becoming a less perfect condenser as the electrode becomes conditioned or as it acquires the condition corresponding to minimum capacity.

The writer has chosen in this paper to regard polarization capacity and the resistance associated with it as being equivalent to a pure capacity and a pure resistance in series. Successful attempts were made, however, to balance the bridge both with a resistance in series with a mica condenser in the arm of the bridge opposed to the polarization cell, and also with a resistance in parallel with the standard condenser. The results were as follows:

Measured values of capacity and resistance when the cell was balanced by a capacity and resistance in series were, respectively,

$$0.0515 \mu f \text{ and } 2840 \text{ ohms.}$$

When C_m and R_m , signifying the corresponding values for the multiple relation, are computed from the above values,

$$C_m = \frac{C_s}{1 + \omega^2 C_s^2 R_s^2} = 0.0274 \mu f$$

and

$$R_m = R_s \left(1 + \frac{1}{\omega^2 C_s^2 R_s^2} \right) = 6070 \text{ ohms.}$$

The values of C_m and R_m as measured directly by means of the bridge were, respectively, $0.0292 \mu f$ and 5920 ohms, in reasonably good agreement with the computed values. The balance or null point was quite distinct in both cases.

TEMPERATURE COEFFICIENT AND CONCENTRATION OF THE ELECTROLYTE

With gold and plain platinum electrodes, conditioned according to the method described above, data were taken for different concentrations of the electrolyte as the temperature was varied over the complete range. The data so obtained are plotted in the curves of Fig. 4, the variation of capacity and

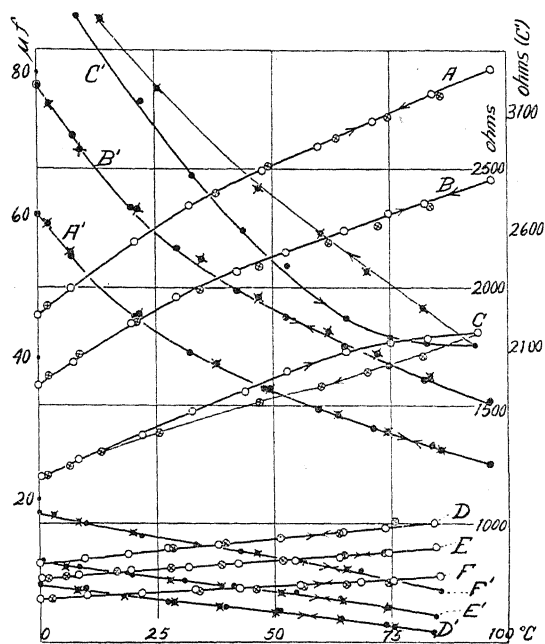


Fig. 4. Curves, capacity-temperature (letters not primed) and resistance-temperature (corresponding, primed letters) for different concentrations of the electrolyte. Curves A, A', D and D' are for 2.42 N concentration; curves B, B', E and E' are for 1.50 N; and curves C, C', F and F' for 0.63 N. The six upper curves are for platinum electrodes and the six lower for gold. For the significance of different kinds of points, see explanation, Fig. 3. The frequency was constant at 1000 cycles per second. All values of capacity are in microfarads per cm² for one electrode, but values of resistance represent the total resistance of the cell. To obtain resistance per cm² for one electrode, the plotted values should be multiplied by 0.0015 for the cases with platinum electrodes and by 0.0174 for the cases with gold electrodes.

the corresponding variation of resistance with temperature for the three different values of concentration being shown for the two kinds of electrodes.

Table I shows results of computations based on the curves of Fig. 4 and the data relating thereto. As is indicated in the table, the temperature coefficient of capacity, defined as

$$(1/C_{18})(dC/dT)_{18},$$

is about twice as much for platinum electrodes as for gold, other conditions being the same. With possibly an exception in the case with platinum electrodes for the 2.42 normal solution, the temperature coefficient for both

TABLE I. *Temperature coefficients of polarization capacity and polarization resistance for different concentrations of the electrolyte.*

Kind of Electrodes Concentration of Electrolyte	Plain Platinum			Gold		
	0.63 N	1.50 N	2.42 N	0.63 N	1.50 N	2.42 N
C_{18}	28.5	44.3	55.3	7.0	10.0	12.6
$(dC/dT)_{18}$	0.29	0.448	0.466	0.0372	0.053	0.067
$(1/C_{18})(dC/dT)_{18}$	0.0101	0.0101	0.0084	0.0053	0.0053	0.0053
R_{18}	4.3*	3.5	2.9	16.7	13.8	12.2
$(dR/dT)_{18}$	-0.045	-0.032	-0.026	-0.067	-0.043	-0.040
$(1/R_{18})(dR/dT)_{18}$	-0.0092*	-0.0089	-0.0089	-0.004	-0.0033	-0.0033

Notes: Values of capacity are in microfarads per cm² for one electrode. Values of resistance are in ohms per cm² of area for one electrode. *N* signifies normal solution (H₂SO₄ in water), i.e., 49 grams of acid per liter of solution. The frequency was constant at 1000 cycles per second.

* This value is somewhat uncertain, due to the fact that the electrodes were not fully conditioned.

Relatively, the values of C_{18} and R_{18} in Table I are accurate to within about 1 percent. Values of $(dC/dT)_{18}$ and $(dR/dT)_{18}$, and, consequently, the values of temperature coefficients, are probably not more accurate than to within 5 percent.

gold and platinum electrodes is independent of concentration for the three values of concentration involved. In other words, C_{18} and $(dC/dT)_{18}$ change in the same manner with respect to changes in concentration.

Also, it may be seen that the values of resistance per unit area of electrode, R_{18} , with platinum are about one-fourth the values for the corresponding concentrations with gold electrodes. On the other hand, values of capacity per unit area are about four times as large with platinum as with gold electrodes for corresponding concentrations. It may be noted from the curves in Fig. 4 that capacity and resistance do not vary linearly with temperature in the cases with platinum electrodes as they do with the gold electrodes.

The value of temperature coefficient of capacity as obtained in this work for platinum electrodes is somewhat less than that computed from the data given by Sheldon, Leitch and Shaw.⁹ The value computed from their data is about 0.02 per degree centigrade when compared to the capacity at a temperature of 18°C.

The degree of variation of the product, capacity of cell times total resistance of cell (regarded as the polarization resistance), is shown in Table II. The corresponding values of the angle of phase difference are also shown in many instances. Although in Table II, the capacity and resistance of the cell were used rather than the values for a single electrode, nevertheless, regarding the capacity and resistance as being in series, the product would not be changed in value in considering the results for a single electrode, for in that case the value of capacity would be double the total capacity of the cell and the value of resistance would be one-half the total resistance of the cell. Since the frequency was constant, Table II also indicates the variations in the tangent of the angle of phase difference for the different conditions represented by the several curves. It may be noted that there is no large

⁹ Sheldon, Leitch and Shaw, reference 1.

variation in the phase difference for any one temperature run. With gold electrodes, the phase difference seems to increase slightly with rising temperature, while with platinum electrodes, for the higher concentrations especially, the phase difference seems to be slightly lower at the higher temperatures. For both kinds of electrodes, the phase difference increases with increase in concentration of the electrolyte.

TABLE II. Variation in product, $C \times R$, with temperature, frequency being constant.

Kind of electrodes	Plain Platinum			Gold		
	0.63 N (H ₂ SO ₄)	1.50 N (H ₂ SO ₄)	2.42 N (H ₂ SO ₄)	0.63 N (H ₂ SO ₄)	1.50 N (H ₂ SO ₄)	2.42 N (H ₂ SO ₄)
Temperature increasing	134 (40°10')	158 (44°48')	162 (45°34')	113 (35°30')	131 (39°27')	142 (41°52')
	137	159	163	115	133	147
	139	160	161	116	136	153
	140 (41°20')	160 (45°15')	162	116	139	156
	140	158	159 (45°3')	117 (36°20')	140 (41°30')	159
	139	157	158	118	141	161 (45°22')
	139	156	158	118	142	160
Maximum temperature	138	154	157	118 (36°30')	143 (41°57')	159 (45°2')
	138 (41°5')	152 (43°40')	155 (44°15')	117	142	
Temperature decreasing	139	152	154	111?	141	167?
	141	153	157	115	141	159
	142	155	159	114 (35°43')	140 (41°20')	157
	143 (42°5')	156	161 (45°27')	114	138	155
	143	158	161	114	137	153
	141	160	163	114	135 (40°22')	150
	139	161 (45°18')	163	113	133	147
Average	139 (41°00')	157 (44°27')	160 (45°10')	115 (36°00')	138 (40°54')	154 (44°8')

Note: The average values of the angle of phase difference are computed from the average values of ($C \times R$).

In Fig. 5 are curves showing the results of attempted runs after the electrodes had been polarized with oxygen or hydrogen, as indicated in the figure. The electrodes were polarized by connecting the two together and

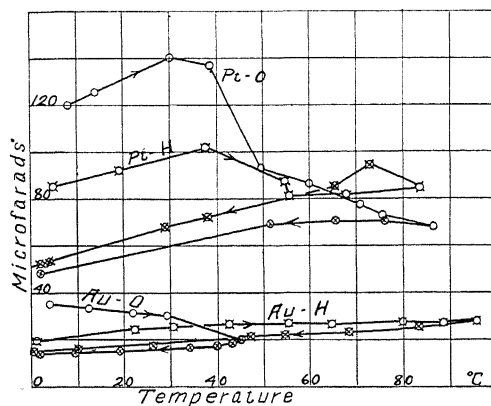


Fig. 5. Curves, capacity versus temperature, for polarized electrodes. The kind of electrodes and type of polarization are indicated in the figure. In all cases, the concentration was 1.46 N and the frequency was 1000 cycles per sec. Values of capacity are in microfarads per cm² for one electrode.

to the appropriate terminal of a direct current source of potential while a comparatively large third electrode was connected to the other terminal. Excepting in the case of gold polarized with oxygen, the capacity increased

regularly on starting the runs, but at temperatures of about 35° or higher there were sudden and irregular decreases in the value of capacity. Such decreases usually occurred simultaneously with the appearance of gas on the faces of the electrodes. Continuing the runs throughout the range of temperatures, the final values of capacity were much lower, yet still somewhat higher than the minimum values.

TEMPERATURE COEFFICIENT AT DIFFERENT FREQUENCIES

Curves, capacity versus temperature, representing measurements at different frequencies, but with the concentration constant, are very similar to those of Fig. 4. The slopes of the curves decrease considerably with increasing frequency. For platinum the temperature coefficient increases with increasing frequency, while the opposite seems to be true in the case with gold electrodes. The results of such tests are given in Table III. As may be seen from the table, both capacity and resistance decrease markedly with increasing frequency (see under C_{18} and R_{18}).

The variation of polarization capacity and resistance with frequency has been the subject of special investigations by Merritt,¹⁰ Jolliffe,¹¹ and Wolff.¹² The results found in this work for variation of capacity with frequency, although representing a comparatively narrow and somewhat lower range of frequencies, are in general agreement with the results of their investigations.

TABLE III. *Temperature coefficient of capacity at different frequencies.*

Kind of Electrode	Plain Platinum				Gold	
	645.0	1290.0	2581.0	3872.0	645.0	2581.0
C_{18}	60.6	42.4	28.2	21.3	14.7	7.6
$(dC/dT)_{18}$	0.487	0.356	0.250	0.205	0.111	0.048
$(1/C_{18})(dC/dT)_{18}$	0.0080	0.0084	0.0088	0.0096	0.0075	0.0063
R_{18}	4.56	3.18	2.0	1.9	15.5	6.5
$(dR/dT)_{18}$	-0.034	-0.028	-0.015	-0.015	-0.083	-0.029
$(1/R_{18})(dR/dT)_{18}$	-0.0075	-0.0088	-0.0075	-0.0088	-0.0053	-0.0045

Notes: Values of frequency are in cycles per second. Values of capacity are in microfarads per cm² for one electrode. Resistance is in ohms per unit area of electrode. The concentration, 1.46 normal, was the same in all cases.

DISCUSSION

It is very well known that temperature affects in a very important way most electrolytic processes. The temperature coefficient of conductivity of sulphuric acid of normal concentration as given in tables by Kohlrausch and Holborn¹³ is about 0.012 per degree centigrade at a temperature of 22°C. Also, the temperature coefficient of fluidity as based on data from tables is positive with a value of about 0.028 per degree centigrade at 15°C. In consideration of the facts that the temperature coefficients of capacity for platinum and gold in sulphuric acid are not the same and that the variation of

¹⁰ Merritt, Phys. Rev. 17, 524 (1921).

¹¹ Jolliffe, Phys. Rev. 22, 293 (1923).

¹² Wolff, reference 4.

¹³ Kohlrausch and Holborn, Leitvermögen der Electrolyte (1916).

capacity with temperature is not linear in the case with platinum, while it is in the case with gold, the temperature coefficients of capacity and resistance are not fully accounted for in variations of conductivity and fluidity with temperature, for if so the coefficients for the two metals would be affected alike.

Knobel and Joy¹⁴ found, with smooth platinum, that increasing the temperature had the effect of decreasing the overvoltage. Overpotential and catalytic activity of metals, according to the work of Rideal,¹⁵ vary inversely, i.e., metals arranged in order of decreasing catalytic activity are also arranged in order of increasing overpotential. Bancroft,¹⁶ also, states that the metals which have a lower overvoltage are those that catalyze the reaction, $2\text{H} \rightarrow \text{H}_2$, while those which have a high overvoltage do not. Among other things, Bancroft also discusses the action of the so-called catalytic poisons in preventing catalysis. Now Wolff¹⁷ has shown that catalytic poisons have the effect of decreasing polarization capacity. It seems quite likely, therefore, that overvoltage, catalytic activity, and polarization capacity are related in an important and probably a very complex way. The decrease in capacity of the electrode as it acquires its stable condition after polishing would mean a corresponding decrease in its catalytic activity. The increase in capacity with temperature would mean an increase in catalytic activity and a reduction in the conditions favorable to overvoltage, as found by Knobel and Joy. It is recognized that in considering polarization capacity in relation to overvoltage one is dealing with much lower values of voltage in the case of polarization capacity, and for so-called minimum capacity, values of voltage which are thought to be strictly reversible.

If polarization capacity and catalytic activity are intimately related, then the results of this paper do not seem to be in full agreement with the work of Bowden and Rideal¹⁸ who found that the specific catalytic activity of the various metals, including platinum, for the electro-deposition of hydrogen suffer only small variations by thermal treatment. Here again, however, the full conditions are not the same, for in this work the capacity was determined by means of a bridge supplied with alternating current and, consequently, not only is the deposition of hydrogen involved, but also the deposition of oxygen and the effect of one on the other after consecutive reversals of the current.

In conclusion, the writer desires to express appreciation of the excellent facilities available at Cornell University, Department of Physics, for doing this work. Thanks are extended to Professor E. Merritt, who approved this problem and under whose direction the work was done, for his interest and many helpful suggestions. The writer is also indebted to Professor C. C. Murdock for his interest in the results of the work and a discussion of their relation to other problems of polarization capacity.

¹⁴ Knobel and Joy, *Trans. Am. Electrochem. Soc.* **44**, 443 (1923).

¹⁵ Rideal, *Jour. Am. Chem. Soc.* **42**, 94 (1920).

¹⁶ Bancroft, *Trans. Am. Electrochem. Soc.* **37**, 21 (1920).

¹⁷ Wolff, unpublished paper.

¹⁸ Bowden and Rideal, *Proc. Royal Soc. of London A* **120**, 80 (1928).

ON THE SOLUTION OF CERTAIN CASES OF THE GENERAL EQUATION OF DIFFUSION

BY R. L. PEEK, JR.
BELL TELEPHONE LABORATORIES, NEW YORK CITY

(Received January 13, 1930)

ABSTRACT

For diffusion in substances for which the conductivity and diffusivity are functions of temperature, the partial differential equation which determines the temperature is non-linear in character. For a certain class of boundary conditions the introduction of an auxiliary function of time and distance reduces this equation to an ordinary differential equation of the second order, in which the temperature and the auxiliary function appear as dependent and independent variables respectively. As this resulting equation can be solved by methods of approximation, the solution to the original equation can be thus obtained.

The conditions under which such an auxiliary function exists are examined and a simple criterion developed by means of which it may be determined whether such a function exists for any particular case. The method is shown to apply to the case of the semi-infinite solid, and the solution of a particular problem of this type (the cooling of a steel ingot) is given. Another case to which the method applies (diffusion in an axially heated cylinder) is considered, and shown to afford a possible method for determining diffusivity as a function of temperature. It is noted that the method developed is available for the solution of problems in the diffusion of matter as well as of those concerned with the diffusion of heat.

THE theory of the diffusion of heat rests upon the assumption that the quantity δQ of heat passing through a plane of area $\delta y \delta z$ in time δt is given by the relation:

$$\frac{\delta Q}{\delta t} = -k \frac{\partial \theta}{\partial x} \delta y \delta z, \quad (1)$$

where $\partial \theta / \partial x$ is the temperature gradient in the direction of the X -axis, and k is the thermal conductivity. When k is taken as a constant, this assumption leads to the well-known differential equation,

$$\frac{\partial \theta}{\partial t} = h^2 \left(\frac{\partial^2 \theta}{\partial x^2} + \frac{\partial^2 \theta}{\partial y^2} + \frac{\partial^2 \theta}{\partial z^2} \right), \quad (2)$$

in which the diffusivity h^2 is the ratio k/cd , c being the specific heat and d the density. If h^2 is taken as a constant, Eq. (2) may be solved for many particular cases by well-known methods.

If k is not a constant, but a function of θ , Eq. (2) no longer applies. The differential equations that then apply for linear and radial flow have been given by many authors; and the general form is easily obtained in a manner analogous to the usual derivation of Eq. (2). The flow into and out of a differential block through the two faces normal to the direction of the X -axis is evidently, from Eq. (1), given by

$$\begin{aligned}\frac{\delta Q}{\delta T_{(x)}} &= -\left(k - \frac{1}{2} \frac{\partial k}{\partial x} \delta x\right) \frac{\partial}{\partial x} \left(\theta - \frac{1}{2} \frac{\partial \theta}{\partial x} \delta x\right) \delta y \delta z \\ &\quad + \left(k + \frac{1}{2} \frac{\partial k}{\partial x} \delta x\right) \frac{\partial}{\partial x} \left(\theta + \frac{1}{2} \frac{\partial \theta}{\partial x} \delta x\right) \delta y \delta z \\ &= \left(k \frac{\partial^2 \theta}{\partial x^2} + \frac{\partial k}{\partial x} \frac{\partial \theta}{\partial x}\right) \delta x \delta y \delta z.\end{aligned}$$

Similar equations apply to the flow into and out of the other two pairs of faces, and the total increment of heat in the differential block is given by the addition of the increments through the three pairs of faces. As the temperature θ is defined by Q/cd , $\delta x \delta y \delta z$, and if k is a function of θ only, there is finally obtained:

$$f(\theta) \frac{\partial \theta}{\partial t} = \left(\frac{\partial^2 \theta}{\partial x^2} + \frac{\partial^2 \theta}{\partial y^2} + \frac{\partial^2 \theta}{\partial z^2}\right) + \frac{1}{k} \frac{dk}{d\theta} \left\{ \left(\frac{\partial \theta}{\partial x}\right)^2 + \left(\frac{\partial \theta}{\partial y}\right)^2 + \left(\frac{\partial \theta}{\partial z}\right)^2 \right\}, \quad (3)$$

where $f(\theta)$ is written for $1/h^2$ or cd/k , as c and d may also be functions of θ . Eq. (3) is the general form of the equation for heat conduction, and reduces to Eq. (2) for the special case where k and h^2 are constants. As is well known, the same equations apply to the diffusion of gases and liquids when θ represents the concentration, k the diffusion constant, and cd the concentration-pressure ratio. The material presented below applies therefore to problems in the diffusion of matter as well as to those dealing with the diffusion of heat.

Due to its non-linear character, Eq. (3) cannot be solved by the methods applicable to Eq. (2). In papers¹ dealing with the experimental determination of k and h^2 will be found discussions of Eq. (3), usually for the case of linear flow [$\partial \theta / \partial y = \partial \theta / \partial z = 0$]. The usual treatment is to employ the solutions of Eq. (2) with approximate corrections applicable to the particular problem. This procedure is facilitated by the use of formal solutions to Eq. (3) such as those obtained by Glage¹ and by Kirchhoff and Hansemann,² among others.

Problems in the interdiffusion of gases have been similarly treated. Boltzmann³ in particular developed formal solutions to Eq. (3) applicable to a number of cases. In the case of the semi-infinite solid, he showed that the solution to Eq. (3) could be expressed formally in terms of the quantity x^2/t only. Advantage has been taken of this relation in the treatment of special cases by Wiedeburg⁴ and Germond.⁵ The procedure given below for the solution of the semi-infinite solid rests upon this same fact: the method will be first discussed in more general terms.

¹ Glage, *Ann. d. Physik* (4) **18**, 904 (1905). This paper gives a critical resume of the classical work in this field.

² Kirchhoff and Hansemann, *Wied. Ann.* **9**, 1 (1880).

³ Boltzmann, *Wien. Ber.* **86**, 63 (1882); *Ann. d. Physik* **53**, 959 (1894).

⁴ Wiedeburg, *Ann. d. Physik* **41**, 675 (1890).

⁵ Germond, *Bull. Am. Math. Soc.* **35**, 460 (1929).

II. The discussion will be limited to the solution of Eq. (3) subject to boundary conditions of the type

$$\begin{aligned}\theta &= c_1 \quad \text{when} \quad F_1(x, y, z, t) = 0, \\ \theta &= c_2 \quad \text{when} \quad F_2(x, y, z, t) = 0.\end{aligned}\quad (4)$$

If θ is so defined, it may be proved that if there exists a function $\Phi(x, y, z, t)$ meeting the following conditions:

$$\begin{aligned}\Phi &= C_1 \quad \text{when} \quad F_1(x, y, z, t) = 0, \\ \Phi &= C_2 \quad \text{when} \quad F_2(x, y, z, t) = 0,\end{aligned}\quad (5)$$

$$\frac{\partial \Phi}{\partial t} = \frac{\left(\frac{\partial \Phi}{\partial x}\right)^2 + \left(\frac{\partial \Phi}{\partial y}\right)^2 + \left(\frac{\partial \Phi}{\partial z}\right)^2}{f_1(\Phi)} = \frac{\frac{\partial^2 \Phi}{\partial x^2} + \frac{\partial^2 \Phi}{\partial y^2} + \frac{\partial^2 \Phi}{\partial z^2}}{f_2(\Phi)}, \quad (6)$$

where $f_1(\Phi)$ and $f_2(\Phi)$ are functions of Φ only, then θ is a function of Φ only, and,

$$(f(\theta) - f_2(\Phi)) \frac{d\theta}{d\Phi} - f_1(\Phi) \frac{d(\log k)}{d\theta} \left(\frac{d\theta}{d\Phi}\right)^2 = f_1(\Phi) \frac{d^2\theta}{d\Phi^2}. \quad (7)$$

For the function θ obtained by integration of Eq. (7) subject to the boundary conditions, $\theta = c_1$ when $\Phi = C_1$, $\theta = c_2$ when $\Phi = C_2$, satisfies Eqs. (4) and also Eq. (3), as the latter, when θ is taken as a function of Φ , reduces to Eq. (7) by virtue of Eqs. (6). Hence θ is the required solution, and the theorem is proved.

In what follows, a function satisfying Eqs. (6) for particular boundary conditions of the type of Eqs. (5) will be termed a resolving function for those boundary conditions.

III. Suppose now that a function θ' has been determined in the above manner for a case of Eq. (3) in which $f(\theta')$ is any function whatever of θ' but in which k is a constant, and the second term to the right of Eq. (3) is therefore zero. Then,

$$\frac{\partial \theta'}{\partial t} = \frac{\frac{\partial^2 \theta'}{\partial x^2} + \frac{\partial^2 \theta'}{\partial y^2} + \frac{\partial^2 \theta'}{\partial z^2}}{f(\theta')}.$$

This is formally identical with the second of Eqs. (6). Substitution for Φ in terms of θ in the first of Eqs. (6) yields:

$$\frac{\partial \theta'}{\partial t} = \frac{\left(\left(\frac{\partial \theta'}{\partial x}\right)^2 + \left(\frac{\partial \theta'}{\partial y}\right)^2 + \left(\frac{\partial \theta'}{\partial z}\right)^2\right) \frac{d\Phi}{d\theta'}}{f_1(\Phi)}.$$

But as Φ is a function of θ' only, $f_1(\Phi)/(d\Phi/d\theta')$ is a function of θ' only. Hence this equation is formally identical with the first of Eqs. (6). There-

fore θ' is itself a resolving function for the particular boundary conditions involved.

It follows that if any resolving function exists for particular boundary conditions, then any solution of Eq. (3) (i.e., θ') when k is constant is, whatever the form of $f(\theta')$, itself a resolving function for these particular boundary conditions.

Applying this theorem to the special case $f(\theta') = 1$, it follows that if any resolving function exists, the solution to this special case is itself a resolving function. But the solutions to this special case are precisely the well-known solutions to Eq. (2) ($k^2 = 1$). Such solutions satisfy the second of Eqs. (6); it is a simple matter to determine by numerical trial if they satisfy the first of these equations. If they do, values of $f_1(\theta')$ vs. θ' may be computed, $f_2(\theta') = 1$, and a solution to Eq. (3) may be obtained by integration of Eq. (7). If they do not, it is proved that no resolving function exists, and the method fails.

The criteria for the use of the method are then that the boundary conditions be of the form of Eqs. (4) and that the known solution θ' for the case $k = \text{constant}$, $f(\theta') = 1$ satisfies both of Eqs. (6).

IV. By actual trial it has been found (in the manner described above) that the method is not applicable to many important cases, such as the diffusion in a slab or cylinder of infinite length when the temperature at the surface is kept constant. It is, however, applicable to the important case of the semi-infinite solid. If in such a solid the initial temperature is θ_0 , while the temperature at the surface $x=0$ is always θ_1 , then Eq. (3) becomes:

$$f(\theta) \frac{\partial \theta}{\partial t} = \frac{\partial^2 \theta}{\partial x^2} + \frac{d(\log k)}{d\theta} \left(\frac{\partial \theta}{\partial x} \right)^2. \quad (8)$$

The problem is then to solve Eq. (8) subject to the conditions,

$$\begin{aligned} \theta &= \theta_0 \quad \text{when} \quad t = 0, \\ \theta &= \theta_1 \quad \text{when} \quad x = 0. \end{aligned} \quad (9)$$

For this problem a resolving function is given by,

$$\Phi = e^{-x/t^{1/2}}. \quad (10)$$

Then from Eqs. (6) and (7), θ is given by integration of

$$\left(\frac{f(\theta) \log \Phi}{2} + 1 \right) \frac{d\theta}{d\Phi} + \Phi \frac{d(\log k)}{d\theta} \left(\frac{d\theta}{d\Phi} \right)^2 + \Phi \frac{d^2 \theta}{d\Phi^2} = 0, \quad (11)$$

subject to the conditions,

$$\begin{aligned} \theta &= \theta_0 \quad \text{when} \quad \Phi = 0, \\ \theta &= \theta_1 \quad \text{when} \quad \Phi = 1. \end{aligned} \quad (12)$$

This integration may be accomplished for any particular case by any of the well-known methods of successive approximations.

This result is of some importance in the solution of physical problems. The most common type of problem in the diffusion of heat involves an initial constant temperature and thereafter the maintenance of another constant temperature on some surface. For all such cases the result for the semi-infinite solid serves as a first approximation, applicable within a high degree of accuracy for an initial time interval sufficiently small. Thus for diffusion in a slab, cylinder, or sphere, the temperature will vary with time and distance from the surface in the same way as for the semi-infinite solid from zero time up to that which the temperature at the center varies by more than the required order of accuracy from its initial value, with the further proviso for the sphere and cylinder that the portion in which the temperature maintains substantially its initial value extend out to a radius beyond which the curvature may be neglected with sufficient accuracy.

V. As an actual example of the method discussed in the preceding section there will be considered the case of the cooling of a large steel ingot, a problem for which the simpler case is discussed by Ingersoll and Zobel, p. 85.⁶ Strictly comparable values of the relations between diffusivity and temperature and between conductivity and temperature were not found in the literature, but data were taken from the Landolt-Börnstein Tables which were thought to be sufficiently representative of a low carbon steel. The diffusivity was taken as that given for Bessemer steel from the data of Kirchhoff and Hansemann,⁷ giving the diffusivity as: $1/f(\theta) = h^2(1 + \beta\theta)$, where $h^2 = 0.1148$ and $\beta = -0.00019$. The conductivity was taken from the mean values given in the Tables⁸ for a 0.64 percent carbon steel, which gave, for the usual approximation of a linear relation: $k = k_0(1 + \alpha\theta)$, where $k_0 = 0.115$ and $\alpha = -0.00046$.

Thus, from Eqs. (11) and (12), the temperature in the block is given by integration of:

$$\frac{d^2\theta}{d\Phi^2} = -\left(\frac{\log \Phi}{2h^2(1+\beta\theta)} + 1\right) \frac{1}{\Phi} \frac{d\theta}{d\Phi} - \frac{\alpha}{1+\alpha\theta} \left(\frac{d\theta}{d\Phi}\right)^2, \quad (13)$$

subject to the boundary conditions which were that $\theta = 800$ when $\Phi = 0$ ($t = 0$), and $\theta = 20$ when $\Phi = 1$ ($x = 0$).

The method of solution employed was that of successive approximations in which the integrations are mechanically obtained by means of an integrator, as described in a paper by Fry.⁹ The work was simplified by taking as a first approximation the well known solution to the problem when h^2 and k are constant, which may be written in terms of Φ as

$$\theta = 800 - \frac{2 \times 780}{\pi^{1/2}} \int_{-(\log \Phi / 2h)}^{\infty} e^{-\lambda^2} d\lambda. \quad (14)$$

In this expression h was taken as having its mean value for the temperature range involved or $(0.1060)^{1/2}$. Due to the discontinuity at $\Phi = 0$ and

⁶ Ingersoll and Zobel, *Mathematical Theory of Heat Conduction*.

⁷ Kirchhoff and Hansemann, *Wied. Ann.* **13**, p. 406 (1881).

⁸ Landolt-Börnstein Tabellen, 5th Ed. p. 1291 (1923).

⁹ T. C. Fry, *Proc. Int. Math. Congress*, Vol. II, p. 405, Toronto (1924).

various associated peculiarities of the equation, some slight modifications in procedure were necessary. Each approximation was made as follows: Given approximations for θ and its first derivative, say θ_n and θ'_n respectively, the corresponding second derivative θ''_n was computed from Eq. (13). This was then integrated to give θ'_{n+1} , the constant of integration being taken such as to give θ'_{n+1} the same value at $\Phi=1$ as that found at this point for θ'_n . In general, this did not make θ'_{n+1} approach zero as Φ approaches zero, a condition which must be satisfied, as is evident from the fact that a function of the type of Eq. (14) is a close approximation to a solution for low values of Φ . Hence θ'_{n+1} was corrected to meet this requirement by taking values of θ proportional to the second term of Eq. (14) up to such a value of Φ as would make this approximation merge into the original curve for θ'_{n+1} without any abrupt change in curvature. The θ'_{n+1} thus corrected

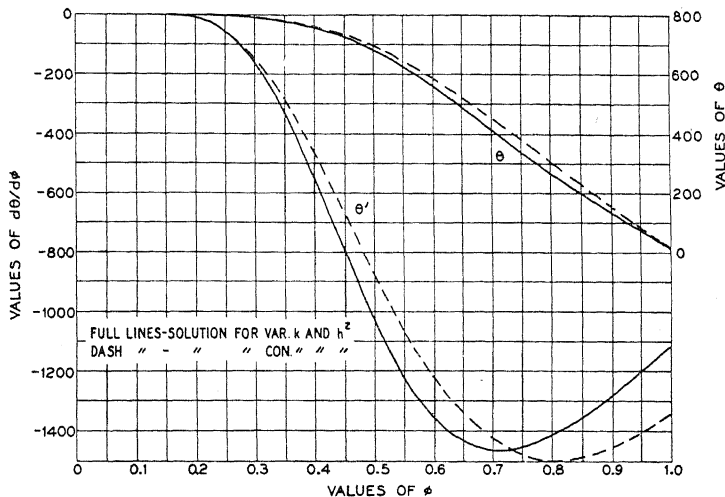


Fig. 1.

was integrated to give θ_{n+1} , the constant of integration being such as to make $\theta_{n+1}=800$ at $\Phi=0$. The difference between 20 and the value of θ_{n+1} at $\Phi=1$, or C , was taken as a correction factor, and a term ΦC added to θ_{n+1} to make it meet both boundary conditions, while the term C was also added to θ'_{n+1} , in accordance with the procedure developed by Fry.⁹ Then θ'_{n+1} was again corrected to make it approach zero as Φ approached zero, by the same method as described above. The values of θ_{n+1} and θ'_{n+1} , thus finally obtained were used to compute θ''_{n+1} and the operation repeated until successive approximations produced no change in θ or θ' .

The solution obtained for the case cited is shown graphically in Fig. 1, in which both θ and θ' are given. The corresponding solution and its first derivative for the case in which the conductivity and diffusivity are constant (the latter taken as $h^2=0.1060$), as given by Eq. (14), are shown in broken lines. It will be seen that the solutions to the two cases differ con-

siderably. To emphasize this difference, Fig. 2 has been prepared, corresponding to Fig. 12, p. 86 of Ingersoll and Zobel,⁶ and giving the rate of cooling ($\partial\theta/\partial t$) at distances of 0.3 cm and 1.0 cm from the face of the block. The broken lines again show the corresponding curves for constant diffusivity and conductivity. It is apparent that consideration of the variation in the conductivity and diffusivity results in a higher maximum rate of cooling than if this variation is neglected.

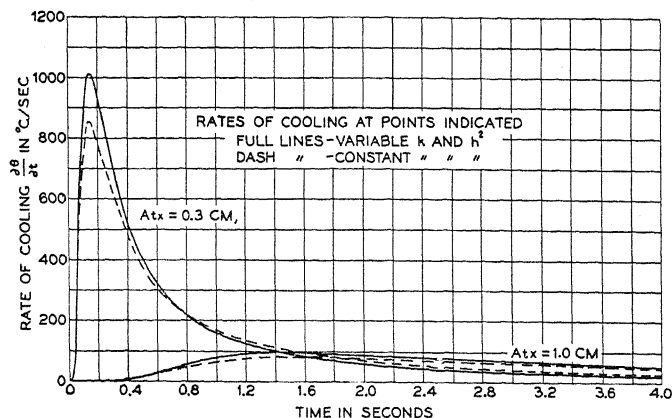


Fig. 2.

VI. Another case in which the method applies is that of a cylinder of infinite length and radius, initially at one constant temperature, of which the axis is thereafter kept at another constant temperature. If x is the radial distance of any point from the axis, the problem is to solve:

$$f(\theta) \frac{\partial \theta}{\partial t} = \frac{1}{x} \frac{\partial \theta}{\partial x} + \frac{\partial^2 \theta}{\partial x^2} + \frac{d(\log k)}{d\theta} \left(\frac{d\theta}{dx} \right)^2, \quad (15)$$

subject to the conditions,

$$\begin{aligned} \theta &= \theta_0 \quad \text{when} \quad t=0, \\ \theta &= \theta_1 \quad \text{when} \quad x=0. \end{aligned} \quad (16)$$

For this case also the Φ of Eq. (10) is a resolving function. From Eqs. (6) and (7), θ is given by integration of

$$\left(\frac{f(\theta) \log \Phi}{2} + \frac{1}{\log \Phi} + 1 \right) \frac{d\theta}{d\Phi} + \Phi \frac{d(\log k)}{d\theta} \left(\frac{\partial \theta}{\partial \Phi} \right)^2 + \Phi \frac{d^2 \theta}{d\Phi^2} = 0. \quad (17)$$

subject to the conditions of Eqs. (12).

Brown and Furnas¹⁰ have discussed the determination of a variable diffusivity by the graphical integration of Eq. (15) for numerical values of the differential terms of this equation in the case of a centrally heated cylinder.

¹⁰ Brown and Furnas, Trans. Am. Inst. Chem. Engineers 18, 295 (1926).

The above development suggests a procedure in which the measurements and computation would be simpler, though the experimental conditions would be more difficult to obtain, as to maintain a constant temperature along the axis would require some method of adjusting the current in the central heating coil in such a way as to fulfill this condition. It would also be necessary to limit the measurements to a temperature range such that the surface never varied appreciably from its initial value. If these conditions are fulfilled Eq. (17) applies, and (assuming k known as a function of θ^*), it is only necessary to take readings from one thermocouple (one value of x), as θ is a function of Φ only, and any value of Φ will be obtained at any x for some value of t . Expressing the values of t in terms of Φ , values of θ vs. Φ are experimentally obtained. Then by graphical differentiation, or numerically by successive differences, values of $d\theta/d\Phi$ and $d^2\theta/d\Phi^2$ may be obtained, and Eq. (17) solved for $f(\theta)$, the reciprocal diffusivity, as a function of temperature.

VII. The development discussed above permits the reduction of the general differential equation of diffusion to a single ordinary differential equation of the second order, which can be readily solved by methods of approximation. The only particular case of major importance to which the method applies is that of the semi-infinite solid, which affords, however, a good approximation to a solution for many other cases within limited ranges of the co-ordinates of time and distance. The form of the differential equation resulting when the method applies is such as to make the solution by the method of successive approximations preferable, and for this graphical methods are more convenient than numerical.

As is apparent in the example given above, solutions obtained by this method when the variations in conductivity and diffusivity are allowed for may differ considerably from those obtained on the assumption that these quantities are constant. Such differences may be particularly apparent in the values obtained for rates of cooling or of temperature gradients, as the example again indicates, and it is in the evaluation of these quantities that most accurate determinations are desirable (*e.g.*, in the casting of metals and glass). It must, however, be admitted that conditions in technical operations seldom approach those of the mathematically ideal problem sufficiently to make such accuracy in calculation significant, and the developments discussed above are more likely to be of practical importance in problems concerned with material diffusion than in those involving heat.

Acknowledgment is due Dr. T. C. Fry of these Laboratories for much helpful criticism of the work reported in this paper.

* This relation would be previously determined by measurements for the steady state, as discussed by Brown and Furnas (reference 10).

LETTERS TO THE EDITOR

Prompt publication of brief reports of important discoveries in physics may be secured by addressing them to this department. Closing dates for this department are, for the first issue of the month, the twenty-eighth of the preceding month; for the second issue, the thirteenth of the month. The Board of Editors does not hold itself responsible for the opinions expressed by the correspondents.

On the Theory of Electrons and Protons

In a recent paper,¹ Dirac has suggested that the reason why the transitions of an electron to states of negative energy, which are predicted by his theory of the electron, do not in fact occur is that nearly all of the states of negative energy are already occupied. Dirac has further shown that the unoccupied states of negative energy have many of the properties of protons; that, for instance, they may be represented by wave functions which would be taken to correspond to a particle of positive charge and positive mass. He has further shown that the mass associated with these gaps is not necessarily the same as that of the electron, and he has suggested the assumption that the gaps are protons. In order to account for the fact that the divergence of the electric field is not, in spite of the infinite electron density, everywhere infinite, Dirac further assumes that only the departures from the normal state in which all negative states are filled are to be counted in computing the charge density for Maxwell's fourth equation

$$\text{div } E = -4\pi\rho. \quad (1)$$

Finally, Dirac is able to account for the validity of the Thomson formula for the scattering of soft light by a free electron, in spite of the fact that the derivation of this formula on his theory of the electron—a derivation which makes explicit use of the transitions to states of negative energy which are now forbidden, is invalid. According to Dirac, the scattering takes place by a double electron jump, in which a negative² electron jumps up to some state of positive energy,

and the original positive electron falls down into the gap left.

There are several grave difficulties which arise when one tries to maintain the suggestion that the protons are the gaps of negative energy, and that there are no distinctive particles of positive charge. In the first place, we can easily see that Dirac's theory requires an infinite density of positive electricity; and since we should expect the de Broglie waves of this charge to be quantized, we should expect some corpuscular properties for the positive charges. The reason why the theory requires an infinite positive charge is this: If the explanation of the scattering of an electron is to be tenable, a negative electron must interact with the electromagnetic field in the way predicted by Dirac's theory of the electron; for otherwise the scheme proposed would not give the Thomson formula. But this means that there must be a term involving the current and charge vector of the negative electrons in the total energy momentum tensor for matter and radiation. Thus by (1), the divergence of the electric field will be everywhere infinite unless there is an infinite density of positive electricity to compensate the negative electrons.

A further difficulty appears when we try to compute the scattering of soft light by a proton. This difficulty is not unconnected with the difference in mass between the electron and proton, and makes it seem improbable that this difference can be explained on the basis suggested by Dirac. For the scattering process must in this case be regarded as a double jump of a single electron, in which a negative electron jumps to some state of positive energy, and then falls back into the hole that is the original proton. Now it is easy to see that the probability of this

¹ P. Dirac, Roy. Soc. Proc. A126, 360 (1930).

² By a negative electron we mean an electron of negative energy.

scattering is determined by precisely the same matrix components as those which give the electron scattering, and that the present theory gives equal scattering coefficients for electron and proton. Of course, the interaction between electrons is omitted in this computation; but the difficulty is this, that such interaction would affect electron scattering and proton scattering in precisely the same way; whereas the Thomson formula requires the latter to be smaller by a factor proportional to the square of the ratio of the masses.

Finally, there is a numerical discrepancy to be noted. According to Dirac's suggestions, the filling of the proton gaps in the distribution of negative electrons should correspond to the annihilation of an electron and a proton, and should thus, under all normal conditions, be a very rare occurrence. Now if we consider for definiteness a free electron in an enclosure in which there are n_p free protons per unit volume, we may readily compute the rate at which the electron should, by the Dirac radiation theory, fall into one of the corresponding gaps. The conservation laws require that at least two quanta be emitted in this process; and it is sufficient to consider jumps in which no more than two quanta are emitted. The details of the calculation will be published elsewhere; if we neglect the interaction of the electron with the negative

electrons we obtain for the mean life time of the electron:

$$T = Gm^2c^3e^{-4}/n_p \quad (2)$$

where G is a numerical constant of the order of unity, e the charge, and m the mass of the electron. Now again it is difficult to see what large errors could be involved in the computation, since the matrix components which give (2) are of precisely the same type as those which give correctly the Thomson formula and the optical transition probabilities of the electron; and (2) gives a mean life time for ordinary matter of the order of 10^{-10} seconds.

Thus we should hardly expect any states of negative energy to remain empty. If we return to the assumption of two independent elementary particles, of opposite charge and dissimilar mass, we can resolve all the difficulties raised in this note, and retain the hypothesis that the reason why no transitions to states of negative energy occur, either for electrons or protons, is that all such states are filled. In this way, we may accept Dirac's reconciliation of the absence of these transitions with the validity of the scattering formulae.

J. R. OPPENHEIMER

The Norman Bridge Laboratory of Physics,
California Institute of Technology,
Pasadena, California,
February 14, 1930.

The Collision Diameter of the Hydrogen Atom

Harteck measured the viscosity of monatomic hydrogen and calculated the collision radius to be $r_H = 1.3 \times 10^{-8}$ cm (r_0 of the first Bohr orbit is 0.53×10^{-8} cm). We have measured the decrease of intensity of a fine beam of monatomic hydrogen in passing through 3.0 cm of mercury vapor at 0.000185 mm Hg and find the decrease of intensity to be 23 percent. If the collisions are supposed to be between elastic spheres the sum of their radii is 6.2×10^{-8} or assuming $r_{Hg} = 1.8 \times 10^{-8}$,

the radius of hydrogen atom is 4.4×10^{-8} . This is larger than would be assumed even on wave mechanics unless there is very considerable resonance interaction between mercury and hydrogen.

E. G. LUNN

F. R. BICHOWSKY

U. S. Naval Research Laboratory,
Anacostia, D. C.,

February 17, 1930.

Excited Radicals in Chemical Compounds

The letter of Mr. D. H. Andrews in your number of December 15th makes the important point it is possible to assign definite frequencies to vibrating groups in the molecule, and that these frequencies are constant, to a first approximation, from molecule to molecule e.g. the value of the vibration fre-

quency of C-H in any molecule will be of the order of 3000 cm^{-1} , altering only slightly with change of environment. Although some of Mr. Andrews' values are open to question, there is a weight of evidence, both from the Raman effect and from infra-red spectra, for the essential correctness of his statement;

the failure to realise it has been the cause of false analyses of the spectra of several polyatomic molecules, in which the frequency of, say, the CO group has been given values varying from 1500 to 200 cm^{-1} .

It is possible, however, to go much further. First, the frequency of a group, which remaining constant in molecules where the chemical environment is the same, can undergo a sharp change to a second value corresponding to a second chemical environment. I was led to this conception from a study of the building-up of the N_2O molecule from NO. The analysis of the vibration-rotation band system of N_2O (to be published shortly) shows that the molecule is linear and symmetrical. The vibration of N-O along the axis of the molecule is 2250 cm^{-1} . Now the frequency of the NO molecule in its normal ($^2\Pi$) state is 1892 cm^{-1} ; the building of the N_2O molecule has brought about a very definite change. A name can be given to this change when it is realized that the frequency of the first excited ($^2\Sigma$) state of NO is 2345 cm^{-1} . The numerical resemblance is striking; and it becomes more than a coincidence when we find that the only other excited state ($^2\Pi$) so far known has a frequency of 1030 cm^{-1} , and that the Raman effect and infra-red spectra of compounds containing the NO group give a value *c.* 1000 without exception. With these frequencies it is possible to fit all the results upon the NO group at present known i.e. a diatomic group within a polyatomic molecule can be described in terms of the excited states of a diatomic molecule.

The results are even more definite when the CO group is considered. In a normal ketone or acid the vibration frequency is *c.* 1600 cm^{-1} . The Raman evidence is contradictory but the infra-red quite convincing. On the other hand, an α -diketone of the form $\text{R}_2\text{C}(\text{CO})_2$

seems, from the careful analysis of the absorption spectra of several compounds of this type by Louis Light of Zürich, to be of the order of 1100 cm^{-1} .

The first three states of the CO molecule are:

<i>x</i>	$^1\Sigma$	2155
<i>a</i>	$^5\Pi?$	1724
<i>d</i>	$^5\Sigma?$	1105

the agreement is satisfactory. The effect of the conjugated system is particularly interesting.

Certain principles may be set down, even at this early stage:

(i) A diatomic group persists throughout a large number of molecules with the same vibration frequency. As Mr. Andrews suggests, this establishes the identity of covalent bindings. The mass of the atoms to which the diatomic groups are attached is of small importance.

(ii) A diatomic group can have several sharply distinct frequencies. Each of these frequencies behaves as defined in (i).

(iii) The frequencies of a diatomic group correspond to the frequencies of excited states of the appropriate diatomic molecule. A frequency corresponding to the frequency of the normal state of the molecule is not usually observed.

At the moment the attempt to put a spectroscopic name to chemical binding must stop with groups bound by covalencies. Clearly the extension of the idea to such problems as the boron hydrides is practicable; if in the B_2H_6 molecule there are B-H groups bound by singlet linkages, then the frequencies of these groups should not coincide with the frequency of any of the states of the ordinary BH molecule bound by a covalency.

Similarly, the kind of linkage shown to exist by Lennard Jones for the normal ($^3\Sigma$) state of the oxygen molecule should be responsible for abnormalities in the way outlined above. There are indications that the C-C binding in C_2H_2 is such a case; if that is true, it will be possible to indulge in a spectroscopic re-naming of the "triple" bond.

C. P. SNOW

Laboratory of Physical Chemistry,
Cambridge, England,
January 27, 1930.

The Glancing Angle of Reflection from Calcite for Silver ($K\alpha_1$) X-rays

We have measured the first order glancing angle at which the $K\alpha_1$ line of silver is reflected from the cleavage planes of calcite

by a method independent of any used by those who have obtained the most reliable results so far. The weighted mean value of

fourteen independent observations reduced to 18°C is $5^{\circ}17'13''.81 \pm 0''.06$.

This value was obtained from spectrograms taken on a new spectrometer specially designed to utilize the displacement method introduced by H. S. Uhler (Phys. Rev. [2] 11, 1-20 (1918)). A full description of the method, instrument and results will be given later.

The value of the wave-length corresponding to the above glancing angle is $0.558238\text{\AA} \pm 0.000002\text{\AA}$, obtained by using 3.02904\AA for the "effective" grating space of calcite (Siegbahn; Spectroscopy of X-Rays, 1924 Edition).

The thermal coefficient of expansion at 18°C for the grating space of calcite obtained from the most reliable sources, without approximations, is $0.0000102\%/^{\circ}\text{C}$. This value differs by about 2% from the generally quoted value originally given by W. Stenström (Dissertation, Lund, 1919) as a sufficient approximation.

It is interesting to note that our value of the glancing angle is $1''.4$ smaller than that given by G. Kellström (Zeits. f. Physik 41, 516 (1927)) for the first order of calcite, viz.

$5^{\circ}17'15''.2$. The probable error of the unweighted mean of Kellström's seven determinations for this order is $\pm 0''.04$. The unweighted mean of his four second order determinations is also larger than ours and has relatively four times this probable error. With such a difference existing one wonders if the grating spaces of the crystal specimens used were the same. We employed an unusually selective piece of calcite which was cleaved from an excellent specimen of Iceland spar contained in the Marsh collection of Yale University.

Our value is larger than those of K. Lang (Ann. d. Physik 75, 489 (1924)), A. Leide (Dissertation, Lund (1925) and A. P. Weber (Zeits. f. Wiss. Photo. 23, 149 (1925)) although coming within $0''.11$ of Lang's and $0''.36$ of Leide's results when their probable errors are added to their respective mean values.

CHARLTON DOWS COOKSEY

DONALD COOKSEY

Sloan Physics Laboratory,

Yale University,

February 11, 1930.

BOOK REVIEWS

Quantum Mechanics. E. U. CONDON AND P. M. MORSE. Pp. 250+xiii, figs. 28. International Series in Physics, McGraw-Hill Book Co., New York, 1929. Price \$3.00.

This is the first book of American authorship on the new science of quantum mechanics and should find a host of readers both here and abroad. It meets the widely felt need for an introductory text making no pretense at completeness, but aiming through numerous illustrative applications and exercises to give the reader a working knowledge of the methods of the quantum theory of today. The authors have kept the work, to use their own words, "on as elementary a plane as possible," but they have not descended to sloppy procedure in their anxiety to make easy reading.

The subject is approached from the standpoint of the statistical interpretation of the Schrödinger theory and the first three quarters of the volume is devoted to an exposition of results obtainable from the Schrödinger wave equation with a minimum of mathematical machinery. A subsequent chapter, however, gives a well written introductory account of the general formulation of the theory by Jordan, Dirac, and von Neuman, which should be helpful to many who have had difficulty in digesting the original papers on this subject.

The rather extensive treatment of diatomic molecules will be most useful to workers in the field of band spectra as there is at present no comprehensive work on the quantum mechanics of molecules. Much of the material in this chapter is derived from the valuable researches of the authors. The reviewer notes with especial pleasure the inclusion of a simplified account of the basic molecular perturbation theory of Born and Oppenheimer worked out directly for the important diatomic case.

The book also contains an interesting chapter on aperiodic phenomena.

The authors lay little emphasis on the philosophical aspect of the quantum mechanics and ignore almost completely many important phases of the subject such as the "electron spin" and the problem of dispersion. These omissions are to be reckoned a virtue rather than a drawback, however, since they enable the authors to deal with the fundamentals of the subject in a leisurely way which will be welcome to the beginner.

EDWIN C. KEMBLE

Outlines of Biochemistry. R. A. GORTNER. Pp. xv and 793. New York, Wiley and Sons; London, Chapman and Hall; 1929. Price \$6.00.

Treatises in biochemistry are the successors of medical textbooks of physiological chemistry; these dealt almost exclusively with mammalian metabolism, foods, enzymes, excreta and the blood; and although when vitamins were recognized and the part played by the secretions of the endocrine glands, these matters were included, the chemistry of the life processes of plants was always beyond their scope. Even with such restrictions on the subject matter, the "conservation of energy" was referred to when dealing with the measurement of animal heat, a formula or two of chemical kinetics got in to ornament the chapter on digestion, and mention was made of the freezing-points of serums and of urine; but—with an eye, no doubt, to the limitations of the medical student—such topics received in general but incidental mention.

It is a far cry from such a book to Professor Gortner's "Outlines." He has a section on the proteins of course, including chapters on the amino-acids and the polypeptides, an up-to-date account of the vitamins written by Professor L. S. Palmer, chapters on the carbohydrates and the fats and oils, and others on the tannins and on the colouring matters of plants; but the first 290 pages of his book are devoted to "The colloidal state of matter." Here the preparation and characteristic properties of colloids are described, their electro-kinetic behaviour, and their behaviour with electrolytes and among themselves; there is a chapter on gels, and one each on hydrogen-ion-concentration, surface-tension, osmotic-pressure, and "the Donnan equilibrium."

It is obvious that in this book the generalizations of physical chemistry are not slipped in as "explanations" of an isolated fact or two, but have the place of honour; in their light the facts of physiology are examined—not mammalian alone, for as might be expected from a professor of agricultural biochemistry the plant receives its due.

To readers of *The Physical Review* the illustrations here afforded of the scope and power of generalizations long familiar should prove intensely interesting. Who that measures vapour-tensions will not enjoy the picture of the cactus on the wall in desert Arizona ten months without rain and sheltered from the dew, or the story of the three-months sojourn of another cactus over sulphuric acid, the account of drought-resisting cereals in Utah, winter-hardy wheat, and the drying-up of earthworms, or the human-interest paragraphs on the granary-weevils' life without a drink, the new oedema diagnosis, and the rigor of our bodies after death? All these and more are brought into the chapter on Gels to illustrate "imbibition" and the distinction between "bound" and "liquid" water; and not as incidental illustrations merely, for they are examined in the light of tables, formulas and charts, and correlated with freezing-points, osmotic-pressures and absorption in the infra-red. Therefore, if any Reader thinks he knows more physics though less biology than Gortner, let him go to it; the door is opened wide.

The sample given above could easily be matched; literature citations show where synoptic papers can be found; it would be a shame to let mere biochemists monopolize the reading of this book.

W. LASH MILLER

Introduction to Physical Optics. JOHN KELLOCK ROBERTSON. Pp. 422, figs 222. D. Van Nostrand Co., New York 1929. Price \$4.00.

This is a text-book which is intermediate in grade between the elementary and the advanced optics texts. A small amount of differential calculus is used, but otherwise the mathematics required consists of the usual trigonometry, algebra, and geometry. A large number of problems are given, the answers to which are found at the end of the book. Several problems are solved in great detail in the text.

A very commendable feature is the use of photographic illustrations of the various optical phenomena such as interference and diffraction bands, and spectra. These show the various types of band systems obtained with different types of apparatus, giving the student a clear impression of the phenomena under discussion. The photographs are all good except the one of interference rings in polarized light.

In trying to be neither too conservative, nor radical, the author seems to overemphasize the conflict between the corpuscular and wave theories of light. Naturally, most of the phenomena treated require the wave theory. The nature of waves and the composition of vibrations is fully and clearly discussed in an early chapter. The principles thus established are later applied to the treatment of interference, diffraction, and elliptical polarization. The Cornu spiral is explained in a graphical, qualitative manner, and is used to explain some of the Fresnel diffraction phenomena.

The quantum theory and the foundations of Bohr's theory of spectra are briefly reviewed. There are also a few paragraphs on wave mechanics and the diffraction of electron waves, which give a rather belated suggestion of the duality of radiation as well as matter. Optical phenomena due to motion are discussed in the closing chapter.

JOSEPH VALASEK

Elementary Differential Equations. THORNTON C. FRY. Pp. x+255, figs. 42. New York, D. Van Nostrand Co., 1929. Price, \$2.50.

This textbook gives a pleasing treatment of its subject of the grade of difficulty that is adapted to junior courses in the better American engineering colleges. It is distinguished by careful presentation of the fundamentals, recognizing that while applications of the subject in physics and engineering are of the highest value, nevertheless, "They are not without their danger, however, if they are used unwisely, for should the student come to rely upon his physical intuition as a substitute for abstract logic, rather than as an aid to it, he would have missed half the benefit of the study." (Preface).

There is a good treatment of operational methods of handling linear equations with constant coefficients, and systems of them, with emphasis on the applications to electrical circuit theory.

E. U. CONDON

Die Grundlage der allgemeinen Relativitätstheorie. A. EINSTEIN. Pp. 64. Fifth unaltered printing. J. A. Barth. Leipzig, 1929.

This is a fifth unaltered printing of Einstein's famous 1916 treatment of the foundations of the general theory of relativity. It was first published, except for the table of contents, as a single article in volume 49 of the *Annalen der Physik*, and was the first systematic treatment of general relativity, providing the complete mathematical and theoretical foundation leading to the three tests of the theory furnished by the rotation of the perihelion of Mercury, the bending of light in passing through the gravitational field of the sun, and the red shift for light from the surface of the sun. The paper is not only a document of the greatest historical interest, but also still furnishes one of the best introductions to general relativity and contains the three conclusions of the theory for which we have the most direct experimental evidence.

RICHARD C. TOLMAN

THE PHYSICAL REVIEW

SEPARATION OF ANGLES IN THE TWO-ELECTRON PROBLEM

By G. BREIT

DEPARTMENT OF PHYSICS, NEW YORK UNIVERSITY

(Received February 3, 1930)

ABSTRACT

Neglecting the spin, two electrons are described in quantum mechanics by means of a wave equation in six variables. It is shown that well-known relations between angular momentum operators make it possible to determine the dependence of the wave function on three variables. The problem is thus reduced from *six* to *three* dimensions. For a state with an assigned "orbital" angular momentum l , say an S , P , D state the dependence of the wave function on three Euler angles is determined by the value of l . The wave function is a linear combination of products of distance and angle functions, the latter depending only on the three Euler angles. The angle functions are well-known solutions of the wave equation for a symmetrical top. The distance functions satisfy wave equations in three variables r_1, r_2, r_{12} or r_1, r_2, θ . The case of P terms is worked out in detail. Equations (10), (25) apply to two electrons having the *same azimuthal quantum number*. Equations (18), (20), (24) describe all the other cases, for instance S and P electrons combining to give 1P and 3P . Triplets are described by (18) and singlets by (20).

TWO electrons are treated in quantum mechanics by means of a six dimensional wave equation. In most atomic problems it is sufficient to consider the two electrons under the influence of a central field of force and to treat all other questions by perturbation methods. It is well known that in this approximation essential simplifications are introduced by the spherical symmetry of the central field of force. The eigenfunctions may be arranged in non-combining systems, each system corresponding to a certain value of the total angular momentum. By considerations of this sort it has been shown that correct space quantization, multiplet intensity relations, selection rules, and anomalous Zeeman effect formulas are consequences of quantum mechanics.†

In the calculations of the two or many electron problem it is customary at present to employ an approximation method such as Hartree's and to

† See in particular E. Wigner, *Zeits. f. Physik* **43**, 624 (1927) and especially p. 640 where the general possibility of (6) below is pointed out. The difference between the present treatment and Wigner's lies in the use of (4) with its known system of eigenfunctions.

consider each electron as subject to the action of a central field of force. In the calculations of the normal energy levels of He, however, Hylleraas¹ found it useful to consider the problem exactly. His calculations apply to the S states, which reduces the problem to a three dimensional one. We shall see that the reduction from six to three dimensions can be always made and that it is an immediate consequence of the spherical symmetry of the field. Even though the solution of a three dimensional wave equation is difficult we believe to have simplified the general problem because the application of variational methods, such as the Ritz method to a six or five dimensional problem is usually out of the question.

Let ψ be the Schroedinger function. Let the coordinates of the electrons be $(x_1, y_1, z_1), (x_2, y_2, z_2)$. By the general theorem of conservation of angular momentum

$$\left[\sum_{x,y,z} \left(y_1 \frac{\partial}{\partial z_1} - z_1 \frac{\partial}{\partial y_1} + y_2 \frac{\partial}{\partial z_2} - z_2 \frac{\partial}{\partial y_2} \right) + l(l+1) \right] \psi = 0 \quad (1)$$

for any state with angular momentum l . Introducing polar coordinates $(r_1, \theta_1, \phi_1), (r_2, \theta_2, \phi_2)$ this becomes

$$\begin{aligned} & \left\{ \left(\sin \phi_1 \frac{\partial}{\partial \theta_1} + \cos \phi_1 \frac{\cos \theta_1}{\sin \theta_1} \frac{\partial}{\partial \phi_1} + \sin \phi_2 \frac{\partial}{\partial \theta_2} + \cos \phi_2 \cot \theta_2 \frac{\partial}{\partial \phi_2} \right)^2 \right. \\ & \quad + \left(-\cos \phi_1 \frac{\partial}{\partial \theta_1} + \sin \phi_1 \cot \theta_1 \frac{\partial}{\partial \phi_1} - \cos \phi_2 \frac{\partial}{\partial \theta_2} + \sin \phi_2 \cot \theta_2 \frac{\partial}{\partial \phi_2} \right)^2 \\ & \quad \left. + \left(\frac{\partial}{\partial \phi_1} + \frac{\partial}{\partial \phi_2} \right)^2 + l(l+1) \right\} \psi = 0. \quad (2) \end{aligned}$$

We now reexpress ψ in terms of Euler angles θ', ϕ', ϕ and r_1, r_2, θ connected by the transformation formulas:

$$\theta' = \theta_1, \quad \phi' = \phi_1$$

$$\begin{aligned} \cos \theta &= \cos \theta' \cos \theta_2 + \sin \theta' \sin \theta_2 \cos (\phi_2 - \phi_1); & \sin \theta_2 \sin \alpha &= \sin \theta' \sin \phi \\ \cos \theta_2 &= \cos \theta' \cos \theta - \sin \theta' \sin \theta \cos \phi; & \sin \theta \sin \alpha &= \sin \theta' \sin (\phi_2 - \phi_1) \\ \cos \theta' &= \cos \theta_2 \cos \theta + \sin \theta_2 \sin \theta \cos \alpha; & \sin \theta \sin \phi &= \sin \theta_2 \sin (\phi_2 - \phi_1) \end{aligned} \quad (3)$$

the notation being throughout as in the first paper of Hylleraas. The angle θ drops out of (2) which reduces itself to

$$\left\{ \frac{\partial^2}{\partial \theta'^2} + \cot \theta' \frac{\partial}{\partial \theta'} + \frac{1}{\sin^2 \theta'} \frac{\partial^2}{\partial \phi'^2} - 2 \frac{\cos \theta'}{\sin^2 \theta'} \frac{\partial^2}{\partial \phi \partial \phi'} + \frac{1}{\sin^2 \theta'} \frac{\partial^2}{\partial \phi'^2} + l(l+1) \right\} \psi = 0. \quad (4)$$

¹ Hylleraas, Zeits. f. Physik 54, 347 (1929); 48, 469 (1928). See also J. C. Slater, Proc. Nat. Acad. 13, 423 (1927); G. W. Kellner, Zeits. f. Physik 44, 91 (1927).

² For derivation see appendix I.

This is a well-known equation, being a special case of the wave equation for a symmetrical top. Its eigenwerte are known to correspond to integral values of l , the value zero being included. The angular momentum about the z axis is represented by the operator

$$M^z = \frac{\hbar}{2\pi i} \left(x_1 \frac{\partial}{\partial y_1} - y_1 \frac{\partial}{\partial x_1} + x_2 \frac{\partial}{\partial y_2} - y_2 \frac{\partial}{\partial x_2} \right) = \frac{\hbar}{2\pi i} \left(\frac{\partial}{\partial \phi_1} + \frac{\partial}{\partial \phi_2} \right) = \frac{\hbar}{2\pi i} \frac{\partial}{\partial \phi'}. \quad (5)$$

If $l(l+1)=0$ there are no eigenfunctions (4) except those which do not depend on θ' , ϕ , ϕ' . Thus for $l=0$ the wave function depends only on r_1 , r_2 , θ or r_1 , r_1 , r_{12} as pointed out by Hylleraas for S states. In all other cases i.e. for P , D , states ψ depends on the angles. Thus for P states ($l=1$) we have the following nine independent eigenfunctions

$$\cos \theta', (1 + \cos \theta') e^{\pm i(\phi + \phi')}, e^{\pm i\phi} \sin \theta', e^{\pm i\phi'} \sin \theta', (1 - \cos \theta') e^{\pm i(\phi - \phi')}.$$

We may say therefore that for any P state

$$\psi = \sum_{i=1}^9 f_i(r_1, r_2, \theta) u_i(\theta', \phi', \phi) \quad (6)$$

where u_1, \dots, u_9 are the above set of nine independent eigenfunctions. Equation (6) is, however, too general because the nine eigenfunctions can be subdivided into three non-combining sets, each set containing three functions, all the functions of a given set depending on ϕ' as $e^{im\phi'}$. According to (5) each set describes such an orientation of the total angular momentum that its component along OZ is $m\hbar/2\pi$. For $m=0$ such a set of functions is

$$\cos \theta', e^{\pm i\phi} \sin \theta'. \quad (6')$$

In (6) therefore, it is permissible to extend the summation only over these three functions if we are interested only in solutions with $m=0$. The legitimacy of using only these three functions is of course a consequence of the invariance of the Hamiltonian under rotations about the z axis. On account of this invariance the result of operating by the Hamiltonian on any term in (6) gives rise to angular functions with the same value of m . In the general expression (6) therefore each set of functions is entirely independent of the other two.

Since the two electrons are equal we have a further subdivision into non-combining term systems. This is the usual subdivision into symmetric and antisymmetric solutions. With this in mind we use Hylleraas' expressions (23), (24) according to which the Schroedinger equation for the energy is

$$\begin{aligned} & \frac{1}{r_1^2} \frac{\partial}{\partial r_1} \left(r_1^2 \frac{\partial \psi}{\partial r_1} \right) + \frac{1}{r_2^2} \frac{\partial}{\partial r_2} \left(r_2^2 \frac{\partial \psi}{\partial r_2} \right) + \frac{1}{r_1^2} \left[\frac{1}{\sin \theta} \frac{\partial}{\partial \theta} \left(\sin \theta \frac{\partial \psi}{\partial \theta} \right) + A_1[\psi] \right] \\ & + \frac{1}{r_2^2} \left[\frac{1}{\sin \theta} \frac{\partial}{\partial \theta} \left(\sin \theta \frac{\partial \psi}{\partial \theta} \right) + A_2[\psi] \right] + 8\pi^2 m \hbar^{-2} (E - V) \psi = 0 \end{aligned}$$

$$\begin{aligned}
A_1[\psi] = & (\cot^2 \theta + 2 \cot \theta \cot \theta' \cos \phi + \cot^2 \theta') \frac{\partial^2 \psi}{\partial \phi^2} + \frac{1}{\sin \theta'} \frac{\partial}{\partial \theta'} \left(\sin \theta' \frac{\partial \psi}{\partial \theta'} \right) \\
& + \frac{1}{\sin^2 \theta'} \frac{\partial^2 \psi}{\partial \phi'^2} + 2 \cot \theta' \sin \phi \frac{\partial^2 \psi}{\partial \theta \partial \phi} - 2 \cos \phi \frac{\partial^2 \psi}{\partial \theta \partial \theta'} - 2 \frac{\sin \phi}{\sin \theta'} \frac{\partial^2 \psi}{\partial \theta \partial \phi'} \\
& + 2 \cot \theta \sin \phi \frac{\partial^2 \psi}{\partial \phi \partial \theta'} - \frac{2}{\sin \theta'} (\cot \theta' + \cot \theta \cos \phi) \frac{\partial^2 \psi}{\partial \phi \partial \phi'}; \quad A_2[\psi] = \frac{1}{\sin^2 \theta} \frac{\partial^2 \psi}{\partial \phi^2} \quad (7)
\end{aligned}$$

On account of spherical symmetry V is a function of r_1, r_2, θ only and does not contain θ', ϕ', ϕ . The functions u_i behave therefore as constant coefficients with the exceptions of the terms $A_1[\psi], A_2[\psi]$. Since by (3) $\sin \theta' \sin \phi = \sin \theta_2 \sin \alpha$, the angular eigenfunction $\sin \theta' \sin \phi$ is seen to be antisymmetric in the electrons 1 and 2. For this reason A_1 and A_2 must produce similar effects on it. In fact it is found that

$$A_1[\sin \theta' \sin \phi] = A_2[\sin \theta' \sin \phi] = -\sin^{-2} \theta (\sin \theta' \sin \phi). \quad (8)$$

We see therefore that the particular linear combination of two of the eigenfunctions for $m=0$, namely $\sin \theta' \sin \phi$ when operated on by the Hamiltonian gives rise to itself only. A possible P state is therefore given by

$$\psi = f(r_1, r_2, \theta) \sin \theta' \sin \phi \quad (9)$$

and the differential equation for f is

$$\begin{aligned}
& \frac{\partial}{r_1^2 \partial r_1} \left(r_1^2 \frac{\partial f}{\partial r_1} \right) + \frac{\partial}{r_2^2 \partial r_2} \left(r_2^2 \frac{\partial f}{\partial r_2} \right) + (r_1^{-2} + r_2^{-2}) \left[\frac{\partial}{\sin \theta \partial \theta} \left(\sin \theta \frac{\partial f}{\partial \theta} \right) - \frac{f}{\sin^2 \theta} \right] \\
& + 8\pi^2 m \hbar^{-2} (E - V) f = 0. \quad (10)
\end{aligned}$$

This differential equation differs from the one for S states only by the term $-(r_1^{-2} + r_2^{-2}) \sin^{-2} \theta$ and it is seen that the determination of its eigenvalues can be carried out by analogous methods. The physical interpretation of the solutions (9) becomes apparent if the perturbation e^2/r_{12} between the two electrons is supposed small. Then (10) is separable. Supposing the separation to take place by

$$f = P_n^{(1)}(\cos \theta) g(r_1, r_2) \quad (10')$$

we obtain

$$\frac{\partial}{r_1^2 \partial r_1} \left(r_1^2 \frac{\partial f}{\partial r_1} \right) + \frac{\partial}{r_2^2 \partial r_2} \left(r_2^2 \frac{\partial f}{\partial r_2} \right) - n(n+1)(r_1^{-2} + r_2^{-2}) f + 8\pi^2 m \hbar^{-2} (E - V) f = 0.$$

This may be considered as the radial part of the Schroedinger equation for two electrons, each being initially in a state with azimuthal quantum number n . The same may be seen from (10') because by (3)

$$\sin \theta \sin \theta' \sin \phi = \sin \theta_1 \sin \theta_2 \sin (\phi_2 - \phi_1)$$

so that the angular part of (10') is a linear combination of products of the type $P_n^1(\cos \theta_1) e^{\pm i\phi_1}$. The solution (9) represents therefore P states which arise either from two 2P or two 2D or two 2F electrons etc. The solutions of (10) may be symmetric or antisymmetric in r_1, r_2 giving the singlet and triplet systems. They include the case of equivalent orbits.

Out of the three functions (6') we have left now only two

$$\cos \theta', \sin \theta' \cos \phi$$

substituting these into (7) it is found that the Hamiltonian operating on one of them gives rise not only to itself but also to the other. Here we must write

$$\psi = f_1 \cos \theta' + f_2 \sin \theta' \cos \phi. \quad (11)$$

Operating on this by (7) we get two simultaneous linear equations in f_1 and f_2 :

$$\begin{aligned} L[f_1] - 2r_1^{-2} \left(f_1 + \cot \theta f_2 + \frac{\partial f_2}{\partial \theta} \right) &= 0 \\ L[f_2] + r_1^{-2} \left(2 \frac{\partial f_1}{\partial \theta} - \sin^{-2} \theta f_2 \right) - r_2^{-2} \sin^{-2} \theta f_2 &= 0 \end{aligned} \quad (12)$$

where

$$\begin{aligned} L[f] &= \frac{\partial}{r_1^2 \partial r_1} \left(r_1^2 \frac{\partial f}{\partial r_1} \right) + \frac{\partial}{r_2^2 \partial r_2} \left(r_2^2 \frac{\partial f}{\partial r_2} \right) \\ &+ (r_1^{-2} + r_2^{-2}) \frac{\partial}{\sin \theta \partial \theta} \left(\sin \theta \frac{\partial f}{\partial \theta} \right) + 8\pi^2 m h^{-2} (E - V) f. \end{aligned} \quad (13)$$

Equations (11), (12) are unsymmetrical in (1) and (2). Making the substitutions

$$F_1 = f_1 + \cot \theta \cdot f_2, \quad F_2 = (\sin \theta)^{-1} f_2 \quad (14)$$

we have

$$\psi = F_1 \cos \theta_1 - F_2 \cos \theta_2 \quad (15)$$

while (12) goes into³

$$\begin{aligned} L[F_1] + \frac{2}{r_1^2} \left(\cot \theta \frac{\partial F_1}{\partial \theta} - F_1 \right) + \frac{2 \partial F_2}{r_2^2 \sin \theta \partial \theta} &= 0 \\ L[F_2] + \frac{2 \partial F_1}{r_1^2 \sin \theta \partial \theta} + \frac{2}{r_2^2} \left(\cot \theta \frac{\partial F_2}{\partial \theta} - F_2 \right) &= 0. \end{aligned} \quad (16)$$

Here F_1, F_2 are functions of r_1, r_2, θ only. Any ψ in (15) must be either symmetric or antisymmetric in (1) and (2). The latter case is obtained if

$$F_2(r_1, r_2, \theta) = F_1(r_2, r_1, \theta) \equiv \tilde{F}(r_1, r_2, \theta). \quad (17)$$

³ For direct derivation see Appendix II.

Letting $F = F_1$ the two equations (16) reduce to a single equation in F viz.

$$L[F] + \frac{2}{r_1^2} \left(\cot \theta \frac{\partial F}{\partial \theta} - F \right) + \frac{2}{r_2^2 \sin \theta} \frac{\partial \tilde{F}}{\partial \theta} = 0. \quad (18)$$

The symmetric solutions are obtained by letting

$$F_2 = -\tilde{F}_1. \quad (19)$$

Here we write $F_1 = G$ and (16) reduces again to a single equation

$$L[G] + \frac{2}{r_1^2} \left(\cot \theta \frac{\partial G}{\partial \theta} - G \right) - \frac{2}{r_2^2 \sin \theta} \frac{\partial \tilde{G}}{\partial \theta} = 0. \quad (20)$$

The only difference between (18) and (20) is in the sign of the last term. This term represents the resonance between the two electrons. In the unperturbed state i.e. if the perturbation term e^2/r_{12} is not important the simplest solutions of (18) are those for which $(\partial F/\partial \theta) = 0$. Then (15) shows that we deal with a 3P term arising from a 2S and a 2P electron while similarly the solutions of (20) give the corresponding 1P terms. In addition to these solutions there are others for the unperturbed case. Thus if we set

$$F = g(r_1, r_2) \cos \theta + \tilde{g}/3$$

we find from (15) that

$$\psi = g(\cos \theta \cos \theta_1 - \cos \theta_2/3) - \tilde{g}(\cos \theta \cos \theta_2 - \cos \theta_1/3).$$

Since

$$\cos \theta \cos \theta_1 - \cos \theta_2/3 = \frac{2}{3} \cos \theta_2 P_2(\cos \theta_1) - \cos \theta_1 \sin \theta_1 \sin \theta_2 \cos(\phi_2 - \phi_1)$$

this angular function is seen to consist of a linear combination of

$$e^{\pm i m \phi_1} P_2^m(\cos \theta_1) \quad \text{and} \quad e^{\pm i m \phi_2} P_1^m(\cos \theta_2).$$

This is a case of 3P and 2D terms combining to give a 3P . In a similar way all other combinations between electrons of unequal azimuthal quantum number resulting in P terms are contained among the solutions of (18).

Summarizing the classifications of all solutions belonging to the subset (6') we may say that (9) and (10) give the P terms arising from electrons which in the unperturbed state have equal azimuthal quantum numbers while (15), (18), (20) give the P terms arising from all other electron combinations.

It will be remembered now that equation (6) contains two more non-combining sets of eigenfunctions corresponding to $m = \pm 1$. The spherical symmetry of the problem enables us to write them down by analogy with those already found. Thus corresponding to (15) and (18) we have now a complete set of orthogonal eigenfunctions

$$\begin{aligned}
u_1 &= (3^{1/2}/4\pi)(F \sin \theta_1 e^{i\phi_1} - \tilde{F} \sin \theta_2 e^{i\phi_2}) \\
&= (3^{1/2}/4\pi)[a \sin \theta' + b(-i \sin \phi - \cos \theta' \cos \phi)]e^{i\phi'} \\
u_0 &= (6^{1/2}/4\pi)(F \cos \theta_1 - \tilde{F} \cos \theta_2) = (6^{1/2}/4\pi)[a \cos \theta' + b \sin \theta' \cos \phi] \quad (21) \\
u_{-1} &= (3^{1/2}/4\pi)(F \sin \theta_1 e^{-i\phi_1} - \tilde{F} \sin \theta_2 e^{-i\phi_2}) \\
&= (3^{1/2}/4\pi)[a \sin \theta' + b(i \sin \phi - \cos \theta' \cos \phi)]e^{-i\phi'} \\
a &= F - \tilde{F} \cos \theta, \quad b = \tilde{F} \sin \theta.
\end{aligned}$$

The normalization being such that

$$\int (F^2 - 2F\tilde{F} \cos \theta + \tilde{F}^2) dV_{r_1, r_2, \theta} = 1; \quad dV_{r_1, r_2, \theta} = r_1^2 r_2^2 \sin \theta dr_1 dr_2 d\theta.$$

These three eigenfunctions belong to the eigenwerte of (18) and are to be used together in solving perturbation problems such as fine structure calculations. Similarly there are three other eigenfunctions for every solution of (20). The remaining three functions are of the type (9). We note that $\sin \theta \sin \phi = R_z/R$ where $R_z = [\tilde{r}_1 \times \tilde{r}_2]$. Forming the combinations $R_z \pm iR_y$ we find this set of functions to be

$$\begin{aligned}
&[(3^{1/2}/4\pi)e^{i\phi'}(i \cos \phi - \cos \theta' \sin \phi), \quad (6^{1/2}/4\pi) \sin \theta' \sin \phi, \\
&(3^{1/2}/4\pi)e^{-i\phi'}(-i \cos \phi - \cos \theta' \sin \phi)]f. \quad (22)
\end{aligned}$$

The differential equations (16), (18) and the corresponding sets of eigenfunctions (21), (22) correspond to essentially different cases and for this reason the variational equations belonging to the two cases are different. We consider the type of solution described by (16) and (21) first. The variational equation belonging to the problem is

$$\delta \int \left\{ \left(\frac{\partial \psi}{\partial x_1} \right)^2 + \dots + \left(\frac{\partial \psi}{\partial z_2} \right)^2 + 8\pi^2 m \hbar^{-2} (V - E) \psi^2 \right\} dx_1 \dots dz_2 = 0 \quad (23)$$

with the equation of condition

$$\int \psi^2 dx_1 \dots dz_2 = 1. \quad (23')$$

Here $dx_1 \dots dz_2$ is the volume element of the six dimensional configuration space. Taking any of the functions (21) the volume element may be reexpressed in terms of $r_1, r_2, \theta, \theta', \phi'$ and the integrations may then be performed over the angles θ', ϕ' in (23) and (23').

The result of the calculation is:⁴

$$\begin{aligned}
&\delta \int \left\{ \left(\frac{\partial F_1}{\partial r_1} \right)^2 - 2 \cos \theta \frac{\partial F_1}{\partial r_1} \frac{\partial F_2}{\partial r_1} + \left(\frac{\partial F_2}{\partial r_1} \right)^2 + \left(\frac{\partial F_1}{\partial r_2} \right)^2 - 2 \cos \theta \frac{\partial F_1}{\partial r_2} \frac{\partial F_2}{\partial r_2} + \left(\frac{\partial F_2}{\partial r_2} \right)^2 \right. \\
&\quad \left. + (r_1^{-2} + r_2^{-2}) \left[\left(\frac{\partial F_1}{\partial \theta} \right)^2 - 2 \cos \theta \frac{\partial F_1}{\partial \theta} \frac{\partial F_2}{\partial \theta} + \left(\frac{\partial F_2}{\partial \theta} \right)^2 \right] + 2r_1^{-2} F_1^2 + 2r_2^{-2} F_2^2 \right\}
\end{aligned}$$

⁴ For derivation see appendix II.

$$\begin{aligned}
& + 2r_1^{-2} \sin \theta F_1 \frac{\partial F_2}{\partial \theta} + 2r_2^{-2} \sin \theta F_2 \frac{\partial F_1}{\partial \theta} \\
& + 8\pi^2 m \hbar^{-2} (V - E) (F_1^2 - 2F_1 F_2 \cos \theta + F_2^2) \} dV_{r_1, r_2, \theta} = 0
\end{aligned} \quad (24)$$

and the equation of condition is

$$\int (F_1^2 - 2F_1 F_2 \cos \theta + F_2^2) dV_{r_1, r_2, \theta} = 1. \quad (24')$$

Performing independent variations of F_1 and F_2 the differential equations (16) follow from (24). Corresponding to (17) and (18) the variational equation (24) gives two different equations, one applying to an antisymmetric ψ and the other to the symmetric one. Each of these involves only one function and its transposed and can be worked out by the same method as used by Hylleraas. It will be noted that the antisymmetric solutions (24) involve combinations of the type $F^2 - 2F\bar{F} \cos \theta + \bar{F}^2$. If $r_1 = r_2$, this vanishes for $\theta = 0$, so that the values of $F(r, r, \theta)$ are not important. On the other hand for the symmetric solutions $G(r, r, \pi)$ are not important. It will be noted also that both the differential equation and the variational one involve simultaneously a function of r_1, r_2, θ and its transposed and that *the dependence on θ is of primary importance in determining the difference between symmetric and antisymmetric solutions.*

The variational equation corresponding to (10) can be written down by inspection and is

$$\begin{aligned}
\delta \int \left\{ \left(\frac{\partial f}{\partial r_1} \right)^2 + \left(\frac{\partial f}{\partial r_2} \right)^2 + (r_1^{-2} + r_2^{-2}) \left[\left(\frac{\partial f}{\partial \theta} \right)^2 + \frac{f^2}{\sin^2 \theta} \right] \right. \\
\left. + 8\pi^2 m \hbar^{-2} (V - E) f^2 \right\} dV_{r_1, r_2, \theta} = 0 \quad (25)
\end{aligned}$$

with the equation of condition

$$\int f^2 dV_{r_1, r_2, \theta} = 1. \quad (25')$$

This differs from the equation used by Kellner and Hylleraas only by the term $(r_1^{-2} + r_2^{-2}) \cdot f^2 / \sin^2 \theta$. Obvious changes of variables to r_1, r_2, r_{12} can of course be made and the elliptic coordinates used by Hylleraas can be introduced here with the same boundary conditions.

Only P terms have been considered here. It is clear, however, that the same can be done for any other value of l . Since closed expressions for the general case are complicated, we do not consider them here.

APPENDIX

(I) Derivation of equation (4)

This can be derived either by the analytical procedure indicated in the text or else by the following geometrical consideration. The first three terms in (2) are squares of infinitesimal rotation operators about the axes x, y, z . The changes in ψ during a rotation are brought about

only through its dependence on θ' , ϕ' , ϕ . We draw two lines ON , OM in the xy plane with azimuths $-\pi/2 + \phi$, ϕ . Resolving a rotation about OX along ON and OM with $ON \perp OM$ the first contributes $\sin \phi' \partial/\partial\theta'$. The second must be compounded as a sum of rotations along OZ and $O(1)$ and give rise to

$$\cos \phi' (\cot \theta' (\partial/\partial\phi') - (\partial/\sin \theta' \partial\phi))$$

The rotation operators are thus found to be

$$\begin{aligned} L_x &= \sin \phi' \frac{\partial}{\partial\theta'} + \cos \phi' \left(\cot \theta' \frac{\partial}{\partial\phi'} - \frac{\partial}{\sin \theta' \partial\phi} \right), \\ L_y &= -\cos \phi' \frac{\partial}{\partial\theta'} + \sin \phi' \left(\cot \theta' \frac{\partial}{\partial\phi'} - \frac{\partial}{\sin \theta' \partial\phi} \right), \\ L_z &= \frac{\partial}{\partial\phi'}. \end{aligned}$$

Equation (4) is then obtained as

$$[L_x^2 + L_y^2 + L_z^2 + l(l+1)]\psi = 0.$$

Usual commutation relations between rotation operators are of course also satisfied by L_x , L_y , L_z .

(II) Derivation of (16) and (24).

On account of spherical symmetry it is sufficient to calculate the variational equation for

$$\psi = F_1 - F_2 \cos \theta = a \cos \theta' + b \sin \theta' \cos \phi$$

where

$$a = F_1 - F_2 \cos \theta, \quad b = F_2 \sin \theta.$$

The equation to be transformed is (23). The volume element is

$$dx_1 \cdots dz_2 = r_1^2 r_2^2 \sin \theta \sin \theta' dr_1 dr_2 d\theta d\theta' d\phi d\phi'.$$

We have

$$\begin{aligned} (\text{grad}_1 \psi)^2 &= \left(\frac{\partial \psi}{\partial r_1} \right)^2 + r_1^{-2} \left[\left(\frac{\partial \psi}{\partial \theta_1} \right)^2 + (\sin \theta_1)^{-2} \left(\frac{\partial \psi}{\partial \phi_1} \right)^2 \right] \\ \frac{\partial \psi}{\partial \theta_1} &= -F_1 \sin \theta_1 + \left(\frac{\partial F_1}{\partial \theta} \cos \theta_1 - \frac{\partial F_2}{\partial \theta} \cos \theta_2 \right) \frac{\partial \theta}{\partial \theta_1} \\ \frac{\partial \psi}{\partial \phi_1} &= \left(\frac{\partial F_1}{\partial \theta} \cos \theta_1 - \frac{\partial F_2}{\partial \theta} \cos \theta_2 \right) \frac{\partial \theta}{\partial \phi_1}. \end{aligned}$$

Remembering now that

$$\left(\frac{\partial \theta}{\partial \theta_1} \right)^2 + \frac{1}{\sin^2 \theta_1} \left(\frac{\partial \theta}{\partial \phi_1} \right)^2 = 1 \quad (a)$$

we have:

$$\begin{aligned} \left(\frac{\partial \psi}{\partial \theta_1} \right)^2 + \frac{1}{\sin^2 \theta_1} \left(\frac{\partial \psi}{\partial \phi_1} \right)^2 &= F_1^2 \sin^2 \theta_1 + \left(\frac{\partial F_1}{\partial \theta} \cos \theta_1 - \frac{\partial F_2}{\partial \theta} \cos \theta_2 \right)^2 \\ &\quad - 2F_1 \sin \theta_1 \frac{\partial \theta}{\partial \theta_1} \left(\frac{\partial F_1}{\partial \theta} \cos \theta_1 - \frac{\partial F_2}{\partial \theta} \cos \theta_2 \right). \end{aligned}$$

Substituting the value for $\partial\theta/\partial\theta_1$ which follows from the first equation (3) and using the second equation (3)

$$\sin \theta_1 \frac{\partial \theta}{\partial \theta_1} = -\sin \theta' \cos \phi$$

Writing further

$$a' = \frac{\partial F_1}{\partial \theta} - \frac{\partial F_2}{\partial \theta} \cos \theta, \quad b' = \frac{\partial F_2}{\partial \theta} \sin \theta$$

we transform the above expression into:

$$F_1^2 \sin^2 \theta' + (a' \cos \theta' + b' \sin \theta' \cos \phi)^2 + 2F_1(a' \cos \theta' + b' \sin \theta' \cos \phi) \sin \theta' \cos \phi.$$

Hence

$$\int_0^\pi \int_0^{2\pi} \int_0^{2\pi} r_1^{-2} \left[\left(\frac{\partial \psi}{\partial \theta_1} \right)^2 + (\sin \theta_1)^{-2} \left(\frac{\partial \psi}{\partial \phi_1} \right)^2 \right] \sin \theta' d\theta' d\phi' d\phi \\ = \frac{(4\pi)^2}{3r_1^2} [F_1^2 + (1/2)(a'^2 + b'^2) + b'F_1].$$

Using the symmetrical expression for the term in r_2^{-2} and replacing all integrals of $(a \cos \theta' + b \sin \theta' \cos \phi)^2$ by $(4\pi^2/6)(a^2 + b^2)$ equation (24) follows at once.

To verify (16) directly we evaluate

$$\frac{\partial^2 \psi}{\partial \theta_1^2} + \cot \theta_1 \frac{\partial \psi}{\partial \theta_1} + \frac{\partial^2 \psi}{\sin^2 \theta_1 \partial \phi_1^2}.$$

Remembering that

$$\left(\frac{\partial^2}{\partial \theta_1^2} + \cot \theta_1 \frac{\partial}{\partial \theta_1} + \frac{\partial^2}{\sin^2 \theta_1 \partial \phi_1^2} \right) \theta = \cot \theta$$

and the relation (a), the above expression reduces to

$$\cos \theta_1 \left[\frac{\partial^2 F_1}{\partial \theta^2} + 3 \cot \theta \frac{\partial F_1}{\partial \theta} - 2F_1 \right] - \cos \theta_2 \left[\frac{\partial^2 F_2}{\partial \theta^2} + \cot \theta \frac{\partial F_2}{\partial \theta} + \frac{2\partial F_1}{\sin \theta \partial \theta} \right]$$

similarly for

$$\frac{\partial^2}{\partial \theta_2^2} + \cot \theta_2 \frac{\partial}{\partial \theta_2} + \frac{\partial^2}{\sin^2 \theta_2 \partial \phi_2^2}.$$

Substituting into Schroedinger's equation, (16) follows on requiring independent vanishing of coefficients of $\cos \theta_1$, $\cos \theta_2$.

AN INTERPRETATION OF PAULI'S EXCLUSION PRINCIPLE

BY E. U. CONDON AND J. E. MACK*

UNIVERSITY OF MINNESOTA, MINNEAPOLIS

(Received February 6, 1930)

ABSTRACT

I. Pauli's exclusion principle can be understood as an instance of the subjectivity of our knowledge. We are built out of only a particular world constructed according to one of the non-combining patterns possible under the laws of quantum mechanics. Therefore we are capable of having sense perceptions of only that world.

II. Dirac's theory of the proton shows why Pauli's principle governs the world.

I.

PROBABLY the most important trend in current physics is that toward the recognition of the fact that our science gives no information about an objective reality wholly independent of ourselves. We are becoming increasingly impressed by the subjectivity of our knowledge. We owe much of this to the work of Bridgman with his emphasis on the unprofitableness of dallying over meaningless questions and his operational formulation of the reality of physical concepts. The rôle played by our subjective limitations on observation of the world about us has been discussed in detail by Heisenberg and by Bohr. We refer to the train of ideas known as Heisenberg's uncertainty principle.

Let us consider what the uncertainty principle did for physics. It came after the fairly complete formulation of the laws of quantum mechanics as we know them to-day. Before the principle the laws were quite definitely stated by Heisenberg, Born, Dirac, Jordan, Schrödinger, Pauli and others. They were stated so definitely that the method of treating special problems was recognised and applied with a good deal of success by a large number of physicists. Therefore, they were valid laws of science, since they met the test of being workable in the hands of physicists in general, and did not rest purely on the genius of the individuals who discovered them. Even without the principle they probably could have attained a universal applicability but we cannot say how that would have been, since, owing to the slowness of diffusion of scientific knowledge, the formal laws were still in the process of becoming the common property of professional physicists when Heisenberg enunciated the principle.

But before he did, even among those who had found the new methods workable and who had contributed to the many successes of the theory, there was a feeling of dissatisfaction, a feeling that the new theory was not understood, perhaps even not understandable. These were disturbing times for we

* National Research Fellow.

did not know why we felt dissatisfied (or perhaps unsatisfied) and so were quite helpless in attempting to remedy the situation. The remedy was provided by Heisenberg in his uncertainty principle. In a sense his famous paper in *Zeitschrift für Physik*, volume 43, has nothing new in it. For it does not alter or add to the formal statement of the laws of quantum mechanics. Nor does it apply them to any specific problem and produce calculations about some aspect of nature which are triumphantly in agreement with somebody's quantitative measurements. What it did do was to relieve that feeling of dissatisfaction. Many a physicist who had been working with the formalism of quantum mechanics felt that he understood it for the first time after he read that paper. Subsequently this satisfaction of understanding was considerably enhanced by the appearance of Bohr's Como lecture simultaneously in *Nature* and *Die Naturwissenschaften*. The title of Heisenberg's paper is significant: he called it the "anschaulich Inhalt" of the new quantum mechanics. It was just that: it was the intuitive, clear, evident content of the theory.

The important feature of this clear and intuitive part of the theory is the deflation of the lords-of-creation attitude of physicists. Wholly rational, detached fellows we thought ourselves (in our naive way), studying objectively the true laws of the external world. We had no concern with unfruitful stuff like metaphysics. Now we know otherwise and are healthily aware of our own organic relation to the traditionally inorganic subject matter of our science.

At present there is another law of nature (empirical, like all laws of nature) intimately connected with quantum mechanics, which we feel that we do not understand. This is Pauli's exclusion principle. We refer to the same feeling of dissatisfaction which was felt about quantum mechanics in general before Heisenberg's paper.

Pauli's principle grew out of empirical spectroscopy and was stated in the form that no two electrons in an atom can have the same set of quantum numbers. A formal place was found for this in the equations of quantum mechanics by Heisenberg, Dirac, Wigner and others. The equations of quantum mechanics showed a remarkable property when applied to the description of a dynamical system consisting of several dynamically similar particles. Such properties are naturally of fundamental importance because of the belief that all electrons are dynamically similar and that they are the fundamental stuff of which all substance is built. This remarkable property may be described by saying that such dynamical systems may exist in $N!$ different classes of states such that if the system exists now in one of these classes then it must exist for all time to come in this same class of states. (N is the number of similar particles in the system.) In other words, quantum mechanics provides, when applied to the dynamical system which is the entire universe, not just one solution but $N!$ possible solutions, which we may call worlds, where N is the total number of electrons in the universe. Since it is an exact conclusion from the postulated exact similarity of all the particles that the universe cannot change from one of these classes of states to

another, our universe must represent a selection from among these possible worlds. Which one? There is one which has the property that it has no possible states characterized by two of the particles' having the same quantum numbers. That one agrees with the world that we know.

That is fine but it leaves us with a lack of understanding of the matter which is, perhaps, akin to the unsatisfied feeling toward quantum mechanics which preceded the discovery of its "anschaulich Inhalt" by Heisenberg. What of the other $N!-1$ possible worlds?

Now we come to our main thesis: The restriction to a world built in accordance with Pauli's principle can be understood as another and extreme instance of the subjectivity of our knowledge. We, physicists, humans, are creatures who are built out of, and therefore are capable of reacting with and having sense perceptions of, only a particular world constructed according to a particular one of the non-combining patterns possible under the laws of quantum mechanics. Because of our own nature we are aware of, or conscious of, only that part of possible reality that is built on our pattern.

Do worlds really exist that are built (of the same electrons as ours) on one of the other patterns but nevertheless according to the laws of quantum mechanics? The question is meaningless in a sense because of our subjective incapacity to be aware of them. It is meaningless for the same reason as is the question, (sometimes asked after an individual has heard, for the first time, an exposition of Heisenberg's uncertainty principle) "Does a particle really have precise position and momentum simultaneously even though we cannot be experimentally aware of precise values for them?"

The situation turns on the meaning to be ascribed to the word "really" in the two questions. We prefer to associate with it the connotation, within the power of human sense perceptions. In that case the answer to both of them is no, as the "even though" clause makes ridiculously self-evident in the case of the second one. But we are reluctant to dismiss the other possible worlds quite so readily as we do simultaneous position and momentum. This is because the other worlds correspond to solutions of the equations of quantum mechanics, whereas there is no place in the structure of the mathematical formalism of quantum mechanics for simultaneous exact position and momentum.

Objective reality these other worlds cannot have, because of our subjective inability to react to them. (Remember that all objective reality is colored by important subjective elements!) This we feel is the simple, evident substratum of the Pauli exclusion principle which provides us with the right to say we "understand" it.

II

The foregoing shows that we can be conscious of only one of the possible worlds. But it throws no light on a possible reason why the real one is the one which obeys Pauli's exclusion principle.

One feels that the type of symmetry represented in our world is especially simple and that there must be some reason for it. It is another instance of an

ancient paradox: out of $N!$ possibilities the chance of the Pauli principle world being the real one seems vanishingly small. But in the matter of building the real world the dice are cast but once and in that one throw the antisymmetric pattern has an equal chance with the others.

Dirac's recent theory of the proton published in the Proceedings of the Royal Society for January, 1930, throws new light on the matter, however. When we spoke in *I* of there being $N!$ different possible worlds according to quantum mechanics, we were speaking of the non-relativistic theory. But the relativistic theory of the electron must represent a surer foundation on which to build cosmologic hypotheses. According to it, electrons can exist in states of negative energy (less than $-mc^2$), as well as in usual states of positive energy (of the order $+mc^2$). We have no experimental evidence of electrons of this sort and so the prediction of such negative energy electrons was regarded as a blemish in the theory. But now the solution to the difficulty is seen in the fact that Pauli's principle governs our world.

We can do no better than quote the crucial paragraph of Dirac's paper:

"The most stable states for an electron (i.e. the states of lowest energy) are those with negative energy and very high velocity. All the electrons in the world will tend to fall into these states with emission of radiation. The Pauli exclusion principle, however, will come into play and prevent more than one electron going into any one state. Let us assume that there are so many electrons in the world that all the most stable states are occupied, or, more accurately, that *all the states of negative energy are occupied except perhaps a few of small velocity*. Any electrons with positive energy will now have very little chance of jumping into negative-energy states and will therefore behave like electrons are observed to behave in the laboratory. We shall have an infinite number of electrons in negative-energy states, and indeed an infinite number per unit volume all over the world, but if their distribution is exactly uniform we should expect them to be completely unobservable. Only the small departures from exact uniformity, brought about by some of the negative-energy states being unoccupied, can we hope to observe."

And now we see why it is that the Pauli principle world is the only one which can be built out of Dirac's relativistic electrons. For it is the only one in which the available states can be filled up. For the others there is no limit to the number of electrons that can occupy a state. The antisymmetric one is the only pattern that has a "bottom." For the others all the electrons in the universe would be drained off into states of indefinitely great negative energy.

THE X-RAY SCATTERING POWERS OF NICKEL
AND OXYGEN IN NICKEL OXIDE

BY RALPH W. G. WYCKOFF

ROCKEFELLER INSTITUTE FOR MEDICAL RESEARCH, NEW YORK CITY

(Received February 6, 1930)

ABSTRACT

Atomic F -curves for the nickel and oxygen atoms in NiO have been obtained from measurements of the intensities of the principal powder reflections of molybdenum, copper and nickel $K\alpha$ radiations. Though the scattering power of oxygen remains nearly constant with respect to NaCl for these wave-lengths, that of nickel shows important variations.

THIS paper forms part of a series of studies of the dependence of the diffracting power of an atom upon the wave-length of the x-rays being scattered. Accurate measurement¹ has shown that with wave-lengths as near together as the $K\alpha$ lines of molybdenum and rhodium the F -values of NaCl are equal for the same $\sin \theta/\lambda$. There is likewise some indication² that the atoms in this crystal do not have very different scattering powers for copper radiation. Recent comparisons of NaCl and metallic silicon³ prove that the ratio of their diffracting powers is nearly the same for molybdenum and for copper $K\alpha$ x-rays. All of these observations are with radiations far removed in frequency from any critical values for the diffracting atoms.

Such a parallelism as that prevailing between NaCl and silicon no longer seems to hold if the comparisons involve metallic copper and iron reflecting molybdenum and copper rays. The experiments already made⁴ with these metals indicate that their scattering powers decrease more rapidly with increasing wave-length than do those of the atoms of NaCl. This conclusion is dependent upon the essential correctness of measured absorption coefficients.

Observations upon NiO avoid such an uncertainty by containing within themselves a comparison of the scattering powers of two atoms—nickel and oxygen. These data consist of determinations of the F -curves of nickel and oxygen using molybdenum, copper and nickel $K\alpha$ radiation. The measurements upon which they are based are spectrometer studies of the intensities of the principal x-ray reflections of powdered NiO. The methods used in obtaining these intensities⁵ and reducing them to atomic scattering powers have been described.

¹ R. W. James and E. M. Firth, Proc. Roy. Soc. 117A, 62 (1927).

² E. Wagner and H. Kulenkampff, Ann. d. Physik 68, 369 (1922).

³ R. W. G. Wyckoff, Zeit. f. Krist. in press (1930).

⁴ A. H. Armstrong, Phys. Rev. 34, 931 (1929).

⁵ A. H. Compton, X-rays and Electrons (New York, 1926) Chap. V; R. W. G. Wyckoff and A. H. Armstrong, Zeit. f. Krist. 72, 319 (1929).

Two different samples of chemically pure green NiO gave results which were identical within the limit of experimental error. In order to suppress the effects of extinction both crystal powders were ground thoroughly in an agate mortar and passed through a 325 mesh per linear inch sieve before being formed into a cake.

Molybdenum radiation was obtained from a water-cooled General Electric tube operated from a synchronous motor-generator-kenetron-condenser

TABLE I. *The relative intensities of powder reflections of nickel oxide.*

Indices	Intensities for $K\alpha$ wave-length of		Nickel
	Molybdenum	Copper	
111	111.8	112.4	129.7
200	159.4	196.1	207.3
220	[100]	[100]	[100]
113	48.9	36.4	42.2
222	29.1	26.4	28.3
400	13.4	10.7	—
133	19.1	—	—
240	28.8	—	—
224	20.5	—	—
333,115	12.5	—	—

set at 30 kv with a current consumption of 5 or 10 ma. The copper and nickel radiations were supplied by Siemens-Phoenix tubes passing 6 ma at 25 kv. The molybdenum rays were rendered essentially monochromatic with a ZrO_2 screen. No attempt was made to filter the x-rays emitted by the copper and nickel target tubes but calculation showed that with the resolution used none of the measured $K\alpha$ spectra was contaminated by other reflections.

TABLE II. *The F -values of powder reflections of nickel oxide.*

Indices	$\sin \theta/\lambda$	$F(Mo K\alpha)$	$F(Cu K\alpha)$	$F(Ni K\alpha)$
111	0.2076	14.13	11.41	13.01
200	.2398	22.60	20.56	22.52
220	.3391	18.28	15.83	16.88
113	.3976	10.76	8.13	9.16
222	.4153	15.12	12.52	13.43
400	.4796	13.65	10.12	—
133	.5223	9.22	—	—
240	.5359	11.65	—	—
224	.5871	10.96	—	—
333,115	.6229	7.96	—	—

The crystal structure of NiO is identical with that of NaCl. Reflections with odd indices therefore represent differences between the contributions of nickel and oxygen atoms, those with even indices (all even order spectra) are due to the cooperation of these two atoms. The relative intensities of the observed reflections for Ni $K\alpha$, Cu $K\alpha$ and Mo $K\alpha$ rays are shown in Table I.

The absolute F -values for molybdenum radiation have been found by comparing the (200) reflection of NiO with (220) of NaCl. A mean of several

determinations using both samples of NiO gave $(200)\text{NiO}:(220)\text{NaCl}=49.6:100$. The apparent accuracy of this ratio is better than 5 percent. The mass absorption coefficient of NiO according to the experiments of Windgardh⁶ is $\mu/\rho=37.93$. If Allen's⁷ value for nickel is used, μ/ρ becomes 37.21. The absorption coefficient of NaCl as provided by Windgardh's data is $\mu=18.21$ ($\rho=2.16$). Of the other quantities⁸ needed to calculate absolute F 's, ρ has been taken as 6.75, $a_0(\text{NiO})=4.17\text{\AA}$, $a_0(\text{NaCl})=5.628\text{\AA}$, $F(220, \text{NaCl})=15.62$. Introduction of these values into the customary expressions leads to the reflection F 's recorded in Table II and Fig. 1. Points on the smooth F -curves drawn through them, when separated by addition and subtraction into

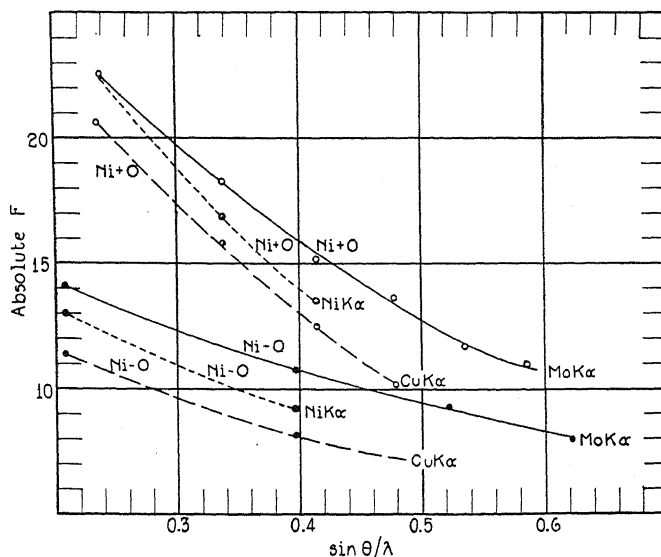


Fig. 1. The reflection F -values observed from NiO using molybdenum, copper and nickel $K\alpha$ radiations.

atomic F -values for nickel and oxygen, give the numbers listed in Tables III and IV and plotted in Fig. 2.

In order to place the F -curves for copper and nickel radiation upon an "absolute" scale for comparison with those for molybdenum x-rays, it has been assumed that $F(220, \text{NaCl})=15.62$ for all three radiations. The absorption coefficients for NiO as calculated by Jönsson's formula⁹ are $\mu=276.8$ for $\text{Cu } K\alpha$ and $\mu=345.1$ for $\text{Ni } K\alpha$. They are in good agreement with existing experimental values. Absorption coefficients for NaCl obtained in the same way are $\mu=161.2$ for $\text{Cu } K\alpha$ and $\mu=196.2$ for $\text{Ni } K\alpha$. Measurements of the

⁶ K. A. Windgardh, *Zeits. f. Physik* 8, 363 (1922).

⁷ S. J. M. Allen, *Phys. Rev.* 28, 907 (1926).

⁸ *Internat. Critical Tables* (New York, 1926) Vol. I p. 343; R. W. James and E. M. Firth, *op. cit.*

⁹ E. Jönsson, *Uppsala Univers. Årsskrift* (1928).

relative intensities of (220) NaCl and (220) NiO have led to the ratios (220)NiO:(220)NaCl=100:57.5 for Cu $K\alpha$ and (220)NiO:(220)NaCl=100:51.8 for Ni $K\alpha$. The reflection F 's calculated from these data are recorded

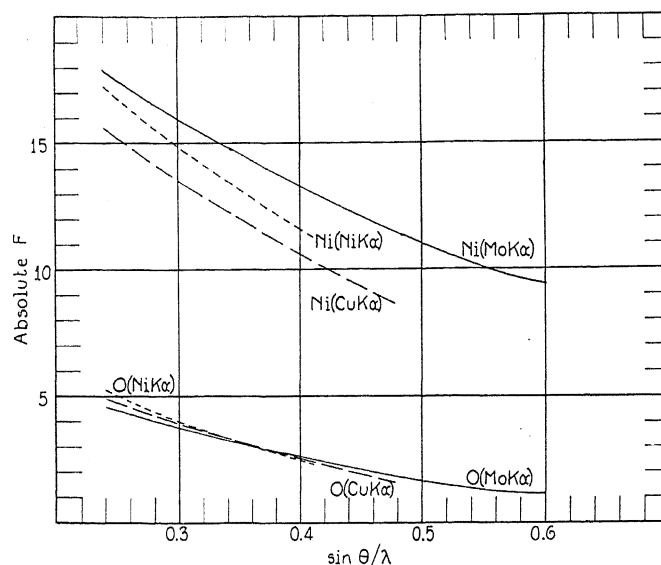


Fig. 2. The F -curves of nickel and oxygen atoms in NiO.

in Table II and plotted in Fig. 1. The atomic F 's derived from them are listed in Tables III and IV and shown graphically in Fig. 2.

TABLE III. Atomic F -values of oxygen in nickel oxide.

$\sin \theta/\lambda$	$F(\text{Mo } K\alpha)$	$F(\text{Cu } K\alpha)$	$F(\text{Ni } K\alpha)$
0.240	4.55	4.87	5.23
.270	4.14	4.42	4.62
.300	3.77	3.96	4.06
.330	3.42	3.52	3.52
.360	3.05	3.10	3.05
.390	2.72	2.67	2.58
.420	2.39	2.27	2.30
.450	2.09	(1.87)	—
.480	1.81	(1.53)	—
.510	1.57	—	—
.540	1.35	—	—
.570	1.22	—	—
.600	1.15	—	—

Note: Values in parentheses in this and the following table are obtained by extrapolating the Ni-O curve of Fig. 1.

A check upon the accuracy of the measurements of this paper can be had by comparing the oxygen F -curves for Mo $K\alpha$ from NiO and¹⁰ MgO. Though

¹⁰ R. W. G. Wyckoff and A. H. Armstrong, Zeits. f. Krist. **72**, 433 (1930).

it is scarcely to be expected that they should be identical, these two curves ought to lie close to one another (Fig. 3).

The most significant feature of these results is the fact that though the oxygen F -curves are nearly identical for the three radiations—or, more accurately, vary in the same manner as does NaCl—relatively large differences exist in the curves for the nickel atoms. Since critical wave-lengths of oxygen

TABLE IV. Atomic F -values of nickel in nickel oxide.

$\sin \theta/\lambda$	$F(\text{Mo } K\alpha)$	$F(\text{Cu } K\alpha)$	$F(\text{Ni } K\alpha)$
0.240	17.95	15.62	17.37
.270	16.94	14.55	16.07
.300	16.03	13.57	14.87
.330	15.16	12.62	13.78
.360	14.33	11.72	12.81
.390	13.54	10.88	11.90
.420	12.79	10.04	11.37
.450	12.09	(9.25)	—
.480	11.41	(8.55)	—
.510	10.81	—	—
.540	10.25	—	—
.570	9.76	—	—
.600	9.39	—	—

are farther from the wave-lengths used than are those of NaCl, the observed slight increase in the oxygen F -curves at low angles with increasing wave-lengths is not contrary to expectation. The F -curves of nickel, lower for copper than for molybdenum radiation, agree with existing data upon copper⁴ and iron in indicating that for atoms having critical frequencies within the experimental range, coherent scattering decreases with increasing wave-

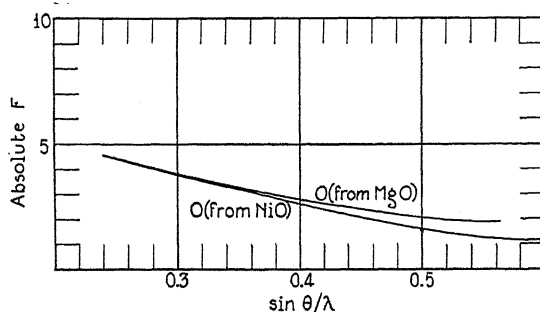


Fig. 3. A comparison of the oxygen F -curves for Mo $K\alpha$ rays as measured in MgO and NiO.

length as this critical range is approached. The greater diffraction of nickel for the nickel than for the copper $K\alpha$ line indicates that this downward trend is broken either some time before or when a wave-length characteristic of the scatterer is reached.

Further experiments are being made with various metals and with several wave-lengths which will bear upon these phenomena.

THE EFFECT OF HYPERFINE STRUCTURE DUE TO
NUCLEAR SPIN ON POLARIZATION OF
RESONANCE RADIATION

BY A. ELLETT

DEPARTMENT OF PHYSICS, UNIVERSITY OF IOWA

(Received February 6, 1930)

ABSTRACT

The existence of hyperfine structure must be taken into account in calculations of the polarization of resonance radiation based upon Heisenberg's extension of the principle of spectroscopic stability. Where the hyperfine structures are due to the existence of a nuclear moment their effect upon the polarization of resonance radiation may be calculated. If the nuclear moment of the thallium atom is $\frac{1}{2}$ (in units of $\hbar/2\pi$) as Schüler and Brück suppose the $\lambda\lambda 3776$ and 5350 lines should show no polarization, while $\lambda 2768$ should show 33.3 to 35.1 percent parallel and $\lambda 3530$ 41.8 to 48.8 percent perpendicular to the electric vector of a plane polarized exciting beam. Sodium resonance radiation excited by plane polarized D_1 and D_2 lines should show 33.3 percent polarization if the nuclear moment is $\frac{1}{2}$ and 16.6 percent if it is 1. The latter value agrees well with 16.3 observed by the writer, but observations on band spectra seem to indicate a higher nuclear moment, according to F. W. Loomis and R. S. Mulliken (Verbal communication to the writer.)

THE success of Back and Goudsmidt¹ in accounting for the hyperfine structure and Zeeman effect of the Bismuth arc spectrum by ascribing a mechanical and magnetic moment to the nucleus of the atom has led to attempts to explain hyperfine structure found in various other spectra in the same manner. Schüler and Brück² have shown that the hyperfine structures of the TII spectrum are probably due to a nuclear moment of $\frac{1}{2}$ (in units of $\hbar/2\pi$) and McLennan, McLay, and Crawford³ have shown that their observations on TI II lend support to this hypothesis. More recently Schüler and Brück⁴ have had some success in unraveling the hyperfine structures of Cd I by supposing that this spectrum is really two superimposed—one without hyperfine structure due to the cadmium isotopes of even atomic number which are supposed to have no nuclear moment, and another with structure due to a nuclear moment ascribed to the odd isotopes.⁵ The idea of nuclear spin has been used also by Jackson⁶ and by Hargreaves⁷ to account for Jackson's observations on the hyperfine structure of Cs I.

¹ Back and Goudsmidt, *Zeits. f. Physik* **43**, 321 (1927); **47**, 174 (1928). Pauli, *Naturwiss.* **12**, 741 (1924) suggested the idea of nuclear spin, but it was not successfully applied to the explanation of hyperfine structures until the paper of Back and Goudsmidt.

² Schüler and Brück, *Zeits. f. Physik* **55**, 575 (1929).

³ McLennan, McLay and Crawford, *Proc. R S A* **125**, 570 (1929).

⁴ Schüler and Brück, *Zeits. f. Physik* **56**, 291 (1929).

⁵ Goudsmidt, *Naturwiss.* **41**, 805 (1929).

⁶ Jackson, *Proc. Roy. Soc. A* **121**, 805 (1929).

⁷ Hargreaves, *Proc. Roy Soc. A* **124**, 568 (1929).

That the existence of hyperfine structures must be taken into account in any comparison of theory and experiment on the polarization of resonance radiation or of radiation excited by electron impact is obvious for the calculation of the polarization in the absence of a magnetic field, based on the idea of spectroscopic stability,⁸ involves the relative intensities of the Zeeman components of the line in *very weak* fields.

All previous calculations of the polarization of resonance radiation have been carried out without taking into account the existence of hyperfine structure. The Zeeman patterns and transition probabilities used have been those calculated for an atomic model without nuclear spin. These intensities are, at least to a first approximation, those which will obtain when the Paschen Back effect of the *hyperfine structure* is complete. There is no reason to expect that calculations made on this basis will show good agreement with experiment and in fact the agreement in general is poor. That hyperfine-structure is responsible for the 80 percent polarization of the $\lambda 2537$ A. U. resonance radiation of mercury has been shown experimentally by MacNair and the writer.⁹

It is not likely that the hyperfine structure of this line is to be accounted for on the hypothesis of nuclear spin alone but in the case of thallium and perhaps sodium the situation is different, and it is interesting to see whether taking into account the nuclear spin will lead to better agreement between theory and experiment.

The present calculations are based on the assumption that the coupling between i , J , and f is of the same character as that between L , S and J in alkali spectra. That is, it is supposed that i , the nuclear moment, combines vectorially with J , the net moment due to the remainder of the atom to give a resultant f in the same way that L and S combine to give a resultant J . This is the assumption used by Back and Goudsmidt¹ and by Schüler and Brück.^{2,4} The relative intensities of the hyperfine lines making up a hyperfine structure pattern (which itself appears as a 'line' save under high revolving power) may be calculated by formulas given by Hill¹⁰ and by Hargreaves.⁷ The relative intensities of the Zeeman components of the hyperfine lines may be calculated by the usual Kronig-Hönl formulas.¹¹ The polarization to be expected in any specified experiment is then calculated by making use of a consequence of the principle of spectroscopic stability first enunciated by Heisenberg.⁸ This extension of the principle of spectroscopic stability may be applied in any case where the experimental situation presents an axis of symmetry, and it states specifically that the introduction of a magnetic field parallel to this axis will not alter the relative probabilities of transitions giving rise to radiation polarized respectively parallel or perpendicular to this symmetry axis. The field is introduced merely to remove the degeneracy which exists in the absence of any field. That is, its purpose is to render

⁸ Bohr, *Naturwiss.* **12**, 1115 (1924); Heisenberg, *Zeits. f. Physik* **31**, 617 (1926).

⁹ MacNair and Ellett, *Phys. Rev.* **31**, 180 (1928).

¹⁰ Hill *Proc. Nat. Acad. Sci.* **15**, 779 (1929).

¹¹ Kronig, *Zeits. f. Physik* **31**, 885 (1925); Hönl, *Zeits. f. Physik* **31**, 340 (1925).

distinct the various magnetic energy levels which coalesce in the absence of a field so that the relative probabilities of transitions between these levels may be calculated. While this hypothetical field must be a strong field in the sense that the degeneracy is removed completely it must at the same time be a weak field so far as the production of Paschen Back effect of the hyperfine structure is concerned. The justification of such procedure then requires that the separation between the various hyperfine structure components of a line should be large compared to the intrinsic breadth of these components. This intrinsic breadth has nothing to do with the breadth of lines as observed in high resolving power spectroscopes; the latter is due to Doppler effect and pressure broadening (collisions) etc. We refer here to the inherent breadth of the line occasioned by imperfect definition of energy levels resulting from the finite life of stationary states.

To calculate the polarization of resonance radiation excited by plane polarized exciting light in the absence of a magnetic field we must imagine a field introduced, its direction being that of the symmetry axis (here the electric vector of the exciting light) so that we may calculate the relative numbers of transitions to the several Zeeman levels into which the upper states involved are split. Then having calculated the relative populations of these levels we determine the relative numbers of return transitions giving rise to radiation polarized parallel or perpendicular to the field. From this we get the polarization of the reemitted radiation and are assured that the value so calculated is that which will obtain when the field is removed.

THALLIUM

The thallium lines arise from transitions shown in the Grotrian diagram, Fig. 1a. Each of the levels shown is split into two when a nuclear moment of $\frac{1}{2}$ is taken into account, and these with the appropriate values of the fine quantum number f , and the permitted transitions are given in Figs. 1b and 2. The values of the transition probabilities are given by Hargreaves⁷—or

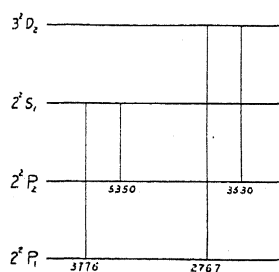


Fig. 1a. Grotrian diagram for thallium.

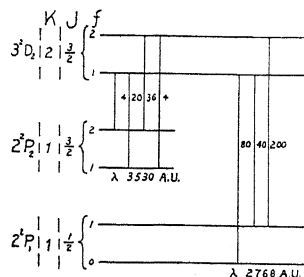


Fig. 1b. Permitted transitions in thallium.

they may be readily computed from the formulas given by Hill.⁹ From the figures it is evident that excitation by $\lambda 3776$ Å. U. will give rise to the emission of this line and also $\lambda 5350$ Å. U. while absorption of $\lambda 2768$ Å. U. excites $\lambda 5350$ Å. U. in addition to itself. In Fig. 2 are shown the Zeeman levels and

transitions involved in the emission of $\lambda\lambda 3776$ and 5350 A. U. Excitation by plane polarized light will excite atoms to those upper energy levels reached by those transitions of $\lambda 3776$ A. U. marked || (parallel) in the figure, the relative numbers of excited atoms in the various upper states depending upon the values of the parallel transitions reaching it and upon the intensity of the incident light of wave-length appropriate to produce these transitions. The question of relative intensities in the exciting radiation need not bother us here however, for no matter what the relative populations of the upper levels the reemitted radiation of each of the aggregates of hyperfine lines composing $\lambda\lambda 3776$ and 5350 A. U. will be unpolarized. That is to say, in each of these aggregates from *each* upper level the chance of returning by a perpen-

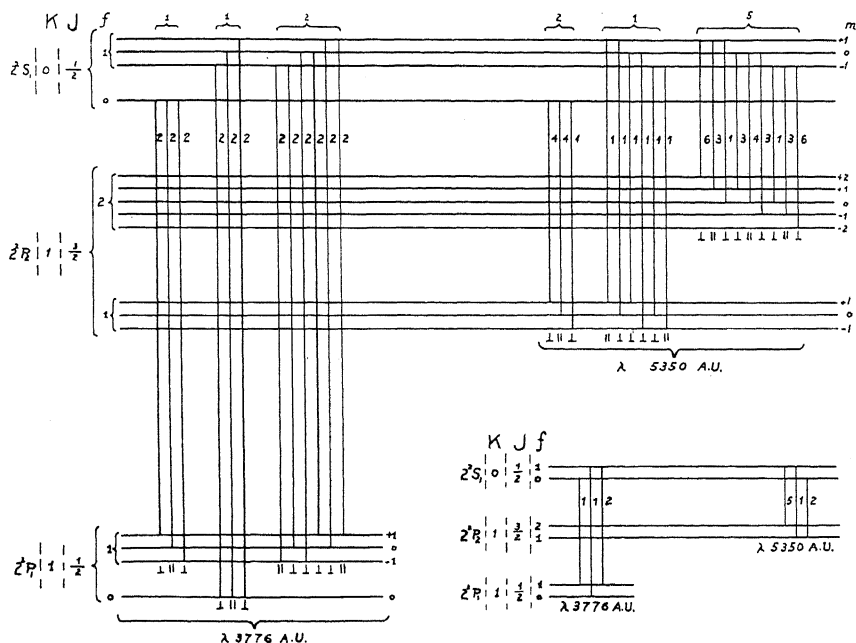


Fig. 2. Permitted transitions in thallium.

dicular transition is twice that of returning by a parallel transition. This leads to no net polarization either parallel or perpendicular to the electric vector of the exciting light—for parallel transitions produce such a distribution of the reemitted radiation as would be produced by a linear oscillator parallel to the electric vector of the exciting light (and also parallel to our imaginary magnetic field) while perpendicular transitions give rise to a distribution such as would be occasioned by a circular oscillator in a plane perpendicular to this.

Figure 3 shows the levels involved in absorption and emission of $\lambda\lambda 2768$ and 3530 A. U. Here the relative population of the upper levels is of some consequence and it becomes necessary to make some assumption regarding the distribution of intensity over the hyperfine structure components of

$\lambda 2768$ A. U. Two cases will be considered — A — that of uniform intensity over the entire absorption pattern, a situation perhaps realizable with a very hot source emitting greatly broadened lines, and — B — that of the theoretical intensity ratios,—such as might be realized with a source run at a temperature low enough so that Doppler broadening will cause no overlap of

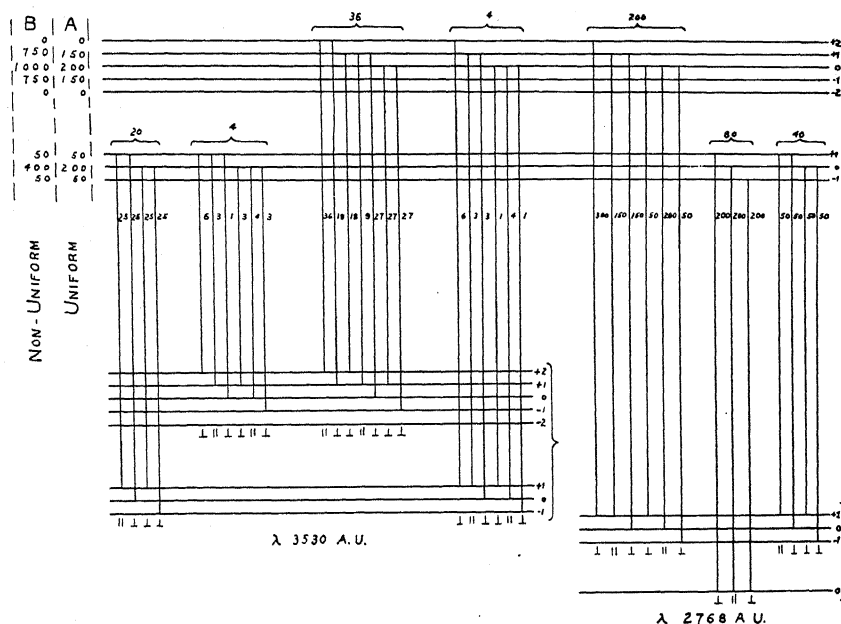


Fig. 3. Levels involved in absorption and emission of $\lambda\lambda 2768$ and 3530 .

hyperfine structure components, and with the density of thallium vapor low enough to eliminate self reversal. In column A of Fig. 3 are given the relative populations of the upper levels for case A and in column B for case B. Table I summarizes the results for these four lines.

TABLE I.

Nuclear moment	i	0	$1/2$		observed
			A	B	
2768	60		33.3	35.1	35 (500°C) 55 (470°C) ^{12a}
3530	75	⊥	41.8 ⊥	48.8 ⊥	30 ⊥ (500°C) 60 ⊥ (470°C) ^{12a}
3776	0		0	0	0 ^{12b}
5350	0		0	0	0 ^{12b}

Observed values^{12a,b} are given in column five, while the values to be expected for an atom without nuclear moment are given in column two.

More recently Schüler and Brück¹³ have advanced the hypothesis that in

^{12a} Gülke, Zeits. f. Physik 56, 524 (1929).

^{12b} Ellett, Nature 114, 931 (1924).

¹³ Schüler and Brück, Zeits. f. Physik 58, 735 (1929).

thallium as well as cadmium⁴ there is a difference of nuclear moments of the isotopes. The presence of an isotope having zero nuclear moment would result in higher values for the polarization, but the presence of such an isotope is not indicated by the spectroscopic data. An isotope with nuclear moment greater than one half probably would lead to even lower values of the expected polarization as a higher nuclear moment means an increased multiplicity of hyperfine structure levels. This might be offset by the changed intensity distribution in the exciting light, as it would be to some extent at least if the components of the hyperfine structure pattern responsible for the polarization should have the same wave-length in the patterns of both isotopes. Whether such a situation exists we cannot say without a more detailed spectroscopic analysis of the thallium hyperfine structures.

SODIUM

For a sodium atom without nuclear moment resonance radiation excited by the D_2 line alone should be 60 percent polarized. When excited by D_1 and D_2 together, using a source such that the effective intensity ratio of the two lines is 2:1 (the theoretical value) the predicted polarization is 50 percent. In 1925 the writer found¹⁴ 16.3 percent for the polarization of resonance radiation excited by both D lines, which corresponds to a value of 20.1 percent for D_2 alone not 24 percent as Datta states.¹⁵ Datta, exciting by means D_2 alone got values as high as 33 percent with the resonating vapor in equilibrium with metallic sodium at 115°C. He supposed that the lower value obtained by the writer was due to higher vapor pressure. This however is not the explanation, for the vapor pressure was actually less than the lowest at which Datta made observations; 95°C and $7.4 \cdot 10^{-8}$ mm. Hg¹⁶ as against his values of 115°C and $4.5 \cdot 10^{-7}$ mm Hg. More recently the experiment has been repeated with a somewhat more powerful source and vapor pressures as low as $1.9 \cdot 10^{-8}$ mm Hg (80°C). The polarization was again found to be 16.3 percent. The reason for the difference between this value and Datta's is not obvious to the writer.

Schüler¹⁷ has observed hyperfine structure of the D lines, and as the hyperfine structure observed in caesium appears to be due to a nuclear moment, I have calculated the polarization to be expected in D line resonance radiation on the assumption of various nuclear moments. In every case the value is less than it is for the atom without nuclear moment. As the sodium hyperfine structure is on a very small scale it has been assumed that the intensity of the exciting light is uniform across the hyperfine structure pattern. This amounts to supposing that the separations in the pattern are small compared to the Doppler line breadth at the temperature of the source. The temperature of the glass walls of the source used by the writer was about 750°C and

¹⁴ Ellett, Jour. Opt. Soc. Am. 10, 427 (1925).

¹⁵ Datta, Zeits. f. Physik, 37, 625 (1926).

¹⁶ Vapor pressures extrapolated from data of Rodebush and De Vries, Jour. Am. Chem. Soc. 47, 2488 (1925).

¹⁷ Schüler, Naturwiss. 16, 512 (1928).

the emission lines have a corresponding breadth, as I have shown by experiments on polarization of resonance radiation in strong magnetic fields.¹⁸

The results of these calculations are summarized in Table II.

TABLE II.

i	0	1/2	1	obs.
D_2	60	40.54	20.5	33 ¹⁴
D_1	0	0	00	00
D_1+D_2	50	33.3	16.6	16.3 ³

In this connection it should be mentioned that observations of alternating intensities in sodium band spectra indicate a quite large nuclear moment,¹⁸ probably greater than one, which probably would lead to even lower values for the polarization.

In conclusion it may be said the presence of hyperfine structure due to nuclear spin cannot be neglected in calculating the polarization of resonance radiation and radiation excited by electron impact. Taking account of such hyperfine structures in certain thallium and sodium lines leads to lower values of the predicted polarization and consequently better agreement between theory and experiment. Experiments on the polarization of resonance radiation may yield the data required for the solution of hyperfine structure problems in cases where direct spectroscopic analysis is impossible, as in the case of overlapping of certain components in the hyperfine structure patterns because of Doppler breadth of the lines.

¹⁸ Ellett, Phys. Rev. 29, 904 (1927).

¹⁸ F. W. Loomis and R. S. Mulliken agree from inspection of Loomis spectrograms of Na₂ bands that i is probably 3/2 or greater. (Verbal statement to the writer). See also Loomis and Wood, Phys. Rev. 32, 223 (1928).

SPECTROSCOPIC EVIDENCE OF TWO TYPES
OF AMMONIA MOLECULE

BY JOSEPH W. ELLIS

PHYSICS DEPARTMENT, UNIVERSITY OF CALIFORNIA AT LOS ANGELES

(Received February 3, 1930)

ABSTRACT

A two-fold difference exists in the equations expressing the anharmonic frequencies arising from vibratory energy changes in ammonia molecules in solution and in gaseous form. The greater coefficient of the n^2 term in the former case, indicating a more rapid approach of the energy terms toward confluence, is assumed to arise from the proximity of the molecules of the solvent. The presence of a constant term of appreciable magnitude in the solution equation is interpreted as measuring the energy required to change the molecule from an α form to a β form of greater potential energy. Chemical support for this latter interpretation is sought in some earlier measurements by Baly and Duncan on the difference in the decomposition rates of ammonia both after immediate evaporation from the liquid and after it had stood for a considerable length of time.

It becomes easier to interpret the Raman spectrum of liquid ammonia, ammonia in aqueous solution and a liquid organic derivative of ammonia, aniline, when the existence of a constant in the infra-red formula is recognized.

BADGER and Mecke¹ and the author² have independently come to the conclusion that the ammonia molecule has a fundamental absorption wavelength near 3μ . This conclusion has been arrived at in each instance by the discovery that there is an anharmonic series of absorption bands with members in the infra-red spectrum below 3μ and in the visible spectrum. The former investigators have photographed the fourth and fifth members of this series in the visible region, using long tubes of gaseous ammonia and a concave diffraction grating to secure high dispersion and resolving power. Out of the complex structure caused by rotational quantum changes they have been able to pick the lines produced by vibrational energy changes alone. They have sought the second and third members in the thermal measurements of Robertson and Fox³ and have used the frequency values of the centers of these unresolved bands. For the first member they have chosen the frequency of maximum absorption in the unresolved Q branch in the record given by Barker.⁴ They have shown that these five frequencies can be fairly well fitted to the following anharmonic formula:

$$\nu_n = 3396n - 60n^2. \quad (1)$$

The author² has used a quartz prism spectrograph to photograph the structureless absorption bands corresponding to the fourth and fifth series

¹ Badger and Mecke, *Zeits. f. Phys. Chem. B* 5, 333 (1929).

² Ellis, *Journal Franklin Inst.* 208, 507 (1929).

³ Robertson and Fox, *Proc. Roy. Soc. A* 120, 128 (1928).

⁴ Barker, *Phys. Rev.* 33, 684 (1929).

members caused by ammonia in aqueous solution. In a similar manner he has also found the weak sixth member in the visible green spectrum. Records of the second and third members have been secured by means of a registering infra-red spectrograph equipped with a thermopile. These latter he has shown retain their positions when carbon tetrachloride replaces water as a solvent. No data for the solution were then available for the first member. For reasons explained in the above reference a wave-length value of 2.916μ was assigned to the initial member of the series.

Although the former reason for selecting this value does not now seem to be well founded, the wave-length value chosen has been shown to be at least approximately correct. To show this a Hilger D 35 infra-red spectrometer equipped with a rock-salt prism was used. A 1 cm cell of ammonia in carbon tetrachloride solution was placed before the slit of the instrument and observations were made on the 3μ region. The difficulty experienced by Robertson and Fox³, namely that the wave-length determination of an absorption maximum is influenced by the variations in the refractive index of the rock-salt prism caused by temperature changes, was experienced here. When, for example, the wave-drum was set for a correct reading with the yellow sodium lines filling the thermopile slit and the instrument allowed to stand for a while with the lamp source radiating near by, the absorption band produced by a 1 mm cell of benzene shifted from its true position of 3.27μ to a value in excess of 3.4μ . Consequently, just prior to a determination of the position of the ammonia band, the reflecting mirror near the prism was so adjusted that when the galvanometer showed a minimum deflection, indicating that the maximum of absorption due to the benzene had been reached, the wave-drum indicated 3.27μ . With this procedure it was found that the ammonia solution band was not at 3.0μ , the position occupied by the gaseous ammonia band, but at 2.9μ .

The frequencies of the six members of the series observed in solution have been shown² accurately to fit the formula:

$$\nu_n = 97 + 3400n - 70n^2. \quad (2)$$

Now in spite of the assertion by Mecke⁵ that there is a good agreement between the bands observed in gaseous ammonia and in solution, a closer examination reveals a significant difference. This difference is two-fold and is revealed in Eq. (2) by the presence of the constant term 97 and by the larger coefficient of the n^2 term, 70 as compared with 60 in Eq. (1). The presence of the constant term arises from the origination of the solution series at 2.9μ rather than at 3μ . The greater coefficient of the quadratic term explains why in the higher series members the wave-lengths of the solution bands become greater than the corresponding bands in the gas. This earlier confluence of the solution series must arise from a more rapid diminution of the force coefficient of the vibrator caused by the proximity of surrounding molecules. In general, however, a less rapid approach of the series members toward confluence would be expected, because this would

⁵ Mecke, Trans. Faraday Soc. 25, 942 (1929).

mean a lesser value for the heat of dissociation of the vibrator. And heats of dissociation evaluated from data obtained from the liquid state should be less than heats of dissociation evaluated from the gaseous state by an amount approximately equal to the heat of vaporization.

Fig. 1 is included to show the difference in the locations of the fifth members of the series in solution and in the gas. The figure shows the solution band approximately symmetrically located between two neon comparison lines, 0.6507μ and 0.6533μ . It has been given the value of 0.652μ . The value given by Mecke and Badger for the analogous gaseous band is 0.647μ , which lies completely outside of the region of absorption in the solution.

The constant term in Eq. (2) has been interpreted² as representing the amount of energy, in wave-number units, required to change the molecule in solution over to a new form before vibration takes place. A chemical investigation carried out a number of years ago by Baly and Duncan⁶ seems to have some bearing upon this subject. These authors showed that

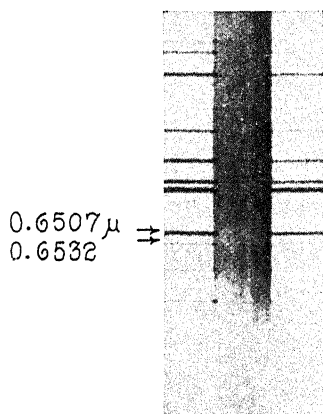


Fig. 1. The 0.652μ absorption band of ammonia in aqueous solution.

ammonia gas which had been slowly evaporated from the liquid or which had stood for some time in contact with the liquid had a certain constant rate of decomposition. The decomposition was effected by thermal energy supplied at a known rate by a heated platinum wire and the decomposition rate was determined from pressure changes in the gas. But when the experiment was repeated upon gas which had been suddenly evaporated from the liquid they found that the decomposition rate was much less than in the previous instance. Furthermore, this rate gradually increased with time. These facts led the investigators to postulate two forms of ammonia molecules, which they designated inactive and active forms, but which we shall designate as α and β forms respectively for reasons which will be apparent presently. The molecules are in the α form when the substance is in the liquid state or in the gaseous state immediately following sudden vaporization. The β form makes up predominantly, or exclusively, the gas which has stood

⁶ Baly and Duncan, Jour. Chem. Soc. **121**, 1008 (1922).

for a considerable length of time. According to these investigators, the decomposition rate of inactive (α) ammonia is lessened because of the use of a portion of the energy supplied by the wire to activate the molecules.

Tronstad⁷ has pointed out that the experimental procedure of Baly and Duncan was similar to that of Bonhoeffer and Harteck in their study of ortho and para hydrogen. He furthermore has stated that Baly and Duncan have not proved the existence of two chemically different types of ammonia molecules, but that their results can be explained equally well on the basis of two forms with different heat conductivities and specific heats. The two types would then be analogous respectively to para and ortho hydrogen.

From considerations of the experimental results of Baly and Duncan it may be concluded that the 97 cm^{-1} term of Eq. (2) represents an energy of "activation." (The assumption is made here that ammonia in solution exists in the α state.) However, in the light of Tronstad's criticism it must be recognized that this activating process may be one in which geometrical and physical changes occur rather than chemical changes.

From the quantitative measurements of Baly and Duncan it would seem that the modified interpretation of Tronstad is the more tenable. Baly and Duncan have shown that in some instances the amount of decomposition is doubled when the β form is used in place of the α form. Under their interpretation then half of the energy supplied by the hot platinum wire must go into energy of activation. Now the energy required to decompose one molecule of NH_3 into NH_2 and H requires some $30,000\text{--}40,000\text{ cm}^{-1}$ which is 300 or 400 times as great as the 97 cm^{-1} energy of activation. But Baly and Duncan state that from 0.5 to 4 percent of the molecules are decomposed during the 20 seconds of observation; and under the assumption that this percentage of molecules decomposes, say into NH_2 and H, there would be required many more molecules than the total number available, to take up the energy of activation.

Following Tronstad's assumption of a greater heat conductivity characterizing the α molecules, the difficulty met with in the discussion of the above paragraph does not enter, for more of the heat than previously could escape to the surrounding constant temperature water bath.

It should be pointed out that Barker,⁸ following Hund, has postulated two forms of ammonia molecule in his interpretation of the doubleness of another fundamental infra-red band of ammonia at 10.5μ . The difference in potential energy between the two types, however, is only 27 cm^{-1} . The approximate equality in intensity of the two components of this double band lead to the conclusion that the two kinds of molecules postulated must exist in the gaseous state with approximately equal abundance. Mecke⁹ also believes that his visible bands which are harmonics of the 3μ fundamental also exhibit a double structure, one set being much weaker than the other. But the frequency difference which he finds is even lower than Barker's 27 cm^{-1} .

⁷ Tronstad, *Zeits. f. Phys. Chem. B* 5, 333 (1929).

⁸ Barker, *Phys. Rev.* 33, 684 (1929).

⁹ Mecke, *Phys. Zeits.* 30, 907 (1929).

The Raman spectrum of ammonia exhibits one, two or three lines corresponding to the 3μ region, the exact locations and number of components depending upon the phase in which the substance exists and upon the individual investigators. Wood¹⁰ and Dickinson, Dillon and Rasetti¹¹ have shown that the Raman frequency corresponding to a rotationless vibrational energy change in the gaseous molecule is 3330 and 3334 cm^{-1} respectively, in good agreement with the 3336 cm^{-1} value obtained by putting n equal to 1 in Eq. (1). The latter investigators¹¹ have shown that liquid ammonia yields two frequencies, 3298 and 3214 cm^{-1} . Daure,¹² however, found in addition to these two frequencies, a third one at 3380 cm^{-1} . His record shows that all three components have approximately equal intensities.

Carrelli, Pringsheim and Rosen¹³ found two frequencies, 3385 and 3312 cm^{-1} , when they used an aqueous solution of ammonia. These authors recognized, however, the possibility that one of these components may have been due to the water solvent.

If the three components found by Daure in the liquid all originate in ammonia molecules, they might be explained by assuming the existence of both the α and β forms of molecule in the liquid state. The components corresponding to greatest, intermediate and least frequency changes could then be correlated with the following energy changes respectively:— α , $0 \rightarrow \beta$, 1; α , $0 \rightarrow \alpha$, 1 or β , $0 \rightarrow \beta$, 1; and β , $0 \rightarrow \alpha$, 1. Here α , 0 designates a vibrationless α type of molecule, β , 1 a β type of molecule vibrating in quantum state 1, etc. The 80 and 90 cm^{-1} frequency differences between the components are comparable to the 97 cm^{-1} term of Eq. (2). However, the failure of Dickinson, Dillon and Rasetti completely to corroborate the findings of Daure raises the question as to whether impurities may have been present in the latter's experiment. Water would be the most likely impurity and water yields at least two Raman bands with frequencies comparable to those given.

Spectroscopically, aniline, $\text{C}_6\text{H}_5\cdot\text{NH}_2$, which is a derivative of ammonia, behaves in a manner similar to its parent substance. The writer has justified his earlier correction¹⁴ to Bell's¹⁵ 2.8μ value for the fundamental N-H band, for he has studied the 3μ region for aniline with the Hilger D35 infra-red spectrometer and has found the band to have its maximum of absorption at 2.9μ . There is a remarkably close agreement between the members of the anharmonic series originating at 2.9μ for aniline and for ammonia in solution. Consequently, a constant term must be included in the aniline series, a fact which has hitherto¹⁴ been overlooked.

Again, the Raman effect in aniline according to Bonino¹⁶ shows a single frequency shift corresponding to a 3.0μ wave-length, rather than to 2.9μ . Thus once more the difference between the Raman frequency and the fundamental infra-red frequency is of the order of 97 cm^{-1} .

¹⁰ Wood, Phil. Mag. **7**, 774 (1929).

¹¹ Dickinson, Dillon and Rasetti, Phys. Rev. **34**, 582 (1929).

¹² Daure, Thesis, Masson et Cie, Paris, (1929).

¹³ Carrelli, Pringsheim and Rosen, Zeits. f. Phys. Chem. B **5**, 333 (1929).

¹⁴ Ellis, Phys. Rev. **33**, 27 (1929).

¹⁵ Bell, Jour. Amer. Chem. Soc. **47**, 2192 (1925).

¹⁶ Bonino, Gazz. chim. Ital. **59**, 668 (1929).

THE AFTERGLOW IN AIR

BY JOSEPH KAPLAN

UNIVERSITY OF CALIFORNIA AT LOS ANGELES

(Received January 6, 1930)

ABSTRACT

It was observed that on passing a weak discharge through the air glow the β bands of nitric oxide were very strongly excited. These bands possess several very interesting properties. They correspond to a transition from the B to the X level of the molecule and the transition B_0-X_0 is very improbable because of the large difference in nuclear separation. These bands have never been reported as being intense in electric discharges and they have been obtained with considerable intensity only in active nitrogen. This present experiment is therefore the first one in which these bands have been observed with great intensity in an electric discharge. The β bands, as observed in the present experiments, correspond to transitions only from the B_0 to the various X vibrational levels, whereas in the afterglow of active nitrogen they correspond to transitions from several B levels to the various X levels. This difference indicates that there are at least two possible methods for exciting these unusual bands and they have been discussed in brief by Kinsey and the author. They are excitation by recombination, and excitation by collisions of the second kind.

INTRODUCTION

THE problem of afterglows has been attacked in a great many different ways in recent years. Of the various afterglows that have been studied the one receiving the most attention has been the afterglow in active nitrogen. The reason for the widespread interest in active nitrogen is readily understood when one considers the many interesting phenomena that have been observed in connection with it. These extend from the field of excitation of spectra by active nitrogen to that of surface chemistry. And because of the large range of action of active nitrogen it has been interesting both as a tool and as a problem in itself. In the present communication it is proposed to discuss some aspects of a much less studied and apparently far less interesting afterglow. The afterglow referred to is the one that is observed when almost any type of discharge is passed through air at pressures around 0.5 mm.

This afterglow was first observed by E. P. Lewis¹ and also studied by R. J. Strutt² during those years in which he made many very valuable contributions to the problem of afterglows. The spectrum of the air glow has not been studied to any great extent and there are no published photographs of it. Herzberg,³ and independently the author,⁴ have photographed the spectrum of the glow and found it to be continuous. Herzberg has reported a

¹ E. P. Lewis, *Ann. d. Physik* (4) 2, 459 (1900).

² R. J. Strutt, *Proc. Phys. Soc.* 23, 66 (1911).

³ Herzberg, *Zeits. f. Physik* 46, 878 (1927).

⁴ Kaplan, *Proc. Nat. Acad. Sciences* 14, 258 (1928).

maximum in the red and a decrease of intensity toward the violet. In addition to the continuous spectrum in the visible, the writer has reported the excitation of the OH band at 3064Å. This band was undoubtedly excited by the active species in the afterglow, but as yet there is no basis for definitely discussing the process of excitation, since no experimental or theoretical work regarding the energy of the active species has appeared. Part of the purpose of the present work was to begin experiments designed for the purpose of studying in more detail than has been done, the nature of this afterglow.

Recently, Herzberg³ and others have revived interest in the air glow by applying to its study a few of the methods that had been used in connection with the nitrogen afterglow. Herzberg has studied the effect of varying the relative amounts of oxygen and nitrogen in the discharge in which the afterglow was produced and also the influence of the condition of the walls of the containing-vessel. Other papers by Majewska,⁵ Majewska and Witold⁶ and Bernard Lewis⁷ report work on the effect of surfaces, the rate of decay of the afterglow and on the mutual effects of nitrogen and oxygen on their afterglows. As the last title suggests, the continuous afterglow in air and in other mixtures of oxygen and nitrogen, has been ascribed to oxygen and several recent writers have suggested that it may simply be a recombination spectrum of atomic oxygen. It is not the purpose of this paper to discuss this point and it will be left for another communication. There is however no conclusive evidence in favor of the recombination hypothesis although the continuous spectrum makes that hypothesis a tempting one.

Another method of attack has recently been applied to the air afterglow by the author. The method, briefly, consists of allowing the active material to pass from the discharge in which it was formed into another discharge through which a very feeble current from a small spark coil is passing. The spectrum in the auxiliary tube is studied and the effect of the active material is noted. Recently Bay and Steiner⁸ have applied this method to active hydrogen, active nitrogen and to a modification of oxygen to which they refer as active oxygen. They used external electrodes and electrodeless ring discharges whereas in the present experiments internal electrodes were used. The method was first used by the author in an attempt to excite atomic nitrogen lines in active nitrogen and it yielded some very interesting results. In the following a brief account will be given of some of the results of the present work.

EXPERIMENTAL METHOD

The afterglow was produced by passing an uncondensed discharge from a 1 kw Thordarsson transformer, giving 20,000 volts in the secondary, through various mixtures of oxygen and nitrogen. The pressure of the gas in the discharge was 0.5 mm and this has been found to be the best pressure

⁵ Majewska, *Zeits. f. Physik* **50**, 372 (1928).

⁶ Majewska and Witold, *Zeits. f. Physik* **48**, 137 (1928).

⁷ B. Lewis, *J.A.C.S.* **51**, 654 (1929); B. Lewis, *J.A.C.S.* **51**, 665 (1929).

⁸ Bay and Steiner, *Zeits. f. Phys. Chemie* **3**, 149 (1929).

for the production of the afterglow. It is interesting to note that 0.5 mm is also about the optimum pressure for the production of atomic hydrogen and active nitrogen. The active material was allowed to pass into another discharge tube, having internal electrodes, and a weak discharge from a small spark coil was allowed to pass through this tube. The spectrum of this discharge was photographed on a Hilger E2 spectrograph and also on a small Gaertner instrument. The auxiliary discharge was sufficiently weak as to make it necessary to expose for about ten hours on the Hilger instrument in order to obtain reasonably intense plates. It is apparently the weakness of the auxiliary discharge that makes the method a valuable one in the study of active materials from discharges.

EXPERIMENTAL RESULTS

Several interesting results were obtained but the only one that is to be here discussed is the excitation of the β bands of nitric oxide. A preliminary note on these results was published in the letter column of the *Physical Review*.⁹ The excitation of these bands with considerable intensity was certainly the most striking effect of the introduction of the active material into the weak discharge. The β bands are of special interest first because they have been obtained with considerable intensity only in the nitrogen afterglow and secondly, because of the large change in moment of inertia between the two levels that are involved in the excitation of these bands.

The β bands were first obtained by E. P. Lewis¹⁰ in active nitrogen. The present experiments are the first ones in which these bands have been excited with great intensity in an electrical discharge. Furthermore, these seem to be the first spectroscopic results, other than the continuous spectrum that was discussed earlier, that have been gotten from the air glow. In what is to follow, the origin of the β bands will be discussed and several questions of interest will be raised.

DISCUSSION

The β bands correspond to the transition from the B level to the X electronic level of the molecule. The X level is the normal level and both the B and X levels are now thought to be $^2\Pi$ levels. Although there will be no occasion in this discussion to refer to the electronic configuration of the two levels involved the older method of identifying the two levels will not be used and they will be referred to as the $^2\Pi$ levels. It is proposed here also to use v instead of n for the vibrational quantum number in accordance with a suggestion contained in a letter¹¹ on band spectrum notation that was recently circulated.

The values of ω_0 for the two $^2\Pi$ levels are 1030 cm^{-1} for the upper one and 1892 cm^{-1} for the lower level. Consequently one should expect an intensity distribution among the bands that is typical of a molecule whose moments

⁹ Kaplan, *Phys. Rev.* **34**, 165 (1929).

¹⁰ E. P. Lewis, *Phys. Rev.* (1) **18**, 125 (1904); *Astrophys. J.* **20**, 49 (1904).

¹¹ O. W. Richardson, *Trans. Farad. Soc.* **25**, 628 (1928).

of inertia in the upper and lower states differ greatly. Barton, Jenkins and Mulliken¹² have studied the intensity distribution among the β bands that were excited in active nitrogen, and they have found that the principal features of the intensity distribution agree with the predictions of the Condon theory. They have also noted some interesting and definite discrepancies between theory and experiment and the occasion will arise later in the paper for mentioning them.

In the present experiments the most intense β bands correspond to the $v'=0$ progression. Transitions from higher ${}^2\Pi$ levels are either very weak or entirely absent in the discharge. Birge¹³ has pointed out that the $v'=0$ progression in the β bands, as excited by active nitrogen, was very intense relative to the higher progression. In the present experiments they seem to be relatively even more intense than they are in active nitrogen. The similarity between the two methods of excitation as indicated by the above point may be interpreted as showing that the mode of excitation in the present experiments may be exactly the same as that occurring in the afterglow of nitrogen. It is not proposed to discuss here the relationship between the excitation of the β bands and the nature of the afterglow. That will be discussed elsewhere. The present experiments have suggested several questions as to the possible ways in which the β bands can be excited and it is those questions that will be briefly discussed here.

The absence of the β bands from the spectra of ordinary discharges through mixtures of nitrogen and oxygen or through nitric oxide, is of course readily accounted for by the Condon theory and is due to the large change in moment of inertia during the transition $B^2\Pi^0 \rightarrow X^2\Pi^0$. The most probable transition from the $X^2\Pi^0$ level by electron impact would probably result in dissociation of the molecule. Now according to ideas advanced by R. J. Strutt, NO_2 is formed in the air afterglow by the oxidation of NO by ozone. It is possible therefore that highly vibrating nitric oxide molecules are formed by the decomposition of NO_2 in the weak discharge and it is these molecules that are excited by electron impact to yield molecules in the $B^2\Pi^0$ level. It is difficult of course to see just why this level should be favored both by this process and by the one in active nitrogen. It is also difficult to reconcile the above suggestion with the absence or weakness of other than the $v'=0$ progressions.

Before calling attention to two other possible modes of excitation another unique property of the β bands will be mentioned. Barton, Jenkins and Mulliken have called particular attention to the fact that progressions higher than $v'=4$ are absent from the β bands excited in active nitrogen. This is especially striking since in absorption bands up to $v'=5$ have been observed. The above mentioned fact may give the clue to the explanation of the excitation of these bands in both afterglows.

The energy necessary for the excitation of the ${}^2\Pi^0$ level from the normal state of the molecule is 5.65 volts. The energy of recombination of NO is

¹² Barton, Jenkins and Mulliken, *Phys. Rev.* **30**, 175 (1929).

¹³ R. T. Birge, *Molecular Spectra in Gases*, p. 141.

now thought to be about 6.6 volts.¹⁴ Consequently it is possible that the energy of recombination of the nitrogen and oxygen atoms is used to excite the β bands. There are several ways in which this energy transfer can be made and a detailed discussion of these possibilities will be given elsewhere. The interesting point to note here is that when it is necessary to excite a molecular level, in which the separation of the two atoms is much larger than in the initial level, there are ways, in which that can be done, that do not involve a transition from the normal to the excited level. In the present case instead of an increase in separation between the nitrogen and oxygen atoms, as would occur if the excitation were from $X^2\Pi^0 \rightarrow B^2\Pi^0$, there is a decrease in separation arising from the recombination of the two atoms. This may account for both the absence of progressions higher than $v'=4$ in the case of active nitrogen, and for the unusual intensity of the $v'=0$ progression in the present experiments as well as in active nitrogen.

One other method remains and attention has already been called to this in an earlier note by Kinsey¹⁵ and the writer. This method is based on the hypothesis that the excitation of bands by collisions of the second kind does not necessarily obey the Condon theory and that large changes in the separation of two atoms can arise when the excitation is brought about in this way. The presence of metastable molecules in active nitrogen makes the above postulate a plausible one, although the energy of the metastable molecules is such as to make difficult the immediate explanation of the several peculiarities in the bands to which attention has been called. There are hardly enough data on the excitation of bands by collisions of the second kind to warrant any hypotheses, but the possibilities are interesting.

¹⁴ Birge, Trans. Farad. Soc. 25, 707 (1929).

¹⁵ Kinsey and Kaplan, Phys. Rev. 33, 114 (1929).

THE INFRA-RED ABSORPTION OF SOME ORGANIC LIQUIDS

BY E. K. PLYLER AND THEODORE BURDINE
UNIVERSITY OF NORTH CAROLINA

(Received February 8, 1930)

ABSTRACT

The infra-red absorption spectra of fourteen organic compounds, including seven alcohols and seven miscellaneous compounds, have been studied in the region from 1μ to 7.5μ . The bands in the region from 1μ to 3μ have been classified as overtones or combination bands of the assumed fundamental bands for the alcohols at about 3.00μ , 3.4μ , 6.8μ , and 9.8μ . By the use of Sappenfield's work for the region from 1μ to 2μ and that of Weniger from 7.5μ to 10μ and the present work a fairly complete idea of the infra-red absorption spectra of the alcohols has been obtained. The intensity relations have been discussed briefly and it was shown that they were in general in accordance with combinations attributed to the different bands. The bands of the miscellaneous organic compounds have been classified, but all the bands have not been included as only the fundamentals at 3.4μ and 6.8μ were used. A probable reason for the similarity of the infra-red spectra of many organic compounds in the region from 1μ to 3μ has been suggested.

INTRODUCTION

AN EXPERIMENTAL study has been made of the infra-red absorption bands of fourteen organic liquids in the region from 1μ to 8μ . The materials used were methyl, ethyl, propyl, butyl, iso-propyl, iso-amyl, and iso-butyl alcohols and m-nitrotoluene, o-nitrotoluene, methyl sulphate, ethyl sulphate, nitromethane, nitrobenzene and ethyl acetoacetate. The purpose of this investigation was to see what similarities existed in the near infra-red absorption bands of some organic liquids of quite different type. Also, it was hoped that several of the more intense bands of each material could be classified as combination bands of the fundamentals.

The infra-red absorption spectra of nearly all the alcohols studied in this work have already been investigated by Weniger¹ in the region from 1μ to 14μ and by Sappenfield² from 1μ to 2μ . The work of Weniger gives one a good representation of the bands to 14μ , but as he used a very thin cell for the entire region many of the smaller bands were not observed. Sappenfield was able, by using cells of different thickness and spectrometer of high resolution, to detect many bands in the region from 1μ to 2μ which had not previously been observed. He classified some of the bands observed by him on the basis of the work of Gapon.³ It was believed that a modification of his classification would be more in accordance with intensity relations. It was thought that it would be of value to extend the experimental observations under high

¹ Weniger, Phys. Rev. **31**, 388 (1910).

² Sappenfield, Phys. Rev. **33**, 37 (1929).

³ Gapon, Zeit. f. Physik **44**, 600 (1927).

resolution beyond the region of 2μ and to classify the bands found by Sappenheim with those of this region.

EXPERIMENTAL PROCEDURE

The apparatus and the method of measurement were essentially the same as used by the writer in a previous investigation.⁴ It was found necessary to use cells of different thickness in order to observe the weaker bands. These cell thicknesses and the effective slit widths are tabulated in Table 1. The

TABLE I. *The cell thicknesses and the effective slit-width at the thermopile for the different parts of the region studied.*

Region	Thickness of cell	Prism used	Effective slit-width
$1.00\mu - 1.25\mu$	1.50 mm	Quartz	0.0060μ
$1.25\mu - 2.00\mu$.7 mm		$.0075\mu$
$2.00\mu - 2.80\mu$.4 mm		$.0150\mu$
$2.80\mu - 3.50\mu$.01 to .001		$.0150\mu$
$5.50\mu - 7.50\mu$.01	Rock-salt	$.155\mu$

thickness of the cells in the region from 2.80μ to 3.50μ and from 5.50μ to 7.50μ varied somewhat for each material studied. For example, in the cases of the alcohols it was necessary to have cells about 0.001 mm in order that 20 percent of the incident beam might be transmitted. These thin cells were made by placing a small drop of the liquid on a microscopic cover glass and then placing another cover glass over this. The cell formed in this manner was then pressed very thin and glued around the edges. An approximate value of the thickness was obtained by observing the change in the interference fringes when the cover glasses were pressed together at the center of the cell. The thicker cells were made by separating glass or rock-salt windows with lead foil or sheet lead. All the materials used in this study except two of the alcohols, which were prepared in the chemical laboratory, were obtained from the Eastman Kodak Laboratories.

RESULTS AND DISCUSSION

The experimental results are represented in Figs. 1 to 6 and a list of the observed bands is given in Table II. The region from 2.8μ to 3.6μ was measured with the rock-salt prism in Fig. 3 and with the quartz prism in Fig. 2. Due to the great effective slit width in the region of 3μ for the rock-salt prism, it was not possible to resolve the bands at 3.00μ and 3.40μ . For the alcohols the region from 3.6μ to 5μ has been included in Fig. 3, but it does not contain any intense bands. Also, any bands of much intensity were not observed for the other materials in this region and results obtained were not included in Fig. 6. The relations found to exist between some of the bands of the alcohols are shown in Table III. The combinations given were calculated on the basis that the intense bands observed at 3.00μ , called ν_1^1 , 3.40μ , ν_1 , 6.90μ , ν_2 , and

⁴ Plyler and Steele, Phys. Rev. 34, 599 (1929).

TABLE II. List of observed bands.

Methyl	Ethyl	Propyl	Alcohols Butyl	Iso-propyl	Iso-amyl	Iso-butyl
2.06 μ	2.03 μ	2.07 μ	2.07 μ	2.06 μ	2.05 μ	2.05 μ
2.27	2.23	2.16	2.18	2.28	2.27	2.10
2.46	2.42	2.27	2.30	2.42	2.39	2.25
2.56	2.54	2.43	2.44	2.54	2.56	2.38
2.92	3.01	2.62	2.60	3.00	3.01	2.50
3.02	3.39	3.01	3.00	3.38	3.42	2.99
3.29	4.31	3.43	3.43	4.22	4.61	3.41
3.42	5.00	4.55	3.22	4.44	5.16	4.52
4.22	5.75	4.91	4.67	5.72	5.69	4.78
4.70	6.11	5.18	5.07	5.98	5.92	5.18
5.42	6.62	5.81	5.93	6.10	6.80	5.86
5.84	6.89	6.06	6.13	6.71	6.96	6.86
6.14	7.04	6.67	6.83	6.91	7.14	7.00
6.73	7.40	6.81	6.95	7.24	7.79	7.88
6.99	7.81	7.91	7.98			
7.38						
7.82						

M-nitro- toluene	O-nitro- toluene	Methyl sulphate	Nitro- methane	Ethyl sulphate	Nitro- benzene	Ethyl acetoacetate
1.15 μ	1.15 μ	1.15 μ	1.12 μ	1.17 μ	1.13 μ	1.17 μ
1.39	1.40	1.38	1.37	1.39	1.29	1.40
1.68	1.67	1.67	1.68	1.71	1.42	1.65
1.98	2.00	1.86	1.82	1.91	1.63	1.92
2.04	2.30	1.97	1.92	2.05	1.80	1.99
2.31	2.41	2.06	2.26	2.30	1.90	2.29
2.47	2.54	2.24	2.41	2.43	2.15	2.40
2.55	3.28	2.37	2.59	3.37	2.44	2.62
3.28	3.39	2.60	3.29	7.20	3.26	3.39
3.42	6.68	3.40	3.41		3.43	5.82
6.57	7.46	7.05	6.37		6.56	7.10
7.40		7.20	7.13		7.36	

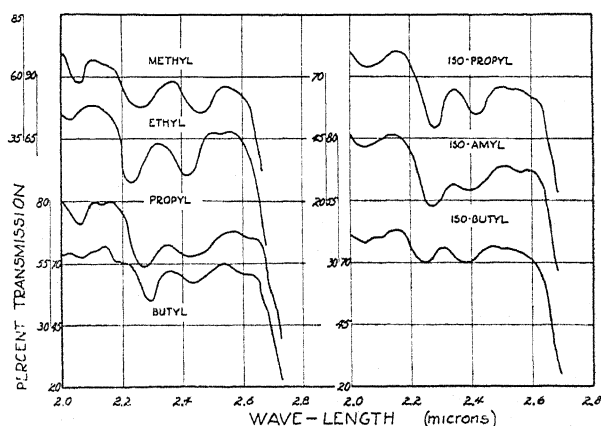


Fig. 1. The percent transmission of methyl alcohol, ethyl alcohol, propyl alcohol, butyl alcohol, iso-propyl alcohol, iso-amyl alcohol and iso-butyl alcohol in the region from 2μ to 2.7μ , the cell thickness being 0.4 mm .

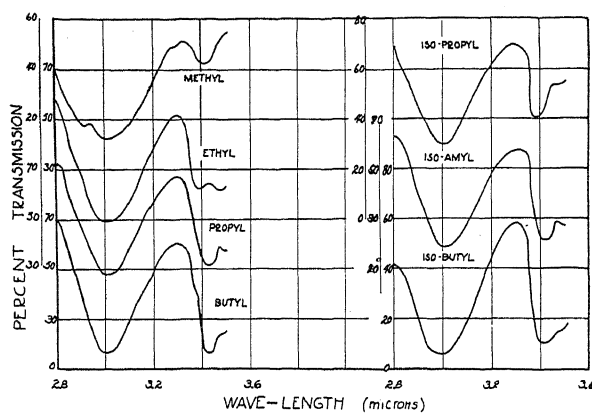


Fig. 2. The percent transmission of methyl alcohol, ethyl alcohol, propyl alcohol, butyl alcohol, iso-propyl alcohol, iso-amyl alcohol and iso-butyl alcohol in the region from 2.8μ to 3.5μ , the cell thickness being from 0.01 to 0.001 mm.

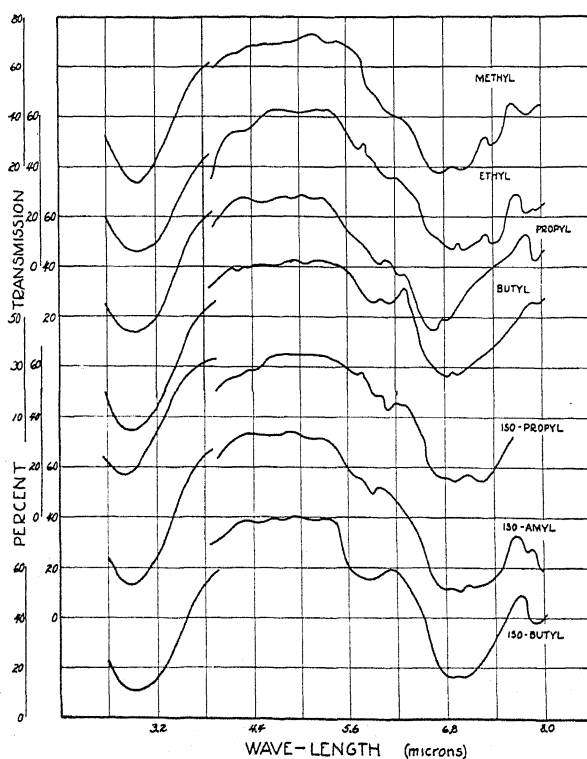


Fig. 3. The percent transmission of methyl alcohol, ethyl alcohol, propyl alcohol, butyl alcohol, iso-propyl alcohol, iso-amyl alcohol and iso-butyl alcohol in the region from 2.8μ to 8μ , the cell thickness being from 0.01 to 0.001 mm.

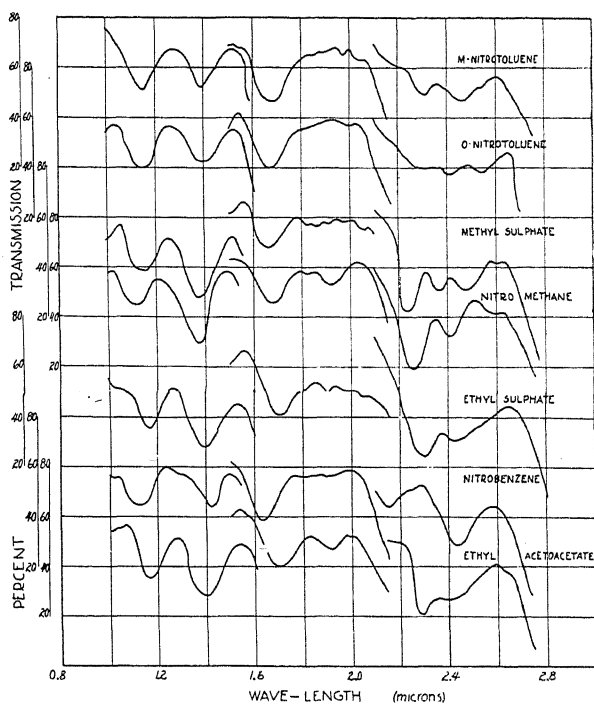


Fig. 4. The percent transmission of m-nitrotoluene, o-nitrotoluene, methyl sulphate, nitromethane, ethyl sulphate, nitrobenzene, and ethyl acetoacetate in the region from 1μ to 2.8μ , the cell thickness being 15 mm from 1μ to 1.25μ , 0.7 mm from 1.25μ to 8.2μ , and 0.4 mm from 2.00μ to 2.8μ .

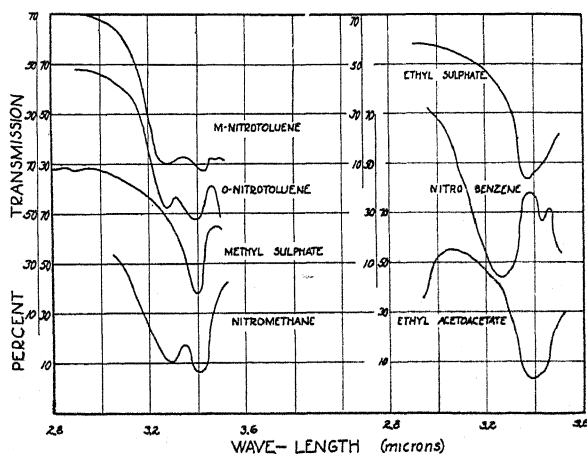


Fig. 5. The percent transmission of m-nitrotoluene, o-nitrotoluene, methyl sulphate, nitromethane, ethyl sulphate, nitrobenzene, and ethyl acetoacetate in the region from 2.8μ to 3.5μ , the cell thickness being about 0.01 mm.

9.8μ , ν_3 , were the fundamental bands. The combinations which the bands are attributed to are made up of only two or three of the fundamentals or their overtones as it is probable that more intense bands will be produced by simple

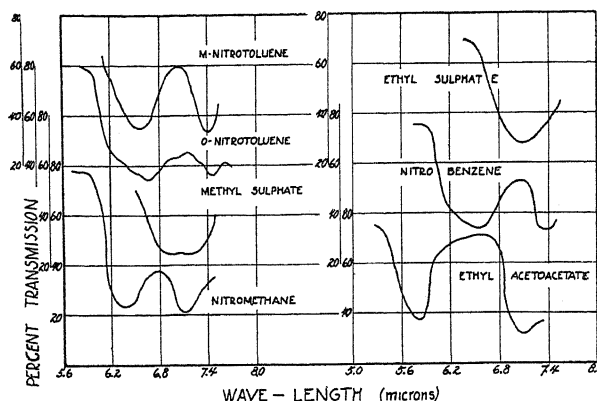


Fig. 6. The percent transmission of m-nitrotoluene, o-nitrotoluene, methyl sulphate, nitromethane, ethyl sulphate, nitrobenzene, and ethyl acetoacetate in the region from 5.5μ to 7.5μ , the cell thickness being about 0.01 mm.

combinations. All the observed bands have not been assigned to combinations as it was found necessary to include up to the fifth or sixth overtone as one of the terms to obtain good agreement between the observed and calculated results. It was believed that the bands at about 1.94μ and 2.60μ

TABLE III. Calculated and observed bands in the alcohols.

	Propyl alcohol		Butyl alcohol		Iso-butyl alcohol	
	obs.	calc.	obs.	calc.	obs.	calc.
$4\nu_1$	0.923μ	0.923μ	0.929μ	0.929μ	0.918μ	0.918μ
$3\nu_1^1$	1.028	1.028	1.032	1.032	1.025	1.025
$\nu_1 + 2\nu_1^1$		1.06		1.06		1.06
$\nu_1^1 + 2\nu_1$		1.11		1.10		1.11
$3\nu_1$	1.198	1.198	1.203	1.203	1.196	1.196
$\nu_1^1 + \nu_1 + \nu_3$		1.37		1.37		1.37
$2\nu_1$	1.53	1.53	1.53	1.53	1.53	1.53
$\nu_1^1 + \nu_1$	1.58	1.60	1.59	1.60	1.58	1.60
$\nu_1^1 + \nu_2 + \nu_3$	1.71	1.71	1.72	1.72	1.71	1.72
$2\nu_1$	1.71	1.76	1.72	1.75	1.71	1.77
$\nu_1 + \nu_2 + \nu_3$		1.84		1.82		1.83
$\nu_1^1 + \nu_2$	2.07	2.08	2.07	2.09	2.10	2.09
$\nu_1 + \nu_2$	2.27	2.27	2.30	2.29	2.25	2.28
$\nu_1^1 + \nu_3$	2.27	2.29	2.30	2.29	2.25	2.29
ν_1^1	3.01	3.05	3.00	3.03	2.99	3.03
ν_1	3.43	3.44	3.43	3.40	3.41	3.47
ν_2	6.73	6.73	6.83	6.85	6.86	6.90
ν_3	9.60	9.60	9.75	9.75	9.75	9.75

which were omitted, were due to a combination including a fundamental beyond 12μ which had not been observed rather than to a combination of the known fundamentals. Fundamental bands have been observed for several

organic compounds in this region and it is probable that they exist for these materials, and if they were known, probably a more complete classification could be made.

By a study of the experimental results it is seen that there is considerable overlapping of the bands in the near infra-red region. Unless high resolution is used the less intense maxima are not observed. Also often a weak band occurs near an intense one and changes the shape of the more intense absorption curve, but does not cause the absorption curve to change sufficiently for it to be detected. This effect is especially noticeable in the alcohols in the region from 1.4μ to 1.6μ .

Sappenfield² has used the suggestion of Ellis⁵ that the organic liquids may be arranged as a series of overtones of the 3.4μ band and thus four of the bands are classified. This classification appears probable and the writer has included it in the present arrangement. The band at 0.92μ was classified as $4\nu_1$ and the band at 1.20μ as $3\nu_1$, and $2\nu_1$ and ν_1 were calculated from these bands. However, as a small error in $4\nu_1$ and $3\nu_1$ would cause a large error in ν_1 it was thought that the observed value of ν_1 was more accurate and it was used in the calculation of the combination bands. In like manner ν_1^1 was checked by using the bands at 1.02μ as $3\nu_1^1$ and 1.53μ as $2\nu_1^1$, but in combination bands the observed value of ν_1^1 was used. It should be noted in some cases there is a considerable difference between the calculated and observed bands in the case of $2\nu_1$ at about 1.75μ . This difference is probably brought about by the fact that the combination $\nu_1^1 + \nu_2 + \nu_3$ also gives rise to a band at near the same wave-length. In the case of tertiary butyl alcohol and secondary butyl alcohol both maxima were found.

By an examination of the results obtained in this work and those obtained by Weniger¹ the intensities of the assumed fundamentals are in the order ν_3, ν_1^1, ν_2 , and ν_1 . Of the combination bands obtained by adding two fundamental bands $\nu_1^1 + \nu_3$ should probably be the most intense and $\nu_1 + \nu_2$ the least intense. However, these two bands fall in the same region of the spectrum and were not separated. The intensity of $\nu_1^1 + \nu_1$ in the region of 1.60μ is somewhat less than the intensity of $\nu_1^1 + \nu_2$ at 2.09μ and the intensity of $\nu_1^1 + \nu_1 + \nu_3$ is less than that of $\nu_1^1 + \nu_1$. The decrease in intensity of the successive overtones of ν_1^1 and ν_1 is large. Due to the considerable overlapping in the bands, it is not possible to make a careful comparison of the intensities of the different combinations, but in the bands where the intensities could be checked the combinations given in Table III were upheld.

In Table IV the assumed fundamentals ν_1 at 3.40μ and ν_2 at 6.80μ and combination bands of M nitrotoluene, methyl sulphate, nitromethane are given. Only slight differences occur for the other materials studied and they have not been included. Since only two fundamentals are known, several of the bands in the near infra-red could not be attributed to simple combinations. They have been omitted for they are possibly due to combinations of ν_1 and ν_2 with bands in the region of 10μ to 12μ and 15μ to 18μ . In these

⁵ Ellis, Phys. Rev. 31, 916 (1928).

regions bands have been shown to exist for several of methyl and ethyl compounds by different observers.⁶

While it must be recognized that the infra-red absorption spectra of each substance are different even though they may be only slightly different chemically, yet the great similarity in the absorption spectra of quite different organic compounds in the region from 1μ to 3μ is readily observed. This similarity in the near infra-red region is probably due to the fact that many

TABLE IV. *Combination bands in nitrotoluene, methyl sulphate and nitrobenzene.*

	M-nitro-toluene		Methyl sulphate		Nitro-benzene	
	obs.	calc.	obs.	calc.	obs.	calc.
$3\nu_1$	1.15μ	$1.15\mu^*$	1.15μ	$1.15\mu^*$	1.13μ	$1.13\mu^*$
$2\nu_1 + \nu_2$	1.39	1.35	1.38	1.35	1.29	1.32
$2\nu_1$	1.68	1.68^*	1.67	1.67^*	1.63	1.63^*
$\nu_1 + \nu_2$	2.21	2.21	2.24	2.29	2.15	2.21
ν_1	3.28	3.27	3.40	3.24	3.26	3.13
$2\nu_2$	3.42		3.40		3.43	
ν_2	6.80	6.80^*	7.05	7.05^*	6.90	6.90^*

* Experimental values used as calculated values.

organic compounds have fundamentals at about 3.3μ and 6.8μ , and in several cases also, fundamental bands are in the region from 8μ to 12μ and from 12μ to 18μ . By the combinations of these bands the near infra-red spectra are somewhat similar in appearance, but in the region from 8μ to longer wavelengths a considerable difference is found in the spectra of similar organic compounds. An examination of the results of Coblentz⁶ shows this for a large number of organic compounds.

⁶ Coblentz, *Investigations of Infra Red Spectra*, Part 1-2, Carnegie Institution of Washington, (1905).

MEASUREMENT OF THE DIELECTRIC CONSTANT AND INDEX OF REFRACTION OF WATER AND AQUEOUS SOLUTIONS OF KCl AT HIGH FREQUENCIES

BY F. H. DRAKE, G. W. PIERCE AND M. T. DOW
CRUFT LABORATORY, HARVARD UNIVERSITY

(Received February 10, 1930)

ABSTRACT

Dielectric constant of distilled water.—The dielectric constant of distilled water was measured with a vacuum tube source of voltage throughout a range of periods extending from about $T=1.31 \times 10^{-8}$ second to $T=8.49 \times 10^{-8}$ second corresponding to vacuum wave-lengths of 3.918 meters to 25.47 meters. The value obtained for the dielectric constant is $\epsilon=78.57$ at 25°C and is independent of the period within the above range of periods.

Temperature coefficient of dielectric constant for distilled water.—The values of the dielectric constant ϵ obtained for various temperatures t between 10°C and 60°C satisfy the empirical equation

$$\epsilon_t = 78.57[1 - 0.00461(t - 25) + 0.0000155(t - 25)^2 \dots].$$

Between 4°C and 10°C the applicability of this equation is somewhat uncertain.

Dielectric constant of conducting solutions.—With distilled water, tap water, and aqueous KCl solutions of conductivity ranging from 0.97×10^7 e.s.u. to 178×10^7 e.s.u., and separating the conduction effects from the dielectric effects, we found the dielectric constant only slightly dependent on the ionic concentration of the solution and nearly the same as that of pure water. The errors of measurement are of the order of 0.1 percent for low conductivities but, because of attenuation, become of the order of 1 percent at the high concentrations of the salt.

Method.—The method employed consists in the measurement of standing electric waves between a pipe and a wire concentrically located within the pipe. The liquid is the dielectric between the wire and the pipe. The frequencies employed were accurately measured by a piezo crystal standardizing a zero beat method, and the half wave-length within the dielectric were obtained by moving a piston in the liquid and observing reactions on the source.

A theoretical discussion of the method is given.

INTRODUCTION

SOON after the discovery of piezoelectric oscillators and their adaptation to the production of constant frequencies of oscillations¹ we began an investigation of waves on wires. The frequencies of an electric oscillator were determined by comparison with the piezoelectric standard and the lengths of the resulting standing waves on two parallel wires were measured. In this way

¹ G. W. Pierce, "Piezoelectric Crystal Resonators and Crystal Oscillators Applied to the Precision Calibration of Wavemeters," *Proc. Am. Acad. of Arts and Sciences* 59, No. 4 (1923). "Piezoelectric Crystal Oscillators Applied to the Precision Measurement of the Velocity of Sound etc." *Ibid.* 60, No. 5 (1925).

an absolute determination of the ratio of the electro-magnetic to the electro-static unit of electric quantity was attempted. After about a year of work on this problem it became apparent that the influence of surrounding objects led to errors and uncertainties which could not be sufficiently reduced with the parallel wire system.

To avoid this stray-field trouble it occurred to us to confine the field to the space between a central wire and a surrounding tube. This apparatus we have now had in operation for several years. The investigation with air or vacuum as the dielectric is not yet good enough for publication since on account of certain small mechanical inequalities of the pipe-system the precision desired has not been attained. We have, however, obtained accuracies better than one-tenth of one percent, and as a by-product to the primary research on the ratio of the units we have employed a similar apparatus in the present investigation.

DETAILS OF THE CONCENTRIC PIPE SYSTEM

The present method of determining the index of refraction of poorly conducting liquids resembles the older well-known scheme of measuring the index by comparing the length of the standing waves on Lecher wires immersed in the liquid with the length of the corresponding air waves. The method is, however, here refined by replacing the wires of the Lecher system by a brass pipe having a copper wire centrally within it along the axis of the pipe, with the solution in the pipe. The pipe and wire are excited by a vacuum tube oscillator at frequencies accurately known by their harmonic relationship with a piezoelectric quartz standard. A movable brass plunger making spring contacts with the pipe and wire and carrying a calibrated rod of the same material above it permits accurate settings at the positions of maximum reaction, which are half a wave-length apart. A sensitive galvanometer, recording changes in the plate current of the oscillator exciting the pipe and wire, indicates the half wave positions as the plunger moves along the pipe. From the known frequencies and the wave-length in the dielectric the velocity of the electric waves in the dielectric is computed.

As a device for producing standing electric waves the system of pipe, wire, and plunger has the outstanding advantage of confining the electric field to the medium between the pipe and wire. Suppose, for example, a set of parallel wires is immersed in a water tank. If the tank is small, an appreciable part of the electric field associated with the charges on the wires may be quite outside the water; difficulties also arise from reflections at the boundaries of the water; and an increase in size of the tank only reduces and does not eliminate these disturbances. For the longer waves in the present experiments the tank would need to be enormous. In the case of the pipe and wire system, on the other hand, the electric currents are confined to the inner surface of the pipe and the outer surface of the wire, so that the electric field has radial symmetry and is completely within the dielectric.

Fig. 1 shows in detail the experimental arrangements adopted. The brass pipe, 3.7 meters long and having an inside diameter of 4.1 cm and a wall-

thickness of 0.32 cm, was mounted vertically against a wall between two neighboring floors of the Cruft laboratory. A hard-drawn copper wire 0.163 cm in diameter was centrally fixed in the pipe held at the lower end by a canvas bakelite cap, and at the upper end by a bakelite strip. In order to make a watertight joint at the lower end, the bakelite cap was screwed to the end of the pipe hard against a thin cardboard gasket which had been boiled in paraffin. The pipe was filled from the top and emptied through a small hole (normally closed with a bakelite plug) in the bakelite cap.

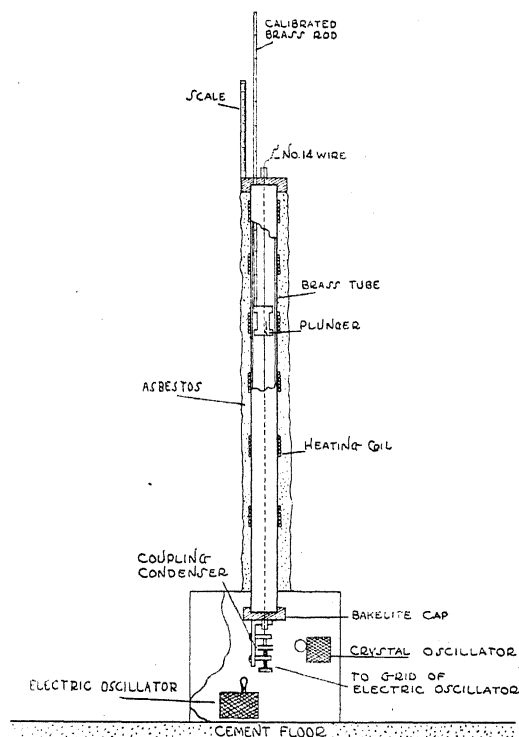


Fig. 1. Arrangement of apparatus.

Two electric oscillators were used to cover the range from 4 to 25 meters vacuum wave-length: one, an oscillator designed particularly for high frequencies, covered the range from 4 to 5 meters; the other, an ordinary Hartley circuit oscillator with parallel plate supply, was used from 5 to 25 meters. These two oscillators and the piezo-electric oscillator, employing a quartz crystal mounted in vacuum, were placed in a sheet iron box at the lower end of the pipe. The pipe protruded below the cover of this box about 10 cm, and made good contact with the cover by means of a bronze flange clamped about the pipe and bolted to the cover. Shielded cables included all electrical connections from the observing position at the top of the pipe to the various oscillators in the box below. The electric oscillator was coupled to the lower end

of the pipe-wire by a single lead through a small condenser, which was variable in order to permit equal coupling at all frequencies. The adjustment to zero beat between the electric oscillator and a harmonic of the crystal oscillator was accomplished by varying a condenser of the electric oscillator for course adjustment; and finally, for fine adjustment, a resistance in the plate circuit of the electric oscillator was varied.

The reflection of waves at the input end occurs principally at the lower surface of the water column, that is, the upper surface of the bakelite cap, due to the large discontinuity in dielectric constants here. The waves are reflected at the other end by a solid brass plunger making spring contact at its lower face with the pipe and wire, and moved by a brass rod 0.6 cm in diameter firmly fixed to the plunger, and upon which are cut marks 50 cm apart. As the piston is moved the current in the plate circuit of the driving oscillator remains constant until the piston is in the neighborhood of a potential node, and then shows a marked change in value as the node is passed due to the reaction of the waves on the oscillator. These nodal positions can be determined with an accuracy of about 0.1 mm with water as dielectric.

STANDARD OF FREQUENCY

The length of a wave in vacuum was computed from the velocity of light and the frequency of the particular harmonic employed. The piezoelectric crystal used as a standard vibrates at a temperature of 25°C with a frequency $f_0 = 5.886 \times 10^6$ cycles per second. In Table I are given the periods and half

TABLE I. *Periods and vacuum half wave-lengths for different harmonics of the crystal standard.*

p	$T \times 10^8$	$\lambda_0/2$	p	$T \times 10^8$	$\lambda_0/2$	p	$T \times 10^8$	$\lambda_0/2$
2	8.49	1273.5	6	2.83	424.5	10	1.70	254.7
3	5.66	849.0	7	2.42	363.9	11	1.54	231.5
4	4.25	636.8	8	2.12	318.4	12	1.41	212.3
5	3.40	509.4	9	1.89	283.0	13	1.31	195.9

wave-lengths in vacuum corresponding to the employed harmonics of this crystal from the second to the thirteenth inclusive. Harmonic numbers are tabulated in the first column under p . The fundamental frequency is characterized by $p = 1$. The periods (T) are in seconds, and the vacuum half wave-lengths ($\lambda_0/2$) are in centimeters.

THEORY

The velocity of propagation of electric waves along coaxial tubes in the ratio of the angular velocity of the exciting current to the retardation angle per unit length of the tubes. That is, if β is retardation angle per unit length of tube, $\omega/2\pi$ the frequency of electric oscillator and v the velocity of electric waves of frequency, $\omega/2\pi$, then

$$v = \omega/\beta. \quad (1)$$

The retardation angle β depends rather simply upon two coefficients of the line: one involving the series resistance and inductance per loop unit length

of the line, and the other involving the capacity and leakage conductance per loop unit.

Let r , l , c , g be respectively resistance, inductance, capacity, and leakage conductance per loop unit of length for the pipe and wire; μ , ϵ be respectively the permeability and dielectric constant of the medium between the pipe and the wire.

$$\begin{aligned}\eta &= r/l\omega \\ s &= g/c\omega \\ f(h) &= + \left(\frac{(1+h^2)^{1/2} + 1}{2} \right)^{1/2} \\ g(h) &= + \left(\frac{(1+h^2)^{1/2} - 1}{2} \right)^{1/2}.\end{aligned}\quad \text{See Footnote 2.}$$

It will be later shown that in these experiments $\eta S < 1$ so that, since $\mu = 1$, the retardation angle β is given by the leaky-line equation:

$$\beta = \frac{\omega}{c'} \epsilon^{1/2} (1 - \eta s)^{1/2} f(h) \quad (2)$$

where

$$h = \frac{\eta + s}{1 - \eta s}$$

c' = ratio of the units.

Since from Maxwell's theory the velocity of electromagnetic waves in vacuum is numerically equal to the ratio of the units (a fact that we have checked experimentally to better than one part in 3000), the index of refraction, corresponding to Eq. (2), is, in view of (1),

$$N = \epsilon^{1/2} (1 - \eta s)^{1/2} f(h). \quad (3)$$

The index N is directly measured in these experiments as the ratio of the wave-length in vacuum to the wave-length in the water.

Eq. (3) then gives a means of calculating the dielectric constant ϵ from values of N and the line coefficients η and s . It will be noted that s and h both involve ϵ through c , the capacity per loop unit of length.

With the object of still further simplifying (3) let us examine the magnitudes of η and s for the actual line. By substitution of the values of g and c in terms of the inner radius of the pipe and the outer radius of the wire it may be shown that

$$s = \frac{2\gamma T}{\epsilon}$$

² Cf. G. W. Pierce, "A Table and Method of Computation etc," Proc. Am. Acad. 57, No. 7 (1922), where these functions, which occur frequently in electromagnetic theory, have been computed and tabulated for values of h between 0 and 250.

where γ is the specific conductivity of the medium between pipe and wire in e.s.u. and T is the period in seconds corresponding to angular velocity ω . Since it is known before hand that ϵ is sensibly independent of frequency, s will be a maximum where the product $T\gamma$ is largest. This occurred in our experiments for waves of period 2×10^{-8} second and for a conductivity of 178×10^7 e.s.u. Since ϵ is approximately 78.5 for water we find

$$s \leq 0.96.$$

The exact value of η for a particular frequency cannot be calculated unless the value of the resistance per loop unit of pipe and wire is known. A value of η sufficiently near the actual value to discuss negligibilities in Eq. (3) may, however, be obtained by assuming that the resistance of the pipe is negligible in comparison with the resistance of the wire.

With this approximation it may be shown, by putting in numerical values, that for the conditions in the present investigation

$$\eta \leq 0.0035$$

and

$$\eta s \leq 0.0034.$$

These results permit considerable simplification in Eq. (3). In the first place, it is evident from inspection of tabulated values of the function $f(h)$ that for all values of h for which $f(h)$ contributes to Eq. (3) a multiplier different from unity the expression for h may be reduced to

$$h = s = 2\gamma T/\epsilon$$

without affecting the accuracy by one part in a thousand. Finally, the maximum error which would be produced by neglecting ηs in comparison with unity under the radical of Eq. (3) will be approximately $\eta s/2$ or about one part in six hundred. But so large an error would occur only for the highest conductivities and lowest frequencies, for which, because of high damping, the accuracy of the experimental determinations is reduced to approximately one part in two hundred; so that the final accuracy of computed observations will not be appreciably affected if we write for all cases in these experiments,

$$N = \epsilon^{1/2} f(h) \quad (4)$$

where

$$h = 2\gamma T/\epsilon$$

Eq. (4) is the theoretical expression for the index of refraction of water and aqueous solutions for the particular frequencies, conductivities, and physical dimensions employed in the work herein described. γ and ϵ are respectively the conductivity in e.s.u. and dielectric constant in e.s.u. of the water or the solution, and T is the period of the electric waves.

MEASUREMENTS OF THE DIELECTRIC CONSTANT OF DISTILLED WATER IN THE RANGE OF PERIODS 1.31×10^{-8} TO 8.49×10^{-8} SECOND

Table II gives a series of results obtained for distilled water at approximately 25°C. The first column contains the number of the harmonic of the

standard crystal oscillator with which the electric oscillator was held at zero beat-frequency. From Table I the corresponding values of the half vacuum wave-length $\lambda_0/2$ are taken and are tabulated in column II. Column III contains the temperature, column IV the measured value of half wave-length in the water at temperature t , conductivity γ ; column V the half wave-length reduced to 25°C by use of the coefficient obtained below; column VI the value of index of refraction N at 25°C. The next to the last column contains approximate values of $2\gamma T/\epsilon$, in which only a rough value of ϵ is needed. For $h=0.0212$, in the top line of the table, the value of $f(h)$ as defined above is 1.00005 and can be replaced by unity. For larger values of $p2\gamma T/\epsilon$ is still nearer unity; so throughout the table the correction for γ is negligible, making ϵ in the last column of this table the same as the square of the sixth column.

TABLE II. *Distilled water, of conductivity $\gamma=0.97 \times 10^7$ e.s.u.*

p	$\lambda_0/2$	t	$\lambda/2(t, \gamma)$	$\lambda/2(25, \gamma)$	$N(25, \gamma)$	$2\gamma T/\epsilon$	ϵ_{25}
2	1273.5	25.5	143.95	143.79	8.856	.0212	78.43
3	849.0	"	95.93	95.82	8.860	.0141	78.50
4	636.8	"	71.89	71.81	8.867	.0106	78.62
5	509.4	"	57.50	57.44	8.868	.0085	78.64
6	424.5	"	47.94	47.89	8.864	—	78.57
7	363.9	"	41.08	41.03	8.868	—	78.64
8	318.4	25.4	35.96	35.92	8.864	—	78.57
9	283.0	"	31.97	31.93	8.864	—	78.57
10	254.7	"	28.77	28.73	8.866	—	78.61
11	231.5	25.7	26.16	26.13	8.861	—	78.52
12	212.3	"	23.97	23.95	8.862	—	78.54
13	195.9	"	22.11	22.09	8.870	—	78.68
Mean = 78.57							Mean departure = ± 0.05

The mean value of ϵ at 25°C is

$$\epsilon_{25} = 78.57 \pm 0.05$$

for distilled water.

MEASUREMENTS OF THE TEMPERATURE COEFFICIENT OF THE DIELECTRIC CONSTANT OF DISTILLED WATER

Water temperatures from 3° to 60°C were obtained by filling the pipe with water just above the freezing point, allowing the pipe to warm slowly to room temperature, taking velocity measurements as different temperatures were reached. For higher temperatures heat was applied to the pipe by passing current through several coils of resistance wire wound around it, as shown in Fig. 1. The pipe was covered with asbestos packing to prevent rapid temperature changes. This precaution, in addition to the stirring produced by moving the plunger, insured a practically uniform temperature throughout the water in the pipe except near the ends, which regions could not be included in the temperature coefficient measurements. The temperature of the water before and after the wave-length measurement was read by a mercury thermometer provided with a cylinder for collecting water and holding it

around the thermometer bulb as the thermometer was raised to read. This method allowed temperatures to be determined within about 0.2°C once the operator developed sufficient speed in pulling up the thermometer and taking readings.

The values obtained for ϵ_t were found to satisfy the empirical equation

$$\epsilon_t = 78.57[1 - 0.00461(t - 25) + 0.0000155(t - 25)^2 \dots]$$

for temperatures between 10° and 60°C , as seen by reference to Fig. 2 where the curve is the curve of the equation and the points are observed values of ϵ_t . Three different vacuum wave-lengths λ_0 were employed, and the points for the three different values of λ_0 all fall near the curve in the specified range of temperatures 10° to 60°C .

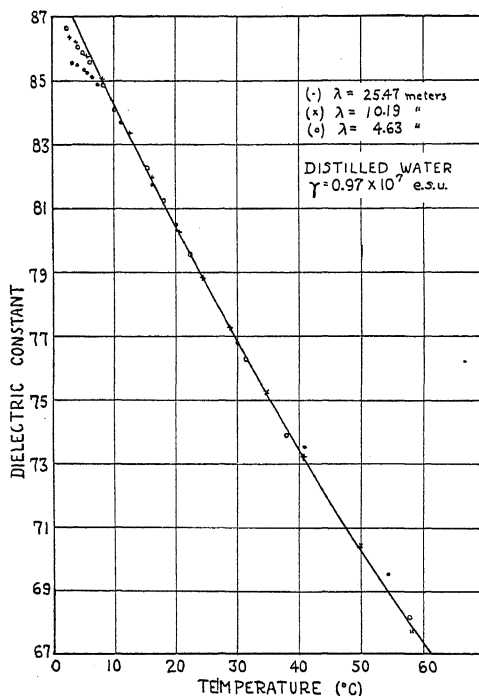


Fig. 2. Locus of empirical equation for the dielectric constant of distilled water as a function of temperature. Observed values for three wave-lengths are included.

For temperatures between 5° and 10°C there is a significant departure from the curve of the equation and the longer wave-lengths seem to give values of ϵ_t departing farther from the curve. These anomalies appear at values of temperature for which the water has anomalous behavior as to density.

INDEX OF REFRACTION AND DIELECTRIC CONSTANT OF TAP WATER AND OF AQUEOUS KCL SOLUTIONS

Tables III, IV, and V give measured values $\lambda/2(t, \gamma)$ of the half wave-length in tap water of conductivity $\gamma = 11.9 \times 10^7$ e.s.u., aqueous KCl-solu-

tion of $\gamma = 47 \times 10^7$ e.s.u. and KCl-solution of $\gamma = 178 \times 10^7$ e.s.u., all measured for the various values of $\lambda_0/2$ indicated in the second column of each table. Using the temperature coefficient formula of the preceding section and ex-

TABLE III. *Tap water, of conductivity $\gamma = 11.9 \times 10^7$ e.s.u.*

p	$\lambda_0/2$	t	$\lambda/2(t, \gamma)$	$\lambda/2(25, \gamma)$	$N(25, \gamma)$	$2\gamma T/\epsilon$	ϵ_{25}
2	1273.5	26.6	142.66	142.16	8.958	0.257	78.95
3	849.0	"	96.14	95.80	8.862	.171	77.91
4	636.8	"	71.73	71.48	8.909	.129	79.04
5	509.4	"	57.36	57.16	8.912	.103	79.26
6	424.5	"	47.93	47.76	8.899	.086	78.85
7	363.9	"	41.12	40.98	8.878	.074	78.66
8	318.4	"	36.01	35.88	8.874	.064	78.55
9	283.0	"	31.98	31.87	8.881	.057	78.71
10	254.7	"	28.83	28.73	8.866	.051	78.45
11	231.5	26.5	26.15	26.06	8.885	.047	78.78
12	212.3	"	23.97	23.89	8.885	.043	78.78
13	195.9	"	22.15	22.08	8.873	.040	78.57
Mean = 78.71 Mean departure = ± 0.23							

TABLE IV. *KCl solution, about 1/270 normal, of conductivity $\gamma = 47 \times 10^7$ e.s.u.*

p	$\lambda_0/2$	t	$\lambda/2(t, \gamma)$	$\lambda/2(25, \gamma)$	$N(25, \gamma)$	$2\gamma T/\epsilon$	ϵ_{25}
2	1273.5	26.6	—	—	—	—	—
3	849.0	"	90.63	90.31	9.401	0.687	79.92
4	636.8	"	68.77	68.53	9.292	.516	81.21
5	509.4	"	55.82	55.62	9.159	.413	80.62
6	424.5	26.8	47.16	46.97	9.038	.344	79.44
7	363.9	"	40.69	40.53	8.977	.294	78.84
8	318.4	26.7	35.79	35.66	8.928	.258	78.45
9	283.0	26.9	31.86	31.73	8.919	.230	78.45
10	254.7	27.1	28.80	28.67	8.884	.207	78.45
11	231.5	27.3	26.15	26.02	8.898	.187	78.15
12	212.3	27.4	23.96	23.83	8.906	.171	78.68
13	195.9	27.3	22.18	22.07	8.877	.159	78.32
Mean = 79.24 Mean departure = ± 0.88							

TABLE V. *KCl solution, about 1/70 normal, of conductivity $\gamma = 178 \times 10^7$ e.s.u.*

p	$\lambda_0/2$	t	$\lambda/2(t, \gamma)$	$\lambda/2(25, \gamma)$	$N(25, \gamma)$	$2\gamma T/\epsilon$	ϵ_{25}
8	318.4	25.6	32.87	32.83	9.698	0.960	78.73
9	283.0	"	29.64	29.60	9.560	.856	78.94
10	254.7	"	27.06	27.02	9.427	.770	78.57
11	231.5	"	24.66	24.63	9.401	.697	79.56
12	212.3	"	22.78	22.75	9.331	.639	79.56
13	195.9	"	21.26	21.23	9.228	.593	78.70
Mean = 79.01 Mean departure = ± 0.33							

tracting the square root we have the approximate relation $\Delta\lambda/\lambda = -0.0023\Delta$ for change of wave-length with change of temperature, and have reduced the measured values of $\lambda/2$ to the values at 25°C recorded in the column marked

" $\lambda/2(25, \gamma)$." Dividing this into $\lambda_0/2$ we obtained $N(25, \gamma)$. Then employing the formula $N = \epsilon^{1/2}f(h)$, which has above been shown to be a correct approximation within the limits of period and conductivity here occurring, we have calculated the values of ϵ given in the last columns of the tables. In examining these results it should be borne in mind that large conductivities and long waves have a higher attenuation and introduce greater difficulties of measurement, which accounts for the fact that departures of readings from their average values are greater with the larger conductivities and with the longer vacuum wave-lengths. (In fact with the solution of Table V the two nodal points necessary for determining the $\lambda/2$ in the solution could not be obtained for $\lambda_0/2$ greater than 318.4 cm). Taking into account these larger sources of error we see that the addition of salts in sufficient quantity to increase the conductivity from 0.97×10^7 to 178×10^7 increases the index of refraction, in

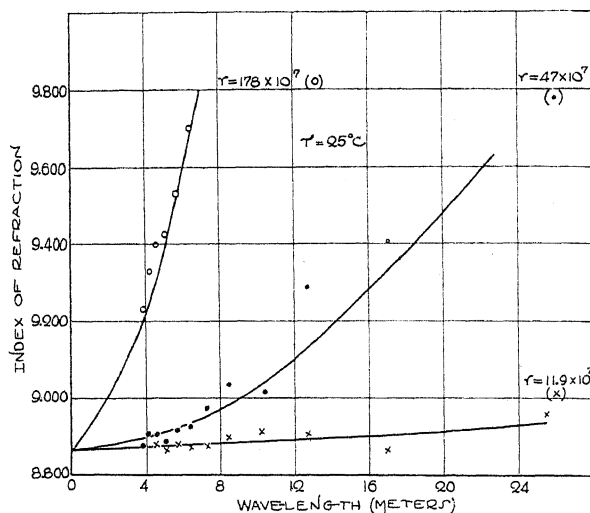


Fig. 3. Theoretical variation of the index of refraction of tap water ($\gamma = 11.9 \times 10^7$) and aqueous solutions of KCl ($\gamma = 47 \times 10^7$ and $\gamma = 178 \times 10^7$) with wave-length, assuming the true dielectric constant ϵ independent of the conductivity. Observed points are included.

a manner dependent on γ and λ_0 , but when the effects of conductivity are eliminated so as to give the true dielectric constant ϵ , the value obtained for ϵ differs from ϵ of distilled water by less than 1 percent. It is not yet known whether this small difference is due to errors introduced by the high attenuation at the higher conductivities; errors which do not arise when water or low-conductivity solutions are employed.

Fig. 3 exhibits graphically as a function of wave-length the values of the index of refraction N taken from the sixth column of Tables III, IV, and V. The smooth curves are the loci of Eq. (4) for the conductivities listed above the tables; and are plotted assuming that ϵ is independent of γ and of the same value as for distilled water. The fact that the observed values lie near these theoretical curves is evidence for the validity of the assumption that ϵ is sensibly independent of γ for the conductivities here employed.

MEASUREMENTS OF THE DIELECTRIC CONSTANTS
OF CONDUCTING MEDIABY JEFFRIES WYMAN, JR.
CRUFT LABORATORY, HARVARD UNIVERSITY

(Received February 10, 1930)

ABSTRACT

It is possible to build small, rigid circuits which have natural periods determined by the medium in which they are immersed. If $T\gamma$, the product of the natural period of the circuit and the conductivity of the medium, is sufficiently small, this period is proportional to the square root of the dielectric constant of the latter. On the basis of this fact measurements have been made of the dielectric constant of water from 0° to 100°C to an accuracy of 0.2 percent or better and covering a range of frequency from $T = 1.4 \cdot 10^{-8}$ to $81 \cdot 10^{-8}$. If $T\gamma$ is not sufficiently small, the period is affected by the conductivity of the medium in a complicated way and cannot be used to obtain the dielectric constant. With the smallest circuits used measurements of the dielectric constants of liquids having conductivities as high as 100 times that of water can be made.

A FEW months ago I became interested in the question of the measurement of the dielectric constants of solutions of certain biological substances, chiefly various proteins which can be prepared in very pure form. Such measurements have an interest in view of existing speculations.¹

The materials in question are for the most part best available in aqueous solution, where they behave like ampholytes containing very weak acid and basic groups.² Under the most favourable conditions concentrated solutions (20–30%) can be obtained having conductivities as low as ten times that of distilled water. They are, moreover, laborious to prepare in more than small quantities. Any method suitable for the study must therefore (1) be appropriate for use with material having a conductivity approaching that of a dilute salt solution and (2) be applicable to small amounts of the substance to be investigated.

The method described in this paper seems to be the simplest and most accurate one which meets these requirements and ought to be generally useful. It has, moreover, some interest in connection with the behaviour of circuits at high frequencies. The following other methods may be mentioned briefly.

The well-known bridge method of balancing the resistance and capacity of a cell containing the unknown liquid for an alternating e.m.f. of fixed frequency has been developed in great detail by Nernst.³ It requires only

¹ Debye, *Polar Molecules*, Chemical Catalogue Co., New York, 1929.

² E. J. Cohn, *Physiological Reviews* 5, 350 (1925).

³ See Nernst, *Zeits. f. Phys. Chemie* 14, 622 (1894). The method has been used by B. B. Turner, *Zeits. f. Phys. Chemie* 35, 428 (1900), to measure the dielectric constant of water and several other liquids. It has also been used by Ratz, *Zeits. f. Phys. Chemie* 19, 94 (1896) and

small amounts of material but it is not suitable for frequencies above about 10^8 sec^{-1} , such as are necessary for measurements on liquids having conductivities much greater than that of distilled water.

Another well-known method makes use of standing waves produced by resonance in parallel wires. The wave-length on the wires is inversely proportional to the square root of the dielectric constant of the surrounding medium provided conductivity effects may be neglected. This method may be used at very high frequencies (greater than $3 \times 10^8 \text{ sec}^{-1}$) in connection with spark oscillators, but it requires considerable amounts of material and its accuracy is not very great.⁴

A modification of this method, developed by Drude, requires much less material; but the accuracy is no greater than that of the original method and there is the disadvantage that the apparatus must be calibrated with known liquids.⁵

One of the earliest of the electrostatic methods is based on a comparison of the attraction between the plates of a condenser charged to a given difference of potential and separated first by air and then by the unknown liquid. The magnitude of the attraction is proportional to the dielectric constant of the medium between the plates. The method has been used successfully with direct and alternating sources of e.m.f. The only apparent objection to it is that it is inconvenient for small amounts of material.⁶

A modification of this method makes use of the torque acting on a small conducting body (Fürth gives this body the form of an ellipsoid of revolution) suspended in the field between the plates of a condenser. The magnitude of this torque is a function of the dielectric constant of the medium separating the plates.⁷

Harrington, *Phys. Rev.* **8**, 581 (1916) on water. More recently it has been used by C. P. Smyth, *Journ. Amer. Chem. Soc.* **49**, 1030 (1927), **50**, 1536 (1928), in the study of organic liquids and liquid mixtures; also by Sack, *Phys. Zeits.* **28**, 199 (1927) in the study of salt solutions.

⁴ This method is based on the work of Lecher and of Blondlot on waves in wires. It was first used by Cohn u. Heerwagen, *Wied. Ann.* **43**, 343 (1891), and later more extensively by Drude, *Wied. Ann.* **55**, 633 (1895); **58**, 1 (1896); **59**, 17 (1896). See also *Zeits. f. Phys. Chemie* **23**, 270 (1897). It has also been used by Marx, *Wied. Ann.* **66**, 603 (1898), Colley, *Phys. Zeits.* **10**, 471 (1909); **10**, 657 (1909); **11**, 324 (1910), Rudop, *Ann. d. Physik* **42**, 489 (1913), Weichman, *Phys. Zeits.* **22**, 535 (1921), and Mie, *Phys. Zeits.* **27**, 792 (1926), for the most part on water. It has been applied by Deubner, *Ann. d. Physik* **84**, 429 (1927) to the study of dilute aqueous salt solutions.

⁵ This method is described by Drude in *Zeits. f. Phys. Chemie* **23**, 270 (1897). The value of the dielectric constants for a large number of substances obtained by the two methods are given. The method has been employed recently by R. Fürth, *Ann. d. Physik* **70**, 63 (1923) for the study of several organic and biological substances, and still more recently by Voigt, *Zeits. f. Physik* **44**, 70 (1927) for obtaining measurements on dilute salt solutions.

⁶ Much of the early work on water and other liquids was carried out by this method: Cohn and Aarons, *Wied. Ann.* **33**, 14 (1888); Tereschin, *Wied. Ann.* **36**, 792 (1888); Heerwagen, *Wied. Ann.* **49**, 272 (1893); Franke, *Wied. Ann.* **50**, 163 (1893). More recently Carman, *Phys. Rev.* **24**, 396 (1924) has revived the method and used it on water at a frequency of 60 cycles. Schmidt, *Phys. Rev.* **30**, 925 (1927), following the procedure of Carman, has applied it to dilute salt solutions.

⁷ The method was used at the suggestion of Nernst by Smale, *Wied. Ann.* **57**, 215 (1897)

A reflection method using polarized waves of very short wave-length (about 3 cm) has been used by Cole⁸ and Merczing⁹ to study the absorption bands of water. It is very inexact and of doubtful validity.

There is a very accurate method based on the principle of standing waves in wires described by Drake Pierce and Dow in a preceding paper of this journal. This method however requires very large amounts of material and is for this reason unsuited to the present requirements.

There is lastly another form of resonance method, which is of more interest in the present connection. A circuit, which we will call the *resonator*, containing the unknown, is brought to resonance with an *oscillator*, maintained at a fixed frequency, by adjustment of a variable condenser. This condenser is calibrated and placed in parallel with the cell or fixed condenser for the unknown, and from its settings when the cell is filled first with air and then with the unknown, the dielectric constant of the latter is calculated. Unfortunately this method is unsatisfactory at high frequencies, owing to stray capacity effects in the resonator. These increase with the frequency and may be expected to change with adjustments of the variable condenser. They can never be determined directly and can only be allowed for by calibration of the whole resonator in terms of known liquids introduced into the cell. This procedure, however, has the following disadvantages: (1) it limits the accuracy and range of all new determinations to that of previous measurements of the standard liquids; (2) it is impossible to get good standards of high dielectric constants (greater than about 30) since water itself is not known to great accuracy; (3) it is constantly necessary to check up on the calibration of the circuit.¹⁰

In order to avoid these difficulties and at the same time profit by the accuracy with which it is possible to make settings by a resonance method it was suggested to me by Professor G. W. Pierce that it might be possible to make a small, rigid resonator which could be entirely immersed in the liquid to be studied, so that all capacities of the circuit would be included alike in the medium. The plan then demands an inversion of the usual procedure of tuning the resonator to the oscillator; instead of this, the frequency of the oscillator is to be varied until it corresponds with the natural period of the resonator, first in air, then in the liquid. These frequencies can then be used to obtain the dielectric constant.

on water. It has been discussed at length by Fürth, *Zeits. f. Physik* 22, 98 (1924). Peckhold, *Ann. d. Physik* 83, 427 (1927), has employed it in the study of salt solutions.

⁸ Cole, *Wied. Ann.* 57, 290 (1896).

⁹ Merczing, *Ann. d. Physik* 33, 1 (1910); 34, 1015 (1911).

¹⁰ Resonance methods of this type have been used by the following observers: Thwing, *Zeits. f. Phys. Chemie* 14, 286 (1894); Niven, *Proc. Roy. Soc.* 85A, 139 (1911); Hyslop, and Carman, *Phys. Rev.* 15, 243 (1920); Preuner and Pungs, *Phys. Zeits.* 20, 543 (1919); Jackson, *Phil. Mag.* 43, 492 (1922); Lattey, *Phil. Mag.* 41, 829 (1921); Kerr, *Journ. Chem. Soc.* 128, 2796 (1926); Williams, *Journ. Am. Chem. Soc.* 48, 1888 (1926) and later; Fritts, *Phys. Rev.* 23, 345 (1924); Walden, Ulrich, and Werner, *Zeits. f. Phys. Chemie* 115, 177 (1925); Kjansky, *Zeits. f. Physik* 52, 743 (1928); Hellmann and Zahn, *Ann. d. Physik* 86, 687 (1928) and Kniekamp, *Zeits. f. Physik* 51, 95 (1928) discuss the method.

After a certain amount of experimentation it was found possible to build compact all metal resonators having natural periods of the desired magnitude. The period of a resonator diminishes with its size, and for a given resonator the period is of course greater in liquids of high dielectric constant. Resonators having a frequency of about 10^8 sec^{-1} in water are small enough to be satisfactorily immersed in 15–20 cc of liquid. This amount of liquid is found to include enough lines of force so that the results are unaffected by parts of the field not included.

The question now arises as to the relation between the natural period of a resonator and the dielectric constant of the medium surrounding it. It is of course well known that if we can treat a circuit as composed of lumped capacity C , inductance L , and resistance R , arranged in series, it will have an impedance given by

$$(R^2 + (L\omega - 1/C\omega)^2)^{1/2}.$$

This will be a minimum at a frequency, called the resonant frequency, given by

$$\omega = 1/(LC)^{1/2}$$

corresponding to the natural period of the circuit.¹¹ If C_0 is the capacity of the circuit in air, and C_1 its capacity in a medium of dielectric constant ϵ , then

$$C_1 = \epsilon C_0.$$

If ω_0 and ω_1 give the corresponding natural periods, then, since L is constant,

$$\epsilon = \omega_0^2 / \omega_1^2. \quad (1)$$

If we could regard our resonators as circuits of lumped capacity, inductance, and resistance, this would make the determination of the dielectric constant

TABLE I. Dielectric constant ϵ of distilled water.

Type of Resonator	Temp.	Frequency	ϵ	ϵ^{*25°
Spiral	21.2	8.147×10^7	79.99	78.62
Cylinder	36.9	4.331×10^7	74.65	78.70
Spiral	38.2	4.344×10^7	74.06	78.51
Cylinder	25.0	2.230×10^7	78.49	78.49
Cylinder	21.3	0.9820×10^7	79.75	78.42
Cylinder	20.0	0.3698×10^7	80.29	78.49
(Cylinder	18.4	0.1396×10^7	84.8	82.4)
				Av. 78.54

* Calculated from temperature data given below.

by the proposed plan very simple. Now there is evidence, to be given below, that we cannot make such an assumption about the resonators; nevertheless

¹¹ We use ω for convenience. It is to be noted that ω , the natural period T , the resonant frequency f , and the corresponding wave-length λ in free space are given by the relations $\omega/2\pi = f = 1/T = 3 \cdot 10^8/\lambda$.

it appears that, if we can neglect the conductivity of the medium, we can still use Eq. (1) to compute the dielectric constant. The justification of this lies in the fact that the results obtained on water with the use of this assumption are consistent among themselves and agree with other observations. The measurements on water were made at various frequencies with a variety

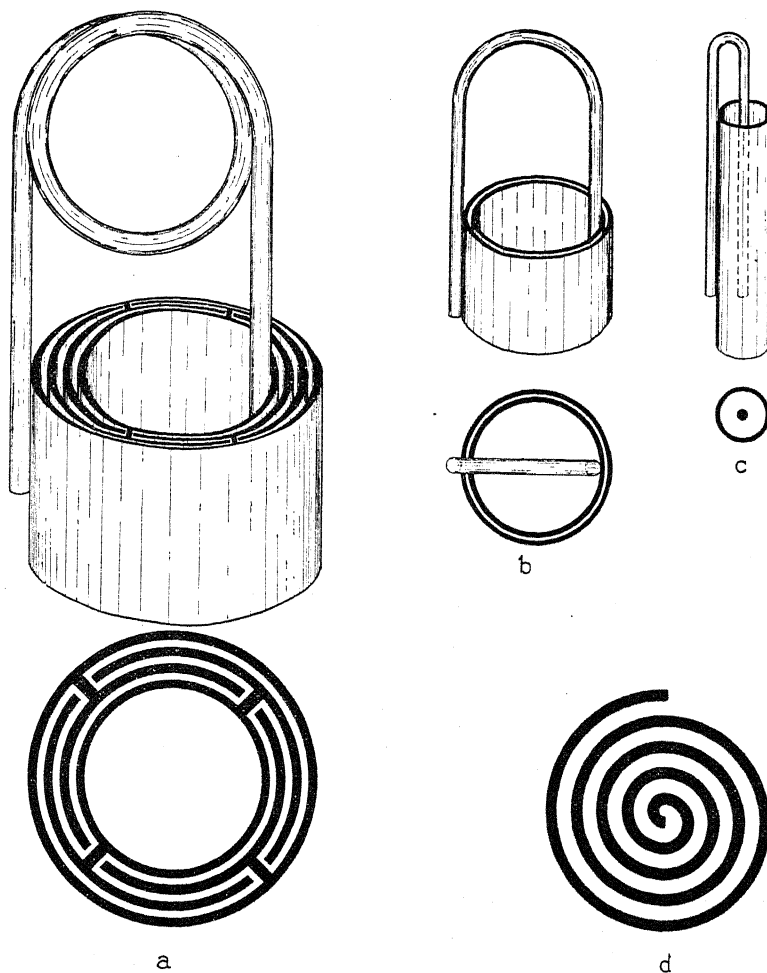


Fig. 1. Types of resonators. a, cylinder type: natural period in air, $8 \cdot 10^{-8}$ sec.; size 13×20 cm. b, cylinder type: natural period, 10^{-8} sec.; size 5×7 cm. c, cylinder type: natural period, $2 \cdot 10^{-9}$ sec.; size $8 \cdot 6$ cm. d, spiral type: natural period, 10^{-9} sec.; diameter, 1.7 cm.

of resonators. Some of these had the form of concentric cylinders and others of spirals. (See Fig. 1.) The results obtained are given in Table I. The values of E were calculated from the observed frequencies by Eq. (1). With one exception they are all in agreement within the experimental error of the determination of the frequencies, and they also agree with values obtained by other methods. The one exception is in the case of the result obtained with

the largest resonator of all at a relatively low frequency. There is no doubt that the discrepancy in this case is due to the effect of conductivity which increases with decreasing frequency and may be expected on theoretical grounds to become evident at about this frequency for water. This close agreement in the values of ϵ is certainly a justification of the application of Eq. (1) to calculate the dielectric constant from the frequency in cases where conductivity of the dielectric may be neglected.

It should be observed in connection with this procedure that it is not possible in all cases to determine $\omega_0 = 2\pi f_0$ directly. If f_1 , the frequency of the resonator in water, is greater than about 1.4×10^7 , $f_0 = \epsilon^{1/2} f_1$ is greater than about 12×10^7 and lies above the upper range of the oscillator—about 12×10^7 . In such cases, however, it is easy to obtain f_0 by determining f_l , the frequency of the resonator in any intermediate liquid l , whose dielectric constant is immediately measured by a larger resonator for which f_0 is known directly. This liquid may be chosen as having low conductivity, and so introduces no trouble on that ground. It need have no especial purity or composition, since its dielectric constant is determined for the occasion. This practice was made use of in determining the values of f_0 for the smaller resonators and is involved in the above determinations of ϵ for water at the higher frequencies. The auxiliary liquid employed was acetone or a mixture of acetone and gasoline. Of course it is evident that each additional measurement of a frequency introduces errors which are accumulated in the final result and such extra steps are to be avoided if possible.

There is no need to describe the vacuum tube oscillator in detail. It was built about a 299X Cunningham tube with the base removed for operation at higher frequencies. The oscillation was set up between the plate and the grid; its frequency was controlled by interchangeable inductances and a rotating condenser driven by a reducing gear and equipped with a dial bearing a vernier. At the lowest frequencies a Hartley circuit was sometimes employed.

The frequency of the oscillator was determined in terms of the frequency of a quartz crystal according to a method described by Pierce.¹² The oscillator was permanently coupled, inductively, with the crystal circuit so as to give audible beats whenever set to the frequency of one of the harmonics of the crystal. These harmonics serve as standard frequencies and are identified by means of a wave meter. From the dial readings of the oscillator corresponding to several nearby harmonics of the crystal, the frequency corresponding to any intermediate setting of the oscillator may be determined by graphical interpolation. The frequency of every setting of the oscillator during the course of a measurement was always obtained directly in this way.

In the above measurements the criterion for resonance was maximum reaction of the resonator on the oscillator. The resonator, suspended by a fine thread in the medium in question, is placed in the field of the oscillator at a distance of 15 to 50 cm from its coil. The frequency of the oscillator is then varied until there is a sudden drop, or rise, in the plate current. This

¹² Pierce, Proc. Amer. Acad. Arts and Sciences 59, No. 4 (1923).

effect on the plate current of the oscillator undoubtedly accompanies a sharp change in the oscillatory current itself and is taken as the indication of maximum reaction. The corresponding frequency of the oscillator is then determined, according to the method just described, without altering the positions of resonator or oscillator. That in the case of water, or any medium whose conductivity may be neglected under the conditions of measurement, the frequency giving maximum reaction back on the oscillator is the same which gives maximum current in the resonator, corresponding to Eq. (1), was determined by means of a resonator containing a hot wire element (described below). It was found in a test case with water that maximum current was induced in the resonator at a wave-length $\lambda = 5.125$ M; whereas maximum reaction on the oscillator occurred at $\lambda = 5.124$ M. This result accords with the applicability of Eq. (1) to settings obtained by the reaction method.

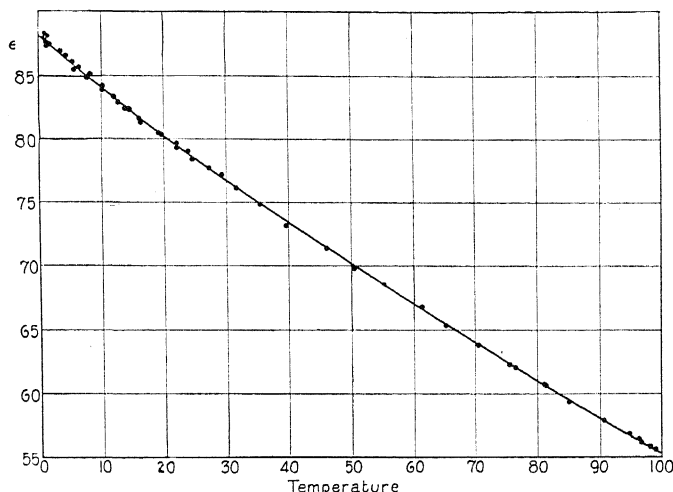


Fig. 2. The dielectric constant of water (ϵ) as a function of temperature.

The sharpness of any resonance setting is of course greater the lower the conductivity of the medium in question. In the case of distilled water the accuracy of a resonance setting at a frequency greater than about 4×10^6 is nearly equal to the accuracy of the determination of the frequency—that is, good to about 0.02 percent. The accuracy of the determination of the resonance frequency itself is thus about 0.04 percent. Any determination of the dielectric constant of water involves the determination of not less than two resonance frequencies, one in air and one in water. The best individual values of the dielectric constant of water obtained by this method are therefore accurate to about 0.1 percent.

The study of water was extended over a range of temperature from about 0°C to 100°C. The results are shown graphically in Fig. 2. The value of the dielectric constant as a function of temperature is expressed with an accuracy equal to that of the experimental results by the equation

$$\epsilon = 78.54[1 - 0.00460(t - 25) + 0.0000088(t - 25)^2] \quad (2)$$

It is gratifying that these values are in good agreement with those obtained by Drake, Pierce, and Dow (preceding paper) over the range of temperature covered by these observers. They are also in reasonably good agreement with the results of earlier observers given in The International Critical Tables.

We now come to the results obtained on dilute salt solutions where conductivity effects are appreciable. Here the situation is much more complicated and shows (1) that the frequencies corresponding to maximum current in the resonator and maximum reaction on the oscillator are different when the conductivity of the dielectric is appreciable, and (2) that the resonators cannot in general be treated as circuits of lumped capacity, resistance, and inductance.

The evidence to support the above statements comes from the use of resonators, already referred to, containing a hot wire element. These resonators are of the cylindrical type. A small section of the metal loop joining the

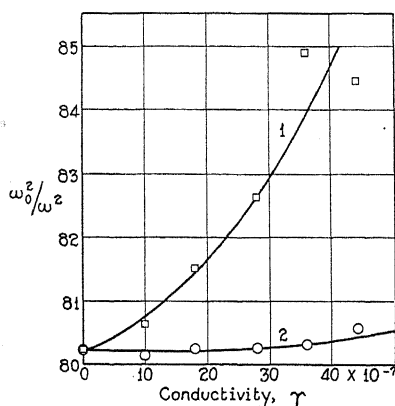


Fig. 3.

two cylinders is removed and replaced by a condensite tube of the same size. This serves to hold the two halves of the resonator rigidly in their former position and at the same time to enclose a piece of 40 gauge copper wire which connects the two cut ends of the loop and restores the connection in the circuit. To the midpoint of this wire are welded the ends of two lengths of 40 gauge wire, one copper and one constantan, which enter through the walls of the tube. These form one junction of a thermo-couple, which is a sensitive detector of any current in the resonator. If the resonator is suspended in water and placed at a distance of two feet from the coil of a power oscillator tuned to the right frequency, sufficient heat is developed in the hot wire to give a full scale deflection of a table galvanometer.

With such a resonator it is possible to tune the oscillator to give either maximum current in the resonator or maximum reaction back on the oscillator. As we have already seen, the two settings are identical for water at a frequency of about 6×10^7 ($\lambda = 5$ M.) When, however, we turn to dilute salt solutions at about the same frequency, the two methods of tuning no longer

give identical results. Instead, the frequency required to produce maximum current in the resonator is greater than that required for maximum reaction on the oscillator, and the difference between the two increases with the conductivity of the solution. This is shown by the results given in Fig. 3. The upper curve corresponds to maximum reaction; the lower to maximum current. It should be noted that a power oscillator was used to get settings by the first method, and the small oscillator to get settings by the second method.

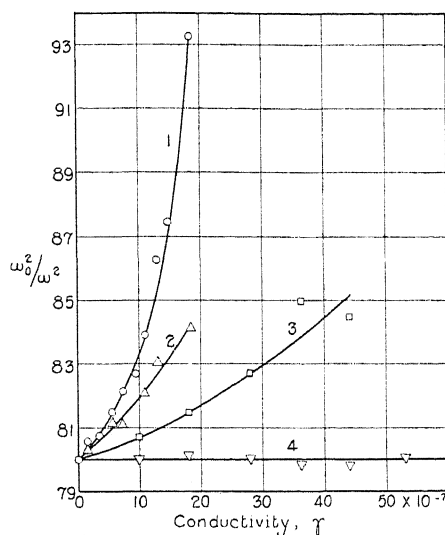


Fig. 4. Values of ω_0^2/ω^2 at varying conductivities obtained by the reaction method of determining resonance. Each curve was made with a different resonator. The natural periods in air of the corresponding resonators, expressed in seconds, are: 1, $11.40 \cdot 10^{-2}$; 2, $5.060 \cdot 10^{-2}$; 3, $1.914 \cdot 10^{-2}$; 4, $1.373 \cdot 10^{-2}$.

Such results are not unexpected in a general way. Suppose we have two circuits 1 and 2, 1 being the oscillator and 2 the resonator. We assume that the circuits are coupled inductively, and that the oscillator is subjected to an impressed E.M.F. of amplitude

$$E = e^{j\omega t}$$

Then, if $Z_1 = R_1 + jX_1$ is the impedance 1, $Z_2 = R_2 + jX_2$ the impedance of 2, and M the mutual induction between them, the complex current amplitudes are given by

$$A_1 = E / [Z_1 - (Mj\omega)^2 / Z_2]$$

$$A_2 = A_1 M j\omega / Z_2.$$

In determining the condition for A_2 maximum, we may certainly neglect changes in A_1 , if circuit 1 is a power oscillator. The frequency ω_2 corresponding to A_2 maximum is then seen to be given by the equation

$$\frac{d}{d\omega} \left(\frac{(R_2^2 + X_2^2)^{1/2}}{\omega} \right) = 0. \quad (3)$$

The determination of ω_1 , corresponding to A_1 maximum, is far less simple, but in general we may expect ω_1 and ω_2 to be different. It is suggestive, however to observe that in the case of a resonator of lumped capacity, inductance, and resistance immersed in a non-conducting medium, we may expect ω_1 and ω_2 to be equal. In this case the impedance of the resonator is $R + j[L\omega - (1/C\omega)]$. Conductivity of the dielectric being negligible, R is simply the resistance of the all-metal circuit, and may be neglected in comparison with L and C . ω_2 is then found to be equal to $1/(LC)^{1/2}$. If, on the other hand, we assume that the condition for A_1 max. is governed primarily by the second term in the denominator, we find that ω_1 is also equal to $1/(LC)^{1/2}$, provided we again neglect R in comparison with L and C .

It is, however, as we have pointed out, impossible to regard the resonators as circuits of lumped capacity, inductance, and resistance when conductivity is appreciable. We will now, in conclusion, consider this point. Values of ω_0^2/ω^2 , the apparent dielectric constant, for dilute salt solutions of various concentrations obtained by the two methods of determining resonance

TABLE II. Values of ω_0^2/ω^2 for solutions of potassium chloride at 20°C.

Resonator 1: $T_0 = 1.914 \cdot 10^{-9}$ sec.				
% conc. KCl	$\gamma \cdot 10^{-7}$	ω_0^2/ω^2	$f(h)$	$f(h)^2 \omega_0^2/\omega^2$
0.000	0.3	80.22	1.000	80.22
.005	10.	80.16	1.001	80.32
.010	18.	80.28	1.001	80.44
.015	28.	80.29	1.004	80.73
.020	36.	80.32	1.006	81.28
.024	44.	80.60	1.009	82.06
.029	53.	80.76	1.013	82.86
.034	62.	80.81	1.017	83.56

Resonator 2: $T_0 = 2.495 \cdot 10^{-9}$ sec.				
% conc. KCl	$\gamma \cdot 10^{-7}$	ω_0^2/ω^2	$f(h)$	$f(h)^2 \omega_0^2/\omega^2$
0.000	0.3	80.22	1.000	80.22
.005	10.	80.19	1.001	80.35
.010	18.	80.01	1.003	80.49
.015	28.	80.62	1.006	81.59
.020	36.	80.62	1.010	82.23
.024	44.	80.89	1.015	83.31

Resonator 3: $T_0 = 6.629 \cdot 10^{-9}$ sec.				
% conc. KCl	$\omega \cdot 10^{-7}$	ω_0^2/ω^2	$f(h)$	$f(h)^2$
0.000	0.3	80.22	1.000	80.22
.001	2.	80.22	1.001	80.38
.002	4.	80.09	1.001	80.25
.003	6.	80.17	1.002	80.49
.004	8.	79.86	1.004	80.50
.005	10.	79.70	1.005	80.50
.006	11.	79.89	1.007	81.02
.008	15.	79.31	1.012	81.22
.010	18.	78.47	1.017	81.15
.012	22.	78.12	1.025	81.11

are shown graphically in Figs. 4 and 5. The values obtained by the reaction method are in general higher than those from the thermal procedure and both sets of results vary among themselves. We will discuss only the latter, where the theory is far simpler. These are given in Table II.

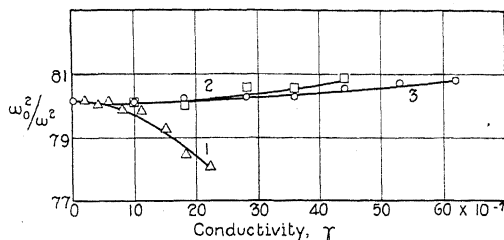


Fig. 5. The same, obtained by the thermal method. Corresponding natural periods in air are: 1, $6.629 \cdot 10^{-9}$; 2, $2.495 \cdot 10^{-9}$; 3, $1.914 \cdot 10^{-9}$.

Let us consider the behavior of an ideal resonator of lumped capacity, inductance, and resistance and compare the predictions with the results given above. Such a circuit placed in a conducting dielectric will behave as if the plates of the condenser were short circuited by a resistance r . If R denote the resistance of the metallic part of the circuit as before, and C and L its capacity and inductance, then it can be shown that the impedance of the circuit suspended in the conducting dielectric is

$$R + \frac{r}{1 + r^2 C^2 \omega^2} + j \left(L \omega + \frac{r^2 C \omega}{1 + r^2 C^2 \omega^2} \right).$$

The frequency corresponding to maximum current amplitude in the resonator may be obtained from Eq. (3) and is given by

$$\omega^2 = \frac{1}{2LC} \left(1 \pm \left(\frac{2LC}{r^2 C^2} + 1 \right)^{1/2} \right),$$

provided we neglect the ratio R/r . Now it can be further shown that for any condenser filled with a medium of dielectric constant ϵ and conductivity γ , the equivalent resistance r between the plates is given by

$$rC = \epsilon / 4\pi\gamma.^{13}$$

Therefore, taking account of the fact that $C = \epsilon C_0$, where C_0 is the capacity of the resonator in air, and that $1/C_0 L = \omega_0^2 = 4\pi^2/T_0^2$, where T_0 is the natural period of the resonator in air, we obtain finally

$$\frac{\omega^2}{\omega_0^2} = \frac{1}{2\epsilon} \left\{ 1 \pm \left(1 + \frac{2}{\epsilon} (2T_0\gamma)^2 \right)^{1/2} \right\}.$$

Since if $\gamma = 0$ this must reduce to $\omega^2/\omega_0^2 = 1/\epsilon$, we discard the $-$ sign before the radical. This result may be compactly expressed by

$$\omega/\omega_0 = f(h)/\epsilon$$

¹³ I am indebted to Professor Pierce for this result.

where $f(h)$ has been tabulated for values of h .¹⁴ If $h=0$, $f(h)=1$. If h is less than about 0.12, $f(h)$ is not greater than 1.001, and ω_0^2/ω^2 is equal to ϵ to an accuracy of 0.2 percent or better.

For distilled water where $\gamma = 3 \times 10^6$ e.s.u., approximately, we should be able to express ϵ by ω_0^2/ω^2 to an accuracy of 0.2 percent in the case all measurements for which T_0 (corresponding to ω_0) is less than 10^{-7} secs, or for which λ_0 , the corresponding wave-length in free space, is less than 30M. For liquids, e.g. salt solutions, for which γ is greater, $f(h)$ increases more rapidly with T_0 and we should be obliged to use smaller resonators having higher natural periods. But the main thing to notice is that as $T_0\gamma$ becomes appreciable and increases, ω_0^2/ω^2 becomes increasingly less than ϵ , according to Eq. (4).

If we attempt to correct the experimental values according to Eq. (4), we obtain the results given in the last column of Table II. Now it is pretty clear that these corrected results cannot give the true values of the dielectric constants of the solutions. The reason for this is that if they did, we should be obliged to assume the dielectric constant to vary with the frequency over the range covered by the measurements and to be greater than that of pure water. The results of Drake, Pierce, and Dow, however, show that the dielectric constant of dilute salt solutions is independent of frequency over the range in which we are interested and is in fact the same as that of water to an accuracy of about 1 percent up to a concentration of 1/70 normal KCl. These results are obtained by a method in which the theory is much simpler and the correction factor known. We are therefore justified in concluding that although the resonators may be treated as circuits of lumped capacity, inductance, and resistance in cases where the conductivity of the dielectric is negligible, i.e., where $T_0\gamma$ is small, they do not in general have the properties of such circuits, but behave in a much more complicated way. It is possible indeed that they are rather to be regarded as lines, if of a complicated type. The analysis of the behavior of even the simplest types of lines is, however, very complex under the circumstances of the above measurements and no attempt has been made to carry it out.

In any case, from the experimental results on the salt solutions, it is clear that we can use ω_0^2/ω^2 directly to express ϵ in the case of frequencies determined by the thermal method up to conductivities many times that of water, provided we use resonators having small natural periods. Table II shows that anomalies begin to appear at conductivities corresponding to values of $T_0\gamma$ for which the correction term $f(h)$, obtained from the analysis of the ideal circuit, begins to become significant. This is not unexpected. It appears that we are safe in equating ω_0^2/ω^2 and ϵ for values of h not greater than about 0.1. This means that if we use a resonator having a natural period in air of about 10^{-9} sec, we can employ the method up to conductivities about 100 times that of water. On the other hand if we make settings by the reaction methods we run into difficulties considerably sooner. Here we are probably safe up to conductivities 20-30 times that of water.

¹⁴ G. W. Pierce, Proc. Amer. Acad. Arts and Sci. 57, No. 7 (1922).

ON THE ANOMALOUS ROTATION OF THE SUN*

BY ROSS GUNN

NAVAL RESEARCH LABORATORY, WASHINGTON, D. C.

(Received February 3, 1930)

ABSTRACT

The requirements of Jeans' theory of the anomalous solar rotation are not in accord with the facts of solar magnetism. A new theory is worked out which attributes the anomaly to atmospheric motions arising from the interaction of ions with the solar magnetic field and an assumed electric field. Observations of the solar atmosphere are made only in those regions where the gaseous pressure is such that the ion free paths are long. Ions of both kinds which execute long free paths in crossed electric and magnetic fields are swept in the same direction and give rise to a mass motion. This superimposed drift of the solar atmosphere is shown to account for the rotational anomaly and the calculated variation of the angular velocity with latitude is of the observed form. The theory requires that the sun possess a radial electric field having a sign and distribution similar to that observed on the earth.

IT HAS been known for nearly 100 years that the measured rotational period of the sun depends upon the latitude of the point selected for observation and that it varies from 25 days at the equator to over 30 days at the pole. Moreover, the value of the period at any given place seems to depend somewhat on the level of the point observed. It has been found that in the solar reversing layer the measured angular velocities at low latitudes, expressed in degrees per day, were given approximately by the relation

$$W = 14^\circ.54 - 3^\circ.50 \sin^2 \lambda \quad (1)$$

where λ is the latitude.

Jeans¹ has proposed a theory to account for the rotation phenomena and he attributes the effects to the braking action of the radiation which filters through the outer solar layers. The final form of his theory requires that the central regions of the sun rotate from ten to fifty times faster than the surface layers and that these layers play only a minor part in the transfer of the radiated angular momentum. It is difficult to establish the existence of high rotational velocities inside the sun from theoretical considerations and it now appears that such a rotation may be improbable. The essential characteristics of the solar magnetic field are known from the work of Hale and his collaborators at Mt. Wilson^{2,3} Observatory. This work established the fact that the distribution of the solar magnetic field at any given level was similar

* Released by the Navy Department.

¹ Jeans, *Astronomy and Cosmogony*, Cambridge Press, 1928.

² Hale, *Astrophys. J.* 38, 31 (1913).

³ Hale, Sears, van Maanen and Ellerman *Astrophys. J.* 49, 1 (1918).

to that of the earth; that the field was limited radially and that the magnetic pole did not coincide with the geographic pole but rotated about it with a period of 31.4 days. These magnetic facts suggest that Jeans' theory of the anomalous solar rotation is incorrect, for if we assume that the rotational velocity changes from layer to layer as we go outward from the core of the sun, then the motion of the magnetic pole with respect to the axis of rotation will set up electrical eddy currents in the moving layers which will tend to bring them into rotational synchronism with the magnetic field. This difficulty would vanish if the magnetic and geographic poles coincided. A still more serious difficulty arises from the fact that on almost any theory of the permanent magnetic field of the sun and earth, as for example, a theory which attributes the field to electrical currents^{4,5}, the magnetic pole would be expected to rotate with the same period as the entire mass. Superimposed on this might be a slow precession but it is unlikely that the solar fields should behave in a manner essentially different from that observed in the case of the earth whose magnetic poles rotate with the period of the entire mass. It thus seems clear that the rotational period of the entire solar mass is 31.4 days and not one-tenth of this as is required by Jeans' theory. The objections to Jeans' theory are of such a nature that the problem has been re-examined. It has been found possible to account for the observations in a simple manner by considering the electromagnetic reactions of the ions in the solar reversing layer.

Mt. Wilson researches demonstrated that the solar magnetic field is essentially similar to that of a uniformly magnetized sphere whose exterior field is limited by some special mechanism. It has been shown that this limitation of the solar field is adequately explained by the diamagnetic properties⁶ of the solar atmospheric ions; for the effective permeability of an ion gas approaches zero under precisely the conditions that exist in the solar reversing layer. It has been argued recently that boundary effects may annul the diamagnetism of the reversing layer, but this view can not be supported. The effect of the boundary has been considered by van Leeuwen⁷ for the case of a metal, who found that the current sheet at the boundary is able to compensate for the volume diamagnetic effect under certain special conditions. She considered the case of short free paths and assumed that the free electrons making up the electron gas were reflected specularly when they collided with the boundary. To meet this condition it is necessary that the boundary be sharp and that the component of the electron momentum normal to the boundary be reversed on impact while the tangential component is preserved. The requirement is satisfied when an electron collides with a heavy ion but when an ion collides with a boundary ion or molecule of its own mass, the normal momentum of the colliding ion is not reversed and boundary currents cannot cancel the volume diamagnetism. Ions play an important part in solar dia-

⁴ Gunn, *Phys. Rev.* **34**, 335 (1929).

⁵ Gunn, *Phys. Rev.* **34**, 1621 (1929).

⁶ Gunn, *Phys. Rev.* **33**, 614 (1929).

⁷ van Leeuwen, *Jour. d. Physique* **2**, 361 (1921).

magnetism and it is clear that van Leeuwen's calculations do not apply there. Moreover, we must note that the sun's atmosphere has no outer boundary and the inner boundary is not sharp so that complete compensation is impossible and we are left with the primary effect—diamagnetism. This general conclusion was pointed out clearly enough in the writer's first paper.⁸ Chapman⁹ has proposed an alternative theory of the radial limitation of the magnetic field but the author has shown¹⁰ that the effect he invokes to explain the phenomena is largely cancelled by another effect which arises from the inhomogeneity of the impressed magnetic field. Moreover, Chapman's theory encounters a serious qualitative difficulty in that the gravitational drift currents of the type he postulates become very small at high solar latitudes where the magnetic field intensity becomes large and nearly parallel to the gravitational acceleration. Thus his theory leads to the conclusion that the magnetic field at a given level near the poles should be much larger than is observed and that a large unobserved stray magnetic field should exist. Diamagnetism on the other hand is equally effective at the poles as at the equator and predicts the same fractional reduction of the initial field at a given ion pressure. This is in accord with observation.

The existence of diamagnetism in the reversing layer and direct spectroscopic evidence both show that the ion free paths in the reversing layer must be longer than the critical free path; that is, they are longer numerically than the radius of the helix generated by the ion as it is caused to spiral about the impressed magnetic field. When this condition is satisfied, other important motions of the nature of ion drifts arise from a combination of an impressed magnetic field with other types of field. These drifts may result from a magnetic field crossed with a gravitational field^{11,12}, an inhomogeneous magnetic field,¹⁰ or an electric field.⁸ The ion drifts and their possible effects have been investigated elsewhere; it is only of importance to note here that the first two effects give rise to ion drifts which are opposite in direction for the positive and negative ions and hence constitute a current while the electric field crossed with a magnetic field acts in such a way as to urge both ions in the same direction and hence is of the nature of a mass movement. When the free paths of the ions and electrons are both longer than their respective critical free paths both drift in the same direction with the same velocity. In certain unobserved regions of the solar atmosphere, however, the free paths of the electrons are longer than their critical radius while the free paths of the ions are less than their own critical value. Thus in this special region electric currents flow which may tend to magnetize or demagnetize the sun according to the direction of the impressed electric field. Such currents may be important in theories of sunspots or of the limitation of the solar magnetic field,

⁸ Gunn, *Phys. Rev.* **32**, 133 (1928).

⁹ Chapman, *Monthly Notices* **89**, 57 (1928).

¹⁰ Gunn, *Phys. Rev.* **33**, 832 (1929).

¹¹ Hulburt, *Phys. Rev.* **33**, 412 (1929).

¹² Chapman, *Monthly Notices* **89**, 57 (1928).

but it is to be noted that the conductivity of this narrow region is moderately large and any electric field must necessarily be small. Our greatest interest in the present paper is in the mass motions of the atmosphere and we therefore assume the sun to have electric as well as magnetic fields and will consider their joint mechanical effects. At the solar equator the direction of the magnetic field is tangential and that of any electric field must be radial. These crossed fields give rise to an equatorial ion drift which is in the same direction for both types of ions and is independent of the charge or mass of the ion. Were neutral molecules present they would presumably be swept along by occasional collisions with ions. It thus seems possible that the observed anomalous rotation of the sun is an effect arising from the movement of the solar atmosphere and is not due to deep seated circulation which seems to be required in earlier ideas regarding the phenomena.

The problem of the electrical state of a rotating heavenly body has been considered by several writers^{13,14,15} and the electrical charge distribution worked out under special assumptions. For example, Rosseland¹³ has pointed out that in the stars loss of charge by radioactive processes might be expected. In addition we may have electrical fields arising from a separation of charge due to (a) gravitational fields¹⁶ (b) temperature gradients (c) radiation pressure (d) pressure gradients¹³ (e) motion in a magnetic field.¹⁵ It seems probable that in the reversing layer (a), (b), and (c) are small compared to the electric fields arising from other causes. A study of the electric fields arising from the motion of the earth in its own magnetic field has been made by Page¹⁵ who assumed that the earth was a uniformly magnetized conducting sphere. Upon working out the consequences of his assumptions he found that electric fields are set up in the high atmosphere which have values such that the ions are swept to the westward with a velocity of the same order of magnitude as the peripheral velocity of the earth. An observer outside the earth watching the ions in the high atmosphere would thus observe an apparent rotational period greater than 24 hours. The entire calculation may equally well be applied to the sun and correction made for the change of magnitude of the quantities due to a larger field and a different type of magnetic distribution. This readjustment does not greatly alter the situation and if the sun is assumed to be unchanged as a whole and free of electric fields in the reversing layer, except those arising from the solar rotation, then an observer on the earth watching an equatorial point in the reversing layer would observe a period of rotation for the layer which is greater than the period of rotation as indicated by the motion of the magnetic pole. This is not in accord with observation and we must conclude that radial electric fields other than that due to rotation in its own magnetic field exist in the solar reversing layer. We shall not enter into a discussion as to the origin of this electric field but simply point out that observation demands its existence. Moreover, as we

¹³ Rosseland, *Monthly Notices* 84, 720 (1924).

¹⁴ Rosseland, *Astrophys. J.* 62, 387 (1925).

¹⁵ Page, *Phys. Rev.* 33, 823 (1929).

¹⁶ Pannekoek, *Bull. Astro. Inst. Netherlands* 19, (1922).

shall see presently, the electric field required is in the same direction, is much smaller, and varies radially in substantially the same manner as the observed electric field of the earth. It is thus consistent with such astrophysical data as are available at the present time.

The mean drift velocity u imposed on both kinds of ions which execute long free paths in crossed electric and magnetic fields is given by

$$u = \frac{E \times H}{H^2} = \frac{E}{H} \sin \beta. \quad (2)$$

Where E and H are in e.m.u. and β is the angle between E and H . We will take H positive northward in the reversing layer at the equator since it coincides in direction with the rotational velocity of the sun and E radially outward. Under this condition a positive value of u corresponds to a westward velocity relative to the surface. According to Mt. Wilson data^{2,3} the magnetic field H at a given atmospheric level and latitude λ is given by

$$H = H_0(1 + 3 \sin^2 \lambda)^{1/2} \quad (3)$$

where H_0 is the value of the equatorial field at the level considered. Thus combining (1) and (2) the superposed angular velocity ω at a given level which arises from the velocity of drift is

$$\omega = \frac{E \sin \beta}{H_0 R [(1 + 3 \sin^2 \lambda)(1 - \sin^2 \lambda)]^{1/2}} \quad (4)$$

where R is the radius of the sun. The diamagnetic layer of the solar atmosphere distorts the permanent magnetic field and the value of β is not readily determined. It is convenient to note that due to diamagnetism the magnetic field is nearly parallel to the surface of the sun in a region 30° on each side of the equator (say) and that the electric field must be radial, so that within the range specified an expansion of Eq. (4) is valid and we may also set $\sin \beta = -1$. Making this substitution, expanding (4) and retaining only the first two terms we have

$$\Omega = \Omega_0 - (E/H_0 R)(1 - \sin^2 \lambda) \quad (5)$$

where Ω is the resultant (observed) angular velocity, Ω_0 the angular velocity as measured by the rotation of the magnetic pole and the last two terms represent the contribution due to the atmospheric drift. In order to account for faster rotation at the equator we must now assume that the required value of E is radially inward or negative. If we set

$$\Omega_0 + (E/H_0 R) = \Omega_0' \quad (6)$$

then (5) becomes

$$\Omega = \Omega_0' - (E/H_0 R) \sin^2 \lambda \quad (7)$$

and agrees in form with the observed relation given in Eq. (1). By selection of the correct value for E ; Eq. (7) gives the exact relation. Thus from Eq. (1) and (7)

$$(E/H_0R) = 7.06 \times 10^{-7} \text{ rad/sec}$$

and taking $R = 6.95 \times 10^{10}$ cm and $H = 25$ gauss we find $E = 0.013$ volts/cm.

There are no data available which contradict the assumption of a radial electric gradient of 0.01 volt/cm in the observed regions of the reversing layer and unless the atmosphere of the sun rotates slower than the magnetic poles we must assume that some kind of an electric field exists which is directed radially inward. The conductivity of the layer in the direction of the electric field has been shown to approach zero⁸ when the electric and magnetic fields are nearly perpendicular as they actually are in the equatorial zone we have considered. There is therefore no reason to suppose that electric charges can readily flow in such a manner as to neutralize the field. Near the poles the electric and magnetic fields approach parallelism and the conductivity increases; thus the electric field distribution in this region is quite different from that at the equator.

The previous calculation of the equatorial electric field was made for an observed level where the magnetic field was taken as 25 gauss. At different values of the magnetic field we might expect different values for the drift velocity. Observations show that deviations do exist but they are not so large that it would be legitimate to assume the electric field constant at all altitudes. A better approximation is suggested by the fact that the drift velocity is observed to be nearly constant with superposed regular variations. On this assumption we have

$$(E/H) = K_1 = 5 \times 10^4 \text{ cm/sec} \quad (8)$$

which requires that E increase with increasing ion pressure in the same manner that H is known to increase. This relation undoubtedly breaks down in the deeper layers of the solar atmosphere. The origin of the electric field is unknown and the distribution cannot now be calculated from independent considerations. The required distribution can be worked out, however, by use of Eq. (8) and earlier results obtained from diamagnetic considerations¹⁰ which gave an approximate relation between the ion density and the magnetic field in the reversing layer. This relation is:

$$N = H^2 / 4\pi kT \quad (9)$$

where N is the ion density, H the magnetic field intensity, k the Boltzmann constant and T the absolute temperature. By the use of observed values for H it was found that the distribution of N was a logarithmic function of the altitude. Making the further assumption that the solar atmosphere was in gravitational equilibrium it was found that the distribution calculated from magnetic data agreed with that required by a gravitational equilibrium distribution when the mean atomic weight of the particles in the reversing

layer was taken as 3.3. A correction for the presence of an electric field was also made but the calculation is not now believed to be valid. In view of the recent work of Unsöld¹⁷ it hardly seems legitimate to talk of equilibrium in the solar atmosphere but if the values of the ion pressure are averaged over a fairly long period the usual expression probably well represents the distribution. On this assumption the ion density n at any level r is given by

$$n = n_0 \exp \left(\frac{-zm_H g(r-R)}{kT} \right) \quad (10)$$

where n_0 is the number of ions per cm^3 at the "surface" of the sun, z the mean atomic weight of the solar ions and R the radius of the sun. We will follow earlier work and assume that the surface of the sun is located at a level where the free paths of the ions are just equal to the radius of the helix generated by an electron as it is caused to spiral about the impressed magnetic field. Extrapolation has shown that the ion pressure at the surface so defined was nearly one half an atmosphere and that the magnetic field intensity was roughly 12,000 gauss. Below this surface the magnetic field is no longer modified by diamagnetism and the electric conductivity is so large that electric fields are negligibly small compared to those outside. Combining (9) and (10) we have

$$H = H_0 \exp \left(\frac{-zm_H g(r-R)}{2kT} \right) \quad (11)$$

where H_0 is the surface magnetic field intensity. We are now able to calculate the difference of potential between the solar surface and outer space. Let this potential difference be ϕ , then from Eq. (8) we have

$$\phi = \int_R^\infty E dr = K_1 \int_R^\infty H dr. \quad (12)$$

The integration is carried out along a path radially outward at the equator which gives by aid of Eq. (11)

$$\phi = \frac{2K_1 H_0 kT}{zm_H g}. \quad (13)$$

Taking therefore $K_1 = 5 \times 10^4$ cm/sec; $H_0 = 1.2 \times 10^4$ gauss; $Z = 3.3$; $m_H = 1.66 \times 10^{-24}$ gm; $g = 2.7 \times 10^4$ cm/sec²; $k = 1.37 \times 10^{-16}$ and $T = 6 \times 10^3$ we get $\phi = 6.6 \times 10^{15}$ e.m.u. or 6.6×10^7 volts. We have pointed out that in the special region where the electron free path is long and the ion free path is short (according to our special definition) the conductivity is moderately large and the electric field must therefore be small. If we assume that the electric field in this region is zero and integrate from the outer edge of the region where H_0 is 280 gauss⁴ out to infinity we find the potential difference to be 1.5×10^6

¹⁷ Unsöld, *Astrophys. J.* 69, 209 (1929).

volts. This is nearly the same potential difference as is observed between the earth and free space. While this calculation cannot be exact since it involves a questionable extrapolation of what may be considered an empirical relation it probably does give a good approximation to the potential difference required to maintain an electric field of the assumed type and distribution.

Special attention should be called to the striking similarity between the the solar magnetic and electric fields and the same fields on the earth. Spectroscopic data show that the solar magnetic field is not unlike that of the earth except for the distortion of the field due to diamagnetic effects in the reversing layer. The requirements in regard to the electric field as deduced in this paper from the observed movements of the solar atmosphere are almost identical with the observed features of the earth's electric field. The earth's electric field in the region of poor electrical conductivity is radially inward, its value drops off with decreasing pressure fairly rapidly in a manner precisely as required in the sun. Moreover the observed potential difference between the surface of the earth and its outer layers is almost identical with that calculated for the sun. The equality of the potentials of the sun and earth seems significant, for conditions on the sun and earth are greatly different and such equality could hardly be expected unless the electric fields arise from the same fundamental mechanism.

A SIMPLE EQUATION FOR THE JOULE-THOMSON EFFECT IN REAL GASES

BY JAMES A. BEATTIE

RESEARCH LABORATORY OF PHYSICAL CHEMISTRY, MASSACHUSETTS INSTITUTE OF TECHNOLOGY

(Received February 1, 1930)

ABSTRACT

Simple approximate relations are given for μC_p and the pressure variation of C_p expressing these quantities as functions of the independent variables p and T . They are derived from the usual thermodynamic relations by use of one form of the Beattie-Bridgeman equation of state, which expresses V as an explicit function of p and T . The values of the Joule-Thomson coefficient μ for air and for ammonia calculated from the relations for μC_p and C_p , equations (10) and (4) respectively, agree well with the observed values in the case of air, and fairly well for ammonia.

The approximate equation for μC_p calculates values of the inversion temperatures of the Joule-Thomson effect in air which are in good agreement with the experimental results.

A VERY sensitive test of an equation of state is the accuracy with which the calculated values of the Joule-Thomson coefficient μ and of the inversion temperatures of the Joule-Thomson effect, at which $\mu = 0$, agree with the experimental results. Keyes¹ has shown that the Joule-Thomson effect in air and carbon dioxide can be calculated by use of his equation of state with good success.

Bridgeman² has derived expressions from the general thermodynamic relations and the Beattie-Bridgeman³ equation of state for μC_p and for the pressure variation of the heat capacity at constant pressure, C_p . The values of μ and of C_p for air computed from these relations agree well with those obtained by Roebuck⁴ from Joule-Thomson measurements which extend from 0 to 280° C and to 220 atmospheres. The equation of state constants used by Bridgeman in this correlation were determined from the compressibility data of Holborn and Schultze.⁵

The values of μ and of the pressure variation of C_p for ammonia calculated⁶ from the expressions obtained by use of the Beattie-Bridgeman equation of state agree well with the experimental results of Osborne, Stimson, Sligh and Cragoe⁷ at the higher temperatures, but the deviations become large at the

* Contribution No. 234.

¹ Keyes, Jour. Amer. Chem. Soc. **43**, 1452 (1921); *ibid.* **46**, 1584 (1924).

² Bridgeman, Phys. Rev. **34**, 527 (1929).

³ Beattie and Bridgeman, Proc. Amer. Acad. Arts and Sci. **63**, 229 (1928).

⁴ Roebuck, Proc. Amer. Acad. Arts and Sci. **60**, 537 (1925).

⁵ Holborn and Schultze, Ann. d. Physik **47**, 1089 (1915); see also Holborn and Otto, Zeits. f. Physik **33**, 1 (1925).

⁶ Beattie, Jour. of Math. and Phys. **9**, 11 (1930).

⁷ Osborne, Stimson, Sligh and Cragoe, Scientific Papers of the Bureau of Standards **20**, 65 (1925).

lower temperatures. The equation of state constants for ammonia used in this comparison were determined from the compressibility measurements of Meyers and Jessup,⁸ which Cragoe⁹ and Osborne, Stimson, Sligh and Cragoe⁷ have shown could be correlated, in part, with the thermal data. The large deviations of the values computed by use of the equation of state from the experimental results at the lower temperatures may be due to either or both of two causes: A slight inconsistency between the thermal and compressibility data, or the failure of the equation of state to reproduce all of the trends of the compressibility data near the saturation line. It should be mentioned, however, that the equation reproduces the compressibility measurements of Meyers and Jessup with an average deviation of 0.043 percent.

The equation of state used for these calculations is:

$$p = \frac{RT}{V} + \frac{\beta}{V^2} + \frac{\gamma}{V^3} + \frac{\delta}{V^4} \quad (1)$$

$$\beta = RTB_0 - A_0 - Rc/T^2$$

$$\gamma = -RTB_0b + A_0a - RB_0c/T^2$$

$$\delta = RB_0bc/T^2$$

where R is the ideal gas constant and A_0 , a , B_0 , b and c are constants for each gas.

The expressions for μC_p and the pressure variation of C_p used by Bridgeman² and by the author⁶ can be derived from the usual thermodynamic relations by use of (1). They are:

$$\mu C_p = \frac{\left[-B_0 + \frac{2A_0}{RT} + \frac{4c}{T^3} \right] + \left[2B_0b - \frac{3A_0a}{RT} + \frac{5B_0c}{T^3} \right] \frac{1}{V} - \frac{6B_0bc}{T^3V^2}}{1 + \frac{2\beta}{RTV} + \frac{3\gamma}{RTV^2} + \frac{4\delta}{RTV^3}} \quad (2)$$

$$C_p = C_p^* - R + (Rc/T^3V) [6 + (3B_0/V) - (2B_0b/V^2)] + \frac{R \{ 1 + [B_0 + (2c/T^3)](1/V) + [-B_0b + (2B_0c/T^3)](1/V^2) - (2B_0bc/T^3V^3) \}^2}{1 + (2\beta/RTV) + (3\gamma/RTV^2) + (4\delta/RTV^3)} \quad (3)$$

where C_p^* is the value of C_p at infinitely low pressures and is a function of the temperature alone. These equations will be called the "complete" relations, since no approximations have been introduced.

Equation (3) can be transformed¹⁰ into the "approximate" expression:

$$C_p = C_p^* + [(2A_0/RT^2) + (12c/T^4)]p; \quad (4)$$

⁸ Meyers and Jessup, *Refrigerating Engineering* 11, 345 (1925).

⁹ Cragoe, *Refrigerating Engineering* 12, 131 (1925).

¹⁰ Beattie, *Phys. Rev.* 34, 1615 (1929).

in which the independent variables are p and T . This relation represents the heat capacity data on air and ammonia almost as well as the "complete" equation (3).

By use of a suitable approximation,¹¹ the equation of state (1) can be written so that V is expressed as an explicit function of p and T :

$$V = \frac{RT}{p} + \frac{\beta}{RT} + \frac{\gamma}{R^2 T^2} p + \frac{\delta}{R^3 T^3} p^2 \quad (5)$$

where β , γ and δ are the functions of the temperature and the equation of state constants given in (1). When the values of the equation of state constants determined for use in equation (1) are substituted into (5), the experimentally measured volumes are calculated very satisfactorily even to 100 atmospheres or over when the temperature is not too near the critical value.

Equation (5) makes it possible to express μC_p and C_p as functions of the independent variables p and T . When the partial differentials in the general thermodynamic relations

$$\mu C_p = T \left(\frac{dV}{dT} \right)_p - V \quad (6)$$

$$\left(\frac{dC_p}{dp} \right)_T = -T \left(\frac{d^2 V}{dT^2} \right)_p \quad (7)$$

are evaluated by (5), and equation (7) integrated between 0 and the variable pressure p , there result:

$$\mu C_p = \left[-B_0 + \frac{2A_0}{RT} + \frac{4c}{T^3} \right] + \left[\frac{2B_0 b}{RT} - \frac{3A_0 a}{R^2 T^2} + \frac{5B_0 c}{RT^4} \right] p - \left[\frac{6B_0 b c}{R^2 T^5} \right] p^2 \quad (8)$$

$$C_p = C_p^* + \left[\frac{2A_0}{RT^2} + \frac{12c}{T^4} \right] p + \left[\frac{B_0 b}{RT^2} - \frac{3A_0 a}{R^2 T^3} + \frac{10B_0 c}{RT^5} \right] p^2 - \left[\frac{10B_0 b c}{R^2 T^6} \right] p^3 \quad (9)$$

It has been shown¹⁰ that the heat capacity of air and ammonia are fairly well represented by the relation (4) which can be obtained from (9) by dropping all terms of higher powers than the first in p . When a similar approximation is made in (8), we obtain a relatively simple equation for μC_p in terms of the variables p and T :

$$\mu C_p = \left[-B_0 + \frac{2A_0}{RT} + \frac{4c}{T^3} \right] + \left[\frac{2B_0 b}{RT} - \frac{3A_0 a}{R^2 T^2} + \frac{5B_0 c}{RT^4} \right] p. \quad (10)$$

The comparisons of the values of μ computed by use of the "approximate" equations (10) and (4) with the experimental results for air and ammonia are given in Tables I and II. For these computations the values of C_p^* for air were calculated by use of (4) from the equation¹²

$$C_p = 0.2405 + 0.000019t$$

¹¹ Beattie, Proc. Nat. Acad. Sci. 16, 14 (1930).

¹² Holborn, Scheel and Henning, "Wärmetabellen". Vieweg, Braunschweig, 1919; p. 58.

where C_p is the specific heat capacity at one atmosphere in 15° calories per gram per degree centigrade and t is in degrees centigrade; the values of C_p^* for ammonia are given by the expression⁷

$$C_p^* = 1.1255 + 0.00238T + \frac{76.8}{T}$$

where C_p^* is in joules(v) per gram per degree centigrade and T is in degrees Kelvin ($^{\circ}\text{C} + 273.1$).

The units of the equation of state constants and those in which the data are expressed are given in the Tables I and II. In the use of equation(4) the reduction factors calculated from data given in International Critical Tables for the term evaluated from the equation of state are: 0.83605 15°-calories/gram per liter-atmospheres/mole for air, and 0.101293 joules (v) per cm^3 -atmospheres for ammonia. The values of C_p derived from (4) were then multiplied by the following reduction factors before use in (10): 1.19609 liter atmospheres/mole per 15° calories/gram for air and 7.5030 cm^3 -meters of mercury per joules (v).

TABLE I. Comparison of the calculated with the observed values of the Joule-Thomson coefficient for air.

Calculations made with Equations (10) and (4).

In units of atmospheres, liters per mole and degrees Kelvin ($T^{\circ}\text{K} = t^{\circ}\text{C} + 273.13$) the values of the constants for air are:

$$R = 0.08206, A_0 = 1.0763, a = 0.01697, \\ B_0 = 0.04070, b = -0.02174, c = 12 \times 10^4.$$

Mol. wt. = 28.960.

Observed values are those of Roebuck.

Temp. °C		0	25	50	75	100	150	200	250	280
Pressure, atm.		Joule-Thomson coefficient, $\mu \times 10^3$, degrees C per atm.								
1	obs.	266	227	189	158	133	93	63	40	30
	obs.-calcd.	-8	1	0	-1	-1	-2	-3	-3	-2
20	obs.	249	212	178	149	124	86	56	35	25
	obs.-calcd.	-6	1	1	1	-1	-2	-4	-4	-3
60	obs.	214	182	153	128	106	71	45	25	16
	obs.-calcd.	-5	-1	0	0	1	-3	-4	-4	-3
100	obs.	178	152	128	107	89	59	35	16	8
	obs.-calcd.	-10	-5	-3	-3	-2	-2	-3	-4	-3
140	obs.	145	124	105	88	72	47	26	9	1
	obs.-calcd.	-16	-11	-7	-4	-4	-2	-2	-2	-2
180	obs.	113	97	83	70	58	37	19	3	-5
	obs.-calcd.	-25	-17	-11	-7	-3	0	1	1	0
220	obs.	81	72	63	54	45	29	13	-2	-11
	obs.-calcd.	-36	-24	-14	-8	-3	-4	5	4	2

The calculated values of μ for air (Table I) agree well with those derived from Roebuck's⁴ data, except at the lowest temperatures, where there are reasons² to believe that the measured values may be in error. The average

deviation of the values calculated by use of the "approximate" relations (10) and (4) is 0.005, whereas Bridgeman² found that the average deviation resulting when the "complete" relations (2) and (3) are used is 0.0035.

TABLE II. *Comparison of the calculated with the observed values of the Joule-Thomson coefficient for ammonia.*

Calculations made with Equations (10) and (4).

In units of atmospheres, cm³ per gram and degrees Kelvin, the values of the constants for ammonia are $R=4.81824$, $A_0=3000$, $a=51.5$, $B_0=0.45$, $b=131$, $c=360 \times 10^6$.

Observed values are those of Osborne, Stimson, Sligh and Cragoe.

Temperature °C	Pressure meters of Hg	μ , °C per meter of Hg		Temperature °C	Pressure meters of Hg	μ , °C per meter of Hg	
		obs.	obs.-calc.			obs.	obs.-calc.
144.95	0.752	1.25	-0.03	30.15	1.527	3.39	.07
	2.323	1.24	-.01		1.532	3.47	.15
110.05	1.512	1.71	.06		1.760	3.42	.12
	10.411	1.70	.25		1.815	3.45	.16
70.05	1.513	2.41	.10		2.308	3.39	.15
52.50	1.303	2.70	-.02		2.326	3.58	.34
	1.518	2.82	.12		4.060	3.64	.58
	2.308	2.78	.14		7.110	3.58	.80
				-5.00	0.392	5.39	.37
					2.307	5.54	1.02
					2.478	5.47	.99
				-12.92	1.475	6.19	1.06
				-18.22	0.394	6.81	.98

The "approximate" equations (10) and (4) lead to values of μ for ammonia (Table II) which are in fair agreement with the experimental results above 30° but in poor agreement at the three lowest temperatures. The same remark⁶ may be made concerning the values calculated by the "complete" equations (2) and (3) with the exception that the agreement is somewhat better throughout. The average deviation for all values at and above 30° C is 0.19 for the "approximate" equation and 0.08 for the "complete."

It is of interest to find out how well the "approximate" relation represents the inversion temperature of the Joule-Thomson effect. This is determined by placing $\mu C_p = 0$, and from (10) we obtain

$$p = - \frac{-B_0 + (2A_0/RT) + (4c/T^3)}{(2B_0b/RT) - (3A_0a/R^2T^2) + (5B_0c/RT^4)} \quad (11)$$

for the relation between the pressure and the inversion temperature. For zero pressure the inversion temperature can be obtained from the relation:

$$-B_0 + \frac{2A_0}{RT} + \frac{4c}{RT^3} = 0. \quad (12)$$

In Figure 1 is given a comparison of the calculated inversion temperature for air determined from (11) by use of the constants given in Table I with the values which Roebuck⁴ derived from his measurements. Figure 1 is a reproduction of Figure 11 of Roebuck's paper with the curve determined by

(11) added. The curves of the inversion temperatures obtained by use of van der Waal's and Dieterici's equations are taken from Roebuck. Comparison of our Figure 1 with Figure 1 of Bridgeman's paper² which gives

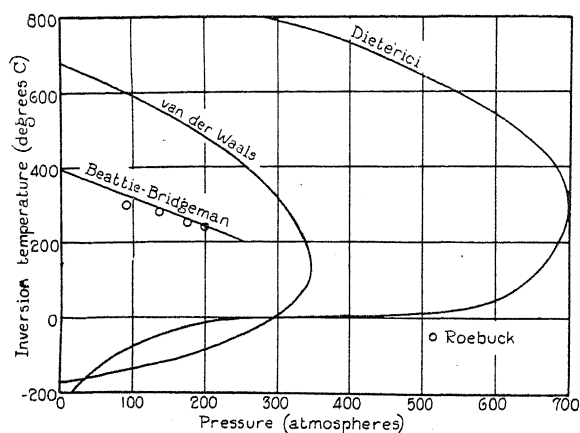


Fig. 1. Inversion temperatures of the Joule-Thomson effect in air.

the curve of the inversion temperatures derived from the "complete" equation shows that the values obtained from the "approximate" equation agree with Roebuck's points as well as those calculated from the "complete" equation.

LETTERS TO THE EDITOR

Prompt publication of brief reports of important discoveries in physics may be secured by addressing them to this department. Closing dates for this department are, for the first issue of the month, the twenty-eighth of the preceding month; for the second issue, the thirteenth of the month. The Board of Editors does not hold itself responsible for the opinions expressed by the correspondents.

Atomic Oxygen as a Reducing Agent

The reducing action of hydrogen peroxide on certain metallic oxides is well known and the analogous reaction might be predicted for atomic oxygen. The authors have spent a considerable amount of time in this laboratory trying to obtain a reducing action by exposing various metallic oxides to a beam of oxygen atoms produced in the electrodeless discharge. No reaction was obtained except in the case of molybdenum trioxide where a reaction was obtained which appears to be identical with the reaction produced by atomic hydrogen. A target which has been covered with a finely divided deposit of molybdenum trioxide, which is light yellow in color, shows the characteristic slate blue trace where the oxygen beam impinges. Not only were traces of atomic hydrogen and atomic oxygen beams produced side by side on the same target, but beams of atomic hydrogen and atomic oxygen were impinged on the same spot in alternation. No change in the appearance of the blue discoloration could be observed on changing from the oxygen to the hydrogen beam, which seems to eliminate the possibility that the reaction with oxygen is the formation of a higher oxide.

Elaborate precautions were taken to free the oxygen from all impurities including water. In order to make certain of the active species the beam was passed through an inhomogeneous magnetic field. The central undeviated line characteristic of atomic oxygen (Phipps and Kurt, Phys. Rev. **34**, 1357, 1929) was readily obtained but no trace of side lines was observed. This is probably due to lack of intensity since the side lines should be fainter than the central line. It may be that the oxygen atom only reacts with the trioxide when it is in the 3P_0 state or it may be of course that the active species is not the atom but an activated molecule, the $^1\Sigma$ state for instance. It should be noted that the molybdenum trioxide is reduced only when it is separated by two slits from the discharge. If only one slit is used or the target is introduced into the discharge the blue coloration disappears almost instantly.

W. H. RODEBUSH

W. A. NICHOLS, Jr.

Laboratory of Physical Chemistry,
University of Illinois,
March 5, 1930.

A Generalization of the Rydberg Formula

On the basis of the old quantum theory it was known that by carrying on a perturbation calculation one arrived successively at the Rydberg and then the Ritz formulas for the terms of a hydrogen-like atom. In the quantum mechanics it has been shown by Hartree (Proc. Camb. Phil. Soc. **24**, 1929) that for an atom with one electron in a central field a generalized Ritz formula holds at least for large values of N . This formula can be written (the series limit is here taken as the zero of frequency).

$$\nu_n = R / (n + \sum_{i=0}^{\infty} q_i \nu_n^i)^2. \quad (1)$$

The ordinary Ritz formula is the approximation obtained when only the first two powers (0 and 1) of ν_n are used. To use more than two constants q_0 and q_1 would make the formula unwieldy and would scarcely help in the complicated cases while in the simpler cases additional constants are unnecessary. The two-constant formula of Ritz is however wholly inadequate to describe certain series of terms especially in the complex atoms.

If one follows the perturbation calculation of the quantum mechanics to two approximations admitting the possibility of more than one optical electron, one is led to suggest a substitute for the Ritz formula which has sometimes important advantages and in the other cases reduces to the Ritz expression. The theoretically derived energy equation can be put into the simple form:

$$\nu_n = R / \left[n + \sum_i p_{in} / (\nu_i - \nu_n) \right]^2 \quad (2)$$

This form involves perhaps a slightly artificial but quite harmless definition of the term for which $i=n$ —so that the first approximation (i.e. Rydberg correction) is taken into account without spoiling the appearance of the formula. For all other terms the ν_i are by no means arbitrary constants but are the observable spectroscopic terms. These as well as the properties of the p_{in} will be described in detail elsewhere. For the present only two remarks will be made.

I. In the most usual case there will be no term difference, ν_i with $p_{in} \neq 0$ small enough to be important. That is, all the terms in the sum can be expanded in powers of ν_n and the ordinary Ritz formula results if one uses only the first two terms in the expansion.

II. If there is more than one electron a possibility arises which has heretofore been left out of account. An electron configuration not belonging to a particular series may have

an energy level for which $\nu_i - \nu_n$ changes sign with varying n while the corresponding p_{in} 's are not zero. The conditions for such a case are too complicated to be described in the present letter further than to say that they are stringent enough to explain why this case is not more common than it is found to be. In the neighborhood of such a ν_i the terms will be given by

$$\nu_n = R / [n + q_0 + P / (\nu_i - \nu_n)]^2 \quad (3)$$

and will show a remarkable irregularity which was first observed by Schrödinger (Ann. d. Physik 77, 1925).

This case which arises, e.g. in Pb I, Ca I, Hg I, Al II, Si III, etc. is possibly the most common form of irregularity and in the past has invariably led to misidentification of terms. If one takes the theory into account and reassigns quantum numbers accordingly the applicability of Eq. (3) is obvious. The term ν_i is incidentally located and because of the conditions on p_{in} is fairly definitely identified.

The chief contribution of this work is the satisfaction one gets from the elimination of an apparent flaw in our notions of line spectra. It permits a temporary relief from the feeling that our present theory is not complete enough.

R. M. LANGER

National Research Fellow,
University of Berlin,
February 14, 1930.

The Reflection of Hydrogen Atoms From Crystals of Lithium Fluoride

The work on the reflection of hydrogen atoms is now being extended to a study of the reflection from LiF crystals. These crystals were grown from the melt by a modification of the method of Ramsperger and Melvin, (Jour. Opt. Soc. 15, 359, 1927). A freshly cleaved surface was mounted in the apparatus formerly used in the study of the reflection from NaCl and KCl, (Frank. Inst. 206, 301, 1928), and bombarded with a sharply defined beam of hydrogen atoms issuing from a discharge tube.

Under favorable conditions the reflection in the specular beam from LiF was as high as 50% of the incident beam, as compared with 5% from NaCl, and 0.5% from KCl. As in the case of the other alkali halides which have been studied, the specularly reflected beam

from LiF is confined to within the same angular breadth as the incident beam.

During the course of the investigation some peculiar fan-shaped patterns consisting of a central spot with radial streamers appeared on the molybdenum oxide coated detecting plate. Simultaneous with the appearance of these patterns the LiF crystal lost its atomic reflecting power and acquired a brownish tinge similar to what is usually observed on glass when bombarded by ions or electrons. If the copper crystal holder was maintained at +110 volts with respect to the surrounding case, these patterns disappeared. Furthermore, it was found that when the crystal holder was insulated similar patterns appeared on the plate even though the crystal was removed from the holder. It was therefore dem-

onstrated that these patterns were due merely to the electrostatic repulsion of the ions in the beam by the charge which accumulated on the crystal and the crystal holder. By applying an electric field across the beam to remove the ions, the fan-shaped patterns disappeared, the crystal remained clear, and its high reflecting power persisted for a long time.

With the discovery of this effect of ion bombardment on the reflecting power of LiF it became of interest to make a reinvestigation of the reflecting power of NaCl and KCl with

the ions removed from the beam. The reflection from these crystals, however, appeared to be unaffected by the ion concentrations present.

The fact that the electrostatic charging of an insulated surface can deflect a beam of ions into irregular patterns, shows that one must be cautious in interpreting any pattern as the diffraction of de Broglie waves when ions or electrons are reflected from insulated crystals.

THOMAS H. JOHNSON

The Bartol Research Foundation,

February 19, 1930.

Multiple Coincidences of Geiger-Müller Tube-Counters

The ordinary method of coincidences [e.g. Bothe and Kolhörster, *Zeits. f. Physik* 56, 751 (1929)] does not make possible the performance of experiments upon the individual very high energy β -particles which presumably give rise to the coincidences between Geiger-Müller tube-counters (*elektronenzählröhre*), chiefly because suitable collimation by slits is nearly impossible in the interesting region of very high energies (10^8 to 10^9 volts) which this new instrument has opened to analytical experimental attack. It occurred to the writer some weeks ago that the observation of the coincidences between *three* tube-counters would make such a study possible. The first two counters would serve as a slit-system, defining a beam and "picking out" individual particles to be observed while the third movable counter would serve to detect these particles after being scattered, deflected by a magnetic field, or otherwise subjected to experimental conditions. Experiments are under way here for obtaining information on the probability of deflection of such extremely fast β -particles in various (small) angles in passing through a scattering block. The theory of multiple scattering indicates that the deflections may be below the practical limits of angular resolution, but even an upper limit, experimentally determined, for such extremely fast particles will be of interest. Other applications are readily devised.

This arrangement has another advantage which may be immediately appreciated—that of increased "resolving power" against accidental coincidences. If the resolving power of the means for determining coincidences between two tube-counters is such that say one out of 200 (residual) counts (a practical

figure) in each individual tube-counter will be accidentally "coincident" within the specified range of resolution, the probability of such an accidental coincidence of *three* tube-counters within the same range of resolution is 1 out of 40,000. The idea of the *multiple*-coincidence method using a series of counters is an obvious extrapolation. Theoretically, any desired degree of freedom from accidental coincidence can readily be obtained, provided, of course, that the efficiency of counting is 100 per cent, as has been shown to be approximately true for β -particles. We do not yet have sufficient data to say how nearly true this is for the very fast particles with which we are dealing. Scattering deflections of the primary particle at the walls of the counters or in the air between counters will set an ultimate limit on the resolution which can be reached in practice even with perfect counting. Secondary effects may also be of importance. The actual resolving power will be less than that calculated on a probability basis also by reason of true coincidences produced only in part of the series of tube-counters by particles not capable of passing through the whole series. There is no doubt, however, that enormously increased resolving power can be obtained by the requirement of multiple instead of paired coincidences. The attainment of very great freedom from accidental coincidences is of greatest importance when it is desired to reduce the solid angle subtended by the tube-counters for true coincidences to a small figure, because of the large number of residual counts in comparison to those due to the very small intensity of the penetrating radiation. The possibility of using the multiple-coincidence method as the basis of a "gamma-ray tele-

scope" for exploring small areas of the sky is being investigated. The intensity of the penetrating radiation is very low for such a purpose if the definition of really small areas is desired unless, of course, later observations show the penetrating radiation to come from particular small areas of the sky rather than uniformly from all directions. An estimate hazarded on the basis of present data, assuming uniform intensity per unit solid angle, gives as the order of magnitude one true coincidence per 1,000 minutes for counters of cross-section 50 cm², subtending one square degree in the sky. Automatic recording of the amount of the penetrating radiation coming from particular areas of the sky, using two tube-counters and a special "coincidence circuit" somewhat similar to that recently published by Bothe [Zeits. f. Physik, 59, 1 (1929)] was begun here early last November. The resolving power (for our circuit between 0.005 and 0.001 second) of such an arrangement without *multiple* coincidences constitutes a severe limitation on the smallness of the area which can be observed.

A few practical notes on a brief oscillographic study of the recovery-time of a tube-counter and associated amplifier-circuits under various conditions may be of interest to others who are using the instrument. The high resistances (5×10^9 ohms) used by Geiger and Müller and others require the tube-counter to operate at a variable voltage, since the time-constant of the circuit is even larger than the average time between counts, whereas lower resistances restrict the range of voltages which give satisfactory counting. By connecting the central wire of the tube-counter directly

to the grid of the amplifier-tube, the recovery-time of the tube-counter may be observed. Oscillograms have been taken using this circuit with resistances from 1 to 5,000 megohms. The recovery-time increases rapidly as the voltage is raised above the minimum critical voltage at which counts begin (which is the same for all values of R), and varies by a factor of perhaps five for different single counts at any given voltage. The average recovery-time (to within five volts of the initial potential on the central wire) varies from perhaps 0.002 second at a voltage midway in the working range (of only a few volts) for $R=1$ megohm, to two seconds or more for $R=5,000$ megohms, where the true working range (actual voltage between central wire and tube) is considerably more than 100 volts. In spite of this very long recovery time of the tube-counter itself, however, a 0.00004 μ f blocking condenser between the tube-counter and the amplifier-grid, and a grid-resistance of 10 megohms, as used by Bothe, gives satisfactory counts on the first amplifier-tube up to several hundred per minute, and the recovery-time of this amplifier-tube is of the order of 0.001 second. The oscillograms using this arrangement show that of two counts 0.01 second apart the second one will be usually missed, but counts 0.1 second apart give ample impulses (UX201A tubes were used). These results could have been safely inferred, but perhaps some interest may be attached to their demonstration by oscillograms.

M. A. TUVE

Department of Terrestrial Magnetism,
Carnegie Institution of Washington,
February 24, 1930.

Temperature Shift of Spectral Lines and Pole Effect in Vacuum Arc

The work of many investigators has shown that the wave-length of most emission lines is a linear function of the total pressure acting when the vapor is in an arc, a furnace, or an absorption tube. It has been considered that the pressure shift per atmosphere is independent of the temperature. This implies that the experimental wave-length of a line from a source operating at constant pressure is independent of temperature. The chief purpose of this note is to report experimental evidence indicating that this view may be incorrect.

Two conclusions may be drawn from previous work: (1) that the wave-length of a line under given conditions of temperature

and pressure is, at least for low values, independent of the partial pressure of the vapor, and (2) that ionic density plays a small part, if any, in the phenomenon of pressure shift. The first is justified by the conclusion of Babcock¹ that pressure shift is independent of changes in vapor density. The second may be justified by consideration of the results of King² and of Füchtbauer, Joos, and Dinkelacker.³ King found a larger pressure shift per

¹ Babcock, *Astrophys. J.* 67, 240 (1928).

² King, *Astrophys. J.* 35, 183 (1912).

³ Füchtbauer, Joos, and Dinkelacker, *Ann. d. Physik* 71, 204 (1923).

atmosphere in the furnace than Babcock¹ found for the same iron lines in the arc. The value of the mean ratio for the pressure shift of lines common to the two lists is 2.3 with an average deviation of 0.3. The second paper reports pressure shifts for $\lambda 2537$ of mercury in absorption at room temperature. These results indicate that molecular density, while not the ultimate cause, is probably the controlling factor in pressure shift.

An increase in pressure at constant temperature indicates an increased density of molecules. This change usually causes an increase in wave-length. A decrease in temperature at constant pressure might be expected to operate similarly.

The core of an iron arc of the Pfund type with cathode below is surrounded by a rather thick envelope of iron vapor and iron oxide dust. In an effort to establish the existence of a temperature shift a layer of this envelope was used by the author as a low temperature source of iron lines, while the central section of the arc with polarity reversed was used as a high temperature source. Two of the three lines selected for this test showed a shift in the direction indicated above, and of the right order of magnitude.

In order to check these results plates were taken of $\lambda 5890$ of sodium. Shifts measured between four different types of sources gave results qualitatively in agreement with that indicated by the previous paragraph. It is considered that neither line asymmetry nor fine structure, as reported by Minkowski⁴ and Schüler⁵ respectively, can account for all the experimental data as easily as the hypothesis here suggested.

⁴ Minkowski, *Zeits. f. Physik* 55, 16 (1929).

⁵ Schüler, *Naturwiss.* 16, 512 (1928).

It therefore seems possible to measure, by means of this phenomenon, effective flame, arc, and furnace temperatures when the pressure is known. Assuming that the wave-length of a line is a linear function of the number of molecules per unit volume, that ionic fields of high value were absent from the sources of Babcock and King, and that the effective temperature of King's furnace was 2000°C , the calculated temperature of the effective emission point of Babcock's iron arc for the lines common to both lists is $5000^{\circ}\text{C} \pm 700^{\circ}\text{C}$.

St. John and Babcock⁶ found that a 6 mm iron arc was practically free from pole effect at pressures below 10 cm. However, an anomalous behavior of the yellow sodium lines has been reported by Kiess.⁷ Both lines showed a shift of 0.004A between absorption in a low pressure tube and emission in a vacuum arc at 6 cm pressure. This indicates either that the pressure shift is non-linear at low pressures or that a positive pole effect existed in the arc used. Two sets of plates of $\lambda 5890$ taken by the author showed a positive pole effect of 0.005A and 0.006A respectively in a carbon arc operated at about 10 cm pressure. Therefore it is suggested that care be used in applying this result of St. John and Babcock to any conditions other than those investigated by them.

All plates were taken at Yale University.

F. T. HOLMES

Department of Physics,

Lehigh University,

Bethlehem, Pa.

February 26, 1930.

⁶ St. John and Babcock, *Astrophys. J.* 42, 231 (1915).

⁷ Kiess, *J.O.S.A. and R.S.I.* 18, 169 (1929).

Emission of Positive Ions From Thoriated Tungsten

In an earlier note, it was reported that tungsten when heated gave off positively charged tungsten ions. The emission from thoriated tungsten has been investigated and in addition to tungsten ions of mass 184, thorium ions of mass 232 and an ion of mass 247 ± 2 have been obtained. This latter ion may be thorium monoxide, although all attempts to reduce it with H_2 have failed. It appears at an estimated temperature of about

2300°C . The alternative explanation is that it is some other extremely stable compound or an element. An x-ray investigation of various thorium sources is under way to settle this last possibility.

H. B. WAHLIN

Laboratory of Physics,

University of Wisconsin,

February 28, 1930.

BOOK REVIEWS

Hydro-und Aeromechanik, Vol. 1. O. TIETJENS. Nach Vorlesungen von L. Prandtl. Pp. 238, figs. 178. Verlag von J. Springer, Berlin, 1929. Price RM 15.

This is a well-written introduction to the Hydro and Aerodynamics of inviscid fluids. The first section, which deals with topics that are of importance in aerostatics, is pleasing to the reader as it opens with brief sketches of the early work of Euler and Stevin on the pressure of fluids and then contains a particularly clear presentation of the statics of the atmosphere and the effect of different atmospheric conditions upon the behavior of a balloon. The section closes with an account of the phenomena of capillarity.

The second section is devoted to the kinematics of liquids and gases. It is pointed out that vortex-lines, stream-lines and paths of particles are not the only lines of kinematical importance because experiments in which foreign matter is introduced into the fluid at some point to render the motion visible have directed attention to the streak-lines (Streichlinien). A method of constructing streak-lines is explained and illustrated by means of diagrams. The section also contains a presentation of the geometry of vector fields and special attention is paid to the kinematical boundary conditions; in particular, the flow near the points of stagnation is discussed in an illuminating way and it is emphasized that liquids and gases are not ideal but only *quasi-continua*.

Section three deals with the dynamics of inviscid fluids and includes important applications of Bernoulli's Equation and Potential Motions. The chapters on vortex-motion and the influence of compressibility are particularly striking and should be of great help to the student who wishes to master the particularly fruitful methods by which Ludwig Prandtl has rejuvenated the science of Hydrodynamics.

H. BATEMAN

La Nouvelle Mecanique des Quanta. GEORGE BIRTWISTLE. Pp. vi+333. Paris, Librairie Scientifique Albert Blanchard, 1929.

This French translation of Birtwistle's book, "The New Quantum Mechanics" is hardly likely to be of much interest to American physicists. The English original¹ was a hasty compilation of the results of the new methods in atomic physics which was useful for reference in regard to formulas although it contributed scarcely anything toward a clear understanding of the theory. The French edition has four appendices by the translators, M. Ponte and Y. Rocard, amounting to 30 pages giving brief accounts of Dirac's relativistic electron theory, the revised electron theory of metals, fluctuations in the new statistics and the so-called "hydrodynamic" interpretation of wave mechanics.

E. U. CONDON

¹ Reviewed in Phys. Rev. 33, 869 (1929).

The Terminology of Physical Science. DUANE ROLLER. Pp. 115, demy 8 vo. Paper cover. University of Oklahoma Press, 1929. Price \$1.00.

Readers of text-books and research reports, and listeners to lectures and recitations are often irritated by non-conformity in the choice of words or in pronunciation. The booklet under review voices the irritation of one such reader and listener. The reviewer sympathizes with the author's state of mind but doubts the feasibility of his proposed reform by proclamation. The chance of success would be greater in this case if the author had not made blunders in etymology, shown little understanding of differences between synonyms, and used his non-scientific English inexpertly. The reader may also be shocked by the author's readiness to

recommend wide departures from standard usage and by his propensity for log-rolling in favor of his colleagues.

In spite of obvious faults of presentation the monograph should prove interesting and stimulating to members of that small group of physicists who wish to improve the intelligibility of their science. The fragmentary remarks on non-technical terms and on technical terms used in half a dozen other sciences are outside the scope of this review.

L. W. McKEEHAN

PROCEEDINGS
OF THE
AMERICAN PHYSICAL SOCIETY

MINUTES OF THE NEW YORK MEETING, FEBRUARY 21 AND 22, 1930

The 162nd regular meeting of the American Physical Society was held in New York City at the Physics Laboratories of Columbia University on Friday and Saturday, February 21 and 22, 1930. The presiding officers were Professor Henry G. Gale, President of the Society, Dr. W. F. G. Swann, Vice-President, Professor John Zeleny and Dr. Arthur E. Ruark.

The Saturday morning session was given over to a Symposium of Photoelectric and Thermionic Phenomena. The speakers were F. L. Mohler, F. K. Richtmyer, William V. Houston, C. E. Mendenhall and G. Wentzel. The titles of their papers appear in the following list of abstracts, numbered 46-50 inclusive. The symposium was attended by over 400 persons.

At the regular meeting of the Council held on Friday, February 21, 1930 twenty-two were elected to membership. *Elected to Membership*: Eugene C. Bingham, Kenneth C. Blanchard, Willard E. Bleick, Leo P. Delsasso, A. M. I. A. W. Durnford, Frank M. Exner, Charles F. Ffolliott, D. A. Fogelsanger, Omer R. Fouts, James D. Hardy, Mituyosi Igari, A. L. Johnson Jr., Wendell R. Koch, Richard H. Lee, William G. Moran, Yoshio Nishina, Luhr Overton, Elmer N. Turnquist, J. S. Webb, Herman G. Wehe, Donald B. Woodbridge and Oliver R. Wulf.

The regular scientific session consisted of 63 papers, Numbers 1, 2, 3, 8, 14, 15, 20, 32, 33, 42, 57 and 58 were read by title. The abstracts of these papers are given in the following pages. An *Author Index* will be found at the end.

W. L. SEVERINGHAUS
Secretary

ABSTRACTS

1. Transient earth currents accompanying the recent Newfoundland earthquake of 1929. RICHARD HAMER, *Acadia University*.—It does not seem to have been recorded hitherto that transient electric and magnetic disturbances were associated with earthquakes. It seems certain that such did accompany the recent earthquake off Newfoundland. Observations, similar or related, of others, besides personal, have been reported supporting the author's contention. The geophysical importance of such a fact is obvious. Several years ago the author proposed to account for variations of the earth's magnetic elements by assuming circulating earth currents. This granted, earth movements would obviously be accompanied by transient electron readjustments. However other possible causes exist; such as temporary readjustments of the electric activity of large mineral deposits and certain strata; also the possible frictional electricity generated due to the relative motion at the long break; and also polarization from fracture or piezoelectric effects on variations of stresses. By induction if not by conduction the temporary

influence of such electrical disturbances was transmitted with a speed approaching that of light in an expanding area around the epicenter. Ordinary seismic waves followed arriving later and later relatively at more distant regions. Thus the author determined the epicenter. The importance of studying earthquakes from this new angle is emphasized.

2. A modification of Wiechert's experiment. T. R. WILKINS AND J. A. WOOD, *University of Rochester*.—Wiechert's single equation method for a direct determination of the speeds of corpuscles has been modified by using a vacuum tube oscillator and an electrostatic deflecting field. This revives an experiment, theoretically very attractive but which has been experimentally extremely difficult. (See J. J. Thomson—Conduction of Electricity through gases.) Since the period of the oscillator can be held very constant, the difficulties experienced by earlier experimenters who used Tesla Coils and large high frequency currents to energize the deflecting fields disappear. The method would seem equally applicable to positive ray analysis or as a general corpuscular filter.

3. Polar molecules—their contribution to energy loss. F. HAMBURGER JR., *Johns Hopkins University*, (Introduced by J. B. Whitehead).—Some discussion has taken place during the last year as to the possible effects of molecular orientation as a source of dielectric loss. The suggestion has been offered that even at frequencies as low as those of commercial power circuits the theory of molecular orientation may be offered as an explanation of at least a portion of the dielectric loss. This paper is an attempt to examine this suggestion on the basis of the Debye theory and the available experimental data. It shows that in the case of glycerine at temperatures of zero and ten degrees Centigrade the loss due to orientation, at frequencies below ten thousand cycles per second, is negligible. Furthermore, it indicates that for the usual insulating oils, the possibility of accounting for even a portion of the dielectric loss observed at commercial frequencies, on the basis of molecular orientation, is remote.

4. Magnetoresistance and elastoresistance in permalloy. L. W. MCKEEHAN, *Yale University*.—A continuation of preliminary work reported by Arnold and McKeehan (Phys. Rev. [2] 23, 114 (1924)). The effect of intensity of tensile stress upon the change in resistance due to magnetization has been observed in straight wires of annealed permalloy over a wide range in composition. Additional studies have been made on specimens containing 45, 77 and 84 percent nickel. In these latter wires the magnetization and resistance have been measured simultaneously. The resistance for a given magnetization is not single-valued, although a symmetrical "hysteresis" loop on the magnetization-resistance plane may cross itself. The magnetic fields were produced by long solenoids and the magnetic field intensity did not exceed 50 gauss in the definitive experiments. Under suitable conditions, however, this field intensity is sufficient for approximate saturation of the magnetoresistance effect. The results lend support to the view that adjacent atoms in a pure ferro-magnetic metal, and—a fortiori—in a ferromagnetic alloy, differ widely in those constraints which determine their dirigibility by externally applied forces.

5. Stabilized oscilloscope with amplified stabilization. FREDERICK BEDELL AND JACKSON G. KUHN, *Cornell University*.—One stage of amplification included in the stabilizing circuit of the Bedell-Reich oscilloscope, which comprises a cathode-ray tube with linear time-axis for observation of periodically varying quantities, extends the range of frequencies through which the curves on the screen of the cathode-ray tube may be stabilized and maintained stationary so that they can be photographed either with camera or contact print. Linearity of time-scale is shown by equality of successive wave-lengths and is controlled by an equalizing adjustment. Although not primarily intended for use beyond the audio range, the instrument has in this way been stabilized above 100,000 cycles. Curves are given showing the use of the instrument for the study of electrical quantities, as in the study of modulation and rectification, the ripple voltages in B-eliminators and filters and the wave-form of different oscillators; also curves obtained with photo-electric cell, showing flicker in candle-power in light sources, and curves, obtained with condenser microphone, showing wave-form of notes from musical instruments, the violin and clarinet. To be published in Review Scien. Instruments, April, 1930.

6. The initial stages of electrical breakdown. J. W. BEAMS AND J. C. STREET, *University of Virginia*.—A Kerr cell method (Beams, *Jour. Franklin Inst.* **206**, 809, (1929)), a simple comparison arrangement and a method making use of a rapidly rotating mirror (Beams, *Phys. Rev.* **33**, 1086 (A) (1929) have been used to determine the average time lag of the spark. The last method has also been used to photograph the different stages of the discharge. The time lag is decreased by ultra-violet light on the cathode, ions in the gap or by increasing the field strength. When a field of 4×10^4 volts/cm is very suddenly impressed, in ordinary air at atmospheric pressure containing the usual number of ions the average time lag is less than 5×10^{-8} sec. In dry filtered air, at atmospheric pressure, from which as many ions as possible were removed by auxiliary fields, 6×10^5 volts/cm could be applied for over 10^{-6} sec. without breakdown. Similar results were obtained with dry filtered hydrogen and nitrogen. Brass ball electrodes were used. The velocity of expansion of the spark is increased with decrease of pressure. At atmospheric pressure, the luminosity near the cathode becomes the most intense in approximately 2×10^{-7} sec. and gives rise to the well-known streamers. However at pressures roughly from 0.008 mm to 0.001 mm the anode luminosity was found to be the most intense.

7. Some new types of electrical discharge in high vacua. R. W. WOOD, *Johns Hopkins University*.—Discharges excited in such high vacua as to be called non-conducting in the usual sense, excited through external electrodes with high frequency oscillators of wave-lengths varying from two to thirty meters. The effects of electric and magnetic fields upon the curious luminous balls and spindle shaped bodies (which have been named "plasmoids" provisionally) have been exhaustively studied, as well as the curious red phosphorescence of the glass which usually appears. Some progress has been made towards the explanation of these discharges by employing stroboscopic methods. The remarkable pressure changes which occur in the sealed off tubes as a result of "clean-up" or gas-evolution have been followed by vibrating quartz fiber mano-meters.

8. Complete dissociation of H_2 . E. U. CONDON, *University of Minnesota*.—It is well known that where nuclear motions are involved mere energy sufficiency does not always make possible processes of excitation by electron impact or light absorption. Usually the critical potential in molecular hydrogen near 30 volts is interpreted as $H_2 \rightarrow H^+ + H^+ +$ two electrons for which the energy needed is $4.4 +$ twice $13.5 = 31.4$ volts. But this cannot be since if both electrons be removed the nuclei possess a mutual potential energy of about 18 volts. Therefore this process should require about 50 volts and when it occurs the protons formed would have kinetic energy of about 9 volts each. Just as Condon and Smyth (*Proc. Nat. Acad.* **14**, 871 (1928)) have interpreted the 11 volt dissociation as due to transitions from the normal state to the repulsive Heitler-London potential energy curve so now it is suggested that the loss at 30 volts is due to transitions from the normal state of H_2 to the repulsive Morse-Stueckelberg curve of H_2^+ in which case the process produces protons having about 6 volts of kinetic energy.

9. The primary ions formed by electron impact in hydrogen. WALKER BLEAKNEY AND JOHN T. TATE, *University of Minnesota*.—The results of a study of the primary products of ionization in hydrogen obtained with a mass spectrograph previously described (*Phys. Rev.* **34**, 157 (1929)) indicate that there are at least three different processes by which an ion may be formed by a single impact with an electron. (1) The molecular ion H_2^+ appears at 15.4 ± 0.1 volts as the result of the removal of one electron. (2) Ionization and dissociation occur simultaneously, yielding the atomic ion H^+ at a minimum potential of 18.0 ± 0.2 volts. (3) At about 30 volts another ion is formed, presumably H^+ , which is characterized by the fact that it has several volts kinetic energy. It appears in the analyzer as a very broad peak and it also has been found to reach a side plate against the influence of a retarding field. The reactions (2) and (3) are much less probable than (1). These effects find a theoretical interpretation in the potential energy curves of Morse and Stueckelberg for the hydrogen molecule, as Condon has pointed out in the preceding paper.

10. The reflection of hydrogen atoms from crystals of lithium fluoride. THOMAS H. JOHNSON, *The Bartol Research Foundation*.—The reflection of hydrogen atoms from crystals

studied at first with NaCl and KCl crystals is now being extended to other alkali halides. The preliminary results with lithium fluoride are interesting in two respects. In the first place a sharply defined specular beam appeared as with the other alkali halides heretofore tried but LiF may, under favorable conditions, reflect up to about fifty percent of the incident beam in the specular direction as compared with 5 percent for NaCl and 0.5 percent for KCl. In the second place it has been found that the reflecting power of LiF is strongly affected by the action of the atomic hydrogen or other products of the discharge tube which is used as the source of the atomic beam. Thus it has been found that a crystal at room temperature, though exposed to atmospheric air and to the molecular hydrogen from the unexcited discharge tube for some time, reflected the atomic beam intensely at first but the reflection had fallen off to one half of its initial intensity in a time of the order of one minute. At higher temperatures the same fatigue occurred but the reflection persisted for longer times up to about an hour.

11. Molecular beams in electromagnetic fields. D. E. OLSHEVSKY, *Yale University*.—A systematic synthetic study of possible arrangements of the vector quantities characteristic of a molecular beam experiment such as field strength, field gradient, molecular moment, velocity of beam and force is made. Known experimental arrangements of Kallman-Reiche, Stern-Gerlach, Rabi and of Clark are thus classified and their features clearly brought out. Analysis yields several new experimental arrangements of interest. Briefly, they are: (a) Reversal of beam direction in Rabi's experiment, the last slit being in the magnetic field and beam coming out of the field, with expected improvement in resolution; (b) Arrangement of field gradient at right angles to field and beam direction with possibility of detecting molecules oriented perpendicular to field; (c) Arrangement with the second slit consisting of two closely spaced, field producing wedges, the beam perpendicularly to the plane of the slit. Arrangement (c) seems to be particularly efficient due to the fact that the beam can be left larger than slit spacing, the second slit serving as a highly efficient microscopical field-producing unit.

12. Recombination of hydrogen-like atoms. E. C. G. STUECKELBERG AND PHILIP M. MORSE, *Princeton University*.—The probability that an electron moving with a velocity of V volts recombines with a hydrogen ion or with an ion having a similar field and resultant nuclear charge Ze to form an atom in a state defined by the quantum numbers n, l is usually expressed by the effective cross section of recombination $q(n, l, Z, V)$ cm². The transition probabilities have been calculated from the matrix elements referring to the two states. A solution of the Schroedinger equation in a Coulomb field giving at large distances a plane wave has been found by Mott and by Temple. With the aid of this function an exact expression for the q 's has been obtained, which decreases monotonically with increasing V . For V small compared to $-E_{n,l}$ (the term value) an asymptotic formula can be used of the form $q(n, l, Z, V) = 1.237 \times 10^{-10} \cdot e^{-4n} \cdot C_{n,l} \cdot Z^2/V$. The values for $C_{n,l}$ have been computed for $l=0$ and $n=1, 2$ and 3 ; for $l=1$ and $n=2$ and 3 . $C_{n,l} \cdot e^{-4n}$ decreases for increasing n and approaches 0 for $n = \infty$. For some of the states the exact expressions for any V have been computed. They show in order of magnitude as well as in functional behavior a fair agreement with the older theories and the experiment. However, this theory can not explain the experiments by Barnes and Davis and it seems that their results must be due to a more complex reaction than simple recombination.

13. A search for critical potentials for electron recombination with Hg^+ . A. M. CRAVATH, (*National Research Fellow*), *Princeton University*.—The discovery by Davis and Barnes (Phys. Rev. **34**, 152 (1929)) that electrons which have just enough energy to ionize He^+ recombine astonishingly rapidly with He^{++} suggested a search for recombination of 10.4 volt electrons with Hg^+ . A cylindrical ring electrode 0.6 cm long, 2.5 cm diameter, was placed in a large Hg vapor arc, pressure 0.01 mm, ions per cm³ up to 1.5×10^{11} . Electrons from a small oxide coated filament along the axis of the cylinder were accelerated in the thin sheath around the filament and then travelled out radially through the nearly equipotential ionized vapor to the cylinder whose potential was positive to the filament but negative to the space. The effect sought was a sharp reduction in the electron current reaching the cylinder when the electron energy passed through 10.4 volts. No effect was found. This may be due to the narrow-

ness to the range of energies for which recombination has a high probability, only a fraction of the electrons in the stream from the filament ($T \sim 1000^\circ\text{K}$) having energies in this range. If this range had been comparable in width to the peaks in Davis and Barnes' experimental curves practically the whole electron stream would have been stopped.

14. Sorting the variables in the crystal structures of certain chromium-nickel alloys. F. C. BLAKE AND JAMES O. LORD, *Ohio State University*.—Microphotographs of certain chromium nickel alloys containing from 63 to 85 percent chromium revealed three phases present. The melts were made in a partial vacuum in crucible of alumina and were practically free from carbon. It was noted in general that after the power for the furnace was shut off but the partial vacuum maintained that the vacuum increased showing that some of the residual gases were being absorbed by the melt. Examination revealed nitrogen present in the melt. One phase was readily found to be body-centered chromium. Further experimentation revealed another phase to be chromium nitride and by the use of proper etching reagents a third phase was found to be chromium nickelide, Cr_2Ni , with ninety-six atoms to the unit cell, the cell consisting of four interpenetrating lattices of nickel with four other interpenetrating lattices of chromium, the lattice being body-centered tetragonal with $a = 10.64\text{\AA}$ and with an axial ratio of 1.040. The density of the tetragonal phase is identical with that of body-centered chromium, viz. 6.93. Both the nickelide and the nitride are very hard and practically insoluble in hot aqua regia, especially the nitride. The lattice of chromium nitride was proved to be close-packed hexagonal with $a = 2.751\text{\AA}$, the axial ratio being 1.605, the unit cell consisting of two atoms of chromium and two of nitrogen. This gives a calculated density for chromium nitride of 7.75. The space group for the nitride is D_3^2 with the two nitrogen atoms interpenetrating. The possibility of a fourth phase being present is discussed.

15. An interesting case of a unit lattice made up of interpenetrating lattices. F. C. BLAKE, *Ohio State University*.—Some of the most interesting and important cases of alloys and solid solutions can be studied only by the powder method, for with several phases present no method has yet been devised for obtaining large single crystals of the phases separately. Indeed the importance of many of the alloys industrially is due to the very fact that their crystallinity consists only of microcrystals. Thus the powder method is the only one available. After considerable effort spent more or less uselessly trying to guess at the structure of a tetragonal chromium nickelide a deliberate attempt was made to see if one could build up synthetically a series of interpenetrating lattices of chromium and nickel which would give the reflection intensities observed. This was found to be possible, the lattice consisting of thirty-two atoms of nickel and sixty-four of chromium and having the property of unusual hardness spoken of by Professor W. H. Bragg (Proc. Royal Inst. XXVI, 6 (1929)) for many-atomed lattices of alloys of copper with aluminum, zinc and tin. The most interesting property of such a lattice is that the first sixteen lines that one might expect to be strong on the powder photograph do not appear at all, in agreement with observation. The space-group of the lattice found is D_{10}^4 , a hemihedral form.

16. The classes of symmetry possible in crystals of elements. R. H. CANFIELD, *Naval Research Laboratory, Anacostia, D. C.* The object of this study is to determine the types of space-lattices possible in crystals composed of atoms of one kind and subject only to mutual central forces, the force between two atoms being zero for only one value of the distance. It is found that the conditions of equilibrium of one atom require that the center of gravity of any group of atoms which lie on the surface of a sphere shall lie at the center of the sphere. This condition of what may be termed "barycentric symmetry" limits the possibilities to 21 out of the 32 recognized classes of symmetry. Equilibrium against a generalized infinitesimal strain of the whole crystal imposes the condition that the principal axes of inertia of all such spherical groups of atoms shall have the same directions, and the principal moments of inertia be in the same proportion. This limits the possible classes still further to the five classes of the cubic system. It is concluded that since there are many exceptions to the latter rule many crystals even of elements cannot be regarded as homopolar in the sense of the first paragraph.

17. Excitation potential of the $L\alpha$ satellites of Ag (47). S. W. BARNES AND F. K. RICHTMYER, *Cornell University*. A precise knowledge of the excitation potentials of satellites should make it possible to distinguish between the Wentzel-Druyvesteyn theory of their origin and the so-called "two-electron jump" theory proposed by one of the present authors. The very meagre data in existence indicate that the excitation potentials of satellites are of the order of 20–40 percent higher than those of the corresponding parent lines. Using a Siegbahn vacuum spectrograph and a transformer-kenotron-inductance voltage supply which gave a ripple of much less than one percent, a series of exposures were made at 7, 6, 5, 4.5 and 4.4 kilovolts, respectively, on the $L\alpha$ line of Ag(47), the excitation potential of which is 3.35 k.v. Satellites were clearly visible on the plates taken at 4.5 k.v. and higher, but were not visible on the plate taken at 4.4 k.v., although the intensity of the parent line on the 4.4 k.v. plate was greater than on that at 4.5 k.v. However, the $L\alpha$ line at 3.8 k.v. shows an unsymmetrical "foot", which may indicate the presence of an unresolved satellite structure. If so, the excitation potential of the satellites may be much lower than 4.4 k.v. Acknowledgment is made of assistance from the Heckscher Research Council of Cornell University.

18. Satellites of $K\alpha$ for the elements Ni(28) to As(33). F. K. RICHTMYER AND E. RAMBERG, *Cornell University*.—The satellites $K\alpha_{3,4}$ of the line $K\alpha$ have been recorded previously from Na(11) to Zn(30) at which point they seemed to disappear. At Zn(30) the N shell begins to grow, which fact, it was previously thought, might be in some way related to the disappearance of the satellites. However, exposures made to bring out the satellite structure of the $K\alpha$ line of the elements Ni(28) to As(33) show that satellites (unresolved on the photographic plate) are clearly visible up to As(33), although they are relatively much less intense than for elements of lower atomic number. Observations by means of the two-crystal spectrometer show that the satellites $K\alpha_{3,4}$ of Cu(29) are clearly resolved into the two components, as is found by the photographic method for lower atomic numbers. These new data fit the Moseley type of graph for satellites proposed by one of the authors (F. K. R., *Phil. Mag.* 6, 76 (1928)). Acknowledgment is made of assistance from the Heckscher Research Council of Cornell University.

19. Position and width of the modified line of the spectrum of scattered x-rays. F. L. NUTTING, *The Drexel Institute, Philadelphia*.—The Compton Shift $\delta\lambda = h/mc(1 - \cos\phi)$ was tested at definite, large scattering angles by two independent methods. (a) *Photographic method*. Using fluorescence radiation before and after for fiducial marks, Mo radiation was scattered at 169 degrees from paraffin for 300 hours (maximum spread of scattering angle 12.5 degrees). The mean value of the shift of the center of gravity of the $K_{\beta\gamma}$ line on microphotometric curves gave $h/mc = 0.0231\text{\AA} \pm 0.00023\text{\AA}$. The shift of the peak of the β line (corrected for the presence of the γ line of 1/7.7 its intensity) gave $h/mc = 0.02376\text{\AA} \pm 0.00023\text{\AA}$. (b) *Ionization method*. Using two narrow cylindrical Mo tubes side by side and a Soller slit to increase intensity and scattering at 170 degrees from graphite (maximum spread of scattering angle 8 degrees), the mean of a large number of runs gave $h/mc = 0.0240\text{\AA} \pm 0.00024\text{\AA}$ for the shift of the K_{α} doublet. *Components*. No definite evidence of components appeared in the mean microphotometric curve, although the fluorescence α doublet was clearly resolved and the angular spread of scattering small.

20. The quantitative application of the irregular doublet law to an isoelectronic sequence. R. A. SAWYER, *University of Michigan*, AND J. E. MACK, *National Research Fellow, University of Minnesota*.—Heretofore the irregular doublet law of x-ray spectroscopy has been applied in isoelectronic sequences only qualitatively. (i.e. $\nu(n, l_1) - \nu(n, l_2)$ is a linear function of Z). Now Wentzel's result $\sigma_1(n, l+1) - \sigma_1(n, l) = 0.58 \cdot 2^{1/2}n$ for the first order screening number σ_1 in x-rays is applied, determining the rate of dependence of the energy of the transition $2s^2 2p^4 \leftarrow 2s 2p^5$ upon the atomic number Z in the fluorine-like sequence, to be $49 \cdot 10^8 \text{ cm}^{-1}$. New experimental results in Na III and Mg IV show it to be $48.01 \cdot 10^8 \text{ cm}^{-1}$. Although such accurate predictions are not generally possible for an arbitrary number of electrons, certain regularities may be used for interpolation in many cases.

21. The quantum theory of x-ray exposures on photographic emulsions. A. P. H. Trivelli, *Eastman Kodak Co.* (Introduced by L. A. Jones.)—The quantum theory of photographic exposures as proposed in 1922 by L. Silberstein had to be given up on account of the fact that the differences in sensitivity of the grains are determined not only by the projective area of the grain; a chemical factor is also entering into it for visible radiation. Kinoshita and Th. Svedberg have showed that every α -particle hitting a silver halide grain makes it developable. The sensitivity of the grain is, therefore, determined by its projective area and the probability that a grain is made developable by exposure to α -particles is given accurately by the equation, $p = 1 - e^{-na}$ (a = projective area, n = number of α -particles). An investigation with L. Silberstein has shown that the same equation holds for x-ray exposures.

22. A theoretical and experimental study of the resonance radiometer. J. D. HARDY, *Johns Hopkins University.* (Introduced by A. H. Pfund.) The voltage sensitivity limit of steady deflection galvanometers, regardless of degree of magnification or precision of manipulation, has been shown to be of the order of 10^{-9} volts. This is the natural sensitivity limit set by the Brownian fluctuations in the suspended system causing a random zero unsteadiness. The calculation has been made for the case of the resonance radiometer (See Abstract of A. H. Pfund, *Science* Feb. 1929) and the results show that this natural limit has been lowered by about one hundred times, that is, to the order of 10^{-11} volts, in the present apparatus with a possibility of still further lowering the limit by mechanical and electrical improvements. Some results are given to show that without much precaution a sensitivity surpassing that heretofore obtainable can be realized and one that is very close to the theoretical limiting value. The smallest energy difference that has been with certainty distinguished is of the order of 10^{-4} ergs per second per square millimeter. A method is described for measuring the speed of response of thermocouples. The average speed of the thermocouples used was found to be 0.2 sec. in air and 2 minutes in vacuum.

23. High dispersion in the infra-red. R. BOWLING BARNES, *Johns Hopkins University.*—For the purpose of comparing the Raman effect with infra-red absorption spectra, the following organic liquids have been measured from 3.1μ to 3.6μ : benzene, toluene, ortho-, meta- and para xylene, ethyl-, butyl-, monochlor-, and monobrombenzene. The spectrometer employed an echelette grating, which had 3600 lines per inch, and which concentrated the energy of a Nernst filament into the region which was investigated. The dispersion of the instrument was such that with the slits each 0.25 mm in width, one "slit width" was approximately $25A^\circ$. The calibration was obtained in terms of the positions of the 5461 line from an auxiliary Hg arc, and the wave-lengths as given are considered accurate to $\pm 0.003\mu$. In every case the bands in this region, due to the C-H vibration, which have hitherto been reported only under low dispersion have been resolved into many component parts. The 3.25μ band of benzene was resolved into three equally strong components lying at 3.231, 3.253 and 3.291μ respectively. The shifts of these bands caused by the various substitutions were studied, and in no case was a shift of over 0.01μ found. Published data on the Raman effect failed to reveal the complexity shown by these absorption spectra.

24. Iodine fluorescence in the infra-red. F. W. LOOMIS, *University of Illinois.*—Oldenberg has photographed in the infra-red the fluorescence spectrum of iodine excited by the mercury arc. The spectrum is chiefly an extension of the well-known series of doublets excited by the green mercury line; but in the neighborhood of the infra-red doublets there appear other lines. Pringsheim attributes these to transitions to the extraordinary new molecular level which he reported. It is now found, however, that they disappear when the yellow lines are filtered from the light of the mercury arc. They should therefore be attributed to the higher members of the fluorescence series excited by the yellow lines. The relatively high intensities of these members is due to their being on the right arm of the Franck-Condon parabola.

25. The relation between Raman spectra and the molecular structure of organic compounds. DONALD H. ANDREWS, *The Johns Hopkins University.*—The following procedure is

proposed for identifying the type of vibration in the molecule to which an observed frequency in a Raman spectrum corresponds. It is assumed that the only forces acting between the atoms in the molecule are those produced by the chemical bonds, and that there is a restoring force if the bond is stretched or if the angle which the bond makes with the other bonds on an atom is altered from the normal equilibrium value. It is also assumed that all non-polar chemical bonds have the same force constants. The different frequencies observed in the Raman spectra may then be considered as due solely to the variation in mass of the atoms concerned and to their space relation to each other, that is, whether they are in a straight chain, a branching chain, a ring, etc. It is possible to calculate in this way the number of Raman lines which should be observed for any compound, and the frequencies they should have. There is fair agreement with the observed spectra, close enough so that the lines can be identified with different types of motion in the molecule, and calculations of specific heat can be made.

26. A theory of zodiacal light. E. O. HULBURT, *Naval Research Laboratory*.—Since solar outbursts which give rise to aurorae and magnetic storms also cause changes in the zodiacal light it is possible that the zodiacal light is mainly sunlight re-emitted by the absorbing particles and not scattered or reflected by them. This permits a reconsideration of an old view that the particles originate in the earth's atmosphere, although the 15 percent polarization of the zodiacal light is left unexplained. Neutral atoms and molecules of the upper fringe of the earth's daytime atmosphere upon collisions of the second kind are ejected upward with velocities around 11 km sec^{-1} to 30,000 or 80,000 km levels where they are ionized by the solar ultra-violet light. Under the action of gravitation, the earth's magnetic field and the pressure of solar radiation, an oblong ring of ions and electrons is formed around the earth in the plane of the ecliptic, the ion densities being fairly low, below 10^3 cm^{-3} ; this gives rise to the zodiacal light. The ring is perhaps 50,000 km distant on the daylight side of the earth. On the night side the ring stretches out to great distances 10^5 or 10^6 km. At its far end ions continually stream away in the direction of the sun's rays, so that the ring merges into a sort of comet's tail which may be the Gegenschein. Quantitative estimates are made throughout which depend on apparently acceptable assumptions of light pressure, time of ionization, etc. The estimates suggest a rate of escape of the earth's atmosphere of perhaps 10^6 ions $\text{cm}^{-2} \text{ sec}^{-1}$, or about 10^{-6} of the atmosphere in 10^6 years.

27. A recording interferometer. C. W. CHAMBERLAIN, *Michigan State College*.—Light from a broad slit, illuminated by an incandescent filament, is collimated and divided into two parts which travel separate paths, one variable in length. The beams are reunited, with their wave fronts parallel, passed through a Wadsworth or constant deviation prism, and viewed through a telescope focussed for infinity. With eyepiece removed circular Fizeau fringes are seen in monochromatic light, when the interfering paths are unequal. With the eyepiece in position, a new type of interference system in white light is brought into view. The continuous spectrum is crossed by sharp dark bands whose positions in the spectrum correspond with the wavelengths for which the interference system is opaque, or the path difference is an odd number of half wave-lengths. The number of bands appearing in an octave is identical with the path difference of the interfering beams, measured in terms of the longest wave. Lines appearing in that portion of the spectrum between 5016 and 6678 of helium correspond to a linear movement of one ten thousandth of a centimeter. In a similar manner, a range of spectrum may be arranged such that a change of one line in the range corresponds to a movement of five hundred-thousandths of an inch or any desired decimal part of an inch or centimeter.

28. An interference method of measuring distance. STUART H. CHAMBERLAIN, *Michigan State College*. (*Introduced by C. W. Chamberlain*).—A collimated beam of white light is divided into two parts, slightly separated and converging toward a mirror, at a distance to be determined. The returning beams, slightly diverging, are received by an interference system which renders them parallel and permits lateral and linear displacements of the parallel wave fronts. The beams are passed through a prism and viewed through a telescope focussed for infinity. A dual system of interference bands is formed; one serviceable for accurately adjusting the

instrument to receive the returning beams, the other to measure the distance between the light source and the distant mirror. The distance is determined by the number of dark bands appearing in a continuous spectrum. The new method substitutes a portable base line measured in wave-lengths of light and an interference method of determining the angle subtended by this base line at the distant mirror for the present method of measuring by means of angles and a fixed base line.

29. On the question of aberration of the light from terrestrial sources and its application to the experiment of Esclangon. N. GALLI-SHOHAT, *Mount Holyoke College*.—The definition of the "relative" ray in the classical ether-theory is usually given by means of two small openings through which light passes. The question is how to direct the moving telescope (two openings)—one system—in order to observe the light traveling along a wave normal in the other system (ether). A more careful analysis of this definition from the standpoint of the cinematics of the question gives the result that the direction of the ray actually observed depends upon the orientation in space, the angle x representing the aberration of light from terrestrial sources being $\beta^2/2 \sin 2\theta_0$, [$\beta^2 = (v^2/c^2)$, $\theta_0 = (\theta_0, v)$]. This method of construction of the relative ray when applied to the experiment of Esclangon gives a satisfactory explanation of the effect observed. The curve calculated for this case, using for the declination of the apex δ 68° , coincides with that given by Esclangon and the values of the right ascension, α and the velocity v of the apex came out as $\alpha = 20^h$ and $v = 200$ km/sec in agreement with modern astronomical data. This second order aberration should also give account for anomalies observed by astronomers and may change the theory of the Michelson-Morley-Miller experiment.

30. Resonance and quenching of the third principal series line of caesium. C. BOECKNER, *Bureau of Standards, Washington D. C.*—A helium discharge is used as a source for the study of the resonance radiation from the third principal series line of caesium. This is possible, due to the coincidence of a strong helium line with the caesium line. In addition to the resonance line, a number of caesium arc lines are observed. These have their origin in lower levels populated by radiation transfers from the initial $4 P_{1/2}$ level. The effect of helium on the fluorescence radiation is studied. It is found that collisions between helium atoms and caesium atoms in the $4 P_{1/2}$ state transfers the latter only to states differing by less than several hundredths of a volt from the initial state. This type of transfer occurs at approximately every kinetic theory collision. Transfers to states differing by as much as 0.18 volts are improbable.

31. The effect of gases on ionization of caesium by line absorption. F. L. MOHLER AND C. BOECKNER. *Bureau of Standards, Washington*.—Measurements consisted of obtaining sensitivity curves for a space charge tube containing caesium at a constant partial pressure when various foreign gases were put in the tube. Hydrogen and nitrogen at pressures of one or two cm reduce the ionization by line absorption to nearly zero. With helium and argon the effects at the fourth and higher lines approach at high pressure values ranging from 60 to 90 percent of the vacuum value but helium increases the effect of the third line. From data on the effects at different pressures we obtain values for the product of the lives of the excited states of caesium and the effective collision areas. This product remains of the same magnitude for different gases and for different excited states.

32. The spectrum of doubly-ionized antimony. R. J. LANG, *University of Alberta*.—The spectrum of the 49 electron atom of antimony consists of term of even multiplicity of which twenty-six have been found as follows: $(s^2 5p)^2 P$, $(s^2 6p)^2 P$, $(s^2 4f)^2 F$, $(s^2 5f)^2 F$, $(5p^3)^4 S$, $(s 5p^2)^4 P^2 D^2 S^2 P$, $(s^2 5d)^2 D$, $(s^2 6d)^2 D$, $(s^2 6s)^2 S$, $(s^2 7s)^2 S$, $(s^2 8s)^2 S$, $(s^2 5g)^2 G$, $(s^2 6g)^2 G$. The ionization potential corresponding to the approximate value of the deepest term $(s^2 5p)^2 P_1 = 200\ 272$ is 24.72 volts. In Sn II the $(s\ 5p^2)^4 P^2 S$ terms are located and also the $(s\ 5p^2)^2 S$ in In I.

33. Nuclear spin and hyperfine structure. H. E. WHITE, *Physikalisch-Technische Reichsanstalt, Berlin, Germany*.—It appears that when hyperfine structure is to be attributed to nuclear angular momentum or spin i , that the relation $\Delta\nu_f : \Delta\nu_f = m_e : 4im_e$, should approximately

hold where $\Delta\nu_g$ is the gross or multiplet structure separation, $\Delta\nu_f$ the hyperfine structure separation, m_k the mass of nucleus and m_e the mass of electron. From a discussion with Dr. Schüller it appears that the hyperfine structure of $\lambda 5486$ in Li II (Zeits. f. Physik **42**, 487 (1927) $^3S_1-^3P_{0,1,2}$, may be accounted for by assigning an angular momentum $i=\frac{1}{2}$ to the nucleus of Li⁷. From the observed hyperfine structure the $^3S_1(1s2s)$ term and the $^3P_2(1s2p)$ term have normal doublet separations of about 0.60 cm^{-1} , and 0.45 cm^{-1} respectively. From the already known relations in hyperfine structure, the $^1P_1(1s2p)$ term should have an inverted doublet separation of about 0.40 cm^{-1} . The gross-structure difference, $^3P_2-^1P_1$, 5700 cm^{-1} as compared with the hyperfine structure difference $\sim 0.85\text{ cm}^{-1}$ gives a ratio of 6700 in good agreement with the theoretical value 6440. Equally as good agreement between theoretical and observed values is found in several other elements. A more detailed explanation will be given in the Physical Reviews.

34. Average lives of lines of mercury triplet 2^3P-2^3S . R. H. RANDALL AND HAROLD W. WEBB, *Columbia University*.—The average life of each of the three components of the mercury triplet $2^3P_{012}-2^3S_1$, when excited by electron impact under conditions involving negligible ionization has been measured. The method used was that previously described (H. W. Webb, Phys. Rev. **24**, 113 (1924)), in which high frequency voltages are applied in phase to the excitation and detecting systems. From the variation of the current with frequency the rate of decay of the radiation after the exciting impact is calculated. The lines were excited in a sealed-off tube with mercury pressures between 0.004 and 0.03 mm. The exciting voltage was less than ten volts. The excitation was such that there was no appreciable concentration in the excited 2^3P states. A specially designed potassium hydride photoelectric cell was used as the detecting system. Optical filters were used to isolate the line under measurement. The results agree with the assumption that the radiation decays exponentially after impact. For the lines $\lambda 4047$ and $\lambda 4358$ the lives were found to be the same within the experimental error (0.75%), viz. $\tau = 5.75 \times 10^{-8}$ sec. The value for $\lambda 5461$ was four times greater, $\tau = 2.37 \times 10^{-7}$ sec. No satisfactory explanation of these results has been found. It is suggested that the fine structure of the lines may be involved.

35. The comet tail bands of carbon monoxide. LOUIS R. MAXWELL, *Research Fellow, Bartol Research Foundation*.—The experimental arrangement described by the writer (Phys. Rev. **32**, 715 (1928)) for measuring the life in the excited states, can be used for determining whether the emitters of band spectra are positive or negative ions or neutral molecules. This method is now applied to the comet tail bands which were produced by impurities in the tube containing helium when excited by 140 volt electrons. The bands experienced a displacement along their length by such an amount as to show clearly that they are produced by positive ions. This confirms the conclusions which have been made in regard to their origin.—By decreasing the pressure to less than 1×10^{-4} mm these bands appeared strongly without the presence of other bands and with the helium spectrum extremely weak. By circulating helium through the tube at 1×10^{-3} mm both spectra were obtainable while further increase of the helium pressure lessened the intensity of the bands until at 2.8×10^{-3} mm they had practically disappeared leaving only the helium spectrum. This effect is opposite in character to the phenomena found by Merton and Barrett and others where small traces of CO in helium at 20 to 60 mm were capable of producing the comet tail bands quite brilliantly.—Since the positions of the bands are altered by the cross-electric field, it is possible to measure their mean life by the method previously used for the mercury spark spectrum.

36. The application of least squares. W. EDWARDS DEMING, *Bureau of Chemistry and Soils, Washington, D. C.*—By writing general relations between the most probable values of observed quantities and of p parameters, it is possible to get a solution to the general problem. The different relations that may exist between the most probable values and the parameters constitute the distinctions between the various types of problems. The general solution takes the form of symmetrical equations. When $p=0$, it reduces to the so-called "method of correlates." For curve fitting, the general solution can be transformed into two sets of equations;

one gives the parameters, the other corrects the observations. Provision is made for cases where the empirical surface must pass through given points. Heretofore it has been customary to throw all the adjustment on to one group of observations and none on to the others—a practice that often contravenes the foundation of least squares and yields unreasonable results, resulting in unjustified criticism of the principle. The present method allows the proper weight of each observation to be used in the adjustment. The corrections give interesting geometrical generalizations of those discussed by the writer in the Proceedings of the London Physical Society for February 15, 1930.

37. Simultaneous irreversible processes. L. ONSAGER, *Brown University*.—A general theorem applying to simultaneous irreversible processes is derived from the assumption that the dynamical laws are symmetrical with regard to past and future. The derivation involves the consideration of fluctuations. The adaptation to processes obeying linear differential equations of the first (or second) order with regard to the time yields an extension of Lord Rayleigh's "principle of the least dissipation of energy." This result provides a satisfactory basis for certain theorems which were originally derived from the consideration of cycles differing from those accepted in thermodynamics in the essential respect that reversible operation is impossible. One of these theorems applies to thermoelectric phenomena (W. Thomson), another to liquid junction potentials in electrolytes (H. v. Helmholtz), a third one to the Soret effect (E. D. Eastman). A new theorem applying to diffusion is also obtained. An external magnetic field disturbs the straight symmetry in past and future (a rotating frame of reference has the same effect). In such cases another symmetry condition connected with a simultaneous reversal of the time and the magnetic field is applicable. On this basis a relation between the Nernst and the Ettingshausen effects, first proposed by P. W. Bridgman and H. A. Lorentz, is confirmed.

38. Thermodynamics of systems with several equilibria. N. RASHEVSKY, *Westinghouse E. and M. Co., East Pittsburgh*.—Further studies on thermodynamical systems having more than one equilibrium constitution for given external conditions, and discussed in a paper presented at the last February meeting, are made. A reversible reaction between two substances which are either dissolved or gaseous, but which in either case are following not the ideal gas laws, but van der Waals' equation, is considered. It is shown that for certain values of temperature, total volume and other external conditions; the free energy of the system, considered as a function of the ratio of the two reacting substances, has *two* minima. Hence, for given external conditions, the system may have two equilibrium concentrations. In other words, the state of the system is not defined by the external conditions alone, but, as has been shown in a previous paper, it depends also on the previous history of the system. We may say that the system possesses hysteresis. Different possible kinds of such a hysteresis and possible application, especially to some biological problems, are discussed.

39. An acoustical analogy of the Schrödinger wave equation. R. B. LINDSAY, *Yale University*.—Investigation is made of the one-dimensional compressional vibrations of an ideal fluid of variable density (in equilibrium under the action of an external force) confined in an infinite tube of bounded but variable cross section. The non-homogeneity is so chosen that the wave velocity is everywhere the same. It is assumed that the ordinary acoustic equations are applicable except as modified by the non-homogeneity and that the cross section is small enough so that transverse motions may be neglected. It is then found that the problem of determining the allowed vibrations in such a tube satisfying the boundary condition that the condensation $s = \delta\rho/\rho_0$ (where ρ_0 is the equilibrium density at any point and $\delta\rho$ the excess density) shall remain analytic, everywhere < 1 and vanish at infinity, is formally equivalent to the problem of solving a one-dimensional Schrödinger wave equation subject to the usual boundary condition. The appropriate density variation and the shape of the tube are shown to be related to the potential energy of the particle whose motion is described by the Schrödinger equation. As illustrations the free particle, the simple harmonic oscillator and the one dimensional hydrogen atom are investigated. It is believed that generalization to three dimensions will prove possible.

40. A general formulation of the uncertainty principle and its classical interpretation. H. P. ROBERTSON, *Princeton University*.—Denoting the mean value of a quantum mechanical variable α in a state ψ by α_0 and its uncertainty or standard deviation by $\Delta\alpha$, the uncertainty principle $\Delta\alpha \cdot \Delta\beta \geq (h/4\pi) |\gamma_0|$, where $(h/2\pi i)\gamma$ is the commutator $\alpha\beta - \beta\alpha$ of α and β , is obtained for general systems, which may include spin. It is found to be a consequence of the more restrictive inequality $\Delta\alpha \cdot \Delta\beta \geq \{[(\alpha\beta)_0 - \alpha_0\beta_0][(\beta\alpha)_0 - \beta_0\alpha_0]\}^{1/2}$. The former result is interpreted classically as meaning that we can only determine that two quantities $\alpha(p, q)$, $\beta(p, q)$ have values lying between $\alpha_0 \pm \Delta\alpha$, $\beta_0 \pm \Delta\beta$ provided the integral invariant $J = |\Sigma(i) \int p_i dq_i|$ taken over the area normal to these four hypersurfaces in phase space is at least of order h .

41. Thomson effect in zinc crystals. L. A. WARE, *University of Iowa*.—The Thomson coefficient, σ , is directly determined for a group of zinc crystal rods with orientations distributed fairly uniformly over the entire possible range of orientations. At 49.5°C, and at 125°C, the values of σ seem to obey the Voigt-Thomson symmetry relation, although not as good a check is obtained at the higher temperature due probably to increased experimental error. The principal values obtained are: at 49.5°C, $\sigma_{\perp} = 0.98 \times 10^{-6}$, $\sigma_{\parallel} = 0.38 \times 10^{-6}$; at 125°C, $\sigma_{\perp} = 2.09 \times 10^{-6}$, $\sigma_{\parallel} = 1.08 \times 10^{-6}$ Cal./coul./degree C. The increase of σ with increased temperature is greater than has been previously reported for polycrystalline zinc but is in approximate agreement with some earlier determinations by the writer. In addition, specific resistivity and temperature coefficient of resistivity are determined.

42. Thermal expansion of copper-nickel-tin alloy. PETER HIDNERT AND W. T. SWEENEY, *Bureau of Standards*.—In 1926 determinations were made at the Bureau of Standards on the linear thermal expansion of a copper-nickel-tin alloy known as Admiralty nickel or Admic. It is claimed that this white nickel alloy resists corrosion and shows good strength at elevated temperatures. The sample, 1-3/10 inches in diameter, was extruded from 1-3/8 inches and finished hard with a 1/16 inch draught after a suitable anneal. The chemical analysis was as follows: Copper 69.57, nickel 28.70, tin 0.91 percent. Scovill Mfg. Co., Waterbury, Conn. prepared the sample and furnished information about the treatment and the chemical composition. The following coefficients of linear expansion were obtained:

Temperature Range	Average Coefficient of Expansion per Degree Centigrade
20 to 100°C	15.2×10^{-6}
100 to 200	15.5
200 to 300	18.0
20 to 200	15.4
20 to 300	16.3

Data on physical properties of this alloy are given in *Mining and Metallurgy* 8, 474 (1927).

43. A new method for measuring the variation of specific heats of gases with pressure. E. J. WORKMAN, *University of Virginia*.—The method determines the ratio of c_p at a high pressure to c_p for the same gas at a pressure of one atmosphere taken as a standard. The continuous flow principle is used in such a way that the necessity for measuring rates of gas flow and heat input is avoided. A stream of gas at high pressure is brought to a temperature t_1 and passed through a heat interchanger acquiring there a temperature t_2 , after which it is throttled to atmospheric pressure, brought to a temperature t_3 and returned to the heat interchanger, where its temperature again becomes t_2 . If there is no heat leakage the ratio of c_p at high pressure to that at atmospheric pressure is equal to $(t_3 - t_2)/(t_2 - t_1)$. Measurements on commercial oxygen taken at a mean temperature of 26°C and pressures ranging from 15 to 100 atmospheres indicate, when corrected, a pressure coefficient in this ratio 0.0017 ± 0.0001 per atm.

44. The effect of hydrogen ion concentration on the measurement of the mean particle size of emulsions. ISABEL C. WEEKS, *The Pennsylvania State College*. (Introduced by Wheeler P. Davey.)—W. P. Davey proposed (Science 64, 252 (1926)) measuring the mean particle size of emulsions by a water-spreading method. The present work investigates the effect on such measurements of the pH ($=1/\log$ concentration of H^+) of the water used. Three emulsions were tested, stabilized with the sodium soaps of myristic, palmitic and stearic acids respectively. The pH was varied from 3.0 to 11.0 by means of buffer solutions. No effect was found traceable to the buffer materials used. At a pH less than 7.0 (i.e. the water is acid) the area of the water-spread emulsion for a given pressure increases with time without reaching an equilibrium value. At a pH greater than 7.0 (i.e. the water is alkaline) the area for a given pressure finally becomes constant with time, but the values are large and depend upon the pH . In every case the emulsion area was corrected for the area covered by pure buffer. At $pH=7.0$ (i.e. the water is neutral) the water-spread emulsion shows a constant area with time for a given pressure, and reaches equilibrium very quickly. Areas found at $pH=7.0$ are therefore taken as the true areas to be used in plotting pressure-area curves for particle-size calculations.

45. Molecular aggregation. A. M. TAYLOR. *Institute of Applied Optics, Rochester, N. Y.* (Introduced by T. R. Wilkins.)—A brief résumé of the lines of evidence by which molecular aggregation in pure liquids may be recognized; from the surface tension, from viscosity, from optical anisotropy, and from the Raman effect. The question of molecular size in the solid state can at present be answered only by x-ray analysis and by comparison of specific heat data with theory. A third method is suggested based on the Vant-Hoff equilibrium equation $d(\log k)/dt = Q/RT^2$. Q is here the differential heat of solution of the solid in a given solvent, while k is the equilibrium constant regulating the exchange between the molecules in the solid and the molecules in the solution; k may be expressed in terms of the change of solubility with temperature. For iodine the method gives I_2 as the molecular size in the solid state; this agrees with x-ray measurements which show that solid iodine has a molecular lattice of I_2 . Lack of data prevents further application of the method at present.

51. Phenomena in oxide coated filaments. E. F. LOWRY, *Westinghouse E. & M. Co., East Pittsburgh*.—It has been suggested in a previous paper that the phenomena of oxide emission might be explained by assuming that the source of electron emission is a layer of metallic barium occluded on the surface of the core metal. The activity of such a filament is characteristic of this composite surface and the peculiar effects met with are due to the diffusion of the electrons through the pores of the oxide coating. In the present paper experiments are described which tend to support this view. Filaments made by vaporizing metallic barium on clean Konel ribbon give emissions of the same magnitude as those coated with oxide in the usual way but approach saturation rapidly while oxide filaments approach saturation very gradually if at all. The "three halves power" law is obeyed exactly by both types. "Bariated" Konel filaments show very little if any "fading" of emission with time, while considerable fading is experienced with oxide filaments, particularly in a certain range of temperatures and with heavy coatings. No activation of these filaments is necessary other than thermal decomposition of the alkaline earth carbonates in vacuum.

52. Density distribution of electron gas in equilibrium with a hot body. A. T. WATERMAN, *Yale University*.—The variation of potential and of electron concentration with distance from a plane emitting surface is investigated, using Poisson's equation and the equilibrium relation between electron concentration and potential in the form $A = A_0 e^{-V^*/kT}$, where A and A_0 are the Fermi A 's outside and inside the hot surface, respectively, and V is the corresponding potential difference. Solutions are found for the equilibrium condition in the absence of applied field and for negative fields, and assuming the electron gas within the body to be degenerate or classical. Results indicate: (1) that on the average an electron is closer to its neighbors than to the surface, except when very close to the latter, and therefore that the image force explanation of the work function is here not applicable; (2) that space charge is quite competent to give the magnitude of the work function; (3) that if the electron concentration within the body

is that of the atoms, the external gas remains degenerate to approximately 10^{-7} cm from the surface; (4) that an applied negative field of the magnitude required for cold field currents materially alters the electron concentration down into the degenerate region. The current obtainable under retarding fields is discussed with a view to estimating the feasibility of experimental proof of the relations established and of the electron concentration within conductors.

53. A space charge interpretation of thermionic work function. RUSSELL S. BARTLETT, *Yale University*.—We try to account for the thermionic work function by the space charge field of electrons streaming out from the surface and turning back in this same field. To account for the increase in thermionic currents in strong electric fields it is necessary that the work function field extend so far out that an escaping electron is much nearer to its neighbors than to the surface. If we extend Fry's space charge analysis, with classical velocity distribution, right down to the surface of the metal, assuming an electron concentration about midway in the range of prediction, we find something resembling saturation currents, a suitable value for the work function, and an increase of current with strong fields agreeing better with experiment (Proc. Roy. Soc. A121, 456 (1928)) than does Schottky's expression depending on image force alone. A first order correction for Fermi-Dirac distribution brings improvement, though the variation of work function with temperature is too great. But the strict application of the Fermi-Dirac statistics for a degenerate gas, with its large zero point energy, should remove that difficulty, and should provide for an explanation of field currents, since the large fields necessary should penetrate into the region of degeneracy.

54. Effective photoelectric work function reduced by weak accelerating fields. W. B. NOTTINGHAM, *Bartol Research Foundation*.—Photoelectric experiments on thin alkali metal films reported (Phys. Rev. 33, 633 and 1081 (1929)) seemed to indicate a nonlinear relation between current and light intensity and a departure from Einstein's photoelectric equation. A study of amplifier-galvanometer systems for measuring small currents (Journal of Franklin Institute, March 1930), showed that the nonlinearity was in the current measuring system. A thin alkali metal film on nickle or platinum changes the work-function (ϕ) of the surface by a small amount, and greatly alters the space distribution of the electric field against which the electron must work in order to escape. This redistribution makes it possible to reduce the effective work-function (ϕ_e) of the surface by applying a small accelerating field. The photoelectric long wave-length limit is a direct measure of ϕ_e . With a retarding field, ϕ_e is greater than ϕ and the Einstein equation gives the relation between ϕ_e and the potential. At zero field, $\phi_e = \phi$ while with an accelerating field, ϕ_e is less than ϕ . For example, ϕ_e has been observed to be reduced by 1.95 volts by the application of an accelerating potential of 4 volts between the electrodes. A further increase in accelerating potential to 750 volts gave a further decrease in ϕ_e of only 0.32 volt.

55. Photoelectric properties of extremely thin films of alkali metals. HERBERT E. IVES AND H. B. BRIGGS, *Bell Telephone Laboratories*.—Films of alkali metal much thinner than those previously studied (Astrophys. J. 60, 209 (1924)) have been investigated by using an electrometer of approximately 100 times the sensitiveness of the galvanometer used before. Attention has been directed to the variation of emission with the angle of incidence and plane of polarization of the exciting light. In agreement with the earlier work, the ratio of emissions for obliquely incident light polarized with the electric vector in and perpendicular to the plane of incidence decreases as the film is reduced in thickness. The new measurements show further that this ratio continues to decrease with film thickness to the value unity, where no variation of emission with angle occurs, and that with further decreases in film thickness, the relationship reverses, ("normal" greater than "selective") and the emission increases with the angle of incidence of the light. It is suggested that when the alkali metal particles become sparsely distributed their absorption of light corresponds to that of a matt surface (Lambert's law). When the particles are still more widely separated, deviation from Lambert's law occurs and the exciting light is in part that reflected from the underlying platinum surface, stronger for light polarized with the electric vector parallel to the surface.

56. Validity of Einstein's photoelectric equation for red sensitive sodium compounds. A. R. OLFIN, *Bell Telephone Laboratories, Inc.*—Using a photoelectric cell specially designed so that the cathode could be sensitized in a side compartment and then slipped into position within a soot-coated nickel anode, stopping potentials were obtained for electrons liberated by highly resolved light of wave-lengths ranging from 3500Å to 8000Å. The cathode consisted of a nickel plate heavily coated with sodium and specially treated with sulphur and air [abstract 57 Bull. Am. Phys. Soc. 4, 2 (1929)]. The anode of such a cell is not sensitive to light, so the voltage at which the emission from the cathode just becomes zero is a measure of the true stopping potential. Plotting the voltages so obtained versus the exciting light frequencies a perfectly straight line is obtained. From the slope of this line, a value of Planck's constant h equal to 6.541×10^{-27} , significant to three figures, is obtained. It is possible with one cell to obtain stopping potentials for electrons released from sodium before and after treating it with sulphur and air. In such cases the voltage at which the photoelectric emission ceases is the same, but after treatment the current saturates at a higher voltage, exhibiting a change in the contact difference of potential of 0.8 volt.

57. Photoelectric cell thermoregulator. F. G. BRICKWEDDE AND R. B. SCOTT, *Bureau of Standards, Washington, D. C.*—Recently a photoelectric cell was used with a thermocouple as the thermosensitive element to make a new kind of thermo-regulator. There are many laboratory problems requiring automatic regulation to which the photoelectric cell can be applied. Photoelectric cell regulators possess great sensitivity, small lag and a wide range of temperatures over which they can be used and be quickly and conveniently adjusted for operation at any desired temperature. The parts of the thermo-regulator are analyzed and it is shown how they can be modified to adapt this regulator to special problems. Improvements are described and causes of trouble pointed out. A photoelectric regulator has been made which will automatically maintain any temperature from 0° to liquid air temperatures constant to 0.001°. It is operated on a 240 volt D.C. power, without batteries, using only one slide wire rheostat with four sliding contacts to furnish all the sources of potential for the photoelectric cell and its amplifier thus making the regulator less expensive and obviating all the inconveniences of run down batteries.

58. Apparatus for maintaining constant low temperatures. R. B. SCOTT AND F. G. BRICKWEDDE, *Bureau of Standards, Washington, D. C.*—A cryostat of improved design for use in the temperature range from 0°C to liquid air temperatures has been constructed. The cryostat bath is contained in a double-walled cylindrical glass vessel surrounded by liquid air, and the amount of refrigeration controlled by varying the air pressure between the walls. Constant temperature is automatically maintained by the use of a photoelectric cell thermo-regulator operating a heating coil on the stirrer tube. Adequate circulation of the liquid, careful heat insulation, and symmetrical distribution of all the parts assure great uniformity of temperature. The temperature is easily adjusted to the desired value and can be maintained constant to 0.001°C. Nonflammable liquids are used for the bath between 0°C and -150°C.

59. Raman spectra excited by the helium hot-cathode arc and a new type of tube for small volumes of liquid. R. W. WOOD, *Johns Hopkins University*.—A hot-cathode helium arc of great brilliancy, carrying three amperes, kindly supplied by the research laboratory of the General Electric Company of Schenectady, has been very successfully used in combination with a filter of nickel oxide glass for the excitation of Raman spectra. Exposures of less than three hours are required as against fifteen hours with the spiral tube which I described last year. A new type of tube for the investigation of volumes of only eight or ten cubic centimeters of liquid has been developed, adapted to the investigation of liquids of low boiling point or solids which liquify below 100°C.

60. The calculation of the specific heats of solid organic compounds from Raman spectra. DONALD H. ANDREWS AND JOHN C. SOUTHARD, *The Johns Hopkins University*.—It seems to be possible to identify the lines in the Raman spectra of a number of organic molecules with

definite modes of vibration in the molecule (see abstract Number 25). This permits the assigning of the correct number of degrees of freedom to each frequency and it is found that the sum of the degrees of freedom so assigned has a value consistent with the number of atoms in the molecule. If we then consider that the various modes of vibration in the molecule act as independent Einstein oscillators, it is possible to employ the frequencies from the Raman spectra and calculate the specific heat of the molecule for any temperature. This has been done for methyl alcohol, ethyl alcohol, benzene, toluene, chlor benzene and brom benzene over the temperature range of 15° to 260°K. The average deviation between the results so calculated and the experimental values is about five percent.

61. Mosaic crystals of elements. R. H. CANFIELD, *Naval Research Laboratory, Anacostia, D. C.*—Assuming that the atoms of a crystal of an element are all exactly alike and exert mutual central forces, and that the force between any two atoms vanishes for only one value of the distance, it is found that the conditions of stability of equilibrium of the crystal against an infinitesimal generalized strain require that certain series of terms in the second derivatives of the energy function shall be greater than zero. If this is granted, it is shown that any translation of a part of the perfect crystal relative to the remainder causes the potential energy of the lattice to increase. Hence all such imperfections are to be regarded as unstable.

62. Selective maxima in the spectral response curves of light-sensitive compounds as a function of valence. A. R. OLFIN, *Bell Telephone Laboratories, Inc.*—Lindemann proposed a formula for computing the frequency of light under excitation by which a substance should yield electrons most readily. This formula, $\nu = (1/2\pi) [(ne^2)/(mr^3)]^{1/2}$, gives the frequency of an electron revolving in an orbit of radius r about a stationary charge ne [m = mass of electron]. The n term is determined by the valence of the substance, a choice of unity for the monovalent alkali metals corresponding to an electron revolving around a singly charged ion. With the normal valence of the alkali metals, Lindemann computed selective frequencies which have been checked by many observers. Under certain conditions, the alkali metals manifest different valences, such, for instance, as those exhibited in the oxide series Na_2O_2 , Na_2O , Na_3O , Na_4O . These compounds are light sensitive and can be prepared in photoelectric cells. Spectral response curves for such cells exhibit all the selective maxima called for by the Lindemann formula when the value of n is chosen to agree with the valence of the metal. Data are presented showing this condition to be general for the other alkali metals, a maximum response to red or infra-red light being dependent upon the formation of a subvalent compound, as a suboxide.

63. The scattering of atomic hydrogen by gases: mercury, argon, oxygen and iodine. E. G. LUNN AND F. R. BICHOWSKY, *Naval Research Laboratory.*—A beam of hydrogen atoms defined by two small holes passes through a gas-filled space and impinges on a plate coated with molybdenum trioxide. The loss in intensity of the beam due to collision of the hydrogen atoms with molecules of the various gases depends on the sum of the radii of the hydrogen atom and the gas molecules. The collision diameter of the hydrogen atom can then be calculated directly and simply by using the known collision diameters of the several gases. While the collision diameter of hydrogen determined by comparison with mercury is about eight Angströms, that calculated from preliminary results on the scattering in argon and oxygen is about two Angströms. Similar measurements in iodine, made uncertain by a fading of the reduced molybdenum oxide due to oxidation by the atomic iodine formed, indicate a collision diameter of over twenty Angströms. The collision diameter is thus a property of the degree of interaction between the colliding particles. This is in accordance with the Heitler and London picture of chemical reaction.

AUTHOR INDEX

- Andrews, Donald H.—No. 25
 ——— and John C. Southard—No. 60
- Barnes, R. Bowling—No. 23
 Barnes, S. W. and F. K. Richtmyer—No. 17
 Bartlett, Russell S.—No. 53
 Beams, J. W. and J. C. Street—No. 6
 Bedell, Frederick and Jackson G. Kuhn
 —No. 5
 Bichowsky, F. R.—see Lunn
 Blake, F. C.—No. 15
 ——— and James O. Lord—No. 8
 Bleakney, Walker and John T. Tate—No. 9
 Boeckner, F.—No. 30
 ——— see Mohler
 Brickwedde, F. G. and R. B. Scott—No. 57
 ——— see Scott
 Briggs, H. B.—see Ives
- Canfield, R. H.—Nos. 16, 61
 Chamberlain, C. W.—No. 27
 Chamberlain, Stuart H.—No. 28
 Condon, E. U.—No. 8
 Cravath, A. M.—No. 13
- Deming, W. Edwards—No. 36
- Galli-Shohat, N.—No. 29
- Hamburger, F. Jr.—No. 3
 Hamer, Richard—No. 1
 Hardy, J. D.—No. 22
 Hidnert, Peter and W. T. Sweeney—No. 42
 Hulburt, E. O.—No. 26
- Ives, Herbert E. and H. B. Briggs—No. 55
- Johnson, Thomas H.—No. 10
- Kuhn, Jackson G.—see Bedell
- Lang, R. J.—No. 32
 Lindsay, R. B.—No. 39
 Loomis, F. W.—No. 24
 Lord, James O.—see Blake
 Lowry, E. F.—No. 51
- Lunn, E. G. and F. R. Bichowsky—No. 63
- Mack, J. E.—see Sawyer
 Maxwell, L. R.—No. 35
 McKeehan, L. W.—No. 4
 Mohler, F. L. and C. Boeckner—No. 31
 Morse, Philip M.—see Stueckelberg
- Nottingham, W. B.—No. 54
 Nutting, F. L.—No. 19
- Olpin, A. R.—Nos. 56, 62
 Olshevsky, D. E.—No. 11
 Onsager, L.—No. 37
- Ramberg, E.—see Richtmyer
 Randall, R. H. and Harold W. Webb—No. 34
 Rashevsky, N.—No. 38
 Richtmyer, F. H.—see Barnes
 ——— and E. Ramberg—No. 18
 Robertson, H. P.—No. 40
- Sawyer, R. A. and J. E. Mack—No. 20
 Scott, R. B.—see Brickwedde
 ——— and F. G. Brickwedde—No. 58
 Southard, John C.—see Andrews
 Street, J. C.—see Beams
 Stueckelberg, E. C. G. and Philip M. Morse
 —No. 12
 Sweeney, W. T.—see Hidnert
- Tate, John T.—see Bleakney
 Taylor, A. M.—No. 45
 Trivelli, A. P. H.—No. 21
- Ware, L. A.—No. 41
 Waterman, A. T.—No. 52
 Webb, Harold W.—see Randall
 Weeks, Isabel C.—No. 44
 Wilkins, T. R. and J. A. Wood—No. 2
 White, H. E.—No. 33
 Wood, J. A.—see Wilkins
 Wood, R. W.—No. 7
 Workman, E. J.—No. 43

THE PHYSICAL REVIEW

PLASMOIDAL HIGH-FREQUENCY OSCILLATORY DISCHARGES IN "NON-CONDUCTING" VACUA

By R. W. WOOD

PHYSICAL LABORATORY, JOHNS HOPKINS UNIVERSITY

(Received February 17, 1930)

ABSTRACT

Plasmoidal discharges. A new type of vacuum tube discharge is described, excited by comparatively low voltage high-frequency oscillations (1.7 meters up to 30 meters wave-length) in which remarkable luminous balls, spindles and pear-shaped bodies are formed. These have been reported in earlier papers in *Nature* and the *Phil. Mag.* A study of the conditions under which these bodies are formed and their behavior in magnetic fields has lead to the conclusion that surface charges play a part in their formation. They have been shown to be built of excited molecules, as their spectra are molecular band spectra (O_2 or CO) and since Langmuir has seen in their formation the possibility of plasma oscillations, such as he observed in the mercury arc; they have been named "plasmoids" provisionally.

Red phosphorescence of the glass wall. This occurs in all of the tubes containing oxygen at very low pressure. It appears to be due to low velocity secondary electrons in combination with excited oxygen. Its behavior in magnetic fields has been studied, and it appears when a plasmoid is deflected against the wall by a magnet. The red phosphorescence does not appear until after the high frequency discharge has operated on the glass for some minutes, becoming finally a bright ruby red. The same glass surface phosphoresces green under the impact of high velocity electrons given off from the inner surface of the glass when the external cathode is excited by higher voltages. It may happen that superposed streaks of red and green phosphorescence may occur simultaneously and they can be separated by a magnetic field.

Clean-up effects. Remarkable clean-up effects have been observed, it being possible to have a tube sealed off from the pump which can be made to show either a pure Balmer spectrum of atomic hydrogen (purple discharge) or the green discharge of molecular oxygen. The pressure changes occurring in the sealed off tubes as the type of spectrum changes have been followed with a vibrating quartz fiber manometer.

Spectroscopic investigation. The spectra of the plasmoids, their dark sheaths, and the less luminous gas in which they are imbedded have been investigated by projecting their images on the slit of a spectroscope. The band spectrum of molecular oxygen is seen in the whole tube, but is concentrated in the plasmoids and diluted in their dark sheaths; atomic lines appear as well, the local concentration being different for singly and doubly ionized oxygen.

General nature of discharge. There are two types of discharge, one at very low potentials, suggesting the Townsend discharge (unmodified by space or surface

charges) and a more brilliant one which comes in suddenly as the potential is gradually raised. Plasmoids, however, appear to form with both types, though their shape and distribution in the tube changes as we pass from one type to the other. External electrodes are used in all cases.

IN THE *Philosophical Magazine* for October, 1929, I gave a short account of some phenomena exhibited by very highly exhausted tubes, excited through external electrodes by comparatively low voltages, at a frequency corresponding to a four meter wave. References were made in this paper to earlier work by Kirchner, who first drew attention to the circumstance that, what is usually called a non-conducting vacuum, is excited to bright luminosity by these very high frequencies at comparatively low potentials. During the past autumn I have made a more careful study of these discharges with an oscillator having a wave-length of 1.75 meters built by A. L. Loomis at his laboratory in Tuxedo, New York, and later on in my own laboratory with other oscillators and sources of high potential. The investigation concerned the general nature of the discharges, their behavior in magnetic fields, and the spectra emitted by them, as well as the very remarkable "clean-up" effects shown.

In the earlier paper reference was made to the curious luminous bodies, balls, spindles and pear shaped forms, which usually appeared in the tubes, and it was shown that these luminous masses were formed of singly ionized molecules, either of oxygen, showing the band spectrum, or CO showing the so called "Comet-tail" spectrum, now known to be due to singly ionized CO molecules. Kirchner's original theory to explain the production of a luminous discharge with a potential of only a few hundred volts in a vacuum impervious to the potential of a large induction coil, was that, at these high frequencies, the electrons made "to and fro" excursions ("pendelt") under the rapidly alternating electric force, increasing enormously their chance of ionizing the rarefied gas by collisions.

While I feel convinced that an oscillatory motion of the electron takes place in the discharges, it appears probable that the matter is more complicated than imagined by Kirchner, for the discharges occur equally well when the position of the electrodes and the dimensions of the tube are such as to make these long to and fro excursions impossible.

It seems highly probable that the comparatively heavy ions remain practically at rest, and the circumstance that the luminous bodies are shown by the spectroscope to be built-up of ionized molecules, while the less luminous regions show atomic line spectra, made it appear probable that a careful study of the movements of these bodies under magnetic and electric forces would throw some light on the nature of the discharge.

It is very probable that surface charges on the glass play a large part, for as I showed in an earlier communication, the deflection of the electrons by a magnetic field, as indicated by the movements of the ruby red phosphorescence patches on the inner wall indicated electrons moving away from the electrodes in their vicinity, and towards the electrodes at the opposite

ends of the tube, the electrodes being near the middle. The end of the tube acted as if it had become a secondary cathode. Surface charges are also indicated by the curious circumstance that if the tubes fail to respond to the oscillator, they usually light up immediately if brushed once with a bunsen flame, or even if a lighted match is brought close to them. We thus have a vacuum tube which can be lighted with a match! I have frequently observed the discharge initiated by striking a match at some distance from the tube the effect being due probably to a modification of the surrounding field. In the earlier work sufficient care was not taken to insure a clean inner surface of the tubes, and the presence of CO masked the clean cut effects obtained in the present work.

We will now consider briefly the phenomena exhibited by one of the tubes during the process of exhaustion and subsequently. A tube of soft glass 2 cm in diameter and 30 cm long is blown round at one end, drawn down at the other for sealing, and exhausted with a Holweck molecular pump. The wires from the oscillator are wound once around the tube, forming ring electrodes. The character of the discharge is profoundly modified by very slight changes in the position of the electrodes as will appear presently. The tube was very carefully cleaned with a boiling solution of KOH followed by chromic acid before sealing it to the pump. When the discharge is first started the spectroscope shows a mixture of nitrogen and hydrogen, the former disappearing as soon as the tube is heated, the water-vapor liberated from the glass driving out the nitrogen. At first the color of the discharge is pink, and the spectroscope shows the secondary spectrum of hydrogen as well as the Balmer lines, but after ten or fifteen minutes of operation, the tube being strongly heated from time to time the color changes to the "fiery purple" characteristic of atomic hydrogen.

At this state it may happen, if the electrodes are properly placed, that the discharge shows periodic changes of intensity, along the tube, as shown in Fig. 1a.

The intensity change is not very marked in the case of hydrogen, but, as we shall see presently with only oxygen in the tube, we may have the condition shown in the lower figures, the spindle shaped luminous bodies giving an appearance suggestive of stationary waves. We may heat and pump continuously for an hour or two, no visible change taking place, the color remaining intense purple, and only the Balmer lines showing in the spectroscope. That we have a nearly pure atomic hydrogen (purple discharge) in a tube at very low pressure with well baked walls, is undoubtedly due to the fact that the very high frequency discharge keeps the hydrogen thoroughly dissociated into atoms. A low frequency discharge under these conditions is nearly white, with the secondary spectrum strong, due to the catalyzing action of the walls as shown in an earlier paper. If now the tube is sealed off from the pump and the discharge continued, a most remarkable change occurs in a few seconds. The color changes to pink and the spectroscope or a direct vision prism shows that the oxygen bands in the red-green part of the spec-

trum are developing rapidly and the Balmer lines fading away. In two or three minutes the last trace of hydrogen vanishes, and the color of the discharge is now bright green. It is important to note that the transition from pure hydrogen to pure oxygen occurs only after the tube has been sealed from the pump, which means that a slight rise of pressure is necessary. An explanation of this very remarkable behavior will be given presently. If the tube is joined to the pump by a fine capillary, the oxygen may develop before the sealing off process, for the pressure in the tube will be higher in this case than with a wider connecting tube. The green luminous bodies are now strongly developed and their position and shape alters with every change in the position of the wire ring electrodes, a change in position of one of them of only a millimeter, giving a complete redistribution as shown in Fig. 1, b and c.



Fig. 1. Appearance of plasmoidal discharges under various conditions.

The tube shown in Fig. 1, b-c was flattened at one end and sucked in, producing a dome shaped bottom, like a wine bottle. This was done to see whether the form of the luminous body would be affected by the contour of the inner surface. A flattening of the green spindle was observed, as shown in the figure. An attempt was made to determine the effect of a change of length of the tube, with fixed electrodes by means of a sliding partition, (a short glass tube closed at one end which fitted snugly within the discharge tube) but a discharge formed on each side of it. A tube was then made with a glass partition fused within it, at the center, each half being exhausted separately. With ring electrodes near one end, *both* compartments were excited to equal luminosity, i.e the glass partition served as an electrode quite as well as the wire rings. The excitation of the second compartment was not due to a stray field, as it appeared only when the wire electrodes encircled the other end of the tube.

The glass near the electrodes phosphoresces with a ruby red color, which is very intense, if the tube has been well baked and thoroughly exhausted. If the baking has been less complete the phosphorescence may not appear.

In this case the green discharge is usually brighter, but the spindles and balls are less pronounced.

RED PHOSPHORESCENCE OF GLASS WALL

The red phosphorescence of the glass walls of electrically excited vacuum tubes appears to have been first noticed and studied by Lilienfeld whose papers will be found in the *Verh. der Deutsch. Phys. Ges.* for 1906-1907. It was observed independently by the author some years later in the long tubes used for extending the Balmer series of hydrogen when oxygen was admitted to them. Gehrke and Reichenbeim attributed it also to oxygen, while Lilienfeld considered it due to slow cathode rays, associated with some other undetermined factor, and from certain observations on the magnetic deflection, considered the hypothesis of positive electrons.

In my own study of the subject with tubes excited in a very different manner from that employed by Lilienfeld and, at the time, in ignorance of Lilienfeld's observations, I arrived at first at quite similar conclusions, and frequently remarked that things would be much simpler of explanation if we could admit the existence of positive electrons! Further study however showed that these were not required, and I believe that progress has been made towards the solution of the mysterious red phosphorescence, though there are still points that require further investigation.

In the first place it has been found that high speed electrons, from a single exterior electrode showered with high potential sparks produce a green fluorescence of the glass in tubes containing oxygen at low pressure, the red phosphorescence being produced by electrons of probably lower velocity, when the electrode is attached to one pole of the high frequency oscillator, operating at comparatively low voltage. In this case no green phosphorescence is observed, but in the former case red phosphorescence in general appears in regions of the tube bombarded by secondary cathode rays of presumably lower electron velocity. I feel convinced also that the presence of excited oxygen molecules in contact with the glass walls is also necessary as will appear presently. This may be the unknown factor mentioned by Lilienfeld.

The glass, moreover, must be acted upon by the discharge for some seconds or minutes before the red phosphorescence appears. In one case a streak of green phosphorescence appeared when the discharge was first started, the color changing to red after a few seconds of operation. If the tube was then rotated on its long axis, so as to bring an "untreated" portion of the glass into the electron stream, the green color appeared again, changing presently to red as before.

If a bright discharge is produced at one end of the tube with a single ring electrode until the glass phosphoresces with a red color, and the ring is moved to the other end of the tube, we have no phosphorescence there, although the discharge is of the same character as before. It is evidently associated with a chemical alteration of the glass.

CHARACTER OF DISCHARGE AND "CLEAN-UP" EFFECTS

The duration of the exhaustion, the amount of baking of tube while on the pump, and the operation of the discharge during the pumping, profoundly influence the subsequent behavior of the tube. With a tube of soft glass joined to the pump by a wide capillary (2 mm) the pumping was continued for 3 hours, during which time it was heated with a bunsen flame about twenty times. The discharge was operating most of the time, the color being intense purple (pure atomic hydrogen). When sealed from the pump, the spectrum changed to one of pure oxygen with about ten minutes of operation. After standing over night the discharge, when first started, was again fiery purple, only the Balmer lines showing, which presently faded away and were replaced by oxygen bands and lines, the color changing to green. This process was repeated over and over again, the transition from oxygen to hydrogen, being accomplished in many cases in a minute or two by heating the tube. We thus have a tube with which we can demonstrate either the spectrum of atomic hydrogen or molecular oxygen at will! With continued repetition of the experiment it was found more and more difficult to obtain the hydrogen stage, and the tube finally reached a condition in which only oxygen bands were shown, and the character of the discharge indicated a higher pressure. Heating the tube caused a momentary trace of the hydrogen lines with the oxygen bands but they faded in a few seconds.

I believe that this behavior may be explained as follows. While the tube is on the pump the oxygen and hydrogen formed by the dissociation of water-vapor coming from the glass, are continuously removed allowing fresh water-vapor to come out of the walls. The spectrum is therefore the line spectrum of hydrogen, which always appears with a discharge in water-vapor at low pressures. A few oxygen lines of relatively feeble intensity appear as well.

If now the tube is sealed off from the pump the pressure rises until a point is reached at which no more water-vapor escapes from the glass, and the hydrogen, formed by the discharge is driven into the glass by the discharge, leaving pure oxygen in the tube. This results in a lowering of the pressure, so that more water-vapor can escape from the wall, if the tube is allowed a rest of a day or two, or heated slightly and we again get the hydrogen lines, until all of the freshly formed hydrogen has been driven back into the glass. Repeating the process over and over again gradually raises the pressure of the oxygen in the tube, water-vapor escapes in smaller quantities and it becomes increasingly difficult to get the hydrogen spectrum as has been mentioned. The alternative explanation of the slow return to the hydrogen state would be to assume that it is the hydrogen and not water-vapor that comes out of the glass. If this were so, the gradual rise of pressure with repetition of the experiment would not occur. A different sequence of events was observed in tubes very thoroughly baked out in an electric furnace.

A tube of Pyrex glass, baked during the pumping operation, at a dull red heat for over an hour in an electric furnace behaved quite differently. This tube was not excited electrically during the exhaustion. When first subjected

to the potential of the oscillator there was only a very pale violet discharge, almost invisible. Red phosphorescence of the glass developed in a few minutes and presently a pale green ball (oxygen) appeared between the electrodes. Heating the tube caused the discharge to become brighter, and balls and spindles of green luminosity appeared but the hydrogen spectrum never appeared.

STUDY OF PRESSURE CHANGES IN "SEALED OFF" TUBES WITH QUARTZ FIBER MANOMETER

It was obvious that a careful study of the pressure changes within the tube during these transitions was most important, and a number of tubes were prepared with quartz fiber manometers, (as used by Haber and Langmuir) by which the changes of pressure within the tube as a result of heating, electrical excitation, and repose could be followed.

These manometers are very easy to prepare, no graded seal being necessary. We have only to draw a fiber 8 or 10 cm long by hand (diameter about that of a very fine hair) drop it into the tube which has a round bottom like a test tube, heat the bottom to the fusing point and then quickly invert the tube, holding it vertical. The fiber will swing to the axis of the tube and remain firmly fixed to the glass. If it is off center, hold the tube horizontally and gently heat the glass at the point of attachment with a small flame until the fiber has sagged to the proper position. The fiber is illuminated by a lamp placed at the side and viewed through a low power microscope with micrometer eye-piece. By gently tapping the tube the fiber is thrown into vibration, and the time for the decrement to half amplitude taken with a stop-watch.

With a tube of soft soda-glass sealed off from the pump, after a one-hour pumping with the discharge operating continuously and repeated heatings (up to the appearance of the *D* lines of sodium) the color was fiery purple and the spectrum that of atomic hydrogen. This indicates water vapor at low pressure in the tube. The vibrating quartz fiber sank to a half amplitude value in 12 seconds. When on the pump the time for half amplitude decrement was 30 seconds. This showed that the pressure had risen after, or during the sealing off process.

The tube was now subjected to the high frequency discharge until the hydrogen spectrum was replaced by that of pure oxygen. The time for half amplitude decrement, which in future we will call H.A.D. was now found to be 30 secs, the same value as when on the pump. After operating for half an hour the time for H.A.D. had decreased to 15 seconds; showing that the oxygen pressure was increasing. The tube was now gently heated with a flame. Purple discharge of hydrogen and time of H.A.D. 7 seconds. Ran discharge until only pure oxygen spectrum. Time of H.A.D. 15 seconds, as before heating.

The inference from these observations is that, under the conditions of these particular experiments in which prolonged heat treatment was not

given to the tube, water-vapor, liberated by heating the tube is completely "cleaned-up" by the discharge, while oxygen formed by the action of the discharge upon the glass or upon water vapor contained within the glass does not "clean-up" but accumulates in the tube with continued operation. This is not the case with a tube subjected to long heat treatment.

With a Pyrex tube the following results were obtained. At the start the spectrum showed both hydrogen lines and oxygen bands. Time of H.A.D. 25 seconds. Heated until discharge white (Balmer lines and band spectra of hydrogen). Time of H.A.D. 4 seconds. We now have a relatively high pressure of water-vapor in the tube. Operating for 1 minute, time of H.A.D. 15 seconds. Operating for 5 minutes, time of H.A.D. 25 seconds. Oxygen spectra only. This indicates that *most* of the oxygen and all of the hydrogen of the original water-vapor present is driven into the glass by the discharge.

With a Pyrex tube baked in a furnace at a dull red heat, with the Holweck pump operating, for over an hour, the time of H.A.D. of the fiber was four minutes and 30 seconds! Discharge at first pale violet, with faint pink fluorescence of the glass. Red fluorescence developed in five minutes with faint green glow of oxygen in the tube. The time of H.A.D. was now 45 seconds. The elimination of water-vapor was evidently fairly complete in this case. Three days later the time of H.A.D. before starting the discharge, was found to have increased to 65 seconds. With the discharge operating the time was 90 seconds, and after running for half an hour it was back to 65 seconds. After 2 1/2 hours of operation by the discharge the time increased to 5 min. 40 secs., indicating a pressure as low as, or lower than when the tube came off the pump. After the lapse of several weeks, the oxygen discharge was strong (green plasmoids) and the time of H.A.D. was eight seconds, which changed to 45 seconds after a one minute operation on the five meter oscillator.

These results show that in a well-baked out tube the oxygen "cleans-up" but that it appears again after the tube has stood for some time, or been subjected to heat. The liberation of oxygen by heat and its rapid "clean-up" by the discharge can be repeated over and over again. Nitrogen and neon, introduced into the tube were rapidly cleaned-up.

GENERAL NATURE OF THE DISCHARGE

Langmuir, from his study of the oscillations which occur spontaneously in a mercury vacuum arc excited by a low voltage direct current, developed a theory based on the hypothesis that a cloud of ions served as a medium in which electrons could oscillate to and fro with a frequency dependent on the density of the ions (i.e. the number in unit volume). A region filled in this way with ions and electrons he called a "plasma," and he suggested to me that very probably the phenomena shown by my tubes were closely related to those which he had observed with the mercury arc. The circumstance that the spectroscopist shows that the luminous balls, spindles and pear shaped bodies are made up of singly ionized molecules, identifies them with Lang-

muir's plasma, (at least this is a plausible hypothesis to make), and on this account I propose, for the present at least, to call them *plasmoids*.

Before taking up in detail the subject of the type of discharge in which the plasmoids are formed, it will be well to consider some effects observed in the same tubes when operated by high potentials of lower frequency, as with hammer interrupter, or intermittent in which the character of the discharge is quite different. Some of the phenomena manifested can be considered to advantage in any effort to formulate a theory of the "plasmoidal" discharges.

DISCHARGE BY "LEAK-TESTER"

This apparatus, sold for therapeutic purposes, and used in physical laboratories for hunting for leaks in vacuum systems, generates a rapidly alternating intermittent potential sufficient to produce a shower of sparks an inch or more in length from its single terminal to any earthed conductor. Excitation of the highly exhausted tubes by this apparatus results in phenomena quite different from those observed with the high-frequency sets.

If the single electrode is applied to the under wall of the tube near one end a patch of green fluorescence is observed above it, and two strips of red

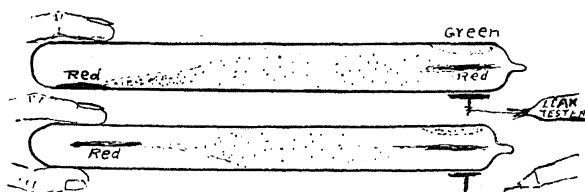


Fig. 2. Red and green phosphorescence patches. Low frequency excitation.

phosphorescence appear along the sides of the tube half way between the electrode and the green patch as shown in Fig. 2. Figs. 2, 3, 5, 7, 12, 13 and 14 are reproduced as "negative" i.e. bright parts of the discharge are black.

If the finger is touched to the upper wall at the opposite end of the tube, a patch of red phosphorescence appears below it on opposite wall. If the thumb is then applied to the wall over the red patch, two red streaks appear on the sides of the tube, half way between the thumb and finger, and if a third finger is applied over one of these it disappears at once and the remaining red streak in the opposite side becomes much brighter. These effects indicate that the red phosphorescence is caused by a discharge of some type, which initially filled the tube uniformly, but which is driven away from those parts of the wall which are "grounded" by an exterior electrode (the finger) and forced against the opposite wall. The depressed "discharge" appears as a faint green glow.

As a substitute for the two fingers and the thumb I wound a "grounded" strip of aluminum around three quarters of the circumference of the tube. The bright red streak appeared along the center of the gap and extended along the wall down the tube towards the electrode. Fig. 3, a.

If a wire, *W* held between the fingers, was brought up towards the red streak from below, the streak was deflected upwards spiraling around to the back of the tube Fig. 3b, while it was deflected downwards if the wire point was brought down from above. If the wire was touched to the outer wall exactly over the center of the red streak, it "forked" into a *Y*, the two branches curving around the wall and uniting at the back. Fig. 3c, very much as would a thin jet of water squirted along the inner wall, and divided into two jets by a small obstacle. The wire had little or no effect if brought up to the red streak in the region of the gap in the aluminum cylinder.

The red streak was also deflected by a magnetic field, upwards or downwards according to the direction of the field. Care was taken to ensure that this deflection was due to the field and not to the mere approach of the metallic mass. The direction of the deflection indicated electrons moving along the inner wall from left to right, i. e. *towards* the electrode.

The deflection by the magnetic field occurred only for that portion of the red streak beyond (to the right of the cylinder). The portion lying between the opposed edges of the $3/4$ cylinder appeared to be held firmly fixed in posi-

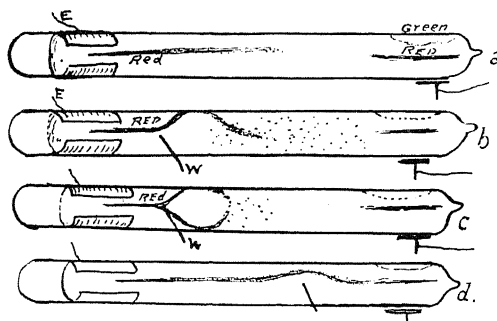


Fig. 3. Deflection of red streak of phosphorescence by grounded wire.

tion by electric forces, while the portion outside was free to move under the influence of the force applied by the magnetic field.

It is worthy of comment, in connection with the forking of the streak into a *Y*, when the point of a wire is placed over it, that the repulsive force due to the wire apparently exerts no influence on the electron (?) stream producing the red phosphorescence streak until it reaches the point immediately under the wire, and that the stream is not driven away from the glass wall towards the axis but merely divided laterally into two streams, which spiral around the tube wall in opposite directions, meeting on the opposite side.

The stream thus appears to have a tendency to stick to the wall, once it has been brought into contact with it by the electric forces set up by the grounded cylinder of aluminum.

In another tube in which the pressure was higher (?) the red streak was bent into an arc by the approach of the wire, i.e., the deflection occurred only in the neighborhood of the wire, as shown in Fig. 3, d. It seems possible that, in this case electron streams from opposite ends of the tube were uniting at the point near the wire. In this case the streak extended nearly down to the

leak-tester and was more sensitive to the approach of an earthed conductor. It was also possible to drive it off the wall entirely, by the approach of an earthed conductor directly above it. A very important observation was made with another tube fitted with the three quarter cylinder of aluminum, and excited at the other end with the leak tester.

The streak of phosphorescence of yellowish color extending out from the gap in the cylinder towards the electrode, appeared to be a mixture of both types, green and red superposed, the latter more easily deflected by the wire or magnet. As the wire was brought up, the red streak was pushed aside, leaving a green streak almost undisturbed, and the same thing could be accomplished with a magnet. When the two streaks were thus separated the original yellow color vanished, being decomposed into its constituents pure red and green. This seems to indicate that we have high velocity electrons giving the green streak, and low velocity electrons, in conjunction with oxygen, giving the red streak. The green streak was visible only in the immediate vicinity of the aluminum cylinder, while the red one extended down the tube nearly to the electrode. If the wire were approached to the tube immediately above the red streak near its end (i.e., at a considerable distance from the gap in the cylinder) it could be made to disappear from the wall and reappear on the opposite wall, the electron stream having been pushed across the axis of the tube. If however the wire was brought up at a point nearer the cylinder the deflected electron stream clung to the wall, curving around the inner wall as a spiral, as has been shown previously (Fig. 2, b).

EXCITATION BY 30 METER OSCILLATOR

The excitation in this case was brought about by simply holding the tube partly within the large coil of copper ribband carrying the oscillatory current. Two large green plasmoids were formed, one at each end, with sharply defined rounded ends facing the ends of the tube and fading away gradually towards the center which were repelled by bringing up the finger to the wall. The tube contained only oxygen at fairly low pressure, but there was no red phosphorescence. On pushing the tube entirely within the coil the discharge vanished, showing that it had been excited by the electric field outside of the coil and not by electro-magnetic induction.

The same tube excited by the "leak-tester" showed only green phosphorescence of the glass with no trace of red. The tube was then excited by the two meter oscillator, and red phosphorescence developed in two or three minutes, accompanied by formation of green plasmoids. This result was due to a partial clean-up of the oxygen i.e., the vacuum was improved.

On exciting again with the leak-tester a red phosphorescence mixed with green in an irregular manner was obtained.

Introduced once more into the coil of the 30 meter oscillator, the projecting end being held with two fingers and the thumb, a single plasmoid formed, tapering to a point on the side towards the finger, and rounded on the end towards the coil. A streak of red phosphorescence formed on the

glass extending from the region between, but not covered by the fingers, to a point opposite the tapered end of the plasmoid. If now the end of a wire held in the fingers was brought up to the wall on the side opposite to that on which the red streak had formed, and near the pointed end of the plasmoid, the latter turned up and joined the red streak, i.e., it was repelled by the wire.

It seemed probable to me that the red streak produced by grasping the tube with the fingers was produced in each case at those moments at which the opposite end of the tube was anode. In the case of the excitation by the leak-tester it will be remembered that red phosphorescence streaks were produced at each end of the tube Fig. 2, a and Fig. 3, a.

If the above hypothesis is correct, the red streaks should not appear simultaneously but in alternation. Examination of an ordinary Geissler tube excited by the leak tester in a waggled mirror showed that its polarity alternated in unison with the vibrations of its small "hammer-break," but the light of the red streaks was not bright enough for a conclusive test in this way, the single images seen in the mirror being rather feeble. A stroboscopic method was therefore adopted, by which the tube could be observed at rest and continuously.

STROBOSCOPIC EXAMINATION OF DISCHARGE

The tube was excited by connecting a single ring of wire, wound around one end of the tube with one pole of a 20,000 volt (60 cycle) transformer. The other end was furnished with an earthed three-quarter cylinder of aluminum foil, as before.

Red phosphorescence appeared close to the ring, and as a red streak in the gap of the cylinder. The tube was viewed through a slot in a card-board disk mounted on the shaft of a synchronous motor operated on the same 60 cycle circuit as the transformer. Only one red patch could be seen at a time, the one visible depending upon the position of the eye as it was moved around the circumference of the disk. This experiment appears to prove that in all of the experiments, in which, with a single electrode at one end of the tube, we have electrons moving from the other end towards the electrode, the motion occurs only at the moments at which the electrode is anode. This applies also I believe to the high frequency experiments, in which plasmoids are formed, and should be taken into account in framing a theory of the formation of the plasmoids. Experiments were also made to ascertain how low a frequency would produce a visible discharge.

If the tube were placed between the poles of a small Holtz machine, no luminosity whatever appeared within the tube, though the potential was high enough to cause sparks to jump around the wall. This same tube, on the five meter oscillator with a potential sufficient to give a spark of only half a millimeter or less, showed a brilliant green plasmodial discharge. A small rotating commutator was now made by pasting tin-foil strips along the edge of a disk of ebonite mounted on the shaft of a small motor. By means of this the steady potential of the Holtz machine could

be converted into an alternating potential. Luminosity appeared within the tube with alternations as low as six per second and reached a maximum at about fifty per second. The discharge vanished as the speed of the commutator increased, for reasons which are not quite clear. Possibly the conductivity became so good that the machine could not build up potential.

THE PLASMOIDS

The study of the plasmoids has been conducted along two quite different lines. (a) Their formation and the changes which they undergo when the form and position of the external electrodes are altered, and their behavior in magnetic fields have been very carefully investigated, with oscillators of different frequencies and with the gas at different pressures. (b) Spectroscopic data have been obtained in regard to the radiations emitted by the plasmoid, by its relatively dark sheath and by the more or less uniformly luminous gas in which it is embedded. It seemed probable that a determination of the distribution in space of singly and doubly ionized atoms and the singly ionized molecules, would be of help in ascertaining the physical processes involved in the plasmoid formation.

There appear to be two distinct types of discharge, one in which the luminosity of the gas is low and the other in which it is high. Plasmoids are formed in both cases, but the transition from one type to the other is abrupt.

This suggests perhaps a transition from a "Townsend discharge," to a glow discharge, space charges and charges on the wall being absent in the former, and the potential drop merely the normal drop from anode to cathode while the "glow discharge" results when ionization becomes more pronounced, and space charges are present.

The transition from one type to the other was well shown in the case of a very highly exhausted tube containing oxygen as the residual gas. It was furnished with two ring electrodes formed of single turns of fine wire wound tightly around the tube.

With the lowest potential capable of exciting a luminous discharge, a pale green disk shaped like a double convex lens appeared midway between the ring electrodes as shown in Fig. 4, a. As the potential increased the disk expanded to the form shown in Fig. 4, b, while a further increase of potential caused the sudden appearance in its place of a much brighter green plasmoid in the form of a prolate spheroid, Fig. 4, c. My first attempt to explain the formation of the plasmoids with their sharply defined smooth surfaces, was along the lines usually followed in accounting for the stratifications in gas discharges, namely that the plasmoid surface represented an ionization caused by electrons which had acquired the requisite velocity after leaving the cathode. This works out well for cases a and b of Fig. 4, for the equipotential surfaces of the ring electrodes are about as shown in Fig. 5 which is a cross section through the rings. At low potentials (as in Fig. 4, a) ionization does not result until the electrons have reached equipotential surfaces 1, and the lenticular luminosity appears in the region between them. At a slightly higher potential the electrons have acquired the requisite velocity

when surface 2 is reached, and the region between these surfaces is luminous as in Fig. 4, b. The sudden production of the spheroidal plasmod at a slightly higher potential may result in part from the formation of negative

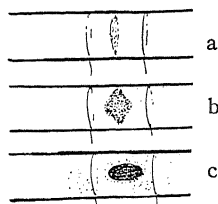


Fig. 4. Change in shape of the plasmod with increasing potential.

charges on the tube wall between the electrodes, but the complete explanation in this case probably requires the introduction of other factors, such for example as the plasma oscillations imagined by Langmuir.

It appears possible that if we could apply a stroboscopic method to these very high frequency discharges we might find that the brilliancy at opposite

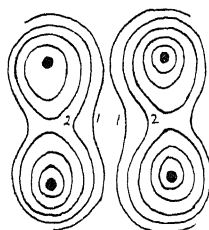


Fig. 5. Equipotential surfaces of ring electrodes.

ends of the plasmod oscillated in unison with the discharge, i. e. the rounded ends facing the ring electrodes became luminous in alternation. My reason for considering this possible was the circumstance that in the case of a short tube excited by introduction into the helix of the thirty meter oscillator two plasmods were formed as shown by Fig. 6. That these occur in alternation

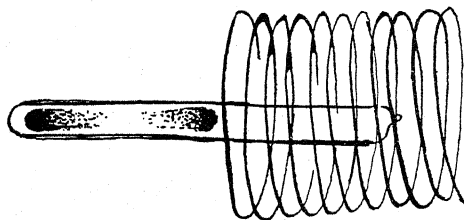


Fig. 6. Plasmods formed with 30 meter oscillator.

and not simultaneously is indicated by the behavior of the discharge at low frequency as examined with the stroboscope. If now the conditions were such as to bring these plasmods closer together we should have the single

spheroidal plasmoid referred to above. The tube in which the lenticular and spheroidal plasmoids formed was excited with the 1.75 meter oscillator by means of two disk electrodes applied on opposite sides of the tube as shown in Fig. 7.

These give a field of simple type, which is easy to calculate, with a potential sufficient to give a spark about half a millimeter long. With a potential giving a spark perhaps half a millimeter in length a brilliant green plasmoid shaped like a double convex lens appeared midway between the electrodes and parallel to them. Fig. 7, a. The plasmoid was surrounded by a dark sheath and two dark arches covered the electrodes as shown in the figure. As the potential was lowered by reducing the filament current, the lenticular disk contracted, remaining very bright however, but suddenly was replaced

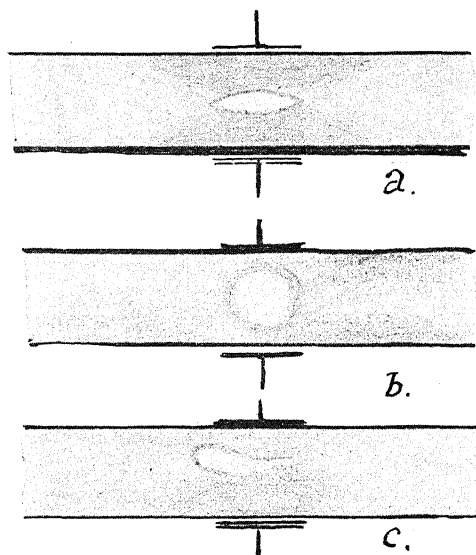


Fig. 7. Change in shape of plasmoids with decreasing potential and magnetic deflection of plasmoid (c).

by a sphere of low luminosity surrounded by a wide dark sheath. Fig. 7, b. If the pole of a small bar magnet was brought up to the wall, in the condition "a" the plasmoid was squeezed to one side and deflected upwards as shown in Fig. 7, c. The magnetic field was such as to deflect downward moving electrons to the left and upward moving ones to the right. The formation of the sphere and disk I am unable to explain.

The development of plasmoids at periodic intervals along the tube, as shown in Fig. 1, I was at first inclined to ascribe to a zig-zag reflection of the electrons from surface charges built up on the inner walls by electron impact. It seemed, however, highly improbable that such sharp localization could be produced in this way, or that a movement of one ring electrode through a distance of only one or two millimeters could cause such a change in the paths of electrons down the tube as to cause a complete redistribu-

tion of the plasmoids in space. Langmuir's theory that the plasmoids are oscillators having a definite frequency of vibration seems to be a much more promising line of attack.

Nevertheless, certain observations have been made which apparently show that a reflection in the manner imagined actually takes place. In a tube at very low pressure, containing only oxygen and excited by a single disk electrode placed close to the outer wall, the following phenomena were observed as the capacity of the condenser in the oscillatory circuit was increased from zero. It must be remembered that with the variable capacity set at zero, the circuit is practically interrupted and the potential is very low if oscillations are present at all. As the capacity is increased a patch of ruby red phosphorescence appears on the upper wall of the tube immediately over the disk, with an area considerably larger than that of the disk, and a second red patch on the lower wall of the same diameter as the disk, as shown in Fig. 8, a.

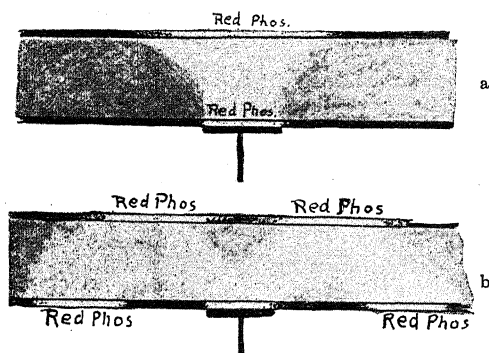


Fig. 8. Reflection of slow electrons by surface charge.

The only way in which I can account for the circumstance that the lower red patch exactly covers the region immediately above the disk electrode is to assume that some of the electrons moving along the lines of force, when the disk is negative fail to reach the upper surface before the field reverses and hence travel backwards along the reversed lines of force to their starting point.

The paths of the electrons through the gas is marked by a faint green luminosity. If the capacity is made slightly greater, which increases the potential, the upper red patch divides at the middle and spreads out, the glass ceasing to phosphoresce immediately above the electrode, and two new red patches appear in the lower wall as shown in Fig. 8, b.

The cause of the division of the electron stream over the electrode results perhaps from the formation of a negative surface charge immediately above the electrode, while the two lower red patches of phosphorescence, appear to be due to the downward deflection of the oblique streams of electrons by negative surface charges at the upper red spots. A slight further increment of capacity results in the sudden birth of two plasmoids to the

right and left of the descending streams. The reversal of the electron stream alluded to above was also indicated in a vertical tube so highly exhausted that practically nothing but red phosphorescence was observed, (with a disk-electrode at the bottom). In the upper two thirds of the tube and at the bottom upward moving electrons were found, while a strong downward stream was indicated by the magnetic concentration of red phosphorescence about one third of the way up. This stream appeared to me to be due to the pulling back of the tail end of the upward electronic blast, when the disk became anode. This case will be alluded to again presently.

If the oxygen is at a slightly higher pressure and we gradually increase the capacity in the oscillating circuit, we get a quite different sequence of events, and can watch the birth of a plasmoid. With a moderate capacity the discharge has the appearance indicated by Fig. 9, a.

Its color is yellow-green of much greater intensity than in the previous case and there is a dark arch over the electrode. The upper wall shows a feeble red phosphorescence, indicating that some of the electrons succeed in reaching it. There are also indications of a segmentation at *A*, which is

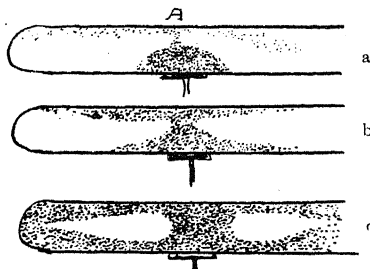


Fig. 9. Birth of a plasmoid.

destined to become the breaking point of the discharge when the plasmoid forms. If now a magnet pole is brought up from the side (of polarity such as would cause upward moving electrons to be deflected to the left) the portion *A* is squeezed to the left and a large and perfectly formed plasmoid develops Fig. 9, b and c.

With an oscillator of five meters wave-length, and a single disk electrode applied to the flat end of the tube the plasmoid development as the capacity of the condenser was increased is illustrated in Fig. 10.

The total capacity of the condenser was about 300 cm and the scale was graduated to equal divisions from 0 to 100. The capacity of the condenser is given below each figure. With the two smallest capacities, the discharge is of the first type and of a very feeble green color, the plasmoid having the shape of a spear-head.

Increasing the capacity to 11 causes a sudden increase in luminosity and two plasmoids form of the shape indicated. With capacity 16 the upper rounded end of the large plasmoid streams up to a point, and at capacity 20 a break to the brighter type of discharge occurs and two sharply defined plasmoids appear at opposite ends of the tube. Two rings of red phosphorescence

appear immediately above and below the lower plasmoid, due probably to reflection of the electrons from charges on the tube wall, or possibly to the upward electron stream from the disk cathode and the downward stream which occurs when the disk becomes anode, a condition mentioned a moment ago. If a magnet pole is brought up to the lower plasmoid, both plasmoids contract and disappear at the same moment, but if the magnet is brought up to the upper one it contracts and vanishes but the lower one remains unaffected.

I think it highly probable, in view of the stroboscopic experiments previously described, that the two plasmoids appear in alternation as the field reverses, the upper plasmoid appearing as a result of a negative charge on

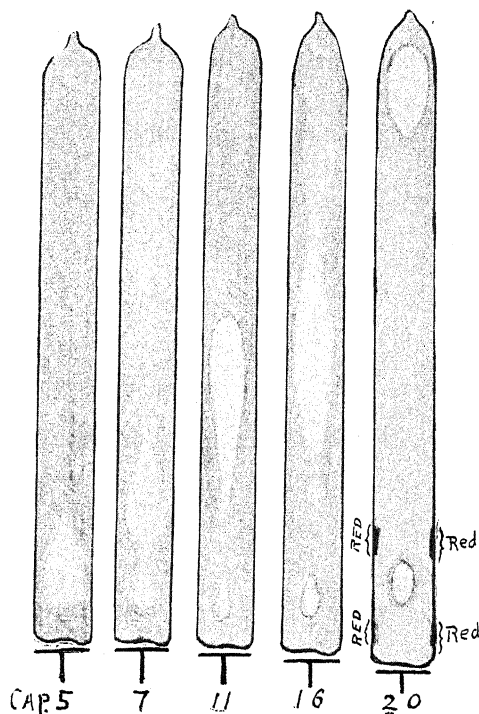


Fig. 10. Plasmoid formation with increasing potential.

the wall of the tube above it, at the moment when the electrode becomes anode. The application of the field at the lower end prevents the electrons, in part at least, from reaching the upper end of the tube, and this probably is responsible for the contraction and disappearance of the upper plasmoid.

The effects of a magnetic field on the plasmoidal discharge is very complicated, due, probably to the circumstance that we have electron streams moving in opposite directions but with different velocities at the same point in the tube. These streams do not of course occur at the same instant but in alternation as the polarity of the oscillator reverses, and they will be deflected in opposite directions by the field. This two-fold deflection is often observed at the center of the tube.

The magnetic field, in some cases, causes the plasmoids to shrink and disappear, in others it causes the birth of plasmoids where none existed previously. It has been found extremely difficult to systematize the multitude of different effects observed, or draw any very definite conclusions from them, and only a few selected examples will be given. The others will be kept on record, as they will be of value in testing any theory of plasmoid formation that may be developed subsequently. It will be best to begin with what appears to be the simplest case, a tube containing oxygen at such low pressure that scarcely any trace of plasmoid occurs. The pale green discharge filling the tube quite uniformly, when excited by a single disk electrode at the base and the five meter oscillator. A small U-shaped magnet was used, much larger than shown in the figure in such a position that the lines of force were perpendicular to the paper in Fig. 11. The intens-

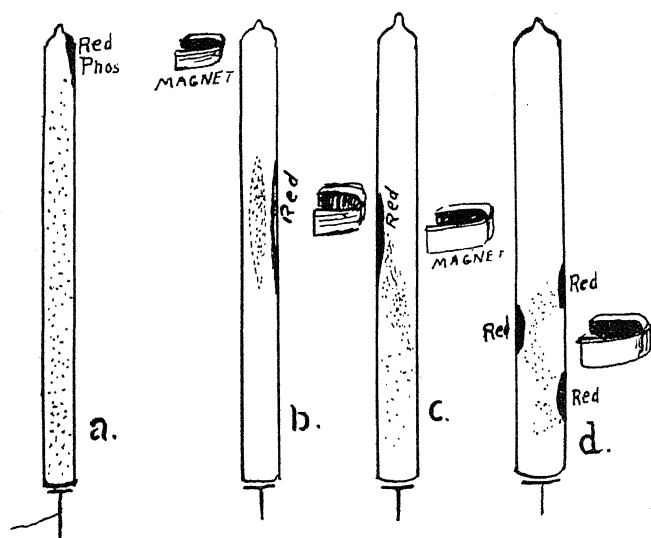


Fig. 11. Magnetic deflection of discharge.

ity of the luminosity fell off gradually towards the top of the tube where it was practically zero. The top of the tube showed a faint red phosphorescence, which was deflected to one side when the magnet was 20 cm from the tube, the direction of the deflection indicating upward moving electrons. On moving the magnet down the tube it was necessary to bring it up closer to cause red phosphorescence on the wall. This indicated that the upward moving electrons had a higher velocity half way down the tube than at the top, due perhaps to a reversal of the field direction during their flight from the disk cathode towards the top of the tube. A small plasmoid formed along the axis of the tube in this stage Fig. 11, b. On bringing the magnet closer to the tube a bright red patch formed on the opposite wall below the magnet, indicating electrons moving down, the plasmoid disappeared and the luminous discharge was pressed against the wall terminating at the spot of red phosphorescence. Fig. 12, c. The inference appears to be that we have at

this point, electrons moving down with a velocity a little greater than that of the electrons moving up, the streams occurring in alternation of course.

On moving the magnet down the tube, two red patches formed on the right hand wall, and one on the left half way between them, Fig. 11, d, and the discharge appeared to zig-zag across the tube as shown. This case is more complicated, and I cannot account for it by considering simply two electron streams moving in alternation in opposite directions with different velocities.

Appearances suggest the formation of surface charges and reflection of the electron streams as in a former case (Fig. 8, b.). Some of the effects described above might be explained by assuming upward moving electrons along the inner wall, the downward stream being at the center, but this seems improbable. We will next consider the case of a tube with oxygen and CO at low pressure in which a white plasmoid formed at the top of the tube with its head pointing downwards as shown in Fig. 12, a.

If the pole of the bar magnet was brought up from behind towards the tail of the plasmoid, it disappeared when viewed from the front but was still visible when viewed from the side, due to its having been spread out

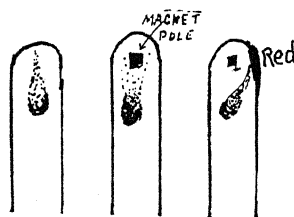


Fig. 12. Magnetic deflection of plasmoid.

into a fan. This would indicate electrons moving both up and down. No phosphorescence of the glass was observed. On bringing the magnet closer a new sharply defined tail formed, and the head of the plasmoid was pulled up; at the same time the tail bent to the right, finally touching the glass forming a patch of red phosphorescence on a closer approach of the magnet. Downward moving electrons were indicated in this case.

With the magnet still closer to the tube a faint red patch appeared on the left hand wall, below the magnet, due to upward moving electrons.

If the magnet was approached immediately below the plasmoid, or even below the bulbous expansion of the tube, the plasmoid contracted and vanished, without suffering displacement.

When the magnet was brought up to the plasmoid shown in Fig. 10, Cap. 11, the upper end was deflected to the right and the lower end to the left red spots forming on the wall, indicating electrons streaming out from the center of the plasmoid through its upper and lower surface. In this case the discharge was of the first type (Townsend?).

In other cases the magnet indicated electron streams flowing into the opposite ends of the plasmoid. Elongated plasmoids were constricted or broken into two, by the magnetic field the broken ends being deflected in

opposite directions against the wall forming red spots, the indication in this case being electron streams flowing out of the broken ends.

It has not been found possible to systematize these observations, doubtless due to the fact that the field, by deflecting electrons, establishes a new condition in the tube (destruction or rupture of a plasmoid and a redistribution of surface charges) and the effects we observe are those produced by the field on this modified discharge. In general I have found that whenever a plasmoid is pushed against the wall by a magnet red phosphorescence is produced.

In the condition shown in Fig. 10, Cap. 20, if the magnet pole is brought up from behind the upper plasmoid, the plasmoid slowly collapses to a point and disappears, red phosphorescence appearing on the left hand wall indicating electrons moving down. The oxygen pressure was higher in this case than in one previously mentioned, in which an upward electron stream was found in the upper two thirds of the tube.

SPECTROSCOPIC STUDY OF PLASMOIDAL DISCHARGE

In this study an image of the discharge was focussed on the spectrograph slit, so that a point-to-point correspondence obtained. It was found that the spectrum of the faintly luminous discharge in which the plasmoids were immersed, (with pure oxygen only in the tube) showed the bands of the

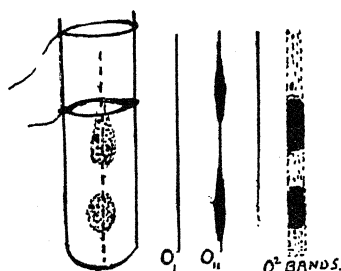


Fig. 13. Distribution of intensity in spectrum lines and bands.

oxygen molecule, and the atomic lines due to OII and OI. The discharge in the single case which we shall consider was produced with the 1.7 meter oscillator with two wire ring electrodes, the plasmoids having the form shown in Fig. 13. The slit covering the portion shown by the dotted line. In this diagram the local intensity of a line is roughly indicated by its width. The atomic line due to OI was of uniform intensity throughout its length, the OII lines showed a slightly greater intensity in the vicinity of the plasmoids, two lines (oxygen triplets) between the green and blue bands were of uniform intensity except at the bottom of the tube, where they were very faint, while the bands due to oxygen molecules were much more intense in the plasmoids, the intensity decreasing abruptly at the plasmoid surface. This shows that in the plasmoid we have a concentration of excited oxygen molecules, while the concentration in its dark sheath is less than in the luminous discharge in which it is embedded.

IONIZATION OF HELIUM BY POTASSIUM POSITIVE IONS

BY RICHARD M. SUTTON AND J. CARLISLE MOUZON
CALIFORNIA INSTITUTE OF TECHNOLOGY, PASADENA

(Received February 18, 1930)

ABSTRACT

A continuation of previous attempts to ionize gases by positive ions has been extended to helium using potassium positive ions as high as 750 volts accelerating potential. At pressures between 0.01 and 0.1 mm there is definite evidence of ionization of helium above 150 or 200 volts accelerating potential. The effect is much smaller than in the gases previously reported, but it may be distinguished from the secondary emission of electrons from the metal parts under action of the positive ions. Great difficulty was encountered in changes of intensity of ionization due to impurities in the helium. Some of the uncertainties in previous work have been removed by changing the relative positions of electrodes.

IN A previous paper by one of us¹ evidence was offered for the ionization of argon and neon by potassium positive ions. It was determined that these positive ions could produce ionization which was distinguishable from other effects produced upon the metals in the tube when the accelerating potential was in excess of 150 volts. An inherited error in calibration of the McLeod gauge used for pressure measurement caused a misstatement in that paper regarding the pressure range over which the effect of ionization is found. The pressure range is nearer 0.005 to 0.1 mm which partially obviates the argument concerning unusually long mean free paths of the positive ions. The indication is that their paths are comparable with, but slightly longer than, the mean free path calculated from kinetic theory data.

This work has been extended to the study of helium in a new tube using electrical connections practically the same as previously described. Fig. 1 shows the tube with its electrical connections. The chief features in which it differs from the previous tube are (1) a ground glass joint by which filament changes may be more easily effected, (2) greater space between collector *S* and grid *G* from which the products of ionization are collected, (3) a flat plate *P* placed only 2 mm above the grid *G* and parallel to it. The ground glass joint is made in two parts, the upper part being coated with graphite, the lower portion coated with stopcock grease and sealed with mercury. A vacuum connection between these two parts minimizes the danger of stopcock grease entering the tube. The filament and cathode leads are mounted in this joint so that the filament may be easily removed and recoated with Kunsman catalyst. The cathode is, as before, a steel cylinder completely enclosing the filament; however, the channel through which the positive ions emerge into the upper part of the tube has been made smaller (1.5 mm diameter) and the hole in the collector through which it projects has been

¹ R. M. Sutton, Phys. Rev. 33, 364 (1929).

made smaller (3 mm diameter) so that the field between collector and grid is more uniform. By placing the grid 2.5 cm above the collector *S*, a larger region is available from which to collect the products of ionization. Furthermore, the region above the grid is greatly reduced from the previous case so that the amount of ionization produced between the grid and upper plate has a negligible effect upon the plate current (I_p) of positive ions. It was found that the reflection of positive ions from the plate was extremely small or negligible so that the V-shaped plate previously used to reduce reflection was eliminated.

The helium used was obtained in moderately pure form from the United States Bureau of Mines at Amarillo, Texas. It was further purified by passing over oxidized copper turnings and charcoal in liquid air until it was spectroscopically pure. As an additional precaution, the helium was passed through

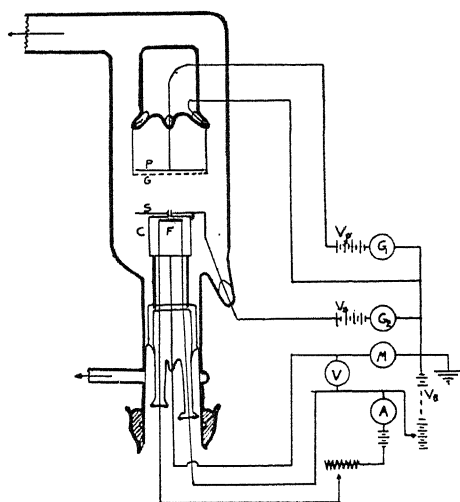


Fig. 1. Experimental tube and connections.

a magnesium discharge tube before its introduction into the experimental tube. The ionization properties of the gas seem to be particularly sensitive to impurities, increasing very materially with amounts of impurity which must be only a few percent of the total gas pressure. It is desired to study this aspect of the ionization more carefully in the future under controlled conditions. Until now, however, the effort has been to work with the purest gas obtainable. Consequently, whenever the gas gave indication of contamination by reason of marked increase of ionization without measurable change of pressure, it was rejected and fresh gas was admitted to the apparatus. This increase may be due in part to ionization of impurities by collision with helium excited by positive ion bombardment.²

The system of measurement consisted in directing the potassium positives through the narrow channel in the cathode into the region between the col-

² G. P. Harnwell, *Phys. Rev.* **29**, 683 (1927).

lector S and plate P . The potential of S was maintained 20 volts positive with respect to the cathode (ground) thus preventing positive ions from reaching the collector directly. Any electrons liberated from the grid or from the cathode under impact of the positive ions would reach S in case they had such initial direction as to enter the field of this collecting potential V_s . It was found that the long narrow channel used in these experiments was the source of a rather large amount of secondary emission of electrons to the collector, especially when the channel was contaminated with potassium from the filament. The secondary emission was, in general, about three times as great as it was in the previous tube. Any electrons liberated by ionization of the gas between S and G are collected on S and show themselves as an additional current in excess of the secondary emission. The primary positive current is measured on the plated P , which is also kept positive (18 volts) to prevent the escape of secondary electrons from the plate into the region between S and G . It will be seen that nei-

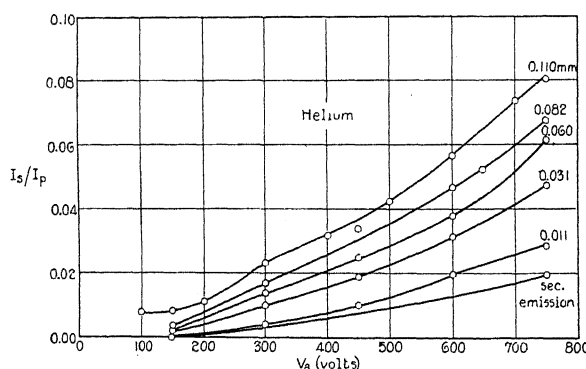


Fig. 2. Ionization in helium at various pressures. Ratio of electron current to collector to positive ion current to plate as function of accelerating potential of positive ions.

ther of these collecting potentials can give electrons energy sufficient to ionize helium and by making the plate potential $V_p = 18$ volts, it was possible to prevent escape of electrons from the plate due to photoelectric effect from radiation produced by excited helium atoms. However, these collecting voltages which are higher than those used in previous work with gases of lower ionizing potentials are in excess of the ionizing potentials of most gases except helium; hence they may be a source of ionization by electrons when impurities are present.

In general, the current to the collector S was measured with a gas pressure of less than 10^{-5} mm and then, without changing other conditions, it was again measured with helium present. A series of measurements of the current to S at different accelerating potentials was made at each gas pressure used, and fresh helium was introduced for each new pressure test. Figure 2 shows a series of curves obtained at various pressures by plotting the electron current to the collector (I_s) divided by the positive ion current to the plate (I_p) as a

function of the accelerating potential of the positive ions. Each curve thus represents the efficiency of ionization at various accelerating potentials for each pressure shown (after subtraction of the current due to secondary emission). The lowest curve was taken with pressure 10^{-5} mm or less. It represents the effect of secondary emission alone. The lowest pressure at which a distinguishable effect due to the presence of helium can be detected is 0.01 mm at which the mean free path of K^+ in helium is approximately one-half the distance between the collector and grid. From .01 to 0.1 mm there is definite evidence of ionization. It will be seen from Fig. 2 that the ionization current plus the secondary emission at 0.11 mm amounts to 8 percent of the initial positive ion stream at 750 volts, and the secondary emission with no gas present is equivalent to approximately 2 percent of this current, which leaves 6 percent as the part due to ionization of the gas assuming that the secondary emission is independent of gas pressure. (This assumption may need some modification inasmuch as the secondary emission in the cathode channel may increase due to scattering of the initial positive beam against the metal). We have no way of determining at present how many impacts each positive ion makes between the collector and grid, so that we are not free to predict or calculate the probability of an impact resulting in ionization. However, it appears to be rather small considering that the positive ions at 750 volts have many times the kinetic energy necessary to ionize helium.

There has been some question as to whether the nature of the discharge through the channel into the upper region of the tube does not change materially with the presence of gas in the tube. This point has been tested by measuring the total current between the cathode and filament under all operating conditions of the tube; the only change in this current due to increase of accelerating potential of the positive ions is such as may be adequately accounted for by the increased secondary emission from the cathode itself under action of the ions up to the potential at which an arc occurs. It is possible, however, that a few positive ions of helium might be formed within this region due to electron impact, and these may emerge into the upper region of the tube to cause collisions with the gas present. It is doubtful whether any such collisions would result in ionization, since the escape of an electron from the combined attraction of two positive helium ions cannot be effected as easily as the escape from the field of a K^+ and an He^+ ion. The chief effect of such helium positive ions in the original beam would be to increase I_p , whereas a decrease in I_p is noted with the presence of the gas. This decrease of I_p upon the introduction of gas may be attributed to a slight cooling of the filament due to conduction, or to retardation of the ions by collision with gas molecules sufficient to prevent their reaching P against the retarding potential of V_p of 18 volts. That part of the decrease of I_p due to stoppage of the initial positive ions obviously causes an abnormally large calculated ratio I_s/I_p . This is particularly evident in the curve for 0.11 mm which does not approach zero as rapidly as do the curves taken at lower pressures. The relatively high ratio at 150 volts is due to almost complete stoppage of the initial positive beam, rather than to a greater amount of ionization at this pressure.

A comparison of results obtained from the present tube with those previously reported was made in a test run on neon. Taking due account of the change of position of electrodes and the increased secondary emission in the present tube, the two tubes give quantitative results in good agreement. Figure 3 summarizes the evidence for argon, neon, and helium. N is the number of electrons per initial positive ion per cm path at 1 mm pressure, calculated at the average of the pressure range, 0.05 mm.³ The increase of N with pressure indicates the possibility of ionization of more than one gas atom

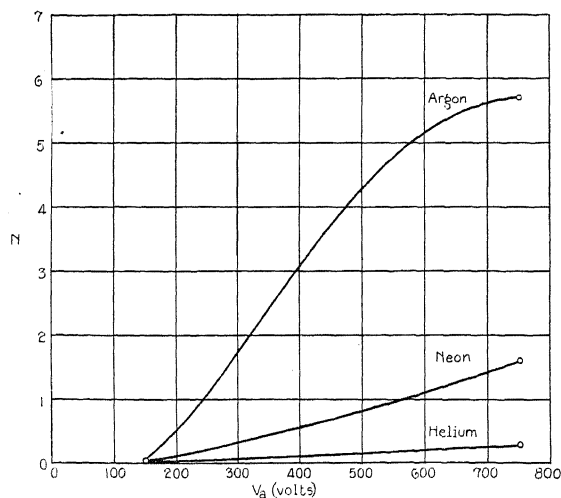


Fig. 3. Comparative ionization of argon, neon, and helium by potassium positive ions. N represents the number of ions formed per positive ion per cm path at 1 mm pressure.

by a single positive. At 0.1 mm pressure each positive ion encounters approximately 15 collisions over a path 3.4 cm long on kinetic theory data. This penetration of the positives is not as great as that previously adduced, due to correction of the pressure measurements, but is still comparable with the magnetic analysis experiments of Durbin, Kennard, and Dempster.⁴

The present work will be continued on the investigation of other gases and different positive ion sources. It seems desirable also to test further the effect of impurities upon ionization of the noble gases.

³ K. T. Compton and C. C. Van Voorhis, *Phys. Rev.* **26**, 436 (1925).

⁴ F. M. Durbin, *Phys. Rev.* **30**, 844 (1927); R. B. Kennard, **31**, 423 (1928); A. J. Dempster **31**, 634 (1928).

ON THE POTENTIAL RELATIONS IN THE STRIATED POSITIVE COLUMN OF ELECTRICAL DISCHARGES THROUGH HYDROGEN

BY JOHN ZELENY

SLOANE PHYSICS LABORATORY, YALE UNIVERSITY

(Received February 17, 1930)

ABSTRACT

The many lined visible spectrum from the striae in the positive column of a discharge through hydrogen must arise from electronic transitions between excited states having energy levels differing by only about 3 volts for the violet lines. The assumption made by others that the light arises from transitions to the ground level from the lowest excited state of 11.5 volts cannot hold because such transitions would give light in the extreme ultra-violet region only. It is necessary to produce excited states at least 3 volts above the lowest excited level. This requires an energy not far below the ionization potential of 16.1 volts. A process is described by which both excitation of molecules to the required levels and ionization might occur at equal intervals throughout the positive column, but a difficulty arises in the fact that the voltage drop between striae under certain conditions is found to be several volts below the ionization potential. It is assumed that the electrons acquire enough energy for ionization in these cases from collisions of the second kind with molecules of some impurity which are in excited states of comparatively low energy levels. Reasons are given for believing that the impurities involved come from the walls of the discharge tube, and that the walls play a very important role otherwise, as well.

THE periodic changes in the electric force along the length of a striated positive column in a discharge tube are usually taken to indicate that there are periodic positions along the column where ionization is taking place. In fact J. J. Thomson¹ postulates that when the positive column becomes striated it does so because under the given circumstances the periodically changing field which accompanies the striated condition permits the replenishment, with the least total expenditure of energy, of the electrons lost along the path of the discharge either by diffusion to the walls of the tube or by attachment to positive ions or neutral molecules. We should accordingly expect the energies acquired by electrons between striae to correspond at least to ionization potentials.

However, the main part of the light coming from the positive column does not have its origin in the recombination of ions, for there is strong evidence² that there is but little recombination in the body of the gas between electrons and positive ions, owing doubtless to the high prevailing speeds of the former. Such union occurs rather at the walls of the tube.

The light from striae in a discharge through hydrogen gives a many lined spectrum and must originate then in *molecules* in excited states. The

¹ J. J. Thomson, Phil. Mag. 8, 1 (1929).

² See R. Seeliger, Phys. Zeits. 30, 329 (1929).

existence of the periodic changes of light intensity which distinguishes the striated state of the positive column points to the energy acquired by electrons between striae as that corresponding to an excitation voltage. Indeed Grottrian³ using a stream of electrons from a hot cathode in mercury vapor has observed a striated discharge with periodic changes of potential of 4.9 volts, corresponding to the lowest excitation level of mercury. Here, however, there was no ionization occurring throughout the volume of the vapor.

When a cold cathode is used ionization as well as excitation of molecules must be taking place in the positive column and there is then a question how the two effects requiring different voltages are produced at the same equal space intervals along a discharge tube. It seems reasonable to assume that the process requiring the higher energy on the part of the electrons, i.e. ionization, determines the potential fall between the striae, and that the excitation of molecules and subsequent radiation from them is an accompanying action of this first process. According to this view when the electrons in their progress through the field have acquired enough energy for excitation some of them will begin to have inelastic collisions with molecules which raise these to excited states. This action will continue until the electrons which have as yet had no collisions of this kind gain enough energy for ionization after which both kinds of inelastic collisions will take place in the same region along the tube. The probability that at any one impact the collision of an electron with a molecule will be an inelastic one is small and hence the process given is a possible one.

The actual linear distance along a discharge tube in which the above two actions take place need be but a minor part of the whole distance between two striae since the energies required for ionization of a hydrogen molecule and for its excitation to states from which visible light may result are not greatly different. To this is added the fact that the mobility of an ion varies inversely as its motion of agitation and so when the electrons have acquired the most energy from the field their progressive speed along the tube will be the least. Accordingly many more impacts than elsewhere will here occur within a given length of the discharge tube and nearly all of the electrons will have their inelastic collisions inside a short length of the tube from which they will then begin a new excursion. Some addition must be made to this process because under some conditions the potential drop between striae is less than the ionization potential.

Compton, Turner and McCurdy⁴, who have expressed views regarding the process of stria formation which in some respects are similar to those above, have assigned an important role to impurities in the gas which are so essential for the appearance of striae in nearly all gases. They postulate that the function of the impurities is, by collisions of the second kind, to restore to the stable form such metastable excited atoms which, having diffused to all parts of the interstria spaces, would otherwise after inelastic impact with comparatively slow electrons give rise to radiations there and thus tend to wash out the visibility of striae.

³ W. Grottrian, *Zeits. f. Physik* **5**, 148 (1921).

⁴ K. T. Compton, L. A. Turner and W. H. McCurdy, *Phys. Rev.* **24**, 597 (1924).

Günther-Schulze⁵ also visualizes the procedure by which the electrons in a discharge tube give up their acquired energy in inelastic impacts within periodic narrow zones in much the same way as that described above, but inasmuch as under some conditions the fall of potential between striae is less than the ionization potential he assumes that the ionization process is not related to stria formation and that ionization arises from a separate set of fast electrons evidence of whose existence has been given from spectroscopic data by Seeliger and Okubo.⁶ Günther-Schulze believes that striae are formed as a result of the inelastic impacts in the narrow zones named of a slower set of electrons which raise the molecules to the lowest excitation level; and seeks support for this view from the fact that under some conditions the energy acquired by electrons between striae in hydrogen has a value nearly equal to this excitation potential. Unfortunately an excitation of molecules to the first levels in hydrogen does not suffice to explain the luminosity of the striae which is observed, as will be shown below.

A comparison of the magnitudes of the energies required for the ionization and for the excitation of hydrogen molecules with the measured potential drops between striae evidently deserves special consideration.

The ionization potential of the hydrogen molecule, which takes place without dissociation, is given⁷ as 16.1 ± 0.2 volts and the energy required to raise a hydrogen molecule to the lowest excited level is given as 11.5 ± 0.4 volts. Above the lowest excitation level there are a large number of other levels extending according to Richardson⁸ to about 15.1 volts.

In the light from striae the visible part of the spectrum must result from transitions between excited states since a transition from any excited state to the $1^1\Sigma$ state would give a line far down in the ultra-violet. To obtain the violet end of the spectrum we must start with an excited state at least 3 volts above the lowest excited level of 11.5 volts, i.e. at 14.5 volts or more.

In some recent measurements⁹ I found the potential drop between striae in hydrogen at pressures below 0.5 mm to be approximately 12 volts and even lower values have been obtained by others. If in this region of pressures the electrons possess only the energy gained directly from the field between adjacent striae, how then is it possible for them to ionize the molecule or to excite it to a sufficiently high level to give rise to the visible spectral lines which are observed? It might be urged that perhaps the ionization in the gas is confined to molecules of traces of impurities having a lower ionization potential than those of hydrogen, but the argument cannot be used to explain directly the production of a hydrogen spectrum. It seems necessary therefore to invoke the aid of some other process. We might postulate, since the electrons are not able to obtain the requisite energy in the potential drop between adjacent striae, that they carry energy from one stria distance into the next,

⁵ A. Günther-Schulze, *Zeits. f. Physik* 31, 1 (1925).

⁶ R. Seeliger and J. Okubo, *Phys. Zeits.* 25, 337 (1924).

⁷ Geiger and Scheel, *Handbuch der Physik*, Vol. 23, p. 749.

⁸ O. W. Richardson, *Proc. Roy. Soc. A*125, 23 (1929).

⁹ J. Zeleny, *Jour. Franklin Inst.*, 209, (1930).

only a part of them losing their energy by inelastic impact in any one stria. It is difficult, however, to imagine how such a process could bring about a periodic appearance of light.

It seems more plausible to assume that the electrons get the energy needed for ionization or excitation, over and above that acquired from the field within a single stria distance, by collisions with molecules of some impurity which are in an excited or metastable state requiring less energy than is requisite to excite a hydrogen molecule. There is good theoretical ground and some direct evidence¹⁰ for the possibility of an electron having its energy increased by this sort of a collision of the second kind. By the presence of traces of impurities of different kinds and in different amounts might be explained the widely different minimum values obtained for the potential drop between striae under different circumstances and by different observers.

In support of the above view it may be mentioned that Pentscheff¹¹ found in very pure hydrogen that, while the potential fall in a stria diminished with reduction of pressure for a constant current, it at no time got below 20 volts, whereas in slightly impure hydrogen it fell to 13 volts under the same circumstances. The pressures used are not stated but if the lowest values of the potential which are given were obtained at pressures below 1 mm, the energy gained between striae by electrons in pure hydrogen were more than sufficient for the ionization of hydrogen molecules, whereas in the impure hydrogen it is necessary to assume that the electrons acquired some energy from secondary processes, such as the one described above, to explain the observations.

Then too, my recent measurements show that when the hydrogen gas was kept stationary and not renewed the energy acquired by electrons in their passage through a stria at any pressure is one to two volts less than when the gas in the discharge tube was being continuously renewed. We should expect a larger amount of impurity to be present in the gas in the first case cited since impurities dislodged from the walls of the tube by the action of the discharge would accumulate in the tube when the gas was not being renewed.

The amount of foreign gas liberated from the walls would naturally depend within some limits on the magnitude and time of action of the discharge current, and according to the view expressed above the potential fall between striae should accordingly diminish as the discharge current is increased. This is actually in accord with my own observations as well as those of Holm, Wehner, and Neubert.¹²

Pentscheff¹¹ also found a decrease in the potential fall between striae with increase of current when impure hydrogen containing mercury vapor and other gases coming from the walls of the tube was used, but when very pure hydrogen was used and great care taken by prolonged treatment to free the

¹⁰ See H. D. Smyth, *Proc. Nat. Acad. Sci.* **11**, 679 (1925).

¹¹ P. B. Pentscheff, *Phys. Zeits.* **7**, 463 (1906).

¹² R. Holm, *Phys. Zeits.* **9**, 558 (1908); F. Wehner, *Ann. d. Physik* **32**, 49 (1910); P. Neubert, *Ann. d. Physik* **42**, 1454 (1913).

metal parts and the walls of the discharge tube of occluded impurities the potential fall between striae rather increased somewhat as the discharge current was increased.

Again, when discharges of the same current density are sent through two tubes of different diameters we might expect the amount of impurity liberated per unit surface of the walls to be approximately the same and inasmuch as the larger of the tubes has a larger ratio of volume to surface the concentration of the impurities liberated from the walls would be greater in the smaller tube. We should then expect the potential fall per stria to be smaller in the smaller tube, and this was found to be the case in my recent measurements.

When the pressure of the gas in a discharge tube is increased a discharge through the tube is less effective in liberating occluded impurities from the walls and such as are liberated form a smaller proportion of the gas than would be the case at a lower pressure. If the amount of these liberated impurities tends to decrease the potential fall between striae then this fall should decrease with decrease of pressure and such was the relation I actually found⁹ both with a stationary gas and with the gas flowing continuously through the discharge tube.

Neubert¹² found that when all spectroscopic traces of mercury disappeared from the discharge through hydrogen the potential fall between striae was 11 volts at the lowest pressure used although previously when this condition was not fulfilled the values obtained were as low as 7.5 volts. Mercury molecules which appear in this instance to lower the potential fall between striae in hydrogen do not possess excitation levels low enough to account for the facts in all cases. However among other likely impurities to be found in discharge tubes there is for example oxygen whose molecules possess metastable states of energy less than 2 volts.

The evidence which has been presented in favor of the view that the liberation of impurities from the walls of the discharge tube by the current is an important factor in determining the variations of the potential fall between striae which have been observed under various conditions, is to be sure for the most part circumstantial evidence.

In connection with the experimental result that the energy acquired by electrons in their motion between two striae increases as the pressure increases, it should be emphasized that there is evidence which indicates that electrons in collisions with molecules may lose more energy than would result from purely elastic collisions and which loss alone I considered in computing the energy acquired by electrons from the observed potential fall between striae. By such greater losses if of the proper magnitude might be explained the increase with pressure in the observed potential drops between striae, but the assumption of these larger losses introduces other difficulties and does not help to explain most of the other observed variations studied.

Another factor that may have some influence on the striated discharge consists of the gas convection currents always present in these discharge

tubes. It is believed however that most of the causes that affect distances and potential drops between striae center about the walls of the tube. These walls, under electronic bombardment during a discharge or with change of pressure or temperature, release occluded molecules of the principal gas and those of foreign substances. They destroy the metastable states of molecules which impinge upon them. They are the seat of the main portion of the recombination of ions and electrons which occurs in the discharge tube, giving rise thereby to electric currents from the axis of the tube towards these walls. Electric charges which collect on the walls influence the electric field in the neighboring gas; and electrons in collision with the walls may lose more or less of their energy depending on the state of the surface of the walls. The differences between the numerical results of different observers on stria distances and the potential fall between striae in discharge tubes can best be accounted for by assuming them due to effects of different conditions at the walls of the tubes. Full equilibrium conditions at the surface of these walls are at best very slow of attainment especially where the gases inside of the body of the glass are concerned. Even if by special treatment such an equilibrium is attained and concordant results obtained in a given case, the nature of the essential elements in equilibrium might still remain unknown.

ON THE DISTRIBUTION IN TIME OF THE SCINTILLATIONS PRODUCED BY THE α -PARTICLES FROM A WEAK SOURCE

BY N. FEATHER*

PHYSICAL LABORATORY, JOHNS HOPKINS UNIVERSITY, BALTIMORE

(Received February 18, 1930)

ABSTRACT

The course of radioactive transformation, which in all known cases takes place in strict conformity with an exponential law of decay, is most satisfactorily explained on the supposition that individual atoms disintegrate in complete independence one of another, so that the disintegrations throughout an extended source constitute a perfectly random series of events. Many observations favor this conclusion, but experiments have recently been described showing that at high concentrations (Kutzner) and also at very low concentrations (preliminary work of Pokrowski) departures may occur. An experiment is here described in which the record of more than 10,000 scintillations produced by the α -particles from a weak source of polonium has been obtained and analysed. A large solid angle was effective, as in Pokrowski's experiments. The various corrections to be applied to the immediate data are discussed: in the present case they were of no importance. There was no evidence to show that the Marsden-Barratt distribution formula was not completely valid under the conditions obtaining.

An investigation was also made of the effect of intense γ radiation on the rate of disintegration in a weak source (Pokrowski), with entirely negative results.

INTRODUCTION

A SERIES of exactly similar point-events separated from one another in time but limited to a prescribed small region of space is defined as a "random" sequence when the probability of occurrence of one such event is the same for equal small intervals of time irrespective of the temporal locations of those intervals. For series comprising point-events separated in space as well as in time, or of line-events having a common focus whilst being separated in time, a further condition must be satisfied if the events are to be considered as taking place "completely at random." In the former case, in any given interval of time, the probability of occurrence of a single event must be the same for equal small elements of volume, irrespective of the spatial locations of such volume elements—and, in the latter, equal probabilities must characterise equal small elements of solid angle about the focus no matter what the directions of the axes of the elementary cones considered.

Radioactive disintegration in an extended source of active material may be regarded as a phenomenon involving line-events originating in foci themselves distributed in space. Now, macroscopically examined, all such cases have been found to exemplify a common transformation law and the customary interpretation of this fact has been based on the assumption that,

* Fellow of Trinity College, Cambridge. Associate in Physics, Johns Hopkins University.

in as far as concerns its time relationships, the ultimate atomic process occurs entirely at random. If this be assumed then the spatial distribution of disintegrating atoms in an extended source must also be a random one—and the observed distribution of directions of particle (or quantum) emission likewise random, for here, whilst preferential directions with respect to natural atomic axes are not excluded, in any practical case the random distribution of atomic axes in space would completely mask such regularities if in fact they were present.

Whilst this is the logical conclusion to be drawn from the usual interpretation of exponential decay, where the analysis is carried down to the behavior of individual atoms, it has been variously maintained that the phenomena observed on the macroscopic scale require no further "explanation" than that the time-distribution of disintegrations in a radioactive source, considered as unit, shall be a random one. From this point of view there remains the possibility that the complete randomness which we have considered may be found lacking under a more penetrating analysis. However unsatisfactory such a contention may appear, from the physical standpoint—and whether or not we hold the view that it is even permissible when the whole range of macroscopic experiments is considered¹—the fact remains that a number of careful experiments has been made and that some of them point to departures from a time-randomness under certain conditions of observation.

For the type of statistical analysis here involved two methods are available, based upon the Bateman² and the Marsden-Barratt³ formulae respectively. In either case a graphical means may be employed in the final comparison of experiment with theory, and, when this is done, conclusions appear more obviously in the latter case, since theoretically a linear function is predicted. But the Bateman type of analysis possesses the compensating advantage that a numerical criterion is afforded of goodness of fit by the dispersion coefficient which may be calculated from the experimental data themselves. Both methods have been used in practice. Kutzner⁴ has made a very thorough analysis of the data afforded by three series of observations automatically recorded under as nearly as possible identical conditions of operation of an electrical point counter. The sole difference between the series (which had reference to 7761, 6907 and 5923 particles, respectively) lay in the surface concentration of polonium in the radioactive source employed. Here there was a factor of 25 times as between conditions in the first and third series, the actual concentrations being roughly 2×10^{-4} , 8×10^{-4} and 5×10^{-3} equivalent milligrams per cm^2 , respectively. With the weakest source no appreciable deviation from perfect time-randomness

¹ In the writer's opinion the only evidence which the macroscopic experiments fail to supply is evidence for the random distribution in space of the disintegrating atoms in a given source. The exponential law of decay may be deduced alike from measurements made on the radiation emitted within a small or a large solid angle about such a source.

² Bateman, *Phil. Mag.* **20**, 704 (1910).

³ Marsden and Barratt, *Proc. Phys. Soc. Lond.* **23**, 367 (1911).

⁴ Kutzner, *Zeits. f. Physik* **44**, 655 (1927).

was found, but, with the other two, deviations quite outside the limits of probable error were set in evidence. In each case dispersion was subnormal (Bateman analysis), there being a marked lack of the longer time intervals between observed disintegrations (Marsden-Barratt analysis). The extent of the discrepancy increased with the surface concentration in the source. Whilst leaving the full interpretation until fresh data had been obtained using large solid angles (only about 1/400 of the total emission was originally employed), Kutzner concluded that his results were in agreement with those of Curie,⁵ who found complete accord between experiment and theory with polonium sources of (apparently) very small concentration. The experimental material in this latter case consisted of 9974 measured time intervals belonging to four distinct series of measurements.

Recently Pokrowski⁶ has published an account of preliminary observations with very weak sources and large solid angles. The concentration employed was about 10^{-7} equivalent milligrams per cm^2 . It is not stated what material was used. Data having reference to 1633 time intervals, analysed by the method of Marsden and Barratt, showed an excess both of the very short and the very long intervals and no real agreement with theory over any appreciable range. In the discussion it was pointed out that new phenomena at small concentrations might be expected if at the higher concentrations mutual action between neighboring nuclei was possible. On account of the fundamental nature of such a suggestion, and because a suitable source of polonium of small concentration was readily available, it was thought worthwhile to make a series of observations parallel to those of Pokrowski, using the scintillation method of registration as he had done. Moreover, the writer did not feel compelled to make the present investigation exhaustive—covering a wide range of surface concentrations—most especially because it is explicitly stated by Pokrowski that his report is merely preliminary in scope. Rather is it intended to put forward this restricted series of results, only, as independent evidence, for what it is worth.

EXPERIMENTAL METHOD AND RESULTS

As a source of α -particles for scintillation experiments polonium is in many respects most suitable: it is not accompanied by appreciable β or γ radiation, and its period is sufficiently long for the decay generally to be negligible. However, when experiments extending over a number of weeks are in question, the latter condition no longer holds⁷ and the desired constancy can be retained only by employing sources of radium *D*, *E* and *F* in equilibrium. Now the writer possessed some pieces of gold leaf exposed to radon in May 1929.⁸ In January 1930 calculation showed that their α -

⁵ Curie, *J. Physique* 1, 12 (1920).

⁶ Pokrowski, *Zeits. f. Physik* 58, 706 (1929).

⁷ The type of "uncorrected" distribution of time intervals which would be obtained in the Marsden-Barratt analysis of data referring to a source of varying activity is one in which very short and very long intervals are each in excess of the number calculated theoretically for a constant source of the same average activity.

⁸ See Feather, *Proc. Camb. Phil. Soc.* 25, 522 (1929).

particle activity was still increasing—but sufficiently slowly for this material to be considered a constant source of α -particles for the present type of experiment over a period of two or three weeks.⁹ It was decided, therefore, to employ it in the work to be described. By placing the gold leaf directly in contact with the zinc sulphide screen a solid angle of approximately 2π radians could simply be attained. Preliminary tests showed, however, that the activity of the source was 5 or 10 times too great for convenient counting. A reduction was made as follows: one surface of a flat piece of glass was very lightly ground with fine emery. A small piece of the activated gold leaf was placed upon the ground surface and, by means of the smooth rounded end of a glass rod, used as a small pestle, was gradually ground to an extremely fine deposit of gold dust which adhered to the roughened surface. The zinc sulphide screen, supported on a microscope cover glass, was then fastened in position in contact with the ground surface. On the free upper surface of the cover glass was fastened a piece of thin aluminum foil, pierced with a hole of approximately 1 mm^2 area, which served to limit the portion of screen under observation. The microscope used was built up of a Watson's Holoscopic objective, of numerical aperture 0.45 and focal length 16 mm, and a low-power eyepiece, giving a field of view of about 8 mm^2 area. The source system was supported so that the hole in the aluminum foil was central in the field of view and, during periods of observation, a dim red light produced a faint illumination of the foil, leaving the central portion of the field relatively dark.¹⁰ The mean interval between scintillations was somewhat greater than 3 sec.¹¹

The record itself was made with the aid of a drum chronograph with magnetically controlled pen, the drum being driven at a uniform rate by the combination of falling weight and centrifugal governor. The uniformity of rate was tested from time to time and found altogether satisfactory. Throughout the presentation of the results, for sake of simplicity, time intervals have been replaced by linear intervals; the conversion factor from the one to the other is 0.921 cm/sec.

Observations were spread over thirteen consecutive days; on each day two or three "sessions"—30 "sessions" in all. During each session "periods of observation" alternated with periods of rest, each, on the average, about a minute and a half in length: in all, 334 "periods of observation." During each period about 30 scintillations were recorded; altogether 10134 "intervals" between scintillations were measured. In the treatment of the records periods were measured to the nearest millimeter and the number of intervals in each period was counted. From this material the mean interval, ω , was determined. Intervals were measured in millimeters and entered in a statistic according to their length. In the first analysis grouping was in millimeter ranges, the elementary group containing those intervals of which

⁹ A more complete statement on this question is reserved for the discussion.

¹⁰ Cf. Chariton and Lea, *Proc. Roy. Soc.* 122A, 304 (1929).

¹¹ From the figures given by Pokrowski it would appear that his field of view had an area of about 70 mm^2 and that the mean interval in his experiments was roughly 0.8 sec.

the length lay between x and $x+1$ mm. Later these groups were combined in sets of three and values of n_x obtained, where n_x now represents the number of intervals of length between $x-1.5$ and $x+1.5$ mm. Values of N_ξ followed immediately from this series of numbers; here N_ξ is the number of intervals of length greater than ξ mm. Now the formula of Marsden and Barratt may be written

$$N_\xi = N_0 e^{-\xi/\omega} \quad (1)$$

or

$$\log_{10} N_\xi = \log_{10} N_0 - (0.4343/\omega)\xi. \quad (2)$$

In our case $N_0 = 10134$ and $\omega = 31.28$ mm. Thus the theoretical distribution leads to the straight line

$$\log_{10} N_\xi = 4.0058 - 0.01388\xi. \quad (3)$$

This line is plotted together with the experimental points in Fig. 1. In Fig. 2 values of $\log_{10} n_x$ are plotted (A).

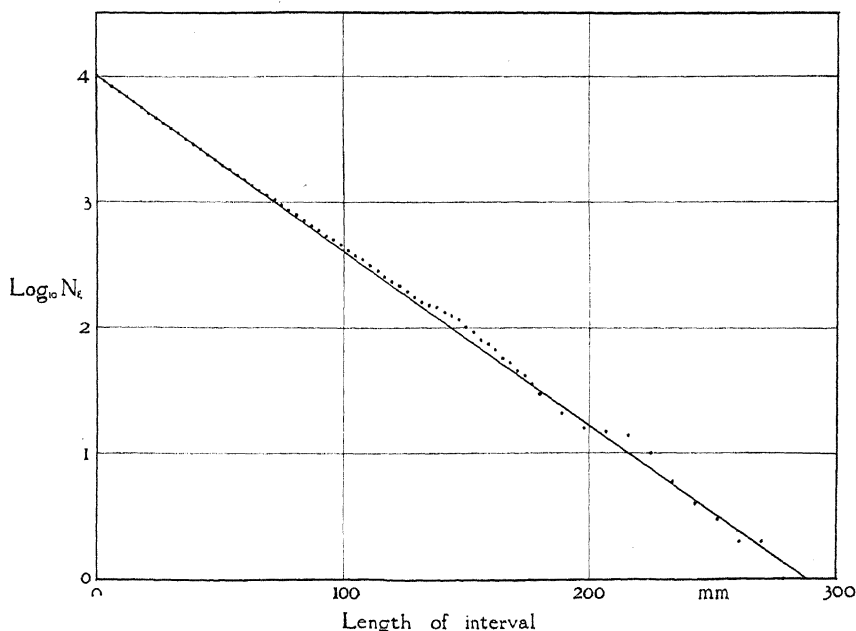


Fig. 1.

To a first approximation

$$n_x = -3(dN_\xi/d\xi)_x. \quad (4)$$

If this relation were strictly correct it is obvious from (1) that the graph of $\log_{10} n_x$ would be a straight line of the same slope as (3). A simple calculation shows that in fact a small correcting term ϵ is involved, depending on the ratio of the "plotting interval" (in this case 3 mm) to the mean length ω (here 31.28 mm), in such a way that

$$n_x = -3(1+\epsilon)(dN_\xi/d\xi)_x. \quad (5)$$

The condition of parallelism therefore remains, but the line as a whole is shifted slightly. Introducing numerical values we have

$$\log_{10} n_x = 2.9875 - 0.01388x. \quad (6)$$

This line is included in Fig. 2 for comparison with the experimental results. The straight line *B*, Fig. 2, corresponds to a plotting interval of 30 mm. Its equation, deduced in like manner to the above, is

$$\log_{10} \nu_x = 4.0039 - 0.01388x. \quad (7)$$

The corresponding points have been obtained by grouping the values of n_x in sets of ten—and the results are presented in this form, also, chiefly in order that they may be more nearly comparable with those of Kutzner, already referred to.

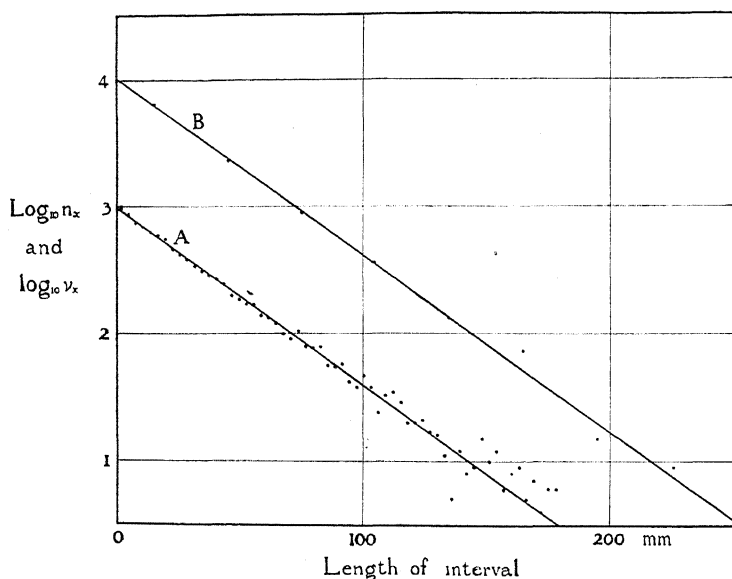


Fig. 2.

DISCUSSION

Any consideration of the results here set forth must be twofold in character: there is the comparison of experiment with theory and, in addition, that of the present experimental results with those of previous investigators. But, before either comparison is made, it is necessary to consider what corrections, if any, should be applied to the crude observational material which the experiment provides—for the points plotted in Figs. 1 and 2 have been deduced without any corrections at all from the measurements of length on the chronograph record. First there is the varying activity of the source, which is entirely apart from any question of imperfection in the methods of registration. Depending upon the extent of this variation the theoretical logarithmic plot will depart more or less from the ideal straight line. At the time of the observations the strength of the source was in-

creasing daily by about 0.205 percent. Columns 1 and 2 of the accompanying table show how observations were spread over the thirty sessions on the thirteen days during which the experiment was in progress. They indicate that the mean interval ω , deduced from the full material, corresponds most probably to the true mean interval on the eighth day. Column 4 gives the true mean interval corresponding to each successive day calculated on this basis and column 3 the observed mean values obtained from the daily observations. Column 5 will be referred to at a later stage in the discussion. With the material which the table provides we may proceed to calculate the theoretical form of $\log_{10} N_t$ in the present experiments, which in the ideal case of the constant source was represented by Eq. (3). For each day's results the theoretical distribution is calculated from Eq. (1) using the

TABLE I.

1	2	3	4	5	1	2	3	4	5
Day	Number of intervals	Mean interval mm	True mean interval mm	Probable error mm	Day	Number of intervals	Mean interval mm	True mean interval mm	Probable error mm
1	381	31.7	31.73	1.6	8	373 268 410	30.2 31.9 28.8	31.28	1.6 1.9 1.4*
2	274 298	33.1 30.1	31.66	2.0 1.7	9	389 392 428	31.7 31.5 29.4	31.22	1.6 1.6 1.4*
3	332 191 261	30.8 32.5 32.6	31.60	1.7 2.4 2.0	10	452 438 407	27.5 30.9 31.1	31.15	1.3* 1.5 1.5
4	282 212	33.2 31.2	31.54	2.0 2.1	11	431 405 421	32.4 33.0 31.1	31.09	1.6 1.6* 1.5
5	104 137 159	27.9 39.5 36.6	31.47	2.7* 3.4* 2.9*	12	469 439	29.2 29.7	31.02	1.3* 1.4
6	352	30.4	31.41	1.6	13	431	30.4	30.96	1.5
7	347 309 342	33.8 35.1 31.6	31.34	1.8* 2.0* 1.7					

appropriate value of ω . The individual distributions are then combined. When this somewhat laborious procedure was carried through it became evident that the greatest departure from the straight line of Eq. (3) was so slight as not to be appreciable on a diagram drawn to the scale of Fig. 1.

The second correction concerns the failure of the method of registration when scintillations succeed one another in rapid succession. It is not that scintillations are missed, but the actual time intervals are distorted on the record obtained. The first point in Fig. 2 (A) has reference to intervals of apparent length less than 3 mm (i.e. intervals shorter than 0.32 sec.): 988 measured intervals were distributed as follows; 0-1 mm, 0; 1-2 mm, 404; 2-3 mm, 584. Assuming, to a first approximation, that the number 988 is the true number of intervals in the three sub-groups in question we should expect a distribution giving 0-1 mm, 340; 1-2 mm, 329; 2-3 mm, 319 inter-

vals, respectively. Thus errors of registration have resulted in an apparent increase of length in the shortest intervals, and this must necessarily have been counterbalanced by an apparent decrease amongst the remainder. The figures quoted do not allow us to make any definite statement about the errors actually committed. At the one extreme is the supposition that in no case has the error been greater than 1 mm. On this basis we should assume that 340 intervals actually between 0 and 1 mm were recorded as between 1 and 2 mm in length, whilst 265 actually between 1 and 2 mm were recorded as between 2 and 3 mm long. At the other extreme is the supposition that all the intervals in the second and third groups in reality were correctly registered, the error lying entirely with the intervals of the first group. Then 75 members of that group could have been wrongly assigned to the second group and the remaining 265 members to the third. From the first point of view, amongst the total number of 10134 measured intervals (including the 988 shortest intervals with their newly assigned lengths) the correction of 605 1 mm errors of underestimation is necessary to rectify the crude distribution: from the second point of view the correction of 75 1 mm and 265 2 mm errors of underestimation is required. On account of the small fractions of the total which these numbers represent the two methods of correction lead to almost identical results. The former transfers 18.9 intervals from $n_{1.5}$ (originally 988), the second 19.4 intervals; these are effectively distributed amongst the various values n_x in gradually decreasing shares as x increases; thus $n_{4.5}$ is increased by 2.9, $n_{7.5}$ by 2.3 intervals, and so on. In Fig. 2(A) the change in position of the first point only is appreciable, as the figure indicates—and obviously to carry this correction to a further approximation is unnecessary.

From the above considerations, therefore, we may conclude that the experimental points of Figs. 1 and 2 and the straight lines accompanying them are entirely comparable: agreement between experiment and theory is to be measured by the closeness of fit of the points and the corresponding straight lines.

It must be admitted at the outset that the fit is good, though hardly as good as in the experiments of Curie.⁵ On the other hand, by comparison with the results of Kutzner,⁴ it will be seen that no such systematic deviations as he observed are in evidence here. It was not to be expected that they should be, since the concentration of active material in the source was smaller than the least concentration which Kutzner employed. Fig. 2 (B)—closely comparable with Figs. 2 (b), 3 (b) and 4 (b) in his paper—shows excellent agreement for the first five points and a non-systematic deviation later. Kutzner's figures likewise have five points closely on the theoretical straight line but, for his two stronger sources at least, the sixth and seventh points lie progressively below the line. Finally, making comparison with Pokrowski's results,⁶ it is evident that no deviation of the order of magnitude of that reported by him is here present, though such deviation as there is in the earlier portion of Fig. 1 is certainly in the same sense as that which he observed. But the order of magnitude is entirely different. It is true that

in the present experiments the surface activity of the source was roughly twenty times as great as in the experiments of Pokrowski, but it must be emphasised that this is a macroscopic comparison. When the phenomenon of aggregation is taken into account it is obvious, for instance, that the size of the mean aggregate does not increase as rapidly as does the mean surface density of deposit during a single activation process, since new centers of aggregation presumably appear continuously throughout the process. Now it is unquestionably the size of the aggregates which is of importance for theories of the mutual action of neighboring atoms. Moreover it is almost impossible to make any *a priori* statement concerning aggregation when the mode of activation is different in the two cases to be compared.

It was pointed out earlier in the discussion that variations in the activity of the source, if sufficiently great, would lead to deviations from the theoretical distribution of the type of which Fig. 1 offers very slight indication and Pokrowski's results very marked evidence indeed. It has already been demonstrated that such changes cannot account for a non-linear relation in the present experiments, but it must be borne in mind that the same effect would be shown with a constant source and a varying efficiency of registration. It is very probable that this explanation is likewise inadequate. Column 5 of Table I gives the probable error in the thirty observed values of the mean interval and asterisks mark those cases in which the latter value differs from the true value (column 4) by more than the probable error. It will be seen that there are ten such cases as against twenty cases of closer agreement than that which the limits of probable error represent. Thus we are dealing with a set of observations more than normally uniform, and it is therefore unlikely that variations in registration efficiency are here in point.

Finally, in order to make sure that simple errors in length measurement were not vitiating the results, the total period of observation was deduced in two ways; first by adding together the measured lengths of the 334 periods, secondly by adding together the measured lengths of the 10134 intervals. In the latter addition the supposition was made that each interval classed as between x and $x+1$ mm in length was actually $x+0.5$ mm long. The first addition led to the value 316988 mm, the second to 317032 mm—a difference of one part in 7200. Moreover, the second sum would be expected to be slightly the larger of the two on account of the simplifying assumption introduced.

A FURTHER EXPERIMENT—THE EFFECT OF INTENSE γ RADIATION

In the account already referred to Pokrowski⁶ has described a very remarkable experiment in which the irradiation of a weak source of radioactive material with γ -rays was found to produce an increase of 45 percent in the frequency of the scintillations observed. X-ray irradiation was reported to produce a similar effect. It was suggested that the possibility of such an effect was intimately connected with the use of a very weak source, in which the hypothetical mutual action of neighboring atoms was too small to be

effective. From this point of view the null result of earlier experiments with stronger sources was obviously explicable.¹²

There should, of course, be an intermediate case with sources a little stronger than Pokrowski's. The writer has carried out the analogous experiment employing a somewhat more concentrated source. To this end the arrangement of the previous investigation was modified in certain particulars; for instance it was no longer thought necessary to employ the maximum possible solid angle and it was recognised that it would be a great convenience to be able to remove the source from time to time. The latter was therefore carried on a rectangular glass plate (a fragment of the original gold leaf was attached to the smooth surface by means of a very thin film of castor oil) which when placed in its holder was maintained in a perfectly definite position, about 1.5 mm distant from the zinc sulphide screen. An area of about 2 mm² of screen was under observation. In the new arrangement the field illumination resulted in the screen being dimly lighted and the rest of the field relatively dark. This is an advantage, for, under sufficiently intense γ -ray irradiation, the screen becomes self-luminous and it is advisable to make conditions in the control experiment as nearly equivalent as possible.

The first comparison was made with a radon tube containing about 25 equivalent milligrams of emanation¹³ placed on the axis of the system about

TABLE II.

1 mg	2	3 mm	4 mm	5
22.2	677	9.05	10.30	565
18.6	667	9.07	10.00	585
16.4	758	8.75	10.79	551
13.5	774	8.31	9.82	654
11.3	742	8.98	9.60	679
9.5	750	8.56	8.97	679
7.9	745	8.76	9.55	698
5.5	766	8.65	9.75	672
4.6	830	8.06	8.91	790
3.8	780	9.13	8.62	720
3.2	783	8.37	9.37	728
2.7	811	8.53	8.57	802
2.3	849	8.16	8.27	898
1.9	816	8.93	8.64	784
Totals	10748			9805

¹² When the present account was in the final stages of preparation Pokrowski's second paper (*Zeits. f. Physik* 59, 427 (1930)) appeared in this country. In it a more detailed point of view is adopted and experimental data, obtained with a source of radium together with its subsequent products, put forward in its support. However, the experiments newly described differ in essential particulars from those of the writer, so that there is at present no basis of comparison. Nevertheless it may be remarked that if, as Pokrowski assumes, this process of induction is "saturated" in the ordinary case of a concentrated source, and if the mechanism is similar to that which he suggests, then the α -particles from such a source would not be homogeneous in velocity, but a distribution of velocities greater than the normal would also be present.

¹³ The writer desires to thank Dr. C. F. Burnam of the Kelly Hospital, Baltimore, for providing him with this material.

3.7 cm distant from the source. The mean length of 1240 intervals recorded with the tube in position was 9.18 mm, 1181 intervals recorded when the tube was removed gave 9.33 mm. Within the probable error of the measurements, therefore, no difference was found. With this arrangement, however, the β and γ -ray luminosity of the screen was almost inappreciable and a further comparison was determined upon with more intense irradiation. The γ -ray tube was moved up in contact with the glass plate supporting the source.¹⁴ Under these conditions the zinc sulphide screen fluoresced brightly and observations with the γ -ray tube in position¹⁵ invariably led to greater values of the mean interval than those carried out when the tube had been removed. It was obvious that scintillations were being missed under the former conditions of observation. Table III summarises the comparisons made on successive days as the activity of the γ -ray tube decayed. A constant geometrical arrangement was used throughout. The strength of the γ -ray source is given in column 1. Columns 2 and 5 show the numbers of intervals

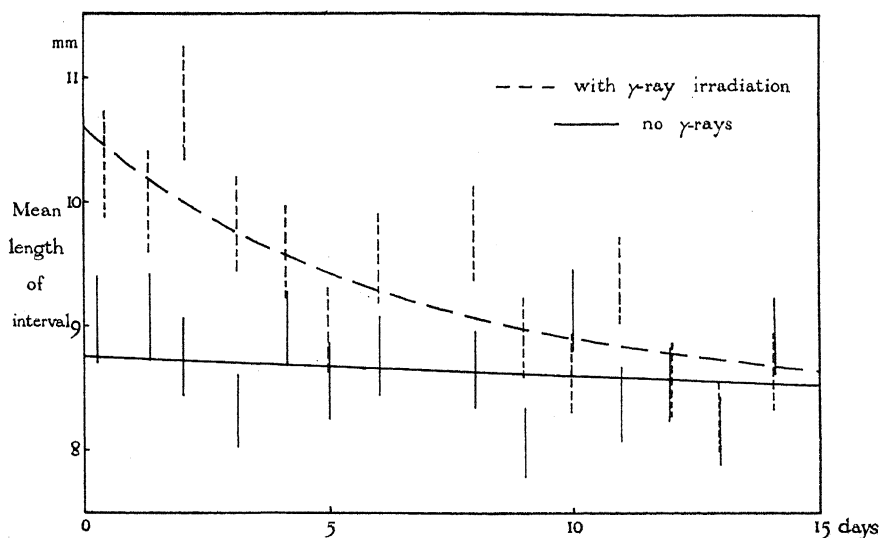


Fig. 3.

measured, in the first case with the γ -ray tube removed, in the second case with the tube in position. Columns 3 and 4 give the values of the mean interval deduced from these measurements. When the γ -ray activity had fallen to 4.6 equivalent milligrams the brightness of fluorescence which it caused was roughly the same¹⁶ as the brightness of artificial illumination employed when the tube was absent; thereafter the very weak fluorescence with the tube in position was supplemented by a certain amount of artificial illumina-

¹⁴ The thickness of the plate was 1.8 mm. The radon tube was contained in a brass case about 0.7 mm thick.

¹⁵ The polonium source was exposed to the γ -rays only during the periods of observation, amounting to about half an hour daily.

¹⁶ This comparison is necessarily inaccurate on account of the difference in quality of the light in the two cases.

tion also. In Fig. 3 the results are shown graphically. The lengths of the vertical lines indicate the magnitude of the probable error in each case. The gradual increase in the α -particle activity of the source during the period of the observations is clearly evident from the decrease in the mean interval determined with the source alone.¹⁷ The broken line, which represents sufficiently well the trend of the apparent activity of the source under γ -ray irradiation, has been drawn in such a way that the difference between corresponding ordinates on this and on the full line, respectively, decreases according to the same law as the activity of the radon tube employed as the source of γ -rays. Whilst no great emphasis is laid on this way of exhibiting the results,¹⁸ it does show at least that, as long as the effect is relatively slight the percentage of scintillations missed when observations are carried out in the presence of intense γ radiation is roughly proportional to the strength of that radiation.

Throughout the present experiments the observed effect of the irradiation of the source has been an apparent decrease in its α -particle activity. It was thought possible, however, that over a short period, during the decay of the γ -ray source employed, an apparent increase would be found. This might have been expected when the intensity of the residual primary β -particles and the secondary electrons produced by the γ -rays was just of the right order of magnitude to give rise to the type of multiple- β -particle scintillations described by Chariton and Lea.¹⁹ Probably the requisite β -particle intensity was reached sometime between the tenth and the fifteenth day, but it is very doubtful indeed whether any trace of this phenomenon has been observed in the present case. Chariton and Lea, observing with a microscope of numerical aperture 0.65, classify this type of scintillation as very faint: it seems likely therefore that, observed with a less powerful microscope, they would only be recorded occasionally when α -particle scintillations were present as well.

In conclusion, therefore, it may be said that no effect has been observed which can in any way be attributed to the induction of disintegration in the polonium nucleus by any of the γ -rays of radium B+C. Very obviously this statement refers only to the concentration of source here employed, but it is interesting to remark that supposing a 10 percent effect had been observed at the beginning of the experiment, when the γ -ray source was most intense, then that would have corresponded to a reaction with the nucleus more than a million times more probable than the recognised types of reaction with the extra-nuclear electrons—and, moreover, this calculation is based on the supposition that γ -rays of all wave-lengths are capable of producing the nuclear change. The factor would be even greater if a selective effect were involved.

¹⁷ In most cases observations with the source alone were carried out immediately after those under conditions of γ -ray irradiation. Occasionally this order was reversed, as may be seen from the figure, but without any systematic difference appearing.

¹⁸ It may be remarked, for comparison with the earlier discussion, that of the 14 points belonging to each curve in Fig. 3, in each case 9 fall within the limits of probable error and 5 fall outside those limits.

¹⁹ Chariton and Lea, *Proc. Roy. Soc.* **122A**, 335 (1929).

THE L SERIES SPECTRA OF THE ELEMENTS FROM CALCIUM TO ZINC

BY C. E. HOWE

DEPARTMENT OF PHYSICS, OBERLIN COLLEGE

(Received February 4, 1930)

ABSTRACT

Using the first inside order of a plane grating (600 lines per millimeter) L lines of the elements Zn, Cu, Ni, Co, Fe, Mn, Cr, V, Ti and Ca have been measured. Separation of the L_α and L_β lines as well as the L_i and L_η is attained by adjusting the grating so that the angle between the inside order and the plane of the grating is small. Under this condition the angular dispersion is given by $(d\alpha/d\lambda) = (1/D\beta)$, where D is the grating space and β the small angle between the plane of the grating and the first inside order. The results obtained are somewhat higher than those obtained by crystal measurements but are entirely consistent with the work of other experimenters. The failure of the L_α and the L_β lines to appear in the case of calcium is in accord with Foote's extension of Stoner's arrangement of the electrons. All measurements are absolute.

THE study and measurement of x-rays of long wave-length have been handicapped by the extensive absorption in air of the rays and by the lack of satisfactory gratings, the grating spaces of ordinary crystals being much too small. The former difficulty has been overcome by the use of vacuum spectrographs; the latter to a certain extent by the use of organic crystals of large grating space. Extensive measurements of L lines in this region have been made by Thoraeus.¹ His work was done with a vacuum spectrograph using crystals of lauric acid ($2d = 54.536\text{\AA}$) and palmitic acid ($2d = 70.98\text{\AA}$). The wave-lengths given in his report are based on the sodium K_α line (11.884\AA). Shearer² has measured the nickel L_α line using the 100 face of a crystal of cane sugar ($2d = 21.1519\text{\AA}$). Unfortunately, however, absorption in the crystal causes a considerable broadening of the spectral lines. It is also quite conceivable that the index of refraction might take on anomalous values due to a resonance frequency of the electrons in the crystal being near the frequency of the x-rays. Under these conditions the application of Bragg's law becomes uncertain even in its corrected form. For these reasons it seems advisable to apply the recently developed method of measuring x-ray wave-lengths from spectra obtained by reflection from a ruled grating to the study of the L lines under discussion.

When Professor A. H. Compton³ showed in 1923 that x-rays could be reflected from plane surfaces at grazing angles smaller than a certain critical angle determined by the index of refraction of the x-rays reflected, he opened

¹ R. Thoraeus, *Phil. Mag.* **1**, 312 (1926); *Phil. Mag.* **2**, 1007 (1926).

² J. Shearer, *Phil. Mag.* **4**, 745 (1927).

³ A. H. Compton, *Phil. Mag.* **45**, 1121 (1923).

up the possibility of using a ruled surface as a grating. Two years later Compton and Doan⁴ obtained x-ray spectra from a ruled reflection grating. In 1926 and 1927 Thibaud,⁵ Osgood,⁶ and Hunt⁷ applied the ruled grating to the study of the spectral region between x-rays and the ultra-violet, Osgood using a concave grating with a Rowland mounting. Since then the grating has been used by a number of investigators⁸ in this field, some making the wave-length determinations from the constants of the apparatus, others by comparison with lines of known wave-length. This method has been used⁹ to compare wave-lengths as measured by crystals with those measured by gratings. The measurements from gratings, using the constants of the apparatus, have been found slightly greater than the crystal measurements.

The general method used in the spectroscopy of soft x-rays has been reviewed by Osgood.¹⁰ The general methods and results of this experiment were briefly presented by the author¹¹ to the American Physical Society. Kellström¹² has reported on measurements of the lines in this same region using outside orders of the spectral lines, comparing them with the K_{α} line of aluminum.

THEORY OF THE EXPERIMENT

In making wave-length measurements in the optical region using a plane reflection grating the formula $n\lambda = D(\sin \phi - \sin \phi')$ is used, n being the order observed, λ the wave-length in centimeters, D the grating space in centimeters, ϕ the angle of incidence and ϕ' the angle of diffraction. In using the plane grating for measurements in the x-ray region it is more convenient to express the wave-length in terms of the grazing angle of incidence θ and the grazing angle of diffraction $\theta \pm \alpha$, the negative sign referring to inside orders, in which case,

$$n\lambda = D[\cos \theta - \cos (\theta \pm \alpha)]. \quad (1)$$

By a simple trigonometric transformation this becomes

$$n\lambda = 2D \sin \frac{2\theta \pm \alpha}{2} \sin \frac{\alpha}{2}. \quad (2)$$

⁴ A. H. Compton and R. L. Doan, Proc. Nat. Acad. Sci. **11**, 598 (1925).

⁵ J. Thibaud, Comptes Rendus **182**, 55 (1926); Comptes Rendus **185**, 62 (1927); Journ. Op. Soc. **17**, 145 (1928).

⁶ T. H. Osgood, Phys. Rev. **30**, 567 (1927); Dissertation, Chicago (1927).

⁷ F. L. Hunt, Phys. Rev. **30**, 227 (1927).

⁸ B. B. Weatherby, Phys. Rev. **32**, 707 (1928). E. Bäcklin, Inaugurald Dissertation, Uppsala Universitets Arsskrift (1928). M. Söderman, Zeits. f. Physik **52**, 795 (1929). C. E. Howe, Proc. Nat. Acad. Sci. **15**, 251 (1929).

⁹ C. P. R. Wadlund, Phys. Rev. **32**, 841 (1928); J. A. Bearden, Proc. Nat. Acad. Sci. **15**, 528 (1929).

¹⁰ T. H. Osgood, Phys. Rev. Supp. **1**, 228 (1929).

¹¹ C. E. Howe, Phys. Rev. **33**, 1088 (1929).

¹² G. Kellström, Zeits. f. Physik **58**, 511 (1929).

Reference to Fig. 1 will help to visualize these angles. The beam of x-rays collimated by the slits, falls on the grating. The zero order is reflected to the point *R*, the first outside order to the point *O* and the first inside order to the point *I*. *P* is in the extended plane of the grating, while *D* is the position of the direct beam when the grating is removed.

It should be noted that the position of the inside order is farther removed from the zero order than is that of the first outside order, indicating greater angular dispersion for the inside order. Differentiating Eq. (1) with respect

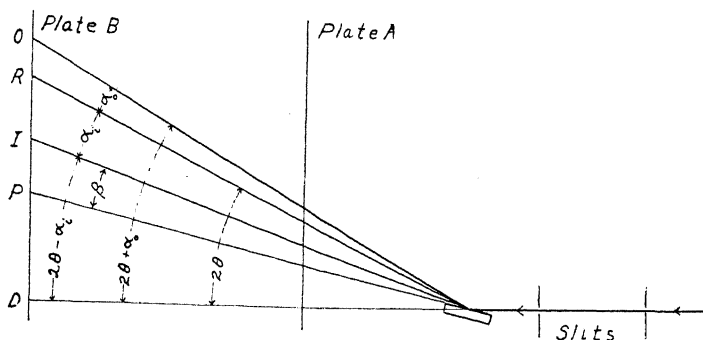


Fig. 1.

to α there is obtained the expression $n(d\lambda/d\alpha) = D \sin(\theta \pm \alpha)$ where, as before, the plus sign refers to outside orders and the minus sign to inside orders. The angular dispersion may be written as

$$\frac{d\alpha}{d\lambda} = \frac{n}{D} \frac{1}{\sin(\theta \pm \alpha)}.$$

It is thus seen that the dispersion is greater for inside orders than for outside orders. By varying θ the position *I* of the inside order may be made as close as desired to the extended plane of the grating. In this way the angle $\theta - \alpha$, which we shall call β , can be made very small, resulting in a large dispersion. For the first inside order

$$\frac{d\alpha}{d\lambda} = \frac{1}{D\beta}. \quad (3)$$

Experimentally it has been found that there is a practical lower limit to the value of β ; otherwise the dispersion could be made greater without limit as the angle β decreases. It is of interest to note that the dispersion is independent of both λ and θ .

For outside orders the theoretical maximum dispersion is obtained when $\sin(\theta + \alpha)$ is a minimum. This is the case when $\theta = 0$. The dispersion for outside orders then becomes (neglecting higher powers of $n\lambda/D$)

$$\frac{d\alpha}{d\lambda} = \frac{1}{D} \left(\frac{D}{2\lambda} \right)^{1/2} n^{1/2}.$$

If r represents the ratio between the dispersion of the first inside order and that of the maximum theoretical value of the n th outside order, then

$$r = \frac{1}{\beta} \left(\frac{2\lambda}{D} \right)^{1/2} \frac{1}{n^{1/2}}.$$

Actually the ratio will be larger than this since it is not possible to make $\theta=0$. In some cases in this experiment the dispersion obtained with the first inside order was equal to twelve times the theoretical maximum for the first outside order. To obtain the same dispersion in an outside order would require going to the 150th order.

THE X-RAY SPECTROGRAPH

Fig. 2 shows a horizontal cross section of the spectrograph and x-ray tube. The body of the spectrograph consisted of a brass tube 8 inches in diameter and 40 inches long. To one end-plate was attached the water-

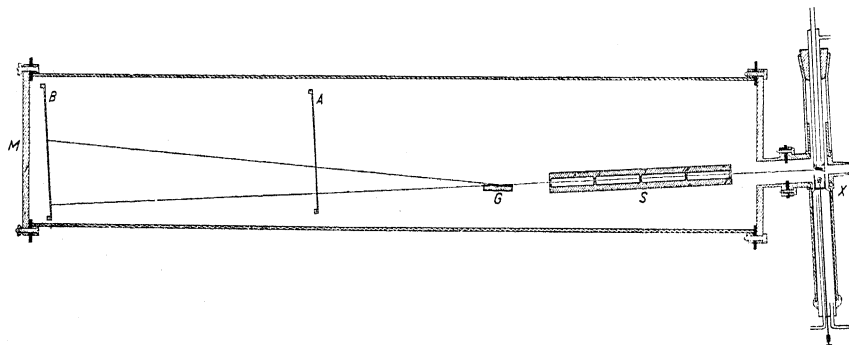


Fig. 2. Horizontal cross-section of the spectrograph and x-ray tube.

cooled metal x-ray tube X . The targets used consisted of small slabs of metal dove-tailed into the face of a water-cooled copper support. The tungsten filament was supported in the center of a water-cooled iron focusing cup.

To the same end-plate was attached a bed-plate on which the slit system, grating support, plate holders etc. were fastened. In order to collimate the rays and to exclude as much of the light from the incandescent tungsten filament as possible, the slit system S consisted of five slits. The two end slits, separated by a distance of 18 centimeters, were 0.05 mm wide; the three intermediate ones, 0.10 mm. By the passage through these slits the intensity of the light was so greatly diminished that it gave little difficulty. No trouble was experienced in the alignment of the slits in as much as the system consisted of two halves, half of each of the several slits being care-

fully machined into each metal piece, the two separate pieces then being clamped together.

The glass grating *G*, ruled 600 lines per millimeter, was mounted on a table which could be turned through any desired angle by means of a train of gears controlled from the rear end of the spectrograph near the end-plate *M*. This table, in turn, was mounted on a slide so that the grating could be removed from the path of the x-rays, this movement also being controlled from the rear end. The mechanism was so constructed that either operation could be performed without disturbing the setting of the other, and also so that definite settings could be reestablished with sufficient accuracy.

The plate holder *A* served to hold a plate which intercepted the lower half of the radiation coming from the grating. The upper half was recorded on a plate placed in the holder *B*. Plate *A* was made perpendicular to the direct beam as follows. One side of the slit system was removed, and a straight iron bar carefully clamped to the other half. With a precision square, *A* was made perpendicular to the bar within a few minutes of arc. *B* was then made parallel to *A* by means of an inside micrometer, this operation serving also to obtain the distance between the two plate holders. This distance was 37.982 cm.

All of the apparatus described thus far was mounted as one unit. It could be removed from the main body of the spectrograph at any time for purposes of adjustment.

After adjustment this unit was placed in the spectrograph, a sulphur-free rubber gasket being placed between the end-plate and the body. Plates (Eastman process) were put in holders *A* and *B*, and the spectrograph evacuated to a pressure of about 2×10^{-4} mm. A pressure considerably lower than this was maintained in the x-ray tube by means of a separate set of mercury vapor pumps. An exposure of from one to twelve hours was made, depending on the intensity of the radiation. After about twenty minutes exposure the reflected beam was covered with a small screen (operated by an electromagnet) to prevent over exposure and fogging. The exposure being completed, air was admitted, the end-plate *M* taken off and the grating removed from the path of the beam. After reevacuation the direct beam was exposed for a minute or two.

A small vessel containing phosphorus pentoxide was kept inside the spectrograph to absorb water vapor. The life of the tungsten filament was increased greatly by having a liquid air trap close to the x-ray tube to take up moisture.

The current through the x-ray tube varied from 15 to 40 milliamperes. Because a transformer having rather high secondary resistance was used it was not practicable to attempt to measure the effective voltage on the target, which was much lower than the inverse voltage across the self rectifying tube. It may be estimated that the effective voltage varied from 4000 to 12000 volts.

THE SPECTRA

Fig. 3 shows typical spectra obtained. These particular spectrograms, having nearly equal values of θ , were selected to show the relative displacement of corresponding lines and the increased dispersion with smaller values of β . The L_α and L_β lines of zinc are not resolved. The corresponding lines

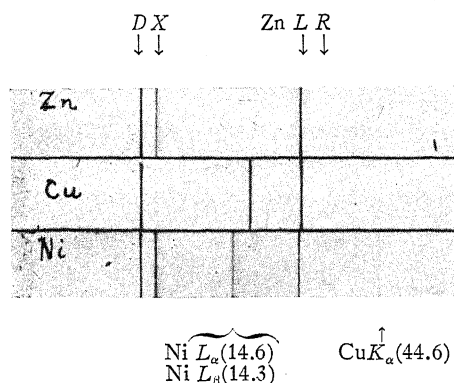


Fig. 3. Typical L series spectra of Zn, Cu and Ni. D is the direct beam, R the reflected beam and X is light diffracted past edge of grating.

of copper overlap, the more intense L_α line being to the left. The lines of nickel are resolved. Since about the same wave-length difference exists between these lines, the spectra show the increase in dispersion as the inside order approaches the plane of the grating. Of the three spectrograms shown only that of nickel is useful in making measurements on the L_β line.

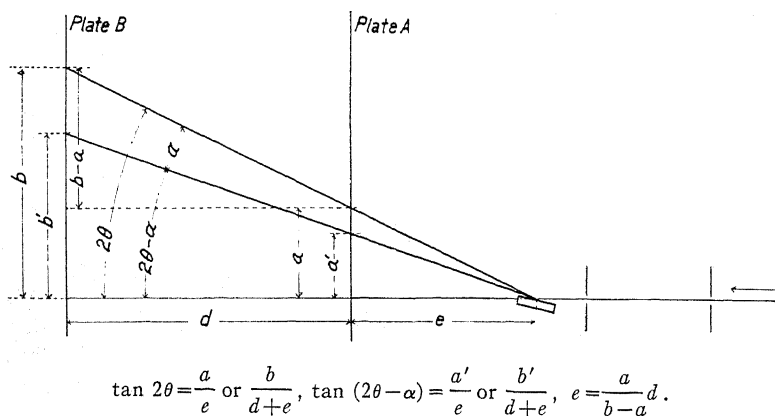


Fig. 4.

It was found that the first inside order from the grating used was much greater in intensity than the outside orders. This fact, combined with the great dispersion obtained with inside orders, contributed greatly to the success of the work. It was also found that the intensity of the L radiation from

the elements studied depended greatly upon the operating conditions of the tube. It was most intense when the temperature of the focal spot was maintained very close to the melting point. With this condition the spot was kept very clean.

The measurement of the plates and the calculation of results can best be described with reference to Fig. 4. The size of the ruled surface (2 cm \times 2 cm), the width of the x-ray beam (approx. 0.1 mm) and the magnitude of the grazing angle (more than $2^{\circ}25'$) make it possible to have the entire beam "reflected" from the ruled surface of the grating. Hence all measurements may be made to the centers of the recorded lines. The positions of the lines on the plates were taken as a mean of at least ten independent settings on a Gaertner comparator. The probable error in the readings was usually less than 0.003 mm. The distance e of plate A from the grating and the angles 2θ and $2\theta - \alpha$ were obtained as indicated. By subtraction α was found and substitution made in Eq. (2) to obtain the wave-length.

The results of the measurements are shown in Table I, which gives both the wave-length in angstroms and the value of $(\nu/R)^{1/2}$.

TABLE I.

Element	$L\alpha_{12}$		$L\beta$		Ll		$L\eta$	
	λ	$(\nu/R)^{1/2}$	λ	$(\nu/R)^{1/2}$	λ	$(\nu/R)^{1/2}$	λ	$(\nu/R)^{1/2}$
30 Zn	12.25	8.63	11.96	8.73	14.02	8.06		
29 Cu	13.37	8.26			15.33	7.71	14.95	7.81
28 Ni	14.62	7.90	14.28	8.00	16.73	7.38	16.36	7.47
27 Co	15.99	7.55	15.64	7.64	18.34	7.05		
26 Fe	17.66	7.18	17.29	7.26	20.25	6.71		
25 Mn	19.55	6.82	19.17	6.89	22.34	6.39		
24 Cr	21.73	6.48						
23 V	24.31	6.12			27.70	5.73		
22 Ti	27.48	5.76						
20 Ca					39.63	4.79		

DISCUSSION

Fig. 5 is a Moseley diagram of the results. The results here given are all higher than those obtained by Thoraues¹ and Shearer.² This is in accord with the results obtained by other experimenters.¹³ Kellström has reported measurements on most of these lines, using outside orders which did not permit the resolution of the α and β lines or of the l and η lines. His values for the α and l lines are less than those reported here. This is, of course, due in part to the added weight of the unresolved β and η lines. However, in the case of the β line at least, the relative intensity is so much smaller than that of the α line that the wave-length determined from the measurement of the unresolved lines is far from the mean of the two component wave-lengths. Comparison of the results of the two experiments is therefore limited. This is further complicated by the fact that Kellström has made his measurements by comparison with the K_{α} line of aluminum as obtained from crystal

¹³ A. H. Compton, Jour. Franklin Inst. 208, 605 (1929).

measurements. This would also make his measurements lower. In view of these considerations the agreement between the two experiments is very satisfactory, with the exception of the l line of calcium for which Kellström

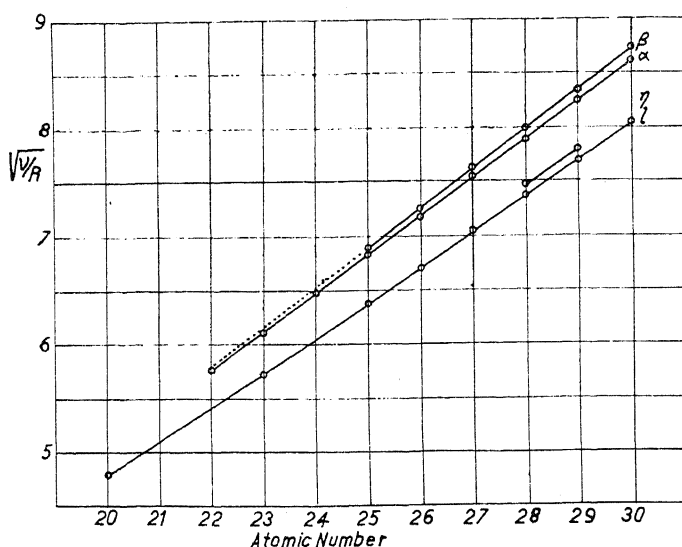


Fig. 5. Moseley diagram for L -series lines.

finds a value three percent higher than the value here given. Unfortunately the author recorded this line on but one plate and could not therefore check this wave-length carefully. In all but a few cases, however, sufficient values were obtained to give a probable error less than 0.01A.

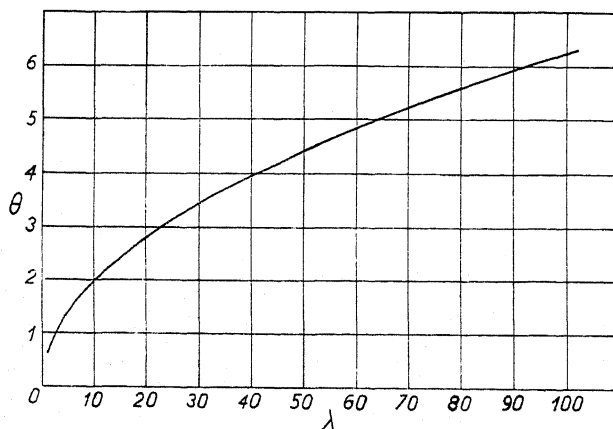


Fig. 6. Values of θ for which the inside order should be in the plane of the grating.

In order to resolve the α and β lines as well as the l and η lines it was necessary to rotate the grating so that the inside orders occurred close to the plane of the grating. Consequently each element required at least two

independent settings; one to resolve the α and β lines, the other to resolve the l and β lines. In order to facilitate this operation the angle θ was calculated for which the inside order should be in the plane of the grating. Fig. 6 shows this value of θ in degrees plotted against the corresponding value of λ in angstrom units. In actual practice θ was made a little larger than this critical value.

For most of the elements in this region the L_α line is really two lines, the $L\alpha_1(M_{33}-L_{22})$ and the $L\alpha_2(M_{32}-L_{22})$. According to Foote's extension of Stoner's arrangement of the electrons the M_{33} level disappears with vanadium and the M_3 level with calcium. This means that neither of the two components of the $L\alpha_{12}$ line should be observed for calcium. Reference to Fig. 1 shows that it was not observed in this experiment although Kellström¹² finds it present. The $L\beta_1(M_{32}-L_{21})$ line should also disappear with calcium.

In conclusion I wish to express my indebtedness to Professor A. H. Compton of the University of Chicago under whose direction the experimental work was done.

THE CYBOTACTIC (MOLECULAR GROUP) CONDITION IN LIQUIDS; THE NATURE OF THE ASSOCIATION OF OCTYL ALCOHOL MOLECULES

BY G. W. STEWART

DEPARTMENT OF PHYSICS, UNIVERSITY OF IOWA

(Received January 15, 1930)

ABSTRACT

In resumé twelve experimental lines of evidence are cited in favor of the adoption of the molecular group theory of the nature of liquids. This theory is assumed in the interpretation of results with octyl alcohols.

The following twenty-two octyl alcohols were used: octanol -1, -2, -3, -4, 2-methyl heptanol -1, -2, -3, -4, 3-methyl heptanol -1, -2, -3, -4, 4-methyl heptanol -1, -2, -3, -4, 5-methyl heptanol -1, -2, -3, 6-methyl heptanol -1, -2, -3.

The value of the effective diameter of the primary normal alcohols is approximately 4.5 Å. With these octyl alcohols the increase for OH and CH₃ in a branch is approximately 0.0 Å and 0.24 to 0.75 Å respectively. When attached to the same carbon atom the increase caused thereby is not noticeable. These results are in fair agreement with previous similar measurements of isomers with other primary alcohols.

Two types of association were found. When the OH group is attached to the end or next to the end of the alcohol molecule, two of these molecules are associated end to end, the lengths of the chains being in the same straight line. On the other hand when the OH group is attached to any other carbon atom, the molecules are associated side by side. This is shown by the planar distances in the direction of the molecule which indicate in the first case the length of two molecules and in the second case the length of a single molecule.

DURING the past four years evidence has been accumulating in favor of the view that in liquids in general there exist temporary, fairly orderly, not sharply defined molecular groups. A brief resumé of that evidence, as an introduction to the present experiments, is opportune. Skepticism concerning the correctness of this conception of molecular groups is natural, since it has formerly been accepted that the molecular motions in a liquid are somewhat independent. Moreover it is known that molecules of a gas, which are certainly not orderly, will give x-ray diffraction haloes.¹

EVIDENCE FOR THE CYBOTACTIC CONDITION

It will be the purpose of this statement of evidence to present the material merely in outline. The reader can easily follow the argument by studying the experimental results mentioned in each case. For the sake of simplicity the references will be limited but the articles to which references are made contain the complete bibliography. It is believed that the evidence establishes the group theory as one worthy of confidence. The chief points will be now enumerated. All the experiments refer to x-ray diffraction.

¹ Debye, Phys. Zeits. 30, 524 (1929); 31, 142 (1930).

1. Scattering centers at random would produce a large scattering near 0° , for in the terms of a wave theory, the nearer the approach to 0° the more nearly the agreement in phase. But crystals and crystal powders would, if ideal, give zero diffraction near but not at 0° . With them, interference would produce zero intensity excepting at angles of regular reflection.² Now it is found that in liquids, in general, we find the diffraction near zero to be similar to that of crystal powders and not to amorphous substances. The author and his co-workers³ habitually approach zero diffracting angle to the limit permitted by the resolving power of the instrument, $24'$, and they find the intensity small and decreasing as 0° is approached.

2. With normal monobasic fatty acids,⁴ one diffraction peak alters its angular position with the number of carbon atoms in the chain in such a manner that the corresponding lengths (computed by Bragg's diffraction law) vary linearly with the carbon content. This is precisely what has been found⁵ with the same fatty acids in solid form and the distances and rate of change are approximately the same in the solids and liquids. Similar causes are presumably operating in the two cases. If the solid is crystalline, the liquid has molecular groups.

3. Comparisons between the solid and liquid diffraction curves show a clear similarity. Of course the diffraction peaks are diffuse as compared with the lines with crystals. But the prominent maxima are similarly located. Krishnamurti⁶ has published comparisons of eight substances. There have also been published lauryl alcohol⁷ and capric acid⁸ diffraction curves. Triphenylmethane shows a like result. The chief maxima of intensity occur apparently at nearly the same angles of diffraction.

4. Binary solutions, where the components are miscible, show not the diffraction intensity maxima of both components, but a modification as of a single liquid. This is analogous to the case of a solid solution,⁹ and can readily be explained by the molecules of the solute participating in the molecular groups of the solvent. This is a reasonable picture of the nature of a solution.

5. The area occupied by the cross-section of a molecule of normal monobasic acids in a surface film on water¹⁰ is the area as computed by measurements within such a liquid assuming the group theory.¹¹ It is also the area computed from similar measurements on primary n-alcohols.¹² The grouping

² Regular reflection occurring at a very small glancing angle less than the critical angle, need not be regarded here.

³ See series of articles by Stewart, Stewart and Morrow, and Stewart and Skinner in *Phys. Rev.* 1927-29.

⁴ Morrow, *Phys. Rev.* **31**, 10 (1928).

⁵ See footnotes in Morrow, reference 4.

⁶ Krishnamurti, *Ind. Jour. Phys.* **III**, II, 225 (1928).

⁷ Stewart and Morrow, *Phys. Rev.* **30**, 232 (1927).

⁸ Morrow, reference 4.

⁹ Krishnamurti, *Ind. Jour. Phys.* **III**, III, 331 (1929); Hertlein, *Zeits. f. Physik* **54**, 341 (1929). Also unpublished results by A. W. Meyer of this laboratory.

¹⁰ Adam, *Proc. Roy. Soc.* **99A**, 336 (1921); **101A**, 452, 456 (1922); **103A**, 676, 687 (1923).

¹¹ Morrow, reference 4.

¹² Stewart and Morrow, reference 7.

of the molecules in such a surface film is acknowledged. Similar dimensions obtained on the interior argues strongly for molecular groups.

6. The group theory leads to simultaneous measurements of two and occasionally three distances. These are in striking consistency and difficult of explanation otherwise. For example, the molecular "diameters" remain constant with increase in the length of the chain.^{11,12} Again, di-n-propyl carbinol gives three distances,¹³ of which two, 4.85 and 4.5 A.U., are consistent with the interpretation that the former is a measurement of the diameter in the direction of the branch and the latter the diameter of the chain perpendicular thereto, or the diameter of the primary n-alcohol.

7. Assuming the group theory, isomers of primary n-alcohols have been measured¹² and these have been found consistent with the usual chemical views as to structure.

8. The effect of temperature on the diffraction in liquids is, in general, similar to that in crystal powders, i.e., a shifting of the maxima to smaller angles, an increase in diffuseness and a decrease in intensity.¹⁴

9. There are two peaks with the primary n-alcohols¹² and only one with n-paraffins.¹⁵ This is in harmony with the group theory. Each series has parallel chains, but the polar molecules produce a longitudinal orderly arrangement that makes possible the second spacing of diffraction centers as found by x-rays.

10. The relative magnitude of the two diffraction peaks in case of the n-alcohols and the saturated normal fatty acids indicate that the intensity obtained by the diffraction from the parallel planes containing the lengths of the chains is much greater than from the parallel planes passing across these chains. Consideration of the structure factor in these two cases shows that a relative magnitude of this order should be anticipated if the group interpretation is correct. The quantitative details of these considerations are not yet published.

11. Quantitatively the dimensions determined by some of the diffraction maxima are much too long to refer to parts of the same molecule and must refer to intermolecular spacing.

12. The integrated intensity in the region of the chief diffraction maximum for solid (powdered crystal) and liquid triphenylmethane (results unpublished), show approximately equal values. It is difficult to see how such coherence could be obtained from a liquid without groups.

These are the more conspicuous lines of argument. But even aside from the evidence, a moment's general consideration indicates the reasonableness of the cybotactic theory. For the molecular forces are evidenced in surface tension, where there is an orderly arrangement, and, with the closeness of approach of molecules in the liquid, these forces must everywhere be of importance. These force fields introduce potentials. From Boltzmann's statistical distribution law the largest number of molecules must be at the

¹³ Stewart and Skinner, *Phys. Rev.* **31**, 1 (1928).

¹⁴ Vaidyanathan, *Ind. Jour. Phys.*, III, III, 391 (1929); E. W. Skinner, not yet published.

¹⁵ Stewart, *Phys. Rev.* **31**, 174 (1928).

least potential. It is then merely a question as to what the possible potentials are. Will the least potential be an orderly periodic arrangement or not? *A priori*, one cannot say, but such considerations would cause one to be ready to adopt the answer favored by experiments. From this view point the above twelve items of evidence seem to lead to the adoption of the cybotactic conception as the best description of the condition of least potential.

X-RAY DIFFRACTION IN OCTYL ALCOHOLS

The present contribution was made possible by Professor E. Emmet Reid of Johns Hopkins University who kindly lent samples of the twenty-

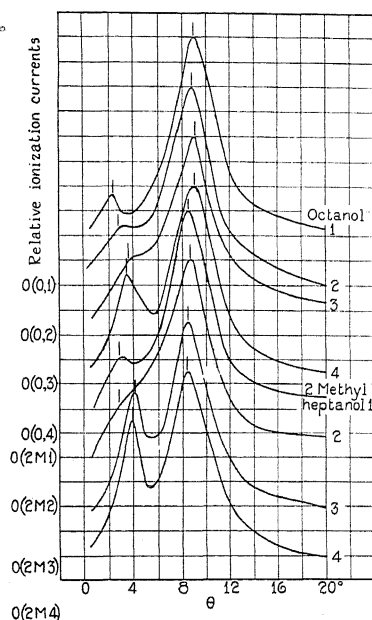


Fig. 1. X-ray diffraction; relative ionization currents of octyl alcohols.

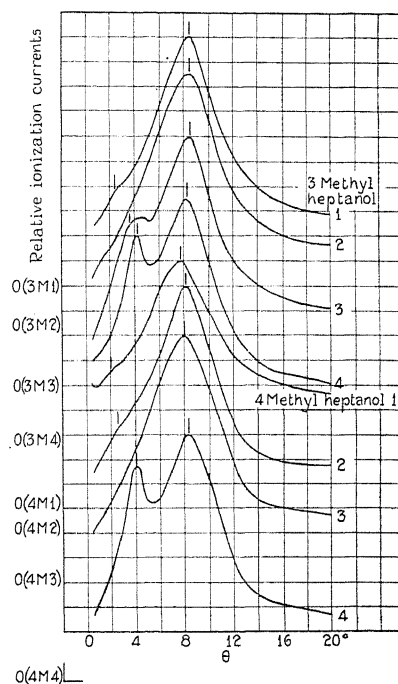


Fig. 2. X-ray diffraction; relative ionization currents of octyl alcohols.

two octyl alcohols made in his laboratory by Messrs. H. B. Glass and G. B. Malore. The following gives a statement of results and conclusions of x-ray diffraction measurements. The description of the apparatus and precautions may be found in one of the earlier articles.¹⁸

In Figs. 1, 2 and 3 are presented the relative ionization currents obtained in a chamber placed at the varying angles of diffraction. In each figure the curves are displaced vertically and each major peak is given the same magnitude. In Fig. 4 are shown the diameters and lengths of the molecules. Bragg's law of crystal diffraction, $\lambda = 2d \sin \theta/2$, wherein λ is the wave-length, d , the separation of planes containing diffraction centers and θ , the angle of dif-

¹⁸ Stewart and Morrow, Phys. Rev. 30, 232 (1927).

fraction, is used. The circle containing a cross is the length of the molecule estimated from the *n*-paraffin chain dimensions obtained in an earlier article.¹⁷

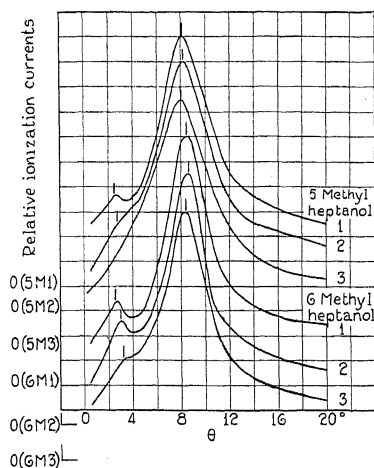


Fig. 3. X-ray diffraction; relative ionization currents of octyl alcohols.

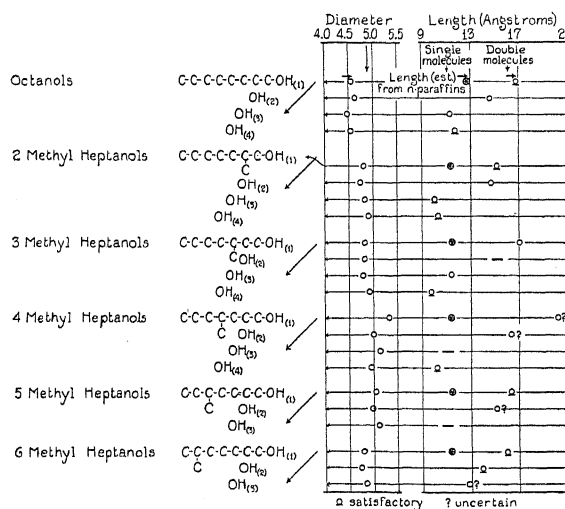


Fig. 4. Effective diameters and comparison of molecular lengths with separation of second set of diffraction planes.

CONCLUSIONS

1. *Molecular diameters.* The effective molecular diameter of octanol-1 is about 4.55×10^{-8} cm (or A.U., indicated merely by A, for the sake of brevity). This is more accurately the mean separation of planes containing parallel

¹⁷ Stewart, Phys. Rev. 32, 153 (1928). The length of a normal paraffin molecule is $1.24n + 2.70$ where *n* is the number of carbons and 2.70 is the length estimated for the two terminal hydrogen atoms. The formula is used for the alcohol molecules, save that *n* does not include the carbon atom in a branch.

molecules and, assuming a square array of the chains in a plane perpendicular thereto, this distance may be interpreted as the effective molecular diameter. It is to be noted that (1) with the group OH in a branch the diameter is not materially increased, (2) with CH₃ in a branch the diameter is increased by approximately 0.24Å for 2-methyl-, 3 methyl- and 6 methyl-heptanol 1, (3) by 0.75Å for 4-methyl-heptanol and (4) by 0.47Å for 5-methyl heptanol. Items (1), (3) and (4) are closely in accord with previous findings on isomers of primary n-alcohols,¹⁸ but the increases noted in (2) are approximately one-half as great. Also, as before, the effect on the diameter of the attachment of OH and CH₃ to the same C atom is not noticeable. The measurements are not in error by more than 0.05Å, but there are other factors to consider. For example the compounds are doubtless not of the highest practicable purity. Also, we are interpreting the grouping in the simplest possible manner, and this picture of the grouping may be only approximately true. Again, the position of the peak in the curve is a statistical result and is not obtained with a *fixed* grouping of molecules.

2. *Association of molecules.* As shown in earlier articles¹⁹ the distance computed from the position of the smaller peak depends upon the length of the molecule but cannot represent the molecular length or an integral value of it because the association produces effective diffraction centers that lie in planes not perpendicular to the molecular lengths. For the primary normal alcohols and the saturated normal fatty acids the distance between the planes was more than the length of the molecule and less than twice this distance. The interpretation was made that two polar groups were associated so that their molecules were placed end to end in the same line. Consequently the effective longitudinal diffraction centers occurred every two molecules. But the planes containing them were not perpendicular to the molecules. Thus the planar distance became less than twice the length of a molecule. In Fig. 4 of this contribution it is noticed that the determination of all the secondary peaks was not possible. But of those obtained, the computed planar distances represented in Fig. 4 convey an interesting result. All the molecules having OH at the end of the molecule or attached to the second C atom, show a distance between planes considerably greater than the computed molecular length and yet clearly less than twice this length. On the other hand when OH is attached elsewhere, the planar distance is approximately the computed molecular length. We hence have here *two different types of association. When the polar group OH is at 1 or 2, the association arranges the molecules end to end in the same line with two polar groups adjoining. When the OH is elsewhere, the associated molecules lie side by side.* This generalization is further verified by the cases of diethyl carbinol and di-n-propylcarbinol.²⁰ The computed molecular length of the former, using the same figures for distance occupied by atoms as described above, is 8.9Å, and the latter 11.38Å, whereas the distances between planes are 8.9Å and 10.5Å, respectively. Considering the

¹⁸ Stewart and Skinner, Phys. Rev. 31, 1 (1928).

¹⁹ Stewart and Morrow, reference 16 (for normal primary alcohols). Morrow, Phys. Rev. 31, 10 (1928), (for saturated normal fatty acids).

²⁰ Stewart and Skinner, reference 18.

inaccuracy of the length computed from atomic dimensions in the molecule, this is clearly an agreement.

3. *Variation in magnitude of secondary peaks.* An interesting variation in relative heights of the secondary maxima can be seen in Figs. 1 to 3. This secondary diffraction peak is the most prominent in the cases of octanol-4, 2-methyl-heptanol-4, 3-methyl-heptanol-4, 4-methyl-heptanol-4; or, in other words, given the position of the methyl group, the secondary diffraction peak is always the greatest with the OH group on the fourth carbon atom. In fact, there is a variation in magnitude through any such set. These are significant facts but their interpretation is not altogether clear. In the first place one must expect the arrangement of atoms to affect the intensity of diffraction (through the much used structure factor, F). As to the major peak, the intensity of diffraction for all is sensibly the same. The experiments required the use of very thin cylindrical glass receptacles, one for each compound. Differences in these and in the sensitivity of the ionization chamber (which is refilled only once in several months), were not large and the results for the magnitude of the diffraction intensity at the major peaks, even including these unavoidable changes mentioned agreed for all the liquids with an average deviation of 17 percent and a maximum deviation from the mean of 30 percent. And this is what should be expected for the changes in structure of these molecules would result in but little change in the structure factor when the molecular length lies in the diffracting planes. Since, then, the magnitude of intensity of the major peaks is of the same order, comparison may be made of the secondary peaks as plotted in Figs. 1, 2, and 3, assuming the major peaks the same magnitude. The difference in secondary peaks is relatively very great. The structure factor for diffracting planes perpendicular to the molecular length, or at any considerable angle, would vary greatly also. Hence this may be in part the explanation of the experimental results. But the second possible explanation is that, although the molecules may lie with lengths parallel, and give well-marked diffraction planes containing these lengths, yet the molecules may not be so regularly arranged for the other set of planes mentioned. The space arrangement longitudinally may not be so perfect. One need not choose between these two factors, for both doubtless exist in important degrees. Computations are at present being made of the probable variation in structure factor, though of course there is much conjecture involved. As to the perfection of the grouping, there now appears some enlightenment through the study of the viscosity of these liquids. In fact, the viscosity is greatest where the secondary peak is greatest. This correlation is doubtless important and will be discussed in a future article by Dr. R. L. Edwards and the author. In the foregoing it must be understood that the cybotactic condition is not one in which the "groups" are definite, having constantly the same constituents, or the same dimensions or spacing. There must be groupings to give the diffraction effects at any instant, but the effect on the ionization chamber is a statistical one.

To Professor E. Emmet Reid for the use of the octyl alcohols and to Mr. H. A. Zahl, research assistant, who is responsible for the data described herein, I wish to express my thanks.

BARKHAUSEN EFFECT II. DETERMINATION OF THE AVERAGE SIZE OF THE DISCONTINUITIES IN MAGNETIZATION

BY RICHARD M. BOZORTH AND JOY F. DILLINGER
BELL TELEPHONE LABORATORIES, NEW YORK, N. Y.

(Received February 12, 1930)

ABSTRACT

When the magnetic field-strength acting on a ferromagnetic material is changed, the magnetization changes discontinuously (Barkhausen effect). These discontinuous changes have been examined in 1 mm wires; an expression is derived and experimental arrangements are described for determining their average size for a given material in a given state of magnetization.

Experimental determinations of the average size have been made for iron (including a single crystal and a hard-drawn wire), nickel, and several iron-nickel alloys (permalloys). The average size is greatest on or near the steepest part of the hysteresis loop. The greatest average size, expressed as the volume of material the magnetization of which must be changed from saturation in one sense to saturation in the opposite sense to produce the same change in magnetization, is much the same for all of the materials examined, the extremes being 1.2×10^{-9} cm³ for annealed iron and 45×10^{-9} cm³ for 50 percent nickel permalloy. This shows that the sizes of the discontinuities do not depend to any considerable extent on the size or kind of crystals.

Criticism is made of previous work on the size of the coherence region, the region within which the change in magnetization is confined. Although the effect of a single discontinuity in magnetization may be detected as far as 10 cm from its source because of the eddy-currents induced, the experimental evidence is consistent with the view that the permanent change in magnetization is confined to the volume in terms of which the size of the discontinuity is measured as stated above, always less than 10^{-6} cm³.

INTRODUCTION

IT IS a well-established fact that when a continuously-varying magnetic field is applied to a ferromagnetic substance, the induction varies not smoothly, but by sharp sudden jumps or "discontinuities." One may interpret it by supposing that the substance is made up of very small regions or "units," each of which is always magnetized to saturation, and that during the magnetization of the sample, the magnetic axes of half of these are reversed, one after another. The volume v of each unit may then be computed from the amount of the corresponding discontinuity. Of course, it may be that the change in the magnetic moment of a unit is less drastic than a complete reversal of all the atomic magnets; in that case, the value of v computed by our formula will be proportionately smaller than the actual volume of the region. However, it is simpler, and we believe also that for discontinuities on the steeper parts of the hysteresis loops it is correct, to interpret v in the first-mentioned manner.

We wish to know the average sizes of these units for as many ferromagnetic materials and as many parts of the magnetization curve as possible. Especially we wish to compare it with the sizes of the crystals on one hand, of the smallest magnetizable atom-groups on the other. For instance, one of us¹ has shown, for a variety of materials, that on the steeper parts of the hysteresis loop nearly all the discontinuities correspond to units larger than 10^{-13} cm³, comprising more than 10^{10} atoms.

In the present work we have obtained data relevant to these questions by determining the average amount of the discontinuities on various segments of the hysteresis-loops of several substances: iron, nickel, several permalloys both annealed and hard-worked, and a single crystal of iron.

THEORY

In our apparatus a slowly and uniformly changing magnetic field acts on the cylindrical specimen *P*, Fig. 1. When a sudden change, characteristic of the Barkhausen effect, occurs in the induction *B* in the sample, an e.m.f.

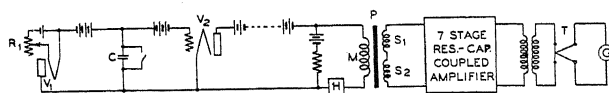


Fig. 1. Diagram of the apparatus.

is induced in one of the search coils *S* which are connected in series opposition to the input of an amplifier. At any instant the e.m.f. impressed on the amplifier is equal to the algebraic sum of the separate e.m.f.'s induced in the two coils. The e.m.f. in each coil is proportional to the dB/dt in the material inside of that coil, consequently when the coils are connected in opposition the e.m.f. acting on the amplifier, and the output current, i , are proportional to the difference between the values of dB/dt within the two coils. Considering dB/dt in one coil to be positive and that in the other to be negative, the difference is $(dB/dt)_1 + (dB/dt)_2$, and the mean value of this sum, or $\overline{dB/dt}$ for the combination, is zero. The thermocouple *T* measures $\overline{i^2}$ (the mean value of i^2) which is then proportional to $\overline{(dB/dt)^2}$. We can now use a statistical relation derived by T. C. Fry,² provided the following assumptions are valid:

(1) The law of superposition holds; that is, the e.m.f. impressed on the amplifier at any time is the algebraic sum of the separate e.m.f.'s induced by separate sudden changes in induction.

(2) The discontinuities are random in character both as to magnitude and time; that is, the magnitude and exact time of beginning of any sudden change in induction is independent of previous changes.

¹ R. M. Bozorth, Phys. Rev. **34**, 772-784 (1929). See also an abstract of the present paper, Phys. Rev. **33**, 1071 (1929).

² T. C. Fry, J. Frank. Inst. **199**, 203-220 (1925).

(3) The form of the induction-vs-time relation is the same for all the impulses produced by the various discontinuities; that is, any impulse is identical with the product of any other by some constant factor.

(4) The time required for the thermocouple reading to reach a steady value is large compared to the duration of a single current impulse but small compared to the gross changes in the output of the amplifier, corresponding to what may be considered changes in the magnetic state of the material.

These assumptions are valid except in relatively minor details. Assumption (2) is not exactly true unless the material inside one search coil has exactly the same magnetic characteristics as that inside the other. In reality materials are not quite homogeneous. Assumption (3) implies that the magnetization in a small volume changes very suddenly but that the e.m.f. induced in the search coil is influenced by the rate of decay of the eddy-currents set up by the change in magnetization. If these small volumes are located at different distances from the axis of the sample, the eddy-currents will decay at slightly different rates and assumption (3) is not strictly correct.

The equation derived by Fry is

$$S = \bar{\nu} \bar{w}, \quad (1)$$

where S is the power expended in the thermocouple, $\bar{\nu}$ the mean number of separate impulses occurring per second, and \bar{w} is the average energy expended in the thermocouple by a single impulse. Obviously,

$$S = \bar{i}^2 R, \quad (2)$$

where R is the resistance of the thermocouple and \bar{i}^2 is the mean square current through it. The mean frequency of the impulses, $\bar{\nu}$, may be expressed in terms of the average volume of material, \bar{v} , the magnetization of which is assumed to change from saturation in one direction to saturation in the other:

$$dB/dt = 8\pi I_s \bar{\nu} \bar{v} / V, \quad (3)$$

where I_s is the saturation value of magnetization and V is the total volume of the sample in which magnetic discontinuities affect the search coils.³ The energy w for one discontinuity is

$$w = \int_0^\infty i_1^2 R dt, \quad (4)$$

where i_1 is the current (a function of time) which would flow in the thermocouple if a single isolated discontinuity occurred in the sample. This current is proportional to the rate of change of induction during this single event,

$$i_1 = A \pi r^2 dB_1 / dt, \quad (5)$$

³ B is used here as an approximation for $B-H$, since in these experiments H is always small compared with B . The apparatus measures changes in $B-H$ rather than in B .

where A is a constant determined by calibrating the apparatus and r is the radius of the sample. Also, for a single impulse the induction will be a function of time,

$$B_1 = \frac{8\pi I_s v}{V} f(\tau), \quad (6)$$

where $f(\tau)$ is the same function of time for all impulses (assumption 3) and is determined by the decay of eddy-currents, and v is the volume which changes in magnetization.

Combining Eqs. (4), (5) and (6), and taking the mean value,

$$\overline{w} = 64\pi^4 A^2 R I_s^2 r^4 (\overline{v^2}/V^2) \int_0^\infty [f'(\tau)]^2 d\tau.$$

Using also Eqs. (1), (2) and (3), and putting $V/\pi r^2 = l$, the length of the specimen which affects the search coils, we have the result

$$\frac{\overline{v^2}}{\overline{v}} = \frac{l \overline{v^2}}{8\pi^2 A^2 I_s r^2 dB/dt \int_0^\infty [f'(\tau)]^2 d\tau}. \quad (7)$$

The function $f(\tau)$ is subject to the condition that $f(\infty) = 1$. Its time derivative, $f'(\tau)$, characterizing the decay of eddy-currents, might be determined experimentally as a function of μ , ρ and r by using a suitable oscillograph to record the wave-form of the current impulses, caused by single Barkhausen discontinuities, which pass through the thermocouple heater. Since the recording of these wave-forms puts a very severe requirement on the oscillograph, and since it is a laborious undertaking in any case to determine $f'(\tau)$ completely in terms of μ , ρ and r , we have used the expression derived by Wwedensky⁴ and supported by experiment. For a spontaneous change in magnetization, we find

$$\int_0^\infty [f'(\tau)]^2 d\tau = \frac{2(10)^9 \rho}{\pi r^2 \mu}, \quad (8)$$

where ρ is the resistivity in ohm-cm, and μ is the permeability which controls the rate of decay of eddy-currents, in this case the reversible permeability or permeability for small alternating fields. Substituting Eq. (8) in Eq. (7),

$$\frac{\overline{v^2}}{\overline{v}} = \frac{l \mu \overline{v^2}}{16\pi(10)^9 A^2 I_s \rho dB/dt}. \quad (9)$$

Wwedensky's expression was derived for a long cylinder the magnetization of which is uniform, consequently Eq. (8) is not strictly applicable to the present problem and must be considered as an approximation. Even if the

⁴ B. Wwedensky, Ann. d. Physik **64**, 609-620 (1921).

sudden change in magnetization occurs entirely within a volume small compared to the cube of the radius of the specimen, the disturbance will spread along the axis of the wire to an extent depending on the permeability, resistivity, and diameter of the wire. The extent of the disturbance, necessary for choosing the proper value of l to be used in equation (9), can be determined as described in the next section.

The ratio \bar{v}^2/\bar{v}^2 is very near unity for most distribution functions, but may in certain cases be very large. One of us¹ has shown that there are very few discontinuities corresponding to volumes several orders of magnitude smaller than the average. Taking this into consideration, we may with reasonable safety extrapolate to the origin the size distribution curve determined by Tyndall⁵ for silicon steel. For the curve so extrapolated we find that $\bar{v}^2/\bar{v}^2 = 0.7$, a value sufficiently close to unity to make \bar{v}^2/\bar{v} , as given by Eq. (9), a reasonably good approximation to \bar{v} , the average volume in which we are interested.

All of the quantities on the right-hand side of Eq. (9) can be determined experimentally without unusual difficulties, as described below.

APPLICATION TO EXPERIMENT

Fig. 1 shows the experimental arrangement for measuring \bar{v}^2 of Eq. (9). The magnetizing coil, M , is 60 cm long; each search coil is 3.8 cm long, 1.7 cm outside diameter, 0.4 cm inside diameter, and is wound with 10,000 turns of No. 40 B.E.S.S. copper wire. The samples are 60 cm long and 1 mm in diameter. The magnetizing coil is supported on rubber bands in a permalloy shield 5 mm thick to protect it from mechanical and magnetic disturbances. The arrangement for changing the magnetic field slowly and uniformly is that described previously.¹ The amplifier is resistance-capacity coupled with resistances of 70,000 ohms and capacities of one microfarad. For the first stage a screened grid vacuum tube is used (Western Electric 246-A), for the next five stages 239-A tubes, and for the last stage a 104-D tube. The amplification may be varied by using different taps on the input resistance of the second stage. The space current of the last tube passes through the primary of a transformer the secondary of which is connected to the heater of a thermocouple. The impedances of the transformer match respectively the impedances of the vacuum tube in the last stage of the amplifier and the heating element of the thermocouple. The thermocouple is connected to a critically damped Moll galvanometer, G , the deflections of which are recorded on photographic paper mounted on a rotating drum. With this arrangement the deflection δ of the galvanometer, as measured on the paper, is proportional to the mean value of the power expended in the thermocouple heating element, i.e., $\delta \propto \bar{v}^2$.

The mean rate of change of induction, dB/dt , is determined by observing dB/dH and dH/dt separately. To determine dB/dH , the two search coils are connected in series aiding to the Moll galvanometer and the field is changed at a uniform rate. The galvanometer deflection, proportional to

⁵ E. P. T. Tyndall, Phys. Rev. 24, 439-451 (1924).

dB/dH , is recorded photographically as before. The calibration is made by integrating the dB/dH -vs.- H curve and comparing it with the total change in B as determined in the usual way with a ballistic galvanometer. Lines indicating predetermined values of H are marked on the paper by flashing a light when the field-strength passes through these values.

The rate of change of field-strength, dH/dt , is determined by noting with a stop-watch the times at which the needle of the milliammeter in the magnetizing circuit passes through chosen positions.

The reversible permeability μ is determined by subjecting the sample to the small sinusoidal field created in a small single-layer "calibrating coil" inside the search coils and magnetizing coil. A measured current, i_s , of frequency 5 cycles/sec is passed through the calibrating coil, the search coils are connected to the amplifier in series aiding and the deflection of the galvanometer, δ_s , noted for a given value of H , the strength of the steady field produced by the magnetizing coil. The calibration for determining μ is made by removing the sample and observing the deflection δ_c , when a larger current, i_c , of the same frequency passes through the calibrating coil. The permeability may then be calculated as follows. The root mean square current passing through the heater of the thermocouple is proportional to the root mean square rate of change of flux threading the search coils. Since δ is proportional to the square of the current,

$$\delta_s^{1/2} = K i_s (\mu A_s + A_c - A_s),$$

and

$$\delta_c^{1/2} = K i_c A_c,$$

where A_s is the cross-sectional area of the sample, A_c that of the calibrating coil, and K a proportionality constant. The permeability is then given by:

$$\mu = \frac{A_c i_c \delta_s^{1/2}}{A_s i_s \delta_c^{1/2}} - \frac{A_c - A_s}{A_s}$$

and must be determined for various values of H . For the coil and samples used, $A_c = 0.083 \text{ cm}^2$ and $A_s = 0.0081 \text{ cm}^2$ so that

$$\mu = \frac{10.2 i_c \delta_s^{1/2}}{i_s \delta_c^{1/2}} - 9.2.$$

The maximum value of the alternating field-strength, calculated from i_s and the number of turns per unit length of the calibrating coil, was kept as low as 0.001 gauss for the more permeable materials.

The values of μ so determined were checked in several cases with those determined with a ballistic galvanometer by measuring ΔB for a change ΔH after several reversals of the field-strength between H and $H + \Delta H$, and extrapolating for the value of $\Delta B/\Delta H$ at $\Delta H = 0$.

The factor A in Eqs. (5) and (9) is the ratio of the current in the thermocouple heater to the rate of change of flux inside the search coils. This is determined by producing a known sinusoidal rate of change of flux in the

calibrating coil and measuring the amplifier output i at the same time. If i_c is the root mean square current in milliamperes through the calibrating coil, f the frequency of the current, n the number of turns of wire per cm, and A_c the cross-sectional area, the root mean square value of the rate of change of flux is

$$(d\phi/dt)_c = 8\pi^2 n A_c f i_c (10)^{-4}$$

and therefore

$$A = \frac{i}{d\phi/dt} = \frac{10^4 i'}{8\pi^2 n A_c f i_c},$$

where i' is the root mean square value of i measured at the same time as i_c . Since i' is proportional to $\delta'^{1/2}$ and i is similarly proportional to $\delta^{1/2}$, we may rewrite Eq. (9) as

$$\frac{\bar{v}^2}{\bar{v}} = \frac{l\mu\delta}{16\pi(10)^9 C^2 I_s \rho dB/dt} \quad (10)$$

where

$$C = \frac{(10)^4 \delta'^{1/2}}{8\pi^2 n A_c f i_c} \quad (11)$$

The calibrating deflection δ' is recorded on the same paper as the deflections δ caused by the Barkhausen discontinuities. Since the value of \bar{C} depends on f directly as expressed by Eq. (11) and indirectly through the frequency

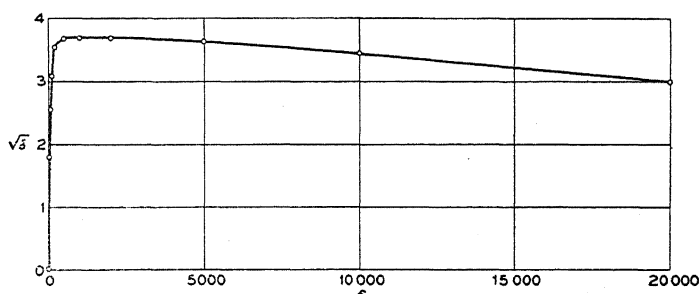


Fig. 2. Frequency characteristics of the apparatus (amplifier, transformer, thermocouple and galvanometer).

characteristics of the apparatus, the amplification was measured for a series of frequencies. At each frequency 0.7 milliampere was passed through a fixed resistance of 0.1 ohm connected to the input of the amplifier in parallel with the search coils, and the deflection of the galvanometer noted. The results are shown in Fig. 2. The range of frequencies shown is sufficient to record accurately the Barkhausen impulses in the materials examined. Calibration was made at the frequency of 60 cycles/sec., and the value of C^2 so obtained has been multiplied by 2 to take account of the lower amplification at this frequency, compared with that in the range of 300 to 5000 cycles.

To determine the length of the sample, l , in which discontinuities will affect the search coils, it is necessary to know how the intensity of a magnetic disturbance decreases with the distance from its source. This was determined experimentally for a disturbance produced by a sinusoidal current flowing in a few turns of fine wire wound directly on a specimen. The law of decay of intensity with distance once determined, it was assumed that the magnetic disturbance caused by a discontinuity in magnetization started at a point and spread along the wire according to this same law. On the basis of this assumption a calculation was made of the change in the observed Barkhausen effect, as measured by the galvanometer deflection δ , when the two search coils (connected in series opposing) were brought closer and closer together,

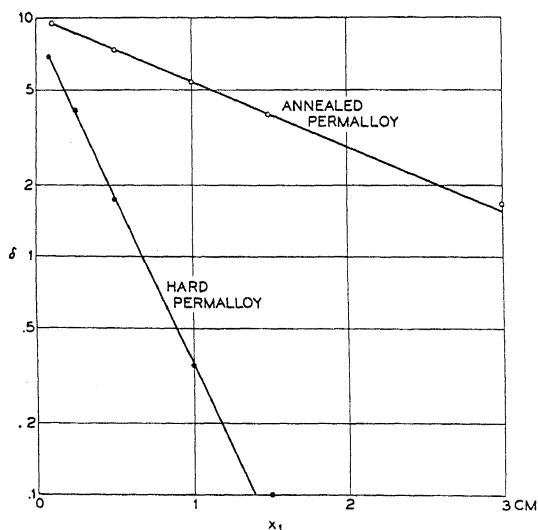


Fig. 3. Decay of magnetic disturbance with distance along wires of different permeabilities.

and this calculation was compared with observation. Ten turns of No. 40 wire were wound closely around the middle of a piece of annealed permalloy containing 81 percent Ni, and a current of 0.5 milliamperes of frequency 35 cycles/sec. was passed through it. Two search coils of 0.15 cm inside diameter and 1.3 cm length were placed at equal distances on each side of the 10-turn coil and the deflection δ_1 of the galvanometer noted for various distances x_1 between the small coil and the centers of the search coils. The results (Fig. 3) show that $\delta_1 = C_1 e^{-ax_1}$, where C_1 and a are constants. Assuming that the rate of change of magnetic flux, $d\phi/dt$, at each point along the sample follows this exponential law, and remembering that $d\phi/dt$ is proportional to $\delta^{1/2}$, we have

$$d(\delta)^{1/2} = C_2 e^{-ax/2} dx \quad (12)$$

for each point along the wire. Since the total effect is obtained by adding the value of $\delta^{1/2}$ contributed by each element along the wire, in a search coil of length l_1 we have

$$\delta_1^{1/2} = \int_{x_1-l_1/2}^{x_1+l_1/2} C_2 e^{-ax/2} dx \quad (13)$$

or

$$\delta_1 = \frac{4C_2}{a^2} (e^{al/4} - e^{-al/4})^2 e^{-ax_1},$$

agreeing with the experimentally determined relation in that $d \ln \delta_1 / dx_1 = -a$. For the sample described above, $a = 0.60$.

Applying Eq. (12) to the Barkhausen effect, we get Eq. (13) for each discontinuity in magnetization which starts at a point in the sample outside of the search coil. For points inside of the search coil,

$$\delta_1^{1/2} = \int_0^{x_1+l_1/2} C_2 e^{-ax/2} dx + \int_0^{x_1+l_1/2} C_2 e^{-ax/2} dx,$$

and integrating for all points on the sample the galvanometer deflection δ is given by

$$\delta^{1/2} = 2 \int_{l_1/2}^{\infty} \delta_1^{1/2} dx_1 + 2 \int_0^{l_1/2} \delta_1^{1/2} dx_1,$$

or,

$$\delta = 16C_2^2 l_1^2 / a^2. \quad (14)$$

To determine the equivalent length l of Eq. (10), used when two search coils are connected in series opposing, δ is recalculated assuming that all impulses originating at points within a length $l/2$ of the specimen affect all turns of one search coil as much as a real impulse occurring within a search coil affects the turns immediately adjacent. This substitutes for Eq. (12),

$$d(\delta)^{1/2} = C_2 dx, \quad (12')$$

for Eq. (13)

$$\delta_1^{1/2} = \int_{x_1-l/2}^{x_1+l/2} C_2 dx = C_2 l, \quad (13')$$

and for Eq. (14)

$$\delta^{1/2} = \int_0^{l/2} \delta_1^{1/2} dx_1 = C_2 l l / 2,$$

or,

$$\delta = C_2^2 l_1^2 l^2 / 4. \quad (14')$$

Comparison with (14) shows that $l = 8/a$ independent of l_1 , the length of each search coil. The value of a is determined experimentally as described above. The data are shown graphically in Fig. 3. A variation in the frequency of the alternating current used in this experiment between 10 and 1000 cycles per

second showed only a slight change in a with frequency. The same experiment was repeated using a hard-drawn wire of the same composition and diameter and a for this sample was found to be 3.22. The ratio of the values of a for these two samples is 5.4, nearly equal to the inverse ratio of the square-roots of their permeabilities, namely $(2510/75)^{1/2} = 5.8$. It is concluded that l is proportional to $\mu^{1/2}$, when the resistivity is constant. If the resistivity ρ varies, l must be proportional to $(\mu/\rho)^{1/2}$ since it is only in the ratio μ/ρ that μ and ρ appear in Maxwell's equations. Using the directly determined value of a for the sample with $\mu = 2510$ and $\rho = 15(10)^{-6}$ ohm-cm, we can therefore finally put

$$l = 1.03(10)^{-3}(\mu/\rho)^{1/2}. \quad (15)$$

A more extensive analysis of the dependence of δ on the distance, y , between the two search coils used in measuring the Barkhausen effect, shows that a may also be determined from the relation between δ and y . Such a determination has been made for one sample and found to agree with the determination as described above.

Combining Eq. (14) with Eq. (10) and designating the ratio \bar{v}^2/\bar{v} by v , we have

$$v = \frac{2.0(10)^{-14}\mu^{3/2}\delta}{C^2 I_s \rho^{3/2} (dB/dH) (dH/dt)} \quad (16)$$

in which all of the quantities are already known or can be determined as described in this section.

THE EXPERIMENTAL RESULTS

The following materials were examined in the form of wires 60 cm long and 0.1 cm in diameter:

Armco iron, hard drawn.

Armco iron, vacuum annealed 2 hrs. at 1000°C, cooled 300°/hr.

Large crystals of Fe⁶.

Nickel, vacuum annealed 2 hrs. at 1100°C, cooled 300°/hr.

Permalloy, 80.5 percent Ni, vacuum annealed 1 hr. at 1200°C, 2 min. at 830°C, cooled about 1000°/min.

Permalloy, 78.1 percent Ni, vacuum annealed 1 hr. at 1100°C, cooled about 1000°/hr.

Permalloy, 50 percent Ni, vacuum annealed 2 hrs. at 1100°C, cooled 300°/hr.

Figs. 4 to 6 show the photographically registered curves dB/dH — $vs.$ — H for annealed iron, permalloy with 80.5 percent Ni, and permalloy with 50 percent Ni. In taking the photographs, as described in the previous section, the field-strength was varied slowly enough to enable the galvanometer to follow the gross changes in dB/dH , but not slowly enough to record the

⁶ We are indebted to Dr. D. Foster of these Laboratories for these crystals. For their preparation and properties, see Phys. Rev. 33, 1071 (1929).

individual discontinuities. It will be noticed that when the Barkhausen effect is large the curve is relatively irregular. Two photographs of each curve are reproduced to show that some irregularities are due to chance and are different in each run, and that some are permanent characteristics of the material and are reproduced during each magnetic cycle. Irregularities of both kinds are present but difficult to detect when hysteresis

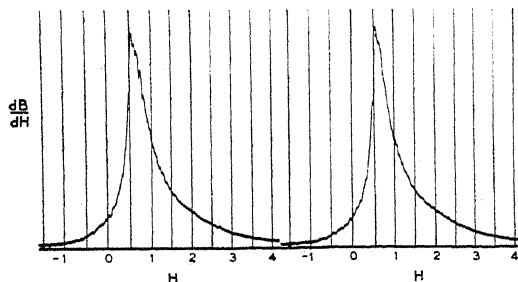


Fig. 4. Galvanometer record of dB/dH for annealed iron.

loops are determined in the usual way with a ballistic galvanometer, small variations from a smooth curve being generally indistinguishable from experimental errors.

The regular procedure was modified slightly for measurements on the large crystals. From a 1 mm wire composed entirely of long crystals, two segments were cut, each 14 cm in length, one containing a single crystal

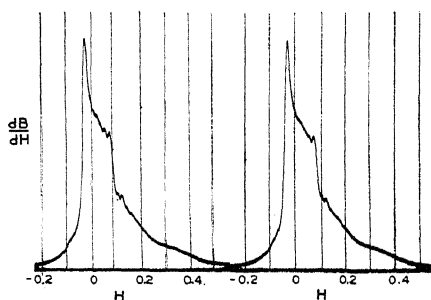


Fig. 5. Galvanometer record of dB/dH for permalloy containing 80.5 percent nickel and 19.5 percent iron.

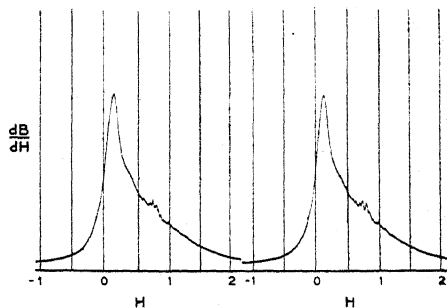


Fig. 6. Galvanometer record of dB/dH for permalloy containing 50 percent nickel and 50 percent iron.

7.2 cm long and the other a single crystal 8.6 cm long, each single crystal occupying the central portion of its segment. The remainder of the two pieces consisted of only four separate crystals, one at each end of the two longest crystals. One search coil was placed around the middle of each of the two segments, the nearest ends of which were 3 cm apart, and measurements of dB/dH , δ , and μ made without moving the specimens of coils.

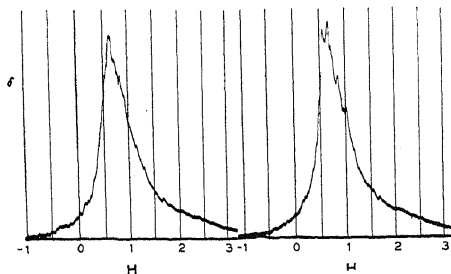


Fig. 7. Record of Barkhausen effect for annealed iron.

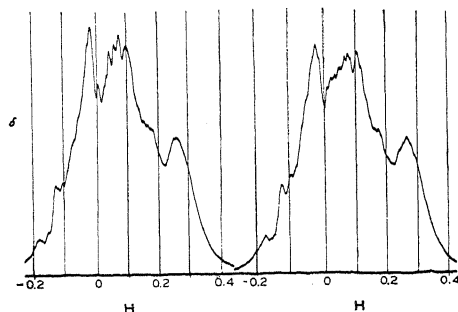


Fig. 8. Record of Barkhausen effect for permalloy containing 80.5 percent nickel and 19.5 percent iron.

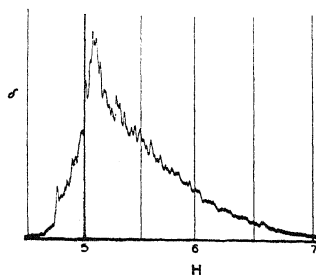


Fig. 9. Record of Barkhausen effect for hard iron.

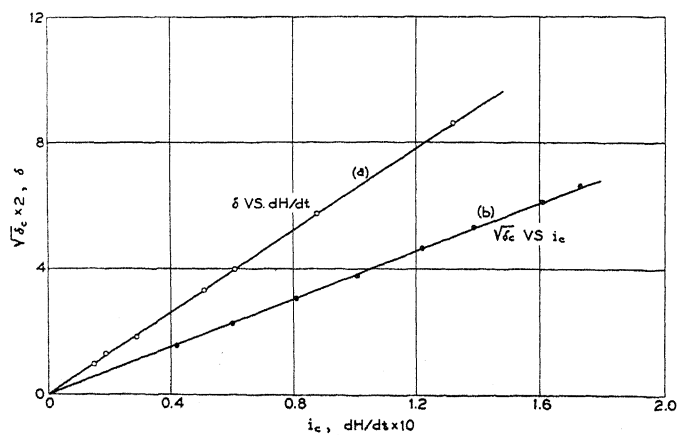


Fig. 10(a) Barkhausen effect in hard permalloy when $H = 4.5$, measured by galvanometer deflection δ , as dependent upon rate of change of field-strength. The linear relation shows that the number of the discontinuities depends only on the amount of change of H , and not on dH/dt .

(b) Calibration curve showing that the deflection δ_0 is proportional to the square of the calibrating current i_c .

These two crystals are so long that the only discontinuities detected by the coils occurred actually in the crystals.

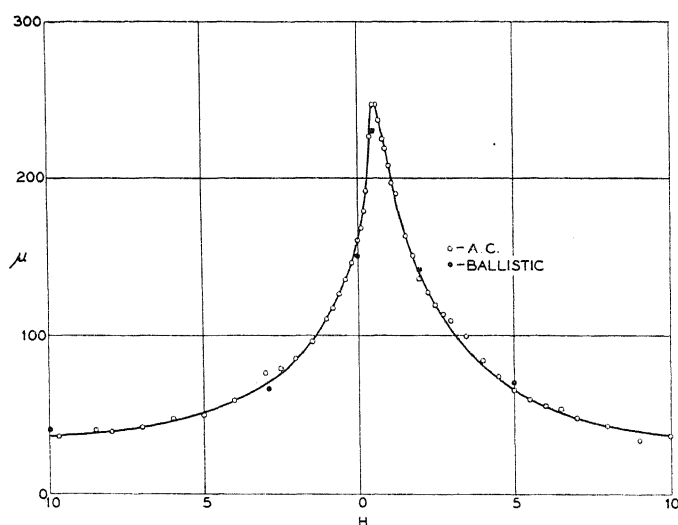


Fig. 11. Comparison of alternating current with ballistic method of determining the permeability for very small alternating fields. The sample is a 1 mm nickel wire, the frequency of the alternating current was 5 cycles/sec., the maximum field-strength during each cycle was 0.006 gauss.

Figs. 7 to 9 are reproductions of the photographically recorded Barkhausen curves, δ -vs. $-H$, for some of the materials listed above. Duplicate

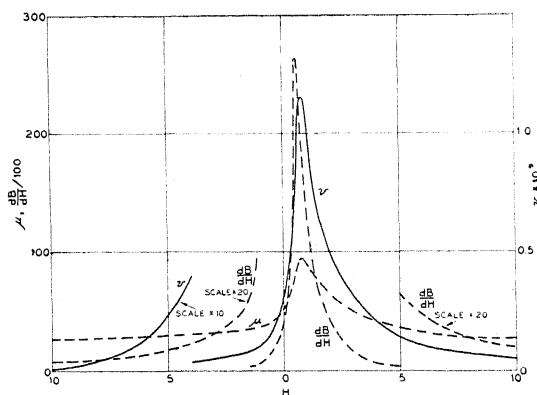


Fig. 12. The average volume, v , of the discontinuities in iron as dependent upon field-strength, and the data used in the determination.

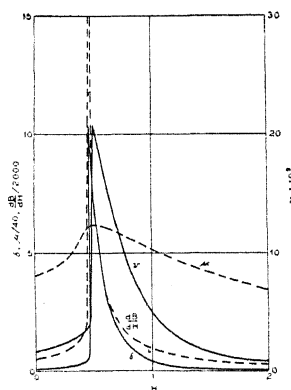


Fig. 13. The v -curve for nickel, and the data from which it was calculated.

runs for annealed iron and permalloy containing 80.5 percent nickel indicate how well the data can be repeated.

According to Eq. (16) the galvanometer deflection δ should be proportional to the rate of change of magnetic field-strength, dH/dt , when the other variables are fixed. Fig. 10(a) shows that this relation was observed, and for

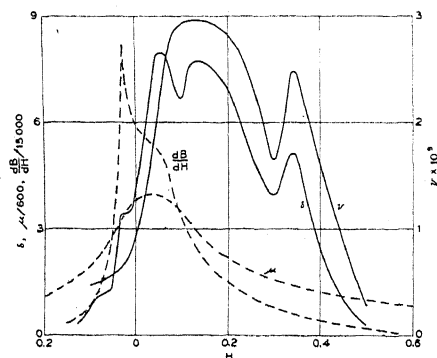


Fig. 14. The v -curve for permalloy containing 80.5 percent nickel and 19.5 percent iron, and the data from which it was calculated.

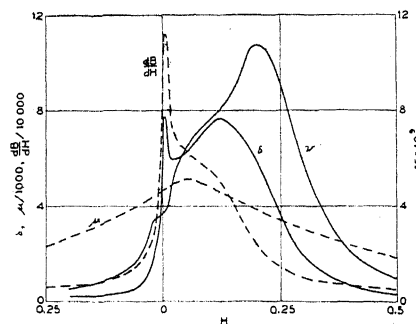


Fig. 15. The v -curve for permalloy containing 78 percent nickel and 22 percent iron, and the data from which it was calculated.

comparison Fig. 10(b) shows the linear relation between the calibrating current, i_c , and the corresponding deflection δ' , which appears in Eq. (11).

Fig. 11 shows an example of a μ -vs.- H curve determined with alternating current of frequency 5 cycles/sec, and for comparison several points determined with a ballistic galvanometer.

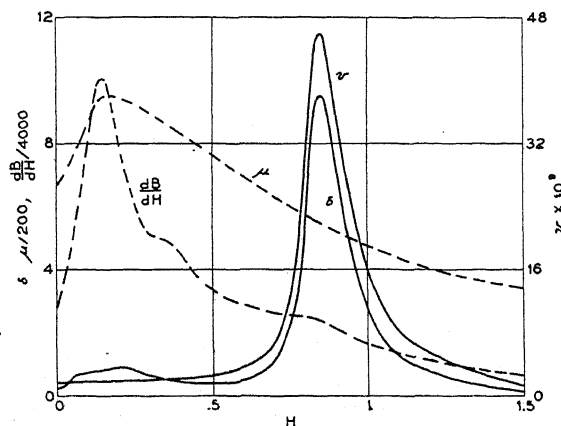


Fig. 16. The v -curve for permalloy containing 50 percent nickel and 50 percent iron, and the data from which it was calculated.

The average volume, v , of the discontinuities in magnetization was calculated in accordance with Eq. (16) for all of the materials. The curves showing v as dependent upon field-strength are shown in Figs. 12 to 18, together with the curves from which the calculations were made. In making

these calculations, small irregularities in the original dB/dH and δ curves were smoothed out, as can be seen for example by comparing Figs. 4, 7, and 12. Finally, Figs. 19 to 25 show how the v -vs.- H curves are placed with respect to the hysteresis loops.

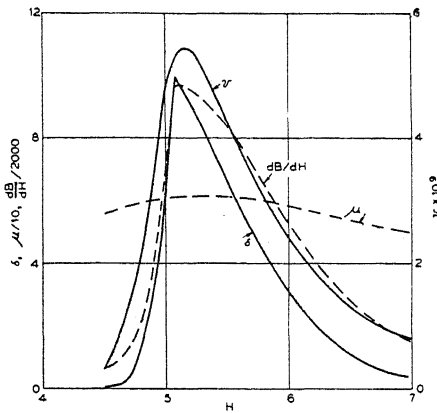


Fig. 17. The v -curve for hard iron, and the data from which it was calculated.

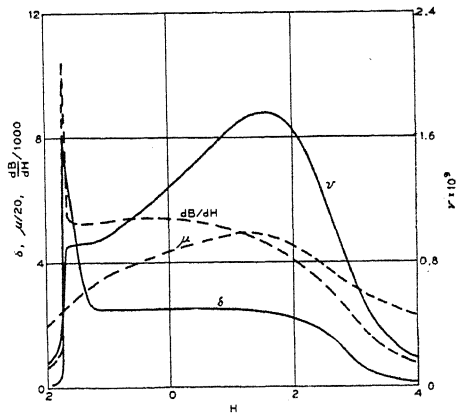


Fig. 18. The v -curve for two single crystals of iron.

DISCUSSION OF THE RESULTS

Figs. 12 to 18, as well as Figs. 19 to 25, show how the average size of the discontinuities varies from one part of the hysteresis loop to another with

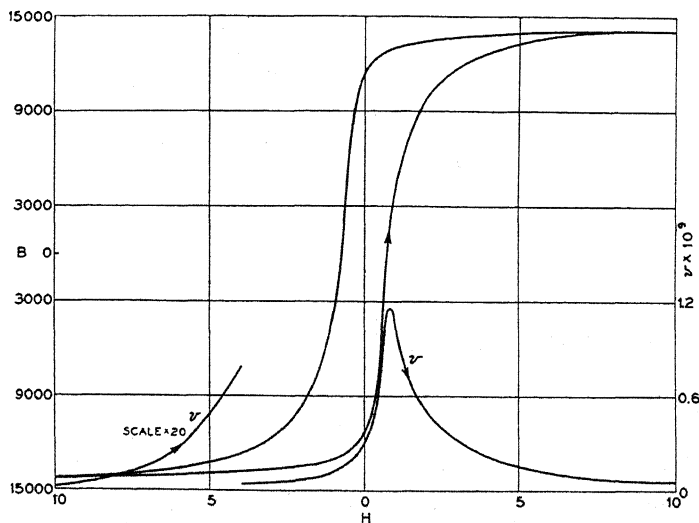


Fig. 19. Hysteresis loop and v -curve for annealed iron.

different materials. The data for annealed iron are more extensive than for the other materials and have been taken over the whole hysteresis loop,

between -10 and $+10$ gauss. When the slope of the hysteresis curve is relatively small, there is some question as to whether the discontinuous changes in magnetization are due to complete magnetic reversals of small

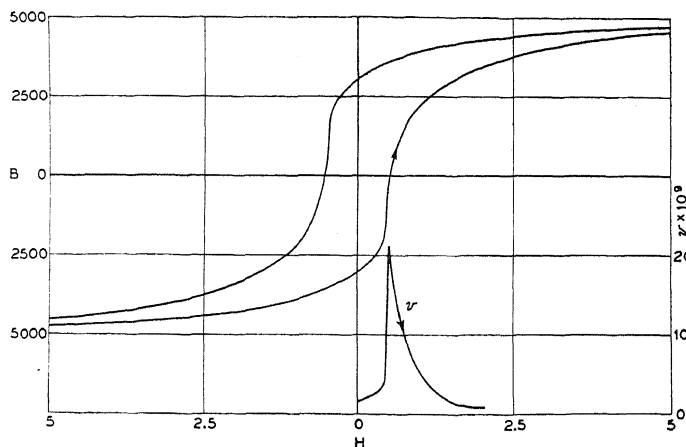


Fig. 20. Hysteresis loop and v -curve for nickel.

parts of the material or whether the reversals are only partially complete, as mentioned in the introduction. Although for this reason the determination of the mean volume of the discontinuities in this case may not be accurate,

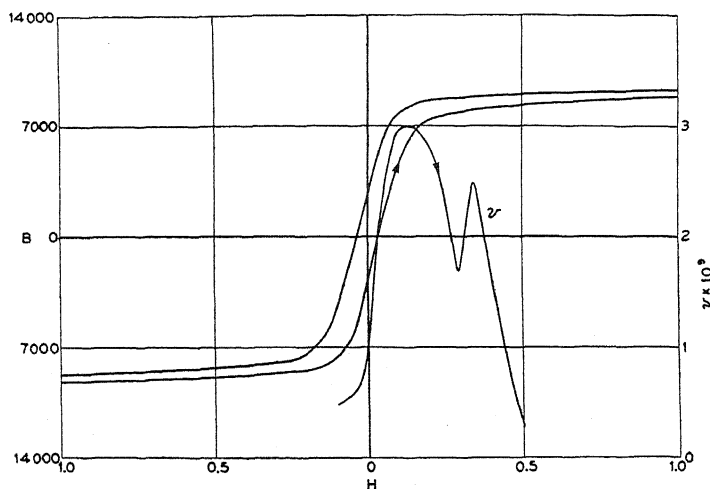


Fig. 21. Hysteresis loop and v -curve for permalloy containing 80.5 percent nickel and 19.5 percent iron.

the data do show, contrary to previous reports, that discontinuities are present throughout the whole cycle. Fig. 26 is a reproduction of the galvanometer record of the Barkhausen effect at the very beginning of the hysteresis

loop for iron, and has been included to show that with sufficiently high amplification the effect is measurable even though dB/dH is as small as 40. It seems possible that the magnetization changes discontinuously in all cases, even

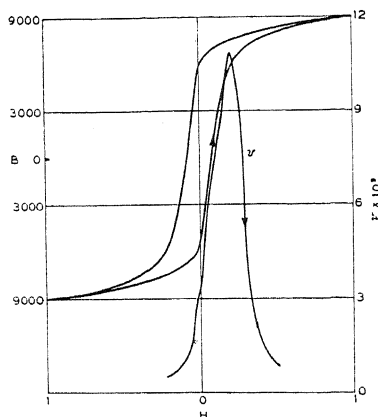


Fig. 22. Hysteresis loop and ν -curve for permalloy containing 78 percent nickel and 22 percent iron.

though the material is nearly saturated, and that the discontinuities have been detected only on the steeper parts of the curve because the amplification available has not been sufficient to detect them on the parts less steep.

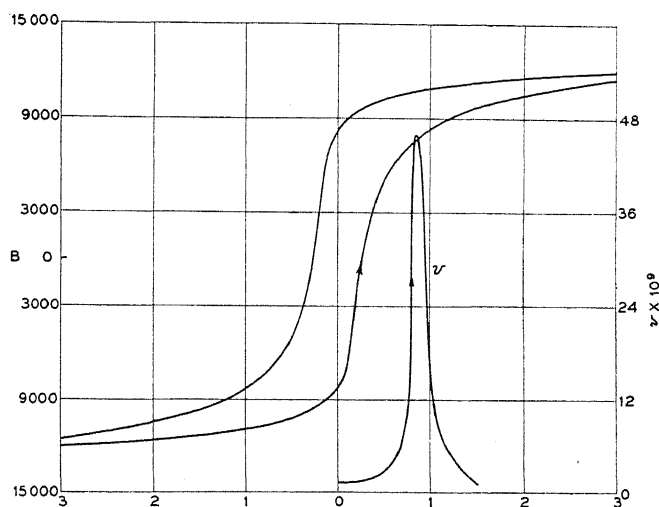


Fig. 23. Hysteresis loop and ν -curve for permalloy containing 50 percent nickel and 50 percent iron.

The average volume of material in which the magnetization changes as a unit is found to have a maximum value of the order of $(10)^{-8}$ or $(10)^{-9}$ cm^3 for the materials examined. The maximum values vary only from 1.2

$(10)^{-9}$ cm³ for iron to $45 (10)^{-9}$ cm³ for permalloy containing 50 percent Ni. These volumes are entirely different in order of magnitude from the volume occupied by the crystals in the "single" crystal specimen, which is much

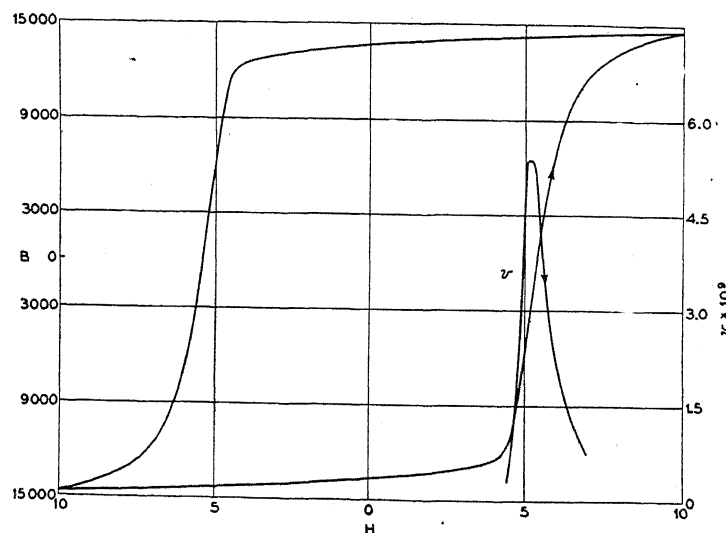


Fig. 24. Hysteresis loop and v -curve for hard drawn iron.

greater; from that occupied by the separate crystals in the hard-worked sample of iron, which is vastly smaller; and also from the volume occupied by a single atom or even by a group of atoms known to be large enough to

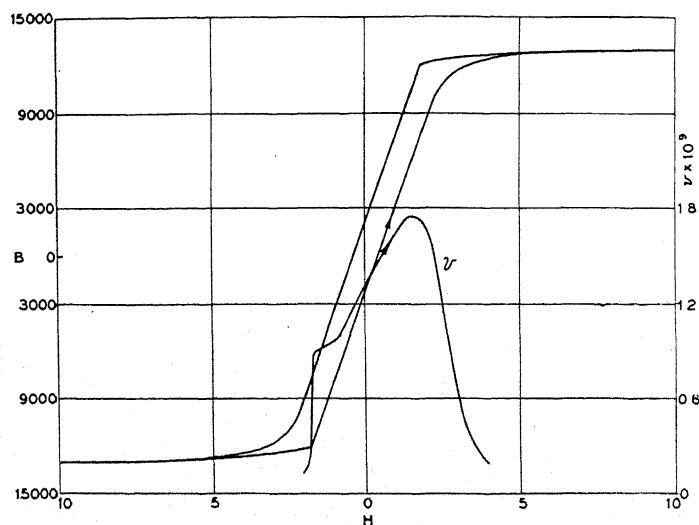


Fig. 25. Hysteresis loop and v -curve for two single crystals of iron.

be oriented by an applied magnetic field, which is very much smaller yet. We regard as a mere coincidence the fact that it is of the same order as the volume occupied by the separate crystals in many well annealed materials.

We conclude that the sizes of the Barkhausen discontinuities are independent of crystal size, and of the nature of the grouping of the atoms of ferromagnetic materials both in respect to the type of lattice upon which the crystal is built, and to the distribution of the different kinds of atoms in alloys.

It is rather surprising at first glance that the computed volumes of the groups should have so nearly the same average value for substances so different. One might expect that, if the magnetization of a group is initiated by the reversal of a single atomic magnet the energy so liberated will aid other magnets to reverse to an extent depending both upon the amount of energy liberated (proportional to the coercive force) and upon the number of other magnets which are about to reverse (proportional to dB/dH). If the coercive force is small and the sides of the hysteresis loop are steep, the initial energy liberated will be small, but there will be a comparatively

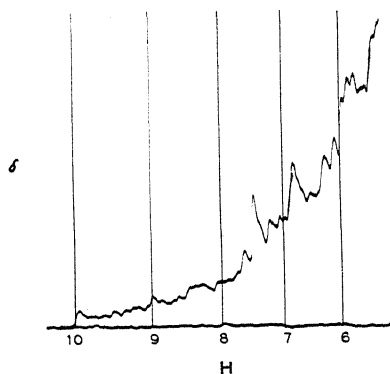


Fig. 26. Barkhausen effect at the beginning of the hysteresis loop for iron, using high amplification

large number of magnets that need but a small disturbance to turn them. If the coercive force is large, the sides of the hysteresis loop are generally less steep. We imagine that these two factors compensate each other, resulting in a relatively constant size of discontinuities in different materials.

The position of the maxima of the v -vs.- H curves for hard and annealed iron and for nickel are near the coercive force, but for the three alloys are definitely displaced to higher values of H . It may be that the positions of these maxima correspond in each case to those for the thermal cooling attending magnetization, observed by Ellwood⁷ for steel at magnetizations near the knee of the hysteresis loop.

Our experiments show that the number and size of the discontinuities do not depend on the rate of change of field-strength. As Fig. 10 shows, δ is accurately proportional to dH/dt and this relation implies that the number and size remain constant. For the same total discontinuous change in B , an increase in the average size of the discontinuities and a consequent decrease in their number would be attended by an increase in the ratio of

⁷ W. B. Ellwood, *Nature* **123**, 797-798 (1929).

δ to dH/dt , in contradiction to our findings. Although this linear relation has been found to hold for all of the specimens we have examined, it may not of course hold for the fine wires examined by Heaps and Taylor⁸, where the linear extent of the discontinuity is comparable with the diameter of the wire.

Pfaffenberger⁹ has reported that the length of the coherence region, within which the discontinuous change is confined, is 3 mm in a steel wire 0.5 mm in diameter. The implication is that during a single discontinuous change in magnetization elementary magnets scattered throughout a volume of about 1 mm^3 are permanently reversed, but that these elementary magnets, if placed next to each other, would occupy a small part, perhaps 10^{-3} , of this volume, corresponding to our volume v . In view of the experiments on the determination of l , described above, we conclude that this 3 mm length is the extent of the region in which the eddy-currents are produced in this sample of steel by the sudden change in magnetization. If Eq. (15) holds for wires 0.5 mm in diameter, we find for Pfaffenberger's sample, using $l/2=0.3$, that $\mu=2.3$. Since Eq. (15) has been established only for wires of radius 0.5 mm, it may be that the more general equation will include some function of the radius. If, for example, the equation is

$$l = 1.03(10)^{-3}(\mu/\rho)^{1/2}r^2/(0.05)^2 \quad (15')$$

we deduce from Pfaffenberger's data that $\mu=10$, a not unreasonable figure for some kinds of steel.

The experiments described above confirm the earlier experiments¹ in showing that for the steeper parts of the hysteresis loop the volume associated with the average discontinuity is very large compared with the dimensions of the atom and seldom involves less than 10^{10} atoms. In annealed materials the average size is comparable with the size of the crystals, but this is regarded merely as a coincidence because the same sized discontinuities are found in hard-worked materials and in a single crystal. The average size is greatest at or near the steepest part of the hysteresis loop and diminishes rapidly as the ends of the loop are approached. The maximum value of the average size (the average size at or near the steepest part of the loop) is about $(10)^{-8} \text{ cm}^3$, corresponding to $(10)^{15}$ atoms, and is much the same in the different materials examined.¹⁰

⁸ C. W. Heaps and J. Taylor, *Phys. Rev.* **34**, 937-944 (1929).

⁹ J. Pfaffenberger, *Ann. d. Physik* **87**, 737-768 (1928).

¹⁰ An interesting paper by F. Preisach, *Ann. d. Physik* **3**, 737-799 (Dec. 1929) has just come to our attention. His experiments support the previous report by one of us¹ that on the steeper parts of the hysteresis loop almost all of the change in magnetization is discontinuous. Our results disagree in one important respect: Preisach states that when the magnetization diminishes from its greatest value (near to saturation) at one end of the loop, no Barkhausen effect is detectable (with a three stage voice-frequency amplifier) and the change is continuous; we have shown that with sufficiently high amplification (seven stages, wide frequency range) the effect is pronounced, as shown in Fig. 26 above. Preisach has shown that the sizes of the discontinuities in fine wires can be markedly changed by straining them, and that in some cases a single discontinuity corresponds to almost the whole possible change in magnetization of the material. We have also observed such discontinuities in fine unstrained wires of permalloy containing 78 percent nickel and 22 percent iron.

MEASUREMENT OF THE INTENSITY OF HIGH
FREQUENCY MAGNETIC FIELDS

BY ROY H. MORTIMORE

DEPARTMENT OF PHYSICS, UNIVERSITY OF IOWA

(Received January 20, 1930)

ABSTRACT

Two methods are developed for the measurement of the intensity of magnetic fields produced by currents of frequencies from 10 to 25 megacycles.

By the first method, the current in a coil is computed from vacuum tube voltmeter readings of potential drop across a standard inductance. The values for current thus obtained are compared with readings of thermo-ammeters in the range for which they are calibrated. For larger currents, the instruments are shunted and calibrated for particular wave-lengths by the standard inductance method. From these known values of current the intensities of the fields which they produce are computed.

By the second method, the e.m.f. induced in a single turn coil placed in the field to be measured is indicated by a vacuum tube voltmeter. The field intensity necessary to induce the observed e.m.f. is computed. Good agreement is found between the results obtained by the two methods.

Improvements are made in vacuum tube voltmeter design which make possible their use in voltage measurements at frequencies as high as 25 megacycles.

Information regarding current distribution in a coil is obtained.

INTRODUCTION

CERTAIN aspects of measuring the intensity of magnetic fields at radio frequency are discussed by a number of investigators. The present work is different from these in that it involves measurements of field intensities in the immediate vicinity of the coil carrying the current and that it includes frequencies as high as 25 megacycles.

Since the audibility of signals in a radio receiving system is a function of the electric and magnetic fields in the vicinity of the receiving antenna, a number of methods of measuring their intensities have been developed. By the use of the siphon recorder, De Groot¹ compared the intensity of static impulses with the intensity of telegraph signals. During the years 1920 and 1921 the Bureau of Standards in an extended series of investigations relative to signal fading used the judgments of 253 observers as to the audibility of the signals in a receiving set as a measure of the intensity of the radiated fields.²

Englund and Friis³ reduced the errors in judging audibility by comparing the intensity of sounds in a receiving set due to the radiated signal with that due to a locally induced e.m.f. of known intensity. Recently, Parlin⁴

¹ De Groot, *Inst. R.E.* 5, 93 (1917).

² *Sci. Pap. B. of S.*, No. 474 (1923).

³ Englund and Friis, *Trans. Am. Inst. E.E.* 46, 492 (1927).

⁴ Parlin, *Phys. Rev.* 33, 432 (1929).

has published the results of measurements of the relative intensity and state of polarization of radiated fields at distances of 40 to 100 meters from the oscillator. One important difference between this work and that of earlier investigators is that the intensity is measured by direct galvanometer deflection instead of indirect judgments.

In all the above investigations, the measurements involve the radiated fields some distance from the oscillator rather than in the immediate vicinity of a coil carrying the current.

In dealing with the variation with frequency of the magnetic permeability of certain iron specimens, Wait⁵ had occasion to measure the intensity of magnetic fields at the center of a solenoid in the range of wave-lengths from 80 to 1700 meters (more recently⁶ in the range from 70 to 120 meters). In this work he used the standard formula $H = 4\pi nb / (b^2 + a^2)^{1/2}$ for the field intensity at the center of a solenoid of radius a and length $2b$. In the development of this formula it is assumed that the current is uniformly distributed in a cylinder whose length and radius correspond to those of the solenoid and whose thickness is vanishingly small. For the present work this formula does not hold since the dimensions of the coils used depart too far from those assumed.

I. THEORY

Computation of field intensity from current. The computation of the intensity of the field about a coil due to a high frequency a.c. in the coil as is done in the case of direct current, is complicated by two factors. First, no instruments are available which will accurately measure high frequency currents of any considerable magnitude; second, the distributed capacity of the coil causes a non-uniformity in the current distribution throughout the coil.

In meeting these difficulties, the measurement of current is accomplished in two ways; first, Weston thermoammeters and thermo-milliammeters with shunts to cover the desired range of current are calibrated at particular frequencies; second, vacuum tube voltmeter readings of the potential drop across standard inductances are taken and from these currents are computed. To eliminate the second complication, a Helmholtz coil of one turn in each section is constructed in which the distributed capacity is sufficiently small that the use of the standard formula⁷ for direct current is permissible.

$$H = 32\pi ni / 5^{3/2} a$$

where n is the number of turns in each section; a is the radius and i is the current in c.g.s. e.m.u.

Computation of field intensity necessary to induce observed e.m.f. in search coil. Since the e.m.f. in a single turn of wire is equal to the rate of change of magnetic flux through the area enclosed by the wire and since the flux is known to vary sinusoidally, the field intensity can be computed if the

⁵ Wait, Phys. Rev. 29, 566 (1927).

⁶ Wait, Phys. Rev. 32, 967 (1928).

⁷ S. G. Starling, Elec. & Mag. p. 57.

induced e.m.f. is known. It is obvious then, that vacuum tube voltmeter readings for e.m.f. induced in a single turn coil substituted in the formula developed below yield values for field intensity. The assumption is made that the intensity is uniform throughout the area enclosed by the coil. Such uniformity is available within a Helmholtz coil.

$$e = d\phi/dt$$

where e is the induced e.m.f. and ϕ the flux through enclosed area. Since a sinusoidal field is assumed ϕ may be written $\phi_0 \sin \omega t$ and

$$e_{\max} = \phi_0 \omega = 2\pi\nu\phi_0$$

But $\phi_0 = H_0 A$

Then $e_{\max} = 2\pi H_{\max} \nu A$ (Or r.m.s. value may be used for e and H)

$H = e/2\pi A \nu$ if e.m.u. are used

$H = E \times 10^8 / 2\pi A \nu$ using volts, gauss and cm^2

Thus we have a formula for H in terms of measurable quantities.

II. APPARATUS

Oscillator. The oscillator which proved most satisfactory includes two triodes in push-pull arrangement. The circuit diagram is shown in Fig. 1. The symmetrical feed-in to the main oscillatory circuit $C_1 L_1$ through C_2 and C_3 produced a comparatively pure sine wave current in L_1 .

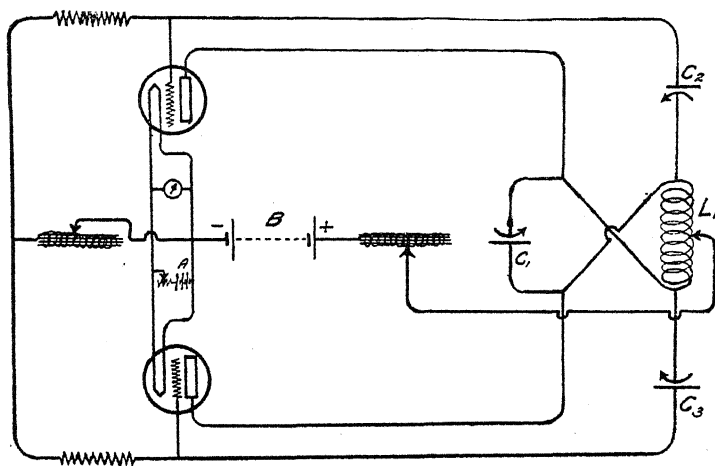


Fig. 1. Oscillator circuit diagram.

The intensity of the output at the first and second harmonics was tested by comparing the readings of the galvanometer of a wave meter tuned to the fundamental with those tuned to the harmonics. The oscillator output was adjusted for full scale deflection of the galvanometer of the wave meter when it was placed several feet from the oscillator. In no case was a deflection of more than a small part of one division (1/100 part of the full scale) noted when the wave meter was tuned to the harmonic frequency and placed one fifth of the above distance from the oscillator.

This circuit is used for three hook-ups. The first, employing seven and one half watt tubes is supplied with seven coils of different numbers of

turns so that a range in wave-length from 5 to 130 meters may be produced. The second, employing fifty watt tubes, covers the range from 5 to 30 meters. The third, employing two hundred fifty watt tubes covers a limited range of 12 to 20 meters.

Pick-up system. The pick-up system in which the current is brought under control is inductively coupled to the oscillator as shown in Fig. 2. L_4 is a one turn coil closely coupled to the output inductance of the oscillator. C_2 and L_5 tune the circuit in which the current is controlled. C_3 and C_1 control the position of the voltage node in circuit C_2L_5 . A_1 and A_3 are thermo-ammeter positions. The position A_2 is used variously to meet different demands. In one Helmholtz coil it serves as a thermo-ammeter position. In another Helmholtz coil and in a 5 turn helix it is supplied with gaps for the plug-in standard inductances.

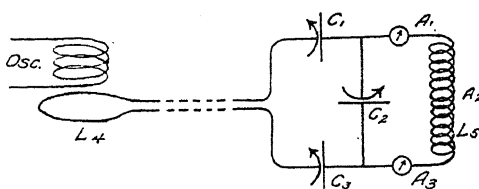


Fig. 2. Pick-up system.

Wave meter. A wave meter including a variable air condenser, an inductance and a Weston thermo-galvanometer to indicate resonance is calibrated by the Lecher wires direct measurement method.⁸ It is provided with different size coils to cover the range in wave-length from 5.7 to 32 meters. It is carefully calibrated throughout this range.

Vacuum tube voltmeter. From the large number of vacuum tube voltmeter circuits which are described in the literature⁹ the three which gave greatest promise of applicability to measurements at high frequencies were selected for investigation. The first circuit tried out is the vacuum tube multiplier described by M. Y. Colby.¹⁰ The attractive features of this circuit are its flexibility, sensitivity and small power absorption. Several calibration curves run at a frequency of 60 cycles gave satisfactory results in the neighborhood of 100 meters. For wave-lengths much shorter than 100 meters difficulties were encountered and below 20 meters the circuit was found unsatisfactory.

The circuit described by James Taylor¹¹ gave promise of satisfactory performance. Many calibration curves run at a frequency of 60 cycles were applied in the range of wave-lengths from 30 to 100 meters. Below 30 meters, however the circuit was not satisfactory since the galvanometer and filament leads are directly connected to the high frequency source.

⁸ A. Hund, Bureau of Standards, Scientific Paper No. 491.

⁹ E. B. Moullin, Radio Frequency Measurements, p. 35. C. R. Cozens, Jour. Sci. Inst. 3, 181. Van Der Bijl, Thermionic Vacuum Tubes, p. 367. Moullin and Turner, Jour. I.E.E. p. 708, Dec. 1922.

¹⁰ M. Y. Colby, Jour. Sci. Inst. 3, 342 (1929).

¹¹ James Taylor, Jour. Sci. Inst. 3, 113 (1929).

The circuit, Fig. 3, which was selected as the most satisfactory for the present work is not found in the literature but has been in use in this laboratory for some time. The deflection of the Leeds and Northrup Galvanometer, G , caused by the d.c. leak off the grid and plate of the vacuum tube is proportional to the charge accumulated thereon. The capacity of C_1 and the resistance of R_1 are not critical but must be sufficiently large as to provide a time constant for the circuit large in comparison with the period of the lowest frequency used. For frequencies greater than 10 megacycles it was found necessary to insert a resistance R_2 to keep the high frequency currents out of the filament battery leads. Since R_2 holds the potential of the galvanometer and filament at the average value of that applied at T_1 (i.e., zero since the applied potential is sinusoidal), the charge on the plate and grid is proportional to the peak value of the potential variation of T_2 rather than the peak value of the potential difference between T_1 and T_2 . This requires that T_1 be attached at or near the voltage node of the circuit containing the

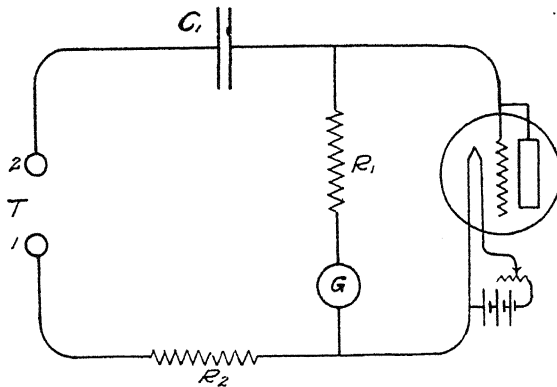


Fig. 3. Vacuum tube voltmeter circuit.

piece of apparatus across which the potential drop is being measured. Fig. 4 shows a typical calibration curve.

From the circuit diagram, Fig. 3, and from the photograph of the instrument, Fig. 5, it is readily seen that an instrument of this type may be designed whose fundamental wave-length is low and which is therefore readily adaptable to high frequency measurements. The total length of wire from T_2 to the grid is 15 cm and the capacity of the vacuum tube is reduced to a minimum by the removal of the base and separation of the leads. To test for the fundamental wave-length of the circuit a thermo-galvanometer was connected across the terminals T , R_2 was shunted by a good conductor and the instrument closely coupled to an oscillator whose output wave-length was varied from 12 to 5.7 meters. No deflection was observed. Similar tests on other instruments whose leads were longer and not so well arranged showed distinct resonance points corresponding to 9 and 16 meters. Thus, it was shown that the natural wave-length of this instrument is somewhat below 5.7 meters.

Helmholtz coils. Two Helmholtz coils were constructed to produce the uniform fields necessary for the search coil method of measurement. The

two differ only in that one is provided with a gap between the turns so that an ammeter may be inserted. The radius of each turn and the distance between the two turns is 8 cm. Substituting these dimensions in the formula (1) for field intensity at the center we get 0.1125 gauss per ampere.

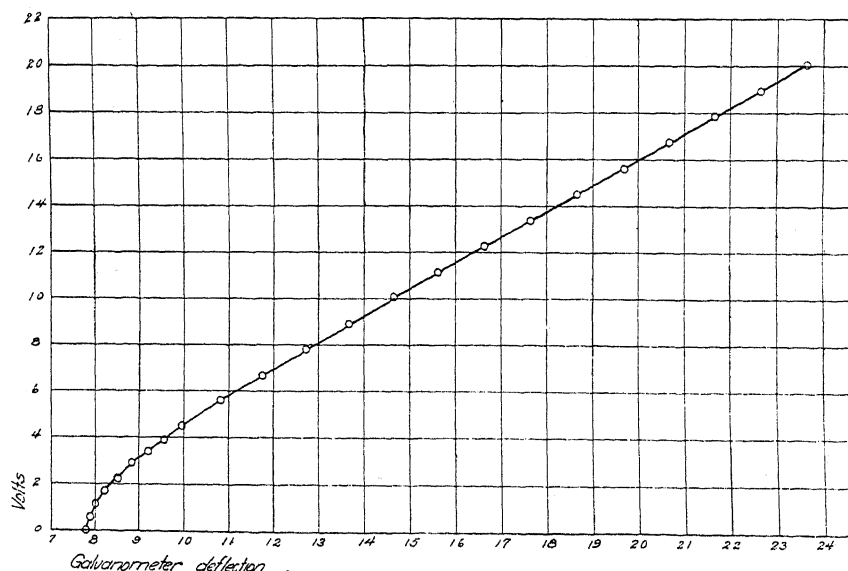


Fig. 4. Vacuum tube voltmeter calibration curve.

Standard inductances. The standard inductances are made from two brass cylinders of different diameters a and b arranged coaxially. One end of each is soldered to the adjacent end of the other by means of a brass disk. To the opposite ends of the two cylinders are attached terminals for plugging

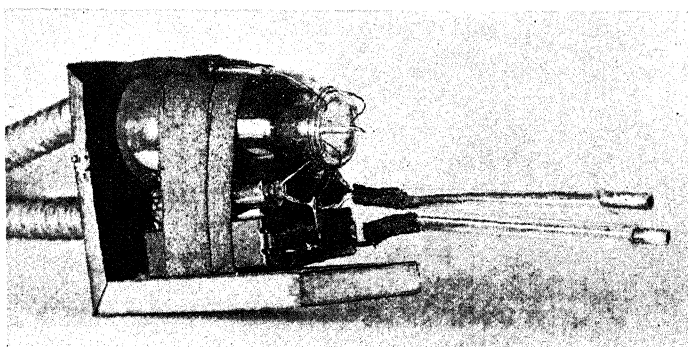


Fig. 5. Vacuum tube voltmeter.

the inductances into the circuit. The numerical value for the inductance was computed from the theory developed in standard texts.¹²

$L = 2 \log_e b/a$ absolute units of inductance per centimeter. Three inductances L_1 , L_2 , and L_3 were constructed; L_1 is 5 cm long, L_2 is 10 cm, L_3 is 15

¹² Starling, Elec. and Mag. p. 308.

cm. In all three b is 1'' and a is 11/32''. The combination L_3 and L_1 providing a length of 10 cm was most often used.

$$L = 10 \times 4.60568 \times 10^3 \log_{10} 1/(11/32) = 0.02137 \text{ henries.}$$

III. PROCEDURE

Measurement of current by potential drop across a standard inductance.

The operation of measuring current by the standard inductance method is carried out as follows: Two standard inductances L_1 and L_3 (previously described) are plugged into the center turn of a five turn helix. A vacuum tube voltmeter is connected across L_1 . The reading, R_1 , of the galvanometer of the vacuum tube voltmeter is taken. L_1 and L_3 are interchanged and the vacuum tube voltmeter reading, R_3 , is taken across L_3 . $R_3 - R_1$ gives the $I\omega L$ drop across a standard inductance whose length is equal to the difference in length of L_3 and L_1 . This subtraction eliminates the end effects, potential variation at T_1 due to improper location of voltage node, pick up by the lead-ins and stray pick up by the vacuum tube voltmeter. From the equation $V = I\omega L$ the corresponding value for current is computed.

Since the standard inductance is essentially a resistance and an inductance in parallel with a capacitance, the potential drop across it is given by the formula:

$$V = I / \{ (r^2 / \omega^4 L^4) + [(1/\omega L) - \omega C]^2 \}^{1/2}$$

For $\lambda = 10$ meters $1/\omega L = 0.247$ and

$\omega C = 0.000981$ which is 0.4% of $1/\omega L$

For $\lambda = 20$ meters $1/\omega L = 0.494$ and

$\omega C = 0.000491$ which is 0.1% of $1/\omega L$

From the equation $r^2 + 4.05^2 = 4.05^2 (1.01)^2$ we get the value 0.57 ohms which resistance added to WL would increase the impedance by 1 percent. This value is very much greater than the resistance of the standard inductance. We may then drop r and ωC from formula (1) which becomes $V = I\omega L$ as it is used in the preceding paragraph.

Ammeter calibration. Since the use of direct reading instruments is more convenient than the use of the vacuum tube voltmeter with standard inductances, the problem of calibrating thermoammeters was considered. This investigation demanded a solution of the problem of current distribution in the coil since it is not safe to conclude that the current passing through one instrument is the same as that passing through another in a different part of the circuit.

The current distribution throughout the Helmholtz coil was first considered. Three Weston milliammeters, all alike, were placed at the positions A_1 , A_2 and A_3 in the pick-up circuit, (see Fig. 2). The oscillator was tuned to different frequencies and the circuit $C_2 L_5$ tuned to resonance with it. Readings were taken at six different wave-lengths from 10 to 30 meters. In all cases when C_1 was larger than C_3 , A_1 read smaller than A_3 and the voltage node in the circuit $C_2 L_5$ was nearer C_3 than C_1 . Greater differences between C_1 and C_3 always resulted in greater difference between A_1 and A_3 and greater shifting of the voltage node. When C_1 was made smaller than

C_3 the reverse changes were observed. These effects both increased with frequency.

When the five turn helix was substituted for the Helmholtz coil the results were similar but slightly more pronounced. A typical set of data is shown here: C_1 , C_2 and C_3 are condenser dial readings in degrees and are essentially proportional to capacities. A_1 , A_2 and A_3 are milliamperere readings.

TABLE I

C_1	C_2	C_3	A_1	A_2	A_3	Voltage node
41	37	10	84	100.1	115.0	Near A_3
21.4	37	20	103	110.2	115.0	
16.8	37	30	112.6	115.0	115.0	
15.5	37	35	113.1	115.0	113.1	At A_2
14.6	37	40	114.3	115.0	113.1	
13.4	37	50	115.0	114.3	110.2	
12.5	37	60	115.0	113.1	107.0	Near A_1
12.0	37	70	115.0	112.6	106.0	
11.6	37	80	115.0	112.0	105.0	

The above investigation brought out clearly the fact that for instrument calibration the unequal current distribution must be allowed for, the position of the voltage node is a very important factor in current distribution and that the voltage node may be shifted as desired by adjusting C_1 and C_3 .

The next step in current measurement was the comparison of current readings by a Weston 115 milliamperere thermo-galvanometer with currents computed from vacuum tube voltmeter readings for potential drop across standard inductances.

Thermo-galvanometers were placed at A_1 and A_3 , the standard inductances L_1 and L_3 were placed at A_2 with the vacuum tube voltmeter across L_1 . When the oscillator had been tuned to the desired wave-length and the pick-up circuit, with the 5 turn helix for L_5 , had been tuned to resonance with it, C_1 and C_2 were adjusted so that the voltage node in L_5 was at the filament lead of the vacuum tube voltmeter. This adjustment also made A_1 read the same as A_3 . By varying the output of the oscillator, A_1 ($=A_3$) was made to read 115 milliamperes. The reading across L_1 was then taken. L_1 and L_3 were interchanged and the voltage across L_3 was read. Let V_i be the difference between these two readings. Let V_i be the values for voltage across L_3-L_2 computed from the formula $V=I\omega L$ assuming $I=0.115$ amps. From the above operations the following data were obtained:

TABLE II.

λ	V_i	V_i	Diff.
30	0.152	0.155	1.9%
28	0.164	0.166	1.2%
26	0.178	0.179	0.5%
24	0.196	0.194	1.0%
22	0.216	0.212	1.9%
20	0.245	0.233	5.1%
18	0.258	0.258	0.0%
16	0.298	0.291	2.3%
14	0.338	0.333	1.5%

The essential agreement of the above and similar data was interpreted to mean that the thermo-galvanometers are reliable for wave-lengths of fourteen meters and larger.

The precision of Weston thermo-ammeters designed for measurement of larger currents when used for high frequencies may be decreased by either of two factors. First, the capacity between the leads and the instrument case may by-pass a certain amount of current and consequently make the instrument read low. Second, the resistance of the heating element does, no doubt, increase with frequency. Since the deflection is proportional to the power (I^2R) consumed in the heating element any increase in R would make the deflection too large for a given current.

The first effect was easily isolated by comparing readings of a given current with the case on with those after the case had been removed. No effect was observed in the range from 10 to 30 meters except for two instruments designed for mounting with their bases flush with the panel. In these instruments the readings were approximately two percent lower at ten meters with cases on than off. These by-passed currents also expressed themselves in form of heat in the cases when the instruments were shunted and large currents passed through them.

The second effect should be more pronounced in instruments designed for larger currents since their heating elements are made of larger wire. In order to test this factor the 115 milliamper meter was compared with the 250; the 250 with the 500 and the 500 with the one ampere. Then instruments were shunted and calibrated at wave-lengths 12, 20 and 26 meters by comparison with the one ampere instruments. In turn these instruments were compared with a 4 ampere Weston thermo-ammeter. It was found to read slightly high at twenty meters seeming to indicate that the second effect was expressing itself.

The final step in instrument calibration was the comparison of the calibrated instruments against standard inductance values. Table III shows the results.

TABLE III.

λ	I_a	I_L	Diff.
26	1 amp.	0.976	0.024
26	2	2.001	0.001
26	3.5	3.58	0.08

Measurement of field intensity by electromotive force induced in search coil. For this set of measurements the pick-up circuit (Fig. 2) was used with the Helmholtz coil at L_s and calibrated ammeters at A_1 and A_3 . A single turn coil 2.5 centimeters in radius made of fine wire was provided with terminals for plugging it into the vacuum tube voltmeter leads. A short piece of wire just long enough to shunt the leads of the voltmeter thus completing the circle was also provided with plug-in terminals. Reading R_1 was taken with the search coil placed coaxially with the Helmholtz coil and at its center. R_2 was taken with the shunt across the voltmeter leads. The differ-

ence $R_1 - R_2$ gave the e.m.f. induced in a coil of one turn and radius 2.5 centimeters. This value substituted in the formula $H = (E \times 10^8) / \omega A$ gave the values of the field intensity in gauss. Values obtained in this way are listed under H_e in Table IV. Simultaneously with the reading of R_1 and R_2 the current in the Helmholtz coil was read from the calibrated ammeters A_1 and A_2 . This reading substituted in the formula $H = 32\pi ni / 5^{3/2} a$ also gave values for field intensity at the center of the Helmholtz coil. Values obtained from this substitution are listed under H_a in Table IV.

TABLE IV.

λ	I (amps.)	H_a (gauss)	H_e	Diff.
100	1.0	0.1125	0.1145	1.8%
90	1.0	.1125	.1116	0.8%
80	.96	.1078	.1074	0.4%
70	.93	.1048	.1046	0.2%
60	.88	.0990	.1033	4.1%
50	.79	.0894	.0885	1.0%
40	.66	.0746	.0732	1.8%
30	.115	.0089	.0092	3.3%
20	2.00	.225	.220	2.1%
20	3.00	.337	.330	2.0%
16	2.00	.225	.225	0.0%
16	3.00	.337	.346	2.6%
12	2.00	.225	.217	3.5%

The measurements in the range from 30 to 120 meters were made before the method of controlling the position of the voltage node and the current distribution had been developed. The same refinement and precautions used in the range below 30 meters applied to this range would have given better agreement.

The essential agreement in the values for field intensity obtained by the two methods provides good evidence of the accuracy of both.

IV. CONCLUSIONS

1. The vacuum tube voltmeter herein described was applied successfully to the measurement of alternating potentials of frequency as high as 25 megacycles.
2. The standard inductance method provides a satisfactory means of measuring alternating currents of frequencies as high as 22 megacycles.
3. Definite information regarding the distribution of current in a coil was obtained.
4. A comparison of thermo-ammeter readings for high-frequency currents with values obtained by the standard inductance method and with readings of similar instruments made possible their calibration for any desired wave-length above 10 meters.
5. The intensity of a magnetic field within a Helmholtz coil may be computed from known currents in the coil.
6. The intensity of a magnetic field may be computed from the vacuum tube voltmeter measure of e.m.f. induced in a single turn search coil placed in the field.

ON THE FUNDAMENTAL CONSTITUTIVE EQUATIONS IN ELECTROMAGNETIC THEORY

BY C. KAPLAN AND F. D. MURNAGHAN
THE JOHNS HOPKINS UNIVERSITY, BALTIMORE

(Received February 14, 1930)

ABSTRACT

The purpose of this paper is to investigate the absolute significance of the well-known constitutive relations in electromagnetic theory, and to see what simplifications are introduced by various assumptions as to the isotropic character of the space-time continuum. The "linear vector function" expressing the linear relationship between the two fundamental electromagnetic tensors $a_{rs} (\equiv \mathbf{B}, c\mathbf{E})$ and $b_{rs} (\equiv -\mathbf{D}, c\mathbf{H})$ is a tensor c_{rs}^{pq} of rank 4 which is covariant and contravariant of rank 2 respectively and is named the "structure-tensor." In order to express mathematically what is meant by the isotropic character of a medium, the notion of orthogonal ennuples is introduced (an orthogonal ennuple defined at a point in space-time enables us to turn the medium in the neighborhood of that point). A tensor is then determined by its invariants with respect to an orthogonal ennuple at the point at which the tensor is taken, rather than by its covariant or contravariant components with respect to the coordinate system of the manifold. The effect of various assumptions as to the isotropic character of space-time on the invariants of the "structure-tensor" c_{rs}^{pq} is investigated and it is found that if space is completely isotropic in the neighborhood of a point P in space-time, then the simple constitutive relations $\mathbf{B} = \mu\mathbf{H}$ and $\mathbf{D} = \epsilon\mathbf{E}$ (with μ and ϵ independent of one another) hold; and that to an observer in space-time this fact is indicated by a time-direction 4-vector issuing from P . Since μ and ϵ are distinct only in places where matter is present we can say that the distribution of matter in space-time is affected by the distribution of these time-direction vectors in space-time. The corresponding constitutive relations $\mathbf{B} = \mu\mathbf{H}$ and $\mathbf{D} = \epsilon\mathbf{E}$ for empty space (where $\mu\epsilon = 1$; Maxwell's relations) are found to hold in the neighborhood of points where these time-direction vectors are absent; i.e. such points are simply geometrical points. The analysis, as introduced in this paper, is a general one and is applied to elasticity theory. Thus the number of distinct coefficients of elasticity appearing in Hooke's law for a transversely-isotropic medium is found to be six instead of five, the reason for this disagreement being that the assumption as to the existence of an energy-density of deformation reduces the number from six to five.

AS IS well known¹ Maxwell's fundamental equations of electromagnetic theory can be very conveniently written in terms of two alternating covariant tensors of rank two (or six-vectors) in space of four dimensions. The first of these, a_{rs} consists of the magnetic induction vector \mathbf{B} and the electric intensity vector \mathbf{E} in such a way that

$$a_{23} = B_x; a_{31} = B_y; a_{12} = B_z; a_{14} = cE_x; a_{24} = cE_y; a_{34} = cE_z \quad (1.0)$$

(c denoting the velocity of light in vacuo) and one set of Maxwell's equations merely expresses the fact that the flux or surface integral of the six-vector

¹A. Sommerfeld, Ann. d. Physik **32**, 749 (1910); **33** 649 (1910.) H. Bateman, Proc. London Math. Soc. **8**, 223 (1910); F. D. Murnaghan, Phys. Rev **17**, 74 (1921).

a_{rs} across any closed spread of two dimensions, imbedded in the given space-time of four dimensions (x, y, z, t) , is zero. The second fundamental six-vector b_{rs} , consists of the electric displacement (or induction) vector D and the magnetic intensity vector H in such a way that

$$b_{23} = -D_x; b_{31} = -D_y; b_{12} = -D_z; b_{14} = cH_x; b_{24} = cH_y; b_{34} = cH_z \quad (1.1)$$

and the second set of Maxwell's equations states that the flux of this six-vector across any closed spread of two dimensions in the given space-time continuum is equal to the volume integral over the space of three dimensions (bounded by the spread of two dimensions) of the current-charge density four-vector. Now, in addition to Maxwell's equations (and quite distinct from them) are certain relations, connecting the four fundamental vectors, B, E, D, H which are known as the constitutive equations. In space free from matter Maxwell made the hypothesis that these constitutive equations were

$$B = H; D = E \quad (1.2)$$

whilst in a material medium these equations were replaced by

$$B = \mu H; D = \epsilon E \quad (1.3)$$

where if the medium is isotropic μ and ϵ are two constants characteristic of the medium and known respectively, as its permeability and specific inductive capacity. If the medium is not isotropic μ and ϵ are linear vector functions so that the equation $B = \mu H$ for instance, is merely an abbreviation for three equations of the form

$$B_x = \mu_{11}H_x + \mu_{12}H_y + \mu_{13}H_z.$$

It is the purpose of the present paper to investigate the general linear relation connecting the two alternating covariant tensors a_{rs} and b_{rs} and to see what simplifications are introduced by various assumptions as to the isotropic character of the space-time continuum. The "linear vector function" expressing this relationship will be a tensor c_{rs}^{pq} of rank four which is covariant of rank two and contravariant of rank two and which may be assumed without any lack of generality, to be alternating in the contravariant and covariant labels separately. Thus we may write

$$b_{rs} = C_{rs}^{\alpha\beta} a_{\alpha\beta} \quad (1.4)$$

where the Greek labels α, β are summation labels and it is supposed that the summation runs over the six pairs 23, 31, 12, 14, 24, 34 formed from the four numbers 1, 2, 3, 4, ($x = x^1, y = x^2, z = x^3, t = x^4$). The most general situation would involve, then, $6 \times 6 = 36$ coefficients c_{rs}^{pq} . The tensor c_{rs}^{pq} which is the analogue of the linear vector function of elementary vector analysis will be called the structure-tensor.

In the section of our paper devoted to the investigation of the effect upon the structure-tensor of various assumptions as to the isotropic charac-

ter of space or space-time, we shall disregard the fact that in the application of our analysis with which we are primarily concerned, i.e., the electromagnetic theory, the tensors a_{rs} and b_{rs} are alternating. The reason for so doing is that a similar analysis is useful in other departments of theoretical physics, e.g. elasticity theory, where the tensors involved are not alternating. In elasticity theory they are symmetric, but it will be convenient not to make any special assumption as to the nature of these tensors until later. The structure-tensor c_{rs}^{pq} will accordingly involve $256 (=16 \times 16)!$ components and the Greek labels in the fundamental relation

$$b_{rs} = c_{rs}^{\alpha\beta} a_{\alpha\beta}$$

are supposed to run, independently, over the values 1, 2, 3, 4.

MATHEMATICAL DESCRIPTION OF ISOTROPY²

In order to express most conveniently what is meant by the isotropic character of a medium we shall suppose an orthogonal ennuple³ (ennuple = n^{ple} ; $n=4$) attached to each point of space-time. Denoting the four vectors of this ennuple by ${}_1\lambda, {}_2\lambda, {}_3\lambda, {}_4\lambda$ any one, ${}_r\lambda$ say, of these will be a contravariant vector whose components are ${}_r\lambda^p$ ($p=1, 2, 3, 4$) and we shall denote the covariant representation of this vector by ${}_r\lambda_p$. Hence we have the relations defining orthogonality

$${}_r\lambda^{\alpha s} \lambda_{\alpha} = \epsilon_r^s \quad (1.5)$$

where the ϵ_r^s are a set of invariants or scalar quantities having the values of the components of the unit tensor δ_r^s ; i.e. $\epsilon_r^s = 0$ if $s \neq r$ and 1 if $s = r$. By means of the tensors ${}_r\lambda$ and ${}_r\lambda$ any tensor may be described in terms of its invariants relative to the ennuple.⁴ For a tensor $A_{s_1 \dots s_k}^{r_1 \dots r_j}$ these are

² T. Levi-Civita, "Absolute Calculus" Ch. 10 sec. 2.

³ By an orthogonal ennuple we mean a pyramid (a generalization of the notion of the trihedron) whose edges are mutually orthogonal. The purpose of fixing a set of four mutually orthogonal directions at every point of our space-time is to provide a mechanism for turning space. Turning the coordinate system simply changes the numbers, for example, which determine a point in space-time.

When we say that any one of the edges of an orthogonal ennuple, the r th say, is presented by a contravariant tensor of rank one ${}_r\lambda$ ($p=1, 2, 3, 4$), we may consider these four components to be the direction cosines of the r th direction with respect to the coordinate system (x) of the space-time continuum. Thus, for example, let us consider a space of three dimensions in which everything is referred to a set of rectangular Cartesian axes and suppose that at any point P a rectangular frame is formed by the tangents (directed in the sense of increasing variables) to the space-polar coordinate curves r = variable, θ = variable and ϕ = variable passing through P . Then the tangent line to the θ = variable curve, for example, is described in the Cartesian coordinate system of our space by three components:

$${}_0\lambda^1 = \cos \theta \cdot \cos \phi; \quad {}_0\lambda^2 = \cos \theta \cdot \sin \phi; \quad {}_0\lambda^3 = -\sin \theta.$$

⁴ For example suppose a space-polar trihedron to be fixed at a point P of space and a vector R determined at this point. Let us suppose that the vector R represents a generalized force. Then this force may be determined by its covariant components ($-\partial\psi/\partial r$, $-\partial\psi/\partial\theta$, $-\partial\psi/\partial\phi$) or by its projections on the directions belonging to the space-polar trihedron at P ,

$$i_{s_1 \dots s_k}^{r_1 \dots r_j} = A_{\sigma_1 \dots \sigma_k}^{\rho_1 \dots \rho_j} i_{\rho_1 \dots \rho_k} \lambda_{\sigma_1}^{r_1} \dots \lambda_{\sigma_k}^{r_j} \quad (1.6)$$

from which it immediately follows that

$$A_{n_1 \dots n_k}^{m_1 \dots m_j} = i_{\beta_1 \dots \beta_k}^{\alpha_1 \dots \alpha_j} \lambda_{\alpha_1}^{m_1} \dots \lambda_{\alpha_j}^{m_j} i_{\beta_1}^{n_1} \dots i_{\beta_k}^{n_k} \quad (1.7)$$

(In deriving which, one uses the elementary theorem of algebra that since the two sets ${}^r\lambda^s$ and ${}^p\lambda_q$ are reciprocal; i.e. ${}^r\lambda^{\alpha s} \lambda_{\alpha}^p = \delta_r^p$, it follows that ${}_{\alpha} \lambda^r \lambda_s^{\alpha} = \delta_s^r$). It follows without difficulty that the tensor relation

$$b_{rs} = c_{rs}^{\alpha\beta} a_{\alpha\beta}$$

is equivalent to a similar relation

$$j_{rs} = K_{rs}^{\alpha\beta} i_{\alpha\beta} \quad (1.8)$$

between the univariants of the tensors involved and it is in terms of the invariants K_{rs}^{pq} of the structure-tensor c_{rs}^{pq} that we shall find it convenient to express the conditions of isotropy.

Suppose now, that at any point of our space-time we have a second ennuple ${}_1\mu, {}_2\mu, {}_3\mu, {}_4\mu$ whose direction-vectors are connected with those of the first set by the relations

$${}^r\mu^p = s_q^{\alpha} \lambda^p \quad (1.9)$$

where the scalar coefficients s_q^p are the elements of an orthogonal matrix. We shall say that the ennuple μ is derived from the ennuple λ by a *rotation* if the determinant of the matrix of the s_q^p is 1 and by a *reflexion* if the determinant of this matrix is -1 . In fact the covariant presentations of the two ennuples are connected by the relation

$$i_{\mu k} = s'^{\alpha} i_{\lambda k} \quad (2.0)$$

where s' is the conjugate matrix to $s (s'^p_q = s^p_q)$ so that for the μ -ennuple to be also orthogonal it is necessary and sufficient that the product of the matrix s by its conjugate s' should be the unit matrix and this is the definition of an orthogonal matrix.

The relation between the invariants of any tensor relative to the λ and μ ennuples follows at once. Thus if we distinguish the invariants of a tensor relative to the μ ennuple from those relative to the λ ennuple by a superposed bar, we have, taking a covariant tensor a_{rs} of rank two as an illustration.

$$\bar{i}_{rs} = a_{\alpha\beta} {}^r\mu^{\alpha} {}^s\mu^{\beta} = a_{\alpha\beta} s_r^{\rho} s_s^{\sigma} \lambda^{\alpha} \lambda^{\beta} = i_{\rho\sigma} s_r^{\rho} s_s^{\sigma}. \quad (2.1)$$

We are primarily interested in the structure-tensor c_{rs}^{pq} and the relation between its invariants relative to the two ennuples is

$$\bar{K}_{rs}^{pq} = K_{\alpha\beta\gamma\delta}^{\epsilon\zeta\eta\theta} s_r^{\epsilon} s_s^{\zeta} s^{\eta} s^{\theta} \lambda^{\alpha} \lambda^{\beta} \lambda^{\gamma} \lambda^{\delta} \quad (2.2)$$

i.e. $(-\partial\psi/\partial r, -(1/r)(\partial\psi/\partial\theta), -(1/r \sin \theta)(\partial\psi/\partial\phi))$. These latter three quantities are invariants with regard to changes in the coordinate system but depend on the particular set of orthogonal directions at P .

The medium will be said to be isotropic (with regard to the structure-tensor c_{rs}^{pq}) relative to the given rotation or reflexion if the invariants \bar{K} of the structure-tensor relative to the new ennuple are the same as its invariants relative to the original ennuple i.e. if

$$\bar{K}_{rs}^{pq} = K_{rs}^{pq}.$$

If the invariants \bar{K} keep their numerical values but change their signs under reflexions the medium will be said to be relatively (as opposed to absolutely) isotropic with respect to the structure-tensor.

ISOTROPY WITH REGARD TO ROTATIONS IN THE COORDINATE PLANES

Now a rotation through a right angle in the 2-3 plane is described by the matrix

$$\begin{array}{c|cccc} & 1\lambda & 2\lambda & 3\lambda & 4\lambda \\ \hline 1\mu & 1 & 0 & 0 & 0 \\ 2\mu & 0 & 0 & 1 & 0 \\ 3\mu & 0 & -1 & 0 & 0 \\ 4\mu & 0 & 0 & 0 & 1 \end{array}$$

so that $s_2^3 = 1$, $s_1^1 = 1$, $s_3^2 = -1$, $s_4^4 = 1$ all the others being zero. Upon substituting these values in the 256 equations

$$K_{rs}^{pq} = K_{\alpha\beta\delta\epsilon}^{pq} s_\epsilon^{\delta\epsilon} s_\delta^{\alpha\beta} s_r^{\alpha\beta} s_s^{\delta\epsilon} \quad (2.3)$$

(which express the assumption that the invariants of the structure tensor are not affected by a rotation through a right angle in the 2-3 plane) we find that many of the invariants of the structure-tensor must be zero; thus if $r = 1$, $s = 1$, $p = 3$, $q = 1$, the only term in the quadruple summation which is different from zero is that for which $\alpha = 1$, $\beta = 1$, $\delta = 2$, $\epsilon = 1$ whence $K_{11}^{31} = -K_{11}^{21}$; similarly $K_{11}^{21} = K_{11}^{31}$ and combining these results we find that $K_{11}^{31} = K_{11}^{21} = 0$. Proceeding in this manner we find that out of the 256 invariants 128 are zero whilst there are 58 relations amongst the remaining 128 so that there are 70 distinct invariants. These may be succinctly displayed in the accompanying table where blanks indicate zero values, and where an abbreviation is introduced for K_{rs}^{pq} . Thus for instance, we write aa for K_{11}^{11} ; ig for K_{31}^{24} and so on. The key to this notation is given by

$$\begin{array}{|cccc|} \hline 11 & 12 & 13 & 14 \\ 21 & 22 & 23 & 24 \\ 31 & 32 & 33 & 34 \\ 41 & 42 & 43 & 44 \\ \hline \end{array} \equiv \begin{array}{|cccc|} \hline a & h & g' & u \\ h' & b & f & v \\ g & f' & c & w \\ u' & v' & w' & d \\ \hline \end{array}$$

TABLE I.

		i															
		11	22	33	44	23	32	31	13	12	21	14	41	24	42	34	43
j	11	aa	ba	ba	da	fa	-fa					ua	u'a				
	22	ab	bb	bc	db	fb	-fb					ub	u'b				
	33	ab	bc	bb	db	fc	-fb					ub	u'b				
	44	ad	bd	bd	dd	fd	-fd					ud	u'd				
	23	af	bf	bf'	df	ff	ff'					uf	u'f				
	32	-af	-bf'	-bf	-df	ff'	ff					-uf	-u'f				
	31							gg	g'g	-g'h'	-gh'			vg	v'g	vh'	v'h'
	13							gg	g'g	-g'h	-gh			vg'	v'g'	vh	v'h
	12							gh	g'h	g'g'	gg'			vh	v'h	-vg'	-v'g'
	21							gh'	g'h'	g'g	gg			vh'	v'h'	-vg	-v'g
	14	au	bu	bu	du	fu	-fu					uu	uu'				
	41	au'	bu'	bu'	du'	fu'	-fu'					uu'	uu				
	24							gv	g'v	g'w	gw			vv	v'v	-vw	-v'w
	42							gv'	g'v'	g'w'	gw'			vv'	v'v'	-vw'	-v'w'
	34							gw	g'w	-g'v	-gv			vv	v'w	vv	v'v
	43							gw'	g'w'	-g'v'	-gv'			vv'	v'w'	vv'	v'v'

In the application of this analysis to electromagnetic theory the table will have 6×6 instead of 16×16 constituents. For isotropy as regards rotation through a right angle in the (2, 3) plane it will read

TABLE IA.

		i					
		23	31	12	14	24	34
j	23	ff			uf		
	31		gg	-gh		vg	-vh
	12		gh	gg		vh	vg
	14	fu			uu		
	24		gv	-gw		vv	-vw
	34		gw	gv		vw	vv

so that sixteen of the invariants are zero and only twelve of the remaining 20 are distinct.

When, on the other hand, the structure-tensor is symmetric in both its covariant and contravariant labels (a state of affairs which will arise when both of the tensors between which it sets up a linear relationship are symmetric) the columns and rows must coincide with the corresponding columns and rows for which the order of the labels is altered so that instead of $100 = 10 \times 10$ ($10 = 4 + 6$) distinct constituents there remain only 28, the table reading as follows:

TABLE IB.

		i									
		11	22	33	44	23	31	12	14	24	34
j	11	aa	ba	ba	da				ua		
	22	ab	bb	bc	db	fb			ub		
	33	ab	bc	bb	db	-fb			ub		
	44	ad	bd	bd	dd				ud		
	23		bf	-bf		ff					
	31						gg	-gh		vg	vh
	12						gh	gg		vh	-vg
	14	au	bu	bu	du				uu		
	24						gv	gw		vv	-vw
	34						gw	-gv		vw	vv

We shall now find the new relations between the 70 distinct invariants of Table I, introduced by a rotation through any angle θ (other than a right angle) in the 2-3 plane. This rotation is described by the matrix

$$\begin{array}{c|cccc} & \begin{array}{c} \rightarrow i \\ 1\lambda \quad 2\lambda \quad 3\lambda \quad 4\lambda \end{array} \\ \begin{array}{c} \downarrow j \\ 1\mu \\ 2\mu \\ 3\mu \\ 4\mu \end{array} & \begin{bmatrix} 1 & 0 & 0 & 0 \\ 0 & \cos \theta & \sin \theta & 0 \\ 0 & -\sin \theta & \cos \theta & 0 \\ 0 & 0 & 0 & 1 \end{bmatrix} \end{array}$$

so that $s_1^1 = s_4^4 = 1$; $s_2^2 = s_3^3 = \cos \theta$; $s_2^3 = \sin \theta$; $s_3^2 = -\sin \theta$.

Upon substituting these values in the equations (2.3) and using the results embodied in Table I, we find the following new relations:

$$\begin{aligned} (a) \quad & 2(K_{22}^{22} - K_{33}^{22} - K_{23}^{23} - K_{32}^{23}) \sin \theta \cos \theta = (K_{23}^{22} + K_{32}^{22}) \\ (b) \quad & 2(K_{22}^{22} - K_{33}^{22} - K_{23}^{23} - K_{32}^{23}) \sin \theta \cos \theta = -(K_{23}^{22} + K_{32}^{22}) \end{aligned}$$

from which we have that $K_{22}^{22} = K_{33}^{22} + K_{23}^{23} + K_{32}^{23}$ and $K_{23}^{22} = -K_{32}^{22}$

$$\begin{aligned} (c) \quad & (K_{22}^{22} - K_{33}^{22} - K_{23}^{23} - K_{32}^{23})(\sin^2 \theta - \cos^2 \theta) \sin \theta \cos \theta = 2K_{23}^{22} \sin^2 \theta \\ (d) \quad & (K_{22}^{22} - K_{33}^{22} - K_{23}^{23} - K_{32}^{23})(\sin^2 \theta - \cos^2 \theta) \sin \theta \cos \theta = 2K_{32}^{22} \sin^2 \theta \end{aligned}$$

so that $K_{23}^{22} = K_{32}^{22}$ which combined with $K_{23}^{22} = -K_{32}^{22}$ gives $K_{23}^{22} = K_{32}^{22} = 0$

$$(e) \quad 2(K_{22}^{22} - K_{33}^{22} - K_{23}^{23} - K_{32}^{23}) \sin \theta \cos \theta = (K_{23}^{22} - K_{32}^{22}) + (K_{22}^{23} - K_{33}^{23})$$

or combined with the results of a , b , and c gives us

$$K_{22}^{23} = K_{33}^{23}.$$

Thus the new relations between the invariants K_{rs}^{pq} introduced by this rotation through an angle θ (excluding 90°) are

$$K_{22}^{22} = K_{33}^{22} + K_{23}^{23} + K_{32}^{23}; \quad K_{23}^{22} = 0; \quad K_{32}^{22} = 0; \quad K_{22}^{23} = K_{33}^{23}.$$

If we include these relations in Table I we shall have the conditions on the invariants for isotropy with regard to a rotation through any angle in the 2-3 plane. There are thus $70 - 4 = 66$ distinct invariants.

Table IA remains unchanged, whilst Table IB (since $K_{23}^{22} = 0$ and $K_{22}^{22} = K_{33}^{22} + 2K_{23}^{23}$) contains only $28 - 2 = 26$ distinct invariants, when we include the rotation through an angle θ .⁵

⁵ We remark that Table IB (disregarding the coefficients involving the 4th index) applies to the case of a tetragonal crystal with one of the edges an axis of symmetry in the sense that the other two edges of the crystal issuing from P and all rays (in the plane of these two edges) which may be made to coincide with either of these edges by a 90° rotation, are equivalent.

If we wish to find the conditions on the invariants for isotropy with regard to a rotation through any angle θ in some other coordinate plane, let us say the 1-2 plane, we may do so by inspection of Table I. We simply replace 23 by 12 and 32 by 21, whilst 1 is replaced by 3; for 3 stands in the same position with respect to 12, as 1 does to 23. For example, the condition $K_{11}^{32} = -K_{11}^{23}$ of table 1 is replaced by the relation $K_{33}^{21} = -K_{33}^{12}$. Similarly, instead of the relations

$$K_{22}^{22} = K_{33}^{22} + K_{23}^{23} + K_{32}^{23}; \quad K_{23}^{23} = K_{32}^{22} = 0; \quad K_{22}^{23} = K_{33}^{23}$$

we have

$$K_{11}^{11} = K_{22}^{11} + K_{12}^{12} + K_{21}^{12}; \quad K_{12}^{11} = K_{21}^{11} = 0; \quad K_{11}^{12} = K_{22}^{12}$$

In this way we may construct a table of invariants such that there will be structural symmetry with regard to any rotation θ in the 1-2 plane.

ISOTROPY WITH REGARD TO COMBINED ROTATIONS IN PLANES 2-3 AND 1-2.

If in addition to symmetry of structure with regard to a rotation through any angle in the 2-3 plane there is structural symmetry with regard to a similar rotation in the 1-2 plane we find without much fresh calculation the table of invariants for structural symmetry in the 2-3 and 1-2 planes. For example the relation $K_{11}^{12} = 0$ of Table I becomes $K_{33}^{23} = 0$ in the table of invariants for the 1-2 plane, both relations holding for the table of invariants for structural symmetry with regard to combined rotations in the 2-3 and 1-2 planes. Proceeding in this way we find that 192 of the 256 invariants are zero whilst of the remaining 64 only 12 are distinct. The following Table II expresses these facts and the symmetry of it shows that there is structural symmetry with regard to combined rotations through any angle in each of the planes 23, 31 and 12.

TABLE II.

	i	11	22	33	44	23	32	31	13	12	21	14	41	24	42	34	43
j	11	aa	ab	ab	da												
	22	ab	aa	ab	da												
	33	ab	ab	aa	da												
	44	ad	ad	ad	dd												
	23					ff	ff'					uf	u'f				
	32					ff'	ff					-uf	-u'f				
	31							ff	ff'					uf	u'f		
	13							ff'	ff					-uf	-u'f		
	12									ff	ff'					uf	u'f
	21									ff'	ff					-uf	-u'f
	14					fu	-fu					uu	uu'				
	41					fu'	-fu'					uu'	uu				
	24							fu	-fu					uu	uu'		
	42							fu'	-fu'					uu'	uu		
	34									fu	-fu					uu	uu'
	43									fu'	-fu'					uu'	uu

with $K_{11}^{11} = K_{22}^{11} + K_{23}^{23} + K_{32}^{23}$

If we include rotations through any angle θ , i.e. the material now possesses an axis of symmetry such that all rays at right angles to this axis are equivalent, the table corresponding to IB contains a less number of coefficients, there being nine in the first case and only six in the second.

Corresponding to Tables IA we have Table IIA with only four distinct invariants and 24, zero.

TABLE IIA.

		$i \rightarrow$	23	31	12	14	24	34
$j \downarrow$	23		$\bar{f}\bar{f}$			uf		
	31			$\bar{f}\bar{f}$			uf	
	12				$\bar{f}\bar{f}$			uf
	14		fu			uu		
	24			fu			uu	
	34				fu			uu

Similarly, when the structure-tensor is symmetric in both its covariant and contravariant labels we have a Table IIB corresponding to Tables IB. Thus

TABLE IIB.

		$i \rightarrow$	11	22	33	44	23	31	12	14	24	34
$j \downarrow$	11		aa	ab	ab	da						
	22		ab	aa	ab	da						
	33		ab	ab	aa	da						
	44		ad	ad	ad	dd						
	23						$\bar{f}\bar{f}$					
	31							$\bar{f}\bar{f}$				
	12								$\bar{f}\bar{f}$			
	14									uu		
	24										uu	
	34											uu

With $K_{11}^{11} = K_{22}^{11} + 2K_{23}^{23}$

there being 78 invariants out of the possible 100 zero, whilst of the remaining 22 only 6 are distinct.

In resumé, the three Tables II, IIA and IIB present the surviving invariants under the assumption that the invariants of the structure-tensor are not affected by a rotation through any angle in the 23, 31 and 12 planes.

We shall now consider the most general orthogonal rotation of the 123-space about the 4th direction. That is, we shall investigate the invariants for structural symmetry about the 4λ -axis.

ISOTROPY WITH REGARD TO A GENERAL ROTATION ABOUT THE λ -AXIS

The general rotation of the 123-space about the 4th direction is given by the matrix

		$\lambda \rightarrow$	1λ	2λ	3λ	4λ
$\mu \downarrow$	1μ		s_1^1	s_1^2	s_1^3	0
	2μ		s_2^1	s_2^2	s_2^3	0
	3μ		s_3^1	s_3^2	s_3^3	0
	4μ		0	0	0	1

Upon substituting these values in the fundamental equations

$$K_{rs}^{pq} = K_{\alpha\beta\gamma\delta}^{\delta\epsilon\zeta\eta} s_{\epsilon}^{p\zeta} s_{\zeta}^{q\eta} s_{\delta}^{\alpha\gamma} s_{\delta}^{\beta\gamma}$$

(using the conditions expressed in Table II) we find the following new relations

$$K_{23}^{14} = \Delta K_{23}^{14}; \quad K_{23}^{41} = \Delta K_{23}^{41}; \quad K_{14}^{23} = \Delta K_{14}^{23}; \quad K_{41}^{23} = \Delta K_{41}^{23}$$

where Δ is the determinant of the matrix of this rotation, namely

$$\Delta = \begin{vmatrix} s_1^1 & s_1^2 & s_1^3 \\ s_2^1 & s_2^2 & s_2^3 \\ s_3^1 & s_3^2 & s_3^3 \end{vmatrix}$$

and since our matrix is an orthogonal one, we have

$$\Delta^2 = 1 \text{ or } \Delta = \pm 1.$$

If $\Delta = +1$ then the rotation characterizes a movement of a rigid body about a fixed point. If $\Delta = -1$ the change of directions involves reflexion together with rotation.

ISOTROPY WITH REGARD TO A GENERAL ROTATION ABOUT A POINT P

We shall now consider the effect on the invariants K_{rs}^{pq} , if in addition to structural symmetry with respect to a general rotation about the λ -direction there is symmetry of structure with regard to a rotation through any angle in, let us say, the 1-4 plane.

Without fresh calculations but simply by inspection of Table I, we see that corresponding to the following relations therein; $-K_{23}^{22} = K_{33}^{23}$; $K_{11}^{33} = K_{33}^{22}$; $K_{33}^{33} = K_{22}^{22}$ we have (for the 1-4 plane) respectively: $K_{11}^{11} = K_{44}^{44}$; $K_{22}^{44} = K_{44}^{22}$; $K_{44}^{11} = K_{11}^{44}$ which when combined with Table II, yield

$$(a) \quad K_{44}^{44} = K_{11}^{11}; \quad K_{11}^{44} = K_{44}^{11} = K_{22}^{11}.$$

Similarly, the relations $K_{41}^{31} = K_{21}^{21}$ and $K_{13}^{31} = K_{12}^{21}$ for the 2-3 plane become respectively, $K_{42}^{42} = K_{12}^{12}$ and $K_{24}^{42} = K_{21}^{21}$ for the 1-4 plane which when taken together with table 2, yield

$$(b) \quad K_{14}^{14} = K_{23}^{23} \text{ and } K_{41}^{14} = K_{32}^{23}.$$

Finally, the relations $K_{31}^{24} = -K_{12}^{43}$, $K_{12}^{42} = -K_{21}^{43}$, $K_{24}^{31} = -K_{34}^{21}$ for the 2-3 plane become respectively $K_{42}^{13} = -K_{12}^{43}$, $K_{43}^{31} = -K_{12}^{34}$, $K_{13}^{42} = -K_{43}^{12}$ for the 1-4 plane which, when combined with Table II, yield

$$(c) \quad K_{23}^{14} = K_{14}^{23}; \quad K_{23}^{41} = -K_{14}^{23}; \quad K_{41}^{23} = -K_{14}^{23}.$$

If now we impose on the invariants K_{ns}^{pq} the conditions that they be unaffected by a general orthogonal rotation of the ennuple (as a whole) about P , the matrix of this rotation being

$$\begin{array}{c|cccc} & 1\lambda & 2\lambda & 3\lambda & 4\lambda \\ \hline 1\mu & s_1' & s_1^2 & s_1^3 & s_1^4 \\ 2\mu & s_2' & s_2^2 & s_2^3 & s_2^4 \\ 3\mu & s_3' & s_3^2 & s_3^3 & s_3^4 \\ 4\mu & s_4' & s_4^2 & s_4^3 & s_4^4 \end{array}$$

we find upon substitution in the fundamental equations $K_{ns}^{pq} = K_{\alpha\beta}^{\delta\epsilon} s'^p s'^q s'^\alpha s'^\beta$ taking into account the conditions expressed by Table II and (a), (b) and (c) above, that the new relation obtained is simple

$$K_{14}^{23} = \Delta \cdot K_{14}^{23}$$

where

$$\Delta = \begin{vmatrix} s_1^1 & s_1^2 & s_1^3 & s_1^4 \\ s_2^1 & s_2^2 & s_2^3 & s_2^4 \\ s_3^1 & s_3^2 & s_3^3 & s_3^4 \\ s_4^1 & s_4^2 & s_4^3 & s_4^4 \end{vmatrix} = \pm 1.$$

These results are best expressed in Tables III, IIIA and IIIB corresponding to Tables II, IIA and IIB. Thus

TABLE III.

j	i															
	11	22	33	44	23	32	31	13	12	21	14	41	24	42	34	43
11	aa	ab	ab	ab												
22	ab	aa	ab	ab												
33	ab	ab	aa	ab												
44	ab	ab	ab	aa												
23					$\frac{ff}{ff'}$	$\frac{ff'}{ff}$					$\frac{fu}{-fu}$	$\frac{-fu}{fu}$				
32													$\frac{fu}{-fu}$	$\frac{-fu}{fu}$		
31						$\frac{ff}{ff'}$	$\frac{ff'}{ff}$									
13																
12									$\frac{ff}{ff'}$	$\frac{ff'}{ff}$						
21															$\frac{fu}{-fu}$	$\frac{-fu}{fu}$
14					$\frac{fu}{-fu}$	$\frac{-fu}{fu}$					$\frac{ff}{ff'}$	$\frac{ff'}{ff}$				
41							$\frac{fu}{-fu}$	$\frac{-fu}{fu}$					$\frac{ff}{ff'}$	$\frac{ff'}{ff}$		
24																
42																
34															$\frac{ff}{ff'}$	$\frac{ff'}{ff}$
43																

with $K_{11}^{11} = K_{22}^{11} + K_{23}^{23} + K_{32}^{23}$

so that there are only four distinct invariants remaining.

TABLE IIIA.

		i					
		23	31	12	14	24	34
j	23	ff			fu		
	31		ff			fu	
	12			ff			fu
	14		fu		ff		
	24			fu		ff	
	34				fu		ff

there being only two distinct invariants K_{23}^{23} and K_{23}^{14} out of 12 different from zero.

TABLE IIIB.

		i									
		11	22	33	44	23	31	12	14	24	34
j	11	aa	ab	ab	ab						
	22	ab	aa	ab	ab						
	33	ab	ab	aa	ab						
	44	ab	ab	ab	aa						
	23					ff					
	31						ff				
	12							ff			
	14								ff		
	24									ff	
	34										ff

with $K_{11}^{11} = K_{22}^{11} + 2K_{23}^{23}$

so that as in table IIB, 78 of the invariants are zero, whilst only two of the remaining 22 are distinct.

APPLICATIONS TO ELECTROMAGNETIC THEORY

a. *Absolute isotropy with regard to a general rotation around the λ -direction.* This means that $\Delta = +1$. Then from Table IIA, we find the relations between the invariants j_{rs} and i_{rs} of the two alternating covariant electromagnetic tensors b_{rs} and a_{rs} respectively:

$$\begin{aligned} j_{23} &= \alpha i_{23} + \beta i_{14}; & j_{31} &= \alpha i_{31} + \beta i_{24}; & j_{12} &= \alpha i_{12} + \beta i_{34} & \text{where } \alpha &= K_{23}^{23}; \beta &= K_{23}^{14}; \\ j_{14} &= \lambda i_{23} + \gamma i_{14}; & j_{24} &= \lambda i_{31} + \gamma i_{24}; & j_{34} &= \lambda i_{12} + \gamma i_{34} & \lambda &= K_{14}^{23}; \gamma &= K_{14}^{14}. \end{aligned} \quad (2.4)$$

Equations (2.4) are relations between the invariants j_{rs} and i_{rs} of the two electromagnetic tensors b_{rs} and a_{rs} respectively and are valid for any Riemannian space of four dimensions R_4 . If, however, we wish to find the corresponding set of relations between the tensor components we must know definitely the ennuple with respect to which the invariants j_{rs} and i_{rs} are taken.

Suppose that the system of coordinates of our R_4 is an orthogonal-curvilinear one for which the fundamental quadratic form is

$$ds^2 = H_1^2(dx^1)^2 + H_2^2(dx^2)^2 + H_3^2(dx^3)^2 + H_4^2(dx^4)^2,$$

and furthermore that the ennuple at P coincides with this reference frame. Then, the relations between the invariants j_{rs} , i_{rs} and the corresponding tensors b_{rs} , a_{rs} are such that

$$j_{rs} = b_{rs}/H_r H_s; \quad i_{rs} = a_{rs}/H_r H_s$$

so that corresponding to equations (2.4) between the invariants j_{rs} and i_{rs} we have the following set of relations between the tensors b_{rs} and a_{rs} :

$$\begin{aligned} \frac{H_1}{H_2 H_3} b_{23} &= \frac{H_1}{H_2 H_3} \alpha a_{23} + \frac{\beta}{H_4} a_{14}; & \frac{1}{H_4} b_{14} &= \frac{H_1}{H_2 H_3} \lambda a_{23} + \frac{\gamma}{H_4} a_{14} \\ \frac{H_2}{H_3 H_1} b_{31} &= \frac{H_2}{H_3 H_1} \alpha a_{31} + \frac{\beta}{H_4} a_{24}; & \frac{1}{H_4} b_{24} &= \frac{H_2}{H_3 H_1} \lambda a_{31} + \frac{\gamma}{H_4} a_{24} \\ \frac{H_3}{H_1 H_2} b_{12} &= \frac{H_3}{H_1 H_2} \alpha a_{12} + \frac{\beta}{H_4} a_{34}; & \frac{1}{H_4} b_{34} &= \frac{H_3}{H_1 H_2} \lambda a_{23} + \frac{\gamma}{H_4} a_{34} \end{aligned} \quad (2.5)$$

We now recall that the tensor a_{rs} consists of the magnetic induction vector \mathbf{B} and the electric intensity vector \mathbf{E} ; whilst the other electromagnetic tensor b_{rs} consists of the electric displacement vector \mathbf{D} and of the magnetic force vector \mathbf{H} . Furthermore, let us suppose that $H_1 = H_2 = H_3 = 1$ and that $H_4 = ic$ i.e. our space-time is a Galilean one. Then equations (2.5) become simply

$$\begin{aligned} -\mathbf{D} &= \alpha \mathbf{B} - i\beta \mathbf{E} \quad \text{and} \quad \frac{1}{i} \mathbf{H} = \lambda \mathbf{B} + \frac{\nu}{i} \mathbf{E} \\ \text{or } \mathbf{D} &= i\beta \mathbf{E} - \alpha \mathbf{B} \quad \text{and} \quad \mathbf{B} = \frac{1}{i\lambda} \mathbf{H} - \frac{\nu}{i\lambda} \mathbf{E} \end{aligned} \quad (2.6)$$

and comparing with the relations $\mathbf{D} = \epsilon \mathbf{E} + \rho \mathbf{B}$; $\mathbf{B} = \mu \mathbf{H} + \delta \mathbf{E}$ we have that $\epsilon = i\beta$, $\mu = 1/i\lambda$, $\rho = -\alpha$ and $\delta = -\gamma/i\lambda$ or $\epsilon\mu = \beta/\lambda$ and $\rho/\delta = \mu\alpha/\gamma$

b. *Absolute isotropy with regard to a general rotation about P.* By definition $\bar{K}_{rs}^{pq} = K_{rs}^{pq}$ and $\Delta = +1$ so that from Table IIIA we have the following relations between the invariants j_{rs} and i_{rs}

$$\begin{aligned} j_{23} &= \alpha i_{23} + \beta i_{14}; & j_{31} &= \alpha i_{31} + \beta i_{24}; & j_{12} &= \alpha i_{12} + \beta i_{34} \\ j_{14} &= \beta i_{23} + \alpha i_{14}; & j_{24} &= \beta i_{31} + \alpha i_{24}; & j_{34} &= \beta i_{12} + \alpha i_{34} \end{aligned} \quad (2.7)$$

where we now have only two distinct invariants $\alpha = K_{23}^{23}$, and $\beta = K_{14}^{23}$. Corresponding to equations (2.6) we have

$$\begin{aligned} \mathbf{D} &= i\beta \mathbf{E} - \alpha \mathbf{B} \quad \text{and} \quad \mathbf{B} = \frac{1}{i\beta} \mathbf{H} - \frac{\alpha}{i\beta} \mathbf{E} \\ \text{or } \mathbf{D} &= \epsilon \mathbf{E} + \gamma \mathbf{B} \quad \text{and} \quad \mathbf{B} = \mu \mathbf{H} + \delta \mathbf{E} \end{aligned} \quad (2.8)$$

where $\mu\epsilon = 1$ (Maxwell's relation for the aether), and $\rho/\delta = \mu$ or $1/\epsilon$.

c. *Relative isotropy with regard to a general rotation about the λ -axis.* That is, $\bar{K}_{rs}^{pq} = -K_{rs}^{pq}$ with $\Delta = -1$. Then in Table IIA $K_{23}^{23} = K_{14}^{14} = 0$ whilst $K_{23}^{14} = -\Delta K_{14}^{23} = K_{14}^{23}$ and $K_{14}^{23} = -\Delta K_{23}^{14} = K_{23}^{14}$ so that the relations between the invariants j_{rs} and i_{rs} are

$$\begin{aligned}j_{23} &= \beta i_{14}; \quad j_{31} = \beta i_{24}; \quad j_{12} = \beta i_{34} \\j_{14} &= \lambda i_{23}; \quad j_{24} = \lambda i_{31}; \quad j_{34} = \lambda i_{12}\end{aligned}$$

where β and λ are distinct invariants (2.9) and corresponding to equations 2.6 we have simply

$$D = i\beta E \text{ and } B = \frac{1}{i\lambda} H \quad (3.0)$$

with $i\beta = \epsilon$ and $i\lambda = 1/\mu$; or $\epsilon\mu = \beta/\lambda$.

Equations (3.0) are precisely the ones we wished to investigate and we see that the conditions necessary for them to be valid are a relatively-isotropic medium round the time-direction vector orthogonal to the space R_3 (considered as a hypersurface in space-time).

The equations $B = \mu H$, $D = \epsilon E$ (where μ , ϵ are distinct) are valid wherever matter is present. Considered from the point of view that our space R_3 is a hypersurface in space-time R_4 , we may say that if matter is present at a point P in our space-time, this fact is made known to an observer (in space-time) by a time-direction ${}_4\lambda$ attached to this point and orthogonal to the hypersurface R_3 .

d. *Relative isotropy with regard to a general rotation about a point P .* Table IIIA with $\bar{K}_{rs}^{pq} = -K_{rs}^{pq}$ and $\Delta = -1$ applies to this case. Corresponding to equations (2.9) we have the following set:

$$\begin{aligned}j_{23} &= \beta i_{14}; \quad j_{31} = \beta i_{24}; \quad j_{12} = \beta i_{34} \\j_{14} &= \beta i_{23}; \quad j_{24} = \beta i_{31}; \quad j_{34} = \beta i_{12}\end{aligned} \quad (3.1)$$

where $\beta = K_{14}^{23}$, which in the special case of coincidence between the ennuple at P and a Galilean reference frame attached to P , become

$$D = i\beta E \text{ and } B = \frac{1}{i\beta} H \quad (3.2)$$

or

$$D = \epsilon E \text{ and } B = \mu H$$

with $\epsilon\mu = 1$ (Maxwell's relation for empty space). We thus see that when the entire space-time is relatively isotropic, i.e. $B = \mu H$ and $D = \epsilon E$ with $\mu\epsilon = 1$, then the fact that *no matter* is present in the neighborhood of the point P (x, y, z, t) is made known to an observer (in space-time) by the absence of a time-direction vector at P , orthogonal to the hypersurface R_3 .

APPLICATIONS TO ELASTICITY THEORY

Hooke's law on the linear dependence of stress on strain when the latter is small, says that each of the six components of the stress at any point of a body is a linear function of the six components of the strain at that point.

Thus at each point of our medium we are provided with two symmetric tensors, the stress tensor T_{rs} and the strain tensor e_{rs} . The linear relation between them is expressed by the equation

$$T_{rs} = c_{rs}^{\alpha\beta} e_{\alpha\beta} \quad (r, s = 1, 2, 3) \quad (3.3)$$

where $c_{rs}^{\alpha\beta}$ may be assumed, without any loss in generality, to be symmetric in the covariant and contravariant indices separately.

Corresponding to the tensor equation (3.2) we have an invariant equation

$$p_{rs} = K_{rs}^{\alpha\beta} q_{\alpha\beta} \quad (3.4)$$

where p_{rs} , $K_{rs}^{\alpha\beta}$ are the invariants of T_{rs} , $c_{rs}^{\alpha\beta}$ respectively, with respect to an orthogonal ennuple attached to the point P at which these tensors are defined.

ABSOLUTE ISOTROPY ROUND AN AXIS

If the medium possesses structural symmetry round an axis we have what is known as *transverse-isotropy*. We find from Table IIB that in this case there are only six distinct invariants. One finds, however, in the literature on the subject that only five independent coefficients are involved in Hooke's law for transverse-isotropy. This disagreement is due to the fact that we have not assumed the existence of an energy-density of deformation, which assumption would lead us to the equation

$$K_{rs}^{pq} = K_{pq}^{rs}$$

and therefore would reduce the number of distinct coefficients of elasticity from six to five. However, we see that as far as Hooke's law is concerned we have six distinct coefficients.

ABSOLUTE ISOTROPY WITH REGARD TO THE ENTIRE SPACE

When the medium possesses structural symmetry round all lines, i.e. there is complete or absolute isotropy, then from Table IIIB (which applies in this case) we see that Hooke's law contains only two independent coefficients of elasticity K_{11}^{11} and K_{23}^{23} which in the familiar notation of Lamé are identified with λ and μ .

THE EQUILIBRIUM BETWEEN MATTER
AND RADIATION

BY LOUIS S. KASSEL*

GATES CHEMICAL LABORATORY, CALIFORNIA INSTITUTE

(Received February 7, 1930)

ABSTRACT

The equilibrium concentration of electrons and protons is recalculated on the basis of Dirac's new theory of the nature of the proton; it is found to be exceedingly small, of the same order of magnitude as had been found in previous calculations.

THERE have recently been a number of attempts to calculate the equilibrium between matter and radiation in the universe.^{1,2,3} There are two difficulties in these calculations; one of these is the generalization of energy and entropy which must be made before the equilibrium state of the entire universe can be treated; this problem has been discussed in particular by Tolman. The other difficulty is the assignment of entropy to a perfect crystal at the absolute zero; it cannot be regarded as entirely certain that this entropy is equal to that of a perfect vacuum, as is assumed. Nevertheless, all calculations agree in yielding for the final equilibrium state one in which the ratio of the energy in the form of matter to that in the form of radiation is exceedingly small; this ratio is dominated by the exponential factor $e^{-mc^2/kT}$ which completely wipes out the effect of all the other factors; the final state of the universe indicated by these calculations is thus one in which there is practically no matter left.

Quite recently Dirac⁴ has proposed a theory of the nature of the proton which seems to call for a new calculation of the equilibrium concentration of matter. Briefly stated, Dirac's theory is that the fundamental unit of matter is the electron; in addition to the usual states in which the electron is observed, there are others in which its mass is negative; in these states its total energy is negative, and in fact becomes more negative as its velocity increases. These negative energy electrons are attracted by ordinary electrons, but ordinary electrons are nevertheless repelled by them. All these properties correspond to solutions of the wave equation of the electron which were previously known, but generally considered extraneous. Dirac proposes the hypothesis that space contains great numbers of these negative energy electrons, which obey the Fermi statistics; the states of lowest energy (highest velocity) are therefore full, but a few of the states of low velocity are not

* National Research Fellow in Chemistry.

¹ Stern, *Zeits. f. Elektrochem.* **31**, 448 (1925); *Trans. Far. Soc.* **21**, 477 (1925-6).

² Tolman, *Proc. Nat. Acad. Sci.* **12**, 670 (1926); **14**, 353 (1928).

³ Zwicky, *Proc. Nat. Acad. Sci.* **14**, 592 (1928).

⁴ Dirac, *Proc. Roy. Soc.* **126A**, 360 (1930).

occupied; these gaps constitute irregularities in the normal arrangement of space, and are observable. It is evident that the gaps will attract ordinary electrons, and be attracted by them; they will also have in effect a positive energy, since they correspond to the absence of a particle of negative energy.

The most natural assumption is that the total number of electrons in the universe is just equal to the number of cells of negative energy; then at the absolute zero every electron would be in the lowest possible state, there would be complete uniformity throughout space, and the universe would be observationally empty. The problem to be solved is simply that of finding the distribution of electrons among the various cells at higher temperatures; we shall confine our solution to a finite region in which there is flat space-time. The problem then differs from the usual applications of the Fermi statistics chiefly in that there are two continuous ranges of energy values. We divide these ranges into intervals in the usual way, and write for the number of cells in the s^{th} interval of the positive energy range

$$Q_s = 4\pi V / h^3 (2m)^{3/2} E_s^{1/2} \Delta E \quad (1)$$

and for the number in the t^{th} interval of the negative energy range

$$Q_t = 4\pi V / h^3 (2M)^{3/2} E_t^{1/2} \Delta E. \quad (2)$$

We have included in these formulae a factor 2 arising from the spin, which we suppose exists for all energies, and in (2) we use the observed proton mass M ; there is some doubt about the correct procedure at this point; $-M$ is what the chemist would call the partial molal (or partial molecular) mass of the electrons of true mass $-m$; it is the right value to use for the change in mass produced in a system by creating the first proton in it; when another proton is created sufficiently close a different value will be needed. The result of our calculations will be that the concentration of matter is exceedingly small, and M therefore is certainly the correct mass for most purposes, though possibly not for ours; it would not make any important change in the results if m did replace M in (2). Also it is unnecessary to use the correct relativistic expressions for (1) and (2), since all cells of large positive kinetic energy are empty, and all those of large negative kinetic energy are full; the number of cells of these kinds will not be correctly given by our result, but this number does not concern us.

The number of distribution of N_s particles among Q_s cells, using the Fermi statistics, is known to be $Q_s! / N_s! (Q_s - N_s)!$ and hence the number of distributions for the entire system, the numbers N_s and N_t being specified, is

$$W = \prod_s \frac{Q_s!}{N_s! (Q_s - N_s)!} \prod_t \frac{Q_t!}{N_t! (Q_t - N_t)!} \quad (4)$$

This is to be a maximum subject to the conditions of conservation of charge and of energy. Proceeding in the usual way we have

$$\sum_s \{ -\log N_s + \log (Q_s - N_s) \} \delta N_s + \sum_t \{ -\log N_t + \log (Q_t - N_t) \} \delta N_t = 0 \quad (4)$$

$$\sum_s \delta N_s + \sum_t \delta N_t = 0 \quad (5)$$

$$\sum_s (E_s + mc^2) \delta N_s - \sum_t (E_t + Mc^2) \delta N_t = 0. \quad (6)$$

Using multipliers e^α and e^β for (5) and (6) we add these three equations and then require each term in the two sums to vanish. Upon rearranging the necessary conditions we have

$$N_s = \frac{Q_s}{e^{\alpha + (E_s + mc^2)\beta} + 1} \quad (7)$$

$$N_t = \frac{Q_t}{e^{\alpha - (E_t + Mc^2)\beta} + 1}. \quad (8)$$

It is easily shown in the usual manner that $\partial E / \partial S = 1/k\beta$ and since thermodynamics requires $\partial E / \partial S = T$, we have as always in this type of calculation

$$\beta = 1/kT. \quad (9)$$

For positive values of α the first term in the denominator of (7) will be very large and (7) may be written approximately

$$N_s = Q_s e^{-\alpha - (E_s + mc^2)/kT}. \quad (10)$$

For values of α not too large the first term in the denominator of (8) will be extremely small and we will have

$$N_t = Q_t \{ 1 - e^{\alpha - (E_t + Mc^2)/kT} \}. \quad (11)$$

We now determine α from the state of electrification of the system. The condition for neutrality is

$$\sum_s N_s = \sum_t (Q_t - N_t) \quad (12)$$

which becomes

$$\sum_s Q_s e^{-\alpha - (E_s + mc^2)/kT} = \sum_t Q_t e^{\alpha - (E_t + Mc^2)/kT}. \quad (13)$$

Upon introducing the values of Q_s and Q_t and replacing the sum by an integral we find

$$(2m)^{3/2} e^{-\alpha - mc^2/kT} \int_0^\infty e^{-E/kT} E^{1/2} dE = (2M)^{3/2} e^{\alpha - Mc^2/kT} \int_0^\infty e^{-E/kT} E^{1/2} dE \quad (14)$$

or

$$e^\alpha = (m/M)^{3/4} e^{(M-m)c^2/2kT}. \quad (15)$$

This value of α is evidently such that the approximations (10) and (11) are justified. Upon inserting (15) and (1) into (10) and integrating we obtain for the number of electrons of positive energy

$$\begin{aligned} N_+ &= \frac{4\pi V}{h^3} (4mM)^{3/4} e^{-(m+M)c^2/2kT} \int_0^\infty e^{-E/kT} E^{1/2} dE \\ &= 2V \left(\frac{2\pi(mM)^{1/2}kT}{h^2} \right)^{3/2} e^{-(m+M)c^2/2kT}. \end{aligned} \quad (16)$$

This then is the number of electrons and also the number of protons which the system contains. It is very closely similar to Stern's result for the number of particles of mass m

$$N = V \left(\frac{2\pi mkT}{h^2} \right)^{3/2} e^{-mc^2/kT}. \quad (17)$$

The vanishingly small amount of matter permitted by this equation has already been pointed out, and our result may be regarded as in some measure supporting the view that if any matter is to be preserved in the final equilibrium of the universe it must be rescued by the tendency of matter toward aggregation. But the evidence of astronomy suggests that the stars are constantly gaining matter in the form of dust and meteors, transforming it into radiation and sending it back into space; this may mean, of course, that the universe cannot save its matter by any device and that it is steadily fading away. On the other hand the evidence of the cosmic rays may be supposed to indicate that in the depths of space radiation is converted back into matter; if this process is occurring it can only mean that the foregoing calculation, and all others of a similar nature, are utterly incorrect.

ON THE INTERACTION OF STARK EFFECT AND ELECTRON SPIN IN ALKALI ATOMS¹

BY VLADIMIR ROJANSKY

WASHINGTON UNIVERSITY, ST. LOUIS, MISSOURI

(Received February 19, 1930)

ABSTRACT

The Stark effect in alkali metal atoms in weak fields is, on the basis of both theory and experiment, a second order effect. It is shown here on the basis of the quantum mechanics that when the second order Stark effect is large enough to be comparable with the multiplet structure, there appears, due to the interaction of the Stark effect and spin, an effect which, in its influence on the multiplet structure, is not unlike the Paschen-Back effect in the magnetic case. It causes a distortion of the multiplet structure and a redistribution of the intensities of the spectral lines.

INTRODUCTION

THE Stark effect in complex atoms has not yet been studied extensively in the light of the quantum mechanics, and some time will probably elapse until its more delicate features will be worked out. However, the general aspects of the effect, especially in case of the alkali atoms, have been worked out, and are confirmed by experiment. A review of this subject was recently given by Ladenburg.²

Experimental data available at present with respect to the alkali atoms in weak electric fields, i.e., fields which produce shifts of the spectral lines small compared to the fine structure separations, show that the effect is quadratic, i.e., that the separations between the Stark components of the energy levels are proportional to the square of the external field F . The quadratic nature of the effect may be inferred theoretically, in a more or less classical manner, as follows³: The valence electron, which does all the radiating, moves in the field due to the nucleus and the inner electrons. This field may be assumed to be central. Since it deviates from a Coulomb field

¹ An abstract of this paper was given in the program of the April, 1929, meeting of the American Physical Society. *Phys. Rev.* **33**, 1084 (1929).

² R. Ladenburg, *Phys. Zeits.* **30**, 369 (1929):

³ This familiar argument is repeated here mostly in order to emphasize that it is not entirely general when the effect of electron spin is considered. For example, it has been shown^{4,5} that the conclusions of such an argument do not agree with the deductions of the quantum mechanics in case of hydrogenic atoms: an insipient linear effect is to be expected in these atoms due to the degeneracy caused by the effects of the electron spin. Though the difficult task of detecting the linear effect directly by experiment has not been carried out, and therefore these deductions of the quantum mechanics remain untested directly, the theory has answered in agreement with experiment a related question, that of the metastability of the $2s$ level in atomic hydrogen.

⁴ R. Schlapp, *Proc. Roy. Soc.* **119A**, 313 (1928).

⁵ V. Rojansky, *Phys. Rev.* **33**, 1 (1929).

the orbit of the electron precesses. Due to the precession the electrical center of the atom coincides, on the average, with the nucleus. If a weak external field is applied in the direction Z the behavior of the system is not appreciably altered, and the time average of the excursion z of the valence electron in the Z direction remains zero. Now, the first order energy correction due to the field is given by the time average of Fz , and since this vanishes effects only of orders higher than the first are to be expected.

Explicit formulas for the Stark effect in alkali atoms were calculated on the Bohr theory by Becker and by Thomas.⁶ With the advent of the quantum mechanics Unsoeld⁷ considered the effect in the light of the new theory for fields insufficient to break down the l -quantization, i.e., for fields which we call weak here. Unsoeld's treatment neglects electron spin, and thus his results should apply strictly only in fields (it is difficult to find a satisfactory adjective for the description of such fields) which are weak if gauged by the effect of l on the energy but are very strong if gauged by the multiplet separations.

The purpose of the present paper is to consider the Stark effect in alkali atoms in weak fields in somewhat greater detail by taking into account the electron spin, and, particularly, to show that as the field becomes sufficiently intense, so that its effects within a doublet become comparable to the doublet separation, there should appear an effect not unlike the Paschen-Back effect in the magnetic case, consisting in a distortion of the multiplet structure and in a redistribution of intensities.⁸

The procedure leading to this conclusion is as follows: The appropriate energy matrix is first set up. Then the approximations to the perturbed energy levels are obtained, not by the general matrix perturbation formulas derived for non-degenerate systems but by actually transforming the energy matrix. In doing this it is found that after the energy matrix has been diagonalized in such a way that no first order terms in F appear off the diagonal it acquires elements whose transition frequencies are those between the components of spin doublets. If, as is the case in light atoms, the spin doublets are narrow the transformed matrix is nearly degenerate⁹ and use of methods applicable to degenerate systems leads then to the effect referred to above.

We adopt, with a few unimportant but convenient exceptions, the terminology and notation used in reference 5.

ENERGY LEVELS

We write the matrix representing the energy of an alkali atom in a weak electrostatic field in the form

⁶ R. Becker, *Zeits. f. Physik* **9**, 332 (1922); W. Thomas, *Zeits. f. Physik* **34**, 586 (1925).

⁷ A. Unsoeld, *Ann. d. Physik* **82**, 390 (1927).

⁸ The theoretical necessity for such an effect in the alkali atoms was recognized by Professor J. H. Van Vleck, who suggested the problem to the writer.

⁹ See Van Vleck's paper "On the σ -Type Doubling and Electron Spin in Diatomic Molecules," *Phys. Rev.* **33**, 467 (1929). In that paper, especially in Section 4, he develops a procedure for handling a system in which a degeneracy appears only in the higher approximations.

$$H = H_0 + H_1 = H_0 + Fez. \quad (1)$$

Here H_0 is the (diagonal) energy matrix of the unperturbed atom, whose elements are the experimental energy levels, which we denote by $H_0(n, m, l, j; n, m, l, j)$, or, for brevity, by $H_0(l, j)$. The additional term $H_1 = Fez$ is the perturbation term due to the external field F , the matrix z representing the z -coordinate of the valence electron. As the elements of z are diagonal in the axial quantum number m , and as transitions involving a change in the principal quantum number n contribute but a negligible part of the total perturbation, we shall be concerned here only with elements of the form $z(n, m, l, j; n, m, l', j')$, which we denote, for brevity, by $z(l, j; l', j')$. In writing the elements it is also convenient to eliminate the inner quantum number j through its relation to the azimuthal quantum number l , i.e., $j = l \pm \frac{1}{2}$ (reference 5 employs the inverse elimination). The expressions for the elements of z can be taken over from the theory of the Stark effect in hydrogenic atoms in weak fields, so long as the valence electron is assumed to move in a central field.¹⁰ These expressions are given explicitly in reference 5. With the abbreviations

$$\begin{aligned} K(\alpha) &= -3a_1 n(\alpha^2 - m^2)^{1/2} / 8Z\alpha, & L(\alpha) &= [n^2 - (\alpha + \frac{1}{2})^2]^{1/2}, \\ M(\alpha) &= -3a_1 n \{ [n^2 - (\alpha + \frac{1}{2})^2] m^2 \}^{1/2} / 4Z\alpha(\alpha + 1), \end{aligned} \quad (2)$$

they are, since $Z = 1$ in arc spectra:

$$\begin{aligned} z(l, l - \frac{1}{2}; l - 1, l - 1\frac{1}{2}) &= 2K(l - \frac{1}{2})L(l - \frac{1}{2}); & z(l, l - \frac{1}{2}; l + 1, l + \frac{1}{2}) &= 2K(l + \frac{1}{2})L(l + \frac{1}{2}); \\ z(l, l + \frac{1}{2}; l - 1, l - \frac{1}{2}) &= 2K(l + \frac{1}{2})L(l - \frac{1}{2}); & z(l, l + \frac{1}{2}; l + 1, l + 1\frac{1}{2}) &= 2K(l + \frac{1}{2})L(l + \frac{1}{2}); \\ z(l, l - \frac{1}{2}; l - 1, l - \frac{1}{2}) &= M(l - \frac{1}{2}); & z(l, l + \frac{1}{2}; l + 1, l + \frac{1}{2}) &= M(l + \frac{1}{2}). \end{aligned} \quad (3)$$

Multiplication of these elements by Fe gives the corresponding elements of the matrix H_1 . Thus for the present purpose the elements of the energy matrix H can be regarded as known.

With these elements on hand one might proceed to calculate the perturbed energy levels of the atom by using the formulas¹¹

$$W^{(1)}(n; n) = H(n; n); \quad W^{(2)}(n; n) = \sum_k \frac{H(n; k)H(k; n)}{h\nu_0(n; k)}; \text{ etc.}, \quad (4a, b, \dots)$$

where n , or k , is the totality of the quantum numbers defining a state, and where $\nu_0(n; k)$ is the transition frequency of the unperturbed system, pre-

¹⁰ With regard to the assumption of a central field for the valence electron see D. R. Hartree, Proc. Camb. Phil. Soc. **24**, 89 (1928), and J. C. Slater, Phys. Rev. **32**, 339 (1928). With regard to the generality of the Kronig's factors see, for example, E. Wigner, Zeits. f. Physik **43**, 644-646, (1927), for the case without spin; as to the effect of including spin see p. 93 of J. v. Neumann and E. Wigner, Zeits. f. Physik **49**, 73, (1928).

¹¹ M. Born, W. Heisenberg, and P. Jordan, Zeits. f. Physik **35**, 557 (1926). Since the diagonal elements of our H contain no F , and the off-diagonal elements are all of the first order, we write the formulas in a simplified way.

sumably known from experiment. The direct application of these formulas to H would yield expressions, quadratic in F , for the Stark effect in alkali atoms. An examination of the transformations leading to formulas (4) will, however, presently show that in the case of alkali atoms such a procedure is not necessarily legitimate, and that for certain values of F the expressions obtained by applying (4) to H are inaccurate.

Formulas (4) are the results of the process of diagonalization of a matrix, assumed to be non-degenerate, by means of appropriate canonical transformations, a process which we shall now consider more closely. The standard procedure is to use a transformation matrix of the form $S = 1 + \lambda S' + \lambda^2 S'' + \dots = 1 + S_1 + S_2 + \dots$. Let H' represent the new energy matrix resulting from the diagonalization of the original matrix H to terms in F^2 . We have:

$$H' = (1 + S_1)H(1 + S_1)^{-1} = (1 + S_1)(H_0 + H_1)(1 - S_1 + S_1^2 - \dots), \quad (5)$$

where $S_1(n; m) = H_1(n; m)/h\nu_0(n; m)$. Neglecting terms in F^3 , we have

$$H'(n; m) = H_0(n; m) + [H_1(m; m) - H_1(n; n)] \frac{H_1(n; m)}{h\nu_0(n; m)} + \sum_k'' \frac{H_1(n; k)H_1(k; m)}{h\nu_0(n; k)},$$

where the double dash is used in Σ'' to indicate that only terms for which $k \neq n$ and also $k \neq m$ are included in the summation. Since the diagonal elements of our H_1 are zero

$$H'(n; m) = H_0(n; m) + \sum_k'' \frac{H_1(n; k)H_1(k; m)}{h\nu_0(n; k)}.$$

The elements of H' are found to correspond to transitions:

$$(l, l - \frac{1}{2}) \rightarrow (l, l - \frac{1}{2}); (l - 2, l - 1\frac{1}{2}); (l - 2, l - 2\frac{1}{2}); (l + 2, l + 1\frac{1}{2}); \text{ and } (l, l + \frac{1}{2});$$

$$(l, l + \frac{1}{2}) \rightarrow (l, l + \frac{1}{2}); (l + 2, l + 1\frac{1}{2}); (l + 2, l + 2\frac{1}{2}); (l - 2, l - 1\frac{1}{2}); \text{ and } (l, l - \frac{1}{2})$$

The elements which will prove of particular interest are:¹²

$$H'(l, l \pm \frac{1}{2}; l, l \pm \frac{1}{2}) = \frac{4F^2 e^2}{h} \left[\frac{K^2(l \pm \frac{1}{2})L^2(l - \frac{1}{2})}{\nu_0(l, l \pm \frac{1}{2}; l - 1, l - 1 \pm \frac{1}{2})} + \frac{K^2(l + 1 \pm \frac{1}{2})L^2(l + \frac{1}{2})}{\nu_0(l, l \pm \frac{1}{2}; l + 1, l + 1 \pm \frac{1}{2})} \right. \\ \left. + \frac{M^2(l \pm \frac{1}{2})}{4\nu_0(l, l \pm \frac{1}{2}; l \pm 1, l \pm \frac{1}{2})} \right] + H_0(l, l \pm \frac{1}{2}) = F^2 A_{3/2 \pm 1/2} + B_{3/2 \pm 1/2}, \quad (7)$$

and

$$H'(l, l \pm \frac{1}{2}; l, l \mp \frac{1}{2}) = \frac{2F^2 e^2 K(l \pm \frac{1}{2})}{h} \left[\frac{L(l \mp \frac{1}{2})M(l \mp \frac{1}{2})}{\nu_0(l, l \pm \frac{1}{2}; l \mp 1, l \mp \frac{1}{2})} \right. \\ \left. + \frac{L(l \pm \frac{1}{2})M(l \pm \frac{1}{2})}{\nu_0(l, l \pm \frac{1}{2}; l \pm 1, l \pm \frac{1}{2})} \right] = F^2 C_{3/2 \pm 1/2}. \quad (8)$$

¹² In (7), or in (8), either the upper or the lower of the double signs is to be taken throughout, the subscripts of A , B , and C included.

Application of (4a) to H' yields, of course, the same results as does application of (4a) and (4b) to H . To show that the latter procedure is not necessarily accurate it suffices to show that it is not always legitimate to apply (4a) to H' . This, however, follows from the appearance in H' of the "troublesome" elements $H'(l, l \pm \frac{1}{2}; l, l \mp \frac{1}{2})$. Since in the alkali atoms the energy differences between states having different azimuthal quantum numbers are much greater than those between the levels of a spin doublet, the transition frequencies corresponding to these troublesome elements are much smaller than those corresponding to other off-diagonal elements of H' . Thus the energy matrix of an alkali atom in a weak electric field, while not strictly degenerate, displays, after being transformed by means of a first order canonical transformation, off-diagonal elements whose perturbing influence cannot be unconditionally disregarded. Formula (4a), on the other hand, disregards entirely the contributions of the off-diagonal elements of a matrix to which it is applied and therefore it cannot be applied directly to H' , unless the troublesome elements are themselves negligible due to an extremely small value of the factor F .

To circumvent this difficulty we shift to methods adapted to handling degenerate systems and seek a new transformation matrix T , such that in the new energy matrix H'' , given by

$$H'' = TH'T^{-1} \quad (9)$$

all the troublesome elements ($\Delta l = 0, \Delta j \neq 0$) vanish. Application of (4a) to H'' is then legitimate, i.e., the diagonal elements of H'' are the required energy levels, correct to terms in F^2 .

To determine just the energy levels it is unnecessary actually to evaluate T , as the diagonal elements of H'' can be found by solving the appropriate secular equation. The procedure is rather simple as in alkali atoms we can neglect the contribution of the elements of H'' which are non-diagonal in l , and can thus treat the interaction of the Stark effect and spin within a given spin doublet separately from that in the other spin doublets. We then obtain for each non-vanishing value of l an independent secular equation of the form

$$\begin{vmatrix} H'(l, l - \frac{1}{2}; l, l - \frac{1}{2}) - W & H'(l, l - \frac{1}{2}; l, l + \frac{1}{2}) \\ H'(l, l + \frac{1}{2}; l, l - \frac{1}{2}) & H'(l, l + \frac{1}{2}; l, l + \frac{1}{2}) - W \end{vmatrix} = 0. \quad (10)$$

The solutions, in terms of the abbreviated notation of (7) and (8), are, (for $l \neq 0$):

$$W(l, l \mp \frac{1}{2}) = \frac{1}{2}(A_1 + A_2)F^2 + \frac{1}{2}(B_1 + B_2) \pm \frac{1}{2} \{ [(A_1 - A_2)F^2 + (B_1 - B_2)]^2 + 4C_1C_2F^4 \}^{1/2}. \quad (11a)$$

The single energy level ($l = 0, j = \frac{1}{2}$) remains unaltered:

$$W(0, \frac{1}{2}) = H'(0, \frac{1}{2}; 0, \frac{1}{2}). \quad (11b)$$

To calculate $W(l, l \mp \frac{1}{2})$ to terms in F^2 we expand the radical in (11a) in powers of F . It is now seen that the consideration of the interaction of the Stark effect and electron spin, embodied in the removal of the "troublesome" elements of H' , leads to a distorted multiplet structure. The distortive effect becomes vanishingly small, of course, when $(A_1 - A_2)F^2$, (the relative shift of the terms of the spin doublet due to the quadratic Stark effect¹³), is negligible compared to $(B_1 - B_2)$, (the spin separation of the doublet in the unperturbed system).

The asymptotic forms of (11a) for small and large values of F are of interest. When F is very small we have, to terms in F^2 :

$$W(l, l \mp \frac{1}{2}) = \frac{1}{2} [(1 \pm 1)B_1 + (1 \mp 1)B_2] + \frac{1}{2} [(1 \pm 1)A_1 + (1 \mp 1)A_2]F^2. \quad (11c)$$

This formula is essentially equivalent to (7). When F is very large the expansion of (11a) becomes, if terms involving reciprocals of F^2 are neglected:

$$W(l, l \mp \frac{1}{2}) = \frac{1}{2} \{A_1 + A_2 \pm [(A_1 - A_2)^2 + 4C_1C_2]^{1/2}\}F^2 \\ + \frac{1}{2} \{(B_1 + B_2) \pm (A_1 - A_2)(B_1 - B_2)[(A_1 - A_2)^2 + 4C_1C_2]^{-1/2}\}. \quad (11d)$$

If the spin separation is assumed to shrink to zero (11d) goes over into the formula of Unsoeld,⁷ as it should.¹⁴

It was the unsatisfactory aspect of H' —its being nearly degenerate—that necessitated the transformation T . But it is seen now that this transformation is indispensable whenever the F^2 terms are comparable with the multiplet structure, quite apart from the fact that the spin doublets are narrow. It is not the "absolute" width of the doublet but its "relative" width, as compared to some unit (such as Fea_1) which measures the effect of the field, that is of importance.

RELATIVE INTENSITIES OF THE STARK COMPONENTS

For a calculation of the relative intensities of the spectral Stark components it is necessary actually to evaluate the matrix T . This is accomplished easiest by again considering singly the matrices of two rows and two columns whose energy determinants are given by (10). The procedure can be simplified still further as follows: The small matrices under consideration are not Hermitian, their two off-diagonal elements being F^2C_1 and F^2C_2 . However, the quantity $(C_1 - C_2)/(C_1 + C_2)$ is very small, of the order of magnitude of the ratio $\nu_0(\Delta l = 0, \Delta j \neq 0)/\nu_0(\Delta l \neq 0)$. We can thus introduce a new quantity C , defined by $C^2 = C_1C_2$, and set $C_1 = C_2 = C$, without reducing the order of accuracy employed in the calculations above. (These approximations are not intrinsically necessary, and are employed only to attain simplicity in the final formulas for the elements of T). When these approximations are made in H' the small matrices become Hermitian, but their eigenvalues are not al-

¹³ In view of (11a) this is only approximately so.

¹⁴ It must be noted that the quantum number which Unsoeld denotes by m is denoted by m_l in the notation of reference 5, adopted here. The quantum numbers denoted by m and by m_l , respectively, in the latter notation are related thus: $m = m_l \pm \frac{1}{2}$.

tered. The indeterminateness in T can now be removed by setting $T\tilde{T}^* = 1$, and the non-vanishing elements of T , written in terms of (7), (11a), and the quantity C , become:

$$\text{for } l=0: \quad T(0, \tfrac{1}{2}; 0, \tfrac{1}{2}) = 1 \quad (12a)$$

$$\text{for } l \neq 0: \quad T(l, l-\tfrac{1}{2}; l, l-\tfrac{1}{2}) = T(l, l+\tfrac{1}{2}; l, l+\tfrac{1}{2}) = F^2 C / \xi, \quad (12b)$$

$$T(l, l+\tfrac{1}{2}; l, l-\tfrac{1}{2}) = -T(l, l-\tfrac{1}{2}; l, l+\tfrac{1}{2}) = [H_1 - W](l, l-\tfrac{1}{2}; l, l-\tfrac{1}{2}) / \xi,$$

where

$$\xi = [F^4 C^2 + \{ [H_1 - W](l, l-\tfrac{1}{2}; l, l-\tfrac{1}{2}) \}^2]^{1/2}.$$

To calculate the relative intensities of the components we may now proceed as outlined in the first paragraph of Section 11 of reference 5, except that instead of the transformation S given there we must use the successive transformations S and T given in the present paper, formulas (5) and (12).

The interaction effect described above is probably not beyond observation in light atoms.

It is a pleasure for the writer to express here his thanks to Professor J. H. Van Vleck for the suggestion of this problem and for the criticism of this work.

ALTERNATING INTENSITIES AND ISOTOPE EFFECT IN THE BLUE-GREEN ABSORPTION BANDS OF Li_2

BY A. HARVEY* AND F. A. JENKINS

DEPARTMENT OF PHYSICS, UNIVERSITY OF CALIFORNIA

(Received February 17, 1930)

ABSTRACT

Term analysis. The analysis of the blue-green Li_2 bands previously given by Wurm is extended by new data obtained with second order plates from the 15-ft. concave grating. The band heads are given by $\nu_k = 20,398.40 + 267.3\nu' - 3.1\nu'^2 - 347.4\nu'' + 2.5\nu''^2$. Wave-numbers of the rotational structure lines of the (0, 1) band are tabulated, and the evaluation of the rotational term-differences in the lower state completely confirms the assignment of this system to the electronic transition ${}^1\Pi \leftarrow {}^1\Sigma$. The molecular constants, as completely re-determined from our data, using a more accurate procedure than that of Wurm, agree closely with his values. The new constants resulting from our work are $F_e' = 1.337 \times 10^{-10} \text{ cm}^{-1}$, $F_e'' = 1.535 \times 10^{-10}$, $\alpha'' = 0.00744$, and $\beta'' = 0.765 \times 10^{-8}$. By means of the final constants and the theoretical equations, an accurate representation of the wave-numbers of the lines of the (0, 0) band is obtained. The origin of this band is found to be $20,395.96 \text{ cm}^{-1}$.

Isotope effect. The vibrational isotope effect is established by the identification of three band heads (1, 0), (2, 0), and (3, 0), due to the less abundant isotopic molecule, Li^6Li^7 , which were found in their calculated positions within the error of measurement. The rotational isotope effect in the (0, 0) band is shown by the detection of two faint line series fitting closely the theoretical equations for the Q and P branches due to Li^6Li^7 .

Alternating intensities The alternation ratio of the intensities of successive lines in the Li_2^7 bands is determined by a new method, depending partly on the theory of intensity distribution in this type of bands given by Mulliken. The best value is found from the Q branches of the (0, 0) and (1, 0) band to be 1.78 ± 0.2 . A less reliable determination from the (0, 1) band gives 1.50. Evidence is given pointing to the true value as 1.67, which corresponds to a nuclear spin of the Li atom of $3/2(h/2\pi)$. This disagrees with the value $\frac{1}{2}(h/2\pi)$ found from hyperfine structure investigations by Schüller and Brück. As required theoretically, the isotope lines due to the unsymmetrical molecule Li^6Li^7 show no alternation.

CERTAIN interesting features of the absorption bands of lithium vapor have recently been discussed by the writers in two preliminary communications.^{1,2} Spectrograms taken with both low and high dispersion showed that with a suitable adjustment of the density of the absorbing vapor, the vibrational and rotational structures of the blue-green system are simple enough to permit the quantum analysis. The close analogy of these bands with the corresponding Na_2 system³ led us to ascribe them to a transition from a ${}^1\Sigma$ normal state to a ${}^1\Pi$ excited state. This is in harmony with the observed simple PQR

* Commonwealth Fund Fellow.

¹ A. Harvey and F. A. Jenkins, Phys. Rev. **34**, 1286 (1929) (Quantum structure, alternating intensities).

² A. Harvey and F. A. Jenkins, Phys. Rev. **35**, 132 (1930), Abstract, (Vibrational isotope effect).

³ F. W. Loomis and R. W. Wood, Phys. Rev. **32**, 223 (1928).

structure of the individual bands, which was verified by applying the combination principle. As was to be expected for a symmetrical molecule, the

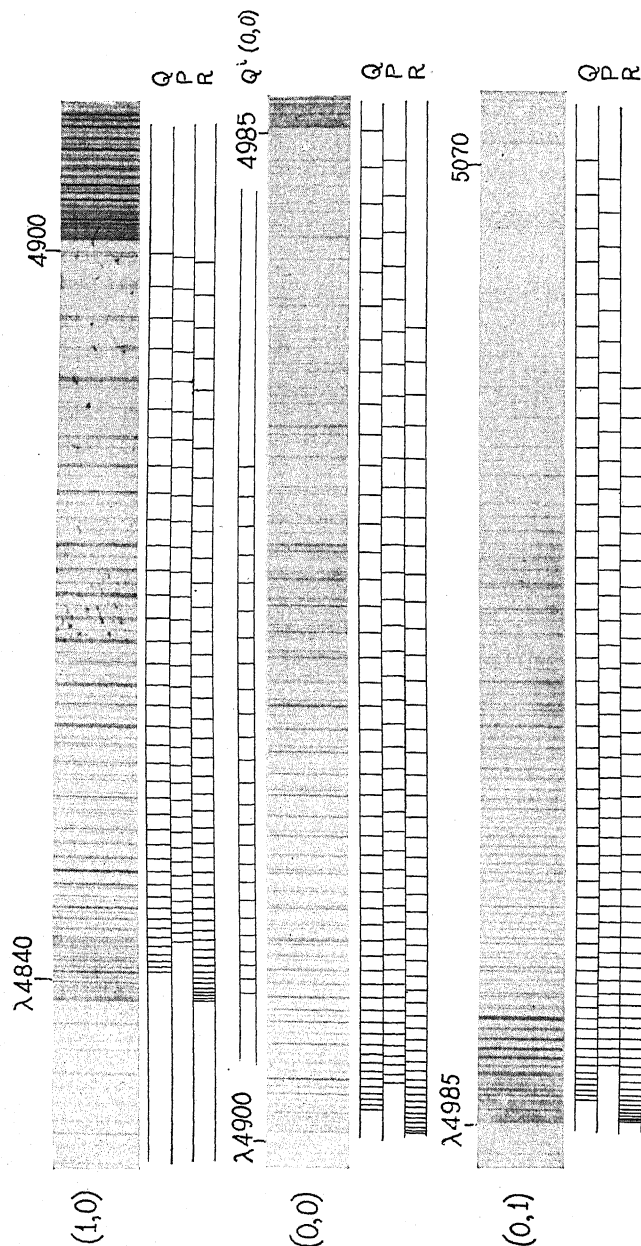


Fig. 1. Three bands of the blue-green system. Length of absorbing column 45 cm, $T=630^{\circ}\text{C}$. Second order of the 15 ft. grating.

intensities of successive lines showed a definite alternation. The alternation factor was estimated as between 1.20:1 and 1.33:1, but for reasons given be-

low the estimate was low. The vibrational isotope effect was also detected.² Li has isotopes of masses 6 and 7 in the proportion of about 1:16 (atomic weight 6.94). Besides the strong bands due to Li^7Li^7 , two weaker systems should be present, due to Li^6Li^7 and Li^6Li^6 , having respectively intensities 1/7.8 and 1/245 that of the strong system. The three most favorably placed band heads of the Li^6Li^7 system were observed. Measurements of heads are difficult in this case, especially at high temperatures, because the head occurs at a very low rotational quantum number. More satisfactory evidence of the isotope effect comes from a study of the rotational effect in the (0, 0) band the results of which will be given in the following section.

Near the completion of our work, two articles by Wurm^{4,5} appeared, dealing with the blue-green and red systems of Li_2 . The agreement of his analysis of the blue-green system with our unpublished results is excellent, not only in the wave-length data, but also in the quantum interpretation and in the resulting molecular constants. In point of self-consistency, our data seem nearly as accurate as those of Wurm, although obtained with somewhat lower dispersion (second order of a 15-ft. grating). This circumstance may be partly due to somewhat more favorable experimental conditions in our case, such as accurate control of the temperature of the electrically heated absorption tube. The spectra obtained in the present work, part of which are shown in Fig. 1, are undoubtedly less confused by the structure of faint underlying bands, since Wurm was only able to analyse the (0, 0) and (1, 0) bands. We have been able to identify the branches of the (0, 1) band without difficulty, thus permitting a check on the combination differences in the lower, as well as in the upper state. Agreements in both states are required to be absolutely certain of a correct analysis.

ISOTOPE EFFECT

Vibrational terms. From measurements of the heads of the blue-green bands an equation for the vibrational structure was derived,¹ which agreed well with that previously given by Wurm.⁴ By suitably weighting the two sets of data, we have adopted the following equation for heads:

$$\nu_h = 20,398.40 + 267.3v' - 3.1v'^2 - 347.4v'' + 2.5v''^2, \quad (1)$$

where v is the true vibrational quantum number, $v = 0, 1, 2 \dots$, formerly called n . In seeking evidence for the vibrational isotope effect, it was apparent that the faintest (Li^6Li^6) system could not be detected, due to the complexity of the spectrum, and to the fact that few of the heads are pronounced. On a low-dispersion spectrogram, taken with a carefully adjusted vapor density, it was, however, possible to find the Li^6Li^7 heads of the (2, 0)₂ and (3, 0) bands, the measured isotope shifts being 4.5 and 6.4 Å toward the

⁴ K. Wurm, *Zeits. f. Physik* **58**, 562 (1929). We had unfortunately overlooked the preliminary notice of this work, (*Naturwissenschaften* **48**, 1028 (1928)), in which a vibrational analysis of the blue-green system is given, and an equation for heads which is in close agreement with that independently derived by us (Ref. 1). Alternation of intensities is also mentioned, but the rotational analysis had not been done.

⁵ K. Wurm, *Zeits. f. Physik* **59**, 35 (1929).

violet, with a possible error of several tenths of a cm^{-1} . The theoretical shifts are most easily found by the following formula.⁶ Denoting by a superscript i quantities appropriate to the Li^6Li^7 bands, this may be written

$$\nu_0^i - \nu_0 = (\rho - 1)(\nu' + \frac{1}{2})\omega_{\nu'}' - (\rho - 1)(\nu'' + \frac{1}{2})\omega_{\nu''}'' \quad (2)$$

where $\rho = (\mu/\mu^i)^{1/2} = 1.040833$. From Eq. (1) we have

$$\omega_{\nu'}' = \omega_e' - 2x_e'\omega_e'(\nu' + \frac{1}{2}) = 270.4 - 2 \times 3.1(\nu' + \frac{1}{2}); \quad \omega_{\nu''}'' = 349.9 - 2 \times 2.5(\nu'' + \frac{1}{2}),$$

assuming that the coefficients apply equally well to band origins. This is justified here because the heads are at a small and nearly constant distance from the origins. The computed shifts in the above two cases are 4.3 and 6.3A, respectively. The (1, 0) isotope head is too close to the main band to be resolved with the prism spectrograph, but on a first order grating plate the attendant (1, 0) head could be measured with difficulty. The observed and calculated shifts in this case were 2.06 and 2.08A. On the red side of the system-origin, the fainter bands are entirely concealed by the Li^7Li^7 bands.

Rotational terms. In identifying the individual lines of the (0, 0) isotope band, more accurate and complete rotational constants of the strong system than those given by Wurm were required. We have therefore made an independent evaluation of these from our data. The wave-numbers of the rotational lines of the (0, 0) and (1, 0) band agree very well with Wurm's published data, although there is a small, nearly constant, discrepancy amounting to about 0.1 cm^{-1} on the average, our values being higher. Measurements of these bands are therefore omitted here, although the constants obtained from them are tabulated below. Table I gives wave-numbers in vacuum for the (0, 1) band, which was not analysed by Wurm, and also shows the agreement of the resulting term-differences, $\Delta_2 F_0'$, with his values from the (0, 0) band.

In the calculation of rotational constants, we have assumed the following expressions for the rotational energy:

$$\begin{aligned} \text{I}\Sigma: F(K) &= B''K(K+1) + D''[K(K+1)]^2 + F''[K(K+1)]^3 \\ \text{I}\Pi: F(K) &= B'[K(K+1) - 1] + D'[K(K+1) - 1]^2 + F'[K(K+1) - 1]^3. \end{aligned} \quad (3)$$

The observed rotational term-differences definitely require the F term, as is evident from Fig. 3 of Wurm,⁴ where it was not taken into account. With the above term formulation, the $R-P$ differences should be given by

$$\Delta_2 F(K) = 4BK + 8DK^3 + 12FK^5, \quad (4)$$

in which some negligible terms have been omitted. By means of the relations

$$D_e = -\frac{4B_e^3}{\omega_e^2}; \quad F_e = \frac{D_e^3}{B_e} \left(2 - \frac{\alpha\omega_e}{6B_e} \right);$$

⁶ The general equation for the vibrational isotope effect has recently been considered by Birge (unpublished work). A sufficiently accurate approximation, in the present case, is given by the formula quoted, a form already used by Patkowski and Curtis, *Trans. Farad. Soc.* 25, 725 (1929).

TABLE I. Absorption lines and combination differences of the (0, 1) band.

K	R(K)	Q(K)	P(K)	$\Delta_2 F_1''(K)$	$\Delta_2 F_0'(K)$	$\Delta_2 F_0'(K)^*$
6	20052.59	20044.63	20037.12		15.47	
7	051.81	042.90	034.78	20.42	17.03	
8	051.14	041.35	032.17	22.29	18.97	
9	050.36	039.37	029.52	24.83	20.84	
10	049.27	037.12	026.31	27.41	22.96	23.046
11	047.95	034.78	022.95	29.79	25.00	25.222
12	046.60	032.17	019.48	32.73	27.12	27.414
13	044.63	029.52	015.22	35.51	29.41	29.733
14	042.90	026.31	011.09	37.92	31.81	31.735
15	040.61	022.95	006.71	40.74	33.90	33.924
16	038.19	019.48	002.16	43.24	36.03	36.148
17	035.68	015.91	19997.37	45.83	38.31	38.350
18	032.73	012.00	992.36	48.54	40.37	40.431
19	029.52	007.81	987.14	51.02	42.38	42.570
20	026.31	003.47	981.71	53.54	44.60	44.649
21	022.95	19998.90	975.98	56.04	46.97	46.792
22	019.17	994.17	970.27	58.66	48.90	48.893
23	015.22	989.16	964.29	61.05	50.93	50.980
24	011.09	984.00	958.12	63.60	52.97	53.055
25	006.71	978.53	951.62	66.21	55.09	55.153
26	002.16	972.96	944.88	68.60	57.28	57.191
27	19997.37	967.17	938.11	71.26	59.26	59.245
28	992.36	961.06	930.90	73.65	61.46	61.310
29	987.14	954.71	923.72	76.06	63.42	63.394
30	981.71	948.27	916.30	78.52	65.41	65.369
31	975.98	941.61	908.62	80.97	67.36	67.338
32	970.27	934.63	900.74	83.40	69.53	69.348
33	963.95	927.52	892.58	86.08	71.37	71.277
34	957.75	920.17	884.19	88.27	73.56	73.315
35	950.98	912.64	875.68	90.75	75.30	75.238
36	944.19	904.90	867.00	92.90	77.19	77.053
37	937.14	896.92	858.08	95.06	79.06	79.119
38	929.97	888.71	849.13	97.49	80.84	81.010
39	922.46	880.30	839.65	99.87	82.81	82.872
40	914.80	871.62	830.10	102.11	84.70	
41	906.86	862.83	820.35	104.45	86.51	
42	898.84	853.86	810.35	106.74	88.49	
43	890.52	844.54	800.12	108.96	90.40	
44	881.88	835.03	789.88	111.15	92.00	
45	873.06	825.47	779.37	113.24	93.69	
46	863.61	815.53	768.64	115.54	94.97	
47	854.87	805.38	757.52	117.03	97.35	
48	845.52	795.02	746.58	119.88	98.94	
49	835.70	784.61	734.99	121.93	100.71	
50	825.47	773.07	723.59		101.88	
51	815.53	762.81				
52	805.38	751.79				
53	795.02	740.31				
54		728.84				

* (0, 0) band, Wurm.

TABLE II. Rotational constants of Li_2^+ molecule.*

	Normal State ($^1\Sigma$)		Excited State ($^4\Pi$)	
	(H. & J.)	(Wurm)	(H. & J.)	(Wurm)
B_0	0.66914 cm^{-1}	0.6694	0.55321	0.5532
D_0	-0.9952×10^{-5}	-0.9865×10^{-5}	-0.9531×10^{-5}	-0.9407×10^{-5}
F_e	1.535×10^{-10}	—	1.337×10^{-10}	—
α	0.00744	—	0.00804	0.0084
β	0.765×10^{-8}	—	-14.48×10^{-8}	-11.7×10^{-8}
I_e	$41.12 \times 10^{-40} \text{ g cm}^2$	—	49.66×10^{-40}	—
r_e	$2.67 \times 10^{-8} \text{ cm}$	—	2.93×10^{-8}	—

* The values of B apply only to P and R branches (cf. text).

$$\beta = \frac{\alpha^2}{6\omega_e} + \frac{20\alpha B_e^2 - 32x_e B_e^3}{\omega_e^2};$$

$$B_v = B_0 - \alpha v = B_e - \alpha(v + \frac{1}{2}); D_v = D_e + \beta(v + \frac{1}{2}); F_v \cong F_e,$$

we have solved Eqs. (4) for the four states $v' = 0, 1; v'' = 0, 1$, by a well-known procedure⁷ involving a number of successive approximations. In this calculation, the vibrational constants from Eq. (1) were used; $\omega_e' = 270.4$, $\omega_e'' = 349.9$, $x_e' = 1.146 \times 10^{-2}$, $x_e'' = 0.7145 \times 10^{-2}$. Table II gives the final constants and a comparison with their values as found by Wurm.

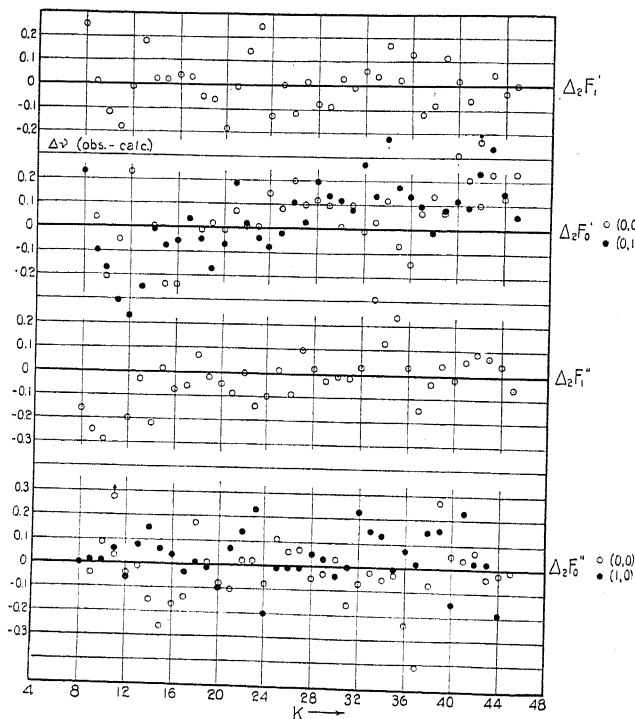


Fig. 2. Deviations (obs-calc) of all rotational term-differences from their values as given by Eq. (4).

Fig. 2 gives the residuals of the available term-differences from those calculated by Eqs. (4) using the above constants. The small linear trend which appears in the $\Delta_2 F_0'$ residuals indicates the necessity for a small constant term in the true expression for $\Delta_2 F$. Such a "secondary ρ " term is justified theoretically, but was not used here since the error is small.

As is expected in a $^1\Pi$ state, the Λ -type doubling of rotational terms causes a small combination defect to appear when an attempt is made to obtain $\Delta_1 F$ values by combinations with the Q branch. This doubling is proportional⁴ to $(K + \frac{1}{2})^2$ and hence the initial terms of the Q branch may also be represented by Eq. (3), using a slightly smaller value of B . Wurm has found

⁷ Method 3 of Birge, "Molecular Spectra in Gases," pp. 173-5.

this difference for the (0, 0) band to be $B_B' - B_A' = 0.00018$, and since our data on the combination defect are in essential agreement with his, we have adopted $B_0' = 0.55303$ for the Q branch.

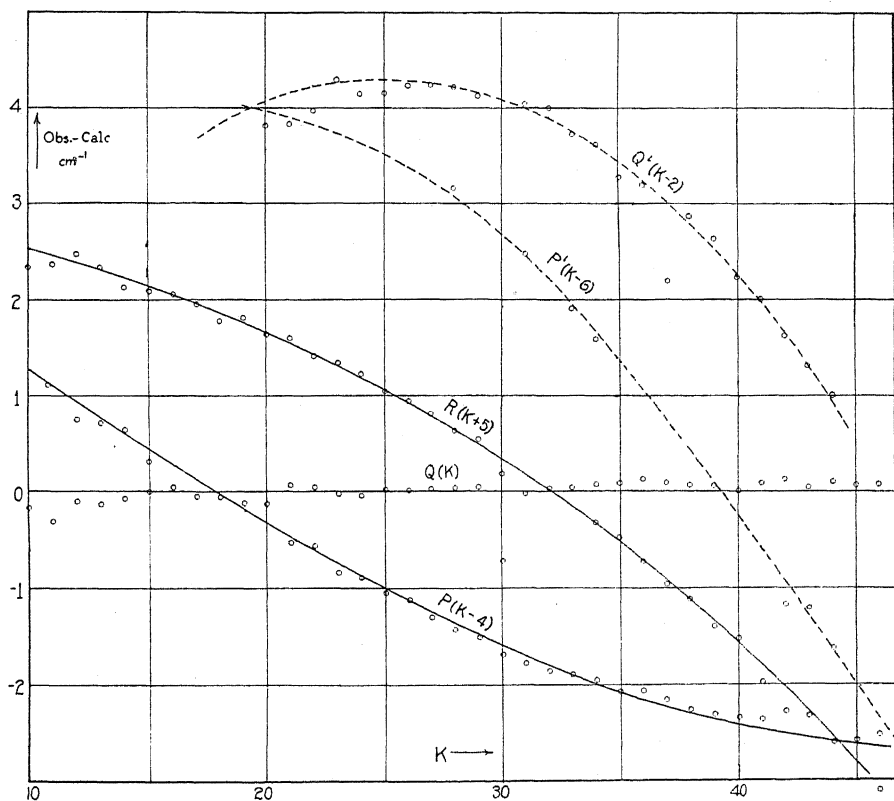


Fig. 3. Differences in wave-numbers of all lines of the (0, 0) band from the calculated Q lines. Solid lines, theoretical values from Eqs. (5); dotted lines, Q and P branches of the (0, 0) isotope band, from Eqs. (6).

A rigorous test of the accuracy of these constants is obtained by finding how well the observed *wave-numbers* of the P , Q and R branches are reproduced by the theoretical formulas:

$$\begin{aligned}
 R(K) &= \nu_0 - \frac{1}{4}C_B + 2B_B'(K + \frac{1}{2}) + (C_B + 4D')(K + \frac{1}{2})^2 + 4D'(K + \frac{1}{2})^3 \\
 &\quad + (E + 12F')(K + \frac{1}{2})^4 + 6F'(K + \frac{1}{2})^5 + G(K + \frac{1}{2})^6, \\
 P(K) &= \nu_0 - \frac{1}{4}C_B - 2B_B'(K + \frac{1}{2}) + (C_B + 4D')(K + \frac{1}{2})^2 - 4D'(K + \frac{1}{2})^3 \\
 &\quad + (E + 12F')(K + \frac{1}{2})^4 - 6F'(K + \frac{1}{2})^5 + G(K + \frac{1}{2})^6, \\
 Q(K) &= \nu_0 - B_A' - \frac{1}{4}C_A + (C_A - 2D')(K + \frac{1}{2})^2 + E(K + \frac{1}{2})^4 + G(K + \frac{1}{2})^6,
 \end{aligned} \tag{5}$$

where $C_A = B_A' - B''$, $C_B = B_B' - B''$, $E = D' - D''$ and $G = F' - F''$. Since the origin ν_0 , is as yet undetermined, this amounts to testing the constancy of ν_0 as computed from the various lines. We find small trends of the order of 0.3

cm.⁻¹ and have taken 20,395.96 as the best average. To show the results of the calculation of wave-numbers of the lines by Eqs. (5), it is convenient to use a graphical method due to Loomis and Wood.³ For this, a plot is made of the differences of every measured line in the band from the calculated values of the *Q* lines. Since the line series in bands of this kind run nearly parallel, the *P* and *R* branches also show on the diagram as series of points lying on a smooth curve. In Fig. 3 is given such a graph for the (0, 0) band. The two solid curves represent the differences of the *calculated R* and *P* lines from the adjacent *Q* lines. The agreement is as close as can be expected. This method of plotting was first used in identifying the branches of the (0, 0) band. It was then found that a number of lines were not accounted for as *P*, *Q* or *R* lines,

TABLE III. Comparison of calculated and observed wave-numbers for the *Q* branches of the Li^7Li^7 and Li^6Li^7 (0, 0) bands.

<i>K</i>	<i>Q</i> (<i>K</i>) calc	<i>Q</i> (<i>K</i>) obs	<i>Q</i> ⁱ (<i>K</i>) calc	<i>Q</i> ⁱ (<i>K</i>) obs
6	20390.53	20390.42		
7	388.91	388.80		
8	387.05	386.98		
9	384.96	384.96		
10	382.64	382.47		
11	380.09	379.78		
12	377.31	377.20		
13	374.29	374.15		
14	371.05	370.97		
15	367.57	367.56		
16	363.86	363.90		
17	359.92	359.86		
18	355.75	355.69	20350.76	20350.52
19	351.35	351.22	346.00	345.62
20	346.72	346.58	340.98	340.72
21	341.86	341.92	335.72	335.73
22	336.76	336.80	330.20	330.03
23	331.44	331.41	324.44	324.26
24	325.89	325.84	318.42	318.32
25	320.11	320.12	312.16	312.08
26	314.10	314.10	305.66	305.61
27	307.86	307.88	298.90	298.82
28	301.40	301.43	291.90	
29	294.70	294.74	284.64	284.66
30	287.78	287.96	277.15	277.25
31	280.62	280.60	269.40	269.35
32	273.25	273.28	261.41	261.41
33	265.64	265.68	253.18	253.01
34	257.80	257.87	244.69	244.67
35	249.74	249.82	235.96	
36	241.47	241.60	226.99	227.07
37	232.94	233.03	217.77	217.86
38	224.20	224.27	208.31	208.27
39	215.23	215.29	198.60	198.62
40	206.04	206.05	188.65	188.59
41	196.62	196.71	178.45	178.42
42	186.97	187.11	168.01	168.01
43	177.10	177.15		
44	167.01	167.12		
45	156.69	156.76		
46	146.15	146.24		
47	135.38	135.34		
48	124.39	124.36		
49	113.18	113.05		
50	101.74	101.65		

and, in fact, a number formed a distinct fourth series, with indications of a fifth. The explanation of these extra branches appears when the positions of the isotope lines of the (0, 0) band of Li^6Li^7 are determined by the theory of the isotope effect. The origin ν_0^i , of this band is, from Eq. (2), 1.635 cm^{-1} lower in wave-number than that of the strong (0, 0) band. Assuming, as is usual, a negligible electronic isotope effect, we may now compute all the lines of the fainter band. It is only necessary to multiply the coefficients of Eqs. (5) by the appropriate powers of ρ , and to insert the new origin. There results:

$$\begin{aligned} R^i(K) &= \nu_0^i - \frac{1}{4}\rho^2 C_B + 2B_B' \rho^2 (K + \frac{1}{2}) + (\rho^2 C_B + 4\rho^4 D') (K + \frac{1}{2})^2 + 4\rho^4 D' (K + \frac{1}{2})^3 \\ &\quad + (\rho^4 E + 12\rho^6 F') (K + \frac{1}{2})^4 + 6F' \rho^6 (K + \frac{1}{2})^5 + \rho^6 G (K + \frac{1}{2})^6, \\ P^i(K) &= \nu_0^i - \frac{1}{4}\rho^2 C_B - 2B_B' \rho^2 (K + \frac{1}{2}) + (\rho^2 C_B + 4\rho^4 D') (K + \frac{1}{2})^2 - 4\rho^4 D' (K + \frac{1}{2})^3 \quad (5') \\ &\quad + (\rho^4 E + 12\rho^6 F') (K + \frac{1}{2})^4 - 6F' \rho^6 (K + \frac{1}{2})^5 + \rho^6 G (K + \frac{1}{2})^6, \\ Q^i(K) &= \nu_0^i - \rho^2 B_A' - \frac{1}{4}\rho^2 C_A + (\rho^2 C_A - 2\rho^4 D') (K + \frac{1}{2})^2 + \rho^4 E (K + \frac{1}{2})^4 + \rho^6 G (K + \frac{1}{2})^6. \end{aligned}$$

The calculated Q^i and P^i branches are shown in Fig. 3 to be in excellent agreement with the two anomalous series, although P^i is rather fragmentary, due to its faintness. With these isotope lines explained, only two measured lines in the (0, 0) band remain unaccounted for, and one perhaps belongs to the R^i branch. This constitutes probably the most exacting test of the theory of the isotope effect yet applied. The numerical accuracy of the agreement appears in Table III. This is within the error of the calculation, and hence discrepancies cannot be taken as indicating that the atomic weights of Li^6 and Li^7 do not differ by integers.

Further confirmation of the isotope character of these lines is found in their failure to show alternating intensities, as discussed below.

ALTERNATING INTENSITIES

The alternation of the intensities of successive lines in each branch already established by the writers,¹ and by Wurm,⁴ is of special interest, since the alternation ratio gives a measure of the spin of the Li nucleus.⁸ To determine the latter, a quantitative measure of the ratio is required. This is particularly difficult in the present case, due largely to the many erratic fluctuations resulting from superpositions with faint underlying structure. There is also the difficulty, at least with our experimental arrangements, that neither the density of vapor nor length of the absorbing column can be found accurately, so that calculations of the absorption coefficients cannot be made, even though the intensities of the absorption lines themselves be correctly evaluated. It was at first thought that the vapor density was low enough for the observed intensities of absorption to be proportional to absorption coefficients, and a preliminary estimate of the ratio was made with this assumption. Density curves were obtained with the Zeiss-Koch recording microphotometer. An example of these curves is given in Fig. 4. In each branch of the (0, 0) band, the average electrometer deflection (background to line center) for the stronger set of lines, those with odd K'' , was compared with

⁸ For a review of this theory see R. S. Mulliken, Trans. Faraday Soc. 25, 634 (1929).

the average deflection for the weaker set. The ratio of these gave 1.2:1. Using the usual law relating densities to intensities, the alternation ratio was estimated as lying between 1.2 and 1.33. Uncertainty in the estimated contrast factor, γ , allowed considerable latitude in this result. Upon repeating the microphotometer curves with a better spectrogram, it was found that, by

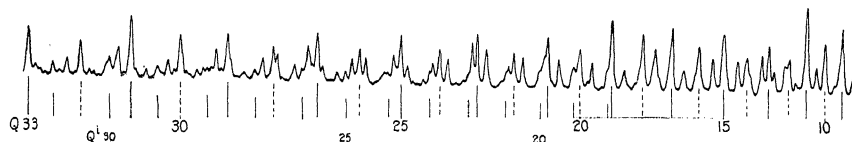


Fig. 4. Microphotometric trace (retouched) of part of the (0, 0) band, showing alternation of intensity in the Q branch of the stronger (Li^7Li^7) band. No alternation is apparent in the weaker branch, Q^2 , due to Li^6Li^7 .

plotting the electrometer throws for a given branch two fairly good curves were obtained, corresponding to the stronger and weaker sets, as shown in Fig. 5. A number of values lie definitely above the general run, and many of these lines are shown by the structure analysis to be blended with other lines of the band. Neglecting these, and giving the smaller values more weight

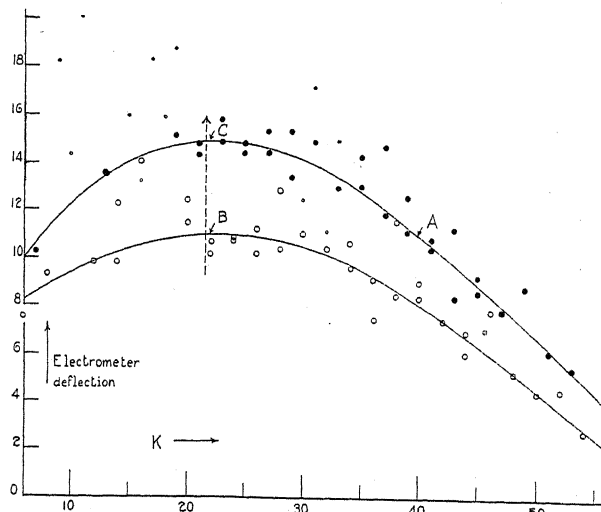


Fig. 5. Height of peaks on microphotometer curves for the Q branches of the (0, 0) and (1, 0) bands as a function of K. To render the two sets of data comparable, that for the (1, 0) band has been multiplied throughout by 0.84. Dots represent the stronger set of lines (K odd) and circles the weaker (K even). Lines known from the analysis to be blends are indicated by small dots or circles. The arrow indicates the theoretical intensity maximum, from Eq. (7). The significance of points A, B and C is discussed in the text.

in drawing the curves, satisfactory curves could be obtained for the Q branches of the three bands studied. The mean ratio of the deflections now becomes about 1.4:1. It will be seen that failure to take into account the evident superpositions tended to render our earlier estimate of the ratio too low.

A new method has now been applied which renders unnecessary the evaluation of absorption coefficients, or determination of γ , since it rests purely on the *equality* of certain intensities. Thus, in Fig. 5, we first determine the value of K for the point A , at which the deflections for the stronger set have fallen to that of the maximum value, B , in the weaker set. Since the blackening is the same at A and B , the intensities are equal at these points. We may then calculate, using the well-established theoretical formulas for intensities in $^1\Sigma-^1\Pi$ bands,⁹ the ratio of intensities of two lines having the K values of points A and B , which ratio is then the required one, because the intensity ratio of points C to A equals that of C to B .

The intensity distribution in the Q branch of a band with $\Lambda'-\Lambda''=+1$ is given, according to Mulliken's formulas,⁹ by

$$I_Q = [2A(K+\frac{1}{2})(K+\Lambda')(K+1-\Lambda')/K(K+1)]e^{-E/kT}$$

or, when $\Lambda'=1$

$$I_Q = A(2K+1)e^{-E/kT}. \quad (6)$$

Since we are dealing with absorption, $E = F''(K)$. This formula has been shown⁹ to be in agreement with experimental data in a number of cases. The corresponding equations for the P and R branches were not of use for the purpose in hand, since the data for these branches, which are roughly half as intense as the Q branch, are not as complete or as consistent. Appreciable deviations of experiment from theory have also been found,⁹ particularly in the case of the P branch. It therefore seems best to restrict ourselves to the Q branches, and to evaluate the alternation ratio from the curves of Fig. 5.

First we may show that Eq. (6) is in agreement with the observed K value of the maximum intensity. Differentiating, and equating to zero:

$$\frac{dI_Q}{dK} = 2Ae^{-E/kT} + A(2K+1)e^{-E/kT} \frac{d}{dK} \left(-\frac{E}{kT} \right) = 0$$

whence we find, inserting for E its value $B''[K(K+1)] + D''[K(K+1)]$,² that, for the intensity maximum,

$$2B''(K+\frac{1}{2})^2 + 4D''(K+\frac{1}{2})^4 = kT. \quad (7)$$

The temperature of the absorption tube was measured by a thermocouple in direct contact with the heavy Ni tube which was covered with asbestos and electrically heated from the outside. For the plate used in this work $T = 630^\circ \pm 10^\circ \text{C} = 903^\circ \text{K}$. Solving Eq. (7), using the B_0'' and D_0'' from Table II, it is found that, for the maximum of intensity, $K = 21.5$. Fig. 5 shows that this is in good agreement with the observed value.

Such a check on the correctness of the theory lends more confidence to the application of the method for determining the alternation ratio outlined above. From Eq. (6) we obtain the ratio of any two lines of the Q branch,

$$I_{Q(K_1)}/I_{Q(K_2)} = \frac{K_1 + \frac{1}{2}}{K_2 + \frac{1}{2}} e^{(E_2 - E_1)/kT}. \quad (9)$$

⁹ R. S. Mulliken, Phys. Rev. 29, 391 (1927).

The stronger lines of the Q branch become equal to the maximum of the weaker set at $K=40$ (point A, Fig. 5). The ratio of intensities at C and A then becomes, from Eq. (6),

$$I_{Q(22)}/I_{Q(40)} = \frac{22 + \frac{1}{2}}{40 + \frac{1}{2}} \exp \left[\frac{1070.62 - 336.04}{903 \times 0.698} \right] = 1.78.$$

A similar evaluation from the (0, 1) band with much less reliable data, and fewer points, gave 1.50. The limit of accuracy of these figures is determined principally by the accuracy with which the curves can be drawn. It is found, however, that the highest possible value for the ratio, corresponding to a reasonable fit with the observed points is 2.0, and the lowest 1.6. The result is also rather sensitive to the value of T assumed. A change of T by 10° changes the ratio by 0.02. We obtained consistent readings of the temperature with the Pt-Pt, Rh thermocouple in various positions along the length of the tube, and it was standardized at the melting point of antimony, 630.5° C. A certain portion of the vapor near the water-cooled ends of the tube must of course have been at a lower temperature, but the vapor density decreases rapidly at this temperature, the absorption with the tube at 580° C being negligible.¹⁰ Hence the effects of the cooler ends should not be great.

According to the theory of alternating intensities in band spectra,⁸ only certain definite values of the alternation ratio are possible. Denoting by i the angular momentum of the Li nucleus in units $\hbar/2\pi$, the statistical weights of successive rational levels contain a factor alternating in the ratio $(i+1)/i$. The nuclear spin, i , may in general be integral or half-integral. In the neighborhood of the observed value we have the following possibilities:

$i = 1$	$3/2$	2
Ratio 2:1	1.67:1	1.50:1

The value 1.67 is within the limit of error of our measurement, but the others are not excluded. In view of relations discussed below, however, they must be regarded as improbable. From eye estimate of intensities by Wurm,⁴ the average ratio of successive lines is 1.7:1, and in the red bands⁵ he estimates the factor to be 2:1.

These results therefore indicate the spin of the Li nucleus to be $3/2$ $\hbar/2\pi$. This is in harmony with some recent generalizations¹¹ which have been drawn by considering all known values of i . For convenience the latter are collected in Table IV.

The conclusion of Heitler and Herzberg¹² that the spin of the electron is not effective in the nucleus, and that the addition of one proton adds or subtracts $\frac{1}{2}$ unit finds strong support in such a table. On this view, an integral value of i would not be expected for Li^7 , nor for any atom with an odd number of protons. One is fairly sure that in Li^7 the α -particle configuration gives a resultant spin of zero; for the He nucleus it is proven by the absence of alter-

¹⁰ Wurm, Ref. 4, estimates absorption to begin at 400° C. We were unable to detect any molecular absorption below 580° C.

¹¹ H. Schüller and H. Brück, *Zeits. f. Physik* **58**, 735 (1929).

¹² W. Heitler and G. Herzberg, *Naturw.* **17**, 673 (1929).

nate lines in the band spectrum that $i=0$. The probable value of $3/2$ in our case may then be interpreted as due to the parallel orientation of the spins of the three remaining protons. It will be seen in Table IV that all atoms with an odd number of nuclear protons heretofore studied have yielded only values of $i=\frac{1}{2}$, $5/2$, and $9/2$, differing by $4/2$. The possible significance of

TABLE IV.

Element	Number of nuclear		Nuclear spin = i	Determined from
	Protons	Electrons		
H	1	0	$\frac{1}{2}$	Band Spectra
He	4	2	0	" "
Li ⁷	7	4	$3/2$	" "
C ¹²	12	6	0	" "
N ¹⁴	14	7	1	" "
O ¹⁶	16	8	0	" "
F	19	10	$\frac{1}{2}$	" "
Na	23	12	$>5/2$	" "
Cl ³⁵	35	18	$5/2$	" "
Mn	55	30	$5/2$	Hyperfine structure
Zn	64	34		} Hyperfine structure Zeeman effect
	66	36	0	
	68	38		
	70	40		
Cd	110	62	0	} Hyperfine structure
	111	63	$\frac{1}{2}$	
	112	64	0	
	113	65	$\frac{1}{2}$	
	114	66	0	
	116	68	0	
I	127	74	$>5/2$	Band spectra
La	139	82	$5/2$	Hyperfine structure
Pr	141	82	$5/2$	" "
Tl	205	124	$\frac{1}{2}$	" "
Bi	209	126	$9/2$	{ Hyperfine structure Zeeman effect

this has been mentioned by White,¹³ but it may be that the absence of intermediate values is due to the scarceness of data for the lighter elements. In a preliminary announcement of their work on the hyperfine structure of the Li II line $\lambda 5485$, Schüler and Brück¹¹ state that the pattern can be completely explained on the assumption that $i=\frac{1}{2}$ for the Li⁷ nucleus. It will be readily seen even upon visual inspection of the bands in Fig. 1, that the alternation ratio of 3:1 required by this is out of the question.

In conclusion, we may mention that a careful examination of the photometric curves has failed to reveal any consistent alternation in the intensities of the lines in the Q branch of the (0, 0) band due to the isotope molecule, Li⁶Li⁷. The ratio of the average height of the peaks for odd K to that of even K was 1.05:1, which means sensible equality when we are dealing with such faint lines. The absence of alternation is of course to be expected for a non-symmetrical molecule, and our result is similar to that obtained by Elliott¹⁴ from his study of the Cl₂ bands.

¹³ H. E. White, Phys. Rev. **34**, 1404 (1929).

¹⁴ A. Elliott, Proc. Roy. Soc. **123A**, 629 (1929).

INTENSITY MEASUREMENTS IN THE
ARC SPECTRUM OF THALLIUM*

BY O. U. VONWILLER

DEPARTMENT OF PHYSICS, UNIVERSITY OF SYDNEY, AUSTRALIA

(Received December 9, 1929)

ABSTRACT

Measurements were made by the photographic method of the ratio of the intensities of the lines $2p_2-2s$, $2p_1-2s$ in the arc spectrum with a current of 1.6 amp. using alloys of lead and thallium in varying proportions. The ratio increased with decreasing concentration of thallium reaching a limit at about 0.01 per cent, the effects of absorption being negligible at this stage. The limiting value for $\overline{a_2^2}/\overline{a_1^2}$ is 0.388, where $I=a^2\nu^4$. Commercial lead was found to have a considerable thallium content making it necessary to use chemically pure lead. Measurements of the ratios of intensities of doublets in the principal series $2s-m p_1$, $2s-m p_2$ were made for $m=4, 5, 6$ and 7 the values obtained for $\overline{a_1^2}/\overline{a_2^2}$ being respectively 4.5, 5.7, 6.4 and 7 of which the last two are very uncertain. The values were found to be independent of concentration of thallium and of the current over a restricted range of tests. The fraction of light transmitted through an antimony film reducer was found to vary with wave-length as follows: λ , 6550, 0.270; λ , 5530, 0.243; λ , 5350, 0.243; λ , 4890, 0.175; λ , 3780, 0.093. The diffraction effects recorded by Shenstone were observed and photometer diagrams are given in illustration.

A CONSIDERABLE amount of work has been done by several investigators on the measurement of intensities of doublets in the arc spectra of the alkalis and a number of interesting and important results have been obtained such as the relations between the ratio of intensities in the doublet, the effective quantum number and the atomic number, found by Sambursky.¹ It is therefore a matter of interest that similar observations should be made with another metal giving doublets but belonging to a different group and for this reason this investigation on the arc spectrum of thallium was commenced.

The method employed was the photographic one developed by Professor Ornstein and in general use in the Physical Laboratory in Utrecht.² A Hilger quartz spectrograph, type E-2, was used with photographic plates of several kinds, namely, Ilford Iso-Zenith, Ortho-Chromatic, Pan-Chromatic and Soft Gradation Pan-Chromatic according to the spectral region being examined.

Density marks were taken on all the plates; these consisted of continuous spectra from a quartz tungsten band lamp, the varying slit method being employed. For the calibration of the lamp and the calculation of the spectral distribution of the energy for the various currents used I am indebted to Mr. D. Vermeulen. With most of the plates for each exposure, both of arc and continuous spectra, two intensities were obtained by means of a reducer placed

* Communication from the Physical Laboratory, the State University of Utrecht.

¹ S. Sambursky, *Zeits. f. Physik*, **49**, 731 (1928).

² L. S. Ornstein, *Proc. Phys. Soc. London* **37**, 334 (1925).

in front of the slit of the spectrometer. This consisted of a quartz plate on half of one surface of which a thin film of antimony had been deposited by evaporation in vacuum. By this means it was possible to overcome the difficulty arising from the very great differences between the intensities of the lines on the plates found with some of the doublets examined though in the case of each pair, by selection of suitable times of exposure and the use of absorbing screens, many comparisons were made using the same half of the spectrum for both lines so that errors due to inequalities in the comparatively narrow spectrometer slit were negligible. The two intensities were used mainly to extend the range of calibration of the plate and as a means of checking the trustworthiness of the work by the parallelism of the two graphs obtained when the photometer records of the density marks were plotted against the logarithms of the slit widths. In all cases the transmission of the antimony screen was determined photographically from the distance between the two curves thus obtained so that the values are free from any error which might be introduced in a direct determination with a somewhat different optical system.

Several of the lines examined, in particular that of wave-length 5350A occur in a region where the sensitiveness of the plate changes to a marked degree for a very small spectral displacement, and special care was needed in the calibration of the plates with the photometer in these cases. It was found that when the plateholder was moved up and down in the camera its path was slightly curved so that if the plate were aligned in the photometer in such a way that the images of a given line in spectra at the top and bottom of the plate passed across the middle of the thermopile slit, the images of corresponding lines in spectra in the middle of the plate were appreciably displaced from this position. The path of the plateholder was, however, reproduced with sufficient exactness when the up and down motion was repeated and errors arising from this were minimized by taking many arc spectra on the plate with not more than two continuous spectra between successive arc spectra. By aligning the plate in the photometer for each successive pair of arc spectra satisfactory records were obtained for the intervening continuous spectra, as was shown by the two graphs being continuous and parallel.

THE DOUBLET $2p_1-2s$, $2p_2-2s$.

The first pairs of lines examined was the first doublet in the Sharp series, $2p_1-2s$, $2p_2-2s$ of wave-lengths 5350.46 and 3775.72. Some difficulty was experienced with these lines because of the feature of plate sensitiveness discussed above and because of the very great disparity between the ratio of intensities of the two lines on the plates and the ratio of the intensities of the continuous spectrum in the same regions. In the final cases with the tungsten band at a temperature of 2750°K the slit widths making the continuous spectrum equivalent to the lines were in the ratio of 40:1, that for the ultra-violet line being the greater. It was found convenient to use in the path of the light a screen consisting of a glass cell containing a dilute aqueous solution of potassium ferrocyanide, which absorbed the ultra-violet to a much greater

extent than the green though of course the same occurred in the case of the continuous spectrum. The fact that the transmission of the antimony reducer was more than 2.5 times as great for the green as for the ultra-violet line was also helpful.

These two lines are strongly reversed when the intensity is at all great and to make a satisfactory determination of the ratio of intensities it was necessary to obtain conditions under which the absorption causing this reversal does not occur.

In the first trials an arc was used between poles made of an alloy of lead and thallium; these were rods, 12 mm in diameter forced into slightly smaller hollows in heavy copper rods. The relative intensities of the two lines were measured using alloys with several different concentrations of thallium it being expected that when the proportion of thallium was reduced the effect of absorption would become less because of the smaller amount of thallium vapor in the arc so that the true value of the ratio would be approached. The current was kept at the same value, 1.5 to 1.6 amp. throughout, the supply voltage being 440. With decreasing concentration it was found that the ratio of intensity of the ultra-violet to the green line increased, this being explained by the absorption being greater in the case of the line of shorter wave-length so that this line should gain relatively when the conditions favored decreased absorption. With the strongest concentrations used, probably 2 or 3 percent thallium, a wide range of values was obtained the explanation of which is the lack of homogeneity of the poles, there being comparatively large regions relatively rich or poor in thallium, so that the arc at different times corresponded with alloys of different concentrations. With smaller concentrations of thallium more regular results were obtained, due probably, in part to a more nearly homogeneous alloy, and in part to the fact that the exposures were longer, minutes instead of seconds, so that various parts of the pole surfaces were in turn the source of the vapor in the arc and a more uniform average value was obtained.

The ratio of intensities was found still to increase with extremely small concentrations and, as it was found at this stage that the commercial lead used in making the alloys contained an appreciable amount of thallium, it became uncertain whether even the dilution in this lead without the addition of any thallium would give the limiting ratio sought. Other specimens of lead examined were found to contain thallium but some "chemically pure" lead was obtained in which the thallium content, if any, was certainly very much smaller so that fresh trials were made in which this lead was used to make the alloys. The results of the experiments with the impure lead are shown in the upper part of Fig. 1, the ordinates being proportional to the ratio of intensities (ultra-violet to green) and the abscissas to the logarithms of the concentration of thallium on an arbitrary scale. The latter are certainly incorrect being based on the assumption that the lead was free from thallium.

As in the first method of producing the arc there was a considerable loss of material through the melting of the poles a new method had to be employed

with the chemically pure lead, especially as it was clear that very small concentrations of thallium would be required, and therefore very long exposures. A Pfund type of arc was used with copper poles, the alloy being placed in a cup shaped hollow on the lower one. The current had the same value as in the earlier experiments, 1.6 amp. Generally it was not found possible to maintain the arc between the upper pole and the alloy for a long time; either the arc would go out or else run to the side of the lower pole. When this occurred the light was at once cut off and the copper cup scraped free of the layer of lead oxide formed on it and a fresh supply of alloy introduced when the arc could be re-started. In this way spectra were obtained in which the copper lines were relatively weak. When the arc passed from copper to copper the thallium lines were still present but of course corresponded with a much smaller concentration of thallium than that in the alloy under examination. It was much easier to maintain a larger current in this way but the small current seemed more likely to give the limiting value for the ratio of intensities.

By this method of experiment consistent results were obtained with various concentrations of thallium and it was found that a point was reached at which a reduction in the proportion of thallium gave no further increase in the ratio of intensities. Several values with very much smaller concentrations confirmed this.

TABLE I. Ratio \bar{a}_2^2/\bar{a}_1^2 for the doublet $=2p_2-2s, 2p_1-2s$ for various concentrations of thallium.

Percentage of thallium	Number of observations	Mean value of \bar{a}_2^2/\bar{a}_1^2	Mean error
0.072	5	0.093	0.009
0.040	3	0.236	0.040
0.087	10	0.372	0.045
0.0051	2	0.395	0.018
0.00143	1	0.382	
0.00024	2	0.388	0.032

The results are given in Table I and shown graphically in the lower part of Fig. 1. The alloys of lower concentration were made by melting stronger ones with lead and the actual numerical values of the concentrations may not be correct because the lead might contain an amount of thallium comparable with that intended in the weakest concentrations and because in melting the product was always less than the sum of the constituents used there being always some loss in which the metals might be in very different proportions from those in which they are placed in the crucible. In the case of the larger concentrations the errors cannot be great and that the concentration became successively less is shown by the fact that the time needed for satisfactory intensities of the lines became greater for each dilution so that there is no room for doubt that the limiting value was attained. On account of the long exposures required with the smallest concentrations—of the order of an hour—the effect of the “continuous spectrum” became relatively great and the value is not very accurate. On the other hand the others are trust-

worthy it being considered for example that the error in that for concentration 0.0087 percent is not more than 2 percent.

In Table I and Fig. 1 the ratio $\overline{a_2^2}/\overline{a_1^2}$ is obtained from the ratio of intensities I_2/I_1 by multiplying by the factor λ_2^4/λ_1^4 , a_1 and a_2 being the amplitudes of the virtual resonators given by the equation $I = a^2\nu^4$.

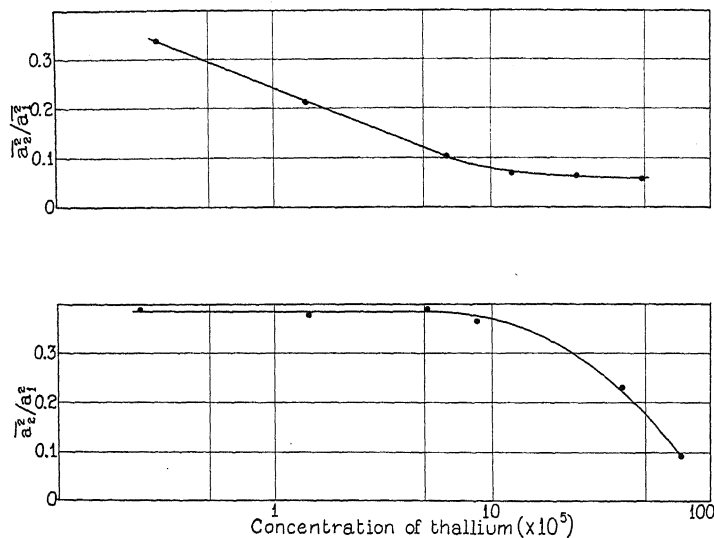


Fig. 1. Values of $\overline{a_2^2}/\overline{a_1^2}$ as a function of thallium concentration.

The values of I_2/I_1 were of course obtained from the ratio determined from the photometer records multiplied by factors for the relative intensities of the lamp radiation at the two regions and for the relative dispersion of the spectrometer.

The limiting values found are

$$I_2/I_1 = 1.56; \quad \overline{a_2^2}/\overline{a_1^2} = 0.388$$

where the suffixes 1 and 2 refer respectively to the line of longer and shorter wave-length.

The last column of Table I gives the mean of the differences between the individual observations and the mean.

THE PRINCIPLE SERIES $2s - mp_1$, $2s - mp_2$.

Measurements were next made of several doublets in this series. The first, occurring in the infra-red could not be attacked by this method but trustworthy determinations were made in the case of the second and third doublets and values were obtained for the fourth and fifth which must be taken simply as indicating the order of the true values as large errors may have been made in their measurement.

The problem is simpler than that of the lines first examined because the separation of the doublets is less and because the effects of absorption are negligible. The Pfund arc was employed, generally with pure thallium though some determinations were made with a lead alloy of 50 percent thallium, and some with a current of 3.5 amp. instead of 1.6, used in most of the work. No appreciable differences were found in the results, justifying the view that the effects of absorption are negligible. That no error was introduced by copper lines in the proximity of lines examined in the case of the first two doublets measured was shown by obtaining spectra of a copper arc with a current of the same value, 1.6 amp., with exposures longer than any used in the measurements. Such lines did not appear, though with a copper arc of 6 amp. copper lines in the neighborhood of the first pair, 6700-6500, were recorded.

The results obtained with these two doublets, recorded below in Table II, show the ratio of intensities, that of shorter wave-length to that of longer, to be distinctly greater for the pair of greater quantum number and attempts were made to obtain values for doublets of higher order. As much longer exposures were needed with these, difficulties arose from the greater continuous spectrum and from the presence of neighboring copper lines not obtained before with the relatively short exposures. Spectra were obtained using poles of carbon and other materials in the hope of obtaining better results. In several cases, mostly with the copper arc, the conditions were such that both lines of one or both doublets were obtained free from appreciable reinforcement from neighboring lines of other elements and of sufficient intensity to allow measurements to be made.

TABLE II. Ratio $\overline{a_1^2}/\overline{a_2^2}$ for doublets in the principal series $2s-mp_1, 2s-mp_2$.

m	Wave-lengths	Number of observations	Mean value of $\overline{a_1^2}/\overline{a_2^2}$	Mean error
4	6549.77 6713.69	8	4.5	0.44
5	5527.90 5583.88	11	5.7	0.92
6	5109.47 5136.84	1	6.4	
7	4891.11 4906.3	3	7	1

The values obtained for the doublets in this series are given in Table II. The ratio of $\overline{a_1^2}/\overline{a_2^2}$ rises with the quantum number but in view of the possibility of large error in the last two values it is impossible to decide whether the values conform with the equation found by Sambursky¹ in the case of the alkalis, namely

$$I_1/I_2 = cn^{a_{eff}}$$

where n_{eff} is the effective quantum number.

As it was impossible for me to remain longer in Utrecht further work could not be done at this stage. It is my intention to continue this investigation on my return to Sydney.

Note 1. The fraction of light transmitted by the antimony screen was determined in the individual cases with an error not exceeding 2 percent. The values, however, were found to vary somewhat according to the part of the screen employed and as it was frequently removed and replaced between the taking of one plate and another a fairly wide range of values was obtained particularly for the shortest wave-length employed. The mean values obtained have some interest and are given in Table III.

TABLE III. *Transmission of antimony film.*

λ	fraction transmitted	λ	fraction transmitted
6549	0.270	4891	0.175
5527	0.243	3776	0.093
5350	0.243		

Note 2. In the first stage of the work there was in many of the photometer records of line 3776 an indication of a companion line on the red side as illustrated in Fig. 2 a. Further examination with altered conditions of the optical system showed that this was a diffraction effect and that similar effects were obtained with many of the intense lead lines. A lack of symmetry of the diffraction pattern in many cases and abnormal intensities of the



Fig. 2. Photometer records of line 3776 showing presence of secondary maxima, (a) obtained with wide spectrometer slit giving unsymmetrical pattern, (b) with narrow slit, nearly symmetrical.

fringes were observed similar to those recorded by Shenstone³ whose paper came to hand while this work was in progress. In Fig. 2b is given a photometer record of line 3776 the spectrum being taken with a fine spectrometer slit. In this case the pattern is symmetrical and measurement of the displacements agree closely with those calculated from the ordinary theory.

In conclusion I wish to express my warm thanks to Professor Ornstein for giving me the opportunity, during my stay in Utrecht, of obtaining an intimate knowledge of the research methods used in his laboratory and in particular for his continued interest and help in this work.

³ A. G. Shenstone, *Phys. Rev.* **34**, 726 (1929).

THE FREQUENCY OF OCCURRENCE OF THE DISINTEGRATIVE-SYNTHESIS OF OXYGEN 17 FROM NITROGEN 14 AND HELIUM

WILLIAM D. HARKINS AND A. E. SCHUH

UNIVERSITY OF CHICAGO AND BELL TELEPHONE LABORATORIES

(Received February 20, 1930)

ABSTRACT

By the use of a modified Wilson-Shimizu apparatus 39000 photographs were taken of the tracks of α -rays in nitrogen. The rays used were those from thorium C and C' as in earlier work in this laboratory. Two disintegrative syntheses were obtained of oxygen of mass 17 and isotopic number 1 by the attachment of the α -particle in each case to the nucleus of an atom of nitrogen. Evidence is presented which shows that the nitrogen atoms which are acted on in this way are in general those of mass 14 and isotopic number 0. The number of disintegrative syntheses per million α -tracks is 8, while the average of this and all other work gives 15. In this work the ratio of the number of inelastic to elastic collisions was smaller than in any earlier work, but this was due largely to the occurrence of an abnormally high number of elastic collisions.

INTRODUCTION

THE procedure now in use for the detection of the synthesis of a heavier atom from two lighter ones is that suggested and used by Harkins and Ryan.¹ They considered that if very fast α -particles were shot into a Wilson cloud-expansion chamber, and if a sufficiently large number of photographs were taken, the mechanism of any atomic disintegrations would be partly revealed. By the use of this method Harkins and Shadduck² found that two disintegrative syntheses of oxygen of mass 17 and isotopic number 1 were obtained by shooting about 250,000 α -rays of 8.6 cm range from thorium C' through nitrogen gas. Although 135,000 tracks of 4.9 cm range were also obtained, the analysis of the forks indicates that only the long range particles were effective in producing disintegrative-syntheses.

This yield of eight such events per million long range tracks is very small, and Kirsch and Petterson consider that the number should be very much higher. While it is true that one or two hydrogen tracks might have escaped observation, it is improbable that this is the case, on account of the method of observation. The 39,000 photographs were projected on a screen, one at a time, usually with two observers present. Every negative which showed a deflection in an α -track was cut out from the film, whether the track of another atom was present or not. All films on which the forks were well defined were segregated, and particular attention was paid to the observation in the other photographs of those deflections which were not so clear, and in which there was any possibility of the occurrence of a disintegra-

¹ W. D. Harkins and R. W. Ryan, J. Am. Chem. Soc. **45**, 2095 (1923).

² W. D. Harkins and H. A. Shadduck, Proc. Nat. Acad. Sci. **2**, 707 (1926).

tion. A second observation of all of the film in order to find deflections which might have been missed earlier, was also made. Pettersson and Kirsch³ consider that short range protons would be more likely to be missed than long range particles, such as are commonly found by the photographic method, but it is our opinion that they should be more easily seen, on account of the increase of ionization with decrease of speed of the particle, within the limits of the range of speed involved.

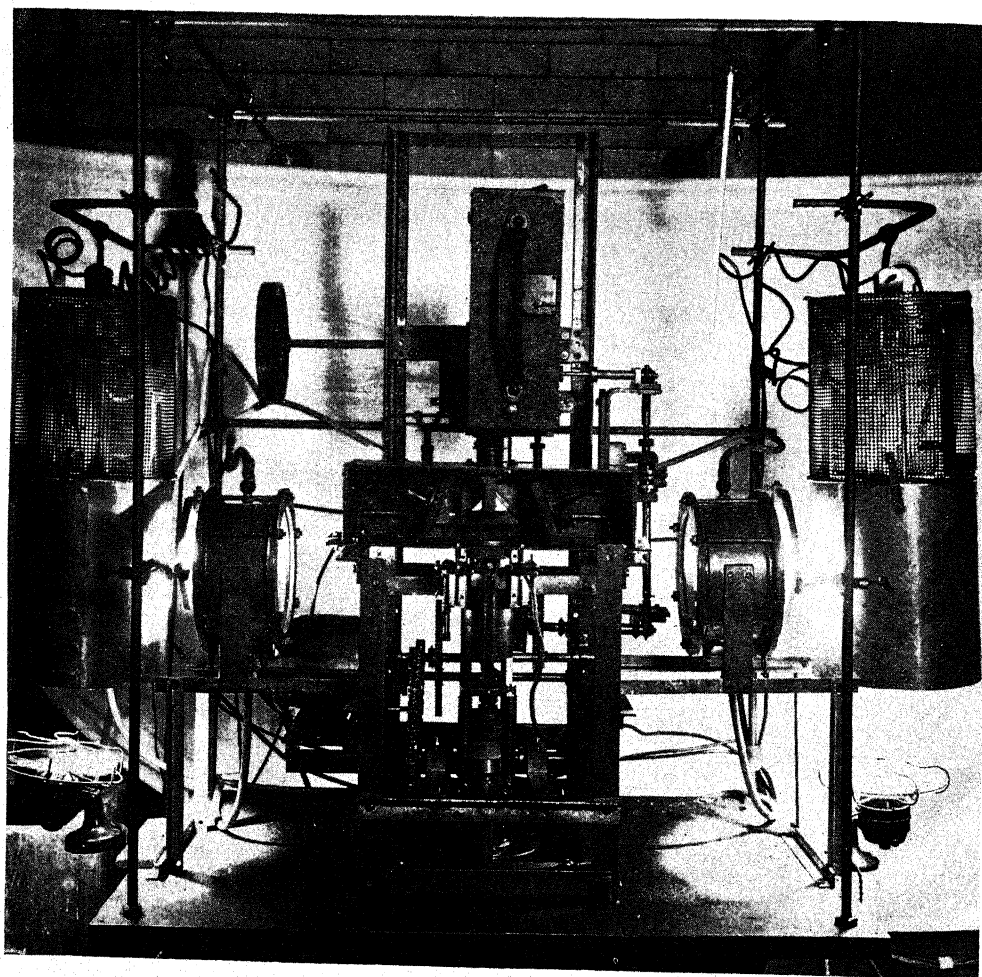


Fig. 1. Modified Shimizu-Wilson apparatus.

EXPERIMENTS ON THE SYNTHESIS OF OXYGEN ATOMS OF MASS 17

The Wilson Cloud-track apparatus used in this laboratory since 1923 was again modified, Fig. 1, and 39,000 photographs, each with two views

³ Pettersson-Kirsch, *Atomzertrümmerung*, p. 139-40.

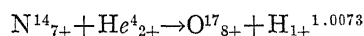
at right angles, were taken. The gas used was nitrogen, and the α -rays were obtained from thorium C and C' as before.

Since the photographs represented about 10 tracks per picture, the number of α -rays used in this work was 390,000, and of these about 250,000 were of long range (8.3 cm) from thorium C'.

From these experiments two disintegrative-syntheses of oxygen 17 were obtained, and one view of one of these is shown in Fig. 2. The remaining range of the α -particle is 6 cm, its velocity 1.86×10^9 cm, and the velocities of the proton and of oxygen 17 are about 3×10^9 cm and 0.31×10^9 cm per second, respectively.

RESULTS AND DISCUSSION

In each of three sets of experiments a quarter of a million α -rays of long range were shot through nitrogen. The yield per million fast α -rays of disintegrative syntheses represented by the following equation



was 8, 29, and 8, respectively for the work of Harkins and Shadduck, of Blackett,⁴ and of the writers.

These results are of somewhat more interest if compared with the number of elastic collisions in which no disintegrative syntheses were involved (Table I).

TABLE I. Number of disintegrative syntheses as related to the number of elastic collisions in which the α -particle was deflected through more than 90° (per million α -rays of 8.6 cm range).

	Elastic collisions	Non-elastic collisions or disintegrative syntheses	Sum
Harkins and Shadduck	22	8	30
Blackett	32	29	61
Harkins and Schuh	100	8	108
	<u>154</u>	<u>45</u>	<u>199</u>

The number of inelastic collisions is about 29 percent as large as the number of collisions in which the α -particle is deflected by an angle greater than 90° . It is apparent, however, that the number of events of either type is too small to give an accurate knowledge of the ratio. In the observations recorded in this laboratory, only about 4 cm of the 8.6 cm range of the fast rays was photographed, but this was the effective region of highest velocity.

Since only about one atom of nitrogen in 800 has an atomic weight of 15 (isotopic number = 1) it is evident, since approximately a fourth of the total number of sharp collisions result in disintegrative syntheses, that the nitrogen affected is in general that of atomic weight 14 and isotopic number 0, which constitutes almost the whole of atmospheric nitrogen.

It seems probable that at least a part of the atoms of mass 17 in atmospheric oxygen are formed by this particular disintegrative synthesis. There is also in the atmosphere a still more abundant oxygen isotope of mass 18

⁴ P. M. S. Blackett, Proc. Roy. Soc. A107, 349 (1925).

and isotopic number 2, which, if formed by an entirely similar process, could only come from the less abundant nitrogen isotope of mass 15.

In this connection it may be noted that while the higher isotopes (17 and 18) of oxygen are very rare in comparison with the 16 isotope, nevertheless, *provided the oxygen of rocks has the same composition as atmospheric oxygen*, these seemingly rare isotopes are actually about as abundant on earth as ordinary nitrogen.

In connection with the problem of the origin of the higher isotopes of oxygen, it would be important to obtain and analyze the band spectrum of oxygen from non-radioactive minerals, and particularly from oxygen compounds present in meteorites. Unfortunately it is difficult to determine the

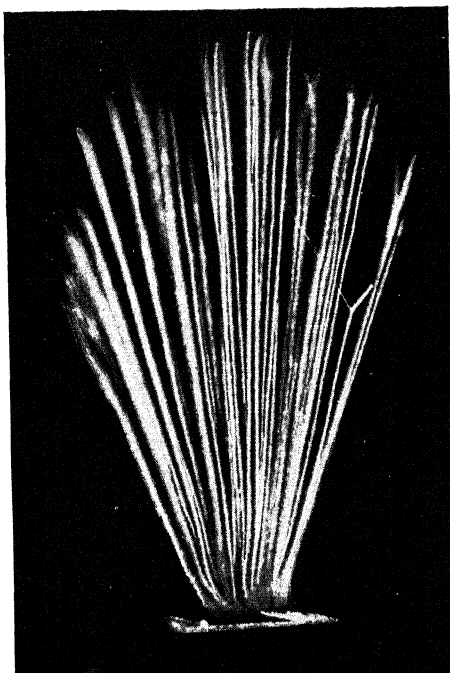


Fig. 2. Disintegrative synthesis of oxygen 17 and hydrogen from nitrogen and helium.

minute amount of the isotope 17 in experiments in the laboratory, since at ordinary pressures the intensity of the absorption band is too small, and the use of high pressures causes a considerable error due to a change in width of the lines and a resultant effect upon the apparent intensity.

Table II gives the abundance of the different atomic species of the elements nitrogen and oxygen as nearly as is now known.

If the oxygen of the earth's crust has the composition of that in the atmosphere, the isotope of mass 17 cannot have been formed entirely by the disintegrative synthesis from nitrogen in any reasonable period unless the amount of radioactive material was formerly very much greater than at present. For example, provided the effective α -rays passed through ni-

TABLE II. *Abundance relations for nitrogen and oxygen and carbon in the twenty-mile crust of the earth (atomic percentage).*

At. No.	Element	Atomic weight	Isotopic	Atomic percentage
8	Oxygen	16	0	57.38
6	Carbon	12 and 13	0 and 1	0.152
8	Oxygen	18	2	0.057
7	Nitrogen	14	0	0.022
8	Oxygen	17	1	0.007
7	Nitrogen	15	1	0.000027

trogen alone, it would require a period of the order of 10^{14} years for the known radioactive material to give the requisite amount of oxygen 17. Since, however, only about one atom in 4,000 in the crust is nitrogen, the period required would be of the order of 10^{18} years, since the stopping power of nitrogen is less than that of the average atom. It would take an extremely large error in the estimated amount of radioactive material in the earth's crust, and in the yield of oxygen 17 from nitrogen, to reduce this period to 10^{16} years, which is very much in excess of the supposed life of the earth. The simplest assumption is that oxygen 17 has been formed by other processes, although there is no need to restrict the time for the formation of this species from nitrogen to the period of existence of the crust of the earth. If oxygen 17 should prove to be very much more abundant in the oxygen of the atmosphere than in that in rocks, then it would be more probable that a considerable fraction has been formed by the disintegrative-synthesis.

The relations of the isotopes of oxygen to the other atomic species, and the relative abundance as well, indicate that the isotope of mass 16 and isotopic number 0 is by far the most stable, while that of mass 17 and isotopic number 1, is by far the most unstable. By analogy the nuclear spin of the zero isotope should be zero, and if recent estimates of the spins for the cadmium isotopes are correct, it seems probable that the spin (in units $h/2\pi$) is also zero for isotope 2, and equal to $1/2$ for the species of isotopic number 1. Thus it seems probable that the oxygen isotope of mass 17 produced by bombardment of a nitrogen nucleus by an alpha-particle, should exhibit a hyperfine structure in its line spectrum, and an alternation of intensities in its band spectrum (alternate lines not missing).

If the nitrogen molecule has a radius of 1.47×10^{-8} then in order to obtain one non-elastic collision, that is one disintegrative synthesis, a fast α -particle would need to shoot through 3.2 billion; to obtain an elastic collision, through five hundred million; and for any collision, through 370 million nitrogen molecules. In each molecule there are two nuclei which may be hit. On this basis the diameter of the nitrogen nucleus is of the order of 10^{-12} cm. This is of the general order of size found by Geiger and Marsden (3.2×10^{-12} cm.) for the nucleus of an atom of gold.

The number of deflections of the α -particle through more than 90 degrees is very large in comparison with the deflection through smaller angles, and in agreement with other work this indicates that the inverse square law does not hold at the small distances of approach between the α -particle and the nucleus of the nitrogen atom.

SOME INVESTIGATIONS INTO THE VELOCITY OF
SOUND AT ULTRA-SONIC FREQUENCIES
USING QUARTZ OSCILLATORS

BY CHARLES D. REID

CRUFT LABORATORY, HARVARD UNIVERSITY

(Received February 10, 1930)

ABSTRACT

The velocity of sound at ultra-sonic frequencies is measured over a frequency range from 40 to 216 kilocycles per second using quartz crystals as sound oscillators. The emitted sound is reflected back upon the source and as its phase changes the plate current of the quartz oscillator goes through a series of maximum values. The distance moved by the sound reflector between these maxima is a half wave-length of the emitted sound.

The velocity is obtained in air free from CO_2 at three values of the relative humidity, dry, 45 percent relative humidity at 20°C , and in air saturated with water vapor at 20°C .

The velocity is found to change with the distance from the source, becoming smaller as the distance becomes greater. This was particularly noticeable at 42 kilocycles.

At a distance of 45 centimeters, all values except those below 60 kilocycles become within 0.03 percent of an asymptotic value of 331.60 meters per second.

The velocity is found to depend upon the number of wave-lengths from the source.

The effect of humidity upon the velocity is found to be expressed by

$$V_H = V_0 + 0.14H$$

where V_0 is the velocity in dry air at 20°C and V_H is the velocity at any relative humidity " H " at 20°C .

THE scope of the present work was intended to include the measurement of sound velocities from about a frequency of 40 kc up to 2000 kc in several ordinary gases. Actually the investigation up to the present has been limited to measurements in air for other problems came by the way which needed solution before the research could be pushed further. As a start it was decided to check the work which had been done in air by Professor Pierce,¹ in particular, to see if the considerable increase in velocity reported by Professor Pierce for the region about 40 kc could be checked. This turned out to be somewhat difficult, and the problem has become a study of the velocity in air in the frequency range from 40 to 216 kilocycles and at various distances from the source. The effect of humidity upon velocity has been studied experimentally. The results seem to shed some light upon the reported increase in sound velocity at 40 kilocycles and indicated that the whole phenomenon is extremely complicated and interesting.

In the following experiments, the control and measurement of four variables constituted the major part of the problem in hand. These were, the

¹ G. W. Pierce, Proc. Am. Acad. of Arts and Sciences 60, No. 5 (1925).

wave-length of the emitted sound; the frequency of this sound; the temperature at which the measurements were made; and finally, the constitution of the medium through which the waves were propagated.

As in Professor Pierce's paper the sound was produced by means of quartz crystals, the use of which has by this time become quite common as frequency-control devices. If quartz crystals are used in conjunction with a vacuum tube circuit of the proper sort, the circuit will oscillate electrically with a frequency determined by one of the natural mechanical periods of vibration of the crystal. Such a circuit based on Figs. 5 and 6 of Professor Pierce's paper is shown in the accompanying diagram, Fig. 1, together with an amplifier.

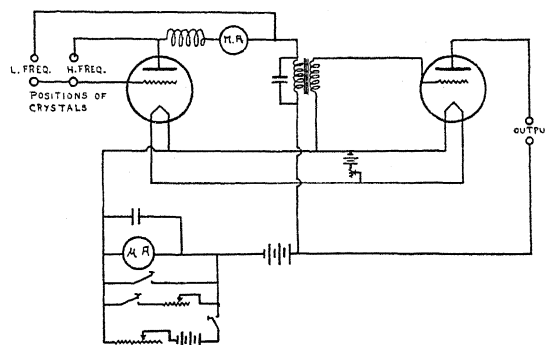


Fig. 1. The oscillating circuit together with the audiofrequency amplifier and microammeter, showing shunting and bucking arrangement for the microammeter.

THE MEASUREMENT OF WAVE-LENGTH

Simultaneously the mechanical motion of the crystal produces longitudinal elastic waves of the same frequency in the medium in which it is situated. To measure the wave-length of such a disturbance a very convenient method is available. It has been found by Professor Pierce that if a solid reflector be moved in a direction perpendicular to the sound emitting face of the crystal so that the sound is reflected back to the crystal face, small changes occur in the plate current of the circuit shown. This current goes through a series of maximum and minimum values as the reflector is moved. The distance between successive maximum values of the current represents a half wave-length of the emitted sound. Since this change is small in comparison with the steady plate current, it may be detected more readily by means of a microammeter which is made to read zero for the normal plate current by means of a local bucking battery and a proper variable resistance. It was also convenient to have a variable shunt and short-circuiting switch, as indicated in the diagram, Fig. 1. Such an arrangement made it possible to use current variations of as little as four microamperes to determine the wave-length.

The position of the reflector was obtained by means of a precision screw of half millimeter pitch provided with a micrometer head divided into 100

parts so that one division on the dial indicates a motion of 0.005 millimeters. This screw was calibrated under actual working conditions by checking against a good standard meter for every five centimeters of length.

THE MEASUREMENT AND CONTROL OF FREQUENCY

The frequency of the sound source was measured in terms of a standard crystal which was kept in a fixed position during any set of measurements. This standard was calibrated directly from the clock at the Harvard Observatory by means of the method of coincidences described by Professor Pierce.² Its frequency was known at any one temperature and its temperature correction was also known. The value of this frequency was close to 421 kilocycles. At any temperature its frequency was known to about three parts in four hundred thousand.

All the crystals used in this experiment had been cut by Professor Pierce and had been ground by him so that they had a frequency such that some harmonic would produce an audible beat with the 421 kc standard. The frequency of this audible beat with the standard was measured on a calibrated

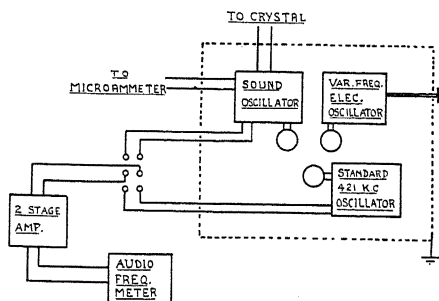


Fig. 2. Relative position of the piezoelectric sound oscillator and the oscillators and amplifiers used in determining the frequency of the sound.

audiofrequency meter and could be determined within two or three cycles per second giving an accuracy better than one part in one hundred thousand in the frequency of the sound source. The harmonic was identified by means of a wave meter.

The control of the frequency offered no difficulty, as the crystals once oscillating continued at constant frequency so long as they were undisturbed. The frequency measured at the beginning and at the end of each run was never significantly different. The disposition of the oscillators is shown in Fig. 2.

THE MEASUREMENT AND CONTROL OF TEMPERATURE

The effect of temperature on velocity was computed from the known relation between velocity and temperature. If one wishes an accuracy of 0.01 percent or better, then the temperature must be measured within 0.05°C.

The temperature was measured by means of a mercury in glass thermometer (No. 6466) divided directly into tenths of degrees centigrade which

² G. W. Pierce, Proc. Am. Acad. of Arts and Sciences 63, No. 1 (1928).

could be read to 0.02°C . This was placed within 10 centimeters of the vibrating air column. Precaution was taken to have it at the same vertical height as the crystal, so that any vertical temperature gradient would be avoided.

This thermometer was compared with a German Standard thermometer (P.T.R. 42547) kept in the Jefferson Coolidge Chemical Laboratory. The thermometer was carefully calibrated against this throughout the range over which it was used. This range was only five degrees in length, viz. 18.00°C . to 23.00°C . Corrections have been applied as they were found in the calibration.

The problem of keeping the air at nearly constant temperature forced the apparatus to be arranged in a manner such that the sound chamber was in a separate room from the operator. This room was only entered when crystals were changed, and its temperature altered very little since the room was below ground level and had no windows and no heating system. During the period over which a single set of measurements were taken, say half an hour, the observed reading on the thermometer seldom changed perceptibly. This thermometer was read from the operator's room by means of a short focus telescope. Since the room was undisturbed and the sound container was metal, it was believed that this observed value indicated accurately the temperature of the enclosed air. This is further substantiated by the fact that on several occasions when air inside was thoroughly stirred, no variation of the reading took place, nor did any occur when the thermometer was forced more deeply into the container.

THE MEASUREMENT AND CONTROL OF HUMIDITY

Professor Pierce had been led to the conclusion that change in humidity produced little effect upon the velocity of sound at these frequencies, but since this is not true at lower frequencies, it was thought advisable to control this factor if possible.

The method used for the determination of humidity was that suggested in International Critical Tables³ depending upon the constancy of the vapor pressure over saturated solutions of various salts. For example, if excess KNO_3 be dissolved in distilled water, the vapor pressure is such that the relative humidity at 20°C is 45 percent. Such a solution was placed inside the sound box while measurements were taken. A hair hygrometer placed in the sound box observed through a window served as an indicator for change in humidity.

When dry air was required the air was pumped through CaCl_2 and then over fused sodium hydroxide which also removed CO_2 . To conserve drying agents and facilitate the drying, the intake of the blower was connected to the sound chamber and thus the same air was passed many times over the drying reagents. Beside this a dish containing P_2O_5 was placed in the container. When air saturated with water vapor was needed, a bubbler was put in series with the pump, and an open dish of distilled water replaced the P_2O_5 . The CO_2 was removed by bubbling the air through a solution of NaOH .

³ International Critical Tables Vol. 1, p. 67

Attention may be called here to the fact that while all results have been reduced to values at 0°C , the amount of moisture present is still referred to 20°C .

ALIGNMENT OF CRYSTAL

In most of the work the crystal was mounted on a platform rigidly attached to the gas container and was made level when the apparatus was in position. Later, a means of tipping the crystal was devised. It was found that the error produced by lack of alignment was small, for when the crystal was deliberately tipped, the change in length of a given number of half-waves was less than would have been predicted by the use of the cosine of the angle. The crystal was set by tipping it up and down until a maximum reaction was obtained with the reflector at a great distance away. In this manner the crystal could be lined within half a degree.

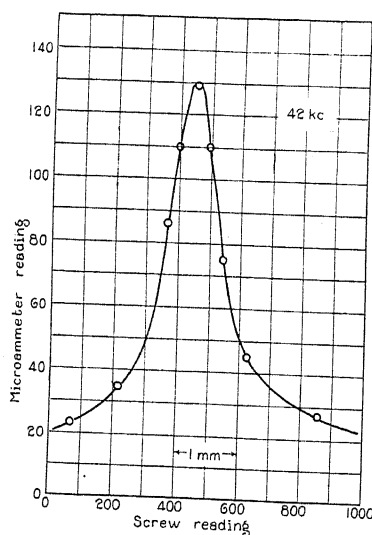


Fig. 3. A typical current peak a short distance from the source at 42 kilocycles per second.

EXPERIMENTAL METHOD FOR LOCATION OF NODAL POSITIONS

While it was possible to measure frequency, temperature, and humidity quite as indicated in the preceding pages, the measurement of the wavelength was a question which turned out to be much more difficult in several respects.

If the readings of the microammeter be plotted against the distance as read by the screw, a series of maxima appear. These maxima will be referred to as "peaks" and the length of a half wave as the distance between two successive peaks.

To obtain the position of the peak with the greatest accuracy, it was impossible to set on it by moving the reflector to the position where the meter gave its largest reading, for it was found that in all cases the top of the peak was flat over a number of scale divisions. This is evident from Fig. 3. To

avoid this, readings on either side of the peak were taken (e.g. when the meter reads "110"). At this point the motion of the needle was great for a small displacement of the piston. Thus the reading can be made with greater accuracy. The mean position of the reflector on the two sides of the peak was taken as its true position.

Back lash existed, but its effect was avoided by taking readings travelling first in one direction and then in the opposite. This also avoided trouble due to change in back lash from point to point. The calibration of the precision screw was also carried out in this manner. Even without any back lash the position of the peak in space is different when the reflector is being moved out from that when the movement of the reflector is in the opposite direction.

Hence a mean position of the reflector going in and out has been taken in every case. The procedure is illustrated by the following readings taken to determine the position of the maximum.

- | | |
|--|---|
| 1. Reflector moving in | 2. Reflector moving out |
| 57707 meter reading increasing | 57732 meter reading increasing |
| 57665 meter reading decreasing | 57764 meter reading decreasing |
| 57686 average | 57748 average |
| 3. Actual position | 4. Difference between two indicated positions |
| 57686 | 57748 |
| 57748 | 57686 |
| 57717 average | 62 divisions |
| 5. Known back lash 48 divisions | |
| 6. Shift of position independent of back lash is 14 divisions. | |

The shift in "6" is not constant, but by using the above method the length of an interval could be determined consistently, with an accuracy dependent upon the frequency of the sound emitter, but seldom with an error of more than ± 3 divisions on the graduated wheel and usually not more than ± 1 .

POSSIBLE PERCENTAGE ERROR

Having dealt with the control and measurement of the four variables concerned, it is interesting to note the accuracy with which sound velocities might be obtained under such conditions. Let us suppose 50 centimeters of the screw could be utilised for measuring purposes and that the maximum points could be located to two divisions on the wheel. The percentage error thus introduced would be 0.004 percent. The frequency can be found to better than one part in thirty thousand and hence introduces a possible error less than 0.003 percent. The temperature can be measured to 0.02°C and thus introduces an error of four parts in one hundred thousand or 0.004 percent. Since the air is kept at a fixed humidity the accumulated percentage error may amount to as much as 0.01 percent.

The work had not progressed very far before it was observed that the number of variables concerned had been underestimated, for with all possible precautions results did not check each other unless taken at exactly the same distance from the vibrating crystal.

PRECAUTIONARY EXPERIMENTS TO PROVE
REALITY OF CHANGE IN WAVE-LENGTH

It must be noted here, that the word "velocity" is used to denote the product of the measured frequency and distance moved by the reflector between alternate "peaks" of current in the plate current of the oscillator. The words "half wave-length" will be used to denote the distance moved by the reflector between peaks.

It was found that velocities computed from measured intervals close to the crystal showed a marked increase in magnitude. While this seems to be true to some extent at all frequencies, the effect is much more marked in the case of 40 kc and most of the experimenting has been done using this frequency.

In order to give an account of these experiments, it will be necessary to describe briefly the apparatus in use at this time. This consisted of a brass box containing two compartments connected by a rectangular opening. In one of these compartments the crystals were arranged on a movable slide in such a way that any crystal which was to be used could be moved to a position where it could radiate sound into the adjoining chamber. This has been designated "the sound chamber." The whole box was mounted on one end of a lathe bed which supported the measuring screw. As a result only a little more than half of the total length could be used for measuring. The reflector was on the end of a piece of one-inch brass tubing which passed through a snug-fitting gland in the end of the sound chamber remote from the crystal. This made a system that was tight enough to prevent very much diffusion of gas from the outside.

The aperture which led from the crystal chamber was larger than the largest crystal face, and hence all radiation from the face entered the sound chamber. The latter had a square cross section 18 centimeters to a side and had a length of about 35 centimeters. The actual interior space was really smaller than this due to the padding.

Padding was always necessary, but no change in it altered the fact that high results were obtained close to the crystal face. The size of the reflector was altered with no results. A felt tunnel was constructed of the same size as the reflector, but this produced no change. A felt pad of cross section equal to that of the sound chamber was fastened to the back of the reflector, and hence the length of the box changed with each setting. Thus any resonant effect due to the fixed size of the sound chamber should be discovered. This also failed to produce any decrease in the wave-length. Two crystals having approximately the same frequency but with different areas of radiating faces were available, both of which produced similar high results.

It was thought that the sagging of the reflector due to its own weight might introduce errors. This would be specially true when the reflection was near the crystal face at which time it hung far out from its support. With this in mind, one of the crystals was set up outside the chamber and the length of groups of waves measured in a region quite close to its face. Then the crystal was moved closer to the lathe bed and the readings repeated. The same in-

crease was noted, but this time the piston hung only half the distance over its support. Thus it was decided that there was no measureable error due to the sagging of the reflector.

At the same time the effect of placing objects in the vicinity of the vibrating column was tried. It was found that even when solid objects were placed but a few centimeters below the direct path of the sound, no noticeable change was made in the position of a particular peak which had been located previously.

Rough measurements made at this time indicated that for all the frequencies used an increase in wave-length could be noted close to the source with or without the container.

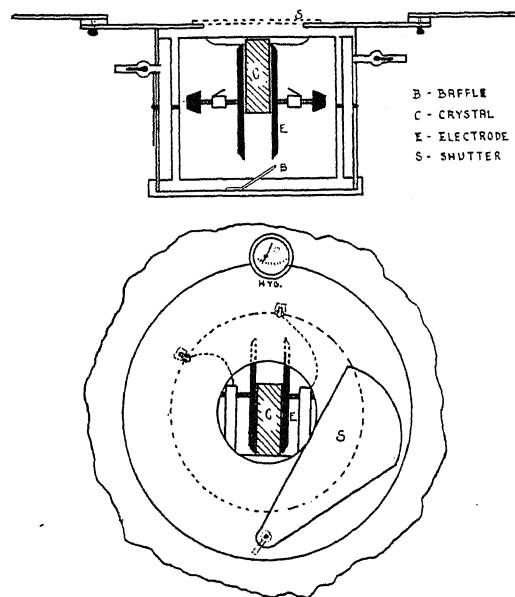


Fig. 4. Two views of the crystal holder and crystal chamber. a. Horizontal section of crystal and holder. b. Elevation of crystal and electrodes as viewed from within sound chamber.

DESCRIPTION OF APPARATUS

As a result of these experiments, it was concluded that the inequalities of the distances between peaks were real and that sound velocity determinations carried out in this way gave values apparently different for different distances from the source and suggested measurements at greater distances from the source. This made it necessary to reconstruct the chamber of the apparatus. The revised disposition of this apparatus has been partly described in the general discussion, but since the revised arrangement has been used for all measurements recorded here, a fuller description is warranted. The revised arrangement consisted of a sound box long enough to permit the use of the full length of the measuring screw, and of sufficient diameter to permit its use without padding the walls. The actual dimensions were 60 centimeters

in length and 45 centimeters in diameter. The crystal holder had circular electrodes whose distance apart could be changed easily. The crystal con-

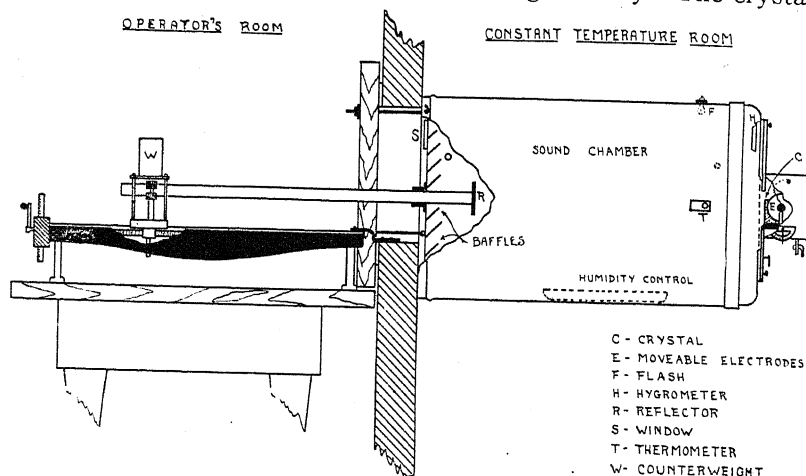


Fig. 5. A general view of the position of the precision screw and sound chamber.

tainer was arranged to permit easy access without opening up the whole sound chamber to the outside air. This was attained by having a slide that could be used to cover the aperture between the crystal chamber and sound box when crystals were to be changed. This slide is shown in the diagram, Fig. 4 by a dotted line. Since the whole container was located in a separate room, the temperature stayed very constant as mentioned.

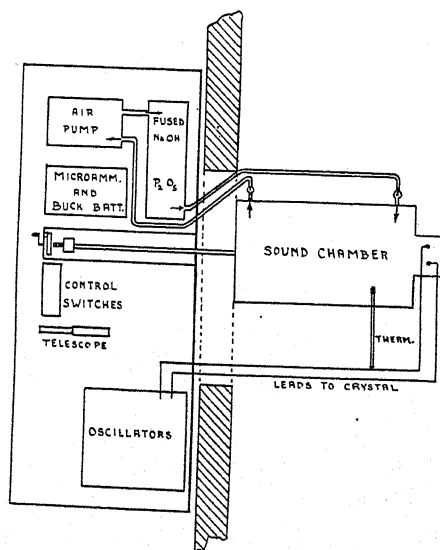


Fig. 6. A plan of all the apparatus.

An attempt was made to shield the lead which went from the piezo-oscillator circuit to the crystal, but the crystals refused to oscillate. The

leads were kept apart for best results. A complete diagram of the apparatus is appended in Fig. 5 and the disposition of the apparatus is shown in Fig. 6.

EXPERIMENTAL METHOD

The procedure for taking data was as follows. The sound oscillator was started, and the switch putting the bucking battery in circuit was closed. This was allowed to run for at least half an hour so that the change in voltage of the bucking battery would not cause the needle of the microammeter to drift. Immediately before the reflector was moved, the temperature of the air was taken, and the beat note with the standard crystal was recorded. Then the position of peaks for equal intervals of from 10 to 50 half waves were recorded as rapidly as could be done conveniently. This completed, the temperature and frequency were taken again, and averaged with the values taken before the run.

METHOD OF USING DATA

The fact that the wave-length changes with position makes it necessary to alter the method of averaging employed previously. The method used by

TABLE I.

Freq. (kc/sec.)	Veloc. (m/sec.)	No. of runs	Distance from source (cm) wave-lengths	
42	333.24	8	12	15
42	332.14	4	20	25
42	332.12	8	32	40
42	332.07	7	40	50
42	331.75	6	53	65
60	332.17	4	12	20
60	331.94	15	29	50
60	331.82	17	40	70
60	331.73	17	52	90
70	332.34	3	12	24
70	331.63	8	30	60
70	331.92	8	40	80
70	331.63	8	51	105
84	331.94	2	20	50
84	331.63	11	29	75
84	331.76	6	35	85
84	331.72	11	51	125
84	331.77	6	51	125
105	331.79	7	17	53
105	331.62	7	32	100
105	331.73	11	40	125
105	331.61	8	49	150
105	331.65	12	49	150
140	331.82	3	16	65
140	331.67	7	32	130
140	331.75	4	32	130
140	331.63	9	32	130
140	331.60	7	49	200
140	331.67	4	49	200
140	331.60	9	49	200

Professor Pierce¹ assumes the presence of equal intervals, the only difference being the experimental uncertainty of measurements. In the present case this is not true except in a limited region for the two highest frequencies used.

The manner in which the results were finally computed was decided after most of the runs were made. The readings were taken as if Professor Pierce's method were to be followed, but the method actually used is described below.

The average wave-length was taken over a distance which could be measured with an accuracy of better than 0.01 percent (viz., three hundred turns of the screw, or 15 cm). *This gave the mean velocity about a point midway between the ends of this interval.* The number of half wave-lengths used was dictated by convenience so long as the total interval did not greatly exceed three hundred turns of the screw. The average was found merely by taking the difference between the end points and dividing by the number of wave-lengths in the interval. When the waves were equal in length in the interval, the average obtained in this way did not differ significantly from that obtained by Professor Pierce's more elaborate method.

The results have been calculated for the most remote 15 centimeters of the screw, then for the next 15 centimeters, and so forth. The distance from the crystal face in wave-lengths at which the results may be considered as average velocities has been listed in Table I. In most cases the 15 centimeter divisions are only approximate as will be seen upon referring to the table.

The results tabulated in Table II are those computed from readings taken over a distance about 15 centimeters in length at an average distance of 45 centimeters from the source.

TABLE II. *Dry air at 0°C. free from CO₂.*

Freq. (kc/sec.)	No. of runs	Velocity m/sec.	Freq. (kc/sec.)	No. of runs	Velocity m/sec.
140	16	331.60	70	8	331.63
105	20	331.63	60	17	331.73
84	17	331.74	42	6	331.75

If this velocity be assumed constant, the maximum variation from the mean is 0.08 meters which is 0.024 percent and is within the limit of error of the experiment.

Taking the average velocity over the same region, remote from the source I have found the following (Table III) for air free from CO₂ at 45 percent humidity at 20°C.

TABLE III. *Air, free from CO₂ at 45 percent relative humidity at 20°C.*

Freq. (kc/sec.)	No. of runs	Velocity m/sec.	Freq. (kc/sec.)	No. of runs	Velocity m/sec.
140	8	332.20	70	8	332.31
105	7	332.27	60	10	332.16
84	8	332.28	42	5	332.38

With the same conditions as above, we have a maximum deviation from the mean of 0.06 meters which is 0.018 percent, which is also within experimental error.

The values of the velocity in air saturated with moisture are not so consistent due to the fact that the crystals would only oscillate for a few minutes in the moist air and measurements were necessarily hurried. This was more serious at low frequencies where more time was needed to make the measurements. Results are given here (Table IV) for four different frequencies. These results were found for the sections of the sound chamber most remote from the crystal.

TABLE IV. *Water saturated air, free from CO₂ at 20°C.*

Freq. (kc/sec.)	No. of runs	Velocity m/sec.	Freq. (kc/sec.)	No. of runs	Velocity m/sec.
140	14	332.97	84	6	332.86
105	8	333.00	42	4	333.34

The maximum variation here is 0.16 meters which gives 0.05 percent, which is a little worse than the other results. The results in Tables II, III, and IV are plotted in Fig. 7.

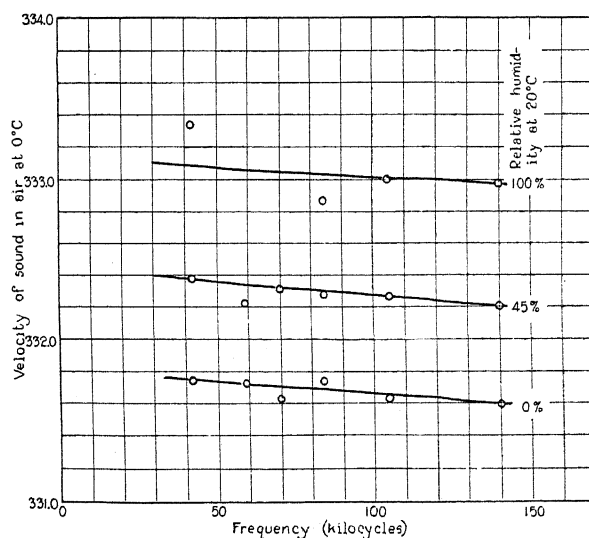


Fig. 7. The velocity of sound in air at 0°C at different frequencies and under different humidity conditions.

By taking the average values at all frequencies for dry, 45 percent humidity, and saturated air we obtain the following velocities in meters per sec.

Dry	45% relative humidity	Wet
331.68	332.27	333.05

These values of the velocity are plotted against the relative humidity at 20°C in Fig. 8. For convenience the actual values of velocity have been reduced to 0°C.

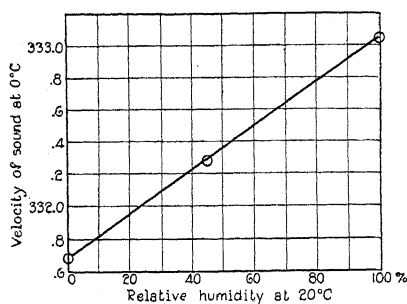


Fig. 8. The relation between the average values of the velocity of sound at all frequencies and the relative humidity at 20°C.

As a result the velocity " V_H " at any relative humidity at 20°C, is related to the velocity " V_0 " in dry air at 20°C by the equation.

$$V_H = V_0 + 0.14H$$

where " H " gives the value of the relative humidity (i.e., that fraction of the amount of moisture which would be required to saturate the air at 20°C).

In addition to the values for the velocity in dry air given in Table II, some further values have been obtained using a so-called direct current amplifier which has been built in order to work at points still more remote from the crystal.

The values tabulated below are the average values taken in a region beyond 40 centimeters from the face.

TABLE V.

Freq. kc/sec.	Velocity at 0°C meters/sec.	Freq. kc/sec.	Velocity at 0°C meters/sec.
216	331.66	70	331.56
140	331.64	60	331.63
105	331.61	54	331.87
84	331.61	42	332.00

As in the preceding work, the values for the low frequencies seem high.

VARIATION OF VELOCITY WITH DISTANCE FROM FACE OF CRYSTAL

The fact still remains that the values of this velocity seem to vary with distance from the crystal, and enough data are available to give some idea of how this variation takes place. In Fig. 9 the values of the velocity are plotted against frequency for intervals at different average distances from the source. In Fig. 10, the same values of the velocity are plotted against the average number of wave-lengths from the source, at which the measurements were made.

From the former plot, it will be seen that as the chosen interval becomes more remote from the source the values of the velocity approach more nearly

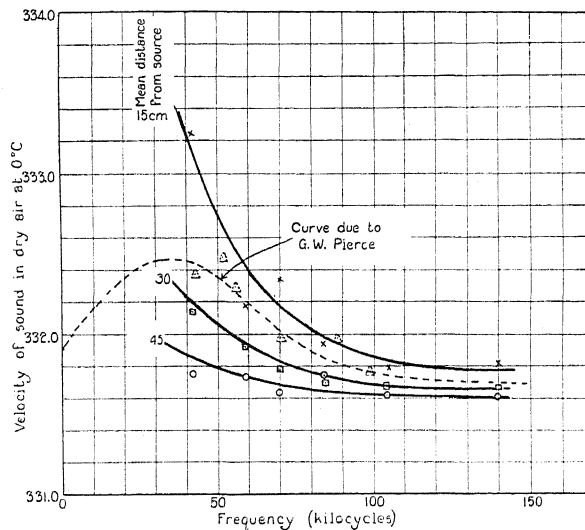


Fig. 9. The relation between the velocity of sound at 0°C and different frequencies to the distance from the sound source at which these measurements were taken.

a common value. The greatest deviations from this common value occur at the lower frequencies.

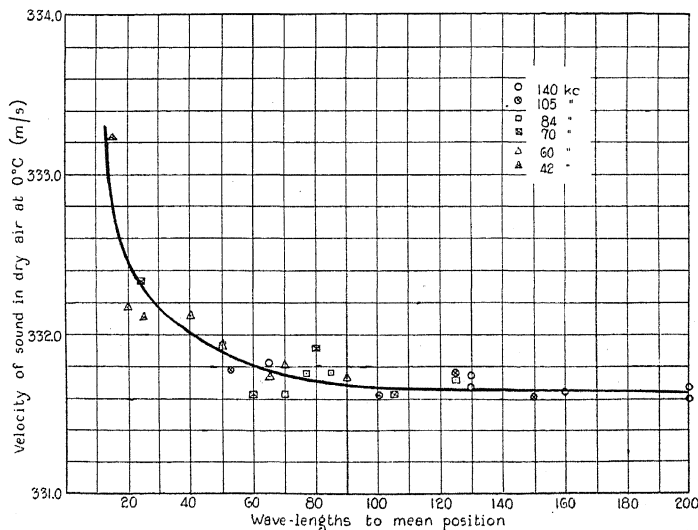


Fig. 10. A curve showing the relation between the velocity of sound, as measured by this method, with the number of wave-lengths from the source, for the frequencies indicated.

It will be seen from Fig. 10 that the size of this deviation depends upon the number of wave-lengths distant from the source at which the measurements are taken.

It will be noted that to obtain the velocity values shown in Fig. 10 it was necessary to make the readings over a considerable distance. For lower frequencies this meant about 40 half waves, while for the frequency of 140 kc this number is of the order of 150 half waves. Hence the closest permissible values at 140 kc will give a mean velocity about 75 wave-lengths away. It will be seen that an increase in velocity in the vicinity of the source would be

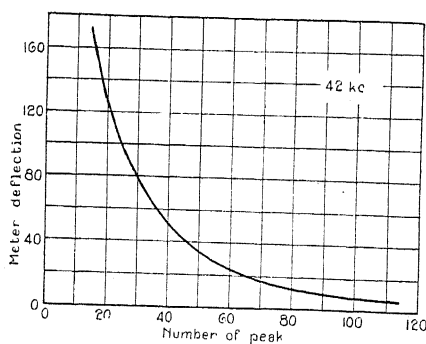


Fig. 11. A plot of the amplitude of 36 consecutive peaks (reading of microammeter against distance) against the number of the peak (starting from the source).

masked in this manner. Thus no real close-up values have been obtained for the higher frequencies. Similar experimental difficulty presents itself at a large number of wave-lengths for the lower frequencies, as the most extreme position at 42 kc was only 80 wave-lengths, and it seems improbable that this is far enough to give the asymptotic value obtained at a great distance.

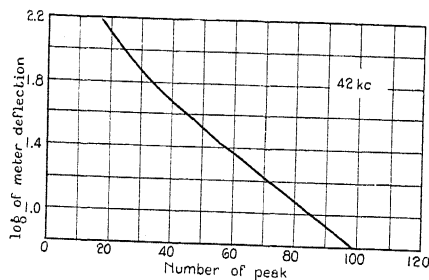


Fig. 12. The logarithm of the deflection plotted in Fig. 11.

Since the velocity close to the source could be studied better by means of the 42 kc crystal, some extra attention has been bestowed upon this. Starting from a position about fourteen half wave-lengths from the source, the next 36 consecutive peaks were plotted (ie., the reading of the microammeter was plotted against the distance), from this point on, every tenth wave was plotted until the 129th half wave was reached.

From these curves a decrement curve, Fig. 11, was plotted to a different scale and also the logarithm of the microammeter deflection, Fig. 12. The latter was very nearly a straight line except for the first few readings. The

decrement was found to be 0.015 per half wave. This is altogether too small to affect the velocity to the extent which is indicated by these experiments.

A graphical examination was made to ascertain the shift in the position of the peak due to this decrement and the effect of the decrement on the position of the peak was found to be negligible. Since the equation of the reaction current was unknown, this was the only available method.

It is worth noting that in addition to the change in wave-length with distance from the source, variations beyond experimental error occur in the separate intervals at the lower frequencies and in extreme cases amount to about 0.5 percent of the length of the interval when this is in the vicinity of the source.

SUMMARY AND DISCUSSION OF RESULTS

An attempt has been made to obtain the value of the velocity of sound at frequencies from 40 kc to 216 kc under conditions simulating outdoors, but at the same time to have greater control over the variables concerned.

Values have been obtained at eight different frequencies for three humidity conditions and at different distances from the source. An apparent rise in wave-length has been noted for regions close to the source, but which at any given position is greater the lower the frequency. As one recedes from the face of the oscillator, the velocities at various frequencies appear to approach a common value. If the velocity as found for all frequencies be plotted against the mean distance from the source in wave-lengths, some relation appears. A study at 42 kc shows that as the reflector recedes from the crystal, the value of the microammeter deflection (the change in plate current in the oscillator) decreases smoothly with a decrement nearly logarithmic, but too small to affect the length of the interval appreciably.

The method employed here has the advantage over tube methods since there is no tube correction to be considered. With the apparatus used, the diameter was equal to sixty of the longest wave-lengths used. This would correspond to a room about 60 feet in diameter for sound of about 1000 cycles.

While it is quite probable that some trouble arose due to reflections from the walls, it is hoped that at some distance from the source such effects are small. Small variations were noted from day to day which may have been due to this cause. Small temperature changes would cause marked alterations in any disturbance of this sort, as the path of wave reflected from the sides of the sound chamber would be much longer than that of the direct beam.

The rise in velocity near the sound source has been observed before. At Chicago in 1905 T. C. Hebb,⁴ working in a large hall with audible sound of wave-length approximately 10 inches, found this same effect. He noted the increase in the wave-length as the source was approached and specifically mentions that it was beyond experimental error. The length of the wave seemed to approach a limit as he reached positions fifty to sixty wave-lengths from the source. A shorter wave-length used seemed to make the trouble less obvious, though it was noted that he was farther from the source to begin

⁴ T. C. Hebb, *Phys. Rev.* 20, 89 (1905).

with and took a greater number of waves for his average length. No explanation was offered save that he thought that his reflecting mirrors were not large enough for the first wave-length he used. Since the above experiment was similar to the present experiment in many ways, it is interesting to note a similar phenomenon was observed.

The cause of this rise in velocity near the source has not been determined definitely so far, but several possibilities present themselves. Regnault found that velocities near the source were high and assumed that this was due to intensity. This can scarcely be true here as the energy radiated as sound is extremely small, for the input to the crystal oscillator, (exclusive of filament) was less than one-tenth of a watt. Some apparent increase would result from the lack of a plane wave system when a comparatively large reflector is used. However the effect is too large to be altogether accounted for by this argument.

An investigation using two crystals with different faces but having the same frequency indicated that the face of the crystal affects the result when the reflector is close to the face. Furthermore it seems probable from some recent work that in the case of higher frequencies no large rise in velocity takes place. A recent experiment showed that this was true when a 54 kc crystal with a small face was used. It is difficult to study the effect of the shape of the crystal face as they are not available in general with differing faces and the same frequency.

It is difficult to see why the reaction in the microammeter should fall off smoothly when passing through a region which must have an elaborate diffraction pattern, unless the reflector was large enough to average out diffraction effects.

The values of the ratio of the specific heats of air deduced from the velocity at 140 kc which seems to be close to the asymptotic velocity, Fig. 10, is 1.4035. This is in good agreement with the average of the best results today, computed from the velocity of sound at audible frequencies.

The average velocity in dry, CO_2 free, air as computed from the values at six frequencies is 331.68 meters per second. This result is felt to be too high, and if measurements at greater distances from the source could be taken for the lower frequencies, it seems that the results ought to decrease to 331.60 meters per second, as this seems to be the asymptotic value.

It will be noted that if the investigator had been limited to any particular region on the screw the results would have indicated, Fig. 9, a higher value for the velocity especially at the lower frequencies. As the interval over which measurements were taken was moved further from the source this increase in velocity becomes less noticeable. A further examination of the data published by G. W. Pierce¹ was undertaken by Professor Pierce and the author and revealed that these measurements were taken in a region extending from the face of the crystal, out to a point about twenty centimeters distant. This will account for the similarity of the shape of the dotted curve, Fig. 9, with those obtained by the writer. Although the numerical values of the velocity are altered by the fact that no correction was made for humidity,

yet the humidity did not change appreciably during the experiments and hence the values lie along a curve similar to those obtained by the present investigator. Notice must be taken that no experimental values have been made below 40 kilocycles per second by this method, either by Professor Pierce or by the writer. The dotted curve, Fig. 9, is merely a reproduction of that published earlier.

The change in the velocity of sound caused by saturation with water vapor at 20°C has been found to be 1.37 meters per second. This agrees very well with values calculated by McAdie⁵ and with values computed by the writer, assuming that the change in velocity is due to change in density only. Some work on this subject at audio frequencies has been done by Barss and Bastille,⁶ but their results gave a change of only 0.57 meters per second.

An examination of Professor Pierce's note-book by Mr. W. J. Cahill has resulted in showing that at that time there was evidence of a change in velocity with humidity which was overlooked. This has been affirmed by Professor Pierce.

It may be added here that this work was done in three parts several months having elapsed between each set, and that the results check well. In one of these intervals the mounting of the standard was changed and recalibrated.

The following conclusions have been reached. The increase in apparent velocity at frequencies around 40 kc grows smaller as the measurements are taken in regions more remote from the source, and, the velocity in this range of frequencies does change with the humidity.

These experiments have been carried out in the Cruft Laboratory under the direction of Professor G. W. Pierce. Further experiments are now under way in this laboratory by the aid of which it is hoped that many of the present difficulties may be cleared up.

⁵ McAdie, *Annals of the Observatory of Harvard College* 86, 107 (1923).

⁶ Barss and Bastille, *Jour. of Math. and Phys. M.I.T.* 2, 210 (1923).

THE VELOCITY OF PROPAGATION OF LONGITUDINAL WAVES IN LIQUIDS AT AUDIO-FREQUENCIES

BY LOUIS GORDON POOLER
COLUMBIA UNIVERSITY, NEW YORK, N. Y.

(Received February 1, 1930)

ABSTRACT

A method for measuring the velocity of propagation of longitudinal waves in liquids is described which is at the same time precise and convenient of application. A column of liquid contained in a cylindrical vertical steel tube was brought into resonance vibration at audio frequency by an electromagnetically excited diaphragm at the bottom. From the solution of the equation of propagation it is shown that when the resonance frequency of the system is the same as that of the diaphragm the reaction of the latter on the system is very small. The height of the column of liquid in the tube was adjusted until its natural frequency nearly corresponded with the predetermined resonance frequency of the diaphragm. The height was then varied slightly and the frequency adjusted until resonance occurred. From several observations of this type the appropriate height corresponding to the resonance frequency of the diaphragm was obtained by interpolation. The velocity of propagation of the longitudinal waves was then calculated from the relation $V=f_0\lambda$, where f_0 is the natural frequency of the diaphragm when clamped in the holder and λ is the wavelength.

Correction for the elasticity of the walls of the tube.—The correction formulas of Korteweg, Lamb and Gronwall were tested experimentally on tubes of different dimensions. The latter was found to give the most satisfactory agreement, the two former being unsuitable for precision measurements.

Measurements.—The velocity of sound was measured in air-free distilled water at 25°C. The average of 52 observations gave for this velocity 1485.4 ± 2.3 m/sec. From this value the bulk modulus, G , and the adiabatic compressibility, κ , were calculated. Curves were plotted illustrating the variation of the velocity of sound with temperature for the range 25°–70°C and with concentration for solutions of NaCl and KCl of different normalities. Curves for the corresponding variations of G and κ are also given.

A. INTRODUCTION

PRECISE determinations of the velocity of sound in liquids by resonance methods at audio-frequencies have not until recently been possible because of the uncertainty regarding the correction required to compensate for the elasticity of the walls of the tube. Wertheim in 1847 observed a large discrepancy between the velocity of sound measured by direct methods in large bodies of water and the velocity calculated from experiments with organ pipes filled with water from the same source. This difference was shown by Helmholtz¹ to be due to a lowering in the wave-velocity caused by yielding of the walls of the tube. Since then several correction formulas for this effect have been developed notably by Korteweg² and Lamb,³ but the approxima-

¹ Helmholtz, *Gesammelte Abhandlungen*, Vol. 1, p. 246.

² D. J. Korteweg, *Wied. Ann.* 5, 525 (1878).

³ H. Lamb, *Memoirs and Proceedings of the Manchester Literary and Philosophical Society* 42, No. 9 (1898).

tions made are not sufficiently close to permit their use in precision measurements. A steel tube 4.32 cm in diameter and having a thickness of wall equal to 0.136 cm when filled with water requires a correction to the measured velocity of sound of 16 and 17 percent according to the Lamb and Korteweg formulas, respectively. Recently Gronwall⁴ has derived a more precise correction formula. This has been tested by the writer under widely varying conditions in experiments described in the present paper.

Previous work on this problem has been done by Dorsing⁵ and Busse.⁶ The former from the measurements on the dust figures in a glass Kundt's tube has calculated the velocity of sound in several liquids with an estimated precision of about one percent; he made use, however, of the Korteweg correction formula. The latter using the same method with some slight improvements measured the velocity of sound in fifteen different liquids and by employing thick walled glass tubes reduced the magnitude of the Korteweg correction.

The purpose of the experiments described in the present paper was to develop a method for measuring the velocity of propagation of longitudinal waves in a liquid at audio-frequencies which would be at the same time precise and convenient of application. Preliminary experiments indicated that it was possible to produce resonance vibrations in a column of water contained in a vertical tube excited at the proper frequency by an electromagnetically driven diaphragm at the bottom, that the frequency which produced a maximum response for a given height of the column could readily be determined, and finally that the resonance curves were very sharp (for air-free water the sound intensity fell away to less than one half its maximum value when the frequency was changed by two or three cycles in the neighborhood of 1000~).

B. APPARATUS

The original apparatus as it appeared when immersed in a thermostatically controlled oil bath is shown diagrammatically in Fig. 1. The steel tube containing the liquid is shown at the left. Its dimensions were: length 101 cm, inside diameter 3.89 cm, outside diameter 6.37 cm. A chromium plated soft iron diaphragm 0.050 cm thick and the magnets from a Western Electric Co. 500 ohm telephone receiver were mounted at the lower end of the tube as shown in Fig. 2. The base consisted of a brass plate screwed over the end of the chamber containing the receiver; the tube itself stood on a horizontal plate fitted with leveling screws. To balance the static weight of the column of liquid and to prevent distortion of the diaphragm, air was admitted to the air-chamber and the pressure measured by means of a water manometer.

Large alterations in the level of liquid in the resonating tube were effected when desired by changing the pressure on the liquid contained in the reservoir and helix of copper tubing shown on the right in Fig. 1. The

⁴ T. H. Gronwall, *Phys. Rev.* **30**, 71 (1927).

⁵ K. Dorsing, *Ann. d. Physik* **25**, 227 (1908).

⁶ W. Busse, *Ann. d. Physik* **75**, 657 (1924).

liquid flowed through a tube from the reservoir, through a needle valve and thence into the resonating tube through a small circular orifice drilled in the steel wall several centimeters above the diaphragm. When the liquid attained the desired height the needle valve was closed to prevent any variation in level during an experiment. Small variations in level were effected by means of a burette which was lowered into the open end of the resonating tube. The height of the column of liquid was measured by the jointed brass rod *A* attached to the scale *B* shown in Fig. 1. The rod had a sharp point on

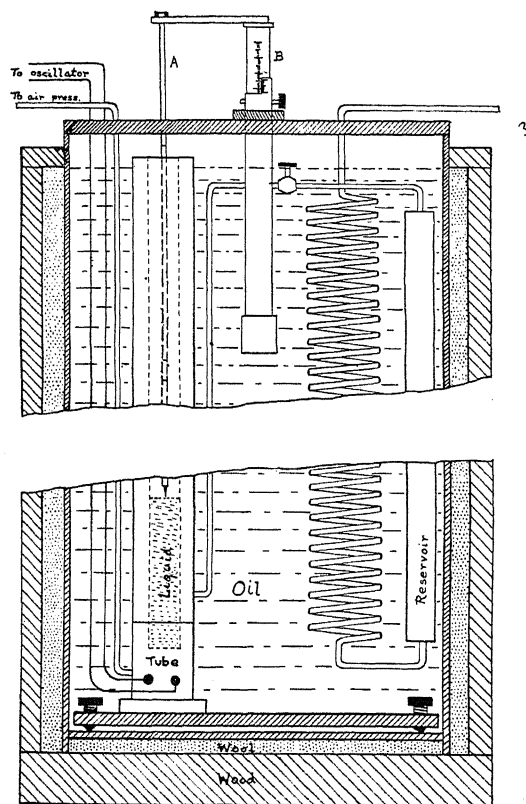


Fig. 1.

Diagram of apparatus.

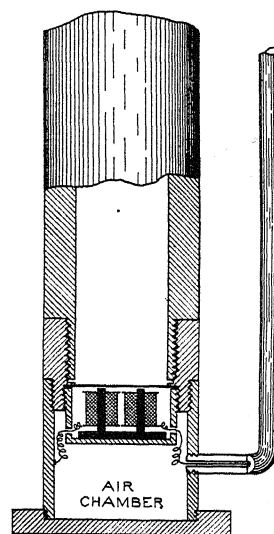


Fig. 2.

the end which upon making contact with the liquid surface closed an electrical circuit thereby producing a signal in a set of head-phones. The scale *B* could be raised or lowered and vertical distances measured with a precision of 0.01 cm by the use of a vernier.

The oscillator, amplifier and detector are shown diagrammatically in Fig. 3. The oscillator was designed to produce a current whose frequency did not vary with small changes in the filament current, B-battery voltage, or variable output. To obtain a circuit with these properties a master oscillator

was used in which the oscillations were excited in the grid circuit and the current was so small that the coils and condensers did not change appreciably in temperature under operating conditions. The plate current in tube *A* (Western Electric Co., Type E) was approximately one milliamper and the B-voltage, 180 volts, was supplied by dry batteries. The master oscillator was transformer-coupled to the amplifier as shown. The tubes *B*₁ and *B*₂ were UX 212 Radiotrons operated from the lighting circuit. The B-voltage was obtained from the two voltage regulator tubes, Radiotron type UX 874, shown at *D*. The oscillating current now amplified to 90–100 milliamperes passed through the tuned filter circuit *G*. The intensity of the output current was regulated by the autotransformer *E*, and then passed through the telephone transformer *F* to the receiver at the bottom of the tube. The oscillator

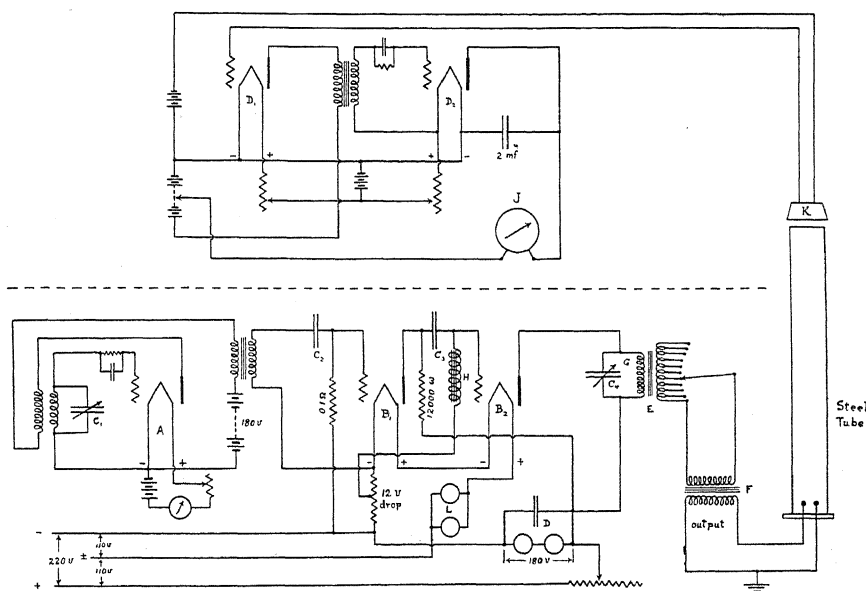


Fig. 3. Diagram of oscillator, amplifier and detector.

covered the range from 660–4500 cycles and the frequency remained appreciably constant throughout the whole range.

The oscillator was calibrated by obtaining the beat note between the current from the oscillator and the current produced in the coils of a telephone receiver by a toothed iron wheel (50 teeth) passing over the poles of the magnet. The shaft on which the toothed wheel revolved was geared (5-1) to a counter and any desired speed of rotation could be obtained by means of cone pulleys and a series resistance in the armature circuit of the motor. To measure the frequency the beat note was reduced to zero and held there and the time of 20,000 revolutions of the toothed wheel was measured with a stop watch. There was no difficulty in measuring the frequency with a precision of better than one tenth of one percent. The change in frequency produced by

varying the filament current of tube *A* by 0.05 amp. was not more than one part in two thousand and a variation of 4 volts in the B-battery did not show a detectable change in frequency.

The variable condenser *C*₁ consisted of a decade condenser, which could be varied in steps of 0.01 μf , in parallel with an air condenser filled with castor oil having a capacity of 0.012 μf . The frequency was determined at 10° and 90° on the scale of the air condenser and since the capacity varies linearly between these points the frequency could be determined for intermediate points by means of the relation

$$f = (b_1 + x b_2)^{-1/2}$$

$$\text{where } b_2 = \frac{f_1^2 - f_2^2}{(x_2 - x_1) f_1^2 f_2^2}$$

$$b_1 = \frac{1}{f_2^2} - x_2 b_2$$

and x_1 and x_2 are the readings on the condenser scale for the frequencies f_1 and f_2 , respectively. This method reduced considerably the number of readings necessary to calibrate the oscillating circuit. The calibration was checked from time to time against a standard. This standard consisted of a fused quartz rod 91.5 cm long which was suspended in a horizontal position by two threads. A small armature of soft iron was cemented to one end of the rod with shellac and a telephone receiver with the diaphragm removed was mounted several millimeters away with the magnets facing the armature. The receiver was excited from the oscillating set and the resonance frequency for the fundamental longitudinal vibration of the rod, 3115.7 ± 0.1 , was checked against the condenser setting.

The frequency of maximum intensity for the sound waves emitted by the column of liquid in the tube could be determined by ear, but the detector shown in Fig. 3 was more satisfactory for the purpose and also furnished qualitative information regarding the shape of the resonance curves. A telephone receiver *K* used as a microphone was placed about one centimeter above the open end of the tube. The current generated by the sound waves was amplified by the tube *D*₁ which was transformer-coupled to the grid of *D*₂. In tube *D*₂ the grid was maintained at a positive potential by connecting it to the positive end of the filament and, therefore it acted as a rectifier. A minimum in the plate current as recorded by the D.C. microammeter *J* indicated a maximum in the intensity of the sound waves incident on the microphone. The same procedure was followed in determining the natural frequency of the diaphragm itself.

C. DIAPHRAGMS

It is necessary to investigate the vibrating system in detail in order to determine the relation between λ the wave-length, f the frequency and V the velocity of propagation of the sound waves in the tube. Lord Rayleigh⁷ has

⁷ Lord Rayleigh, *Theory of Sound*, Vol. II, p. 158 *et seq.*

shown that for the case of forced vibrations of a fluid contained in a circular cylinder the waves ultimately become plane if $\lambda \geq 3.413 R$, where R is the radius of the tube, and that if the source of vibration be symmetrical with respect to the axis the waves ultimately become plane for a smaller value of λ than the one given by the above expression. The condition for plane waves was amply satisfied in this investigation and the law of reciprocity permits us to consider the waves produced by the vibrations of the diaphragm as equivalent to the waves produced by the forced vibrations of a piston. The wave equation for this case has the form

$$\frac{d^2 u}{dt^2} = V^2 \frac{d^2 u}{dz^2} + \frac{4}{3} \nu \frac{d^3 u}{dz^2 dt} \quad (1)$$

where u is the particle displacement, ν the kinematic coefficient of viscosity for the liquid and V represents the velocity of propagation in the tube. To determine the boundary conditions, G the bulk modulus of the liquid is defined by the equation $G = \rho V^2$, where ρ is the density of the liquid. The axis of z coincides with the axis of the tube; for the diaphragm $z=0$ and for the surface of the liquid $z=l$.

The boundary conditions for the propagation of a longitudinal wave along the axis of the tube require that at the free surface of the liquid the sum of the elastic and viscous stresses parallel to z vanish, namely,

$$G \frac{du}{dz} + Q \rho \frac{d^2 u}{dz dt} = 0 \quad \text{for } z=l; \quad (2)$$

and that at the surface of the liquid in contact with the diaphragm the pressure must be equal on the two sides, hence

$$\pi_0 e^{int} = K u + m \frac{d^2 u}{dt^2} + G \frac{du}{dz} + Q \rho \frac{d^2 u}{dz dt} \quad \text{for } z=0, \quad (3)$$

where $Q = 4\nu/3$; K is the stiffness per unit area and m the effective mass per unit area of the diaphragm and π_0 is the amplitude of the pressure. The displacement at all points in the system varies harmonically with the time and

$$u = A_1 e^{int + (\alpha + i\beta)z} + A_2 e^{int - (\alpha + i\beta)z} \quad (4)$$

will be a solution of (1), where

$$\alpha = \frac{1}{2} \frac{n^2 Q}{V^3} \quad (5)$$

$$\beta = \frac{n}{V}$$

provided $n^2 Q^2 / V^4$ is small compared with unity. The constants A_1 and A_2 are to be evaluated from the equations expressing the boundary conditions at $z=0$ and $z=l$.

From Eqs. (1) to (4) the following equation for the displacement u_l at the surface of the liquid can be found without trouble

$$|u_l|^2 = \frac{\pi_0^2}{(M^2 + P^2) \left\{ \left(\frac{1}{4} \frac{n^4 l^2}{V^6} + Nl \right) Q^2 + \cos^2(\phi - \epsilon) \right\}} \quad (6)$$

where

$$M = n\rho V, \quad P = K - mn^2, \quad N = \frac{P}{P^2 + M^2} \cdot \frac{1}{2} \cdot \frac{n^4 \rho}{V^4}$$

$$\phi = \beta l = \frac{n}{V} l, \quad \epsilon = \arctan \frac{M}{P}$$

Consider now the case of resonance $|u_l|^2 = \max$. Neglecting for the moment the term in Q^2 in the denominator on the right hand side of Eq. (6), $|u_l|^2$ will be a maximum when $\cos(\phi - \epsilon) = 0$, i.e. when

$$\phi - \epsilon = m\pi - (\pi/2)$$

where m is the number of half waves in the tube. For resonance, therefore, the relation between V , l and the resonance frequency of the system will be

$$f = \frac{V}{2l}(m + \eta) \quad (7)$$

or

$$V = \frac{2l}{T(m + \eta)} \quad (8)$$

where $T = 1/f$, and

$$\eta = \frac{\epsilon}{\pi} - \frac{1}{2} = \frac{1}{\pi} \left\{ \arctan \frac{n\rho V}{K - mn^2} \right\} - \frac{1}{2}. \quad (9)$$

At the resonance frequency of the diaphragm $K - mn^2 = 0$, hence $\eta = 0$, and

$$f_0 = \frac{V}{2l} m = \frac{V}{\lambda} \quad (10)$$

where f_0 is the resonance frequency of the diaphragm when clamped in the holder.

The effect of the term in Q^2 in shifting the maximum of $|u_l|^2$ represents the effect of viscosity on the resonance frequency of the system. It can easily be shown that this shift of the resonance frequency is but a fraction of the width of the resonance curve at half maximum. In the present experiments this corresponds to less than one cycle.

In the above discussion the give of the walls of the tube is ignored, but for the purpose in view Eq. (10) is nevertheless, sufficiently accurate. It is evident that f_0 is the frequency at which the measurements are best taken. for in this case, and in this case only, does the simple relation $V=\lambda f$ apply.

In the absence of sufficient knowledge regarding the constants of the diaphragm only qualitative information can be obtained from Eqs. (8) and (9). Fortunately, however, this information is sufficient to allow Eq. (10) to be tested experimentally. The manner in which V varies with T in Eq. (8) is shown in Table I where $T_1 > T_0 > T_2$.

TABLE I.

Period	$P = K - mn^2$	$\epsilon = \arctan M/P$	η	V
T_1	positive	$\epsilon < \pi/2$	negative	$V_1 > V$
T_0	0	$\epsilon = \pi/2$	0	$V_0 = V$
T_2	negative	$\epsilon > \pi/2$	positive	$V_2 < V$

In the preliminary experiments to test Eq. (10) two diaphragms D_1 ($f_0 = 1269 \sim$) and D_2 ($f_0 = 2590 \sim$) were investigated over a wide range of frequencies. The relation between the height of the column of liquid l ($=\lambda/2$) and the period for resonance is shown in a much exaggerated form by the curves in Fig. 4. The exaggeration is necessary as the curve is nearly a straight line throughout its entire length except near the extremities.

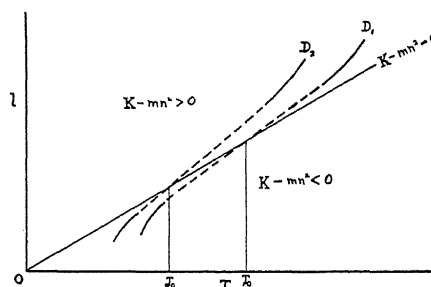


Fig. 4. Relation between height of the column of liquid and the period of resonance.

Inspection of these curves shows that they are in accord with the results predicted in Table I. It may also be observed that the tangents to the curves at the point for which $T = T_0$ pass through the origin; this is in agreement with Eqs. (8) and (9) as can easily be shown.

TABLE II.

Diaphragm	f_0	$\lambda/2$	$V = \lambda f$
D_1	1269	57.53 cm	1460 m/s
D_2	2590	28.07	1455

The observations which determine the shape of the curves in Fig. 4 were taken at the same temperature and with the same tube in both cases,

so that a comparison of the diaphragms can be made without requiring a correction for temperature or for the yielding of the walls of the tube. The observed data for $f=f_0$ and the calculated values of V are given in Table II.

A further experimental test of the equations is possible when the height of the column of liquid in the tube corresponds to several half wave-lengths. From Eq. (8) it is seen that unless $\eta=0$; $l_1=\lambda/2$, $l_2=\lambda$, and $l_3=3\lambda/2$ will not be in the ratio 1:2:3, since there will not be an integral number of half waves in the tube. Hence, the values of V obtained from l_1 , l_2 and l_3 should differ as m takes on successive integral values. A typical set of curves for this case is shown in Fig. 5 and Table III contains the data from another experiment of this type made with diaphragm D_2 .

TABLE III.

m	f_0	l	$\lambda/2$	Av. $\lambda/2$
1	2590	28.07 cm	28.07 cm	28.12 cm
2	2590	56.30	28.15	
3	2590	84.40	28.13	

D. METHOD OF EXPERIMENTATION AND TREATMENT OF DATA

The procedure followed in making a complete run on a given liquid was as follows:

1. The tube was placed in position, (see Fig. 1), the point of contact between the diaphragm and the measuring rod was determined and the reading on the vertical scale recorded.
2. The natural frequency f_0 of the diaphragm was determined by the method described under B.
3. The variable condenser in the oscillating set was adjusted for a frequency slightly higher than f_0 and the liquid admitted to the tube until the resonance height, $l=\lambda/2$, was reached.
4. The system was then left undisturbed for about 10 minutes to make certain that thermal equilibrium was established and the resonance frequency was then carefully determined and the height of the column of liquid measured.
5. Several cc of the liquid were then withdrawn from the tube and the resonance frequency was again determined and the new height measured.
6. This process was continued until four or five determinations had been made for frequencies slightly above and below f_0 .
7. In the investigation of diaphragms the procedure described in 3 to 6, corresponding to the resonance height $l_1=\lambda/2$, was then repeated for $l_2=\lambda$ and $l_3=3\lambda/2$.

The results of these experiments were then used as follows:

1. From the vertical heights recorded for contact between the measuring rod and the surface of the liquid the different lengths of the column were determined.
2. The condenser readings were expressed as reciprocals of the frequency.

3. A curve was plotted using the height of the column of liquid as ordinate and the period of vibration as abscissa.

4. The point corresponding to the natural period of the diaphragm was located on the curve and the height of the column at this point determined.

5. The velocity of propagation of the longitudinal waves in the liquid was then calculated from Eq. (10).

A typical set of curves for l_1 , l_2 , and l_3 plotted in accordance with the above method are shown in Fig. 5. The points indicated by the circles represent the experimental observations.

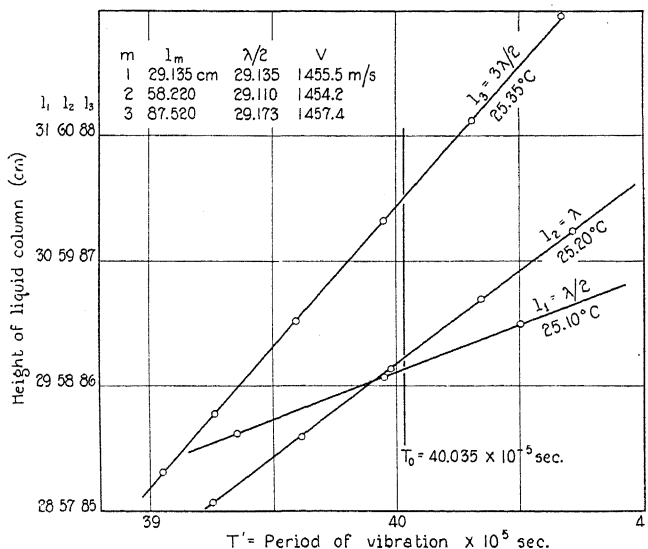


Fig. 5. Typical curves for l_1 , l_2 and l_3 .

E. THE GRONWALL CORRECTION FORMULA

The correction formulas of Korteweg and Lamb assume that the liquid completely fills the tube, thus introducing a requirement which in the present investigation would obviously be quite inconvenient to fulfill. Gronwall, however, considers the case where the liquid under observation only partly fills the tube, while the tube itself is supposed to be in a tank filled with another liquid, as would be the case when the tube is placed in a constant temperature bath.

The boundary conditions can all be satisfied experimentally, including that for the surface of separation between liquid and diaphragm, viz. $p=0$ at $z=0$ (reference 4, Eq. (31)), which is automatically satisfied for f_0 the natural frequency of the clamped diaphragm, except for the small viscous stress Qp ($d^2u/dzdt$). Gronwall's results show that B the observed velocity of the longitudinal waves in the liquid as obtained from Eq. (10) is related to V_0 their velocity in an unlimited body of the liquid by the equation

$$V_0 = \frac{V}{1-\delta} \quad (11)$$

where

$$\delta = y + 2y^2 + \left(7 - \frac{\pi^2}{3}\right)y^3 + \left(30 - \frac{7\pi^2}{3}\right)y^4 + \dots$$

For thick walled tubes

$$y = \frac{\rho V^2}{E} \left(\frac{b^2 + a^2}{b^2 - a^2} + \sigma \right) \quad (12)$$

and for thin walled tubes

$$y = \frac{\rho V^2}{E} \left[\frac{2}{3} \left(\frac{b^2 + a^2}{b^2 - a^2} + \sigma \right) + \frac{1}{3} \left(\frac{1}{2\sigma} - 1 \right) \frac{a}{b-a} \right] \quad (13)$$

where ρ is the density of the liquid, E and σ are Young's modulus and Poisson's ratio, respectively, for the material of the tube and a and b are the inner and outer radii.

The correction for the elasticity of the walls of the tube given by Eq. (11) was investigated for three tubes made of mild steel by the extrusion process. The dimensions are given in Table IV. The correction factors for the different tubes were computed, taking E for mild steel as 2.08×10^{12}

TABLE IV.

Tube	a	b	$b-a$	$1/1-\delta$
I	1.945 cm	3.185 cm	1.240 cm	1.0285
II	1.938	2.225	0.287	1.0771
III	2.024	2.160	0.136	1.1675

dynes/cm² and σ as 0.3. The quantity y was obtained from Eq. (12) for tubes I and II and from Eq. (13) in the case of tube III. A comparative analysis of an experiment with the three tubes containing air-free distilled water, using the same diaphragm and $l = \lambda/2$ is given in Table V. The diaphragm holder, Fig. 2, was so constructed that the tube did not come in contact with the diaphragm, hence, changing the tube did not alter the clamping at the boundary and f_0 was the same in each case.

TABLE V.

Tube	V (Eq. (10))	V (Correct.)	Temp.	V at 25°C [*]
I	1453.4 m./s.	1494.8 m./s.	24.8°C	1495.6 m./s.
II	1384.9	1491.7	25.6	1489.8
III	1277.6	1491.6	24.85	1492.1

The agreement between the calculated velocity of sound in the three tubes when corrected by Gronwall's formula is very good, but thin tubes require such a large correction that an appreciable error may be introduced

^{*} The temperature corrections have been made from a least square solution applied to forty observations taken between 23° and 30°C on air-free distilled water.

by uncertainty in the value of E , consequently tube I and two shorter tubes of the same dimension were used.

F. THE ASCOLOY TUBE

In the measurements made with tube I great difficulty was encountered from rusting and freshly distilled water showed traces of rust after having been in the tube for several hours at 25°C. When measurements were made at high temperatures it was necessary to keep the water in the tube over a period of many hours and the rusting became so serious that steps were taken to prevent it. The difficulty was finally overcome by chromium plating the diaphragm and by making a new tube of approximately the same dimensions from a stainless steel manufactured by the Allegheny Steel Co. under the trade name of Ascoloy 22. This tube had the dimensions $a=1.945$ cm, $b=3.155$ cm, $b-a=1.210$ cm, length 40 cm, $E=1.97 \times 10^{12}$ dynes/cm² and $\sigma=0.3$. The tube was designed for observations on $l=\lambda/2$ and since only a slight variation in the level of the liquid was required, the small hole in the wall was eliminated. In the new tube (tube V) the liquid was introduced through the open end and small changes in level were effected with the burette.

Tube V showed no signs of corrosion even with the most concentrated salt solution, but the calculated value of V for air-free distilled water was about 1/2 of one percent lower than the value previously obtained using tube I. Careful investigation showed that this difference in the value of V could only be explained by the influence of the hole in the wall. To test this point a small steel plug was made which just filled the hole and observations were taken with the plug in and then with it out. A definite lowering in the value of V was observed when the hole was plugged. Four sets of readings gave an average lowering of 6.2 m./s. and a new tube without a hole made from tube I gave results which agreed with those obtained from tube V within the limits of precision.

G. RESULTS

Following the method outlined above the velocity of sound was measured in air-free distilled water at 25°C and from 30° to 70°C at intervals of ten degrees, and in solutions of NaCl and KCl for different concentrations at 25°C.

TABLE VI.⁹

Diaphragm	Thickness	Res. Freq.	No. of Read's.	Av. Vel. at 25° C.
D ₁	0.031 cm	1269	3	1498.0 m./s.
D ₂	0.0505	2590	15	1494.2
D ₃	0.048	2318	4	1494.8
D ₄	0.052	2715	6	1492.5
		Height of Column	No. of Read's.	Av. Vel. at 25°C.
		$\lambda/2$	20	1492.2 m./s.
		λ	14	1493.1
		$3\lambda/2$	10	1494.1

⁹ The values of V in Table VI have not been corrected individually for the effect discussed in Section F.

1. *Air-free distilled water.* The value of V for air-free distilled water obtained with four different diaphragms at their respective resonance frequencies and with the same diaphragms, D_1 excepted, for $l=\lambda/2, \lambda, 3\lambda/2$ are given in Table VI.

The average of 47 observations on tube I with air-free distilled water at 25°C gave for the velocity of sound 1493.2 m./s. Correcting this value for the effect of the hole discussed under Section F and including 5 additional observations made with tube V gives for the velocity of propagation of the longitudinal waves in an unlimited body of the liquid

$$V_0 = 1485.4 \pm 2.3 \text{ m/s.}^{10}$$

From this value of V_0 and the relation $G = \rho V_0^2$ we can obtain the bulk modulus and the adiabatic compressibility of water.

$$G = 2.2000 \times 10^{10} \text{ dynes/cm}^2.$$

$$\kappa = 1/G = 4.5455 \times 10^{-11} \text{ cm}^3/\text{dyne}.$$

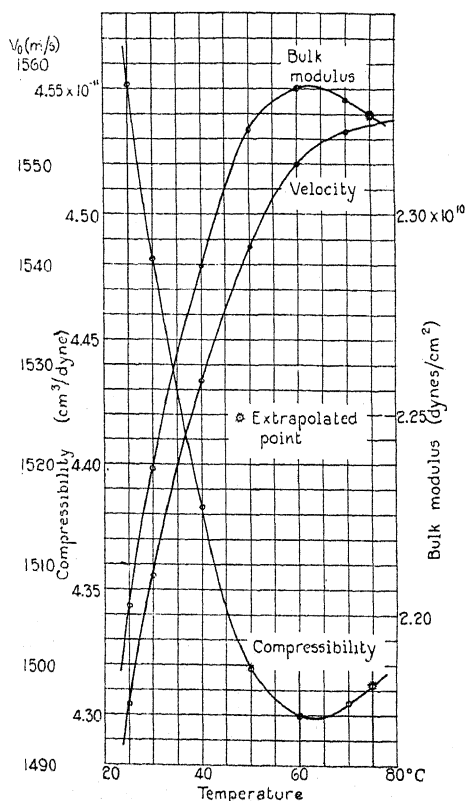


Fig. 6. G , V_0 and κ as functions of the temperature.

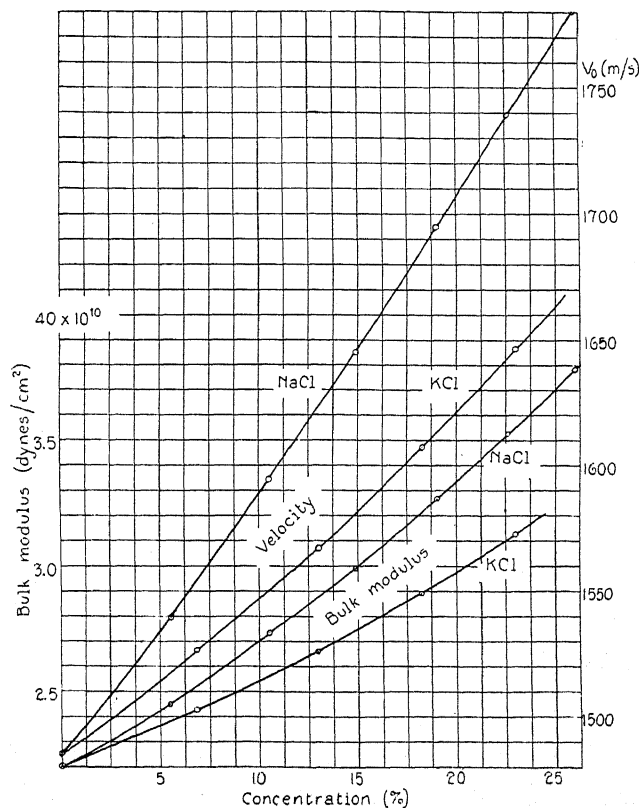
¹⁰ L. G. Pooler, Phys. Rev. 31, 157 (1928). In a note presented at the Chicago meeting of the Physical Society in Nov. 1927 the value was given as 1493.2 m/s. The effect of the hole in the wall of tube I was subsequently discovered.

Measurements on the velocity of sound, bulk modulus and compressibility at different temperatures taken from two experiments using tube I in which the agreement between corresponding values of V_0 was remarkably

TABLE VII.

Temp.	Av. V_0	G	κ
25°C	1486.0 m./s.	2.2018×10^{10} dynes/cm ²	4.5417×10^{-11} cm ³ /dyne
30	1498.7	2.2362	4.4716
40	1518.3	2.2872	4.3721
50	1531.6	2.3208	4.3088
60	1539.8	2.3311	4.2898
70	1543.1	2.3284	4.2947
Extrapolated point			
75	1544.2	2.3248	4.3014

close are given in Table VII. The curves in Fig. 6 have been plotted from these data and exhibit the variation of the measured quantities with the temperature.

Fig. 7. Variation of V_0 and bulk modulus with concentration.

Above 70°C the column of liquid could not be maintained in a state of vibration long enough to permit taking the necessary observations. This

phenomenon was apparently caused by the liquid boiling under reduced pressure as bubbles of gas could be seen adhering to the walls of the tube below the surface. When they were removed by stirring the liquid column came into resonance only to cease again in a very abrupt manner after several minutes.

2. *Salt solutions.* The velocity of sound was measured in aqueous solutions of NaCl and KCl for different normalities up to saturation using tube V. The results are given in Table VIII and the curves in Fig. 7 illustrate the variation in V_0 and the bulk modulus with the concentration.

TABLE VIII.

Concentration			Density	V_0 at 25°C	G	κ
NaCl	1N	5.5%	1.036	1539.4 m/s.	2.455×10^{10} dy./cm ²	4.073×10^{-11} cm ³ /dy.
	2N	10.5	1.072	1593.8	2.723	3.672
	3N	14.9	1.105	1644.8	2.989	3.345
	4N	19.0	1.137	1695.1	3.267	3.061
	5N	22.6	1.165	1739.6	3.526	2.837
	6N	26.0	1.194	1780.1	3.784	2.643
KCl	1N	6.9	1.041	1526.5	2.426	4.123
	2N	13.0	1.081	1567.7	2.657	3.764
	3N	18.3	1.119	1607.7	2.892	3.458
	4N	23.0	1.151	1647.2	3.123	3.202

H. DISCUSSION

The results obtained with air-free distilled water indicate that the method is one of high precision for the measurement of the velocity of sound in liquids and solutions and that much valuable information can be gained regarding the bulk modulus and the compressibility. The coefficient of viscosity enters into Eq. (6), but due to the excessively complicated relation which must exist at the boundary between the liquid and the tube it is doubtful if any information regarding it can be obtained from experiments of this type. It is felt that the limits of precision of this method have not as yet been reached and that with some further small refinements to the apparatus, the value of the velocity of sound can be measured to better than one tenth of one percent.

Recently two papers by Hubbard and Loomis¹¹ have appeared which present the results of an experimental determination of the velocity of sound in liquids at high frequencies (around 500,000~). The precision of their measurements is extremely high and they find that at the frequencies used the effect of the yielding of the walls of the tube can be completely neglected. The results of the present investigation correspond closely with theirs as regards the shape of the velocity-temperature curve and the velocity-concentration curves, but the measurements at audio frequencies are in all cases about one percent lower than at 500,000~. They were unable to obtain satisfactory readings at supersonic frequencies above 40°C while

¹¹ Hubbard and Loomis, *Phil. Mag.* **5**, 1177 (1928); Loomis and Hubbard, *J.O.S.A.* **17**, 295 (1928).

in the present investigation it was possible to continue observations up to 70°C before the column of liquid ceased to resonate. This difference can easily be explained when it is recalled that in a longitudinal wave the variation in pressure at a node is proportional to the frequency, and hence in their experiments ebullition would commence at a lower temperature.

The position of the maximum in the curve for the bulk modulus and the corresponding minimum in the compressibility curve at 63°C shown in Fig. 6 is in good agreement with the temperature found by other experimenters using entirely different methods. This peculiar behavior of the compressibility is fully discussed from the thermodynamical aspect in a paper by Bridgman¹² in which experiments with water at different temperatures and under static pressures up to 1200 kg/cm² are described.

The progress of this research indicates that many interesting facts can be discovered from measurements on the velocity of sound in liquids and particularly in solutions. It is hoped that through further experiments of this kind it may be possible, in the near future, to throw some light on the subject of dissolved substances in general and to derive an expression for the relation between the compressibility and the diminution in volume which occurs when many substances dissolve. The method also lends itself to a study of the rate of chemical reaction for cases in which the velocity of sound differs for the reacting liquids and the product of the combination.

The writer wishes to express his appreciation of the kindness of Dr. Wenté and the late Dr. I. B. Crandall of the staff of the Bell Telephone laboratories who furnished the thick diaphragms used in these experiments and to Professor Colin G. Fink in whose laboratory the diaphragms were chromium plated; and also to acknowledge his indebtedness to Professor A. P. Wills whose advice and encouragement have been of great assistance during the progress of this research.

¹² P. W. Bridgman, *Proc. Amer. Acad. of Arts & Sci.* **48**, 309 (1912).

THE DIELECTRIC CONSTANT AND THE MOLECULAR STRUCTURE OF CS_2

By C. T. ZAHN

PALMER PHYSICAL LABORATORY, PRINCETON UNIVERSITY

(Received February 20, 1930)

ABSTRACT

By the radio frequency heterodyne method previously developed measurements have been made of the dielectric constant of CS_2 at various pressures and temperatures. The molecular polarization is shown to be independent of temperature and therefore the electric moment is zero. The previous value published tentatively is shown to be in error. The structure of the CS_2 molecule can now be considered to be rectilinear and symmetrical. The value for the molecular polarization obtained is $P = 22.36$.

Comparisons with other data are given, and some convenient modifications in the experimental method and in the interpretation of dielectric constant data are described.

IN A recent article of this review Dr. J. B. Miles together with the author¹ gave values for the dielectric constant and the electric moment of CO , COS , CS_2 , and H_2S . The results then obtained indicated a small electric moment for the CS_2 molecule which seemed to be in contradiction to Williams'² results from the study of solutions. The experiments on CS_2 were accompanied by two chief difficulties. First, the apparatus was not adapted to the study of hot vapors, since part of the gas system was always at room temperature and it was therefore possible to work only at pressures below about one-third of an atmosphere. Secondly, the solubility of the CS_2 in the small amount of grease collected around the stopcocks made the results on CS_2 somewhat questionable. For these reasons the values for CS_2 were given only tentatively in the above mentioned article and it was there promised to make more conclusive measurements in the near future. Since then the apparatus has been adapted to work with hot vapors by Dr. J. B. Miles in collaboration with the author, and measurements have been made on CS_2 under excellent experimental conditions.

While this work was in progress there appeared an article by Ghosh, Mahanti, and Mukherjee³ on the dielectric constant and the molecular structure of CS_2 and N_2O , in which the moments of CS_2 and N_2O were found to be zero. The experiments described in the present article verify the conclusion that CS_2 has no appreciable electric moment but the value of the molecular polarization obtained is not in sufficiently close agreement with that of the above mentioned observers. It therefore seems worth while to give a full discussion of the present work.

¹ C. T. Zahn and J. B. Miles, Jr., *Phys. Rev.* **32**, 497 (1928).

² J. W. Williams, *Phys. Zeits.* **29**, 177 (1928).

³ P. N. Ghosh, P. C. Mahanti, and B. C. Mukherjee, *Zeits. f. Physik* **58**, 145 (1929).

EXPERIMENTAL METHOD AND MODIFICATIONS

The radio frequency heterodyne null method was used as previously described and applied to the measurement of a considerable number of gaseous substances.⁴ In the present arrangement of the apparatus there is one stopcock, which is separated from the gas system by liquid CS₂ in the manometer described,⁴ and should therefore not be so likely to introduce impurities even if grease were used in the seal. In order to make perfectly certain of this the grease was replaced by P₂O₅. The CS₂ used was taken from the same purified specimen as used before.¹

Some convenient modifications have been made in the method of interpretation of the dielectric constant data as follows. The dielectric constant should obey Debye's equation:

$$3\left(\frac{\epsilon-1}{\epsilon+2}\right)vT = AT + B$$

where ϵ is the dielectric constant, v is the specific volume referred to the *ideal* volume under S.P.T. conditions, T is the absolute temperature, and A and B are constants.

$$B = \frac{4\pi N_0}{3k} \mu^2 \text{ or } \mu = 1.099_8 \times 10^{-18} B$$

where N_0 is Loschmidt's number, the ideal number of molecules per cc under S.P.T. conditions, $2.705_6 \times 10^{19}$, k is Boltzmann's constant, $1.370_9 \times 10^{-16}$, and μ is the electric moment of the molecule.

In previous experiments it has been customary to determine the difference between the dielectric constants at atmospheric pressure and at approximate vacuum, and to determine the value of v by the van der Waal equation in its approximate form:

$$v = \frac{RT}{p} \left\{ 1 - \frac{(a/vp) - b}{v} \right\}$$

using for v on the right hand side its approximate or ideal value RT/p . This method of calculation is convenient if the dielectric constant is measured at only one pressure. A more satisfactory way to determine $(AT+B)$ is to make measurements of $\Delta\epsilon$ over the whole range of pressure available, and at the same time to test the Clausius-Mossotti relation: $(\epsilon-1)/(\epsilon+2) :: \text{density}$. At a fixed temperature the polarization would be accurately proportional to p only for an ideal gas so that plotting $3(\epsilon-1)/(\epsilon+2)$ against p would not give a straight line. If we plot against p' , the *ideal* pressure which the gas would have at the given temperature and density, we should obtain a straight line of slope $3[(\epsilon-1)/(\epsilon+2)] V/RT$. The value of p' can be

⁴ C. T. Zahn, Phys. Rev. **24**, 400 (1924); C. P. Smyth and C. T. Zahn, Jour. Amer. Chem. Soc. **47**, 2501 (1925); C. T. Zahn, Phys. Rev. **27**, 329 (1926); C. T. Zahn, Phys. Rev. **27**, 455 (1926); C. T. Zahn and J. B. Miles, Jr., Phys. Rev. **32**, 497 (1928); J. B. Miles, Jr., Phys. Rev. **34**, 964 (1929).

calculated as follows. Van der Waal's equation can be rewritten approximately:

$$v = \frac{1}{\frac{p}{RT} \left\{ 1 + \frac{p}{RT} \left(\frac{a}{RT} - b \right) \right\}} \equiv \frac{RT}{p'}$$

which defines:

$$p' = p \left\{ 1 + \frac{p}{RT} \left(\frac{a}{RT} - b \right) \right\}.$$

Hence the effect of the van der Waal constants is to introduce into the actual pressure relation a small quadratic term which can be taken into account by plotting against p' as above mentioned. The final value of $(AT+B)$ is got by multiplying the slope by RT^2 . This is done for a range of temperatures and the values plotted against T . The resulting straight line gives A as the slope and B as the intercept from which the moment is determined. If the molecule studied has no fixed moment then the values of $3(\epsilon-1)/(\epsilon+2)$ should be constant, and it is not necessary to draw the Debye line in order to determine A . It is only necessary to average the experimental values of $3[(\epsilon-1)/(\epsilon+2)]v$, which are approximately equal for the different temperatures used.

The above method of plotting has another advantage as follows. In a previous paper the author has mentioned the fact that it is impossible to make a reading for the dielectric constant at vacuum because the condenser plates are then so perfectly insulated thermally that a small but very disturbing temperature difference can be set up between them. It is then necessary to extrapolate to vacuum in order to find the actual value of $(\epsilon-1)$. The apparatus can always be so adjusted that the difference values of $(\epsilon-1)$ are approximately the actual values. These values can be divided by the corresponding approximate values of $(\epsilon+2)$ and then $3\{\Delta(\epsilon-1)/\epsilon+2\}$ can be plotted against p' . The linear extrapolation should be very accurate since the correction due to the factor $(\epsilon+2)$ is usually small and, in fact, often negligible. It is easily seen that the factor $\epsilon+2$ has the effect of introducing a small quadratic term in the value of $\epsilon-1$ as a function of the pressure since

$$3 \left\{ \frac{\epsilon-1}{\epsilon+2} \right\} :: p' \text{ or } (\epsilon-1) :: p' \left(1 + \frac{\epsilon-1}{3} \right)$$

and $(\epsilon-1)$ on the right hand side may be set proportional to p' approximately.

For a considerable number of gases there seems to be no question concerning the validity of the Clausius-Mossotti relation. On the other hand there have been performed a number of experiments⁵ in which anomalies

⁵ M. Jona, *Phys. Zeits.* 20, 14 (1919); C. T. Zahn, *Phys. Rev.* 27, 329 (1926); K. Wolf, *Phys. Zeits.* 27, 588, 830 (1926); K. Wolf, *Ann. d. Physik* 83, 884 (1927); F. Maske, *Phys. Zeits.* 28, 533 (1927); J. B. Miles, Jr., *Phys. Rev.* 34, 964 (1929).

have occurred, particularly in the case of vapors near the condensation point. These anomalies have been attributed to two causes, association and actual condensation on the condenser plates. The author has performed experiments to show that both these effects exist; for example, for water vapor. In the case of water vapor condensation on the condenser plates is accompanied by electrical conductivity which can be measured directly. The existence of such effects, whether they be due to association or condensation, or both can be detected by pressure curves such as those described above. If they are found to exist they can usually be eliminated by working at sufficiently low pressures.

TABLE I.

$T^{\circ}\text{K}$	p cm Hg	p' cm Hg	$3\left\{\frac{\Delta(\epsilon-1)}{\epsilon+2}\right\}\times 10^6$	$3\left\{\frac{\epsilon-1}{\epsilon+2}\right\}\frac{10^6}{p'}$	$3\left\{\frac{\epsilon-1}{\epsilon+2}\right\}v\times 10^6$	P
325.1 ₁	14.21	14.25	477	from curve		
	25.33	25.44	835			
	34.42	34.63	1134			
	44.47	44.82	1479			
	53.72	54.23	1779			
	64.49	65.23	2147			
	64.57	65.31	2149			
	53.76	54.27	1782			
	43.82	44.16	1454			
	34.96	35.18	1143			
	24.37	24.48	793			
	15.92	15.96	494			
				2518	2997	
391.7 ₀	15.21	15.23	305			
	28.93	29.03	697			
	48.81	49.09	1247			
	50.27	50.57	1264			
	30.40	30.51	748			
	15.81	15.84	330			
				2088	2995	
489.2 ₂	14.64	14.66	385			
	22.63	22.67	558			
	33.45	33.53	787			
	43.06	43.19	983			
	52.95	53.15	1199			
	61.71	61.98	1384			
	52.95	53.15	1199			
	43.37	43.50	987			
	33.81	33.89	763			
	24.35	24.39	541			
	15.00	15.02	334			
				1666	2985	
322.3 ₁	13.69	13.72	618			
	24.16	24.26	964			
	33.37	33.57	1284			
	43.26	43.60	1614			
	52.87	53.37	1942			
	62.15	62.85	2264			
	53.13	53.63	1957			
	43.54	43.88	1618			
	33.47	33.67	1286			
	24.10	24.20	958			
	14.15	14.18	633			
				2538	2995	
					2993, mean	22.36

EXPERIMENTAL RESULTS

In the present measurements on CS_2 complete pressure curves were obtained at four different temperatures in order to insure the absence of such effects. In Table I are shown the experimental values obtained. The fourth column contains the difference readings, $3[\Delta(\epsilon-1)/(\epsilon+2)]$, referred to a fixed point of the experimental condenser system for convenience

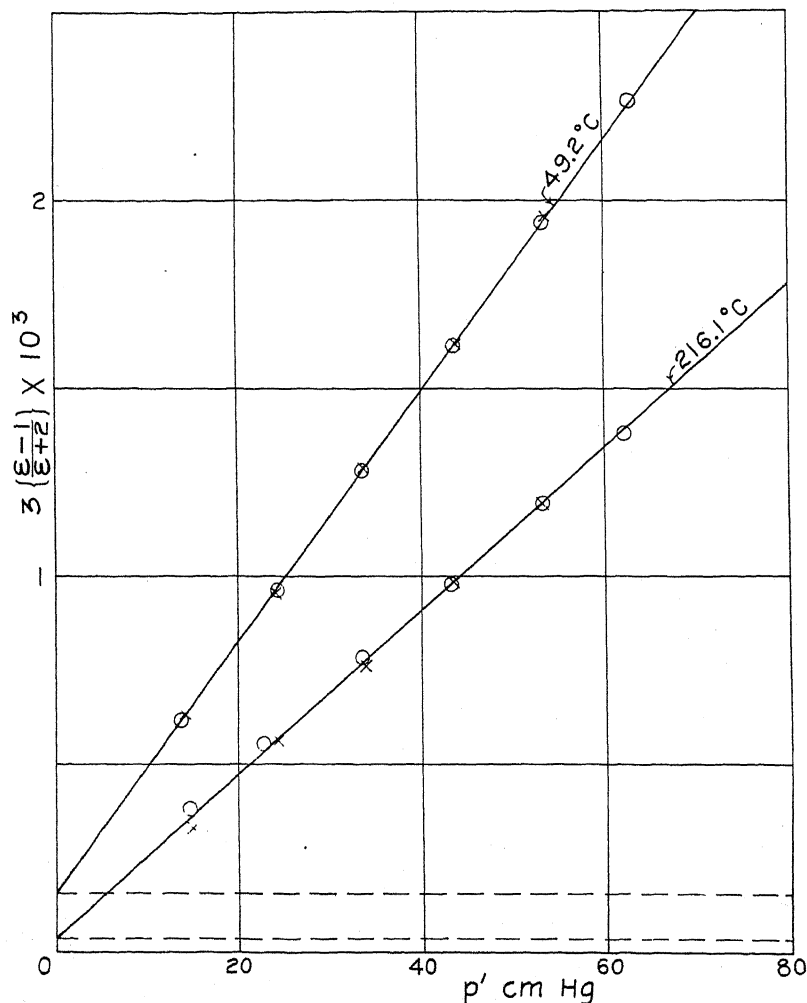


Fig. 1. Variation of polarization with pressure, p' .

in the calculations. The circuits are always adjusted to give the vacuum reading at approximately this fixed point, so that there is no appreciable error introduced in the value of the slope of the pressure curves. A table of calculated values or an accurately drawn chart then serves to facilitate the calculations of ϵ . The true values of $3\{\epsilon-1/\epsilon+2\}$ are measured from the zero values obtained by extrapolation on the curves. In Fig. 1 the values

of $3[\Delta(\epsilon-1)/(\epsilon+2)]$ are plotted against p' and the true values are measured from the horizontal zero lines. For the calculation of p' values of the van der Waal constants were obtained from Kaye and Laby: $a=0.02316$ and $b=0.00343$. Only two of the four sets of data are plotted here for illustration, the best and the worst. The pressure runs were always repeated in the reverse direction in order to eliminate the effect of errors caused by any drifts in the condenser system not due to the CS₂. The part of the readings for increasing pressure is marked by circles; and the part for decreasing pressure, by crosses. The line for the temperature 49.2°C is remarkably well reproduced, while that for 216.1°C shows a slight drift, which is eliminated in the drawing of the line. The strict linearity of these pressure curves indicates that there is no appreciable association or surface condensation throughout the total observed range of pressure.

The last column of Table I contains the value of the molecular polarization. P , or the total induced electric moment per gram-molecule of the substance, calculated from the mean value in the preceding column. $(\epsilon-1)/(\epsilon+2)v$ is the moment or polarization due to N_0 molecules; therefore P can be obtained from the values in the sixth column as indicated by:

$$P = (n/3N_0) \times 3 \left\{ \epsilon - 1/\epsilon + 2 \right\} v = 7.4716 \times 10^3 \times 3 \left\{ \epsilon - 1/\epsilon + 2 \right\} v$$

where n is Avogadro's number, $6.064_4 \times 10^{23}$. The values of the constants, n , N_0 , L , and k used in these calculations are those given by Birge.⁶

Since the values in the last two columns of Table I are independent of temperature within the limits of experimental error, as mentioned above it is not necessary to draw a Debye line in order to determine the constant A . The results can be summarized by: $A=0.002993$ or $P=22.36$, and $\mu=B=0$.

COMPARISONS WITH OTHER DATA

The result $\mu=0$ is in accord with the observations of Ghosh, Mahanti, and Mukherjee,⁴ but the value of A given by them is 0.002912, about three percent lower than the above value. The discrepancy may be due to a calibration error in either of the two sets of experiments. It is believed by the author that the calibration of the apparatus used for the measurements given here is accurate to a fraction of a percent. Evidence substantiating this has been pointed out by Stuart⁷ and by the author.⁸ Furthermore the value of A for air given by the above mentioned authors is 0.0005797, about one percent higher than that obtained by the author,⁹ 0.000572, and deviates in the opposite direction to that required to explain the discrepancy in the values for CS₂. A part, if not all, of the deviation could be explained by the failure of the above mentioned authors to take into account the departures of the gas from the ideal law. At atmospheric pressure this amounts

⁶ R. T. Birge, Phys. Rev. Supplement, 1, 1 (1929).

⁷ H. A. Stuart, Zeits. f. Physik 47, 457 (1928).

⁸ C. T. Zahn and J. B. Miles, Jr., Phys. Rev. 32, 497 (1928).

⁹ C. T. Zahn, Phys. Rev. 24, 400 (1924).

to about two percent in such a direction as to increase the values given. Their values of $(\epsilon - 1)$ agree remarkably well for different temperatures, but if they worked at approximately constant density of gas the above mentioned correction would probably not sensibly alter this agreement. In addition there is an unimportant error of a small fraction of a percent introduced by the neglect of the factor $(\epsilon + 2)$. They also give the value of $n_\infty^2 = 1.002956$, taken from Graetz's handbook which is *higher* than their value $\epsilon = 1.002912$. Now deviations between n_∞^2 and ϵ are usually in the opposite direction¹⁰ because the extrapolation to n_∞ is usually done from the visible spectrum neglecting the infra-red terms which have been shown to be of importance in the case of CO_2 . In the case of CO_2 the refractivity has been measured over the entire range from the ultra-violet through the infra-red. Fuchs¹¹ has extrapolated for n_∞^2 taking into account the infra-red terms and obtains a value differing from the author's value of ϵ by less than one-tenth percent. If the extrapolation had been done without considering the infra-red terms, a value too small would have been obtained. It is therefore difficult to explain experimental observations of ϵ which are smaller than the value of n_∞^2 extrapolated from the visible. In the case of CS_2 one would expect ϵ to be larger than such values of n_∞^2 all the more because it has been definitely shown to be the case for its structurally similar compound CO_2 . As additional confirmation of the value given here Williams' value of P , as given by Errera,¹⁰ is 22.2 as compared with the value of 22.36. The small deviation is in the direction to be expected from data cited by Errera.¹² For the above reasons it is believed that the above mentioned value of $\epsilon = 1.002912$ is about three percent too low.

MOLECULAR STRUCTURE

In the previously cited article¹ the authors discussed values for the electric moment of CO , CO_2 , COS , and CS_2 , with reference to molecular structure. Since in that discussion the moment for CS_2 was tentatively considered to be 0.33×10^{-18} c.g.s. e.s.u., the discussion should be somewhat modified. The moment of COS was found to be 0.65×10^{-18} ; and that of CO , 0.10×10^{-18} . Therefore one would expect the moment of CS to be of the same order as that of COS , and the value of the moment of CS_2 as there found would have to correspond to an approximately linear structure, or to a truly linear structure of the unsymmetrical type suggested by Heisenberg. Since the moment of CS_2 is now definitely proven to be zero the situation is simplified. CO_2 has been shown by Stuart⁷ to have a rectilinear structure since it has no electric moment and for other reasons which he has pointed out. The similar compound CS_2 has now been shown to have no electric moment, and we can therefore consider with a high degree of probability that its structure is rectilinear.

¹⁰ For an excellent discussion of this see: J. Errera, "Polarization Diélectrique."

¹¹ O. Fuchs, *Zeits. f. Physik* **46**, 519 (1928).

¹² Errera, reference 10, p. 68.

THE VARIATION OF DIELECTRIC CONSTANT WITH
TEMPERATURE. I. THE ELECTRIC MOMENTS OF
THE CARBON BISULPHIDE AND NITROUS
OXIDE MOLECULES*

BY CHRISTIAN H. SCHWINGEL AND JOHN WARREN WILLIAMS
LABORATORY OF PHYSICAL CHEMISTRY, UNIVERSITY OF WISCONSIN

(Received February 8, 1930)

ABSTRACT

An apparatus has been described which makes it possible to determine dielectric constants of gases and vapors and their dependence on temperature over a range of several hundred degrees. The electric moments of gaseous carbon bisulphide and nitrous oxide have been measured and found to be zero. These results indicate a linear arrangement of the three atoms forming each molecule.

IN RECENT years the study of the constitution of simple polar and non-polar molecules has attracted much attention. There have become available physical methods, among them the dipole theory of Debye,¹ which enable one to determine at least the relative positions of the atoms forming the simpler molecules, and also to say something concerning the symmetry of more complicated ones. In this connection the configuration of the carbon dioxide molecule is of interest. The results of x-ray studies on the solid² indicated without any question a linear and symmetrical arrangement of the three atoms which make up the molecule. For a long time, however it was thought that the molecule possessed a finite electric moment, suggesting a triangular arrangement of the atoms for the molecule in the gaseous condition. This conclusion appeared to be substantiated by molecular spectra data, and it was not until Stuart³ showed its electric moment to be zero that the linear and symmetrical model was accepted for the vapor as well.

There are other triatomic molecules for which electric moment data have been reported in the literature, and in certain cases where rather small values have been reported, the possibility existed that these values were indistinguishable from zero, because of experimental difficulties. Thus an electric moment of magnitude, $\mu = 0.33 \times 10^{-18}$ e.s.u., was reported by Zahn and Miles⁴ for the carbon bisulphide molecule, although liquid carbon bisulphide had previously been successfully used as a non-polar solvent for the determination of the electric moment of a number of dissolved molecules.⁵ Again,

* This paper is an abstract of a part of the thesis of C. H. Schwingel submitted in partial fulfillment of the requirements for the degree of Doctor of Philosophy.

¹ Debye, Handbuch d. Radiologie VI, 597 (1925). Polar Molecules, Chemical Catalog Co., New York, (1929).

² Mark, Zeits. f. Elektrochem. 31, 523 (1925).

³ Stuart, Phys. Zeits. 47, 457 (1928).

⁴ Zahn and Miles, Phys. Rev. 32, 497 (1928).

⁵ Williams and Ogg, Jr. Amer. Chem. Soc. 50, 94 (1928).

nitrous oxide shows such a similarity with carbon dioxide in its physical behavior⁶ that one might expect it to be non-polar in character as well.

The purpose of this article is to present the results of an experimental study of the temperature variation of the dielectric constant of the vapors of carbon bisulphide and nitrous oxide, and to show that their electric moments do not differ from zero by more than 0.05×10^{-18} in the case of N_2O and by more than 0.02×10^{-18} in the case of CS_2 .[†] The apparatus and method used are briefly described later.

RESULTS

Debye has shown how one may have a dielectric constant, or rather a portion of it that varies with the absolute temperature if it be assumed that there exist permanent electrical dipoles in the molecules. This theory has been amply verified in recent years, so it is only necessary here to give its mathematical result. The total polarization is given by the equation

$$P = \frac{\epsilon - 1}{\epsilon + 2} \cdot \frac{M}{d} = \frac{4\pi}{3} N \left[\gamma' + \frac{\mu^2}{3kT} \right] \quad (1)$$

where ϵ is the dielectric constant; M the molecular weight; d the density; N is Avogadro's number; γ' is—a constant; μ the electric moment of the molecule; k the Boltzmann constant; T the absolute temperature; $(4\pi/3) N\gamma'$ is the polarization due to deformation of the molecule and $(4\pi/3) (N\mu^2/3kT)$ is the polarization due to orientation of the molecule. In the case of gases and vapors this equation may be written with sufficient accuracy in the following form:

$$\begin{aligned} \frac{\epsilon - 1}{4\pi} \cdot \frac{M}{Nd} &= \gamma' + \frac{\mu^2}{3kT} = a + \frac{b}{T} \\ \text{i.e. } \frac{\epsilon - 1}{4\pi} \cdot \frac{m \cdot T}{d} &= aT + b = D \end{aligned} \quad (2)$$

where m = mass of the molecule in question.

In this equation the function D is a linear function of T . The slope of the line gives the polarization due to deformation, while the "y" intercept ($T=0$) gives the value of the electric moment squared divided by $3k$, that is, $b = \mu^2/3k$.

The nitrous oxide used was of hospital purity and triple distilled. It was dried thoroughly with P_2O_5 before each determination.

The carbon disulphide, Baker's C.P. analyzed, was allowed to stand over P_2O_5 for several days before use. On distillation high and low-boiling fractions were discarded. It was later distilled directly into the apparatus.

⁶ Langmuir, Jr. *Amer. Chem. Soc.* **41**, 1543 (1919).

[†] The experimental work reported herein was practically complete when an article by Ghosh, Mahanti and Mukherjee, *Zeits. f. Physik* **58**, 200 (1929) appeared in which it was found that both nitrous oxide and carbon bisulphide had zero moments. Thus the results of the two investigations are entirely in agreement.

The results of the experimental work are given by Fig. 1 which has, in turn, been constructed from the data given in Tables I and II. All measurements were made at constant pressure. The simple gas law was used to

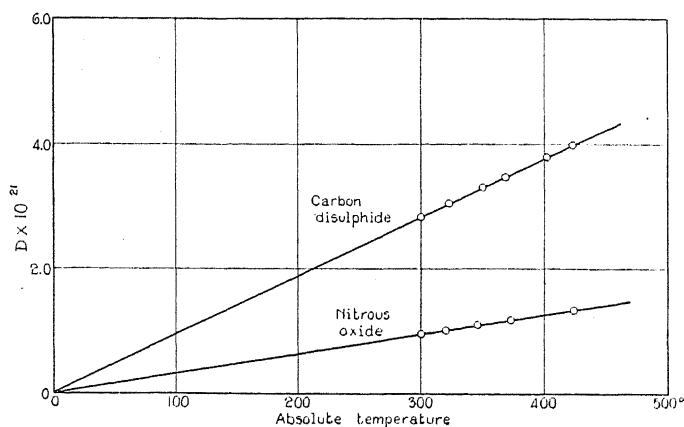


Fig. 1.

calculate the dielectric constant of the gas at 760 mm Hg pressure. The error involved in this method of procedure was proven to be well within the limit of the experimental error of the final result for the electric moments of the molecules.

TABLE I. Summary of data (Carbon disulphide).

T°	$(\epsilon-1)10^{-5}$ (760 mm)	$D \times 10^{21}$	$P = \frac{(\epsilon-1)M}{3d}$
301.6	290	2.84	24.0
322.6	275	3.07	24.2
350.0	250	3.29	23.9
369.8	237	3.45	24.0
400.1	219	3.76	23.9
424.3	206	3.98	23.9

From equation of straight line (Fig. 1), $b = 0.001 \times 10^{-21} = \mu^2/3k$ or $\mu^2 = 3 \times 1.37 \times 0.001 \times 10^{-37} = 0.00041 \times 10^{-36}$, $\mu = 0.020 \times 10^{-18}$ e.s.u.

TABLE II. Summary of data (Nitrous oxide).

T°	$(\epsilon-1)10^{-6}$ (760 mm)	$D \times 10^{21}$	$P = \frac{(\epsilon-1)M}{3d}$
301.0	993	0.965	8.17
320.5	921	1.02	8.07
347.3	850	1.11	8.10
374.0	780	1.19	8.10
425.6	693	1.35	8.06

From equation of straight line (Fig. 1), $b = 0.007 \times 10^{-21} = \mu^2/3k$ or $\mu^2 = 3 \times 1.37 \times 0.007 \times 10^{-37} = 0.00288 \times 10^{-36}$, $\mu = 0.05 \times 10^{-18}$ e.s.u.

EXPERIMENTAL METHOD*

The method used for the determination of the dielectric constants at the various temperatures was similar to that presented by Pungs and Preuner⁷ and later improved upon by Zahn,⁸ Stuart,³ Sanger,⁹ and others.

Two loosely coupled oscillating circuits, I and II, (Fig. 2) were used to generate constant frequencies, n_1 and n_2 . These frequencies, when coupled to a detector, give the frequency $n_d = n_1 - n_2$, which may be detected in the receiver of the detector circuit.

It is evident that a variation of capacity in either circuit will change n_d . If the frequency of circuit II is kept constant, then any change in the frequency of circuit I, due to the change in capacity of C_x , can be detected in

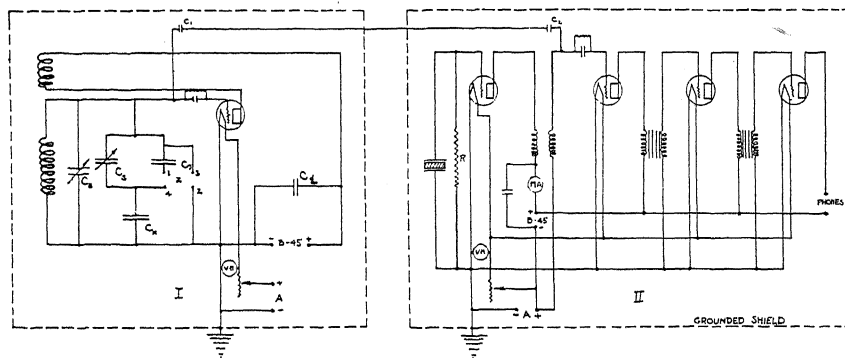


Fig. 2.

the receiver and brought back to the frequency of n_2 by means of a capacity C_s . Circuit I has in series with the gas condenser C_x , a fixed condenser C_v of much greater capacity, and a precision variable condenser C_s . The total capacity is kept constant, determined by the method of counting beats produced in the receivers of the detector circuit. The total capacity of the circuit is changed only by the change in the value of C_x , due to the admission of gases into the previously evacuated condenser; and this is compensated for by means of a change in C_s .

The following equation gives the total series capacity

$$\text{Total capacity} = (1/C_x) + (1/C_v + C_s) \quad (3)$$

If ΔC_x equals the change in capacity due to the admission of gas, and if ΔC_s is the change necessary to bring the circuit to the original frequency of circuit II, then

$$\frac{1}{C_x + \Delta C_x} + \frac{1}{C_v + C_s + \Delta C_s} = \frac{1}{C_x} + \frac{1}{C_v + C_s} \quad (4)$$

* A diagram of the apparatus without any description was included in an article submitted in June 1929 by one of us (J. W. W.) to the Fortschritte der Chemie, Physik und physikalischen Chemie as part of a discussion of this and related subjects. It is published as Band 20, Heft 5, 1930.

⁷ Pungs and Preuner, Phys. Zeits. 20, 543 (1919).

⁸ Zahn, Phys. Rev. 24, 400 (1924).

⁹ Sanger and Steiger, Helv. Phys. Acta. 1, 369 (1928), et. al.

Solving for ΔC_x , there is obtained

$$\Delta C_x = \frac{C_x^2 \cdot \Delta C_s}{(C_y + C_s)^2 + (C_y + C_s + C_x) \Delta C_s} \quad (5)$$

This can be written with sufficient accuracy

$$\Delta C_x = \frac{C_x^2 \Delta C_s}{(C_y + C_s + \frac{1}{2} \Delta C_s)^2}$$

If the condenser C_y is very large compared to C_x then a small change ΔC_x will necessitate a large change ΔC_s to bring the circuit to the initial frequency. The frequency of circuit II is kept constant by means of a thermally protected quartz plate.

The electrical connections employed are shown in the figure referred to above. The vacuum tubes were all of the UX 301 type, operated at voltages considerably below rating. It was found that a potential of 4 volts for the oscillating tubes produced the most constant conditions of frequency. The detector tube and amplifiers were operated at full rating. A plate potential of 45 volts was used in all cases. All connections were carefully soldered, and it was found advisable to remove all filament rheostats and voltmeters. The entire apparatus was fastened rigidly in place and thoroughly shielded. Separate shields were used for circuits I and II. Inductances were bakelite tubes wound with silk covered copper wire.

Capacity measurements were made at a frequency of 498.6 kilocycles, corresponding to a wave-length of approximately 600 meters. This frequency was kept constant by means of a quartz crystal, ground and calibrated at the laboratories of the General Radio Company, Cambridge, Mass. For constant conditions of operation, it was found necessary to separate the two circuits by several feet, the only coupling being the single wire as shown in the diagram. Under favorable temperature conditions in the room, the frequency would remain constant to a tenth of a scale division for several minutes, or show a regular increase of several tenths per minute and could be corrected for accordingly. The beats produced in the receiver were amplified by means of two stages of transformer coupled amplification, the zero reading being taken as twenty beats in ten seconds. Capacity C_s was a standard precision condenser of 500 $\mu\mu\text{f}$ capacity, manufactured and calibrated in the laboratories of the General Radio Company. A mica condenser, C_y was calibrated to the latter as standard. All condensers, as well as the entire apparatus, were protected from thermal fluctuations by means of proper insulation.

Gas condenser C_x , was a specially constructed fixed air condenser, made for this particular purpose by the Cardwell Manufacturing Corporation. It is shown diagrammatically in Fig. 3. The construction was of brass and heavily gold plated. The twenty-three plates, each spaced approximately 3 mm, were held in position by means of two strips of Mycalex, the strips being placed as far as possible outside the electrostatic field. The added

capacity correction is negligible, due to their size and position, amounting to not more than 0.2 percent of the total capacity.

This capacity, C_z , was mounted inside a rigidly constructed brass drum (internal diameter, six inches) one terminal of the condenser being grounded to it, and the other leading out through the central glass tube which was used for the entry and removal of gases, and which also contained the thermocouple well. The gas tight drum, containing the condenser, was bolted to the inside of an oil bath, and the capacity when assembled was approximately 444 μmf . The assembly of condenser and thermostat, consisting of (1) thermo-regulator, (2) heater, (3) gas-tight drum, (4) opening for thermocouple, (5) entrance for gas, (6 and 7) condenser terminals, and (8) stirrer, is shown in Fig. 3 and need not be detailed further.

The temperature control bath was a large galvanized iron vessel, insulated completely with "balsam wool," and filled with cotton seed oil. It was kept at constant temperature by means of a heater constructed of nichrome

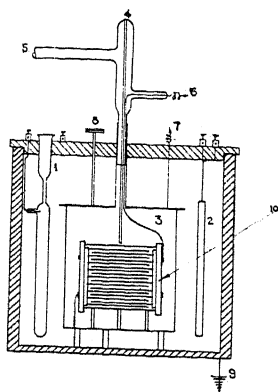


Fig. 3.

wire wound on a grid of "transite." This was immersed directly in the oil. The ordinary make and break type mercury regulator was found satisfactory for keeping the temperature constant to within 0.1° for values up to 100°C , and to within 0.2° for higher temperatures. A calibrated copper-constantan couple placed in close proximity to the condenser served to determine the temperatures. It was found that the temperature became constant after about ten minutes from the time of the gas entry.

In order to evacuate the apparatus, a Hy-Vac oil pump was employed in connection with a water pump. The water pump was used only for the initial clearing out of vapors that might be absorbed by the oil in the pump. In the case of carbon disulphide vapors, and other oil soluble vapors, the system was flushed out thoroughly several times with carbon dioxide, each time evacuating to about 2 cm by means of a water pump. After several of these flushings, the Hy-Vac pump was connected and the system evacuated to 0.01 mm or better. The oil in the pump was changed at frequent intervals. For pressure measurements, a modified U-type manometer was used.

Fig. 4 shows the method used for allowing gases and vapors to enter the condenser chamber. In the case of organic liquids it was necessary to lubricate the stopcocks with a paste made of very finely precipitated silicon dioxide, phosphoric anhydride, and phosphoric acid. This mixture was found to be very satisfactory, having no appreciable vapor pressure, and lasting for the duration of a determination. Outlets *g* and *f* were attached to the oil pump and water pump respectively; and *d* was the connection to the condenser chamber. Stopcock *c* was used to allow the entrance of gases, while *a* was the bulb used for holding the liquids which were allowed to evaporate into the system. Liquids were allowed to evaporate into the system until the partial pressure, as read on the manometer, was slightly less than saturation for room temperature; consequently no condensation could take place in the system.

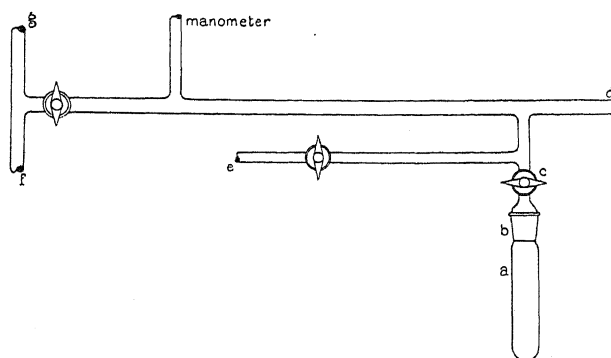


Fig. 4.

To determine the absolute values of the dielectric constants, it was necessary to determine the capacities of all condensers and lead wires.

The capacity of the gas condenser was determined before and after every series of measurements. This was accomplished by means of a mercury switch *z*, Fig. 2. By connecting 1 and 3, the fixed condenser C_y is short circuited. Then C_x and C_s are connected in series and C_s adjusted to fixed frequency corresponding to capacity C_s' . Then C_x was short circuited by connecting 2 and 4, and C_s adjusted to the original beat frequency, or, in other words, until the original capacity had been reached. Calling the new position C_s'' , the equation of the series capacity will be,

$$\frac{1}{C_s''} = \frac{1}{C_x + X} + \frac{1}{C_s'} \quad (6)$$

where X is the capacity of the lead wire from C_x to C_s and to z . Solving

$$C_x + X = \frac{C_s' \cdot C_s''}{C_s' - C_s''} = C. \quad (7)$$

The value for X , calculated from radio formulae was $10.6 \mu\mu f$, with a maximum variation of $2 \mu\mu f$. This amounts to not more than 0.5 percent of the total capacity.

The values for the dielectric constants were calculated according to the equation,

$$\epsilon - 1 = \frac{\Delta C_x}{C - X} \quad (8)$$

where C_x is the capacity before the admission of vapor, including X , the lead capacity.

Combining Eqs. (5), (7), and (8)

$$\epsilon - 1 = \frac{C^2}{(C_v + C_s + \frac{1}{2}\Delta C_s)^2} \cdot \frac{\Delta C_s}{C - X} \quad (9)$$

Errors in the determination of C_x amount to not more than 0.5 percent, in C_v not more than 1.5 percent, and in ΔC_x not more than 1.5 percent. Since errors in the temperature and pressure measurements are small in comparison, the total error in a dielectric constant determination will not be more than 1.5 percent.

For determining values of ΔC_s , the system was flushed out several times and evacuated. After constant temperature conditions were attained, C_s was adjusted to the beat frequency, twenty in ten seconds. Having taken the reading of C_s' , the cock was opened to allow the gas or vapor to enter the condenser chamber. When constant temperature conditions had again been attained C_s was adjusted to the capacity corresponding to the original beat frequency, C_s'' . The reading C_s' and the difference between C_s' and C_s'' or ΔC_s were substituted in formula (9), along with predetermined values of C , C_v and X . By this means $\epsilon - 1$ is evaluated directly. Any slight drift in C_s must have been predetermined, and taken into consideration.

For each temperature, five to eight readings were taken, evacuation taking place each time. The time for a single temperature measurement amounted usually to approximately eight hours.

In order thoroughly to test our apparatus the electric moment of the ethyl ether molecule was determined. The result, $\mu = 1.12 \times 10^{-18}$ e.s.u., is in perfect agreement with the recent and now commonly accepted results of Sanger¹⁰ and of Stuart.¹¹ The electric moment of carbon dioxide was also found to be zero.

CONCLUSIONS

The results of this article, with those of Ghosh, Mahanti, and Mukherjee, demonstrate that carbon bisulphide and nitrous oxide do not have finite electric moments.

To explain this fact the simplest assumption is to assign a linear and symmetrical arrangement to the three atoms which form the molecule. It is not our intention, however, to conclude that these are necessarily rigid molecules with which we are dealing. A complete knowledge of the vibration-rotation and rotation spectra of a molecule is also of particular importance in such a study, and these data are unfortunately not available at this time.

¹⁰ Sanger, *Leipziger Vortrage*, 1929.

¹¹ Stuart, *Zeits. f. Physik* **51**, 490 (1928).

THE NUMERICAL DETERMINATION OF CHARACTERISTIC NUMBERS

BY W. E. MILNE

DEPARTMENT OF MATHEMATICS, UNIVERSITY OF OREGON

(Received February 24, 1930)

ABSTRACT

A method is developed for the numerical calculation of characteristic energy levels in cases where the wave equation contains, or can be reduced so as to contain, a single space variable. The procedure consists in the numerical integration of an auxiliary differential equation for several chosen values of the energy, after which the characteristic values are obtained by interpolation. The method is one of considerable generality so far as the form of the differential equation is concerned, and is capable of giving any preassigned degree of accuracy.

1. The entrance of wave mechanics into modern physics gives new interest to boundary value problems associated with linear differential equations, especially those problems treated by Weyl¹ and others which have to do with the Sturm-Liouville equation

$$\frac{d}{dx} \left[p(x) \frac{dy}{dx} \right] - q(x)y + \lambda \rho(x)y = 0 \quad (1)$$

in the intervals $0 < x < \infty$ or $-\infty < x < \infty$. A problem of particular physical interest is the determination of those characteristic values of λ (eigenwerte) for which (1) possesses solutions that are finite at both ends of the interval.² In several important special cases the complete analytical solution of this problem is known,³ but in other instances it is necessary to resort to approximate methods.

The object of this note is to describe a numerical procedure for obtaining the characteristic values of λ belonging to the equation

$$\frac{d^2 u}{dx^2} + G(x, \lambda)u = 0. \quad (2)$$

Equation (1) can be reduced to this form by the substitution $y = up^{-1/2}$, provided p has first and second derivatives and does not vanish in the interval.

¹ Weyl, *Mathematische Annalen* **68**, 220 (1910), and *Göttinger Nachrichten*, (1910), p. 442. Hilb, *Mathematische Annalen* **76**, 333 (1915). Milne, *Trans. Amer. Math. Soc.* **30**, 797 (1928).

² Schrödinger, *Ann. d. Physik* **79**, 361 (1926). See p. 363. Kemble, *Phys. Rev. Supplement* **1**, 157 (1929), see p. 177.

³ Cf. e.g. Kemble, reference 2, pp. 183-186. Condon and Morse, *Quantum Mechanics*, (McGraw-Hill, 1929) Chapter II.

Equation (2) contains as a special case the wave equations of the type

$$\frac{d^2u}{dx^2} + \frac{8\pi^2\mu}{h^2} [W - V(x)]u = 0, \quad (3)$$

as is seen by setting

$$\lambda = \frac{8\pi^2\mu W}{h^2}$$

and

$$G(x, \lambda) = \lambda - \frac{8\pi^2\mu}{h^2} V(x).$$

Equation (2), however, is considerably more general than (3).

With regard to $G(x, \lambda)$ we assume that $\partial G / \partial \lambda$ exists and is positive, that $G(x, \lambda)$ is continuous in x , that when $|x|$ is sufficiently large $G(x, \lambda)$ is negative for the values of λ under consideration, and (if the interval is $0 < x < \infty$) $\lim_{x \rightarrow 0} G(x, \lambda) = -\infty$.

2. For simplicity we consider only the case in which the interval is $-\infty < x < \infty$. Let x_0 be a value of x in the interval, and let $u_1(x)$ and $u_2(x)$ be two solutions of Eq. (2) satisfying the conditions

$$\begin{aligned} u_1(x_0) &= 1, & u_2(x_0) &= 0, \\ u_1'(x_0) &= 0, & u_2'(x_0) &= a \neq 0. \end{aligned} \quad (4)$$

The constant a is arbitrary and in any particular case is to be determined so as to make the numerical work as simple as possible. These solutions satisfy the well-known identity

$$u_1(x)u_2'(x) - u_2(x)u_1'(x) \equiv a. \quad (5)$$

Let a function $w(x)$ be defined by the equation

$$w(x) = [u_1^2(x) + u_2^2(x)]^{1/2} \quad (6)$$

By differentiating this equation twice, eliminating $u_1''(x)$ and $u_2''(x)$ by means of (2), and simplifying with the aid of (5) we find that the function $w(x)$ satisfies the simple differentiation equation

$$\frac{d^2w}{dx^2} + G(x, \lambda)w - \frac{a^2}{w^3} = 0. \quad (7)$$

Now the general solution of (2) can be expressed in the form

$$u(x) = Cw(x) \sin \left\{ a \int_{x_0}^x w^{-2} dx - \alpha \right\}, \quad (8)$$

in which C and α are arbitrary constants. Since with the given hypotheses $w(x)$ does not approach zero at either end of the interval, it is clear that a solution satisfying the desired conditions at both ends of the interval can be found if and only if

$$\frac{a}{\pi} \int_{-\infty}^{\infty} w^{-2} dx = n \quad (9)$$

in which n is a positive integer.

3. Now the integral

$$N = \frac{a}{\pi} \int_{-\infty}^{\infty} w^{-2} dx \quad (10)$$

is an increasing function of λ , so that if we select k values of λ for which this integral is finite (values of λ for which N is infinite belong to the continuous spectrum and do not interest us here), say $\lambda^1 < \lambda^2 < \dots < \lambda^k$, we obtain k values of N , say $N_1 < N_2 < \dots < N_k$. If an integer n lies in the interval $N_1 < n < N_k$, we may use the method of interpolation to obtain approximately the corresponding value of λ , $\lambda = \lambda_n$, which will be precisely the n -th characteristic value of λ counted in order of magnitude.

To put this plan into execution we proceed as follows:

First, we solve Eq. (7) with the initial conditions $w(x_0) = 1$, $w'(x_0) = 0$ for each of the k values of λ , $\lambda^1, \lambda^2, \dots, \lambda^k$. For this purpose we may use any one of several well-known methods for the numerical integration of differential equations.

Second, using in turn each of the solutions now obtained, we evaluate by numerical quadrature the integral (10) and get the k values of N , N_1, N_2, \dots, N_k .

Lastly, we obtain by interpolation the values of λ corresponding to each integer in the interval N_1 to N_k .

When the characteristic value of λ has been found it is then possible to integrate (7) using this value of λ and then obtain the corresponding wave function itself by means of (8). As a matter of fact, however, it will generally be easier to obtain $w(x)$ and $\int_0^x w^{-2} dx$ by interpolation from the computations already performed.

Naturally the speed and accuracy of the method depend largely on good judgment in the selection of the trial values $\lambda^1, \lambda^2, \dots, \lambda^k$. This is perhaps best illustrated by means of an example.

4. We take as an illustrative example the differential equation

$$\frac{d^2 u}{dz^2} + \frac{8\pi^2 \mu}{h^2} [W - kz^4] u = 0,$$

which upon the substitutions

$$z = \frac{h^{1/3}}{(8\pi^2 \mu k)^{1/6}} x,$$

$$\lambda = \left[\frac{64\pi^4 \mu^2}{h^4 k} \right]^{1/3} W,$$

reduces to

$$\frac{d^2u}{dx^2} + (\lambda - x^4)u = 0.$$

For simplicity we choose $x_0 = 0$, $a = \lambda^{1/2}$, so that equation (7) becomes

$$\frac{d^2w}{dx^2} + (\lambda - x^4)w - \lambda w^{-3} = 0, \quad (11)$$

with the initial conditions $w = 1$, $w' = w'' = w^{(3)} = w^{(4)} = w^{(5)} = 0$ at $x = 0$. The desired solution is even, so that we need to compute it for positive values of x only.

The critical values of λ are evidently positive, and when n is large their order of magnitude can be obtained from the formula⁴

$$\pi n = \lambda_n^{3/4} \int_0^1 s^{1/4} (1-s)^{-1/2} ds + R_n,$$

in which R_n is bounded. This gives

$$\lambda_n = n^{4/3} [2.184 + E/n]$$

where E is bounded. It appears, therefore, that λ_1 will probably lie somewhere between 1 and 4, so we choose the four trial values $\lambda^1 = 1$, $\lambda^2 = 2$, $\lambda^3 = 3$, $\lambda^4 = 4$, and calculate the solution of (11) for each of these values. The method actually used was that described by the author elsewhere.⁵ With the aid of a calculating machine and Barlow's Tables the integration can be done rapidly. The values of $1/w^2$ and $1/w^3$ are read directly in the columns headed "square" and "cube" respectively. We retained only enough significant figures in w to give $1/w^2$ to four places of decimals. The first one of the four computations is shown below to illustrate the general method. The integrals

$$I(\lambda) = \int_{-\infty}^{\infty} w^{-2} dx = 2 \int_0^{\infty} w^{-2} dx$$

were found with the calculating machine, using Weddle's rule and were checked with Simpson's rule. They proved to be as follows:

λ	$I(\lambda)$	ΔI	$\Delta^2 I$	$\Delta^3 I$
1	3.0469			
2	3.1090	621		
3	3.1719	629	8	
4	3.2362	643	14	6

⁴ Milne, Trans. Amer. Math. Soc. 31, 907-918 (1929), see formula (25) p. 914.

⁵ Milne, Numerical Integration of Ordinary Differential Equations, Amer. Math. Monthly 33, 455 (1926).

From (8), since $a = \lambda^{1/2}$, we get

$$\lambda_n = [\pi n / I(\lambda)]^2$$

and by a few trials find from this that the values of the first two characteristic numbers are

$$\lambda_1 = 1.0605$$

$$\lambda_2 = 3.7998.$$

COMPUTATION I. $\lambda = 1$.

x	w	w'	w''	$[x^4 - 1]$	$1/w^3$	$1/w^2$
0	1.0000	.0000	.0000	-1.0000	1.0000	1.0000
.1	1.0000	.0000	.0001	-.9999	1.0000	1.0000
.2	1.0000	.0001	.0016	-.9984	1.0000	1.0000
.3	1.0000	.0005	.0081	-.9919	1.0000	1.0000
.4	1.0001	.0021	.0252	-.9744	.9997	.9998
.5	1.0005	.0061	.0605	-.9375	.9985	.9990
.6	1.0015	.0151	.1238	-.8704	.9955	.9970
.7	1.0038	.0322	.2258	-.7599	.9886	.9924
.8	1.0084	.0620	.3798	-.5904	.9752	.9833
.9	1.0168	.1104	.6016	-.3439	.9513	.9673
1.0	1.0314	.1853	.9114	.0000	.9114	.9400
1.1	1.0551	.2966	1.341	.4641	.8514	.8983
1.2	1.0924	.4590	1.940	1.0736	.7671	.8380
1.3	1.1493	.6930	2.792	1.8561	.6587	.7570
1.4	1.2344	1.031	4.039	2.8416	.5316	.6563
1.5	1.3606	1.522	5.924	4.0625	.3971	.5402
1.6	1.5467	2.251	8.859	5.5536	.2703	.4181
1.7	1.8232	3.353	13.57	7.3521	.1650	.3008
1.8	2.2377	5.067	21.34	9.4976	.0893	.1997
1.9	2.8706	7.803	34.58	12.0321	.0423	.1213
2.0	3.856	12.32	57.83	15.0000	.0175	.0673
2.1	5.440	20.01	100.4	18.4481	.0062	.0338
2.2	8.058	33.66	180.7	22.425	.0019	.0154
2.3	12.60	58.74	338.6	26.98	.0005	.0063
2.4	20.57	106.9	661.6	32.18		.0024
2.5	36.5	230.0	1387.	38.06		.0007
2.6	60.	410.0				.0003

$$\int_{-\infty}^{\infty} w^{-2} dx = 3.0469 \text{ by Weddle.}$$

$$3.04688 \text{ by Simpson.}$$

LETTERS TO THE EDITOR

Prompt publication of brief reports of important discoveries in physics may be secured by addressing them to this department. Closing dates for this department are, for the first issue of the month, the twenty-eighth of the preceding month; for the second issue, the thirteenth of the month. The Board of Editors does not hold itself responsible for the opinions expressed by the correspondents.

Growth of Zinc Crystals

In two recent papers by Goetz and Hasler¹ and Goetz² reference is made to a paper by Mr. A. G. Hoyem³ and myself on the growth of zinc crystals. Since certain conclusions are drawn which are based on a misconception of one point in our work I would like to point out that for crystals of the same diameter, drawn at the same rate, the height of the column of liquid zinc just below the crystal is *always the same*, regardless of the temperature of the molten zinc. It is of course obvious that the higher the latter temperature the greater the blast of cooling gas that must be used. Too feeble a gas blast for the molten zinc temperature causes an increase in the height of the liquid zinc column but also a *reduction of the diameter of the crystal*. Mr.

Hoyem and I therefore felt justified in considering the excess of temperature of molten zinc (in the crucible) above the melting point of zinc as proportional to the temperature gradient in the liquid column as long as crystals of only one diameter were grown and at a single rate. Our paper would have had little point otherwise.

E. P. T. TYNDALL

Department of Physics,
University of Iowa
March 7, 1930

¹ A. Goetz and Maurice F. Hasler, Proc. Nat. Acad. **15**, 646 (1929).

² A. Goetz, Phys. Rev. **35**, 193 (1930).

³ A. G. Hoyem and E. P. T. Tyndall Phys. Rev. **33**, 81 (1929).

The Spark Spectrum of Ruthenium

During last year we undertook the analysis of the spectrum Ru II. The fundamental multiplets were very easily discovered, but further progress was stopped by the insufficient accuracy of the measures. Accurate measures will shortly be made and the analysis extended. In the meantime it is perhaps of interest to give a table of the low terms. The table includes the electron configuration, designation and value of each low term. The odd terms are not given, but comprise $^6P^o$, D^o , F^o and $^4P^o$, D^o , $F^o(d^6p)$.

Table of low terms of Ru II.

d^7 $^4F_{4\frac{1}{2}}$	0.0
" $^4F_{3\frac{1}{2}}$	1523.0
" $^4F_{2\frac{1}{2}}$	2494.0
" $^4F_{1\frac{1}{2}}$	3104.2
" $^4P_{2\frac{1}{2}}$	8256.8
" $^4P_{1\frac{1}{2}}$	8477.4

d^6s $^6D_{4\frac{1}{2}}$	9151.5
d^7 $^4P_{\frac{1}{2}}$	9373.6
d^6s $^6D_{3\frac{1}{2}}$	10150.6
" $^6D_{2\frac{1}{2}}$	10851.8
" $^6D_{1\frac{1}{2}}$	11303.6
" $^6D_{\frac{1}{2}}$	11604.1
" $^4D_{3\frac{1}{2}}$	19378.7
" $^4D_{2\frac{1}{2}}$	20514.9
" $^4D_{1\frac{1}{2}}$	21246.2
d^7 $^2F_{2\frac{1}{2}}$	21557.8
d^6s $^4D_{\frac{1}{2}}$	21645.5
d^7 $^2F_{3\frac{1}{2}}$	22289.0

Measurements of the Zeeman effect indicate that the g -values are very close to the normal Landé values.

It will be noticed that $(d^7)^2F$ is reinverted as is predicted by Goudsmit's theory.

W. F. MEGGERS
A. G. SHENSTONE

March 11, 1930

X-Rays Generated by Three Element Tube

The character of the x-rays generated by a specially designed three element tube was studied. This tube consisted of two filaments placed symmetrically with respect to a ring anode. The two filaments were maintained at the same potential and the electrons accelerated to the anode by a high voltage, 15,000 volts A.C. in these experiments, applied between the filaments and the anode. When the filament current was increased sufficiently, the anode current became limited by space charge and the tube started to oscillate; in this condition, the electrons oscillate back and forth through the anode.

While oscillations were present, the tube became a very efficient producer of x-rays, in the anode region. The average wave-length of these x-rays, as measured by their absorption coefficient in thin metal foils was less than 0.8Å. This indicates that either the efficiency of exciting continuous x-rays with a wave-length corresponding to the full voltage applied to the electrons is very great or that the tube can emit x-rays with a wave-length

shorter than that calculated from the voltage impressed between the anode and the filaments. The hardness of the x-rays may be due either to very high voltage oscillations in the tube which increases the energy of the electrons striking the anode or it may arise from the mutual interaction of the electron streams from the two filaments in the space surrounding the anode where the electron concentration is very high. A pin-hole picture of the source of the x-rays showed that the x-rays were generated in a space charge sheath surrounding the glass wall and extending into the space around the anode. In all these measurements, the pressure in the tube was less than 10^{-6} mm of Hg.

With one filament heated, i.e. no oscillations in the tube, no x-rays could be detected for the same anode current and voltage.

ARTHUR BRAMLEY

Bartol Research Foundation
Swarthmore, Pa.

March 8, 1930.

Regularities in Radioactive Nuclei

While reading an interesting paper by Barton (Phys. Rev. 35, 408 (1930)) on "A New Regularity in the List of Excited Nuclei," it occurred to us that it would be interesting to look for a similar regularity in radioactive nuclei. (The symbols we shall use in discussing this addition to his work will be those of Barton's paper, and for brevity will not be redefined here.) We plotted P against E for these nuclei assuming that the mass numbers of the actinium family are secured from those of uranium 238 by the subtraction of an integral number of α particles with mass number 4. Plotted in this way an approximate center of symmetry exists at (P, E) equal to (220, 134) which is thorium emanation. There are 34 points in this diagram, some of which are double because two radioactive nuclei fall at the same point in a number of cases. It is necessary to add 5 points to the diagram in order to complete the symmetry so that the symmetry of this "cluster" compares favorably with Barton's non-radioactive clusters. It seems, therefore, that we are justified in adding another cluster to the three which he found.

The uranium-radium-actinium family and the thorium family each form independent symmetrical clusters about the same point.

There is some uncertainty as to whether the mass number of a protactinium should be 230 as we have assumed it to be, 231, or 232. If its mass number should be 232, the actinium family and the thorium family diagrams would coincide except that (232, 141) must be added to the thorium family and (228, 140) must be added to the actinium family, and thus the actinium and thorium families would be symmetrical about the point (220, 134). The uranium-radium family would be approximately symmetrical about the point (224, 137), but the symmetry would not be so great as it is when all families are plotted together with the protactinium taken with mass number 230. If protactinium is taken with mass number 231 then the actinium family will be symmetrical about (219, 133), the thorium family would be symmetrical about (220, 134), and the uranium-radium family would have its lesser symmetry about the point (224, 137); but if all families were plotted on the same dia-

gram, the appearance of symmetry would be destroyed. It seems that all these families should be plotted on the same diagram in order to make comparisons with Barton's clusters which include all possible "radioactive families" of these non-radioactive elements.

Assuming for the sake of argument that this radioactive cluster exists, it indicates that Barton's suggested mechanism for the origin of his clusters is improbable, for his mechanism cannot be applied to the radioactive cluster. A primordial element of mass number 440 and 268 nuclear electrons cannot be postulated. Moreover, we know that the radioactive atoms do not originate by the decomposition of such a primordial element. The symmetry of this cluster is determined by regularities in the radioactive decomposition series and, therefore, the suggestion immediately arises that Barton's clusters may consist of radioactive series of nuclei with very long lives. From Aston's data (Proc. Roy. Soc. A115, 487 (1927)) on packing fractions, it is easy to see that considerable radioactivity might be possible in the (124, 72) cluster because for the general decreasing packing fractions with decreasing mass number in this region. Only a very feeble radioactivity or none at all would be possible in the (80, 45) clusters because these atoms are so near the minimum of the packing frac-

tion curve. Rubidium whose isotopes are (85, 48) and (87, 50) and belong to this cluster has been reported to be slightly radioactive. The lowest cluster with center at approximately (25, 13) could not be radioactive at all because the packing fraction curve has a negative slope. It seems to us that the symmetry of these 4 clusters is probably not due to the process of formation of the nuclei at all, but merely represents some stability relationship or some nuclear exclusion principle. At sufficiently high temperatures and pressures atoms of high packing fraction and high mass number would be stable and probably in the genesis of the elements under such conditions the possible permitted nuclei would be formed. In the radioactive cluster we merely see a spontaneous process which results in a transient excitation of these same possible permitted nuclear configurations.

It is interesting to note that the centers of these 4 clusters are at atomic numbers 12(?), 35, 52 and 86 which are very near the atomic numbers of the inert gases neon, krypton, xenon and the emanations. We have no idea whether this approximate agreement has any significance.

HAROLD C. UREY
HELEN JOHNSTON

Department of Chemistry,
Columbia University,
March 22, 1930.

BOOK REVIEWS

The Kinematical Design of Couplings in Instrument Mechanisms. A. F. C. POLLARD, A. R. C. S., A. M. I. E. E., Professor of Instrument Design at the Imperial College of Science and Technology. Pp. 64, figs. 25. Adam Hilger, Ltd., London, England, 1929. Price 4s. 6d.

This book is an application to instrument design of the law of kinematics that six constraints are necessary to fix a rigid body. The author defines the terms used in the book, states the principles of kinematical design, and cites examples of the application of these principles to the design of instruments recently built by Adam Hilger Ltd., W. G. Pye and Co., Cambridge Instrument Co., E. Leitz, and others. Machine tool design of instruments depends too largely on the machines used in construction and on past experience, too little on kinematical principles, whereas kinematical design places first importance on these principles. By the latter method the forces on various members of an instrument are determined, the proper number of constraints applied, the materials decided upon, the so-called point contacts on the guiding surfaces expanded to withstand the pressures involved, and the allowable fits or clearances determined. This results in a stable instrument, in a reduction of variance in the instrument, in simpler and more economical manufacture because the workmanship is expended in the production of accurate geometrical forms rather than accurate fits, and permits the introduction of small adjustments which are often of great importance. Though this book is not intended as a complete text, it adequately sets forth the principles of the subject. It should be of great value to those who construct, repair, or use precision instruments.

Since reading the book this reviewer has applied these principles to the design of a comparator and an adjustable lamp support for the recording galvanometer of a microphotometer. A study of some of our present apparatus indicates that changes indicated by kinematical design would be very desirable. Accurate steel balls, which are easily and cheaply procurable, are widely used in these designs.

C. W. GARTLEIN

Handbuch der Experimentalphysik, Vol. IX, Part 1. High and Low Temperature by H. VON WARTENBERG; Liquefaction of Gases by H. LENZ; Heat Conduction by OSCAR KNOBLAUCH and H. REIHER; Heat Radiation by W. WIEN and C. MÜLLER. Pp. 484, figs. 50. Akademische Verlagsgesellschaft, Leipzig, 1929. Price, bound RM 44.60.

The first section by Wartenberg is a detailed listing of the means for obtaining and methods of measuring high and low temperatures.

The second section by Lenz on the liquefaction of gases is a very excellent discussion, both qualitative and quantitative, of the whole problem. The thermodynamic aspect of the fundamental gas theory is given in detail. The literature of the experimental side of the theory is completely given with interesting abstract and comment. The experimental work and data for air are given particular attention and their application to the liquefier problems carried right through. The writer knows of no such treatment anywhere in English.

The various technical methods used for liquefying air are described in their physical, not their engineering aspect. The liquefaction of H and He are described in connection with the actual installation at the few places where they have been carried out.

A short treatment on separation or purification of gases by fractional distillation—oxygen and nitrogen from air, hydrogen from various mixtures, helium from natural gas—completes the section.

The section on heat transfer is opened by Oscar Knoblauch with a discussion on heat conduction. After a brief introduction to the analytical situation, the experimental methods with some results are described for the metals especially with reference to the Wiedeman and Franz relation; for poorly conducting bodies with special reference to economically important materials; for single crystals, for liquids and for gases.

The second part, heat transfer by convection (Reiher), covers the very complex and important subject especially in its engineering aspect of the transfer of heat between solid bodies by a moving fluid. Both the analytical and experimental aspects are given in considerable detail, especially the case of transfer through tubing in various arrangements.

The third part discusses radiation as a means of heat transfer without duplication seriously of the later section. The fourth part discusses some important applications of the previous discussion.

The third and final section of the volume is by W. Wien and C. Müller on heat radiation, of which Wien writes the larger part. They cover the general theory, thermodynamical and statistical; experimental technique, sources, measuring instruments, units, black body, light pressure; experimental test of the theory and measurement of the radiation constants; energy distribution in the spectrum. The mass of references seems to cover all the important work.

J. R. ROEBUCK

Wave Mechanics, Being One Aspect of the New Quantum Theory. H. T. FLINT. Pp. ix+117. E. P. Dutton, New York. Price, \$1.25.

This little book, which has just (March 1930) been received for review has a preface dated December 1928. It is probably the poorest of the books which have appeared on this subject. It is of about the scope of Biggs' little book on wave mechanics.

Chapter 1 and 2 present the analogy between optics and mechanics and arrive at the wave equation in much the same way as Schrödinger did in the second of his famous series of *Annalen der Physik* papers.

The Schrödinger relativistic equation is given and the erroneous formula for the hydrogen fine structure to which it leads is presented. Then the author says, "It is apparently of no purpose to discuss the accuracy of the formula just obtained . . ." and does not tell the reader that the formula is wrong and how the electron spin hypothesis corrects it and improves Sommerfeld's original theory of the fine structure!

Chapter 4 purporting to review the diffraction by crystals and gases of electron waves, is very bad. Three of the book's 19 figures are devoted to the old uncertain results of Davisson and Kunsman while not a single mention is made of the work of Davisson and Germer! Then three more figures are devoted to Dymond's work on scattering in helium although Harnwell had shown that these results were due to secondary effects and published his work during 1928. Then follow about ten pages about G. P. Thomson's electron diffraction work still with no reference to the earlier work of Davisson and Germer.

The last fifth of the book is devoted to an account of attempts to connect Ψ with the general relativity theory which are certainly among the least important of the recent developments especially since they were carried out without reference to the electron spin problem which Dirac showed (winter, 1927) was inseparably connected with relativistic effects. I can find no mention of electron spin in the whole book.

Now the reason for setting these things out so fully is this: The publishers wrote to me a year ago for criticism of this book and paid me well for it. I told them much the same as I have written here and recommended that the book be revised before being issued in this country. But I suppose that was too much trouble so they prefer to offer to the physicists of America, at a price of more than 1 cent per 8×14 cm type page, a book which is very much out of date, misleading in spots, and ignores completely one of the finest pieces of experimental work done in the past decade.

E. U. CONDON

Bandenspektren auf experimenteller Grundlage. RICHARD RUEDY. Pp. vi+124, figs. 62. Sammlung Vieweg, Heft 101/102, 1930. Price RM 9.60.

Progress in the field of band spectra, since the publication, in 1926, of the National Research Council Bulletin "Molecular Spectra in Gases," has been both extensive and important. As a result, there is a real demand for an up-to-date account, but the knowledge and the time required to prepare a really adequate monograph on this very complex subject are

so great that even the leading workers in the field have shrunk from the task. The volume under review cannot be said to satisfy the demand. It is written in text book style,—that is, categorically, with no references to original literature, save for a brief list on the last two pages, of which no mention is made elsewhere. The reviewer feels that the subject is still too new for this style of treatment, and that the general reader is likely to get a false impression from it. A large portion of the volume is devoted to a detailed description of the fine structure, of various types of bands. This will be of interest mainly to the prospective research worker but the precise definitions and directions, so necessary for successful work, are in general not included. The most valuable feature of the book is the many diagrams, mainly taken with more or less adaptation from the original literature.

The nomenclature of band spectra is now undergoing a complete revision, and preliminary evidences appear in this volume, where two different symbols for the same quantity are sometimes used indiscriminately. In this matter of nomenclature, just one point will be mentioned. It has recently been agreed to use v as the vibrational quantum number (the former n). Professor Mulliken and the reviewer are now suggesting the use of $u = v + 1/2$, so that $u = 0$, or $v = -1/2$, for the hypothetical state of zero vibration. Ruedy retains n with its former meaning, and defines $v = n + 1/2$, so that his v is our u . He then makes the error of defining *his* v as the vibrational quantum number.

RAYMOND T. BIRGE

Handbuch der Experimental Physik, Band VIII, 2. Teil. Wärmeausdehnung, Zustandsgrößen und Theorien der Wärme. Pp. xii+766, 17.1×24.1 cm, Akademische Verlagsgesellschaft M. b. H., Leipzig, 1929. Price, bound RM 76.

Not much more can be attempted in a necessarily short review of a book of this character and extent than a summary of the nature of the contents.

The thermal expansion of solids and liquids is treated in 72 pages by Valentiner. Not only are the conventional experimental methods described with the aid of a number of diagrams but the theoretical significance of such measurements is made plainer by a discussion of the laws of expansion proposed by Debye and Grüneisen.

The thermal parameters (Thermische Zustandsgrößen) of gases at moderate and low pressures are discussed by Otto in an article of 161 pages. This includes a discussion of the experimental methods of determining the p - v - t relations for gases, together with the experimental results, dealing particularly with the experiments of Amagat. There is a very useful section on equations of state, with a reproduction of the 56 most important such equations that have been proposed. A very short section is given on gaseous mixtures.

The thermal parameters of liquids, solids and gases under high pressures are treated in 155 pages in an article written by myself and translated by Lenz. This article is by intention mostly concerned with my own experiments, and deals with the compressibility of liquids, gases, and solids as a function of pressure and temperature, melting phenomena and polymorphic transitions under high pressure. There is a short concluding section on the absorption of gases by liquids at pressures of a few hundred kg/cm².

Adsorption phenomena of gases and vapors on solid surfaces are treated in 100 pages by Glaser. Not only is the experimental material presented, but there is a welcome discussion of the thermodynamics of adsorption.

Vapor pressure measurements are discussed in 76 pages by Harteck. This includes the conventional material, and also such recent material as methods of determining the vapor pressure of involatile substances like tungsten or carbon. There is a section on hygrometry, which perhaps might not be looked for under the general heading.

The kinetic theory of gases and vapors is treated in 144 pages of Przibram. Such an article on a theoretical subject might perhaps not be expected in a Handbuch ostensibly devoted to experimental topics, but the emphasis is throughout on the experimental aspects, and for this reason it will be found to be a most useful supplement to the ordinary theoretical discussions by statistical methods. The discussions of recent direct methods of determining the actual velocity of gas molecules and demonstrating the Maxwellian velocity distribution are to be especially commended.

The concluding article is a short one of 22 pages by Herzfeld on certain consequences for physical chemistry of Nernst's heat theorem, dealing mostly with transition and reaction phenomena, with a discussion of the chemical constant.

P. W. BRIDGMAN

Molecular Spectra and Molecular Structure. A General Discussion held by the Faraday Society, September 1929. Price 15/6.

This volume consists of a collection of forty papers on molecular spectra and molecular structure given before the Faraday Society, September 1929, at the University of Bristol. The contributions are grouped into three parts, Band Spectra in the Visible and Ultra-Violet Regions, The Raman Effect and Infra-Red Spectra which latter part is subdivided into sections dealing with Solid Bodies, Liquids and Gases. Each division is opened by an introductory paper which presents the subject and gives something of the historical development. This is then followed by a series of original papers dealing with researches on particular phases of the problem.

It is difficult to summarize the individual papers since the problems they treat are so diversified. The reviewer can only call attention to some few which appear to him to be more outstanding. In the first section we find an attempt to provide a uniform Nomenclature for Diatomic Molecular Spectra introduced by O. W. Richardson, Band Spectra and Atomic Nuclei by R. S. Mulliken, a paper on Chemical Binding by F. Hund, a general paper on the Electronic Structure of Diatomic Molecules by J. E. Lennard-Jones and papers describing particular diatomic molecules by R. C. Johnson, O. W. Richardson, and W. E. Curtis. R. T. Birge contributes two papers, The Determination of Heats of Dissociation by Means of Band Spectra and Recent Work on Isotopes in Band Spectra.

The second part is opened with a paper by Professor Sir, C. V. Raman and is followed among others by articles by R. W. Wood and J. C. McLennan. The section on Infra-Red Spectra is well represented by some thirteen papers including, On the Infra-Red Spectra of Gases under High Dispersion by E. F. Barker and C. F. Meyer, and The Absorption Spectrum of Ammonia Gas in the Near Infra-Red by R. Mecke and R. M. Badger.

This volume issued by the Faraday Society will prove useful in three ways. The introductory articles are for the most part excellent and serve as a survey of the whole field of molecular spectra. The original contributions are valuable as such and give a good account of the most recent work on the subject. All the papers seem to be well supplied with citations of earlier work and since there are so many of them, on so many different phases, the whole collection may profitably be used for purposes of reference.

DAVID M. DENNISON

The Science of Voice. DOUGLAS STANLEY. Pp. 327, Carl Fisher Inc., 430 S. Wabash Avenue, Chicago. 1929.

This book was apparently written principally for the use of teachers and students of singing and speaking. It is divided into three parts. First, a physical introduction written in rather elementary form and in such a way that teachers and students with a moderate understanding and interest in physical principles might profit by it. The second part called "Vocal Technic" contains a description in physical terms of what the author considers to be a mechanism of the various terms used in vocal art. For a physicist without musical experience who is interested in the meaning attached by musicians to such terms as "register," "breath control," "the vibrato," "slur," "shakes," "staccato," etc., this second section is very suggestive in a manner which seems to be unique in such treatises. The third section on "musicianship and interpretation" is addressed almost entirely to musicians.

R. L. WEGEL

THE PHYSICAL REVIEW

ON THE USE OF THE ENERGY-MOMENTUM PRINCIPLE IN GENERAL RELATIVITY

BY RICHARD C. TOLMAN

NORMAN BRIDGE LABORATORY, CALIFORNIA INSTITUTE OF TECHNOLOGY,
PASADENA, CALIFORNIA

(Received December 20, 1930)

ABSTRACT

The primary purpose of this article is to obtain from the general relativity form of the energy-momentum principle certain new consequences which are needed for later work that the author has in mind. In addition, it is the intention to give at the same time a somewhat comprehensive and coherent treatment of the principle and its consequences, which it is hoped will increase the confidence and facility of physicists in the use of this important part of the general theory of relativity. In carrying out the investigation, it has seemed desirable for English readers, to take Eddington's "Mathematical Theory of Relativity" as a starting point, and this has incidentally led to a new form of deduction for certain consequences of the energy-momentum principle that were already known.

After presenting the energy-momentum principle in the form discovered by Einstein and showing its application to the case of the conservation of energy in an isolated system, an important expression is derived which gives the total densities of energy and momentum in the form of a divergence. This expression is equivalent to one previously obtained by Einstein but on account of the starting point adopted is derived and expressed in terms of the quantities $g^{\mu\nu}$ and $g_{\alpha}^{\mu\nu}$ instead of the $g^{\mu\nu}$ and $g_{\alpha}^{\mu\nu}$. Following this, the limiting values at large distances from an isolated material system are obtained for the quantities $g^{\alpha\beta}\partial\mathcal{E}/\partial g_{\gamma}^{\alpha\beta}$ and $g^{\alpha\beta}\partial\mathcal{E}/\partial g_{\gamma}^{\alpha\beta}$. These values, which have considerable use, have not previously received explicit expression. This is followed by a deduction from our present starting point of Einstein's famous relation $U=m$ between the energy and gravitational producing mass of an isolated system. An important expression is then obtained which gives the energy of a quasi-static isolated system in the form of an integral which has to be extended only over the portion of space actually occupied by matter or radiation. This expression has not previously received a satisfactory derivation. The result is used to obtain an expression for the energy of a spherical distribution of a perfect fluid, and it is then shown that this expression, in the case of a sphere of ordinary material, approaches in a sufficiently weak field to the classical expression for energy including the potential gravitational energy. This result is not only intrinsically useful, but also shows for a particular case that a higher order of approximation to the general relativity value for total energy is obtained by including the classical gravitational energy than by going at once to flat space-time as is often done. Finally, a general consideration is given to the problem of determining the conditions imposed on those changes from one static state to another which could occur in a non-isolated system forming part

of a larger static system, without changing the distribution of matter and radiation outside the boundary and without contravening the energy-momentum principle as applied to the system as a whole.

§1. INTRODUCTION

IN ACCORDANCE with Einstein's development of the general theory of relativity, the relativity analogues of the classical principles of the conservation of energy and momentum are to be obtained with the help of integration from the well-known differential equation¹

$$\frac{\partial}{\partial x_\nu}(\mathfrak{T}_\mu^\nu + t_\mu^\nu) = 0 \quad (1)$$

where \mathfrak{T}_μ^ν is the tensor density of material energy and momentum and t_μ^ν is the pseudo-tensor density of potential gravitational energy and momentum. Considering x_4 to be the time-like coordinate, equation (1) leads to the three equations for the conservation of momentum with $\mu = 1, 2, 3$, and leads to the equation for the conservation of energy with $\mu = 4$.

Taking for illustration the latter case, multiplying the equation by $dx_1 dx_2 dx_3$, and integrating over the system of interest, we obtain with some rearrangement of terms

$$\begin{aligned} \frac{\partial}{\partial x_4} \iiint (\mathfrak{T}_4^4 + t_4^4) dx_1 dx_2 dx_3 \\ = - \iiint \left[\frac{\partial}{\partial x_1} (\mathfrak{T}_4^1 + t_4^1) + \frac{\partial}{\partial x_2} (\mathfrak{T}_4^2 + t_4^2) + \frac{\partial}{\partial x_3} (\mathfrak{T}_4^3 + t_4^3) \right] dx_1 dx_2 dx_3 \end{aligned}$$

and by performing the indicated integrations on the right hand side this can be rewritten in the form

$$\begin{aligned} \frac{\partial}{\partial x_4} \iiint (\mathfrak{T}_4^4 + t_4^4) dx_1 dx_2 dx_3 \\ = - \iint \left| \mathfrak{T}_4^1 + t_4^1 \right|_{x_1}^{x_1'} dx_2 dx_3 - \iint \left| \mathfrak{T}_4^2 + t_4^2 \right|_{x_2}^{x_2'} dx_1 dx_3 - \iint \left| \mathfrak{T}_4^3 + t_4^3 \right|_{x_3}^{x_3'} dx_1 dx_2 \quad (2) \end{aligned}$$

where the limits of integration are denoted by x_1, x_1' etc. The result states that the rate of change with the time (x_4) in the value of the integral on the left hand side of the equation can be calculated from the conditions prevailing at the boundary of the system of interest as given by the right hand side of the equation. The equation can thus be regarded as a statement of the energy principle provided we define the energy of the system by the expression

$$U = \iiint (\mathfrak{T}_4^4 + t_4^4) dx_1 dx_2 dx_3. \quad (3)$$

And a similar treatment for the components of momentum can be obtained by taking $\mu = 1, 2, 3$.

¹ See for example Eddington, "The Mathematical Theory of Relativity." Cambridge 1923, equations (59.2) and (59.3).

Owing to the fact that equations (1) and (2) are not tensor equations and that the quantity t_μ^ν is not a true tensor density, considerable doubt as to the validity of the above formulation of the energy principle was at one time expressed² and perhaps to some extent still exists.³ It can be shown, nevertheless, that the equations have the necessary fundamental property of being true in all sets of coordinates, and a completely satisfactory justification of the formulation was finally given by Einstein in 1918.⁴

Since that time, however, the interest of mathematical physicists has been largely turned to other matters, and the methods and results of applying the energy-momentum principle have not been particularly investigated. It is the purpose of the present article to consider some of these methods and results not only because of their intrinsic importance, but also because of certain further applications which the writer has in mind.

In carrying out the investigation we shall use, as far as may be, the notation adopted by Eddington in his "Mathematical Theory of Relativity", and shall base our deductions on equations given by him. This choice of starting point necessitates some duplication of results which have previously been obtained by other methods, but seems desirable owing to the familiarity of English readers with Eddington's treatise and owing to the excellence of the detailed and coherent treatment which he has given.

In the immediately following section, §2, we shall first give Einstein's method of applying the above energy principle to an isolated material system. In §3 we shall then obtain a very useful formula which expresses the total density of energy and momentum as an ordinary divergence; the formula is equivalent in import to one already obtained by Einstein but because of our choice of starting point differs in method of derivation and form of expression. Following this, in §4, we shall deduce the limiting values at large distances from such an isolated system of certain functions of the gravitational field; these values are necessary for our further work and have not previously received explicit expression. In §5 we shall then be able to give a deduction from our present basis of Einstein's relation between the total energy and gravitational mass of an isolated material system. In §6 we shall deduce an extremely important equation expressing the total energy of an isolated system by an integral which has to be extended only over that portion of space which is actually occupied by matter or radiation; this equation

² Schroedinger, *Phys. Zeits.* 19, 4 (1918); Bauer, *ibid.* 19, 163 (1918).

³ Thus, for example, Eddington (reference 1, pp. 135-136) objects to the fundamental significance of the equation $\partial/\partial x_\nu (\mathfrak{T}_\mu^\nu + t_\mu^\nu) = 0$ on the ground that t_μ^ν is not a true tensor density, and appears to regard the introduction of the equation as an unfortunate pandering to an immoral desire to obtain by hook or crook some kind of conservation laws in the mechanics of general relativity. It should be remarked, however, that the appropriate criterion for the fundamental significance of equations should not be that they are written in tensorial form but that they are written in covariant form so as to be true in all sets of coordinates. All tensor equations are indeed covariant equations, but this does not exclude the possibility of covariant equations, such as the one above, which are not tensorial. To assume the contrary would be the fallacy of the Dormouse in Alice in Wonderland, who said:—"I breathe when I sleep" is the same thing as "I sleep when I breathe."

⁴ Einstein, *Berl. Ber.* 1918, p. 448.

has not previously received a satisfactory derivation. In the following section, §7, we shall use this equation to obtain an expression for the total energy of a distribution of perfect fluid having spherical symmetry. And in §8 we shall show that, on making the gravitational field weaker, the above expression approaches the classical expression for the energy of such a sphere including the classical value for its potential gravitational energy; the result is an intrinsically useful one and also shows for a particular case that a higher order of approximation to the general relativity value for total energy is obtained by including the classical gravitational energy than by neglecting the gravitational energy entirely as has hitherto often been done. Finally in §§9, 10 we shall consider the application of the general energy-momentum principle to changes occurring within a region which forms part of a larger system, and in §11 shall make some concluding remarks.

§2. THE CONSERVATION OF ENERGY IN AN ISOLATED SYSTEM

Let us now first consider the application of the energy principle to those changes which can take place within a limited system without producing any changes in the gravitational field outside of a sufficiently distant boundary located in the free space surrounding the system. Such a system will be called an isolated one. In this case, we can easily show that the general energy principle, as given by equation (2), can be interpreted as leading to the conservation of energy within the boundary taken.

For the tensor density of matter and energy \mathfrak{T}_μ^ν , occurring in equation (2), we can write from the equation of definition⁵

$$\mathfrak{T}_\mu^\nu = \sqrt{-g} g_{\alpha\mu} T^{\alpha\nu} = \sqrt{-g} g_{\alpha\mu} \rho_0 \frac{dx_\alpha}{ds} \frac{dx_\nu}{ds} \quad (4)$$

where ρ_0 is the proper density of matter. And since we take the boundary which encloses the system as located in free space the density ρ_0 will there be zero, so that it is evident that the quantities \mathfrak{T}_4^1 , \mathfrak{T}_4^2 and \mathfrak{T}_4^3 , occurring on the right hand side of equation (2), will themselves have the value zero at the boundary.

Furthermore, the pseudo-tensor density of potential energy is defined in terms of the Lagrangian function \mathfrak{L} and the cosmological constant Λ by the equation⁶

$$t_\mu^\nu = \frac{1}{16\pi} \left\{ g_\mu^\nu \mathfrak{L} - g_\mu^{\alpha\beta} \frac{\partial \mathfrak{L}}{\partial g^{\alpha\beta}} \right\} + \frac{\Lambda}{8\pi} g_\mu^\nu \sqrt{-g}. \quad (5)$$

The quantity g_μ^ν , however, is equal to zero with $\mu \neq \nu$, and the symbol $g_4^{\alpha\beta}$ is a short hand for $\partial(g^{\alpha\beta}\sqrt{-g})/\partial x_4$ and hence is equal to zero at the boundary enclosing our system, if the gravitational field at that boundary is not changing with the time as postulated. Hence the quantities t_4^1 , t_4^2 , and t_4^3 ,

⁵ See Eddington, reference 1, equation (53.1).

⁶ See Eddington, reference 1, equation (59.4). The additional term in Λ , when the cosmological term is not neglected, can easily be shown necessary. Compare Einstein, reference 4, equation (18).

occurring on the right hand side of equation (2), will also be zero at the boundary with which we have enclosed the system.

Hence using a system of coordinates such that the limits of integration coincide with the boundary enclosing the system,⁷ it is evident that the terms on the right hand side of equation (2) will all of them become zero and the energy principle for this particular case will reduce to the conservation of energy

$$\frac{\partial}{\partial x_4} \iiint (\mathfrak{T}_4^4 + t_4^4) dx_1 dx_2 dx_3 = 0$$

or

$$U = \iiint (\mathfrak{T}_4^4 + t_4^4) dx_1 dx_2 dx_3 = \text{const.} \quad (6)$$

§3. THE DENSITIES OF MOMENTUM AND ENERGY EXPRESSED AS DIVERGENCES

In order to make use of this interesting result, it will now be necessary to make a rather lengthy digression by deducing certain useful lemmas in this and in the following section. In the present section we shall show the possibility of expressing the total density of momentum or energy as an ordinary divergence in accordance with the equation⁸

$$8\pi(\mathfrak{T}_\mu^\nu + t_\mu^\nu) = \frac{\partial}{\partial x_\gamma} \left(-g^{\alpha\nu} \frac{\partial \mathfrak{L}}{\partial g_\gamma^{\mu\alpha}} + \frac{1}{2} g_\mu^\nu g^{\alpha\beta} \frac{\partial \mathfrak{L}}{\partial g_\gamma^{\alpha\beta}} \right). \quad (7)$$

To prove this equation will be a very tiresome business, justified only by the importance of the result. To carry out the demonstration we shall have to make use of a large number of well established results which we shall now give.

For the density of material energy and momentum we shall use the fundamental equation connecting it with the metrical properties of the field⁹

$$-8\pi\mathfrak{T}_\mu^\nu = \mathfrak{G}_\mu^\nu - \frac{1}{2} g_\mu^\nu \mathfrak{G} + \Lambda g_\mu^\nu \quad (8)$$

where \mathfrak{G}_μ^ν is the tensor density corresponding to the contracted Riemann-Christoffel tensor and Λ the cosmological constant. For the density of potential energy and momentum we shall use the equation of definition already given above

$$16\pi g_\mu^\nu = g_\mu^\nu \mathfrak{L} - g_\mu^{\alpha\beta} \frac{\partial \mathfrak{L}}{\partial g_\nu^{\alpha\beta}} + 2\Lambda g_\mu^\nu \quad (9)$$

⁷ With a system of coordinates chosen so that some of the limits of integration do not fall on the boundary, the quantities $[\mathfrak{T}_4^4 + t_4^4]_{x_4}$ etc. will not necessarily be zero. Compare §9.

⁸ This equation is equivalent in import to equation (18) given by Einstein, *Berl. Ber.* 1916, p. 1115. It differs in form since we are regarding \mathfrak{L} as a function of the $g^{\mu\nu}$ and $g_\alpha^{\mu\nu}$ instead of as a function of the $g^{\mu\nu}$ and $g_\alpha^{\mu\nu}$.

⁹ See Eddington, reference 1, equation (54.71).

where the Lagrangian function \mathfrak{L} is defined in terms of the Christoffel symbols by the equation¹⁰

$$\mathfrak{L} = \sqrt{-g} g^{\alpha\beta} \left(\{ \alpha\gamma, \epsilon \} \{ \beta\epsilon, \gamma \} - \{ \alpha\beta, \gamma \} \{ \gamma\epsilon, \epsilon \} \right). \quad (10)$$

In accordance with this definition it is possible to show that \mathfrak{L} can also be expressed as a function of the quantities

$$g^{\alpha\beta} = g^{\alpha\beta} \sqrt{-g} \quad \text{and} \quad g_{\gamma}^{\alpha\beta} = \frac{\partial}{\partial x_{\gamma}} (g^{\alpha\beta} \sqrt{-g}) \quad (11)$$

and will then have the differential coefficients¹¹

$$\frac{\partial \mathfrak{L}}{\partial g^{\alpha\beta}} = - \left(\{ \alpha\gamma, \epsilon \} \{ \beta\epsilon, \gamma \} - \{ \alpha\beta, \gamma \} \{ \gamma\epsilon, \epsilon \} \right) \quad (12)$$

and¹²

$$\frac{\partial \mathfrak{L}}{\partial g_{\gamma}^{\alpha\beta}} = - \{ \alpha\beta, \gamma \} + \frac{1}{2} g_{\alpha}^{\gamma} \{ \beta\epsilon, \epsilon \} + \frac{1}{2} g_{\beta}^{\gamma} \{ \alpha\epsilon, \epsilon \}. \quad (13)$$

Further important properties of the Lagrangian function, relating it to the metrical properties of the field, are given by the equation¹³

$$G_{\mu\nu} = \frac{\partial}{\partial x_{\gamma}} \frac{\partial \mathfrak{L}}{\partial g_{\gamma}^{\mu\nu}} - \frac{\partial \mathfrak{L}}{\partial g^{\mu\nu}} \quad (14)$$

and¹⁴

$$\mathfrak{G} = \frac{\partial}{\partial x_{\gamma}} \left(g^{\alpha\beta} \frac{\partial \mathfrak{L}}{\partial g_{\gamma}^{\alpha\beta}} \right) - \mathfrak{L}. \quad (15)$$

Finally, the quantity $g_{\gamma}^{\alpha\beta}$ may be expressed in terms of the Christoffel symbols by the equation¹⁵

$$g_{\gamma}^{\alpha\beta} = \sqrt{-g} \left(- \{ \delta\gamma, \alpha \} g^{\delta\beta} - \{ \delta\gamma, \beta \} g^{\delta\alpha} + \{ \gamma\delta, \delta \} g^{\alpha\beta} \right). \quad (16)$$

We are now ready to proceed to the derivation of equation (7). Combining equations (8) and (9) we have

$$8\pi(\mathfrak{T}_{\mu}^{\nu} + t_{\mu}^{\nu}) = - \mathfrak{G}_{\mu}^{\nu} + \frac{1}{2} g_{\mu}^{\nu} \mathfrak{G} + \frac{1}{2} g_{\mu}^{\nu} \mathfrak{L} - \frac{1}{2} g_{\mu}^{\alpha\beta} \frac{\partial \mathfrak{L}}{\partial g_{\nu}^{\alpha\beta}}$$

¹⁰ See Eddington, reference 1, equation (58.1).

¹¹ See Eddington, reference 1, equation (58.51).

¹² See Eddington, reference 1, equation (58.52). We have written the expression in a symmetrical form which is equivalent to Eddington's unsymmetrical form.

¹³ See Eddington, reference 1, equation (58.6).

¹⁴ See Eddington, reference 1, equation (58.8).

¹⁵ See Eddington, reference 1, the equation immediately following (58.72).

Substituting (14) and (15) we obtain

$$8\pi(\mathfrak{T}_\mu^\nu + t_\mu^\nu) = -g^{\alpha\nu} \frac{\partial}{\partial x_\gamma} \frac{\partial \mathfrak{L}}{\partial g^{\mu\alpha}} + g^{\alpha\nu} \frac{\partial \mathfrak{L}}{\partial g^{\mu\alpha}} + \frac{1}{2} g_\mu^\nu \frac{\partial}{\partial x_\gamma} \left(g^{\alpha\beta} \frac{\partial \mathfrak{L}}{\partial g^{\alpha\beta}} \right) - \frac{1}{2} g_\mu^{\alpha\beta} \frac{\partial \mathfrak{L}}{\partial g^{\alpha\beta}}$$

and this can evidently be rewritten in the form

$$8\pi(\mathfrak{T}_\mu^\nu + t_\mu^\nu) = \frac{\partial}{\partial x_\gamma} \left(-g^{\alpha\nu} \frac{\partial \mathfrak{L}}{\partial g^{\mu\alpha}} + \frac{1}{2} g_\mu^\nu g^{\alpha\beta} \frac{\partial \mathfrak{L}}{\partial g^{\alpha\beta}} \right) + g_\gamma^{\alpha\nu} \frac{\partial \mathfrak{L}}{\partial g^{\mu\alpha}} + g^{\alpha\nu} \frac{\partial \mathfrak{L}}{\partial g^{\mu\alpha}} - \frac{1}{2} g_\mu^{\alpha\beta} \frac{\partial \mathfrak{L}}{\partial g^{\alpha\beta}}. \quad (17)$$

Comparing this result with equation (7), we see that our deduction will be completed if we can now show that the sum of the last three terms is equal to zero. To accomplish this we must substitute for the quantities occurring in these three terms their explicit values in terms of the Christoffel symbols as given by equations (12), (13) and (16). Doing so we obtain

$$\begin{aligned} & g_\gamma^{\alpha\nu} \frac{\partial \mathfrak{L}}{\partial g^{\mu\alpha}} + g^{\alpha\nu} \frac{\partial \mathfrak{L}}{\partial g^{\mu\alpha}} - \frac{1}{2} g_\mu^{\alpha\beta} \frac{\partial \mathfrak{L}}{\partial g^{\alpha\beta}} \\ &= \sqrt{-g} [-\{ \delta\gamma, \alpha \} g^{\delta\nu} - \{ \delta\gamma, \nu \} g^{\delta\alpha} + \{ \gamma\delta, \delta \} g^{\alpha\nu}] [-\{ \mu\alpha, \gamma \} + \frac{1}{2} g_\mu^\gamma \{ \alpha\epsilon, \epsilon \} + \frac{1}{2} g_\alpha^\gamma \{ \mu\epsilon, \epsilon \}] \\ &\quad + \sqrt{-g} g^{\alpha\nu} [-\{ \alpha\gamma, \epsilon \} \{ \mu\epsilon, \gamma \} + \{ \alpha\mu, \gamma \} \{ \gamma\epsilon, \epsilon \}] \\ &\quad - \frac{1}{2} \sqrt{-g} [-\{ \delta\mu, \alpha \} g^{\delta\beta} - \{ \delta\mu, \beta \} g^{\delta\alpha} + \{ \mu\delta, \delta \} g^{\alpha\beta}] [-\{ \alpha\beta, \nu \} + \frac{1}{2} g_\alpha^\nu \{ \beta\epsilon, \epsilon \} \\ &\quad + \frac{1}{2} g_\beta^\nu \{ \alpha\epsilon, \epsilon \}] \\ &= \sqrt{-g} [\{ \delta\gamma, \alpha \} \{ \mu\alpha, \gamma \} g^{\delta\nu} - \frac{1}{2} \{ \delta\mu, \alpha \} \{ \alpha\epsilon, \epsilon \} g^{\delta\nu} - \frac{1}{2} \{ \delta\alpha, \alpha \} \{ \mu\epsilon, \epsilon \} g^{\delta\nu} \\ &\quad + \{ \delta\gamma, \nu \} \{ \mu\alpha, \gamma \} g^{\delta\alpha} - \frac{1}{2} \{ \delta\mu, \nu \} \{ \alpha\epsilon, \epsilon \} g^{\delta\alpha} - \frac{1}{2} \{ \delta\alpha, \nu \} \{ \mu\epsilon, \epsilon \} g^{\delta\alpha} \\ &\quad - \{ \gamma\delta, \delta \} \{ \mu\alpha, \gamma \} g^{\alpha\nu} + \frac{1}{2} \{ \mu\delta, \delta \} \{ \alpha\epsilon, \epsilon \} g^{\alpha\nu} + \frac{1}{2} \{ \alpha\delta, \delta \} \{ \mu\epsilon, \epsilon \} g^{\alpha\nu} \\ &\quad - \{ \alpha\gamma, \epsilon \} \{ \mu\epsilon, \gamma \} g^{\alpha\nu} + \{ \alpha\mu, \gamma \} \{ \gamma\epsilon, \epsilon \} g^{\alpha\nu} \\ &\quad - \frac{1}{2} \{ \delta\mu, \alpha \} \{ \alpha\beta, \nu \} g^{\delta\beta} + \frac{1}{4} \{ \delta\mu, \nu \} \{ \beta\epsilon, \epsilon \} g^{\delta\beta} + \frac{1}{4} \{ \delta\mu, \alpha \} \{ \alpha\epsilon, \epsilon \} g^{\delta\nu} \\ &\quad - \frac{1}{2} \{ \delta\mu, \beta \} \{ \alpha\beta, \nu \} g^{\delta\alpha} + \frac{1}{4} \{ \delta\mu, \beta \} \{ \beta\epsilon, \epsilon \} g^{\delta\nu} + \frac{1}{4} \{ \delta\mu, \nu \} \{ \alpha\epsilon, \epsilon \} g^{\delta\alpha} \\ &\quad + \frac{1}{2} \{ \mu\delta, \delta \} \{ \alpha\beta, \nu \} g^{\alpha\beta} - \frac{1}{4} \{ \mu\delta, \delta \} \{ \beta\epsilon, \epsilon \} g^{\delta\nu} - \frac{1}{4} \{ \mu\delta, \delta \} \{ \alpha\epsilon, \epsilon \} g^{\alpha\nu}] \\ &= 0 \end{aligned}$$

where the value zero arises, after some changes in dummy suffixes, from the mutual cancellation of all terms, as can easily be verified by noting that the terms have been labelled in such a way that those which destroy each other are given the same number.

Combining this result with equation (17), we now complete the derivation of the original equation (7), which it was the purpose of this section to prove.

§4. THE LIMITING VALUES OF CERTAIN QUANTITIES AT LARGE DISTANCES FROM AN ISOLATED MATERIAL SYSTEM

As a further preparation for our later considerations we shall now obtain the limiting values at large distances from an isolated material system for the quantities $g^{ab}(\partial\mathfrak{L}/\partial g^{ab})$ and $g^{a4}(\partial\mathfrak{L}/\partial g^{a4})$ which occur on the right hand side of equation (7). To do this we recall that we have defined an isolated system in §2, in such a way that the changes taking place within the system do not produce changes in the gravitational field outside of a sufficiently distant boundary. Therefore, at a sufficient distance from an isolated system the gravitational field will be static and spherically symmetrical, and we can use for it the well known Schwarzschild solution. Hence placing the system in the neighborhood of the origin of a set of coordinates x, y, z, t , which approach Galilean coordinates at large distances we can write for the line element the approximate Schwarzschild expression¹⁶

$$ds^2 = -(1+2m/r)(dx^2+dy^2+dz^2) + (1-2m/r)dt^2$$

where the constant m is the mass of the system and r is an abbreviation for $(x^2+y^2+z^2)^{1/2}$.

Since the above expression gives the form taken by the Schwarzschild solution in a particular kind of quasi-Galilean coordinates, it is evident that later results, which are dependent on the present section, will also be originally derived in the form which they assume in these particular coordinates, and their translation into the language of other systems of coordinates must be undertaken with due cognizance of their method of derivation. Furthermore, the above expression is an approximate one, valid at distances large enough so that terms of the order $(m/r)^2$ can be neglected, and yet at the same time small enough so that the curvature of the universe as a whole, as given by the cosmological term, can be neglected. Hence those later considerations which are dependent on this section will primarily apply only to systems which are small compared to the total dimensions of the universe, even though of course still very large compared with ordinary terrestrial dimensions.

Returning to our approximate expression for the Schwarzschild line element we may now write for the components of the fundamental metrical tensor, the values

$$\begin{aligned} g_{11} &= g_{22} = g_{33} = -[1+2m/r] & g_{44} &= [1-2m/r] \\ g^{11} &= g^{22} = g^{33} = -\frac{1}{[1+2m/r]} & g^{44} &= \frac{1}{[1-2m/r]} \\ g_{\mu\nu} &= g^{\mu\nu} = 0 \quad (\mu \neq \nu) & \sqrt{-g} &= [1+2m/r]^{3/2} [1-2m/r]^{1/2} \end{aligned} \quad (18)$$

To calculate the desired quantities from these expressions for the metrical tensor, we shall first need the values of the Christoffel symbols. These are defined by the equation¹⁷

¹⁶ See Eddington, reference 1, equation (46.15).

¹⁷ See Eddington, reference 1, equation (27.2).

$$\{\mu\nu, \sigma\} = \frac{1}{2} g^{\sigma\lambda} \left(\frac{\partial g_{\mu\lambda}}{\partial x_\nu} + \frac{\partial g_{\nu\lambda}}{\partial x_\mu} - \frac{\partial g_{\mu\nu}}{\partial x_\lambda} \right)$$

which evidently reduces under our circumstances to

$$\{\mu\nu, \sigma\} = \frac{1}{2} g^{\sigma\sigma} \left(\frac{\partial g_{\mu\sigma}}{\partial x_\nu} + \frac{\partial g_{\nu\sigma}}{\partial x_\mu} - \frac{\partial g_{\mu\nu}}{\partial x_\sigma} \right) \quad (\text{not summed})$$

and taking μ, ν , and σ as *different* indices we obtain the four cases

$$\begin{aligned} \{\mu\mu, \mu\} &= \frac{1}{2} g^{\mu\mu} \frac{\partial g_{\mu\mu}}{\partial x_\mu} \\ \{\mu\mu, \nu\} &= -\frac{1}{2} g^{\nu\nu} \frac{\partial g_{\mu\mu}}{\partial x_\nu} \\ \{\nu\mu, \mu\} &= \{\mu\nu, \mu\} = \frac{1}{2} g^{\mu\mu} \frac{\partial g_{\mu\mu}}{\partial x_\nu} \\ \{\mu\nu, \sigma\} &= 0. \end{aligned} \tag{19}$$

We are now ready to proceed to our calculations. Under our circumstances we may evidently write

$$g^{\alpha\beta} \frac{\partial \mathfrak{L}}{\partial g_1^{\alpha\beta}} = \sqrt{-g} \left(g^{11} \frac{\partial \mathfrak{L}}{\partial g_1^{11}} + g^{22} \frac{\partial \mathfrak{L}}{\partial g_1^{22}} + g^{33} \frac{\partial \mathfrak{L}}{\partial g_1^{33}} + g^{44} \frac{\partial \mathfrak{L}}{\partial g_1^{44}} \right).$$

Substituting the values given by equation (13), this becomes

$$\begin{aligned} g^{\alpha\beta} \frac{\partial \mathfrak{L}}{\partial g_1^{\alpha\beta}} &= \sqrt{-g} \left(-g^{11} \{11, 1\} + \frac{1}{2} g^{11} \{1\epsilon, \epsilon\} + \frac{1}{2} g^{11} \{1\epsilon, \epsilon\} \right. \\ &\quad \left. - g^{22} \{22, 1\} - g^{33} \{33, 1\} - g^{44} \{44, 1\} \right) \end{aligned}$$

and introducing the values of the Christoffel symbols given by equations (19) it reduces to

$$\begin{aligned} g^{\alpha\beta} \frac{\partial \mathfrak{L}}{\partial g_1^{\alpha\beta}} &= \frac{1}{2} \sqrt{-g} \left(g^{11} g^{22} \frac{\partial g_{22}}{\partial x} + g^{11} g^{33} \frac{\partial g_{33}}{\partial x} + g^{11} g^{44} \frac{\partial g_{44}}{\partial x} \right. \\ &\quad \left. + g^{22} g^{11} \frac{\partial g_{22}}{\partial x} + g^{33} g^{11} \frac{\partial g_{33}}{\partial x} + g^{44} g^{11} \frac{\partial g_{44}}{\partial x} \right). \end{aligned}$$

Finally, substituting the values for the components of the metrical tensor given by equations (18), and, because of the large distances under consideration, neglecting quantities of the order m/r in comparison with unity, we easily obtain

$$g^{\alpha\beta} \frac{\partial \mathfrak{L}}{\partial g_1^{\alpha\beta}} = -2 \frac{\partial}{\partial x} \left(\frac{2m}{r} \right) + \frac{\partial}{\partial x} \left(\frac{2m}{r} \right) = \frac{2m}{r^2} \frac{\partial r}{\partial x}.$$

From considerations of symmetry it is evident that we shall also have similar expressions in y and z , and introducing the direction cosines for the radius vector we may evidently write

$$g^{\alpha\beta} \frac{\partial \mathfrak{L}}{\partial g^{\alpha\beta}_1} = \frac{2m}{r^2} \cos(nx), \quad g^{\alpha\beta} \frac{\partial \mathfrak{L}}{\partial g^{\alpha\beta}_2} = \frac{2m}{r^2} \cos(ny), \quad g^{\alpha\beta} \frac{\partial \mathfrak{L}}{\partial g^{\alpha\beta}_3} = \frac{2m}{r^2} \cos(nz) \quad (20)$$

while the value of the fourth quantity $g^{\alpha\beta}(\partial \mathfrak{L} / \partial g^{\alpha\beta}_4)$ will not be needed for our later work.

Turning now to the second of the quantities of interest mentioned at the beginning of this section, we may evidently write with the help of equations (18), (13) and (19)

$$g^{\alpha 4} \frac{\partial \mathfrak{L}}{\partial g^{\alpha 4}_1} = \sqrt{-g} g^{44} \frac{\partial \mathfrak{L}}{\partial g^{44}_1} = -\sqrt{-g} g^{44} \{44, 1\} = \frac{1}{2} \sqrt{-g} g^{44} g^{11} \frac{\partial g^{44}}{\partial x}$$

or, to the same order of approximation as before, we obtain

$$g^{\alpha 4} \frac{\partial \mathfrak{L}}{\partial g^{\alpha 4}_1} = -\frac{m}{r^2} \cos(nx), \quad g^{\alpha 4} \frac{\partial \mathfrak{L}}{\partial g^{\alpha 4}_2} = -\frac{m}{r^2} \cos(ny), \quad g^{\alpha 4} \frac{\partial \mathfrak{L}}{\partial g^{\alpha 4}_3} = -\frac{m}{r^2} \cos(nz). \quad (21)$$

§5. RELATION BETWEEN THE ENERGY AND MASS OF AN ISOLATED SYSTEM

We are now ready to return to our discussion of the energy principle by giving a deduction from our present basis of Einstein's relation between the energy and mass of an isolated material system. Using the quasi-Galilean coordinates described in the last section, we may write for the energy of the system, in accordance with equation (6),

$$U = \iiint (\mathfrak{T}_4^4 + t_4^4) dx dy dz$$

and this quantity will be constant independent of the time t as shown in §2, provided the boundary of the region of integration is taken sufficiently distant from the system. Substituting the value for total energy density given by equation (7), we can now rewrite our expression for the energy in the form

$$U = \frac{1}{8\pi} \iiint \frac{\partial}{\partial x_\gamma} \left(-g^{\alpha 4} \frac{\partial \mathfrak{L}}{\partial g^{\alpha 4}_\gamma} + \frac{1}{2} g^{\alpha\beta} \frac{\partial \mathfrak{L}}{\partial g^{\alpha\beta}_\gamma} \right) dx dy dz.$$

Taking the boundary of the region of integration as a sphere with its center at the origin of coordinates, using Gauss's theorem to transform to a surface integral, and substituting at the distant boundary the three values for the term in parenthesis found in the previous section as given by equations (20) and (21), this can evidently be rewritten in the form

$$U = \frac{1}{8\pi} \iint \frac{2m}{r^2} [\cos^2(nx) + \cos^2(ny) + \cos^2(nz)] dS \\ + \frac{1}{8\pi} \frac{\partial}{\partial t} \iiint \left(-g^{\alpha 4} \frac{\partial \mathfrak{L}}{\partial g^{\alpha 4}_4} + \frac{1}{2} g^{\alpha\beta} \frac{\partial \mathfrak{L}}{\partial g^{\alpha\beta}_4} \right) dx dy dz.$$

Since, however, both U and the surface integral on the right hand side of the equation are constants independent of the time,¹⁸ it is evident that the second term on the right hand side of the equation must be zero, as the volume integral in the second term could not continue to change permanently at a constant rate with the time. Hence evaluating the surface integral, we easily obtain for an isolated system the simple relation

$$U = m \quad (22)$$

where U is Einstein's expression for the energy of the system, and m is the mass which must be substituted into the Schwarzschild solution to give the gravitational field at large distances. This appropriate result is itself no mean justification for Einstein's formulation of the energy principle.

§6. THE ENERGY OF A QUASI-STATIC ISOLATED SYSTEM EXPRESSED BY AN INTEGRAL EXTENDING ONLY OVER THE OCCUPIED SPACE

For certain purposes both of the expressions for the energy of an isolated system, $\iiint (\mathfrak{T}_4^4 + t_4^4) dx dy dz$ and m , are sometimes unsatisfactory, the first because the integration has to be extended over a region large compared with the actual system, owing to the fact that t_4^4 is in general not zero in free space, and the second because it gives no method of computing the energy from the actual distribution of matter or radiation within the system. For a particular class of systems, which we shall call quasistatic, a more usable expression can be obtained.

Starting once more with our fundamental equation (6) for the energy of an isolated system, we write

$$U = \iiint (\mathfrak{T}_4^4 + t_4^4) dx dy dz$$

where we again use the quasi-Galilean coordinates defined in §4. Substituting the expression for the density of potential energy t_4^4 given by equation (9) this can be rewritten in the form¹⁹

$$U = \iiint \left(\mathfrak{T}_4^4 + \frac{\mathfrak{L}}{16\pi} - \frac{1}{16\pi} g^{\alpha\beta} \frac{\partial \mathfrak{L}}{\partial g^{\alpha\beta}} \right) dx dy dz$$

and introducing the expression for \mathfrak{L} given by equation (15) this becomes

$$U = \iiint \left[\mathfrak{T}_4^4 - \frac{\mathfrak{G}}{16\pi} + \frac{1}{16\pi} \frac{\partial}{\partial x_\gamma} \left(g^{\alpha\beta} \frac{\partial \mathfrak{L}}{\partial g^{\alpha\beta}} \right)_\gamma - \frac{1}{16\pi} g^{\alpha\beta} \frac{\partial \mathfrak{L}}{\partial g^{\alpha\beta}} \right] dx dy dz.$$

¹⁸ The quantity m must be a constant, since it determines the gravitational field at the distant boundary, and by our definition an isolated system produces a constant gravitational field at the distant boundary.

¹⁹ We omit the cosmological term in the expressions for t_4^4 and \mathfrak{T} since our present considerations already contain the assumption that the system is small compared with the total dimensions of the universe.

Substituting now for \mathcal{G} the well-known expression¹⁹

$$\mathcal{G} = 8\pi\mathfrak{T} = 8\pi(\mathfrak{T}_1^1 + \mathfrak{T}_2^2 + \mathfrak{T}_3^3 + \mathfrak{T}_4^4)$$

writing the third term of the integrand out in full, and combining with the last term, we then easily obtain

$$\begin{aligned} U = & \frac{1}{2} \iiint (\mathfrak{T}_4^4 - \mathfrak{T}_1^1 - \mathfrak{T}_2^2 - \mathfrak{T}_3^3) dx dy dz \\ & + \frac{1}{16\pi} \iiint \left[\frac{\partial}{\partial x} \left(g^{\alpha\beta} \frac{\partial \mathfrak{Q}}{\partial g^{\alpha\beta}_1} \right) + \frac{\partial}{\partial y} \left(g^{\alpha\beta} \frac{\partial \mathfrak{Q}}{\partial g^{\alpha\beta}_2} \right) + \frac{\partial}{\partial z} \left(g^{\alpha\beta} \frac{\partial \mathfrak{Q}}{\partial g^{\alpha\beta}_3} \right) \right] dx dy dz \quad (23) \\ & + \frac{1}{16\pi} \iiint g^{\alpha\beta} \frac{\partial}{\partial t} \left(\frac{\partial \mathfrak{Q}}{\partial g^{\alpha\beta}_4} \right) dx dy dz. \end{aligned}$$

The second integral on the right hand side of this equation can be evaluated, however, by taking the boundary of the region of integration as a sphere, transforming to a surface integral and substituting at the distant boundary the values given by equations (20). We thus easily obtain $m/2$ as the value of the second integral and since for an isolated system this is itself equal by equation (22) to $U/2$ as shown in the preceding section, we can rewrite equation (23) in the form

$$U = \iiint (\mathfrak{T}_4^4 - \mathfrak{T}_1^1 - \mathfrak{T}_2^2 - \mathfrak{T}_3^3) dx dy dz + \frac{1}{8\pi} \iiint g^{\alpha\beta} \frac{\partial}{\partial t} \left(\frac{\partial \mathfrak{Q}}{\partial g^{\alpha\beta}_4} \right) dx dy dz \quad (24)$$

Finally, let us now define a quasi-static system as one in which changes with the time are taking place sufficiently slowly so that the last term in this equation can be neglected in comparison with the others, as will of course be exactly true in case we are only interested in the energy of the system at times when it is in a quiescent state of temporary or permanent equilibrium. We can then write as the desired expression²⁰ for the energy of an isolated quasi-static system

$$U = \iiint (\mathfrak{T}_4^4 - \mathfrak{T}_1^1 - \mathfrak{T}_2^2 - \mathfrak{T}_3^3) dx dy dz \quad (25)$$

²⁰ This expression for energy was first given by Nordström, *Proc. Amster. Acad.* **202**, 1080 (1918). The derivation given for the expression, however, was unsatisfactory since it was made to depend on an equation which the author ascribed to von Laue without any citation of the place of publication nor statement as to its range of validity. I have myself not been able to find the source of this expression and Professor von Laue has informed me by letter that he has been unable to find such an expression in the second volume of his book on relativity, does not know how he could have arrived at such an equation, now where else he might have set it forth, and is inclined to believe that Nordström must have been in error concerning the reference. Attention should also be called in this connection to the limited range as to the nature of the system and the choice of coordinates which will make equation (25) valid.

where it is evident from the equation of definition

$$T^{\mu\nu} = \rho_0 \frac{dx_\mu}{ds} \frac{dx_\nu}{ds}$$

that the integration has to be extended only over the region actually occupied by matter or radiation.

§7. ENERGY OF A SPHERE OF PERFECT FLUID.

We may now use equation (25) to calculate the energy of a spherical distribution of perfect fluid in a static state of stable or metastable equilibrium.

Continuing to use our quasi-Galilean coordinates x, y, z, t , we may evidently write the line element for our spherically symmetrical and static system in the form

$$ds^2 = -e^\mu (dx^2 + dy^2 + dz^2) + e^\nu dt^2 \quad (26)$$

where μ and ν are functions of $r = (x^2 + y^2 + z^2)^{1/2}$ and independent of t . In accordance with this line element we have for the components of the fundamental metrical tensor

$$\begin{aligned} g_{11} = g_{22} = g_{33} &= -e^\mu & g_{44} &= e^\nu \\ g^{11} = g^{22} = g^{33} &= -e^{-\mu} & g^{44} &= e^{-\nu} \\ g_{\rho\sigma} = g^{\rho\sigma} &= 0 \quad (\rho \neq \sigma) & \sqrt{-g} &= e^{\frac{3\mu+\nu}{2}}. \end{aligned} \quad (27)$$

For the tensor of energy and momentum for a perfect fluid we have the well known equation²¹

$$T^{\rho\sigma} = (\rho_{00} + p_0) \frac{dx_\rho}{ds} \frac{dx_\sigma}{ds} - g^{\rho\sigma} p_0 \quad (28)$$

where ρ_{00} and p_0 are the proper *macroscopic* density and proper pressure of the fluid as measured by local observers, and the quantities (dx_ρ/ds) are *macroscopic* velocities. For our case the macroscopic velocities will all be zero except for the case $\rho = \sigma = 4$ and we shall then have

$$\left(\frac{dt}{ds} \right)^2 = g^{44} = e^{-\nu}$$

so that the surviving components of the energy tensor will be

$$T^{11} = T^{22} = T^{33} = e^{-\mu} p_0 \quad T^{44} = e^{-\nu} \rho_{00}$$

or lowering suffixes

$$T_1^1 = T_2^2 = T_3^3 = -p_0 \quad T_4^4 = \rho_{00} \quad (29)$$

Multiplying these results by $\sqrt{-g}$ to change to tensor densities and substituting in equation (25), we now obtain for the energy of a steady spherical distribution of perfect fluid

²¹ See Eddington, reference 1, equations (54.81) and (54.82).

$$U = \iiint (\rho_{00} + 3p_0) e^{\frac{3\mu+p}{2}} dx dy dz. \quad (30)$$

We also have, moreover, the general relation

$$dV_0 ds = \sqrt{-g} dx_1 dx_2 dx_3 dx_4$$

where dV_0 is the element of proper three dimensional volume, and in our case this reduces to

$$dV_0 = e^{\frac{3\mu+p}{2}} dx dy dz \frac{dt}{ds} = e^{3\mu/2} dx dy dz$$

so that equation (30) can be rewritten in the extremely simple form

$$U = \int (\rho_{00} + 3p_0) e^{\nu/2} dV_0 = \int (\rho_{00} + 3p_0) \sqrt{g_{44}} dV_0. \quad (31)$$

§8. APPROXIMATE EXPRESSION FOR THE ENERGY OF A SPHERE OF FLUID IN A WEAK GRAVITATIONAL FIELD

We shall now investigate the value of this expression, for the energy of a sphere of perfect fluid, under circumstances where the gravitational field is weak enough so that the Newtonian theory of gravitation is approximately valid. Such a condition can of course be achieved by taking the quantity of matter in the sphere sufficiently small.

Under these circumstances the line element will approach that for flat space-time and we may write the components of the metrical tensor in the form

$$g_{\mu\nu} = \delta_{\mu\nu} + h_{\mu\nu} \quad (32)$$

where the quantities $\delta_{\mu\nu}$ are the Galilean values for the components of the metrical tensor, ± 1 or 0 , and the quantities $h_{\mu\nu}$ are *small* deviations therefrom. With these values for the components of the metrical tensor, however, we may easily obtain a well-known relation between h_{44} and the Newtonian gravitational potential Ψ .

To do this let us consider the behavior of a test particle placed at the point of interest and then allowed to move freely under the action of the gravitational field. In accordance with the theory of relativity the motion of this free particle must correspond to a geodesic in space-time and hence be governed by the equation²²

$$\frac{d^2 x_\alpha}{ds^2} + \{\mu\nu, \alpha\} \frac{dx_\mu}{ds} \frac{dx_\nu}{ds} = 0. \quad (33)$$

Since the particle starts from rest, however, the initial "velocities" dx_μ/ds and dx_ν/ds will all be zero except with μ or $\nu = 4$, and taking first the case of $\alpha = 1$, the above equation will reduce at the beginning of the motion to

²² See Eddington, reference 1, equation (49.42).

²³ See Eddington, reference 1, equation (28").

$$\frac{d^2x}{ds^2} + \{44, 1\} \left(\frac{dt}{ds} \right)^2 = 0. \quad (34)$$

Furthermore, we have for a particle at rest

$$ds^2 = g_{44} dt^2 = (1 + h_{44}) dt^2 \approx dt^2 \quad (35)$$

and in general

$$\{44, 1\} = \frac{1}{2} g^{\lambda 1} \left(\frac{\partial g_{4\lambda}}{\partial x_4} + \frac{\partial g_{4\lambda}}{\partial x_4} - \frac{\partial g_{44}}{\partial x_\lambda} \right)$$

which for our case reduces with sufficient approximation to

$$\{44, 1\} = \frac{1}{2} \frac{\partial g_{44}}{\partial x} = \frac{\partial}{\partial x} \left(\frac{h_{44}}{2} \right). \quad (36)$$

So that substituting (35) and (36) in (34) and writing the analogous equations with $\alpha = 2$ and 3 , we easily obtain for the initial acceleration of the test particle the equations

$$\frac{d^2x}{dt^2} = -\frac{\partial}{\partial x} \left(\frac{h_{44}}{2} \right), \quad \frac{d^2y}{dt^2} = -\frac{\partial}{\partial y} \left(\frac{h_{44}}{2} \right), \quad \frac{d^2z}{dt^2} = -\frac{\partial}{\partial z} \left(\frac{h_{44}}{2} \right). \quad (37)$$

We note at once that $(h_{44}/2)$ satisfies the same differential equations of motion as the gravitational potential Ψ in the ordinary Newtonian theory, and since h_{44} tends to zero at large distances may now write

$$\frac{h_{44}}{2} = \Psi \quad (38)$$

provided we make the usual convention that the gravitational potential shall be zero at infinity. This equation connects the relativity and Newtonian methods of treatment, providing the gravitational field is weak enough to permit the use of the older method.

In addition to this equation, we shall also need to use a value for a certain integral which was known in the Newtonian theory but is sufficiently unfamiliar so that we shall now derive it. The integral in question is $3 \int p dV$, where p is the pressure within the fluid and the integration is to be taken over the volume V of the whole sphere. We write

$$3 \int p dV = 3 \int_0^R 4\pi r^2 p dr$$

where R is the radius of the sphere, and by partial integration obtain

$$\begin{aligned} 3 \int p dV &= 4\pi r^3 p \Big|_0^R - \int_0^R 4\pi r^3 dp \\ &= - \int_0^R 4\pi r^3 dp \end{aligned}$$

where the first term has been dropped since r is zero at one limit and p at the other. It is evident, however, that the quantity $-4\pi r^2 dp$ is the total radial force acting outwards on the spherical shell of material dM_r lying between the radii r and $r+dr$ and hence can be equated to the gravitational attraction acting on this shell which gives us

$$3 \int p dV = \int_0^R \frac{M_r}{r} dM_r.$$

Moreover, the quantity on the right hand side of this equation is obviously the work that would be necessary to remove the material of the sphere to infinity and hence the negative of its potential energy. So that we can finally write

$$3 \int p dV = - \int \frac{\rho \Psi}{2} dV \quad (39)$$

where the integral on the right hand side of the equation is a well-known expression for potential energy, ρ being the density of material and Ψ the gravitational potential.

We are now ready to return to equation (31) which gave as an exact expression for the total energy of the sphere

$$U = \int (\rho_{00} + 3p_0) \sqrt{g_{44}} dV_0.$$

In accordance with equations (32) and (38) we can write as approximately valid in the case of a weak field

$$\sqrt{g_{44}} = (1 + h_{44})^{1/2} \approx 1 + \frac{h_{44}}{2} = 1 + \Psi.$$

And this can be substituted above to give

$$U = \int \rho_{00} dV_0 + \int \rho_{00} \Psi dV_0 + 3 \int p_0 dV_0 + 3 \int p_0 \Psi dV_0.$$

In the case of a weak gravitational field, however, the potential Ψ is everywhere small compared with unity and for the case of ordinary matter in a weak gravitational field²⁴ p_0 is small compared with ρ_{00} . Hence the last term in the above expression may be dropped entirely and the next two preceding terms simplified by omitting the subscripts $(_0)$ which specify a proper system of coordinates for the measuring of quantities. The result then becomes

$$U = \int \rho_{00} dV_0 + \int \rho \Psi dV + 3 \int p dV$$

²⁴ This is not true for radiation where $p_0 = \rho_{00}/3$, so that our present considerations apply to a sphere in which the density of ordinary matter is large compared with that of radiation, which is of course the case for which the Newtonian potential energy was known.

and introducing the value of $3\int p dV$ given by equation (39), we finally obtain as an approximate expression for the energy of a sphere of perfect fluid in a weak gravitational field

$$U = \int \rho_{00} dV_0 + \int \frac{\rho \Psi}{2} dV. \quad (40)$$

In satisfactory agreement with older theory, the energy thus consists of two parts,—the first being the total proper energy of the material out of which the sphere is composed, and the second the well-known Newtonian expression for its potential gravitational energy.

As far as the writer is aware, this is the first case in which it has been shown that Einstein's exact relativity expression for the energy of a system is more closely approximated by including the Newtonian potential energy than by going at once to flat space-time. It is hoped that the reasonableness of this result will lead to increased confidence in the use of the energy-momentum principle in general relativity.

§9. THE INTERPRETATION AND USE OF THE ENERGY-MOMENTUM PRINCIPLE IN THE CASE OF NON-ISOLATED SYSTEMS

So far, the applications of the energy-momentum principle, which we have considered in the foregoing, have dealt with the conservation of energy for an isolated system enclosed within a distant boundary located in the free space surrounding the system, and these applications have been made largely in order to illustrate the reasonableness of Einstein's formulation of the principle. In applying the theory of relativity to the phenomena of nature, however we may often be interested in using the energy-momentum principle to give us information as to the changes which could take place within a limited region which forms part of a larger system. Hence in the present section we shall consider the interpretation and use of the energy-momentum principle when applied to such non-isolated systems, and in the following section we shall discuss specifically the changes which the energy-momentum principle would allow in the distribution of matter within a certain kind of non-isolated system.

Let us return to the fundamental differential equation, true in all sets of coordinates, which was given in §1

$$\frac{\partial}{\partial x_\mu} (\mathfrak{T}_\mu^\nu + t_\mu^\nu) = 0 \quad (41)$$

where \mathfrak{T}_μ^ν is the tensor density of material energy and momentum and t_μ^ν the pseudo-tensor density of potential gravitational energy and momentum. Taking x_4 to be the time like coordinate, this equation will lead to the momentum principles with $\mu = 1, 2, 3$ and to the energy principle with $\mu = 4$. For our present purposes, however, we shall leave μ unspecified since the following considerations are general enough to apply to the energy-momentum principle as a whole.

Multiplying the above equation by $dx_1 dx_2 dx_3$, and integrating over the system of interest we obtain with some rearrangement of terms

$$\begin{aligned} & \frac{\partial}{\partial x_4} \iiint (\mathfrak{T}_\mu^4 + t_\mu^4) dx_1 dx_2 dx_3 \\ &= - \iiint \left[\frac{\partial}{\partial x_1} (\mathfrak{T}_\mu^1 + t_\mu^1) + \frac{\partial}{\partial x_2} (\mathfrak{T}_\mu^2 + t_\mu^2) + \frac{\partial}{\partial x_3} (\mathfrak{T}_\mu^3 + t_\mu^3) \right] dx_1 dx_2 dx_3 \end{aligned}$$

and, by performing the indicated integrations on the right hand side, this can be rewritten in the form

$$\begin{aligned} & \frac{\partial}{\partial x_4} \iiint (\mathfrak{T}_\mu^4 + t_\mu^4) dx_1 dx_2 dx_3 \\ &= - \iint \left[\mathfrak{T}_\mu^1 + t_\mu^1 \right]_{x_1}^{x_1'} dx_2 dx_3 - \iint \left[\mathfrak{T}_\mu^2 + t_\mu^2 \right]_{x_2}^{x_2'} dx_1 dx_3 - \iint \left[\mathfrak{T}_\mu^3 + t_\mu^3 \right]_{x_3}^{x_3'} dx_1 dx_2 \end{aligned} \quad (42)$$

where the limits of integration for the spatial variables x_1, x_2, x_3 are to be chosen so as to include the system of interest.

Equation (42) as written is true in all sets of coordinates, owing to its immediate dependence on the covariant equation (41). The interpretation and use of the equation, however, are often simplified if we choose coordinates in such a way that the limits of integration which must be taken in order to include the system of interest actually lie on the boundary surface which separates the region in question from its surroundings. Thus for example quasi-Galilean coordinates x, y, z with the limits of integration x to x' , y to y' , and z to z' lying on the boundary of the system, are usually preferable for our present purposes to polar coordinates r, θ, ϕ , with the origin inside the system and the limits of integration 0 to r , 0 to π and 0 to 2π , in which case r is the only limit actually lying on the boundary. The increased simplicity of the properly chosen coordinates arises from the fact that the right hand side of equation (42) is then completely determined solely by the values assumed at the boundary by the quantities $\mathfrak{T}_\mu^i, t_\mu^i$ etc. and is not dependent on their values within the system.

Having chosen coordinates in the way suggested, the interpretation of equation (42) becomes very simple. The equation now states that the rate of change with time x_4 of the volume integral on the left hand side of the equation is equal to the quantity on the right hand side, whose value is entirely determined by the conditions prevailing at the boundary of the system. The left hand side of the equation can then be interpreted as the rate of change with the time of a component of the total momentum of the system, with $\mu = 1, 2, 3$, or the rate of change of the energy of the system, with $\mu = 4$; and the right hand side of the equation can be interpreted as the flux of momentum or energy through the boundary.

The use of equation (42) will also be facilitated by the suggested choice of coordinates, when we are interested in some process which takes place within our system under circumstances such that we have definite information as to

the values of the quantities $\mathfrak{T}_\mu^1, t_\mu^1$ etc. at the boundary of the system, but do not have definite information as to the values they may assume in the interior of the system during the course of the process which interests us. In the following section we shall use coordinates of the kind suggested without further remark.

§10. APPLICATION OF THE ENERGY-MOMENTUM PRINCIPLE TO THE STATIC STATES OF A SYSTEM

Having thus obtained an indication as to the interpretation and use of the energy-momentum principle in the case of non-isolated systems, we shall now apply the principle to determine what restriction it would impose on the form of line element within a system which could exist in different static states. To solve this problem we apply the energy-momentum principle to the following process.

We start with a non-isolated system which together with its surroundings is originally in some given static state such that none of the components of the metrical tensor are changing with the time x_4 . Without altering the metric or the distribution of matter and radiation outside of the system, we then assume a change to take place in the distribution of matter and energy inside the system in such a way that the system ultimately arrives in some new possible static state. In the absence of the detailed knowledge, which would permit us to describe the exact mechanism of the internal process that takes place, we now inquire into the restrictions which the energy-momentum principle, as applied to the system as a whole, would impose on the changes in the form of line element inside the system which could accompany such a process.

The first condition on the possible changes in the line element is imposed by the hypothesis that the metric and the distribution of matter and radiation outside the system are not to be changed by the process, this hypothesis being introduced since our interest will lie in those changes which could take place solely within the system without affecting anything in the outside surroundings. As an immediate result of the assumption that the metric is not to be changed outside of the system, it is at once evident that the process must produce no change in the values at the boundary of the components $g_{\mu\nu}$ of the metrical tensor and their first differential coefficients $\partial g_{\mu\nu}/\partial x_\alpha$. And as a result of the assumption that the distribution of matter and radiation is not to be changed outside of the system, it is evident that the energy-momentum tensor $T^{\mu\nu}$ will remain unchanged at the boundary since it is completely determined by the distribution of matter and radiation in accordance with the equation of definition

$$T^{\mu\nu} = \rho_0 \frac{dx_\mu}{ds} \frac{dx_\nu}{ds}. \quad (43)$$

The second condition on the possible changes in the line element is imposed by the requirement that the process taking place within the system shall agree with the energy-momentum principle as applied to the system as a whole. This condition is given by our previous equation

$$\begin{aligned} & \frac{\partial}{\partial x_4} \iiint (\mathfrak{T}_\mu^4 + t_\mu^4) dx_1 dx_2 dx_3 \\ &= - \iint \left| \mathfrak{T}_\mu^1 + t_\mu^1 \right|_{x_1}^{x_1'} dx_2 dx_3 - \iint \left| \mathfrak{T}_\mu^2 + t_\mu^2 \right|_{x_2}^{x_2'} dx_1 dx_3 - \iint \left| \mathfrak{T}_\mu^3 + t_\mu^3 \right|_{x_3}^{x_3'} dx_1 dx_2. \end{aligned} \quad (44)$$

To apply this equation, we note that at the start of the process when the system is in its original static state, the left hand side of the equation is obviously equal to zero since none of the quantities involved can be changing with the time. Thus at the start of the process the values at the boundary of the quantities $\mathfrak{T}_\mu^1 \cdots t_\mu^3$ must be such as to make the right hand side also equal to zero. The quantities \mathfrak{T}_μ^1 , \mathfrak{T}_μ^2 and \mathfrak{T}_μ^3 , however, are determined by the $g_{\mu\nu}$ and $T^{\mu\nu}$ and the quantities t_μ^1 , t_μ^2 and t_μ^3 by the $g_{\mu\nu}$ and $\partial g_{\mu\nu}/\partial x_\alpha$, and hence in accordance with the last paragraph the values which they assume at the boundary will not change during the process. The result is that both sides of equation (44) remain equal to zero throughout the process, and the condition imposed by the energy-momentum principle reduces to the requirement of constant energy and components of momentum for the system as given by the equation

$$\iiint (\mathfrak{T}_\mu^4 + t_\mu^4) dx_1 dx_2 dx_3 = \text{const.} \quad (45)$$

To investigate the effect of this condition on the possible changes in line element which could occur, we shall now reexpress the integrand by substituting for it the expression given by equation (7) in §3. We thus obtain

$$\iiint \frac{\partial}{\partial x_\gamma} \left(-g^{\alpha 4} \frac{\partial \mathfrak{L}}{\partial g^{\mu\alpha}} + \frac{1}{2} g_\mu^4 g^{\alpha\beta} \frac{\partial \mathfrak{L}}{\partial g^{\alpha\beta}} \right) dx_1 dx_2 dx_3 = \text{const.} \quad (46)$$

In this equation, however, the suffix γ is a dummy and the term with $\gamma=4$ will be zero at the beginning and end of our process, since by hypothesis the system is at these times a static one and the rate of change of all quantities with respect to the time x_4 is zero. Hence, writing the summation out in full and performing the possible integrations with respect to x_1 , x_2 and x_3 which are indicated, we can now express the condition imposed on the form of the line element by stating that for the static states at the beginning and end of the process we must have the relation

$$\begin{aligned} & \iint \left| -g^{\alpha 4} \frac{\partial \mathfrak{L}}{\partial g^{\mu\alpha}} + \frac{1}{2} g_\mu^4 g^{\alpha\beta} \frac{\partial \mathfrak{L}}{\partial g^{\alpha\beta}} \right|_{x_1}^{x_1'} dx_2 dx_3 \\ &+ \iint \left| -g^{\alpha 4} \frac{\partial \mathfrak{L}}{\partial g^{\mu\alpha}} + \frac{1}{2} g_\mu^4 g^{\alpha\beta} \frac{\partial \mathfrak{L}}{\partial g^{\alpha\beta}} \right|_{x_2}^{x_2'} dx_1 dx_3 \\ &+ \iint \left| -g^{\alpha 4} \frac{\partial \mathfrak{L}}{\partial g^{\mu\alpha}} + \frac{1}{2} g_\mu^4 g^{\alpha\beta} \frac{\partial \mathfrak{L}}{\partial g^{\alpha\beta}} \right|_{x_3}^{x_3'} dx_1 dx_2 = \text{const.} \end{aligned} \quad (47)$$

where the limits of integration x_1, x_1' etc. lie on the boundary of the system. The quantities occurring in the integrands of this equation, however, are completely determined by the values of the components $g_{\mu\nu}$ of the metrical tensor and their first differential coefficients, as can be verified from equations already given in this article. Hence the condition imposed by the energy-momentum principle has already been met by our previous requirement necessary to preserve the metric outside that the values at the boundary for the $g_{\mu\nu}$ and their first differential coefficients should not be changed by the process.

Hence, noting the restriction given in §9 as to the kind of coordinate systems that we employ, we can now state the following otherwise general conclusion. Let us start with a non-isolated system, which together with its surroundings is originally in some given static state, and consider that some process then takes place which leaves the metric and the distribution of matter and radiation outside the system unaltered but changes the matter and radiation inside the system in such a way that we finally arrive in some new static state. Assuming no detailed knowledge as to the nature of the internal process that has occurred, but applying the energy-momentum principle to the system as a whole, we then find that the requirements imposed by the energy-momentum principle on the possible changes in line element within the system are to be met by the condition that the components $g_{\mu\nu}$ of the metrical tensor and their first differential coefficients $\partial g_{\mu\nu}/\partial x_a$ are to retain their values unaltered at the boundary.²⁵

§11. CONCLUSION

This concludes the material which it was desired to present in the present article. It is hoped that the general coherence of the treatment and the specific satisfactory result, as to the inclusion of the ordinary Newtonian expression for potential gravitational energy in the case of a fluid sphere in a weak gravitational field, will increase the confidence with which the energy principle is used in general relativity.

Some apology should perhaps be offered for the great length of the two preceding sections on the application of the energy principle to the changes that may take place within a limited region which forms part of a larger system. There are, however, a number of points connected with the development which have seemed puzzling enough to warrant a detailed exposition and the final conclusion is one of considerable usefulness.

It should perhaps also be remarked that we have not treated in the foregoing any questions which involve the energy of the closed universe as a whole since these deserve separate consideration.²⁶

²⁵ In connection with the formulation of this section, I have been greatly helped by discussions with my colleague Dr. J. Robert Oppenheimer, for which I wish to thank him, also in this place.

²⁶ See Einstein, Berl. Ber. 1918, p. 452, and Tolman, Proc. Nat. Acad. 14, 348 (1928).

ON THE USE OF THE ENTROPY PRINCIPLE
IN GENERAL RELATIVITY

BY RICHARD C. TOLMAN

NORMAN BRIDGE LABORATORY, CALIFORNIA INSTITUTE OF TECHNOLOGY, PASADENA

(Received December 30, 1929)

ABSTRACT

The main purpose of this article is to use the extension of thermodynamics to general relativity, previously proposed by the author, to obtain expressions which will give the criteria for the thermodynamic equilibrium of a static gravitating system in a readily applicable mathematical form. After restating the principle chosen by the author as the general relativity analogue of the second law of thermodynamics, and showing once more that it is a natural covariant generalization of the ordinary second law of thermodynamics, the principle is then applied to finite systems in general and to adiabatic systems having no flux of matter or heat at the boundary. The mathematical conditions for thermodynamic equilibrium are then obtained for the case of any finite static system, and a specially useful form for these conditions is obtained for the case that the system has spherical symmetry.

§1. INTRODUCTION

IN SEVERAL previous articles, I have attempted an extension of thermodynamics to general relativity¹ and have tried to make certain applications of this extension.² The main purpose of the present article is to prepare for certain further applications which I propose to make.

The postulate, which must be taken in work of this kind as the general relativity analogue of the ordinary first law of thermodynamics, is evidently Einstein's generalized energy-momentum principle, which reduces in flat space-time to the ordinary laws of the conservation of energy and momentum, and is a principle which certainly must not be violated by any thermodynamic changes which may take place. The use of this principle has already been discussed in some detail in the preceding article in this journal,³ and, those conclusions drawn from it, which will be necessary for the present considerations.

The postulate which was chosen as the general relativity analogue of the second law of thermodynamics was a new one, which was justified, so far as may be, by showing it to be a natural covariant generalization of the ordinary second law of thermodynamics in flat space-time. In the present article we shall be especially interested in the method of applying this principle to determine the equilibrium conditions for a finite system in a static state.

¹ Tolman, Proc. Nat. Acad. 14, 268 (1928); *ibid.* 14, 701 (1928).

² Tolman, Proc. Nat. Acad. 14, 348 (1928); *ibid.* 14, 353 (1928).

³ Tolman, Phys. Rev. 35, 875 (1930).

⁴ See reference (3) last paragraph of §10.

In the immediately following section, §2, we shall again state the postulate chosen as the general relativity analogue of the second law of thermodynamics in the form which it assumes for an infinitesimal region, and show again by way of review that it is a natural covariant generalization of the ordinary second law of thermodynamics valid in flat space-time. In §3, we shall obtain by integration the form taken by the principle in the case of a finite system in general, and then more especially in the case of an adiabatic system having no flux of matter or heat at the boundary. Following this we shall consider, in §4, the conditions for thermodynamic equilibrium in the case of a finite static system, and finally, in §5, we shall consider a specific form in which these conditions for equilibrium can be put in case the system under consideration has spherical symmetry.

§2. THE GENERALIZED SECOND LAW OF THERMODYNAMICS

To state the postulate which was taken as the general relativity analogue of the second law of thermodynamics, we shall first define the *entropy vector* at a given point in space-time, by the equation

$$S^\mu = \phi_0 \frac{dx_\mu}{ds} \quad (1)$$

where ϕ_0 is the *proper density of entropy* at the point in question as measured by a local observer, and dx_μ/ds is the *macroscopic velocity* of matter at that point. Corresponding to this vector, we also have the *entropy vector density* given by the equation

$$\mathfrak{S}^\mu = S^\mu \sqrt{-g} = \phi_0 \sqrt{-g} \frac{dx_\mu}{ds} \quad (2)$$

The second law postulate can then be stated in the form

$$\frac{\partial \mathfrak{S}^\mu}{\partial x_\mu} dx_1 dx_2 dx_3 dx_4 \geq \frac{dQ_0}{T_0} \quad (3)$$

where dQ_0 is the *heat measured in proper coordinates* flowing through the boundary into the infinitesimal region and during the infinitesimal time denoted by $dx_1 dx_2 dx_3 dx_4$, and T_0 is the *proper temperature* at the boundary.

To show that expression (3) is covariant, we rewrite it by a well-known transformation in the form

$$(S^\mu)_\mu \sqrt{-g} dx_1 dx_2 dx_3 dx_4 \geq \frac{dQ_0}{T_0} \quad (4)$$

The quantity $(S^\mu)_\mu$, however, is the contracted covariant derivative of S^μ and is known to be an invariant, while $\sqrt{-g} dx_1 dx_2 dx_3 dx_4$ and dQ_0/T_0 are also obviously invariants so that both sides of expression (4) are tensors of rank zero, and the requirement of covariance is met in the simplest possible way.

To show that expression (3) reduces to the ordinary requirements of the second law in the limiting case of flat space-time, we first rewrite it with the help of (2) in the form

$$\frac{\partial}{\partial x_\mu} \left(\phi_0 \sqrt{-g} \frac{dx_\mu}{ds} \right) dx_1 dx_2 dx_3 dx_4 \geq \frac{dQ_0}{T_0}. \quad (5)$$

In flat space-time, however, using Galilean coordinates x, y, z and t , we shall have $\sqrt{-g}=1$, and writing out the indicated summation in full, we obtain with some rearrangement in the order of terms

$$\begin{aligned} \frac{\partial}{\partial t} \left(\phi_0 \frac{dt}{ds} \right) dx dy dz dt \\ \geq - \left[\frac{\partial}{\partial x} \left(\phi_0 \frac{dx}{ds} \right) + \frac{\partial}{\partial y} \left(\phi_0 \frac{dy}{ds} \right) + \frac{\partial}{\partial z} \left(\phi_0 \frac{dz}{ds} \right) \right] dx dy dz dt + \frac{dQ_0}{T_0} \end{aligned}$$

and this can evidently be rewritten as

$$\begin{aligned} \frac{\partial}{\partial t} \left(\phi_0 \frac{dt}{ds} \right) dx dy dz dt \\ \geq \left[\frac{\partial}{\partial x} \left(\phi_0 \frac{dt}{ds} \frac{dx}{dt} \right) + \frac{\partial}{\partial y} \left(\phi_0 \frac{dt}{ds} \frac{dy}{dt} \right) + \frac{\partial}{\partial z} \left(\phi_0 \frac{dt}{ds} \frac{dz}{dt} \right) \right] dx dy dz dt + \frac{dQ_0}{T_0}. \quad (6) \end{aligned}$$

In accordance, however, with the special theory of relativity, valid in flat space-time, entropy is an invariant for the Lorentz transformation, so that entropy density will be affected by the Lorentz-Fitzgerald factor of contraction ds/dt in such a way that we can make the substitution

$$\phi = \phi_0 \frac{dt}{ds} \quad (7)$$

where ϕ is the density of entropy in the particular set of Galilean coordinates that are being used. Furthermore, since heat and temperature have the same transformation factors on the basis of the special theory, we may also substitute

$$\frac{dQ}{T} = \frac{dQ_0}{T_0}. \quad (8)$$

Hence, using u, v, w to denote the components of ordinary velocity dx/dt etc. we can finally rewrite expression (6) in the form

$$\frac{\partial \phi}{\partial t} dx dy dz dt \geq - \left[\frac{\partial}{\partial x} (\phi u) + \frac{\partial}{\partial y} (\phi v) + \frac{\partial}{\partial z} (\phi w) \right] dx dy dz dt + \frac{dQ}{T}. \quad (9)$$

This expression, however, evidently states the essence of the ordinary second law of thermodynamics, since it requires that the actual increase of entropy occurring in the time dt in the infinitesimal volume $dx dy dz$ cannot be less

than the total entropy brought in from the outside by the flux of matter and the flow of heat.

Our postulate as to the general relativity analogue of the second law has thus been justified both by the fact of its expression in covariant form and by its reduction in the limiting case of flat space-time to the ordinary second law of thermodynamics. The justification, thus presented, is of course in no sense a complete proof of the validity of the postulate taken. Covariance and agreement with the form of the second law valid in the special theory of relativity are necessary but not sufficient requirements for determining the new form of the second law. The new postulate must be regarded as a real generalization containing an element not present in the special theory of relativity, and the ultimate complete justification of the postulate must be dependent on the agreement between the conclusions that can be drawn from it and actual experimental or observational facts.

§3. APPLICATION OF THE ENTROPY PRINCIPLE TO FINITE SYSTEMS

To apply the new principle to the changes taking place in a finite system, let us start with the principle in the form given by expression (5), and taking x_1 , x_2 and x_3 as being the space-like coordinates, integrate over the spatial region of interest. If we carry out such an integration, using coordinates such that the limits of integration necessary to include the whole system fall on the actual boundary which separates the system from its surroundings, it is evident that the summation of dQ_0/T_0 over the interior of the system will cancel out, since any heat entering a given element of volume is abstracted from neighboring elements, so that we shall only have to consider the heat entering the system from its surroundings. Hence dividing equation (5) through by dx_4 , writing out the indicated summation, and performing the suggested integration, we obtain with some rearrangement in the order of terms

$$\begin{aligned} \frac{\partial}{\partial x_4} \iiint \left(\phi_0 \sqrt{-g} \frac{dx_4}{ds} \right) dx_1 dx_2 dx_3 \\ \cong - \iiint \left[\frac{\partial}{\partial x_1} \left(\phi_0 \sqrt{-g} \frac{dx_1}{ds} \right) + \frac{\partial}{\partial x_2} \left(\phi_0 \sqrt{-g} \frac{dx_2}{ds} \right) \right. \\ \left. + \frac{\partial}{\partial x_3} \left(\phi_0 \sqrt{-g} \frac{dx_3}{ds} \right) \right] dx_1 dx_2 dx_3 + \sum \left(\frac{1}{T_0} \frac{dQ_0}{dx_4} \right)_{\text{Boundary}}. \end{aligned}$$

The last term on the right hand side of this expression is the total value taken over the boundary of the system of the quantity $(1/T_0) (dQ_0/dx_4)$, and by performing the indicated integrations the other terms on this side of the expression can also be seen to depend solely on quantities whose values are determined by conditions at the boundary, provided we continue to use, as suggested above, a set of coordinates so chosen that the limits of integration necessary to include the whole of the system actually lie on the boundary. We obtain

$$\begin{aligned}
\frac{\partial}{\partial x_4} \iiint \left(\phi_0 \sqrt{-g} \frac{dx_4}{ds} \right) dx_1 dx_2 dx_3 \geq & \int \int \left| \phi_0 \sqrt{-g} \frac{dx_1}{ds} \right|_{x_1}^{x_1'} dx_2 dx_3 \\
& - \int \int \left| \phi_0 \sqrt{-g} \frac{dx_2}{ds} \right|_{x_2}^{x_2'} dx_1 dx_3 - \int \int \left| \phi_0 \sqrt{-g} \frac{dx_3}{ds} \right|_{x_3}^{x_3'} dx_1 dx_2 \\
& + \sum \left(\frac{1}{T_0} \frac{dQ_0}{dx_4} \right)_{\text{Boundary}}
\end{aligned} \tag{10}$$

where the limits of integration at the boundary of the system are denoted by x_1, x_1' etc.

This expression (10) may be regarded as a general statement of the second law of thermodynamics as applied to finite systems, and defining the entropy of the system by the equation

$$S = \iiint \left(\phi_0 \sqrt{-g} \frac{dx_4}{ds} \right) dx_1 dx_2 dx_3 \tag{11}$$

the expression can be interpreted as giving the relation which must hold between the rate at which the entropy of a finite system is changing with the "time" x_4 , and those conditions existing at the boundary which determine the flux of matter and the flow of heat.

For the case of an adiabatic system with no flow of heat through the boundary, and in addition with the quantities dx_1/ds , dx_2/ds and dx_3/ds equal to zero at the boundary, so that there is no flux of matter between the system and its surroundings, expression (10) reduces to

$$\frac{\partial}{\partial x_4} \iiint \left(\phi_0 \sqrt{-g} \frac{dx_4}{ds} \right) dx_1 dx_2 dx_3 \geq 0. \tag{12}$$

In accordance with this expression, the entropy of an adiabatic system of the kind described can only increase or remain constant with increases in the time x_4 .

§4. THERMODYNAMIC EQUILIBRIUM IN A STATIC SYSTEM

We shall now investigate the conditions for thermodynamic equilibrium in a static system. To do this we must examine the changes which could take place from one static state to another without violating either the energy-momentum principle or the entropy principle as applied to the system as a whole.

Consider a system which together with its surroundings is originally in some given static state, such that none of the components $g_{\mu\nu}$ of the metrical tensor are changing with the time, and furthermore such that there is no flow of heat nor macroscopic flux of matter or radiation at any point. Without alteration in the metric or the distribution of matter and radiation outside of the system we then assume some change to take place in the distribution of matter and radiation inside the boundary in such a way that the system ultimately arrives in some new possible static state. Assuming no detailed

knowledge of the exact nature of the internal process which occurs, we now inquire into the restrictions which the energy-momentum principle and the entropy principle applied to the system as a whole would impose on the change in state.

In accordance with a conclusion obtained in my previous article on the energy-momentum principle,⁴ the restrictions imposed by this principle on the possible changes in line element within the system are to be met by the condition that the components $g_{\mu\nu}$ of the metrical tensor and their first differential coefficients $\partial g_{\mu\nu}/\partial x_\alpha$ are to retain their values unaltered at the boundary. These restrictions, coming from considerations of the energy-momentum principle, must be applied as part of the thermodynamic criteria for determining the possible changes in state.

Turning now to the entropy principle, we note that the process under consideration has been so chosen that the change is an adiabatic one of the kind described in the preceding section, since by hypothesis the flow of heat and macroscopic flux of matter are everywhere zero at the start and remain so at the boundary while the process is under way; hence we can at once apply expression (12) to the process. We thus obtain as the restriction imposed by the entropy principle the requirement that the entropy as defined by equation (11) shall not be decreased by the process. This restriction must be applied as giving the remaining thermodynamic criteria for determining the possible changes in state.

The considerations of the last two paragraphs immediately make it evident that the condition for the thermodynamic equilibrium of a static system, with no flow of heat or flux of matter at any point, is that the entropy of the system as given by equation (11) shall be the maximum that can be obtained without violating the boundary conditions furnished from considerations of the energy-momentum principle. Stating this conclusion more specifically by the use of the calculus of variations, we may now give as the condition of thermodynamic equilibrium in a static system of the kind described above

$$\delta \iiint \phi_0 \sqrt{-g} \frac{dx_1}{ds} dx_2 dx_3 = 0 \quad (13)$$

under the subsidiary condition holding *at the boundary of the system*

$$\delta g_{\mu\nu} = \delta \left(\frac{\partial g_{\mu\nu}}{\partial x_\alpha} \right) = 0 \quad (14)$$

where it is to be remembered that the conclusions have been derived using a system of coordinates such that the limits of integration necessary to include the whole of the system of interest fall on the actual boundary which separates the system from its surroundings.

§5. EQUILIBRIUM IN A STATIC SYSTEM HAVING SPHERICAL SYMMETRY

As just mentioned the conditions given by equations (13) and (14) have been derived using a system of coordinates such that the limits of integration

necessary to include the whole of the system fall on the actual boundary separating it from its surroundings. In the case of a system having spherical symmetry, it is possible, however, to translate these results into a system of polar coordinates, and thus put them into a more convenient form for use.

Let us take a static system of the kind discussed above, with no flow of heat nor macroscopic flux of matter or radiation at any point, and having spherical spatial symmetry, and let us initially make use of a set of coordinates x, y, z, t with the center of symmetry at the origin of the three equivalent spatial axes x, y and z . Such a set of coordinates is of the kind used in deriving the restrictions given by equations (13) and (14).

The line element for our system in these coordinates can evidently be written in the form

$$ds^2 = -e^\mu (dx^2 + dy^2 + dz^2) + e^\nu dt^2 \quad (15)$$

where the exponents μ and ν are independent of the time t , and on account of the spherical symmetry depend on the coordinates x, y and z in such a way that they are expressible as functions of $(x^2 + y^2 + z^2)^{1/2}$.

In accordance with this line element we have

$$g_{11} = g_{22} = g_{33} = -e^\mu \quad g_{44} = e^\nu$$

$$\sqrt{-g} = e^{\frac{3\mu + \nu}{2}} \quad (16)$$

and since there is no macroscopic flux of matter or radiation, we have the value zero for all the macroscopic velocities dx_μ/ds except for the case $\mu = 4$, and then have

$$\frac{dx_4}{ds} = \frac{dt}{ds} = e^{-\nu/2}. \quad (17)$$

Substituting the values given by equations (16) and (17) into equations (13) and (14) we then have as the requirement for thermodynamic equilibrium in our present coordinates

$$\delta \iiint \phi_0 e^{3\mu/2} dx dy dz = 0 \quad (18)$$

under the subsidiary condition holding at the boundary of the system

$$\delta\mu = \delta \left(\frac{\partial\mu}{\partial x_\alpha} \right) = \delta\nu = \delta \left(\frac{\partial\nu}{\partial x_\alpha} \right) = 0. \quad (19)$$

These requirements, however, can now easily be translated into polar coordinates r, θ and ϕ by setting

$$\begin{aligned} x &= r \sin \theta \cos \phi \\ y &= r \sin \theta \sin \phi \\ z &= r \cos \theta \end{aligned} \quad (20)$$

and noting that the condition of spherical symmetry makes it possible to take μ and ν as functions of r alone

$$\mu = \mu(r) \quad \nu = \nu(r). \quad (21)$$

The requirements for thermodynamic equilibrium then evidently become

$$\delta \iiint \phi_0 e^{3\mu/2} r^2 \sin \theta dr d\theta d\phi = 0 \quad (22)$$

under the subsidiary condition

$$\delta\mu = \delta\mu' = \delta\nu = \delta\nu' = 0 \quad (23)$$

where the primes indicate differentiation with respect to r , and the limitation given by (23) is to be applied at the actual boundary separating the system from its surroundings rather than at the limits of integration which must be given to the new variables in order to include the region of interest.

Finally if we take the region of interest as being a spherical shell contained between the constant radii r_1 and r_2 , we can evidently rewrite equations (22) and (23) in the form

$$\delta \left[4\pi \int_{r_1}^{r_2} \phi_0 e^{3\mu/2} r^2 dr \right] = 0 \quad (24)$$

under the subsidiary condition

$$\delta\mu = \delta\mu' = \delta\nu = \delta\nu' = 0 \quad (\text{at } r_1 \text{ and } r_2). \quad (25)$$

It is believed that this form of the conditions of equilibrium will be found an easy and useful one to employ.

ON THE WEIGHT OF HEAT AND THERMAL EQUILIBRIUM IN GENERAL RELATIVITY

BY RICHARD C. TOLMAN

NORMAN BRIDGE LABORATORY, CALIFORNIA INSTITUTE OF TECHNOLOGY,
PASADENA, CALIFORNIA

(Received December 30, 1929)

ABSTRACT

In accordance with the special theory of relativity all forms of energy, including heat, have inertia and hence in accordance with the equivalence principle also have weight. The purpose of the present article is to investigate the thermodynamic implications of the idea that heat has weight. In particular an investigation is made to see if a temperature gradient is a necessary accompaniment of thermal equilibrium in a gravitational field, in order to prevent the flow of heat from regions of higher to those of lower gravitational potential.

A preliminary non-rigorous treatment of this problem is first given by attempting to modify the classical thermodynamics only to the extent of associating with each intrinsic quantity of energy an additional amount of potential gravitational energy. In this way an expression is obtained for increase in equilibrium temperature with decrease in gravitational potential which, however, could in any case only be correct as a first approximation in a weak gravitational field. A discussion of the uncertainties and lack of rigor of this preliminary treatment is then given and the necessity pointed out for a rigorous treatment based on the principles of general relativity.

A rigorous relativistic treatment is then undertaken using the extension of thermodynamics to general relativity previously presented by the author. The system to be treated is taken as a static spherical distribution of perfect fluid which has come to gravitational and thermodynamic equilibrium. The principles of relativistic mechanics are first applied to such a system in order to obtain results needed in the later work. And it is then shown that these *mechanical* principles themselves are sufficient to determine the temperature distribution as a function of potential in the simple case of black-body radiation. The principles of relativistic thermodynamics are then applied to this same case of pure black-body radiation and the same expression for temperature as a function of potential obtained by the *thermodynamic* as by the mechanical treatment. This may be regarded as giving some measure of check on the validity of the proposed relativistic thermodynamics.

Following this, a thermodynamic treatment is given for the temperature distribution in the more general case of matter and radiation and a result found which harmonizes with that for radiation alone. A treatment is then given to the distribution of a perfect monatomic gas in a gravitational field both on the assumption that the total number of atoms must remain constant and on the assumption of the ready interconvertibility of matter and radiation. In the latter case the same dependence of concentration on temperature is obtained as was found by Stern and by the author for the case of flat space-time.

Using a system of coordinates such that the line element for the sphere of fluid takes the form

$$ds^2 = -e^u(dr^2 + r^2 d\theta^2 + r^2 \sin^2 \theta d\phi^2) + e^v dt^2$$

the general result for the relation between gravitational potential and equilibrium temperature T_0 as measured by a local observer in proper coordinates can be given by the equation

$$\frac{d \ln T_0}{dr} = - \frac{1}{2} \frac{dv}{dr}$$

This equation reduces in the case of a weak field to that obtained by the preliminary non-rigorous treatment, and gives a very small change of temperature with position in fields of ordinary intensity. The result, however, is one of great theoretical interest, since constant temperature throughout any system which has come to thermal equilibrium has hitherto been regarded as an inescapable thermodynamic conclusion. It is also not out of the question that the effect might sometime be of experimental or observational importance.

§1. INTRODUCTION

ONE of the most important results of the special theory of relativity was the relation between the total energy of a system U and its inertial mass m , given by Einstein's equation

$$U = mc^2 \quad (1)$$

where c is the velocity of light. In accordance with this equation we must ascribe the property of inertia to energy. For ordinary matter, however, we are in the possession of very exact experimental results showing a proportionality between inertia and weight, and hence the question at once arises whether we must also ascribe to energy the property of weight.

As early as 1911, in developing those ideas which finally led to the general theory of relativity, Einstein¹ considered this question, as to the weight of energy, and showed by a simple application of the equivalence hypothesis that the property of weight must indeed also be ascribed to energy if we are to maintain the postulated equivalence between behavior in a homogeneous gravitational field and behavior with reference to a set of uniformly accelerated axes. The later more complete developments of the general theory of relativity have shown that the Newtonian concept of the weight of a body as a force acting on it when placed in a gravitational field, is an idea which is only suitable for the treatment of slow-moving particles in weak gravitational fields. Nevertheless, these more complete developments of the general theory of relativity have completely confirmed the fundamental nature of the idea that weight must be ascribed to energy, since they have shown in any case that all forms of energy will be subject to the same gravitational action when placed under the same conditions in a gravitational field. Furthermore, in the case of weak enough fields and slow enough motions so that the Newtonian concepts may still be taken as approximately valid, the general theory of relativity has shown that the gravitational force F acting on any quantity of energy U will be given as would be expected by the simple equation

¹ Einstein, *Ann. d. Physik* **35**, 898 (1911).

$$F = (U/c^2)g \quad (2)$$

where g is the acceleration due to gravity.

If we accept the conclusion that energy has weight, it is evident that we must also ascribe weight to energy in the form of heat, and hence must expect to find thermodynamic consequences of the new idea. Thus considering for example cases where the Newtonian approximation is valid, we might expect the flow of heat from a place of higher to a place of lower gravitational potential to be accompanied by a decrease in potential energy, and this in turn would lead us to suspect that the condition of thermal equilibrium in a gravitational field might involve higher temperatures at the lower gravitational levels in order to prevent any thermal flow. It is the purpose of the present article to investigate the thermodynamic consequences of this idea that heat has weight, making use of principles obtained in an extension of thermodynamics to general relativity which I have already given.²

In the immediately following section, §2, we shall first consider a preliminary treatment of temperature equilibrium in the case of a system in such a weak gravitational field that we shall feel warranted in trying to apply the Newtonian concept of gravitation as a first approximation. And in §3, we shall examine the inadequacies of this preliminary treatment and show the necessity for the more rigorous treatments to follow. In §4, we shall then prepare for the rigorous general relativity treatment by applying the principles of relativistic mechanics to a spherical distribution of perfect fluid to obtain results which will be needed in the later developments. And in §5, we shall show that these purely mechanical results are alone sufficient to determine the temperature distribution in the simple case of a spherical distribution of pure radiation. In §6, we shall then briefly restate that result of the earlier extension of thermodynamics to general relativity which is necessary for our present considerations and then apply it in §7 to this same special case of pure radiation, and show that the same results are also obtained from the thermodynamic as from the purely mechanical treatment; this may be regarded as furnishing a partial confirmation of the correctness of the new system of relativistic thermodynamics. Following this, in §8, we shall use our relativistic thermodynamics to obtain a general equation for the distribution of temperature in any spherical mass of gravitating fluid, which has come to equilibrium. In §9, we shall then consider the equilibrium distribution of matter in a gravitational sphere of fluid; in particular the cases of a perfect monatomic gas, both when in equilibrium with radiation and when the total number of atoms is constant, will be treated. Finally in §10, we shall make some concluding remarks.

§2. PRELIMINARY TREATMENT OF TEMPERATURE EQUILIBRIUM IN A WEAK GRAVITATIONAL FIELD

To obtain a preliminary non-rigorous treatment of the temperature equilibrium in a weak gravitational field, we shall endeavor to apply the

² Tolman, Proc. Nat. Acad. 14, 268 (1928); *ibid.* 14, 701 (1928); This Journal, 896, *ibid.*

principles of the classical thermodynamics, modified only by assuming that the force of gravity will act on any quantity of energy U as though it had a weight, in the Newtonian sense, corresponding to its inertial mass U/c^2 . Under these circumstances a quantity of energy which has the intrinsic magnitude U , when measured at the zero of gravitational potential at a great distance from bodies producing a gravitational field, will be assumed to have associated with it the potential energy $U\Psi/c^2$ when brought to a point where the gravitational potential has the value Ψ .

Consider now an isolated sphere of material which is held together by its own gravitational attraction, but has a small enough mass so that the gravitational field is everywhere weak. In accordance with the classical thermodynamics, this system should be in equilibrium provided it has the maximum entropy S consistent with its total energy U . To determine the temperature distribution which corresponds to these conditions, let us then consider a small variation in temperature distribution, leaving unaltered, however, the amount of substance of each component in each element of volume dV . For the variation in total entropy we shall write

$$\delta S = \int \frac{\delta u}{T} dV \quad (3)$$

where T is the temperature at the point where the element of volume dV is located, δu is the change in the intrinsic energy density at that point produced by the variation in temperature, and the integration is to be taken over the whole volume of the system. On the other hand for the variation in the total energy of the system, we shall write

$$\delta U = \int \left(1 + \frac{\Psi}{c^2} \right) \delta u dV \quad (4)$$

where Ψ is the gravitational potential at the point in question.

Setting equation (3) equal to zero as the condition that the entropy be a maximum, and equation (4) equal to zero as the subsidiary condition of constant energy, and combining by the method of Lagrange, we obtain

$$\int \left[\frac{1}{T} - \lambda \left(1 + \frac{\Psi}{c^2} \right) \right] \delta u dV = 0 \quad (5)$$

where λ is a constant undetermined multiplier, and this equation can only be true for arbitrary variations δu , if we have

$$\frac{1}{T} = \lambda \left(1 + \frac{\Psi}{c^2} \right) \quad (6)$$

which is the desired expression giving the distribution of the temperature T throughout the system as a function of the gravitational potential Ψ .

Differentiating this equation with respect to the radius r , to obtain an expression for the rate of change of the temperature with distance from the center of the gravitating sphere, we have

$$-\frac{1}{T^2} \frac{dT}{dr} = \frac{\lambda}{c^2} \frac{d\Psi}{dr}$$

and substituting the expression for λ which can be obtained from (6), we obtain

$$\frac{d \ln T}{dr} = -\frac{(1/c^2)(d\Psi/dr)}{1+\Psi/c^2} = -\frac{d}{dr} \ln \left(1 + \frac{\Psi}{c^2} \right) \quad (7)$$

or since by hypothesis the field is weak enough so that Ψ/c^2 is small compared with unity we have approximately

$$\frac{d \ln T}{dr} = -\frac{1}{c^2} \frac{d\Psi}{dr} = -\frac{g}{c^2} \quad (8)$$

where g is the acceleration due to gravity.

For the case of a field of vanishing gravitational intensity with g negligible, the result degenerates into the usual condition for thermal equilibrium, $T = \text{constant}$. Furthermore, owing to the magnitude of the velocity of light the percentage change in temperature with height would be very small in fields of any ordinary intensity. Thus in a gravitational field having the strength of that at the surface of the earth we should have approximately

$$\frac{d \ln T}{dr} = -10^{-17} \text{ cm}^{-1}.$$

§3. INADEQUACY OF THE PRELIMINARY TREATMENT

The foregoing treatment contains of course many inadequacies and uncertainties, which can only be removed by a rigorous treatment of the problem from the point of view of general relativity. In the first place, in accordance with the classical thermodynamics, we have assumed maximum entropy and constant energy as the criteria of equilibrium for an isolated system, without any certain knowledge as to the form or even the validity of such principles in the presence of a gravitational field. Equation (3) for the entropy assumes it to depend on what we have called the intrinsic energy but the justification for this is by no means clear. Equation (4) for the energy, on the other hand, even if satisfactory for the case of weak gravitational fields,³ can certainly not be regarded as correct in general when we recall the great modifications in the nature of the energy principle which have to be introduced in the theory of general relativity. Furthermore, it should be noted that we have given no very clear definition of the quantities temperature T and intrinsic energy density u which occur in the equations, although we might perhaps guess that we should take the values of these quantities as measured by local observers using proper coordinates. In addition, even the interpretation of the quantity dV appears dubious when we recall the differences between pro-

³ See §8 in the article already referred to, This Journal, 888, for a satisfactory approximate treatment of the energy of a sphere of perfect fluid in a weak gravitational field.

per volume and coordinate volume which occur in the general theory of relativity.

It is hence abundantly evident that we cannot regard the results of the preceding section as having any certainty of validity, unless indeed we can show them to be an approximation in weak fields for conclusions which can be obtained from a more rigorous general relativity treatment. In what follows we shall now turn our attention to the general relativity treatment of the distribution of temperature and matter in a sphere of gravitating fluid which has come to thermodynamic equilibrium.

§4. THE RELATIVITY MECHANICS OF A SPHERICAL DISTRIBUTION OF PERFECT FLUID

As a preparation for our later work we must first consider the application of the mechanics of general relativity to a static distribution of perfect fluid having spherical symmetry. For a sufficiently general line element for such a system we may evidently write

$$ds^2 = -e^\mu (dr^2 + r^2 d\theta^2 + r^2 \sin^2 \theta d\phi^2) + e^\nu dt^2 \quad (9)$$

where the conditions that the system is to be static and spherically symmetrical are fulfilled if μ and ν can be taken as functions of r alone.

The components of the metrical tensor corresponding to this line element are evidently

$$\begin{aligned} g_{11} &= -e^\mu, & g_{22} &= -e^\mu r^2, & g_{33} &= -e^\mu r^2 \sin^2 \theta, & g_{44} &= e^\nu \\ g^{11} &= -e^{-\mu}, & g^{22} &= -\frac{e^{-\mu}}{r^2}, & g^{33} &= -\frac{e^{-\mu}}{r^2 \sin^2 \theta}, & g^{44} &= e^{-\nu} \\ g_{\rho\sigma} &= g^{\rho\sigma} = 0 \quad (\rho \neq \sigma) & \sqrt{-g} &= e^{\frac{3\mu+\nu}{2}} r^2 \sin \theta \end{aligned} \quad (10)$$

and the components of the contracted Riemann-Christoffel tensor corresponding to this metrical tensor have already been worked out and are known to have the values⁴

$$\begin{aligned} G_{11} &= \mu'' + \frac{\nu''}{2} + \frac{\mu'}{r} - \frac{\mu'\nu'}{4} + \frac{\nu'^2}{4} \\ G_{22} &= \frac{3}{2} r\mu' + \frac{r\nu'}{2} + \frac{r^2\mu''}{2} + \frac{r^2\mu'^2}{4} + \frac{r^2\mu'\nu'}{4} \\ G_{33} &= G_{22} \sin^2 \theta \\ G_{44} &= -e^{\nu-\mu} \left[\frac{\nu''}{2} + \frac{\nu'}{r} + \frac{\mu'\nu'}{4} + \frac{\nu'^2}{4} \right] \\ G_{\rho\sigma} &= 0 \quad (\rho \neq \sigma) \end{aligned} \quad (11)$$

⁴ See Eddington, "The Mathematical Theory of Relativity," Cambridge 1923. The results in question can be obtained by setting $\lambda = \mu$ in Eddington's equations (43.5).

where the primes indicate differentiation with respect to r . Raising suffixes with the help of the values of the metrical tensor (10), and substituting into the fundamental equation

$$-8\pi T_\sigma^\sigma = G_\sigma^\sigma - \frac{1}{2}g^\sigma_\sigma G \quad (12)$$

which connects the energy-momentum tensor T_σ^ρ with the metric we can then obtain, after a simple calculation, for the separate components of T_σ^ρ

$$\begin{aligned} -8\pi T_1^1 &= e^{-\mu} \left[\frac{\mu' + \nu'}{r} + \frac{\mu' \nu'}{2} + \frac{\mu'^2}{4} \right] \\ -8\pi T_2^2 &= -8\pi T_3^3 = e^{-\mu} \left[\frac{\mu'' + \nu''}{2} + \frac{\mu' + \nu'}{2r} + \frac{\nu'^2}{4} \right] \\ -8\pi T_4^4 &= e^{-\mu} \left[\mu'' + \frac{2\mu'}{r} + \frac{\mu'^2}{4} \right]. \end{aligned} \quad (13)$$

On the other hand in the case of a perfect fluid the energy tensor is known to depend on the properties of the fluid in accordance with the equation⁵

$$T_{00} = (\rho_{00} + p_0) \frac{dx_\rho}{ds} \frac{dx_\sigma}{ds} - g^{\rho\sigma} p_0 \quad (14)$$

where ρ_{00} is the proper *macroscopic* density of energy in the fluid, p_0 its proper pressure and the quantities dx_ρ/ds are *macroscopic* "velocities." Since we assume a static condition in our fluid, these "velocities" will all be zero except for the case ρ or $\sigma = 4$, and in accordance with the line element (9) will then have the value $dx_4/ds = e^{-\nu/2}$. Hence noting the values for $g^{\rho\sigma}$ given by equations (10) we obtain for the separate components of $T^{\rho\sigma}$

$$T^{11} = e^{-\mu} p_0, \quad T^{22} = \frac{e^{-\mu}}{r^2} p_0, \quad T^{33} = \frac{e^{-\mu}}{r^2 \sin^2 \theta} p_0, \quad T^{44} = e^{-\nu} \rho_{00} \quad (15)$$

or lowering suffixes with the help of the metrical tensor (10) we have

$$T_1^1 = T_2^2 = T_3^3 = -p_0 \quad T_4^4 = \rho_{00}. \quad (16)$$

Comparing these results with those given by equations (13) we can now write

$$p_0 = \frac{e^{-\mu}}{8\pi} \left[\frac{\mu' + \nu'}{r} + \frac{\mu' \nu'}{2} + \frac{\mu'^2}{4} \right] \quad (17)$$

$$p_0 = \frac{e^{-\mu}}{8\pi} \left[\frac{\mu'' + \nu''}{2} + \frac{\mu' + \nu'}{2r} + \frac{\nu'^2}{4} \right] \quad (18)$$

$$\rho_{00} = -\frac{e^{-\mu}}{8\pi} \left[\mu'' + \frac{2\mu'}{r} + \frac{\mu'^2}{4} \right] \quad (19)$$

⁵ See Eddington, reference 4, equations (54.81) and (54.82).

as expressions connecting the proper pressure p_0 and proper macroscopic density ρ_{00} with the metric. The reason that we obtain two separate expressions (17) and (18) connecting the pressure with the metric lies in the fact that the line element (9) with which we have started is sufficiently general to apply to any static distribution having spherical symmetry, while our later assumption of a perfect fluid involves at each point of the fluid an equality between the stresses in the radial and tangential directions.

Adding equations (17), (19), and (18) taken twice we obtain

$$(\rho_{00} + 3p_0) = \frac{e^{-\mu}}{8\pi} \left(v'' + \frac{2v'}{r} + \frac{\mu'v'}{2} + \frac{v'^2}{2} \right)$$

and this can be rewritten in a form which will later prove useful

$$8\pi(\rho_{00} + 3p_0)e^{\frac{3\mu+\nu}{2}}r^2 = e^{\frac{\mu+\nu}{2}} \left(v'' + \frac{2v'}{r} + \frac{\mu'v'}{2} + \frac{v'^2}{2} \right) r^2 = \frac{d}{dr} (e^{\frac{\mu+\nu}{2}} v' r^2). \quad (20)$$

We are now ready to apply the principles of mechanics to our system, in accordance with the fundamental equation of relativity mechanics which can be written in the form.⁶

$$\frac{\partial \mathfrak{T}_\sigma^\rho}{\partial x_\rho} - \frac{1}{2} \mathfrak{T}^{\alpha\beta} \frac{\partial g_{\alpha\beta}}{\partial x_\sigma} = 0 \quad (21)$$

Considering first the case $\sigma = 1$, substituting values for the tensor *densities* of energy and momentum obtained from (15) and (16) through multiplication by $\sqrt{-g}$, and substituting for $g_{\alpha\beta}$ from (10), we can write

$$\begin{aligned} \frac{\partial}{\partial r} (-p_0 \sqrt{-g}) - \frac{1}{2} (e^{-\mu} p_0 \sqrt{-g}) \frac{\partial}{\partial r} (-e^\mu) - \frac{1}{2} \left(\frac{e^{-\mu}}{r^2} p_0 \sqrt{-g} \right) \frac{\partial}{\partial r} (-e^\mu r^2) \\ - \frac{1}{2} \left(\frac{e^{-\mu}}{r^2 \sin^2 \theta} p_0 \sqrt{-g} \right) \frac{\partial}{\partial r} (-e^\mu r^2 \sin^2 \theta) - \frac{1}{2} (e^{-\nu} \rho_{00} \sqrt{-g}) \frac{\partial}{\partial r} (e^\nu) = 0 \end{aligned}$$

and substituting the value $\sqrt{-g} = r^2 \sin \theta e^{\frac{3\mu+\nu}{2}}$ given in (10), this is easily found to reduce to the form

$$\frac{\partial p_0}{\partial r} = -\frac{\rho_{00} + p_0}{2} \frac{\partial \nu}{\partial r} \quad (22)$$

which furnishes us with a very simple and useful expression for the change in pressure with radius. The equation may be regarded as the general relativity analogue of the Newtonian equation

$$\frac{dp}{dr} = -\rho \frac{d\Psi}{dr}$$

where ρ is now expressed in terms of mass per unit volume, and indeed can be shown to reduce to this in case the gravitational field is weak and the sys-

⁶ See Eddington, reference 4, equation (55.6).

tem consists of ordinary matter with the pressure p_0 negligible compared with the density ρ_{00} .

It is also of interest to note that equation (22) can alternatively be derived by combining equations (17), (18) and (19), without the use of the mechanical principle given by equation (21). The mechanical principle and the equality of the two different expressions for pressure thus imply the same restrictions on the pressure distribution within the sphere.

Returning now to the mechanical equation (21) and considering the cases $\sigma=2$ and $\sigma=3$, it is easy to show by a similar method to the one just used that we obtain the results

$$\frac{\partial p_0}{\partial \theta} = \frac{\partial p_0}{\partial \phi} = 0 \quad (23)$$

as was to be expected.

Finally, considering the case $\sigma=4$, we obtain by substitution into (21)

$$\frac{\partial}{\partial t}(\rho_{00} \sqrt{-g}) - \frac{1}{2} \mathfrak{T}^{\alpha\beta} \frac{\partial g_{\alpha\beta}}{\partial t} = 0$$

and since by our hypothesis of a static system the $g_{\alpha\beta}$ are independent of the time t , we have the result

$$\frac{\partial \rho_{00}}{\partial t} = 0 \quad (24)$$

the proper density remaining constant with time at each point in the distribution, in complete agreement with our original assumption of a static system

§5. MECHANICAL TREATMENT OF TEMPERATURE DISTRIBUTION IN THE CASE OF RADIATION

In the case of a spherical distribution of pure black-body radiation such as might surround a gravitating sphere of denser matter, relativistic mechanics without a resort to relativistic thermodynamics will be sufficient to determine the temperature distribution. This arises because of the simple relations in the case of black-body radiation directly connecting the thermodynamic quantity temperature with the mechanical quantities energy density and pressure.

For the energy density and pressure of black-body radiation we can evidently write in accordance with well known equations

$$\rho_{00} = aT_0^4 \quad (25)$$

and

$$p_0 = \frac{1}{3} aT_0^4 \quad (26)$$

where a is the Stefan-Boltzmann constant and T_0 is the *proper* temperature, as measured by a local observer, located at a point where ρ_{00} and p_0 are the proper macroscopic energy density and proper pressure of the radiation.

Substituting these expressions into our mechanical equation (22), we at once obtain as exact relativistic expressions for the temperature distribution within a field of radiation

$$\frac{d \ln T_0}{dr} = -\frac{1}{2} \frac{d\nu}{dr} \quad (27)$$

or

$$T_0 = C e^{-\nu/2} \quad (28)$$

where C is a constant of integration. Furthermore, in the case of weak enough fields so that the Newtonian theory of gravitation is a sufficient approximation, equation (27) can be shown to reduce to

$$\frac{d \ln T_0}{dr} = -\frac{1}{c^2} \frac{d\Psi}{dr} = -\frac{g}{c^2} \quad (29)$$

in agreement with equation (8) obtained by our preliminary treatment. The qualitative nature of this result is entirely reasonable since it is evident that the pressure of radiation must increase as we go to lower gravitational levels in order to support the increasing amount of the radiation above, and in the case of pure radiation such an increase in pressure can only be the result of an increase in temperature.

It is a matter of great interest that we have thus been able to determine, by a straightforward application of relativity mechanics without any resort to the new relativistic thermodynamics, the effect of gravity on temperature distribution in the particular case of a field of pure radiation. We have thus obtained in a rather unimpeachable manner a justification in at least one case for our original general idea, as expressed in §1, that the condition of thermodynamic equilibrium under the action of gravitation would involve higher temperatures at lower gravitational levels in order to prevent the downward flow of heat, and shall be ready to expect similar effects of gravitational action on temperature in more complicated cases whose solution will involve our new system of relativistic thermodynamics.

§6. THE THERMODYNAMIC CONDITIONS FOR EQUILIBRIUM

To prepare for our thermodynamic treatment, we may now restate the conditions for equilibrium in a static system obtained in the previous development of relativistic thermodynamics.⁷ Using the polar coordinates adopted in §4 of this article, these conditions took the form that the general relativity expression for the entropy of the system lying within the spherical shell between the constant radii r_1 to r_2 should be a maximum in accordance with the variational equation

$$\delta \left[4\pi \int_{r_1}^{r_2} \phi_0 e^{3\nu/2} r^2 dr \right] = 0 \quad (30)$$

under the subsidiary condition coming from consideration of the energy-momentum principle

⁷ See in particular §5 in the article in *This Journal*.

$$\delta\mu = \delta\mu' = \delta\nu = \delta\nu' = 0 \quad (\text{at } r_1 \text{ and } r_2) \quad (31)$$

where μ and ν are the exponents occurring in our expression for the line element, and the quantity ϕ_0 occurring in equation (30) is the proper density of entropy.

§7. THERMODYNAMIC TREATMENT OF TEMPERATURE DISTRIBUTION IN THE CASE OF RADIATION

Let us now make use of the thermodynamic method to obtain a treatment of temperature distribution in the case of radiation. To do this we can re-express the entropy density ϕ_0 occurring in equation (30) in terms of energy density ρ_{00} , and by means of our previous relation connecting energy density with the metric can obtain the condition for maximum entropy in a form in which it depends explicitly on the metrical variable μ and its differential coefficients. The variation indicated in equation (30) can then be performed and the subsidiary conditions imposed by equation (31) on the variable μ easily introduced.

For the proper density of entropy ϕ_0 in terms of the proper temperature T_0 we can evidently write in accordance with the well known properties of black-body radiation

$$\phi_0 = \frac{4}{3} a T_0^3 \quad (32)$$

where a is the Stefan-Boltzmann constant. Combining this with equation (25), connecting the energy density with temperature, we obtain

$$\phi_0 = \frac{4}{3} a^{1/4} \rho_{00}^{3/4} \quad (33)$$

and using equation (19) which connects the energy density with the metric we can write

$$\phi_0 = -\frac{4a^{1/4}}{24\pi} e^{-3\mu/4} \left[\mu'' + \frac{2\mu'}{r} + \frac{\mu'^2}{4} \right]^{3/4}. \quad (34)$$

Substituting this into equation (30) and dividing out the constant factors, we finally obtain as the condition of maximum entropy in terms of the metrical variable μ

$$\delta \int_{r_1}^{r_2} \left(\mu'' + \frac{2\mu'}{r} + \frac{\mu'^2}{4} \right)^{3/4} e^{3\mu/4} r^2 dr = 0 \quad (35)$$

under the condition

$$\delta\mu = \delta\mu' = 0 \quad (\text{at } r_1 \text{ and } r_2). \quad (36)$$

Performing the variation indicated in equation (35) we obtain

$$\begin{aligned} \int_{r_1}^{r_2} \left[\frac{3}{4} \left(\mu'' + \frac{2\mu'}{r} + \frac{\mu'^2}{4} \right)^{-1/4} \left(\delta\mu'' + \frac{2}{r} \delta\mu' + \frac{\mu'}{2} \delta\mu' \right) e^{3\mu/4} \right. \\ \left. + \frac{3}{4} \left(\mu'' + \frac{2\mu'}{r} + \frac{\mu'^2}{4} \right)^{3/4} e^{3\mu/4} \delta\mu \right] r^2 dr = 0 \quad (37) \end{aligned}$$

and resubstituting the expression for energy density given by equation (19) this can be rewritten in the simpler form

$$\int_{r_1}^{r_2} \left[\frac{e^{(\mu/2)} r^2}{\rho_{00}^{1/4}} \left(\delta\mu'' + \frac{2}{r} \delta\mu' + \frac{\mu'}{2} \delta\mu' \right) - 8\pi \rho_{00}^{3/4} e^{3\mu/2} r^2 \delta\mu \right] dr = 0$$

Noting, however, in accordance with equation (36) that $\delta\mu'$ and $\delta\mu$ are equal to zero at the limits r_1 and r_2 this can evidently be transformed in the usual manner with the help of partial integrations, dropping terms that become zero at the limits, to the following form containing $\delta\mu$ alone.

$$\int_{r_1}^{r_2} \left[\frac{d^2}{dr^2} \left(\frac{e^{\mu/2} r^2}{\rho_{00}^{1/4}} \right) - 2 \frac{d}{dr} \left(\frac{e^{\mu/2} r}{\rho_{00}^{1/4}} \right) - \frac{d}{dr} \left(\frac{e^{\mu/2} r^2}{\rho_{00}^{1/4}} \frac{\mu'}{2} \right) - 8\pi \rho_{00}^{3/4} e^{3\mu/2} r^2 \right] \delta\mu dr = 0. \quad (38)$$

This equation, however, can be true for arbitrary variations $\delta\mu$ only if the quantity in the square brackets is equal to zero, and this can evidently be rewritten to give us

$$\frac{d}{dr} \left\{ e^{\mu/2} r^2 \frac{d}{dr} \left(\frac{1}{\rho_{00}^{1/4}} \right) \right\} = 8\pi \rho_{00}^{3/4} e^{3\mu/2} r^2. \quad (39)$$

And substituting the relation between energy density ρ_{00} and temperature T_0 given by equation (25), this becomes

$$\frac{d}{dr} \left\{ e^{\mu/2} r^2 \frac{d}{dr} \left(\frac{1}{T_0} \right) \right\} = 8\pi \frac{\rho_{00}}{T_0} e^{3\mu/2} r^2. \quad (40)$$

To solve this equation for T_0 as a function of r , we note that in the case of radiation we have $8\pi\rho_{00}=4\pi(\rho_{00}+3p_0)$ and substituting equation (20) we can then rewrite (40) in the form

$$\frac{d}{dr} \left\{ e^{\mu/2} r^2 \frac{d}{dr} \left(\frac{1}{T_0} \right) \right\} = \frac{e^{-\nu/2}}{T_0} \frac{d}{dr} \left\{ e^{\mu/2} r^2 \frac{d}{dr} (e^{\nu/2}) \right\}$$

or

$$\left(\frac{1}{T_0} \right)^{-1} \frac{d}{dr} \left\{ e^{\mu/2} r^2 \frac{d}{dr} \left(\frac{1}{T_0} \right) \right\} = (e^{\nu/2})^{-1} \frac{d}{dr} \left\{ e^{\mu/2} r^2 \frac{d}{dr} (e^{\nu/2}) \right\}. \quad (41)$$

Postponing a more general discussion of the solution of this equation until the next section, §8, where the equation again occurs, we note at once that a particular solution of the equation is given by

$$T_0 = C e^{-\nu/2} \quad (42)$$

where C is a constant of integration and this equation for the temperature distribution in a field of radiation which has come to equilibrium under the action of gravity is exactly the same as equation (28) which we obtained in §5. Hence in this simple case of radiation, where a mechanical treatment can be given, the thermodynamic and the mechanical treatment of temperature

distribution under the action of gravity lead to the same result. This can be regarded as some confirmation of the validity of the system of relativistic thermodynamics which I have proposed.

§8. TEMPERATURE DISTRIBUTION IN THE GENERAL CASE OF ANY PERFECT FLUID

Let us now consider the application of our condition for a maximum of the relativistic expression for entropy

$$\delta \left[4\pi \int_{r_1}^{r_2} \phi_0 e^{3\mu/2} r^2 dr \right] = 0 \quad (43)$$

to a determination of the temperature distribution in the general case of any perfect fluid. To apply this equation it will be convenient to note that $4\pi e^{3\mu/2} r^2 dr$ is evidently the *proper* spatial volume lying in the spherical shell between r and $r+dr$. This can be seen from the general relation for the element of proper spatial volume

$$dV_0 ds = \sqrt{-g} dx_1 dx_2 dx_3 dx_4$$

which, in the case of our system and line element (9), gives

$$dV_0 = e^{\frac{3\mu+\nu}{2}} r^2 \sin \theta dr d\theta d\phi \frac{dt}{ds} = e^{3\mu/2} r^2 \sin \theta dr d\theta d\phi.$$

And if we integrate this over all values of θ and ϕ , we obtain

$$V_0 = 4\pi e^{3\mu/2} r^2 dr \quad (44)$$

for the proper spatial volume lying between r and $r+dr$, where V_0 is of course an infinitesimal quantity.

Under these circumstances, since ϕ_0 is the proper density of entropy, we may evidently write

$$S_0 = 4\pi \phi_0 e^{3\mu/2} r^2 dr \quad (45)$$

as an expression for the entropy, as measured in proper coordinates, associated with the material lying between r and $r+dr$. As this quantity of entropy is measured in proper coordinates, it will evidently obey the classical laws of thermodynamics and may be taken as a function of temperature T_0 , volume V_0 and number of molecules $N_1, N_2 \dots N_n$ of the n different components which are necessary to specify the composition, in the way ordinarily employed in thermodynamics.

We are now ready to investigate the temperature distribution in our fluid. To do this let us consider the effect of a variation in the temperature T_0 and volume V_0 associated with the shell r to $r+dr$, keeping the composition of the material in this shell unaltered, that is holding $N_1 \dots N_n$ constant. Under these conditions, we shall have in accordance with the principles of ordinary thermodynamics

$$\delta S_0 = \frac{\delta U_0}{T_0} + \frac{p_0}{T_0} \delta V_0 \quad (46)$$

and in accordance with equations (44) and (45) this can evidently be written in the form

$$\delta(4\pi \phi_0 e^{3\mu/2} r^2 dr) = \frac{\delta(4\pi \rho_{00} e^{3\mu/2} r^2 dr)}{T_0} + \frac{p_0}{T_0} \delta(4\pi e^{3\mu/2} r^2 dr). \quad (47)$$

Substituting this in equation (43) for the maximum of the relativistic expression for entropy we now obtain

$$4\pi \int_{r_1}^{r_2} \left[\frac{\delta(\rho_{00} e^{3\mu/2})}{T_0} + \frac{p_0}{T_0} \delta(e^{3\mu/2}) \right] r^2 dr = 0 \quad (48)$$

which gives the condition for a maximum of the relativistic entropy in a form which can be made to depend solely on the variation of the metrical variable μ and its derivatives, by substituting for the energy density ρ_{00} its values as given by equation (19). Doing so we obtain

$$\int_{r_1}^{r_2} \left[-\frac{1}{2T_0} \delta \left\{ e^{\mu/2} \left(\mu'' + \frac{2\mu'}{r} + \frac{\mu'^2}{4} \right) \right\} + \frac{4\pi p_0}{T_0} \delta(e^{3\mu/2}) \right] r^2 dr = 0 \quad (49)$$

Performing the indicated variations, we have

$$\begin{aligned} \int_{r_1}^{r_2} \left[-\frac{e^{\mu/2}}{2T_0} \left(\delta\mu'' + \frac{2\delta\mu'}{r} + \frac{\mu'}{2} \delta\mu' \right) - \frac{e^{\mu/2}}{4T_0} \left(\mu'' + \frac{2\mu'}{r} + \frac{\mu'^2}{4} \right) \delta\mu \right. \\ \left. + \frac{12\pi p_0}{2T_0} e^{3\mu/2} \delta\mu \right] r^2 dr = 0. \end{aligned}$$

Noting, however, that the variations are to be carried out in accordance with equation (31) which gives $\delta\mu' = \delta\mu = 0$ at r_1 and r_2 , the first term in the integrand can evidently be transformed in the usual manner with the help of partial integrations, dropping terms that become zero at the limits, to a form depending on $\delta\mu$ alone; and the second term in the integrand can be simplified by resubstituting equation (19) for the energy density ρ_{00} . We thus obtain

$$\int_{r_1}^{r_2} \left[\frac{d^2}{dr^2} \left(\frac{e^{\mu/2} r^2}{T_0} \right) - 2 \frac{d}{dr} \left(\frac{e^{\mu/2} r}{T_0} \right) - \frac{d}{dr} \left(\frac{e^{\mu/2} r^2}{T_0} \frac{\mu'}{2} \right) - \frac{4\pi(\rho_{00} + 3p_0)}{T_0} e^{3\mu/2} r^2 \right] \delta\mu dr = 0.$$

This equation can be true, however, for arbitrary variations $\delta\mu$ only if the term in square brackets is equal to zero, and this can evidently be rewritten to give us

$$\frac{d}{dr} \left\{ e^{\mu/2} r^2 \frac{d}{dr} \left(\frac{1}{T_0} \right) \right\} = \frac{4\pi(\rho_{00} + 3p_0)}{T_0} e^{3\mu/2} r^2 \quad (50)$$

and substituting equation (20), we finally obtain as an expression connecting T_0 with the coordinate r and the metrical variables μ and ν

$$\frac{d}{dr} \left\{ e^{\mu/2} r^2 \frac{d}{dr} \left(\frac{1}{T_0} \right) \right\} = \frac{e^{-\nu/2}}{T_0} \frac{d}{dr} \left\{ e^{\mu/2} r^2 \frac{d}{dr} (e^{\nu/2}) \right\}. \quad (51)$$

This differential equation for T_0 is the same as equation (41) which we got when we applied the thermodynamic method to pure radiation. A first integral for this equation can be written in the form

$$\frac{d \ln T_0}{dr} = -\frac{1}{2} \frac{d\nu}{dr} + \frac{B e^{-\frac{\mu+\nu}{2}}}{r^2} T_0 \quad (52)$$

where B is a constant of integration, and substituting equation (22) this can be written as

$$\frac{d \ln T_0}{dr} = \frac{1}{\rho_{00} + p_0} \frac{dp_0}{dr} + \frac{B e^{-\frac{\mu+\nu}{2}}}{r^2} T_0.$$

If, however, we now assume on physical grounds that at the center of the sphere $r=0$, we have dT_0/dr and dp_0/dr equal to zero, T_0 not equal to zero and the other functions of r finite, it is evident that the constant of integration B must be equal to zero.⁸ Under these circumstances the second integral of our equation is then easily seen to be

$$T_0 = C e^{-\nu/2} \quad (53)$$

where C is a second constant of integration.

This result is exactly of the same form as that obtained for radiation alone and that is a satisfactory outcome since our method of derivation did not involve the assumption that any matter at all was necessarily present. The equation gives a definite relation connecting the equilibrium temperature in a gravitational field with the variable ν which is itself determined in a known way by the gravitational field. The general nature of the result can perhaps be more easily appreciated by redifferentiating equation (53) with respect to r and substituting equation (22). We then obtain

$$\frac{d \ln T_0}{dr} = -\frac{1}{2} \frac{d\nu}{dr} = \frac{1}{\rho_{00} + p_0} \frac{dp_0}{dr} \quad (54)$$

and can at once see that temperature and pressure will increase together as we go towards the center of the sphere. It is also of interest to note once more the approximation

$$\frac{d \ln T_0}{dr} = -\frac{1}{c^2} \frac{d\Psi}{dr} = -\frac{g}{c^2}$$

⁸ It would be interesting to investigate the possibility of solutions of physical interest with $B \neq 0$.

valid in weak enough fields so that the Newtonian method is applicable, and this is the same equation as was obtained in our preliminary non-rigorous treatment.⁹

§9. THE DISTRIBUTION OF MATTER IN A SPHERE OF PERFECT FLUID

The principles of relativistic thermodynamics which we have used in the preceding section should be sufficient to give us information not only as to the temperature distribution in a sphere of fluid but also as to the equilibrium distribution of matter. To obtain such information let us return once more to our condition for a maximum of the relativistic expression for entropy

$$\delta \left[4\pi \int_{r_1}^{r_2} \phi_0 e^{3\mu/2} r^2 dr \right] = 0. \quad (55)$$

In using this equation to determine the distribution of temperature, we considered the result of varying the temperature as a function of r , holding constant the number of molecules $N_1 \cdots N_n$ of each of the different components of the system in each spherical shell lying between r and $r+dr$. To determine the distribution of matter, on the other hand, we may hold the temperature constant and consider the result of varying the composition of the layers. As simple illustrations, we shall apply this method to a system consisting of a mixture of a perfect monatomic gas and radiation, both on the assumption that radiation and matter are interconvertible, and on the assumption that the total number of molecules in the system cannot be varied.

For the proper density of entropy of a mixture of perfect monatomic gas and radiation, we may evidently write in accordance with well known equations

$$\phi_0 = N_0 k \ln \frac{CT_0^{3/2}}{N_0} + \frac{4}{3} a T_0^3 \quad (56)$$

where N_0 is the number of molecules in unit volume as measured in proper coordinates by a local observer, T_0 is the proper temperature, k and a are respectively the Boltzmann constant and Stefan constant, and C is a constant so chosen that the starting points for the measurement of the entropy of matter and radiation will be in agreement.

If now we vary the proper concentration of molecules N_0 holding the temperature T_0 constant, we obtain

$$\delta \phi_0 = \left(k \ln \frac{CT_0^{3/2}}{N_0} - k \right) \delta N_0. \quad (57)$$

On the other hand for the proper density of energy we evidently have

$$\rho_{00} = N_0 m c^2 + \frac{3}{2} N_0 k T_0 + a T_0^4 \quad (58)$$

⁹ As a justification for the results of this section, my colleague Dr. J. Robert Oppenheimer has kindly pointed out to me that the relation which I have obtained between temperature and gravitational potential is a necessary one if the Planck radiation law is to hold at different gravitational levels.

where m is the rest mass of one molecule and c the velocity of light, $-mc^2$ thus being the internal energy and $(3/2)kT_0$ the average kinetic energy per molecule. Hence, holding the temperature constant as before, and varying N_0 we obtain

$$\delta\rho_{00} = (mc^2 + \frac{3}{2}kT_0)\delta N_0 \quad (59)$$

and by combining equations (57) and (59) we can express the variation in the density of entropy in terms of the variation in density of energy in the form

$$\delta\phi_0 = \frac{k \ln CT_0^{3/2}/N_0 - k}{mc^2 + 3/2kT_0} \delta\rho_{00}$$

or

$$\delta\phi_0 = f(N_0, T_0) \delta\rho_{00} \quad (60)$$

where for simplification we have written $f(N_0, T_0)$ as an abbreviation for the coefficient of $\delta\rho_{00}$.

Since $\delta\rho_{00}$, however, can be expressed as a function of the metrical variable μ , we can now return to our equation (55) for maximum entropy and write as a condition for equilibrium

$$4\pi \int_{r_1}^{r_2} [\delta\phi_0 e^{3\mu/2} + \frac{3}{2}\phi_0 e^{3\mu/2} \delta\mu] r^2 dr = 0$$

or substituting equation (60)

$$4\pi \int_{r_1}^{r_2} [f(N_0, T_0) e^{3\mu/2} \delta\rho_{00} + \frac{3}{2}\phi_0 e^{3\mu/2} \delta\mu] r^2 dr = 0 \quad (61)$$

and substituting in turn the value of ρ_{00} in terms of the metrical variable give by equation (19) we obtain

$$\begin{aligned} \int_{r_1}^{r_2} \left[-\frac{1}{2}f(N_0, T_0)e^{\mu/2} \left(\delta\mu'' + \frac{2}{r}\delta\mu' + \frac{\mu'}{2}\delta\mu' \right) \right. \\ \left. + \frac{1}{2}f(N_0, T_0)e^{\mu/2} \left(\mu'' + \frac{2\mu'}{r} + \frac{\mu'^2}{4} \right) \delta\mu + 4\pi\frac{3}{2}\phi_0 e^{3\mu/2} \delta\mu \right] r^2 dr = 0. \end{aligned}$$

Noting as in previous sections, however, that the variations are to be carried out in accordance with equation (31) which gives $\delta\mu' = \delta\mu = 0$ at r_1 and r_2 , the first term in the integrand can evidently be transformed in the usual manner with the help of partial integrations, dropping terms that become zero at the limits, to a form depending on $\delta\mu$ alone; and the second term in the integrand can be simplified by resubstituting equation (19) for the energy density ρ_{00} . We thus obtain

$$\begin{aligned} \int_{r_1}^{r_2} \left[\frac{d^2}{dr^2} \{ f(N_0, T_0) e^{\mu/2} r^2 \} - 2 \frac{d}{dr} \{ f(N_0, T_0) e^{\mu/2} r \} \right. \\ \left. - \frac{d}{dr} \left\{ f(N_0, T_0) e^{\mu/2} r^2 \frac{\mu'}{2} \right\} + 4\pi \{ 2f(N_0, T_0)\rho_{00} - 3\phi_0 \} e^{3\mu/2} r^2 \right] \delta\mu dr = 0 \end{aligned}$$

and combining the first three terms this can be rewritten in the form

$$\int_{r_1}^{r_2} \left[\frac{d}{dr} \left\{ e^{\mu/2} r^2 \frac{d}{dr} f(N_0, T_0) \right\} + 4\pi \{ 2f(N_0, T_0) \rho_{00} - 3\phi_0 \} e^{3\mu/2} r^2 \right] \delta\mu dr = 0. \quad (62)$$

This equation has resulted from an application of the condition for maximum relativistic entropy under the subsidiary condition, given by equation (31), which satisfies the requirements of the energy-momentum principle. In case we assume the ready interconvertibility of matter and radiation no further subsidiary conditions need be introduced. On the other hand, if we are interested in what might be only a temporary condition of equilibrium reached in a length of time such that the total number of molecules could not change, we must evidently add as a further subsidiary condition

$$\delta \left[4\pi \int_{r_1}^{r_2} N_0 e^{3\mu/2} r^2 dr \right] = 0 \quad (63)$$

where N_0 is the proper concentration of molecules and as we saw above $4\pi e^{3\mu/2} r^2 dr$ is the proper volume in the spherical shell lying between r and $r+dr$.

Performing the indicated variation, keeping of course the temperature constant as in the previous variation, and substituting the value for δN_0 given by equation (58), we obtain

$$4\pi \int_{r_1}^{r_2} \left[\frac{e^{3\mu/2}}{mc^2 + (3/2)kT_0} \delta\rho_{00} + \frac{3}{2} N_0 e^{3\mu/2} \delta\mu \right] r^2 dr = 0.$$

This equation, however, is of the same general form as (61) above, and can be treated by the same methods which led from (61) to (62), and will then evidently reduce to

$$\int_{r_1}^{r_2} \left[\frac{d}{dr} \left\{ e^{\mu/2} r^2 \frac{d}{dr} \left(\frac{1}{mc^2 + (3/2)kT_0} \right) \right\} + 4\pi \left\{ \frac{2\rho_{00}}{mc^2 + (3/2)kT_0} - 3N_0 \right\} e^{3\mu/2} r^2 \right] \delta\mu dr = 0. \quad (64)$$

Equations (64) and (62) may now be combined by the method of Lagrange to give us a single condition

$$\int_{r_1}^{r_2} \left[\frac{d}{dr} \left\{ e^{\mu/2} r^2 \frac{d}{dr} \left(f(N_0, T_0) + \frac{\lambda}{mc^2 + (3/2)kT_0} \right) \right\} + 4\pi \left\{ 2 \left(f(N_0, T_0) + \frac{\lambda}{mc^2 + (3/2)kT_0} \right) \rho_{00} - 3\phi_0 - 3\lambda N_0 \right\} e^{3\mu/2} r^2 \right] \delta\mu dr = 0$$

where λ is a constant undetermined multiplier, whose value will be zero in case equilibrium between matter and radiation is established, since the additional condition (63) will then not be needed. This equation, however, can only be true for arbitrary variations $\delta\mu$, if the quantity in square brackets

is equal to zero. Hence, resubstituting the value of $f(N_0, T_0)$ given by equation (60) we have as our final differential equation

$$\frac{d}{dr} \left\{ e^{\mu/2} r^2 \frac{d}{dr} \frac{k \ln CT_0^{3/2}/N_0 - k + \lambda}{mc^2 + (3/2)kT_0} \right\} = 4\pi \left\{ 3\phi_0 + 3\lambda N_0 - 2 \frac{k \ln CT_0^{3/2}/N_0 - k + \lambda}{mc^2 + (3/2)kT_0} \rho_{00} \right\} e^{3\mu/2} r^2 \quad (65)$$

where $\lambda=0$ in case the equilibrium between matter and radiation is established.

We have thus obtained a second order differential equation connecting the thermodynamic quantities concentration N_0 and temperature T_0 with the coordinate r . We have already found in the previous section, §8, however, equations for T_0 as a function of r , and hence the present equation requires that N_0 be such a function of T_0 as not to disagree with the previous results. We shall then suggest as an expression for the dependence of N_0 on T_0 and hence implicitly on r

$$k \ln \frac{CT_0^{3/2}}{N_0} - k + \lambda = \frac{mc^2}{T_0} + \frac{3}{2}k \quad (66)$$

or

$$N_0 = C e^{\lambda/k - 5/2} T_0^{3/2} e^{-mc^2/kT_0}$$

and test the suggestion by substituting into (65). Doing so, we obtain

$$\frac{d}{dr} \left\{ e^{\mu/2} r^2 \frac{d}{dr} \left(\frac{1}{T_0} \right) \right\} = 4\pi \left\{ 3\phi_0 + 3\lambda N_0 - \frac{2\rho_{00}}{T_0} \right\} e^{3\mu/2} r^2.$$

Comparing the first form of equation (66), however, with the expression for ϕ_0 given by (56), and introducing the expression for ρ_{00} given by (58), we obtain

$$\begin{aligned} \frac{d}{dr} \left\{ e^{\mu/2} r^2 \frac{d}{dr} \left(\frac{1}{T_0} \right) \right\} &= 4\pi \left\{ \frac{3N_0 mc^2}{T_0} + \frac{15}{2} N_0 k - 3\lambda N_0 + 4a T_0^3 \right. \\ &\quad \left. + 3\lambda N_0 - 2 \frac{N_0 mc^2}{T_0} - 3N_0 k - 2a T_0^3 \right\} e^{3\mu/2} r^2 \\ &= 4\pi \left\{ \frac{N_0 mc^2 + (3/2)N_0 k T_0 + a T_0^4 + 3(N_0 k T_0 + (a/3)T_0^4)}{T_0} \right\} e^{3\mu/2} r^2 \\ &= 4\pi \frac{(\rho_{00} + 3p_0)}{T_0} e^{3\mu/2} r^2 \end{aligned} \quad (67)$$

since the gas pressure is evidently $N_0 k T_0$ and the radiation pressure $\frac{1}{3}aT_0^4$. And this equation is exactly the same as our general equation (50) for the dependence of temperature on the coordinate and metric as obtained in the previous section §8. Hence our suggested expression equation (66) for the dependence of the concentration on temperature can be accepted as

satisfying the information previously obtained as to the dependence of temperature on the metric, and thus as a satisfactory solution of the problem of the distribution of a perfect monatomic gas in a gravitational field.

It is also significant to point out that equation (66) can be subjected to another test, since this expression for the proper concentration of the gas makes it possible to calculate the partial pressure of the gas and by combining with the partial pressure of radiation, then examine the dependence of total pressure on the radius r to see if it agrees with the purely mechanical equation $dp_0/dr = -(\rho_{00} + p_0)v'/2$, obtained in §4. And as a matter of fact equation (66) does lead to this result.¹⁰

Finally, it is interesting to compare the dependence of proper concentration on proper temperature given by equation (66) with the result obtained for the equilibrium concentration in flat space-time by Stern¹¹ and myself.¹² Taking the case where equilibrium between matter and radiation has been established, we have $\lambda = 0$ and equation (66) can be written

$$N_0 = (Ce^{5/2}) T_0^{3/2} e^{-mc^2/kT_0}$$

which agrees with my previous result as it stands, and agrees with the Stern result if we assign to the constant term $(Ce^{5/2})$ the not necessarily correct value which Stern obtained for it. Hence the conclusion can again be stated, owing to the great magnitude of the negative exponent for reasonable values of m and T , that the equilibrium concentration would be extremely small unless the constant term could be shown to have an enormous magnitude.

§10. CONCLUSION

In accordance with the special theory of relativity and the equivalence principle all forms of energy, including heat, must be regarded as having both inertia and weight, and the purpose of the present article has been to investigate, in as consequent a manner as may be, the thermodynamic implications of the notion that heat has weight. The most striking result of the investigation has been the discovery of a definite relation connecting gravitational potential with the distribution of temperature throughout a system which has come to thermodynamic equilibrium.

Qualitatively, the increase in equilibrium temperature which was found to accompany decrease in gravitational potential, may be regarded as due to the necessity of having a temperature gradient to prevent the flow of heat from places of higher to those of lower potential energy; and quantitatively, a first approximation to the magnitude of this temperature gradient was

¹⁰ It may seem strange that this purely mechanical equation holding within the interior of the system should be derivable from the application of thermodynamics to the system as a whole. The result, however, is the relativity analogue to the equation for change in pressure with height obtained by Gibbs ("Scientific Papers," Longmans, Green 1906, equation 230, p. 145) in his thermodynamic treatment of the conditions of equilibrium under the influence of gravity. Indeed the whole treatment of this article may be regarded as the relativistic extension of this part of Gibbs' work.

¹¹ Stern, *Zeits. f. Elektrochem.* **31**, 448 (1925); *Trans. Farad. Soc.* **21**, 477 (1925-26).

¹² Tolman, *Proc. Nat. Acad.* **12**, 670 (1926).

obtained by modifying the classical thermodynamics merely by ascribing to each given intrinsic quantity of energy the right additional quantity of potential gravitational energy. For a rigorous treatment, however, it was obviously necessary to investigate the whole problem from the standpoint of general relativity, and this was done using the extension of thermodynamics to general relativity which I have previously given. In this way it was possible to obtain what appears to be a rigorous equation connecting equilibrium temperature with gravitational potential. In addition in the case of black-body radiation it was possible to test the thermodynamic method, since the same temperature distribution in the case of this simple system was also obtained by the use of relativistic mechanics, without the necessity for the use of the new relativistic thermodynamics.

This discovery of a dependence of equilibrium temperature on gravitational potential must be regarded as something essentially new in thermodynamics, since uniform temperature throughout any system which has come to equilibrium has hitherto been taken as an inescapable part of thermodynamic theory. The new result hence has a very considerable theoretical interest, and even though the effect of gravitational potential on temperature may usually be extremely small the result may sometime be of experimental or observational interest.

THE DETERMINATION OF ELECTRON DISTRIBUTIONS FROM MEASUREMENTS OF SCATTERED X-RAYS

BY ARTHUR H. COMPTON

RYERSON PHYSICAL LABORATORY, UNIVERSITY OF CHICAGO

(Received March 5, 1930)

ABSTRACT

A calculation based on classical electromagnetic theory is made of the intensity of the x-rays scattered by an atom in which the electrons are arranged with random orientation and with arbitrary radial distribution. Conversely an expression is derived for the radial distribution of the electrons in an atom, assuming that they have random orientation. This expression has the form of a Fourier integral, which can be evaluated from observed intensities of the scattered x-rays for different wave-lengths and angles.

A comparison of this calculation with Wentzel's quantum theory of x-ray scattering suggests the introduction of a certain correction factor to express more nearly the intensity of the modified rays. It is also noted that the interpretation of $\psi\bar{\psi}$ as a probability of the occurrence of an electron leads to the correct value for the intensity of total scattered x-rays.

As an example of the application of the new method of calculation, Barrett's experimental data for the scattering of x-rays by helium are analyzed to give the distribution of the electrons in the helium atom. The resulting distribution is in close agreement with the value calculated by Pauling on the basis of wave mechanics, but differs by more than the probable experimental error from the electron orbits given by Bohr's theory.

1. INTRODUCTION

IT IS well known that the intensity of the x-rays scattered at small angles may be considerably greater than is anticipated on the assumption that each electron in the scattering material acts independently of the other electrons. When the scattering of x-rays by solids and liquids is considered, at least a part of this "excess scattering" may be ascribed to the interference between the rays scattered by neighboring atoms. In the case of gases, however, such interference is negligible, since the phases of the rays scattered by neighboring molecules are random. It has nevertheless long been recognized¹ that groupings of the electrons in the atoms themselves should result in some excess scattering in the forward direction. Calculations of the intensity of the scattered x-rays for typical electron distributions have in fact been made by Debye,² Schott,³ the writer,⁴ Glocker⁵ and others. The converse problem of determining the electron distribution corresponding to an observed angular

¹ D. L. Webster, Phil. Mag. **25**, 234 (1913); C. G. Darwin, Phil. Mag. **27**, 325 (1914).

² P. Debye, Ann. d. Physik **46**, 809 (1915).

³ G. A. Schott, Proc. Roy. Soc. **96**, 695 (1920).

⁴ A. H. Compton, Washington University Studies, **8**, 98 (1921).

⁵ R. Glocker, Zeits. f. Physik **5**, 54 (1921).

distribution of scattered x-rays has not however been attempted. We shall in the present paper obtain a solution of this problem which applies to certain important cases, and illustrate its application by determining the electron distribution in atoms of helium.

Because of the very important information which can thus be obtained regarding atomic structures, the problem would doubtless have been long ago pressed to a solution had it not been for an obstinate theoretical difficulty. Calculations of the effect of interference on the intensity of x-ray scattering are based upon the classical electron theory and electrodynamics. In the course of these x-ray diffraction studies, however, it became evident⁶ that these classical theories are inadequate to supply a complete solution of the problem of the intensity of scattered rays. The problem was accordingly "laid on the table" until a new quantum dynamics should be developed which would be able to supply a more reliable solution. Recently Wentzel⁷ has shown how the wave mechanics may be applied to this problem, and from his discussion it appears that the classical electron theory itself should give results which are not greatly in error.

In the meantime, closely allied problems have been successfully attacked on the basis of classical electron theory. In our studies of the diffraction of x-rays by crystals, which is of course only a special case of the general problem of x-ray scattering, application of the usual wave theory has enabled us to arrive at satisfactory arrangements of the atoms in the crystals, and has recently been used to determine also electron distributions in the atoms.⁸ We have every reason to believe that the information supplied by this work regarding atomic arrangements is reliable, and even the electron distributions found by its use are too satisfactory to admit any major error in the method of analysis. Similarly the classical wave diffraction theory has been successfully applied to the x-ray study of molecular shapes and sizes of liquids,⁹ and very recently also to the study of interatomic distances in gaseous molecules.¹⁰ We are thus encouraged to undertake again a more detailed analysis of the scattering of x-rays by gases, on the basis of classical theory. The results of this analysis will then be compared with Wentzel's conclusions, to see what modifications are necessary in light of quantum mechanics.

2. INTENSITY OF THE X-RAYS SCATTERED BY A GROUP OF ELECTRONS HAVING A RANDOM ANGULAR DISTRIBUTION

Let us suppose that an atom has Z electrons whose distances from the nucleus are at any instant $r_1, r_2 \dots r_s$, and whose angular distribution is random. We imagine that this atom is traversed by an x-ray wave propagated

⁶ A. H. Compton, Bull. Nat. Res. Council No. 20, p. 10 (1922).

⁷ G. Wentzel, Zeits. f. Physik 43, 1 and 779 (1927).

⁸ For summaries of the latter work, cf. e.g., A. H. Compton, "X-rays and Electrons," Chapter V, or W. L. Bragg, "Electrons et Photons," report of the Fifth Solvay Congress, Paris (1928).

⁹ For a summary of this work, cf. e.g., G. W. Stewart, Phys. Rev. Supp., Jan., 1930.

¹⁰ P. Debye, L. Bewilogua and F. Ehrhardt, Phys. Zeits. 30, 84 (1929); Ber. Sächsischen Ak. d. Wiss. zu Leipzig 81, 29 (1929).

along the X axis, and that the forced oscillations of the electrons give rise to a scattered wave at an arbitrary distant point P at an angle ϕ . If A_e is the amplitude of the electric vector and δ the phase at P of the wave scattered by an electron coincident with the nucleus, the electric vector due to the n^{th} electron in the group is (Fig. 1),

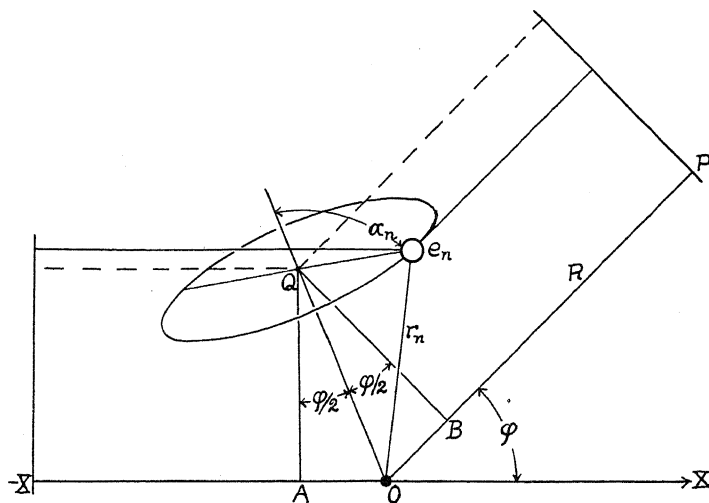


Fig. 1.

$$E_n = A_e \cos \left\{ \delta - (2\pi/\lambda) 2r_n \cos \alpha_n \sin (\phi/2) \right\}, \quad (1)$$

where $2r_n \cos \alpha_n \sin (\phi/2)$ is the total difference in path¹¹ between the ray scattered from e_n and that scattered from O , and α_n is the angle between Oe_n and the line OQ which bisects the angle $-XOP$. Equation (1) may be written

$$E_n = A_e \cos (\delta - x_n), \quad (2)$$

where

$$x_n = (4\pi r_n / \lambda) \cos \alpha_n \sin (\phi/2). \quad (3)$$

The total electric vector due to all the electrons in the atomic group is then,

$$E = \sum_1^Z E_n = A_e \sum_1^Z \cos (\delta - x_n). \quad (4)$$

Let us choose the origin of time such that the phase of the wave scattered from O is $\delta = pt$, where $p = 2\pi\nu$ is the phase frequency of the incident wave. The electric vector at the instant t is then, from Eq. (4),

$$\begin{aligned} E &= A_e \sum_1^Z \cos (pt - x_n) \\ &= A_e \sum_1^Z (\cos pt \cos x_n + \sin pt \sin x_n). \end{aligned} \quad (5)$$

¹¹ Cf. e.g., A. H. Compton, "X-rays and Electrons," p. 385.

The intensity of the scattered ray at this instant is however proportional to E^2 , say bE^2 , or,

$$I_i = bA_e^2 \left\{ \sum_1^Z (\cos pt \cos x_n + \sin pt \sin x_n) \right\}^2. \quad (6)$$

When this expression is averaged over a complete cycle, from $t=0$ to $t=2\pi/p$, all the terms in the summation disappear except those of the form

$$\cos x_m \cos x_n + \sin x_m \sin x_n,$$

and we find for the intensity averaged over a cycle,

$$I_\alpha = \frac{1}{2} bA_e^2 \sum_1^Z \sum_1^Z (\cos x_m \cos x_n + \sin x_m \sin x_n). \quad (7)$$

For a single electron, this becomes

$$I_e = \frac{1}{2} bA_e^2. \quad (8)$$

As Thomson has shown,¹² for unpolarized x-rays

$$I_e = \frac{Ie^4}{2m^2R^2c^4} (1 + \cos^2 \phi), \quad (9)$$

where I is the intensity of the primary beam traversing the electron, e , m and c have their usual significance, and R is the distance from O to P . Equation (7) may thus be written,

$$I_\alpha = I_e \sum_1^Z \sum_1^Z (\cos x_m \cos x_n + \sin x_m \sin x_n). \quad (10)$$

Since we have assumed that the electrons have random angular distribution, we must now average this intensity over all angles α_n . The probability that any α will lie between α and $\alpha + d\alpha$ is for random orientation $\frac{1}{2} \sin \alpha d\alpha$. Writing then

$$x_n = z_n \cos \alpha_n, \quad (11)$$

where

$$z_n = (4\pi r_n / \lambda) \sin (\phi/2), \quad (12)$$

the probable contribution to the intensity due to the orientations α_n is

$$\begin{aligned} dI_\alpha = I_e \left\{ \sum_1^Z \sum_1^Z \sum_{m \neq n} \frac{1}{2} [\cos (z_m \cos \alpha_m) \cos (z_n \cos \alpha_n) \right. \\ \left. + \sin (z_m \cos \alpha_m) \sin (z_n \cos \alpha_n)] \times \sin \alpha_m \sin \alpha_n d\alpha_m d\alpha_n \right. \\ \left. + \sum_1^Z \frac{1}{2} [\cos^2 (z_n \cos \alpha_n) + \sin^2 (z_n \cos \alpha_n)] \sin \alpha_n d\alpha_n \right\}. \end{aligned}$$

¹² J. J. Thomson, *Conduction of Electricity through Gases*, 2nd Ed., p. 325; or cf. "X-rays and Electrons," p. 60.

Integrating over all values of α_m and α_n this takes the simple form,

$$I_r = I_e \left\{ Z + \sum_1^Z \sum_{m \neq n}^Z \frac{\sin z_m}{z_m} \frac{\sin z_n}{z_n} \right\}. \quad (13)$$

Equation (13) represents the scattering by electrons arranged at fixed distances $r_1, r_2 \dots$ from the nucleus, but with random orientations.

As an example of the application of this formula, consider the case of an atom with two electrons, both at a distance $r=a$ from the center, but with random orientations. We may write equation (13) in the form

$$S \equiv \frac{I_r}{ZI_e} = 1 + \frac{1}{Z} \sum \sum_{m \neq n} \frac{\sin z_m \sin z_n}{z_m z_n}, \quad (14)$$

which in the present case becomes,

$$S = 1 + \left(\frac{\sin z_a}{z_a} \right)^2. \quad (15)$$

A graph of this expression is shown in Fig. 2 by the solid line. This may be compared with scattering by two electrons separated by a fixed distance $2a$, which is given by the expression¹³

$$S = 1 + \frac{\sin 2z_a}{2z_a}, \quad (16)$$

and is represented in the figure by the broken line.

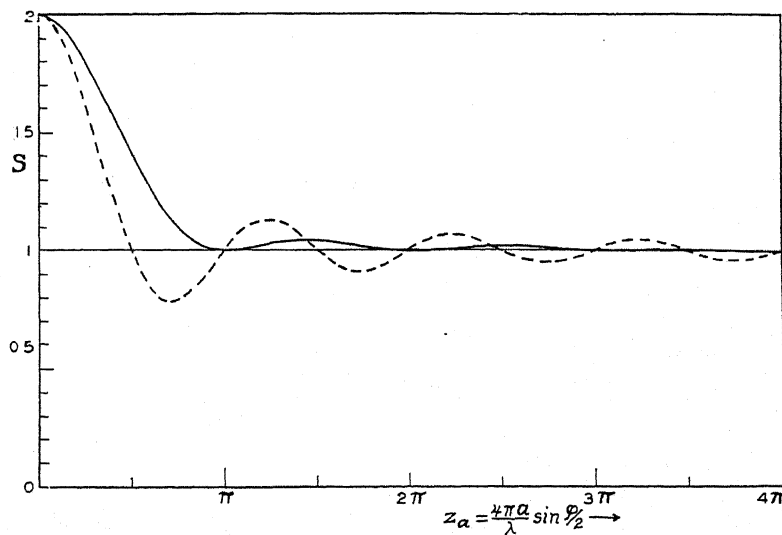


Fig. 2. Relative scattering per electron for an atom of two electrons. Solid line, both electrons at radius a and random orientation. Broken line, electrons at opposite ends of diameter $2a$.

¹³ P. Debye, reference 2, or "X-rays and Electrons," p. 72.

If the probability that any one electron shall lie between r and $r+dr$ is $u(r)dr$, and if this probability is the same for every electron, we have,

$$dI_s = I_e \left\{ Z + \sum \sum_{m \neq n} \frac{\sin kr_m \sin kr_n}{k^2 r_m r_n} u(r_m) u(r_n) dr_m dr_n \right\},$$

where

$$k \equiv z_m/r_m = (4\pi/\lambda) \sin(\phi/2). \quad (17)$$

Since $u(r_m)$ assumed the same for all electrons, the integral of this expression may be written,

$$I_s = I_e Z + I_e \sum \sum_{m \neq n} \left\{ \int_0^a u(r) \frac{\sin kr}{kr} dr \right\}^2,$$

where a is the maximum radius of the atom.

Since

$$\sum_1^Z \sum_{m \neq n}^Z 1 = Z^2 - Z,$$

$$I_s = I_e \left\{ Z + (Z^2 - Z) \left[\int_0^a u(r) \frac{\sin kr}{kr} dr \right]^2 \right\}. \quad (18)$$

For the relative scattering per electron we thus have

$$S = \frac{I_s}{ZI_e} = 1 + (Z - 1) \left\{ \int_0^a u(r) \frac{\sin kr}{kr} dr \right\}^2. \quad (19)$$

Expressions (13) or (18) may be applied to calculate the intensity of the rays scattered by an electron group, according as the electrons are at fixed distances from the center of the atom, or as they have a continuous radial distribution.

According to equation (18), I_s should never fall below ZI_e , since the term representing the interference is always positive. In this respect our calculation differs from that of Debye,² who considers electrons at fixed distances from each other, of which equation (16) is the simplest example.

3. COMPARISON WITH RESULTS OF QUANTUM MECHANICS.

Wentzel's equation (3a) for the intensity of the modified scattered rays¹⁴ may be written in the form

$$I_{unm} = I_e \left\{ \int \sum_n 4\pi r_n^2 \rho_n \frac{\sin kr}{kr} dr \right\}, \quad (20)$$

where $\sum \rho_n = \sum u_n$,² the electrical charge distribution in electronic units, the subscript indicating the n^{th} quantum number. Noting that $\sum 4\pi r^2 \rho_n$ is numerically equal to our $Zu(r)$, this may be written

$$I_{unm} = I_e \cdot Z^2 \left\{ \int u(r) \frac{\sin kr}{kr} dr \right\}^2. \quad (21)$$

¹⁴ G. Wentzel, reference 7, p. 781.

His equation (4a) for the intensity of the modified scattered rays (uncorrected for the change of wave-length) may similarly be written

$$I_{\text{mod}} = I_e \left\{ Z - \sum \left[\int 4\pi r^2 \rho_n \frac{\sin kr}{kr} dr \right]^2 \right\}. \quad (22)$$

The total intensity of the scattered rays thus becomes,

$$\begin{aligned} I_s &= I_{\text{unm}} + I_{\text{mod}} \\ &= I_e \left\{ Z - \sum \left[\int 4\pi r^2 \rho_n \frac{\sin kr}{kr} dr \right]^2 + Z^2 \left[\int u(r) \frac{\sin kr}{kr} dr \right]^2 \right\}. \end{aligned} \quad (23)$$

This expression becomes identical with equation (18) if

$$4\pi r^2 \rho_n = u(r). \quad (24)$$

We have noted above that

$$\sum_1^Z 4\pi r^2 \rho_n = Zu(r), \quad (25)$$

whence relation (24) holds if

$$\sum_1^Z 4\pi r^2 \rho_n = Z \cdot 4\pi r^2 \rho_n, \quad (26)$$

i.e. if the charge distribution for every electron is the same. This is precisely the assumption on which equation (18) is derived. Wentzel, in his numerical calculation of equation (22) takes

$$\rho_n = u_n^2 \quad (27)$$

as the charge density for the n th electron, instead of

$$\rho_n = (1/Z) \sum_1^Z u_n^2, \quad (28)$$

which is the equivalent of (26). This introduces a slight difference between the results of his calculation and that of ours. It would seem however that relation (28) is in better accord with present interpretation of quantum mechanics than is (27), and if its validity is admitted, our classical equation (18) becomes identical with Wentzel's quantum equation (23).

This comparison shows that if we interpret $\sum u_n^2 dx dy dz$ as the electric charge in the volume element, the scattering which we calculate is the *unmodified* scattering (eq. 21). If, however, we interpret it as the probability that a discrete electron will be present in the volume element, as we have done in deriving equation (18), we calculate the *total* scattering. Since the total scattering is experimentally observed, it would seem that the latter interpretation has the better physical justification.

In his derivation of equation (22), Wentzel has assumed the limiting case of very long wave-lengths, for which the scattering by a free electron is identical with that calculated on the classical theory. For shorter wave-lengths

Breit¹⁵ and Dirac¹⁶ have shown that the intensity of the modified rays from free electrons is reduced in the ratio

$$\frac{I_{\text{mod}}}{I_{\text{class}}} = \left(\frac{\lambda}{\lambda'} \right)^3 = (1 + \gamma \text{vers } \phi)^3, \quad (29)$$

where λ and λ' are the wave-lengths of the primary and the modified ray respectively, and $\gamma = h/mc\lambda$. We may accordingly expect to get a closer approximation to the intensity of the modified scattering if we multiply equation (22) by equation (29), or using the equivalent part of equation (18),

$$I_{\text{mod}} = Z I_e (1 - F^2/Z^2) (1 + \gamma \text{vers } \phi)^{-3}. \quad (30)$$

Similarly¹⁷

$$I_{\text{unm}} = I_e F^2, \quad (31)$$

where

$$F = Z \int_0^a u(r) \frac{\sin kr}{kr} dr, \quad (32)$$

which is identical with the so-called "atomic structure factor."

A convenient method of comparing the experiments with the theoretical calculations is thus to multiply the observed intensity of the modified rays by the factor $(1 + \gamma \text{vers } \phi)^3$, and add to the observed intensity of the unmodified rays. The resulting value

$$I_s' = I_{\text{mod}} (1 + \gamma \cos \phi)^3 + I_{\text{unm}} \quad (33)$$

may then be compared directly with the value of I_s derived by the classical equation (18).

4. ANALYSIS OF SCATTERING DATA TO DETERMINE RADIAL ELECTRON DISTRIBUTION

If the distribution of the electrons is spherically symmetrical, as we have assumed, we may represent the probability that an electron will lie between r and $r + dr$ by a Fourier sine series of the form,

$$u(r) = A_1 r \sin \pi r/a + A_2 r \sin 2\pi r/a + \dots + A_n r \sin n\pi r/a + \dots \quad (34)$$

Substituting this value of $u(r)$ in equation (19) we get,

$$S = 1 + (Z - 1) \left[\sum_n \int_0^a \frac{A_n}{k} \sin \left(n\pi \frac{r}{a} \right) \sin (kr) dr \right]^2. \quad (35)$$

If the scattering I_s is evaluated for $k = n\pi/a$, i.e., by equation (17) for

$$\sin (\phi/2)/\lambda = n/4a, \quad (36)$$

¹⁵ G. Breit, Phys. Rev. **27**, 242 (1926).

¹⁶ P. A. M. Dirac, Proc. Roy. Soc. **111**, 405 (1926). This relation (29) presumably does not hold for wave-lengths so short that the velocity of the recoil electron approaches c . In this case the formula of Klein and Nishina presents a closer approximation.

¹⁷ It is interesting that the ratio $I_{\text{mod}}/I_{\text{unm}}$ is expressed by equations (30) and (31) in terms of interference. It was early suggested by the writer (Phil. Mag. **46**, 910 (1923)) that this ratio might be thus expressed, as an alternative to the more obvious description developed later by Jauncey, in terms of the ratio of the energy of recoil of the scattering electron to its binding energy in the atom. Wentzel¹⁷ shows that equivalent expressions of the ratio I_u/I_m may be made in terms of either interference or energy of recoil.

where a is an assumed maximum radius, all integrals in the sum of equation (35) vanish except the n th, giving

$$S_n = 1 + (Z - 1) \left[\frac{1}{4} \frac{a^2}{k^2} A_n^2 \right]. \quad (37)$$

Thus

$$A_n = \pm \frac{2k}{a} \left\{ \frac{S_n - 1}{Z - 1} \right\}^{1/2}. \quad (38)$$

Corresponding to each value of S_n we thus determine the n th term of the Fourier series (34), and thus eventually the value of $u(r)$.

Our series (34) has in it an arbitrary radius a , and in evaluating the series the data for only certain arbitrarily chosen values of k are employed. If this arbitrary radius is made large, the values of k which are used come closer together, and our series approaches the Fourier integral,

$$u(r) = r \int_0^\infty B \sin(\pi r x) dx, \quad (39)$$

where

$$x \equiv n/a = (4/\lambda) \sin(\phi/2), \quad (40)$$

according to equation (36), and

$$B \equiv A_n a = 2\pi x \left\{ \frac{S_x - 1}{Z - 1} \right\}^{1/2}. \quad (41)$$

If instead of the probable position of a single electron, we wish to find the probable number of electrons between r and $r+dr$, we have only to multiply $u(r)$ by the number of electrons per atom, giving by equation (34)

$$U(r) = Zu(r) = Zr \sum_1^\infty A_n \sin n\pi r/a, \quad (42)$$

or by (39),

$$U(r) = Zr \int_0^\infty B \sin(\pi r x) dx. \quad (43)$$

It is interesting to compare equation (42) with the similar series expressing the radial distribution of electrons in the atoms of a crystal,¹

$$U(r) = 8\pi \frac{r}{D^2} \sum_1^\infty n F_n \sin 2\pi n \frac{r}{D}. \quad (44)$$

We note that a of equation (42) corresponds to $D/2$ of (44), since both quantities represent the assumed outer limit of the atom. The series are accordingly identical if $2\pi(r/a^2)nF_n = ZrA_n$. Using the value of A_n given by (38), and noting that $D = 2a = (n\lambda/2) \sin \frac{1}{2}\phi$, this means that

$$F_n = Z \left\{ \frac{S_x - 1}{Z - 1} \right\}^{1/2}. \quad (45)$$

This expression enables us to compare the " F " curves obtained from crystal reflection with the data given by scattering experiments.

¹⁸ A. H. Compton, "X-rays and Electrons," p. 164. An integral identical in form with (43), but representing the electron distribution in atoms of a crystal, has been given by G. E. M. Jauncey and W. D. Claus, Phys. Rev. **32**, 20 (1928).

5. TESTS OF THE METHOD OF ANALYSIS

Before applying equation (43) to the interpretation of experimental data, it will be of interest to study its application to certain cases where the solution is known.

a. Consider the intensity distribution described by equation (15). From equations (15) and (41) we have

$$B = \pm (2/a) \sin \pi x a. \quad (46)$$

Substituting this value in (43), since $Z = 2$,

$$U = 4(r/a) \int_0^\infty \sin(\pi a x) \sin(\pi r x) dx. \quad (47)$$

This integral is zero,¹⁹ except when $r = a$, in which case its value becomes infinite, indicating a concentration of the electrons at the distance $r = a$ from the nucleus, in accord with the original assumption on which (15) was based.

b. An atom of four electrons, each of whose probability of lying between r and $r + dr$ is $u(r) = 2r/a^2$ between $r = 0$ and $r = a$, and is zero beyond $r = a$.

By equation (19) we find,

$$S = 1 + 3 \left\{ \frac{2(1 - \cos \pi x a)}{\pi^2 x^2 a^2} \right\}^2. \quad (48)$$

From (41) then,

$$B = \pm \frac{4}{\pi x a^2} (1 - \cos \pi x a),$$

and equation (39) becomes,

$$u(r) = 4 \frac{r}{a} \left\{ \int_0^\infty \frac{\sin \pi r x}{\pi a x} dx - \int_0^\infty \frac{\cos \pi a x \sin \pi r x}{\pi a x} dx \right\}. \quad (49)$$

The value of the integrals is²⁰ $1/2a$ for $[r < a]$, and 0 for $[r > a]$, whence

$$\begin{aligned} u(r) &= 2r/a^2 & [r < a], \\ &= 0 & [r > a], \end{aligned} \quad (50)$$

as initially assumed.

These tests check the accuracy of the mathematical analysis. They of course say nothing, however, regarding the validity of our physical assumptions of spherical symmetry and of independence of the positions of the various electrons in the atomic groups.

6. ELECTRON DISTRIBUTION IN HELIUM

The formulas that have been developed above are directly applicable only to the scattering of x-rays by gases, in which case the interference effect due to neighboring molecules is negligible. In the case of the noble gases we are also free from interference between adjacent atoms, since the gases are mona-

¹⁹ At any point when $r \neq a$ the integral is strictly speaking indeterminate; but its average value over a finite range of x is zero.

²⁰ B. O. Peirce, "A Short Table of Integrals" (1910) nos. 484 and 485.

tomic, and according to current theories the probable electron distributions should be spherically symmetrical as we have assumed in our calculations. Fortunately recent experiments by Barrett²¹ supply sufficient information regarding the scattering by helium to yield valuable information.

In Barrett's Fig. 7 he compares the scattering by helium with that by hydrogen, which he finds identical with that calculated from the Breit-Dirac quantum formula for the range investigated. With an effective wave-length of 0.49A, he finds that helium and hydrogen scatter equally, within experimental error, at angles greater than 60°, but that at 40°, 30° and 20° the scattering by helium is greater by the ratios 1.025, 1.08 and 1.26 respectively. These values are indicated by the circles in Fig. 3, where $S \equiv I_s/ZI_e$ is plotted against x . At sufficiently small angles the phase difference between the rays from the two electrons in helium must be negligible, in which case our theory demands that the value of S must approach 2. For small values of x the phase

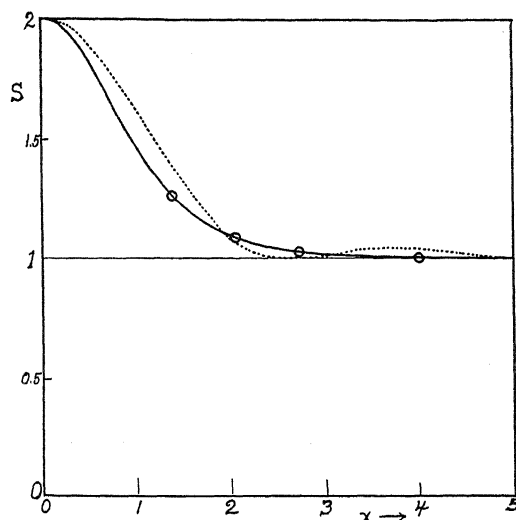


Fig. 3. Solid line, relative scattering by helium, based on Barrett's data (circles). Broken line, calculated scattering by Bohr type helium atom.

differences are small quantities of the first order; but the amplitudes, being proportional to the cosines of the phase differences, are affected only in the second order of small quantities.²² Thus the S curve must leave the $x=0$ axis parallel to the x axis, and must initially be of a parabolic form.²³ We can thus interpolate the S curve between $x=0$ and $x=1.4$ with some degree of assurance as indicated by the solid line.

This S curve can be transformed into a B curve by the help of equation (41), giving the result shown in Fig. 4. Here again the values given by the experimental data are shown by the circles.

²¹ C. S. Barrett, Phys. Rev. 32, 22 (1928).

²² This may be seen by finding the maximum value of E from equation (5) for small values x_n . This maximum is unaffected to the first power of x_n , but is reduced by terms containing x_n^2 .

²³ These conclusions are valid only if the atom is not of infinite extent.

For values of x greater than 3 the experiments suggest that B gradually approaches zero.²⁴ The values of the integral U are not much affected by the exact manner of this approach as long as it is slow and continuous. For con-

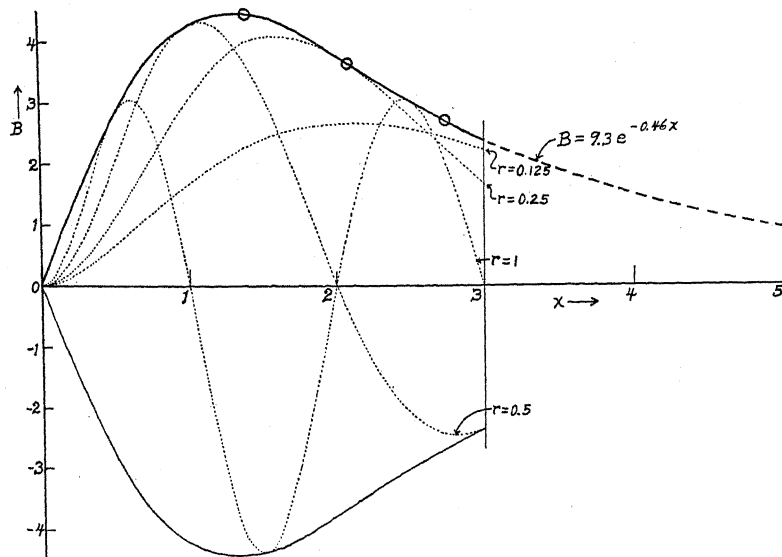


Fig. 4.

venience, therefore, we may assume that beyond some arbitrary value of x , say x_1 , B may be expressed by

$$B = be^{-ax} \quad [x > x_1]. \quad (51)$$

In order that at $x = x_1$ the values of B and dB/dx shall be continuous, we must have

$$a = - \left(\frac{1}{B} \frac{dB}{dx} \right)_{x_1} \quad (52)$$

and

$$b = B_1 e^{ax_1} \quad (53)$$

In order to evaluate $U(r)$ for a definite value of r we must determine the integral,

$$\Phi = \int_0^\infty B \sin(\pi r x) dx. \quad (54)$$

This may be separated into two parts,

$$\Phi_1 \equiv \int_0^{x_1} B \sin(\pi r x) dx, \quad (55)$$

and

$$\Phi_2 \equiv \int_{x_1}^\infty B \sin(\pi r x) dx. \quad (56)$$

²⁴ B must approach zero for large values of x unless the electron density at the center of the atom is infinite.

The first part Φ_1 may be evaluated graphically, by plotting $B \sin (\pi r x)$ for various values of r , as indicated by the dotted lines of Fig. 4, and integrating from O to x_1 with a planimeter. Φ_2 may be determined by substituting in equation (56) the value of B given in equation (51) and integrating, which gives

$$\Phi_2 = B_1 \frac{a \sin \pi r x_1 + \pi r \cos \pi r x_1}{a^2 + \pi^2 r^2}. \quad (57)$$

From Fig. 4 we find for helium, if $x_1=3$, $B_1=2.36$ and $a=0.46$, whence the value of Φ_2 may be determined for any desired value of r .

As typical examples, we have the following values (Table I):

TABLE I.

r	Φ_1	Φ_2	$\Phi = \Phi_1 + \Phi_2$	$U = Zr\Phi$
1.125A	5.75	1.64	7.39	1.85
0.25	8.16	-0.42	7.74	3.87
0.5	3.14	-0.35	2.79	2.79
1.0	0.86	-0.70	0.16	0.32

The resulting values of U plotted against r are shown in Fig. 5 by the solid line.

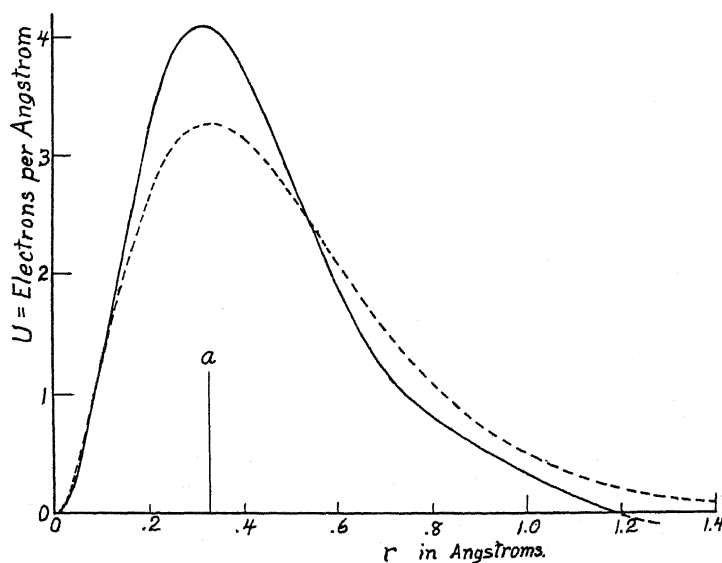


Fig. 5. Radial electron distribution in helium. Solid line, based on Barrett's x-ray scattering data. Broken line, Pauling's calculation from wave mechanics. a =radius of Bohr orbits.

It is of great interest to compare the "observed" distribution with that calculated theoretically. According to the Bohr-Sommerfeld theory, the elec-

trons in helium should both traverse approximately circular orbits with unit angular momentum, the radius of the orbits being given by

$$a = h^2 / [4\pi^2 e^2 m (Z - s)]. \quad (58)$$

where h , e , m and Z have their usual significance, and s is the "screening constant" of each electron on the other, having a value²⁵ of approximately $s = 0.39$. Using the usual values of the constants, we thus find $a = 0.33\text{\AA}$. It will be seen that this value falls very close to the radius of maximum electron density as shown in Fig. 5.

If we assume that the two electrons are on a spherical surface of fixed radius $r = 0.33\text{\AA}$, the intensity of the scattered rays should be given by equation (15). The values of s thus calculated are shown by the dotted line Fig. 3. The differences between this dotted curve and the experimental points are considerably greater than the probable experimental error. Yet it is not impossible that a combination of heterogeneous x-rays such as Barrett used and the presence of incoherent rays (Compton scattering) at the large angles might flatten out the dotted curve to resemble the experimental one.

The distribution found from this analysis of Barrett's scattering data is however in striking agreement with that calculated on Schrödinger's wave mechanics. Thus Pauling²⁵ has shown that the radial electron distribution in helium can be expressed to a close approximation by

$$U(r) = Zr^2 X^2, \quad (59)$$

where for helium in the normal state he finds,

$$X = u_{1,0} = -2 \left(\frac{Z - s}{a_0} \right)^{3/2} e^{-\xi/2} \quad (60)$$

$$a_0 = h^2 / 4\pi^2 e^2 m = 0.53\text{\AA},$$

$$Z = 2$$

$$s = \text{screening const} = 0.39$$

$$\xi = 2(Z - s)r/a_0.$$

Substituting these values in equation (59) we get the U curve shown by the dotted line of Fig. 5. The striking similarity between this distribution predicted by the quantum theory and that coming from our interpretation of the scattering experiments is the more convincing when it is noted that there are no arbitrary constants available to make the two curves correspond. This agreement is a strong argument in favor of a continuous electron distribution, as predicted by the wave-mechanics, as opposed to the Bohr quantum theory of definite orbits.

²⁵ Cf. e.g. L. Pauling, Proc. Roy. Soc. A114, 181 (1927).

TWO NOTES ON THE PROBABILITY OF RADIATIVE TRANSITIONS

BY J. R. OPPENHEIMER

NORMAN BRIDGE LABORATORY, PASADENA

(Received March 4, 1930)

ABSTRACT

In 1 we compute the rate at which electrons and protons should, on Dirac's theory of electrons and protons, annihilate each other; this gives a mean life time for matter of the order of 10^{-10} sec.

In 2 we compute by Dirac's radiation theory the relative probability of radiative and radiationless transitions; we obtain an expression substantially equivalent to that derived by Heisenberg and Pauli.

I

AN ELECTRON satisfying Dirac's linear wave equation will very rapidly lose energy to the electromagnetic field. If the electron is free, it must lose this energy by radiating at least two quanta, in order that energy and momentum may be conserved in the process. If the electron is bound, e.g. in an atom, transitions in which only one quantum is radiated can occur, since there are then other particles present which can take up the necessary momentum. But these transitions are rare compared with the two-quantum transitions, which, as is well known, may be expected according to the theory to occur at an infinite rate. Now Dirac has suggested¹ that the reason why these transitions do not in fact occur is that the states of negative energy are filled; and this suggestion leads to a satisfactory understanding of the validity of the scattering laws derived from his wave equation. But according to Dirac not all of the states of negative energy are full; there are a few gaps in the distribution for negative electrons nearly at rest; and thus transitions to states of negative energy should not be quite excluded. Dirac further suggests that the empty states of negative energy are protons; and thus the filling of these states should correspond to the annihilation of an electron and a proton. This should occur very rarely; and if Dirac's suggestion were correct, we should expect to find a very small value for the corresponding transition probability. In this note we shall compute this transition probability on the basis of the present theory.

This computation cannot be made theoretically unique and certain until the grave difficulties introduced by the inequality of electron and proton masses are resolved; and this resolution seems to demand an essential advance² in the theory. The chief ambiguity for the present work arises from the fact that the energy radiated by the conversion of a stationary positive elec-

¹ P. A. M. Dirac, Roy. Soc. Proc. A126, 360 (1930).

² J. R. Oppenheimer, Phys. Rev. 35, 461 (1930).

tron into a stationary negative electron is $2mc^2$; whereas the energy liberated by the annihilation of a stationary electron and a stationary proton should be $(m + M_P)c^2$. We shall make the computation without explicit recognition of the difference in mass of electron and proton; this gives a transition probability which is absurdly large, and which is not appreciably reduced by the substitution of $m + M_P$ for $2m$ in the final formula.

Let us consider for definiteness an enclosure of volume V in which there is one free electron, and one gap in the negative energy distribution; and let both the electron and the gap be at rest. If electron and proton have in fact a relative velocity v , then our result will be in error by terms of the relative order $(v/c)^2$. For the wave equation of the electron we write

$$\{W/c + \alpha_0 mc + (h/2\pi i)[\alpha_1(\partial/\partial x) + \alpha_2(\partial/\partial y) + \alpha_3(\partial/\partial z)]\}\psi = 0 \quad (1)$$

We take the matrices $||\alpha_\mu(\rho\sigma)||$ in the form

$$\begin{aligned} ||\alpha_1(\rho\sigma)|| &= \begin{vmatrix} 0 & 0 & 0 & 1 \\ 0 & 0 & 1 & 0 \\ 0 & 1 & 0 & 0 \\ 1 & 0 & 0 & 0 \end{vmatrix}; & ||\alpha_2(\rho\sigma)|| &= \begin{vmatrix} 0 & 0 & 0 & i \\ 0 & 0 & -i & 0 \\ 0 & i & 0 & 0 \\ -i & 0 & 0 & 0 \end{vmatrix} \\ ||\alpha_3(\rho\sigma)|| &= \begin{vmatrix} 0 & 0 & 1 & 0 \\ 0 & 0 & 0 & -1 \\ 1 & 0 & 0 & 0 \\ 0 & -1 & 0 & 0 \end{vmatrix}; & ||\alpha_0(\rho\sigma)|| &= \begin{vmatrix} 1 & 0 & 0 & 0 \\ 0 & 1 & 0 & 0 \\ 0 & 0 & -1 & 0 \\ 0 & 0 & 0 & -1 \end{vmatrix} \end{aligned} \quad (2)$$

The normalized solutions corresponding to momenta p, q, r , and energy W given by

$$(W/c)^2 = m^2c^2 + p^2 + q^2 + r^2 \quad (3)$$

may then be written

$$\begin{aligned} \psi_3^\alpha &= 0; \\ \psi_4^\alpha &= \frac{(mc + W/c)e^{2\pi i/h(px+qy+rz)}}{[(mc + W/c)^2 + p^2 + q^2 + r^2]^{1/2}V^{1/2}} \\ \psi_1^\alpha &= \frac{-(p + iq)e^{2\pi i/h(px+qy+rz)}}{[(mc + W/c)^2 + p^2 + q^2 + r^2]^{1/2}V^{1/2}}; \\ \psi_2^\alpha &= \frac{re^{2\pi i/h(px+qy+rz)}}{[(mc + W/c)^2 + p^2 + q^2 + r^2]^{1/2}V^{1/2}} \end{aligned}$$

and

$$\begin{aligned} \psi_4^\beta &= 0; & \psi_3^\beta &= \psi_4^\alpha \\ \psi_1^\beta &= -\psi_2^\alpha; & \psi_2^\beta &= \tilde{\psi}_1^\alpha. \end{aligned} \quad (4)$$

The two wave functions for α and β give electrons with spin oriented parallel and antiparallel respectively to the z axis.

For the initial state of the electron we take

$$W = E_0 = h\nu_0 = mc^2; \psi_1^0 = \psi_2^0 = 0; \psi_3^0 = e^{2\pi i \gamma} (2V)^{-1/2}; \psi_4^0 = (2V)^{-1/2} \quad (5)$$

similarly for the final state we take

$$\begin{aligned} W = E^e = -h\nu_0 = -mc^2; \quad \psi_3^e = \psi_4^e = 0; \\ \psi_1^e = e^{2\pi i \delta} (2V)^{-1/2}; \quad \psi_2^e = (2V)^{-1/2}. \end{aligned} \quad (6)$$

Here γ and δ are independent indeterminate phases; if in the final results we average over these, we shall have assumed random orientations for the spins of both initial and final states; and with this understanding both (5) and (6) may be regarded as spherically symmetric.

We shall need also the wave functions for states with

$$p = q = 0; r = \pm mc; W = \pm (2)^{1/2} mc^2.$$

These are

$$\psi_2^\alpha = \psi_4^\alpha = 0; \psi_1^\alpha = \frac{-re^{\pm 2\pi i mcx/h}}{mcV^{1/2}(4 \pm 2(2)^{1/2})^{1/2}}; \psi_3^\alpha = \frac{(1 \pm (2)^{1/2})e^{\pm 2\pi i mcx/h}}{V^{1/2}(4 \pm 2(2)^{1/2})^{1/2}}$$

and

$$\psi_1^\beta = \psi_3^\beta = 0; \psi_2^\beta = -\psi_1^\alpha; \psi_4^\beta = \psi_3^\alpha. \quad (7)$$

Initially there is to be no radiation present; the electron is in the state (0). The probability amplitude at a later time t that a quantum of frequency ν , momentum \mathbf{p} , and electric vector polarized along the unit vector \mathbf{e} , shall have been emitted, and that the electron shall have jumped to a state of momentum \mathbf{P} , energy $h\bar{\nu}$, and polarization of spin $\tau = \alpha, \beta$, is then

$$\phi(\mathbf{p}, \mathbf{e}; \mathbf{P}, \bar{\nu}, \tau) = -v(0; \mathbf{p}, \mathbf{e}, \bar{\nu}, \tau) \frac{1 - e^{2\pi i(\nu + \bar{\nu} - \nu_0)t}}{\nu + \bar{\nu} - \nu_0}. \quad (8)$$

Here $v(0; \mathbf{p}, \mathbf{e}, \bar{\nu}, \tau)$ is the matrix component for the transition in question of the interaction energy between the electron and the light quantum field. This vanishes except when $\mathbf{P} = -\mathbf{p}$, and for $\mathbf{P} = -\mathbf{p}$ has the value

$$ec(2\pi/\nu hV)^{1/2} \left(\sum_{l=1}^3 \epsilon_l \alpha_l e^{-2\pi i/h(\mathbf{p} \cdot \mathbf{r})} \right) 0; \bar{\nu}, P, \tau; \text{ with } \bar{\nu}^2 = \nu_0^2 + \nu^2 \quad (9)$$

where

$$\left(\sum_{l=1}^3 \epsilon_l \alpha_l e^{-2\pi i/h(\mathbf{p} \cdot \mathbf{r})} \right) 0; \bar{\nu}, P, \tau$$

is the matrix component corresponding to the electronic transition

$$(0) \rightarrow (\bar{\nu}, P, \tau)$$

of the component of the vector

$$\mathbf{a} e^{-2\pi i/h(\mathbf{p} \cdot \mathbf{r})}$$

parallel to \mathbf{e} .

The probability amplitude that the electron should have jumped to state (e), and that a second quantum of frequency ν' , momentum \mathbf{p}' , and polarization along $\boldsymbol{\varepsilon}'$ should have been emitted, vanishes except when $\mathbf{p}' = -\mathbf{p} = \mathbf{P}$, and for $\mathbf{p}' = \mathbf{P}$ has the value

$$\phi(\mathbf{p}, \boldsymbol{\varepsilon}, \mathbf{p}', \boldsymbol{\varepsilon}'; e) = \frac{2\pi e^2 c^2}{h\nu V} \sum \left\{ \frac{1 - e^{2\pi i(\nu - \bar{\nu} - \nu_0)t}}{\nu - \bar{\nu} - \nu_0} - \frac{1 - e^{4\pi i(\nu - \nu_0)t}}{2(\nu - \nu_0)} \right\}$$

with

$$\begin{aligned} \sum = & \sum_{\bar{\nu}} \sum_t \left\{ \left(\sum_{l=1}^3 \epsilon_l \alpha_l e^{-2\pi i/h(\mathbf{p}, \mathbf{r})} \right)_{0; \bar{\nu}, P, \tau} \left(\sum_{l=1}^3 \epsilon'_l \alpha_l e^{2\pi i/h(\mathbf{p}, \mathbf{r})} \right)_{\nu, P, \tau; e} \right. \\ & \left. + \left(\sum_{l=1}^3 \epsilon'_l \alpha_l e^{2\pi i/h(\mathbf{p}, \mathbf{r})} \right)_{0; 0, P, \tau} \left(\sum_{l=1}^3 \epsilon_l \alpha_l e^{-2\pi i/h(\mathbf{p}, \mathbf{r})} \right)_{0, P, \tau; e} \right\} (\nu + \bar{\nu} - \nu^{-1}) \end{aligned} \quad (10)$$

This grows large only for $\nu \sim \nu_0$, $\bar{\nu} \sim \pm (2)^{1/2} \nu_0$; and here the first term in the bracket may be neglected.

To evaluate \sum for $\nu = \nu_0$, $\bar{\nu} = \pm (2)^{1/2} \nu_0$, we may without loss of generality take \mathbf{p} along z , since both initial and final wave functions are effectively spherically symmetric. We may further take, again without loss of generality, $\boldsymbol{\varepsilon}$ along x . There are then two cases to consider, with $\boldsymbol{\varepsilon}'$ along x and along y respectively. For these cases we have in turn

$$\begin{aligned} \sum = & \sum_{\bar{\nu} = \pm (2)^{1/2} \nu_0} \sum_{\tau = \alpha, \beta} \bar{\nu}^{-1} \left\{ \left[\int dV \sum_{\rho, \sigma} \bar{\psi}_{\sigma}^{\bar{\nu}, P, \tau} e^{-2\pi i/c \cdot \nu_0 z} \alpha(\sigma \rho) \psi_{\rho}^0 \right] \right. \\ & \left. \left\{ \int dV \sum_{\rho, \sigma} \psi_{\sigma}^e e^{2\pi i/c \nu_0 z} \left\{ \begin{matrix} \alpha_1(\sigma, \rho) \\ \alpha_2(\sigma, \rho) \end{matrix} \right\} \psi_{\rho}^{\bar{\nu}, P, t} \right\} \right. \\ & \left. + \left\{ \int dV \sum_{\rho, \sigma} \bar{\psi}_{\sigma}^{\nu, P, \tau} e^{2\pi i/c \cdot \nu_0 z} \left\{ \begin{matrix} \alpha_1(\sigma, \rho) \\ \alpha_2(\sigma, \rho) \end{matrix} \right\} \psi_{\rho}^0 \right\} \left\{ \int dV \sum_{\rho, \sigma} \bar{\psi}_{\sigma}^e e^{-2\pi i/c \cdot \nu_0 z} \alpha_1(\sigma, \rho) \psi_{\rho}^{\bar{\nu}, P, \tau} \right\} \right] \right\}. \end{aligned} \quad (11)$$

If we use (2) and (7) this gives us

$$\begin{aligned} \sum &= 0 \text{ for } \boldsymbol{\varepsilon}' \parallel x \\ \sum &= (-i/2\nu_0)(1 + e^{2\pi i(\gamma - \delta)}) \text{ for } \boldsymbol{\varepsilon}' \parallel y. \end{aligned} \quad (12)$$

From this we conclude that the probability of an emission is proportional to the square of the sine of the angle between the electric vectors of the two quanta.

Now there are $2\nu_0^2(V/c^3)$ components of the radiation field per unit solid angle per unit frequency about ν_0 ; the direction of propagation of one quantum can vary over a hemisphere; but when this is fixed polarization, frequency and direction of propagation of the other quantum are determinate. Thus we get the total chance of an emission at time t by integrating the absolute value of the square of ϕ (averaged over γ and δ) over a hemisphere of solid angle and all frequencies, and multiplying by $2\nu_0^2(V/c^3)$; thus

$$\begin{aligned}
\sum_{p, \epsilon} \int d\gamma \int d\delta |\phi(p, \epsilon, -p, \epsilon'; c)|^2 \\
= \frac{4\pi\nu_0^2 V}{c^3} \frac{e^4 c^4 \cdot 4\pi^2}{h^2 \nu_0^2 V^2} \frac{1}{2\nu_0^2} \int_0^\infty \frac{d\nu |1 - e^{4\pi i(\nu - \nu_0)t}|^2}{4(\nu - \nu_0)^2} \\
= t \cdot \frac{16\pi^4 e^4 c}{h^2 \nu_0^2 V} \int_{-\infty}^\infty \frac{1 - \cos x}{x^2} dx \\
= t \cdot \frac{16\pi^5 e^4}{m^2 c^3 V}.
\end{aligned} \tag{13}$$

The mean life time of an electron in a proton density of n_P protons per unit volume is thus

$$T = \frac{m^2 c^3}{16\pi^5 e^4 n_P} \sim \frac{5 \times 10^{10}}{n_P} \text{ sec.} \tag{14}$$

It should be observed that the retention of the terms for $\bar{\nu} = -2^{1/2}\nu_0$ in the expression (11) for \sum , may be justified by an argument similar to that used by Dirac to validate the scattering formulae. For although the electron cannot jump to this state of negative energy, because it is already filled, there is a double transition which gives just the same terms in \sum , and in which first a negative electron in the state $(-2^{1/2}\nu_0, P, \tau)$ jumps to a state near the state (0), and then the original positive electron jumps down from the state (0) to the state $(-2^{1/2}\nu_0, P, \tau)$; in either transition either of the two quanta may be emitted.

If we try to correct (13) to take account of the fact that the energy radiated should be $(m + M_P)c^2$ and not $2mc^2$, we get in place of (14)

$$T' = \frac{(m + M_P)^2 c^3}{64\pi^5 e^4 n_P} \sim \frac{5 \times 10^{16}}{n_P} \text{ sec.} \tag{15}$$

Both (14) and (15) give an absurdly short mean life time for matter. With $n_P = 10^{25}$ we get

$$T \sim 5 \times 10^{-15}; \quad T' \sim 5 \times 10^{-9}.$$

Of course the protons and electrons of matter are not in general free, nor uniformly distributed, nor at rest. But we should hardly expect their agglomeration into nuclei, or even atoms, to reduce appreciably the mean transition probability, since this would mean essentially an increase in the effective n_P to be used. In any case (14) or (15) should apply roughly to electrons and protons in a discharge tube.

II

In their paper on the relativistic treatment of the interaction of radiation and matter, Heisenberg and Pauli point out that according to their theory the radiationless transitions of the quantum mechanics may always be expected

to be accompanied by transitions which correspond to a change in the material system and the emission of at least one quantum of light.³ So, for example, in the Auger jumps, in the ionization of an atom in an electric field, in the capture of electrons by alpha-particles, and in the radioactive decay of nuclei, the energy of the liberated particles should show a certain diffuseness; and energy is only conserved by the emission of an appropriate continuous distribution of light. Heisenberg and Pauli derive an expression for the probability of such transitions involving radiation; they show that this probability is small, compared with that of the radiationless transitions, of the order

$$e^2/hc (v/c)^2.$$

They apply this result to the problem of radioactive disintegration, where the escape of the alpha and beta particles may be roughly schematized as a diffusion through a high wall of potential energy; and they obtain so an explanation of the sharp definition of the energies of alpha-particles, and the great diffuseness of the beta spectrum. The non-appearance of the gamma radiation, which, on this theory, should accompany beta-ray disintegration, remains unexplained.

In this note we shall compute the relative probability of such radiative transitions on the basis of the Dirac radiation theory. For this probability we obtain an expression which, in the approximation to which the calculations of H. P. were carried, should agree with the results of that calculation. In our formula certain terms appear which were deliberately neglected in H. P.; and further this formula is applicable to a slightly more general group of problems than that of H. P., which cannot strictly be applied to any of the problems mentioned above except that of the Auger jumps; but except for these minor modifications our result reduces to that of H. P.; and it gives the same predictions when applied to the theory of radioactive disintegration. The present work is rather simpler than that on the basis of the more general theory.

For the occurrence of radiationless transitions it is essential that the material system (and we shall call this the "atom") be in a quasistationary state of an energy equal to the energy of some aperiodic motion of the system. Let the wave equation for the atom,—which may be written in the configuration space, and without explicit reference to the radiation field, to the order $(v/c)^2$ —be

$$(H - h\nu)\psi_v = 0. \quad (16)$$

Let the initial state have the energy

$$E_0 = h\nu_0 \quad (17)$$

and be given by a wave packet which satisfies the equation

$$(H - V - h\nu_0)\psi_0 = 0. \quad (18)$$

³ W. Heisenberg and W. Pauli, *Zeits. f. Physik* **56**, 1 (1929); cited as H. P.

The wave packets for the quasistationary aperiodic states of the atom we call θ_ν ; they satisfy

$$(H - V' - h\nu)\theta_\nu = 0; E = h\nu \quad (19)$$

and shall be normalized to $d\nu$. Then the probability of a radiationless transition to the continuum is given, to the first order in the small quantity λ_0/ν_0 , by

$$\lambda_0 = 4\pi^2/\hbar^2 |V_{\nu_0}|^2; V_{\nu_0} = \int d\tau \delta_{\nu_0} V \psi_0. \quad (20)$$

(The integral over $d\tau$ is to be taken over the configuration space of the atom.)

Now let there be no radiation present initially. Since the atom has energy levels lower than E_0 , it can make radiative transitions to these states; Dirac's radiation theory gives us, for the probability per unit time per unit frequency ν_s of the radiation, for this transition

$$\lambda_s d\nu_s = 16\pi^2 \nu_s d\nu_s / 3\hbar c^3 | \dot{P}_{\nu_0-\nu_s, 0} |^2$$

with

$$\dot{P}_{\nu_0-\nu_s, 0} = \int d\tau \bar{\theta}_{\nu_0-\nu_s} \dot{P} \psi_0 \quad (21)$$

where \dot{P} is the time rate of change of the electric moment of the atom. (With Dirac's linear Hamiltonian for the electron it will be

$$\sum_R e_k \mathbf{a}^k$$

where e_k is the charge on the k 'th particle, and the \mathbf{a}^k s are the Dirac matrices, and the summation is to be taken over all particles.)

Now when V is not very small, (21) gives us only a very poor approximation for the probability of the corresponding transitions. Somewhat inaccurately we may say that the system can reach the same final state by a double jump, in which, e.g., the atom goes over into some arbitrary state in the continuum, and then—but there is no interval between the jumps,—jumps to the final state and emits a quantum. In this process of course only the total energy of the system is conserved, and that only when one considers the double jump as a single process. This is the effect treated by H. P.; and to obtain it we have only to carry the perturbation theory a step farther than was necessary for the derivation of (20) and (21).

The Dirac wave equation for the probability amplitude ϕ for the whole system, taken as a function of the state, which for brevity we describe by the single index ν , of the atom, and the number $N_{\nu s}$ of quanta of frequency ν_s , polarization p , and given direction of propagation, is

$$\begin{aligned}
- h/2\pi i \cdot \partial/\partial t \phi(\nu, N_{sp}) &= \sum_{\nu' N'_{sp}} H(\nu, N_{sp}; \nu' N'_{sp}) \phi(\nu', N'_{sp}) \\
&= \int d\nu' V'_{\nu\nu'} \phi(\nu', N_{sp}) + V_{\nu 0} \phi(0, N_{sp}) \\
&+ \int d\nu' \sum_{s' p'} N_{s' p'}^{1/2} \nu_{s' p'}^{1/2} (\mathbf{e}_{s' p'} \cdot \dot{\mathbf{P}}_{\nu\nu'}) \phi(\nu', N_{sp} - \delta_{ss'} \delta_{pp'}) \\
&+ \int d\nu' \sum_{s' p'} (N_{s' p'} + 1)^{1/2} \nu_{s' p'}^{1/2} (\mathbf{e}_{s' p'} \cdot \dot{\mathbf{P}}_{\nu\nu'}) \phi(\nu', N_{sp} + \delta_{ss'} \delta_{pp'})
\end{aligned} \quad (22)$$

with

$$\kappa_{sp} = h/2\pi c^3 \sigma_{sp}.$$

Here σ_{sp} is the number of components of the radiation field of given polarization per unit frequency about ν_s per unit solid angle for the direction of propagation; and \mathbf{e}_p is a unit vector parallel to the electric vector of the component sp . The summation \sum_{sp} , and the product \prod_{sp} infra, are to be taken over all the components of the field.

If we take for our initial conditions for ϕ

$$\begin{aligned}
\phi(\nu, N_{sp}) &= 0 \\
\phi(0, N_{sp}) &= \prod_{sp} \delta(N_{sp}, 0) e^{-2\pi i \nu_0 t}
\end{aligned} \quad (23)$$

and put these values in (7), we find in first approximation

$$\begin{aligned}
\phi_1(\nu, N_{sp}) &= \prod_{sp} \delta(N_{sp}, 0) V_{\nu_0} \frac{e^{-2\pi i \nu t} - e^{-2\pi i \nu_0 t}}{h(\nu - \nu_0)} \\
&+ \sum_{s' p'} \delta(N_{s' p'}, 1) \prod_{s'' p''} \delta(N_{s'' p''}, 0) \nu_{s' p'}^{1/2} \nu_{s'' p''}^{1/2} (\mathbf{e}_{s' p'} \cdot \dot{\mathbf{P}}_{\nu\nu_0}) \frac{e^{-2\pi i (\nu + \nu_{s'}) t} - e^{-2\pi i \nu_0 t}}{h(\nu + \nu_{s'} - \nu_0)}
\end{aligned} \quad (24)$$

In Π' the factor for $s'' = s'$, $p'' = p'$ is to be omitted.

If one puts this expression (24) for ϕ_1 in (22), integrates the equation to obtain the second approximation $\phi_2(\nu, N_{sp})$, and takes the sum over all components of the field

$$\sum_p \int d\nu_s \int d\omega_s |\phi_2(\nu, 1_{sp})|^2,$$

this gives the probability that the system has, at time t emitted a quantum of frequency near $\nu_s = \nu_0 - \bar{\nu}$, and made a transition to a state in the continuum of energy near $h\bar{\nu}$. The coefficient of t in this expression gives the transition probability for transitions to a state in the range $\bar{\nu}$ to $\bar{\nu} + \Delta\bar{\nu}$:

$$\lambda_s(\bar{\nu}) \Delta\bar{\nu} = \frac{16\pi^2 \nu_s \Delta\bar{\nu}}{3c^3 h^3} \left| h \dot{\mathbf{P}}_{0\nu} - \int \frac{d\nu' V_{0\nu'} \dot{\mathbf{P}}_{\nu'\bar{\nu}}}{\nu_0 - \nu'} - \int \frac{d\nu' \dot{\mathbf{P}}_{0\nu'} V'_{\nu'\bar{\nu}}}{\bar{\nu} - \nu'} \right|^2. \quad (25)$$

The first term in the bracket is the direct emission given by (21) and neglected by H. P.; the remaining terms differ from those of H. P. (132) only by having

V' in place of V . When ψ_0 and θ_v are characteristic functions of the same equation, these terms reduce to those given in H. P.

It should be observed that both (25) and H. P. (132) are derived as approximations; in particular, the momentum of the light quantum, and terms of higher order in v/c , are neglected in both computations. The retention of this momentum leads to the same modification in (25) and H. P. (132); and so does the retention of terms of the fourth order in v/c . But in higher orders only the method of H. P. can be used, since then no equation of the form (16) holds for the atom, and it is necessary to work directly from the more general equations of quantum electrodynamics, and take more complete account of the retardation of the forces between the particles of the atom.

To obtain the order of magnitude of the total radiative transition probability for radioactive disintegrations, we may observe that V and V' may be expected to be of the same order of magnitude as $h\nu_0$, and we integrate (25) for all frequencies ν_s up to ν_0 ; this gives

$$\lambda_s = \int_0^{\nu_0} \lambda_s(\bar{\nu}) d\bar{\nu} \sim v^2 \nu_0^2 e^2 / c^3 h \left| \int d\tau \bar{\theta}_v \psi_0 \right|^2. \quad (26)$$

The ratio of this to (20) gives the relative probability that radiation will be emitted in the disintegration:

$$\lambda_s / \lambda_0 \sim e^2 / hc \cdot (v/c)^2 \quad (27)$$

in agreement with H. P. (133). From (25) it is clear that only a much more detailed knowledge of θ_v and ψ_0 and of the form of the Hamiltonian H in (16) than is at present available can give us any precise value for λ_s / λ_0 .

The application of (27) enables us to estimate the relative probability of radiative and radiationless capture of electrons from atoms by an alpha particle, and gives for the ratio of the probabilities 10^{-6} , in agreement with the more detailed calculations of the effect.

BOUNDARY CONDITIONS AND THE MEANING OF WAVE GROUPS IN WAVE MECHANICS

BY H. A. WILSON

RICE INSTITUTE, HOUSTON, TEXAS

(Received January 29, 1930)

ABSTRACT

Reasons are given for believing that the boundary conditions at a discontinuity in the potential (V) in wave mechanics may be $\phi_1 = \phi_2 \mu^{1/2}$ and $\phi_1 d\phi_1/dx = \phi_2 d\phi_2/dx$. Here ϕ is the wave function and μ the ratio of the group velocities. With these boundary conditions the waves are either completely transmitted or completely reflected according as the energy E is greater or less than V . The particles therefore need not be supposed to enter the region in which $V > E$ where their velocities would be imaginary and their kinetic energies negative. It is suggested that the group of waves associated with a particle should be identified with the particle and that the energy and momentum of the particle are the energy and momentum of the group of waves. When the group is stopped or absorbed it contracts to small dimensions and so becomes a particle.

IN THE applications of wave mechanics to the theory of thermionics and of the disintegration of atomic nuclei the boundary conditions at a discontinuity in the potential have been considered and it is customary to suppose that the wave function ϕ and its first derivative must be continuous at the discontinuity.

Consider the case of a particle with energy E moving along x in the positive direction and suppose that its potential energy is zero for $x < 0$ and equal to V' for $x > 0$ so that there is a discontinuity in the potential at $x = 0$. The usual wave equations in this case are

$$\begin{aligned} \frac{d^2\phi}{dx^2} + k^2 E \phi &= 0, & x < 0 \\ \frac{d^2\phi}{dx^2} + k^2 (E - V') \phi &= 0, & x > 0. \end{aligned}$$

As a solution we may take, as usual, when $E > V'$,

$$\begin{aligned} \phi_1 &= a e^{-ikE^{1/2}x} + b e^{ikE^{1/2}x}, & x < 0 \\ \phi_2 &= c e^{-ik(E-V')^{1/2}x}, & x > 0. \end{aligned}$$

To determine b and c in terms of a it is usual to suppose that $\phi_1 = \phi_2$ and $d\phi_1/dx = d\phi_2/dx$ at $x = 0$. We then get $b = a(1 - \mu)/(1 + \mu)$ and $c = 2a/(1 + \mu)$ where $\mu = [(E - V')/E]^{1/2}$ which is equal to v_2/v_1 where v_1 is the group velocity for $x < 0$ and v_2 that for $x > 0$.

The condition $\phi_1 = \phi_2$ at $x = 0$ gives $a + b = c$. This equation is not obviously correct. Consider two points A and B one at $x = -d$ and the other at $x = +d$. Since there is a discontinuity in the potential at $x = 0$, so that the group velo-

city v_1 for $x < 0$ changes to v_2 for $x > 0$, it is not clear that the chance that the particle is in an element dx at A should become equal to the chance that it is in a dx at B as d is diminished indefinitely. This is so because A and B are on opposite sides of the discontinuity even when $d = 0$.

To determine the correct boundary conditions at $x = 0$ we may begin by considering a case in which the potential varies gradually from 0 to V' near $x = 0$ and then make the distance in which the change from 0 to V' takes place small.

Let a train of waves moving along x in the positive direction be represented by $\phi = A e^{-ikB}$ where A and B are functions of x which we shall suppose to be real quantities. ϕ must satisfy the wave equation

$$\frac{d^2\phi}{dx^2} + k^2(E - V)\phi = 0$$

where E is the total energy and V the potential energy of the particle. Substituting the above value of ϕ in this equation we get

$$\frac{1}{A} \frac{d^2A}{dx^2} - k^2 \left(\frac{dB}{dx} \right)^2 - ik \left(\frac{d^2B}{dx^2} + \frac{2}{A} \frac{dA}{dx} \frac{dB}{dx} \right) + k^2(E - V) = 0$$

Hence we must have $d^2B/dx^2 + (2/A) (dB/dx) (dA/dx) = 0$ which gives $C = A^2 dB/dx$ where C is a constant. It will be noted that this result is exact not merely an approximation. Also

$$\frac{1}{A} \frac{d^2A}{dx^2} - k^2 \frac{c^2}{A^4} + k^2(E - V) = 0. \quad (1)$$

Now let $A = A_1 + (A_2 - A_1)/(\epsilon^{-\alpha x} + 1)$ where α is a positive constant. This makes $A = A_2$ where αx is large and positive and $A = A_1$ where αx is large and negative. Thus A changes from A_1 to A_2 in the region near $x = 0$ and if we suppose α to become infinite then we shall have $A = A_1$ for $x < 0$ and $A = A_2$ for $x > 0$.

Substituting this value of A in (1) and putting $c = A_1^2 E^{1/2}$ we get

$$V = \frac{\alpha^2(A_2 - A_1)(\epsilon^{-\alpha x} - 1)\epsilon^{-\alpha x}}{k^2(A_2 + A_1\epsilon^{-\alpha x})(1 + \epsilon^{-\alpha x})^2} + E \left\{ 1 - \left(\frac{A_1(1 + \epsilon^{-\alpha x})}{A_2 + A_1\epsilon^{-\alpha x}} \right)^4 \right\}.$$

According to this when αx is large and negative then $V = 0$ and when αx is large and positive then $V = E \{ 1 - (A_1/A_2)^4 \} = V'$.

Thus if α is supposed large this solution of the wave equation gives the variation of A with x when the potential changes rapidly near $x = 0$ from the constant value zero when x is negative to the constant value V' when x is positive.

The value of B can be found if desired since $C = A^2 dB/dx$ but since $\phi \bar{\phi} = A^2$ it is not required.

Put $\alpha^2 = \beta k^2 E$ where β is a constant and also let $y = \epsilon^{-\alpha x}$. The expression for V above then becomes in the case when $A_2 = 2A_1$.

$$V = E \left\{ \frac{\beta y(y-1)}{(2+y)(1+y)^2} + 1 - \left(\frac{1+y}{2+y} \right)^4 \right\}$$

¹ An approximate result equivalent to this is well known.

The expression $y(y-1)/(2+y)(1+y)^2$ has a maximum value equal to about 0.08 when $y=3.3$. $\{(1+y)/(2+y)\}^4$ is then about 0.4 so that β may be made equal to 4 without danger of V becoming greater than E . Fig. 1 shows the variation of A with $2kE^{1/2}x$ when $A_2=2A_1$ and $\beta=4$. Fig. 2 shows the corresponding variation of V/E with $2kE^{1/2}x$ and Fig. 3 shows the variation of V/E with $2(2)^{1/2}kE^{1/2}x$ with $\beta=8$. In Fig. 3 V/E becomes greater than unity.

It appears that, in this case, with $\beta=4$, practically all the changes in A and V takes place in a range of $2kE^{1/2}x$ equal to about 5. Thus if d denotes the thickness of the layer in which the potential changes then we have $d=5/2kE^{1/2}$. For electrons $k=4\times 10^{13}$ and $E=1.6\times 10^{-12}P$ where P is the potential difference in volts equivalent to E . Hence $d=5\times 10^{-8}/P^{1/2}$. The wave-length λ of the waves associated with an electron is given by $\lambda=12.25/P^{1/2}$ so that $d=0.4\lambda$. Thus if $P=10$ volts then $d=2\times 10^{-8}$ cm and if $P=1$ volt then $d=5\times 10^{-8}$ cm. In the case considered V' is equal to $15E/16$. It appears that the potential does not become greater than E in a layer similar to those on the surface of metals for which V' is about 10 volts and d about 5×10^{-8} cm.

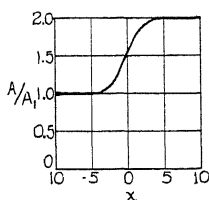


Fig. 1.

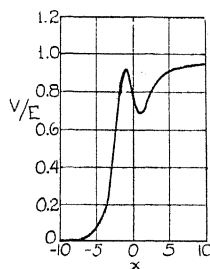


Fig. 2.

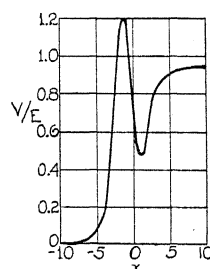


Fig. 3.

When V' is equal to $15E/16$ then the ratio of the group velocities $\mu = v_2/v_1 = \frac{1}{4}$ so that $b = a(1-\mu)/(1+\mu)$ is equal to $3a/5$. Hence $b^2a^2 = 9/25$ so that $9/25$ of the electrons should be reflected back if the boundary conditions $\phi_1 = \phi_2$ and $d\phi_1/dx = d\phi_2/dx$ are correct. But as we have just seen when V changes from 0 to $15/16$ of E in a distance of about half a wave-length there is no reflection. This suggests that the boundary conditions should be modified so as to make the reflection zero when $E > V'$.

The equation $V' = E\{1 - (A_1/A_2)^4\}$ gives $A_2/A_1 = (v_1/v_2)^{1/2}$ or $A_2 = A_1\mu^{1/2}$.

For $x < 0$ let $\phi_1 = a\epsilon^{-ikE^{1/2}x}$ so that $A_1 = a$ and $B = E^{1/2}x$. It then follows that for $x > 0$ $\phi_2 = (a/\mu^{1/2})\epsilon^{-ik(E-V')^{1/2}x}$.

It appears therefore that in the equations

$$\phi_1 = a\epsilon^{-ikE^{1/2}x} + b\epsilon^{+ikE^{1/2}x}$$

$$\phi_2 = c\epsilon^{-ik(E-V')^{1/2}x}$$

we must have $b=0$ and $c=a/\mu^{1/2}$, if there is no reflexion when V' is less than E .

According to this the boundary condition $\phi_1 = \phi_2$ at $x=0$ must be replaced by $\phi_1 = \phi_2 \mu^{1/2}$. The condition $d\phi_1/dx = d\phi_2/dx$ cannot then be correct. Since the number of particles falling on the surface at $x=0$ must be equal to the number leaving it we must have $a^2 v_1 = b^2 v_1 + c^2 v_2$ or $a^2 - b^2 = c^2 \mu$. The condition $\phi_1 = \phi_2 \mu^{1/2}$ gives $a + b = c \mu^{1/2}$ so that $a - b = c \mu^{1/2}$. This requires that $\mu^{1/2} d\phi_1/dx$ should be equal to $d\phi_2/dx$ or that $\phi_1 d\phi_1/dx = \phi_2 d\phi_2/dx$. This suggests that the correct boundary conditions at the discontinuity may be $\phi_1 = \phi_2 \mu^{1/2}$ and $\phi_1 d\phi_1/dx = \phi_2 d\phi_2/dx$. These conditions give $a + b = c \mu^{1/2}$ and $(a+b)(a-b) = c^2 \mu$. These equations have two solutions which are $b = 0$ and $c = a/\mu^{1/2}$ and $c = 0$ and $b = -a$. The first solution as we have seen is the one to use when $E > V'$ so that then $\phi_1 = a e^{-ikE^{1/2}x}$, $\phi_2 = (a/\mu^{1/2}) e^{-ik(E-V')^{1/2}x}$ so that all the particles go through the plane $x=0$ exactly as in classical theory. The other solution is clearly the one to use when $V' > E$ so that then $\phi_1 = a e^{-ikE^{1/2}x} - a e^{ikE^{1/2}x}$, $\phi_2 = 0$ so that all the particles are reflected back at $x=0$ exactly as in classical theory.

Thus if the boundary conditions at a discontinuity are $\phi_1 = \phi_2 \mu^{1/2}$ and $\phi_1 d\phi_1/dx = \phi_2 d\phi_2/dx$ then when $V' > E$ the waves are reflected completely at the discontinuity so that the particles need not be supposed ever to enter the region in which $V' > E$ where their kinetic energy is negative. This seems to the writer to be a very strong argument in favor of these boundary conditions.² It is very difficult to imagine any sort of physical meaning which can be attached to the idea of a particle with an imaginary velocity and a negative kinetic energy.

The writer now proposes to bring forward some considerations with regard to the nature of wave groups in wave mechanics. The view proposed is perhaps unorthodox and may not meet with approval but it seems to the writer to be worth considering.

It was originally suggested by Schroedinger that the wave function ϕ could be interpreted by supposing that the density of the electricity is proportional to $\phi \bar{\phi}$. This view has been replaced, at least in many cases, by the idea that the chance that an electron is in an element of volume dv is proportional to $\phi \bar{\phi} dv$. According to the original idea the electron in standing waves was at rest but was spread out over the whole volume occupied by the waves. A moving electron was spread out over a moving group of waves. According to the later view the electron is presumably somewhere in the standing waves or group but its location and motion, if any, are unknown. According to the first view the electron when it appears somewhere as a minute particle must have contracted from its state of diffusion over the waves. This necessary contraction seems to me to be of fundamental importance, as will be explained below.

Although according to the present view the motion of an electron in standing waves cannot be determined it seems to the writer to be nevertheless allowable to suppose that it must move from one point to another,

² Nordheim (Proc. Roy. Soc. A December 3, 1928) concludes that practically all the electrons having $E > V'$ escape from a metal because of the effect of the image forces in rounding off the discontinuity.

when it does move, along some definite path. That is, it will not do to suppose that it disappears at one point and appears at another without occupying the intermediate positions.

Another possible view, very similar to Schroedinger's original suggestion, is that the group of waves and the electron are identical and that when the group is stopped or absorbed and appears at a point the group of waves contracts to small dimensions and so becomes a particle.

If we suppose that a particle is associated with or is a group of waves of length l then it is easy to show that l diminishes when the velocity v of the group diminishes. This idea is not new but it does not seem to have attracted much attention.

According to Heisenberg's uncertainty principle we have $\delta E \delta t = h$, roughly at least, where δE is the uncertainty in the energy of the particle and δt that in its time of passing a given point. If v is the group velocity then we have $\delta t = l/v$ and since $E = h\nu$ where ν is the frequency of the waves we get $l = v/\delta\nu^2$ where $\delta\nu$ is the uncertainty in the frequency ν . There seems to be no reason to suppose that δE or $\delta\nu$ should vary as the group moves along so that we may conclude that the group length l should be approximately proportional to the group velocity v . Thus if the group enters a field of force in which it is gradually slowed down we should expect l to become smaller and to become very small on a surface where the group velocity is zero. It does not become zero at this point because owing to the uncertainty in E there is some uncertainty in the position of the surface in question.

Darwin's solution⁴ of the motion of a group in a uniform force field does not indicate such a variation of l which must mean that his solution involves a variation of $\delta\nu$ with v so that $v/\delta\nu$ remains constant or rather only varies to the extent demanded by the uncertainty in v . It seems to the writer that $\delta\nu$ should be supposed constant and so l should vary with v . Thus when a group is brought to rest it becomes very small or we may say that it becomes a particle. If preferred we may say that the group contracts onto the particle in it which is so located in a nearly definite position when the group stops. According to this we should expect the group and particle to come to rest approximately on a surface at which $E - V = 0$ and so either to remain on such a surface or else to move back into the region where $E > V$. We should not expect the particle to penetrate into the region where $V > E$ where its kinetic energy would be negative. It seems to the writer that this is as it should be. When a mathematical theory indicates that particles in a certain region would have imaginary velocities and negative kinetic energies then the proper conclusion to draw is that the particles do not go into that region. Of course when there is uncertainty in E then the position of the surface $E - V = 0$ is subject to a corresponding uncertainty. This conclusion is supported by the results obtained above on the motion of electrons through a discontinuity or near discontinuity in the

³ This result is given by H. T. Flint, Proc. Roy. Soc. A, December 2, 1929.

⁴ Darwin, Proc. Roy. Soc. A, December 1, 1927.

potential. The electrons and the waves also are probably reflected unless $E > V'$.

Bridgman's suggestion that the negative sign on the kinetic energy of particles inside the region where $V > E$ is merely the "bar sinister" on particles which have got in improperly is similar to Rutherford's suggestion that particles somehow leak through a potential hump although they have not got enough energy to get over it. In my opinion it is better to suppose that they do not get into regions where $V > E$ in any case.

It seems worth while to point out that the conclusion that particles can enter regions in which $V > E$ may be due to the assumption that the energy E can have a definite value with zero uncertainty. It seems probable that there should always be some uncertainty in E so that any one particular solution of the wave equation $\Delta\phi + k^2(E - V)\phi = 0$ for an exact value of E does not really represent a possible state of things. Such solutions correspond to a group of waves of infinite length, since $l = \hbar v / \delta E$, and if the group is really of finite length then they are merely approximations. When the region occupied by the waves is of atomic dimensions the group may be long enough to overlap itself many times and so the solution for a group of infinite length is a good approximation. But there should be some uncertainty in E so that the particle may have enough energy to go through the surface $E - V = 0$ of the approximate solution⁵ without its kinetic energy becoming negative.

Consider the case of an electron moving normally between two parallel plane surfaces at which it is reflected back. As in the theory of the discontinuity with $V' > E$, if we suppose the group length to be infinite, we may take $\phi\bar{\phi} = 4a^2 \sin^2 kE^{1/2}x$. Thus we have nodal planes half a wave-length apart on which $\phi\bar{\phi} = 0$. The distance between the parallel reflectors must be a multiple of the half wave-length. The chance that the electron is between any pair of adjacent planes is then $\lambda/2 d$ where d is the distance between the reflectors. We do not know where the electron is but it is supposed to be moving backwards and forwards between the reflectors with uniform velocity v . It is therefore supposed to pass through the nodal planes one after another. But on these planes $\phi\bar{\phi} = 0$ so that the chance that the electron is at any nodal plane is zero. It cannot therefore be supposed to be moving with uniform velocity and so passing through the nodal planes.⁶ We may if we like suppose a large number of electrons present all having the same energy and so all having nodal planes in the same positions.

Wiener's experiments on standing light waves may be considered in this connection. The particles are then photons instead of electrons. He showed by means of a thin photographic film that there were nodal planes half a wave-length apart at which the film was unaffected. If the photons were moving towards and away from the mirror they would pass through the

⁵ The exact solution, of course, would be the sum of a number of the solutions for particular values of E each multiplied by a suitable factor.

⁶ The argument here is directed against the *assumption* that the electron is moving with uniform velocity v .

film whatever its distance from the mirror and so the film would be equally affected at any distance. The fact that the film is affected between the nodal planes shows that the photons get there but the fact that it is not affected on the nodal planes shows that the photons do not pass through the nodal planes.

In the opinion of the writer, if the idea that a group of waves contains a particle is retained, then these considerations about standing waves make it necessary to suppose that in standing waves the particle is at rest. This amounts to a partial return to Schroedinger's original idea. In the case of a large number of particles being reflected normally we must suppose that they are arranged in layers between the nodal planes. The way in which such an arrangement could be brought about can be easily imagined.

Consider a group of waves of length l containing one particle⁷ and suppose that the particle is at a distance d from the front of the group. If the group is reflected normally the reflected waves will meet the particle when it is at a distance $d/2$ from the mirror. The particle will then stop since it is in standing waves and it will remain stopped for a time $(l-d)/v$ and will then move away with the reflected waves. According to this the waves must convey the momentum $2mv$ which the particle loses to the mirror. It is therefore necessary to suppose that the waves of wave mechanics are not merely waves of probability but that they are real physical waves which can convey energy and momentum. In fact it would seem to be best to regard the energy and momentum of a particle as the energy and momentum of its group of waves. When the group is stopped the energy and momentum appear on the particle or the group becomes a particle.

It will be observed that according to this when a particle is reflected back at a discontinuity in the potential in which $V' > E$ the particle does not get to the discontinuity at all unless it happens to be exactly at the front of its group of waves.⁸ Hence even if we suppose that the waves do penetrate through the discontinuity with amplitude falling off exponentially on the other side the particle need not be supposed ever to go through. For example we might suppose that the particle is always located at the crest of a wave and so is never exactly at the front of the group.

To represent a moving particle it is necessary to have a moving group of waves. Standing waves do not represent moving particles. Any solution of the equation $\Delta\phi + k^2(E - V)\phi = 0$ which represents standing waves may be said to be a group of waves at rest. For example when an electron is captured by a proton the group of the electron may be said to form the waves of the resulting hydrogen atom. The electron group contracts to atomic dimensions in this case. The electron group is of finite length and so must have uncertainty in its energy which should persist in the energy of the atom formed.

⁷ Particle here may mean either electron or photon. The groups associated with photons are of finite length which indicates uncertainty in the frequency and energy just as for electrons.

⁸ The particle is supposed to be somewhere in its group. To assume that it is at a distance d from the front of the group does not involve the assumption that d can be determined experimentally.

The standing waves may be said to be the particle but if it is desired to suppose that there is a particle somewhere in the standing waves then since it should be at rest it seems natural to suppose that it is on the surface $E - V = 0$ or else in a region where V is constant. If the particle remains at rest on the surface $E - V = 0$ or anywhere in a field of force it cannot be supposed to be acted on by the field of force. It is therefore necessary to suppose that fields of force do not act directly on the particles but merely alter the wave velocity. This of course is implied by the accepted method in wave mechanics which is to calculate the effect of the force field on the waves and not on the particles.

According to what has been said above the waves should not be supposed to go into the regions where $V > E$ but should be reflected at the surface $E - V = 0$ or else it should be supposed that $\phi\bar{\phi}dv$ is only proportional to the probability that a particle is in dv when $E \geq V$ at dv . The integral $\int \phi\bar{\phi}dv$ should in this case be made equal to unity when taken only over the region in which $E \geq V$. A third alternative which seems to the writer very plausible is to suppose that the energy E has enough uncertainty in its value to account for the chance that the particle may be in the region where $V > E$. That is we suppose $E = E_0 \pm \delta E$ and if a particle is found where $V > E_0$ then δE is equal to $V - E_0$ at least.

The second or third alternatives seem at the moment to be the more acceptable but it may be worth while to mention that the energy levels of the hydrogen atom may be very simply obtained by supposing that spherical waves are reflected at the surface $E - V = 0$ and so form standing waves.

Since in the hydrogen atom the wave velocity is equal to $E/(2m(E + e^2/r))^{1/2}$ the time T required for spherical waves to move from the nucleus to a sphere of radius $-e^2/E$ and back is given by

$$T = 2 \int_0^{-e^2/E} \frac{[2m(E + e^2/r)]^{1/2}}{E} dr = -\frac{\pi e^2}{E} \left(\frac{2m}{-E} \right)^{1/2}.$$

We may suppose that $T = n/\nu$ where ν is the frequency of the standing waves and n is an integer and that $E = -h\nu$ so that $E = -2\pi^2 m e^4 / n^2 h^2$ as usual.

One of the difficulties in optical theory is to see how the energy and momentum of the waves can become concentrated at points when the light is absorbed. The view that the waves have no energy or momentum is not satisfactory because for example it is difficult to see how waves with no energy could be reflected by a mirror. Reflexion requires the electrons all over the surface of the mirror to oscillate with the frequency of the light. The hypothesis of virtual oscillators in the mirror is also very unsatisfactory. A similar difficulty is present in the wave theory of electrons. The waves are diffracted as though they had uniformly distributed energy but appear as electrons when absorbed. According to what has been said above this difficulty may be to some extent removed by supposing that the wave groups contract to small dimensions when stopped. This process of contraction is made possible by the increase in the wave velocity as the group velocity

diminishes. The wave velocity becomes infinite when the group velocity becomes zero so that the group can contract very rapidly as it stops. It seems reasonable to suppose that the same thing happens with light as with electrons. When light is moving in empty space the wave and group velocities are equal but in the intense fields inside atoms we may suppose that the group velocity is diminished and the wave velocity increased. It is nevertheless very difficult to imagine a group occupying many cubic feet to be absorbed by an electron. If it is supposed that when the photon in a group is slowed down the wave velocity all over the group becomes very large and infinite when the photon stops then it is possible to imagine a very large group to contract very rapidly onto the photon. Even if we admit such sudden group contractions to be possible great difficulties remain. For example we have to explain why some groups are reflected and others not and how a group can be reflected without giving up any energy to the mirror.

As we have seen above a group of waves associated with a particle of energy E is either completely transmitted or completely reflected at a discontinuity in the potential according as $E > V'$ or $E < V'$. This suggests that the group associated with a photon must be either completely transmitted or completely reflected by a mirror. If the energy and momentum of photons and electrons are in the wave groups associated with them then it is necessary to suppose that these groups never divide into two and so must be either completely reflected or completely absorbed. In the case of photons exceptions to this may be supposed possible since a single photon may be imagined to give rise to two or more photons having the same total energy as the original one. The classical theory of reflexion must then be supposed to give the probability that a wave group and its photon are reflected together and not merely the chance that the photon is reflected.

The view suggested is therefore that a particle such as a photon or electron is practically identical with the group of waves associated with it. The energy and momentum are spread out over the group and not concentrated at a point. When the group is stopped or absorbed it contracts to small dimensions and so becomes a particle. The group cannot be divided by reflexion or by passing through a small aperture in an opaque screen but must be either all stopped or all get through. The group of waves must be regarded as a material entity and wave theory must be regarded as an approximation in so far as it now seems to require wave groups to be divided by reflexion and other similar processes which do not involve any change of frequency.

The writer does not claim to have removed the difficulties in optical and mechanical wave theory but he hopes that the above discussion may help to make the serious nature of these difficulties clearer.

THE HEAT OF DISSOCIATION OF CARBON MONOXIDE

BY JOSEPH KAPLAN

UNIVERSITY OF CALIFORNIA AT LOS ANGELES

(Received January 15, 1930)

ABSTRACT

The author's method for calculating the heat of dissociation of nitrogen, has now been applied to carbon monoxide. For both N_2 and CO the method agrees with the best values obtained by other methods. Using the present value of 10.3 volts for the heat of dissociation of CO, the dissociation products of the molecule are discussed for several electronic levels. In this way it is shown that the recent value of 1.3 volts for the energy of the metastable 1D_2 state in oxygen, obtained by McLennan and Crawford, agrees best with the present work.

IN A short paper that appeared last March,¹ the writer has calculated the heat of dissociation of nitrogen and found it to be equal to 9.0 volts. In a paper on the determination of heats of dissociation by means of band spectra, Professor R. T. Birge² has called attention to the difficulty of determining definitely the most probable value of D for N_2 . At the same time however he has given what is in his opinion the best value of the heat of dissociation of N_2 and that value is 9.1 volts. Since the method used by the writer yielded a value which is in such good agreement with the one given by Birge, it will be of some interest to try the same method for some other molecule. One of the cases that is of immediate interest is that of carbon monoxide.

It is now generally recognized that the bands of the third positive group of carbon arise in transitions from the b to the a level, and that only the $v'=0$ progression has been observed.³ The same reason for the non-appearance of higher progressions can be given here as was given for the fourth positive group of nitrogen. If the value of ω_0x for the b level of CO is very large, then the heat of dissociation in that level will be very small and dissociation will occur when the total energy of the molecule in the b level is only slightly greater than its electronic energy. It may be that ω_0x is of such a magnitude that not even a single discrete vibrational state exists, in which the total energy of the molecule is less than the heat of dissociation.

If one uses the above reasoning as a basis, it is then possible to determine the heat of dissociation, since the products of dissociation from the b level have been theoretically predicted to be a normal carbon atom and a normal oxygen atom.⁴ It immediately follows that the heat of dissociation of CO is either equal to or only slightly greater than the electronic energy in the b level. This energy is equal to 10.35 volts, so that the heat of dissociation of CO must

¹ Kaplan, Proc. Nat. Acad. Sci. **15**, 226 (1929).

² Birge, Trans. Farad. Soc. in press.

³ Birge and Sponer, Phys. Rev. **28**, 259 (1926).

⁴ R. C. Johnson, Trans. Farad. Soc. **15**, 649 (1929).

be almost equal to 10.35 volts. It is interesting here to remark that the value given by Birge in his Faraday Transactions paper is equal to 10.3 volts. The agreement between the present method and the method used by Birge is extremely satisfactory. The fact, that the fourth positive group of N_2 and the third positive bands of CO are the two outstanding examples of bands for which there is only one v' progression, certainly indicates that the present explanation is worth consideration.

The new value of D will now be applied to a brief discussion of some recent ideas regarding carbon monoxide. Johnson has given a very extensive discussion of the carbon monoxide molecule in his Faraday Society paper, and in particular he has discussed tentatively the dissociation products from the various electronic states of the molecule.

If the present value of 10.3 volts is to be accepted then it follows that at least one of the dissociation products from the electronic states that lie above 10.3 volts, must be in an excited state. Using the formerly accepted value of 11.2 volts for D , Johnson has already made the above statement for the c level. In view of the present lower value for D , the same statement must now apply to the b' level, the dissociation products of which were predicted to be a normal carbon and a normal oxygen atom.

One of the most interesting levels, from the point of view of the ideas presented in this paper, is the F level. The value of ν_e for this level is 99,730 cm^{-1} and ω_0 and ω_0x are 1914 cm^{-1} and 198 cm^{-1} , respectively. The F level is thus an example of a molecular level having a very high value for ω_0x , as compared with the values of ω_0x for nearly all of the known molecular levels. Because of the large ω_0x , a linear extrapolation of the vibrational levels, associated with the F level, yields a small and probably a fairly accurate heat of dissociation. The heat of dissociation is equal to 0.57 volts and the total energy in the F level is 12.88 volts. The difference between this and the heat of dissociation yields 2.5 volts as the energy of the two products of dissociation. Since the products of dissociation from this level are predicted to be a 1D_2 carbon atom and a 1D_2 oxygen atom, the sum of the energies of 1D_2 in carbon and in oxygen must be equal to 2.5 volts and this is probably a fairly good estimate of the sum.

One other state that possesses a fairly high value of ω_0x is the B level and a linear extrapolation yields a value of 2.8 volts as the heat of dissociation for this level and a value of 3.2 volts for the energy of the dissociation products. This extrapolation is longer than the one for the F level and is undoubtedly less trustworthy, probably being too high. Once again the products of dissociation are predicted to be a 1D carbon and a 1D oxygen atom, so that if the assumption is made that the error in the extrapolation is about 25 percent then the lower value is not far from being correct. A 25 percent error in a linear extrapolation of the above magnitude is not unusual in the determination of heats of dissociation from band spectra.

Two values for the difference $^3P-^1D_2$ in oxygen have been suggested. One of these is about 1.95 volts, suggested independently by L. A. Sommer⁵

⁵ L. A. Sommer, *Zeits. f. Physik* 51, 451 (1928).

and the author,⁶ and the other is 1.3 volts, obtained by McLennan and Crawford.⁷ It is difficult, in view of the theoretical predictions regarding the F level, to accept the higher of the two values, because then the difference $^3P - ^1D_2$ in carbon would have to be only about 0.6 volts. A comparison of carbon with the spectroscopically similar atoms N^+ and O^{++} ⁸ makes such a low value highly improbable. On the other hand the 1.3 volt value of McLennan and Crawford is a very reasonable one, since that would make the 1D level of carbon possess a value of about 1.2 volts and this is much more reasonable than the lower one of 0.6 volts.

The main purpose of this paper has been to point out the fact that the assumption, that the b level is extremely anharmonic, yields a very good value for D . Consequently a more detailed discussion of evidence regarding the energy in the 1D_2 state of the oxygen atom would be out of place here and will be left for another communication.

⁶ Kaplan, Phys. Rev. 33, 638 (1929).

⁷ McLennan and Crawford, Nature 124, 874 (1929).

⁸ Bowen, Astrophys. J. 67, 1 (1928).

THE BAND SPECTRUM OF SILVER CHLORIDE

BY BROOKS A. BRICE

NEW YORK UNIVERSITY, UNIVERSITY HEIGHTS

(Received March 10, 1930)

ABSTRACT

Analysis of vibrational structure. —The electronic band system of AgCl extending from $\lambda 3124$ to $\lambda 3400$ has been obtained in emission and absorption, the latter under high dispersion. A complete vibrational quantum analysis has been carried out, giving the following formula for the heads of the bands of the molecule $\text{Ag}^{107}\text{Cl}^{35}$:

$$\nu = 31574.4 + 275.0\nu' - 6.20\nu'^2 - 0.133\nu'^3 - 342.4\nu'' + 1.163\nu''^2.$$

The data give $\omega_e'' = 343.6 \text{ cm}^{-1}$, $\omega_e' = 281.0$, and $\nu_e = 31606.9 \text{ cm}^{-1}$. Vibrational quantum numbers have been assigned to Franck and Kuhn's data for AgBr and AgI.

Isotope effects. —The vibrational isotope effect was observed for both the Cl and the Ag atoms. The complete spectrum consists of four overlapping systems due to the four possible isotopic molecules. The order of magnitude of the isotope shift for the Cl isotope effect was 1 to 30 cm^{-1} ; for the Ag isotope effect, 1 to 4 cm^{-1} . The agreement of observed shifts with those calculated from the equations recently derived by Birge (not yet published) is close.

Energies and products of dissociation. The heats of dissociation of the AgCl molecule are $D_0'' = 3.11$ volts in the normal state, $D_0' = 0.31$ volt in the excited state. The energy of excitation of the atoms resulting by dissociation from the excited state is 1.10 ± 0.12 volt. This value can be explained if it is assumed that $^2D'$ states exist in Ag as in Cu and Au. It is concluded that the silver halides dissociate from the excited state into a silver atom in a $^2D'$ state and a halogen atom in the metastable $^2P_{1/2}$ state.

INTRODUCTION

THE spectrum of silver chloride vapor consists of a system of single-headed bands in the ultra-violet, all the bands being shaded toward the red. These bands were first obtained by Franck and Kuhn¹ in absorption and fluorescence. Their work was concerned chiefly with a study of the type of molecular binding of the silver halides AgI, AgBr, and AgCl. Their results indicate that these molecules are of the "atom-molecule" type, in contrast to the alkali halide "ion-molecule" type. AgCl gave only a discontinuous band spectrum, whereas AgBr and AgI each showed a single continuous spectrum in addition to bands. The heats of dissociation of AgI and AgBr were calculated from the long wave-length limit of the continuous spectrum assuming that the product of dissociation from the excited state were a normal silver atom and an excited halogen atom. The heats of dissociation were also found independently by extrapolation of the fluorescence series. But for AgCl no direct calculation was possible by either method. The authors were not able to assign vibrational quantum numbers for any of these band systems. No mention was made of an isotope effect.

¹ Franck and Kuhn, *Zeits. f. Physik*, **43**, 164 (1927); **44**, 607 (1927).

In the present research, a complete vibrational quantum analysis of the AgCl band spectrum has been made. Accurate determinations of the heats of dissociation of the molecule in both the normal and the excited states lead to new conclusions as to the products of dissociation of the silver halides. In addition, the vibrational isotope effect of both atoms simultaneously has been obtained.² This is the first time the silver isotope effect has been obtained in spectra.

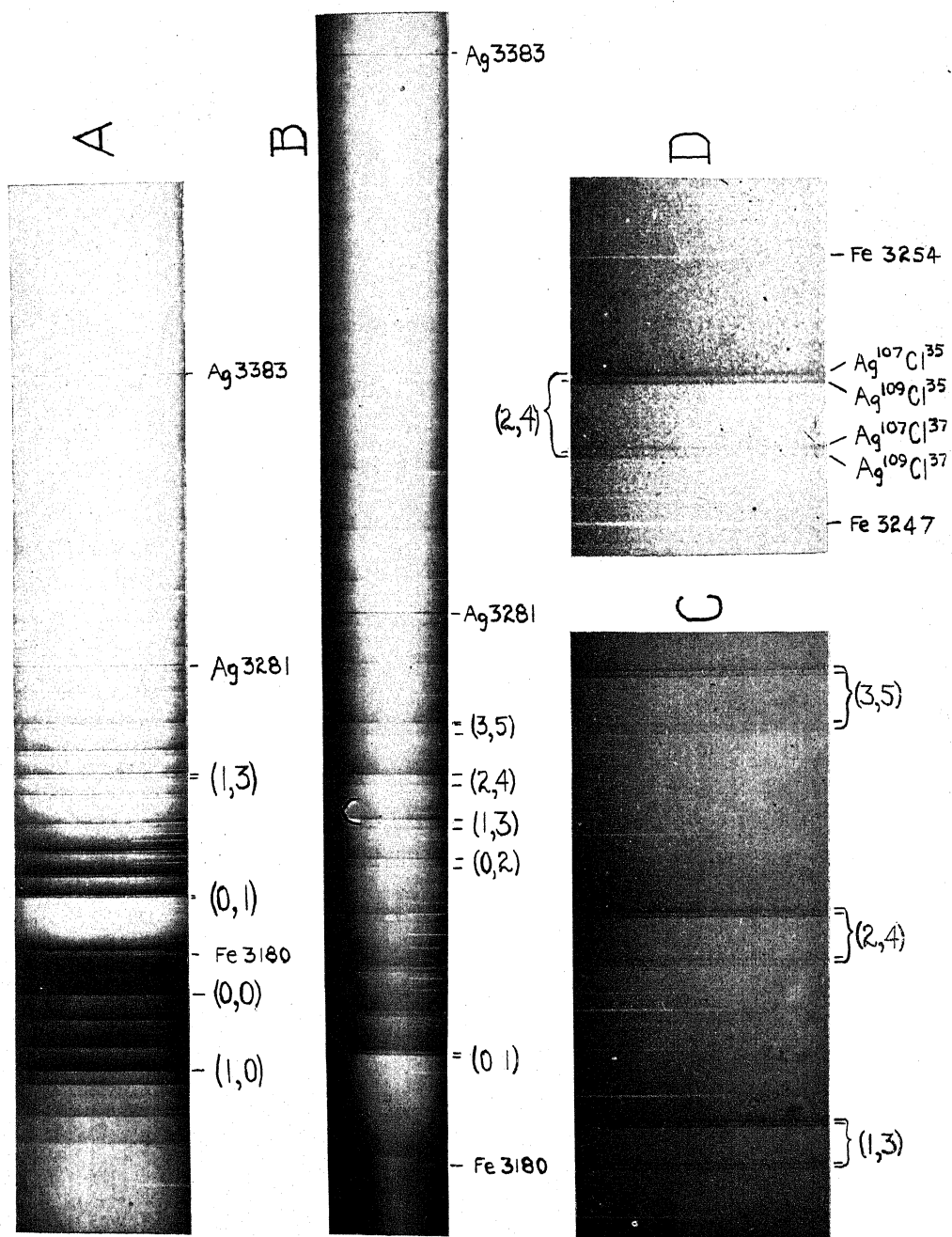
EMISSION SPECTRUM

The silver chloride band spectrum was obtained in emission³ by viewing the region immediately above a long silver electrode covered with fused AgCl, in a high voltage discharge in hydrogen at about 1 mm pressure. Photographs were made with a quartz Hilger E2 spectrograph. The small number of bands appearing in emission permitted a ready assignment of vibrational quantum numbers. The heads of the following bands were obtained in emission: (0, 0), (1, 0), (0, 1), (1, 1), (2, 1), (1, 2), (3, 2), (2, 3), (3, 4). Of the bands recorded by Franck and Kuhn, those which do not fit into this assignment can be shown to belong to the fainter isotope molecule AgCl³⁷. In order to extend the observations of the isotope effect and to obtain accurate values for

TABLE I. Wave-lengths and wave-numbers of observed heads. F. & K., bands observed by Franck and Kuhn.

(v', v'')	Ag ¹⁰⁷ Cl ³⁵		Ag ¹⁰⁹ Cl ³⁵		Ag ¹⁰⁷ Cl ³⁷		Ag ¹⁰⁹ Cl ³⁷		F. & K.
	λ	ν	λ	ν	λ	ν	λ	ν	
(2, 0)	—	—	—	—	3114.60	32077.0	—	—	32096
(3, 1)	3124.17	31999.3	—	—	3124.79	31992.9	—	—	32005
(4, 2)	3135.10	31887.7	—	—	3135.39	31884.7	—	—	—
(1, 0)	3139.70	31841.0	—	—	3140.15	31836.4	—	—	31845
(2, 1)	3147.93	31757.7	—	—	—	—	—	—	31760
(3, 2)	3157.48	31661.7	—	—	—	—	—	—	31663
(0, 0)	3166.21	31574.4	—	—	—	—	—	—	31579
(1, 1)	3173.35	31503.4	—	—	3173.60	31500.9	—	—	31506
(2, 2)	3181.95	31418.2	—	—	3181.59	31421.8	—	—	31426
(0, 1)	3200.81	31233.1	—	—	3200.07	31240.3	—	—	31243
(1, 2)	3208.03	31162.8	—	—	3207.14	31171.4	—	—	31174
(2, 3)	3216.26	31083.0	—	—	3215.28	31092.5	3215.16	31093.7	31094
(3, 4)	3225.79	30991.2	—	—	3224.46	31004.0	—	—	30998
(0, 2)	3235.98	30893.7	3235.82	30895.2	3234.50	30907.8	3234.31	30909.6	30908
(1, 3)	3243.18	30825.0	3242.97	30827.0	3241.50	30841.0	3241.31	30842.8	30833
(2, 4)	3251.35	30747.6	3251.14	30749.6	3249.47	30765.4	3249.24	30767.6	30755
(3, 5)	3260.77	30658.8	3260.52	30661.2	3258.63	30678.9	3258.35	30681.5	30667, 30687
(4, 6)	3271.76	30555.8	3271.46	30558.6	3269.26	30579.2	3268.98	30581.8	30564
(1, 4)	3278.63	30491.8	3278.33	30494.6	3276.23	30514.1	3275.91	30517.1	30495
(2, 5)	3286.77	30416.3	3286.48	30418.9	3284.15	30440.5	3283.87	30443.1	30422
(3, 6)	3296.20	30329.3	3295.87	30332.3	3293.30	30356.0	3292.94	30359.3	30335, 30366
(4, 7)	3307.14	30228.9	3306.82	30231.8	3303.91	30258.5	3303.49	30262.3	30235, 30262
(2, 6)	3322.77	30086.7	3322.42	30089.9	—	—	—	—	—
(3, 7)	3332.14	30002.1	3331.73	30005.8	—	—	—	—	30008
(4, 8)	3343.11	29903.7	3342.70	29907.4	—	—	—	—	29912
(4, 9)	3379.55	29581.2	3379.10	29585.2	—	—	—	—	29590
(5, 7)	—	—	—	—	—	—	—	—	30443
(5, 8)	—	—	—	—	—	—	—	—	30118
(5, 9)	—	—	—	—	—	—	—	—	29795
(6, 10)	—	—	—	—	—	—	—	—	29655
(3, 8)	—	—	—	—	—	—	—	—	29689
(5, 10)	—	—	—	—	—	—	—	—	29475
(6, 11)	—	—	—	—	—	—	—	—	29327
(4, 10)	—	—	—	—	—	—	—	—	29270
(5, 11)	—	—	—	—	—	—	—	—	29161
(6, 12)	—	—	—	—	—	—	—	—	29014
(5, 12)	—	—	—	—	—	—	—	—	28839
(6, 13)	—	—	—	—	—	—	—	—	28694

² B. A. Brice, Phys. Rev. **34**, 1227 (1929) (Letter).³ B. A. Brice, Phys. Rev. **33**, 1090 (1929) (Abstract).



SILVER CHLORIDE ABSORPTION

Fig. 1.

the heats of dissociation, it was considered worth while to photograph AgCl vapor in absorption under high dispersion.

ABSORPTION SPECTRUM

The absorption spectrum was obtained by passing white light from a tungsten quartz lamp through AgCl vapor. The salt was heated to about 900°C in an open quartz tube 2 ft long surrounded by an electric furnace. Photographs were taken using a 21 ft concave grating, giving a dispersion of 2.5 Å/mm in the first order and 1.3 Å/mm in the second order. The grating* is mounted according to Paschen in a temperature-controlled room. The photographs are reproduced in the accompanying plate. Photograph *A* shows the first order spectrum, *B* the second order; the enlargements *C* and *D* illustrate in more detail the isotope effect, showing the four heads composing each band. The comparison spectrum is that of an iron arc, the standard wave-lengths being taken from Kayser's Handbuch Vol. VII.

Table I gives the wave-lengths in air of the observed heads. The corresponding wave-numbers are corrected to vacuum by using Kayser's table. The values recorded are the mean of two independent measurements on a first order plate and one on a second order plate. The heads given by Franck and Kuhn are also recorded for comparison. It is evident that their measurements are from 3 to 10 cm⁻¹ too high.

VIBRATIONAL ANALYSIS

Throughout this paper the notation used will be as far as possible consistent with that proposed recently by Mulliken for the general theory of band spectra, and that proposed by Birge⁴ for the isotope theory. The *true* vibrational quantum number is integral, $v=0, 1, 2, \dots$; the *effective* quantum number is half-integral, $u=v+\frac{1}{2}$. Subscripts *e* refer to the vibrationless but impossible state for which $u=0$; subscripts 0 refer to the lowest possible vibrational state, for which $u=1/2$.

The possible energy levels of a non-rotating molecule are given by

$$G_u = \omega_e(u - x_e u^2 + y_e u^3 + \dots) \quad (1)$$

where ω_e is the mechanical vibration frequency for vanishingly small amplitude. The wave-numbers of the origins of the bands in the spectrum are

$$\nu = \nu_e + \omega_e'(u' - x_e' u'^2 + y_e' u'^3 + \dots) - \omega_e''(u'' - x_e'' u''^2 + y_e'' u''^3 + \dots) \quad (2)$$

where ν_e corresponds to the electronic energy change, and is defined as the origin of the band system. The classical vibration frequency is obtained from Eq. (1) by differentiation: $\omega_u = dG_u/du$. But experiment yields values of $\omega_{u+1/2}$, which is the spacing of the energy levels. From Eq. (1)

$$\omega_{u+1/2} = G_{u+1} - G_u = \omega_e u [1 - 2x_e(u + \frac{1}{2}) + 3y_e(u + \frac{1}{2})^2 + \dots] \quad (3)$$

* The Anderson grating used at present in this mounting is the property of Townsend Harris Hall, College of the City of New York.

⁴ R. T. Birge, unpublished work.

If the data are sufficient, a plot of the observed spacings $\omega_{u+1/2}$ against $u + \frac{1}{2}$ can be used to determine the constants of Eq. (2). The value of ω_u for any value of u can then be obtained from the resulting curve by interpolation or extrapolation. Eq. (2) will then represent the origins (or heads, in practice) of the observed bands.

It is found experimentally that for non-polar molecules the $\omega_u:u$ curve is linear for low values of u , and that extrapolation of the linear part to $u = u_0$ when $\omega_u = 0$ leads to a fairly reliable determination of the heat of dissociation.⁵ This gives $u_0 = \omega_e / 2x_e\omega_e$. Geometrically the heat of dissociation is given by the area under the $\omega_u:u$ curve:

$$D_e = \int_0^{u_0} \omega_u du = \frac{1}{2} \frac{\omega_e^2}{2x_e\omega_e} \quad D_0 = \int_{1/2}^{u_0} \omega_u du = \frac{1}{2} \frac{\omega_0^2}{2x_e\omega_e} \quad (5), (6)$$

Eq. (5) gives the heat of dissociation referred to the equilibrium state. Eq. (6) is the *true* heat of dissociation, referred to the lowest possible vibrational state. There will be a value D_0'' for dissociation by vibration from the normal state, and a value D_0' for the excited state.

Fig. 2 shows the observed heads of the most abundant molecule $\text{Ag}^{107}\text{Cl}^{35}$ arranged in the customary array which determines the true assignment of vibrational quantum numbers, and which yields the experimental values of $\omega_{u+1/2}''$ and $\omega_{u+1/2}'$. The intensity distribution here is characteristic of molecules having a small change in moment of inertia on electronic transition.

$v'' \backslash v'$	0	1	2	3	4	5	6	7	8	9	10	11	12	13
0	(10)	(9)	(3)											
1	(9)	(5)	(9)	(5)	(2)									
2	(2)	(8)	(4)	(8)	(4)	(1)	(1)							
3		(3)	(7)		(3)	(3)	(1)	(1)						
4			(2)				(2)	(1)	(0)	(0)	(0)			
5								(0)	(0)	(0)	(0)	(0)		
6											(0)	(0)	(0)	(0)

Fig. 2. Assignment of vibrational quantum numbers. Numerals indicate estimated intensities. Dotted circles are additional bands observed by Franck and Kuhn.

Table II contains the values of ω_u for corresponding u , including both the experimental, and the extrapolated and interpolated values, which are needed later for calculating the isotope shifts. In Fig. 3 the $\omega_u:u$ curves for the most abundant molecule are A'' , A' . The curve A' for the excited state is not a straight line.

⁵ Birge and Sponer, *Phys. Rev.* **28**, 259 (1926). See also *Bull. Natl. Res. Council*, No. 57 (1926), p. 131; R. T. Birge, *Trans. Far. Soc.* **25**, 707 (1929).

TABLE II. Values of ω_u .

u	$\text{Ag}^{107}\text{Cl}^{35}$		$\text{Ag}^{109}\text{Cl}^{35}$		$\text{Ag}^{107}\text{Cl}^{37}$		$\text{Ag}^{109}\text{Cl}^{37}$	
	ω_u''	ω_u'	ω_u''	ω_u'	ω_u''	ω_u'	ω_u''	ω_u'
0	343.6	281.0	342.4	—	336.0	276	—	—
$\frac{1}{2}$	342.4	275.0	341.3	275	334.9	270	—	—
1	341.3	268.3	—	—	—	263.6	—	—
$1\frac{1}{2}$	340.2	262	339.0	262	332.7	257	—	—
2	339.0	255.1	—	255.0	332.5	251.1	—	250.7
$2\frac{1}{2}$	337.8	249	336.8	249	330.5	245	—	—
3	336.5	242.8	—	242.4	329.9	238.5	—	238.4
$3\frac{1}{2}$	335.5	235	334.5	235	328.3	231.3	—	—
4	334.3	226.4	332.4	226.2	327.0	223.2	325.9	222.5
$4\frac{1}{2}$	333.2	217	332.2	217	326.2	214	—	—
5	331.9	206 ?	330.7	—	325.0	—	324.5	—
$5\frac{1}{2}$	330.8	194 ?	330.0	194	324.0	—	—	—
6	329.6	173 ?	328.9	—	322.9	—	322.2	—
$6\frac{1}{2}$	328.5	—	327.8	—	321.8	—	—	—
7	327.1	—	326.7	—	320.7	—	319.5	—
$7\frac{1}{2}$	326.2	—	325.6	—	319.6	—	—	—
8	325.2	—	324.4	—	—	—	—	—
$8\frac{1}{2}$	323.8	—	323.3	—	317.4	—	—	—
9	322.5	—	322.2	—	—	—	—	—
$9\frac{1}{2}$	321.5	—	—	—	—	—	—	—
$10\frac{1}{2}$	319.2	—	—	—	—	—	—	—
$11\frac{1}{2}$	316.8	—	—	—	—	—	—	—
$12\frac{1}{2}$	314.5	—	—	—	—	—	—	—

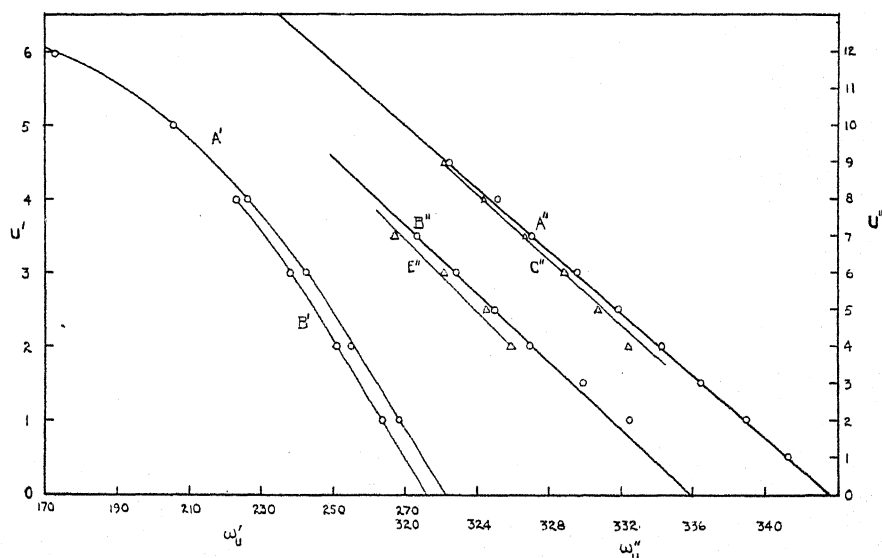


Fig. 3. u_u : u curves: A'' normal, A' excited state of $\text{Ag}^{107}\text{Cl}^{35}$; B'' normal, B' excited state of $\text{Ag}^{107}\text{Cl}^{37}$; C'' normal state of $\text{Ag}^{109}\text{Cl}^{35}$; E'' normal state of $\text{Ag}^{109}\text{Cl}^{37}$.

The equation representing the heads of the bands for the molecule $\text{Ag}^{107}\text{Cl}^{35}$, from Eq. (2) and the above data is:

$$\nu = 31574.4 + 275.0\nu' - 6.20\nu'^2 - 0.133\nu'^3 - 342.4\nu'' + 1.163\nu''^2 \quad (7)$$

The value of u'' for which the spacings of the levels becomes zero is $u_0'' = 148$. By Eq. (5), $D_e'' = 25390 \text{ cm}^{-1} = 3.13$ volts; by Eq. (6), $D_0'' = 3.11$ volts. The latter is the true heat of dissociation of the molecule $\text{Ag}^{107}\text{Cl}^{35}$. Its accuracy is estimated as ± 0.10 volt. This agrees closely with the value 3.1 volts taken from thermochemical data.*

For the excited state, extrapolation of the $\omega_u:u$ curve is somewhat uncertain. It is safe to assume however that a maximum value will be set by extrapolating a straight line drawn through the first three points. This gives $D_0' = 0.33$ volt. A lower limit may be set by calculating the area under the actual curve, using the empirical equation. This gives 0.28 volt. Hence we may take $D_0' = 0.31 \pm 0.02$ volt.

THEORY OF THE ISOTOPE EFFECT

The theory of the vibrational isotope effect, first formulated by Mulliken,^{5a} has recently been applied in a form more convenient for calculation of isotope shifts in bands of high vibrational quantum numbers by Gibson,⁶ Patkowski and Curtis,⁷ and R. T. Birge.⁴ Professor Birge has given a thorough discussion of the applicability of this method, and has kindly made his results available to the writer in advance of their publication. In the following, his notation will be followed, and some of his equations given. Superscripts i will refer to the "isotope" or less abundant molecule, while letters without superscript will denote the "main" or more abundant molecule.

The vibrational energy of a non-rotating molecule as given by Mulliken^{5a} is $G_u = f(u\mu^{-1/2})$ where $\mu = M_1M_2/M_1 + M_2$, the effective or reduced mass of the molecule, M_1 and M_2 being the relative masses of the two atoms composing the molecule. If an isotope of one of the atoms is present, the reduced mass of the isotope molecule is μ^i , and if we let $\rho = (\mu/\mu^i)^{1/2}$ the vibrational energy of this molecule is $G_u^i = f(u\rho\mu^{-1/2})$. Hence for a given value of u , regardless of the functional form of G_u given by Eq. (1), we obtain G_u^i by replacing u by $u\rho$. Writing Eq. (1) for the isotope molecule:

$$G_u^i = \omega_e[u\rho - x_e\rho^2u^2 + y_e\rho^3u^3 + \dots] \quad (8)$$

Subtracting Eq. (1) from Eq. (8) we obtain the general form of the isotope shift, as given by Birge:

$$G_u^i - G_u = \omega_e[(\rho - 1)u - (\rho^2 - 1)x_eu^2 + (\rho^3 - 1)y_eu^3 + \dots] \quad (9)$$

When an electron transition occurs, this becomes, in terms of the wave numbers of the origins of the bands,

* Taken from ref. 1.

^{5a} R. S. Mulliken, Phys. Rev. **25**, 119 (1925).

⁶ G. E. Gibson, Zeits. f. Physik **50**, 692 (1928).

⁷ Patkowski and Curtis, Trans. Far. Soc. **25**, 725 (1929).

$$\begin{aligned} \nu_0^i - \nu_0 = \Delta\nu_0 = & (\rho - 1)(\omega_e' u' - \omega_e'' u'') \\ & - (\rho^2 - 1)(\omega_e x_e' u'^2 - \omega_e'' x_e'' u''^2) \\ & + (\rho^3 - 1)(\omega_e y_e' u'^3 - \omega_e'' y_e'' u''^3) + \dots \end{aligned} \quad (10)$$

Eq. (10) can be used for calculating the direction and magnitude of the isotope shift when the data are sufficient to give an analytic function representing the bands. This is more general than Loomis's Eq. (7)⁸ and is in terms of half integral quantum numbers.

As shown by Birge, an approximate equation can be written for Eq. (9):

$$G_u^i - G_u = (\rho - 1)\omega_u u. \quad (11)$$

This gives, on transition,

$$\Delta\nu_0 = (\rho - 1)(\omega_u' u' - \omega_u'' u''). \quad (12)$$

The advantage of Eq. (12) is that it can be used independently of any functional form of G_u . It is necessary only to know the values of ω_u for the band whose isotope shift is to be calculated. The value of ω_u may be read directly from the $\omega_u:u$ curve, or interpolated linearly between $\omega_{u+1/2}$ and $\omega_{u-1/2}$, which are obtained directly from the spectrum.

This theory shows that the isotope effect is zero at the true origin of the band system. It also shows that the isotope shift does not increase uniformly as u increases. For, by differentiating Eq. (9) and equating the result to 0, a maximum value of the shift for a certain value $u = u_c$ is obtained. In case the $\omega_u:u$ curve is linear, u_c is approximately $1/2u_0$. The theory shows further that the apparent heats of dissociation D_e and D_e^i are equal. Geometrically, the $\omega_u:u$ curves for the main molecule and the isotope molecule cross each other at $u = u_c$, and the area under each is the same since $u_0/u_0^i = \rho$ and $\omega_e^i/\omega_e = \rho$. But the true heats of dissociation D_0 and D_0^i are not the same. The theory has been verified by Patkowski and Curtis⁷ by application to the bands of ICl, and by Birge⁴ to ICl and Cl₂, both of which involve isotope effects in the region of relatively high quantum numbers.

ISOTOPE EFFECT IN AgCl

The $\omega_u:u$ curves for the four isotopic molecules Ag¹⁰⁷Cl³⁵, Ag¹⁰⁹Cl³⁵, Ag¹⁰⁷Cl³⁷, and Ag¹⁰⁹Cl³⁷ are shown in Fig. 3. The curves for the excited states of the two Ag isotope molecules are not shown, since they almost coincide with the other two curves. The curves A'' and B'' for the normal states of the first set of Cl isotope molecules are very nearly parallel and show no intersection. But this is to be expected, since the extrapolated value of u_0'' was 148, and therefore u_c is about 74. However, the extrapolated values of ω_e for these molecules are in the ratio $336/343.6 = 0.978$, in close agreement with the calculated value of $\rho = 0.9794$. Also, for the strong pair of silver isotope bands, curves C'' and A'' , the ratio $\omega_e^i/\omega_e = 342.4/343.6 = 0.997$ in close agreement with $\rho = 0.9977$. However, due to the slight uncertainty in determining the

⁸ Bull. Natl. Res. Council, No. 57 (1926) p. 262.

TABLE III. *Isotope shifts.*

(v', v'')	$\text{Ag}^{107}\text{Cl}^{37} - \text{Ag}^{107}\text{Cl}^{35}$				$\text{Ag}^{109}\text{Cl}^{37} - \text{Ag}^{109}\text{Cl}^{35}$	
	$\rho - 1 = -0.020577$				$\rho - 1 = -0.020672$	
	$\Delta\nu$ obs	I $\Delta\nu$ calc	II $\Delta\nu$ calc	III $\Delta\nu$ calc	$\Delta\nu$ obs	$\Delta\nu$ calc
(2, 0)	—	-9.28	-8.27	—	—	—
(3, 1)	-6.5	-6.42	-6.39	-8.08	—	—
(4, 2)	-3.0	-2.72	-2.94	-5.77	—	—
(1, 0)	-4.6	-4.56	-4.57	-4.81	—	—
(2, 1)	—	-2.31	-2.30	-3.10	—	—
(3, 2)	—	+0.45	+0.49	-1.12	—	—
(0, 0)	—	+0.70	+0.69	+0.67	—	—
(1, 1)	+2.5	+2.41	+2.39	+2.13	—	—
(2, 2)	+3.5	+4.57	+4.58	+3.89	—	—
(0, 1)	+7.2	+7.67	+7.67	+7.70	—	—
(1, 2)	+8.6	+9.29	+9.24	+9.14	—	—
(2, 3)	+9.5	11.35	11.37	10.77	—	—
(3, 4)	12.8	13.93	13.92	12.67	—	—
(0, 2)	14.3	15.84	14.54	14.68	14.4	14.56
(1, 3)	15.9	16.08	16.08	16.09	15.8	16.08
(2, 4)	17.7	18.04	18.06	17.69	18.0	18.03
(3, 5)	20.3	20.51	20.56	19.51	20.4	20.52
(4, 6)	23.4	23.86	23.63	21.63	23.3	23.86
(1, 4)	22.0	22.77	22.76	22.94	22.6	22.78
(2, 5)	24.2	24.63	24.65	24.51	24.1	24.65
(3, 6)	26.7	27.03	27.04	26.30	26.9	27.04
(4, 7)	29.6	30.25	31.94	28.36	30.3	30.29
(2, 6)	—	31.14	31.15	31.28	—	—
(3, 7)	—	33.42	33.47	33.03	—	—

TABLE III (continued)

(v', v'')	$\text{Ag}^{109}\text{Cl}^{35} - \text{Ag}^{107}\text{Cl}^{35}$		$\text{Ag}^{109}\text{Cl}^{37} - \text{Ag}^{107}\text{Cl}^{37}$	
	$\rho - 1 = -0.002264$		$\rho - 1 = -0.002360$	
	$\Delta\nu$ obs	$\Delta\nu$ calc	$\Delta\nu$ obs	$\Delta\nu$ calc
(1, 2)	—	—	—	1.04
(2, 3)	—	—	1.2	1.27
(3, 4)	—	—	—	1.55
(0, 2)	1.7	1.60	1.8	1.63
(1, 3)	1.9	1.77	1.8	1.81
(2, 4)	1.9	1.99	2.2	2.02
(3, 5)	2.3	2.26	2.4	2.29
(4, 6)	2.6	2.62	2.6	2.66
(1, 4)	2.5	2.50	3.0	2.56
(2, 5)	2.7	2.71	2.5	2.76
(3, 6)	3.0	2.97	3.1	3.03
(4, 7)	2.9	3.33	3.8	3.38
(2, 6)	3.3	3.43	—	3.49
(3, 7)	3.3	3.68	—	3.75
(4, 8)	3.8	3.95	—	4.09
(4, 9)	4.2	4.71	—	—

proper slopes, it cannot be verified from the data that D_e is the same for all the molecules and D_0 different.

Curves A' and B' for the excited states of the first set of Cl isotope bands apparently show approach of intersection. The value of u_0' could not be accurately determined, but probably lies between 15 and 23. Hence the cross-over value u_c' is probably just outside the range of observation.

Table III contains the observed and calculated isotope shifts. Values of $\Delta\lambda$ were calculated from the mean of the observed displacements from the original measurements of the plates, and not the difference between the mean wave-lengths of Table I. The observed $\Delta\nu$ were calculated from these $\Delta\lambda$. The values of $\rho - 1$ are also recorded in this table for the four sets of isotope bands. The main molecule in each case is written in italics. For the first set of Cl isotope bands, the calculated values of $\Delta\nu_0$ were obtained in three ways for comparison: column I using the approximate Eq. (12), column II the analytic Eq. (10), and column III the old equation $\Delta\nu = (\rho - 1)\nu_u$ where ν_u is the difference between the wave-numbers of the head of the main molecule and ν_e , the origin of the band system. All three methods agree about equally well for most of the shifts. But Eqs. (10) and (12) are superior when high values of u' are involved. The old equation gives very poor agreement for bands having a high u' and low u'' . This is to be expected, since III should agree asymptotically with I and II for low quantum numbers, and the greatest departure of III should occur when u is relatively high, as it is here in the excited state. The observed values of u in the normal state are relatively low.

The shifts for the other sets of isotope bands were calculated by Eq. (12). The observed shifts for the Ag isotopes are somewhat erratic due to the smallness of separation of the heads and their lack of sharpness, as well as their faintness in some cases. The results here confirm the existence of two isotopes of silver, of relative mass 107 and 109.

PRODUCTS OF DISSOCIATION

It has been shown by Franck,⁹ Dymond,¹⁰ and others that when absorption of light by an "atom-molecule" results in dissociation by vibration from the excited state, at least one of the resulting atoms is excited. From a study of the $\omega_u:u$ curves in the normal state, Birge and Sponer¹¹ showed it quite probable that most molecules in dissociating by vibration from the normal state yield two normal atoms. The difference between the total energy (measured from the normal state) required to dissociate the molecule in the two cases should correspond to the amount of excitation of the resulting atoms. Hence, if a continuous spectrum exists which corresponds to the convergence limit of the $u'' = 0$ progression of the vibration bands, then by subtracting the lowest excitation energy in one of the resulting atoms from the long wave-length limit of this continuum, a value for the normal heat of dissociation D_0'' is obtained. For example, this was done by Dymond for I_2 .

⁹ J. Franck, Trans. Far. Soc. 22, 536 (1925).

¹⁰ Dymond, Zeits. f. Physik 34, 553 (1925).

¹¹ Birge and Sponer, see ref. 5.

Conversely, if it is possible from the data for a given molecule to determine the heats of dissociation in both the normal and excited states, it is sometimes possible to find the states of the atoms resulting by dissociation.

In their work on the silver halides, Franck and Kuhn¹ report a continuous spectrum for AgI overlapping the discontinuous bands, and showing a maximum at $\lambda 3170$. The long wave-length edge is variable with temperature and pressure. Assuming a normal silver atom and an excited (metastable) iodine atom formed by dissociation, and adding to this atomic energy the thermochemical value of D_0'' , they obtained an energy value agreeing approximately with the observed long wave-length limit at $\lambda 3740$. It appears to the writer that the use of the long wave-length limit of this continuum is in this case not at all reliable. Furthermore, the writer's conclusions as to the products of dissociation differ from Franck and Kuhn's. The use of the maximum at $\lambda 3170$, which is on the high frequency side of the bands, would give close agreement. The same criticism would apply to AgBr. No continuous spectrum appeared with AgCl.

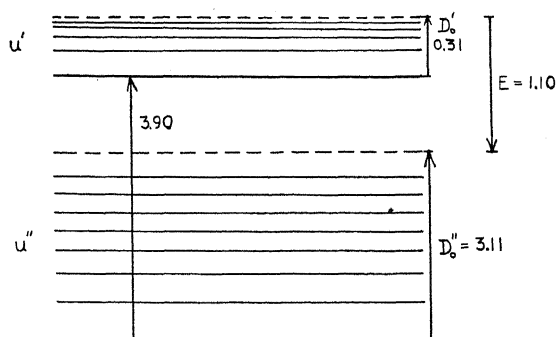


Fig. 4. Energy relations in AgCl.

Fig. 4 summarizes the results obtained in the present paper for AgCl. $D_0'' = 3.11 \pm 0.10$ volts, $D_0' = 0.31 \pm 0.02$ volt, and the energy corresponding to the (0, 0) band is 3.90 volts. This leaves 1.10 ± 0.12 volts as the electronic excitation of the atoms resulting by dissociation. In accounting for this energy, several possibilities must be examined. If the products are: (1) Ag^+ and Cl^- , the resultant energy would be the ionization potential of Ag minus the electron affinity of Cl, or $7.53 - 4.1 = 3.42$ volts. (2) Normal Ag and excited Cl; the separation $^2P_{1/2} - ^2P_{3/2}$ in the normal state of Cl is 0.11 volt. This is the process which would be assumed consistent with Franck and Kuhn's conclusions. Other levels in the Cl atom may be excluded because of their high energy. (3) Excited Ag and normal Cl; this case was barred by Franck because of the large separation between the 2P and 2S levels of silver. (4) Both atoms excited.

The present results definitely exclude cases (1) and (2) even allowing a wide limit of error. However, (3) and (4) may be considered. Now in both Cu and Au there exist 2D states between the 2P and 2S states, due to terms based

on the d^9 s configuration of the ion.¹² The lines of the Ag spectrum have not been completely classified, but since Ag stands between Cu and Au in the periodic table, it is a plausible assumption that these low-lying states exist also in Ag.¹³ If the silver halides dissociate into a normal halogen atom and a silver atom in this metastable $^2D(d^9s^2)$ state, then the electronic energy obtained as indicated in Fig. 4 should be *constant* for all three silver halides.

The writer has succeeded in assigning vibrational quantum numbers to Franck and Kuhn's data¹ for AgI and AgBr. This assignment is shown in

AgI

$v \backslash v''$	0	1	2	3	4	5	6	7	8	9	10	11	12	13
0	×	×	×	×	×	×	×	×		×	×	×	×	×
1	×	×	×			×	×	×						
2	×													
3	×													
4	×													

AgBr

$v \backslash v''$	0	1	2	3	4	5	6	7	8	9	10	11	12	13
0	×	×	×	×	×	×	×	×	×	×	×	×		
1			×		×	×	×	×	×					
2			×	×	×	×	×	×	×	×				
3														

Fig. 5. Assignment of vibrational quantum numbers to AgI and AgBr.

Fig. 5, which includes both absorption and fluorescence bands. Approximate equations representing the bands are as follows:

$$\begin{aligned}\text{AgI: } \nu &= 31153 + 127.5v' - 5.7v'^2 - 205.7v'' + 0.57v''^2, \\ \text{AgBr: } \nu &= 31421 + 179.4v' - 9.5v'^2 - 249.4v'' + 0.83v''^2.\end{aligned}$$

This gives for AgI, $\omega_0'' = 205.7 \text{ cm}^{-1}$ and $\omega_0''x'' = 0.57$, and for AgBr $\omega_0'' = 249.4$, $\omega_0''x'' = 0.83$. These agree with the values deduced by Birge from Franck and Kuhn's data, 205.8, 0.56, 247.2, and 0.81 respectively.¹⁴ On account of the uncertainty of the measurements, the $\omega_u: u$ curves are uncertain, and the heats of dissociation obtained by this data are not very accurate. But it is certain that the heats of dissociation in the excited states are very small and therefore a large error in determining them by extrapolation will not affect the results appreciably.

¹² Grotian, *Graphische Darstellung von Atomen . . . I*, p. 73, II, p. 44, 51, A. G. Shonstone, *Phys. Rev.* **28**, 449 (1926) Cu.

¹³ But the d^{10} s configuration of Ag is expected to be more stable for Ag than for Cu or Au. See Hund's "Spectrallinien" p. 169-170; also R. Ruedy, *Jour. de Phys. et le Radium* **10**, 129 (1929); also *Trans. Far. Soc.* **25** (Dec. 1929) p. 752 (Bengtsson and Hulthén). For evidence of instability see J. Kaplan *Zeits. f. Phys.* **52**, 883 (1929).

¹⁴ *Int. Crit. Tables*, Vol. V, p. 411 (Birge's table).

As in Fig. 4 we may now calculate approximately the resulting electron excitation E of the dissociation products by the sum $\nu_0 + D_0' - D_0'' = E$, where ν_0 represents the energy corresponding to the (0, 0) band. For AgBr and AgI we will use the thermochemical values¹⁴ for D_0'' and the extrapolated values from the above analysis for D_0' .

$$\text{AgCl: } 3.90 + 0.31 - 3.11 = 1.10$$

$$\text{AgBr: } 3.88 + 0.11 - 2.6 = 1.39$$

$$\text{AgI: } 3.85 + 0.09 - 2.0 = 1.94$$

The resulting values of E are thus not constant. But if we now subtract from these values of E the ${}^2P_{1/2} - {}^2P_{3/2}$ separation in the normal states of the halogens, which are respectively 0.11, 0.46, 0.94 volt¹⁵ we obtain for E in the three cases 0.99, 0.93, 1.00 volt respectively, which is now very nearly constant. This indicates that the silver halides dissociate from the excited state into a silver atom in a ${}^2D(d^9s^2)$ state and a halogen atom in the ${}^2P_{3/2}$ state.

As in Cu and Au, combinations may occur in the silver atom between the 2P and these ${}^2D'$ terms. Assuming the ${}^2D'$ level to be 0.99 ± 0.1 volt, or $8000 \pm 800 \text{ cm}^{-1}$, above the normal 2S level, we would expect a line in the Ag spectrum at $4400 \pm 150 \text{ \AA}$ for the transition ${}^2P_{3/2} - {}^2D_{3/2}'$. There are several fairly strong unclassified lines in this region. Referring to Kayser's Handbuch Vol. VII, the two lines $\lambda 4888.3 (2u)$ and $\lambda 4677.9 (4u)$ have a wave-number separation 920 cm^{-1} , which agrees with the 2P doublet separation. They are the only lines found giving this difference. Hence it is possible that they correspond to transitions ${}^2P_{3/2} - {}^2D_{1/2}'$ and ${}^2P_{1/2} - {}^2D_{1/2}'$ in Ag. The next line of the same type as these two is $\lambda 4396.3 (2u)$. If this is the ${}^2P_{3/2} - {}^2D_{3/2}'$ line, this leaves 7731 cm^{-1} or 0.955 volt for the ${}^2D' - {}^2S$ separation. This is in close agreement with the above value $E = 0.99$ volt deduced from the band spectrum of AgCl. Extrapolations such as were made in obtaining this value should be done cautiously. But even allowing a wide limit of error, the conclusions seem to be unaffected.

The above agreement may indeed be accidental, and awaits further testing by the final analysis of the Ag spectrum,* and by more accurate work on the band spectra of AgI and AgBr. The latter will be carried out by the author in the near future.

In conclusion, the writer expresses much appreciation for the valuable suggestions and constant interest of Dr. F. A. Jenkins, under whom this work was begun. I also am greatly indebted to Professor R. T. Birge for use of his manuscript on the vibrational isotope effect. Suggestions and interest of Dr. F. W. Loomis, and Dr. G. Breit were also helpful.

¹⁵ L. A. Turner, Phys. Rev. 27, 397 (1926).

* Dr. A. G. Shenstone has kindly informed me that his recent work on the Ag spectrum predicts these ${}^2D(d^9s^2)$ terms to be near 30000 cm^{-1} , close to the 2P terms, with a doublet separation of about 5000 cm^{-1} . He believes that the lines mentioned above are due to the terms ${}^4P^{\circ}D^{\circ}F^{\circ}(d^9sp)$ combining with ${}^4D(d^9s, s)$, though he has not as yet been able to identify them. If this is correct, the value of E obtained by the writer remains unexplained.

THE RELATION BETWEEN THE INTENSITY AND POSITION
OF THE OVERTONES OF SOME ORGANIC LIQUIDS

BY P. E. SHEARIN

UNIVERSITY OF NORTH CAROLINA

(Received February 20, 1930)

ABSTRACT

A theoretical study of the intensity relations of the overtones of some organic liquids has been made with a view of determining whether there exists a relation between the intensity and position of overtones. A brief summary of some of the work that has been done by other observers is included. By the graphical method the intensities of the first and second overtones of some liquids were measured. These results, together with the ratio of the intensities of the first and second overtones and also a list of the products of this ratio times the correction factor, x , are given in a table. Values are also listed for three diatomic gases, the intensities having been obtained by other observers and the ratio of these intensities times the correction factor being calculated in this work. For both the liquids and the gases the product of the ratio of the intensities of the first and second overtones and the correction factor, x , is of the same order of magnitude and, in consideration of the errors involved, appears to be constant.

A STUDY of the intensity relations of the overtones of some polyatomic molecules in the liquid state has been made with the purpose of determining whether there exists any relation between the relative intensities of the overtones and the correction factor as applied to the position of the bands. The position of an overtone is given by the relation, $\nu_n = n\nu_0(1 - nx)$, where ν is the frequency of the overtone, n the number of the overtone, ν_0 the theoretical frequency of the fundamental band and x the correction factor. Some calculations have already been made on the intensity relations for the fine structure of gases by several observers. Dennison¹ has, through the aid of the correspondence principle, computed the intensities of certain infra-red bands in order to gain information concerning the structure of the molecule. He computed the intensities of harmonic bands of some diatomic molecules—HCl, HBr and HF. Since some of the constants used in the calculations depend upon a knowledge of the fine structure of the bands, the method could not be used generally. In order to check the results, the relative intensities of overtones were obtained from experimental curves by taking for each band the maximum value of the absorption coefficient, α , rather than the actual value of the integral, $\int_0^\infty \alpha d\nu$.

The intensities of bands of symmetrical triatomic molecules and of axially symmetrical molecules with four atoms were studied by making certain assumptions concerning the relative positions of the atoms in the molecule, and it was found that the experimental and theoretical values were of the same order of magnitude.

¹ Dennison, Phil. Mag. 1, 195 (1926).

Tolman² made some calculations of intensities of lines by graphical integration under the experimental curve for the absorption coefficient, and also by making the approximation of putting the integral, $\int_0^\infty \alpha_\nu d\nu$, proportional to the product of the maximum value of α_m and the spectral width, $\Delta\nu$, at which the value of α has sunk to one half its maximum value. This relation may be denoted by the following equation:

$$\int_0^\infty \alpha_\nu d\nu = K\alpha_m\Delta\nu.$$

Dennison,³ in a more recent paper, has investigated the intensities and shapes of absorption lines of HCl. Formulae for comparing the relative intensities of a set of lines were developed. The area under the curve was measured in relative absorption times waves per cm.

The studies which have been briefly outlined above were all made upon the fine structure of the bands of gases. In the case of liquids this fine structure overlaps to such an extent that the individual lines cannot be observed at all, but only their envelope, which may be considered as the addition of all the separate lines in the band. In order to obtain the intensity of such a band the integral $\int_0^\infty \alpha_\nu d\nu$, was evaluated by the graphical method. The area under the curve was divided into a number of very narrow strips. The area of each strip was measured, and the sum of the areas of the rectangles taken as the area under the curve. The original curves were plotted in percent transmission as a function of spectrometer settings rather than in the coefficient of absorption as a function of waves per cm; however, the percent transmission was changed to coefficient of absorption by plotting a curve for each cell thickness showing relative transmission as a function of the coefficient of absorption. The relation between the relative transmission, I/I_0 , the coefficient of absorption, α , and cell thickness, d , is given by the following equation: $\alpha = [\log(I/I_0)]/d$. In another curve the spectrometer settings were plotted against waves per cm. The dimensions of the small rectangles were found in terms of percent transmission and spectrometer settings. Each value was then changed to absorption coefficient or to waves per cm as the case might be. The curves which were used were greatly enlarged by projecting them on a piece of coordinate paper by means of a projection lantern.

Although a large number of measurements of infra-red bands have been made, most of them have been taken with prism spectroscopes of low resolving power and large slit width. The true shape of the band is lacking due to the width of the slit, and the true position of the band cannot be determined accurately due to the low resolving power of the instrument. The emphasis has been placed upon the position of the bands rather than upon their true shape. These and other inaccuracies make many curves which have been observed, useless for intensity calculations. However, in the work of Spence^{4,5},

² Tolman, *Phys. Rev.* **23**, 693 (1924).

³ Dennison, *Phys. Rev.* **31**, 503 (1928).

⁴ Easley, Fenner and Spence, *Astrophys. J.* **67**, 185 (1928).

⁵ Spence and Easley, *Phys. Rev.* **34**, 730 (1929).

and his associates the absorption bands of several organic liquids have been measured with great accuracy. Their measurements were made with a grating spectrometer of slit width 0.25 mm. The settings were made with an accuracy corresponding to 0.5Å. A grating with 10,000 lines to the inch was used up to 2μ . From this point on it was necessary to use a grating with 2,500 lines per inch. The entire range was gone over with cells of 1.4 cm, 0.7 cm, and 0.15 cm thickness. The absorption of the cell walls was compensated for by having two quartz plates of the same thickness of the cell walls to place in the beam of light when the cell was removed.

The relative intensity of the first and second harmonic bands of six different liquids as obtained by Spence and his associates was computed. Only six^{4,5} were used since the remainder of the curves were very irregular. It was thought that some of these irregularities might have been due to overlapping of other bands.

If overtones exist for an harmonic oscillator, the ratio of frequencies of the successive harmonics to the fundamental should be 2:3:4, etc. Due to the anharmonic oscillation, strong overtones or harmonics occur in some substances, and their frequencies are found to be in the ratio $2\nu_0(1-2x):3\nu_0(1-3x):4\nu_0(1-4x)$, etc., where x is a correction factor. The correction factor, x , and the relative intensity of the harmonics are both functions of the anharmonicity of the oscillation, so it seems probable that there should be some definite relation between the two. That this is the case is shown by the present work. The results of the calculations are listed in Table I. There are

TABLE I. *The intensity of the first and second harmonics of certain liquids and gases and the ratio of these intensities times the correction factor, x . (ρ_2^2 = intensity of first harmonic. ρ_3^2 = intensity of second harmonic.)*

Substance	ρ_2^2	ρ_3^2	Thickness of cell	ρ_2^2/ρ_3^2	x	(Ratio) (x)
CHCl ₃	352.62	97.50	1.4 cm	3.616	.0213	.082
CHCl ₃	388.60	97.50	.7*	3.986	.0213	.085
CHBr ₃	271.48	91.14	1.4	2.998	.0293	.088
CHBr ₃	189.22	91.14	.7*	2.076	.0293	.061
CH ₂ Cl·CHCl ₂	363.40	84.48	1.4	4.302	.0174	.075
CHBr ₂ CHBr ₂	377.32	195.88	1.4	1.926	.0391	.075
CHBr ₂ CHBr ₂	376.70	195.88	.7*	1.923	.0391	.075
CCl ₃ CHCl ₂	103.28	18.98	1.4	5.441	.0171	.093
CHCl ₂ CHCl ₂	143.38	51.74	1.4	2.789	.0201	.056
CO				14.3	.006	.086
HCl				5.0	.017	.085
HBr				5.8	.013	.075

* 0.7 cm applies to the first harmonics only.

also listed in this table values for CO, HBr and HCl. The relative intensities of the overtones for these three substances were taken from the work of other observers^{6,7}. The value for the relative intensity of the first and second overtones of CO is due to C. Schaefer and M. Thomas,⁶ the value of x being given

⁶ C. Schaefer and M. Thomas, *Zeits. f. Physik* 12, 330 (1923).

⁷ B. Burmeister, *Verh. d. D. Phys. Ges.* 40, 589 (1913).

by Burmeister.⁷ For HCl and HBr the values of x were computed from the work of Schaefer and Thomas. Using this and the value for the relative intensity of the fundamental and first overtone as given by Brinsmade and Kemble,⁸ the relative intensity of the first and second overtones was computed by means of the equation for x as given by Dennison.¹

Some very interesting relations can be noted in these results. In general as the value of x increases the ratio of the intensities of the first and second overtones decreases, or, in other words, as x increases the intensity of the harmonic band increases. The last column shows the product of the ratio and the value of x . It can be seen that this product is approximately a constant for the bands under consideration. The largest variation is in the value of $\text{CHCl}_2\text{CHCl}_2$. This discrepancy was not accounted for. The variation of the other values is well within the range of experimental error. The values for the three diatomic molecules, CO, HBr and HCl, as obtained by other observers are in excellent agreement with the results as obtained for the liquids.

In order to check the accuracy of the method used, the intensity of the first overtones of three different liquids was measured from the band obtained from a different cell thickness. The two values checked very closely except in the case of CHBr_3 . There evidently was some error in the drawing of the curve for cell thickness of 0.7 cm. By reference to these curves⁴ it can be seen that this band does not follow the form of the band for 1.4 cm cell thickness. For CHCl_3 the values checked very closely, and for $\text{CHBr}_2\text{CHBr}_2$ the check was almost perfect. The original bands did not extend to the 100 percent line, and some error was necessarily involved in the extrapolation of the bands to this line, but since the value of α is very small in this part of the band the error is not very great. In order to determine what possible error might be involved, one pair of curves was extrapolated in two ways, one extrapolation making the area much larger and the other making it much smaller than probable. It was found that the difference between the two areas amounted to about 10 percent.

While no general conclusion can be drawn from these results until a larger amount of data is available, yet it appears that, for the substances under consideration at least, the ratio of intensities of the first and second harmonic bands times the correction factor is approximately a constant.

The writer is indebted to Dr. E. K. Plyler who suggested the above problem.

⁸ J. Brinsmade and E. C. Kemble, *Proc. Nat. Acad.* 3, 420 (1917).

THE MAGNETIC SUSCEPTIBILITY OF RUBIDIUM

BY C. T. LANE*

MACDONALD PHYSICS LABORATORY, MCGILL UNIVERSITY

(Received February 27, 1930)

ABSTRACT

In view of the theoretical interest involved in Pauli's theory of paramagnetism, the author has reinvestigated the magnetic susceptibility of rubidium. The metal used is subjected to double distillation in vacuum to ensure purity. The technique employed for this is fully described. The susceptibility is determined at nine different field strengths ranging from approximately 9 to 25 kilogauss. No variation in the susceptibility of more than 2 percent is observed over this range. The estimated error in the mean value of the susceptibility is between 2 and 3 percent. The uniformity of the susceptibility, accordingly, shows absence of serious ferromagnetic impurity. The mean value of the mass susceptibility is found to be $+0.217 \times 10^{-6}$ at 20°C , the Pauli theoretical value being $+0.32 \times 10^{-6}$. A table is included showing the results found by all other investigators on this subject. The bearing of the results on the Pauli theory is discussed briefly.

I. INTRODUCTION

THE quantum statistics of an electron gas, first proposed by Fermi, has, in the hands of Sommerfeld, Pauli and many others, yielded much interesting information concerning the electrical and optical properties of metals. More particularly Pauli has applied these statistics to the calculation of the susceptibility of the alkali metals.¹ The agreement between theory and experiment in the case of the metals Na, K and Cs is, considering the nature of the Pauli calculation, quite remarkable.² In the case of rubidium however, upon which, up to the present work, three independent measurements have been made³ very wide differences exist both between one another and the theoretical result. From the point of view of divergence from the theory rubidium appears to be distinctly "anomalous," and this is the more remarkable when it is seen that the allied element caesium is in good agreement with the theoretical value.

The author has accordingly made a new determination of the susceptibility of this element applying the methods used in his previous work on this subject. The results of this investigation are communicated in the following pages.

II. PREPARATION OF THE METAL

The rubidium metal was supplied by Messrs. Eimer and Amend, New York, and stated to be "chemically pure." Nevertheless it was felt that fur-

* National Research Fellow, Canada.

¹ W. Pauli, *Zeits. f. Physik* **41**, 81 (1927).

² C. T. Lane and E. S. Bieler, *Proc. Roy. Soc. Can.* **22**, 117 (1928); C. T. Lane, *Phil. Mag.* **8**, 354 (1929).

³ M. Owen, *Ann. d. Physik* **37**, 657 (1912); W. Sucksmith, *Phil. Mag.* **2**, 21 (1926); McLennan, Ruedy and Cohen, *Proc. Roy. Soc. A* **116**, 468 (1927).

ther purification would be desirable especially since it is highly important to avoid even minute traces of ferromagnetic substances. Accordingly the metal was subjected to double distillation in vacuum.

Figure 1 shows, schematically, the apparatus by which this was accomplished. The necessary high vacuum was produced by a Langmuir mercury pump, backed with a Cenco "Hy-vac" pump. The former had attached to it the usual liquid air trap (L) consisting of a bulb of nut charcoal.

The distilling apparatus proper consisted of bulbs B_1 and B_2 fitted with a charging tube F and a ground glass stopper W . The specimen tube, into which the distilled metal is received is shown at S . The latter consists of a thin-walled glass tube, of uniform bore (about 0.4 mm) and some 18 cm long.

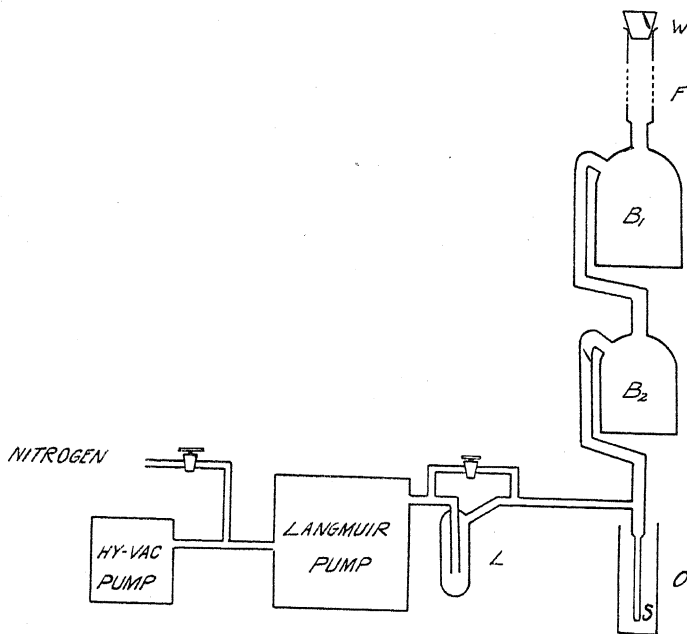


Fig. 1. Diagram of apparatus.

The diameter of the tube was uniform to within 1/5 percent. The whole apparatus was constructed of Pyrex glass.

The metal was received from the makers in 1 gr lots packed in a heavy oil. The tubes containing the metal were broken under petroleum ether, and the metal washed in two separate baths of the same material, and then quickly introduced into the charging tube F . While the charging was in progress a stream of nitrogen was kept flowing through the distilling apparatus. When the requisite amount of metal had been placed in F the nitrogen was cut off, the stopper W replaced and the whole apparatus pumped down. The metal was then melted into bulb B_1 and the tube F sealed off. An electric furnace was now placed over bulb B_1 and the metal gently distilled into bulb B_2 . Bulb B_1 was then sealed off from B_2 and the operation repeated until about half the metal in B_2 was distilled into the specimen tube S . The latter was

kept in an oil bath at a temperature of about 70°C. This was allowed to cool down to room temperature, and then was sealed off from the main apparatus. The distillation process took about two hours to perform.

III. METHOD OF MEASUREMENT

The Gouy method⁴ for measuring the susceptibility was used wherein the specimen in the form of a long cylinder is suspended between the poles of an electromagnet, the axis of the former being perpendicular to the lines of force. The downward pull on the cylinder is given by the relation

$$P = \frac{1}{2} \chi A d (H_1^2 - H_0^2)$$

where P is the force in dynes; χ the mass susceptibility; A the cross sectional area cylinder in cm²; d the density of specimen in gr per cc; H_1 the field in gauss in the magnet gap; and H_0 the field in gauss at the other extremity of the cylinder. The pull P was measured with a balance accurate to 1/50 mg. The magnetic field was produced by a large Weiss electromagnet provided with water cooling arrangements. An aluminum housing was built around the magnet in order to shield the specimen from draughts. The former was provided with a celluloid front through which the specimen could be observed at all times. A thermometer could also be observed through this window. The water control allowed a very constant temperature to be maintained in the housing. The measurements were carried out at about 20°C.

Due to the fact that the glass tube containing the metal is diamagnetic a blank test had to be performed upon it, at the various field strengths used. After the measurement had been made on the metal, the tube was cleaned out and re-exhausted of air and the blank test made at the same temperature as the original measurement.⁵

The magnetic field was measured by means of a null method, developed by the author, which has been fully described previously.⁶ A survey of the field in the vicinity of the magnet showed H_0^2 to be negligible compared to H_1^2 .

IV. RESULTS

The results of the measurement are given in Table I below, in each case the specific or mass susceptibility is quoted. In the first column is given the value of the exciting current in the magnet, in the second the force P corrected for the effect of the glass container and in the third and fourth the magnetic field intensity and mass susceptibility respectively. The density of rubidium (1.53) is the value quoted in "International Critical Tables."

The susceptibility is seen to be constant over the field range used (approximately 19 kilogauss) to within about 2 percent which is within the experimental error.

⁴ Stoner, "Magnetism and atomic structure," p. 40.

⁵ This latter point is important since the susceptibility of glass varies greatly with temperature. Some rough tests on the glass used here (Pyrex) indicated that it had a temperature coefficient of approx. $\frac{1}{3}\%$ per degree C. The temperatures at which the two measurements were made agreed to within 1°C. See in this connection Gerlach and Little, *Zeits. f. Physik* 52, 464 (1928).

⁶ C. T. Lane, reference 2.

TABLE I. *Mass-susceptibility of rubidium (20°C).*

Current in Magnet Coils (Amps.)	Force (<i>P</i>) Milligrams	Magnetic Field gauss	Mass susceptibility
3.0	1.92	9400	$+0.21_5 \times 10^{-6}$
3.6	2.71	11160	0.21 ₆
4.2	3.75	13150	0.21 ₅
4.8	4.97	15020	0.22 ₀
5.5	6.30	17040	0.21 ₆
6.2	7.90	19060	0.21 ₆
7.0	9.47	20950	0.21 ₅
9.0	12.50	23830	0.21 ₉
12.0	14.24	25300	0.22 ₁

Mean value $+0.21_7 \times 10^{-6}$
 Area cross section specimen = 0.1288 cm²
 Density = 1.53 gms per cc.

Owen⁷ has shown that if iron be present in the specimen we should have the following relation between susceptibility and field strength, viz.

$$x = x_0 + \sigma/H$$

where x is the measured susceptibility; x_0 the "iron free" value of susceptibility; σ the saturation intensity of magnetization (per unit mass) of the uncombined iron impurity; and H the magnetic field intensity. The susceptibility should therefore decrease with increasing field according to an hyperbolic law if any noticeable ferromagnetic impurity be present. The susceptibility should be independent of field strength if no noticeable impurity exists, as is the case in the present experiment.

In Table II the various experimental results on rubidium are collected, together with the theoretically predicted value. The estimated accuracy of the present measurement is between 2 and 3 percent.

TABLE II. *Various results on mass-susceptibility of rubidium.*
(All values to be multiplied by 10^{-6})

Observer	Owen 18°C	Sucksmith 0°C	McLennan, Ruedy, Cohen	Author 20°C	Pauli (calculated)
Mass susceptibility	+0.07	+0.07	+0.17	+0.21 ₇	+0.32

V. DISCUSSION

It is seen that the result found by McLennan, Ruedy and Cohen is in close agreement with the present work. The divergence between these results and those of Owen and Sucksmith may perhaps be accounted for by the fact that in the latter experiments no especial precautions were taken to ensure purity in the specimens used.

The most remarkable feature is the wide difference between the experimental and calculated values, especially in view of the fact that the agreement between theory and experiment in the case of Na, Rb and Cs is remarkably

⁷ M. Owen, reference 3.

close; nowhere differing by more than 10 percent of the calculated value. In this respect, then, rubidium seems to be anomalous.

We may recall that the Pauli formula for the susceptibility is

$$x = 12(\pi/3)^{2/3} \mu_0^2 n^{1/3} m_0 h^{-2} d^{-1} = 2.21 \times 10^{-14} n^{1/3} / d$$

where x is the mass susceptibility; n the number of free electrons per cc; d the density of the substance; μ_0 the value of the Bohr magneton; and m_0 and h have their usual significance. The only factor in this formula which might conceivably be incorrect is n , the number of free electrons per unit volume. Pauli makes the reasonable assumption that this is equal to the number of atoms per unit volume. Now in order to bring the theoretical value into agreement with the observed it would be necessary to suppose that n is actually about one-third its present accepted value, or rather, for some reason, only about one-third the number of free electrons per cc contribute to the paramagnetism. Of course we should not expect very close agreement with the Pauli formula since the latter neglects certain factors which should contribute to the susceptibility, viz.: (I) the diamagnetic effect of the atom cores; (II) a possible diamagnetic "induction" effect of the free electrons. We are at present unable to make any definite statement about the magnitude of these effects since no satisfactory theory for them has appeared.⁸ All we can say is that the Pauli formula should produce higher values than those observed.

In any event the Pauli theory can only be considered as provisional since in its present form it is quite unable to account for at least two important observed facts, namely, the observations of McLennan, Ruedy and Cohen on the variation of susceptibility with orientation in single crystals of zinc and cadmium⁹ and also on the observations of the author on the sudden change in susceptibility in passing over from the solid to the liquid state in the case of caesium.¹⁰

On the other hand, it must be remembered that it is the only theory in existence which even remotely gives the correct values for the susceptibility of the alkali metals, and further it accounts for that remarkable experimental fact that the susceptibility of the alkali metals (for a given state) is independent of the temperature.

In conclusion it gives me great pleasure to thank Dr. A. S. Eve, F. R. S. for his continued interest in this work. I am indebted also to Mr. H. G. I. Watson, Lecturer in Physics, for his aid in some of the numerical work.

⁸ Cf. L. Rosenfeld, *Naturwissenschaften* **17**, 49 (1929). In this paper Rosenfeld has estimated the diamagnetic effect of the cores as a function of the "lattice potential" (V_0) of the metal. The quantity V_0 is estimated from G. P. Thomson and Rupp's data on electron beam diffraction experiments. Since only the order of the quantity V_0 is known the correction appears rather uncertain. In any event no data whatever exist for the alkali metals.

⁹ McLennan, Ruedy and Cohen, *Proc. Roy. Soc. A* **121**, 9 (1928). In this paper the authors have apparently neglected to make a correction for the susceptibility of air which would have the effect of somewhat lowering their values. The values quoted for an isotropic crystal aggregate of Zn and Cd should be decreased by approximately 2.5 and 2.6 percent respectively. This brings their result into much better agreement with previous measurements.

¹⁰ C. T. Lane, reference 2.

SECONDARY ELECTRONS FROM CONTAMINATED SURFACES

BY PAUL L. COPELAND
STATE UNIVERSITY OF IOWA
(Received February 21, 1930)

ABSTRACT

Surface fields.—Small quantities of grease, or condensed vapors, or foreign metal upon a metallic surface have in the past been the cause of many spurious electrical effects. Stuhlmann and Compton cite a spurious contact potential difference of some 60 volts. Using electron reflection and secondary emission as a tool, some of the properties of such surfaces have been investigated. The results indicate that surface fields are set up retarding the reflected electrons.

Insulating layers.—New evidence is found for a sudden breakdown of the insulation of oils in thin films which has been investigated by Brüninghaus and by Watson and Menon. The bearing of the present results on suggested interpretations of the effect is briefly discussed.

THE fields in the neighborhood of incandescent filaments have been investigated^{1,2} through a study of characteristics of the saturation curve. In the present investigation an attempt is made to study the fields in the neighborhood of cold metallic surfaces. The currents used are obtained by reflection and secondary emission of electrons at the surface to be studied.

APPARATUS

The apparatus used is shown in Fig. 1. A filament, F , (of 7 mil tungsten wire) is placed at the center of a molybdenum cylinder, C , the diameter

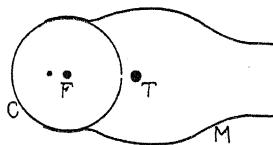


Fig. 1. Apparatus.

of which is about 1 cm. Electrons emitted by the filament are accelerated toward the cylinder by an applied potential. Some pass out through the slit (of width 0.25 mm) and strike the target, T , which is placed directly before it. The target consists of a second tungsten wire.

The potential of the cylinders, C and M , may be below that of the target, giving a field tending to prevent the escape of reflected electrons, or above it tending to accelerate them in their escape. With the cylinders at low potential, the escape may be almost entirely avoided; with C positive, the number

¹ Irving Langmuir, G. E. Rev. 23, 503 (1920).

² Becker and Mueller, Phys. Rev. 31, 431 (1928).

of electrons leaving may be greater than the primary ones which hit and the current to the target be actually positive.

The tungsten wire used for a target was in the earlier experiments a 10 mil and in the later experiments a 20 mil filament. This form of target was selected to facilitate the application of rather intense, homogeneous fields at its surface. With such a target, however, there is the danger that the full primary current will not strike it and, more serious, that the fraction which does strike it will vary as the field is changed. Fig. 2 shows the results of experiments performed to investigate this question. The current to the target was observed for different settings of the target near the slit as it was moved transverse to the slit. The numbered divisions correspond to motions of the target of approximately $1/7$ cm or 0.056 in. transverse to the slit.

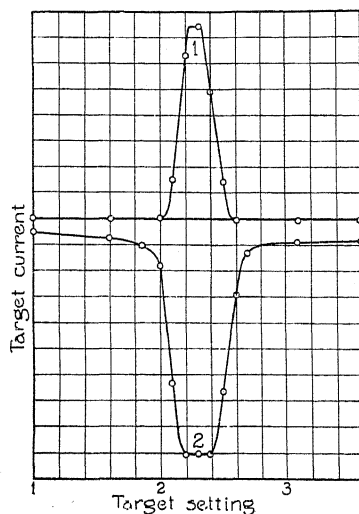


Fig. 2. Electron beam.

The curves in Fig. 2 show the results for a 20 mil target. The impacting speed was such as to produce large secondary emission in each case—in curve 1 this emission was allowed to leave; in curve 2 the field prevented secondary emission. In curve 1 the cylinders were maintained at a potential of 240 volts positive and the target 142 volts positive with respect to the source, F . Between the target and its surroundings was a potential difference of 98 volts, the field being in such a direction as to aid electrons in leaving the target. There is no current to the target until it comes into the direct electron beam from the slit. It rapidly approaches a maximum value and maintains this value while the target is moved about $1/7$ mm transverse to the slit.

In the second curve, the target is 142 volts positive, but the cylinders have been lowered to 60 volts positive with respect to the source. The general shape of the curve is much the same as before except that the current is reversed in sense. The flat plateau on both of these curves indicates that the

target is larger than the electron beam and hence receives the full current for a number of settings. This result would be expected from the dimensions involved. When using a 20 mil filament, the target is enough larger than the beam so that the primary current can be considered constant as the field about the target is changed. Probably also a 10 mil target receives nearly all of the current through the slit.

INFLUENCE OF THE SURFACE ELECTRIC FIELD ON SECONDARY EMISSION

To investigate the fields present at the surface of the target, the current carried by the target was observed as a function of the applied field, all the other conditions being held as nearly constant as possible. A given potential,³ which for any single curve was held constant, was applied between the filament and the target. The effect of variation of secondary emission with bombarding velocity was thus eliminated. In the curves which follow, the abscissas give the potential of the cylinders, *C* and *M*, relative to the target. The ordinates give the net current to the target. Electron currents to the target are plotted as negative.

In the investigation of surface fields, a tungsten wire, without any special treatment whatever, was fastened in place as a target. The current to the target was then measured for different fields determined by the potential of the cylinders relative to the target, and the resulting curve was plotted. The target was then cleaned by heating it to incandescence,⁴ and after this the observations of target current against cylinder potential were repeated. The difference in the shape of the two curves thus obtained indicates the influence of the impurities eliminated by the heating.

The curve indicated as number 1 in Fig. 3 was obtained soon after the target had been cleaned through heating it by an electric current. At the left of the curve, the negative current is not increasing; very few of the electrons are reflected with sufficient velocity to overcome these high retarding fields. As the potential of the cylinders is raised, an increasing number of electrons leave the target; this decreases the net current. The increase of the return current is particularly rapid when the retarding field is removed, for this enables the slow speed electrons to leave. Finally, the net current is reversed in sign; more electrons leave the target than strike it. In addition, then, to the electrons of the original beam which have been reflected, there must be others in the return current liberated by ionization at the surface. The positive current comes to a maximum value at once. This saturation of the secondary current with low positive potentials is exactly what we should expect; all the secondary electrons are able to leave the target if no field retards their escape.

The case is different, however, for targets which have surface contamination. The second curve indicated in Fig. 3 is one obtained just before the

³ It was found that electrons of 100 volts energy produced secondary currents of suitable value, and in the curves which follow, the source was maintained 100 volts negative with respect to the target unless some other value is given.

⁴ Such high temperatures were later found to be unnecessary for the removal of the impurities causing the pronounced effects observed.

heating of the target. The most significant feature is the poor saturation of the positive current. This must be due to retarding fields in the neighborhood of the target surface; otherwise we would expect all electrons emitted to be able to leave the target. This poor saturation appears to be the analogue of that observed for composite surfaces in thermionic emission. This has been explained as an effect of the fields in the neighborhood of the filament surface. Somewhat similar fields must exist here.

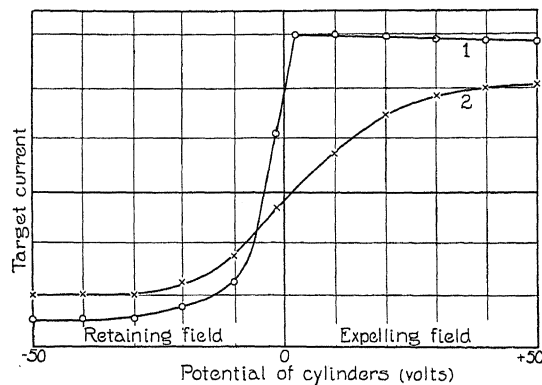


Fig. 3. Influence of electric field on secondary emission.

An attempt was made to observe by the present method fields due to thorium on a tungsten filament. That a surface field exists about an incandescent filament partly covered with thorium is known from saturation characteristics in thermionic emission. The results in the case of reflected electrons, however were not decisive. The effect of thorium on the saturation curve does not appear to be as pronounced as that due to the more easily volatilized impurities responsible for the above results.

INSULATING PROPERTY OF THIN OIL FILMS

The erratic behavior of metal surfaces contaminated by slight quantities of oil or wax have been at various times observed. Stuhlmann and Compton⁵ in attempting to account for abnormally high velocities of photoelectrons showed that slight quantities of wax vapor could result in surface charges, sometimes as high as 60 volts, which acted in some respects as a contact difference of potential. A real contact potential difference of this amount is hardly plausible, and it would seem likely that the results are to be attributed to an insulating layer which was charged as high as sixty volts before the insulation broke down.

In the present experiment in the case of extreme contamination by oil particles, an interesting kind of "one way conduction" was observed which can be explained as due to an insulating layer. In the apparatus used for this experiment, the target was fastened onto wires entering the vacuum system

⁵ Stuhlmann and Compton, *Phys. Rev.* **2**, 199 (1913).

through a stop-cock. Oil was placed around the top of the stop-cock; the stop-cock was then raised slightly from its socket, and the oil was injected into the system as a spray. The curve of Fig. 4, obtained after such treatment, follows the axis for a considerable range of potentials. The number of electrons striking the target in this range just equals the number leaving it. This rather striking result was confirmed by repeating the treatment several times.

To explain this we must suppose that the oil forms an insulating layer on the surface of the target which breaks down at some critical potential, apparently about 50 volts. The difficulty is that with retarding fields, even for small values of these fields, a negative current is indicated. To explain the entire curve on the basis of a continuous insulating layer would demand the assumption of some sort of one way conduction in the layer.

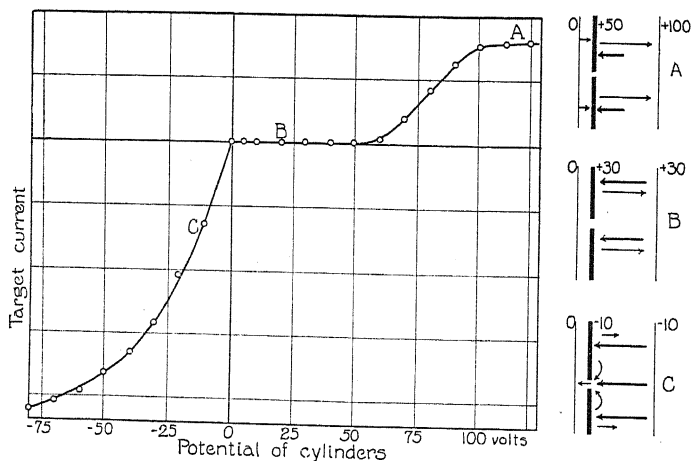


Fig. 4. Insulation due to oil film.

The curve can, however, be explained on two assumptions: first that the surface is only partially covered with minute droplets of oil, and second that these insulate only below some critical potential of about 50 volts; the insulation then breaks down. This leads to the insulation observed for small accelerating fields, which corresponds to the region *B* of the curve. The oil surface is raised by the more than one hundred percent reflection up to the potential of the cylinders,⁶ and after this the secondary equals the primary current. The total current is zero. At higher potentials, such as in the region *A*, the insulation breaks down; electrons are supplied through the layer, and more than one hundred percent secondary current results. As soon as the potential of the cylinders has been reduced below that of the target, the primary and secondary currents find a way to the clean metal somewhat as

⁶ See Fig. 3. The zero of current for the contaminated surface closely approaches the zero of the applied field. The zero of current does not usually fall more than five volts from the zero of applied potential. It should be noted that the argument used here does not depend upon the zero of current being exactly at the zero of the applied field.

shown in the lower sketch at the right of Fig. 4. This accounts for the negative currents indicated in the region C.

The apparent breakdown potential of this thin film is interesting. It has been known, of course, for some time that vaseline and other oils, which are ordinarily good insulators, may be used in thin films on electrical contacts to lower the resistance. The assumptions made above concerning this thin film and its breakdown potential appear to be in substantial agreement with the results of a number of rather detailed investigations^{7,8} in which thin films (about 10μ thick) were included between two conducting planes to which a potential difference was applied. This was a simple and direct method of investigation; the results obtained could be interpreted quantitatively at once. The results obtained in the present experiment are of a more complicated nature; exact quantitative interpretations are perhaps impossible. The present verification of the effect, however, has some advantages. The results

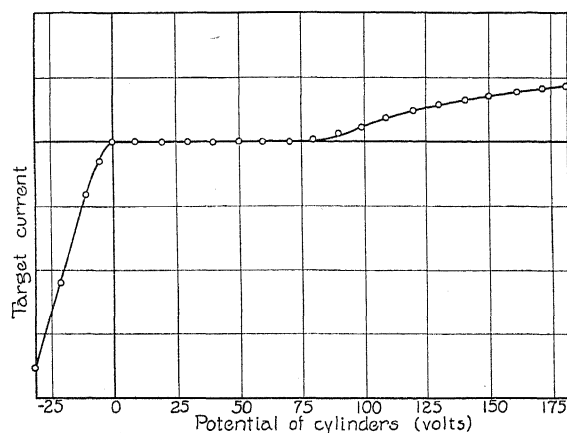


Fig. 5. Insulation at lower bombarding potentials.

of the present experiment eliminate the objection (possible in the case of the previous investigations although perhaps unfair in view of the care with which they were performed) that the breakdown obtained might be due to small projections of metal completing the circuit between the plates. In this experiment, small projecting areas are assumed to exist to explain the shape of the curves obtained. The breakdown, however, is evident; the positive current observed depends upon ionization over very considerable areas of the target surface to which the charge must be supplied through the oil. By the same argument, the experiment would seem to indicate something as to the nature of the phenomenon, because an explanation of the above results seems to demand the assumption of conductivity in the film over considerable areas. Some theories⁹ have treated the conductivity as quite local.

⁷ L. Brünighaus, *Comptes Rendus*, **188**, 1386-88 (1929).

⁸ H. E. Watson and A. S. Menon, *Roy. Soc. Proc.* **123**, 185-202 (1929).

⁹ A. Gyemant, *Phys. Zeits.* **30**, 33-58 (1929).

It is probable, however, that the general electronic bombardment of the oil surface causes the disturbance to become quite general over the film. If, for instance, the theory of Güntherschulze¹⁰ is correct and the breakdown is due to the movement of the ions in the film producing strong local heating with evaporation and the formation of gas bubbles in which the discharge takes place, it may be that the heating or the ionization produced by the impact of an electron would make such a breakdown more probable. The impact of electrons of the primary beam does in fact influence the breakdown. If the energy of the electrons striking the surface is greater than 100 volts, the breakdown occurs at a lower potential than indicated in Fig. 4. If the incident electrons are slow, the breakdown occurs at a higher potential. Fig. 5 shows the results for a bombarding velocity corresponding to 70 volts difference between the target and source. The curve follows the axis for a greater range of cylinder potentials than the curve of Fig. 4. The effect is even more pronounced at lower bombarding potentials.

In the present experiment, discharge does not occur between two metallic electrodes. The conduction appears to be from the metal to the surface of the film from which the charge may be dislodged only by electronic impact. The present results suggest that the conduction is continuous and general for the bombarded parts of the film.

CONCLUSIONS

The experiments reported here lead to the conclusions:

1. Strong fields are set up in the neighborhood of a contaminated surface retarding the escape of reflected electrons.
2. In extreme cases of oil contamination the impurities form an insulating film which breaks down at some critical value of the applied field.
3. The breakdown potential of a given film varies with the energy of the incident electrons.
4. The conductivity observed in these films appears to be rather general and continuous.

The writer wishes to thank the members of the staff of the Department of Physics of the State University of Iowa for their interest and assistance. Thanks are especially due to Professor J. A. Eldridge who suggested and directed the investigation.

¹⁰ A. Güntherschulze, *Jahrbuch d. Radioakt. u. Elektr.* 19, 92 (1922).

THOMSON EFFECT IN ZINC CRYSTALS

BY L. A. WARE

PHYSICS LABORATORY, UNIVERSITY OF IOWA

(Received March 4, 1930)

ABSTRACT

The *Thomson coefficient*, σ , is directly determined for a group of zinc crystal rods with orientations distributed fairly uniformly over the entire possible range. At 49.5°C and at 125°C the values of σ seem to obey the Voigt-Thomson symmetry relation, although not as good a check is obtained at the higher temperature on account of increased experimental error. The principal values obtained are:

$$\begin{array}{l} \text{At } 49.5^\circ\text{C, } \sigma_{\perp} = 0.98 \times 10^{-6} \text{ cal.} \cdot \text{coul.}^{-1} \cdot \text{deg.}^{-1} \\ \quad \sigma_{\parallel} = 0.38 \times 10^{-6} \text{ " " " } \\ \text{At } 125^\circ\text{C, } \sigma_{\perp} = 2.09 \times 10^{-6} \text{ " " " } \\ \quad \sigma_{\parallel} = 1.08 \times 10^{-6} \text{ " " " } \end{array}$$

The values at 49.5°C are found to compare favorably with values for polycrystalline zinc calculated from Sommerfeld's theory of conduction, (0.32×10^{-6} cal. · coul.⁻¹ · deg.⁻¹), and found by Borelius experimentally, (0.88×10^{-6} cal. · coul.⁻¹ · deg.⁻¹). The increase of σ with increased temperature is greater than has been previously reported for polycrystalline zinc but is in approximate agreement with some earlier determinations by the writer. In addition, *specific resistivity* and *temperature coefficient of resistivity* are determined.

INTRODUCTION

ABOUT two years ago the writer determined directly values of the Thomson coefficient for a few zinc single crystals¹ of orientations² near 0° and 90°. The main emphasis in this earlier work was placed on the variation of σ , the Thomson coefficient, with temperature, although it was possible to make some comparison with values of $(\sigma_{\perp} - \sigma_{\parallel})$ computed from the previously published thermal e.m.f. determinations of Linder,³ Bridgman,⁴ and Grüneisen and Goens.⁵ Following the work just mentioned, some determinations of σ were made at a single temperature, (about 50°C), on a group of crystals covering a wider range of orientations, particularly with a view to checking the Voigt-Thomson symmetry relation for the Thomson coefficient. These crystals were a by-product of the investigations of Tyndall⁶ and of Hoyem and Tyndall⁷ and were therefore grown under somewhat different conditions and

¹ M. S. Thesis. University of Iowa, 1927; not published.

² Orientation, for a hexagonal crystal, is defined as the angle between the main crystallographic axis and the length of the specimen.

³ E. G. Linder, Phys. Rev. **26**, 486 (1925); **29**, 554 (1927).

⁴ P. W. Bridgman, Nat. Acad. Sci. Proc. **11**, 608 (1925); Proc. Amer. Acad. Sci. **61**, 101 (1926).

⁵ Grüneisen and Goens, Zeits. f. Physik **37**, 378 (1926).

⁶ E. P. T. Tyndall, Phys. Rev. **31**, 313 (1928).

⁷ A. G. Hoyem, and E. P. T. Tyndall, Phys. Rev. **33**, 81 (1929).

throughout a rather long period of time. It is certain also that the zinc came from several lots (although of the same kind of zinc). In view of other work done recently in this laboratory, it is not now surprising that such a miscellaneous series of crystals failed to give very consistent results. In particular σ was not determined as a definite function of the orientation. A third series covering a good range of orientations was therefore prepared by Mr. Hoyem. The crystals were made consecutively, were grown at the same rate, were of very nearly the same diameter, and the zinc came from only one original container. The material was Kahlbanm's best zinc. The work reported herein consists mainly of a direct determination of the Thomson coefficient at two temperatures (49.5°C and 125°C) for each crystal of this last series. From these data it is possible to check the usual thermodynamic theory of thermoelectricity and to test the Voigt-Thomson symmetry relation directly for σ .

In addition the specific resistance at 20°C and the temperature coefficient of resistivity were measured, mainly as tests for purity of the zinc, freedom of the crystals from strain, etc.

APPARATUS AND EXPERIMENTAL PROCEDURE

The Thomson coefficient was measured in the fashion described by Nettleton⁸ with some slight modifications which are described below. In this method the two ends of the specimen, which is a short wire or rod, are kept at constant, but different temperatures. At the same time a current, I_1 , is passed in such a direction through the specimen that the Thomson effect causes a generation of heat. If this current is reversed the temperature at the center of the specimen will decrease slightly, as the Thomson heat is now being subtracted. If, however, on reversal, a suitable increase in the current, to I_2 , is made an extra generation of Joulean heat compensates for the previous loss and the temperature remains unchanged. The apparatus is designed to measure directly the difference between I_2 and $I_1 (=i_0)$ and to detect, with a bolometer coil and a Wheatstone bridge, any change in temperature at the center of the crystal, so that the state of zero-change may be found. Let R represent the resistance of the crystals, U , the difference in temperature between the two ends, and J , the constant 4.18 joules per calorie. Then, as Nettleton has shown, the Thomson coefficient, σ , will be given by the equation, $\sigma = i_0 R / JU$ cal. · coul.⁻¹ · deg.⁻¹ provided certain conditions are satisfied. It is believed that all these are satisfied in the present work except that the crystals were made longer than Nettleton considered because of their very low resistance. The heat insulation was improved greatly, however, over previous methods and it seems certain that the equation is satisfactory for the lengths and diameters used.

To determine the specific resistance, ρ , and the temperature coefficient of resistivity, α , curves were plotted for resistance against temperature between room temperature and 110°C. For a linear relationship between resistance and temperature, α is given by;—

⁸ H. R. Nettleton, Proc. Phys. Soc. Lond. **34**, 77 (1921); **29**, 59 (1916).

$$\frac{1 - p}{t_2 p - t_1}$$

in which $p = R_1/R_2$; R_1 and R_2 being resistances measured at temperatures t_1 and t_2 respectively. The specific resistance at any temperature is given by:

$$\rho = RM/\delta L^2$$

where R is the resistance at the desired temperature, M is the mass of the crystal, δ is the density, and L is the length. The resistance measurements were made by the usual potentiometer method, the crystal being immersed in a constant temperature oil-bath heated by an electric heating coil. The bath could be adjusted easily for any temperature between room temperature and 125°C . In this case, room temperature to 110°C was used as the range.

Fig. 1 shows the arrangement of apparatus used to measure the Thomson coefficient. The details of the terminals H and C will be considered with Fig. 3. In Fig. 1, H represents the hot end of the crystal and C , the cold. V is

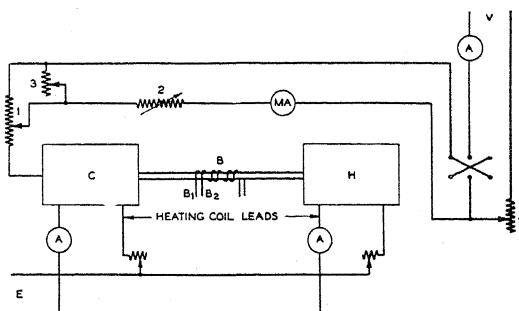


Fig. 1. Apparatus wiring diagram.

a source of 12 volts for which storage batteries were used so that the current would be as uniform as possible. B_1 and B_2 represent the two bolometer coils wound around the middle third of the crystal for the purpose of detecting a change in temperature when the current through the crystal is reversed. Apparently only one coil was used by Nettleton, but the use of two coils in opposite arms of the Wheatstone bridge was adopted on account of the increased sensitivity. The bridge is shown in Fig. 2. Actually the windings of B_1 and B_2 are interspaced as shown in Fig. 1 although shown separated in Fig. 2 to render the electrical connections clearer. In Fig. 1 the resistance 1 is about 10 ohms, 2 is a 500 ohm resistance box adjustable to 0.1 ohm, 3 is a rheostat of 2000 ohms, and 4, which controls the main current, is 47 ohms. The switch S is especially constructed to be very rapid and of very low resistance. E is a source of 110 volts A.C. supplying the heater coils at both ends of the crystal.

Fig. 3 presents the method of producing the constant temperatures at the ends of the crystals. Brass blocks were turned down to make the pieces A and

B, each about one inch in diameter and 1.5 inches long. *A* was threaded into the end of the basin *C* so that the crystal could be directly connected to it. An opening *D* was made in *A* to facilitate the circulation of water. On *A*, a heating coil was wound of No. 24 Karma wire and leads taken out. The heating coil was used to melt the solder for the purpose of either putting the crystal in place or removing it. A screen partition, *E*, was placed as shown to prevent the ice getting into the stirrer. This arrangement maintained the cold end of the crystal very constantly at about one degree above 0°C . At *H*, a double

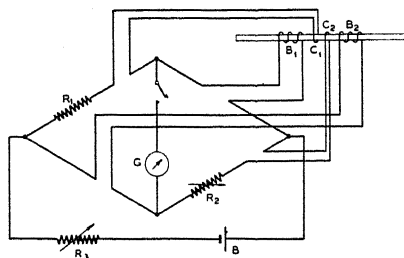


Fig. 2. Wheatstone bridge connection.

cylinder was used with heat insulating powder in the space *F*. The block, *B*, was similar in all respects to *A*, it being threaded into the end of the cylinder, and having a heating coil for the double purpose of mounting the crystal and heating the enclosure to a constant temperature when readings were being made. During an experiment the space, *G*, was filled with water and maintained by the heater at very nearly the boiling point. The thermometer, *T*, was used to read the temperature. By keeping the current about 0.9 ampere, *B* could be maintained at a remarkably uniform temperature for about three hours. Thus was obtained a very satisfactory method of maintaining a tem-

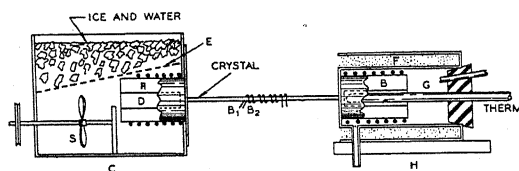


Fig. 3. Details of hot and cold terminals.

perature difference of about 97°C for a considerable length of time and it proved to be a much better method than that used later in obtaining the results for an average temperature of 125°C .

The details of the bridge circuit are shown in Fig. 2. Here, R_1 is a fixed resistance of about 6 ohms which, with as much of the wiring as possible, was inclosed in a heat insulated box. R_2 is a resistance made up of shunts across a coil, similar to R_1 , and in series with a slide wire resistance of 0.1 ohm capable of adjustment to about 0.01 ohm. The function of the two coils, B_1 and B_2 , has

been described already. The compensating coils, C_1 and C_2 , are used to decrease the drift of the galvanometer due to the change of resistance of the leads to B_1 and B_2 . B_1 , B_2 , and R_2 as well as R_1 are all about 6 ohms resistance. The bolometer coils and compensators were constructed of No. 40 copper wire silk insulated. The Wheatstone bridge thus arranged proved to be much more sensitive than the arrangement used in the previous work, which contained only one bolometer coil and no compensating coils.

For the purpose of determining σ at the average temperature of 125°C it was necessary to make a few minor changes in the arrangement shown in Figs. 1 and 3. In Fig. 1 the source, V , was reversed as well as all the meters contained in the circuit. A little inspection will demonstrate that this allows the measurement of positive σ^* if H and C are also interchanged. In this case the method of heating H was unchanged, it being, as before, maintained near the boiling point of water. However, the ice water in C was removed and polarine oil was substituted. The heating coil on A was brought into use and the temperature of the oil maintained at about 150°C . Here it was rather difficult to maintain the temperature sufficiently constant, a condition which slowed the procedure somewhat. The temperature at the hot end of the crystal was measured by a sensitive thermometer placed in the opening, D . The readings of the thermometers at both ends of the crystal were checked by means of thermocouples connected to the face of A and B near the ends of the crystal. It was found that the temperature gradient determined from the readings of the thermometers differed from the actual gradient by about 2 percent. In computing the results, a suitable correction was, of course, made.

Measurements on the crystals were taken as follows. First a crystal is carefully cut to about 9 cm length, weighed, and to each end is soldered, by a very small amount of solder, a small copper wire, at about the middle of the wire, so that its two ends can serve as current and potential leads, respectively, for the resistance measurements. The crystal is then suspended in the oil bath, the heater in the oil bath is adjusted for the desired temperature, and the assembly is allowed to stand until the temperature, as indicated on a calibrated thermometer, is steady. A current of 0.3 ampere is then sent through the crystal and the P.D. read on the potentiometer. The current is reversed and readings made again. The average of four readings, (two in each direction), gives sufficient data to determine the resistance at this particular temperature. This is repeated for six or seven different temperatures and a curve plotted from which ρ and α can be determined.

After these data have been obtained the crystal is taken from the oil bath, the leads unsoldered, and two bolometer coils wound on at the center as indicated above. The heaters A and B of Fig. 3 are then started and when sufficiently hot the crystal is soldered closely against the face of A and B as there indicated. It is necessary in this procedure to be very careful not to strain the crystal. When the crystal has been fastened in place and the bolometer and compensating coils have been connected to the bridge, kieselguhr is

* σ is positive if heat is generated for current flow down the temperature gradient.

packed into the space between *A* and *B* and around the crystal to a radius of about 5 cm. Over this is packed a considerable amount of cotton and the apparatus is ready for the establishment of a temperature gradient. The space, *G*, is filled with water, and with the thermometer in place the current is established through the heater, *B*. It is given a high value at first and as the temperature approaches 98° or 99°C it is reduced to 0.9 ampere, where it is left. In the meantime, with the current shut off in *A*, the container is filled with water, the screen put in place, and the space above the screen filled with cracked ice. The stirrer is then started and the whole assembly is allowed to attain a steady state. As it begins to approach such a state the currents through the Wheatstone bridge and through the crystal are established. A determination of the balancing current, i_0 , is made as follows: Referring to Fig. 1, it is seen that with the switch, *S*, to the left the main current divides, part going through the crystal and part through the milliammeter, M.A. When *S* is thrown to the right all the line current goes through the crystal. Thus the current through the crystal has been increased on reversal and if the rheostats 1 and 3 are correctly adjusted, the milliammeter, for any particular setting of resistance 2 and the main current, will read the same for either position of the switch, *S*. In this case the reading of the milliammeter is the i_0 required in the working equation. Thus it is necessary first to adjust resistances, 1 and 3, (Fig. 1), so that the milliammeter reads the same for both positions of *S*, then, if the system is otherwise balanced, some value of i is tried and the bridge, (Fig. 2), is adjusted for left position of *S*. Switch *S* is then thrown to the right and if the bridge indicates a decrease of temperature at the center of the crystal, i is increased, and the procedure repeated until it is just determinable that the current, i , is too low. A similar process is gone through with i being successively reduced from a value initially too high. The balancing current, i_0 , is the mean of these two limiting values of i . The difference between these two values is generally less than 10 percent of i_0 .

The procedure for the determination of σ at the higher temperature, 125°C, is similar to that at 49.5°C. However, in this case it should be pointed out that it was not so easy to maintain a constant temperature at the hot end. This introduced a certain amount of unsteadiness, and a corresponding decrease in the reliability of the results.

RESULTS

The experimental results are exhibited graphically in Figs. 4 and 5. The specific resistance will be considered first. It is plotted in Fig. 4 against the square of the cosine of the orientation. This plot should yield a straight line since the validity of the Voigt-Thomson law for specific resistance of zinc crystals has been established, particularly by Bridgman.* The solid straight line shown is that for data recently obtained by Bridgman.⁹ It is actually drawn by him through the lowest of his points, in spite of the fact that the

* The Voigt-Thomson symmetry relation states that the thermo-electric effects in crystals plotted against the square of the cosine of the angle of orientation should yield a straight line.

⁹ P. W. Bridgman, Proc. Am. Acad. Arts and Sc. 63, 351 (1929).

scattering of his observations is about half as great as that shown in Fig. 4. This procedure is justified by his discovery that any very slight strain raises the resistance of a zinc crystal. Five of the writer's crystals were therefore rechecked with the purpose of determining what effect resulted from intentional slight strains. The points so obtained are indicated by triangles. In two cases the resistivity changed and it increased. Of the three crystals which

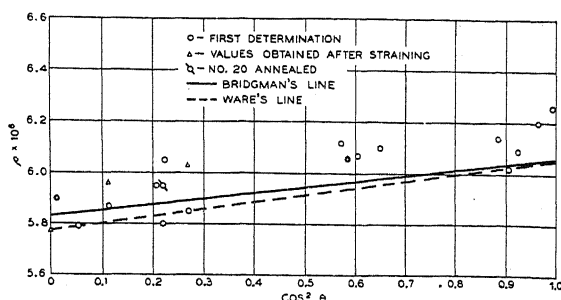


Fig. 4. Specific resistivity in ohms per cm^3 plotted against $\cos^2\theta$.

did not change in resistivity, two already had high values and the other probably was not very much strained as it was a 90° crystal and therefore stiff. The greatest increase was about 3 percent. It will be noted also that the value for crystal No. 20, ($\rho = 5.8 \times 10^{-6}$, $\cos^2\theta = 0.22$) has increased due to annealing. However, this crystal has shown very inconsistent results in other respects. Following the idea of Bridgman that the lowest values are more probably correct, the dashed straight line has been drawn through four low

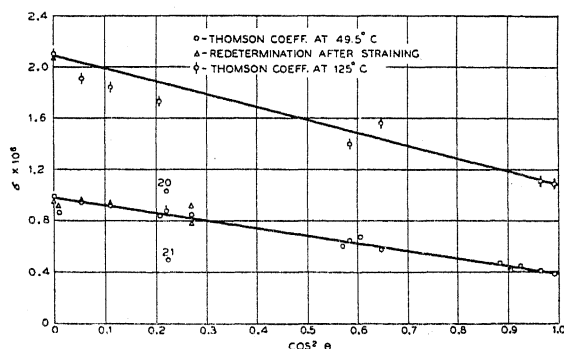


Fig. 5. The Thomson coefficient in $\text{cal.} \cdot \text{coul.}^{-1} \cdot \text{deg.}^{-1}$ as a function of $\cos^2\theta$.

points neglecting the point for crystal No. 20. The values of ρ obtained from this line for $\cos^2\theta = 0$ and $\cos^2\theta = 1$ are: $\rho_{\perp} = 5.78 \times 10^{-6}$, $\rho_{\parallel} = 6.05 \times 10^{-6}$. These given for $(\rho_{\parallel} - \rho_{\perp})$, 0.27 whereas Bridgman obtains 0.23. Bridgman's ratio $\rho_{\parallel}/\rho_{\perp}$ is 1.04 while the values above yield 1.05. Grüneisen and Goens obtain 1.08. The agreement with Bridgman in the matter of specific resistance and the effect of strains is quite satisfactory.

The variation of resistance with temperature, between 20°C and 110°C is for all but four of the crystals accurately linear. These four show only a very slight deviation. The temperature coefficient, α , was therefore computed in the manner explained above. The values of α lie between 0.00413 and 0.00437 and show no very certain variation with orientation. The average value is 0.00425, a value about 2 percent higher than that obtained by Bridgman.

The values of the Thomson coefficient for both 49.5°C and 125°C are presented in Fig. 5. If the best straight line is drawn through the points for 49.5°C it will be found that the deviation from the line is, in all except two cases, within the experimental error. These two cases are those of crystals No. 20 and No. 21, ($\theta = 62^\circ$). No. 20 has already been mentioned in the case of resistivity as being anomalous and here it is seen that even at 125°C the value of σ is lower than for 49.5°C. Also, No. 20 was annealed, as mentioned before, and the same value for σ was again obtained at 49.5°C. There was no visible evidence of No. 20 or No. 21 being different from the other crystals and the explanation of their deviation is not readily apparent.

Although a straight line has been drawn through the points for 125°C, the writer does not claim that the data afford a test of the Voigt-Thomson symmetry relation at this temperature. The deviations from the line as drawn are no greater, however, than the experimental error at this temperature. Moreover the value of $(\sigma_\perp - \sigma_\parallel)$, obtained from this line and stated just below agrees as well with indirectly determined values as is the case at 49.5°C.

The values of σ_\perp and σ_\parallel at 49.5°C are 0.98×10^{-6} cal. · coul.⁻¹ · deg.⁻¹ and 0.38×10^{-6} cal. · coul.⁻¹ · deg.⁻¹ respectively. Thus a value of $(\sigma_\perp - \sigma_\parallel)$, 0.60×10^{-6} cal. · coul.⁻¹ · deg.⁻¹ results. From the relation, $(\sigma_\perp - \sigma_\parallel) = T \frac{d^2 E}{dT^2}$, Bridgman⁹ obtains 0.661×10^{-6} , Grüneisen and Goens,⁵ 0.622×10^{-6} , and Linder,³ 0.521×10^{-6} cal. · coul.⁻¹ · deg.⁻¹. At 125°C the writer obtains the value 1.01×10^{-6} cal. · coul.⁻¹ · deg.⁻¹ as compared with Bridgman's⁹ 0.813×10^{-6} , Grüneisen and Goens' 1.12×10^{-6} , and Linder's 0.795×10^{-6} cal. · coul.⁻¹ · deg.⁻¹. Borelius and Gunneson¹⁰ have made measurements on several polycrystalline metals and obtain for zinc at 49.5°C, 0.885×10^{-6} cal. · coul.⁻¹ · deg.⁻¹. Taking $\sigma_{54.5}$ as representative of σ in polycrystalline zinc, the writer obtains 0.78×10^{-6} cal. · coul.⁻¹ · deg.⁻¹. The difference in purity of the material used by the various investigators may well account for the rather wide range of values obtained.

In general it can be said that the observation of Bridgman concerning resistivity is substantiated. The average value of α obtained is slightly higher than that given by Bridgman and there appears to be a somewhat greater difference between α_\perp and α_\parallel than that which Bridgman finds. The values of $(\sigma_\perp - \sigma_\parallel)$ for 49.5°C agree with those calculated by the thermodynamic formula from the previously observed thermal e.m.f. vs. temperature curve. The Voigt-Thomson relation is supported within the limits of error by the data on $\sigma_{49.5}$. The data on σ_{125} are presented for what they may be worth.

Sommerfeld,¹¹ by an extension of his theory of electrical conduction, has

¹⁰ G. Borelius and F. Gunneson, *Ann. d. Physik* **65**, 520 (1921).

¹¹ A. Sommerfeld, *Zeits. f. Physik* **47**, 143 (1928).

developed an equation for the Thomson coefficient which to the first approximation is:

$$\sigma = \frac{2\pi^2}{3} \frac{m k^2 T}{e h^2} \left[\frac{8\pi}{3n} \right]^{2/3}$$

which is seen to be dependent on T , the absolute temperature, and n , the number of atoms per cc, only as variables. This, calculated for zinc, gives, at 49.5°C , $0.32 \times 10^{-6} \text{ cal.} \cdot \text{coul.}^{-1} \cdot \text{deg.}^{-1}$, a value agreeing, in order of magnitude with existing data.

No theory has been developed for the Thomson effect in single crystals, although Houston¹² has extended his work in this direction.

The writer wishes to express his thanks to Dr. E. P. T. Tyndall, under whose direction this work was undertaken, for his help and encouragement at all times. He wishes also to thank Mr. Hoyem for so kindly consenting to grow the crystals used in this work. Thanks are also extended to members of the department for their advice and suggestions.

¹² W. V. Houston, *Zeits. f. Physik* **48**, 449 (1928).

E.M.F., RESISTANCE, AND CAPACITANCE PHENOMENA IN
PHOTOVOLTAIC CELLS CONTAINING GRIGNARD
REAGENTS

BY H. E. HAMMOND

UNIVERSITY OF MISSOURI

(Received February 10, 1930)

ABSTRACT

E.m.f., resistance, and polarization capacitance have been measured in light-sensitive cells containing ether solutions of Grignard reagents in an effort to determine whether the known voltage variations with illumination are due to ionization changes or to electrode-film variations. Voltage alterations with illumination or x-ray irradiation are described. Resistance variations with illumination are found in ethylmagnesium bromide cells but not in phenylmagnesium bromide cells until a "forming" process has been carried out. Solvation changes seem to offer a more reasonable explanation than ionization changes. Capacitance changes seem unrelated to resistance or voltage changes. Unsymmetrical resistances are noted in several cases. Capacitances as high as 7 mf per cm² of electrode area have been found. Film thicknesses are estimated to be of approximately molecular dimensions, greater for benzene-ring compounds than for short-chain compounds. Voltage variations are thought to be due to phenomena taking place on or very near electrode surfaces.

THE Becquerel effect is the name applied to an alteration of the electromotive force of a voltaic cell upon exposure of the cell to light. Originally found by Becquerel¹ to take place in a cell having platinum or silver plates coated with a silver halide and immersed in dilute sulphuric acid, the effect was later discovered by Rigollot² to exist with solutions of fluorescent dyes. Now the effect is known to be very common. Through the work of Nichols and Merritt,³ Hodge,⁴ and others, the effect has been shown to be located at or very near the electrode surface in the case of the dye solutions. Goldmann⁵ offered a theory based on the photoelectric effect. Baur⁶ proposed a photochemical theory for the effect, which has been upheld by Garrison,⁷ Tucker,⁸ and Russell⁹ among others. A reasonably comprehensive survey of the work carried on with solutions in water and in absolute alcohol is presented by Lifschitz and Hooghoudt.¹⁰

¹ E. Becquerel, *Compt. Rend.* 9, 145 (1839).

² M. H. Rigollot, *Compt. Rend.* 116, 878 (1893).

³ Nichols and Merritt, *Phys. Rev.* 19, 415 (1904).

⁴ P. Hodge, *Phys. Rev.* 28, 25 (1909).

⁵ A. Goldmann, *Ann. d. Physik* 27, 449 (1908).

⁶ E. Baur, *Zeits. f. Phys. Chemie* 63, 683 (1908).

⁷ A. D. Garrison, *Jour. Phys. Chem.* 28, 334 (1924).

⁸ C. W. Tucker, *Jour. Phys. Chem.* 31, 1357 (1927).

⁹ H. W. Russell, *Phys. Rev.* 32, 667 (1928).

¹⁰ Lifschitz and Hooghoudt, *Zeits. f. Phys. Chemie* 128, 87 (1927).

A number of papers have been published on the luminescence of Grignard compounds, organo-magnesium halides, under suitable conditions.^{11,12} Kondyrew¹² showed that cells containing ether solutions of ethylmagnesium bromide produced an e.m.f. He also measured the temperature-resistance coefficient. Such cells show the Becquerel effect.^{11,12} Considerable work, much of it as yet unpublished, has been done by others on the variation of the e.m.f. of Grignard cells with changes in illumination, in wave-length of light used, in temperature, etc.

The primary purpose of this investigation was to uncover new evidence as to whether the photovoltaic effect in Grignard cells took place on or near the electrodes or in the body of the electrolyte. A photoelectric effect should produce a change in the conductivity of the solution and an alteration in an electrode film might cause a detectable change in the cell capacitance. The method employed contemplated tests of many such cells, first as to the nature and magnitude of e.m.f. alterations, second as to the existence and magnitude of any resistance and capacitance changes under exposure to light or to x-rays. The results obtained suggested a further investigation of certain of the effects of electrolysis on these cells, a feature not originally planned. Certain interesting results were obtained.

Most of the cells were made up in one-inch test tubes with the electrodes mounted on glass tubes passing through rubber stoppers. The supporting wires were either of the same materials as the electrodes or else the electrodes were long enough to keep the wires out of the solutions. A few H-cells with one electrode in each arm were used. Some cells hermetically sealed in glass were made, since it was desired to test whether the properties were retained for a long time, if the evaporation of the ether was prevented. The Grignard reagents were made in an atmosphere of nitrogen, but in the solution there may be formed an etherate of the magnesium halide. It has not been possible to determine how far these etherates influenced the actions noted. The compounds used were phenylmagnesium bromide, ethylmagnesium bromide, the corresponding iodides, and bromo-ethylmagnesium bromide. These compounds were used because previous work by others had shown that they gave the largest photovoltaic responses. Various concentrations and electrode combinations were used.

The cells were mounted in a constant-temperature water bath packed in sawdust in a large light-proof box provided with a window and sliding shutter. Each cell was in a separate stall. A shielded cable ran from the cell-box to a selector panel by which any cell could be connected to the measuring apparatus. A 1000-watt lamp was used as the light source and the light was concentrated upon the cell under test by means of a large glass lens. An x-ray tube was also available.

¹¹ Dufford, Nightingale, and Gaddum, *Jour. Am. Chem. Soc.* **49**, 1858 (1927).

¹² R. T. Dufford, *Jour. Opt. Soc. Amer.* **18**, 17 (1929) and R. T. Dufford, *Phys. Rev.* **33** 119 (1929).

¹³ N. W. Kondyrew, *Ber. D. Deutsch. Chem. Gesell.* **58**, 464 (1925).

The other resistances and capacitances are parts of the modified Wagner ground. The parenthetical correction factor in Eq. (1) is usually near enough to unity to be safely neglected, but in some of the cells tested here it was found to be as low as 0.75. Eq. (2) made possible the computation of the cell capacitance from data obtained during the measurement of the cell resistance. It can be seen that the balance conditions are functions of the frequency of the bridge current. Since the oscillators both gave out several harmonics, it was never possible to obtain complete silence in the phones, but merely to balance out the fundamental.

A number of tests were made which indicated that the resistance measured by the bridge was the electrolytic resistance and was very slightly affected, if at all, by films on the electrodes. For example, tests showed that variations of the distance between electrodes produced proportional changes in the resistance.

When an approximate value of the cell-resistance was known, bridge readings could be taken every minute. Potentiometer readings were taken at one-minute or half-minute intervals. Usually cells were illuminated for five minutes and then allowed to remain dark for an equal period.

The tests made can be classified under four general headings, which will be discussed in turn.

(a) *The effects of illumination and mechanical agitation on e.m.f.* Every cell was tested in this way. Ordinarily the entire cell was illuminated. With H-cells, tests were also made by illuminating separate electrodes or the cross-bar. In a few cases, a slit was placed in front of a straight cell so that a narrow ribbon of light passed parallel to the electrode surface or merely through the solution. Tests were made with varying degrees of mechanical agitation. As most of this part of the work was a repetition of what had been done by others, only the general conclusions will be given.

The e.m.f. was greatly affected by agitation of the cell and by polarization. The photovoltaic effects occurred without noticeable temperature changes. Oscillations of e.m.f., due to some unknown cause, took place even in the dark. Any change in the electrode surface caused an e.m.f. change, for example, exposing the electrode to air for a moment, cleaning the surface, etc. E.m.f. changed with age of the cell, partly because of concentration changes and partly no doubt because of slow electrolysis by minute leakage currents. Cells sealed in glass retained properties for many months but the e.m.f. varied and also the magnitude of the photovoltaic response. Light affected the potential of a given electrode almost invariably in the same way. Illumination of the electrolyte alone produced very small effects, possibly due to scattered light reaching the electrodes. In a few cases readings closely spaced showed that the light-e.m.f. effect involved two or three successive alterations. These were shown, by illuminating first one electrode and then the other by means of the narrow slit, to take place part near one electrode and part near the other, but very little, if any, in the body of the liquid. These tests, in general, favored the belief that the voltage phenomena are mainly localized near the electrodes. As a whole, these

conclusions are in agreement with those given in papers by the writer's colleague, R. T. Dufford, already quoted^{11,12} or soon to be published.

(b) *Measurements of e.m.f. as affected by irradiation with x-rays.* The general results obtained upon exposing certain cells to a beam of x-rays have already been reported in a brief note.¹⁵ Although they gave some promise as a means of measuring x-ray intensities, there were uncertainties about their behavior which need clearing up. This x-ray response differed from that produced by visible light in magnitude and frequently in sign, indicating that it was a different sort of action. Fig. 2 is a typical graph.

(c) *Measurements of e.m.f., resistance, and capacitance of cells as affected by visible light or by x-rays.* The accuracy of resistance measurements was about 0.1 percent, while that of the capacitance measurements was about

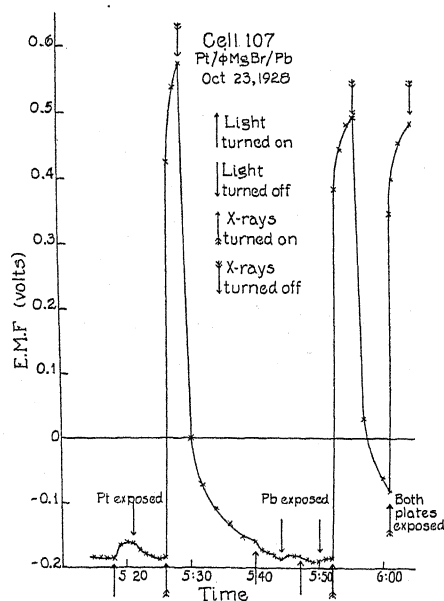


Fig. 2. E.m.f. as affected by light and x-ray illumination.

1 percent. Values of the cell-capacitances found by this bridge agreed with those indicated by a Leeds and Northrup Farad Bridge. All the cells studied carefully were of the test-tube type with electrodes about 5 mm apart. Platinum electrodes were of 1 cm² area, most of the others were of 5 cm² area. Resistance of a cell ranged between 500 and 20,000 ohms, capacitance from 0.4 to 35 mf.

Seven cells contained phenylmagnesium bromide with various electrode combinations. None of these cells showed any change in resistance upon exposure to light when the cells were new, but one, with platinum and copper electrodes, developed such sensitivity after about six months. The light-induced change was a drop of about 1 percent in resistance, recovery taking

¹⁵ R. T. Dufford and H. E. Hammond, Phys. Rev. 33, 124 (1929).

place in an equal period. Temperature rise produced an increased resistance which persisted as long as the cell was observed, indicating that the light effect was a different phenomenon.

Two cells filled with ethylmagnesium iodide gave no definite light-resistance response.

Four cells contained ethylmagnesium bromide. These were all symmetrical cells with electrodes of aluminum, platinum, copper, and sodium respectively. These cells showed lower resistances than those containing phenylmagnesium bromide. The resistances decreased and the capacitances increased with age in general. A single cell with platinum and aluminum electrodes and containing bromo-ethylmagnesium bromide showed a high

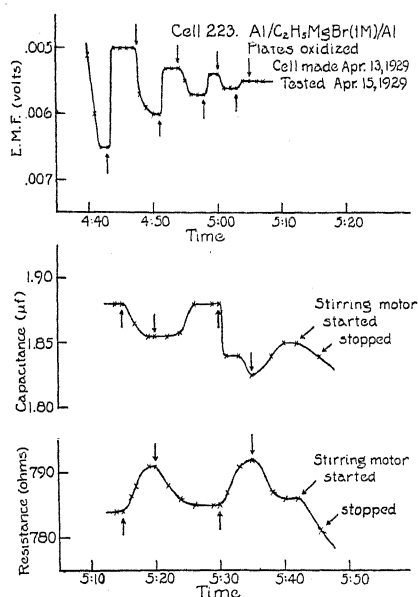
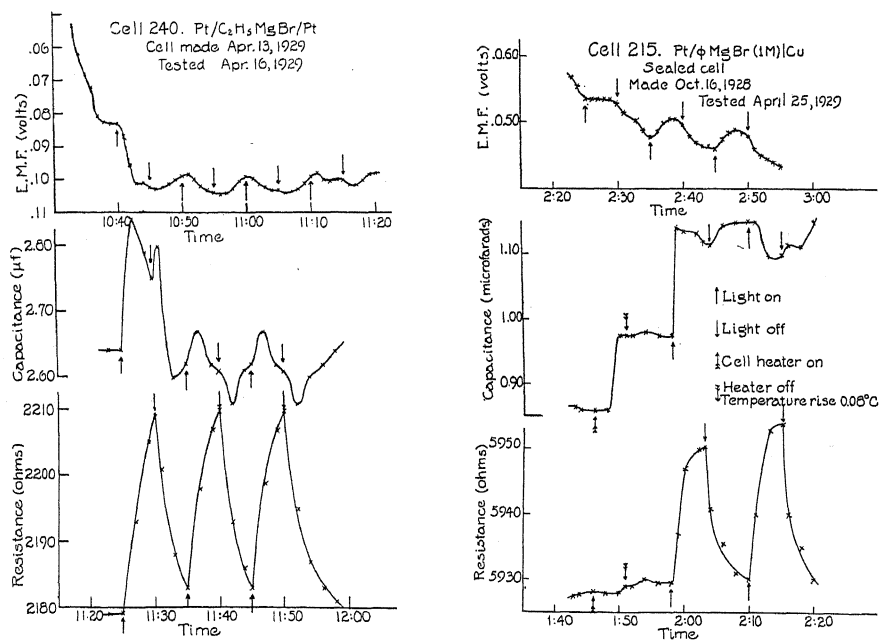


Fig. 3. Effect of light on e.m.f., resistance and capacitance. Upward-pointing arrows indicate when light was turned on; downward-pointing arrows when light was turned off. The same notation is followed in succeeding figures.

initial resistance, which became smaller with age, while the capacitance increased. All these cells showed an increase of about 1 or 2 percent in resistance during five minutes illumination, followed by recovery in an equal period of darkness. The changes in resistance could be detected within a few seconds after turning on or off the light. Resistance changes due to temperature rise could not be detected so soon and the changed value usually persisted after the temperature had come back to the original level. Furthermore, these light-induced changes were not in the same sense as those due to temperature rise in all cases. Figs. 3, 4, and 5 show typical sets of results. It was not possible to trace any general interrelation between the changes in e.m.f., resistance, and capacitance when the cells were illuminated. Fig. 4 shows the only example found of any apparent regular relation between

the capacitance values and the presence or absence of light on the cell. This relation existed for only a part of the test, as can be seen.

No tests of specific resistance were made for the Grignard solutions, but the values must be high in view of the high resistances compared with the cell dimensions. Secular variations in resistance ran as high as 50 or 60 percent, while the light-induced changes never exceeded 2 percent. The former changes were not reversible, the latter were. The photoelectric hypothesis is not tenable as some of the light-induced changes were increases in resistance. Neither does it seem reasonable to attribute a voltage variation of from 10 to 50 percent to a process which caused a resistance change of only 1 or 2 percent. The secular changes in resistance were undoubtedly due to chemical changes in the cell composition, evidences of which sometimes be-



Figs. 4 and 5. Effect of light on e.m.f., resistance, and capacitance.

came evident to the eye as time went on. The writer believes that the light-induced resistance changes were due to temporary and reversible variations in solvation of the ions rather than in percentage of ionization. These data, therefore, served to strengthen the idea that the voltage phenomena are due to changes near the plate surfaces, but the lack of any consistent relation between the capacitance changes and the presence or absence of light did not give any definite evidence to locate the seat of action on the surface itself.

Operation of the x-ray apparatus caused so much noise in the phones that the bridge could not be balanced while the cell was being irradiated. If the resistance or capacitance was affected by x-rays, the effect did not persist long enough to be measured after the apparatus was shut off.

As the high-frequency bridge current sometimes altered the e.m.f. of the cells, the potentiometer tests were always made first and the bridge measurements as soon as possible thereafter.

(d) The development of light-resistance sensitivity in one phenylmagnesium bromide cell after several months suggested that electrolysis of these cells might yield some interesting results. The high values of the capacitance per unit area in several of the cells also increased the belief that interesting data of that sort might be found by an application of the electrolytic or "forming" process. Although this feature was not a part of the program originally outlined, it was hoped that something bearing on the general question might be developed.

Electrolysis of ether solutions shows some features not common to aqueous solution. Ollar¹⁶ showed that in certain cases hydrogen was evolved at both electrodes, but he offered no explanation. Only a few papers¹⁷ have yet been published upon the electrolysis of Grignard reagents but work along that line is now being done. It is not possible to say just what happened in the cells treated in this paper, except that in some cases magnesium in the "tree" form was deposited on the cathode. Most of the deposit fell off the plate as soon as the current ceased, but the plate area may have been increased enough to account for at least a part of the increase in capacitance always noted. Luminescence has been observed during electrolysis, sometimes on the anode, sometimes on the cathode, sometimes on both plates.

In the electrolysis, a current of a few milliamperes at 15 volts was passed for 15 minutes through the phenylmagnesium bromide cells in the same direction as the current they generated. With the lower-resistance ethylmagnesium bromide cells 5 volts was applied for 5 minutes. With the first-mentioned type, the process resulted uniformly in decreased resistance, increased capacitance, and a light-resistance sensitivity where none had existed before. In the presence of light a decrease in resistance took place, while in a period of darkness equal to that of the illumination the original resistance was recovered. The ethylmagnesium bromide cells all developed capacitances 2 to 6 times the former values, but the resistance varied differently in different cells. No special change in light-resistance sensitivity was observed, except a small diminution in the magnitude.

Figs. 6 and 7 show results of tests with one cell of each type. Again no general relation was found between e.m.f., resistance, and capacitance changes under illumination. No resistance or capacitance effects were noted under x-ray irradiation.

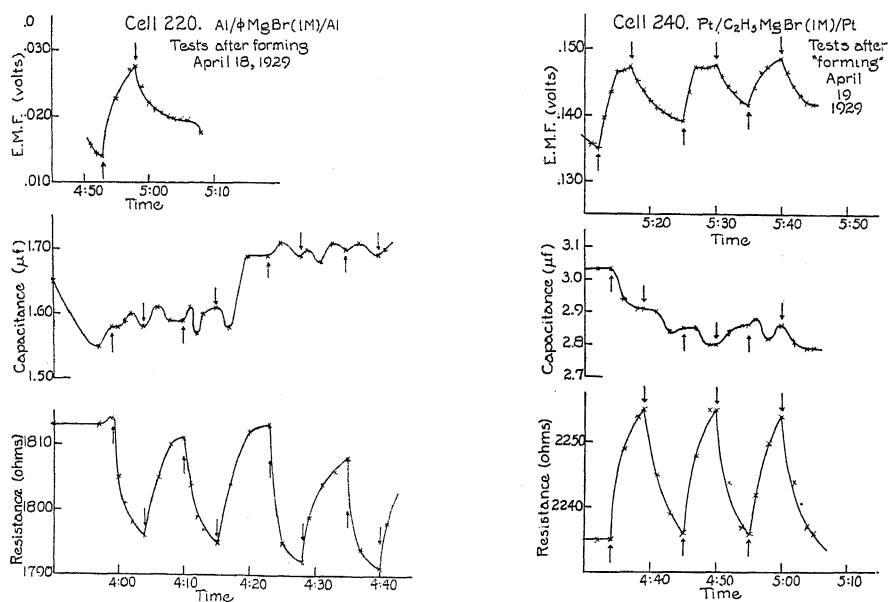
In several cases, cells measured with an ordinary d.c. Wheatstone bridge showed asymmetrical resistances somewhat like those shown by aluminum rectifiers, but the asymmetry was not so pronounced. In one case, the resistances to currents in opposite directions were 8000 and 16000 ohms respectively, while in another the figures were 2600 and 19000 ohms, the higher resistance being uniformly offered to a current opposite to the "forming"

¹⁶ A. Ollar, Thesis, University of Missouri (1926).

¹⁷ L. W. Gaddum and H. E. French, *Jour. Am. Chem. Soc.* **49**, 1295 (1927).

current. The aluminum rectifier stops a current flowing in the same direction as the forming current. The cells which showed this characteristic had aluminum plates and contained phenylmagnesium bromide. Such differences of resistance are not great enough to be of practical use.

One other interesting point remains to be discussed, but lack of exact knowledge of the chemistry of these cells forces rather vague conclusions. Films on aluminum in electrolytic condensers have been found to have thicknesses ranging from 10^{-2} to 5×10^{-6} cm and the dielectric constant was estimated as 14.5.¹⁸ Assuming a value of 1 for the dielectric constant in the present cases, film thicknesses have been computed for two cells which showed very large capacitances. An ethylmagnesium bromide cell gave over 7 mf per cm^2 after "forming". For $k = 1$, the film thickness was 1.2×10^{-8}



Figs. 6 and 7. Effect of light on e.m.f., resistance and capacitance.

cm. A phenylmagnesium bromide cell with copper plates showed about the same capacitance per unit area and the thickness figures were 8×10^{-8} cm. These figures are of the order of interplane distances in crystals, so it is possible that the films are single layers of molecules or a few such layers. It may be noted that the thickness attributed to the film in phenylmagnesium bromide, a benzene-ring compound, is greater than that found for ethylmagnesium bromide, a short-chain compound, as might be expected. The very large capacitance per unit area, 7 mf per cm^2 , is worthy of note. If these thickness figures are near the truth, it seems strange that regular light-capacitance effects were not found, especially in view of the fact that other evidence seems to indicate that the photovoltaic effect is dependent upon condition of the electrode surface.

¹⁸ H. O. Siegmund, Trans. Am. Elect. Chem. Soc. 53, 203 (1928).

The following conclusions may be drawn.

(a) The conclusions of others as to variations in the e.m.f. of Grignard cells with age, with mechanical agitation, and with illumination are corroborated. The evidence seems to locate the seat of the phenomena at or near the surfaces of the electrodes.

(b) Several types of cells gave large voltage responses when exposed to x-rays and also showed large changes in current through a high-resistance circuit during such irradiation. The phenomenon is apparently a different one from the photovoltaic effect in the same cells.

(c) The resistance and polarization capacitance of a number of cells have been measured by means of a high-frequency bridge. Cells containing phenylmagnesium bromide showed no light-resistance response when freshly made, some containing ethylmagnesium bromide and one containing bromoethylmagnesium bromide did. This has been shown not to be a temperature effect. Some cells showed an increase of 1 or 2 percent in resistance when illuminated and some a decrease of about the same percentage, but a given cell was consistent. These results made a general photoelectric theory untenable and also indicated that the rather large voltage variations were not of the same origin as the resistance changes. The small reversible changes in conductivity were laid to alterations in solvation of the ions rather than to changes in ionization percentage. Such capacitance changes as were found seemed unrelated to other phenomena.

(d) A "forming" or electrolytic process was carried out with several cells containing phenylmagnesium bromide and ethylmagnesium bromide. The former then showed a light-resistance sensitivity. After the process, larger capacitances were observed in all cases, but no regular light-capacitance response.

Asymmetrical resistances, smaller than those in aluminum rectifiers, were found in a few cells.

Capacitances as high as 7 mf per cm² were found. Assuming a value of unity for the dielectric constant of the films, the probable thickness of the films was estimated to be of the order of the diameter of a molecule or a small multiple of that diameter. The thickness was greater for a benzene-ring compound than for the short-chain compounds used.

No effects on resistance or capacitance due to x-ray irradiation were detected.

In general, the evidence supports the belief that the voltage variations with illumination must be attributed to phenomena near enough to the electrodes to be affected by changes on their surfaces. The capacitance effects were inconclusive as to whether light-induced effects occurred in the films.

The writer expresses his sincere gratitude to Mr. R. T. Dufford, at whose suggestion the investigation was attempted and whose assistance and advice have been invaluable in carrying out the work; also to Professor O. M. Stewart for suggestions as to the bridge circuit and for the provision of the necessary apparatus and materials.

THERMAL CONVECTION

By R. W. BABCOCK

DE PAUW UNIVERSITY, GREENCASTLE, INDIANA

(Received March 8, 1930)

ABSTRACT

The differential equations which apply to slow steady convective motion of a viscous fluid are the standard equations of hydrodynamical theory, combined with equations expressing the law of thermal interchanges in a moving fluid. Approximate solutions are found following the method outlined by Oberbeck (*Ann. d. Physik*, 1879, p. 271). A comparative study of the exact solution of a special system of non-linear ordinary equations and the Oberbeck approximate solution shows that the magnitude of the constants in the system controls the rate of convergence of the approximation, and often produces divergence. Solutions with graphs of temperature and velocity fields have been computed for special cases of cylindrical and plane boundaries with sinusoidal impressed boundary temperatures. If this temperature has a vertical gradient only, the Oberbeck method produces a null solution, corresponding to equilibrium in stratified layers. Arithmetical solutions for common liquids at ordinary temperatures show that the Oberbeck solutions diverge unless the gradient is much too small to be easily applied in laboratory practice.

ANALYTIC solution of the problems of convection in fluids presents extreme difficulty. No methods have been devised for the exact solution of the differential equations, which are non-linear, and must be solved subject to complicated boundary conditions.

Free convection in a fluid consists of the motions produced by gravity throughout its volume due to changes in its density caused by variations in temperature. This paper presents approximate solutions of certain special cases of steady free convection, produced by temperature differences maintained at the fixed boundaries of the fluid.

If expressions are formed to represent: (1) the flow of momentum; (2) the flow of mass; (3) the flow of energy throughout any volume chosen in the fluid, and terms of second order are neglected, the resulting equations are

$$(dV/dt) - \alpha gT + (1/\rho)\nabla p - \nu\nabla^2 V = 0, \quad (1)$$

$$\text{div } V - \alpha dT/dt = 0, \quad (2)$$

$$(dT/dt) - h^2\nabla^2 T = 0. \quad (3)$$

The symbol g denotes a vector of magnitude $|g| = 32.2 \text{ ft/sec.}^2$ whose direction is upward.

The simplest cases are the flow of a liquid between two infinite parallel plane plates (Fig. 1), and between two infinitely long vertical concentric circular cylindrical pipes (Fig. 2). In both of these cases, the velocity equation reduces to $\nabla^4 u = 0$, and the temperature equation to

$$\alpha gT + \nu\nabla^2 u = 0. \quad (4)$$

When temperatures $\pm t$ are maintained on the plane plates, whose equations are $y = \pm a$, the solutions are

$$u = -\frac{\alpha g t}{6 a \nu} (y^3 - a^2 y), \quad (5)$$

$$T = ty/a. \quad (6)$$

For the cylinders whose radii are 1 and e , upon whose boundaries are maintained temperatures respectively of 0 and 0.5, the solutions are (using the physical constants of water)

$$u = 4.126 [r^2 - 1 - \log r (1.849 - 0.615 r^2)], \quad (7)$$

$$T = 0.5 \log r. \quad (8)$$

In both these cases, it is seen that the temperature is exactly what would be produced by conduction alone in a rigid body filling the space now occupied by the flowing liquid and having the same physical constants.

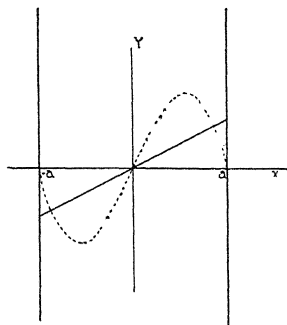


Fig. 1. T , solid curve; u , dotted curve.

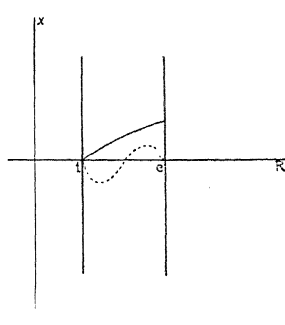


Fig. 2. T , solid curve; u , dotted curve.

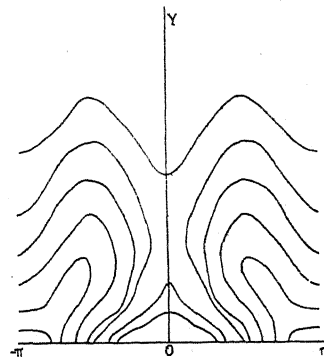


Fig. 3. Temperature field and isothermal lines.

For the solution of other cases, this paper follows the rule for approximation of such equations which was developed by Oberbeck.¹ This method reduces the analysis to equations of the type $\nabla^2 f(x, y, z) = F(x, y, z)$ subject to proper boundary conditions. Oberbeck, in his paper, starts the approximate analytic solution of the convection of a liquid between two concentric spherical shells, which are maintained at different constant temperatures, computing the first velocity terms and the second temperature term. He does not consider conditions of convergence of the solution.

To check Oberbeck's method of solution, a pair of similar simultaneous ordinary differential equations,

$$\frac{d^2 \Psi}{dx^2} - a \frac{dT}{dx} = 0, \quad (9)$$

$$\frac{d^2 T}{dx^2} - b \frac{dT}{dx} \cdot \frac{d\Psi}{dx} = 0, \quad (10)$$

¹ Oberbeck, Ann. d. Physik, 1879, S 271.

may be solved and the results computed numerically for various values assigned to a and b . The exact solution, subject to boundary values, $T(0) = -\alpha$, $T(l) = \alpha$, $\Psi(0) = \Psi(l) = 0$, is

$$\Psi = \frac{2}{b} \log \left[\cos \frac{Bl}{2} \sec B \left(x - \frac{l}{2} \right) \right], \quad (11)$$

$$T = \frac{2B}{ab} \tan B \left(x - \frac{l}{2} \right), \quad (12)$$

where B is the first positive root of the transcendental equation $B \tan (Bl/2) - (\alpha ab/2) = 0$. For $\alpha abl^{-1} = 0.25$, the Oberbeck type of series approximations converge rapidly toward the Maclaurin expansions of the exact solution; for $\alpha abl^{-1} = 1$, the convergence is slow; and for $\alpha abl^{-1} = 5$, divergence of the series is obtained. Any approximation, therefore, to equations of type of Eqs. (1), (2), (3), must depend for their convergence upon the values of their physical constants. Since these are restricted in a problem involving laboratory experiments, the analytical question of convergence prescribes the amount of temperature difference which may be applied. In the numerical computation of the following cases, the physical constants of glycerine have been chosen. These examples have been set up so that the Z -axis is a line of symmetry, and all the equations have but two independent variables.

Whenever the liquid is assumed to be absolutely incompressible so that $\text{div } V = 0$, and cartesian coordinates are used, a "current function" Ψ is formed such that

$$u = \partial \Psi / \partial y, \quad v = -\partial \Psi / \partial x. \quad (13)$$

Eqs. (1), (2), (3), then become

$$h^2 \nabla^2 T = \frac{\partial T}{\partial x} \frac{\partial \Psi}{\partial y} - \frac{\partial T}{\partial y} \frac{\partial \Psi}{\partial x}, \quad (14)$$

$$\nabla^4 \Psi = \frac{\alpha g}{\nu} \frac{\partial T}{\partial x}, \quad (15)$$

subject to $\Psi = \partial \Psi / \partial n = 0$, and $T = T(x, y)$ at the boundary surfaces. Two such cases are studied in detail.

(A) A half-space above the plane $y = 0$ upon whose surface $T(x, y) = t \cos x$ is maintained. The following solutions are obtained:

$$T = te^{-y} \cos x + \frac{\alpha g t^2}{128 h^2 \nu} [2 + e^{-2y} \{ (2y^2 + y) \cos 2x - (4y^2 + 4y + 2) \}] \quad (16)$$

$$\Psi = -\frac{\alpha g t}{8 \nu} y^2 e^{-y} \sin x - \frac{\alpha^2 g^2 t^2}{24576 h^2 \nu^2} e^{-2y} \sin 2x (4y^4 + 4y^3 + 3y^2). \quad (17)$$

The temperature and velocity fields are shown in Figs. 3 and 4. The limiting temperature approached high up in the space is not zero, but a definite positive value, $\alpha g t^2 / 64 h^2 \nu$, the heat having been carried upward by the convection currents and not brought down again as rapidly.

(B) The space between two infinite horizontal plane plates whose equations are $y = \pm l$, upon both of which $T(x, y) = t \cos x$ is maintained. When l is chosen as 3, and t as 0.5, the principal temperature term is $0.0496 \cosh y \cos x$, and

$$u = -10^{-3} \sin x [0.28y^2 \sinh y - 1.08y \cosh y + 0.74 \sinh y], \quad (18)$$

$$v = 10^{-3} \cos x [0.28y^2 \cosh y - 1.64y \sinh y + 2.38 \cosh y]. \quad (19)$$

The temperature and velocity fields are shown in Figs. 5 and 6. In both these cases the velocity fields show a jet-like streaming above the warm portions of

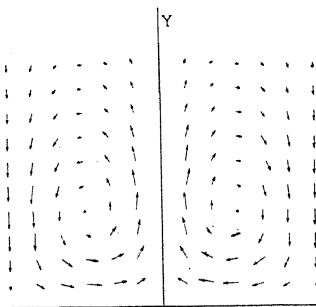


Fig. 4. Velocity field.

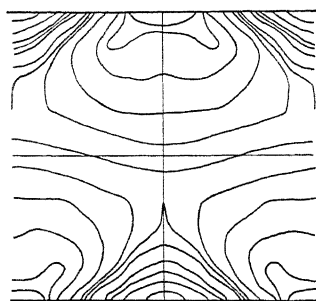


Fig. 5. Temperature field and isothermal lines.

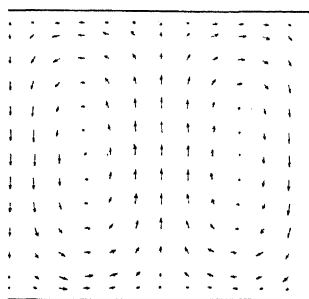


Fig. 6. Velocity field.

the boundary. This is of the same type as that observed by Nelson² in his experiments in convection. The boundary temperatures are different in his work, so that only a qualitative check is obtainable here.

Using polar coordinates, analytic solutions may be computed for impressed boundary temperatures more readily adaptable to laboratory conditions. In the following examples the container is assumed to be an infinite horizontal circular cylinder, the initial line chosen as the upward radius, the vectorial angle running counterclockwise. Eqs. (14) and (15) when transformed to this system of coordinates are

$$\frac{\partial T}{\partial \rho} \cdot \frac{\partial \Psi}{\rho \partial \theta} - \frac{\partial T}{\rho \partial \theta} \cdot \frac{\partial \Psi}{\partial \rho} = h^2 \nabla^2 T, \quad (20)$$

$$\nu \nabla^4 \Psi + \alpha g \left(\sin \theta \frac{\partial T}{\partial \rho} + \cos \theta \frac{\partial T}{\rho \partial \theta} \right) = 0, \quad (21)$$

² Nelson, Phys. Rev. 23, 94 (1924).

where the radial and tangential components of velocity are

$$R = \partial\Psi/\rho\partial\theta, \quad \Theta = -\partial\Psi/\partial\rho. \quad (22)$$

As usual, the boundary conditions prescribe the temperature maintained on the surface, and cause the velocity to vanish there.

(A) The first case discussed in this coordinate system is an impressed boundary temperature $T = t \sin \theta$. This may be considered as the temperature impressed in a large metal block, across which a linear horizontal temperature gradient is constantly maintained. Temperature within the block near the boundary has not been measurably changed by the convection within the cylinder.

The first approximation to the velocity is a pure rotation, the current function being

$$\Psi_1 = -\frac{\alpha g t}{64\nu}(1 - \rho^2)^2 \quad (23)$$

the same solution which was found by Love³ in the deformation of a circular plate clamped at the circumference under uniform pressure. The temperature and velocity fields, approximated to another term, are shown in Figs. 7 and 8. This velocity field shows regions of "dead water" which have been observed under similar laboratory conditions.

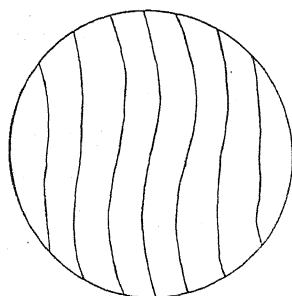


Fig. 7. Temperature field and isothermal lines.

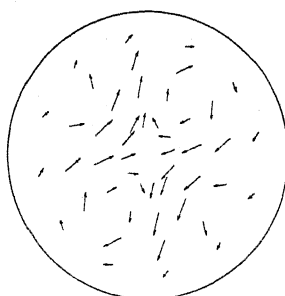


Fig. 8. Velocity field.

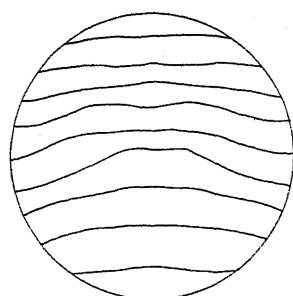


Fig. 9. Temperature field and isothermal lines.

For this case, a complete solution which does not include an assumption of the incompressibility of the liquid shows that the difference between the two types of solution consists of terms occurring only after the second approximations to temperature and velocity, and that these differences are of relative magnitude 10^{-3} . The analytic solution in this case is much more tedious. The values of the fluid pressure due to the convection current must be found, and the added accuracy of the solution occurs only in those terms which are of such size as to be entirely outside the range of experimental observation. The full solution is then neither a necessary nor an efficient method of attacking the problem.

(B) If a pure vertical gradient of any sort is impressed in the boundary temperatures, no motion is determined from the analytic solution. This represents equilibrium in the liquid, which is stable or unstable if the sign of the

³ Love, *Mathematical Theory of Elasticity*, 3d ed., p. 490.

upward gradient is positive or negative. The body of liquid stratifies in horizontal layers. In order to consider an approximate solution, one of two choices must be made: (1) assume a form of initial velocity; (2) assume an initial temperature which does not have a pure vertical gradient such as $T_0 = (t\rho \cos \theta)/a + kf(\rho, \theta)$, where $f(a, \theta) = 0$ to satisfy the boundary conditions. Either of these choices is so arbitrary that the solutions obtained do not compare with facts which could be observed. Two choices for $f(\rho, \theta)$ are studied here, both of which have radial symmetry. These are (1) $f(\rho, \theta) = (kt/a)(a - \rho)$ and (2) $f(\rho, \theta) = (kt/a^2)(a^2 - \rho^2)$. The temperature and velocity fields are compared. The two sets are shown in Figs. 9, 10, 11, and 12. In both cases, the

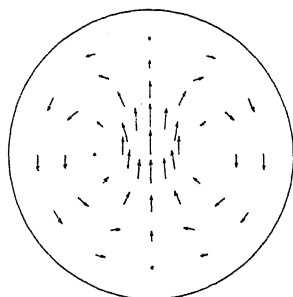


Fig. 10. Velocity field.

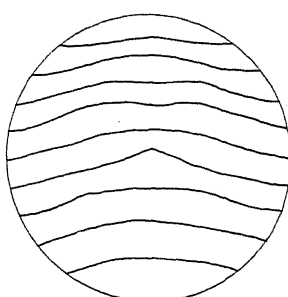


Fig. 11. Temperature field and isothermal lines.

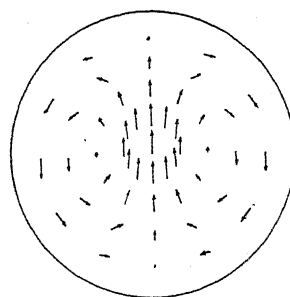


Fig. 12. Velocity field.

whole problem approaches a null solution as the parameter k is made infinitesimal, so that neither presents a satisfactory approximation to the desired result. There is, however, a tendency for the corrections to the temperatures to equalize and thus become independent of the specific form chosen for $f(\rho, \theta)$.

Since Eqs. (14) and (15) are non-linear, the sum or difference of two solutions is not a new solution. This prevents the use of the usual type of uniqueness proof to assume a second solution and show that the difference of the two solutions vanishes identically. The essential accuracy of the approximations must be checked through experiment.

In all the particular examples studied, it is, of course, necessary to study carefully the question of the convergence of the series obtained:

$$T = T_0 + \alpha T_1 + \alpha^2 T_2 + \dots, \quad (24)$$

$$\Psi = \alpha \Psi_1 + \alpha^2 \Psi_2 + \dots. \quad (25)$$

For a liquid having a low viscosity, like alcohol or water, the sufficient condition for convergence requires the amplitude of the impressed temperature not to exceed about 10^{-4} degrees per centimeter of the horizontal cylinder. Such values are useless for comparison with any type of experiment. For a much more viscous liquid, such as glycerine, the amplitude of the impressed temperature may be as large as 10^{-1} degrees per centimeter radius. Even this restricts the usefulness of the Oberbeck method to such an extent as to render it practically useless as a comparison with laboratory results. The computations here show the dependence of the analytic solution upon the physical constants of the particular problem. They also determine the small amount of error obtained by assuming the absolute incompressibility of the liquid and demonstrate the fact that these corrections may be neglected, thus materially shortening the computations, which are laborious under the most favorable conditions.

LETTERS TO THE EDITOR

Prompt publication of brief reports of important discoveries in physics may be secured by addressing them to this department. Closing dates for this department are, for the first issue of the month, the twenty-eighth of the preceding month; for the second issue, the thirteenth of the month. The Board of Editors does not hold itself responsible for the opinions expressed by the correspondents.

*On the Mechanism of "Atomization"

So far as the writer knows no adequate explanation has been offered of the phenomenon of liquid "atomization." Scheubel¹ has, indeed, given some interesting and instructive spark pictures of the process as it occurs in the carburetor throat, but not much direct information can be derived from them except at fairly low air speeds. The fact, however, that the phenomenon can be used with confidence in the design of many machine elements,—that certain results may be expected to attend certain conditions,—is tacit declaration that the process has a definite physical background.

If, given a quantity of liquid which at one time exists as a single comparatively large mass, and a moment later is observed to be in the form of a very great number of very small discrete drops, we merely make the assumption that there must be an intermediate stage in which fine ligaments are formed, of such diameter that they will disintegrate into drops of the observed size, we can account for this phenomenon on the basis of Rayleigh's theory of jet disintegration and certain recent observations of the size of the drops formed when a liquid is atomized. This assumption seems reasonable, since time and temperature considerations exclude the possibility of evaporation and subsequent recondensation; it seems necessary, since it will appear very improbable that the existence of such fine ligaments can ever be directly demonstrated; and it is hoped to show that it is sufficient.

Rayleigh² thus explained the disintegration of a jet which we shall identify with the ligament mentioned in the preceding paragraph: He considered the jet as an infinitely long cylinder of liquid initially in equilibrium under the influence of the tension of its

envelope, and investigated the efficiency of various types of disturbance in upsetting this equilibrium. He found that

$$\alpha = \alpha_0 e^{qt} \quad (1)$$

where α and α_0 are amplitudes, at times t and 0, respectively, of a disturbance symmetrical with reference to the cylinder axis; e is the Napierian base; and

$$q = \left(\frac{8T}{\rho D^3} \right)^{\frac{1}{2}} \cdot F \quad (2)$$

In Eq. (2), T and ρ represent the liquid's surface tension and density, respectively:

D is the diameter of the undisturbed filament; and F is a (dimensionless) function of Z , the ratio length/diameter. The denominator of this fraction is the same as D above, while its numerator is the distance along the jet between two adjacent points in the same phase of vibration.

When α grows to $D/2$ the filament breaks.

The function F has been investigated by Rayleigh² and by the present writer.³ As a result it follows that the effective value of F may be taken as about 0.34 at $Z=4.5$. For this value of Z it also follows that the diameter d of a spherical drop will be about twice D , the diameter of the cylindrical segment from which the drop is formed.

Hausser and Strobl⁴ and Sauter⁵ found,

* Publication approved by the Director of the Bureau of Standards of the U.S. Department of Commerce.

¹ F. N. Scheubel, *Jahrbuch der W. G. L.* p. 140 (1927).

² Rayleigh, *Proc. Lon. Math. Soc.* 10, 4, (1879).

³ Castleman, *Nature* 114, 857, (1924).

⁴ Hausser and Strobl, *Zeits. tech. Phys.* 5, 154 (1924).

⁵ J. Sauter, *Zeits. V.D.I.* 72, 1572 (1928).

for water atomized in a high speed air stream, a mean value of d of about 6×10^{-4} cm, while Woltjen⁶ found about the same for oil atomized by "airless" injection into a high pressure bomb. Taking 10^{-3} cm as an upper limit, we have 5×10^{-4} cm for D , so that Eq. (2) gives $q = 740,000 \text{ sec.}^{-1}$ for water atomized in a high speed air stream.

Now, it is very difficult, if not impossible, to estimate the value of α_0 precisely. The molecular diameter is, however, of the order of 10^{-7} cm⁷ so it seems legitimate to place about 10^{-8} cm as a lower limit. To cut through a ligament 5×10^{-4} cm in diameter, α must grow to $D/2 = 2.5 \times 10^{-4}$ cm. The necessary time is, by Eq. (1), $t = (1/q) \ln \alpha/\alpha_0 = (1/M_q) \log_{10} \alpha/\alpha_0 = 1/73,000 \text{ sec.}$ (approx.). This would correspond to a motion of about

2 millimeters of the *air* stream in the throat of the carburetor of an automobile engine turning over at high speed; or of about 1 mm of the spray 0.0005 sec. after injection at 8000 lbs/in², into a chamber held at 200 lbs/in² (N.A.C.A. Report #268).

The above gives *upper* limits of the possible lengths of these fine ligaments. Small wonder that they have never been observed!

R. A. CASTLEMAN, JR.

Bureau of Standards,
March 15, 1930.

⁶ Woltjen, Dissertation, Tech. H.S. at Darmstadt (1925) (Data taken from N.A.C.A. Tech. Memo. #403, pp. 19-22).

⁷ Rayleigh, Phil. Mag. 48, 331 (1899).

The Atomic Weights of Hydrogen and Helium.

Eddington (Proc. Roy. Soc. A126, 696, 1930) has obtained a new theoretical value of $1/137$ for the fine structure constant α . This agrees much better with observational data than his previous value of $1/136$. He also reaches the very interesting conclusion that in a *rigid system* of protons and electrons, there should be a proportional loss of mass equal to α . The most rigid system of this kind now known is the alpha-particle, and the loss of mass, assuming the alpha-particle to be absolutely rigid, agrees more closely with the theory than is indicated in Eddington's paper. In fact, on this assumption, an atomic weight of 1.00777 ± 0.00002 for hydrogen (see Birge, Phys. Rev. Suppl. 1, 1, 1929) leads to 4.00166 as the calculated atomic weight of helium. As I have noted (footnote 12a, page 21, loc. cit.) the best chemical value for this latter quantity is now 4.0018. Because of the newly discovered isotopes of oxygen, Aston's mass spectrograph value of 4.0022 should be lowered about one part in 10,000 (page 69, loc. cit.) and then agrees precisely with the chemical value. Hence the observed and calculated values of the atomic weight of helium differ by only one part in 30,000, and this may be

taken to indicate that the alpha-particle is in fact very nearly "rigid."

This correlation of the fine structure constant with the "packing effect" in an alpha-particle has already been suggested, on a purely empirical basis, by Lunn (Phys. Rev. 20, 1, 1922) and has been revived by Witmer (Nature 124, 180, 1929). In this earlier work, the predicted decrease in mass was given as $\alpha/(1+\alpha)$, but this differs by an entirely negligible amount from the present predicted decrease of α .

If the nucleus of the isotope oxygen "16" is a non-rigid system composed of four such "rigid" alpha-particles, the mass of this nucleus should be four times the mass of an alpha-particle, diminished by the mass-equivalent of the binding energy of the four alpha-particles. The atomic weight of the isotope oxygen "16" is 15.9984 (one part in 10,000 less than 16.0000), and one thus obtains 0.0082 atomic weight units (or one part in 1950 of the total mass) as the mass-equivalent of the binding energy. This seems to be a reasonable value.

RAYMOND T. BIRGE

University of California,
March 25, 1930.

A New Unified Field Theory and Wave Mechanics

In your issue of January 1st 1930, you published a preliminary notice of a paper on the above subject by the present writer. A few more words of explanation thereof, not included in the paper itself seem called for.

The fundamental postulate is that the unobservable is non-existent. This is familiar in wave mechanics, but is now applied for the first time to relativity.

Since the metric tensor of space time is

defined logically in terms of an unobservable N -dimensional pseudo-Euclidean space, for classical relativity, by our postulate the definition is impossible. For us the metric tensor becomes a perfectly arbitrary set of ten functions of the space-time coordinates, available for descriptive purposes. The old analogy with the intrinsic properties of two-dimensional curved surfaces can be dropped and surpassed. The metric tensor is defined only by transfer according to a certain rule from an initial point, and its increments are not perfect differentials; it depends upon the track along which the rule has been applied. Such a tensor is sufficient to give definite magnitude to the elements of the vector lines in the vector field defined by another transfer rule applied to a vector. As already pointed out these vector lines become the known orbit equations when the simplest derivable definite tensor function is used to describe the electric field.

This is a distinct improvement on the theory of Kaluza and Klein which introduces an unknowable fifth dimension directly into the equations, apart from the others required for the logical definition of the metric.

It has been found necessary to abandon the

hope that the theory might lead to quantised orbits round atomic nuclei; but this is not necessary, for there is no longer any inconsistency with wave mechanics. Thus classical electromagnetic theory was based on the concept of a local singularity with definite position and velocity; but no such singularity is at the basis of the present theory. The new point of view is this: If local singularities exist, then their tracks can be described by means of the vector line theory, but if the uncertainty in the position or velocity of such singularities becomes significant, the method will no longer be useful, and statistical methods appropriate to the case must be used. There is thus no longer any inconsistency, it is merely a matter of convenience in description.

We may finally claim to have cleared up the apparent inconsistencies between the field theory and the atomic theory, and set the former on the same satisfactory philosophical basis as the latter.

WILLIAM BAND

Yenching University,
Peping, China,
February 28, 1930.

The Carbon Dioxide Theory of the Ice Ages

It was pointed out long ago by Tyndall, (Phil. Mag. 22, 277 (1861)), that changes in the carbon dioxide content of the atmosphere might be a controlling factor in the cause of ice ages. The suggestion was generally accepted for many years but more recently writers have denied its importance, for example Angström, Ann. d. Physik 6, 172 (1901), Humphreys, ("Physics of the Air," pages 564 and 602 (1929)), Abbot and Foule, (Smithsonian Institution, Annals Astrophys. Obs. 2, 172 (1908)), Jeffreys, ("The Earth," page 263 (1924)) and Simpson (Nature 124, 988 (1929)) and "Past Climates," page 9 (1929)). These writers have used the single blanket argument, which in its simplest form may be stated as follows: If all the energy leaving a hot body is absorbed by one blanket the cooling rate will not be reduced by increasing the number of blankets. Since water vapor is practically completely absorbant for the radiation in the CO_2 absorption bands, they argued that changing the amount of CO_2 in the atmos-

phere would not affect the climate of the earth.

The argument of course is not correct. For example, the temperature T degrees Kelvin of a body warmed by a constant supply of energy f ergs $\text{cm}^{-2} \text{sec}^{-1}$ and cooled by radiation through an absorbing sheath containing n molecules, in a 1 cm^3 column through the sheath, of atomic absorption coefficient α for the radiation, is given by

$$T^4 = f(1 + \alpha n) / a\sigma, \quad (1)$$

where a is the absorption coefficient of the surface of the body and σ is the Stefan-Boltzmann constant. From (1) it is seen that T increases with n for all values of n . Calculations for the carbon dioxide and the water vapor in the upper atmosphere, using (1) and taking into account the shift of the spectral distribution curve of the radiation as it passes through the atmosphere, etc., show that a 70 percent decrease in the carbon dioxide will cause a decrease of more than 6 percent in the radiation entering the lower atmosphere, (Terr. Mag. and Atmos. Elec.

33, 253 (1928)). This decrease alone will account for a temperature drop of about 6°C at the earth's surface. When to this 6° is added decreases associated with decreased humidity, decreased wind action in providing a cooled insulating layer and increased reflection of sun's rays accompanying the extension

of ice fields we would expect a temperature drop such as would be associated with an ice age. It is hoped to develop these ideas to some extent in a future paper.

H. B. MARIS

Naval Research Laboratory,
March 31, 1930.

BOOK REVIEWS

Magnetism. EDMUND C. STONER. viii + 117 pp. 20 figs. E. P. Dutton and Co., New York 1930. Price: \$1.10.

This little book is one of a series by English physicists which propose to supply the advanced student of physics in general with condensed accounts of recent progress in specialized branches of his subject. The general preface by O. W. Richardson emphasizes the utility of these monographs to those preparing for examinations. The present exemplar is well written and is thoroughly up-to-date in all that relates to the theory of magnetism and to the experimental basis upon which it rests, that is to theory and experiment in diamagnetism, paramagnetism and ferromagnetism in high magnetic fields. Ferromagnetism in weak magnetic fields—including the Barkhausen effect—is not so happily treated. This is no doubt because this part of the subject is still, as the author clearly states, almost without a theoretical structure to connect its phenomena. Aside from four misprints, a slight mistake regarding the magnetostriction of nickel-iron alloys on page 88, and a general tendency to use sub-visible subscripts, the reviewer finds nothing in which the author, editor, and publisher have been remiss. The practice of omitting the name of each investigator with whose conclusions the author disagrees is novel but commendable.

L. W. MCKEEHAN

Acoustics of Buildings. F. R. WATSON. Second Edition, Pp. 165, Figs. 69. John Wiley & Sons, New York, 1930. Price \$3.00.

This is a second edition of Professor Watson's book first published in 1923, and is intended for that rapidly growing group of persons who have to deal with the practical problems of architectural acoustics. For this reason the emphasis throughout is laid upon the application of the developments in this field during the last thirty years to the control of acoustic conditions rather than upon a detailed account of the underlying principles and theory.

The first section of the book concerns itself with the problems of Auditorium Acoustics, particularly with the calculation and control of reverberation. Numerous illustrations and examples of the use of the reverberation formula both in the design of new rooms and in the correction of existing rooms are given. The most important addition made in the revision of this section of the book is a table of sound absorption coefficients of commercial materials used for acoustical correction, and one giving the absorbing power of opera chairs of various types. The author's position on the question of optimum reverberation times as a function of the size of the auditorium is somewhat equivocal. Thus a graph is given showing what the author considers the optimum time computed by the well-known Sabine formula increasing linearly with the logarithm of the volume from 0.8 to 2.05 seconds as the volume is increased from 1,000 to 1,000,000 cubic feet. In a subsequent paragraph under the heading "Ideal Auditorium Acoustics" appears the statement "The second condition (for ideal acoustics) is that the auditorium should be made as dead as out doors for the benefit of the auditors." The reader interested in the acoustical design of a new room is left in doubt as to whether to install absorbent material so as to give the "optimum reverberation time," or to try to approximate the "ideal" condition of out of doors where sound reflection is nil. The difference is one of considerable practical importance.

There are no important additions to the material given in the earlier edition in the section devoted to sound proofing in buildings, although numerous references to recent original work on this phase of the subject are added.

Considered even as a vehicle for the conveyance of practical information, one feels that the author frequently errs on the side of brevity and over simplification. This is particularly true in some of the illustrative diagrams. Thus to represent sound of wave-length of the order of two feet as being reflected in a parallel beam from a parabolic mirror with an aperture of five feet and reflected again geometrically from a plain surface of small dimensions is to neglect the complicated standing wave pattern that must result in such a case from interference and diffraction, and measurements based on such a simplified picture of the phenomenon must be open to serious question.

Taken as a whole the book is a concise, almost summary, statement of the principal facts of architectural acoustics as they were known at the time of the publication of the first edition of the book. To include the considerable mass of data that have been accumulated in the last five years would call for more rewriting than could be included in a revision of the first edition.

PAUL E. SABINE

Molekelbau. F. HUND. Pp. 38, 7 figs. and 3 tables. Part of Band VIII, *Ergebnisse der exakten Naturwissenschaften*, Julius Springer, Berlin, 1929.

This is a valuable compact summary of the progress made to date (i.e., spring of 1929) in the theory of molecular structure from the standpoint of the wave mechanics. The emphasis is laid on the qualitative features of the problem and no attempt is made to consider the mathematical arguments involved. The bibliography is comprehensive. The attention of persons interested in this review may also be called to the "Zusammenfassende Bericht" on homopolar chemical binding by W. Heitler in the *Physikalische Zeitschrift* for March, 1930, and to the articles on the "Interpretation of Band Spectra" by Mulliken now appearing in *Reviews of Modern Physics*.

E. C. KEMBLE

THE PHYSICAL REVIEW

THE ELECTRON DISTRIBUTION OF MAGNESIUM OXIDE

By E. O. WOLLAN

RYERSON PHYSICAL LABORATORY, UNIVERSITY OF CHICAGO

(Received March 16, 1930)

ABSTRACT

The *intensity of x-rays reflected* from powdered crystals of magnesium oxide was measured for all lines out to $\theta = 45^\circ$. The values of the structure factor, F , were calculated and plotted against $\sin \theta$. Using the values of F from this curve as coefficients in Compton's Fourier series, the *radial electron distribution for the atoms of magnesium and oxygen* was determined. The electron distribution curves for these atoms are very similar to Havighurst's curves for sodium chloride and sodium fluoride. Although it has been generally conceded that crystals of the magnesium oxide type are polar in form, the data here included are more in line with their being non-polar crystals. However, it is not believed possible from x-ray reflection data to prove definitely this point.

INTRODUCTION

THE intensity of reflection of the K_α line of molybdenum has been measured for powdered crystals of magnesium oxide. The structure factor curves have been calculated, and the electron density in the crystal and the radial electron distribution in the atoms of magnesium and oxygen have been determined, using the Fourier Series worked out by A. H. Compton.¹ Besides being able to determine the distribution of the electrons in the atoms, the total number of electrons associated with each point of the space lattice can thus be found. This should make it possible to decide whether the crystal is in a polar or non-polar form. In the work of Bragg, James, and Bosanquet, sodium chloride was concluded to be polar and Havighurst has concluded that several crystals with which he worked were of this form. In general the evidence seems to favor this view for crystals of the sodium chloride type, but it can hardly be said to be conclusive.

Magnesium oxide has been chosen for analysis, not only for the interest in determining the electron distribution in the atoms of magnesium and oxygen, but also because it is a very suitable substance for showing the state of ionization of the atoms in the space lattice.

¹ A. H. Compton, "X-Rays and Electrons."

EXPERIMENTAL PROCEDURE

The accuracy with which intensity measurements can be made with powdered crystals is limited to some extent by the difficulty of obtaining a strictly homogeneous beam of x-rays of sufficient intensity. It was found that the method used by Havighurst² was most suitable for obtaining accurate results, especially at large angles, where the intensity is very weak. This method is essentially that first used by W. H. Bragg,³ and consists in utilizing the focussing effect of randomly oriented crystals pressed into a flat plate, and the use of zirconium oxide filters for cutting out the K_β and K_γ lines and a greater part of the general radiation. The arrangement of the author's apparatus is shown in Fig. 1. A molybdenum target x-ray tube was operated at a potential of 35 kv and 35 m.a., supplied by a transformer with full wave rectification.

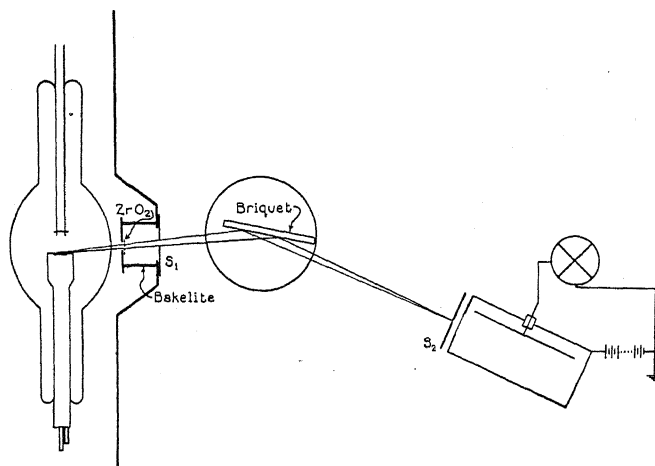


Fig. 1. Diagram of apparatus

The pure magnesium oxide powder was pressed into a brass ring two inches in diameter. The mass per cm² of the powder was made just great enough for practically total absorption of the K_α lines of molybdenum. In this way some of the general radiation of shorter wave-length was not effective in scattering and increasing the continuous background.

The slits used in front of the ionization chamber were accurately measured to be of such width that when the briquet was moved through some predetermined increment of arc (generally five to ten minutes) the slit, S₂, moved through its own width. In this way all the reflected energy was received in the ionization chamber.

The ionization current was measured with a Compton electrometer, having a sensitivity of from five to ten meters per volt. The rate of deflection of the electrometer needle was taken at each increment of arc corresponding

² R. J. Havighurst, Phys. Rev. **28**, 832, (1926).

³ W. H. Bragg, Proc. Phys. Soc. London, **33**, 222 (1921).

to the width of the slit, S_2 . The reciprocals of these readings were plotted as ordinates against the angle θ and the intensity of the line was taken as proportional to the sum of the ordinates above the base line. If the increments are small the intensity is also proportional to the area under the curve. Different widths of slits, S_2 , were found to give results in satisfactory agreement.

Table I, column three, gives the average of the relative intensity measurements where the intensity of the (200) reflection has been taken equal to 100.00. The measurements have been extended to about $\theta = 45^\circ$. This is as far as the spectrometer could conveniently be used.

TABLE I. *Measured values of F for magnesium oxide.*

Plane	Sin θ	Rel. Int.	F
111	0.1464	8.55	2.92
200	0.1691	100.00	13.40
220	0.2390	55.10	10.15
311	0.2804	5.80	2.78
222	0.2929	15.20	8.20
400	0.3380	6.00	6.94
331	0.3684	2.53	2.51
420	0.3780	13.20	5.92
422	0.4140	8.72	5.35
511	0.4392	1.07	1.73
333			
440	0.4782	1.71	4.00
531	0.5000	0.83	1.41
600	0.5071	3.31	3.78
442			
620	0.5344	1.84	3.22
533	0.5542	0.25	1.29
622	0.5606	1.30	3.00
444	0.5856	0.37	2.90
551	0.6036	0.19	0.90
711			
640	0.6095	0.89	2.60
642	0.6324	1.40	2.52
553	0.6492	0.16	0.71
731			
800	0.6762	0.12	2.21
733	0.6918		
644	0.6970	0.80	2.05
820			
822	0.7172	0.48	1.86
660			

STRUCTURE FACTOR DETERMINATIONS

Darwin⁴ and A. H. Compton⁵ have derived equations which relate structure factor and the integrated intensity of x-rays reflected from powdered crystals.

When the relative intensity measurements have been made by reflection from a briquet of powder as they were in this case, the equation for calculating the relative values of the structure factor, F , takes the simple form

⁴ C. G. Darwin, Phil. Mag. **43**, 827, (1927).

⁵ A. H. Compton, Phys. Rev. **9**, 29, (1917).

$$F^2 = \frac{P_s \sin \theta \sin 2\theta}{j (1 + \cos^2 2\theta)} \quad (1)$$

where P_s is the intensity of the reflected beam measured on some arbitrary scale, j is the number of planes cooperating in producing the intensity P_s , and 2θ is the angle between the primary and the reflected beam. F^2 is the square of the structure factor in which the Debye⁶ temperature factor, $\exp [(b^2 \sin^2 \theta) / \lambda^2]$, is included. The reasons for the inclusion of the Debye factor in the value of F have been pointed out by Havighurst.²

The relative values of F can be placed on an absolute scale by comparing the intensity of some line of the substance to be analyzed with the intensity

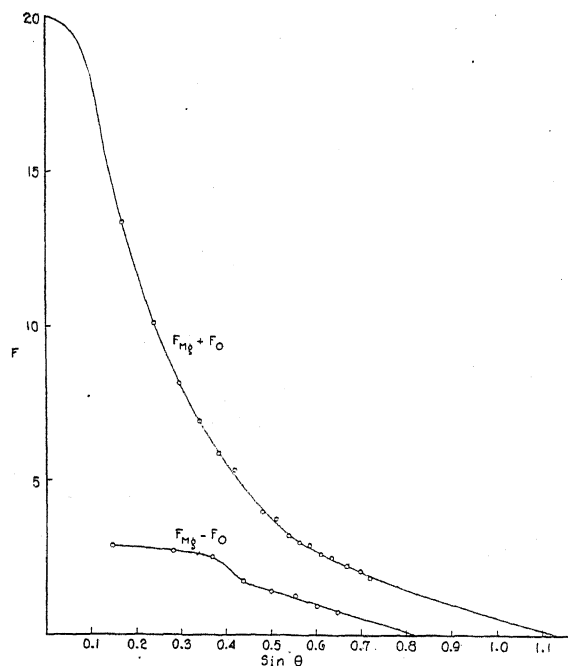


Fig. 2. Structure factor curve for MgO.

of a line of a substance for which the absolute value of F has been directly determined. The absolute value of F for the (220) reflection of sodium chloride has been measured by James, Bragg and Bosanquet⁷ on single crystals, and corrected for secondary extinction. Their value of $F=15.75$, has been used as a standard for placing the relative F values of magnesium oxide on an absolute basis.

Table I, column IV gives the absolute values of F for all the lines measured, where F (220) was found equal to 10.15 by comparison with the same reflection from sodium chloride.

⁶ P. Debye, *Verh. d. D. Phys. Ges.* **15**, 678, (1913).

⁷ W. L. Bragg, James, and Bosanquet, *Phil. Mag.* **42**, 1, (1921).

Fig. 2 shows the F curves plotted from the above values of F . The upper curve is due to even order reflections and corresponds to $F_{Mg} + F_O$, while the lower curve corresponds to $F_{Mg} - F_O$. The values of F for the separate atoms can be found from the relations

$$\begin{aligned} F_{Mg} &= \frac{1}{2}(F_{Mg} + F_O) + (F_{Mg} - F_O) \text{ and} \\ F_O &= \frac{1}{2}(F_{Mg} + F_O) - (F_{Mg} - F_O). \end{aligned} \quad (2)$$

Since magnesium and oxygen are bivalent and have atomic numbers of 12 and 8, respectively, the ions would have 10 electrons each. This means that for ions the lower F curve is dependent on the different electron distributions and not on the number of electrons in the two ions. If the scattering centers are neutral atoms this curve would be a function of both the distribution and the number of electrons.

ELECTRON DISTRIBUTION CURVES

For the determination of the radial electron distribution curves the equation derived by Compton was used. This is a one dimensional Fourier series and much easier to evaluate than the three dimensional series of Duane. The series has the form

$$U = \frac{8\pi r}{D^2} \sum_1^{\infty} n F_n \sin \frac{2\pi n r}{D} \quad (3)$$

where U is equal to the number of electrons per Angstrom and r is the distance from the center of the atom in Angstroms. If both sides of this equation are multiplied by dr and integrated from 0 to $D/2$ one gets an expression for Z , the total number of electrons in the atom included between these limits,

$$Z = -2 \sum_1^{\infty} (-1)^n F_n. \quad (4)$$

In calculating the electron distribution curves for magnesium and oxygen, spherical symmetry has been assumed in the atoms, and the values of F were read directly from the F curves, assuming a grating space of 2.5Å for the sake of convenience in calculations. This gives a series of only seven terms, but it was found that the distribution in the K and L shells was only very slightly different if a larger number of terms were used.

TABLE II. Values of F from F -curves on basis of $D=2.5\text{\AA}$.

Indices	Sin θ	$(F_{Mg} + F_O)$	$(F_{Mg} - F_O)$	F_{Mg}	F_O
111	0.142	15.00	2.92	8.96	6.04
222	.284	8.40	2.76	5.58	2.82
333	.426	5.10	2.00	3.55	1.60
444	.568	2.94	1.14	2.04	0.90
555	.710	1.94	0.44	1.19	0.75
666	.852	1.24	0.00	0.62	0.62
777	.994	0.60	0.00	0.30	0.30

Table II gives the values of $F_{Mg} + F_O$ and $F_{Mg} - F_O$ which have been taken from the F curves of Fig. 2 and the values of F_{Mg} and F_O , which have been calculated with the aid of Eq. (2). Using these values of F as coefficients in the series 3, given above, the electron distribution curves of magnesium and oxygen have been plotted in Figs. 3 and 4.

MAGNESIUM

Fig. 3 shows the curve for the radial electron distribution in magnesium. The area under the curve corresponding to the K and L shells is about 9.5 electrons, unless a part of the adjoining hump is included. If the distribution is calculated on the basis of $D = 5.00\text{\AA}$ the area under this part of the curve is 10 electrons and its distribution is very nearly the same with a slightly better resolution of the hump at $r = 0.5\text{\AA}$. The distribution in these shells is very similar to Havighurst's⁸ curves for sodium in NaCl and NaF, except that in this case the average distance of the electrons from the nucleus is less.

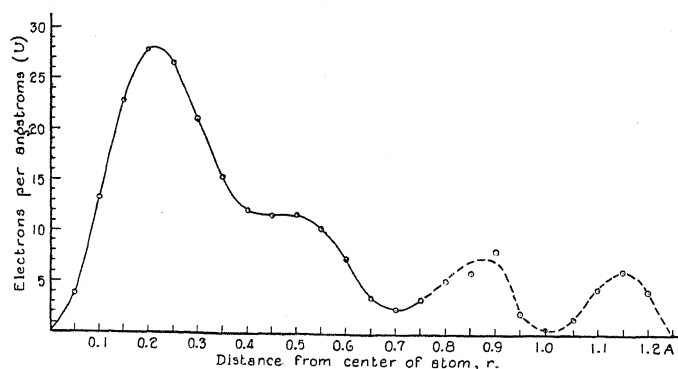


Fig. 3. Electron distribution in Mg.

This could be expected from the fact that magnesium has a higher atomic number and also that the grating space of Mg is less than for either of the other two substances mentioned.

In this curve there is also an indication of the two valence electrons, and these, as might be expected, are more loosely bound than the other electrons. Little significance can be placed in the positions of these humps, however, since they are not the same when calculated on the basis of $D = 5.0\text{\AA}$.

The total number of electrons in the atom, according to this analysis is 11.50. This is the area under the curve and also the value as given in Table II, calculated from Eq. (4). In all cases the area under the curve checks the value from Eq. (4) as, of course, should be the case if no error is made in working out the Fourier series. The existence of only 11.50 electrons using the F values corresponding to $D = 2.5\text{\AA}$ and 11.04 electrons for $D = 2.424\text{\AA}$ indicates that some of the electron atmosphere is at a distance greater than

⁸ R. J. Havighurst, Phys. Rev. **29**, 1, (1927).

$D/2$ from the nucleus, beyond which the series does not hold, since it drops to zero at this value.

OXYGEN

Fig. 4 shows the radial electron distribution curve for oxygen. Here the electron shells in oxygen have areas corresponding to 3, 3.5 and 1.5 electrons with a small erratic variation near $D/2$. The fact that the humps do not represent an integral number of electrons may be due to experimental error,

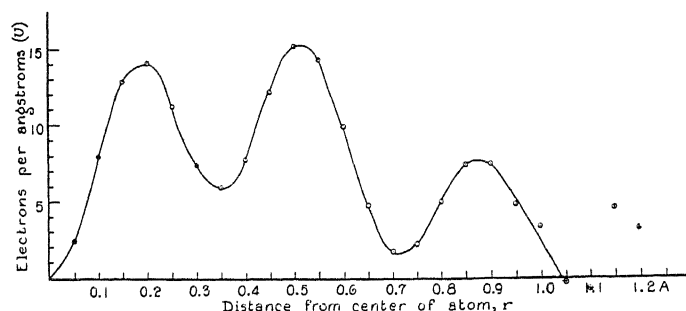


Fig. 4. Electron distribution in O.

but there is no reason, from the idea of elliptic and interpenetrating orbits, that the distributions should be made up of humps representing integral numbers of electrons.

The total area under the curve is equal to 8.7 electrons, which also checks the value in Table II, as calculated from Eq. (4). This curve for oxygen closely resembles Havighurst's curve for fluorine.

ELECTRON DENSITY IN THE MgO CRYSTAL

Compton has derived a series which represents the number of electrons in a plane at any height above some atomic layer. This series has the form

$$P = \frac{Z}{a} + \frac{2}{a} \sum_{n=1}^{\infty} \left(F_n \cos 2\pi n \frac{z}{a} \right) \quad (5)$$

where P is equal to the number of electrons per Angstrom, z is the distance above the reference plane in Angstroms, and Z is the total number of electrons per molecule of the substance.

Using the values of F_{111} , F_{222} , etc., given in Table I and the value of F_{666} extrapolated from the F curve, as coefficients in this series and plotting P against z/a , one gets the curve shown in Fig. 5.

It will be noticed that the electron density does not fall to zero between the atoms. This means that the atoms overlap, and in order to tell how many electrons belong to each atom it is necessary to extrapolate the curve of one atom into the space of the other. This, in general, can be only a good guess; but in this case there is considerable difference in the size of the humps, and the most obvious extrapolation would be to give magnesium more electrons

than oxygen. In Fig. 5 extrapolations have been made for the two extreme cases of the neutral atom and the ion. The broken line shows how the curve can be extrapolated to give Mg 12 electrons and oxygen 8 electrons, while the dot and dash line gives the ions with 10 electrons each. From the fact that the radial electron distribution curves for magnesium do not contain 12 electrons between 0 and $D/2$, however, one is led to the conclusion that the valence electrons of magnesium spend part of the time nearer to the nucleus of oxygen than to that of the magnesium atom. It is, however, probable that the distribution for large values of r in the radial distribution

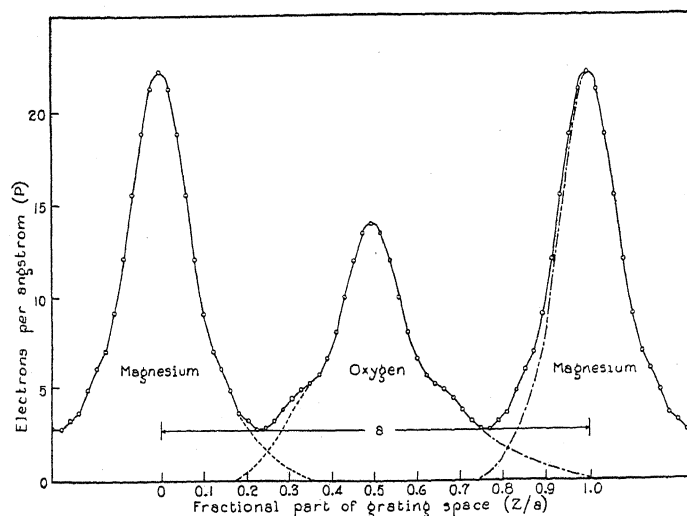


Fig. 5. Electron density in MgO.

curves, is no more reliable than a logical extrapolation of the curves in Fig. 5.

Using the table of F values worked out by Havighurst as coefficients in series 4, the total number of electrons associated with the atoms in various crystals has been determined and the results are shown in Table III. It will be seen that the analysis of these data by the use of Compton's series leads to no definite conclusions regarding the state of ionization of the atoms in the crystals considered.

TABLE III.

Mg		O	
$D = 2.5\text{\AA}$	$Z = 11.52$	$Z = 8.70$	
2.424\AA	$Z = 11.04$	$Z = 8.42$	
5.00\AA	11.56	8.34	
Havighurst's Data			
NaCl	NaF	CaF ₂	LiF
$Z_{\text{Na}} = 10.82$	$Z_{\text{Na}} = 10.48$	$Z_{\text{Ca}} = 19.04$	$Z_{\text{Li}} = 1.42$
$Z_{\text{Cl}} = 17.54$	$Z_{\text{F}} = 9.12$	$Z_{\text{F}} = 10.46$	$Z_{\text{F}} = 8.38$

CONCLUSION

There seems to be fairly good agreement in the data of different observers for the distribution of the electrons in the *K* and *L* shells of various atoms. For magnesium there is no overlapping of these shells for neighboring atoms. In the shells of larger radius, where there is overlapping of the electrons for the two or more atoms considered, it is quite likely that the analysis of the distribution is less reliable.

From the data at hand, one is hardly justified in drawing definite conclusions regarding the location and the behavior of the valence electrons in the atoms of crystals. To say that an atom is ionized in the crystal presumably means that the electrons are revolving about the nucleus of the other atom. Since a large portion of each atom overlaps its neighbor, this implies that the analysis can detect whether an electron scattering at a point near the nucleus of one atom is actually revolving about the nucleus of the other. This can, at best, be only a good guess as to what is actually occurring.

The calculation of the distribution of diffracting power in some direction in the crystal is considerably more straightforward. Hence, a curve of the type of that shown in Fig. 5 would be more reliable than the radial distribution curves. In the case of magnesium oxide it would be easier to extrapolate this curve to give 12 and 8 electrons to the atoms of magnesium and oxygen, respectively, than to make an extrapolation giving these atoms each 10 electrons.

Since there is a considerable amount of overlapping of the neighboring atoms, it would be more reasonable to conclude from the data at hand that the valence electrons are shared by the atoms of magnesium and oxygen and that neither of the conclusions regarding the existence of ions or neutral atoms in the points of the crystal lattice is altogether correct.

In conclusion, the writer wishes to express his appreciation to Professor A. H. Compton for his helpful suggestions throughout the work.

PREDISSOCIATION OF DIATOMIC MOLECULES
FROM HIGH ROTATIONAL STATESBY D. S. VILLARS AND E. U. CONDON
UNIVERSITY OF MINNESOTA, MINNEAPOLIS

(Received March 12, 1930)

ABSTRACT

Instability of molecules in high rotational states, as observed especially in HgH and AlH, is a phenomenon whose quantum-mechanical explanation is closely analogous to that of the radioactive disintegration of atomic nuclei. The heat of dissociation of AlH from its normal state is estimated to be 3.07 volts.

THE observations of Henri¹ and his school, that certain band systems apparently pass progressively from a discontinuous to a continuous character in such a manner as to indicate that the emitting molecules lose their rotational quantization before they lose their vibrational quantization, has been ascribed to a "predissociation" by various writers. The generally accepted mechanism for this process is that proposed by Bonhoeffer and Farkas,² who assume, in accordance with quantum mechanics, that there may occur a radiationless transition of the molecule in a definitely quantized rotational and vibrational state, to another electronic state for which the same total energy places the molecule in the continuous energy range corresponding to dissociation. When the probability of transition from the quantized level to the dissociated state is high, the average life of the molecule may become less than a rotational period of the molecule so the corresponding band is diffuse. But there is an additional mechanism for predissociation which also is a consequence of quantum mechanics which has not been mentioned before, so far as we are aware.

It is known that the set of rotational quantum levels associated with the same vibrational quantum number may extend up to values of the total energy in excess of the amount necessary to dissociate the molecule in that electronic state. Such sets of rotational levels however do not extend upward indefinitely but are often observed to break off rather suddenly. In at least one instance, that of aluminum hydride, the last two or three levels broaden out so that lines involving them become faint because their energy is spread out more on the photographic plate. This phenomenon has been interpreted by Mulliken,³ Hulthén,⁴ and Ludloff⁵ as due to an instability of the molecule arising from the high rotation. What has been lacking is an

¹ Henri, *Photochemie* (1919); *Structure des Molécules* (1925).

² Bonhoeffer and Farkas, *Zeits. Phys. Chem.* **134**, 337 (1927).

³ Mulliken, *Phys. Rev.* **25**, 509 (1925).

⁴ Hulthén, *Zeits. f. Physik* **32**, 32 (1925), **50**, 319 (1928).

⁵ Ludloff, *Zeits. f. Physik* **39**, 526 (1926).

account of the nature of the instability and the reason that it sets in when it does.

Franck and Sponer⁶ have advanced the view that the phenomena both of the sudden termination of such sets of rotational levels and the broadening of the last few levels, are to be interpreted as Bonhoeffer and Farkas have suggested. Oldenberg,⁷ from classical ideas alone, has criticized this paper of Franck and Sponer. He points out that the potential energy governing the radial motion of a molecule that is rotating with quantum number, m , is equal to

$$U_m(r) = U_0(r) + \frac{h^2}{8\pi^2\mu} \frac{m(m+1)}{r^2}$$

where $U_0(r)$ is the potential energy for the non-rotating molecule and is determined by the electronic state. Since for large r , $U_0(r)$ becomes constant more rapidly than r^{-2} approaches zero, the function $U_m(r)$ is positive for large values of r and will show, for m not too great, a minimum followed by a maximum at greater nuclear separation. This behavior is illustrated by Fig. 1 which represents the curves (Morse⁸) for HgH.

The similarity of the curves with those that lie at the basis of quantum mechanics of radioactive disintegration⁹ is evident. Hence the general properties of the wave equation which were so successful in that field are applicable here. The formula for the mean time of remaining essentially in the range of the periodic classical motion near the minimum, before going over into the range of the aperiodic classical motion extending from beyond the maximum to infinity, there developed for the atomic nucleus, is here applicable to the dissociation of molecules by rotation. We do not expect accurate results from it, both because it is based on an approximate integration of the wave equation, and because it requires an accurate knowledge (which we do not have) of $U_0(r)$ for the larger values of r . In principle, however, we have the means of inferring from the $U_0(r)$ curve, which is inferred from the energy levels, the exact maximum value of the rotational energy which can give levels effectively sharp in radiative transitions. These are the ones for which the mean life, τ , of the molecule before it "leaks" through the hump in the potential energy curve is large compared with 10^{-8} sec, which is the mean life needed to provide a sharp line in spectroscopic instruments of the resolving power actually available to experimenters.

Oldenberg has shown that there will be no trace of any discrete level structure for any value of m greater than the one for which $U_m(r)$ has a horizontal inflection point. (An *integral* value of m may not give a horizontal inflection point, m is regarded here as a continuous variable). He also mentions that owing to the existence of the so-called zero-point vibration energy the actual

⁶ Franck and Sponer, *Göttinger Nachr.*, p. 241 (1928).

⁷ Oldenberg, *Zeits. f. Physik* **56**, 563 (1929).

⁸ Morse, *Phys. Rev.* **34**, 57 (1929).

⁹ Gurney and Condon, *Phys. Rev.* **33**, 127 (1929).

values of m will not extend this far. But there is another factor to consider: the level in question must be sufficiently below the maximum of the $U_m(r)$ that the mean life before leakage is large compared to the mean life before radiation. It is clear why the rotational levels associated with the second vibrational quantum state cannot extend as high as those associated with the

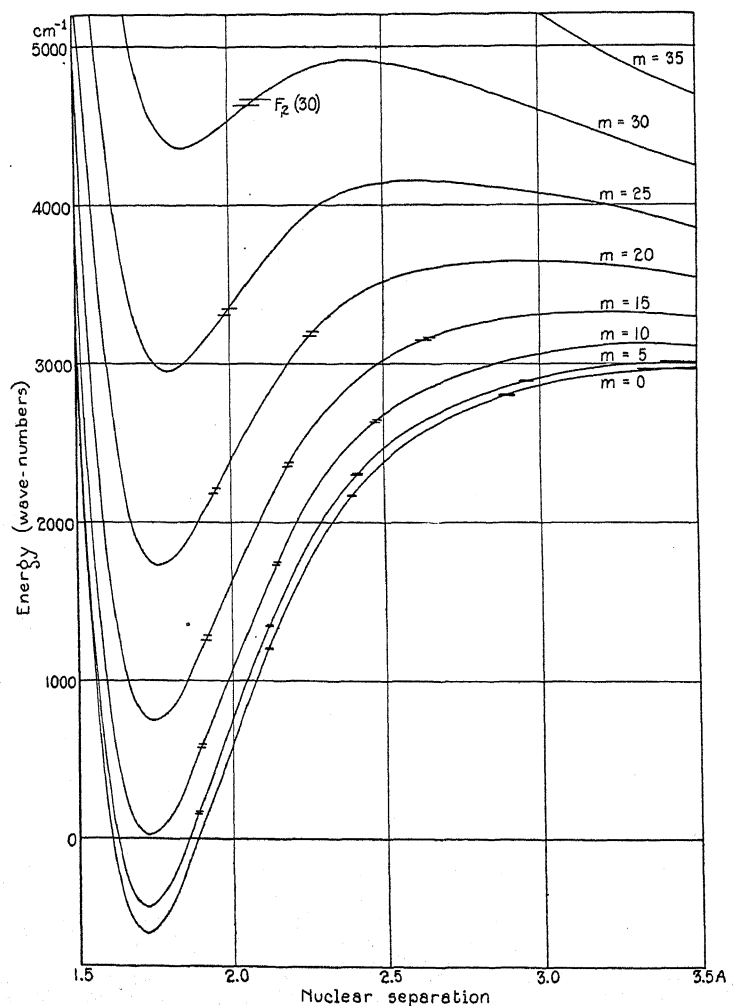


Fig. 1. Rotational vibrational (Morse) curves for HgH (normal $^2\Sigma$ state.) The designation $F_2(30)$ refers to the upper of the two doublet levels on the $m=30$ curve.

first; they are always higher above the minimum of the $U_m(r)$ curve because of the extra vibrational energy and therefore the requirement that they be sufficiently below the maximum of $U_m(r)$ can only be satisfied for smaller values of m . This behavior is nicely illustrated by the levels of HgH plotted by Franck and Spomer in their Fig 2.⁶

This behavior is also shown by the excited electronic state of AlH concerned in the band system studied by Eriksson and Hulthén.¹⁰ Here only two vibrational levels are known so that the heat of dissociation cannot be found by the usual method of extrapolation of vibration levels, due to Birge and Sponer.¹¹ Fig. 2 shows the range of rotational energy associated with the zero and one vibrational levels of this electronic level. Comparing this figure with the analogous one for HgH, we do not hesitate to say that the dissociation energy for excited AlH must lie below the lowest fuzzy level and above the one quantum vibration level with zero rotation. This puts it probably within the range of the braces around "D" in the figure, that is,

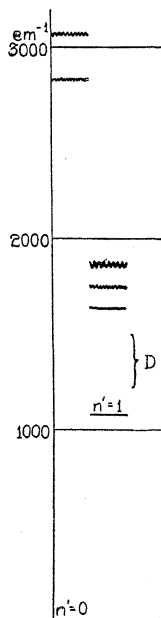


Fig. 2. Predissociation levels in the excited $^2\Pi$ state of AlH.

it is close to 0.17 ± 0.02 volts. This is the quantity called "y" in Table I of Mulliken's¹² study of band spectra of diatomic hydrides. Hence the heat of dissociation from the normal state is 3.07 volts. This is essentially the conclusion of Franck and Sponer, though from different theoretical considerations.

Oldenberg¹³ is of the opinion that the radiationless transfers in the nuclear separation coordinate violate Franck's principle because they call for a fairly large "sudden" alteration in the nuclear separation. We feel that this is an attempt to push the Franck idea beyond the limits of its validity. The

¹⁰ Eriksson and Hulthén, *Zeits. f. Physik* **34**, 786 (1925).

¹¹ Birge and Sponer, *Phys. Rev.* **23**, 259 (1926).

¹² Mulliken, *Phys. Rev.* **33**, 730 (1929).

¹³ Reference 7, p. 573.

principle is simply an easily visualized rule describing approximately what quantum mechanics will predict. The connection with quantum mechanics has already been developed.¹⁴ The principle has to do with the nuclear motions accompanying electron transitions and not with the nuclear motions when there is no change of electronic state.

A rough calculation for HgH was made, using a Morse function for $U_0(r)$,

$$U_0(r) = 2990 + 3592e^{-6.25(r-r_0)} - 7184e^{-3.125(r-r_0)},$$

where energy is measured in cm^{-1} and distance in 10^{-8} cm. The zero-point vibrational energy was arbitrarily taken as one-half the difference between the two lowest vibrational levels. The quantity ω_e was taken as 1528.8 cm^{-1} . These assumptions are somewhat arbitrary but are the best that can be made. The half-breadth of a line is given by

$$\Delta\nu/c = 1/4\pi\tau c,$$

(compare Pauli, *Handbuch der Physik*, vol. 23, p. 70). With the formula for mean life from Gurney and Condon¹⁵, the half-breadth of the line with rotation quantum number thirty and zero vibration comes out to be 39 cm^{-1} . Actually this level gives rise to a sharp line, but a slight change in the form of the $U_0(r)$ curve, entering the exponent of the formula for τ will make it be sharp, so we conclude that insufficient knowledge of the $U_0(r)$ function does not justify further calculations at present.

¹⁴ Condon, *Phys. Rev.* **32**, 858 (1928).

¹⁵ Reference 9, p. 133.

NEW MEASUREMENTS ON THE FOURTH POSITIVE
BANDS OF CARBON MONOXIDE

BY L. B. HEADRICK AND G. W. FOX

UNIVERSITY OF MICHIGAN PHYSICS LABORATORY

(Received March 19, 1930)

ABSTRACT

New measurements of that part of the fourth positive band system of carbon monoxide between 2174A and 1280A have been made from plates photographed with a one-meter vacuum spectrograph. Low voltage arc excitation was used. The densities of the band edges were determined from a microphotometric trace. A few new band edges lying below the fourth positive system are reported. In general the measurements here reported are in good agreement with the wave-lengths published by Birge.

INTRODUCTION

THE fourth positive band system of carbon monoxide extending from 2800A to about 1280A has been measured in parts by a number of investigators at different times. Birge¹ describes the work previous to 1926 and analyzes data taken by Deslandres, Bair, Duncan, Lyman and Leifson. Recently Estey² discusses the papers on CO subsequent to 1926 and reports new measurements on that part of the fourth positive system lying between 1970A and 2800A.

In the course of some work with a vacuum spectrograph, measurements were made on the part of the fourth positive system of CO lying between 1280A and 2174A. It seems advisable to report these results at this time to give a more complete set of new measurements for this important band system.

EXPERIMENTAL DETAILS

The bands were photographed with a one-meter vacuum spectrograph of the design described by Sawyer.³ Two plates were made; one of short exposure for microphotometer records and the other of longer exposure for wave-length determinations.

A low voltage arc in CO containing a trace of hydrogen was used to excite the bands. The gas pressure was 0.5 mm of mercury, current 10 to 12 m.a. and potential difference 22 volts. An enlargement of one of the plates extending from 2090A to 1150A is shown in Fig. 1. A microphotometric trace of the same plate, made on a Moll self-recording microphotometer is shown in Fig. 2. The densities of the band edges and lines given in Table II and

¹ Birge, Phys. Rev. **28**, 1157 (1926).

² Estey, Phys. Rev. **35**, 305 (1930).

³ Sawyer, J.O.S.A. **15**, 305 (1927).

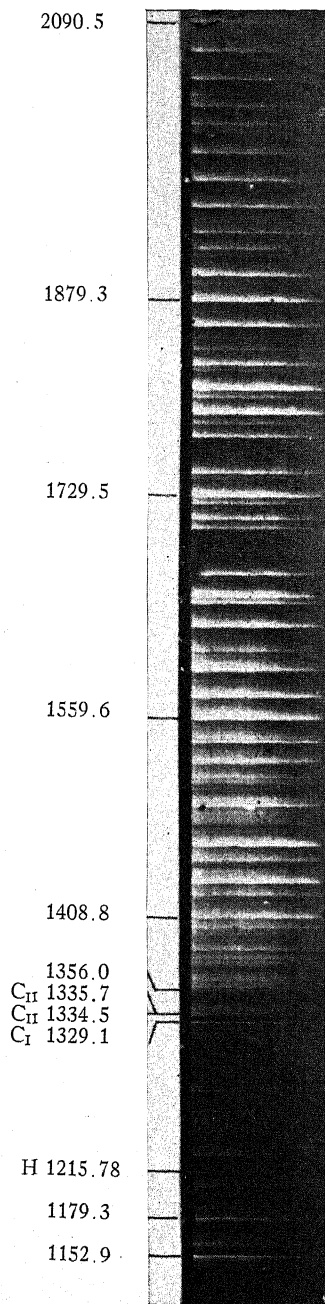


Fig. 1. The fourth positive band system of CO.

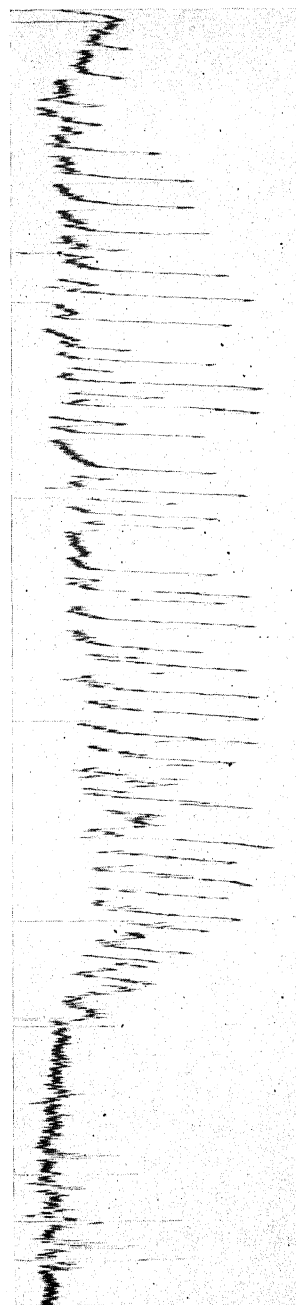


Fig. 2. A microphotometer record of part of the fourth positive band system of CO. from 2090.5A to 1280.6A. Including the hydrogen line 1215.78A, several carbon lines and bands of CO at 1179.3 and 1152.9A.

Table III were obtained from this trace by use of the relation,⁴ density = $\log d/(d-h)$, where d is the total galvanometer deflection in the absence of a line and h is the height of the peak on the trace corresponding to a band edge or line.

The carbon line 2479.29 was used as a standard for the measurements of the bands from 2173.8A to 1595.8A. The hydrogen line 1215.78A was used as a standard for the measurements from the lower wave-length end of the plate up to 1611.5A. The measurements from the two standard lines overlapped for several bands near 1600A. The two measurements obtained in this way for the same edges checked within 0.2A.

The grating constant varied somewhat over the region photographed. The best values for it were previously determined experimentally by Dr. J. E. Mack. Table I gives these values for the regions over which they may be applied.

TABLE I.

Grating constant Angstroms/mm	Wave-length range
17.49	2332.2A—1970.0A
17.47	1970.0A—1729.5A
17.46	1729.5A—1597.4A
17.44	1597.4A—1025.7A

RESULTS

The measurements on the band edges, their densities as obtained from the microphotometer record, and their identification as assigned by Birge¹ are given in Table II. Some of the weaker band edges could not be measured on the plate but they appear on the photometer record in Fig. 2. A few new unidentified bands which apparently belong to the fourth positive system of CO are included in Table II.

TABLE II.

λ (A)	ν (cm ⁻¹)	Density $\times 10^4$	n'	n''
2173.8	* 46002.8		5	13
2150.9	46492.8		4	12
2138.1	46770.9		7	14
2129.1	46968.9		3	11
2107.9	47439.7		2	10
2090.5	47835.0	0.5	5	12
2068.3	48348.7	0.7	4	11
2046.9	48854.4	0.5	3	10
2042.9	48949.5	0.3		
2034.9	49142.2	0.7	6	12
2026.3	49351.3	1.4	2	9
2012.4	49691.2	0.7	5	11
2006.4	49839.8	0.4	1	8
1990.8	50230.3	1.6	4	10

⁴ Hughes and Lowe, Phys. Rev. 21, 292 (1923).

TABLE II (continued).

$\lambda(\text{\AA})$	$\nu(\text{cm}^{-1})$	Density $\times 10^4$	$n'n$	n''
1970.0	50761.7	2.8	3	9
1950.0	51281.5	2.6	2	8
1930.6	51797.1	3.0	1	7
1918.0	52129.5	1.4	4	9
1912.8	52279.9	0.5	0	6
1897.8	52692.0	4.0	3	8
1879.2	53214.4	6.1	2	7
1859.3	53782.5	4.8	1	6
1850.1	54050.8	0.3	4	8
1841.3	54309.8	1.3	0	5
1829.9	54646.9	4.0	3	7
1827.6	54715.7	0.8	6	9
1810.8	55223.0	7.6	2	6
1804.9	55404.7	1.9	5	8
1792.4	55790.8	7.5	1	5
1784.9	56026.8	1.3	4	7
1772.9	56403.8	3.4	0	4
1747.1	57238.7	3.8	2	5
1743.5	57356.2	0.7	5	7
1729.5	57820.8	6.1	1	4
1723.7	58013.4	2.2	4	6
1712.2	58403.4	3.9	0	3
1704.8	58658.9	3.1	3	5
1684.9	59350.0	0.4	5	6
1669.7	59891.7	3.9	1	3
1647.8	60687.3	4.0	3	4
1629.6	61366.3	6.9		
1611.5	62055.9	3.1	4	4
1597.4	62603.7	6.9	0	1
1595.8	62665.3	1.6	6	5
1576.8	63421.6	7.1	2	2
1559.6	64120.6	7.0	4	3
1545.3	64712.8	3.5	0	0
1542.4	64835.7	6.9	3	2
1525.7	65542.0	5.3	2	1
1515.7	65977.9	2.5	7	4
1510.4	66206.3	1.8	4	2
1492.6	66997.2	6.0	3	1
1480.2	67556.6	1.5	5	2
1463.4	68333.3	9.0	4	1
1452.2	68859.6	4.9	6	2
1435.3	69671.4	6.4	5	1
1425.8	70136.5	4.7	7	2
1408.8	70981.4	4.8	6	1
1401.0	71378.1	2.5	8	2
1384.0	72256.9	2.7	7	1
1378.0	72566.8	1.5	9	2
1373.7	72796.1	0.9	11	3
1363.3	73350.4	1.1		
1356.0	73746.3	0.4	10	2
1316.0	75986.7	0.3		
1299.3	76965.7	0.2		
1280.5	78091.4	0.2		

In Table III are given the wave-lengths of the C_I and hydrogen lines which were used as standards to measure the band edges. A few other C_I and C_{II} lines which were used to check the measurements are also given in this table. Measurements of four strong unidentified band edges below the fourth positive system are included. Three of these band edges may be seen

on the microphotometric trace, one just to the left of the hydrogen line. The other two at the right of this line are marked. The fourth one at 1025.7A is not shown on the trace. This was the shortest wave-length edge observed.

TABLE III.

λ (Å)	ν (cm ⁻¹)	Density $\times 10^4$	Remarks
1335.7	74866.8	0.3	C _{II} line
1334.53	74932.2	0.2	" "
1037.02	96430.1		" "
1329.1	75238.9	1.0	C _I line
2479.29	40334.1		" "
1215.78	82254.5	1.6	Hydrogen
1228.2	81422.6	0.7	
1179.3	84793.9	2.8	band
1152.9	86733.3	3.3	edges
1025.7	97496.3		

These edges probably belong to the absorption systems of Hopfield and Birge,⁵ corresponding to transitions from excited states, above those giving rise to the fourth positive system and the normal state.

⁵ Hopfield and Birge, Phys. Rev. 29, 922 (1927).

ABSORPTION BANDS OF AMMONIA GAS
IN THE VISIBLE

BY RICHARD M. BADGER

GATES CHEMICAL LABORATORY, CALIFORNIA INSTITUTE OF TECHNOLOGY

(Received March 4, 1930)

ABSTRACT

The article describes an investigation of the absorption spectrum of ammonia gas in the visible region. At 5490Å an absorption region was found which was too weak for a complete investigation with the means at hand. On a second band at 6474Å measurements on 57 lines are given, and the structure of the band is discussed. These two bands are the fifth and fourth overtones of an ammonia band at 3μ . Some interesting alternations of intensity are pointed out, and comparison is made with other ammonia bands of the same harmonic series. Some features of other portions of the ammonia spectrum are discussed in connection with the bands here investigated.

INTRODUCTION

IT WAS recently shown by Badger and Mecke¹ that molecular band spectra of the vibration-rotation type, corresponding to higher members of a harmonic series with a fundamental in the infra-red, may be photographed in the near infra-red or visible regions with the large dispersion of a long focus grating. In the case particularly investigated (ammonia gas) it was found that a complexity of structure was revealed which could only be surmised from the existing investigations on bands lying further in the infra-red and beyond the reach of photographic methods.

Recently, information concerning the spectra of diatomic molecules has been accumulating at a very rapid rate, so that the more important features of this type of spectrum are now quite well understood. Our knowledge of polyatomic molecules is in a much less satisfactory state, and up to the present only relatively small portions of the complete spectrum originating in any molecule of this type have been submitted to anything like a complete analysis.

The study of the vibration-rotation type of band with the relatively high resolution permitted by photography seems to offer important possibilities in the solution of the general problem, and a program for the investigation of a number of the simpler polyatomic molecules by this method has consequently been undertaken.

In the case of certain molecules it has been found that different vibration-rotation bands of the same molecule may have a very different appearance, even in the case of bands of the same harmonic series. Theoretical reasons for this on the basis of symmetry considerations have been discussed by Hund.²

¹ Badger and Mecke, *Zeits. f. phys. Chem.* **5**, 333 (1929).

² Hund, *Zeits. f. Physik* **43**, 805 (1927).

One of the most interesting cases of the kind mentioned is found in ammonia, which is a relatively simple molecule and one whose spectrum might be expected to be capable of treatment. At 3μ there is a band which has been investigated by Stinchcomb and Barker³ and has been interpreted by Dennison⁴ as due to a molecular vibration in which the change of electric moment is perpendicular to the symmetry axis. The harmonics of this band are relatively strong as shown by Badger and Mecke,¹ who investigated the fourth and located the fifth members of the series. The two bands of the series which have been studied present considerable difference in appearance and have several features of which the explanation is not immediately evident.

It is the purpose of the investigation described in this paper, as a part of the general program mentioned above, to extend the investigation of this harmonic series to higher members with the expectation that a comparison of several bands, and especially of the intensity alternation of each, will lead to an understanding of the nature of the various rotational and vibrational levels involved.

EXPERIMENTAL PROCEDURE

The ammonia gas used in the investigation was a synthetic product and was confined in a steel absorption tube 280 cm long, closed at the ends with plate glass windows. Gas pressures of from one to five atmospheres were employed, but increasing the pressure did not seem to have great advantage, probably due to a broadening of the absorption lines. The source of illumination was a tungsten lamp.

The majority of the exposures were made with a six inch grating of ten foot radius of curvature. This grating gives intense spectra in the first order in the red, and has great freedom from ghosts. Some exposures were also made using the second order of a twenty-foot grating.

When using the ten-foot grating the exposures were made on a process panchromatic film which was very contrasty and fine grained. The exposure times ranged from ten to thirty minutes. Development was carried as far as possible without introducing excessive developer fog. When using the second order of the large grating it was necessary to use a faster film, which unfortunately was less contrasty than the process film, so that only the stronger lines showed up in the exposures. An iron arc calibration spectrum was photographed on each of the films.

Since, at best, the absorption bands studied are very weak, and direct measurements on the films were difficult, as all but the most intense lines disappear under the microscope of a comparator, the following procedures were used in working up the results.

(1) Enlargements of several different films were made on contrast paper. Measurements were made on each with a scale, and the results compared.

³ Stinchcomb and Barker, *Phys. Rev.* **33**, 305 (1929).

⁴ Dennison, *Phil. Mag.* **1**, 195 (1926).

(2) The best film (most contrasty, free from blemishes) was microphotometered and measurements made on the record plate.

(3) Enlargements from four of the best films were made on contrast film and superposed (see Oldenberg, *Zeits. f. Physik*, **58**, 722 (1929)) and measurements made on the resulting composite picture. It is remarkable how this procedure averages out small defects in the plates and intensifies lines which on a single plate would be pronounced doubtful.

TABLE I. *The ammonia band at 6474A.*

$\lambda(\text{\AA})$	$\nu(\text{cm}^{-1})$	I	$\lambda(\text{\AA})$	$\nu(\text{cm}^{-1})$	I
6419.5	15573.1	0	{6472.4}	{15445.9}	
			{6474.0}	{15442.0}	9
{6422.2}	{15566.7}	0	{6474.7}	{15440.5}	
{6423.3}	{15564.1}		{6475.7}	{15438.2}	
{6425.5}	{15558.6}	0	{6478.8}	{15430.6}	6
{6426.5}	{15556.2}	1	{6479.6}	{15428.7}	
{6427.8}	{15553.1}	?			
{6428.6}	{15551.1}	?	6483.2	15420.1	6
{6429.7}	{15548.5}	?			
6431.8	15543.4	1	{6485.3}	{15415.3}	
			{6485.8}	{15414.0}	?
{6434.5}	{15536.9}	5	{6486.9}	{15411.5}	
{6435.6}	{15534.3}				
6438.2	15527.9	10	{6488.5}	{15407.7}	5
			{6489.5}	{15405.2}	
6442.5	15517.7	9	6492.4	15398.4	1
6446.2	15508.6	8	{6494.9}	{15392.5}	4
			{6495.9}	{15390.0}	
{6449.5}	{15500.9}	7	{6498.2}	{15384.6}	?
{6450.4}	{15498.6}		{6499.3}	{15382.0}	7
6453.1	15492.1	2	{6501.0}	{15377.9}	?
6455.4	15486.7	2	{6501.8}	{15376.0}	?
6457.4	15481.9	3	6506.6	15364.7	6
			6510.9	15354.6	1
{6460.1}	{15475.2}	0	6512.9	15349.8	3
{6460.8}	{15473.7}				
{6363.6}	{15466.9}	0	6514.9	15345.1	?
{6364.7}	{15464.4}		6517.1	15340.1	?
{6364.9}	{15463.7}	0	6519.9	15333.3	2
{6365.6}	{15462.2}				
{6367.9}	{15456.7}	0	6522.7	15326.8	?
{6368.2}	{15456.1}		6525.9	15319.4	1
6370.3	15451.0	?			
			{6528.0}	{15314.4}	?
			{6529.4}	{15311.2}	?

EXPERIMENTAL RESULTS

In this work two absorption regions were investigated corresponding to the fifth and sixth harmonics of the band at 3μ . At 6474A a band was found

with a broad *Q* branch, an *R* branch with four intense lines and several rather weak ones, and several irregularly spaced absorption maxima in a *P* branch. The most distinguishing features of the band are the four strong lines of the *R* branch.

In the region at 5490A, evidences of absorption were obtained in all of a number of exposures. The absorption lines were so weak, however, as to be of the same order as non-uniformities in the emulsion of the film, and although the center of the absorption band seemed to lie at about 5490A, the *Q* branch could not be identified with certainty. Consequently no data are given for this band.

In Table I is given a summary of the measurements on the ammonia band at 6474A. The lines for which an intensity is given are well assured as real by several measurements. The lines designated by a point of interrogation are very weak and are possibly somewhat uncertain. Included in braces are broader regions of absorption which are incompletely resolved into lines, but have maxima of absorption at the wave-lengths given. They have possibly a more complex structure than that indicated. All of the lines in the spectrum are rather broad, but this does not seem to be due to a lack of dispersion or resolving power in the means employed, since the spectrograms taken with the second order of the 20 ft. grating showed no better resolution than those taken with the first order of the 10 ft. grating. To secure complete resolution of the lines one would probably have to work at very low gas pressures and a correspondingly long absorption path.

DISCUSSION OF THE RESULTS

In Figure 1 is given for purposes of comparison a diagrammatic representation of three of the ammonia bands of the series with fundamental at 3μ . In the case of the band at 6474A the curve is adapted from a microphotometer investigation of the best spectrogram obtained. The vertical lines represent the position of absorption maxima as taken from the various measurements. The dotted lines indicate the less certain maxima. The band at 7919A is reproduced from the work of Badger and Mecke¹ and the curve for the band at 3μ is adapted from the figure given by Barker and Stinchcomb.³

Below the first two bands is indicated a provisional arrangement of the lines into "series." Each series includes all the lines where one of the quantum numbers characterizing the rotational states, say τ , makes the particular transition $\tau' \rightarrow \tau''$, the other quantum number, say j , making all possible transitions (with the restriction of course that $\Delta\tau$ and $\Delta j = 0 \pm 1$). In the case of the two harmonic bands all of the intense lines, at least, fit into five of these series. Higher series may also be present but the lines of these will nearly coincide with those of the series given, the first and sixth series coinciding, and so on. For the band at 6474A the assignment is possibly in some cases ambiguous owing to incomplete resolution of the lines.

From the figure the following characteristic features are evident. First of all one may note that the bands at 7919A and 6474A include many double

lines with a separation of the two components which is perhaps constant within experimental error, since the resolution is not complete. In general it seems to be the weaker lines which are so resolved, and it is not impossible that the broadness of the stronger lines conceals a similar structure, though in a few cases the stronger lines are relatively sharp and apparently single.

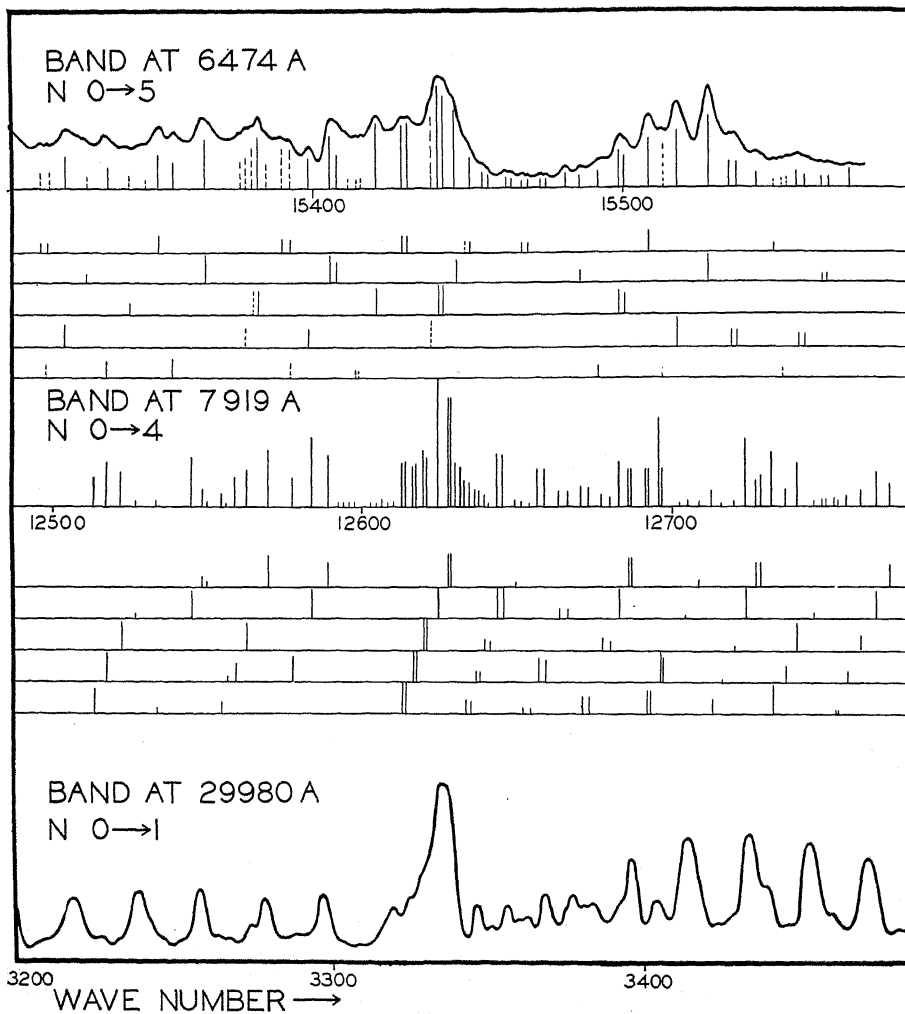


Fig. 1. Two harmonic bands of ammonia and the fundamental band at 3μ .

Badger and Mecke suggested as an explanation of the doubling that the ammonia molecule becomes slightly unsymmetrical as the amplitude of vibration increases. An alternative explanation has been offered by Barker⁵ on the basis of a slight difference in the energy values corresponding to the symmetric and anti-symmetric eigenfunctions representing an oscillational state, this

⁵ Barker, *Phys. Rev.* **33**, 684 (1929).

difference arising from the possibility of the nitrogen atom passing through the plane of the three hydrogen atoms. Barker interprets the bands here considered as due to an oscillation in which all the atoms of the molecule approach each other simultaneously. As the amplitude of this vibration increases the potential energy increases, as the nitrogen atom approaches the plane of the hydrogen, also rises, and the difference between energy levels corresponding to the two types of eigenfunction should decrease. Consequently the doubling of levels might be appreciable only in the lowest energy state, and the doubling of the bands would thus be nearly constant through the harmonic series. This is indeed in agreement with the data. However, it seems very questionable whether the bands here under consideration are due to the type of oscillation mentioned, first on account of the great intensity of transitions in which $\Delta\tau \neq 0$, and secondly on account of the convergence of the bands. An extrapolation of the harmonic series yields a dissociation energy of 6.0 volts, which is much less than that required for the complete separation of the molecule into its atoms (about 12 volts) which would result from the vibration in question. Dennison⁴ in a treatment of the vibrations of the ammonia molecule by means of normal coordinates, concluded that the 3μ band arose from an oscillation perpendicular to the symmetry axis. But it is possible that even for this kind of oscillation one should expect a similar situation for the doubling of the vibrational levels.

It is striking that no very appreciable convergence in any series in any of the bands is observed. Furthermore, as one must expect from this fact, the spacing of the lines in a series is sensibly constant for all of the bands, having the approximate mean value 19.88 cm^{-1} for the band at 7919A and 19.74 cm^{-1} for the band at 6474A, corresponding to a moment of inertia of $2.78 \times 10^{-40} \text{ gm. cm}^2$ or $2.80 \times 10^{-40} \text{ gm. cm}^2$, respectively, about an axis perpendicular to the axis of symmetry. It would be very interesting to observe whether the other moment of inertia (about the symmetry axis) is not appreciably changed by the oscillation, as seems not improbable, but the accuracy of measurement scarcely suffices for this. The probable value for this quantity is $3.49 \times 10^{-40} \text{ gm. cm}^2$ if one assumes a flat pyramidal structure for the ammonia molecule.

A particularly striking feature of the two harmonic bands is the alternation of intensity in each series. There seems to be a great tendency for alternate lines to be weak or to fall out altogether, and an alternation is also observed for corresponding lines through successive series. The irregularity of spacing in the *P* branch of the 3μ band suggests that the strong lines here do not all belong to the same series, and that greater resolution would disclose a similar condition in this case. Indeed this band seems quite similar to the harmonic at 6474A except that certain series which in the former are quite weak have in the latter become of intensity comparable with the strongest series.

For purposes of clarity the five series of the two harmonic bands have been represented in Figure 2 by means of a scheme similar to that which is frequently used in representing electronic bands. The diagonal lines sloping

to the left indicate the transitions giving rise to the P branches, and those sloping to the right to the R branches. J' and J'' are the probable values of the quantum number associated with the larger spacing of the band structure, in the normal and excited states respectively. The absolute values of the other quantum number τ for the several series are somewhat in doubt. The thickness of the diagonal lines represents roughly the intensity of the observed transitions, and as in Figure 1, broken lines indicate doubtful cases. At the bottom of the figure are shown the kinds of transitions which are especially characteristic of the two bands.

In the case of the band $N, 0 \rightarrow 4$ the results indicate that the rotational levels are alternately of two kinds in both lower and upper states, one of these kinds being considerably the more probable. For the band $N, 0 \rightarrow 5$ the

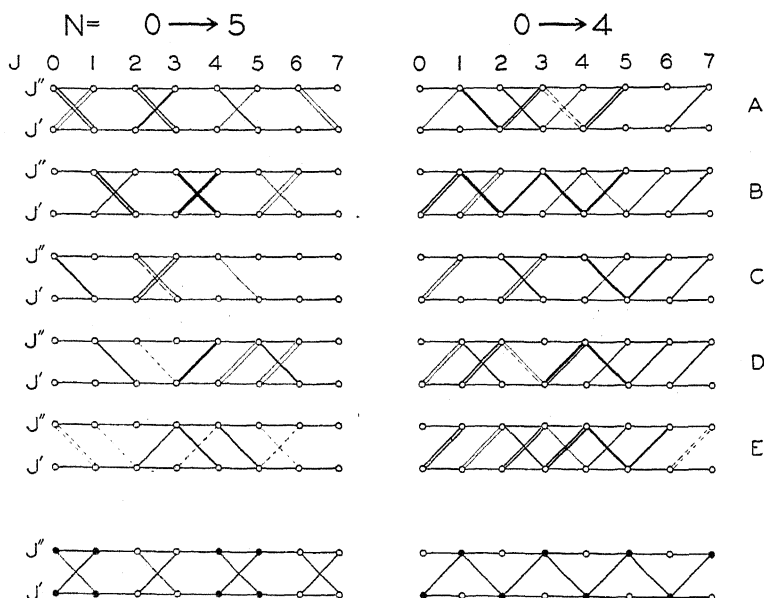


Fig. 2. Scheme of transitions in the ammonia harmonic bands.

situation seems to be quite different and the explanation is not obvious. In neither case is the condition quite what would seem to be predicted by the considerations of Hund.²

In this connection it is not out of place to make some remarks on certain other ammonia bands. At 10μ there is an absorption region which is produced by another type of molecular vibration. This band has been investigated by Barker,⁵ who finds a double band of apparently simple structure. According to Barker's analysis this band comprises two component bands, each of which consists of a Q branch and simple P and R branches corresponding to the transitions $\Delta j = \pm 1, \Delta \tau = 0$. There is no appreciable convergence of the lines, and one component has a spacing of 20.2 cm^{-1} the other of 18.7 cm^{-1} . This would mean that the band is produced by two kinds of ammonia mole-

cule whose moments of inertia are the same in the upper and lower states but appreciably different from that of the lower state involved in the bands at 3μ etc. In other words these bands do not have a common lower level.

It seems to the writer, however, that the absorption curve may equally well be interpreted in a slightly different way, but one which is much more satisfactory when one considers its connection with the other data. The following analysis of the 10μ band is accordingly suggested.

TABLE II. *The ammonia band at 10μ . (from the data of Barker⁶).*

Band at 10.7μ or 933 cm^{-1}					Band at 10.3μ or 966 cm^{-1}			
ν_R	$\Delta\nu$	ν_P	$\Delta\nu$	Initial j	ν_R	$\Delta\nu$	ν_P	$\Delta\nu$
				14	1250	19		
				13	1231	18	711	18
				12	1213	15	729	21
		726	20	11	1198	19	750	20
1158	18	746	16	10	1179	18	770	19
1140	21	762	19	9	1161	18	789	19
1119	20	781	18	8	1143	18	808	20
1099	22	799	18	7	1125	19	828	21
1077	21	817	22	6	1106	19	849	19
1056	20	839	17	5	1087	18	868	21
1036	21	856	18	4	1069	20	889	20
1015	20	874	21	3	1049	20	909	19
995	—	895	16	2	1029	20	928	21
—	—	911	22	1	1009	—	949	17
955	22			0	—	—		
Mean $\Delta\nu = 19.6\text{ cm}^{-1}$					Mean $\Delta\nu = 19.3\text{ cm}^{-1}$			
Weighted mean $\Delta\nu = 19.83\text{ cm}^{-1}$					Weighted mean $\Delta\nu = 19.66\text{ cm}^{-1}$			

There is only one region of the absorption curve which does not fit this analysis as well as that given by Barker, and that is the weak maximum at 981 cm^{-1} which should include two maxima at about 975 cm^{-1} and 987 cm^{-1} . It seems, however, that a more complete resolution of this region is necessary to decide definitely which interpretation is the correct one.

In the interpretation here suggested, the band at 933 cm^{-1} converges slightly in the P branch, which indicates a decrease of moment of inertia perpendicular to the symmetry axis, in the activated state. This is not surprising if one considers the type of vibration probably responsible for this band. The three hydrogen atoms are presumed to separate at the same time as the nitrogen atom is approaching their plane. The oscillation should be considerably nonharmonic with a tendency for the nitrogen atom to linger near the plane of the hydrogen atoms, causing a decrease of average moment of inertia as the amplitude of vibration increases.

The suggested interpretation of this band gives within experimental error the same moment of inertia for the normal state as that obtained from the other data.

In a study of the pure rotation spectrum of ammonia Badger and Cartwright⁶ found an apparent convergence of the lines toward shorter wave-

⁶ Badger and Cartwright, *Phys. Rev.* **33**, 692 (1929).

lengths. This spectrum consists of lines produced when j increases by unity, τ remaining constant. If this convergence is not real the molecular moment of inertia calculated from the lines of shorter wave-length, which were those most accurately measured, is the same as that calculated from the vibration rotation bands. But if the interpretation given for the doubling of these bands is the correct one, one should expect that the pure rotation lines are all double with components of perhaps unequal intensity. In this case it could appear that the unresolved lines were somewhat unequally spaced. A similar effect would not be observed, of course, in the case of the Raman spectrum.

At this point the author wishes to express his thanks to Professor J. Anderson of the Mount Wilson Solar Observatory of the Carnegie Institution for the loan of the ten-foot grating which made the investigation possible; and to Dr. Edison Pettit of the same institution for the microphotometer measurements.

EVIDENCE FOR QUANTIZATION FROM THE ELECTRIC POLARIZATION OF ACETIC ACID VAPOR

BY C. T. ZAHN

PALMER PHYSICAL LABORATORY, PRINCETON UNIVERSITY

(Received March 24, 1930)

ABSTRACT

The dielectric constant of acetic acid vapor was measured at various pressures and temperatures. The results indicate a departure from Debye's theory which suggests an internal transition, with respect to temperature variation, from one type of single molecule to another. Near saturation there was detected a small amount of association of a kind increasing the molecular polarization. The anomaly is discussed from the point of view of the new quantum mechanics and it is suggested as an explanation that the effect is due to a transition from one state to a higher state of vibration associated with the OH group. The data are interpreted in terms of the proposed extension of Van Vleck's theory given in the following note. The Raman frequencies given by Dadiou and Kohlrausch indicate that the fundamental vibration frequency due to the OH group is of such a value as to produce transitions of quantum state in precisely the observed region of temperature. This is in agreement with the proposed theory, particularly since molecular polarization measurements in general indicate that the OH group always has associated with it a large electric moment.

The electric moment of the acetic acid molecule cannot be calculated accurately but the data indicate roughly a transition from 1.4×10^{-18} in the ground state to an average value greater than 1.7×10^{-18} c.g.s. e.s.u. in the upper states.

A discussion is given of the anomalous behavior of other physical properties of the vapor, regarding it as a statistical distribution of molecules, surrounded by different force fields associated with the change in electric moment. The possibility of attributing previously observed discrepancies between refractivities and the optical parts of the dielectric polarization to the above mentioned type of quantization is suggested.

IN THE measurement of the dielectric constant of vapors there have occurred occasional apparent deviations¹ from Debye's theory. These deviations are detected by a departure from linearity of the curve obtained by plotting the product of the molecular polarization and the absolute temperature against the absolute temperature itself. They occur always near the saturation point of the vapor, i.e., at low temperatures or high pressures. For this reason they have been attributed to association or adsorption on the condenser material. An associated molecule would give an increased contribution to the "optical" term of Debye's equation and a change in the "orientational" term corresponding to either an increased or a decreased electric moment.² The existence of association is to be detected by studying

¹ M. Jona, *Phys. Zeits.* **20**, 14 (1919); C. T. Zahn, *Phys. Rev.* **27**, 329 (1926); K. Wolf, *Phys. Zeits.* **27**, 588 (1926); K. Wolf, *Ann. d. Physik.* **83**, 884 (1927); F. Maske, *Phys. Zeits.* **28**, 533 (1927); J. B. Miles, Jr. *Phys. Rev.* **34**, 964 (1929).

² L. Ebert, *Zeits. f. Physik. Chem.* **113**, 1 (1924).

the variation of the polarization with pressure. Absorption could be detected in the same manner, but there is sometimes introduced a complication due to accompanying conductivity between the condenser plates. An anomaly of the latter type was observed by the author³ in the case of water vapor at room temperature. The effect seemed to set in sharply at about one-third the saturation pressure. This adsorption was explained qualitatively by the attraction of the dipole molecule for its image in the adsorbing surface. As the molecule approaches the surface its potential energy is lowered until it touches the surface. The ratio of the pressure at the surface to that far from the surface is obtained by the Boltzmann distribution law. When the pressure in the body of the vapor reaches a certain value, that on the surface reaches saturation and adsorption follows. Originally it was thought that the observed effect was due to the direct dielectric effect of the layer of water on the condenser plates. This required about 200 layers of water. Later experiments were made by K. Wolf on this effect, and it was shown that there is considerable conductivity between the plates of the condenser. The author has also made measurements of this conductivity which show that the observed apparent increase in dielectric polarization may be largely due to the indirect effect of conductivity across the thin layer of water adsorbed on the quartz insulators used. It is impossible to say how much of the effect is due to each of the three causes, association, adsorption layer on the plates, and conductivity across the insulators. Fraser⁴ has shown by measurements of the polarization of light reflected from the adsorbing surface of glass that about 5 layers of water are present at saturation. Therefore in the case of water vapor the effect must be almost entirely due to conductivity and possibly association. Only in case there is no observable conductivity can one be sure that a variation in molecular polarization with pressure is due to association (or chemical reaction).

All the above effects can usually be eliminated by working at pressures considerably below saturation, when one is interested in the polarization of single molecules.⁵ In cases where there is no appreciable leakage in the condenser the anomalies can be used to obtain information concerning the forces causing association.⁶ On account of the general anomalous behavior of the physical properties of acetic acid vapor it was thought that measurements of its dielectric constant might prove of interest, particularly since it is known definitely to associate in the gaseous state. By making pressure runs at each temperature and using only the linear, or low pressure parts, the polarization corresponding to the single molecules can be obtained. The Debye line obtained from these data should enable one to calculate the electric moment of the molecule and thus to obtain an idea of the magnitude of the moment characteristic of the carboxyl group. The upper or high pressure parts of the curves should give an idea of the nature of the association.

³ C. T. Zahn, *Phys. Rev.* **27**, 329 (1926).

⁴ J. H. Fraser, *Phys. Rev.* **33**, 97 (1929).

⁵ c.f. C. T. Zahn, *Phys. Rev.* **35**, 848 (1930)

⁶ P. Debye, "Polar Molecules," p. 41.

EXPERIMENTAL RESULTS

The experiments here described were made by the same method used by the author in a series of previous investigations.⁷ Pressure curves were obtained at eleven different temperatures in the range 20–220° C. In Fig. 1 are shown two typical pressure curves, one for a high temperature, and the other for a low temperature where the gas was nearer saturation. The high temperature curve shows no departure from linearity and therefore no as-

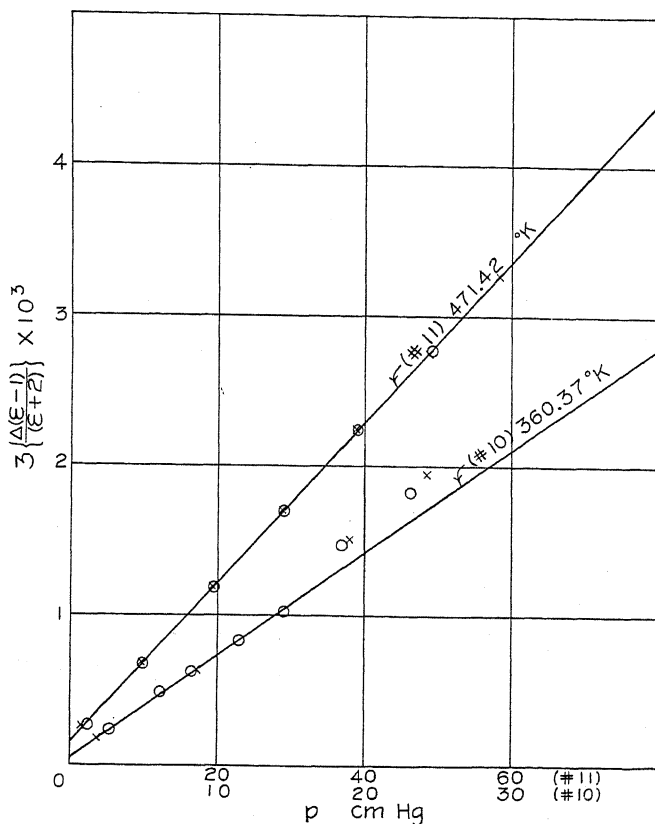


Fig. 1.

sociation. The low temperature curve has a linear portion at the lower pressures and an anomalous increase of the polarization for the higher pressure, near saturation. Leakage tests showed no appreciable conductivity. Therefore there is association of such a nature that the electric moment is increased.

A more interesting feature of the results is seen when an attempt is made to plot a Debye line. In Table I are given the data taken from the lower portions of the pressure curves where the effect of association is negligible. For economy in space the individual pressure data are not included. In

⁷ C. T. Zahn, Phys. Rev. **24**, 400 (1924), C. T. Zahn, Phys. Rev. **35**, 848 (1930).

column III is given the limiting slope of the pressure curve in the lower part for pressures expressed in atmospheres. This gives the value of $(\epsilon-1) 10^6$ corresponding to an atmosphere of single molecules. Column IV gives values of $3(\epsilon-1/\epsilon+2) (1/p_{at})$; and column V, values of $3(\epsilon-1/\epsilon+2) v \cdot 10^6$ where

TABLE I.

No.	T°K	$\frac{\epsilon-1}{p_{at}} \cdot 10^6$	$3 \left(\frac{\epsilon-1}{\epsilon+2} \right) \frac{10^6}{p_{at}}$	$3 \left(\frac{\epsilon-1}{\epsilon+2} \right) v \cdot 10^6$	$3 \left(\frac{\epsilon-1}{\epsilon+2} \right) vT$	P
1	410.84	4767	4760	7165	2.94 ₀	53.5
2	491.44	3742	3737	6724	3.30 ₄	50.2
3	357.78	5246	5235	6860	2.45 ₀	51.2
4	341.13	5461	5452	6809	2.32 ₃	50.8
5	389.64	5044	5036	7184	2.79 ₉	53.7
6	320.85	5791	5782	6792	2.17 ₉	50.7
7	450.09	4340	4334	7142	3.21 ₄	53.3
8	297.51	6764	6756	7359	2.18 ₉	55.0
9	493.86	3728	3724	6733	3.32 ₅	50.3
10	360.37	5246	5235	6907	2.48 ₉	51.6
11	471.42	4068	4063	7013	3.30 ₆	52.3

v is calculated from the ideal gas law $v = T/273.13 p_{at}$. The van der Waal correction would probably amount to about one percent. This correction was not made because of the lack of data. Column VI gives the ordinates for the Debye line:

$$3 \left(\frac{\epsilon-1}{\epsilon+2} \right) vT = AT + B.$$

Column VII gives values of the molecular polarization P , i.e., the value of $(\epsilon-1/\epsilon+2)$ corresponding to a gram molecule of single acetic acid molecules.

In Fig. 2 are plotted the values of columns VI and VII of the table. According to Debye's theory the upper curve should be a straight line of slope A and intercept B . The lower curve should be of the form:

$$P :: A + (B/T).$$

It is obvious that this is far from the case and that there is here represented a departure from Debye's theory which is due neither to association nor to conducting layers. Apart from the linearity of the pressure curves in their lower parts, if there were association, it would be practically absent at the higher temperatures and the upper portion of the curve of Fig. 2 would approach the supposed true Debye line. Then the anomalous *decrease* of $3(\epsilon-1/\epsilon+2)vT$ for the lower temperatures would have to be attributed to association corresponding to *reduced* electric moment. On the other hand the pressure curves near saturation indicate that association occurs in such a way as to *increase* the electric moment of the molecule. Therefore an explanation of the departure from the Debye line based on the assumption of association leads to a contradiction.

The values for the lowest temperature, given in the table and shown in Fig. 2, were obtained under very difficult experimental conditions because of

the low vapor pressure, and are therefore subject to a much greater probable error. Association may not be completely eliminated. The slight rise in the upper curve is probably not correct, but the rise in the lower curve is probably only a little too great but definitely existing.

During the investigation it was thought that the observed anomalies could be due to an indirect effect of a small amount of water in the acid specimen. In order to test this supposition an especially pure specimen, of

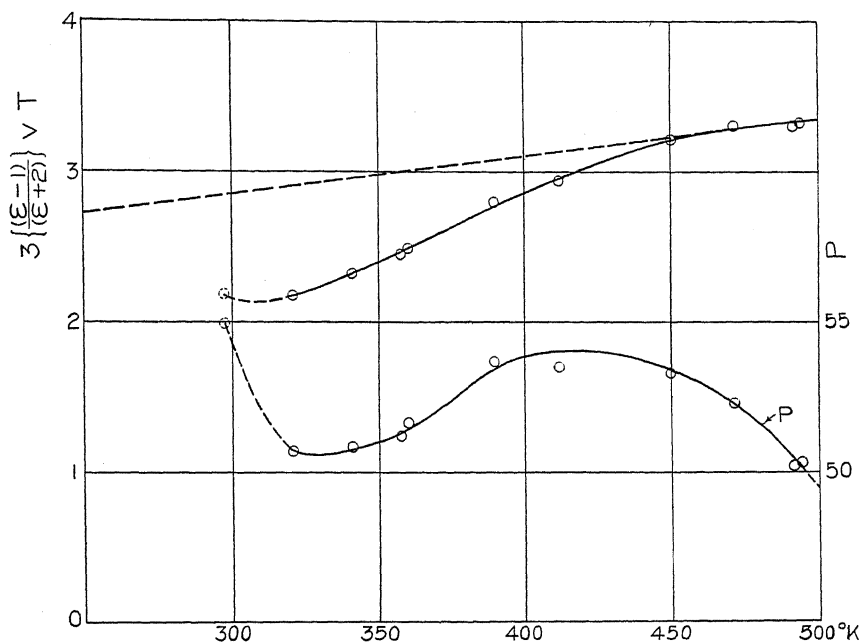


Fig. 2.

fusion point 16.6°C , was prepared and measurements were repeated at extreme temperatures. No appreciable difference was observed between the two specimens. In any case if the effect of water vapor is only its direct effect it would require a considerable amount to produce an appreciable change in the dielectric constant, since the two substances have nearly the same dielectric constant.

EVIDENCE FOR QUANTIZATION

The curves in Fig. 2 indicate roughly a transition from one value of A and B in the Debye equation to another. Since the pressure curves are linear this must correspond to an internal change in the molecule. On the quantum theory such a change would be a change from one stationary state to another, or to a redistribution among several states, according to the Boltzmann theorem. Van Vleck⁸ has given a general derivation of the Debye formula in the new quantum mechanics. The Debye formula is found

⁸ J. H. Van Vleck, *Phys. Rev.* **29**, 729 (1927); *Phys. Rev.* **30**, 31 (1927).

to hold for temperatures such that $h\nu \ll kT$ where $h\nu$ is the energy spacing of the rotational levels or other low energy levels. This means that deviations due to rotational quantization are small when T is such that the above inequality holds. To a second approximation the effect of rotational quantization gives the formula:

$$3 \left(\frac{\epsilon - 1}{\epsilon + 2} \right) = A + \frac{B}{T} - \frac{C}{T^2}$$

Van Vleck has calculated the constant C in terms of the moments of inertia of the molecules and the components of the electric moment along the principal axes of inertia. When $T = h\nu/k$ the deviations are considerable and the above second approximation is not sufficient, of course. Debye⁹ calls this latter temperature the "characteristic" temperature and finds that for HCl it is 14.7°K. At 0°C the correction due to rotational quantization is only about 2 percent, and it would be difficult to detect departures from the Debye formula unless measurements could be made near the characteristic temperature.

One can let each energy transition $h\nu$ define a temperature such that $h\nu = kT$. In this sense a transition in the region of $T = 400^\circ\text{K}$ could certainly not be attributed to rotational quantization since it would require a moment of inertia many times smaller than that of HCl. Van Vleck in his derivation of the Debye equation assumes that the electric moment of the molecule is invariant with respect to all quantum numbers producing low or medium frequency transitions. There are many substances which have vibrational energies in the region of measurable temperatures. If one admits the possibility of different "fixed" electric moment in different vibrational states the general behaviour of the curves in Fig. 2 can be explained as due to the statistical distribution in these states. In a note to follow Van Vleck's theory has been generalized to include such an assumption and Debye's formula is replaced by:

$$3 \left(\frac{\epsilon - 1}{\epsilon + 2} \right) = A + \frac{[\sum_v B_v e^{-h\nu_v/kT}]/[\sum_v e^{-h\nu_v/kT}]}{T}$$

This does not include the small correction due to rotational quantization. The B of Debye's equation is replaced by a statistically averaged B over all vibrational states. The same is true of the square of the electric moment since it is proportional to B .

In case the changes in the electric moment μ are due to a single type of vibration the various overtones ν_v will be spaced relatively far apart on the temperature scale, and in the region of temperature around a particular value of ν the transition will be roughly as from one value of ν to one other value. The higher energy states will exist in only small amounts. The general shape of the distribution curve in the two states according to the Boltzmann theorem is like the upper curve of Fig. 2. If the overtones be taken into

⁹ P. Debye, "Polar Molecules," p. 150.

account the shape of the curve is only slightly changed in this region. Judging from such a distribution curve one would expect the transition frequency $h\nu$, to correspond to a temperature in the region from 420–450°K.

RELATION TO RAMAN SPECTRUM

Dadiou and Kohlrausch¹⁰ have investigated the Raman spectrum of acetic acid in the liquid state and give lines of the following wave-numbers: 440 (0); 618 (1); 890 (4); 1430 ($\frac{1}{2}$); 1656 (1); and 2935 (4). Salant and Sandow¹¹ have shown that for HCl there is a small shift of the infra-red lines on passing from the liquid to the vapor states on account of the Lorentz force in the liquid. The frequency in the gaseous state was found to be of the order of 4 percent higher. This would not alter the following qualitative discussion. In the sense defined by $h\nu = kT$ these lines lie at temperatures: 307; 432; 622; 998; 1157; and 2050°K. Of these lines the only one definitely in the region of observed temperatures is the second at 432°K. This is a moderately strong line and is attributed by the above mentioned authors to the OH group of the molecule. This is in excellent agreement with what would be expected from the existing data on electric moments.¹² The OH group is known to have associated with it a large electric moment and therefore the Raman line associated with this group would be the most likely to produce changes in electric moment. The other lines in the Raman spectrum excepting the overtones of the OH line which are not sufficiently strong to appear, would probably cause only very small changes in electric moment. There may be also a small effect on the electric moment due to vibrations associated with the CO group, if the corresponding value of $h\nu$ is near the observed temperature region.

If the potential energy function associated with the vibration is unsymmetrical about the minimum point, the average nuclear separations may be quite different for the different quantum states. Accompanying this the electric moment might have quite different values, particularly in cases of weak bonds such as exist in large organic molecules. On the other hand it is just here that one would expect interaction between rotation and vibration or centrifugal expansion; and that the sum rules, discussed by Van Vleck in connection with the high frequency or optical part of the susceptibility, might be invalidated. It does not seem impossible that such disturbing effects might be small even if the electric moment is altered by the vibration. As another possibility, in a complicated organic molecule there might be more than one minimum value of the potential energy of vibration with fairly strong binding forces around each one of them. For example, in the case of the ammonia molecule, the potential energy of the nitrogen nucleus along the axis of the molecule is probably symmetrical, or nearly symmetrical, with respect to the plane of the hydrogen triangle and there exist two minima

¹⁰ A. Dadiou and K. W. F. Kohlrausch, *Monatsch. f. Chem.* **52**, 220 (1929).

¹¹ E. O. Salant and A. Sandow, *Phys. Rev.* **35**, 214 (1930).

¹² H. A. Stuart, *Phys. Zeits.* **31**, 80 (1930).

on opposite sides of the triangle. In an organic molecule such a bond might be unsymmetrical and hence give rise to two distinct energy levels.

In connection with the above mentioned high frequency part of the dielectric susceptibility there are in progress in this laboratory observations of the refractivity of acetic acid vapor under the same conditions of pressure and temperature as the present observations. These observations may indicate whether any of the temperature variation is due to the failure of the sum rules which are called upon to prove the invariance of the high frequency term with temperature. They should also be of interest in connection with the association of the vapor near saturation. An observed variation with temperature could also be due to a variation in refractivity from one vibration state to another.

ELECTRIC MOMENT

On account of the inability to resolve completely the effects of the different states and of the lack of accurate knowledge of the Raman frequency for the vapor, it is impossible to obtain from the present observations an *accurate* knowledge of the electric moment in either state. Using a value of the refractivity obtained from the liquid one can calculate roughly the effective electric moment at the various temperatures. This is, of course, the root mean square electric moment. The calculation indicates that the average moment varies from 1.4 to 1.7×10^{-18} c.g.s. e.s.u. The lower value is probably not far from the value corresponding to the ground state. At the highest temperature there are still present a considerable number of the molecules in the ground state, which would necessitate a moment still greater than 1.7×10^{-18} for the upper state.

C. P. Smyth has recently made measurements¹³ of the molecular polarization of acetic acid solutions in benzene and in ether from 0 to 30°C. The values for the solution in benzene are in general abnormal. A calculation using the refractivity of acetic acid as above indicates an average moment of 0.7×10^{-18} . This may be due to a special type of association in the liquid state. For the solution in ether the behavior is normal and there is probably very little association as indicated by partition coefficient measurements. The value of the moment calculated by Smyth for this solution is 1.40×10^{-18} . At temperatures from 0 to 30°C all the molecules are probably in the ground state of vibration, judging from the curve of Fig. 2. The lower limit previously calculated from this curve, 1.4, is in good agreement with Smyth's value.

PHYSICAL PROPERTIES

In addition to the anomalous behavior here described acetic acid has long been known to behave anomalously with respect to van der Waal's equation. The value of $(RT_k d_k)/(Mp_k)$, which for most vapors is around 3.88, is abnormally high for acetic acid vapor, 4.99. Also Nasini¹⁴ has recently measured

¹³ To be published in the Jour. Amer. Chem. Soc.

¹⁴ A. G. Nasini, Phil. Mag. 52, 596 (1929).

the viscosity of acetic acid vapor at pressures of the order of 5 mm Hg and at temperatures from 90 to 250°C. At such low pressures there is no appreciable association, yet the temperature-viscosity curve shows at lower temperatures an opposite shape to those of other non-associated compounds.

If the interpretation of the behavior of acetic acid here suggested is correct it seems that the above mentioned deviations could be explained by the fact that such a vapor must be considered as a mixture of molecules surrounded by different force fields and distributed statistically. Any physical property depending on these force fields, such as van der Waal forces, mean free path, mobility, viscosity, etc., would be expected to behave abnormally with respect to temperature variation.

This effect of the variation of electric moment with vibrational state may be of some small importance even in molecules such as HCl where Debye's theory is apparently obeyed. If the vibration frequencies are not near the observed temperature region and if the moment is slightly different for different quanta of vibration, there may still be a first order linear correction to be applied. This would not alter the linearity of the Debye line but would give a slightly erroneous electric moment, and an erroneous value of the "optical" part, A , of the susceptibility. In a number of cases¹⁵ where the electric moment is large there have been discrepancies between the value of A and the refractivity. A is usually higher than the refractivity. In the case of the halogen hydrides the discrepancy is larger the larger the electric moment. These discrepancies have been discussed by various authors, notably Van Vleck,¹⁶ without obtaining a satisfactory explanation. For the case of HCl Van Vleck has made calculations to show that the effect of the vibrational spectrum on the dielectric constant is negligibly small. It should be noted in this connection that he has assumed an electric moment fixed with respect to the vibrational quantum number. In the case of CO₂ Fuchs¹⁷ has shown that the atomic vibration frequencies are necessary for the extrapolation of the refractivity to infinite wave-length, and that the value so extrapolated agrees well with the polarization obtained from electrical measurements. The discrepancies then may be due either to an error in the refractivity by the failure to include the atomic vibration frequencies when they are important, or to an erroneous value of A caused by vibrational quantization, when there is a variable electric moment, and possibly to a much smaller extent by the rotational quantization. There may also be a temperature effect on the high frequency part A caused by the failure of the sum rules for molecules with loose bonds; and the value of A obtained from dielectric constant data on the assumption that it is constant would be in error.

¹⁵ C. T. Zahn, *Phys. Rev.* **24**, 400 (1924).

¹⁶ J. H. Van Vleck, *Phys. Rev.* **30**, 44-46 (1927).

¹⁷ O. Fuchs, *Zeits. f. Physik* **46**, 519 (1928).

AN EXTENSION OF VAN VLECK'S THEORY OF DIELECTRIC POLARIZATION

By C. T. ZAHN

PALMER PHYSICAL LABORATORY, PRINCETON UNIVERSITY

(Received March 24, 1930)

ABSTRACT

The experimental data in the preceding paper show a departure from the Debye equation:

$$\left\{ \frac{\epsilon - 1}{\epsilon + 2} \right\} \frac{1}{d} = A + \frac{B}{T}$$

suggesting an effect of vibrational quantization where the electric moment depends on the vibrational quantum number. Van Vleck assumed the electric moment fixed for all states of low energy and thus did not admit the above possibility. In the following note it is shown that Van Vleck's theory can easily be extended to include the effect of such vibrational quantization which may occur in the region of observed temperatures. Debye's equation no longer holds in its simple form. In a sense it can be regarded to hold if the vapor be considered as a mixture of molecules statistically distributed in the vibration states.

THE following is simply an extension of Van Vleck's¹ theory of dielectric polarization and differs from his treatment only in the degree of restriction of the assumptions. He considers all the quantum numbers effective on the molecule to be divided into three classes, n , j , and m . The index n includes all quantum numbers whose effect is such that $h\nu \gg kT$; the index j , such that $h\nu \ll kT$, excluding the axial quantum number; and m , the axial quantum number for which also $h\nu \ll kT$. n may include electronic and vibrational quantum numbers; j , inner, rotational, and spin; and m , axial. In many vapors there are vibrational states for which $h\nu \sim kT$. As Van Vleck states, under his assumption of invariant "fixed" moment, these states, which correspond to linear oscillators, would cause no temperature variation; but they will be important under the present assumptions. For this reason there will be included an index v for the cases where $h\nu \sim kT$. This will be considered to correspond to some of the vibrational states.

Considering, as did Van Vleck, the electric moment matrix of typical element,

$$M_z(nvj m; n'v'j'm') e^{2\pi i \nu(nvj m; n'v'j'm') t}$$

the dielectric susceptibility can be written:

$$\chi = \frac{N}{F} \frac{\sum_{vj m} M_z^{(F)}(nvj m; nvj m) e^{-W^{(F)}(nvj m)/kT}}{\sum_{vj m} e^{-W^{(F)}(nvj m)/kT}} \quad (1)$$

where all the molecules are assumed to be in the ground state indicated by n . The perturbation theory gives, to the first power in F :

¹ J. H. Van Vleck, Phys. Rev. **29**, 727 (1927).

$$M_z^{(F)}(nvjm; nvjm) = M_z(nvjm; nvjm) - \frac{2F}{h} \sum_{n'v'j'm'} \frac{M_z(nvjm; n'v'j'm')^2}{\nu(nvjm; n'v'j'm')} \quad (2)$$

and

$$W^{(F)}(nvjm) = W(nvjm) - FM_z(nvjm; nvjm). \quad (3)$$

Substituting (2) and (3) in (1) gives:

$$\left\{ \begin{aligned} \chi &= \frac{N}{F} \frac{\sum_{vjm} M_z(nvjm; nvjm) e^{-W(nvjm)/kT}}{\sum_{vjm} e^{-W^{(F)}(nvjm)/kT}} \end{aligned} \right. \quad (a)$$

$$+ \frac{B}{kT} \sum_{vjm} |M_z(nvjm; nvjm)|^2 e^{-W(nvjm)/kT} \quad (b) \quad (4)$$

$$- \frac{2B}{h} \sum_{vjm; n'v'j'm'} \frac{|M_z(nvjm; n'v'j'm')|^2 e^{-W(nvjm)/kT}}{\nu(nvjm; n'v'j'm')} \quad (c)$$

where:

$$B \equiv N / \sum_{vjm} e^{-W(nvjm)/kT}. \quad (5)$$

4(a) vanishes because there is no residual electrifications for the field intensity $F=0$. (4) can now be written:

$$\left\{ \begin{aligned} \chi &= \frac{B}{kT} \sum_{vjm} |\mu_z(vjm; vjm)|^2 e^{-W(nvjm)/kT} \end{aligned} \right. \quad (a)$$

$$- \frac{2B}{h} \sum_{vjm; v'j'm'} \frac{|\mu_z(vjm; v'j'm')|^2}{\nu(nvjm; nv'j'm')} e^{-W(nvjm)/kT} \quad (b) \quad (6)$$

$$- \frac{2B}{h} \sum_{vjm; n'v'j'm' (n', v' \neq n, v)} \frac{|M_z(nvjm; n'v'j'm')|^2}{\nu(nvjm; n'v'j'm')} e^{-W(nvjm)/kT} \quad (c)$$

where for the low frequency elements $M_z(nvjm; nv'j'm') \equiv \mu_z(vjm; v'j'm')$ for separate treatment. For a fixed value of v 6(b) can be grouped in pairs and by approximate expansion put into the same form as 6(a) and included under a general summation (c.f. Van Vleck). Then (6) becomes:

$$\left\{ \begin{aligned} \chi &= \frac{B}{kT} \sum_v \sum_{jm; j'm'} |\mu_z(vjm; v'j'm')|^2 e^{-W(nvj)/kT} \end{aligned} \right. \quad (a)$$

$$- \frac{2B}{h} \sum_v \sum_{jm; n'v'j'm' (n', v' \neq n, v)} \frac{|M_z(nvjm; n'v'j'm')|^2}{\nu(nvjm; n'v'j'm')} e^{-W(nvjm)/kT} \quad (b) \quad (7)$$

where $W(nvjm) \equiv W(nvj)$ since the m separations are small.

On account of the high degree of spectroscopic stability $\sum_{mm'} |\mu_z(vjm; v'j'm')|^2$ is invariant of the direction of space quantization and can be written $\frac{1}{3} \sum_{mm'} |\mu(vjm; v'j'm')|^2$. If the energy spacings due to j and m are small compared to those associated with v and n then for 7(b) $\nu(nvjm; n'v'j'm') \rightarrow \nu(nv; n'v')$ and $W(nvjm) \rightarrow W_v$. This latter requirement may not always be satisfied in actual cases, particularly with reference to the index v , but will

probably be met in most cases. Also $\sum_{jm} |\mu(vjm; vj'm')|^2$ is the diagonal element $\mu^2(vjm)$ of the μ_v^2 matrix. This fixed moment is assumed independent of (jm) , but not of v as in Van Vleck's treatment.

All these facts together with (7) and (5) give:

$$\chi = \frac{\sum_v N \{ \alpha_v + (\mu_v^2/3kT) \} e^{-W_v/kT}}{\sum_v e^{-W_v/kT}} \quad (8)$$

where

$$\alpha_v \equiv -\frac{2}{3h} \sum_{jm; n'v'j'm' (n', v' \neq n, v)} \frac{|M_z(nvjm; n'v'j'm')|^2}{\nu(nv; n'v')}$$

represents the high frequency terms. As Van Vleck has shown α_v will be independent of temperature if the sum rules for absorption are applicable. These rules, according to Dirac, should be easily extended to any molecules for which the internal coupling forces give rise to pure precessions and not to distortions such as centrifugal expansion. On the other hand it is in just such molecules where the binding is weak and the electric moment depends on the state of vibration that the effects of centrifugal expansion would be expected. Therefore it is possible that each α_v depends on the temperature to a small extent in case the sum rules break down. The high frequency term then is subject to three possible causes of small temperature variation: redistribution amongst the α_v for different vibration states, a breaking down of the sum rules, and the effect of j quantization which was neglected in setting $W(nvjm) = W(nv)$ and $\nu(nvjm; n'v'j'm') = \nu(nv; n'v')$.

Further α_v is probably nearly independent of v for the following reasons. It has long been known that the law of additivity of atomic refractivities holds fairly well except in molecules with polar bonds. Therefore one would expect that α_v would not change very much in going from one vibration state to another if the accompanying changes in electric moment were only a small fraction of the total fixed moment. Still this effect might be much greater than that due to the breaking down of the sum rules or to the j quantization. If we do make the assumption that α_v is independent of v (8) becomes:

$$\chi = N \left\{ \alpha + \frac{\sum_v (\mu_v^2/3kT) e^{-W_v/kT}}{\sum_v e^{-W_v/kT}} \cdot \frac{1}{T} \right\} \quad (9)$$

or:

$$\chi = A + \frac{\sum_v B_v e^{-W_v/kT}}{\sum_v e^{-W_v/kT}} \cdot \frac{1}{T} \quad (10)$$

where the constants A and B_v correspond to those in Debye's equation. In these equations the effect of rotational quantization is neglected. This has been discussed by Van Vleck, Debye, and others for the low frequency term. As a first approximation there is introduced a term $(-C/T^2)$ in the expression for χ .

In conclusion the author wishes to express his indebtedness to Dr. G. Breit for the opportunity to discuss with him several aspects of this problem.

ON A NEW PHOTOELECTRIC EFFECT
IN ALKALI CELLS

BY ERICH MARX

DEPARTMENT FOR RADIOPHYSICS, PHYSICAL INSTITUTE, UNIVERSITY OF LEIPZIG

(Received March 13, 1930)

ABSTRACT

If two monochromatic beams fall simultaneously on an alkali electrode, a new photoelectric effect is shown as follows: If the intensity of the high frequency light ν_1 is sufficient to establish the limiting potential corresponding to the Einstein law, the presence of any component of lower frequency ν_2 diminishes the potential according to the following equation

$$R = c (n_2/n_1) \cdot (\nu_1/\nu_2)(\nu_1 - \nu_2)h/e$$

where R is the potential decrease and n_2/n_1 the ratio of the electronic emission of the two components, measured by the test cell itself. A tentative explanation of the phenomenon is advanced.

I.

IN A preliminary note to *Die Naturwissenschaften*¹ I have described a new photoelectric effect in alkali cells. The existence of this effect was denied by Olpin.² In the present article we present the essential experiments on which the original note was based.

The effect is as follows. If light of frequency ν falls on a potassium surface the limiting potential V is given by Einstein's law $h(\nu - \nu_0) = e \cdot V$, where ν_0 is the long wave limit and h the Planck constant; $h\nu_0$ is equal to the contact potential of the potassium in the cell. If the insulation of the electrodes is sufficient, and the light intense enough, the limiting potential should depend only on the shortest radiation which is contained in the incident beam.

Our experiments show conclusively that if white light falls on a highly evacuated potassium cell, which is so constructed that the anode is shielded from all light, direct as well as reflected, a limiting potential is reached. If now a blue glass filter is put in the path of the incident light, the limiting potential is increased. Since the filter cannot possibly add light of higher frequency, it is obvious that we are dealing with a new phenomenon. The limiting potential is consequently diminished by the presence of the long wave radiation.

At the Breslau meeting of the Deutschen Physikalischen Gesellschaft in January of this year, I demonstrated this effect by two different experiments. In the first experiment light passing through a small diaphragm was permitted to fall on the photoelectric cell, until a constant potential was shown by the string electrometer connected to the cell. A neutral gray

¹ Marx, *Die Naturwissenschaften* 17, 806-807 (1929).

² A. R. Olpin, *Phys. Rev.* 35, 112 (1930).

filter was then interposed. No change was shown by the electrometer demonstrating that the conditions of light intensity and insulation were fulfilled. When I replaced the gray filter by a blue filter the electrometer showed an increased potential, although the intensity of the incident light was diminished to $1/5$ by the blue filter. In the second experiment the incident

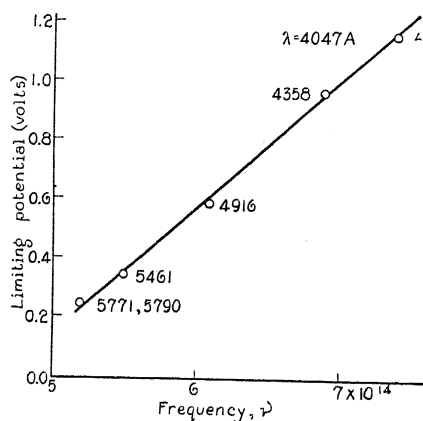


Fig. 1. Dependence of electrometer potential on the wave-length.

light was split into two beams. In the path of one beam an orange filter (Schott filter OG 2) was placed and in the path of the other a blue filter (BG 4) was placed. When the blue beam alone was permitted to fall on the cell, the electrometer showed a constant potential, but when the orange beam also was permitted to fall on the cell the electrometer potential decreased to a new constant value.

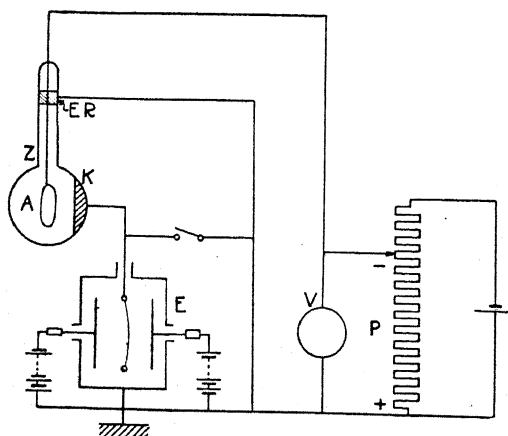


Fig. 2. Compensation device for measuring the limiting potential.

In my first experiment I demonstrated the effect by subtracting long wave-length light from the original beam; in the second experiment I demonstrated the same effect by adding orange light to the beam.

II. The effect shown by the above qualitative experiments has been investigated completely and quantitatively by A. H. Herbert Meyer and myself using a double monochromator in place of the glass filters. We found without exception that whenever the cell is illuminated simultaneously with a shorter and a longer wave-length beam, that the electrometer potential is less than if the cell is illuminated by a shorter wave-length beam alone.

We next investigated our photoelectric cell. Fig. 1 shows the dependence of electrometer potential on the wave-length. The linear dependence and the slope of the line are completely in agreement with the best experimental

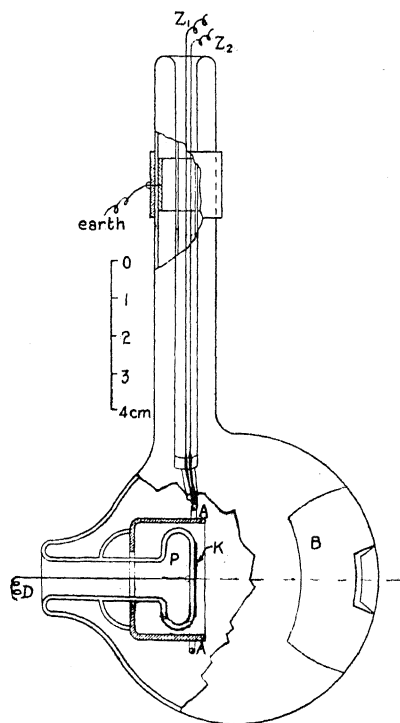


Fig. 3. Diagram of cell.

values of h and e . We used two different methods for these investigations both of which were different from the known pioneer method of Millikan. In the first method we measured the deflections of a string electrometer, in the second method, we used a compensation device, shown in Fig. 2. V is a precision voltmeter. The two methods were in complete agreement, but the compensation method has the advantage of introducing a guard ring. This compensation method is superior to the other mentioned with respect to accuracy and rapidity of measurement. The cell used for this purpose was of the kind sketched in Fig. 3. The tube was evacuated as well as could be done in the presence of potassium. The potassium layer

K was deposited on the platinized front of the glass mushroom P . The contact was established by the wire D . The anode AA formed an almost complete annular ring, with contacts by the lead wire Z_1Z_2 . This arrangement permitted us to heat the anode. The shield G was made of black glass which protected the anode from all reflected and scattered light. The interior surface of the bulb was covered with a very thin potassium layer. B was a tin

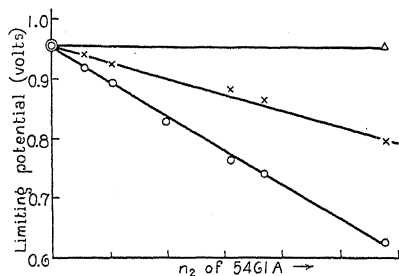


Fig. 4. Dependence of limiting potential for three different intensities of 4358 Å when mixed with various intensities of 5461 Å.

foil covering on the outer surface, in which a rectangular opening was cut. It was electrically connected with the interior surface and the cathode K , all of which was kept at earth potential. The compensating potential was applied to the anode only. This form of cell gave the very satisfactory results of Fig. 1.

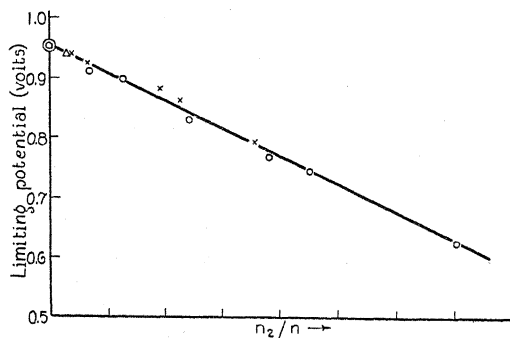


Fig. 5. Dependence of limiting potential upon the ratio of the intensity of the components.

Although it is not necessary to shield the anode in order to demonstrate the qualitative effect of light mixtures, it is necessary to do so if we wish to obtain quantitative results. The precautions which must be taken in order to obtain results of highest accuracy will be discussed by Mr. A. H. Herbert Meyer in his thesis, which will soon be published.

III. After obtaining the results plotted in Fig. 1 we then investigated the effect of light mixtures.

Fig. 4 shows the dependence of the limiting potential for three different intensities of the blue line 4358 Å, when mixed with various intensities of

the green line 5461A. By intensities we mean the amount of light which results in electronic emission. The three blue intensities were 139 erg/sec, 11.4 erg/sec and 5.8 erg/sec. It is to be noticed that when no green light was admitted, the electrometer showed exactly the same potential. When green light was admitted the limiting potential depends not only upon the intensity of the green line but also upon the intensity of the blue line. The

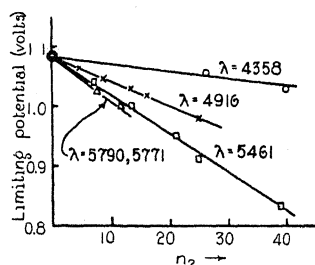


Fig. 6. Dependence of limiting potential of $\lambda 4047$ when mixed with various intensities of different longer wave-lengths.

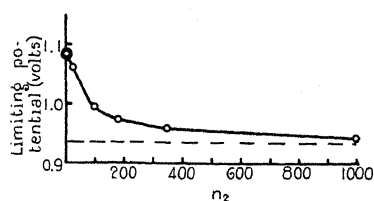


Fig. 7. Dependence of the limiting potential of $\lambda 4047$ upon the intensity of $\lambda 4358$ up to very high intensities.

dependence is linear. This can be more conveniently shown in Fig. 5 by plotting the potential against n_2/n_1 as is done for all data contained in Fig. 4.

IV. We next tried the effect of varying the frequencies of the long wavelength component, keeping the frequency and intensity of the high frequency component constant. For a high frequency component we chose the line 4047A, since this is the highest frequency in the mercury spectrum which glass transmits with sufficient intensity.

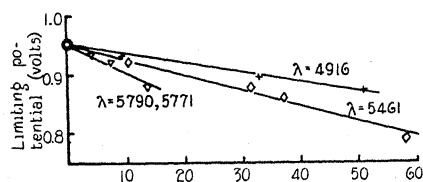


Fig. 8. Dependence of limiting potential of $\lambda 4351$ when mixed with various intensities of different longer wave-lengths.

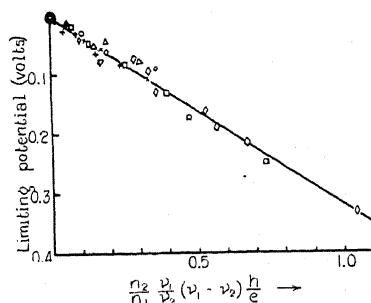


Fig. 9.

In Fig. 6 we have plotted the limiting potentials for this line when mixed with various intensities of the lines $\lambda\lambda 4358, 4916, 5461$ and $5790-5771A$. It is evident that in all cases we get a linear dependence. The intensities were determined by a helium cell before and after measurement of the limiting potential in our test cell. This helium cell had already been compared with our test cell and a thermocouple at various frequencies.

If the intensity of the low frequency components is increased still more, keeping the intensity of the short wave component constant, a point is reached where the linear dependence ceases. The curve approaches asymptotically to the value it would have for the pure low frequency component (Fig. 7).

Fig. 8 is exactly the same as Fig. 6 except that in this case we used the line $\lambda 4358\text{\AA}$ for high frequency component in place of $\lambda 4047\text{\AA}$.

V. As may be seen from the linear form of the curve of Fig. 9, all our observations can be fairly well represented by a straight line. The lowering of the limiting potential is therefore given by

$$R = \text{const.} \frac{n_2 \nu_1}{n_1 \nu_2} (\nu_1 - \nu_2) \frac{h}{e}$$

where n_2/n_1 is the ratio of the intensities of the components and ν_1 and ν_2 are the frequencies of the shorter and longer wave-length components, respectively.

VI. In the Einstein law the $h\nu_0$ term which represents the work of emission is independent of the frequency of the light which falls on the photoelectric substance for a given substance. We could therefore expect this work

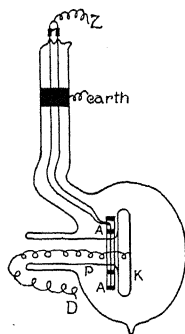


Fig. 10.

to be constant for light mixtures. The obvious explanation of the effect which we have observed would be that the anode is emitting electrons and therefore the equilibrium potential is lowered. This was the first point that we tested by constructing a cell, in shape of a dumbbell, in one side of which was the anode ring and in the other the potassium. The diameter of the anode was so large, that none of the light which passed through the connecting tube could fall on the anode. It was therefore completely shielded from both direct and reflected light. The possibility of explaining the observed effect by assuming an electron emission on the anode is very nearly excluded. In order to make absolutely certain of this point we constructed the cell shown in Fig. 10. In this cell the anode lies behind the cathode and is still further shielded from it by black glass which half incloses the anode. This cell gives exactly the same results as the cell which was used in this

investigation. Due, however, to the unfavorable form of the field in the cell it took too long actually to use this cell in the investigation. We have, however, tried such a cell in which potassium was replaced by sodium. This sodium cell behaves exactly like the potassium cell. This does not agree with the results in the letter mentioned above.

VII. The explanation of the determination of the limiting potential by light of long wave-length is the following. As a result of the general distribution of velocities, as given by Ramsauer, it follows that in the case of limiting potential there must be, even with monochromatic light, a distribution of space charge extending over the whole distance between anode and cathode. The magnitude of the space charge is determined by capacity and limiting potential. This gives all the conditions necessary and sufficient for the theory.

The integration of the Poisson equation gives the variation of the distribution of the space-charge as a function of the frequency. Now, if long-wave light is incident along with short-wave light, then the space charge resulting from the long-wave light (just as the charging of the illuminated electrode) can only be generated at cost of the electrons, set free by the short-wave light. Since each electron which is released returns to the illuminated electrode, the number of electrons produced by light of frequencies ν_1 and ν_2 is equal to the number n_1 and n_2 respectively which is present in the space between anode and cathode. The ratio n_1/n_2 of the electrons, produced per second from frequencies ν_1 and ν_2 , determines therefore the proportion in which the electrons generated by these frequencies take part in the emission and are present in the space charge. If by illumination with short-wave light alone the limiting potential was attained, then this will sink, when the repressing of the electrons generated by short-wave light has advanced to such a degree, that the number of electrons released per second is no longer sufficient to charge up the illuminated electrode to the limiting potential. The limiting potential then approaches asymptotically the limiting potential of the long-wave light as in diagram 7.

The publication of the complete theory follows in the near future.

OSCILLATIONS IN THE GLOW DISCHARGE IN NEON

BY GERALD W. FOX

DEPARTMENT OF PHYSICS, UNIVERSITY OF MICHIGAN

(Received February 26, 1930)

ABSTRACT

Radio-frequency oscillations consisting of one or two fundamentals together with a series of harmonics for each fundamental have been observed in large current glow discharges in neon. The observed frequencies lie in the range from approximately 1.5×10^4 to 2×10^5 cycles per second. The oscillations are very sensitive to pressure changes, their frequency increasing rapidly with decreasing gas pressure. The oscillation frequency also increases markedly with increasing current. The frequency is quite independent of resistance in series with the discharge.

The suggestion is made that the oscillations are due to the presence of a reversed electric field in the negative glow of the discharge.

INTRODUCTION

OSCILLATIONS in gaseous discharges have been observed for many years. As far back as 1876, Spottswode¹ reported observing intermittent electric discharges in gas filled tubes. More recently the work of Whiddington,² Appleton,³ Penning,⁴ Webb and Pardue,⁵ Tonks and Langmuir,⁶ and others have brought this phenomenon to the fore, with the result that many new and interesting data have come to light. The present paper deals only with glow discharges in neon.

APPARATUS AND METHOD

The discharge tube is shown in Fig. 1. The over all length was approximately 50 cm, of which the central section was a quartz tube 22 cm long and 2 cm in diameter. The two Pyrex bulbs contained respectively the heavy copper anode, *P* and the barium-oxide coated cylindrical nickel cathode, *C*. The cathode was indirectly heated by radiation from a 20 mil tungsten spiral inside. A close fitting glass sleeve diminished gas diffusion to the back of the anode so that only the front was effective. Ground joints, deKhotinsky sealed, connected the central quartz section to the two end bulbs. These joints were water cooled. The tube voltage was supplied through series resistance by a 600 volt storage battery.

The usual arrangement of pressure gauges and pumping equipment made up the vacuum system. The discharge tube itself was at all times isolated

¹ Spottswode, Proc. Roy. Soc. May 18 (1876).

² Whiddington, Engineering, 120, 20 (1925)

³ Appleton, Phil. Mag. 45, 879 (1923).

⁴ Penning, Phys. Zeits. 27, 187 (1926).

⁵ Webb and Pardue, Phys. Rev. 32, 946 (1928).

⁶ Tonks and Langmuir, Phys. Rev. 33, 195 (1929).

from the pumping system by a liquid air immersed charcoal trap close to the anode bulb, and a second liquid air trap nearer the pumps. At no time throughout the period of the experiments did the discharge show the presence of mercury vapor.

The detection scheme was essentially the same as that used by Webb and Pardue.⁵ A regenerative detector circuit and a one stage audio amplifier worked admirably. The current through the discharge tube flowed through a

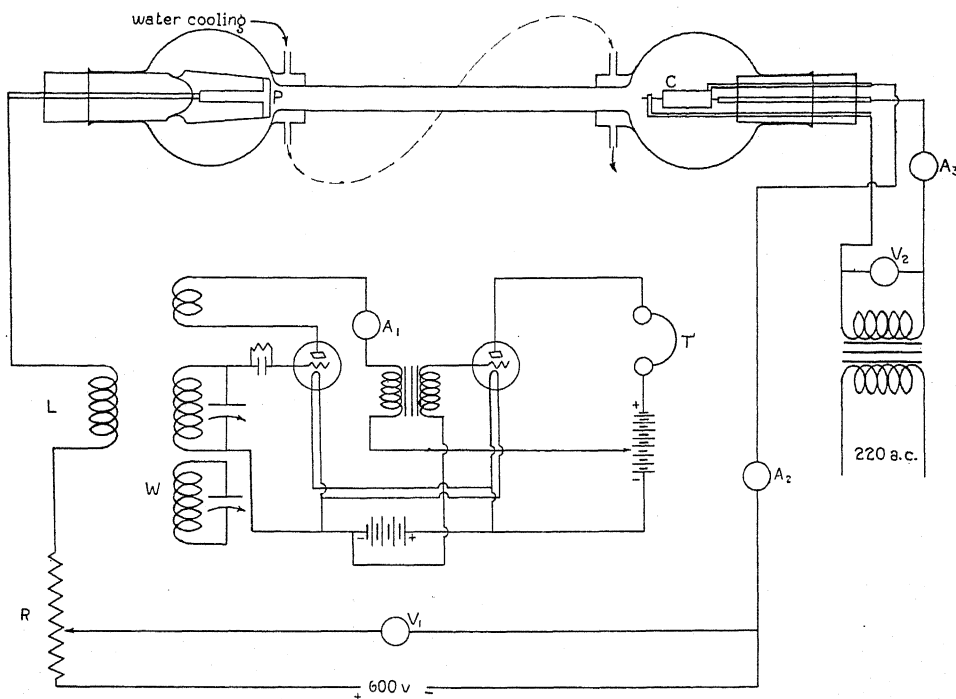


Fig. 1. Diagram of apparatus.

five turn coil of heavy wire which was very loosely coupled to the input of the detector tube. The frequency of the discharge was determined through the method of beats. On zero beat the frequency was measured by a loosely coupled wavemeter.

RESULTS

1. *Frequencies present at a given pressure.*

Data taken in a large number of runs show that several frequencies were present in the discharge at the same time. These frequencies appear to be multiples of a fundamental frequency. The pick up circuit allowed complete covering of a wave-length range of 24000 meters to 100 meters. Throughout this range a large number of frequencies were found. Table I shows one typical run and Table II another. It will be noticed that these are for different tube currents and gas pressures.

TABLE I. *Observed frequencies in glow discharge in neon.* (Tube current 1 ampere, tube voltage 170 volts, Gas pressure 0.52 mm Hg).

Wave-length (meters)	Frequency (cycles/sec)	Order
19800	15151	1
9540	31446	2
6580	45592	3
3960	75757	5
2830	106007	7
2480	120968	8
1990	151753	10
1800	166666	11

TABLE II. *Observed frequencies in glow discharge in neon.* (Tube current 3 amperes, tube voltage 165 volts, gas pressure 1.8 mm Hg).

Wave-length (meters)	Frequency (cycles/sec)	Order
15460	19404	1
7700	38961	2
5150	58252	3
3900	76923	4
3080	97402	5
2580	116279	6
2200	136363	7
1930	155440	8

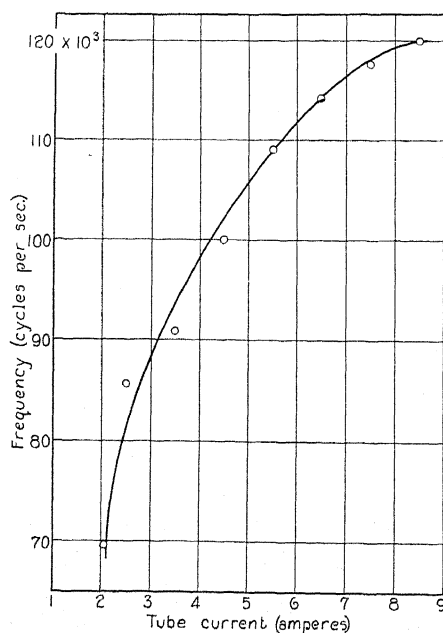


Fig. 2. Typical curve showing variation of oscillation frequency with tube current in neon.

2. Variation of frequency with tube current.

The curve shown in Fig. 2 is typical of the frequency variation with tube current. The frequency at first rose rapidly with the increase in current; then more slowly. However, it never reached a condition where it no longer changed with increase in current. At some current value there was always an abrupt change, the frequency stopping suddenly and some other fundamental appearing with its corresponding series of harmonics.

3. Variation of frequency with pressure.

The discharge frequency was extremely sensitive to pressure changes. Even the slight pressure fluctuations caused by raising or lowering the mercury in the McLeod gauge were enough to vary the beat note as heard in the

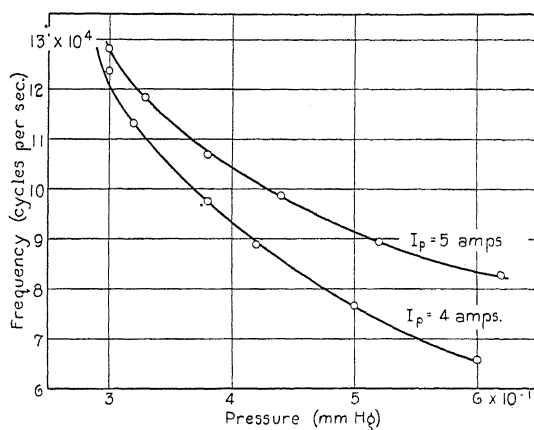


Fig. 3. Variation of oscillation frequency with gas pressure in neon.

telephone receivers as much as a thousand cycles. Fig. 3 shows typical frequency-pressure curves. The frequency rose very rapidly as the pressure was lowered to 0.2 mm of mercury. Below 0.2 mm it became increasingly difficult to maintain oscillations. Their regularity disappeared and, although even at 0.01 mm for some current values the discharge could be made to oscillate, conditions were very uncertain.

4. Oscillations independent of series resistance.

Table III shows that the oscillation frequency is not a function of the series resistance.

TABLE III. Independence of oscillations of series resistance. (Tube current = 3 amperes, pressure = 0.57 mm).

Total voltage	Tube voltage	Series resistance (ohms)	Frequency
500	175	108	88495
325	175	47	88235
230	175	18	87915
190	165	8	88626

These data were taken within a period of five minutes. The discharge was off only long enough to allow decreasing the total battery voltage.

DISCUSSION

The oscillations here investigated exist only when the discharge is perfectly steady with a uniform positive column. They are entirely unaffected by any capacitance or inductance in parallel with the discharge. In Appleton's³ work on ionic oscillations the inference is made that oscillations occur in sharply defined striae. In the work of Webb and Pardue⁵ the oscillations do not exist so long as sharply defined striae are present but begin when diffusion between adjacent striae takes place and continue until a uniform glow fills the tube. In both the investigations mentioned the tube currents were small, of the order of a few hundred milliamperes at most, while in this investigation the tube currents varied from one ampere to as much as twenty amperes. Oscillations consisting of one or two fundamentals and numerous harmonics were present for any current in this range providing the pressure was not too low.

In their theory of plasma-ion oscillations Tonks and Langmuir⁶ have developed an expression for the frequency of ionic oscillations. The limiting value is given by:

$$\nu = e^2 \left(\frac{n}{\pi m} \right)^{1/2} . \quad (1)$$

Under the conditions of their experiments the limiting value for mercury vapor comes out to be about 1.5×10^6 cycles per second. According to their theory the plasma-ion type of oscillation is likely to go over into electric-sound waves, whose frequency may extend up to 6.5×10^5 per second. The frequencies observed in this investigation fall in this range. The variation of frequency with gas pressure is in general agreement with the curves of Webb and Pardue.⁵

It seems very certain that the type of oscillation herein described does not depend on series resistance. As shown in Table III there is a negligible frequency change for different values of series resistances. In fact the discharge has an entirely positive characteristic since it will run steadily with no series resistance at all, except the very small value due to lead wires from the storage batteries, provided the total voltage across the tube does not exceed by more than a few volts the usual drop across the tube (about 170 volts for this tube). The cathode temperature is not affected appreciably by positive ion bombardment but is wholly controlled by radiation from the heater coil.

Compton and Eckert⁷ have shown that oscillations may exist in discharges of the low voltage arc type when there is a high resistance in series with the arc. As the voltage across the tube increases to the ionization potential of the gas, the arc strikes. The negative space charge surrounding the filament is at once neutralized by the positive gas ions. Bombardment of the filament in-

⁷ Compton and Eckert, *Phys. Rev.* **24**, 97 (1924).

creases its temperature, thereby further increasing the emission and hence the arc current. But the resulting large IR drop in the series resistance lowers the voltage across the tube. This constitutes one type of oscillation. The glow discharge is not greatly different from a low voltage arc except for the long positive column. One might expect, therefore, a similar explanation of the origin of the oscillations, but the evidence is against this.

At all times during the experiments, the interesting flashes described by Aston and Kikuchi⁸ and Whiddington² were present. The suggestion is made that the ionic high frequency oscillations are modulated by these rather low frequency pulsations, since on zero beat a note of about 150 cycles was always

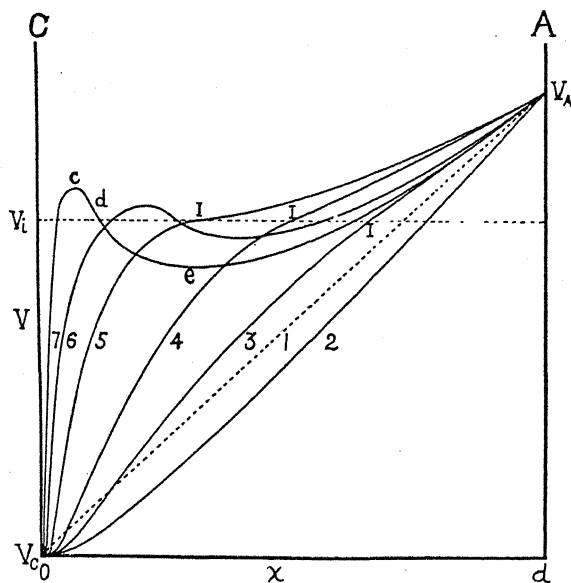


Fig. 4. The effect of increasing amounts of ionization on the distribution of potential between two parallel electrodes one of which is a source of electrons. Curve 1 shows the electrostatic distribution, curve 2 the distribution in the presence of space charge from electrons, and the remaining curves the distribution in cases of successively increasing amount of ionization at the ionizing potential V_i . (From Compton, Turner and McCurdy.)

heard. This is roughly the frequency of the flashes. It is to be noted also that these flashes only occurred in the positive column. Examined by the aid of a rotating mirror they appeared very bright from anode to Faraday dark space, where they disappear. The light of the negative glow is entirely uniform.

The question of the origin of the oscillations is a puzzling one. It seems possible that they originate in the Faraday dark space. A small bar magnet moved about in the vicinity of the discharge had very slight effect except in the region of the Faraday dark space where its motion changed the oscillation frequency very markedly.

⁸ Aston and Kikuchi, *Proc. Roy. Soc. A* **98**, 50 (1920).

In their theory of the glow discharge, Compton, Turner, and McCurdy⁹ have shown the possibility of a reversed field in the region of the negative glow, especially in cases where there is large ionization. As shown in Fig. 4, increasing ionization leads finally to the potential distribution shown in curve 7. There is no reason to suppose conditions should not become even more exaggerated until the potential of the gas in the negative glow should actually be higher than the potential of the gas in the negative end of the positive column. Compton and Eckert¹⁰ have shown this possibility for the case of the low voltage arc. The suggestion seems reasonable that this reversed field is the cause of the ionic oscillations. The positive ions fall through the potential gradient at the cathode end of the positive column with gradually increasing speed, in spite of numerous collisions, until they run into the reversed field which sends them back toward the anode. A back and forth motion of the positive ions results which constitutes the ionic oscillation.

⁹ Compton, Turner and McCurdy, *Phys. Rev.* 24, 597 (1924).

¹⁰ Compton and Eckert, *Phys. Rev.* 25, 139 (1925).

THE CONDUCTIVITY OF A HIGH FREQUENCY DISCHARGE IN HYDROGEN*

BY CHARLES J. BRASEFIELD
UNIVERSITY OF MICHIGAN

ABSTRACT

Measurements were made of the voltage between electrodes necessary to produce a current of 100 milliamperes in the discharge for gas pressures between 0.005 mm and 1.0 mm and for frequencies of oscillation between 1.25 and 20 million cycles per second (wave-lengths between 240 and 15 meters). It was found that the discharge has its maximum conductivity when operated at a frequency of 15 million cycles (20 meters) and a pressure of 0.015 mm. A theory of the mechanism of the high frequency discharge indicates that under these conditions, an electron makes an inelastic collision with a gas molecule every electronic mean free path having been under the influence of the electric force for one half cycle. The theory also indicates that for any frequency of oscillation greater than 15 million cycles, both the electric force and the gas pressure for which the conductivity is a maximum, will increase directly with the frequency of oscillation.

INTRODUCTION

THERE are essentially two methods by which a high frequency discharge can be obtained in a rarefied gas without the use of internal electrodes. The first method consists in surrounding the discharge tube by an inductance coil through which high frequency currents are passed. In the second method, high frequency voltages are applied to external electrodes of sheet metal which are attached to the outside of the discharge tube. As for the first method, it has been shown ^{1,2,3} that unless the high frequency currents in the inductance coil are very large, (such as are obtained with damped oscillations), the electric forces producing the discharge are principally the electrostatic forces between the ends of the coil. In other words, for small currents the two methods of excitation are fundamentally the same. On the other hand, the second method has the advantage of greater simplicity and flexibility. For this reason, the second method was used in the work about to be described.

It is well known that a high frequency discharge is profoundly affected by changes in gas pressure and frequency of oscillation. It therefore should be of interest to discover at what pressure and frequency of oscillation the discharge will function most efficiently. One way of doing this would be to study the variation in the striking potential or the minimum maintaining potential of the discharge as the pressure and frequency of oscillation are

* Publication of the Research Organization of the Grigsby-Grunow Company, Chicago, Illinois.

¹ J. S. Townsend and R. H. Donaldson, *Phil. Mag.* 5, 178 (1928).

² C. J. Brasefield, *Phys. Rev.* 34, 1392, 1627 (1929).

³ K. A. MacKinnon, *Phil. Mag.* 8, 605 (1929).

varied. Hayman⁴ has made such measurements for helium and neon while C. and H. Gutton⁵ have done the same for hydrogen. In some preliminary experiments the writer attempted to reproduce Guttons' results, but found that it was practically impossible to make any reliable measurements of the striking potential of the discharge because of the difficulty in determining at just what potential the discharge struck. In an effort to obtain results which would have more significance, the problem was attacked from a different angle. It was proposed to study the conductivity of the discharge, that is, the voltage between electrodes necessary to produce a given current in the gas. Such an investigation would clearly show under what conditions the high frequency discharge operates most efficiently.

APPARATUS AND PROCEDURE

The apparatus used to produce the high frequency oscillations was essentially the same as that described in a previous paper.⁶ The discharge tube was 90 cm long, 4.5 cm internal diameter while the electrodes surrounding it were of sheet copper 4 cm wide. It was found that the conductivity of the discharge could be measured with greatest accuracy when the distance between electrodes was 40 cm. If the electrodes were much farther apart than this then there was an appreciable leakage current between the high potential electrode and the standard used to support that end of the tube. On the other hand, if the electrodes were too close together, the capacity current between electrodes became appreciable. For pressures below 0.2 mm a continuous flow of pure hydrogen was maintained through the tube while above 0.2 mm the gas was stagnant.

Instead of applying the total voltage of the high frequency generator to the electrodes, one electrode was connected to ground through a 0-120 high frequency milliammeter. The experimental procedure consisted simply in measuring the voltage between electrodes which was necessary to produce a current of 100 milliamperes through the tube, for different frequencies of oscillation and different gas pressures. The voltage between electrodes, which is equal to the voltage across one of the condensers of the tank circuit, was calculated from the formula $E = I/2\pi fC$ where I is the tank current in amperes, f the frequency of oscillation and C the capacity in farads of one of the two equal tank condensers. The tank current was measured by a 0-10 Weston radio frequency ammeter (thermocouple type) which is guaranteed by the makers to be accurate within one percent of full scale deflection. The amplitude of the electromotive force between electrodes is $E(2)^{1/2}$. Measurements were made for frequencies of oscillation corresponding to 15, 20, 25, 30, 40, 50, 60, 80, 100, 120, 160, 200, and 240 meters.

RESULTS

Fig. 1 shows, for a few typical frequencies of oscillation, the relation between gas pressure, and the voltage between electrodes which is necessary to

⁴ R. L. Hayman, *Phil. Mag.* 7, 586 (1929).

⁵ C. and H. Gutton, *Comp. Rend.* 186, 303 (1928).

⁶ C. J. Brasefield, *Phys. Rev.* 35, 92 (1930).

produce a current of 100 milliamperes through the tube. Fig. 2 shows the variation with frequency of oscillation of the minimum voltage necessary to produce a current of 100 milliamperes. It can be seen from Fig. 2 that the high frequency discharge in hydrogen has its maximum conductivity at frequencies of oscillation between 10 and 15 million cycles (i.e. between 20 and 30 meters) and at gas pressures between 0.035 and 0.015 mm. Operating the discharge under these conditions of maximum conductivity, it was possible to obtain a current as large as 300 milliamperes at 20, 25, and 30 meters. This current was, of course, limited only by the output of the high frequency generator.

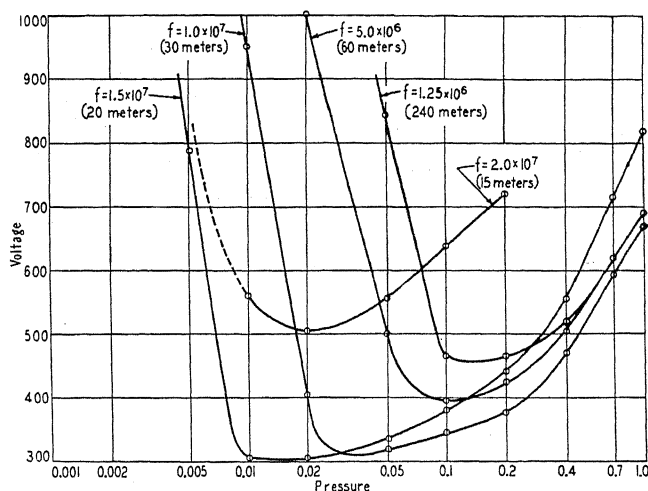


Fig. 1. Variation with gas pressure (in mm of mercury) of the voltage between electrodes necessary to produce a current of 100 milliamperes.

It can be seen from Fig. 1 that at very low pressures, the discharge is most conducting when operated at 20 meters. Using this frequency of oscillation and applying the full voltage of the high frequency generator to the electrodes it was found possible to obtain a faint white luminous discharge at pressures even as low as 10^{-6} mm. This discharge was accompanied by a blue fluorescence of the glass at the ends of the tube and by a red fluorescence of the glass at irregular spots along the tube. These spots were evidently due to bombardment of the walls of the tube by a stream of electrons for they could be shifted by moving one's finger in their neighborhood or by the presence of a magnet. The discharge itself at these low pressures seemed to be due to a beam of electrons moving along the axis of the tube, for it could be deflected by the presence of one's finger. However, no peculiarly shaped luminous bodies of gas such as Wood⁷ observed using ultra high frequencies, were ever seen.

⁷ R. W. Wood, Phys. Rev. **35**, 658 (1930).

DISCUSSION

It is not difficult to explain, qualitatively, the shape of the curves of Fig. 1. In order to maintain a stable high frequency discharge, the electrons in the discharge must satisfy two conditions. In the first place, they must produce positive ions by collision with gas molecules within a distance which is in general not greater than a few electronic mean free paths and within a time which is not greater than one-half the period of the oscillation. The second condition is, of course, that at the time of collision, the electron must have a

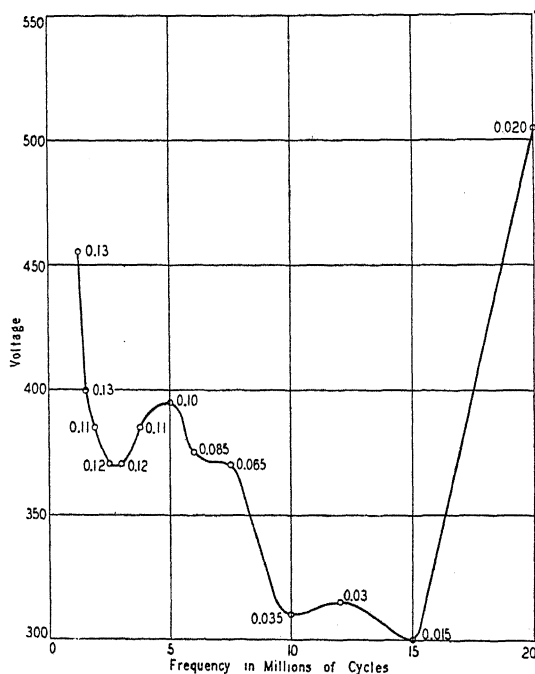


Fig. 2. Variation with frequency of oscillation of the minimum voltage necessary to produce a current of 100 milliamperes. Numbers along curve represent the pressure corresponding to the minimum voltage.

velocity sufficient to ionize a gas molecule. Now at relatively high pressures, the mean free path of the electron is small. Hence if an electron is to attain ionizing velocity in this small distance, the applied electric force must be large. On the other hand, at low pressures the mean free path of the electron is large, so that the electric force must be large in order that the electron can make a collision with a gas molecule within one-half the period of the oscillation. Between these two extremes will be a pressure at which a smaller electric force will enable the electron to satisfy the two conditions simultaneously. These points of maximum conductivity are shown in Fig. 1.

To explain the variation in the conductivity with the frequency of oscillation (Fig. 2) requires a more detailed study of the mechanism of the high

frequency discharge. The motion of an electron in a high frequency electric field can be represented by the equation

$$mx'' = eE_0 \sin 2\pi ft \quad (1)$$

where E_0 is the amplitude of the electric force and f is the frequency of oscillation. Integrating, we get the velocity at any time t ,

$$v_t = \frac{e}{m} \frac{E_0}{2\pi f} (1 - \cos 2\pi ft) \quad (v_0 = 0). \quad (2)$$

Integrating once again, we get the distance the electron goes in time t

$$d = \frac{e}{m} \frac{E_0}{4\pi^2 f^2} (2\pi ft - \sin 2\pi ft). \quad (3)$$

From Eq. (2) it is evident that for a given E_0 and f , the electron will have its maximum velocity after a time $t = 1/2f$, that is, after it has been under the influence of the electric force for one half cycle. If this terminal velocity is sufficient to ionize a gas molecule and if the distance which the electron has gone in one half cycle (given by Eq. (3)) is at least one mean free path, then the high frequency discharge will be operating under the most favorable conditions possible.

Let us consider the mechanism of a high frequency discharge operating at a frequency of 20 million cycles per second (15 meters). The electron velocity given by Eq. (2) must also satisfy the equation

$$\frac{1}{2}mv^2 = eV \quad (4)$$

where V is at least 16 volts. As a matter of fact, a previous investigation⁶ has shown that to maintain a stable high frequency discharge in hydrogen, the electron velocity must probably be at least 21 equivalent volts. Assuming this value for V and substituting the corresponding value of v in Eq. (2), we find that an electric force of amplitude $E_0 = 9.7$ volts per cm acting on an electron for one half period ($t = 1/2f$) will give it enough energy to ionize a hydrogen molecule. This, then, is the minimum electric force capable of maintaining a discharge at 15 meters; moreover, a discharge will not occur for this value of E_0 unless the distance gone by the electron is at least one mean free path. Substituting $E_0 = 9.7$ in Eq. (3) we find that the distance which the electron goes in one half period is 3.39 cm. From Fig. 2 we see that the pressure corresponding to maximum conductivity at 20 million cycles is 0.02 mm. The electronic mean free path at this pressure is 3.5 cm, which compares favorably with the distance 3.39 cm which the electron goes in one-half period.

Hence we have shown that at 20 million cycles the high frequency discharge in hydrogen has its maximum conductivity at 0.02 mm pressure because at this pressure a minimum electric force of amplitude 9.7 volts per cm is sufficient to allow an electron to make an inelastic collision with a hydrogen molecule in one mean free path having been under the influence of the elec-

tricfield for onehalf cycle. At this point of maximum conductivity the potential difference between electrodes is 505 volts. Dividing this by the distance between electrodes, 40 cm, and multiplying by $2^{1/2}$ we get an apparent electric force of amplitude 17.8 volts per cm. This is entirely compatible with the theoretical value of 9.7 volts per cm. For the potential difference between electrodes consists of two parts. The first is the drop in potential in the body of gas and the second is the drop in potential at the electrodes. Since there is at present no means of estimating the magnitude of this second factor, all that can be said is that the apparent electric force represents the upper limit of the true electric force in the gas.

Let us now consider a high frequency discharge operating at 15 million cycles per second (20 meters). Assuming as before $V=21$ volts, we find that a minimum electric force of amplitude $E_0=7.3$ volts per cm acting on an electron for one half period will give it enough energy to ionize a hydrogen molecule. Substituting this value of E_0 in Eq. (3), we find the distance which the electron goes in one half period is 4.53 cm. This compares favorably with the electronic mean free path of 4.65 cm at the pressure corresponding to maximum conductivity at 15 million cycles. Moreover, the electric force at 15 million cycles is less than the electric force at 20 million cycles. This explains why the conductivity of the discharge is greater at 15 million cycles.

At both 20 and 15 million cycles, we have seen that the mechanism of the high frequency discharge under conditions of maximum conductivity consists in an electron making an inelastic collision with a gas molecule every electronic mean free path having been under the influence of the electric force for one half cycle. If this were also the mechanism of the discharge at frequencies less than 15 million cycles, then we would expect to find that both the voltage and pressure corresponding to maximum conductivity would be less than at 15 million cycles. Since Fig. 2 shows that at frequencies less than 15 million cycles, both the voltage and pressure corresponding to maximum conductivity are greater than the voltage and pressure at 15 million cycles, we must conclude that the mechanism of the discharge at frequencies less than 15 million cycles is different from the mechanism at frequencies greater than 15 million cycles. Using Eqs. (2) and (3) we find that the difference in mechanism is due primarily to the fact that below 15 million cycles, the electron makes an inelastic collision before it has been under the influence of the electric force for an entire half period. The shape of the curve of Fig. 2., combined with a rough calculation, suggests that between 15 and 12 million cycles the electron makes an inelastic collision having been under the influence of the electric force for one third cycle; between 12 and 10 million cycles for one fourth cycle; between 10 and 7.5 million cycles for one fifth cycle; between 7.5 and 6.5 million cycles for one sixth cycle; between 6.5 and 5 million cycles for one seventh cycle; between 5 and 3 million cycles for one eighth cycle; and between 3 and 1.25 million cycles the electron makes an inelastic collision having been under the influence of the electric force for only one ninth cycle. Since the time during which the electron is under the influence of the electric field is becoming shorter, the electric force must be increased in order

that the electron can attain ionizing velocity. On the other hand, it is evident that the even fractions of a cycle will be more efficient in producing ions than the odd fractions. This explains the maxima and points of inflection of Fig. 2.

If the conditions described in the last paragraph give a true picture of the mechanism of the discharge at frequencies below 15 million cycles, then the number of electronic mean free paths involved in an inelastic collision increases as the frequency of oscillation decreases. Thus for maximum conductivity at 10 million cycles, the electron makes an inelastic collision in a little more than one mean free path; at 5 million cycles in about 3 mean free paths; and at 1.25 million cycles in about 15 mean free paths.

The reason for the sharp break in the curve at 15 million cycles is probably due to the fact that 0.015 mm pressure is the lowest pressure at which sufficient ions can be produced to sustain a current of 100 milliamperes. Hence if the current through the tube were decreased, we might expect to find maximum conductivity at some frequency less than 15 million cycles and some pressure less than 0.015 mm. As yet, experiments have not been undertaken to verify this.

In conclusion, it has been shown that the conductivity of a high frequency discharge in hydrogen is greatest when the frequency of oscillation is 15 million cycles per second and the gas pressure is 0.015 mm because the discharge is operating most efficiently under these conditions. For, under these conditions, an electron is undisturbed for one complete half cycle of the electric field, and at the end of this time it has gone exactly one mean free path so that it can make an inelastic collision with its maximum velocity. Moreover, even though at 20 million cycles and 0.02 mm pressure, the mechanism of the discharge is the same (i.e. the electron goes exactly one mean free path in one half cycle) the electric force required is greater than at 15 million cycles. Finally, at frequencies of oscillation greater than 20 million cycles, if the mechanism of the discharge is the same as at 15 and 20 million cycles (which appears very probable), it is possible to predict from Eqs. (2) and (3), first, that the electric force at maximum conductivity will increase directly with the frequency of oscillation and second, that the gas pressure at maximum conductivity will also increase directly with the frequency of oscillation.

The writer wishes to express his appreciation to the Grigsby-Grunow Company of Chicago, Illinois, for whom this investigation has been carried out. He is also indebted to several members of the Department of Physics for their interest in this work and especially to Mr. J. S. Owens who assisted in the experimental work.

ON THE CATHODE OF AN ARC DRAWN IN VACUUM

BY R. TANBERG

RESEARCH DEPARTMENT, WESTINGHOUSE ELECTRIC AND MANUFACTURING CO.
EAST PITTSBURGH, PA.

(Received December 23, 1929)

ABSTRACT

It has been found that the cathode is the only electrode which contributes vapor for the maintenance of an electric arc under very low gas pressure.

The velocity of this vapor was determined by two methods. Method 1 consisted of measuring the force of reaction of the vapor on the cathode and the rate of vaporization of the cathode material. Method 2 consisted of determining the force exerted by the vapor on a vane suspended in front of the cathode spot and the rate of vapor condensation on the vane.

Both these methods gave a vapor velocity of the order of 16×10^5 cm/sec. A temperature of around $500,000^\circ$ K results when this value for the cathode vapor velocity is substituted for c in the equation: $\frac{1}{2}mc^2 = 3KT/2$.

INTRODUCTION

A SERIES of experiments with electric arcs drawn in vacuum indicated that a jet of high-speed vapor is ejected from the cathode region of such an arc.¹ A description will be given in the following paper of an attempt to obtain quantitative data on the velocity of this cathode vapor.

For the sake of simplicity the word "vacuum arc" will be used as representing an electric arc under an air pressure of the order of a few microns. The exact pressure will be given in each particular case wherever this is of interest.

DESCRIPTION OF EXPERIMENTS

An electric arc can be drawn even in very high vacuum by separating two metal contacts carrying current of the order of a few amperes.

The arc is drawn initially in the vapor given off by the vaporization of the metal at the point of last contact² and may be maintained by the vapor which after contact separation continues to be given off from the contact surface.

A number of preliminary experiments suggested that a jet of metal vapor with considerable velocity was emitted from the cathode region. A knowledge of the velocity of this vapor jet is not only of value in connection with the determination of the temperature of the cathode region, but will also enable us to get a better quantitative picture of the conditions in the vacuum arc in general. Accordingly an investigation was undertaken based upon the following experiments:

1. Measurement of the force of reaction of the vapor on the cathode. Knowing the amount of metal vapor evaporated per unit time the velocity can be calculated.

¹ R. Tanberg, *Nature*, Sept. 7, 371 (1929).

² J. Slepian, *Journ. A.I.E.E.*, October, 1926, p. 930.

2. Determination of the momentum imparted by the vapor to a vane suspended in front of the cathode. Knowing the amount of vapor condensed on the vane per unit time the vapor speed can be obtained.

In Fig. 1 is shown the apparatus used for the tests outlined under #1 above. The copper cathode, *c*, consisted of a short copper cylinder, 0.6 cm

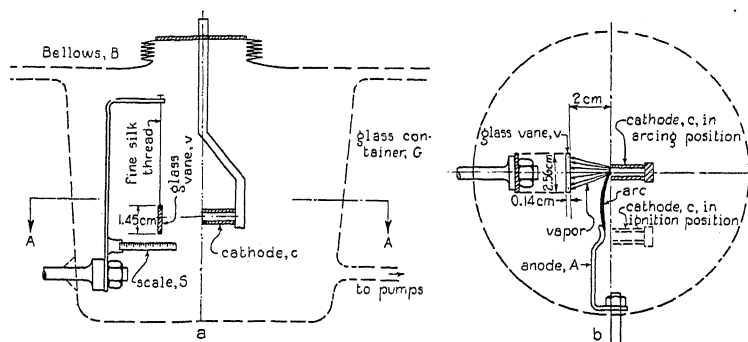


Fig. 1. Apparatus for determination of cathode vapor speed.

diameter, on the end surface of which the cathode spot was located. A quartz tubing fitted tightly around the copper cylinder in order to limit the motion of the cathode spot. The cathode was fastened to a strip of aluminum which was suspended by two fine molybdenum wires from a suitable supporting frame mounted directly on the negative terminal leading through the wall of

TABLE I. Results of vapor speed determinations by cathode reaction tests.

1 Test	2 Arc current (amps)	3 React. force (uncorr.) (gm)	4 Electrostatic force (gm)	5 Electrodynamic force (gm)	6 Total correction for electrodynamic and electrostatic forces grams	7 % of uncorr. react. force
353	11	198×10^{-3}	6.1×10^{-3}	4.8×10^{-3}	+ 1.3	0.66
352	16	265×10^{-3}	8.9×10^{-3}	10.3×10^{-3}	- 1.4	0.53
354	19	367×10^{-3}	10.6×10^{-3}	14.5×10^{-3}	- 3.9	1.06
355	19	367×10^{-3}	10.6×10^{-3}	14.5×10^{-3}	- 3.9	1.06
356	32	485×10^{-3}	18.0×10^{-3}	41.0×10^{-3}	-23.0	4.7

8 React. force (corr.) (gm)	9 gm/sec. evap. from cathode	10* (C ²) ^{1/2} cm/sec.	11 T° abs. temper. at cathode
199.3×10^{-3}	0.17×10^{-3}	16.3×10^5	6.8×10^5
263.6×10^{-3}	0.25×10^{-3}	14.6×10^5	5.45×10^5
363.1×10^{-3}	0.30×10^{-3}	16.8×10^5	7.25×10^5
363.1×10^{-3}	0.30×10^{-3}	16.8×10^5	7.25×10^5
$462. \times 10^{-3}$	0.49×10^{-3}	13.1×10^5	4.37×10^5

* Based upon figures in column 8 and 9.

the arcing chamber. The pressure in the arcing chamber varied between 0.2×10^{-3} mm Hg at the beginning of the arcing to around 10×10^{-3} mm Hg at the finish. The arc current was supplied to the cathode through an iron wire which dipped into a pool of mercury, *P*, electrically connected with the negative terminal.

Thus the cathode was suspended so it would swing freely back and forth in a plane vertical to the cathode surface. The deflection was measured on a scale, *S*, located underneath the cathode. The instrument was calibrated for cathode deflection against the corresponding force on the cathode surface.

The arc was formed by contact between the cathode and anode as indicated in Fig. 1b. As soon as the arc was playing the anode was moved to about 1.5 m away from the cathode. The deflection of the cathode during the arcing was of considerable magnitude and quite steady and could, therefore, be read with good accuracy on the scale provided for that purpose.

The results of a series of typical tests are compiled in Table I. Column 3 gives the force on the cathode as a function of the arc current given in column 2. Column 9 gives the amount of vapor in grams per second leaving the cathode during the arcing.

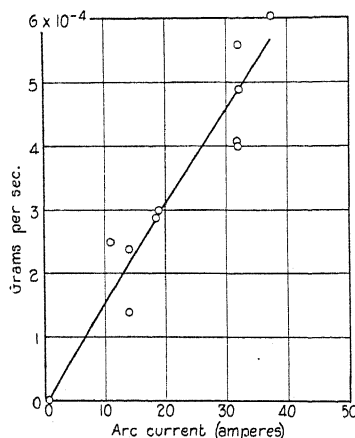


Fig. 2. Vaporization of copper cathode by arc in vacuum.

These last values are taken from the curve in Fig. 2 which is based upon a separate series of tests made under identically the same conditions as those existing during the measuring of the cathode reaction force. The cathode was weighed before and after each test and the time duration of the arcing was noted, thus determining the rate of vaporization of the cathode material.

Column 10 contains the root mean square velocities of the vapor leaving the cathode, calculated from the data given in columns 8 and 9 using the formula:-

$$(C^2)^{1/2} = 1.39K/m$$

where

K = force in dynes on cathode.

m = mass in grams per second of metal evaporated from the cathode.

$(C^2)^{1/2}$ = root mean square velocity in cm/sec. of vapor leaving the cathode.

The development of this formula will be found in the appendix to this paper.

Considering the conditions under which the tests were made it is evident that the results should be corrected for possible radiometric, electrodynamic and electrostatic forces. A discussion of these corrections can also be found in the appendix.

The values of the cathode reaction force obtained when the above mentioned corrections are taken into account will be found in column 8 in Table I.

As will be seen later by the calculation of the corresponding temperature, the vapor velocities obtained are very high compared with what could be expected from conservative estimates of the temperature existing at the cathode. It was, therefore, thought desirable to check the results by the vane deflection method already referred to.

This was made with the apparatus shown in Fig. 3a and b. The cathode, *c*, was of the same design (copper cylinder surrounded by quartz tube) as

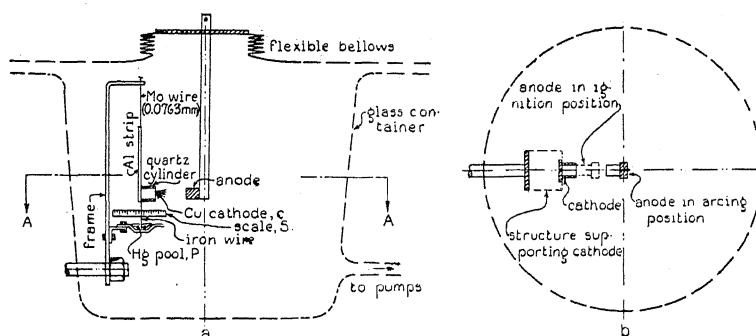


Fig. 3. Apparatus for measuring cathode vapor speed.

used in the previous experiments. It was fastened to a metal rod which could be moved from outside the vacuum by means of the flexible bellows, *B*. The same pressure was maintained during these experiments as during the cathode reaction tests just described. The arc was formed by moving the cathode to touch the anode as indicated in Fig. 3b. As soon as the arc was playing, the cathode was moved back in front of the glass vane, *v*, consisting of a square piece of Pyrex glass. This was suspended by two fine silk threads from a supporting frame indicated in the figure. The deflection of the vane was read directly on the scale, *S*, and the force necessary to deflect the vane as a function of the deflection was determined.

During a test the arc would play between the cathode and anode as indicated in Fig. 3b, while the vapor would be projected from the cathode spot directly against the vane deflecting this according to the momentum imparted to it by the impinging molecules.

The presence of this jet of high-speed vapor was not only evident from the definite deflection of the vane, but could also be realized visually by the sharply defined, faintly luminous, cone-shaped region, extending from the cathode spot to the vane. The results of these tests are given in Table II.

TABLE II. Results of vapor speed determination by deflecting vane method.

1 Test	2 Arc current (amps.)	3 Force on vane (gm)	4 Vapor condensed (gms/sec.) on vane	(C ²) ¹ / ₅ cm/sec. R.M.S. vapor velocity
366	14.2	64×10^{-3}	42.6×10^{-6}	20.8×10^5
369	16.0	64×10^{-3}	53.7×10^{-6}	16.6×10^5
367	18.0	94×10^{-3}	65×10^{-6}	20.1×10^5

The velocities in column 5 in this table were calculated by the same formula as previously used for calculating the vapor velocities from the cathode reaction tests, while m (column 4), representing the amount of metal vapor condensed on the vane per second, was obtained from the curve in Fig. 4, which is based upon direct measurements. It will be seen that the values for the cathode vapor speed obtained by this method agree quite well in the order of magnitude with the values obtained by the previous method.

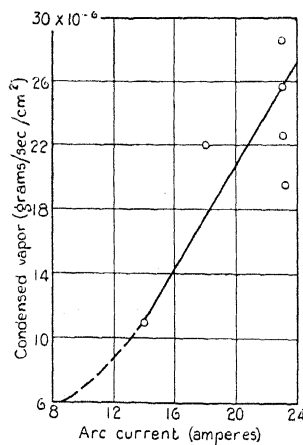


Fig. 4. Condensation of copper vapor on collector 2 cm from cathode.

When judging these results it must be remembered that it is practically impossible to prevent the cathode spot from traveling on the cathode surface. The amount of vapor hitting the vane may, therefore, vary somewhat with the location of the cathode spot.

The discussion in the appendix of possible corrections to these measurements will show that the effects from radiometric pressure, electrostatic fields etc., can be entirely neglected.

CALCULATION OF TEMPERATURE CORRESPONDING TO THE MEASURED VAPOR VELOCITIES

The knowledge of the speed with which the metal vapor is ejected from the cathode region enables us to calculate at least the order of magnitude of the temperature at the cathode by the well-known relations between the average

kinetic energy and the absolute temperature of the molecules in a gas. It is believed to be justified to use in this connection the equation applying to three degrees of freedom of the molecule:

$$\frac{1}{2}m' \cdot C^2 = 3kT/2 \quad (1)$$

where m' is the molecular mass in grams; C^2 is the mean square of the velocity of the molecules in cm/sec.; k is Boltzmann's gas constant in erg/°Abs. and T is the absolute temperature.

The justification for using this form of the temperature-kinetic energy equation is the good agreement it gives with experimental results when applied to Stern's³ and Eldridge's⁴ measurements on velocities of molecules emitted from a hot metal surface under low gas pressure.

Substituting in Eq. (1) the values for the molecular velocities given in Table I give temperatures as shown in column 11.

GENERAL DISCUSSION OF RESULTS

As will be realized, these temperatures are far in excess of even the most extreme temperatures ever measured in connection with any physical phenomenon of any duration. One must, however, remember that the space close to the cathode of an electric arc constitutes a very small volume with a large energy input where one, from only conservative estimates, could expect exceedingly high temperatures.

A similar case with large energy input into a small space constitutes the interesting experiments made by J. A. Anderson⁵ with electrically exploded wires, during which he obtained estimated temperatures of 300,000°C.

CONCLUSION

The temperature existing at the cathode spot determined from the velocity of the cathode vapor is of the order of 500,000°K.

If this extreme temperature is confirmed by other investigators, our present ideas of what takes place at the cathode of a vacuum arc must be revised. The cathode region would then offer an excellent opportunity to study the very interesting physical conditions which must exist in a location with such an enormous temperature.

The writer wants to express his thanks to Dr. J. Slepian for the encouragement he has received from him during the preparation of this paper.

APPENDIX

Calculation of vapor velocities. A molecule will exert an impulse

$$\int K' dt = m' \cdot u \quad (2)$$

³ Stern, Zeits. f. Physik 2, 49 (1920).

⁴ Eldridge, Phys. Rev. 30, 931 (1927).

⁵ J. A. Anderson, Astrophys. J. p. 37. Jan. (1920).

on any surface which it is either leaving or striking. In this equation:

K' = force in dynes.

m' = mass in grams of the molecule.

u = component of velocity of molecule in cm/sec. perpendicular to surface.

The probability that a molecule in the vapor shall have a velocity component lying between u and $u+du$ is: $f(u) \cdot du$ assuming a certain velocity distribution. If n is the number of molecules per cm³ of the vapor, the number of these which has a velocity lying between u and $u+du$ is: $n \cdot f(u) \cdot du$. The total number of molecules per cm² per second leaving the cathode region with velocities lying within this particular interval must therefore be:

$$\Delta\gamma = u(n \cdot f(u) \cdot du) \cdot \text{molecules/sec.} \quad (3)$$

where u = velocity perpendicular to the surface in cm/sec.

The force exerted by these molecules on the cathode per cm² is (from Eqs. (2) and (3)). $K' = (m' \cdot u) \cdot (u \cdot n \cdot f(u) \cdot du)$.

$$K' = m' \cdot n \cdot u^2 \cdot f(u) \cdot du. \quad (4)$$

The total force per cm² of molecules leaving the cathode:

$$K = m' \cdot n \int_0^{\infty} u^2 \cdot f(u) \cdot du. \quad (5)$$

By changing integration limits:

$$K = m' \cdot n \cdot \frac{1}{2} \int_{-\infty}^{+\infty} u^2 \cdot f(u) \cdot du.$$

If u^2 denotes the mean square of the velocity component perpendicular to the surface:

$$K = \frac{1}{2} m' \cdot n \cdot u^2. \quad (6)$$

Since the vapor density $m' \cdot n$ is not practical to determine it is necessary to express this term by the amount of vapor leaving the cathode. The total number of moles per cm² leaving the cathode per second is found by integrating Eq. (3) from 0 to ∞ : $\gamma = n \int_0^{\infty} u \cdot f(u) \cdot du$. if $|\bar{u}|$ denotes the average numerical value of the perpendicular component of velocity we have: $\gamma = \frac{1}{2} n \cdot |\bar{u}|$. Thus the total mass of the atoms leaving the cathode per second is: $A \cdot m' \cdot \gamma = A \cdot m' \cdot (\frac{1}{2} n \cdot |\bar{u}|) = m$ or

$$A \cdot m' \cdot n = 2 \frac{m}{|\bar{u}|} \quad (7)$$

where m is total loss of cathode material during one second of arcing and A is the area of the cathode spot in cm². Making Eq. (6) apply to the whole

⁶ Richardson, "The Emission of Electricity from Hot Bodies" Edition 1921, pages 155 and 177.

cathode spot by multiplication with the cathode spot area "A" and combining it with Eq. (7) gives

$$K = (\bar{u}^2 / |\bar{u}| m). \quad (8)$$

There is reason⁶ to believe that the fundamental equations of Maxwell's velocity distribution theory can be used in connection with the conditions considered here. We can, therefore, substitute in equation (8) $\bar{u}^2 = \frac{1}{3} \bar{C}^2$ and $|\bar{u}| = \frac{1}{2} \bar{C}$ which gives: $K = \frac{2}{3} C^2 / C (C^2)^{1/2} m$ according to the Maxwellian velocity distribution function:

$$(C^2)^{1/2} / C = 1.08.$$

Hence:

$$(C^2)^{1/2} 1.39 K / m \quad (9)$$

which is the formula used for calculating the values given for the root mean square velocities in columns 10 and 5 in Tables I and II respectively.

The conditions at the vane are somewhat more complicated than assumed above because the existence of a Maxwellian velocity distribution in the gas at the vane surface may be questioned. However, the application of Eq. (9) to the data obtained from the vane deflection experiments will undoubtedly give values representing the correct order of magnitude of the R. M. S. velocity of the vapor striking the vane.

The values given in column 5 Table II which are calculated from Eq. (9) must therefore only be considered as serving the purpose of a rough check on the velocity values given in Table I.

DISCUSSION OF POSSIBLE CORRECTIONS TO VANE DEFLECTION TESTS

a. Radiometric effect—Due to the brilliancy of the cathode spot it was thought possible that the deflection of the vane during the experiments may have been affected by radiometric pressure. The tests recorded in Table III indicate, however, quite conclusively that the effect of radiometric pressure on the vane deflection must be of such small magnitude as to be negligible.

TABLE III. Showing that variations in gas pressures do not affect the deflection of the vane.

1 Test	2 Arc current (amps.)	3 Distance cathode-anode (cm)	4 Pressure before test	(mm Hg) after test	5 Force on vane (gm)	Remarks
456	2.30	2.0	0.9×10^{-3}	56×10^{-3}	94×10^{-3}	vane deflect.
457	"	"	63×10^{-3}	64×10^{-3}	130×10^{-3}	did not vary
458	"	"	0.2×10^{-3}	13×10^{-3}	130×10^{-3}	with press.
459	"	"	0.2×10^{-3}	12×10^{-3}	94×10^{-3}	increase
460	"	"	0.2×10^{-3}	16×10^{-3}	130×10^{-3}	
461	"	"	0.2×10^{-3}	8.5×10^{-3}	130×10^{-3}	

During these experiments the gas pressure was measured by a McLeod gauge before and after each test allowing sufficient time for the pressure to equalize all through the vacuum system. The time required for equalization

was very short since all tube connections were dimensioned so as to give a large ratio of diameter to tube length.

The pumps were shut off during each experiment. Since the leakage of the system was found to be negligible, the increase in pressure during each test represents gas given off from the electrode during the arcing.

Thus during test #456 which lasted several seconds the pressure increased from 0.9×10^{-3} mm Hg to 56×10^{-3} mm Hg but the deflection of the vane remained constant around the value given in column 5 in spite of the fact that the radiometric effect within the same pressure interval according to data by Westphal⁷ should be expected to increase ten fold.

The difference in pressure at the end of tests 460 and 457 in Table III does not reveal any change in the force on the vane while the corresponding change in radiometric pressure according to Westphal's experiments should be about 28 percent.

A similar analysis of the other tests recorded in Table III points just as conclusively to the fact that the radiometric pressure on the vane can be entirely neglected during the writer's experiments.

b. Accumulation of charge on vane. If the vapor consisted of ions of one sign it would charge the vane up to a potential of the same sign as the charge on the vapor particles. The magnitude of this charge would increase until a sufficient field was set up to reflect the vapor particles back against the cathode. The momentum imparted to the vane by the vapor under such conditions would be about twice the momentum delivered to the vane if the particles condensed. It is, therefore, necessary to determine if such a reflection actually can have taken place during the tests recorded in the Tables I, II and III.

During a series of experiments the vapor from the cathode spot was made to condense on a metal plate which was kept under different potentials relative to the cathode. The metal plate was located in the same relative position to the cathode and anode as the vane during the previous experiments. The potential was varied between 0 and +60 volts without producing any effect upon the amount of condensed vapor.

Since the R. M. S. velocity of the vapor (15×10^5 cm/sec.) corresponds to about 74 volts assuming singly-ionized Cu atoms, this potential interval should have been sufficient to show some changes in condensation had the vapor when reaching the vane been charged.

CORRECTIONS TO CATHODE REACTION TESTS

a. Radiometric effect: From the discussion in connection with the vane experiments it is probably safe to assume that the radiometric effect is negligible also at the cathode outside of the cathode spot proper. This assumption is justified on account of the extremely steep temperature gradient existing at the cathode spot which will limit the high temperature area to the spot itself.

⁷ Westphal, Zeits. f. Physik 1, 92 (1920).

It remains, however, to be proved that the radiometric pressure at the cathode spot also will be of such small magnitude as to be negligible.

Knudsen⁸ gives the following formula for the radiometric force as a function of temperature and gas pressure:

$$K = \frac{1}{2}p \cdot \left(\frac{T_1}{T_2} - 1 \right) \quad (10)$$

where K is the radiometric force in grams/cm²; p is the gas pressure in grams/cm², and T_1 and T_2 are absolute temperatures.

The good agreement obtained by Knudsen between experimental and calculated values within the pressure range existing during the writer's arcing experiments justifies the use of this formula in calculating the radiometric force at the cathode of the vacuum arc.

Assuming a temperature at the cathode of 700,000°K and a temperature of the surrounding parts of 300°K gives:

$$K = 328 \times 10^{-3} \text{ grams/cm}^2$$

from Eq. (10) for a pressure equal to 10×10^{-3} mm Hg. If we assume that the current density of 7200 amp/cm² found by Güntherschultze⁹ for cathode spots on iron under atmospheric pressure also holds for a vacuum arc the cathode spot of a 20 amp. arc will have an area of 2.8×10^{-3} cm². Thus the total force on the cathode spot due to radiometric effects under the conditions specified will not exceed 0.92×10^{-3} grams/cm².

A comparison with the forces actually measured on the cathode spot shows that the radiometric effect also in this case can be entirely neglected.

b. Electrostatic force on the cathode. On account of the cathode drop an electrostatic force will be exerted on the cathode during the arcing in such a direction as to tend to move it into the arc. Since the cathode drop is known to be concentrated in a very small distance from the cathode surface the electrostatic force may be of such magnitude that it can not be neglected.

If S is the area in cm² over which the electric field extends at the cathode and E the field strength in absolute units per cm, the force in dynes exerted on the cathode is (assuming a dielectric constant = 1) $F = S \cdot E^2 / 8 \cdot \pi$.

Observations of the Stark effect¹⁰ indicates a field strength at the cathode surface of the order of 10^5 volts/cm. Since the field at the edge of the cathode spot probably falls off very rapidly it should be correct to substitute for S in the above equation the area of the cathode spot determined from the current density observed by Güntherschultze.⁹ The values thus obtained are given in column 4 Table I.

c. Electrodynamic forces. Due to the form of the current path in the apparatus shown in Fig. 1 an electrodynamic force can be expected to act upon the suspended cathode during the arcing, tending to increase its deflection. The correction for this will be found in column 5, Table I.

⁸ Knudsen, Ann. d. Physik 32, 809 (1910).

⁹ Güntherschultze, Zeits f. Physik 11, 74 (1922).

¹⁰ R. Seeliger, Physik der Gasentladungen, Leipsig, p. 282 (1927).

THE REFLECTION OF LITHIUM IONS FROM METAL SURFACES

BY R. B. SAWYER

RYERSON PHYSICAL LABORATORY, UNIVERSITY OF CHICAGO

(Received March 22, 1930)

ABSTRACT

A study has been made of the reflection of lithium ions from reflectors of platinum foil and of nickel crystals deposited on tungsten foil. Movable ground joints in the tube were completely eliminated in order to prevent contamination of the reflector surfaces by grease. Readings were taken with both cold and hot reflectors. Spodumene was used as a source of ions and reflection was studied in the meridian plane only.

Superposed on a diffuse scattering of ions were two reflected beams. One was reflected nearly specularly, as found by Read and by Gurney, the angle of maximum reflection, however, being independent of accelerating potential. The other beam appeared only at voltages above 200 and was composed of ions most of which had retained 80 percent or more of their original energy. This beam was found between the incident beam and the normal to the surface, at angles independent of the accelerating potential up to 700 volts. This independence of angle on voltage forbids diffraction interpretations. A tentative explanation consists in supposing specular reflection from the (110) planes of the nickel crystals, but the agreement is not entirely satisfactory.

THE reflection of lithium and potassium ions from a platinum surface has been investigated by Read,¹ and that of lithium, potassium, and caesium from platinum by Gurney.² Both found considerable reflection from a clean platinum surface, the maximum occurring at an angle somewhat larger than that corresponding to specular reflection. Since an extremely clean reflector seemed to be necessary in order to obtain appreciable reflection, it was desirable to continue the study, making every effort to avoid contamination of the reflector, especially by grease vapor. The discovery of electron diffraction by crystals³ and the work of Ellett and Olson⁴ on reflection of neutral atoms by crystals suggested a trial of crystal surfaces as reflectors of positive ions.

APPARATUS

The tube used is shown in Fig. 1 and Fig. 2. A tiny crystal of spodumene, *S*, on an electrically heated platinum strip was used as a source of lithium ions.⁵ These were accelerated to the drum, *B*, and a portion passed through holes 1 mm in diameter, and entered the cylinder, *A*, which had a 3 mm slot cut around it to admit them. After striking the reflector, *T*, those ions which

¹ Read, Phys. Rev. 31, 629, (1928).

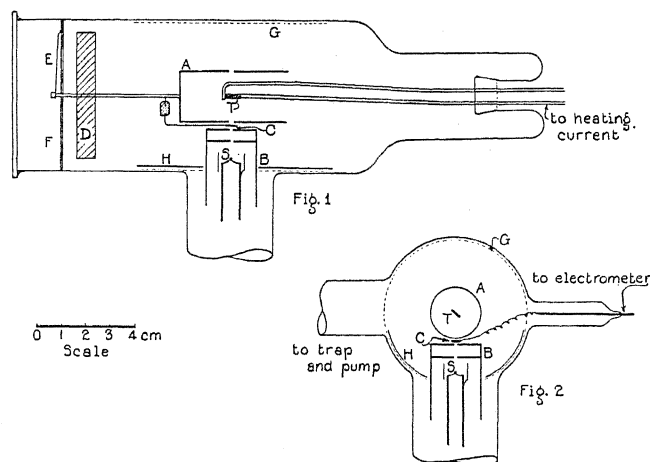
² Gurney, Phys. Rev. 32, 467 (1928).

³ Davisson and Germer, Phys. Rev. 30, 705 (1927).

⁴ Ellett and Olson, Phys. Rev. 31, 643 (1928).

⁵ Read, reference 1, p. 629.

were reflected at any given angle could be caught by the collector, *C*, which was a 2 mm \times 7 mm nickel strip rigidly fastened by means of a Pyrex bead to the axis of the cylinder, *A*. The collector-cylinder system was mounted in a supporting framework (not shown in the figure) so that it could be rotated from the outside of the tube by an electromagnet applied to the soft iron armature, *D*. The angle at which the collector was set was indicated by a pointer, *E*, moving over a graduated circle, *F*. The collector was connected to a string electrometer by a flexible lead. The positive ion current from the collector was balanced by a negative current from an ionization chamber.⁶ The central part of the tube was shielded by a gauze, *G*, and an additional screen, *H*, of sheet metal was placed around the bottom part of the tube in order to prevent the escape of any positive ions from the source except



Figs. 1, 2. Construction of tube.

through the holes in the top of the drum, *B*. The cylinder and framework supporting it were grounded through the same lead as the screen, *H*, but the gauze, *G*, had a separate ground connection. Neither of these ground leads is shown in the figure. Tungsten wires were used for sealing through the Pyrex.

The reflector was either a 5/16 in. \times 3/8 in. strip of platinum-iridium foil (10 percent iridium) 0.0005 in. thick, or a 1/8 in. \times 3/8 in. strip of tungsten foil, kindly supplied Dr. W. E. Forsythe, upon which nickel crystals had been deposited by evaporation, according to the method of Rupp.⁷ He states that the minute crystals so formed are oriented with their (111) planes parallel to the surface of the backing foil. The platinum foil was mounted so as to be kept always under slight tension by a tungsten spring, while the heavy nickel wires supporting the nickel crystal reflector had enough elasticity to keep the tungsten foil taut. In either case the reflector could be heated electrically to any temperature desired. Except as otherwise noted, all metal parts were made of nickel.

⁶ Read, reference 1, p. 630.

⁷ Rupp, *Ann. d. Physik* 1, 801 (1929).

Spodumene proved to be so satisfactory a source of lithium ions that the stem supporting the source and drum was sealed permanently into the side tube. A useful life of from 75 to 100 hours for one crystal was not unusual. One end of the main tube was ground off and closed by a glass plate waxed on with ordinary red sealing wax, care being taken to keep the wax on the outside of the tube. Contamination by grease vapors was thus entirely eliminated and that by vapors of wax reduced to a very small amount.

Originally a small Faraday cylinder was used as a collector. It was found that the measured ion current to such a cylinder was sensibly the same no matter whether the ions struck the inside of the cylinder or the bottom outside. It has been noted by others⁸ that the reflection of positive ions almost disappears at normal incidence. Furthermore, a particularly clean surface seems to be necessary to secure much reflection at any angle, and no pains were taken to secure this degree of cleanliness of the collector. Hence, since the ions would be incident normal to the collector and the collector was not especially cleaned, one would not expect loss of ions by reflection even from a simple strip. Experience bears out this conclusion. The cylinder was later replaced by a strip because it took up less space.

METHOD

The accelerating potential could be applied in two parts: one between the source and the drum, the other between the cylinder and the reflector, drum and cylinder both being grounded. The field between cylinder and reflector served both to accelerate primary ions moving toward the reflector and to retard reflected ions leaving it. Thus by making the source 30 volts positive and the reflector 20 volts negative with respect to the drum and cylinder, the ions caught by the collector would have struck the reflector with an energy of 50 volts and would have retained 20 volts or more after impact. These will be designated as 50-20 volt ions.

It is true that with this arrangement the ions are in a field of force while they are being reflected and this may conceivably influence the reflection somewhat. The geometry of the tube was such that the field between the cylinder and the reflector was, to a rough approximation, radial, and the velocities of the reflected ions should not have been greatly altered by it as regards direction. Furthermore, when a reading was being taken the field around the cylinder was not distorted by the presence of the collector, since its potential at such a time was always zero. One disadvantage of this method is that the field between the cylinder and the reflector focuses the incident beam to some extent, so that even though the ion current getting through the holes in the drum remains constant, the number of ions striking the reflector is greater the greater the potential difference between it and the cylinder. Thus for the higher retarding potentials, i.e., larger fractions of total accelerating potential applied between cylinder and reflector, the current to the reflector is actually increased.

⁸ Gurney, reference 2, p. 472, and his quotation of Jackson, *Phys. Rev.* **28**, 524 (1926).

An alternative method would be to keep the drum, cylinder, and reflector all at ground potential, applying the whole accelerating field between the source and the drum, and the retarding field between the cylinder and collector. This has two disadvantages. In the first place, the field in the immediate vicinity of the collector tends to change the direction of approaching ions, deflecting them so that some which should strike the collector now miss it entirely. In the second place, this method involves placing the whole collector-electrometer system at a positive potential, sometimes comparatively high, with the consequently greater likelihood of insulation leaks. All of the data in this paper were obtained with the first arrangement.

The procedure in taking a series of readings was as follows. The desired accelerating and retarding potentials were applied and the source was heated for several minutes until the emission became steady. The total ion current getting through the holes in the drum was measured by turning the collector so as to cover the holes. This current was kept as nearly constant as possible and was checked occasionally during a run, little difficulty being found in maintaining constancy. The heating current through the reflector was adjusted to give the desired temperature and the collector then rotated so as to collect ions reflected at various angles. The width of the collector subtended an angle of about 9.5° at the center of the reflector, and in taking readings settings were made at 10° intervals. The pressure was kept as low as possible, being of the order of 10^{-6} mm. If the reflector were at any temperature higher than that of a just visible red heat, it was found necessary to apply to it a negative potential of 2 or 3 volts in order to suppress positive ion emission from the reflector itself.

RESULTS

In general, the reflector gave more intense reflection when hot than when cold, though little change was observed as the temperature was raised beyond a medium red. In most of the following work a medium red heat was used. It is probable, as Read and Gurney suggested, that the increased reflection when hot was due to the removal of surface films of gas or grease. Read reported that within a few seconds after the heating current was turned off no reflection could be detected, while Gurney publishes a curve showing that the intensity of reflection decreased to 0.4 of its initial value during the first minute after heating was stopped. With the tube used in this investigation it was found that the intensity was 0.9 of its original value after an interval of 8 minutes, in one instance, and even after 20 minutes it had sunk only to $0.86 I_0$.

When only small retarding fields were applied so that ions of all but the very lowest velocities were collected, reflection was found as shown in Figs. 3-6. The figures show the incident beam coming from the right, and the length of the radius vector from the center of the reflector to any point on a curve is proportional to the intensity of reflection at that angle. The broken lines marked *N* and *S* show, respectively, the normal to the surface and the angle of specular reflection.

The reflection from platinum, Fig. 3, shows much the same sort of distribution as reported by Read and Gurney, but there are several points of difference. Apparently there was considerably more diffuse scattering at small

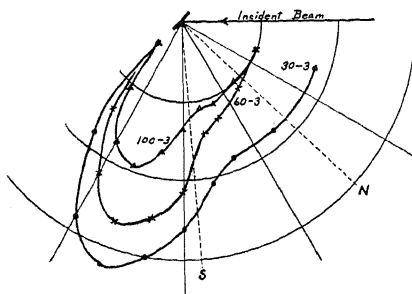


Fig. 3. Reflection from platinum, angle of incidence 43°. Small retarding potentials.

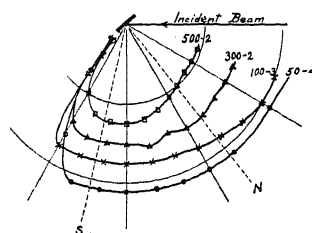


Fig. 4. Reflection from nickel, angle of incidence 51.5°. Small retarding potentials.

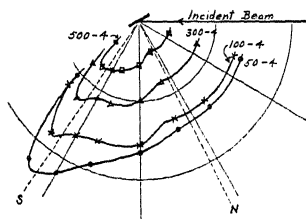


Fig. 5. Reflection from nickel, angle of incidence 62.5°. Small retarding potentials.

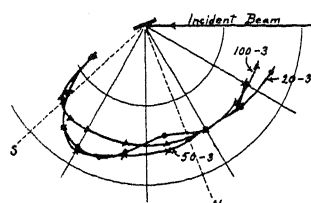


Fig. 6. Reflection from nickel, angle of incidence 69°. Small retarding potentials.

angles than was found by either Read or Gurney. There is a rather broad peak in each curve, the maximum falling at a larger angle than specular reflection would give. Contrary to the findings of Read, the position of this maximum did not change with a change in the accelerating potential.

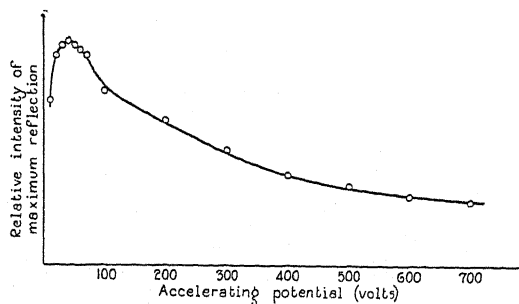


Fig. 7. Reflection from nickel, angle of incidence 62.5°.

The curves for a nickel crystal reflector, Figs. 4-6, show hardly any peaks in some cases. Where they do occur they are not as prominent as with the platinum reflector, and fall much more nearly at the specular angle.

The relation between the intensity of the maximum and the accelerating potential is shown in Fig. 7 for a nickel reflector with a primary beam incident at 62.5° . The maximum in the neighborhood of 40 volts agrees with the results of Read and Gurney for platinum.

Figs. 8-13 are curves for larger retarding potentials. These curves show directly the angular distribution of all reflected ions having more than a certain amount of energy. For instance, the 50-20 volt curve of Fig. 8 shows the distribution of ions which originally had an energy of 50 volts and which retained 20 volts or more after reflection. For low accelerating potentials these curves show a progressive shift of the maximum toward larger angles as the retarding potential is increased, indicated in Fig. 8. This shows that the ions which were the least deviated from their original directions were apt to have higher velocities than those which were deflected through larger angles. This corroborates the result obtained by Gurney.

From a set of curves such as Fig. 8 or Fig. 9 it is possible to get some idea of the velocity distribution of the ions as well as their distribution in angle.

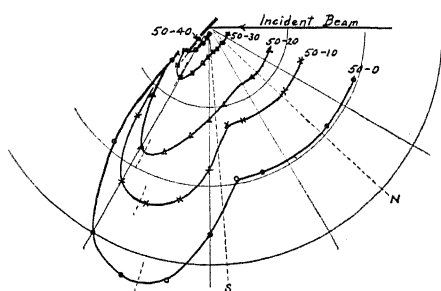


Fig. 8. Reflection from platinum, angle of incidence 43° . Large retarding potentials.

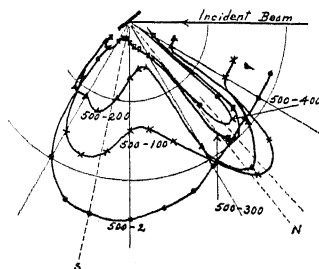


Fig. 9. Reflection from nickel, angle of incidence 51.5° . Large retarding potentials.

Thus in Fig. 9 it is seen that there is a fairly well-defined beam of ions coming off at an angle just inside the normal to the surface, and the ions composing the beam seem to have retained a large part of their original energy. The fact that some of the curves for large retarding potentials show a greater intensity than those for smaller retarding potentials at a given angle may be explained by the focusing effect of the field between the cylinder and the reflector, as before mentioned. Increasing the retarding potential accentuates the specularly reflected peak, though reducing its intensity, at the same time bringing into marked prominence the high velocity beam which must previously have been obscured by general, low velocity scattering. It should be noted that the position of this new peak, as shown in Figs. 10-13, is unaffected by a change in the accelerating potential of the incident ions up to 700 volts, the largest used. This is not particularly apparent in Fig. 11. While the number of voltages used for an angle of incidence of 62.5° was not as large as might be desirable to locate accurately the position of the new peak, careful examination of all the data taken leads to the conclusion that the maximum was located at about 5° inside the normal, as shown by the 250-150 volt curve.

However, the accuracy of measurement was hardly sufficient to locate the maximum within 5° .

The peak near the normal was not observed with accelerating voltages below 200 volts and increased in prominence as the accelerating potential was raised. Its position so near the normal to the surface at once suggested that it might be due to the condensation of ions upon the surface and their subsequent evaporation, according to the theory of Langmuir⁹ and Frenkel.¹⁰ This would result in a cosine distribution with a maximum along the normal. However, it would hardly be expected that the ions would evaporate with such high velocities as were observed, if, indeed, they evaporated as ions at

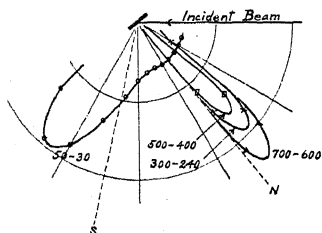


Fig. 10. Reflection from nickel, angle of incidence 51.5° . Large retarding potentials.

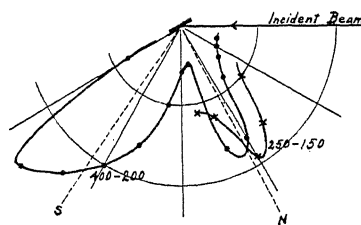


Fig. 11. Reflection from nickel, angle of incidence 62.5° . Large retarding potentials.

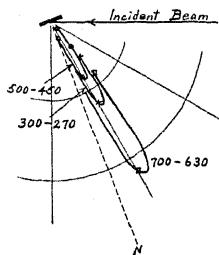


Fig. 12. Reflection from nickel, angle of incidence 69° . Large retarding potentials.

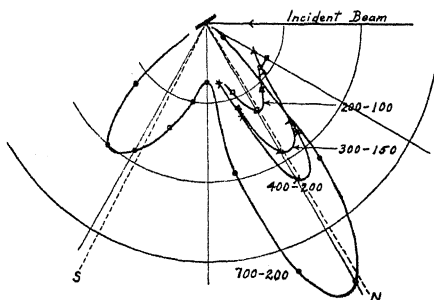


Fig. 13. Reflection from platinum, angle of incidence 59° . Large retarding potentials.

all. The sharpness of the peak, too, did not suggest a cosine law. As a further check on the adsorption—re-evaporation idea, the effect was tried of changing the density of the ion stream, since the work of Cockcroft¹¹ indicated that stream density was an important factor in molecular condensation. However, it seemed to be impossible to make the peak either appear or disappear simply by changing the ion current. In one trial, using a voltage below that at which the peak appeared, an increase in the current by a factor of thirty failed to produce a peak.

A hot reflector gave the effect better than a cold one. It was not observed

⁹ Langmuir, *Phys. Rev.* 8, 149 (1916).

¹⁰ Frenkel, *Zeits. f. Physik* 26, 117 (1924).

¹¹ Cockcroft, *Proc. Roy. Soc. A*119, 293 (1928).

at all with a nickel crystal reflector at an angle of incidence of 42° or with platinum at 44° .

When the larger accelerating potentials were used there sometimes appeared to be an emission of secondary electrons from the reflector. It was usually possible, by the application of a suitable magnetic field, to prevent these from reaching the collector and yet to leave the positive ions practically unaffected.

DISCUSSION

The reflected beam of ions coming off near the normal to the surface and having nearly the same velocity as the incident ions is the most interesting result of this study. It would be most natural to try to attribute it to positive ion diffraction were it not for the fact that the position of the beam is independent of the accelerating potential. The wave-length associated with a 200 volt lithium ion would be expected to be approximately 0.01A. Although it is difficult to predict the behavior to be expected of a complex ion when it strikes a crystal surface, specular reflection would seem to be as likely as anything else. A consideration of the possibilities of such reflection from various planes in the nickel crystals shows that, of those having the largest atom densities, only the (110) planes could give specular reflection at approximately the observed angles. Table I shows the angles observed and calculated. Having no accurate knowledge of the crystal structure of the platinum reflector, it is impossible to calculate the reflection as in the case of the nickel crystals.

TABLE I. *Reflection from nickel crystals. All angles measured from the normal to the surface.*

Angle of incidence on (111) planes	Angle of Reflection		Difference
	Calculated from (110) planes	Observed	
51.5°	19.5°	8.5°	+11.0°
62.5°	8.5°	5.5°	+3.0°
69.0°	2.0°	9.0°	-7.0°

One argument against the hypothesis of reflection by the (110) planes is that the differences between observed and calculated values of the angles show a systematic trend in one direction. However, the number of different angles tried was not sufficient to permit drawing a definite conclusion. The reflected beam was so nearly normal to the surface as to suggest the possibility that more accurate measurements might show it to lie exactly along that direction. A rough test of the relative satisfactoriness of the two suppositions—reflection by the (110) planes or reflection along the normal—is found by applying the method of least squares, though here again a greater number of angles would be desirable. This method gives little choice between the two hypotheses, the slight difference being in favor of the first mentioned.

The writer wishes to acknowledge his indebtedness and express his appreciation to Professor A. J. Dempster, who proposed the problem and whose suggestions proved extremely valuable, and to Mr. K. S. Woodcock, who assisted in taking some of the data and making the drawings.

THE ZODIACAL LIGHT AND THE GEGENSCHN AS
PHENOMENA OF THE EARTH'S ATMOSPHERE.*

BY E. O. HULBURT

NAVAL RESEARCH LABORATORY

(Received March 14, 1930)

ABSTRACT

A quantitative atmospheric theory of the zodiacal light and the gegenschein is developed. Neutral particles sprayed out in all directions from the earth's atmosphere are ionized at 50,000 to 70,000 km levels by the ultra-violet light of the sun. Because of the wobble of the earth's magnetic field with the rotation of the earth ions near the equatorial plane stay for some time at these high levels to form a ring around the earth, ions at high latitudes fall quickly back to the earth to give aurorae. The gravitational magnetic drift of the ions forces the ion ring into a long oval stretching out away from the sun to 10^6 km. The pressure of the sunlight warps the oval into the plane of the ecliptic and makes the ions stream out like a comet's tail. The ions are fluorescent; they absorb the sun's ultra-violet light and emit a part of the absorbed energy as visible light. The oval ring is the zodiacal light; the comet tail ion stream is the gegenschein. The zodiacal cones in December are somewhat to the south of the cones in June; the evening cone is south and north of the morning cone in March and September, respectively. These theoretical inferences are in qualitative accord with observation. The theory suggests that the spectrum of the zodiacal light and the gegenschein be different from that of sunlight.

Quantitative estimates lead to a low ion density in the zodiacal ring, less than 10^3 ions cm^{-3} and to a rate of escape of the terrestrial atmosphere of 10^6 particles $\text{cm}^{-2} \cdot \text{sec}^{-1}$ or 10^{-6} of the entire atmosphere in 10^6 years. These are perhaps under-estimates. The theory indicates that helium escapes more rapidly than the other gases because of its lightness and higher ionization potential. This may account for the small amount of helium in the atmosphere, which is regarded as being surprisingly low in the face of the estimated large rate of supply from the earth.

Variations in the zodiacal light, from the observations of Jones in 1853-1855 and of more recent observers, are shown to occur usually during magnetic storms. Similarly Barnard's observations of the variations in the gegenschein fall in with magnetic disturbances, although more data are needed to establish the connection clearly. The variations are in accord with the atmospheric theory.

INTRODUCTION

SHORTLY after sunset when the evening twilight has gone the zodiacal light appears as a faint cone of light in the west rising upward from the horizon, with a similar cone in the east before dawn.¹ At their apexes the cones narrow to a band which extends across the sky from one apex to the other. Thus the phenomenon is spoken of as a "band" of luminosity. The

* Published with the permission of the Navy Department.

¹ For general descriptions of the zodiacal light and the gegenschein see Newcomb, *Encyclopaedia Britannica*, 13th ed., Vol. 28, page 998; Schmid, "Das Zodiakallicht," Hamburg, 1928; Bayldon, *Pub. Ast. Soc. of the Pacific* 12, 13 (1900); and references cited throughout the present paper.

band lies closely, but not exactly, along the plane of the ecliptic. It is usually less bright than the milky way and may be seen on any clear night when there is no disturbing illumination such as the moon, planets, the milky way, artificial lights, etc. At an angle of 30° from the sun, the closest angle to the sun at which the light can be seen when observed in the eastern or western sky, the band is about 40° wide.² The width of course is rather indefinite for the band is brightest near its center and fades into obscurity at the edges. Newcomb³ and Barnard⁴ in north latitudes around 45° during the midnight hours of the summer solstice observed a glow passing from the west to the east along the north horizon. They concluded that this was the zodiacal band, for it could not have been ordinary twilight because the sun was more than 18° below the horizon, and that therefore the band was about 70° wide along the sun's axis. With increasing angular distance from the sun the band decreases in width and in brightness. At 90° from the sun it is about 20° wide and at 150° about 10° wide. At 180° , the point directly opposite the sun, there is a faint knot of luminosity, sometimes appearing as a swelling in the zodiacal band, called the "gegenschein"⁵. Attempts to measure the parallax of the zodiacal band have always led to values close to zero, but, what is very curious, often negative. The parallax of the gegenschein, as determined by simultaneous observations in the northern and southern hemispheres, was found⁶ to be zero within an error of 1° or 2° . Therefore the zodiacal light and the gegenschein have been considered to be far away, beyond the moon, or farther.

The zodiacal light is supposed to be sunlight scattered or reflected or emitted by particles in the plane of the ecliptic. Whether the particles come from the atmosphere or the earth or are planet dust widely scattered through the solar system is an unsettled question, although probably the planet dust theory is more generally held at the present time. Recently the physics of the outer fringe of the atmosphere⁷ of the earth was developed, primarily for the purpose of the theory of aurorae and magnetic storms. At the time it was realized that the ideas might be brought to bear on the zodiacal light. Just how this was to be done was not clear until it was noticed (Hulburt, Amer. Phys. Soc. Bul. Dec. 30, 1929) that the fluctuations in the zodiacal light occurred at the same time as the magnetic disturbances. This indicated at once that the planet dust theory was open to objection and pointed the way to the development of the atmospheric theory. It is the purpose of this paper to give the evidence for the connection between the zodiacal light changes and magnetic storms and to describe a theory of zodiacal light based on the action of molecules and ions in the outer fringe of the terrestrial atmosphere. The theory offers an explanation of many features of the zodi-

² Hall, Monthly Weather Review 34, 126 (1906).

³ Newcomb, Astrophys. Jr. 22, 209 (1905).

⁴ Barnard, Astrophys. Jr. 23, 168 (1905).

⁵ Barnard, Popular Astronomy 7, 169 (1899): 27, 109 (1919).

⁶ Scarle, Astrophys. Jr. 8, 244 (1898).

⁷ Maris and Hulburt, Phys. Rev. 33, 412 (1929).

acal light and the gegenschein which the planet dust theory is inadequate to explain.

In company with almost all who have written about the zodiacal light we shall use extensively the classical observations⁸ of Reverend George Jones USN, made for the most part in north latitudes 10° to 30° while on a voyage on the Pacific Ocean. From April, 2, 1853, to April 22, 1855, he observed the light every night, weather and other things permitting, and sketched on a chart of the heavens the zodiacal light as he saw it. The drawings, 341 in number, and their descriptions were published; they are by far the most complete and extensive series available. The observations are of gold, and whereas some writers, among them Jones himself, have wondered at apparent inconsistencies we have found that it is just these variances which fall in with the pattern of the theory, Jones wrote in his introduction, "I have put down all, exceptions and incongruities as well as others, not feeling authorized to omit any portion; for who can say, in a new science, that what seem to be exceptions are not a part of the general rule."

2. *Abnormalities in the zodiacal light and magnetic storms.* It was recognized long ago by Humboldt, Arago, Birt and others^{8,9} that the zodiacal light is at times variable in intensity the entire body of the light alternately weakening for a few minutes and strengthening again. That the zodiacal light is often unusually intense during epochs of strong aurorae has been known for a long time. For example, in 1881 Groneman⁹ referred to the fact as of common knowledge. Aurorae are known to occur in general during periods of magnetic disturbance, but no one has been interested in examining the exact relations with the zodiacal light. Turning to Jones' observations we find that occasionally he noticed and commented on fluctuations in the intensity of the zodiacal light; the entire body of the light grew brighter and dimmer in a period of two or three minutes. In a few cases he recorded an unusually wide spread of the zodiacal luminosity. One of his descriptions is as follows, "The changes were a swelling out, laterally and upwards, of the Zodiacal Light, with an increase of brightness in the Light itself; then, in a few minutes, a shrinking back of the boundaries, and a dimming of the Light; the latter to such a degree as to appear, at times, as if it was quite dying away; and so back and forth for about three quarters of an hour;" We have plotted these abnormalities on a qualitative scale in dots as ordinates against the dates as abscissas; a portion of the plot is given in Fig. 1. The magnetic storms observed at The Greenwich Observatory¹⁰ are plotted as short lines in the figure; 1, 2, and 3 mean a storm of moderate, strong and very strong intensity respectively. It is seen that the zodiacal light abnormalities occurred, usually during magnetic disturbances. To summarize the data: There were 27 magnetic storms, or groups of storms, in the period of Jones' observations, 17 of which were followed by cases of unusual zodiacal

⁸ Jones, United States Japan Expedition, Vol. III, Washington, 1856. "Observations on the Zodiacal Light."

⁹ Groneman, Archives Néerlandaises, Tome XVI.

¹⁰ Maunder, Monthly Notices, Roy. Ast. Soc. 65, 2 and 540 (1904-5).

light. There were 10 storms with no zodiacal light observations because of clouds, etc., and 10 instances when the zodiacal light might be regarded as abnormal with no accompanying magnetic storms.

A few more recent observations may be mentioned. Pachine¹¹ in Russia observed the zodiacal light to be remarkably brilliant and to exhibit fluctuations on January 28, 1911 at 6:30 p. m. The light appeared normal during the following days. The preceeding days were cloudy but the clouds were unusually illuminated and he concluded that the exceptional zodiacal brilliance began on the 25th. We do not know whether or not the illumination of the clouds might have been due to an aurora. A four-day magnetic storm of intensity 2 began at 4 hr, G. M. T., on January 24, 1911. Fluctuations in

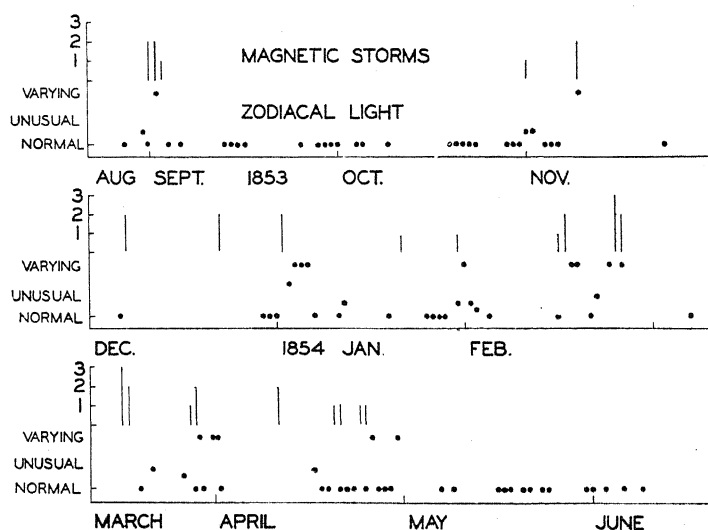


Fig. 1. The dots are the zodiacal light observations of Jones, the vertical lines are the magnetic storms.

the zodiacal light were observed by Hanahan¹² in South Carolina on February 4 and 13 and on March 5, 1913. The storms in this period were January 29 (1), February 13 (1), 24 (1), and March 13 (2). The fluctuations on February 13 fall in with a magnetic storm, the others do not. The zodiacal light was very brilliant on March 21, 1927, according to a photograph by Graff¹³. The period was one of magnetic activity, a seven-day magnetic storm lasting from March 13 to 20 of intensity 2 on March 16 and 1 on March 20. Fluctuations in the zodiacal light were seen simultaneously by two observers Kamei and Oraki¹⁴ at widely separated points in Japan on November 3, 1929, at about 3 A. M. local time. A magnetic disturbance set in on November 2 at 23 hr,

¹¹ Pachine, *Bul. Société Astronomique* 27, 68 (1913).

¹² See note by Glanville, *Pop. Ast.* 37, 493 (1929).

¹³ Graff, *Grundriss der Astrophysik*, page 481, Teubner, (1928.)

¹⁴ See note by Glanville, *Pop. Ast.* 38, 124 (1930).

G. M. T., rose to intensity 2 on November 3 and continued with decreasing violence through November 6.

Of course abnormalities in the zodiacal light may at times be due to local causes, such as variations in haze, etc., rather than to changes in the light itself, and in such cases there would be no connection between the zodiacal light behavior and magnetic disturbances. The foregoing facts, however, support the conclusion that the connection is genuine and this suggests that the zodiacal light is influenced by the same solar emission which gives rise to magnetic storms. All in all, the data indicated that the zodiacal manifestation occurred within less than two days after the storm began, sometimes it was observed a day or a few hours before the storm (see the theoretical discussion of section 13).

3. *The energy, polarization and spectrum of the zodiacal light.* The energy $\cdot \text{cm}^{-2} \cdot \text{sec}^{-1}$ received at the earth from all the stars, from the total night sky (the non-polar aurora) and from the total zodiacal region was found¹⁵ to be equal to that of 1440, 0.08 and 0.08 stars, respectively, of magnitude 1 on the Harvard visual scale. The energy of starlight at the earth is $3 \times 10^{-3} \text{ erg} \cdot \text{cm}^{-2} \cdot \text{sec}^{-1}$ and therefore that of the night sky and the zodiacal luminosity each amounts to $0.08 \times 3 \times 10^{-3} \div 1440 = 1.7 \times 10^{-7} \text{ erg} \cdot \text{cm}^{-2} \cdot \text{Sec}^{-1}$. Assuming the zodiacal region to occupy 10^{-1} of the area of the sky, the energy emitted per $\text{cm}^{-2} \cdot \text{sec}^{-1}$ from the zodiacal region on the average is of the order of $10^{-6} \text{ erg} \cdot \text{cm}^{-2} \cdot \text{sec}^{-1}$. This means that the zodiacal region is ordinarily about 10 times as bright as the sky would be if there were no stars.

The zodiacal light was observed to be partially polarized,¹⁶ about 15 per cent. Early observers¹⁷ found that the spectrum of the zodiacal light was similar to that of sunlight, as well as could be judged from visual observations. More recently Fath¹⁸ photographed the spectrum with a 12 hour exposure, from 3 to 4 A. M. for 12 days. The spectrum from $\lambda 5000$ to 3900\AA was 2.2 mm long. Two absorption lines could be seen on the plate. Fath wrote, "A comparison of this plate with one of the sky spectrum taken with the same slit-width shows these lines to be *G* and the blend of *H* and *K* of the solar spectrum. These are the only two lines shown on the sky comparison plate within the limits of the spectrum obtained on the zodiacal light plate. There is no indication of bright lines on any of the spectrograms of the zodiacal light. Thus insofar as spectra of such low dispersion and resolving power can be trusted, we would seem to have good evidence to support the claim that the zodiacal light is reflected sunlight."

4. *The planet dust theory of the zodiacal light.* This theory assumed that there are dust particles in a flat lens shaped region with the sun at the center spreading out in the plane of the ecliptic well beyond the orbit of the earth. The particles were not molecules of a gas, for due to diffusion and light pressure molecules would not stay near the plane of the ecliptic. The particles

¹⁵ Van Rhyn, *Astrophys. Jr.* 50, 356 (1919).

¹⁶ Wright, *Amer. Jr. of Sci. and Arts* 7, 451 (1874).

¹⁷ Smyth, *Trans. Roy. Soc. Edinburgh* 20, 489 (1852).

¹⁸ Fath, *Lick Obs. Bul.* 5, 141 (1909).

were considered to be small solid bodies each moving in its independent orbit around the sun. It was suggested that they were small meteoroids of the solar system, possibly remnants of the spray and dust from the large splash which inaugurated our planet system.¹⁹ The particles were assumed to reflect the sunlight, particles 1 mm in diameter and 5 miles apart of albedo 0.07, the albedo of the moon, being sufficient to account for the observed zodiacal luminosity.²⁰ Light reflected from minerals such as granite, clay, etc., was found to be partially polarized.¹⁶

Since the zodiacal light undergoes fluctuations in intensity it follows that all of the light can not be reflected sunlight. For the sunlight, at least in that portion of the spectrum accessible to us, does not fluctuate very much, the short period (a few hours or a day) variations²¹ of the solar constant being usually less than 10 per cent, whereas the variations in the zodiacal light intensity, although not measured, would perhaps be of the order of hundreds of percent. Therefore the planet dust theory, if it be retained at all, requires some fundamental modification not heretofore contemplated.

5. *The atmospheric theory of the zodiacal light.* As described in the following pages the atmospheric theory assumes that fast flying atoms or molecules are sprayed out in all directions from the sunlit hemisphere of the earth which, after a number of hours, are ionized by the ultra-violet light of the sun. Under the action of solar radiation pressure and the earth's magnetic and gravitational fields ions at levels beyond 30,000 km form a sort of oblong ring around the earth approximately in the plane of the ecliptic. The ions absorb sunlight in the far ultra-violet region of the spectrum and re-emit a portion of the absorbed energy as visible light. This is the zodiacal light. This view encounters two difficulties at the outset, namely, the light might be expected to be unpolarized and the spectrum should be different from that of sunlight. The first difficulty may be got round for the present by suggesting that the fluorescence radiation might be polarized to some extent and by expressing the wish that the polarization observations be repeated. The difficulty with the spectrum is more serious, so serious in fact that if future observations show that the zodiacal spectrum is that of sunlight the atmospheric theory in the form given here will fall to the ground. We may remark that the solar corona and certain comet tails exhibited a spectrum more of less continuous which, in part at least, was not that of sunlight.²²

6. *The ion spray to distances of 70,000 km.* In the earlier paper, reference 7, paragraph 3, it was shown that beyond 450 km above sea-level there were about 10^{-16} molecules and atoms in a 1cm^2 column of the atmosphere. These dance up and down, being knocked upward by thermal impacts from below and falling back under gravity, with practically no collisions except at the 450 km level where they experience 10^{14} collisions per sec. The thermal ve-

¹⁹ Jeans, "Astronomy and Cosmogony," page 400, (1928).

²⁰ Russell, Dugan and Stewart, "Astronomy," Vol. 1, page 359 (1926).

²¹ Annals of the Astrophys. Obs. of the Smithsonian Institution, IV, pages 17 and 207 (1922).

²² Reference 20, pages 439 and 507; Slipher, Lowell Obs. Bul. 52; etc.

locities are hardly greater than 2 km sec^{-1} and the levels reached by the particles are on the average not above 2000 km. It was assumed that 2×10^6 of the collisions were of the second kind, *i. e.* collisions with excited atoms or molecules, which gave the particles velocities as great as $10 \text{ km} \cdot \text{sec}^{-1}$ (See reference 7 for a more detailed discussion.) In the present case the assumption is extended to include 2×10^7 collisions which result in velocities as high as 12 or 13 $\text{km} \cdot \text{sec}^{-1}$. Thus $10^7 \text{ cm}^{-2} \cdot \text{sec}^{-1}$ fast moving atoms or molecules move out from the earth. They are ionized by the ultra-violet light of the sun in a time t given by the relation $t = a/I_0 (1 - e^{-\beta})$, (reference 7, equation (1)) where a is the ionization potential of the atom or molecule, I_0 is the energy of the sun in the ionizing wave-lengths and β is the atomic absorption coefficient. β is defined in the usual way by

$$I = I_0 e^{-\beta y x}, \quad (1)$$

where I is the intensity of the light after passing through x cms of atoms or molecules of density y . It is assumed that the sun is quiet, *i. e.* no aurorae or

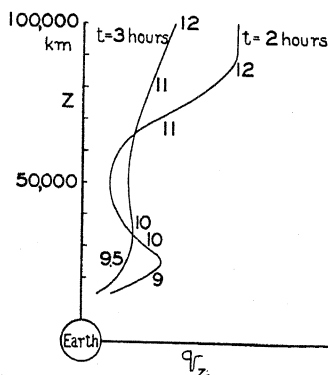


Fig. 2. The rate of supply q_z of ions as a function of the distance from the earth.

magnetic storms, and that its spectrum is that of a black body at 6000°K . The energy in the region from 725 to 750A of the solar spectrum falling $\text{cm}^{-2} \cdot \text{sec}^{-1}$ on the earth is 10^{-4} erg. With this value for I_0 , with $\beta = 3 \times 10^{-11}$ and with $a = 3.1 \times 10^{-11}$ ergs, corresponding to 20 volts, t is 3 hours.

Assuming always 3 hours for the time of ionization, the heights z where the neutral atoms were ionized were calculated for various values of v the velocity of projection from the 300 km level of the earth's atmosphere. For example, an atom with $v = 9.7 \text{ km} \cdot \text{sec}^{-1}$ reaches $z = 31,800 \text{ km}$ in 2.6 hours and falls back to 31,400 km in 0.4 hours where it is ionized; with $v = 10, 10.3$ and $11 \text{ km} \cdot \text{sec}^{-1}$ the atoms are ionized at $z = 39,800, 48,000$ and $70,000 \text{ km}$ respectively. The v, z curves were plotted for $t = 3$ hours and $t = 2$ hours. Assuming that the velocities are equally distributed among the high flying atoms, in which case the number of atoms with a specified energy is proportional to the square root of the energy, the rate of production q_z of ions cm^{-3} was determined from the slopes of the v, z curves. The q_z, z curves are given

in Fig. 2 for $t = 2$ and 3 hours, q_z being in arbitrary units; the numbers written along each curve are the values of v of the atom which became ionized at the ordinate z . It is seen that q_z is greater at heights above 50,000 km than at lower heights. Since v can not go on increasing indefinitely q_z must grow less somewhere and we may assume that q_z reaches a maximum between 50,000 and 80,000 km and falls to low values at greater distances. The foregoing calculations can only be regarded as illustrative, but they serve to show that hypotheses, perhaps not unreasonable ones, of the sort which have been made lead to a rate of ion production which does not fall off rapidly with increasing z and which may even increase with z for a time.

In order to determine the distribution of the high flying ions around the earth it is assumed that the number of fast moving atoms or molecules emitted from each cm^2 of the surface of the high atmosphere in a direction ϕ is proportional to $\cos \phi \cos i$, where ϕ is the angle with the normal to the surface

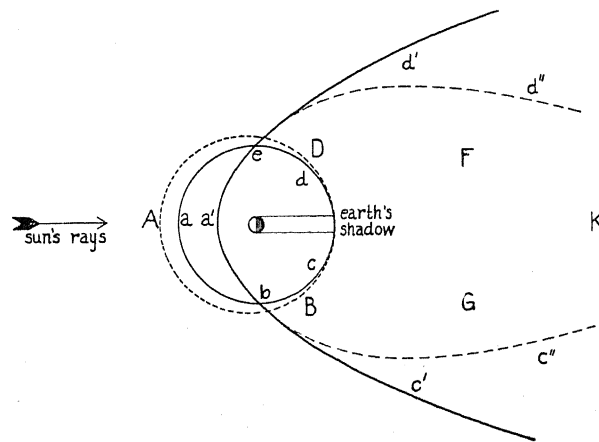


Fig. 3. Cross section of the zodiacal ion ring in the plane of the earth's equator.

and i is the angle of incidence of the sunlight on the surface. Let q_θ be the total number of fast moving particles emitted from the day hemisphere in a direction at an angle θ with the sun's rays. The relation between q_θ and θ is thus the same as that which expresses the distribution of light reflected from a perfectly diffusing hemisphere or the variation of the intensity of moonlight with the phase of the moon. The relation is

$$q_\theta = q_0(1 + \cos \theta)/2, \quad (2)$$

where q_0 is the value of q_θ for $\theta = 0$. The q_θ, θ curve is a cardioid. In Fig. 3, $abcde$ is a circle around the earth in the plane of the equator with a radius of 50,000 km. From this circle as a base q_θ , calculated from (2), is measured outward and forms the curve ABD . This curve represents the rate of supply of high flying atoms and molecules, and hence of ions, at the high levels in the plane of the equator. Rotating the curve about AK as an axis forms a figure which represents the rate of supply of the high flying ions around the

earth. Although (2) is an approximation, it is exact enough for our purposes. It assumes that the radius of the earth is small compared to 50,000 km, thereby neglecting the earth's shadow and giving values of q_0 greater than zero in the shadow, except for $\theta = 180^\circ$. No ions can be formed in the shadow but ions can get there because some fast flying atoms shoot over the poles of the earth, become ionized and follow along a magnetic line into the shadow.

7. *The ion ring around the earth.* It is assumed that the earth is electrically neutral at all points. Therefore any electric fields which exist are generated by the ions themselves and the motions of the ions at distances beyond several radii of the earth are approximately independent of the rotation of the earth on its axis²³, i.e. are the same whether the earth rotates or not. The centrifugal force due to the motion of the earth in its orbit around the sun is small and is neglected. When the neutral particles are ionized the ions and electrons thus formed are guided by the earth's magnetic field. They fall

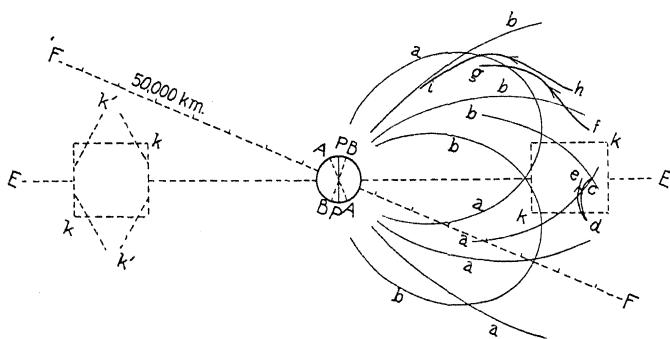


Fig. 4. A section in the plane through the center of the earth normal to the sun's rays; kk or $k'k'$ is the zodiacal ion ring.

toward the earth along the magnetic lines of force under gravity and they drift across the magnetic field because of gravity, the positive ions going east and the negative electrons west. Dealing first with their fall we take into account the wobble of the magnetic field with the rotation of the earth. The magnetic axis makes an angle of about 20° with the geographic axis; the fact that the magnetic pole does not pass exactly through the center of the earth is of no consequence in the present discussion. In Fig. 4 PP is the geographic axis, AA is the magnetic axis with its magnetic lines given by curves a and BB is the magnetic axis 12 hours later with its magnetic lines b . The figure is in the plane through the center of the earth normal to the sun's rays. EE marks the plane of the earth's equator, and FF and EE mark the plane of the ecliptic at equinox and solstice, respectively; the angle between EE and FF is 23° . At equinox PP is in the plane of the drawing of Fig. 4, at solstice PP is tilted 23° out from the plane of the drawing.

An ion at c , Fig. 4, with an initial zero velocity component along the magnetic field H , falls under gravity along a number of slightly different curved

²³ Page, Phys. Rev. 33, 823 (1929).

paths depending on the time of day at which it starts to fall. One of the curved paths is given by cde , Fig. 4; the ion reaches e after about a day, and takes roughly a week to fall 20,000 km. Although the general path is cde , the actual path may be a spiral with a radius ρ which depends upon v , the velocity component across H , according to

$$\rho = mv/He. \quad (3)$$

m and e are the mass and charge of the ion, respectively; electromagnetic units are used throughout the paper. At 50,000 km with $v = 10 \text{ km} \cdot \text{sec}^{-1}$ ρ is 50 km for a nitrogen atomic ion, and is less for lighter ions as helium. Therefore ρ is small compared to the distances under consideration and in general the ions move along their paths in relatively tight spirals. An ion at f , Fig. 4, falls along the path fg reaching g in 1 day; an ion at h falls along hi and reaches the earth in less than a day. Thus the speed with which ions leave any level is a minimum on the earth's equator EE and increases rapidly on either side of EE . Since the rate of supply of ions at any level in the plane of Fig. 4 is constant the ion density y at a given level is a maximum at EE and falls off on either side by perhaps an order of magnitude or more at 20° from EE . Further, ions formed at the, say, 30,000 km level will remain there a shorter time than those formed at the 60,000 km level because of the greater gravitational attraction of the earth at the lower levels. This combined with the rate of supply curves of Fig. 2 indicates that the ion density y in the levels below 50,000 km down to perhaps 20,000 km may be much less than from 50,000 to 70,000 km.

Therefore the ions congregate into a ring around the earth lying roughly in the plane of the equator on the daylight side of the earth; on the night side, as is shown in sections 9 and 10, the ring is warped off the equatorial plane approximately into the plane of the ecliptic and is stretched out into a long oval by light pressure and by magnetic gravitational actions. Illustrative equivalent cross-sections of the ring at $\theta = 90^\circ$ are shown by kk , Fig. 4. These are sketched 20° wide and 20,000 km deep, the actual cross-section is perhaps more like $k'k'$, Fig. 4; at $\theta = 0^\circ$ the width is about 70° (section 9).

The total number of ions y_1 in any cross-section of the ring 1 cm thick is equal to $q\theta t$, where t is the time the ions remain there. Since t is a constant with respect to θ we have from (2)

$$y_1 = y_0(1 + \cos \theta)/2, \quad (4)$$

where y_0 is the value of y_1 at $\theta = 0$. An outflow of 10^7 high flying atoms $\text{cm}^{-2} \cdot \text{sec}^{-1}$ from the earth means a supply of 10^5 ions and electrons $\cdot \text{cm}^{-2} \cdot \text{sec}^{-1}$ into the portion of the ring nearest the sun, i.e. $q_0 = 10^5$. If t is ten days or 10^6 sec. there are 10^{11} ions in an average 1 cm^2 column out through the ring. With an equivalent cross section 20,000 km wide and 20,000 km deep the average ion and electron density y is 50, and y_0 is 2×10^{20} . At $\theta = 90^\circ$ $y = 25$ and $y_1 = 10^{20}$. With such low densities there are practically no collisions, for the free path of an ion is 10^{14} cm. The ion densities are so low that it seems doubtful that the presence of the ions and electrons could be detected by experiments

with wireless waves. It also seems doubtful that the diamagnetism²⁴ of the ions has any great effect upon the earth's magnetic field in the zodiacal region, although the field may be distorted to some extent.

It is assumed that ions absorb the solar ultra-violet radiation from $\lambda 900$ to 1000\AA , or an equivalent amount. The energy received at the earth in this spectrum region is $1 \text{ erg} \cdot \text{cm}^{-2} \cdot \text{sec}^{-1}$, as calculated for a quiet sun at 6000 K . Assuming the atomic absorption coefficient β for the radiation to be 10^{-12} , the energy absorbed by the 10^{11} ions is $10^{-1} \text{ erg} \cdot \text{sec}^{-1}$. If 10^{-5} of the absorbed energy is emitted as visible light the ion ring emits $10^{-6} \text{ erg} \cdot \text{cm}^{-2} \cdot \text{sec}^{-1}$, which is the observed value of the zodiacal luminosity (section 3).

8. *Radiation pressure.* The numerical assumptions of section 7 lead at once to a value for the radiation pressure on the zodiacal ions. The force of the radiation on y ions of mass m is $my\dot{p}$, where \dot{p} is the acceleration. If the energy flux of the radiation is I_0 the energy absorbed by the y ions is $I_0\beta y$ and the energy density of the absorbed radiation is $I_0\beta y/c$, where c is the velocity of light. Then $my\dot{p} = I_0\beta y/c$, or

$$\dot{p} = I_0\beta/mc. \quad (5)$$

With $I_0 = 1 \text{ erg} \cdot \text{cm}^{-2} \cdot \text{sec}^{-1}$, $\beta = 10^{-12}$ and $m = 2.3 \times 10^{-23}$ grams, as for a nitrogen atomic ion, \dot{p} is $1.5 \text{ cm} \cdot \text{sec}^{-2}$. For helium and hydrogen atomic ions \dot{p} is 5.2 and $20.8 \text{ cm} \cdot \text{sec}^{-2}$, respectively. The solar gravitational acceleration g_s is $0.6 \text{ cm} \cdot \text{sec}^{-2}$ at the earth. Therefore \dot{p} is greater than g_s by perhaps an order of magnitude. This is keeping with the observed streaming away in the direction of the sun's rays of the particles in comets' tails. The motion indicated that in some cases the radiation repulsion was 12 times the solar gravitational attraction.²⁵

In this paper we do not encounter any ionic velocities so great that the absorption coefficients and radiation pressure are influenced by Doppler effects, as Milne²⁶ found in dealing with stellar atmospheres. We may state without giving the calculations that light pressure and scattering effects calculated from the Rayleigh scattering formula are entirely negligible compared to the absorption and fluorescence processes which we have assumed.

Atomic absorption coefficients of order 10^{-11} or 10^{-12} as assumed in sections 6 and 7 may be too high, although one can not be very sure about it. Various theories²⁷ indicate values of β of order 10^{-15} to 10^{-17} near the heads of the principal series of hydrogenic atoms. Observations²⁸ on the lines and continuous spectrum near the heads of the principal series of the alkali metals give β of the order of 10^{-19} . In the ozone molecular band²⁹ β is 10^{-17} at about 2500\AA , and in the oxygen molecular band β is greater than 10^{-17} at 1500\AA ,

²⁴ Gunn, Phys. Rev. 33, 614 (1929), equation (12).

²⁵ Chambers, "The Story of the Comets," page 37, 1910.

²⁶ Milne, Monthly Notices, Roy. Ast. Soc. 86, 459 (1925-26).

²⁷ Kramers, Phil. Mag. 46, 836 (1923); Eddington, "The Internal Constitution of the Stars," equation 166.8; Pannekoek, K. Akad. Amsterdam, Proc. 29, 1165 (1926); etc.

²⁸ Mohler, Phys. Rev. Sup. 1, 216 (1929), and references therein.

²⁹ Fabry, Proc. Phys. Soc. London 39, 1 (1926).

as judged from Lyman's³⁰ spectrograms of the oxygen band. One can not be very certain that these values of β give a correct idea of the order of magnitude of β in the far ultra-violet for the atmospheric atoms, which are probably helium, nitrogen and oxygen. However, in the present case we are not restricted to a definite assumption about β ; we require that the product βI_0 have certain specified values. If β should be less than 10^{-12} we can increase the assumed value of I_0 , which is of course permissible within limits.

9. *The ion ring on the side of the earth near the sun is compressed toward the earth and on the side away from the sun is stretched out to a great distance.* It has been shown⁷ that long free path ions, no matter what their velocities are, under the combined action of gravity and the earth's magnetic field move at right angles to these two vectors with a velocity w given approximately by

$$w = mg \sin \phi / He, \quad (6)$$

the positive ions going eastward and the negative ions and electrons westward. ϕ is the angle between g and H ; w is a maximum at the equator and decreases rapidly at high latitudes. The drift of the ions and electrons constitutes an electric current flowing eastward around the earth if the circuit is complete. If the circuit is not complete electric fields are built up which react on the motion of the ions. At the surface of the earth $w = 4.6 \text{ cm} \cdot \text{sec}^{-1}$ for a singly charged nitrogen atomic ion at the equator, and is $1/26,000$ of this or practically zero, for the electron. The eastward current i , due to the drift velocity w , is $i = y_1 ew$ where y_1 is the total number of ions in a cross-section of the ring 1 cm thick in a plane passing through the earth's axis. Since g and H are proportional to z^{-2} and z^{-3} , respectively, z being the distance to the center of the earth, $w = 4.6z/z_0$, where $z_0 = 6400 \text{ km}$ is the radius of the earth, and $i = 4.6ey_1/z_0$. With $e = 1.59 \times 10^{-20}$

$$i = 1.14 \times 10^{-28} z y_1. \quad (7)$$

We note in passing that this current causes a negligibly small magnetic field at the earth. With $y_1 = 2 \times 10^{20}$ and $z = 50,000 \text{ km}$, i from (7) is 10^3 amperes. The current causes a magnetic field at the earth less than 10^{-5} gauss, which is probably inappreciable.

In order that the zodiacal ion ring be in a steady state the drift current i must be a constant through all cross-sections of the ring. Therefore from (7) zy_1 should be a constant. The values of y_1 are given by (4) and hence

$$z = A/(1 + \cos \theta), \quad (8)$$

where A is a constant. The z, θ curve from (8) is the curve for the steady state and is shown by $c'ba'ed'$, Fig. 3. The branches bc' and ed' meet at infinity. This is wrong; actually they join at a finite distance. The error arises from the fact that (8) is derived through (4) from (2) which gives no ions at $\theta = 180^\circ$. As explained in section 6 there are ions at all values of θ , and hence z in (8) is always finite. Therefore, the branches of the steady state

³⁰ Lyman, *Astrophys. Jr.* 27, 87 (1908).

curve will be something like bc'' and ed'' . The curve is quite different from the circular ring $abcde$ in which the ions are produced. Therefore the ions immediately and continually flow from the circle to distribute themselves in the curve $c''ba'ed''$ although because of radiation pressure they probably never attain this distribution. The process is similar to that worked out³¹ for the ions in the lower atmospheric levels from 100 to 200 km and is as follows:

Suppose that the ring were circular as $abcde$, Fig. 3, and that y_1 were given by (4). i would not be constant around the ring. Due to the drift w positive ions accumulate on the side b of the ring leaving a negative accumulation on side e . This gives rise to an electric field E' from the b to the e side of the ring. E' is in such a direction that, combined with H , it causes the charged particles of both signs to move at right angles to E' and H with a velocity $v' = E'\sin\phi/H$, where ϕ is the angle between E' and H . The movement together with the wobble of the earth's magnetic field (section 7) causes ions in or near the equatorial plane to move away from the sun roughly parallel to the equatorial plane. Thus ions and electrons formed in the region bae , Fig. 3, flow toward $ba'e$. If the ring has an angular width of 20° at $\theta = 90^\circ$ then at a' , i.e. at $\theta = 0$, because of its greater proximity to the earth and its greater supply and less loss of ions than $\theta = 90^\circ$, the ring may have an angular width of as much as 70° , in agreement with the observations of Barnard³ and Newcomb.⁴ Likewise ions and electrons formed at $bcd e$, Fig. 3, stream toward $c''GFd''$ maintaining their concentration in the equatorial plane, the motion being modified by radiation pressure after they get beyond 100,000 km (section 10). The flow or streaming of the ions away from the sun is a maximum at the equator and falls off rapidly at the higher latitudes. Therefore the details of the ion movements brought out here do not disturb the aurora theory⁷ but offer helpful additions to the theory which will be considered in a future paper.

To work out E' and v' exactly throughout the region $BGFD$, Fig. 3, is intricate. Approximate calculations show that the ions and electrons stream away from $BcdD$ about as rapidly as they are produced and that v' becomes less as z increases; beyond $z = 100,000$ km v' is negligible compared with the effects of radiation pressure. An average v' of order 1 km sec^{-1} from $z = 50,000$ km to $100,000$ km is indicated.

10. *Radiation pressure causes the zodiacal ions and electrons to stream away in or near to the plane of the ecliptic.* The accelerations due to the pressure of solar radiation at the earth were estimated in section 9 to be 1.5, 5.2 and $20.8 \text{ cm} \cdot \text{sec}^{-2}$, respectively, for a nitrogen, helium and hydrogen atomic ion; these are also the values of the earth's gravitational accelerations at about 210,000, 96,000 and 45,000 km, respectively. The solar gravitational attraction is just cancelled, or nearly so, by the centrifugal force due to the velocity of the earth in its orbit around the sun and may be neglected. Thus ions and electrons which are formed in the region $bcd e$, Fig. 3, and which move out in

³¹ Hulburt, Phys. Rev. 34, 1167 (1929).

the equatorial plane with velocity v' find themselves subjected to a radiation pressure parallel to the ecliptic plane which beyond, say, $z=100,000$ km is equal to or greater than the earth's gravitational attraction.

In order to find out what happens to these particles we must examine the motion of a neutral ion cloud of finite size in a magnetic field H acted on by a constant force F , F being normal to H . Take H along the X -axis and F along the Y -axis. Then the ions drift along the Z -axis with a velocity F/He , the positive and negative ions going in opposite directions. As a result of the drift a separation of charge occurs which causes an electric field E along Z in such a direction that, combined with H , it causes the ions of both signs to move in the direction of F with a velocity v . The energy acquired from F goes into the kinetic energy η of the ions and the energy ξ of the electric field. At all times $v=E/H$. $\eta=mv^2y/2$ and $\xi=E^2/8\pi c^2$. Therefore $\xi/\eta=2H^2/8\pi c^2my=2.85H^2/y$. With H two or three orders of magnitude less than y , as in the present problem, ξ/η is less than 10^{-4} . Thus the energy taken by the field E is small compared to that of the moving ions. Therefore the ion cloud moves across the magnetic field under the action of the force approximately as it would if there were no magnetic field. This of course can not keep up indefinitely. For, as they recede from the earth the ions reach a region where the magnetic field is so small that the simple formulas used in the foregoing sentences become invalid. Actually the ion progresses along a cycloidal path and $v=E/H$ is approximately the average velocity of progression. The approximation breaks down when the radii ρ , equation 3, of the loops of the cycloid become comparable with the size of the ion cloud. This occurs at about $z=500,000$ km for a radiation pressure acceleration $p=5 \text{ cm}\cdot\text{sec}^{-2}$ and an ion cloud 50,000 km across. At this distance the ions commence to progress away from the sun more slowly than they would if their acceleration were constantly $5 \text{ cm}\cdot\text{sec}^{-2}$, their motion being in large cycloidal loops. At greater distances, beyond 10^6 km, the earth's magnetic field becomes inappreciable, the ion paths straighten out and the ions move away under light pressure.

We now make use of what has been said about the motion of the zodiacal ions and electrons and give some numerical calculations. Ions formed on the day side of the earth for the most part do not drift to the night side. For an ion at a or a' , Fig. 3, hardly stays there more than 10^6 sec (section 7) before falling back to the earth; its drift velocity w is of the order $10^2 \text{ cm}\cdot\text{sec}^{-1}$, and in 10^6 sec it drifts eastward only 1000 km, which does not take it very far around the ion ring. Therefore the ions on the night side of the earth practically all come from those formed in the region bcd , Fig. 3. Consider ions and electrons at b , Fig. 3, at winter solstice; these are at the intersection of the planes of the equator and the ecliptic. Due to the combined effects of a light pressure acceleration $p=5 \text{ cm}\cdot\text{sec}^{-2}$ in the ecliptic plane and an average velocity $v=1 \text{ cm}\cdot\text{sec}^{-1}$ in the equatorial plane out to $z=100,000$ km, and zero beyond this (v' being due to E' which arises from the gravitational magnetic drift w , section 9) the ions move in 3×10^4 sec or 8.3 hr away from the sun to a position about 49,500 km from and 12,000 km south of the ecliptic. After

this v' becomes negligible and the accelerations which act on the ions are p and g , g being the acceleration of the earth's gravitational attraction. In the next 4×10^4 sec or 11.2 hr the ions move away from the sun to z about 400,000 km, at this distance having a velocity around 3 or 4 km·sec⁻¹. The component of the vector $p+g$ toward the line AK , Fig. 3, is about 0.5 cm·sec⁻², and thus the ions progress about 4000 km toward AK . The ions then continue to progress away from the sun with a lessened acceleration until z is perhaps 10^6 km, at the same time they bear in slightly closer to AK . After this the effect of the earth's magnetic field becomes inappreciable and the ions stream away with the full light pressure acceleration p . The earth's shadow has practically no effect on the motion, the ions in the shadow moving along with those in full sunlight. This is because the ions in the shadow are few compared with those in the sunlight, since the cross-section of the shadow is small compared with that of the ion cloud, and because the ions in the

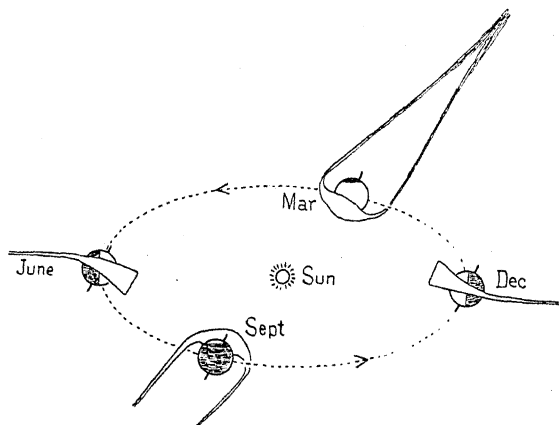


Fig. 5. The zodiacal ion ring at various seasons of the year.

sunlight move by setting up the electric field E , which acts equally on the sunlit and the dark ions.

11. *Comparison of the atmospheric theory of the zodiacal light with observation.* The results of the theory of the zodiacal ions worked out in sections 5 to 10 are represented in Fig. 5. The figure is not drawn to scale. On the daylight side of the earth the zodiacal ion ring is wide and follows the plane of the earth's equator. On the night side the ring is narrow, is warped off the equatorial plane roughly on to the ecliptic plane and trails off to a great distance. Referring to the portions of the zodiacal band at roughly $\theta = 90^\circ$ to 130° from the sun it is seen from Fig. 5 that both the morning and evening zodiacal cones should appear somewhat to the south of the ecliptic near winter solstice and to the north of the ecliptic near summer solstice. Around spring equinox the evening cone should be to the south and the morning cone to the north of the ecliptic, with a reversed position of the cones at autumn equinox. Fig. 6 gives a plot obtained from Jones' observations.⁸ The ordinates are the positions in degrees to the north or south of the ecliptic of

the center of the zodiacal cone for $\theta = 90^\circ$ to 130° at solstice and 70° to 130° at equinox, approximately; the dots and crosses refer to the evening and morning cones, respectively. The course of the dots and crosses is in accord with the theoretical deductions. The dots and crosses are together at the solstices, those at winter solstice being below those at summer solstice; the crosses are above the dots at spring equinox and below the dots at winter equinox. The observations of Cassini⁸ made in 1685 to 1687 are plotted in Fig. 6, the circles being the evening observations and the triangles the morning observations. They agree well with those of Jones, as Jones himself remarked. The magnetic storms, shown by the vertical lines in Fig. 6, are discussed in section 13.

Although the march of the crosses and dots of Fig. 6 is in qualitative agreement with the present theory, there is a quantitative discrepancy. At equinox the morning and evening cones are separated in latitude by

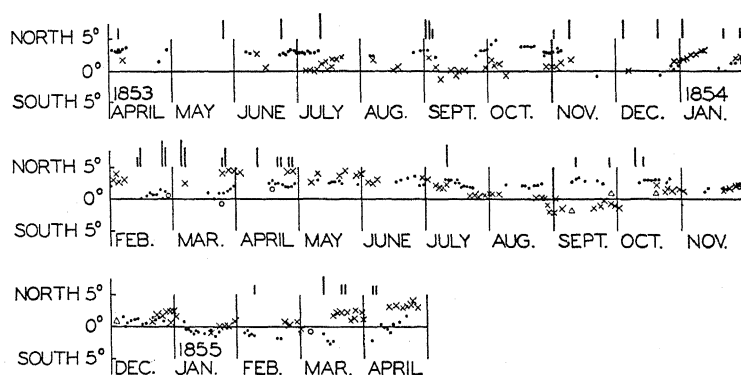


Fig. 6. Positions in degrees to the north or south of the ecliptic of the evening and morning zodiacal cones, shown by dots and crosses, respectively, from the observations of Jones. The observations of Cassini are shown by circles, evening, and triangles, morning.

about 5° , whereas if the cones lie partly along the earth's equatorial plane the separation should perhaps be greater than 5° , but not more than 46° . Whether the discrepancy is serious or whether it will disappear upon further attention to theory or observation can not be said at the present time. On the other hand the north and south shift of the cones of about 5° from winter to summer solstice agrees with the theory. If one plots from Jones' drawings the positions of the apexes of the zodiacal cones to the north or south of the ecliptic the points show the same general trend as those of Fig. 6, but much less pronounced and with many irregularities due no doubt to observational errors. The average deviation of the apexes from the ecliptic is less than 2° . This would be expected on the present view for the apexes of the cones are light from zodiacal ions which are probably more than 100,000 km away.

The dots and crosses of Fig. 6 are on the average about 2° to the north of the ecliptic, whereas one would expect the average over a year to be on the ecliptic. In explanation we follow a suggestion of others⁹ and make use of

the fact that the atmospheric transmission due to haze, etc., decreases toward the horizon. Thus if the ecliptic and the zodiacal cones had a slant, say, to the south of the vertical with the horizon, an observer would place the zodiacal cones too far to the north. Any traces of twilight would accentuate the error, although Jones avoided errors from twilight by making most of his observations after the sun was 18° below the horizon. The correction due to the slant of the cones shifts the points of Fig. 6 generally southward and therefore is qualitatively in the right direction to bring their average close to the ecliptic, without however disturbing the equinox and solstice relations brought out in the last paragraph. In more detail, from April to December, 1854, the zodiacal cones slanted in general to the south; the points of Fig. 6 in this period should therefore all be shifted a degree or so southward. In January, 1855, the ecliptic was nearly vertical and the points need no correction. In February the correction is northward on both dots and crosses, in March is zero for the crosses and slightly northward for the dots, and in the latter part of April is southward again for all the points. Thus we find a simple explanation of the curious fact^{1,2,9} that in general observers in northern and southern latitudes have recorded the zodiacal cones to the north and the south of the ecliptic, respectively. From the foregoing analysis of Jones' observations it seems that it is not the latitude of the observer but the slant of the cones with the horizon that is important.

From Fig. 5 one can see how Jones and other observers sometimes got an apparent negative parallax of the zodiacal cones. At equinox the observer found himself south of the ecliptic in, say, the evening. He recorded the position of the evening cone against the stars. By the rotation of the earth on its axis he was carried to the north of the ecliptic in the morning and recorded the position of the morning cone. Upon comparing the two results he found to his surprise that the zodiacal cone had apparently moved with him from the south to the north of the ecliptic. Thus the parallax came out zero or negative, which is to be expected on the present view because the evening and morning cones are two different portions of a warped zodiacal band.

From the observations of Serpieri, Heis, Weber and others (see reference 9) as well as from those of Jones it seems to be an accepted fact that the zodiacal cones are longer at solstice than at equinox. The present theory does not provide an explanation of this. Qualitatively, at any rate, it does not point with any clearness to marked seasonal variations in the shape of the cones. The theoretical calculations of the motions of the zodiacal ions have been pretty rough and it is possible that many details, and perhaps important ones, have escaped us.

12. *Moon zodiacal light.* Here we have to deal with conclusions so incomprehensible on any theory that we think they are in error. Nor are we the first to think this, for Newcomb¹ commented on Bayldon's¹ observations as follows, "He (Bayldon) also describes the moon as adding to the zodiacal light in her first and last quarters, a result so difficult to explain that it needs confirmation." To give a typical experiment; the observer an hour or two after sunset could see as usual the western zodiacal cone but ordinarily he

could not see the zodiacal band extending across the sky down to the eastern horizon. The moon was about to rise in the east and he thought that he could see the zodiacal band near the eastern horizon. He concluded that this was due to an illumination of the zodiacal particles by the moonlight. However, the intensity of moonlight at the earth is 10^{-6} of that of sunlight and the conclusion would be that the brilliance of the zodiacal cone or band which is barely discernable when illuminated by sunlight is perceptibly increased by light 1,000,000 times weaker. The moon zodiacal light observations were made when the moon was less than 10° , and usually less than 5° , below the horizon. Therefore moon twilight would certainly have interfered with the observations and perhaps moon twilight was all that the observer saw. Jones recorded 13 moon zodiacal light observations and by chance 8 of these were during magnetic storms when the zodiacal light might have been unusually brilliant, because of the solar activity and not because of the moon.

On the present theory the moon, being about 380,000 km from the earth, moves through the zodiacal ions in the region *K*, Fig. 3. At 10,000 km from the center of the moon the acceleration of the moon's gravitation is 5 cm sec^{-2} , which is comparable with the light pressure acceleration. Therefore the moon might sweep a hole through the zodiacal ions probably less than 20,000 km in diameter. The magnetic moment of the moon may be estimated³² to be considerably less than 10^{-2} of that of the earth and the effect of the moon's magnetic field on the ions is probably inappreciable beyond 1000 km from the moon compared to that of light pressure. The hole in the zodiacal ions caused by the moon would be difficult to observe, being wrongly oriented to the terrestrial observer, and being healed quickly by the ion flow would not be expected to give rise to zodiacal or gegenschein variations which could be detected.

13. *Zodiacal light variations and solar outbursts.* The effects of sunlight in producing the zodiacal ions and in stimulating them to emit light, which have been described for a quiet sun, are accentuated during solar outbursts. According to the ultra-violet light theory⁷ of aurorae and magnetic storms the solar outburst is a flare of ultra-violet light. The ultra-violet flare would in general be expected to increase the number of the zodiacal ions and the intensity of their fluorescence. We make no attempt here to enter into a complete discussion of the complicated effects which the flare might produce, but a few simple cases are of interest. The zodiacal ion ring on the day side of the earth might be compressed toward the earth because I_0 is increased and t is decreased during the flare (section 6). Therefore the portion of the ring from $\theta = 0$ to 90° might be widened during a magnetic disturbance. Apparently this is what happened during the latter part of June 1853 according to Jones' observations. The position and shape of the ring on the night side of the earth would not be expected to be greatly changed by the flare. In keeping with this idea the magnetic storms are shown by vertical lines in Fig. 6, and it is seen that the course of the dots and crosses is on the whole undisturbed during the magnetic storms.

³² From equation (12), Gunn, Phys. Rev. 34, 335 (1929).

A flickering of the intensity of the ultra-violet wave-lengths of the flare which cause the fluorescence of the zodiacal ions would cause pulsations in the entire body of the zodiacal light, as are observed. Various types of flares would be expected to occur (see the discussion of an earlier paper³³), in particular, the ionizing wave-lengths might be feeble compared to the fluorescent wave-lengths. This might occur at any time or when the flare was warming up to storm intensity. In the first case there might be zodiacal light changes with no accompanying magnetic storm, and in the second case the zodiacal light variation would be followed by the magnetic storm. Instances of both these possibilities are found in the data of section 2. For example, the zodiacal light fluctuations of November 3, 1929, (section 2) were seen at about 3 A.M. and the magnetic storm began 4 hours later. Similarly, auroral displays and vagaries in the propagation of wireless waves are known³³ to occur before a magnetic storm at times. The Radio Division of this Laboratory has noticed on a few occasions that wireless communication was very unusual several days before a magnetic storm; the storm was actually predicted in advance, the feeling at the time being that the prediction was about as certain as a weather prediction.

14. *The gegenschein.* The ions which stream away from the region *bcde*, Fig. 3, form a sheet mainly in the ecliptic plane extending throughout the region *BGKFD*, which seen edge-on is the zodiacal band. The ion densities are somewhat greater near the boundaries *bc''* and *ed''* of the sheet than in the interior regions. As shown in section 10 the boundaries swing into some extent toward the line *AK*, and at about $z = 0.5 \times 10^6$ km the ions progress more slowly away from the earth until $z = 10^6$ km is reached, whereupon they stream away with the full light pressure acceleration like the particles of a comet's tail. Thus looking end-on at the ion stream the terrestrial observer sees it as a patch of greater luminosity on the zodiacal band. This is the gegenschein. If the cross-section of the stream were 100,000 km in width along the ecliptic and 40,000 km high and if the equivalent optical distance were 10^6 km, the patch would be 6° wide along the ecliptic and 3° high, as seen from the earth, and its parallax as determined by two observers 20,000 km apart would be 1° . These values agree with observation^{5,6}; Barnard⁵ stated that the brighter portion of the gegenschein is about 7° in diameter fading insensibly into the night, the luminosity sometimes being perceptible to a diameter of more than 30° . The present theory of the gegenschein is of course quite different from the meteorite theory of Gylden and of Moulton.³⁴

That the gegenschein may be a comet tail appendage of the terrestrial atmosphere was mentioned long ago by Arrhenius, Evershed and others.¹ Barnard⁵ suggested that the atmosphere surrounding the earth acts as a lens to give a concentration of light somewhere along the line *AK*, Fig. 3. This would make a spot of illumination if there were particles there to be illuminated. Exact calculations are difficult but approximate ones show that the con-

³³ Hulburt, Phys. Rev. 34, 344 (1929).

³⁴ Moulton, "Celestial Mechanics," page 305 (1914).

centration of the light due to the lens, or refraction, effects probably occurs beyond $z = 0.5 \times 10^6$ km and that the concentration is not very great, perhaps about the same as the effects of diffraction. The apex of the cone of the earth's geometrical shadow is at $z = 1.37 \times 10^6$ km.

The present theory gives no clear indication of marked seasonal variations in the appearance of the gegenschein, but Barnard⁵ found that the gegenschein "undergoes singular changes in form and that these changes are periodic with the seasons." To explain Barnard's observations we turn to the magnetic storms. In a time of solar quiescence the gegenschein would be a small spot elongated into the zodiacal band along the ecliptic. During a magnetic storm the spot would be larger for the number of gegenschein ions and their fluorescent light would be increased. From 73 observations extending over 15 years Barnard concluded that the gegenschein was large and round in February, March (especially in the latter part of the month), April, August, September, the first part of October, and November. It was small and elongated along the ecliptic in January, July and the latter part of October. The milky way interfered with observations in June and December, and there were few observations in May. These facts are pictured in Fig. 7.

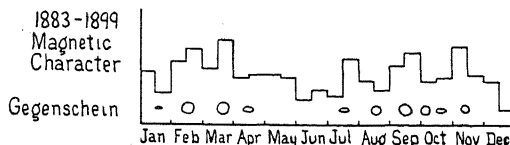


Fig. 7. Average magnetic character curve and Barnard's observations of the gegenschein for the years from October 1882 to February 1899.

Barnard made the 73 observations of the gegenschein from October 1883 to February 1899. We have added together all the magnetic storms for the first and last halves of each month throughout this period and have plotted the results in the broken curve of Fig. 7. In the addition storms of intensity 1, 2, 3 and 4 counted as 1, 2, 3 and 4, respectively. The curve is a magnetic character curve for the 15 years. It is seen that very roughly the gegenschein was large during epochs of magnetic storms and small during magnetic calm. The magnetic character curve has an ill defined maximum near equinox and a minimum near solstice, and thus has a sort of seasonal period. Fig. 7 can not be regarded as offering convincing evidence of a connection between magnetic storms and changes in the gegenschein. Further evidence would be desirable. It suggests, however, that the seasonal variations in the gegenschein were perhaps due to solar disturbances rather than to the tilt of the earth's axis.

15. *The rate of escape of the earth's atmosphere.* Zodiacal ions and electrons in the region *BDFG*, Fig. 3, which get beyond roughly 100,000 km move away under the solar radiation pressure. They do not come back to the earth. The zodiacal light and the gegenschein are the last fleeting evidences of particles which are leaving the earth never to return. If 1/10 of the high flying atoms

and molecules pass into space *via* the zodiacal band and the gegenschein, there is a loss of 10^6 particles $\cdot \text{cm}^{-2} \cdot \text{sec}^{-1}$ from the atmosphere, or 10^{-6} of the entire atmosphere in 10^6 years. This is, if anything, an under-estimate, but a rate of escape of this amount, or even two or three orders of magnitude greater, seems small and open to no objection on general cosmogonical grounds.

We may go a step farther. Geophysicists³⁵ have found a difficulty in explaining the smallness of the amount of helium, 10^{13} atoms in a 1 cm^2 column, present in the earth's atmosphere. They estimate that the average acid rock sets free helium at the rate of 10^7 atoms of helium per year per gram of rock, and therefore that, say, 100 grams of acid rock per cm^2 would in 10,000 years produce the 10^{13} helium atoms. Thus in the long periods of geological time much more helium would be produced than is found to exist, especially so since no processes are recognized which would remove the helium by absorption back into the crust of the earth. The present theory points a way out of the difficulty in that it suggests that helium may escape from the atmosphere more rapidly than the other gases. For helium atoms, being lighter, will be sprayed away from the earth with greater velocities than the heavier nitrogen or oxygen molecules and atoms. More energy is required to ionize helium than the other gases and hence the helium particles reach much greater distances from the earth before being ionized and swept away by radiation pressure. Therefore, compared with oxygen or nitrogen ions, few of the fast flying helium ions return to the earth, and the rate of escape of the helium into space may be of the same order of magnitude as the rate of supply from the earth.

³⁵ Holmes, Geological Mag. 2, 60 (1915), and references given in Jeffreys, "The Earth."

POLAR MOLECULES, THEIR CONTRIBUTION
TO ENERGY LOSS IN DIELECTRICS

BY F. HAMBURGER, JR.

SCHOOL OF ENGINEERING, JOHNS HOPKINS UNIVERSITY

(Received March 8, 1930)

ABSTRACT

Recently suggestion has been made that even at frequencies as low as those of commercial power circuits the theory of molecular orientation may serve as an explanation of at least a portion of the dielectric energy loss. This paper is an attempt to examine this suggestion on the basis of the Debye theory and the available experimental data. It reaches the following conclusions:

(a) The contribution of molecular orientation to the energy loss at frequencies below ten thousand cycles per second is negligible at the temperatures of zero and ten degrees Centigrade, for glycerine.

(b) For temperatures higher than ten degrees the contribution becomes still smaller and in all probability vanishes.

(c) The probability that any substantial portion of the normal dielectric loss found in the usual insulating oils, at commercial frequencies, may be accounted for on the basis of the Debye theory, is remote.

(d) In order to determine the effect of the dipoles in their contribution to dielectric loss, very accurate determinations of the dielectric constant must be made, especially for those substances that show small changes in dielectric constant with temperature and frequency.

INTRODUCTION

THE principle interest in Debye's theory of polar molecules has centered in its explanation of hitherto anomalous behavior of dielectric constant as related to temperature and frequency, and in the light it has thrown on the groupings within the molecules of compounds and mixtures. Little attention has been given to the necessary energy dissipation associated with the oscillation of polar molecules in an electric field. These losses, in absolute energy values, are relatively unimportant within the luminous range of frequencies although their close interrelation with absorption and anomalous dispersion is well understood. Under certain conditions, however, it is to be expected that an energy maximum will be encountered at some lower frequency. In general these maxima should occur at frequencies which are still relatively high, as related to those pertaining to the electric systems of practice, with the possible exception of those of radio transmission. There is in fact an increasing tendency in the literature of dielectric loss to invoke the frictional oscillation of the Debye polar molecule in explanation of the loss phenomenon. There is some evidence that this may be true, in part at least, within the upper range of radio frequencies. Some authors^{1,2} however

¹ D. W. Kitchin, *Trans. A. I. E. E.* **48**, April (1929).

² D. W. Kitchin, and Hans Müller, *Phys. Rev.* **32**, 979 (1928).

have attempted to extend the application of the theory, in the matter of energy loss, even to the low alternating frequencies of commercial power circuits. This paper is an effort to examine this last proposal from the standpoint of the theory and the available experimental data. It reaches the conclusion that there is little probability that in any of the materials as commonly used for insulation, any appreciable part of the observed dielectric loss is to be accounted for by the oscillation of polar molecules.

In his discussion of anomalous dispersion and absorption Debye³ considers the effects of dipole oscillation in periodic electric fields. He develops the distribution function of the moments and shows that the mean moment of the molecules is a complex number. The meaning of the complex moment is that there is a difference in phase between the moment and the external force. This difference in phase between the field intensity and polarization is accompanied by energy absorption. Since the moment is complex the molar polarization and hence the dielectric constant are complex. The dielectric constant must therefore be of the form

$$\epsilon = \epsilon' - j\epsilon''.$$

This means that in a dielectric under alternating stress, instead of having a current that is 90 degrees ahead of the voltage in phase, we also have a component of current which is in phase with the electromotive force and therefore causes an energy loss. The constant ϵ' is the 90 degree component and is the value that is usually determined by ordinary bridge methods. Considering a condenser in an electric circuit, Debye shows that $\epsilon' = C/C_0$, where C_0 is the capacity of an empty condenser and C is the capacity of the same condenser with a dielectric. The in-phase or loss component is ϵ'' where $\epsilon'' = 1/\omega WC_0$ and we consider the condenser in question as having no losses and having a capacity C shunted by a resistance W . The energy loss may therefore be expressed in terms of the phase defect angle Φ so that $\tan \Phi = \epsilon''/\epsilon'$.

It is natural to expect that under the influence of a periodic electric field the polarized molecules will tend to oscillate following the direction of the field. In a liquid dielectric this rotational motion would take place in a more or less viscous medium and the motion of the dipoles through this medium would be opposed by friction and so lag in phase behind that of the field. Heat would be generated which we observe as energy loss. This energy loss is that which would contribute the phase defect angle mentioned above.

Bearing in mind that the polar oscillation takes place during the period of free motion of kinetic agitation, we must conclude that the variations and losses in question would generally be associated only with frequencies relatively high. The theory however has recently been invoked by Kitchin and Müller to explain the phenomena observed in low frequency fields. Kitchin suggests in fact that the orientation of the molecules in a field of frequency as low as 60 cycles per second may account for at least a portion of the observed energy loss. From the relation of the time interval of molecular orientation with the kinetic activity it would appear that the orientation in a low fre-

³ P. Debye, *Polar Molecules*, The Chemical Catalog Company, 1929.

quency field would be such that there would be no phase difference between the field intensity and the polarization and hence no energy absorption.

METHOD OF ATTACK

As mentioned above the energy loss can be expressed in terms of the phase defect angle, that is,

$$\tan \Phi = \epsilon''/\epsilon'$$

Debye derives the following expressions for ϵ' and ϵ'' ;

$$\epsilon' = \epsilon_0 + \frac{\epsilon_1 - \epsilon_0}{1 + [(\epsilon_1 + 2)/(\epsilon_0 + 2)]\omega^2\tau^2}$$

$$\epsilon'' = (\epsilon_1 - \epsilon_0) \frac{[(\epsilon_1 + 2)/(\epsilon_0 + 2)]\omega\tau}{1 + [(\epsilon_1 + 2)/(\epsilon_0 + 2)]\omega^2\tau^2}$$

In these equations the values ϵ_0 , ϵ_1 and τ are constants for a given material at a given temperature, the value of ω is 2π times the frequency. The quantity τ is known as the relaxation time of the liquid and is the time required for all the molecules to revert to a random state after the removal of the impressed field. The dielectric constant ϵ_0 is the dielectric constant at very high frequency and the constant ϵ_1 is the dielectric constant for zero frequency. It is readily seen that if the constants ϵ_0 , ϵ_1 and τ are known it is possible to calculate from the above two equations the values of ϵ' and ϵ'' , and hence the phase defect angle, for any frequency.

TABLE I.

Temp. °C	Frequency Cycles/sec.	ϵ_1	ϵ_0	τ $\times 10^9$	Normal pf	Power Factor due to dipole	% Normal pf due to dipole
Glycerine							
0	60	37.38	6.72	1.28	0.0566	0.00000175	0.0031
0	100	"	"	"	0.0939	0.00000298	0.0032
0	1000	"	"	"	0.6866	0.0000298	0.0043
0	10^4	"	"	"	0.9944	0.000298	0.030
0	10^5	"	"	"	0.9999	0.00298	0.298
0	10^6	"	"	"	1.0000	0.0298	2.98
0	6×10^6	"	"	"	1.0000	0.1742	17.42
0	3.15×10^7	"	"	"	1.0000	0.6051	60.51
0	9.74×10^7	"	"	"	1.0000	0.6667	66.67
10	60	44.51	5.22	47.3	0.0297	0.000001	0.00337
10	100	"	"	"	0.0492	0.00000169	0.00343
10	1000	"	"	"	0.4432	0.0000169	0.00381
10	10^4	"	"	"	0.9802	0.000169	0.0172
10	10^5	"	"	"	0.9998	0.00169	0.169
10	10^6	"	"	"	1.0000	0.01689	1.69
10	10^7	"	"	"	1.0000	0.1659	16.59
10	10^8	"	"	"	1.0000	0.7646	76.46
n-Propyl alcohol							
-60	60	32.79	2.747	2.46	—	0.00625	—
-60	6.0×10^6	"	"	"	—	0.5028	—
-60	3.16×10^7	"	"	"	—	0.7443	—
-60	9.74×10^7	"	"	"	—	0.4751	—

It should be possible to determine these three constants by measuring ϵ' for three different values of ω and solving three simultaneous equations. Therefore from data taken at three frequencies it is possible to calculate, for any frequency, the contribution of molecular orientation to the energy loss in a dielectric. We can therefore show the importance or lack of importance of such a contribution at low frequency.

A search of the literature in an effort to find data that would permit such calculations to be carried out revealed only a meagre amount of suitable material. The data from which the calculations, given below, were made were taken from the work of Mizushima.⁴ On the basis of his observations on glycerine the calculations shown in Table I were made. The table gives the energy loss in terms of power factor.

RESULTS OF CALCULATIONS

The column headed "normal power factor" was calculated as a basis for comparison. This is the power factor due to dielectric constant and resistivity and is approximately the value that would be obtained by the usual bridge measurements at low frequency. The calculation was made on the basis of the following formula,

$$\tan \theta = (18 \times 10^{11}) / (f \epsilon' \rho)$$

In this formula θ is the phase angle, f is the frequency in cycles per second, ϵ' is the dielectric constant and ρ is the resistivity in ohms per cm³.

The results show that for glycerine the dipole contribution to the energy absorption is negligible for frequencies below ten thousand cycles, both for zero and ten degrees Centigrade. Furthermore, at the low frequency of 60 cycles per second their contribution is only three thousandths of one percent, a quantity entirely out of the range of accuracy of ordinary loss measurements. These results are strikingly brought out in Figure 1 where the value of power factor, for glycerine, is plotted against frequency. From Mizushima's data it is immediately apparent that for temperatures above ten degrees Centigrade the effect of the orientation becomes still smaller and certainly vanishes for low frequency.

Table I also gives some results on n-propyl alcohol and shows the small value of the power factor for 60 cycles compared to the high frequency value. The data are for -60°C and no resistivity values being available for this temperature, it was not possible to calculate the "normal power factor." However, it would appear that for temperatures near that of room, where the viscosity of the alcohol would be considerably less than at -60°C , the loss would be considerably less and would probably disappear for 60 cycles.

The paper by Kitchin¹ gives curves of dielectric constant and power factor against temperature for wood resin. The curves given are for 10^7 , 10^6 and 60 cycles per second and the suggestion was made on the basis of these curves and the curves of viscosity and dielectric loss for the same material. It would appear that these three measurements should permit calculation of the dipole

⁴ San-ichiro Mizushima, *Bull. Chem. Soc. Japan* 1, 47, 83, 115, 143, 163 (1928).

contribution. Such a calculation was attempted but was not satisfactory, since the observed changes in dielectric constant were too small. The calculations depend on differences in the value of the dielectric constant and it is thus evident that accurate determinations of that quantity are essential. Furthermore, it was necessary to take the data from the published curves which are not reproduced with sufficient fidelity. This was apparent from the fact that the same curves published in two different papers^{1,2} were not in entire agreement.

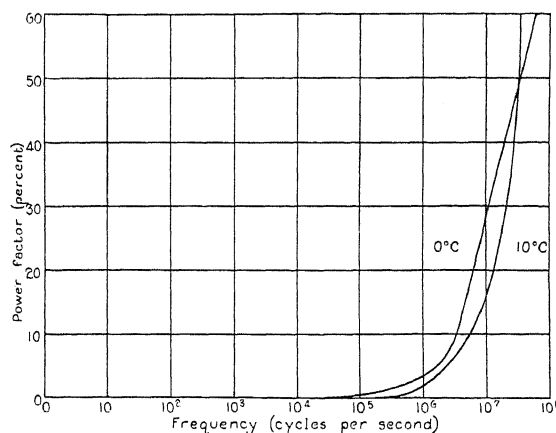


Fig. 1. Power factor due to molecular orientation. Glycerine at 0°C and 10° C. (Calculated curve.)

The "normal power factor" calculated as indicated above is probably somewhat smaller than that which would actually be measured since the calculation made on this basis takes no account of energy loss due to the "absorption" that is observed in short time studies of dielectrics. A recent paper by Whitehead⁵ shows beyond doubt that dielectric absorption in certain cases accounts for at least 95 percent of the dielectric loss. Taking this property into account, the dipole contribution would be even smaller than indicated in the last column of Table I, where the dipole contribution is given in percent of the "normal power factor."

EFFECTS IN INSULATING OILS

The suggestion of Kitchin, that the phenomenon of molecular orientation might account for energy absorption at 60 cycles was made with the idea of applying the theory to dielectrics used in commercial insulation. No other data in connection with such insulation are available from which calculations, similar to those made for glycerine, could be made.

So far as the commercial insulating oils are concerned there are certain general facts that enable us to estimate the possible effects of dipole orientation. It is obvious that in order to apply the theory to any liquid dielectric

⁵ J. B. Whitehead, Jour. Frank. Inst. 208, No. 4, October (1929).

the liquid must first of all be polar, that is, possess an electric moment. Probably the most used insulating oil is the well-known "transil" or transformer oil. This oil is a straight chain hydrocarbon and certainly possesses very small polarity, if it has any at all. It is certain that for this particular material dipole orientation plays no part in the energy loss.

As for the other insulating oils, particularly those used in high voltage impregnated paper cables, the lack of fundamental knowledge as to their molecular structure makes it impossible to estimate with any degree of precision the possible effects of orientation. The fact that the dielectric constant of this type of oil is always small, in the range of from say 2 to 3, and the dielectric constant of materials of the nature of glycerine is from ten to twenty times as large indicates that the effect of molecular orientation must necessarily be considerably smaller in such oils than in glycerine. And as we have shown the energy loss due to molecular orientation, at low frequency, is negligible for glycerine; it would seem safe to assume therefore that it should certainly be negligible for the insulating oils.

The author wishes to express his appreciation to Dr. J. B. Whitehead and to Dr. K. F. Herzfeld for their helpful suggestions during the preparation of this paper.

LETTERS TO THE EDITOR

Prompt publication of brief reports of important discoveries in physics may be secured by addressing them to this department. Closing dates for this department are, for the first issue of the month, the twenty-eighth of the preceding month; for the second issue, the thirteenth of the month. The Board of Editors does not hold itself responsible for the opinions expressed by the correspondents.

Possibility of Determining the Energy of the Cosmic β -Particles by Magnetic Deflection

In a recent letter to this section, Tuve¹ has pointed out how the scope of the Bothe and Kolhörster² coincidence method of investigating high-velocity β -particles can be greatly enlarged by making use of multiple coincidences in three or more electron-counting-tubes instead of the usual method of counting coincidences in only two counters. As Tuve has shown, there are two important advantages in this method: (1) a pair of counters can be used to define a beam of β -particles which is subsequently picked up by a third counter after being scattered, deflected by a magnetic field or otherwise experimented upon, and (2) the number of multiple coincidences occurring by chance can be reduced to a much smaller fraction of the true coincidences, making it possible to work with a beam of much smaller angle than can be used with only two counters.

When Tuve's note appeared, the writer had begun an experiment based on exactly these considerations in an attempt to obtain further information on the nature of the cosmic β -particles discovered by Skobelzyn³ and investigated by Bothe and Kolhörster.² It is planned to attempt a magnetic deflection of these particles, for such an experiment would test the possibility that they may be protons as well as give a direct measure of their energy. Definite knowledge of their energy distribution would be of assistance in deciding whether these particles are the actual cosmic rays or are of a secondary nature.

It may be of interest to describe an experimental arrangement, (at present under construction), by means of which it appears feasible to measure the energy of β -particles (or protons) having energy up to the value of 10^9 electron-volts which these particles are estimated to have. A pair of Geiger-Müller⁴

tube-counters will be used to "collimate" a beam of the particles, which are then passed through a region of strong magnetic field and are finally detected by a third counter placed at a suitable distance. By counting the number of particles which produce a triple coincidence in passing through all three counters, and by arranging the third counter to be suitably movable with respect to the axis of the apparatus, it will be possible to measure the deflection of the beam if sufficient deflection can be obtained. Calculation shows that with counting tubes of sufficient area and subtending a large enough solid angle to keep the intensity high enough to be measurable, a very strong magnetic field is necessary. Furthermore, on account of the necessity of using large counters, (our present "collimating" tubes are 4.4 cm in diameter and 27 cm long), this field must be produced over a considerable volume. These difficulties may be overcome by a device suggested by Skobelzyn,³ who points out that magnetic deflection of particles of such enormous penetrating power can be produced by passing them directly through a magnetized iron bar. By this method it will be possible to produce a magnetic induction of about 20,000 over a sufficient volume. The loss of energy of the rays in passing through the 15 cm of iron which will be used is not serious since particles of 10^9 e-volts energy can be expected to experience a loss of only about 12 percent.

¹ M. A. Tuve, Phys. Rev. 35, 651, (1930).

² W. Bothe and W. Kolhörster, Zeits. f. Physik 56, 751, (1929).

³ D. Skobelzyn, Zeits. f. Physik 54, 686, (1929).

⁴ H. Geiger and W. Müller, Phys. Zeits. 29, 839, (1928).

A widening of the beam due to straggling in the iron is estimated to be negligible for particles of such high energy. Calculation shows that by choice of suitable geometrical conditions and under the assumption of a magnetic induction of 20,000 over a 15 cm path a deflection equal to the width of the beam (about 8 cm) can be obtained for β -particles with the assumed energy of 10^9 e-volts. A somewhat smaller but still detectable deflection can be expected for protons of the same

energy. Intensity considerations indicate that under these conditions the number of true triple coincidences will be sufficient to be measurable by a few hours of registration and that the number of such coincidences occurring by chance can be reduced to a small fraction of the true ones.

L. M. MOTT-SMITH

Department of Physics, Rice Institute.
Houston, Texas,
April 2, 1930.

Magnetic Moment of the Sulfur Molecule

It is perhaps an open question as to whether the oxygen molecule is singly or doubly bound. According to Heitler and London the $^3\Sigma$ state indicates a singly bound molecule but Heitler and Herzberg have suggested that the second valence may reside in the exchange degeneracy of the electron orbits without involving the spins.

In the case of the sulfur molecule S_2 the evidence is more definite. Sulfur does not often form double bonds, and the fact that sulfur is a solid at ordinary temperatures and even in the vapor state is largely polymerized, indicates that the S_2 molecule is highly unsaturated. A $^3\Sigma$ state is to be expected.

The magnetic moment of the S_2 molecule has been determined in this laboratory and the prediction is confirmed. Since most of the S_2 molecules are in states of high rotational energy it would not be expected that the field would break the coupling between

the spins and the rotational axis. Under these circumstances only a widening of the molecular beam in the inhomogeneous field would occur and this result has been obtained in the experiments. In some cases however a faint satellite line on the side of the broadened central image has been observed. This line is on the side next the knife edge where the field is strongest. It seems probable that the field is strong enough here to uncouple the spins from the rotational axis in those molecules in the lower rotational states. If this is the case then the line is one of the three to be expected from a $^3\Sigma$ molecule with strong field quantization.

E. J. SHAW

T. E. PHIPPS

W. H. RODEBUSH

Laboratory of Physical Chemistry,
University of Illinois,
April 9, 1930.

Raman Spectra from Sulfur Dioxide

In view of the increasing interest which is being shown in the spectra of polyatomic molecules, we desire to report the results of some Raman effect measurements on sulfur dioxide. The material used was taken from a commercial tank; it was passed over phosphorus pentoxide to dry it and then condensed in a heavy walled Pyrex glass tube 2 cm in diameter and 20 cm long. During the condensation care was taken to exclude moisture; but no further purification than drying was considered necessary since the commercial product is ordinarily much better than 99 percent pure. When this glass tube was nearly filled with liquid, it was sealed off and subsequently used for the light-scattering experiments.

The Raman spectra were obtained with a mercury arc and the plates calibrated with

TABLE I. *Scattered lines from liquid SO₂.*

Frequency of modified line	Intensity	Frequency of exciting line	Frequency shift
24182.5	v.f.(diffuse)	24705.5	523.0
23560.4	st.	24705.5	1145.1
23371.2*	med.	24516.1	1144.9
23366.1*	weak (diff.)	24705.5	1339.4
22412.5	weak (diff.)	22938.1	525.6
21893.7	v.f.	23039.1	1145.4
21847.8	f.	22995.3	1147.5
21791.4	v.st.	22938.1	1146.7
21597.4	med. (diff.)	22938.1	1340.7

* These two lines overlapped on the plates; separate measurement was attempted since one line was much sharper than the other.

an iron arc. The apparatus and method of measurements were substantially the same as previously used in the case of liquid ammonia (Dickinson, Dillon and Rasetti, *Phys. Rev.* **34**, 582 (1929)). The results of the measurements are given in Table I. The frequencies of modified lines in cm^{-1} , given in the first column, are averages obtained from several plates. Reduction of the calibrating wave-lengths to vacuo has been made.

These modified lines show the existence of three shifts with the following average values; 524.3 cm^{-1} , weak (diffuse); 1145.9 cm^{-1} , strong; 1340.1 cm^{-1} , medium (diffuse). The last two of these shifts agree, within the limits of error, with the frequencies of the two

strongest absorptions by gaseous sulfur dioxide found by Coblenz (Carnegie Institute Publication, No. 35, p. 177) in the infrared. The smallest shift lies outside of the range of Coblenz's measurements. It is of interest to recall that such direct agreement between Raman shift and infrared absorption frequency has not been found in the cases of carbon dioxide and carbon disulfide whose molecules have points of similarity with those of sulfur dioxide.

ROSCOE G. DICKINSON
S. STEWART WEST

Gates Chemical Laboratory,
California Institute of Technology,
March 31, 1930.

On the Reason for Pauli's Exclusion Principle

It is generally recognized nowadays that physics deals primarily with one aspect of human experience; thus has the philosophical contention of Berkeley and Kant become after a century one of the presuppositions of our science. It was substantially this principle that led Heisenberg, first to his quantum mechanics, and then to the Indetermination Principle.

An interesting attempt has been made by Condon and Mack (*Phys. Rev.* **35**, 579, 1930) to find in the same principle the ground for Pauli's exclusion rule. It is suggested that human beings are themselves in an antisymmetric quantum state and that for this reason we can perceive only those material structures which are likewise in an antisymmetric state; hence, for us, the apparent validity of the exclusion rule. By implication there may exist all round us another set of physical systems in non-antisymmetric states without our being able to perceive them at all; presumably (if I understand correctly) there may also exist another race of humans who are experimenting upon those other systems but who, not being quantum-mechanically antisymmetric, can no more perceive us than we can perceive them.

An adequate proof seems to be lacking, however, that such possibilities are actually contained in quantum mechanics; certainly they are not among the familiar results of the theory. If, for example, an "antisymmetric" atom were to encounter a "symmetric" one under a law of interaction that is symmetrical in the electrons of each, then it follows from "resonance" theory that the

first atom could never bump the second one into an antisymmetric state, nor could the second bump the first into a symmetric state; each atom would retain its initial character. There is, however, no indication that each would simply pass by as if the other were not there at all. The photons emitted by symmetric atoms would also, on current theory, be indistinguishable from photons of the same size emitted by other atoms and so should be observable. Since the same considerations hold for systems of any size, no reason is apparent why an antisymmetric physicist should be unable to perceive at all a symmetric world, or, perceiving it, to form an antisymmetric (?) concept of its symmetry.

The same consideration seems applicable at first sight to Condon and Mack's alternative suggestion that the non-antisymmetric electrons may all have vanished from our ken into Dirac states of negative energy, which for such electrons form a set having no "bottom." It remains to be shown that the endless dropping of these electrons into ever greater depths of the abyss would have no effect upon our instruments. Perhaps they are physically imperceptible just as an electron or photon with infinite positive energy has a zero coefficient of absorption and so is physically non-existent. I hope the authors of the paper will give us an exact mathematical analysis of this point.

E. H. KENNARD

Department of Physics,
Cornell University,
April 4, 1930.

Influence of Accelerating Fields on the Photoelectric and Thermionic Work Function of Composite Surfaces.

With an accelerating potential of 22.5 volts, Ives and Olpin (Phys. Rev. **34**, 117, (1929)) found that the long wave-length limit of an alkali metal film on platinum progressed toward the red as the film thickness increased, reached a maximum and then receded when the film was made very thick. Experiments by the writer with a twenty volt accelerating potential confirm this result with the exception that the long wave-length limits observed were more than 1000 Angstrom units farther into the infra-red than those reported by Ives and Olpin. Although there is an optimum film thickness, as pointed out above, when an accelerating field is applied, such is not the case at *zero field*. Lowering the accelerating field causes the optimum thickness to increase until at zero field the long wave-length limit has been observed to change progressively from that of the background metal to that of the alkali metal *without a maximum excursion* and regression.

This investigation has also been carried over into the field of thermionics using a type T thoriated tungsten filament with a small carbon content. With an activation temperature of 1920°K, a test temperature of 1230°K and a test accelerating potential of 20 volts, the thermionic current increased to a maximum of 98×10^{-6} amp. per cm^2 at the end of 90 minutes activation. This time of activation had produced the optimum thickness. With continued activation the thermionic current decreased until at 280 minutes an equilibrium condition was produced with a current of 59.3×10^{-6} amp. per cm^2 . This observation is thus exactly analogous to that reported for the photo-electric effect. Judging by abstract 62 of the forthcoming meeting at Washington this phenomenon has also been

observed by W. H. Brattain who deposited the thorium on tungsten from an external source but made no mention of the importance of the accelerating field. In order to prove that an excess film thickness had caused the decrease in emission described above, the activation temperature was raised and the emission was observed to *increase* with time of activation reaching new equilibrium values for each temperature. At a temperature of 2085°K the rates of evaporation and diffusion were so balanced as to keep the surface covered to just the optimum thickness for maximum thermionic emission which was 98×10^{-6} amp. per cm^2 . Further increase in temperature reduced the thermionic emission indicating that the equilibrium condition of the surface corresponded to a film thickness less than the optimum. Tests with *lower* accelerating potentials showed that the optimum thickness depended on the test potential and moved toward thicker films as the potential was decreased until at practically zero field the maximum emission of 40.5×10^{-6} amp. per cm^2 was attained after 200 minutes of activation at 1920°K and practically no decrease in emission was produced by continued activation. These experiments, showing such close relationships between the thermionic and photoelectric behaviour of thin films, lend support to the theory that the "thermionic" and "photo-electric" electrons in these experiments come from the same family, presumably the "free" electrons.

W. B. NOTTINGHAM

Bartol Research Foundation,
Swarthmore, Pa.,
April 17, 1930.

Capture of Electrons by Alpha-Particles

The important experiments of A. H. Barnes on the above subject reported in the Phys. Rev. for Feb. 1, 1930, render rather interesting the theory of x-ray emission independent of temporary excitation suggested in a recent letter of the writer's in the Phys. Rev., since the latter gives a very simple explanation of the dependence of electron capture on the relative velocity; the result of those experiments.

According to the theory, if the relative velocity is such that relative kinetic energy is $E = h\nu_n$ corresponding to a natural frequency of the alpha-particle, then there is a probability that the electron will penetrate to the n -level, radiate the energy $h\nu_n$ and emerge from the field of the nucleus with a zero relative velocity; the probability of capture is thus equal to that when the initial relative velocity is zero. On the other hand if the

initial relative velocity is not one of the critical values the electron will penetrate to a level n such that $h\nu_n$ is less than the relative kinetic energy, and finally emerge with a finite relative velocity, thus reducing the probability of capture.

On this theory therefore we should expect the energy to be radiated in two separate and independent frequencies, one being governed by the relative velocity of the electron and the alpha-particle, and the other by the probability laws pertaining to the capture of stray electrons.

Further, if this suggestion is true, we should

X-Ray Emission Independent of Temporary Excitation

The usual explanation of Kramer's rule is that only when an incident electron has an incident minimum energy $eV = h\nu_x$ is it able to remove an electron from the X level of an atom; in the subsequent refilling of the level the X -radiation is emitted. Kramers in particular has studied the results of this assumption, and has explained to some extent the intensity distribution of the continuous spectrum by means of the statistics of collision between free electrons and temporarily ionized atoms.

But may we point out that an electron is given, over and above any initial energy, sufficient extra kinetic energy due to the attraction of the nucleus, to remove the X electron at a head-on collision. If the electron impacts are perfectly elastic, then their masses being equal they merely interchange velocity, and the ejected electron eventually emerges with an energy equal to the initial energy of the incident electron. No radiation is emitted. If the impact is not perfectly elastic, then the ejected electron emerges with less energy, and the incident electron, instead of remaining in the X orbit, may be carried out to a level n where $eV > h\nu_n$, and radiation of frequency $\nu_x - \nu_n$ will be emitted when it drops back into the vacant X level. Both these processes can occur even when the

expect that when the relative energy was not a critical value, then there should appear a finite percentage of electrons with a velocity nearly, but not quite, equal to the velocity of the alpha-particles, and independent of the initial velocity of the electron beam, or nearly so. This point could be tested by the first experimental tube of A. H. Barnes, using a magnetic separation of the various particles in the beam emerging from the collision region.

WILLIAM BAND

Physics Department,
Yenching University, Peking,
March 15, 1930.

energy $eV < h\nu_x$, contrary to experimental data.

To avoid this dilemma I would propose the following hypothesis. That an incident electron cannot penetrate to the n level of an atom unless (a) that level is vacant, or failing this, (b) the electron has sufficient initial energy $eV = h\nu_n$ to carry it out again into free space after radiating the energy $h\nu_n$ appropriate to the n level. That this energy is automatically emitted whenever an electron penetrates to that level, but that it may be emitted either in the fundamental frequency ν_n or else as a spectrum of frequencies $(\nu_n - \nu_{n+k})$, $(\nu_{n+k} - \nu_{n+k+i})$, etc.

The initial energy of the incident electrons is thus itself directly changed into radiation, and no temporary excitation of the atom is required.

It seems that the experimental facts force us to this position, but although it is an interesting move back towards the classical theory, it is nevertheless obvious that the wave mechanics will be required to give it a satisfactory theoretical basis.

WILLIAM BAND

Physics Department,
Yenching University,
Peking, China.
March 10, 1930.

Motion of Positive Ions through Gases

In a previous paper¹ the writer published the results of some experiments on slow moving heavy alkali ions passing through light gases at low pressures. The method used is that of Dempster.² The ions pass through a slit into the space 3 mm wide between the pole pieces of a magnet. The ions move in the

magnetic field in a semi-circular path, passing out through a second slit into a faraday chamber, where they give up their charge to an

¹ R. B. Kennard, Phys. Rev. 31, 423 (1928).

² A. J. Dempster, Phys. Rev. 11, 316 (1918) et seq.

electrometer. From the curves showing the change in electrometer current with changing gas pressure and magnetic field, conclusions were drawn concerning the mean free path, neutralization, scattering, and loss of velocity of the ions in passing through the gas in the system.

Cox³ using the same method with lithium ions passing through mercury gas, questions the possibility of distinguishing between scattering and neutralization. He assumes that the number of ions scattered along the slot between the pole pieces would be negligible compared to the number scattered into the pole pieces and so lost. Scattering would therefore have the same effect as neutralization; that is, at the higher gas pressures there would be a decrease in the peaks of the curves obtained, without a broadening of the base of the curves to both sides. This assumption is valid in the case of light ions in a heavy gas, but it is not necessarily valid for a heavy ion passing through a light gas. In fact a study, based on the kinetic theory, of the space distribution of the once-scattered ions, shows that scattering should have been observed in three of the four cases investigated by the writer.

Cox assumes that in a collision between an ion and a gas atom, the ion rebounds from the atom as from an immovable sphere. This is a legitimate approximation in the case of lithium ions making impacts with mercury atoms, since the mass of the atom is twenty-nine times the mass of the ion. It is however not valid when the mass of the ion is of the same order or greater than the mass of the atom. If M_1 is the mass of the ion and M_2 the mass of the gas atom or molecule, conservation of energy and momenta give for the scattering angle ϕ as a function of the angle of impact θ ,

$$\phi = \cot^{-1} \left[\frac{M_1}{M_2} \csc 2\theta - \cot 2\theta \right], \quad (1)$$

and for the fractional loss of velocity of the ion,

$$\frac{\bar{c}-c}{\bar{c}} = 1 - 1/(\cos \theta + \sin \phi \cot \theta). \quad (2)$$

From Eq. (1) and its derivative, the maximum scattering angle can be found, namely:

³ I. W. Cox, Phys. Rev. 34, 1426 (1929).

$$\phi_{(\max)} = \cot^{-1} \left(\left(\frac{M_1}{M_2} \right)^2 - 1 \right)^{1/2}. \quad (3)$$

The maximum scattering angle for caesium in hydrogen is 51'-46"; for caesium in helium 1°-31'; for sodium in hydrogen 5°; for caesium in argon 17°-10'.

In the apparatus used by the writer the slits were 3×1 mm and the semicircular path from the first to the second slit was 112 mm. The maximum displacement of the once-scattered ions in the plane of the second slit is therefore: for caesium in hydrogen 1.71 mm; caesium in helium 3.4 mm; sodium in hydrogen 9.9 mm, and caesium in argon 35.6 mm.

The statistical distribution of the once-scattered ions in the plane of the second slit is determined by:

- (1) the equation between ϕ and θ ;
- (2) the fact that collisions are equally probable at all points in the path;
- (3) the probability of a collision occurring between θ and $\theta+\Delta\theta$ is given by $p = \sin 2\theta\Delta\theta$;
- (4) In a constant magnetic field, the proportional decrease in the radius of curvature of the path is equal to the proportional decrease in velocity.

When the range of scattering angle is small, due to the large ratio of M_1/M_2 , the pattern produced by the scattered ions cannot be calculated on the assumption that the ions are all scattered on the center line of the stream. By dividing the ion stream into elementary streams and the normal plane at the second slit into elementary areas, the distribution of the ions over the plane of the second slit is given by the summation of the contribution of each of the stream elements to each area element.

A single distribution function involving all the above factors has not as yet been found. However, a close approximation of the distribution of the scattered ions can be obtained by graphic methods. In this manner the proportion of once-scattered ions that will fall on an area 3×1 mm adjacent to the second slit has been determined. It is for caesium in hydrogen 14%; caesium in helium 11%; sodium in hydrogen 6.5%, and caesium in argon 1.6%. When the magnetic field is increased so that the undeviated ions just fail to pass the second slit, the above proportion of once-scattered ions will pass through the

slit and register as current to the electrometer. In all cases but that of caesium in argon this proportion is sufficient to give a measurable current. No current was however observed. The slight evidence for sodium in hydrogen occurs for ions that have had, on an average, many more than one collision.

The failure to find small angle scattering by the method used would indicate that the collisions between the ions and the gas molecules or atoms are not governed by the simple assumption of the kinetic theory. (1) The force between the ion and the molecule may be a function of the distance, as indicated by Cox. This would increase the proportion of ions scattered at very small angles but would not affect the maximum scattering angle. (2) The collisions may not be perfectly elastic, part of the energy being converted into radia-

tion. (3) The collision may involve something analogous to friction, resulting in a spin of either the molecule, the ion, or both.

Further experiments are needed which will determine the distribution in angle of the scattered ions and the loss of velocity for different angles of scattering. From the results of such experiments one may expect more definite information as to what happens when a moving ion comes close enough to a relatively stationary atom or molecule to suffer a change in the direction and magnitude of its velocity.

RALPH B. KENNARD

Department of Physics,
Robert College,
Constantinople, Turkey,
April 5, 1930.

Certain Effects Accompanying Electron Diffraction

Results on electron diffraction by a copper crystal, for normal incidence on a (100) face, have previously been reported by the writer.¹ With two exceptions, all of the expected diffraction beams which are the x-ray analogues in the two principal azimuths, and in the range below 250 volts were found. In addition, 20 sets of beams were found, 12 of which satisfy the conditions required by a wave of one-half the length given by $\lambda = h/mv$, or by a double grating spacing. It was pointed out that these beams must be due to the structure of the crystal since most of them appear in the (111) azimuth. These beams appeared not to be due to gas. Hendricks² has suggested that these "additional" beams are best accounted for by assuming a simple-cubic surface structure with the dimensions of the face-centered structure, and that those "additional" beams not accounted for by this arrangement may be some which have their maximum development in some minor azimuth closely adjacent to the ones in which observations were made. The structure suggested by Hendricks had previously been considered, but did not appear feasible at that time, since the azimuths of the beams not accounted for by this arrangement had been checked and found to be the same as the azimuths in which observations were made. However, there is still the possibility that the "additional" beams may consist of more than one type and that more

than one hypothesis will be necessary to account for all of them. As Hendricks pointed out, if the simple-cubic structure is present, then reflection from other possible crystal planes, such as (521) should occur. A search for such beams should then be of value in deciding this question.

During the past several months the measurements above described have been repeated for a new crystal made of exceptionally pure copper. The crystal was made by slowly lowering the molten copper, contained in a pure graphite mold, through a temperature gradient in an atmosphere of hydrogen. The results obtained with the second crystal are in accord with those previously obtained with the first crystal. These results were obtained after outgassing the crystal in a high vacuum for many hours at such red-heat temperatures that considerable copper evaporated from the surface of the crystal. Wolf³ has recently obtained results which confirm the above observations. For the second crystal *all* of the expected diffraction beams in the two principal azimuths and in the region below 325 volts have been observed. A search for the

¹ H. E. Farnsworth, *Phys. Rev.* **34**, 679 (1929).

² S. B. Hendricks, *Phys. Rev.* **34**, 1287 (1929).

³ Karl Wolf, Private communication.

(521) beam above referred to showed it to be present, and hence confirms the hypothesis of a simple-cubic structure.

After obtaining the above observations, the second crystal was then heated at temperatures considerably higher than those previously used, in fact, so near the melting point that in about 10 minutes sufficient copper evaporated from the crystal to make the surrounding glass tube practically opaque to visible light. After 30 minutes of heating at this temperature, with one exception, the "additional" beams occupying the positions required by the simple-cubic structure had decreased in intensity to about 10 to 20 percent of their former values so that only the stronger beams were observable. However, further heating for periods of several hours at the higher temperature failed to further decrease the intensity of these stronger beams. (The crystal has been outgassed at various red-heat temperatures for about 35 hours.) It is thus obvious that these "additional" beams are due to a surface structure. Exposing the crystal while red hot to pressures of hydrogen up to 2 mm Hg failed further to decrease the intensity of these "additional" beams. Hence if this surface structure consists of gas, the last traces of it are much more difficult to remove than in the case of a nickel surface, as found by Davisson and Germer.⁴ There is still the possibility that this surface layer is composed of copper atoms, the thickness of which is a function of heat treatment. Very recently the crystal has been exposed to the atmosphere for several days. Then, subsequent to moderate heating at red heat in a vacuum for only a few minutes, it was found to give the same diffraction pattern as originally. With further heating the surface appears to be quickly brought back to its final state, although complete observations on this point have not yet been obtained. This result substantiates the possibility of a gas or oxide layer.

During the course of the above observations certain beams have been found which require a refractive index of unity. A search for other weak beams of this nature reveals a whole series of such beams which accompany the intense diffraction beams as satellites. In many cases these satellites are so close to the main beams that they are not completely resolved, and hence are not observed by the usual method of taking colatitude curves for

various primary voltages. In these cases their presence is detected by varying the primary voltage in small steps, and measuring the current to the Faraday collector, whose angular position is adjusted for the maximum of the beam at each reading, while the total primary current is held constant for the entire set of observations.

In the (100) azimuth the satellites which accompany the 4 first-order beams below 325 volts all occur within 2 volts of the theoretical values for unit refractive index; that of one second-order beam occurs within 11.9 volts; that of the other second-order beam is missing. In the (111) azimuth, the satellites of 3 first-order beams are within 2.7 volts of theoretical values; that of the other first-order beams below 325 volts is within 7.3 volts; those of 2 second-order beams are within 5 volts; that of the other second-order beam is within 19.5 volts; that of 1 third-order beam is within 5 volts. The intensities of the satellites are between 10 and 20 percent of those of the main diffraction beams at the lowest voltages, and decrease to an unmeasurable amount at about 325 volts.

It is significant that with but one exception all of the first-order beams fall well within the observational error of the required value for unit refractive index. For the exceptional case in which the voltage difference is 7.3, it should be pointed out that the voltage of the main beam which the satellite accompanies is also several volts from the expected position, indicating an error of the same sign as that of the satellite, and it is the corresponding beam in the second-order whose satellite differs by 19.5 volts from the theoretical value. The voltage of this second-order main beam is also several volts from the expected position, indicating an error of the same sign as that of the satellite. Satellites of the higher-order beams are less certain, but since the higher-order beams are relatively weak and occur only at the higher voltages, this may perhaps be expected. Although the satellites are not present until after a certain amount of red-heat treatment of the crystal, they were observed previous to the final rigorous heating at temperatures very near the melting point. In fact, at least two of the beams obtained with the first crystal are of this type.

⁴ Davisson and Germer, *Phys. Rev.* 30, 705 (1927).

The satellites are as sharp in voltage and colatitude angle as the main diffraction beams, and are not confined to large colatitude angles. Hence, they are not due to a two-dimensional surface grating. Two possibilities suggest themselves. First: a surface contraction of the crystal lattice. Lennard-Jones and Dent⁵ have computed the contraction of the lattice at the (100) boundary of crystals of the NaCl type. They found that the contraction is confined almost entirely to the top layer, and is only of the order of 5 percent. Further, they obtain a decrease in the interatomic spacing in the surface layer of the order of 5 percent. Thus, on the basis of these computations, the depth contraction would be insufficient to account for the shift of some of the beams, and the decrease in the interatomic spacing in the surface layer would produce a marked displacement of the beams from the plane grating lines on which they are found. In addition, the contraction necessary varies from 17.5 percent for the lowest voltage beams to less than 5 percent for the higher voltage beams, and there is no evident reason why a contraction should be such as to make the apparent refractive index exactly unity. Second: a penetration of the incident electron through several layers of the crystal before its velocity is appreciably altered under the action of the inner potential of the crystal. This view is, of course, contrary to the present conception, and, while it would account for observations similar to the above for a single lattice, there is some uncertainty in explaining on this basis the presence of the above satellites previous to the removal of most of the surface lattice.

Additional observations which, however, appear in accord with this view are the following. Simultaneously with the weakening of the "additional" beams requiring a simple-cubic structure, there appeared a new set of beams on the $\frac{1}{2}$ -order lines in both the (100) and (111) azimuths indicating that the surface layer on the crystal was changing in structure from a single-spaced simple cubic to a double-spaced face-centered cubic. Further, the positions of these latter beams are such as to require a refractive index of approximately

unity while those due to the simple-cubic structure require a refractive index *greater than unity*. There is also a shift in the voltage of the beams due to the simple-cubic structure as their intensity decreases, such as to decrease the refractive index. Observations on the structure formed by the condensation of hydrogen on the crystal show that hydrogen forms in two different lattices depending on the pressure of the hydrogen while the lattice is formed. At small pressures (less than 0.5 mm Hg) a relatively thin double-spaced face-centered structure is formed; at larger pressures (2 mm Hg) a thicker single-spaced simple-cubic structure takes its place. The beams for the first structure require a refractive index of approximately unity while those of the second structure require one *greater than unity*. This second structure is extremely unstable and reverts to the first structure in the course of a few minutes under the bombardment of the low-velocity primary electrons. The presence of hydrogen on the surface does not decrease the intensity of the main diffraction beams as is the case for air.

A careful examination of the observations on the "additional" beams requiring a simple-cubic structure shows in some cases the presence of satellites of these beams requiring a refractive index close to unity.

Taking into account the various types of diffraction beams outlined above, there are still a few very weak beams observed with the first copper crystal which cannot be classified. It was found, however, that during the course of the heat treatment of the second crystal, most of these weak beams disappeared before the decrease in intensity of the "additional" beams requiring a single-spaced simple-cubic structure occurred. They may, therefore, be attributed to a slight trace of some other form of surface structure which was not identified.

H. E. FARNSWORTH

Department of Physics,
Brown University,
Providence, R. I.,
April 19, 1930.

⁵ Lennard-Jones and Dent, Proc. Roy. Soc. 121A, 247 (1928).

Absorption and Emission Spectra in the Region $\lambda 600-1100$.

Lyman discovered the resonance series of helium several years ago. I have repeated his work and in addition have studied the

ultraviolet light emitted by helium, and by helium mixed with other gases. The following is a preliminary report of many new

phenomena observed.

A region, $\lambda 600\text{--}\lambda 1000$, of very strong continuous light has been discovered in helium. This is best observed in a condensed discharge. The short wave-length limit of the continuous source found by Lyman and Schumann is about $\lambda 900$. The new continuous spectrum is the only one known in the region $\lambda 600\text{--}900$. This continuous spectrum is an isolated one, and on this account its second order is also very useful. With this light as a background, absorption bands have been observed in this region. Among these is a new system of bands in hydrogen. The 0-0 band of this system is $\lambda 842$, and the electronic levels concerned in its production are the normal level and a new one 14.7 volts above it. A progression of eight bands have been observed. These new bands are much stronger than the *A-B* and the *A-C* absorption bands previously found by Dieke and Hopfield.

Strong absorption bands in this region have been obtained also in nitrogen and oxygen. I have not yet examined any of these in great detail. There are several scores of them forming perhaps many systems. They are especially interesting for in this region of high frequency one expects to find bands with high electronic quantum numbers, bands concerned with double electronic transitions and possibly even bands of ionized molecules.

An examination of a small part of these spectra shows clearly six bands in a region unmixing with others. They are $\lambda\lambda 722$, 694, 682, 675, 671 and 669. These bands form approximately a Rydberg series. Since they occur in absorption they are probably due to electronic transitions from the normal level, and their limit of convergence, 18.58 volts, is the ionizing potential of the molecule. The form of the series, the spacing of the bands and the experimental conditions all point to helium (He_2) as the source of these bands. From the above measurements the

effective quantum number of the lowest level is 0.853. This is one unit less than the value of the number for the $2S^1\Sigma$ term of helium found by Curtis and others.

The resonance series of the helium atom discovered by Lyman has been extended to nine members which is two more than were observed by him. I have observed the first line self-reversed and lying in what appears to be a strong band several angstroms wide. This resonance line was obtained in five orders and the fourth and fifth orders have been photographed against iron standards. Its wave-length measured in the fifth order is $\lambda 584.358$ I.A. reduced to vacuum. This value is about 0.04A lower than that given by Lyman. The band at $\lambda 600$ was observed under certain conditions, and there have been found also some new emission bands in this region probably due to helium.

In a mixture of helium and hydrogen thirteen members of the Lyman series have been observed. This more than doubles the known length of the series. Two very interesting things are evident from the spectrograms. One is that the Lyman series shows a much smaller intensity gradient when produced in an excess of helium than when produced with only atomic hydrogen present in the discharge tube. The other is that in an excess of helium an anomalous intensity occurs in the line $\lambda 972$ of hydrogen. This line, the third member of the series, is much weaker than the lines near it. It is in fact only as strong as the sixth line. If this anomaly has its source in the four-quantum state of the atom one would expect a similar weakening of H_β of the Balmer series. This phenomenon is now being investigated. If this found to be true in the visible series it would be a parallel to the case of the spectra of *M*-type stars in which H_γ is weaker than H_β .

JOHN J. HOPFIELD

University of California, Berkeley
April 20, 1930

BOOK REVIEWS

Technische Mechanik. L. FÖPPL, Pp. 189+x, figs. 117. Akademische Verlagsgesellschaft, Leipzig, 1929. Price bound, RM 19.75.

This book constitutes part 2 of mechanics in the "Handbuch der Experimentalphysik," many references being made to A. Hass' "Mechanik der Massenpunkte und der starren Körper" which appeared as part 1.

The text contains an elementary presentation of the simpler problems of applied mechanics, the author's endeavor being to impart to the reader a clear understanding of the principles underlying the subject rather than to furnish him with information alone. Although the treatment is quite elementary, the author uses the calculus freely and introduces scalar and vector products without much explanation of their meaning. The topics treated are statics, kinematics, dynamics of particles, dynamics of groups of particles, dynamics of rigid bodies, impulse, friction, in the order given. The book is exceptionally well illustrated by line drawings and halftones.

LEIGH PAGE

Intermediate Dynamics and Properties of Matter. R. A. HOUSTOUN. Pp. 138, figs. 139. Longmans Green and Co., London, 1929. Price \$1.25.

This text constitutes the first part of a series on Intermediate Physics of which the sections on Heat, Light and Electricity and Magnetism have already been published. Elementary algebra and trigonometry are used, but no calculus. The topics are well selected and clearly treated, although one may object to the time-honored but meaningless definition: "The mass of a body is the quantity of matter in it." A number of simple problems are placed at the end of each of the twelve chapters, and a list of Oxford and Cambridge Schools examination questions together with answers to problems at the end of the book.

LEIGH PAGE

Foundations of Potential Theory. O. D. KELLOGG. Pp. 384+ix. Julius Springer, Berlin, 1929. Price bound RM 21.40.

This excellent treatise on potential theory is based on two courses, one elementary and the other advanced, which the author has given at Harvard. In the first quarter of the book the subject is treated in a fairly elementary manner, with applications to gravitational theory, electrostatics, magnetostatics and the flow of heat. It is, perhaps, unfortunate that the author feels constrained to follow the convention of defining the potential in a gravitational field as the negative of the potential energy per unit mass, as this procedure necessitates a revision of the definition when elements which repel as well as attract are taken into consideration, causing needless confusion on the part of the student as to the proper sign to be used. The author avoids the use of vector notation, writing (X, Y, Z) for the vector whose rectangular components are represented by the three capitals, and employs the notation, grad, div, curl in preference to Gibbs' significant symbols.

The last three-quarters of the book is more mathematical in character. The restrictions on the validity of Gauss' and Stokes' theorems are carefully examined and these theorems are proved under broad conditions, a study is made of Laplace's equation with applications to electrostatics, and the development of functions in series of spherical harmonics and in Fourier series is investigated. The last part of the book is concerned with the establishment of existence theorems, particular attention being paid to the Dirichlet problem and its investigation by the use of integral equations.

Exercises in the form of problems are interspersed through the text, and an index and a brief bibliography are appended. The book should prove very valuable, particularly to those who are interested in the rigorous development of the subject of potential theory.

LEIGH PAGE

Atoms, Molecules, and Quanta. ARTHUR E. RUARK AND HAROLD C. UREY. First edition, 1930. Pp. xvii+765+25 (indices), 6×9 in. McGraw-Hill Book Co., New York, Price \$7.00.

This is the second book of the International Series in Physics, F. K. Richtmeyer, Consulting Editor, which was inaugurated last fall by the "Quantum Mechanics" of Condon and Morse. It bids fair to become the long needed prototype of Sommerfeld's *Atombau* for the English language. Written with a double purpose, the first part (Chap. I–XIV) is intended to satisfy the needs of those who are approaching the study of atomic and molecular structure for the first time, while the latter part attempts to furnish the initiated with an up-to-date account of the theoretical and experimental aspects of quantum mechanics.

The chemical influence of one of the authors is strongly suspected (and approved) by the reviewer in reading the significant statement in the preface, "On the other hand, a very large number of physicists and chemists do not wish to eliminate models from their modes of thought, nor to rely entirely on mathematical connections between their observations. In the past these models have consisted of particles, moving on selected orbits. . . . It is only human nature to construct a new picture of a hidden mechanism as soon as an old one is discarded." It is with this view point that the authors devote the first eleven chapters to a complete discussion of the orbital theory of the atom. After a historical development of the fundamentals of atomic theory, with a careful description of experimental details, a very good chapter entitled "Review of Dynamical Principles" is inserted. This is distinguished by many clarifying illustrative examples. Then follows a consideration of hydrogenic atoms and their spectra. It is to be regretted that the authors have not seen fit to adhere to the Gibbs system of vector notation and have preferred the German. Chapter VI on general theorems of the older quantum theory (such as the correspondence principles, the adiabatic principle and a justification of the Bohr quantum conditions) is a parenthesis interrupting the continuity of the treatment of spectra and would have been better placed in the appendix along with relations between average kinetic and potential energies, quantum integral evaluation, phase and group velocities, mathematical manipulation of functions arising in the wave mechanics, Maxwell's equations, Larmor's theorem, radiation from a moving charge and the relativity transformation. The subsequent chapters then develop spectroscopic theory, the climax occurring in chapter X where the general theory is illustrated by an actual typical multiplet spectrum (Cr). The theory of molecular spectra is expounded in Chapter XII, which comprises some eighty pages. The discussion of this subject is divided into three parts, the first dealing with infrared spectra (18 pages), the second with electronic bands (50 pages) and the last with spectra from polyatomic molecules. The discussion of the spectra of diatomic molecules is quite satisfactory. A paragraph is devoted to the relation between the different systems of nomenclature (five in addition to that of the authors) now in use. The inclusion of polyatomic spectra is especially welcome, as this is the first serious attempt at a critical treatment in any treatise beyond the statement that they are too complicated and that too little is known concerning them. The first or elementary part of this book winds up with a presentation of the present status of critical potential measurements and experiments involving collisions of the second kind.

The second part of the book starts off with a chapter on wave mechanics, followed by its application to hydrogenic atoms. An intelligible chapter is then devoted to an exposition of matrix mechanics, which it seems we must understand in spite of the almost insurmountable difficulties experienced in obtaining important results (without the aid of Schrödinger's method), because of the persistence of theoretical physicists in interjecting surreptitiously into their discussions the phrase, "The matrix components of such and such." A couple of paragraphs are also given of Dirac's formulation of quantum dynamics and his theory of q numbers. The general theory of quantum dynamics is next developed in its relation to Heisenberg's uncertainty principle. The transformation theory of Dirac is also given. Chapter XIX takes up the conditions occasioned by equivalence degeneracy and discusses He, H_2 and H_2^+ and the symmetry properties of diatomic molecules consisting of equivalent nuclei. As most of the material in chapter XX on spectral intensities is derived from classical theory, that involving quantum mechanics being merely quoted without proof, it seems that this chapter is out of place and should have been presented earlier in the first part along with spectroscopy,

perhaps immediately following the chapter on band spectra. The book ends with a presentation of the Davisson and Germer effect, and allied matters.

The authors have not discussed the quantum mechanical aspects of radioactivity, statistics, valence, nor group theory. The book is well illustrated, but tables of data for the use of the experimental worker are rather scarce. This, however, is probably beyond the scope of such a treatise. Although the arrangement in places is not ideal, the wealth of material seems to be well indexed and the book is therefore highly recommended for reference use in clearing up knotty theoretical points.

D. S. VILLARS

Lehrbuch der Chemischen Physik. A. EUCKEN. Pp. xvi and 1037, 250 figures. Akademische Verlagsgesellschaft, m.b.H., Leipzig 1930. Price bound RM 56.

Eucken's book which appeared in its first edition in 1922 with 492 pages, has grown with this third edition into a volume of double the size and has changed its name from a text-book in physical chemistry to a text-book in chemical physics, making the emphasis on the physical side even stronger than it had been in the first edition. A number of features which were characteristic of the first edition have survived. Among them is the general plan which consists in dividing the book into two parts, the first presenting the phenomena from the standpoint of the theory of heat and occupying about 600 pages. The second, under the title "Structure of Matter," occupies the rest.

The first part is divided according to subjects. Each chapter falls then into usually four parts: presentation of the experimental facts, treatment with the method of thermodynamics, explanation with the help of kinetic theory and practical applications. In the whole treatment of the first part it is characteristic that the modern views are introduced rather early. But as a concession to the reader the somewhat crisp statements of the first edition have been elaborated and perhaps from the standpoint of the theoretical physicist lose something of their original precision.

The first chapter is an introduction presenting the first and second law, the general ideas of the kinetic theory, Maxwell's distribution law and even the statistical interpretation of entropy. The Reviewer thinks it a pity that Eucken has relinquished the name of "free energy at constant pressure" for $U - TS + pv$ which he had adopted in his first edition in agreement with Lewis and Randall and has gone back to the historical name introduced by Gibbs.

The following chapters treat ideal gases, then solid bodies. In this latter chapter a rather full treatment of the specific heat of solids is given and accordingly the quantum theory of specific heats is introduced already here. The next chapter on real gases gives more concerning the corrections for the reduction to the ideal gas state than is usual. Chapters on liquids and on the laws concerning the change of state follow in which the empirical relations, the new thermodynamics, kinetic theory and general statistics are discussed very completely. The next chapters deal with the more chemical equilibria, first for ideal gases then for condensed solutions of all types. It is in these chapters and the following where the growth compared with the first edition is largest. Formerly Eucken had referred the reader for these more conventional subjects to other books but since this time even these old-fashioned questions have advanced so much that an extended treatment seems necessary. This applies especially to the theory of strong electrolytes which was almost completely missing in the first German edition, but had been added to the English translation by Jette and La Mer. An almost completely new chapter follows on surface phenomena, dealing with adsorption and the highly important question of surface potentials.

The next three chapters treat of irreversible processes, namely diffusion, electrical phenomena, among which are to be mentioned a treatment of electrokinetics which play such an important part in biology, and finally on chemical kinetics. It is in this last subject that the American reader will feel some gaps. Especially he will be astonished that the name of H. S. Taylor does not occur.

The whole treatment in this first part is admirably suited to teach the subject in its many sides. There are a number of small points where the opinion of the Reviewer differs with that of the author in this as well as in the second part.

The subject of the second part makes the task of the writer particularly difficult, because the more intricate problems of theoretical physics, the theory of line and especially band spectra have gained a large importance for the chemists as the only method of gaining a knowledge of some molecules which can not be prepared in large amounts. Accordingly one must make available to the physico-chemist the methods to analyze spectra without forcing him to go through all the difficult calculations of the theory. In this Eucken has been highly successful.

After an introduction giving the general properties of electrons and nuclei and radioactivity, he treats first the general quantum principles for emission and absorption of energy and then he goes on to describe the characterization of optical and x-ray spectra, including the new quantum theory but without giving too many mathematical details. The Pauli principle leads to the periodic system and a description of the possible spectral terms.

The next chapter deals with the properties of molecules, their spectra, the application to specific heats—the hydrogen problem is included. The calculation of the heat of dissociation concludes this subject. There is then a chapter on optical refraction and polarization in which field the measurement of dipole-moments has given considerable insight into the structure of organic molecules. Finally the nature of the chemical valence is discussed, the unipolar bond is explained according to the new quantum theory (Heitler and London), while for the polar compound the older theory of Kossel is given. The properties of crystals, determination of their structure and the question of the forces holding them together are treated next with mention of the theory of metals at the end.

Summing up, the book is a treatment of the most interesting chapters of physics, written for chemists who have the necessary endurance to master the difficulties which can not be avoided.

KARL F. HERZFELD

Inorganic Chemistry for Colleges. WILLIAM FOSTER. Pp. viii+837. Figs. 212. D. Van Nostrand Company, New York, 1929. Price \$3.90.

Since the author has written this book for students of second year chemistry, the treatment is much more complete and comprehensive than most of the text-books for college chemistry. The author follows a different yet worthwhile arrangement of subject matter, and divides the book into four parts: I. Introduction, II. Non-metals, III. Metals, IV. Supplementary—carbon compounds.

It is in Part I that the greatest departure from standard practice occurs. Following an excellent historical introduction the author considers such fundamentals as the laws of chemical combination, the atomic theory, the gas laws, the kinetic theory, and the internal structure of crystals. These are well presented and very nicely illustrated. Radioactivity and the radioactive elements are then studied in some detail so that an experimental foundation is laid for the study of atomic structure and the classification of the elements. This concludes the first section of the book.

The second part of the book covers in a fairly complete way the chemistry of the non-metallic elements. In addition the subject of solutions follows the chapter on the chemistry of water. Ionization, ionic theory, the properties of acids, bases, and salts as well as oxidation and reduction are also considered in this section which is concluded by a chapter on colloid chemistry. In the work on colloids, the author makes the mistake of using $\mu\mu$ for $m\mu$. This is one of the very few errors in the book. The third section deals with the chemistry of the metallic elements together with a chapter on electrochemistry. As stated by the author, part four is supplementary and may be used or not as the teacher sees fit. It is an introduction to the study of organic chemistry. Ten pages of well chosen problems appear at the end of the book as well as a useful appendix of tables.

The book as a whole is very well written and should prove valuable as a text for second year students. The presentation of radioactivity and atomic structure before consideration of the chemistry of the elements is being advocated more and more by teachers of college chemistry. The author places his book in the forefront of those adopting this style of presentation. The format of the book is good and it is excellently illustrated.

L. H. REYERSON

THE PHYSICAL REVIEW

SPACE-DISTRIBUTION OF X-RAY PHOTOELECTRONS EJECTED FROM THE *K* AND *L* ATOMIC ENERGY-LEVELS

BY CARL D. ANDERSON

CALIFORNIA INSTITUTE OF TECHNOLOGY, PASADENA, CALIFORNIA

(Received April 2, 1930)

ABSTRACT

A C.T.R. Wilson expansion-chamber was used to study the space-distribution of photoelectrons ejected from a gas by monochromatic x-rays. In agreement with Auger, and Watson and Van den Akker a more isotropic space-distribution was found for electrons ejected from the *L* energy-levels than for those ejected from the *K* energy-level. The distribution of the electrons from the *L* energy-levels became less isotropic with an increase in frequency of the incident radiation. For a given radiation, the average forward momentum of the electrons from the *K* energy-level was found to decrease with an increase in the binding energy of the parent atom. Within experimental error, however, for electrons from the *K* energy level, even for different binding energies, the average forward momentum remained the same for a given velocity of ejection of the electron. The average forward momentum of electrons from the *L* energy-level was greater than that for electrons from the *K* energy-level for a given velocity of ejection. The space-distribution of electrons from the *K* energy-level was in fair accord with the recent results of quantum mechanics.

THE longitudinal space-distribution of photoelectrons ejected from a gas by x-rays has been extensively studied by means of the C. T. R. Wilson expansion-chamber by several investigators.^{1,2} The general shape of the distribution curve for electrons ejected from the *K* energy-level and the dependence on the frequency of the incident radiation has been determined, and are in approximate agreement with the recent quantum mechanical expressions.^{3,4,5,6} Results so far published for the space-distribution of electrons ejected from the *L* energy-levels are rather meager. Auger⁷ and Watson and Van den Akker⁸ have shown, however, that a more isotropic

¹ E. J. Williams, J. M. Nuttal and H. S. Barlow, Proc. Roy. Soc. A121, 611 (1928).

² M. P. Auger, C.R. 187, 1141 (1928).

³ A. Sommerfeld, Atombau und Spektrallinien, Wellenmechanischer Ergänzungsband.

⁴ G. Wentzel. (Communicated in Lecture Series of Norman Bridge Laboratory.)

⁵ A. Carrelli, Zeits. f. Physik 56, 694 (1929).

⁶ S. E. Szczeniowski, Phys. Rev. 35, 374 (1930).

⁷ M. P. Auger, C.R. 188, 447 (1929).

⁸ E. C. Watson and J. A. Van den Akker, Proc. Roy. Soc. A126, 138 (1929).

space-distribution exists in this case. In the present work, the distribution of electrons ejected from the L energy-levels is found to become less isotropic as the frequency of the incident radiation is increased.

The C. T. R. Wilson expansion-chamber employed in this investigation was essentially that described by Simon and Loughridge.^{9,10} Only minor refinements were effected to insure greater accuracy in the data obtained.

Simple filtering of the general radiation obtained from an x-ray tube was found to produce radiation not sufficiently monochromatic so other means of monochromatizing the x-rays were employed. Monochromatism

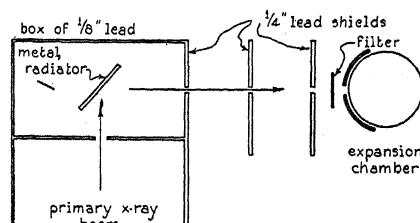


Fig. 1. Fluorescence radiator as source of monochromatic x-rays.

was insured, in one instance, by the selection of the $K\alpha$ line of molybdenum by means of a calcite crystal spectrometer. For the other frequencies, the secondary fluorescence radiation from a metal plate, irradiated by primary x-rays from a tungsten-target Coolidge type tube, was collimated to a narrow beam and passed into the expansion chamber (Fig. 1). A. H. Compton¹¹ has shown the fluorescence radiation obtained in this manner to be very homogeneous, having 99 percent of its energy in the characteristic K line-radiation of the metal radiator.

The wave-lengths of the x-rays used in this investigation are given in Table I together with the metal radiator employed in three cases.

TABLE I.

Source	Monochromatizer	λ
M ₀ target tube	Calcite spectrometer	0.71 Å
W " "	Silver radiator	0.56 Å
W " "	Palladium radiator	0.59 Å
W " "	Tin radiator	0.49 Å

The relatively faint $K\beta$ lines of palladium were filtered out by means of a ruthenium filter. The presence of the $K\beta$ lines in the other cases was not objectionable.

The longitudinal space-distribution curves, representing the density of emission per unit angle of the photoelectrons as a function of the angle between the direction of ejection and the forward direction of the x-ray beam, were plotted in a number of cases to show the effect of the energy level from

⁹ A. W. Simon and D. H. Loughridge, Jour. Opt. Soc. 13, 679 (1926).

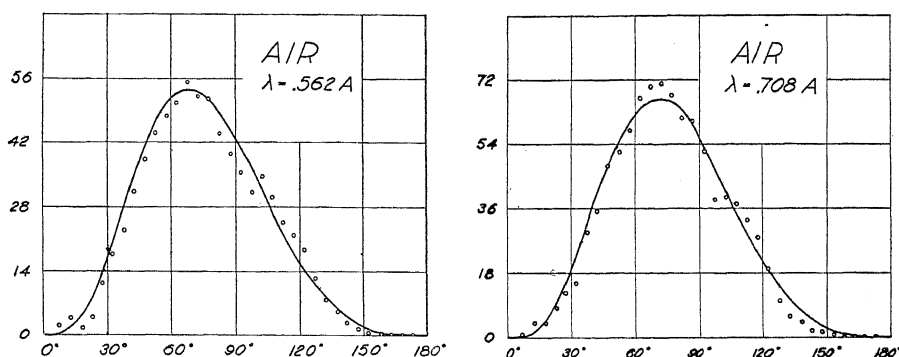
¹⁰ D. H. Loughridge, Phys. Rev. 30, 488 (1927).

¹¹ A. H. Compton, Proc. Nat. Acad. 14, 549 (1928).

which the electron is taken, and also the effect of a change in the frequency of the incident radiation.

In Figs. 2 and 3 are plotted the results obtained respectively from measurements on 272 tracks in air produced by radiation of 0.71A and on 200 tracks in air produced by radiation of 0.56A. Each small circle represents the number of electrons ejected in a 15° interval the point being plotted at an angle corresponding to the center of the interval. Points are plotted every 5° and therefore represent overlapping intervals.

In order to study the distribution where the binding energy was of appreciable magnitude, C_2H_5Br was introduced into the expansion-chamber in an atmosphere of hydrogen. The photoelectrons were produced by radiation of 0.59A, most of them being ejected from the *K* shell of the bromine



Figs. 2 and 3. Space distribution of photoelectrons ejected from air.

atom. About 64 percent of the energy of the incident radiation was required to remove the electron from the atom, the remaining 36 percent appearing as kinetic energy. The secondary and tertiary photoelectrons could easily be distinguished from one another due to the difference in path length.* Photoelectrons ejected from levels other than the *K* level of bromine or from light atoms could be distinguished by their long path length and hence omitted in the measurements. Thus, only the photoelectrons having their origin in the *K* shell of bromine were included. Fig. 4 represents the distribution curve plotted as before for 233 tracks of electrons ejected from the *K* level of bromine by radiation of 0.59A.¹²

For the study of the distribution of electrons ejected from the *L* energy levels, CH_3I was introduced into the chamber in an atmosphere of hydrogen and photoelectrons produced by radiation of 0.71A and 0.49A emission, being from the *L* levels of iodine. The results of measurements on 200 tracks formed by radiation of 0.71A are shown in Fig. 5. In agreement with the work of Auger the curve is broader than that found for the *K* electrons indicating a

* The ratio of the number of secondary to tertiary photoelectrons was found to be 2.5 in agreement with Auger [Ann. de Physique 6, 229 (1926)] and Wentzel [Zeits. f. Physik 43, 524 (1927)].

¹² C. D. Anderson, Phys. Rev. 34, 547 (1929).

more isotropic distribution. The small circles as before represent the experimental points. Fig. 6 represents the distribution of 264 photoelectrons ejected from the L levels of iodine by radiation of 0.49A. The curve here is narrower

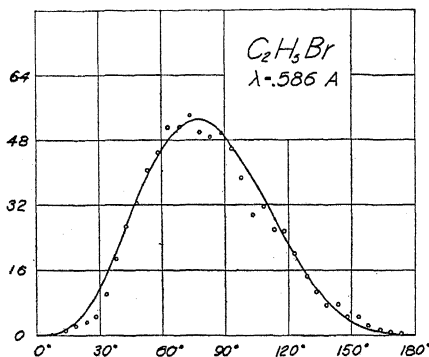
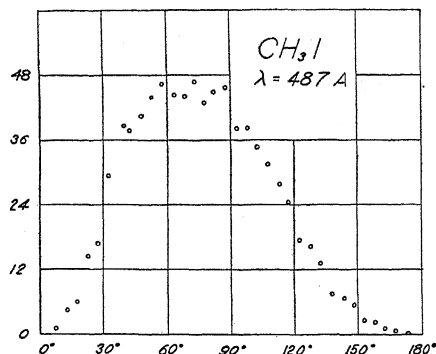
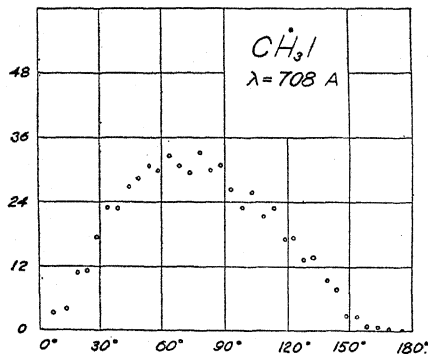


Fig. 4. Space distribution of photoelectrons ejected from K energy-level of bromine.

than in Fig. 5, indicating a decrease in the isotropy of the distribution with an increase in the frequency of the incident radiation. Watson and Van den Akker⁸ have shown that photoelectrons ejected from the L_{11} and L_{111} energy levels have a space-distribution more isotropic than those from the K and L_1 energy levels, and Robinson and Cassie¹³ have found the relative number of



Figs. 5 and 6. Space distribution of photoelectrons ejected from L energy-levels of iodine.

L_1 electrons ejected to increase with an increase in the frequency of the incident radiation. The narrower distribution curve of Fig. 6 may then be explained by the presence of a greater proportion of L_1 electrons than is the case for the curve of Fig. 6.

A theoretical expression derived recently by Wentzel¹⁴ on the basis of quantum mechanics,

$$P(\theta) \propto \frac{\sin^3 \theta}{\left[1 - \frac{v}{c} \cos \theta + \frac{h\nu}{2mc^2}\right]^4} \quad (1)$$

¹³ H. R. Robinson and A. M. Cassie, Proc. Roy. Soc. A113, 296 (1926-27).

¹⁴ G. Wentzel, reference 4.

gives the probability of ejection per unit angle of a photoelectron from the K energy level as a function of the angle, θ , between the direction of ejection and the forward direction of the x-ray beam, where v represents the velocity of ejection, ν the frequency of the incident radiation, and h , m , and c are the customary physical constants.

The solid-line curves of Figs. 2, 3 and 4 represent $P(\theta)$ with the proper values of ν and v inserted, the curves being plotted on a scale to conform to the experimental points. No analogous theoretical expression has as yet been published for the probability of ejection of a photoelectron from the L levels.

The observed asymmetry of the distribution about a plane normal to the x-ray beam may be compared with the theory in several ways.¹⁵ The value of $\cos \theta$ averaged over all the photoelectron tracks, a quantity proportional to the average forward momentum of the photoelectrons may be computed as follows

$$\overline{\cos \theta} = \frac{\int_0^\pi P(\theta) \cos \theta d\theta}{\int_0^\pi P(\theta) d\theta} = \frac{4}{5} \frac{v}{c} + \dots \quad (2)$$

if only first order terms in v/c are retained. The observed and calculated values of the mean of $\cos \theta$ are listed in Table II.

TABLE II.

Energy Level	Gas	λ	$\overline{\cos \theta}$ (obs.)	$\overline{\cos \theta}$ (calc.)
K	Air	0.71 A	0.182	0.210
K	Air	0.56 A	0.210	0.235
K	C_2H_5Br	0.59 A	0.133	0.138
L	CH_3I	0.71 A	0.230	
L	CH_3I	0.49 A	0.255	

The average forward momentum of the K electrons for a given radiation decreases with an increase of the binding energy of the parent atom. Within experimental error, however, K electrons of the same initial velocity have the same average forward momentum. It is to be noted, moreover, that in accord with the results of Auger and Watson and Van den Akker for a given velocity of ejection, the L electrons have an average forward momentum greater than that of the K electrons. The difference in behavior of the K and L electrons is more marked for the lower frequencies of incident radiation. The asymmetry to be expected on theoretical grounds for the L electrons has not as yet been brought to light.

The bi-partition angle, θ_b , the half-angle at the apex of a cone which divides the photoelectrons into two groups of equal numbers, is defined by Eq. (3). Calculation of $\cos \theta_b$ shows it to be equal to v/c to a first approximation. The experimental and calculated values of $\cos \theta_b$ are given in Table III.

¹⁵ Williams, Nuttall and Barlow, reference 1.

$$\int_0^{\theta_b} P(\theta) d\theta = \int_{\theta_b}^{\pi} P(\theta) d\theta. \quad (3)$$

TABLE III.

Energy Level	Gas	λ	$\cos \theta_b$ (obs.)	$\cos \theta_b$ (calc.)
<i>K</i>	Air	0.71 A	0.242	0.262
<i>K</i>	Air	0.56 A	0.292	0.294
<i>K</i>	C ₂ H ₅ Br	0.59 A	0.191	0.173
<i>L</i>	CH ₃ I	0.71 A	0.174	
<i>L</i>	CH ₃ I	0.49 A	0.242	

For a given value of v/c the bi-partition angle for electrons ejected from the *L* energy-levels seems to occur nearer 90° than for those from the *K* energy-level, in agreement with the conclusions of Auger.^{2,7}

The ratio, of the number of electrons ejected forward of the plane normal to the x-ray beam, to the number ejected backward, ρ , is given by Eq. (4):

$$\rho = \frac{\int_0^{\pi/2} P(\theta) d\theta}{\int_{\pi/2}^{\pi} P(\theta) d\theta} = \frac{2 + 3 \frac{v}{c}}{2 - 3 \frac{v}{c}} + \dots \quad (4)$$

The observed and calculated values of ρ are given in Table IV.

It is to be noted that no marked difference was found in the behavior of ρ for the *K* and *L* electrons.

TABLE IV.

Energy Level	Gas	λ	ρ (obs.)	ρ (calc.)
<i>K</i>	Air	0.71 A	2.17	2.30
<i>K</i>	Air	0.56 A	2.39	2.58
<i>K</i>	C ₂ H ₅ Br	0.59 A	1.74	1.70
<i>L</i>	CH ₃ I	0.71 A	2.00	
<i>L</i>	CH ₃ I	0.49 A	2.30	

In conclusion I wish to express my gratitude to Professor R. A. Millikan and Professor E. C. Watson for their interest in this work.

Note added in proof:

Since this article was written, G. Schur [Ann. d. Physik, 4, 441, (1930)] has published a theoretical expression for the space-distribution of photo-electrons ejected from the *L* energy-levels of an atom. For the longitudinal space-distribution he finds,

$$P(\theta) \propto \sin^3 \theta + \frac{4\nu}{c} \sin^3 \theta \cos \theta \left(1 - \frac{I_L}{h\nu} \right) + \frac{I_L \sin \theta}{h\nu + 3I_L} \left\{ 1 + \frac{8I_L}{h\nu} \sin^2 \theta + \frac{2\nu}{c} \cos \theta \left(1 + 2 \sin^2 \theta \left(1 + \frac{11I_L}{h\nu} \right) \right) \right\} \quad (5)$$

where I_L represents the mean value of the binding energy of the L energy-levels, and the other quantities remain as defined above.

Calculation of the average value of $\cos \theta$ for L electrons, in the manner carried out above for K electrons, leads to the following results:

TABLE V.

Energy level	Gas	λ	$\overline{\cos \theta}$ (obs.)	$\overline{\cos \theta}$ (calc.)
L	CH_3I	0.71 A	.23	.17
L	CH_3I	0.49 A	.25	.22

The agreement here is not satisfactory, the observations seeming to indicate a greater average forward momentum of the photoelectrons than the theory.

Calculation of ρ , defined as above, leads to the following results:

TABLE VI.

Energy level	Gas	λ	ρ (obs.)	ρ (calc.)
L	CH_3I	0.71 A	2.0	1.9
L	CH_3I	0.49 A	2.3	2.4

With regard to ρ , experiment and theory are in fair accord.

A decrease in the isotropy of the space-distribution curve for L electrons, with an increase in the frequency of the incident radiation, as was found above, is also to be expected from the theory. The ratio of the number of L_{II} and L_{III} electrons to the L_I electrons is given by

$$\frac{L_{II} + L_{III}}{L_I} = \frac{I_L}{h\nu + 3I_L} \left(3 + 8 \frac{I_L}{h\nu} \right) \quad (6)$$

which for this case, leads to:

TABLE VII.

Energy level	Gas	λ	Relative proportion of	
			L_I Electrons	L_{II} and L_{III} Electrons
L	CH_3I	0.71 A	67%	33%
L	CH_3I	0.49 A	72%	28%

For the harder radiation then, due to the greater proportion of L_I electrons ejected, a slightly less isotropic distribution is to be expected.

HYPERFINE STRUCTURE IN NEUTRAL MANGANESE, $Mn I$.

By H. E. WHITE* AND R. RITSCHL

PHYSIKALISCH-TECHNISCHE REICHSANSTALT, BERLIN

(Received March 5, 1930)

ABSTRACT

Observations. The hyperfine structure patterns of some 30 or 40 lines in the spectrum of $Mn I$ have been photographed by means of a prism spectrograph and silvered Fabry-Perot etalons. A tube, designed by Schüler, and operated at liquid air temperatures, has been used as a light source for most of the lines and a king vacuum furnace for the others. Patterns of from 2 to 6 components are found, some degrading in intensity and intervals toward low frequencies and others toward higher frequencies.

Interpretation. The strictly LS coupling in the well-known multiplet structure of $Mn I$, and Ji coupling in the hyperfine structure enable vector diagrams to be drawn for the space quantization of each valence electron with respect to the nucleus. Some of the hyperfine structure terms are computed directly from observed term differences while others are computed from the observed diagonal components. The normal state ${}^6S_{5/2}(3d^5 4s^2)$ is found to be quite narrow, whereas the metastable ${}^6D(3d^5 4s)$ terms show the widest separations. While the hyperfine structure intervals for any given term are proportional to $\cos(Ji)$, the total separations are approximately determined by $\cos(Si)$, the l values of the electrons contributing but very little.

Theoretical computations. A study of the vector diagrams for the different multiplet terms shows quite definitely that while the hyperfine structure is determined primarily by the coupling between the $4s$ electron and the nucleus, the remaining valence electrons must also be taken into account. The hyperfine structure formula given by Goudsmit and Bacher for the interaction between an s electron spin and the nuclear spin is extended so as to include not only the spins of all of the valence electrons but their l values as well. From the derived general formula and the observed hyperfine structure term separations, coupling constants to be associated with each electron have been computed. While the energy of interaction between electron spin s and nuclear spin i is given by $ais \cos(is)$ the energy of interaction between electron l value and nuclear spin i is given by $a'il \cos(il)$.

THE hyperfine structure in the spectral lines of neutral manganese was investigated in this laboratory by Janicki¹ some twenty years ago and later verified by Wali-Mohammed.² An analysis of the gross or multiplet structure of $Mn I$ was first given by Catalan,³ some of the terms being later assigned to definite electron configurations by Hund.⁴ A more complete analysis of the gross structure has been given by Russell⁵ and by McLennan,

* National Research Fellow.

¹ Janicki, Ann. d. Physik 29, 833 (1909).

² Wali-Mohammed, Astrophys. J. 39, 198 (1914).

³ Catalan, Phil. Trans. Roy. Soc. London 223, 127 (1923).

⁴ Hund, Linienspektren, p. 161, 1927.

⁵ Russell, Astrophys. J. 66, 184 (1927).

McLay and Crawford.⁶ Since the *hfs*⁷ of many of the lines is observed to have the same general appearance as that found in a number of other elements (for example, praseodymium, lanthanum, iodine, and bromine) it was hoped that an analysis of the *hfs*, at the expense of the well-known *gs*, would not only verify the interpretation of *hfs* given previously by one of the authors,⁸ but at the same time to lead to some conclusions concerning *hfs* in general.

APPARATUS AND MEASUREMENTS

A Zeiss three-prism constant deviation spectrograph, with a large glass optical system specially constructed for fine-structure work, was used in conjunction with quartz Fabry-Perot etalons for photographing the *hfs*. In order to eliminate self-reversal of resonance lines and at the same time to

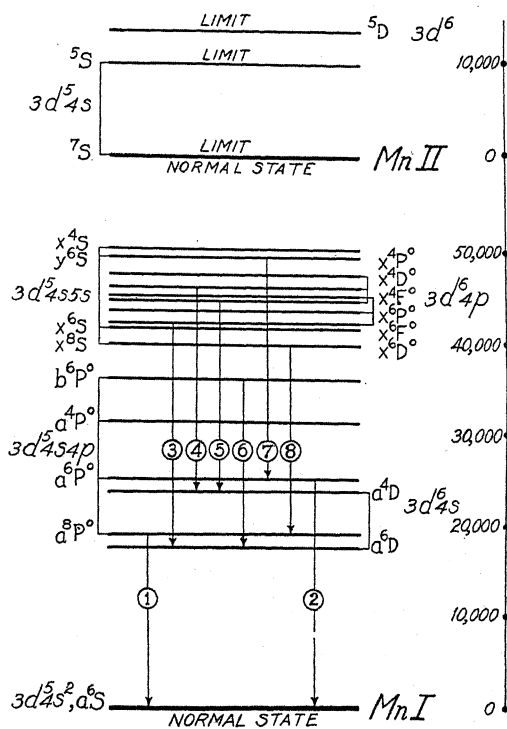


Fig. 1. Term scheme of neutral manganese, Mn I.

produce very sharp lines, a metal discharge tube, operated at liquid air temperatures, has been used. Prior to publication, the design and operation of this tube was very kindly submitted to the authors by Dr. Schüler.⁹ The manganese lines were excited in a discharge of argon by placing small pieces

⁶ McLennan, McLay and Crawford, Trans. Roy. Soc. Canada 20, 15 (1926).

⁷ The words hyperfine structure and gross structure will be abbreviated by *hfs* and *gs* respectively.

⁸ White, Phys. Rev. 34, 1404 (1929); Proc. Nat. Acad. Sci. 16, 68 (1930).

⁹ Schüler, Zeits. f. Physik 59, 149 (1930).

TABLE I. Measured hfs -components in $Mn I$.

Mult. No.	Design.	λ μ	$\Delta\lambda_1$ $\Delta\mu_1$	$\Delta\lambda_2$ $\Delta\mu_2$	$\Delta\lambda_3$ $\Delta\mu_3$	$\Delta\lambda_4$ $\Delta\mu_4$	$\Delta\lambda_5$ $\Delta\mu_5$	Total $\Delta\lambda$ Total $\Delta\mu$
1	${}^6S_{3/2} - {}^8P_{3/2}^0$	5394.677	+ .0325	+ .0285	+ .0230	+ .0200	+ .0111	+ .1151
	${}^6S_{3/2} - {}^8P_{3/2}^0$	18531.65	- .1116	- .0979	- .0790	- .0687	- .0381	- .3953
	${}^6S_{3/2} - {}^8P_{3/2}^0$	5432.555	+ .0306	+ .0247	+ .0198	+ .0133		+ .0884
2	${}^6S_{3/2} - {}^8P_{3/2}^0$	18402.45	- .1036	- .0836	- .0671	- .0450		- .2993
	${}^6S_{3/2} - {}^8P_{3/2}^0$	4030.760	+ .0155	+ .0133	+ .0104	+ .0079	+ .0052	+ .0523
	${}^6S_{3/2} - {}^8P_{3/2}^0$	24802.23	- .0930	- .0798	- .0624	- .0474	- .0312	- .3138
3	${}^6S_{3/2} - {}^8P_{3/2}^0$	4033.074	+ .0142	+ .0127	+ .0090	+ .0060		+ .0419
	${}^6S_{3/2} - {}^8P_{3/2}^0$	24788.01	- .0873	- .0781	- .0553	- .0369		- .2576
	${}^6S_{3/2} - {}^8P_{3/2}^0$	4034.489	+ .0145	+ .0117	+ .0077			+ .0339
	${}^6S_{3/2} - {}^8P_{3/2}^0$	24779.31	- .0891	- .0719	- .0473			- .2083
	${}^6D_{3/2} - {}^6D_{3/2}^0$	4018.108	- .0192	- .0155	- .0129	- .0100		- .0651
	${}^6D_{3/2} - {}^6D_{3/2}^0$	24880.32	+ .1188	+ .0959	+ .0799	+ .0619		+ .4029
	${}^6D_{3/2} - {}^6D_{3/2}^0$	4035.730	- .0159	- .0135	- .0107			- .0507
	${}^6D_{3/2} - {}^6D_{3/2}^0$	24771.69	+ .0976	+ .0829	+ .0657			+ .3113
	${}^6D_{3/2} - {}^6D_{3/2}^0$	4041.366	- .0165	- .0140	- .0116	- .0093	- .0060	- .0574
	${}^6D_{3/2} - {}^6D_{3/2}^0$	24737.15	+ .1010	+ .0857	+ .0710	+ .0569	+ .0367	+ .3513
	${}^6D_{3/2} - {}^6D_{3/2}^0$	4048.760	- .0146	- .0125	- .0098			- .0369
	${}^6D_{3/2} - {}^6D_{3/2}^0$	24691.97	+ .0890	+ .0763	+ .0598			+ .2251
	${}^6D_{3/2} - {}^6D_{3/2}^0$	4055.553	- .0142	- .0122	- .0099	- .0070		- .0481
	${}^6D_{3/2} - {}^6D_{3/2}^0$	24650.62	+ .0863	+ .0742	+ .0602	+ .0426		+ .2925
	${}^6D_{3/2} - {}^6D_{3/2}^0$	4063.533	- .0133	- .0102	- .0082			- .0364
	${}^6D_{3/2} - {}^6D_{3/2}^0$	24602.18	+ .0807	+ .0619	+ .0492			+ .2209
	${}^6D_{3/2} - {}^6D_{3/2}^0$	4079.245	- .0139	- .0110	- .0082			- .0436
	${}^6D_{3/2} - {}^6D_{3/2}^0$	24507.44	+ .0834	+ .0660	+ .0492			+ .2616
	${}^6D_{3/2} - {}^6D_{3/2}^0$	4079.428	- .0197					- .0197
	${}^6D_{3/2} - {}^6D_{3/2}^0$	24506.34	+ .1182					+ .1182
	${}^6D_{3/2} - {}^6D_{3/2}^0$	4082.947	- .0112	- .0091	- .0070			- .0273
	${}^6D_{3/2} - {}^6D_{3/2}^0$	24485.22	+ .0672	+ .0546	+ .0420			+ .1638
	${}^6D_{3/2} - {}^6D_{3/2}^0$	4083.639	- .0109					- .0326
	${}^6D_{3/2} - {}^6D_{3/2}^0$	24481.07	+ .0654					+ .1956

TABLE I (continued).

4	$4D_{1\frac{1}{2}} - 4D_{\frac{3}{2}}^0$	4453.013 22450.42	+ .0172 - .0867			+ .0172 - .0867
	$4D_{\frac{1}{2}} - 4D_{\frac{3}{2}}^0$	4472.793 22351.14	- .0229 + .1145	- .0162 + .0810		- .0391 + .1955
	$4D_{\frac{3}{2}} - 4D_{1\frac{1}{2}}^0$	4490.078 22265.10	- .0235 + .1165			- .0235 + .1165
	$4D_{3\frac{3}{2}} - 4F_{3\frac{3}{2}}^0$	4709.704 21226.83	+ .0133 - .0599			+ .0420 - .1893
5	$4D_{2\frac{1}{2}} - 4F_{2\frac{1}{2}}^0$	4727.462 21147.10	+ .0152 - .0697			+ .0421 - .1883
	$6D_{4\frac{1}{2}} - 6P_{3\frac{1}{2}}^0$	5341.070 18717.64	- .0628 + .2201	- .0530 + .1857	- .0438 + .1535	- .2170 + .7605
	$6D_{3\frac{1}{2}} - 6P_{3\frac{1}{2}}^0$	5407.432 18487.97	- .0552 + .1888	- .0445 + .1522		- .1627 + .5564
	$6D_{3\frac{1}{2}} - 6P_{2\frac{1}{2}}^0$	5420.368 18443.82	- .0581 + .1976	- .0467 + .1589	- .0348 + .1184	- .1846 + .6279
6	$6D_{2\frac{1}{2}} - 6P_{3\frac{1}{2}}^0$	5457.468 18318.44	- .0508 + .1705	- .0408 + .1369		- .1423 + .4777
	$6D_{2\frac{1}{2}} - 6P_{2\frac{1}{2}}^0$	5470.640 18274.33	- .0545 + .1821	- .0435 + .1453		- .1484 + .4958
	$6D_{2\frac{1}{2}} - 6P_{1\frac{1}{2}}^0$	5481.395 18238.48	- .0662 + .2203	- .0512 + .1704	- .0365 + .1215	- .1539 + .5122
	$6D_{1\frac{1}{2}} - 6P_{2\frac{1}{2}}^0$	5505.877 18157.38	- .0484 + .1597	- .0413 + .1362		- .1189 + .3922
	$6D_{1\frac{1}{2}} - 6P_{1\frac{1}{2}}^0$	5516.773 18121.52	- .0748 + .2458	- .0498 + .1636		- .1246 + .4094
	$6D_{\frac{1}{2}} - 6P_{1\frac{1}{2}}^0$	5537.749 18052.88	- .1116 + .3640			- .1116 + .3640
	$6P_{3\frac{1}{2}}^0 - 6S_{2\frac{1}{2}}^0$	4061.744 24613.03	- .0326 + .1975	- .0290 + .1757	- .0210? + .1272?	- .1066? + .6458?

of manganese metal in the tube, the discharge itself taking place in a small cylinder, 2 cm long and 1 cm in diameter, working as a Paschen hollow cathode, in the bottom of the tube. The light from the discharge was reflected into a horizontal position by a plane mirror and then brought to focus on the slit of the spectrograph. With a current of 100 to 200 m.a. at about 2500 volts d.c., exposure times at 4000Å ranged from 1 to 5 minutes. In the absence of hydrogen, and at the right pressure, the manganese lines were stronger than those of argon. With silvered quartz mirrors, separated by invar rings 5, 7.5, 10, 12, and 15 mm in thickness, placed between the collimating lens and the prisms, a resolving power of nearly one million at 4000Å has been obtained. The mirrors were silvered in vacuum by evaporation from electrically heated silver filaments, a method developed previously by one of the authors.¹⁰ While the lines photographed have the same appearance as those found in praseodymium,¹¹ they are in general about one-fifth to one tenth as wide and vary in number from one to six components.

An energy level diagram of Mn I is given in Fig. 1. Each *gs*-multiplet, for which the *hfs* has been studied, is shown by a transition arrow and assigned a number for reference in Tables I and II. All of the lines except those in multiplets numbered six and seven, have been photographed with the light source at liquid air temperatures, thus enabling the *hfs* $\Delta\lambda$'s in Tables I and II to be given to four decimal places. The last two multiplets, numbers six and

TABLE II. Measured *hfs*-components in Mn I.

Mult. No.	Design	λ ν	Total $\Delta\lambda$ Total $\Delta\nu$	Mult. No.	Design	λ ν	Total $\Delta\lambda$ Total $\Delta\nu$
4	$^4D_{3\frac{1}{2}} - ^4D_{2\frac{1}{2}}^0$	4414.887 22644.29	+ .0264? - .1352?	4	$^4D_{1\frac{1}{2}} - ^4D_{2\frac{1}{2}}^0$	4498.897 22221.45	sharp
	$^4D_{2\frac{1}{2}} - ^4D_{1\frac{1}{2}}^0$	4436.358 22534.70	+ .0226 - .1148		$^4D_{2\frac{1}{2}} - ^4D_{3\frac{1}{2}}^0$	4502.223 22205.01	+ .0244 - .1204
	$^4D_{3\frac{1}{2}} - ^4D_{3\frac{1}{2}}^0$	4451.578 22457.66	+ .0274 - .1383	7	$^6P_{1\frac{1}{2}}^0 - ^6S_{2\frac{1}{2}}$	4057.959 24635.99	- .0792 + .4810
	$^4D_{2\frac{1}{2}} - ^4D_{2\frac{1}{2}}^0$	4464.679 22391.76	+ .0236 - .1184		$^6P_{2\frac{1}{2}}^0 - ^6S_{2\frac{1}{2}}$	4059.399 24627.26	- .0850 + .5160
	$^4D_{1\frac{1}{2}} - ^4D_{1\frac{1}{2}}^0$	4470.142 22364.40	sharp				

seven, were photographed using as a light source a King vacuum furnace operated at about 2000°C. Fortunately these two multiplets show the widest *hfs* in Mn I, thus making it possible to resolve some of the patterns at this temperature. The manganese lines were brought out much stronger than is usually obtained from such a furnace by applying a potential of 120 volts d.c. between a small anode and the heating element of the furnace.¹² The anode is

¹⁰ Ritschl, Verhand. d. Deutsch. Phys. Ges. (3), 10, 33 (1929).

¹¹ White, Phys. Rev. 34, 1397 (1929).

¹² Schüller, Zeits. f. Physik 37, 728 (1926).

here placed coaxial with and extends half way through the heated graphite tube of the furnace.¹⁰ Since the relative intensities of the components in each pattern are always found to decrease regularly toward longer or shorter wave-lengths, the wave-length and frequency number of only the strongest component in each pattern is given in column three. The wave-lengths and frequency numbers of the other components may be obtained by adding or subtracting, as the case may be, the $\Delta\lambda$'s and $\Delta\nu$'s given in columns four, five, six, seven and eight. Where only the first two, three, or four components of a group are resolved, the end of the group has been measured. The total

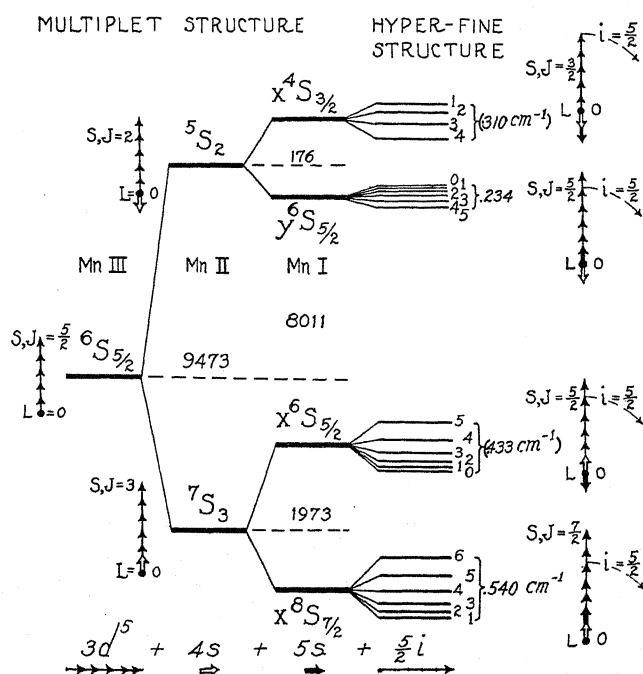


Fig. 2. Hyperfine structure terms and space quantization vectors for the electron configuration $3d^5 4s 5s$.

width of each pattern is given in the last column. In general the measurements given by Janicki¹ are in good agreement with those in Tables I and II. The additional component which Janicki found on the short wave-length side of $\lambda\lambda 4030, 4033$ and 4034 is very probably a self-reversal effect of each hfs -component, and, is not found on any of our plates. At liquid air temperatures very sharp and well-resolved patterns of these three lines have been photographed. As reported by Janicki, $\lambda\lambda 6021, 6016$, and 6013 appear sharp. Although these lines are quite strongly excited at liquid air temperatures and are visually seen to be quite narrow, they have not been photographed due to the extremely long exposures necessary at this wave-length.

Owing to an early mistake in the width of an etalon ring, the computations reported in a brief note, "Letters to the Editor" in the Physical Review,¹³ are

¹³ White and Ritschl, Phys. Rev. 35, 208 (1930).

in error. The $\Delta\lambda$'s and $\Delta\nu$'s for the two lines there given may be corrected by multiplying by a factor of 1.25.

THE COMPUTATION AND INTERPRETATION OF THE *HFS*-TERM SEPARATIONS

There are two distinct and characteristic systems of multiplet terms in the arc spectrum of manganese, as may be seen from Fig. 1; (a) a system of *normal* multiplet terms built upon the 5S and 7S ($3d^54s$) terms of Mn II, which in turn are built upon the 6S ($3d^6$) term of Mn III, and (b) a system of inverted multiplet terms built upon the inverted 5D ($3d^6$) term of Mn II. It has been indicated previously⁸ that the *hfs* of manganese is in good agreement with the

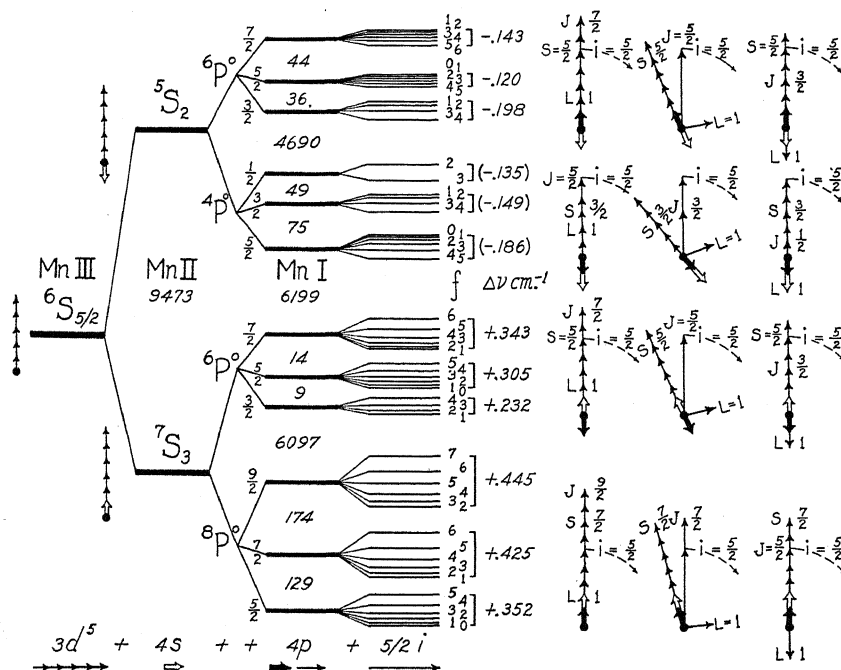


Fig. 3. Multiplet structure terms, *hfs*-terms, and space quantization vectors for the electron configuration $3d^5 4s 4p$.

interpretation of *hfs* in other elements. Here in manganese, as in many other elements, the deep penetrating and tightly bound *s* electron is found to play an important role. The coupling of a *4s* electron with the resultant of six other valence electrons is observed to give the widest *gs*-separations while its strong coupling with the nucleus gives rise to the widest *hfs*-separations. Fortunately, *LS* coupling in the *gs* and *Ji* coupling in the *hfs* is quite rigidly held to, thus enabling vector diagrams for the space quantization of the *s* and *l* values for each valence electron to be quite accurately drawn. It has also been previously shown⁸ that the total *hfs*-separation of a *gs*-term should be approximately proportional to $\cos(is)$, where *s* is the spin of the deeply penetrating and tightly bound *s* electron, and *i* is the nuclear spin momentum. Since this proportionality is taken for the vector position $\cos(Ji) = 1$, where

$\cos(is) = \cos(Js)$, it may be stated that for each gs -term where $\cos(Js)$ is *positive*, the hfs -terms are *normal*, and where $\cos(Js)$ is *negative* the hfs -terms are *inverted*.

At the left in Fig. 2 the building up of the x^4S , x^6S , y^6S , and x^8S ($3d^54s5s$) terms of Mn I is shown starting with the parent term 6S ($3d^5$) of Mn III. This is done in order to show the direction taken on by the spins of the $4s$ and $5s$ electrons in each gs -term and to show the shift in energy due to the inversion (with respect to the electron resultant J) of either the $4s$ or $5s$ electron. At the right in Fig. 2, it may be seen that when the $4s$ electron spin is parallel with J , $\cos(Js_{4s})$ positive, the hfs -terms are *normal*, and when oppositely directed, $\cos(Js_{4s})$ negative, the hfs -terms are *inverted*. Space quantization of i with J and s is only shown for the position of largest f value.

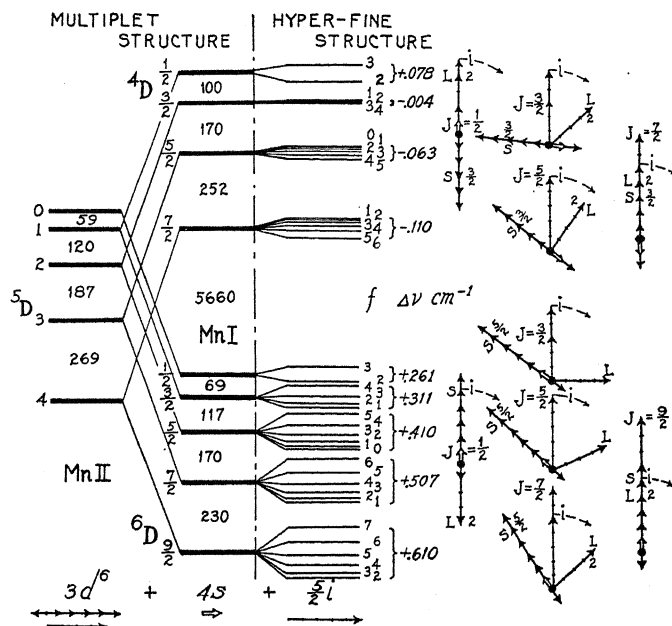


Fig. 4. Hyperfine structure terms and space quantization vectors for the electron configuration $3d^5 4s$.

The building up of the a^4P^0 , a^6P^0 , b^6P^0 , and a^8P^0 ($3d^5 4s 4p$) terms in Fig. 3 is quite similar to that of the x^4S , x^6S , y^6S and x^8S terms in Fig. 2. The addition of a $4p$ electron, with quantum number $s = \frac{1}{2}$ and $l = 1$, in place of a $5s$ electron, with $s = \frac{1}{2}$ and $l = 0$, however, splits both 5S and 7S ($3d^5 4s$) of Mn II into six levels in place of two. The vector diagrams for each level are given at the right in Fig. 3. For each gs -level of a^4P^0 and b^6P^0 , $\cos(Js_{4s})$ negative, the hfs -terms are *inverted*, whereas, for a^6P^0 and a^8P^0 , $\cos(Js_{4s})$ positive, the hfs -terms are *normal*.

Starting with the inverted 5D ($3d^5$) term of Mn II at the left in Fig. 4, the addition of a $4s$ electron splits each level into two levels resulting in the *inverted* multiplet terms a^4D and a^6D ($3d^5 4s$). Here again for $\cos(Js_{4s})$ negative, the hfs -terms are *inverted*, while for $\cos(Js_{4s})$ positive they are *normal*.

The stepwise inversion of the *hfs* in the four terms of a^4D follows directly from the stepwise change from positive $\cos(Js_{4s})$ in $a^4D_{3/2}$ to negative $\cos(Js_{4s})$ in $a^4D_{5/2}$.

Each spectral line in manganese is in reality a tiny multiplet. Several characteristic types of these *hfs*-multiplets are shown in Figs. 5 and 6. A new Zeiss microphotometer, having variable magnification, has been used to obtain density curves from the best plates, copies of which are shown at the bottom of the figures. From the total width of lines of the type shown in Fig. 5, it is obvious why only the *diagonal* lines have been resolved and measured. The intervals between the *diagonal* lines give only the difference between the

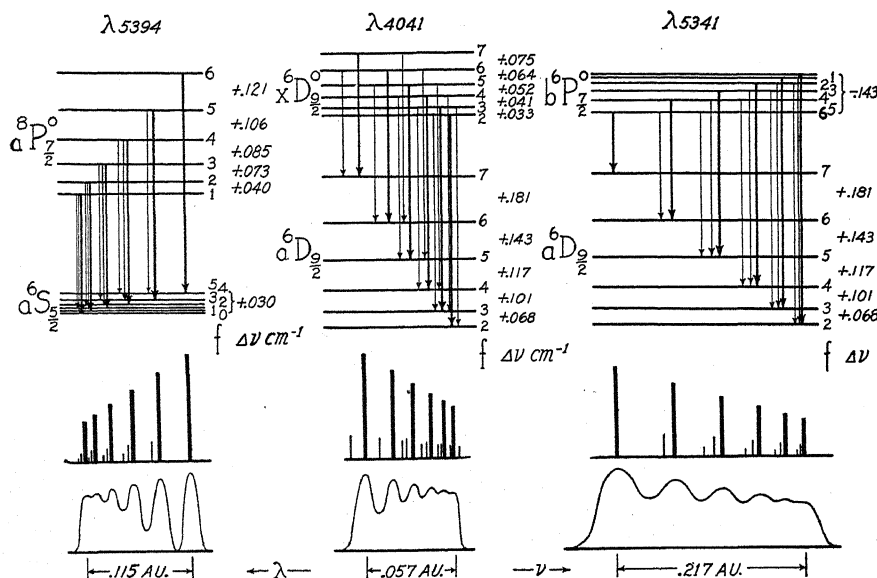


Fig. 5. Hyperfine structure patterns in neutral manganese. $\lambda\lambda 5394$ and 4041 taken at liquid air temperatures and $\lambda 5341$ taken from a vacuum furnace.

set of levels above and the set below. It should here be pointed out that the total width of $\lambda 4041$ is only 0.057\AA . It was hoped, therefore, in a wide pattern of lines like $\lambda 5341$, Fig. 5, that the *off diagonal*, or faint lines, could be observed. Since the *gs*-multiplet to which this line belongs was so weakly excited in the Schüller tube, and at the same time lies in a region of the spectrum where photographic plates are rather insensitive, the vacuum furnace was resorted to. The only trace of the *off diagonal*, or faint lines, in any of the *hfs*-multiplets has been found in the lines $a^8P^0_{4\frac{1}{2}, 3\frac{1}{2}, 2\frac{1}{2}}, -x^8S_{3\frac{1}{2}}$. All three lines of this *gs*-multiplet, $\lambda\lambda 4823, 4783$, and 4754 , are shown in Fig. 6. Even though the extremely narrow patterns of these lines have not been completely resolved, their interpretation is quite unambiguous since their general appearance verifies the order and magnitude of the *hfs*-term separations of a^8P^0 and x^8S arrived at from other considerations. What has actually been measured is indicated at the bottom of the figure. The five *off diagonal* lines on the low frequency side of $\lambda 4783$ fortunately fall almost together and can be

measured as a single strong component. With the measured separations between this component and the first two diagonal components and, making the valid assumption that the Landé interval rule is in operation, the x^8S , and in turn the a^8P^0 , hfs -term separations can be approximately computed. With this as a start, the total separation of the normal state $^6S_{5/2}$ ($3d^54s^2$) is determined from the two resonance lines $\lambda\lambda 5394$ and 5432 to be about 0.030 cm^{-1} . The separations for $a^6P^0_{3/2, 2/2, 1/2}$ are then determined from $\lambda\lambda 4030$, 4033 , and 4034 . While the hfs -patterns of $^6D-^6D^0$ and $^4D-^4D^0$ ($3d^64s-3d^64p$)

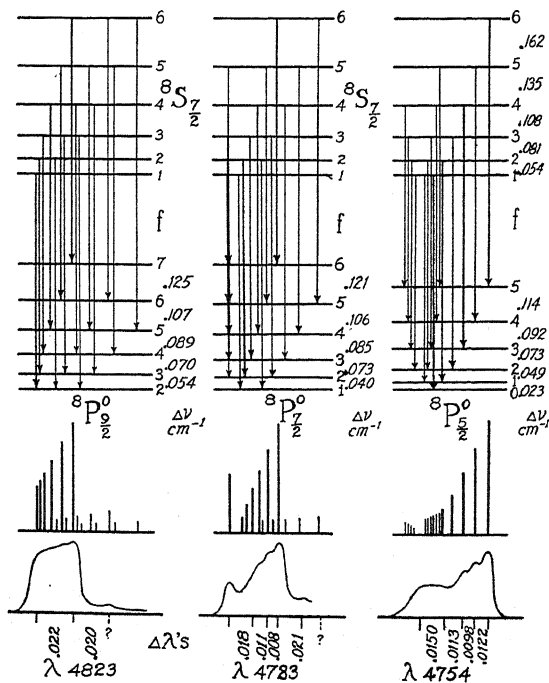


Fig. 6. Very narrow hyperfine structure patterns in the octet system of manganese taken at liquid air temperatures.

have been obtained at liquid air temperatures, none of them resolve the *off diagonal* components that must certainly be there. From the measured differences between the different patterns of a multiplet, however, a clue to the hfs -separations is obtained. The successive differences, for example, between the $\Delta\nu$'s of $\lambda\lambda 4018$, 4055 and 4083 as compared with the successive differences between the $\Delta\nu$'s of $\lambda\lambda 4079$, 4055 and 4035 show that the a^6D ($3d^64s$) separations are about two and one-half times as wide as those of x^6D^0 ($3d^64p$). Even though relations of this kind can only give, at best, an approximation to the true separations, it has been necessary to use such relations to compute the separations for a^6D , b^6P^0 , a^4D , x^6D^0 and x^4D^0 . The gs -terms and hfs -term intervals are given in Table III.

THEORETICAL INTERPRETATION

It has quite generally been observed that the widest hfs -separations are due to the strong coupling between the spin of a single s electron and the nu-

TABLE III. *hfs-term intervals, Mn I.*

Term	Value	$\Delta\nu_1$	$\Delta\nu_2$	$\Delta\nu_3$	$\Delta\nu_4$	$\Delta\nu_5$	Total $\Delta\nu$
$a^8S_{2\frac{1}{2}}$	59937.47	+ .010	+ .008	+ .006	+ .004	+ .002	+ .030
$x^8S_{3\frac{1}{2}}$	20506.13	+ .162	+ .135	+ .108	+ .081	+ .054	+ .540
$x^8S_{2\frac{1}{2}}$	18533.50	+ .144	+ .115	+ .087	+ .058	+ .029	+ .433
$y^8S_{2\frac{1}{2}}$	10524.27	- .078	- .062	- .047	- .031	- .016	- .234
$x^4S_{1\frac{1}{2}}$	10346.03	- .138	- .103	- .069			- .310
$a^8P_{4\frac{3}{2}}^0$	41232.09	+ .125	+ .107	+ .089	+ .070	+ .054	+ .445
$a^8P_{3\frac{3}{2}}^0$	41405.80	+ .121	+ .106	+ .085	+ .073	+ .040	+ .425
$a^8P_{2\frac{3}{2}}^0$	41534.98	+ .114	+ .092	+ .073	+ .049	+ .023	+ .352
$a^6P_{3\frac{3}{2}}^0$	35135.24	+ .103	+ .088	+ .068	+ .051	+ .033	+ .343
$a^6P_{2\frac{3}{2}}^0$	35149.46	+ .097	+ .086	+ .061	+ .041	+ .020	+ .305
$a^6P_{1\frac{3}{2}}^0$	35158.16	+ .099	+ .080	+ .053			+ .232
$b^6P_{3\frac{3}{2}}^0$	24167.53	- .044	- .037	- .030	- .019	- .013	- .143
$b^6P_{2\frac{3}{2}}^0$	24211.65	- .040	- .032	- .022	- .008		- .120
$b^6P_{1\frac{3}{2}}^0$	24247.40	- .100	- .060	- .038			- .198
$a^4P_{2\frac{1}{2}}^0$	28936.41	- .062	- .050	- .037	- .025	- .012	- .186
$a^4P_{1\frac{1}{2}}^0$	28861.11	- .066	- .050	- .033			- .149
$a^4P_{\frac{1}{2}}^0$	28812.58	- .135					- .135
$a^6D_{4\frac{3}{2}}$	42885.17	+ .181	+ .143	+ .117	+ .101	+ .068	+ .610
$a^6D_{3\frac{3}{2}}$	42655.50	+ .160	+ .123	+ .103	+ .073	+ .048	+ .507
$a^6D_{2\frac{3}{2}}$	42485.96	+ .142	+ .111	+ .083	+ .053	+ .021	+ .410
$a^6D_{1\frac{3}{2}}$	42368.98	+ .128	+ .104	+ .079			+ .311
$a^6D_{\frac{3}{2}}$	42300.28	+ .261					+ .261
$a^4D_{3\frac{1}{2}}$	36640.81	- .033	- .028	- .022	- .016	- .011	- .110
$a^4D_{2\frac{1}{2}}$	36388.29	- .021	- .017	- .013	- .008	- .004	- .063
$a^4D_{1\frac{1}{2}}$	36217.00	- .002	- .001	- .001			- .004
$a^4D_{\frac{1}{2}}$	36118.69	+ .078					+ .078
$x^6D_{4\frac{3}{2}}^0$	18148.04	+ .075	+ .064	+ .052	+ .041	+ .033	+ .265
$x^6D_{3\frac{3}{2}}^0$	18004.88	+ .065	+ .052	+ .042	+ .034	+ .022	+ .216
$x^6D_{2\frac{3}{2}}^0$	17883.78	+ .062	+ .050	+ .037	+ .025	+ .012	+ .186
$x^6D_{1\frac{3}{2}}^0$	17793.97	+ .057	+ .043	+ .028			+ .128
$x^6D_{\frac{3}{2}}^0$	17738.89	+ .092					+ .092

clear spin i , and also that the observed intervals follow the Landé interval rule. Since the classical quantum mechanics have yielded interval rules which agree so well with observations in *gs*-multiplets, Goudsmit and Bacher¹⁴ have extended them to some of the simpler cases in *hfs*. The Landé interval rule for separations between two states f and $(f+1)$ is, as in *gs*, given by $\Delta\nu = A(f+1)$, where f is the resultant of i and J , and A is an observed proportionality constant. The total separation of a multiplet term is given by

$$\Delta\nu = mA \quad (1)$$

where $m = \sum f$'s minus the smallest f .

Assuming the cosine law for the interaction energy of any two electronic angular momentum vectors, the energy of interaction between an s electron spin and the nuclear spin, i , as shown by Goudsmit and Bacher and others, may be written

$$a i s \cos(is). \quad (2)$$

Since i and s are constants, a is a constant to be associated with the electron, its value depending upon how strongly the electron spin is coupled with the nucleus spin.

¹⁴ Goudsmit and Bacher, Phys. Rev. 34, 1501 (1929).

In the case of an s electron and an arbitrary other electron, in LS coupling,

$$a_1 i s \overline{\cos(i s_1)} = a_1 i s_1 \cos(i j) \cos(j s) \cos(s s_1) = A i j \cos(i j) \quad (3)$$

where in terms of the quantum mechanics cosines

$$A = a_1 \frac{s(s+1) + s_1(s_1+1) - s_2(s_2+1)}{2s(s+1)} \cdot \frac{j(j+1) + s(s+1) - l_2(l_2+1)}{2j(j+1)} \quad (4)$$

and is the A of Eq. (1). The subscripts denote the s and arbitrary electron respectively. As pointed out by Goudsmit and Bacher, this expression for A , which is also applicable in the case where an s electron is added to a more general electron configuration, takes into account only the interaction between the s electron and the nucleus and neglects the interaction of the other valence electrons. A study of the vector diagrams and hfs shown in Figs. 2, 3, and 4 shows quite definitely that while the total hfs -separations depend primarily upon the $4s$ electron, the remaining valence electrons also make some contribution, and in some cases almost equal the contribution of the $4s$ electron. We may extend Eq. (4) in such a way that it is applicable to p , d , and f electrons as well as to s electrons. This is done by assuming that the electron has only a spin s and that its l vector is associated with the remaining valence electrons. This total *remainder* is then thought of as a parent term R_1 to which an electron spin S_1 alone is added to give the resultant multiplet term under consideration. Eq. (4) is then written

$$A = a_1 \frac{S(S+1) + S_1(S_1+1) - S_{R_1}(S_{R_1}+1)}{2S(S+1)} \cdot \frac{J(J+1) + S(S+1) - L_{R_1}(L_{R_1}+1)}{2J(J+1)} \quad (5)$$

Here S_1 may represent the spin of one or more electrons and a_1 the coupling constant associated with S_1 . Making the valid assumption that the energy of interaction between an l vector and the nuclear spin i is given by

$$a i l \cos(i l) \quad (6)$$

the l vectors of each valence electron may be taken into account by replacing each S and L of Eq. (5) by L and S respectively. Taking into account all of the electrons we get the general expression

$$A = \sum_n a_n \frac{S(S+1) + S_n(S_n+1) - S_{R_n}(S_{R_n}+1)}{2S(S+1)} \cdot \frac{J(J+1) + S(S+1) - L_{R_n}(L_{R_n}+1)}{2J(J+1)} + \sum_n a_n \frac{L(L+1) + L_n(L_n+1) - L_{R_n}(L_{R_n}+1)}{2L(L+1)} \cdot \frac{J(J+1) + L(L+1) - S_{R_n}(S_{R_n}+1)}{2J(J+1)} \quad (7)$$

For n valence electrons this gives A in terms of $2n$ constants. With seven valence electrons in manganese the fourteen constants are readily reduced to

TABLE IV. *hfs-coupling constants. Electron configurations 3d⁵4s4p and 3d⁵3s².*

Term	Total $\Delta\nu$	$R_1 R_2 R_3 R_4$	m_A	A			a_1 4s ₂	a_2 4p ₂	a_3 4p ₁	a_4 3d _{5/2}
$a^8P_{43/2}^0$	+ .445	$^7P^7P^8S^3P$	25A	+ a_1 1/9	+ a_2 1/9	+ a_3 2/9	.120	.019	.006	.002
$a^8P_{33/2}^0$	+ .425	$^7P^7P^8S^3P$	20A	+ a_1 59/441	+ a_2 59/441	+ a_3 4/63	.124	.021	.006	.002
$a^8P_{23/2}^0$	+ .352	$^7P^7P^8S^3P$	15A	+ a_1 9/49	+ a_2 9/49	- a_3 2/7	.110	.018	.006	.002
$a^6P_{33/2}^0$	+ .343	$^5P^7P^6S^1P$	20A	+ a_1 1/7	- a_2 5/49	+ a_3 2/7	.112	.020	.006	.002
$a^6P_{23/2}^0$	+ .305	$^5P^7P^6S^1P$	15A	+ a_1 31/175	- a_2 31/245	+ a_3 4/35	.113	.018	.006	.002
$a^6P_{13/2}^0$	+ .232	$^5P^7P^6S^1P$	9A	+ a_1 7/25	- a_2 1/5	- a_3 2/5	.105	.020	.006	.002
$b^8P_{33/2}^0$	- .143	$^7P^5P^6S^1P$	20A	- a_1 5/49	+ a_2 1/7	+ a_3 2/7	.125	.018	.006	.002
$b^8P_{23/2}^0$	- .120	$^7P^5P^6S^1P$	15A	- a_1 31/245	+ a_2 31/175	+ a_3 4/35	.112	.021	.006	.002
$b^8P_{13/2}^0$	- .198	$^7P^5P^6S^1P$	9A	- a_1 1/5	+ a_2 7/25	- a_3 2/5	.137	.018	.006	.002
$a^4P_{33/2}^0$	- .186	$^5P^5P^4S^3P$	15A	- a_1 3/25	- a_2 3/25	+ a_3 2/5	.118	.019	.006	.002
$a^4P_{23/2}^0$	- .149	$^5P^5P^4S^3P$	9A	- a_1 11/75	- a_2 11/75	+ a_3 4/15	.118	.019	.006	.002
$a^4P_{13/2}^0$	- .135	$^5P^5P^4S^3P$	3A	- a_1 1/3	- a_2 1/3	- a_3 2/3	.118	.019	.006	.002
$a^6S_{23/2}$	+ .030	1S_0	15A	+ a_4						.002

TABLE V. *hfs-coupling constants. Electron configuration 3d⁴5s.*

Term	Total $\Delta\nu$	$R_1 R_2 R_3$	mA	A	a_1 4s _s	a_2 5s _s	a_3 3d ⁴ _s
$x^3S_{3/2}$	+ .540	$7S^7S^4S$	20A	$+a_1 \frac{1}{7}$.149	.030	.002
$x^3S_{1/2}$	+ .433	$5S^7S^1S$	15A	$+a_1 \frac{1}{5}$.156	.030	.002
$y^3S_{3/2}$	- .234	$7S^5S^1S$	15A	$-a_1 \frac{1}{7}$.165	.030	.002
$x^3S_{1/2}$	- .310	$5S^5S^2S$	9A	$-a_1 \frac{1}{5}$.156	.030	.002

TABLE VI. *hfs-coupling constants. Electron configuration 3d⁶4s.*

Term	Total $\Delta\nu$	$R_1 R_2 R_3$	mA	A	a_1 4s _s	a_2 3d ⁶ _s	a_3 3d ⁶ _l
$a^6D_{4/2}$	+ .610	$5D^2D^6S$	25A	$+a_1 \frac{1}{9}$.159	.011	.004
$a^6D_{3/2}$	+ .507	$5D^2D^6S$	20A	$+a_1 \frac{37}{315}$.158	.011	.004
$a^6D_{2/2}$	+ .410	$5D^2D^6S$	15A	$+a_1 \frac{23}{175}$.153	.011	.004
$a^6D_{1/2}$	+ .311	$5D^2D^6S$	9A	$+a_1 \frac{13}{75}$.153	.011	.004
$a^6D_{1/2}$	+ .261	$5D^2D^6S$	3A	$+a_1 \frac{7}{15}$.154	.011	.004
$a^4D_{3/2}$	- .110	$5D^2D^4S$	20A	$-a_1 \frac{3}{35}$.156	.011	.004
$a^4D_{1/2}$	- .063	$5D^2D^4S$	15A	$-a_1 \frac{13}{175}$.156	.011	.004
$a^4D_{1/2}$	- .004	$5D^2D^4S$	9A	$-a_1 \frac{1}{25}$.156	.011	.004
$a^4D_{1/2}$	+ .078	$5D^2D^4S$	3A	$+a_1 \frac{1}{5}$.156	.011	.004

three or four since five $3d$ electrons may be treated as a unit. The electron configuration $3d^5 4s 4p$, for the terms shown in Fig. 3, will here be used as an example. For the $4s$ electron with l value 0, only one constant, a_1 of Table IV, is to be determined. The contribution of a $4p$ electron with s value $\frac{1}{2}$ and l value 1 is represented by two constants, a_2 and a_3 respectively. The five $3d$ electrons, considered as a unit, have a spin value $2\frac{1}{2}$ and an l value 0 and may therefore be treated as a single s electron with spin $2\frac{1}{2}$ and represented by one constant, a_4 , Table IV.

The values of the a 's in the last four columns of Table IV may be computed from the $\Delta\nu$'s of Table III in the following manner. From Eqs. (1) and (7) and the total $\Delta\nu$'s we get for

$$a^6S_{21}, + 0.030 = 15(\quad + a_4) \quad (8)$$

$$a^8P_{43}^0, + 0.445 = 25(a_1 1/9 + a_2 1/9 + a_3 2/9 + a_4 5/9) \quad (9)$$

$$a^8P_{23}^0, + 0.352 = 15(a_1 9/49 + a_2 9/49 - a_3 2/7 + a_4 45/49) \quad (10)$$

$$a^6P_{31}^0, + 0.343 = 20(a_1 1/7 - a_2 5/49 + a_3 2/7 + a_4 5/7). \quad (11)$$

From the four simultaneous equations the four constants a_1 , a_2 , a_3 , and a_4 can be determined. Since a_3 and a_4 are small as compared with a_1 and a_2 they are assumed the same for all of the terms in Table IV and are set in italics. The constant a_3 for $^8P_{43}^0$ for example, is the mean of six values, taking each time Eq. (9) and one of the six equations from the $^6P^0$ terms. The a_1 's for the $4s$ electron are then computed independently for each term, so that the four constants following each term give the total $\Delta\nu$ in column two. Since the $\Delta\nu$'s for the a^4P^0 terms have not been observed they have been computed from the mean values of the a 's of the other nine P^0 terms. A method similar to that used for the P^0 terms has been used to determine the a 's for the D and S terms of the electron configurations $3d^5 4s 5s$ and $3d^5 4s$ respectively. The results are shown in Tables V and VI.

It is to be expected that the value of a_1 for the $4s$ electron obtained from each term of each electron configuration would be nearly the same. It is likewise to be expected that a_4 of Table IV and a_3 of Table VI would have nearly the same value. Attempts to alter any one set of a 's or $\Delta\nu$'s is found to alter other sets of a 's or $\Delta\nu$'s in such a way as to make conditions worse. Just how much, from the theoretical standpoint, a_1 ($4s$) should be changed by a change in the electron configuration, for example from $3d^5 4s 4p$ to $3d^5 4s$, is difficult to determine. The agreement between the a_1 's within each of the electron configurations is as good as can be expected.

The narrow hfs -separations in the 4D terms of Fig. 4 and the wide separations in the 6D terms show that the coupling of the six $3d$ electrons with the nucleus almost neutralizes that of the $4s$ electron. This same effect is also found in the b^6P^0 terms of Fig. 3. It should here be stated that preliminary calculations of a_1 , a_2 , and a_4 for the first nine terms of Table IV, omitting the l value of the $4p$ electron a_3 , indicated that the inclusion of the l value would give more constant values of a_1 and a_2 .

A study of Figs. 2, 3, and 4 and a comparison of these figures with Tables IV, V, and VI shows that only a few of the interesting relations to be found between the hfs and the gs of manganese have been pointed out above. This investigation has been carried on at Professor Paschen's laboratory at the Physikalisch-Technische Reichsanstalt, Berlin.

MEAN LIVES OF LINES OF MERCURY TRIPLET $2^3P_{012} - 2^3S_1$

BY ROBERT H. RANDALL

PHYSICS LABORATORIES, COLUMBIA UNIVERSITY

(Received April 4, 1930)

ABSTRACT

The mean life of each of three lines coming from the same upper level in the mercury atom has been measured. The triplet $2^3P_{012} - 2^3S_1$ was excited by electron impact under conditions involving negligible ionization and concentration of excited atoms. The method was that previously described by Webb, in which high frequency voltages are applied in phase to the excitation and detecting systems. The lines were excited in a sealed-off tube with mercury pressures between 0.004 and 0.03 mm. The exciting voltage was less than ten volts. The excitation was such that there was no appreciable concentration in the $2P$ states. A specially designed potassium-hydride photoelectric cell was used as the detecting system. Optical filters were used to isolate the line measured. The results agree with the assumption that the radiation decays exponentially after impact. For the lines $\lambda 4047$ and $\lambda 4358$ the lives were found to be the same within the experimental error (0.75 percent) viz. $\tau = 5.75 \times 10^{-8}$ secs. The value for $\lambda 5461$ was four times greater, $\tau = 2.37 \times 10^{-7}$ secs. The agreement between the lives of $\lambda 4047$ and $\lambda 4358$ supports the quantum assumption that lines coming from the same level in the atom have the same life. Collins has found that under certain exciting conditions the fine-structure of $\lambda 5461$ is anomalous as compared to $\lambda 4047$ and 4358 . It is suggested that the longer life found for $\lambda 5461$ may be explained by considering the fine structure of the 2^3S_1 level. The results are then consistent with the above assumption.

INTRODUCTION

FROM the relation between the mean life, τ_n , of an excited atomic state and the Einstein probabilities for transitions to all possible lower states,

$$\tau_n = \left(\sum_m A_m^n \right)^{-1}$$

it is generally assumed that all spectral lines originating in the same upper level in the atom have the same life.¹ Direct experimental evidence on this point is scarce.

While Kerschbaum² has measured τ for a number of spectral lines, using Wien's canal-ray method, and has found equal lives for lines originating in the same upper level, in agreement with the Einstein assumptions, he also found, in general, equal lives for *all* the arc lines of any one element. This last is hardly to be expected, as Maxwell³ has pointed out, since the sum of the transition probabilities, upon which the lives depend, is not necessarily the same for every level in the atom.

The present investigation was undertaken to test further the validity of the Einstein assumptions by measuring the mean lives of each of several

¹ Pauli, Handbuch der Physik, V. 23, p. 11.

² H. Kerschbaum, Ann. d. Physik **83**, 287 (1927).

³ L. R. Maxwell, Phys. Rev. **34**, 199 (1929).

lines coming from the same upper level, but under simpler excitation conditions than obtained in Kerschbaum's measurements. The lines were excited by simple electron impact at voltages below ionization. The mercury $2^3P_{012} - 2^3S_1$ triplet, $\lambda\lambda 5461, 4358$ and 4047 , was chosen because the intensity of the lines and their wide wave-length separation favored the application of the particular method of measurement used. Since levels higher than the 2^3S_1 were not excited to any appreciable extent, the conditions were less complicated than where high voltage excitation is used, as in Wien's canal-ray method. Voltage and pressure conditions were such as to make it unlikely that absorption and re-emission played any part in the persistence of the radiation.

METHOD

The method of measurement employed was a modification of that previously used in this laboratory.⁴ The excitation was produced by electron impact excited by alternating voltages in such a way that there was excitation during only the positive half cycle. A voltage of the same frequency and phase was applied to a photoelectric detecting system, so that only radiation reaching the photoelectric surface in the positive half cycle was effective; during the negative half cycle the photoelectrons were held in the surface. As the frequency was increased, the total excitation being held constant, the photoelectric current decreased, owing to the persistence of the radiation, some of which then reached the photoelectric surface in the negative half cycle. From the form of the curve, the value of the mean life τ of the radiation was calculated, assuming that radiation excited at the time $t=0$ falls off according to the law e^{-kt} .

APPARATUS

The details of the apparatus are shown in Fig. 1. The excitation was produced in an evacuated vessel of Pyrex, containing electrodes C, G, G' and O . The hot cathode C , for which we are indebted to Dr. A. W. Hull of the General Electric Company, was equipotential, consisting of an oxide-coated nickel cylinder with an internal tungsten heater. Electrodes G and G' , comprising the accelerating system, were in the form of two concentric cylinders of 1.6 mm mesh nickel gauze, with a difference in radius of 2.0 mm. For most of the measurements grids G and G' were connected together just outside the cell and used as a single electrode which we shall call GG' . The outer cylindrical electrode O , of sheet nickel, had a window covered with gauze to allow the passage of the radiation.

All metal parts were pre-outgassed. Before sealing off, the excitation cell was baked for several hours at 450°C , the filament sensitized and a strong arc operated for an hour. Later tests indicated that accumulated gas did not exceed 10^{-4} mm of mercury.

The mercury vapor pressure in the excitation cell was controlled by a mercury well at the bottom, kept in a water-bath whose temperature was

⁴ H. W. Webb, Phys. Rev. **24**, 113 (1924); F. G. Slack, Phys. Rev. **28**, 1, (1926); H. W. Webb and H. A. Messenger, Phys. Rev. **33**, 319 (1929).

held constant to 0.1°C . The body of the tube was superheated to about 80°C .

The detecting system, containing electrodes P , H and W , was a specially constructed photoelectric cell placed at a distance of 8 cm from the excitation cell. The potassium-covered electrode P was a nickel cylinder, supported on a long re-entrant glass tube to increase the electrical leakage path. Surrounding P was a cylindrical nickel gauze electrode H . Against the walls was a third cylindrical grid, which in addition to removing the photoelectrons quickly, served as a flashing electrode in forming the sensitive potassium-hydride surface. During the flashing process electrode H was slid to one end of the cell, allowing a more uniform discharge between W and P and preventing the formation of a light sensitive surface on H .

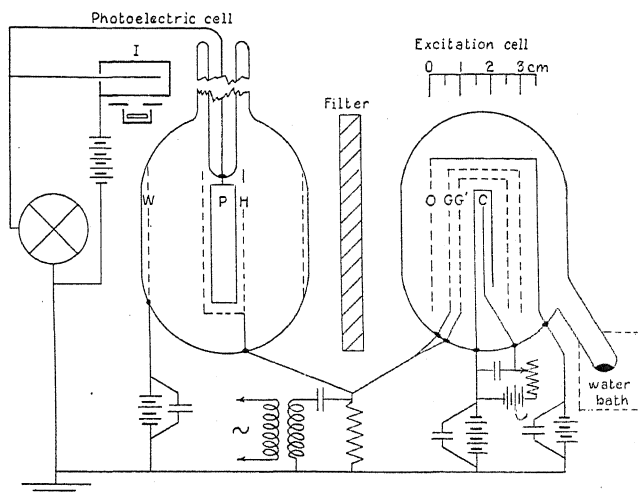


Fig. 1. Schematic diagram of apparatus and electrical circuits.

The metal parts were pre-outgassed and the cell which was of Pyrex, was baked out before distilling in the potassium. The hydrogen necessary for the flashing process was thoroughly pumped out before sealing off. The gas pressure in the cell after sealing off was below 10^{-4} mm mercury.

An electric heater on the electrometer lead prevented internal electrical leakage due to the formation of a film of potassium. Occasionally, after standing, a strong reverse photoelectric current from the grid H was found, due probably to a thin potassium film. This effect soon disappeared, however, after exposure to the heat of the excitation cell.

Corning glass filters were used between the excitation cell and the photoelectric cell to isolate each of the three lines; filters nos. G 555-Q and G 34-Y for $\lambda 5461$; nos. G 585-L and G-38 for $\lambda 4358$; and nos. G 586-A and G 38-L for $\lambda 4047$.

Photographs of a mercury arc taken through the filter for $\lambda 5461$ and for $\lambda 4358$, made certain that under the conditions of excitation of this experiment, the transmission of one filter for either of the other two lines, or for any other line likely to be excited, was less than 1 percent of the transmission

for the desired line. The radiation transmitted by the filter for $\lambda 4047$ also included the line $\lambda 4078$, but was otherwise monochromatic. White⁵ and Crozier⁶ have found that under excitation conditions similar to those of this experiment, $\lambda 4078$ was considerably weaker than $\lambda 4047$. A study of the results of the present investigation showed that the presence of the small quantity of $\lambda 4078$ did not affect the measurement of the life of $\lambda 4047$.

There was always a considerable steady photoelectric current, due to the light from the hot cathode of the excitation cell. This was balanced out by means of a radio-active leak, I , Fig. 1, controlled by a variable lead shutter over the opening of the metal box containing the active material.

The filament was heated by an 8 volt storage battery while all other d.c. voltages were furnished by small dry cells. The alternating voltages were supplied by air-core transformers coupled to the 60 cycle lighting circuit

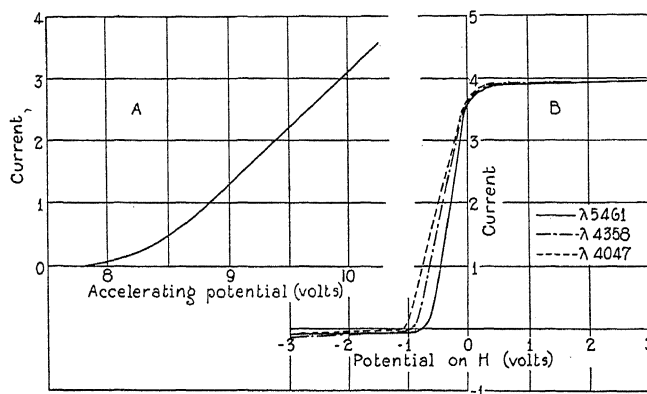


Fig. 2. Curve A, a typical excitation curve ($\lambda 4358$). Curve B, photoelectric characteristics.

or to a vacuum-tube oscillator of variable frequency. The voltages were applied to the experimental cells across a nearly non-inductive resistance of about 45 ohms, one end of which was connected directly to the grids H and GG' . In the case of the high frequencies supplied by the oscillator this resistance formed part of a tuned circuit which helped to insure a pure impressed sine wave. The alternating voltages were measured with a vacuum-tube voltmeter. The frequencies were measured with a wave-meter.

A Compton quadrant electrometer with a sensitivity of about 3000 mm per volt was used to measure the photoelectric current.

EXPERIMENTAL AND RESULTS

Fig. 2 shows the steady current characteristics of the exciting and of the detecting systems which it was necessary to know in calculating the lives of the radiations. The excitation curve (A) was taken with the filter for $\lambda 4358$ in place, and shows how the photoelectric current varied with the accelerating voltage between GG' and C , the voltage between H and P being held constant. The voltage conditions were $P=0.0$, $H=2.0$, $W=6.0$, $GG'=0.0$, $O=-3.0$, and C variable between 0.0 and -10.5 volts.

⁵ D. R. White, Phys. Rev. 28, 1125 (1926).

⁶ W. D. Crozier, Phys. Rev. 31, 800 (1928).

The curve for $\lambda 4358$ shows that this radiation appeared at about the theoretical voltage 7.7 and that the variation of the photoelectric current was roughly linear for higher voltages up to 10.5 volts. Excitation curves taken with each of the other two filters were found to have exactly the same shape as that shown for $\lambda 4358$, agreeing with the results of White⁵ and Crozier.⁶ The line $\lambda 4078$ should theoretically come in at 7.9 volts. There was, however, no evidence of complexity in the excitation curve found for $\lambda 4047$, indicating that $\lambda 4078$ was considerably weaker than $\lambda 4047$.

The photoelectric characteristics Fig. 2 (B) were taken with each of the three filters separately, maintaining a constant voltage between GG' and C

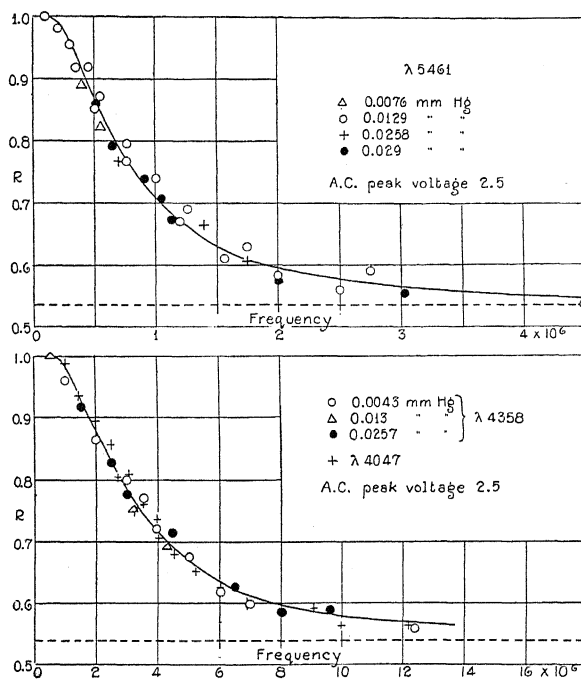


Fig. 3. R -frequency curves.

and varying the voltage between H and P . The ordinates are proportional to the photoelectric currents in each case and have been reduced to the same saturation current for comparison. The voltage conditions for the curves shown were $GG' = 0.0$, $C = -9.0$, $O = -3.0$, $P = 0.0$, and H variable between -3.0 and 3.0 volts. The three curves show that for these wave-lengths the cell was practically unidirectional and that a change of only a volt in the potential on H was sufficient to produce saturation. The shift in the stopping voltage is the only marked variation of the photoelectric characteristic with wave-length.

The curves from which the lives of the radiations were determined were obtained by applying alternating voltages, of the same peak value and phase, to GG' and H simultaneously and measuring the photoelectric current at different frequencies. The curves in Fig. 3 are typical of those obtained.

The abscissas are the frequencies. The ordinates are proportional to the photoelectric currents and represent in each case the ratio R of the current obtained with a high frequency to that obtained with a low frequency, 60 cycles, for which the effect of the persistence of the radiation was negligible. The ratio R was used instead of the actual photoelectric current to avoid error due to changes in the sensitivity of the photoelectric cell.

The d.c. voltage conditions for the curves shown were $GG'=0.0$, $C=-7.5$, $O=-3.0$, $P=0.0$, $H=0.0$ and $W=6.0$. The peak value of the alternating voltage applied to GG' and H was 2.5, so that the accelerating voltage varied between 5 and 10 volts. Measurements were taken at several different pressures, varying between 0.004 and 0.03 mm of mercury, as indicated in the figure. In the case of $\lambda 4047$ the different pressures are not specified on the graph, for the sake of clearness, but the points for this line were taken over the same pressure range as for $\lambda 4358$. Pressures below 0.004 mm in the case of $\lambda 4047$ and 4358, and below 0.007 mm in the case of $\lambda 5461$, could not be used since there was then insufficient energy to give a measurable photoelectric current, while with pressures much above 0.03 mm trouble was experienced with the arc striking.

It is important for this method of measurement that the impressed alternating voltages be of approximately sine form. The tests for wave-form described in earlier papers, were made for each frequency and indicated that up to the highest frequency it was possible to use, 1.2×10^7 cycles, no error was introduced due to faulty wave-form.

The solid lines shown with the experimental points in Fig. 3 were calculated in a manner similar to that discussed in earlier papers. It was assumed that the radiation excited at any time $t=0$ falls off according to the exponential law e^{-kt} . Since the excitation was approximately linear with the voltage, the excitation during the positive half cycle approximated the form of the positive half of a sine curve. Also the photoelectric cell was nearly unidirectional and saturated quickly with a reversal of the voltage. It was therefore possible to find a simple approximate analytic expression for R as a function of the frequency f

$$R = \frac{K^2 + 2\pi^2 f^2}{K^2 + 4\pi^2 f^2}.$$

To this approximate expression certain correction terms, amounting to about 10 percent had to be added to take care of the fact that the photoelectric cell did not saturate instantaneously with a reversal of the voltage, and also the fact that excitation did not begin immediately with positive values of the alternating voltage. Since these correction terms were complicated and involved quantities determined empirically from the excitation and photoelectric characteristics, they are of no special interest here. With very high frequencies R approached a limiting value determined by the photoelectric characteristics and the amplitude of the applied alternating voltages. This is shown in Fig. 3 (a) and (b) by a horizontal dotted line.

By trial, a value of K was found such that the calculated curve best fitted the experimental points. The agreement was such as to justify the assumption of an exponential decay. For $\lambda 5461$, K was found to be $4.23 \times 10^6 \text{ secs.}^{-1}$; the mean life of the radiation, τ , was then $1/K$ or $2.37 \times 10^{-7} \text{ secs.}$ The same K was found for $\lambda 4358$ and for $\lambda 4047$, viz. $1.74 \times 10^7 \text{ secs.}^{-1}$, giving a mean life for each of these lines of $5.75 \times 10^{-8} \text{ secs.}$ The life of $\lambda 5461$ was therefore closely four times that of $\lambda 4358$ and 4047 .

The precision of measurement for τ was about 4 percent. In order to see how closely the lives of $\lambda 4358$ and $\lambda 4047$ agreed, a fixed frequency of 3×10^6 cycles was used and a large number of alternate measurements of R were taken by simply interchanging the filters, the electrical conditions remaining the same. The same value of R was found for both lines to within the experimental error 0.75 percent, indicating the same value of K for the two lines to within that precision.

Measurements were taken using a peak value for the alternating voltage of 1.1 instead of 2.5. This resulted in a slightly different form for the calculated R -frequency curve. The experimental points lay on the calculated curve, however, and the values of K which best fitted the data agreed in every case with those found using a peak voltage of 2.5, to within the experimental error.

Using Corning glass filter no. G-586-AW, measurements were made on the mean life of another group of lines, which included the singlet $2^3P_1 - 3^1D_2$, $\lambda 3663$, and the triplet $2^3P_1 - 3^3D_{1,2,3}$, $\lambda \lambda 3650, 3654$ and 3662 . These lines could not be separated optically and the life measured was for the composite radiation. It was found impossible to obtain a complete R -frequency curve, since the radiation was apparently short-lived and it was necessary to go to very high frequencies before the photoelectric current began to decrease. Enough of the curve was obtained from which to estimate a value for the mean life of the radiation of $2.4 \times 10^{-8} \text{ secs.}$, certain to within 10 percent. The curve was too incomplete, however, to be able to determine whether there were different lives for the different components of the radiation.

DISCUSSION

There was some question as to the purity of the radiation reaching the photoelectric cell when using the filter for $\lambda 4047$. The theoretical voltages at which $\lambda 4047$ and $\lambda 4078$ come in are 7.7 and 7.9 respectively. Both White⁵ and Crozier,⁶ however, found no appreciable intensity for $\lambda 4078$ under 8.4 volts. From a study of their voltage-intensity curves for these lines, the change in the peak value of the alternating voltage from 1.1 to 2.5 volts which changed the peak of the excitation voltage from 8.6 to 10.0 volts, would be expected to increase the average intensity of $\lambda 4078$, as compared to that of $\lambda 4047$, several times. If the intensity of $\lambda 4078$ were comparable to that of $\lambda 4047$, a change in the peak voltage should result in different R -frequency curves, providing the life of $\lambda 4078$ were appreciably different from that of $\lambda 4047$. No such change was noted, indicating either that the intensity of $\lambda 4078$ was too low to give a measurable photoelectric current; or that if $\lambda 4078$ were present to any considerable extent, its life was very

nearly that of $\lambda 4047$. In either case the measured life must be approximately the true life of $\lambda 4047$.

A study of the results for all three lines, $\lambda\lambda 5461, 4358$ and 4047 , leads to the conclusion that the results were not affected by absorption and re-emission of the radiation, but that the lives measured are actually those of the single atomic processes. It has been shown that for $\lambda 2537$ these absorption and re-emission processes play an important part in the persistence of the radiation emitted by excited mercury vapor, even down to pressures of 0.0002 mm of mercury.⁷ It is also known that under certain conditions large concentrations of excited atoms in the 2^3P_1 and the metastable 2^3P_0 state exist in the vapor and considerable absorption of $\lambda 4358$ and $\lambda 4047$ results.⁸ The subsequent re-emission of all three lines, $\lambda\lambda 4047, 4358$ and 5461 by atoms so excited to the 2^3S_1 level would cause persistence of the radiation in the vapor, beyond the mean life of the single atomic processes.

That such absorption processes did not occur to any measurable extent in the present experiment is evident from the fact that no change in the mean life resulted from varying the pressure and the exciting alternating voltages. Increasing the pressure should increase the concentration of atoms excited to the 2^3P_1 and 2^3P_0 states and as a consequence there should be greater persistence of the lines under study, if absorption processes were playing a part. The concentration of atoms in the 2^3P_1 and 2^3P_0 states would also be greater when the peak voltage of 2.5 was used than with the peak voltage of 1.1 , since in the former case the population in these states would be augmented by the return of electrons from upper states excited by the higher accelerating voltages.

A further test for effects due to absorption was made by varying the voltage on the outer electrode O in the excitation cell between the limits -8.0 and 0.0 volts. This had the result of increasing the total number of excited atoms produced in the positive half cycle, as O was made less negative, and this change should have increased the probability of any quantum of radiation being absorbed by an excited atom before escaping from the vapor. Again, some of the curves were taken with the two accelerating grids, G and G' connected together; for other curves only the inner grid served as an accelerating grid, the outer of the pair being connected to the electrode O . This change also affected the total concentration of excited atoms and should therefore have affected any persistence due to absorption.

The lives measured were, however, found to be independent of any of these pressure or voltage changes, indicating that they are the true mean lives of the corresponding single atomic processes.

The results show identical lives for $\lambda\lambda 4047$ and 4358 . This is strong evidence in support of the assumption that lines coming from the same upper level in the atom have the same life. While the fact that $\lambda 5461$ was found to have quite a different life than the other two lines may be interpreted as evidence that the Einstein relation is not valid, it is believed that a much more reasonable explanation will be found in the fine-structure of the lines.

⁷ H. W. Webb and H. A. Messenger, *Phys. Rev.* **33**, 319 (1929).

⁸ C. Fuchtbauer, *Phys. Zeits.* **21**, 635 (1920); R. W. Wood, *Proc. Roy. Soc. A* **106**, 679, (1924), *Phil. Mag.* **50**, 774 (1925), *Phil. Mag.* **4**, 406 (1927).

These fine-structure components have been carefully studied. Under the conditions obtaining in a strong arc $\lambda 5461$ has at least twelve distinct components; $\lambda 4358$ at least twenty; and $\lambda 4047$ at least nine. Ruark⁹ has proposed a fine-structure energy level scheme which supposes a triple fine structure for the 2^3S_1 level as well as a triple fine structure for each of the $2P$ levels, and which accounts for about $\frac{2}{3}$ of the components found in the arc. Some experiments of Collins,¹⁰ however, have shown that the fine structure of these lines is much simpler when the lines are optically excited than in the strong arc. He excited the lines in a resonance tube placed next to a mercury arc. Atoms were excited to the 2^3S_1 level by the successive absorption of $\lambda 2537$ and $\lambda 4358$. About half the components found in a strong arc appeared in the case of $\lambda \lambda 4358$ and 4047 , while only *one* of the many arc components of $\lambda 5461$ appeared. When nitrogen was introduced into the resonance tube little change was noted in the fine structures of $\lambda \lambda 4358$ and 4047 , but to the single component of $\lambda 5461$ was added one other equally strong component.

These results indicate a certain anomalous character for $\lambda 5461$ as compared to the other two lines. It suggests that under certain excitation conditions, quite different upper fine-structure levels may be involved in the case of $\lambda 5461$ than in the case of $\lambda \lambda 4047$ and 4358 , and that the lives measured in the present investigation may therefore be the lives characteristic of these different sub-levels. It is, however, not possible to say whether a single one of these sub-levels is involved in the case of each of the lines or whether the result, in each case, is the average life of lines coming from a group of sub-levels. The precision of the method is such that if a radiation were made up of two components of about equal intensity, the complexity could be detected if their lives differed by more than 30 percent. Again, if there were two components of widely different lives, the complexity could be detected as long as the intensity of one component was not less than 10 percent that of the other. Since there was no evidence of complexity from the curves, it was concluded either that one fine-structure component predominated in the case of each of the three lines, or that if several strong components were excited in each case, they had about equal lives.

A study of the fine structure of these lines under conditions of excitation somewhat similar to those of this investigation is being undertaken in this laboratory.

It is interesting to note that Wien,¹¹ using his canal-ray method, found a value for the mean life of $\lambda 4358$ of 1.82×10^{-8} secs. No explanation can be offered for the difference between the value of the mean life found here and Wien's result. It should be pointed out, however, that the type of excitation was quite different for the two experiments, Wien using high voltages, while here the exciting voltage was always below ionization.

The author wishes to express his thanks to Professor H. W. Webb, who suggested this problem, for his continued help and advice throughout the experiment.

⁹ A. E. Ruark, *Phil. Mag.* **1**, 977 (1926).

¹⁰ E. H. Collins, *Phys. Rev.* **32**, 753 (1928).

¹¹ W. Wien, *Ann. d. Physik* **73**, 483 (1924).

THE HYDROGEN ATOM IN THE STARK EFFECT

BY FRANCIS G. SLACK

DEPARTMENT OF PHYSICS, VANDERBILT UNIVERSITY

(Received April 4, 1930)

ABSTRACT

Characteristics of the hydrogen atom wave function, which show the statistical distribution of electronic charge with respect to the nucleus and electric field, are computed for the first five quantum states. The results are tabulated and are represented graphically for one state as an example. The average coordinates of the electronic charge are also computed and included in the tabulation.

EXPERIMENTS¹ with hydrogen canal rays in an electric field show phenomena apparently dependent upon the statistical distribution of the electronic charge with respect to the nucleus and to the electric field.² This statistical "distribution of charge" or "electronic configuration" is dependent on the wave functions of the various states of the hydrogen atom, as indicated by Schrödinger.³

In the following paper we compute and present in tabular and graphical form certain characteristics of the electronic configuration of the hydrogen atom wave function, namely, the statistical total charge in certain regions between which this charge reduces to zero, and the average coordinates of the total electronic charge with respect to the nucleus. These are computed from Schrödinger's³ expressions for the Stark effect, using unperturbed wave functions in the case of a vanishingly small field.⁴ No attempt is made to place any special significance or meaning on the computed values further than has been done⁵ and it is unnecessary to choose from among the several points of view already expressed by various authors.⁶

We start with the Schrödinger wave equation for the hydrogen atom in an electric field of strength F :

$$\Delta\psi + \frac{8\pi^2m}{h^2} \left(E + \frac{e^2}{r} - eFz \right) \psi = 0$$

and insert the parabolic coordinates $\lambda_1, \lambda_2, \phi$ where: $x = (\lambda_1 \lambda_2)^{1/2} \cos \phi$, $y = (\lambda_1 \lambda_2)^{1/2} \sin \phi$, and $z = 1/2(\lambda_1 - \lambda_2)$. The field has the direction of $+z$,

¹ J. Stark, *Berliner Berichte* 20 (1913); H. Lunelund, *Ann. d. Physik* 45, 517 (1914); R. Wierl, *Ann. d. Physik* 82, 563 (1927).

² F. G. Slack, *Ann. d. Physik* 82, 576 (1927).

³ E. Schrödinger, *Ann. d. Physik* 80, 437 (1926).

⁴ Condon and Morse, "Quantum Mechanics" p. 125.

⁵ Condon and Morse, "Quantum Mechanics" p. 28.

⁶ Ruark and Urey "Atoms, Molecules, and Quanta" p. 537; A. Sommerfeld, *Phys. Zeits.* 30, 866 (1929).

i.e. the direction of the axis of the λ_2 parabolas. The wave function (ψ) satisfying this equation under these conditions is given by Schrödinger as:

$$\psi_{k_1 k_2 m} = \lambda_1^{m/2} \lambda_2^{m/2} e^{-(\lambda_1 + \lambda_2)/2na_0} L_{m+k_1}^m \left(\frac{\lambda_1}{na_0} \right) L_{m+k_2}^m \left(\frac{\lambda_2}{na_0} \right) e^{\pm im\phi}$$

where $n = (k_1 + k_2 + m + 1)$ is the total quantum number, k_1 and k_2 are parabolic quantum numbers and $(m+1)$ is the equatorial quantum number. L_{m+k}^m is the m th derivative of the $(m+k)$ th Laguerre polynomial. $a_0 = \hbar^2/4\pi^2 me^2$ the radius of the first Bohr orbit of the hydrogen atom. Forming the product of the wave function (ψ) with its conjugate ($\bar{\psi}$) we obtain the "electronic charge density" or "electronic probability"

$$\rho = \psi\bar{\psi} = \lambda_1^m \lambda_2^m e^{-(\lambda_1 + \lambda_2)/na_0} \left[L_{m+k_1}^m \left(\frac{\lambda_1}{na_0} \right) \right]^2 \left[L_{m+k_2}^m \left(\frac{\lambda_2}{na_0} \right) \right]^2.$$

For normalization² we introduce the factor C so that $\int_{\phi=0}^{2\pi} \int_{\lambda_1=0}^{\infty} \int_{\lambda_2=0}^{\infty} C \rho dv = e$ where $dv = 1/4(\lambda_1 + \lambda_2) d\lambda_1 d\lambda_2 d\phi$ is the volume element and e is the total extra-nuclear or electronic charge. We determine

$$C = \frac{k_1! k_2! e}{\pi (na_0)^{2m+3} [(m+k_1)!]^3 [(m+k_2)!]^3 n}.$$

Thus we obtain a final normalized expression for the integral of ρdv where we may evaluate over any set of limits to determine $e_{\text{limits}} = \iiint C \rho dv$ within their boundary. This being the integral of "charge density" multiplied by volume element we designate it by e_{limits} and have:

$$e_{\text{limits}} = \iiint \frac{C}{4} (\lambda_1 + \lambda_2) \lambda_1^m \lambda_2^m e^{-(\lambda_1 + \lambda_2)/na_0} \left[L_{m+k_1}^m \left(\frac{\lambda_1}{na_0} \right) \right]^2 \left[L_{m+k_2}^m \left(\frac{\lambda_2}{na_0} \right) \right]^2 d\lambda_1 d\lambda_2 d\phi$$

where the limits $\int_{\phi=0}^{2\pi} \int_{\lambda_1=0}^{\infty} \int_{\lambda_2=0}^{\infty}$ will give a total electronic charge e . However on substituting concrete values of the quantum numbers and evaluating the Laguerre polynomials it is seen that for certain values of λ_1 and λ_2 the expression for ρ vanishes. Along these parabolas the "charge density" and hence the charge is zero. This gives us natural limits or boundaries within which we shall evaluate the integral. (The expression is degenerate in regard to the angular coordinate (ϕ) and thus has axial symmetry about an axis parallel to the impressed field. Integration over this coordinate then always introduces the factor 2π .)

As an example we introduce the quantum numbers for one substate and carry through the integration. Thus for the state $2-1-2$, $n=5$, $k_1=2$, $k_2=1$ and $m=1$ we have:

$$e_{2-1-2 \text{ limits}} = \int_{\lambda_1} \int_{\lambda_2} \frac{C\pi}{2} (\lambda_1 + \lambda_2) \lambda_1 \lambda_2 e^{-(\lambda_1 + \lambda_2)/5a_0} \left[L_3^1 \left(\frac{\lambda_1}{5a_0} \right) \right]^2 \left[L_2^1 \left(\frac{\lambda_2}{5a_0} \right) \right]^2 d\lambda_1 d\lambda_2$$

$$= \frac{C\pi}{2} \int_{\lambda_1} \int_{\lambda_2} (\lambda_1 + \lambda_2) \lambda_1 \lambda_2 e^{-(\lambda_1 + \lambda_2)/5a_0} \left[-3 \left(\frac{\lambda_1}{5a_0} \right)^2 + 18 \left(\frac{\lambda_1}{5a_0} \right) - 18 \right]^2 \left[2 \left(\frac{\lambda_2}{5a_0} \right) - 4 \right]^2 d\lambda_1 d\lambda_2.$$

The roots of $[-(\lambda_1/5a_0)^2 + 6(\lambda_1/5a_0) - 6]$ are $\lambda_1 = 6.34a_0$ and $\lambda_1 = 23.66a_0$, and the root of $[(\lambda_2/5a_0) - 2]$ is $\lambda_2 = 10a_0$ and thus the expression under the integral will vanish along the three parabolas fixed by these values of λ_1 and λ_2 as well as for $\lambda_1 = 0$ or $\lambda_2 = 0$ and for $\lambda_1 = \infty$ or $\lambda_2 = \infty$. These four λ_1 parabolas intersected by the three λ_2 parabolas will divide the region surrounding the nucleus into six regions⁷ bounded by the limits:

$$\begin{aligned} e_1 &= \int_{\lambda_1=0}^{6.34a_0} \int_{\lambda_2=0}^{10a_0} ; e_2 = \int_{\lambda_1=0}^{6.34a_0} \int_{\lambda_2=10a_0}^{\infty} ; e_3 = \int_{\lambda_1=6.34a_0}^{23.66a_0} \int_{\lambda_2=0}^{10a_0} ; \\ e_4 &= \int_{\lambda_1=6.34a_0}^{23.66a_0} \int_{\lambda_2=10a_0}^{\infty} ; e_5 = \int_{\lambda_1=23.66a_0}^{\infty} \int_{\lambda_2=0}^{10a_0} ; \\ e_6 &= \int_{\lambda_1=23.66a_0}^{\infty} \int_{\lambda_2=10a_0}^{\infty} . \end{aligned}$$

Substituting its values as given for C and integrating in this particular case we have:

$$\begin{aligned} e_{2-1-2 \text{ limits}} &= \frac{e}{2^3 \cdot 5^6 \cdot 6a_0^5} \left\{ \left[-\frac{\lambda_1^6}{125a_0^3} e^{-\lambda_1/5a_0} \right. \right. \\ &+ \frac{6}{25a_0} \lambda_1^5 e^{-\lambda_1/5a_0} - \frac{18}{5a_0} \lambda_1^4 e^{-\lambda_1/5a_0} - 180a_0 \lambda_1^2 e^{-\lambda_1/5a_0} \\ &- 1800a_0^2 \lambda_1 e^{-\lambda_1/5a_0} - 9000a_0^3 e^{-\lambda_1/5a_0} \left. \right] \text{limits} \left[-\frac{\lambda_2^3}{5a_0} e^{-\lambda_2/5a_0} + \lambda_2^2 e^{-\lambda_2/5a_0} \right. \\ &- 10a_0 \lambda_2 e^{-\lambda_2/5a_0} - 50a_0^2 e^{-\lambda_2/5a_0} \left. \right] \text{limits} + \left[-\frac{\lambda_1^5}{125a_0^3} e^{-\lambda_1/5a_0} + \frac{7}{25a_0^2} \lambda_1^4 e^{-\lambda_1/5a_0} \right. \\ &- \frac{20}{5a_0} \lambda_1^3 e^{-\lambda_1/5a_0} + 12\lambda_1^2 e^{-\lambda_1/5a_0} - 60a_0 \lambda_1 e^{-\lambda_1/5a_0} - 300a_0^2 e^{-\lambda_1/5a_0} \left. \right] \text{limits} \\ &\left. \left[-\frac{\lambda_2^4}{5a_0} e^{-\lambda_2/5a_0} - 20a_0 \lambda_2^2 e^{-\lambda_2/5a_0} - 200a_0^2 \lambda_2 e^{-\lambda_2/5a_0} - 1000a_0^3 e^{-\lambda_2/5a_0} \right] \text{limits} \right\} . \end{aligned}$$

and on substituting the above limits we have: $e_1 = 0.0055 e$; $e_2 = 0.0820 e$; $e_3 = 0.0187 e$; $e_4 = 0.0219 e$; $e_5 = 0.1907 e$; $e_6 = 0.6792 e$; as shown in Table I and in Fig. 1-g.

⁷ F. G. Slack, Ann. d. Physik 80, 582 (1927). The statement that there will always be $(n-m)$ regions given here is incorrect. This holds only for the special cases $k_1=0$ or $k_2=0$ where there are no intersecting parabolas for which ρ disappears. The number of regions in the general case is given by $(k_1+1)(k_2+1)$.

TABLE I.

n	$k_1-k_2-(m+1)$	(k_1+1) (k_2+1)	Limits for λ_1	Limits for λ_2	Limits	\bar{x}	\bar{z}
1	0-0-1	1	0- ∞	0- ∞	e	1.178 a_0	0
2	0-0-2	1	0- ∞	0- ∞	e	4.418 a_0	0
	1-0-1	2	0-2 a_0 2 a_0 - ∞	0- ∞ 0- ∞	0.0786 e 0.9210 e	3.825 a_0	3.0 a_0
3	0-0-3	1	0- ∞	0- ∞	e	9.664 a_0	0
	1-0-2	2	0-6 a_0 6 a_0 - ∞	0- ∞ 0- ∞	0.1213 e 0.8787 e	7.975 a_0	4.5 a_0
	2-0-1	3	0-1.76 a_0 1.76 a_0 -10.24 a_0 10.24 a_0 - ∞	0- ∞ 0- ∞ 0- ∞	0.0296 e 0.102 e 0.868 e	7.310 a_0	9.0 a_0
	1-1-1	4	0-3 a_0 0-3 a_0 3 a_0 - ∞ 3 a_0 - ∞	0-3 a_0 3 a_0 - ∞ 0-3 a_0 3 a_0 - ∞	0.0025 e 0.1364 e 0.1364 e 0.716 e	9.792 a_0	0
4	0-0-4	1	0- ∞	0- ∞	e	16.91 a_0	0
	1-0-3	2	0-12 a_0 12 a_0 - ∞	0- ∞ 0- ∞	0.183 e 0.817 e	16.92 a_0	6.0 a_0
	2-0-2	3	0-5.06 a_0 5.06 a_0 -18.8 a_0 18.8 a_0 - ∞	0- ∞ 0- ∞ 0- ∞	0.038 e 0.175 e 0.787 e	17.46 a_0	12.0 a_0
	3-0-1	4	0-1.664 a_0 1.664 a_0 -9.176 a_0 9.176 a_0 -25.16 a_0 25.16 a_0 - ∞	0- ∞ 0- ∞ 0- ∞ 0- ∞	0.0147 e 0.0583 e 0.095 e 0.831 e	11.46 a_0	18.0 a_0
	1-1-2	4	0-8 a_0 0-8 a_0 8 a_0 - ∞ 8 a_0 - ∞	0-8 a_0 8 a_0 - ∞ 0-8 a_0 8 a_0 - ∞	0.0179 e 0.172 e 0.172 e 0.638 e	17.48 a_0	0
	2-1-1	6	0-2.34 a_0 0-2.34 a_0 2.34 a_0 -13.66 a_0 2.34 a_0 -13.66 a_0 13.66 a_0 - ∞ 13.66 a_0 - ∞	0-4 a_0 4 a_0 - ∞ 0-4 a_0 4 a_0 - ∞ 0-4 a_0 4 a_0 - ∞	0.00178 e 0.0595 e 0.0148 e 0.124 e 0.155 e 0.645 e	16.78 a_0	6.0 a_0
5	0-0-5	1	0- ∞	0- ∞	e	26.16 a_0	0
	1-0-4	2	0-20 a_0 20 a_0 - ∞	0- ∞ 0- ∞	0.2155 e 0.7844 e	26.45 a_0	7.5 a_0
	2-0-3	3	0-10 a_0 10 a_0 -30 a_0 30 a_0 - ∞	0- ∞ 0- ∞ 0- ∞	0.0918 e 0.1409 e 0.7673 e	24.65 a_0	15.0 a_0
	3-0-2	4	0-4.68 a_0 4.68 a_0 -16.53 a_0 16.53 a_0 -38.80 a_0 38.80 a_0 - ∞	0- ∞ 0- ∞ 0- ∞ 0- ∞	0.0341 e 0.0337 e 0.0413 e 0.8909 e	24.84 a_0	22.5 a_0
	4-0-1	5	0-1.625 a_0 1.625 a_0 -8.730 a_0 8.730 a_0 -22.77 a_0 22.77 a_0 -46.88 a_0 46.88 a_0 - ∞	0- ∞ 0- ∞ 0- ∞ 0- ∞ 0- ∞	0.0093 e 0.0218 e 0.0523 e 0.2075 e 0.7090 e	15.72 a_0	30.0 a_0
	3-1-1	8	0-2.08 a_0 0-2.08 a_0 2.08 a_0 -11.47 a_0 2.08 a_0 -11.47 a_0 11.47 a_0 -31.45 a_0 11.47 a_0 -31.45 a_0 31.45 a_0 - ∞ 31.45 a_0 - ∞	0-5 a_0 5 a_0 - ∞ 0-5 a_0 5 a_0 - ∞ 0-5 a_0 5 a_0 - ∞ 0-5 a_0 5 a_0 - ∞	0.00092 e 0.0336 e 0.0095 e 0.0690 e 0.0182 e 0.1064 e 0.1617 e 0.6003 e	24.80 a_0	15.0 a_0
	2-2-1	9	0-2.930 a_0 0-2.930 a_0 2.930 a_0 -17.07 a_0 2.930 a_0 -17.07 a_0 17.07 a_0 - ∞ 17.07 a_0 - ∞ 17.07 a_0 - ∞	0-2.930 a_0 2.930 a_0 - ∞ 17.07 a_0 17.07 a_0 - ∞ 0-2.930 a_0 2.930 a_0 - ∞ 17.07 a_0 17.07 a_0 - ∞ 17.07 a_0 - ∞	0.00063 e 0.00682 e 0.0732 e 0.00682 e 0.01905 e 0.1322 e 0.0732 e 0.1322 e 0.5560 e	26.85 a_0	0
	2-1-2	6	0-6.34 a_0 0-6.34 a_0 6.34 a_0 -23.66 a_0 6.34 a_0 -23.66 a_0 23.66 a_0 - ∞ 23.66 a_0 - ∞	0-10 a_0 10 a_0 - ∞ 0-10 a_0 10 a_0 - ∞ 0-10 a_0 10 a_0 - ∞	0.0055 e 0.0820 e 0.0187 e 0.0219 e 0.1907 e 0.6792 e	29.25 a_0	7.5 a_0
	1-1-3	4	0-15 a_0 0-15 a_0 15 a_0 - ∞ 15 a_0 - ∞	0-15 a_0 15 a_0 - ∞ 0-15 a_0 15 a_0 - ∞	0.0296 e 0.1886 e 0.1886 e 0.5931 e	27.20 a_0	0
6	0-0-6	1	0- ∞	0- ∞	e	37.41 a_0	0
7	0-0-7	1	0- ∞	0- ∞	e	50.66 a_0	0

Similar evaluations⁸ have been made for all possible quantum combinations through $n=5$ and thus the configurations are given for the initial and final states resulting in several of the spectral lines of the Lyman, Balmer, and Paschen series for which the most reliable observations have been made. The results of the computations are given in Table I. In column 1 is given the total quantum number $n=(k_1+k_2+m+1)$. In the second column the values of k_1 , k_2 , and $(m+1)$ are given, in the third column the value of $[(k_1+1)(k_2+1)]$ or the number of regions into which the space about the nucleus is divided by the parabolas for which ρ disappears. Columns 4 and 5 give respectively the limits of the integrations over λ_1 and λ_2 in units of $a_0=0.528 \times 10^{-8}$ cm, while column 6 gives the results of the integration over these limits in terms of the total electronic charge e . Since the general expressions are symmetrical with respect to k_1 and k_2 results are given only for those combinations resulting in zero or positive values of (k_1-k_2) .

Also in order to convey pictorially the form of the configurations we show in Fig. 1 to scale ($a_0=0.528 \times 10^{-8}$ cm) the various possible configurations for the total quantum number $n=5$ with the exception of the substate $k_1=k_2=0$, $(m+1)=5$ which results in a toroidal charge in a single region about the nucleus. The solid line parabolas are those for which $\rho=\psi\bar{\psi}=0$ and they are plotted to the rectangular coordinates x and z where the $+z$ direction, the axis of the λ_2 parabolas, is the positive direction of the electric field. The nucleus is at the origin. The figures represent sections in the xz plane and the values of e_{limits} given are the average electronic charge contained in the total volume obtained when the areas shown are revolved about the z axis. The value of \bar{z} the average z coordinate⁹ of the electronic charge as shown in each figure is computed from the general expression $\bar{z}=3/2na_0(k_1-k_2)$. This is also given in column 8 of Table I. For the states with k_1 and k_2 interchanged that is for states $k_1=0$, $k_2=1$, $(m+1)=4$; $k_1=0$, $k_2=2$, $(m+1)=3$; etc. the configurations will be identical to those shown but with the direction of the electrical field reversed.

The values of \bar{x} or the average x coordinates of the charge in any plane are not so easily determined since the expression

$$\bar{x} = \iiint C \rho x dv = \int_0^\infty \int_0^\infty \int_0^{2\pi} C \rho (\lambda_1 \lambda_2)^{1/2} \cos \phi \frac{1}{4} (\lambda_1 + \lambda_2) d\lambda_1 d\lambda_2 d\phi$$

involves fractional exponents and the general integral may be expressed only as a series. For any individual quantum state however the expression may be reduced to a series with a finite number of terms of the form $\int_0^\infty \lambda^P e^{-\lambda/na_0} d\lambda$ which are readily evaluated. The integration results in the common gamma function. The angle ϕ is set equal to zero and \bar{x} thus is the distance from the z axis to the cylindrical shell, concentric with the z axis, which divides the

⁸ Thanks are due to Messrs. Frank Burns and T. C. Butler of Vanderbilt for the evaluation of certain of these integrals.

⁹ F. G. Slack, Ann. d. Physik 80, 579 (1927).

¹⁰ Thanks are due to Professor J. S. Morrel of Vanderbilt University.

electronic charge in half. Or as shown in Fig. 2, drawn for the state 3-1-1 the values of \bar{x} and \bar{z} determine a ring which locates the average position of

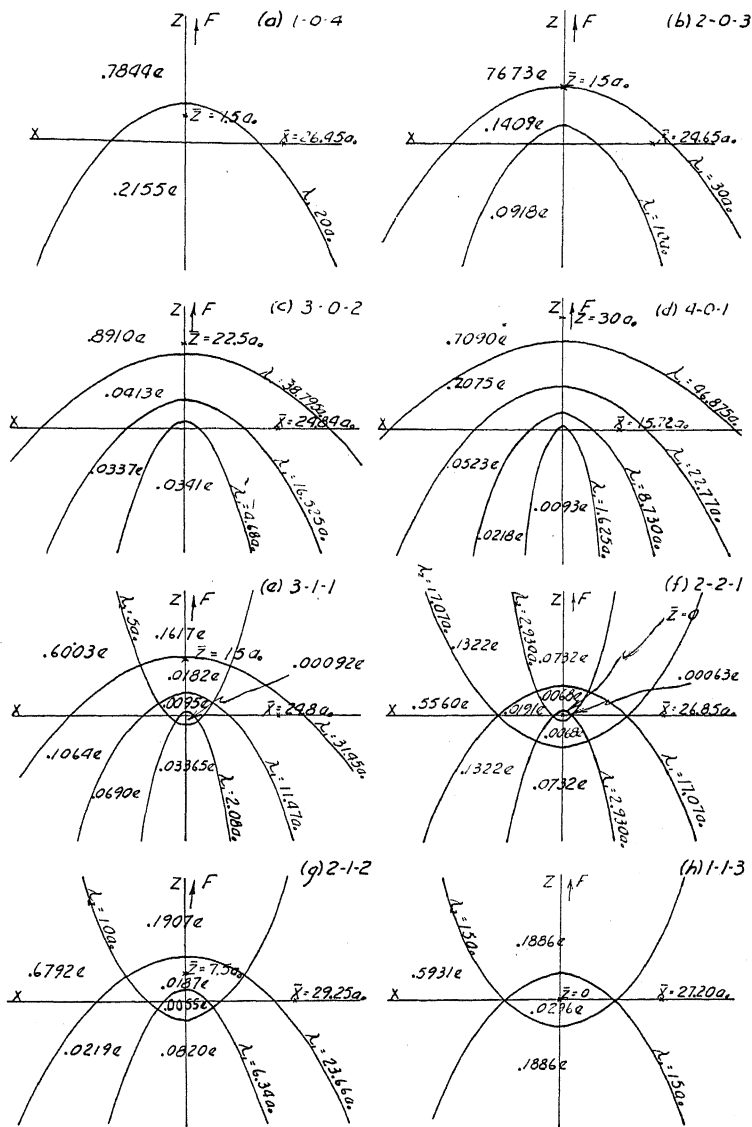


Fig. 1. Electronic configuration for quantum state $n=5$.

the electronic charge with respect to the nucleus. The values of \bar{x} are given in column 7 of Table I and shown on the x axis in the figures of Fig. 1.

Attention is called to the point that for the quantum states 0-0-1, 0-0-2, etc. (i.e. for $k_1=k_2=0$, the circular orbits of the Bohr atom) the

values of \bar{x} are not $n^2 a_0$ as in the Bohr atom but for $n=1$, $\bar{x}=1.178a_0$, $n=2$, $\bar{x}=4.4178a_0$ and for $n=5$, $\bar{x}=26.16a_0$ etc. In general for $k_1=k_2=0$ we have

$$\bar{x}_n = \frac{(2n+1)!(2n-1)!\pi a_0}{2^{4n} n! [(n-1)!]^3}.$$

This arises from the degeneracy of the system in the case of the unperturbed atom.

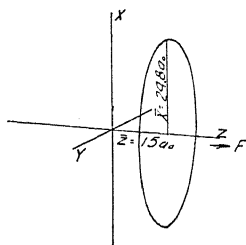


Fig. 2. Location of average electronic charge for state 3-1-1.

As stated in the introductory paragraph calculations of this type have been used by the author to explain the intensity dissymmetry found between the long and short wave components of the hydrogen canal ray light in an electric field parallel to the motion of the beam. It appears to the author that it should be possible to explain the discrepancies between the intensity ratios found by Mark and Wierl¹¹ and those calculated on the Schrödinger theory on the basis of impact probability computed from the above given configurations. This problem and that of polarization in hydrogen canal-ray light due to impact are now under investigation from this point of view.

¹¹ H. Mark and R. Wierl, *Zeits. f. Physik* 53, 526 (1929); 55, 156 (1929); 57, 494 (1929).

A POSSIBLE ORIGIN OF THE BAND AT 2540 IN THE SPECTRUM OF MERCURY VAPOR

BY R. ROLLEFSON

UNIVERSITY OF WISCONSIN, MADISON

(Received March 26, 1930)

ABSTRACT

It can be shown that the band at 2540A in the spectrum of mercury vapor can be accounted for on the basis of a molecule with low energy of dissociation, in agreement with the work of Koernicke who used this band to determine the heat of dissociation of Hg_2 . Certain possibilities are suggested for explaining the high value of the heat of dissociation obtained by Mrozowski.

MUCH of the recent work on the spectrum of mercury vapor has concerned itself with the fluted bands lying between 3000 and 1850A, especially those to the short wave-length side of the resonance line 2536A. By assuming these bands to be due to Hg_2 , and correlating the electronic levels involved with certain atomic levels, Mrozowski¹ has been able to obtain a value for the heat of dissociation of Hg_2 in the normal electronic state, using an extrapolation to obtain the band convergence point. The values obtained ranged between about 10 and 20 k cal/mol, depending on which band was used, but the indication was that the result should be nearer 20 than 10 since the lowest value was obtained by using a long extrapolation and hence was less reliable than the others. Using a different method, the study of the change in absorption by Hg vapor of three lines in the cadmium spark, 2144A, 2573A, and 2749A, as a function of the temperature, he obtained approximately 17 k cal/mol. These results are of a different order of magnitude from the ones obtained by Franck and Grottrian² (1 k cal/mol) and later by Koernicke³ (1.4 k cal/mol). The latter investigators, however, made use of the decrease in intensity of absorption in a definite band, that at 2540, with increasing temperature. It is the purpose of this note to show that this band at 2540, which was used by Koernicke in his determination of the heat of dissociation of Hg_2 , may be rather easily accounted for if we assume his small value for the energy of dissociation to be correct. We thus have two self consistent groups of phenomena which seem to contradict one another.

Considerations concerning the type of molecule one would expect to result from the union of two closed-shell atoms would seem to indicate that it should have a small energy of binding. If one considers a configuration consisting of two such atoms, attracting and repelling forces may each be expected to vary inversely as a high power of the distance between them,

¹ Mrozowski, *Zeits. f. Physik* 55, 338 (1929).

² Franck and Grottrian, *Zeits. f. techn. Physik* 3, 194 (1922).

³ Koernicke, *Zeits. f. Physik* 33, 219 (1925).

due to the high degree of symmetry of the atoms. If, then, we should plot the potential energy of the configuration as a function of the nuclear separation (following Franck) we should obtain a curve similar to I, Fig. 1. Such a sharp curvature of the potential energy curve indicates that the frequency of vibration in the zeroth vibrational state would be comparatively large, hence the energy of this lowest level might well be nearly that necessary for dissociation. In fact this ground state might be the only existing vibrational state connected with the lowest electronic level of Hg_2 . A case similar to this has already been treated according to the new quantum mechanics by Peierls,⁴ who also suggested the possibility of the application of his results to homopolar molecules with polarization binding. The latter is very probably what is dealt with in the case being considered, that of a molecule formed

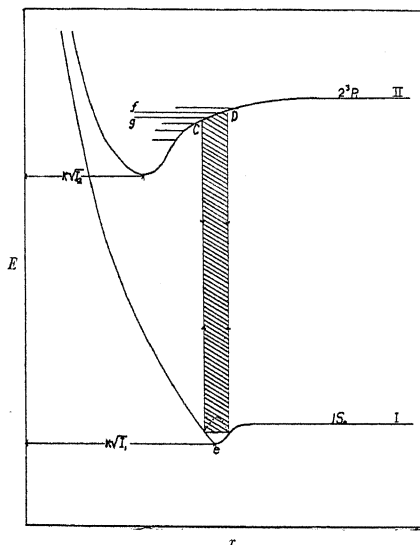


Fig. 1

by the union of two unexcited mercury atoms. Thus curve I, with only one vibrational level may be taken to represent the ground level of such a molecule.

With one atom excited, however, conditions would be somewhat changed. The polarizability and hence the binding force would be greater, and consequently the internuclear distance corresponding to equilibrium would be diminished, resulting in a potential energy curve similar to II and a smaller moment of inertia for the molecule. Applying the Franck-Condon principle for determination of the intensity of bands, we may represent the most probable transitions by the shaded area in the diagram. The number of intense bands would then be determined by the number of vibrational levels between C and D. Then, since a decrease in the moment of inertia is involved in the transition, these bands would be shaded toward shorter wave-lengths. If, for

⁴ Peierls, *Zeits. f. Physik* 58, 59 (1929).

instance, there were two vibrational levels f and g between C and D , we should have two bands, sharp on the long wave-length side and shaded toward the resonance line 2536, and if the energy difference between f and g were small, the two bands would be partially superposed. This is in complete agreement with what has been observed by Wood and Voss.⁵ Thus the band at 2540 can be accounted for by assuming a low heat of dissociation for unexcited Hg_2 , and this same band, when studied by Koernicke's method indicates that neutral Hg_2 has that low heat of dissociation.

In the light of the above it may be well to consider again the results of Mrozowski. Although the consistency of the results he obtained argues in favor of his interpretation, still it seems reasonable to assume that agencies other than Hg_2 contribute to the absorption by mercury vapor in the regions he used for determining the heat of dissociation. In the case of the line 2573 for instance, it is possible that Hg_2 is responsible for none of the absorption, but that what occurred was an interaction of radiation and impact, that is, absorption during collision, such as has already been discussed by Oldenberg,⁶ or absorption by quasi-molecules as discussed by Born and Franck.⁸ A possible explanation of the fact that the fluted bands indicate a large energy of dissociation may be that the bands do not involve a transition to or from the lowest electronic level of a molecule composed of two unexcited mercury atoms. For example Walter and Barratt⁷ have been able to obtain the fluted band between 3000 and 2600 only when oxygen was present in the absorption tube. This band has the variation in intensity characteristic of a triatomic molecule, with no sharp edges such as one would expect in a band due to a diatomic molecule, and may be due to Hg_2O . The other bands used by Mrozowski may be due to a mercury molecule, but not necessarily the same type of molecule which gives rise to 2540.

The writer acknowledges his indebtedness to Professors C. E. Mendenhall and G. Wentzel for helpful criticism in the writing of this note.

⁵ Wood and Voss, Proc. Roy. Soc. **A119**, 698 (1928).

⁶ Oldenberg, Zeits. f. Physik **51**, 605 (1928).

⁷ Walter and Barratt, Proc. Roy. Soc. **A122**, 201 (1929).

⁸ Born and Franck, Zeits. f. Physik **31**, 411 (1925).

THE IONIZATION OF HYDROGEN BY SINGLE ELECTRON IMPACT

BY WALKER BLEAKNEY

PHYSICAL LABORATORY, UNIVERSITY OF MINNESOTA

(Received April 11, 1930)

ABSTRACT

From an analysis of the theoretical potential energy curves for the H_2 molecule as outlined by Condon the theoretical predictions for the types of ions resulting from primary impacts with electrons are described. These predictions include the formation of H_2^+ at 15.25 volts, H^+ at 17.9 volts, H_2^{2+} at about 30 volts which then dissociates with several volts kinetic energy, and H_2^{3+} at about 50 volts which also dissociates with kinetic energy. Using a mass spectrograph the experimental results of a study of the primary ions in hydrogen indicate the formation of H_2^+ at 15.4 ± 0.1 volts, H^+ at 18.0 ± 0.2 volts, and H^+ at 26 to 30 volts, the last having various amounts of kinetic energy.

Curves are given showing the relative number of each of these types of ions from which it appears that at the higher velocities about 92 percent of the total number of ions formed is of the H_2^+ type, 1 percent of the H^+ corresponding to the 18 volt potential, and 7 percent of the H^+ having kinetic energy. The probability of ionization for all types together as a function of the electron velocity is given by a curve, plotted to an arbitrary scale, which exhibits a well-defined maximum at 60 volts.

INTRODUCTION

THE ions produced by electron impact in hydrogen have been studied by the method of positive ray analysis so many times and by so many investigators that it might, at first sight, seem useless to try to make much more progress in this direction. As early as 1916 Dempster¹ designed a mass spectrograph with which he studied the ions produced in hydrogen by 800 volt electrons. Since that time somewhat similar experiments have been carried out by Smyth,² Hogness and Lunn,³ Kallmann and Bredig,⁴ Dorsch and Kallman,⁵ and Brasefield.⁶ The consensus of opinion of these observers is that their experiments have failed⁷ to show that any ion other than H_2^+ may result from a single impact with an electron. The evidence from the experiment to be described⁸ points toward a different conclusion. Moreover certain aspects of the theory of the hydrogen molecule predict several possible modes of production of the H^+ ion at a single impact.

¹ A. J. Dempster, *Phil. Mag.* **31**, 438 (1916).

² H. D. Smyth, *Proc. Roy. Soc. A* **105**, 116 (1924), and *Phys. Rev.* **25**, 452 (1925).

³ T. R. Hogness and E. G. Lunn, *Proc. Nat. Acad. Sci.* **10**, 398 (1924), and *Phys. Rev.* **26**, 44 (1925).

⁴ H. Kallmann and M. A. Bredig, *Zeits. f. Physik* **34**, 736 (1925), and *Zeits. f. Physik* **43**, 16 (1927).

⁵ K. E. Dorsch and H. Kallmann, *Zeits. f. Physik* **44**, 565 (1927).

⁶ C. J. Brasefield, *Phys. Rev.* **31**, 52 (1928).

⁷ In their first papers both Smyth, and Hogness and Lunn (see references 2 and 3) reported H^+ as a primary process but later both reported these results as inconclusive.

⁸ W. Bleakney and J. T. Tate, *Phys. Rev.* **35**, 658 (1930) (Abstract).

THEORY

Before the present experiment was undertaken Professor Condon drew up an outline of the results one might expect to find in making an e/m analysis of the primary ions in hydrogen. The essential ideas of this outline have been discussed by Condon,⁹ and Condon and Smyth,¹⁰ and the particular points pertinent to the present experiment will be reviewed here in some detail.

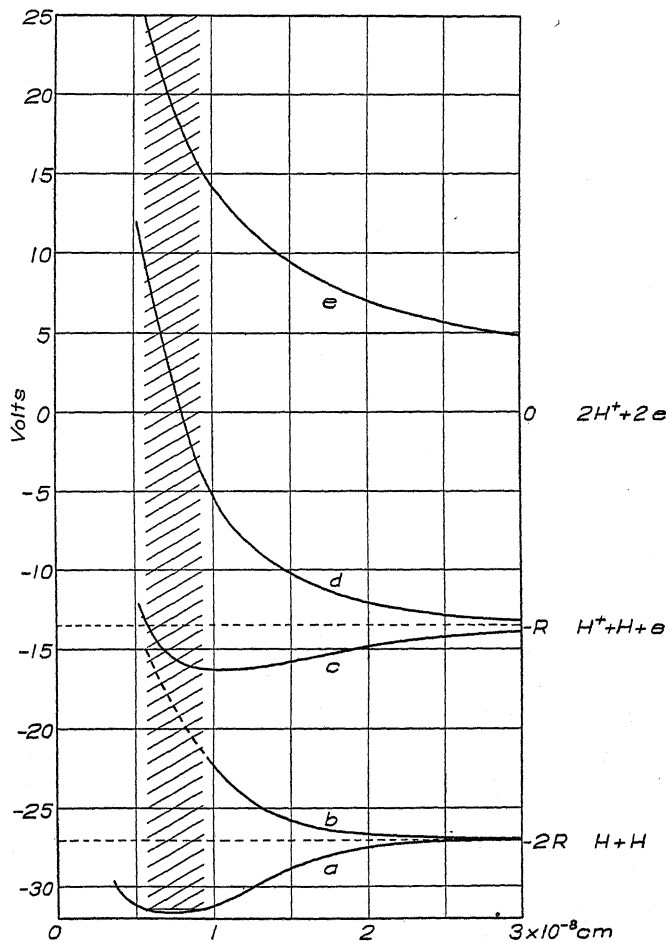


Fig. 1. Potential energy curves for the H_2 molecule.

In Fig. 1 are represented some of the theoretical potential energy curves for the hydrogen molecule. The potential energy in volts is plotted as a function of the nuclear separation in Angstrom units. Curves a and b represent the two solutions for the problem of bringing two H atoms in the normal state near each other to form an H_2 molecule as calculated by Sugiura¹¹ from the theory of Heitler and London.¹² Curve a has been altered slightly in order to

⁹ E. U. Condon, Phys. Rev. 35, 658 (1930) (Abstract).

¹⁰ E. U. Condon and H. D. Smyth, Proc. Nat. Acad. Sci. 14, 871 (1928).

¹¹ Y. Sugiura, Zeits. f. Physik 45, 484 (1927).

¹² W. Heitler and F. London, Zeits. f. Physik 44, 455 (1927).

fit the data as given by Birge and Jeppesen¹³ and b has been lowered somewhat in the dotted region. In like manner curves c and d represent the two solutions for the problem of the formation of the H_2^+ molecular ion from a normal H atom and a proton. Curve c is that calculated by Burrau¹⁴ and d is from the paper by Morse and Stueckelberg.¹⁵ Curve e represents the potential energy of the H_2^{++} molecule due to the Coulomb force of repulsion between the two protons. The width of the shaded band corresponds to the range of nuclear separations executed by the hydrogen molecule in its lowest vibrational state.¹⁶ The effect of rotational energy has been disregarded since it would add the same amount of energy to all the curves.

Now if a normal H_2 molecule is transformed by an electron impact from its lowest energy level on a to one of the states represented by the other curves it will, according to the Franck-Condon principle, suffer meanwhile little change in nuclear separation. Immediately after the transition, therefore, there is a high probability that the point representing the energy state of the molecule will lie within the shaded area. Hence, transitions are represented in this diagram by vertical or nearly vertical jumps from one state to another. Transitions from the normal to the state b would result in subsequent dissociation into two normal atoms each having several volts kinetic energy. This transition has no significance in the present experiment since only ions are measured. A jump to the state c results in the ordinary H_2^+ ion which should, according to this scheme, occur at 15.25 to 17.9 volts with various amounts of vibrational energy. An inspection of the figure shows that there is a small chance of a transition to a point on this curve which lies above the dotted line and the molecule in this state would then dissociate. Hence a small number of H^+ ions should be predicted at potentials above 17.9 volts. From 27 to 40 volts should be required to raise the molecule from its normal state to that represented by curve d where dissociation would occur into a normal H atom and a proton each having from 5 to 11 volts kinetic energy. Finally to strip both electrons from the H_2 molecule at a single blow should require from 46 to 56 volts and the two protons would then fly apart each with 7.5 to 12.5 volts kinetic energy. Between the last two stages there are many other transitions possible as a result of which the molecule would dissociate into a proton and an excited atom. Summarizing, then, the theory would predict the following primary reactions;

- | | |
|--|-----------------|
| 1. $H_2 \rightarrow H_2^+ + e$ | 15.4—17.9 volts |
| 2. $H_2 \rightarrow H^+ + H + e$ | 17.9—18.0 volts |
| 3. $H_2 \rightarrow H^+ + H + e + \text{kinetic energy}$ | 27 —40 volts |
| 4. $H_2 \rightarrow 2H^+ + 2e + \text{kinetic energy}$ | 46 —56 volts. |

APPARATUS AND PROCEDURE

The apparatus was the same as that used for the study of mercury ions¹⁷ and the details will therefore not be given here. In the present experiment the

¹³ R. T. Birge and C. R. Jeppesen, *Nature* **125**, 463 (1930).

¹⁴ Burrau, *Kgl. Danske Vid. Selskal. Math-fys. Med.* **7**, 14 (1927).

¹⁵ P. M. Morse and E. C. G. Stueckelberg, *Phys. Rev.* **33**, 932 (1929).

¹⁶ For the details of this theory see E. U. Condon, *Phys. Rev.* **32**, 858 (1928).

¹⁷ W. Bleakney, *Phys. Rev.* **34**, 157 (1929) and *Phys. Rev.* **35**, 139 (1930).

flow method was used, the hydrogen being admitted to the system through a palladium tube. This tube was surrounded on the outside with hydrogen at atmospheric pressure and its temperature was maintained at the required value by an electric heating element. The rate of flow of the gas into the apparatus could be regulated by adjusting the rheostat controlling the heating current. The pressure of the gas in the ionization chamber was not measured but it was estimated to be in all cases in the neighborhood of 10^{-3} mm Hg. A trace of mercury vapor was allowed to remain in the apparatus for calibration purposes.

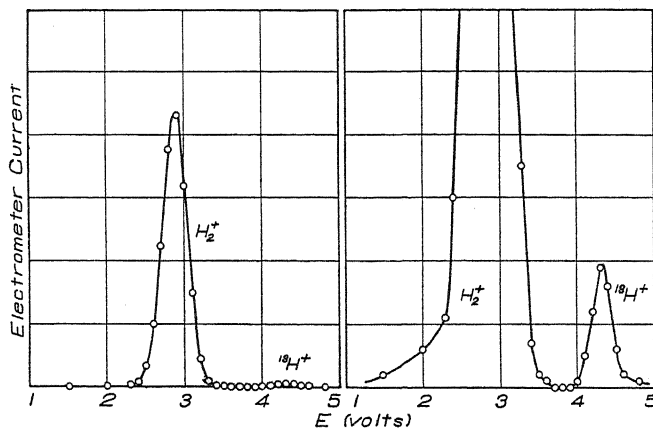


Fig. 2. A typical e/m analysis curve. Electron velocity = 150 volts. The second curve is the first magnified 40 times.

EXPERIMENTAL RESULTS

Primary ions in hydrogen. Figure 2 illustrates an e/m analysis curve for hydrogen ions produced by 150 volt electrons. The symbol $^{18}\text{H}^+$ is used to designate the atomic ion which begins to appear at 18 volts. The two curves represent the same data but in the second the ordinates have been expanded forty times. These two ions have at the instant of formation very little kinetic energy compared to that given them by the analyzing fields. In Fig. 3 is shown another peak obtained when the field V_2 ordinarily used to draw out the positive ions was made 1 volt per cm negative. In this case all the ordinary ions were prevented from reaching the analyzing chamber but those having high kinetic energy reached the collector. The number, however, was small and it was necessary to increase the sensitivity of the electrometer considerably in order to detect them at all. It will be noticed that the peak is very broad compared to those in Fig. 2. The second curve in Fig. 3 represents the maximum height of this peak as a function of the electron velocity. It is evident that weak ionization sets in at about 26 volts and becomes quite strong at 30 volts. This ion will be designated by the symbol $^{30}\text{H}^+$. These results can only be interpreted as *primary* processes. No trace of secondary reactions such as the formation of H_3^+ could be found.

Critical potentials for ionization. The ionization potentials for H_2^+ and $^{18}\text{H}^+$ obtained by plotting the heights of the peaks as functions of the electron velocity in volts are shown in Fig. 4. The Hg^+ ion is included in order to

determine one point on the voltage scale assuming its ionization potential to be 10.4 volts. In this figure the curve for $^3\text{H}^+$ was obtained by measuring with a galvanometer the positive current reaching the plate, to which the

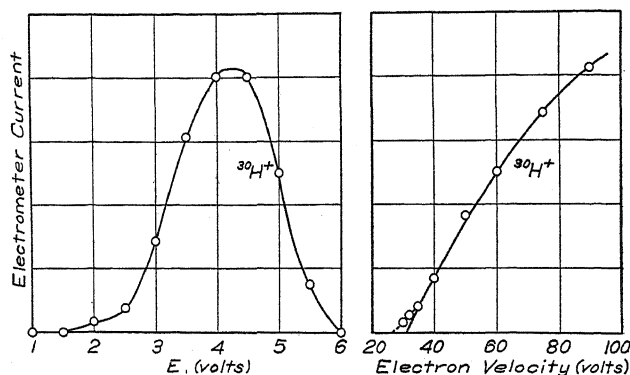


Fig. 3. A broad peak due to the initial high velocity of the ions. The second curve shows the ionization potential.

total positive ion current is ordinarily measured, against a small retarding field. This curve checks closely the one shown in Fig. 3 which was obtained in a different way. It would indicate that the critical potential for the forma-

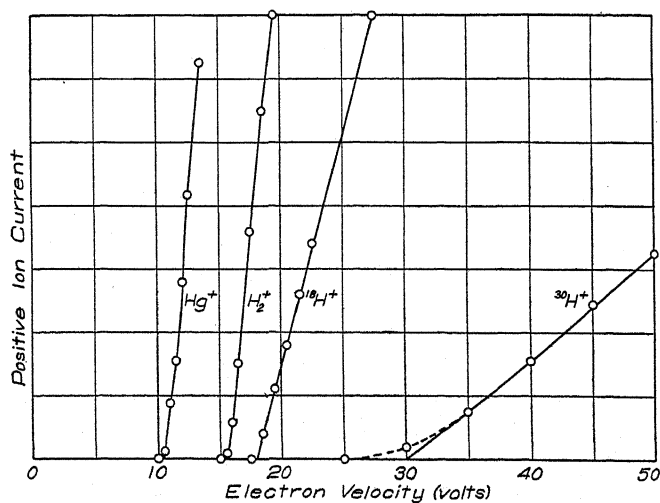


Fig. 4. Ionization potentials.

tion of this ion is about 26 volts while strong ionization of this type sets in from 30 to 35 volts. A summary of these results may be expressed in the following way.

Process	Predicted	Observed
1. $\text{H}_2 \rightarrow \text{H}_2^+ + e$	15.25 volts	15.4 ± 0.1 volts
2. $\text{H}_2 \rightarrow \text{H} + \text{H}^+ + e$	17.9	18.0 ± 0.2
3. $\text{H}_2 \rightarrow \text{H} + \text{H}^+ + e + \text{kin. energy}$	27.	$26 \pm 1.$

These conclusions constitute a striking confirmation of the theory.

Relative numbers of the different ions. The number of $^1\text{H}^+$ ions relative to the number of H_2^+ ions was determined by finding the relative areas¹⁸ under the peaks in the e/m analysis curves. Such a procedure was unsuitable, however, for determining the relative number of those ions having kinetic energy

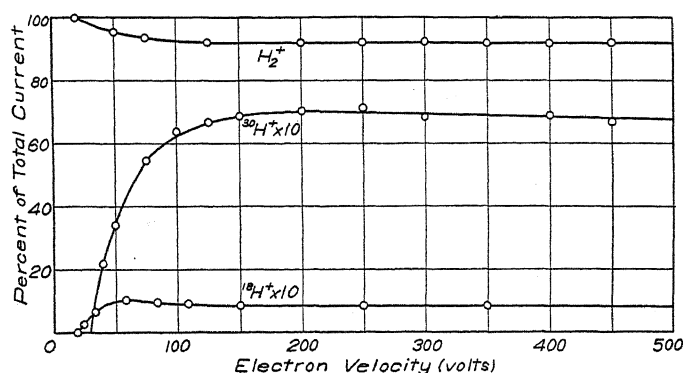


Fig. 5. Relative intensity of the different types of ions.

since only a small fraction is shot out in the direction of the analyzer. A rough estimate of their intensity was made in the following manner. The total positive ion current was measured with the galvanometer in the usual way and then the field V_2 was reversed so that only ions having kinetic energy

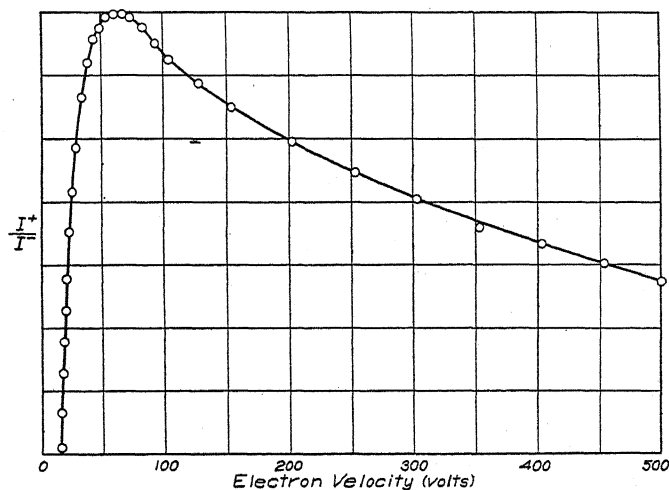


Fig. 6. Efficiency curve for hydrogen.

could reach the plate. This number reaching the plate was plotted as a function of the retarding field and the curve so obtained extrapolated to zero field. Knowing the solid angle subtended at the electron beam by the plate and assuming cylindrical symmetry the fraction of the total current due to those ions having kinetic energy was calculated. The results are shown in Fig.

¹⁸ For a discussion of the assumption that the numbers are proportional to the areas see the second paper of reference 17.

5 where the ordinates for $^{18}\text{H}^+$ and $^{30}\text{H}^+$ have each been multiplied by ten. The curve for $^{30}\text{H}^+$ may include ions having kinetic energy as a result of some transition other than the 30 volt variety but it is believed that these are relatively very small in number.

Efficiency of ionization. Since in this experiment the pressure of the gas was not measured the efficiency of ionization could only be determined within an arbitrary constant factor. The result is given by the ratio of the electron current to the total positive ion current plotted as a function of the electron velocity. The curve, Fig. 6, shows a well-defined maximum at 60 volts. From the previous data it may be concluded that over ninety percent of the total number is made up of H_2^+ ions.

There is a marked difference between the shape of this curve and that reported by Compton and Van Voorhis¹⁹ in that the maximum appears at a much lower electron velocity and the curve falls off more rapidly beyond this point. Qualitatively the agreement with the data of Hughes and Klein²⁰ is good.

DISCUSSION

It is believed that the results of this experiment yield, at present, the most direct evidence for the existence of those repulsive forces represented by the potential energy curves for the H_2^+ ion. It will be recalled that such an energy state is contrary to the concepts of the classical theory which predicts only a force of attraction. Indirectly these results also lend support to the reality of the other repulsive curves predicted by the quantum theory.

The determinations of the critical potential for the formation of H_2^+ as made by a large number of observers²¹ cluster about a mean value of about 16.0 volts. That found in this experiment, 15.4 volts, is lower than any experimentally determined value known to the writer but it is believed that the method lends itself to greater accuracy than any of the previous methods. The close agreement with the theory lends support to this view. As Condon⁹ has pointed out, it is now impossible in the light of the theory and these experiments to interpret the critical potential near 30 volts which has been reported by Krüger,²² Horton and Davies,²³ and Vencov²⁴ as double ionization accompanied by dissociation. In the present work a search was made for the 50 volt transition resulting in H_2^{++} but only slight evidence for its existence could be found. An effort is being extended in this laboratory to throw more light on this question with an apparatus designed to measure the velocity distribution of high velocity ions.

The author is greatly indebted to Professors E. U. Condon and John T. Tate for their many helpful suggestions.

¹⁹ K. T. Compton and C. C. Van Voorhis, *Phys. Rev.* **26**, 436 (1925) and *Phys. Rev.* **27**, 724 (1926).

²⁰ A. L. Hughes and E. Klein, *Phys. Rev.* **23**, 450 (1924).

²¹ For a compilation of these values see the paper by Hogness and Lunn, *Phys. Rev.* **26**, 44 (1925).

²² T. Krüger, *Ann. d. Physik* **64**, 288 (1921).

²³ F. Horton and A. C. Davies, *Phil. Mag.* **46**, 872 (1923).

²⁴ S. Vencov, *Comptes Rendus* **189**, 27 (1929).

ELECTRON ENERGY LOSSES IN MERCURY VAPOR

BY CASTLE W. FOARD

STATE UNIVERSITY OF IOWA, IOWA CITY

(Received March 31, 1930)

ABSTRACT

An improved magnetic spectrum method was used to determine the energy losses sustained by slow speed electrons in mercury vapor. Electron energies up to 60 volts were used, the main region of interest being from 0 to 25 volts. The energy losses detected, below that required for ionization, were; 4.9, 5.4, 6.7, 7.7, 8.8, 9.8 volts. These correspond to practically all the transitions of a valence electron from the basic 1S level up to each of the higher levels to 4P. No evidence of other losses such as are observed by the photoelectric method were found. At voltages above 10.4, the ionization potential, electrons seem to be able to give up any quantity of energy in excess of that required for ionization, the higher losses being favored. A very interesting loss of 11.07 volts has been found, which has not been recorded heretofore. It begins to be resolved at about 18 volts, and grows steadily with increasing voltage in much the same manner as the 6.7 volt loss. It is thought that this loss involves the simultaneous displacement of both valence electrons from their normal levels.

THE pioneer work on inelastic impacts of electrons with mercury atoms, by Franck and Hertz,¹ showed that the energy lost by the electron is quantized. At first there appeared to be but one type of inelastic impact, that in which the loss of energy was equivalent to a drop in potential of 4.9 volts. Since that time, three other types of losses have been found by this or similar methods.^{2,3,4} The photoelectric method, developed by Franck and Einsporn,⁵ is also capable of giving us an insight into the phenomena of impacts. The number of critical potentials found by this latter method is quite large—eighteen, in the work referred to, and a still larger number in the later work of Jarvis.⁶ Some of these critical potentials have been shown^{7,8} to be due to other effects than resonance collisions: but there has persisted a discrepancy between the results of each of these methods, not only with each other, but with the results of spectroscopic study.^{9,10,11,12,13}

¹ Franck and Hertz, *Verh. d. Deut. Phys. Ges.* **16**, 457 (1914).

² Mohler, Foote, and Meggers, *Phys. Rev.* **10**, 101 (1917).

³ Eldridge, *Phys. Rev.* **20**, 456 (1922).

⁴ Whitney, *Phys. Rev.* **34**, 923 (1929).

⁵ Franck and Einsporn, *Zeits. f. Physik* **2**, 18 (1920).

⁶ Jarvis, *Phys. Rev.* **27**, 808 (1926).

⁷ Webb, *Phys. Rev.* **24**, 113 (1924).

⁸ Messenger, *Phys. Rev.* **28**, 962 (1926).

⁹ Hertz, *Naturwissenschaften* **11**, 778 (1923).

¹⁰ Eldridge, *Phys. Rev.* **23**, 685 (1924).

¹¹ White, *Phys. Rev.* **28**, 1125 (1926).

¹² Valasek, *Phys. Rev.* **29**, 817 (1927).

¹³ Crozier, *Phys. Rev.* **31**, 800 (1928).

It seemed highly desirable that the inelastic impact method, which, in the past, has given the most meager results, should be improved, with a view to determining which of the impacts involve actual quantized energy losses to the electrons. For this purpose, the method used by Whitney⁴ has certain points of advantage over other methods. The electrons which have lost energy are spread out into a velocity spectrum, and can be collected, group by group, without mutual interference. This makes possible the use of greater sensitivity, in the search for the less probable types of losses. While Whitney was primarily interested in the excitation functions of the more probable impacts, his failure, under apparently favorable conditions, to detect the losses observed by the photoelectric method increased the difficulty of a reconciliation between results of the two methods.

A possible explanation of this discrepancy, as Whitney points out, would be that the types of losses which he does not find, are very improbable, except when the electron has little more than the amount of energy required for the excitation. Since Whitney's apparatus was quite insensitive to very slow electrons, we can see how these collisions involving a total loss of energy, would, under this hypothesis, have escaped detection. We therefore set about to remove this limitation by increasing the sensitivity of the Whitney method for slow speed electrons, and at the same time, to improve the resolving power. An additional end has been gained by a change of procedure which allows the energy losses to be read directly in volts from an accurate potentiometer, rather than by means of a calibration curve.

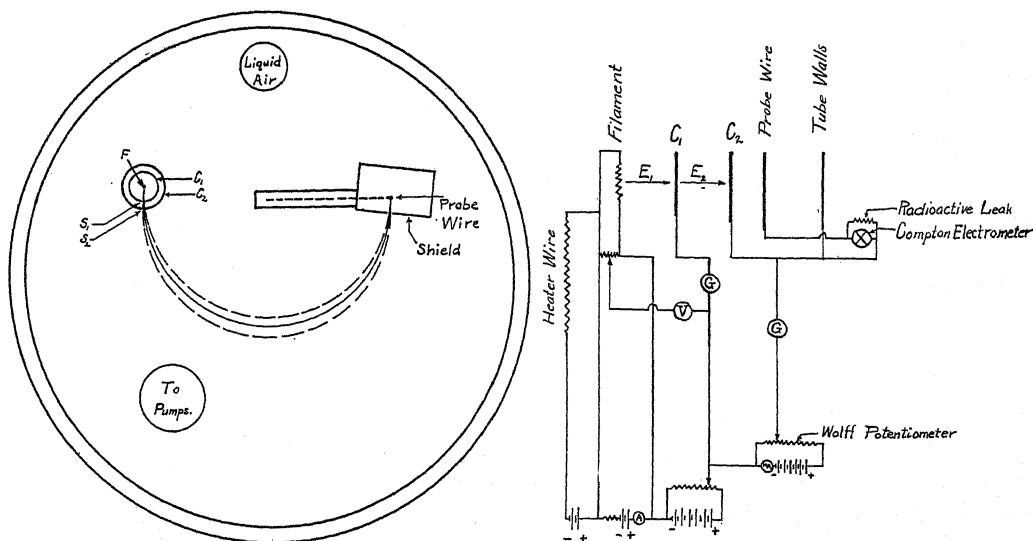
APPARATUS

The apparatus is pictured in Figs. 1 and 2. Electrons evaporating from the unthoriated tungsten filament F , are attracted toward the concentric cylinder C_1 , during which time they may make elastic or inelastic impacts with the atoms of mercury vapor which fills this region. A sample of the electrons arriving at the cylinder pass through the slit S_1 . The second cylinder, C_2 , allows us to control the speed with which the electrons emerge from S_2 . In the electric field free region outside the cylinders, the electrons are spread into a velocity spectrum by means of a uniform transverse magnetic field produced by a large pair of Helmholtz coils. Electrons having some definite speed, determined by the strength of the magnetic field used, will converge at a point 180° distant from S_1 , along an arc of a circle of 5 cm radius. Here they are collected by a probe wire which is shielded from stray electrons. A Compton quadrant electrometer, shunted by a radioactive leak, measures the current to the probe, which is of the order of 10^{-11} amp.

The vacuum tube was made entirely of brass, $3/8$ " thick, 20 cm diameter, and 22 cm long. The only metal parts of other material were the inner (molybdenum) cylinder and the tungsten filament. Two small glass windows and a reentrant liquid air trap, used in freezing out the mercury vapor from the outside region, were carefully shielded with brass wire gauze. The vacuum was kept below 10^{-5} mm, and liquid air traps employed constantly. The mercury vapor was introduced into the impact chamber from a furnace

heated reservoir maintained at various temperatures from 90° to 118° , depending on the pressure desired. The vapor pressure, under these conditions, is hard to estimate, since diffusion through the slit S_1 and the temperature of the impact chamber play an uncertain role; from the probability of certain types of losses, the pressure seemed to be of the order of 0.1 mm.

While a number of changes have been made, the tube, as described above, is essentially of the same type as that employed by Whitney. The chief point of difference lies in the addition of the auxiliary accelerating cylinder, C_2 . By means of this cylinder, the speed of the electrons may be adjusted so that any particular group may be focused on the probe wire, without changing the magnetic field.



Figs. 1 and 2. Plan of apparatus and electrical circuit.

PROCEDURE

In Whitney's method, the electrons emerging from C_1 with various residual speeds, were collected, group by group, by varying the magnetic field. In the present work, the procedure was somewhat different. All of the electrons collected were made to travel the circular path to the probe, with the same speed, regardless of how much energy they had lost. This was accomplished by accelerating them enough between C_1 and C_2 to just make up for their loss in energy at impact. For example, the 6 volt curve in Fig. 4 was taken as follows. E_1 , the potential on C_1 , was set at 6 volts, the desired impact speed. E_2 , the difference of potential between C_2 and C_1 , was set at (say) 2 volts. The magnetic field was then adjusted for maximum probe current, i.e., for 8 volt electrons. E_2 was then varied from 0 to 8 volts, in convenient steps of, generally, 0.1 volt, and the data recorded directly on graph paper. Those electrons which have lost none of their initial 6 volts, will require but two volts to be brought to the probe wire: but those which

have lost 4.9 volts at an inelastic impact, will require that much more energy, or a total of 6.9 volts acceleration between the cylinders, in order to have the proper speed to be collected. The no-loss electrons then have, of course, 10.9 volts, and hence move in too large a circle to interfere. If the arbitrary two volt initial value of E_2 be neglected in plotting, the abscissas of the peaks give the values of the energy losses directly in volts, and the ordinates, approximately the relative probability of each type of impact, at a particular impact speed. The width of the peaks is due to several causes, such as velocity distribution in the original electron stream, imperfect focusing, and finite width of probe.

Fig. 3 shows the degree to which this method was successful in improving the sensitivity for slow speed electrons. The first curve is similar to that

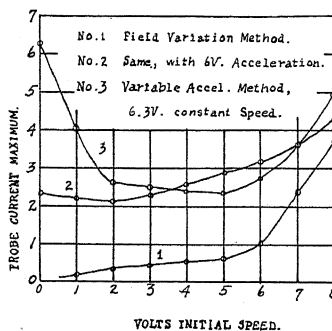


Fig. 3. Efficiency of collection of electrons as a function of their voltage.

published by Whitney, and shows the efficiency of collection of electrons, in the absence of the auxiliary cylinder. Curve 2 shows that, when this cylinder is inserted and maintained at a potential 6 volts above that of the first cylinder, the slow electrons are collected much better than before. In making curve 3, the new method of procedure was used. The total speed of collection was always 6.3 volts, but the speed with which they emerged from S_1 is varied from 0 upward. Slow electrons are still more favored than in the preceding curve, but the direct-reading characteristic of the new method is an additional advantage.

RESULTS

Fig. 4 shows the type of curves that are obtained with electron energies below ionization. The 4.9 volt loss, which is the predominant one up to 9 volts, begins to show itself at as low as 4 volts. In that curve, it appears to be a loss of only 4.3 volts, rather than 4.9 volts. These two illusions, the detection of a loss at too low a voltage, and the apparent smallness of the loss are traceable to the rather large velocity distribution—amounting to about 1.6 V.—which is here present. Since the potential E_1 is measured with respect to the center of the emitting portion of the filament, a certain share of the electrons may well have enough more energy than the average, to be able to lose 4.86 V. After this loss, a subsequent addition of less than 4.86 V. would

be required in order to collect them at the normal speed. This effect is most prominent for the types of losses which increase most rapidly in the vicinity of their critical potentials. The occurrence of a loss by an electron which apparently does not have that much energy might also be due to impacts occurring between the two cylinders, after the electron has acquired part of the added potential E_2 , though this is not considered likely.

At an impressed voltage of 5.2, an energy loss of 5.4 V. is clearly discernible, anticipated in voltage for the same reason as in the case of 4.9. A 6.7 V. loss is seen in the 6.5 volt curve, anticipated less than 4.9 was, and probably less than 5.4 would have been, had the latter not been partly obscured by the 4.9 V. peak.

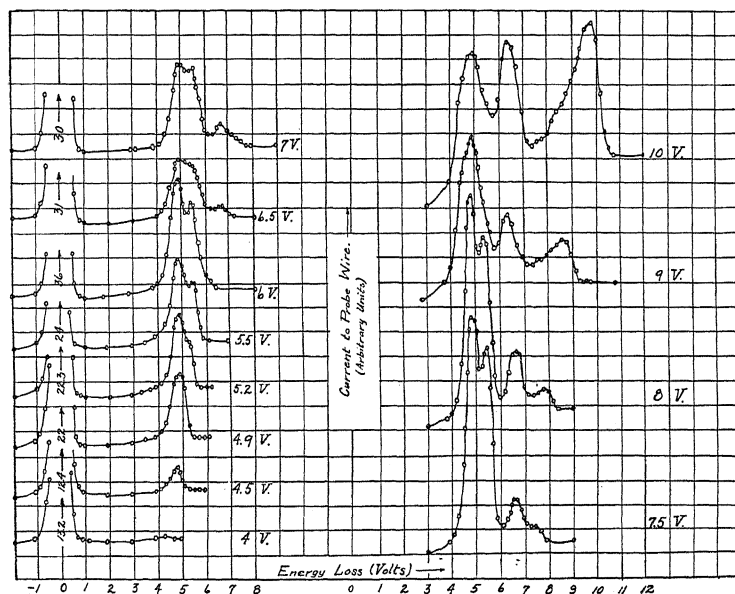


Fig. 4. Energy losses in Hg below ionization.

The failure of previous users of the inelastic impact method, to find a loss of 7.7 V., or 7.9 V., corresponding to transitions of the valence electron from the 1S to the 2s or 2S levels, has been a serious criticism of the completeness of the results to be obtained by this method. These levels are separated by approximately a volt on either side, from all other levels, and upward transitions to them should be easily observable, if their probability is at all large. That such a loss does occur is seen from the curves of Fig. 4, beginning with the one for 7.5 V. The probability of the loss, while always small, rises to a maximum and falls off to insignificance within two or three volts of its critical potential. The exact loss could not be determined with much accuracy, but appears to be 7.7 V., though 7.9 might also be present. It is interesting to note that Crozier¹³ found that the intensity of the downward transitions from

$2s$ to $2p_{2,3}$, changed in a similar manner, while transitions from $2S$ had but one-third the probability in comparison.

The well-known loss of 8.8 V., and a loss of 9.8 V., sometimes observed, but attributed to two successive 4.9 V. losses, complete the list of losses less than that required for ionization. These may be seen better in Fig. 5, at impact speeds above ionization, because of their increased probabilities of occurrence. At 41 V., the 9.8 V. peak is at least as large as the single 4.9 V. peak, while the multiple collision peaks involving one or more 6.7 V. loss, are, quite properly, but a small fraction of the size of the single loss peak. This

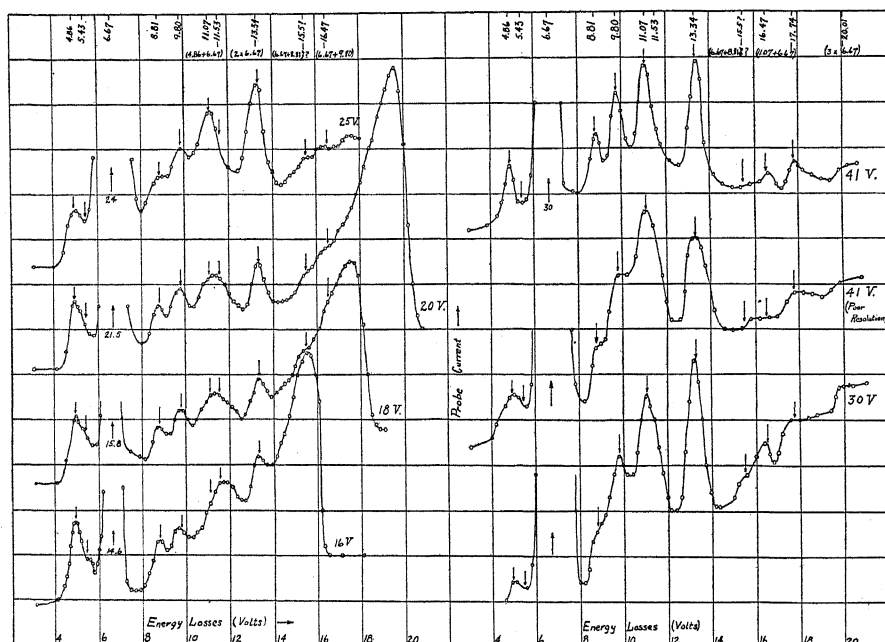


Fig. 5. Energy losses in Hg at higher electron voltages.

consideration, along with a study of the change of size of the 9.8 V. loss with change of vapor pressure, leaves little doubt of its interpretation as a single impact loss.

IONIZATION

In all the curves taken with impact speeds above about 10 V., the threshold current, upon which the inelastic impact peaks are superimposed, rises rapidly in the vicinity of the region indicating total energy loss. It falls again, of course, at a distance beyond the total loss value, equal to half the velocity distribution. In other words, this rather large group of electrons appears to lose any amount of their energy from about that required for ionization up to total loss, the great bulk of them being in the latter category. The absolute number of these electrons is probably a great deal less than would be inferred from the size of the peak, because of the facility of collec-

tion of slow electrons, as previously explained. It was suspected that these slow electrons might have lost their energy at reflection from the walls of one of the cylinders. To test this, the furnace was cooled to 25°C, when the slow speed peak persisted to a certain extent, while the inelastic impact peaks practically vanished. The conclusion derived from this was that a part of the effect was due to reflected electrons from the cylinder walls, but that the major portion was to be attributed to some kind of a loss involving the mercury vapor, presumably associated with ionization. Eldridge³ came to the conclusion that, at ionization, both the impacting electron and the electron born of ionization had but a negligible amount of energy. What to do with the extra loss of energy is a moot question. Some later authors have supposed a sharing of the surplus energy by the two electrons: on this hypothesis, the current due to this source should be symmetrical about a line midway between total loss and ionizing loss; this is decidedly a different distribution than that observed here. This is, admittedly, an unsatisfactory way to leave the problem, but additional information is needed before a better interpretation can be made by this method.

ENERGY LOSSES ABOVE IONIZATION

When relatively high potentials are being used, and the losses under investigation are but a fraction of the total electron energy, it becomes very advantageous to be able to use a retarding potential between the two cylinders C_1 and C_2 , rather than an accelerating one, as was described in the investigation of losses near their critical potentials. Consider, for instance, the two curves in Fig. 5, marked 41 V. The upper curve was taken with a magnetic field set to collect 15.1 V. electrons to the probe wire. In order to collect the electrons which have lost no energy at impact, a retarding potential of 25.9 V. must be applied between the cylinders. As this retarding potential is reduced, which is equivalent to *increasing* the *accelerating* potential in the previous cases, electrons which have lost more and more energy are brought into focus and measured. This results in a controllable increase in the percent separation of the groups of electrons, with an accompanying increase in resolving power which is very desirable. The lower 41 V. curve was taken with a field set for 27.2 V. electrons, and hence with less retarding potential. The one-volt separation between the 8.8 and 9.8 V. losses is now but one-half the fraction of the whole path speed that it was before, and the peaks are no longer separated. With no retarding potential, the resolution was extremely bad. This improvement in resolution has been accomplished at the sacrifice of fidelity in the measurement of probabilities, in which we are not so much concerned in the present paper.

The chief point of interest in the curves of Fig. 5, is the 11.07 V. loss, which is seen to rise to an importance second only to that of the 6.7 V. loss, at this voltage. Its value may be observed very accurately, due to the presence of peaks of known value on either side of it, so that the value given is probably accurate to within 0.03 V. It makes its appearance at a potential unfavorable to its detection, because of the presence of the peak due to the

double impact loss $4.9+6.7$. Rising steadily from about 18 V., where the masking peak drops rapidly, this loss becomes so prominent that, at 41 V., we even see a peak due to the double impact $11.07+6.67$.

Several possible interpretations for this type of energy loss have been studied. No combination of the known losses in either the arc or the spark systems would give this value. Moreover, when the vapor pressure is changed, the size of the peak remains proportional to the single impact peaks rather than to the double impact peaks, which decrease more rapidly. It is therefore thought to involve but a single impact. If this were a *critical potential* method, a delay in the appearance of the loss until the energy of impact was somewhat above the amount required for ionization, might be interpreted as a delay in the process of ionization until some conservative force be overcome: but here, we are measuring the actual amount of the energy lost by the electron, regardless of the total energy possessed. Hence, some other type of quantized loss would have to accompany ionization, in order to account for the excess energy. According to the HgII energy values of Carroll,¹⁴ the simultaneous ionization and spark excitation to the lowest level would involve 16.8 V. Even then, it is doubtful whether the loss would be quantized, because of the possibility of energy sharing by the two electrons, as in ordinary ionization.

The most likely interpretation so far found, seems to be that of simultaneous excitation of both valence electrons in the same atom, without ejection of either. So little is known concerning this interesting type of excitation, that a complete verification of this theory is not to be expected at this time. Sawyer¹⁵ has classified four lines in mercury, which he attributes to such double transitions, and from them, arrives at the values of the three lowest "*p*'" levels.^{16,17} The lowest of these has a wave number of -7860 (negative, because it lies above the ionization level), so that excitation to this level ($1S-p_3'$) would require 11.35 V. This is 0.28 V. more than that found in the present work, which is far too great a difference to be attributed to experimental error in either method. Sawyer points out, however, that this level was determined by a single line, which might have a different interpretation; the other, and higher levels have as many as three transitions observable, and hence are much less in doubt. It is possible that a reclassification of these lines, with a lower level in mind, might bring about a better agreement.

CONCLUSIONS

The energy losses observed in this work are; 4.9, 5.4, 6.7, 7.7, 8.8, 9.8, and 11.07 V.—all save the last named one being those predicted on spectroscopic grounds. The circumstances of the appearance of 7.7 both increase confidence in the data given by the inelastic impact method, and explain the

¹⁴ Carroll, Phil. Trans. 225, 357, A 634 (1926).

¹⁵ Sawyer, J.O.S.A. 13, 432 (1926). For pioneer work on *p*' levels see the following articles.

¹⁶ Wentzel, Phys. Zeits. 24, 106 (1923); 25, 182 (1924).

¹⁷ Russell and Saunders, Astrophys. J. 61, 8 (1925).

difficulty of detection of certain losses. Failure to detect 4.7 V. losses is attributed to the extremely large probability and rapid rise of the 4.9 V. loss, together with a rather large velocity distribution. Excitation to the 3S and to all of the "4" levels, involving about 9.2 and 9.5 V. losses, are thought to be even less probable than 7.7 V., and hence not detected. The unexplained losses of the photoelectric method were not observed, although they should have been, had they represented actual quantized losses of electronic energy of any appreciable probability. The energy loss at ionization is not quantized. The new loss, of 11.07 V., is thought to represent new data opening up the question of p' energy levels and simultaneous excitation of two valence electrons. The present method has not yielded spark terms, but may do so, if ionization be accomplished prior to the excitation dealt with here.

In conclusion, the author wishes to express his appreciation for the help and encouragement given him by the staff of the physics department of the University of Iowa, and especially for the constant and generous guidance of Professor J. A. Eldridge.

THE MOTION OF SLOW POSITIVE IONS IN GASES

BY JAMES S. THOMPSON

RYERSON PHYSICAL LABORATORY, UNIVERSITY OF CHICAGO

(Received April 1, 1930)

ABSTRACT

Positive caesium ions with velocities of 3.5 to 600 equivalent volts have been studied in hydrogen and helium. No absorption of the ions in the apparatus used is found for pressures below 0.01 mm of mercury. For the higher velocities this absence of absorption persisted for pressures as high as 0.05 mm of mercury. In all cases the ions were retarded in passing through the gas and there is an approximate probability distribution of ion energies about an average retarded value. The retardation in all cases is found to be proportional to the pressure. For Cs^+ ions in helium the percent loss of initial energy varies from 11.5 for 400 volt ions to 55 for ions of 3.5 volts initial energy. Similar results are found for hydrogen. Values of the constant, h , of the error curve which are characteristic of a particular distribution are given for various velocities and pressures. An interpretation of the absence of scattering and the retardation of the ions is given on the basis of elastic collisions between ion and gas molecule. It is found that no absorption of the Cs^+ ions would be expected until the pressures are high enough to give rise to multiple scattering. The data on retardation give values of the radius of the Cs^+ ion as: 1.78A in helium and 3.09A in hydrogen. The slowing up of the ions offers an explanation of the large absorption of Cs^+ in helium found by Ramsauer and Beeck. Probability considerations show that for increasing velocities the energy loss per collision found in the present experiments is less than that to be expected on the basis of elastic collisions.

The absorption of Li^+ ions has been studied by three methods for velocities of 20 to 900 equivalent volts. The coefficients of absorption, C , representing the effective absorbing cross section have been determined by two methods. The general dependence of C on the ion velocity is the same for the two types of apparatus used, but the values of C are found to depend on the dimensions of the absorbing chamber. The results have led to the interpretation of scattering in which forces other than those due to elastic collisions are effective. No general retardation of the Li^+ ions was found. Values of C found by Ramsauer and Beeck are interpreted in terms of the dimensions of their apparatus. It is concluded that no absolute significance may be attached to values of atomic radii determined from measurements of this kind.

WHEN a beam of positive ions moves through a column of gas there is in general a weakening of the bundle which may be due to a number of different processes of interaction between ion and gas molecule. Neutralization of the ions, either from the capture of a free electron or an ionization of the gas molecule, scattering or a combination of these effects will contribute to a decrease in intensity. In addition, any retardation of the ions may show itself as an absorption unless precautions are taken in the experimental method of measurement. It is customary to express any absorption of the ion bundle in the relation:

$$N = N_0 e^{-xp/760L} \quad (1)$$

where N is the intensity of the beam after passing through a distance, x , of the gas at pressure p ; N_0 the intensity of the incident ions, and L the absorption coefficient, also referred to as the mean free path under standard conditions. Writing L in terms of the radii of the ion and gas molecule,

$$\begin{aligned} L &= 1/\pi n(R_{ion} + R_{mol})^2, \text{ or} \\ C &= \pi(R_1 + R_2)^2 = 1/Ln \end{aligned} \quad (2)$$

where C may be termed the effective absorbing cross section. Most of the experiments on absorption of positive ions have yielded in effect values for L and C .

A study of the motion of hydrogen and helium ions in helium has been made by Dempster using his positive ray apparatus.¹ He found that protons with velocities corresponding to potential differences of 14 to 900 volts passed through many helium atoms without neutralization and with slight changes of velocity and direction; while 900 volt helium ions in helium were absorbed much more readily and showed a mean free path but little greater than the kinetic theory value. These were the first experiments of this kind with low velocity positive ions.

Durbin² and Ramsauer and Beeck³ have studied the slow alkali metal ions in various gases and found in most cases abnormally long free paths varying up to ten times the kinetic theory value. Their experimental methods would not distinguish the three causes of absorption mentioned above.

Kennard⁴ modified the method used by Durbin and Ramsauer and Beeck, and by measuring the ions of various velocities which passed through the gas column was able to detect a change in velocity as well as any weakening due to other causes. He found that for 90 volt Cs^+ ions in hydrogen there was a decrease in speed equivalent to 1.3 volts per collision, but no evidence of scattering or neutralization, for pressures up to 0.008 mm of mercury. Slowing up was also observed for 35 and 90 volt Cs^+ ions in both hydrogen and helium with only a slight weakening of the bundle due to other causes. For Cs^+ in argon no slowing up was observed but there was a rapid absorption of the bundle with pressure, which Kennard interpreted as due to neutralization.

Recently, Cox⁵ has shown from experiments with Li^+ ions in mercury vapor that for gas-ion combinations which show no definite change in speed of the ion, the chief cause of absorption is scattering. The velocities were from 18 to 300 equivalent volts. For the ions of higher velocity range—10,000 to 50,000 equivalent volts—there is evidence of some scattering but the velocity losses are less than one-half of one percent.^{6,7}

¹ Dempster, *Phil. Mag.* 7, Series 13, 115, (1926).

² Durbin, *Phys. Rev.* 30, 844 (1927).

³ Ramsauer and Beeck, *Ann. d. Physik* 87, 1 (1928).

⁴ Kennard, *Phys. Rev.* 31, 423 (1928).

⁵ Cox, *Phys. Rev.* 34, 1426 (1929).

⁶ G. P. Thomson, *Proc. Roy. Soc.* 102, 197 (1922).

⁷ Koenigsberg and Kutschewski, *Ann. d. Physik* 161, 37 (1912).

Thus it appears that the entire problem of positive ion absorption is quite complex and depends not only on the gas-ion combinations, but on the velocity, gas pressure, apparatus and method used and other experimental variables. For heavy ions passing through light gases at moderate velocities the predominant effect seems to be a slowing up of the ion bundle, whereas for a light ion in a heavy gas the chief cause of absorption is due to scattering. Intermediate cases may show a combination of both effects; for example, Kennard found that for Na^+ ions with a velocity of 455 volts in hydrogen, there was a small but definite slowing up, together with an absorption probably due to scattering. As pointed out by Cox, it seems evident that the importance of any absorption process due to scattering, and, in some cases, of that due to retardation is dependent on the dimensions of the apparatus used and the method of measurement. Thus, the absorption constants usually calculated from such measurements have no absolute significance and cannot be interpreted in terms of any atomic process.

The purpose of the experiments to be described was: first, to make a more complete study of the motion of Cs^+ ions in hydrogen and helium, particularly in the region of low velocities, and, secondly, to investigate the process of absorption of a light ion in a light gas as typified by Li^+ ions in helium; and to study any dependence of this absorption on velocity.

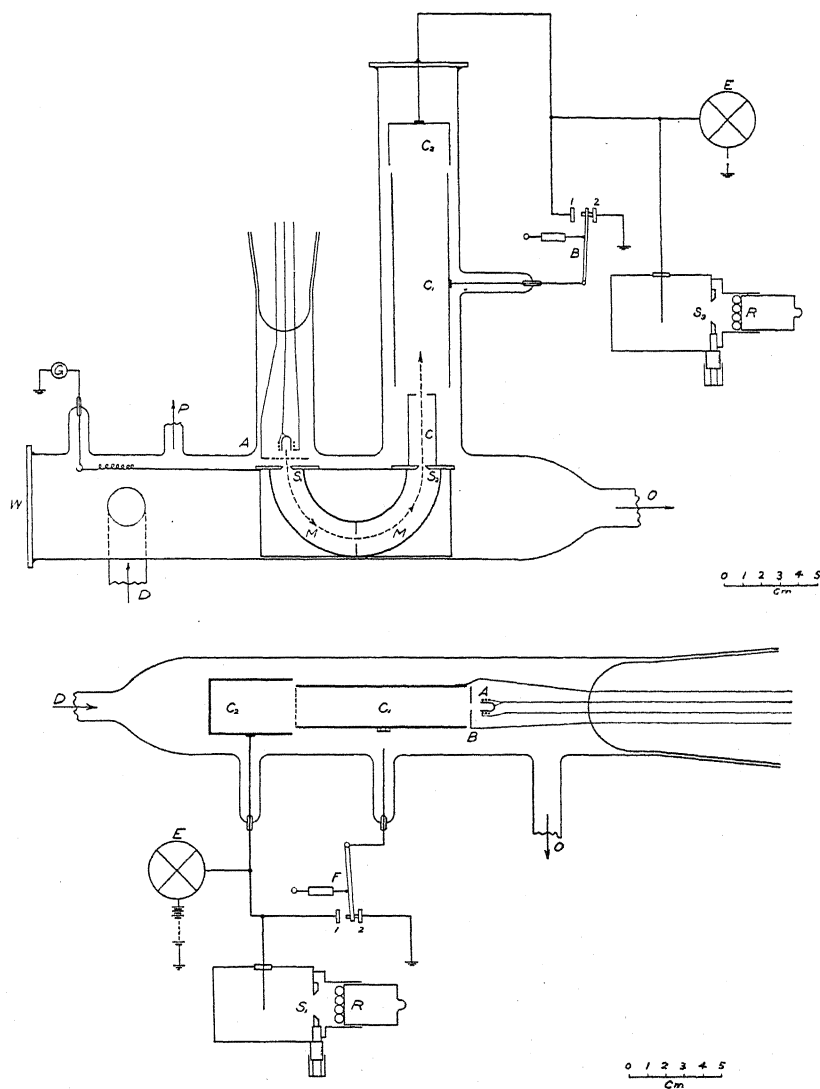
CAESIUM IN HYDROGEN AND HELIUM

The results obtained by Kennard for 35 and 90 volt Cs^+ ions have been obtained for 100 and 200 volt ions in helium. The apparatus used is based on Dempster's method of positive ray analysis and is shown in Fig. 1.⁸ The cylinder *C* was removed in some experiments and a single collector mounted above the slit, S_2 . The ion source contained in the furnace, *A*, is made positive with respect to the slit S_1 , the emission current being held constant and measured with the galvanometer *G*. The ion beam enters the magnetic field and by varying the magnet current, is swept across the slit S_2 , after traversing the gas-path S_1MMS_2 . The dimensions of the path through the armature were, $3.0 \times 10 \times 112$ millimeters. The resultant intensity through S_2 is then measured by balancing the current to the collector against the ionization current from the RaE tubes shown at *R*. A Compton electrometer, *E*, adjusted to a sensitivity of 2500 divisions per volt was used as a null indicator. Helium was introduced into a reservoir by allowing it to pass slowly through a charcoal trap immersed in liquid air; after this preliminary purification the gas was admitted to the apparatus through a drying tube, a fine capillary and a second charcoal trap which was also kept at liquid air temperature. The gas was tested by observing the spectrum with a hand spectroscope, the lines showing distinctly on a dark background.

The gas enters the tube at *D* and is kept in circulation through the apparatus. Various pressures are established by adjusting the rate of pumping of the mercury diffusion pumps connected at *O*. An ionization gauge was

⁸ Dempster, Phys. Rev. 11, 316 (1918).

used in some experiments to show when steady gas pressures were attained, all final measurements being made with McLeod gauge attached at P . For a definite pressure and emission current the current through S_2 is measured as a function of the magnet current, four or five such curves being taken for a single accelerating potential.



Figs. 1 and 2. Diagram of apparatus.

The type of curves obtained are the same as those of Kennard and are shown in Fig. 2. For increasing pressures the peaks of the curves are seen to be shifted in the direction of lower ion velocities, the general symmetry of the curves being retained about the shifted peak. Within the limits of

experimental variation, the areas under these curves remain constant, showing that in traversing the gas-path S_1MMS_2 all the ions of various velocities reach the collector. Kennard observed this behavior for Cs^+ ions in hydrogen and helium for 35 and 90 volts velocities. He concluded that there was a general slowing up of the Cs^+ ions, and for pressures up to 80×10^{-4} mm of mercury, due to the constancy of the areas, that there was no neutralization or scattering of the bundle.

This behavior of Cs^+ ions for the velocities used in the above method indicated the possibility of isolating a single process of interaction between ion and gas molecule and of studying this process over a range of conditions in which it was operative.

In the procedure outlined above it is essential that the emission of ions through S_1 be held constant over a considerable period of time in order that the complete curves of Fig. 3 may be obtained for several gas pressures. This difficulty together with that of obtaining sufficient intensity with low velocity ions limited the range of the method. Also in establishing the equality of the areas under the curves shown, it is difficult to determine the exact range of the base line.

Experiments were tried with the two-cylinder method shown drawn to scale in Fig. 1 and used by Cox in experiments on Li^+ ions in mercury vapor.⁵ Here the ion bundle is accelerated to S_1 as before and bent through 180° in the magnetic field. The collimating slit C directs the beam up the axis of the cylinders C_1 and C_2 . Measurements to detect any absorption were made by first connecting C_1 and C_2 together with the switch B in position (1); then C_1 was grounded and those ions which had travelled over the extra gas-path of length C_1 were collected and measured in C_2 . Both values are determined with the balance method described. No absorption in C_1 for Cs^+ ions in helium was observed for velocities of 25 to 600 volts and pressures up to 0.013 mm of mercury. Here again the difficulty of obtaining sufficient intensity limited the range.

In order to study the behavior of Cs^+ more directly and over a range of velocities not possible with the magnetic methods described, a third tube was constructed and shown drawn to scale in Fig. 2. Tubes of similar construction have been used by Mayer,⁹ Akesson¹⁰ and Eldridge¹¹ in experiments on electron velocity distribution.

The source of ions was contained in the small electric furnace shown at A . The ions were accelerated to the slit B , passed through a field-free space within the nickel cylinder, C_1 , 9.2 cm long and were collected in the Faraday cylinder C_2 . The gas entered at D and was kept in circulation through the tube, various pressures being established by adjusting the rate of pumping of the mercury diffusion pumps connected at O . Pressures were measured with a McLeod gauge connected first at O and later, in order

⁹ Mayer, Ann. d. Physik **64**, 451 (1921). Also P. Lenard; Wien's "Handbuch der Experimental Physik" XIV, 170, (1927).

¹⁰ Akesson, Lund's Arsskrift **12**, 11 (1916).

¹¹ Eldridge, Phys. Rev. **20**, 456 (1922).

to insure that no pressure gradient affected the measurements, to the central tube which supports the electrode above *F*. Helium was purified as in the experiments outlined above; hydrogen was admitted through a heated platinum tube sealed into the glass line and about which was circulated commercial hydrogen at atmospheric pressure.

In experiments with a tube of this type a particularly pure source of ions was essential as no magnetic separation was possible. This source was found in the mineral pollucite which is essentially a caesium aluminum silicate containing 27 percent caesium ($\text{H}_2\text{O} \cdot \text{Cs}_2\text{O} \cdot \text{Al}_2\text{O}_3 \cdot 9\text{SiO}_2$). The

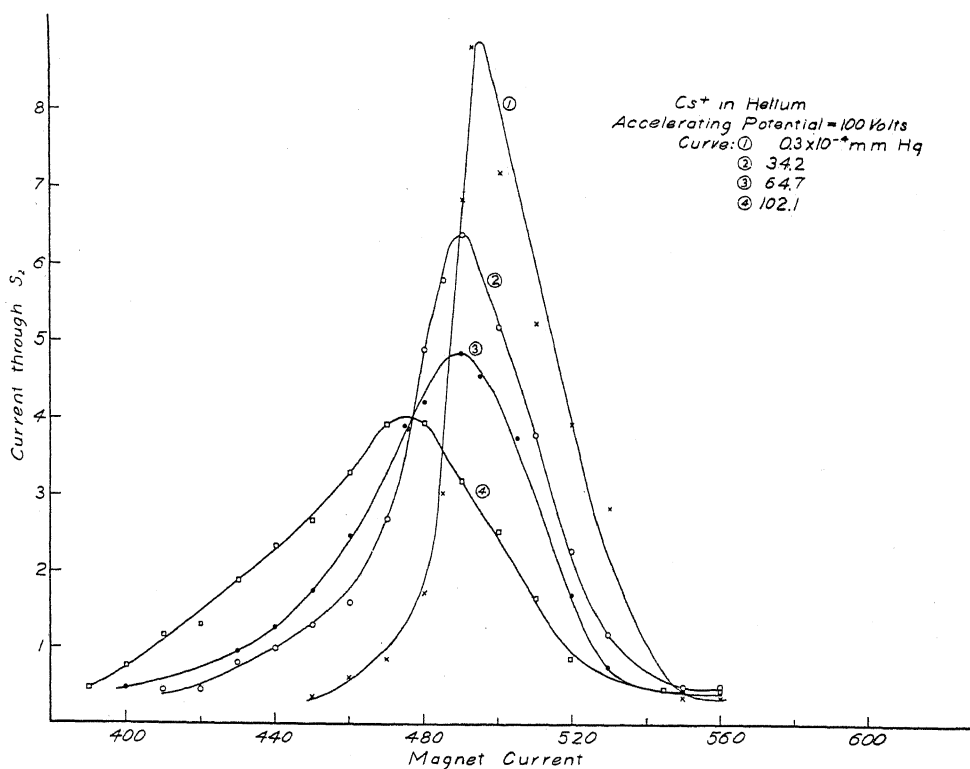


Fig. 3

mineral is powdered and packed into the small resistance-wound furnace made of steel tubing 5 mm long and about 2.5 mm inside diameter. In some instances the mineral was mixed with powdered iron to make it conducting and allow it to fuse more readily. It was found that the substance could not be fused on a platinum strip as is the case with the lithium source, spodumene. This source was prepared and always placed in the magnetic analyzing apparatus before use and examined for other ions. No emission other than Cs^+ was detected for temperatures considerably above those normally used. At a dull red heat a very strong and steady emission of Cs^+ ions was obtained. The experimental tube and source were baked out thoroughly for several hours before use.

It was thought that the process of interaction of Cs^+ ion with hydrogen and helium was one of pure retardation, but to make certain of this, experiments were first tried to detect any weakening or absorption of the ion bundle due to causes other than slowing up. For this purpose the gauze shown on the end of C_1 in Fig. 2 was removed. The central electrode supported C_1 at the center, the ground connection through the stem being removed. By connecting the switch F in position 1, the total ion current to $(C_1 + C_2)$ was observed. Then with C_1 grounded, by moving F to position 2, the ions which reached C_2 after traversing the gas-path through C_1 were measured. As in the first type of tube both currents were measured by the balanced electrometer arrangement, intensities being proportional to the slit widths, S_1 . Measurements of the ratio, $C_2/(C_1 + C_2)$ were taken for increasing pressures in the tube so that any weakening of the beam was detectable in a decrease in this ratio. For very low velocity ions this ratio was not equal to unity for low pressures because of the divergence of the bundle caused by the field between A and B so that some of the ions hit the wall of C_1 . However, in all cases, values of the ratio were obtained for several pressures so that any real absorption could be observed.

In this way it was found that for pressures less than 0.01 mm of mercury, no appreciable absorption of the Cs^+ ions in hydrogen and helium took place for velocities of 3.5 to 600 equivalent volts. For velocities above 10 volts this absence of absorption persisted for pressures even higher than 0.03 mm of mercury. Below 10 volts and for pressures above 0.01 mm of mercury a definite weakening of the bundle set in and increased rapidly with the pressure. This absorption is probably due to the effects of multiple scattering as the number of collisions with the slow moving ions is increased, and is discussed later.

Thus for a considerable range of velocity and pressure the Cs^+ ions are not deviated appreciably from their path, making it possible to study the slowing up effect as an individual process over this range.

The arrangement used for observing the retardation of the ions is shown also in Fig. 2. The ions are accelerated as before, by applying a positive potential to A ; B and C_1 are grounded as shown; the ions pass through the field-free space C_1 , and are collected in the Faraday cylinder, C_2 . In some experiments a grounded shield was placed around the two cylinders but this was not used in general as the ion path is well shielded as shown and the grounded cylinder provided an extra leakage path. Any retardation takes place over the gas-path, AC_2 , measured from the ion source to the far end of the collector C_2 or 14.2 cm. With a constant pressure in the tube, increasing retarding potentials are placed on C_2 through the electrometer as shown. This potential is applied with respect to the gauze on C_1 , which gives a more uniform distribution of the field. The current to C_2 is then observed as a function of the retarding voltage. Hence, only those ions with velocities greater than or equal to the retarding potentials will be recorded in C_2 . In this way the velocity or energy distribution of the retarded ions was measured for various pressures. Curves of this type are shown in Fig. 4, which shows

the distribution for 6.4 volt Cs^+ ions in helium at the pressures given. Another set for 100 volt Cs^+ ions in hydrogen is shown in Fig. 5. In both these sets except for the lowest pressure the actual curve drawn represents the theoretical energy distribution fitted to the experimental data as explained below. The points shown were determined experimentally as described. Similar sets were taken for velocities ranging from 3.5 to 600 volts in both hydrogen and helium. Any point on these curves is proportional to the number of ions retaining energies equal to or greater than the corresponding voltages. In all such curves the distribution at low pressure was always taken as

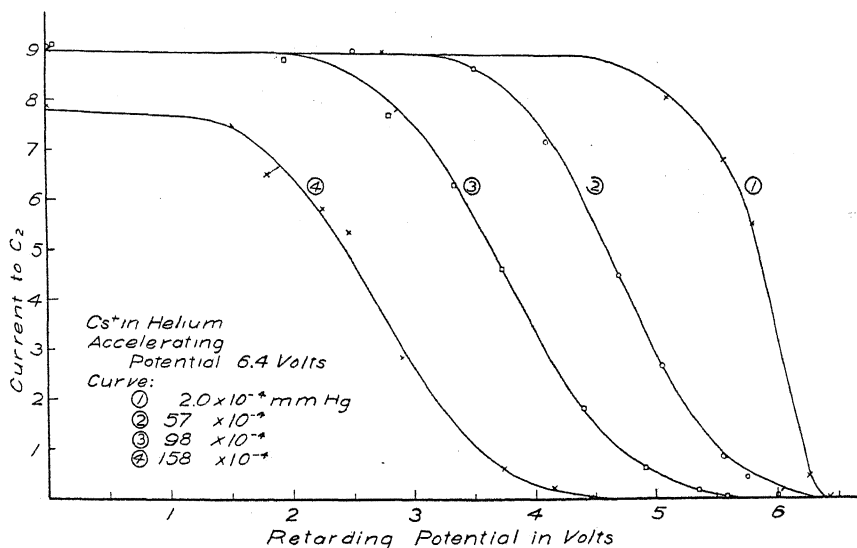


Fig. 4

a control, since here the distribution of energies should be approximately homogeneous. The points shown in the curves of Figs. 4 and 5 were not corrected for small changes in the emission current at the various pressures so that no significance is to be attached to the absolute values of the ordinates shown. As explained above, separate experiments were made to determine any change in the current to C_2 with pressure.

By integration of curves of the form

$$y = ke^{-h^2x} \quad (3)$$

it was found that the resulting curve could be fitted to the experimental points, indicating that when the ions reached the collector there was an approximate probability distribution of energies about the average retarded value. This distribution is what would be expected from probability considerations, due to some ions making more collisions, and some less than the average number in completing the path, L . Each point on the curves of Figs. 4 and 5 represents the number of ions found to retain energies equal to or greater than the corresponding voltage. For a value of the retarding voltage,

V_R , the number of ions retaining energies greater than V_R would be expected to be given by

$$I = k \int_{V_R}^{\infty} e^{-h^2 V^2} dV$$

the constant, h , depending on the particular distribution. In order to obtain the value of h , which is characteristic of a particular energy distribution, we may consider the expression:

$$P = \frac{h}{\pi^{1/2}} \int_0^{V-V_0} e^{-h^2(V-V_0)^2} d(V-V_0) \quad (4)$$

for the probability that an ion will retain an energy between V_0 and V . Here V_0 is the average retarded velocity, represented in the experimental curves

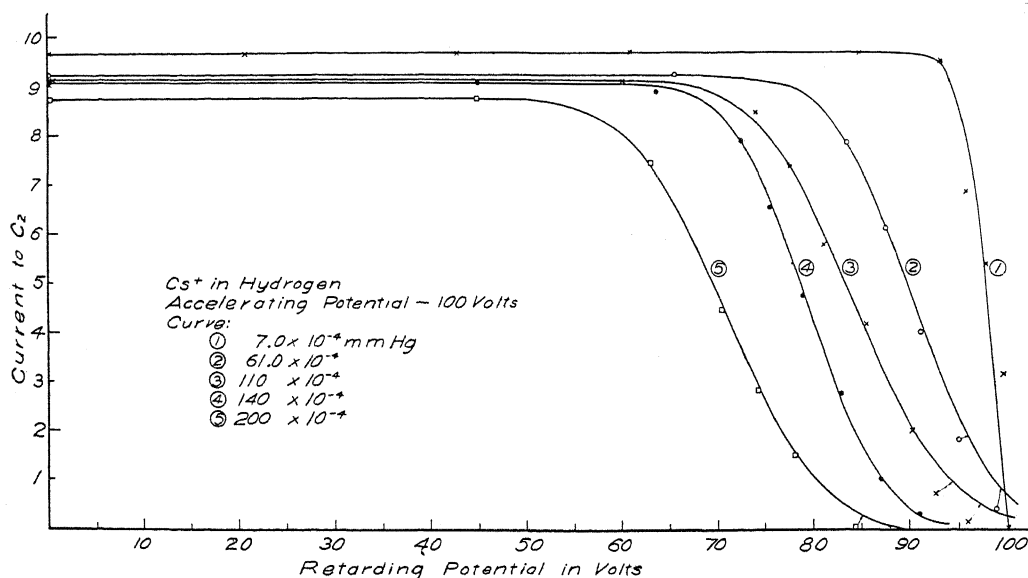


Fig. 5

(Figs. 4 and 5) by the half ordinate, and corresponding to the peak value of the error curve. The constant, h , may be conveniently found by observing the energy, V_1 , at which the probability is one-fourth as indicated in Figs. 6 and 7. Setting:

$$h(V - V_0) = z$$

we then have that:

$$P = \frac{1}{\pi^{1/2}} \int_0^z e^{-z^2} dz = \frac{1}{4}$$

for $z = z_1 = h(V_1 - V_0)$. As, $z_1 = 0.477$, $h = 0.477/(V_1 - V_0)$.

If n is the average number of collisions, the probability of an ion making a number greater than n but less than, $n + z(2n)^{1/2}$ is:

$$\frac{1}{\pi^{1/2}} \int_0^z e^{-z^2} dz.$$

If the energy loss per collision were constant, $z(2n)^{1/2}$ would be proportional to $(V - V_0)$, or z/h . That is, we should expect h^2 to be inversely proportion-

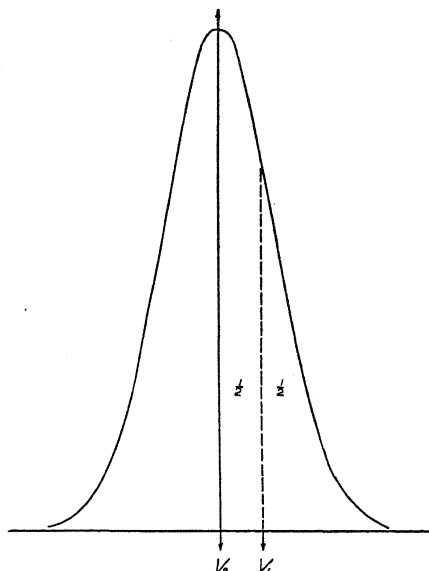


Fig. 6

al to the number of collisions, the pressure, or the average energy lost by the ions, which is $(V_i - V_0)$, V_i being the initial velocity. Thus for a constant

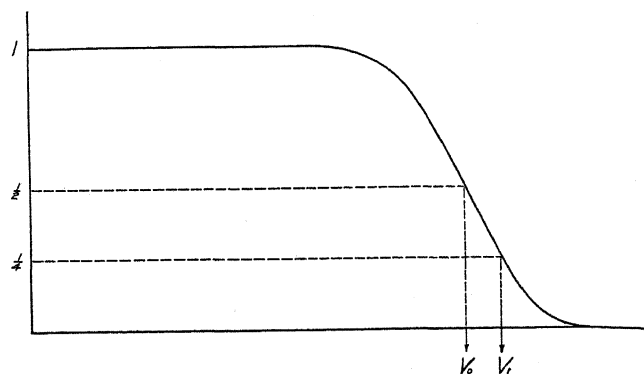


Fig. 7

energy loss per collision, $h(V_i - V_0)^{1/2}$ would be constant. If $h(V_i - V_0)^{1/2}$ is less with ions of high velocity, it signifies that the energy loss per collision is less in this case.

In the case of the 6.4 volt Cs^+ ions in helium at a pressure of 98×10^{-4} mm of mercury, the dispersion, $(V_1 - V_0)$ was 0.55 and $h = 0.87$; $h(V_i - V_0)^{1/2} = 1.41$. Values of h calculated from the experimental data, together with the quantity, $h(V_i - V_0)^{1/2}$ are shown for various velocities and pressures in the Table I. From the values of h given in the table, the expected energy distribution may be calculated and compared with the experimental results. The theoretical curve is obtained for any particular distribution by the use of the proper h in the integral of Eq. (4). The resulting curves are shown for two initial velocities in Figs. 4 and 5 together with the experimental points. It is seen that the agreement is in general better for the low velocity ions and for the higher

TABLE I. Cs^+ in helium.

Initial velocity V_i	Pressure $\times 10^4$ mm mercury	V_0	$(V_1 - V_0)$	h	$h(V_i - V_0)^{1/2}$
3.5	57.0	2.24	0.31	1.54	1.73
	83.0	1.97	0.33	1.45	1.79
	110.0	1.45	0.32	1.49	2.14
6.4	57.0	4.70	0.45	1.06	1.38
	72.5	4.35	0.53	0.90	1.29
	98.0	3.75	0.55	0.87	1.41
	126.0	3.20	0.55	0.87	1.55
	158.0	2.78	0.49	0.97	1.84
9.3	52.0	6.57	0.95	0.50	0.826
	110.0	5.15	0.99	0.48	0.976
30.0	60.0	24.40	3.05	0.157	0.372
	97.0	21.80	3.00	0.159	0.455
	163.0	19.70	2.40	0.199	0.64
60.0	60.0	51.50	4.00	0.119	0.347
	116.0	45.60	4.90	0.097	0.368
	167.0	41.30	3.90	0.122	0.528
100.0	50.0	88.00	5.70	0.084	0.291
	85.0	80.50	6.60	0.072	0.318
	150.0	70.80	7.00	0.068	0.368
200.0	88.0	170.00	13.50	0.035	0.192
	168.0	151.00	14.00	0.034	0.238
	242.0	132.00	15.00	0.032	0.264
400.0	52.0	370.00	15.00	0.032	0.175
	90.0	343.00	21.00	0.023	0.174
	160.0	333.00	22.00	0.022	0.180
	220.0	293.00	27.00	0.018	0.186
590.0	76.0	570.00	16.00	0.030	0.134
	242.0	487.00	33.00	0.014	0.142
<i>Cs⁺ in hydrogen</i>					
3.5	46.0	2.36	0.31	1.54	1.65
	65.0	1.90	0.35	1.36	1.72
	108.0	1.17	0.33	1.45	2.21
13.5	40.0	11.40	0.60	0.79	1.14
	96.0	9.20	1.00	0.48	1.00

TABLE I. Cs^+ in hydrogen (Continued).

Initial velocity V_i	Pressure $\times 10^4$ mm mercury	V_0	$(V_i - V_0)$	h	$h (V_i - V_0)^{1/2}$
30.0	40.0	27.7	1.00	0.48	0.728
	65.0	26.1	1.60	0.30	0.592
	100.0	23.7	2.00	0.24	0.603
	215.0	18.5	2.20	0.22	0.746
	270.0	15.5	1.70	0.28	1.060
60.0	57.0	55.0	2.00	0.24	0.537
	75.0	52.5	2.80	0.17	0.466
	160.0	44.4	3.60	0.13	0.514
	290.0	35.0	3.50	0.14	0.700
100.0	61.0	90.5	4.50	0.11	0.340
	110.0	84.4	5.34	0.089	0.352
	140.0	79.5	4.20	0.113	0.520
	220.0	71.0	5.30	0.090	0.485
200.0	61.0	183.2	7.30	0.065	0.266
	90.0	177.2	8.80	0.054	0.258
	131.0	170.0	7.50	0.064	0.350
	216.0	151.0	9.40	0.051	0.357

pressures. On the high velocity side of the curves the points were obtained with much less precision.

The values of h given in the table are seen to decrease with increasing voltage and the values of $h(V_i - V_0)^{1/2}$ are not constant as would be expected

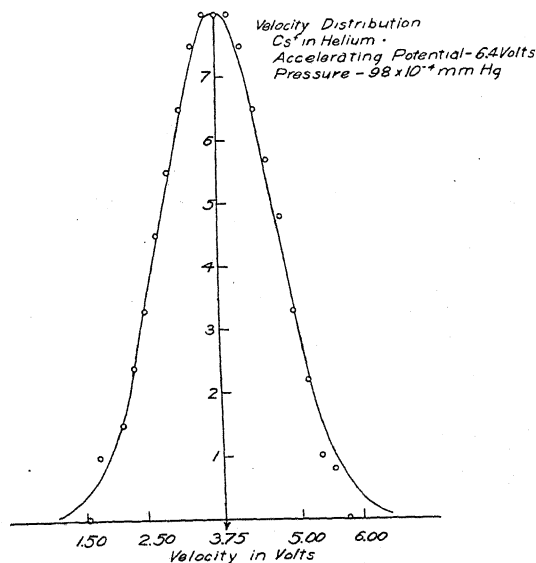


Fig. 8

if the energy loss per collision were the same for ions of all velocities. As explained above the decrease is what would be expected if the energy loss per collision decreases with the high velocity ions. In hydrogen, the consistently

larger values of h than in helium for corresponding voltages indicate that in this gas there is less loss of energy per collision.

The actual error curve distribution for the case of 6.4 volt Cs^+ ions in helium for a pressure of 98×10^{-4} mm of mercury is shown in Fig. 8. The full line represents the theoretical distribution of the velocities for curve (3) of Fig. 4. Here V_0 is 3.75 volts and V_1 is 4.30 volts; the points shown are obtained by graphical differentiation of the experimental curve.

Each of the curves in Figs. 4 and 5 represents a new distribution of energies about a most probable energy V_0 which is that corresponding to the half ordinate. The difference then between the applied potential and this half ordinate energy gives the retardation of the ions for the pressure shown. For each applied potential this retardation has been plotted as a function of the

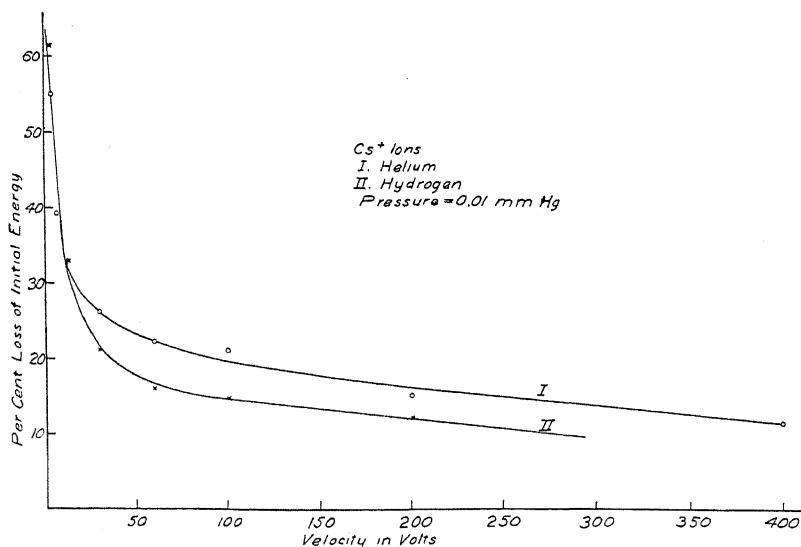


Fig. 9

pressure and is found to be linear over a wide range. This slowing up took place over the gas-path AC_2 measured from the furnace source to the far end of the collector, C_2 , or 14.2 cm. From the curves the retardation for 0.01 mm of mercury was obtained since for this pressure no absorption was found. Fig. 9 shows this retardation, expressed as a percent loss of initial energy, as a function of the initial velocity in volts. Points for 600 volt ions, not shown on the curves, would fall on the lower linear portion if extended. The loss in helium is seen to be greater over most of the range as might be expected for the gas molecule of greater mass, especially if the interpretation is that of mechanical collisions. In both cases the loss decreases with increasing velocity. This is in agreement with the data cited for canal rays of 10,000 volts and more which show less than one-half of one percent loss of energy.^{6,7} Below forty volts the curves rise rather rapidly and tend to merge; extending them to the axis of ordinates indicates that the maximum loss for this pressure would be about 66 percent.

These results suggest an interpretation of the results of Ramsauer and Beeck³ for Cs^+ ions in helium that differs from their conclusions. In their experiments the apparatus used was similar to that described in connection with Fig. 1, except that the dimensions were much smaller. The method of observations was to hold the magnetic field constant and observe the weakening of the bundle for several gas pressures. Referring to Fig. 3, this is seen to be equivalent to observing the intensities along a vertical line drawn through the peak value of the lowest pressure curve used. It is evident that this method of observation would show an apparent absorption for the retarded ions. From their results, Ramsauer and Beeck calculate what is designated as the "Wirkungsquerschnitt," which is the value $1/L$ from Eq. (1), reduced to 1 mm of mercury. For Cs^+ ions in helium, they find a considerable absorption of the ions for velocities of 1 to 10 volts; for instance, reducing their values in terms of the effective cross section, C , gives a value of $11.3 \times 10^{-1} \text{ cm}^2$ for ions of 9 volts velocity; or in terms of the mean free path, $L = 33 \times 10^{-6}$

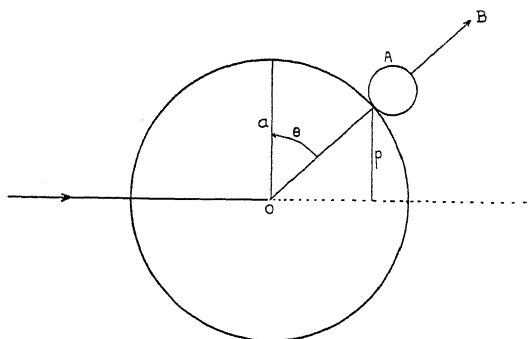


Fig. 10

cm under standard conditions. These values show a large opposing cross section of ion against molecule, whereas for the pressures used by Ramsauer and Beeck,³ no real absorption at all was observed in the present experiments. Fig. 9 shows that 9 volt Cs^+ ions suffer a loss in velocity of about 35 percent, which, as explained above, would account for the large value of C found by Ramsauer and Beeck.³ No relation to atomic constants can be attached to the values of C and to the various values of atomic radii calculated therefrom as they are at once seen to depend on the dimensions of the apparatus and the experimental method used. Thus the mechanism of absorption is of primary importance in the interpretation of these measurements.

It is of interest to compare the results for caesium ions with what would be expected on the basis of elastic collisions between ion and gas molecule. In Fig. 10 consider a Cs^+ ion moving forward with a velocity V among helium atoms at rest. If an elastic collision occurs with the helium atom at A , this atom is projected along OAB with a velocity, $2V \sin \theta$, provided the mass of the Cs^+ ion is very large compared to that of helium. Since the ratio is 133/4 we may take this velocity as a first approximation. The equality of momenta

in a transverse direction shows that the Cs^+ ion then receives a velocity at right angles to its direction equal to:

$$V' = 2V \sin \theta \cdot \cos \theta \cdot 4/133.$$

The angle made by the ion with its original direction is then,

$$\phi = V'/V = 8/133 \cdot \sin \theta \cos \theta$$

since V is only slightly altered. Now the number of collisions in the range, p to $p+\Delta p$ as shown in the figure is proportional to the area presented in the direction, V , i.e., to $2\pi p \Delta p$. Since the total number of collisions is proportional to, πa^2 , where a is the radius of the Cs^+ ion, we may write for the average angle of scattering,

$$\Phi = \frac{1}{\pi a^2} \frac{8}{133} \cdot \int_0^a \frac{p}{a} \left(1 - \frac{p^2}{a^2}\right)^{1/2} \cdot 2\pi p \cdot dp$$

where, from Fig. 10 $\cos \theta = p/a$ and $\sin \theta = (1 - p^2/a^2)^{1/2}$. This upon integration gives,

$$\Phi = \pi/133 = 0.023 \text{ radians.}$$

The maximum angle of scattering, for $\theta = 45^\circ$, gives

$$\phi_{max} = 0.030 \text{ radians.}$$

In the apparatus used, an ion would always reach the collector unless deflected by more than $10/92$ or 0.11 radians. Thus single scattering is unable to produce a weakening of the bundle. Experimentally, no weakening was observed until the pressure was made high enough to give rise to multiple scattering.

We may also calculate the energy loss to be expected on the basis of elastic collisions. In the Fig. 10 let m equal the mass of the helium atom and M the mass of the Cs^+ ion. On the basis of elastic collisions, the energy lost by the Cs^+ ion is equal to the amount gained by the helium atom, or,

$$\Delta E_0 = \frac{1}{2}m(2V \sin \theta)^2$$

for the loss due to a collision at angle, θ . The ratio of this loss to the initial kinetic energy of the Cs^+ ion is then,

$$\frac{\Delta E_0}{E_0} = \frac{\frac{1}{2}m(2V \sin \theta)^2}{\frac{1}{2}MV^2} = \frac{16}{133} \sin^2 \theta.$$

In travelling a distance, L , the average fractional loss per collision may be written, referring to Fig. 11 as:

$$\frac{\Delta E}{E} = \frac{1}{\pi a^2 L n} \int_0^{\pi/2} \{ (2\pi a \cos \theta)(a \sin \theta d\theta) L n \} \left(\frac{16}{133} \sin^2 \theta \right) = \frac{8}{133}$$

where, $a = r_1 + r_2$, the sum of the ion and atom radii; and, n = the number of helium atoms per cc for the pressure considered.

The energy remaining after, $\pi a^2 L n$ collisions may then be written as,

$$\left\{1 - \frac{\Delta E}{E}\right\} = \left\{1 - \frac{8}{133}\right\}^{\pi a^2 L n}. \quad (6)$$

From Fig. 9 we may obtain a value of the percent loss of initial energy of the Cs^+ ion for the smallest velocity observed. The value for helium is 55 percent for 3.5 volt ions. In Eq. (6),

$$L = 14.2 \text{ cm}$$

$$n = 3.48 \times 10^{14} \dots (p = 0.01 \text{ mm of mercury})$$

so that,

$$a = r_{\text{Cs}} + r_{\text{He}} = 2.88 \text{ \AA}.$$

Viscosity measurements give for the radius of the helium atom, $r_{\text{He}} = 1.10 \text{ \AA}$, so that we should expect a value for the radius of the Cs^+ ion,

$$r_{\text{Cs}} = 1.78 \text{ \AA}.$$

Herzfeld¹² gives values of r_{Cs^+} which vary from 0.83 to 2.36 \AA depending on the method of measurement. The radius of the xenon atom obtained from

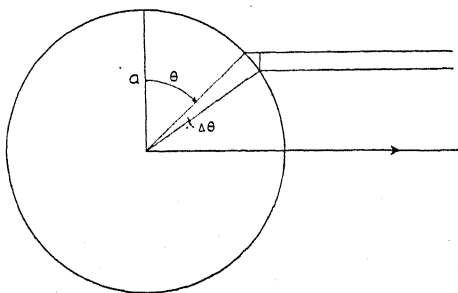


Fig. 11

viscosity measurements is 2.44 \AA . Similar calculations for hydrogen, where $\Delta E/E = 4/133$ and the percent loss was 61.5, gave a value,

$$a = r_{\text{Cs}} + r_{\text{H}_2} = 4.55 \text{ \AA}.$$

A value for r_{H_2} from viscosity measurements quoted by Jeans as 1.36 \AA leaves for the radius of the Cs^+ ion,

$$r_{\text{Cs}} = 3.19 \text{ \AA}.$$

For ions of greater initial energy the percent loss decreases. This disagrees with the elastic collision interpretation which would make the percent loss a constant. We must conclude that at higher velocities the interaction at a collision of a Cs^+ ion with a helium or hydrogen molecule is different from

¹² Geiger Scheel, "Handbuch der Physik," Band XXII, 386, 1926.

that considered in the kinetic theory of gases and that less energy is lost than would be the case, were the collisions elastic.

LITHIUM IONS IN HELIUM.

With low velocity Li^+ ions in helium the change in the curves produced by increasing pressure was entirely different from that found in Cs^+ ions. We shall find that with the light ion, small angle scattering is the predominant phenomenon, whereas with the heavy Cs^+ ions, scattering was inappreciable in comparison with process of retardation. By using several different experimental arrangements it has been possible to establish the type of absorption that occurs over the range of velocities studied, namely 20 to 930 equivalent volts.

METHOD I

The apparatus used has been described in connection with the experiments with caesium and is shown drawn to scale in Figs. 1 and 2. In this method the cylinders C_1 and C_2 were replaced as before with a single Faraday cylinder, mounted above S_2 . The slit S_1 varied between 1 and 2 mm and in several instances runs were taken with this slit entirely removed.

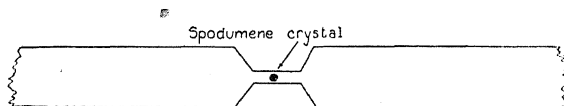


Fig. 12

In Kennard's experiments the ion sources used were the positive ion iron catalysts supplied by Kunsman. These catalysts usually emit Na^+ and K^+ to an appreciable extent together with an ion possibly arising from the insulating cement of the furnace. This necessitates the assumption that the total emission current held constant and measured with the galvanometer G , is also constant in its composition throughout the series of observations. In order to obviate this difficulty the mineral spodumene (used by Hundley¹³) was investigated for purity in emission. A small crystal, less than 0.2 mm in diameter, was melted down on the center of a constricted platinum filament as shown in Fig. 12. This strip is mounted horizontally over the slit S_1 and replaced the furnace source at A (Fig. 1). At low temperatures in vacuum this source showed a large emission of Na^+ and K^+ but continued heating at a yellow heat removed these ions to less than one-half of one percent. By treating the substance in this way a very pure source of Li^+ was obtained, which in many cases could be used for 100 hours or more, with good intensity and constant emission. Due to the small value of the emission current to S_1 , an electrometer shunted with a high resistance replaced the galvanometer G in most of the experiments in an attempt to attain greater accuracy of observation. Since the method used depends on Eq. (1), the emission current N_0

¹³ Hundley, Phys. Rev. 30, 864 (1927).

must be constant and proportional to the actual ion current passing through S_1 . The current actually recorded represents the total ion current through S_1 as well as to neighboring metal parts connected to the magnet armature. It was not possible, with this arrangement, to determine whether the actual current through the slit remained constant, but it was assumed that a constant fraction of the total emission current entered S_1 . This assumption is not entirely justified as spreading of the beam may occur due to the admission of

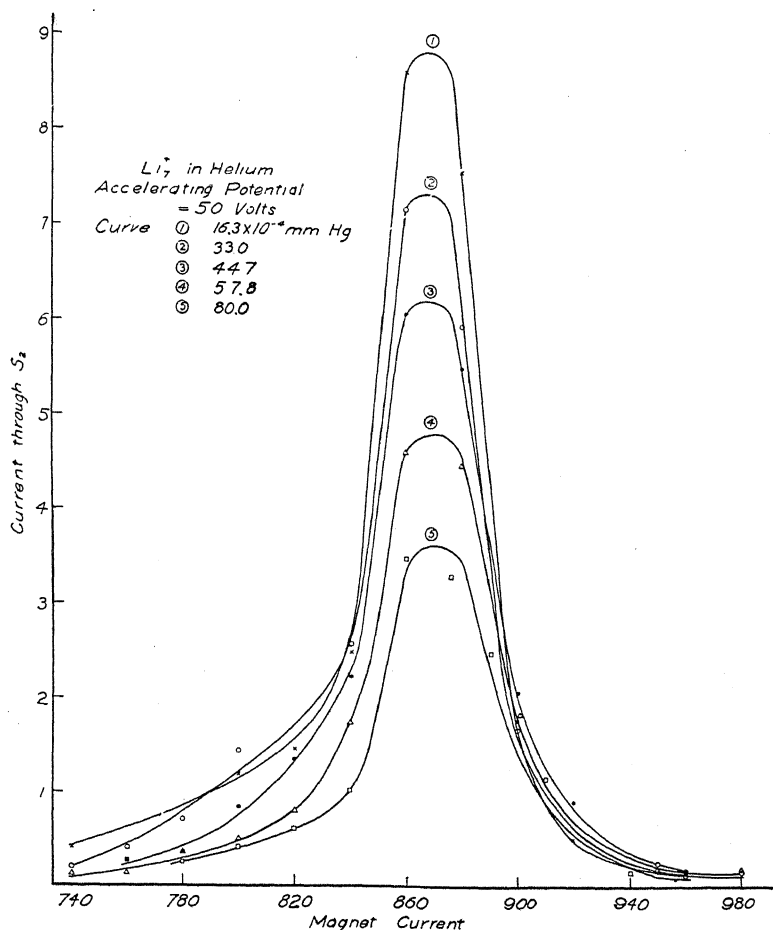


Fig. 13

gas, or the actual character of the emission from the source may change, giving a bundle of varying divergence. This indefiniteness accounts partially for the variation of the absorption coefficients obtained by this method, although no difficulty was found in getting reasonable checks.

The method of procedure is the same as that of Kennard and has been outlined above. The type of curves obtained for five different pressures with a constant accelerating potential is shown in Fig. 13 for Li^+ ions of 50 equiva-

lent volts. Sets of curves of this type were taken for velocities varying from 20 to 931 volts and for each velocity at least three such sets were obtained. From each pair of pressures of each set of curves, the value of the mean free path, L , was determined, making use of Eq. (1). The gas path was 11.2 cm in length, so that L was given by:

$$L = 11.2 \times (p_2 - p_1) / 760 \times 2.30 \times \log \frac{N_1}{N_2}.$$

From Eq. (2), C is then obtained, where,

$$C = \pi(R_{Li} + R_{He})^2 = 1/Ln$$

and

$$n = 2.70 \times 10^{19}.$$

Values of C are shown as curve I, Fig. 14 for ion velocities ranging from 20 to 500 equivalent volts; a value of C for 931 volts is not shown on the curve, but

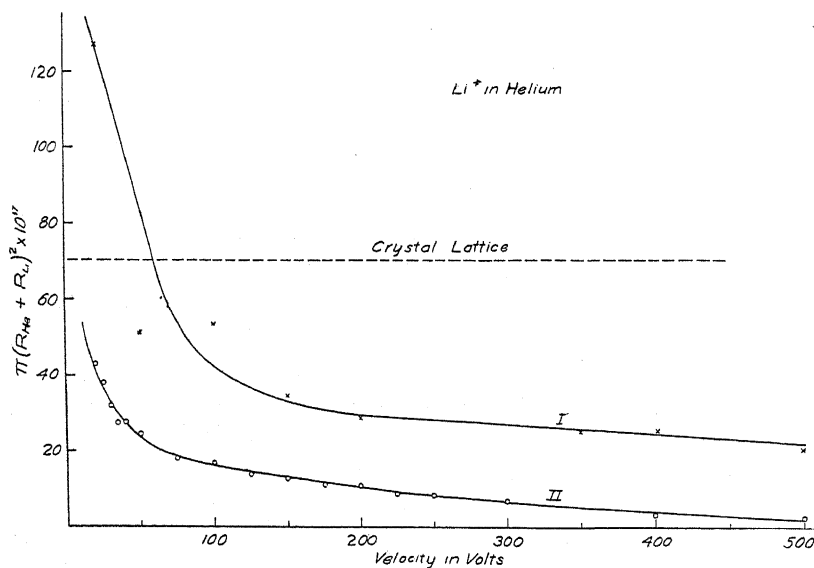


Fig. 14

has a value of $9.5 \times 10^{-17} \text{ cm}^2$, and would fall on the lower linear portion if extended. Using kinetic theory values of the atomic radii as,

$$R_{He} = 1.10 \times 10^{-8} \text{ cm} \text{—viscosity measurements}$$

and, $R_{Li} = 0.41 \times 10^{-8} \text{ cm}$ —crystal lattice data we find for C , $C = 70.1 \times 10^{-17} \text{ cm}^2$ and this value is shown as a dotted line in Fig. 14. In terms of the mean free path, the values of L found vary from about one-half the kinetic theory value at 20 volts to almost eight times this at 931 volts. Reducing Ramsauer and Beeck's values of the "Wirkungsquerschnitt" for Li^+ and helium in terms of C we find for 16 volt ions,

$$C = 42 \times 10^{-17} \text{ cm}^2.$$

This value is about one-third of that found in the present experiments which, from the curve, would give 130×10^{-17} . The difference is accounted for by the dimensions of their apparatus, which had several times the angular aperture used in the present experiments. It has been found that the rate of absorption of the lithium ions depends strongly on the dimensions of the measuring chamber, which indicates that the process is one of scattering. On this basis a considerably smaller value of C would be expected for the wider apertures used by Ramsauer and Beeck.³ As in the experiments of Cox, the interpretation of the behavior of Li^+ in helium as due to scattering is strengthened from the results obtained with a second type of apparatus.

METHOD II

This method has been used by Cox and described by him in detail for the case of lithium ions in mercury vapor.⁵ The experimental tube is shown in Fig. 1, where the dimensions of the various parts are drawn to scale. Measurements of C and L are based on Eqs. (1) and (2), where the length of the absorbing gas path is equal to 11.3 cm. For a given pressure, the total ion current (N_0), to C_1 and C_2 is measured by connecting these two cylinders together with the switch B in position (1). Then with B in position (2), C_1 is grounded and the value of N is measured as the ion current to C_2 . This method allows a more rapid determination of N and N_0 and eliminates the problem of measuring the emission current to S_1 . Values of C and L were determined from observations at three different gas pressures. In all cases the currents to $C_1 + C_2$ and to C_2 were equal for the lowest pressures attainable (10^{-5} mm of mercury). This equality was attained by means of the collimating slit, C , placed over the emergent slit S_2 , which directed the ions up the axes of the cylinders; in this way none of the ions struck the cylinder C_1 at low pressures.

The values of C determined in this way are shown plotted against the ion velocity in Fig. 14, curve II. It is seen that the general shape of this curve is identical with that obtained with Method I, but that in all cases the values of C are smaller. In both cases the values of C rise sharply for velocities below 40 volts, in the one case rising to a value over twice that calculated from kinetic theory values and in the second case approaching the crystal lattice value for low velocities. The dimensions of the absorbing paths for the two methods correspond to those used by Cox and while the actual values of C are smaller, as might be expected with the lighter gas, the same change in these values is found for the two types of apparatus. These results show that the most reasonable interpretation of the process is that of scattering in which forces other than those of elastic collisions come into play. For the large scattering apertures of Method II, a much larger cone of rays may pass over the absorbing path than for Method I, where the angular opening was several times smaller and many more of the ions were lost through deflections to the walls of the chamber. It has been shown by Dempster⁵ that the rate of absorption may show a strong dependence on the dimensions of the apertures, provided some law of force other than that of elastic collisions is effective.

Experiments on the scattering of the Li^+ ions were also tried, using the apparatus shown in Fig. 2. Results obtained for several velocities confirm the conclusions reached above,—that the absorption of the ions is due to scattering and depends on the dimensions of the absorbing chamber and of the collector. Velocity distribution curves were also obtained for Li^+ in helium by the method of retarded potentials, used with Cs^+ ions. This distribution for 50 volt Li^+ ions is shown in Fig. 15. It is seen that the shapes of these curves

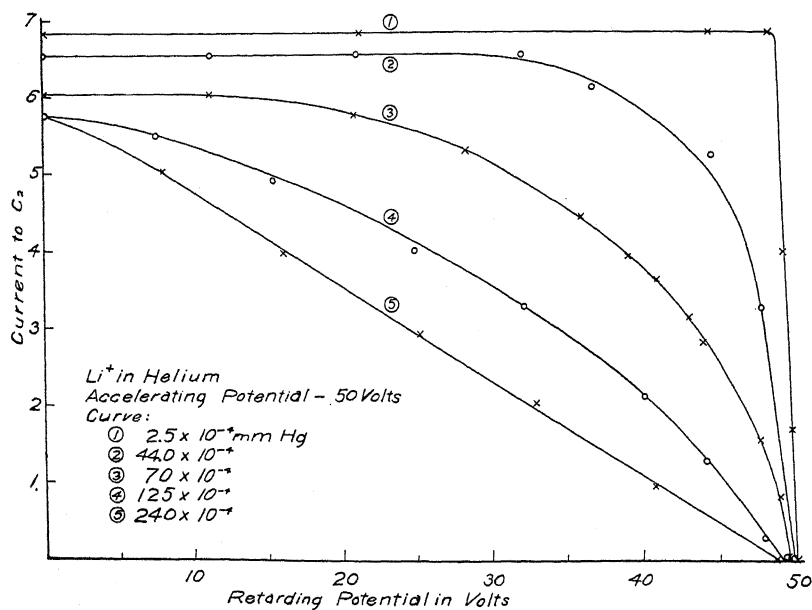


Fig. 15

are quite different from those obtained with Cs^+ ; they do not shift to the left as a whole and some of the ions appear to retain approximately their full initial velocity. The decrease in the number of ions of any particular velocity with pressure is probably due to a decrease in the forward component as a result of scattering, so that we have an "absorption" process which involves only a scattering of the ion bundle as distinct from retardation.

Professor A. J. Dempster suggested the experiments reported on in this paper. The writer is indebted to him for the theory of retardation of the Cs^+ ions as well as for invaluable suggestions and advice regarding experimental procedure and interpretation of results.

THE ABSORPTION COEFFICIENT FOR SLOW
ELECTRONS IN GASES

By C. E. NORMAND

DEPARTMENT OF PHYSICS, UNIVERSITY OF CALIFORNIA

(Received April, 1, 1930)

ABSTRACT

The absorption coefficient has been measured in H_2 , He, A, Ne, N_2 , and CO for electrons with velocities corresponding to from 0.5 to 400 volts. As a result of the high resolving power of the apparatus fine structure was found in the curves of all the gases. A minimum in the absorption coefficient curve was found in every case at velocities between 0.7 and 1.1 (volts)^{1/2}. A lack of agreement between the present measurements at velocities below 2 volts and recent results of Ramsauer and Kollath appears to be due to a difference of about 0.5 volts in the velocity scales of the two sets of observations.

THE absorption coefficients for slow electrons in hydrogen, helium, argon, neon, nitrogen, and carbon monoxide have been rather definitely established by the investigations of Ramsauer,^{1,2} Brode,³ and Bruche.^{4,5,6} Measurements in each of these gases have been made by two or more observers. The object in redetermining the absorption coefficient curves for these gases was two-fold: first to detect any fine structure in the curves which might be brought out by the use of an apparatus having a velocity resolving power higher than had previously been used, and second to extend the measurements as far as possible into the low velocity region.

APPARATUS AND METHOD

The apparatus and method employed in this experiment were essentially the same as used by Brode in determining the absorption coefficient in gases.³ The apparatus used in producing the electron beam was the one used by Brode in his determinations of the absorption coefficient in mercury⁷ and the alkali metal vapors.⁸ Except for the tungsten filament the apparatus was constructed entirely of tantalum. The electron source was a 3 mil tungsten filament placed along the axis of a cylinder 7 mm in diameter. The electrons were accelerated to the cylinder. A narrow beam of these electrons passed through a longitudinal slit 0.2 mm wide and 5 mm high in the cylinder, and was bent by a magnetic field into a circular path defined by a system of

¹ C. Ramsauer, *Ann. d. Physik* **64**, 513 (1921).

² C. Ramsauer, *Ann. d. Physik* **66**, 546 (1921).

³ R. B. Brode, *Phys. Rev.* **25**, 636 (1925).

⁴ E. Bruche, *Ann. d. Physik* **82**, 912 (1927).

⁵ E. Bruche, *Ann. d. Physik* **83**, 1066 (1927).

⁶ E. Bruche, *Ann. d. Physik* **84**, 279 (1927).

⁷ R. B. Brode, *Proc. Roy. Soc. A* **125**, 134 (1929).

⁸ R. B. Brode, *Phys. Rev.* **34**, 673 (1929).

four slits. The last slit of this system was 1 mm wide and 10 mm high. Electrons passing through this last slit entered a collector and were measured by a high sensitivity galvanometer placed between the collector and ground. The reading, I , of this galvanometer was taken as a measure of the intensity of the beam at the end of its path.

The initial intensity of the electron beam was taken as proportional to the total emission, M , from the slit in the cylinder which surrounded the filament. That this proportionality holds, even at low velocities, throughout the pressure range used is shown by the fact that the logarithm of the ratio of I to M is a linear function of the pressure. Fig. 1 shows several examples, taken in helium, of this linear relation. The consistency with which the points fall on a straight line is also an indication of the experimental accuracy of the determinations of the absorption coefficient at these low velocities.

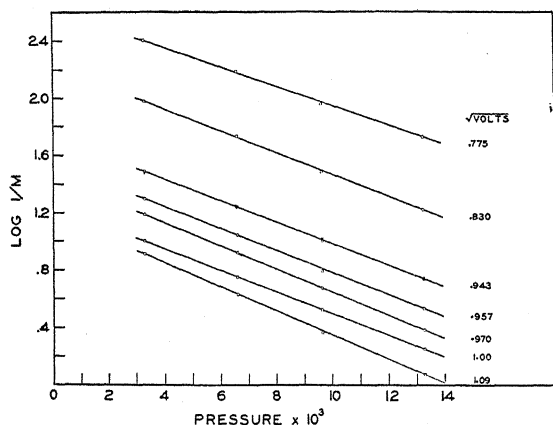


Fig. 1. Log of ratio of maximum current I at collector to total current M from slit in cylinder as a function of pressure, for low velocity beams in helium.

Due to the potential drop in the filament and the contact e.m.f. between the tantalum cylinder and the tungsten filament the applied potential will not give the true velocity of the electrons. The true velocity was determined from the magnetic field required to bend the electron beam into the circular path defined by the slit system of the apparatus. If r is the radius of this path, H the magnetic field strength in gauss, and V the energy of the electrons in equivalent volts, $H \cdot r = 3.3 V^{1/2}$. Since r is a constant of the apparatus the electron velocity in root volts is proportional to the magnetic field strength or to the current, I_h , producing the magnetic field. Working with acceleration potentials of 100 volts or more, where the filament drop and the contact e.m.f. were negligible, the square root of the accelerating potential when plotted against I_h gave a straight line passing through the origin, Fig. 2. From the slope of this line the velocity corresponding to any value of I_h could be calculated. For accelerating potentials below 25 volts the influence of the filament drop and the contact e.m.f. becomes appreciable causing the points to lie above the straight line which gives the true velocity.

As a check of this method of velocity determination retarding potential curves were taken at a number of velocities between 0.5 and 1.2 volts. With a given accelerating potential I_h was varied until I was a maximum. From this value of I_h the velocity of the electrons was calculated. A retarding

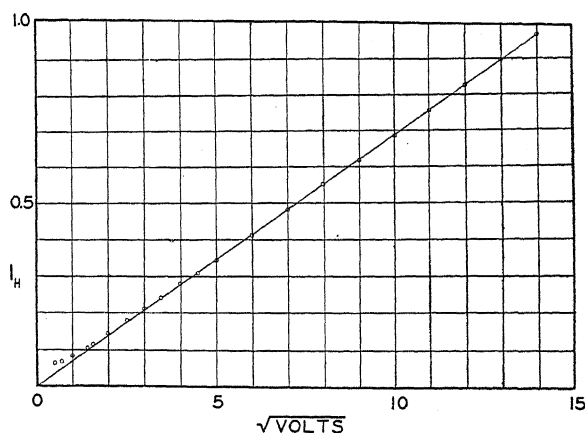


Fig. 2. Deflecting magnetic field current I_h as a function of the square root of the accelerating potential.

potential was then applied between the collector and ground and the values of I corresponding to measured increasing values of the retarding potential were recorded. The points of inflection of the curves obtained by plotting the collector current, I , against the retarding potential give the velocity of the electrons. Four of these curves are shown in Fig. 3. The vertical lines indicate the velocity as calculated from the deflecting magnetic field

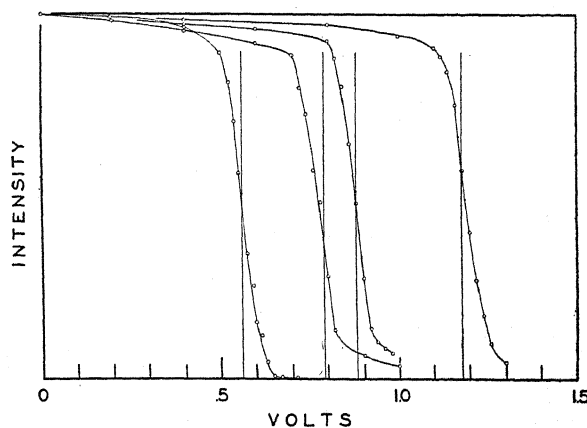


Fig. 3. Intensity of electron current arriving at collector as a function of retarding potential applied between collector and ground.

current I_h , Fig. 2. For six velocities between 0.5 and 1.2 volts the mean deviation of the values as measured by the two methods was 0.014 volts.

These retarding potential curves give also a measure of the velocity resolving power of the apparatus. The width of the half maximum of the

electron velocity distribution curves is found to be 0.035, 0.040, 0.031, 0.030 volts^{1/2} for mean velocities equivalent to 0.56, 0.79, 0.88, 1.18 volts respectively. From the dimensions of the apparatus the maximum variation of the velocity of the electrons passing through the last slit should be about 3 percent of the mean velocity.

RESULTS

The results are shown in Figs. 4 to 9 where the absorption coefficient, α , is plotted as a function of the electron velocity in volts^{1/2}. The previous results of Brode, and Bruche, are also given. All the observed values of α have been plotted in each case. The consistency of the results is shown by the fact that many of the points taken on different days agree within less than one percent. α is expressed in square centimeters per cubic centimeter of the gas at 0°C and a pressure of 1 mm of Hg.

Hydrogen was prepared by the electrolysis of barium hydroxide and was further purified and dried by passage over heated copper and through a phosphorous pentoxide tube. The general form of the curve agrees well with the results of Bruche. A small secondary maximum in the curve appears at 2.2 volts^{1/2}, and at 1.55 volts^{1/2} a sharp peak similar to those observed by Brode in the alkali metal vapors is superimposed on the broad maximum previously observed. A distinct minimum occurs at 1.1 volts^{1/2} beyond which the curve rises rapidly with decreasing velocity.

Helium was purified by slow passage through a charcoal trap immersed in liquid air, the trap having been previously baked at 500°C. At the higher velocities the results are in good agreement with those of Brode. The maximum, however, occurs at a velocity lower than determined by Brode and Bruche and appears as two distinct and almost equal maxima. Beyond the second maximum is a minimum at 0.92 volts^{1/2} and for still lower velocities the curve rises slightly.

Argon was purified by a magnesium arc. There are indications of fine structure between 4.5 and 5.5 volts^{1/2}. The minimum is at about 0.8 volts^{1/2}.

Neon, purchased as 99.5 percent pure, was used without further treatment. The value of α increases steadily to a maximum at about 5 volts^{1/2}. From here the curve drops irregularly to a final minimum at 0.85 volts^{1/2}.

Nitrogen was prepared by the decomposition of sodium azide on being heated. The curve has a small maximum at 12 volts^{1/2}, pronounced fine structure between 2 and 3 volts^{1/2} and a very large and sharp maximum at 1.5 volts^{1/2}. A slight nick occurs at 1.2 volts^{1/2} and a final minimum is reached at slightly below 1 volt.

Carbon monoxide was prepared by the decomposition of formic acid on being dropped into hot sulphuric acid, and was dried by passage through a phosphorous pentoxide tube. The results are in very good agreement with those of previous observers. The similarity between the CO and N₂ curves is seen to persist even in the fine structure.

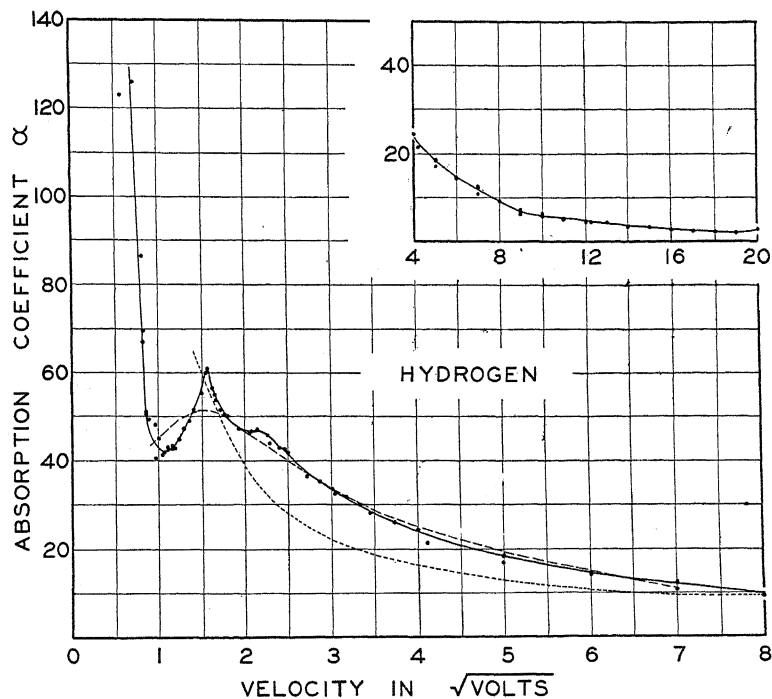


Fig. 4. The absorption coefficient α for electrons in hydrogen as a function of the velocity of the electrons.

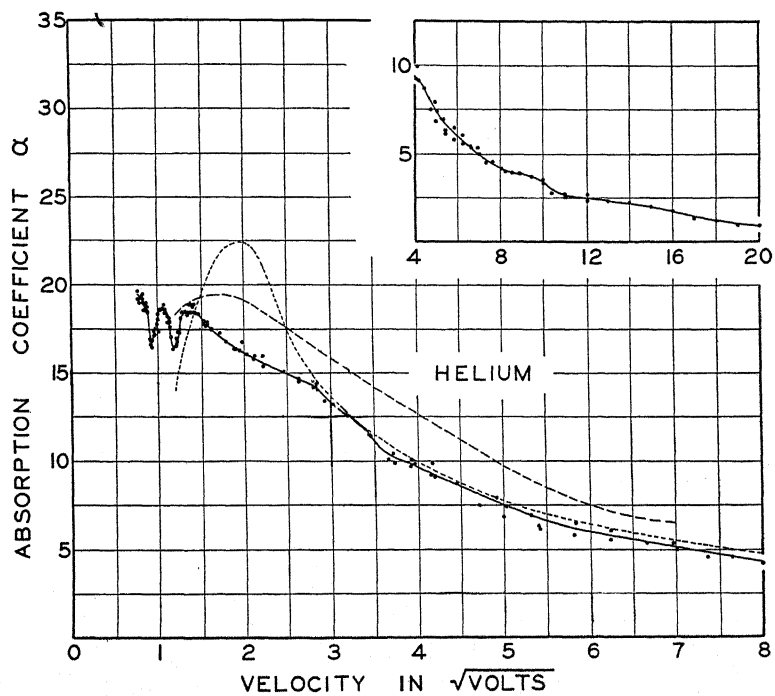


Fig. 5. The absorption coefficient α for electrons in helium as a function of the velocity of the electrons.

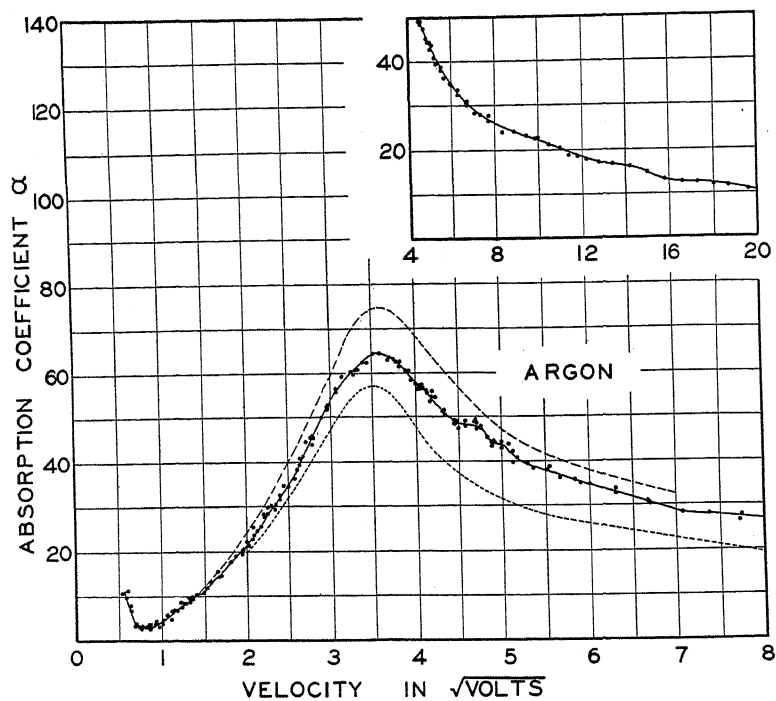


Fig. 6. The absorption coefficient α for electrons in argon as a function of the velocity of the electrons.

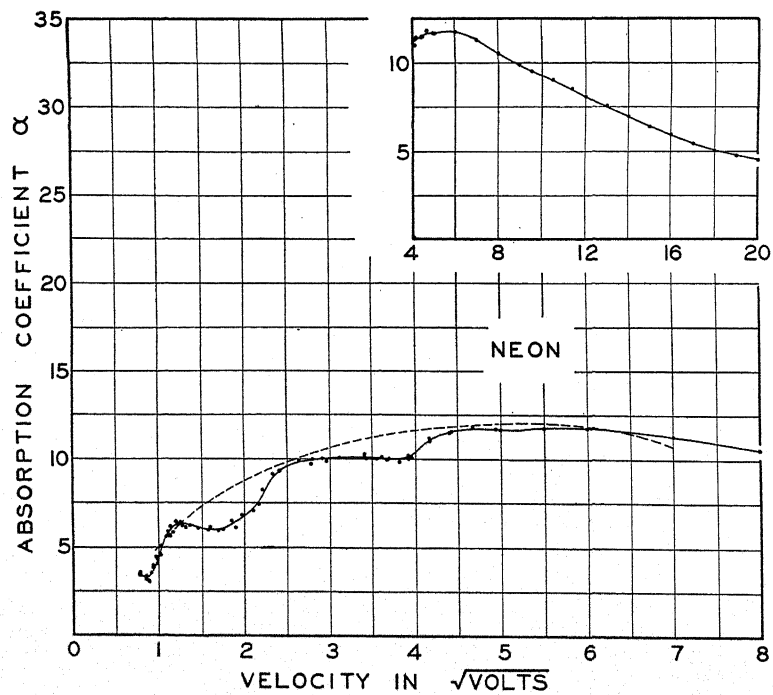


Fig. 7. The absorption coefficient α for electrons in neon as a function of the velocity of the electrons.

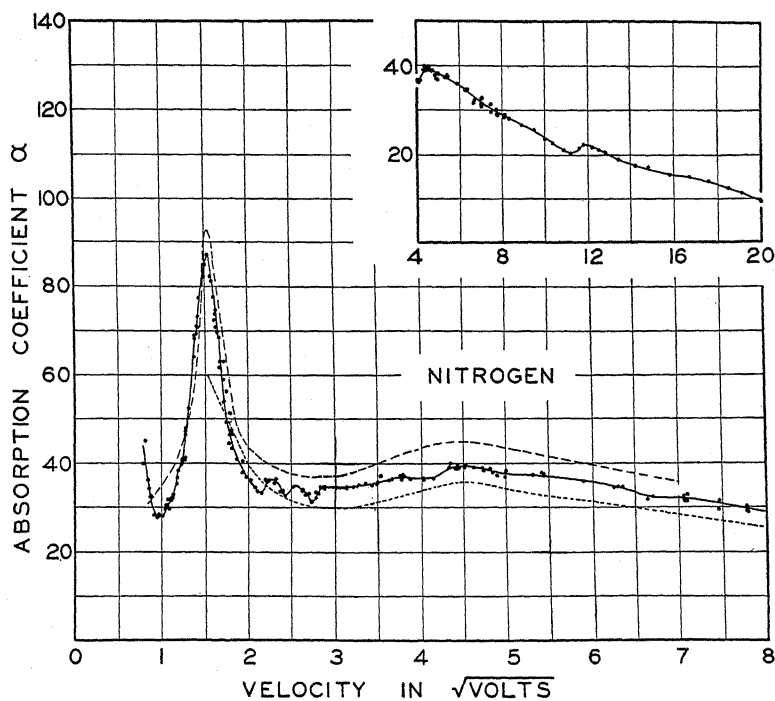


Fig. 8. The absorption coefficient α for electrons in nitrogen as a function of the velocity of the electrons.

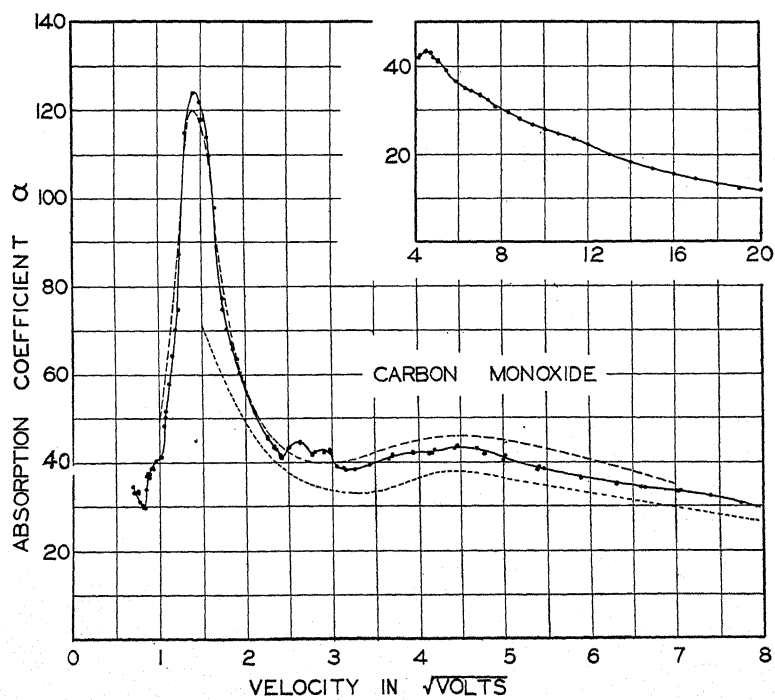


Fig. 9. The absorption coefficient α for electrons in carbon monoxide as a function of the velocity of the electrons.

LOW VELOCITY RESULTS

For velocities below 1 volt the intensity of the electron beam drops off very rapidly with decreasing velocity. Somewhat greater intensity and extended range toward lower velocity was obtained by applying an accelerating potential of about 1.5 to 2 volts and then retarding the electrons to the desired velocity. The values of α obtained with and without the auxiliary

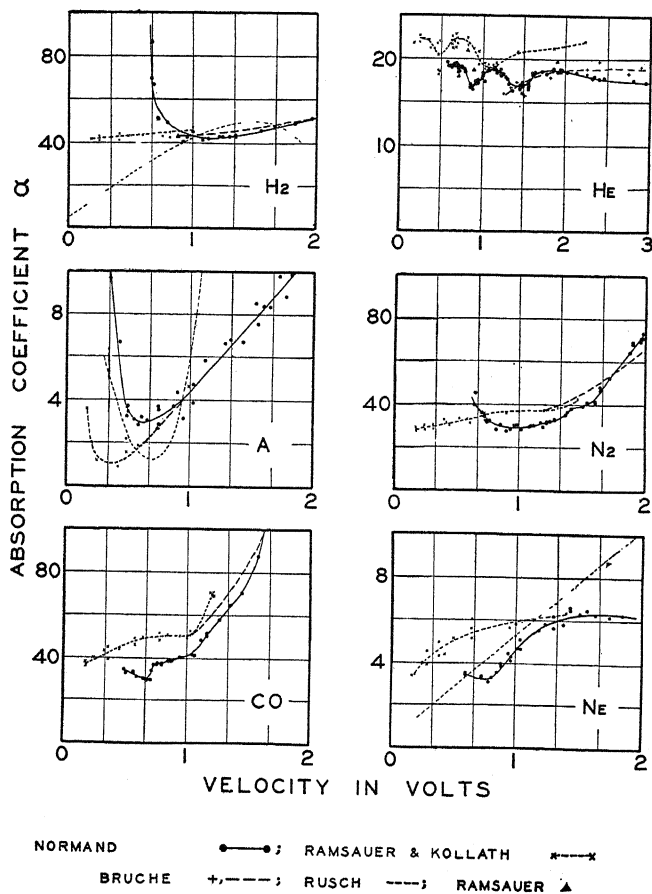


Fig. 10. The absorption coefficient α for very slow electrons in H_2 , He, A, Ne, N_2 , and Co as a function of the energy of the electrons in volts.

retarding potential were identical. The rapid diminution of intensity, however, rendered impossible the determination of α for velocities lower than about 0.5 volts except in the case of argon where measurements were extended to about 0.3 volts.

The results of these measurements for velocities below 2 volts, (3 volts in the case of He), are given in Fig. 10 together with the recent results of Ramsauer and Kollath,^{9,10} the earlier results of Bruche,¹¹ and the points

⁹ C. Ramsauer and R. Kollath, Ann. d. Physik 3, 536 (1929).

¹⁰ C. Ramsauer and R. Kollath, Ann. d. Physik 4, 91 (1929).

¹¹ M. Rusch, Phys. Zeits. 26, 748 (1925).

obtained by Ramsauer¹ in his first measurements. Here α is plotted as a function of the electron energy in equivalent volts rather than of electron velocity, volts^{1/2}. In no case is the agreement with Ramsauer and Kollath as good as might be expected from the accuracy of the measurements in each case.

A comparison of the results in the case of helium is especially interesting. The actual magnitude of the values of α given here are about 17 percent smaller than those given by Ramsauer and Kollath. Neglecting this difference in magnitude, which is of little importance, the two curves are seen to be nearly identical if Ramsauer and Kollath's velocities are increased by about 0.4 volts or if the velocities in this paper are decreased by the same amount. The agreement with the results obtained by other observers is seen to be better for the values of velocity given in this paper than for those given by Ramsauer and Kollath.

What has been said about the disagreement of the values of the velocity for helium is equally true for all the other gases measured. The magnitudes of the coefficient are in somewhat closer agreement but the volt scale is still displaced by about 0.4 to 0.6 volts. As already described, the velocity has been carefully checked throughout these measurements. Ramsauer and Kollath have also checked their velocities by both the retarding potential and the magnetic deflection method. The most probable source of the discrepancy would appear to be a contact e.m.f. The thin sheet tantalum parts of the apparatus used in this experiment were spotwelded together. The apparatus was baked at 500°C for several hours and the tantalum parts were heated to a bright yellow with an induction furnace. At no time were unsteady conditions such as reported by Ramsauer and Kollath observed. The apparatus of Ramsauer and Kollath was constructed of brass and placed under an evacuated bell-jar. The unsteady conditions arising from contact e.m.f.s between the parts of the apparatus made necessary the complete dismantling of the apparatus and the scraping of all metal surfaces at intervals of about 10 days. By this treatment steady and repeatable measurements were obtained with their apparatus.

The author wishes to express his indebtedness to Professor R. B. Brode for proposing this investigation, for his many helpful suggestions, and for his interest throughout the work.

ON THE CONCENTRATION OF METASTABLE MERCURY ATOMS

BY E. GAVIOLA

INSTITUTO DE FISICA, LA PLATA UNIVERSITY, ARGENTINA

(Received March 26, 1930)

ABSTRACT

The concentration of metastable atoms in presence of 3 mm nitrogen obtained using the measurements of Stuart seems to be in contradiction with a calculation given here using observations of Wood. The contradiction disappears if the different statistical weights of the levels 2^3P_1 and 2^3P_0 are taken in account. Corrected curves for the number of metastable atoms as functions of the foreign gas pressure are given for CO, H₂O, N₂, A and He which are to replace the corresponding curves of the previous paper. It is shown that the assumption of the author that by high primary light intensities the number of metastable atoms increases only with the square root of the intensity is strikingly supported by measurements of Wood.

THIS paper is a continuation of a previous one¹ by the author "On life and concentration of metastable atoms and the quenching of mercury resonance radiation." The concentration of metastable mercury atoms produced by collisions of resonance ones optically excited with nitrogen (or other foreign gas molecules) can be calculated numerically from the well-known fact that the introduction of a few mm of nitrogen into the vessel containing the mercury vapour (illuminated by a quartz mercury lamp) produces a many-fold increase in the intensity of the visible mercury lines emitted as fluorescence by the vapour. R. W. Wood² observed increases of the intensity of the green line 5461 ranging from 16 to 32 times. He interpreted this increase as due to the accumulation of metastable atoms when nitrogen is present and he was able to show experimentally by means of the absorption of the line 4046 that metastable atoms actually were present in large amounts. Let us now calculate numerically how many metastable atoms were present in the experiments of Wood, repeated and extended afterwards by the author.³

I

The green line 5461 is emitted by the 2^3S_1 level and its intensity in fluorescence which we will call J_{5461} is equal to

$$J_{5461} = A_{5461} \cdot N_s \quad (1)$$

if A_{5461} is the Einstein spontaneous transition probability and N_s the number of atoms in the level 2^3S_1 . This level can be reached when mercury vapour alone is in the fluorescence vessel ("vacuum" case) practically only³ through

¹ E. Gaviola, Phys. Rev. **34**, 1373 (1929).

² R. W. Wood, Phil. Mag. **50**, 761, 774 (1925); **4**, 466 (1927).

³ E. Gaviola, Phil. Mag. **6**, 1167 (1928).

the absorption of the line 4358 of the arc on the part of the the resonance atoms in the level 2^3P_1 , the number of which we call N_1^0 . It is therefore possible to write

$$N_s(\text{vacuo}) = \frac{1}{c} N_1^0 \cdot I_{4358} \cdot B_{4358} \cdot \tau_s \quad (2)$$

where I_{4358} is the intensity of the line 4358 of the primary light source, B_{4358} its Einstein absorption coefficient and τ_s the mean life of the atoms N_s .

If a few mm pressure of nitrogen gas are admitted to the vessel containing the saturated mercury vapour, many resonance atoms are brought down by collisions with nitrogen molecules to the metastable level 2^3P_0 where owing to

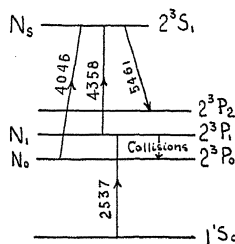


Fig. 1. Diagram of transitions.

is long life they accumulate until a concentration is obtained which, as the absorption experiments show is many times larger than the one of resonance atoms. The level 2^3S_1 is reached now practically only by the absorption of the line 4046 of the primary lamp on the part of the metastable atoms N_0 and consequently

$$N_s(\text{gas}) = 1/c \cdot N_0 \cdot I_{4046} \cdot B_{4046} \cdot \tau_s. \quad (3)$$

It may be thought that the admission of nitrogen might also disturb the atoms in the level 2^3S_1 diminishing their number as a result of collisions, in which case formula (3) would give too large numbers. But according to recent results of Hanle and Richter⁴ it takes at least 80 mm pressure of nitrogen to produce noticeable influence upon the level 2^3S_1 . Formula (3) is therefore correct for all pressures below 80 mm and as our pressures do not exceed 10 mm we can quietly use it. Combining (1) with (2) and with (3) and dividing we obtain

$$J_{5461}(\text{gas})/J_{5461}(\text{vacuo}) = N_0/N_1^0 \cdot I_{4046}/I_{4358} \cdot B_{4046}/B_{4358}.$$

This ratio was photographically measured and found to be equal to 32 in Wood's earlier experiments, therefore

$$N_0/N_1^0 = 32 \cdot I_{4358}/I_{4046} \cdot B_{4358}/B_{4046}. \quad (4)$$

Now, the ratio I_{4358}/I_{4046} of the intensities of the blue and violet lines of the arc has been repeatedly measured and found to be equal to 2. As both lines

⁴ W. Hanle and E. F. Richter, Zeits. f. Physik 54, 816 (1929).

are emitted by the same upper level, the ratio of their intensities gives at the same time the relation of the values of their corresponding Einstein emission coefficients A_{4358} and A_{4046} if that value is not falsified by absorption or reversal of the lines before they leave the mercury lamp. As that ratio is the same for the lines of the primary lamp when the discharge is magnetically deflected against the wall of the tube as for the secondary fluorescence light in the case of "vacuo" when practically no reabsorption can take place, one can write with confidence

$$A_{4358}/A_{4046} = 2 = I_{4358}/I_{4046}. \quad (5)$$

Between the coefficients A and B there is a relation

$$A = B \cdot 2h\nu^3/c^2 \cdot q_1/q_2 \quad (6)$$

where q_1 and q_2 are the statistical weights of the lower and upper levels respectively. The statistical weights of the levels 2^3P_0 , 2^3P_1 and 2^3S_1 are 1, 3 and 3, therefore for 4358 $q_1/q_2 = 1$ and for 4046 $q_1/q_2 = 1/3$. We can then write

$$A_{4358}/A_{4046} = 2 = B_{4358}/B_{4046} \cdot (\nu_{4358}/\nu_{4046})^3 \cdot \frac{1}{3}$$

and since $(\nu_{4358}/\nu_{4046})^3 = 0.8$ we obtain

$$B_{4358}/B_{4046} = 7.5.$$

Introducing the now known numerical values in formula (4) we have finally

$$N_0/N_1^0 = 32 \times 2 \times 7.5 = 480. \quad (7)$$

That means that when a few mm of nitrogen are present in the tube the number of metastable atoms is 480 times larger than the number of resonance atoms when no nitrogen is present. This last number can be easily obtained numerically if the intensity of the primary line 2537.5 is known. N_1^0 is for instance equal to one if 10^7 light quanta are absorbed per second in the volume element considered (since the life of 2^3P_1 is 10^{-7} sec.).

II

In a former paper of mine on the same subject¹ I have made a numerical calculation of the ratio N_0/N_1^0 as a function of the foreign gas pressure for different gases (and among them for nitrogen) using the measurements of Stuart for the quenching of resonance radiation and some other experimental data. Now, Fig. 5 of that paper indicates that for a pressure of about 3 mm of nitrogen (which was the pressure used by Wood to obtain a 32 fold increase of the green line) the ratio N_0/N_1^0 ought to be about 1200. This number is nearly three times larger than the one obtained above. It is therefore necessary to solve this contradiction. This we shall here do. The values of my former paper were all calculated neglecting the fact of the different statistical weights of the levels 2^3P_1 and 2^3P_0 .⁵ If we take this fact into account, none of the previous formulas is changed but the value α which

⁵ Dr. H. Beutler kindly called my attention to this point.

indicates the ratio N_0/N_1 for the case of thermal equilibrium and is given by the formula

$$\alpha = q_0/q_1 \cdot e^{w/kT} \quad (8)$$

where q_0 and q_1 are the statistical weights of the levels 2^3P_0 and 2^3P_1 respectively and w their energy difference, this value α becomes three times smaller than it was assumed to be in the previous paper because $q_0/q_1 = 1/3$. For the same reason the constants b and E_0 of Table I of that paper are three times too small. If we recalculate now the curves for N_0/N_1^0 as a function of

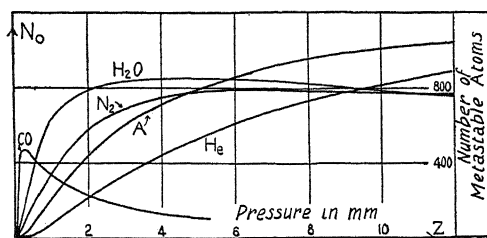


Fig. 2. Number of metastable atoms as a function of the foreign gas pressure if 10^7 quanta are absorbed per second.

the pressure of foreign gases using three times larger values for b and E_0 and a three times smaller α we obtain the curves reproduced in Figs. 2 and 3 which are to take the place of Figs. 5 and 6 of the previous paper. We see in Fig. 2 that the number N_0/N_1^0 for about 3 mm nitrogen pressure has reduced itself to about 700. This number is still larger than the one obtained independently in the first part of this paper but we have to remember that the number 480 corresponds to the experimental conditions of Wood while the number 700

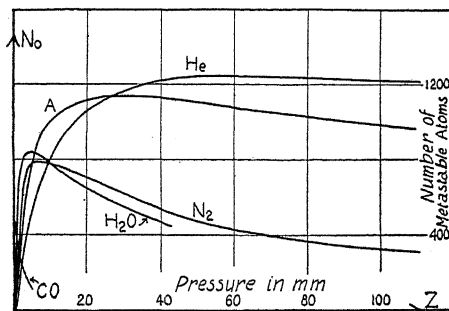


Fig. 3. Number of metastable atoms as a function of the foreign gas pressure for $N_1^0 = 1$ (10^7 quanta absorbed per second).

to those of Stuart. The main difference between the experimental conditions of both observers was that Wood used a considerably larger primary light intensity. As I have shown in the previous paper N_0 increases for large primary light intensities not proportional to the intensity itself but to the

square root of it, while N_1^0 grows on linearly. The relation N_0/N_1^0 must therefore become smaller for large intensities, as in the case of Wood. An interesting confirmation of this result is given by the measurements of Wood himself. In his earlier experiments⁶ he obtained as said above a 32 fold increase of the green line by the admission of nitrogen. After that he increased his primary light intensity considerably by pressing the arc discharge against the wall with a magnetic field. The increase of the green line was now at best only 15 fold.⁷ The ratio N_0/N_1^0 had decreased therefore (compare formulas (4) and (7)) to 225. Since the decrease of N_0/N_1^0 for large intensities is due to collisions between two metastable atoms which destroy both of them (one is excited to a higher level, the other becomes normal) the above result is a striking hint at the fact that the probability of such collisions (collision-section) must be rather large.

⁶ R. W. Wood, *Phil. Mag.* 50, 761 (1925).

⁷ R. W. Wood, *Phil. Mag.* 4, 485 (1927).

THE MOST PROBABLE 1930 VALUES OF THE
ELECTRON AND RELATED CONSTANTS

BY ROBERT A. MILLIKAN

NORMAN BRIDGE LABORATORY OF PHYSICS, CALIFORNIA INSTITUTE, PASADENA

(Received April 8, 1930)

ABSTRACT

The conclusions are reached that: (1) No such empirical oil-drop formula as that suggested by H. A. Wilson can be valid, (2) It is highly improbable that the spectroscopic fine structure constant can be a whole number—either 136 or 137, (3) The most probable 1930 values of e , N , and h , are the same as in 1917, corrections due merely to new determinations of the velocity of light and the absolute value of the ohm being alone needed. These values so corrected are

$$e = (4.770 \pm 0.005) \times 10^{-10} \quad h = (6.547 \pm 0.011) \times 10^{-27} \quad N = (6.064 \pm 0.01) \times 10^{23}.$$

(4) If Lewis and Adam's theoretical equation is considered valid the probable errors are much smaller than the foregoing estimates.

THE first purpose of this paper is to comment on Professor H. A. Wilson's "Note on the Value of the Electric Charge,"¹ in which he concludes that "the oil-drop experiments do not definitely exclude" a value of e one percent higher than 4.774×10^{-10} ; the second purpose is to express an individual 1930 judgment, with the reasons therefor, as to the best values of these constants in view of all that has been done to date in the way of their exact evaluation; the third purpose is briefly to discuss the mutual restrictions which the theorists and the experimentalists impose upon each other; and the fourth is to present evidence bearing on Eddington's contention that the spectroscopic fine-structure constant is a whole number.

I. OIL-DROP METHOD'S PRECISION

If there were nothing more to the oil-drop work than the finding of some empirical equation that would reproduce the experimental data published in my 1917 paper,² then the statement quoted above might have some justification; but the experimental facts are, first, that Professor Wilson's empirical equation merely fits the relatively *short portion* of the oil-drop curve which corresponds to these data, and shoots above a considerable number of *observed points* farther down on the curve, that is, corresponding to smaller values of $1/pa$, then runs into the axis at a point much higher than these observed points permit; second, that it departs very largely from the *observed curve* at its upper end, that is, for large values for $1/pa$. For not only has the complete oil-drop curve from very low to very high values of $1/pa$ been worked out empirically so that we know by experiment

¹ H. A. Wilson, Phys. Rev. **34**, 1493 (1929).

² R. A. Millikan, Phil. Mag. **34**, 1 (1917).

that no such equation as that given by Professor Wilson is valid, but also—and this is more important—in view of a group of papers, some by myself,³ partly experimental and partly theoretical, and a masterly one by Epstein,⁴ *we now know precisely why Stoke's law of fall breaks down*, and why the law of fall embodied in the oil-drop equation takes its place.

I shall later in the paper have reason to insist that the theorist is bound to build his theories so that they do not collide head on with experimental facts; but at this point my insistence is that the experimentalist is not justified in setting up an empirical equation which makes Nature behave in a way which established and well verified theory tells him that she cannot behave. With this my comment upon Professor Wilson's paper is ended, and possibly no further remarks on e , h , and N would be needed had not Professor Zwicky's recent work on the secondary or block-structure of crystals gone far toward clearing the atmosphere surrounding these constants since Birge's masterly review⁵ of last July appeared. This may perhaps justify the following brief historical review and new appraisal of where these constants now seem to me to stand.

II. CHANGES IN e , h , AND N IN FOURTEEN YEARS

Fourteen years ago, at the conclusion of seven years of work on the experimental evaluation of these three constants, the electron, the Avogadro number, and Planck's quantum of action, the following were published as the most reliable values then attainable:²

$$\begin{aligned} e &= 4.774 \pm .005 \times 10^{-10} \\ h &= 6.547 \pm .006 \times 10^{-27} \\ N &= 6.062 \pm .006 \times 10^{-23} \end{aligned} \tag{1}$$

and these values have been incorporated into most of the tables and texts compiled since that time; but quite recently some uncertainty has arisen, and there has been a widespread discussion of these constants, stimulated, in the first instance, by Eddington's theoretical suggestion as to what ought to be the value of the spectroscopic fine-structure constant, and in the second place by the more recent experimental work of Bäcklin,⁶ Wadlund,⁷ and Bearden⁸ on the comparison of x-ray wave-lengths as determined by ruled gratings and by crystals. After this discussion, the following is where the matter now stands from the viewpoint of an experimentalist,—that is, the man who is engaged in making the measurements themselves and who has the feeling and the judgment that possibly only the observer can have about the relative reliability of the readings involved.

³ R. A. Millikan, Phys. Rev. **21**, 67 (January 1923); also **21**, 217 (March 1923); also **22**, 1 (July 1923).

⁴ P. S. Epstein, Phys. Rev. **23**, 710 (June 1924).

⁵ Raymond T. Birge, Phys. Rev. Supplement **1**, 1 (1929).

⁶ E. Bäcklin, "Absolute Wellenlängenbestimmungen der Röntgenstrahlen," Uppsala Dissertation, 1928.

⁷ A. P. R. Wadlund, Proc. Nat. Acad. Sci. **14**, 588 (1928), and Phys. Rev. **32**, 841 (1928).

As to the electron, I think it is generally agreed that the oil-drop method still remains the chief, if not the sole, reliance of the physicist, so far as directness, reliability, and precision are concerned, in arriving at its value. I had myself hoped, and expected, that the comparison of wave-lengths as determined by ruled gratings and by crystals would lead to greater precision in the fixing of both N and e , but I now feel sure that both (1) the experimental results obtained by this method, and (2) Zwicky's theoretical work (Proc. Nat. Acad. March, 1930) on the secondary structure of crystals, show that this method cannot have anything like the reliability which we had hoped that it would show, and therefore that all of the methods which depend upon crystal grating-space, as computed from density and N , had better be left out of the accounting.

† No new work has been done by the oil-drop method that is comparable in elaborateness nor precision with that published in 1917, but the fundamental constants entering into that method, such as the velocity of light and the value of the ohm, have been redetermined within that period, so that *the 1917 data, treated precisely as it was then treated, but combined with Michelson's new value of the velocity of light, namely, 2.99796 instead of 2.999, and the absolute value of the ohm* (my international volts thus are raised 1 part in 2000 to reduce them to absolute volts) *yields*

$$e = (4.770 \pm .005) \times 10^{-10} \text{ absolute electrostatic units}^9 \quad (2)$$

in place of $(4.774 \pm .005) \times 10^{-10}$. *The foregoing is, then, merely the old oil-drop value of e brought up to date by inserting new values of the velocity of light and the value of the ohm.*

‡ This value of the electron is also that at which Birge finally arrives as a result of his survey of the whole field of fundamental constants. It is true that he reanalyzes for himself my individual oil-drop readings and weights them so that he gets from them the value 4.768 ± 0.005 in place of my value

⁸ J. A. Bearden, Proc. Nat. Acad. Sci. 15, 528 (1920).

⁹ The following quotation is made from an article published in Science on May 10, 1929:

"The reason I have not heretofore made the foregoing readjustment in my value of e is, first, that it is of no particular significance any way, since it is in any case within the limits of my estimated uncertainty; and, second, that I have until recently doubted its legitimacy.

"In the presentation of the best values of widely used physical constants I have heretofore questioned the wisdom, or even the correctness, of making a differentiation between so-called international units and absolute units before a suitably authorized international commission had recognized that difference, since otherwise such differentiation would rest merely upon some individual's *estimate* of the superior reliability of some particular new determination or determinations over the weighted mean of the whole series of determinations used by the international commission which in 1908 and 1911 fixed upon the international units. However, Professor Raymond T. Birge has called my attention to the fact that in view primarily of the close agreement between new determinations of the absolute value of the ohm by F. E. Smith (Phil. Trans., 1914) and Grüneisen and Giebe (Ann. d. Physik, 1920), the compilers of tables have actually recently begun to make the foregoing differentiation. It is because of this fact and because of Michelson's undoubted new precision in the measurement of the velocity of light that I have thought it worth while to begin herewith to recognize the effect of these changes upon the value of e ."

4.770 ± 0.005 , a result that is so much nearer mine than my experimental uncertainty that I am quite content—indeed gratified—but I may perhaps be pardoned for still preferring my own graphical weightings, since I thought at the time, and still think, that I got the best obtainable results in that way from my data. The person who makes the measurements certainly has a slight advantage in weighting over the person who does not, and the *graphical method by which I got at my final estimated uncertainty* is, I think, in the hands of the experimenter himself more dependable than least squares. A glance at the 1917 paper will show that I used least squares only to exhibit how well my observed points were distributed about my final graphically chosen *line*. Birge actually chooses for his final value my own foregoing value, 4.770, instead of 4.768, because he attaches enough weight to Wadlund's work to induce him to push the latter value up by 2 parts in 5000. Wadlund's work, however, must now, I think, be thrown entirely out of account, both because Bearden's repetition of it yielded a full percent of divergence from it and because Zwicky's theoretical block-structure work indicates that the method itself involves up to a percent of uncertainty.

The photoelectric evaluation of h , as reported in this same 1917 article, was $(6.56 \pm 0.03)10^{-27}$, but *it was definitely stated in that article* that the value of this constant derived from the Bohr equation

$$R_{\infty} = \frac{2\pi^2 e^5}{h^3 c^2 e/m} \quad (3)$$

was in my judgment the most reliable value then obtainable, the value then resulting from inserting in the foregoing equation $e = 4.774$ and $e/m = 1.767$ was as given in that paper

$$h = (6.547 \pm 0.01) \times 10^{-27} \quad (4)$$

Birge, from his recently published survey, comes to precisely this 1917 value with practically the same estimated error, namely, 0.008, so that these fourteen years have not changed at all the final result as to h . The reason that h remains unchanged while my e suffers a slight decrease is that the new work done by Babcock¹⁰ and Houston¹¹ changes e/m as spectroscopically determined to 1.761, while the value used in the 1917 computations was 1.767, and this change just balances the foregoing change in e . The present numerical equation is

$$h = \left[\frac{2\pi^2 (4.770 \times 10^{-10})^5}{109737.42 (2.99796 \times 10^{10})^2 (1.761 \times 10^7)} \right]^{1/3} = 6.5471 \times 10^{-27} \text{ erg. sec.} \quad (5)$$

The Avogadro number Birge estimates as 6.064 ± 0.006 in place of the 1917 value, namely, 6.062 ± 0.006 . In view of the estimated error in both cases the difference of course has no significance whatever. The reason the agreement is so good is that new work on the electro-chemical equivalent

¹⁰ Babcock, Phys. Rev. 33, 268 (1929).

¹¹ Houston, Phys. Rev. 30, 608 (1927).

leads Birge to choose to modify the Faraday constant in such a way as nearly to offset the influence of the slight change in e on the value of N .

So far, then, as the foregoing estimates by both Dr. Birge and myself are to be depended upon, the last fourteen years have introduced no change into the values of e , h , and N as experimentally determined, save the insignificant one in e due to new precision in the velocity of light and the value of the ohm.

III. THEORETICAL RELATIONSHIPS

What, then is to be said of the demands that the theorists have made upon the relations of these constants? This is a very important and a very interesting question. There are two such relations to be considered, one brought forward by Lewis and Adams¹² in 1914 and one by Eddington¹³ in 1929. With respect to the first, I have nothing to add to Birge's comments, except to emphasize them. Lewis and Adams, from their theory of ultimate rational units arrive at the following relation between h , c , and e :

$$\frac{hc}{2\pi e^2} = 8\pi \left(\frac{8\pi^5}{15} \right)^{1/3}. \quad (6)$$

It will be seen that the right side of this equation involves no physical measurements whatever. It has the value 137.348. The left side, which is Eddington's spectroscopic fine-structure constant $1/\alpha$, contains three physically measured quantities, and if the values $e=4.770 \times 10^{-10}$, $h=6.547 \times 10^{-27}$, and $c=2.99796 \times 10^{10}$ be inserted, *it yields 137.29 in exceedingly close agreement with the right side.*

This Lewis and Adams theoretical relationship is introduced here merely to emphasize the fact that if it is correct, then without recourse to any experiment at all the spectroscopic fine-structure constant—the left side of the foregoing equation—cannot possibly be a whole number, as contended by Eddington. Also, the remarkable agreement of the left side with the demands of the right side lends rather extraordinary experimental credentials to the Lewis and Adams relationship, although I believe that in other particulars it has not behaved itself so well.

But, turning next to experiment alone, what has it to say as to Eddington's suggestion that the spectroscopic constant $1/\alpha$ ought to be a whole number? The number he originally suggested was 136, but, as Birge pointed out, this suggestion was in irreconcilable conflict, first, with the oil-drop results on e ; second, independently of e , it was in conflict with Houston's and Babcock's determinations of the spectroscopic value of e/m ; and, third, it collided with Lewis and Adams' equation. The combined weight of this attack was so great that Eddington's suggestion could not possibly be entertained, provided the principle be admitted that the theorist cannot be permitted to ignore the facts in building his theories.

Quite recently, however, Eddington has changed the theoretical value of his fine-structure constant, still keeping it a whole number, but now

¹² G. N. Lewis and E. Q. Adams, *Phys. Rev.* **3**, 92 (1914).

¹³ A. S. Eddington, *Proc. Roy. Soc. A* **122**, 358 (1929).

making it 137^{14} instead of 136. This might perhaps remove the clash with my experimental oil-drop work, for if h were kept at 6.547 and e pushed up to 4.775—a change only a trifle outside the limits of my estimated experimental uncertainty— $1/\alpha$ would come down from 137.29 to 137. But quite independently of the oil-drop work on e , Eddington would still be in what appears to be an irreconcilable clash with the spectroscopic measurements on e/m and the following series of measurements on the ratio of h/e . To see this, write with Birge the spectroscopic equation in the following form:

$$R_{\infty} = \frac{\alpha^2 \left(\frac{e}{h} \right) 1}{2 \frac{e}{m}}.$$

This fits perfectly with $1/\alpha = 137.29$, $e = 4.770$, $h = 6.547$, and $e/m = 1.761$.

If, then, α^2 is to be pushed up the 0.42% necessary to make $1/\alpha$ equal to 137, then if e/h remains constant, e/m , spectroscopically determined, must go up 0.42%. But e/m , spectroscopically determined, and it is this mode of evaluation which obviously must be used for substitution in a spectroscopic equation, is now known to about one part in a thousand, for not only are both Babcock's and Houston's published determinations extraordinarily precise, but Houston and his associates inform me that the new independent determination that they are now making appears to check with the other two. If, then, there is no flexibility in e/m , the factor e/h must go down 0.42% or h/e up 0.42% to match the 0.42% rise in α^2 .

Now h/e has been determined by four different methods, none of which involve the properties of crystals: (1) the photoelectric method; (2) the ionizing potential method; (3) the c_2 , or Wien displacement-law method; and (4) the σ , or Stefan-Boltzmann-law method. *Not one of these methods will permit h/e to go up 0.42%.* The best result to date by the photoelectric method—which involves simply the equation $h\nu = eV$ —is probably my 1916 value of h/e for sodium; for the length of the line, the slope of which gives h/e , was several times greater than that used by other observers, and in addition the currents were large and stopping potentials accurately determined. The value of h as published both in my 1916¹⁵ and 1917¹⁶ papers, and in "The Electron"¹⁷ (1917) was $(6.56 \pm 0.03) \times 10^{-27}$, and this remains the value when absolute units, Michelson's new c , and $e = 4.770$ are used. Lukirsky and Prilezaev's recent determination¹⁸ made with the metals Al, Zn, Sn, Ni, Cd, Cu, and Pt yields a mean 6.543×10^{-27} , and there has just appeared a paper by Olpin¹⁹ which yields $h = 6.541 \times 10^{-27}$ "significant to three figures." I shall take the mean of these three, 6.560 and 6.543 and 6.541 namely 6.548, as the most probable value of h which combines with $e = 4.770$ to make the best photoelectric value of h/e .

¹⁴ A. S. Eddington, Proc. Roy. Soc. A126, 696 (1930).

¹⁵ Millikan, Phys. Rev. 7, 373 (1916).

¹⁶ Millikan, Phil. Mag. 34, 14 (1917).

¹⁷ Millikan, "The Electron" (1917), p. 227.

¹⁸ Lukirsky and Prilezaev, Zeits. f. Physik 49, 236 (1928).

¹⁹ A. R. Olpin, Phys. Rev. 35, 670 (1930).

The ionizing potential method, also involving merely $h\nu = eV$ is most accurately used by Lawrence,²⁰ who gets, corresponding to $e = 4.770$, the value $h = 6.560 \pm 0.015$.

I have nothing to add to Birge's estimates of h/e from the Wien Displacement Law method, which corresponds to $h = 6.548 \pm 0.015$. The equation here is $c_2 = hc/k$ where k is determined from, and is proportional to e , so that h/e has here the same error as c_2 and $c_2 = 1.432 \pm 0.003$ cm deg.

The Stefan-Boltzmann Law method does not yield h/e directly, but it does give, through Planck's equation, $h/k^{4/3} \propto \sigma^{1/3}$ and although the variation in the experimental values of σ is large, since the error in $h/k^{4/3}$, or $h/e^{4/3}$, is only one-third that in σ , I am willing to accept Birge's estimate that the probable error in the value of h corresponding to $e = 4.770$ as given by this method is $h = (6.539 \pm 0.010) \times 10^{-27}$.

The mean of the values 6.548, 6.560, 6.548, and 6.539 by these four methods is 6.549, which is very close to my 1917 value 6.547, and *the foregoing analysis shows how extraordinarily unlikely it is that h/e can go up the 0.42% necessary to permit $1/\alpha$ to be 137*, as Eddington wishes it to be, so that even when the theoretical evidence from Lewis and Adam's equation is entirely discarded the *experimental situation alone* renders it highly improbable that Eddington's conclusion can be correct.

If, however, the experimental credentials which have thus far developed for Lewis and Adam's relation are considered significant, then the values of e , h , and N are probably considerably more accurately known than the foregoing estimates of probable experimental error indicate. If both Eqs. (5) and (6) are to be considered correct, then, since (5) is of the form $h/e^{5/8} \propto 1/e/m$, and (6) of the form $h/e^2 = \text{constant}$, when I compare them with the experimental limits of error of h/e I find that the possible range of variation in e , h , and e/m is very small indeed, and I should then write the most probable values of e , h , and e/m as follows:

$$\begin{aligned} e &= (4.769 \pm 0.001) \times 10^{-10} \\ h &= (6.547 \pm 0.001) \times 10^{-27} \\ e/m &= (1.7595 \pm 0.001) \times 10^7. \end{aligned}$$

It will be interesting to see whether new experimental work can check this prediction as to the value of e/m .

However, in view of the theoretical uncertainty in Lewis and Adams' relation, I think it safer not to depend at all upon it, and hence to continue to write, as representing the best 1930 experimental situation, the 1917 values merely corrected for volts and for speed of light, namely,

$$\begin{aligned} e &= (4.770 \pm 0.005) \times 10^{-10} \\ h &= (6.547 \pm 0.010) \times 10^{-27} \\ N &= (6.064 \pm 0.006) \times 10^{-23}. \end{aligned}$$

²⁰ E. O. Lawrence, Phys. Rev. 28, 947 (1926).

THE UNIFORM POSITIVE COLUMN OF AN ELECTRIC DISCHARGE IN MERCURY VAPOR

BY THOMAS J. KILLIAN

THE MASSACHUSETTS INSTITUTE OF TECHNOLOGY, CAMBRIDGE, MASS.
and

THE RESEARCH LABORATORY, GENERAL ELECTRIC CO., SCHENECTADY

(Received January 11, 1930)

ABSTRACT

Uniform positive column of an electric discharge in mercury vapor. The uniform positive column was studied in a long circular cylindrical tube by means of the Langmuir probe electrode method. Measurements were made of the space potentials, random electron current densities, and the electron temperatures along the axis and across a diameter of the tube at vapor pressures ranging from 0.27 baryes to 7.13 baryes. The mobility of the electrons was obtained and the results interpreted in terms of the mean free path of the electrons by Langevin's expression for mobility.

($\mu = 0.75e\lambda/m\bar{v}$) These mean free paths were in fair agreement with those obtained in angular scattering experiments by other investigators. The rate of generation of positive ions per electron was obtained from measurements of the positive ion current to the walls and the total number of electrons per unit length of tube. With the probabilities of ionization for electrons of various velocities obtained by other observers, it is found that at vapor pressures above 1.4 baryes the ionization is accounted for by the direct impacts with neutral atoms of electrons whose velocity distribution is Maxwellian. At lower vapor pressures it seems necessary to assume the presence of a larger number of higher speed electrons than is present in a Maxwellian distribution. The ratio of the concentrations of electrons at any two points on a diameter satisfies the Boltzmann equation. As the temperature of the electrons is lowered from 38,000°K to 19,900°K by raising the pressure of the mercury vapor the energy delivered to the walls by the recombination of positive ions and electrons decreases from 48 percent to 14 percent of the total input. Since less than 0.03 percent is lost through elastic collisions of electrons and atoms the remainder of the energy goes into excitation.

I. INTRODUCTION

THE electrical conditions in an ionized gas are completely determined when the densities of the electrons and ions and their distributions of velocities are known at every point within the discharge. The velocity distributions must of course be known both in direction and magnitude. From the densities of the electrons, negative ions and positive ions, n_e , n_n , and n_p respectively, the variation of the electric field can be obtained by means of Poisson's equation. A single integration of this equation gives the field at any point while a double integration the potential at the point. The currents to and the potentials of the various electrodes and walls of the tube furnish the boundary conditions necessary for the complete solution. The current densities of the electrons and ions, I_e , I_n , and I_p , can be determined in any direction at any point from the densities of the electrons and ions and the laws of their distribution of velocities. It is not difficult to understand why

the behavior of some discharges is so complicated since any of the variables may vary in time as well as in space.

In order to gain a general idea of the mechanism of gaseous discharges an investigation should be made of the simplest sort of discharge. In the positive column conditions are primarily dependent upon the pressure and nature of the gas and the current carried by the discharge and not upon the nature and position of the electrodes and the walls of the tube. If, furthermore, the positive column be studied in a long circular cylindrical tube, conditions will not only be constant along its length but in the absence of any transverse magnetic field there will also be radial symmetry. The uniform positive column of a mercury arc was studied in such a tube by means of the Langmuir probe electrode method.^{1,2,3}

The most common type of velocity distribution occurring in nature is the random type known as the Maxwellian distribution. It has been found from an analysis of the volt-ampere characteristics of small electrodes placed in the positive column of a discharge that the free electrons move with a Maxwellian distribution of velocities in nearly random directions.^{1,2,4} A small electrode, placed in the discharge, will repel electrons from its neighborhood and collect positive ions when it is negatively charged. Electrons with energies greater than V_e , where V is the potential of the collector below that of the space and e the charge of an electron, can, however, reach the collector. As the potential of the collector is increased a greater number of the more slowly moving electrons will be collected. Since these electrons have a Maxwellian distribution of velocities the ratio of their concentrations in two regions differing in potential by an amount V is given by the Boltzmann equation

$$n'/n = e^{V_e/kT} \quad (1)$$

where k is the Boltzmann constant and T the temperature of the electrons. Since the velocity distribution is not affected by a retarding field the random current densities are in the same ratio as the electron concentrations. It is thus seen that the logarithm of the electron current to a small collector varies linearly with the voltage of the collector and that the rate of change of the logarithm of the electron current with respect to the voltage is e/kT , where e/k is 11,600 degrees per volt and T is the temperature of the electrons in degrees absolute. This relation is only true when the collector is negative with respect to the space. If the field is an accelerating one the current increases more slowly and according to different laws.³ Thus there is a transition at space potential. If the probe is a small one the break may be sharp enough to fix the space potential as in Fig. 5. When the collector is at space potential there is no sheath about it and its presence does not affect the discharge. Hence the random electron current, I_e , can be obtained by dividing

¹ I. Langmuir, Jour. Frank. Inst. 196, 751 (1923).

² I. Langmuir and H. Mott-Smith, Gen. Elec. Rev. 27, 449, 538, 616, 762, 810 (1924).

³ H. Mott-Smith and I. Langmuir, Phys. Rev. 28, 727 (1926).

⁴ I. Langmuir, Phys. Rev. 26, 585 (1925).

the electron current to the collector at this point by the area of the collector. According to kinetic theory the density of electrons in terms of their temperature and random current is given by

$$n_e = \frac{4I_e}{ev} = \left(\frac{2\pi m}{kT} \right)^{1/2} \frac{I_e}{e} = 4.03 \times 10^{13} \frac{I_e}{T^{1/2}} \quad (2)$$

where I_e is in amperes per cm^2 . There is a second method of finding the space potential which consists in analysing the electron current to a collector when it exerts an accelerating field.^{2,3}

Since the fields existing in the positive column are very small the density of positive ions is very nearly equal to that of the electrons, but due to their much higher mobility the electron current is from 200 to 400 times the positive ion current.

The positive ions do not appear to have a Maxwellian distribution of velocities but seem to obtain their velocities from the fields they move through after being formed.⁵ Therefore the positive ion current to a collector is a measure of the number of positive ions formed per second in a region drained by the collector and surrounded by a surface of maximum potential. This surface will be somewhat blurred due to the thermal energy of the positive ions which is probably very nearly equal to that of the gas molecules.

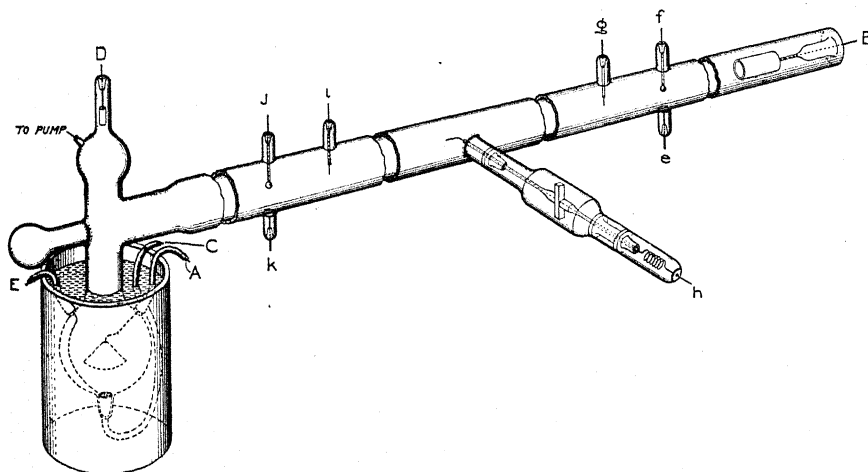


Fig. 1. Mercury vapor tube with various collectors.

II. METHOD

The tube used in the experiments is represented in Fig. 1. The long cylindrical portion in which the positive column was studied is 6.2 cm in diameter and 140 cm long. Anode *A*, which is above the pool of mercury which served as a cathode, is cone-shaped to prevent the blast of mercury from the cathode spot from affecting the pressure in the tube. Anode *B* consists of an

⁵ L. Tonks and I. Langmuir, *Phys. Rev.* **34**, 876 (1929).

open molybdenum cylinder 5.1 cm long and 3.18 cm in diameter. Probe wires *i* and *g*, 61.1 cm apart, are 3 mil tungsten wires of area 0.0311 cm^2 each. The nickel collectors *f* and *j*, 7.6 cm respectively from *g* and *i* are approximately spherical and of area 1.22 cm^2 and 1.15 cm^2 respectively. The disks *e* and *h* bent to conform with the curvature of the walls and fitting closely against them are each of area 1.99 cm^2 . The movable collector *h* consists of a 4 mil tungsten wire of 0.061 cm^2 area.* It can be moved by magnetic control across a diameter of the tube and also be turned to make any angle with the axis of the tube. In the present experiments it was kept parallel to the axis of the tube.

Before any experiments were made the electrodes were heated by means of a high-frequency coil and the tube allowed to run several days with a large current while being exposed to the radiation of several radiant heaters in order to drive out any water vapor or other occluded gases which might be present. Throughout all of the experiments the tube was being constantly exhausted by means of a two-stage Langmuir condensation pump and the vacuum was always such that a distinct click might be heard when the mercury was slowly raised in the McLeod gauge. The vapor pressure of the mercury in the tube was controlled by means of a water bath about the cathode bulb. When the temperature of the bath was above that of the room, mercury was prevented from condensing in the tube by means of small heating coils on each of the appendices and by exposing the whole tube to the radiant heaters.

In order to insure stable operation resistances were placed in series with *A* and with *B*. In all of the runs the current to *A* was held between 4 and 5 amperes. Sometimes a small current was drawn to *D* but the effect of this upon the stability was negligible. Complete voltage current characteristics were taken of each of the collectors at various vapor pressures. At each of these vapor pressures complete characteristics were made with *h* at different points across the tube.

Large rectangular coils, placed above and below the tube, furnished a means of obtaining a transverse magnetic field. The effects of this transverse field upon the positive column were studied and will be reported in a later paper. In the present experiments the current through the coils was only such as to cancel the effect of the earth's field.

III. EXPERIMENTAL RESULTS

Complete runs were made with the water bath about the cathode at 1.4°C , 18.6°C and 38.6°C . Using the methods of Langmuir and Mott-Smith² the random electron currents, electron densities and temperatures, and the

* After these experiments and others involving much higher current densities had been carried out, it was found that the probe wire *h* had been sputtered so that it varied from 0.0028 inches in diameter at one end to 0.004 inches at the bend into the glass tube. Since the experiments which would cause the most severe sputtering were performed after most of the runs reported here were made it is believed that the area of this probe wire was very close to 0.061 cm^2 when these runs were made.

space potentials were obtained from the semi-log plots of the electron current to the collector and the voltage of the collector for the probe wires i , g and h . Due probably to the small thickness of the sheaths about the probe wires better results were obtained by this method of analysis than from an analysis of the electron currents to the probe wires when they exert an accelerating field and the current to them is limited by orbital motion. In most of these runs the drift current through the tube, i_w , was held at 5 amperes. With smaller currents the agreement of the results obtained by each of the methods was very good. In each case the electron current to the collector was found by adding to the observed current the positive ion current to the collector at this voltage. This positive ion current was found by extrapolating to higher

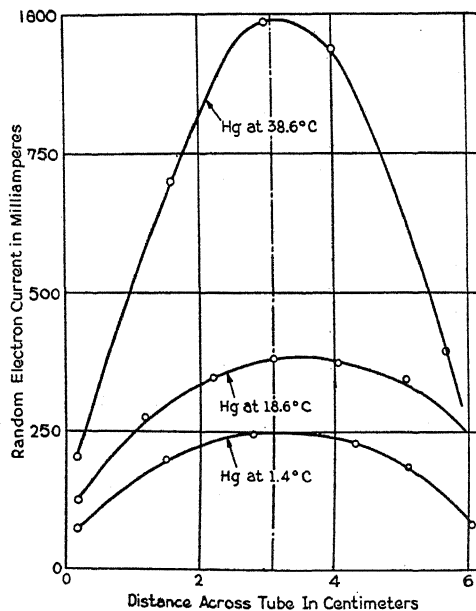


Fig. 2. Variation of the random electron current across the tube at different vapor pressures. Drift current, 5 amperes.

voltages the positive ion currents obtained at voltages so low that practically no electrons were collected.²

The vapor pressure of mercury was found from the data of Knudsen⁶ and also that of Poindexter.⁷ Since he has taken Knudsen's values at 0°C the values are very similar in the range here considered.

The positive ion current densities to the walls of the tube were obtained by plotting $(i_+)^{1/2}$ against $\nu^{1/2}$ where i_+ is the positive ion current to one of the disk-shaped collectors and $\nu = V^{3/2} [1 + 0.0247(T/V)^{1/2}]$. Here V is the voltage of the collector below that of the space and T is a factor which takes into account the initial velocities of the positive ions on entering the sheath and is about 10,000. If the positive ions had a Maxwellian distribution, T

⁶ Knudsen, Ann. d. Physik **29**, 179 (1909).

⁷ F. E. Poindexter, Phys. Rev. **26**, 859 (1925).

would correspond to their temperature in degrees absolute. Values of the shape factor equal to 1.36 ± 0.17 agreeing fairly well with the values Langmuir and Mott-Smith⁸ found were obtained over a thirty-fold range in vapor pressure.

In Fig. 2 the variation of the random electron current across the tube is represented as measured by h . It is seen that there is a large variation

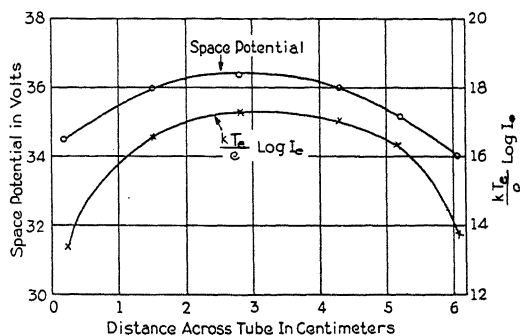


Fig. 3. Comparison of space potential with $kT_e/e \log I_e$. Cathode bulb at 1.4°C. p , 0.264 baryes.

in this random current. In Figs. 3 and 4 are the space potentials at these points. The electrons move in a retarding field in going from the axis of tube toward the walls. If their density at any point is determined by the Boltzmann equation the space potential curve should be identical with that of the variation of $kT_e/e \log I_e$ across the tube. It is seen that this is very

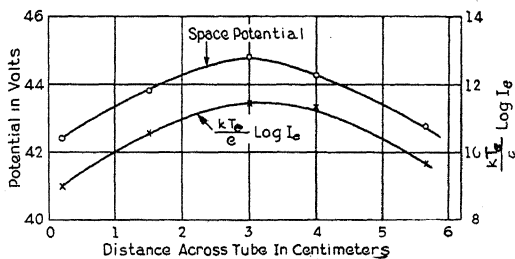


Fig. 4. Comparison of space potential curve with $kT_e/e \log I_e$. Cathode bulb at 38.6°C. p , 7.13 baryes.

nearly true at 38.6°C. Except for the points near the walls the agreement at 1.4°C is also within the experimental error. Also the semi-log plots of the voltage-current characteristics taken at different points along the diameter should lie on the same straight line as far as the space potential, where a break occurs. This is seen to be the case in Fig. 5. Here the cathode bulb was at 38.6°C where the best results were obtained.

⁸ I. Langmuir and H. Mott-Smith, Gen. Elec. Rev. 27 541 (1924).

IV. MOBILITY OF THE ELECTRONS

If the density of electrons at a distance r from the axis is n_e the total number of electrons per unit length of tube is

$$N_e = 2\pi \int_0^R n_e r dr \quad (3)$$

where R is the radius of the tube. If v_x is the average drift velocity of the electrons toward the anode the total electron drift current is

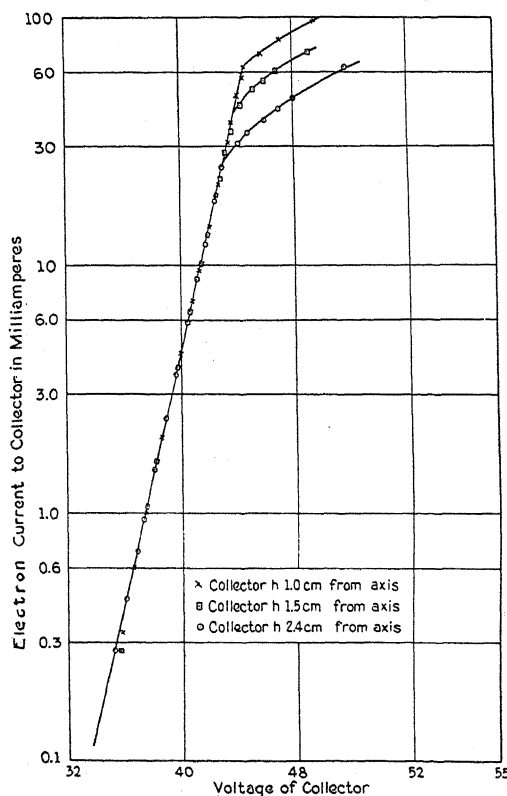


Fig. 5. Semi-logarithmic plot of the electron current to h against its voltage for various positions of h . Temperature of cathode bulb, 38.6°C . Drift current, 5 amperes.

$$i_- = N_e e v_x \quad (4)$$

Since the current carried by electrons is 300 or 400 times that carried by positive ions the current to the anode B , i_x , can be assumed to be equal to the electron drift current. The mobility of the electrons is given by

$$\mu_- = \frac{v_x}{X} = \frac{i_x}{N_e e X} \quad (5)$$

where X is the longitudinal potential gradient. Assuming the speed gained between successive collisions to be small compared with the average speed of the electrons Langevin⁹ has derived an expression for the mobility of electrons given by

$$\mu_- = 0.75e\lambda/m\bar{v} \quad (6)$$

where λ is the mean free path of the electrons in the gas, m the mass of an electron and \bar{v} the average speed.

Since $\bar{v} = (8kT/\pi m)^{1/2}$ it is possible to combine Eqs. (5) and (6) and obtain

$$\lambda = \frac{(8kTm)^{1/2}i_x}{0.75(\pi)^{1/2}N_e e^2 X} = 2.94 \times 10^9 \frac{i_x T^{1/2}}{N_e X} \quad (7)$$

where T is the temperature of the electrons in degrees absolute, i_x the drift current in amperes and X the longitudinal voltage gradient. N_e was obtained by a graphical integration of Eq. (3), n_e being found by means of Eq. (2). In Column 4 of Table I are the values of the mean free path of electrons in mercury vapor for three different vapor pressures. In reducing to λ_1 , the mean free path at 1 barye and 20°C, it was assumed that the temperature of the gas molecules was 50°C. The kinetic theory value of the mean free path (i.e. $4(2)^{1/2}$ times the mean free path of gas molecules) is usually taken to be about 20 cm at this temperature and pressure.¹⁰ Since, however, the mean free path is dependent upon the velocity of the electrons this value cannot be expected to apply very accurately.

TABLE I

Temperature of Cathode Bulb °C	Pressure of Hg baryes	T_e °K	λ from Eq. (7) cm	λ_1 cm	λ_1' from Eq. (8) cm
1.4	0.27	38,000	27.6	6.78	12.9
18.6	1.38	27,500	5.7	7.14	9.6
38.6	7.13	19,900	1.46	9.45	8.3

The angular scattering of low-velocity electrons in mercury vapor has been studied by various investigators whose results can be interpreted in terms of the mean free path of the electron.^{11,12,13,14} A comparison of the temperature of the electrons in Table I, Column 3, and λ_1 in Column 5 seems to show that as the velocity of the electrons is increased there is a small increase in the effective diameter of the molecules. Minkowski¹¹ seems to have observed this Ramsauer effect for electrons whose velocities were less than an equivalent volt. Beuthe,¹³ using the Ramsauer method, studied the absorption of low-velocity electrons and found that as the velocity decreased

⁹ Langevin, Ann. de Chemie et de Physique 81, 5, 245 (1905).

¹⁰ S. Dushman, Hochvakuumtechnik, 1926.

¹¹ R. Minkowski, Zeits. f. Physik 18, 258 (1923).

¹² L. R. Maxwell, Proc. Nat. Acad. Sci. 12, 509 (1926).

¹³ H. Beuthe, Ann. d. Physik 84, 949 (1928).

¹⁴ T. J. Jones, Phys. Rev. 32, 459 (1928).

the absorption increased to a maximum at about 3 volts and then fell off to about 1/6 of this maximum value at 1 volt. Jones¹⁴ using the Ramsauer and another method could find no evidence of this effect in mercury vapor. The results he obtained by his second method are very close to those obtained by Maxwell.¹² If the mean free path of an electron is given as a function of its velocity, i.e. $\lambda(v)$, then the mean free path of electrons with a Maxwellian distribution of velocities at a temperature T is given by

$$\lambda' = 4\pi \left(\frac{m}{2\pi kT} \right)^{3/2} \int_0^\infty e^{-mv^2/2kT} v^2 \lambda(v) dv. \quad (8)$$

Using the values of $\lambda(v)$ as found by Maxwell¹² and reducing the mean free paths found from Eq. (8) to the mean free path, λ'_1 , at 1 barye and 20°C it is seen by a comparison of these values in Column 6 with those in Column 5 that the two vastly different methods of obtaining the mean free path give results in fair quantitative agreement, although the free paths as obtained by each method vary differently with the temperature of the electrons.

One of the assumptions made in the derivation of Eq. (6) is that the speed gained between collisions is small compared with the average speed of the electrons. This is not true at the lower vapor pressures. The average distance the electrons move in the direction of the electric field between collisions, as Compton¹⁵ has shown is given by

$$s = \mu E \lambda / \bar{v} = 0.75 \lambda^2 e X / m \bar{v}^2. \quad (9)$$

The average energy gained between collisions is therefore $\Delta U = Xs$ and since $\bar{v}^2 = 0.849 c^2$ and $eU = \frac{1}{2} mc^2$ the average energy gained between collisions is

$$\Delta U = 0.441 \lambda^2 X^2 / U. \quad (10)$$

This varies from 1.5 percent of the average energy of the electrons when the cathode bulb is at 38.6°C to 12 percent when it is at 1.4°C. However, the degree of the agreement between the values of λ_1 and λ'_1 is an indication of the extent to which the simple classical kinetic theory considerations, which underlie the Langevin mobility equation and the calculation of the free path, are applicable to this case.

V. RATE OF GENERATION OF POSITIVE IONS

a. Experimental. If I_+ is the positive ion current density to the walls, the total positive ion current to the walls per unit length of tube is $2\pi R I_+$ and since the recombination of positive ions with electrons is negligible within the positive column, the number of ionizing collisions per electron per second is given by

$$\alpha = 2\pi R I_+ / e N_e. \quad (11)$$

The values of α as obtained from Eq. (11) are in row 8 of Table II.

b. Theoretical. Consider unit length of tube containing N_e electrons with a Maxwellian distribution of velocities corresponding to a temperature T . Let the gas in the tube have a pressure p and temperature T_g . An electron of

¹⁵ K. T. Compton, Phys. Rev. 22, 333 (1923).

velocity v has an energy of V volts where $\frac{1}{2}mv^2 = Ve$. The probability, P , of such an electron making an ionizing collision in going unit distance is dependent only upon the velocity of the electron and the nature and density of the gas. For an electron of velocity v the probability is given by $P = P'(n/n') = P'(pT'_g/p'T_g)$ where P' is the probability of an ionizing collision per cm path at pressure p' and temperature T'_g . These probabilities have been studied for different gases including mercury vapor by Compton and Van Voorhis¹⁶ and for mercury vapor by Jones¹⁷ and by von Hippel.¹⁸

The probability that an electron of velocity v will make an ionizing collision in one second is Pv . The number of electrons whose velocities lie between v and $v+dv$ is

$$N_e f(v) dv = 4\pi N_e \left(\frac{m}{2\pi kT} \right)^{3/2} v^2 e^{-mv^2/2kT} dv. \quad (12)$$

Hence, the number of positive ions formed per second by electrons whose velocities are between v and $v+dv$ is given by

$$N_e P f(v) v dv = 4\pi N_e \left(\frac{m}{2\pi kT} \right)^{3/2} P v^3 e^{-mv^2/2kT} dv. \quad (13)$$

If v be replaced by $(2Ve/m)^{1/2}$ the number of positive ions formed per second by electrons whose energies lie between V and $V+dV$ is found to be

$$N_e P F(V) dV = 8\pi N_e \left(\frac{m}{2\pi kT} \right)^{3/2} \frac{e^2}{m^2} P V e^{-eV/kT} dV. \quad (14)$$

In the case of mercury it has been found that the probability of ionization for electrons of less than 30 volts, varies linearly with the difference between the energy of the impinging electron and that required to ionize. Thus if V is less than V_i , P is zero but if V is greater than V_i but less than $3V_i$ we may write $P = \beta(V - V_i)$. Since, however, very few electrons have energies greater than $3V_i$ the total number of positive ions formed per second per cm is approximately

$$\nu_p = 8\pi N_e \left(\frac{m}{2\pi kT} \right)^{3/2} \frac{e^2}{m^2} \beta \int_{V_i}^{\infty} (V - V_i) V e^{-eV/kT} dV. \quad (15)$$

Integrating this expression and dividing by the total number of electrons per unit length of tube, the number of positive ions formed per second by each electron is found to be

$$\begin{aligned} \alpha' &= \beta \left(\frac{8kT}{\pi m} \right)^{1/2} e^{-eV_i/kT} \left(V_i + \frac{2kT}{e} \right) \\ &= 6.24 \times 10^5 \beta T^{1/2} e^{-eV_i/kT} \left(V_i + \frac{2kT}{e} \right) \end{aligned} \quad (16)$$

¹⁶ K. T. Compton and C. C. Van Voorhis, Phys. Rev. **26**, 436 (1925); **27**, 724 (1926).

¹⁷ T. J. Jones, Phys. Rev. **29**, 822 (1927).

¹⁸ A. von Hippel, Ann. d. Physik **87**, 1035 (1928).

In order to find out how much Eq. (16) is in error due to the fact that Eq. (15) is integrated to infinity, Eq. (15) may be integrated from $3V_i$ to infinity and the contribution to α' of electrons whose energies are greater than $3V_i$ found. This contribution, α'_1 , divided by α' gives the maximum relative error made in assuming that the expression for the probability holds to infinity. It is found that

$$\frac{\alpha'_1}{\alpha'} = e^{-2V_i e/kT} \left\{ \frac{(6eV_i^2/kT) + 5V_i + (2kT/e)}{V_i + (2kT/e)} \right\}. \quad (17)$$

Since $V_i = 10.4$ volts, α'_1/α' varies from 0.00018 for T equal to $20,000^\circ\text{K}$ to 0.033 for T equal to $40,000^\circ\text{K}$. Thus the error made in integrating Eq. (15) from V_i to infinity is small.

From the work of Compton and Van Voorhis¹⁶ β is given by $0.20 p/T_g$ while from that of Jones¹⁷ it is equal to $0.28 p/T_g$ where p is in baryes and T_g in degrees Kelvin. The values of α' as found by substituting these two values of β in Eq. (16) are in row 9 of Table II. It is seen that at higher vapor pressures the ionization within the positive column may be accounted for by the impacts with neutral atoms of electrons whose velocity distribution is Maxwellian. However at 1.4°C it would appear that only about 40 percent of the positive ions are produced by these electrons. At this low pressure with the mean free path of the electrons several times the diameter of the tube there is probably very little cumulative ionization.

A more acceptable explanation of the relatively large values of α found at low pressures as compared with the calculated values, is to assume that the excess ionization is due to "high-speed" electrons, not belonging to the Maxwellian group considered above. At 0.27 baryes the random current is only 4.3 times the drift current so that there are probably present more "high-speed" electrons than there would be if the electrons were moving in random directions with a Maxwellian distribution corresponding to $38,000^\circ\text{K}$.

In the experiments of Compton and Van Voorhis¹⁶ and also in those of Jones¹⁷ a measured current of electrons of a given speed was passed through an ionizing chamber and the number of positive ions produced measured. For electrons whose energies lay between 10 and 30 volts the effect of the fields necessary to collect the positive ions was less in the arrangement of Jones than in that of Compton and Van Voorhis.

When an electron ionizes an atom it will not only lose an amount of energy corresponding to the ionization potential but will in general divide its energy with the new electron formed. Then the average energy of the two electrons is half of the surplus energy. The impinging electron and that formed by ionization will be considered secondary electrons. The total surplus energy delivered per second to these secondary electrons is given by

$$W' = 8\pi N_e \left(\frac{m}{2\pi kT} \right)^{3/2} \frac{e^3}{m^2} \int_{V_i}^{\infty} PV(V - V_i) e^{-eV/kT} dV. \quad (18)$$

To find the average energy transferred per ionizing collision Eq. (18) is divided by the number of ionizing collisions per second and the average energy of the secondary electrons is found to be

$$\bar{V} = \frac{kT}{e} \left\{ \frac{eV_i + 3kT}{eV_i + 2kT} \right\}. \quad (19)$$

If \bar{V}_e is the average energy of the primary electrons ($e\bar{V}_e = 3kT/2$) the following results are obtained

$$\begin{array}{ll} T=0 & \bar{V}=0.667\bar{V}_e \\ T=10,000^\circ\text{K} & \bar{V}=0.714\bar{V}_e \\ T=40,000^\circ\text{K} & \bar{V}=0.797\bar{V}_e \\ T \rightarrow \infty & \bar{V} \rightarrow \bar{V}_e \end{array}$$

The secondary electrons would have a Maxwellian distribution of velocities if the probability of ionization were independent of the energy of the impinging electron. However, since this probability increases with the energy of the electrons there exists among the secondaries a surplus of higher-speed electrons and a deficiency of the lower-speed ones. Since the rate at which a Maxwellian distribution is reestablished among the electrons decreases with decreasing vapor pressures¹⁹ the discrepancies between the values of α and α' at 0.27 baryes may in part be due to this surplus of higher-speed electrons at this pressure.

TABLE II. Summary of results. Diameter of tube = 6.2 cm.

1. Bulb temperature	°C	1.4	18.6	38.6
2. Pressure of Hg vapor	baryes	0.27	1.38	7.13
3. Drift current	amperes	5.0	5.0	5.0
4. Longitudinal potential gradient (X)	volts cm ⁻¹	0.0932	0.196	0.311
5. Electron temperature (T)	°K	38,000	27,500	19,900
6. $2\pi \int_0^R n_e r dr$	N_e	11.1×10^{11}	21.8×10^{11}	45.7×10^{11}
7. Positive ion current density to the walls of tube (I_+)	milliamperes cm ⁻²	0.356	0.45	0.505
8. Rate of production of positive ions per electron from Eq. (11)	α	41,000	25,800	13,800
9. Rate of production of positive ions per electron from Eq. (16)	α'	14,600	16,900	12,600
	$\beta=0.20 p_0/T_0$	20,400	23,600	17,600
	$\beta=0.28 p_0/T_0$			
10. Random electron current in the direction of the axis ($2\pi \int_0^R I_{er} dr$)	amperes	21.5	35.8	64

* Tonks and Langmuir⁸ derive an expression for α for a cylindrical mercury discharge at low pressures gives by $\alpha = 703.1 T_e^{1/2}/R$. The values of α obtained by means of this expression are: at 1.4°C, 44,200; at 18.6°C, 37,500; at 38.6°C, 32,000.

VI. ENERGY BALANCE

The power input per unit length of tube is

$$W = Xi_x \quad (20)$$

¹⁹ A. F. Dittmer, Phys. Rev. 28, 507 (1926).

where X is as before the longitudinal potential gradient and i_z the drift current in the tube. Part of this energy is delivered to the walls by the recombination of positive ions and electrons, by the absorption of radiation and by the diffusion of metastable atoms to the walls and part goes into radiation which escapes from the tube. The total energy delivered to the walls by the recombination of a positive ion and an electron is the sum of the energy of recombination and the energies of the combining electron and positive ion. Since the electrons are moving in a retarding field their average energy expressed in volts is $2kT/e$. Therefore the total energy delivered to the walls per second by recombination is

$$W_r = 2\pi R I_+ (V_i + 2kT/e + \bar{V}_p) \quad (21)$$

where \bar{V}_p is the average energy of the positive ions. The positive ions acquire most of their energy in the sheath close to the walls. The potential of the walls must be such as to make the current of electrons equal to that of the positive ions. It is therefore that at which zero current flows to a small collector against the walls such as e or k . The potential of a point on the axis opposite e or k can be found from the longitudinal gradient and the space potentials at i or g . Thus the difference between the potentials of points on the axis and the walls opposite can be found. Combining this with the results obtained by means of collector h as given in Figs. 3 and 4 the total variation of potential across a diameter of the tube can be found. Since the temperature of the electrons is constant the rate of production of positive ions at any point is proportional to the electron density. The energy acquired by a positive ion from the time it is formed until it recombines at the walls is equal to the difference between the potentials at the point where it was formed and that at which it recombined. At very low vapor pressures when the probability of a collision is very small it will deliver all this energy to the walls. However, even if it does make collisions and lose energy to gas molecules they in turn will deliver it to the walls. As a first approximation the longitudinal potential gradient may be neglected and the average energy delivered to the walls due to the fields the positive ions move in is given by

$$\bar{V}_p = \frac{2\pi\alpha \int_0^R n_e V_r r dr}{2\pi\alpha \int_0^R n_e r dr} = \frac{2\pi \int_0^R n_e V_r r dr}{N_e} \quad (22)$$

where V_r is the difference between the potentials at r and R and n_e is the electron density at r . \bar{V}_p was obtained graphically from Eq. (22) and found to vary from 7.3 volts at 38.6°C to 14.5 volts at 1.4°C. The fraction of the power input delivered to the walls ($F_r = W_r/W$) by the recombining ions and electrons is in the fourth column of Table III. It is seen that this fraction increases rapidly with the temperature of the electrons.

By multiplying the frequency of collisions between electrons and gas molecules by the average loss of energy per electron per elastic collision the energy lost by the electrons per second through elastic collisions can be found.

When the energy of electrons is much greater than that of the gas molecules Compton¹⁵ has shown that the average fraction of energy lost at an elastic collision is $2m_e/M$. Using the values of mean free paths as found from Eq. (7) and given in column 4 of Table I, the fraction, F_e , of the power input delivered by the electrons to the gas molecules by elastic collisions was found. It is seen from column 5 of Table III that this energy is very small and may be neglected.

TABLE III. Fraction of power input delivered to the walls by the recombination of positive ions and electrons. Arc current = 5 amperes.

Temp. of cathode bulb °C	Temp. of electrons T °K	Power input per unit length W watts	Fraction to walls F_r	Fraction to gas molecules by elastic impacts F_e
1.4	38,000	0.466	0.483	2.8×10^{-5}
18.6	27,500	0.98	0.233	4.0×10^{-5}
38.6	19,900	1.55	0.136	2.5×10^{-4}

In order to obtain a rough idea of the efficiency of excitation it may be assumed that the remainder of the energy input goes into raising the mercury atoms from the normal 1^1S_0 to the 2^3P_1 state, which excitation requires 4.9 volts. This state is between the two metastable states 2^3P_0 at 4.66 volts and 2^3P_2 at 5.43 volts. Making this assumption the average number of resonance collisions per electron per second, α_r , and per atom per second, a_r , can be found. These values are given in the third and fourth columns of Table IV. Using the values of the mean free path found by means of Eq. (7) the probability of ionization, P'_i , and that of resonance, P'_r , can be obtained. These values are given in the fifth and sixth columns of Table IV.

TABLE IV

Temp. of cathode bulb °C	Temp. of electrons °K	Number of resonance collisions per electron per second α_r	Number of resonance collisions per atom per second a_r	Probability of ionization on collision P'_i	Probability of excitation on collision P'_r
1.4	38,000	2.78×10^6	1690	0.0091	0.063
18.6	27,500	4.41×10^6	1030	0.0014	0.024
38.6	19,900	3.74×10^6	354	0.00023	0.0062

Few data are available on the probability of excitation on collision in mercury vapor. Sponer²⁰ found the average efficiency to be about 0.004 for the excitation of mercury atoms by electrons of from 5 to 6 volts energy. Using a different value for the total number of impacts made by the electrons Hertz²¹ recalculated her results and obtained 0.03 for the average efficiency.

VII. DISCUSSION OF RESULTS

The free electrons in the uniform positive column move in nearly random directions with a Maxwellian distribution of velocities. This distribution

²⁰ H. Sponer, *Zeits. f. Physik* **7**, 185 (1921).

²¹ G. Hertz, *Zeits. f. Physik* **32**, 298 (1925).

is being continually disturbed by the loss of higher-speed electrons to the walls and by excitation and ionization. This continuous loss of energy by the electrons is supplied to the drift current by the longitudinal field and in some manner is transferred to the electrons so that they keep their Maxwellian distribution. No satisfactory explanation of the mechanism by which this distribution is maintained has yet been offered. There is evidence that it may be due to oscillations.^{22,23} In any event it has been shown that the temperature corresponding to this distribution of velocities is one of the most important characteristics of the discharge. It determines the ionization and excitation efficiencies of the electrons. Furthermore, since the electrons have a Maxwellian distribution of velocities their concentrations satisfy the Boltzmann equation.

The mobility of the electrons was measured and by means of the Langevin equation the results were interpreted in terms of the mean free path of the electrons. Over a twenty-five fold range of vapor pressures the mean free paths found in this way, when reduced to the values at 1 barye and 20°C, were within 30 percent of each other. It was true even when the mean free path appeared to be five or six times the diameter of the tube. This is probably because the electrons make specular reflections at the walls. Their momentum is unchanged except for the component perpendicular to the walls, which is reversed.

The rate of production of positive ions seems to be accounted for by direct impacts with neutral atoms of the higher-speed electrons of the Maxwellian group when the vapor pressure is greater than 1.4 baryes. At 0.27 baryes only about one half of the ionization can be accounted for in this way. The small ratio of the random to the drift current probably accounts for the additional high-speed electrons.

It is seen that as the temperature of the electrons is lowered from 38,000°K to 19,900°K by raising the pressure the percentage of the energy delivered to the walls by the recombination of positive ions and electrons decreases from 48 to 14.

There are several sources of error in this work which are difficult to eliminate. The space potentials are probably accurate to within two-tenths of a volt. The random electron currents may be in error due to the fact that some electrons are reflected when the collector is at space potential. However, the results of Farnsworth²⁴ show that this coefficient of reflection must be very small under these conditions. The electron temperatures in the tube were usually within 1500°K of each other as measured by any collector during a run. It is therefore believed that the probable error is within five percent.

The author wishes to express his appreciation for the many suggestions and kind assistance of Dr. I. Langmuir and Dr. L. Tonks of the Research Laboratory of the General Electric Company at Schenectady where this work was done. He is also grateful for the considerable aid rendered by Professor K. T. Compton of Princeton University.

²² I. Langmuir, *Proc. Nat. Acad. Sci.* **14**, 627 (1928).

²³ L. Tonks and I. Langmuir, *Phys. Rev.* **33**, 195 (1929).

²⁴ H. E. Farnsworth, *Phys. Rev.* **25**, 41 (1925).

ABSORPTION OF RESONANCE RADIATION IN MERCURY VAPOR

BY ANCIL R. THOMAS

VALPARAISO UNIVERSITY, VALPARAISO, INDIANA

(Received April 8, 1930)

ABSTRACT

The theories of absorption in mercury vapor of mercury resonance light of wave-length 2536.7A as formulated by Malinowski and H. A. Wilson are briefly reviewed. It is well established that the absorption coefficient for resonance radiation increases as the number of absorbing atoms decreases. This is probably due to a Doppler effect in the radiating vapor. To diminish the influence of the Doppler effect a jet of mercury vapor was used, and the resonance radiation coming from it was investigated. A series of measurements of the absorption coefficient of this light is given. The maximum atomic absorption coefficient observed is 10.22×10^{-13} , nine times as large as any previously observed. It is shown that Malinowski's assumptions are not in accord with the observed effects.

INTRODUCTION

A NUMBER of people^{1,2,3,4,5,6} have investigated the properties of mercury resonance light of wave-length 2536.7A since it was first discovered by R. W. Wood.⁷ The writer⁸ assisted in one such investigation in which the atomic absorption coefficient was measured. The atomic absorption coefficient, γ , is defined by the equation

$$I = I_0 e^{-\gamma n_a} \quad (1)$$

where I_0 is the intensity of the light as it enters the cell, I the intensity as it leaves it and n_a is the number of absorbing atoms per cm^2 of the cell. As the number of absorbing atoms changed from 1.35×10^{12} to 87.6×10^{12} per cm^2 of the absorption cell the atomic absorption coefficient changed from 11.2×10^{-14} to 2.53×10^{-14} . Several investigators have observed this variation in the absorption coefficient. The cause appears to be the non-homogeneity of the resonance line for in the case of a perfectly homogeneous radiation γ should be constant. Consequently, the values of γ are to be regarded only as average values for the atoms involved.

¹ A. v. Malinowski, Ann. d. Physik **44**, 935 (1914).

² C. Fuchtbauer, G. Joos, and O. Dinkelacker, Ann. d. Physik **71**, 222 (1923).

³ W. Orthmann, Ann. d. Physik **78**, 601 (1925).

⁴ F. Goos and H. Meyer, Zeits. f. Physik **35**, 803 (1926).

⁵ M. Schein, Ann. d. Physik **85**, 257 (1928).

⁶ P. Kunze, Ann. d. Physik **85**, 1013 (1928).

⁷ R. W. Wood, Phil. Mag. **23**, 696 (1912).

⁸ A. L. Hughes and A. R. Thomas, Phys. Rev. **30**, 466 (1927).

FORMER THEORIES

The Doppler effect predominates among the various effects⁹ proposed to account for the width of spectrum lines, particularly when the pressure is low, as it is in mercury vapor at room temperature. It has been shown that the visibility in interference patterns^{10,11} is the same as one would expect if the entire width were due to the Doppler effect.

The shift in wave-length $\delta\lambda$ due to the Doppler effect is given by

$$\frac{\delta\lambda}{\lambda} = \frac{v}{c} \quad (2)$$

from which we get that

$$v = \frac{c\delta\lambda}{\lambda} = \beta\delta\lambda \quad (3)$$

where β is a constant. The number of atoms with any particular component of velocity along the line of emission is given by the formula from kinetic theory,

$$dn = Ke^{-v^2/\alpha^2} dv. \quad (4)$$

The intensity, dI , of the light at any particular wave-length, separated from the center of the line by a wave-length difference $\delta\lambda$, is proportional to the

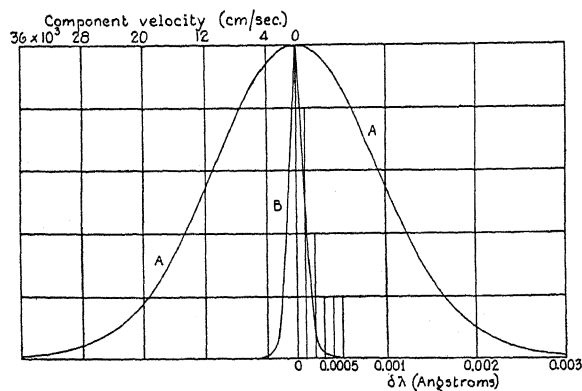


Fig. 1. Distribution of energy in the resonance line. Curve A shows the distribution in the ordinary resonance line, curve B, the distribution in the line used in this experiment.

number of atoms, dn , which have the proper component of velocity, v , to give this wave-length. We then have that

$$dI \propto dn \propto e^{-v^2/\alpha^2} dv \propto e^{-(\beta\delta\lambda)^2/\alpha^2} d(\delta\lambda) \quad (5)$$

⁹ Rayleigh, Phil. Mag. 29, 274 (1915).

¹⁰ A. A. Michelson, Astrophys. J. 3, 251 (1896).

¹¹ Buisson and Fabry, Jour. d. Physique 2, 442 (1912).

where ν and also $\delta\lambda$ varies from $-\infty$ to $+\infty$. This distribution is shown graphically in Fig. 1, curve *A*, when the emitting vapor is at a temperature of 293°K.

Malinowski¹, assuming this line form, has worked out an expression for I/I_0 in terms of n_a (see Eq. (1)). He also assumes that the ability of the atoms in an infinitely thin layer to absorb light of any particular wavelength will be given by

$$k_\nu = k_0 e^{-\nu^2/\alpha^2} \quad (6)$$

where k_0 represents the ability of the atoms to absorb the very center of the line. This equation results from assuming that an atom in the absorption cell can absorb light only near the wave-length which it, itself, can emit, and also that this band over which it can absorb light is very narrow with respect to the entire line. (If, in accordance with the strict quantum theory, we suppose that the correspondence between $\delta\lambda$ and ν must be exact it is evident that there can be no absorption for as we narrow down the velocity range in which an atom must be in order to absorb light of a particular wavelength the number of atoms available for such absorption approaches zero.¹²) On these assumptions Malinowski shows that the absorption coefficient for the very center of the line is the square root of two times the observed value for a cell which is infinitely thin. The atomic absorption coefficient for the very center of the line should, then, also be the square root of two times the observed value for a very thin cell. A reasonable extrapolation of the values secured by Hughes and Thomas gives $\gamma = 12 \times 10^{-14}$ for an infinitely thin layer of vapor and $\gamma_0 = 17 \times 10^{-14}$. If his ideas are correct, it is evident that, if the importance of the Doppler effect could be reduced greatly, the observed atomic absorption coefficient should approach γ_0 , that is, the square root of two times the former value observed for an infinitely thin layer of atoms. Also the coefficient should remain constant for all cell thicknesses.

H. A. Wilson¹³ has also proposed a theory which is applicable in this case. He assumed that the atom absorbs as a simple linear oscillator, the equation of motion of which may be taken to be

$$m\ddot{x} + k\dot{x} + \mu x = Fe \quad (7)$$

where m is the mass of the vibrating particle, k the viscous resistance to the motion at unit velocity, μ a constant, F the electric intensity in the light at the atom, which may be taken as equal to $F_0 \cos pt$, e the charge on the particle and x the displacement of the particle. From this he deduces that

$$\gamma = \frac{\gamma_0}{1 + (4m^2/k^2)q^2} \quad (8)$$

where γ_0 is the atomic absorption coefficient for exact resonance, γ that for a departure from exact resonance given by a frequency difference q (which

¹² A. L. Hughes and A. R. Thomas, *Phys. Rev.* **30**, 472 (1927).

¹³ H. A. Wilson, *Proc. Roy. Soc. A* **118**, 362 (1928).

corresponds to $\delta\lambda$ as used above). He then assumed that the energy distribution in the incident line was given by $Ae^{-\beta^2 a^2}$ which is the form appropriate for a Doppler effect but does not demand this explanation for the finite width of the line. With this added he shows that

$$\gamma_0 = \frac{1}{(n_a)^{1/2}} \left(\log \frac{I_0}{I} \right) \frac{m}{\beta k} \quad (9)$$

when n_a is not too small. Wilson showed that this fitted Hughes and Thomas' results when n_a was greater than about 10^{13} . It is implied in the derivation of Eq. (8) that the emission line is broader than the absorption line.

Both theories predict that if the width of the resonance line could be reduced the observed absorption coefficient should increase and Malinowski's work specifies the amount of this increase. Also according to Malinowski the absorption coefficient should not change with cell thickness. An experimental test of these predictions is described on the following pages.

DISTRIBUTION OF ENERGY IN INCIDENT LIGHT

The most feasible method of reducing the width of the resonance line which presented itself was to use a jet of mercury vapor as a source of resonance light. If the light is taken out at right angles to the jet the component velocities of the atoms in the line of emission will be quite small. The jet was diaphragmed so that five degrees was the maximum angle that any atom's path could make with the line of centers of the diaphragms. The distribution of energy in the radiation from such a jet was computed and the results plotted graphically in Fig. 1, curve *B*. While this distribution curve cannot be represented accurately by a curve of the form e^{-v^2/α^2} , we may, however, find a curve of this form which is roughly superposable on the distribution curve, and so find a value for the "most probable velocity," α , in a direction perpendicular to the jet. This turns out to be about one tenth of the value of the most probable velocity in isotropic mercury vapor at room temperature. This means that laterally its effective temperature as measured by the component velocity of the atoms is about 0.31 times its real temperature, that is 90°K .

APPARATUS AND PROCEDURE

The source of light was a vertical quartz mercury arc. It was kept cool by circulating distilled water around it. Ice was kept in the water most of the time to prevent heating. The current for the arc was supplied by a generator floating across a bank of storage batteries. A preliminary test showed that about four amperes through the arc gave the greatest amount of light from the resonance lamp. The central part of the arc was deflected to the front of the tube by an electro-magnet excited by the same current that was used in the arc. Under these circumstances the arc ran very steadily. No fluctuations could be noticed in the course of an entire day's work.

The light from this arc was focused into a resonance lamp constructed of Pyrex glass shown in Fig. 2. *A* is a cross section, *B* is a vertical section.

Light, not absorbed in the jet, continued into the horn, H_1 , (see Fig. 2A) where it was lost by multiple reflection. The resonance light taken out through the window, W , had the horn H_2 as a background so that any stray light returning from H_1 could not get out in the same direction as the resonance light. The most careful tests made showed no light of this sort whatever. An intensity much less than one percent of the resonance light could have been detected. The jet (see Fig. 2B) was diaphragmed as shown, the upper diaphragm being merely a slight constriction in the tube. The walls of the tube were cooled with solid CO_2 as was the reentrant tube, R , on which the mercury in the jet condensed. A heater, T , to increase the strength of the jet was not used as the jet proved to be quite strong enough without it.

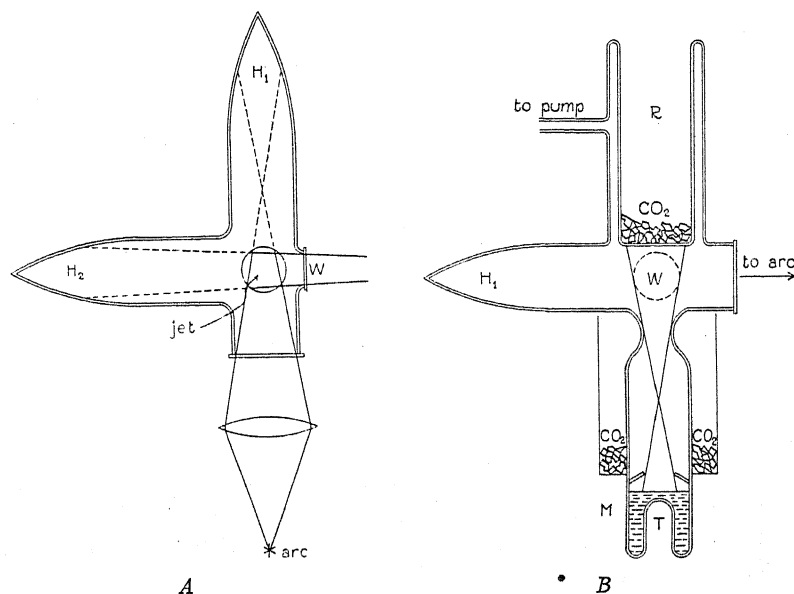


Fig. 2. The resonance lamp used. A is a cross section, B, a vertical section.

Moreover the amount of stray vapor, the atoms of which were moving at random, was greatly increased by heating the mercury. In the final experiment practically the whole of the lamp was surrounded by solid CO_2 in order to diminish the amount of stray vapor as much as possible. In a former unpublished investigation¹⁴ with potassium a method for securing quite strong jets was developed. A diaphragm was placed very near the liquid metal surface, M , and the walls of the tube were kept cool as close down to this diaphragm as possible. By this method it was possible to secure jets several times as strong as is possible with the metal in the bottom of just a straight tube with no diaphragm near the surface of the liquid metal.

The remainder of the apparatus was arranged as in Fig. 3. The resonance light passed through the absorption cell C , on through a quartz lens L , a

¹⁴ Done with L. C. Van Atta.

variable rotating shutter S , and into a photoelectric cell. The active material in the photoelectric cell was aluminum. It was filled with helium to about one mm pressure after the surface had been sensitized by a discharge through hydrogen as is done in making an alkali hydride surface. A potential of 200 volts was used on the cell. The sensitivity to mercury resonance radiation was about seventy five times that of the untreated vacuum cell. The absorption cell, C , consisted of a glass tube 1.622 cm long to which quartz windows were sealed. A side tube contained a drop of mercury. The pressure in the cell and thus the number of absorbing atoms was controlled by cooling the side tube. The absorption cell was fixed so that it could be shifted

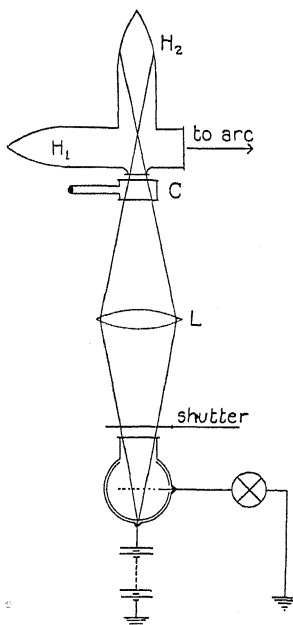


Fig. 3. Arrangement of the apparatus.

out of the beam and the electrometer current secured without the cell. The transmission of the cell was approximately matched by the variable rotating shutter and the actual transmission secured by interpolation. The mercury was all frozen out of the cell and its transmission secured by the same method as well as by comparing it with a previously calibrated screen. The transmission was 0.69. Calling the amount of light getting through the cell with the side tube cooled by solid CO_2 I_0 , and the amount at any other temperature I then the fraction transmitted by the vapor will be I/I_0 .

RESULTS

The experimental values for I/I_0 are shown in Fig. 4 plotted against the temperature of the side tube. A smooth curve was drawn through the experimental points and values read off this for purposes of computation. These

values are listed in Table I. The temperatures of the side tube are listed in column one and the corresponding values for I/I_0 in column two. The next column gives the values of the natural logarithms of I_0/I .

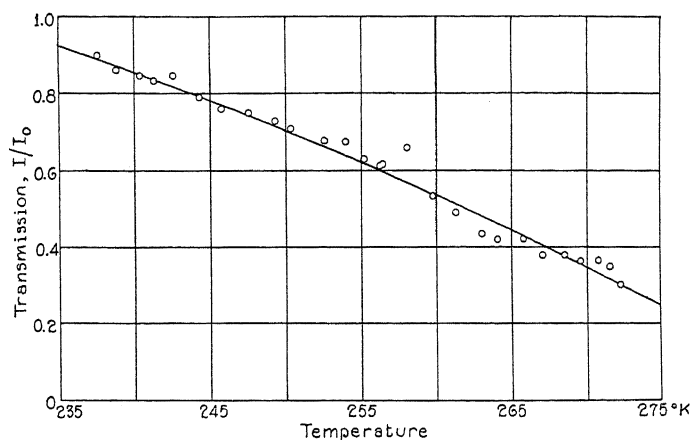


Fig. 4. Ratio of transmitted to incident radiation for various temperatures of mercury vapor.

To determine the atomic absorption coefficient we have to calculate the number of atoms involved in the absorption in each case. This must be calculated from the pressure. The fourth column gives the pressures of the

TABLE I.

Temp. °K	I/I_0	$\log I_0/I$	p in side tube in mm	p in cell in mm	n_a	γ
235	0.915	0.0888	1.45×10^{-6}	1.62×10^{-6}	8.71×10^{10}	10.22×10^{-13}
240	0.862	0.1484	3.09	3.41	18.36	8.08
245	0.792	0.2332	6.30	6.89	34.06	6.29
250	0.715	0.3355	12.3	13.3	71.63	4.68
255	0.628	0.4652	23.2	24.9	133.8	3.48
260	0.538	0.6200	42.8	45.4	244.4	2.54
265	0.444	0.8118	76.2	80.1	431.0	1.88
270	0.344	1.0671	133.	139.	745.3	1.43
275	0.240	1.4271	228.	235.	1266.	1.13

mercury vapor in the side tube for the corresponding temperatures recorded in the first column. The vapor pressures of mercury at different temperatures given in the International Critical Tables were used in this computation. As the same absorption cell was used which Hughes and the writer used in their former investigation the relations deduced at that time can be used. The pressure, p , in the absorption cell and the pressure, p_m , in the side tube are connected by the relation

$$\frac{p}{p_m} = \left(\frac{T}{T_m} \right)^{1/2} \quad (10)$$

where T and T_m are the temperatures of the absorption cell and the side tube respectively. The pressures in the absorption cell, as corrected by this equation, which takes care of thermal transpiration, are listed in column five.

The number of absorbing atoms, n_a , per cm^2 of the cell is connected with the pressure, p , by the equation

$$n_a = (5.38 \times 10^{16})p. \quad (11)$$

The values of n_a are listed in column six. The atomic absorption coefficient, γ , is calculated according to Eq. (1) and listed in column seven. This is an average value for all the atoms present in the absorption cell although it is not absolutely certain that they are all active in absorbing the light.

The atomic absorption coefficient which, according to Malinowski's theory, should have been almost constant for all values of n_a , is shown plotted against n_a in Fig. 5, curve *A*, along with the values of the atomic

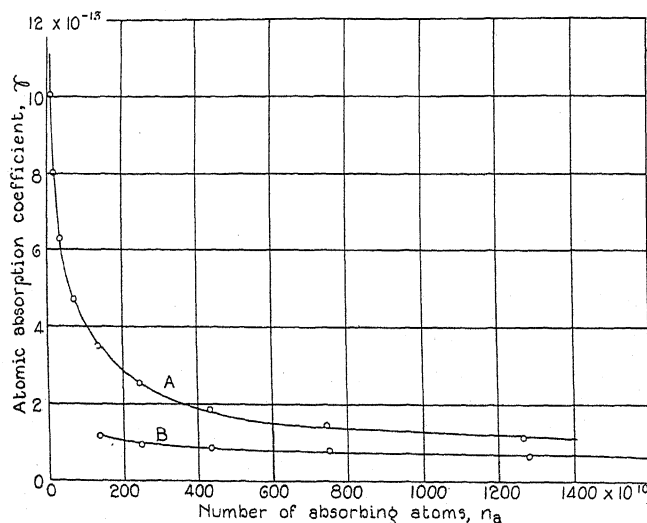


Fig. 5. Variation of the atomic absorption coefficient with the number of absorbing atoms. *A* is the curve secured in this experiment, *B*, that secured by Hughes and Thomas.

absorption coefficient from the previous work, curve *B*. The coefficient is definitely not a constant and it is certainly several times greater than the square root of two times any possible extrapolation of the former curve to an infinitely thin cell.

TABLE II.

n_a	$\frac{1}{(n_a)^{1/2}} \log_e \frac{I_0}{I}$	$\frac{(n_a + 6 \times 10^{10})^{1/2}}{n_a} \log_e \frac{I_0}{I}$
8.71×10^{10}	3.01×10^{-7}	3.91×10^{-7}
18.36	3.46	3.99
34.06	3.83	4.13
71.63	3.96	4.13
133.8	4.02	4.11
244.4	3.97	4.01
431.0	3.91	3.94
745.3	3.91	3.92
1266.	4.01	4.02

According to H. A. Wilson's theory, $1/(n_a)^{1/2} \log I_0/I$ should be constant for values of n_a which are not too small. These values are tabulated in Table II column 2. It is seen that they are practically constant for values of n_a greater than about 50×10^{10} . Wilson also proposed an empirical expression which is constant for all values of n_a and by means of which γ for an infinitely thin cell can be deduced. It is

$$\frac{(n_a + K)^{1/2}}{n_a} \log_e \frac{I_0}{I} = C. \quad (12)$$

It is seen that it goes over into the theoretical relation when n_a is large. Values of C are tabulated in Table II, column 3. From it γ for the infinitely thin cell is given by $C/K^{1/2}$ which for this case is 16.33×10^{-13} . This is thirteen times greater than the value secured (1.25×10^{-13}) when the same relation is applied to the results of Hughes and Thomas and about sixty per-cent greater than the maximum experimental value obtained in this experiment, (viz. 10.22×10^{-13}).

DISCUSSION

As the light from the jet is much more absorbable than that from an ordinary resonance lamp the distribution of energy in the line must be very different from the ordinary distribution, certainly the line must be much more homogeneous, probably as homogeneous as light from a discharge tube cooled in liquid air (disregarding, for the moment, the fact that actually all the atoms would be condensed). It would seem from this that the Doppler effect controls emission for no other effect presents itself which will be affected by the jet sufficiently to explain, even qualitatively, the observed effects. It is evident that Malinowski's assumption that the absorption and emission lines have the same width is not justified for we do not get his predicted results. A consideration of these results points to the conclusion that the emission line must be wider than the absorption line, otherwise the absorption coefficient would not increase rapidly as the number of atoms, n_a , diminishes. Since there are good reasons, already mentioned, for believing that the width of the emission line is determined by the Doppler effect, we must, therefore, conclude that, because the absorption line is apparently narrower than the emission line, the width of the absorption line is not controlled by the Doppler effect. It appears, since H. A. Wilson's theory applies to these results, that we may consider the mercury atoms, as far as absorption goes, behaving like simple linear oscillators. It does not seem possible, at present, to interpret the results of these absorption experiments in such a way as to give a satisfactory and consistent picture of the processes involved in emission and absorption of resonance radiation.

The above work was done at Washington University, St. Louis, Mo. The writer wishes to thank Dr. A. L. Hughes for especial assistance and advice given during the course of the experiment. Also he wishes to thank Mr. C. A. Reinhart, instrument maker, for help in the construction of apparatus.

THE DISPERSION FORMULA AND RAMAN EFFECT
FOR THE SYMMETRICAL TOP

BY MORRIS MUSKAT

THE GULF COMPANIES, PITTSBURGH, PA.

(Received March 28, 1930)

ABSTRACT

Schroedinger's theory of dispersion is applied to the symmetrical top. The dipole of the top is assumed to lie along the axis of symmetry, and the wave-length of the incident light to be large as compared with the dimensions of the top. An explicit expression is derived for the index of refraction of a gas composed of symmetrical tops, as a function of the frequency of the incident light. As the perturbed eigenfunction is a linear function of only 3 unperturbed eigenfunctions, the dispersion formula, for a given state, consists of only 2 terms.

The moments for the Raman effect transitions for the symmetrical top are also computed. Simple closed expressions are obtained, again because of the simplicity of the perturbed eigenfunctions. The polarization of the Raman variations is computed with the result that the unshifted lines are unpolarized whereas for the shifted lines: $|m_z|^2/|m_x|^2 = 4/3$.

THE importance of the symmetrical top for the interpretation of molecular spectra makes it of interest to derive the dispersion formula and Raman effect intensities for this mechanical system. Kronig and Rabi,¹ Reiche and Rademacher,² Manneback,³ and Condon,⁴ have developed the theory of the unperturbed state of the top, and its Stark and Zeeman effects. However, explicit expressions have not been yet given for the interaction of the top with time varying fields.

As a mechanical system, the top is defined by the fact that two of its moments of inertia are equal to A , and are unequal to the moment of inertia, C , about the axis of symmetry. It is considered as a rigid system. A dipole, of moment μ , lies along the axis of symmetry and interacts with a small periodic field, $E_0 \cos 2\pi\nu t$, directed along the Z axis, fixed in space.

The wave mechanical treatment of dispersion and Raman transitions is well known, being given originally by Schroedinger.⁵ This treatment in which the dispersion phenomena are considered as pulsating Stark effects, is valid if the wave-length of the incident light is large as compared to the dimensions of the atomic or molecular system; the application made here will also assume that we are dealing with relatively long wave-lengths.

¹ Kronig and Rabi, *Phys. Rev.* **29**, 262 (1927).

² Reiche and Rademacher, *Zeits. f. Physik* **39**, 444 (1926); **41**, 453 (1927).

³ Manneback, *Phys. Zeits.* **28**, 72 (1927).

⁴ Condon, *Phys. Rev.* **30**, 781 (1927).

⁵ Schroedinger, *Ann. d. Physik* **81**, 109 (1926).

THE DISPERSION FORMULA

We may begin with the well-known expression for the "partial density" to be associated with two states, j and j' , of the system perturbed by the radiation:

$$\begin{aligned} \psi_j \psi_{j'}^* = e^{2\pi i/h(W_{j'} - W_j)t} & \left[u_{j'} u_{j'}^* + e^{2\pi i \nu t} \left\{ u_{j'}^* \sum_r c_{jr}^+ u_r + u_j \sum_r c_{j'r}^* u_r^* \right\} \right. \\ & \left. + e^{-2\pi i \nu t} \left\{ u_{j'}^* \sum_r c_{jr}^- u_r + u_j \sum_r c_{j'r}^{*+} u_r^* \right\} \right]. \end{aligned} \quad (1)$$

In this equation, W_j is the eigenvalue of the unperturbed j state, and u_j is the corresponding unperturbed eigenfunction. The c_{jr} are proportional to the matrix elements of that part of the potential energy of the system that is due to the perturbing field. The * indicates the complex conjugate. If we refer the top to the Eulerian angles θ , ϕ , and χ , the c_{jr} in our case are given by:

$$\begin{aligned} c_{jr}^\pm &= \frac{-\mu E_0 A C^{1/2}}{2(W_j - W_r \pm h\nu)} \int_0^{2\pi} \int_0^{2\pi} \int_0^\pi u_j u_r^* \cos \theta \sin \theta d\theta d\phi d\chi \\ &\equiv \frac{-\mu E_0 z_{jr}}{2(W_j - W_r \mp h\nu)}. \end{aligned} \quad (2)$$

Following Manneback, the eigenfunctions u_j may be expressed as:

$$u_j \equiv u_{jnm} = e^{i(n\chi + m\phi)} y_{jnm}(x), \quad (3)$$

where n , m are quantum numbers associated with χ and ϕ , $x = \cos \theta$, and the y_{jnm} are an orthogonal set of functions satisfying the equation:

$$\frac{d}{dx} \left[(1-x^2) \frac{dy_{jnm}}{dx} \right] - \frac{m^2 - 2mnx + n^2}{1-x^2} y_{jnm} + j(j+1) y_{jnm} = 0. \quad (4)$$

n and m are integral and range independently from $-\infty$ to $+\infty$; j is integral and $\geq |n|$, $|m|$. Furthermore, the y_{jnm} satisfy a recurrence relation of the form:

$$x y_{jnm} = A(jnm) y_{j+1,nm} + B(jnm) y_{jnm} + C(jnm) y_{j-1,nm}. \quad (5)$$

It follows, then, that in our case the c_{jr} vanish unless the values of n and m are the same for both states j and r . They also vanish unless $|j-r| \leq 1$.

When in Eq. (1) we set $j'=j$, we have the "density" determining the dispersion produced by the (jnm) state. The form of (3) and the above remarks about the c_{jr} permit us to rewrite Eq. (1) in the form:

$$\psi_j \psi_j^* = u_j u_j^* + 2 \cos 2\pi \nu t \left[u_j^* \sum_r u_r (c_{jr}^+ + c_{jr}^-) \right]. \quad (6)$$

In this equation the values of n and m are the same in all the terms and hence are omitted from the subscripts. The dispersion moments are now:

$$m(jnm) = m_z = \mu \int \cos \theta \psi_j \psi_j^* d\tau. \quad (7)$$

The moments $m_x = \mu \int \sin \theta \psi_i \psi_i^* d\tau$ and $m_y = -\mu \int \cos \theta \sin \theta \psi_i \psi_i^* d\tau$ are obviously zero. Introducing the matrix elements z_{jr} , defined in Eq. (2), we get for the time varying part of m_z in which alone we are interested:

$$m(jnm) = 2\mu^2 E_0 \cos 2\pi\nu t \sum_r z_{jr}^2 \frac{(W_j - W_r)}{h^2\nu^2 - (W_j - W_r)^2}. \quad (8)$$

Now it may be shown from the formulae given by Manneback that the coefficients in Eq. (5) have the following values:

$$A(j, n, m) = \frac{1}{j+1} \left(\frac{\{(j+1)^2 - m^2\} \{(j+1)^2 - n^2\}}{(2j+1)(2j+3)} \right)^{1/2};$$

$$B(jnm) = \frac{mn}{j(j+1)}.$$

$$C(jnm) = A(j-1, n, m).$$

These give the explicit values of the only non-vanishing matrix elements z_{jr} , which are, clearly:

$$z_{j, j+1} = A(jnm); \quad z_{j, j} = B(jnm); \quad z_{j, j-1} = C(jnm). \quad (10)$$

Recalling that the eigenvalues of the symmetrical top are given by:

$$\frac{8\pi^2 A}{h^2} W_{jnm} = j(j+1) + \left(\frac{A}{C} - 1 \right) n^2, \quad (11)$$

and setting $\eta = -8\pi^2 A\nu/h$, we finally get for m_z :

$$m_z = \frac{32\pi^2 \mu^2 A E_0}{h^2(2j+1)} \cos 2\pi\nu t \left[\frac{\{(j+1)^2 - n^2\} \{(j+1)^2 - m^2\}}{(j+1)(2j+3) \{4(j+1)^2 - \eta^2\}} - \frac{(j^2 - n^2)(j^2 - m^2)}{j(2j-1)(4j^2 - \eta^2)} \right]. \quad (12)$$

As the state (j, n) has a $2j+1$ fold degeneracy in the quantum number m , we must use for our dispersion formula the average of m_z over m , i.e. the value: $\bar{m}_z = (1/2j+1) \sum_{m=-j}^{+j} m_z$. And noting that $\sum m^2 = j(j+1)(2j+1)/3$, where $|m| \leq j$, we get:

$$\bar{m}_z = \frac{32\pi^2 \mu^2 A E_0}{3h^2(2j+1)} \cos 2\pi\nu t \left[\frac{(j+1)^2 - n^2}{4(j+1)^2 - \eta^2} - \frac{(j^2 - n^2)}{4j^2 - \eta^2} \right]. \quad (13)$$

For the state: $j=0$, we must use:

$$\bar{m}_z = m_z = \frac{32\pi^2 \mu^2 A E_0 \cos 2\pi\nu t}{3h^2(4 - \eta^2)}. \quad (13a)$$

We therefore have the result that the index of refraction, r , for a gas in which there are N molecules, of the type of the symmetrical top, per unit volume, and all of which are in the (j, n) state, is given by:

$$\frac{r^2 - 1}{r^2 + 2} \cong \frac{r^2 - 1}{3} \cong \frac{2}{3}(r - 1) = \frac{128\pi^3\mu^2AN}{9h^2(2j+1)} \left[\frac{(j+1)^2 - n^2}{4(j+1)^2 - \eta^2} - \frac{j^2 - n^2}{4j^2 - \eta^2} \right]. \quad (14)$$

For an ensemble of molecules with a thermal equilibrium distribution the index of refraction will be:

$$r^2 - 1 = \frac{128\pi^3\mu^2AN}{3h^2} \frac{\left[\frac{1}{4 - \eta^2} + \sum_{-\infty}^{+\infty} n \sum_{|n|}^{\infty} j \left\{ \frac{(j+1)^2 - n^2}{4(j+1)^2 - \eta^2} - \frac{j^2 - n^2}{4j^2 - \eta^2} \right\} e^{-W_{jn}/kT} \right]}{\sum_{-\infty}^{+\infty} n \sum_{|n|}^{\infty} j(2j+1) e^{-W_{jn}/kT}} \quad (14a)$$

If we denote $h/8\pi^2A$ by ν_k , and if we put in the value of W_{jn} from Eq. (11), (14a) may be rewritten as:

$$r^2 - 1 = \frac{256\pi^3\mu^2NA}{3h^2} \frac{\sum_{-\infty}^{+\infty} n \sum_0^{\infty} p \left\{ \frac{(|n|+p)^2 - n^2}{4(|n|+p)^2 - (\nu/\nu_k)^2} \right\} \sin h - \frac{h\nu_k}{kT} (|n|+p) e^{-h\nu_k/kT \{ (A/C-1)n^2 + (|n|+p)^2 \}}}{\sum_{-\infty}^{+\infty} n \sum_0^{\infty} p (2|n| + 2p + 1) \exp - \left\{ \left(\frac{A}{C} - 1 \right) n^2 + \{ |n| + p \} (|n| + p + 1) \right\} \frac{h\nu_k}{kT}} \quad (15)$$

These formulae are simply special cases of the Kramers-Heisenberg general dispersion formula. And as is to be expected, the two terms in (14) are those corresponding to the only two possible transitions, involving radiation, from the (jnm) state of the unperturbed top.

THE RAMAN TRANSITIONS

To get the intensities of the Raman effect radiations we must compute the moments:

$$m_z = \mu \int \cos \theta \psi_{jnm} \psi_{j'n'm'}^* d\tau \quad (16)$$

$$m_x \pm im_y = \mp \mu i \int \sin \theta e^{\pm i\phi} \psi_{jnm} \psi_{j'n'm'}^* d\tau. \quad (17)$$

From (1), (3) and our remarks about the c_{jr} we immediately get the following selection rules:

$$\left. \begin{aligned} m_z(jnm; j'n'm') &= 0, \text{ unless: } n' = n; m' = m. \\ m_x + im_y(jnm; j'n'm') &= 0, \text{ unless: } n' = n; m' = m + 1. \\ m_x - im_y(jnm; j'n'm') &= 0, \text{ unless: } n' = n; m' = m - 1. \end{aligned} \right\} \quad (18)$$

We may now express the form of the moments as:

$$m(jnm; j'n'm') = \mu e^{2\pi i/h(W_{j'} - W_j)t} \left[q_{jj'} + e^{2\pi i\nu t} \left\{ \sum_r (c_{jr}^+ q_{rj'} + c_{j'r}^- q_{jr}) \right\} + e^{-2\pi i\nu t} \left\{ \sum_r (c_{jr}^- q_{rj'} + c_{j'r}^+ q_{jr}) \right\} \right] \quad (19)$$

where for m_z , $q_{jj'} = z_{jj'}$, as defined in Eq. (2); and for $m = m_x \pm im_y$, $q_{jj'} = \mp i \int \sin \theta e^{\pm i\phi} u_j u_{j'}^* d\tau$. The problem that remains is that of obtaining the values of the $q_{jj'}$ and putting them into Eq. (19).

From Eqs. (2) and (10) we see that the only non-vanishing moments m_z are: $m_z(j; j \pm 2)$ and $m_z(j; j \pm 1)$. Upon putting into (19) the values of the matrix elements as given in Eqs. (9) and (10), we get for these moments:

$$m_z(j; j+2) = \frac{-8\pi^2 \mu^2 E_0 A e^{+2\pi i/h(W_{j+2,n} - W_{j,n})t}}{h^2(j+1)(j+2)(2j+3)} \left(\frac{\{(j+2)^2 - n^2\} \{(j+2)^2 - m^2\} \{(j+1)^2 - n^2\} \{(j+1)^2 - m^2\}}{(2j+1)(2j+5)} \right)^{1/2} \left[\frac{e^{2\pi i \nu t}}{\{\eta - 2(j+1)\} \{2(j+2) - \eta\}} - \frac{e^{-2\pi i \nu t}}{\{2(j+2) + \eta\} \{2(j+1) + \eta\}} \right] \quad (20)$$

$$m_z(j; j+1) = \frac{\mu e^{2\pi i/h(W_{j+1,n} - W_{j,n})t}}{j+1} \left(\frac{\{(j+1)^2 - m^2\} \{(j+1)^2 - n^2\}}{(2j+1)(2j+3)} \right)^{1/2} \left[1 - \frac{16\pi^2 \mu E_0 A m n}{h^2 j(j+2)} \left\{ \frac{e^{2\pi i \nu t}}{\eta \{\eta - 2(j+1)\}} + \frac{e^{-2\pi i \nu t}}{\eta \{\eta + 2(j+1)\}} \right\} \right]. \quad (21)$$

$m_z(j; j-2)$ is to be obtained from $m_z(j; j+2)$ by replacing j by $j-2$ and taking the conjugate; and similarly we get $m_z(j; j-1)$ from $m_z(j; j+1)$ by replacing j by $j-1$ and taking the conjugate.

To evaluate the matrices $q_{jj'}$ from $m_x \pm im_y$ we have to compute integrals of the form: $\int_0^\pi \sin^2 \theta y_{jnm} y_{j'n'm'} d\theta$. For this purpose we make use of the results of Reiche and Rademacher. If we compare the present notation with theirs we find that we have the following relation for the integrals in question:

$$4\pi^2 AC^{1/2} \int_0^\pi \sin^2 \theta y_{jnm} y_{j'n'm'} d\theta = 2L_{a,b,l} / (J_{a,b,l} J_{a',b',l'})^{1/2} \quad (22)$$

where the $L_{abl, a'b'l'}$ and J_{abl} are integrals evaluated by Reiche and Rademacher, the latter being normalization integrals. The parameters a, b, l , are defined by:

$$a = |m+n|; b = |m-n|; l = j - \frac{a+b}{2}.$$

In addition to the selection rules of Eq. (18) we must take account of the four following cases possible for the change: $|m' - m| = 1$.

- a) $\Delta a = +1; \Delta b = +1$; b) $\Delta a = +1; \Delta b = -1$; c) $\Delta a = -1; \Delta b = +1$; d) $\Delta a = -1; \Delta b = -1$.

The Δ_s refer to the difference of the value of the parameter between the primed and unprimed states. Different integrals $L_{a,b,l, a'b'l'}$ must be used for these four cases. It turns out, however, that all four cases give the same final result, so that here only case a will be considered.

For this case, we have, according to Reiche and Rademacher:

$$L_{a+1, b+1, l'} = 0 \text{ for } l' < l-2 \text{ and } l' > l. \quad (23)$$

The non-vanishing integrals have the values:

$$\begin{aligned} & \frac{L_{a, b, l}}{a+1, b+1, l} / (J_{a, b, l} J_{a+1, b+1, l})^{1/2} \\ = & \frac{1}{2l+a+b+2} \left(\frac{(l+a+1)(l+b+1)(l+a+b+1)(l+a+b+2)}{(2l+a+b+1)(2l+a+b+3)} \right)^{1/2} \\ & \frac{L_{a, b, l}}{a+1, b+1, l-1} / (J_{a, b, l} J_{a+1, b+1, l-1})^{1/2} \\ = & \frac{(b-a)(l(a+b+l+1))^{1/2}}{(2l+a+b)(2l+a+b+2)} \quad (24) \\ & \frac{L_{a, b, l}}{a+1, b+1, l-2} / (J_{a, b, l} J_{a+1, b+1, l-1})^{1/2} \\ = & \frac{1}{(2l+a+b)} \left(\frac{l(l-1)(l+b)(l+a)}{(2l+a+b-1)(2l+a+b+1)} \right)^{1/2}. \end{aligned}$$

In these formulae, the following values of the parameters are to be used:

For: $m' = m+1$, $a = n+m$, $b = m-n$, $l = j-m$.

For: $m' = m-1$, $a = -n-m$, $b = n-m$, $l = j+m$.

When these substitutions are made in the values of the integrals and finally in Eq. (17), the results are the following:

$$\begin{aligned} m_x \pm im_y = & \frac{j'=j+2}{h^2(j+1)(j+2)(2j+3)} \left(\frac{\{(j+2)^2-n^2\} \{(j+1)^2-n^2\} \{(j+1)^2-m^2\}^{1/2}}{(2j+1)(2j+5)} \right) \\ & \cdot ((j+m+3)(j \pm m+2))^{1/2} \left\{ \frac{e^{2\pi i \nu t}}{\{\eta-2(j+1)\} \{2(j+2)-\eta\}} - \frac{e^{-2\pi i \nu t}}{\{\eta+2(j+1)\} \{\eta+2(j+2)\}} \right\} \\ m_x \pm im_y = & \frac{j'=j+1}{(j+1)} \mp i \mu e^{2\pi i/h(W_{j+1, n} - W_{j, n})t} \left(\frac{\{(j+1)^2-n^2\} (j \pm m+2)(j \pm m+1)^{1/2}}{(2j+1)(2j+3)} \right) \\ & \left[1 \mp \frac{8\pi^2 \mu A E_0}{h^2 j(j+2)} n(j \pm 2m) \left\{ \frac{e^{2\pi i \nu t}}{\eta \{\eta-2(j+1)\}} + \frac{e^{-2\pi i \nu t}}{\eta \{\eta+2(j+1)\}} \right\} \right] \\ m_x \pm im_y = & \frac{j'=j-2}{h^2(j-1)(2j-1)} \pm \frac{8\pi^2 \mu^2 i A E_0 e^{2\pi i/h(W_{j-2, n} - W_{j, n})t}}{(2j-3)(2j+1)} \left(\frac{\{(j-1)^2-n^2\} (j^2-n^2)(j^2-m^2)(j \mp m-1)(j \mp m-2)^{1/2}}{(2j-3)(2j+1)} \right) \\ & \left[\frac{e^{2\pi i \nu t}}{(2j+\eta) \{2(j-1)+\eta\}} + \frac{e^{-2\pi i \nu t}}{\{2j-\eta\} \{2(j-1)-\eta\}} \right] \quad (25) \end{aligned}$$

The value for $j' = j-1$, is to be obtained from that for $j' = j+1$ by replacing in the expression for the latter j by $-j-1$.

As in the case of m_x , all the moments $m_x \pm im_y$ vanish for which $|j-j'| \geq 3$. It should be noted that as $m_x - im_y = 0$, for $m' = m+1$, $m_x + im_y = 2m_x = 2im_y$; and as $m_x + im_y = 0$, for $m' = m-1$, $m_x - im_y = 2m_x = -2im_y$.

Formally, we can express the general moment $m(jnm; k'n'm')$ as:

$$m(j; k) = m(\nu_{jk}) e^{2\pi i \nu_{jk} t} + m(\nu + \nu_{jk}) e^{2\pi i (\nu + \nu_{jk}) t} + m(\nu - \nu_{jk}) e^{-2\pi i (\nu - \nu_{jk}) t} \quad (26)$$

where $m(\nu)$ is the moment oscillating with the frequency ν , and $\nu_{jk} = (W_k - W_j)/h$. To get the intensities of transitions for these particular

frequencies, we must pick out from the general expression of Eq. (26) the "partial moments" oscillating with that frequency. We thus see immediately that all the $m(\nu_{jk})$ vanish for $|\Delta j| = 2$. This simply means that there is no "unshifted" Raman lines for such transitions; and this is to be expected, since there are no spontaneous transitions for the unperturbed top, for which $|\Delta j| = 2$. To get the total intensities we must know the squares of the resultant moments, given by:

$$R(\nu) = |m_x(\nu)|^2 + |m_y(\nu)|^2 + |m_z(\nu)|^2 \quad (27)$$

From the previous equations we find that:

$$\left. \begin{aligned} R(\nu + \nu_{j,i+2}) &= \frac{64\pi^4 \mu^4 A^2 E_0^2 \{ (j+2)^2 - n^2 \} \{ (j+1)^2 - n^2 \} \{ (j+1)^2 - m^2 \}}{h^4 (j+1)^2 (2j+3)^2 (j+2)(2j+1) \{ \eta - 2(j+1) \}^2 \{ 2(j+2) - \eta \}^2} \\ R(\nu + \nu_{j,i+1}) &= \frac{64\pi^4 \mu^4 A^2 E_0^2 n^2 \{ (j+1)^2 - n^2 \} \{ j^4 + 3j^3 + 2j^2 - 2j^2 m^2 + 9m^2 + 3m^4 \}}{h^4 (j+1)^2 j^2 (2j+1)(2j+3)(j+2)^2 \eta^2 \{ \eta - 2(j+1) \}^2} \\ R(\nu_{j,i+1}) &= \frac{\mu^2 \{ (j+1)^2 - n^2 \}}{(2j+1)(j+1)} \\ R(\nu + \nu_{j,i-2}) &= \frac{64\pi^4 A^2 E_0^2 \mu^4 \{ (j-1)^2 - n^2 \} \{ j^2 - n^2 \} \{ j^2 - m^2 \}}{h^4 j^2 (j-1)(2j-1)(2j+1)(2j+\eta)^2 \{ 2(j-1) + \eta \}^2} \end{aligned} \right\} \quad (28)$$

In the above, the values of R are not listed for the Raman lines of frequency $\nu - \nu_{jk}$. But these may be obtained from those given by replacing η by $-\eta$ wherever it occurs. It may be noted that the values of R for the unshifted lines are independent of m ; this is in agreement with the observation of Reiche and Rademacher that none of the squared moments of the unperturbed top depend on m .

We have finally to sum the given values of R over m , since the unperturbed top is degenerate with respect to m . Using the value of

$$\sum_{|m| \leq j} m^4 = \frac{j}{15} (j+1)(2j+1)(3j^2 + 3j - 1)$$

we get

$$\begin{aligned} I(\nu + \nu_{j,i+2}) &\equiv \sum_{|m| \leq j} R(\nu + \nu_{j,i+2}) \\ &= \frac{64\pi^4 \mu^4 A^2 E_0^2 \{ (j+2)^2 - n^2 \} \{ (j+1)^2 - n^2 \}}{3h^4 (j+1)(j+2)(2j+3) \{ \eta - 2(j+1) \}^2 \{ 2(j+2) - \eta \}^2} \\ I(\nu + \nu_{j,i+1}) &= \frac{448\pi^4 \mu^4 A^2 E_0^2 n^2 \{ (j+1)^2 - n^2 \}}{15h^4 j (j+1)(j+2) \eta^2 \{ \eta - 2(j+1) \}^2} \\ I(\nu_{j,i+1}) &= \frac{\mu^2 \{ (j+1)^2 - n^2 \}}{(j+1)} \\ I(\nu + \nu_{j,i-2}) &= \frac{64\pi^4 \mu^4 A^2 E_0^2 \{ (j-1)^2 - n^2 \} \{ j^2 - n^2 \}}{3h^4 j (j-1)(2j-1)(2j+\eta)^2 \{ 2(j-1) + \eta \}^2} \end{aligned} \quad (29)$$

For $j' = j - 1$, we replace the values of j in the expression for I for $j' = j + 1$ by $-j - 1$ and change the sign. Again, the values for I for $\nu - \nu_{jk}$ are to be obtained from the above by replacing η by $-\eta$, wherever it occurs.

These formulae permit a computation of the intensities of any Raman line emitted or absorbed by a gas whose molecules are of the type of symmetrical tops.

It is of interest to note that in none of these formulae for the Raman moments or for the dispersion by a single state, does the moment of inertia C enter. This might be expected, however, since as observed by Manneback, C does not enter in the corresponding formulae of the Stark effect, and our dispersion theory deals essentially with a pulsating Stark effect. But to formally remove the effect of the moment of inertia C we must make $n = 0$. This makes the top equivalent to the three dimensional rotator. And in fact, putting $n = 0$, in our dispersion formulae reduces them to those derived by Debye⁶ for the rotator. When we put in $n = 0$ in the expression for the Raman moments we see that there will be no Raman lines, with the shift in frequency, for the transitions occurring in the unperturbed state of the rotator; on the other hand, there will be the shifted Raman lines for the transitions that violate the selection rule of the unperturbed rotator, and which are induced by the incident light. This fact may be considered as a special case of the same rule which has been shown by a number of authors to hold in the rotational fine structure of the Raman spectra of diatomic molecules.

Finally we may compute from Eqs. (20), (21), and (25) the polarization of the Raman radiations. The result is that for the unshifted lines we get:

$$|m_x|^2 = |m_y|^2 = |m_z|^2. \quad (30)$$

For the shifted lines, however, we do get a polarization, given by:

$$|m_x|^2 = |m_y|^2 = \frac{3}{4} |m_z|^2. \quad (30a)$$

The writer is indebted to Dr. A. E. Ruark for the opportunity of discussing with him questions arising in this problem.

⁶ Debye; *Polar Molecules*, p. 165.

THE LOCATION OF THE ELECTROMOTIVE FORCE IN
THE PHOTOVOLTAIC CELL

BY W. NORWOOD LOWRY

DEPARTMENT OF PHYSICS, CORNELL UNIVERSITY

(Received April 8, 1930)

ABSTRACT

1. A method was developed to utilize a 4-element vacuum tube to measure small potential differences.
2. The so called photovoltaic e.m.f. appears to be a modification of the electrolyte with light, there being no indication of any effect due to the direct illumination of the electrode or the boundary region between the electrode and the electrolyte.
3. In certain types of experiments with these cells, current measurements cannot be regarded as a quantity proportional to e.m.f.
4. The e.m.f. of the photovoltaic cell increases with the concentration of the electrolyte.

INTRODUCTION

IT IS well known that when two similar electrodes are placed in a suitable electrolyte and one of the electrodes is illuminated while the other is kept in the dark, an e.m.f. is produced. Goldmann¹ attributed the phenomena to a photoelectric effect arising from the illumination of the boundary between the electrode and the electrolyte. Grumbach² introduced near one electrode of a dark cell a small amount of previously irradiated electrolyte and obtained an effect, thus showing that the e.m.f. produced was due, at least in part, to a change or modification of the electrolyte with light.

Murdock³ devised a means whereby the electrolyte flowed by the electrode in such a way that the electrolyte could be irradiated before, while, or after flowing by the electrode, and like Grumbach found the effect largely due to some change in the electrolyte. But in addition having found that the steady state current increased suddenly when the electrode first entered the edge of the illuminated region, he was led to believe that there might be some effect superimposed upon that due to photo-chemical change, when the boundary between the electrode and the electrolyte was irradiated.

Subsequent workers^{4,5} have felt that certain variations in their results might arise from an effect other than the photochemical change of the electrolyte.

The original purpose of this present work was to devise a means of finding some of these variations if they existed, and, if found, to study them.

¹ A. Goldmann, *Ann. d. Physik* **27**, 449 (1908).

² A. Grumbach, *Comptes Rendus* **176**, 88 (1923).

³ C. C. Murdock, *Proc. Nat. Acad. Sci.* **12**, 504 (1926).

⁴ W. Rule, *Proc. Nat. Acad. Sci.* **14**, 272 (1928).

⁵ H. W. Russell, *Phys. Rev.* **32**, 667 (1928).

APPARATUS AND GENERAL DISCUSSION

The apparatus used in the first part of this investigation has been patterned after that of Murdock,⁶ but with some modifications. Briefly, platinum electrodes in the form of long narrow strips were sputtered diametrically opposite on the outside of a pyrex test tube 18×150 mm. Pyrex was used as it was found less likely to crack than the soft glass test tubes, when copper wires were soldered to the top of the platinum films. The sputtered films were about 130×6 mm. After the Cu wires were soldered, the test tubes were covered with bakelite lacquer down to about 8 mm from the end of the film. This left the electrode itself exposed, with dimensions of about 8×6 mm. The rest of the platinum film served only as a conducting lead to the soldered wire. Except for very thin electrodes the platinum leads were the same density as the electrodes, as it was found that cells made in this way stood up over longer periods than those previously used,³ due to the tendency of the bakelite lacquer (used to insulate the lead from the electrolyte) to chip off from the glass with the thicker films, and that higher resistance was not objectionable, in making e.m.f. measurements.

Considerable care was taken with the sputtering process, a special sputtering jar being designed so as to eliminate as far as practicable the occlusion of undesirable gases in the films. A G.E. 10 kv, 100 m.a. D.C. generator was used, which permitted very close control of current and voltage while sputtering. The test tubes were first thoroughly cleaned. After sputtering they were aged slowly by heating to a temperature ranging between 300–360°C for several hours; then they were slowly cooled, lacquered, dried in air, and baked at 135°C. Of the 32 cells made in this way, only a few were found, when first tried, to have a dark e.m.f. of such a magnitude as to prohibit their use.

The test tube was slipped over a vertical brass tube covered with felt so as to hold the test tube snugly, but permit of its rotation about the brass tube. A small rectangular window was cut in the lower end of the brass tube, and a beam of light, caused to pass down the brass tube, was reflected through the window by means of a mirror placed at a 45° angle just behind it. By turning the test tube, the electrode, which was slightly smaller than the window, could be brought directly in front of the window, or on either side of it, through a range of more than 180°, and by a suitable scale and index the position of the electrode in respect to the window could be determined. The test tube was placed in a cylindrical glass bottle (painted black to exclude external light) containing the electrolyte, rhodamine B in absolute alcohol. The mouth of the bottle was just large enough to give about 2 mm clearance around the test tube, in order to reduce evaporation. This bottle was mounted on a rotator, driven by a synchronous motor through a reduction gear, assuring constant speed of rotation. The bottle with its electrolyte thus rotated concentrically about the test tube with its electrodes.

⁶ C. C. Murdock and D. W. Murdock, *Trans. of the Faraday Soc.* **23**, part 5, 593 (1927).

Filters were used to vary the intensity of illumination. They consisted of photographic plates exposed for different lengths of time and developed in the usual manner. The transmission of the filters as well as the electrodes was measured photometrically. In every case the light passed through a water cell to remove the infra red radiation.

All concentrations of electrolyte are given as percent of rhodamine B by weight in absolute alcohol.

Using a similar cell, Murdock obtained the curve previously published³ by plotting the current against the position of the electrode in respect to the window. The current was measured by a high sensitivity galvanometer in series with a suitable resistance, after a steady state had been obtained. He pointed out that his results were in agreement with Grumbach's,² but that the change in slope of the curve at the points where the electrode began to be directly illuminated indicated that some effect other than photochemical change might exist. He also showed that the effect was dependent

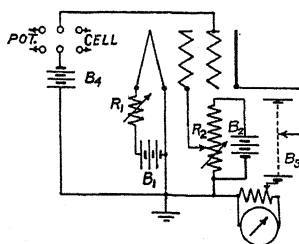


FIG. 1

upon the shape of the electrode and that polarization⁶ played an important rôle.

It was felt that the actual e.m.f. produced might not be directly proportional to the residual current that he measured. Therefore it was decided to utilize a potential measuring instrument, that would not draw current.

A Compton type quadrant electrometer was used in the major part of the work, but on account of its long period another device was developed. This consisted of a specially constructed 4-element vacuum tube, built by Osram in Berlin, connected as shown in Fig. 1. The purpose of this tube was to act as a voltage amplifier for the small potentials measured, and by means of the 4th element or "space charge grid" to effectively prevent current being drawn from the source. The filament is surrounded by a helical "space charge grid," which is enclosed by a second helical control grid, with a lead brought out through an amber bushing in the top of the tube. The cylindrical plate is just outside of the control grid. The 4 elements are nearly concentric. B_1 , B_2 and B_3 are storage batteries of 6, 6, and 24 volts respectively. B_4 consists of 3 standard cells, which were used because of the necessity to maintain a constant negative bias in series with the e.m.f. to be measured. Plug type resistance boxes were used for R_1 and R_2 to eliminate variable contact resistance. A highly insulated mercury contact switch was used to quickly connect either the potentiometer or cell circuits

to the measuring system. A galvanometer having a sensitivity of 25,000 megohms was connected in the plate circuit through an Ayrton shunt and an auxiliary resistance to critically damp it.

In operation the control grid was made more negative than its floating potential to prohibit electron current. The space charge grid was made positive (from 2 to 3 volts) in respect to the filament in order to shield the control grid from positive ions. An extremely hard tube, operation of filament at 40 percent of normal temperature, and low plate potential (18 to 22 volts) all contributed to reduce positive ion current. Leakage was reduced by precautions in the insulation of the control grid lead coming out through the top of the tube, and the use of ceresine wax to insulate every lead and piece of apparatus in the circuit. A galvanometer having a sensitivity of 25,000 megohms used at a distance of 3 meters from the scale showed no trace of a deflection when connected in series with the control grid circuit. It should indicate any current greater than 10^{-13} amperes.

E.m.f. measurements were made by noting the change in plate current when the source of potential was connected in series with the standard cells so as to make the control grid more negative.

Sensitivity could be varied by changing R_1 , R_2 , B_3 or B_4 . After proper adjustments were once made R_1 and R_2 were the only controls needed. The system was used with a sensitivity between 3000 and 4000 mm per volt, although 5200 mm per volt was obtained. With suitable amplification higher sensitivities should be possible.

For very small values the e.m.f. was found to be nearly linear with scale deflections.

The advantages of the system lie in the short period of the galvanometer, and freedom from the usual electrometer adjustments.

The disadvantages may be summed up as follows:

1. It was difficult to make comparative measurements over long periods of time due to slight fluctuations in battery voltages.
2. Changes in room temperature changed the constants of the circuit.
3. The tube was found to be photoelectric. (This was taken care of by covering the tube with a metal shield and grounding it.)
4. Special precautions had to be taken against leakage currents.
5. The system was extremely sensitive to high tension discharges or arcs.
6. The filament of the tube had to be burned several hours before using the system.

EXPERIMENTAL

The electrolyte rotating with the bottle had a small region illuminated as it passed in front of the window. The test tube was adjusted vertically while assembling so that the front electrode was symmetrically placed in front of the window. By moving the test tube about the axis of the brass tube, the horizontal position of the electrode in respect to the window could be altered, and thus the electrolyte could be irradiated before, while in contact with, or after passing by the electrode. This arrangement per-

mitted a study of the effect when the boundary region between the electrode and electrolyte was illuminated, as well as the condition when the electrode was displaced from the window so that the effect was produced by the previously irradiated electrolyte flowing by the electrode. The scale which indicated the position of the electrode in respect to the window was arranged to read in millimeters displacement.

There were four variable factors: (1) speed of rotation of electrolyte; (2) thickness of sputtered films; (3) intensity of illumination; and (4) con-

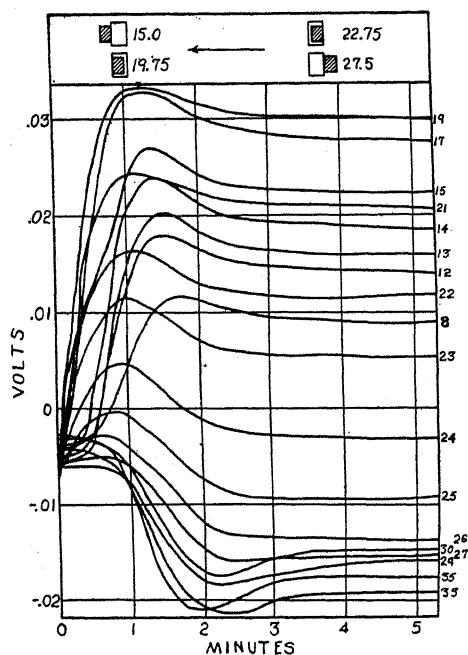


FIG. 2

Opposite electrodes	35 percent
Electrode transmission	20.8 r.p.m.
Speed of rotation	2.19 percent
Concentration of electrolyte	4-element vacuum tube system
Method of measurement	

In this experiment a square electrolyte bottle was used.

centration of rhodamine B in the electrolyte. In order to make a thorough study of the effect many sets of data were obtained in which three of these factors were held constant and the fourth varied.

Two distinct types of cell were used in this part of the work. (1) The electrodes were arranged opposite each other, and were of the same length. (2) The back electrode, while opposite, was from 3 to 4 cm above the front one. Hereafter the former will be referred to as a cell with "opposite" electrodes, and the latter as one with "staggered" electrodes. With staggered electrodes the irradiated material from the window should stream around

an annulus the height of the window, and should not come in contact with the back electrode, except for vertical diffusion.

The following curves show a few results which are representative of many sets of data taken. The white rectangles represent the window and the shaded ones the electrode, and the numbers the scale readings for the positions shown. The arrows indicate the direction in which the electrolyte flowed by the window.

Fig. 2 is a set of curves showing the relation between e.m.f. and time for various positions of the electrode in respect to the window. The numbers along the right hand side of the curve represent the positions of the electrode, the scale being laid off so that each unit represented a movement of 1 mm in respect to the window.

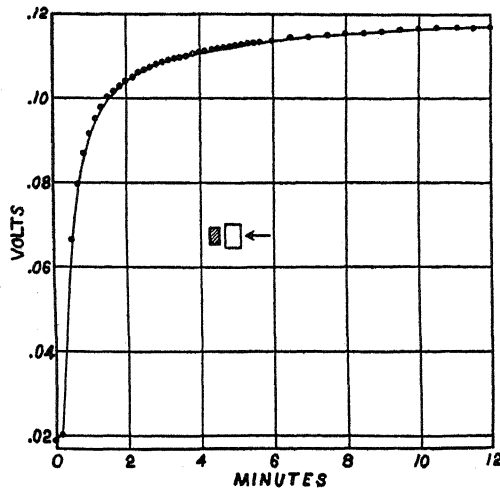


FIG. 3

Staggered electrodes	
Electrode transmission	11 percent
Speed of rotation	49.5 r.p.m.
Concentration of electrolyte	2.19 percent
Method of measurement	4-element vacuum tube

The cell was allowed to rotate in the dark until only a small dark e.m.f. was present; then time was measured from the beginning of illumination. This procedure was repeated for each curve. These shown are only part of the total number of time curves thus studied. No attempt has been made to indicate the points, as the curves were drawn free hand through practically all of them.

They show that after a time a steady state value of e.m.f. is obtained for each position of the electrode. The shape of the curves can be accounted for. If the electrode is at the left of the window, a certain time will elapse before the irradiated material will be carried around to the electrode. When it reaches this point, there will be a sudden rise in the e.m.f. Later some of the material will be carried around to the back electrode giving a differential

effect, and causing a decrease in the e.m.f. As one would expect, the maximum effect is found when the electrode is part way across the window and moving from left to right, because, as the electrode more nearly covers the window, the intensity of illumination is decreased by the electrode itself. When the electrode is at the left of the window the effect grows smaller since diffusion carries away some of the changed material. When the electrode is at the right of the window the back electrode receives the modified material first, which accounts for the negative e.m.f., and which of course is much smaller on account of diffusion as stated above. It is interesting to note that as the electrode approaches the window in either direction

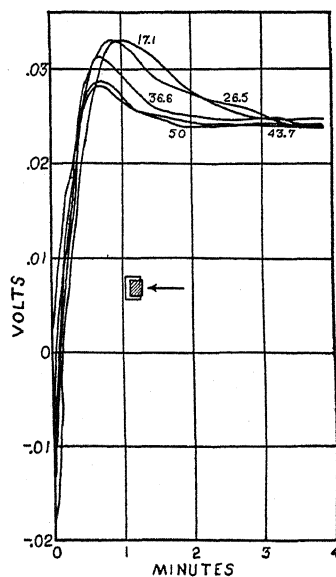


FIG. 4

Opposite electrodes	
Electrode transmission	35 percent
Concentration of electrolyte	2.19 percent
Method of measurement	4-element vacuum tube system

the maximum effect for each curve, which is either a positive or a negative e.m.f., occurs sooner. This represents the time required for the largest amount of changed material to reach the front electrode. It will also be observed that the steady state e.m.f. occurs in a shorter time as the electrode approaches the window. This latter fact was observed in all subsequent experiments.

Fig. 3 represents a curve similar to those in Fig. 2 except "staggered" electrodes were used. The approximate position of the electrode is shown by the diagram, and the arrow shows the direction of flow of the electrolyte. As might be expected, no maximum is found, but the e.m.f. builds up to the steady state value.

Fig. 4 shows a set of e.m.f.—time curves for varying speeds of rotation. The diagram shows the position of the electrode in respect to the window for all curves, and the arrow shows the direction of flow of electrolyte. Numbers on curves represent speeds of rotation. These curves show that the steady state of e.m.f. is independent of speed, within the limits tried. It is also seen that the maximum point is reached in shorter time as the speed increases; this result would be expected from the discussion of Fig. 2. The curves were drawn free hand through practically all of the points.

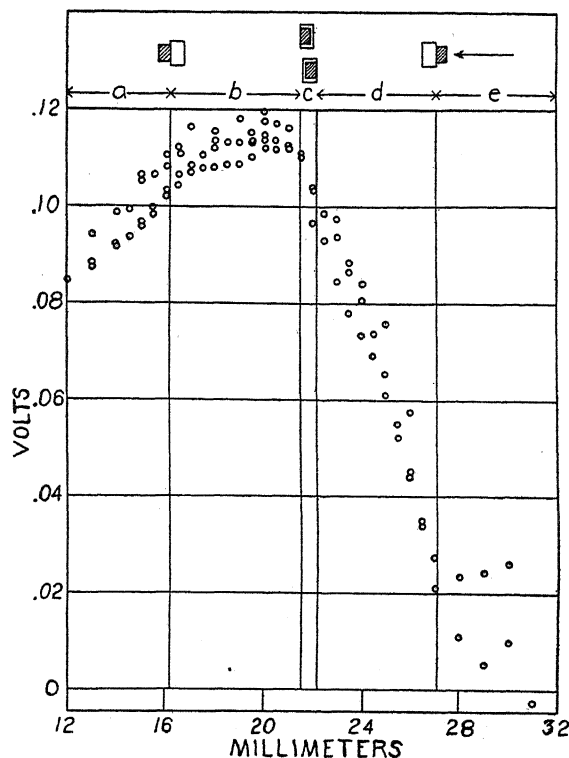


FIG. 5

Opposite electrodes	
Electrode transmission	9 percent
Speed of rotation	21.6 r.p.m.
Concentration of electrolyte	2.46 percent
Method of measurement	4-element vacuum tube system

Fig. 5 shows the relationship between e.m.f. and position of electrode in respect to window. Each point was taken after a steady state e.m.f. had been reached. The points were not taken on consecutive electrode positions, but at random positions over different parts of the scale. The variations are small when it is considered that the time for taking these data was several hours, and that the voltages used for controlling the vacuum tube system were bound to fluctuate some in this period. The diagrams at the top show the positions of the electrode and the vertical lines on the curve

indicate these positions. This arrangement is similar to that of Murdock,³ the regions *a*, *b*, *c*, *d*, and *e* representing respectively: electrolyte illuminated before passing electrode; electrode partially illuminated; electrode completely illuminated; electrode partially illuminated; and electrolyte illuminated after passing electrode. The arrow shows the direction of flow of the electrolyte.

Fig. 6 shows two curves plotted with positions of electrode in respect to e.m.f. Curve *B* was obtained by reversing the direction of rotation of the electrolyte from that in *A*, the lettered arrows indicating the respective directions of electrolyte rotation. In this case data were taken for consecu-

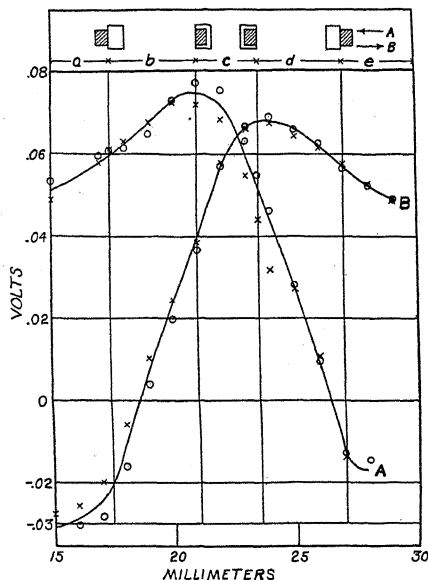


FIG. 6

Opposite electrodes	
Electrode transmission	14.5 percent
Speed of rotation	19.9 r.p.m.
Concentration of electrolyte	2.46 percent
Method of measurement	Compton electrometer

tive electrode positions, and as a check were again taken consecutively back over the scale. The circles represent increasing scale readings for electrode positions, and the crosses, the return or decreasing scale readings. The symmetry of the two curves is quite marked. Murdock³ was unable to obtain this symmetry when making current measurements, which failure he attributed to the shape of the electrode.

Fig. 7 is another group of curves taken in a similar manner to those in Fig. 6. In this case the intensity of illumination was varied by filters, the other factors being kept constant. Curves *A*, *B*, and *C* represent intensities of 3 percent, 17 percent, and 100 percent respectively. The circles and crosses again have the same meaning as in Fig. 6.

DISCUSSION

If there is an e.m.f., due to the illumination of the electrode or the boundary between the electrode and the electrolyte, measurable with the instruments used, superimposed upon that due to a photo-chemical change

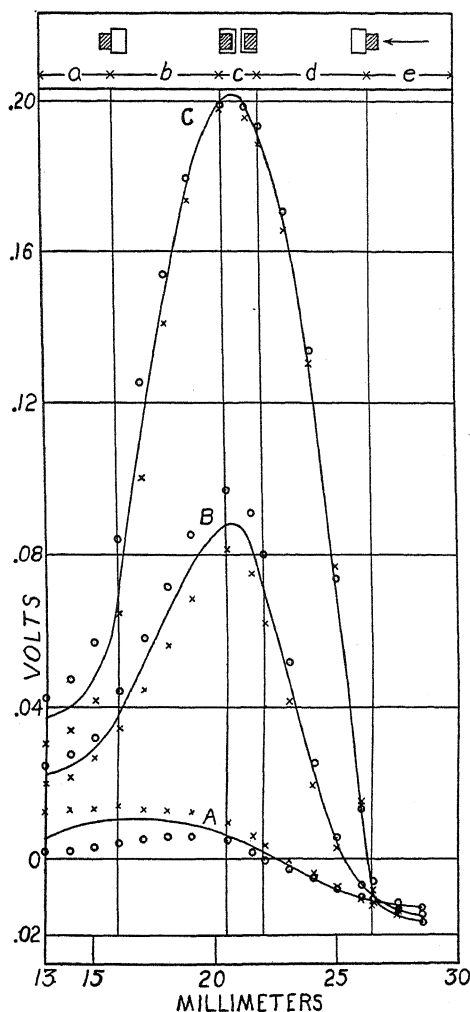


FIG. 7

Opposite electrodes	
Electrode transmission	24 percent
Speed of rotation	14.9 r.p.m.
Concentration of electrolyte	4.2 percent
Method of measurement	Compton electrometer

of the electrolyte, one would expect to find an abrupt change of slope on going from a dark to an illuminated region. A study of Figs. 5, 6 and 7 reveals no such change. Many similar sets of data were taken in which one

of the four factors before mentioned was varied and in every case a smooth curve resulted in going from region "a" to region "b."

This regularity leads to the viewpoint that the phenomenon is due entirely to the modification of the electrolyte with light, and that the effect follows the laws of the concentration cell theory. If one calls the original material *A* and the modified material due to light, *B*, then the e.m.f. will depend upon the difference in concentrations of *B* at the two electrodes, and this has been shown to be a function of $\log C_1/C_2$, where C_1 and C_2 are the concentrations of *B* at the electrodes.

In these cells the concentration of material *B* should be some function of three variable factors: (1) the intensity of the light; (2) time of illumination; and (3) the concentration of material *A*. According to the concentration cell theory, one would expect the effect to increase with these three factors. Rule⁴ has shown that the e.m.f. is a function of the intensity and time of illumination. In an earlier experiment⁷ by him and independently by Mrs. Junkins,⁸ it was found that a maximum effect occurred for a particular concentration of material *A*, and any further increase in concentration of material *A* gave a decreased effect.

From the results in the rotational experiments of the present work in which concentrations were varied, and from the concentration cell theory, it was felt that the effect must increase with the concentration of material *A*. Accordingly ten rhodamine B solutions of varying strengths were made up in small bottles, and in turn were slipped over a test tube with the electrode placed directly in front of the window and the electrolyte at rest. Fig. 8 shows the results where e.m.f. was plotted against time, the numbers on the right hand side of the curves being percent concentrations of rhodamine B. It is seen that the effect increases with the concentration. It was later found that the solution became saturated a little above 8 percent. While care was used in making up the solutions, the concentrations were not afterward checked gravimetrically, as in the case of the former experiments with the rotating electrolyte, and may be slightly in error. In Fig. 9 the data were secured by subtracting the dark e.m.f.'s observed at the beginning of each time curve from the values obtained after ten minutes irradiation. It is quite evident that there is no maximum value for any particular concentration below saturation. Goldmann,¹ while making current measurements, found no maximum sensitivity for any particular concentration. In Rule's experiment⁷ using fluorescein, e.m.f. was measured against concentration, but the electrode was illuminated through the electrolyte. For very dilute solutions not much light would be absorbed in the outer layers of the electrolyte, but on increasing the concentration more and more light would be absorbed. Hence there would be a particular concentration for any given intensity of illumination where the intensity of light near the electrode (and therefore material *B*) would be a maximum. Mrs. Junkins⁸ illuminated the

⁷ W. Rule, *Phil. Mag.* 1, 532 (1926).

⁸ R. Y. Junkins, *Phys. Rev.* 18, 402 (1921), May 1929.

electrolyte through a semi-transparent electrode, as in the present work, but used current measurements as an indication of the effect with concentration, and found that for rhodamine B the maximum value occurred near 3 percent. Subsequent workers^{3,5} used this value, believing it to give a maximum effect. Probably the current measurement was affected by polarization, and the rate of diffusion of polarizing material, which constitutes a quantity proportional to the current measured, must have attained a maximum value at 3 percent concentration.

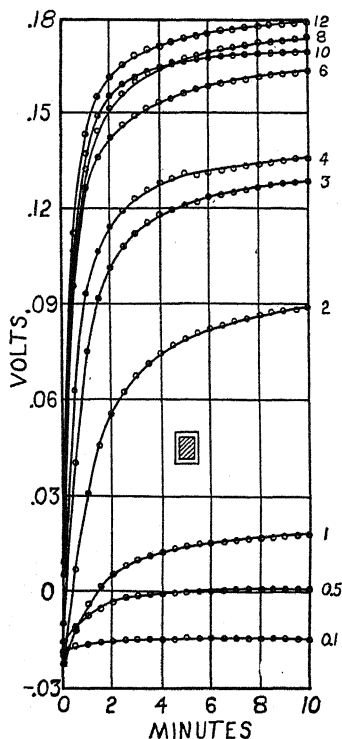


FIG. 8

In Figs. 5, 6, and 7 it will be observed that in region "e" the values of e.m.f. fluctuate. This is probably due to the fact that the effect is small, and that some light gets to the electrode by scattering and reflection, even though the electrode is at the right of the window, and in this position the back electrode begins to receive some of the irradiated material first. Diffusion also carries some of the new material to the front electrode against the direction of rotation. The fluctuation was observed in all of the data taken. It was also found that a greater length of time was always necessary to reach a steady state condition in this region. This effect was more marked in those curves where the intensity of light or the concentration of electrolyte was very small.

Rule,⁴ using uranine, found at the beginning and end of illumination a small e.m.f. opposite in sign from the major effect. Russell,⁵ working with rhodamine, did not actually observe a reversal, but found that the values of e.m.f., for a short interval of time after illumination began, departed somewhat from the theory he had developed, leading him to believe that some effect similar to the one found by Rule might be superimposed upon that due to photo-chemical change. Grumbach² also observed reversals.

Such an effect would not be compatible with the theory that an e.m.f. due to a pure concentration cell was the only one present, so a careful investigation was deemed advisable. In getting the data for Figs. 8 and 9, readings at the exact beginning and end of illumination were noted for each concentration, but no such effect was observed. Several different types of cell holders were used with rhodamine B and uranine at different concentra-

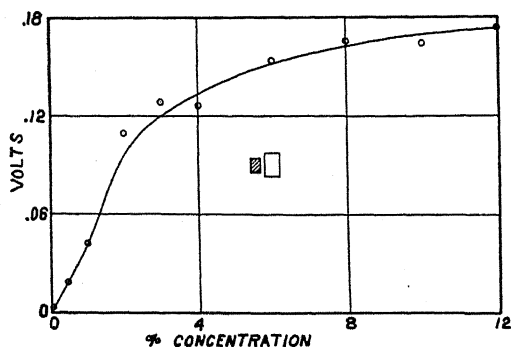


FIG. 9

tions. No reversal was found either at the beginning or end of illumination, even when a cell was made up and used in exact accordance with the method of Rule,⁴ though the growth-time curves were found to agree consistently with his.

REMARKS

In all of the rotational experiments, in which e.m.f. was plotted against position of electrode in respect to the window, no break in the slope of the curve was found when the electrode first entered the illuminated region. As stated before, in the case of current measurements such a break has been observed. Contradictory to the results of another investigator, no reversal of e.m.f. was observed at the beginning or end of illumination in taking the growth-time curves of a cell. Both of these small effects had been previously interpreted as due to the illumination of the electrode or a region very close to it, and had been thought to be superimposed upon the main effect arising from a photo-chemical change of the electrolyte. The results of the present work thus lead to the viewpoint that there is no auxiliary effect produced by directly irradiating the electrode.

The failure to find a break in the curve when the electrode first entered the illuminated region can be attributed to the fact that e.m.f., instead of

current measurements were made. Likewise the discrepancy between the results of the present work and that of Mrs. Junkins, in which sensitivity of the effect with increasing concentrations was studied, can be explained in the same way. Therefore, it is inferred that current measurements are not satisfactory for studying some of the phenomena occurring in this type of cell, especially in these particular cases mentioned where it was evidently assumed that the current was proportional to the e.m.f. A possible explanation might be that this disagreement in results was linked with some peculiarity of the polarization present in current measurements.

The author wishes to express his appreciation to Professor C. C. Murdock, who suggested the original problem and contributed many suggestions and valuable criticism during its progress. Also to Professors Ernest Merritt and R. C. Gibbs in particular, and to other members of the Physics staff in general, who made helpful suggestions in regard to the work.

THE VISCOSITY OF COMPRESSED GASES

BY JAMES H. BOYD, JR.†

DEPARTMENT OF CHEMICAL ENGINEERING, MASSACHUSETTS INSTITUTE OF TECHNOLOGY

(Received April 7, 1930)

ABSTRACT

New data and a new theory for the viscosity of compressed gases are presented. Data for nitrogen, hydrogen and a mixture of these gases are given, in the calculation of which, the "end effects" are not neglected as has been done in the past. Previous viscosity data are of doubtful validity owing to neglect of this factor. The theory is based on an analogy between the kinetic pressure and viscosity of a gas and is derived using an equation of state of the Lorentz type. Allowance is made for the difference between the viscosity and compressibility covolumes. The theory is substantiated experimentally and further confirmed by the recalculation of other data on the variation of Reynolds' criterion with the pressure, which is here shown to be constant. The mixture data offer a direct opportunity of comparing the Lorentz and linear rules for the calculation of the covolume of a mixture from the covolumes of the components and such comparison indicates that the Lorentz rule is not to be preferred. The substantiation of the new theory is the first direct proof of the validity of the separate treatment of the kinetic and cohesive pressures in the equation of state.

I. INTRODUCTION

THE viscosity coefficient of a gas is defined as the time rate of the net transfer of momentum across an imaginary, plane unit-surface in the interior of a flowing gas when there is a unit velocity gradient normal to the plane surface and normal also to the direction of gas flow. The statement is often encountered that the viscosity of gases is independent of the pressure. At atmospheric pressure and less this is substantially true and is confirmed experimentally but for high pressures theory predicts and experiment concurs in giving greater values of the gas viscosity.

A number of theories of the viscosity at high gas densities have been advanced and Meyer,¹ Brillouin² and Batschinski³ have attempted solutions of this problem. Far more significant are the investigations of Jäger,⁴ H. B. Phillips⁵ and Dubief⁶ who employed equations of state of the van der Waal type in their derivations. H. B. Phillips' paper is of particular interest in view of certain generalizations made concerning the effect of intermolecular forces on gas properties.

† Research Assistant, Research Laboratory of applied chemistry.

¹ Meyer, *Kinetic Theory of Gases*, 2 Ed., Eng. Trans., Longmans, Green and Co., 1899.

² Brillouin, *Leçon sur la Viscosité*, II, p. 132, Villiers, Paris, 1907.

³ Batschinski, see Bingham, *Fluidity and Plasticity*, pp. 142-152, McGraw Hill, New York, 1922.

⁴ Jäger, *Wien. Sitz. Ber.* 150, 2A, 15 (1896); 108, 2A, 447 (1899).

⁵ H. B. Phillips, *J. Math. and Phys.*, M. I. T. 1, 42 (1921).

⁶ Dubief, *J. de Phys. et Rad.* 7, 402 (1926); *Compte Rendus* 180, 1164 (1925); 182, 688 (1926).

In the experimental field Warburg and von Babo⁷ and P. Phillips⁸ determined the viscosity of gaseous carbon dioxide at pressures exceeding one hundred atmospheres and for several temperatures. Wildhagen,⁹ in his study of the flow of compressed air, measured the viscosity of air at room temperature for pressures up to two hundred atmospheres. All of the writers cited used some form of the transpiration method. In all of these investigations end effects were neglected.

The transpiration method of determining viscosity coefficients is that most readily adapted to use at high pressures. This method is based on Poiseuille's law for isothermal viscous flow which may be expressed

$$\Delta p = \frac{k_c M}{\rho} \mu \quad (1)$$

where Δp is the pressure drop in centimeters of mercury at 0°C, occasioned by the flow of M grams per second of an incompressible fluid of viscosity μ and density ρ through a tube of circular section whose dimensions determine the value of k_c . The density and viscosity are in c.g.s. units and k_c equals $8L/13.596 g\pi r^{4*}$ where L and r are the length and radius respectively in centimeters of the tube and g is the gravitational acceleration. When Eq. (1) is integrated assuming the ideal gas laws and an isothermal expansion there results

$$p_1^2 - p_2^2 = 2RTk_c M \mu \quad (2)$$

Here p_1 and p_2 are the upstream and downstream pressures respectively, R the gas constant and T the absolute temperature.

Neither of these equations may be applied directly to experimental data as they neglect "end effects" which are caused by losses in the kinetic energy of the fluid due to changes in the cross-section of the path of flow. As a result the observed pressure difference is greater than it would be were there no such loss. Accordingly Eqs. (1) and (2) should be modified as otherwise the calculated values of the viscosity coefficients would be high. End effects are discussed by Brillouin,¹⁰ Fisher,¹¹ Rapp,¹² Bingham,¹³ Benton,¹⁴ Walker, Lewis and McAdams,¹⁵ and by Trautz and Weizel.¹⁶ The majority of these writers agree, on reducing their results, that the proper form for the end correction is

⁷ Warburg and von Babo, *Ann. d. Physik* **17**, 390 (1882).

⁸ P. Phillips, *Proc. Roy. Soc. Lon.* **87a**, 48 (1912).

⁹ Wildhagen, *Z. Angew. Math. u. Mech.* **3**, 181 (1923).

* The coefficient of slip is negligible and has been omitted here.

¹⁰ Brillouin, reference 2, pp. 117-124.

¹¹ Fisher, *Phys. Rev.* **32**, 216 (1911).

¹² Rapp, *Phys. Rev.* **2**, 263 (1913).

¹³ Bingham, *Fluidity and Plasticity*, p. 17.

¹⁴ Benton, *J. Ind. Eng. Chem.* **11**, 623 (1919).

¹⁵ Walker, Lewis and McAdams, *Principles of Chemical Engineering*, p. 90, 2nd Ed., McGraw Hill, New York, 1927.

¹⁶ Trautz and Weizel, *Ann. d. Physik* **48**, 799 (1915).

$$\Delta p_e = \frac{k_e M^2}{\rho} \quad (3)$$

where Δp_e is the end effect pressure drop and k_e is the end effect constant. Eqs. (1) and (2) accordingly become

$$\Delta p = \frac{k_c M \mu}{\rho} + \frac{k_e M^2}{\rho} \quad (4)$$

$$p_1^2 - p_2^2 = 2RT(k_c M \mu + k_e M^2) \quad (5)$$

It is of interest to consider the effect of a change in density of a given gas on the magnitude of the end correction when the latter is negligible at atmospheric pressure. Assume that the pressure drop due to the viscous action of the gas is relatively small and constant and that the viscosity is independent of the density. Eq. (4) is sufficient for this estimate since at the higher pressures the gas density is substantially constant throughout the apparatus. For these conditions M/ρ is constant and therefore the end correction, $k_e M^2/\rho$, is linear in density. For density variations of several hundred-fold the end correction may well be of the order of ten to twenty percent. This approximation shows that all previous high pressure investigations are of questionable quantitative significance in view of the neglect of end effects.

II. THE EXPERIMENTAL METHOD

The transpiration method was used in this investigation and consisted in measuring the pressure drop occasioned by the isothermal flow of a gas of known density at a measured rate through a metal capillary whose constants, k_c and k_e , were determined by direct calibration. This necessitated relatively large amounts of the gases and so precluded the use of highly purified materials. Hydrogen and nitrogen of the highest commercial purity obtainable were used in these experiments.

The capillary used in these experiments was a steel tube about a meter long and roughly 0.025 cm in internal diameter. It was immersed in a stirred water bath thermostat whose temperature was read from calibrated thermometers fully immersed. The temperature variation seldom exceeded 0.2°C and generally was within 0.1°C which was adequate for these experiments. The calibration of the capillary for k_c and k_e will be described later. A metal capillary was used to insure isothermal flow.

The pressure-drop measurements were made with a new type of high pressure manometer. In principle, the instrument consisted of a mercury filled manometer whose arms were of widely different diameters thus giving practically the entire pressure differential in the smaller arm. The change of the mercury level in the smaller arm was detected by successively making and breaking an electrical circuit by means of a platinum tipped screw rod which was insulated from the body of this apparatus. The relative travel of the rod was determined by measuring the distance between its upper end and

a fixed reference plane by means of a micrometer depth gauge. A galvanometer indicated the completion of the circuit through which a feeble current flowed whose source was a thermocouple immersed in ice and water. This very feeble current was desirable to minimize arcing on breaking the circuit. The pressure differential was calculated from the difference between the flow and zero or no-flow readings. In this calculation corrections were made for the drop in mercury level in the larger arm, the gas density, and the temperature variation of the mercury density.

The gas density was computed from the temperature and pressure of the gas flowing. Pressures were measured with a dead weight piston gauge of the type developed by Keyes¹⁷ and his coworkers. The gas temperature was taken to be that of the bath and the density was calculated from these data using Bartlett's¹⁸ compressibility factors. No attempt was made to

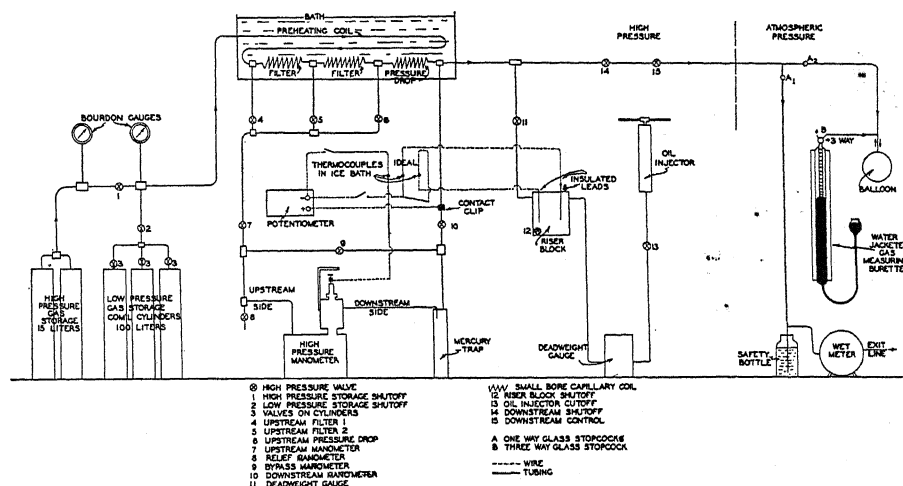


Fig. 1. Diagrammatic sketch of viscosity apparatus.

correct the gas density for the water vapor present since its concentration was very low as has been shown by Bartlett.¹⁹

The transpiration rate was determined by expanding the compressed gas and passing it into an exhausted rubber balloon for an observed time interval measured with a calibrated, split-second stop watch. The gas was then drawn into a water jacketed burette and measured at known temperature and pressure. From these data and the gas composition the transpiration rate was calculated.

The gas mixture was made up in a small holder, allowed to stand for several hours, compressed and then analyzed. The same method of compression was used for the pure gases to obtain pressures exceeding 150 atmospheres.

¹⁷ Keyes, and Dewey, *J. Opt. Soc. Am. and Rev. Sci. Instr.* **14**, 491 (1927).

¹⁸ Bartlett, *J.A.C.S.* **49**, 687 (1927); **49**, 1955 (1927).

¹⁹ Bartlett, Cupples and Tremearne, *J.A.C.S.* **50**, 1275 (1928).

The apparatus is shown diagrammatically in Fig. 1. The gas flowed from the storage cylinders through a preheating coil of relatively large capillary tubing and then through two fine steel capillaries employed as dust filters before entering the pressure drop capillary. These capillaries were all immersed in the bath. On leaving the pressure-drop capillary the gas passed through a needle control valve and was reduced to atmospheric pressure. Care was taken that steady viscous flow was maintained during experiments.

The capillary constant k_c was determined by low pressure transpiration experiments which were calculated by Eq. (5) inspection of which shows that $(p_1^2 - p_2^2)/M$ is linear in M . Actually Eq. (5) ignores the effect of the acceleration of the gas in the capillary but since the data plotted by the

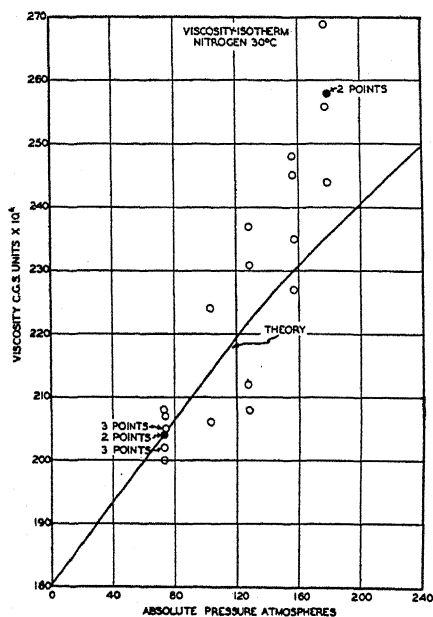


Fig. 2.

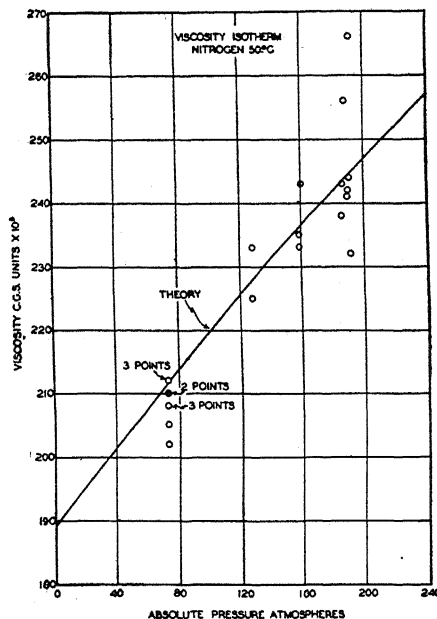


Fig. 3.

above method were linear the value of k_c was readily calculated on obtaining the intercept by extrapolation to zero gas flow. A very satisfactory check was given by an alternative method based on the determination of the volume of the capillary. This latter procedure required the weight, length and average external diameter of the tubing and further necessitated the determination of the density of the steel in the tubing. From these data k_c was calculated. The excellent agreement of the results obtained by these two separate methods gave great confidence in the validity of the transpiration method for this calibration. The distention of the capillary by changes in temperature and pressure which, if appreciable, would affect the value of the constant, was found to be negligible for the ranges of temperature and pressure employed here. A supplementary transpiration calibration for k_c

was required because of a very slight rusting of the interior walls of the capillary. This rusting was due to the condensation of small amounts of water vapor from the compressed gas which occurred on increasing the pressure in the capillary above that in the supply cylinder from which the gas was drawn. This was avoided in subsequent experiments by performing them in the order of their descending pressures. After establishing this procedure check transpiration calibration experiments showed the value of k_c to be unchanged.

The constant k_c was determined by means of high pressure transpiration experiments which were calculated with Eq. (4) which is linear in $\Delta p \cdot \rho / M$ versus M . The slope of such a plot gave the value of k_c . Here the use of

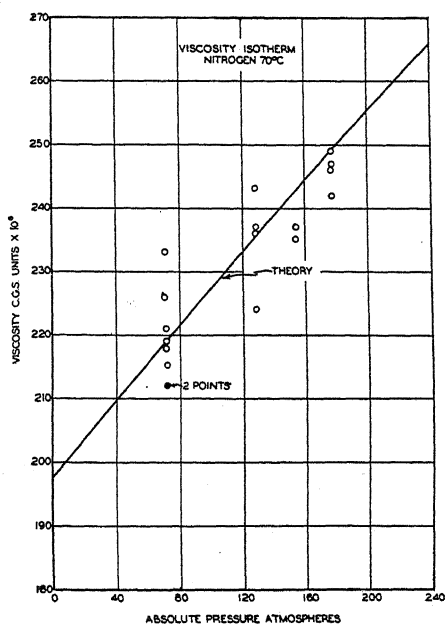


Fig. 4.

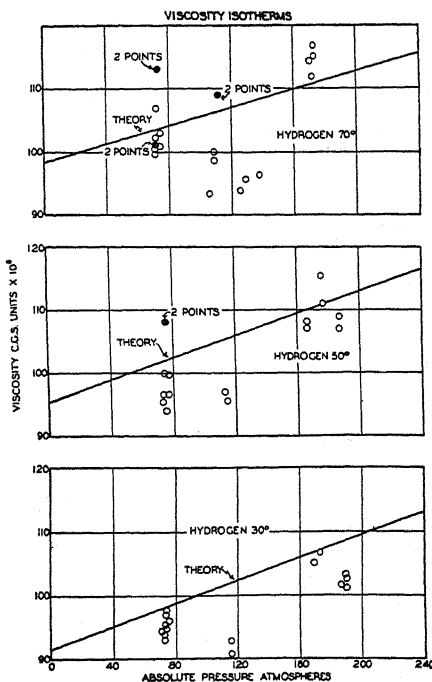


Fig. 5.

Eq. (4) simplified the calculations and was valid because at high pressures the gas density was substantially constant throughout the apparatus. This constancy of the density required that the linear velocity of flow in the capillary also be constant, and thus the acceleration effect previously mentioned was eliminated in the high pressure experiments. Experiments with nitrogen were made proving that the constant is independent of the temperature and pressure ranges covered here. Further experiments with hydrogen checked the value so determined and showed it to be independent of the gas employed. The magnitude of k_c exceeds that predicted from theory but this is believed due to a divergence between the actual experimental conditions and those postulated in the theoretical derivations. In any case this does not invalidate the results reported here.

In the high pressure experiments the system was brought under pressure by permitting the gas to flow through the capillaries to the *downstream* side of the differential manometer, under the mercury seal and into the upstream side. When the pressure was equalized throughout the system the by-pass valve and then the upstream valve were opened. The zero reading was then made after which the screw rod was run up the riser well to a point above the approximate mercury level expected in the experiment. Gas flow at the desired rate was obtained with the downstream control valve. The by-pass valve was then closed and twenty minutes allowed to insure a steady flow

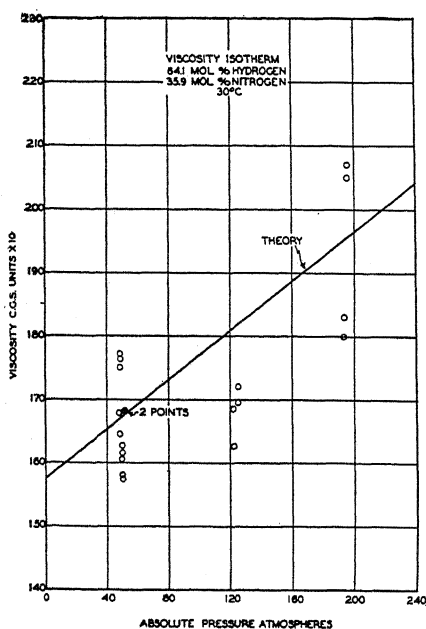


Fig. 6.

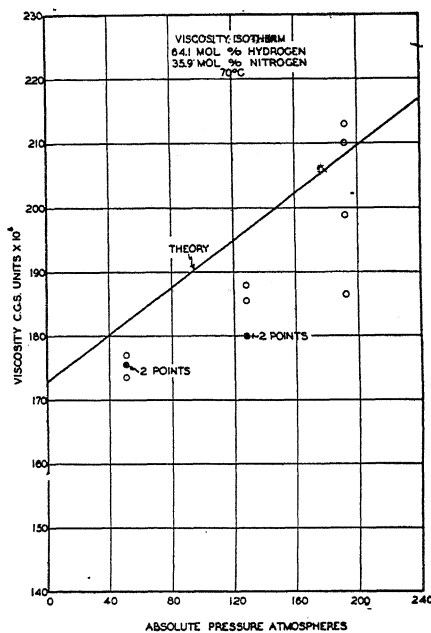


Fig. 7.

before manometer readings were taken. In each case the mercury approached its equilibrium position from below thus tending to introduce a compensation of errors. The gas was then passed into the balloon during an observed time interval after which manometer readings were again made and the average of the initial and final readings was taken for computation. The pressure was next measured by means of the dead weight piston gauge. The bath temperatures were noted during each experiment. The volume of the gas in the balloon was then determined at atmospheric pressure and room temperature. These data permitted the calculation of the viscosity coefficients.

III. EXPERIMENTAL RESULTS

Viscosity coefficients for nitrogen and hydrogen were obtained at 30°, 50° and 70°C for pressures from 75 to 180 atmospheres. Similar data were obtained for a mixture containing 64.1 mol percent of hydrogen and 35.9

TABLE I. *Viscosity data, nitrogen.*

30°C		50°C		70°C	
Absolute Pressure Atm.	Viscosity c.g.s. units ×10 ⁶	Absolute Pressure Atm.	Viscosity c.g.s. units ×10 ⁶	Absolute Pressure Atm.	Viscosity c.g.s. units ×10 ⁶
178.8	258	191.0	232	176.9	246
178.8	244	191.0	266	176.9	242
177.6	258	189.8	242	176.9	247
177.6	256	189.8	244	176.9	249
176.9	269	188.0	241	154.1	237
176.9	276	188.0	256	154.1	235
156.8	235	185.5	238	127.5	224
156.8	227	185.5	243	127.5	236
156.2	245	158.7	243	126.7	243
156.2	248	158.5	235	126.7	237
128.4	231	158.5	233	71.5	219
128.4	237	128.4	225	71.5	221
128.4	208	128.4	233	71.5	215
128.4	212	73.2	208	71.5	212
103.6	224	73.2	212	71.5	218
103.6	206	73.0	210	71.5	212
74.3	207	72.9	212	70.4	226
74.1	205	72.7	205	70.4	233
73.7	202	72.7	208		
73.5	200	72.4	208		
73.5	202	72.4	210		
73.5	204	72.1	212		
73.5	205	72.1	203		
73.5	205				
73.3	204				
73.0	208				
73.0	202				

TABLE II. *Viscosity data, hydrogen.*

30°C		50°C		70°C	
Absolute Pressure Atm.	Viscosity c.g.s. unit ×10 ⁶	Absolute Pressure Atm.	Viscosity c.g.s. units ×10 ⁶	Absolute Pressure Atm.	Viscosity c.g.s. units ×10 ⁶
191.7	102.5	186.8	107.0	173.4	115.0
191.7	101.2	186.8	109.0	172.8	116.8
189.8	103.4	176.1	111.0	172.1	112.7
188.0	101.6	175.5	115.6	171.7	115.8
172.8	106.2	165.7	107.7	138.5	98.4
169.1	105.2	164.8	107.8	128.7	96.7
116.3	92.8	113.8	95.7	125.6	94.8
115.9	90.8	113.2	96.8	112.5	109.0
104.0	98.7	76.9	99.7	112.1	109.0
103.3	102.0	76.7	96.7	108.7	100.0
74.7	95.8	75.7	108.0	107.6	98.8
74.2	97.7	75.7	108.0	105.8	93.5
74.0	95.6	75.0	94.2	74.7	103.0
73.6	94.8	75.0	100.0	74.6	101.0
73.6	97.6	73.5	96.6	73.7	113.7
73.6	94.6	73.4	95.5	73.5	113.7
73.5	93.0			72.7	101.3
73.3	94.7			72.7	101.4
				72.0	102.4
				71.7	107.0
				71.5	101.6
				71.2	99.5

TABLE III. *Viscosity data.*
64.1% Hydrogen—35.9% Nitrogen

30°C		70°C	
Absolute Pressure Atm.	Viscosity c.g.s. units $\times 10^6$	Absolute Pressure Atm.	Viscosity c.g.s. units $\times 10^6$
195.9	205	192.4	187
195.9	207	192.4	199
194.4	183	192.1	210
194.4	180	192.1	213
124.9	172	128.4	188
124.9	170	128.4	180
122.2	163	127.8	186
122.2	168	127.8	180
50.4	168	51.0	176
50.4	168	51.0	173
50.2	163	50.7	175
50.2	161	50.7	177
50.1	158		
50.1	158		
49.2	177		
49.2	160		
48.7	175		
48.7	176		
48.0	164		
48.0	168		

mol percent of nitrogen at 30° and 70°C for a somewhat greater pressure range.

The new viscosity data are presented in Tables I to III and are shown graphically in Figs. 2 to 7 inclusive.

IV. A NEW VISCOSITY THEORY

In the theory of the equation of state it has been customary to regard the hydrostatic pressure as the net effect of a kinetic (distending) pressure and of a cohesive pressure. The kinetic pressure of a gas is defined as the time rate of the transfer of momentum across an imaginary plane unit surface in the interior of the gas. The viscosity coefficient is, by definition, the time rate of the *net* transfer of momentum in a flowing gas across a similar unit plane when there is a unit velocity gradient normal to the plane surface and normal also to the direction of gas flow. Thus the viscosity and kinetic pressure are similar phenomena whose origin is in the molecular motion and therefore it is logical that the kinetic pressure and the viscosity may be treated by the same analytical method.

Of the quantitative equations of state that of Beattie and Bridgeman²⁰ has had marked success in reproducing the observed pressures of a number of gases for wide ranges of temperature and pressure. Application of this equation to the computation²¹ of the specific heat and Joule-Thomson coefficients of compressed air has shown good agreement between theory and experiment. The derivation of the equation is based on the two main assump-

²⁰ Beattie and Bridgeman, Proc. Am. Acad. Sci. 63, 229 (1928).

²¹ Bridgeman, Phys. Rev. 34, 527 (1929).

tions that the kinetic and cohesive pressures may be treated separately and that the law of intermolecular force be such that it diminish rapidly with distance.

Their evaluation of the kinetic pressure is of interest here. The kinetic pressure of a perfect gas is calculated on the basis of a rectilinear free path, but the existence of intermolecular forces, as in a real gas, alters the linearity of the free path and increases the molecular migration in the gas interior. H. B. Phillips²² on general considerations has pointed out this is so regardless of the nature and law of such forces and, further, that this is independent of the size of the molecules. Beattie and Bridgeman employ a slight modification of H. B. Phillips' method of calculating the kinetic pressure of a real gas and obtain

$$P_a = \bar{p}RT(1 + r) = P_i(1 + r) \quad (6)$$

where P_a and P_i are the pressures of the actual and ideal gases respectively, \bar{p} is the density, R the gas constant, T the absolute temperature, and r the fractional increase in the molecular migration relative to an ideal gas owing to the intermolecular forces. Further, r is a function of the density and covolume

$$r = B_0\bar{p}(1 - b\bar{p}) \quad (7)$$

where B_0 is the covolume in liters per mol, b a characteristic constant of the gas and the density is in mols per liter. These authors also correct the kinetic pressure to allow for the change in the time of molecular encounter with temperature and the complete expression for the kinetic pressure now is

$$P_a = P_i(1 + r)(1 - \epsilon) \quad (8)$$

where ϵ is the encounter factor and equals $c\bar{p}/T^3$, c being another characteristic constant of the gas. Eq. (8) is of the form first derived by Lorentz in his calculation of the kinetic pressure.

In adapting this equation to viscosity theory the viscosity coefficients are substituted for the kinetic pressure terms. It is well known that for isothermal pressure changes at low densities the viscosity of a gas is independent of the density. Thus the viscosity of a real gas at low densities is substantially that of a perfect gas, μ_0 . For high densities the viscosity coefficient of a real gas, μ , corresponds to P_a . In the equation of state the covolume, B_0 , is obtained from compressibility data. Among others, Jeans²³ and Keyes²⁴ have remarked that the compressibility covolume differs from that obtained from viscosity data. Therefore it is consistent and desirable in a viscosity theory to use the viscosity covolume, B_0' and further the relative density effect on the viscosity covolume should be the same as for the compressibility covolume and in addition the time of encounter factor

²² H. B. Phillips, reference 5.

²³ Jeans, *The Dynamical Theory of Gases*, pp. 282, 326, 4 Ed., University Press, Cambridge, 1925.

should be identical for both the kinetic pressure and viscosity. The viscosity equation is then

$$\mu = \mu_0(1 + r)(1 - \epsilon). \quad (9)$$

The constants b and c are the same as before and are derived from compressibility data. The term B_0' is evaluated from the relation given by Keyes²⁵ which on reducing to units employed here is

$$B_0' = \left(\frac{3.159 \times 10^{-7} (M_w^{1/2})}{D} \right)^{3/2} \quad (10)$$

where M_w is the molecular weight and D is a constant in Sutherland's equation

$$\mu_0 = \frac{DT^{1/2}}{1 + C/T}. \quad (11)$$

The relation cited for the calculation of the viscosity covolume requires that the covolume be independent of the temperature which is true for gases obeying Sutherland's Law.

So far the theory has been implicitly limited to pure gases but as Beattie and Bridgeman's equation of state has been found valid²⁶ for mixtures the viscosity theory is readily extended to this case also, provided that μ_0 for the mixture be known. The constants B_0' , b and c for the mixture are calculated from those for the components by the rule of linear combination, where

$$\begin{aligned} B_{0' mix} &= \Sigma(B_{0i}' X_i) \\ b_{mix} &= \Sigma(b_i X_i) \\ c_{mix} &= \Sigma(c_i X_i), \end{aligned} \quad (12)$$

and X_i is the mol fraction of component (1) in the mixture. The viscosity theory is now complete.

The theory derived here is based on the analogous treatment of the kinetic pressure and viscosity of a real gas and uses a viscosity covolume instead of a compressibility covolume which, it is assumed, density changes affect in exactly the same way. The viscosity covolume, B_0' , is calculated from the constants in Sutherland's equation and so it is assumed to be independent of the temperature. The time of encounter factor should be the same in the two cases. By a suitable combination of the constants of the components the theory is applicable to mixtures.

V. DISCUSSION OF RESULTS

Examination of the tabulated results shows that the data prove beyond question that, at high densities, the viscosity of a gas is not independent of

²⁴ Keyes, Z. Phys. Chem. Cohen Fest Band, 709 (1927).

²⁵ Keyes, Chem. Rev. 6, 210 (1929).

²⁶ Beattie, J. Am. Chem. Soc. 51, 19 (1929).

the density. The maximum relative increase in the viscosity observed for nitrogen is 25 percent, for hydrogen is 10 percent and for the mixture is 20 percent. The increase in viscosity is not as great as might have been expected on the basis of previous work which however is believed to be of gravely questionable validity in view of the neglect of end effects.

The absolute accuracy of the calculated coefficients is not all that could be desired. Errors in the computed values of the viscosity and in the constants, k_0 and k_∞ , are due to errors of observation and the presence of impurities in the gases used. This latter factor is significant in the case of hydrogen as its viscosity at low pressures and its density are both extremely sensitive to traces of impurities. This source of error is not significant for nitrogen and the mixture. The method of calculation is of itself not conducive to accuracy since it involves the taking of differences and so the error in the calculated viscosities is generally greater than that of the observations.

TABLE IV. *Comparison of theory with experiment for nitrogen.*
 B_0 compressibility = 0.05046 Beattie and Bridgeman
 B_0' viscosity = 0.0421*

Pressure Atm.	No. of Experi- mental Points	30°C		
		Observed Mean	Viscosity Coefficients c.g.s. units $\times 10^6$ Viscosity Covolume Compr. Covolume	
1	—	181*	—	—
73	11	204	204	212
103.6	2	215	214	220
128.4	4	222	222	237
156.8	4	240	229	248
176.9	6	260	235	257
50°C				
1	—	189.5*	—	—
73	10	209	212	220
128.4	2	229	228	244
158.5	3	237	236	256
188	8	246	244	267
70°C				
1	—	198*	—	—
71.5	8	219.5	219	224
126.7	4	235	236	242
154.1	2	236	243	252
176.9	4	246	249	259

* Calculated from Sutherland's constants derived by least squares by Dr. F. G. Keyes after a critical survey of the literature and transmitted to the author in a private communication. The values of these constants were

	C	$D \times 10^6$
Nitrogen	101.3	1.386
Hydrogen	35.8	0.588

The new data afford a test of the theory derived above which is graphically shown in Figs. 2 to 7. The time of encounter factor was neglected in all calculations as for the least favorable case, lowest temperature and highest density, the correction is less than one percent for nitrogen and is much less for hydrogen. Numerical comparison of the mean observed and calculated viscosity coefficients for nitrogen are given in Table IV. Both viscosity and compressibility covolumes were used in computing the viscosities.

In general there is excellent agreement between experiment and theory when the viscosity covolume is used, but with the compressibility covolume there is a progressively greater difference between the observed and calculated values. The evidence is decidedly in favor of the new theory using the viscosity covolume and the three discrepancies between theory and fact are all attributed to experimental error. In the 30° isotherm two thirds of the maximum pressure is attained without introducing a trend in the comparison and the disagreement is attributed to experimental error. The discrepancy in the 70° isotherm occurs at a point where but two experimental values were available so the disagreement here is not regarded as serious.

A numerical comparison for the hydrogen data is not given as the graphical comparison shows reasonably good agreement in view of the sensitivity of the hydrogen density and low pressure viscosity to traces of impurities. The hydrogen data are of a confirmatory nature.

The mixture data are of especial interest in that they are believed to be the first data of this nature and they afford the opportunity of a direct comparison of the linear and Lorentz²⁷ rules for the calculation of the covolume of a mixture from those of the components. This comparison is particularly significant in view of the appreciable difference in magnitude of the covolumes of the components. The Lorentz rule of combination for a binary mixture is

$$B'_{0\text{ mix}} = B'_{01}X^2 + B'_{012}(1 - X_1)X_1 + B'_{02}(1 - X_1)^2 \quad (13)$$

where X_1 is the mol fraction of component one and

$$B'_{012} = [\frac{1}{2}(B'_{01})^{1/3} + \frac{1}{2}(B'_{02})^{1/3}]^3 \quad (14)$$

The calculated and observed values are given in Table V. A slight but not significant trend in favor of the Lorentz rule is shown. The highly desirable

TABLE V. Comparison of the Lorentz and linear rules for mixtures.
64.1% Hydrogen—35.9% Nitrogen
30°C

Pressure Atm.	No. of Exper. Points	Mean Obs.	Viscosity Coefficients c.g.s. units $\times 10^6$	
			Calc. Lorentz	Calc. Linear
1	—	158*	—	—
49.4	8	166.4	167.0	167.3
123.5	4	168.1	181.5	182.0
195.	4	193.1	195.5	196.0
70°C				
1	—	173*	—	—
51	4	175.3	181.8	182.0
128	4	183.5	196.7	197.3
192	4	202	207.9	208.5

* By interpolation from data of Kleint, Landolt-Bornstein-Roth Tabellen, 5 Ed., Berlin 1923.

²⁷ Lorentz, Wied. Ann. 12, 127, 660 (1881).

simplicity of the linear rule leads to its recommendation here. A plot of the theoretical (using the linear rule) and observed values gives good agreement as shown in Fig. 7.

Further confirmation of the theory is obtained by a recalculation of Wildhagen's²⁸ data which purport to show a variation of Reynolds' criterion with the pressure. This quantity is defined by the equation

$$M/r\mu = \text{constant} \quad (15)$$

and the variation claimed above is in contradiction with a vast amount of experimental evidence which has shown that the value of the criterion is independent of the fluid employed.

Viscosities were computed with the new viscosity theory and values of Reynolds' criterion recalculated for Wildhagen's data. The results are given in Table VI and yield a constant for Reynold's criterion which is strong evidence in support of the new viscosity theory. The chief source of error in

TABLE VI. Recalculations of Wildhagen's values for Reynold's criterion for compressed air.

Pressure Atm.	40	80	120	160	200
<i>Values of viscosity coefficients $\times 10^6$</i>					
Wildhagen (Mean of A and B)	195	224	235	268	321
Calculated from Viscosity Theory	192	205	218	230	242
<i>Reynold's criterion</i>					
Wildhagen (Mean of A and B)	2000	1835	1910	1763	1526
Calculated from Viscosity Theory	2030	2010	2060	2050	2025

Wildhagen's results lies in the neglect of end effects and may attain the order of thirty percent at high densities. The magnitude of the end effects in the cases of Warburg and von Babo²⁹ and of P. Phillips³⁰ is not easy to estimate but is believed to be of the order of at least ten per cent on the basis of previous considerations.

The author wishes to acknowledge his appreciation of the financial aid given him by the Research Laboratory of Applied Chemistry and the committee on Graduate Courses and Scholarships of the Massachusetts Institute of Technology. He is particularly grateful to Dr. T. E. Warren for his assistance and to Dr. J. A. Beattie for his many helpful suggestions. Further, the author wishes to thank Drs. W. K. Lewis, F. G. Keyes and P. K. Frolich for their advice and criticism.

²⁸ Wildhagen, reference 9.

²⁹ Warburg and von Babo, reference 7.

³⁰ P. Phillips, reference 8.

LETTERS TO THE EDITOR

Prompt publication of brief reports of important discoveries in physics may be secured by addressing them to this department. Closing dates for this department are, for the first issue of the month, the twenty-eighth of the preceding month; for the second issue, the thirteenth of the month. The Board of Editors does not hold itself responsible for the opinions expressed by the correspondents.

A New System of Bands in Carbon Monoxide

A new system of CO bands have been obtained when a trace of CO was excited in a long atomic hydrogen tube. Under the best conditions of the experiment, the spectrum of CO showed features that are usually obtained when a trace of CO is excited in the presence of the inert gases.

Under low dispersion, the new bands resemble the third positive group and its two associated groups, 5B and 3A. Each band apparently contains six heads and in addition shows the complex structure that is typical of the above mentioned multiple-headed bands of CO. Because of this striking resemblance it was suspected that the final level of these new bands coincides with the final level of the third positive group and its two associated groups. Only three of the new bands have been found and the separations of similar heads show that they correspond to transitions from an initial level (that may be called "e") to the $v=1, 2$, and 3 levels associated with the "a" level. A rough measurement of these heads has been made

and they have been found to have wavelengths 2518A, 2630A and 2750A, yielding a value of ν_e for the initial level of 88954 cm^{-1} . This value depends of course on the assumption that the upper level is the zero vibrational state.

The failure of these bands to appear under ordinary conditions shows that the initial level must be either a metastable quintet state or a triplet or singlet state. It has not been possible to excite the Cameron bands in the present conditions and this, together with the fact that the Cameron bands have been obtained only very weakly under the best conditions that have been found, shows that intercombinations are very improbable. Until further evidence is available it seems that the most probable identity of the new "e" level is as a metastable quintet state.

JOSEPH KAPLAN

University of California,
Los Angeles, California,
April 25, 1930.

Boundary Conditions in Wave Mechanics

In the April 15 issue of this Journal¹ H. A. Wilson attempts to construct a Schrödinger equation whose solutions shall be known and represent the case of an electron approaching a potential barrier. He neglects to state the interpretation of his procedure explicitly; there are two possible, the second of which is probably the one intended, and I discuss the first only as a basis for the second.

The first interpretation depends on the assumption that any function $F(x, E)$ x =coordinate, E =total energy of the electron) is the solution of some problem in wave

mechanics. The assumption is obviously false, but a proof of its falsity will clarify the discussion of the second interpretation. It is true that a differential equation,

$$\phi'' + k^2(E - V)\phi = 0 \quad (1)$$

can always be found such that $\phi = F(x, E)$ is a solution for any value of E . While this is superficially identical with the Schrödinger equation, it usually differs from the latter in the fundamental fact that V , the potential energy, depends on E , the total energy of the electron. The fact that V is independent of E is one of the fundamental postulates of the Schrödinger theory, hence

¹ Wilson, Phys. Rev. 35, 948 (1930).

only those functions $F(x, E)$ which yield a V independent of E can be considered as solutions of a wave-equation.

The alternative interpretation suppose that V in Eq. (1) is really independent of E , but dependent on another parameter (call it W) which happens to be numerically equal to E ; but then $F(x, E)$ is not in general a solution of (1), but only if $E=W$. The original goal (the construction of a wave-equation, all of whose solutions shall be known) has thus been missed. To put it in another way, $F(x, E_1)$ and $F(x, E_2)$ are solutions of two different wave-equations, corresponding to two physical systems which differ in both their potential and total energies. In order to obtain a complete set of solutions for any one physical problem (single value of the parameter W) it will be necessary to find a function $\phi(x, E, W)$.

This function may satisfy the condition $\phi(x, E, E) = F(x, E)$, but there are other solutions which do not, since electrons may move in either of two directions along the x -axis. The conclusion is that Wilson has not found a complete set of characteristic functions for a given system, but rather one particular function for each of a large number of systems. This seriously restricts the generality of his results.

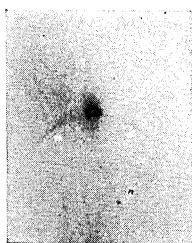
Turning to these, the only one I shall discuss is the conclusion that electrons are not reflected by a potential barrier if their total energy is greater than the maximum value of the potential energy. From the foregoing remarks it follows that this is true for only one particular value of E , and it becomes of interest to find the physical reason for the distinction enjoyed by this particular value of E . This becomes apparent on an examination of Figs. (2) and (3) reference 1, which represent the potential energy, i.e., qualitatively the index of refraction of the de Broglie waves. It is seen that the optical problem analogous to this dynamical one is that of an etalon consisting of one very thin plate placed at a distance of $\frac{1}{4}$ wave-length in front of a much thicker plate. Elementary optical considerations show that such an etalon will not reflect any light but will transmit all of it. If the wave-length of the incident light be changed (variation of E) keeping the separation between the plates constant (fixed W) this situation will change, and for some other wave-length, the reflection will be complete, the transmission zero.

CARL ECKART

University of Chicago,
April 29, 1930.

Photographic Record of First Order Diffraction of Hydrogen Atoms by a Lithium Fluoride Crystal

I have recently obtained a photographic record of the diffraction pattern resulting from the reflection of a beam of monatomic hydrogen atoms from a crystal of lithium fluoride.



The atom beam, which was of nearly circular cross section, was incident upon the crystal at an angle of 30° from grazing and the plane of incidence made an angle of 45° with the cleaved edges. In this position rows of similar ions run parallel and perpen-

dicular to the plane of incidence with a spacing between two consecutive rows of 2.835\AA . The reflected atoms were recorded on a plane surface coated with MoO_3 which was placed perpendicular to the plane of incidence and parallel to the incident beam.

The atoms of the beam were moving with the velocities of thermal agitation in equilibrium at a temperature of about 200°C . Their deBroglie wave-length $\lambda = h/mv$ had a distribution corresponding to the Maxwellian velocity distribution with the most probable wave-length equal to 0.89\AA .

A diffraction pattern appeared on the plate reproduced in the figure which satisfies the cross grating formulae

$$\cos \theta_0 - \cos \theta = n\lambda/d$$

$$\cos \phi_0 - \cos \phi = m\lambda/d$$

where θ and ϕ are, respectively, the angles between any beam and the parallel and perpendicular rows of ions on the surface of the

crystal. The subscript 0 refers to the incident beam. The beams corresponding to $n=0$, $m=\pm 1$ were the most intense and are reproduced quite clearly. They appear in the figure as the parabolic intersection of the detecting plate with the cone $\theta=\theta_0$. The positions of calculated maxima of intensity corresponding to $\lambda=0.89\text{\AA}$ are opposite the white dots and agree well with the observed maxima.

The beams corresponding to $m=0$, $n=\pm 1$ were possibly visible on the original plate but were too faint to reproduce. The maximum corresponding to $n=+1$ is calculated to be at the upper dot but that corresponding to $n=-1$ lies below the plane of the crystal.

THOMAS H. JOHNSON

Bartol Research Foundation,
April 23, 1930.

BOOK REVIEWS

Photo-Processes in Gaseous and Liquid Systems, R. O. GRIFFITH AND A. McKEOWN. Pp. 690. figs. 52. Longmans, Green and Co., London and N. Y., 1929. Price \$8.50.

The authors have brought together in one volume two subjects which have usually been dealt with separately: spectroscopy and photochemistry. Their purpose in presenting the former as an introduction to experimental photochemistry will be generally recognized and approved. The importance of such a ground-work is evident in that the entire first half of the book is concerned with the nature of radiation, series and band spectra, the application of the quantum theory to atomic structure, excitation, spectral absorption of atoms, life of the excited state, molecular spectra, fluorescence and chemiluminescence. This material has been treated not only with all the clarity which is essential in presenting the fundamental principles to chemists, but with a directness and simplicity that may recommend itself to any one interested primarily in this field.

The second half of the book deals with photochemical processes and presents a very careful review of the most important literature. The authors have been generous in their treatment of the views and hypotheses which have been put forward in support of various reaction mechanisms. One chapter is devoted to photochemical reactions in general, two to Einstein's law and photochemical reaction mechanisms, one to the hydrogen-chlorine and carbon monoxide-chlorine reactions, one to photo-sensitization and one to photochemical catalysis and inhibition, temperature coefficient and after effects. An appendix of four and a half pages is devoted to chemical effects of X-rays, alpha-particles and electrons, which affords a brief summary of the field and serves to show that the three quite different agents of chemical activation have common ground in ionization at one stage of the process.

S. C. LIND

Jetziger Stand der grundlegenden Kenntnisse der Thermoelektrizität. C. B. BENEDICKS. Special reprint of 42 pages from volume VIII of *Ergebnisse der exakten Naturwissenschaften*, Julius Springer, Berlin, 1929.

It is so unusual that the Physical Review should be asked to write a review of one of the single articles in the series of the "Ergebnisse" that one looks for some special feature in the situation in explanation, and indeed on reading the article one feels that only special considerations could account for its publication in the series at all. It is well known that in 1916 Benedicks discovered certain thermoelectric phenomena which he claimed rounded out the classical scheme of thermoelectric effects embraced in the Seebeck, Peltier, and Thomson effects, and also that this claim has been received with considerable scepticism, and that the consensus of opinion has been unfavorable. Benedicks has always defended his ideas. In the last few years several papers by other authors have appeared not unfavorable to Benedicks views, and this has apparently impressed the editors of the *Ergebnisse* as lending sufficient interest to the whole subject to justify an invitation to Benedicks to expound from the beginning his whole argument, which he does. It seems to me unfortunate that this new exposition by Benedicks embraces very little new material, and in fact does not discuss at all recent developments which entirely alter the significance of his whole point of view. For example, the relation between Benedicks' "phoretic" theory of conduction in metals and his thermoelectric ideas is expounded. If the ideas of the phoretic theory are to be taken seriously today, one has a right to expect some discussion of the connection between them and the wave mechanics picture of conduction, but wave mechanics is not mentioned.

Perhaps the briefest characterization of Benedicks' position is that he does not accept as correct the law of Magnus, which states that the thermal e.m.f. of a couple depends only on the temperatures of the two junctions, and not on the details of the temperature distribution in the two homogeneous branches. Benedicks fails to recognize that as a general statement applied to solid metals this "law" of Magnus is reduced to a purely academic position in view

of our new knowledge of thermoelectric phenomena in single crystals (as I stated in a paper in 1926), because it is now recognized that there may be thermoelectric currents in a single crystal of a non-cubic metal in which there are temperature differences. It follows that in any ordinary bar or wire of a non-cubic metal in which the size of the individual grains is appreciable, the law of Magnus would not be expected to hold. If I understand Benedicks' position correctly, he would say that this is not the sort of thing he understands by his effect, but he would expect the e.m.f. in an infinitely thin single crystal rod to depend on the manner of temperature distribution along the rod. It follows, therefore, that Benedicks' experiments should now be performed with material so chosen as to rule out this newly recognized possibility, but Benedicks' gives no consideration at all to this sort of thing. It is perhaps significant that he found by far his largest effects in graphite, which is non-cubic.

Benedicks' other experimental evidence leaves me personally unconvinced. I still am confident that an experiment which I made some time ago with liquid mercury to show the non-existence of his effect in mercury constitutes a valid objection, and I have since then tried without success to duplicate his experiment on the temperature difference between two ends of a long wire of constantan carrying a current. (This experiment has not been published.) Finally there is the fact that it has not been possible to find numerical magnitudes for any properties of metals connected with the new effect, neither has it been possible to introduce the constants of the new effect into any thermodynamic discussion or to show their quantitative connection with other phenomena.

The reader cannot but be pleased with the undogmatic attitude of Benedicks in describing his measurements and his ideas. Should any one else be predisposed to examine this subject by independent experiment, he should be fully conscious of the enormous difficulty of eliminating or correcting for all extraneous effects, such as those arising from stresses inevitably associated with temperature gradients in solids, and getting a clean cut proof of the existence of the effect.

P. W. BRIDGMAN

La Théorie de la Relativité et la Mécanique Céleste, Tome II, JEAN CHAZY. 258 pp. Gauthier-Villars et Cie, Paris, 1930. Price fr 60.

This is the second volume of the work of this author on the theory of relativity and celestial mechanics.

In the first volume the author has assumed the Schwarzschild line element as the starting point for investigating the problems of celestial mechanics, and has given from this basis a discussion of the motions of the planets and the curvature of light in passing the sun. The volume includes a detailed chapter on the calculations of Le Verrier and Newcomb on the motions of the planets.

In the present volume, the author presents an exposition of the fundamental principles of general relativity, and proceeding from this basis obtains the results of particular interest for celestial mechanics. These include a derivation of the Schwarzschild line element and the line element inside a fluid sphere, approximate methods for the solution of gravitational problems, a treatment of the effect of the rotation of the attracting mass on the motion of a particle, a discussion of the problem of n bodies with application to the motion of the planets, a treatment of the motion of the moon, and a discussion of the cosmological line elements of Einstein and de Sitter.

RICHARD C. TOLMAN

THE PHYSICAL REVIEW

THE PENETRATION OF A POTENTIAL BARRIER BY ELECTRONS

BY CARL ECKART

RYERSON PHYSICAL LABORATORY, UNIVERSITY OF CHICAGO

(Received April 21, 1930)

ABSTRACT

A potential barrier of the kind studied by Fowler and others may be represented by the analytic function V (Eq. (1)). The Schrödinger equation associated to this potential is soluble in terms of hypergeometric functions, and the coefficient of reflection for electrons approaching the barrier with energy W is calculable (Eq. (15)). The approximate formula,

$$1 - \rho = \exp \left\{ - \int \frac{4\pi}{h} (2m(V - W))^{1/2} dx \right\}$$

is shown to agree very well with the exact formula when the width of the barrier is great compared to the de Broglie wave-length of the incident electron, and $W < V_{\max}$.

THE "failure" of the law of conservation of energy in quantum dynamics, as evidenced by the penetration of an electron through a region of space in which its potential energy is greater than its total energy, has been advanced as the explanation of several phenomena. Gamow,¹ Gurney and Condon,² and others have discussed it in relation to the Geiger-Nuttall law of the radioactive decay constants; Fowler and Nordheim³ in its relation to the lowering of the thermionic work-function by surface impurities, and to the emission of electrons from cold metals under the influence of strong fields.

The mathematical discussions in these papers have all been based either on a potential function which has discontinuous derivatives, or else on approximate treatments involving asymptotic (i.e., divergent) series. It is therefore of some interest to note that there is an analytic function which represents some of the types of potential barriers which have been discussed and whose associated Schrödinger equation is soluble. This function is

$$V(x) = -A\xi/(1 - \xi) - B\xi/(1 - \xi)^2, \quad \xi = -\exp(2\pi x/l), \quad (1)$$

¹ G. Gamow, *Zeits. f. Physik* 51, 204 (1928).

² R. W. Gurney and E. U. Condon, *Phys. Rev.* 33, 127 (1929).

³ R. H. Fowler, *Proc. Roy. Soc. A* 122, 36 (1929), A117, 549 (1927). L. Nordheim, *Zeits. f. Physik* 46, 833 (1928).

in which x is the cartesian coordinate, and A , B , and l are constants. The graphs of this function for various values of A and B are shown in Fig. 1. It is seen to approach zero for large negative values of x and a constant value

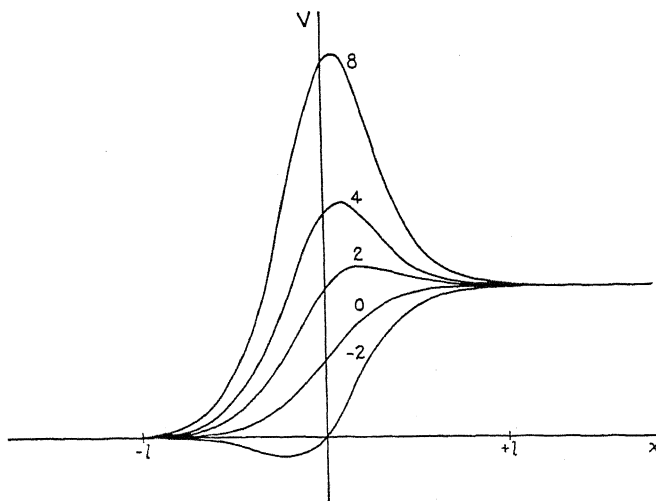


Fig. 1. Graphs of the function $V(x)$. The numbers on the curves are the values of B/A .

A for large positive values. The width of the transition region is, practically speaking, $2l$. When $|B|$ is greater than $|A|$ it possesses an extremum at

$$x_m = \frac{l}{2\pi} \log [(B + A)/(B - A)],$$

whose height is

$$V(x_m) = V_m = (A + B)^2/4B. \quad (2)$$

In the following, it will be assumed that $B \geq 0$ so that the extremum is a maximum, when it exists at all.

The wave equation governing the dynamical problem of an electron moving under the action of this potential is

$$\frac{d^2u}{dx^2} + \frac{8\pi^2m}{h^2} \{A\xi/(1-\xi) + B\xi/(1-\xi)^2 + W\}u = 0 \quad (3)$$

or if differentiation with respect to ξ be indicated by an accent

$$\xi^2 u'' + \xi u' + \frac{2ml^2}{h^2} \{A\xi/(1-\xi) + B\xi/(1-\xi)^2 + W\}u = 0. \quad (4)$$

This equation⁴ is of the hypergeometric type, and its solutions may therefore be written down at once in terms of the hypergeometric series:⁵

⁴ Special cases ($A=0$, and $B=0$) of this equation were discussed in the Colloquium at Pasadena by Professor P. Epstein in 1925, the occasion being the work of Epstein and Robertson on the reflection of radio waves by the Heaviside layer.

⁵ F. Klein, Ueber die hypergeometrischen Reihen, (Göttingen, 1894) pp. 3-7. A. R. Forsythe, Treatise on Differential Equations, (2^d, one vol. ed.) (New York, 1888) p. 185.

$$F(a, b, c, y) = 1 + \frac{a \cdot b}{1 \cdot c} y + \frac{a(a+1) \cdot b(b+1)}{1 \cdot 2 \cdot c(c+1)} y^2 + \dots \quad (5)$$

Before proceeding to study the exact solutions, it will be well to consider their asymptotic behavior for very large positive and negative values of x . In both cases, the potential is practically constant and therefore the solutions should be monochromatic de Broglie waves to a first approximation. For large negative values of x the wave-length will be $\lambda = h/(2mW)^{1/2}$, for large positive values, $\lambda' = h/(2m(W-A))^{1/2}$. It may be assumed that $W \geq A$, since the interest in the other case is not very great. The solution may be specified even more precisely if we confine ourselves to the case in which the electrons are incident on the barrier from $x = -\infty$. Then there will be a single (transmitted) wave

$$\exp(2\pi i x/\lambda') = (-\xi)^{i\beta}, \quad \beta = l/\lambda' \quad (6)$$

for large positive values of x , and two waves (incident and reflected) for large negative values of x :

$$a_1 \exp(2\pi i x/\lambda) + a_2 \exp(-2\pi i x/\lambda) = a_1(-\xi)^{i\alpha} + a_2(-\xi)^{-i\alpha}, \quad \alpha = l/\lambda. \quad (7)$$

As will be shown, the condition that the exact solution reduce approximately to these values for large values of x , suffices to determine it uniquely, and also to determine the constants a_1 and a_2 . The quantity $\rho = |a_2/a_1|^2$ is the reflection coefficient, whose value is required for the applications mentioned in the first paragraph.

In working with the hypergeometric series, Eq. (5), it must be borne in mind that it converges only for $|y| < 1$. It then appears that of the twenty-four well-known ways⁶ in which solutions of the hypergeometric equation can be expressed in terms of $F(a, b, c, y)$, only eight converge for large values of ξ ($x > 1$); of these only four approach $(-\xi)^{i\beta}$ (the other four approaching $(-\xi)^{-i\beta}$) when $|\xi|$ increases indefinitely. The four solutions approaching $(-\xi)^{i\beta}$ are only formally different, so that it suffices to study any one of them; we single out the form

$$u = (1 - \xi)^{i\beta} (\xi/\xi - 1)^{i\alpha} F\left[\frac{1}{2} + i(\alpha - \beta + \delta), -\frac{1}{2} + i(\alpha - \beta - \delta), 1 - 2i\beta, 1/(1 - \xi)\right] \quad (8)$$

in which α and β have the values of Eqs. (6) and (7) and δ is to be defined immediately. If we define a quantity C by the relation $(2mC)^{1/2} = h/2l$, it becomes possible to write

$$\alpha = \frac{1}{2}(W/C)^{1/2}, \quad \beta = \frac{1}{2}[(W - A)/C]^{1/2}, \quad (9)$$

and the quantity δ is then defined by

$$\delta = \frac{1}{2}[(B - C)/C]^{1/2}. \quad (9a)$$

⁶ Klein, pp. 76-80; Forsythe, pp. 189-194.

C is the energy of an electron whose de Broglie wave-length is $2l$, the total width of the region of variable potential.

The function u of Eq. (8) obviously approaches $(-\xi)^{i\beta}$ for large values of ξ , since $F(a, b, c, 0) = 1$. Its value for very small values of ξ cannot be determined at once, however, since the series $F(a, b, c, 1)$ diverges. It is necessary to have recourse to the so-called process of analytic extension, and to express u in terms of series which do converge for small values of $|\xi|$. The result of the analytic extension of the hypergeometric series has been known, practically speaking, since the times of Euler and Gauss; it is summarized in the formula⁷ for compounding two hypergeometric series:

$$\begin{aligned} y^a(1-y)^c F(a+b+c, a+b'+c, 1+a-a', y) \\ = \phi(c, c')(1-y)^c y^a F(a+b+c, a+b'+c, 1+c-c', 1-y) \\ + \phi(c', c)(1-y)^{c'} y^a F(a+b+c', a+b'+c', 1+c'-c, 1-y) \end{aligned} \quad (10)$$

where

$$\phi(c, c') = \frac{\Gamma(1+a-a')\Gamma(c'-c)}{\Gamma(1-a'-b-c)\Gamma(-a'-b'-c)} \quad (11)$$

This equation is an identity for those values of y for which all the series converge, and may be used as a definition of $F(a, b, c, y)$ for $|y| > 1$, $|1-y| < 1$. If we set y equal to $1/(1-\xi)$, $a = -a' = -i\beta$, $b = -b' = \frac{1}{2} + i\delta$, $c = -c' = i\alpha$, and

$$\begin{aligned} a_1 &= \frac{\Gamma(1-2i\beta)\Gamma(-2i\alpha)}{\Gamma[\frac{1}{2} + i(-\alpha - \beta - \delta)]\Gamma[\frac{1}{2} + i(-\alpha - \beta + \delta)]}, \\ a_2 &= \frac{\Gamma(1-2i\beta)\Gamma(+2i\alpha)}{\Gamma[\frac{1}{2} + i(\alpha - \beta - \delta)]\Gamma[\frac{1}{2} + i(\alpha - \beta + \delta)]}, \end{aligned} \quad (12)$$

it reduces to

$$\begin{aligned} u &= a_1(\xi/\xi - 1)^{i\alpha}(1-\xi)^{i\beta} F[\frac{1}{2} + i(\alpha - \beta + \delta), \\ &\quad -\frac{1}{2} + i(\alpha - \beta - \delta), 1 + 2i\alpha, \xi/(\xi - 1)] \\ &+ a_2(\xi/\xi - 1)^{-i\alpha}(1-\xi)^{i\beta} F[\frac{1}{2} + i(-\alpha - \beta + \delta), \\ &\quad -\frac{1}{2} + i(-\alpha - \beta - \delta), 1 - 2i\alpha, \xi/(\xi - 1)]. \end{aligned} \quad (13)$$

The two series on the right side of this equation converge when $|\xi/(\xi-1)| < 1$ hence certainly when $|\xi| < \frac{1}{2}$. For very small values of ξ the value of u may be computed from this equation, and is seen to be exactly the expression of Eq. (7) with a_1 and a_2 defined by Eqs. (12). Eqs. (8) and (13) thus define the function u for all real values of x ; it may readily be shown that it satisfies⁸ Eq. (4), and is finite, continuous, and possesses continuous derivatives

⁷ Klein, pp. 88-91; Forsythe, pp. 194-201.

⁸ For it is a linear function of two of Kummer's twenty-four solutions (cf. reference 6).

throughout this range. It is therefore the wave-function we are seeking, and the coefficient of reflection is hence

$$\rho = \left| \frac{a_2}{a_1} \right|^2 = \left| \frac{\Gamma[\frac{1}{2} + i(\delta - \beta - \alpha)] \Gamma[\frac{1}{2} + i(-\delta - \beta - \alpha)]}{\Gamma[\frac{1}{2} + i(\delta - \beta + \alpha)] \Gamma[\frac{1}{2} + i(-\delta - \beta + \alpha)]} \right|^2 \quad (14)$$

since $|\Gamma(2i\alpha)/\Gamma(-2i\alpha)|$ is obviously 1.

In the numerical evaluation of this formula the two cases, δ =real and δ =imaginary, are to be distinguished. These two cases are separated by the condition $B=C$; since B will in general be of the order of magnitude of W , the case of a real δ corresponds to a potential barrier whose region of inhomogeneity is wide compared to the wave-length of the incident electron (cf. Eq. (9)) while an imaginary δ corresponds to a narrow region of inhomogeneity.

If δ is real, the arguments of all the gamma-functions have the form $\frac{1}{2} + iv$, where v is real. It is known that⁹

$$|\Gamma(u + iv)| = \Gamma(u) \exp[-P(u, v)]$$

and that

$$\exp[P(\frac{1}{2}, v)] = [\cosh(\pi v)]^{1/2}.$$

Hence

$$\begin{aligned} \rho &= \frac{\cosh[\pi(\delta - \beta + \alpha)] \cosh[\pi(\delta + \beta - \alpha)]}{\cosh[\pi(\delta - \beta - \alpha)] \cosh[\pi(\delta + \beta + \alpha)]} \\ &= \frac{\cosh[2\pi(\alpha - \beta)] + \cosh[2\pi\delta]}{\cosh[2\pi(\alpha + \beta)] + \cosh[2\pi\delta]}. \end{aligned} \quad (15)$$

If δ is imaginary, both the numerator and denominator of Eq. (14) have the form

$$|\Gamma(u + iv)\Gamma(1 - u + iv)|$$

with $u = \frac{1}{2} + |\delta|$. Now,

$$\exp[P(u, v) + P(1 - u, v)] = [(\cosh 2\pi v - \cos 2\pi u)/2 \sin^2 \pi u]^{1/2}$$

and hence

$$\rho = \frac{\cosh[2\pi(\alpha - \beta)] + \cos[2\pi|\delta|]}{\cosh[2\pi(\alpha + \beta)] + \cos[2\pi|\delta|]}. \quad (15a)$$

The two Eqs. (15) and (15a) are identical, if it be remembered that

$$\cosh[2\pi\delta] = \cos[2\pi|\delta|]$$

⁹ The formulae regarding $\Gamma(u + iv)$ which are used in the following are all to be found on pp. 23-25 of N. Nielsen, *Handbuch der gammafunktion*, (Leipzig, 1906).

when δ is imaginary; the separate derivation of the two is necessary, however, for $|\Gamma(u+iv)|$ is not an analytic function. The expressions for ρ are plotted in Fig. 2 for $B=8A$ and various values of l .

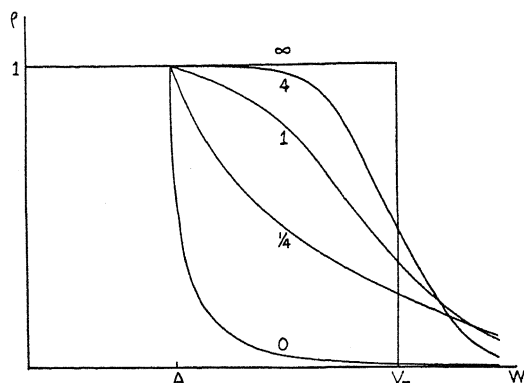


Fig. 2. Graphs of the reflection coefficient. The numbers are the values of A/C .

It is instructive to compare this expression for the reflection coefficient with the values which have been obtained by other writers. If $W < V_m$, the expression

$$1 - \rho = \gamma \exp \left\{ -\frac{4\pi}{h} \int (2m(V - W))^{1/2} dx \right\} \quad (16)$$

has been used, in which the integral is to be extended over all values of x for which $V > W$, and $\gamma \sim 1$. It may be shown that this is a valid approximation to Eq. (15) when l is very large, C very small. In this case, α and β become very large, so that

$$\cosh [2\pi(\alpha \pm \beta)] \sim \frac{1}{2} \exp [2\pi(\alpha \pm \beta)]$$

and $\delta \sim \frac{1}{2}(B/C)^{1/2}$. Hence, approximately,

$$\rho = \frac{1 + \exp [\pi(W^{1/2} - (W - A)^{1/2} - B^{1/2})/C^{1/2}]}{1 + \exp [\pi(W^{1/2} + (W - A)^{1/2} - B^{1/2})/C^{1/2}]}$$

The argument of the exponential in the denominator of this expression is very much greater than 1 when $W \gg V_m$, and very much less than -1 when $W \ll V_m$. Hence

$$\rho = \exp [-\pi(W^{1/2} + (W - A)^{1/2} - B^{1/2})/C^{1/2}] \quad (17)$$

when $W \gg V_m$, and

$$(1 - \rho) = \{1 - \exp[-2\pi((W - A)/C)^{1/2}]\} \exp [\pi(W^{1/2} + (W - A)^{1/2} - B^{1/2})/C^{1/2}]$$

when $W \ll V_m$. When l is very large, therefore, ρ is practically zero if $W > V_m$ and practically 1 if $W < V_m$; these formulae are valid except when $|W - V_m| \sim C$. Comparing the second of Eqs. (17) with Eq. (16) it is seen that the latter is verified if

$$-\frac{4\pi}{h} \int (2m(V - W))^{1/2} dx = \pi(W^{1/2} + (W - A)^{1/2} - B^{1/2})/C^{1/2}.$$

The integral on the left is readily evaluated by the method of residues,¹⁰ and does prove to be equal to the right side of the equation.

For very small values of l (C very large) $\cosh 2\pi\delta$ approaches -1 regardless of B and

$$\cosh 2\pi(\alpha \pm \beta) = 1 + \pi^2[W^{1/2} \pm (W - A)^{1/2}]^2/8C$$

so that

$$\rho = [W^{1/2} - (W - A)^{1/2}]^2/[W^{1/2} + (W - A)^{1/2}]^2.$$

In this limit, therefore, all effect of the maximum of potential function vanishes and the reflection coefficient has the value characteristic of a rectangular potential barrier of infinite width,¹¹ and height A .

For values of W very much larger than A , B , or C ,

$$\cosh [2\pi(\alpha - \beta)] \sim 1, \quad \cosh [2\pi(\alpha + \beta)] \sim \frac{1}{2} \exp [2\pi(W/C)^{1/2}],$$

so that

$$\rho = [1 + 2 \cosh (2\pi\delta)] \exp [-2\pi(W/C)^{1/2}].$$

For $W \leq A$ the reflection coefficient is always unity, as may be most readily deduced from general principles.

¹⁰ See, e.g., A. Sommerfeld, *Atombau*, (4th Ed. 1924), p. 772.

¹¹ See, e.g., W. Heisenberg, *Physical Principles of the Quantum Theory* (in course of publication.)

THE QUANTUM MECHANICS OF ELECTRONS IN CRYSTALS

BY PHILIP M. MORSE

PALMER PHYSICAL LABORATORY, PRINCETON, N. J.

(Received April 18, 1930)

ABSTRACT

A general solution is developed for the motion of electrons in the potential field of the nuclei in a crystal lattice. As usual the energy interaction terms due to nuclear vibration and to the presence of other electrons are neglected; they are to be included later by approximation methods.

It is shown for low energies the wave function becomes a linear combination of the atomic wave functions, the allowed energies approximating the discrete atomic levels; and for high energies the wave function approaches that of the free electron, with the allowed energies a nearly continuous range. However, for electrons coming into the crystal from outside, the crystal becomes impenetrable for those electronic wave-lengths and directions analogous to the beams producing Bragg and Laue beams in x-rays.

The solution is computed for a simple form of potential lattice, and the results are shown to be in quantitative agreement with the experimental results of Davisson and Germer. The phenomenon they call anomalous dispersion is shown to be a natural consequence of the characteristics of the wave function.

INTRODUCTION

THE problem of determining the behavior of electrons in crystals has applications in several types of phenomena: in the scattering of electrons from metal surfaces, instanced by the experiments of Davisson and Germer,¹ of G. P. Thomson and others; and in the behavior of metallic conductors.

The first problem in the study of the theory of any of these phenomena is the study of a single electron in a crystal lattice made up of atomic nuclei fixed at their equilibrium centers. The perturbation terms due to nuclear vibration and to the presence of other electrons must then be dealt with by approximation methods.

The simplest possible assumption for the unperturbed electron is that used by Sommerfeld,² the wave function being approximately like that of a field-free electron:

$$\psi_e(W) = N_e \exp i(W)^{1/2}(ax + by + cz) \quad (1)$$

where W is $8\pi^2\mu/\hbar^2$ times the electronic kinetic energy inside the crystal, and a , b and c are the direction cosines of the electronic motion. This type

¹ This work was begun under the supervision of Dr. Davisson, at the Bell Telephone Laboratories. The writer wishes to express his appreciation of the help the Laboratories in general, and Drs. Davisson and Germer in particular, have given him. He also has obtained many helpful suggestions from Professor E. Wigner.

² Sommerfeld, *Zeits. f. Physik* 47, 1, (1928).

of wave function is most nearly correct for the most loosely bound electrons, but is not sufficiently correct, even for them, to explain the experiments of Davisson and Germer.

The other type of approximation is to consider the electron behavior as primarily determined by the electric fields of the crystal nuclei. Since the potential wall between the atoms is not infinite, there is a finite probability of an electron belonging originally to one nucleus to change to any other nucleus. This means that in equilibrium the wave function for the electrons in the crystal will be any one of the large number of linear combinations of terms, each term representing the electron in the n th quantum state about the s th nucleus.³ This is an example of equivalence degeneracy similar to the simple case of the hydrogen molecular ion, and as a result the energy level corresponding to the n th quantum state of a free atom will be split into a large number of very slightly separated levels; in fact, if the crystal is considered infinite in extent, the levels of the free atom will be spread into bands of allowed energies which may or may not be separated from their neighbors by bands of forbidden energies. Of course the wave functions for the electron will be somewhat modified by this proximity of other nuclei, and Bloch⁴ has used a wave function which becomes, for an infinitely large crystal:

$$\psi_e(E) = N_e \exp i(W)^{1/2}(ax + by + cz) \cdot u(W_a)$$

where E is a function of W and W_a , and u is a linear combination of wave functions representing the electron about the various nuclei with an energy W_a .

This assumption is fairly good for the more tightly bound electrons, in the inner orbits, but for the loosely bound ones, the ones contributing most to the electric conductivity, the field due to the nucleus is so greatly distorted by the neighboring atoms that the undisturbed atomic functions are not particularly good approximations.

At any rate, whatever the potential function happens to be, it can always be represented by the three dimensional Fourier series of the type

$$V = -\frac{h^2}{8\pi^2\mu} \sum_{l,m,n=-\infty}^{\infty} A_{lmn} \exp i(l\alpha x + m\beta y + n\gamma z) \quad (2)$$

where $\alpha, \beta, \gamma = 2\pi/(d_x, d_y, d_z)$, where the d 's are the lengths of sides of the unit lattice cell in the x, y and z directions respectively. The A 's are chosen so that V is real and $A_{000} = 0$. This series is applicable to the cubic, tetragonal and orthorhombic systems of lattices, and the generalization to the other systems is obvious. The wave function for such a potential will be obtained, and its properties investigated, in this paper.⁵

³ Heisenberg, *Zeits. f. Physik* **49**, 619 (1928). A very good resumé of the subject is given by Slater, *Phys. Rev.* **35**, 509 (1930).

⁴ Bloch, *Zeits. f. Physik* **52**, 555 (1928).

THE WAVE FUNCTION

A somewhat less general, but considerably simpler form of potential function

$$V = -\frac{\hbar^2}{8\pi^2\mu} \left[\sum_{l=-\infty}^{\infty} \alpha^2 A_{xl} e^{il\alpha x} + \sum_{m=-\infty}^{\infty} \beta^2 A_{ym} e^{im\beta y} + \sum_{n=-\infty}^{\infty} \gamma^2 A_{zn} e^{in\gamma z} \right] \quad (3)$$

will first be considered. The crystal will at first be considered as infinite in extent, and the average potential as zero, so that $A_{x0} = A_{y0} = A_{z0} = 0$. If the electronic energy is $\hbar^2 W / 8\pi^2\mu$ then the Schrodinger equation which must be satisfied can be separated into three equations of the type

$$\Xi'' + \left(W_x \alpha^2 + \alpha^2 \sum_l A_{xl} e^{il\alpha x} \right) \Xi = 0 \quad (4)$$

where $W_x \alpha^2 + W_y \beta^2 + W_z \gamma^2 = W$. The complete wave function is $\Psi = \Xi(x) \cdot H(y) \cdot \Omega(z)$, where the equations for H and Ω are similar to Eq. (4).

The independent variables are now changed to $\xi, \eta, \zeta = \alpha x, \beta y, \gamma z$ and then all three equations have the form

$$\Xi'' + (W_x + \sum_l A_{xl} e^{il\xi}) \Xi = 0. \quad (5)$$

The solution of this equation was given by Hill,⁶ and is

$$\Xi = N \cdot e^{ik_x \cdot \xi} \cdot \sum_{r=-\infty}^{\infty} b_{xr}(k_x) \cdot e^{ir\xi} \quad (6)$$

where k_x and the b 's are to be determined. k_x is given by the equation

$$\sin^2 \pi k_x = \sin^2 \pi (W_x)^{1/2} \cdot \square(0) \quad (7)$$

where $\square(0)$ is the infinite determinant

$$\begin{vmatrix} \dots & \dots & \dots & \dots & \dots & \dots & \dots \\ \dots & \frac{-A_{x,-1}}{1-W_x} & 1 & \frac{-A_{x,1}}{1-W_x} & \frac{-A_{x,2}}{1-W_x} & \frac{-A_{x,3}}{1-W_x} & \frac{-A_{x,4}}{1-W_x} \dots \\ \dots & \frac{-A_{x,-2}}{-W_x} & \frac{-A_{x,-1}}{-W_x} & 1 & \frac{-A_{x,1}}{-W_x} & \frac{-A_{x,2}}{-W_x} & \frac{-A_{x,3}}{-W_x} \dots \\ \dots & \frac{-A_{x,-3}}{1-W_x} & \frac{-A_{x,-2}}{1-W_x} & \frac{-A_{x,-1}}{1-W_x} & 1 & \frac{-A_{x,1}}{1-W_x} & \frac{-A_{x,2}}{1-W_x} \dots \\ \dots & \frac{-A_{x,-4}}{4-W_x} & \frac{-A_{x,-3}}{4-W_x} & \frac{-A_{x,-2}}{4-W_x} & \frac{-A_{x,-1}}{4-W_x} & 1 & \frac{-A_{x,1}}{4-W_x} \dots \\ \dots & \frac{-A_{x,-5}}{9-W_x} & \frac{-A_{x,-4}}{9-W_x} & \frac{-A_{x,-3}}{9-W_x} & \frac{-A_{x,-2}}{9-W_x} & \frac{-A_{x,-1}}{9-W_x} & 1 \dots \\ \dots & \dots & \dots & \dots & \dots & \dots & \dots \end{vmatrix}$$

⁵ Equations similar to those considered here were discussed by Bethe, Ann. d. Physik 87, 55 (1928), but no solution was obtained, Peierls, Ann. d. Physik 4, 121 (1930) gets an approximate solution, Strutt, Ann. d. Physik 86, 319 (1928) discussed a one-dimensional case.

⁶ Hill, Acta Mathematica 8, 1 (1886).

This determinant can be expanded into a convergent series of the form

$$\begin{aligned} \square(0) = & 1 - (C_{11}A_{x1}^2 - C_{12}A_{x1}^4 + C_{13}A_{x1}^6 \cdots) \\ & - (C_{21}A_{x2}^2 \cdots) \cdots \\ & + (C_{121}A_{x1}^2A_{x2} - C_{122}A_{x1}^4A_{x2} + \cdots) \\ & - (C_{131}A_{x1}^3A_{x3} \cdots) + \cdots \\ & + (C_{1231}A_{x1}A_{x2}A_{x3} \cdots) + \cdots \end{aligned} \quad (8)$$

The values of some of the C 's as functions of W_x are given in Fig. (1).⁷ When the series of A 's converge at least as rapidly as $A_{xn} = 1/2^n$, this expansion

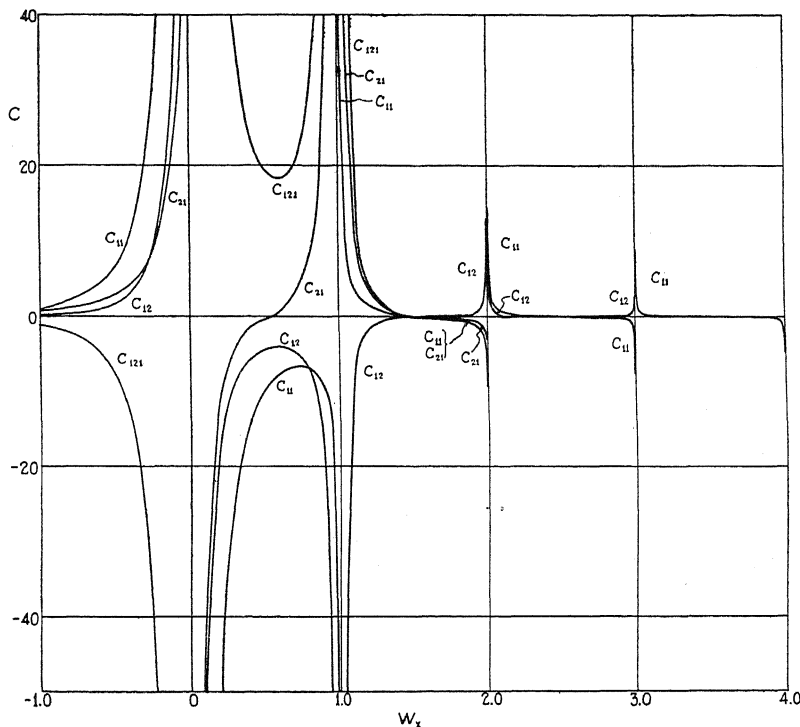


Fig. 1. Values of some of the coefficients in the expansion of $\square(0)$.

is accurate to one part in a thousand if only the terms written above are used.

The b 's are obtained by solving the equations

$$[(k_x + r)^2 - W_x]b_{x,r} - \sum_{l=-\infty}^{\infty} A_{xl}b_{x,r-l} = 0 \quad (9)$$

where r can have any integral value from plus to minus infinity.

⁷ The writer is very much indebted to Mr. B. L. Snavely for computing the values of a number of the functions discussed in this paper.

A generalization of Hill's arguments shows that a solution of the Schrodinger equation using the general potential function given in Eq. (2) will be of the form

$$\psi = N \exp i(\kappa_x x + \kappa_y y + \kappa_z z) \sum_{r,s,t=-\infty}^{\infty} B_{rst} \exp i(r\alpha x + s\beta y + t\gamma z) \quad (10)$$

where the relations between the κ 's are given by the equation

$$S(\kappa_x, \kappa_y, \kappa_z; \alpha, \beta, \gamma) = S(aW^{1/2}, bW^{1/2}, cW^{1/2}; \alpha, \beta, \gamma) \cdot \square(0, 0, 0,) \quad (11)$$

where $\square(0, 0, 0,)$ is a determinant similar to $\square(0)$. The function

$$S(x, y, z; \alpha, \beta, \gamma) = (x^2 + y^2 + z^2) \prod'_{l,m,n=-\infty}^{\infty} \left[1 - \frac{2l\alpha x + 2m\beta y + 2n\gamma z - x^2 - y^2 - z^2}{l^2\alpha^2 + m^2\beta^2 + n^2\gamma^2} \right]$$

where the infinite product does not include the term for which $l=m=n=0$, and a , b and c are the direction cosines which the electronic motion would have if all the A 's were zero. For a two-dimensional case $S(x, y; \alpha, \beta)$ is the product of the elliptic functions $H(x+iy) \cdot H(x-iy)$, where the periods of these functions are $K=\alpha/2$ and $K'=\beta/2$. For the one-dimensional case discussed by Hill, $S(x; \alpha)$ is $\sin^2(\pi x/\alpha)$ as given in Eq. (7). The B 's are given by the equations

$$[(\kappa_x + r\alpha)^2 + (\kappa_y + s\beta)^2 + (\kappa_z + t\gamma)^2 - W]B_{r,s,t} + \sum_{l,m,n} A_{lmn} B_{r-l, s-m, t-n} = 0.$$

Expression (10) is of natural form; that of a free electron whose direction cosines of motion are proportional to κ_x , κ_y and κ_z , multiplied by a function representing the distortion of the wave function due to the periodic variation of the potential function. For low energies this distorting function will be a Fourier expansion of one of the linear combinations of atomic wave functions discussed earlier. In this case Eq. (9) is the form used by Bloch.

One property of (9) must be emphasized, however. The coefficients κ_x , κ_y , κ_z , in the "field-free-electron" factor are not equal to $W^{1/2}(a, b, c)$ as they would be if the A 's all equalled zero, as for Eq. (1). For values of $a(W)^{1/2}$ near $l\alpha/2$, or $b(W)^{1/2}$ near $m\beta/2$, or $c(W)^{1/2}$ near $n\gamma/2$ (i.e., near the singular points of the determinant or near the maximum points of the function S) the κ 's differ considerably from the values $(W)^{1/2}(a, b, c)$, and for certain ranges become complex.

In crystals of infinite extent, the values of W and a , b and c for which any of the κ 's become complex are not allowed; for in these cases the wave function contains a real exponential factor which becomes infinite at plus or minus infinity. Even in the case of finite crystals, it is seen that the amplitude of wave functions for which a κ becomes complex is negligible in the interior of the crystal. Thus for crystals of size greater than, say, a thousand atoms along a side, electrons with energies for which a κ is complex are not present inside the crystal.

This means that the periodic variation of potential inside the crystal creates bands of forbidden energies inside the crystal, even for electronic energies greater than the maximum potential energy, a somewhat surprising result. However, this only means that when electrons outside a crystal have energies such that their wave-number components are integral multiples of the reciprocal lattice spacing, they are reflected strongly back at the surface of the crystal. That this is true experimentally has been shown by Davisson and Germer.

These bands of forbidden energies are very wide for low energies, but become very narrow for higher energies. In other words, the allowed bands of energy are very narrow for low energies, corresponding quite closely to the atomic levels; but for energies larger than the maximum potential energy nearly every energy is allowed. Thus the general solution shows a gradual transition from purely atomic states to states of the free electron, as general considerations have shown it should.

A SIMPLE EXAMPLE

It will be of interest to examine in detail the solution for a very simple form of potential variation. The form

$$V = -\frac{\hbar^2}{8\pi^2\mu} [2\alpha^2 A_x \cos \alpha x + 2\beta^2 A_y \cos \beta y + 2\gamma^2 A_z \cos \gamma z] \quad (12)$$

is not a particularly good approximation to the lattice field, but its solution is not too difficult, and the quantitative check of the computed results with experiment leads one to believe that it is not too bad an approximation when dealing with electrons of high energy. It is, of course, a very poor approximation for the low energy, "bound" electrons, and care should be used in applying its results.

The three Schroedinger equations which must be solved are Matthieu equations

$$\Xi'' + (W_x + Ae^{i\xi} + Ae^{-i\xi})\Xi = 0. \quad (13)$$

The solution is the generalized Matthieu function,⁸ of the form given in Eq. (6), where the values of k_x are given by Eq. (7) when $A_{x1}=A_{x-1}=A$, and $A_{xn}=A_{x-n}=0$, for n greater than unity, in the determinant $\Delta(0)$.

The values of k_x^2 as a function of A and W_x are shown by means of the contour map in Fig. 2. The shaded areas are the values of A and W_x where k_x is complex. It is to be noticed that these areas are larger the larger A is, and are smaller the larger W_x is. The area included between the diagonal dotted lines radiating from $A=W_x=0$ represents the values of W_x less than the maximum and greater than the minimum potential energy. The values of the contours for k_x^2 are equal to the values of W_x when $A=0$, as would be expected. The narrowing of the unshaded bands of energy as A increases

⁸ E. C. G. Poole, Proc. Lond. Math. Soc. 20, 374 (1921); B. van der Pol and M. J. O. Strutt, Phil. Mag. 5, 18 (1928).

illustrates the transition from the continuous allowed levels when $A = 0$ to the discrete levels when A is infinite.

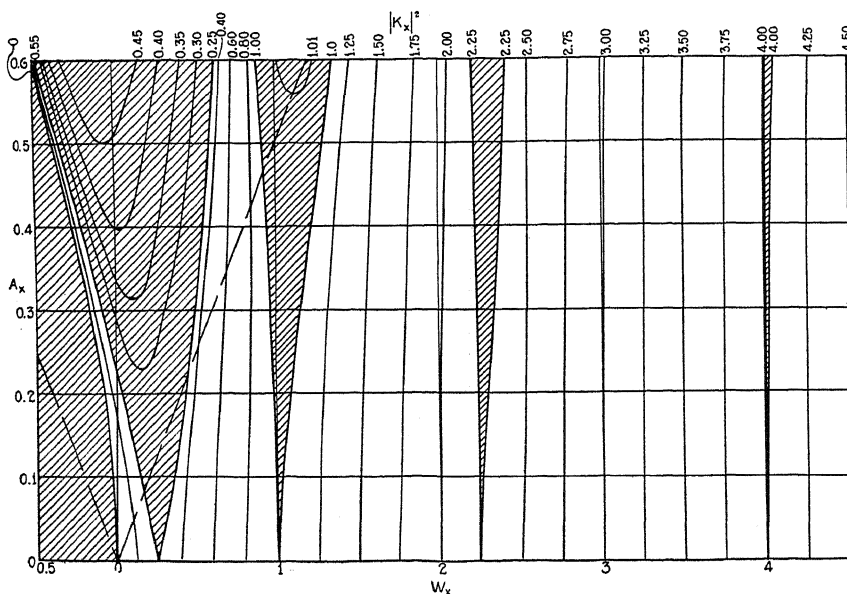


Fig. 2. Values of k_x^2 as a function of A and W_x . Shaded portions represent areas where k_x is complex and equals $(n/2) + ig(W_x)$, where g is real.

The difference between the character of the levels for one atom and for an infinite lattice is shown in Fig. 3. Curve (a) gives the potential energy cross section for a single "atom" with its discrete set of allowed levels, and

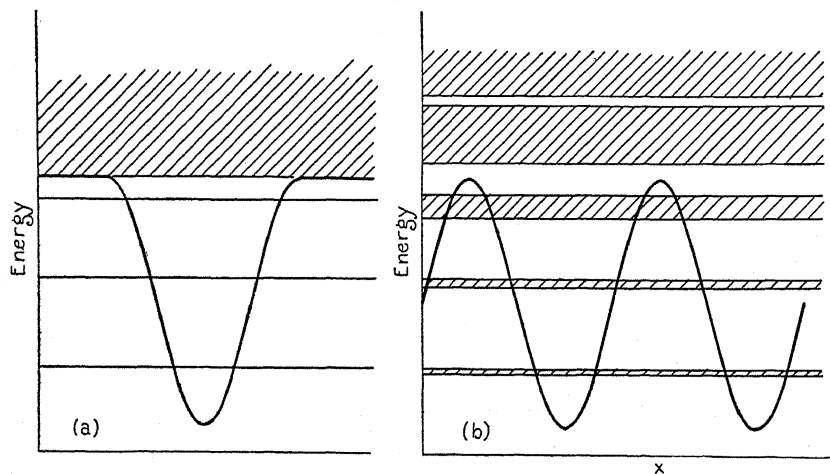


Fig. 3. Potential function and allowed energies for a single "atom" and for a crystal of infinite extent. Horizontal lines represent discrete levels, and shaded areas represent continuous allowed bands.

curve (b) gives the potential function for an infinite lattice with its bands of allowed levels.

The difference between W_x and the real values of k_x for a given value of A can be given by considering W_x as a function of k_x and defining

$$f_x(k_x) = W_x(k_x) - k_x^2. \quad (15)$$

Values of f_x for real values of k_x are given in Fig. 4 for a particular value of A .

The value of A will be chosen to be $1/4$ for the calculations below, since for this value, and for a lattice spacing of 3.5 Angstrom units, the difference between the maximum and minimum potential energy in the crystal will be about 36 electron volts, a reasonable variation.

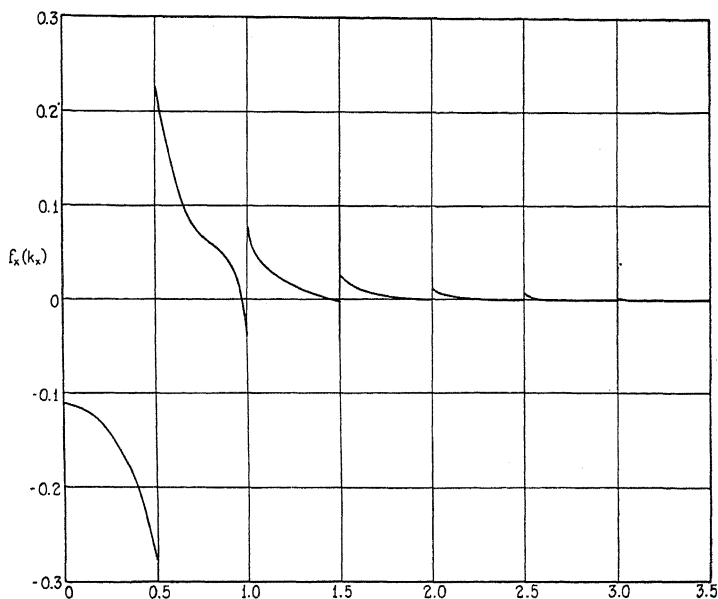


Fig. 4. Values of $f(k_x)$ for real values of k_x , for $A=1/4$.

The Fourier coefficients, $b_{xn}(k_x)$, can next be computed by means of Eq. (9), which in this special case can be transformed⁹ into one or the other of the following continued fractions

$$\frac{b_{x,r}}{b_{x,r+1}} = \frac{A}{S_r - \frac{A^2}{S_{r-1} - \frac{A^2}{S_{r-2} - \dots}}} \quad (16)$$

$$\frac{b_{x,r}}{b_{x,r-1}} = \frac{A}{S_r - \frac{A^2}{S_{r+1} - \frac{A^2}{S_{r+2} - \dots}}}$$

⁹ E. C. G. Poole, Proc. Lond. Math. Soc. 20, 382 (1921).

where $S_r = (k_x + r)^2 - W_x$. Values of b_{xr} are computed in terms of b_{x0} and the value of b_{x0} adjusted so that $\sum_r b_{xr}^2 = 1$, for normalization purposes. Values of the b 's for $A = 1/4$ for various real values of k_x are shown in Fig. 5.

It can be shown in general, by symmetry arguments, that when $k_x = n/2$ (n an integer) $b_{x,r} = \pm b_{x,-n-r}$. In intermediate cases, as is seen in the curves, b_{x0} is very much larger numerically than any of the other b 's.

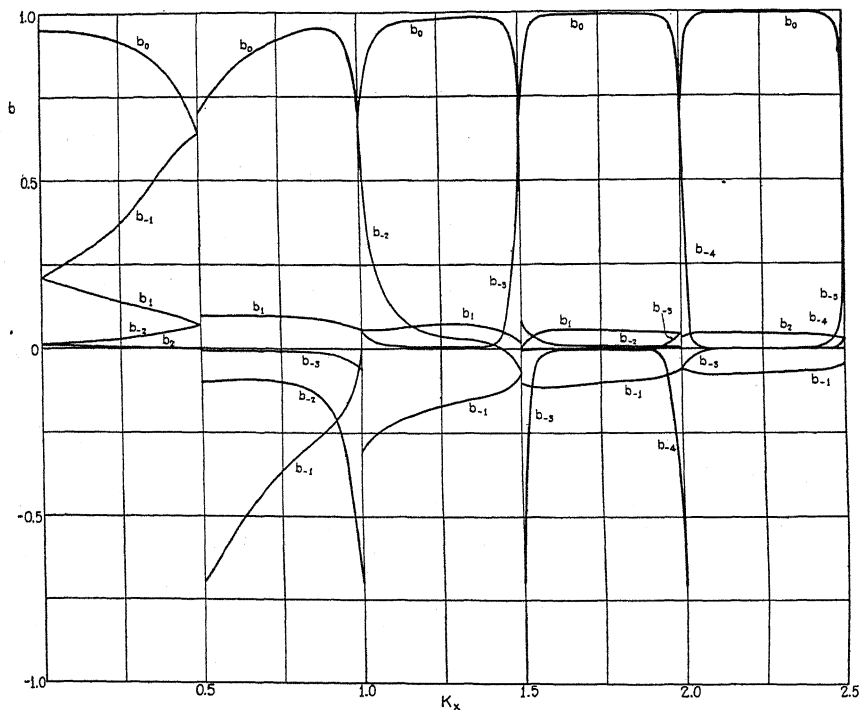


Fig. 5. Values of the Fourier coefficients $b_r(k_x)$ for real values of k_x , for $A = 1/4$. Coefficients not shown in this figure are negligibly small.

SCATTERING FROM CRYSTAL SURFACES

Thus for this simple case it is possible to obtain an exact solution for the motion of electrons inside a potential lattice. Let us see how nearly these results check with experiments with electrons of high energies.

Such experiments have been chiefly concerned with the scattering of electrons from the surface of a crystal. A simple model of this experiment would be a plane electron wave of kinetic energy $\hbar^2 E / 8\pi^2 \mu$ outside the crystal. If the potential outside is zero, that inside will be $\hbar^2 V_0 / 8\pi^2 \mu$ plus the V given in Eq. (12), since the average potential inside the crystal is less than that outside. The values of the W 's used will then be such that $W_x \alpha^2 + W_y \beta^2 + W_z \gamma^2 = W = E + V_0$.

The wave function inside the crystal (positive values of x) will be given by the product of three factors similar to Eq. (6). Then, since the wave

function must be continuous in value and normal gradient at the crystal surface, the wave function outside must be

$$\begin{aligned} \Psi_0 = & \sum_{m,n=-\infty}^{\infty} C_{mn} \exp i \{ [E - (k_y + m)^2 \beta^2 - (k_z + n)^2 \gamma^2]^{1/2} \cdot x \\ & + (k_y + m) \beta y + (k_z + n) \gamma z \} \\ & + \sum_{m,n=-\infty}^{\infty} D_{mn} \exp i \{ - [E - (k_y + m)^2 \beta^2 - (k_z + n)^2 \gamma^2]^{1/2} \cdot x \\ & + (k_y + m) \beta y + (k_z + n) \gamma z \} \end{aligned} \quad (18)$$

where the C terms represent beams impinging on the surface and the D terms represent beams coming from the surface. But to fit the case we were considering, where there was only one incident beam with the direction cosines a , b and c , we must make all the C 's equal to zero except, say, C_{00} , and then make $b^2 E = k_y^2 \beta^2$ and $c^2 E = k_z^2 \gamma^2$. To do this we must introduce other internal beams, due to the secondary internal reflections from the surface.

Then the complete wave function inside the crystal is

$$\begin{aligned} \Psi_i = & \sum_{r,s=-\infty}^{\infty} F_{rs} \exp i [k_x(rs) \alpha x + (k_y + r) \beta y + (k_z + s) \gamma z] \\ & \cdot \sum_{l,m,n} B_{lmn}(rs) \cdot \exp i (l \alpha x + m \beta y + n \gamma z) \end{aligned} \quad (19)$$

where $B_{lmn}(rs) = b_{xl}(k_x(rs)) \cdot b_{ym}(k_y + r) \cdot b_{zn}(k_z + s)$, and where F_{00} , the coefficient of the primary internal beam, can be taken as unity. The value of $k_x(rs)$ is determined by the value of $W_x(rs)$, where

$$\alpha^2 W_x(rs) = E + V_0 - (k_y + r)^2 \beta^2 - (k_z + s)^2 \gamma^2 - \beta^2 f_y(k_y + r) - \gamma^2 f_z(k_z + s).$$

No negative value of k_x is included, since the other boundary of the crystal is considered as being at x equals positive infinity, and no beams reflected from its surface are present.

The intensity of these secondary internal rays is determined by $|F_{rs}|^2$ and will be shown to be small compared to $|F_{00}|^2$. Since also the B 's decrease rapidly (except for special cases considered later) for increasing l , m , n , to a good approximation we can neglect all except the $B_{l00}(rs)$ for every beam except the primary one, where $r = s = 0$.

Then the boundary conditions determining the relative magnitudes of the D 's and F 's for all C 's equal to zero except C_{00} are, approximately

$$\begin{aligned} C + D_{00} &= \sum_l B_{l00}(00) \\ & \quad \sum_l (k_x + 1) \alpha B_{l00}(00) \\ C - D_{00} &= \frac{\sum_l (k_x + 1) \alpha B_{l00}(00)}{(E - k_y^2 \beta^2 - k_z^2 \gamma^2)^{1/2}} \end{aligned} \quad (20)$$

for the incident and primary reflected and refracted beams. Here $C = C_{00}$ and $k_x = k_x(00)$ for brevity. Also

$$D_{rs} = \sum_l [B_{lrs}(00) + F_{rs} B_{l00}(rs)]$$

$$-D_{rs} = \frac{\sum_l [(k_x + l) B_{lrs}(00) + F_{rs} (k_x(rs) + l) B_{l00}(rs)] \alpha}{(E - (k_y + r)^2 \beta^2 - (k_z + s)^2 \gamma^2)^{1/2}} \quad (21)$$

for the secondary beams outside and inside, since all the other C 's are zero.

These equations will hold to a good approximation except in the special cases when F_{rs} becomes of the same order of magnitude as F_{00} (this can only happen when $B_{lrs}(00)$ is of the same order as $B_{000}(00)$, and then not necessarily). In this case the D 's other than D_{rs} will be small anyhow, and the resulting inaccuracy in the determination of the reflected intensities will be small even in this special case.

Then the ratio between the incident current of electrons and the regularly reflected current is

$$\left| \frac{D_{00}}{C} \right|^2 = \frac{\left| \sum_r [(a(E)^{1/2}/\alpha) - k_x - r] b_{xr}(k_x) \right|^2}{\left| \sum_s [(a(E)^{1/2}/\alpha) + k_x + s] b_{xs}(k_x) \right|^2} \quad (22)$$

When k_x is not near half integral values, it is nearly equal to $(a^2 E + V_0)^{1/2}/\alpha$, and b_{x0} is the only not-negligible b_x . Then the formula reduces to

$$\left| \frac{D_{00}}{C} \right|^2 = \left[\frac{a(E)^{1/2} - (a^2 E + V_0)^{1/2}}{a(E)^{1/2} + (a^2 E + V_0)^{1/2}} \right]^2$$

which is the intensity of reflection when $A=0$. That is, except for special values of k_x , the crystal behaves as though it were a hollow of uniform potential $-\hbar^2 V_0/8\pi^2\mu$ with no periodic potential variation at all.

When $k_x = n/2$, however, we have seen that $b_{x,s} = \pm b_{x,-s-n}$, and substituting $-(s+n)$ for r in Eq. (22) it is seen that

$$\left| \frac{D_{00}}{C} \right|^2 = \left[\frac{\pm \sum_s [(aE^{1/2}/\alpha) + (n/2) + s] b_{xs}}{\sum_s [(aE^{1/2}/\alpha) + (n/2) + s] b_{xs}} \right]^2 = 1.$$

For the complex values of k_x , $|D_{00}/C^2| = 1$, but there is a change of phase on reflection. That is, the crystal is perfectly reflecting for every value of electronic energy and direction of incidence which has a value of W_x for which k_x is a half integer or is complex. These values of W_x for any value of A are represented by the shaded areas in Fig. 2.

Of course in an actual crystal the reflected intensity for these values of W_x will be considerably less than unity, because a number of electrons will interact with the crystal atoms as they traverse the lattice. In any case, however, the maximum reflection intensity will be for values of W_x somewhere within the shaded areas in Fig. 2, and can be represented by the equation

$$W_{zn} = (n^2/4) + G_n(A) \quad (23)$$

where G is a small quantity compared to $1/4$, except for the case $n = 1$.

When the incident electron stream is normal to the crystal surface, $W_y = f_y(0)$ and $W_z = f_z(0)$, since k_y and k_z must both equal zero. Equation (18) reduces to

$$W_z \alpha^2 = E + V_p$$

where $V_p = V_0 - \beta^2 f_y(0) - \gamma^2 f_z(0)$, which is larger than V_0 since the $f(0)$'s are negative quantities.

In this case the relative intensity of the reflected beam will be a maximum when

$$E_n = (n^2 \alpha^2 / 4) + \alpha^2 G_n(A) - V_p \quad (24)$$

from Eq. (23). The ideal curve for a typical case is given in Fig. 6. In the actual case, as was previously pointed out, the maxima are less than unity and probably decrease in height for increasing n , since the peaks are narrower and the chance of losing energy is greater. The experimental curves of Davisson and Germer¹⁰ for nearly normal incidence show just such characteristics.

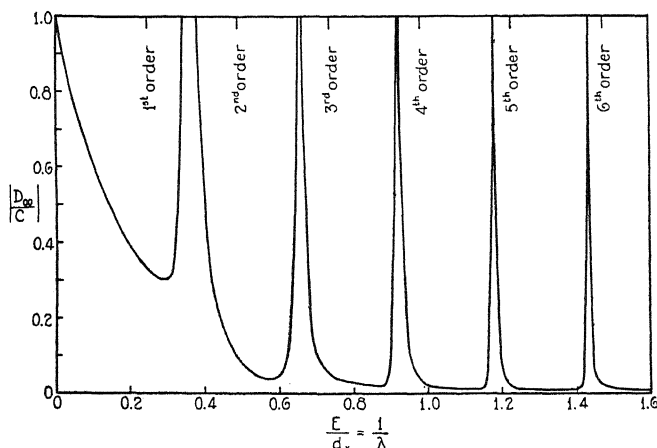


Fig. 6. Relative intensity of the regularly reflected beam as a function of the electronic wave number. The incident beam is normal to the 111 surface of a nickel crystal. Lines marked 1st order, etc., indicate positions of strong x-ray reflection for the same crystal.

There will also be the other scattered beams represented by the coefficients D_{mn} in Eq. (19) whose direction cosines will be $(E - m^2 \beta^2 - n^2 \gamma^2)^{1/2} / E^{1/2}$, $m\beta / E^{1/2}$ and $n\gamma / E^{1/2}$, whose relative intensities will vary with E , but will in general be much smaller than unity.

For an obliquely incident beam whose plane of incidence is parallel to the z axis we have

$$W_z \alpha^2 = E \cos^2 \theta + V_a - \beta^2 f_y \left(\frac{E^{1/2} \cdot \sin \theta}{\beta} \right)$$

¹⁰ Davisson and Germer, Proc. Nat. Acad. Sci. 14, 622 (1928).

where $V_a = V_0 - \gamma^2 f_z(0)$ is larger than V_0 but smaller than V_p , and where θ is the angle of incidence.

The values of θ and E for a regularly reflected beam of maximum intensity will be such that

$$W_{zn} \alpha^2 = (n^2 \alpha^2 / 4) + \alpha^2 G_n(A)$$

similarly to Eq. (23). Substitution in the equation for $W_{zn} \alpha^2$ gives

$$E_n \cos^2 \theta_n = (n^2 \alpha^2 / 4) - V_n + \beta^2 f_y \left(\frac{(E_n)^{1/2} \sin \theta_n}{\beta} \right) \quad (25)$$

where $V_n = V_a - \alpha^2 G_n$, and where E_n and θ_n signify the values of E and θ for maximum regular reflection. Since the quantity f_y is small for most values of its argument (see Fig. 4) we see that the wave-length $1/E_n^{1/2}$ plotted against $\cos \theta_n$ gives in general a straight line going through the origin. However since f_y is large and discontinuous for values of E_n and θ_n near where

$$E_n^{1/2} \sin \theta_n = m\beta/2 \quad (26)$$

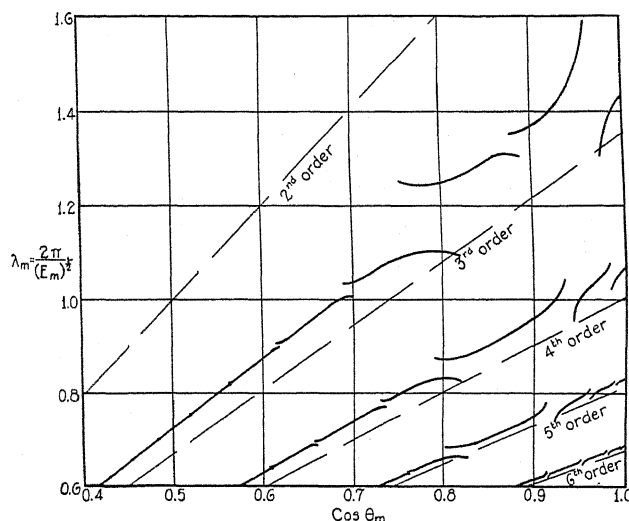


Fig. 7. Values of electronic wave number and angle of incidence of electron beam for strong regularly reflected beam. The crystal is nickel, the surface the 111 plane. Broken lines indicate positions of analogous x-ray reflection.

the curve deviates from a straight line near these values, and is discontinuous. A curve of $1/E_n^{1/2}$ against $\cos \theta_n$ for values of α , β and A corresponding to a nickel crystal is shown in Fig. 7.¹¹

¹¹ The analysis here has been for the case when the crystal surface is the 100 plane, perpendicular to a crystal axis. In the experiments of Davisson and Germer, the crystal surface was the 111 plane, oblique to the crystal axes. In this case, both f_x and f_y vary, and although the discontinuities are of the same character as that given above, their shape is more complicated. Eqs. (25) and (26) still hold, however, if α and β are now considered as the distance between atom planes parallel and perpendicular to the surface, respectively, and $\Phi(E_n^{1/2} \sin \theta_n / \beta)$, a function of f_x and f_y , be substituted for f_y in Eq. (25). Fig. 7 has been computed by means of these revised equations.

When the experimental curves¹² for this case are studied it is seen that not only is the general form of the curves similar, discontinuities and all, but that the positions of the discontinuities correspond. The shape of the curves near the discontinuities does not fit exactly, but if a better approximation to the actual potential function were used in the calculations, the correspondence would probably be better.

The physical explanation of these discontinuities is that for $E_n \sin^2 \theta_n = m^2 \beta^2 / 4$ there is resonance, and therefore strong damping, in the y direction, and nearly all the electrons are reflected back in a direction exactly opposite to the incident beam, leaving none to be regularly reflected. This phenomenon was given the tentative name of "anomalous dispersion" by Davisson and Germer, and in a way this term is correct, for it is due to a simultaneous resonance of the x and y components of the electronic wave number, and a consequent damping out of the wave function in the interior of the crystal.

The other scattered beams in the x, y plane come off at angles ϕ_m , where

$$\sin \phi_m = \sin \theta + m\beta/E^{1/2}. \quad (27)$$

It can be seen from Eq. (21) that their relative intensities will be

$$\left| \frac{D_{m0}}{C} \right| = \left| \frac{b_{ym}(E^{1/2} \sin \theta)}{b_{y0}(E^{1/2} \sin \theta)} \times \frac{\sum_{rs} (k_x' + s - k_x - r) b_{xr}(k_x) \cdot b(k_x')}{\sum_{ln} \left(k_x' + l + \frac{E^{1/2} \cos \Phi}{\alpha} \right) \left(k_x + n + \frac{E^{1/2} \cos \theta}{\alpha} \right) b_{xn}(k_x) b_{xl}(k_x')} \right|^2 \frac{E \cos^2 \theta}{\alpha^2}$$

where k_x' is the $k_x(m0)$ of the beam reflected back into the crystal at the surface, and is a function of the energy W_x' , where

$$\alpha^2 W_x' = E + V_a - (E^{1/2} \sin \theta + m\beta)^2 - \beta^2 f_y \left(\frac{E^{1/2} \sin \theta}{\beta} + m \right)$$

These secondary internal beams will make a slight change in the magnitude of the primary internal beam, but this can be neglected. The quantity b_{ym} is only large when $E^{1/2} \sin \theta$ is near the value $-m/2$, corresponding to reinforcement due to the y, z planes of atoms, and, when E and θ also satisfy Eq. (23), corresponding to the case of "anomalous dispersion" of the regularly reflected beam. The quantity $|D_{m0}/C|^2$ also shows other maxima analogous to the various Laue beams in x-ray scattering.

CONCLUSION

Thus it has been seen that for high energy electrons even the simple potential function used above gives results in good accordance with experiment. This accordance becomes less and less good as we consider electrons with less and less energy, and the results probably do not fit at all for the

¹² Davisson and Germer, Proc. Nat. Acad. Sci. 14, 624 (1928). Later (unpublished) curves show a more complete agreement.

tightly bound electrons in the inner atomic shells, where the allowed energies are narrow bands very slightly different from the simple discrete atomic levels. For these electrons, also, the interaction between electrons cannot be neglected.

However for those electrons whose energy is greater than $-\hbar^2 V_0/8\pi^2\mu$ it seems likely that the results of the simple case discussed above will be indicative. So that while this simple case will not tell us anything about ferromagnetism, for instance, or of any other crystal property which depends on the inner bound electrons, it may be of help in discussing those properties which depend primarily on the high energy free electrons, such as electric conductivity. We have seen that for the still higher energy electrons used in scattering experiments, the agreement with experiment is very good.

When the stationary states inside a crystal of finite size (say a rectangular one whose edges are Ld_x , Md_y , Nd_z respectively, where L , M and N are integers) are considered, it is seen that the wave functions are

$$\psi_{rst} = \frac{(2)^{1/2}}{(L^2d_x^2 + M^2d_y^2 + N^2d_z^2)^{1/2}} \sum_{l,m,n} B_{lmn}(r,s,t) \sin \left[\left(\frac{r}{2L} + l \right) \alpha x + \left(\frac{s}{2M} + m \right) \beta y + \left(\frac{t}{2N} + n \right) \gamma z \right]$$

where the fractions $r\alpha/2L$, $s\beta/2M$ and $t\gamma/2N$ (r , s , t integers) replace the variables κ_x , κ_y and κ_z , and where the B 's are normalized so that $\sum_{l,m,n} B_{lmn}^2 = 1$. From this it can be seen that the distribution of electrons in terms of $r^2\alpha^2/L^2$, $s^2\beta^2/M^2$, $t^2\gamma^2/N^2$ is a normal Fermi one. But, since the energy is a complicated function of these quantities, the electron distribution in energy is different from that of the completely free electron.

AN EXTENSION OF HOUSTON'S AND SLATER'S
MULTIPLY RELATIONS

By S. GOUDSMIT

DEPARTMENT OF PHYSICS, UNIVERSITY OF MICHIGAN

(Received April 21, 1930)

ABSTRACT

Expressions giving the change in the positions of the energy levels with change in electron coupling are derived. The change in g -values is discussed also. The method of derivation is a short-cut of the rigorous detailed method and therefore simpler. One knows the form of the equations of which the desired energies must be roots. The coefficients of these equations are determined by the known results for extreme couplings. This method does not always give all coefficients, but even in complicated cases useful relations between the energy levels are found.

FOR the case of two electrons one of which is in an s -state, Houston¹ obtained expressions for the four resulting levels for any coupling strength. Houston considered the coupling and the spin-orbit interaction as perturbations and calculates by quantum mechanics the first order perturbations to the energy. He also derived expressions for the g -values and for the intensities to show their variation with change of coupling.

As soon as one removes the restriction that one of the two electrons is in an s -state the method used by Houston becomes very complicated. Dr. Laporte has informed me that one can apply Houston's results to configurations like p^5s and d^9s by considering the p^5 and the d^9 group as if it were a single p , or d electron and by taking, in addition, the spin orbit interaction with a negative sign. This remark led to the considerations outlined in this paper.

It is possible to get the main results and often even the complete results of the detailed theory as used by Houston by a simplified procedure. One knows from perturbation theory exactly what type of equations will be obtained for the first order perturbations to the energy. Furthermore one knows from simple considerations of the vector model the energies in extreme (j, j) coupling and in the extreme Russell-Saunders coupling.² In the latter case the results of the vector model have to be supplemented with the results derived by Slater³ which give relations among the distances of various multiplets of a configuration. Our knowledge of these extreme cases is sufficient to fix the most important coefficients, sometimes all coefficients, in the general equation for the energy perturbation.

¹ W. V. Houston, Phys. Rev. **33**, 297 (1929).

² Extreme (j, j) coupling means no interaction between the electrons, extreme Russell-Saunders coupling large interaction, much larger than the interaction between spin and orbit.

³ J. C. Slater, Phys. Rev. **34**, 1293, (1929).

From the formulas obtained in this way one hopes to be able to predict the position of unknown levels but in this respect the results are rather disappointing. First of all one must not forget that we consider only the first order perturbation; thus neither the coupling nor the spin-orbit interaction may be too large. This excludes the very light and the very heavy elements. In the former the singlet-triplet and similar distances are often of the same order as the total energy, in the latter this is the case for multiplet separations. But much worse for their use as predictors of levels is the special form which most of the resulting expressions have. Consider for instance a triplet and a connected singlet level. If one knows the singlet and two levels of the triplet one can predict with great accuracy the position of the third triplet level. This great accuracy, however, is due to the fact that this triplet level is not displaced very much in going from one extreme coupling to the other. A mere guess would have given a fair result. In practice, on the contrary, one always knows the triplet and wants to know the position of the singlet. Its variation in position with change of coupling is very large and a small error in the known triplet causes a large error in the predicted position of the singlet. Of course the percentage error one makes in predicting the triplet level is the same as for the singlet level, but for the latter this corresponds to a much larger absolute error in position. In general the predictions will be most accurate if the singlet is not very far away from the triplet. It is to be regretted that in practice one just always needs the cases where the prediction is most unusable! What is said here for the simple example of a singlet and a triplet holds also for more complicated cases.

Before demonstrating the method by examples we will describe the general equation for the energy perturbation mentioned above. Let us denote the perturbation energies by X_1, X_2, \dots . For instance in the case of two electrons X_1 is the coupling energy, X_2 and X_3 are the spin orbit interactions⁴ for both electrons, X_4 might be the energy in an external magnetic field in case we want the g -values, etc. If, in the configuration which we consider, a certain value of the total moment J occurs for n levels, their energy perturbations E will be the roots of an equation of the n th degree, homogeneous in E and all the X 's.

$$E^n + E^{n-1}\sum a_k X_k + E^{n-2}\sum b_{kl} X_k X_l + E^{n-3}\sum c_{klm} X_k X_l X_m + \dots = 0. \quad (1)$$

It is obvious that only in a few cases our knowledge of the extreme couplings is sufficient to determine *all* the unknown coefficients. But we can be glad that such rather simple cases form quite an interesting group for which there is a large amount of known material and which is also of some interest with regard to the prediction of levels.

In more complicated cases not all coefficients can be found. For example, the coefficients of products of different X 's are often not obtainable by our method. But even if we know only the first coefficient, that of E^{n-1} , it gives

⁴ We neglect the interaction between the one spin and the other orbit. See W. Heisenberg. *Zeits. f. Physik* 39, 499 (1926).

us interesting information. This coefficient is the sum of the roots, with the negative sign, and is, as we see from (1), a linear function of the perturbation energies. From this one can derive relations among the energies similar to the constancy of g -, Γ -, and intensity sum rules.

DEMONSTRATION OF THE METHOD BY EXAMPLES

The configuration p^4 . As we are dealing with equivalent electrons we have only one coupling parameter X and one parameter to measure the spin orbit interaction, which will be denoted by A . This configuration gives rise to one level with $J=1$, two with $J=2$ and also two with $J=0$. In the extreme

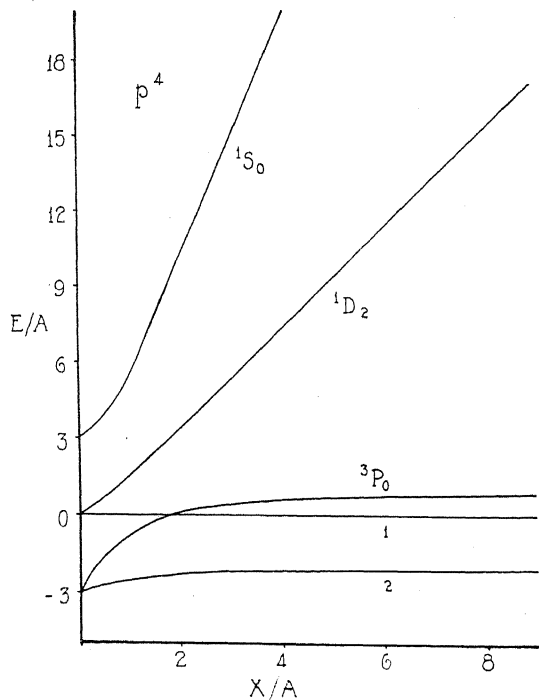


Fig. 1. Change in coupling for configuration p^4 .

Russell-Saunders coupling they would be arranged in an inverted $3P$, a $1D$ and a $1S$. The total separation of the triplet is equal to the doublet separation which one of the p electrons would show if it alone were present.⁵ We will measure the energies in wave number units and for convenience put the ideal triplet separation equal to $3A$. The arrangement in the extreme (j, j) coupling can be found as follows.⁶ The lowest state will have as many electrons as are allowed by the Pauli principle with their individual $j = \frac{1}{2}$. Thus in this state there are two electrons with $j = \frac{1}{2}$ and the remaining two have $j = 1\frac{1}{2}$,

⁵ S. Goudsmit, Phys. Rev. 31, 946 (1928).

⁶ L. Pauling and S. Goudsmit, The Structure of Line Spectra, McGraw-Hill 1930, page 256.

giving rise to one level with $J=2$ and another with $J=0$. Next higher will be the state with one electron with $j=\frac{1}{2}$ and three with $j=1\frac{1}{2}$, producing two levels with $J=0$ and 1. The distance between these levels and the former group will be just the doublet separation of one of the p electrons, as just one changed its j from $\frac{1}{2}$ to 1 and this is again the distance which we call $3A$. Finally again $3A$ higher lies one level with $J=0$ which results from all four electrons having $j=1\frac{1}{2}$. In Figure 1 the left side represents the extreme (j, j) coupling, the right side tends to the extreme Russell-Saunders coupling. As reference level we will take the single level with $J=1$ and give the other levels by their distance E from this level.⁷ Our equations (1) are thus for this example:

$$\begin{aligned} J = 1: E_1 &= 0 \\ J = 0: E_0^2 + E_0(aX + bA) + cX^2 + dXA + eA^2 &= 0 \\ J = 2: E_2^2 + E_2(pX + qA) + rX^2 + sXA + tA^2 &= 0. \end{aligned} \quad (2)$$

Now for $X=0$, in the extreme (j, j) coupling the results must be

$$X = 0: E_0 = -3A \text{ and } +3A; E_2 = 0 \text{ and } -3A.$$

From this follows immediately for the coefficients:

$$b = 0, e = -9; q = 3, t = 0.$$

In the extreme Russell-Saunders coupling we consider first the finite roots.

$$X \text{ large: } E_0 = +A; E_2 = -2A.$$

This gives

$$c = 0, d = -a; r = 0, s = 2p.$$

The large roots in that case will be

$$E_0 = -aX; E_2 = -pX.$$

They represent the 1S_0 and the 1D_2 . Now we need the result obtained by Slater in his above quoted paper, informing us that in the extreme Russell-Saunders coupling the order of the levels is as in our Fig. 1 and that the distance between 3P and 1S is $5/2$ times that between 3P and 1D . If we thus put $-p=2$, we must take $-a=5$ in order to agree with those results. The total set of expressions for p^4 thus becomes

$$\begin{aligned} J = 1: E_1 &= 0 \\ J = 0: E_0^2 - 5XE_0 + 5XA - 9A^2 &= 0 \\ J = 2: E_2^2 - (2X - 3A)E_2 - 4XA &= 0. \end{aligned} \quad (3)$$

For practical purposes it is easiest to choose A as the unit of energy as is done in Fig. 1. The figure shows the interesting crossing over of the triplet

⁷ In some cases the formulas become somewhat simpler if one chooses the center of gravity of a multiplet or of all the levels as reference level, but in practice it is easier to do it the way it is done here.

levels with $J=0$ and $J=1$. This explains for instance the partial inversion of this triplet as observed in tellurium.⁸ With this same example we can check our expressions. The sum of observed E 's for the levels with $J=0$ is $5X = -44 + 18441 = 18397$. For the levels with $J=2$ this sum is equal to $2X - 3A$ and is observed to be $-4751 + 5808 = 1157$. It follows

$$X = 3680 \quad A = 2068, \quad X/A = 1.78.$$

The energies calculated with these values are:⁹

$J = 0$ calc.	- 13	obs.	- 44
	+ 18410		+ 18441
$J = 2$	- 4970		- 4751
	+ 6127		+ 5808.

Figure 2 represents the interval ratio of the triplet as a function of X/A . This figure may be useful to predict roughly the singlets if one knows the trip-

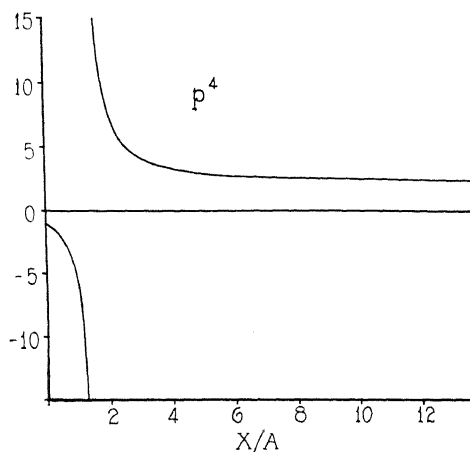


Fig. 2. Interval ratio for $p^4 \ ^3P$ for change from (j,j) to Russell-Saunders coupling.

let in cases near the Russell-Saunders coupling. In such an extreme one may take for A one third of the observed total triplet. The triplet intervals must be known with accuracy however and it is therefore impossible to do this in the very important case of the oxygen spectrum. Assuming the interpretation of the auroral line to be correct, we can predict the position of the singlets with respect to the triplet and find (this time referred to the lowest level 3P_0):

$$^1D_2 = 11984 \quad ^1S_0 = 29909$$

which is very near the estimate of McLennan and Crawford.¹⁰

⁸ J. C. McLennan and M. F. Crawford, *Nature* **124**, 874 (1929).

⁹ As was said above one can check the formulas in such a way as to make them come out either in good or rather bad agreement with the experiments. The way it is done here, however, is probably the least objectionable, being between the two.

¹⁰ They give 10587 and 28512 which again proves that for predictions of this kind the intuition of an experienced spectroscopist is at least as good as any formula. *Nature* **124**, 874 (1929).

The configuration p^2 . Figures 3 and 4 give the result for this configuration. As was to be expected it differs from p^4 only in the sign¹¹ of the coefficients of A . Here there is not such an interesting crossing over of levels as in the p^4 case. The total triplet distance is the same in both extreme couplings, but in between it is somewhat *larger*, which is the remarkable fact discovered by Sawyer and Humphreys.¹² It does not check, however, quantitatively.

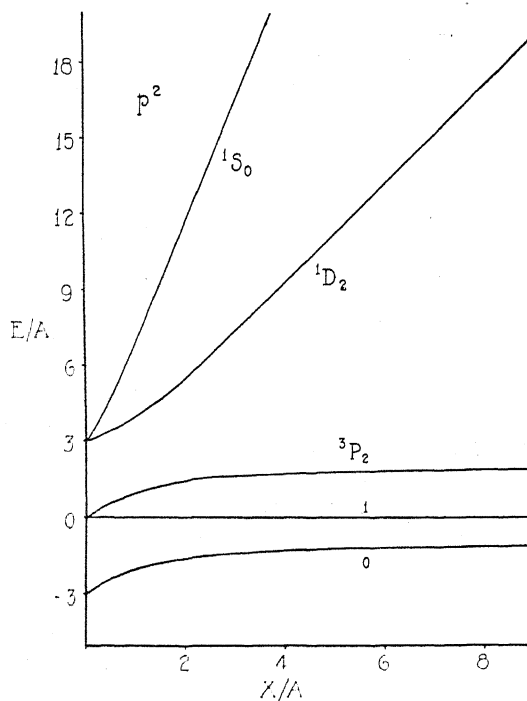


Fig. 3. Change in coupling for configuration p^2

We find a good fitting example in Sn I. By the same method used in the example for p^4 one obtains:

$J = 0$	calc. - 1633	obs. - 1692
	+ 15412	+ 15471
$J = 2$	+ 1649	+ 1736
	+ 7008	+ 6921.

The configuration p^3 . This configuration gives one level with $J = 2\frac{1}{2}$ one with $J = \frac{1}{2}$ and three with $J = 1\frac{1}{2}$. In the extreme Russell-Saunders coupling they

¹¹ It might perhaps have been better to take A negative in the case of p^4 and then the formulas for both cases would have been identical.

¹² R. A. Sawyer and C. J. Humphreys, Phys. Rev. **32**, 582 (1928). The explanation which I suggested at that time and which is mentioned in that article is now of course to be considered as pure nonsense.

form a 4S , a 2D and a 2P , the first one being the lowest and from Slater's paper we obtain that their distances are in the ratio 3:2. From the theory of multiplet separations⁵ we know that in the ideal case the 2D and 2P would show no multiplet splitting at all. For the extreme (j, j) coupling we find¹³ a lowest level with $J=1\frac{1}{2}$, a distance $3A$ higher we find three levels with $J=\frac{1}{2}, 1\frac{1}{2}$ and $2\frac{1}{2}$. Finally again $3A$ higher there is the third level with $J=1\frac{1}{2}$. We will choose the level with $J=2\frac{1}{2}$ as reference level. For the level with $J=\frac{1}{2}$ we

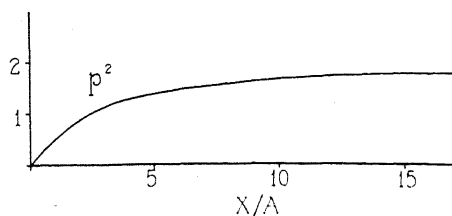


Fig. 4. Interval ratio of $p^2 \ ^3P$ for different strengths of coupling.

expect a linear equation but for the three levels with $J=1\frac{1}{2}$ we must have a cubic equation. Writing down these equations with unknown coefficients gives us:

$$\begin{aligned} J = 2\frac{1}{2}: E_{2\frac{1}{2}} &= 0 \\ J = \frac{1}{2}: E_{\frac{1}{2}} &= pX + qA \\ J = 1\frac{1}{2}: E_{1\frac{1}{2}}^3 + E_{1\frac{1}{2}}^2(aX + bA) + E_{1\frac{1}{2}}(cX^2 + dXA + eA^2) \\ &+ fX^3 + gX^2A + hXA^2 + iA^3 = 0. \end{aligned} \quad (4)$$

It is easily found that the coefficient q for $E_{\frac{1}{2}}$ must be 0. With regard to Slater's result we will most conveniently choose $p=2$. For $J=1\frac{1}{2}$ we have the following known roots:

$$\begin{aligned} X = 0: \quad E_{1\frac{1}{2}} &= -3A, 0, +3A. \\ X = \text{large}: \quad E_{1\frac{1}{2}} &= -3X, 0, 2X, \text{ from Slater's results.} \end{aligned}$$

This gives

$$\begin{aligned} i &= 0, & b &= 0, & e &= -9; \\ f &= 0, & a &= 1, & c &= -6. \end{aligned}$$

We still can determine two more coefficients by remembering that the doublets in the extreme Russell-Saunders case must have zero separation. This means that their levels must fall together even if we take the first order terms of A into account for large X . From this it follows that

$$d = 0 \quad \text{and} \quad g = 0.$$

I see no way, however, to find the coefficient h by the method used here. The final equations are thus

¹³ Pauling and Goudsmit, reference 6, 256.

$$J = 2\frac{1}{2}: E_{2\frac{1}{2}} = 0$$

$$J = \frac{1}{2}: E_{\frac{1}{2}} = 2X$$

(5)

$$J = 1\frac{1}{2}: E_{1\frac{1}{2}}^3 + XE_{1\frac{1}{2}}^2 - (6X^2 + 9A^2)E_{1\frac{1}{2}} + hXA^2 = 0.$$

The first coefficients tell us that the sum of the levels with $J=1\frac{1}{2}$ is half the distance of the level with $J=\frac{1}{2}$, all referred to $E_{2\frac{1}{2}}$. In As for instance we find $E_{\frac{1}{2}}=7271=2X$ and the sum for $J=1\frac{1}{2}$ is 3580 which indeed checks very well.¹⁴ No good agreement can be found in Bi and in N, in the former case A and in the latter X is probably too large for a first order perturbation calculation to be sufficient.

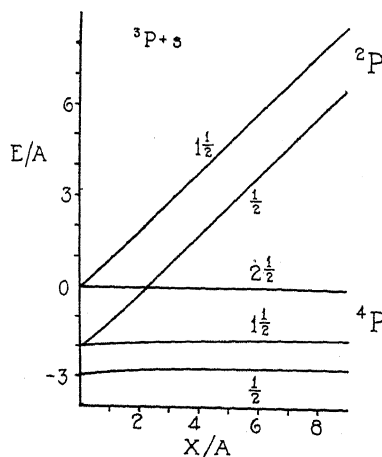


Fig. 5. Addition of an s -electron to a 3P -state for different strengths of coupling.

The configuration ${}^3P+s$ and similar ones. It sometimes occurs that an electron is added to a very regular multiplet state of the next ion for which the connected multiplets of the same configuration are far away. Under such circumstances one may sometimes consider this multiplet as a state in itself and neglect the presence of the other states of the configuration. For such cases we can derive expressions for the variation of the levels with coupling, if we assume that the multiplet state to which the electron is added does not change at all. We will demonstrate this with the simplest example, a 3P state with an added s -electron. In the extreme (j, j) coupling we find the triplet itself, slightly split up by the addition of the electron, as shown at the left of Figure 5. The total triplet separation we put equal to $3A$. In the extreme Russell-Saunders coupling we obtain a 4P and a 2P . The theory of multiplet separations¹⁵ tells us that the separations in the quartet are $5/3 A$ and A , and the doublet separation is $2A$. With the method described before one now finds, choosing the level with $J=2\frac{1}{2}$ for reference, the following equations:

¹⁴ As the doublets in this example are small it proves Slater's relations rather than our formulas.

¹⁵ For this case see S. Goudsmit and C. J. Humphreys, Phys. Rev. 31, 960 (1928).

$$\begin{aligned}
 J = 2\frac{1}{2}: E_{2\frac{1}{2}} &= 0 \\
 J = 1\frac{1}{2}: E_{1\frac{1}{2}}^2 - (X - 2A)E_{1\frac{1}{2}} - 5/3AX &= 0 \\
 J = \frac{1}{2}: E_{\frac{1}{2}}^2 - (X - 5A)E_{\frac{1}{2}} - 8/3AX + 6A^2 &= 0.
 \end{aligned}
 \tag{6}$$

Though these formulas may give the qualitative change very well, one can hardly expect a quantitative agreement except perhaps in a few extreme cases. Sb I is an example where the 2P overlaps partially with the 4P as shown in the left of Fig. 5.

It is not difficult to obtain the formulas for the addition of an s -electron to any multiplet, but if a p - or d - electron is added, it becomes much more complicated.

The configurations d^2 and d^8 . As final examples in this paper we shall give the results for these configurations. They can be treated simultaneously and will differ in the sign of A , which will be positive for d^2 and negative for d^8 . The levels arising from these configurations are

two	with $J=4$
one	with $J=3$
three	with $J=2$
one	with $J=1$
two	with $J=0$.

We shall use the single level with $J=3$ as reference level. In the extreme Russell-Saunders coupling one finds 3F , 3P , 1G , 1D , 1S . The distances of the centers of gravity of the various multiplets in the extreme Russell-Saunders coupling from the center of gravity of the 3F , to which our reference level belongs, will be denoted by

$$\begin{aligned}
 ^3F \text{ to } ^3P &= \alpha X \\
 ^1G &= \beta X \\
 ^1D &= \gamma X \\
 ^1S &= \delta X.
 \end{aligned}$$

From Slater's results one obtains among the coefficients the following relations (for d^2 only):

$$\begin{aligned}
 \alpha &= 15 - 15t \\
 \beta &= 12 + 2t \\
 \gamma &= 5 + 9t \\
 \delta &= 22 + 27t.
 \end{aligned}
 \tag{7}$$

In these expressions t is a new parameter, which from Slater's estimates is about $1/4$. Slater showed for this configuration that the coupling energy depended upon two integrals, which will be different from case to case. These two integrals determine our coefficients. In d^8 and many other configurations more integrals enter combined in such a complicated way that no simple relations between the coefficients exist.

To determine as many coefficients as possible in our final formulas we must again take into account the first approximation in A for large X . This means that though the multiplets are far apart, we do not neglect their own splitting up, which, by the way, we know exactly from multiplet separation theory. We take the doublet separation for a single d -electron equal to $5A$. The total separation for the 3F in the extreme Russell-Saunders coupling is then $7A$, and for the 3P it is $3A$. Remembering that the distances expressed in X are between the centers of gravity one finds the following energies in the extreme cases:

$$\begin{aligned}
 J = 3: & \quad E_3 = 0, \text{ reference level.} \\
 J = 0: X = 0: & \quad E_0 = 5A, -5A \\
 & \quad X \text{ large:} \quad (\alpha X - A), (\delta X + A) \\
 J = 1: & \quad E_1 = \alpha X \\
 J = 2: X = 0: & \quad E_2 = 0, +5A, -5A \\
 & \quad X \text{ large:} \quad -3A, (\alpha X + 2A), (\gamma X + A) \\
 J = 4: X = 0: & \quad E_4 = 0, +5A \\
 & \quad X \text{ large:} \quad +4A, (\beta X + A).
 \end{aligned}$$

The following expressions are the final results. One sees again that one coefficient in the cubic equation for $J=2$ could not be determined by our method.

$$\begin{aligned}
 J = 3: E_3 &= 0 \\
 J = 0: E_0^2 - (\alpha + \delta)XE_0 + \alpha\delta X^2 + (\alpha - \delta)XA - 25A^2 &= 0 \\
 J = 1: E_1 &= \alpha X \\
 J = 2: E_2^3 - (\alpha + \gamma)XE_2^2 + [\alpha\gamma X^2 - (2\alpha + \gamma)XA - 25A^2]E_2 \\
 &\quad + 3\alpha\gamma X^2A + hXA^2 = 0 \\
 J = 4: E_4^2 - (\beta X + 5A)E_4 + 4\beta XA &= 0
 \end{aligned} \tag{9}$$

THE ZEEMAN EFFECT

The application of an external magnetic field may be treated by the addition of a perturbation parameter to our formulas. We denote the field strength by H , expressed in the right units so as to obtain wave numbers in our equations.¹⁶ We then add terms with H to all our coefficients, but as we are only interested in the results for weak fields, we need consider the terms in the first power¹⁷ of H only. We shall discuss the simple case in which the energy is given by a quadratic equation. One can easily extend it to more

¹⁶ For this purpose the wave-number shift of the normal Zeeman effect must be chosen as the unit.

¹⁷ Taking into account all the powers of H would lead to the study of the Paschen-Back effect, which has been done in great detail by C. G. Darwin, Proc. Roy. Soc. A115, 1 (1927).

complicated cases but it is then in general impossible to determine all the necessary coefficients by our method. Equation (1) we will now write

$$E^2 + E(x + pH) + y_2 + qzH = 0. \quad (10)$$

In this equation x , y_2 and z stand symbolically for the linear and quadratic functions of the other perturbations, such as X and A . We assume that x and y_2 are completely known from the problem without field. The term in H^2 has been purposely omitted. We know that the field splits each level into a number of levels with different values of the magnetic quantum number M , but for our purpose we consider only an arbitrarily chosen value for this number. If E' and E'' were the energy levels without field, they become in the field

$$E = E' + Mg'H \text{ and } E'' + Mg''H.$$

Substituting these values in (10) leads at once to

$$g' = -\frac{pE' + qz}{2E' + x} \text{ and } g'' = -\frac{pE'' + qz}{2E'' + x}. \quad (11)$$

There originally stood Mg' and Mg'' , but just because M enters here merely as a proportionality factor we can put it equal to 1 irrespective of the fact whether this is in reality possible value for M or not. From the first part of this paper we have

$$x = -E' - E''.$$

Substituting this and adding the two g -values shows

$$g' + g'' = -p. \quad (12)$$

This is the well-known g -sum rule for this simple case and it tells us at once the value of the coefficient p . The coefficients q of the linear function z of the other perturbation parameters has not such a simple meaning but can always be found by means of the known g -values in extreme couplings.

In our example of the configuration p^4 we find for instance

$$\text{for } J = 2 \quad g = \frac{5/2E - 3X + 7/2A}{2E - 2X + 3A} = \frac{5/2E' - 3X + 7/2A}{E' - E''}. \quad (13)$$

For p^2 one obtains again the same formulas but with the sign of A reversed.

CONCLUSION

We have illustrated our method of deriving relations between multiplets by various examples. Needless to say it is possible to apply it to many more cases than have been mentioned here. For instance it is clear that the formulas derived by Houston can be easily obtained by our method.

In a following paper a few more cases will be treated and the formulas will be applied to the available spectroscopic material. It is actually surprising

that in many instances they are not so very bad after all and even the discrepancies may prove to be of interest.¹⁸

The intensities can be treated by a similar procedure as used in this paper especially since we now know the intensity formulas for the extreme (j, j) coupling from the recent paper by Bartlett.¹⁹

This and the following paper, I hope, will contribute a little bit to the understanding of spectra with intermediate coupling. The fact that so few of such spectra have been analysed at present is certainly only due to a lack of theoretical knowledge of their structure, for the classification of these spectra can not be so very much harder than for multiplet spectra. But one must not look for multiplets in spectra where there are not such structures and one perhaps ought to start by abolishing the use of multiplet notations in those cases, where they are, in the main, meaningless and misleading.

¹⁸ Compare a paper by Laporte and Inglis treating important examples of the d^2s and p^2s configurations, as was mentioned at the beginning of this article. This issue, p. 1337.

¹⁹ J. H. Bartlett, Phys. Rev. 35, 229 (1930).

RESONANCE SEPARATIONS IN CONFIGURATIONS OF TYPE p^5s and d^9s

BY O. LAPORTE AND D. R. INGLIS

DEPARTMENT OF PHYSICS, UNIVERSITY OF MICHIGAN

(Received April 21, 1930)

ABSTRACT

Considerations concerning the invariance of the configurations p^5s and d^9s with changing coupling lead to application of Houston's formulas to the cases p^5s and d^9s with negative A and X values. The expressions thus obtained are tested on the separations and g values of numerous spectra. The agreement is satisfactory.

AS IS well known the separations of the levels within a configuration depend upon influences of two kinds: firstly those of relativistic origin obeying a $(Z-\sigma)^4$ law and secondly those depending upon the coupling between the electrons. Although through the researches of Goudsmit¹ and Slater² the niveau distances are known in the extreme cases of pure Russell-Saunders and of pure $\{jj\}$ coupling, the transition stage has heretofore been investigated only for simple configurations of two electrons one of which is in an s state. The formulas of this case were given by Houston.³

For pure $\{LS\}$ coupling such a configuration yields a triplet and a singlet term with inner quantum numbers $l-1, l, l+1$ and l ; the total separation of the triplet term which is given by the Sommerfeld formula

$$\frac{\Delta\nu}{R} = \frac{\alpha^2(Z-\sigma)^4}{n^3l(l+1)} \quad (1)$$

is small compared with the distance between the two terms. Here A denotes the so-called interval factor, n and l are the quantum numbers of that electron which is not in the s state; Z is the nuclear charge, σ the screening number and $R\alpha^2$ a universal constant with the value 5.82. The position of the middle triplet level is fixed by Landé's interval rule.

In the other extreme case of pure $\{jj\}$ coupling the four levels are arranged in two narrow doublets with the distance (1) from each other. All one knows from elementary considerations about the transition is that the change in coupling will not affect the distance between levels whose inner quantum numbers occur only once, like $l-1$ and $l+1$.

If we define the centroid of the triplet term in the well-known way by

$$\Gamma(J) = \frac{1}{2}A(J(J+1) - l(l+1) - 2),$$

then the general formulas of Houston for the transition from $\{LS\}$ to $\{jj\}$ coupling may be written:

¹ S. Goudsmit, Phys. Rev. 31, 946 (1928).

² J. C. Slater, Phys. Rev. 34, 1293 (1929).

³ W. V. Houston, Phys. Rev. 33, 297 (1929).

$$\left. \begin{aligned} \Gamma_1(l) &= A \left\{ \frac{X-1}{2} + \frac{1}{2}((X+1)^2 + 4l(l+1))^{1/2} \right\} \\ \Gamma(l+1) &= Al \\ \Gamma_2(l) &= A \left\{ \frac{X-1}{2} - \frac{1}{2}((X+1)^2 + 4l(l+1))^{1/2} \right\} \\ \Gamma(l-1) &= -A(l+1) \end{aligned} \right\} \quad (2)$$

X is the parameter which describes the transition; for $X = \infty$ we obtain pure $\{LS\}$, for $X=0$ pure $\{jj\}$ coupling.

MODIFICATION OF HOUSTON'S FORMULAS

The application of these formulas to configurations of type p^5s and d^9s suggested itself to the authors for two reasons: firstly the inner quantum numbers are the same as in the cases ps and ds , and secondly it follows from the above mentioned considerations of Goudsmit, that the configurations p^5 and d^9 yield regardless of coupling 3P and 3D terms the separation of which is given by (1). The only difference is that these terms possess a negative A value, *i.e.* they are inverted. In (2) a negative A value would mean that (for large X) the singlet lies below the triplet term—which is almost never the case. Upon changing the sign of X also, it is seen however that the singlet term and the middle triplet level change places. Thus a negative X as well as a negative A brings about the desired arrangement with an inverted triplet term and a singlet level above it. If then $-X=X'$ and $-A=A'$ with $X', A' > 0$ are introduced into (2) we obtain:

$$\left. \begin{aligned} \Gamma_2(l) &= A' \left\{ \frac{X'+1}{2} + \frac{1}{2}((X'-1)^2 + 4l(l+1))^{1/2} \right\} \\ \Gamma(l-1) &= A'(l+1) \\ \Gamma_1(l) &= A' \left\{ \frac{X'+1}{2} - \frac{1}{2}((X'-1)^2 + 4l(l+1))^{1/2} \right\} \\ \Gamma(l+1) &= A'l. \end{aligned} \right\} \quad (3)$$

For positive X' the magnitude of the four Γ values is in the order in which they are given above. It is readily seen that for large or small X' values, that is to say complete $\{LS\}$ or complete $\{jj\}$ coupling, the levels have indeed the position required.

All that has been said about the separations holds *mutatis mutandis* for the g values of the Zeeman effect. Due to the principle of the permanency of the g sums the g values of the outer triplet levels (with inner quantum numbers $l \pm 1$) are independent of the coupling. They remain unaltered and thus offer nothing new. The g values of the middle triplet level and the singlet level however are obtained from Houston's expressions by introducing $-X = X' > 0$. Thus the following formulas are arrived at:

$$\left. \begin{aligned} g_2(l) &= 1 + \frac{1}{2l(l+1)} + \frac{X' - 1}{2l(l+1)((X' - 1)^2 + 4l(l+1))^{1/2}} \\ g_1(l) &= 1 + \frac{1}{2l(l+1)} - \frac{X' - 1}{2l(l+1)((X' - 1)^2 + 4l(l+1))^{1/2}} \end{aligned} \right\} \quad (4)$$

COMPARISON WITH DATA

A vast amount of spectroscopic material can be interpreted by means of the equations (3), because levels of type p^5s and d^9s occur in a series of well investigated spectra of rare-gas type and of Ni, Pd and Pt type.⁴ Fortunately these spectra have lost their Russell-Saunders character almost completely. The comparison with the data was carried out in the following manner. First from the distance $\Gamma(l-1) - \Gamma(l+1) = A'(2l+1)$ the values of A' were obtained. Then by means of the second and fourth equation (3) the position of the centroid was determined. Finally two independent values of X' were calculated from Γ_2 and Γ_1 by means of the formula

$$X'_{1,2} = \frac{\Gamma_{1,2}}{A'} - \frac{l(l+1)}{(\Gamma_{1,2}/A') - 1} \quad (3')$$

in order to avoid giving preference to either level. The agreement of these two determinations is a measure for the degree of accuracy with which (3) represent the measured separations.

The following Tables I and II give the numerical values for the levels of type p^5s and d^9s respectively. The first and second columns contain symbols

TABLE I.

Spectrum	Configuration	$^1P_1 - ^3P_0$	$^3P_0 - ^3P_1$	$^3P_1 - ^3P_2$	A'	X_2	X_1	g_2	g_1
Ne I	$2p^53s$	1070.1	359.3	417.4	258.9	5.75	5.78	1.036	1.464
Ne I	$2p^54s$	153.7	584.0	194.8	259.6	1.33	1.35	1.220	1.280
Ne I	$2p^55s$	50.1	693.6	84.6	259.1	0.53	0.53	1.291	1.209
Ne I	$2p^56s$	21.7	738.6	42.7	260.4	0.24	0.25	1.314	1.186
Ne I	$2p^511s$	3.28	775.5	4.70	260.1	0.04	0.03	1.331	1.169
Na II	$2p^53s$	2481.0	592.0	765.5	452.8	7.17	7.14	1.023	1.477
Mg III	$2p^53s$	3688	977	1216	731	6.86	6.60	1.026	1.464
A I	$3p^54s$	846.2	803.1	606.8	470.0	3.09	3.11	1.101	1.399
A I	$3p^56s$	64.7	1236.5	77.1	471.2	1.56	0.25		
A I	$3p^57s$	9.23	1393.7	48.3	477.7	0.05	0.12		
A I	$3p^58s$	18.5	1452.5	-21.0	473.0	0.13	-0.07		
A I	$3p^59s$	8.61	1420.2	11.1	473.1	0.03	0.08		
K II	$3p^54s$	1312.0	1912.5	730.0	880.8	2.69	1.54	1.16	1.34
K II	$3p^55s$	291.8	1734.1	417.4	716.8	0.99	0.99	1.251	1.249
Ca III	$3p^54s$	1985.0	1681.4	1383.5	1021.7	3.38	3.45	1.087	1.413
Ca III	$3p^55s$	355.9	2462.3	563.4	1041.9	0.85	1.10	1.252	1.248
Kr I	$4p^55s$	655.0	4274.9	945.0	1740.0	0.920	0.915	1.257	1.243
Xe I	$5p^56s$	988.3	8141.6	977.6	3043.1	0.80	0.51	1.281	1.219

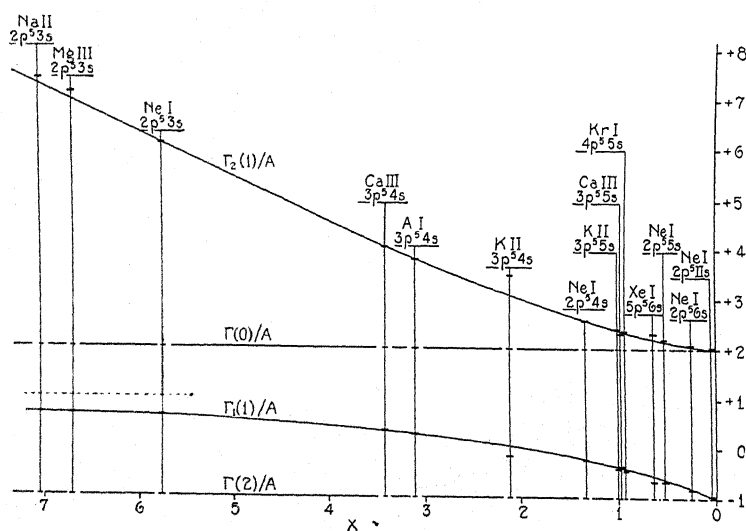
⁴ The sources of data on the Ni-, Pd-, and Pt-like spectra are listed in a paper by J. E. Mack, Phys. Rev. **34**, 18 (1929). Other sources are: Cu: G. Kruger; Phys. Rev. **34**, 1122 (1929). Ne: F. Paschen and R. Goetze, Seriensysteme der Linienspektren, 1922. Na: O. Laporte, Nature **121**, June 16 (1928). Mg: J. E. Mack and R. A. Sawyer, Science **68**, 306 (1928). A: K. W. Meissner, Zeits. f. Physik **39**, 172 (1926); **40**, 839 (1926). K, Ca: I. S. Bowen, Phys. Rev. **31**, 497 (1928). Kr: W. F. Meggers, T. L. de Bruin, C. J. Humphreys, B. S. Journ. Res. **3**, 129 (1929).

for the spectra and configurations in question. In the third, fourth and fifth columns the separations of the four levels are given in cm^{-1} . The sixth column contains the values of the interval factor A' . The seventh and eighth columns

TABLE II.

Spectrum	Configu- ration	$^1D_2 - ^3D_1$	$^3D_1 - ^3D_2$	$^3D_2 - ^3D_3$	A'	X_2	X_1	g_2	g_1
Ni I	$3d^9 4s$	1696.8	833.3	675.0	301.66	7.90	8.12	1.015	1.152
Ni I	$3d^9 5s$	150.4	1322.2	184.1	301.26	1.06	1.11	1.082	1.085
Cu II	$3d^9 4s$	2266.0	1151.2	918.5	413.94	7.73	8.02	1.015	1.151
Cu II	$3d^9 5s$	281.7	1748.7	320.9	413.9	1.44	1.38	1.077	1.090
Cu II	$3d^9 6s$	95.7	1935.7	133.9	413.9	0.54	0.57	1.091	1.076
Cu II	$3d^9 7s$	51.1	2001.6	69.6	414.2	0.29	0.29	1.095	1.071
Zn III	$3d^9 4s$	2650	1576	1178	551	6.93	7.09	1.018	1.148
Ga IV	$3d^9 4s$	2937	2120	1455	715	6.14	6.26	1.022	1.027
Ge V	$3d^9 4s$	3180	2796	1740	907	5.42	5.46	1.027	1.139
Pd I	$4d^9 5s$	1627.8	2338.9	1191.0	706	3.92	4.26	1.051	1.115
Ag II	$4d^9 5s$	2306.5	3017.7	1557.1	915	4.89	4.32	1.034	1.132
Cd III	$4d^9 5s$	2652.4	3866.0	1900.1	1153.2	3.91	4.08	1.040	1.127
In IV	$4d^9 5s$	2871	4912	2196	1422	3.51	3.67	1.044	1.122
Sn V	$4d^9 5s$	3025	6142	2478	1724	3.15	3.27	1.049	1.117
Pt I	$5d^9 6s$	3364.3	9356.1	775.9	2026	2.96	0.73		
Au II	$5d^9 6s$	1855.3	10125.2	2601.5	2545.3	1.53	2.05	1.070	1.096
Hg III	$5d^9 6s$	2679	12377	3179	3111	1.76	2.05	1.068	1.098
Tl IV	$5d^9 6s$	2916	15277	3588	3773	1.56	1.87	1.071	1.127

give the two values of X' as calculated from (3'), and finally in the ninth and tenth columns the g values are listed which were computed from (4) using an average X' .

Fig. 1. Values of Γ/A' plotted against X' .

In Fig. 1 and 2 the values of Γ/A' are plotted against X' for the configurations p^5s and d^9s . Obviously by dividing with A' we free ourselves of the dependance upon the spin doublet of the preceding ion and are then in a position to study the dependence of the separations upon X' alone.

The bad agreement in the case of platinum is probably due to the fact that our equations (3) which are only the result of a first order calculation do not hold in the case of very large A' values which are comparable with the ionization potential $d^9s - d^9$. We thus understand the better agreement for the higher isoelectronic analogues of Pt I, namely Au II, Hg III, etc.

On the other hand the total lack of agreement for the higher series members $3p^56s$ to $3p^59s$ of A I renders doubtful the identifications of the combinations involved. The same might be said of $3p^54s$ of K II.

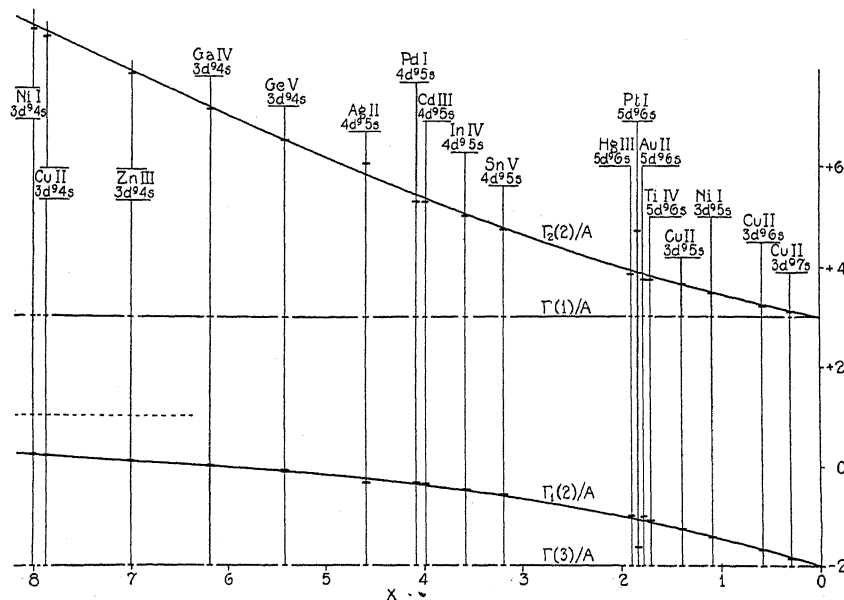


Fig. 2. Values of Γ/A' plotted against X' .

It is interesting to study the dependence of X' upon Z for a group of isoelectronic spectra. It seems that after some initial irregularities X' varies almost linearly with Z .

The only spectrum in which a comparison of the equations (4) with the experiment is possible, is Ne I. In this spectrum the g values of the singlet and the middle triplet level of $2p^53s$ were measured by Back.⁵ The following Table III gives the comparison of experimental and theoretical values.

TABLE III.

	observed (Back)	calculated Table II.	calculated {LS} coupling	calculated {jj} coupling
g_2	1.034	1.036	1.000	1.300
g_1	1.464	1.464	1.500	1.200

The agreement is excellent. Many attempts have been made in the past to compute the g values of these Ne levels, but naturally only the values in limiting cases were obtained.

⁵ E. Back, Ann. d. Physik 76, 329 (1925).

SINGLET-TRIPLET INTERVAL RATIOS FOR sp , sd , sf , p^5s AND d^3s CONFIGURATIONS*

BY E. U. CONDON AND G. H. SHORTLEY

UNIVERSITY OF MINNESOTA

(Received April 29, 1930)

ABSTRACT

A systematic comparison of the known data on the singlets and triplets arising from sp , sd , sf , p^5s and d^3s configurations with the theory of Houston shows that the theory gives a good account of the deviations from the Landé interval rule which accompany departure from Russell-Saunders coupling. There are numerous significant discrepancies, however. Writing 1L_l and $^3L_{l+1}$, 3L_l , $^3L_{l-1}$ with $L=P, D, F$, when $l=1, 2, 3$ for the term values, we plot as abscissa $(^3L_{l-1}-^3L_{l+1})/|^3L_l-^1L_l|$ and $(^3L_{l-1}-^3L_l)/(^3L_l-^3L_{l+1})$ as ordinate if $(^3L_l-^1L_l)$ is positive, otherwise the reciprocal of this quantity. Houston's equations (12) give functional relations between these interval ratios which are compared with the experimental values.

HOUSTON¹ has worked out an approximate quantum mechanical theory of the relation of the triplet interval ratio to the singlet-triplet interval for two electron configurations in which one of the electrons is in an s state, but the comparison he makes with experimental data gives one very little idea as to just how accurate the theory is. The purpose of the present paper is therefore to make a systematic comparison of the available data with Houston's theory.

If we write the terms of a singlet-triplet system as 1L_l , $^3L_{l+1}$, 3L_l , $^3L_{l-1}$, with $L=P, D, F$, when $l=1, 2, 3$, Houston's equations (12) give the following relative term values in terms of the parameter X , which is the ratio of the exchange perturbation integral to the perturbation theory integral which measures the spin energy. (The first classification applies to $X > 0$, the second to $X < 0$):

$$\begin{aligned} ^1L_l, ^3L_l &= -\frac{1}{2}(X-1) - \frac{1}{2}\{(X+1)^2 + 4l(l+1)\}^{1/2} \\ ^3L_{l+1} &= -l \\ ^3L_l, ^1L_l &= -\frac{1}{2}(X-1) + \frac{1}{2}\{(X+1)^2 + 4l(l+1)\}^{1/2} \\ ^3L_{l-1} &= l+1. \end{aligned}$$

Fig. 1. illustrates the behavior of these intervals. With X large and positive the triplet has the Landé interval and the singlet is high above the triplet as at a . As X approaches zero the levels approach coincidence in pairs as at b ; and with X large and negative we again have the Landé interval with the singlet far below the triplet as at c .

* This paper was presented at the Washington meeting of the American Physical Society, April 24, 1930.

¹ W. V. Houston, Phys. Rev. 33, 297 (1929).

The theoretical curves of Figs. 2 and 3 are plotted as follows: For abscissa is used $(^3L_{l-1} - ^3L_{l+1}) / |^3L_l - ^1L_l|$. For the lower curve, $X > 0$, the ordinate is $(^3L_{l-1} - ^3L_l) / (^3L_l - ^3L_{l+1})$, which goes from $l/(l+1)$ with abscissa zero, to zero with abscissa one. For the upper curve, $X < 0$, the ordinate

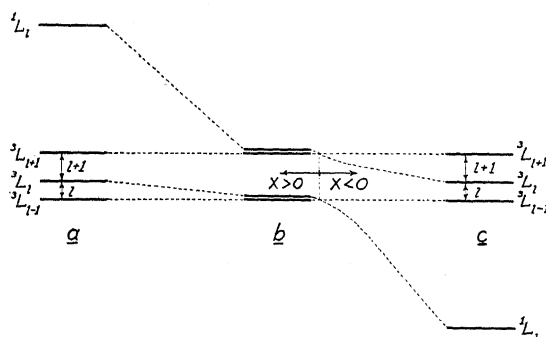


Fig. 1. Diagram illustrating the behavior of the singlet-triplet intervals. (a) X large and positive. (b) X very small and positive. (c) X large and negative.

is the reciprocal of this, $(^3L_l - ^3L_{l+1}) / (^3L_{l-1} - ^3L_l)$, which goes from zero with abscissa one to $(l+1)/l$ with abscissa zero. The fact that the abscissa starts increasing (to $(l+\frac{1}{2})/(l(l+1))^{1/2}$ at $X = -1$) shows that $^1L_l - ^3L_l$ becomes less than the whole spread of the triplet until the ordinate equals $1/2l$ at $X = -2$.

TABLE I. Coordinates.

† indicates a point which is not plotted on account of large probable error (see text).
* indicates a point which does not fall within the limit of Figs. 2 and 3.

Elem.	Config.	Abs.	$sp(X > 0)$ Ord.	Sources
Al II	3s3p	0.0084	0.493	Int. Crit. Tab.
	4p	0.0293	0.481	
	5p	0.1145	0.445	
Ba I	6s6p	0.2301	0.422	Int. Crit. Tab.
	7p	0.1410	0.420	
	8p	0.1181	0.619	
C I	3s2p	0.0527	0.499	Proc. Roy. Soc. A118, 43
Ca I	4s4p	0.0179	0.494	Int. Crit. Tab.
	5p†	0.1253	0.110	
Cd I	5s5p	0.1315	0.462	Int. Crit. Tab.
	6p	0.1695	0.406	
	7p	0.202	0.355	
	8p	0.211	0.378	
	9p	0.219	0.367	
Ga II	4s4p	0.0604	0.478	Phys. Rev. 34, 714
	5s4p	0.1476	0.424	
Ge I	5s4p	0.719	0.177	Phys. Rev. 31, 786
	6s4p	0.914	0.095	
Ge III	4s4p	0.0818	0.465	Phys. Rev. 34, 698
	5p	0.276	0.366	
Hg I	6s6p	0.436	0.382	Int. Crit. Tab.
	7p	1.035	0.094	
	8p	0.952	0.056	
Mg I	3s3p	0.0046	0.487	Int. Crit. Tab.
N II	3s2p	0.680	0.235	Proc. Roy. Soc. A114, 662
	4s2p	0.135	0.437	
	5s2p	0.305	0.373	
O III	3s2p	0.0658	0.458	Proc. Roy. Soc. A118, 43
Pb I	7s6p	0.972	0.032	Phys. Rev. 33, 301
Pb III	6s6p	0.600	0.274	Phys. Rev. 34, 397
Sb IV	5s5p	0.278	0.388	Phys. Rev. 34, 402
Si I	4s3p	0.221	0.395	Zeits. f. Phys. 40, 530
Sn I	6s5p	0.918	0.074	Phys. Rev. 30, 574
Sn III	5s5p	0.230	0.407	Int. Crit. Tab.
	6p	0.598	0.226	
Sr I	5s5p	0.0808	0.474	Int. Crit. Tab.
	6p	0.607	0.395	
Te V	5s5p	0.323	0.366	Phys. Rev. 34, 402
Tl II	6s6p	0.528	0.316	Phys. Rev. 35, 236
	7p	0.403	0.088	
Zn I	4s4p	0.0406	0.489	Int. Crit. Tab.
	5p	0.0507	0.475	
	6p	0.0589	0.464	
	7p	0.0666	0.456	
	8p	0.0651	0.464	
	9p†	0.0739	0.514	
Yt II	5s5p	0.321	0.380	Bur. Stand. J. of Res. 2, 738
Elem.	Config.	Abs.	$sp(X < 0)$ Ord.	Sources
Al II	3s6p*	0.1045	2.193	Int. Crit. Tab.
Ca I	4s6p	0.0140	1.950	Int. Crit. Tab.
Hg I	6s9p*	0.3935	5.356	Int. Crit. Tab.
	10p*	0.1273	7.135	
	11p*	0.1131	8.73	
Sr I	5s7p*	0.0902	2.100	Int. Crit. Tab.
Elem.	Config.	Abs.	$p^{ss}(X < 0)$ Ord.	Sources
A I	3p ⁴ s	0.854	0.756	Zeits. f. Phys. 40, 839
	6s	1.008	0.0578	
	7s	1.021	0.0282	
	9s	1.002	0.0078	
Ca III	3p ⁶ 4s	0.814	0.823	Phys. Rev. 31, 501
	5s*	1.109	0.269	
K II	3p ⁶ 4s	0.819	0.383	Phys. Rev. 31, 501
	5s	1.063	0.241	
Kr I	4p ⁶ 5s	1.058	0.221	B. S. J. Res. 3, 154
Na II	2p ⁶ 3s	0.442	1.293	Phys. Rev. 31, 967

TABLE I (continued)

Ne I	2p ³ s	0.544	1.161	Int. Crit. Tab.
	5s	1.047	0.122	
	6s	1.027	0.0578	
	7s	1.017	0.0322	
	8s	1.010	0.0211	
	9s	1.006	0.0125	
	10s	1.003	0.0084	
	11s	1.001	0.0061	
Xe I	5p ⁶ s	0.999	0.120	B. S. J. Res. 3, 756

Elem.	Config.	Abs.	sd (X > 0) Ord.	Sources
Ba I	6s5d	0.258	0.476	Int. Crit. Tab.
Ca I	4s3d	0.0237	0.640	Int. Crit. Tab.
	5d†	0.0258	0.607	
	7d†	0.712	0.750	
Cr V	4s3d	0.1678	0.525	Phys. Rev. 33, 542
Lu II	6s5d	0.490	0.363	Bul. Am. Ph. Soc. Apr. 10, 1930, 11
*Pb III	6s5d	0.220	0.466	Phys. Rev. 34, 397
Sb IV	5s5d	0.258	0.628	Phys. Rev. 34, 402
	6d	0.562	0.683	
Sc II	4s3d	0.0718	0.616	Sci. Papers, Bur. Stand. 22, 329
	5s3d	0.301	0.483	
Sn III	5s5d	0.250	0.659	Int. Crit. Tab.
	6d	0.129	0.610	Phys. Rev. 34, 402
Sr I	5s4d	0.083	0.600	Int. Crit. Tab.
	6d	0.409	0.398	
Te V	5s5d	0.257	0.616	Phys. Rev. 34, 402
Ti III	4s3d	0.1031	0.592	Astro. J. 69, 13
V IV	4s3d	0.1335	0.558	Phys. Rev. 33, 542
Yt II	5s4d	0.272	0.506	B. S. J. Res. 2, 738
	6s4d	0.996	0.124	

Elem.	Config.	Abs.	sd (X < 0) Ord.	Sources
Ba I	6s6d	0.0485	1.228	Int. Crit. Tab.
	7d	0.0456	0.438	
	8d	0.0284	1.190	
	9d	0.0746	1.595	
	10d†	0.0324	4.61	
Ca I	4s4d	0.0207	1.474	Int. Crit. Tab.
	6d†	0.0544	1.200	
Cd I	5s5d	0.1074	1.555	Int. Crit. Tab.
	6d	0.0621	1.414	
	7d	0.0553	1.388	
	8d†	0.0454	6.000	
Ga II	4s4d	0.0096	1.360	Phys. Rev. 34, 714
	5s4d	0.0029	1.416	
	6s4d	0.0022	1.125	
Ge III	4s4d	0.0099	1.505	Phys. Rev. 34, 697
Hg I	6s6d*	1.510	0.585	Int. Crit. Tab.
	7d	1.018	0.923	
	8d	0.808	1.051	
	9d	0.717	1.438	
	10d	0.653	0.556	
Pb III	6s5d	0.250	2.145	Phys. Rev. 34, 397
Sr I	5s5d	0.183	1.520	Int. Crit. Tab.
	7d	0.273	1.195	
	8d	0.163	1.250	
	9d	0.298	1.271	

Tl II	6s6d	0.532	1.384	Phys. Rev. 35, 236
	7d	0.237	1.173	
	8d*	0.118	1.861	
Zn I	4s4d	0.0283	1.618	Int. Crit. Tab.
	5d†	0.0128	1.818	
Yt II	5s5d	0.0533	1.509	B. S. J. Res. 2, 738

Elem.	Config.	Abs.	sd (X < 0) Ord.	Sources
Ag II	4d ⁹ s	0.862	0.526	Phys. Rev. 31, 317
	6s	1.022	0.0896	
Au II	5d ⁹ s	1.062	0.2569	Phys. Rev. 34, 19
Cd III	4d ⁹ s	0.886	0.4916	Phys. Rev. 31, 778
Cu II	3d ⁹ s	0.605	0.798	Phys. Rev. 29, 386
	5s	1.018	0.1835	
	6s	1.018	0.0692	Phys. Rev. 34, 1128
	7s	1.010	0.0348	
Ga IV	3d ⁹ s	0.708	0.686	Phys. Rev. 31, 750
Ge V	3d ⁹ s	0.759	0.622	Phys. Rev. 31, 750
Hg III	5d ⁹ s	1.033	0.2568	Phys. Rev. 34, 19
In IV	4d ⁹ s	0.913	0.447	Phys. Rev. 31, 778
Ni I	3d ⁹ s	0.596	0.810	Phys. Rev. 29, 386
	5s	1.024	0.1393	
	6s	1.016	0.0519	Phys. Rev. 34, 828
Pd I	4d ⁹ s	0.890	0.510	Phys. Rev. 29, 386
	6s	1.018	0.065	
Pt I	5d ⁹ s	0.796	0.0829	Phys. Rev. 34, 19
	7s	1.001	0.0374	Phys. Rev. 34, 190
Tl IV	5d ⁹ s	1.042	0.235	Phys. Rev. 34, 19
Zn III	3d ⁹ s	0.652	0.748	Phys. Rev. 30, 381

Elem.	Config.	Abs.	sf (X > 0) (not plotted) Ord.	Sources
Al II	3s4f†	0.0978	0.750	Int. Crit. Tab.
	5f	0.0506	0.783	
	6f	0.0573	0.777	
	7f	0.0389	0.761	
	8f	0.0118	0.657	
	9f†	0.0049	0.750	
	10f†	0.0030	0.786	
	11f†	0.0016	0.667	
	12f†	0.0019	0.800	
*Ge III	4s4f	1.384	0.275	Phys. Rev. 34, 697
Sn III	5s4f	0.0556	0.378	Int. Crit. Tab.
	5f	0.0312	0.357	Phys. Rev. 30, 574
Sr I	5s4f†	0.0056	0.630	Int. Crit. Tab.
	5f†	0.0113	0.889	
	6f†	0.1765	0.049	
	7f†	0.314	0.165	

Elem.	Config.	Abs.	sf (X < 0) (not plotted) Ord.	Sources
Ba I	6s4f	0.0046	1.014	Int. Crit. Tab.
	5f	0.0847	4.34	
	6f	0.0092	1.594	

* S. Smith, Phys. Rev. 34, 397 (1929) has a question as to which of two singlets belong to this configuration. These are both listed, one for $X > 0$, plotted with a question mark and one for $X < 0$, which tell off the graph.

† The singlet is within the triplet.

A fairly complete search of the literature was made and the points plotted on Figs. 2 and 3. The coordinates are tabulated in the accompanying tables together with a brief reference to the source of the data. No points were plotted for which any of the intervals were less than 2.5 cm^{-1} , since the accuracy of these points did not seem to be sufficient for a fair comparison with the theory. Such points are listed in the table with a dagger (†). Those points

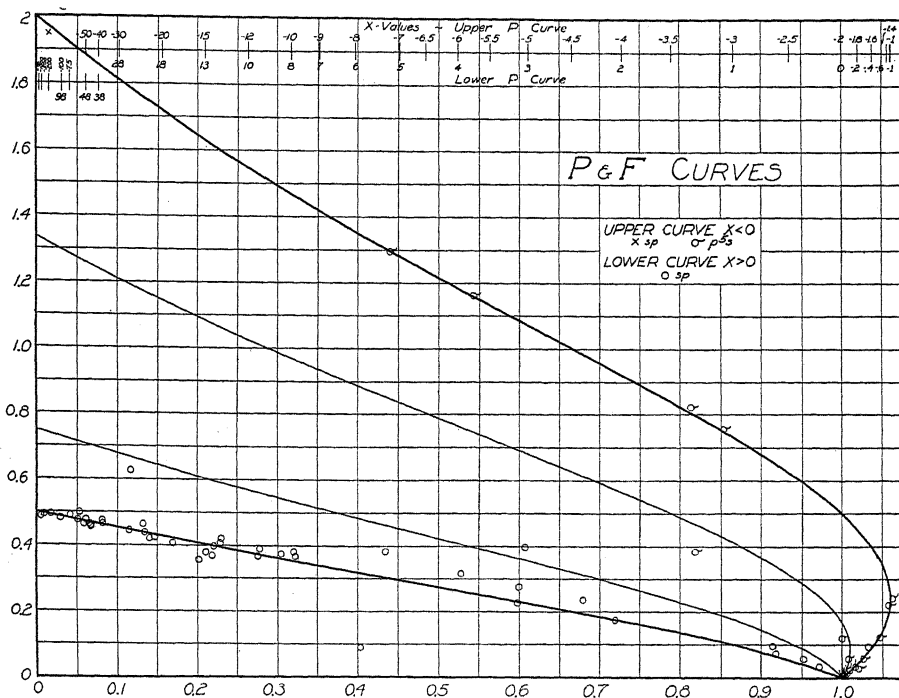


Fig. 2. P and F curves showing sp and $p's$ points. (F curve is drawn lightly and no points plotted.)

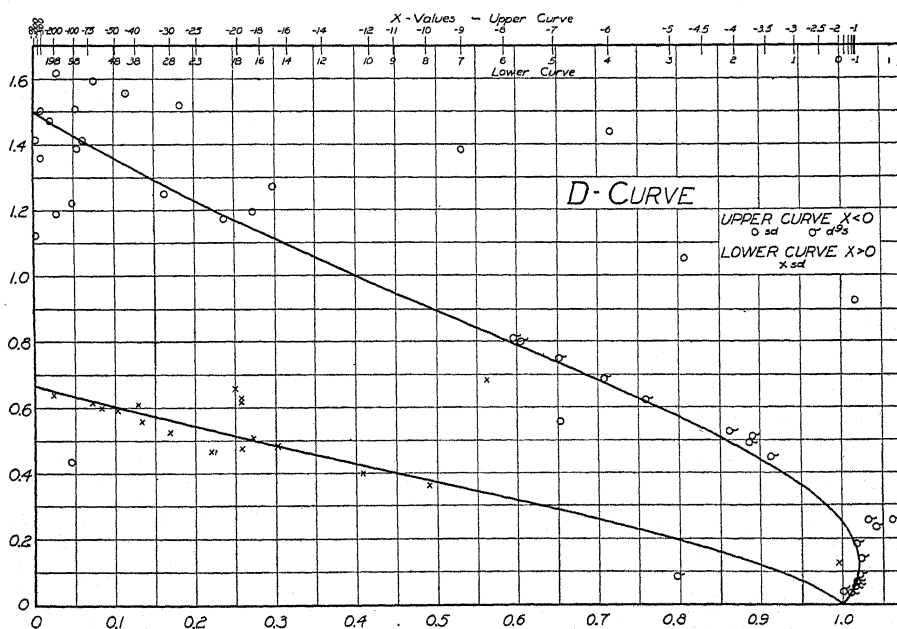


Fig. 3. D curve showing sd and $d's$ points.

whose coordinates fell off the graph are listed with an asterisk (*). No sf points were plotted because there were just a few clustered near Russell-Saunders coupling.

It is found that the theory works well for p^5s and d^9s configurations, in which we are one p or d electron short of a closed shell, except that the whole system of lines is inverted. These points all fall on the upper curves.

Pb III² and Tl II³ have sf configurations in which 3F_3 and 1F_3 are on opposite sides and outside of the $^3F_2 - ^3F_4$ interval. A similar thing happens in the case of the $3p^5 8s$ configuration of A I⁴. These partially inverted triplets might have been plotted with negative ordinates on our graphs.

As to the accuracy with which the points fit the theory, it can be said that in general the d^9s and p^5s fit best, sp and sd for $X > 0$ next, and sp and sd for $X < 0$ poorest. Also in general, elements of high atomic number show especially pronounced disagreements. The disagreements are to be regarded provisionally as cases in which the second-order perturbations are not negligible rather than as essential defects in the basic theory.

² S. Smith, Phys. Rev. 34, 397 (1929).

³ S. Smith, Phys. Rev. 35, 236 (1930).

⁴ A. Meissner, Zeits. f. Physik 40, 839 (1927).

INTENSITIES OF VIBRATION-ROTATION BANDS WITH
SPECIAL REFERENCE TO THOSE OF HClBY J. L. DUNHAM¹

RVERSON PHYSICAL LABORATORY, UNIVERSITY OF CHICAGO

(Received April 19, 1930)

ABSTRACT

Intensity formula for vibration bands. The intensities of vibration bands depend on certain matrix elements of the electric moment of the molecule. The electric moment of a diatomic molecule is a function of the nuclear separation and must be expanded in a power series about the equilibrium point. Matrix elements are calculated by perturbation methods for the fundamental and first two harmonic bands of the vibration spectrum, and it is found that, to a first approximation, for the n^{th} harmonic it is necessary to consider the $(n+1)^{\text{th}}$ power in the series expansion of the electric moment, and higher powers for better approximations. The formulas for the fundamental and first harmonic are given to a second approximation. The matrix elements are also calculated from wave functions due to Morse for a diatomic molecule, and it is shown that there is a negligible difference between the two methods of calculation for small quantum numbers. Formulas are also given for the ratio of the intensity of the first two harmonic bands to that of the fundamental.

Application to HCl. The formulas derived in the first part are applied to the case of HCl which is the only molecule for which the intensities of the vibration bands have been measured with any precision. New data from wave-length measurements of Meyer and Levin are used and the value of the coefficient of the quadratic term in the power series expansion of the electric moment is found. It is found that two values of this coefficient would give the same intensities and no satisfactory way of resolving the ambiguity is available. Numerically it is found that if the electric moment $p = p_e + p_e' \xi + p_e'' \xi^2/2$, then $p_e'' = 0.070 \times 10^{-18}$ or 4.56×10^{-18} e.s.u.

INTRODUCTION

I HAVE recently shown² that the ratio of the measured intensities of the fundamental and harmonic bands of HCl in the near infrared can be predicted quantitatively assuming Morse's³ vibrational wave function analysis and also that the electric moment of the molecule is a linear function of the nuclear separation. Morse's potential function is not as general as a simple power series expansion of the potential function about the equilibrium point and so there has been some question as to what effect the difference between these forms for the potential function would have on the predicted intensities. It is the purpose of the present paper to compare the intensity formulas obtained from both potential functions and also to consider the effect on the intensities of higher terms in the power series expansion of the electric moment. Briefly stated the results are that the intensity formulas derived by the two methods give numerical results which differ by less than the experi-

¹ National Research Fellow.

² J. L. Dunham, Phys. Rev. **34**, 438 (1929).

³ P. M. Morse, Phys. Rev. **34**, 57 (1929).

mental error of the measurements, and that the inclusion of higher terms in the electric moment is, in general, necessary. The numerical agreement obtained previously does not have a unique interpretation. Either it is an indication that for HCl the coefficient of the quadratic term is very small indeed, or it is due to a cancellation of terms. The first part of the paper will deal with the derivation of the intensity formulas based on the two potential functions and with a comparison of these formulas; the second part will consider their application to the numerical results for HCl.

PART I

The ratio of the intensities of two corresponding lines in different bands has been shown to be⁴

$$\frac{\alpha_{nm}}{\alpha_{jk}} = \frac{\nu_{nm} \left(\frac{P_{nm}}{P_{jk}} \right)^2}{\nu_{jk}} \quad (1)$$

where α_{nm} is the intensity of the line $n \rightarrow m$ and ν_{nm} is its frequency. P_{nm} is the matrix component of the electric moment associated with the line $n \rightarrow m$ and will hereafter be called the *intensity integral*. It is calculated from the expression

$$P_{nm} = \int p(r) R_n(r) R_m(r) dr \quad (2)$$

where $p(r)$ is the electric moment of the molecule and is a function of r , the nuclear separation, and $R(r)$ is the radial part of the wave function. If we expand $p(r)$ in a power series about the equilibrium point ($r=r_e$) and change to the dimensionless variable $\xi = (r-r_e)/r_e$, we have

$$p(\xi) = p_e + p_e' \xi + \frac{p_e''}{2} \xi^2 + \frac{p_e'''}{6} \xi^3 + \dots \quad (3)$$

where $p_e' = (dp/d\xi)_{\xi=0}$ etc., and, correspondingly

$$P_{nm} = p_e' \xi_{nm} + \frac{p_e''}{2} \xi_{nm}^2 + \frac{p_e'''}{6} \xi_{nm}^3 + \dots \quad (4)$$

where $\xi_{nm}^i = \int \xi^i R_n R_m r_e d\xi$, is the $(n\ m)^{\text{th}}$ component⁵ of the matrix ξ^i .

The expansion of the potential function about the equilibrium point can be written as

$$U = \frac{h\omega_e}{2\theta^2} (\xi^2 + a_1 \xi^3 + a_2 \xi^4 + a_3 \xi^5 + \dots) \quad (5)$$

where ω_e is the frequency of a classical oscillation for very small amplitudes, $\theta^2 = h/4\pi^2 \omega_e I_e \ll 1$, I_e is the moment of inertia of the molecule, and a_1 , a_2 and a_3 are arbitrary constants which can be determined from the frequencies of the

⁴ This formula was given in reference 2, p. 448. The material for its derivation is given very concisely by E. C. Kemble, Phys. Rev. 25, 1 (1925); where the only change to be made by the new quantum mechanics is that on p. 6. \bar{M}^2 is to be replaced by P_{nm}^2 .

⁵ This expansion of P_{nm} is not to be confused with the expansion of charge distribution into dipoles and multipoles. This entire analysis concerns only the dipole radiation.

lines.^{6,7} The first term gives the potential of a simple harmonic oscillator, for which the wave functions are known, but the wave functions of the more general case must be calculated by perturbation methods. Fues⁷ has calculated the energy levels by this method and has given a formula for evaluating all of the integrals required in the perturbation calculation so that the details of the analysis will not be reproduced here. Suffice it to say that the perturbed wave functions are calculated by straight forward application of perturbation methods and from them the intensity integrals are obtained by Eq. (4).

The intensity integrals for the fundamental and the first two harmonic bands are found to be

$$P_{01} = \frac{p_e' \theta}{(2)^{1/2}} \left[1 + \theta^2 \left(\frac{11}{16} a_1^2 - \frac{3}{4} a_2 - \frac{5\rho'' a_1}{4} \right) \right] \quad (6)$$

$$P_{02} = \frac{p_e' \theta^2}{2(2)^{1/2}} \left[(a_1 + \rho'') + \theta^2 \left(\frac{243}{32} a_1^3 - \frac{111}{8} a_1 a_2 + 5a_3 \right. \right. \\ \left. \left. + \rho'' \left(\frac{3}{32} a_1^2 - \frac{15}{8} a_2 \right) - \frac{3a_1 \rho'''}{2} \right) \right] \quad (7)$$

$$P_{03} = \frac{p_e' \theta^3 (3)^{1/2}}{4} \left[\frac{3a_1^2 + 4a_2}{8} + a_1 \rho'' + \frac{\rho'''}{3} \right] \quad (8)$$

where $\rho'' = p_e''/p_e'$ and $\rho''' = p_e'''/p_e'$. The formulas for P_{01} and P_{02} have been carried out to a second approximation, and the formula for P_{03} has been given to show how higher derivatives of p enter into the intensity integrals for higher harmonics. There are no reliable intensity measurements for any second harmonic bands so far as I am aware, and consequently P_{03} has been given only to a first approximation.

Mensing and Dennison⁸ have obtained by perturbation methods similar to those used here a formula for the intensity ratio of the harmonic to the fundamental band based on the first terms of Eqs. (6) and (7) but omitting the term in ρ'' , and Fues⁹ has given formulas for the intensity integrals to a first approximation, using Kratzer's potential function, which are closely related to the first terms in Eqs. (6), (7) and (8), but omitting ρ'' and ρ''' . However, the fact that ρ'' enters into the first term of P_{02} in Eq. (7), and that both ρ''' and ρ'' enter into P_{03} , shows that in general these terms cannot be neglected even to a first approximation. Generalizing from the above equations it seems that for the band $(0 \rightarrow n)$ it is necessary to consider at least the first n terms in Eq. (4).¹⁰

⁶ E. C. Kemble, Journ. Opt. Soc. Am. **12**, 1 (1926).

⁷ E. Fues, Ann. d. Physik. **80**, 367 (1926).

⁸ Note by D. M. Dennison at the end of a paper by Meyer and Levin, Phys. Rev. **34**, 44 (1929). L. Mensing, Zeits. f. Physik **36**, 814 (1926).

⁹ E. Fues, Ann. d. Physik **81**, 281 (1926).

¹⁰ The reason for this can be seen quite simply by considering the case of P_{02} in the following fashion. The wave functions are those of an harmonic oscillator made slightly asymmetrical by the anharmonicity of the potential function. The integrand of ξ_{02} is composed of

It turns out that because the expressions for P_{nm} are even or odd in θ , it is necessary to carry the perturbation process two steps farther for each new term in θ added to P_{nm} , a behavior very like that found by Fues for the energy levels.

The frequency ratios which are necessary to calculate the intensity ratios (see Eq. (1)) are given by $\nu_{02}/\nu_{01} \cong 2(1-x)$ and $\nu_{03}/\nu_{01} \cong 3$ and the formula for x (which is the coefficient of the quadratic term in the vibrational energy level formula) as given by Fues⁷ or Kemble⁸ is $x = 3h[5a_1^2/4 - a_2]/16\pi^2\omega_e I_e$ so that the intensity ratios are given by

$$\frac{\alpha_{02}}{\alpha_{01}} = \frac{\theta^2}{2} \left[(a_1 + \rho'')^2 + \theta^2 \left(\frac{103}{8} a_1^4 - \frac{51}{2} a_1^2 a_2 + 10 a_1 a_3 \right. \right. \\ \left. \left. + \rho'' \left(\frac{53}{4} a_1^3 - 27 a_1 a_2 + 10 a_3 \right) + \rho''^2 \left(\frac{23}{8} a_1^2 - \frac{3 a_2}{2} \right) \right. \right. \\ \left. \left. + \frac{5 a_1 \rho''^3}{2} - 3 a_1^2 \rho''' - 3 a_1 \rho'' \rho''' \right) \right] \quad (9)$$

$$\frac{\alpha_{03}}{\alpha_{01}} = \frac{9}{8} \theta^4 \left[\frac{3 a_1^2 + 4 a_2}{8} + a_1 \rho'' + \frac{\rho'''^2}{3} \right]. \quad (10)$$

The derivation of the formulas for P_{01} , P_{02} and P_{03} using the wave functions derived by Morse³ is similar to the calculation of P_{02} given in reference 2, with the exception that the terms in ρ'' and ρ''' require evaluation of integrals of the type $\int e^{-kx} x^{k-i-1} (\log x)^n dx$. This offers no difficulty as they can be obtained by $(n-1)$ -fold differentiation with respect to i of the formula for the integral with $n=1$. Since we are using only small quantum numbers and since $k=1/x \gg 1$ it is possible to expand the logarithms and radicals appearing in the expressions for P_{nm} ¹¹ in terms of $1/k=x$. This simplifies these expressions considerably.

$$P_{01} = \frac{p_e'(x)^{1/2}}{ar_e} \left[1 + x \left(\frac{1}{2} + \frac{5\rho''}{2ar_e} \right) \right] \quad (11)$$

$$P_{02} = \frac{p_e'x}{ar_e(2)^{1/2}} \left[\left(1 - \frac{\rho''}{ar_e} \right) + x \left(\frac{3}{2} + \frac{2\rho''}{ar_e} - \frac{3\rho'''}{a^2r_e^2} \right) \right] \quad (12)$$

$$P_{03} = \frac{p_e'x^{3/2}}{ar_e} \left(\frac{2}{3} \right)^{1/2} \left[1 - \frac{3\rho''}{2ar_e} + \frac{\rho'''}{2a^2r_e^2} \right]. \quad (13)$$

the product of two wave functions both of which are nearly even functions, and of ξ which is an odd function, so that the *integrand* as a whole is nearly odd. Consequently in the *integral* there is nearly complete cancellation, it being saved from vanishing only by the slight asymmetry of the wave functions. Now ξ is a first order small quantity to begin with, because for low quantum numbers the wave functions are appreciable only for a small range of ξ about $\xi=0$, so ξ_{02} is a second order small quantity. On the other hand the integrand of ξ_{02}^2 is nearly even, all three factors being nearly even, so that there is no cancellation, but, since ξ^2 is a second order small quantity, the value of ξ_{02}^2 is of the second order too, and therefore of the same order of magnitude as ξ_{02} .

¹¹ Unfortunately in reference 2, Eq. (13) was incorrectly printed. The factor $A_0 A_2 k^{k-3}$ should be replaced by $[(k-2)(k-5)/2a^2]^{1/2}$.

From these the intensity ratios can be calculated at once.

$$\frac{\alpha_{02}}{\alpha_{01}} = x \left[\left(1 - \frac{\rho''}{ar_e} \right)^2 + x \left(1 + \frac{4\rho''^2}{a^2r_e^2} - \frac{5\rho''^3}{a^3r_e^3} - \frac{6\rho'''}{a^2r_e^2} + \frac{6\rho''\rho'''}{a^3r_e^3} \right) \right] \quad (14)$$

$$\frac{\alpha_{03}}{\alpha_{01}} = 2x^2 \left[1 - \frac{3\rho''}{2ar_e} + \frac{\rho'''}{2a^2r_e^2} \right]. \quad (15)$$

We are now in a position to compare the intensity ratio formulas given by the perturbation method with those given by Morse. This is best done by expanding Morse's potential function in powers of ξ about $\xi=0$ giving

$$U = Da^2r_e^2 \left(\xi^2 - ar_e\xi^3 + \frac{7}{12}a^2r_e^2\xi^4 - \frac{1}{4}a^3r_e^3\xi^5 \right). \quad (16)$$

There are only two assignable constants in this expression, D and a , whereas in Eq. (5) all the terms have arbitrary coefficients. That is to say there are certain relations connecting the coefficients of all the higher terms in Morse's potential with that of the first term. Now if we impose these relations on the coefficients a_1 , a_2 and a_3 in Eqs. (9) and (10), we find that we get exactly Eqs. (14) and (15), so that any numerical differences in the values of intensities calculated by these two methods would be entirely due to slight differences between the potential functions assumed and not to any difference in the mathematical analysis. It has been pointed out by Fues^{7,8} that since the harmonic oscillator has no continuous spectrum and since the perturbing terms in the energy go to infinity for large values of ξ , intensity calculations based on this perturbation procedure are not to be relied upon. The identity of the two analyses shown here, however, proves that for low quantum numbers and to the approximations used, the absence of a continuous spectrum in the perturbation analysis has no effect upon the intensities.

A word should be said about the relative accuracy of the two methods. Although for accurate calculations the perturbation method is more precise than Morse's, because the potential function assumed can be fitted to any given molecule more accurately, nevertheless, for first approximations Morse's formulas are to be preferred. The reason is that the first term in Eq. (9) takes into account only the first perturbing term in the potential function, whereas the first term in Eq. (14) contains contributions from higher terms in the potential function as well. In other words Morse's intensity formula converges the more rapidly of the two, so that its *first term* is a better approximation than that of the perturbation formula.¹² For HCl, the numerical difference between the two second approximations is considerably less than the experimental error of the observed intensities. For gases like CO and NO where x is materially smaller than for HCl, the difference is very small even for the first order terms.

¹² Of course perturbation methods could be applied to Morse's wave functions to obtain a more accurate intensity formula, but there is no need of this here in view of the relatively large experimental error.

PART II

We are now ready to turn to a consideration of the numerical values for HCl. Unfortunately there are no accurate data on the intensities of vibration-rotation bands for any other diatomic molecule, as data from imperfectly resolved bands observed with only one tube length or only one pressure are not in the least reliable for intensity measurements.

I have measured the intensity of several lines in the harmonic band of HCl² and shown that the observed ratio of the intensity of that band to the intensity of the fundamental band as observed by Bourgin¹³ is 0.0161. The probable error of this ratio depends on the probable error of the measured intensities of both bands. The probable error of the harmonic is given (reference 2, p. 445) as 6 percent and Bourgin gives 25 percent as the "precision limits" of his measurements. Interpreting "precision limits" as a figure which the true error is unlikely to exceed, or that there is, say, but one chance in ten of the true error being greater than 25 percent, the probable error for the fundamental turns out to be 10 percent.¹⁴ The probable error of the ratio is given by the square-root of the sum of the squares of the separate errors,¹⁴ which is 12 percent. Thus we have for the observed value of the intensity ratio

$$\frac{\alpha_{02}}{\alpha_{01}} = 0.0161 \pm 0.0019. \quad (17)$$

Dennison,⁹ on the basis of observations of Meyer and Levin, has estimated the ratio of these intensities as 0.021 ± 0.004 , which agrees, within the limits of error, with the value just given. Dennison's estimate, however, is based on the measurements of one or at most two tube-lengths and so cannot be considered to be as accurate as the value given in Eq. (17).

To compare this value with the theoretical expressions for intensity it is necessary to substitute in Eqs. (9) or (14) the values of the measurable constants of HCl. Meyer and Levin⁹ have recently published the results of new measurements of the wave-lengths of the HCl bands under higher dispersion than had previously been obtained and Colby¹⁵ has derived the values of the various molecular constants from their data. These values differ appreciably from the constants used in reference 2. They are:¹⁶

$$\begin{aligned} I_e &= 2.613 \times 10^{-40} \text{ gm cm}^2 & a &= 1.710 \\ \omega_e &= 2988.7 \text{ cm}^{-1} & a_1 &= -2.34 \\ x &= 0.01725 & a_2 &= 3.62 \\ r_e &= 1.276 \times 10^{-8} \text{ cm} & a_3 &= -2.60 \\ \theta^2 &= 0.00709 \end{aligned}$$

¹³ D. C. Bourgin, *Phys. Rev.* **29**, 794 (1927).

¹⁴ R. T. Birge, *Phys. Rev. Supp.* **1**, 1 (1929), esp. p. 4.

¹⁵ W. F. Colby, *Phys. Rev.* **34**, 53 (1929).

¹⁶ The values given are obtained by averaging the results for the two isotope components which is sufficiently accurate for our purposes. The value of a_3 has been obtained by using the value of $a^3 r_e^3/4$ (i.e. the value of a_3 according to Morse's analysis, cf. Eq. (16)). a_3 is a small term occurring only in a second order correction so that a more precise evaluation is not necessary.

Substituting these values in Eqs. (9) and (14) we have:

$$\frac{\alpha_{02}}{\alpha_{01}} = (0.0194 - 0.0166\rho'' + 0.00355\rho''^2) \quad (\text{Pert}) \quad (18)$$

$$(-0.0015 + 0.0008\rho'' + 0.00026\rho''^2 - 0.000147\rho''^3 - 0.000414\rho''' + 0.000177\rho'''\rho'')$$

$$\frac{\alpha_{02}}{\alpha_{01}} = (0.0173 - 0.0159\rho'' + 0.00364\rho''^2) \quad (\text{Morse}) \quad (19)$$

$$(+0.0003 + 0.00025\rho''^2 - 0.000143\rho''^3 - 0.000376\rho''' + 0.000173\rho'''\rho'')$$

In Eqs. (18) and (19) the two terms in θ appearing in Eqs. (9) and (14) have been kept separate to show that the formula from Morse's analysis converges more rapidly than the other so that its first term may be considered a better approximation than that of Eq. (9). If the two terms are combined, it is easy to see that the difference between the two second approximations cannot be greater than 2 percent, as none of the major terms differ by more than that amount.

In these equations the only unknowns are ρ'' and ρ''' . Unfortunately we cannot evaluate both of these constants from one equation, as the method of successive approximations would not yield very significant results for ρ''' in view of the relatively large experimental error. Consequently we shall use only the first terms and solve only for ρ'' . Now, as we have seen, if we are going to use only the first term, Eq. (19) is more accurate than Eq. (18) so that we shall use the former in calculating ρ'' , which gives us:

$$\rho'' = \begin{matrix} 0.066 \pm 0.13 \\ 4.30 \pm 0.13 \end{matrix} \quad (20)$$

there being two values because the first term of Eq. (19) is quadratic in ρ'' . Now $p'' = p_e''/p_e'$ and, for a known value of p_e' determines p_e'' . Using the value of p_e' found by Bourgin¹³ ($p_e' = 1.06 \times 10^{-18}$ e.s.u.) we have for p_e''

$$p_e'' = \begin{matrix} 0.070 \times 10^{-18} \\ 4.56 \times 10^{-18} \end{matrix} \left. \vphantom{\begin{matrix} 0.070 \times 10^{-18} \\ 4.56 \times 10^{-18} \end{matrix}} \right\} \text{e.s.u.} \quad (21)$$

p_e'' is the coefficient of the quadratic term in the expansion of $p(\xi)$ about $\xi=0$ and consequently is a measure of the "curvature" of the electric moment at that point.

The fact that one of the values of p_e'' is zero (within experimental error) shows why in my previous paper on this subject² a calculation of the intensity ratio assuming a linear electric moment gave results in good agreement with the observed value. This correspondence, however, cannot be used to show that p_e'' is negligible because we have just seen that a value of p_e'' which is a good sized positive quantity (a negative quantity if p_e' is negative) also gives

the correct value for the intensity ratio, and there is no way, using only intensity data, to distinguish between these two values of p_e'' .

A similar ambiguity arises in the case of p_e' where, because of the quadratic dependence of the intensity on the electric moment, it is not possible to determine the sign of p_e' from intensity measurements alone. This ambiguity in the sign of p_e' leads to a sort of double ambiguity in p_e'' because a change of sign of p_e' changes the sign of p_e'' as determined from Eq. (20). This, of course, does not affect that value of p_e'' which is practically zero, but the other greater value may apparently have either sign depending on that of p_e' .

It has always been assumed that the electric moment of HCl is linear and that p_e' is positive in the region about the equilibrium point. These were natural assumptions when HCl was supposed to dissociate into ions, but in recent years, it has been shown that HCl probably dissociates adiabatically into neutral atoms,¹⁷ which means that at least for large values of r , the electric moment decreases with increasing nuclear separation. This surely means that the curvature of the electric moment is appreciable somewhere, and there is no reason why it should be negligible at the equilibrium point, so that we cannot rule out the larger value of p_e'' until there is more detailed information on the form of p as a function of r . As far as the sign of p_e' is concerned, it is probably positive. The position of the hydrogen nucleus when at equilibrium, is generally considered to be inside the M shell of the chlorine atom and so we may assume that its distorting influence on the chlorine atom, and consequently the electric moment of the molecule, is not at its greatest, and hence p is still increasing with r .¹⁸ This is a very rough sort of reasoning but owing to our complete ignorance about the detailed processes responsible for setting up electric moments in molecules with atomic binding, it is the only sort of reasoning that we can apply to the data at present.

¹⁷ V. Kondratjew, *Zeits. f. Physik* **48**, 583 (1928); R. Samuel, *Zeits. f. Physik* **49**, 95 (1928); F. London, *Zeits. f. Physik* **46**, 455 (1928) esp. p. 472 et seq.; Franck und Kuhn, *Zeits. f. Physik* **43**, 164 (1927) esp. p. 169.

¹⁸ Assuming that the electric moment at r_e is near its maximum and has a positive slope, the most probable value of p_e'' is the small one (nearly zero) because the other implies a large positive curvature which is impossible in the neighborhood of a maximum. However the assumption that r_e is near the maximum is too questionable to warrant definite predictions and the whole matter may be complicated by subsidiary maxima in the electric moment for values of r less than r_{max} .

THE RAMAN EFFECT IN HCl GAS

BY R. W. WOOD AND G. H. DIEKE
JOHNS HOPKINS UNIVERSITY, BALTIMORE

(Received April 23, 1930)

ABSTRACT

Improvements in the experimental conditions made it possible to get much better pictures of the Raman effect of HCl-gas than before. The results are in perfect agreement with what is predicted by the dispersion theory.

THE first report of the Raman effect in the case of a gas at atmospheric pressure was published by R. W. Wood in *Nature*, February 2, 1929, where it was shown that hydrochloric acid gas contained in a long glass tube mounted in contact with a Cooper-Hewitt glass mercury arc, the whole surrounded by a reflecting cylinder of highly polished sheet aluminum, gave a Raman line excited by the Hg 4046 line, the frequency difference corresponding to an infrared line in the position of the "missing line" of the absorption band at 3μ . In the following number of *Nature*, Rasetti announced the discovery of the Raman lines of CO and CO₂ also at atmospheric pressure.

The experiments in HCl were more fully described in the *Phil. Mag.* for April 1929 and it was shown that the 4358 Hg line was accompanied by a series of close companions, corresponding to rotations of the HCl molecule, and it was further shown that the infrared frequencies corresponding to these lines were of very nearly the same wave-length as the *alternate* lines observed by Czerny. An interpretation of these results was given by several investigators independently.² Rasetti¹ studied with great success the Raman effect of other diatomic gases at atmospheric or higher pressures.

With the same tube, and with a platinum diaphragm as was employed in the earlier experiment, but with a recently constructed spectrograph equipped with two interchangeable camera lenses, one a large Steinheil portrait objective (F2.5) and the other a Cooke objective of one meter focus, some superior spectrograms of the Raman effect in HCl have been obtained.

A better alignment of the tube was secured and greater precautions taken to exclude all parasitic light. Six, or possibly seven rotation bands appeared on the long wave-length side of Hg 4355 and three (anti-Stokes) on the other side. Rotation bands also appeared on both sides of the 4046 line, but the "Q branch" line excited by 3650–3655 and 3663 appeared in triplicate mixed in with these rotation bands.

¹ F. Rasetti, *Nature* **123**, 205, 757 (1929). *Proc. Nat. Acad. Sci.* **15**, 234, 515, (1929). *Phys. Rev.* **34**, 367 (1929).

² G. H. Dieke, *Nature* **123**, (1929). F. Rasetti reference 1. E. L. Hill and E. C. Kemble, *Proc. Nat. Acad. Sci.* **15**, 387 (1929), and others. All these papers are simply an interpretation of the formulas of the dispersion theory developed first by Kramers and Heisenberg in 1925.

An enlargement of the entire spectrum is reproduced in Fig. 1. and a highly enlarged portion of the part showing the *Q* branch excited by 4046 and the rotation bands to the right and left of the 4358 line in Fig. 2.



Fig. 1. Enlargement of entire spectrum.

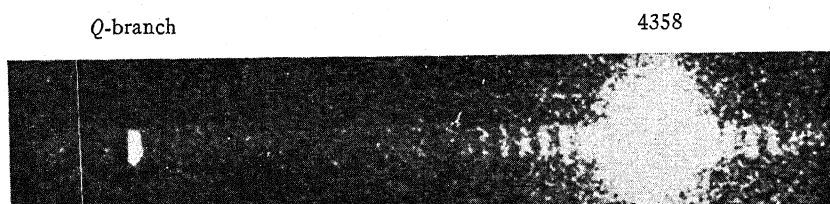


Fig. 2. Highly enlarged portion of spectrum.

INTERPRETATION OF THE RESULTS

The Raman effect of HCl furnishes an excellent opportunity to compare the theoretical predictions with the experimental results, for the HCl molecule is very simple, and furthermore we know its entire infrared absorption spectrum. The situation is therefore much more favorable than for the organic molecules, the exact structure of which is generally not known, so that it is impossible to say what we ought to expect theoretically.

The experimental data are given in Table I.

TABLE I.

λ	$\Delta\nu$	Transition	$\Delta\nu$ infrared
—	—	0→2	62.69
4377.60	101.1	1→3	104.29
85.6	142.7	2→4	146.03
94.2	187.5	3→5	187.45
4402.4	229.4	4→6	228.87
10.4	271.0	5→7	270.03
18.6	312.9	6→8	311.23
26.5	353.0	7→9	352.23
4314.7	143.8	4→2	146.03
23.8	183.3	5→3	187.45
31.2	232.2	6→4	228.87
4581.8	2886.0	j→j	2885.4*

* This line is excited by $\lambda 4047$. The corresponding line excited by $\lambda 4358$ would fall in a region where the plate is very insensitive. The infrared datum is the zero line of the absorption band at 3.4μ . The wave-length of the Raman *Q*-branch has been taken from the previous work because the dispersion was then greater. We find now a value about 3 cm^{-1} less, but think it less reliable.

The first column gives the observed wave-lengths of the Raman lines. The second column gives the frequency differences with the exciting line $\lambda 4358$.

In the third column we find the rotational transitions in the molecule to which the lines correspond, and the fourth column gives a comparison with the infrared data (see farther down).

The dispersion theory of Kramers and Heisenberg³ published in 1925 contains, as is well known now, a complete theory of the Raman effect. The more rigid radiation theory of Dirac leads essentially to the same formulae. The essential feature of this theory is, that the intensity of a Raman line which corresponds with a transition of the molecule from the level a to the level b , has no connection at all with the transition probability between these two levels, which would determine the intensity of the corresponding absorption line. In order to find the intensity of a Raman line we must consider virtual transitions with a certain third level c . If this level c can be reached in an ordinary transition from both the levels a and b , the Raman line is allowed. The Raman line can therefore be considered as the difference between two lines of the molecule, one of which must be an absorption line. The theory gives further the exact intensities of the lines expressed in terms of the transition probabilities between the different levels of the molecule, but we need not go here into details of the theory.

If we consider now a HCl molecule in its normal electronic and vibrational state and with a value j of the rotational quantum number, we have to consider first the possible absorption transitions in order to find which Raman lines we have to expect. In any transition the change of j can be only zero or ± 1 . From the theory of the spectra of diatomic molecules it is well known⁴ that those states to which the molecule can go if $\Delta j=0$ are of a different nature from those for which $\Delta j=\pm 1$.

Let us consider the latter ones first. The molecule would be either in a state with $j+1$ or with $j-1$ after the virtual absorption act. It has to fall back in a virtual emission act to the *normal* electronic level, and the change of j can only be ± 1 in this transition. After the emission of the Raman line the molecule can therefore only be in a state with the rotational quantum number j or $j\pm 2$. If we take into account also those virtual absorption acts for which $\Delta j=0$, (such transitions would occur when the upper electronic state is a Π -state), nothing will be changed in this result. For in the virtual reemission act j must remain likewise unchanged, so that in this particular kind of Raman transition no change of j can occur. As we have to take the sum over all possible third levels c , our result is that in any Raman transition j can change only zero or ± 2 . As for any infrared absorption line of HCl we must have $\Delta j=\pm 1$, we see that not a single Raman line can correspond to an absorption line.

As was shown by Van Vleck⁵ the possible changes of the vibrational quantum number are zero or ± 1 only, even if intermediate levels c with high

³ H. A. Kramers and W. Heisenberg *Zeits. f. Physik* **31**, 681 (1925).

⁴ E. Hulthén, *Zeits. f. Physik* **46**, 349 (1927). R. de L. Kronig *Zeits. f. Physik* **46**, 814 (1928).

⁵ J. H. Van Vleck, *Proc. Nat. Acad. Sci.* **15**, 754 (1930).

values of the vibrational quantum number are taken into account. A higher electronic level of the HCl molecule than the normal one is as yet unknown. From the behavior of similar molecules we have reason to expect that an absorption act will result in such a case into dissociation. There seems to be no reason why these dissociated states cannot act in just the same way as the discrete levels as intermediate states in the Raman effect. The considerations which determine the selection rule for j hold just as well for this kind of transition. It may be expected that the probability for the ultraviolet absorption is much greater than that for the infrared absorption so that the transitions via the dissociated states play the most important part in the Raman effect of HCl. But other factors ought also to be considered, so that this point cannot be settled yet with the present material.

If the vibrational quantum number does not change, we can notice only a change ± 2 of the rotational quantum number for $\Delta j = 0$ gives the unmodified line. If j increases two units we have what is called the normal Raman

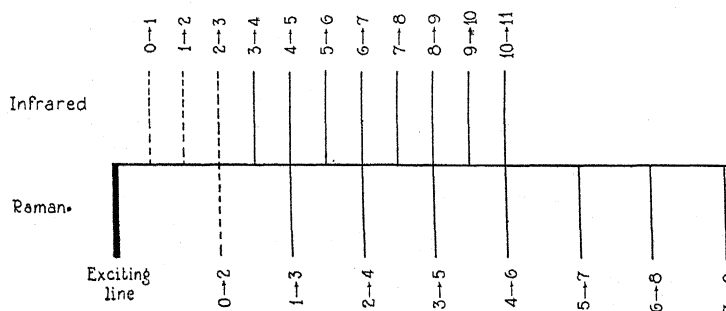


Fig. 3. Diagram showing the connection between the Raman and the infrared rotational spectrum of HCl.

effect,⁶ i.e., lines on the red side of the directly scattered line and as the table shows, the transitions up to $7 \rightarrow 9$ have been observed except the first one which would come too close to the strong unmodified line so that it cannot be detected. We can obtain the same rotational differences also from the infrared data of the vibrational rotational bands *nl*. as differences $R(j-1) - P(j+1)$ of lines of the *R*- and *P*-branch, and these differences are given in the fourth column of the table.⁷ The agreement is as good as it can be expected from measurements of such faint lines.

In the former communication and in the beginning of this paper it was mentioned that these lines correspond with alternate lines of the rotational absorption band in the far infrared observed by Czerny.⁸ But this correspondence is only accidental as can be seen immediately from Fig. 3 in which

⁶ A sequence for which in the Raman effect $j \rightarrow j+2$ is called an *O*-branch. It would be similar to an ordinary *P*-branch with double spacing. Similarly a sequence of lines for which $j \rightarrow j-2$ is called an *S*-branch.

⁷ Taken from C. F. Meyer and A. A. Levin, *Phys. Rev.* **34**, 44 (1929).

⁸ M. Czerny *Zeits. f. Physik* **34**, 227 (1925); **44**, 235 (1927).

both the Raman and the far infrared absorption spectrum of Czerny are plotted and the corresponding transitions indicated. The fact that the Raman lines coincide with alternate infrared lines is only due to the fact that the rotational energy can be represented with good approximation by $Bj(j+1)$, from which follows that the Raman lines due to the transitions $j+1 \rightarrow j-1$ coincide with the absorption lines $2j+1 \rightarrow 2j$. This agreement is not exact as one would find deviations if one takes into account also the higher terms in the rotational energy. These deviations are however too small to be noticeable with the accuracy of the present observations.

The conditions for the observation of the Raman lines corresponding to transitions $j \rightarrow j-2$ (anti-Stokes lines, *S*-branch) were much less favorable, as the first lines are covered by the companions of $\lambda 4358$. However, the three lines given in the table can clearly be recognized. Obviously the distance of a line $j \rightarrow j-2$ from the unmodified line must be the same as that for the line $j-2 \rightarrow j$. The intensity of the $j \rightarrow j-2$ transition seems to be less than that of the $j \rightarrow j+2$ transition. This asymmetry can also be accounted for theoretically. For a $\Sigma \rightarrow \Sigma$ transition the probability for a transition $j+1 \rightarrow j$ is equal to that for $j \rightarrow j+1$ and proportional to $j+1/2$. For a Raman transition the intensity is determined by expressions in which the product of the probabilities for the virtual absorption and emission act occur. Therefore for a transition $j \rightarrow j-2$ the intensity would be proportional to $(j-1/2)(j-3/2)$ whereas for the transition $j \rightarrow j+2$ the intensity would be proportional to $(j+1/2)(j+3/2)$. That means that a line of the *O*-branch must be stronger than the line of the *R*-branch which has the same initial state, and that is in agreement with the observed intensities.

If the vibrational quantum number increases one unit, we have to expect transitions $j \rightarrow j+2$ (*O*-branch) $j \rightarrow j-2$ (*P*-branch) and $j \rightarrow j$ (*Q*-branch). The *O* and *P* branches were too weak to be noticeable on the plates, which indicates that a Raman transition in which the vibrational quantum number increases one unit is *much* less probable than the transition in which it remains unchanged in accordance with Van Vleck's calculations. All the lines of the *Q*-branch fall so close together that they cannot be separated and are seen as one somewhat diffuse line. As the moment of inertia is larger in the final state of the Raman transition (on account of the stronger vibration) the *Q*-branch ought to be degraded towards the exciting line, i.e. towards the violet. It can clearly be seen on the plate that this is actually the case.

THE PHOTOELECTRIC AND THERMIONIC PROPERTIES
OF PLATINUM COATED GLASS FILAMENTS

BY A. KEITH BREWER

FERTILIZER AND FIXED NITROGEN INVESTIGATIONS BUREAU OF CHEMISTRY AND SOILS
WASHINGTON, D. C.

(Received April 21, 1930)

ABSTRACT

The photoelectric and thermionic properties of platinum sputtered glass filaments are discussed, special attention being given to the effect of temperature, and to electrolysis of potassium through the glass to or from the sputtered coating. When electrolysis is away from the surface, the photoelectric threshold is independent of the temperature up to 450° and is close to 2720Å. With electrolysis toward the surface the threshold remains at 2720Å up to 260°C above which it shifts toward the red with rising temperature, reaching a maximum value of about 4300Å at 410°C . Electrolysis produces identical effects on the photoelectric and thermionic emissivity for electrons; the effect on positive ion emission is similar, also, except that a peculiar maximum in the emissivity occurs for a specific electrolysis potential. Ultraviolet radiation has no effect on the thermionic emission of electrons or positive ions from this type of filament.

IN A recent article from this Laboratory by F. G. Cottrell, C. H. Kunsman and R. A. Nelson¹ a new method was presented for the production and control of positive ions. The present paper is a continuation of this study, and deals with the photoelectric and low temperature thermionic phases of the problem.

APPARATUS

The type of emitter chosen for this research consisted of a platinum filament over which a thin layer of potassium glass* was fused, the diameter being about 1.5 mm. A reserve supply of potassium was provided by immersing the filament in molten potassium nitrate and electrolyzing potassium through the glass onto the filament; the potassium formed a golden brown layer over the filament surface. The emitting surface was a thin layer of platinum deposited on the glass by cathode sputtering; short distances at the ends were kept free to insulate the platinum coating from the filament. Electrical contact to the platinum coating was made by twisting a fine platinum wire tightly around the filament. With this type of filament, potassium could be electrolyzed to or from the platinum coating as desired by placing a suitable potential (V_E) between the coating and the filament.

A schematic drawing of the apparatus is shown in Fig. 1. The temperature of the filament was given by a thermocouple twisted about the coating. The emission currents were read with a Compton electrometer shunted with a

* A donation of the Corning Glass Works.

¹ Cottrell, Kunsman and Nelson, J. O. S. A. 20, 152 (1930), and in press.

high resistance leak and potentiometer, which enabled currents to be read from 10^{-15} to 10^{-10} amps. The collecting electrode was made of copper, while the filament supports were made of nickel or tungsten. Ultraviolet light was admitted through a 1 inch quartz window with a graded glass seal.

A Hilger monochromatic illuminator was used to resolve the light of a hot mercury arc of the Uviarc type operating at 75 volts and 1.85 amps. The intensities of the various lines were measured with a Hilger thermopile, using the same slit width as that used in the photoelectric measurements, namely 0.5 mm.

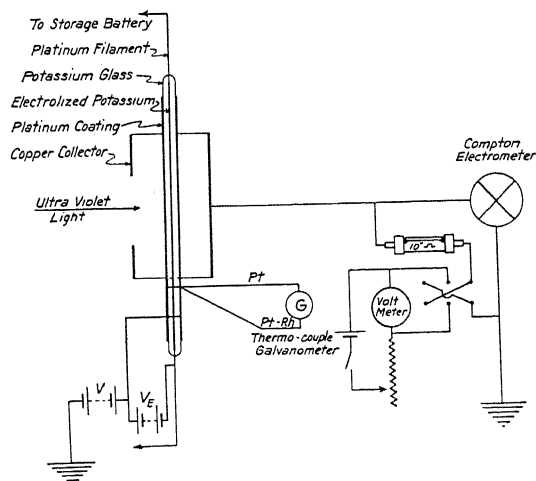


Fig. 1. Diagram of apparatus.

The nature of the filament did not permit of a systematic outgassing process. The pressure in all cases, however, was below the sticking point of mercury in the McLeod gauge (10^{-6} mm of Hg).

RESULTS

Photoelectric emissivity. In determining the photoelectric threshold the current per unit of light intensity method was used. Corning glass filters and direct radiation from the arc were used also where greater intensity was needed.

The factors investigated in this research were (1) the effect of the electrolysis potential between the coating and the filament on the threshold, and on the emissivity; (2) the effect of temperature on the threshold, and on the rate of electrolysis; (3) the effect of electrolysis on the characteristics of the wave-length—current intensity curve, and (4) the effect of ultraviolet light on the thermionic emissivity of both electrons and positive ions.

The effect of an electrolysis potential (V_E) on the photoelectric activity is shown by line A of Figure 2.

It will be noted that the emissivity for λ 2653 is changed by an order of 30 fold, when V_E is changed from 1.5 v. negative to 3.0 v. positive. These

voltages, however, are not corrected for the fall of potential along the filament which for this temperature was about 3.0 v., the filament drop being negative to the coating. The zero, therefore, should be moved 1.5 v. to the right in Fig. 2, to give the correct electrolysis potential.

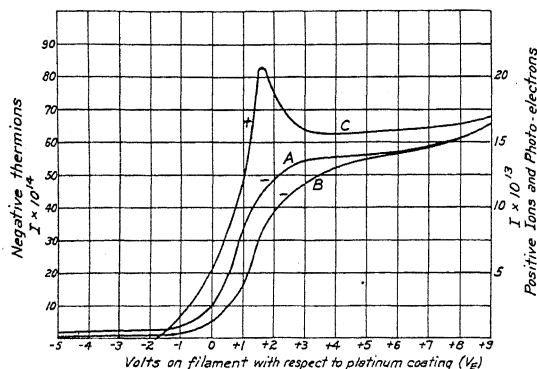


Fig. 2. A. Photoelectric emission, $\lambda 2653$, temp. 337°C ; B. Thermionic emission of electrons, temp. 632°C ; C. Thermionic emission of positive ions, temp. 422°C .

In these experiments a constant difference of potential of 45 volts was maintained between the coating and the collector. Saturation was obtained at slightly less than 2 volts and showed no change up to 135 volts.

The effect of temperature on the rate of electrolysis is shown in Figure 3.

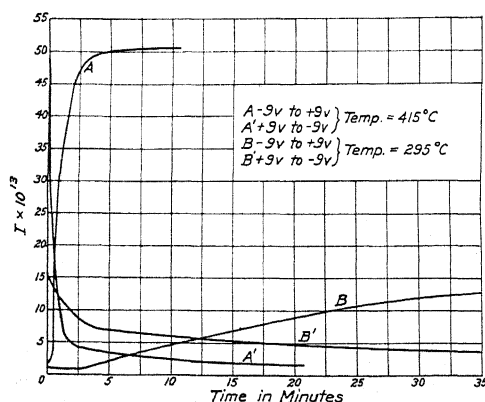


Fig. 3. Effect of temperature on the rate of electrolysis.

It will be noted that at 295°C one hour is required for a steady state to be reached when the electrolysis potential is changed from 9 v. positive to 9 v. negative, or vice versa. At 415°C steady conditions are reached in about 4 minutes, while at higher temperatures the change is too rapid to be measured. At 260° no effect could be observed from changing the electrolysis potential, as is illustrated by line C of Figure 4.

A lag exists between the time when V_E is made positive and when an increase in photoelectric activity is observable, the duration of the lag decreasing with rising temperature. On the other hand, the emissivity falls off rapidly the instant a negative electrolyzing potential is applied.

The effects of temperature and electrolysis potential on the threshold and on the specific activity for various wave-lengths are illustrated in Fig. 4.

Line *C*, as has just been stated, represents the current per unit intensity at 260°C for $V_E = +9$ v. and $V_E = -9$ v. This is the lowest temperature at which an electrolysis effect could be observed. These results were obtained with a fresh filament. After the filament had been worked in at temperatures up to 400°C the threshold shifted to a position represented by line *D*.

The long wave-length limit for a worked-in filament with $V_E = -9$ volts was very close to 2720 Å, as is shown by line *D*. After the filament was

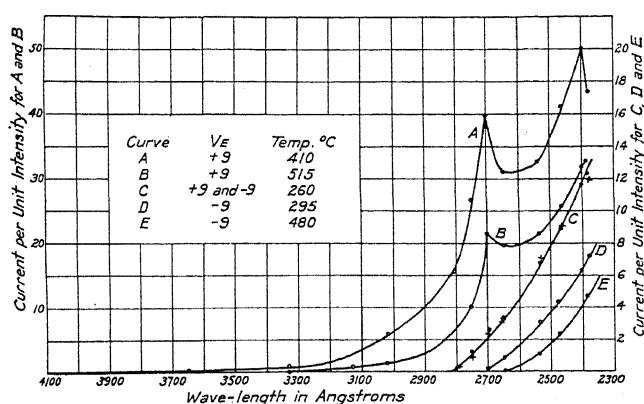


Fig. 4. Effects of temperature and electrolysis potential on the threshold and on the specific activity for various wave-lengths.

once worked in, the temperature coefficient became zero for all temperatures up to 425°C. At temperatures above 425°C the threshold shifted downward as is shown by line *E*, the shift increasing with the temperature.

The electrolysis of potassium to the surface (V_E positive) at temperatures above 260°C results in an enhanced photoelectric activity increasing with V_E as is shown by line *A* of Fig. 2, and with temperature, as is shown by comparing lines *A* and *B* of Fig. 3. The increase in emissivity is accompanied by a nearly corresponding shift in the threshold toward the red.

The conditions for maximum threshold are shown by line *A* of Fig. 4, in which case it was just possible to detect a photoelectric current with $\lambda 4350\text{Å}$. As the temperature was raised above 260°C, the threshold moved from about 3130 Å to 4350 Å, at 425°C. The exact value depended on the previous treatment of the filament, being higher when the filament had been cooled down with a strong positive electrolyzing potential applied. At temperatures above 425°C the threshold again shifted toward shorter wave-lengths, and the shape of the line became more regular as is shown by

line *B* of Fig. 4. At visibility the threshold shifted to about 3050Å. The shift in the neighborhood of redness is due to the combined effect of temperature and fatigue, for the total emissivity cannot be restored by lowering the temperature.

The specific photoelectric activity is apparently abnormally high in the region around 2700Å and 2400Å as is shown by the breaks in curves *A* and *B*. These irregularities are more pronounced for fresh filaments and when electrolysis to the surface has just been increased by raising the temperature or by increasing the electrolysis potential.

The long wave-length limits, as determined above, were checked with Corning filters using the direct radiation from the arc. At 280° the photoelectric current was about 10^{-10} amp. when the light direct from the arc was passed through 12 mm of Pyrex, which should cut out $\lambda 3022\text{Å}$, and fell to 1.1×10^{-13} amps. for a 3.5 mm Noviol O filter, and to about 10^{-15} for 7 mm, which should exclude most of $\lambda 3650\text{Å}$; the threshold is, therefore, very close to 3600Å. When the temperature was raised to 310°, the photoelectric current increased 4-fold.

The effect of fatigue is especially noticeable at high temperatures; the total activity can be reduced to a third of its initial value by holding the filament at redness for a period of minutes. The activities can usually be restored by reversing the sign of V_E and electrolyzing potassium ions away from the coating. Filaments have also been restored by washing in water and alcohol, and then lightly annealing with a small blue flame.

The thermionic emission of electrons. The thermionic emission of electrons from a fresh surface was detectable at temperatures above 425°C for positive electrolyzing potentials. The effect of V_E on the current is shown by line *B* of Fig. 2. The fall of potential along the filament is not corrected for in the graph; making this correction would shift the entire line 2 volts to the left.

The work function curves obeyed the Richardson equation fairly well, yielding a value for b of about 4×10^4 . No significance can be applied to this value, however, since the character of the surface definitely changed with temperature.

Special tests were made to detect an enhancement of the thermionic emission in the presence of ultraviolet light. These tests were carried out by balancing out the photoelectric current with the leak potentiometer, while the thermionic current was observed, and then by balancing out the thermionic current and measuring the photo-electric emissivity. Both general and monochromatic radiation were used. No effect of the ultraviolet light could be observed either in the temperature at which thermionic emission became detectable or in the magnitude of the thermionic currents.

The thermionic emission of positive ions. The emission of positive ions became detectable at 270°C. This is very close to the temperature where the photoelectric measurements showed the electrolysis potential to become operative.

The effect of V_E on the positive ion emission at 422°C is shown by line *C* in Fig. 2. The fall of potential along the filament is such that the entire

line should be shifted 1.5 volts to the left, bringing the peak of the curve at approximately $V_E = 0$.

Curve *C* is distinctly different from curves *A* and *B* in that it shows a critical value of V_E at which the maximum ion current is obtained.

The positive ion currents between 270°C and 450°C agree very well with those reported by Cottrell, Kunsman and Nelson, except that the value of ϕ computed from the Richardson equation is higher by about 0.5 volts. The high work function at the low temperature is to be expected from the fact that the rate of electrolysis also increases with temperature, thus increasing the available supply of possible ions at the surface.

A test for the photoelectric emission of positive ions was made, using direct radiation from the arc in which light of wave-lengths below the threshold of the copper collector was screened out by Corex A Blue Purple filters. No photoelectric emission of positive ions could be detected.

DISCUSSION OF RESULTS

The fact that the emission of electrons thermally and by ultraviolet light are both affected by electrolysis to and from the surface becomes doubly interesting when the characteristics of curves *A* and *B* of Fig. 2 are considered. By making the necessary corrections for zero potential, it will be seen that the two curves are identical in form and position. This is a further proof for the contention that the same group of electrons in the metal contribute to photoelectric and thermionic emission,² and is in line with the results of DuBridge³ and of Warner⁴ who have shown that the work functions for the two types of emission are identical.

Line *C* for positive ion emission is also very similar to lines *A* and *B* for electron emission, except for the fact that it contains an optimum value of V_E . It will be noted that the photoelectric activity increases rapidly at the value of V_E where positive ion emission becomes detectable.

The similarity between the positive ion and electron curves as well as the presence of an optimum electrolysis voltage for positive ions is readily explained by applying to the Richardson equation the intrinsic force concept previously outlined by the writer.^{5, 6, 7}

In the equation $i = ne(kT/2\pi M)^{1/2}e^{-b/T}$, n is the number of possible positive ions per unit volume at the surface of the emitter, while b is a measure of the work done in bringing such an ion through the surface region. From this it follows that any process which decreases n or raises b will decrease the positive ion current.

The electrolysis of positive ions away from the surface ($-V_E$) decreases the value of n ; line *C* of Fig. 2 shows that the positive ion emission is not de-

² Sommerfeld, *Zeits. f. Physik* **47**, 1 (1928).

³ DuBridge, *Phys. Rev.* **31**, 236 (1928).

⁴ Warner, *Proc. Nat. Acad. Sci.* **13**, 56 (1927).

⁵ Brewer, *Proc. Nat. Acad. Sci.* **12**, 560 (1926).

⁶ Brewer, *Proc. Nat. Acad. Sci.* **13**, 592 (1927).

⁷ Brewer, *J. Phys. Chem.* **32**, 1006 (1928).

tectable for large negative values of V_E . The increase in the positive ion current as shown on the graph from $V_E = -1.75$ to $V_E = +1.5$, is without doubt due to an increase in the value of n .

The accumulation of an element of large atomic diameter such as potassium on the surface should, according to the intrinsic force concept, increase the value of b for positive ion emission just as it decreases b for negative emission. The decrease in emissivity beyond the critical value of V_E is due, therefore, to an increase in the thermionic work function for positive ions occasioned by the accumulation of potassium at the surface. Thus the electrolysis of potassium to the surface increases both n and b for positive ion emission, the observed emission curve being a resultant of these two effects.

The fact that an electrolysis potential larger than 3 volts positive has only a small effect on the emissivity, as may be seen from Fig. 2, raises the question as to the nature of the potassium on platinum surface. A condition such as this may result either from the surface being completely covered with potassium at this point, or from a state of polarization being reached in the surface layer which prevents a further accumulation of potassium.

Two facts may be mentioned which indicate that a state of polarization exists and that the surface does not become covered with free potassium. First, in Fig. 3 it will be seen that the emissivity drops markedly the instant a negative electrolyzing potential is applied. Had the surface been covered with a layer of potassium, lines A' and B' should have shown a time lag. The second fact is that it was never possible to obtain the threshold for pure potassium, the values found always lying between that for potassium and platinum. It would seem, therefore, that the surface can best be considered as a surface solution of potassium in platinum rather than a deposit of potassium on platinum.

The writer's best thanks are due Dr. C. H. Kunsman for his interest and advice, and Mr. R. A. Nelson for constructing the filament and rendering other valuable assistance.

THE ROLE OF THE CORE METAL IN
OXIDE COATED FILAMENTS

By E. F. LOWRY

WESTINGHOUSE RESEARCH LABORATORIES, EAST PITTSBURGH

(Received March 14, 1930)

ABSTRACT

Temperature-power relations have been determined for numbers of oxide coated filaments. Part of these filaments had cores of platinum-10% iridium and others had cores of "Konel," an alloy of nickel, cobalt, iron and titanium. Oxide coated Konel is a much better radiator than oxide coated platinum-iridium which causes a considerable difference in their temperature-input power characteristics. Nevertheless, emission measurements show that oxide coated Konel filaments yield higher electron emissions than oxide coated platinum-iridium under the same conditions of filament power. Experimental proof is also given that these filaments need no activation other than the decomposition of the alkaline earth carbonates to oxides in vacuo. The enormous difference shown between the emission characteristics of these two types of oxide filament necessitates the conclusion that the core metal has a definite function other than simply a mechanical support for the alkaline earth oxides.

Suggested mechanism of thermionic emission from oxide coated filaments. In order to account for this difference, a modification is suggested in existing ideas concerning the mechanism of emission from this type of cathode. This modification consists in assuming that the source of emission is the composite layer formed by occlusion of alkaline earth metal on the surface of the core and that the electrons emitted diffuse through the interstices in the oxide coating into the vacuum space. Argument is presented to show that this explanation will also account for other peculiarities in the behavior of oxide cathodes. (1) The decay of emission during life may be explained by a slow sintering of the coating and a consequent closing of these pores. (2) De-activation of the filament by over-heating may be attributed to the same cause. (3) Non-saturation may be due to a pseudo-space charge formed by occlusion of electrons on the surface of the coating particles.

INTRODUCTION

SINCE the discovery by Wehnelt¹ in 1904 of the exceedingly large electron emissions obtainable from glowing calcium oxide, this type of hot cathode has steadily become of greater and greater importance both for use in various thermionic devices and as a copious source of electrons in work of purely scientific interest. This popularity has followed closely upon necessary improvements in technique, resulting in a much greater degree of uniformity from filament to filament as well as in a constant improvement in their efficiency. An inspection of the values of the work function for the alkaline earth oxides obtained by various investigators in the chronological order in which their results were obtained is an excellent proof of this improvement. A table of this sort is appended for which we are indebted to Espe.²

¹ Wehnelt. Ann. d. Physik 14, 425-468 (1904).

² Espe, Wissenschaftliche Veröffentlichungen aus dem Siemens Konzern, 5, 29-46 (1927).

Observer	Material	$d\phi$ (volt)	$d\phi'$ (volt)
Wehnelt 1904	{ CaO BaO	3.67 3.85	
Horton 1907	CaO	4.11	
Deiningen 1908	CaO	3.76	
	{ CaO SrO	3.48 3.87	
Jentzsch (1908)	BaO	3.58	
Schneider (1912)	CaO	3.45	
Cook and Richardson (1913)	CaO	2.4	
Germerhausen (1916)	CaO	2.54	
	{ CaO BaO 50%	3.28-3.94	
Wilson (1917)	{ SrO 50% BaO 50%	2.02-2.16	
	{ SrO 25% CaO 25%	2.34-2.59	
Arnold (1920)	BaO + SrO	1.67-2.05	
Davisson and Germer (1923)	BaO + SrO	1.79	
	{ CaO SrO	2.4 2.15	
Spanner (1924)	BaO	1.85	
Koller (1925)	{ BaO 60% SrO 40%		1.04
Rothe (1926)	(Five Commercial Tubes)	0.64-1.24	
	{ CaO SrO	1.93 1.43	1.77 1.27
Espe (1926)	BaO	1.11	0.99

As a result of the composite nature of this type of cathode the phenomena attendant upon its use are quite complicated and of a somewhat different nature than those found upon examination of pure metallic cathodes. This complexity has given rise to several schools of thought in regard to the mechanics of electron emission from this class of material. It has been held:

1. That the emission is derived from the oxide *per se*,
2. That it is the result of a chemical reaction within the coating, and
3. That the emission comes from a layer of metallic barium on the surface of the oxide coat.

To the best of the author's knowledge the effect of the base or core metal has always been held to be negligible or has been entirely ignored. This is, perhaps, a natural consequence of the various ideas concerning the nature of the oxide emission which have been held up to the present and to the fact that nearly all students of this subject have used platinum as the core metal to the exclusion of everything else. Schottky and Rothe in Vol. 13, chapter IX page 227 of the Wein-Harms Handbuch der Experimental Physik (1928) have summed up the situation very nicely as follows: "Aus einer der ersten Untersuchungen der Oxydemission durch F. Deiningen geht hervor, dass diese (i.e., the work functions for various oxides) unabhängig von dem Material des Glühdrahtes und eine charakteristische Eigenschaft des betreffenden Oxyds ist, wie es auch allen unseren Anschauungen über die Wirkung von Oberflächenschichten entspricht."

Results which have been obtained in this laboratory indicate that the core metal does play a very important rôle in the behavior of this type of hot cathode and therefore that the explanations stated above are misleading as to the true nature of this emission, or at best, are inadequate. It is the purpose of this paper to set forth proofs that the core metal has a vital function in the phenomena of oxide emission. It is also our purpose to suggest an explanation of the mechanics of emission which will take into account this newly discovered factor as well as conform to the demands of their better known but equally important characteristics.

With the advent of the oxide coated filament into common use in radio receiving tubes, it became an economic necessity to find a satisfactory substitute for platinum-iridium as the core metal. Dr. Dayton Ulrey of this laboratory suggested that nickel was the logical metal to begin with. Experiment showed that quite as good emissions could be obtained from oxide coated nickel filaments as had ever been gotten from the oxide coated platinum filaments then in use. The subsequent almost universal adoption of this material for commercial use has entirely corroborated the results obtained by the author at that time.

The search for a satisfactory platinum substitute was not abandoned with the proof that nickel could be used with equally good results. A metal having a higher tensile strength at red heat and above was desirable to insure longer life before burn out as well as less danger of breakage.

An alloy of nickel, cobalt, iron and titanium was found to meet these requirements and also to give excellent thermionic results when coated with oxides of the alkaline earths in the usual way. This alloy has received some publicity of late under the name "Konel."

During the course of investigation of oxide coated Konel filaments in commercial tubes of the UX-112 type it was noted that the brightness temperature of these filaments appeared to be considerably lower than that of similar oxide coated platinum filaments operating at the same power per unit area. This observation seemed to call for a careful study of the relative operating temperatures of these two types of filaments, since neither theory nor experience could account for the effect noticed. This investigation was carried out in the manner described in the succeeding paragraphs.

EXPERIMENTAL METHOD AND RESULTS

The filaments used during the course of this investigation have all been of the type used in UX-281 Radiotrons. Both the platinum-10% iridium (referred to hereafter in this paper simply as platinum) and the Konel filaments were coated in the same fashion. Several applications of a water paste consisting of equal parts of BaCO_3 and SrCO_3 were baked on the ribbon in an atmosphere of CO_2 . This carbonate coating was subsequently decomposed to oxide in vacuo during the outgassing process of the tube to be examined. Since all data given are averages obtained from a rather large number of filaments made from different spools of ribbon and coated at different times, their exact dimensions are irrelevant. Their approximate dimensions were

27 cm length by 0.06 cm width. Both the platinum and the Konel filaments had practically the same areas and resistance characteristics. This equality of area insures equal space charge limitations when mounted in tubes whose anodes are all of the same size. The filaments were mounted *M* fashion in standard UX-281 tubes save that for the temperature investigation no anodes were included. No corrections for cooling effects of the leads and hooks have been applied since a careful test showed that this effect was negligible when plotting the temperature of the center of the filament against the power input to the filament.

This test was carried out on a tube in which were mounted two filaments as shown in Fig. 1. These filaments were taken from the same spool of coated ribbon but were of different lengths. They were connected in series

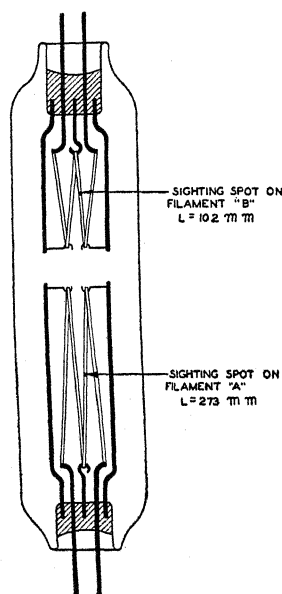


Fig. 1. Diagram of tube.

so that by subtracting the voltage drop through the shorter filament from that through the longer one the power loss in the uniformly heated central portion of the longer filament could be calculated. Further calculation showed that the end cooling on a filament of this length was responsible for an error in the curves of about 3 degrees in the lower range of temperature and about 1 degree in the upper range. The target for optical pyrometer observations on the base metal was formed by carefully scraping the coating from one side of the ribbon at the center of one of the middle legs of each filament for a space about equal to the width of the filament. Brightness temperature observations were made on this spot as well as on the surface of the coating at a point immediately adjacent to this bare area. Two Leeds & Northrup optical pyrometers calibrated against standard lamps furnished by Dr. Forsythe of Nela Park were used for this work, the results of

which are shown in Fig. 2. It may be well to call attention to the fact that each point plotted is an average of five separate observations and each point of a group was found for a different filament. A check test was run recently on two of the filaments previously studied using a different pyrometer. The results of this check are indicated by crosses. It seems entirely safe to conclude from the results shown that the brightness temperature curves given here are not in error by more than $\pm 5^\circ\text{C}$.

Obviously, we are interested in the true temperature of the core metal and not particularly in that of the surface of the coating. In order to calculate the true temperature of the Konel filaments it became necessary to find the value of its spectral emissivity at $\lambda = 0.65\mu$ in the temperature region under investigation. This was accomplished by the spiral filament

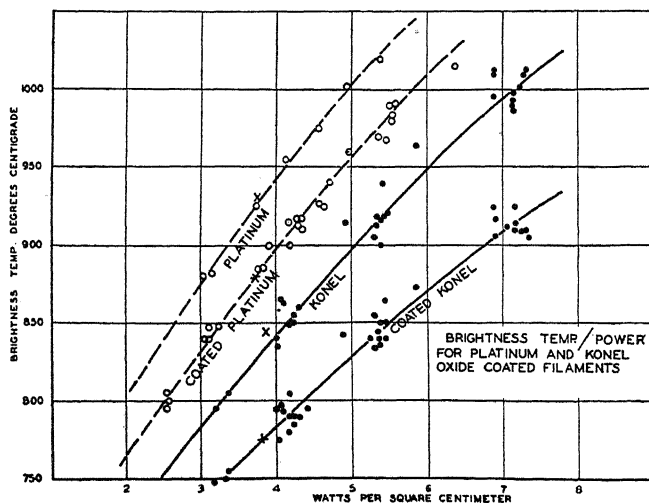


Fig. 2.

method described by Shackelford³ with the result that a value of 83% was found for this factor. Foote and Fairchild⁴ give this correction factor for platinum as 33% and for iridium as 30%. A rough calculation of the spectral emissivity of the coatings yields a value of the order of 25%. This value is of course only approximate since the difference in temperature between the surface of the coating and that of the base metal is not precisely known, although it can at the most be a matter of only 10 to 15 degrees C. Furthermore, these coatings, although appearing pure white by reflected light are quite porous as well as translucent, with the result that the above value is probably high.

By applying the proper correction factors to the curves of Fig. 2 we arrive at the values shown in Fig. 3 which refer of course to the true temperature

³ Shackelford, Phys. Rev. 8, 470-478 (1916).

⁴ Foote & Fairchild, Symposium on Pyrometry, Am. Inst. Mining & Met. Eng. 338, (1920).

of the metal cores as a function of the power supplied to the filaments in watts per cm^2 .

The difference in temperature between oxide coated platinum and Konel filaments operating under like conditions of power input is readily explained. Konel becomes considerably oxidized during the coating process described above and hence is a much better radiator than platinum. The oxide coating, although a poor radiator, allows an appreciable amount of the radiation from the core to escape owing to its porosity and translucence. As a result the energy radiated is dependent upon the nature of the core

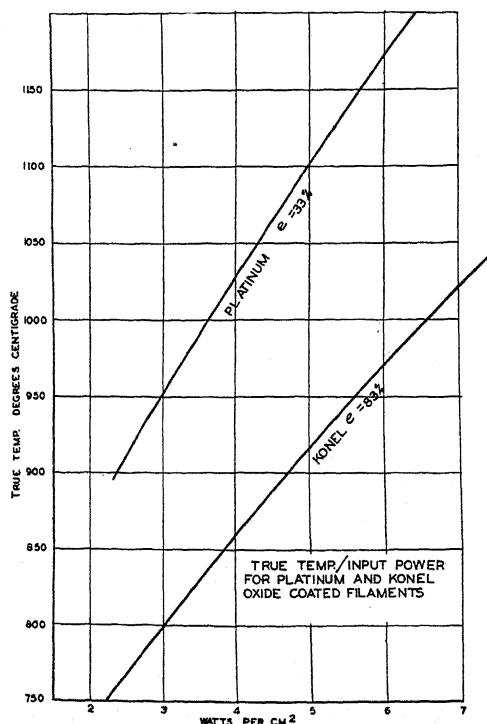


Fig. 3.

to a considerable extent and is not limited entirely by conduction through and radiation from the surface of the coating.

In Fig. 4 are shown some space current measurements made with UX-281 Radiotrons using similar filaments to those used in the tests described above save that these filaments have a length of approximately 17 cm. In fact, some of them were taken from the same spools of coated ribbon. These curves are also averages for numbers of tubes and show that when the currents are limited by emission rather than by space charge the values for oxide coated Konel are higher than for oxide coated platinum operating at the same power per unit area. It must be borne in mind that the results given here are to be considered as typical of this particular kind of coating. It is possible that different results might be obtained with, for example,

the barium azide method of coating. The whole process of making oxide filaments, coating them with oxides and their subsequent treatment on the pumps is of the nature of an art only to be acquired through long practice. The author would, therefore, hesitate to comment on the results to be obtained by some distinctly different process of coating. The filaments used

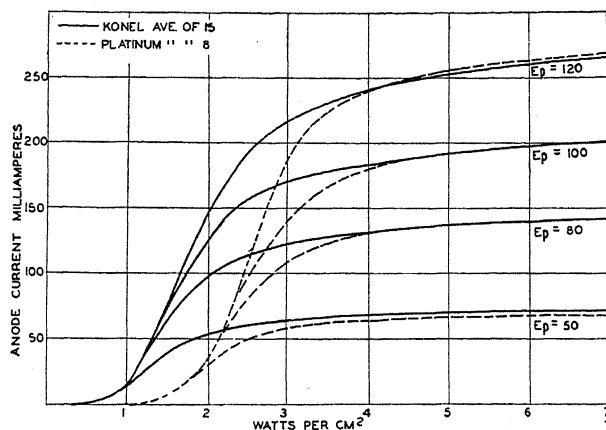


Fig. 4.

throughout this work were good representative samples of commercial oxide coated filament. The tubes used were also representative in every way, their only difference from commercial tubes being that the most extreme care was used in getting the highest obtainable vacuum in each one to obviate the possibility that any appreciable part of the space currents obtained was due

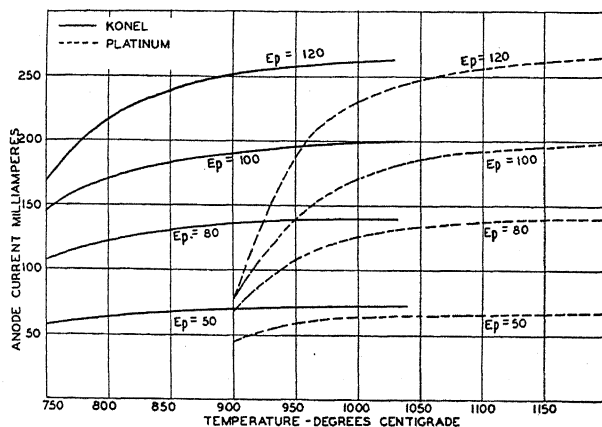


Fig. 5.

to the presence of gas. The normal value of emission for UX-281 Radiotrons is 0.170 amperes at $E_p=100$ volts and a power input of approximately 4 watts per cm².

The results of the previous curves have been combined to obtain the results shown in Fig. 5. Here are shown the space current values obtained

at various anode voltages plotted against the temperature of the filaments in degrees C. It here becomes obvious that the core metal has an enormous effect on the thermionic activity of the coating. It is readily seen from these curves that the same anode current may be obtained from oxide coated Konel at 775°C. as can be obtained from platinum coated with the same oxides at 950°C. This is the phenomenon which we believe is new and for which we offer a possible explanation in the succeeding pages.

THE MECHANICS OF EMISSION

As mentioned in the introductory matter of this paper, at least three distinctly different explanations of the mechanics of emission from oxide coated filaments have been set forth in the past. None of them take into account any function of the core metal other than as a mechanical support for the thermionically active oxides and as a means of furnishing the necessary thermal energy to them in a convenient manner. The experimental facts stated in the foregoing pages make it imperative that the role of the core metal be recognized and its effect explained. It is obvious that such an explanation must also be in accord with other phenomena peculiar to this type of cathode. Some of these phenomena are:

1. The formation process.
2. Destruction of activity by overheating.
3. Decay of activity with life.
4. Non-saturation.

The explanation most in favor during recent years has been that offered by Koller,⁵ Espe,⁶ Rothe⁷ and others in which it is assumed that the source of activity is a layer of metallic barium on the surface of the oxide coating. Espe argues that this barium is formed by electrolytic decomposition of the oxide coating and that the barium diffuses to the surface of this coating where it serves as emission centers. The explanation submitted herein is a modification of this idea in that it is believed that the emission arises from a layer of metallic barium occluded on the surface of the core metal or alloyed with it. This modification seems necessary in that if the emission arises from the oxide itself or from barium "emission centers" on the surface of the coating, the thermionic activity of such filaments should be unaffected by the nature of the core. In such case both platinum and Konel oxide filaments should be equally active at like temperatures. This obviously is far from the fact.

In a way, it is immaterial to the argument at hand as to just the method by which the barium is produced. If it is formed by electrolytic decomposition according to Espe,⁶ the barium ions would be positively charged and have a natural tendency to migrate toward the core. As a matter of fact this is probably the method by which a constant supply of barium on the core is maintained after the initial "activation."

⁵ Koller, Phys. Rev. 25, 671, (1925).

⁶ Espe, reference 2.

⁷ Rothe, Zeits. f. Physik 36, 737-758 (1926).

It is also possible that metallic barium is formed by positive ion bombardment under certain conditions of activation. This explanation does not, however, account satisfactorily for a maintenance of a barium supply under high vacuum conditions.

With the type of coating used by the author in the course of this work it is, however, entirely probable that the barium is formed either by thermal decomposition of the carbonates in vacuo or by the reducing action of the metallic core. Figure 6 shows a curve of the behavior of a typical filament during the course of an experiment to prove this point. Tube #X2410 containing Konel filament #125-386 was baked at 400°C in the usual way, after which the metal parts of the tube were thoroughly outgassed in a high

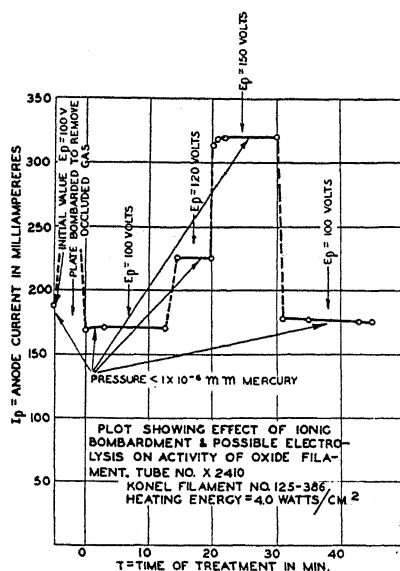


Fig. 6.

frequency furnace. The only heating received by the filament up to this time was that due to radiation from the hot anode. An instantaneous measurement of emission was then made and yielded a value of 5×10^{-6} amp. at a filament power input of 4 watts per cm^2 and an anode voltage of 100 volts. The filament was then heated at 8.5 watts per cm^2 for several minutes and then at 5-6 watts per cm^2 until the gas pressure in the tube had been reduced to less than 1×10^{-5} mm of mercury. During this treating out of the filament no anode voltage was applied and the plate was cold except for radiation absorbed from the filament. Another instantaneous determination of the emission now gave 0.186 amperes under the same test conditions as before. Subsequent treatment of various kinds gave no improvement as is indicated by the curve, which is self explanatory. This behavior is typical of this type of filament when properly handled. Similar results have been obtained with oxide coated platinum filaments, so the results described can-

not be ascribed to the kind of base metal used. Since a certain amount of vaporization of the barium from the core is to be expected at operating temperature especially in the case of platinum filaments, it is quite likely that the supply of barium is replenished by some such process as the electrolytic decomposition of the oxide coating. It certainly is not essential however to their initial activation. Again we must insist that this applies only to coatings of the type used in this work. If the carbonates are converted to oxide by long continued heating in the air and not converted in vacuo as in this case, an activation process of some length does have to be followed to bring the filaments up to normal activity.

Evidence of this and also of the fact that the emission is due to metallic barium was obtained in an experiment similar to the one just described in which the filament was burned in air at low pressure for a short time after it had been tested as above with identical results. The burning in air had the result of enormously reducing its activity (to about 5×10^{-6} amp.) and it was only by heating it for some hours in high vacuum with a constant application of 200 volts on the anode that its activity was restored to the same order of magnitude that it had originally.

A necessary consequence of our hypothesis is that the electrons leaving the emitting layer must diffuse through the interstices in the oxide coating. This consequence presents no serious difficulties. Indeed, it offers a solution to some of the perplexing problems connected with the behavior of this type of cathode. At best, the electrical resistivity of these oxide coatings is very high even at glowing temperatures. In fact, Dr. C. T. Ulrey of the Research Laboratory of the Westinghouse Lamp Company during the course of some yet unpublished work has not been able to obtain a discontinuity in the space current curve for such filaments when the anode was made to approach the filament until it actually touched the surface. Furthermore, these coatings are very porous. When viewed through a microscope they have the appearance of a light fluffy fall of snow. It seems reasonable to suppose therefore that the escaping electrons may diffuse through this oxide layer which, however, does offer some impedance to their progress. Suppose now that this coating should become more compact so that its pores are partially closed. The natural consequence would be that the apparent activity of the filament would be measurably impaired. This is precisely the type of phenomenon that does occur. It is well known that glowing the filament for a comparatively short interval of time at a considerable overvoltage will practically ruin its emission. It has been the author's experience at least that a filament which has been so mistreated cannot, in general, be reactivated to anything like its original characteristics. It is also true that such filaments will, after such reactivation as is possible, yield large emissions if very high anode voltages are applied. The net result of such an overheating of a filament is essentially to increase the impedance of the tube by an appreciable amount. This we believe to be caused by a partial closing of the pores of the coating. Preliminary microscopic examination of some such filaments actually showed a sintering or glazing of the coating until it had the appearance of a crackled enamel.

Exactly similar behavior is shown by filaments whose activity has gradually decreased during a long period of use. Such worn out filaments always retain an appreciable amount of coating. In fact, a fairly close inspection shows that they still possess nearly as thick a layer of oxide as they had initially. In this case also large emissions may be drawn if sufficiently high anode voltages are applied.

If the loss of activity in these cases were due solely to a loss of metallic barium due to vaporization it should be possible to cause these filaments to regain all their initial activity by electrolysis or by positive ion bombardment. As stated above it is rarely if ever that it is possible to do this.

The process of electron diffusion through a porous, poorly conductive coating may also explain the phenomenon of non-saturation which is commonly met with in this type of cathode. It follows logically that large numbers of electrons will become enmeshed in the pores of the coating or occluded on the surface of the particles of poorly conducting material composing it. It is quite possible also that the numbers of electrons so entrapped will vary somewhat with the anode voltage applied. This process will give rise to an effect similar to a negative space charge within the confines of the coating itself. The space currents obtainable then at any given anode voltage and filament temperature represent the number of electrons per second it is possible to drag out of or through this negative charge built up within the coating layer. The result will be that much higher anode voltages will be required to approach a saturation than if this pseudo space charge did not exist. At temperatures in the neighborhood of 1000°C the electron emission from these filaments is so enormous that it is next to impossible to obtain anything approaching saturation owing to the very considerable heating effects of the emission itself. At these temperatures also the conductivity of the coatings will be increased appreciably affording a better opportunity for the electron charge to leak off.

CONCLUSIONS

In view of the experimental results presented in the foregoing pages, we are forced to accept the fact that the base or core metal does affect appreciably the electron emission from the alkaline earth oxides. This situation in turn demands a modification of existing ideas concerning the mechanism of emission from oxide cathodes.

An hypothesis is offered concerning this mechanism in which:

1. The source of emission is assumed to be a layer of metallic barium (or other alkaline earth metal) occluded on the surface of the base metal or alloyed with it. In this case the constants of the well-known Richardson equation must be characteristic of the composite surface.
2. The electrons emitted from this composite surface must diffuse through the pores of the coating.
3. The coating in turn, as a function of its porosity, offers considerable impedance to the progress of the electrons.

4. The occlusion of electrons on the particles of the coating sets up a pseudo space charge effect which serves to explain the phenomena of non-saturation as well as the fading of emission during short periods of operation.

5. The gradual decay in activity of coated filaments during life is due to a slow sintering of the coating resulting in a closing of its pores and a consequent increase in the impedance offered to the passage of electrons. A similar process occurs if the filament is strongly glowed for a comparatively short interval of time with or without anode voltage.

It is admitted that no crucial tests of this explanation have been offered with the exception of that showing the pronounced influence of the core metal; which, of course, is the effect which makes the above modification in existing ideas necessary. Numerous experimental investigations are now under way in this laboratory which have been designed as tests of the various assumptions made herein. It is hoped that these tests will be far enough along to permit of their publication in this magazine in the near future.

In conclusion, the author wishes to express his gratitude to Dr. C. T. Ulrey of the Westinghouse Lamp Company Research Dept. and to Drs. D. L. Ulrey and N. Rashevsky of this laboratory for their interest and for the helpful suggestions received from them during the progress of this work.

ON THE THEORY OF THE SOLAR CORONA*

BY E. O. HULBURT

NAVAL RESEARCH LABORATORY

(Received April 17, 1930)

ABSTRACT

The outer atmosphere of the sun is assumed to be composed mainly of ions and electrons which are actuated by gravitation, radiation pressure and the magnetic field of the sun. By distillation along the lines of magnetic force the particles collect in the lower latitudes of the solar outer atmosphere and by their diamagnetism reduce the magnetic field approximately to zero in this region, leaving a stray field at the poles. Thus the polar plumes, prominent during sun-spot minima, are regarded as owing their form to the magnetic field of the sun. Whereas the wide spreading structureless coronal luminosity extending out from the lower latitudes is due to an accumulation of ionization which reduces the magnetic field to a low value and permits the radiation to blow the particles out to great distances. During maximum solar activity there is sufficient ionization of the outer atmosphere to reduce the magnetic field to a low value even at the poles, and hence the outer atmospheric spray extends roughly equally in all directions, in accord with the appearance of the corona.

DURING minimum solar activity the corona spreads out from the sun between latitudes about 50° north and south as shown in Fig. 1.¹ In this region the luminosity is mainly structureless, with of course irregularities such as clouds and prominences. The polar plumes are short and well defined. During maximum solar activity the corona extends more or less equally in all directions, as in Fig. 2,² with no marked polar plumes. At times the luminous streams ejected from the active latitudes around 40° give the corona roughly the outline of a square. The material of the corona is considered to be very attenuated, for comets have been observed to pass through it without being damaged.² The coronal particles were found, from Doppler effects, to be moving outward from the sun³ with velocities around 20 km sec^{-1} . In the present paper the assumption is made that the outer atmosphere of the sun is composed of ions and electrons, and it is shown that the particles, due to the influence of gravitation, radiation pressure, and the magnetic field of the sun, form an atmosphere which has approximately the observed shape of the corona.

From measurements of the Zeeman effect of spectrum lines in the chromosphere Hale⁴ has shown that the magnetic field of the sun is similar to that of a uniformly magnetized sphere. The magnetic field around a uniformly

* Published with the permission of the Navy Department.

¹ Slocum, *Astrophys. J.* **64**, 145 (1926).

² Mitchell, "Eclipses of the Sun" (1924).

³ Russell, Dugan and Stewart, "Astronomy" **2**, 509 (1927).

⁴ Hale, *Astrophys. J.* **38**, 31 (1913); Hale, Sears, van Maanen and Ellerman, *Astrophys. J.* **47**, 1 (1918).

magnetized sphere is drawn in Fig. 3. The magnetic field of the sun was found to decrease along the radius, falling from 55 gauss to less than 10 gauss in a distance of a few hundred kilometers measured radially outward.⁴ Gunn⁵ explained the radial degradation of the magnetic field by means of the diamagnetism of the long free path ions and electrons in the chromosphere; various drift currents may add to or subtract from the diamagnetic effect but perhaps not to a great extent.

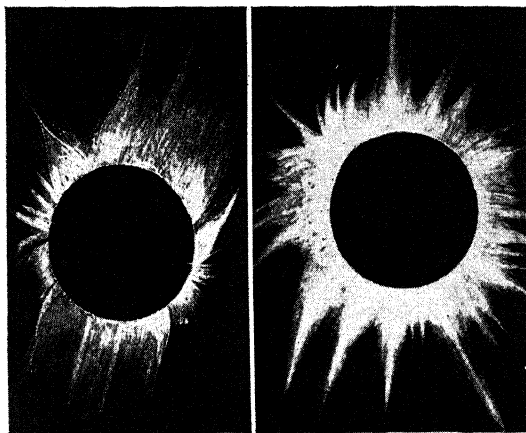


Fig. 1.

Fig. 2.

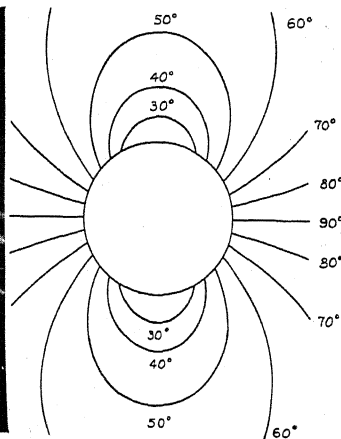


Fig. 3.

Fig. 1. Drawing of the eclipse of January 24, 1925, near minimum solar activity.

Fig. 2. Drawing of the eclipse of August 30, 1905, near maximum solar activity.

Fig. 3. Magnetic field of a uniformly magnetized sphere.

If a region contains γ long free path ions or electrons per cm^3 and if H is the impressed magnetic field in the region, the ions and electrons by their diamagnetism cause a reduction in H . The condition that H be reduced to a small value is expressed by⁵

$$\gamma \geq H^2/4\pi kT, \quad (1)$$

where T is the absolute temperature of the ions and k is the Boltzmann constant 1.371×10^{-16} erg deg⁻¹. Although accurate enough for the present discussion (1) is an approximation, for it neglects the possible warping of the field H by the diamagnetic cloud.

In order for diamagnetism to exist we must have

$$\gamma \geq \rho, \quad (2)$$

where γ is the free path of the ion and ρ is the radius of gyration of the ion about H . Assuming that all the particles are ions of mass m , diameter $\sigma = 3 \times 10^{-8}$ cm and velocity v ,

$$\rho = mv/He, \quad (3)$$

⁵ Gunn, Phys. Rev. 33, 614 (1929), 35, 635 (1930).

and

$$\gamma = 1/(2)^{1/2} \pi y \sigma^2. \quad (4)$$

From (1) with T of order 10^4 °K and with H of order 10^{-3} , 10^{-4} and 10^{-5} gauss at various regions of the corona y can not be greater than 10^6 , 10^4 and 10^2 , respectively. From (2) it follows that the ions can not reduce the field to zero, for if H is very small ρ from (3) is so large that (2) is not satisfied. For example, with m of order 10^{-23} grams and v of order 10^5 cm sec $^{-1}$ H can not be reduced by the diamagnetism of the ions to less than 10^{-7} , 10^{-9} and 10^{-11} gauss for $y = 10^6$, 10^4 and 10^2 , respectively. However, this slight remnant of the magnetic field is of no interest here, for it does not influence the motion of the coronal ions appreciably.

It is assumed that the outer regions of the chromosphere are composed mainly of ions and electrons, each cm 3 containing approximately an equal number of positively and negatively charged particles, and that the particles are forced outward by radiation pressure with velocities around 20 km sec $^{-1}$. A mechanism of radiation pressure has been discussed by Milne⁶ and need not be described here. The diamagnetism of the ions reduces the solar magnetic field to small values in the outer chromosphere. Let us suppose that the magnetic field outside of the chromosphere were that of a uniformly magnetized sphere, as Fig. 3, with a value of, say, 1 gauss at chromospheric levels at the equator. The positive and negative ions and electrons, forced out by radiation pressure, follow along the lines of magnetic force in tight spirals; with $m = 10^{-23}$ grams, $v = 2 \times 10^6$ cm sec $^{-1}$ and $H = 1$ gauss ρ from (3) is 12.6 meters, which is very small compared to distances in the corona. In general, wherever the magnetic field is more or less normal to the radiation pressure the ions accumulate sufficiently to break down the field. Thus the charged particles ejected between the latitudes 50° north and south are constrained to move in the space between the 50° magnetic line, Fig. 3, and the sun. They accumulate in this space until by their diamagnetic action they reduce the magnetic field to very small value, practically to zero. From (1) with T of order 10^4 °K and $H = 1$ gauss y is 10^{11} . Therefore, when y reaches 10^{11} the guiding action of H is destroyed. The ions thereupon steam out from the sun in the lower latitudes to form a structureless luminosity similar to that of Fig. 1.

In polar latitudes the lines of magnetic force are nearly parallel to the force of radiation pressure. The ions slide out along the lines of force without hindrance and large ion densities in the polar regions of the corona are not built up. Therefore the corona in the polar zones does not extend to such great distances from the sun as it does in the lower latitudes. The polar magnetic field is not destroyed; it guides and is outlined by the flying ions. Thus the short polar coronal plumes are formed, as are observed during solar quiescence, Fig. 1. During maximum solar activity we may suppose that sufficient numbers of ions are ejected to wipe out the magnetic field in the coronal regions at all latitudes, thereby permitting the coronal ions to move out more or less uniformly in all directions, as in Fig. 2.

⁶ Milne, Monthly Notices, Roy. Ast. Soc. **87**, 697 (1926-27).

The solar latitudes around 40° are the regions of greatest activity, the eruptions being in general more frequent there than in other areas of the solar surface. It is possible that enough ions may be emitted to reduce H to zero above the 40° line, Fig. 3, and yet because of a less rapid supply of ions in latitudes below 40° , H may be appreciable in the lower latitudes within the coronal regions bounded by the 40° line. Thus the present view is not incompatible with Deslandres' hypothesis⁷ that H is of the order 10^{-7} gauss. The hypothesis was advanced to explain the curvature of certain solar protuberances, on the idea that the material of the eruption carried an excess charge, either positive or negative, and therefore in its progress across the magnetic field would move in a curved path. The hypothesis may, however, not be necessary, for in certain cases, at least, asymmetrical radiation pressure, as suggested by Pike,⁸ may cause the curvature of the prominences. The curious twining and curvature occasionally observed in the long coronal streamers and filaments may be evidence of remnants of the distorted magnetic field.

The total brightness of the corona is about 10^{-6} of that of the sun, and the luminosity falls off roughly with the inverse fourth to sixth power of the distance from the center of the sun². The ions and electrons of the coronal atmosphere are pushed out from the chromosphere by radiation pressure, the pressure acting mainly on the ions which, by their electrostatic attraction, drag the electrons along with them. The ions absorb the sunlight, thereby being subjected to radiation pressure, and reemit a portion of the absorbed energy as coronal light. The radiation pressure acceleration⁹ p is given by

$$p = I\beta/mc, \quad (5)$$

where I is the energy flux of the sunlight which is absorbed by the ion with ionic absorption coefficient β , m is the mass of the ion and c is the velocity of light. If a fraction f of the absorbed energy is reemitted as coronal radiation I_c , then

$$I_c = f\beta I\gamma_c, \quad (6)$$

where γ_c is the total number of ions in the corona.

The total energy flux in all wave-lengths from the solar surface is 6.2×10^{10} erg cm^{-2} sec^{-1} . Assuming that 10^{-3} of this, corresponding to the energy in the ultraviolet region from about 1500 to 1800A, is absorbed by ions of mass $m = 10^{-23}$ grams and absorption coefficient $\beta = 5 \times 10^{-16}$, I is 6.2×10^7 and p from (5) is 10^4 cm sec^{-2} . This is somewhat greater than the solar gravitational attraction acceleration 2.75×10^4 cm sec^{-2} , which is as it should be if the coronal ions are forced out from the sun by radiation pressure. If the ion density y is 10^6 ions cm^{-3} in the outer chromosphere and falls off with the inverse fifth power of the distance from the center of the sun, γ_c is about 10^{40} ions. With these values and with $f = 10^{-5}$ in (6) I_c is 3×10^{27} erg sec^{-1} . The total

⁷ Deslandres, *Comptes Rendus* 189, 413 (1929).

⁸ Pike, *Monthly Notices, Roy. Ast. Soc.* 88, 3 (1927).

⁹ Cf. Hulburt, *Phys. Rev.* 35, 1098 (1930), section 8.

radiation I_s emitted by the sun amounts to 3.7×10^{33} erg sec⁻¹. Thus the coronal energy I_c is 10^{-6} of I_s in accord with observation.

Equations (5) and (6) are valid no matter what processes of light absorption and emission are assumed, i. e. whether the processes are those of fluorescence, Raman radiation, resonance scattering,¹⁰ etc. On the other hand, Anderson's¹¹ very startling theory of the corona makes quite a different set of hypotheses and therefore uses equations different from (5) and (6). The theory assumes that positive electricity is continually annihilated in the sun leaving the sun negatively charged, that the excess negative electrons are driven out mainly by electrostatic forces to form a pure electron atmosphere around the sun and that the coronal light is the solar radiation scattered from this atmosphere. As far as can be seen the considerations advanced in the foregoing paragraphs in explanation of the geometrical form of the corona will hold equally well on Anderson's theory as on a radiation pressure theory. Probably a final decision about the constitution of the coronal atmosphere can not be reached as long as the origin of the lines in the spectrum of the corona remains unknown.

In conclusion the present paper can hardly be regarded as offering a quantitative theory of the corona. It presents a few quantitative ideas about the processes which may be important in the corona and thus furnishes a framework on which to build a quantitative theory. To work out the ideas in more exact detail promises to be a difficult problem, entirely apart from the fact that the development will have to deal as best it can with many unknown quantities and uncertainties of assumption.

¹⁰ Unsöld, *Zeits. f. Physik.* 46, 765 (1928).

¹¹ Anderson, *Zeits. f. Physik* 42, 475 (1927), 41, 51 (1927).

DISTRIBUTION OF NON-REACTING FLUIDS IN THE GRAVITATIONAL FIELD

BY MORRIS MUSKAT

RESEARCH DEPARTMENT, THE GULF COMPANIES

(Received March 28, 1930)

ABSTRACT

The paper consists essentially of an analysis of the equations given by Lewis and Randall for the distribution of non-reacting ideal fluids in a gravitational field. When the fluids are incompressible a formal solution is obtained, for a mixture of any number of constituents. But it has not been possible to put it into a form convenient for numerical application. The ratios of the concentrations of any constituent at the top to that at the bottom of a vertical column of the mixture are given explicitly, both for incompressible and compressible fluids. When all the molar volumes of the various fluids are equal the equations are solved completely and lead to a *relative* barometric distribution, and in the particular case of ideal gases, to individual barometric distributions. The physical meaning of this is briefly discussed. The case of binary mixtures is treated in detail, and numerical examples are given, first for a mixture of two paraffins, and secondly for a dilute solution of NaCl in water which is equivalent to an ideal solution of liquids. As is to be expected, the effect is extremely small, and in the first case only one tenth as large as is given by a simple barometric formula.

I. INTRODUCTION

ALTHOUGH we might predict, *a priori*, that the effect of gravity in causing a variation with height in the composition of a mixture of non-reacting fluids is but a slight one, it is of interest to have explicit theoretical expressions for this effect. As yet, this has not been attained in the general case of a mixture of any number of constituents: however, the problem of a binary mixture of two ideal fluids has been completely solved and some results of interest have been obtained for the general case. These results and the general problem will be discussed in the following.

Gouy and Chaperon¹ first, and later Duhem² and van der Waals³ considered binary mixtures thermodynamically, but they do not present explicit formulae for the results. Even earlier, however, Gibbs⁴ derived the general conditions of equilibrium for a mixture of any number of fluids, but he applied them only to the ideal gas mixture. The conditions of Gibbs are:

- (a) The temperature, T , be uniform throughout the mixture;
- (b) $\mu_i + gz = \text{constant}$ (1)

where μ_i is the intrinsic potential of the i^{th} constituent, and z is the height above a fixed horizontal plane.

- (c) $d\phi = -g\rho dz$ (2)

¹ Gouy and Chaperon, Ann. Chimie Physique 12, 384 (1887).

² Duhem, Jour. de Physique 7, (1888).

³ van der Waals, Die Continuität des Gasförmigen und Flüssigen Zustandes, II, p. 30.

⁴ Gibbs, Thermodynamics, p. 146 and p. 159.

where $p = p(z)$ is the pressure at z , and $\rho = \rho(z)$ is the density of the mixture at z .

II. THE DIFFERENTIAL EQUATIONS FOR THE EFFECT

The general differential equations for the effect were then set up by Lewis and Randall.⁵ Their method is the following:

Considering any constituent separately, the i^{th} for example, the second law of thermodynamics requires that under equilibrium conditions throughout the mixture

$$dF_i = \frac{\partial F_i}{\partial z} dz + \frac{\partial F_i}{\partial p} dp + \frac{\partial F_i}{\partial \bar{n}_i} d\bar{n}_i + \sum_j \frac{\partial F_i}{\partial \bar{n}_j} d\bar{n}_j = 0, \quad (3)$$

where $F_i = F_i(p, z, T, \bar{n}_i, \bar{n}_j)$ is the partial molal free energy of this constituent and $\bar{n}_i = \bar{n}_i(z)$ is its mol fraction. This is obviously equivalent to Gibb's condition (1).

Clearly, if w_i is the i^{th} molar mass,

$$\frac{\partial F_i}{\partial z} = w_i g, \quad (4)$$

and by the second law of thermodynamics,

$$\frac{\partial F_i}{\partial p} = \bar{V}_i \quad (5)$$

where $\bar{V}_i = \bar{V}_i(p)$ is the partial molal volume for the i^{th} constituent.

Now for ideal solutions, to which the present considerations will be restricted, \bar{V}_i is by definition equal to the i^{th} molar volume, V_i , at the pressure p and temperature T . This is a consequence of the criterion that an ideal solution must obey the law of additivity of volumes. Also, in this case,

$$\frac{\partial F_i}{\partial \bar{n}_j} = 0, \quad j \neq i \quad \frac{\partial F_i}{\partial \bar{n}_i} = \frac{RT}{\bar{n}_i} \quad (6)$$

where R is the gas constant, per mol. Combining (2), (4), (5) and (6) with (3):

$$\frac{d\bar{n}_i}{dz} = \frac{\bar{n}_i g}{RT} [\rho v_i - w_i] \quad i = 1, 2, \dots, r \quad (7)$$

if there are r constituents. This is the final form given by Lewis and Randall.

To get the explicit solution to the problem under consideration, the system of simultaneous equations (7) must be integrated, since the composition is essentially given by the \bar{n}_i . In principle, (7) would be immediately integrable in the case of incompressible fluids, except for the term $\rho = \rho(z)$ which must be determined from the equations together with the \bar{n}_i . This difficulty is not serious in itself, since $\rho(z)$ may be expressed in terms of the \bar{n}_i , and in this way eliminated; for, by definition,

$$\rho = \sum_i w_i \bar{n}_i \quad (8)$$

⁵ Lewis and Randall, Thermodynamics, p. 242.

where n_j is the number of mols of the j^{th} constituent per cc of mixture. Also, the definition of the ideal mixtures implies that

$$\sum_i v_j n_j = 1. \quad (9)$$

Hence

$$\rho = \frac{\sum_i w_j n_j}{\sum_i v_j n_j} = \frac{\sum_i w_j \bar{n}_j}{\sum_i v_j \bar{n}_j}. \quad (10)$$

Alternatively, (10) may be derived from the equations (7) themselves: by adding the equations (7) and noting that by definition

$$\sum_i \bar{n}_j = 1 \quad (11)$$

$$\sum_i \frac{d\bar{n}_j}{dz} = \frac{d}{dz} \sum_i \bar{n}_j = 0 = \frac{g}{RT} \left[\rho \sum_i v_j \bar{n}_j - \sum_i w_j \bar{n}_j \right]$$

which is identical with (10).

Putting (10) into (7), the latter becomes a system of non-linear coupled equations:

$$\frac{d\bar{n}_i}{dz} \sum_j v_j \bar{n}_j = k \bar{n}_i \sum_j \bar{n}_j (v_i w_j - v_j w_i) \quad (12)$$

where $k = g/RT$; $\rho_i = w_i/v_i$.

III. INTEGRATION OF THE EQUATIONS

The general system (12) has not been integrated completely, except in the case of a binary mixture. However, when all the v_i are equal, (12) or (7) can be solved exactly for a mixture containing any number of constituents.

Returning to (7), its integral is, clearly:

$$\bar{n}_i = c_i e^{-k w_i z + k \int v_i \rho dz} \quad (13)$$

and hence

$$\frac{\bar{n}_i}{\bar{n}_j} = \frac{n_i}{n_j} = \frac{c_i}{c_j} e^{kz(w_j - w_i) + k \int \rho (v_i - v_j) dz}. \quad (14)$$

However, as $\rho(z)$ is unknown until the \bar{n}_i themselves are known, (13) or (14) do not give the solution to the problem in a form which can be applied to any specific case. If the v_i are taken to be constant, ρ can be eliminated from (12), giving

$$\frac{(\bar{n}_i)^{1/v_i}}{(\bar{n}_j)^{1/v_j}} = \frac{(c_i)^{1/v_i}}{(c_j)^{1/v_j}} e^{kz(\rho_j - \rho_i)}. \quad (15)$$

But, although there is yet the relation (11) to be imposed on the \bar{n}_i , the system (15) cannot in general be solved for the \bar{n}_i .

On the other hand, for the special case where

$$v_i = v_j = \dots = v, \text{ for all values of } z, \quad (16)$$

(14) gives

$$\frac{\bar{n}_i}{\bar{n}_j} = \frac{n_i}{n_j} = \frac{c_i}{c_j} e^{kz(w_j - w_i)}. \quad (17)$$

This equation clearly implies that

$$\bar{n}_i = c_i e^{-kzw_i + \phi(z)}, \quad (18)$$

$$n_i = c_i e^{-kzw_i + \psi(z)}. \quad (19)$$

Applying (11) to (18)

$$\bar{n}_i = \frac{c_i e^{-kzw_i}}{\sum_j c_j e^{-kzw_j}} \quad (20)$$

and applying (9) to (19)

$$n_i = \frac{c_i e^{-kzw_i}}{v \sum_j c_j e^{-kzw_j}}. \quad (21)$$

From (2), (8), and (21) it now follows that

$$\int v dp = RT \log \sum_j c_j e^{-kzw_j}. \quad (22)$$

If v is known as a function of p , (22) will give p , and hence v as a function of z . This, when put into (21), gives n_i explicitly as a function of z . The constants c_i may then be determined, in principle, by applying the conditions that:

$$\int_0^h n_i dz = N_i \quad (23)$$

where z is measured from the bottom of the vessel containing the mixture and h is the height of the free surface above $z=0$; N_i is the total number of mols of the i th constituent in the mixture.

If v is not a function of p , (21) itself gives the final solution to the problem, after the determination of the c_i by (23).

It may seem that (16) is a very strong restriction upon the mixture constituents. Nevertheless, the important case where these constituents are perfect gases satisfies (16). For the molar volume is the same for all perfect gases at a given temperature and pressure, and they obviously form "ideal mixtures." In fact, for perfect gases

$$v_i = v_j = \dots = v = \frac{RT}{p}. \quad (24)$$

When this is put in (22), it gives

$$p = \text{const.} \sum_j c_j e^{-kzw_j}. \quad (25)$$

Thus, by applying again (24), (21) becomes:

$$n_i = n_0 e^{-kzw_i}. \quad (26)$$

This is the ordinary barometric formula derived quite differently by Gibbs, though usually tacitly assumed without explicit justification. Here, it results from a very special case of the general equations.

In addition to the case of perfect gases, (16) would be satisfied by a set of non-reacting liquids whose molar volumes happen to be the same, or nearly the same, since the liquids may be taken as incompressible. (21) is the complete solution under these circumstances.

Finally, the fact that we get the barometric formula (17) under the assumption that all the v_i are equal, whereas, when this assumption is not made the distribution law is quite different, is of added interest in that it suggests the physical basis of the effect under consideration. If we mix a number of substances whose molecules interact in no way with each other, it is clear that a barometric distribution of the type given by (17) will result, since before mixing each had a barometric distribution. Hence, variations from barometric distributions must be related to the interactions between the molecules. For the present purposes, we may consider a molecule and its field of force to be characterized by its "effective volume," i.e., the volume per molecule in the ensemble, and we note that the assumption of ideal mixtures means that, on mixing at constant pressure and temperature, these effective volumes are not changed.

If, then, to a homogeneous substance is added another with molecules of the same effective volumes, it is apparent that to the original molecular type the added ones will be indistinguishable, in the matters of collisions and perturbing forces, from molecules of their own kind, and vice versa. The effect will be essentially that of increasing the total number of molecules of either kind. Thus, we should expect the *relative* distribution to be barometric, as it was before mixing. Only for ideal gases will the individual distributions be barometric, but the relative distributions in all such cases will be of the type given by (17).

On the other hand, when the effective volumes of the added molecules are different from that of the original kind, the added molecules will exert different forces upon those originally present from those which the latter exert between themselves. Under these circumstances, we cannot expect even the relative distributions to remain as they were before mixing. Hence, in this general case we may get a distribution quite different from that given by (17). In fact, for the example given below of a binary mixture in which the effective volumes differ by a factor of about 2, we find that the distributions given by (15) and that given by a barometric formula may differ by a factor of 10.

Thus, in this qualitative way we can understand the physical basis for the analytical simplicity involved in the assumption of equal molecular volumes for all the molecular species.

Before discussing in detail the binary liquid mixture, it may be of interest to examine (15) further. If (15) be written as

$$\frac{(\bar{n}_1)^{1/v_1}}{(\bar{n}_i)^{1/v_i}} = c_j e^{kz(\rho_j - \rho_1)} \quad c_1 = 1 \quad (15')$$

and if $s \equiv (\bar{n}_1)^{1/v_1}$, then

$$\frac{s^{v_j}}{\bar{n}_j} = c_j^{v_j} e^{kz v_j (\rho_j - \rho_1)}$$

and

$$\bar{n}_j = 1 - \bar{n}_1 - \sum_l \bar{n}_l = 1 - s^{v_1} - \sum_l \frac{s^{v_l}}{c_l^{v_l} e^{kz v_l (\rho_l - \rho_1)}}$$

so that

$$\sum_j \frac{s^{v_j}}{c_j^{v_j} e^{kz v_j (\rho_j - \rho_1)}} = 1 \quad (27)$$

This is an equation for s as a function of z . Provided the c_j were known, it could be readily solved numerically for any value of z . But as the c_j are implicitly determined by (23), it is very difficult to express them directly in terms of the N_i . However, if, in the particular problem under consideration, the object is to study the variation in composition from an assumed composition at a given height, (27) will suffice. As

$$c_j = \frac{[\bar{n}_1(h)]^{1/v_1}}{[\bar{n}_j(h)]^{1/v_j}} e^{-kh(\rho_j - \rho_1)}, \quad (28)$$

the composition assumed at the height h , will give the c_j , and (27) will then give the composition at any other height.

Finally, it should be pointed out that, both for incompressible and compressible fluids, the ratio of the concentrations f_i , defined as the mol-fraction, of any constituent at the top to that at the bottom of the vessel containing the mixture, can be found in the general case. Considering first the incompressible fluids, if h be the height of the vessel and M the total mass of the mixture for the volume of unit section of height h , then (13) taken between the limits 0, h , gives

$$\frac{\bar{n}_i(h)}{\bar{n}_i(0)} = \frac{f_i(h)}{f_i(0)} = e^{-kw_i h + kv_i M} \equiv A_i. \quad (29)$$

If an average density be defined by $\bar{\rho} = M/h$, then

$$\frac{f_i(h)}{f_i(0)} = A_i = e^{kv_i h (\bar{\rho} - \rho_i)}. \quad (30)$$

Thus, if $\rho_i < \bar{\rho}$, the composition of the i th constituent at the top is greater than that at the bottom and, conversely, if $\rho_i > \bar{\rho}$. This of course, would be expected.

If the fluids are compressible, we may consider their molar volumes, v_i , to be given as a function of the pressure. In this case, applying (2) to (13), we get

$$\bar{n}_i = c_i e^{-kz w_i - k/a \int v_i(p) dp}. \quad (13')$$

We may consider $\int v_i(p) dp = b_i(p)$ as known. Then, taking (13') between the limits 0 and h , we get:

$$\frac{\bar{n}_i(h)}{\bar{n}_i(0)} = \frac{f_i(h)}{f_i(0)} = e^{-k w_i h - k/g [b_i(p_0) - b_i(p_0 + M_0)]} f(h) \equiv f_0. \quad (30a)$$

For any particular case, the expressions for $b_i(p)$ may be put into (30a) and the actual ratios of the concentrations may then be determined numerically.

IV. THE BINARY MIXTURE

We shall first treat the binary mixtures of incompressible fluids. In this case, (15) does permit of an explicit solution. Letting

$$\left. \begin{aligned} t &= \frac{\bar{n}_1}{\bar{n}_2} = \frac{n_1}{n_2} \\ \bar{n}_1 &= \frac{t}{1+t}; \quad \bar{n}_2 = \frac{1}{1+t} \end{aligned} \right\} \quad (31)$$

then

Hence, by (15)

$$\frac{1}{v_1} \log t + \left(\frac{1}{v_2} - \frac{1}{v_1} \right) \log (1+t) = \text{const} + k z (\rho_2 - \rho_1). \quad (32)$$

Now from (29) and (11)

$$A_1 \bar{n}_1(0) + A_2 \bar{n}_2(0) = 1$$

which, combined again with (11), gives

$$\left. \begin{aligned} t(0) &= \frac{1 - A_2}{A_1 - 1} \equiv t_0 \\ \bar{n}_1(0) &= \frac{1 - A_2}{A_1 - A_2}; \quad \bar{n}_2(0) = \frac{A_1 - 1}{A_1 - A_2} \end{aligned} \right\} \quad (33)$$

so that

$$\frac{1}{v_1} \log \frac{t}{t_0} + \left(\frac{1}{v_2} - \frac{1}{v_1} \right) \log \frac{1+t}{1+t_0} = k z (\rho_2 - \rho_1). \quad (34)$$

As t_0 is known, (34) gives explicitly the variations of the composition t with z . The density of the mixture is then

$$\rho = \frac{w_1 t + w_2}{v_1 t + v_2}. \quad (35)$$

The actual magnitude of the effect may be more directly inferred from the extreme values of the concentrations $\bar{n}_1(0)$ and $\bar{n}_2(0)$, given by (33) and (29), or by the extreme values of the density. These latter are easily found to be by (35), (33), and (29)

$$\left. \begin{aligned} \rho(0) &= \frac{w_1 - w_2 + w_2 A_1 - w_1 A_2}{v_1 - v_2 + v_2 A_1 - v_1 A_2} \\ \rho(h) &= \frac{A_1 A_2 (w_2 - w_1) + A_1 w_1 - A_2 w_2}{A_1 A_2 (v_2 - v_1) + A_1 v_1 - A_2 v_2} \end{aligned} \right\} \quad (36)$$

Referring to (23), we let $N_1/N_2 = c$, and noting that $N_1 w_1 + N_2 w_2 = M$, $N_1 v_1 + N_2 v_2 = h$, A_1 and A_2 take the values

$$A_1 = e^{k v_1 v_2 (\rho_2 - \rho_1) h / v_1 c + v_2}; \quad A_2 = A_1^{-c}. \quad (37)$$

Thus, $\rho(0)$ and $\rho(h)$ can be expressed directly in terms of c and h . For comparison with these formulae, we may note the expression for the composition which would be given by a barometric distribution. This latter is

$$t^1 = \frac{n_1}{n_2} = \frac{N_1 w_1 (1 - e^{-k w_2 h})}{N_2 w_2 (1 - e^{-k w_1 h})} e^{k (w_2 - w_1) z}. \quad (38)$$

We see that here the molar volumes V do not enter at all. Yet, this is in complete agreement with our physical picture of the phenomenon, according to which a barometric distribution implies that all the molar volumes are equal and hence do not explicitly affect the distribution. The fact that c does not enter in the expressions as $\rho(h)/\rho(0)$ is simply a corollary of the same reasoning.

The forms of (36) and (37) indicate that the effects of gravity, which we have been considering, should be entirely beyond experimental observations for any reasonable values of h . The following computation will give an example of the actual magnitude of the effect. We consider a mixture of two members of the paraffin series, heptane and octodecane, mixtures of which are very nearly "ideal." Let the temperature be 293°K. The data are

$$\begin{aligned} w_1(\text{heptane}) &= 100.12; \quad \rho_1 = 0.684; & v_1 &= 146.374 \\ w_2(\text{octodecane}) &= 254.30; \quad \rho_2 = 0.777; & v_2 &= 327.284 \end{aligned}$$

Let $c=1$. The computation gives for

$$\begin{aligned} h=100 \text{ meters: } \rho(0) &= 0.74834 \\ &\rho(h) = 0.74818 \\ h=1000 \text{ meters: } \rho(0) &= 0.74901 \\ &\rho(h) = 0.74750. \end{aligned}$$

The composition variation according to (34) is plotted in Fig. 1 and, for comparison, is added the composition curve which would be given by the barometric formula (38).

It is of interest to observe that, for this case at least, the incorrect barometric formula would indicate a rather appreciable variation of composition, whereas the equation (34) gives a quite negligible variation.

As a final example, it may be mentioned that, since a dilute solution is equivalent to an "ideal" mixture, the present formulae may be applied to such a case as a dilute solution of NaCl in water. Thus, if $c = 100$, $T = 300^\circ\text{K}$.

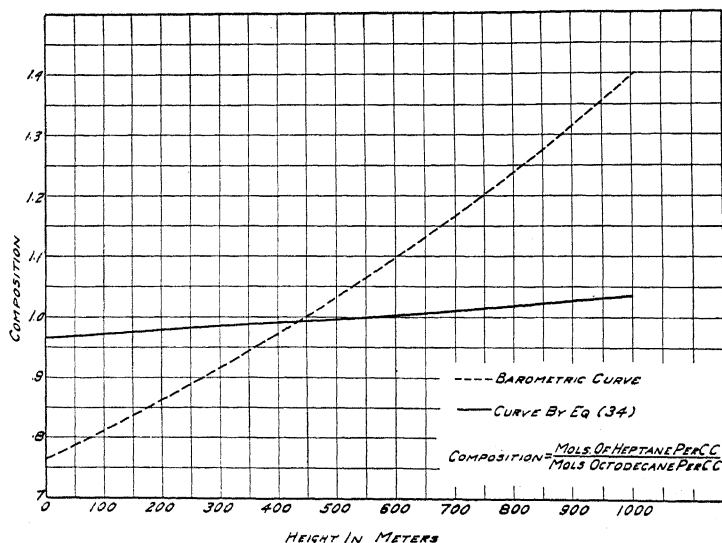


FIG. 1.

$$w_2(\text{NaCl}) = 58.457; \quad \rho_2 = 2.17; \quad v_2 = 26.939$$

$$w_1(\text{H}_2\text{O}) = 18.016; \quad \rho_1 = 1.00; \quad v_1 = 18.016$$

the extreme values for $\rho(0)$ and $\rho(h)$ are, for a depth of 1000 meters,

$$\rho(0) = 1.01809$$

$$\rho(h) = 1.01571$$

again with a difference clearly insignificant.

Hence, it may be generally concluded that, except at very low temperatures or on a planet or star with a considerably higher gravitational constant, gravity cannot produce any appreciable variation with depth in the composition of a fluid mixture. It is possible, however, that in a centrifuge *effective* gravity constants may be obtained such as to make the effect observable.*

Finally, we shall outline the method of treating binary mixtures of compressible fluids. We note that equation (13') implicitly gives the distribution function, in the general case, except for the constants c_i . For the binary case, these constants may be determined as follows:

We know that at $z=0$, $p = Mg + p_0$ where M is the total mass of the liquid in the column of height, h , and unit cross section; also, at $z=h$, $p = p_0$. We therefore have

* This possibility was kindly suggested to us by Dr. A. G. Loomis of this laboratory.

$$\left. \begin{aligned} \bar{n}_1(0) &= c_1 e^{-k/gb_1(Mg+p_0)}; & \bar{n}_2(0) &= c_2 e^{-k/gb_2(Mg+p_0)} \\ \bar{n}_1(h) &= c_1 e^{-k[b_1(p_0)/g+w_1h]}; & \bar{n}_2(h) &= c_2 e^{-k[b_2(p_0)/g+w_2h]}. \end{aligned} \right\} \quad (39)$$

As $\bar{n}_1(0) + \bar{n}_2(0) = 1$ and $\bar{n}_1(h) + \bar{n}_2(h) = 1$, c_1 and c_2 can be expressed directly in terms of the known constants of the mixture, if we put into the above expressions the proper forms of the functions $b_1(p)$ and $b_2(p)$.

We next determine the pressure, p , by the relation;

$$c_1 e^{-w_1 z + b_1(p)} + c_2 e^{-w_2 z + b_2(p)} = 1. \quad (40)$$

When it is difficult to obtain an algebraic solution of this equation, for $p = p(z)$, a graphical solution will always be possible. When $p(z)$ is known, it may be put back into (13'), and we shall then have the desired solution to the problem, namely, the mol-fractions \bar{n}_i as a function of z . The individual molar concentrations, n_i , are then given by the general relation, already used in Eq. (20):

$$n_i = \frac{\bar{n}_i}{\sum_j \bar{n}_j v_j}. \quad (41)$$

With the aid of these formulae, $\bar{n}_i(z)$ and $n_i(z)$ may be determined for any particular case of a binary mixture of compressible fluids. Of course, the mixture of incompressible fluids is a special case of these, but the previous development has been given as it illustrates more clearly the general problem of the incompressible fluids.

The writer is indebted to Dr. P. D. Foote and Mr. W. O. Smith for suggesting this problem and to Drs. A. E. Ruark and L. Shereshefskey for the opportunity of discussing the problem with them.

THE RECOMBINATION OF IONS IN AIR AND OXYGEN
IN RELATION TO THE NATURE OF GASEOUS IONS

BY OVERTON LUHR

PHYSICAL LABORATORY, UNIVERSITY OF CALIFORNIA

(Received April 14, 1930)

ABSTRACT

Coefficient of recombination of ions produced by x-rays as a function of the age and initial concentration of the ions. Measurement of the coefficient of recombination of ions in air and oxygen has been continued, with an improved form of the apparatus previously described by L. C. Marshall. Marshall's results in air have been checked, showing a sharp initial drop in the coefficient α for short time intervals ascribed to initial non-random distribution of the ions. Further measurements at longer time intervals have been made, using a new system of calculation whereby α is found as a function of τ , the age of the ions, rather than t , the total time of recombination. In this case α does not drop to a constant value of about 0.8 to 0.9×10^{-6} as indicated by Marshall's results, but continues to drop off to values of 0.5 to 0.6×10^{-6} after the ions have aged for one second, and 0.3 to 0.4×10^{-6} after two seconds. This is for a high initial concentration of ions of about 3.5×10^8 ions per cm^3 . With an initial concentration of 1.55×10^8 ions per cm^3 , α drops only to 1.15×10^{-6} after a time of one second. In pure oxygen the values of α are in general higher than the corresponding ones for air, although they become equal at low initial concentrations.

Interpretation of results and the absolute value of the coefficient in air. The results may be explained by assuming that heavy slow-moving ions are formed in increasing amounts as time goes on by reaction with impurities present. The faster ions are constantly being removed at a high rate by recombination, leaving the slow ions behind with a resulting increasingly low coefficient of recombination. It is possible that the ionizing agent produces nitric oxides, O_3 or H_2O_2 , which load up the ions. It is impossible to set accurately an absolute value of α in air, due to two disturbing factors: initial non-random distribution producing abnormally high values of α at short time intervals, and the loading up of the ions with impurities producing abnormally low values of α at long time intervals. At a time where these two factors have a minimum effect α has the value $1.4 \pm 0.1 \times 10^{-6}$, which is set as the closest approximation to an absolute value.

INTRODUCTION

RECENTLY in this laboratory L. C. Marshall¹ measured the coefficient of recombination of ions in air and argon using a new direct method with x-rays as a source of ionization. His results showed that the coefficient α given by the equation $dn/dt = -\alpha n^2$ is not a constant as has generally been supposed with a value about 1.6×10^{-6} for air but is a function of three factors: (1) the time of x-ray exposure t' ; (2) the initial ion concentration n_0 ; (3) the time of recombination t . He found that α dropped from a value of 4.0×10^{-6} at short times of recombination to an apparent nearly constant value of about 0.8 or 0.9×10^{-6} at time intervals of about one second. Also, the value of α was in general higher for short times of x-ray exposure and small

¹ L. C. Marshall, Phys. Rev. **34**, 618 (1929).

initial concentrations of ions. The high values at short time intervals were shown by experiment and also by the theory of Loeb and Marshall^{2,3} to be due to the initial non-random distribution of the ions which results from their formation in pairs along a β -ray track. The theory indicates that after a time interval of about 2.25×10^{-8} seconds, the value of α should become constant since by that time the ions would attain random distribution due to their heat motions.

The work has been continued by the writer in air and oxygen with essentially the same apparatus as that used by Marshall, although with important improvements in some details and particularly using a new method of measurement and calculation. These results show that the value of α does not become constant after a short time as indicated by Marshall's results but continues to fall off quite rapidly as the ions become older. This leads to important conclusions concerning the nature of gaseous ions.

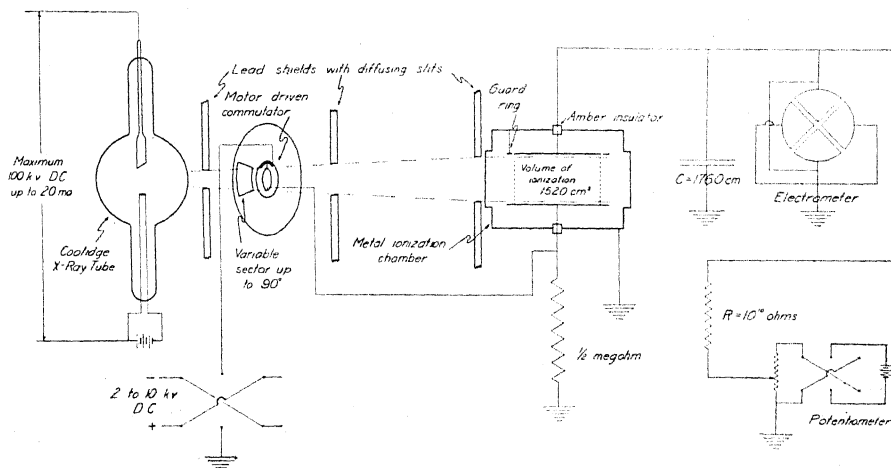


Fig. 1. Diagram of apparatus.

METHOD OF MEASUREMENT

The apparatus and system of measurement has previously been described by Marshall.¹ The essential features are shown in Fig. 1. D.C. potential is applied to the Coolidge x-ray tube by means of a transformer, kenotrons and filter system not shown in the diagram. The x-rays pass through a solid brass rotating disk which has a variable sector from 0° to 90° cut in it, thus producing a flash in the metal ionization chamber. The beam of x-rays is defined by three lead slits and passes through almost two meters of air and an aluminum window before reaching the chamber. The beam is thus sharply defined and nearly homogeneous. The shaft carrying the sector also carries an adjustable commutator by which potentials of 1000 to 10,000 volts may

² L. B. Loeb and L. C. Marshall, Jour. Franklin Inst. 207, 371 (1929).

³ L. B. Loeb, Trans. Am. Electrochem Soc. LV, 131 (1929).

be applied to the lower plate of the chamber. The high field almost instantly sweeps all the ions of one sign to the upper plate at any desired time after the x-ray beam has been cut off by the brass disk. The lower plate is also connected to ground through a one-half megohm resistance so that its potential becomes zero immediately after the brush breaks contact with the commutator segment.

Since the upper plate must also be kept at zero potential during the flash time and time of recombination, a neutralizing mechanism is used to prevent a charge from building up on the plate and electrometer system as a result of the repeated flashes of x-rays. For this the alternate system described by Marshall is used. A current of opposite sign to that collected on the upper plate of the chamber is forced through the high resistance leak R by means of a voltage applied from a potentiometer. Thus, when the electrometer deflection is zero, the two currents are neutralizing each other and the voltage

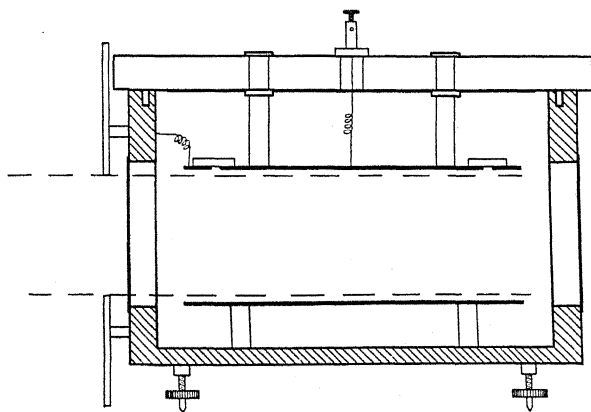


Fig. 2. Ionization chamber.

read directly from the potentiometer will be proportional to the ionic current.

It may be noted that difficulty was encountered in constructing a high resistance leak of the order of 10^{10} ohms which would remain constant over a period of several hours. Experiment showed that an India ink line drawn on typing paper and enclosed in an airtight vessel containing a small amount of P_2O_5 to remove the moisture, was satisfactory. Such a leak exhibits no polarization and stays constant well within 0.5 percent.

The only major change made in the apparatus used by Marshall was the substitution of a new ionization chamber allowing much greater volume of ionization (See Fig. 2). It consists of rectangular brass plates in a heavy brass box fitted with aluminum windows through which the x-ray beam passes. An important feature of the chamber is the plate glass cover to which the upper plate and guard ring are attached by means of amber insulators. The cover is sealed on by means of stopcock grease, a double seal with a groove between being employed to prevent the diffusion of stopcock grease vapor

into the chamber. The stopcock grease is employed only in the outer seal, all excess grease being forced either outside or into the groove. The total volume of ionization is 1520 cm³ compared to 63 cm³ in Marshall's apparatus. The advantages of this large volume are: (1) the ionic currents are much larger and can be measured more accurately; (2) the volume can be determined more accurately and diffusion plays a smaller though still appreciable role. In this connection it may be noted that the x-ray beam extends well beyond the sides of the plates; so that only diffusion toward the plates must be considered; not that toward the sides or ends.

The air and oxygen used in the ionization chamber were purified according to standard technique, all dust, moisture, CO₂ and organic vapors being removed by passage through glass wool, CaCl₂, sodium calcium hydrate, P₂O₅, and two liquid air traps. Special care was taken to remove organic substances by cleaning the metal chamber thoroughly with cleaning solution.

In calculating α the integrated form of the well-known equation,

$$\frac{dn}{dt} = -\alpha n^2 \quad (1)$$

is used, where n is the number of ions of either sign per cm³. Integration gives:

$$\alpha = \frac{1}{t} \left(\frac{1}{n} - \frac{1}{n_0} \right) \quad (2)$$

where t is the time of recombination, n_0 is the number of ions per cm³ at $t=0$ and n is the number of ions left after time t . Inserting the experimental constants Eq. (2) becomes:

$$\alpha = \frac{1.59 \times 10^{-19} RNV}{\epsilon} \frac{1}{t} \left(\frac{1}{r} - \frac{1}{r_0} \right) \quad (3)$$

where R is the value of the high resistance leak in ohms, N is the number of revolutions per second of the commutator, V is the volume of ionization, ϵ is the e.m.f. of the neutralizing potentiometer battery in volts, and r and r_0 are the direct potentiometer readings at the time $t=t$ and $t=0$ respectively.

In the method of calculation one important change is made from that used by Marshall who measured n_0 the number of ions at the instant the x-ray flash was cut off, then n the number left after varying time intervals t . α was calculated between these two limits thus giving an average value over the whole time of recombination. In the present work values of n_0, n_1, n_2, \dots are measured at short intervals of time 0, t_1, t_2, \dots . Then α may be calculated between any two of these intervals. That is, Eq. (2) becomes of the form:

$$\alpha = \frac{1}{t_p - t_q} \left(\frac{1}{n_p} - \frac{1}{n_q} \right). \quad (4)$$

This allows α to be studied as a function of the age of the ions rather than as a function of the time of recombination after the x-rays are cut off. Setting τ as the average age of the ions over any period of recombination $t_p - t_q$ and assuming $\tau = 0$ at $t = 0$ we have:

$$\tau = t_q + \frac{t_p - t_q}{2}. \quad (5)$$

If $t_p - t_q$ is a short time interval compared to the maximum time allowable at any particular commutator speed, τ is a fairly accurate measure of the age of the ions and the variation of α with τ can be studied.

RESULTS

The first series of runs were taken as a check on Marshall's work and show results similar to his, α being plotted as a function of t the time of recombination (see Fig. 3). Each succeeding run was taken with the commutator speed one-half that of the previous run. These show the sharp initial drop due to the non random distribution of the ions with the apparent flattening out of

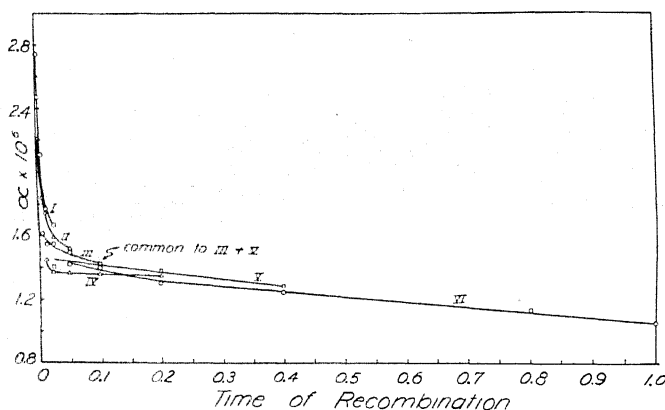


Fig. 3. First six runs corrected for diffusion.

the curves at longer time intervals. The final value at one second is about 1.03×10^{-6} compared to Marshall's value of 0.9×10^{-6} . This is due to a very short time of exposure (0.01562 seconds which was kept constant throughout the series of runs by narrowing the sector) and a resulting low initial concentration of the ions. The matter of initial concentration is important even at long time intervals as will be seen later.

All later runs were taken by measuring n at short intervals of time thus making it possible to calculate α as a function of τ the age of the ions, as well as a function of t the time of recombination. All the curves (Fig. 5) show without exception a continued drop in α up to a time of two seconds, the maximum time which could be studied. At the end of these long time intervals α still shows no indication of becoming constant although the slope of the curves gradually decreases.

Fig. 4 shows a comparison for one particular run of the two methods of calculating α . In the upper curve, α is plotted as a function of the time of recombination, in the lower curve as a function of τ the age of the ions. In the lower curve α drops more sharply than in the upper. In other words, Marshall's results gave an average high value of α rather than the true value at any particular time. However, on the magnified scale of Fig. 4, α still drops quite sharply even with Marshall's method of calculating, while it appeared to be nearly constant on the scale used in Fig. 3.

Values of α calculated as a function of τ do not lie as close to a smooth curve as those calculated as a function of t . (See Fig. 4). This is because α is obtained for comparatively small differences in the potentiometer readings, especially at the later time intervals when the concentration of ions

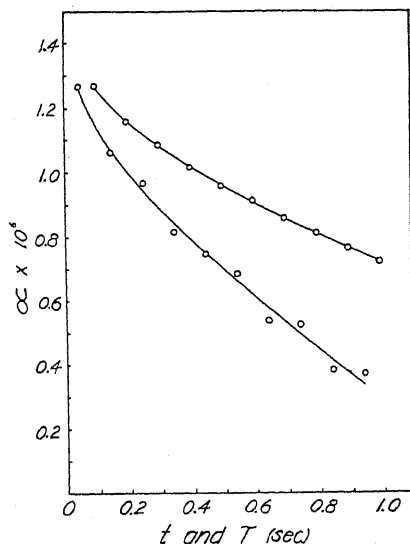


Fig. 4. Comparison of two methods of calculating α .

has become small and very little recombination takes place. Thus small errors in the potentiometer readings may result in large errors in the calculated values of α . However, the points show a definite trend in every case. This is more important than the absolute values since a final definite value of α does not seem to exist.

Fig. 5 shows the complete results for all the runs taken over the longer time intervals in air and oxygen. α is plotted against τ , the age of the ions, and the curves are all averages of values taken from two or more runs which may vary by considerable amounts due to an overcorrection for diffusion at the longer time intervals which will be discussed later. The dotted lines show the results in oxygen and the full lines those for air.

Curve I is a run taken with the commutator revolving at the rate of two revolutions per second; curve II, one revolution per second; curve III 0.5 revolutions per second; curve IV 0.25 revolutions per second; all at rather

high initial ion concentrations varying from 2.5 to 3.5×10^6 ions per cm^3 . Curve V is taken in air at 0.5 revolutions per second corresponding to curve III, only in this case the initial concentration was reduced to 1.55×10^6 ions per cm^3 compared to 3.5×10^6 for curve III. As can be seen, the values of α for the low concentration are much higher than those for high concentration although the slope of the curve is approximately the same in each case.

Curves VI, VII and VIII are those for pure oxygen; VI corresponding to III for air, VII corresponding to V and VIII corresponding to IV. Curve VI is much higher than the corresponding curve III for air at the same initial concentration. For low concentrations the oxygen and air curves (V and VII) are approximately the same although the points do not fall on a smooth curve due to the extreme difficulty of measuring the coefficient accurately at these low concentrations. The trend is very definite however,

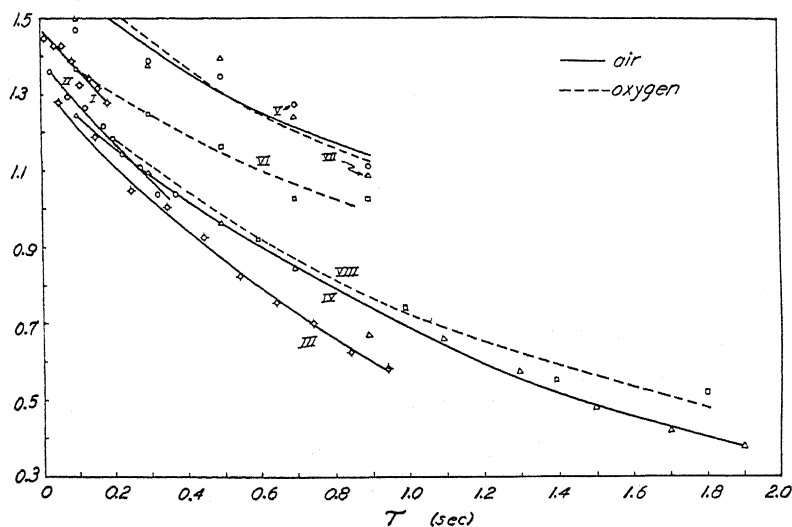


Fig. 5. Complete results for all runs taken over the longer time interval in air and oxygen.

and shows the slope to be about the same as for the curves taken at higher concentrations. Curve VIII for the longest time intervals in oxygen is only slightly higher than the corresponding curve IV for air although there is a distinct difference.

One question which must be considered in connection with these results is the correction for diffusion. Two types of runs were made: one with the beam of x-rays grazing though not touching the plates; so that the whole volume between the plates was ionized; and another with the beam about one centimeter from the plates. In general if no diffusion correction is made, the values of α obtained in each case are nearly the same. If, however, correction is made for diffusion, the values are higher when the beam is one centimeter from the plates, especially at the longer time intervals. This results from the fact that the correction is in the opposite direction in the two cases.

For the case when the beam grazes the plates, a certain number of ions diffuse to the plates during the time of recombination and are thereby lost. This loss is in addition to the loss due to recombination. The number lost by diffusion may be calculated, and this number then added to the measured value n_p at the time t_p to give the true value due to recombination alone. The number diffusing to the plates in time $t_p - t_q$ is given by

$$2n_p A [(\overline{\Delta x})_p - (\overline{\Delta x})_q] \text{ where } (\overline{\Delta x})_p = \left(\frac{4Dt_p}{\pi} \right)^{1/2} \text{ and } (\overline{\Delta x})_q = \left(\frac{4Dt_q}{\pi} \right)^{1/2}$$

n is the number of ions per cm^3 of either sign, A is the area of each plate, $\overline{\Delta x}$ is the average distance an ion diffuses in the time t derived from the Brownian movement equation,² and D is the coefficient of diffusion having a value about 0.047. The number

$$2n_p A \left[\left(\frac{4Dt_p}{\pi} \right)^{1/2} - \left(\frac{4Dt_q}{\pi} \right)^{1/2} \right]$$

being added to the measured value of n_p serves to reduce the uncorrected value of α by as much as ten percent.

Marshall has derived a rather complicated equation for the case when the beam is some distance from the plates but this is not readily applicable when α is calculated as a function of τ rather than t . In this paper therefore, a correction is made assuming a swelling of the volume of ionization due to diffusion which gives approximately the same results as Marshall's equation. In calculating α at any time τ the volume is assumed to be:

$$V = V_0 + 2A(\overline{\Delta x})_\tau = V_0 + 4A \left(\frac{D\tau}{\pi} \right)^{1/2}.$$

Since V occurs in the numerator of Eq. (3) this increases the value of α over that calculated without the diffusion correction.

From the fact that the diffusion correction throws the values of α as much as twenty percent apart at the longest time intervals there is apparently an overcorrection for this effect in the equations and values used. This would follow if the coefficient of diffusion becomes less for the ions remaining after long time intervals. Other factors may further reduce the actual rate of diffusion, but from a kinetic theory standpoint a correction like that indicated is necessary. As it does not seem justifiable to omit the correction, all the results are calculated in this manner and the average of the two types of runs is taken in plotting the curves in Fig. 5. The absolute value of α in the curves may be too high or too low by several percent especially for large values of τ since the correction for the case when the beam is one centimeter from the plates is greater than for the case when the beam is grazing the plates. However, the important fact remains that in every case, no matter whether a diffusion correction is made or not, the value of α still drops off continuously with the aging of the ions.

SUMMARY OF RESULTS AND CONCLUSIONS

From the curves in Fig. 5 the behavior of α may be summed up as follows:

(1) α is not a constant as has always been supposed, but beyond the sharp initial drop due to the non-random distribution of the ions, the curves continue to drop indefinitely as the ions age. At the end of one second the value of α is 0.5 to 0.6×10^{-6} ; at the end of two seconds, 0.3 to 0.4×10^{-6} .

(2) The lower the initial concentration of ions, the higher the value of α after random distribution has been attained. The value for an initial concentration of 1.55×10^6 ions per cm^3 drops to about 1.15×10^{-6} at the end of a second compared to about 0.6×10^{-6} when the initial concentration is 3.5×10^6 ions per cm^3 . However, the slope of the curves is about the same in each case.

(3) The values of α in pure oxygen are in general higher than the corresponding ones in air although they become equal when the initial concentration of the ions is small. The slope of the curves is still the same indicating that the same type of aging effect is taking place.

At first glance it would seem impossible to explain these results by any reasonable assumption. *However, the whole situation becomes clear at once if it is supposed that as time goes on some of the ions form clusters with the impurities present.*

Although special care was taken to remove organic vapors such as ether, alcohol, stopcock grease, etc., which are known to affect the nature of the ion, the number of these heavy molecules present was probably comparable to the number of ions. In addition, water vapor may be present coming from the walls of the metal chamber and there is the possibility that the intense hard x-rays form small quantities of nitric oxides, O_3 or H_2O_2 . Any of these impurities might form large ion clusters in increasing quantity during the time of measurement. The method is particularly sensitive to impurities as the small, fast moving ions are removed first by recombination leaving the heavier ions as time goes on. Hence α drops continuously.

The supposition that impurities formed by the x-rays form clusters is in agreement with the work of Tyndall, Grindley and Sheppard,⁴ also that of Erikson.⁵ Erikson showed definitely that the presence of β -rays from radium emanation tubes formed impurities which hastened the aging of the ions so that clusters formed in about 0.001 second. Passage of the gas through a metal ionization chamber which had not been thoroughly cleaned also hastened the aging although to a lesser degree. If neither the β -rays or metal ionization chamber were present there was no appreciable aging effect up to 0.1 second.

Since measurements of the coefficient of recombination in pure oxygen give in general higher values than in air, it would seem that the extremely low values in air are due in part to nitric oxides. The fact that low initial ion concentrations give higher values of α than high initial concentrations is

⁴ Tyndall, Grindley and Sheppard, Proc. Roy. Soc. A121, 125 (1928).

⁵ H. A. Erikson, Phys. Rev. 34, 635 (1929).

further evidence that clusters of some sort are forming and that the more intense the ionizing agent the more impurities there are present to retard recombination.

It has always been a moot question as to the true nature of ions in gases of normal purity such as are used in this experiment. Practically the only evidence on this subject is from mobility measurements. Erikson's well-known aging of the positive ions gives an indication of clustering and Loeb's measurements in mixtures show definitely that clustering occurs in some gases. Apparently in other gases the ions may consist of single molecules or at any rate small aggregates. However, the evidence from mobility measurements is incomplete in two respects: first because the measurements are generally made within a time interval of less than one tenth of a second after the ions are formed, and second because the mass factor is an unimportant one in mobility; i.e., the mobility is decreased very little by a considerable increase of mass.

The coefficient of recombination measurements are more reliable since in this case the ions can be studied up to time intervals of two seconds after they have had a chance to collide with all kinds of impurities and the faster ions have been weeded out by recombination. In addition, the mass factor is much more important than in mobility or diffusion. On J. J. Thomson's⁶ theory of recombination which Loeb and Marshall² have shown to be a correct approach to the problem, α is proportional to the velocity of thermal agitation of the ions. The velocity of thermal agitation is in turn inversely proportional to the square root of the mass. The better of two equations as given by Loeb and Marshall after inserting the various constants turns out to be:

$$\alpha = 1.9 \times 10^{-5} \left(\frac{273}{T} \right)^{3/2} \left(\frac{1}{M} \right)^{1/2} \epsilon$$

where T is the absolute temperature, M is the molecular weight of the ions, and ϵ is the probability that recombination will occur if the ions approach each other within a defined distance d . For the case of air or oxygen at room temperature and 760 mm pressure the theory gives ϵ a value of about 0.9 which, however, may be too high. T is about 295° so that the equation reduces to:

$$\alpha = 1.51 \times 10^{-5} \left(\frac{1}{M} \right)^{1/2}.$$

If α has a value of 0.4×10^{-6} which is the lowest observed in this work, it turns out that M the molecular weight of the ions is about 1400. This seems unreasonably high but is not inconceivable if there were a large cluster of heavy molecules. The equation, however, is correct only to the roughest approximation and probably gives high values of α . As a result, the mass, which varies inversely as the square of α may be much less than 1400.

⁶ J. J. Thomson, *Conduction of Electricity through Gases*, III Edition, Cambridge 1928.

The only conclusion which can safely be drawn is that little is actually known concerning the nature of gaseous ions, but that in gases of normal purity that are ordinarily used in gas ion work, clusters of large mass are formed, due probably to the effect of the ionizing agent. The process of cluster formation and weeding out of the faster ions by recombination continues for at least two seconds after the ions are formed. The exact nature and true mass of these clusters cannot be accurately determined owing to the lack of a completely satisfactory theory.

The absolute value of α in air. It appears to be of considerable interest to know the absolute value of α in air for use in numerous calculations. It is evident from the results in this paper that there are two factors which make it impossible to set an accurate absolute value. The first factor is the initial non-random distribution of the ions which produces very high apparent values of α at short time intervals and the second is the loading up of the ions with impurities and selective recombination which produces abnormally low values of α at long time intervals. Probably the closest approach to an absolute value is at a time when the ions have nearly attained random distribution but clustering and elimination of the faster ions has not yet played a major role. In other words, a point must be chosen on the curves in Fig. 3 where the sharp drop in α ends and the more gradual steady drop due to clustering begins. Such a point appears to lie between 0.05 and 0.1 seconds where the value of α is $1.4 \pm 0.1 \times 10^{-6}$. This is not much different from the commonly accepted value of 1.5 or 1.6×10^{-6} which has been determined by earlier investigators under conditions where, in general, these important disturbing factors have not been detected, or at any rate not clearly differentiated. The value of 1.4×10^{-6} for air may then be used with some degree of confidence under conditions where the ions have attained random distribution but have not aged more than one-tenth of a second.

In conclusion, the writer wishes to express his appreciation to Dr. Marshall who designed and constructed the fundamental parts of the apparatus; to Mr. G. P. Kraus of the shop who accomplished a difficult piece of work in building the ionization chamber; and to Mr. N. E. Bradbury who assisted in taking some of the later readings. Particularly, the writer wishes to thank Professor Loeb for his unfailing interest in the work and for his suggested explanation of the experimental results.

At present, the measurements are being continued in other gases, particularly argon and hydrogen.

LETTERS TO THE EDITOR

Prompt publication of brief reports of important discoveries in physics may be secured by addressing them to this department. Closing dates for this department are, for the first issue of the month, the twenty-eighth of the preceding month; for the second issue, the thirteenth of the month. The Board of Editors does not hold itself responsible for the opinions expressed by the correspondents.

Reflection of Positive Ions by Crystals

Further experiments on the reflection of hydrogen positive rays from crystals similar to those described in The Physical Review for December 1, 1929 have shown that the phenomenon is more complex than might have been expected. More than a hundred photographs showing reflected rays have been obtained under various conditions, and show several features of interest. Great differences have been found in the reflecting powers of different samples of calcite. Two were found that gave strong reflected rays when the glancing angle was less than two degrees. The images obtained on Schumann plates placed at right angles to the beam may be properly termed reflection patterns, as they show considerable complexity, vary in a regular manner with the angle of incidence, and can be reproduced at will with the same setting of the crystal and speed of the rays. Six other calcite crystals gave reflection patterns containing fewer lines or lines on a fogged background. Reflected rays were also observed with a diamond which was kindly loaned by Dr. D. Cooksey. A natural cleavage face of this diamond had been used in experiments on the reflection of gamma-rays. A highly polished face gave indistinct patterns on a fogged background. Clear lines were obtained from two other faces, one of which was the natural cleavage face, and the other a face that had been cut and appeared rough due to the saw marks. No reflected rays were found in a few trials with rock-salt galena and magnetite.

The strongest parts of the patterns are produced by rays that have energies corresponding to more than six thousand volts. Slower rays may be present in the original bundle, as shown by a positive ray analysis, but they are not reflected as strongly as the

faster rays. With a low potential on the discharge tube, the reflection pattern lacks certain of the parts that appear with high potentials. A positive-ray analysis of the ions reflected from one of the calcite crystals showed that in addition to the hydrogen atoms previously reported, all the positive ions in the original bundle are present in the reflection patterns, viz.: hydrogen molecules, triatomic hydrogen molecules and heavier ions that are probably oxygen atoms. With the present resolution the various ions are superimposed in the streaks or lines formed by the reflected rays of various velocities.

The dependence of the angle of deviation by the crystal on the energy of an ion rules out the possibility of ascribing the reflection to the deviation of particles by electrostatic forces which would require the reflected rays of various velocities to lie in a plane and to have angles of deviation inversely proportional to the energies of the particles. In most cases the reflected rays of different velocities do not lie in planes as they give curved images on the plate and in the cases where a straight line is formed the deviation is not inversely proportional to the energy but is a linear function of the reciprocal of the velocity. Charges would not be expected to accumulate on the crystal because of the secondary electrons liberated by the bombardment of metal parts near it and its uncharged condition is shown by the fact that those rays which just pass over the crystal without hitting it are undeflected. The small penetration of ions into matter as compared with electrons of the same equivalent wave-length suggests that energy changes at the surface or inside the crystal will have to be taken into account in a complete theory. The important factor in determining the angles may be a quantity

analogous to a refractive index which would depend on the energy of the ion and its alterations.

Small changes in the angle at which the incident rays hit the crystal produce a regular series of changes in the directions of the deflected rays. At nearly grazing incidence on one of the calcite crystals with the rays parallel to an edge of the cleavage rhomb there was a fan-shaped arrangement of the reflected rays in eight or more radial lines of different intensities. As the angle was made steeper the lines formed by the reflected rays of various velocities shifted towards the normal to the crystal surface and became curved the intensities altered and new curved lines appeared at the sides making the patterns more complex and more symmetrical. This change was produced by an increase of

only one degree. With a second calcite crystal which was turned so that at grazing incidence the rays made an angle of about fifteen degrees with an edge of the cleavage rhomb clear patterns were obtained which had an unsymmetrical character. These patterns as well as those from the diamond also changed in a regular manner with small increases in the angle of incidence. The dependence of the angles of reflection on the angle of incidence and on the velocity of the rays suggests very strongly that a theory of the phenomenon will have to contain other elements besides particles and the forces exerted on them by electric and magnetic fields.

A. J. DEMPSTER

University of Chicago
April, 1930.

High-Voltage Tubes

We have found that the internal shattering and puncturing of Pyrex high voltage tubes of the cascade type described in the Physical Review of January 1 is entirely eliminated if the glass is "heat-worked" throughout. Since last autumn we have been using tubes made by blowing a series of "bubbles" which comprise the cascade sections at proper intervals along a piece of Pyrex tubing using a glass lathe for holding the work. In other respects the tube construction and shielding have been similar to that previously described except that tungsten instead of wax seals were used and the electrodes were shorter. Shattering and puncture finally occurred with most of our tubes in the necks between bulbs ("bubbles") although such tubes were operated to over 1600 kilovolts by careful "seasoning" and by short-circuiting sections which shattered before these had progressed to actual puncture. It was then found that if the glass tubing was first worked at all points (by heating and alternately blowing and contracting as in working a glass seal or joint) and then formed into bubbles and necks and the electrodes assembled no shattering took place when the tube was used. In two months of very severe tests on a series of such "heat-worked" tubes we have not been able to produce any shattering or puncturing with our Tesla coil voltages. One such tube of 14 sections, 135 cm overall, was operated up to 1950 kolovolts (at about one spark per second) where gassing set in due to slightly contaminated electrodes. This

type of limitation by gas is the only one we experience with these tubes and our vacuum technique can be improved considerably when higher voltages are desired. An ionization-gauge near the pumps usually reads about 10^{-6} mm Hg equivalent air-pressure. We find that every tube which is assembled using reasonable precautions against contamination especially by water-vapor, can be relied on to go to voltages of 1,000 to 2,000 kilovolts, depending on the number of sections, the ground-point, and the success in avoiding contamination, which usually shows up as a discoloration of the out-gassed electrodes.

These tubes have been operated as high as 1500 kilovolts without a potentiometer, that is, with all except the end-electrodes electrically floating. We made the accidental discovery on several occasions that some of our potentiometer units had been broken while we were running a tube, without our knowing of their failure until afterwards, no trouble having been noted with the tube. When all of the potentiometer units were removed, the tube still operated without severe flashing, although the voltage-distribution was obviously very non-uniform. Brasch and Lange (Naturwiss. January 3, 1930) have already reported the successful operation of a somewhat similar "floating-electrode" tube. Whether or not a filament is used in a tube makes no detectable difference in its behavior or flashing, at least up to 1500 kilovolts at one spark per second, nor has any effect of the filament

been noted with 120 sparks per second up to 800 kilovolts, which voltage has happened to be the maximum available with 60-cycle excitation of the condenser at the time of these tests, due to temporary power-limitations.

We are now using tubes of 12 sections placed inside of a Tesla coil 6 inches in diameter and 38 inches long, each electrode being connected to a tap on the winding of the coil. The coil itself shields the tube from ground, and distributes the voltage. A tube of this type, *with one end grounded*, has been operated to 1900 kilovolts at one spark per second, and to 1600 kilovolts at 120 sparks per second, at which voltage the tube oper-

ated perfectly; primary power was again the limitation. Insulation difficulties are also serious at these voltages above ground. Experiments are in progress on direct measurements of the output from these tubes of the expected radiations and "rays" of radioactive energy-equivalents, the results of which we hope to report shortly.

M. A. TUVE
L. R. HAFSTAD
O. DAHL

Department of Terrestrial Magnetism,
Carnegie Institution of Washington,
May 6, 1930.

Photoelectric Effect and the *J* Phenomenon

In the issue of the Physical Review for May 1, 1930, appears a paper by E. Marx describing "A new photoelectric effect in alkali cells" wherein that author investigates changes produced in the limiting potential acquired by an insulated alkali electrode, by varying the composition of the incident radiation. Although these experiments constitute the first systematic study of the phenomenon in the optical region, an analogous investigation was carried out with x-rays some years ago by C. G. Barkla. I quote from one of the latter's notices (Nature, March 27, 1926, p. 448)—"The ionization produced by a heterogeneous beam of x-rays in a gas, or the electronic emission from a metal plate, (measured by ionization outside the plate) may be abruptly and enormously increased either by (a) superposing on that beam a very feeble radiation of slightly shorter wave-lengths, or (b) by taking away from the complex radiation a very small amount of the radiation of longer wave-lengths, as by filtering; that is, either by adding higher frequency radiations to or eliminating lower frequency radiations from the beam, the same effect is produced; namely, a sudden large increase in the ionization. The magnitude of a sudden increase may be from 100 to 150 percent of the original magnitude. This is the *J* ionization produced by the *J* photoelectric emission accompanying the *J* absorption."

Since the independent variable (composition of the incident radiation) is the same for both cases, they deal presumably with the same effect, and it should be legitimate to compare the results, although an extrapolation from the optical to the x-ray region must be made with caution. This comparison is

difficult, since it is unlikely that the experimental arrangements were the same for both. In Marx's work, the alkali electrode was insulated, and the removal of some of the red from an incident beam of white light caused an increase in the limiting potential acquired. On the other hand, in Barkla's experiment, the photoelectric plate was probably kept at a constant potential, and he observed that the removal of some of the long wave-length radiations from the beam of x-rays caused an increase in the ionization due to photoelectrons. Barkla interprets his result as a manifestation of some unexplained interaction between the component radiations in the incident beam, which causes a fundamental change in the amount or in the nature of the photoelectric emission. This is not necessarily inconsistent with the experiments of Marx, but it is not one of the assumptions of the tentative theory which he offers. Other possible suppositions as to Barkla's experimental arrangement lead also to conclusions which are at variance with the theory of Marx. At present all that can be deduced is that the four items (a) the experiments, (b) the theory of Marx, (c) the experiments, (d) the theory of Barkla, are not consistent.

I am not aware that Barkla's observation has ever been verified. It is possible that a series of varied experiments of this nature might throw some light on the elusive *J* phenomenon.

THOMAS H. OSGOOD

Department of Physics,
University of Pittsburgh,
Pittsburgh, Pennsylvania,
May 15, 1930.

The Origin of O^{17}

In the Physical Review of April 1 Harkins and Schuh have considered the possibility of all the O^{17} atoms in the earth's crust and atmosphere having been formed by close collisions of alpha-particles with the nuclei of nitrogen atoms as revealed by the cloud tracks. Assuming that the ratio $O^{17}:O^{16}$ atoms is the same in the crust as in the atmosphere and that the known nitrogen and radium contents are uniformly distributed in the crust they estimate that the necessary lapse of time would have been about 10^{18} years which is an impossibly great age for the earth.

At about the same time the writer made (Minnesota Technol. 10, 240 (1930)) a similar calculation for the atmosphere alone by using its known radon content of 10^{-10} curie per cubic meter. The result is about 10^{14} years required. Since this also represents an apparently excessive age one is inclined to seek auxiliary means of production. A former content of U-Ra-Rn higher than at present suggests itself but seems improbable as one would then expect to find higher Pb:U ratios than those actually found in nature.

From Harkins and Schuh's calculation it is evident that oxygen liberated from the crust would diminish the relative content of O^{17} in the atmosphere. However if instead of a uniform distribution of uranium and nitrogen in the crust we consider concentration in the form of high grade uranium ore and an enhanced concentration of nitrogen in the ore the rate of O^{17} production would be increased. Hillebrand (W. F. Hillebrand U. S. Geol. Survey Bull. 78, 43 (1891); Am. J. Sci. 40, 384 (1890)) did find a striking association of nitrogen and uranium. Whether this could be a large source of O^{17} would of course depend on the size of such deposits. This would be difficult to estimate and it appears unnecessary to consider it further in this connection since the following simple considerations show it to be highly improbable that any important fraction of O^{17} in the atmosphere can have been

generated on the earth either in the crust or in the atmosphere itself by alpha-ray bombardment.

About 100,000 alpha-particles are required for each nuclear encounter with nitrogen. Therefore the ratio of He to O^{17} generated would be 100,000 He:1 O^{17} . In the atmosphere the actual ratio is about 1 He:5 O^{17} . We can hardly conceive any natural process that would have achieved a change of 500,000 fold in the ratio of the two gases.

If we reverse the calculation and assume with Jeans (Jeans' Dynamic Theory of Gases, 1921, p. 345-6) no diffusion of helium away from the upper atmosphere then for 100,000 He atoms there would be only one O^{17} atom of the assumed origin, or only about two millionths of the O^{17} atoms actually found by the band spectrum method.

As a matter of fact there are good reasons for believing that at least several fold as much helium has diffused "out at the top" as now remains, since that many fold have been liberated into the atmosphere by erosion, etc. The writer would point out that Jeans' denial of loss by diffusion is based wholly on thermal diffusion; whereas light gases like hydrogen and helium in the upper atmosphere can absorb radiation which upon conversion into translational energy would give them a velocity quite beyond that corresponding to thermal equilibrium with the surroundings and thus allow their escape. This process would therefore raise the O^{17} ratio by lowering the helium. While it may have taken place to an extent several times the present helium content of the atmosphere, it would be difficult to believe that it might have occurred to an extent of 500,000 fold, which would be necessary to have established the present He: O^{17} ratio.

S. C. LIND

School of Chemistry,
University of Minnesota,
May 9, 1930.

Paschen-Back Effect on the Line Spectra of Solids

In a work which we shall publish soon,¹ we have been able to assign a number of the lines of the spectrum of Gd^{+++} in the crystal $GdCl_3 \cdot 6H_2O$ to definite energy levels. These levels have been fixed by studying the spectrum under various conditions, namely, observing how the lines shift their position with the

temperature, observing their polarization, the corresponding lines of the crystal $GdBr_3$.

¹ Freed and Spedding, Nature 123, 525 (1929).

Freed and Spedding, Phys. Rev. 34, 945 (1929).

$6\text{H}_2\text{O}$, and the behavior of the spectrum in a magnetic field.

The lines that are decomposed by a relatively weak magnetic field invariably break up in two components which are equal in intensity and are symmetrically displaced from the position of the original line. However, dissymmetries occur with stronger fields when the levels produced by the magnetic field approach each other. The dissymmetry in the intensities is especially pronounced. Some of the lines become much stronger while others become weaker, practically vanishing in some cases. A number of the lines coalesce and it has been found impossible to force any crossing with the maximum field at our disposal.

This work was done with a crystal of

$\text{GdCl}_3 \cdot 6\text{H}_2\text{O}$ at room temperature. The dissymmetries would undoubtedly have been different at other temperatures as the intervals between the energy levels are then different² and consequently the intervals and the interactions between the magnetic levels would no longer be the same.

SIMON FREED

FRANK H. SPEDDING

Chemical Laboratory,
University of California,
Berkeley, California

May 17, 1930

² Freed and Spedding, *Phys. Rev.* **34**,
945 (1929).

BOOK REVIEWS

Einführung in die Geophysik, II, Erdmagnetismus und Polarlicht, Wärme—und Temperaturverhältnisse der Obersten Bodenschichten, Luftelektrizität, von A. NIPPOLDT, J. KERRANEN, E. SCHWEIDLER. Pp. 388, figs. 130. Julius Springer, Berlin, 1929. Price RM 35. (bound).

The first part on the earth's magnetism and aurorae and the third part on the electricity of the lower atmosphere treat the subjects in pretty much the same way as most other handbooks have done. Brief and adequate discussions are given of what is known about the permanent magnetic field of the earth and its variations, of magnetic storms, of aurorae, of the earth's electric charge, of the potential gradient, ionization and electric current in the lower atmosphere, and of thunderstorms and their electrical effects. The older theories of the phenomena are well presented with, in some cases, an appraisal of the successes and the shortcomings of the theories. The high atmosphere is hardly touched upon, there is almost no mention of wireless wave phenomena. The second part deals in detail with the temperature of the upper few feet of the surface of the land. Temperatures of the soil and of snow are given at various latitudes, on mountains, etc., for various hours of the day and seasons of the year. Some of the results are interpreted with the aid of the mathematics of heat conduction theory.

E. O. HULBURT.

Einführung in die Geophysik, III, Dynamische Ozeanographie, von A. DEFANT. Pp. 222, figs. 87. Julius Springer, Berlin, 1929. Price RM 19.80 (bound).

"Distilled by the sun, kneaded by the moon," swept by the winds, the sea swirls, upwells and drifts in great streams and small eddies. The investigation, both experimental and theoretical, of these movements and of the causes which produce them, that is dynamical oceanography. Hydrodynamics as developed by Lamb dealt for the most part with homogeneous fluids. It was V. Bjerkness, perhaps, who laid the theoretical foundation of dynamical oceanography in his papers on the dynamics of heterogeneous fluids.

In the volume under review are chapters on the statics and kinematics of the sea, the general dynamics of ocean currents, stationary currents in a stratified ocean, convection currents, ocean circulation, waves and tides. A satisfying glimpse is given of the facts gathered by many expeditions on the sea. The mathematics are simple and are applied directly to the analysis of the water movements. Original references are given throughout. One could wish for an English translation of the treatise, for the subject deserves a wider attention in this country than it has received.

E. O. HULBURT

Traité de Polarimétrie. GEORGES BRUHAT. Pp. xvi+448, 250 figs. Editions de la Revue d'Optique théorique et Instrumentale, Paris, 1930. Price, 65 francs.

The volume is limited to the study of the phenomena of rotatory polarization and the apparatus which serves to measure it. The first part of the book contains detailed discussion of apparatus and technique. The second part is on the phenomena of natural rotation, magnetic rotation, and dispersion of rotation, including circular dichroism in the regions of absorption. This is a very useful handbook for all who have occasion to use the polariscope, whether for chemical analysis, or for the study of the phenomena of rotatory dispersion, circular dichroism, or magneto-optic rotation. The literature is made readily referable by the 882 references. The printing is good, but the binding is poor.

J. VALASEK

The Use of the Microscope. JOHN BELLING. Pp. xi+315, 28 figs. McGraw-Hill Book Company, New York, 1930. Price \$4.00.

The many common imperfections of microscope images are described, their causes are given, and the adjustment for optimum high-power microscopy are discussed. The intro-

ductory chapter is planned so that it summarizes the entire text in a form convenient for reference. At the end of the text is a list of 200 review questions and a glossary of microscope terms. Users of microscopes will find many useful suggestions in this volume.

J. VALASEK

Wien-Harms Handbuch der Experimental Physik. Vol. X. G. HOFFMAN—Das Elektrostatische Feld. W. O. SCHUMANN—**Hochspannungstechnik.** Akademische Verlagsgesellschaft m.b.H. Leipzig 1930. Price RM 55 (bound).

G. HOFFMANN. *Das Elektrostatische Feld.* Pp. 345.

Standard texts on electricity and magnetism consider electrostatics as an excuse for the introduction of some of the methods of mathematical physics. As a result little space is ordinarily devoted to the experimental side of the subject. It is very refreshing to see in the present volume a detailed and adequate presentation of the many interesting phenomena connected with static electric fields and of the experimental methods employed in their study. A concise introduction including historical references, definitions of quantities and units, and the most important formulae for capacities constitutes the first section. This is followed by a description and by the theory of instruments. Among these the electrometer is treated in particular detail with definite information concerning the sensitivity and performance of various types. A chapter is devoted to methods of measurement. A general survey of the data on properties of dielectrics is accompanied by a brief description of the current theories and a discussion of the experimental methods used. The experimental facts about the temperature dependence of the dielectric constant and the results of the theory, phenomena of dielectric absorption, volta effect, pyro- and piezo-electricity, conduction through dielectrics are brought up to date.

W. O. SCHUMANN. *Hochspannungstechnik.* Pp. 199.

Essentially a survey of the main points in high voltage engineering. Few books on this subject being available at present this is a very welcome section of the Handbuch. It is of particular interest to see the methods of German engineering practice. On account of the rapid development which took place since the completion of the manuscript much of the recent work has been referred to only in bibliographical addenda, and the volume is therefore already somewhat out of date. The presentation of the older developments is however very clear and contains the essential features of high voltage high power engineering. It is especially pleasing to see a discussion of the theory of dielectric breakdown both from the point of view of physics and of practical electrical engineering.

Both sections are very well illustrated with photographs and diagrams. The index is good and even the spelling of American names is almost correct.

G. BREIT

The Physics and Chemistry of Surfaces. NEIL KENSINGTON ADAM. Pp. 332+x. Figs. 45 Oxford University Press, 114 5th Ave., New York, 1930. Price, bound, \$6.00.

For some time, surface tension has been considered as one of the most classical, and accordingly for many most uninteresting parts of physics. Now this field has, thanks mainly to the author of the above book, to Harkins and Langmuir, and to the investigations of heterogeneous catalysis, developed into a flourishing branch which gives us many new results, up to now mostly concerning the properties of organic molecules and of crystal surfaces. This book is a very good account of this development, written with an eye on the chemist—even the industrial chemist.

Starting with a short chapter on definitions, it deals in the second chapter with films of insoluble substances. Adam distinguishes four types corresponding to two-dimensional crystals, liquids, compressed gases (the latter two are not sharply separated) and rarefied gases. In the solid films, long chain compounds have their active groups immersed in water while the long chains stand out, closely packed, similar to the arrangement in bulk crystals (Chapter III). In the gaseous films, the molecules seem to lie flat.

The next chapter deals with films of soluble substances and contains an interesting account of the nature of soap films.

Then follows a chapter (V) on the result of surface tension measurements, while a critical survey of the experimental methods is given in chapter IX with sufficient detail for the actual

performance of the experiments and their evaluation. This detailed description occurs also in other chapters and should be very valuable to non-specialists who want to use surface tension measurements. An attempt of a kinetic explanation of Eötvös' rule seems to be at least incomplete because it does not consider the fact that surface tension is only due to the *deviations* from the conditions in the interior.

The sixth chapter describes the behavior of an interface liquid-solid ("wetting"), followed by a chapter on lubrication. Both of these chapters show interestingly, how very practical questions can be better understood with increasing knowledge of molecular properties. Besides the technical problems mentioned above, Adam touches cleaning and dyeing, flotation of ores and (as already in chapter IV) emulsification and the influence of films thereon.

The eighth chapter, on adsorption on solids and its connection with chemical reactions and catalysis, can of necessity contain only a selection of topics. It starts out with the "sensitive patches" of Langmuir and Taylor, the marked increase in activity by mixing catalysts, and the methods for measuring the "microscopic surface" of a solid. Next the work of Langmuir on the theory of absorption and the behavior of gas films, which has already become classical in the good sense, is discussed, followed by selected organic reactions catalysed by metals. Then comes the discussion of charcoal and a little later some very interesting work on the catalytic properties of bacteria. The importance of adsorbed anions on the photosensitivity of silver bromide is then discussed. One wonders at the absence of a reference to the pioneer work of Fajans and his school. Finally, the theoretical calculation of surface tension in salts is discussed.

K. F. HERZFELD

Dipolmoment und Chemische Struktur. Edited by P. P. DEBYE. Leipziger Vorträge 1929. Pp. 134 + viii, 35 figs. S. Hirzel, Leipzig, 1929. Price Rm 9.

Elektrische Dipolmomente von Molekülen. I. ESTERMANN. Pp. 49, 20 figures, 7 tables. Part of Band VIII, *Ergebnisse der exakten Naturwissenschaften*, Julius Springer, Berlin, 1929.

Dipolmoment und Molekularstruktur. H. SACK. Pp. 60, 8 figures, 19 tables. Part of Band VIII, *Ergebnisse der exakten Naturwissenschaften*, Julius Springer, Berlin, 1929.

The first of the three titles reviewed contains lectures given at a Symposium on the connection between the dipolemoment and the chemical structure of molecules, held at the University of Leipzig in the summer of 1929, the two others are articles on the same subject from Volume 8 of *Ergebnisse der exakten Naturwissenschaften* and can not be purchased separately.

The determination of dipolemoments can be carried out in different ways: (a) By determining the temperature change of the dielectric constant ϵ in the gaseous state, which follows rigorously Debye's formula, if the exact equation of state is used in evaluating (R. Sängner, Zurich), (b) By investigating the deflection of a molecular ray, which is broadened if dipoles are present (I. Estermann, Hamburg).

In this way it is proved that pentaerythrite $C(CH_2OH)_4$ as gas has a moment and therefore the groups CH_2OH are not arranged in a regular tetraeder. (c) By investigating dilute solutions, where all associated molecules are broken up. Following ϵ to higher concentrations and at different temperatures, one can draw conclusions concerning the degree of association and compare them with vapor pressure and viscosity (I. Errera, Brussels).

(d) By subtracting the effects of electronic and ionic (or atomic) polarization from the total polarization (L. Ebert, Würzburg). The former can be determined from measurements of solids sufficiently far from the melting point, the electronic contribution also from the refractive index. To see how large the ionic polarization (displacement of the ions as a whole) is, Errera investigates salt crystals, while K. Hojendahl (Kopenhagen) uses the theory of Born-Landé concerning the forces in the crystal.

The results (Estermann, Errera, Sack, Ebert) show that one can with fair accuracy ascribe definite dipole moments to certain groups in organic compounds and that the resultant moment of a molecule with more than one of these groups can approximately be calculated as a result of a vectorial addition of the moments of each group as predicted by J. J. Thomson. It seems very probable from the results that the benzene ring is flat. The situation is more complicated in the case of groups like C-O-H where the valence bonds form an angle. Here the possibility of rotation of the dipole (lying along OH) around the C-O bond arises. Ebert dis-

cusses in much detail the transition between oscillation and free rotation as well as the question of an influence of the temperature on the apparent value of the dipole.

F. Hund (Leipzig) explains the results of the new quantum mechanics concerning the shapes of simple inorganic molecules.

K. L. Wolf (Karlsruhe) treats two auxiliary methods for solving doubts, which might occur in the interpretation of dipole measurements. These methods are first an observation of the Kerr effect and the depolarisation of scattered light, which are both connected with the unsymmetry of the molecule, and secondly the measurement of the shift of absorption bands for different compounds.

Finally W. Hückel (Freiburg) discusses the influence of the dipole on reaction velocities, especially in so far as there is a connection between the dipole moment and the heat of dissociation or activation of one of the parts of the dipole itself or a neighboring dipole.

K. F. HERZFELD

ERRATUM

AMERICAN PHYSICAL SOCIETY

PROCEEDINGS OF THE NEW YORK MEETING

Through an oversight the titles of the invited papers presented at the Symposium on photoelectric and thermionic phenomena were omitted from the program of the meeting as printed in the March 15, 1930 issue (Phys. Rev. 35, 656, 1930). On page 668 the following should be inserted after abstract 45:

SYMPOSIUM ON PHOTOELECTRIC AND THERMIONIC PHENOMENA

46. Photoelectric ionization of gases. F. L. MOHLER, *Bureau of Standards*.
47. Photoelectric multiple ionization by x-rays. F. K. RICHTMYER, *Cornell University*.
48. The quantum theory of the photoelectric and thermionic effects in metals. WILLIAM V. HOUSTON, *California Institute of Technology*.
49. The influence of surface conditions on the photoelectric effect. C. E. MENDENHALL, *University of Wisconsin*.
50. The velocity distribution of x-ray photoelectrons. DR. G. WENTZEL, *University of Zürich*.

PROCEEDINGS
OF THE
AMERICAN PHYSICAL SOCIETY

MINUTES OF THE WASHINGTON MEETING, APRIL 24-26, 1930

The 163rd regular meeting of the American Physical Society was held in Washington, D. C., On Thursday, Friday and Saturday, April 24-26, 1930. The Thursday and Friday sessions were held at the Bureau of Standards in the East Building and the Industrial Building. The Saturday sessions were held at the National Academy of Sciences. The presiding officers were Professor Henry G. Gale, President of the Society, Dr. W. F. G. Swann, Vice-President of the Society, and Professors John T. Tate, Harold W. Webb, and L. P. Sieg. On Thursday afternoon and Friday morning there were sessions devoted to papers on "Applied Physics."

On Friday evening there was a dinner for the members of the Society and their friends in the Gold Room of the Washington Hotel. President Gale presided and the speakers were Professors R. A. Millikan, G. F. Hull, Gregor Wentzel, Karl T. Compton and Doctors W. F. G. Swann and L. W. Nordheim. There were 257 guests at the dinner.

At the regular meeting of the Council held on Friday, April 25, 1930, thirty-five candidates were elected to membership. *Elected to Membership:* William Alter, John C. Batchelor, Ralph D. Bennett, John F. Blackburn, George W. Bloemendal, R. M. Buffington, H. R. Byerlay, Stuart Campbell, Shih-Chang Chen, Frank Coleman, T. C. Hardy, R. C. Hartsough, Curtiss R. Haupt, James A. Hootman, Frederick L. Hunter Jr., Franklin S. Irby, Hubert M. James, Carl Kaplan, Horace H. Lagerpusch, S. Lehrman, Leon B. Linford, Ellice McDonald, R. F. Morris, S. M. Naudé, Mr. Parker, John R. Patty, Herbert B. Roese, Oscar Siedman, Caspar V. Shapiro, Johannes A. Van den Akker, Claude C. Van Nuys, Bertram E. Warren, Carl J. Wiggers, Hugh C. Wolfe and Henry H. zur Burg.

The regular program of the American Physical Society consisted of 114 papers, numbers 1, 9, 15, 47, 48, 64, 65, 66, 74, 84, 105, 106, 107, 110 and 113 being read by title. The abstracts of the papers are given in the following pages, An Author Index will be found at the end.

W. L. SEVERINGHAUS, *Secretary*

ABSTRACTS

1. Distribution of non-reacting fluids in the gravitational field. MORRIS MUSKAT, *Gulf Research Laboratory Pittsburgh*.—The paper consists essentially of an analysis of the equation given by Lewis and Randall for the distribution of non-reacting ideal fluids in a gravitational field. When the fluids are incompressible a formal solution is obtained, for a mixture of any number of constituents. But it has not been possible to put it into a form convenient for numerical computation. The ratios of the concentrations of any constituent at the top to that

at the bottom of a vertical column of the mixture are given explicitly, both for incompressible and compressible fluids. When all the molar volumes of the various fluids are equal, the equations are solved completely and lead to a *relative* barometric distribution, and in the particular case of ideal gases, to individual barometric distributions. The physical meaning of this is briefly discussed. The case of binary mixtures is treated in detail, and numerical examples are given, first for a mixture of two paraffins, and secondly for a dilute solution of NaCl in water, which is equivalent to an ideal solution of liquids. As is to be expected, the effect is extremely small, and in the first case it is only one tenth as large as is given by a simple barometric formula.

2. **Capillary retention of liquids in assemblages of homogeneous spheres.** W. O. SMITH, PAUL D. FOOTE, P. F. BUSANG. *Gulf Research Laboratory, Pittsburgh.*—The pore space is an assemblage of uniform spheres was initially filled with liquid. After very slow drainage the amount of liquid retained by the spheres was experimentally measured. The liquid is retained in the form of rings at the contacts of adjacent spheres. The radii of curvature of the ring surfaces are computed in terms of surface tension, grain radius and pressure drop across the liquid-vapor interface, permitting calculation of the volume retained per sphere contact. The number of contacts per unit volume of spheres is obtained from porosity measurements using the theory developed earlier. (Phys. Rev. **34**, 1271 (1929).) Computed and observed data on the total volume of retained liquid are in agreement.

3. **The mechanism of "atomization."** R. A. CASTLEMAN, JR., *Bureau of Standards.*—The process of liquid "atomization" is in wide and important commercial use; yet, so far as the writer knows, no adequate explanation of its mechanism has been offered. The fact, however, that the phenomenon can be used with confidence in the design of machine and other details seems to be sufficient indication of a recognized definite physical background. If we assume that a necessary step in "atomization" is the drawing off, from the unatomized liquid, of ligaments of such size that they will eventually draw up into drops of the size observed in the spray, it appears that a satisfactory explanation of the phenomenon can be obtained by combining Rayleigh's theory of jet disintegration with some recent drop size measurements. For analysis shows that the degree of instability of ligaments of the necessary size is so great that direct observation of either the initial disturbances or even of the ligaments themselves seems improbable. The above assumption appears to be reasonable, necessary and sufficient.

4. **Wind pressure on cylindrical stacks.** H. L. DRYDEN AND G. C. HILL, *Bureau of Standards, Washington, D. C.*—A summary is given of the published model experiments on the wind pressure on cylinders and of some additional experiments (a) on model cylinders in the wind tunnel, (b) on a large cylinder in the natural wind, and (c) on the power plant stack in the natural wind. The object is to provide a basis for estimating the average wind pressure on stacks and other cylindrical structures at known wind speeds. The conclusions are as follows: 1. The wind pressure on a stack at a given wind speed is a function of the ratio of the height of the stack to its diameter and possibly of the roughness of the surface. 2. Model experiments can not be directly utilized because of a large scale effect. 3. Provision for a wind load equivalent to 20 pounds per square foot of projected area at a wind speed of 100 miles per hour is a safe procedure for stacks whose exposed height does not exceed ten times the diameter. 4. The local values of the pressure may require consideration in the design of thin-walled stacks of large diameter.

5. **Airfoils of circular-arc section for use at high speeds.** L. J. BRIGGS AND H. L. DRYDEN, *Bureau of Standards, Washington, D. C.*—Experiment has shown that the airfoil sections used in the design of airplane propellers change their aerodynamical properties as the relative air speed approaches the speed of sound. The component of the force in the direction of the airstream (the drag) increases more rapidly than the square of the airspeed, and the component normal to the airstream (the lift) less rapidly. In some earlier measurements, an airfoil which was a segment of a circular cylinder was found to give good results. The present measurements were undertaken to survey the field more thoroughly and to investigate the effect of

rounding the sharp edges. The effect of a moderate rounding was found to be small. At speeds above 0.95 of the speed of sound the circular-arc sections are more efficient than the usual types. At low speeds, (0.5 of the speed of sound), the thick circular-arc sections are much less efficient, but the thin circular-arc sections compare more favorably with the usual types. For propellers operating at high tip-speeds it would be advantageous to use circular-arc sections in the outer parts of the blade.

6. Absorption and velocity of high frequency sound in oxygen. W. H. PIELEMEIER, *Pennsylvania State College*.—Deviations of the experimentally determined absorption and velocity values from their theoretical values in air suggest their determination in oxygen and nitrogen at the same frequencies. The acoustic interferometer and torsion vane methods are used. The torsion vane method is the more reliable but the interferometer makes it possible to make simultaneous measurements of absorption and velocity. The theoretical value of K , the absorption constant, is given by the equation, $K = A/\lambda^2$, where A has the value 0.000365 for oxygen at 20°C. The experimental K is defined by the equation, $I = I_0 e^{-Kx}$. The frequency variation of the above deviations can readily be shown by comparing the theoretical value of A , 0.000365, with the observed values. At 1215 kilocycles the radiometer method gave 0.00039. With the interferometer 0.00031 was obtained. At 655.5 kilocycles the radiometer and interferometer both gave 0.00055. Dulong's value for V_0 , the velocity at 0°C, of audible sound in oxygen, is 317.2 m/sec. At 1215 and at 655.5 kilocycles the values are 317.1 and 317.4 m/sec respectively. The value given by Laplace's formula is 315.0 m/sec.

7. Influence of the walls enclosing a sounding air column upon the tone quality. DAYTON C. MILLER AND JOHN R. MARTIN. *Case School of Applied Science*.—Three organ pipes are provided, the first made of wood which sounds the tone of $G_2 = 192$. Two other pipes having the same internal dimensions are made of zinc about 0.5 millimeters thick. One of the zinc pipes is surrounded by a zinc case to form a double walled pipe, with spaces two centimeters wide between the walls. These two pipes have the same pitch, giving a tone a little flatter than $F_2 = 173$. When the single walled zinc pipe is blown in the ordinary manner, its sound has the usual tone quality. By touching this pipe on the outside, extraordinary changes in tone quality can be produced with the formation of inharmonic partial tones, the ratios of which are 1:2.06:2.66. When the double walled pipe has the space between the walls filled with a liquid the pitch is $E_2 = 153$. If the liquid is allowed to flow out gradually, the tone quality changes conspicuously during the process with the formation of inharmonic partials having the ratios 1:2:2.9. These experiments indicate that the material of which a musical wind instrument is made may have an important effect upon the tone quality.

8. The excitation of overtones of shear vibrations in Y cut quartz plates. J. R. HARRISON, *University of Pittsburgh*.—It is well known that Y cut quartz plates will function as resonators and oscillators with shear vibrations giving rise to transverse waves in the direction of the Y axis. (W. G. Cady, *Phys. Rev.* 29, 617, (1927).) Also it is not difficult to excite the odd overtones, i.e., those frequencies which are approximately odd multiples of the fundamental frequency. With a new type of crystal mounting it has been found possible to excite the even overtones also. To excite the second overtone, a three electrode crystal mounting is used. This mounting consists of two flat electrodes covering the two XZ plane surfaces of the plate and also a frame shaped electrode about one-third as thick as the crystal plate. This third electrode fits around the crystal plate like a frame and is symmetrically disposed with respect to the flat electrodes in the XZ planes. The frame shaped electrode allows fields to be applied between it and the electrodes in the XZ planes in opposite directions. To accomplish this, the flat electrodes are connected together serving as one terminal and the frame shaped electrode as the second terminal. By using two flat electrodes and three frame shaped electrodes, the fourth overtone can also be excited. Similarly, mountings can be constructed for exciting the higher overtones.

9. Torsion of rhombic prisms and of cylinders in the elastic and plastic state. JAKOB KUNZ, *University of Illinois*.—The corresponding problems for isotropic bodies are at first

solved by means of the stress function. The new problems are then reduced to the older ones by means of linear transformations of the variables. The plastic flow is then determined for the elliptic cylinder in a closed form, which however could not be found for the plastic rectangular prism.

10. Some applications of the theory of plastic deformations of ductile metals. A. NADAI, *Westinghouse Elect. Mfg. Co. East Pittsburgh*. (Introduced by S. M. Kintner).—A brief account will be given of the principal conditions which are available to express the equilibrium of stress in the plastic state of ductile metals. These conditions will be discussed for the case of rotational symmetry in a plastic body. As an example several cases of plastic flow in a thick walled cylinder subjected to high internal pressure with and without longitudinal expansion will be treated. The distribution of stress during yielding is given for a long cylinder and for a flat ring both subjected to radial pressure. How yielding and the plastic deformation spread through the walls of the cylinder will be shown.

11. The flarimeter: a clinical instrument for testing circulatory fitness. P. V. WELLS, *Medical Department, The Prudential Insurance Company of America*.—Forced expiration at constant lung pressure of 20 mm provides the most convenient means of placing the circulatory system under standard load. The response in systolic blood pressure is maximum at rates about 36 cc/sec. Among normals, the blow should exceed 50 seconds; its decrease measures shortness of breath, the leading symptom of an impaired heart muscle. The blood pressure normally rises 20 mm in 45 sec, 40 mm before the impulse to breathe stops the blow. The Flarimeter is a simple durable, reproducible, inexpensive, portable instrument designed to enable an individual to perform such a standard test. A 200 cc/sec orifice is also provided, its length of blow giving an accurate measure of vital capacity (the volume of a maximum single expiration). Some investigators have believed the vital capacity to be a measure of shortness of breath because it is so reduced in heart disease. But after exercise the vital capacity is not reduced, while the small orifice blow is shortened to a third of normal length, showing that it is a much better measure of shortness of breath.

12. Suggested explanation of Michelson-Morley-Miller experiment. N. GALLI-SHOHAT, *Mount Holyoke College*.—The complete theory of Michelson-Morley-Miller experiment leads to two effects: one due to the phase difference, another to the "rotation" of the waves produced by reflections from the moving mirrors. P. Epstein has given an estimation of this last effect and has found it too small to be discovered. However, his estimation was based on the orbital velocity of the earth, 30 km/sec, while the velocity of the solar system in space is much greater. Thus if one makes an estimation of the "rotational" effect for $v=300$ km/sec. one gets a displacement about 0.2 fringes in agreement with what Professor Miller has observed under the conditions of his experiment. This suggests the following assumptions: *Phase effect is fully compensated (Lorentz contraction); effect actually discovered by Miller is a rotational effect due to the aberration X' observed by Esclangon and discussed in the previous paper.* Rotational effect is assumed to be proportional to the horizontal component of X' , being $\beta l \cos \theta$ ($\sin^2 \theta - \cos^2(\theta - z)$)^{1/2} = $[\theta = (\theta_1 l), Z\text{-zenith}]$. The curves, representing the variation of the azimuth of the maximum effect and its magnitude, computed for Mt. Wilson, using the apex-declination 68° agrees with the curves given by Miller; the agreement being most striking for the data 1925.

13. The magnetic moment of the lithium nucleus. S. GOUDSMIT AND L. A. YOUNG, *University of Michigan*.—The hyperfine structure observed by Schüler in ionized lithium is of the same order of magnitude as the multiplets in that spectrum. This has led to the belief that the magnetic moment of the nucleus must be of the same order of magnitude as that of an electron. However, the hyperfine structure is produced by the deeply penetrating 1s electron whereas the multiplet separation is due to the outside 2p electron. These two should thus not be compared and indeed rough calculations show that a nuclear magnetic moment of only a few proton units is sufficient to account for the hyperfine structure. The considerations of H. E. White on lithium as well as other hyperfine structures (Phys. Rev. 35, 441 (1930)) are

incorrect since he erroneously compares them with singlet-triplet and other "Austausch" separations. His error is caused by a misinterpretation and a too literal application of the vector model.

14. Possibility of bringing mean life directly into Schroedinger equation for the hydrogen atom. A. BRAMLEY AND ALLEN C. G. MITCHELL, *Bartol Research Foundation*.—The possibility of bringing an expression for the mean life of an atom in a given state directly into the wave equation for the hydrogen atom with relative motion of the nucleus, has been investigated. A solution for the electron and proton in their mutual coulomb field has been found which contains a damping term β occurring in the time factor of the equation for

$$\Psi_m^t = \Psi_m \exp (2\pi i/h)(E_m + i\beta)t.$$

The value of the constant β is determined from the condition, that if the atom is in the state designated by eigenwert E_m for the electron at time $t=0$, then the probability of making a transition to any other state in all time is unity; or expressed analytically

$$\sum_n \alpha_{mn} \int M_{mn} dt = 1$$

where M_{mn} is the matrix moment of the transition. This leads to a value of β_m (reciprocal of mean life) which is proportional to $[\sum_n \{ \int x u_m u_n^* dx dy dz \}]^2$. This expression is similar to the expression derived by Sagiura from the Correspondence Principle for the value of the mean life.

15. Life and radius of the metastable mercury atom. M. L. POOL, *Ohio State University*.—The experimental arrangement described by the writer (Phys. Rev. 33, 22, (1929)) has been altered in order to lend itself more easily to mathematical treatment. A quartz resonance cell containing mercury vapor at 25°C is placed between two high speed disks which interrupt the total radiation from two symmetrically placed water-cooled and magnetically controlled quartz mercury arcs. A few millimeters of purified nitrogen and a trace of water vapor is admitted into the resonance cell and slowly moved over hot copper and copper oxide. The life of the 2^3P_0 state is measured by the rate of decrease of the absorption of 4047 with increasing time-wait after optical excitation of the mercury vapor. Extrapolation to zero nitrogen pressure gives a natural life of about 2×10^{-8} sec. Admixtures of argon at low nitrogen pressures prevented rapid diffusion of the metastable atoms to the walls of the tube. A treatment of the life-time similar to that outlined by Zemansky (Phys. Rev. 34, 213 (1929)) gives the radius of the metastable atom to be 2.4 to 3.0×10^{-8} cm depending on the pressure of the admixed nitrogen.

16. Interval rule for sp, sd, sf configurations. E. U. CONDON AND G. H. SHORTLEY, *University of Minnesota*.—A systematic comparison of the known data on the singlets and triplets arising from sp, sd, sf configurations with the theory of Houston (Phys. Rev. 33, 297 (1929)) shows that the theory gives a good account of the deviations from the Landé interval rule which accompany departure from Russell-Saunders coupling. There are numerous significant discrepancies, however. Writing 1L_l and $^3L_{l+1}$, 3L_l $^3L_{l-1}$ with $L=P, D, F$, when $l=1, 2, 3$ for the term values, we plot as abscissas $(^3L_{l-1} - ^3L_{l+1}) / |^3L_l - ^1L_l|$ and $(^3L_{l-1} - ^3L_l) / (^3L_l - ^3L_{l+1})$ as ordinate if $(^3L_l - ^1L_l)$ is positive, otherwise the reciprocal of this quantity. Houston's equations (12) give functional relations between these interval ratios which are compared with the experimental values.

17. The resonance of (B-A) bands of the hydrogen molecule. HUGH H. HYMAN, *Union College*.—Photographs of the extreme ultraviolet spectrum (λ 1100A to 11640A) have been taken, using a vacuum spectrograph made available to the author at the University of California. A three inch grating, 15000 lines per inch with a three meter focal length, was used, giving a resolving power of 0.1A and a dispersion of 2.76A per millimeter in the second order. The fine structure of sixty eight bands of the first resonance (B-A) system has been studied. The moment of inertia of the normal (A) state is found to be 0.4673×10^{-40} g.cm², the nuclear

separation, 0.7500×10^{-8} cm. In the first excited (*B*) state the moment of inertia is given as 1.4225 g.cm² and the nuclear separation as $1.308_4 \times 10^{-8}$ cm. Resulting constants leave no doubt but that the *B* state is also the lower state of bands found in the visible and studied by Richardson and Davidson. The proof of the connection between the ultraviolet system and the visible system leads to the conclusion reached by Birge that the ionization potential of the hydrogen molecule is 15.34 volts to within a few hundredths of a volt.

18. Regularities in the spectra of lutecium. WILLIAM F. MEGGERS AND BOURDON F. SCRIBNER, *Bureau of Standards*.—A study of the arc and spark spectra of lutecium (71 Lu) resulted in the separation of the lines into 3 distinct classes: (1) those characterizing neutral atoms, constituting the Lu_I spectrum; (2) those due to singly ionized atoms, the Lu_{II} spectrum and (3) a small number of lines ascribable to doubly ionized atoms, the Lu_{III} spectrum. Regularities have been discovered in each of these spectra. The normal state of neutral Lu atoms is represented by a 2D spectral term arising from the electron configuration (s^2d); its levels are separated by 1993.9 wave-numbers. The normal state of Lu⁺ atoms is described by $^1S(ss)$, and metastable terms 1D , $^3D(ds)$, $^3F'(dd)$ have also been established. The relative values are as follows:

$$\begin{aligned} ^1S &= 0.0, & ^3D_1 &= 11796.1, & ^3D_2 &= 12435.2, & ^3D_3 &= 14199.0, \\ ^1D_2 &= 17332.5, & ^3F'_2 &= 29406.7, & ^3F'_3 &= 30889.1, & ^3F'_4 &= 32503.7. \end{aligned}$$

A $^2S(s)$ term describes the normal state of Lu⁺⁺ atoms; a $^2D(d)$ term has levels at 6304.3 and 8648.1. There is no evidence that *f*-electrons play any part in the production of the spectra; it is concluded that the fourteen *f*-electrons in Lu form a closed shell of considerable stability.

19. The spark spectrum of cobalt (Co II). J. H. FINDLAY, *Princeton University*.—A further examination of the Co II spectrum, based on the previous work of Meggers (*Journ. Wash. Ac. Sci.* 18, No. 12, 1928), has been made. A magnetic analysis shows that Meggers' classification of the terms $d^7p^5F^0$, $^5D^0$ should be interchanged, except for the term $^5F_5^0$. Since Meggers' results were obtained from intensity rules, the author's $^5F^0F^0$ and $^5F^0D^0$ multiplets show irregular intensities. The strongest lines in these multiplets are, respectively, 5F_n $^5F_{n-1}$ and 5F_n $^5D_n^0$. The magnetic analysis also shows that Meggers' terms 3D should be d^7s^5P and that his $^3P^0$, $^3D^0$, and $^3F^0$ should be partly $d^7p^5P^0$ and $^5D^0$. In addition, the terms d^7s^3F , $d^7p^3D^0$, $^3F^0$, $^3G^0$, $^5S^0$, and the lowest terms d^8 3F have been found. The location of the second member of the $d^7s^5F^0F$ series gives an I. P. of 16.9 volts from d^7s to d^7 and 17.3 volts from d^8 to d^7 , in practically exact agreement with the predictions of Dr. H. N. Russell.

20. A surplus level in the arc spectrum of palladium. A. G. SHENSTONE, *Princeton University*.—The spectrum Pd I has been so thoroughly analyzed that the positions of all the structures to be expected are known. One even level, k_1 of Bechert and Catalan, is apparently not explainable in terms of the Hund theory unless it is a hyperfine structure component of $d^45d^3P_1$. That explanation is extremely improbable since (1) it makes the hyperfine structure greater than the fine structure and (2) no other levels are known to have structure. The lines due to k_1 are peculiar in being the only diffuse lines in Meggers' list which extends from $\lambda 4500$ to $\lambda 9200$.

21. Spectra of gases lighted with strong discharges. E. O. HULBURT, *Naval Research Laboratory*.—Spectra of condensed discharges through hydrogen at pressures up to several cms of mercury showed, as usual, the Balmer lines merging into the continuous spectrum. With increasing strength of the discharge the Balmer lines widened, the higher members of the series disappeared and the continuous spectrum became more intense, until with 1 microfarad at 15 kilovolts (the method of J. A. Anderson, *Astrophys. J.* 51, 37 (1920)) there were no Balmer lines left at all, only the continuous spectrum and some absorption lines due to aluminum from the electrodes, etc. Helium, oxygen and nitrogen exhibited similar changes, i.e., with increasing intensity of discharge in helium the lines gave way to a continuous spectrum, and in oxygen and nitrogen the molecular bands gave way to spark lines and these in turn to a continuous spectrum. The continuous spectra from all the gases were alike. The intensity

distribution across the continuous spectrum was rather even and hardly that of a black body. In the strong discharges the external characteristics of the atoms were pretty well effaced and the conditions approached those in the interior of a star.

22. Excitation processes in the hollow cathode discharge. R. A. SAWYER, *University of Michigan*.—The negative glow inside a hollow cathode in a rare gas discharge has often been used to excite metallic spark spectra. The excitation is largely due to collisions of the second kind between gas and metal atoms and ions. The exact processes may be inferred from the observed highest term excited and from maxima or abnormal intensities in the metallic spectrum. The available data have been examined. In general only those processes occur in which the metal can be excited to some term in the spark spectrum with gain or loss of only a small amount of kinetic energy to balance the reaction equation. If the metal has a low vapor pressure or sputters poorly cathodically the metal atoms in the normal state or a low metastable state if any will be excited by collisions with gas ions and metastable atoms. If the metal has a high vapor pressure metal ions will enter the reactions. In intermediate cases metal ions may or may not enter depending on conditions. The limit of excitation is fixed by the possible reaction yielding the greatest energy; the other possible reactions may produce maxima in the spectra.

23. Collisions of the second kind and their effect on the field in the positive column of a glow discharge in mixtures of the rare gases and mercury vapor. O. S. DUFFENDACK AND L. B. HEADRICK, *University of Michigan*.—Measurements were made of the electric field in the positive column in mixtures of helium-neon, helium-argon, neon-argon, in all proportions and mixtures of each of these gases with mercury vapor. Spectrograms were taken of the radiation from the positive column for each of these mixtures. The electrical and spectral characteristics of the positive column in mixtures of monatomic gases can be explained in terms of collisions of the second kind between the metastable atoms or the ions of one gas and the neutral or the metastable atoms of the other. The necessary condition for a large effect to be produced by a small amount of one gas added to another is that there exists a close resonance between the metastable states of the main gas and the ionized or excited states of the added gas. The introduction of only 0.15% argon into neon produced a marked increase in the electric field and the spectrum emitted changed completely from neon I to argon I, while the addition of 10% neon to argon had practically no effect.

24. Secondary emission from nickel in a neon discharge. W. UYTERHOEVEN AND M. C. HARRINGTON, *Princeton University*.—Continuing experiments on the secondary emission from a negatively charged metal collector placed in a neon discharge (Science 70, 586, 1929) we obtained additional evidence of a secondary electron current amounting to about 40% of the total current. With the experimental arrangement described before, a perforated collector with a Faraday box behind it, (Phys. Rev. 35, 438, 1930) an estimate can be made of the electron emission due to metastable atoms. This is found to be much more important than the part due to ion impact, namely about 30 to 35% of the total current. When this is deducted from the total secondary emission, values for the number of electrons liberated per incoming positive ion can be estimated. This comes out of the same order of magnitude (10%) as the values determined directly by Penning (Physica 8, 13, 1928).

25. The effect of intense electric fields on the photoelectric behavior of thin potassium films. ERNEST O. LAWRENCE AND LEON B. LINFORD, *University of California*.—Photoelectric thresholds of thin films of potassium on tungsten were observed at 5620Å with fields drawing the electrons from the surface of 260 volts/cm. Increasing the applied fields shifted thresholds towards the red, for example, to 5880Å by a field of 26,000 volts/cm. It is calculated from the data that at distances between $7(10^{-7})$ cm and $12(10^{-7})$ cm of such surfaces the field is entirely the Schottky image field while at greater distances the field exceeds the image field, indicating patched surfaces. Films of potassium on thick layers of oxygen on tungsten show no dependence on fields, indicating either that ion layers exist more than 300 atom diameters from the metal surface which produce fields greater than the Schottky field or that such surfaces are rough. Poor current saturation indicates the latter as more probable. Potassium on a thin oxide layer

has a threshold farthest to the red and exhibits dependence on applied fields assignable to image forces alone. Wentzel's wave mechanics theory of the photoelectric effect is verified in the respects that the whole photoelectric sensitivity curve shifts with the threshold and that the maximum sensitivity occurs at a frequency $3/2$ the threshold frequency.

26. A representation of the dynamic properties of molecules by mechanical models. C. F. KETTERING, L. W. SHUTTS AND D. H. ANDREWS, *General Motors Corporation*.—Mechanical models have been constructed to represent the dynamical systems found in the molecule. Assuming that the intramolecular forces lie along lines associated with the chemical bonds and that for small vibrations they obey Hook's law and have the mechanical character of spiral springs, it is possible to get a picture of the forces and masses which can be represented on a large scale by steel balls and spiral springs. Models have been constructed for some of the simpler nonpolar molecules. They are found to have characteristic frequencies which correspond very closely to the frequencies observed in the Raman spectra and it is possible by this means to identify the Raman lines with definite types of motion of particular atoms in the molecule. This substantiates the view that Raman lines correspond very closely to characteristic fundamental molecular frequencies.

27. The fluorescence spectrum of benzene. F. ALMASY, *University of Zurich*, AND C. V. SHAPIRO, *Cornell University*. (Introduced by R. C. Gibbs).—Using an improved technique, the fluorescence spectrum of benzene, excited by the radiation from a quartz Hg arc, has been photographed with a Hilger E_1 spectrograph, whose dispersion in the region under investigation is 3Å per mm. Wave-length measurements were made from an Fe spark comparison spectrum. The data so obtained are in excellent accord with those for the absorption spectrum in the range over which the two overlap. An energy level diagram is proposed which accounts for the majority of the bands on the assumption that the electronic origin of the system lies at 37489 cm^{-1} (see following abstract). The vibrational frequencies are 923 cm^{-1} for the excited state and 998 and 160 cm^{-1} for the normal state.

28. Electronic transitions in the spectra of benzene. C. V. SHAPIRO, R. C. GIBBS AND J. R. JOHNSON, *Cornell University*.—A review of the available data on the absorption and emission spectra of benzene, together with new data on the absorption of the vapor at higher concentrations, leads to the definite conclusion that only two electronic transitions need be assumed in setting up an adequate energy level scheme, as opposed to the recent suggestions of 5 and 3 respectively, by Austin and Black, (*Phys. Rev.* 35, 457 (1930)) and by Black, (*Nature*, 125, 274 (1930)). These two values are 37489 and 38612 cm^{-1} and are identical with those previously assigned by Henri, *Structure des Molecules*, Paris, (1925), pp. 109, 110. The observed fluorescence spectrum is confined solely to the first of these two systems, while the absorption spectrum is distributed between the two, though showing a much greater intensity in the second. The Tesla luminescence spectrum is very similar to the fluorescence spectrum, except that a few bands corresponding to the most intense of the absorption bands of the second system, do appear.

29. Polarization of sensitized fluorescence. ALLAN C. G. MITCHELL, *Bartol Research Foundation*.—The question of whether or not angular momentum of optical electrons is conserved on a collision of the second kind between an excited mercury atom and a cadmium atom has been investigated. It is well known that under certain conditions mercury resonance radiation is almost completely polarized. It is also known that an excited mercury atom can give its energy to a cadmium atom causing this atom to emit its resonance line $\lambda\ 3261$. In this experiment a mixture of Hg and Cd vapors was radiated by light from a quartz-mercury arc (giving the unreversed 2537Å Hg line). The electric vectors of the exciting light were in the X - Z plane. The Hg-Cd mixture was in a magnetic field (300 gauss) directed in the y direction. The fluorescence from the mixture was observed through a Savart Plate and Nicols prism in the X direction. Under the conditions of the experiment (low pressures of Cd and Hg vapors) the fluorescent light consisted of the 2537Å line of Hg and the 3261Å line of Cd. The Cd line was unpolarized whereas the Hg line was polarized. Had the polarization been carried over on collision one would have expected the Cd line to be polarized in the same direction as the Hg line.

30. The chemiluminescence of metallic sodium. JAY W. WOODROW AND R. M. BOWIE, *Iowa State College*.—It has been known for a long time that metallic sodium and potassium will give off a faint bluish glow when a fresh surface is exposed to the air. This has been attributed to direct oxidation upon contact with the oxygen in the air. A careful check of this effect, however, has shown that it is mostly, if not entirely, due to the water-vapor present. A special apparatus was constructed by means of which it was possible to feed into a gas chamber a fine thread of metallic sodium which always had a fresh surface. When carbon-dioxide or oxygen which had been bubbled through water was passed into this chamber, the sodium thread glowed quite brightly. The effect appeared to be as prominent for the moist carbon-dioxide as for the moist oxygen. On the other hand neither dry oxygen nor dry carbon-dioxide gave an effect which could be detected by the eye even after a half hour in absolute darkness, while at the same time a freshly cut surface of sodium, used as a check, was clearly visible in open air.

31. An electrical method of determining the gelation temperature of starch. E. C. McCracken, *Iowa State College*.—During an investigation of the electrical properties of the potato, it was observed that there was a discontinuity in the resistance-temperature curve. As the potato was heated by an electric current passing directly through it, a sudden decrease in the resistance took place at a temperature between 87° and 88°C. This effect was undoubtedly due to a disruption of the starch grains. Chapman and others have concluded from measurements with the viscometer that this phenomenon takes place at a temperature near 90°C. The electrical resistance method has been found to be quicker, simpler and more accurate for determining this gelation temperature than that in which the viscometer is used.

32. Absorption of ultraviolet light by lacquer films. W. P. DAVEY AND D. C. DUNCAN, *The Pennsylvania State College and Hercules Powder Co.*—Absorption tests on a series of nitro-cotton films, film solutions and their various individual ingredients yielded the following results: None of the films showed selective absorption. They were completely opaque to radiation of wave-length less than about 3300Å. Absorption decreased markedly with increasing wave-length, becoming inappreciable for wave-lengths greater than 4000Å. The absorption was found to be quite independent of viscosity, nitrogen content and such plasticizers as were used. The limitation of transmission to wave-lengths greater than 3300Å was found to be due to ester gum, a constituent common to all of the films. The nitrocotton constituent was quite transparent to wave-lengths greater than 3000Å. Similarly, tests on a series of cellulose acetate films, film solutions and their various individual ingredients yielded no evidence of selective absorption. In this series there was no close correlation between the absorption characteristics of the dried films and the solutions from which the films were made. This was found to be due to the fact that the absorption of the solvents present masked that of the other ingredients. Absorption of solvent-free cellulose acetate films for wave-lengths greater than 2900Å was found to be due to the particular plasticizer used.

33. Transmission of ultraviolet radiation by lake water. CHARLES D. HODGMAN, *Case School of Applied Science*.—Pure water, relatively transparent to the ultraviolet, is rendered less so by the presence of small quantities of dissolved salts and organic materials such as occur in natural river and lake waters. The extent to which ultraviolet radiation, either from the sun or from artificial sources, penetrates such media is of interest for many reasons. A series of measures of the transmission of unfiltered water from Lake Erie, made by the sector photometer and quartz spectrograph for a thickness of 2 cm shows a relatively low transmission ranging from about 74 percent at 0.40 μ to 12 percent at 0.22 μ . Determinations are in progress for water from the same source after filtration and as taken from the city water supply as well as from other sources.

34. Measurement of intensity of helium lines with voltage using a photoelectric device. JOSEPH RAZEK AND PETER J. MULDER, *University of Pennsylvania*.—The variation of intensity with exciting voltage for the lines 6678, 5876, 5016, 4713, 4471, of the helium arc spectrum has been measured using the automatic photoelectric spectrophotometer described by Mulder and Razek before the Ithaca Meeting of the Optical Society of America in Oct. 1929. It was found

the results on $6678(1^1P-2^1D)$, $5878(1^1P-2^3D)$, $5016(1^1S-2^1P)$, $4471(1^1P-3^3D)$ were generally smooth curves, differing somewhat from the results of Hughes and Lowe, (Proc. Royal Soc. A104, 1923 Pg. 480) whereas $4713(1^1P-3^3S)$ shows undoubted maxima near the critical exciting potentials consistent with the results reported by Cornog, (Phys. Rev. 32, 746-752 (1928)). The radiation was developed in a spherical equipotential space 20 cm in diameter, formed of a hollow copper ball. The equipotential cathode and grid from a commercial power tube formed the internal structure, the sphere itself being the anode. The filament, grid and outer sphere were connected to the positive of a battery, with the cathode as the only part inside the sphere at a lower potential. This resulted in a very uniform potential inside the sphere. Direct light from the cathode was cut out by means of a diaphragm on the window in the sphere through which the light was examined. Arc currents as high as 300 milliamperes were obtained with 50 volts across the tube.

35. Further experiments with an automatic photoelectric spectrophotometer. PETER J. MULDER AND JOSEPH RAZEK, *University of Pennsylvania*.—The automatic photoelectric spectrophotometer described by Razek and Mulder before the Optical Society of America, October 1929, has been satisfactorily applied to a series of problems, some of which are detailed. Certain changes in the instrument made possible operation at about ten times the former sensitivity when desired. In this way differences in very dark samples, having an intrinsic brightness of only a few percent, can be readily shown. By a series of tests on biological pigments, the instrument was shown to be admirably suited for testing any solutions that change color rapidly. Three records were taken on an acid hematin solution in six minutes, showing three different stages in its light transmitting property. Records have also been obtained on a 1% solution of oxyhemoglobin in water, both when fresh and when reduced. One record was obtained showing the oxyhemoglobin in the act of reduction. The effect of surface gloss of the sample was tested and found to be negligibly small. All records mentioned, and various other interesting color analyses will be shown.

36. Pictures in relief made with a large diameter lens. HERBERT E. IVES, *New York City*.—Pictures showing relief through a large range of angles and distances of observation (parallax panoramagrams) have heretofore been made by the use of a moving lens, and an opaque line grating slightly separated from the sensitive plate, both plate and grating also being moved in some schemes. All moving parts may be eliminated if a single stationary large diameter lens is substituted for the small moving lens, and provided (a) the transparency positive is placed in front of the grating instead of behind it, (b) the image is given a single inversion, as by a mirror, (c) a grating is used for viewing which has a slightly greater line spacing than the taking grating. The resulting relief pictures are visible through the angle subtended by the lens from the object. The method has the advantages of simplicity of apparatus and manipulation, and of greatly shortened exposure time.

37. Alloys for vacuum-tight glass-metal joints. BY D. E. OLSHEVSKY, *Yale University*.—Joints between materials possessing different physical properties constitute an essential feature of much apparatus involving high vacuum. A glass-metal solder joint occupies—as far as assembling and disassembling is concerned—a position intermediate between direct metal-glass seal and the classical ground joint. In an attempt to find suitable solders ternary alloys of Pb, Sn and Bi were investigated first and characteristic breakages occurring some time after solidification were found to be due to little hard crystals growing out of the interface and pressing against the surface of glass. Several alloys laying on straight lines $E-Pb$, $E-Sn$ and $E-Bi$ as well as in the $E-e_1$, $E-e_2$, and $E-e_3$ valleys (Int. Crit. Tables, v. II, p. 418) were investigated by pouring into Pyrex tubing moulds. An alloy lying on the $E-Pb$ straight line (Pb 50, Bi 37.5, Sn 12.5) was found to possess small glass cracking tendency. This is attributed to separation of soft Pb crystals on cooling. In agreement with the above, alloys obtained by shifting from the eutectic of Pb-Bi-Sn-Cd on a straight line toward the Pb corner (as Pb 31.1, Sn 12.5, Bi 47, Cd 9.4) were also found to have no tendency to burst glass, even in thin layers between glass and metal. The vacuum-tightness of the alloys is still unsatisfactory and joints must be backed by cement for high vacuum work. The joints proved in actual service to be mechanically strong, rigid, vacuum tight and replaceable. Further study is in progress.

38. Studies in contact rectification, II. The cupric sulfide-magnesium junction. MILTON BERGSTEIN, J. F. RINKE, AND C. M. GUTHEIL, *Research Laboratory, P. R. Mallory & Co., Inc.*—The commercial cupric sulfide-magnesium rectifier junction consists of a disk of heat-treated, compressed, cupric sulfide powder contacted with the suitably oxidized face of a magnesium disk. The efficiency of the rectifier unit increases with operating temperature within usual working limits. The phenomenon of "reverse rectification" (i.e. rectification in the direction opposed to normal) is related to the a.c. voltage across the junction. Oscillograms show that there is formation of a film which possesses resistive properties in one direction, that the film may be partially destroyed by continued passage of current in the conductive direction, that application of sufficient voltage in the resistive direction causes re-formation of the film in less than 0.004 sec., that there is no battery effect or thermoelectric effect sufficient to account for rectifying properties, and that formation of the film is probably electrothermic rather than electrolytic in origin.

39. The effect of cyclones and anticyclones upon the intensity of radio signals. R. C. COLWELL, *West Va. University*.—Observations made up by the signal variation of station KDKA at Pittsburgh have shown that the signal intensity increases after nightfall provided there is a low pressure area between Pittsburgh and Morgantown. Hence an increasing intensity after nightfall is an indication of cloudy or stormy weather the next day. An area of high pressure between Pittsburgh and Morgantown will cause the night signal to decrease, so that this type of signal curve indicates fair weather. If the low pressure area passes south of Morgantown, it does not effect the signal. Such a low pressure brings rain with an east wind changing to north and a storm of this kind is unpredictable by observations upon a station to the north of the observer. As with the barometer, the readings indicate weather conditions twenty-four hours in advance.

40. Reflection of radio waves from the surface of the earth. LAL C. VERMAN, *Cornell University*. (*Introduced by E. Merritt.*)—The reflection of an elliptically polarized electromagnetic wave from partially conducting and perfectly conducting surfaces is studied in detail. It is shown that in either case the interference of incident and reflected waves gives rise to a pseudo-stationary wave field above the surface of the reflector. This field is bodily propagated along the horizontal projection of the direction of the incoming wave with a velocity greater than that of light, i.e. $c/\sin \alpha$, where α is the angle of incidence. The resultant electric and magnetic vectors at any given point above the reflector describe two field ellipses lying in two different planes, whose orientation vary with height. This fact is made the bases of experimental measurements.

It is found that the 43 meter wave from WIZ, located in New Brunswick, N. J., holds its polarization and angle of incidence constant during morning hours at Ithaca, N. Y. The rapid fading that accompanies the signal is to be attributed to amplitude fluctuations. Observations on this station are analyzed on the basis of the above theory to obtain the angle of incidence and the polarization of the incoming wave. Polarization is found to be generally elliptical.

41. The x-ray fiber structure of alloys containing precipitated crystals. CHARLES S. BARRETT, *Naval Research Laboratory, Washington, D. C.*—Dahl, Holm, and Masing (*Wiss. Veröffentlich. Siemens-Konzern* 8, 154–185, 1929) prepared cold drawn wires of Be in solid solution in Cu which showed [111] and [100] directions along the wire axis. Annealing these at 350° precipitated a compound of CsCl structure with both [110] and [100] directions in the axis of the wire, the first of which is "a typical crystal position for (fibred) body-centered lattices." Their comparison to ordinary body-centered fibering is without significance because the precipitate was absent when the wire was drawn. The preferred orientation of the precipitate is not due to processes of slip in the precipitate itself, but is due to the precipitate forming with definite orientation on certain planes of the solid solution. Young (*Proc. Roy. Soc. A* 112, 630, 1926) observed such a relation of orientation in meteorites. Similarly, a solid solution of Ag in Al (21.3% Ag) precipitates on (111) planes, with (00.1) hexagonal close-packed precipitate planes parallel to (111) solid solution planes and with [11.0] and [110] directions in these planes parallel, as determined by an analysis of x-ray diffraction from wires.

42. An x-ray determination of crystal orientation in silver sheet, produced by cold rolling. CLEVELAND B. HOLLABAUGH, *The Pennsylvania State College*. (Introduced by Wheeler P. Davey.)—Sheet silver, 99.9%, free from preferred orientation was rolled in 2 1/4 inch rolls and the orientations determined after each pass using the method of Davey, Nitchie and Fuller. (Mines and Met. Tech. Pub. 243, E, 88.) Two symmetrical orientations were found which were independent of the technique of rolling. To picture the resulting preferred orientation, visualize a face-centered cube, with the cube face parallel to the surface of the sheet and with the face diagonal in the direction of rolling. Using the other face diagonal as an axis, rotate the cube until this diagonal makes an angle of not less than 10° , nor more than 42° with the surface. Allow this cube to be rotated at random about the rolling direction as an axis. Any point in this random rotation is within the preferred ranges, provided the face diagonal is in its range of positions. In one of the preferred orientations the direction of rotation is such as to raise that end of the face diagonal which points to the end of the foil entering the rolls first. The other orientation lowers this end of the face diagonal.

43. Radial-asterism in multi-crystalline materials. C. NUSBAUM, *Case School of Applied Science*.—The phenomenon of radial asterism as seen in a Laue photograph of a distorted single crystal is generally attributed to internal strain, whether the strain is produced by a uniform bending moment, compression or tension. It is thus a suitable means for the detection of the presence of internal strains in multi-crystalline materials. A study has been made of radial asterism in such iron samples when subjected to a variable but uniform bending moment. The results are qualitative in nature but are related to the magnitude of the distortion.

44. An x-ray study of very pure iron. O. L. ROBERTS. *The Pennsylvania State College*.—Iron, from chemically pure ferric nitrate, (Baker's Analyzed), was precipitated as the hydroxide and reduced to the metallic state by oxygen-free, dry hydrogen. The metallic powder was pressed into wire form, sintered and swaged. This should give a strictly carbon-free iron. Spectroscopic tests show that the iron is especially free from these impurities. Diffraction patterns were obtained at various temperatures close to the recalcence temperature so as to find the lowest temperature which would cause the change from the body centered to face centered cubic structure. The whole apparatus, including photographic film, was inclosed in an atmosphere of hydrogen. Grain growth was found to take place to a large extent. Face centered cubic structure exists at 921°C .

45. The effect of an electric field on the x-ray diffraction pattern of a liquid. RONALD L. MCFARLAN, *University of Chicago*.—An investigation is made of the effect produced on the x-ray liquid diffraction pattern by an electric field so designed as to give the Kerr effect for the liquid under examination. The liquid diffraction pattern is obtained by replacing the crystal of a Bragg spectrometer with a cell containing the liquid. The electric field is applied approximately normal to the x-ray beam. Under a potential gradient of 9 kv per cm nitrobenzene shows a 2.3 percent increase in the intensity of the diffraction peak, while for a gradient of 5 kv per cm it shows an 0.8 percent increase. Benzene, which shows no Kerr effect for the type of field used, gives a 0.3 percent decrease in peak intensity, the potential gradient being 9 kv per cm. The probable error in all these cases is 0.3 percent. There is thus indicated a small but detectable tendency of the nitrobenzene molecules toward a definite orientation with respect to the electric field.

46. X-ray diffraction in water 2° to 98°C : The nature of molecular association. G. W. STEWART, *State University of Iowa*.—X-ray diffraction ionization curves of water show (1) the presence of two definite peaks corresponding to the separation of diffraction planes of 3.27A and 2.11A; (2) the practically constant diffraction intensity of one peak over the temperature range, 2° to 98°C as compared with the gradual disappearance of the second peak with increasing temperature; (3) correspondence in angle of diffraction between these peaks and the chief diffraction intensities with ice crystals; and (4) the increase of peak width with increasing temperature with a movement indicating less distance of planes. It is difficult to reconcile these results with what was formerly regarded as the alteration, in complexity of

the water molecule. The simplest explanation emphasized by all the experiments in x-ray diffraction in liquids, is that the so-called molecular complexity is the arrangement of molecules in more or less orderly groups with intermolecular forces of distinct magnitude. With temperature increase the nature of the group changes, one set of planes becoming more poorly defined because of more slippage and less orderly arrangement. The alteration in grouping is also shown by the decrease in distance between planes. The group arrangement (cybotactic condition) describes the nature of what has formerly been termed "association" and what is now regarded by Longinescu as "molar concentration."

47. **Electron distribution in the chlorine ion.** G. G. HARVEY AND G. E. M. JAUNCEY, *Washington University, St. Louis*.—Jauncey and Claus (Phys. Rev. 31, 717 and 32, 12 (1928)) have obtained theoretical F values for the chlorine ion in rocksalt from the assumption of a Bohr model in which the Compton effect has been taken into account according to the method of Jauncey (Phys. Rev. 29, 757 (1927)). These theoretical values were in fair agreement with the experimental values. It occurred to the writers to subject both the Jauncey and Claus theoretical F curve and the experimental F curve for chlorine to a Fourier analysis, thus obtaining a U curve. The U curves for different values of D , the grating space, calculated from the experimental F values are independent of the value of D used, being practically superposable. Such is decidedly not the case with the theoretical curves, the general shape changing as well as the peaks shifting. This seems to show that the Compton effect cannot be taken account of in the way proposed by Jauncey and supports the theoretical finding of Waller (Phil. Mag. 4, 1228) and Wentzel (Zeits. f. Physik 43, 1 and 779) that a Schrodinger charge density may be assumed for the atom and the Compton effect disregarded in calculating F values.

48. **Temperature effect in diffuse scattering of x-rays from rocksalt.** W. D. CLAUS, *Washington University, St. Louis*. (Introduced by G. E. M. Jauncey.)—According to Debye (Ann. d. Physik 43, 49 (1914)), the intensity of x-rays diffusely scattered in a direction ϕ from a crystal should be equal to that scattered from an amorphous substance, multiplied by the temperature factor $(1 - e^{-M})$. Experiments by Jauncey (Phys. Rev. 20, 421 (1922)) show that the intensity scattered is proportional to $\sin(\phi - \theta) / \{\sin(\phi - \theta) + \sin \theta\}$ as predicted, where θ is the crystal angle. Experiments are at present being conducted to test the temperature effect. In the temperature range 295° to 135°K, a decrease of approximately 50 percent in intensity is to be expected (depending on slightly different assumptions used in calculation) for $\phi = 30^\circ$ and 60° . Results to date indicate a decrease of not more than 5 percent, in no wise comparable to the expected effect.

49. **Spectroscopic analysis of scattered x-rays.** J. A. BEARDEN, *Johns Hopkins University*.—Davis and his collaborators using a double crystal spectrometer have found a fine structure in the spectra of scattered x-rays. Several investigators using a single crystal method have failed to find any fine structure. The present experiment is a repetition of Davis' experiment using a double crystal spectrometer on the unmodified line. Greater scattered x-ray intensity has been obtained by using a line focus tube and placing the scattering blocks of aluminum and graphite about 5 mm from the focal spot. Two wave-lengths were used, the $K_{\alpha_1}K_{\alpha_2}$ line of silver and the $K_{\alpha_1}K_{\alpha_2}$ line of copper. The capacity of the electrometer system was about 12 cm and the sensitivity of the electrometer 20,000 scale dimension per volt. No fine structure lines of one tenth the intensity of the K_{α_2} line have been observed. Chemical analysis of the scattering blocks showed no trace of copper or silver as an impurity. Measurements have also been made on the Compton shift which agree very closely with the equation $\delta\lambda = (h/mc)(1 - \cos \theta)$.

50. **Scattering of x-rays and the distribution of electrons in helium.** ARTHUR H. COMPTON, *University of Chicago*.—An analysis of the theory of scattering of x-rays by monatomic gases makes it possible to express the probable distribution of the electrons in the atom as a Fourier integral. To evaluate this integral it is necessary to know the intensity of scattering of x-rays of known wave-length at different angles. With data recently obtained by C. S. Barrett the distribution of electrons in atoms of helium gas is thus determined. This distribution agrees

satisfactorily with that calculated by Pauling from wave-mechanics but differs by more than the experimental error from that predicted from Bohr's theory.

51. A direct-reading two-crystal spectrometer for x-rays. F. K. RICHTMYER, S. W. BARNES AND E. RAMBERG. *Cornell University*.—The two-crystal spectrometer developed by Bergen Davis and others provides a means of obtaining monochromatic x-rays of high intensity. Such a spectrometer, reading wave-lengths directly in angstroms, has been constructed, using the principle described by Nicholas (*J.O.S.A. & R.S.I.* **14**, 61, Jan. 1927) for the single crystal instrument. Details of construction and adjustment are described; and sources of error are discussed. The instrument is capable of absolute measurement of wave-lengths, with very high precision.

52. A vacuum spectrograph for the precision measurement of x-rays of long wave-length. CARL E. HOWE, *Oberlin College*.—The spectrograph has four unique features which make it fitted for precision measurements. (1) A slit system, consisting of five slits each one thousandth of an inch wide, excludes optical light and gives excellent collimation of the x-rays. (2) An x-ray tube with interchangeable targets, mounted on a micrometer slide enables the focal spot to be readily lined up with the fixed slit system. (3) A universal grating support permits the plane grating to be set at any desired angle and to be removed in vacuo from the path of the x-rays without disturbing any adjustments. (4) A set of two parallel plate holders at a fixed and known distance apart, placed at right angles to the slit system, permits accurate measurements of angles from the lines recorded on the two plates at different distances from the grating. The slit system and grating support are mounted as one unit which may be completely removed from the rest of the spectrograph for the purpose of making adjustments.

53. An instrument for high-voltage x-ray spectrography and radiography. FREDERICK SILLERS, JR., *Follansbee Bros. Co.* (*Introduced by Wheeler P. Davey*).—The increasing application of the x-ray diffraction method of crystal analysis to the study of materials of construction has led to the desire, in certain fields, for a more rapid method of obtaining results. Such a method may involve the adoption of higher voltages than are now in general use for this type of work. An instrument suitable for use with these higher voltages (in the neighborhood of 200 kv) will be described. The instrument consists essentially of a lead-lined drum equipped with four pin-hole or slit diffractometers, as well as an opening for radiographic exposures. It is adapted to a standard 200 kv installation employing a Coolidge tube. The instrument is so designed that comparable intensities of x-rays at all four diffractometers are available, rendering practicable the comparison of different patterns. Through the use of the present instrument x-ray spectrograms, by direct transmission, of coarse-grained polycrystalline material; e.g., high-silicon sheet steel about 0.02 in. thick for electrical uses, may be obtained in less than an hour. If radiographs are desired during the course of any study, they may be obtained by rotating the tube 90° on its axis.

Points to be discussed deal with strained materials, intensifying screens, optimum voltage, intensity variations, and radiography of fine effects.

54. The dielectric constants of aqueous KCl solutions. ALLEN ASTIN, *National Research Fellow, The Johns Hopkins University*.—Probable causes of the many discrepancies in existing data on the dielectric constants of aqueous electrolyte solutions have been determined and methods of either eliminating them or correcting for them worked out. It is shown that by use of a voltage resonance method, (Jezewski, *Zeits. f. Physik* **48**, 123 (1928)); (Kneikamp, *Zeits. f. Physik* **51**, 95 (1928)); (Lattey and Gatty, *Phil. Mag.* **7**, 985 (1929)) and (Astin, *Phys. Rev.* **34**, 300 (1929)), the necessary corrections are considerably simplified. The voltage resonance curve is also shown to be symmetrical, regardless of the amount of damping. The corrected results show that the dielectric constants of aqueous KCl solutions from concentrations of 0.00025N to 0.01N are no different from that of water, at least within the limit of error of the measurements. The probable error of the corrected results is 2 parts in 1000 at 0.001N. and 6 parts in 100 at 0.01N. The uncorrected results show an apparent decrease of the dielectric constant similar to that reported by most other observers. The magnitude of this apparent

decrease may be varied by changing either the frequency, the size of the test condenser or the dimensions of the leads. The lowering of the dielectric constant in solutions which was predicted by Hückel (Phys. Zeits. 26, 93 (1925)) is much smaller than any reported experimentally and is too small to be detected with the limit of error reported here. Frequency employed is 1.8×10^6 .

55. Time lag in changes of electrical properties of rubber with temperature and pressure. ARNOLD H. SCOTT, *Bureau of Standards*.—When the temperature of rubber is suddenly (within five minutes) changed from one value to another, the electrical properties do not at once assume their final values. Two hours or more may be required for the dielectric constant, power factor, and resistivity to become constant. Part of the data for one specimen are given in the following table:

Time after specimen reaches 150°C (125° Change) Minutes	Dielectric Constant	Power Factor Percent	Equilibrium Temp. corre- sponding to dielectric constant and power factor
3	3.07	2.96	107°C
15	3.52	7.83	120
25	3.83	8.87	128
63	4.32	6.22	144
155*	4.39	4.42	150

* (Equilibrium)

This time lag was studied with specimens of several compositions from soft to hard rubber following temperature changes varying in amount from 75 to 125°C. Data on the time lag with pressure were obtained on only one specimen using pressures between 1 and 700 atmospheres. Twenty-four hours were required for the electrical properties to become constant.

56. Changes in the specific resistance of aluminum. G. E. DAVIS AND GILBERT GREENWOOD, *University of Rochester*.—Measurements on aluminum wires confirm previous investigations concerning the increase of specific resistance with cold-working. Tammann attempted to explain this increase by assuming particle orientation. Such orientation has since been found in the fibrous texture of drawn wires. This explanation, however, requires anisotropic electrical properties of the metallic crystals. Such anisotropy is most unlikely in cubically crystallized aluminum. Furthermore aluminum wires, annealed until the increase in specific resistance is lost, show distinctly fibrous texture. The increase in specific resistance has sometimes been ascribed to lattice distortions caused by the stresses of cold working. v. Arkel investigated such distortions by the effects produced in Debye-Scherrer photographs. The α -lines in such photographs are actually doublets ($K\alpha_1$ and $K\alpha_2$), the sharpness of resolution of which decreases with increasing lattice distortion. Aluminum, completely annealed or cold-worked to different degrees, always shows a sharp resolution of these doublets. Distortions of the v. Arkel type cannot, therefore, be responsible for the increased resistance. Dehlinger discussed distortions extending throughout very minute regions of the lattice—possibly only along the surfaces of the particles. Such distortions would not cause a decrease in the sharpness of the doublets, and might be responsible for the increased specific resistance.

57. Contact resistance and microphonic action. F. S. GOUCHER, *Bell Telephone Laboratories*.—An experimental study of single contacts between granules of microphone carbon, the contact forces being of the order of 1 dyne. For established contacts Ohm's Law is obeyed up to 0.1 volt. The resistance decreases with increase of temperature, the temperature coefficient of resistance being of the same order of magnitude as that of solid carbon wires produced by a heat treatment which is similar to that used in the preparation of the microphone carbon.

Above 0.1 volt (up to 1.0 volt) there are departures from Ohm's Law which can be accounted for by the theory of contact temperature as a function of voltage when a reasonable value of the Wiedemann Franz ratio for carbon is assumed. The conclusion is that the conducting portions of such contacts are carbon to carbon. The temperature coefficient of resistance of a contact varies in a reproducible, but non-systematic manner as the resistance is changed in a reversible resistance force cycle. This shows that new surfaces having coefficients different from the average value are inserted into or removed from the circuit during the cycle.

58. **A theory of the resistance of alloys.** L. W. NORDHEIM, *University of Goettingen* (Introduced by *Alpheus W. Smith.*)—According to the new (Sommerfeld-Houston-Block) theory of metallic conductivity any resistance in a conductor is due to an imperfection of the crystal lattice. Thus the ordinary resistance is due to the heat motion of the atomic ions, and, therefore, is essentially dependent on the temperature, and vanishes at the absolute zero point. In alloys an additional disturbance is introduced because of the irregular distribution of the constituents. This disturbance can be calculated and gives the additional resistance, which is independent of temperature. Most facts about the resistance of alloys are easily explained by this picture. Formulae are given for the simplest cases, which are in good agreement with experiment.

59. **Shot effect of the emission from oxide cathodes.** H. N. KOZANOWSKI (Introduced by *N. H. Williams, University of Michigan.*)—Fluctuations in the electron space current from barium-strontium oxide cathodes at low accelerating potentials are many times as large as those observed in the case of currents from metallic emitters. When space charge is obliterated by the use of high accelerating potentials, the true value of the electronic charge, as predicted by Schottky, is obtained. The results indicate that at low accelerating potentials, positive ions leave the emitter, and travel into the space charge region under the action of the reverse space charge field. Due to the low mobility of the positive ion, large groups of electrons are affected by each positive ion, thus causing large, sudden variations in the space charge. A tube containing a tungsten filament and a Kunsmann emitter surrounded by a cylindrical collector gives the normal shot effect when only the tungsten is heated. The same abnormally high values observed with the barium-strontium emitter are obtained with this tube with a low accelerating potential when positive ions emitted from the Kunsmann emitter interact with the electron space charge around the tungsten filament. Even in this case, the true value of the electronic charge is obtained when the space current is temperature limited.

60. **Effect of positive ion shot effect on space charge limited electron currents.** LLOYD P. SMITH, *Cornell University.*—A transcendental equation has been derived which relates the electron current between two parallel plane electrodes (one of which is a hot cathode emitting positive ions as well as electrons, and the other is a collecting electrode at a potential positive with respect to the cathode) to the total positive ion emission as well as the difference of potential between the electrodes, their distance apart, etc. Curves have been plotted which give the electron current to the collecting electrode as a function of the total positive ion current at various collector voltages. From such relations, the variation in the electron current produced by statistical variations in the positive ion emission can be obtained. Such variations are large compared to the ordinary shot effect. This is to be expected since a positive ion moves relatively slowly through the space charge region liberating a group of electrons during one transit. From the curves it is possible to obtain the difference of potential between the electrodes, at which the fluctuations of the positive ion current produce the greatest variation in the electron current.

61. **Studies of abnormal shot effect in gaseous discharges.** JOHN S. DONAL, JR., *University of Michigan.* (Introduced by *N. H. Williams.*)—Space charge limited electron currents from hot filaments have been found to exhibit extremely abnormal fluctuations when the tube contained argon gas. The abnormality is due to the release of groups of electrons from the space charge region by the positive argon ions. A detailed study has been made of the variation of the abnormal fluctuations with the field, filament temperature and gas pressure, the results

have obvious application to the elimination of extraneous noises in vacuum tubes. Positive ion currents of the order of one microampere have been obtained from tungsten filaments undergoing attack by oxygen. These ions, when trapped in the minimum of potential surrounding a hot cathode, produce very abnormal fluctuations in space charge limited electron currents. An expression for the resulting shot voltage has been developed, which permits the calculation of the average anode current increase due to each positive ion, and the average time of life of the ions in the space charge region. When the positive ions are accelerated to a cold cathode, an abnormal shot voltage is obtained which is unusual in being independent of the positive ion current.

62. Effect of adsorbed thorium on the thermionic emission from tungsten. WALTER H. BRATTAIN, *Bell Telephone Laboratories*.—The thermionic emission from a tungsten ribbon filament on which thorium was deposited, has been investigated. The thorium was derived from a thorium filament placed parallel to one face of the tungsten ribbon. For each successive equal amount of thorium deposited, the corresponding increase in the logarithm of the emission, for a given temperature of the tungsten ribbon, was smaller and smaller until the emission reached a maximum. Continued deposition of thorium caused the emission to decrease and finally approach a stationary value. Further investigation indicated that migration of the thorium to the back side of the tungsten ribbon took place at an appreciable rate at 1500°K. At approximately 1800°K. there was definite evidence of diffusion of thorium into the tungsten ribbon. At higher temperatures, the thorium evaporated from the tungsten surface.

63. The ion-grid theory of the decrease in work function for composite surfaces. J. A. BECKER, *Bell Telephone Laboratories*.—When electropositive atoms are adsorbed on electro-negative surfaces, some of the atoms are ionized. These adsorbed ions act like a positively charged grid very close to the cathode. For a large plane surface, this ionic grid produces strong fields close to the surface but only small fields at larger distances. As a result, the work function is reduced by $4\pi\sigma l$ and the emission current saturates as well as it does for clean surfaces. σ = charge per cm^2 ; l = distance of ions above surface. In most experiments, however, the surface consists of irregularly oriented facets or else the ions form clusters due to the presence of electronegative gases. In these cases the distribution of the fields is greatly dependent upon the size of the facets or clusters. Computation shows that for small applied fields, the work function is decreased by a fraction of $4\pi\sigma l$. As the applied field increases, this fraction increases and the emission current increases much more rapidly than for clean surfaces. For large fields, the current saturates as well as or even better than for clean surfaces. Numerous experimental observations are accounted for by the finite extent of the ion-grid.

64. Grid glow tube relays. D. D. KNOWLES AND S. P. SASHOFF, *Westinghouse Elec. & Mfg. Co., East Pittsburgh*.—The name Grid Glow Tubes applies to a line of gaseous discharge glow and arc tubes, the breakdown of which is controlled by means of a grid. They are, then, essentially relays having a discontinuous grid-voltage plate-current characteristic. These tubes are made in two general types: tubes with a cold cathode and tubes in which the negative electrode is a hot filament—the characteristics of both types being similar. Grid Glow Tubes have been made in sizes ranging from a few milliamperes of plate current up to several hundred amperes. They can be filled with one of the inert gases neon, argon, or helium or with mercury vapor. A study of the behavior of these devices must necessarily include that of the type of circuit in which they are to be used. A series of curves plotted for both a.c. and d.c. voltages on the plate, a.c. and d.c. grid bias and various self biasing schemes are given. The effect of phase shift between the grid and plate voltages when alternating current is used is also illustrated.

65. The radioactivity of Stone Mountain. JAMES A. HOOTMAN AND W. S. NELMS, *Emory University*.—The radioactive content of the waters which issue from the base of the unique geological formation known as Stone Mountain (Georgia) was determined. Tests were made of a number of large springs well distributed around the base of the mountain, and of other shallower sources above and below the 1000 foot level. The method employed was the Schmidt

Shaking Method, in which a known volume of water is thoroughly shaken with a known volume of air in a closed container. The resulting mixture of air and radium emanation is then pumped into an electroscope, and the rate of fall of the leaf is a measure of the radioactivity of the water. The electroscopes were calibrated by means of the Duane and Laborde formula, and corrections were made for temperature and pressure. This method has been shown by Ramsey to have an accuracy of about 3%. A majority of the springs tested were highly radioactive, the value for the highest being $15,980 \times 10^{-12}$ Curies per litre. This value is nearly twice the maximum reported by Boltwood for forty-four radioactive springs, and more than half as large as the maximum reported by Lester for one-hundred-seventy-eight mineral waters of Colorado.

66. The measurement of the intensity of gamma rays of radium in *r*-units. OTTO GLASSER AND V. B. SEITZ, *Cleveland Clinic Foundation*.—Determinations of the intensity distribution of gamma-rays were made under various experimental conditions with a condenser intensitometer previously described. By using small ionization chambers and a system unaffected by penetrating radiations the difficulties usually encountered in such measurements were greatly reduced. The intensities obtained are given in *r*-units.

67. Disintegration constant of actino-uranium and ratio of actinium to uranium. ALOIS F. KOVARIK, *Yale University*.—With data of Fenner-Piggot and of Aston for broggerite, Karlhus, Norway, and also Aston's 206, 207, 208 line intensities in common lead mass spectrum in conjunction with my age formula (Phys. Soc., April 1929) amounts of common lead and AcD are calculated. AcD, uranium, and actinium: uranium ratio (3%) lead to $\lambda = 2.5 \times 10^{-9} \text{ yr}^{-1}$ or $T = 2.7 \times 10^8 \text{ yr}$. Boltwood's 8% (N. Car. uraninite), Hahn-Meitner's 3% (pitchblende) and others, including recent work of Wildish, indicate a variation of the ratio with age of mineral. Considering actino-uranium an isotope of uranium initially in correct proportion to UI, the ratio should vary and 400 million years difference in the age of the minerals will bring Boltwood's and Hahn-Meitner's values into agreement. Furthermore, calculation of this ratio for the age of Keystone, S. D., uraninite (1462 million years) gives 0.6% and for Sinyaya Pala, Carelia, uraninite (1852 million years) gives 0.25%. The latter values receive a check if AcD is practically the only lead isotope left after subtracting RaG and ThD from the total. Broggerites and cleveites do not give such a check because considerable amount of common lead is present.

68. An attempt to detect deBroglie waves of hydrogen atoms. THOMAS H. JOHNSON, *Bartol Research Foundation*.—Earlier work on the reflection of atomic hydrogen from NaCl failed to reveal deBroglie wave diffraction patterns. This was not unexpected because of the low intensity of the specular reflection and the great intensity of the diffuse background, arising principally from the reemission of adsorbed atoms. Lithium fluoride presents a much more favorable opportunity for detecting the wave character of atomic hydrogen. The specular beam is very intense and there is no reemission of monatomic hydrogen. The MoO_3 detecting plate therefore records only elastically reflected atoms. First order surface-grating bands from the LiF lattice were expected with abrupt maxima separated from the specular beam by 20° to 30° . These bands were found, showing that the total number of atoms going into any one is certainly less than 5% of the number in the specular beam. If the crystal was heated to 600° C a diffuse band appeared extending asymmetrically to about 20° on either side of the specular beam. With the crystal at room temperature this largely disappeared.

69. Satellites of electron diffraction beams. H. E. FARNSWORTH, *Brown University*.—While investigating electron diffraction by a copper crystal, for normal incidence on a (100) face, certain beams have been found which require a refractive index of unity. A search for other weak beams of this nature reveals a whole set of such beams which accompany the intense diffraction beams. In many cases these satellites are so close to the regular beams that they are not completely resolved, and hence are not observed by the usual method of measurement. In the (100) azimuth the satellites which accompany the 4 first-order beams below 325 volts all occur within 2 volts of the theoretical values for unit refractive index;

that of one second-order beam occurs within 11.9 volt; that of the other second-order beam is missing. In the (111) azimuth, the satellites of 3 first-order beams are within 2.7 volts of theoretical values; that of the other first-order beam below 325 volts is within 7.3 volts; those of 2 second-order beams are within 5 volts; that of the other second-order beam is within 19.5 volts; that of 1 third-order beam is within 5 volts. These satellites are as sharp in voltage and colatitude angle as the main diffraction beams, and are not confined to large colatitude angles. Hence they are not due to a two-dimensional surface grating. The significance of these diffraction beams is discussed.

70. The capture of electrons by alpha-particles. A. H. BARNES, BERGEN DAVIS AND H. L. HULL, *Columbia University*.—Abstract of this paper is withheld for revision by the authors.

71. Absorption of sodium vapor in the extreme ultraviolet. S. A. KORFF AND J. L. NICKERSON, *Princeton University*.—Employing a vacuum spectrograph, sodium vapor was examined for absorption in the region from 1300 to 300 Angstrom units, against a background of many lines. Vapor pressures used ranged up to 1 mm of Hg. No broad absorption peaks were observed in this region. Extremely narrow peaks would not be distinguishable, however, by this test. This region includes the point at twice the series limit, or 1205.9 Angstrom units. In general, sodium vapor was found to be almost perfectly transparent to radiation in the observed range.

72. Most probable 1930 value of the electron and related constants. R. A. MILLIKAN, *California Institute of Technology*.—This paper discusses, in the light of Zwicky's results on the block structure of crystals, the reliability of old and new measurements on the relations of e and h , and by combining experimental and theoretical considerations assigns most probable 1930 values to these constants.

73. The nature of cosmic radiation. L. F. CURTISS, *Washington, D. C.*.—Two Geiger-Müller tube counters placed vertically above each other show, in addition to accidentals, coincidences which have been ascribed to cosmic rays. Absorption experiments by Bothe and Kohlhörster indicate that these rays are corpuscular. The author has made observations with the poles of a large electromagnet between two counters, recording the number of coincidences with and without the magnetic field. With the field used of 7000 gauss over an area 24 cm in diameter, a parallel beam of 10^9 volt electrons which passes through the upper counter would be deflected sufficiently just to miss the lower counter in spite of the fact that the $H\rho$ for such electrons is approximately 3×10^6 . Since the radiation is actually diffuse with a maximum in the vertical direction, using two counters one can expect only a slight decrease in the coincidences if they are caused by high-speed electrons. However, if they are due to ultra γ -rays, no such effect should be observable. Making the theoretical allowance for accidentals, a decrease of the order of 25% has been observed in the coincidences which may be attributed to cosmic radiation. This confirms the existence of a corpuscular radiation of very high energy.

74. The absorption of acetylene and ethylene in the near infrared. RICHARD M. BADGER, *California Institute of Technology*. (Introduced by Richard C. Tolman).—The absorption spectra of gaseous acetylene and ethylene have been investigated photographically in the region 6800A–9200A. In the case of acetylene a band with very sharp lines, and showing marked intensity alternation was found, with center at about 7886A. It resembles a band found by Levin and Meyer at 3.0μ , of which it is probably a harmonic, but shows strong convergence on the short wave length side indicating a considerable increase in the average moment of inertia due to oscillation. In the case of ethylene a band was found with center at about 8706A which apparently also shows convergence, but which has a rather complex structure. An investigation of the structure of these bands is in progress.

75. The effect of high pressure on the near infra-red absorption spectra of certain liquids. J. R. COLLINS, *Cornell University*.—The state of polymerization of liquids composed of polar molecules is supposed to depend on the temperature, pressure, etc. The near infra-red absorption

bands of these substances, which are due to molecular vibrations, should be affected by changes in the state of polymerization, and hence also by changes in the temperature, etc. Experiments have shown that changes in the temperature changed the spectral position and intensity of absorption bands of water and certain alcohols, while the bands of benzene, a nonpolar substance, were unaffected by changes of temperature. The present experiments are measurements of the absorption of water, methyl alcohol, and iso amyl alcohol as examples of polar substances, and of toluene as a nonpolar substance, when these substances were subjected to pressures up to 5000 atmospheres. The pressure chamber was designed by P. W. Bridgeman and the measurements were made in the Jefferson Laboratory at Harvard University. No change was found in the position of any of the absorption bands studied. The conclusion is made that, in this pressure range, the state of polymerization does not depend on the pressure.

76. Bismuth-black and its applications. A. H. PFUND, *Johns Hopkins University*.—If a bit of bismuth be evaporated from a spiral of incandescent tungsten wire in a space evacuated to a pressure of about 0.25 mm of mercury, the bismuth is deposited as an intensely black film. For visible light, the diffuse reflectivity of "bismuth-black" is but one sixth that of camphor black. Tests have shown that bismuth-black films which are opaque to visible light, transmit and reflect at normal incidence, less than 1% of infra-red radiation out as far as 13μ . It was decided to use this new material on the receiving areas of delicate thermopiles, radiometer vanes, etc. Quite apart from the blackness and small heat capacity of bismuth-black, a further advantage is gained because of the circumstance that the most delicate surfaces may be blackened without the least danger of harming them. Because of the fineness of the particles, films of bismuth-black on plate glass reflect specularly at grazing incidence. Films which are rough at all angles of incidence may be produced by depositing, first, an extremely thin (grayish) film of soot from burning camphor upon which the bismuth-black is subsequently thrown down. It appears that the soot particles act as centers of condensation and, as a result, the bismuth-black is built up in the form of minute pyramids. Delicate surface bolometer's were made by forming a layer of nitrocellulose so thin as to show first-order Newton's colors. Upon this film was deposited a highly reflecting film of bismuth. The best attainable vacuum—less than 10^{-4} mm Hg—was required. This film was an excellent conductor for electricity. Air was then admitted so as to raise the pressure to 0.25 mm and the absorbing film of bismuth-black was thrown down. This general mode of procedure is being applied to the construction of thermopiles.

77. The effect of aberrations in limiting the resolving power of infra-red spectrometers. R. BOWLING BARNES AND A. H. PFUND, *Johns Hopkins University*.—Because of the increasing demand for high dispersion infra-red measurements, it seems timely to call attention to some of the difficulties which arise when very small "slit-widths" are used, and to a method of overcoming them. In the usual spectrometer, concave mirrors must be used off the optic axis, and unless these are parabolized along the proper axes, noticeable aberrations are present. Due to astigmatism and coma the slit image is broad and accompanied by a diffuse wing. If the eye is placed behind S_2 , and the grating viewed in monochromatic light only a small portion of it will be illuminated, the jaws of the narrow slit having blocked out the light from some parts. One then, never gets the advantage of the full aperture, and the spectrum used is very impure. By a method somewhat similar to that described by Pfund (*J.O.S.A.*, April 1927), spherical mirrors of aperture $f \cdot 4$ can be used along the optic axis, and to full advantage. The radiation, after falling upon each of the spherical mirrors, M_1 and M_3 , is reflected along the axis to the plane mirrors, M_2 and M_4 respectively. These mirrors, containing oversized slits at their centers, are placed just in front of the slits S_1 and S_2 , and are inclined to the optic axes at the desired angles. With this arrangement the eye looking through S_2 , sees the entire grating filled with light no matter how narrow the slits are made. This is a necessary result if one wishes to work with very small "slit-widths".

78. On the theory of the Brownian motion. L. S. ORNSTEIN, *University of Utrecht, Holland* AND G. E. UHLENBECK, *University of Michigan*.—Using a method first indicated by Ornstein (*Proc. Acad. Amst.* 21, 96, 1917) the mean values of all the powers of the velocity

u and the displacement s of a free particle in Brownian motion are calculated. It is shown that $u = u_0 \exp(-\beta t)$ and $s = u_0/\beta [1 - \exp(-\beta t)]$ where u_0 is the initial velocity and β the friction coefficient divided by the mass of the particle, follow the normal Gaussian distribution law. For s this gives the exact frequency distribution corresponding to the exact formula for S^2 of Ornstein and Fürth. Discussion is given of the connection with the Fokker-Planck partial differential equation. By the method exact expressions are obtained for the square of the deviation of a harmonically bound particle in Brownian motion as a function of the time and the initial deviation. Here the periodic, aperiodic and overdamped cases have to be treated separately. In the last case, when β is much larger than the frequency and for values of $t > \beta^{-1}$, the formula takes the form of that previously given by Smoluchowski.

79. A test of the Dalton-Gibbs law of partial pressures. LOUIS J. GILLESPIE. *Massachusetts Institute of Technology (Introduced by F. G. Keyes).*—According to Gibbs' formulation the pressure of a gaseous mixture equals the sum of the partial pressures, $P = \sum_i p_i$, when p_i is conceived as the pressure of pure gas 1 that would just prevent the gas 1 in the mixture from escaping through a membrane permeable to it alone. This can be shown equivalent to the statement: The "density" (or concentration) of a gas is the same at equilibrium on either side of a membrane permeable to it alone. Examination of the data of Larson and Black and of Lurie and Gillespie shows the following: (1) The mole fraction of ammonia mixed with 3:1 hydrogen-nitrogen mixture at temperatures from -20 to $+20^\circ$ C, and of ammonia mixed with nitrogen at 45° , is greater than that calculated from the Gibbs formulation, by an amount that increases with the pressure at low pressures (50 atm. plus). (2) In the case of the hydrogen-nitrogen mixtures the difference appears to pass through a maximum at 100-300 atmospheres. (3) The difference may reach 25% of the observed mole fraction. (4) Considered as a possible basis for the thermodynamic treatment of gaseous equilibrium the Gibbs formulation must be regarded as approximate, like its analog, the fugacity rule of Lewis and Randall.

80. A rational basis for the thermodynamic treatment of mixtures of real gases. JAMES A. BEATTIE, *Massachusetts Institute of Technology.*—In the treatment of the thermodynamic properties of gas mixtures several assumptions are necessary. It is now found that two assumptions suffice: One relates to the isothermal variation of the energy of pure gases and the other to the isothermal variation of the ratio of the equilibrium pressure of a gas in a mixture to the total pressure multiplied by the mole fraction of the gas. From these two assumptions it can be shown that at infinitely low pressures the following relations hold for all real gases: (1) The laws of Boyle and Avogadro, (2) the energy, entropy, heat content and thermodynamic potentials of a mixture of gases are equal to the sums of the corresponding quantities for the component gases existing each by itself with the same value of its volume, temperature and chemical potential as in the gas mixture; (3) the energies and heat capacities of gases and gas mixtures are functions only of the temperature; (4) $p_v = nRT$ for pure gases and $p_v = \sum_i (n_i)RT$ for gas mixtures where T is thermodynamic temperature.

81. A thermodynamic theory of excitation of nerves. N. RASHEVSKY, *Westinghouse Elec. & Mfg. Co., East Pittsburgh, Pa.*—In their ionic theory of nervous excitation, W. Nernst (Pflügers Archiv, 122, 275, 1908) and A. V. Hill (Journal of Physiology, 40, 190, 1910) considered the motion of ions near a membrane, correspondingly between two membranes. Though the last case, worked out mathematically by Hill, accounts for the general features of the experimental excitation time curve, it does not account, without additional hypothesis, for the fundamental fact that the rate of increase of the exciting current is of prime importance. In the present paper, it is first pointed out that the boundary conditions, used in the mathematical treatment of Hill, cannot correspond to physically real cases, and a modified treatment is considered. Furthermore, it is shown that not only the general shape of the excitation time curve, but also the dependence on the rate of change of the exciting current, can be accounted for by purely thermodynamical considerations, which do not involve any special hypothesis about the ionic mechanism of excitation, and are based on considerations of systems with several equilibria.

82. The energy of dissociation of normal Cd_2 . J. G. WINANS AND R. ROLLEFSON, *University of Wisconsin*.—Kapusinski and Jablonski (Zeits. f. Physik 57, 692, 1929) give an interpretation of the Cd absorption flutings between $\lambda 2825$ and 2590 which yields 1.0 volts for the dissociation energy of normal Cd_2 . From an interpretation of the Cd absorption band at $\lambda 2212$ Winans (Phil. Mag. 7, 555, 1929) obtained 0.20 volts for this dissociation energy. Walter and Barrett found that cadmium vapor from which electronegative elements had been excluded failed to show the $\lambda 2825$ – 2590 flutings but still gave the 2212 band in absorption. They attributed the flutings to impurities in the cadmium and the 2212 band to cadmium molecules. The value of the dissociation energy obtained from the flutings is therefore doubtful. Also one should not expect an energy of dissociation as high as one volt for molecules like Cd_2 . Since cadmium is a closed shell atom, a molecule formed by the union of two unexcited Cd atoms must be held together by polarization forces only. That such forces are too small to account for a large energy of dissociation of Cd_2 is made very plausible by consideration of the fact that the alkaline earths and helium which have a similar electronic configuration show no molecular absorption. The work of Koernicke on Hg_2 indicates that the energy of dissociation of such molecules is of the order of 0.1 volts.

83. The composition of the interior of the earth. A. A. BLESS, *University of Florida*.—The high density of the whole earth as compared with the density of the crust is usually accounted for by the hypothesis that the core of the earth is composed of iron. This hypothesis is inadequate for a number of reasons, the chief of which is that it gives an iron content for the earth much too high compared with the abundance of this element in the sun or in other stellar bodies. Without introducing such a radical hypothesis the high density of the interior of the earth may be explained as being due to the ionization of the materials composing the core, the ionization being produced by the collision of atoms moving with the high velocity of thermal agitation. A temperature sufficient to cause ionization by collision would be reached at a depth of 2000 miles if the temperature gradient observed near the surface remains constant for this distance. At a comparatively short distance from the surface the high temperature would cause decomposition of molecules. The permanent gases so liberated would form an envelope around elements which are solid at ordinary temperatures, these elements forming the core. The ionization of the material of the core by decreasing the size of the atom, would increase the density sufficiently to account for the observed mass of the earth. The suggested distribution of the material gives the proper value for the moment of inertia of the earth, and is also in qualitative agreement with data concerning the propagation of seismic waves.

84. Striations and magnetic effect in electrodeless discharges. J. TYKOCINSKI-TYKOCINER AND JACOB KUNZ, *University of Illinois*.—Electrodeless tubes filled with H_2 (0.01 mm Hg) were placed in the field of a coil with high frequency currents (3000–12000 kc.) of constant amplitude. Striations appearing in pairs were observed. Their number decreases with current density. Moving a tube away from a flat spiral coil is equivalent to decreasing the density of the discharge current, consequently the number of striations increases. At a certain critical distance the striations pass through a transitory stage of irregular movements to and fro and disappear then altogether giving place to a uniform glow. Striations were also obtained with the axis of the tube directed perpendicularly to the axis of the exciting coil, showing that the striations are not necessarily connected with ring discharges. A magnetic field applied perpendicularly to the axis of the tube produces a rotational deflection of each striation clockwise and perpendicular to the direction of the magnetic field. This deflection may be interpreted by the Biot-Savart action of the magnetic field on the radial component of currents formed by carriers moving spirally with increasing radii around the axis of the tube and directed outward. A similar interpretation is applicable to striations produced by high frequency discharges in tubes supplied with inner or outer electrodes.

85. High frequency electrodeless discharge characteristics. OTTO STUHLMAN, JR., M. D. WHITAKER, M. L. BRAUN, *University of North Carolina*.—These discharges are classed as primarily due to electrostatic and to electromagnetic fields. Excitation by damped and by un-

damped frequencies are considered. The investigation involved the production of a glow discharge in mercury vapor as a function of frequency, pressure, current, and visual intensity. With a predominant electrostatic excitation and damped frequencies no simple relation was found to exist between visual intensity of the discharge and pressure, current, or frequency. However, consistent irregularities, characteristic of the gas and the mode of excitation, were obtained. With continuous wave and predominant electromagnetic excitation the minimum currents necessary to initiate, and necessary to sustain, the glow discharge were investigated at pressure ranging from 0.1 to 2.0 mm. For each frequency there exists a critical pressure at which the current through the coil required to initiate the glow discharge, and the current required to sustain it, are at minimum values. The ratio of these two currents is not constant for all pressures, but generally increases with increase in pressure. A characteristic arc transition from spark discharge at high pressure to arc discharge at lower pressures, occurred near 0.025 mm.

86. Relative intensities of arc and spark lines of the electrodeless discharge in mercury vapor. O. P. HART AND O. STUHLMAN, JR., *University of North Carolina*.—Excitation of discharge took place in a 12.5 cm spherical bulb placed inside a helical coil 14.5×44 cm when the latter was supplied with damped high frequency current. Three sets of spectrograms were taken—(A) Radiation intensity as a function of pressure with frequency and potential constant. (B) Intensity as a function of frequency with potential and pressure constant. (C) Intensity as a function of potential with frequency and pressure constant. Spectrogram series (A) showed that as the pressure was decreased (0.026 to 0.0005 mm) the intensity of the arc lines increased, whereas the intensity of the spark lines decreased. Series (B) showed that as the frequency of the excitation current was increased the intensity of the arc lines increased. No spark lines were observed at low pressures (0.0002 mm). Series (C) showed that as the potential between the terminals of the coil was increased the intensity of the arc lines increased. No spark lines appeared at this pressure (0.0002 mm). At low pressure and with increasing potential the triplet 4358, 5460, 4047 first appeared followed by the singlets 5790, 4347, 3906 in order of decreasing intensities.

87. Time lags in spark discharges at high overvoltages. J. C. STREET, *University, Va.*—Further studies of the long time lags in dry filtered gases at high overvoltage, first reported by Beams and Street (Phys. Rev. 35, 658 A), have been made. Surge potentials were applied and the time lags were measured by a comparison method. Several enclosed gaps were constructed and tested, care being taken to remove the residual ions. In each case for air, nitrogen or hydrogen at atmospheric pressure the lags remained longer than 10^{-6} sec. until fields of about 3×10^5 volts per cm were reached. With an increase to 3.3×10^5 volts per cm the lags became less than 5×10^{-8} sec. The magnitude of the field, at which the transition from long to short lags begins, is little affected by increase in pressure, amounting only to about 3.4×10^5 volts per cm at three atmospheres. On the other hand it is remarkably increased by a previous treatment consisting of discharges between the electrodes at reduced pressures in hydrogen. After this procedure, fields of 6×10^5 and 5×10^5 volts per cm for spherical electrodes of brass and steel respectively were required to produce lags shorter than 10^{-6} sec. Fields of the same order of magnitude as those just mentioned were required to produce a spark under the same circuital conditions in high vacuum between the same electrodes.

88. A direct measurement of the velocity of cathode rays. CHARLOTTE T. PERRY AND E. L. CHAFFEE.—The method used in this experiment makes no assumptions as to the law of deflection of moving electrons in magnetic and electric fields but measures the time of flight of the electrons directly in their passage over a distance of about 75 cm. Electrons are projected through a long tube by a potential E . In their journey they pass through two very localized alternating electric fields. These deflecting fields are produced by a very high frequency oscillator connected so that the fields are 180° out of phase. Only those electrons which pass when the fields are zero reach the end of the tube. The time required to travel the distance between fields is an even multiple of the half period of oscillation of the fields. The accuracy of determination of velocity is better than 0.1% and results are given for various driving voltages E .

89. The ionization of helium and neon by electron impact. PHILIP T. SMITH AND JOHN T. TATE, *University of Minnesota*.—The total positive ion current per electron per centimeter path has been measured as a function of the energy of the impacting electrons up to 3000 volts in neon and up to 4500 volts in helium, using a modified Jones type of apparatus (T. J. Jones, *Phys. Rev.* **29**, 822 (1927)). Both helium and neon exhibit well-defined maxima which occur at 110 and 170 volts respectively. The ratio of the positive ion current to the electron current per centimeter path reduced to 1 mm pressure and 0°C at the maxima was 1.256 for helium and 3.056 for neon. At 3000 volts the ratio was 0.172 for helium and 0.605 for neon. It was found that for energies from about 500 volts to 3000 volts the efficiency of ionization of neon is a linear function of V^{-1} , where V is the energy of the impacting electrons in volts. In helium the efficiency is a linear function of $V^{-1/2}$ from about 500 to 2000 volts. Beyond 2000 volts the efficiency approaches a linear function of V^{-1} . The empirical formula

$$3.383 (V_0/V)^{1/2} \left[1 - \exp \left(-\frac{54V_0}{V} \right) \right]^{1/2} \left[1 - \exp \left(-\frac{V - V_0}{2.28V_0} \right) \right]$$

expresses the efficiency of ionization of helium, within the experimental error, from the ionization potential V_0 to 4500 volts. The above results were free from any effects due to secondary electrons, and were independent of the pressure, electron current, and the magnetic field.

90. The absorption coefficient for slow electrons in gases. C. E. NORMAND AND R. B. BRODE, *University of California*.—The absorption coefficients or the effective collision cross sections have been measured in H_2 , He, Ne, A, N_2 and CO for velocities of the electrons from 0.5 to 400 volts. With a higher resolution of velocity a fine structure in the absorption coefficient curves has been found for all of these gases. At the lowest velocities, about 0.5 volts, all of the curves are rising with decreasing velocity. The minimums in the absorption coefficients occur between 0.5 and 1.2 volts for these gases. Ramsauer and Kolloth (*Ann. d. Physik* **4**, 91 (1930)) have reported minimums for He and A and none for the other gases. Their scale of velocity is, however, in disagreement with the velocities measured here, being 0.5 volts lower. When adjusted for this difference the data are in agreement.

91. Heating of a cathode by positive gas ions, and their "accommodation coefficient." C. C. VAN VOORHIS AND K. T. COMPTON, *Princeton University*.—Positive ions of helium, neon or argon were produced by a low voltage arc at low pressure and were made to bombard a spherical molybdenum collector with regulated velocities up to 140 volts. The resulting heating of the collector was measured by a thermal junction and found to be *considerably less* than the product of current by bombarding voltage. The problem was to account for the undetected remainder of the energy. Both calculations and experimental tests showed that this cannot possibly be explained as the result of part of the apparent ion current actually consisting of secondary electron emission or of ions losing energy at collisions with molecules. After making all such corrections, we are still forced to conclude that a fraction of the kinetic energy of the incident ions is carried away by ions (atoms) after neutralization. The fractions of their energies delivered to the cathode by the ions are the following "accommodation coefficients": He 0.4 to 0.5, Ne 0.7, A 0.8, which are strikingly similar to the gas kinetic values. There are a number of interesting applications of this discovery.

92. Angle and energy distribution of electrons rebounding from gaseous molecules. A. L. HUGHES AND J. H. McMILLEN, *Washington University, St. Louis*.—The distribution of electrons rebounding at definite angles from gaseous molecules was investigated. An electrostatic re-focusing arrangement was used to analyse the energies of the electrons. In helium, it was possible to identify the following energy losses at several angles, 21.12, 22.97, and 23.62 volts for a primary electron beam of 100 volts, but not the 19.77 and 20.55 volt losses. The number of electrons, rebounding without loss of energy, was measured for different angles of rebound (7° to 80°) from argon, helium, and molecular hydrogen molecules, and for various energies (50 to 15) volts. In almost all cases, the number decreased rapidly as the angle in-

creased. The higher the energy of the electrons, the more rapidly did the number fall off with increasing angle. The steepness of the curves increases as we go from argon to helium to hydrogen for the slower electrons. For the faster electrons their curves are practically superposable.

93. An attempt to detect collisions between photons. G. E. M. JAUNCEY AND A. L. HUGHES, *Washington University, St. Louis*.—It has been shown that if two photons, of identical frequency, moving along paths making an angle of 120° with each other, collide, and produce one photon travelling forward along the line bisecting the 120° angle, and another photon traveling in the opposite direction, the frequency of the photon traveling forward must be 1.707 of the frequency of the original photons (Hughes and Jauncey, *Phys. Rev.* **33**, 290 (1929)). This suggested the following experiment. Two beams of sunlight (one suitably deflected by a mirror), filtered through red glass, were passed through lenses 10 inches in diameter, so that the beams, whose axes made an angle of 120° with each other, intersected at a common focus. As the diameter of the beams at the focus amounted to only 4 mm, great concentration of light was obtained. The point of intersection of the beams was examined through a green filter with the eye which had been rested in total darkness for periods up to an hour. No light was detected. It was estimated that if the photon has a cross section, effective for the type of collision here contemplated, it must be less than 10^{-11} cm.

94. On the principle of Huyghens. G. E. UHLENBECK, *University of Michigan*.—Attention is called to the general formula:

$$\int_0^\infty d\nu \int_{-\infty}^{+\infty} f(\xi) \sin \nu(x - \xi) d\xi = P \int_{-\infty}^{+\infty} \frac{f(\xi)}{x - \xi} d\xi$$

where P denotes Cauchy's principal value. An exact (not published) proof of this has been given by Droste, when $f(\xi)$ fulfills the Dirichlet conditions. One has to compare this with the Fourier's integral theorem:

$$\int_0^\infty d\nu \int_{-\infty}^{+\infty} f(\xi) \cos \nu(x - \xi) d\xi = \pi f(x).$$

By integrating the wave equation in n dimensions $(\partial^2/\partial t^2 - \Delta_n)\psi = 0$ with given initial values for ψ and $\partial\psi/\partial t$ according to the method of Fourier-Cauchy, one can show that the curious difference between the formula's (1) and (2) reflects the well-known fact that the principle of Huyghens is not valid in spaces with n even number of dimensions and valid in spaces with an odd number.

95. The Stark effect near the series limit. JANE DEWEY, *University of Rochester*.—The number and position of the lines appearing near the limit in a hydrogen-like spectrum have been investigated on the Bohr theory, extending the work of Robertson and the writer (*Phys. Rev.* **31**, 973 (1928)). From a study of the limiting cases, for which the complete equation can be handled more easily than in the general case, it appears that only orbits with principal quantum number less than a given number (approximately $43/F^{1/4}$) are periodic in the presence of a field. The region in which both lines and continuous spectrum appear is due to the large displacement of the lines. The outer components of the last group of lines appearing in a field of 1 e.s.u. per centimeter are displaced 50 cm^{-1} . For small fields the position of all the lines is given correctly by the perturbation theory if the second order terms are taken into account, as lines for which the series would not converge do not appear. The large displacements and large number of lines which appear near the series limit in a field make it probable that the lines observed in discharges in this region are the central components of the group of lines having the same principal quantum numbers and that the other components are spread over the background by the stray fields necessarily present. The apparent sharpness of the lines is thus not a criterion for no spreading out of the lines and an experimental investigation of the effect would be very difficult as it would probably not be possible to maintain a field sufficiently constant to observe the higher series members distinct from one another.

96. Zeeman effect in the calcium hydride band spectra. WILLIAM W. WATSON AND WILLIAM BENDER, *Yale University*.—The Zeeman effect in the red CaH bands has been investigated at several field strengths to 30,000 gauss, with a dispersion of 2.1 Å per mm. For $K < 7$ in the $^2\Sigma \rightarrow ^2\Sigma$ system, the P_1 and R_1 lines (parallel S) are unaffected at all fields, while the P_2 and R_2 lines (anti-parallel S) mostly become diffuse doublets shading away from the no-field position. All P_1 and R_1 lines of higher K value have at low fields only a strong, broad component shifted to the red with the extreme edge at about $\Delta\nu_{\text{norm}}$, the breadth decreasing as K increases. At 30,000 gauss a broad weak violet component appears. The P_2 and R_2 lines with $K > 8$ are merely broadened to the violet, the overall width being approximately $\Delta\nu_{\text{norm}}$. The lines of low K values in the $^2\Pi \rightarrow ^2\Sigma$ band give field patterns as expected from Hill's theory. For $K > 22$, the lines involving F_1 states rapidly broaden out, and for highest K values are of negligible intensity. The lines arising from F_2 levels, remain sharp and strong for all high rotational states, but shifted to the violet by about $1/2(\Delta\nu_{\text{norm}})$. These effects can be explained by a consideration of the "rho-type" doubling involved.

97. Electro-optical modifications of light waves. L. H. STAUFFER, *University of California* (Introduced by Ernest O. Lawrence).—Broadening of the satellites of the Hg green line $\lambda 5461$ was observed when the light passed between the plates of a Kerr cell on which was impressed a varying E.M.F. having a frequency of $2 \times 10^7 \text{ sec}^{-1}$. The E.M.F. was obtained by superposing the output of a vacuum tube oscillator upon a steady potential of about 7000 volts. The maximum oscillator voltage was about 5000 volts. With this voltage the fine structure of the Hg green line became so diffuse that two satellites having a separation of 0.045 Å were scarcely resolved by the Lummer-plate. The broadening was observed to increase rapidly with the oscillator voltage. The observed effect is predicted by the classical electromagnetic theory and constitutes a proof of the generalized Doppler principle. The high frequency voltage effects a rapid variation of the refractive index of the nitrobenzene in the Kerr cell which in turn produces a corresponding variation in optical path, giving the source a virtual velocity. The observed broadening is in agreement with the predictions of classical theory.

98. The electric double refraction in gases. J. W. BEAMS AND E. C. STEVENSON, *University of Virginia*.—A method for the study of the electric double refraction or Kerr effect in gases as a function of pressure has been devised. Light of known frequency was passed through a Nicol prism, between two parallel metal plates, through a second Nicol prism and into a photoelectric cell. The two Nicols and the metallic plates across which the electric potential was applied were inclosed in a heavy steel tube with glass ends. As a result, the Kerr effect in the gas could be studied at a few hundred atmospheres pressure without introducing errors due to strains in the windows. Intense electric fields could also be employed because of the large value of the dielectric strength of the gas at high pressures. The precision of the method was limited only by the precision with which the potential across the plates could be measured. The results indicate that in the case of CO_2 the Kerr constant per molecule does not change by as much as 2 percent between 15 and 45 atmospheres pressure at 21°C . An easily measurable Kerr effect was observed in O_2 and N_2 at 100 atmospheres pressure.

99. Spontaneous temperature changes accompanying magnetization in steel. W. B. ELLWOOD, *Columbia University*.—The purpose of this experiment is to determine the dissipation of energy accompanying magnetization in iron by observing the change in temperature of a test specimen produced by a change in the magnetizing force at consecutive intervals in a single cycle of magnetization. The test specimen is in the form of an ellipsoid consisting of 104 bars of #57 drill rod alternate with 104 similar copper rods arranged in coaxial concentric cylinders. One hundred and two thermocouples in series are constructed by connecting adjacent copper and steel bars with 3 mm lengths of constantan and copper wire. Adequate thermal insulation isolates the specimen from the magnetizing solenoid in which it is placed. A temperature change of 3×10^{-6} degrees Centigrade can be detected. The specimen is put in a cyclic magnetic state and allowed to come to thermal equilibrium. On traversing the hysteresis loop from $+290$ to $+20$ gauss, heat is evolved by the iron and is measured as an increase in temperature.

On further demagnetization from +20 to -6 gauss the iron cools suddenly. From -6 to -90 gauss, the iron heats most rapidly. Increase of the field to -290 gauss is accompanied by cooling of the iron. Temperature-magnetization curves for various other magnetic paths are described.

100. The propagation of large Barkhausen discontinuities along wires. K. J. SIXTUS AND L. TONKS, *General Electric Co.*—Preisach has shown that by applying increasing tension or torsion to a wire of nickel iron alloy, the Barkhausen discontinuities in magnetization become larger and larger. Finally, at a tension near to the elastic limit, a rectangular hysteresis loop is produced whose discontinuous change in magnetization includes 97 percent of the whole difference between positive and negative saturation. Langmuir suggested that this sudden change in magnetization starts at a nucleus from which it propagates along the wire. Investigation based on this view shows that the nucleus forms in a uniform field at a somewhat variable critical field strength, and at different points along the wire, depending apparently on uncontrolled factors. The nucleus can be made to form at a definite point, however, by applying locally a small additive field, and the discontinuity will then propagate into the uniform portion of the field, the strength of which can be smaller than the critical field strength. The velocity of propagation increases for a given sample with increasing field strength and tension. A 10% Ni-90% Fe wire of 0.038 cm diameter showed velocities up to 14000 cm sec⁻¹

101. The mobilities of ions in moist and dry air. JOHN ZELENY, *Yale University*.—Using the method recently described (Phys. Rev. 34, 310, 1929) the distribution of mobilities of aged ions in *dry air* has been determined and the values for moist air remeasured because of a neglected correction. The dissymmetry in the distribution of mobilities around the most numerous kind noted in the previous paper for *negative ions* in moist air, was found more pronounced in air dried by calcium chloride. In air dried further by passage through coils and filters immersed in liquid air a second distinct group of negative ions constituting about 35 percent of the total number and having a peak mobility of about 1.45 cm/sec was partially resolved. Under the last conditions the positive ion distribution curve also shows some dissymmetry indicating a possible group with a peak mobility of about 1.5 cm/sec. The mobility of the ions at the main peak of the distribution curve *decreased* for *positive ions* from 1.36 cm/sec for air with a water content of about 2 mg/liter to 1.05 cm/sec for the driest air used. Under similar circumstances the mobility of the *negative ions increased* from 2.08 cm/sec to 2.45 cm/sec. The existence of the two groups of negative ions is ascribed to a difference in size of the ion clusters arising from a difference in constitution at or near their centers.

102. Restriking of short a.c. arcs. F. C. TODD AND T. E. BROWNE, JR., *Westinghouse Elec. and Mfg. Co., East Pittsburgh*.—The restriking after zero current of short a.c. arcs with melting electrodes and of rapidly moving arcs with cold electrodes was investigated with a cathode ray tube of the Braun type. Long exposure photographs and observations of the volt-ampere traces on the fluorescent screen show the effect of the electrode vapor on the magnitude and variation of the restriking voltage. Brass, copper, iron, tungsten, and carbon were used as hot electrodes. The restriking characteristics of rapidly moving cold electrode arcs are influenced by the condition of the electrodes, magnitude of the driving magnetic field, and rate of rise of the voltage after current zero.

103. Extinction of short a.c. arcs between brass electrodes. T. E. BROWNE, JR. AND F. C. TODD, *Westinghouse Elec. and Mfg. Co., East Pittsburgh*.—Results are given which show that the dielectric recovery after current zero of short, stationary, a.c. arcs between brass electrodes is similar to that of cold-electrode arcs previously investigated and described. These results also show that the rate of recovery of dielectric strength of hot-electrode arcs after a current zero *may be greatly increased* by reducing, within limits, the electrode separation. An explanation is suggested on the basis of ionic diffusion to the electrode surfaces and the deionizing action of blasts of metal vapor from the boiling electrodes.

104. Problems suggested by an uncertainty principle in acoustics. G. W. STEWART, *State University of Iowa*.—At the suggestion of Professor A. Landé the principle adopted is

$\Delta\nu \cdot \Delta t \sim 1$, where ν is the intrinsic frequency of an acoustic signal and Δt is its time duration. Applying this principle one finds that it is consistent with experiments on the change in ν in the vibrato and the failure to detect it by ear, with recorded tests on minimum perceptible differences in frequency, and with the minimal time for tone perception. The problems suggested by the principle are: (1) variations in Δt and $\Delta\nu$ by an artificial vibrato with aural observations of detectable $\Delta\nu$, (2) redetermination of minimum perceptible differences in frequency as dependent upon Δt and (3) an examination of Δt required for tone perception with varied values of $\Delta\nu$ required for so-called tone perception.

105. The dispersion formula and Raman effect for the symmetrical top. MORRIS MUSKAT, *Gulf Research Laboratory Pittsburgh*.—Schroedinger's theory of dispersion is applied to the symmetrical top. The dipole of the top is assumed to lie along the axis of symmetry, and the wavelength of the incident light to be large as compared with the dimensions of the top. An explicit expression is derived for the index of refraction of a gas composed of symmetrical tops, as a function of the frequency of the incident light. As the perturbed eigenfunction is a linear function of only three unperturbed eigenfunctions, the dispersion formula, for a given state, consists of only two terms. The moments for the Raman effect transitions for the symmetrical top are also computed. Simple closed expressions are obtained, again because of the simplicity of the perturbed eigenfunctions. The polarization of the Raman radiations is computed with the result that the unshifted lines are unpolarized, whereas for the shifted lines, $|m_z|^2/|m_x|^2 = 4/3$.

106. The measurement of the variation in intensity of the helium lines with voltage by means of selected filters and a photoelectric cell. PETER J. MULDER AND JOSEPH RAZEK, *University of Pennsylvania*.—A method has been developed by which the variations in the intensity of individual spectrum lines can be measured without resolution through a spectroscope, making use of a photoelectric cell and the recording amplifier described by Razek and Mulder as part of their automatic spectrophotometer (other paper, this meeting). This method has its application in the spectrophotometry of weak sources. We have used the method to study the variation of intensity of helium arc lines with voltage. The deflection of the amplifier galvanometer with various filters of known transmission coefficients for the lines to be measured interposed successively in the beam is noted. Assuming that all the energy recorded is limited to n lines, and that n filters are used, n equations soluble for ϕ_a of the form $L_a = a_1\phi_1 + a_2\phi_2 + \dots + a_n\phi_n$ can be written, where L_a is the total light intensity as recorded with filter a interposed, $a_1 \dots a_n$ are the appropriate filter transmission coefficients, and $\phi_1 \dots \phi_n$ are the intensities of the lines multiplied by a factor depending on the wave-length sensitivity of the cell. To increase accuracy, more filters may be used and a reduction made to n normal equations by Gauss' method. In our work the helium lines were treated in four groups to reduce computation. The results generally checked with those obtained independently by a direct method.

107. The polarization and the electric moment of tung oil. A. A. BLESS, *University of Florida*.—The dielectric constant of a solution of tung oil in benzene of different concentrations was measured for three frequencies 10^6 , 4×10^6 , 10^8 , using an electrical resonance method. The molar polarization of the solutions was calculated by the aid of the Clausius-Mosotti relation. The molar polarization proved to be a linear function of the mole fraction of tung oil, showing that the interaction of the polar molecules is in this case negligible. The polarization of the pure oil was found to be -364 cc, giving an electric moment of 2.195 e.s. units. The values found are substantially the same for each of the three frequencies for which the electric constant was measured.

108. Methods of acoustic interferometry for the measurement of velocity and absorption of sound in gases. J. C. HUBBARD, *Johns Hopkins University*.—In the well known acoustic interferometer of Pierce (Proc. Am. Acad. 60, 271, 1925) the piezoelectric plate serves at the same time as generator of electric and acoustic oscillations. In order to eliminate the crystal as an essential part of the power circuit and use it only as a source of sound waves, thus to secure greater adaptability to the study of sound velocity and absorption over a range of temperatures and pressures, the writer has applied the method of forced piezoelectric vibrations used in the

sonic interferometer for liquids developed in collaboration with Mr. A. L. Loomis (Phil. Mag. June, 1928; J.O.S.A., Oct. 1928). The audible beat note of two Hartley circuits is adjusted in unison with a tuning fork, one of the circuits being provided with a secondary coil connected to the electrodes of the piezoelectric plate of the interferometer system. Cyclic variation of beat note as the gas column is lengthened is compensated by a vernier condenser in the exciting circuit, from the readings of which the velocity and attenuation of the sound in the gas are deduced. Acknowledgment is made to the Rumford Fund of the American Academy of Arts and Sciences, and to Mr. A. L. Loomis for the use of quartz plates.

109. Independence of x-ray absorption on temperature. J. A. BEARDEN, *Johns Hopkins University*.—Measurements have been reported (Read, Phys. Rev. **27**, 373 and Phys. Rev. **28**, 898) which indicated a change in the absorption coefficient of x-rays with change in temperature of the absorbing screen. Due to the theoretical importance of this effect the measurements have been repeated with much higher precision than was obtained in the previous work. The present method consists in comparing the intensity transmitted by two screens, first with both screens at the same temperature (about 24°C) and then with one screen raised to a higher temperature while the other was retained at 24°C. It can be shown that the percent change due to the expansion of the hot screen should be equal to $2\alpha T\mu\chi$ where α is the linear expansion of the metal, μ the linear absorption coefficient of the transmitted beam, and χ the thickness of the screen. By making χ and μ large the expected change due to expansion in the present experiments was equal to 10 to 18 percent at 600°C. Measurements with wave-lengths from 0.4Å to 1.5Å showed no change from the expected change due to expansion.

110. On the heat of formation of molecular oxygen. L. C. COPELAND (*National Research Fellow in Chemistry*) (Introduced by E. C. Kemble, *Harvard University*).—Molecular oxygen at pressures of 0.1 mm to 0.4 mm has been dissociated by the electrodeless discharge. The percent dissociation in the flowing gas was determined from pressure measurements on the high pressure side of a set of small orifices, using Knudsen's formula. Palladium black freshly deposited on a platinum surface has been shown to cause total recombination. A calorimeter consisting of such a surface fastened to a Beckmann thermometer and calibrating resistance coil with Woods metal was used to measure the energy of recombination. It has also been shown that the palladium black surface, poisoned with mercury vapor, or a shiny platinum surface do not cause total recombination. Several preliminary experiments have been made with about twenty-five percent dissociation at a rate of flow of 0.75 cc per minute.

111. On the mechanism of very absorbable radiation emitted by compressed crystalline substances under high potentials. ISAY A. BALINKIN, *University of Cincinnati* (Introduced by S. J. M. Allen).—Following the work of Reboul, the emission from specially designed "radiating cells" was studied photographically. Powdered alum with the average size of the grains 0.0032 in. was subjected to a pressure of 300 kg/cm² in an atmosphere of 55% relative humidity. Under a potential difference of 5000 volts the emission from the cell was completely absorbed by celluloid, $t=0.13$ mm, and only partially absorbed by cellophane, $t=0.02$ mm. This corresponds to a range between very soft x-rays and short ultraviolet. A similar effect on the photographic film can be obtained by passing a spark discharge in an electrostatic field of about 1000 volts per centimeter in which the negative and positive ions are separated and then drawn into a recombination chamber. A Bunsen flame as an ionizing agent under the same circumstances, produces the same effect. The mechanism of the radiation emitted by the "radiating cell" under high potentials is explained by the external recombination of the ions which were produced in the interstices of the compressed crystalline substance. The wave-length of the emitted radiation corresponds to the ionization potentials of oxygen and nitrogen as given by the relation, $h\nu = Ve$. For a value of 14 volts, $\lambda=900\text{Å}$ which agrees with the results given by the experiment.

112. A 21 ft. vacuum spectrograph for intensity measurements in the Schumann region. GEORGE R. HARRISON, *Stanford University*.—A 21 ft. concave grating ruled by Wood with 15,000 lines per inch and having a very bright first order has been mounted in vacuum for use in the Schumann region. The case consists of a 20 ft. vanadium steel tube of 16 inch internal

diameter, closed with tinned bronze castings. Three oil pumps exhaust this volume of 863 liters to 0.01 mm pressure in two hours; four large steel condensation pumps using n-dibutyl phthalate trapped with CO_2 lower the pressure to less than 10^{-4} mm in three more hours after 50 hours of outgassing with the pumps off. The camera box holds 4 x 16 inch plates or films, recording at one setting a range of 900A with a dispersion of 2.7A per mm. Thirty exposures to different sources can be made without destroying the vacuum. The instrument, designed particularly for making intensity measurements on multiplets of multiply ionized atoms using the photometric methods developed by Leighton and the author for the Schumann region, has only been used to photograph the region 2200-1300A thus far; the strength of the spectrum indicates that 1000A should be reached without difficulty

113. Photographic record of the first order diffraction of hydrogen atoms by a lithium fluoride crystal. THOMAS H. JOHNSON, *Bartol Research Foundation*—A beam of hydrogen atoms was reflected from a cleaved surface of a crystal of lithium fluoride at an angle of incidence of 30° . The plane of incidence made an angle of 45° with the cleavage edges of the crystal. In addition to the specularly reflected beam, first order beams appeared on the MoO_3 detecting plates having the positions calculated from the wave-length $\lambda = h/mv$ and from the grating spacing of the rows of similar ions.

114. Double crystal spectra of scattered x-rays. NEWELL S. GINGRICH, *University of Chicago*.—To get high scattered intensity, two molybdenum metal x-ray tubes of small diameter were used with a graphite scattering block between them. A total current of 95 m.a. at 50 k.v. was used. The effective scattering angle was about 109 degrees. Successive spectra taken in the neighborhood of the $K\alpha$ lines are not identical, since the experimental error is relatively large when measuring weak ionization currents. Nevertheless it can be said from the spectra obtained that the intensity of any fine structure line in the unmodified spectrum is probably not greater than 10 or 15 percent that of the $K\alpha$ line. The spectrum of the modified $K\alpha$ lines is observed at the position calculated from the equation $\delta\lambda = 0.0243 (1 - \cos \phi) \lambda$. No evidence is found of fine structure lines in the modified spectrum as reported by Davis and Purks.

AUTHOR INDEX

- Almasy, F. and C. V. Shapiro—No. 27
 Andrews, D. H.—see Kettering
 Astin, Allen—No. 54
- Badger, Richard M.—No. 74
 Balinkin, Isay A.—No. 111
 Barnes, A. H., Bergen Davis and H. L. Hull—No. 70
 Barnes, R. Bowling and A. H. Pfund—No. 77
 Barnes, S. W.—see Richtmyer
 Barrett, Charles S.—No. 41
 Beams, J. W. and E. C. Stevenson—No. 98
 Bearden, J. A.—Nos. 49, 109
 Beattie, James A.—No. 80
 Becker, J. A.—No. 63
 Bender, William—see Watson
 Bergstein, Milton, J. F. Rinke and C. M. Gutheil—No. 38
 Bless, A. A.—Nos. 83, 107
 Bowie, R. M.—see Woodrow
 Bramley, A. and A. C. G. Mitchell—No. 14
 Brattain, Walter H.—No. 62
 Braun, M. L.—see Stuhlman
 Briggs, L. J. and H. L. Dryden—No. 5
 Brode, R. B.—see Normand
 Browne, T. E., Jr.—see Todd
 ——— and F. C. Todd—No. 103
 Busang, P. F.—see Smith
- Castleman, R. A., Jr.—No. 3
 Chaffee, E. L.—see Perry
 Claus, W. D.—No. 48
 Collins, J. R.—No. 75
 Colwell, R. C.—No. 39
 Compton, Arthur H.—No. 50
 Compton, K. T.—see Van Voorhis
 Condon, E. U. and G. H. Shortley—No. 16
 Copeland, L. C.—No. 110
 Curtiss, L. F.—No. 73
- Davey, W. P. and D. C. Duncan—No. 32
 Davis, Bergen—see Barnes
 Davis, G. E. and Gilbert Greenwood—No. 56
 Dewey, Jane—No. 95
 Donal, John S., Jr.—No. 61
 Dryden, H. L. and G. C. Hill—No. 4
 ——— see Briggs
 Duffendack, O. S. and L. B. Headrick—No. 23
 Duncan, D. C.—see Davey
 Ellwood, W. B.—No. 99
 Farnsworth, H. E.—No. 69
- Findlay, J. H.—No. 19
 Foote, Paul D.—see Smith
- Galli-Shohat, N.—No. 12
 Gibbs, R. C.—see Shapiro
 Gilliespie, Louis J.—No. 79
 Gingrich, Newell S.—No. 114
 Glasser, Otto and V. B. Seitz—No. 66
 Goucher, F. S.—No. 57
 Goudsmit, S. and L. A. Young—No. 13
 Greenwood, Gilbert—see Davis
 Gutheil, C. M.—see Bergstein
- Harrington, M. C.—see Uyterhoeven
 Harrison, George R.—No. 112
 Harrison, J. R.—No. 8
 Hart, O. P. and O. Stuhlman, Jr.—No. 86
 Harvey, G. G. and G. E. M. Jauncey—No. 47
 Headrick, L. B.—see Duffendack
 Hill, G. C.—see Dryden
 Hodgman, Charles D.—No. 33
 Hollabaugh, Cleveland B.—No. 42
 Hootman, James A. and W. S. Nelms—No. 65
 Howe, Carl E.—No. 52
 Hubbard, J. C.—No. 108
 Hughes, A. L. and J. H. McMillen—No. 92
 ——— see Jauncey
 Hulburt, E. O.—No. 21
 Hull, H. L.—see Barnes
 Hyman, Hugh H.—No. 17
- Ives, Herbert E.—No. 36
- Jauncey, G. E. M.—see Harvey
 ——— and A. L. Hughes—No. 93
 Johnson, J. R.—see Shapiro
 Johnson, Thomas H.—Nos. 68, 113
- Kettering, C. F., L. W. Shutts and D. H. Andrews—No. 26
 Knowles, D. D. and S. P. Sashoff—No. 64
 Korff, S. A. and J. L. Nickerson—No. 71
 Kovarik, Alois F.—No. 67
 Kozanowski, H. N.—No. 59
 Kunz, Jakob—No. 9
 ——— see Tykociner
- Lawrence, Ernest O. and Leon B. Linford—No. 25
 Linford, Leon B.—see Lawrence
- McCracken, E. C.—No. 31
 McFarlan, Ronald L.—No. 45

- McMillen, J. H.—see Hughes
 Martin, John R.—see Miller
 Meggers, Wm. F. and Bourdon F. Scribner—
 No. 18
 Miller, Dayton C. and John R. Martin—No. 7
 Millikan, R. A.—No. 72
 Mitchell, Allen C. G.—see Bramley
 — No. 29
 Mulder, Peter J. and Joseph Razek—Nos. 35,
 106
 — see Razek
 Muskat, Morris—Nos. 1, 105
- Nadai, A.—No. 10
 Nelms, W. S.—see Hootman
 Nickerson, J. L.—see Korff
 Nordheim, L. W.—No. 58
 Normand, C. E. and R. B. Brode—No. 90
 Nusbaum, C.—No. 43
- Olshevsky, D. E.—No. 37
 Ornstein, L. S. and G. E. Uhlenbeck—No. 78
- Perry, Charlotte T. and E. L. Chaffee—No. 88
 Pfund, A. H.—No. 76
 — see Barnes
 Pielemeier, W. H.—No. 6
 Pool, M. L.—No. 15
- Ramberg, E.—see Richtmyer
 Rashevsky, N.—No. 81
 Razek, Joseph and Peter J. Mulder—No. 34
 — see Mulder
 Richtmyer, F. K., S. W. Barnes and E. Ram-
 berg—No. 51
 Rinke, J. F.—see Bergstein
 Roberts, O. L.—No. 44
 Rollefson, R.—see Winans
- Sashoff, S. P.—see Knowles
 Sawyer, R. A.—No. 22
 Scott, Arnold H.—No. 55
 Scribner, Bourdon F.—see Meggers
 Seitz, V. B.—see Glasser
 Shapiro, C. V.—see Almasy
- R. C. Gibbs and J. R. Johnson—No.
 28
 Shenstone, A. G.—No. 20
 Shortley, G. H.—see Condon
 Shutts, L. W.—see Kettering
 Sillers, Frederick, Jr.—No. 53
 Sixtus, K. J. and L. Tonks—No. 100
 Smith, Lloyd P.—No. 60
 Smith, Philip T. and John T. Tate—No. 89
 Smith, W. O., Paul D. Foote and P. F.
 Busang—No. 2
 Stauffer, L. H.—No. 97
 Stevenson, E. C.—see Beams
 Stewart, G. W.—Nos. 46, 104
 Street, J. C.—No. 87
 Stuhlman, Otto, Jr., M. D. Whitaker and
 M. L. Braun—No. 85
 — see Hart
- Tate, John T.—see Smith, P. T.
 Todd, F. C. and T. E. Browne, Jr.—No. 102
 — see Browne
 Tonks, L.—see Sixtus
 Tykociner, J. T. and Jakob Kunz—No. 84
- Uhlenbeck, G. E.—No. 94
 — see Ornstein
 Uyterhoeven, W. and M. C. Harrington—No.
 24
- Van Voorhis, C. C. and K. T. Compton—No.
 91
 Verman, Lal C.—No. 40
- Watson, William W. and William Bender—
 No. 96
 Wells, P. V.—No. 11
 Whitaker, M. D.—see Stuhlman
 Winans, J. G. and R. Rollefson—No. 82
 Woodrow, Jay W. and R. M. Bowie—No. 30
- Young, L. A.—see Goudsmit
- Zeleny, John—No. 101

THE PHYSICAL REVIEW

POSSIBLE EFFECTS OF NUCLEAR SPIN ON X-RAY TERMS

BY G. BREIT

DEPARTMENT OF PHYSICS, NEW YORK UNIVERSITY

(Received May 5, 1930)

ABSTRACT

It is shown that magnetic moments of nuclei are likely to cause small but presumably measurable separations of x-ray terms. A nucleus having a spin of $9/2$ (in units of $\hbar/2\pi$) and a magnetic moment $9/2$ in protonic units should cause the K terms of the heaviest elements to split into two components separated by about 22 volts. Such separations require for their detection a resolving power of 4200. For lighter elements the effect is relatively smaller. The same nuclear spin and magnetic moment would cause a separation of only 0.9 volts in Mo which would require for its detection a resolving power of 1.9×10^4 .

The calculations are made using Dirac's equation for a single electron without approximations. The effect of electrons in another shell, however, is neglected. It is estimated to be very small for a single K electron. If the observation of hyperfine structures in the K series of the heavier elements proves feasible, it should offer a simple means of determining magnetic moments of nuclei having a known spin.

THE hyperfine structure of spectral lines is at present attributed to the nuclear spin. The quantitative theory of the effect has been worked out by Hargreaves, Fermi, Goudsmit and Bacher and by Casimir.¹ A quantitative application of the theory is simple in a few cases such as e.g. the Li^+ hyperfine structure. For most spectra it is necessary to use approximate solutions for the electronic eigenfunctions which are at present usually carried out by the Hartree method. Quantitative determinations of the nuclear magnetic moment become, therefore, difficult. An examination of Fermi's result shows however that the order of magnitude of the effect can be expected to be much larger for the spectral terms in the x-ray region than for visible spectra. The absolute value of the splitting of an s term due to a single electron is according to Fermi

$$(F) \quad (8\pi/3)[(2k+1)/k]\mu\mu_0\psi^2(0)$$

where k is the angular momentum of the nucleus, μ its magnetic moment, μ_0 the Bohr Magneton, and $\psi(0)$ is the value of the Schroedinger function

¹ J. Hargreaves, Proc. Roy. Soc. A124, 568 (1929). E. Fermi, Zeits. f. Physik 60, 320 (1930). S. Goudsmit and R. F. Bacher, Phys. Rev. 34, 1501, (1929). S. Goudsmit and L. A. Young, Nature, March 22, (1930).

at $r=0$. For large atomic numbers the value of $\psi(0)$ for a $(1s)K$ electron is large. In fact it is seen that $\psi^2(0)$ must increase as the cube of the reciprocal of the radius of the K orbit i.e., as Z^3 where Z is the atomic number. The energy of the K level increases only as Z^2 so that the splitting $\Delta\nu$ increases more rapidly than the term value ν . The values of the magnetic moments of the nuclei are not known at present and so it is necessary to be content with approximate estimates using the known orders of magnitude derived from hyperfine structure observations in the visible region. Making such estimates it is found that for heavy elements the separation $\Delta\nu$ may be expected to be of the order of $1/5000$ of the frequency of the K line. The double crystal spectrometer developed by Bergen Davis appears to offer at least a possibility of observing such separations. The main purpose of this note is to call attention to the possibility of determining the magnetic moments of the nuclei by means of observations of the hyperfine structure of the lines in the K series. Corresponding effects in the L and M series are estimated to be smaller, though not necessarily beyond the range of experimental accuracy.

In order to form proper estimates for the case of x-rays it is necessary to perform somewhat more precise calculations than those of Fermi. The inaccuracy of his method lies in the fact that $E + (Ze^2/r) + mc^2$ is replaced by $2mc^2$. This is a good approximation as long as the region of large values of Ze^2/r is relatively small and as long as $E \sim mc^2$. Both of these conditions are satisfied for the lighter elements. The approximate dimensions of the regions in which the eigenfunction is appreciable are then of the order of 10^{-8} cm while $e^2/r > mc^2$ only if $r < 2.5 \times 10^{-13}$ cm. For the heavier elements this is not so because the charge density is more concentrated and Ze^2/r is greater for the same r . It thus becomes necessary to use exact solutions of Dirac's equation as a starting point in the calculation of the perturbation due to the magnetic moment of the nucleus.

Using Gordon's form of the solution of the Dirac equation for a Coulomb field of force² it is seen that for s terms of a single electron any set of four ψ_i 's can be expressed as a linear combination of the following two sets

$$(I) \quad \begin{aligned} \Psi_1 &= ((i/r) \cos \theta \phi_1, (i/r) \sin \theta e^{i\phi} \phi_1, \phi_2/r, 0) \\ \Psi_2 &= ((i/r) \sin \theta e^{-i\phi} \phi_1, -(i/r) \cos \theta \phi_1, 0, \phi_2/r) \end{aligned}$$

where ϕ_1, ϕ_2 are two functions (denoted by Gordon as ψ_1, ψ_2) given by

$$(G) \quad \phi_1 = (1 - E/mc^2)^{1/2} (\sigma_1 - \sigma_2); \quad \phi_2 = (1 + E/mc^2)^{1/2} (\sigma_1 + \sigma_2)$$

where $\sigma_1 = c_0^{(1)} e^{-k_0 r} r^\rho F(-n' + 1, 2\rho + 1; 2k_0 r); \quad \rho = (1 - \alpha^2)^{1/2}$

$$\sigma_2 = c_0^{(2)} e^{-k_0 r} r^\rho F(-n', 2\rho + 1; 2k_0 r); \quad \alpha = 2\pi Ze^2/\hbar c$$

$$F(\alpha, \beta; x) = 1 + \frac{\alpha x}{1\beta} + \frac{\alpha(\alpha+1)x^2}{2\beta(\beta+1)} + \dots; \quad k_0 = (2\pi mc/\hbar) [1 - (E/mc^2)^2]^{1/2}$$

$$c_0^{(1)}/c_0^{(2)} = -n'/[1 + \alpha(1 - (E/mc^2)^2)^{-1/2}]; \quad E/mc^2 = [1 + \alpha^2/(n' + \rho)^2]^{-1/2}$$

Here $n' = 0, 1, 2, \dots$ for $(1s), (2s), \dots$ terms.

² W. Gordon, Zeits. f. Physik **48**, 22 (1928).

In particular for (1s) terms $c_0^{(1)}/c_0^{(2)}=0$ and σ_2 contains only one term.

The perturbation function due to the magnetic moment of the nucleus we take to be the same as Fermi's

$$w = (e/r^3) \vec{a} [\vec{y} \times \vec{r}].$$

The unperturbed orthogonal Eigenfunctions can be taken to be

$$\begin{aligned} &u_k^{(1)}, u_{k-1}, \dots, u_{-k}^{(1)} \\ &u_k^{(2)}, \dots, u_{-k+1}^{(2)}, u_{-k}^{(2)} \end{aligned} \quad (1)$$

corresponding to angular momenta

$$(k + \frac{1}{2}, k - \frac{1}{2}, \dots, -k - \frac{1}{2})(h/2\pi)$$

To every angular momentum in the direction of the Z axis there correspond in general two unperturbed functions. Each of these is a rectangular matrix. The superscripts (1), (2) indicate whether Ψ_1 or Ψ_2 of I are used. Thus the function $u_{k-l}^{(1)}$ has for elements zeros in the first l rows; Ψ_1 stands with its four elements in the l th row, and the remaining elements are zero. This is exactly as in Fermi's article. We remark that in the secular determinant we can have matrix elements only between such functions which are in the same vertical column of (1).

There are two multiple roots of the secular determinant one of which occurs $2k+2$ and the other $2k$ times. The functions at the extreme right and left correspond to the first of these two roots. This can be calculated first and the remaining root can be ascertained by obtaining the diagonal elements of the subdeterminant formed by the combinations of any other vertical pair in (1). The first root is therefore $\int u_k^{*(1)} w u_k^{(1)} d\tau$. This integral sign is of course understood to include in it a summation over the indices of the matrix eigenfunctions. The operations μ are on the columns and the operations α are on the rows. We are therefore only interested in that part of $w u_k^{(1)}$ which on performing the operations μ involves the index k . This part is due to μ_z and is $(e\mu/r^3) (x\alpha_y - y\alpha_x) u_k^{(1)}$. The remaining operation is entirely on Ψ_1 . Performing it and substituting in the integral it is found that

$$w_1 = \int u_k^{(1)*} w u_k^{(1)} d\tau = (16\pi/3) e\mu \int_0^\infty (\phi_1 \phi_2 / r^2) dr \quad (2)$$

This is therefore one of the roots. The sum of the two roots is $\int [u_{k-1}^{(1)*} w u_{k-1}^{(1)} + u_k^{(2)*} w u_k^{(2)}] d\tau$, with the same understanding about the integral as before. The calculation of the first term in brackets is the same as before with the difference that a factor $(k-1)/k$ is introduced. In the second term the result (2) is obviously obtained but with opposite sign due to the occurrence of Ψ_2 instead of Ψ_1 . The sum of the two roots is therefore

$$w_1 + w_2 = -w_1/k. \quad (3)$$

Hence

$$\Delta\nu = w_1 - w_2 = ((2k+1)/k) w_1. \quad (4)$$

The difference between this result and Fermi's can be expressed by saying that Fermi's

$$\psi^2(0) \rightarrow (2e/\mu_0) \int_0^\infty (\phi_1 \phi_2 / r^2) dr = - (8\pi mc/h) \int_0^\infty (\phi_1 \phi_2 / r^2) dr.$$

Equation (4) is practically exact for any s term; in a Coulomb field the only approximation made being that of supposing the effect of the nuclear magnetic moment to be small.

In applying (4) it must be remembered that ϕ_1, ϕ_2 are supposed to be normalized in such a way that

$$4\pi \int (\phi_1^2 + \phi_2^2) dr = 1 \quad (5)$$

as is obvious from (I). For (1s) terms

$$\phi_1 = -C[1 - (E/mc^2)]^{1/2} e^{-k_0 r}; \phi_2 = C[1 + (E/mc^2)]^{1/2} e^{-k_0 r}. \quad (6)$$

These expressions are substituted into (4), the normalization constant C being determined by (5). The integrals are expressible by means of the Γ function. Using $\Gamma(x+1) = x\Gamma(x)$ and the relations G it is found that the exact quantity which replaces Fermi's $\psi^2(0)$ is (see (4'))

$$(4\pi mc/h)^3 (\alpha^3/8\pi) [2\rho^2 - \rho]^{-1}. \quad (7)$$

Here the first two factors are Fermi's $\psi^2(0)$, and the factor in brackets is a correction due to relativity effects brought in by this calculation.* Substituting (7) into (F)

$$\begin{aligned} \Delta\nu &= 0.0169Z^3(k + \frac{1}{2})(1840\mu/2k\mu_0)[2\rho^2 - \rho]^{-1} \text{ cm}^{-1} \\ &= 2.08(Z/100)^3(k + \frac{1}{2})(1840\mu/2k\mu_0)[2\rho^2 - \rho]^{-1} \text{ volts.} \end{aligned} \quad (8)$$

In order to estimate the order of magnitude of the effect we suppose that $k=9/2$ and that $1840\mu=2k\mu_0$. We find for

	U	Bi	W	Mo
$Z =$	92	83	74	42
$\Delta\nu =$	22.5	12.6	7.31	0.896 volts
$\nu_{K\alpha} =$	(9.395	7.436	5.912	$1.734) \times 10^4$ volts
$\nu_{K\alpha}/\Delta\nu =$	4175	5911	8092	19361

Of these elements Bi is known³ to have a nuclear spin 9/2. It is clear from the above table that for the heavier elements the separation is sufficiently large not to be confused with chemical effects and that the resolving power tabulated in the last row is sufficiently small to make the possibility of experimental detection of $\Delta\nu$ at least hopeful.

In a similar way the separation of 2s terms has been worked out. In this case the correction factor to Fermi's formula is

$$[2/(1 + \rho)]^{3/2} [1 + (2\rho + 2)^{1/2}] \cdot [\rho(4\rho^2 - 1)]^{-1}.$$

* In fact it is readily found that $\psi^2(0) = 1/\pi a_0^3 n^3$ where $a_0 = \hbar^2/(4\pi^2 m Z e^2)$ and n is the total quantum number.

³ E. Back and S. Goudsmit, *Zeits. f. Physik* **43**, 321 (1927); **47**, 174 (1928).

This correction factor is even larger than that derived for 1s electrons. For U it is 3.94. Neglecting screening the splitting of the L_{11} level of U can be expected to be $3.94/2.78 \times (1/8) = 1/5.64$ of the K level splitting. For the lighter elements this fraction approaches $1/8$. It is presumably much less accurate however to apply the present method of calculation to the L electrons because screening effects must be more important here. Their importance may be expected to be least for the heaviest elements. The order of magnitude of the splitting of the L_{11} level of U supposing its nucleus to have a spin $9/2$ and a magnetic moment $9/2$ proton units is 4.0 volts. The frequency of the $L_{11}-M_{21}$ line of the L series is 1221×13.55 volts. For the L series $\nu/\Delta\nu$ is therefore also of the order 4150. This estimate is, however, not as accurate as the one for the K series on account of the screening effects. It is mentioned here only because it is of interest to see that the same order of magnitude of the splitting can be expected for both series and because the L series is more accessible experimentally.⁴

The writer is very grateful to Dr. E. Wigner for an interesting discussion.

⁴ A single observation of the fine structure separation of the K levels gives only $(2k+1)\mu/k$. In order to obtain μ it will be necessary to determine k either by optical means (band spectra, hyperfine structure) or else by observing multiplicities of other X terms, or perhaps by intensity measurements of the hyperfine structure components in the K series.

ON THE REFLECTION OF THE $K\alpha$ LINE OF CARBON FROM A GLASS MIRROR

BY JEAN THIBAUD

LABORATOIRE DE PHYSIQUE DES RAYONS X, PARIS

(Received January 14, 1930)

ABSTRACT

The author recalls previous experiments which he tried in order to determine the limiting angle of total reflection from a glass grating, for a set of radiations between 20 and 65Å, making a slight correction to a recent work of E. Dershem on the reflection of the $K\alpha$ line of carbon. In the case of glass, with $\lambda=44.9\text{Å}$, if we take into account the discontinuities of absorption in the dispersive medium, the Kallman-Mark dispersion formula leads us to a result ($\delta=1-n=5.73\times 10^{-3}$) of the same order as the Drude-Lorentz simplified formula. The reflected intensity from the mirror is calculated from the angle of incidence, account being taken of the absorption. The result is then compared with the experimental curve given by Dershem for the $K\alpha$ line of carbon, and shows that it is possible to determine the critical angle of total reflection from glass ($\theta_m=6^\circ 12'$) and the refractive index ($\delta=1-n=5.84\times 10^{-3}$).

IN a previous work,¹ I have endeavored to determine the critical angle θ_m of total reflection for a beam of soft x-rays (wave-length between 20 and 65Å) by varying the glancing angle of incidence of the beam upon a glass grating and measuring the angles $\theta_{1/2}$ at which the intensity of each line of the spectrum had decreased to one-half value. The conclusions were then: *a.* The reflected intensity does not *suddenly* decrease for a certain angle θ_m : instead of this limit in total reflection, we find for the reflected intensity a somewhat *flattened* curve, the shape of which may be computed by using the Fresnel formulae and taking into account the intense absorption of soft x-rays in the medium.² *b.* An increase in the flattening of the reflection curve is observed, with increase of the wave-length (from $\lambda=45\text{Å}$ to $\lambda=65\text{Å}$). *c.* The $\theta_{1/2}$ angles of half-decreased intensities increase in proportion to the wave-length λ . They are equal to several degrees. $\delta=1-n$ (n =index of refraction) therefore varies as the square of λ .

The simplified form of the Drude-Lorentz dispersion formula seems to be verified:

$$\delta = \frac{e^2}{2\pi m} \frac{N}{c^2} \lambda^2, \quad (1)$$

if we add a numerical coefficient 0.5 in the calculation of $\theta_{1/2}$.

Recently E. Dershem³ has determined the curve connecting the reflected intensity with the glancing angle of incidence for the $K\alpha$ line of carbon and a glass mirror. He concludes that his measures do not confirm my previous

¹ Thibaud, Comptes rendus, 187, 219 (1928).

² Cf: especially: J. Thibaud, Annales Soc. Scientifique Bruxelles, Series B, 48, 167 (1928).

³ E. Dershem, Phys. Rev. 34, 1015 (1929).

results. A mistake has crept in Dershem's paper regarding his interpretation of my results. The θ_m angles in my numerical table are not connected with the complete disappearance of the reflected line (I have assumed for θ_m almost the same number as for the measured angle $\theta_{1/2}$). I insisted rather (see for instance reference 2) upon the gradual decrease of the intensity with increase of angle, and upon the great difficulty of locating with some definiteness the critical angle of total reflection.

The only difference between Dershem's results and mine is that the decrease as a function of the angle in the intensity diffracted by a grating seems more rapid than when determined from an ordinary glass mirror. Prins⁴ has made a remark on this subject. A grating seems thus less fit for an accurate determination of θ_m . At another place⁵ Dershem says that the shape of the curve makes it difficult to determine the limiting angle θ_m and that, on the other hand, it seems doubtful to him whether the index of refraction may be computed from the simplified Drude-Lorentz formula. I wish to discuss further these two points.

1. Kallman and Mark have changed, for the case of x-rays, the dispersion formula as quoted in Eq. (1) into another expression, which takes into account the presence of critical frequencies in the dispersive medium:

$$\delta = \frac{e^2}{2\pi m} \sum \frac{N_i}{\nu^2} = 1 + \frac{\nu_i^2}{\nu^2} n \left(1 - \frac{\nu^2}{\nu_i^2} \right) \quad (2)$$

and which seems to be correctly verified with ordinary x-rays.⁶

I have already pointed out⁷ that the results as computed from Eq. (2) in the case of about 50Å x-rays, the absorption discontinuities being taken into account, show but little difference from the numbers given by the simplified formula (1): the atomic "resonators" for the wave-length considered effect no important disturbance of index.

Let us consider with especial care the case of the reflection of the $K\alpha$ carbon line ($\lambda = 44.9\text{\AA}$) from an ordinary glass mirror.

If we take into account⁸ the K and L discontinuities of the different constituents of glass (Si, O, Na, Ca, etc.), we find by using formula (2):

$$\delta = 5.73 \times 10^{-3},$$

whereas formula (1) would give:

$$\delta = 7.08 \times 10^{-3}$$

which is quite of the same order.

The discrepancy between the results of the two formulae becomes appreciable only for wave-lengths very near (1 or 2Å) to an L , or especially an

⁴ Prins, *Nature*, Sept. 7, 1929.

⁵ Reference 3, p. 1020.

⁶ A. Larsson, *Dissertation*. Uppsala (1929).

⁷ Thibaud et Soltan. *Journ. de Physique* 8, 494 (1927) and: Thibaud, *Phys. Zeits.* 29, 259 (1928).

⁸ The calculation will appear very soon in the *Journ. de Physique*.

M or N discontinuity of one of the constituent elements of the reflecting mirror. But for glass and ordinary metals, the latter case is reached only for radiations of more than 100Å.

2. Reflected intensities may be computed from angles, in the case of a medium strongly absorbing for the radiation, by using the Fresnel equations relative to the components of incident and reflected radiations, which are parallel to the mirror plane. In the case of a complex index⁹

$$n' = (1 - \delta) - i\kappa$$

(κ =extinction coefficient; $\kappa = \mu\lambda/4\pi$; μ =absorption coefficient for λ in the medium). We thus arrive at an expression of the ratio A of reflected and incident intensities as a function of the angle θ ,

$$A = \frac{(1+m)^2 + 2(m^2 + a^2)^{1/2} + 2(1+m)[2(m^2 + a^2)^{1/2}]^{1/2} + a^2 \cos \phi/2}{(1+m)^2 + 2(m^2 + a^2)^{1/2} - 2(1+m)[2(m^2 + a^2)^{1/2}]^{1/2} \cos \phi/2} \quad (3)$$

in which: $\theta = (1+m)\theta_m$; $a = \lambda/2\delta = \mu\lambda/4\pi\theta_m^2$; $\tan \phi = -a(1-\delta)/m$; $\pi < \phi < 2\pi$. The graphic representation of (3) is given on Fig. 1 for different values of the coefficient a between 0.01 and 1.

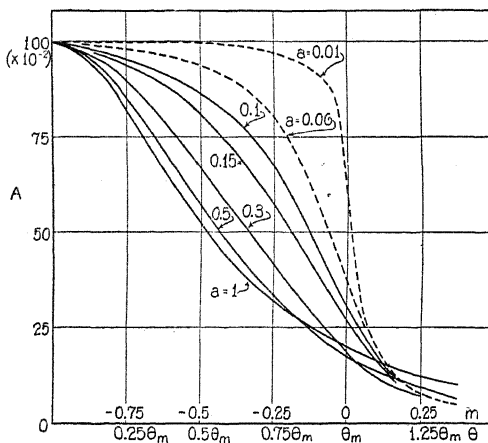


Fig. 1.

It is easy to see, with formula (3), that the reflecting power A_0 connected with the angle $\theta = \theta_m$, goes through a minimum ($A_0 = 0.17$) for $a = 0.5$. Thus, for wave-lengths much longer than 45Å and very strong absorptions μ , one would notice an *increase* in the reflected intensity for angles $\theta > \theta_m$.

The curves show that, in the neighborhood of $a = 0.5$, the reflecting power A_0 suffers only small variations, around 20 percent, and that for $\theta_{1/2} = 0.5\theta_m$, the reflected intensity is about one-half of incident intensity.

In the case of the reflection of the $K\alpha$ line of carbon, from a glass mirror, we have no accurate measurements of the absorption coefficient μ of glass.

⁹ See also: R. Forsler, *Helv. Phys. Acta* **1**, 18 (1927). and J. Prins, *Zeits. f. Physik* **47**, 479 (1928).

The most probable value, as concluded particularly from unpublished measurements of Holweck, is $\mu = 10^5$. If we adopt the above computed value $\delta = 5.73 \times 10^{-3}$, we find: $a = 0.31$.

One may notice a close similarity between the curve $a = 0.3$ (Fig. 1) as computed from (3), with the experimental curve of reflection given by Dershem. For $a = 0.3$ we find $A_0 = 0.19$. The angle θ for which the reflected intensity is reduced to 19 percent of initial intensity is equal, on Dershem's curve to $6^\circ 12'$. It is the critical angle θ_m of total reflection of the $K\alpha$ carbon line from glass. The corresponding value of the index is:

$$\delta = \frac{\theta_m^2}{2} = 5.84 \times 10^{-3}.$$

It is therefore possible to determine, from the experimental curves of reflection, the limiting angle and the refractive index $n = 1 - \delta$. The result is in good accord with the value as deduced from the Kallman and Mark formula (2) ($\delta = 5.73 \times 10^{-3}$). It follows moreover that the extinction coefficient, in the case of the $K\alpha$ line of carbon and glass, is approximately: $\kappa = \alpha \times 2\delta = 3.5 \times 10^{-3}$.

Lastly the curves show that the desired limiting angle θ_m is almost double the angle $\theta_{1/2}$, and thus we find the reason a 0.5 coefficient was to be introduced in my previous researches when θ_m was (arbitrarily) taken equal to $\theta_{1/2}$.

MOLYBDENUM *L*-SERIES WAVE-LENGTHS
BY RULED GRATINGS

By J. M. CORK

DEPARTMENT OF PHYSICS, UNIVERSITY OF MICHIGAN

(Received May 12, 1930)

ABSTRACT

With plane ruled gratings having 30,000 lines per inch and 14,400 lines per inch and grating to photographic plate distances up to a meter in length in vacuo, about 160 plates were taken of the Mo *L*-series lines. The wave-lengths for $L\alpha_1$, and $L\beta_1$, as given by Siegbahn using a gypsum crystal are 5.3943Å and 5.1658Å. If a calcite crystal were employed and approximate correction made for refraction, wave-lengths 5.3960Å and 5.1674Å should be expected, whereas the average of the ruled grating measurements gave 5.4116Å and 5.1832Å. A comparison of the two values leads to an apparent value of the electronic charge 4.8162×10^{-10} e.s.u., being slightly higher than Bearden's value using Cu *K* lines. The possibility of the variation being due to anomalous variation in the refractive index of the crystal is discussed.

THE possibility of the absolute determination of x-ray wave-lengths by means of ruled diffraction gratings, has now been demonstrated.¹ The most precise results so far obtained² indicate that x-ray wave-lengths determined by the ruled grating method are somewhat longer than when determined by the crystal reflection method. Unfortunately, however, agreement regarding the magnitude of this discrepancy is still lacking. Since this wave-length difference may be given the interpretation that the Avogadro number, used in calculating the dimensions of the unit cell in the fundamental crystal lattice, was in error and hence also the value of the electronic charge, its importance is evident. In comparing wave-length values obtained by the two methods, the results from the crystal method should first be corrected for the index of refraction of the crystal. For long wave-lengths, that is, crystals of large lattice constant, this correction is appreciable and it may be further complicated at certain wave-lengths by anomalous effects.

It was the original intention in this investigation to report on the *L* series wave-lengths for the metallic elements from Mo 42 to Ba 56 and several plates were taken for each of these elements, but in view of the significance of the results it was considered more important at this time to carry out an exhaustive study with one of the elements. For various reasons molybdenum was chosen for the target material.

Granting a certain error in setting upon a spectral line in the measurement of the photographic plates, the overall accuracy is increased by having the final result depend upon large distances upon the photographic plate. For a

¹ Compton and Doan, Proc. Nat. Acad. Sci. 11, 598, 1925; Thibaud, Comptes rendus, 182, 55, (1926).

² Wadlund, Phys. Rev. 32, 841, (1928); Bäcklin, Dissertation, Upsala, 1928, Bearden, Proc. Nat. Acad. Sci. 15, 528, (1928).

given wave-length, two main factors contribute to the distance between lines on the photographic plate, namely, the grating constant (i.e. distance between adjacent ruled lines) and the distance between grating and photographic plate. For large displacements the grating constant should be small and the distance between grating and photographic plate large. The dispersion also depends to a slight extent upon the value of the incident grazing angle employed, being greatest when this angle is least. The use of inside spectral orders, that is, those lying between the regularly reflected beam and the diffracted beam parallel to the grating, has been proposed,³ since it leads to very large dispersion when the diffracted beam becomes parallel to the grating. Although this method is eminently satisfactory to show fine structure in this narrow region, its value in the absolute determination of wave-length must not be overestimated. The use of sufficiently large incident angles to give linear displacements on the plate comparable with those of high outside orders is prohibited due to the critical grazing angle for the grating material.

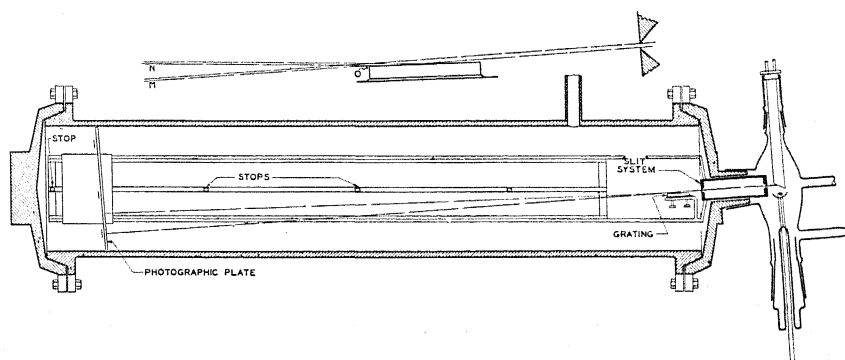


Fig. 1. Diagram of spectrometer and x-ray tube as viewed from above.

APPARATUS

For this wave-length region the complete spectrometer must be in a vacuum with no absorbing layer between the x-ray tube and diffraction chamber. Fig. 1 is a schematic drawing of spectrometer and x-ray tube as viewed from above. The x-ray tube was made of glass and provided with a water-cooled target. The cathode was an activated platinum spiral. Both cathode and anode were removable by ground glass joints. The tube as a whole was mounted on the end of the brass spectrometer tube by a ground glass to metal joint.

Radiation from the target was collimated by parallel slits so as to be incident upon the grating at grazing angles from ten to forty minutes of arc. The slits were approximately 0.05 mm in width and were adjustable in distance from 12 cm to 24 cm. In the adjustment of the grating, part of the collimated beam was allowed to miss the grating surface, giving a

³ Howe, Phys. Rev. 35, 717 (1929).

beam direct to the photographic plate one edge of which was sharply defined by the shadow of the grating edge.

The photographic plate is carried by a plate holder in such a position that the direct beam is incident upon it normally. The plate holder travels upon a heavy grooved track carefully adjusted for parallelism. Four definite positions for stopping are provided by allowing the carriage to make contact with stops, the distances between which were accurately measured upon the same comparator used for the photographic plates. Two positions would have sufficed to determine the distance between plate and grating by triangulation. The photographic plates were changed by removing a metal cap from the end of the spectrometer tube, fitted by ground metal joint.

The slit system, grating and plate holder bed were all a single rigidly connected unit which could be removed completely from the tube without disturbing the adjustment. The containing brass tube had a diameter of 21 cm and a length of 110 cm. The x-ray tube and spectrometer chamber were evacuated by separate mercury vapor pumps with liquid air traps, although gas could pass freely between them through the slit system. The spectrometer tube and the end brass castings were tinned inside and out by immersion for a short time in a bath of molten tin.

The mounting for the grating was provided with adjusting screws so that the grating could be tilted in any direction. In the present investigation four different glass gratings were employed. Three of these were nominally ruled 30,000 lines per inch by Professor R. W. Wood at Johns Hopkins University, while the fourth was a 14,400 line per inch grating ruled at this University by Professor E. F. Barker and Mr. Weyrich.

CALCULATION

The fundamental grating relationship for constructive interference is

$$n\lambda = \pm d[\cos \theta - \cos \phi]$$

where θ is the small grazing incident angle and ϕ is the angle between the diffracted beam and the grating surface. The distance in Angstroms between adjacent ruled lines on the grating is represented by d , and n represents the spectral order. For the regularly reflected beam θ and ϕ are equal, while for outside orders, ϕ exceeds θ and the plus sign is used, whereas for inside orders ϕ is less than θ and the sign is negative.

The dispersion for a given setting of θ then (for outside orders) becomes:

$$\frac{\partial \phi}{\partial \lambda} = \frac{n}{d \sin \phi}.$$

This is not independent of θ since for smaller values of θ the value of ϕ and hence $\sin \phi$ for any particular wave-length becomes smaller.

In the upper part of Fig. 1 is shown an enlarged sketch of the grating with the direct and reflected beam. It is evident that the ray m in the direct beam and the ray n in the reflected beam have a common origin in the edge of the

grating at 0. Thus by measuring on the photographic plate the distance between outside edges of direct and reflected lines and dividing by the distance between the grating edge and photographic plate the $\tan 2\theta$ and hence θ is at once determined.

The origin of the spectral lines is not the edge of the grating but an effective diffracting center which may be as much as a millimeter farther from the plate if a 2 mm width of the ruled surface is employed. To determine the distance between the photographic plate and the effective grating centre, the following procedure is carried out. With some particular x-ray source, spectrograms are obtained for the photographic plate in each of the four positions. By measuring the distance between any pair of these lines sufficiently far apart on any two of the plates and solving by similar triangles the origin or effective center may be located. While two positions would be sufficient, in most cases all four positions were used for confirmation of results. Such spectra for three positions for a molybdenum target are shown in Fig. 2.

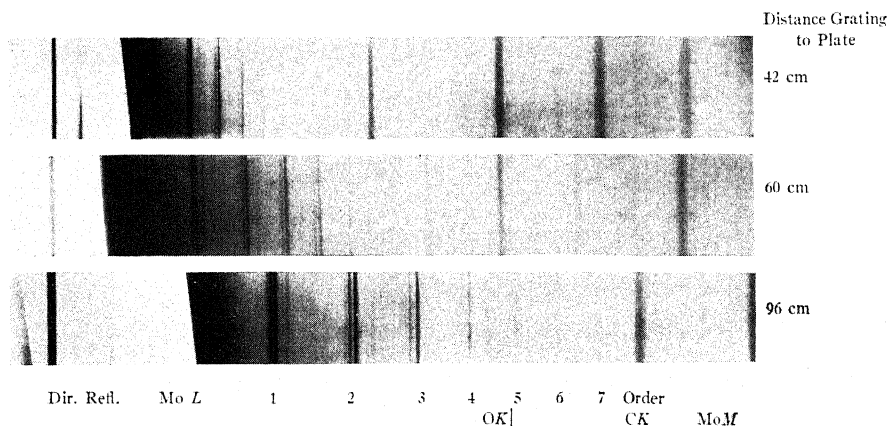


Fig. 2.

Now to calculate wave-lengths, the distance between the outside edge of the direct beam and each spectral line is measured on the comparator. This distance in each case divided by the respective normal plate to grating distance gives $\tan (\theta + \phi)$ and hence the ϕ for any spectral line. Since θ is already calculated for all of the lines the approximate value of λ is at once determined. The term approximate is used, since the edge of a line may be somewhat altered in position by growth of blackening due to over exposure. This does not, however, lead to any error in the final result because the spectral line is observed in many orders, thus on the molybdenum plates shown in Fig. 2 seven orders are available for calculation. Now if the wave-lengths as calculated from the various orders show a systematic variation, the results may be made concordant by the addition or subtraction of a small amount from all observed distances of the spectral lines from the edge of the direct beam. Experience shows that errors in the value of θ by as much as $15''$ of arc,

would automatically be corrected by this same operation, leading always to the same final values of λ when agreement between the various orders is obtained. Thus a real error in the exact location of the edge of the direct beam or of the incident angle θ need, if not too large, produce no appreciable error in final results, if several orders of some spectral line are available on the plate. In making the wave-length calculations, particularly in obtaining the cosines of the small angles, the fifteen place 'Andoyer—Tables Trigonométriques' is invaluable.

RESULTS

The grating constant for the 30,000 line gratings was determined by an optical spectrometer using the strong lines in the mercury arc spectrum as known wave-lengths. The result of this experiment gave the number of lines per inch as 30,011 or d equal to 8,463.3 Angstrom units. This is somewhat at variance with the result obtained by Thibaud⁴ for gratings from the same source, namely 29,972 lines per inch or d equal to 8,477 Angstrom units. This latter value would lead to even longer wave-lengths than those recorded in this paper.

Since the ruling machine was available on which the 14,400 line grating was ruled, it became possible to determine the constant for this grating in another way. This machine employed a wheel having 720 teeth mounted on the head of a screw whose pitch was nominally 1/20 of an inch. If the pitch of the screw therefore were accurately determined this would give the width of 720 lines. A special steel bar was prepared and ruled with light lines, one for every ten revolutions of the screw. This scale was then calibrated in terms of the International meter. The result showed the pitch of the ruling machine screw in the part used to be very uniform and to be 0.050008 inch, such that there were 14,397.6 lines per inch or a value of d equal to 17,641.8 Angstrom units. In all, about 160 plates were taken on molybdenum using the different gratings with different adjustments on each, as well as various plate to grating distances. The average of all calculations are given in Column 1 in the following Table I in Angstrom units.

TABLE I.

	Grating Measurement	Gypsum crystal	Calcite crystal (Calc.)	Corrected for crystal refraction
$\lambda_{\text{MoL}\alpha_1}$	5.4116	5.3943	5.3967	5.3960
$\lambda_{\text{MoL}\beta_1}$	5.1832	5.1658	5.1681	5.1674

The values obtained by the crystal method using a gypsum crystal are given in column 2.* Siegbahn and Hjalmar⁵ have shown that if the ratio

⁴ Thibaud, J.O.S.A. and R.S.I. 17 145 (1928).

* The values of λ published in the abstract of a paper presented at the Chicago meeting of the American Physical Society, Nov., 1930, were, by error, these values from Siegbahn with which the experimental values were compared to obtain the value of e therein given.

⁵ Siegbahn and Hjalmar, Nature 115, 85, (1925).

$d_{\text{calcite}}/d_{\text{gypsum}}$ be obtained with different wave-lengths, a variation in this quantity from 0.39976 at 1A to 0.39959 at 5.5A is observed, with anomalous peaks at 3.06A and 5.01A corresponding to the *K* absorption edges of calcium and sulphur respectively. This relationship may then be employed to calculate what the wave-lengths of the Mo *L* lines would be if measured by a calcite crystal since for gypsum, $d=7.578\text{A}$, was used at all wave-lengths. Such results are given in column 3. These values may now be corrected for the deviation to the Bragg law due to ordinary refraction in the crystal, by the approximate formula, as follows:

$$\lambda = \lambda' \left[1 - 5.4 \frac{\rho d^2}{n^2} \cdot 10^{-6} \right]$$

where λ' denotes the apparent wave-length, n the spectral order, ρ and d the density and lattice constant of the crystal respectively. For calcite this gives a correction factor of 0.014 percent for the first order spectra. Such results are recorded in column 4, and are the values to be compared with those of column 1.

It should be noted that the ratio $d_{\text{calcite}}/d_{\text{gypsum}}$ changes by as much as one half of a tenth of a percent for wave-lengths from 1A to 5A. This variation is of the nature of a difference effect and it may well be possible that the variation in calcite alone may be much greater than this.

The dispersion formula showing the effect of wave-length change upon the index of refraction as developed from polarization theory is as follows:

$$\delta = \mu - 1 = \frac{e^2}{2\pi m} \sum \frac{N_e}{\nu_e^2 - \nu_x^2}$$

where μ represents the index of refraction, N the total number of mobile electrons per cm^3 , N_e the number of electrons per cm^3 having the natural frequency ν_e and ν_x represents the x-ray frequency. For x-rays in which ν_x is large compared with ν_e , the quantity δ is negative leading to a correction to the Bragg law as shown above, i.e. true wave-length less than apparent. Now as the x-ray wave-length increases or as the frequency decreases, the value of δ becomes more negative but upon passing through the *K* absorption limit of calcium the contribution of the calcium *K* electrons changes from negative to positive and at longer wave-lengths δ may actually become positive, in which case the true wave-length will be greater than the apparent.

If possibilities of error due to this variable refractive index be overlooked, the values of column 1 may be compared with column 4 to determine what would be implied regarding the value of the electronic charge. The value of the electronic charge as determined by the oil drop method as corrected by Birge⁶ for best values of the viscosity of air, velocity of light and transformation factors to change from International to absolute electrostatic units is $4.768 \pm 0.005 \times 10^{-10}$ abs. e.s.u. Tempering this value by the consideration of Wadlund's result from x-rays, the most probable value was

⁶ Birge, Phys. Rev. Sup. 1, 40, (1929).

given as $(4.770 \pm 0.008) \times 10^{-10}$ e.s.u. However, in the most accurate determination by calculation, of a fundamental crystal lattice, namely that of calcite by Compton, Beets and DeFoe,⁷ the Avogadro number was assumed to be $(6.0594) \times 10^{23}$ which combined with Birge's most probable value of the Faraday, $(2.89270 \pm 0.00021) \times 10^{14}$ e.s.u. means that e was assumed to be 4.7739×10^{-10} e.s.u. The calcite lattice constant as so computed agreed exactly with the value as used by Siegbahn in his wave-length determinations, namely 3.02904 Å at 18°C.

For the α_1 line the wave-length by ruled grating is 0.288 percent greater than the corrected crystal measurement, while for the β_1 line a difference of 0.304 percent is observed. The average of these values gives for the electronic charge the apparent value of 4.8162×10^{-10} e.s.u. and for the Avogadro number $(6.0062) \times 10^{23}$. This value of the electronic charge is thus even larger than Bearden's value of 4.804×10^{-10} e.s.u. obtained by CuK wave-lengths.

The explanation of this effect as due to a surface contraction as discussed by Zwicky⁸ is unlikely. Such contractions are supposed to be only a few atomic layers deep and certainly many hundred atomic planes must cooperate in the x-ray reflection even up to 5 Angstroms. Also there is good agreement between crystal measurements by the transmission and reflection methods. Furthermore, a surface contraction would have to be interpreted as increasing the discrepancy rather than decreasing it, since instead of multiplying the observed $\sin \theta$ by an average d one should use the smaller surface d .

Attempts to explain the effect by altering the general grating formula for the case of grazing incidence, narrow grating width and ruling defects seem to prove inadequate for differences as large as observed.

⁷ Compton, Beets and DeFoe, *Phys. Rev.* 25, 625 (1925)

⁸ Zwicky, *Proc. Nat. Acad. Sci.* 15, 253 (1929).

THE INDEPENDENCE OF X-RAY ABSORPTION
ON TEMPERATURE

BY J. A. BEARDEN

JOHNS HOPKINS UNIVERSITY, BALTIMORE

(Received May 12, 1930)

ABSTRACT

If the absorption coefficient of x-rays is dependent upon the temperature of the absorber it is pointed out that the effect can be made easily measurable by increasing the thickness of the absorber. Using this method in which the thickness was made very great, measurements have been made on Al, Cu, Fe, Ni, Ag, and Pb. Heterogeneous x-rays were used with voltages from 30 to 80 k.v., also the monochromatic x-ray lines $K\alpha_{1,2}$ of silver and copper were used. All measurements showed no effect of temperature on the absorption coefficients within the probable error involved in the thermal expansion coefficients.

It is also pointed out that the effect of temperature on the absorption of x-rays and γ -rays, as found by previous investigators, was probably due to an error in the determinations of the linear absorption coefficient. When their results are corrected, using the absorption coefficient of the beam transmitted by the absorber, the results are in agreement with the present experiments.

MEASUREMENTS have been reported^{1,2} which indicated a change in the atomic absorption coefficient of x-rays with a change in the temperature of the absorbing screen. In the first¹ series of these measurements using the direct x-rays from a Coolidge tungsten x-ray tube and absorbing screens of Al, Cu, Fe, Ni, Ag, and Pb an increase in the atomic absorption coefficient was observed as the temperature of the absorber was increased. The increase was about 0.2 percent per 100°C up to temperatures near the melting point of the absorber. The second² series of measurements were made using narrow bands of x-rays of various wave-lengths absorbed in Ag and Ni. For some wave-lengths the absorption was greater than the normal absorption and for others it was less. Similar observations³ have been made using γ rays and absorbers of Pb, Fe, Sn, and Al. In each case it was found that the absorption coefficient increased with an increase in the temperature of the absorber. For both γ -rays and x-rays, if the change in absorption is expressed as a linear function of the temperature as $\mu' = \mu(1 + \beta T)$ where μ' and μ are the linear absorption coefficients of the absorber when hot and cold respectively it is found that β is proportional to the thermal expansion coefficient of the absorber.

Existing theories of absorption of x-rays and γ -rays offer no explanation of such an effect. Thus the effect offers a critical experimental check on the theoretical correctness of absorption theories. The present experiments were

¹ Read, Phys. Rev. 27, 373 (1926).

² Read, Phys. Rev. 28, 898 (1926).

³ Bastings, Nature CXIX, 51 (1927), Phil. Mag. 7, 337 (1929).

undertaken with the purpose of making more accurate observations of the change in absorption of x-rays with various wave-lengths and absorbing screens.

METHOD

The expected change in the intensity transmitted by the absorber when cold and hot due to the thermal expansion of the absorber may be calculated as follows:

Let I_0 , I_c and I_h be the intensities of the direct x-ray beam, the beam transmitted by the absorber when cold, and when hot respectively.

Then $I_c/I_0 = e^{-\mu_c x}$

and

$$\frac{I_h}{I_0} = e^{-\mu_h x / (1 + \alpha T)^2} \quad (1)$$

where μ_c and μ_h are the linear absorption coefficients of the absorber when cold and hot respectively, x the thickness, and αT the linear expansion of the absorber. The ratio of intensity transmitted by the absorber when cold and hot is then

$$\frac{I_h}{I_c} = e^{(\mu_c - \mu_h)x + 2\mu_h \alpha T x} \quad (2)$$

For a heterogeneous beam μ_c and μ_h refer to the effective linear absorption coefficient of the beam transmitted by the absorber when cold and hot respectively. This of course would have to be measured by using absorbers of the same material and extrapolating to a thickness equal to the thickness x of the absorber used in Eq. (2). The percentage change in transmitted x-ray intensity is

$$\frac{I_h - I_c}{I_c} = (\mu_c - \mu_h)x + 2\mu_h \alpha T x \quad (3)$$

in this equation μ is really μ_h but since μ and μ_h cannot differ by more than 0.1 percent, the use of the normal absorption coefficient introduces practically no error in the value of $(I_h - I_c)/I_c$.

From Eq. (3) it will be seen that the greatest change in x-ray intensity will be for an absorber of maximum thickness x . Experimentally one must make x such that I_c and I_h are easily measured. For direct radiation from an x-ray tube the area of the collimating slits can be made very great and correspondingly x made larger. In the case of x-rays reflected from a crystal the area is very limited but with water cooled x-ray tubes where the x-ray intensity is very great x can still be made large. It will be noticed in Eq. 3 that a measurement of the intensity I_0 which may be 1000 times I_c or I_h is not needed. In the present experiments I_c and I_h were measured using two exactly similar pieces of metal for the absorbing screen so placed on an eccentric that either could be inserted in the path of the x-ray beam. One piece was placed in a furnace and the other kept at room temperature. After a series of measurements of I_c and I_h had been made the two absorbers

were interchanged and a new set of readings taken. This procedure was adopted to make it possible to obtain I_c and I_h without a time lag and without a change in temperature of slits, sensitivity of electrometer, etc. Previous experiments^{1,2,3} have indicated that

$$(\mu_c - \mu_h)x = \mu_h \alpha T$$

so if one makes x large enough to make $(I_h - I_c)/I_c = 0.1$ or larger the effect of such a change in absorption would change the x-ray intensity by 5 percent or more. Such a change in intensity can be easily measured.

APPARATUS

The high voltage outfit consisted of a regular high voltage transformer (165 k.v. 500 m.a.) connected to a four kenetron full wave rectifier. The kenetrons and all filament transformers were immersed in oil in order to reduce the corona discharge. The source of a.c. was a motor generator set (15 k.w.) with the field of the generator connected to a large capacity storage battery. With this arrangement it was possible to hold the primary a.c. constant to 0.2 percent over a long period of time. Two x-ray tubes were used, one was a water-cooled copper target Coolidge tube, the other a water-cooled silver target Coolidge tube. A thin window (0.01 mm al.) was provided

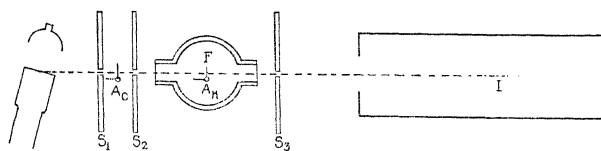


Fig. 1. Diagram of apparatus as used with heterogeneous x-rays. For the $K\alpha_{1,2}$ lines of Ag and Cu a calcite crystal was inserted between S_3 and the ionization chamber.

for the copper target tube to reduce the absorption of the characteristic copper x-rays. The x-ray tubes were operated at 20 to 40 m.a. and 25 to 80 k.v.

The ionization chamber was 7.5 cm in diameter and 30 cm long filled with argon. The electrometer (Compton type) was mounted directly above the chamber in order to reduce the electrical capacity. The sensitivity of the electrometer was about 10,000 division per volt.

The furnace was made up from a heavy wall copper tube 7 cm long with copper top and bottom (Fig. 1). The tube was insulated with asbestos on the top and sides and was heated with a gas flame from the bottom. The openings for the x-rays to pass through were made by inserting brass tubes into the side of the furnace and covering the ends of the tubes with aluminum (0.01 mm thick). The furnace was filled with hydrogen to prevent oxidation of the absorbing screens. The temperature was measured with a 600°C mercury in glass thermometer, placed so the bulb of the thermometer was very near the absorbing screen. The absorbing screen was mounted on a rod (Fig. 1) so it could be placed in or out of the path of the x-rays by rotating the supporting rod from outside the furnace. A long arm was attached to the supporting rod outside the furnace and a stop arranged so the absorber could be rotated

back into exactly the same position for each measurement. A similar method was used for moving the cold absorber in and out of the x-ray beam. In the case of the thin foils it was found necessary to use a frame (made of the same material as the absorber) to hold the absorbers so they would not bend or warp when heated. This was accomplished by making two frames and placing the foil between the frames and then fastening the frames to the rotating support.

METHODS OF MAKING MEASUREMENTS

Three types of radiation were used. First, the copper $K\alpha_{1,2}$ line and the silver $K\alpha_{1,2}$ line reflected from calcite; secondly, the direct rays from the copper and silver targets operated at voltages from 20 to 80 k.v. and third, the direct ray from these tubes filtered through copper and aluminum. The disposition of the apparatus is shown in Fig. 1. The slits were made of lead in the usual manner and were protected by sheets of asbestos from the heat given off by the furnace so that no appreciable expansion took place. When the heterogeneous rays from the tube were used, the slits were 4 mm wide and 2 cm high. In the case of the x-rays reflected from calcite the slits were 1 mm wide and 2 cm high. It will also be noticed that an expansion or shift of slits cannot effect the results taken by this method of comparison. The cold absorber A was placed perpendicular to the x-ray beam. With the furnace cold the angular position of the absorber B in the furnace was adjusted until it absorbed the same amount (to within 1 percent) of x-rays as the absorber A outside the furnace. The furnace was then heated to 600°C and allowed to cool to room temperature again. A series of measurements (usually 10) were then made, alternately placing the absorber A and B in the path of the rays. The furnace was then raised to a temperature 90 to 100°C above room temperature. A series of measurements similar to those made above were then made. This process was repeated advancing the temperature in steps of 90 to 100°C for each series until a temperature of 600°C (except in the case of Pb) had been reached. The process was then reversed and the temperature lowered in similar steps and similar measurements taken until the furnace was brought back to its original temperature (room temperature).

The intensity transmitted by each absorber was never exactly the same so a small correction factor (less than 1 percent) had to be applied in order to obtain the true values of I_c and I_h . The absorption coefficient μ in Eq. (3) was measured by placing A or B in the path of the x-ray beam and then adding thin layers of the same material in the path of the x-ray beam and measuring μ for each layer. By extrapolation the value of μ was obtained for 0 thickness of added absorbers which was the value used in Eq. (3).

The values for the thermal expansion coefficients used were taken from the tables of Landolt and Börnstein, 5th edition.

RESULTS

The results for the heterogeneous x-rays are plotted in the graphs of Fig. 2, in which the values of $I_h - I_c/I_c$ are plotted against the temperature of the

absorber. The solid line is calculated from Eq. (3) in which the term $(\mu_c - \mu_h)x$ has been neglected. The dotted line was calculated assuming that

$$(\mu_c - \mu_h)x = \mu\alpha T$$

which seemed to fit with the experimental measurements of previous experiments.^{1,2,3} The circle represents the experimental values obtained in the

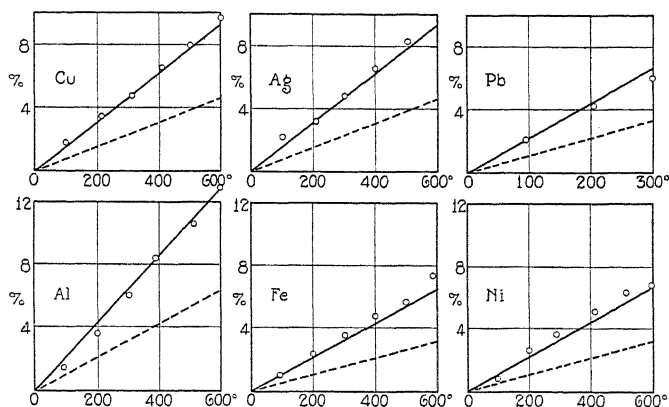


Fig. 2. The experimental points (small circles) were determined with heterogeneous x-rays from a Cu target operated at 50 kv. The solid line is drawn assuming no temperature effect on absorption of x-rays.

present work. It will be seen that the experimental points lie on the solid line within the error of the measurements and the error which must be present in

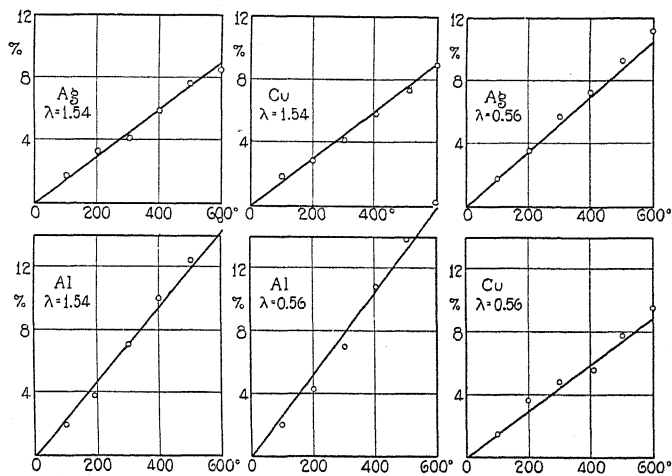


Fig. 3. Same as Fig. 2 except the monochromatic $K\alpha_{1,2}$ lines of Ag and Cu were used.

the thermal expansion coefficients. In the case of aluminum and copper the experimental points seem to be a little higher than the solid line but there

are differences in the thermal expansion coefficients given by various experimenters which would account for the difference observed here. The results using the monochromatic wave-length $K\alpha_{1,2}$ of copper and silver absorbed in silver, aluminum and copper are shown in Fig. 3. In each case the experimental points, as above, agree with the theoretical curve within the error of the measurements and the error involved in the thermal expansion coefficient.

Similar results were obtained using x-rays filtered through copper and aluminum. The x-ray measurements are believed to be more accurate than the thermal expansion coefficients are known. Thus the method may be conveniently used to measure the change in the thermal expansion coefficients with change in temperatures.

DISCUSSION AND CONCLUSION

The change in absorption found by Read in his first experiments¹ using a heterogeneous x-ray beam is undoubtedly due to the use of the wrong absorption coefficient μ in Eq. (3). He measured μ by removing the absorber and measuring I_0 of the direct beam. This gives a value of μ which is entirely too high. It is clear from the way in which Eq. (3) is derived that the correct μ is the μ of the transmitted beam and not that obtained by using the I_0 of Eq. (1). If this were not the case, the change in absorption with temperature would be a function of the thickness of the absorbing screen which obviously cannot be true.

The error in the second series of measurements² is not so apparent. In these measurements, narrow bands of wave-lengths were used so the above effect would be greatly reduced. These measurements seemed to be somewhat erratic and some undetected experimental error must have been present. Precision absorption measurements are extremely difficult to make so that an error of a fraction of 1 percent is easily made. In the measurements of Bastings³ on the temperature coefficient of γ -ray absorption he derives an equation

$$\beta = \frac{n'\mu'd'(1 + 2\alpha T) - n\mu d}{n\mu d T} \quad (4)$$

in which n is the number of atoms per cc, μ is the linear absorption coefficient, d the thickness of the absorber, α the thermal expansion coefficient, T the temperature of the absorber, and the prime letters refer to the absorber when hot. This equation also neglects the change in effective wave-length of the heterogeneous γ -rays in passing through an absorber. Even though there were no change in absorption with temperature it can be shown that Eq. (4) would give $\beta \propto \alpha$ which is what Bastings observes. Substituting the results of Bastings in Eq. (3) using an estimated value of μ from other sources gives no temperature effect within the error of the calculation.

Thus one is lead to the conclusion that there is no effect of temperature on the absorption of x-rays or γ -rays within the error of the present determinations of the thermal expansion coefficient.

THE EFFECT OF AN ELECTRIC FIELD ON THE X-RAY DIFFRACTION PATTERN OF A LIQUID

BY RONALD L. MCFARLAN

RYERSON PHYSICAL LABORATORY, UNIVERSITY OF CHICAGO

(Received April 28, 1930)

ABSTRACT

An investigation is made of the effect produced on the x-ray liquid diffraction pattern by an electric field so designed as to give the Kerr effect for the liquid under examination. The liquid diffraction pattern is obtained by replacing the crystal of a Bragg spectrometer with a cell containing the liquid. The electric field is approximately normal to the x-ray beam. Nitrobenzene is found to show an increase in peak intensity, on applying the field, ranging from four to seven times the probable error of observation, while benzene shows no observable effect. For the type of field used nitrobenzene shows a large Kerr effect, while benzene shows only a slight effect. Theoretical considerations indicate that this effect cannot be due to molecular orientation alone, but that an increase in the regularity of the spatial distribution of molecular scattering centers must occur.

INTRODUCTION

THE form of the x-ray liquid diffraction pattern is usually interpreted as being primarily due to the arrangement of the molecules in the liquid, the arrangement of the atoms in the molecule and the electrons in the atom producing secondary effects. To the space array of molecules producing this pattern one worker has given the name cybotaxis.¹ In attempting to derive a theoretical expression for the observed distribution of intensity in the liquid diffraction pattern Prins² assumes that;

1. The electricity (average electron density) is distributed continuously in each molecule.
2. This electricity vibrates in the plane of incidence of the x-ray wave.
3. The phases of the emitted partial waves from all the elementary volumes must be added in order to calculate the intensity of the diffracted ray for any particular angle of diffraction.

Starting with these assumptions Prins arrives at the following formula for the intensity of the scattered rays as a function of the angle of diffraction.

$$I(s) = N\bar{A}^2 + N\bar{A}^2 \int_0^\infty dr 4\pi r^2 g(r) \frac{\sin sr}{sr} \quad (1)$$

where $s = 4\pi/\lambda \sin \phi/2$, ϕ is the angle of diffraction, r represents the distance from a fixed but arbitrary center, and N is the number of molecules which scatter the x-rays. The scattering power A of a rigid molecule is thought of as localized at this center. The average of the scattering power over all possible

¹ Stewart and Morrow, Phys. Rev. 30, 232 (1927).

² J. A. Prins, Zeits. f. Physik 56, 617 (1929).

orientations of the molecule is indicated by the horizontal line above A . The function $g(r)$, first introduced by Zernicke and Prins,³ describes the distribution of molecular scattering centers throughout the liquid, and is defined in such a way as to make $4\pi r^2 dr g(r)$ represent the probability that a molecular center will lie between a distance r and $r+dr$ from a fixed but arbitrary center. The first term on the right-hand side of Eq. (1) gives the intensity due to N molecules scattering independently. The second term takes account of the interference between the rays scattered by the different molecules, and may have a negative sign.

It is a well-known phenomenon of optics that if certain liquids are placed in a strong electric field they become slightly double-refracting, behaving somewhat like a uniaxial crystal. This experiment was originally performed by J. Kerr,⁴ and is known as the Kerr effect. It has, perhaps, been most successfully explained by the orientation hypothesis as developed, by Langevin Born, and others.⁵ According to this hypothesis when an electric field is applied across a liquid an asymmetry is produced in it as a result of a tendency of the molecules to orient themselves in a definite direction with respect to the field because of the electric moment associated with each molecule. Two factors may contribute to the presence of this moment. In the first place the molecule may not be equally polarizable in all directions, and consequently will endeavor to set itself so that its axis of maximum polarizability is turned parallel to the field. Secondly, there may be a permanent moment associated with the molecule. Both factors are usually present.

Now, if an electric field applied across a liquid produces in the molecules a tendency to orient themselves in a particular direction with respect to the field, and consequently produces an asymmetry in the liquid it might be expected that the angular distribution of the intensity of the scattered x-rays would be altered. Since the liquid diffraction pattern is primarily molecular in origin there are two possibilities to be considered. The first is the effect which the electric field would have on the scattering of the molecules considered separately, while the second is the effect on the distribution of molecular scattering centers throughout the liquid.

CALCULATION OF THE ANTICIPATED EFFECT

The effect of the field on the molecules scattering separately can be considered in the following manner. Assume that the molecules are diatomic, that they have a permanent moment m , and that the scattering power of each atom is located at its center. Then, referring to Fig. 1, the scattered intensity due to the electric vector of the incident beam which is parallel to the plane XOP will be⁶

$$I_{11} = 4\beta A_\phi^2 \cos^2 \left(\frac{4\pi a}{\lambda} \sin \frac{\phi}{2} \cos \alpha \right) = 4\beta A_\phi^2 \cos^2 (x \sin \alpha)$$

³ Zernicke and Prins, *Zeits. f. Physik* **41**, 184 (1927).

⁴ J. Kerr, *Phil. Mag.* **50**, 337 (1875).

⁵ Cf. P. Debye, *Marx Handbuch der Radiologie*, Vol. VI, p. 754

⁶ A. H. Compton, *X-rays and Electrons*, Appendix IV, p. 384.

where $2a$ represents the distance between the atomic centers, $A_\phi = zAe^2 \cos \phi / rmc^2$, z represents the number of scattering electrons in each atom, ϕ is the angle of diffraction, β is a constant defined by $I = \beta A^2$ and $x = 4\pi a / \lambda \sin \phi / 2$.

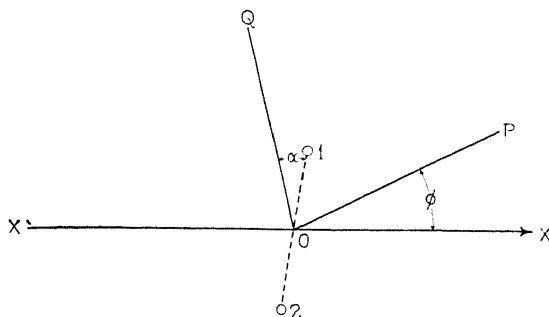


Fig. 1.

If an electric field of strength E is applied in the direction OQ the probability that the moment m will lie in a solid angle $d\Omega = \sin \alpha d\alpha d\psi$ is, according to the Boltzmann-Maxwell law

$$\frac{1}{4\pi} e^{mE \cos \alpha / kT} \sin \alpha d\alpha d\psi.$$

The average intensity of I_{11} that is scattered in the direction ϕ on applying the field E is then

$$\begin{aligned} I_{11} &= \frac{4\beta A_\phi^2}{4\pi} \int_{\psi=0}^{\psi=2\pi} \int_{\alpha=0}^{\alpha=\pi} \cos^2(x \cos \alpha) e^{mE \cos \alpha / kT} \sin \alpha d\alpha d\psi \\ &= 2\beta A_\phi^2 \left[P(x) + \frac{m^2 E^2}{2k^2 T^2} Q(x) \right] \end{aligned}$$

where

$$P(x) = 1 + \frac{\sin 2x}{2x}, \quad Q(x) = \frac{1}{6} + \frac{\sin 2x}{2x} \left[1 + \frac{1}{4x^2} \right] - \frac{\cos 2x}{2x^2},$$

and powers of mE/kT greater than the second are neglected. Following the usual method the total intensity of the scattering at an angle ϕ is found to be

$$I_\phi = 2ZI_e \left[P(x) + \frac{m^2 E^2}{2k^2 T^2} Q(k) \right] \quad (2)$$

where I_e is the scattering at an angle ϕ due to a single electron. It will be seen that the effect should be proportional to the square of the field applied. A similar calculation was carried out for a model of the nitrobenzene molecule in which five CH groups and one NO₂ group were evenly spaced on the circumference of a ring. It was assumed that these groups scattered as units, and that the ring possessed a permanent moment due to the asymmetry produced by the NO₂ group. An intensity formula analogous to Eq. (2) was obtained and as in Eq. (2) $P(x)$ and $Q(x)$ were found to be of approximately

the same order of magnitude. In order to estimate the relative importance of the additional term introduced because of the presence of the electric field let E be taken as 5 k.v. per cm, one of the values used in this experiment, let m be given the value 3.9×10^{-18} e.s.u. as determined by polarization measurements,⁷ let T be taken as 300°K , and k given its usual value 1.39×10^{-16} . The value of $m^2 E^2 / 2kT^2$ then becomes of the order of 10^{-6} . It would thus seem that the effect of the field on the scattering of the molecules considered independently would be very small, probably too small to be detected by the usual methods of measuring intensity.

On the other hand the optical effect of the electric field on the liquid is to make it act as if it were a uniaxial crystal. If the electric field tends to arrange the molecules into something approximating crystalline structure the second term on the right-hand side of Eq. (2) would be affected, in that the distribution function would correspond to an increased regularity in the spatial arrangement of the scattering centers. The effect on the diffraction pattern would be an increase in the intensity of the peak, and also a sharper peak. Thus in looking for an effect of the electric field on the liquid diffraction pattern it would appear best to investigate the peak intensity with and without the field. This has been done in the following experiment.

EXPERIMENTAL PROCEDURE

The cell in which the liquids were put for investigation is shown in Fig. 2. The window was made of cellophane 0.025 mm thick, on the inner side of

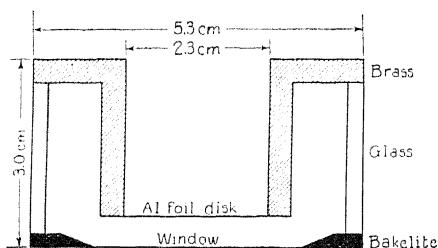


Fig. 2. Diagram of cell.

which aluminum leaf 0.00065 mm thick was fastened. The high potential was applied to the aluminum leaf by means of the electrode E , Fig. 3, and a strip of aluminum foil leading from the electrode to the inner side of the window. Separated from the window by a distance of 3.5 mm was a heavy aluminum foil disk which was grounded by means of the earthed brass back of the cell. The x-rays entering through the window were scattered by the liquid lying between the window and the aluminum foil disk. In this way the field was given the direction OQ of Fig. 1 with respect to the x-ray beam. Fig. 3 illustrates the arrangement of the apparatus used.

In order to apply the field as nearly at right angles to the x-ray beam as possible, since the Kerr effect is observed when the light beam is traveling

⁷ P. Debye, *Polar Molecules*, p. 54.

normal to the field, the ordinary Bragg crystal reflection method was used to obtain the x-ray diffraction pattern. The incident x-ray beam was collimated by a Soller slit set each slit of which was 9 cm long, 1.5 cm high, and 0.045 cm wide. Attached to the front of the ionization chamber and rotating with it was another slit set with slits 6 cm long, 1.5 cm high, and 0.022 cm wide. An adjustable slit, kept at a width of about one mm, was placed between the second slit set and the celluloid window of the ionization chamber. This slit system served to prevent the rays scattered either by the cellophane-aluminum window, or the aluminum disk at the back of the cell from entering the ionization chamber. The chamber was filled with methyl bromide at atmospheric pressure, and the ionization currents were measured by a Compton electrometer adjusted to a sensitivity of 10,000 mm divisions per volt at a scale distance of 3 meters. Unfiltered x-rays obtained from a molybdenum-target tube operated at 35 k.v. and 32 milliamperes were used. The current supplied to the x-ray tube was rectified by means of a full-wave balanced-circuit kenotron rectifier.

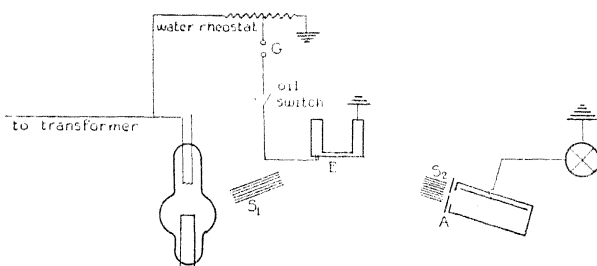


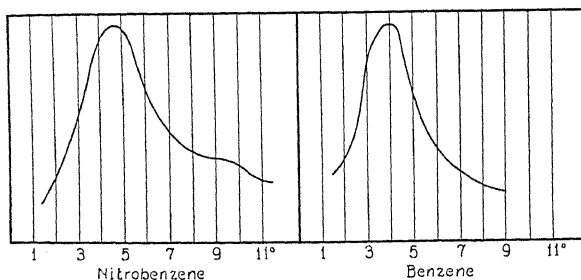
Fig. 3. Arrangement of apparatus.

Since the Kerr effect is most prominent when the electric field consists of a rapid succession of short, sharp peaks it was thought best to look for the effect with the same type of field. In order to synchronize the peaks of the applied field with the peaks of the voltage across the x-ray tube the same high voltage source was used for both. The voltage applied to the cell was stepped down by means of a water rheostat. The peaks of the electric impulses across the cell were sharpened by means of a spark gap, across which a jet of air was blown, inserted between the rheostat and the cell. This device permitted the use of higher fields, and also gave a field more nearly like that used in observing the Kerr effect for nitrobenzene.

With this arrangement the liquid diffraction curves shown in Fig. 4 and Fig. 5 were obtained. These curves do not differ appreciably from the diffraction curves obtained by other methods. They show the same approach toward zero scattering at small angles of diffraction, and the same principal maximum of intensity. The nitrobenzene curve appears to be somewhat broader than the benzene curve.

To observe the effect of the electric field on the diffraction pattern the cell and ionization chamber were set at angles corresponding to the diffraction

peak. The following procedure was observed in taking all readings. The field was applied across the cell, and 45 sec. later an observation of the intensity was made. The field was then removed, and 45 sec. were allowed to



Figs. 4 and 5. Diffraction curves.

elapse before the reading without the field was taken. Alternate readings, with and without the field, were taken in this way for nitrobenzene and benzene.

RESULTS

The results obtained are shown in Table I. The + sign is used to indicate an increase in peak intensity on applying the field, the - sign a de-

TABLE I.

Liquid	Field Applied	Intensity Change	Probable Error
Nitrobenzene	5 kv per cm	+0.8 percent	0.2 percent
Nitrobenzene	9 kv per cm	+2.3 percent	0.3 percent
Nitrobenzene	14 kv per cm	+2.0 percent	0.8 percent
Benzene	9 kv per cm	-0.3 percent	0.3 percent

crease. The probable error listed in each case is the probable error of the arithmetic mean as computed in the ordinary way from least squares theory. The values given for nitrobenzene under fields of 5 k.v. per cm and 9 k.v. per cm, and for benzene represent the average of 100 pairs of readings taken as described above. The change in intensity listed for nitrobenzene under a field of 14 k.v. per cm is the average of 37 pairs of readings, the breaking down of the cell preventing further observations at this voltage. With so strong a field it was difficult to obtain steady conditions, and the results are not as reliable as the others listed.

The same type of field was used for all observations. With this type of field benzene shows only a slight Kerr effect. As is seen the change in peak intensity for benzene is not significant, and is in the direction of lesser instead of greater intensity. This lack of any definite shift for benzene rules out the possibility that the effect observed for nitrobenzene might be due to mechanical causes such as the bending of the cellophane window as a result of electrostatic forces of attraction.

The increase in peak intensity for nitrobenzene appears to be a function of the potential drop across the cell. On the basis of the observations made for the two lower voltages it might appear as if the effect varied approximately as the square of the potential applied. Further experiment is necessary, however, to decide this point definitely. But it is reasonably certain that over a range of field strengths less than 9 k.v. per cm the effect increases with increasing field strength. The observations made at 14 k.v. per cm are not sufficiently accurate to permit any definite conclusions to be drawn from them.

CONCLUSIONS

Since the observed changes in intensity range from four to seven times the probable error, and as mechanical effects do not produce them it seems reasonably certain that the type of electric field described above produces an increase in the peak intensity of the nitrobenzene diffraction pattern. This change is a function of the strength of the field applied, and from the data now available appears to vary as the square of the field strength over a range of potential gradients less than 9 k.v. per cm.

The effect is far larger than would be expected from the orientation of the molecules considered as scattering separately. It would thus appear that molecular orientation alone is not capable of producing the observed change. If, however, the effect of the field is to bring about a more orderly arrangement of the molecular scattering centers with an increased regularity in the spatial distribution of these centers then such an effect as that observed might be expected. Such a tendency toward a crystalline arrangement was the explanation originally advanced by Kerr to account for the effect he observed.

It is possible that the effect just described is not associated with the Kerr effect, and that the correlation obtained for nitrobenzene and benzene is due to the large difference in their permanent moments. Liquids are known with permanent moments of the same order of magnitude as nitrobenzene but which do not show a Kerr effect of the same order of magnitude. Experiments with some of these liquids are desirable in order to gain further information regarding this point.

In conclusion the author wishes to express his appreciation to Professor A. H. Compton for his very helpful advice and his constant interest in the problem.

THE RESOLVING POWER OF CALCITE FOR X-RAYS AND THE NATURAL WIDTHS OF THE MOLYBDENUM $K\alpha$ DOUBLETBY SAMUEL K. ALLISON AND JOHN H. WILLIAMS
UNIVERSITY OF CALIFORNIA, BERKELEY

(Received May 14, 1930)

ABSTRACT

The half widths at half maximum of the rocking curves in parallel positions of the double x-ray spectrometer have been observed for the first five orders of reflection of $\text{MoK}\alpha_1$ from calcite. The calculated half widths for a single crystal have been compared with the theoretical results of Darwin and Ewald. The observed values are of the same order of magnitude as the theoretical, but slightly larger (1.4 times as large in the first order).

The rocking curve widths in 8 anti-parallel positions for $\text{MoK}\alpha_1$ at 50 k.v. have been observed. Geometric corrections arising from the vertical spread of the beam have been applied. The half width at half maximum of $\text{MoK}\alpha_1$ has been found to be 0.147 X.U. corresponding to an energy width of 3.6 volts. The variation of this width with voltage from 25 to 50 k.v. has been studied, and no significant variation found. The half width at half maximum of $\text{MoK}\alpha_2$ at 50 k.v. was observed in 2 positions and found to be 0.161 X.U., the corresponding energy width being 3.9 volts. The observed difference between α_1 and α_2 is close to the experimental error and may not be real. The observed values are 2.5 times as great as the width to be expected from a classical electronic oscillator damped by its electromagnetic radiation.

The computed life of the excited K state of molybdenum is 1.8×10^{-16} seconds. No evidence of fine structure of $\text{MoK}\alpha_1$ or α_2 was obtained.

THIS paper is a report of experiments performed with the double x-ray spectrometer recently constructed in this laboratory. Experiments analogous to those described here have been carried out by Davis and Stempel,¹ Wagner and Kuhlenkampff,² Ehrenberg and Mark,³ Ehrenberg and von Susich,⁴ Davis and Purks,⁵ and Allison.⁶ These experiments will be discussed later in connection with various topics in this report.

APPARATUS

The double spectrometer with which these results were obtained has been described elsewhere.⁷ Constants of the spectrometer, some of which were

¹ Davis and Stempel, *Phys. Rev.* **17**, 608 (1921), **19**, 504 (1922).

² Wagner and Kuhlenkampff, *Ann. d. Physik* **68**, 369 (1922).

³ Ehrenberg and Mark, *Zeits. f. Physik* **42**, 807 (1927).

⁴ Ehrenberg and von Susich, *Zeits. f. Physik* **42**, 823 (1927).

⁵ Davis and Purks, *Proc. Nat. Acad. Sci.* **13**, 419 (1927), **14**, 172 (1928), *Phys. Rev.* **34**, 181 (1929).

⁶ S. K. Allison, *Phys. Rev.* **34**, 176 (1929).

⁷ Williams and Allison *J.O.S.A. and R.S.I.* **18**, 473 (1929). Opportunity is taken here to point out some errors in this paper. The equation on page 474 is only approximately true, the correct expression being Eq. (1) of the present paper. On page 475 the tube holding the slits is stated to be 35 cm long whereas it actually is 30 cm. It is also stated that "the horizontal width of the slits can be adjusted to give the maximum resolving power" whereas the resolving power of the double spectrometer is independent of the slits mentioned.

not previously given, are as follows: distance from the focal spot of the x-ray tube to the first crystal (crystal *A*), 53 cm; distance between the axes of crystals *A* and *B*, 19 cm; distance from the axis of crystal *B* to the ionization chamber window, 4.5 cm; length of the ionization chamber, 40 cm; diameter of the chamber, 4.3 cm. The ionization chamber was filled with a mixture of ethyl bromide and argon at partial pressures of 17 cm and 59 cm respectively. The slit for admitting x-rays into the ionization chamber was 3 mm wide.

Two slit systems were used simultaneously which will be referred to as the horizontal and vertical slits respectively. The vertical slits limited the spread of the beam in a horizontal plane (more generally, a plane perpendicular to the axes of rotation of crystals *A* and *B*). The horizontal slits limited the spread of the beam in a vertical plane (one including the axes of rotation). The vertical slits were 30 cm apart and each 1.5 mm in width. The horizontal slits were 30.95 cm apart. The widths used for them will be given later.

Molybdenum target tubes supplied by the General Electric Company for crystal analysis work were used. In these tubes the face of the target is normal to the impinging electron beam which lies in the long axis of the tube. The radiation used in the spectrometer was taken at a glancing angle of 8° from the target face. It will be shown later that this is not the most desirable arrangement for the double spectrometer. The tubes were cooled by pumping kerosene through the targets.

The high potential for operating the tubes was supplied by a 550 cycle transformer-kenotron-capacity set in which the calculated voltage fluctuations at 50 k.v. and 20 milliamperes tube current were 1.8 percent. The voltages were read on a high voltage electrostatic voltmeter which had been calibrated by measuring the short wave-length limit of the continuous spectrum.

The electrometer has been described in a previous paper.⁷

The calcite crystals used were freshly cleaved from an optically clear parallelepiped whose surfaces were cleavage planes, by placing a razor blade as accurately as possible parallel to the cleavage direction and tapping it sharply with a light hammer. The faces from which the x-rays were reflected were the fresh faces from a single fracture and were rhombs whose sides were 1.9 cm long. These faces were not by any means optically flat. Close inspection showed that the fracture had not been all in one plane but that there were very thin "steps" on the crystal face. The holders for the crystals could be slipped out of the dove-tailed guides⁸ and replaced in them without changing the orientation of the crystals more than about 10 seconds of arc about a vertical axis. The crystals were removed in this manner after each set of readings and placed in a dessicator over dehydrated calcium chloride and a few sticks of sodium hydroxide. This was done to safeguard the fresh surfaces from attack by acid fumes which might be in the

⁸ See reference 7, Fig. 2 p. 476. The springs *K* were unhooked, and *E* and its superstructure slid out of *F*.

air. There was no evidence of deterioration of the surfaces during the period of observation.

A thermometer which could be read to a few hundredths of a degree centigrade was placed over the spectrometer and read at frequent intervals while working in anti-parallel positions.

ADJUSTMENTS

It is convenient to speak of a "central ray" which may be defined as a ray passing through the geometric centers of the slit apertures. The adjustment of the instrument must insure the following conditions.

- (1) The central ray must pass through the center of the focal spot of the x-ray tube.
- (2) The central ray must intersect the reflecting surface of crystal *A* near its geometric center.
- (3) The axis of rotation of crystal *A* must intersect the central ray at the point where the ray intersects *A*'s surface.
- (4) The axis of rotation of crystal *A* must lie in its reflecting surface.
- (5) The central ray, after reflection from crystal *A*, must intersect the reflecting face of crystal *B* near its geometric center.
- (6) The axis of rotation of crystal *B* must intersect the central ray at the point where the ray intersects *B*'s surface.
- (7) The axis of rotation of crystal *B* must be parallel to that of *A*.
- (8) The axis of rotation of crystal *B* must lie in its reflecting surface.
- (9) The central ray after reflection from crystal *B*, must enter the ionization chamber through the center of its slit and pass down the long axis of the chamber.

A necessary condition for the fulfillment of these requirements is that the central ray, the focal spot of the tube, the geometrical centers of the reflecting faces of the crystals and the axis of the ionization chamber lie in the same (horizontal) plane. This is accomplished partly in the original construction of the instrument and partly in the judicious placing of the crystals on their holders.

The spectrometer was levelled by means of levelling screws. The reflecting face of *A* was made vertical as follows. A cathetometer carrying a horizontal slit system was set up about 150 cm from the axis of *A*. The cathetometer was used merely as a rigid support for the slit system. The horizontal slit system of the cathetometer could be rotated about a horizontal axis until its central ray was horizontal to within 30 seconds of arc. This was accomplished by means of a sensitive spirit level. A parallel beam of light from an arc-lens combination was sent through the slits carried by the cathetometer and reflected from crystal *A*. The cathetometer was set in such a position that the reflected beam from the surface of *A* almost coincided with the incident beam. By means of a set screw in the crystal holder,⁹ *A* was tilted about a horizontal axis until the beam reflected from it was in the same horizontal plane as the

⁹ See reference 7, Fig. 2 476. *R* is the set screw referred to here.

incident beam. Due partially to the step-like structure of the cleavage surfaces previously mentioned, the reflected beam was not perfectly defined and this allowed an error of perhaps 2 minutes of arc to remain in the verticality of *A*.

The vertical slit system of the spectrometer was then made vertical by a plumb line or by setting an accurate right angle on the upper flat surface of the spectrometer and sighting past its vertical arm through the slits. The mechanism for closing the jaws of the vertical slits was such that they necessarily opened symmetrically about the central ray. The slits were then made about 0.05 cm wide and a beam of light from an arc sent into the spectrometer. This beam was observed on a ground glass or other translucent material after it had passed the axis of crystal *A*. Crystal *A* was then translated horizontally and rotated about its vertical axis until the ground glass showed that its face, when parallel to the light beam, extended just halfway into it. The crystal was then rotated through 180°. In this new position it did not, in general, again bisect the beam. Half of the adjustment necessary was taken up by rotation of the slit system about a vertical axis and half by translation of *A* horizontally and rotation about its vertical axis. *A* was then rotated through 180° again and the process repeated. By this method requirements (2), (3), and (4) of the preceding list could be satisfied.

In the adjustment of crystal *B* it was assumed that in the construction of the instrument requirement (7) has been met. It will be seen that this uncertainty may be a cause of error in the curves obtained in parallel positions. Crystal *A* was removed from the spectrometer. Crystal *B* was made vertical by the cathetometer method, and the arm carrying *B*'s axis of rotation (this arm revolved about the axis of *A*) was set so that the beam of light from the spectrometer slits passed approximately over *B*'s axis. The accurate adjustment was made similarly to that of *A* by repeated rotations of *B* through 180°. In this case the arm carrying the axis of *B* and the horizontal translation of *B* were adjusted until the surface of *B* was half-way across the beam at positions 180° apart. In this way requirements (5), (6), (7), and (8) were satisfied. In subsequent settings of the instrument the arm carrying the axis of *B* was rotated through twice the angle that the crystal *A* was turned around its axis.

The ionization chamber was set by noting where the beam of light entered its window. Later the position corresponding to requirement (9) was more accurately found by moving the ionization chamber across the reflected beam of x-rays from crystal *B* and setting it at the center of the angular range through which radiation entered its window.

When the adjustments of crystals *A* and *B* and the preliminary adjustment of the ionization chamber had been made the x-ray tube and horizontal slits were put in place. By means of a fluorescence screen it was ascertained that the x-ray beam (which in the actual experiments had a rectangular cross section about 0.15×0.1 cm at crystal *A*) was horizontal. The vertical slits were then further narrowed and the instrument used as a single crystal spectrometer with only crystal *A* in use. An emission line of the target was

found and the x-ray tube shifted horizontally until the maximum intensity was obtained. This made certain that the central ray passed through the most intense part of the focal spot of the tube.

PURPOSE OF THE EXPERIMENTS

The purpose of the experiments can best be understood by a brief outline of the theory of the instrument. A notation for the double spectrometer has been suggested by the authors in a previous paper.¹⁰ This notation has been of the greatest service in guiding the course of the experiments and will be retained. A fundamental expression for the instrument is that the dispersion D may be written as follows:

$$D \equiv \frac{d\theta_B}{d\lambda} = \frac{n_A}{2d \cos \theta_A} + \frac{n_B}{2d \cos \theta_B} \quad (1)$$

in which the meaning of the symbols and the convention as to sign of n_B have been previously given.¹⁰ n_A is to be considered always positive. n_B is negative when the first incident and last reflected rays are on opposite sides of the first reflected ray,¹¹ otherwise it is also positive. A setting of the instrument is described by giving the values of n_A and n_B in the form (n_A, n_B) and of the wave-length reflected. Eq. (1) is derived by differentiation of the Bragg law and addition of the dispersions of the crystals.

The second equation for the double spectrometer that we shall consider here gives the observed width of the rocking curve for any line in the spectrum at any setting of the instrument. We will temporarily assume that geometric widths due to slit heights and deviations of the crystals from verticality have been made negligibly small. We then have¹²

$$W = (W_A^2 + W_B^2 + D^2 W_\lambda^2)^{1/2}. \quad (2)$$

In this equation, W represents the half width at half maximum in angular measure of the observed rocking curve, W_A the half width at half maximum in angular measure of the curve (assumed Gaussian error curve) representing the intensity of reflection from crystal A as a function of the deviations from the Bragg angle, W_B is the analogous quantity for crystal B , D is defined in (1) and W_λ is the half width at half maximum of the line in question in linear measure. In the derivation of (2) it is assumed that the line has a Gaussian error curve distribution of intensity.

From Eqs. (1) and (2) it is seen that the positions of the double spectrometer naturally fall into two classes, so-called parallel and anti-parallel positions. Parallel positions are distinguished by having $D=0$, or $n_B = -n_A$. If $D=0$ in Eq. (2) we see that the observed width is due to the angular range through which a crystal may be turned and reflect a single wave-length, in

¹⁰ Allison and Williams, *Phys. Rev.* **35**, 149 (1930). The interpretation of negative values of D from Eq. (1) is also found here.

¹¹ Schwarzschild, *Phys. Rev.* **32**, 162 (1928).

¹² Schwarzschild, reference 11. This equation may be obtained by combining Eqs. (43) and (45) of his paper. Important special cases of this equation had been previously developed by Ehrenberg and Mark, reference 3.

other words, the widths in such positions are closely related to the limit of resolution of the instrument. Anti-parallel positions have $D \neq 0$ and are all positions for which $n_A \neq -n_B$. From Eq. (2) it is seen that the rocking curves in such positions include, in addition to the factors giving the widths in parallel positions, contributions from the widths of the spectrum lines themselves.

RESULTS IN PARALLEL POSITIONS

If $D = 0$ in Eq. (2), it becomes

$$W = (W_A^2 + W_B^2)^{1/2}. \quad (3)$$

If we now assume that $W_A = W_B = W_c$ we may write this

$$W = 2^{1/2} W_c \quad (4)$$

where W is the observed width and W_c the interference pattern width from a single crystal.

We have investigated the values of W for the reflection of $\text{MoK}\alpha_1$ in the first five orders from the cleavage face of calcite. If the adjustments previously described were not perfect, there would be an appreciable width to the rocking curve in these positions due to geometric causes, that is, there would be a width even if the width of the interference pattern of the crystals were zero. It has been shown by Schwarzschild¹³ that this width would be

$$\delta\theta'_B = \frac{2\phi(\delta_A + \delta_B)}{\cos \theta} \quad (5)$$

where $\delta\theta'_B$ is the angular range in parallel positions through which crystal B may be turned and yet reflect some of the radiation sent to it by A . δ_A and δ_B are the angular deviations of the reflecting faces of crystals A and B from verticality, θ is the glancing angle, (the same for both crystals) and ϕ is one half of the maximum angle between any two rays in a plane parallel to the axes of rotation of the crystals. Eq. (5) is derived on the assumption that the axes of rotation of crystals A and B are parallel.

In our experiments it was found that the widths of the rocking curves in parallel positions were very sensitive to deviations from verticality of the crystals. The method of setting for verticality previously described was not sufficiently accurate in general to produce the narrowest curves. The following procedure was adopted. The face of crystal A was set vertical within the limits of accuracy of the cathetometer method. (The reflected light beam was somewhat sharper from A than from B). Crystal B was then set vertical within the limits of error and a rocking curve taken. B was then rotated in small steps¹⁴ around a horizontal axis (a minute of arc at a time) and rocking curves taken for each position until a minimum width was found. If at this position δ_A and δ_B are zero, then from Eq. (4) the width observed should be

¹³ Schwarzschild, reference 11. see Eq. (24) of his paper in which $R = 2(\delta_\alpha + \delta_\beta)/\cos \theta$ and $\phi = s/L$

¹⁴ See the figure mentioned in reference 9. The screw R is used.

independent of ϕ . Several experiments were made to test this by changing the value of ϕ after the position of minimum width had been found. ϕ was varied by varying the width of the horizontal slits. The maximum value of ϕ was limited by the height of crystal *B* and was about 0.015.

TABLE I. Minimum half width at half maximum in parallel positions as a function of ϕ . $\text{MoK}\alpha_1$.

Position	ϕ	Observed <i>W</i> seconds
(1, -1)	.015	3.0
(1, -1)	.012	3.0
(2, -2)	.015	1.0
(2, -2)	.0072	1.1
(2, -2)	.0054	.90

Table I shows that from a value of ϕ of 0.0054 to a value of 0.015 the changes in the width of the rocking curve observed were within the limit of error to which a given experiment could be duplicated. The low intensity of reflections such as (4, -4) and (5, -5) made the use of the larger value of ϕ very desirable and Table I seems to justify this procedure.

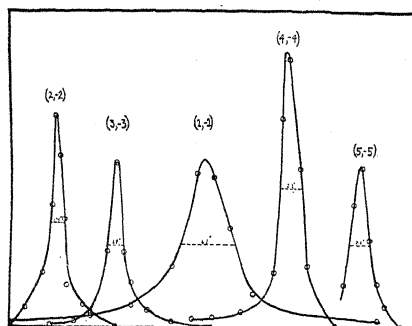


Fig. 1. Observed rocking curves in parallel positions. Ordinates are proportional to ionization currents, abscissae to angular settings of crystal *B*. The vertical scale is not the same for all the curves.

Fig. 1 shows some of the rocking curves obtained, and in Table II the half widths at half maximum, together with the values of W_c calculated from Eq. (4) are listed.

TABLE II. Minimum half widths at half maximum in parallel positions. $\text{MoK}\alpha_1$

Position	<i>W</i> (seconds)	<i>W_c</i> (seconds)
(1, -1)	3.0	2.1
(2, -2)	.90	.64
(3, -3)	.95	.67
(4, -4)	1.1	.78
(5, -5)	1.2	.88

DISCUSSION OF RESULTS IN PARALLEL POSITIONS

Sources of error. Probably the most important source of error in the values of Table II arises from a possible lack of parallelism of the vertical axes around which *A* and *B* were rotated. Unfortunately the apparatus was designed in such a manner that these axes were rigid with respect to each other and no adjustment could be made. Other sources of error are (1) irregularities in the slow motion screw moving *B*; (2), temperature differences between crystals *A* and *B*. No evidence of irregular motion of *B* was obtained; rotation in regular steps of one-half second of arc seemed possible. Although variations in the temperature of the room of a few tenths of a degree centigrade sometimes occurred while a curve was being taken, the possibility of significant temperature difference between the two crystals (19 cm apart) seems excluded.

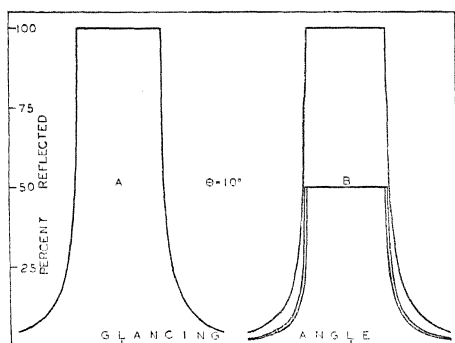


Fig. 2. A. Theoretical reflection curve from a perfect crystal for polarized x-rays (Eq. (6) and (7) and (8), or Eq. (9) and (7) and (8)). B. Theoretical reflection curve for unpolarized rays. The innermost curve represents the reflection of the component whose electric vector lies in the plane of incidence. The intermediate curve represents reflection of radiation polarized so that its electric vector lies perpendicular to the plane of incidence. The outermost curve is the sum of these components.

Comparison with theory of a perfect crystal. The reflection of plane waves from a so-called perfect or ideal crystal in which there is no warping or mosaic structure has been theoretically studied by Darwin¹⁵ and Ewald.¹⁶

Plane, monochromatic waves fall on an idealised crystal made up of electrons lying on planes separated by a constant distance. The radiation is polarized in such a plane that the electric vector lies perpendicular to the plane of incidence. Fig. 2a shows the intensity of reflection to be expected as a function of glancing angle. The curve is symmetrical about a glancing angle which may be obtained from that calculated by Bragg's law by correcting for the index of refraction. The extent of the region of 100 percent reflection is given by

$$\Delta\theta = 4\delta \operatorname{cosec} 2\theta \quad (6)$$

¹⁵ Darwin, Phil. Mag. 27, 325 and 675, (1914).

¹⁶ Ewald Phys. Zeits. 26, 29 (1925).

where $\Delta\theta$ is the range of glancing angle θ ; δ is the deviation of the index of refraction from unity. Outside the region of perfect reflection, the intensity falls off rapidly. The equation of the curve in these regions is given by

$$I_{\theta'-\theta} = I_0 \left(\frac{\Delta\theta}{2(\theta' - \theta) + (4(\theta' - \theta)^2 - \Delta\theta^2)^{1/2}} \right)^2, \quad \theta' - \theta > \frac{1}{2}\Delta\theta \quad (7)$$

$$I_{\theta'-\theta} = I_0 \left(\frac{\Delta\theta}{2(\theta' - \theta) - (4(\theta' - \theta)^2 - \Delta\theta^2)^{1/2}} \right)^2, \quad \theta' - \theta < -\frac{1}{2}\Delta\theta \quad (8)$$

where $I_{\theta'-\theta}$ is the intensity at a glancing angle θ' , I_0 is the incident intensity, and $\Delta\theta$ is defined by Eq. (6). If $I_{\theta'-\theta}/I_0$ is set equal to $\frac{1}{2}$ in Eq. (7), and the half width at half maximum calculated it is found to lie at a value of $\theta' - \theta$ equal to $1.06\Delta\theta/2$.

If the incident radiation is plane polarized in such a manner that the electric vector lies in the plane of incidence, the analogous equation to Eq. (6) is

$$\Delta\theta = 4\delta \cot 2\theta. \quad (9)$$

The radiation used in these experiments was a characteristic emission line of the target, known to be unpolarised. We may consider the unpolarised incident light resolved into two components, with electric vectors parallel and perpendicular to the plane of incidence. The intensity of each one of these components will be half the incident intensity. The reflection curve for unpolarised incident rays will then be the sum of two curves given by Eqs. (6) and (9) and the Eqs. (7) and (8) appropriate to each. Such a curve is shown in Fig. 2b.

The half width at half maximum for the unpolarised curve will be slightly greater than $2\delta \operatorname{cosec} 2\theta$ by a factor which approaches 1.06 as the glancing angle is decreased and falls off to unity at larger glancing angles. As will be seen later this correction is less than the uncertainty in the structure factors involved and will therefore be disregarded.

For a real crystal, the electrons are of course not situated on equidistant planes but are distributed throughout the structure. In this case the formula for the half width at half maximum for unpolarised radiation becomes

$$2F\delta \operatorname{cosec} 2\theta/Z \quad (10)$$

where

$$F = \sum_i F_i e^{2\pi ni(hx_i + ky_i + lz_i)}. \quad (11)$$

In the preceding equations, F is the structure factor, or equivalent reflecting power of the Z electrons in the unit cell of the crystal, F_i is the ionic structure factor, n is the order of reflection, h, k, l are the Miller indices of the plane, and x_i, y_i, z_i are the coordinates of the atom i in the unit cell.¹⁷ The unit cell of

¹⁷ Our thanks are due Professor Linus Pauling for his aid in calculating the structure factors given here.

calcite contains two molecules of CaCO_3 . Its sides are not parallel to those of a natural cleavage parallelepiped, so that the Miller indices of a plane in the true unit and the cleavage unit are not the same. The cleavage plane, which has indices (100) in the cleavage unit, has indices (211) in the true unit,¹⁸ and these are the values to use in Eq. (11) for hkl . The ionic structure factors for calcium and oxygen were taken from Bragg and West.¹⁹ The ionic structure factor for carbon was assumed to be one-fourth of that for oxygen. The calculation of the structure factors used is indicated in Table III.

TABLE III. Structure factors for (100) planes of calcite for $\text{MoK}\alpha_1$.

Order	$(\sin \theta)/\lambda$	F_{Ca}	F_{C}	F_{O}	F
1	0.165	15.1	1.8	6.6	$2(F_{\text{Ca}} + F_{\text{C}} + F_{\text{O}}) = 47.0$
2	.330	10.5	.9	3.3	$2(F_{\text{Ca}} + F_{\text{C}}) - 2F_{\text{O}} = 16.2$
3	.495	7.6	.4	1.7	$2(F_{\text{Ca}} + F_{\text{C}} + F_{\text{O}}) = 19.4$
4	.660	5.9	.2	.9	$2(F_{\text{Ca}} + F_{\text{C}}) + 6F_{\text{O}} = 17.6$
5	.825	4.5	.1	.5	$2(F_{\text{Ca}} + F_{\text{C}} + F_{\text{O}}) = 10.2$

The theoretical half widths at half maximum for the unpolarised $\text{MoK}\alpha_1$ radiation from calcite may now be found by inserting the values of F from Table III in Eq. (10), using $Z=100$. The value of δ taken from A. H. Compton²⁰ is 1.84×10^{-6} . In this way the theoretical values of Table IV were obtained, in which experimental values due to Davis and Purks²¹ are included.

TABLE IV. Comparison of theoretical and observed values of W_c (Eqs. (10) and (4)). $\text{MoK}\alpha_1$

Order	W_c Theory Eq. (10)	W_c Exp. Eq. (4)	W_c Davis and Purks
1	1.5 sec.	2.1 sec.	1.6 sec.
2	.28	.64	.45
3	.22	.67	
4	.16	.78	
5	.08	.88	

The values of Table IV are shown graphically in Fig. 3. It is seen that the crystal reported by Davis and Purks has very nearly the predicted half width for a perfect calcite crystal, while those used in this investigation were less perfect on this criterion. It is interesting to note that the theory gives results which agree well with experiment for the widths of the curves, although it is known that the intensity predictions are not verified.

¹⁸ Strukturbericht of the Zeits. für Krystallographie, pp. 292-295.

¹⁹ Bragg and West, Zeits. f. Krystallographie **69**, 118 (1928).

²⁰ A. H. Compton, X-rays and Electrons, p. 218 Table VII-2.

²¹ Davis and Purks Phys. Rev. **34**, 181 (1929). These investigators state that their observed widths are less than those predicted for a perfect crystal. They used a theoretical formula, however, in which an effective width had been calculated for the purpose of expressing the reflected energy as the product of the incident intensity by this effective region of 100% reflection.

RESULTS IN ANTI-PARALLEL POSITIONS

In the nomenclature which we have adopted for the instrument, D is finite in anti-parallel positions. The total geometrical width in anti-parallel positions is given by the formula

$$\delta\theta_B = \frac{1}{2}D\lambda\phi^2 \quad (12)$$

in which $\delta\theta_B$ is the *total* angular range through which crystal B can be turned while reflecting the wave-length λ .²² Since what we have measured is the half width at half maximum, the correction for geometric width should not be the entire amount of Eq. (12). The purely geometric rocking curve corresponding to Eq. (12) is not symmetrical about its maximum.²³ Its shape depends on the

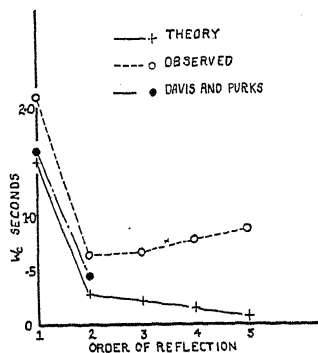


Fig. 3. Comparison of observed and calculated values of the half width at half maximum of the reflection curve from calcite.

intensity of the bundle of parallel rays passing through the slits and making an angle α with the central ray in a vertical plane relative to that of the bundle of rays proceeding parallel to the central ray. This will be referred to as the variation of intensity with vertical divergence of the beam. If the widths of the horizontal slits are h_1 and h_2 , ($h_2 \geq h_1$), and the distance between them is L ,

$$\phi = (h_1 + h_2)/2L. \quad (13)$$

ϕ calculated from Eq. (13) gives the upper limit of α . If we neglect variations of intensity in the focal spot itself, we may assume that the intensity of a parallel bundle of rays is proportional to its cross-section area. This gives

$$I_\alpha = I_0 \text{ for } 0 < \alpha < (h_2 - h_1)/2L \quad (14)$$

$$I_\alpha = I_0(h_1 + h_2)(1 - \alpha/\phi)/2h_1 \text{ for } h_2 - h_1/2L < \alpha < \phi. \quad (15)$$

²² Eq. (12) occurs in Schwarzschild's paper as $\frac{1}{2}(\tan\theta_1 \pm \tan\theta_2)\phi^2$. It does not, of course, express the entire geometric width if the crystal faces and axes are not vertical. The percentage contribution to the geometric width from lack of verticality is much less in anti-parallel than in parallel positions due to the preponderating influence of the natural line breadths. In our experiments it was found by trial that using the cathetometer and horizontal slits we could set the crystals so nearly vertical that the minimum width was obtained at once in anti-parallel positions, although, as has been previously stated, this was not true in parallel positions. For this reason we do not include a term involving verticality corrections in Eq. (12)

²³ See Schwarzschild, reference 11, p. 166, Fig. 3b curve D. This curve corresponds to a function $I_\alpha = I_0(\phi - \alpha)$, or to horizontal slits of equal width.

In the preceding equations, I_α is the intensity of a bundle of parallel rays having a vertical angular divergence α ; I_0 is the intensity of the bundle of rays parallel to the central ray. Due to geometric causes alone, as crystal B is rotated from the position in which the central ray makes the angle of best reflection for a certain wave-length, other vertically divergent rays also can make this glancing angle and be reflected. If ξ is the angular deviation of crystal B from the position of reflection for the central ray, and α the vertical divergence of the bundle of rays making the correct angle for reflection at ξ ,

$$\xi = \frac{1}{2}D\lambda\alpha^2 \quad (16)$$

We wish to find the value of ξ at which this geometric rocking curve comes to half maximum. If we set $I_\alpha/I_0 = \frac{1}{2}$ in Eq. (16) and solve for $\alpha_{1/2}$ we find

$$\alpha_{1/2} = h_2\phi/(h_1 + h_2) \quad (17)$$

and substitution in Eq. (16) gives

$$\xi_{1/2} = \frac{1}{2}D\lambda\phi^2 \left\{ \frac{h_2}{h_2 + h_1} \right\}^2. \quad (18)$$

In correcting our results for geometric width in anti-parallel positions we have subtracted the values of $\xi_{1/2}$ calculated from Eq. (18) from our observed full widths at half maximum.

The temperature correction. In their paper on the natural widths of x-ray lines Ehrenberg and von Susich noted effects on the widths of the rocking curves in anti-parallel positions which they ascribed to a change in temperature of the crystals while the readings were being taken. It is easily shown that

$$d\theta_B/dT = -a\lambda D \quad (19)$$

where $d\theta_B$ is the angular range on crystal B corresponding to a temperature change dT . The negative sign has the same interpretation as that previously given.¹⁰ a is the linear expansion coefficient of calcite in a direction perpendicular to the cleavage planes,²⁴ which is 1.04×10^{-5} . For the reflection of $\text{MoK}\alpha_1$ in the (1, 1) position Eq. (19) gives $d\theta_B/dT = -0.51$ seconds of arc

TABLE V. Half widths at half maximum for $\text{MoK}\alpha_1$ at 50 kv.

TABLE V. <i>Ray widths at ray maximum for MoKα_1 at 50 kv.</i>									
$\lambda = 707.768 \text{ X.U.}$		$d = 3.02904 \text{ \AA.}$							
Position (n_A, n_B)	$ D $ "/X.U.	h_1 cm	h_2 cm	ξ_3	W	W_A	W_B	no. aver- aged	W_λ
(1, -2)	35.748	.23	.43	.63"	6.4"	2.1"	.64"	1	}.154 X.U.
(1, -2)	35.748	.10	.23	.17	6.0	2.1	.64	3	
(2, -1)	35.748	.10	.23	.17	6.5	.64	2.1	1	
(1, 1)	68.572	.10	.23	.34	11.2	2.1	2.1	4	.155
(1, -3)	74.777	.10	.23	.36	11.4	2.1	.67	2	.148
(1, 2)	104.32	.10	.23	.51	15.0	2.1	.64	5	.139
(2, 1)	104.32	.10	.23	.51	14.8	.64	2.1	1	.138
(2, 2)	140.07	.23	.30	1.2	19.7	.64	.64	3	.136
(1, 3)	143.34	.10	.23	.70	19.8	2.1	.67	2	.135
Weighted average of $W_\lambda = 0.147 \text{ X.U.}$									
Corresponding energy width 3.63 volts.									

²⁴ Siegbahn, Phil. Mag. 37, 601, (1919).

per degree centigrade. During the readings in the anti-parallel positions, the thermometer was frequently read. The change of temperature during the observations was never over 0.5°C . Accordingly we have made no temperature corrections to our results.

We have investigated the half widths at half maximum of the rocking curves for $\text{MoK}\alpha_1$ for as many positions of the instrument as were conveniently possible with the intensity available. The results are shown in Table V.

The values of W_λ in column 10 of Table V are in general averages of several trials, the number of trials being given in column 9. In taking the averages we have weighted our results according to our estimate of their reliability. Some of the curves taken are shown in Fig. 4.

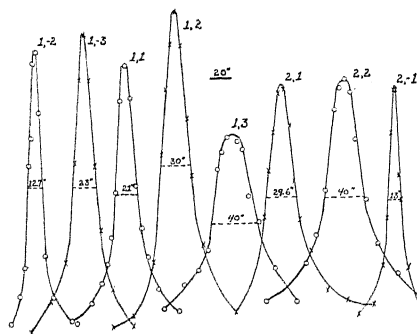


Fig. 4. Observed rocking curves in anti-parallel positions for $\text{MoK}\alpha_1$ at 50 k.v. Ordinates are proportional to ionization currents, abscissae to angular settings of crystal B . The vertical scale is not the same for all the curves.

We have investigated the half width at half maximum of $\text{MoK}\alpha_1$ as a function of voltage from the excitation voltage up to 50 k.v. If part of the observed width is due to satellites arising from multiply ionized states of the atom the width should depend on the voltage. The results are given in Table VI. The details given in Table V are omitted, although all corrections were made.

TABLE VI. Variation of width of $\text{MoK}\alpha_1$ with voltage. All observations in (1,1) position.

Voltage	W_λ
25.0 kv	0.143 X.U.
37.0	.162
46.2	.150
50.0	.155

We have also investigated the width of the line $\text{MoK}\alpha_2$ in the (1, 1 and (1, 2) positions as shown in Table VII. It was assumed that the crystal widths W_a and W_b were the same as had been measured for $\text{MoK}\alpha_1$.

TABLE VII. Half widths at half maximum for $\text{MoK}\alpha_2$ at 50 k. v.

Position (n_A, n_B)	$\lambda = 712.078 \text{ X. U.}$			ξ_1	W	$d = 3.02904 \text{ \AA.}$			W_λ
	$\frac{D}{\text{"/X.U.}}$	h_1 cm	h_2 cm			W_A	W_B	no. of observa- tions	
(1,1)	68.572	0.10	0.23	0.34"	12.2"	2.1"	2.1"	5	0.169X.U.
(1,2)	104.36	.10	.23	.52	16.2	2.1	.64	5	.151

Weighted average of $W_\lambda = 0.161 \text{ X.U.}$
Corresponding energy width 3.92 volts.

DISCUSSION OF RESULTS IN ANTI-PARALLEL POSITIONS

We shall first discuss the results given in Table V. It is seen that in positions in which D varies from 35.748 to 143.34 seconds per X. U. the half width at half maximum W_λ varies from 0.155 X. U. (if we disregard the single observation at (2, -1)) to 0.135 X. U. or a variation of about 13 percent. This variation is not random, however; there is a distinct trend toward lower values of W_λ with higher values of D . A systematic error is therefore indicated. We are not certain where this systematic error lies, but offer the following hypotheses (1). The actual shape of the lines differs from the Gaussian error curve shape sufficiently to make Eq. (2) inapplicable; (2) The effect is due to the finite size of the focal spot.

It is possible to calculate the size of focal spot which would explain the effect. Due to the fact that during the measurement of a line, crystal A is left stationary, the radiation reflected by B at various values of ζ must come from different parts of the target. This effect is increased for higher values of D (broader curves) and by the fact that the radiation was taken at a glancing angle of 8° from the target face. Let us assume that the adjustments have been correctly made and that therefore when crystal B is reflecting the tip of the peak for a line, the radiation reflected comes from the most intense part of the focal spot. As B is rocked to either side of this position, the radiation reflected will have a different initial intensity if the focal spot is finite in extent. We have calculated that if the distribution of intensity in the focal spot in the particular tube used is such that at a distance of 0.43 mm from the center of the spot the intensity has fallen to $\frac{1}{2}$ that at the center, a 10 percent decrease in rocking curve width in the (2, 2) position can be explained. This corresponds to a diameter of 0.86 mm for the most intense part of the focal spot. The region of discoloration of the target appeared to be about 2.5 mm in diameter so that this explanation does not seem obviously impossible. If in later work it is found that this decrease of wave-length width with increasing D persists when a broad focus tube is used and rays taken at a large glancing angle from the target this explanation must be abandoned.

From Table VI we conclude that there is no significant variation of the width of $\text{MoK}\alpha_1$ from 25 kv to 50 kv. The excitation voltage is 19.945 kv, but from intensity considerations it was not possible to take measurements below 25 kv. This indicates that the observed width is not due to satellites.

We obtained no evidence of satellites of $\text{MoK}\alpha_1$ or α_2 from our experiments.²⁵

Table VII indicates that the width of $\text{MoK}\alpha_2$ is slightly greater than $\text{MoK}\alpha_1$. The observed difference between the widths of the two lines is however close to the experimental error and we cannot positively assert that there is a difference in width.

The half width at half maximum to be expected from the classical theory of an oscillating electron damped by the electromagnetic radiation emitted is²⁶

$$\Delta\lambda = \frac{2\pi e^2}{3mc^2} \quad (20)$$

where e is the electronic charge in e.s.u., m the electronic mass and c the velocity of light. Eq. (20) gives $\Delta\lambda = 5.9 \times 10^{-13}$ cm. Our measured value of W_λ for $\text{MoK}\alpha_1$ is 1.47×10^{-12} or 2.5 times as large. If we call τ the time required for the vibrations of the electron to decrease to $1/e$ of their initial amplitude,

$$\tau = \frac{3mc\lambda^2}{4\pi^2 e^2} = \frac{\lambda^2}{2\pi c} \frac{1}{\Delta\lambda} \quad (21)$$

Using $\Delta\lambda = 1.47 \times 10^{-12}$ we find $\tau = 1.8 \times 10^{-16}$ seconds, which gives the order of magnitude of the life of a molybdenum atom excited to the K state.

Ehrenberg and Mark,³ using diamond crystals, found $W_\lambda = 0.204$ X. U. for $\text{MoK}\alpha_1$ and 0.199 for $\text{MoK}\alpha_2$. Ehrenberg and von Susich⁴ found, using calcite, $W_\lambda = 0.19$ X. U. for $\text{MoK}\alpha_1$. These observations were made using only the (1, 1) and (1, -1) positions.

Davis and Purks²⁵ observed the rocking curves in the (2, 2) and (3, 3) positions but did not give a definite value to the line width as they interpreted their curves as being composed of satellites. The present results may be considered as an extension of the work of Ehrenberg and Mark and Ehrenberg and von Susich. Their results are confirmed in the sense that a line width in excess of the classically predicted value was found. The lower value found here may be partially due to the limitation of the vertical divergence of the x-ray beam.

²⁵ Davis and Purks, *Proc. Nat. Acad. Sci.* **14**, 172 (1928). Allison and Williams, *Phys. Rev.* **35**, 149 (1930).

²⁶ W. C. Mandersloot, *Jahrb. der Radioakt. und Elektron.* **13**, 16 (1916), A. H. Compton, *X-rays and Electrons*, p. 56. The expression given here corresponds to full width at half maximum.

THE VIBRATIONAL QUANTUM ANALYSIS OF THE
BLUE-GREEN BANDS OF MAGNESIUM OXIDE

By P. N. GHOSH, P. C. MAHANTI AND B. C. MUKHERJEE

UNIVERSITY COLLEGE OF SCIENCE AND TECHNOLOGY, CALCUTTA

(Received March 14, 1930)

ABSTRACT

The paper deals with the assignment of the vibration quantum numbers of the violet degrading system of the magnesium oxide bands. The frequencies of vibration for infinitesimal amplitude are found to be 716 cm^{-1} and 751 cm^{-1} for the upper (initial) and lower (final) states respectively. The heat of dissociation as calculated from the extrapolation of the $\omega^2:n$ curve is nearly 5.8 volts.

INTRODUCTION

A REVIEW of the studies of the band spectrum of magnesium oxide has been given by Kayser¹ till the year 1910. Since then there has been no further investigation of the bands which are found to lie in the red, green and ultraviolet regions.

Lecoq² was the first to observe the bands of MgO in the green region. The bands lying in this as well as in the two other regions have been measured by Eder,³ Brooks,⁴ Olmstedt⁵ and others. They excited these bands either by sparking through a solution of magnesium chloride, or by burning magnesium ribbon in air, or by burning the salts in an oxy-hydrogen flame or by arcing or sparking between magnesium electrodes in oxygen at reduced pressure.

The necessity of the presence of oxygen in the production of these bands has been shown by Dewar⁶ and also by Brooks.⁴ These bands were found to come out in the presence of air and CO₂ but would completely disappear when nitrogen or hydrogen was substituted. Even when the sparking between the magnesium electrodes was continued for a long time in the atmosphere of CO₂, these bands would gradually become fainter and finally disappear.

By using a new method of excitation, we have obtained the bands lying in the blue and green regions but the bands in the ultraviolet region observed by Olmstedt did not come out.

So far no relations, either empirical or theoretical, have been found among the various heads of the magnesium oxide bands. The object of the present paper is to obtain the vibrational quantum analysis of the bands com-

¹ Kayser, *Handbuch der Spectroscopie*, 5, 717 (1920).

² Lecoq, *Spectres Lumineux*, Paris, 1874.

³ Eder, *Beiträge zur Photochemie und Spectral Analysis*, 1904, pp. 410.

⁴ Brooks, *Proc. Roy. Soc. A80*, 218 (1908); *Nat. Acad.* 78, 198 (1908).

⁵ Olmstedt, *Zeits. f. Wiss. Photogr.* 4, 255 (1906).

⁶ Dewar, *Proc. Roy. Inst.* 9, 204 (1882).

posing the blue-green system. The rotational structure of these bands shall be treated in a later communication.

EXPERIMENTAL

A quartz spectrograph (Model E 1 of Adam Hilger) of the Littrow type has been used in the investigation. The burning of magnesium ribbon in air or in an atmosphere of oxygen is certainly the most natural way of exciting the oxide bands for they come out only during the combination of magnesium with oxygen. But the magnesium ribbon while so burning forms a flocculent white oxide which glows in the light and becomes a source of continuous radiation. To avoid this, a mixture of powdered magnesium metal and nitrate of magnesium in suitable proportions was used. This mixture, on being ignited, produces an explosive flash and quickly disperses away the flocculent oxide. In this case it was found that the spectrum showed a larger number of bands than when magnesium ribbon was simply burned in air or in the atmosphere of oxygen. The heat generated during the flash was enough to melt a platinum wire (about a millimeter in thickness) which was used as the sparking arrangement. The flash so produced was focussed by a quartz lens on the slit of the spectrograph and the number of flashes required for

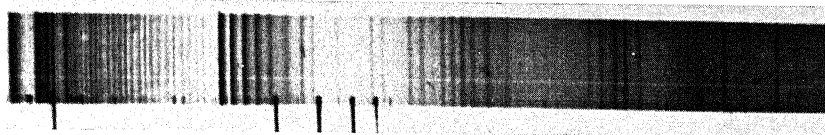


Fig. 1.

an exposure depended on the sensitiveness of the photographic plate in the region in which the bands were photographed. From a preliminary observation, these bands were found to lie between the regions $\lambda 5210$ and $\lambda 4700$. Ilford Special Process Panchromatic Plates were used which gave the best results in these regions.

The comparison lines for calculating the wave-lengths were obtained from a Pfund iron arc. They were photographed on either side of the bands. The standard wave-lengths used were those of Meggers, Kiess and Burns. Actual measurements of the band-heads were done on a Hilger comparator. On account of a general diffuse character of some of the bands and high magnifying power of the comparator used, difficulties were encountered in the correct location and measurement of the weak bands. It is, however, very well known that it is the identification and location of the "null" or "zero" line in an individual band, which is of more importance than that of its head or edge, in arranging the bands into various n' and n'' progressions. Unless the line structure of a band be studied under sufficient dispersion, the "null" line can hardly be located. Thus the frequency of the head may be taken to fit the various progressions. This, however, will produce some error. R. S. Mulliken⁷ is in favour of setting the cross-wire of the comparator on the point

⁷ R. S. Mulliken, *Phys. Rev.* 26, 2 (1925).

of maximum blackening for each band as it reduces the uncertainty in locating a band-head. This procedure has been adopted by us in the measurements of the bands where possible. No where within the range of our measurements could we find a band in which the head could be distinguished from the "null" line either by a gap in the shading or even by a mere lightening—so the method of indirectly calculating the null lines from the observed bands could not be applied.

ANALYSIS OF MgO BANDS

A visual inspection of the plate indicates that the bands near about λ 5211 have been resolved inspite of the low dispersion of the quartz spectrograph in this region. They have, however, been identified to be the hydride bands of magnesium. Considerable difficulty was, therefore, met with in locating the oxide bands lying in this region. It is, however, found that the bands at λ 5007 come out very easily, even when magnesium ribbon is simply burned in air. This fact seems to be in agreement with the intensity measurements and with the excellent reproduction of Eder and Valenta ("Atlas typischer Spektren," Wien, 1928). Hence they were taken as the O-sequence.

WAVE-LENGTH DATA

The results of the present measurements together with the data of the previous investigators are given in the following table.

TABLE I.

		Authors			Previous investigators		
n'	n''	$\lambda_{\text{air}}(\text{\AA.})$	ν (Vac)	O—C	Eder λ (R.S.)	Brooks λ (R.S.)	Morse λ (R.S.)
0	1	5190.91	19,259	-1.00	5190.60 (1)	5191.00	
1	2	5177.18	19,310	2.00	5177.23 (1)		
2	3	5162.99	19,363	1.00	5162.81 ($\frac{1}{2}$)	5162.00	
3	4	5148.50	19,418	-4.00	5145.87 ($\frac{1}{2}$)	5145.00	
4	5	5130.34	19,486	0.00	5130.34 ($\frac{1}{2}$)		
5	6	5113.47	19,551	3.00			
6	7	5097.95	19,610	1.00	5096.02 (1)		
7	8	5085.42	19,659	-4.00			5086.50
8	9	5072.64	19,708	1.00			5072.00
0	0	5007.13	19,966	-1.00	5007.44 (10)		
1	1	4996.84	20,007	4.00	4996.85 (8)		
2	2	4986.32	20,049	2.00	4986.23 (6)		
3	3	4975.51	20,093	-3.00	4974.81 (4)		
4	4	4962.40	20,146	-2.00	4962.45 (3)		
5	5	4949.19	20,200	-1.00	4949.30 (2)		
6	6	4935.20	20,257	5.00	4935.01 (1)		
7	7	4923.80	20,304	2.00	4923.65 (1)		
8	8	4913.40	20,347	-1.00	4913.37 ($\frac{1}{2}$)		
9	9	4903.35	20,388	-3.00	4903.36 ($\frac{1}{2}$)		
10	10	4892.82	20,432	2.00			
1	0	4826.12	20,715	0.00		4826.00	
2	1	4818.92	20,746	2.00		4820.00	
3	2	4810.96	20,780	0.00		4811.00	
4	3	4801.93	20,819	-2.00		4802.00	
5	4	4790.95	20,867	2.00		4791.00	
6	5	4780.72	20,911	1.00		4781.00	
7	6	4771.08	20,954	0.00		4771.00	
8	7	4761.78	20,994	0.00			

To start with, the band at λ 5007.13 was taken as the 0-0 band and the rest of the band system was then arranged into the Deslandre's progressions according to the criterion of Heurlinger and Kratzer for the assignment of the vibrational quantum numbers. The vibrational isotopic effect was looked for but no evidence of it was obtained.

The equation in terms of the parameters n' and n'' capable of representing the position of the measured heads is given below.

$$\nu_n = 19,967 + (751n' - 3.06n'^2) - (716n'' - 5.96n''^2).$$

CALCULATION OF THE HEAT OF DISSOCIATION

Having made the assignment of the vibration quantum numbers for the system of bands, the average values of each ΔG_n , i.e., ω^n for the two progressions were calculated and plotted as a function of n . The interval between successive vibrational levels in the lower electronic state is zero when $n' = 125$, i.e. when $751 - 6n' = 0$. The area on the $\omega^n:n$ diagram therefore gives 5.80 volts, which is the heat of dissociation of MgO(gas) into Mg(gas) and O(gas).

DISCUSSION

Mecke,⁸ Mulliken,⁹ Birge¹⁰ and Hund¹¹ have shown that the band spectra of diatomic molecules bear a simple systematic relationship with the line spectra of atoms having similar outer electronic configuration. In the case of these it has been definitely proved by Dewar and by Brooks as well that the presence of oxygen is essential to produce these bands. Their emitter, may therefore be legitimately assumed as the oxide of magnesium. The band spectra of MgO will then resemble the line spectra of argon since they have the same outer electronic configuration. The ground state is therefore a singlet 1S -state in both cases, and in the excited states, one would get singlets and triplets. Hence the MgO bands would be singlets and triplets in character.

There, however, remains the other possibility that the emitter of these bands may be MgO^+ . If so, the band spectra would resemble the line spectra of ionized argon atom or of the normal chlorine atom. In either case, they would be doublet in structure.

But in the region in which these bands lie, the quartz spectrograph has a low dispersion and hence the separation of the bands into doublets or triplets could not be detected. We, therefore, reserve our opinion about the nature of the emitter till the line analysis of each individual band is made.

Our best thanks are due to Professor Birge for kindly sending us his monograph for the rapid calculation of the least squares solution of a polynomial, which has been of great use in our investigation.

⁸ Mecke, *Phys. Zeits.* **25**, 597 (1924); *Zeits. f. Physik* **28**, 261 (1924); **31**, 709, (1925).

⁹ Mulliken, *Nat. Acad. Proc.* **12**, 144 (1926); *Phys. Rev.* **28**, 19 and 32 (1928).

¹⁰ Birge, *Nat. Acad. Proc.* **12**, 146 (1926).

¹¹ Hund, *Zeits. f. Physik* **40**, 742 (1927); **42**, 93 (1927).

THE ZEEMAN EFFECT IN THE OH BANDS

BY GERALD M. ALMY

JEFFERSON PHYSICAL LABORATORY, HARVARD UNIVERSITY

(Received April 19, 1930)

ABSTRACT

Apparatus and experimental procedure. The Zeeman effect in the $^2\Sigma \rightarrow ^2\Pi$ OH bands in the near ultraviolet has been photographed with a 21-foot grating at 7 field strengths, varying from 5000 gauss to 34000 gauss. Up to 22000 gauss a discharge in water vapor was used as the source. Two types of quartz tubes were employed, one viewed laterally, the other end-on and placed between rectangular pole-faces. At high fields the Back-box arc, operating in water vapor, was employed.

Nature of the OH bands. The structure of the bands is briefly reviewed. New data on the satellite lines are presented, from which the ρ -type doubling in the $^2\Sigma$ states for which $v=0$, and 1, is found to be $0.216 (K + \frac{1}{2})$. Wave-number data on the hitherto unobserved $^{PP}P_{21}$ branch are also given. The agreement between the calculated and observed wave numbers, as well as the Zeeman effect, establishes the identity of this branch.

Theoretical calculation of the Zeeman patterns in OH. Hill's theory of the Zeeman effect in doublet states is applied to OH. In the $^2\Pi$ state the molecule behaves in the field as though quite rigid, symmetrical patterns being produced. The exact treatment of a $^2\Sigma$ molecular state, is given here for the first time. This state gives rise to large magnetic energy patterns which are shown in diagrams, as are also the resulting Zeeman spectrum patterns. The variety of ordering of the magnetic levels in the two states involved is the cause of strange patterns, consisting, for all lines except those near the origin, of a narrow concentrated part and a wide diffuse part.

Results and comparison with the theory. The results of observations on the Zeeman patterns are given in tables and diagrams and quantitatively compared with the theoretical expectations. The lines are treated in three groups, (1) lines near the origin, whose fine structure is resolved, (2) lines of intermediate J'' whose patterns were completely observed, (3) lines of larger J'' . The agreement with the theory is satisfactory.

INTRODUCTION

THE theory of the effect of a magnetic field on molecular spectra of the doublet type has been discussed in a recent paper by Hill.¹ At the same time the observations of Crawford and the writer² on the Zeeman effect in the $^2\Pi \rightarrow ^2\Sigma$ MgH band at 5211A were correlated quantitatively with the theory with generally satisfactory results. In the present paper the Zeeman effect in the $^2\Sigma \rightarrow ^2\Pi$ OH bands in the near ultraviolet is similarly treated, particular attention being paid to the (0,0) band at 3064A.

From a spectroscopic point of view the OH molecule differs from the MgH in two essential respects. First, the $^2\Pi$ state in OH is distinctly more rigid, or nearer case (a), as is indicated by the greater doublet separation in

¹ E. L. Hill, Phys. Rev. **34**, 1507 (1929).

² G. M. Almy and F. H. Crawford, Phys. Rev. **34**, 1517 (1929).

the bands;³ second, the $^2\Sigma$ state in OH is obviously a doublet state (ρ -type doubling) for it gives rise to observable satellite branches accompanying the main branches. These satellites permit definite measurements of the magnitude of the doubling.⁴ This definite knowledge of the $^2\Sigma$ state enables one to predict quantitatively how it will be affected by the magnetic field. As a result, the appearance of the OH bands in the field can be more definitely calculated than the MgH, especially for the higher rotational lines. Hence the agreement with the theory is more significant than in the case of MgH.

The Zeeman effect in OH has been extensively investigated by Fortrat.⁵ His report included a qualitative description of the Zeeman patterns as well as numerical data on displacements from the no-field positions. He made observations at fields of about 5000, 20000, and 40000 gauss on the six branches of each of the bands, (0,0) at 3064Å and (0,1) at 3122Å. He reported that the effect was the same in perpendicular and parallel polarizations. His measurements of displacements (obtained by reference to iron lines) showed odd fluctuations which he thought greater than the experimental error. He did not discuss the resolvable fine structure of the patterns near the origin, except the doublet from the first line in the P_1 and Q_1 branches, nor did he give any data on the unresolved parts of the patterns. Moreover, he did not publish measurements on the weak $^{RR}R_{21}$ branch beyond the head of the band, which furnishes the most certain data on widths of patterns. It is probable that much of this information was to be found on Fortrat's plates but that in the absence of a theory to guide the work it was not recognized as useful. In view of the rather better experimental conditions at hand, it was thought worth while to repeat the investigation of OH. Information was secured on most of the points left in doubt by Fortrat's paper.

The present paper deals, in the first section, with the experimental procedure employed in photographing the Zeeman effect in the OH bands. In the second section, in which the nature of the states giving rise to the bands is discussed, some new data on the satellite branches and a hitherto unobserved non-satellite branch ($^{PP}P_{12}$) are given. The third section contains a discussion of the theoretical behaviour of the two states in the field, according to Hill's results, and the last, a detailed comparison of the observed and theoretical patterns.

³ The position which a molecular state occupies in the range from case (a) to case (b) is specified by its "coupling constant," λ . For normal case (a) λ is $+\infty$, for inverted case (a), $-\infty$. For case (b) λ is 0 or $+4$. Hence the $^2\Pi$ state in OH ($\lambda \approx -6.9$) is considerably more removed from the nearer case (b) than in MgH ($\lambda \approx +5.7$). For the theory of multiplet molecular states, see E. L. Hill and J. H. van Vleck, Phys. Rev. **32**, 250, (1928).

⁴ In order to account for the observed doublet widths in MgH at large rotational speeds, it is necessary to assume a considerable ρ -type doubling in the $^2\Sigma$ state. No satellites appear, however, as might be expected, since their theoretical intensity near case (b) is very low. Hence one has no way of determining uniquely the amount of the ρ -type doubling. It was assumed to be zero in the work on the Zeeman effect, which led, of course, to a discrepancy between the observed and theoretical patterns. The discrepancy is discussed in Footnote 13.

⁵ R. Fortrat, Jour. de Physique et le Rad. **5**, 20 (1924).

APPARATUS AND EXPERIMENTAL PROCEDURE

The apparatus used in this work, except for the light sources, was that employed in previous work in this laboratory on the Zeeman effect in bands.^{2,6} Two types of source were used, an uncondensed discharge in water vapor and the Back-box arc, operating in water vapor at low pressure. The spectrum from the former is freer from impurities but the tubes employed could not be used at very high fields.

Two discharge tubes were used. The first one, made of quartz, had a capillary 4 mm in internal diameter and 5 cm in length. It was mounted vertically between the flat-tipped conical polepieces of the electromagnet. A stream of water vapor from a bulb containing freshly boiled, distilled water was pumped continuously through the tube, the flow being controlled, as suggested by Jack,⁷ by means of a 1 mm capillary tube, about 10 cm long, in the inlet of the tube. With a $\frac{1}{2}$ -kw transformer, a discharge could not be forced through the tube at fields exceeding about 20000 gauss. It was necessary to cool the tube with an air blast. The OH spectrum produced was very weak. A 20-hour exposure just under 20000 gauss gave a spectrum of excellent definition and purity, though of only fair intensity. A similar exposure was required to get the no-field comparison spectrum.

The difficulty of faintness of source was overcome by using a tube which could be viewed end-on, between polepieces with rather large rectangular faces (3×13.5 cm). The polepieces, which were made in the laboratory shop, were designed in accordance with the theory of polepieces given by Du Bois,⁸ in such a way as to give the largest field consistent with the necessary homogeneity. The maximum field attainable with a pole separation of one cm was

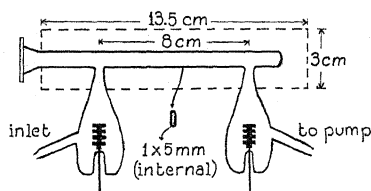


Fig. 1. Construction of the end-on quartz discharge tube. The rectangle shows the size and relative position of the pole-faces. The capillary between the side tubes was flattened, as shown in the section, in order to concentrate the discharge.

about 24000 gauss. That the field was satisfactorily uniform was shown by the sharpness of the Hg atomic line Zeeman patterns, obtained with Hg in the discharge tube. The construction of the discharge tube and its position in the magnetic field is shown in Fig. 1. The tube was made of quartz. The window on the end was fastened with deKhotinsky cement. The whole tube was cooled with a blast of cold air, and water was allowed to drop slowly on a bit of cotton wrapped around the tube just back of the window. The water

⁶ E. C. Kemble, R. S. Mulliken, and F. H. Crawford, *Phys. Rev.* **30**, 448 (1927).

⁷ D. Jack, *Proc. Roy. Soc. A* **115**, 373 (1927).

⁸ H. Du Bois, *Ann. d. Physik, und Chemie* **42**, 934 (1913).

vapor was supplied as before and a more powerful transformer used. With this arrangement the intensity was increased at least ten-fold over that previously obtained.

With the end-on tube, usable photographs were taken at the following fields; 4900 gauss, 1 set of plates; 12900 gauss, 2 sets of plates; 18000–22000 gauss, 4 sets of plates. Two of the exposures near 20000 gauss were extended to 24 hours to bring out the weak RR_{21} branch lying beyond the head of the band at 3064Å. At lower fields this branch was obtained satisfactorily in much less time (7 hours at 12900 gauss).

At high field strengths the Back-box with brass electrodes was used. Water vapor was pumped through the box, the pressure being less than 1 cm Hg. A satisfactory photograph was obtained in about 8 hours, with a field of 33600 gauss. The RR_{21} branch was not obtained.

The most intense spectra were obtained in the second order of the 21-foot grating, where the dispersion is 0.93Å per mm. The third order was usable in some cases. Photographs were taken of the three bands, 3064Å, 2811Å, 3122Å. A no-field comparison spectrum of the bands and the iron arc spectrum were photographed on each set of plates. Eastman Speedway plates were used. The patterns were measured with the aid of a Wolz comparator.

The field strengths were determined, when a discharge tube was the source, from the Zeeman patterns of the Hg atomic lines at 4047Å and 4358Å. These were obtained by introducing a drop of mercury into the tube and exposing a properly placed plate for a few minutes. When the Back-box was used the field was determined from the Zn triplet, 4680Å, 4722Å, 4811Å, whose Zeeman patterns were photographed in a few minutes with brass electrodes in the box.

NATURE OF THE OH BANDS

The OH bands consist of six strong branches forming three branches of doublets, several satellite branches, and two weak branches arising from extraordinary transitions in which K changes by two units instead of one. Mulliken⁹ has discussed the structure of the bands and given a diagram showing the arrangement of levels in both states as well as the transitions which produce the first line in each branch.

The $^2\Pi$ state is inverted, having a coupling constant (λ , or Mulliken's $\Delta E/B$) equal to -6.9 . The doublet character of the main branches arises from the fact that there are two energy levels associated with each value of K in the $^2\Pi$ state. These states, whose J values are $K \pm \frac{1}{2}$, correspond to the two possible orientations of S and K . The doublet difference decreases from about 125 cm^{-1} at the origin to about 30 cm^{-1} at $K'' = 20$. Each level also shows appreciable Λ -type doubling which, however, does not enter into a consideration of the Zeeman effect.¹

The $^2\Sigma$ state shows a pronounced ρ -type doubling which increases linearly with K . As in the $^2\Pi$ state there are two levels associated with each value of K , whose J values are $K \pm \frac{1}{2}$. The origin of this doubling, considered

⁹ R. S. Mulliken, Phys. Rev. **32**, 388 (1928).

especially by Van Vleck,¹⁰ lies presumably in a combination of (1) a magnetic moment due the rotating nuclei themselves, and (2) a rotational distortion of the electronic motions, also resulting in a magnetic moment along the axis of rotation. Both should produce effects proportional to $K + \frac{1}{2}$. This doubling gives rise to the satellite branches accompanying the main branches. These satellites result from transitions in which ΔJ is not equal to ΔK , as is true for the main branches. The results of several investigations of these satellites have been discussed by Mulliken, who concludes that the width of the ρ -type doublet is $0.22 K$, for the lowest vibrational state.

Since the satellites in the (1,0) band at 2811A have not been reported, and because some uncertainty was expressed by Mulliken in his value of the ρ -doubling constant (0.22), it may be worth while to include here measurements on the satellites, made on the comparison spectra. Table I gives

TABLE I. Displacements in cm^{-1} of satellite lines from main branch lines, arranged according to the value of K in the $^2\Sigma$ state. These displacements are the amounts of the ρ -type doubling in this state. The mean displacements are plotted in Fig. 2 from which the best value of the doublet constant may be obtained.

K	P_2	Q_1	Q_2	R_1	Mean displacement
(0,0) band at 3064A					
1			+0.28		0.28
2	+0.50	-0.49		-0.45	.48
3	.77	.73		.73	.74
4	.99	1.00		.98	.99
5		1.24		1.18	1.21
6	1.44	1.45	1.42	1.37	1.42
7	1.58		1.64		1.61
8		1.88	1.86		1.87
9	2.14	2.10	2.00		2.08
10	2.32	2.28			2.30
11			2.45		2.45
12		2.82	2.60		2.71
14		3.12	3.12		3.12
(1,0) band at 2811A					
2	+0.43		+0.39		0.41
3	.62			-0.67	.64
4	.94	-0.96	.89	.91	.93
5	1.15	1.11			1.13
6	1.40		1.34		1.37
7	1.60	1.56	1.61		1.59
8	1.86	1.78		1.83	1.82
9	2.05			1.99	2.02
10	2.21				2.21

the displacements of the satellites from the main branch lines. The (0,0) band at 3064A furnishes the data on the lowest vibrational state ($^2\Sigma^{(0)}$), the (1,0) band at 2811A on the next higher ($^2\Sigma^{(1)}$). The average values of these displacements are plotted against K in Fig. 2. The data indicate, though none too conclusively, that the ρ -doubling is proportional to $K + \frac{1}{2}$, rather than K , agreeing with Van Vleck's prediction. Within experimental error the doubling in either vibrational state is equal to $0.216 (K + \frac{1}{2})$.

¹⁰ J. H. Van Vleck, Phys. Rev. 33, 467 (1929).

A search was also made for the ${}^{PP}P_{12}$ branch of the (0,0) band which Mulliken predicts should be somewhat stronger than the ${}^{RR}R_{21}$ branch. It is situated in the midst of the bands at 3064A and 3122A and observation

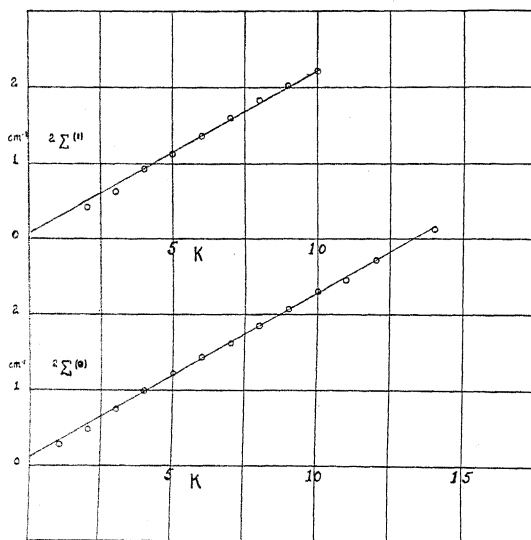


Fig. 2. Average displacement of satellites in the (1, 0) band (above), and the (0,0) band, plotted against K . The ordinate thus gives the amount of ρ -type doubling in the ${}^2\Sigma$ state involved in each band. From the intercept of the solid, averaging line on the vertical axis it appears that the displacements are proportional to $K + \frac{1}{2}$, rather than K , and that for both states it is about $0.216(K + \frac{1}{2})$.

is difficult. As can be seen from Mulliken's energy level diagram the positions can be calculated by the relation:

$${}^{PP}P_{12}(J) = Q_2(J) - \Delta_2 F_2'(J-1) + 0.216(J-1)$$

where

$$\Delta_2 F_2'(J-1) = F_2'(J) - F_2'(J-2)$$

and 0.216 is the ρ -type doubling constant. $\Delta_2 F_2'$ was obtained from Mulliken's data on the ${}^{RR}R_{21}$ branch and $Q_2(J)$ from Fortrat's table of wave numbers. The results of these calculations appear in Table II together with the observed wave numbers of what are believed to be the lines of this branch. The agreement is good. This assignment is substantiated by the Zeeman effect of these lines, which will be discussed later. The observed intensities in this branch are about the same as those of the ${}^{RR}R_{21}$ branch and decrease rapidly with increasing J .

THEORETICAL CALCULATION OF THE ZEEMAN PATTERNS IN OH

The theory of the Zeeman effect in doublet bands has been discussed in terms of the quantum mechanics by Hill.¹ He has obtained an expression in closed form for the magnetic energy of ${}^2\Pi$, ${}^2\Delta$, . . . molecular states ranging from case (a) to case (b). Qualitatively, the predicted behavior in

TABLE II. Wave numbers of ${}^{PP}P_{12}(J)$. When a line coincides with a main branch line the latter is put in parentheses. The intensity scale is arbitrary.

J	Calculated cm^{-1}	Observed cm^{-1}	Intensity (Obs.)
$1\frac{1}{2}$	32253.29	$(P_2(2\frac{1}{2}))$	
$2\frac{1}{2}$	186.11	$(Q_1(12\frac{1}{2}))$	
$3\frac{1}{2}$	113.50	32113.38	6
$4\frac{1}{2}$	036.02	036.10	6
$5\frac{1}{2}$	31954.89	31954.90	—
$6\frac{1}{2}$	870.04	$(P_1(11\frac{1}{2}))$	
$7\frac{1}{2}$	781.51	$(Q_2(18\frac{1}{2}))$	
$8\frac{1}{2}$	690.31	$(P_2(12\frac{1}{2}))$	
$9\frac{1}{2}$	596.00	31595.85	3
$10\frac{1}{2}$	498.97	498.88	2
$11\frac{1}{2}$	399.07	$(Q_2(23\frac{1}{2}))$	
$12\frac{1}{2}$	296.96	31296.78	1
$13\frac{1}{2}$	192.25	192.26	$\frac{1}{2}$

the field of the ${}^2\Pi$ state of OH is that of a rigid molecule. Each level (J, K) breaks up into $2J+1$ magnetic sublevels, symmetrically placed about the no-field energy. Their positions are quantitatively given by Hill's Eq. (12):¹¹

$$W(\Lambda, K, J, M) = B \left\{ (J + \frac{1}{2})^2 - \Lambda^2 + \beta(\Lambda^2 + \frac{1}{2}) \right. \\ \left. \pm \frac{1}{2} [(2J+1)^2(1-\beta)^2 + \Lambda^2(\lambda + \beta)(\lambda - 4 + 5\beta)]^{1/2} \right\} \quad (1)$$

where the two signs are to be associated with the two states for which $J = K \mp \frac{1}{2}$, $B = h/8\pi^2 cI$, and $\beta = (\Delta\nu_n/B) M/J(J+1)$.

In the paper referred to, Hill treated the ${}^2\Sigma$ state as if it consisted of two coincident levels, neglecting the ρ -type doubling. Such a state should become, in the field, a doublet of twice normal separation, arising from the energy of the spin in the field. This procedure was justifiable in the case of MgH, since its bands have no satellites from which the ρ -type doubling can be estimated.⁴ In OH, however, the ${}^2\Sigma$ state possesses, as has been discussed, a ρ -type doubling equal to $0.216(K + \frac{1}{2})$. At a field of 20000 gauss ($\Delta\nu_n = 0.94 \text{ cm}^{-1}$) the ρ -type doubling is considerably less at the origin than $\Delta\nu_n$, but it increases linearly with K , becoming considerably greater than $\Delta\nu_n$ rather early in the band. Near the origin, therefore, we may expect a molecular Paschen-Back effect, with the spin parallel or anti-parallel to the field, giving a doublet of twice normal width. But since the interaction energy which gives rise to the ρ -type doubling still remains, each member of this twice normal doublet should be "spread out" to approximately the ρ -type doublet width, the pattern consisting of $2J+1$ closely spaced levels. On the other hand, as K increases, and the ρ -type doublet width becomes much greater than $\Delta\nu_n$, S and K tend to preserve their orientation when in the field. Each member of the no-field doublet splits into $2J+1$ magnetic levels. Their separations from the no-field position run from about $+\Delta\nu_n$

¹¹ The OH molecule is sufficiently rigid that the δ term in Hill's complete Eq. (22) is negligible. This reduces (22) to (12). In Eq. (12) the terms in the square of the field also turn out to be negligible so that the Zeeman energy level pattern for the ${}^2\Pi$ state is sensibly symmetrical about the no-field position. In the calculations on MgH Hill's Eq. (22) had to be used.

to $-\Delta\nu_n$, since the magnetic energy is largely that of spin and field, with that of nuclear rotation and field making little contribution.

Precisely this behavior is predicted in the following quantitative treatment of the $^2\Sigma$ state. This treatment is due to Dr. Hill, and I owe him thanks for permission to set it down here. Since the p -type doubling is a small effect, compared with other interactions in the molecule, we may treat the motion in the $^2\Sigma$ state as case (b) (i.e., K and S precess regularly about J), perturbed by the magnetic field. Assuming that the perturbation energy is due to the interaction of S and H , it has the form,

$$H_1 = 2\Delta\nu_n(S \cdot H). \quad (2)$$

The matrix elements of this perturbation function may be written:

$$\begin{aligned} H_1(K_1, M; K_1, M) &= \Delta\nu_n \frac{M}{K + \frac{1}{2}} = \Delta\nu_n \alpha, \quad \text{where } \alpha = \frac{M}{K + \frac{1}{2}} \\ H_1(K_1, M; K_2, M) &= H_1(K_2, M; K_1, M) = \Delta\nu_n(1 - \alpha^2)^{1/2} \\ H_1(K_2, M; K_2, M) &= -\alpha\Delta\nu_n \end{aligned}$$

where K_1 corresponds to $J = K + \frac{1}{2}$, K_2 to $J = K - \frac{1}{2}$. Let $W(K_1) - W(K_2) = \nu_0$ (energy expressed in cm^{-1}).¹² The energy determinant is,

$$\begin{vmatrix} -\frac{\nu_0}{2} - \alpha\Delta\nu_n - W & \Delta\nu_n(1 - \alpha^2)^{1/2} \\ \Delta\nu_n(1 - \alpha^2)^{1/2} & \frac{\nu_0}{2} + \alpha\Delta\nu_n - W \end{vmatrix} = 0,$$

where the origin for W is the mid-position of the no-field doublets. The solution of this determinant is,

$$W = \pm \frac{1}{2} \{ \nu_0^2 + 4\alpha\nu_0\Delta\nu_n + 4\Delta\nu_n^2 \}^{1/2} \quad (3)$$

where the upper sign goes with $J = K + \frac{1}{2}$, the lower with $J = K - \frac{1}{2}$. From (3) the magnetic energy levels may be calculated. The two extreme levels in the K_1 state need separate treatment, since for them, $M = K + \frac{1}{2}$, and the non-diagonal terms vanish. Since the upper left term in the determinant is associated with the K_2 state, only the single lower right term remains. Hence the energies for these two extreme magnetic levels of the K_1 state are simply,

$$W = \frac{\nu_0}{2} \pm \Delta\nu_n. \quad (4)$$

Calculations at 12900, 20000, and 33600 gauss of the magnetic energy levels in the two states of OH have been carried through by means of Eqs. (1)

¹² In the $^2\Sigma$ states of some molecules $W(K_1)$ is less than $W(K_2)$, in which case the appropriate change in the sign of ν_0 must be made. The assignment of the two roots of Eq. (3) to the two no-field levels is also changed.

and (3). In the $^2\Pi$ state the values, $\lambda = -6.9$, $B = 18.47$, given by Mulliken, were used. In the $^2\Sigma$ state the ρ -type doubling (ν_0 in Eq. (3)) was supposed to be $0.22 K$. As shown above, the subsequent more careful consideration

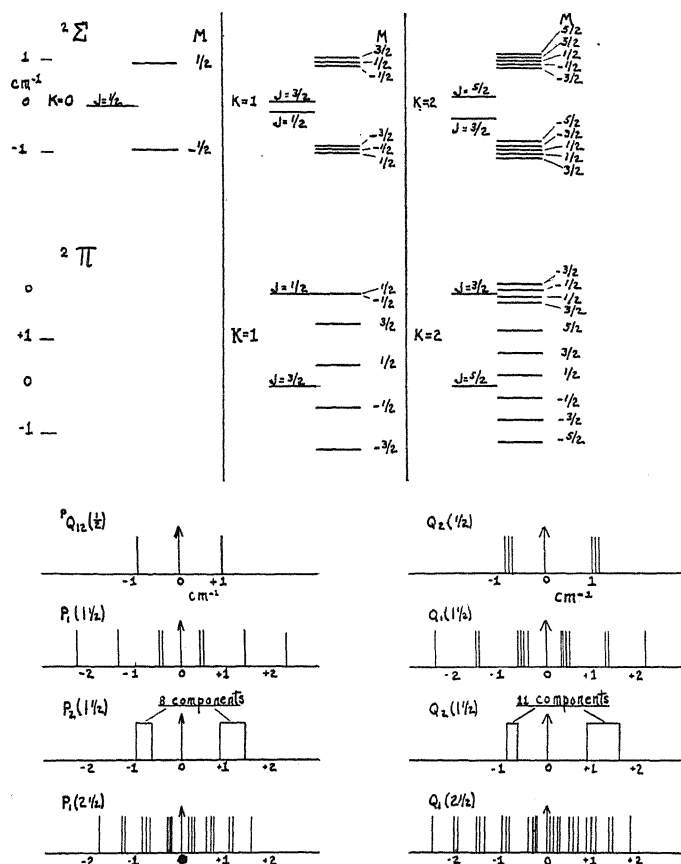


Fig. 3. Magnetic energy levels at 20000 gauss in OH $^2\Sigma$ and $^2\Pi$ states of low values of K , and some of the resulting Zeeman patterns. In each group of energy levels the no-field energies are shown at the left, the energies in the field at the right. In the Zeeman patterns the grouping in clusters is due to the fact that M may change by 0 or ± 1 . Hence, since the spacing is quite close in the $^2\Sigma$ state, three lines may fall close together. These groups are not resolvable at attainable fields, but appear as broadened lines on the plates, their intensities roughly proportional to the number in the group. Parts of all of these patterns (except $P_2(1\frac{1}{2})$ and $Q_2(1\frac{1}{2})$) are observed as resolved (Table III). In the $Q_1(2\frac{1}{2})$ pattern, for example, the five low-frequency groups are resolved at 33600 gauss, while the high-frequency part appears as a broad faint band, consistent with the fairly uniform distribution of components in this figure. All intervals are to scale except the $^2\Sigma \rightarrow ^2\Pi$ interval and the $^2\Pi$ no-field doublet interval.

of the satellites indicates that this doubling is, more precisely, $0.216 (K + \frac{1}{2})$. However, since the change would make differences of much less than 0.1 cm^{-1} in any of the computed patterns, it was not thought worth while to repeat the calculations.

The magnetic energy levels in both states for a field of 20000 gauss are plotted in Figs. 3 and 4. Fig. 3 shows the fine structure in the two states for low values of K , and, below, the Zeeman patterns of some of the early lines, when all permissible transitions ($\Delta M = \pm 1, 0$) are considered. Fig. 4 shows the magnetic energy of the extreme levels ($M = \pm J$) in each state, plotted as a function of K . The fictitious level, $M = 0$, serves merely to locate the center of the number of levels, but, since J is half integral, does not correspond to a real level. In the $^2\Sigma$ state the magnetic energy is calculated with reference to the center of the no-field doublets. The energy separations

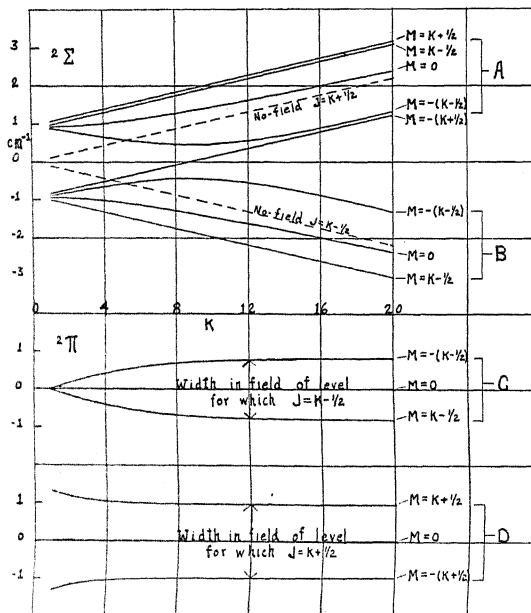


Fig. 4. Magnetic energies at 20000 gauss of the $^2\Sigma$ and $^2\Pi$ states of OH, plotted as a function of K . The levels omitted are quite uniformly spaced between the center "levels" ($M = 0$) and the extreme levels ($M = \pm J$). The broken lines show the no-field $^2\Sigma$ levels, the distance between them being the amount of the ρ -type doubling. The Zeeman patterns in Fig. 6 are obtained by considering the transitions between the groups of this figure, taking into account the proper changes in K and M during the transition.

of the latter are given by the distance between the broken lines. Due to the peculiar behavior near the origin of the level for which $M = -(K + \frac{1}{2})$ the levels $M = \pm(K - \frac{1}{2})$ in the upper group are also shown.

In a consideration of the Zeeman spectrum patterns resulting from this arrangement of energy levels, the order of these levels is very significant. Thus, in the group A (Fig. 4) of the $^2\Sigma$ state the level, $M = K + \frac{1}{2}$ is at the top whereas in group B the level $M = -(K - \frac{1}{2})$ is at the top. This is to be expected for large values of K since in A the spin is parallel to the nuclear rotation ($J = K + \frac{1}{2}$), and thus parallel to the field when $M = +J$. In B, on the other hand, the spin is anti-parallel to K , and parallel to the field when

$M = -J$. These states are highest in their respective groups because the magnetic energy is mostly due to the interaction of spin and field. The calculations show that this ordering of energy levels holds continuously to low values of K , where, however, S is to be thought of as quantized independently in the field (molecular Paschen-Back effect).

Similar considerations as to the arrangement of the energy levels apply to the ${}^2\Pi$ state. The difference in the two groups, for which $J = K \pm \frac{1}{2}$, is shown in Fig. 4, C and D . In C the spin is anti-parallel to K , and the state for which $M = -(K - \frac{1}{2})$ has the greatest energy. In D , spin and K are parallel and the state for which $M = K + \frac{1}{2}$ has the greatest energy.

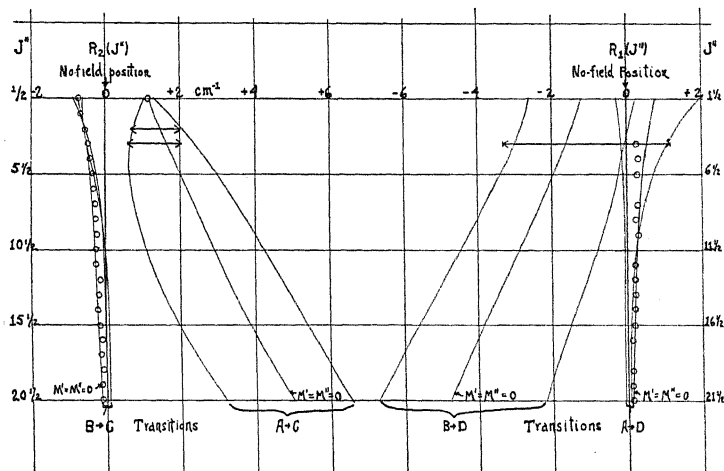


Fig. 5. Zeeman patterns of the R branches in the OH bands at 20000 gauss. The values of J'' are so arranged that the intersection of a horizontal line with the curves gives the outline of a pattern of a no-field R doublet. Two things may be particularly noted: (1) the great difference in width, except near the origin, of the two parts of the pattern of a line, due to the arrangement of magnetic levels in the two states (cf. Fig. 4 and text), (2) the appearance, at intermediate values of J'' , of the "center line" ($M' = M'' = 0$) outside of what would ordinarily be the extreme components. The circles show the observed positions of the narrow intense parts, the two-headed arrows the widths of the observable broad faint parts.

From the energy level diagram of Fig. 4 the outlines of the Zeeman spectrum patterns may be obtained. As an example, the patterns of the R_1 and R_2 branches in a field of 20000 gauss are shown in Fig. 5. Displacement from the no-field position is plotted horizontally and J'' , vertically. The extreme components and the center of the number of components ($M' = M'' = 0$) of any line are the intersections of the curves shown with a horizontal line at the corresponding value of J'' . The curious effect of one wide and one narrow part of each pattern is due to the arrangement of energy levels in the two states, just discussed. Thus the transitions $B \rightarrow C$ and $A \rightarrow D$ (cf. Fig. 4) result in close clusters of components near the no-field position, because the magnetic effect in one state undoes that in the other, when one considers the transition. But for the transitions $A \rightarrow C$ and $B \rightarrow D$ the displacements in the two states add, giving the extremely wide, and con-

sequently faint, parts of the patterns. In the narrow groups $B \rightarrow C$ and $A \rightarrow D$ it is also to be noted that, except near the origin, the center line, for which $M' = M'' = 0$, falls outside the components which would ordinarily be the extreme edges of the pattern. In other words, each of these groups folds back on itself. The components not shown fall, in all cases, fairly uniformly between the center line and the "extreme" components.¹³

In anticipation of the results to be discussed in the following section, it may be said that the circles in Fig. 5 represent the observed positions of the intense narrow parts of the patterns and the two-ended arrows the observed widths of the more diffuse parts of the patterns.

The theoretical patterns of the Q and P branches are, except for small differences in widths, like those of the R branch. The general appearance of the calculated patterns at 12900 and 33600 gauss is the same as that shown for 20000 gauss. Widths and displacements are different, of course, and roughly proportional to the field.

RESULTS AND COMPARISON WITH THE THEORY

A description of the general features of the Zeeman effect in the OH bands will be given and, where feasible, a quantitative account and comparison with the theory. The lines may be considered in three groups, (1) the lines near the origin for which the fine structure is resolved, (2) a number of intermediate lines for which complete patterns are observable, including lines in the $^{RR}R_{21}$ and $^{PP}P_{12}$ branches, and (3) the lines with larger values of J'' , for which only the intense parts of the patterns are observed. Quantitative observations were made extensively only on the (0,0) band at 3064A. Qualitative observations and a few measurements indicated that the (0,1) band at 3122A and the (1,0) band at 2811A behave in very much the same manner.

Fine structure of the lines near the origin. The calculated patterns of several lines near the origin are shown in Fig. 3. It is seen that the fine structure patterns increase rapidly in complexity as one proceeds from the origin. Only branches subscribed "1" have patterns which one might expect to resolve beyond the relatively coarse doubling to be observed in most of the patterns. The numerical description of the patterns observed and comparison with the theory is contained in Table III.

As predicted, $Q_2(\frac{1}{2})$, $R_2(\frac{1}{2})$, $^PQ(\frac{1}{2})$ become doublets of twice normal separation. The doublets of the first two of these lines are unsymmetrical with

¹³ A consideration of the ρ -type doubling would account for the discrepancies appearing in the Zeeman patterns of the high rotational doublets of MgH (Ref. 2). The Zeeman pattern of such a doublet consisted, at 16000 gauss, of an intense part filling the no-field doublet interval and on either side a somewhat fainter, narrow "wing." The central part corresponds to the broad parts of the patterns in OH (Fig. 5), though in MgH they overlapped. The wings correspond to the narrow parts of the OH patterns. (Their faintness was due to the fact that the Paschen-Back effect was setting in.) Thus both the too large width of the central part (according to the previous theory) and the too small width of the wings, as well as the too large no-field doublet width (Cf. Footnote 4), would be accounted for by a consideration like the above for OH of the ρ -type doubling in the $^2\Sigma$ state.

TABLE III. *Fine structure of lines near the origin. Values given are displacements in cm^{-1} from the no-field position of the line in question. The question mark indicates that the pattern overlaps with another, the identity of the component being uncertain.*

Line	12,900 gauss		20,000 gauss		33,600 gauss	
	Obs.	Calc.	Obs.	Calc.	Obs.	Calc.
$PQ_{12}(\frac{1}{2})$	-0.70 + .52	-0.60 + .60	-0.93	-0.94 + .94		-1.58 +1.58
$P_1(1\frac{1}{2})$	-0.75 - .20 + .34	-1.45 -0.88 - .28 + .28 + .88 +1.45	-1.36 -0.51 + .36	-2.28 -1.39 -0.44 + .44 +1.39 +2.28	-0.84	-3.78 -2.31 -0.74
$P_1(2\frac{1}{2})$					-2.80? -2.17? -1.29 -0.35 + .40	-2.91 -2.09 -1.27 -0.42 + .29
$Q_2(\frac{1}{2})$	-0.59	-0.46 + .75	-0.81	-0.80 +1.08	-1.45	-1.44 +1.73
$Q_1(1\frac{1}{2})$	-1.57 -0.93 - .20 + .37 + .80	-1.53 -0.96 - .22 + .25 + .81 +1.31	-2.36 -1.46 - .43 + .53	-2.41 -1.55 - .55 + .40	-4.20 -2.39 - .57	-3.94 -2.43 - .80 + .66 +2.21 +3.67
$Q_1(2\frac{1}{2})$					-4.03? -3.09 -2.28 -1.30 -0.38 + .28	-3.91 -3.08 -2.24 -1.38 -0.47 + .32
$R_2(\frac{1}{2})$	-0.46 + .74	-0.42 + .86	-0.78 +1.14	-0.75 +1.17	-1.28 +2.00	-1.47 +1.81
$RR_{21}(1\frac{1}{2})$	-0.24 + .52 +1.17 +2.03?	-1.16 -0.57 -0.05 + .61 +1.25 +1.82	+0.00 + .92 +1.74 +2.52	-2.12 -1.13 -0.03 + .87 +1.65 +2.51		

respect to the no-field position. Such asymmetry, which appears throughout the band, is due to the fact that the Zeeman energy levels in the $^2\Sigma$ states are symmetrical with respect to the mid-points of the p -type doublet levels, while a no-field line arises from a level displaced from a mid-point by $0.108 (K + \frac{1}{2})$. The agreement between theory and observation for these lines is not too good. Measurement is difficult in the Q_2 and R_2 doublets because of the prominence of the satellite line in the no-field spectrum of each. It is nearly as intense as the no-field line and barely resolved from it.

No more patterns are resolved in the branches with subscript "2". But the more open patterns of the early lines of the branches with subscript "1" are resolved, where observable. The agreement with theory is generally good.

The intensities fall off rapidly as one proceeds outward from the components nearest the no-field line. This corresponds to the decreasing number of members of the close groups in the theoretical pattern. Data on the first line of the $^{RR}R_{21}$ branch is also given, though the pattern is so faint as to be barely observable on the plates. This pattern is noteworthy because of the unusually large shift of the whole pattern with respect to symmetry about the no-field position. This shift is due to the fact that the ρ -type doubling in the $^2\Sigma$ state for this line is larger than in other lines with the same final J .

Patterns of lines of intermediate J ". Several of the lines of intermediate J " are so situated that the complete patterns may be observed. The appearance of these patterns is just what would be expected from Fig. 5. Thus the branches with subscript "2" consist of two separated parts, one (the low-frequency) fairly sharp, intense, and less displaced than the other, which is wide and faint. On the other hand, the pattern of a line with subscript "1" consists of two contiguous parts, the high-frequency part being intense, fairly sharply defined, and narrower than the fainter low-frequency part. The fainter part of each type of pattern becomes rapidly too weak to observe as one proceeds out in the band, though on one plate at 20500 gauss the complete patterns of $Q_2(12\frac{1}{2})$ and $Q_1(12\frac{1}{2})$ could be observed. The numerical description of these patterns is contained in Table IV. Some are reproduced in Fig. 6.

In this group should be included the observable lines of the $^{RR}R_{21}$ branch. This branch, being beyond the head of the band, offers excellent opportunity

TABLE IV. Quantitative description of patterns of lines with intermediate J ". Only patterns which could be fairly completely observed are included. Measurements are given to the nearest 0.05 cm^{-1} .

a. Lines with subscript "1".

Field	Line	Total width		Width		Intense part Position with respect to no-field	
		Obs.	Calc.	Obs.	Calc.	Obs.	Calc.
20000	$P_1(5\frac{1}{2})$	3.7	4.0	1.6	1.4	+0.45	+0.6
	$P_1(6\frac{1}{2})$	3.2	4.0	1.7	1.2	+ .3	+ .5
33600	$P_1(5\frac{1}{2})$	Indef.		2.4	2.7	+0.9	+1.2
	$P_1(6\frac{1}{2})$	"		2.0	2.5	+ .7	+1.1
20000	$Q_1(4\frac{1}{2})$	4.2	4.0	1.5	1.4	+0.0	+0.6
	$Q_1(5\frac{1}{2})$	4.4	4.1	1.4	1.2	+ .1	+ .5
	$Q_1(6\frac{1}{2})$	4.5	4.1	1.3	1.0	+ .3	+ .4
	$Q_1(9\frac{1}{2})$	4.9	4.2	sharp	.5	+ .25	+ .2
	$Q_1(12\frac{1}{2})$	4.6	4.7	"	.4	+ .25	+ .15
33600	$Q_1(4\frac{1}{2})$	6.45	6.70	2.75	2.75	+1.0	+1.2
	$Q_1(5\frac{1}{2})$	5.8	6.65	2.35	2.45	+0.85	+1.1
	$Q_1(6\frac{1}{2})$	6.25	6.65	2.25	2.25	+ .85	+1.0
	$Q_1(9\frac{1}{2})$	6.3	6.7	1.9	1.7	+ .7	+ .7
20000	$R_1(4\frac{1}{2})$	4.5	4.1	1.3	1.2	+0.5	+0.5
33600	$R_1(4\frac{1}{2})$	6.1	6.8	2.2	2.4	+ .9	+1.2

TABLE IV (continued)

b. Lines with subscript "2". (Positions measured with respect to no-field positions.)

Field	Line	High-frequency part of pattern				Low-frequency part of pattern			
		Position		Width		Position		Width	
		Obs.	Calc.	Obs.	Calc.	Obs.	Calc.	Obs.	Calc.
20000	$P_2(3\frac{1}{2})$	+1.45	+1.3	1.7	1.5	-0.65	-0.6	0.9	0.5
	$P_2(4\frac{1}{2})$	+1.5	+1.5	2.2	1.8	-.55	-.5	.95	.45
	$P_2(6\frac{1}{2})$	+2.0	+1.7	3.0	2.1	-.4	-.4	.7	.3
33600	$P_2(3\frac{1}{2})$	+1.9	+2.0	2.1	2.1	-1.1	-1.3	1.05	1.1
	$P_2(4\frac{1}{2})$	+2.1	+2.1	2.8	2.65	-1.0	-1.2	1.2	1.1
	$P_2(6\frac{1}{2})$	Indef.	+2.3	Indef.	3.3	-0.9	-1.0	1.1	1.1
20000	$Q_2(3\frac{1}{2})$	+1.4	+1.45	1.65	1.6	-0.35	-0.6	1.0	0.4
	$Q_2(6\frac{1}{2})$	+1.6	+1.9	3.0	2.5	-.3	-.35	.8	.3
	$Q_2(8\frac{1}{2})$	+2.0	+2.2	2.35	2.9	-.25	-.25	—	.3
	$Q_2(10\frac{1}{2})$	+2.3	+2.5	2.6	3.2	-.25	-.2	1.0	.3
	$Q_2(11\frac{1}{2})$	+2.6	+2.75	2.9	3.3	-.2	-.2	1.1	.3
	$Q_2(12\frac{1}{2})$	+2.8	+3.0	3.1	3.4	-.2	-.2	1.0	.3
33600	$Q_2(3\frac{1}{2})$	Too faint to measure				-1.0	-1.2	0.9	0.7
	$Q_2(6\frac{1}{2})$					-0.8	-0.9	1.2	0.7
	$Q_2(8\frac{1}{2})$					-.65	-.75	1.0	.6
	$Q_2(10\frac{1}{2})$					-.6	-.6	1.0	.6
	$Q_2(11\frac{1}{2})$					-.55	-.55	1.2	.6
	$Q_2(12\frac{1}{2})$					-.55	-.5	1.0	.6
20000	$R_2(2\frac{1}{2})$	+1.35	+1.25	1.3	1.3	-0.65	-0.6	sharp	0.1
	$R_2(3\frac{1}{2})$	+1.35	+1.25	1.4	1.45	-.55	-.5	sharp	.1
33600	$R_2(2\frac{1}{2})$	+1.8	+2.05	1.75	1.8	-1.25	-1.15	1.0	0.6
	$R_2(3\frac{1}{2})$	+1.85	+2.20	2.1	2.45	-1.05	-1.05	0.8	.65

Notes to Table IV. 1. The data at 20000 gauss are the average of measurements on 4 sets of plates between 18200 and 20700 gauss, the measurements being adjusted to 20000 gauss, assuming the effects proportional to the field in this range.

2. Since the width of a no-field line, as determined by the blackened portion of the plate, is about 0.5 cm^{-1} , measured widths of less than 1 cm^{-1} , say, have little meaning. In a well-exposed part of a pattern, the observed width might easily be 0.5 cm^{-1} greater than the actual width, or range of wave number, of the part. The negative parts of the Q_2 patterns, however are definitely wider than expected from the theory.

3. In both $P_2(6\frac{1}{2})$ and $Q_2(6\frac{1}{2})$ the observed high-frequency part at 20000 gauss is abnormally wide.

TABLE V. Quantitative description of the Zeeman patterns of the $^{RR}R_{21}$ branch, and comparison with the theory. The values at 20000 gauss are figured to the nearest 0.05 cm^{-1} . Observations at 18200 and 20500 were adjusted to 20000 gauss, assuming that the effect was proportional to the field, and averaged.

Field	J''	Total width		Position of negative edge with respect to no-field line		Position of positive sharp comp. with respect to no-field line	
		Obs.	Calc.	Obs.	Calc.	Obs.	Calc.
12900	$2\frac{1}{2}$	2.86	2.89	-1.40	-1.31	+1.35	+1.40
	$3\frac{1}{2}$	2.95	2.85	-1.38	-1.25	1.49	1.48
	$4\frac{1}{2}$	2.89	2.96	-1.18	-1.25	1.62	1.63
	$5\frac{1}{2}$	3.06	3.06	-1.22	-1.23	1.81	1.79
20000	$2\frac{1}{2}$	4.4	4.3	-1.9	-2.05	1.4	Indef.
	$3\frac{1}{2}$	4.3	4.2	-2.0	-1.95	1.45	1.4
	$4\frac{1}{2}$	4.35	4.2	-1.85	-1.95	1.4	1.35
	$5\frac{1}{2}$	4.3	4.2	-1.85	-1.9	1.4	1.35
	$6\frac{1}{2}$	4.3	4.25	-2.0	-1.9	1.3	1.35

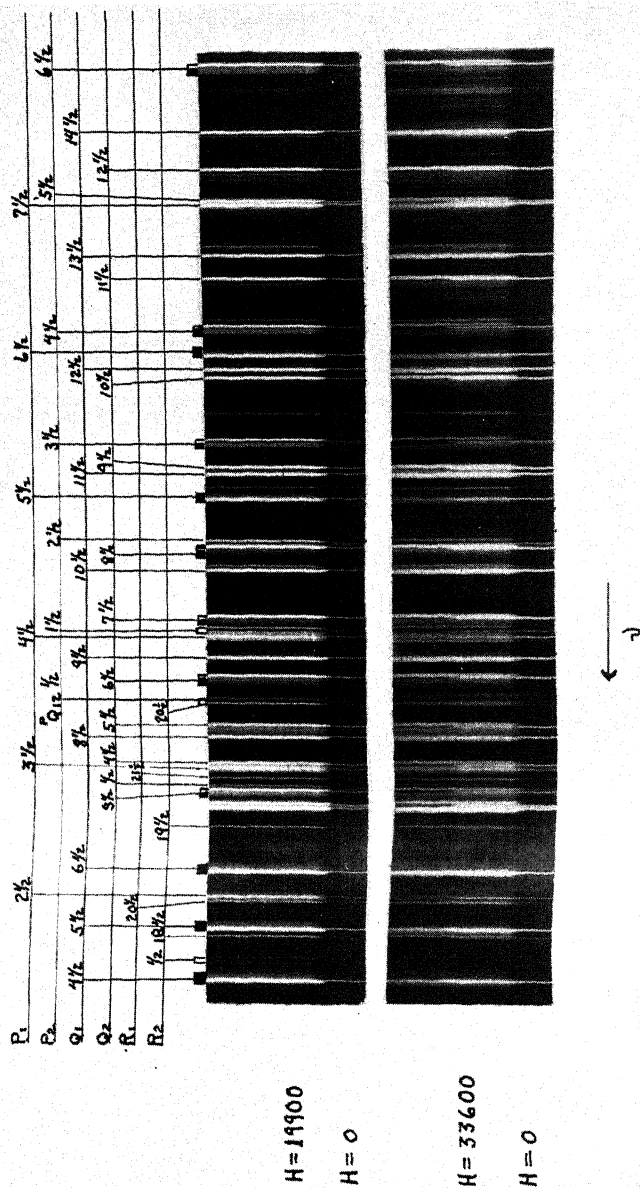


Fig. 6. Reproductions of a part of the 3064A band, at two fields, together with the no-field comparison spectra. The patterns at the lower field are labelled with the usual line notation, and those at the higher field can be identified by comparison. The effects, such as doubling, broadening, and displacement are seen to be roughly proportional to the field. As representative patterns, $P_2(3\frac{1}{2})$, $Q_1(6\frac{1}{2})$, $Q_2(6\frac{1}{2})$, $R_1(20\frac{1}{2})$, $R_2(\frac{1}{2})$ might be suggested. Some satellites can be seen in the no-field spectrum, e.g. in $P_2(3\frac{1}{2})$, $P_2(4\frac{1}{2})$, $P_2(6\frac{1}{2})$, on the high frequency side of the main branch line. There are a great many apparently spurious lines, especially on the high field plate.

for observation, but is very weak. Only 6 or 7 lines were obtained with sufficient intensity to measure accurately. The Zeeman pattern of each of these consists of a broad sharp-edged pattern which is divided into two parts, a broad low-frequency part and a sharper high-frequency part whose sharpness increases with increasing J'' . This is exactly the calculated behavior. The two parts have about the same maximum intensity, in contrast to the

TABLE VI. Zeeman patterns of $^{PP}P_{12}$ branch.

Field	J''	Total width (cm ⁻¹)		Position of negative edge with respect to no-field position (cm ⁻¹)	
		Obs.	Calc.	Obs.	Calc.
12900	$3\frac{1}{2}$	2.15	2.4	-1.3	-1.3
	$4\frac{1}{2}$	2.25	2.7	-1.4	-1.45
20000	$3\frac{1}{2}$	3.4	3.75	-1.7	-1.95
	$4\frac{1}{2}$	3.4	4.1	-1.8	-2.15

patterns of the main branch lines. In the latter the intensity of the concentrated part is much greater than that of the wider part, as one would expect. The results of observation and the comparison with theory are contained in Table V.

Of the lines ascribed to the $^{PP}P_{12}$ branch only two have Zeeman patterns sufficiently intense and in the clear to permit definite measurements. These

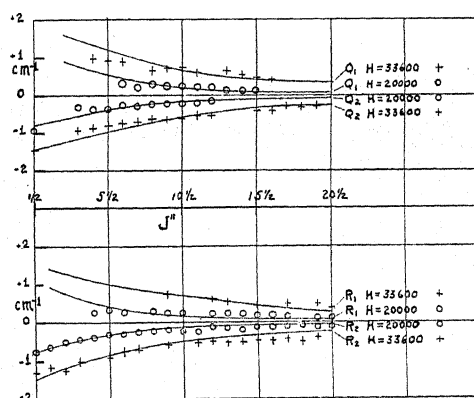


Fig. 7. Displacements of the narrow intense parts of the patterns of Q and R branches. The solid curves give the calculated displacements as estimated from plots like Fig. 5. The crosses and circles are the observed displacements.

two, $J'' = 3\frac{1}{2}$ and $J'' = 4\frac{1}{2}$, have been observed at 12900 and 20500 gauss. The total width and position with respect to no-field of these patterns is in fair agreement with the theory (Table VI). The intensity distribution, however, is surprising. For the calculations indicate a fairly uniform distribution of components from edge to edge of the pattern, while the observed pattern consists of two parts, a low-frequency narrow part and a high-fre-

quency wider part, with possibly a faint band between. Other lines assigned to this branch apparently have the characteristic wide patterns, but they are partly obscured by other lines. Since there are no other lines in this spectral region which show such width of pattern, the Zeeman effect substantiates the assignment of these lines to the $^{PP}P_{12}$ branch.

Lines with large values of J'' . The Zeeman patterns of lines with large values of J'' theoretically consist of the concentrated slightly displaced part and the wide diffuse part (Fig. 5). The latter is too weak to photograph. The intense sharp part, however, may be followed apparently as far as the band itself. Hence the Zeeman spectrum looks almost like the no-field spectrum, except for a slight broadening and a small displacement of each line, positive for those branches subscribed "1", negative for those subscribed "2". The displacements of these intense parts in the Q and R branches is plotted in Fig. 7. The P branches behave similarly. The solid curves show the calculated displacements. The behavior of the R branches at 20000 gauss is also shown in Fig. 5. Several patterns of large J'' are reproduced in Fig. 6.

I am glad to express my gratitude to Professor E. C. Kemble for suggesting this problem, to Dr. F. H. Crawford for advice and criticism throughout the work, and to Dr. E. L. Hill for many discussions of the application of the theory of the Zeeman effect. I am also very grateful to the laboratory technicians, particularly Mr. H. W. Leighton, for assistance in the manufacture of apparatus. It should also be mentioned that a large part of the apparatus used in this work was acquired through the generosity of the Milton Fund of Harvard University.

THE ZEEMAN EFFECT IN THE RED CaH BANDS

BY WILLIAM W. WATSON AND WILLIAM BENDER

SLOANE PHYSICS LABORATORY, YALE UNIVERSITY

(Received May 1, 1930)

ABSTRACT

The Zeeman effect in the red ${}^2\Pi \rightarrow {}^2\Sigma$ and ${}^2\Sigma \rightarrow {}^2\Sigma$ CaH bands, together with new satellite branches in the ${}^2\Pi \rightarrow {}^2\Sigma$ system, are reported. Field strengths up to 30,000 gauss were employed, the dispersion of the large concave grating in a parallel light mounting being about 2.1 Å per mm.

Satellite series in the ${}^2\Pi \rightarrow {}^2\Sigma$ bands.—The ${}^0P_{12}$ satellite branches are measured for both the A and A' bands. These frequencies together with certain combination relations fix the hitherto uncertain J numbering in the Q branches, and hence the size of the Λ -type doubling. This doubling is very large (70 cm^{-1} at $K=34\frac{1}{2}$) and of opposite sign to that usually found in other bands.

Zeeman effect in the ${}^2\Pi \rightarrow {}^2\Sigma$ bands.—General agreement with the pattern blocks predicted by Hill's theoretical formulas for the lower K' states is found. Intensity variations with increasing field strength are described. For $K' > 19$, where the no-field spin doublet components come together and cross over, uncoupling effects occur. Only the transitions from anti-parallel S and K in the ${}^2\Pi$ state to parallel S and H in the ${}^2\Sigma$ state, and from parallel S and K to antiparallel S and H persist. The displacements of these components are proportional to H^2 . At 30,000 gauss the high K components in the P_1 branch broaden out and go rapidly to zero intensity, but the P_2 field components remain narrow and strong. With complete uncoupling by this "strong field," these components are probably the transitions from parallel S and H in the ${}^2\Pi$ state to parallel S and H in the ${}^2\Sigma$ state. For the highest K levels, these high-field P_2 components are displaced farther from the no-field position and become more diffuse, suggestive of an approach to Hund's case d .

Zeeman effect in the ${}^2\Sigma \rightarrow {}^2\Sigma$ bands.—Contrary to the usual findings for bands of this type, broad and prominent Zeeman patterns here occur for $K' > 8$ which are quite similar to those found in a ${}^2\Pi$ state. The explanation is probably that an appreciable magnetic moment is created in the upper $4s\sigma^2 3d\sigma^2 {}^2\Sigma$ state by the increasing component of L along the rotational axis.

INTRODUCTION

A THEORETICAL treatment of the Zeeman effect in doublet band spectra has recently been published by E. L. Hill,¹ and the formula for the magnetic field patterns have been nicely verified by Almy and Crawford² for the case of the MgH ${}^2\Pi \rightarrow {}^2\Sigma$ band system. This theory considers molecules which can be classed under Hund's cases (a) and (b) or for cases intermediate between (a) and (b), neglects "rho-type" doubling, and considers the only uncoupling effect to be that on the electron spin. There are examples of diatomic molecules, however, where the rho-type doubling becomes very large, and where the coupling of the electronic orbital angular momentum to the rotational axis would be accompanied by a magnetic

¹ E. L. Hill, Phys. Rev. **34**, 1507 (1929).

² G. M. Almy and F. H. Crawford, Phys. Rev. **34**, 1517 (1929).

moment in that direction. In the $\lambda 6389^2\Sigma \rightarrow ^2\Sigma$ and $\lambda 7000^2\Pi \rightarrow ^2\Sigma$ CaH bands, for which these effects become very large, the Zeeman effect predicted by Hill's theory is to be expected, then, for the lower rotational states, but for the highest rotational states new magnetic field patterns should be found. Measurements of this perturbing effect of an external field should increase our knowledge of the dynamics of molecules exhibiting such a very large ρ -type and Λ -type doubling.

The analysis of Hulthén,³ together with Mulliken's⁴ discussion of these data, demonstrate the marked distortion increasing with the rotation in these CaH bands. In the upper electronic state of the $^2\Sigma \rightarrow ^2\Sigma$ band the orientation energy of the spin S with respect to the nuclear rotation axis, as measured by the separation of the F_1 and F_2 terms, is exceptionally large, the rotational doublets being separated even at the origin of the band by 1.3 cm^{-1} . Also the usual relation for $^2\Sigma$ states, $F_1 > F_2$, is reversed in this case. In the $^2\Pi$ state of the $\lambda 7000$ band the Λ -type doubling is very large (see below), thereby indicating a large L_{perp} (component of orbital angular momentum L perpendicular to the electric axis of the molecule), and the usual $^2\Pi$ state relation, $F_2(J) > F_1(J+1)$, which does hold for low J values is reversed for $J > 19\frac{1}{2}$. The ρ -type doubling in the common lower $^2\Sigma$ state is small, as in most $^2\Sigma$ states.

EXPERIMENTAL PROCEDURE

Our source was an intermittent d.c. arc in a modified Back chamber mounted on the pole faces of a large water-cooled Weiss electromagnet. The moving electrode was a small block of metallic calcium mounted on a tungsten wire, while the fixed electrode was a thin copper strip insulated from the pole face by a piece of mica. The arc was struck in a hydrogen atmosphere at from 5 to 10 cm pressure, and since the arc chamber was not absolutely vacuum tight, a stream of hydrogen gas from a tank was pumped slowly through the apparatus during the exposures. It was necessary to renew the calcium electrode at frequent intervals during each run. The bands were photographed in the second order of a large concave grating mounted in parallel light, the dispersion being approximately 2.1 \AA per mm.

The $\lambda 6389$ band was photographed with Eastman panchromatic plates hypersensitized by an ammonia bath. Plates were taken with field strengths of 14,000, 24,600 and 29,950 gauss with no polarizing prism in the path, and at 29,950 gauss in the perpendicular and parallel polarizations separately, with the exposure times up to 12 hours when the Nicol prism was used. The $\lambda 7000$ band was recorded on Eastman 40 and panchromatic plates dyed with dicyanin. Field strengths of 10,500 and 30,000 gauss were used, the times of actual exposure on the slit running to 18 hours. On every plate in addition to the field exposure a no-field comparison and an iron arc spectrum were photographed. The strength of the magnetic field was determined by measurements of the patterns of the Zn triplet $\lambda\lambda 4680, 4722$, and 4811 .

³ E. Hulthén, Phys. Rev. 29, 97 (1927).

⁴ R. S. Mulliken, Phys. Rev. 30, 138 (1927), and 32, 388 (1928).

NEW SERIES AND MAGNITUDE OF Λ -TYPE DOUBLING IN ${}^2\Pi \rightarrow {}^2\Sigma$ BAND

The J values assigned by Hulthén³ to the lines in the P and R branches of the $\lambda 7000$ band are correct when reduced by $\frac{1}{2}$ unit in order to agree with the quantum mechanics numbering. But since it is apparent from Hulthén's data that the ordinary PQR combination relation does not even hold approximately, and since no (1, 0) or (0, 1) band seems to be available for combination checking purposes, the J numbering in the Q branches has been heretofore undetermined. Now our spectrograms indicate that all the satellite series to be expected in a ${}^2\Pi_{ab}$ state⁵ are present and with fair intensity in this band. In particular the ${}^0P_{12}$ satellite branch⁶ proceeds to the red from the P branch head in a region clear of other lines. The frequencies of the lines in this branch can be calculated from the relation⁷

$${}^0P_{12}(J) = Q_1(J-1) + [F_1''(J-1) - F_2''(J-2)] - [F_2''(J) - F_2''(J-2)]_{(1)} \\ = Q_1(J-1) + 0.045(J - 1\frac{1}{2}) - \Delta_2 F_2''(J-1).$$

The second term on the right side of this equation involves the empirical rule for the separation of the spin components in the lower state of these bands,⁵ while the $\Delta_2 F_2''$ values can be taken directly from Hulthén's tables. The proper Q_1 frequencies to so combine with these F'' differences as to give the observed satellite branch lines can be thus uniquely determined, and the important point is that this fixes the J numbering of the Q_1 branch and hence the exact course of the Λ -type doubling in the F_1' levels. Table I

TABLE I. ${}^0P_{12}$ Series in (0,0) and (1,1) CaH ${}^2\Pi \rightarrow {}^2\Sigma$ bands.
(0,0) or A band (1,1) or A' band

J	ν calc.	ν obs.	ν calc.	ν obs.
$11\frac{1}{2}$	14231.68	14231.58		
$12\frac{1}{2}$	18.66	18.62		
$13\frac{1}{2}$	06.17	05.88		
$14\frac{1}{2}$	193.77	193.48		
$15\frac{1}{2}$	81.55	81.36		
$16\frac{1}{2}$	69.69	69.61	14209.91	14209.78
$17\frac{1}{2}$	58.23	58.08	198.66	198.55
$18\frac{1}{2}$	47.12	46.94	87.81	87.54
$19\frac{1}{2}$	36.21	36.07	77.28	76.92
$20\frac{1}{2}$	25.86	25.61	66.92	66.75
$21\frac{1}{2}$	15.78	15.49	56.97	56.60
$22\frac{1}{2}$	06.02	05.72	47.36	
$23\frac{1}{2}$	096.53	96.36	38.17	37.84
$24\frac{1}{2}$	87.64	87.35		
$25\frac{1}{2}$	78.97	78.68		
$26\frac{1}{2}$	70.73	70.51		
$27\frac{1}{2}$	62.56	62.70		

⁵ Cf. R. S. Mulliken, Phys. Rev. 32, 388 (1928) for a detailed account of the various possible branches in ${}^2\Pi \rightarrow {}^2\Sigma$ transitions.

⁶ We are using, throughout, the notation recommended by R. S. Mulliken in his forthcoming article in this journal on standardized notation for description of molecular spectra. This branch would be designated formerly as ${}^PP_{12}$.

⁷ Compare level diagram in ref. 5. Note particularly that the ${}^0P_{12}$ and Q_1 transitions are from the same A sublevels in the upper state.

gives the wave-numbers of the observed ${}^0P_{12}$ lines for both the (0, 0) and (1, 1) bands together with their calculated values from Eq. (1). The agreement of the observed and calculated frequencies can only be produced by increasing Hulthén's J numbering in the Q_1 branch of the (0, 0) band (his A band) by $1\frac{1}{2}$ units, and in the Q_1 branch of the (1, 1) band (his A' band) by $\frac{1}{2}$ unit. Two new Q_1 lines should be added to Hulthén's tabulation for the A band; $Q_1(\frac{1}{2})$ 14393.31 and $Q_1(1\frac{1}{2})$ 14396.71. These are clearly present and of good intensity on our plates. Because of the confusion of stronger lines in the short wave-length side of these bands, the accurate measurement of the corresponding ${}^5R_{21}$ is rendered difficult. Fragments of this branch have been located, however, and seem to indicate similarly that Hulthén's J numbering in the Q_2 branch should also be raised $1\frac{1}{2}$ units. In computing the magnitude of the Λ -type doubling in the F_1' terms we use the relation

$$\begin{aligned} & [R_1(J) - Q_1(J)] - [Q_1(J+1) - P_1(J+1)] \\ &= F_{1B}'(J+1) - F_{1A}'(J) - F_{1A}'(J+1) + F_{1B}'(J) \\ &\cong F_{1B}'(J+\frac{1}{2}) - F_{1A}'(J+\frac{1}{2}). \end{aligned} \quad (2)$$

Table II gives in condensed form the course of this doubling, showing that for the lowest J levels the doubling increases in the usual fashion;⁸ but that at $J=6\frac{1}{2}$ the separation of these sublevels begins to decrease, becomes

TABLE II. Λ -type doubling in F_1' levels of (0,0) ${}^2\Pi \rightarrow {}^2\Sigma$ band calculated from Eq. (2).

J	$F_{1B}'(J+\frac{1}{2}) - F_{1A}'(J+\frac{1}{2})$	J	$F_{1B}'(J+\frac{1}{2}) - F_{1A}'(J+\frac{1}{2})$
$1\frac{1}{2}$	+2.04	$11\frac{1}{2}$	-0.54
$2\frac{1}{2}$	2.66	$12\frac{1}{2}$	-1.76
$3\frac{1}{2}$	3.06	$14\frac{1}{2}$	-4.61
$4\frac{1}{2}$	3.26	$19\frac{1}{2}$	-14.00
$5\frac{1}{2}$	3.27	$24\frac{1}{2}$	-25.89
$6\frac{1}{2}$	3.06	$29\frac{1}{2}$	-53.38
$9\frac{1}{2}$	1.45	$34\frac{1}{2}$	-69.71
$10\frac{1}{2}$	+0.53		

zero at $J=11\frac{1}{2}$, and increases to very large negative values for the highest rotational levels. The F_2' levels proceed apparently in much the same way, although usually⁸ F_2 levels show an almost negligible Λ -type doubling.

This large rotational doubling in the Π state is evidence for a very considerable growth in L_{perp} . There is reason therefore for supposing that the effect of an external magnetic field on these high rotational levels would be a variation of that for cases a to b .

THE ZEEMAN EFFECT IN THE ${}^2\Pi \rightarrow {}^2\Sigma$ BAND

We will consider the effect of the magnetic field first for the lines of low and intermediate K values, and then for the high rotation lines. For the lines in the first group the CaH molecule is intermediate between case a and case b , and Hill's theory should give a good description of the observed patterns. Since the ρ -type doubling is small in the lower ${}^2\Sigma$ state, the only effect of the field in this state should be to uncouple the spin S from its weak coupling with K , so that these levels all become sharp doublets of separation

⁸ J. H. Van Vleck, Phys. Rev. **33**, 467 (1929). R. S. Mulliken, Phys. Rev. **33**, 507 (1929).

$2\Delta\nu_{\text{norm}}$. In general one must make a detailed computation with Hill's equation (22), the constants for our $^2\Pi$ state being $B=4.3\text{ cm}^{-1}$, $\lambda=+19\text{ cm}^{-1}$, $\Lambda=1$. Since for no line have we observed the resolved magnetic fine structure due to all the possible values of M , the magnetic quantum number, it is only necessary to calculate the position and overall widths of the blocks of unresolved components in the patterns by using $M=+J$, 0, and $-J$. These patterns we have calculated for $K'=3$, 10, and 18. For $K'=18$, and even for $K'=10$, Hill's energy equation considerably overestimates the width of the spin doublet interval, since it does not consider ρ -type doubling, and therefore complete quantitative agreement with the observations is not to be expected. The details of the comparison, together with some observations on lines with approximately these K' values are presented in Table III. Figs. 1 and 2 show graphically this comparison for $K'=3$ and 10.

TABLE III. Comparison of observed and calculated patterns for low and intermediate values of K in $^2\Pi \rightarrow ^2\Sigma$ band.

(In this and the other tables + indicates field radiation to the higher frequency side, - to the lower frequency side, of the no-field position.)

Lines	Patterns																										
$P_1(2\frac{1}{2}), (4\frac{1}{2})$ $(5\frac{1}{2}), (6\frac{1}{2})$	$K'=1$ to 5 $H=10,500$ gauss, $\Delta\nu_n=0.49$ cm ⁻¹ . Theory predicts at $K'=3$ a symmetrical doublet, with 0.98 cm ⁻¹ between centers of the two component blocks, separation between "inside" edges 0.61 , width of each component 0.38 ; Obs. doublet width																										
$Q_1(2\frac{1}{2}), (4\frac{1}{2}), (5\frac{1}{2})$ $R_1(2\frac{1}{2}), (3\frac{1}{2})$	<table><tr><th>K'</th><th>P</th><th>Q</th><th>R</th><th></th></tr><tr><td>1</td><td>0.78</td><td></td><td></td><td rowspan="5">Measurements from center to center showing that since obs. width < theoretical, inside edges are stronger. Components same intensity for $K'=1$ and 2, but red component then becomes stronger, and at $K'=5$ is much stronger than violet component.</td></tr><tr><td>2</td><td></td><td>0.84</td><td></td></tr><tr><td>3</td><td></td><td></td><td>0.71</td></tr><tr><td>4</td><td>0.83</td><td>0.70</td><td>0.74</td></tr><tr><td>5</td><td>0.80</td><td></td><td></td></tr></table>	K'	P	Q	R		1	0.78			Measurements from center to center showing that since obs. width < theoretical, inside edges are stronger. Components same intensity for $K'=1$ and 2, but red component then becomes stronger, and at $K'=5$ is much stronger than violet component.	2		0.84		3			0.71	4	0.83	0.70	0.74	5	0.80		
K'	P	Q	R																								
1	0.78			Measurements from center to center showing that since obs. width < theoretical, inside edges are stronger. Components same intensity for $K'=1$ and 2, but red component then becomes stronger, and at $K'=5$ is much stronger than violet component.																							
2		0.84																									
3			0.71																								
4	0.83	0.70	0.74																								
5	0.80																										
	$H=30,000$ gauss, $\Delta\nu_n=1.41$. Calculated pattern wide diffuse doublet, approx. symmetrical about no-field position; roughly in agreement with obs. $P_1(4\frac{1}{2})$ pattern. - components inside edge at -0.89 ; obs. -0.94 . Violet block's outermost edge at $+1.93$; obs. $+2.06$. Other two edges obscured. Q_1 lines also become diffuse doublets but the intensity distribution is very different: the two blocks are of equal intensity, whereas at the lower field strength the "wings" are more intense; maximum intensity in each block is near the inner edge, nearest the no-field position. Red component's maximum at -0.72 , violet's at $+0.79$, whereas predicted inside edges are -0.89 and $+0.85$ cm ⁻¹ .																										
$P_1(11\frac{1}{2}), (12\frac{1}{2})$ $(13\frac{1}{2})$ $Q_1(10\frac{1}{2}), (13\frac{1}{2})$ $P_2(9\frac{1}{2}), (10\frac{1}{2}), (11\frac{1}{2})$ $Q_2(13\frac{1}{2})$	$K'=9$ to 14 $H=10,500$. Calculated patterns are doublets. F_1 states: calculated inside edge of red component at -0.08 for $K'=10$; obs. -0.09 -0.08 , -0.14 for $P_1(11\frac{1}{2})$, $P_1(12\frac{1}{2})$, and $Q_1(10\frac{1}{2})$ respectively. Width of red components: calc., 0.78 ; obs., 0.39 , 0.35 , and 0.30 respectively—i.e., obs. blocks much narrower than calculated width. P_1 and R_1 violet components of negligible intensity, but in $Q_1(10\frac{1}{2})$ the violet component is weaker than the red component but is present starting at the red component and extending to $+0.51$, against the theoretical max. displacement $+0.90$. F_2 states: Predicted doublets are approximately symmetrical with respect to no-field line, have components narrower, 0.48 cm ⁻¹ , and separated by 0.98 cm ⁻¹ between centers for $K'=10$. Observed patterns in good agreement with theory. Violet or "wing" components much stronger than red components and narrower than predicted.																										

TABLE III (continued).

	K'	Observed F_2 Patterns		
		Doub. width	Component widths	
P_2	9	0.85	-0.37	+0.28
Q_2	14	0.79	-0.46	+0.31

$H=30,000$. F_1 states: Lines should become broad symmetrical doublets in field according to theory. P_1 and R_1 patterns not present; probably too weak and diffuse. Q_1 lines become strong broad doublets, narrowing with increasing K , and whose inside edges nearest the no-field line are much the stronger parts of the patterns. For $K'=10$ these maxima are at -0.50 and $+0.55$ as against computed inside edges for the blocks at -0.28 and $+0.30$. The red "wing" components are just as intense as the violet components.

F_2 states: Calculated field doublets are symmetrical, have inside edges farther from no-field position, and have narrower component blocks. All in agreement with observations, but obs. components much narrower than predicted, hence quite intense; also two components are equally strong.

P_2 component separations from no-field line.

K'	Calc.	Obs. -	Obs. +
9		1.14 to 1.62	1.08 to 1.37
10	0.74 to 2.08	1.15 to 1.45	1.05 to 1.34
11		1.17 to 1.57	0.98 to 1.31

$K'=18$

$P_1(19\frac{1}{2})$
 $Q_1(18\frac{1}{2})$
 $P_2(18\frac{1}{2})$
 $R_2(16\frac{1}{2})$

$H=10,500$. According to theory all lines become doublets in the field; the F_1 patterns with very narrow components separated by 0.96 . Actually only the red "wing" components can be seen; in $P_1(19\frac{1}{2})$ from -0.08 to -0.43 ; in $Q_1(18\frac{1}{2})$ from $+0.01$ to -0.29 , although theory has this component at -0.48 .

F_2 patterns are calculated to be more diffuse doublets with but 0.21 cm^{-1} between inside edges and center of components at -0.48 and $+0.50$. For $P_2(18\frac{1}{2})$ only violet component observed from $+0.07$ to $+0.38$. $R_2(16\frac{1}{2})$ becomes a doublet with strong violet component from $+0.16$ to $+0.46$ and very weak red component at -0.27 . Theory predicts no-field spin doublet separation 15.8 cm^{-1} , whereas experimentally it is but 2.5 cm^{-1} .

$H=30,000$. Theory predicts widely separated doublets (2.82 cm^{-1}) with components narrow for F_1 patterns. These are not observed. No P_1R_1 field radiation is apparent and the Q_1 pattern is broad and diffused into adjacent patterns. F_2 patterns predicted to be broad diffuse doublets with inside edges at -0.32 and $+0.35$ and centers at -1.30 and $+1.52$ for the red and violet components respectively.

Observed F_2 patterns for $K'=18$

$P_2(18\frac{1}{2})$	-0.86 to -1.30	+0.94 to +1.67
$R_2(16\frac{1}{2})$	-0.86 to -1.30	+1.22 to +1.61

Both components intense and considerably narrower than the computed widths.

Some of the more striking features of the observed patterns should be emphasized. In agreement with the theory, all of these lines apparently become doublets in the field, each component of the doublet of course being in reality a block of $2J+1$ unresolved lines, but the observed doublet width is always less than that predicted. This smaller width may be caused by the relative faintness of the outer portions of the patterns. At $10,500$ gauss, for all except the very lowest K' values, the intensity is almost entirely in the red components for the P_1 , Q_1 , R_1 patterns and in the violet components for

the P_2 , Q_2 , R_2 patterns. These are the transitions from parallel S and K in the $^2\Pi$ state to the $M_s = +\frac{1}{2}$ level in the $^2\Sigma$ state and anti-parallel S and K to $M_s = -\frac{1}{2}$ respectively, and correspond to the "wings" of Almy and Crawford's

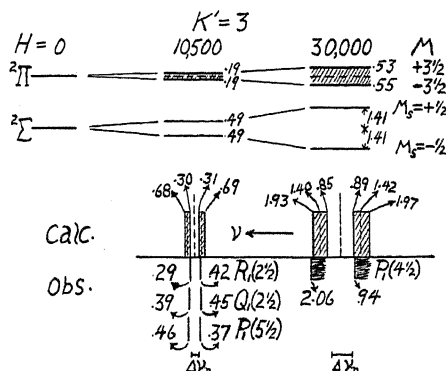


Fig. 1. Calculated splitting of the energy levels and the resulting Zeeman patterns for lines with $K'=3$ from Hill's theoretical equation (ref. 1). Of the observed lines, $P_1(4\frac{1}{2})$ and $R_1(2\frac{1}{2})$ have $K'=3$, while for $Q_1(2\frac{1}{2})$, $K'=2$ and $P_1(5\frac{1}{2})$ has $K'=4$. The corresponding P_2 , Q_2 , R_2 lines are too weak to observe. Since at 10,500 gauss the field components are narrow, only a measurement of the center of the component in each case was made. At 30,000 gauss due to overlapping patterns only the measurements given on the $P_1(4\frac{1}{2})$ line pattern could be made, but the observations indicate widths for the blocks approximately in agreement with the predictions.

MgH patterns.² The components arising from the other two possible transitions⁹ we shall refer to as the "inside" components. At 30,000 gauss, however, both components are equally strong for all the patterns measured (P_2 , R_2 ,

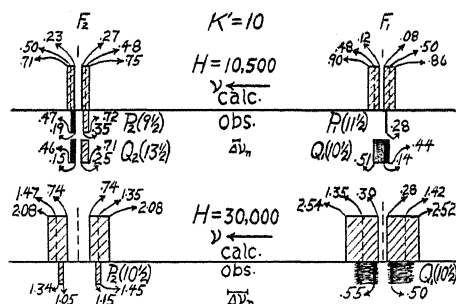


Fig. 2. Comparison of calculated and observed patterns for lines with $K'=10$. The $P_1(11\frac{1}{2})$, $Q_1(10\frac{1}{2})$ and $P_2(10\frac{1}{2})$ lines all have $K'=10$. For $P_2(9\frac{1}{2})$, $K'=9$, while for $Q_2(13\frac{1}{2})$ $K'=14$. At 10,500 gauss the "outside" components are much stronger (indicated by solid black) than the inside (shaded) components. At 30,000 gauss the P_2 components are narrower than predicted, the Q_1 components are strongest at their edges nearest the no-field line position, and both components are in all cases of equal intensity.

Q_1), thus indicating that, because the no-field spin doublet separation is still considerably greater than $\Delta\nu_n$, the coupling of S in the $^2\Pi$ state has not been

⁹ Cf. the excellent diagrams illustrating the relation between the possible transitions and the components in ref. 2.

broken down by the field. The intense concentration of the patterns of the Q_1 lines as contrasted with the apparent absence of field radiation for the P_1 and R_1 lines, however, is difficult to explain. The enlargement of a portion of this band in Fig. 3 illustrates some of these pattern changes.

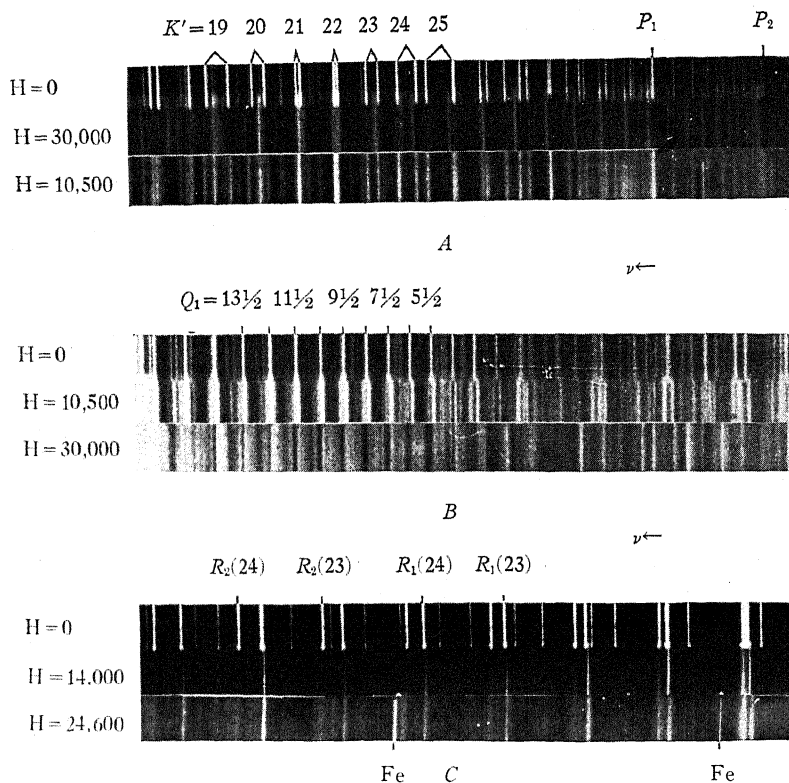


Fig. 3. Enlargements 9 times. A shows the "cross-over" region in the P branches of the $^2\Pi \rightarrow ^2\Sigma$ band. It is evident that for $K' > 24$ both the P_1 and P_2 lines for $H = 10,500$ gauss have "inside" component blocks equally strong, but that for $H = 30,000$ gauss the P_1 field radiation has broadened out and become of negligible intensity, although the P_2 components are strong. In the reproduction P_1 and P_2 denote the heads of the two branches in the no-field strip. In B note the greater intensity of the field components on the long wave length side for $H = 10,500$ gauss as compared to the equal intensity of the two field components for $H = 30,000$ gauss. In the latter case the greater intensity of the field blocks at their inside edges is evident. C gives some of the patterns for high K values in the $^2\Sigma \rightarrow ^2\Sigma$ band. The R_2 line patterns and the weak components of the R_1 lines on the high frequency side are of insufficient intensity to be brought out well in the reproduction. The breadth of the no-field lines in C is due to over exposure.

For $K' \geq 19$ where the no-field spin doublet components come close together and then cross over, making $F_1'(J+1) > F_2'(J)$, prominent and interesting "second-order" or Paschen-Back effects appear. These effects are summarized in Table IV and are illustrated in Fig. 3A for the P_1 , P_2 lines only. That a "strong field" uncoupling of S is here taking place is evidenced by first, the fact that the wing components decrease to zero intensity

TABLE IV. Magnetic field patterns at and beyond the cross-over in the P branch spin doublets in the $^2\Pi \rightarrow ^2\Sigma$ band.

K'	10,500 gauss. $\Delta\nu_n = 0.49 \text{ cm}^{-1}$
19	Practically all the intensity in the "wings". $P_1(20\frac{1}{2})$ wing at -0.28 , $P_2(19\frac{1}{2})$ wing at $+0.33$. Very little shading between the lines.
20	Now wings are weaker and the other two "inside" components have appeared. Reckoning from the P_2 line: P_1 wing at -2.07 , P_1 no-field, -1.64 ; inside components fused from -1.36 to -0.44 , P_2 wing $+0.51$.
21	Wings have disappeared. P_1 no-field at -0.57 , strong field component -0.52 to -0.29 , weaker fused field radiation from strong component to $+0.13$.
22	No-field lines have now crossed over. Field pattern one strong broad block approximately width of original spin doublet separation, 0.51 . No wings.
23	Fused inside components now separated because spin doublet separation is greater. P_2 no-field at 0.0 , P_2 component at $+0.07$, P_1 component $+1.45$, P_1 no-field $+1.54$. These P_1 and P_2 field components are equally strong. No wings. Succeeding P_1 and P_2 lines to the ends of the branches similarly affected.
	30,000 gauss. $\Delta\nu_n = 1.41 \text{ cm}^{-1}$
19	Reckoning all separations from the P_2 no-field line position in each pattern: Weak shading in field starts at P_1 no-field, -2.83 , and goes to strong band component starting at -0.91 and ending -0.41 , P_2 wing from $+1.74$ to $+2.20$.
20	Weak shading from -1.82 to strong component starting at -1.00 and ending -0.65 . P_1 no-field position is -1.64 . No evidence now of P_2 wing.
21	Rather strong shading begins sharply at -1.08 and extends to the strong, narrower field component at -0.24 . P_1 no-field position is -0.57 . No wings.
22	Lines have crossed. Strongest field line and $P_2(22\frac{1}{2})$ position at 0.00 , with field radiation extending rather intense to a strong edge at $+0.85$. P_1 position is $+0.51$. No wings.
23	Weaker fused field radiation starts at -0.35 and extends to $+1.94$. Edges of this block are well defined. Strong field component at $+0.45$ superposed. P_1 position is $+1.54$.
24	Strong field component at $+0.54$ with weaker field radiation solid from here to $+2.88$. P_1 position is $+2.50$.
25	Strong field component at $+0.74$. Broad weak field radiation for the P_1 from $+1.75$ to $+4.47$. P_1 position is $+3.53$. From here on to the P_1 head, the P_1 field radiation is very diffuse and weak causing the whole background to be slightly blackened. The strong P_2 field component blocks continue out to the P_2 head, the displacements from the no-field positions for the next four lines being $+0.65$, $+0.69$, $+0.75$ and $+0.73$, or about $\frac{1}{2}\Delta\nu_n$. For the last lines near the head, the displacements are a little greater, averaging $+0.80 \text{ cm}^{-1}$ for $K' = 36, 37, 38$, and the components are becoming definitely broader and more diffuse.

and the inside components come in strong as the spin doublet separation goes to zero. This is to be interpreted as due to the uncoupling of S from its interaction with the internal field directed along the rotational axis in the molecule, the F_2 state in which S and K are anti-parallel being replaced by the parallel orientation of S and the field H , while the F_1 state or parallel S and K is replaced by the state in which S lies anti-parallel to H .¹⁰ S and K are then separately quantized with respect to the field, giving the quantum numbers M_S and M_K . Since only the inside components representing transitions for which $M_S = 0$ occur for all levels of higher K , we infer that this uncoupling is complete. Second, the displacement of the strong P_2 field components seems to be almost exactly proportional to H^2 rather than to H as in the usual first-order Zeeman effects.

The difference between the patterns of the P_1 and P_2 lines at 30,000 gauss in this uncoupling process is striking. The one inside field component

¹⁰ Reference 1, p. 1513.

of the P_2 lines is rather narrow and intense, whereas the field radiation associated with the P_1 lines in the interval from $K'=20$ to 25 becomes increasingly broader and weaker, and for $K' > 25$ is too weak to detect. Apparently the transition from parallel S and H in the $^2\Pi$ state is very much more probable when the field is "strong" than that from the anti-parallel S and H , indicating an instability of this anti-parallel orientation.

Also to be especially noticed are the increasing separation and increasing diffuseness of these high field P_2 components for the highest K levels. This would seem to be related to the exceptionally large Λ -type doubling and consequent relatively large L_{perp} . The electric axis of the molecule at these highest rotational levels is probably becoming less effective in orienting the L , with the result that Λ is no longer a good quantum number. There is a close approach to the case d type of coupling, and the resulting changes in the magnetic moment are reflected in the broadening of these last field patterns.

THE ZEEMAN EFFECT IN THE $^2\Sigma \rightarrow ^2\Sigma$ BAND

Neglecting p -type doubling, $^2\Sigma \rightarrow ^2\Sigma$ bands should exhibit no first order Zeeman effect, for the field merely completely uncouples the spin S in both states, and with $\Delta M_S = 0$ accurately holding, no displacement of the spectrum lines is to be expected. The very pronounced p -type doubling in the $\lambda 6389$ CaH band, however, indicates a considerable energy of orientation of S with respect to an internal field directed along the rotational axis in the

TABLE V. Summary of magnetic field measurements in the $\lambda 6389$ $^2\Sigma \rightarrow ^2\Sigma$ CaH band.
($H_1 = 14,000$ gauss, $\Delta\nu_n = 0.66$. $H_2 = 24,600$ gauss, $\Delta\nu_n = 1.16$. $H_3 = 29,950$ gauss, $\Delta\nu_n = 1.41$)

K' 1 to 7	Measurements and Remarks		
	P_1 and R_1 lines (parallel S) unaffected by field $R_2(1\frac{1}{2})$ becomes a doublet in field, components at -0.35 and $+0.55$ for H_2 and -0.36 and $+0.88$ for H_3		
	Other R_2 lines are affected by field but patterns are confused with other radiation P_2 lines are doubled in field:		
K'	H_1	H_2	H_3
1	-0.42, -0.29, +0.62	-0.67 to -0.27, no + comp.	-0.67 to -0.21, no + comp.
2	-0.87 to -0.26, +0.29 to +0.54	-0.28, no + comp.	—
3	-1.02 to -0.18, +0.22 to ?	diffuse + comp.	—
4	-0.74 to -0.12, +0.35 to +0.87	diffuse + comp. ?	from -0.24 shaded to red, strong and from +0.53 shaded to violet, weak
For $K'' > 8$ all of the R_1 and R_2 lines have the patterns as given below for a few samples:			
	R_1	R_2	
12	H_1 -0.60 to -0.25 and shades to +0.93	H_2 -1.34 to -0.20 and +0.28 to +0.91 + and - components same strength	H_3 -1.74 to -0.25 and +0.42 to ? These single blocks shading to the violet from the no-field position constitute the full R_2 pattern
15	-comp. at -0.44 no + comp.	-1.15 to -0.19 strong, and +0.37 to ? weak	
21	-comp. at -0.35 no + comp.	-1.05 to -0.25 strong, and +0.49 to ? very weak	-1.29 to -0.29 strong, and +0.34 to ? weak 0.00 to +1.49 ($K' = 23$:) 0.00 to +0.64
25	-comp. at -0.34 no + comp.	-0.91 to -0.47 strong, with +0.36 to ? very broad and weak	-1.24 to -0.37 strong, with + comp. very weak 0.00 to +1.50 ($K' = 24$:) 0.00 to +0.58

upper electronic state. One might anticipate a rather large and unique Zeeman effect in this band, then, and so there is. In Table V we list briefly some of our measurements, and in Fig. 3C an enlargement of a portion of one of the spectrograms illustrates the principal pattern types obtained. The measurements are confined mostly to the R branch lines, since the overlapping of the patterns from the rather closely packed lines in the P branches makes their analysis hopeless at this dispersion.

It will be noticed that the P_1 and R_1 lines of low K values are unaffected by the field, but that the P_2 and R_2 lines become rather broad doublets. At about the level $K'=8$ the field patterns change, and take on a form which they retain out to the highest K level observed. The R_1 lines (parallel S and K) become rather diffuse doublets, the red and violet components being at first of about the same intensity, and with the outer edge of each component at about $\Delta\nu_n$ displacement from the no-field position. As K increases, however, the violet component becomes much weaker and the red component becomes narrower and somewhat stronger. The characteristic pattern for all the corresponding R_2 lines (anti-parallel S and K), on the other hand, is just one block of unresolved lines, shading from the no-field position toward higher frequency for an interval of about $\Delta\nu_n$. All patterns appear in both polarizations, although the widths and intensities are perhaps different on the two plates.

These patterns for the higher rotational levels are quite similar to those found in a $^2\Pi$ state for which there is a normal magnetic moment associated with the component of L in the direction of the electric axis. In the upper $^2\Sigma$ electronic state of this $^2\Sigma \rightarrow ^2\Sigma$ band there is a large magnetic interaction energy between S and an internal field directed along the nuclear rotational axis. This field must be due to a component of L in this direction, the order of magnitude of this component being at least a full unit of angular momentum, for one can interpret these patterns as being the superposition of the pattern due to the symmetrical top on a partial uncoupling of the spin S . The width of the blocks of lines forming the components in the patterns decreases with increasing K , as they should. And the strength of the $-$ components for the R_1 lines and the $+$ components for the R_2 lines is just as found in the $^2\Pi \rightarrow ^2\Sigma$ band, for these components originate in the "wing" transitions which we have discussed above.

It is not probable that this magnetic moment in this $^2\Sigma$ state could be due to nuclear rotation, for then one would expect similar very large p -type doubling in all $^2\Sigma$ states of this and like molecules. Now there is other reason to believe that the outer electron configuration in this $^2\Sigma$ state¹¹ is $4s\sigma^23d\sigma$, this level being derived from the low-lying $3D$ level of the Ca atom. Since $L=2$ (due to the d electron) and the effect of the electric axis is small ($\lambda=\sigma=0$), there is a good chance that the component of L along the perpendicular axis can become large. The accompanying magnetic moment and rather large coupling energy with the S then account for the Zeeman patterns observed.

¹¹ R. S. Mulliken, Phys. Rev. **33**, 730 (1929).

THE INFRARED ABSORPTION OF SOME ORGANIC LIQUIDS
UNDER HIGH RESOLUTIONBY R. BOWLING BARNES
JOHNS HOPKINS UNIVERSITY

(Received April 30, 1930)

ABSTRACT

For the purpose of comparing the Raman effect with infrared absorption spectra, the following organic liquids have been measured from 3.1μ to 3.6μ : benzene, toluene, ortho-, meta- and para-xylene, ethyl-, butyl-, monochlor-, and monobromobenzene. The spectrometer employed an echelette grating, which had 3600 lines per inch, and which concentrated the energy of a Nernst filament into the region which was investigated. The dispersion of the instrument was such that with the slits each 0.25 mm in width, one "slit width" was approximately 25\AA . The calibration was obtained in terms of the positions of the 5461 line from an auxiliary Hg arc, and the wave-lengths as given are considered accurate to $\pm 0.003\mu$. In every case the bands in this region, due to the C-H vibration, which have hitherto been reported only under low dispersion have been resolved into many component parts. The 3.25μ band of benzene was resolved into three equally strong components lying at 3.231 , 3.253 and 3.291μ respectively. The shifts of these bands caused by the various substitutions were studied, and in no case was a shift of over 0.01μ found.

DURING the past two years much has been said concerning a new method of infrared analysis, the Raman effect. Much importance is attached to it, for it offers a very convenient mode of attacking many problems of molecular structure. However, its usefulness depends upon the accuracy of its theoretical interpretation, and the manner in which this latter agrees with experimental evidence. As a direct result of this, all work previously done in the infrared has taken on an added importance, that of furnishing means of investigating and testing the theory of this effect.

The technique of the Raman effect has developed so rapidly that the photographs taken now, are all made under high resolution and hence show considerable detail. These results must be compared with such infrared measurements as may be found in the literature, and since these latter wave-lengths are usually known to a rather low degree of accuracy, such comparisons are not fair and in most cases can be only qualitative. So, in order to obtain any quantitative checks between the two phenomena, it seems necessary that many absorption measurements be made with the highest resolution obtainable.

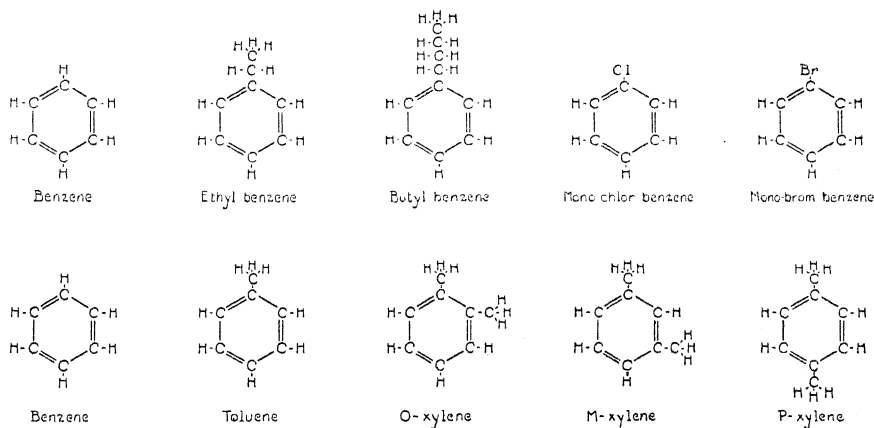
The complete theory of the Raman effect is contained in the theory of dispersion as outlined by Kramers as early as 1925. Further calculations by Dirac,¹ based upon the more recent form of quantum mechanics lead to the same results as those stated in the papers by Kramers and Heisenberg.²

¹ Dirac, Proc. Roy. Soc. A114, 710 (1927).

² Kramers and W. Heisenberg, Zeits. f. Physik 31, 681 (1925).

Here we learn that the intensity of a Raman line is determined in an entirely different manner from that of an absorption line. Between any two energy levels, say A_1 and A_2 , the presence or absence of an absorption line is completely determined by the value of the transition coefficient (a_{12}). However, in the expression for the intensity of the Raman line, this coefficient does not enter, but in its place the transition coefficients to a third level, say B , which can combine with both A_1 and A_2 . Thus it is possible to have, between A_1 and A_2 , either an absorption line or a Raman line, or both, depending on the values of the transition coefficients (a_{12}), (a_{1b}) and (a_{2b}). Further, in case both exist, the intensities are to be entirely independent of each other. That this interpretation is correct, cannot be doubted in view of the beautiful manner in which it agrees (in the case of the simple molecules) with the experimental results obtained by Rasetti, McLennan and McLeod and Wood. In HCl, Wood finds that the so called "missing line" occurs as a rather strong Raman line. It was shown by Kemble and Hill³ that this was in perfect ac-

TABLE I. STRUCTURAL FORMULAE OF COMPOUNDS STUDIED



cord with the theory. In the case of more complex molecules further corroboration comes from the work of Coblenz⁴ on CCl_4 , and of many other experimenters.

It seems well to emphasize here, the fact that one must not expect to find a one-to-one correspondence between absorption and Raman spectra. In spite of the many theoretical papers on the question regarding the difference between the two, experimentalists frequently refer to the fact that absorption lines "predicted" by the Raman effect do not appear in absorption measurements. Only if we know the energy diagram for a given substance, can we really predict from the Raman spectra just what lines shall occur in the absorption spectra. And in the case of the complex molecule usually studied by Raman investigators, these energy schemes are entirely unknown.

³ Kemble and Hill, Proc. Nat. Acad. Sci. **15**, 387 (1929).

⁴ W. W. Coblenz, Bull. Amer. Phys. Soc. **4**, No. 2 (1929).

It is out of the question therefore to expect, as is very frequently done, that strong Raman lines will be found corresponding to each of the intense absorption lines, and vice versa.

It is clear then, that infrared measurements which can state wave-lengths with the same degree of accuracy as those on Raman photographs, will be of great interest. And so, as a step in this direction, we offer here a study of the C-H vibration in the case of the following nine organic liquids whose structural formulae are given in Table I: benzene, toluene, ortho-, meta- and para-xylene, ethyl- butyl-, monochlor-, and monobrom-benzene.⁵ It is hoped that these results will be useful in connection with the Raman study of the same compounds made by Wood,⁶ for his plates show that this band is in every case quite complex in its structure.

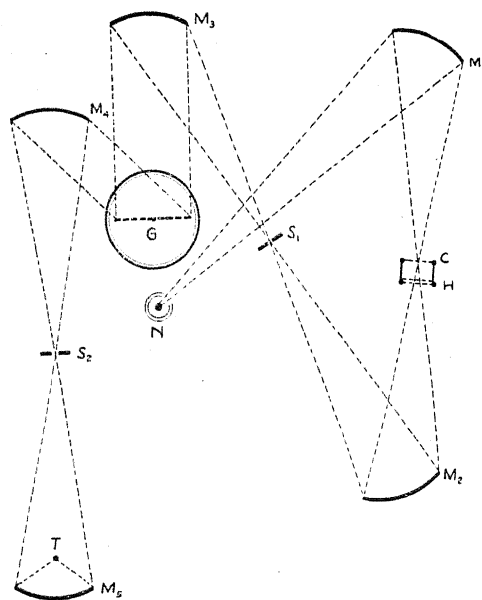


Fig. 1. Plan of apparatus.

APPARATUS

A plan of the grating spectrometer, which was used is given in Fig. 1. Radiation from a Nernst glower, operated on a 110-volt storage battery at 0.35 amp., was focussed upon the absorption cell, *C*. After passing through this, it was focussed upon *S*₁, the first slit. *M*₃ then collimated the beam and directed it to *G*, the eschelette grating. The diffracted beam was then focussed upon *S*₂, after which it was finally concentrated upon the thermopile *T*, by the mirror *M*₅.

Attention is called to several novel features included in this spectrometer. In the major part of these investigations a new type absorption cell was used,

⁵ R. B. Barnes, *Nature* **124**, 300 (1929), *Bull. Amer. Phys. Soc.* **5**, 10 (1930).

⁶ R. W. Wood, *Phil. Mag.* **7**, 858 (1929).

instead of the customary one of rock-salt. As is shown in Fig. 2(b), this cell consisted of a brass cup so designed that the layer of the liquid to be examined would be contained between the two microscope cover glasses, b and b' . This thickness could be varied at will, and very easily measured, for a metal "thickness gauge" could be temporarily inserted between the plates, while the horizontal tubes were being sealed in place with sodium silicate. Such a cell has a high uniform transparency in this region, and eliminates the inconveniences caused by evaporation of the solution and fogging of salt plates. The use and design of this new cell was suggested by Dr. Pfund.

The grating was a chromium plated echelette⁷ ruled in this laboratory, and concentrated most of the energy in the desired region. Having 3600 lines

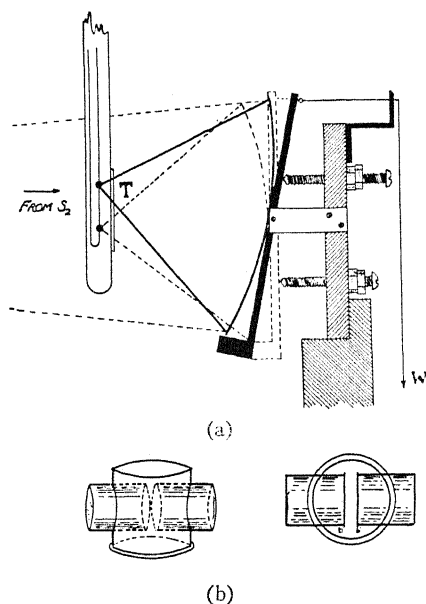


Fig. 2. Absorption cell and thermocouple mounting.

per inch, and being 3 inches wide, it had a theoretical resolving power of over 10,000, as compared with about 170 for a 3-inch salt prism, the type usually used in this region. Since a grating, however, superposes orders, the effect of the second order 1.5μ radiation had to be determined. A water cell, which had zero transmission beyond 3μ was used. This had a transparency of about 70 percent at 1.5 to 2.0μ . By making measurements with and without this shutter in place, the second order effect was readily detected and due allowance made for it in the calculations.

The thermocouple was a compensating one made of Hutchings alloys.⁸ This was used in series with a high-sensitivity Leeds and Northrup galvanometer of 5 sec. period. The scale distance was about 5 m, and the deflections

⁷ R. W. Wood, *Phil. Mag.* 7, 742 (1929).

⁸ A. H. Pfund, *J.O.S.A.* 15, 69 (1927).

were read to 0.5 mm. By means of the arrangement shown in Fig. 2(a) a double deflection method, somewhat analogous to that used by Pfund,⁹ was employed. By raising the weight, W , the radiation was focussed upon the lower junction of the thermocouple instead of the upper junction, and a deflection in the opposite direction was obtained. Readings were taken of deflections to the right, left and again to the right, thus eliminating the troublesome zero shift and at the same time realizing a double sensitivity and a greater accuracy.

The calibration was obtained by placing a mercury arc in front of S_1 and observing the positions of the grating as the first eight orders of the 5461 line fell upon S_2 . The grating settings were determined by observing the image of a lamp filament, reflected by a small mirror which rotated with the grating. By plotting the grating settings against the respective wave-lengths a perfectly straight calibration curve was obtained. Before and after each set of absorption measurements were made, this was checked at two points. In no case did the image of the filament fail to fall at its appointed place by as much as 0.5 mm, where a distance of 1 mm indicated a change of wave-length of 0.0028μ . The accuracy of the calibration was therefore better than 0.0014μ .

For each setting of the spectrometer we recorded a set of galvanometer deflections, C , for the radiation passing through the absorption cell; a set for transmission through an empty cell, E ; and finally a set while the water shutter H , was in place. By dividing $(C-H)$ by $(E-H)$ we obtained directly the percentage transmission for the wave-length indicated by the grating setting.

RESULTS AND DISCUSSION

The wave-lengths as stated below are believed to be accurate to less than $\pm 0.003\mu$. Throughout most of the work the two slits were kept at a separation of 0.25 mm. The mercury yellow lines in the 6th order were separated on the face of S_2 by 1.2 mm, which indicated that the "slit-width" must have been very nearly 0.0025μ . Except in regions where a more careful check upon the location of some particular band was desired, readings were taken at intervals of 0.0070μ . Even when these intervals were halved, the author realizes that much of the band structure has been missed.

Fig. 3 shows a comparison of the absorption of benzene and four methyl substitutions. In Fig. 4 we have compared benzene with ethyl-, butyl-, chlor- and brom-benzene. In these curves we have plotted as ordinates the percentage transmission, and while the numerical values are not given, as the curves are each based upon a different zero line, the percentages run in each curve from about 95% to 25 or 30%. The structural formulae of the various compounds, showing the position of the C-H linkages, are given in Table I. Table II gives a list of all the observed bands. The samples used in every case are the same as those used by Dr. Wood in his Raman work, and are of a very high degree of purity.

⁹ A. H. Pfund, Pub. of Allegheny Observatory 111, No. 6 (1913).

TABLE II. Wave-lengths of observed bands.

Benzene	Toluene	O Xylene	M Xylene	P Xylene	Ethyl- Benz	Butyl- Benz.	Mono- Chlor Benzene	Mono- Brom Benzene
*3.036 μ	*3.163 μ	*3.193 μ	*3.193 μ	*3.186 μ	*3.186 μ	*3.178 μ	*3.156 μ	*3.133 μ
*3.096	3.238	3.261	3.276	3.231	3.238	3.238	*3.186	*3.163
*3.163	3.261	3.283	3.291	3.291	3.261	3.261	3.253	*3.186
*3.186	3.276	3.313	3.313	3.308	3.298	3.298	3.268	3.261
3.231	3.298	3.366	*3.328	*3.328	*3.328	*3.328	3.298	3.298
3.253	*3.343	3.396	3.381	3.366	3.366	3.381	*3.328	*3.328
3.291	*3.358	3.418	3.396	3.396	3.411	3.411	3.366	3.396
*3.351	3.388	3.456	3.426	3.411	3.456	3.501	3.426	3.426
3.456	3.426	3.473	3.441	3.426	3.478	3.546	3.441	3.478
3.501	3.478	3.501	3.486	3.486	3.568	—	3.456	3.493
—	3.583	3.666	3.658	3.658	—	—	3.478	—

* Bands due to the absorption of water vapor in the atmosphere. More recent investigations, in which better resolution was obtained, have revealed the fact that several of the bands listed in Table II, and which occur in Figs 3 and 4 as very small minima, are due to atmospheric absorption. It is possible also, that in regions where the C-H bands are of about the same intensity as the water-vapor bands, there may be some little uncertainty as to the exact locations of the former due to imperfect resolution. However, in the cases of the stronger C-H bands which I discussed above, this effect plays a negligible role. A complete account of this more recent work is very soon to be published.

In this series of benzene derivatives, we have an excellent opportunity to study and observe the effects of various substitutions and of molecular arrangement and symmetry in causing a shift in the frequency of particular bands. Since benzene is the parent of all of the compounds studied we call especial attention to its characteristic bands.

The C-H band of benzene is always reported at 3.25 μ in the literature.¹⁰ In this work we have it clearly resolved into three components of approximately the same intensity lying at 3.231 μ , 3.253 μ and 3.291 μ respectively. We shall follow these bands throughout all of these compounds. Benzene shows other weaker bands as can be seen from Table II. In this discussion however, we shall deal only with the strongest bands in each of the compounds.

In the case of toluene, we find in the literature¹⁰ a single band at 3.34 μ , indicating a shift, due to the substitution of the methyl group of 0.09 μ . From curve (b) of Fig. 3 it can be seen that this is not at all the case. All three of the benzene C-H vibrations persist, each having been shifted by 0.007 μ only, and are found at 3.238 μ , 3.261 μ and 3.298 μ respectively. The intensities of the two bands of shorter wave-length have been noticeably decreased, while the band at 3.291 μ is still quite strong. The vibrations of the C-H within the methyl group have apparently introduced rather strong bands at 3.276, 3.343, 3.428 and 3.478 μ besides other weaker ones. These facts suggest that the presence of the other two H atoms in the CH₃ group makes possible several modes of C-H vibration other than those possible in benzene.

In the xylenes we find many interesting changes. Orthoxylene is very unsymmetrical with respect to benzene, and so we expect the substitution

¹⁰ W. W. Coblentz, *Astrophys. J.* 20, 207 (1924); *Carnegie Inst. of Wash.* No. 35, 1 (1905).

to have a greater effect on the benzene vibrations than in the case of toluene. In the meta form, the effect should be smaller, and in paraxylene we would expect it to be nearly the same as that in toluene, or possibly less. By examining curves (c), (d), and (e) of Fig. 3 this is seen to be the case. In orthoxylene there is only one band which closely checks the benzene vibrations, the 3.253μ band occurring here at 3.261μ again. In paraxylene on the

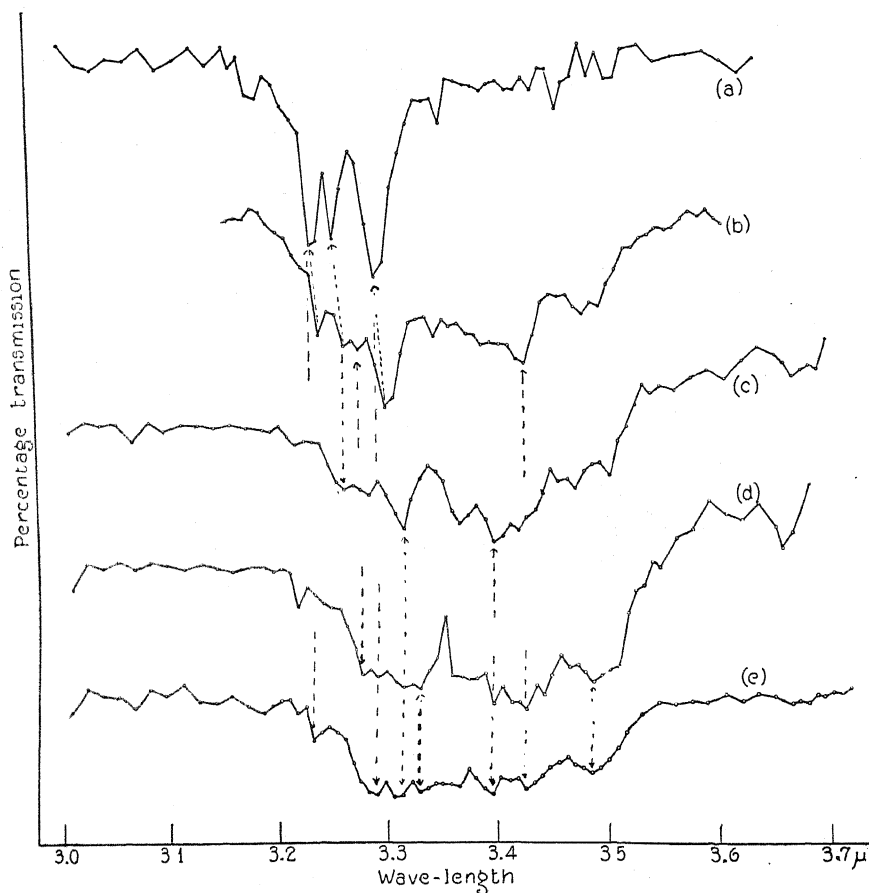


Fig. 3. Absorption curves. (a) benzene (b) toluene (c) orthoxylene (d) metaxylene (e) paraxylene. Thickness, 0.05 mm.

other hand, we find the 3.231μ and the 3.291μ bands recurring with no shift at all.

Since the strong 3.426μ band of toluene, does not appear in orthoxylene, while it does in the meta- and para- forms, we are inclined to look for a mutual effect of the two neighboring CH_3 groups. We find bands at 3.313μ , 3.396μ and 3.486μ occurring almost exactly in all three forms of xylene, while they are entirely absent in toluene, or to say the least, they occur in entirely new locations, again seeming to point to a mutual effect of the two groups.

The cases of ethyl- and butyl- benzene are somewhat similar. In each, we find the three benzene bands each shifted by 0.007μ . Their intensity changes are relatively the same as in the case of toluene. Just as we expected, the other bands, occurring in these two compounds, which are apparently due to the C-H vibrations within the ethyl- and butyl groups, are found at

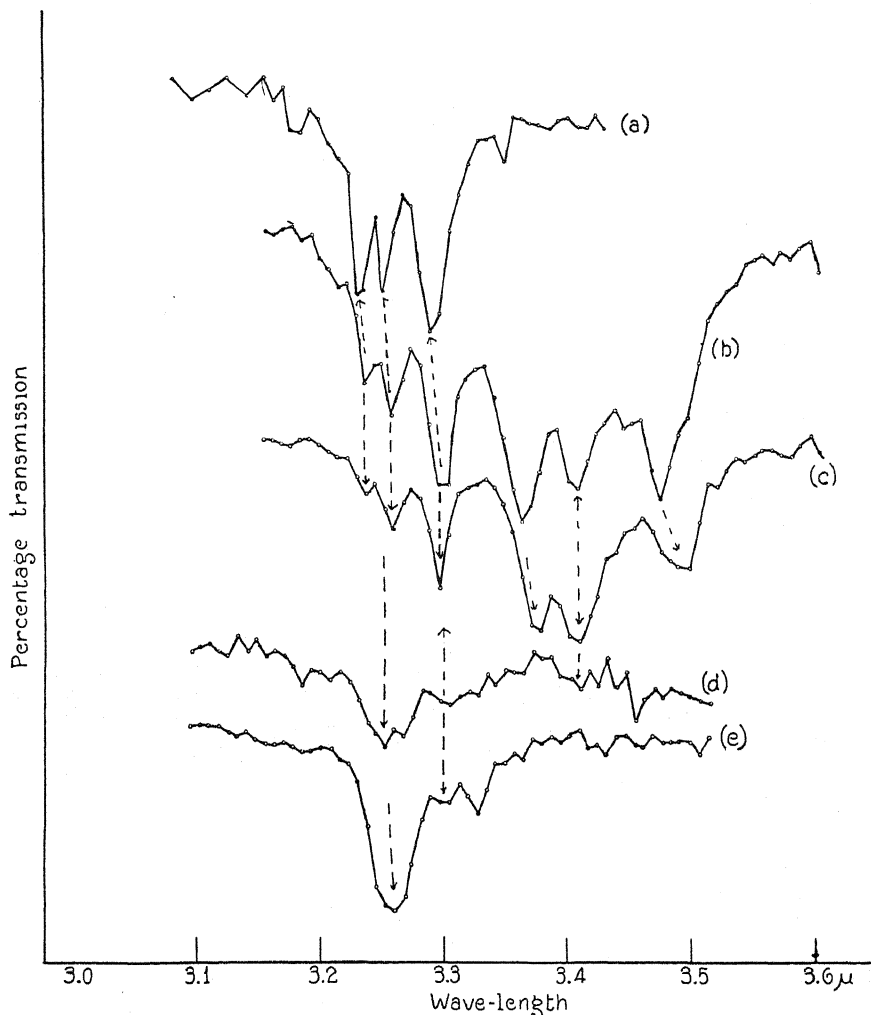


Fig. 4. Absorption curves. Thickness 0.05 mm. (a) benzene (b) ethyl benzene (c) n-butyl benzene (d) monochlor benzene (e) mono-brombenzene.

entirely different wave-lengths in the two cases. This is probably due to a different mutual effect in the two cases.

It is interesting to note that in methyl-, ethyl- and butyl-benzene, whose molecular weights are respectively 92, 106 and 134, the vibrations of the C-H bond in the benzene radical, have been shifted by the same amounts, namely

0.007μ . It must be remembered that 0.007μ is the interval between the spectrometer readings and so the actual shift might even be slightly less than that indicated.

In chlor- and brom- benzene we have a different type of substitution-namely, a single heavy atom instead of a group of C's and H's. Here, the 3.23μ band is absent entirely; the 3.253μ band occurs in each; the 3.291μ vibration appears in each at 3.298μ , and for the first time has its intensity very greatly decreased. Literature¹⁰ gives for each one single band at 3.25μ , with that for brom-benzene being much the stronger of the two, in close agreement with these results.

CONCLUSIONS

If we notice in every case the combined effect of the intensity changes and of the new vibrations introduced by the substitutions, we find that the result is just that necessary to cause the center of the absorption region to agree nicely with the wave-lengths given in the lower resolving power work recorded in literature.¹⁰

Apparently we can follow a particular band through the series of substitutions, noting the shifts and intensity changes which it suffers. We can see the mutual effect of the neighboring atoms upon the C-H radicals, and we can note distinct changes, dependent upon the symmetry of the molecule, as we progress for instance from benzene through toluene, ortho- and metaxylene to paraxylene.

It is thought that from these results, supplemented by further experimental data on temperature effects which we are at present assembling, we shall be able to work out the energy levels of these compounds.

The author wishes to express his sincere appreciation to Dr. Pfund, Dr. Herzfeld, and Professor Wood, who have been very helpful in aiding this work.

QUANTUM KINETICS AND THE PLANCK EQUATION

BY GILBERT N. LEWIS

DEPARTMENT OF CHEMISTRY, UNIVERSITY OF CALIFORNIA

(Received May 13, 1930)

ABSTRACT

With the same system that Einstein employed, the Planck equation should issue directly from kinetic principles without the aid of the theory of induced emission. The three fundamental laws of physico-chemical kinetics are (1) the law of entire equilibrium, (2) the law of the duality of elementary processes (or the equality of direct and reverse transition probabilities), (3) the law of equal *a priori* probabilities. It is shown that all three follow from the law of the symmetry of time, and furthermore, that the first and third of these laws are both derivable from the second.

From one of these laws, from the equation of Boltzmann, and from the number of quantum positions in a Hohlraum within a given range of frequency, the equation of Planck is immediately derived. Finally, there is a brief discussion of the more general case of thermal equilibrium in a Hohlraum when the number of photons is permanently or temporarily restricted, resulting in a state of *gray* rather than of *black* radiation.

IN THE justly famous paper in which Einstein¹ derived the Planck equation, he first introduced that coefficient of induced emission which has played so large a part in recent physics. Without in any way minimizing the value of this conception, which indeed seems necessary to an understanding of radiation from the standpoint of field-theory, one may doubt whether it was necessary, or even legitimate, to combine this method of treatment with a totally different method based upon the kinetics of light quanta, or photons; especially as Einstein's treatment seems to be incompatible with the principle of the symmetry of time, which we shall discuss presently.

It should be possible to obtain the laws of radiation by methods of two distinct types. Let us not risk misunderstanding by calling these the method of the wave and the method of the particle. Let us rather say that the first has its analogy in classical electromagnetics, in which a radiating particle is conceived to be immersed in, and in equilibrium with, a field, while the second has its analogy in the classical methods of kinetic theory, such as that of Guldberg and Waage, whereby the radiating atoms may be regarded as reacting with the atoms of light. Einstein borrowed from both types, but we shall see that it is possible by the second type of method alone to obtain, in a remarkably simple way, Planck's law of radiation, without otherwise departing from Einstein's procedure.

THE LAWS OF QUANTUM KINETICS DERIVED FROM THE SYMMETRY OF TIME

In a paper which is being published in *Science*, I show what remarkable conclusions may be drawn from the simple law, that in the domain of physical

¹ Einstein, *Phys. Zeits.* 18, 121 (1917).

science it is impossible to distinguish between past and future. If this law had been recognized, many of the errors of classical physics would have been avoided, such as the doctrine of Clausius that entropy tends toward a maximum, the theory that energy is radiated in a continuous expanding spherical shell, and the associated use of the retarded potentials. To present problems the law of the symmetry of time finds its most interesting applications in the study of quantum transitions, into which all physico-chemical processes may be resolved.

In discussing thermal equilibrium a special assumption has sometimes been employed which is not derivable from thermodynamics. It has been called the principle of detailed balancing, or of microscopic reversibility, or of entire equilibrium, and has usually been regarded as of useful, but limited, applicability. However, in the paper² in which I spoke of it as the principle of entire equilibrium, I proposed that it be regarded as a universal law, valid throughout physics and chemistry. This view was unacceptable to many physicists on the ground that the principle could not apply to cases in which radiation is involved. I think it will be apparent as we proceed that these very cases illustrate in a most satisfactory manner the value and the scope of the principle.

We may regard a physico-chemical system as passing through a succession of well defined quantum states for the whole system, which may be numbered (each degenerate state being separately listed). If the succession of these several quantum states is followed over a period of time long enough to be representative, we say that we are dealing with an equilibrium, and we may inquire how frequently one of these quantum states is reached; how long, on the average, it lasts, and what the chance is of a transition to any other given state.

The law of entire equilibrium demands that on the average the transition from state j to state k will occur just as often as the transition from k to j , or in other words, that the chance of going from j to k is equal to the reverse chance. The chance of going from j to k is equal to the chance p_j that the system is in the state j , multiplied by the intrinsic probability ϕ_{jk} that when it is in state j it will go over in unit time to state k . The law of entire equilibrium then states that,

$$p_j \phi_{jk} = p_k \phi_{kj}. \quad (1)$$

The reason that I felt convinced of the universality of the law of entire equilibrium was that it is directly derivable from the principle of symmetry in time. If it should fail at any point it would be the only known case in the whole of physical science in which time appears as unsymmetrical. The argument is simple: If in any system we should find $p_j \phi_{jk} > p_k \phi_{kj}$, $p_k \phi_{kl} > p_l \phi_{lk}$, $p_l \phi_{lj} > p_j \phi_{jl}$, we might still have equilibrium, but it would be of a cyclic character. We could state as a law for this system that the succession of states is chiefly in the direction $jkljk \dots$. Now reversing time, we should be obliged to describe the chief sequence as $jlkjl \dots$, a different law.

² G. N. Lewis, Proc. Nat. Acad. Sci. 11, 179, 422 (1925).

I shall not enter here upon the somewhat more difficult but equally binding, proof, which I give in my other paper, that the law of the symmetry of time also requires the equality of the intrinsic transition probabilities in two directions, namely,

$$\phi_{jk} = \phi_{kj}. \quad (2)$$

This, the most fundamental law of quantum kinetics, has hitherto received no name, except in so far as it has occasionally been confused with the law expressed in Eq. (1). It may be called the law of the duality of elementary processes, in order to indicate that the transition from j to k , and the transition from k to j , are not two separate physical entities, but the same entity regarded from two points of view.

By combining Eqs. (1) and (2), we find

$$p_i = p_k. \quad (3)$$

This is the principle known as the equality of *a priori* probabilities. These three equations, all of which may be derived from the law of the symmetry of time, underlie the whole theory of physico-chemical kinetics.

Both of the other two laws may be obtained from the law of duality, in the following manner. If we say that the probability of finding a system in a given state is determined by the probability of entering that state, and by the probability of leaving it, this means that all the p 's are determined when all the ϕ 's are given. The equations which suffice for such determination are evidently the ones which express the fact that in the long run the system enters as often as it leaves a given state. Thus,

$$\begin{aligned} p_1\phi_{12} + p_1\phi_{13} + \cdots p_1\phi_{1N} &= p_2\phi_{21} + p_3\phi_{31} + \cdots p_N\phi_{N1} \\ p_N\phi_{N1} + p_N\phi_{N2} + \cdots p_N\phi_{N(N-1)} &= p_1\phi_{1N} + p_2\phi_{2N} + \cdots p_{(N-1)}\phi_{(N-1)N} \end{aligned}$$

Of these N equations the last may obviously be derived algebraically from the remainder, but since the system must always be in one of the states, we have the further equation,

$$p_1 + p_2 + \cdots p_N = 1.$$

We therefore still have N equations, and these must be independent if the p 's are determined by the equations. Hence the solution is unique. Now, employing Eq. (2), we see that a solution, and therefore the only solution, is obtained by making the p 's equal. Thus we obtain Eq. (3) from Eq. (2), and from these Eq. (1) follows.

THE DERIVATION OF THE PLANCK EQUATION

Let us consider the same system that was discussed by Einstein, namely a Hohlraum of volume V , and temperature T , in which there is a single atom which may exist in the two quantum states A and B , the energy of the latter being greater in the amount $h\nu$. In systems of this simple character it is possible to express the quantum state of the whole system by describing separately the quantum states of its several parts. Thus we may completely describe this system by saying whether the atom is in state A or B , and by giving

the complete quantum state of the radiation. The latter may also be simplified by setting up a set of skeleton quantum positions, or cells, and giving the number of photons in each skeleton position, or cell.

The number dn of these cells lying within a given energy range $h\nu$ has now been obtained by several very different methods, all of which lead to the same result, namely,

$$dn = \frac{8\pi V\nu^2}{c^3} d\nu. \quad (4)$$

By making V indefinitely large, dn can be kept large, however small the range $d\nu$. Indeed, the Planck equation, to which Eq. (4) leads, is strictly valid only for a Hohlraum of infinite volume.

A completely specified individual state of the system is given when we know whether the atom is in state A or B , and when we know the number of photons in each of the skeleton positions or cells. The relative probability that the atom will be in state B or A , we shall assume, with Einstein, to be given by the following equation (although later we shall further consider its validity).

$$\frac{p_B}{p_A} = e^{-h\nu/kT} \quad (5)$$

From Eqs. (4) and (5), and with one of the preceding equations, we may obtain in a variety of ways the equation for black-body radiation. The very simple method which I shall give here I owe in part to a kind communication from Professor L. Brillouin, who has consistently maintained the applicability of the fundamental laws of kinetics to radiative processes.

Let us pick out one particular cell, Q , which corresponds to the energy emitted by state B . Let us then consider a process by which the atom changes from B to A , while the number of photons in cell Q changes from an initial value, m , to $m+1$, all the remaining radiation being unchanged. This may be expressed as

$$B, Q_m \rightarrow A, Q_{m+1}.$$

Calling the two complete states I and II, we have from Equation (3)

$$p_I = p_{II}.$$

The probability p_I is equal to the probability p_B , that the atom will be in state B , multiplied by the independent probability q_m , that cell Q has m photons; so also for the second state, and we may write

$$p_B q_m = p_A q_{m+1}. \quad (6)$$

Combining this equation with Eq. (5) we now have a result which concerns the radiation alone, and tells the relative probability of having $m+1$ and m photons in a given cell, namely,

$$\frac{q_{m+1}}{q_m} = e^{-h\nu/kT}.$$

If then q_0 represents the chance that cell Q has no photons, q , the chance that it has one, and so on,

$$q_0 + q_1 + q_2 + \dots = 1 = q_0(1 + e^{-h\nu/kT} + e^{-2h\nu/kT} + \dots). \quad (7)$$

If the cell Q has no photons, it has zero energy, with one photon it has the energy $h\nu$, with two photons $2h\nu$, so that \bar{E} , the probable energy of the cell, is

$$\bar{E} = q_0 h\nu (e^{-h\nu/kT} + 2e^{-2h\nu/kT} + \dots).$$

Eliminating q_0 by means of the previous equation,

$$\bar{E} = \frac{h\nu(e^{-h\nu/kT} + 2e^{-2h\nu/kT} + \dots)}{(1 + e^{-h\nu/kT} + e^{-2h\nu/kT} + \dots)}, \quad (8)$$

and by carrying out the indicated division we find,

$$\bar{E} = h\nu(e^{-h\nu/kT} + e^{-2h\nu/kT} + \dots) = \frac{h\nu}{e^{h\nu/kT} - 1}. \quad (9)$$

Multiplying \bar{E} by the number of cells lying in the range $d\nu$, from Eq. (4), we find the energy dE lying within this range,

$$dE = \frac{8\pi V h\nu^3 d\nu}{c^3} \frac{1}{e^{h\nu/kT} - 1}. \quad (10)$$

In this straightforward derivation of the Planck equation from simple kinetic principles there is no suggestion of "induced emission," which, I should like to repeat, may appear as a very real phenomenon when the same system is studied from the standpoint of field-theory, but is not a consideration that properly belongs to the kinetic mode of treatment.

Both Eq. (5) and Eq. (10) represent states of thermal equilibrium in the presence of an unlimited supply of photons. It is, however, perfectly possible to find processes by which photons interchange energies, and thus establish thermal distribution with respect to frequencies, without changing the number of photons. In case the concentration of photons of each frequency is less than that of black radiation, we may speak of *gray* radiation. Such a distribution I regard as a true and permanent case of equilibrium. Others who deny this will still admit that such a state may persist for a long time. Such equilibria, whether permanent or temporary, are susceptible to thermodynamic treatment.

In the presence of such a gray equilibrium of radiation, the atom at a given temperature will be less often in state B than when black radiation is present, and we may correct Eq. (5) by writing

$$\frac{\dot{p}_B}{\dot{p}_A} = \gamma e^{-h\nu/kT}, \quad (11)$$

where γ may be a function of temperature as well as of the number of photons per unit volume. Using this equation in place of Eq. (5), we obtain the expression for the distribution of energy in gray radiation, which I have previously derived more rigorously,³ namely,

$$dE = \frac{8\pi V h\nu^3 d\nu}{c^3} \frac{1}{(1/\gamma)e^{h\nu/kT} - 1} \quad (12)$$

³ G. N. Lewis, Proc. Nat. Acad. Sci. 13, 471 (1927).

A CONTRIBUTION TO THE QUANTUM MECHANICAL
THEORY OF RADIOACTIVITY AND THE DISSOCIA-
TION BY ROTATION OF DIATOMIC MOLECULESBY OSCAR KNEFLER RICE¹

INSTITUT FÜR THEORETISCHE PHYSIK DER UNIVERSITÄT, LEIPZIG

(Received February 26, 1930)

ABSTRACT

In the recent theory of radioactive decay, and also, as is shown, in the theory of dissociation of a diatomic molecule by the acquisition of rotational energy, there occurs a potential energy curve which has the following shape, as we go, say, from left to right. At the left the potential energy is very high, it then comes down to a minimum, increases to a maximum, and again falls off to an asymptotic value. The problems connected with such a curve are of two types. First, we may be given a particle in the region near the minimum, in an energy level which lies below the maximum, and wish to find the chance that it appear by a quantum mechanical process in the region on the other side of the maximum. Second, we wish to find how the "discrete states" in the neighborhood of the minimum are "broadened" by the continuum on the other side of the maximum. To solve these problems we first find the stationary eigenfunctions. By means of them the width and shape of the "broadened discrete levels" are found immediately. We then use these eigenfunctions to set up a wave packet, or, rather, we show how nature may set up a wave packet, which enables us to solve the first of the problems mentioned. The result justifies the use of complex eigenvalues for the solution of the problem.

INTRODUCTION

THE theory of radioactive decay, recently proposed by Gurney and Condon,² and independently by Gamow³ makes use of a potential energy curve of the type shown in Fig. 1 (solid curve), the wave equation being of the form

$$d^2\psi/dx^2 + (8\pi^2M/h^2)(E - U)\psi = 0. \quad (1)$$

The alpha-particle is supposed to be originally in some energy level such as E between x_2 and x_3 . There is then a finite probability of its appearing to the right of x_1 which gives the chance of disintegration of the radioactive atom.

Curves of much the same general characteristics also occur in the case of molecules, and can be used to explain the phenomenon of dissociation by rotation; i.e. one can use them to show how rotational energy can cause a diatomic molecule to dissociate. This explanation was given by Oldenberg,⁴ but as his work was not put into quantum mechanical form, and as a little more information may be obtained when this is done, it seems worth while to devote a paragraph to indicating how this may be done.

¹ National Research Fellow.

² Gurney and Condon, *Nature* **122**, 439 (1928); *Phys. Rev.* **33**, 127 (1929).

³ Gamow, *Zeits. f. Physik* **51**, 204 (1928).

⁴ Oldenberg, *Zeits. f. Physik* **56**, 563 (1929).

One begins with the wave equation of a rotating and oscillating diatomic molecule, and, in the usual way, separates out the variables which give the orientation of the molecule. One thus obtains a wave equation in r , the dis-

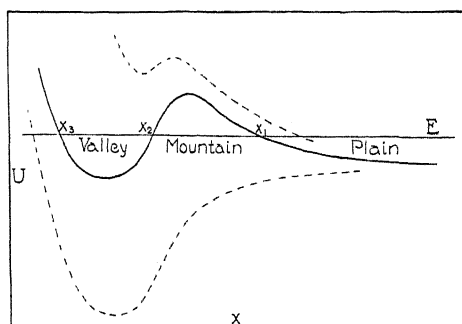


Fig. 1.

tance between the two nuclei. If we let $F=rR$, where R is the part of the eigenfunction which depends on r , this equation is⁵

$$d^2F/dr^2 - j(j+1)F/r^2 + (8\pi^2M/h^2)(E - U_0)F = 0$$

where j is the rotational quantum number, M the reduced mass, E the eigenvalue, and U_0 the potential energy, which is a function of r . The term $j(j+1)/r^2$ when multiplied by $h^2/8\pi^2M$ acts exactly like an addition to the potential energy⁶ and we may replace $U_0 + (h^2/8\pi^2M)j(j+1)/r^2$ by an effective potential energy U , getting an equation like (1). When $j=0$ the curve has the usual form of the potential energy curve for a molecule (lower dotted curve in Fig. 1). As j increases the curves become like the solid curve of Fig. 1, and finally when j is quite large they are like the upper dotted curve of Fig. 1, the valley becoming shallower and finally disappearing altogether.⁷ Now, as we shall see, we can in a certain sense speak of discrete states in the valley, corresponding to an oscillation of the molecule in this region, and we see that the number of discrete states in the valley grows less and less until at last there are no more. Thus if a molecule is in a certain vibrational state, this state will disappear, and the molecule will dissociate, if j exceeds a certain value. This is the phenomenon observed in the case of mercury hydride, and the explanation does not differ greatly from that given by Oldenberg.

For energy levels such as E between the top of the mountain and the level of the plain, the problems which occur in the case of radioactivity will have an analog in the case of molecules. In the case of radioactivity what we observe is that a system starting in the valley goes through the mountain and appears in the plain. In the case of molecular spectra we actually observe another phenomenon. We find that the discrete states in the valley will be broadened

⁵ Fues, *Ann. d. Physik* 80, 371 (1926).

⁶ See Gamow and Houtermans, *Zeits. f. Physik* 52, 509 (1928).

⁷ The curves of Fig. 1 are quite schematic. For curves drawn to scale see Oldenberg, *l.c.*

in the same sense as in the case of predissociation,⁸ and one in fact observes diffuse rotation lines.

The problem which concerns the rate at which particles appear on the plain, and which, as noted, is of particular interest in the case of radioactivity, has been considered by a number of investigators. In the original papers of Gurney and Condon, and Gamow, no attempt was made to put this calculation on a rigorous basis. Numerous articles have appeared since, attempting to do this.⁹ Among the various methods used the introduction of complex eigenvalues offers to my mind the most elegant solution of this problem which has appeared so far. This very ingenious procedure gives very reasonable results. Still the idea of a complex eigenvalue is a rather unusual one. The method also includes the assumption that the decomposition is proceeding in just the same way as if it had been going on for an infinite length of time. This is also not an unreasonable assumption but it can be avoided; at the same time the use of complex eigenfunctions can be justified, and new light thrown on the significance of the whole process by the method we propose to use.

METHOD OF ATTACK

First of all we shall consider the entire system to be enclosed in a large box, to avoid the necessity of considering a continuum. Then we shall find the stationary eigenfunctions. In general it will be found that the part of the eigenfunction on the plain will be great compared to that in the valley. As we pass through certain energies, however, the relative size of the part inside will increase, reach a maximum and fall off again. To avoid circumlocution we shall refer to these energies as "discrete levels." They will in general occur near an energy where we would expect a discrete level to be if the curve rose continuously to the right of the valley. Since there is a finite energy range over which the part of the eigenfunction in the valley has a relatively large size these discrete levels are "broadened."

We wish now to investigate how our system can appear in a "discrete state," and what it means to say that we start out with our system in the valley, and calculate the probability that it will get out on the plain. To do this we suppose that the system was originally in some real discrete state which might or might not be part of the system of states belonging to the potential energy curve of Fig. 1, but from which no escape from the valley into the plain is possible. We will call the eigenfunction of this state ψ_0 and its energy E_0 . Now our system is subjected to a perturbation which causes it to appear in one of the states belonging to the curve of Fig. 1. There is a cer-

⁸ Rice, *Phys. Rev.* **33**, 748 (1929). And see Schrödinger, *Sitzungsber. Preuss. Akad. Wiss.*, (1929) 668.

⁹ Kudar, *Zeits. f. Physik* **53**, 61, 95, 134 (1929); **54**, 297 (1929); Gamow and Houtermans, *Zeits. f. Physik* **52**, 496 (1928); Gamow, *Zeits. f. Physik* **53**, 601 (1929); Fowler and Wilson, *Proc. Roy. Soc. A* **124**, 493 (1929). See also v. Laue, *Zeits. f. Physik*, **52**, 726 (1928); Sexl, *Zeits. f. Physik* **54**, 445 (1929); **56**, 62, 72 (1929); Born, *Zeits. f. Physik*, **58**, 306 (1929); Atkinson and Houtermans, *Zeits. f. Physik* **58**, 478 (1929); Sexl, *Zeits. f. Physik* **59**, 579 (1930). Relativity treatment, Möller, *Zeits. f. Physik*, **55**, 451 (1929).

tain probability that it will land in some one of these states, of energy E , say, which is near some discrete energy, E_d . The eigenfunction of energy E (not including the exponential time factor) will be called $\psi(E)$. The wave packet which is formed by systems jumping from the state to the states $\psi(E)$ will be of the form

$$\psi = \sum a(E)\psi(E) \exp(-2\pi iEt/h)$$

where $a(E)$ is a constant coefficient for any E , and the sum is taken over all allowable values of E , which form a continuous set within the limits allowed by the box.

As a typical example, we shall consider the case where the perturbation which sets up the wave packet ψ for us is due to the action of monochromatic light,¹⁰ of a frequency somewhere near $E_d - E_0$ which difference we will suppose great¹¹ compared to the "breadth" of the discrete state at E_d . Now we have said that we will have the wave packet produced by monochromatic light. But if light is to be strictly monochromatic we have to shine it in for an infinitely long time. There would be no sense in making any calculation for a process which occurs after such an excitation. In fact there would be no process to calculate. The system after the excitation by light would simply be in one of the stationary states $\psi(E)$. We can, however, shine in light of a given frequency for a short time. It is of particular interest to have it shine in for so short a time that any of the states $\psi(E)$ over a considerable range of energies in the neighborhood of E_d may be excited, and short enough so that no appreciable difference in phase of the exponential factor for the various states $\psi(E)$ in the expression for ψ can arise.¹² The matrix component of the perturbation for the excitation by light from state ψ_0 to a state $\psi(E)$ is proportional to the matrix component,¹³ $P_{0E} = \int_0^\infty \psi_0 P \psi(E) dx$, where P is the electrical polarization expressed as a function of x . The $\psi(E)$ must be normalized. $a(E)$ will be proportional to P_{0E} and to find out how P_{0E} depends on E we must make a certain assumption regarding the integral which gives it. We assume that all appreciable contributions to this integral come from the range

¹⁰ Rice, Phys. Rev. **34**, 1454 (1929).

¹¹ The assumption that $E_d - E_1$ should be great compared to the width of the discrete state at E_d was also made in the previous work, Ref. 9, but it was forgotten to mention it explicitly there. This assumption was necessary to show that a_n in Eq. (5) of that article is proportional to P_{n0} ; it makes $E_n - E_0$ practically independent of E_n' over the important range of E_n' .

¹² As in the case previously considered (Ref. 10, see p. 1458) it seems safe to replace this condition by the statement that the time of illumination must be short compared to the time of decomposition, i.e. in this case the average life of a particle in the valley before it escapes into the plain. If the time of illumination is so short that more than one discrete state is excited the various decompositions from the various states may all be treated separately provided the energy between two discrete states is great compared to the breadth of a discrete state, a condition which must be fulfilled anyhow. This will also presumably be the case, if the perturbation is due to any other cause, provided it lasts for such a short time that no appreciable decomposition takes place in this time. The point is, as we shall see, that the wave packet starts in the neighborhood of the valley, and if the time of the perturbation is short enough, it will not, during that time, get out of the valley.

¹³ Dirac, Proc. Roy. Soc. **A112**, 674 (1926).

of x in the valley, because ψ_0 is supposed to have appreciable values only in the valley. In the immediate neighborhood of any given discrete level in the valley, the shape of the part of $\psi(E)$ which is in the valley or the amplitude of the part in the plain will not vary greatly with the energy over a small energy range, but the ratio which we call B , of the magnitude of the valley part of $\psi(E)$ (for some definite value of x , say x^1) to the amplitude of the plain part will vary greatly with the energy. Let us designate the maximum of B as B_1 . Then B/B_1 (which does not depend on x^1) is equal to the ratio¹⁴ P_{0E}/P_{0E_1} because the normalization makes all $\psi(E)$ alike in the plain.^{14a} The coefficient $a(E)$ is proportional to P_{0E} hence to P_{0E}/P_{0E_1} , hence to B/B_1 . Therefore, neglecting a constant factor, ψ becomes

$$\psi = \sum (B/B_1) \psi(E) \exp(-2\pi i E t / \hbar) \quad (2)$$

where the summation is over all allowable values of E . Now it will later be seen that this equation results in the total amount of material in the plain at $t=0$ being zero or almost so, but as time goes on, matter appears in the plain, and the amount of material in the valley suffers an exponential decrease.

If E_0 is greater than E_d so that the wave packet is set up by emission of light the above will also hold.

CALCULATION OF THE STATIONARY EIGENFUNCTION

If ψ now is the stationary eigenfunction for some definite energy E , it has been shown that for regions when $|E - U|$ is not too small, and the slope of the U vs. x curve not too great, that the solutions of the wave equation can be written in the form¹⁵ (disregarding constant factors)

$$\psi = \begin{matrix} \sin \\ (E - U)^{-1/4} \text{ or } \left\{ \kappa \int (E - U)^{1/2} dx \right\} \\ \cos \end{matrix} \quad (3)$$

for $U < E$, and

$$\psi = (U - E)^{-1/4} \exp \left\{ \pm \kappa \int (U - E)^{1/2} dx \right\} \quad (4)$$

for $U > E$, where $\kappa = (8\pi^2 M / \hbar^2)^{1/2}$.

In the immediate neighborhood of such a point as x_1 these solutions do not hold. The question now arises as to what happens if we start with some given solution in the mountain to the left of x_1 , and go through x_1 into the plain. On the assumption that the side of the mountain is long and straight, Kramers¹⁶ has shown that, if we start with the solution

$$(U - E)^{-1/4} \exp \left\{ -\kappa \int_x^{x_1} (U - E)^{1/2} dx \right\}$$

far to the left of x_1 , after going through x_1 and getting far to the right the solution has become

¹⁴ E_d is not a well defined energy and we could take it as that value of the energy for which B is a maximum. We prefer, however, to designate the latter energy as E_1 .

^{14a} The matter of normalization is explained in more detail after Eq. (17). See also Ref. 8, p. 749.

¹⁵ See, e.g., Nordheim, *Zeits. f. Physik* **46**, 842 (1927).

¹⁶ Kramers, *Zeits. f. Physik* **39**, 828 (1926).

$$2(E-U)^{-1/4} \cos \left\{ \kappa \int_{x_1}^x (E-U)^{1/2} dx - \pi/4 \right\}.$$

This means that the particular solution of the differential equation which has the one form to the left of x_1 has the other form to the right. We express this by using the following notation:

$$(U-E)^{-1/4} \exp \left\{ -\kappa \int_x^{x_1} (U-E)^{1/2} dx \right\} \xleftrightarrow{x_1} 2(E-U)^{-1/4} \cos \left\{ \kappa \int_{x_1}^x (E-U)^{1/2} dx - \frac{\pi}{4} \right\} \quad (5)$$

Putting in the limits is equivalent to evaluating the constant of integration, the integral being a function of x . Kramers and Ittman¹⁷ also point out that

$$(U-E)^{-1/4} \exp \left\{ \kappa \int_x^{x_1} (U-E)^{1/2} dx \right\} \xleftrightarrow{x_1} -(E-U)^{-1/4} \sin \left\{ \kappa \int_{x_1}^x (E-U)^{1/2} dx - \frac{\pi}{4} \right\} \quad (6)$$

Zwaan¹⁸ points out that the relation (5) holds whether the side of mountain is long and straight or not, if we can go from a region where the approximations of the type (4) hold to a region where the approximations of the type (3) hold, *via* a path in the complex plane along which the solutions are of the general type $(E-U)^{-1/4} \exp \left\{ i\kappa \int_{x_1}^x (E-U)^{1/2} dx \right\}$ and which crosses the curve along which argument of $\int_{x_1}^x (E-U)^{1/2} dx$ is $\pi/2$ at a point where the absolute value of $\int_{x_1}^x (E-U)^{1/2} dx$ is large.¹⁹

In similar manner we also have

$$2(E-U)^{-1/4} \cos \left\{ \kappa \int_x^{x_2} (E-U)^{1/2} dx - \frac{\pi}{4} \right\} \xleftrightarrow{x_2} (U-E)^{-1/4} \exp \left\{ -\kappa \int_{x_2}^x (U-E)^{1/2} dx \right\} \quad (7)$$

and

$$-(E-U)^{-1/4} \sin \left\{ \kappa \int_x^{x_2} (E-U)^{1/2} dx - \frac{\pi}{4} \right\} \xleftrightarrow{x_2} (U-E)^{-1/4} \exp \left\{ \kappa \int_{x_2}^x (U-E)^{1/2} dx \right\}. \quad (8)$$

Now if we multiply the left hand side of expression (5) by the factor $\exp \left\{ \kappa \int_{x_2}^{x_1} (U-E)^{1/2} dx \right\}$ which we will call $\theta/2$ we see that it coincides exactly with the right hand side of expression (8). Likewise if we multiply the left

¹⁷ Kramers and Ittman, *Zeits f. Physik* 58 222 (1929)

¹⁸ Zwaan: *Intensitäten im Ca-Funkenspektrum*, Thesis, Utrecht (1929), p. 35. I am indebted to Dr. F. Bloch for calling my attention to this work.

¹⁹ Kramers and Ittman state that (6) can be derived in the same way.

hand side of (6) by $2\theta^{-1}$ it coincides with the right hand side of (7). Thus we have established a connection between the solutions to the left of x_2 and to the right of x_1 . We see, in fact, that

$$-(E-U)^{-1/4} \sin \left\{ \kappa \int_x^{x_2} (E-U)^{1/2} dx - \frac{\pi}{4} \right\} \\ \longleftrightarrow_{x_2 \text{ and } x_1} \theta(E-U)^{-1/4} \cos \left\{ \kappa \int_{x_1}^x (E-U)^{1/2} dx - \frac{\pi}{4} \right\} \quad (9)$$

and

$$(E-U)^{-1/4} \cos \left\{ \kappa \int_x^{x_2} (E-U)^{1/2} dx - \frac{\pi}{4} \right\} \\ \longleftrightarrow_{x_2 \text{ and } x_1} -\theta^{-1}(E-U)^{-1/4} \sin \left\{ \kappa \int_{x_1}^x (E-U)^{1/2} dx - \frac{\pi}{4} \right\}. \quad (10)$$

The actual eigenfunction in the valley must consist of a linear combination of the left hand sides of (9) and (10). If the eigenfunction in the valley is

$$(E-U)^{-1/4} \left[\cos \left\{ \kappa \int_x^{x_2} (E-U)^{1/2} dx - \frac{\pi}{4} \right\} \right. \\ \left. + b \sin \left\{ \kappa \int_x^{x_2} (E-U)^{1/2} dx - \frac{\pi}{4} \right\} \right] \quad (11)$$

the same eigenfunction in the plain is

$$-(E-U)^{-1/4} \left[\theta^{-1} \sin \left\{ \kappa \int_x^{x_1} (E-U)^{1/2} dx - \frac{\pi}{4} \right\} \right. \\ \left. + b \theta \cos \left\{ \kappa \int_{x_1}^x (E-U)^{1/2} dx - \frac{\pi}{4} \right\} \right] \quad (12)$$

THE SHAPE OF THE BROADENED DISCRETE STATE

In order that the solution of the wave equation should be an eigenfunction it must satisfy a certain condition to the left of x_3 . It is probably good enough to assume that to the left of x_3 the solution must decrease exponentially in absolute value as we go to the left,¹⁶ and the solution to the left of x_3 will therefore be of the form $(U-E)^{-1/4} \exp \left\{ -\kappa \int_x^{x_3} (U-E)^{1/2} dx \right\}$. Now

$$(U-E)^{-1/4} \exp \left\{ -\kappa \int_x^{x_3} (U-E)^{1/2} dx \right\} \\ \longleftrightarrow_{x_3} 2(E-U)^{-1/4} \cos \left\{ \kappa \int_{x_3}^x (E-U)^{1/2} dx - \frac{\pi}{4} \right\} \quad (13)$$

(11) must be the same as the right hand side of (13), and it can be made the same as follows. We can easily at any time adjust the amplitude of (11) or (13) so that they will be the same. But we have to adjust the phase of (11)

so that it will coincide with (13). This is done by choosing the value of b . At some energy, say for example at E_1 , the value of b will be zero. Then under the mountain we have only the decreasing exponential. The value E_1 will therefore be approximately the same as an eigenvalue of the wave equation if the curve for U increased indefinitely to the right. Kramers¹⁶ has shown that the condition that E_1 should be the energy of such a discrete state is

$$\kappa \int_x^{x_2} (E_1 - U)^{1/2} dx = n\pi \quad (14)$$

when $n = 1/2, 3/2, 5/2, \dots$. The phase of the right hand side of (13) (starting from x) is less than that of the first term of (11), at some E not too distant from E_1 , by

$$\kappa \int_{x_1}^{x_2} (E - U)^{1/2} dx - \kappa \int_{x_1}^{x_2} (E_1 - U)^{1/2} dx. \quad (15)$$

The amount that the phase of (11) is less than that of its first term is $\tan^{-1}b$. Thus, since (13) and (11) must be alike,

$$b = \tan \left\{ \kappa \int_{x_1}^{x_2} (E - U)^{1/2} dx - \kappa \int_{x_1}^{x_2} (E_1 - U)^{1/2} dx \right\}. \quad (16)$$

Now if the breadth of the "broadened discrete state" is to be narrow compared to the distance between two discrete states, it means that over the "width" of the discrete state (15) must be small compared to π . We assume it so small that we may write

$$\begin{aligned} b &= \kappa \int_{x_1}^{x_2} (E - U)^{1/2} dx - \kappa \int_{x_1}^{x_2} (E_1 - U)^{1/2} dx \\ &= (E - E_1) \frac{\partial}{\partial E} \kappa \int_{x_1}^{x_2} (E - U)^{1/2} dx \end{aligned} \quad (17)$$

which we set $= b'(E - E_1)$. The derivative is taken for $E = E_1$. It is important to note that b' is positive.

We now wish to find how the value of b affects the relative size of the eigenfunction in the valley and on the plain. For large values of x we know that U takes on some asymptotic value, which we can without loss of generality take as 0. Then (12) also has an asymptotic form. In the limiting case when the box is large this part of (12) will determine the normalization, as the integral of ψ^2 over the plain can always, by taking the plain long enough, be made large compared to the integral across the valley. We make $\int_0^\infty \psi^2 dx = 1$. The amplitude of the sinusoidal function represented by (12) is (for large values of x where $U=0$) equal to $(\theta^{-2} + b^2 \theta^2)^{1/2} E^{-1/4}$. To satisfy the normalization conditions the amplitude must be $(2/x_\infty)^{1/2}$ where x_∞ is the largest possible value²⁰ of x . To normalize we therefore multiply (12) by $(\theta^{-2} + b^2 \theta^2)^{-1/2} E^{1/4}$

²⁰ Giving x a largest value allows in an idealized way for the fact that the system is in a box.

$(2/x_\infty)^{1/2}$. Now (11) must also be multiplied by the same thing, so its amplitude becomes $(1+b^2)^{1/2}(E-U)^{-1/4}(\theta^{-2}+b^2\theta^2)^{-1/2}E^{1/4}(2/x_\infty)^{1/2}$. But if b is small so that (17) holds, then it will also be negligible compared to 1. So the amplitude of (11) becomes

$$(E-U)^{-1/4}(\theta^{-2}+b^2\theta^2)^{-1/2}E^{1/4}(2/x_\infty)^{1/2}.$$

If we divide this expression by its value when $E=E_1$, and hence $b=0$, we get an expression which will no longer depend on the particular value of x between x_2 and x_3 , and which will in fact be just equal to the quantity B/B_1 which appeared in Eq. (2). We thus find (assuming that E and θ do not vary appreciably over the range of E included in a broadened discrete state):

$$B/B_1 = (1+b^2\theta^4)^{-1/2} = [1+b'^2(E-E_1)^2\theta^4]^{-1/2}. \quad (18)$$

The shape of the broadened discrete state is found by plotting

$$(B/B_1)^2 = [1+b'^2(E-E_1)^2\theta^4]^{-1} \quad (19)$$

against E . The width w of the state we may define as the energy over which $(B/B_1)^2$ has the value $\frac{1}{2}$ or greater, or twice the absolute value of $E-E_1$ for which $(B/B_1)^2 = \frac{1}{2}$. Thus

$$w = 2/b'\theta^2. \quad (20)$$

THE SETTING-UP OF THE WAVE PACKET; THE RATE OF DECAY; PROOF OF ASSUMPTION OF COMPLEX EIGENVALUES

For a very large box the summation in Eq. (2) can be replaced by an integration, which is surely allowable, as it will be seen that the integrand has no singular points. Eq. (2) thus becomes

$$\psi = \int_{-\infty}^{\infty} (B/B_1)\psi(E) \exp(-2\pi i Et/h) dE/\epsilon \quad (21)$$

where ϵ is the distance between energy levels, and is equal to $2\pi E^{1/2}/\kappa x_\infty$ where x_∞ is the largest possible value of x . It is only possible to integrate thus from ∞ to $-\infty$ because only a small range of E 's contributes appreciably. To find ψ for $x \gg x_1$ we substitute for $\psi(E)$ in (21) the expression (12) with $U=0$ which must however be multiplied, as noted, by $(\theta^{-2}+b^2\theta^2)^{-1/2}E^{1/4}(2/x_\infty)^{1/2} = \theta(B/B_1)E^{1/4}(2/x_\infty)^{1/2}$. To find $\psi(E)$ for $x_3 < x < x_2$ we use (11) multiplied by the same thing. We will, however, find it convenient to multiply (11) and (12) through by $-\theta(B/B_1)E^{1/4}\epsilon$, instead, which is permissible for the following reasons: ψ itself is not normalized, and we can always further multiply or divide (11) and (12) by any factor which does not depend on E . And in the range of values of E which contribute importantly in the integral (21) we may regard ϵ as constant. $E^{1/4}$, $(E-U)^{1/4}$, and θ are also practically constant. So (11) gives, when thus multiplied and substituted in (21) remembering (17) and (19):

$$\psi = -\frac{E_1^{1/4} \theta}{(E_1 - U)^{1/4}} \left[\int_{-\infty}^{\infty} \frac{\cos \left\{ \kappa \int_x^{x_2} (E - U)^{1/2} dx - \frac{\pi}{4} \right\} \exp(-2\pi i E t / h)}{1 + b'^2 \theta^4 (E - E_1)^2} dE \right. \\ \left. + \int_{-\infty}^{\infty} \frac{b'(E - E_1) \sin \left\{ \kappa \int_x^{x_2} (E - U)^{1/2} dx - \frac{\pi}{4} \right\} \exp(-2\pi i E t / h)}{1 + b'^2 \theta^4 (E - E_1)^2} dE \right] \quad (22)$$

For great values of x we can substitute $\kappa E^{1/2} x + \zeta$ for $\kappa \int_x^{x_2} (E - U)^{1/2} dx - \pi/4$ in (12). We simply let ζ be the difference between these two expressions, this difference being constant for large values of x . Then we multiply (12) by the same expression as we multiplied (11) by, and get

$$\psi = \int_{-\infty}^{\infty} \frac{[\sin \{ \kappa E^{1/2} x + \zeta \} + \theta^2 b'(E - E_1) \cos \{ \kappa E^{1/2} x + \zeta \}] \exp(-2\pi i E t / h)}{1 + b'^2 \theta^4 (E - E_1)^2} dE \quad (23)$$

We assume that the important range of E in this integral is so small that ζ is the same for all the states in this range. We now proceed to evaluate (23).

We substitute $(E - E_1) + E_1$ for E , and $E_1^{1/2} + (E - E_1)/2E_1^{1/2}$ for $E^{1/2}$, as this is allowable for the small values of $E - E_1$ which contribute to the integral. The latter substitution gives the cosine and the sine of the sum of the two angles $\kappa E_1^{1/2} x + \zeta$ and $(\kappa/2E_1^{1/2})(E - E_1)x$. These are reduced by the usual trigonometric formulas. We also write $\exp(-2\pi i E t / h) = \exp(-2\pi i E_1 t / h) [\cos \{ 2\pi(E - E_1)t/h \} - i \sin \{ 2\pi(E - E_1)t/h \}]$. One thus gets a number of parts of the integral which drop out because they are antisymmetrical about the point $E - E_1 = 0$. The rest of the expression becomes

$$\psi = \exp(-2\pi i E_1 t / h) \left[\int_{-\infty}^{\infty} \frac{\sin \{ \kappa E_1^{1/2} x + \zeta \} \cos \{ (\kappa/2E_1^{1/2})(E - E_1)x \} \cos \{ 2\pi(E - E_1)t/h \}}{1 + b'^2 \theta^4 (E - E_1)^2} d(E - E_1) \right. \\ - b' \theta^2 \int_{-\infty}^{\infty} \frac{(E - E_1) \sin \{ \kappa E_1^{1/2} x + \zeta \} \sin \{ (\kappa/2E_1^{1/2})(E - E_1)x \} \cos \{ 2\pi(E - E_1)t/h \}}{1 + b'^2 \theta^4 (E - E_1)^2} d(E - E_1) \\ - i \int_{-\infty}^{\infty} \frac{\cos \{ \kappa E_1^{1/2} x + \zeta \} \sin \{ (\kappa/2E_1^{1/2})(E - E_1)x \} \sin \{ 2\pi(E - E_1)t/h \}}{1 + b'^2 \theta^4 (E - E_1)^2} d(E - E_1) \\ \left. - i b' \theta^2 \int_{-\infty}^{\infty} \frac{(E - E_1) \cos \{ \kappa E_1^{1/2} x + \zeta \} \cos \{ (\kappa/2E_1^{1/2})(E - E_1)x \} \sin \{ 2\pi(E - E_1)t/h \}}{1 + b'^2 \theta^4 (E - E_1)^2} d(E - E_1) \right]$$

The four integrals we shall designate respectively as I_1, I_2, I_3, I_4 . Another trigonometric reduction gives $I_1 = \frac{1}{2} [\sin \{ \kappa E_1^{1/2} x + \zeta \}] (I_1^+ + I_1^-)$ and $I_2 = \frac{1}{2} [\sin \{ \kappa E_1^{1/2} x + \zeta \}] (I_2^+ + I_2^-)$, where

$$I_1^{\pm} = \int_{-\infty}^{\infty} \frac{\cos \{ [(\kappa/2E_1^{1/2})x \pm 2\pi t/h](E - E_1) \}}{1 + b'^2 \theta^4 (E - E_1)^2} d(E - E_1)$$

and

$$I_2^{\pm} = \int_{-\infty}^{\infty} \frac{(E - E_1) \sin \{ [(\kappa/2E_1^{1/2})x \pm 2\pi t/h](E - E_1) \}}{1 + b'^2 \theta^4 (E - E_1)^2} d(E - E_1)$$

I_1^+ and I_1^- are to be found from Pierce's Tables²¹ and I_2^+ and I_2^- can readily be found by differentiating I_1^+ and I_1^- with respect to the proper parameter $(\kappa/2E_1)^{1/2}x \pm 2\pi t/h$. Now it will be found (as b' is positive) that the contributions from I_1^+ and I_2^+ cancel each other in the expression for ψ , as do also the contributions from I_1^- and I_2^- when $(\kappa/2E_1)^{1/2}x > 2\pi h/t$. When, however, $(\kappa/2E_1)^{1/2}x < 2\pi h/t$ the latter add. We can treat I_3 and I_4 in a similar way. So ψ is zero for $(\kappa/2E_1)^{1/2}x > 2\pi h/t$ and for $(\kappa/2E_1)^{1/2}x < 2\pi h/t$ we have

$$\begin{aligned} \psi &= (\pi/b'\theta^2) [\sin(\kappa E_1^{1/2}x + \zeta) - i \cos(\kappa E_1^{1/2}x + \zeta)] \\ &\quad \exp \left\{ [(\kappa/2E_1)^{1/2}x - 2\pi t/h]/b'\theta^2 \right\} \exp(-2\pi i E_1 t/h) \\ &= (\pi/b'\theta^2) \exp \left\{ i(\kappa E_1^{1/2}x - 2\pi E_1 t/h - \pi/2 + \zeta) \right\} \exp \left\{ [(\kappa/2E_1)^{1/2}x - 2\pi t/h]/b'\theta^2 \right\} \end{aligned} \quad (24)$$

We see that this represents a wave going in the positive direction with the particle velocity $(2E_1/M)^{1/2}$, and with an amplitude determined by the second exponential factor for values of x up to the place where $(\kappa/2E_1)^{1/2}x = 2\pi t/h$ after which it breaks off. The wave shows an exponential decrease with time and just the proper exponential increase with distance to insure that the amount of matter in the wave is conserved. This is exactly like the outward going wave of Kudar's,⁹ which resulted from the use of complex eigenvalues, except that his did not break off, but continued out to infinity in space and negative infinity in time.

We shall now evaluate (22). The sine and cosine of $\kappa \int_x^{x_2} (E - U)^{1/2} dx - \pi/4$ are roughly periodic functions of E , but we know that in the important range of E the functions have gone through a small fraction of a period, as we are considering a discrete state that is narrow compared to the distance between two discrete states. We can therefore consider the sine and cosine terms as constant factors in the integration of (22). We write $\exp(-2\pi i E t/h)$ in sine and cosine form, as before, substitute in (22), note that some of the parts of the resulting integral drop out because of antisymmetry of the part of the integrand about $E - E_1 = 0$, integrate the remaining terms, which involve integrals of the type already met with, and get

$$\begin{aligned} \psi &= - [\exp(-2\pi i E_1 t/h)] [(E_1^{1/4}\theta)/(E_1 - U)^{1/4}] \\ &\quad [(\pi/b'\theta^2) \cos \left\{ \kappa \int_x^{x_2} (E_1 - U)^{1/2} dx - \pi/4 \right\} \exp(-2\pi t/hb'\theta^2) \\ &\quad - i(\pi/b'\theta^4) \sin \left\{ \kappa \int_x^{x_2} (E_1 - U)^{1/2} dx - \pi/4 \right\} \exp(-2\pi t/hb'\theta^2)]. \end{aligned} \quad (25)$$

Since the distance between two discrete states is by (17) and (14) of the order of $1/b'$ and since, if w is to be small compared with this, θ^2 must, by (20), be large compared to 1, the last term in the expression (25) is negligible, and we are left with

$$\begin{aligned} \psi &= - [\exp(-2\pi i E_1 t/h)] E_1^{1/4} \theta (E_1 - U)^{-1/4} (\pi/b'\theta^2) \\ &\quad \cos \left\{ \kappa \int_x^{x_2} (E_1 - U)^{1/2} dx - \pi/4 \right\} \exp(-2\pi t/hb'\theta^2), \end{aligned} \quad (26)$$

²¹ Pierce, "A short Table of Integrals," Ginn and Co., Formula 490.

a standing wave, except for the exponential decrement with time. Actually, if we consider terms of higher order, the wave function in the valley will not be expected to be merely a standing wave with exponential decrement with time.

Now if the mountain is not too thick through (i.e. if $x_1 - x_2$ is not too great)²² we may find the expression for ψ in the mountain the same way as we found it for ψ in the valley. We simply assume that $\exp\{\kappa \int_{x_2}^x (U - E)^{1/2} dx\}$ does not vary over the effective range of $E - E_1$, and this is, in fact included in the assumption we have already made that θ does not vary appreciably over this range. The integrations are then readily performed. We get an expression which again contains the factor $\exp(-2\pi i E_1 t / h - 2\pi t / h b' \theta^2)$. Also just to the right of x_1 , (23) does not give an exact expression for ψ . The difference between the true value of ψ and that given by (23) will, however, not be appreciably different from 0 for any great distance to the right of x_1 , and for this range we may also assume that $\kappa \int_{x_1}^x (E - U)^{1/2} dx$ does not vary appreciably with E over the range w , or at least that it is a linear function of $E - E_1$. In either case it is easily seen that the expression for ψ will contain the factor $\exp(-2\pi i E_1 t / h - 2\pi t / h b' \theta^2)$. Thus we see that the assumption of a complex eigenvalue is at least approximately correct, and that the smaller w is the better the approximation is. It also depends on the relations (9) and (10). It is also, of course, necessary that t should not be too small.

The rate of decay, γ , of ψ^2 is of course given by twice the real factor of t in this exponential time factor. We have²³

$$\begin{aligned} \gamma &= 4\pi / h b' \theta^2 \\ &= \frac{\pi}{h} \left(\frac{\partial}{\partial E} \kappa \int_{x_2}^{x_1} (E - U)^{1/2} dx \right)^{-1} \exp \left\{ -2\kappa \int_{x_2}^{x_1} (U - E)^{1/2} dx \right\}. \end{aligned} \quad (27)$$

It is seen from (20) that

$$w / \gamma = h / 2\pi \quad (28)$$

the same relation that held in the case of predissociation, where we have a different type of interaction between discrete and continuous states.²⁴

GENERALIZATION OF THE RESULTS

Our results so far are somewhat unsatisfactory inasmuch as the general validity of the relations (5), (6), (7) and (8) depends upon the properties of $E - U$ considered a function of x when x is a complex variable, which are a little hard to investigate in a general way, or upon the assumption that the

²² In order for the discrete state not to be too broad, θ must be great. The condition just cited states that a sufficient portion of this greatness must be caused by the height rather than the breadth of the mountain. If the mountain and the valley are of somewhat the same width the required condition will be sufficiently well fulfilled.

²³ This expression agrees with that of Kudar, *Zeits. f. Physik* **53**, 99 (1929) also that of Fowler and Wilson, *l.c.*, in the exponential part, but not in the factor. The difference is probably due to the fact that Kudar and Fowler and Wilson considered a type of potential energy curve to which Kramer's approximation method could hardly apply.

²⁴ Ref. 10, p. 1457.

mountain-sides are long and straight. We may, however, show that the general character of the results depends only on the broadening of the discrete state being sufficiently small so that any given solution of the wave equation does not change its general character in that range. For then we may assume that a particular solution in the plain (far to the right of x_1) is connected with a particular type of solution in the mountain and in the valley. Thus the two solutions $E^{-1/4} \frac{\cos}{\sin}(\kappa E^{1/2}x + \zeta)$ are connected with solutions in the mountain and valley which do not change much over the range of energies in the width of the discrete state. This will be true no matter what value we choose for ζ . Let us choose ζ so that if $E=E_1$ the eigenfunction in the plain becomes $E^{-1/4} \sin(\kappa E^{1/2}x + \zeta)$. For any other value of E the eigenfunction in the plain is

$$[E^{-1/4} \sin(\kappa E^{1/2}x + \zeta) + gE^{-1/4} \cos(\kappa E^{1/2}x + \zeta)]/(1 + g^2)^{1/2}. \quad (29)$$

If $E-E_1$ is small enough g can be written as a linear function of $E-E_1$ say $g'(E-E_1)$ and in general it may be expected to be of the order of $b'\theta^2(E-E_1)$ as before, but the general character of the results, and the possibility of the use of complex eigenvalues do not depend on this. (The sign of g' is important but is surely the same as that of $b'\theta^2$.) Since we assume that the range of $E-E_1$ is so small that the shape of the eigenfunction in the valley is not affected we see that $(B/B_1)^2$ is given by $1/[1+g'^2(E-E_1)^2]$, hence all our previous results follow with g' substituted for $b'\theta^2$. Except, therefore, for this substitution we see that our results depend only on general properties of the solutions of the wave function, and not on their specific form.

I wish to thank Professor W. Heisenberg and Dr. F. Bloch for discussing this problem with me. I am informed by Dr. Bloch that much the same thing has been worked out independently by Professor Kramers, though without indicating, as is done here, how the wave packet is probably formed in nature.

PERTURBATIONS IN MOLECULES AND THE THEORY OF PREDISSOCIATION AND DIFFUSE SPECTRA. II

BY OSCAR KNEFLER RICE¹

INSTITUT FÜR THEORETISCHE PHYSIK DER UNIVERSITÄT, LEIPZIG

(Received March 8, 1930)

ABSTRACT

Further consideration is given to the problems which arise when the continuum of one electronic state of a diatomic molecule occurs in the same range as the discrete states of another electronic state. In the finding of electronic states and the potential curves which go with them certain approximations must be made; a better approximation can then be obtained by quantum mechanical perturbation theory. The discrete states are broadened, and this will appear, inasmuch as spectral lines involving these states are broadened. In this paper the shape of the broadened spectral lines is found, certain properties of the perturbation matrix are considered, and a wave packet is set up or rather one such as would be set up by nature is used to give all the details of a radiationless transition from a discrete state to the overlying continuum.

SHAPE OF A SPECTRAL LINE IN CASES OF PREDISSOCIATION

THE simple result obtained in the preceding paper² for the shape of the absorption line in the case of radioactive decay and other similar processes, suggests that it would be well to try to obtain an explicit result for the shape of the line in the case of predissociation, for purposes of comparison. The shape of line could of course be calculated from the expressions in the first paper with the above title³ (hereafter referred to as (I)), but it turns out that these can be somewhat simplified.

In this paper it was shown that the absorption coefficient over a broadened spectral line (see Abstract above) as a function of $E - E_1$ (called $-E$ in (I)) where E is the energy of the light absorbed and E_1 the energy of the center of the line, is proportional to K^2 , where

$$K^2 = \left(\frac{1}{(\epsilon/2 + \beta)^2} + \frac{1}{(3\epsilon/2 + \beta)^2} + \dots + \frac{1}{(\epsilon/2 - \beta)^2} + \frac{1}{(3\epsilon/2 - \beta)^2} + \dots \right)^{-1} \quad (1)$$

where ϵ is the distance between unperturbed continuous levels⁴ (the system being in a box) and where β is a parameter given by the equation⁵

¹ National Research Fellow.

² Rice, Phys. Rev. preceding paper in this issue.

³ Rice, Phys. Rev. **33**, 748 (1929).

⁴ ϵ can of course be varied arbitrarily by varying the size of the box, but in any given problem can be regarded as a constant. None of the results depend on it in any essential particular, and it will always cancel out of expressions for things which are experimentally determinable. Nevertheless it has been found very convenient to treat the system as if contained in a box, so the continuous levels really become a very close-spaced set of discrete ones, and we shall continue to do so.

⁵ (I), Eq. (26), since $v_{ed} = v_{de}$ (see Rice, Phys. Rev., **34**, 1459 (1929), especially footnote 19).

$$E - E_1 = -2\beta A v_{ed}^2 \quad (2)$$

where $A = (\pi/2\epsilon\beta) [2 \cot(2\pi\beta/\epsilon) - \cot(\pi\beta/\epsilon)]$ and v_{ed} is the component of the perturbation matrix giving the interaction between the discrete level and the continuous levels. Now A is easily reduced to the form $-(\pi/2\epsilon\beta) \tan(\pi\beta/\epsilon)$, hence (2) becomes

$$E - E_1 = (v_{ed}^2 \pi / \epsilon) \tan(\pi\beta/\epsilon) \quad (3)$$

Eq. (1) can also be further reduced as follows. A was originally expressed as an infinite series,⁶

$$\left(\frac{1}{\beta^2 - (\epsilon/2)^2} + \frac{1}{\beta^2 - (3\epsilon/2)^2} + \dots \right)$$

which is equal to

$$\frac{1}{2\beta} \left(\frac{1}{\epsilon/2 + \beta} + \frac{1}{3\epsilon/2 + \beta} + \dots - \frac{1}{\epsilon/2 - \beta} - \frac{1}{3\epsilon/2 - \beta} - \dots \right).$$

From this and (1) we see that K^{-2} is equal to $-2d(\beta A)/d\beta = (\pi/\epsilon)^2 \sec^2(\pi\beta/\epsilon)$. Disregarding the constant factor, the absorption coefficient is given as a function of β/ϵ by $(K\pi/\epsilon)^2 = [\sec^2(\pi\beta/\epsilon)]^{-1} = [1 + \tan^2(\pi\beta/\epsilon)]^{-1}$. By (3) this becomes

$$(K\pi/\epsilon)^2 = 1/[1 + 4(E - E_1)^2 w^{-2}] \quad (4)$$

where $w = 2\pi v_{ed}^2/\epsilon$ is the width of the line. Hence the shape of the broadened discrete line is the same in the case of predissociation as in the case of radioactive decay or dissociation by rotation.

SOME PROPERTIES OF THE EIGENFUNCTIONS AND PERTURBATIONS

In previous work on the rate of predissociation⁷ it has never as yet been possible to follow the wave of dissociating molecules in the same way as in the preceding paper we have followed the wave of departing alpha particles in the case of radioactivity or the dissociating molecules in the case of dissociation by rotation. We are now in a position to do this in the case of predissociation. First we must consider certain properties of the eigenfunctions and perturbations involved.

To get the unperturbed eigenfunctions we first hold the distance, r , between the nuclei fixed, and solve the wave equation for the electrons and the rotation of the nuclei. We can write this equation in the following form

$$(H_\Theta - U_m)\Theta_m = 0 \quad (5)$$

H_Θ is the Hamiltonian⁸ with respect to the electrons and the rotation, Θ_m

⁶ See (I), Eq. (23), and text just after (23).

⁷ Wentzel, *Phys. Zeits.* 29, 333 (1928); Kronig, *Zeits. f. Physik* 50, 360 (1928); Rice, *Phys. Rev.* 34, 1451 (1929).

⁸ We use the following system of coordinates. We refer everything to a set of axes which pass through the center of gravity of the system as a whole. But in the case of the nuclei we use

is an eigenfunction, U_m an eigenvalue with quantum numbers designated collectively as m . We then set up arbitrarily the following wave equation for a function $F_{m,k}$ of r :

$$\begin{aligned} d^2 F_{m,k}/dr^2 + \kappa^2 (E_{m,k} - U_m) F_{m,k} &= 0 \\ \kappa^2 &= 8\pi^2 M/h^2 \end{aligned} \quad (6)$$

where M is the reduced mass, h Planck's constant $E_{m,k}$ an eigenvalue of (6), U_m being the eigenvalue (a function of r) previously found from (5).

instead of the six rectangular coordinates, the three coordinates of the center of gravity of the nuclei, the two coordinates ϕ and θ giving the direction of the line joining the nuclei, and r . The coordinates of the center of gravity of the two nuclei are counted among the electronic and rotational coordinates. Now if r is so large that interaction between the two atoms forming the molecule is negligible (a case which will later be of importance) then the potential energy function for any given ϕ and θ will depend on $x_1 - \alpha r l$, $y_1 - \alpha r m$, $z_1 - \alpha r n$, $x_2 - \alpha r l$, \dots , where l , m , and n are the direction cosines of the line joining the nuclei, α is a constant depending on the relative masses of the two nuclei and on which nucleus the electron in question is (αr being the distance to the given nucleus from the center of gravity of the nuclei), and $x_1, y_1, z_1, x_2, \dots$, are the coordinates of the electrons, and also on the coordinates of the center of gravity of the nuclei, but not otherwise on r than as noted above, provided the coordinates of the system have values at all probable. Therefore the eigen-function Θ_m will depend upon r only in like manner. From this we see that any function of Θ_m and its derivatives when integrated over all coordinates except r , ϕ , θ will very approximately be independent of r . For we can always substitute the variables $x_1 - \alpha r l$ for the original variables, and $d(x_1 - \alpha r l)$ for dx_1 for constant r . Further integration over ϕ and θ of course leaves the expression independent of r .

Note added in proof: Since Footnote 8 may not be clear it may be well to explain it in more detail. The reason that Θ_m involves r only in the form $x_1 - \alpha r l$ when r is large is as follows. A partial differentiation with respect to x_1 is the same as a partial differentiation with respect to $x_1 - \alpha r l$. So if in finding our eigenfunction we first hold ϕ and θ fixed as well as r we get an eigenfunction depending only on $x_1 - \alpha r l$, etc., and the coordinates of the center of gravity of the nuclei. We call this eigenfunction N and will omit subscripts. For the dependence on ϕ and θ we multiply by a spherical harmonic, Y . The NY form a complete orthogonal set in terms of which the Θ_m can be expanded. The perturbation matrix components are found in much the same way as the others (v_{ss} and v_{st}) in this paper, and are due to the fact that the terms

$$\frac{1}{r^2 \sin^2 \theta} \frac{\partial}{\partial \theta} \left(\sin \theta \frac{\partial}{\partial \theta} \right) + \frac{1}{r^2 \sin^2 \theta} \frac{\partial^2}{\partial \phi^2}$$

in the Hamiltonian must operate on the whole expression NY instead of just on Y , since l , m , and n which are involved in N depend on ϕ and θ . We have

$$\partial N / \partial \theta = -\alpha r (\partial l / \partial \theta) \partial N / \partial (x_1 - \alpha r l),$$

and correspondingly for the second derivative, etc. Wherever the second partial derivatives of N with respect to $x_1 - \alpha r l$, etc., occur a factor r^2 cancels the r^{-2} in the perturbation operator, and subsequent integration over x_1 , etc., removes the dependence on r in the way discussed near the end of footnote 8. The terms in a perturbation matrix component involving only a first derivative of N will contain r to the minus first power, hence will be small for large r . Therefore, for large r , the coefficients of the of NY 's in the expression for Θ_m will not involve r and Θ_m will depend on r only as stated.

Another remark we should like to make is this. The coordinates of the actual distance of an electron to its nucleus (if X_0 , etc., are the coordinates of the center of gravity of the nuclei) are $x_1 - \alpha r l - X_0$ and the potential energy depends more directly on this quantity than on $x_1 - \alpha r l$, but this does not matter for our purposes.

As the unperturbed eigenfunction we use $\Theta_m F_{m,k}/r$. This is the usual procedure for molecules, it being generally conceded that it gives the energy levels of molecules to a good approximation.⁹

The unperturbed eigenfunction obviously obeys the equation:

$$(F_{m,k}/r)(H_\Theta - U_m)\Theta_m - \kappa^{-2}(\Theta_m/r)d^2F_{m,k}/dr^2 - (\Theta_m/r)(E_{m,k} - U_m)F_{m,k} = 0 \quad (7)$$

Since H_Θ and $E_{m,k}$ and U_m contain no derivatives with respect to r we may write

$$H_\Theta(\Theta_m F_{m,k}/r) - \kappa^{-2}(\Theta_m/r)d^2F_{m,k}/dr^2 - E_{m,k}(\Theta_m F_{m,k}/r) = 0 \quad (8)$$

The actual Hamiltonian for the system, however, is

$$H = H_\Theta - \kappa^{-2}\left(\frac{\partial^2}{\partial r^2} + \frac{2}{r}\frac{\partial}{\partial r}\right). \quad (9)$$

The actual wave equation, therefore, if it operates on $\Theta_m F_{m,k}/r$ contains the extra terms¹⁰

$$- \kappa^{-2}[(F_{m,k}/r)(\partial^2\Theta_m/\partial r^2) + (2/r)(\partial\Theta_m/\partial r)(dF_{m,k}/dr)]. \quad (10)$$

Now to get the real solution of the wave equation we can expand in terms of the $\Theta_m F_{m,k}/r$ which form an orthogonal set.¹⁰ We can treat the $\Theta_m F_{m,k}/r$ as solutions of equations like (8) and use the extra terms in setting up a perturbation matrix, (10) being considered as the result of an operator acting in a special way on $\Theta_m F_{m,k}/r$.

Now in the case of predissociation we expand the perturbed eigenfunction in terms of a $\Theta_m F_{m,k}/r$ belonging to a discrete state,¹¹ which we will call simply ψ_d , and a set of continuous ones, which belong to another electronic level, and which we designate as $\Theta_c F_{c,i}/r$ where i runs over the set of continuous states. It is to be noted that the continuous property arises from the $F_{c,i}$'s, as Θ_c for all r 's is a discrete eigenfunction of (5).

The perturbed eigenfunction, ψ'_n may thus be written as a linear function of the unperturbed, thus:¹²

$$\psi'_n = S_{dn}\psi_d + \Theta_c \sum_i S_{in} F_{c,i}/r. \quad (11)$$

For large values of r the first term of (11) gives no appreciable contribution, hence for this case

$$\psi'_n = \Theta_c \sum_i S_{in} F_{c,i}/r = \Theta_c F'_n/r \quad (12)$$

⁹ Born and Oppenheimer, Ann. d. Physik **84**, 457 (1927).

¹⁰ Perturbations of this nature were first set up in practically this form by Slater, Proc. Nat. Acad. Sci. **13**, 423 (1927), which should be seen for details. Our formulation differs only in that we have put the r part of the eigenfunction in the form $F_{m,k}/r$.

¹¹ Only one discrete state is to be considered, for we assume as throughout that any other discrete states which interact with the set of continuous states we are interested in are so far away in the term spectrum that their effect may be neglected. Also, of course we consider that the given discrete state interacts with only one set of continuous ones. See (I) pp. 751-2.

¹² (I), Eq. (29) It has been, unfortunately, necessary to change the notation somewhat.

where $F_n' = \sum_i S_{in} F_{c,i}$. The perturbed wave equation may be written

$$(H - E_n')\psi_n' = 0 \quad (13)$$

where E_n' is the corresponding eigenvalue.

This gives, for large r , using (9) and (12)

$$H\Theta(\Theta_c F_n'/r) - \kappa^{-2}(\Theta_c/r)d^2 F_n'/dr^2 - E_n'(\Theta_c F_n'/r) - \kappa^{-2}(F_n'/r)\partial^2 \Theta_c/\partial r^2 - \kappa^{-2}(2/r)(\partial \Theta_c/\partial r)(dF_n'/dr) = 0. \quad (14)$$

We now proceed to reduce (14) to an equation in F_n' . To do this we first multiply through by r , then by Θ_c and integrate over all values of the electronic and rotational coordinates. (We call the volume element $d\tau'$.) We remember that $\int \Theta_c H \Theta_c d\tau' = U_c$ and note that¹³ $2\int \Theta_c (\partial \Theta_c/\partial r) d\tau' = \int (\partial \Theta_c^2/\partial r) d\tau' = (d/dr) \int \Theta_c^2 d\tau' = d1/dr = 0$, since the Θ_m are an orthogonal set. Further we set $\kappa^{-2} \int \Theta_c (\partial^2 \Theta_c/\partial r^2) d\tau' = I_c$. Eq. (14) thus becomes

$$d^2 F_n'/dr^2 + \kappa^2(E_n' + I_c - U_c)F_n' = 0 \quad (15)$$

For large distances, r , the integral I_c must be independent of r , because for large distances r the molecule is separated into atoms which do not interact appreciably. Θ_c will always be affected the same way by a displacement, dr , regardless of what r is, provided it is large enough (see footnote 8). Eq. (15) shows us that F_n' satisfies a wave equation of the usual type for a problem of one degree of freedom, and hence is a sinusoidal function of the usual type.

CONCERNING THE PERTURBATION MATRIX AND THE PERTURBATION PROBLEM

Before we proceed further we must introduce some considerations about the perturbation matrix. The diagonal matrix component for a given continuous state is by (10) remembering that the r part of the volume element is $r^2 dr$ (we substitute c for m in (10)—also we write s for k to correspond to the notation used in previous papers—unfortunately we cannot make the correspondence complete, as in this paper it has been necessary to use two subscripts):

$$v_{ss} = -\kappa^{-2} \int_0^\infty F_{c,s}^2 dr \int \Theta_c (\partial^2 \Theta_c/\partial r^2) d\tau' - 2\kappa^{-2} \int_0^\infty F_{c,s} r (dF_{c,s}/dr) dr \int \Theta_c (\partial \Theta_c/\partial r) d\tau'$$

For the method of setting up this expression Slater's article¹⁰ can be consulted. The last term vanishes since $\int \Theta_c (\partial \Theta_c/\partial r) d\tau' = 0$ as noted above. Remembering the definition of I_c we find

$$v_{ss} = - \int_0^\infty F_{c,s}^2 I_c dr.$$

¹³ Kronig, l. c., p. 355.

Now I_c approaches a constant value for large r . Let us call this value I_{c1} . Then $I_c = I_c' + I_{c1}$ where I_c' differs from zero only for small r , and there will be of the order of I_{c1} . From the orthogonal properties of the $F_{c,s}$ we see that

$$v_{ss} = - \int_0^\infty F_{c,s}^2 I_c' dr - I_{c1}. \quad (16)$$

In similar manner, for two different continuous states s and t belonging to the same electronic-rotational state c , we get, remembering the orthogonal properties of the $F_{c,s}$

$$v_{st} = - \int_0^\infty F_{c,s} F_{c,t} I_c' dr.$$

Therefore the contributions to v_{st} come from a range in which r is small, and our previous deductions that v_{st} is small enough to be neglected are valid.¹⁴ The same deductions hold for the first term of the right of (16). Hence, very approximately

$$v_{ss} = - I_{c1} \quad (17)$$

The method of handling cases where v_{ss} is not small has already been indicated.¹⁴ In fact, it consists simply in adding v_{ss} (which is practically independent of s) to the corresponding energy $E_{c,s}$ and proceeding exactly as before. Now suppose instead of (6) we write (for the case $m=c$ and $k=s$)

$$d^2 F_{c,s} / dr^2 + \kappa^2 (E_{c,s} - U_c - v_{ss}) F_{c,s} = 0 \quad (18)$$

Then $E_{c,s} + v_{ss}$ takes the place of $E_{c,s}$ ($m=c$, $k=s$) as eigenvalue in Eq. (6). We could therefore take (18) as the unperturbed equation for the electronic-rotational state c , and otherwise disregard v_{ss} . This is the most convenient way of handling the problem, for the relations between the eigenvalues of (18) and the perturbed eigenvalues E_n' will be just the same as the relation between the eigenvalues of (6) and the E_n' *would have been* were v_{ss} actually 0, and this relationship has been deduced in the previous work.

The relationship is as follows. Between every two eigenvalues of (18) lies a value E_n' . Let us denote as $E_{c,n}$ the eigenvalue of (18) which is just above the particular value E_n' . Then from the original definition¹⁵ of the quantity β which appeared earlier in the paper

$$E_{c,n} - E_n' = \beta + \epsilon/2. \quad (19)$$

THE WAVE PACKET FOR THE DISSOCIATING MOLECULES

Now it has been shown¹⁶ that the wave packet for the dissociation from the discrete state into the overlying continuum is given by

¹⁴ (I), Appendix I. Correction, Phys. Rev. **34**, 1462.

¹⁵ (I), p. 755.

¹⁶ Rice, Phys. Rev. **34**, 1451 (1929).

$$\psi = \sum_n S_{dn} \psi_n' \exp(-2\pi i E_n' t / h) \quad (20)$$

where $S_{dn} = K/v_{cd}$. For values of r large compared to atomic sizes, we have from (12), (4), and (20)

$$\psi = \frac{\epsilon \Theta_c}{\pi v_{cd} r} \sum_n \frac{F_n' \exp(-2\pi i E_n' t / h)}{[1 + 4(E_n' - E_1)^2 / \omega^2]^{1/2}} \quad (21)$$

We shall now find the relation between the F_n' and the eigenfunctions $F_{c,s}$ of Eq. (18). The latter may be written in the following form for large r

$$F_{c,s} = \sin \{ \kappa(E_{c,s} - U_c - v_{ss})^{1/2} r + \zeta_s \} \quad (22)$$

where ζ_s is a phase constant. The condition that $F_{c,s} = 0$ at $r = r_1$ where r_1 is the largest value r can take (the system being in a box) requires

$$\sin \{ \kappa(E_{c,s} - U_c - v_{ss})^{1/2} r_1 + \zeta_s \} = 0. \quad (23)$$

But the quantum condition in the neighborhood of $r=0$ requires that ζ_s should be the same¹⁷ for all s . At any rate this will be practically true over a range of energies greater than the small breadth, w , of the broadened discrete state. It would always be exactly true if U_c were constant for small r , as well as large, (i.e. if (22) actually held for small r), and the smallest value r could take were 0. Now since F_n' obeys the equation (15) we have for large r

$$F_n' = \sin \{ \kappa(E_n' - U_c - v_{ss})^{1/2} r + \zeta_n' \} \quad (24)$$

F_n' must be 0 at $r = r_1$ so

$$\sin \{ \kappa(E_n' - U_c - v_{ss})^{1/2} r_1 + \zeta_n' \} = 0 \quad (25)$$

Eq. (25) will obviously be satisfied if

$$\zeta_n' = \zeta_s + \kappa(E_{c,n} - U_c - v_{ss})^{1/2} r_1 - \kappa(E_n' - U_c - v_{ss})^{1/2} r_1 \quad (26)$$

(see Eq. (23) and see also just before Eq. (19) for definition of $E_{c,n}$). Now as the difference between the quantities $(E_{c,n} - U_c - v_{ss})^{1/2}$ and $(E_n' - U_c - v_{ss})^{1/2}$ is very small¹⁸ we may write it as $\frac{1}{2}(E_{c,n} - E_n')$ $(E_{c,n} - U_c - v_{ss})^{-1/2}$ or, by (19) as $\frac{1}{2}(\beta + \epsilon/2) (E_{c,n} - U_c - v_{ss})^{-1/2}$. Now $\epsilon = 2\pi\kappa^{-1}(E_{c,n} - U_c - v_{ss})^{1/2} r_1^{-1}$. So we see that

$$\begin{aligned} \zeta_n' &= \zeta_s + \pi\beta/\epsilon + \pi/2 = \zeta_s + \pi/2 + \tan^{-1} \{ (E_n' - E_1)\epsilon/\pi v_{cd}^2 \} \\ &= \zeta_s + \pi/2 + \tan^{-1} \{ 2(E_n' - E_1)/w \} \end{aligned} \quad (27)$$

by (3) and remembering that $w = 2\pi v_{cd}^2/\epsilon$. We thus get an expression for ζ_n' which can be used in evaluating F_n' . Now

$$\sin \{ x + \tan^{-1} y \} = (\sin x + y \cos x) (1 + y^2)^{-1/2}.$$

¹⁷ Or differ only by multiples of π . We can choose that they should be all the same.

¹⁸ It may be made as small as we please by making r_1 large.

Using this formula we get from (24), (27), and (21)

$$\psi = \frac{\epsilon\Theta}{\pi v_{cd}r} \sum_n \frac{[\sin\{\kappa(E_n' - U_c - v_{cs})^{1/2}r + \zeta_s + \pi/2\} + [2(E_n' - E_1)/w]\cos\{\kappa(E_n' - U_c - v_{cs})^{1/2}r + \zeta_s + \pi/2\}]\exp(-2\pi i E_n t/\hbar)}{1 + 4(E_n' - E_1)^2/w^2}.$$

The sum over n can be converted to an integral with respect to E_n' , and then, except for the factor $1/r$, which merely means that here we have taken all three dimensions of space into account, and so have a spherical wave, the part which involves r has exactly the same form as Eq. (23) of the preceding paper. We thus have a wave of dissociating particles of exactly the same type as before, with exponential decrement with time bearing the same relation to the width of the discrete state, in fact the same in all details. There is thus a complete analogy in results between these two different types of decompositions. Also the part of the wave for small r can be handled as in the preceding paper, since for small r the eigenfunctions will not vary appreciably over a small range of energies.

I wish to express my thanks to Professor Heisenberg for his interest in this work, and helpful discussion.

CONCERNING THE ABSORPTION METHOD OF INVESTIGATING
 β -PARTICLES OF HIGH ENERGY: THE MAXIMUM
ENERGY OF THE PRIMARY β -PARTICLES OF
MESOTHORIUM 2.

BY N. FEATHER*

PHYSICAL LABORATORY, JOHNS HOPKINS UNIVERSITY, BALTIMORE

(Received April 30, 1930)

ABSTRACT

For the primary β -particles of radium C, radium E and mesothorium 2 the maximum effective mass range, R , has been determined in paper and aluminum by the method of Chalmers. In the two former cases the maximum energy of the particles, E , is known, and these results and earlier data lead to the relation

$$R = 0.511E - 0.091$$

for $E > 0.7$. Here R is measured in grams/cm² and E in millions of electron volts. For mesothorium 2, $R = 0.955 \pm 0.015$ gm/cm², so that the maximum energy of the particles is $2.05 \pm 0.03 \times 10^6$ electron volts. Reasons are advanced for employing the empirical relation above quoted rather than results obtained with particles of a single velocity, as in the experiments of Varder and Madgwick, in the interpretation of absorption measurements made upon primary β -particles.

INTRODUCTION

THE earliest recognition of the emission of two distinct types of corpuscular radiation from radioactive material followed immediately upon the adoption of absorption methods of investigation; continuously throughout the development of the subject these methods have been applied afresh in the study of the radiations from the β -ray bodies. Beyond a general qualitative analysis, however, they provide little information which admits of easy interpretation. We now know, for example, that exponential absorption reflects no fundamental property of the different natural radiations—and, in consequence, exponential absorption coefficients have lost much of their significance. Moreover most of the early work was directed toward their determination.

And yet, despite this indefiniteness, absorption measurements do provide, simply and without ambiguity, the maximum effective range, in the medium employed, of the particles submitted to analysis. Now it is of considerable interest to determine the maximum energy appearing as kinetic energy in each of the cases of β -particle disintegration and it is evident that absorption measurements make this determination possible when the necessary data relating effective range with the energy of the particle are available. Such data in fact exist, and already the method has been applied to the β -ray bodies of the active deposit of thorium by Chalmers¹ and to those of the active

* Fellow of Trinity College, Cambridge; Associate in Physics, Johns Hopkins University.

¹ Chalmers, Proc. Camb. Phil. Soc. 25, 331 (1929).

deposit of actinium by Sargent.² But the data in question, upon which the interpretation of these experiments depends, in themselves are ambiguous: the ranges in aluminum given by Madgwick³ are more than 10 percent greater than the corresponding ranges as determined by Varder.⁴

Eddy⁵ has recently made a more detailed study of the absorption of β -particles of somewhat less energy than those with which we are here chiefly concerned and has concluded that the discrepancies between the results of Varder and Madgwick are to a large extent due to the different arrangements of ionization chamber which these authors employed. This conclusion, coupled with the fact that the conditions obtaining in absorption measurements on the complete natural radiations are quite different from those effective in the two investigations under discussion, makes a review of the precise relevance of the data of Varder and Madgwick to the present problem of considerable interest. The results of each investigator show that the effective range is a linear function of the energy of the particle for values of the energy greater than 0.65 million electron volts, or formally

$$R = aE + b \quad (1)$$

for $E > 0.65$ (million electron volts). Varder's data for aluminum are best represented by $a = 0.469$, $b = -0.071$, R being expressed in grams/cm²; Madgwick's figures by $a = 0.552$, $b = -0.097$. It is to be expected that a similar relation must apply to the conditions of experiment in the primary β -particle case also, but it should be pointed out that the relation in question no longer connects the effective range with the energy for particles initially homogeneous in velocity, but rather it relates the maximum effective range with the maximum energy when particles of continuously varying energy are present. It is very probable that this circumstance makes the determination of the effective range more independent of the conditions than it appears to be in the case of particles of a single velocity,⁶ but obviously it cannot result otherwise than that the maximum effective range which is measured should be determined by the highest energy particles present in the beam. Nevertheless there is no simple reason for believing this range to be precisely the same as the effective range determined by extrapolation from the absorption curve taken under any arbitrary conditions with β -particles of that unique limiting velocity. For the purposes of interpretation of experiments performed upon the full natural β -radiation from different substances we ought in preference to employ a calibration curve determined under closely comparable conditions. Such a curve may be obtained by applying the absorption method to the determination of the maximum effective range of the β -particles from bodies which have already been studied in greater detail by the method of magnetic spectroscopy.

² Sargent, Proc. Camb. Phil. Soc. 25, 514 (1929).

³ Madgwick, Proc. Camb. Phil. Soc. 23, 970 (1927).

⁴ Varder, Phil. Mag. 29, 725 (1915).

⁵ Eddy, Proc. Camb. Phil. Soc. 25, 50 (1929).

⁶ A necessary condition for the truth of this statement is that the continuous spectrum of velocities should have a sharply defined upper limit. This seems to be the case: cf. Chalmers, reference 1, p. 337, Gurney, reference 9, p. 549.

The experiments of Chalmers¹ and Gurney⁷ provide the first point on such a curve. Chalmers fixed the maximum effective range of the β -particles of thorium C at 0.98 gm/cm² of aluminum whilst Gurney showed that the maximum energy of the particles was 2.18×10^6 electron volts. The first portion of the present work is devoted to the determination of the maximum effective range of the radium E β -particles and of those of radium C. The limiting energies to which these ranges correspond are known from the measurements of Madgwick,⁸ and Gurney,⁹ respectively. Then two more points are added to the curve and the most probable values of the constants a and b of Eq. (1) may be determined.

The second part of the work consists in a similar absorption experiment upon the primary β -particles of mesothorium 2 and the newly determined range-energy relation makes possible its interpretation.

GENERAL EXPERIMENTAL ARRANGEMENT

The β -ray electroscope used in all the measurements consisted of a gold leaf system suspended in the usual manner at the center of a cubical aluminum case of 11 cm edge and 3 mm thickness of wall. In the base of the electroscope a hole 7.5 cm square was closed with aluminum foil weighing 6.5 mg/cm². The electroscope was supported on a wooden stand with a space of 24 cm between its base and the surface of the bench. A wooden slide could be inserted in various positions below the base of the instrument. This slide carried both the active material and the absorbing foils. The former was placed at the bottom of a shallow cylindrical hole (depth 1.1 cm, diameter 3.2 cm) cut in the slide and the latter, in the form of sheets 5 cm square, were placed upon the slide so as to cover the hole symmetrically. In most cases the slide was inserted in the highest position, and in these circumstances the source was about 3.5 cm below the base of the electroscope. In all the experiments the decay of the source and the varying density of the air in the electroscope were corrected for by making frequent measurements under standard conditions of absorption. In general the mean of ten independent observations was obtained for each point plotted on an absorption curve. Adopting this routine it was not found necessary to employ a magnetic field to separate β - and γ -ray effects, even in the case of radium C where the latter effect is very pronounced, and indeed it is the writer's opinion that the avoidance of such a method is much to be preferred whenever that is possible, for it is difficult to estimate the effect of the stray magnetic field on the γ -ray ionization in the electroscope in any of the simpler experimental arrangements that have been used.

EXPERIMENTAL RESULTS. PART I

Radium E. Madgwick⁸ has determined the upper limit of the continuous spectrum of the β -particles of radium E as 1.07×10^6 electron volts energy. This is the datum with which our range measurements are to be combined.

⁷ Gurney, Proc. Roy. Soc. 112A, 380 (1926).

⁸ Madgwick, Proc. Camb. Phil. Soc. 23, 982 (1927).

⁹ Gurney, Proc. Roy. Soc. 109A, 540 (1925).

Absorption methods have, in fact, already been applied to the determination of the range in this case. In 1912 Gray¹⁰ first pointed out¹¹ the phenomenon of an end point to the β -particle absorption with a source of radium E. His measurements lead to an effective mass range between 0.45 and 0.49 gm/cm² of paper. Douglas¹² extended the measurements to other absorbing media and gave 0.474 and 0.460 gm/cm² for the effective ranges in paper and aluminum respectively. But the sources employed were weak and the logarithmic method of extrapolation was used to fix the range. It was thought worthwhile to repeat the determinations¹³ with a stronger source employing the method of simple extrapolation of Chalmers. This method has been adopted as standard throughout.

The results are shown in Fig. 1. They refer to a source of radium D, E and F in equilibrium¹⁴ deposited by evaporation on a small platinum dish. The

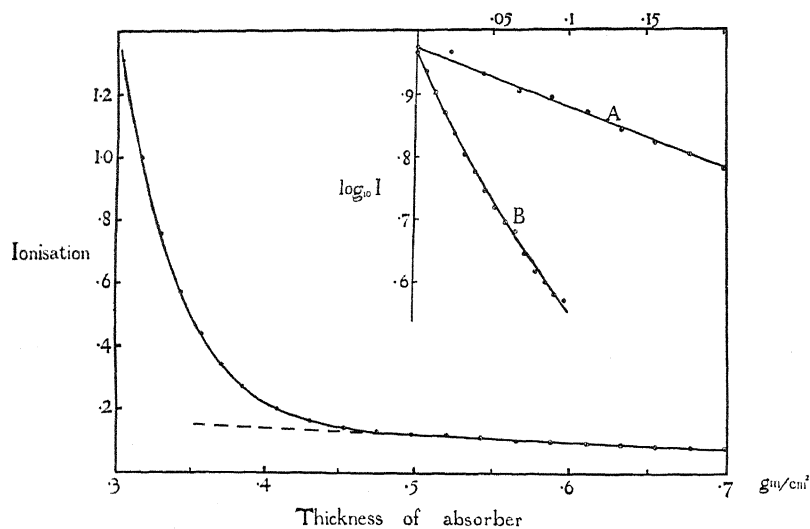


Fig. 1. Radium E.

weight of deposit, more than 1 cm² in extent, was a few milligrams only. Unwhitened paper was used as absorber and the maximum effective mass range in this medium may be taken as 0.475 ± 0.005 gm/cm².

A simple experiment was also made upon the radiation unabsorbed by this thickness of material. The source was covered with sheets of paper repre-

¹⁰ Gray, Proc. Roy. Soc. 87A, 487 (1912); Trans. Roy. Soc. Canada 16 III, 125 (1922).

¹¹ The end point is clearly shown in absorption curves published by Schmidt in 1907 (Phys. Zeits. 8, 362 (1907)).

¹² Douglas, Trans. Roy. Soc. Canada, 16 III, 113 (1922).

¹³ Absorption measurements by Aston (Proc. Camb. Phil. Soc. 23, 935, (1927)) and by Fournier and Guillot (Comptes rendus 189, 1079 (1929)) also have reference to a region including the β -particle end point but, being concerned chiefly with the weak γ -radiation, permit of no accurate range values being drawn from them.

¹⁴ The writer wishes to thank Dr. C. F. Burnam of the Kelly Hospital, Baltimore, for a supply of old radon tubes from which this material was extracted.

senting (together with the air gap and the base of the electroscope) 0.499 gm/cm^2 of absorber. Aluminum foils were then added and the further progress of the absorption followed. The curve *B*, Fig. 1, exhibits these results, the logarithm of the corrected ionization being plotted against the foil thickness. Curve *A* represents the parallel case where the absorption was in paper throughout. A mass absorption coefficient of $2.3 \text{ cm}^2/\text{gm}$ is a sufficiently good approximation here; the initial absorption in aluminum, however, is roughly five times as great, for equal mass of absorber. This is what we should expect if the absorption were chiefly photoelectric, and the numerical values also suggest that the effective radiation is for the most part the very soft component, probably the *LX*-radiation of radium D, for which a mass absorption coefficient of $16.5 \text{ cm}^2/\text{gm}$ in aluminum is accepted as correct.¹⁵ The smaller value ($11.3 \text{ cm}^2/\text{gm}$) found with the present arrangement is to be attributed largely to the fact that the first 0.5 gm/cm^2 of paper has already reduced this soft component to about a quarter of its original intensity, so that the influence of the less intense though harder components is no longer negligible. It is of interest to record that the last point on the curve *B*, representing the smallest ionization current involved in this series of measurements, yet represents a current about forty times as great as the natural leak of the electroscope effective at the time.

Radium C. The primary β -particles of this body comprise a continuous spectrum of energies having a sharp upper limit at 3.15×10^6 electron volts (Gurney⁹). On the other hand no data have hitherto been available concerning the maximum effective range of these particles as determined in the present type of experiment. The problem here presented is considerably more difficult than in the case of radium E, on account of the very great intensity of the γ -radiation from radium C and of the rapid decay of this body. The latter difficulty may be overcome by using a radon tube as a β -particle source, although this procedure increases the γ -ray effect, by adding the γ -rays of radium B to those of its subsequent product. Moreover the radiation thus added is in general much less penetrating than the latter, and it is the softer components of the radiation which constitute the greater source of error. An attempt was made to minimise this effect in the arrangement finally adopted.

A small glass bulb, about 3 mm in diameter, originally containing about 800 equivalent milligrams of radon was employed as the source of β -particles at the stage when its activity had fallen to a few thousandths of its initial value.¹⁶ In this way the points of Fig. 2 were obtained. The absorbing material consisted of aluminum to the extent of 1.012 gm/cm^2 placed directly over the source, with sheets of paper for the remainder. By using the aluminum it was hoped to cut down the softer components of the γ -rays to reasonable proportions whilst the use of paper for the rest of the absorption was governed by considerations of ease of manipulation and of the sharper type of absorption

¹⁵ Rutherford and Richardson, *Phil. Mag.* **26**, 324 (1913). Curie and Fournier, *Comptes rendus* **176**, 1301 (1923).

¹⁶ For this material also the writer is indebted to Dr. Burnam.

limit thereby obtained. Moreover Chalmers failed to find any appreciable difference between the mass ranges of the thorium C β -particles in paper and aluminum. The equivalence of these materials in this respect has been assumed in the present experiments. The walls of the radon tube were not negligibly thin and an estimate of their thickness was made in two ways, by direct weighing, and by a subsequent absorption experiment after the lapse of a few weeks, when the radium E β -particles were responsible for the greater proportion of the ionisation as measured through small thicknesses.¹⁷ The difference

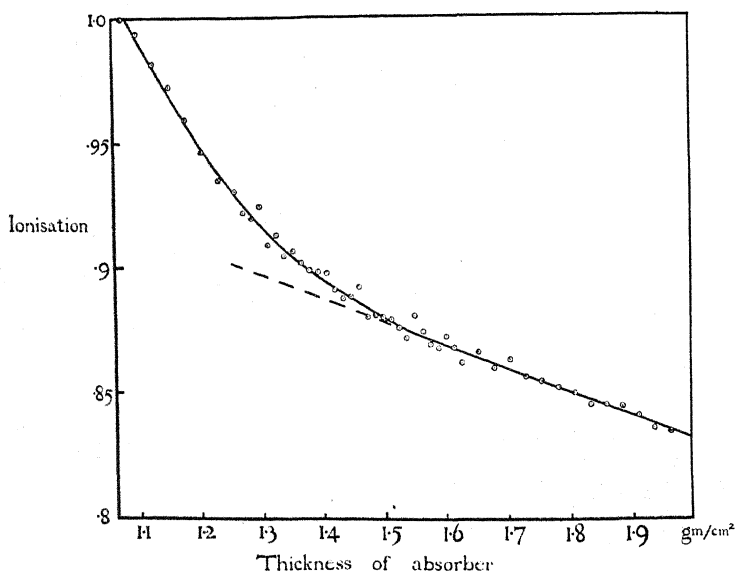


Fig. 2. Radium C.

between the apparent maximum effective range of these particles as determined with this source and in the direct experiments on radium E described above was attributed to absorption in the glass walls of the bulb. Both methods suggested an equivalent thickness of glass of 0.03 gm/cm^2 . So corrected the maximum effective mass range of the primary β -particles of radium C in aluminum or paper may be given as $1.54 \pm 0.02 \text{ gm/cm}^2$, as indicated in the figure.

The range-energy relation. The data which are to be employed in constructing our calibration curve are given in Table I.

TABLE I. Data used in constructing calibration curve.

Source of β particles	Maximum energy electron volts $\times 10^{-6}$	Maximum effective mass range gm/cm ²
RaE	1.07	0.475
ThC	2.18	0.98
RaC	3.15	1.54

¹⁷ The final decay of the emanation originally contained in the bulb is responsible for the production of about 0.3 equivalent milligrams of radium D, E, and F.

Within experimental error this material is consistent with a linear relation such as that given by Eq. (1) and is best represented by the straight line

$$R = 0.511E - 0.091 \quad (2)$$

which, by analogy with the relations of Varder and Madgwick, may probably be regarded as valid for values of E greater than 0.7 (million electron volts). It may be remarked that the present straight line occupies a position intermediate between those of Varder and Madgwick—and it may be pointed out that the results of Eddy occupy a similar position in the region of smaller energies where the curve is no longer linear. But the intention of any very close comparison between the present results and results having reference to particles of a single velocity has already been disclaimed, so that no primary importance is attached to this apparent agreement. Moreover, not only was the work of Eddy concerned with particles of a single velocity, but it was carried out by the method of electrical counting, providing a further reason for caution in its comparison with the results of ionization measurements.

EXPERIMENTAL RESULTS. PART II

Mesothorium 2. The β -particles of mesothorium 2 have been studied by Yovanovitch and d'Espine¹⁸ by the direct deviation method of magnetic spectroscopy. These authors suggest that the high energy limit of the continuous spectrum occurs in the region of 1.6 million electron volts energy. It is not unreasonable to suppose, from a knowledge of the general characteristics of the method, however, that this represents merely a lower limit to the maximum energy of the particles.¹⁹

The difficulties in the way of absorption measurements with mesothorium 2 are similar to those obtaining with radium C: there are γ -rays of considerable intensity and the pure substance is of fairly rapid decay. The broad scheme of the experiments, therefore, was first to determine an absorption curve in full detail with a source of mesothorium 1 and 2 in equilibrium and then to make confirmatory tests with a small number of selected thicknesses of absorber and a source of pure mesothorium 2, in order to be certain that the main features of the former curve, in the region of the β -particle end point at least, were due to the latter body alone.

A solution of mesothorium 1, freed from radiothorium by repeated precipitation with iron, and from a large fraction of the ammonium chloride which accumulates as a result of such operations, was allowed to stand so that the thorium X should decay. Being neutralized the solution was electrolysed with platinum anode and silver cathode at a temperature of about 90°C.²⁰

¹⁸ Yovanovitch and d'Espine, *J. de Physique*, **8**, 276 (1927).

¹⁹ For a constant value of the field the dispersion decreases rapidly as the energy of the particles increases, and this, together with the peculiarities of photographic registration, must necessarily introduce considerable distortion. Both in the case of the primary β -particles of radium C and for those of radium E this method has given too low a value for the maximum energy (2.74×10^6 electron volts in the former case and 0.94×10^6 in the latter).

²⁰ Meitner, *Phys. Zeits.*, **12**, 1097 (1911).

Mesothorium 1 and 2 were obtained together, the latter in about 90 percent of its equilibrium amount. The silver plate (about 2 cm² in area), carrying the deposit on one surface only, was enclosed in an airtight container to prevent the diffusion of emanation. A thin sheet of mica was employed for the upper face of the vessel which fitted neatly in the whole cut in the electroscope slide already described. Since originally the mesothorium was extracted directly from monazite, radium was known to be present as "impurity." But the duration of the previous heat treatment of the solution, and of the electrolysis, was such that immediately after its preparation the β -particle source could be regarded as free from all contamination except by radium element itself. Provided, therefore, that measurements were carried out within the

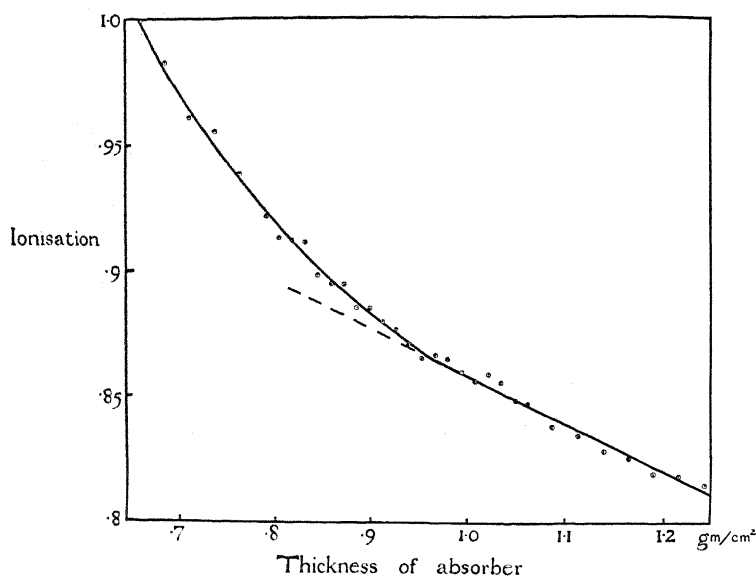


Fig. 3. Mesothorium 2.

first 24 hours after the source was prepared they were unlikely to be seriously affected by the growing β -particle activity arising from the active deposit of radium.

The results of measurements with this source are shown in Fig. 3, the last measurement being completed 22 1/2 hours after the source was obtained on the plate. As in the experiment on radium C roughly the first two-thirds of the absorption was in aluminum—a thickness of 0.646 gm/cm² of this metal being succeeded by sheets of paper. In an attempt to detect any possible effect of the gradual building up of radium C in the source during the period of observation measurements were made in the following order, namely through

44, 40, , 0,
 11, 15, , 27,
 2, 6, , 42,
 29, 25, , 13

sheets of paper, in turn. This sequence was, of course, interrupted periodically to permit of measurements with a standard absorber in place. It will be seen from the figure that no such effect as was sought was observed.²¹ In this way the β -particle end point was fixed at 0.955 ± 0.015 gm/cm² and it only remained to confirm its identification with the maximum effective mass range of the primary β -particles of mesothorium 2 by an independent experiment.

A source of mesothorium 2 was prepared in the usual manner by precipitation with a trace of iron from a solution containing mesothorium 1 and 2 in equilibrium. Three thicknesses of absorber, corresponding respectively to the first and last points in Fig. 3 and to the point nearest the absorption discontinuity, were chosen and two sets of measurements made, separated in time by about 3 1/2 hours. Table II contains the results.

TABLE II. Results

Thickness of absorber gm/cm ²	Relative ionizations	
	(1)	(2)
0.660	1.000	1.000
0.952	0.867	0.870
1.241	0.825	0.824

The decay of activity, corresponding to a half period of 6.4 hours, showed that the source was sufficiently pure for the test to be conclusive, and the figures given, when compared with the values 1.000, 0.868, 0.812 read directly from the curve, establish the identity which was in question. The exact agreement in the second instance is probably fortuitous but it is obvious first of all that no appreciable amount of unrecognized radioactive impurity was present in the original source, and secondly that any γ -rays emitted by mesothorium 1 were of little or no consequence in the measurements made with that source.

Inserting the value 0.955 gm/cm² for R in Eq. (2) we have $E = 2.05$ million electron volts and consequently, as the result of these experiments, may adopt this as the most probable value for the maximum energy of the primary β -particles of mesothorium 2. As was pointed out earlier in the discussion, a value considerably in excess of that given by Yovanovitch and d'Espine was almost to be expected.

Finally, in addition to acknowledgements already made, the writer wishes to record his appreciation of help received from the Rumford Fund of the American Academy of Arts and Sciences, a grant from which made possible the purchase of the mesothorium employed in these researches.

²¹ Further measurements were made on the source at three different absorptions within the range of the figure after 4 and 10 days, respectively. Also a rough absorption curve extending over this range was determined for a source of radium B+C in equilibrium. All the measurements could be explained simply by assuming that 8.7 percent of the ionization through 0.66 gm/cm² of aluminum at the end of 4 days, and 17.0 percent at the end of 10 days, was due to the β and γ -rays of radium B+C which had grown in the interim.

THE MOTION OF ELECTRONS IN CARBON MONOXIDE

By H. B. WAHLIN

DEPARTMENT OF PHYSICS, UNIVERSITY OF WISCONSIN

(Received May 5, 1930)

ABSTRACT

With the same data as were presented in an earlier paper it is shown that K. T. Compton's theory of electron mobilities holds within the limits of experimental error for high pressures and low fields, provided it is assumed that the energy loss of the electrons on impact with the molecules is greater than that due to momentum transfer.

The electron mean free path in CO has been calculated and, when the electrons are in thermal equilibrium with the gas, is 0.069 cm at a pressure of 1 mm.

I

IN AN earlier paper¹ it was shown that the mobility of electrons in CO can be represented as a function of the field strength and the pressure by an equation of the form

$$u = \frac{a}{P(B + x/p)^{1/2}}$$

with a high degree of accuracy. It is only for low fields that a systematic deviation from this equation appears.

Later, K. T. Compton² showed that from theoretical considerations, the mobility should be given by

$$u = \frac{0.815e\lambda}{m^{1/2}[\alpha T + (\alpha^2 T^2 + 1.76\lambda^2 e^2 x^2/f)^{1/2}]^{1/2}} \quad (1)$$

That this equation is applicable to the mobility of electrons in H₂ and He (at least for low fields and high pressures) has been shown by the writer.³

It was in order to test the validity of the Compton equation when applied to CO that the calculations submitted herewith were undertaken. The data are the same as were used in the earlier paper.

The method used in obtaining the data was the Rutherford alternating potential one for determining mobilities and has been described in detail earlier.

The Compton equation may be written in the form

$$u = \frac{a}{[1 + (1 + Bx^2)^{1/2}]^{1/2}}$$

¹ H. B. Wahlin, Phys. Rev. **21**, 517 (1923).

² K. T. Compton, Phys. Rev. **22**, 333 (1923).

³ H. B. Wahlin, Phys. Rev. **27**, 558 (1926).

If the electron is moving under the action of a sine wave alternating field the velocity in the direction of the field at any instant is, according to this equation,

$$\frac{dy}{dt} = \frac{aX \sin 2\pi nt}{[1 + (1 + BX^2 \sin^2 2\pi nt)^{1/2}]^{1/2}}$$

Imposing the condition that during one half cycle of the alternating field the electrons shall travel a distance d (the distance between the plates in the Rutherford method) we get on reducing the elliptic integral obtained and solving for n

$$n = \frac{a(2r)^{1/2}}{\pi d(B)^{1/2}} 2[E(k, \phi) - F(k, \phi)] \quad (2)$$

where $r = (BX^2 + 1)^{1/2}$, $k = \left(\frac{r+1}{2r}\right)^{1/2}$, $\phi = \sin^{-1}\left(\frac{r-1}{r+1}\right)^{1/2}$

and X is the peak value of the field corresponding to the voltage intercept of the mobility curves.

This equation may be verified directly with the data at hand.

Placing $A = 16,800$ and $B = 0.005$ it is seen that at a pressure of 722 mm good agreement between the experimental results and the theoretical curve

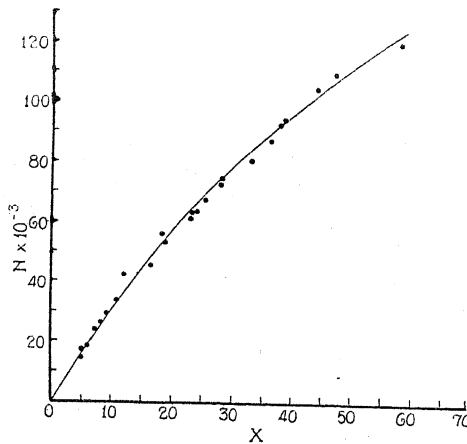


Fig. 1.

calculated from Eq. (2) is obtained. (Fig. 1). Here the points are experimental and show the relation between the frequency and the effective value of the field.

Fig. 2 shows the comparison between theory and experiment for a pressure of 500 mm. Here A and B have been corrected for the change in λ with pressure, assuming that λ varies inversely as the pressure.

At a pressure of 250 mm the agreement is good for low fields (Fig. 3). In fields above 35 volts/cm a systematic deviation appears—*viz.* the mobility

decreases more rapidly with field strength than is to be expected on the basis of the theory. This deviation is best ascribed to the beginning of the Ramsauer effect.

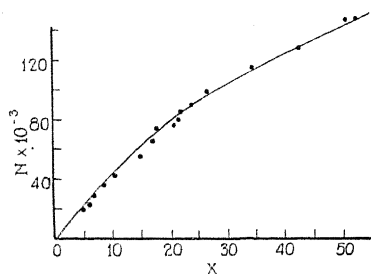


Fig. 2.

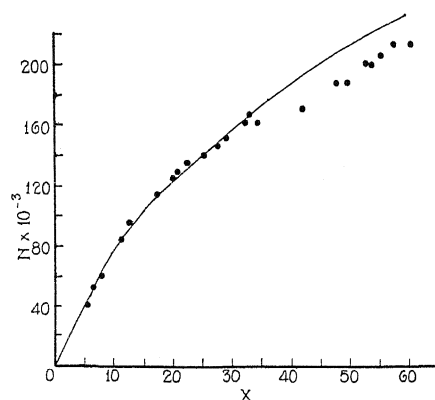


Fig. 3.

A comparison of theory and experiment may also be made as follows. If it is assumed that the mobility is independent of the field strength, it is possible to calculate the mobility from the relation

$$k = \pi n d^2 / 2^{1/2} V$$

where n is the frequency, d the distance between the plates, and V the r.m.s. value of the alternating voltage of the intercept of the mobility curves.

The value calculated from this equation for the case of electrons will be an average mobility defined so that the average velocity with a mobility k shall be the same as the average velocity determined from Compton's equation. This may be written

$$\int_0^d dy = \int_0^{1/2n} kX \sin 2\pi n t dt = \int_0^{1/2n} \frac{aX \sin 2\pi n t dt}{[1 + (1 + BX^2 \sin^2 2nt)^{1/2}]^{1/2}}$$

Integrating and solving for k we get

$$k = \frac{a(2r)^{1/2}}{X(B)^{1/2}} [2E(k, \phi) - F(k, \phi)].$$

Here r , k , ϕ and X have the same significance as in Eq. 2 above.

Fig. 4 shows the relation between the theoretical and experimental values of k at a pressure of 722 mm. In plotting the curve the same values of A and B were used as in the calculation of n .

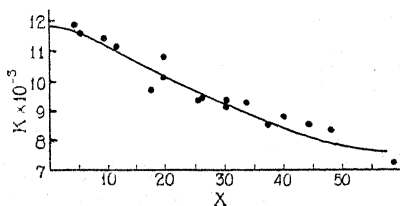


Fig. 4.

II

The limiting mobility for zero field will be given by $u = A/2^{1/2}$. Substituting the known value of A in this equation, the limiting mobility found is 11,900 cm/sec/volt/cm, at a pressure of 722 mm.

From this value of u the electron free path may be calculated using the theoretical relation $u = 0.75e\lambda/m\bar{c}$. The value thus calculated, placing $\bar{c} = 1.065 \times 10^7$ cm/sec (the thermal electron velocity at room temperature), is 0.069 cm at a pressure of 1 mm.

This value is 1.75 times the value calculated from the kinetic theory molecular free path, assuming the electron free path to be $4(2)^{1/2}$ the molecular one. It is also 1.68 times the electron free path in H_2 , whereas the kinetic theory prediction is that it should be less. It seems impossible therefore to apply molecular free path data to the calculation of electron free paths. This is also borne out by the results on N_2^4 in which it was found that the electron free path is 2.55 times the predicted value.

III

The value of B used in the calculations above is much smaller than the value calculated on the assumption that the impacts of the electrons with the molecules are elastic. For this case the expression for B becomes

$$B = \frac{1.76\lambda^2 e^2 M}{2\alpha^2 T^2 m}$$

assuming $f = 2m/M$ where m is the electronic and M the molecular mass. This expression gives

$$B = 0.278$$

whereas the value found above is 0.005.

On the basis of Compton's theory one must conclude one of two things: Either the electrons do not reach their terminal thermal energy under the action of a sine wave field, or the fraction of its energy that an electron loses on impact with a CO molecule is greater than it would be if the loss were due to momentum transfer only. In the case of N_2 and H_2 referred to above, it was shown that any error due to a non-terminal state is negligible, and it seems reasonable to conclude that this will also be the case for CO. The second alternative is therefore the more probable.

⁴ H. B. Wahlin, Phys. Rev. 23, 169 (1924).

THE MAGNETIC SUSCEPTIBILITY OF GASES

I. PRESSURE DEPENDENCE

BY FRANCIS BITTER*

NORMAN BRIDGE LABORATORY OF PHYSICS, PASADENA, CALIFORNIA

(Received April 28, 1930)

ABSTRACT

A method is described for measuring the magnetic susceptibility of gases which has certain advantages over those used by previous observers. With such an apparatus, it is found that the volume susceptibility of CO_2 , N_2 and H_2 is proportional to the pressure. Deviations from proportionality of the type observed by Glaser are found in the above gases upon introducing water vapor as an impurity in amounts probably less than a few hundredths of a percent.

IN ATTEMPTING to interpret the results of magnetic observations on matter, it is difficult to determine what effects are due to the molecules themselves, and what due to their interaction with each other. Because of this, results obtained with gases may be interpreted with most confidence, since in this case, isolated molecules without interaction are most nearly approximated. The fundamental quantity to be observed is K , the volume susceptibility, which measures the average induced moment per cc. Classical mechanics and quantum theory agree in predicting

$$K = \left(\frac{a}{T} + b \right) \frac{p}{T} \quad (1)$$

or

$$K = cp. \quad (2)$$

a is a positive constant which is zero if there is no permanent magnetic moment in the molecule, and b is a negative¹ constant which measures the distribution of electric charge in the molecule. The experiments described below were undertaken to check Eq. (2). In a future communication I hope to take up the absolute values of the constants a and b , and their interpretation for various gases.

The proportionality between the volume susceptibility and the pressure must be established before any interpretation of the constants a and b can be undertaken as it is equivalent to the statement that the molecules in a gas do behave as isolated units with only thermal interactions to establish thermodynamic equilibrium. The first attempt to verify Eq. (2) experimentally was made by Glaser^{2,3,4} who found that it held only for O_2 and atomic

* National Research Fellow.

¹ b may, for polyatomic molecules, be positive, though no such case has actually been observed or even suggested. See, for instance, J. H. Van Vleck, *Phys. Rev.* **31**, 597 (1928).

² A. Glaser, *Ann. d. Physik* **75**, 459 (1924).

³ A. Glaser, *Ann. d. Physik* **78**, 641 (1925-6).

⁴ A. Glaser, *Ann. d. Physik* **1**, 814 (1929).

diamagnetic gases, but that for CO_2 , CO , N_2 and H_2 certain characteristic deviations occurred. Subsequently, Lehrer,⁵ Hammar,⁶ and Vaidyanathan^{7,8} repeated this work, and found no anomalies of the type reported by Glaser. Hammar in a further paper⁹ suggested that the effect observed by Glaser might be due to the absorption of water vapor on the test body by means of which measurements are carried out, as he once found the effect, but made it disappear again by renewing the P_2O_5 in his cleaning train. Further Buchner¹⁰ showed that small temperature differences, if present, in the various parts of Glaser's measuring apparatus, might account for the observed phenomenon. Thereupon, Glaser in a brilliant series of papers^{11,12,13} succeeded in showing that by introducing small amounts (1%) of O_2 in CO_2 , he could produce a mixture which satisfied Eq. (2), but that with greater concentrations of O_2 anomalies reappeared; that in all probability adsorbed water vapor on his test body could not produce the effects observed; and that thermal disturbances were not present in his apparatus in a sufficient degree to influence his observations. From these results he deduces, and this is the weak point in his arguments, that other observers *had* O_2 as an impurity in their gases in just sufficient amounts (1% for CO_2) to hide the anomaly.

According to these papers, the relevant factors are small impurities of O_2 and H_2O . For the sake of completeness, let us add molecular orientation, which was first considered by Glaser himself, and two further ones whose influence has been tacitly neglected: excited states and ions. Molecular orientation in fields of the order of magnitude of those at present in use is not understandable¹⁴ on the basis of our present conception of the laws governing the behavior of molecules in a magnetic field, and may therefore be dismissed until the other possibilities are definitely disposed of. The presence of any radiation in the apparatus other than black-body radiation corresponding to the temperature of the gas under observation would destroy thermodynamic equilibrium and invalidate Eq. (2). As a matter of fact, excess of incoming radiation would produce an effect of the type observed by Glaser, though as nearly as one can calculate, it should be much smaller. Exact computations are impossible, as the electrical constitution of excited states is unknown. Actual observation on N_2 under various conditions of illumination ranging from almost complete darkness to very intense illumination of the gas between the pole pieces of the magnet gave no effect of the order of magnitude of that observed by Glaser. Further, the presence of 2 mg of radium within a few cm of the test body (see diagram of the apparatus in Fig. 1) gave no

⁵ E. Lehrer, *Ann. d. Physik* **81**, 229 (1926).

⁶ G. W. Hammar, *Proc. Nat. Acad. Sci.* **12**, 594 (1926).

⁷ V. I. Vaidyanathan, *Ind. Journal Phys.* **1**, 183 (1926).

⁸ V. I. Vaidyanathan, *Phil. Mag.* **5**, 380 (1928).

⁹ G. W. Hammar, *Proc. Nat. Acad. Sci.* **12**, 597 (1926).

¹⁰ H. Buchner, *Ann. d. Physik* **1**, 40 (1929).

¹¹ A. Glaser, *Ann. d. Physik* **2**, 233 (1929).

¹² A. Glaser, *Ann. d. Physik* **3**, 1119 (1929).

¹³ A. Glaser, *Ann. d. Physik* **4**, 82 (1930).

¹⁴ F. Bitter, *Phys. Zeits.* **30**, 501 (1929).

change in the deflections of the order of magnitude of those to be expected if the Glaser effect is to be explained on the basis of the anomalous behavior of ions which are, of course, always present unless very elaborate precautions are taken.

Experimentally, then, the problem reduces itself to the determination of the effect of small amounts of impurities. To settle this question definitely for all possible impurities in varying amounts in all the gases on which observations have been made would require a very long investigation. In the following, I have gone only part way. The results obtained experimentally are that,

(1) CO_2 , N_2 and H_2 in which certainly not more than traces of H_2O and O_2 are present obey Eq. (2).

(2) A mixture of CO_2 and about 11% O_2 when dried as efficiently as possible, obeys Eq. (2).

(3) CO_2 , N_2 and H_2 , when contaminated by small amounts of H_2O (probably less than a few hundredths of a percent) do not obey Eq. (2), but give deviations of the type observed by Glaser.

The proof of these statements is contained in the rest of this report. Assuming their correctness, the present state of our knowledge concerning the applicability of Eq. (2) is summed up on the following statements.

Both linearity and departure from linearity have been observed in pressure susceptibility curves on samples CO_2 , N_2 and H_2 considered pure by the observers. The one observer, Glaser, who consistently obtains departure from linearity finds that linearity can be produced in CO_2 by critical amounts of O_2 impurity. He assumes that a similar effect exists for N_2 and H_2 and assumes that the samples used by other observers are contaminated with just this critical amount of impurity. Presumably, this critical amount of impurity would vary from gas to gas. The above assumption is possibly applicable to some observations, but it is certainly very improbable that it applies to all. It is certainly not applicable to the observations reported in this paper, since spectroscopic evidence is given that the purifying train removed all observable traces of O_2 from N_2 . Further, since the purifying train removed O_2 from N_2 satisfactorily, it probably did so equally well for H_2 and CO_2 . Further, since a mixture consisting of CO_2 and 11% of O_2 showed linearity, it is impossible to contend that this linearity was due to a 1% O_2 contamination. This much of the evidence seems straightforward, and disposes of the assumption that linearity in all observations is due to a critical O_2 impurity. The interpretation of the remainder of the evidence, that the addition of water vapor to the above gases gives anomalous effects, is not so clear. It shows merely that Glaser's results may be due to water vapor. But it is also conceivable that other substances might have a similar effect, and it is quite possible though highly improbable, that Glaser's results are due to some still undetermined and unsuspected cause. Taking the evidence all in all, however the following conclusions seem most plausible: that dry gases and gas mixtures obey Eq. (2); and that Glaser's anomalies are due to the presence of water vapor in his measuring apparatus.

It should be noticed that the mechanism by which H_2O influences the magnetic behavior of gases is by no means specified; it need not be adsorption in the test body, and in the light of Glaser's¹² work probably is not. It is, however, known that small amounts of H_2O do produce anomalous effects in gases. (For instance, ion mobilities¹⁵). This might suggest a clustering of gas molecules around H_2O molecules. Further the absence of any anomaly in argon and neon in Glaser's apparatus might be explained by assuming that these gases because of their chemical inertness do not cluster around H_2O molecules. However, such assumptions need experimental verification, and further discussion at present is useless. One more fact should, however, be observed, and that is that Glaser's arrangements for drying his gases are, as nearly as one can tell from his publications, extremely good, especially in his purifying train for H_2 , where the last unit is a liquid air trap containing charcoal! The only way in which any vapor could possibly contaminate this H_2 is if it were introduced in transferring the gas from the cleaning train to the apparatus (a step which is not described in his papers) or from the walls and ground joints of the apparatus itself.¹⁶ The latter is probably the only possibility, as in order to explain the fact that Glaser can repeat his results over and over again, a constant source of impurities would have to be assumed.

DESCRIPTION OF THE EXPERIMENTS

The method used in the measurements described below is essentially that employed by Glaser,² Hammar⁴ and Vaidyanathan.⁷ It consists in measuring the torque exerted by a gas on a solid body suspended in an inhomogeneous magnetic field. This solid body, called the test body, was constructed as shown in Fig. 1*a* and *b*. It is entirely of Pyrex glass with fused joints. At the bottom of a glass rod is a cylindrical vessel divided radially into four equal chambers. Two of these, *A*, had small holes in them to permit the surrounding gas to enter. The other two, *B*, could be sealed off. In this particular set of experiments, they were first exhausted, and sealed at *C'*. Then *C'* was dipped into liquid air, and they were sealed off at *C*. Above this test body was a small glass rod *D* so mounted that it could be either moved vertically or rotated horizontally around the stem of the test body. A small spring of tungsten wire was attached to hold it in place in any given position. If the test body with a vacuum in all four quadrants, is suspended between the pole-pieces of a magnet, it will be in equilibrium in some position which is adjustable by moving *D*. Actually *D* was moved and the suspension twisted until the test body would hang as nearly as possible with the dividing walls parallel and perpendicular to the line joining the pole pieces, both when the

¹⁵ H. Erikson, *Phys. Rev.* **34**, 635 (1929).

¹⁶ In one of his papers,¹² Glaser performed two experiments to show that water vapor does not enter his apparatus at this point. One consisted in showing that P_2O_5 was not attacked in a tube sealed to his system near the measuring apparatus; the other consisted in showing that a glass rod which changed its resistance when water vapor was adsorbed on its surface, did not do so in the course of a series of measurements. One can only say that these measurements are not quantitative and until one knows how little water vapor can be detected, no inference can be drawn.

magnet was on and off. If now, with the field on, a gas is admitted to the chambers *A*, the test body will evidently be deflected in such a way that *A* will approach the pole-pieces if the gas is paramagnetic, or recede from them if it is diamagnetic. The advantage of this test body over that used by Glaser is that it is made entirely of diamagnetic glass, and consequently, the

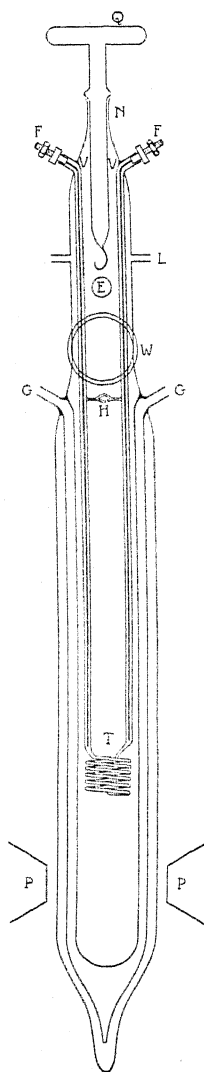


Fig. 2. Diagram of apparatus.

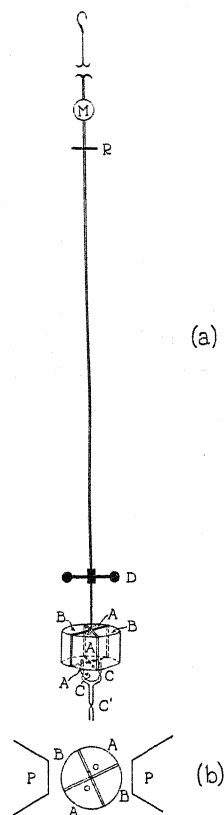


Fig. 1a. and 1b. Diagram of test body.

magnetic forces acting on it are practically independent of the temperature. The advantage over Hammer's test body lies in its symmetry, so that the magnetic forces acting on it do not have to be compensated by a large twist of the supporting fiber. In this way, the zero position (position of rest in a vacuum) is made practically independent of the field strength and of

the temperature. M is a mirror by means of which changes in position are read off on a scale 3 meters away. The suspension consisted of two small quartz hooks with a fiber drawn out between them. The test body hangs in the chamber shown in Fig. 2. The lower part is a Dewar flask. Liquid air or other condensed gases may be admitted at G into a chamber surrounded by a vacuum. In the present investigation, the chamber G contained air at room temperature. The inner chamber in which the test body was suspended had four openings; E , for admitting gases was fused to the purifying train; W , where a large plane window was sealed on with picein; and the lid, sealed at L and N with picein. N was introduced to lower and raise the test body, as the method of drawing the fiber made it impossible to predetermine its length to more than approximately 1 cm. To the lid were fused the glass tubes V terminating in a spiral of small thin tubing containing a platinum wire used as a resistance thermometer with terminals at F . H is a glass collar drawn in perspective which, when the test

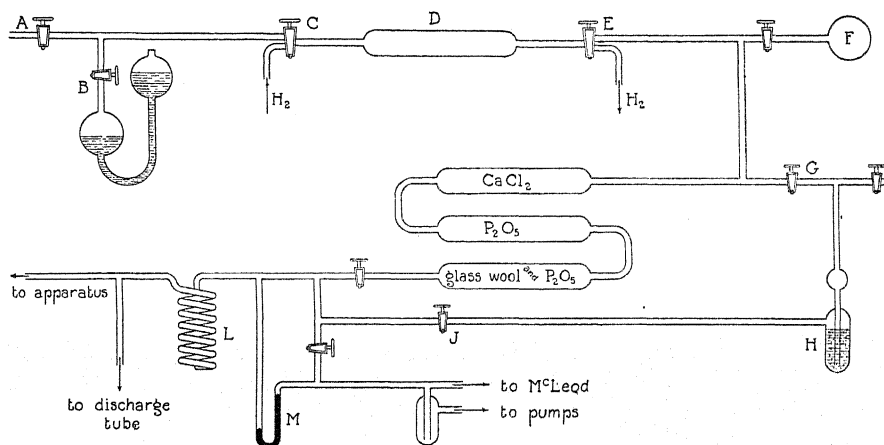


Fig. 3. Diagram of cleaning train.

body was in place, came just below R , Fig. 1*a*, so that if in lowering the system into its container the fiber should break, the test body would be caught by H instead of dropping to the bottom of the container.

For the preliminary experiments the purifying train was very simple, consisting of a small quartz furnace, containing copper wire, a tube containing CaCl_2 and finally a liquid air trap. With this apparatus, the effect of light and γ -rays was investigated, and found to have no influence on the shape of the pressure susceptibility curves, as mentioned above. The gases used were taken from steel cylinders under pressure. The first measurements were made on CO_2 and the curves in Fig. 4 obtained. The liquid air trap was, of course, not in operation. The system was so slow in coming to rest that before proceeding with the measurements, a small damping coil of copper wire was attached to the rod D , Fig. 1a. This greatly improved the accuracy with which readings could be made. The next measurements were made with N_2 , and the curves in Fig. 5 repeated several times, alternately

with and without liquid air. These experiments indicated that the critical factor was purification and that probably the water vapor given off by the CaCl_2 ¹⁷ (which has a partial pressure of about 0.3 mm) was responsible for the departures of the observations from linearity, since the introduction

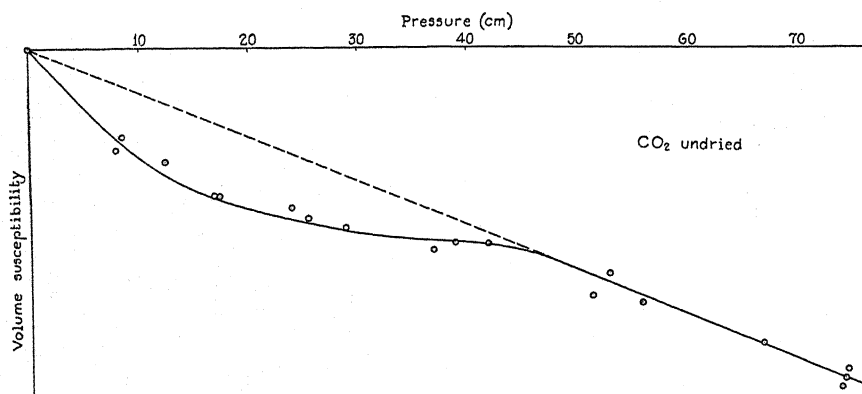


Fig. 4. Pressure susceptibility curve of undried CO_2 .

of a liquid air trap gave readings along a straight line. Consequently, the cleaning train was rebuilt with a view to carefully checking the effect of impurities. The system built is shown in Fig. 3. The tank containing the gas to be measured is connected to the system at *A*. *B* is a gasometer containing

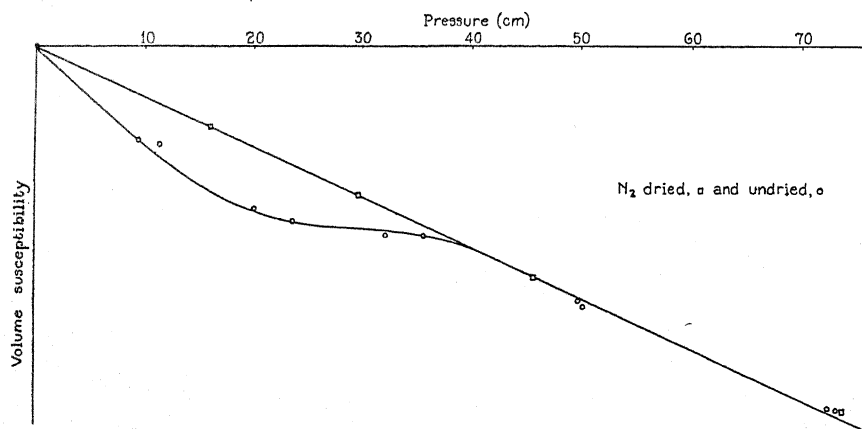


Fig. 5. Pressure susceptibility curves. \square and \circ N_2 .

pump oil, and was a great convenience in admitting the gases. *D* is a quartz tube 60 cm long and 2.5 cm in diameter filled with copper wire. At either end the tube was fused to short pieces of smaller tubing and these sealed with

¹⁷ This CaCl_2 was in the system while adjustments were being made, and had already taken up a good deal of water. The partial pressure of 0.3 mm is given in A. Goetz, *Physik und Technik des Hochvakuum*, p. 114, Second Edition.

sealing wax to the two way stopcocks *C* and *E*. The tube *D* was first covered with asbestos, then wound with chromel resistance wire in such a way that the near end from the point of view of gas entering the system could be kept red hot, while the far end did not glow at all. *F* is a bulb containing O_2 for measurements on gases mixed with O_2 . From this point, there were two approaches to the measuring apparatus. One went through a wash bottle *H* containing an 85% mixture of H_2SO_4 and H_2O whose specific gravity was 1.775. Such a mixture has according to the Landolt Bernstein Tables a vapor pressure of 0.15 mm. This path could be isolated from the system by means of the stopcocks *G* and *J*, and these were not opened until the first measurements with dry gases were finished. The other path went through three drying tubes, each about 1 meter long and 2–3 cm in diameter. The first contained $CaCl_2$, the second P_2O_5 , and the third P_2O_5 spread on glass wool. At this point the two paths joined again and were connected through a large stopcock to the pumps, a McLeod gauge, a mercury manometer, and to the apparatus through a glass spiral containing approximately 2 meters of glass tubing which could be immersed in liquid air. Immediately before the measuring apparatus a small discharge tube with a quartz window was fused to the system, so that a photograph of the spectrum of every gas could be taken immediately after a measurement. The procedure in filling a gas was to pump out the whole apparatus from *E* on, except for the measurements with dry gases, in which the wash-bottle *H* was not evacuated. In about 10 minutes the pressure could be reduced to 10^{-3} mm. The oil in the gasometer was sucked up to the stopcock *B*, which was then closed. The gas to be measured was then blown through the apparatus from *A* and out at *E*. Then the furnace *D* was heated and H_2 flushed over the copper to activate it. Then more gas was flushed through from *A* to remove the H_2 . Then *E* was closed and *B* opened until the gasometer was full, when the stopcock *A* was closed. Then by opening *E*, gas could be let into the measuring apparatus from the gasometer. In this way the system could be filled without applying a vacuum to the reducing valve on the gas tank. Before beginning measurements the apparatus was filled and evacuated two or three times. The magnet was operated by a bank of storage batteries, giving 21 amperes and the current kept constant to about 0.01%. The coils were immersed in transformer oil which was cooled with water circulation, so that with the above current, the magnet was at a temperature only a few degrees above room temperature.

With this equipment the experiments were resumed. The first gas examined was CO_2 . The results of three runs are shown in Fig. 6. The gas went through the drying tubes at the rate of about 2 liters an hour. The spiral *L* was at room temperature. Although the points are somewhat scattered about the line drawn in the figure, there can be little doubt that they lie along a straight line. All measurements on CO_2 were complicated by the fact that in spite of the damping, the test body would continue to swing over a range of a few tenths of a millimeter for some time, usually about 1/2 hour, sometimes longer, and these swings were not perfectly regular. The

effect was especially large at atmospheric pressure. Apparently the swinging would die down and then suddenly start up again. This effect was observed only with CO_2 , not with a vacuum, or air, or O_2 or N_2 or H_2 in the apparatus. The observed points on Fig. 6 at atmospheric pressure are indicated by a line, as no single definite deflection could be obtained. Further, the zero

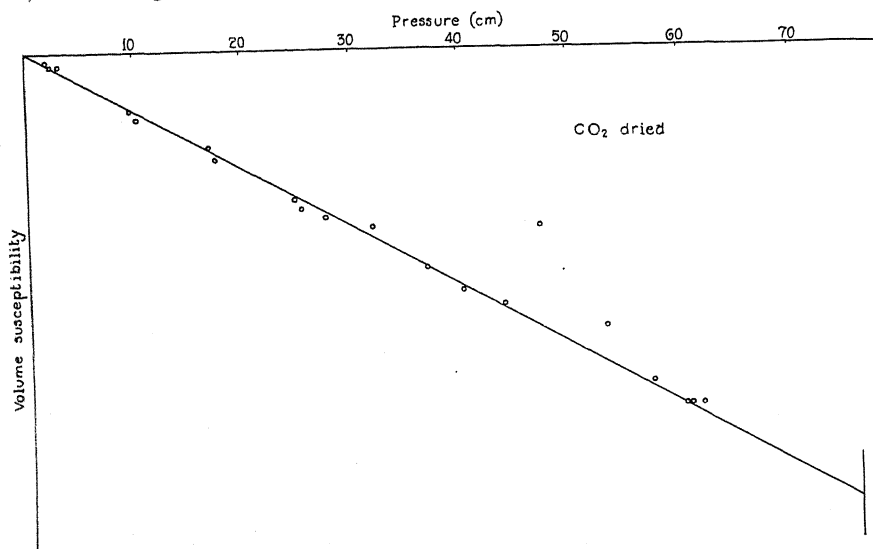


Fig. 6. Pressure susceptibility curve of dried CO_2 .

position of the apparatus did change between runs, as observed by Glaser in his papers. The cause of this zero-shift has not been determined. I am of the opinion that it is due to the changes in adsorbed layers on the test body, and hope eventually to build an apparatus that can be baked out to

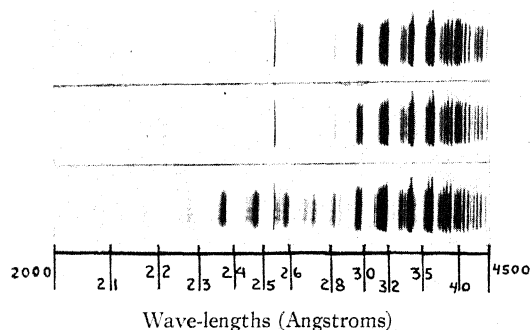


Fig. 7. N_2 band spectrum in varying degrees of purity.

test this point. The next measurements were made on N_2 with and without a liquid air trap, and three runs gave points lying on a straight line at least as closely as the points in Fig. 5. The spectroscopic photographs for N_2 proved to be the only useful ones. With CO_2 and H_2 , small impurities of O_2 and H_2O did not show. The spectrograph used was a small one made by Hilger with a quartz prism for use in the ultraviolet. In Fig. 7, are repro-

ductions of sample photographs. All three photographs were given the same exposure, 30 secs, with the same current and were taken with a gas pressure of about 3 cm in the discharge tube.

The first photograph was taken with N_2 passed over the hot copper, $CaCl_2$, P_2O_5 and the liquid air trap. In the second, the liquid air trap was removed. In the third, the liquid air trap was replaced but the furnace which heated the copper turned off. In the first picture, the NO bands are entirely absent. In the second, they begin to appear. This means that the water vapor which has passed all three drying tubes is sufficient, on dissociation, to produce a detectable amount of NO. The NO bands in the third photograph are due entirely to the O_2 present in the gas, as it comes from the tank, all water having been absorbed¹⁸ in the liquid air trap. A gas analysis showed that the N_2 in the tank contained only 0.6% of O_2 .

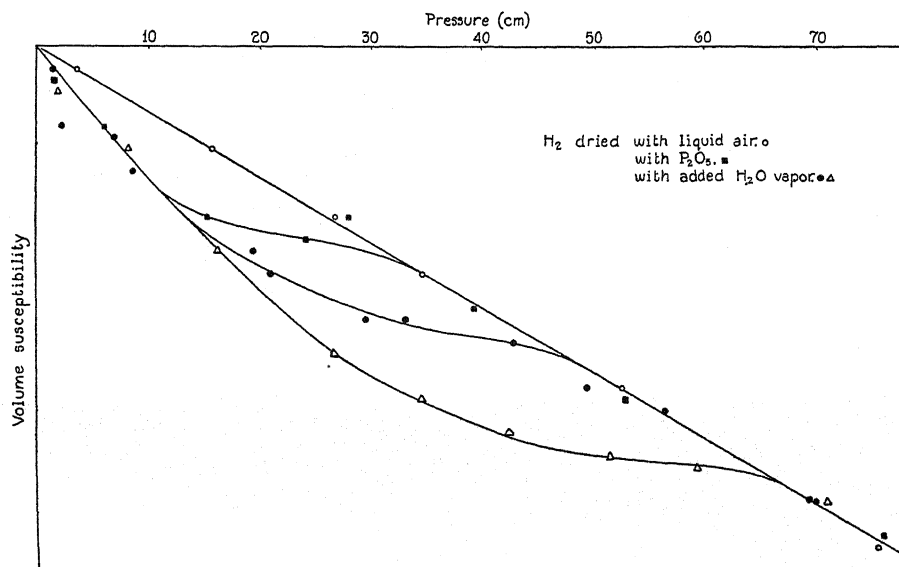


Fig. 8. Pressure susceptibility curves of H_2 with varying amounts of water vapor.

The next measurements were made on H_2 dried over P_2O_5 , but not with liquid air. This gave a very small Glaser effect. Upon the introduction of liquid air, however, a further run gave a perfectly straight line. The interpretation of this seems very straightforward; namely, that in spite of preliminary flushings over the copper in the furnace, this was not completely reduced, and that therefore, the H_2 entering the drying tubes contained more water vapor than any of the gases previously used; if this is so, it follows that a drying train, in all 3 meters in length, left sufficient amounts of water vapor in the gas to be detectable. It is also interesting to note that the one gas in

¹⁸ With longer exposure times the NO bands would appear even on photographs of N_2 as pure as I could make it. That this was due to the heating of the electrodes could be shown by taking two photographs of 30 secs duration each immediately after each other. The second showed NO bands, while the first did not. This sets a lower limit to the amount of water vapor detectable, but this is surely very small, as P_2O_5 has a vapor pressure of 10^{-4} mm and ice at liquid air temperatures 10^{-7} mm. See Goetz.¹⁷

which Hammar observed a Glaser effect was H_2 , which, for the reasons given above, probably contained more water vapor than either N_2 or CO_2 . The view that the H_2 leaving the furnace was very wet is further substantiated by the next measurements. The liquid air was removed and the gas admitted to the apparatus via the wash bottle *H*. The first runs gave very large Glaser effects, as in the lower curve in Fig. 8, but after considerable flushing, it was possible to repeat several times the curve in Fig. 8, which showed an intermediate Glaser effect. If the gases were saturated in the wash bottle, this corresponds to a water vapor pressure of .15 mm.

The results obtained so far seemed fairly conclusive, except for CO_2 , where it might conceivably be contended that the straight line in Fig. 6 is due to just that amount of O_2 (1%) impurity which according to Glaser destroys the anomaly. The first argument against such a view is that the furnace certainly purified N_2 so that nothing like 1% of O_2 was left as an impurity, and that consequently, there is every reason to believe that it

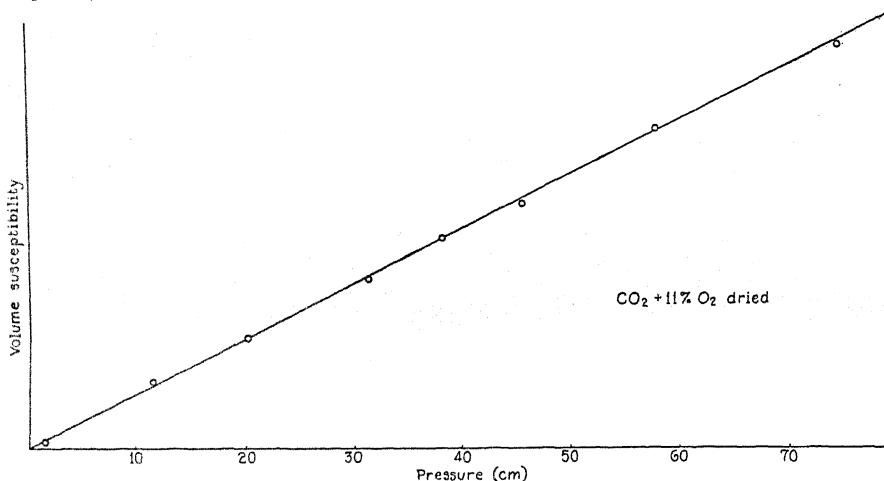


Fig. 9. Pressure susceptibility curve of the mixture 89% CO_2 + 11% O_2 .

did the same for CO_2 . The problem can, however, be attacked from another angle. According to Glaser,¹¹ the paramagnetic mixture of CO_2 plus about 11% O_2 should definitely show an anomaly at low pressures. This was tried with the gas dried in the train described above, and the observations indicated no such effect. The results are plotted in Fig. 9. The concentration of O_2 in this experiment was calculated on the basis of the relative deflections for the mixture and pure CO_2 . Deflection for CO_2 plus O_2 / Deflection for pure CO_2 = $+7.5 / -9.0 = -.83$. According to Glaser, an anomaly should certainly be observed for O_2 concentrations corresponding to values of the above ratio between $-.9$ and 0 . This effectively disposes of the argument that normal behavior of CO_2 is due to a 1% O_2 impurity, since such normal behavior is found in a mixture which certainly contains much more than 1% of O_2 .

In conclusion, I wish to take this opportunity of expressing my appreciation of the very beautiful work done by Mr. William Clancy in blowing the glass parts of the apparatus previously described.

LETTERS TO THE EDITOR

Prompt publication of brief reports of important discoveries in physics may be secured by addressing them to this department. Closing dates for this department are, for the first issue of the month, the twenty-eighth of the preceding month; for the second issue, the thirteenth of the month. The Board of Editors does not hold itself responsible for the opinions expressed by the correspondents.

Scattering of Alpha-Rays and High Speed Electrons in Radial Fields

Wentzel,¹ Sommerfeld,² and Mitchell,³ among others, have derived by the wave mechanics first approximation formulae for elastic scattering of alpha-rays and high speed electrons in spherically symmetrical fields. They all use Born's perturbation method and differ from each other only in their assumptions as to the potential fields that represent the scattering system. The fundamental expression, however, from which their particular scattering formulae may be derived, by the special assumptions as to the potential functions, may be written as:

$$c \quad \left| \frac{\psi_1}{\psi_0} \right| = \frac{K^2}{rEv} \int_0^\infty \rho V(\rho) \sin \rho u d\rho \quad (1)$$

where $|\psi_1/\psi_0|$ is the absolute value of the ratio of the amplitude of the scattered alpha-ray or electron wave at a large distance r from the scattering atom, to that of the incident wave, and is a function of the argument u . E is the energy of the particle, M its mass, and $K^2 = 8\pi^2 ME/h^2$; $u = 2K \sin \theta/2$ where θ is the angle of scattering. $V(\rho)$ is the potential energy of the particle when it is at a distance ρ from the center of the scattering system.

A Coulomb potential $V(\rho)$ should theoretically lead to the Rutherford scattering formula, but as it gives a divergent integral, Wentzel assumed that $V(\rho) = (A/\rho)^{-\alpha\rho}$. Sommerfeld made essentially the same assumption, though he justified it physically by deriving it from the wave mechanical model of a nucleus screened by its electrons concentrated in the K shell. Mitchell, supposed the electrons to be distributed as in the Thomas-Fermi statistical theory of the heavier atoms. These various assumptions

do lead to scattering formula which differ from the Rutherford formula only to the extent that the $V(\rho)$ assumed differ from the Coulomb value.

As experimentally it is definitely established that deviations from Rutherford's formula do occur, Sommerfeld,² Kirchner,⁴ and Mott⁵ have attributed these deviations to the electron distributions about the nuclei of the scattering atoms, and consequent deviations from the Coulomb potential. These authors have computed by Eq. (1) the scattering to be expected from certain types of potential function and have compared them with the observed scattering. But since we are after all more interested in a direct determination of the potential field and electron distribution within an atom than in merely checking observed with predicted scattering formulae according to assumed types of potential field, we propose to reverse the problem heretofore considered. Thus we propose to determine directly the potential field $V(\rho)$ and the electron distribution from the observed scattering.

This problem can be solved; in principle, by applying Fourier's reciprocal theorem to Eq. (1); we then obtain:

$$V(\rho) = \frac{2rE}{\pi K^2 \rho} \int_0^\infty v \left| \frac{\psi_1}{\psi_0} \right| \sin \rho u dv \quad (2)$$

The classical charge density σ is then given by:

¹ G. Wentzel, Zeits. f. Physik 40, 590 (1927).

² A. Sommerfeld, Ergänzungsband, p. 226.

³ A. C. G. Mitchell, J. of Franklin Institute.

⁴ F. Kirchner, Naturwiss. Jan. 24, 1930.

⁵ N. F. Mott, Nature, Dec. 28, 1929.

$$\sigma = \frac{-1}{4\pi\epsilon} \Delta^2 V = \frac{-rE}{2\pi^2 K^2 \epsilon \rho \partial} \frac{\partial^2}{\partial \rho^2} \int_0^\infty \left| \frac{\psi_1}{\psi_0} \right| \sin \rho u d\rho \quad (3)$$

where ϵ is the charge of the alpha-particle or electron.

Although physically u and hence $|\psi_1/\psi_0|$ is only defined for $0 \leq v \leq 2K$, the integration in (2) and (3) implies that the functional form of $|\psi_1/\psi_0|$ is to be used, as derived from the experimental curves. And even when the integration can only be carried out graphically, the region for $u > 2K$ may be safely neglected anyway except for very small y values of ρ , since K will always be at least of the order of 10^9 for any case to which the present approximation applies. In fact, the major difficulty in carrying out the integrations is for small values of u , for these give the largest contribution to the integrals, while at the same time the values of $|\psi_1/\psi_0|$ for small values of u will be the most uncertain since accurate scattering measurements at small angles are very difficult. Computations are now being made to test the possibility of making reasonable extrapolations and deriving reasonable distributions by equations (2) and (3).

We may point out, too, that Eq. (3) gives the net charge distribution, of both the nuclear positive charge and the enveloping electronic charge. Thus to the extent that the data can be obtained with accuracy and the integration carried out accurately, it will afford a means of studying the charge distribution of the nucleus as well as of the electrons. Heretofore, the nucleus has been considered as a point charge so that σ would have meaning only for $\rho > 0$ and then give the electron density only. From our present point of view we need make no such assumption,

but rather determine simultaneously the positive and negative charge distribution which gives the resultant scattering $|\psi_1/\psi_0|$. Of course, if σ turns out to be negative for all $\rho > 0$ it would be proof that the nucleus is essentially a point charge, but we do not have to assume this to begin with.

It is of interest to note that if we assume the Rutherford scattering formula: $|\psi_1/\psi_0| = A/v^2$, we immediately get from Eq. (2) the Coulomb potential, and avoid Wentzel's convergence difficulty. It is easily verified also that using Sommerfeld's formula: $|\psi_1/\psi_0| = A/v^2 + d^2$ we get his expression for $V(\rho)$.

Finally, it may be observed that our point of view of reversing the problem of scattering as heretofore considered, may also be applied to the interpretation of x-ray scattering intensities. In this problem, the structure factor, F , which determines the interference of the scattered rays and depends on the charge distribution of the scattering atom, may be expressed as:

$$F = \frac{\lambda}{4\pi \sin \epsilon} \int_0^\infty \frac{U(r)}{r} \sin \left| \frac{4\pi r \sin \theta}{\lambda} \right| dr \quad (4)$$

where $U(r)/4\pi r^2$ is the charge density, assumed to have spherical symmetry, at a distance r from the center of the scattering system, θ is the angle of reflection, and λ is the wave-length. An inversion of this integral will again give directly the charge distribution as an integral of the same type as (2) with the observable function, F , in the integrand.

MORRIS MUSKAT

Gulf Research Laboratory,
Pittsburgh, Pa.,
May 31, 1930

Nuclear Electrons

It has been suggested by Heitler and Herzberg (Naturwissenschaften 17, 673, 1929) to explain the observations of Rasetti (Proc. Nat. Acad. Sci. 15, 515, 1929) on the Raman effect in N_2 that the electron in the nucleus loses its spin and its contribution to the statistics of the nucleus. If all the nuclear particles (electrons as well as protons) are effective in determining whether the nuclear spin factor makes the total Ψ function symmetrical or antisymmetrical in the nuclei, there is great difficulty (cf. R. S. Mulliken, Trans. Faraday Soc. 25, 644, 1929) in explaining the

fact that in the Raman spectrum of N_2 the transitions between the even rotational levels are the stronger, whereas for H_2 the Raman lines representing transitions between odd rotational levels are more intense. For both H_2 and N_2 have a $^1\Sigma$ normal state, built up out of two equal atoms in S states, each with an odd number of nuclear particles (1 for the H atom, 21 for the N atom). And therefore, since for both molecules $\Lambda = 0$, and since the electron configurations are in both cases composed of closed shells, making ΣL_r for the external electrons an even number, one would

expect the odd K levels to be the stronger levels, symmetrical in the nuclei.

If, however, only the nuclear protons have a spin, then the interchange of electrons in the two nuclei does not affect the symmetry of the Ψ function. Consequently the nuclear spin factor will make the total Ψ function either symmetrical or antisymmetrical in the nuclei, according as the number of protons is even or odd. But the stronger K levels should always be symmetrical in the nuclei with respect to the nuclear spin factor, and so a rule that Ψ must be symmetrical in the nuclei if the number of protons is even, antisymmetrical in the nuclei if the number of protons is odd, would require that the even K levels be stronger in N_2 (14 protons) and the odd K levels be stronger in H_2 (1 proton). There is then no contradiction with previous conclusions as to the electronic configuration of the normal state for N_2 and H_2 . Furthermore, there is now also agreement with the 2:1 alternating intensity ratio found in the N_2^+ bands, for this ratio requires a nuclear spin $= 1 \cdot h/2\pi$ for the N atom, which is to be interpreted as a parallel orientation of the spins of the two protons in excess of α -particle configurations. The nuclear spin $= 3/2 \cdot h/2\pi$ recently reported by Harvey and Jenkins (Phys. Rev. 35, 789, 1930) is, as they sug-

gest, additional evidence in support of the view that the spin of the electron is not effective in the nucleus.

In this connection it is interesting to recall that the radius of a non-rotating Lorentz electron of mass $8.994(10)^{-28}$ gm calculated on classical electromagnetic theory is $1.88(10)^{-13}$ cm, whereas that of a Lorentz electron with a spin of a half quantum which has a mean mass equal to the figure above is $3.98(10)^{-9}$ cm. On the other hand, a Lorentz proton of mass $1.661(10)^{-24}$ gm has a radius of $1.02(10)^{-16}$ cm if it has no rotation and a radius of $2.15(10)^{-12}$ cm if it is assumed to have a half quantum of spin. If the radius of the nucleus is of the order of magnitude of 10^{-12} cm as suggested by experiments on the scattering of α -rays, these figures indicate that the size of a spinning electron is too great to permit its inclusion in the nucleus. It may be for this reason that nuclear electrons have no spin. The dimensions of a spinning proton, on the other hand, are of the same order of magnitude as those of the nucleus.

LEIGH PAGE
WILLIAM W. WATSON

Sloane Physics Laboratory,
Yale University,
May 21, 1930.

Concerning the Existence of a New Term in Hg I

T. Takamine¹ and T. Suga have recently made an excellent photographic investigation of the near infrared spectrum of Hg. On their spectrograms they find two new series of lines given by $X-m^3S_1$ and $X-m^3D_3$ having a common final term of value 15299 cm^{-1} . They state that this new term is of the nature of a P term but that other evidences would certainly be necessary before its reality is established. It is the purpose of this note to present other evidence which supports their assumption.

All of the lines of longer wave-length—except two (outside of the region covered)—necessary to complete the two series appear on the writer's² records of this spectrum and were reported as unclassified lines. These two series with the writer's additions are tabulated below. The value of X is taken as

¹ T. Takamine and T. Suga, Sc. Pap. I. P. C. R., No. 232, 13, (1930).

² E. D. McAlister, Phys. Rev. 34, No. 8, Oct. 15 (1929).

Sharp Series

Diffuse Series

λ_{vac}	ν	ν_{calc}	Int. ²	λ_{vac}	ν	ν_{calc}	Int. ²
15300A	6536	—6534	30.	—	—	2547	—
19705	5075	5077	4.2	12131A	8243	8245	3.3
10711	9336	9332	1.1	9245T	10817	10818	—
8786T	11381	11384		8198T	12198	12201	
7979T	12532	12532		7678T	13024	13027	
7552T	13241	13239		7370T	13568	13562	
7294T	13710	13707		7175T	13937		
7126T	14033			7045T	14195		
				6948T	14393		

15297 cm^{-1} since this gives a closer agreement between observed and calculated frequencies when the writer's additions are included. Fowler's term values are used. Takamine's lines are marked with a T.

Of particular interest is the first line (negative ν_{calc}) of this "sharp" series $\lambda = 15300\text{\AA}$ (λ_{vac} Paschen³) which is one of the strong lines in the infrared spectrum of Hg. Paschen⁴ attempted to use it as the first line of another series but this attempt failed to gain recognition. It does not fit into the once-ionized Hg scheme and appears much too strong in the arc spectrum to be a spark line. Hence this assignment of it to Takamine's series seems quite reasonable.

The deviations from the calculated values are somewhat larger than is desirable but the discrepancies are probably due to the difficulty of accurate wave-length measurements in this region. The intensity² (mm deflection) of the first three lines in the "sharp" series and of the second line in the "diffuse" series

are particularly convincing as to the correctness of the present assignment. The writer has inserted in the "diffuse" series a line $\lambda_{\text{air}} = 9243\text{\AA}$ appearing on Takamine's pictures which he did not include. This line appears as a sharp line on all of Takamine's pictures while most of the others in this series are diffuse or "washy." This must be why Takamine does not include it. However the photographic method undergoes an enormous change in sensitivity between this line and the others in this series, and also the other lines appear much sharper on his one hour exposure than they do on the 10 hour one. It thus seems likely that this line really belongs to the series.

E. D. McALISTER

Physics Department, University of Oregon,
Eugene, Oregon,
May 31, 1930.

³ Paschen, Ann. d. Physik 27, 558 (1907).

⁴ Paschen, Ann. d. Physik 29, 663 (1909).

Boundary Conditions in Wave Mechanics Reply to Criticism

Mr. Eckart's letter in the May 15th issue of the Physical Review about my paper of April 15th on the above subject seems to call for some reply. If the potential varies sufficiently gradually from the constant value zero to a constant value V' then there is no reflexion and if there is no reflexion for a particular wave-length there will be none for any shorter wave-length. My calculation showed that there may be no reflexion at the layers on the surfaces of metals because the thickness of these layers may be sufficient to allow the potential variation to be sufficiently gradual for this when $E > V'$. According to this the usual boundary conditions at a discontinuity may not be applicable to these layers. I therefore suggested new boundary conditions giving no reflexion when $E > V'$ which can therefore be used with these layers when they give no reflexion with $E > V'$.

I also suggested that these new boundary conditions may be correct for an actual discontinuity if such a thing can exist.

Mr. Eckart suggests that the absence of reflexion is due to the potential variation acting like an étalon with a spacing of one quarter-wave length. The distance in which the potential changes may be made any multiple or fraction of a wave-length, without reflexion, by suitably changing the constant β so that I do not think the action is really at all analogous to that of an étalon.

I quite agree with what Mr. Eckart says about the very limited generality of the solution of the wave equation which I obtained.

H. A. WILSON

Rice Institute.
Houston, Texas,
June 6, 1930.

Ionization Potential of Carbon

The ionization potential of carbon was estimated as 11.2 volts by Fowler and Selwyn (Proc. Roy. Soc. A118, 34, 1928). The basis for this estimation was the C I spectrum which they arranged into series for the first time and a comparison of this spectrum, which was not extensive enough for accuracy, with that of the related spectra of N II and O III.

In my work on the helium continuous spectrum (Phys. Rev. 35, 1113, 1930) I had noticed that a series of lines shone brightly in the ultraviolet when the stopcock grease contaminated the helium. I followed up this observation by purposely introducing carbon monoxide into the helium with the result that the spectrum of C I has been greatly

extended in the vacuum region and some new features of this spectrum observed. In this note I shall deal only with a small phase of the data now on hand, namely that concerned with the ionization potential of carbon. The fuller treatment is reserved for the complete paper that will be published when the examination of these data is finished.

The most obvious feature of the new ultraviolet spectrum is that it contains three series of multiplets that converge to the same three-fold limit, the $^3P_{0,1,2}$ of the atom. These have been measured to eight members and form the basis of the present determination of the ionization potential of normal carbon. The series multiplets are not resolved after the first three members so one has to deal with diffuse lines for the higher terms. Fortunately, however, the middle series is much stronger than the other two. It stands out like a ridge in the mist and is easily measured. It is the middle series that has been used for the calculation of the terms and the ionization potential.

The following is a list of the "ridge" groups: $\lambda 1649.93$ (2), (uncertain if C I), 1277.53 (5)

seen as triplet in second order; 1193.17 (5), 1158.02 (4); 1139.80 (3); 1129.12 (2); 1122.32 (1); and 1117.68 (0). The series limit is $A = 90834 \text{ cm}^{-1}$ and the effective quantum numbers for the above lines are 1.905; 2.955; 3.952; 4.948; 5.949; 6.952; 7.955; and 8.970. It is seen that this is very nearly a Rydberg series. The values are not too smoothly arranged but are as good as the nature of these unresolved multiplets when superimposed on two other converging groups might be expected to yield.

Using the known values of the separations of the lowest 3P term of C I, and assuming that the above limit refers to its center of gravity, the term values have been calculated to be $^3P_2 = 90817.7$, $^3P_1 = 90845.2$ and $^3P_0 = 90860$. The metastable levels 1D and 1S listed by Fowler and Selwyn lie 1.179 volts and 2.593 volts respectively above the 3P_0 state, and the ionization potential of the carbon atom from the 3P_0 , lowest normal state, is 11.217 volts.

JOHN J. HOPFIELD

University of California,
May 23, 1930.

The Ultraviolet Light Theory of Aurorae and Magnetic Storms

The ultraviolet light theory of aurorae and magnetic storms¹ contained some unsettled points and some conclusions in disagreement with observation. The further development of the theory of the outer atmosphere² and the recognition of an effect hitherto unseen have now automatically removed the discrepancies. So that the theory, with no change in the original assumptions, begins to assume a more finished appearance. The new effect has emerged directly from the results of Page.³ Page showed, on the assumption of an earth with no excess charge, that the long free path ions in the upper atmosphere would drift westward. We now point out that the westward drift is hindered by collisions of the ions with the neutral molecules of the atmosphere which move approximately with the earth's rotation. As a result of the hindrance there is a displacement of positive ions to polar regions and negative ions to equatorial regions. This sets up an electric field which, together with the earth's magnetic

field, causes the high flying ions to move partially with the angular velocity of the earth. They descend into the 50° to 70° latitudes during the evening hours to cause aurorae and the diurnal variation phase of the world wide magnetic storms. With the new values of the electrical conductivity² of the upper atmosphere the diurnal variation phase is seen to be due to the gravitational magnetic drift currents set up by the polar ionic concentrations. Agreement is secured throughout with the observations. The second phase of the world wide magnetic storm is found to arise mainly from reactions in the atmosphere rather than to induced currents in the earth.

E. O. HULBURT

Naval Research Laboratory,
Washington, D. C.,
May 28, 1930.

¹ Phys. Rev. **33**, 412 (1929), **34**, 344 (1929).

² Phys. Rev. **34**, 1167 (1929), **35**, 240 (1930).

³ Page, Phys. Rev. **33**, 823 (1929).

BOOK REVIEWS

Elementare Quantenmechanik. M. BORN AND P. JORDAN. Pp. 434. J. Springer, Berlin, 1930. Price bound RM 29.80.

This book appears in the "Struktur der Materie" series edited by Born and Franck as the second volume of the former's well-known "Vorlesungen über Atommechanik." Written by the founders of the matrix mechanics, it is the first book on the subject to give a systematic and thorough account of the formulation of quantum mechanics by matrix methods.

The guiding view-point is expressed in the preface: "We are convinced that the true connection of the classical and the new mechanics lies not so much in the formal similarity of the wave-mechanical differential equations and boundary value problems with the methods of classical mechanics of continua, as in the correspondence principle of Niels Bohr; we see in the new mechanics the rigorous working out of Bohr's program."

The authors have succeeded in giving an admirably clear account of the subject from this standpoint. After chapters devoted to mathematical methods and the basic ideas of quantum mechanics there is a valuable chapter devoted to theorems on angular momentum from the standpoint of invariance under the rotation group. The chapter on perturbation theory gives a full account of dispersion theory including natural optical activity and the Kerr and Faraday effects. The two remaining chapters are devoted to the statistical interpretation of quantum mechanics and the quantized electromagnetic wave approach to radiation theory.

The notation is unwieldy and shows perhaps the richest efflorescence of subscripts, superscripts and diacritical marks that has yet blossomed in any physical treatise. Can we hope to understand nature in terms of equations like

$$2 U_{\rho\rho}^{(k)(rr)} = - \sum_{l=1}^{k-1} \sum_{j,r} U_{\rho r}^{(l)+(r j)} U_{r\rho}^{(k-l)(j r)} .$$

The notation devised by Dirac for his forthcoming book is much simpler and it is to be hoped that it rather than that of this book, will be the one to find general acceptance.

The book is to be recommended as the most important that has thus far appeared on the subject. The word elementary in the title has to be taken more in the sense of fundamental and first principles, rather than simple, easily understood and suitable for a first introduction to the subject.

E. U. CONDON

AUTHOR INDEX TO VOLUME 35

References with (A) are to abstracts of papers presented at meetings of the Physical Society and references with (L) are to Letters to the Editor.

- Adams, John Mead. Origin of snowflakes—113(L)
 ——— Photographs of single crystals of ice, grown from the vapor—136(A)
- Allison, Fred and Edgar J. Murphy. A magneto-optic method of chemical analysis—124(A)
 ——— and Edgar J. Murphy. Evidence of the presence of element 87 in samples of pollucite and lepidolite ores—285(L)
- Allison, Samuel K. and John H. Williams. Experiments on the reported fine structure and the wavelength separation of the $K\beta$ doublet in the molybdenum x-ray spectrum—135(A), 149
 ——— and John H. Williams. Resolving power of calcite for x-rays and the natural widths of the molybdenum $K\alpha$ doublet—1476
- Almasy, F. and C. V. Shapiro. Fluorescence spectrum of benzene—1422(A)
- Almy, Gerald M. Zeeman effect in the OH bands—1495
 ——— F. H. Crawford, and E. L. Hill. Zeeman effect in $\lambda 5211$ MgH band—124(A)
- Anderson, Carl D. Space-distribution of x-ray photoelectrons ejected from the K and L atomic energy-levels—1139
- Andrews, Donald H. Relation between Raman spectra and the molecular structure of organic compounds—662(A)
 ——— and John C. Southard. Calculation of the specific heats of solid organic compounds from Raman spectra—670(A)
 ——— (See Kettering, C. F.)—1422(A)
- Arnott, E. G. F. (See Smyth, H. D.)—126(A)
- Austin, Allen. Dielectric constants of aqueous KCl solutions—1428(A)
- Austin, J. B. and Ian Armstrong Black. Emission spectrum of benzene in the region 2500–3000A—452
- Babcock, Harold D. New absorption band of atmospheric oxygen and the vibrational frequency of the normal molecule—125(A)
- Babcock, R. W. Thermal convection—1008
- Bacher, R. F. (see Goudsmit, S.)—127(A), 129(A)
- Badger, Richard M. Absorption of acetylene and ethylene in the near infrared—1433(A)
 ——— Absorption bands of ammonia gas in the visible—1038
- Balinkin, Isay A. On the mechanism of very absorbable radiation emitted by compressed crystalline substances under high potentials—1443(A)
- Band, William. A new relativity theory of the unified physical field—115(L)
 ——— A new unified field theory and wave mechanics—1015(L)
 ——— Capture of electrons by alpha-particles—1128(L)
 ——— X-ray emission independent of temporary excitation—1129(L)
- Barnes, Arthur H. Capture of electrons by alpha-particles—217
 ——— Bergen Davis and H. L. Hull. Capture of electrons by alpha-particles—1433(A)
- Barnes, R. Bowling. High dispersion in the infrared—662(A)
 ——— Infrared absorption of some organic liquids under high resolution—1524
 ——— and A. H. Pfund. Effect of aberrations in limiting the resolving power of infrared spectrometers—1434(A)
- Barnes, S. W. and F. K. Richtmyer. Excitation potential of the $L\alpha$ satellites of Ag(47)—661(A)
 ——— (see Richtmyer)—1428(A)
- Barrett, Charles S. X-ray fiber structure of alloys containing precipitated crystals—1425(A)
- Bartlett, James H., Jr. Relative intensities of supermultiplet lines—229
- Bartlett, Russell S. A space charge interpretation of thermionic work function—669(A)
- Barton, Henry A. A new regularity in the list of existing nuclei—408
- Bateman, H. Variable flow in pipes—177
 ——— Book review—654
- Beams, J. W. Spectral phenomena in spark discharges—24
 ——— and E. C. Stevenson. Electric double refraction in gases—1440(A)
 ——— and J. C. Street. Initial stages of electrical breakdown—658(A)
- Bearden, J. A. Independence of x-ray absorption on temperature—1443(A)
 ——— Spectroscopic analysis of scattered x-rays—1427(A)

- Beattie, James A.** Simple equation for the Joule-Thomson effect in real gases—643
 ——— A rational basis for the thermodynamic treatment of mixtures of real gases—1435(A)
- Becker, J. A.** Ion-grid theory of the decrease in work function for composite surfaces—1431(A)
- Bedell, Frederick and Jackson G. Kuhn.** Stabilized oscilloscope with amplified stabilization—657(A)
- Bender, William** (see Watson, William W.)—1440(A), 1513
- Bergstein, Milton, J. F. Rinke and C. M. Gutheil.** Studies in contact rectification. II. Cupric sulfide-magnesium junction—1425(A)
- Bichowsky, F. R.** (see Lunn, E. G.)—563(L), 671(A)
- Birge, Raymond T.** Vibrational isotope effect—133(A)
 ——— Atomic weights of hydrogen and helium—1015(L)
 ——— Book review—872
 ——— (see King, A. S.)—133(A)
- Bitter, Francis.** Magnetic susceptibility of gases. I. Pressure dependence—1572
- Black, Ian Armstrong** (see Austin, J. B.)—452
- Blake, F. C.** An interesting case of a unit lattice made up of interpenetrating lattices—660(A)
 ——— and **James O. Lord.** Sorting the variables in the crystal structures of certain chromium-nickel alloys—660(A)
- Bleakney, Walker.** A study of the ions produced in mercury vapor by electron impact—123(A)
 ——— Probability and critical potentials for the formation of multiply charged ions in Hg vapor by electron impact—139
 ——— Ionization of hydrogen by single electron impact—1180
 ——— and **John T. Tate.** Primary ions formed by electron impact in hydrogen—658(A)
- Bless, A. A.** Composition of the interior of the earth—1436(A)
 ——— Polarization and the electric moment of tung oil—1442(A)
- Blodgett, Katharine B.** (see Langmuir, Irving)—478
- Bloomenthal, Sidney.** Vibrational quantum analysis and isotope effect for the lead oxide band spectra—34
 ——— (see Christy, Andrew)—46
- Boeckner, C.** Resonance and quenching of the third principal series line of caesium—664(A)
 ——— (see Mohler, F. L.)—664(A)
- Bowie, R. M.** (see Woodrow, Jay W.)—1423(A)
- Boyd, James H., Jr.** Viscosity of compressed gases—1284
- Bozorth, Richard M. and Joy F. Dillinger.** Barkhausen effect. II. Determination of the average size of the discontinuities in magnetization—733
- Bramley, Arthur.** X-rays generated by three element tube—869(L)
 ——— and **Allen C. G. Mitchell.** Possibility of bringing mean life directly into Schroedinger equation for the hydrogen atom—1419(A)
- Brasefield, Charles J.** Electron velocities in a high frequency discharge in hydrogen—92, 122(A)
 ——— Conductivity of a high frequency discharge in hydrogen—1073
- Brattain, Walter H.** Effect of absorbed thorium on the thermionic emission from tungsten—1431(A)
- Braun, M. L.** (see Stuhlman, Otto, Jr.)—1436
- Breit, G.** Separation of angles in the two-electron problem—569
 ——— Possible effects of nuclear spin on x-ray terms—1447
 ——— **M. A. Tuve and O. Dahl.** A laboratory method of producing high potentials—51
 ——— (see Tuve, M. A.)—66
 ——— Book review—1411
- Brennen, Herbert J.** Nernst heat theorem—121(A)
 ——— A new equation of state—129(A)
 ——— Use of homogeneous coordinates in physics and chemistry—294(A)
- Brewer, A. Keith.** Photoelectric and thermionic properties of platinum coated glass filaments—1360
- Brice, Brooks A.** Band spectrum of silver chloride—960
- Brickwedde, F. G. and R. B. Scott.** Photoelectric cell thermoregulator—670(A)
 ——— (see Scott, R. B.)—670(A)
- Bridgman, P. W.** Book reviews—873, 1301
- Briggs, H. B.** (see Ives, Herbert E.)—669(A)
- Briggs, L. J. and H. L. Dryden.** Airfoils of circular-arc section for use at high speeds—1416(A)
- Brode, Robert B.** Effective collision cross-section of cadmium and zinc atoms for slow electrons—134(A), 504
 ——— (see Normand, C. E.)—1438(A)
- Brown, Joseph G.** Electric space charge in the lower atmosphere—135(A)
 ——— Variation of the electric potential gradient in the lower atmosphere—135(A)
- Browne, T. E. Jr. and F. C. Todd.** Extinction of short a.c. arcs between brass electrodes—1441(A)
 ——— (see Todd, F. C.)—1441(A)
- de Bruyne, Norman A.** Temperature dependence of field currents—172
- Bryan, A. B. and C. W. Heaps.** Magnetostriction measurements using a heterodyne beat method—298(A)
- Burdine, Theodore** (see Plyler, E. K.)—605
- Busang, P. F.** (see Smith, W. O.)—1416(A)
- Canfield, R. H.** Inhomogeneities in crystals—114(L)
 ——— Stability of metallic crystal lattices—530

- Canfield, R. H. Classes of symmetry possible in crystals of elements—660(A)
 ——— Mosaic crystals of elements—671(A)
- Cartwright, C. Hawley. Black bodies in the extreme infrared—415
- Castlemen, R. A., Jr. On the mechanism of "atomization"—1014(L), 1416(A)
- Chaffee, E. L. (see Perry, Charlotte T.)—1437(A)
- Chamberlain, C. W. A recording interferometer—663(A)
- Chamberlain, Stuart H. An interference method of measuring distance—663(A)
- Child, C. D. Absorption of light by flames containing sodium—294(A)
- Christy, Andrew and Sidney Bloomenthal. Fine structure analysis of the bands in the *A* and *D* systems of lead oxide—46
- Claus, W. D. Temperature effect in diffuse scattering of x-rays from rocksalt—1427(A)
- Collins, J. R. Effect of high pressure on the near infrared absorption spectra of certain liquids—1433(A)
- Collins, T. R. D. (see Fagan, H. D.)—421
- Colson, DeVer. Voltage-intensity relations of the cadmium spectra—294(A)
- Colwell, R. C. Effect of cyclones and anti-cyclones upon the intensity of radio signals—1425(A)
- Compton, A. H. Efficiency of x-ray fluorescence—127(A)
 ——— Determination of electron distributions from measurements of scattered x-rays—925, 1427(A)
- K. T. Compton (see Van Voorhis, C. C.)—1438(A)
- Condon, E. U. Complete dissociation of H_2 —658(A)
 ——— and J. E. Mack. An interpretation of Pauli's exclusion principle—579
 ——— and G. H. Shortley. Singlet-triplet interval ratios for *sp*, *sd*, *sf*, *p^s*, and *d^s* configurations—1342, 1419(A)
 ——— Book reviews—567, 654, 872, 1588
 ——— (see Villars, D. S.)—1028
- Constant, F. W. Microstructure of some magnetic alloys of high platinum concentration—116(L)
- Cooksey, Charlton Dows and Donald Cooksey. Glancing angle of reflection from calcite for silver ($K\alpha_1$) x-rays—564(L)
- Cooksey, Donald. (see Cooksey, Charlton Dows)—564(L)
- Copeland, L. C. On the heat of formation of molecular oxygen—1443(A)
- Copeland, Paul L. Secondary electrons from contaminated surfaces—293(A), 982
- Cork, J. M. Absolute measurement of certain x-ray wave-lengths—128(A)
- Cork, J. M. Molybdenum *L* series wave-lengths by ruled gratings—1456
- Cox, I. W. Absorption of lithium ions in mercury vapor—123(A)
- Cravath, A. M. A search for critical potentials for electron recombination with Hg^+ —659(A)
- Crawford, F. H. (see Almy, G. M.)—124(A)
- Cunningham, H. L. (see Woodrow, Jay W.)—125(A)
- Curtiss, L. F. Nature of cosmic radiation—1433(A)
- Dahl, O. (see Breit, G.)—51
 ——— (see Tuve, M. A.)—1406(L)
- Dasannacharya, Balebail. Polarization of x-rays from thin aluminum anticathodes—129(A)
- Davey, W. P. and D. C. Duncan. Absorption of ultraviolet light by lacquer films—1423(A)
- Davis, Bergen. Limiting resolving power of a crystal grating—209(L)
 ——— (see Barnes, A. H.)—1433(A)
- Davis, G. E. and Gilbert Greenwood. Changes in the specific resistance of aluminum—1429(A)
- Deming, W. Edwards. Application of least squares—665(A)
- Dempster, A. J. Deflection of hydrogen positive rays by calcite—298(A)
 ——— Reflection of positive ions by crystals—1405 (L)
- Dennison, David M. Book review—874
- Dershem, Elmer. Index of refraction and absorption coefficient of gold for the $K\alpha$ line of carbon—128(A)
 ——— and Marcel Schein. Intensity of reflection of the $K\alpha$ line of carbon from a quartz surface—292(A)
- Dewey, Jane M. Intensity maxima in the continuous helium spectrum—155
 ——— Stark effect near the series limit—1439(A)
- Dickinson, Roscoe G. and S. Stewart West. Raman spectra from sulfur dioxide—1126(L)
- Dieke, G. H. (see Wood, R. W.)—1355
- Dillinger, Joy F. (see Bozorth, Richard M.)—733
- Donal, John S., Jr. Studies of abnormal shot effect in gaseous discharges—1430(A)
- Dow, M. T. (see Drake, F. H.)—613
- Drake, F. H., G. W. Pierce and M. T. Dow. Measurement of the dielectric constant and index of refraction of water and aqueous solutions of KCl at high frequencies—613
- Dryden, H. L. and G. C. Hill. Wind pressure on cylindrical stacks—1416(A)
 ——— (see Briggs, L. J.)—1416(A)
- Duffendack, O. S. and L. B. Headrick. Collisions of the second kind and their effect on the field in the positive column of a glow discharge in mixtures of the rare gases and mercury vapor—1421(A)
 ——— (see Thomas, C. H.)—72

- DuMond, Jesse and Harry Kirkpatrick. Multiple crystal x-ray spectrograph—136(A)
 — (see Kirkpatrick)—136(A)
 Duncan, D. C. (see Davey, W. P.)—1423(A)
 Dunham, J. L. Intensities of vibration-rotation bands with special reference to those of HCl—1347
 Dunnington, Frank G. (see Lawrence, Ernest O.)—134(A), 396
 Eckart, Carl. Boundary conditions in wave mechanics—1298(L)
 — Penetration of a potential barrier by electrons—1303
 Edwards, R. L. and G. W. Stewart. Dependence of viscosity in liquids upon the molecular space arrangement as shown by x-ray diffraction—291(A)
 Ellett, A. Specular reflection of atoms from crystals—293(A)
 — Effect of hyperfine structure due to nuclear spin on polarization of resonance radiation—588
 Ellis, Joseph W. Doublets in the vibration spectrum of cyclohexane—437(L)
 — Spectroscopic evidence of two types of ammonia molecule—595
 Ellwood, W. B. Spontaneous temperature changes accompanying magnetization in steel—1440 (A)
 Estey, Roger S. New measurements in the fourth positive CO bands—309
 Fagan, H. D. and T. R. D. Collins. Peltier and Thomson effects for bismuth crystals—421
 Farnsworth, H. E. Certain effects accompanying electron diffraction—1131(L)
 — Satellites of electron diffraction beams—1432(A)
 Feather, N. On the distribution in time of the scintillations produced by the alpha-particles from a weak source—705
 — Concerning the absorption method of investigating β -particles of high energy: the maximum energy of the primary β -particles of mesothorium 2—1559
 Findlay, J. H. Spark spectrum of cobalt (Co II)—1420(A)
 Foard, Castle W. Electron energy losses in mercury vapor—293(A), 1187
 Foote, Paul D. (see Smith, W. O.)—1416(A)
 Fox, Gerald W. Oscillations in the glow discharge in neon—1066
 Fox, G. W. (see Headrick, L. B.)—1033
 Freed, Simon and Frank H. Spedding. A comparison of the reflection spectra of $\text{SmCl}_3 \cdot 6\text{H}_2\text{O}$ at room temperature and at that of liquid air with its absorption spectra at low temperatures 212(1.)
 Freed, Simon and Frank H. Spedding. Paschen-Back effect on the line spectra of solids—1408(L)
 Froman, Darol K. Young's modulus determined with small stresses—120(A), 264
 Galli-Shohat, N. On the question of aberration of the light from terrestrial sources and its application to the experiment of Esclangon—664(A)
 — Suggested explanation of Michelson-Morley-Miller experiment—1418(A)
 Gartlein, C. W. Book review—871
 Gaviola, E. On the concentration of metastable mercury atoms—1226
 Ghosh, P. N., P. C. Mahanti and B. C. Mukherjee. Vibrational quantum analysis of the blue-green bands of magnesium oxide—1491
 Gibbs, R. C. (see Shapiro, C. V.)—1422(A)
 Gillespie, Louis J. A test of the Dalton-Gibbs law of partial pressures—1435(A)
 Gingrich, Newell S. Double crystal spectra of scattered x-rays—1444(A)
 Glasser, Otto and V. B. Seitz. Measurement of the intensity of gamma-rays of radium in r -units—1432(A)
 Goetz, Alexander. On mechanical and magnetic factors influencing the orientation and perfection of bismuth single-crystals—193
 Goucher, F. S. Contact resistance and microphonic action—1429(A)
 Goudsmit, S. A remark, on hyperfine structure—436(L)
 — Predictions of manganese hyperfine structure—440(L)
 — An extension of Houston's and Slater's multiplet relations—1325
 — and R. F. Bacher. Relations between hyperfine structure separations—127(A)
 — and R. F. Bacher. Paschen-Back effect of hyperfine structure—129(A)
 — and L. A. Young. Magnetic moment of the lithium nucleus—1418(A)
 Greenwood, Gilbert. (see Davis, G. E.)—1429(A)
 Gunn, Ross. Electrodynamical damping in pulsating stars—107, 295(A)
 — On the anomalous rotation of the sun—635
 Guthel, C. M. (see Bergstein, Milton)—1425(A)
 Hafstad, L. R. (see Tuve, M. A.)—66, 1406(L)
 Hall, Harvey and J. R. Oppenheimer. Why does molecular hydrogen reach equilibrium so slowly?—132(A)
 Hamer, Richard. Transient earth currents accompanying the recent Newfoundland earthquake of 1929—656(A)
 Hamburger, F., Jr. Polar molecules—their contribution to energy loss—657(A), 1119

- Hammond, H. E.** E.m.f., resistance and capacitance phenomena in photovoltaic cells containing Grignard reagents—998
- Hardy, J. D.** A theoretical and experimental study of the resonance radiometer—662(A)
- Harkins, William D.** Atomic stability as related to nuclear spin—434(L)
- and **A. E. Schuh.** Frequency of occurrence of the disintegrative-synthesis of oxygen 17 from nitrogen 14 and helium—130(A), 809
- Harnwell, Gaylord P.** Note on electron scattering in atomic and molecular hydrogen—285(L)
- Harrington, M. C.** (see Uytterhoeven, W.)—124(A), 438(L), 1421(A)
- Harrison, George R.** Equivalent temperatures in the electric arc as measured by multiplet intensities—133(A)
- A 21 ft. vacuum spectrograph for intensity measurements in the Schumann region—1443(A)
- (see Leighton, Philip A.)—134(A)
- Harrison, J. R.** Excitation of overtones of shear vibrations in Y-cut quartz plates—1417(A)
- Hart, O. P. and O. Stuhlman, Jr.** Relative intensities of arc and spark lines of the electrodeless discharge in mercury vapor—1437(A)
- Harvey, A. and F. A. Jenkins.** Blue-green absorption bands of Li_2 —132(A), 789
- Harvey, G. G. and G. E. M. Jauncey.** Electron distribution in the chlorine ion—1427(A)
- Headrick, L. B. and G. W. Fox.** New measurements on the fourth positive bands of carbon monoxide—1033
- (see Duffendack, O. S.)—1421(A)
- Heaps, C. W.** (see Bryan, A. B.)—298(A)
- Herzfeld, Karl F.** Surface heat of charging—248
- Book reviews—1137, 1411, 1412
- Hesthal, Cedric E.** Intensity relations in some of the stronger multiplets of chromium I and chromium II—126(A)
- Hidnert, Peter.** Thermal expansion of Carboly—120(A)
- and **W. T. Sweeney.** Thermal expansion of lead—296(A)
- and **W. T. Sweeney.** Thermal expansion of copper-nickel-tin alloy—667(A)
- Hill, E. L.** (see Almy, G. M.)—124(A)
- Hill, G. C.** (see Dryden, H. L.)—1416(A)
- Hodgman, Charles D.** Transmission of ultraviolet radiation by lake water—1423(A)
- Hoffacker, J. V.** Construction of a master clock with light controlled contacts—121(A)
- Hollabaugh, Cleveland B.** An x-ray determination of crystal orientation in silver sheet, produced by cold rolling—1426(A)
- Holmes, F. T.** Temperature shift of spectral lines and pole effect in vacuum arc—652(L)
- Hootman, James A. and W. S. Nelms.** Radioactivity of Stone Mountain—1431(L)
- Hopfield, John J.** Absorption and emission spectra in the region $\lambda 600-1100$ —1133(L)
- Ionization potential of carbon—1586(L)
- Houston, William V.** Method of calculating complex spectra—136(A)
- Quantum theory of the photoelectric and thermionic effects in metals, (title)—1414
- Howe, Carl E.** The *L* series spectra of the elements from calcium to zinc—717
- A vacuum spectrograph for the precision measurement of x-rays of long wave-lengths—1428(A)
- Howell, Lynn G.** (see Johnston, Morris)—274
- Hubbard, J. C.** Methods of acoustic interferometry for the measurement of velocity and absorption of sound in gases—1442(A)
- Huggins, M. L. and Ruth Parrish.** Valence electrons in the diamond—136(A)
- Hughes, A. L. and J. H. McMillen.** Angle and energy distribution of electrons rebounding from gaseous molecules—1438(A)
- (see Jauncey, G. E. M.)—1439(A)
- Hulburt, E. O.** Ionization in the upper atmosphere variation with longitude—240
- Zodiacal light and the gegenschein as phenomena of the earth's atmosphere—295(A), 663(A), 1098
- On the theory of the solar corona—297(A), 1379
- Spectra of gases lighted with strong discharges—1420(A)
- Ultraviolet light theory of auroras and magnetic storms—1587(L)
- Book reviews—1410
- Hull, H. L.** (see Barnes, A. H.)—1433(A)
- Hummel, A.** (see Kunz, J.)—123(A)
- Hyman, Hugh H.** Resonance of (*B-A*) bands of the hydrogen molecule—1419(A)
- Inglis, D. R.** (see Laporte, O.)—1337
- Ives, Herbert E.** Pictures in relief made with a large diameter lens—1424(A)
- and **H. B. Briggs.** Photoelectric properties of extremely thin films of alkali metals—669(A)
- Jauncey, G. E. M. and A. L. Hughes.** An attempt to detect collisions between photons—1439(A)
- (see Harvey, G. G.)—1427(A)
- Jenkins, F. A.** Fine structure of the beryllium fluoride bands—315
- (see Harvey, A.)—132(A), 789
- Johnson, J. R.** (see Shapiro, C. V.)—1422(A)
- Johnson, Thomas H.** Reflection of hydrogen atoms from crystals of lithium fluoride—650(L), 658(A)

- Johnson, Thomas H.** Photographic record of first order diffraction of H atoms by a lithium fluoride crystal—1299(L), 1444(A)
 ——— An attempt to detect de Broglie waves of hydrogen atoms—1432(A)
- Johnston, Helen** (see Urey, Harold C.)—869(L)
- Johnston, Norris and Lynn G. Howell.** Sedimentation equilibria of colloidal particles—274
- Kaplan, C. and F. D. Murnaghan.** On the fundamental constitutive equations in electromagnetic theory—763
- Kaplan, Joseph.** Heat of dissociation of oxygen—436(L)
 ——— Afterglow in air—600
 ——— Heat of dissociation of carbon monoxide—957
 ——— A new system of bands in CO—1298(L)
- Karapetoff, Vladimir.** Relativity transformation of an oscillation into a traveling wave, and de Broglie's postulate in terms of velocity angle—127(A)
- Kassel, Louis S.** Persistence of velocity and the theory of second order gas reactions—261
 ——— Equilibrium between matter and radiation—778
- Kemble, E. C.** Book reviews—566, 1018
- Kennard, E. H.** Shatter oscillations, their nature and theory—428
 ——— On the reason for Pauli's exclusion principle—1127(L)
- Kennard, Ralph B.** Motion of positive ions through gases—1129(L)
- Kettering, C. F., L. W. Shutts and D. H. Andrews.** A representation of the dynamic properties of molecules by mechanical models—1422(A)
- Kievit, Ben Jr. and Geo. A. Lindsay.** Fine structure in K x-ray absorption spectra—292(A)
- Killian, Thomas J.** Uniform positive column of an electric discharge in mercury vapor—1238
- King, A. S. and R. T. Birge.** Carbon isotope, mass 13—133(A)
- Kinsey, E. L.** Effect of dilution upon the Raman spectra of nitric acid—284(L)
- Kirkpatrick, Harry** (see DuMond, Jesse)—136(A)
 ——— and Jesse DuMond. Adjustments and tests of the multiple crystal x-ray spectrograph—136(A)
- Knipp, Charles T.** (see Sparks, F. M.)—259, 297(A)
- Knowles, D. D. and S. P. Sashoff.** Grid glow tube relays—1431(A)
- Korff, S. A.** Scattering of light in sodium vapor—435(L)
 ——— and J. L. Nickerson. Absorption of sodium vapor in the extreme ultraviolet—1433(A)
- Kovarik, Alois F.** Disintegration constant of actino-uranium and ratio of actinium to uranium—1432(A)
- Kozanowski, H. N.** Shot effect of the emission from oxide cathodes—1430(A)
- Kuhn, Jackson G.** (see Bedell, Frederick)—657(A)
- Kunz, Jakob.** A relation between the Compton effect and the diffraction by electrons—129(A)
 ——— Torsion of rhombic prisms and of cylinders in the elastic and plastic state—1417(A)
 ——— and A. Hummel. Ionization efficiency of electrons in potassium vapor—123(A)
 ——— (see Tykocinski-Tykociner, J.)—1436(A)
- Lane, C. T.** Magnetic susceptibility of rubidium—977
- Lang, R. J. and R. A. Sawyer.** Spectrum of singly ionized indium—126(A)
 ——— Second spark spectrum of antimony and a note on the first spark spectrum of tin—445
 ——— Spectrum of doubly-ionized antimony—664(A)
- Langer, R. M.** Generalization of the Rydberg formula—649(L)
- Langmuir, Irving, Saunders MacLane and Katharine B. Blodgett.** Effect of end losses on the characteristics of filaments of tungsten and other materials—478
- Laporte, Otto.** On the origin of the line absorption spectra of the rare earths—130(A)
 ——— and D. R. Inglis. Resonance separations in configurations of type p^5s and d^9s —1337
- Lawrence, Ernest O. and Frank G. Dunnington.** On the early stages of electric sparks—134(A), 396
 ——— and Leon B. Linford. Effect of intense electric fields on the photoelectric behavior of thin potassium films—1421(A)
- Leighton, Philip A. and George R. Harrison.** Photographic photometry in the extreme ultraviolet—134(A)
- Lewis, Gilbert N.** Quantum kinetics and the Planck equation—1533
- Lind, S. C.** Book review—1301
 ——— The origin of O^{17} —1408(L)
- Lindsay, Geo. A.** (see Kievit, Ben Jr.)—292(A)
- Lindsay, R. B.** An acoustical analogy of the Schrodinger wave equation—666(A)
- Linford, Leon B.** (see Lawrence, Ernest O.)—1421(A)
- Loeb, Leonard B.** Ionic mobilities in Cl_2 and in Cl_2 -air mixtures—137(A), 184
- Loomis, F. W.** Iodine fluorescence in the infrared—662(A)
- Lord, James O.** (see Blake, F. C.)—660(A)
- Lowry, E. F.** Function of the base metal in oxide-coated filaments—121(A)

- Lowry, E. F.** Phenomena in oxide-coated filaments—668(A)
—— Role of the core metal in oxide-coated filaments—1367
- Lowry, W. Norwood.** Location of the electromotive force in the photovoltaic cell—1270
- Luhr, Overton.** Recombination of ions in air and oxygen in relation to the nature of gaseous ions—1394
- Lunn, E. G. and F. R. Bichowsky.** Collision diameter of the hydrogen atom—563(L)
—— and F. R. Bichowsky. Scattering of atomic hydrogen by gases: mercury, argon, oxygen and iodine—671(A)
- McAlister, E. D.** Concerning the existence of a new term in Hg I—1585(L)
- McCracken, E. C.** An electrical method of determining the gelation temperature of starch—1423(A)
- McFarlan, Ronald L.** An x-ray study of molecular orientation in the Kerr effect—211(L)
—— Effect of an electric field on the x-ray diffraction pattern of a liquid—1426(A), 1469
- McKeehan, L. W.** Magnetoresistance and elastoresistance in permalloy—657(A)
—— Book reviews—654, 1017
- McMillen, J. H.** (see Hughes, A. L.)—1438(A)
- Mack, J. E. and R. A. Sawyer.** Sodium and magnesium spark lines in the far ultraviolet, and the quantitative application of the irregular doublet law to isoelectronic sequences—299, 661(A)
—— Book review—118
—— (see Condon, E. U.)—579
- MacLane, Saunders** (see Langmuir, Irving)—478
- Mahanti, P. C.** (see Ghosh, P. N.)—1491
- Maris, H. B.** Carbon dioxide theory of the ice ages—1016(L)
- Martin, John R.** (see Miller, Dayton C.)—1417(A)
- Marx, Erich.** On a new photoelectric effect in alkali cells—1059
- Maxwell, Louis R.** Comet tail bands of carbon monoxide—665(A)
- Meggers, William F. and Bourdon F. Scribner.** Regularities in the spectra of lutecium—1420(A)
—— and A. G. Shenstone. Spark spectrum of ruthenium—868(L)
- Mendenhall, C. E.** Influence of surface conditions on the photoelectric effect, (title)—1414
- Meyer, A. Wesley.** X-ray scattering by mixtures of organic liquids—291(A)
- Miller, Dayton C. and John R. Martin.** Influence of the walls enclosing a sounding air column upon the tone quality—1417(A)
- Miller, W. Lash.** Book review—566
- Milikan, R. A.** Most probable 1930 values of the electron and related constants—1231, 1433(A)
- Milne, W. E.** Numerical determination of characteristic numbers—863
- Mitchell, Allan C. G.** Polarization of sensitized fluorescence—1422(A)
—— (see Bramley, A.)—1419(A)
- Mohler, F. L.** Photoelectric ionization of gases, (title)—1414
- Mohler, F. L. and C. Boeckner.** Effect of gases on ionization of caesium by line absorption—664(A)
- Morse, Philip M.** Quantum mechanics of electrons in crystals—1310
—— (see Stueckelberg, E. C. G.)—116(L), 659(A)
- Mortimore, Roy H.** Measurement of the intensity of high frequency magnetic fields—753
- Mott-Smith, L. M.** Possibility of determining the energy of the cosmic beta-particles by magnetic deflection—1125(L)
- Mouzon, J. Carlisle** (see Sutton, Richard M.)—694
- Mukkerjee, B. C.** (see Ghosh, P. N.)—1491
- Mulder, Peter J. and Joseph Razek.** Further experiments with an automatic photoelectric spectrophotometer—1424(A)
—— and Joseph Razek. Measurement of the variation in intensity of the helium lines with voltage by means of selected filters and a photoelectric cell—1442(A)
—— (see Razek, Joseph)—1423(A)
- Murdock, Carleton C.** Form of the x-ray diffraction bands for regular crystals of colloidal size—8
- Murnaghan, F. D.** (see Kaplan, C.)—763
- Murphy, Edgar J.** (see Allison, Fred)—124(A), 285(L)
- Muskat, Morris.** Dispersion formula and Raman effect for the symmetrical top—1442(A), 1262
—— Distribution of nonreacting fluids in the gravitational field—1384, 1415(A)
—— Scattering of alpha-rays and high speed electrons in radial fields—1583(L)
- Nadai, A.** Some applications of the theory of plastic deformations of ductile metals—1418(A)
- Naudé, S. M.** An isotope of nitrogen, atomic weight 15—130(A)
- Nelms, W. S.** (see Hootman, James A.)—1431(A)
- Nicholas, Warren W.** Efficiency of production of continuous spectrum x-rays—128(A)
- Nichols, W. A. Jr.** (see Rodebush, W. H.)—649(L)
- Nickerson, J. L.** (see Korff, S. A.)—1433(A)
- Nordheim, L. W.** A theory of the resistance of alloys—1430(A)
- Normand, C. E.** Absorption coefficient for slow electrons in gases—1217
—— and R. B. Brode. Absorption coefficient for slow electrons in gases—1438(A)
- Nottingham, W. B.** Effective photoelectric work function reduced by weak accelerating fields—669(A)

- Nottingham, W. B. Influence of accelerating fields on the photoelectric and thermionic work function of composite surfaces—1128(L)
- Nusbaum, C. Radial-asterism in multi-crystalline materials—1426(A)
- Nutting, F. L. Position and width of the modified line of the spectrum of scattered x-rays—661(A)
- Olpin, A. R. Effect of red light on stopping potentials of photoelectrons liberated by blue light—112(L)
- Validity of Einstein's photoelectric equation for red sensitive sodium compounds—670(A)
- Selective maxima in the spectral response curves of light-sensitive compounds as a function of valence—671(A)
- Olshchinsky, D. E. Molecular beams in electromagnetic fields—659(A)
- Alloys for vacuum-light glass-metal joints—1424(A)
- Olson, Howard. An observed periodicity in the packing fraction—213(L)
- Onsager, L. Simultaneous irreversible processes—666(A)
- Oppenheimer, J. R. Note on the theory of the interaction of field and matter—461
- On the theory of electrons and protons—562(L)
- Two notes on the probability of radiative transitions—939
- (see Hall, Harvey)—132(A)
- Ornstein L. S. and G. E. Uhlenbeck. On the theory of the Brownian motion—1434(A)
- Osgood, Thomas H. Photoelectric effect and the J phenomenon—1407(L)
- Ostensen, Floyd C. Voltage intensity of $\lambda 2537$ in mercury—286(L)
- Page, Leigh—Book reviews—287, 1135
- and William W. Watson. Nuclear electrons—1584(L)
- Parrish, Ruth (see Huggins, M. L.)—136(A)
- Peek, R. L. Jr. On the solution of certain cases of the general equation of diffusion—554
- Perry, Charlotte, T. and E. L. Chaffee. A direct measurement of the velocity of cathode rays—1437(A)
- Pfund, A. H. Bismuth-black and its applications—1434(A)
- (see Barnes, R. Bowling)—1434(A)
- Phipps, T. E. (see Shaw, E. J.)—1126(L)
- Pielemeyer, W. H. Absorption and velocity of high frequency sound in oxygen—1417(A)
- Pierce, G. W. (see Drake, F. H.)—613
- Pietenpol, W. B. and H. H. Scott. Surface tension of molten glass at temperatures near the melting point—296(A)
- Plyler, E. K. and Theodore Burdine. Infrared absorption of some organic liquids—605
- Pool, M. L. Life and radius of the metastable mercury atom—1419(A)
- Pooler, Louis Gordon. Velocity of propagation of longitudinal waves in liquids at audio-frequencies—832
- Poulter, Thos. C. A glass window mounting for withstanding pressures of 30,000 atmospheres—297(A)
- Ramberg, E. (see Richtmyer, F. K.)—661(A), 1428(A)
- Randall, Robert H. Mean lives of lines of mercury triplet 2^3P_{012} — 2^3S_1 —1161
- and Harold W. Webb. Average lives of lines of mercury triplet 2^3P — 2^3S —665(A)
- Rashevsky, N. Thermodynamics of systems with several equilibria—666(A)
- A thermodynamic theory of excitation of nerves—1435(A)
- Razek, Joseph and Peter J. Mulder. Measurement of intensity of helium lines with voltage using a photoelectric device—1423(A)
- (see Mulder, Peter J.)—1424(A), 1442(A)
- Reid, Charles D. Some investigations into the velocity of sound at ultrasonic frequencies using quartz oscillators—814
- Reyerson, L. H. Book review—1138
- Reynolds, Neil B. Schottky effect and contact potential measurements on thoriated tungsten filaments—158
- Rice, O. K. A contribution to the quantum mechanical theory of radioactivity and the dissociation by rotation of diatomic molecules—1538
- Perturbations in molecules and the theory of predissociation and diffuse spectra. II.—1551
- Richardson, D. E. Resistance of an electrolytic conductor at various frequencies—297(A)
- Richtmyer, F. K. and E. Ramberg. Satellites of $K\alpha$ for the elements Ni(28) to As(33)—661(A)
- S. W. Barnes and E. Ramberg. A direct-reading two-crystal spectrometer for x-rays—1428(A)
- (see Barnes, S. W.)—661(A)
- Photoelectric multiple ionization by x-rays, (title)—1414
- Rinke, J. F. (see Bergstein, Milton)—1425(A)
- Ritschl, R. (see White, H. E.) 208 (L), 1146.
- Roberts, O. L. An x-ray study of very pure iron—1426 A
- Robertson, H. P. A general formulation of the uncertainty principle and its classical interpretation—667(A)

- Rodebush, W. H. Third law of thermodynamics—210(L)
—— and W. A. Nichols Jr. Atomic oxygen as a reducing agent—649(L)
—— (see Shaw, E. J.)—1126(L)
Roebuck, J. R. Porous plug measurements with air—121(A)
—— Book review—871
Rojansky, Vladimir. On the interaction of Stark effect and electron spin in alkali atoms—782
Rollefson, R. A possible origin of the band at 2540 in the spectrum of mercury vapor—1177
—— (see Winans, J. G.)—1436(A)
Roller, Duane. Photoelectric behavior of solid and liquid mercury—122(A)
Ruedy, Richard. On the active nitrogen glow—125(A)
—— Rectifier characteristics and detection diagrams—129(A)
—— Changes in the ozone concentration of the atmosphere—295(A)
Sabine, Paul E. Book review—1017
Salant, E. O. and A. Sandow. On the vibration frequencies of HCl and HBr in the liquid state—214(L)
Salkover, Meyer. Unified field-theory and Schwarzschild's solution—I 209(L), II 214(L)
Sandow, A. (see Salant, E. O.)—214(L)
Sashoff, S. P. (see Knowles, D. D.)—1431(A)
Sawyer, C. B. and C. H. Tower. Rochelle salt as a dielectric—269
Sawyer, R. A. Excitation processes in the hollow cathode discharge—1421(A)
—— (see Mack, J. E.)—299, 661(A)
—— (see Lang, R. J.)—126(A)
Sawyer, R. B. Reflection of lithium ions from metal surfaces—124(A), 1090
Schein, Marcel (see Dershem, Elmer)—292(A)
Schuh, A. E. (see Harkins, William D.)—130(A), 809
Schwingel, Christian H. and John Warren Williams. Variation dielectric constant with temperature. I. Electric moments of the carbon bisulphide and nitrous oxide molecules—855
Scott, Arnold H. Time lag in changes of electrical properties of rubber with temperature and pressure—1429 (A)
Scott, H. H. (see Pietenpol, W. B.)—296(A)
Scott, R. B. and F. G. Brickwedde. Apparatus for maintaining constant low temperatures—670(A)
—— (see Brickwedde, F. G.)—670(A)
Scribner, Bourdon F. (see Meggers, William F.)—1420(A)
Seitz, V. B. (see Glasser, Otto)—1432(A)
Shapiro, C. V., R. C. Gibbs and J. R. Johnson. Electronic transitions in the spectra of benzene—1422(A)
Shapiro, C. V. (see Almasy, F.)—1422(A)
Shaw, E. J., T. E. Phipps, and W. H. Rodebush. Magnetic moment of the sulfur molecule—1126(L)
Shearin, P. E. Relation between the intensity and position of the overtones of some organic liquids—973
Shenstone, A. G. A surplus level in the arc spectrum of palladium—1420(A)
—— (see Meggers, W. F.)—868(L)
Shortley, G. H. (see Condon, E. U.)—1342, 1419(A)
Shutts, L. W. (see Kettering, C. F.)—1422(A)
Sillers, Frederick Jr. An instrument for high-voltage x-ray spectrography and radiography—1428(A)
Sixtus, K. J. and L. Tonks. Propagation of large Barkhausen discontinuities along wires—1441(A)
Skinner, E. W. Diffraction of x-rays in liquids and the effect of temperature—128(A)
Slack, Francis G. Hydrogen atom in the Stark effect—1170
Slater, J. C. Note on Hartree's method—210(L)
—— Cohesion in monovalent metals—509
Smith, Lloyd P. Emission of positive ions from tungsten and molybdenum—381
—— Effect of positive ion shot effect on space charge limited electron currents—1430(A)
Smith, Philip T. and John T. Tate. Ionization of helium and neon by electron impact—1438(A)
Smith, Stanley. An extension of the spectrum of Tl II—235
Smith, W. O., Paul D. Foote and P. F. Busang. Capillary retention of liquids in assemblages of homogeneous spheres—1416(A)
Smyth, H. D. and E. G. F. Arnott. Excitation of certain nitrogen bands by positive ion impact—126(A)
Snow, C. P. Excited radicals in chemical compounds—563(L)
Southard, John C. (see Andrews, Donald H.)—670(A)
Sparks, F. M. and Charles T. Knipp. Change of spacing of positive column striations with temperature—259, 297(A)
Spedding, Frank H. (see Freed, Simon)—212(L), 1408(L)
Stauffer, L. H. Electro-optical modifications of light waves—1440(A)
Stearns, J. C. An x-ray search for the origin of ferromagnetism—1,292(A)
Stern, Otto. Diffraction of molecules—298(A)
Stevenson, E. C. (see Beams, J. W.)—1440(A)
Stewart, G. W. Extent of noticeable cybotactic condition in a liquid as exhibited by triphenol-methane—291(A)
—— Two different types of association of alcohol molecules in the liquid state—296(A)

- Stewart, G. W.** The cybotactic (molecular group) condition in liquids; the nature of the association of octyl alcohol molecules—726
 — Problems suggested by an uncertainty principle in acoustics—1441(A)
 — X-ray diffraction in water 2 to 98°C: Nature of molecular association—1426(A)
 — (see Edwards, R. L.)—291(A)
- Stewart, O. M.** Book review—287
- Street, J. C.** Time lags in spark discharges at high overvoltages—1437(A)
 — (see Beams, J. W.)—658(A)
- Stueckelberg, E. C. G. and Philip M. Morse.** Recombination of electron and alpha-particle—116(L)
 — and Philip M. Morse. Recombination of hydrogen-like atoms—659(A)
- Stuhlman, O. Jr.** (see Hart, O. P.)—1437(A)
 — M. D. Whitaker and M. L. Braun. High-frequency electrodeless discharge characteristics—1436(A)
- Sutton, Richard M. and J. Carlisle Mouzon.** Ionization of helium by potassium positive ions—694
- Swann, W. F. G.** Relativity and aether drift—127(A), 336
- Sweeney, W. T.** (see Hidnert, Peter)—296(A), 667(A)
- Swenson, H. N.** Intensity measurements in neon spectrum—126(A)
- Szczeniowski, S.** Spatial distribution of photoelectrons—122(A), 347
- Tanberg, R.** On the cathode of an arc drawn in vacuum—294(A), 1080
- Tate, John T.** (see Bleakney, Walker)—658(A)
 — (see Smith, Philip T.)—1438(A)
- Taylor, A. M.** Molecular aggregation—668(A)
- Taylor, John B.** Reflection of beams of the alkali metals from crystals—375
- Thomas, Ancil R.** Absorption of resonance radiation in mercury vapor—1253
- Thomas, C. H. and O. S. Duffendack.** Anode spots and their relations to the absorption and emission of gases by the electrodes of a Geissler discharge—72
- Thompson, James S.** Slow caesium ions in hydrogen and helium—123(A)
 — Motion of slow positive ions in gases—1196
- Thibaud, Jean.** On the reflection of the $K\alpha$ line of carbon from a glass mirror—1452
- Tolman, Richard C.** On the use of the energy-momentum principle in general relativity—875
 — On the use of the entropy principle in general relativity—896
- Tolman, Richard C.** On the weight of heat and thermal equilibrium in general relativity—904
 — Book reviews—568, 1302
- Todd, F. C. and T. E. Browne, Jr.** Restricting of short a. c. arcs—1441(A)
 — (see Browne, T. E. Jr.)—1441(A)
- Tonks, L.** (see Sixtus, K. J.)—1441(A)
- Tower, C. H.** (see Sawyer, C. B.)—269
- Trivelli, A. P. H.** Quantum theory of x-ray exposures on photographic emulsions—662(A)
- Tuve, M. A., G. Breit and L. R. Hafstad.** Application of high potentials to vacuum-tubes—66
 — Multiple coincidences of Geiger-Muller tube-counters—651(L)
 — (see Breit, G.)—51
 — L. R. Hafstad, and O. Dahl. High-voltage tubes—1406(L)
- Tykocinski-Tykociner, J. and Jakob Kunz.** Striations and magnetic effect in electrodeless discharges—1436(A)
- Tyndall, E. P. T.** Growth of zinc crystals—868(L)
 — and W. W. Wertzbaugher. Magnetic properties of thin films of cobalt—292(A)
- Uhlenbeck, G. E.** On the principle of Huyghens—1439(A)
 — (see Ornstein, L. S.)—1434(A)
- Urey, Harold C. and Helen Johnston.** Regularities in radioactive nuclei—869(L)
- Uytterhoeven, W. and M. C. Harrington.** Secondary emission from metals by impact of metastable atoms and positive ions—124(A), 438(L)
 — and M. C. Harrington. Secondary emission from nickel in neon discharge—1421(A)
- Valasek, J.** Structure of certain K series emission lines—291(A)
 — Book reviews—567, 1410
- Vallarta, M. S.** Unified field theory and Schwarzschild's solution: a reply—435(L)
- Van Voorhis, C. C. and K. T. Compton.** Heating of a cathode by positive gas ions, and their "accommodation coefficient"—1438(A)
- Verman, Lal C.** Reflection of radio waves from the surface of the earth—1425(A)
- Villars, D. S. and E. U. Condon.** Predissociation of diatomic molecules from high rotational states—1028
 — Book review—1136
- Vonwiller, O. U.** Intensity measurements in the arc spectrum of thallium—802
- Wagner, Paul Berthold.** Secondary electrons of high velocity from metals bombarded with cathode rays—98
- Wahlin, H. B.** Motion of electrons in carbon monoxide—122(A), 1568

- Wahlin, H. B. Emission of positive ions from thoriated tungsten—653(L)
- Warburton, F. W. Will the magnetic pole vanish?—292(A)
- Ware, L. A. Thomson effect in zinc crystals—667(A), 989
- Waterman, A. T. Density distribution of electron gas in equilibrium with a hot body—668(A)
- Watson, William W. (see Page, Leigh)—1584(L)
- and William Bender. Zeeman effect in the calcium hydride band spectra—1440(A), 1513
- Webb, Harold W. (see Randall, R. H.)—665(A)
- Weeks, Isabel C. Effect of hydrogen ion concentration on the measurement of the mean particle size of emulsions—668(A)
- Wegel, R. L. Book review—874
- Weld, LeRoy D. Analysis of cosmic-ray observations—295(A)
- Wells, P. V. Flarimeter: a clinical instrument for testing circulatory fitness—1418(A)
- Wentzel, G. Velocity distribution of x-ray photoelectrons, (title)—1414
- Wertzbaurgher, W. W. (see Tyndall, E. P. T.)—292(A)
- West, S. Stewart (see Dickinson, Roscoe G.)—1126(L)
- Whitaker, M. D. (see Stuhlman, Otto Jr.)—1436(A)
- White, H. E. Nuclear spin and hyperfine structure—441, 664(A)
- and R. Ritschl. Hyperfine structure in the spectra of neutral manganese—208(L)
- and R. Ritschl. Hyperfine structure in neutral manganese, Mn I—1146
- Wilkins, T. R. and J. A. Wood. A modification of Wiechert's experiment—657(A)
- Williams, John H. (see Allison, Samuel K.)—135(A), 149, 1476
- Williams, John Warren (see Schwingel, Christian H.)—855
- Wilson, H. A. Boundary conditions and the meaning of wave groups in wave mechanics—948; reply to criticism—1586(L)
- Winans, J. G. and R. Rollefson. Energy of dissociation of normal Cd_2 —1436(A)
- Wold, P. I. Mass-weight ratio of metals under strain—296(A)
- Wollan, Ernest O. Electron distribution in magnesium oxide—127(A), 1019
- Wood, J. A. (see Wilkins, T. R.)—657(A)
- Wood, R. W. Raman spectra excited by the helium hot-cathode arc and a new type of tube for small volumes of liquid—670(A)
- Plasmoidal high-frequency oscillatory discharges in "non-conducting" vacua—658(A), 673
- and G. H. Dieke. Raman effect in HCl gas—1355
- Woodrow, Jay W. and R. M. Bowie. Chemiluminescence of metallic sodium—1423(A)
- and H. L. Cunningham. Absorption spectrum characteristic of vitamin A—125(A)
- Workman, E. J. A new method for measuring the variation of specific heats of gases with pressure—667(A)
- Wyckoff, Ralph W. G. Reflecting powers of atoms for x-rays of different wave-lengths—215(L)
- X-ray scattering powers of nickel and oxygen in nickel oxide—583
- Wyman, Jeffries Jr. Measurements of the dielectric constants of conducting media—623
- Young, L. A. (see Goudsmit, S.)—1418(A)
- Zahl, Harold A. Reflection of zinc atoms from NaCl crystals—293(A)
- Zahn, C. T. Dielectric constant and the molecular structure of CS_2 —848
- Evidence for quantization from the electric polarization of acetic acid vapor—1047
- An extension of Van Vleck's theory of dielectric polarization—1056
- Zartman, I. F. A direct measurement of molecular velocities—134(A)
- Zeleny, John. On the potential relations in the striated positive column of electrical discharges through hydrogen—699
- Mobilities of ions in moist and dry air—1441(A)
- Zimmerman, E. E. Influence of temperature on polarization capacity and resistance—543
- Zwicky, F. Inhomogeneities in crystals (a reply)—283(L)

ANALYTIC SUBJECT INDEX TO VOLUME 35

References marked (A) are to abstracts of papers presented at meetings of the American Physical Society, those marked with (L) refer to letters to the Editor.

Aberration of light

From terrestrial sources, N. Galli-Shohat—664(A)

Absorption of light

Hg vapor, resonance radiation, A. R. Thomas—1253

Lacquer films, ultraviolet, W. P. Dewey, D. C. Duncan—1423(A)

Lake water, ultraviolet, C. D. Hodgman—1423(A)

Liquids, near infrared, effect of pressure, J. R. Collins—1433(A)

Na vapor, 300–1300A, S. A. Korff, J. L. Nickerson—1433(A)

Na vapor in flames, C. D. Child—294(A)

Organic liquids, infrared, E. K. Plyler, T. Burdine—605; R. B. Barnes—662(A), 1524

Organic liquids, intensity and position of overtones, P. E. Shearin—973

$\text{SmCl}_2 \cdot 6\text{H}_2\text{O}$, comparison with reflection at high and low temperatures, S. Freed, F. H. Spedding—212(L)

Various bodies, $\lambda > 50\mu$, C. H. Cartwright—415

Vitamin A, characteristic, J. W. Woodrow, H. L. Cunningham—125(A)

Acoustics

Absorption and velocity of high frequency sound in oxygen, W. H. Pielemeier—1417(A)

Absorption and velocity of sound in gases, interferometer method, J. C. Hubbard—1442(A)

Analogue of Schroedinger wave equation, R. B. Lindsay—666(A)

Tone quality, influence of walls—D. C. Miller, J. R. Martin—1417(A)

Uncertainty principle, problems, G. W. Stewart—1441(A)

Velocity in liquids at audio-frequencies, L. G. Pooler—832

Velocity of ultrasonic waves, C. D. Reid—814

Aerodynamics (see also Hydrodynamics)

Airfoils of circular cross-section, L. J. Briggs, H. L. Dryden—1416(A)

Wind pressure on cylindrical stacks, H. L. Dryden, G. C. Hill—1416(A)

Afterglow

Air, production and characteristics, J. Kaplan—600

Nitrogen, R. Ruedy—125(A)

Alpha-particles

Recombination with electrons; measurements, A. H. Barnes—217; A. H. Barnes, B. Davis, H. L. Hull—1433(A); explanation, W. Band—1128(L); theory, E. C. G. Stueckelberg, P. M. Morse—116(L), 659(A)

Scattering in radial fields, M. Muskat—1583(L)

Scintillations, time distribution, from weak source, N. Feather—705

Anode spots

In Geissler tube, relation to absorption and emission of gases, C. H. Thomas, O. S. Duffendack—72

Arcs (see also Discharge of electricity in gases, Spark discharge)

A.c., between brass electrodes, extinction, T. E. Browne, Jr., F. C. Todd—1441(A)

A.c. restriking, F. C. Todd, T. E. Browne, Jr.—1441(A)

Temperature, from multiplet intensities, G. R. Harrison—133(A)

Vacuum, cathode characteristics, R. Tanberg—294(A), 1080

Vacuum, pole effect, temperature shift of spectra, F. T. Holmes—652(L)

Astrophysics

Anomalous rotation of sun, R. Gunn—635

Pulsating stars, electrodynamic damping, R. Gunn—107, 295(A)

Solar corona, theory, E. O. Hulburt—297(A), 1379

Atomic beams

Alkali metals, reflection from crystals, J. B. Taylor—375

Hydrogen, attempt to detect de Broglie waves, T. H. Johnson—1432(A)

Hydrogen, collisions in Hg vapor, radius of atom, E. G. Lunn, F. R. Bichowsky—563(L)

Hydrogen, diffraction by LiF crystal, T. H. Johnson—1444(A); 1299(L)

Hydrogen, reflection from calcite, A. J. Dempster—298(A), 1405(L)

Hydrogen, reflection from LiF crystals, T. H. Johnson—650(L), 658(A)

Hydrogen, scattering by Hg, A, O₂, I₂, E. G. Lunn, F. R. Bichowsky—671(A)

- Oxygen, as reducing agent, W. H. Rodebush, W. A. Nichols, Jr.—649(L)
- Reflection, specular, from crystals, A. Ellett—293(A)
- S, magnetic moment, E. J. Shaw, T. E. Phipps, W. H. Rodebush—1126(L)
- Zn, reflection from NaCl, H. A. Zahl—293(A)
- Atomic weights**
- H and He, R. T. Birge—1015(L)
- Packing fraction, periodicity, H. Olson—213(L)
- Atomization**
- Mechanism, R. A. Castlemen, Jr.—1014(L), 1416(A)
- Atmospheric electricity**
- Auroras and magnetic storms, theory, E. O. Hulburt—1587(L)
- Ionization in upper atmosphere, variation with longitude, E. O. Hulburt—240
- Potential gradient in lower atmosphere, variation, J. G. Brown—135(A)
- Space charge in lower atmosphere, J. G. Brown—135(A)
- Barkhausen effect**
- Propagation along wires, K. J. Sixtus, L. Tonks—1440(A)
- Size of discontinuities, R. M. Bozorth, J. F. Dillinger—733
- Beta-particles**
- From mesothorium 2, maximum energy, N. Feather—1559
- Biophysics**
- Excitation of nerves, theory, N. Rashevsky—1435(A)
- Flarimeter, for testing circulatory fitness, P. V. Wells—1418(A)
- Vitamin A, absorption of light, characteristic, J. W. Woodrow, H. L. Cunningham—125(A)
- Black body**
- Bismuth-black, properties, A. H. Pfund—1434(A)
- For $\lambda > 50\mu$, C. Cartwright—415
- Book reviews**
- Adam, Neil Kensington, The Physics and Chemistry of Surface—1411
- Belling, John, The Use of the Microscope—1410
- Benedicts, C. B., Jetziger Stand der grundlegenden Kenntnisse der Thermoelektrizität—1301
- Birtwistle, George, La Nouvelle Mecanique des Quanta—654
- Born, M., and P. Jordan, Elementare Quantenmechanik—1588
- Bruhat, Georges, Traite de Polarimetrie—1410
- Chazy, Jean, La Theorie de la Relativite et la Mecanique Celeste—1302
- Condon, E. U. and P. M. Morse, Quantum Mechanics—566
- Debye, P., Dipolmoment und Chemische Struktur—1412
- Einführung in die Geophysik, II, Erdmagnetismus und Polarlicht, Wärme—und Temperaturverhältnisse der Obersten Bodenschichten, Luftelektrizität, von A. Nippoldt, J. Keränen, E. Schweidler—1410
- Einführung in die Geophysik, III, Dynamische Ozeanographie, von A. Defant—1410
- Einstein, A., Die Grundlage der allgemeinen Relativitätstheorie—568
- Ergebnisse der Exakten Naturwissenschaften, Jetziger Stand der grundlegenden Kenntnisse der Thermoelektrizität—1301
- Estermann, I., Elektrische Dipolmomente von Molekülen—1412
- Eucken, A., Lehrbuch der Chemischen Physik—1137
- Flint, H. T., Wave Mechanics, Being One Aspect of the New Quantum Theory—872
- Föppl, L., Technische Mechanik—1135
- Foster, William, Inorganic Chemistry for Colleges—1138
- Fry, Thornton C., Elementary Differential Equations—567
- Gortner, R. A., Outlines of Biochemistry—566
- Griffith, R. O. and A. McKeown, Photo Processes in Gaseous and Liquid Systems—1301
- Handbuch der Experimental Physik, Band VIII, 2 Teil, Warmausdehnung, Zustandsgrossen und Theorien der Wärme—873
- Handbuch der Experimental Physik, Band IX, 1 Teil, High and Low Temperature by H. von Wartenberg, Liquefaction of Gases by H. Lenz, Heat Conduction by Oscar Knoblauch and H. Reiher, Heat Radiation by W. Wien and C. Muller—871
- Houstoun, R. A., Intermediate Dynamics and Properties of Matter—1135
- Hund, F., Molekelbau—1018
- Kellogg, O. D., Foundations of Potential Theory—1135
- Mason, Max and Warren Weaver, The Electromagnetic Field—287
- Molecular Spectra and Molecular Structure. A General Discussion Held by the Faraday Society, September, 1929—874
- Müller-Pouille, Lehrbuch der Physik, 11 aufl., 2 band, Lehre von der Strahlenden Energie (Optik) 2 hälfte, 1 and 2 teil, Karl Wilhelm Meissner, editor—118
- Pollard, A. F. C., The Kinematical Design of Couplings in Instrument Mechanisms—871
- Robertson, John Kellock, Introduction to Physical Optics—567

- Roller, Duane, The Terminology of Physical Science—654
- Ruark, Arthur E. and Harold C. Urey, Atoms, Molecules, and Quanta—1136
- Ruedy, Richard, Bandenspektren auf experimenteller Grundlage—872
- Sack, H., Dipolmoment und Molekularstruktur—1412
- Stanley, Douglas, The Science of Voice—874
- Stoner, Edmund C., Magnetism—1017
- Terry, Earle M., Advanced Laboratory Practice in Electricity and Magnetism—287
- Tietjens, O., Hydro-und Aeromechanik, Vol. I—654
- Wien-Harms, Handbuch der Experimental Physik Vol. X, G. Hoffman, Das Elektrostatistische Feld; W. O. Schumann, Hochspannungstechnik—1411
- Watson, F. R., Acoustics of Buildings—1017
- Brownian motion**
Theory, L. S. Ornstein, G. E. Uhlenbeck—1434(A)
- Capillary action** (see **Surface tension**)
- Cathode rays** (see **Electrons**)
- Chemical analysis**
Magneto-optical method, F. Allison, E. J. Murphy—124(A); application to search for element 87—285(L)
- Chemical reactions**
Reducing action of atomic oxygen, W. H. Rodebush, W. A. Nichols, Jr.—649(L)
Second order, effect of persistence of velocities. L. S. Kassel—261
- Chemiluminescence**
Na, effect of moisture, J. W. Woodrow, R. M. Bowie—1423(A)
- Clock**
Master, with light-controlled contacts, J. V. Hoffacker—121(A)
- Cohesion**
In monovalent metals, theory, J. C. Slater—509
- Collision diameter** (see also **Electrons in gases, Ions**)
Of hydrogen atom, E. G. Lunn, F. R. Bichowsky—563(L)
- Colloids**
Emulsions, particle size, influence of p_H , I. C. Weeks—668(A)
Sedimentation equilibria of particles, N. Johnston, L. G. Howell—274
Gelation temperature of starch, E. C. McCracken—1423(A)
- Compton effect** (see also **X-rays, diffraction**)
Position and width of modified line, F. L. Nutting—661(A)
- Relation to electron diffraction, J. Kunz—129(A)
- Conductivity, thermal** (see **Thermal conductivity**)
- Contact potentials**
Thoriated tungsten, N. B. Reynolds—158
- Cosmic rays**
Analysis of observations, L. D. Weld—295(A)
Method of measuring energy by magnetic deflection, L. M. Mott-Smith—1125(L)
Method of study, M. A. Tuve—651(L)
Nature, L. F. Curtiss—1433(A)
- Crystals and crystal structure**
Ag sheet, cold rolled crystal orientation, C. B. Hollabaugh—1426(A)
Alloys containing precipitated crystals, C. S. Barrett—1425(A)
Alloys, magnetic, of high Pt content, microstructure, F. W. Constant—116(L)
Alum, radiation emitted under pressure in electric field, I. A. Balinkin—1443(A)
Bi, methods of forming, factors influencing orientation and perfection effect of magnetic field, A. Goetz—193
Calcite, grating space, C. D. Cooksey, D. Cooksey—564(L)
Colloidal crystals, x-ray diffraction bands, theory, C. C. Murdock—8
Cr-Ni alloys, variables, F. C. Blake, J. O. Lord—660(A)
Electron distribution, theory, P. M. Morse—1310
Fe, radial asterism, C. Nusbaum—1426(A)
Fe, very pure, x-ray study, O. L. Roberts—1426(A)
GdCl₃·6H₂O, line spectra, Paschen-Back effect, S. Freed, F. H. Spedding—1408(L)
Ice, grown from vapor, J. M. Adams—136(A)
Inhomogeneities, theory, R. H. Canfield—114(L); reply, F. Zwicky—283(L)
Mosaic crystals of elements, R. H. Canfield—671(A)
Possible symmetries, R. H. Canfield—660(A)
Stability of lattices, theory, R. H. Canfield—530
Unit lattice of interpenetrating lattices, example, F. C. Blake—660(A)
Zn, method of growth, E. P. T. Tyndall—868(L)
- Cybotactic State**
Alcohols, G. W. Stewart—296(A), 726
Liquids, organic, mixtures, A. W. Meyer—291(A)
Liquids, organic, temperature effect, E. W. Skinner—128(A)
Resumé of evidence, A. M. Taylor—668(A)
Triphenolmethane, G. W. Stewart—291(A)
Viscosity relations, R. L. Edwards, G. W. Stewart—291(A)

- Water, molecular association, G. W. Stewart—1426(A)
- Dielectric constant and properties**
Acetic acid vapor, C. T. Zahn—1047
Conducting media, J. Wyman, Jr.—623
CS₂ and NO, temperature variation, electric moments, C. H. Schwingel, J. W. Williams—855
CS₂ vapor, C. T. Zahn—848
Energy losses, effect of polar molecules, F. Hamburger, Jr.—657(A), 1119
H₂O and KCl solutions, high frequencies, F. H. Drake, G. W. Pierce, M. T. Dow—613
KCl solutions, A. Austin—1428(A)
Polarization, extension of Van Vleck's theory, C. T. Zahn—1056
Rochelle salt, temperature effect, C. B. Sawyer, C. H. Tower—269
Rubber, temperature and pressure variation, time lag, A. H. Scott—1429(A)
Tung oil, polarization and electric moment, A. A. Bless—1442(A)
- Diffraction of atoms** (see Atomic beams)
Diffraction of electrons (see Electrons, diffraction)
Diffraction of molecules (see Molecular beams)
Diffraction of radiation (see X-rays, diffraction)
Discharge of electricity in gases (see also Arc, Spark)
Anode spots, relation to absorption and emission of gases, C. H. Thomas, O. S. Duffendack—72
Cathode characteristics, R. Tanberg—294(A), 1080
Cathode heating by He⁺, Ne⁺, A⁺, C. C. Van Voorhis, K. T. Compton—1438(A)
Excitation processes in hollow cathode, R. A. Sawyer—1421(A)
H₂, high frequency, conductivity, C. J. Brasefield—1073; electron velocities—92, 122(A)
High frequency, characteristics, O. Stuhlman, Jr., M. D. Whitaker, M. L. Braun—1436(A)
H₂, striations, potential relations, J. Zeleny—699
Hg, positive column, T. J. Killian—1238
Ne, oscillations, G. W. Fox—1066
Ne, secondary electrons from Ni, W. Uytterhoeven, M. C. Harrington—1421(A)
Plasmoidal, high frequency oscillatory discharges, R. W. Wood—658(A), 673
Rare gases and Hg vapor, positive column, collisions of second kind, O. S. Duffendack, L. B. Headrick—1421(A)
Shot effect, abnormal, J. S. Donal, Jr.—1430(A)
Striations, temperature variation of striations, F. M. Sparks, C. T. Knipp—259, 297(A)
Striations and magnetic effect in electrodeless discharges, J. Tykocinski-Tykociner, J. Kunz—1436(A)
- Dispersion of light**
By symmetrical top-like molecules, theory, M. Muskat—1442(A), 1262
- Dissociation**
Diatomic molecules, by rotation, O. K. Rice—1538
H₂, by electron impact measurement, W. Bleakney, J. T. Tate—658(A), 1180; theory, E. U. Condon—658(A)
Predissociation of diatomic molecules, D. S. Villars, E. U. Condon—1028
- Dissociation, heat of** (see also Molecular structure and constants)
AgCl, from spectra, B. A. Brice—960
AlH, from spectra, D. S. Villars, E. U. Condon—1028
Cd₂, J. G. Winans, R. Rollefson—1436(A)
CO, from spectra, J. Kaplan—957
O₂, from spectra, J. Kaplan—436(L)
O₂, heat of formation, L. C. Copeland—1443(A)
- Double refraction**
Electrical, in gases, J. W. Beams, E. C. Stevenson—1440(A)
- Earth** (see Geophysics)
- Elasticity**
Metals, mass-weight ratio under strain, P. I. Wold—296(A)
Plastic deformation of ductile metals, A. Nadai—1418(A)
Shear vibrations in quartz, overtones, J. R. Harrison—1417(A)
Tensile stress and conductivity, in permalloy, L. W. McKeehan—657(A)
Torsion of rhombic prisms and cylinders, J. Kunz—1417(A)
Young's modulus for small stresses, D. K. Froman—120(A), 264
- Electrical conductivity and resistance**
Al, changes with working, G. E. Davis, G. Greenwood—1429(A)
Alloys, theory, L. W. Nordheim—1430(A)
Contact resistance, microphonic action, F. S. Goucher—1429(A)
Electrolytes, variation with frequencies, D. E. Richardson—297(A)
Permalloy, effect of stress and magnetic field, L. W. McKeehan—657(A)
- Electrical discharge in gases** (see Discharge of electricity in gases)
- Electric moment** (see Dielectric constant)
- Electrolytic phenomena**
E.m.f. location in photovoltaic cells W. N. Lowry—1270

- E.m.f. resistance, capacitance in photovoltaic cells, H. E. Hammond—998
 Polarization capacity and resistance temperature effect E. E. Zimmerman—543
 Resistance at various frequencies D. E. Richardson—297(A)
- Electromagnetic theory**
 Constitutive equations C. Kaplan F. D. Mur-naghan—763
 Interaction of field and matter J. R. Oppenheimer—461
 Magnetic poles F. W. Warburton—292(A)
- Electrons**
 Density distribution in equilibrium with hot body, A. T. Waterman—668(A)
 Distribution in atoms and molecules, from x-ray scattering: He, A. H. Compton—925, 1427(A); Cl, G. G. Harvey, G. E. M. Jauncey—1427(A); MgO, E. O. Wollan—127(A), 1019
 Equilibrium concentration in universe, L. S. Kassel—778
 Motion in crystals, theory, P. M. Morse—1310
 Nuclear, spin, L. Page, W. W. Watson—1584(L)
 Relation to protons, theory, J. R. Oppenheimer—562(L)
 Photoelectric (see **Photoelectric effect**)
 Recombination with alpha-particles: measurements, A. H. Barnes—217; A. H. Barnes, B. Davis, H. L. Hull—1433(A); explanation, W. Band—1128(L); theory, E. C. G. Stueckelberg, P. M. Morse—116(L), 659(A)
 Recombination with Hg^+ , search for critical potentials, A. M. Cravath—659(A)
 Scattering in radial fields, M. Muskat—1583(L)
 Valence, in diamond, M. L. Huggins, R. Parrish—136(A)
 Velocity, direct determination, T. R. Wilkins, J. A. Wood—657(A); C. T. Perry, E. L. Chaffee—1437(A)
- Electron, charge**
 Most probable value, R. A. Millikan—1433(A), 1231
- Electrons, diffraction**
 Crystals, quantum theory, P. M. Morse—1310
 Cu crystal, H. E. Farnsworth—1131(L); satellites—1432(A)
 Relation to Compton effect, J. Kunz—129(A)
- Electrons in gases**
 Absorption coefficients, collision diameters: Cd and Zn vapors, R. B. Brode—134(A), 504; H_2 , He, A, Ne, N_2 , CO, C. E. Normand, R. B. Brode—1438(A), 1217
 Energy losses: H_2 , analysis of ions, W. Bleakney, J. T. Tate—658(A), 1180; He, Ne, ionization efficiencies, P. T. Smith, J. T. Tate—1438(A); Hg vapor, C. W. Foard—293(A), 1187; Hg vapor, analysis of ions, W. Bleakney—123(A), 139; K vapor, ionization efficiencies, J. Kuns, A. Hummel—123(A)
 Mobility and velocity: in CO, H. B. Wahlin—122(A), 1568; in H_2 , high frequency discharges, C. J. Brasefield—92, 122(A)
 Scattering, angular distribution: H and H_2 , G. P. Harnwell—285(L); He, A, H_2 , A. L. Hughes, J. H. McMillen—1438(A)
- Electrons in metals**
 Alloys, resistance, theory, L. W. Nordheim—1430(A)
 Field currents, temperature dependence, N. A. de Bruyne—172
- Electrons, photoelectric (see Photoelectric effect)**
Electrons, scattered (see Electrons in gases)
- Electrons, secondary**
 From Au, Ag, Al when bombarded by 16–40 Kv cathode rays, P. B. Wagner—98
 From contaminated surfaces, P. L. Copeland—293(A), 982
 From Ni, by impact of metastable atoms and positive ions, W. Uytterhoeven, M. C. Harrington—124(A), 438(L), 1421(A)
- Electrons, thermionic (see Thermionic emission of electrons)**
- Electro-optical effects**
 Modification of light waves by electrical oscillations on Kerr cell, L. H. Stauffer—1440(A)
- Element 87**
 Presence in pollucite and lepidolite, F. Allison, E. J. Murphy—285(L)
- Emulsions**
 Particle size, effect of pH , I. C. Weeks—668(A)
- End losses**
 Effect on characteristics of filaments, I. Langmuir, S. MacLane, K. Blodgett—478
- Faraday effect**
 Lag, method of chemical analysis, F. Allison, E. J. Murphy—124(A); search for element 87, F. Allison, E. J. Murphy—285(L)
- Ferromagnetism**
 Origin, magnetic and silicon steel, J. C. Stearns—1, 292(A)
- Field currents**
 Temperature dependence, N. A. de Bruyne—172
- Fine structure (see also Hyperfine structure)**
 BeF bands, F. A. Jenkins—315
 PbO bands, A. Christy, S. Bloomenthal—46
 Mo $K\beta$ doublet, S. K. Allison, J. H. Williams—135(A), 149
- Flarimeter**
 For testing circulatory fitness, P. V. Wells—1418(A)

Fluorescence

- C₆H₆, spectrum, F. Almasy, C. V. Shapiro—1422(A)
 Cs, third principal series line, C. Boeckner—664(A)
 Iodine, infrared, by Hg arc, F. W. Loomis—662(A)
 Sensitized, polarization, A. C. G. Mitchell—1422(A)
 X-rays, efficiency, A. H. Compton—127(A)

Gases

- Equation of state, H. J. Brennen—129(A)
 Persistence of molecular velocities, second order reactions, L. S. Kassel—261

Geiger-counters

- Multiple coincidences, M. A. Tuve—651(L)

Gelation temperature

- Starch, method of determination, E. C. McCracken—1423(A)

Geophysics (see also Atmospheric electricity)

- Composition of earth interior, A. A. Bless—1436(A)
 Earth currents, transient, and earthquake, R. Hamer—656(A)
 Ice ages, CO₂ theory, H. B. Maris—1016(L)
 Ozone concentration in atmosphere, R. Ruedy—295(A)
 Zodiacal light, theory, relation to magnetic storms, E. O. Hulburt—295(A), 663(A), 1098

Gravitation

- Mass-weight ratio of metals under strain, P. I. Wold—296(A)

Heat conductivity (see Thermal conductivity)**Heat of Dissociation (see Dissociation, heat of)****Huyghens principle**

- Applicability, G. E. Uhlenbeck—1439(A)

Hydrodynamics

- Distribution of non-reacting fluids in gravitational field, M. Muskat—1415(A), 1384
 Shatter oscillations in liquids, nature and theory, E. H. Kennard—428
 Thermal convection, R. W. Babcock—1008
 Variable flow in pipes, theory, H. Bateman—177

Hyperfine structure

- Effect on polarization of resonance radiation, A. Ellett—588
 Error in literature, S. Goudsmit—436(L)
 Mn I, observations and theory, H. E. White, R. Ritschl—208(L), 1146
 Mn, predictions, S. Goudsmit—440(L)
 Paschen-Back effect, S. Goudsmit, R. F. Bacher—129(A)
 Relations between separations, theory, S. Goudsmit, R. F. Bacher—126(A)
 Relation to nuclear spin, theory, H. E. White—441, 664(A)

Intensities in spectra

- Cd, voltage relations, D. Colson—294(A)
 Cr I, Cr II, multiplets, C. E. Hesthal—126(A)
 HCl, vibration-rotation bands, J. L. Dunham—1347
 He, continuous, maxima, J. M. Dewey—155
 He, variation with voltage, J. Razek, P. J. Mulder—1423(A), 1442(A)
 Hg, electrodeless discharge, O. P. Hart, O. Stuhlman, Jr.—1437(A)
 Hg λ 2537, variation with potential, F. C. Osten-sen—286(L)
 In Schumann region, vacuum spectrograph, G. R. Harrison—1443(A)
 Li₂, isotope effect, A. Harvey, F. A. Jenkins—789
 Multiplets, temperatures of arc, G. R. Harrison—133(A)
 Ne, multiplets, measurements, H. N. Swenson—126(A)
 Super-multiplet lines, theory, J. H. Bartlett, Jr.—229
 Ti I, measurements, O. U. Vonwiller—802

Interference

- Method of measuring distance, S. H. Chamberlain—663(A)

Interferometer

- Recording, C. W. Chamberlain—663(A)

Ionization by Impact

- H₂, by electrons, analysis of ions, W. Bleakney, J. T. Tate—658(A), 1180
 H₂, by electrons, theory, E. U. Condon—658(A)
 He, by K⁺ ions, Richard M. Sutton, J. C. Mouzon—694
 He, Ne by electrons, efficiency 0–5000 volts, P. T. Smith, J. T. Tate—1438(A)
 Hg, by electrons, efficiency of production of Hg⁺, Hg²⁺, Hg³⁺, Hg⁴⁺, Hg⁵⁺, W. Bleakney—123(A); 139
 K vapor, by electrons, efficiency, J. Kunz, A. Hummel—123(A)

Ionization by radiation (see Photoionization)**Ions**

- Accommodation coefficient, He⁺, N⁺, A⁺, on Mo surface, C. C. Van Voorhis, K. T. Compton—1438(A)
 Diffraction, H⁺ by crystals, A. J. Dempster—298(A), 1405(L)
 Motion in gases, excitation of spectra, Hg⁺ in N₂, H. D. Smyth, E. G. F. Arnott—126(A)
 Motion in gases, ionization, K⁺ in He, R. M. Sutton, J. C. Mouzon—694
 Motion in gases, neutralization, retardation, scattering, R. B. Kennard—1129(L); Cs⁺, Li⁺ in H₂ and He, J. S. Thompson—123(A), 1196; Li⁺ in Hg vapor, I. W. Cox—123(A)

- Recombination coefficient, air and oxygen, O. Luhr—1394
- Recombination with electrons, Hg^+ , A. M. Cravath—659(A)
- Reflection; H^+ from crystals, A. J. Dempster—298(A), 1405(L); Li^+ from metals, R. B. Sawyer 124(A), 1090
- Thermionic emission (see **Thermionic emission of positives**)
- Velocity, direct determination, T. R. Wilkins, J. A. Wood—657(A)
- Ions, mobility**
- In Cl_2 and Cl_2 -air mixtures, L. B. Loeb—137(A), 184
- In moist and dry air—J. Zeleny—1441(A)
- Isotopes**
- Ag and Cl, from AgCl band spectra, B. A. Brice—960
- C_{18} , from band spectra, A. S. King, R. T. Birge—133(A)
- Li, from band spectra, A. Harvey, F. A. Jenkins—789
- Metals, magneto-optical effect, F. Allison, E. J. Murphy—124(A)
- N_{18} , from band spectra, S. M. Naude—130(A)
- O_{17} , disintegrative synthesis, W. D. Harkins, A. E. Schuh—130(A); origin, S. C. Lind—1408
- Pb, effect in PbO bands, S. Bloomenthal—34
- Regularities in nuclei, H. A. Barton—408; in radioactive nuclei, H. C. Urey, H. Johnston—869(L)
- Vibrational shift in band spectra, R. T. Birge—133(A)
- Joule-Thomson coefficient**
- Air, J. R. Roebuck—121(A)
- Real gases, simple equation, J. A. Beattie—643
- Kerr effect**
- Alternating fields, modulation of light wave, L. H. Stauffer—1440(A)
- In gases, pressure variation, J. W. Beams, E. C. Stevenson—1440(A)
- X-ray study of molecular orientation, R. L. McFarlan—211(L), 1426(A), 1469
- Kinetic theory of gases**
- Equation of state, H. J. Brennan—129(A)
- Molecular velocities, direct measure, I. F. Zartman—134(A)
- Persistence of velocities, second order gas reactions, L. S. Kassel—261
- Light waves**
- Modification by electrical oscillation on Kerr cell, L. H. Stauffer—1440(A)
- Huyghen's principle, applicability, G. E. Uhlenbeck—1439(A)
- Luminescence**
- Chemiluminescence of Na, J. W. Woodrow, R. M. Bowie—1423(A)
- Magnetic fields**
- High frequency, intensity measurements, R. H. Mortimore—753
- Magnetic storms (see Geophysics)**
- Magnetic properties**
- Barkhausen effect, propagation along wires, K. J. Sixtus, L. Tonks—1440(A); size of discontinuities, R. M. Bozorth, J. F. Dillinger—733
- Bi, influence of magnetic field on crystal formation, A. Goetz—193
- Co, thin films, E. P. T. Tyndall, W. W. Wertzbaugher—292(A)
- Ferromagnetism, search for origin, J. C. Stearns—1, 292(A)
- Moment of Li nucleus, S. Goudsmit, L. A. Young 1418(A)
- Moment of sulphur molecule, E. J. Shaw, T. E. Phipps, W. H. Rodebush—1126(L)
- Permalloy, effect of stress on resistance in magnetic field, L. W. McKeehan—657(A)
- Rb, susceptibility, C. T. Lane—977
- Steel, temperature changes accompanying magnetization, W. B. Ellwood—1440(A)
- Susceptibility of gases, pressure dependence, Francis Bitter—1572
- Magneto-optical effects**
- Faraday effect, lag, search for element 87, F. Allison, E. J. Murphy—285(L)
- Method of chemical analysis, F. Allison, E. J. Murphy—124(A)
- Magnetostriction**
- Measurements by heterodyne method, A. B. Bryan, C. W. Heaps—298(A)
- Mathematics**
- Least squares, application, W. E. Deming—665(A)
- Matter**
- Electrons and protons, theory; J. R. Oppenheimer—562(L)
- Equilibrium with radiation in universe, L. S. Kassel—778
- Interaction with field, J. R. Oppenheimer—461
- Mechanics, quantum**
- Boundary conditions, meaning of wave groups, H. A. Wilson—948; criticism, C. Eckart—1298(L); reply, H. A. Wilson—1586(L)
- Characteristic energy levels, method of calculation, W. E. Milne—863
- Cohesion in metals, J. C. Slater—509
- Complex spectra, calculation, W. V. Houston—136(A)

- Dielectric polarization, extention of Van Vleck's theory, C. T. Zahn—1056
- Dispersion and Raman effect for symmetrical top, M. Muskat—1442(A), 1262
- Electrons and protons, J. R. Oppenheimer—562(L)
- Electrons in crystals, P. M. Morse—1310
- Field theory, W. Band—1015(L)
- Hartree's method, J. C. Slater—210(L)
- Intensities of super-multiplet lines, J. H. Bartlett, Jr.—229
- Interaction of field and matter, J. R. Oppenheimer—461
- Mean life of excited states, A. Bramley, A. C. G. Mitchell—1419(A)
- Nuclear spin and hyperfine structure, H. E. White—441, 664(A)
- Nuclear spin, effect on x-ray terms, G. Breit—1447
- Ortho and para-hydrogen, equilibrium rate, H. Hall, J. R. Oppenheimer—132(A)
- Recombination of alpha-particles and electrons, E. C. G. Stueckelberg, P. M. Morse—116(L)
- Recombination of electrons with H-like atoms, E. C. G. Stueckelberg, P. M. Morse—659(A)
- Pauli's exclusion principle, interpretation, E. U. Condon, J. E. Mack—579; origin, E. H. Kennard—1127(L)
- Penetration of potential barrier by electrons, C. Eckart—1303
- Predissociation and diffuse spectra, O. K. Rice—1551
- Predissociation of diatomic molecules, D. S. Villars, E. U. Condon—1028
- Quantum kinetics and the Planck equation, G. N. Lewis—1533
- Radiative transitions, probability, J. R. Oppenheimer—939
- Radioactivity and dissociation by rotation, O. K. Rice—1538
- Relativity, W. Band—1016(L)
- Rydberg formula, generalization, R. M. Langer—649(L)
- Schrödinger equation, acoustical analogy, R. B. Lindsay—666(A)
- Separation of angles in two-electron problem, G. Breit—569
- Spatial distribution of photoelectrons, S. E. Szczeniowski—122(A), 347
- Stark effect and electron spin in alkali atoms, V. Rojansky—782
- Stark effect near series limit, J. Dewey—1439(A)
- Stark effect of H atom, F. G. Slack—1170
- Uncertainty principle, general formulation, H. P. Robertson—667(A)
- Mechanics, statistical**
- Brownian motion, theory, L. S. Ornstein, G. E. Uhlenbeck—1434(A)
- Electron density distribution in equilibrium with hot body, A. T. Waterman—668(A)
- Metastable atoms**
- Excitation of spectra, R. A. Sawyer—1421(A)
- Fluorescence, sensitized, A. C. G. Mitchell—1422(A)
- Hg, concentration, E. Gaviola—1226
- Hg, life and radius, M. L. Pool—1419(A)
- Hg mixed with rare gases, effect on field in positive column, O. S. Duffendack, L. B. Headrick—1421(A)
- Ne, impacts on Ni, secondary electrons, W. Uyterhoeven, M. C. Harrington—124(A), 438(L), 1421(A)
- Meteorology**
- Cyclones and anticyclones, effect on radio, R. C. Colwell—1425(A)
- Ice ages, CO₂ theory, H. B. Maris—1016(L)
- Origin of snow flakes, J. M. Adams—113(L)
- Ozone concentration in atmosphere, R. Ruedy—295(A)
- Methods and instruments**
- Acoustics interferometry, J. C. Hubbard—1442(A)
- Alloys for vacuum-tight glass-metal joints, D. E. Olshevsky—1424(A)
- Bismuth-black as absorber of radiation in bolometers and thermopiles, A. H. Pfund—1434(A)
- Chemical analysis, magneto-optic method, F. Allison, E. J. Murphy—124(A)
- Clock, master, with light-controlled contacts, J. V. Hoffacker—121(A)
- Flarimeter for testing circulatory fitness, P. V. Wells—1418(A)
- For determining gelation temperature of starch, E. C. McCracken—1423(A)
- For directly measuring corpuscular velocities, T. R. Wilkins, J. A. Wood—657(A); I. F. Zartman—134(A)
- For making pictures in relief, Herbert E. Ives—1424(A)
- For maintaining low temperatures, R. B. Scott, F. G. Brickwedde—670(A)
- For measuring intensity of high frequency magnetic fields, R. H. Mortimore—753
- For producing high potentials, G. Breit, M. A. Tuve, O. Dahl—51
- Glass window mounting for pressures of 30,000 atmospheres, T. C. Poulter—297(A)
- High voltage x-ray spectrography and radio-graphy, F. Sillers, Jr.—1428(A)
- Infrared spectrometer, resolving power, R. B. Barnes, A. H. Pfund—1434(A)

- Interferometer, recording, C. W. Chamberlain—663(A)
- Measuring distance, interference method, S. H. Chamberlain—663(A)
- Oscilloscope, stabilized, F. Bedell, J. G. Kuhn—657(A)
- Photometer, photoelectric, P. J. Mulder, J. Razez—1424(A)
- Photometry, photographic, in extreme ultraviolet, P. A. Leighton, G. R. Harrison—134(A)
- Radiometer, resonance, J. D. Hardy—662(A)
- Rectifier characteristics, R. Ruedy—129(A)
- Relays, grid-glow tubes, D. D. Knowles, S. P. Sashoff—1431(A)
- Specific heats of gases, variation with pressure, E. J. Workman—667(A)
- Spectrograph, vacuum, for intensity measurements in Schumann region, G. R. Harrison—1443(A)
- Spectrograph, vacuum, x-ray, C. E. Howe—1428(A)
- Spectrometer, x-ray, two-crystal, F. K. Richtmyer, S. W. Barnes, E. Ramberg—1428(A)
- Thermoregulator, photoelectric, F. G. Brickwedde, R. B. Scott—670(A)
- Vacuum tubes, high-voltage, M. A. Tuve, L. R. Hafstad, O. Dahl—1406(L)
- X-ray spectrograph, multiple crystal, J. DuMond, H. Kirkpatrick—136(A), adjustments and tests, H. Kirkpatrick, J. DuMond—136(A)
- Michelson-Morley experiment**
- Relation to relativity, W. F. G. Swann—127(A), 336
- Suggested explanation, N. Galli-Shohat—1418(A)
- Microphone**
- Microphone action and contact resistance, F. S. Goucher—1429(A)
- Mobility of ions** (see *Ions, mobility*)
- Molecular beams**
- Diffraction by crystals, O. Stern—298(A)
- In electromagnetic fields, D. E. Olshevsky—659(A)
- Velocities, direct measure, I. F. Zartman—134(A)
- Molecular structure and constants** (see also *Spectra, molecular*)
- AgCl, heat of dissociation, B. A. Brice—960
- Aggregation in solid state, from solubility, A. M. Taylor—668(A)
- Be F, from bands, F. A. Jenkins—315
- Cd₂, heat of dissociation, J. G. Winans, R. Rollefson—1436(A)
- CO, heat of dissociation, J. Kaplan—957
- CO, heat of dissociation, moment of inertia, R. S. Estey—309
- CS₂, dielectric constant and structure, C. T. Zahn—848
- CS₂, NO, electric moments, G. H. Schwingel, J. W. Williams—855
- H₂, para and ortho, equilibrium time, H. Hall, J. R. Oppenheimer—132(A)
- Mechanical model to represent dynamic properties, C. F. Kettering, L. W. Shutts, D. H. Andrews—1422(A)
- NH₃, two types, spectroscopic evidence, J. W. Ellis—595
- O₂, heat of dissociation, J. Kaplan—436(L)
- O₂, heat of formation, L. C. Copeland—1443(A)
- Organic compounds, relation to Raman effect, D. H. Andrews—662(A)
- PbO, rotational constants, nuclear separation, A. Christy, S. Bloomenthal—46
- Sulphur, magnetic moment, E. J. Shaw, T. E. Phipps, W. H. Rodebush—1126(L)
- Multiplets** (see also *Spectra, atomic*)
- Extension of Houston's and Slater's relations, S. Goudsmit—1325
- Nuclear structure**
- Disintegrative synthesis of oxygen, W. D. Harkins, A. E. Schuh—130(A), 809
- Electron spin, L. Page, W. W. Watson—1584(L)
- Li, magnetic moment, S. Goudsmit, L. A. Young—1418(A)
- Nuclear spin and hyperfine structure, H. E. White—441, 664(A)
- Packing fraction, periodicity, H. Olson—213(L)
- Regularities in list of nuclei, H. A. Barton—408
- Regularities in radioactive nuclei, H. C. Urey, H. Johnston—869(L)
- Stability and nuclear spin, W. D. Harkins—434(L)
- Oscilloscope**
- Stabilized, with amplified stabilization, F. Bedell, J. G. Kuhn—657(A)
- Packing effect**
- Periodicity in packing fraction, H. Olson—213(L)
- Paschen-Back effect**
- In hyperfine structure, S. Goudsmit, R. F. Bacher—129(A)
- Pauli's exclusion principle**
- Interpretation, E. U. Condon, J. E. Mack—579; origin, E. H. Kennard—1127(L)
- Peltier effect**
- Bi crystals, Thomson effect, H. D. Fagan, T. R. D. Collins—421
- Photoelectric effect**
- Alkali metals, properties, H. E. Ives, H. B. Briggs—669(A)

- And *J* phenomenon, T. H. Osgood—1407(L)
Hg, solid and liquid, characteristics, D. Roller—122(A)
K, thin films, effect of intense electric fields, E. O. Lawrence, L. B. Linford—1421(A)
Na compounds, red sensitive, validity of Einstein's law, A. R. Olpin—670(A)
Pt coated glass filaments, characteristics, A. K. Brewer—1360
Selective maxima as function of valence, A. R. Olpin—671(A)
Spatial distribution of electrons, theory, S. E. Szczeniowski—122(A), 347
Spectrophotometer, P. J. Mulder, J. RazeK—1424(A)
Stopping potentials, effect of red light, A. R. Olpin—112(L); E. Marx—1059
Thermoregulator, F. G. Brickwedde, R. B. Scott—670(A)
Threshold, temperature variation, K. F. Herzfeld—248
Work function, reduction by weak fields, W. B. Nottingham—669(A), 1128(L)
X-ray, fluorescence yield, A. H. Compton—127(A)
X-ray, space distribution of *K* and *L* electrons, C. D. Anderson—1139
- Photography**
Photometry in extreme ultraviolet, P. A. Leighton, G. R. Harrison—134(A)
Stereoscopic, H. E. Ives—1424(A)
X-ray, quantum theory of exposures, A. P. H. Trivelli—662(A)
- Photoionization**
Cs, by line absorption, effect of gases, F. L. Mohler, C. Boeckner—664(A)
- Photometry**
Photoelectric, P. J. Mulder, J. RazeK—1442(A)
Photographic, in extreme ultraviolet, P. A. Leighton, G. R. Harrison—134(A)
- Photons**
Collisions between, attempt to detect, G. E. M. Jauncey, A. L. Hughes—1439(A)
- Photovoltaic cells**
E.m.f., resistance capacitance, H. E. Hammond—998
Location of e.m.f., W. N. Lowry—1270
- Plasmoidal discharges** (see **Discharge of electricity in Gases**)
- Piezoelectric effect**
Rochelle salt, characteristics, C. B. Sawyer, C. H. Tower—269
- Polarization of radiation**
Fluorescence, sensitized, A. C. G. Mitchell—1422(A)
Resonance radiation, effect of hyperfine structure, A. Ellett—588
X-rays from thin Al, B. Dasannacharya—129(A)
- Pole effect**
In vacuum arc, F. T. Holmes—652(L)
- Porous plug experiment**
Air, measurements, J. R. Roebuck—121(A)
Real gases, theory, J. A. Beattie—643
- Potentials, critical** (see also **Spectra**)
Ag $L\alpha$ satellites, S. W. Barnes, F. K. Richtmyer—661(A)
Carbon, ionization, from spectra, J. J. Hopfield—1586(L)
 H_2 , ionization, analysis of ions, W. Bleakney, J. T. Tate—658(A), 1180
 Hg^+ , recombination with electrons, A. M. Cravath—659(A)
Hg vapor, electron energy losses, C. W. Foard—293(A), 1187
Hg vapor, formation of multiply charged ions, W. Bleakney—123(A), 139
In II, ionization, spectra, R. J. Lang—126(A)
Sb III, term values, R. J. Lang—445, 664(A)
Ti II, ionization, S. Smith—235
- Potentials, high**
Application to vacuum tubes, M. A. Tuve, G. Breit, L. R. Hafstad—66, 1406(L)
Method for producing, G. Breit, M. A. Tuve, O. Dahl—51
- Pressures, high**
Glass window for withstanding, T. C. Poulter—297(A)
- Power factor** (see **Dielectric constant and properties**)
- Proceedings of the American Physical Society**
Chicago Meeting, November 29 and 30, 1929—119
Stanford Meeting, December 7, 1929—132
Des Moines Meeting, December 30 and 31, 1929—289
New York Meeting, February 21 and 22, 1930—656; erratum—1414
Washington Meeting, April 24 to 26, 1930—1415
- Protons**
And electrons, theory, J. R. Oppenheimer—562(L)
Equilibrium concentration in universe, L. S. Kassel—778
- Radiation**
Emitted by compressed alum in electric field, I. A. Balinkin—1443(A)
Equilibrium with matter in universe, L. S. Kassel—778
From heated glass, extreme infrared, C. H. Cartwright—415

Radio

- Intensity, effect of cyclones and anti-cyclones, R. C. Colwell—1425(A)
- Reflection from earth's surface, L. C. Verman—1425(A)

Radioactivity

- Disintegration constant of actino-uranium, ratio Ac to U, A. F. Kovarik—1432(A)
- Gamma-ray intensity of radium, O. Glasser, V. B. Seitz—1432(A)
- Mesothorium 2, maximum energy of beta-particles, N. Feather—1559
- Of Stone Mountain, J. A. Hootman, W. S. Nelms—1431(A)
- Origin of O_{17} , S. C. Lind—1408(L)
- Quantum mechanical theory, O. K. Rice—1538
- Synthesis of O_{17} from N, W. D. Harkins, A. E. Schuh—130(A), 809
- Rate of transformation, N. Feather—705
- Regularities in radioactive nuclei, H. C. Urey, H. Johnston—869(L)

Radiometer

- Resonance, theory and practice, J. D. Hardy—662(A)

Raman effect

- Excited by He arc, new methods, R. W. Wood—670(A)
- For symmetrical top-like molecules, theory, M. Muskat—1442(A), 1262
- HCl, R. W. Wood, G. H. Dieke—1355
- HCl and HBr (liquid) vibration frequencies, E. O. Salant, A. Sandow—214(L)
- HNO_3 , effect of dilution, E. L. Kinsey—284(L)
- Organic compounds, relation to molecular structure, D. H. Andrews—662(A)
- Organic liquids, R. B. Barnes—662(A), 1524
- Solid organic compounds, specific heats, D. H. Andrews, J. C. Southard—670(A)
- SO_2 spectra, R. G. Dickinson, S. S. West—1126(L)

Recombination

- Alpha-particles and electrons, measurements, A. H. Barnes—217; A. H. Barnes, B. Davis, H. L. Hull—1433(A); explanation, W. Band—1128(L); theory, E. C. G. Stueckelberg, P. M. Morse—116(L), 659(A)
- Ions and electrons, Hg^+ , A. M. Cravath—659(A)
- Ions and ions, air and oxygen, O. Luhr—1394

Rectifiers

- Characteristics, R. Ruedy—129(A)
- Contact, cupric sulphide-magnesium junctions, M. Bergstein, J. F. Rinke, C. M. Gutheil—1425(A)

Reflection of corpuscles

- Alkali metal atoms, from crystals, J. B. Taylor—375

Atoms, from crystals, A. Ellett—293(A)

H atoms, attempt to detect de Broglie waves, T. H. Johnson—1432(A)

H atoms from LiF crystal, T. H. Johnson—1299(L), 1444(A)

H^+ , by crystals, A. J. Dempster—298(A), 1405(L)

Li^+ from metal surfaces, R. B. Sawyer—124(A), 1090

Molecules, diffraction by crystals, O. Stern—298(A)

Zn atoms from NaCl, H. A. Zahl—293(A)

Reflection of light

$SmCl_3 \cdot 6H_2O$ comparison with absorption at high and low temperatures, S. Freed, F. H. Spedding—212(L)

Refractive index

H_2O and KCl solution at high frequencies, F. H. Drake, G. W. Pierce, M. T. Dow—613

Au, for $C K\alpha$ x-rays, E. Dershem—128(A)

Relativity

Aberration of light from terrestrial sources, N. Galli-Shohat—664(A)

Field and matter, interaction, J. R. Oppenheimer—461

General, energy-momentum principle, R. C. Tolman—875; entropy principle—896; weight of thermal equilibrium—904

Michelson-Morley experiment, suggested explanation, N. Galli-Shohat—1418(A)

Relation to aether drift, W. F. G. Swann—127(A), 336

Transformation of oscillation to travelling wave, de Broglie's postulate, V. Karapetoff—127(A)

Unified field theory and wave mechanics, W. Band—1015(L)

Unified field theory, Schwarzschild's solution, M. Salkover—I 209(L), II 214(L), reply, M. S. Vallarta—435(L)

Unified physical field, W. Band—115(L)

Resolving power

Calcite, for x-rays, S. K. Allison, J. H. Williams—1476

Crystal grating, limits, B. Davis—209(A)

Resonance radiation

Cs, third principal series line, quenching, C. Boeckner—664(A)

Hg, absorption in Hg vapor, A. R. Thomas—1253

Polarization, effect of hyperfine structure, A. Ellett—588

Scattering of light (see also Raman effect)

In Na vapor, S. A. Korff—435(L)

Schottky effect (see also Photoelectric effect, Thermionic emission)

Thoriated tungsten, N. B. Reynolds—158

Sedimentation

Equilibria of colloidal particles, N. Johnston, L. G. Howell—274

Shatter oscillations

Nature and theory, E. H. Kennard—428

Shot effect

Abnormal, in gas discharge, J. S. Donal, Jr.—1430(A)

Of positive ions, effect on space charge limited electron current, L. P. Smith—1430(A)

Oxide-coated filaments, H. N. Kozanowski—1430(A)

Snow flakes

Origin, J. M. Adams—113(L)

Solar physics

Anomalous rotation of sun, R. Gunn—635

Spark discharge

Early stages, time of appearance of spectra, temperature, ion concentration, E. O. Lawrence, F. G. Dunnington—134(A), 396

Initial stages, time lag in characteristics, J. W. Beams, J. C. Street—658(A)

Time differences in appearance of spectrum lines, J. W. Beams—24

Time lags at overvoltages, J. C. Street—1437(A)

Specific heats

Gases, variation with pressure, E. J. Workman—667(A)

Solid organic compounds from Raman spectra, D. H. Andrews, J. C. Southard—670(A)

Spectra, atomic

Alkali atoms, Stark effect and electron spin, theory, V. Rojansky—782

C I, ionization potential, J. J. Hopfield—1586(L)

Cd, voltage-intensity relations, D. Colson—294(A)

Co II, analysis, J. H. Findlay—1420(A)

Complex spectra, method of calculating, W. V. Houston—136(A)

Cr I, Cr II, intensities in multiplets, C. E. Hesthal—126(A)

Cs, resonance and quenching of third principal series line, C. Boeckner—664(A)

Excitation, in hollow cathode, R. A. Sawyer—1421(A)

GdCl₂·6H₂O, line spectra from solid, S. Freed, F. H. Spedding—1408(L)

H, variation with pressure and capacitance, E. O. Hulburt—1420(A)

He, H, N, O, 600–1100 Å, J. J. Hopfield—1133(L)

He, continuous, intensity maxima, J. M. Dewey—155

He, intensities, J. Razek, P. J. Mulder—1423(A)

He, intensity-voltage relations, P. J. Mulder, J. Razek—1442(A)

Hg, average lives of 2^3P-2^3S triplet, R. H. Randall, H. W. Webb—665(A)

Hg, intensity potential relations for $\lambda 2537$, F. C. Ostensen—286(L)

Hg $2^3P_{012}-2^3S_1$, mean lives, R. H. Randall, H. W. Webb—665(A), 1161

Hg, relative intensities in electrodeless discharge, O. P. Hart, O. Stuhlman, Jr.—1437(A)

Hg I, new term, E. D. McAlister—1585(L)

Hyperfine structure and nuclear spin, H. E. White—441, 664(A)

Hyperfine structure, error in literature, S. Goudsmit—436(L)

Hyperfine structure, Paschen-Back effect, S. Goudsmit, R. F. Bacher—129(A)

Hyperfine structure, relations between separations, S. Goudsmit, R. F. Bacher—126(A)

In II, measurements and classification, R. J. Lang—126(A)

In spark discharge, time of appearance of lines, J. W. Beams—24

Interval ratios, rule for *sp*, *sd*, *sf*, configurations, E. U. Condon, G. H. Shortley—1419(A), 1342

Li, magnetic moment of nucleus, S. Goudsmit, L. A. Young—1418(A)

Lu, regularities, W. F. Meggers, B. F. Scribner—1420(A)

Mn, hyperfine structure, H. E. White, R. Ritschl—208(L)

Mn I, hyperfine structure, H. E. White, R. Ritschl—1146

Mn, prediction of hyperfine structure, S. Goudsmit—440(L)

Multiplets, extension of Houston's and Slater's relations, S. Goudsmit—1325

Multiplets, intensities, temperature of arcs, G. R. Harrison—133(A)

Na III, Mg IV, Mg V, for ultraviolet, new levels, irregular doublet law, J. E. Mack, R. A. Sawyer—229, 661(A)

Ne, intensities, H. N. Swenson—126(A)

Pd, surplus level, A. G. Shenstone—1420(A)

Rare earths, origin of line absorption spectra, O. Laporte—130(A)

Resonance separations in p^5s and d^5s configurations, O. Laporte, D. R. Inglis—1337

Ru I, analysis, W. F. Meggers, A. G. Shenstone—868(L)

Rydberg formula, generalization, R. M. Langer—649(L)

Sb III, Sn II, classification, R. J. Lang—445, 664(A)

SmCl₃·6H₂O, reflection and absorption, S. Freed, F. H. Spedding—212(L)

Spark discharge, time of appearance of lines, E. O. Lawrence, F. G. Dunnington—134(A), 396

- Stark effect near series limit, J. Dewey—1439(A)
 Super-multiplet lines, intensities, J. H. Bartlett, Jr.—229
 Temperature shift and pole effect in vacuum arc, F. T. Holmes—652(L)
 Tl I, intensity measurements, O. U. Vonwiller—802
 Tl II, extinction and analysis, S. Smith—235
Spectra, molecular (see also **Raman effect**)
 Acetylene, ethylene, 6800-9200A, R. M. Badger—1433(A)
 AgCl, analysis, B. A. Brice—960
 Air, afterglow, J. Kaplan—600
 BeF, wave-lengths, analysis, molecular constants, F. A. Jenkins—315
 CaH, red bands, Zeeman effect, W. W. Watson, W. Bender—1440(A), 1513
 Cd₂, heat of dissociation, J. G. Winans, R. Rollefson—1436(A)
 C₆H₆ fluorescence, F. Almasy, C. V. Shapiro—1422(A)
 C₆H₆, electronic transitions, C. V. Shapiro, R. C. Gibbs, J. R. Johnson—1422(A)
 C₆H₆, emission 2500-3000A, J. B. Austin, I. A. Black—452
 CO, comet tail bands, emitter, L. R. Maxwell—665(A)
 CO, fourth positive bands, new measurements and classification, R. S. Estey—309
 CO, fourth positive bands, wave-lengths, L. B. Headrick, G. W. Fox—1033
 CO, new band system, J. Kaplan—1298(L)
 Cyclohexane, vibration doublets, J. W. Ellis—437(L)
 Excited radicals in compounds, constancy of vibration frequencies, C. P. Snow—563(L)
 H₂ absorption 600-1100A, J. J. Hopfield—1133(L)
 H₂, (B-A) bands, resonance, H. H. Hyman—1419(A)
 HCl, vibration-rotation bands, intensities, J. L. Dunham—1347
 Hg band at 2540, origin, R. Rollefson—1177
 Iodine, fluorescence, infrared, by Hg arc, F. W. Loomis—662(A)
 Isotope shift, R. T. Birge—133(A)
 Li₂, blue-green absorption, A. Harvey, F. A. Jenkins—132(A), 789
 MgH, λ 2511 band, Zeeman effect, G. M. Almy, F. H. Crawford, E. L. Hill—124(A)
 MgO, blue-green, analysis, P. N. Ghosh, P. C. Mahanti, B. C. Mukkerjee—1491
 N₂, afterglow, R. Ruedy—125(A)
 N₂, excited by positive ion impact, H. D. Smyth, E. G. F. Arnott—126(A)
 NH₃, absorption in visible, R. M. Badger—1038
 NH₃, evidence of two molecular types, J. W. Ellis—595
 OH bands, Zeeman effect, G. M. Almy—1495
 O₂, atmospheric new absorption band, H. D. Babcock—125(A)
 Organic liquids, absorption, infrared, E. K. Plyler, T. Burdine—605
 Organic liquids, C-H vibration, Raman effect, R. B. Barnes—662(A)
 Organic liquids, intensity and position of overtones, P. E. Shearin—973
 PbO, fine structure analysis, A. Christy, S. Bloomenthal—46
 PbO, quantum analysis and isotope effect, S. Bloomenthal—34
 Predissociation from high rotational states, D. S. Villars, E. U. Condon—1028
 SmCl₃·6H₂O, reflection and absorption, S. Freed, F. H. Spedding—212(L)
Spectra, reflection
 SmCl₃·6H₂O, comparison with absorption, S. Freed, F. H. Spedding—212(L)
Spectrograph, Spectrometer
 Infrared, resolving power, R. B. Barnes, A. H. Pfund—1434(A)
 Vacuum, for intensity measurements in Schumann region, G. R. Harrison—1443(A)
 X-ray, two-crystal, F. K. Richtmyer, S. W. Barnes, E. Ramberg—1428(A)
 X-ray, multiple crystals, J. DuMond, H. Kirkpatrick—136(A); adjustments and tests, H. Kirkpatrick, J. DuMond—136(A)
 X-ray, vacuum, C. E. Howe—1428(A)
Stark effect
 Alkali atoms, electron spin, theory, V. Rojansky—782
 Hydrogen atom, theory, F. G. Slack 1170
 Near series limit, J. Dewey—1439(A)
Stars (see **Astrophysics**)
Sun (see **Astrophysics**)
Surface tension
 Glass, molten, W. B. Pietenpol, H. H. Scott—296(A)
 Retention of liquids in assemblages of homogeneous spheres, W. O. Smith, P. D. Foote, P. F. Busang—1416(A)
Susceptibility, magnetic (see **Magnetic properties**)
Thermal conductivity
 Solution of general equation for certain cases, R. L. Peek, Jr.—554
Thermal convection
 In fluids, R. W. Babcock—1008
Thermal expansion
 Carbonyl, measurements, P. Hidnert—120(A)

- Cu-Ni-Sn alloy, P. Hidnert, W. T. Sweeney—667(A)
- Pb, measurement, P. Hidnert, W. T. Sweeney—296(A)
- Thermal radiation**
Of glass for $\lambda > 50\mu$, C. H. Cartwright—415
- Thermionic emission of electrons**
Composite surfaces, work function, effect of fields, W. B. Nottingham—1128(L); ion-grid theory, J. A. Becker, 1431(A)
Electron density distribution in equilibrium with hot body, A. T. Waterman—668(A)
From various filaments, effect of end losses, I. Langmuir, S. MacLane, K. B. Blodgett—478
Oxide-coated filaments, characteristics, E. F. Lowry—668(A), role of base metal, E. F. Lowry—121(A), 1367; shot effect, H. N. Kozanski—1430(A)
Pt-coated glass filaments, characteristics, A. K. Brewer—1360
Relation to surface heat of charging, K. F. Herzfeld—248
Shot effect, abnormal, in Ne gas, J. S. Donal, Jr.—1430(A)
Thoriated tungsten, variation with extent of thoriation, W. H. Brattain—1431(A); contact e.m.f., Schottky effect, N. B. Reynolds,—158
Work function, space charge interpretation, R. S. Bartlett—669(A)
- Thermionic emission of positives**
From thoriated tungsten, H. B. Wahlin—653(L)
From W and Mo, characteristics, L. P. Smith—381
Shot effect, effect on space charge limited electron currents, L. P. Smith—1430(A)
- Thermodynamics**
Dalton-Gibbs law, test, L. J. Gillespie—1435(A)
Entropy in general relativity, R. C. Tolman—896
Equation of state for gases, H. J. Brennen—129(A)
Excitation of nerves, theory, N. Rashevsky—1435(A)
Homogeneous coordinates, uses, H. J. Brennan—294(A)
Joule-Thomson effect, theory, J. A. Beattie—643; measurements with air, J. R. Roebuck—121(A)
Mixtures of real gases, theory, J. A. Beattie—1435(A)
Nernst heat theorem, H. J. Brennen—121(A)
Simultaneous irreversible processes, L. Onsager—666(A)
Systems with several equilibria, N. Rashevsky—666(A)
Third law, W. H. Rodebush—210(L)
- Thermoelectric properties**
Bi crystals, Peltier and Thomson effects, H. D. Fagan, T. R. D. Collins—421
- Thermoregulator**
For low temperatures, R. B. Scott, F. G. Brickwedde—670(A)
Photoelectric, F. G. Brickwedde, R. B. Scott—670(A)
Thomson effect in Zn crystals, L. A. Ware—667(A), 989
- Thomson effect** (see **Thermoelectric properties**)
- Transitions, radiative**
Probability, theory, J. R. Oppenheimer—939
- Ultrasonic waves**
Velocity measurements, C. D. Reid—814
- Uncertainty principle**
In acoustics, G. W. Stewart—1441(A)
Formulation and classical interpretation, H. P. Robertson—667(A)
- Vacuum tubes**
For high-voltages, M. A. Tuve, G. Breit, L. R. Hafstad—66; M. A. Tuve, L. R. Hafstad, O. Dahl—1406(L)
Grid-glow tube relays, D. D. Knowles, S. P. Sashoff—1431(A)
- Valence**
Valence electrons in diamond, location, M. L. Huggins, R. Parrish—136(A)
- Viscosity**
Dependence on molecular space arrangement, R. L. Edwards, G. W. Stewart—291(A)
Of compressed gases, J. H. Boyd, Jr.—1284
- Voltmeter**
Vacuum tube, improvements, R. H. Mortimore—753
- Wave equation**
Huyghens principle, G. E. Uhlenbeck—1439(A)
- Work function** (see **Thermionic emission**)
- X-rays, absorption**
Au, for $K\alpha$, E. Dershem—128(A)
Temperature independence, J. A. Bearden—1443(A), 1463
- X-rays, diffraction, reflection and scattering** (see also **Compton effect**)
Alcohols, molecular association, G. W. Stewart—296(A), 726
Alcohols, relation to viscosity, R. L. Edwards, G. W. Stewart—291(A)
Calcite, glancing angle for $AgK\alpha$, C. D. Cooksey, D. Cooksey—564(L)
Compton effect, position and width of modified line, F. L. Nutting—661(A)
Crystals of colloidal size, form of bands, theory, C. C. Murdock—8
Diamond, Valence electrons, M. L. Huggins, R. Parrish—136(A)
Fe crystal, magnetized and unmagnetized, J. C. Stearns—1, 292(A)

- Fe, Ni, Cu atoms, R. W. G. Wyckoff—215(L)
 Glass, C. $K\alpha$ line, J. Thibaud—1452
 He, distribution of electrons, A. H. Compton—1427(A)
 Liquids, effect of electric field, R. L. McFarlan—211(L), 1426(A), 1469
 Liquids, organic mixtures, A. W. Meyer—291(A)
 Liquids, organic, temperature effect, E. W. Skinner—128(A)
 Magnetite and silicon steel, magnetized and unmagnetized, J. C. Stearns—1
 MgO, electron distribution, E. O. Wollan—1019
 NaCl, electron distribution in Cl, G. G. Harvey, G. E. M. Jauncey—1427(A)
 NaCl, temperature effect, W. D. Claus—1427(A)
 Ni, O, in NiO, R. W. G. Wyckoff—583
 Quartz, C $K\alpha$, E. Dershem, M. Schein—292(A)
 Spectra, N. S. Gingrich—1444(A)
 Spectroscopic analysis, J. A. Bearden—1427(A)
 Theory, relation to electron distribution in atoms, A. H. Compton—925, 1427(A)
 Triphenylmethane, G. W. Stewart—291(A)
 Water, molecular association, G. W. Stewart—1426(A)
- X-rays, emission**
 Efficiency, W. W. Nicholas—128(A)
 From three-element tube, A. Bramley—869 (L)
 Mechanism, W. Band—1129(L)
- X-rays, fluorescence**
 Efficiency, A. H. Compton—127(A)
- X-rays, photoelectric effect**
 Relation to J phenomenon, T. H. Osgood—1407(L)
 Space distribution of K and L electrons, C. D. Anderson—1139
- X-rays, photographic effect**
 Theory, A. P. H. Trivelli—662(A)
- X-rays, polarization**
 From thin Al anticathode, B. Dasannacharya—129(A)
- X-rays, refraction**
 Au, for $K\alpha$, E. Dershem—128(A)
- X-rays, spectra and Spectroscopy**
 Absolute measure of wave-lengths, J. M. Cork—128(A)
 Ag $L\alpha$ satellites, excitation potential, S. W. Barnes, F. K. Richtmyer—661(A)
 By double crystal, N. S. Gingrich—1444(A)
 Ca, Cr, Mn, Co, Ni, Cu, Zn, K absorption, fine structure, B. Kievit, Jr., G. A. Lindsay—292(A)
 Cu, Mo, Ag K lines, structure, J. Valasek—291(A)
 Effect of nuclear spin on term values, theory, G. Breit—1447
 Instrument for high-voltage, F. Sillers, Jr.—1428(A)
 $K\alpha$ satellites of Ni I As, F. K. Richtmyer, E. Ramberg—661(A)
 Limiting resolving power of crystal grating, B. Davis—209(L)
 L series, Ca to Zn, measurements, C. E. Howe—717
 Mo $K\alpha$, natural width, S. K. Allison, J. H. Williams—1476
 Mo $K\beta$ doublet, separation and fine structure, S. K. Allison, J. H. Williams—135(A), 149
 Mo L series, wave-lengths by ruled grating, J. M. Cork—1456
 Scattered x-rays, N. S. Gingrich—1444(A)
 Spectrograph and radiograph, F. Sillers, Jr.—1428(A)
 Spectrograph, multiple crystal, J. DuMond, H. Kirkpatrick 136(A); adjustments and tests, H. Kirkpatrick, J. DuMond—136(A)
 Spectrograph, vacuum, C. E. Howe—1428(A)
 Spectrometer, two-crystal, F. K. Richtmyer, S. W. Barnes, E. Ramberg—1428(A)
- Young's modulus**
 Under small stresses, D. K. Frohman—120(A), 264
- Zeeman effect**
 CaH bands, W. W. Watson, W. Bender—1440(A), 1513
 Hyperfine structure, Paschen-Back effect, S. Goudsmit, R. F. Bacher—129(A)
 $GdCl_3 \cdot 6H_2O$, line spectra of solid, Paschen-Back effect, S. Freed, F. H. Spedding—1408 (L)
 MgH $\lambda 5211$ band, G. M. Almy, F. H. Crawford, E. L. Hill—124(A)
 OH bands, G. M. Almy—1495
- Zodiacal light**
 Theory, E. O. Hulburt—295(A), 663(A), 1098